Volume Editor: Zvi Rappoport

The Chemistry of
Anilines

Part 1
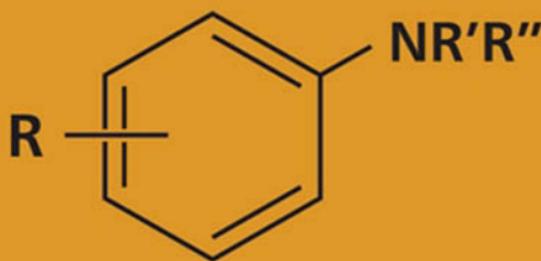
The chemistry of
Anilines

Patai Series: The Chemistry of Functional Groups

A series of advanced treatises founded by Professor Saul Patai and under the general editorship of Professor Zvi Rappoport

The **Patai Series** publishes comprehensive reviews on all aspects of specific functional groups. Each volume contains outstanding surveys on theoretical and computational aspects, NMR, MS, other spectroscopic methods and analytical chemistry, structural aspects, thermochemistry, photochemistry, synthetic approaches and strategies, synthetic uses and applications in chemical and pharmaceutical industries, biological, biochemical and environmental aspects.
To date, over 110 volumes have been published in the series.

Recently Published Titles

The chemistry of the Cyclopropyl Group (Volume 2)
The chemistry of the Hydrazo, Azo and Azoxy Groups (Volume 2, 2 parts)
The chemistry of Double-Bonded Functional Groups (Volume 3, 2 parts)
The chemistry of Organophosphorus Compounds (Volume 4)
The chemistry of Halides, Pseudo-Halides and Azides (Volume 2, 2 parts)
The chemistry of the Amino, Nitro and Nitroso Groups (2 volumes, 2 parts)
The chemistry of Dienes and Polyenes (2 volumes)
The chemistry of Organic Derivatives of Gold and Silver
The chemistry of Organic Silicon Compounds (2 volumes, 4 parts)
The chemistry of Organic Germanium, Tin and Lead Compounds (Volume 2, 2 parts)
The chemistry of Phenols (2 parts)
The chemistry of Organolithium Compounds (2 volumes, 3 parts)
The chemistry of Cyclobutanes (2 parts)
The chemistry of Peroxides (Volume 2, 2 parts)
The chemistry of Organozinc Compounds (2 parts)
The chemistry of Anilines (2 parts)

Forthcoming Titles

The Chemistry of Organomagnesium Compounds

The Patai Series Online

Starting in 2003 the **Patai Series** is available in electronic format on Wiley InterScience. All new titles will be published as online books and a growing list of older titles will be added every year. It is the ultimate goal that all titles published in the **Patai Series** will be available in electronic format.
For more information see under **Online Books** on:

www.interscience.wiley.com
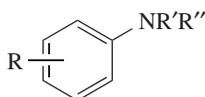
The chemistry of
Anilines

Part 1

Edited by

ZVI RAPPOPORT

The Hebrew University, Jerusalem

2007

Other Wiley Editorial Offices

John Wiley & Sons Inc., 111 River Street, Hoboken, NJ 07030, USA

Jossey-Bass, 989 Market Street, San Francisco, CA 94103-1741, USA

Wiley-VCH Verlag GmbH, Boschstr. 12, D-69469 Weinheim, Germany

John Wiley & Sons Australia Ltd, 42 McDougall Street, Milton, Queensland 4064, Australia

John Wiley & Sons (Asia) Pte Ltd, 2 Clementi Loop #02-01, Jin Xing Distripark, Singapore 129809

John Wiley & Sons Canada Ltd, 6045 Freemont Blvd, Mississauga, ONT, L5R 4J3, Canada

Wiley also publishes its books in a variety of electronic formats. Some content that appears
in print may not be available in electronic books.

Dedicated to

Itzik and **Tzipi**

and to

Silvio

Contributing authors

Daniella Vasconcellos Augusti	Agriculture National Laboratory/MG, Av. Romulo Joviano s/n, CEP 33600–000, Pedro Leopoldo/MG, Brazil, PO BOX 35/50. Fax: +55 31 3661 2383; e-mail: daniella.lanagro@yahoo.com.br
Rodinei Augusti	Department of Chemistry, Federal University of Minas Gerais—UFMG, 31270 901 Belo Horizonte, MG, Brazil. Fax: +55 31 34995700; e-mail: augusti@ufmg.br
Fabiola Barrios-Landeros	Department of Chemistry, Yale University, P.O. Box 208107, New Haven, Connecticut 06520 8107, USA.
Marcos N. Eberlin	ThoMSon Mass Spectrometry Laboratory, Institute of Chemistry, State University of Campinas, 13084 971 Campinas, SP, Brazil. Fax: +55 19 3521 3073; e-mail: eberlin@iqm.unicamp.br
Luciano Forlani	Dipartimento di Chimica Organica 'A. Mangini', University of Bologna, Viale Risorgimento 4, 40136, Bologna, Italy. Fax: +39 051 2093654; e-mail: forlani@ms.fci.unibo.it
Ryszard Gawinecki	University of Technology and Life Sciences, Faculty of Chemical Technology and Engineering, Seminaryjna 3, PL 85 326, Bydgoszcz, Poland. Fax: +48 52 3749005; e-mail: gawiner@utp.edu.pl
John F. Hartwig	Department of Chemistry, University of Illinois, 600 South Matthews Avenue, Urbana, Illinois, 61801, USA. Fax: +217 244 9248; e-mail: jhartwig@uiuc.edu
Jan S. Jaworski	Faculty of Chemistry, Warsaw University, 02-093 Warszawa, Poland. Fax: +48 22 822 5996; e-mail: jaworski@chem.uw.edu.pl
Marek K. Kalinowski	Faculty of Chemistry, Warsaw University, 02-093 Warszawa, Poland. Fax: +48 22 822 5996; e-mail: mkalin@chem.uw.edu.pl
Alla V. Koblik	ChemBridge Corporation, Malaya Pirogovskaya str., 1, 119435 Moscow, Russia. e-mail: semiluk@chembridge.ru
Erkki Kolehmainen	Department of Chemistry, P.O. Box 35, FIN-40014, University of Jyväskylä, Finland. Fax: +358 14 2602501; e-mail: ekolehma@jyu.fi

Ikchoon Lee   Department of Chemistry, Inha University, Inchon
                            402-751, Korea. Fax: +82 32 8654855; e-mail:
                            ilee@inha.ac.kr

Joel F. Liebman   Department of Chemistry and Biochemistry, University of
                            Maryland, Baltimore County, 1000 Hilltop Circle,
                            Baltimore, Maryland 21250, USA. Fax: +1 410 455 2608;
                            e-mail: jliebman@umbc.edu

Sergei M. Lukyanov   ChemBridge Corporation, Malaya Pirogovskaya str., 1,
                            119435 Moscow, Russia. Fax: +495 956 49 48; e-mail:
                            semiluk@chembridge.ru

Yizhak Marcus   Department of Inorganic and Analytical Chemistry, The
                            Hebrew University of Jerusalem, Jerusalem 91904, Israel.
                            Fax: +972 2 6585341; e-mail: ymarcus@vms.huji.ac.il

Minh Tho Nguyen   Department of Chemistry and Institute for Nanoscale
                            Physics and Chemistry, University of Leuven,
                            Celestijnenlaan 200F, B-3001 Leuven, Belgium. Fax: +32
                            16 32 7992; e-mail: minh.nguyen@chem.kuleuven.be

Borys Ośmiałowski   University of Technology and Life Sciences, Faculty of
                            Chemical Technology and Engineering, Seminaryjna 3, PL
                            85 326, Bydgoszcz, Poland. Fax: +48 52 3749005;
                            e-mail: borys.osmialowski@people.pl

Valery A. Ozeryanksii   Department of Organic Chemistry, Rostov State
                            University, Zorge str., 7, 344090, Rostov-on-Don, Russian
                            Federation. Fax: +7 863 2975146; e-mail:
                            vv_ozer2@rsu.ru

Alexander F. Pozharskii   Department of Organic Chemistry, Rostov State
                            University, Zorge str., 7, 344090, Rostov-on-Don, Russian
                            Federation. Fax: +7 863 2975146; e-mail:
                            apozharskii@rsu.ru

Shashank Shekhar   Department of Chemistry, Yale University, P.O.
                            Box 208107, New Haven, Connecticut 06520 8107, USA.

Qilong Shen   Department of Chemistry, Yale University, P.O.
                            Box 208107, New Haven, Connecticut 06520 8107, USA.

Suzanne W. Slayden   Department of Chemistry, George Mason University, 4400
                            University Drive, Fairfax, Virginia 22030, USA. Fax: +1
                            703 993 1055; e-mail: sslayden@gmu.edu

Dae Dong Sung   Department of Chemistry, Dong-A University, Busan
                            604-714, Korea. Fax: +82 51 2007259; e-mail:
                            ddsung@dau.ac.kr

Anthony S. Travis   Sidney M. Edelstein Center for the History and
                            Philosophy of Science, Technology and Medicine, The
                            Hebrew University of Jerusalem, Edmond J. Safra
                            Campus, Givat Ram, Jerusalem 91904, Israel. Fax: +972
                            2 6586709; e-mail: travis@cc.huji.ac.il

Jye-Shane Yang   Department of Chemistry, National Taiwan University,
                            Taipei, Taiwan (ROC), 10617. Fax: +886 2 23636359;
                            e-mail: jsyang@ntu.edu.tw

Jacob Zabicky   Department of Chemical Engineering, Ben-Gurion
                                 University of the Negev, P.O. Box 653, Beer-Sheva
                                 84105, Israel. Fax: +972 8 6472969; e-mail:
                                 zabicky@bgu.ac.il

Grażyna Maria Wójcik   Institute of Physical & Theoretical Chemistry, Wrocław
                                 University of Technology, Wyb. Wyspiańskiego 27,
                                 50-370 Wrocław, Poland. Fax: +071 483203364; e-mail:
                                 grazyna.m.wojcik@pwr.wroc.pl

Foreword

This is the second volume in 'The Chemistry of Functional Groups' series that deals with an aromatic functional group, following on from *The Chemistry of Phenols* published in 1993.

In the modern world there is no chemical functional group that has a longer and more varied history than the aromatic amino group. The organized scientific study of aromatic amines advanced greatly from the mid-1840s when August Wilhelm Hofmann began to develop his ammonia type theory. In this the simplest member, aniline, and its derivatives were expressed, by analogy, as compounds in which hydrogen atoms of ammonia were successively replaced by other atoms or groups of atoms. The study of these compounds, now conveniently labeled as anilines, received a tremendous stimulus after 1856, when the teenaged chemical inventor William Henry Perkin discovered the first aniline dye, later known as mauve. During the second half of the 19th century the anilines revolutionized the study of chemistry, led to the inauguration of industrial research laboratories and helped forge academic-industrial collaborations. As agents of modernity, anilines and their derivatives forced changes in patent law, fostered technology transfer and stimulated the emergence of the modern chemical industry. They contributed to the discovery of pharmaceutical products and new agrochemicals. Hence, there is reason enough for a historical review of the role of the anilines in the development of what was undoubtedly the first high-tech science-based industry, especially since 2006 marks the 150th anniversary of the beginning of the chemical industry based on anilines, following Perkin's discovery.

The two parts of the present volume consist of 17 chapters written by experts from 10 countries. They start with historical background, followed by chapters on the theory, structure, thermochemistry, photophysics and photochemistry and electrochemistry of anilines, on their mass spectrometry, NMR spectra and analysis and on their modern syntheses by transition metal catalysed processes. Other chapters deal with their rearrangements, their reactivity as nucleophiles, their use as solvatochromic probes, their hydrogen bonded complexes, and their versatile uses in the chemical industry, and the relevant topic of toxicity and environmental aspects. A chapter on a special group of anilines—the proton sponges—ends the book.

A few promised chapters on the acidity of anilines, on polyanilines and on radical cations of triarylamine and phenylenediamine were not delivered. We hope to include these chapters in a future supplementary volume.

The literature coverage of most chapters is up to 2005.

I would be grateful to readers who draw my attention to mistakes or to missing topics in the present volume.

Jerusalem   Zvi Rappoport
October, 2006

The Chemistry of Functional Groups
Preface to the series

The series 'The Chemistry of Functional Groups' was originally planned to cover in each volume all aspects of the chemistry of one of the important functional groups in organic chemistry. The emphasis is laid on the preparation, properties and reactions of the functional group treated and on the effects which it exerts both in the immediate vicinity of the group in question and in the whole molecule.

A voluntary restriction on the treatment of the various functional groups in these volumes is that material included in easily and generally available secondary or tertiary sources, such as Chemical Reviews, Quarterly Reviews, Organic Reactions, various 'Advances' and 'Progress' series and in textbooks (i.e. in books which are usually found in the chemical libraries of most universities and research institutes), should not, as a rule, be repeated in detail, unless it is necessary for the balanced treatment of the topic. Therefore each of the authors is asked not to give an encyclopaedic coverage of his subject, but to concentrate on the most important recent developments and mainly on material that has not been adequately covered by reviews or other secondary sources by the time of writing of the chapter, and to address himself to a reader who is assumed to be at a fairly advanced postgraduate level.

It is realized that no plan can be devised for a volume that would give a complete coverage of the field with no overlap between chapters, while at the same time preserving the readability of the text. The Editors set themselves the goal of attaining reasonable coverage with moderate overlap, with a minimum of cross-references between the chapters. In this manner, sufficient freedom is given to the authors to produce readable quasi-monographic chapters.

The general plan of each volume includes the following main sections:

(a) An introductory chapter deals with the general and theoretical aspects of the group.

(b) Chapters discuss the characterization and characteristics of the functional groups, i.e. qualitative and quantitative methods of determination including chemical and physical methods, MS, UV, IR, NMR, ESR and PES—as well as activating and directive effects exerted by the group, and its basicity, acidity and complex-forming ability.

(c) One or more chapters deal with the formation of the functional group in question, either from other groups already present in the molecule or by introducing the new group directly or indirectly. This is usually followed by a description of the synthetic uses of the group, including its reactions, transformations and rearrangements.

(d) Additional chapters deal with special topics such as electrochemistry, photochemistry, radiation chemistry, thermochemistry, syntheses and uses of isotopically labeled compounds, as well as with biochemistry, pharmacology and toxicology. Whenever applicable, unique chapters relevant only to single functional groups are also included (e.g. 'Polyethers', 'Tetraaminoethylenes' or 'Siloxanes').

This plan entails that the breadth, depth and thought-provoking nature of each chapter will differ with the views and inclinations of the authors and the presentation will necessarily be somewhat uneven. Moreover, a serious problem is caused by authors who deliver their manuscript late or not at all. In order to overcome this problem at least to some extent, some volumes may be published without giving consideration to the originally planned logical order of the chapters.

Since the beginning of the Series in 1964, two main developments have occurred. The first of these is the publication of supplementary volumes which contain material relating to several kindred functional groups (Supplements A, B, C, D, E, F and S). The second ramification is the publication of a series of 'Updates', which contain in each volume selected and related chapters, reprinted in the original form in which they were published, together with an extensive updating of the subjects, if possible, by the authors of the original chapters. Unfortunately, the publication of the 'Updates' has been discontinued for economic reasons.

Advice or criticism regarding the plan and execution of this series will be welcomed by the Editors.

The publication of this series would never have been started, let alone continued, without the support of many persons in Israel and overseas, including colleagues, friends and family. The efficient and patient co-operation of staff-members of the Publisher also rendered us invaluable aid. Our sincere thanks are due to all of them.

The Hebrew University   SAUL PATAI
Jerusalem, Israel   ZVI RAPPOPORT

Sadly, Saul Patai who founded 'The Chemistry of Functional Groups' series died in 1998, just after we started to work on the 100th volume of the series. As a long-term collaborator and co-editor of many volumes of the series, I undertook the editorship and I plan to continue editing the series along the same lines that served for the preceeding volumes. I hope that the continuing series will be a living memorial to its founder.

The Hebrew University   ZVI RAPPOPORT
Jerusalem, Israel
May 2000

Contents

List of abbreviations used

Ac	acetyl (MeCO)
acac	acetylacetone
Ad	adamantyl
AIBN	azoisobutyronitrile
Alk	alkyl
All	allyl
An	anisyl
Ar	aryl
Bn	benzyl
Bu	butyl (C_4H_9)
Bz	benzoyl (C_6H_5CO)
CD	circular dichroism
CI	chemical ionization
CIDNP	chemically induced dynamic nuclear polarization
CNDO	complete neglect of differential overlap
Cp	η^5-cyclopentadienyl
Cp*	η^5-pentamethylcyclopentadienyl
DABCO	1,4-diazabicyclo[2.2.2]octane
DBN	1,5-diazabicyclo[4.3.0]non-5-ene
DBU	1,8-diazabicyclo[5.4.0]undec-7-ene
DIBAH	diisobutylaluminium hydride
DME	1,2-dimethoxyethane
DMF	*N,N*-dimethylformamide
DMSO	dimethyl sulfoxide
ee	enantiomeric excess
EI	electron impact
ESCA	electron spectroscopy for chemical analysis
ESR	electron spin resonance
Et	ethyl
eV	electron volt
Fc	ferrocenyl
FD	field desorption

FI	field ionization
FT	Fourier transform
Fu	furyl(OC_4H_3)
GLC	gas liquid chromatography
Hex	hexyl(C_6H_{13})
c-Hex	cyclohexyl(c-C_6H_{11})
HMPA	hexamethylphosphortriamide
HOMO	highest occupied molecular orbital
HPLC	high performance liquid chromatography
i-	iso
ICR	ion cyclotron resonance
Ip	ionization potential
IR	infrared
LAH	lithium aluminium hydride
LCAO	linear combination of atomic orbitals
LDA	lithium diisopropylamide
LUMO	lowest unoccupied molecular orbital
M	metal
M	parent molecule
MCPBA	*m*-chloroperbenzoic acid
Me	methyl
MNDO	modified neglect of diatomic overlap
MS	mass spectrum
n	normal
Naph	naphthyl
NBS	*N*-bromosuccinimide
NCS	*N*-chlorosuccinimide
NMR	nuclear magnetic resonance
Pen	pentyl(C_5H_{11})
Ph	phenyl
Pip	piperidyl($C_5H_{10}N$)
ppm	parts per million
Pr	propyl (C_3H_7)
PTC	phase transfer catalysis or phase transfer conditions
Py, Pyr	pyridyl (C_5H_4N)
R	any radical
RT	room temperature
s-	secondary
SET	single electron transfer
SOMO	singly occupied molecular orbital

t-	tertiary
TCNE	tetracyanoethylene
TFA	trifluoroacetic acid
THF	tetrahydrofuran
Thi	thienyl(SC_4H_3)
TLC	thin layer chromatography
TMEDA	tetramethylethylene diamine
TMS	trimethylsilyl or tetramethylsilane
Tol	tolyl(MeC_6H_4)
Tos or Ts	tosyl(*p*-toluenesulphonyl)
Trityl	triphenylmethyl(Ph_3C)
Xyl	xylyl($Me_2C_6H_3$)

In addition, entries in the 'List of Radical Names' in *IUPAC Nomenclature of Organic Chemistry*, 1979 Edition, Pergamon Press, Oxford, 1979, p. 305–322, will also be used in their unabbreviated forms, both in the text and in formulae instead of explicitly drawn structures.

Anilines: Historical background

ANTHONY S. TRAVIS

Sidney M. Edelstein Center for the History and Philosophy of Science, Technology and Medicine, The Hebrew University of Jerusalem, Edmond J. Safra Campus, Givat Ram, Jerusalem 91904, Israel
Fax: +972 2 6586709;   e-mail: travis@cc.huji.ac.il

I. INTRODUCTION

One-hundred-and-fifty years ago, in March 1856, a teenaged chemical inventor in London, England, discovered in his makeshift home laboratory a process that converted aniline, made in two steps from coal-tar benzene, into a purple dyestuff, or colorant. The young man was William Henry Perkin, assistant to the German chemist August Wilhelm Hofmann, then head of the Royal College of Chemistry. From Perkin's single serendipitous discovery the anilines went on to become a generic class of organic chemicals that would make tremendous contributions to material well-being. Quite apart from providing routes to synthetic dyestuffs—that were also called 'anilines'—pharmaceuticals, products for the processing of rubber, and new polymers, the anilines revolutionized the study of chemistry, led to the inauguration of industrial research laboratories, and helped forge academic–industrial collaborations. It is difficult to convey now the day-to-day excitement that infused the academic and industrial laboratories that pursued the anilines during the half century following Perkin's discovery. The endeavor made reputations and attracted the greatest stars of organic chemistry, including August Wilhem Hofmann, Adolf Baeyer and Emil Fischer. No less profound were the economic and political consequences. The anilines and their derived colorants, as agents of modernity, forced changes in patent law, fostered technology transfer, stimulated the emergence of the modern chemical industry and decimated cultivation of dye-yielding plants. Aniline products contributed to the growth of Germany as a major economic power, to the extent that successors to the early coal-tar dye companies enabled Germany to wage world war twice in the 20th century. After the aniline dye industry was adopted by the US, from 1915, its mode of applied research led to the discovery of synthetic polymers and new agrochemicals. Apart from the intrinsic chemical interest in the early story of aniline and its products, these few facts make a compelling reason for the inclusion of a historical introduction to the anilines.

In this chapter, with its emphasis on historical events and chemists engaged in both academic and industrial investigations, first names of participants are given wherever possible. Also, many trivial and common names of products are retained, in order to aid understanding of the historical literature and earlier textbooks. Several are still in common usage, particularly for the aminonaphthalenesulfonic acids that are known by special names rather than by their structural designations. In accord with common usage, lower case letters are used for what have become both generic and trademark names, such as Bismarck brown, chrysoidine, mauve, mauveine and rosaniline. However, capitals are used for arcane names, to avoid confusion, for example, between Benzidin and benzidine, as well as for more recent trade names, mainly for products introduced from around 1940.

This chapter also revisits some of the major chemical firms of former times that were completely transformed at the end of the 20th century. Reflecting the former importance of, and prestige associated with, aromatic amines, a number included the word Aniline in their corporate titles, notably, in Germany, Badische Anilin- & Soda Fabrik (BASF) and Aktiengesellschaft für Anilinfabrikation (AGFA), in the US, General Aniline and Film (GAF) and National Aniline & Chemical Co. (NACCO), and in the UK, CIBA's Clayton Aniline Company Limited. Extensive and ongoing historical studies into the aniline dye industry are today stimulated by the fact that it was the first high-technology industry, and became the exemplar of all science-based industries. Moreover, and despite the decline in its use for colorants, the manufacture of aniline is still carried out on a vast scale for the production of polyurethanes.

II. IDENTIFYING ANILINE

The feebly basic oil that we now call aniline (**1**) was perhaps first handled, though not identified, during the 18th century by the French chemists and dye experts Jean Hellot

(in 1740) and Lepileur d'Apligny. The raw material for their experiments was the leaf of the indigo plant that afforded a blue dye. What is certain is that in 1826, by destructive distillation of indigo (2), the German chemist Otto Unverdorben isolated a substance that he called Krystallin. During the next 15 years the same base would be independently obtained by several investigators. Friedrich Ferdinand Runge in 1834 extracted what he called Cyanol, or Kyanol, from coal tar. The indigo connection remained important. In 1841, Jean Baptiste André Dumas established a formula for the indigo colorant (C_8H_5NO), and Auguste Laurent and Otto Linné Erdmann independently isolated the oxidation products isatin (3) and isatic acid[1] (Scheme 1).

SCHEME 1

Laurent and Erdmann oxidized isatin, from which they obtained anthranilic acid (4). Carl Julius Fritzsche (also known as Iulii Federovich Fritsshe) in 1840 subjected anthranilic acid to alkaline distillation and obtained 'a powerful base, devoid of oxygen', that he called Anilin, from anil, the Portuguese word for indigo, which in turn had been derived from Arabic and Sanskrit. In 1842, the Russian chemist Nikolai N. Zinin reduced, with hydrogen sulfide, Nitrobenzid (nitrobenzene) to what was called Benzid (also Benzidam,

and later Benzidin) (Scheme 1). Fritsche drew attention to the identities of Anilin and Benzid. From nitronaphthalene, Zinin obtained Naphthalid (an aminonaphthalene). During 1844–1846 he reported reduction of dinitrobenzene to diaminobenzene with ammonium sulfide, reduction of dinitronaphthalene and the synthesis of the diaminobiphenyl (benzidine) from nitrobenzene. Zinin also reported azoxybenzene[2].

Zinin was a former student at Giessen of Justus Liebig, who investigated the chemical constitution of indigo, as well as other natural products. Liebig also undertook studies into novel raw materials from which useful products might be derived. Of particular interest around 1840 was the vast amount of coal-tar waste available from coal-gas works and distilleries. Ernst Sell, a former student of Liebig, owned a coal distillery and sent samples of the tar to Giessen for further study. It was Liebig's practice to assign research projects to his students, including, around 1837, August Wilhelm Hofmann (Figure 1). Hofmann extracted several nitrogen-containing oils from coal tar by trituration with acid. He showed that of these bases the one present in greatest abundance was identical with the product earlier obtained from isatin and Zinin's Benzidin. Hofmann preferred the name Krystallin, but the chemical community chose aniline (though aminobenzene, phenylamine, as well as the more modern benzeneamine have been used). Hofmann's results were published in 1843 and became the foundation for his life's work and international reputation[3].

Among many other experiments that Hofmann undertook with aniline was treatment of the indigo-derived base with chlorine. He identified the products. They were used to demonstrate that the two main rival theories of chemical combination were entirely compatible. These were the electrochemical theory of attraction of Jöns Jacob Berzelius and the substitution theory of Jean Baptiste André Dumas. This work was published in 1845 when Hofmann was at Bonn[4]. Hofmann then moved on to synthesis of aniline in
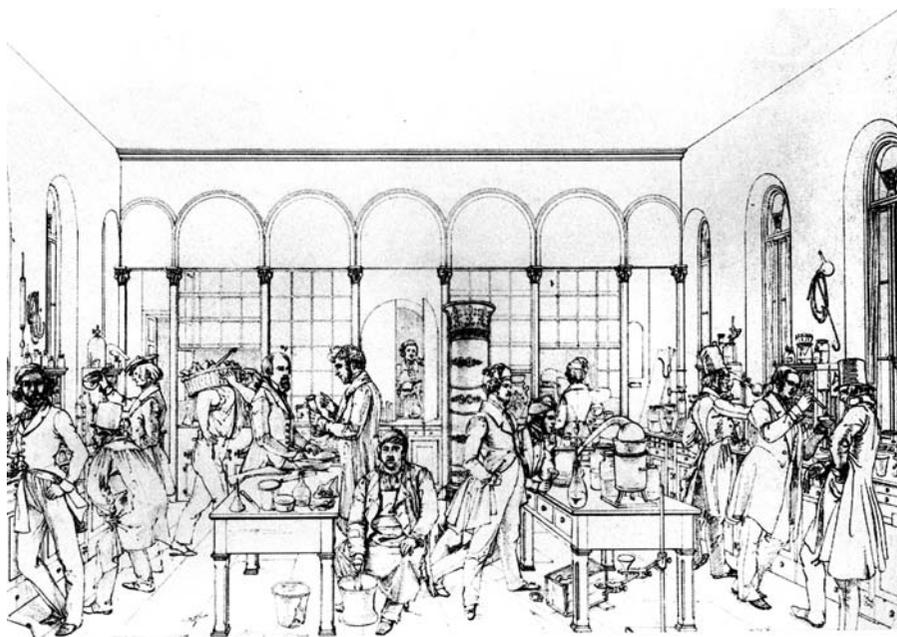
FIGURE 1. The Giessen laboratory of Justus Liebig, *ca* 1840. August Wilhelm Hofmann at extreme right (with top hat). Edelstein Collection

two steps from coal-tar benzene, first nitration, second reduction. He also collaborated with Liebig and others in an attempt to produce a quinine substitute.

In 1845 also, at Liebig's instigation, Hofmann moved to London to head the new Royal College of Chemistry. There he continued his studies into aniline and its reactions. Through this work he made major contributions to constitutional formulae. At that time, thirteen years before quadrivalent carbon was drawn, there were no modern structural formulae, only so-called type formulae. These indicated chemical constitutions and were used as a system of classification. Type formulae were based on simple compounds, such as water and methane. Significantly, Adolphe Wurtz had indicated that methyl and ethyl amines might be considered derivatives of ammonia. Hofmann extended this to organic bases in general, by comparing aniline with ammonia, and also with a compound discovered in 1834 by Liebig and called melamine. Hofmann demonstrated that the three hydrogens of ammonia, and those of the ammonium radical, could be replaced to give primary, secondary and tertiary amines, and quarternary ammonium derivatives. From these results he developed what in 1850 he would call the ammonia type theory. With this, it was now possible to classify organic bases using a formula that, as with the other type formulas, separated one atom, in this case nitrogen, with a bracket from other atoms and groups of atoms. Thus aniline was an ammonia derivative in which one hydrogen was replaced by what we now call an aryl group. This is in keeping with the modern definition of aromatic amines, in which the remaining two hydrogens are replaceable by aryl or alkyl groups[5].

III. THE ANILINE DYES

Despite the availability of methods for extracting aniline from coal tar, this source hardly provided an abundant supply of the aromatic amine. Some chemists worked on the development of the two-step synthesis from coal-tar benzene. They included Hofmann's assistant Charles Blachford Mansfield, who pioneered the separation by distillation of coal-tar hydrocarbons, undertook nitration of benzene, and reduction of the nitrobenzene, probably by the method of Zinin. Mansfield's experiments came to an abrupt end early in 1855 when, while preparing samples for the Paris International Exhibition, a still in his laboratory caught fire. He was badly burned and died in hospital a few days later.

Hofmann introduced to the college a new method for reducing nitrobenzene, based on the use of iron and glacial acetic acid as the source of reducing hydrogen, as first described by André Béchamp in 1854. It was put to good use by several of Hofmann's students, including William Henry Perkin, who had entered the college in 1853, at the age of fifteen (Figure 2). Perkin showed a remarkable industriousness. In 1856, he created the first synthetic dye made from aniline. It is worth considering how he got there.

In the mid-1850s, there was great interest in quinine, much needed to control malaria among the British colonists. Hofmann reasoned that it might be synthesized from coal-tar naphthalene. Perkin decided, instead, to start with allyltoluidine, through oxidative condensation. The reaction, undertaken at home in his primitive laboratory during the 1856 Easter vacation, failed. However, he wisely decided to repeat the experiment using the simplest aromatic amine, aniline, that was known to be sensitive to the action of oxidants. The result of treating it with dichromate was a mixture from which an alcoholic extract colored a piece of silk a brilliant, and persistent, purple. It spread like an uncontrollable stain, coloring everything that it touched. This triggered an immediate response. Perkin recognized the potential as a dyestuff, particularly since the color was not fugitive, as was the case for other important purple dyes, namely the semi-synthetic murexide (Roman purple) and lichen-derived products. The teenaged inventor filed a patent for his process, resigned from the college and, with the backing of his brother and father, set up a

6

FIGURE 2. August Wilhelm Hofmann and students at the Royal College of Chemistry, London, *ca* 1855. William Henry Perkin is in the back row, fifth from right. Edelstein Collection

JOURNAL OF THE SOCIETY OF ARTS.
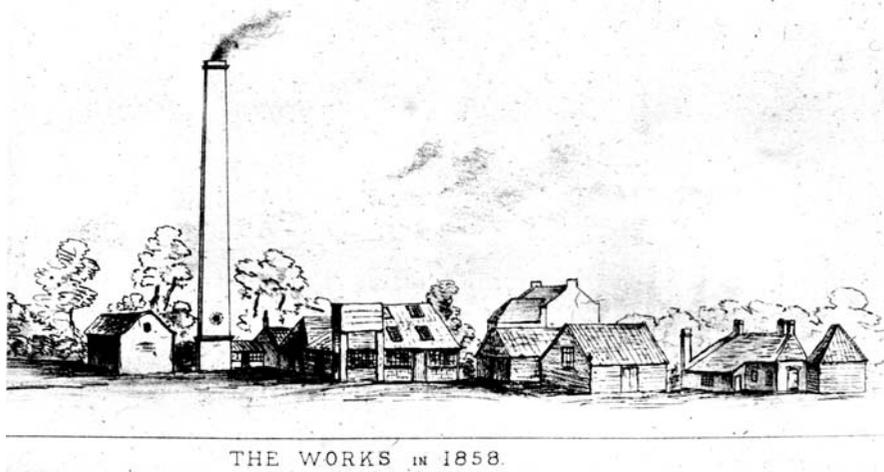
THE WORKS IN 1858.

FIGURE 3. The works of Perkin & Sons, Greenford Green, northwest London, 1858. From a sketch by William Henry Perkin. Edelstein Collection

small factory at Greenford Green, northwest of London, to manufacture his novel product (Figure 3). There from 1858, coal tar was distilled to provide a mixture of aromatic hydrocarbons, mainly, if not exclusively, it was believed, benzene. By successive nitration of benzene to nitrobenzene, with mixed sulfuric and nitric acids, reduction of the nitro compound to aniline, with iron and acid, and oxidation, the colorant was obtained. The working conditions in the small buildings were far from salubrious. Originally the nitration and reduction apparatus was made of glass, but soon hand-cranked horizontal iron reactors were introduced. The aniline purple was a success with silk dyers, and once a number of fixing agents, or mordants, for cotton, were developed, the highly fashionable synthetic colorant, originally marketed as Tyrian purple, was quickly adopted by calico printers. By 1859, the aniline-derived colorant was the main color of fashion among the ladies of Britain and France. The English gave the aniline purple a new name, mauve, from the French word for the mallow flower. Perkin prepared crystalline salts of the principal component of his colorant, which in 1863 he called mauveine[6]. The correct structure, **5**, was established only in 1994[7], showing how mauveine arose from the presence of toluidines in the impure aniline.

Commercial success made a fortune for Perkin (Figure 4). It also stimulated further investigations into reactions of aniline that might yield other colorants. At the end of 1859, an aniline red (**6**), made by treating what was believed to be aniline alone with stannic chloride, was discovered in Lyon by François Emmanuel Verguin. A more successful process was discovered by two of Hofmann's former students in London, Henry Medlock and Edward Chambers Nicholson (Figure 5), who independently treated aniline with arsenic acid. The red colorant was known as fuchsine in France and magenta in England. Nicholson, a partner in the London chemical manufacturing firm of Simpson, Maule
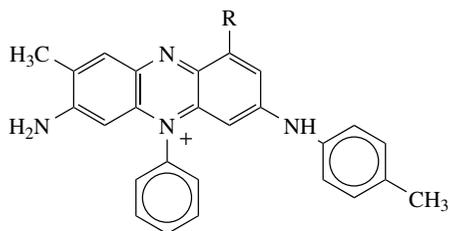
mauveine
(Tyrian purple, aniline purple)
R = H
R = CH₃ (minor component)
(5)
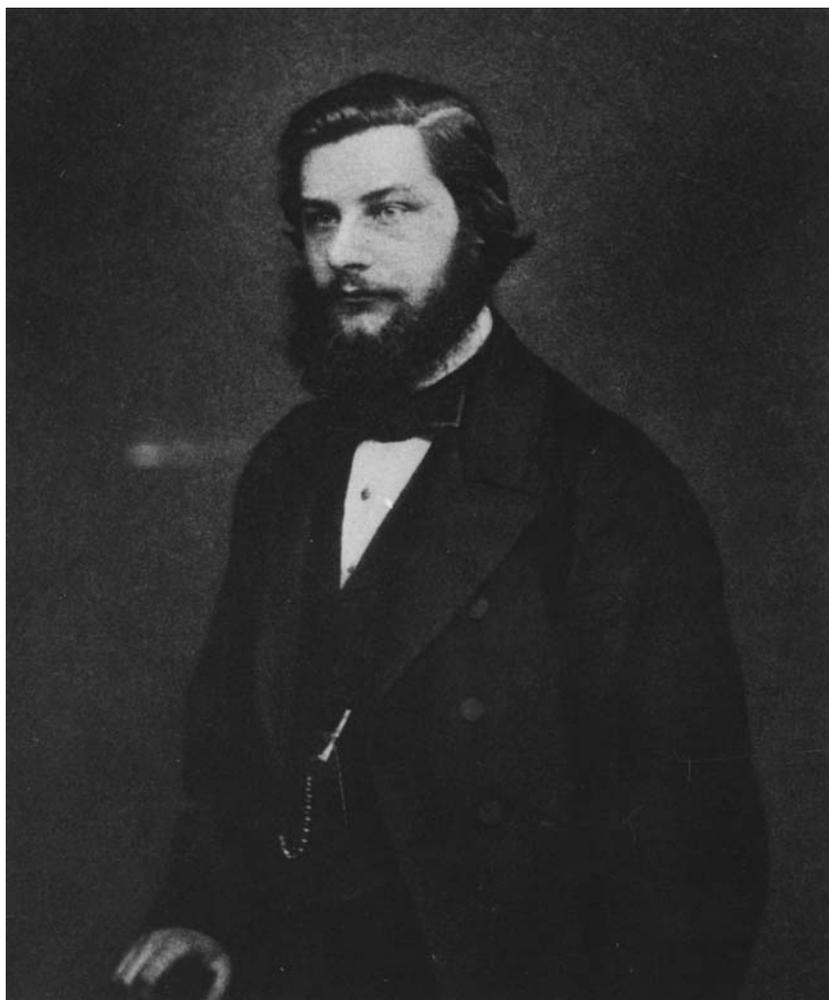
FIGURE 4. William Henry Perkin (1838–1907), in 1860. Edelstein Collection

FIGURE 5. Edward Chambers Nicholson (1827–1890). Edelstein Collection

& Nicholson, developed processes for the successful bulk production of nitrobenzene and aniline in batteries of closed iron reactors fitted with power-driven stirrers (Figure 6). For aniline, Nicholson adopted the Béchamp reduction process and introduced steam into the reaction mixture by employing a hollow stirrer tube. The product aniline was obtained by distilling with steam after the addition of lime. Within a few years the standard reduction mixture became iron filings and hydrochloric acid. Production improvements and better quality benzene enabled aniline to be obtained in 90–95% yield.

Hofmann's great interest in aniline dyes began in 1860, when one of his 1858 publications was used as evidence in a French patent dispute concerning alleged infringement of monopoly rights related to aniline red[8]. The publication stated that a red color appeared when aniline was treated with carbon tetrachloride, and therefore, it was claimed, Hofmann was the scientific discoveror of aniline red. Soon after, he was called in as a consultant to aid Simpson, Maule & Nicholson. In 1861, Hofmann began to investigate this firm's aniline red, from which he obtained a number of salts. Analysis indicated that it was a

FIGURE 6. Early reactors for conversion of benzene to nitrobenzene (left) and reduction of nitrobenzene to aniline (right). (Charles Girard and Georges de Laire, *Traité des dérivés de la houille*, Paris: G. Masson, 1873, plate II)

condensation product of three anilines. Hofmann called the free base rosaniline (1862)[9]. Intriguingly there were two more carbon atoms than condensation of three anilines would allow (6). Their presence could not then be explained.

The new aniline dye companies in Europe displayed their wares at the 1862 London International Exhibition, where Hofmann, as juror, acquired a number of samples. They included a blue (7) discovered, almost by chance, by two French chemists working near London in 1861. It had first appeared when excess aniline was erroneously added to the aniline red reaction mixture. E. C. Nicholson in 1862 treated the aniline blue with sulfuric acid to yield a more valuable product, the soluble alkali blue, later better known as CI [Colour Index] Pigment Blue 61. In May 1863, Hofmann found that the aniline blue was a substitution product of aniline red in which three phenyl groups had replaced three hydrogens (Scheme 2). This immediately suggested that other substituted derivatives might be made and perhaps even provide new aniline dyes. Alkylation with ethyl iodide showed that this was indeed correct. Hofmann achieved stepwise replacement of three hydrogens to afford colorants that were, successively, reddish violet, violet blue and then violet, what were soon known as the Hofmann's violets (8). Hofmann next turned to the aniline red process, and found that the colorant was formed not from aniline alone

$$C_{20}H_{19}N_3 \cdot HCl \quad + \quad 3C_6H_5NH_2 \quad = \quad C_{20}H_{16}(C_6H_5)_3N_3 \cdot HCl \quad + \quad 3NH_3$$

rosaniline salt   +   aniline   =   salt of aniline blue

                                                   (7)

aniline red
(magenta, fuchsin)

               (6)

SCHEME 2. Formation of salt of aniline blue, constitutional formulas, 1860s (**7**)

FIGURE 7. Manufacture of aniline blue by phenylation (arylation) of amino groups in aniline red (magenta, fuchsine), 1860s. Edelstein Collection

$$N_3, H_2O \left\{ \begin{array}{l} C_6H_4 \\ (C_7H_6)_2 \\ H_3 \end{array} \right. \longrightarrow N_3, H_2O \left\{ \begin{array}{l} C_6H_4 \\ (C_7H_6)_2 \\ (C_6H_5)_3 \end{array} \right.$$

aniline red   aniline blue
(Verguin, 1859)   (Girard and de Laire, 1861)

(6)   **(7)**

$$N_3, H_2O \left\{ \begin{array}{l} C_6H_4 \\ (C_7H_6)_2 \\ (C_2H_5)_3 \end{array} \right.$$

aniline violet(s)
(Hofmann, 1863)

(8)

SCHEME 3. Modified ammonia type constitutional formulas for aniline dyes

but from a mixture of aniline and toluidine (its isomers were identified only later). This explained the presence of the two additional carbon atoms in the formula of aniline red. Hofmann then returned to the various derivatives of the red. He was intrigued by the fact that while it had not been possible to prepare phenyl-substituted anilines in the laboratory, industrialists were producing phenyl derivatives of aniline red (Figure 7). Degradative distillation of Hofmann's violets gave ethylated aniline, confirming that the violets were made by replacing hydrogens. More significant was the fact that basic oils

$$
\left.\begin{array}{c} C_6H_5 \\ C_6H_5 \\ H \end{array}\right\} N
$$
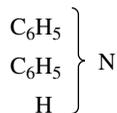
diphenylamine,
ammonia type formula

(9)

from aniline blue under the same degradative conditions gave diphenylamine, the simplest diaryl amine **9**. Therefore, Hofmann reasoned, the aniline red, blues and violets were all members of a family based on his modified ammonia type (Scheme 3). Given the circumstances, particularly the lack of understanding of the constitutions of aromatic substances, the drawing up of partial constitutional formulas based on the ammonia type was a major breakthrough. In the published formulas, superscript primes indicated the number of replaceable hydrogens. This form of notation had been introduced in the 1850s and contributed to ideas about valency, a term introduced in 1865, as was Kekulé's benzene ring theory. Hofmann's formulas became essential guides for further research and stimulated the early emergence of theory-based chemical invention[10]. Even at this stage, Hofmann realized that the introduction of aryl and alkyl groups involved replacement of amino group hydrogens.

Though the synthetic dye industry was based in England and France, the new discoveries were quickly copied in Germany and Switzerland. The outcomes of patent litigation in Paris and London led to the decline of the British and French industries and, because of the absence of a comprehensive patent system in the German states, assisted the growth of the German dye industry, including forerunners of AGFA, BASF, Bayer and Hoechst.
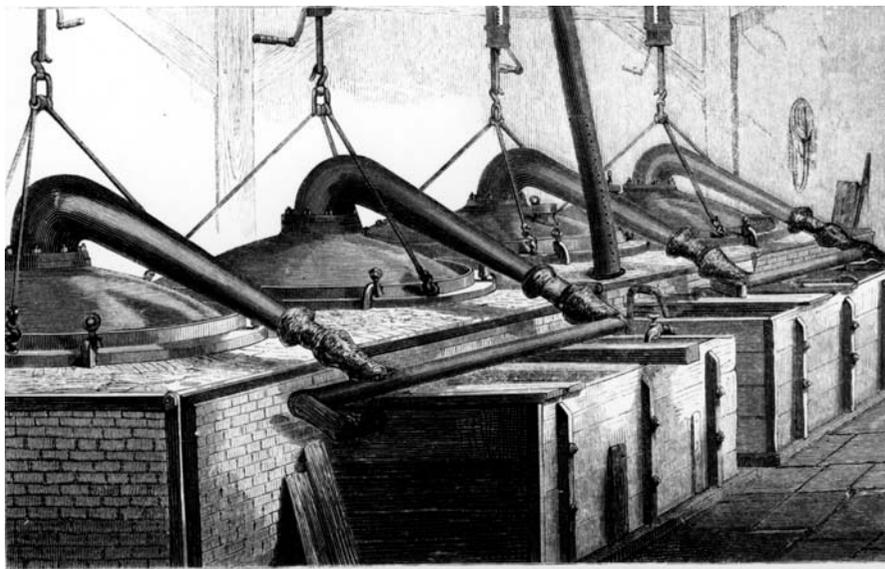
FIGURE 8. Plant for distillation of *N*,*N*-dimethylaniline, 1860s. Edelstein Collection

Swiss entrepreneurs, including those whose enterprises would later be known as CIBA and Geigy, also benefited from the absence of a patent system. The patent suits in England and France and environmental difficulties created by the waste of dye-making did, however, encourage new ways of making aniline dyes. Thus from 1866, the hydrogens of the amino group in aniline were replaced in industrial processes by alkylation and phenylation to provide intermediates, the *N*-alkylated and *N*-phenylated anilines, respectively, that were to become important in dye manufacture (Figure 8). These intermediates enabled the circumvention of patent monopolies, since they could be converted directly into violets and blues, respectively. The processes also avoided the use of arsenic acid, the main oxidant used to prepare aniline red, the original intermediate from which the blues and violets were obtained. Severe environmental problems arising from the use of arsenic acid brought about its replacement by nitrobenzene, based on Jean Théodore Coupier's process (1867). This led to the discovery of the black colorant called nigrosine. From 1865, the year in which Hofmann left London to take up a post as professor at the University of Berlin, the synthetic dye industry, based on aniline, that had originated in England and flourished for a time in France, moved increasingly to Germany, aided, as we shall see, by the benzene ring theory, the creation of a modern industrial infrastucture and a novel patent system[11].

IV. TECHNOLOGY TRANSFER

The one individual most responsible for the transfer of aryl amine science and technology to Germany was Heinrich Caro (Figure 9). This German textile colorist and chemical inventor, while working in Manchester at the firm of Roberts, Dale & Co. during 1859–1866, adopted mechanized equipment for manufacture of nitrobenzene and aniline and developed an alternative oxidation process for mauve. Caro's training as a colorist in the calico (cotton) printing industry enabled him to fully appreciate the technical challenges of dye application, and through this he facilitated the smooth transition from natural to artificial colorants. Among his many achievements in Manchester, which included a reputation among English and Scottish dye users that would be put to good use in Germany, was the development of an aniline black, extracted from the residue of his mauve process[12]. Elsewhere in Lancashire aniline black processes were invented, one by John Lightfoot that involved direct application of aniline during the cotton printing process, and another by Frederick Crace Calvert[13,14]. The latter was less successful, though the product, known as emeraldine, would come to prominence with the development of polyanilines in the 1990s.

At the end of the 1850s, Roberts, Dale & Co. had set out to capture some of the synthetic dye market. This was achieved with varying degrees of success between 1860 and 1866 by exploiting colorant-producing reactions of aniline, toluidines (methylanilines), naphthylamine and phenol. By 1864, through Caro's network of contacts, the firm had accumulated a remarkable selection of German chemists and colorists, including Hofmann's former assistant in London, Carl A. Martius. The main effort was presided over by the John Bull-like figure of John Dale senior who, on arriving at the works laboratory each day, would reputedly ask: 'Well Dr. Martius, well Caro, have you got anything fresh to show me?'[15]. The investigations and inventions based on aniline and its congeners carried all the hallmarks of a new high-technology industry in the making. By the mid-1860s, through these and other endeavors, mauve had been displaced by the newer aniline dyes. However, mauve saw extensive use in wallpaper and paper printing and, through Caro's efforts, in the printing of postage stamps, probably its last commercial application[16].

Manufacture of the aniline red with arsenic acid underwent extensive improvement at Roberts, Dale & Co. in the hands of the German chemist and colorist August Leonhardt, who developed a process for recovery and reuse of the arsenic acid. This overcame the

FIGURE 9. Heinrich Caro (1834–1910). Edelstein Collection

sort of environmental problems that had created difficulties in France and Switzerland. Leonhardt's process was so successful that he continued to promote its introduction after returning to Germany, first with Meister, Lucius & Co. (later Hoechst), then in partnership with Leo Gans, making aniline dyes for Cassella and, finally, for his own company established at the end of the 1870s. Leonhardt claimed advantages over Coupier's nitrobenzene oxidation process that had found great favor after 1870. In particular, Leonhardt noted that the acidic conditions under which Coupier's process was conducted caused rapid destruction of the expensive wrought iron reactors, which was not the case when the less corrosive arsenic acid was used[17].

Following the protracted patent litigation in London, the production of aniline red, blues and violets was controlled by Simpson, Maule & Nicholson. This stimulated Caro to investigate alternative processes and different reactions of aniline and other amino compounds, as well as coal-tar phenol (carbolic acid), then recently available in Manchester as a pure product, following the work of Crace Calvert. During 1862, Caro showed great interest in the reactions of phenol that afforded colorants, particularly the red known as rosolic acid, made from phenol, oxalic acid and sulfuric acid. Caro's collaborator was the chemist James Alfred Wanklyn. The studies of Caro and Wanklyn on both phenol- and aniline-based colorants and their formulas would turn out to be critically important contributions to the eventual structural elucidation of the aniline dyes. This happened after Caro, through his close familiarity with rosolic acid, aniline dyes and the diazo reaction, was enabled to make a singularly major contribution to the chemical understanding of the constitutions of both aniline and phenol dyes. The results showed unequivocally that the constitutions of rosaniline (the base of aniline red) and rosolic acid were similar. Wanklyn speculated that both rosaniline and rosolic acid (and their derivatives) belonged to what he called the 'ethylene type'.

In 1864, ethylene was first expressed graphically in its modern form with a double bond connecting the two carbon atoms ($CH_2=CH_2$). This was adopted by Wanklyn to represent the constitutional formula of rosaniline (**6**), and made public in September of that year at the annual meeting of the British Association for the Advancement of Science, held in Bath. Wanklyn's ethylene-type formula showed two carbon atoms separated from the four hydrogen atoms by a bracket[18]. The ethylene type, unlike other type formulas, was used only to express the constitutions of coal-tar dyes. Wanklyn argued that the constitutions of the members of the rosaniline series could be expressed by his ethylene type by virtue of known reduction and replacement reactions. Thus he compared the conversion of **6** into colorless leucaniline (**10**) with the ready reduction of ethylene (ethene) (**11**) to ethane (**12**), both of which involved the addition of two hydrogen atoms (Scheme 4)[19−21].

Wanklyn stated, as would Hofmann a few weeks later, that the replaceable hydrogens in rosaniline were attached to nitrogen. In other words, both chemists confirmed the presence of free amino-group hydrogens that were replaceable by alkylation or arylation. Wanklyn suggested how his ethylene type could also be used to express the constitution of rosolic acid (**13**), such that three molecules of phenol condensed through the uptake of two carbon atoms from oxalic acid. Wanklyn's main contribution was in suggesting, in two separate presentations at Bath, the rosolic acid−rosaniline relationship. The link was through the decomposition of diazo compounds with water which, as Caro found, took place if the temperature was allowed to rise above 10 °C. Instead of the usual nitrogen-containing colored precipitates, nitrogen-free compounds were obtained[22] (Scheme 4).

Soon after, Caro played the leading technical and scientific role, mainly based on aryl amines, in the growth of Badische Anilin- & Soda-Fabrik, better known as BASF. This firm was founded in 1865 in Mannheim to manufacture aniline red and its derivatives, as well as other coal-tar dyes. Caro returned to Germany at the end of 1866 and acted as a consultant to BASF, prior to joining that firm in 1868, by which time it had relocated to nearby Ludwigshafen, on the west bank of the River Rhine. Early in 1869, Caro became

$$
C_2 \begin{cases} HNC_6H_5 \\ HNC_6H_5 \\ HNC_6H_5 \\ H \end{cases}
\qquad
C_2 \begin{cases} H \\ H \\ H \\ H \end{cases}
$$

rosaniline   ethylene (type)

(6)   **(11)**

$$
C_2 \begin{cases} HNC_6H_5 \\ HNC_6H_5 \\ HNC_6H_5 \\ H \\ H \\ H \end{cases}
\qquad
C_2 \begin{cases} H \\ H \\ H \\ H \\ H \\ H \end{cases}
$$

leucaniline   hydride of ethylene (ethane)

(10)   **(12)**
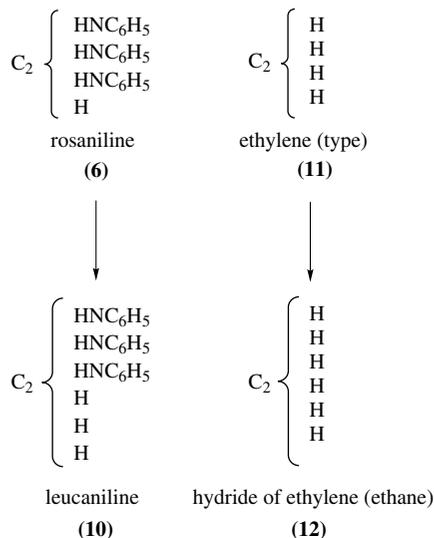
SCHEME 4. Alfred Wanklyn's ethylene-type constitutional formulas

$$
C_2 \begin{cases} C_6H_4OH \\ C_6H_4OH \\ C_6H_4OH \\ H \end{cases}
$$

rosolic acid

(13)
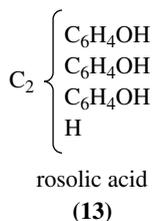
involved in industrialization of a process for synthetic alizarin, the commercially important colorant previously obtained from the root of the madder plant. The starting point was coal-tar anthracene, which was converted into anthraquinone, followed by sulfonation, then fusion with alkali under pressure to afford alizarin as well as various co-products, some that also became commercial dyes. The importance of the alizarin process was that its inventors, Carl Graebe and Carl Liebermann, and its investigators, Caro and Adolf Baeyer, through their extensive studies, gave tremendous support to the benzene-ring theory. This led to the modern structural formulas for naphthalene and anthracene. The very early adoption of the benzene-ring theory by German chemists, particularly those involved in industrial problem solving, initiated the long period of massive competitive advantage held by the German dye and chemical industry[23–26].

Apart from Hofmann and Caro, several German chemists and colorists who had worked in the English aniline dye industry returned to their homeland from the mid-1860s. Some, however, did not. Among the latter was Ivan Levinstein (Figure 10), who emigrated from Berlin to Salford, near Manchester, in 1864, and set up in business to manufacture aniline, its salts, and aniline red and derivatives. Soon he moved to Blackley, Manchester, to found what in 1926 would become a major facility of Imperial Chemical Industries (ICI).
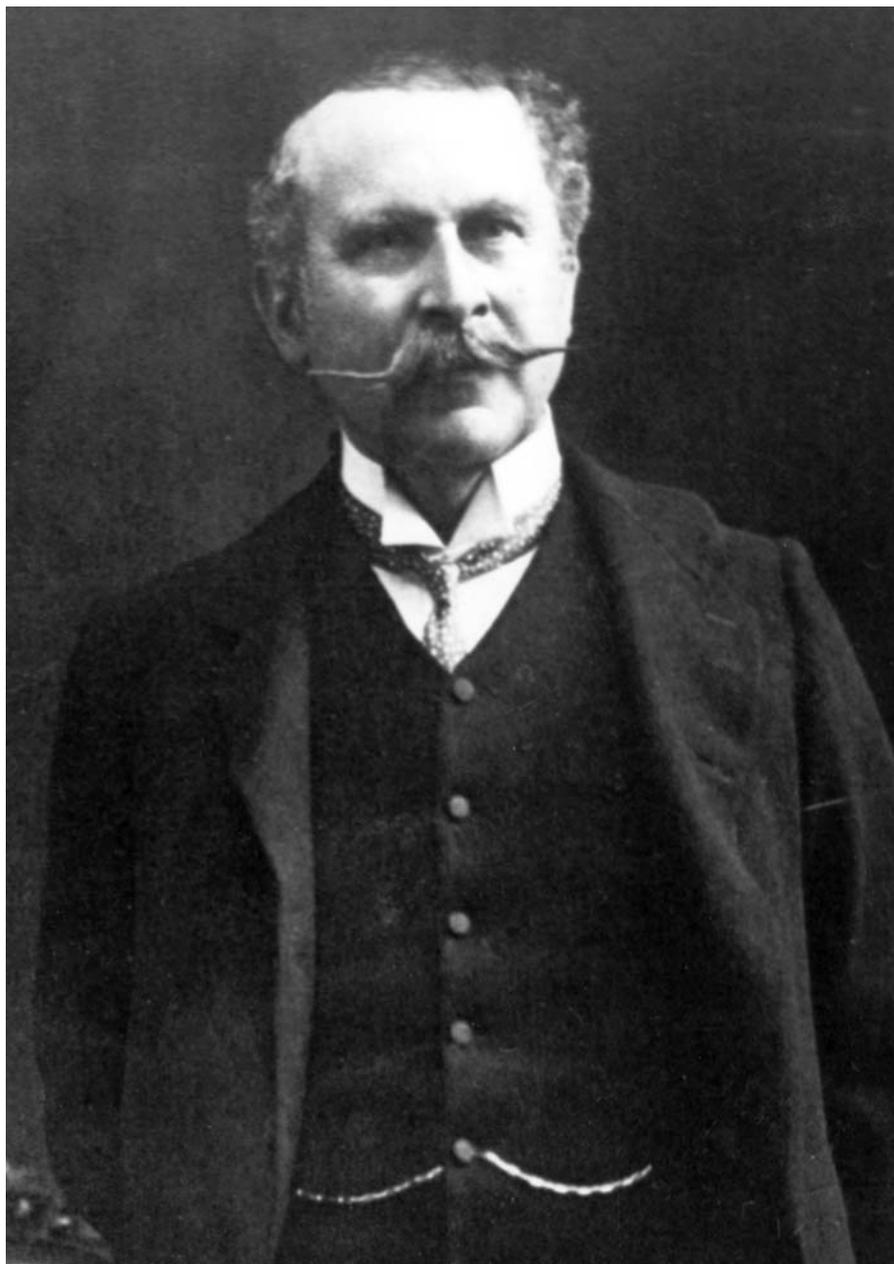
FIGURE 10. Ivan Levinstein (1845–1916). Edelstein Collection

V. AZO DYES AND THEIR INTERMEDIATES

The next major phase in dye invention involved the development of anilines into azo dyes. Two members of this class (though not known as such), one made from *m*-phenylenediamine **(14)** (from 1972 referred to by *Chemical Abstracts* as *m*-benzenediamine), that yielded a brown **(15)**, later corrected to **15a**, and another from aniline, that yielded a yellow **(16)**, were discovered by C. A. Martius while working as assistant to Hofmann in 1863 (Scheme 5). After Martius joined Caro at Roberts Dale & Co. later in the year,
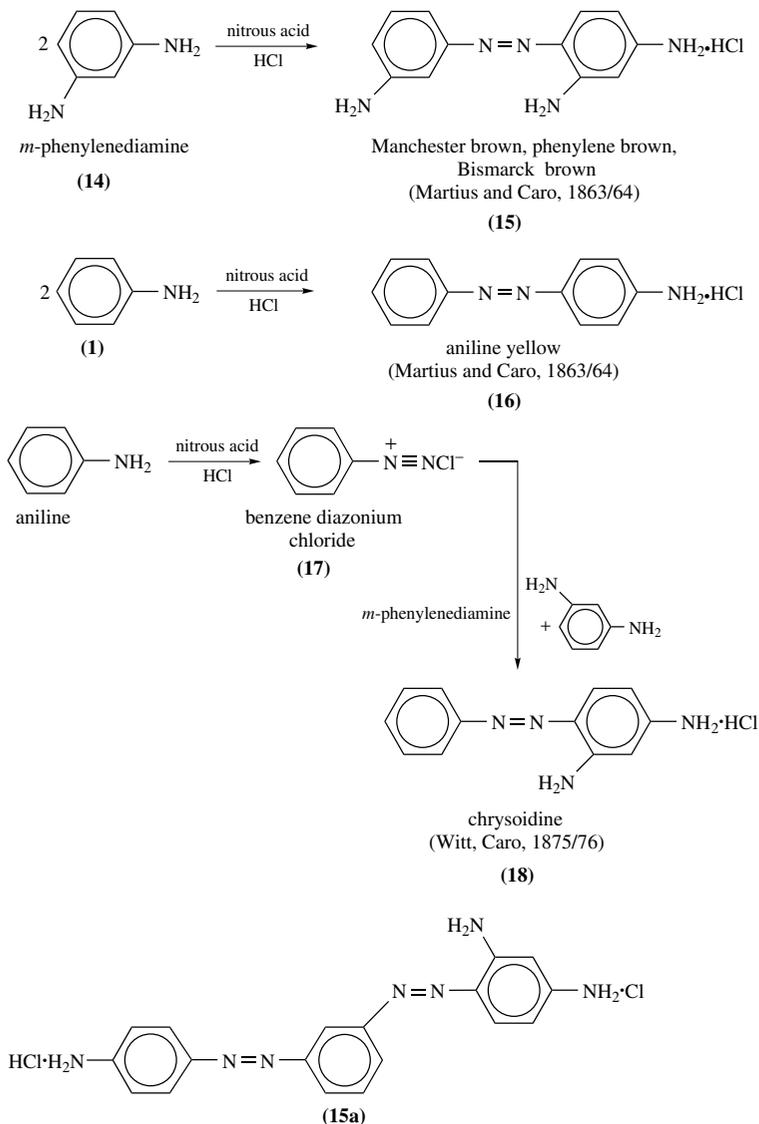
SCHEME 5. The first azo dyes, and modern formula for Bismark brown **(15a)**

15 was marketed as Manchester, or phenylene, brown (from the 1870s it was known as Bismarck brown). Caro also extended this reaction to develop a process for induline. Very little was known about the constitutions of these products, although patents for the processes had been filed in London.

Azo compounds are formed by the coupling of an amino or phenolic compound with a diazonium intermediate (or nowadays ion), for example benzene diazonium chloride (**17**), that contains the diazonium group, $-N_2^+$. The diazonium intermediates are formed by the diazo reaction, namely the action of nitrous acid on aromatic amino compounds, known since 1858 through the work of (Johann) Peter Griess. Because many aromatic amino and phenolic compounds were known by the 1870s, it was possible to synthesize a myriad of combinations, which explains in part the diversity of azo dye chemistry. This was enhanced by the coupling of more than two components to generate large molecules containing two or more azo groups. However, this could not be achieved until the nature of the reaction was fully understood.

The phenylene brown and aniline yellow developed by Caro and Martius in the 1860s were manufactured by the reaction involving single amines, *m*-phenylenediamine (**14**), to afford the brown (**15**), or aniline to afford the yellow (aminoazobenzene) (**16**). That the coupling components could be different aryl amines from the starting amines was not apparent. Kekulé, however, understood that this change was an intermolecular one involving coupling of two components, aniline and its diazo intermediate[27,28].

Though Kekulé also established the correct structural formula for the azo grouping, Griess and others did not immediately accept this. There was also the practical problem of the explosive nature of diazo compounds. In 1875, Otto N. Witt, working at the aniline dye factory of Williams, Thomas & Dower, near London, speculated, on the basis of the yellow **16** having one free amino group and the brown **15** having three amino groups, that a similar colorant with two amino groups would exist. This was probably in connection with his development of a theory of color and constitution, based on what were to be called chromophores, that determined the character of the dye. The molecular arrangement, or nucleus, containing the chromophore, he called the chromogen. The chromogen required an auxochrome, a salt-forming group, that conferred the property of a dye[29–31]. His hunch was correct, and he made the new dye from two different aromatic amines, aniline, converted into diazobenzene, and *m*-phenylenediamine (**14**) (Scheme 5). The orange precipitate offered potential as a dye[32]. Witt, however, did not patent his discovery. Instead he shared its secrets with Caro at BASF, who had been working on a similar product.

In April 1876, Caro met Witt and Griess in London, where they discussed the new results. A few weeks later, on 13 May, Queen Victoria and the Empress of Germany opened the 'Special Loan Exhibition at the South Kensington Museum', in London. Williams, Thomas & Dower was one of the exhibitors, and placed on display a sample of Witt's new orange dye. Caro analyzed the product and identified it as 2,4-diaminoazobenzene (**18**), which was almost identical to one of his own products that Griess had investigated. The new BASF product, based on Caro's process, was chrysoidine, an instant success, and because of that a considerable scientific and commercial curiosity. Like Witt, Caro also did not file a patent or apply for monopoly rights in any of the German states.

Martius, by now a partner in the AGFA firm of Berlin, obtained a sample of chrysoidine (**18**) and handed it over to his consultant, A.W. Hofmann (Figure 11), for scientific investigation. In January 1877, Hofmann published details of the constitutions, as well as the methods of preparation, for **18**, phenylene brown (**15**) and the related aniline yellow (**16**), much to the chagrin of Caro and his colleagues[33–36]. Soon it was shown that phenylene, or Bismarck brown (**15**), was in fact a bisazo compound **15a** (Scheme 6).

Hofmann had thus demonstrated to chemists the existence of another family of synthetic dyestuffs, though this time the constitutional formulas used in his publications came

FIGURE 11. August Wilhelm Hofmann (1818–1892). Edelstein Collection
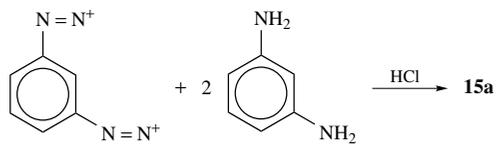
SCHEME 6. Revised synthesis of Bismarck brown (**15a**)

very close to the structural formulas. Next came what was described as a technological sensation, the soluble sulfonic acid derivatives of azo dyes. The pioneer was François Zacharie Roussin, who prepared azo compounds based on sulfanilic acid, naphthol and N,N-dimethylaniline, to yield yellow colorants. Again, no patents were filed for these 'Roussin oranges' that were an immediate success when sold in France during 1876–1877 by the Poirrier firm, of Paris. Caro opined that the products of Roussin were acid dyestuffs of pathbreaking new technical effect. They rapidly displaced certain natural dyestuffs.

From this time dye research in the German aniline dye industry flourished. Caro later described azo dye research and development as scientific mass production. The most important activity was the invention of key aryl amine intermediate compounds for use in the coupling reaction, and for this endeavor structural studies were essential. Caro extended the range of the new azo dyes into the reds with his invention of fast red AV (**19**) in July 1877. This was based on his reasoning that two naphthalene-based components in the azo compound would give a red. To achieve this he used diazotized 1-naphthionic acid (4-amino-1-naphthalenesulfonic acid) (**20**)[37].

At the turn of the 1870s Heinrich Baum at Hoechst separated the various isomers of sulfonated naphthol compounds. Isolation of β- or 2-naphthol (**21**), its conversion to R acid (**22**) and G acid (**23**) and the separate use of them as intermediates for azo dyestuffs gave much clearer shades (Scheme 7). As had been the case with the alizarin dyes, the importance of understanding isomerism in technical work became critical to further progress.
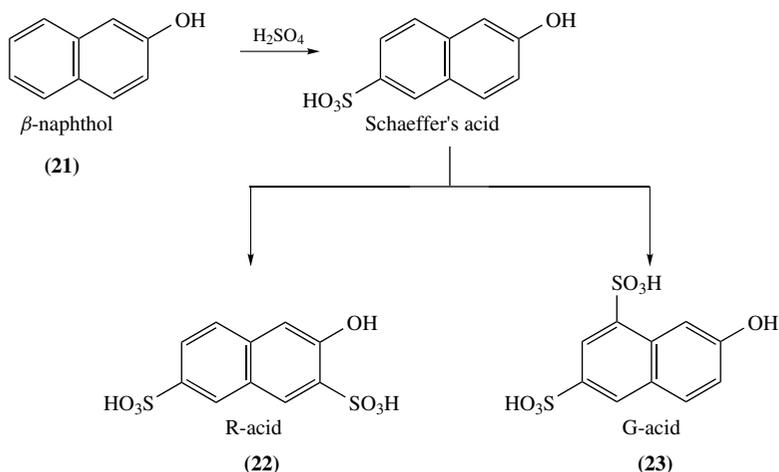
SCHEME 7. Conversion of β-naphthol to G and R acids via Schaeffer's acid

By 1884, seven years after the inauguration of the first German patent law, 9,000 azo dyestuffs were covered by German patents. Diversity, ease of manufacture and profitability stimulated research for new azo dyestuffs. A major endeavor involved the synthesis of other suitable naphthalene intermediates (Scheme 8). Caro made important contributions to this field, partially in collaboration with his friend Peter Griess in England. At BASF, research led to several important innovations in the field of intermediates and, unexpectedly, even to aniline dyes. Caro invented acid magenta and converted naphthols into naphthylamines. During 1879, with his assistant Robert Holdmann, Caro made available β- or 2-naphthylamine (**24**), previously a laboratory curiosity reported in 1875 by Liebermann and Scheiding[38,39]. Despite the great inventiveness of Heinrich Caro and his
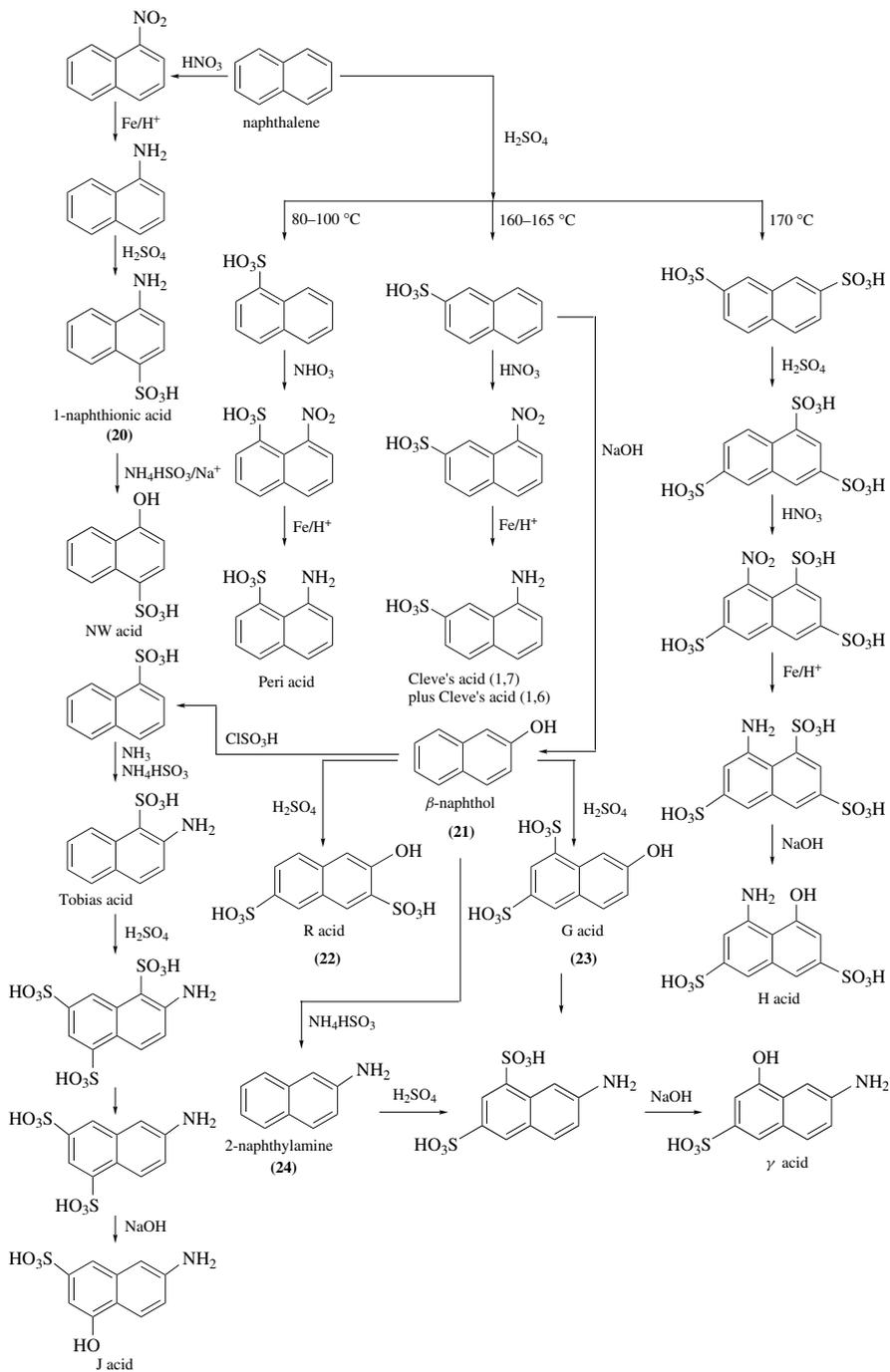
SCHEME 8. Aminonaphthalene sulfonic acids

colleagues at BASF, other companies, most notably Hoechst, Bayer and AGFA, invented better colorants and generated greater profits from the azo dye business[40].

Azo dyes based on the aromatic intermediate benzidine were invented in 1884. These were the first synthetic dyes that adhered to cotton fabrics without the need for a fixing agent (mordant). For this reason they were known as direct or substantive dyes. The first member was discovered by Paul Böttiger, at Bayer. From benzidine **(25)** and naphthionic acid **(20)** he obtained a red bisazo dyestuff **(26)**[41]; see Scheme 9.

Böttiger, however, kept the details to himself. He left Bayer and filed a patent for his new process. Leading companies, including Hoechst and BASF, lost the opportunity to
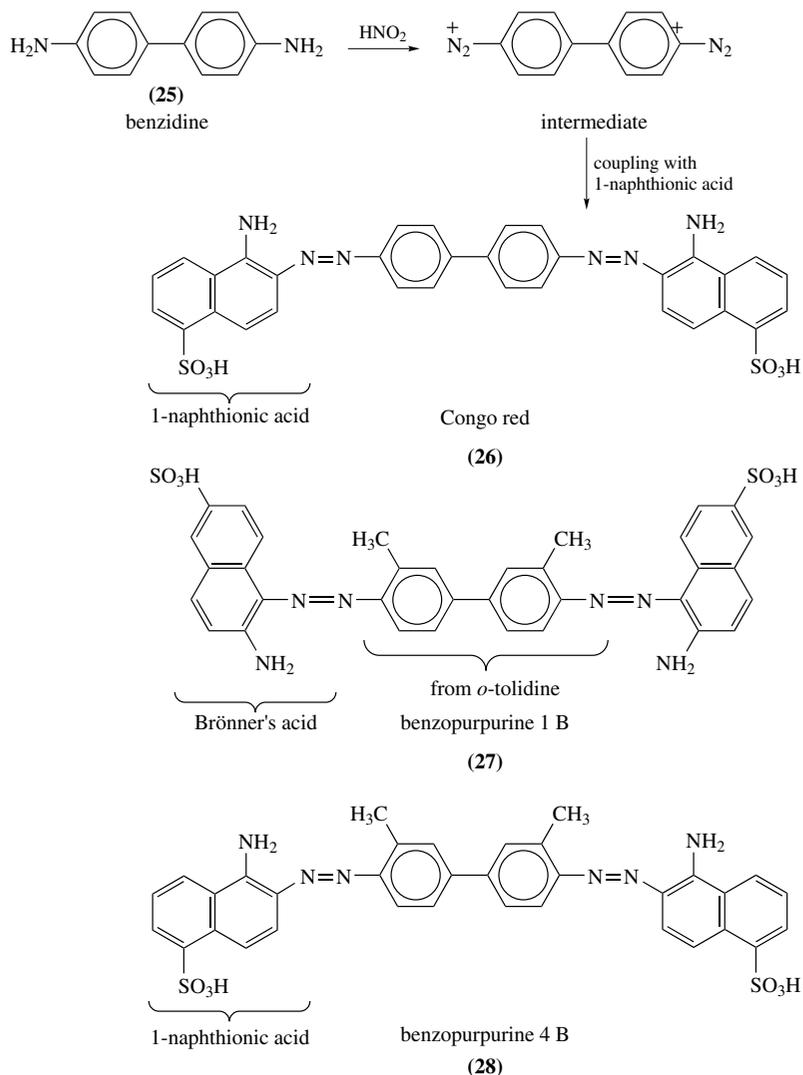
SCHEME 9. Synthesis of benzidine and tolidine azo dyes

exploit the new range from the start because of the poor acid fastness of this first dye. Direct dyeing with benzidine-derived dyes, however, made the fortunes of Bayer and AGFA. The first product, named Congo red **(26)**, transformed modern azo dye chemistry.

Structural studies required elegant procedures that enabled unambiguous assignment of substituents in the aromatic rings of important intermediates, particularly those based on naphthalene. The technical development of the reactions used for the synthesis of intermediates was often complex. It was these aspects of industrial azo dye chemistry that would contribute most to the establishment of industrial research laboratories in the German chemical industry. However, there were notable contributions from English chemists, such as Henry E. Armstrong, who aided Caro in the study of naphthylamines, particularly over questions concerning isomerism, that impacted on patent litigation.

VI. PATENT LAW IN GERMANY

The Germans succeeded in the discovery, invention and marketing of synthetic dyes because of their mastery of the use of formal knowledge, the introduction in 1877 of a comprehensive patent system and, as a result, the inauguration of dedicated industrial research laboratories. They also relied on novel business strategies based increasingly upon the power of 'conventions', or cartels, and 'communities of interests' (which were officially endorsed in 1888). In other words, they created the infrastructure that they needed. The process included the fostering of higher education, since the search for new dyestuffs and intermediates required qualified research chemists[42]. This provided career opportunities for the students and assistants of Baeyer and Hofmann, as well as enhancing the status of chemistry to hitherto unprecedented levels. In this section we explore how the influence of dye discovery on the patent system of Germany impacted on the dynamics of business cooperation and technical collaboration. The events described here comprise the pre-history of an important area of modern European patent law, one in which the aryl amine colorants played a decisive role.

In 1874, Hofmann and Martius, of AGFA, joined the Vorstand of the Deutscher Patentschutz-Verein, chaired by Werner Siemens, and, soon after, Hofmann through publication disclosed the constitution of Caro's fluorescein derivative, known as eosin[43]. This, as with Hofmann's publication of the constitution of chrysoidine, meant that he claimed to be the scientific discoverer of the dye. Witt, in angry response, claimed priority for inventing the process for azo dyes and the new orange by citing the brief description of his product in the London exhibition catalog. Hofmann, however, declared that the days of protection of scientific inventions through secrecy were numbered: 'The time of the Arcanists is over. Whosoever, in the last quarter of the nineteenth century, provides his colleagues with a chemical puzzle must be prepared to see it solved, sooner or later'[44]. ['Die Zeit der Arcanisten ist vorüber. Wer in dem letzen Viertel des neunzehnten Jahrhunderts seinen Fachgenossen ein chemisches Räthsel aufgeben will, der muss sich schon darauf gefasst machen, dass diesses Räthsel frührer oder später gerathen wird'.]

Significantly, the Reichstag was then in the process of approving the new patent law that covered chemical processes, rejecting an earlier proposal for product protection alone. The comprehensive patent law was passed in 1877 to serve the needs of the new German Empire. Now chemical manufacturers were obliged to protect discoveries and encourage inventiveness. This was achieved through the establishment of industrial research laboratories, focusing on intermediates and dyes, a new feature of industrial society, organized and managed on a large scale, and soon institutionalized. Discoveries protected by strong patent law generated profits; profits supported new and expensive research programs. The German firms filed patents in all countries where patent systems existed[45].

However, many problems remained, including the need to deal with speculative patents. In 1884, AGFA filed a patent for the substantive dye Congo red **(26)**. It was soon followed

by the Bayer company's version called benzopurpurine (27). This group of aryl amine colorants, soon collectively known as benzopurpurines, including 27 and 28, were to become the main topic of industrial research and of patent litigation for over a decade (Scheme 9)[46]. The reason was, quite simply, the economic significance, since cotton dyeing and printing were the most important applications of dyes. The benzopurpurines were investigated by inventors in Germany and, to a lesser extent, in England and the US, who filed blanket patents for processes that specified a variety of intermediates, some that had not even been prepared. In any case, mixed products resulted from many of the processes specified, which created considerable confusion. This left the patent system open to abuse or, at best, uncertainty[47].

By 1886 the situation had become so unclear in Germany that an Imperial Commission was charged with revising the patent law. Heinrich Caro's wide experience in patent litigation during the 1880s enabled him to play a not inconsiderable role in the formulation of the new ruling as it applied to organic chemicals. He also contributed to the more fluid legal concept of an inventive idea, rather than a chemical process or product. In the case of the benzopurpurines, the inventive idea was the new technical effect of direct attachment to cotton. The revised patent law came into effect on 1 October 1891, and cleared up much confusion with an unambiguous ruling that extended a patent for a chemical process to the products of that process[48].

After 1880, most of the British synthetic dye industry was lost to Germany. From the end of the decade the Manchester dye-maker Ivan Levinstein lobbied for patent law reform and commercial protectionism in Britain[49]. Following the introduction of German-made synthetic indigo in 1897, he implored dyers and printers of his adoptive country to support the colonial trade in the natural dyestuff. He is given much credit for the steps leading to the British Patent Act of 1907[50].

As for Switzerland, leading representatives of its dye industry, forerunners of CIBA and Geigy, managed to overturn attempts to introduce a patent system, particularly in 1882 and 1886. It was only after German firms, who supplied the Swiss with intermediates and were angered by the extent of unlicensed copying of their inventions, threatened to withhold supplies of intermediates early in the 20th century, that the Swiss introduced a patent law.

VII. ANILINE RED AND THE STRUCTURES OF ANILINE DYES

Despite the economic importance of rosaniline (aniline red, magenta) (6) and its derivatives during the 1860s and after, there was no clear structural information about aniline-derived colorants, at least until 1878. Then, through the joint work of the cousins Emil and Otto Fischer, the search for the parent compound of 6 was successfully concluded with publication of the modern structures for aniline dyes. The Fischers' starting point had been Caro and Wanklyn's work on 6 and rosolic acid (13).

The research began in 1876, when Emil Fischer (Figure 12) discovered phenylhydrazine, later employed in the structural elucidation of sugar molecules, and, with Otto, synthesized the hydrazine derivative of rosaniline. Then, via the diazo intermediate, they introduced hydroxyl groups. These groups were removed to yield the hydrocarbon 'mother substance'. The Fischers reacted pure aniline with p-toluidine (29) to yield pararosaniline (30), which was degraded with nitrous acid and alcohol to afford the mother substance, triphenylmethane (31). From this they determined that rosaniline was a homologue of triaminotriphenylmethane (pararosaniline) (30). Two years later, in 1878, the Fischers produced 30 from triphenylmethane, proving the correctness of their structural formula (Scheme 10). This enabled new pathways from anilines to dyestuffs, through condensations with novel reagents, particularly phosgene (COCl$_2$), benzaldehyde and formaldehye[51].
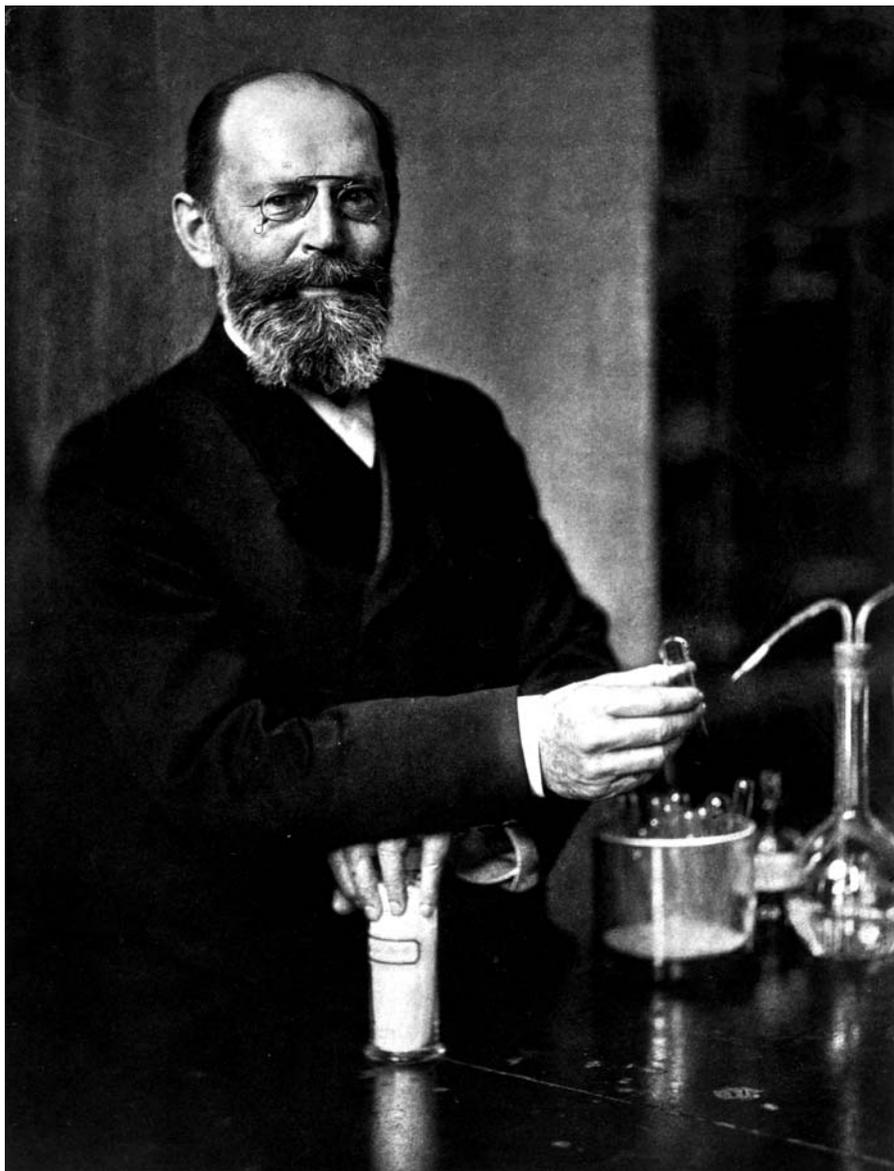
FIGURE 12. Emil Fischer (1859–1919). Edelstein Collection

The *N*-substituted anilines, available since the mid-1860s, became important inter-
mediates in the manufacture of both the new triarylmethane and the azo colorants.
N,*N*-Dimethylaniline **(32)** was used by Caro to synthesize the thiazine dye methylene
blue **(33)**, the first colorant for which a patent was granted under the new German patent
law (Scheme 11). In 1877, Otto Fischer achieved the synthesis from benzaldehyde and **32**
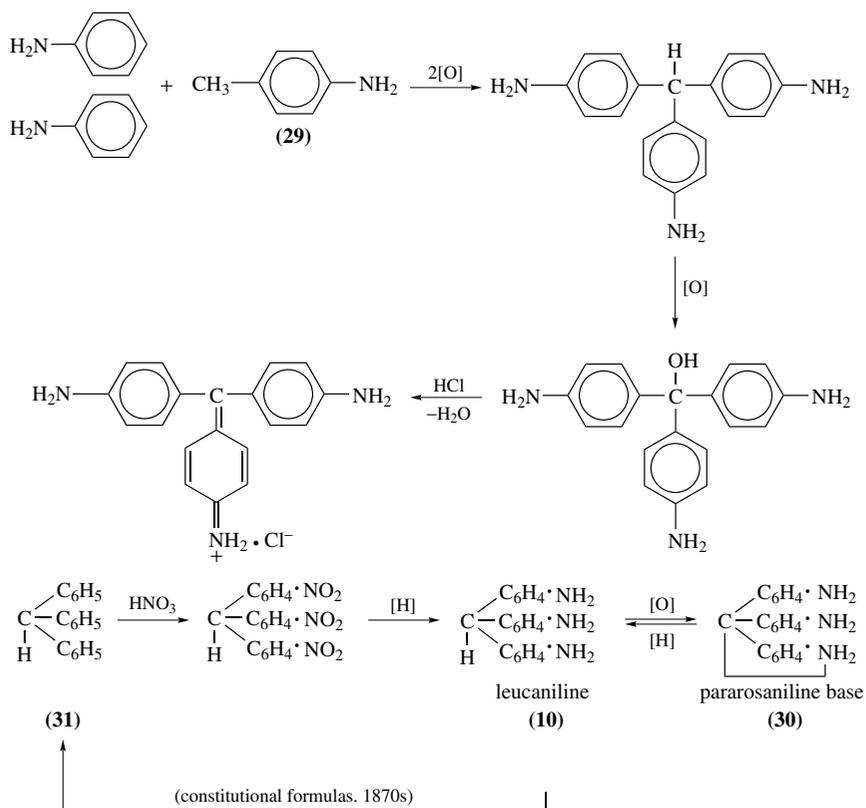
SCHEME 10. Structure of rosaniline dyes (E. and O. Fischer, 1878)
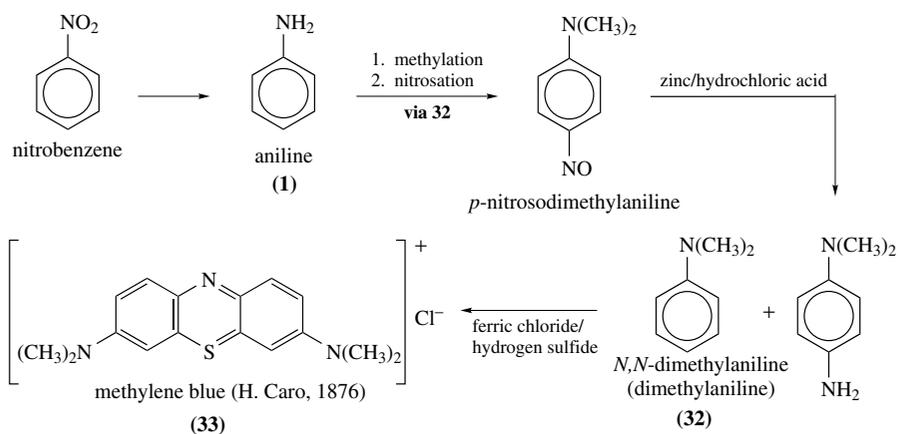
SCHEME 11. Methylene blue, thiazine dye
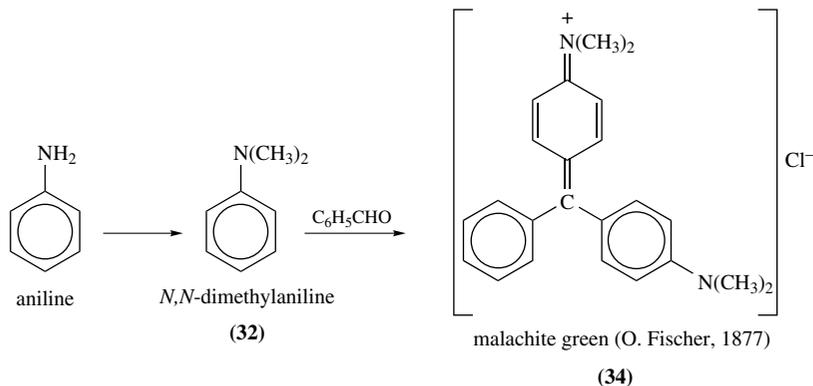
SCHEME 12. Malachite green, triphenylmethane dye
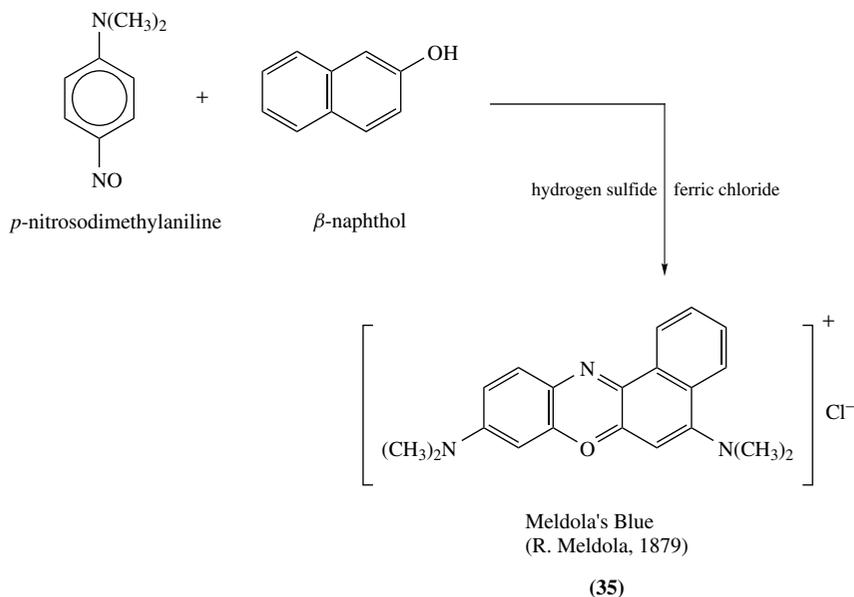
SCHEME 13. Meldola's blue, oxazine dye

of malachite green **(34)** (Scheme 12). In London, Raphael Meldola (Figure 13), at Brooke, Simpson & Spiller (successor to Simpson, Maule & Nicholson), discovered a number of novel products, including, in 1879, the first oxazine dye, Meldola's blue **(35)** (Scheme 13). In 1883, Alfred Kern, of the CIBA-forerunner Bindschedler & Busch, employed phosgene in the synthesis of a new aniline dye, crystal violet, which is hexamethylpararosaniline **(36)**. The process was complicated and not fully mastered. During 1883–1884, Caro

FIGURE 13. Raphael Meldola (1849–1915). Edelstein Collection

improved the reaction. Combination of one molecule of phosgene with two molecules of **32** yielded the intermediate Michler's ketone **(37)** which, with phosphorus oxychloride (POCl$_3$) and **32**, gave **36** (Scheme 14)[52,53].
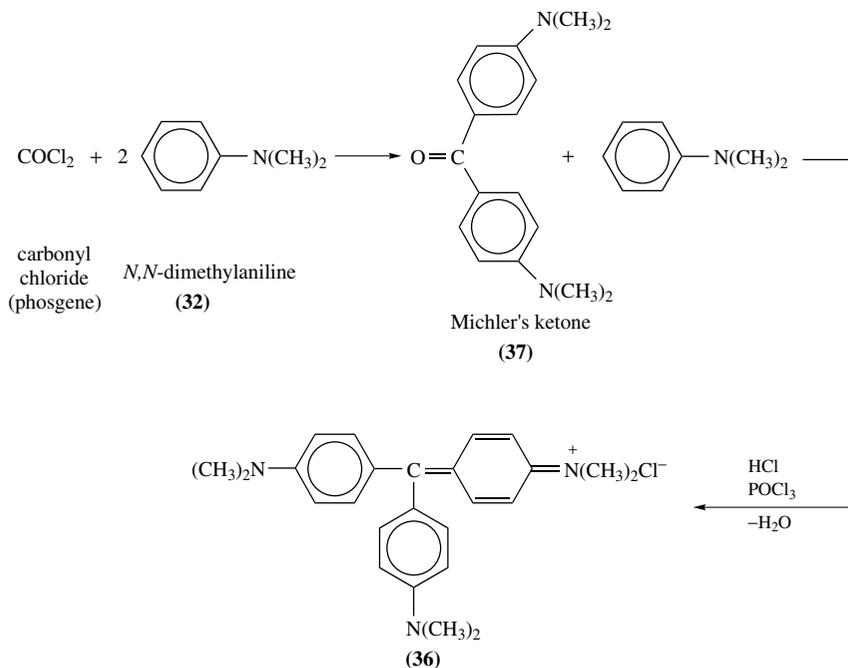
SCHEME 14. Caro's process for crystal violet, 1884

In 1880, Otto Fischer synthesized rosaniline (aniline red) from *para*-nitrobenzaldehyde. However, the process was not of commercial value due to the difficulty in converting the colorless, reduced, leuco intermediate into the dyestuff. This was a problem with all novel syntheses of aniline red before 1900. Pararosaniline continued to be made by nitrobenzene oxidation of anilines, at least until around 1940, when condensation of aniline with formaldehyde came into more general use.

Traugott Sandmeyer's 1896 discovery of acid glaucine red **(38)** led to the colorant better known as peacock blue, later employed extensively in multicolor printing. It came to prominence in the 1930s, with the introduction of flushed color production that enables retention of the required degree of fineness of pigment particles and provides uniform dispersion (Scheme 15)[54,55].

VIII. CONTRIBUTIONS TO ACADEMIC CHEMISTRY

During the five decades commencing 1840, chemists established a comprehensive chemistry of aromatic amines. Aniline was characterized by its feeble basicity and sensitivity to oxidants, the latter explaining why the colorless, odorless pure liquid darkens on exposure to air and light. It also takes on a characteristic odor. Methods of laboratory preparation
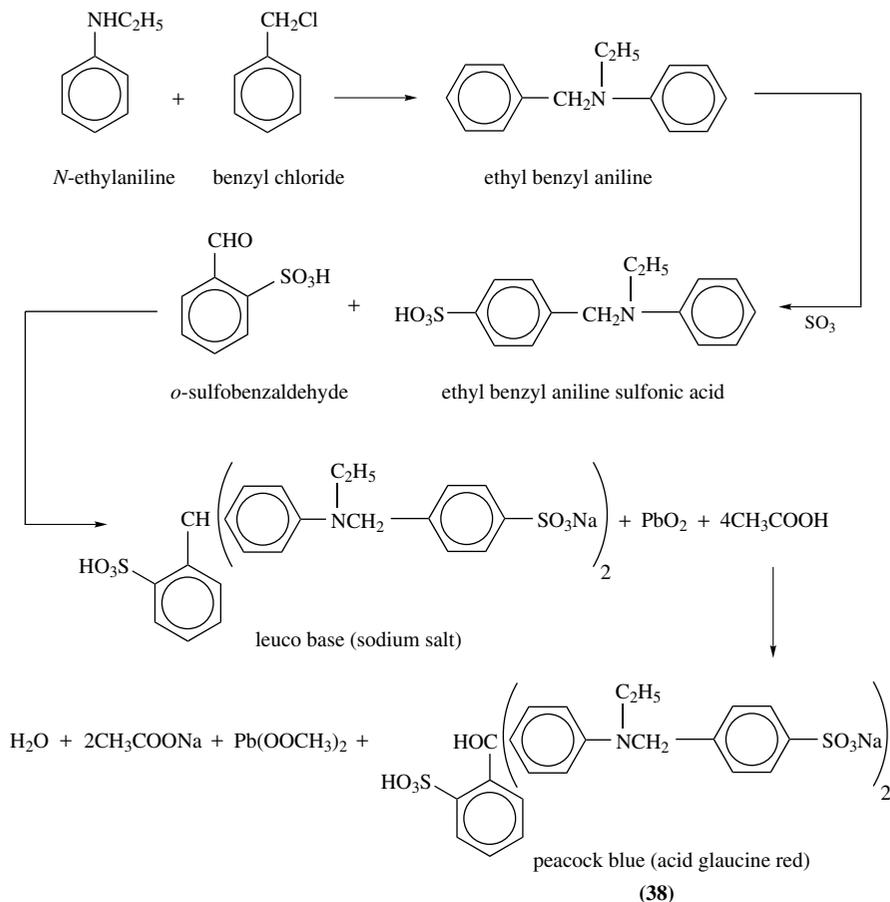
SCHEME 15. Synthesis of peacock blue

of aryl amines from nitro precursors, including selective reductions, were established. The early methods based on reduction of the corresponding nitro compounds, generally nitrobenzene and nitrotoluenes, involved a variety of reducing agents, including zinc and hydrochloric acid, tin or stannous chloride and acid, iron and hydrochloric acid, and alcoholic ammonium sulfide. The influence of chemists who were in some way connected with the development of anilines and their conversion into dyes is seen in the many reactions that bear their names, or through which they have strong associations, including Armstrong, Béchamp, Baeyer, Caro, Meldola, Witt and Zinin. They appeared in practically all organic chemistry textbooks published until the 1950s[56–59].

The test for aniline, involving treatment with bleaching powder, affording a deep violet that soon changed to red, was named after Runge. The method of Griess gave diazonium intermediates, which was the main difference in behavior as compared to aliphatic amines. The coupling reaction with aromatic amines and phenols was well developed, mainly due

to industrial interest. The anilines underwent ring-substitution or addition, according to the conditions. They were readily halogenated, nitrated and acetylated (to anilides). The tertiary amine N,N-dimethylaniline **(32)** with nitrous acid gave p-nitrosodimethylaniline, which on reduction yielded p-amino-N,N-dimethylaniline, an intermediate used in the synthesis of methylene blue and Meldola's blue.

Hofmann established a route to higher homologues of aromatic amines by intramolecular rearrangement of N-alkylated anilines, a reaction that was of great theoretical and technical importance. In 1870, he reported the conversion of an acid amide into an amine, with loss of one carbon. In 1881, he discovered that when the degradation was carried out with sodium hypochlorite or hypobromite, the yields of primary amines were excellent. This is the Hofmann degradation, or reaction, that takes place via formation of isocyanate[60].

Sandmeyer in 1884 found that replacement of the diazonium group by halogen was catalyzed by cuprous chloride or bromide. It is a good route to o- and p-chlorotoluenes and m-nitrochlorobenzene. Gattermann in 1890 used copper powder to permit milder conditions. Methods were available for synthesis of benzidine and its congeners, a variety of aminoanthraquinones and acyl derivatives of aryl amines.

Later methods for synthesis of aniline, some developed in the 20th century, involved heating phenol with the double compound of zinc chloride and ammonia, treating an aromatic carboxylic acid with hydrazoic acid or sodium azide, and reduction of nitrobenzene by either electrochemical methods or with hydrogen and Raney nickel catalysts. These routes were generalized to the synthesis of other aryl amines. Secondary amines included diphenylamine **(8)**, from heating aniline with aniline hydrochloride, and N-methylaniline **(39)**, the outcomes of dye-making processes. Likewise tertiary amines were made by adapting processes developed in the search for synthetic dyes: The diamines were important in dye manufacture. In 1894, the inexpensive sulfide, or sulfur, dyes, made by the action of sulfur and sodium sulfide on aniline and phenols, were introduced.

Consensus on nomenclature had been reached by the 1890s. Aniline was the parent of its derivatives, though sulfonic acids were considered derivatives of benzene, such as aminobenzenesulfonic acid. The prefix amino- was added to naphthalene and its derivatives. Many trivial names came into use, particularly for aminonaphthalenesulfonic acids, found in both academic and industrial research laboratories. Though IUPAC convention now numbers amino aryl compounds according to the parent hydrocarbon, the earlier system of numbering has often been retained, since some names include the positions of substituents at carbon atoms numbered according to the older systems.

IX. ANILINES FOR EXPLOSIVES

Dye intermediates were early on adapted to the production of explosives. While most modern explosives are aromatic nitro compounds, ancillary products incorporate amino groups. Of interest here are two tetranitroanilines. Tetryl (2,4,6-trinitrophenyl-N-methylnitramine, or N,2,4,6-tetranitro-N-methylaniline) **(40)** is employed as a booster for TNT. It can be made from N-methylaniline **(39)**, or the cheaper N,N-dimethylaniline **(32)**, since the latter loses one methyl group on oxidation. An alternative route, introduced in World War II, starts with conversion of dinitrochlorobenzene into dinitro-N-methylaniline, which is then nitrated. The explosive tetrotyl is 70% tetryl and 30% TNT.

TNA, 2,3,4,6-tetranitroaniline **(41)**, is a detonator in explosives. The product and the process for its synthesis were invented by the German-British chemist Bernard J. Flürscheim, who from 1905 had investigated nitroanilines. In 1913, he sold rights to his process to Verona Chemical Company, of Newark, New Jersey. Though the process was not then adopted, the development work enabled Verona to commence the manufacture of aryl amines. The original manufacturing process for TNA was similar to those employed
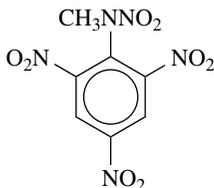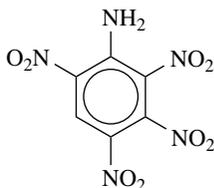
(39)   (40)   (41)

in production of anilines. Benzene was nitrated to dinitrobenzene, which was selectively reduced to *meta*-nitroaniline (MNA). This crystallized out from sulfuric acid as the sulfate salt, and was then nitrated to afford TNA. Final operations, particularly drying, had to be carried out with care[61].

Reduction of the 2-nitro in 2,4,6-trinitrophenol yields picramic acid, 2-amino-4,6-dinitrophenol. It is highly explosive but safe to handle when wet. It was also an important intermediate in dye manufacture. Centralite, a stabilizer in smokeless powders, is made from monoethylaniline.

X. INDUSTRIAL RESEARCH

Another of Heinrich Caro's achievements was the introduction of the industrial research laboratory as a formal business unit at BASF. Eventually, each main operating department had a laboratory that increasingly became the domain of highly qualified chemists who engaged in research, analysis and process development. Academic consultants, particularly Adolf Baeyer, played important roles as inventors for BASF and other German firms. It was through industrial collaboration that in 1883 Baeyer could first draw the almost correct modern structural formula for indigo (42). At the end of the 1880s, Caro oversaw the construction of a central research laboratory at Ludwigshafen (Figure 14). Its purpose was to deal with research and development (R&D) and the protection of BASF patents. Later, the departmental research laboratories became the more active sites of discovery and invention, often because they were more closely connected to particular types of products and end uses, and also because they were sometimes better able to foster new directions and diversification. The latter included, at BASF, nitrogen products, high-pressure processes and synthetic rubber. This set a pattern that was closely followed in all science-based chemical and pharmaceutical industries during most of the 20th century. Coal-tar anilines acted as the crucible of discovery for most synthetic organic chemicals[62–65].
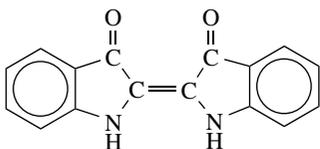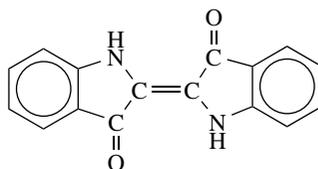
A. Baeyer, 1883   modern structure, 1928

(42)   (2)

While these developments were noted in Europe and the US, little action was taken outside of Germany to improve industrial research and industrial–academic collaboration. British chemist Raphael Meldola's experience in the English synthetic dye industry
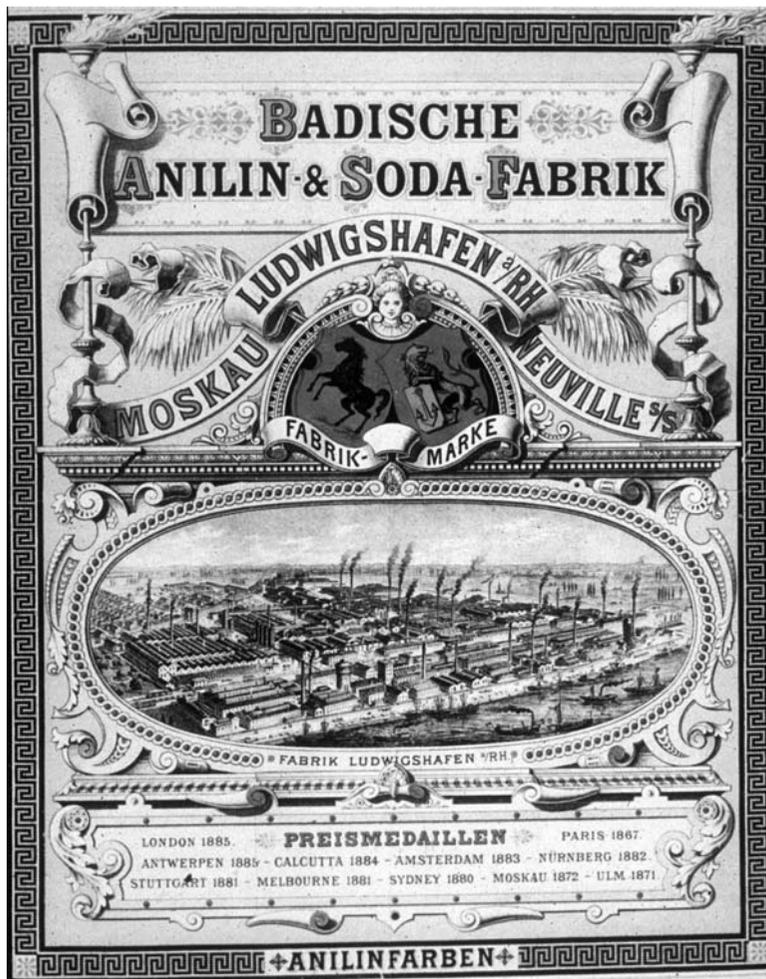
FIGURE 14. Title page of BASF price list for aniline dyes, 1896. BASF Archives

enabled him to understand its several failings, particularly lack of investment and research, which in turn were the outcomes of what he perceived to be inadequate education and training. From 1886, he lobbied for improved scientific education, though without success.

It was the outbreak of war with Germany in August 1914, and the almost immediate crisis caused by the shortage of dyestuffs—mostly made in Germany—in Britain that brought the lobbying for a British science-based organic chemical industry to the fore. Dyestuffs and their intermediates used in the manufacture of explosives were now classified as strategic materials. The British public was informed of proposals for a national aniline dye industry under government control. In November 1914, Ivan Levinstein's former patent lawyer, Lord John Fletcher Moulton, an accomplished scientist in his own right, and Arthur G. Green, of Leeds University, began negotiations on behalf of the British government with three main firms, including Levinstein Ltd, with the intention of outright

purchase of one or more of them. Shortly afterwards, Moulton became involved in munitions manufacture, which involved procuring supplies of TNT. However, he arranged for the amino product TNA (41) to be manufactured in the US. Flürscheim assisted the Aetna company in this endeavor, until the factory blew up. TNA manufacture was then taken up, and improved, at the newly-founded Calco Chemical Company, of Bound Brook, New Jersey[66].

Meldola was appointed a member of the Board of Trade Committee on the Supply of Chemical Products. In 1915 he became chairman of the advisory councils of the newly formed British Dyes Ltd, and of the forerunner of the Department of Scientific and Industrial Research. At that time, indigo was one of the many important synthetic dyes suddenly no longer available from German factories.

XI. INDIGO

During the 1870s and 1880s, Adolf Baeyer and other academic chemists derived considerable scientific benefits from collaborations with Caro and other leading industrial chemists. Caro provided Baeyer with information about potentially interesting reactions and novel products that became topics for academic research. Foremost among the problems of structural elucidation was, in both scientific and commercial terms, that of indigo. This great scientific puzzle of the 19th century was taken up by Baeyer. With its solution, Baeyer also contributed to an understanding of the phenomenon of tautomerism, and arrived at the modern formula for indigo. The technical problems, particularly a synthetic route based on a low-cost starting material, however, eluded both Baeyer and Caro. Nevertheless, the eventual success of artificial indigo was based on researches that Baeyer had commenced at the Gewerbeinstitut in Berlin in 1865, on encouragement from and collaboration with Caro in the mid-1870s, and on Baeyer's agreements with both BASF and Hoechst at the beginning of the 1880s[67].

Until the early 1880s, Caro was the principal industrial participant, even though the process he scaled up on the basis of Baeyer's research was a commercial failure. It was, nevertheless, part of the tremendous science-based commitment towards the industrial replication of important natural products. Baeyer was able to establish in 1883 that the intermediate product of the indigo degradation was pseudo-indoxyl, not indoxyl. It was this work that enabled him to draw the modern structure for indigo (42), in a letter to Caro, dated 3 August 1883[68].

The industrial manufacture of indigo is based on two processes developed by Carl Heumann in 1890 at Zurich Polytechnic. They make use of aryl amines derived from the abundant hydrocarbons benzene and naphthalene. The former process involves aniline; the latter proceeds via anthranilic acid (o-aminobenzoic acid) (4). In 1897, BASF and Hoechst in Germany were the first firms to manufacture synthetic indigo. The BASF process, in use until the late 1920s, converted phthalic anhydride into phthalimide with ammonia. The phthalimide was then treated with alkali and chlorine to yield anthranilic acid by the Hofmann reaction. Anthranilic acid was then condensed with chloroacetic acid to afford phenylglycine-o-carboxylic acid, which on fusion with alkali gave indoxyl (43). Indoxyl oxidizes in air to indigo (Scheme 16). The Hoechst process was based on reaction of aniline with chloroacetic acid to give N-phenylglycine, which on fusion with alkali afforded indoxyl. The yield of the original Heumann process was about 10%. It was increased to 75% in 1901 when Johannes Pfleger of Deutsche Gold- und Silberscheidanstalt (Degussa) added sodamide at the fusion step[69] (Scheme 17).

Certainly the successful manufacture of synthetic indigo would not have been so readily realized but for the joint work of Baeyer and Caro, which also contributed towards Baeyer's Nobel Prize (1905). It brought about the end of the British monopoly on the
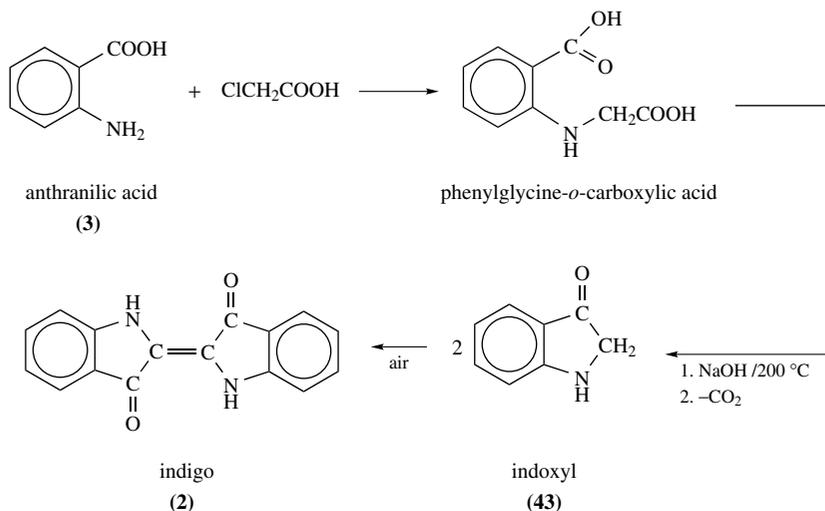
SCHEME 16. BASF process for indigo, 1897
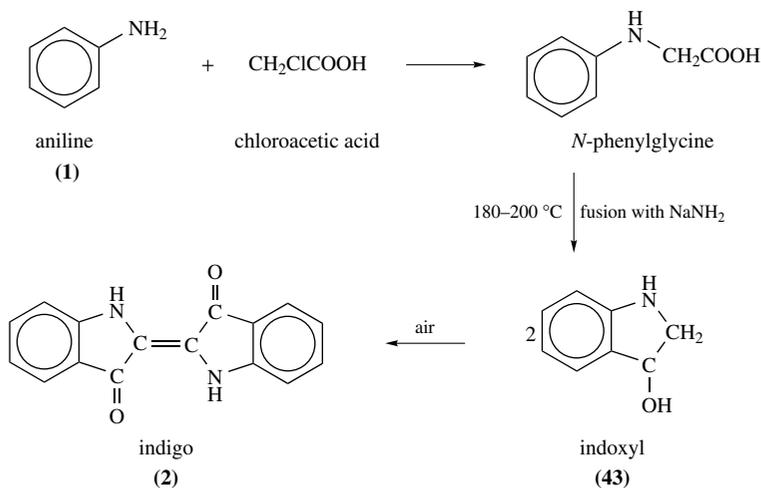
SCHEME 17. Hoechst process for indigo, 1901

natural product, known as the 'king of dyestuffs' (Figure 15). Well before 1910, the cultivation of the indigo plant in India and elsewhere had collapsed[70]. Demand for synthetic indigo remained strong, even after it was displaced by other, less fugitive, synthetic colorants. In 1936 alone, 18 million lbs. were manufactured in the US. Modern versions of the Heumann processes are still in use.

British-made synthetic indigo was produced by Levinstein Ltd in 1916 at the sequestered Ellesmere port factory of Hoechst, where the antiseptic acriflavine (44) and novocaine (45) were also produced. During World War I, Levinstein's highly qualified technical team, led by Arthur Green, developed close links with academic institutions. In November 1918,

FIGURE 15. Gathering the indigo crop, India, around 1900. Aniline was first obtained from indigo, prior to isolation of the aromatic amine from coal tar and synthesis from benzene. Cultivation of the natural product declined following the introduction of synthetic indigo by BASF and Hoechst in 1897. Edelstein Collection

H_2N N NH_2
Cl CH_3

(44)

$COOCH_2CH_2N(C_2H_5)_2$

H_2N

novocaine (procaine)

(45)
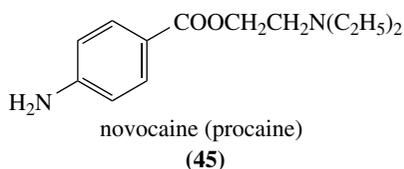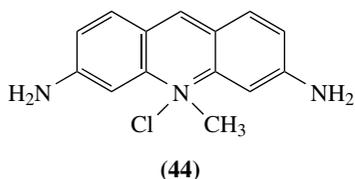
Levinstein Ltd was merged, under government influence, with British Dyes Ltd to form the British Dyestuff Corporation Ltd[71].

XII. AMINOANTHRAQUINONE VAT DYES

In 1901, René Bohn, head of the BASF alizarin laboratory, applied the indigo reaction conditions to 2-aminoanthraquinone **(46)** and discovered a blue colorant that he named indanthrone, from 'indigo' and 'anthraquinone'. He then obtained the same product more directly from **46**. Later known as indanthrene blue RS **(47)**, it was the first of the anthraquinone vat dyes, more correctly anthraquinonoid vat dyes, also known as indanthrene dyes (Scheme 18). With this innovation, three types of anthraquinone dyes became available: mordant (such as alizarin), acid (Robert E. Schmidt, at Bayer, 1894) and vat.
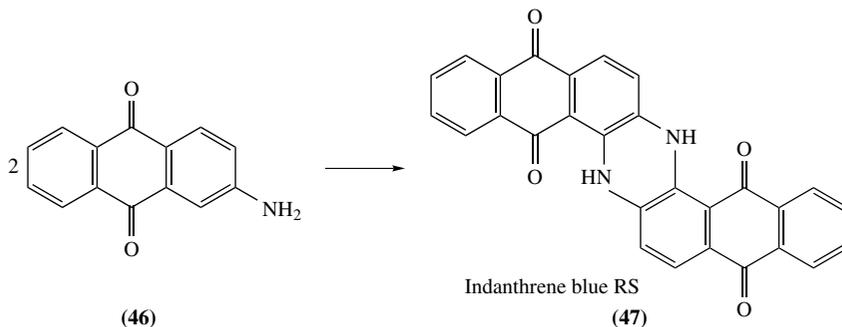
SCHEME 18

Chemists at the rival Bayer company established the structure: Indanthrone consists of two anthraquinone units joined through a heterocyclic bridge containing two nitrogens. This enabled industrial research laboratories to discover anthraquinone-based intermediates for other vat dyes. In 1904, an assistant of Bohn synthesized benzanthrone (48), later an important intermediate in processes involving aminoanthraquinone-derived colorants[72].

(48)
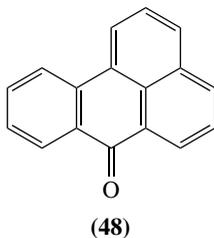
The novel vat dyes encouraged the development of processes for obtaining the important intermediate 1-aminoanthraquinone (49). The reaction involves replacement of the sulfonic acid group in anthraquinone-1-sulfonic acid by the amino group. It is achieved by heating the sulfonate with aqueous ammonia in the presence of sodium arsenate, which oxidizes the sulfite liberated to sulfate.

The research leading to this process was important since sulfonation at the 1-position was difficult to achieve until Schmidt at Bayer and Iljinsky in Russia independently discovered that the presence of mercury led to the formation of the 1-sulfonic acid, rather than the expected 2-sulfonic acid. The former could then be readily converted into 49 by amination in the presence of arsenic. Typical reactions, as discovered by W. Mieg at Bayer in 1910, include condensation of 49 with 1-chloroanthraquinone (50) to yield dianthrimide 51, which is readily converted into cyclic carbazole C.I. Vat Green 9 (52) (Scheme 19). Schmidt converted N-methyl 1-aminoanthraquinone (53) into a quinone analogue of 48, to which was attached a heterocyclic ring. Bromination followed by reaction with 46 gave Algol red B (54) (Scheme 20). Schmidt developed other Algol vat dyes by acetylation and benzoylation of aminoanthraquinones, including Algol red 5 (55). During 1913, chemists at AGFA reacted aniline with bromaminic acid, 1-amino-4-bromoanthraquinone-2-sulfonic acid, to yield a dye that colored wool blue. After Hoechst took over further developments,

1-aminoanthraquinone (49) 1-chloroanthraquinone (50) 1,1'-dianthrimide (51)

4,4'-diamino-1,1'-dianthrimide 4,4'-dinitro-1,1'-dianthrimide

4,4'-dibenzamido-1,1'-dianthrimide (52)
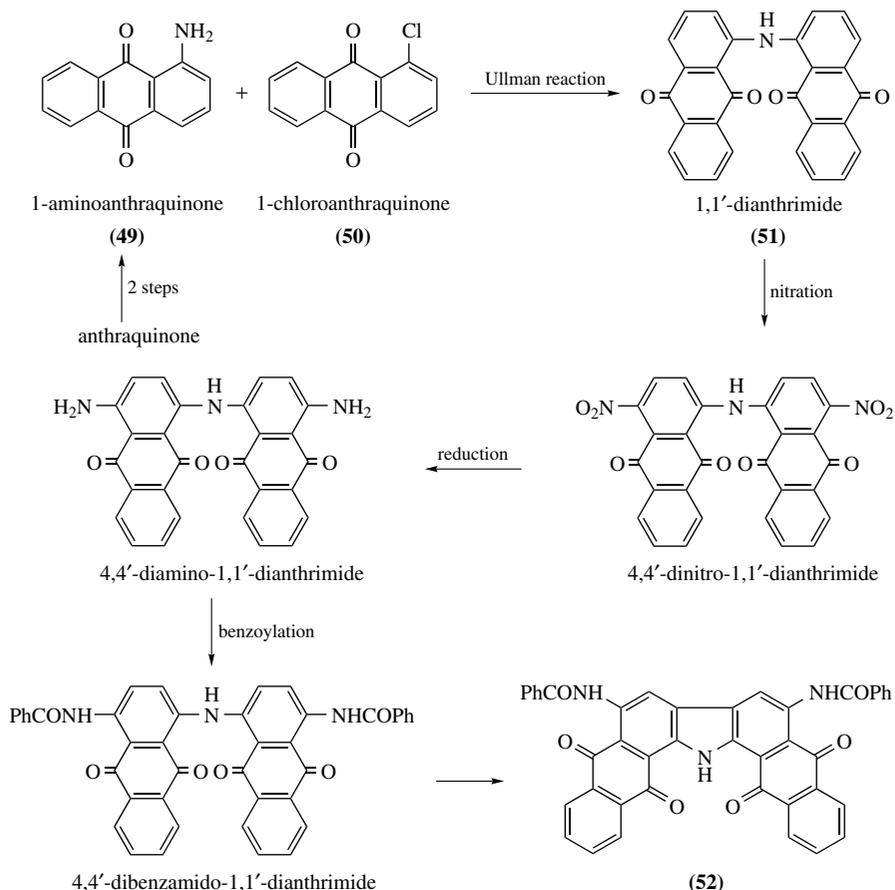
SCHEME 19. Synthesis of C.I. Vat Green 9 (vat olive R)

a range of extremely successful wool dyes, fast to light and perspiration, was introduced, including alizarin sapphirol A, alizarin direct blue A2G, anthralan blue FR and supranol brilliant blue G. In 1924, W. Eckert and H. Greune at Hoechst found that condensation of *o*-dianiline (*o*-phenylenediamine) **(56)** with 1,4,5,8-naphthalenetetracarboxylic acid **(57)** yielded imidazole derivatives **58** and **59**, members of a group of extremely bright and fast vat dyes (Scheme 21). A. Wolfram converted acetylaminoanthraquinone into a derivative of indanthrenazine, later used as a route to indanthrene blue RS **(47)**[73].

The vat dyes, though expensive, in part because they required multistep syntheses, quickly became popular because of their resistance to light and washing. They were widely used in curtains, shirting fabrics, toweling and beachware. Throughout much of the 20th century, dye manufacture was generally dominated by azo and vat dyes. The market for the relatively expensive vat dyes, however, was far greater in the US than in Europe.
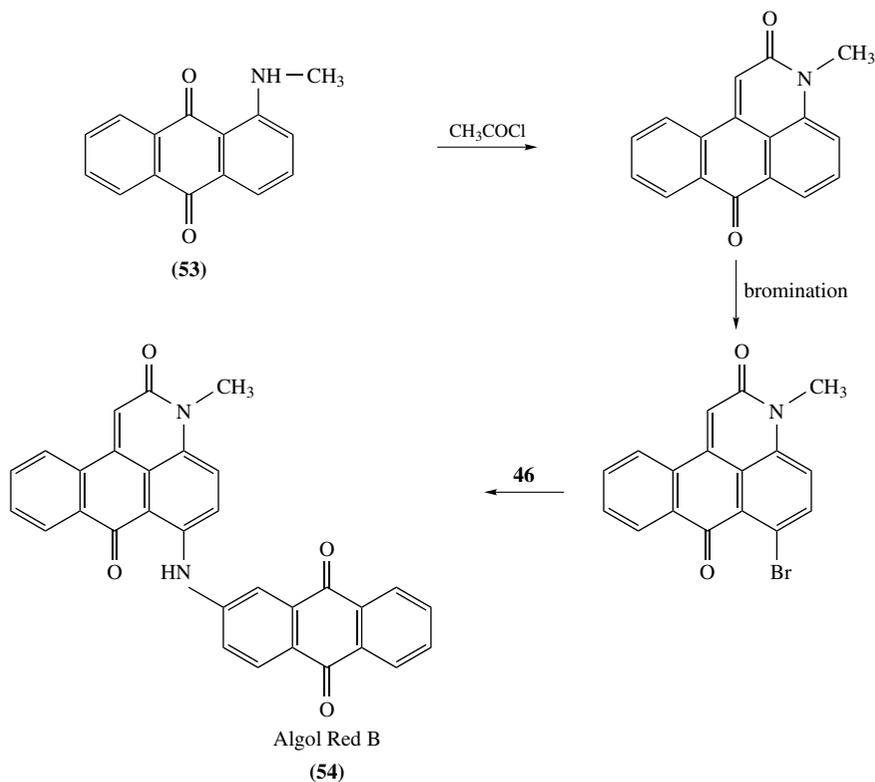
SCHEME 20. Synthesis of Algol red B

N,N-dibenzoyl-1,4-diaminoanthraquinon
Algol red 5 G

(55)
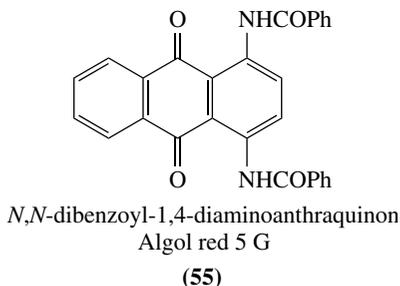
Greune worked on another interesting reaction. He condensed 3-amino-*N*-ethylcarba-zole **(60)** with chloranil **(61)**, and then heated the product in nitrobenzene to afford the first dioxazine pigment **62** (Scheme 22). This led to other condensations with aromatic amines, and a range of products that included sulfonated dyes for dyeing silk, wool, cellulose and viscose a very fast blue. Finally, naphthol AS, 2-hydroxy-3-naphthanilide **(63)** and similar products were developed mainly at Griesheim Elektron from 1909. These were applied direct to the fiber, which was then treated with a diazonium compound to afford fast bright colors that were resistant to light and cleaning. From 1930, research was

1,4,5,8-naphthalene-
tetracarboxylic acid

(56)   (57)   *trans*   *cis*
      (58)   (59)

SCHEME 21

(60)   (61)

(62)
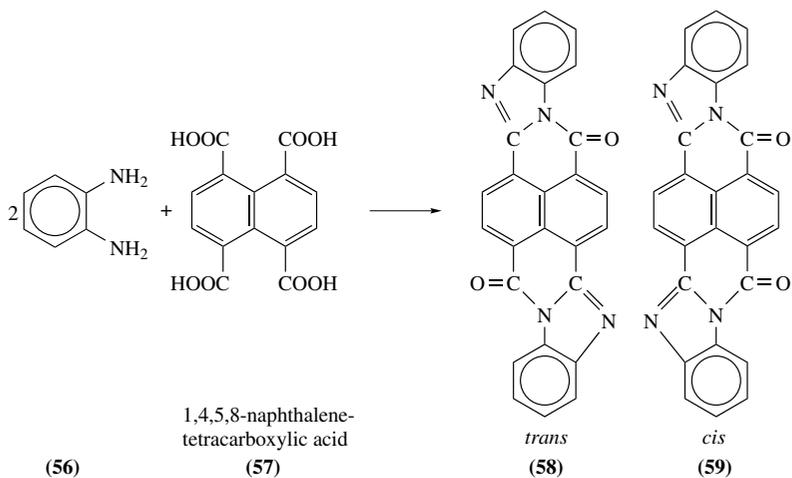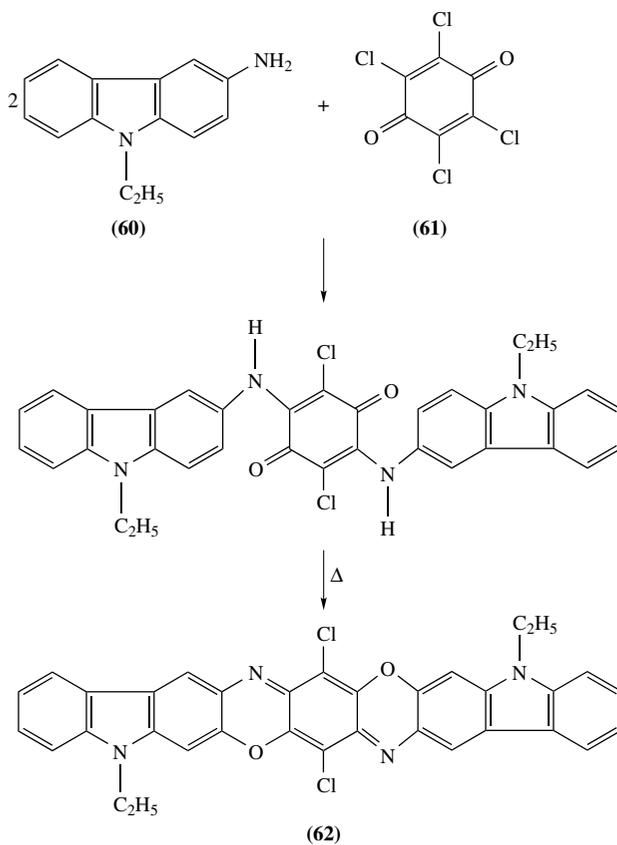
SCHEME 22
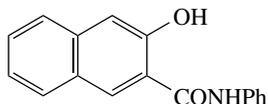
naphtol AS
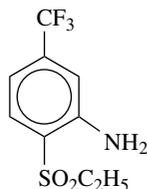
(63)   **(64)**

undertaken into trifluoromethyl derivatives of naphtol AS colorants. Apart from a useful shift towards yellow, brighter, faster colors were obtained with, for example, 1-amino-5-trifluoromethyl-2-ethylsulfonylbenzene **(64)**.

XIII. THE UNITED STATES SYNTHETIC DYE INDUSTRY

The first decade of the 20th century marked the end of half a century of remarkable inventiveness in aniline products and synthetic dyestuffs that had started with William Perkin's 1856 discovery of the aniline dye known as mauve. Through intensive research and development, control of patents and aggressive marketing, the industry was dominated by German manufacturers, such as BASF, of Ludwigshafen (Figure 16), and Bayer, of Leverkusen. Before 1914, the US possessed around seven manufacturers of synthetic dyes (one at Rennselaer owned by Bayer), none of great significance; the extensive textile industry of the US relied on imports of foreign, mainly German, synthetic dyes. This latter source was reduced to a trickle at the outbreak of World War I as a result of restrictions on exports from Germany and the British blockade on transatlantic German merchant shipping. The last German-made dyes arrived in the US through normal channels at the end of April 1915[74]. This led to expansion of the then tiny US synthetic dye industry, from which emerged that nation's modern organic chemicals industry.

American chemical and textile firms began the large-scale production of coal-tar intermediates. E.I. du Pont de Nemours & Co., Inc., of Wilmington, Delaware, better known as

FIGURE 16. BASF, Ludwigshafen, showing interior of indigo building. BASF Archives.

DuPont, shared information with the Levinstein firm in Manchester, England. The Calco Chemical Company, founded in 1915 mainly to manufacture intermediates, resorted to German textbooks, an American academic consultant and industrial chemists[75,76]. Calco, through trial and error—a great deal of both—and a government contract for TNA **(41)**, built up expertise in intermediates manufacture. The Grasselli Chemical Company commenced sulfur dye manufacture at Linden, New Jersey, in 1915, and purchased the Bayer facility in 1919. This was the forerunner of the General Aniline & Film Corporation.

Dow Chemical Company embarked on the manufacture of synthetic indigo in 1916. In October 1917, not long after the US entered World War I, Congress passed the Trading-with-the-Enemy Act, and the Office of Alien Property was established. The act enabled the Federal Trade Commission to issue licenses for the use of German patents, particularly dyestuffs and pharmaceutical products based on coal-tar intermediates. The US was now a major player in the business of making anilines and their products.

After the war, Calco (Figure 17) and other American start-ups were able to share the spoils of German inventions when the sequestered German patents were made available through an organization called the Chemical Foundation, Inc. This appropriation of intellectual property rights was part of the war booty that America had sequestered after Congress suspended the privilege of monopoly accorded to German patents. In the US during 1920, some one-hundred factories produced 88 million lbs. of dyes, which was fifteen times the output in 1914. They were aided by extension of a 1916 tariff on German dyes, and through passage of the temporary Dye and Chemical Control Act in 1921[77]. A further aid to the US dye industry was the surplus war gas phosgene, that before 1915 was mainly imported, and cost $1.50 a pound. It was now available in abundance at 10 to 15 cents a pound. Combined with N,N-dimethylaniline it yielded Michler's ketone, the silvery flake-like intermediate from which malachite green, auramine, crystal violet, Victoria blue and other colorants were manufactured.

Capabilities were built up in the transformation of patent recipes and new knowledge into useful products. During the 1920s, there were opportunities to gather ideas from Europe, such as amino resin processes, and for Calco and DuPont to absorb American firms with the requisite proprietary knowhow. Meantime, in Germany, I.G. Farben was formed in 1925 by the merger of Bayer, BASF and Hoechst (later incorporating AGFA, Griesheim and Cassella), following a loose association created in 1916. The British Dyestuffs Corporation became part of ICI, founded in 1926, in response to German events.

Since Calco's activities encompassed practically every sector of chemical manufacture involving anilines, commencing with intermediate, dye and explosive manufacture during World War I, it will frequently be used here, through these products, to delineate the rise of important sectors of the modern US organic chemicals industry. After Calco was acquired by American Cyanamid in 1929, new products based on aryl amines were invented (Figure 18).

During the 1930s the United States took second place, after Germany, as major manufacturer of coal-tar intermediates and dyes. Coal-tar chemistry advanced beyond dyestuffs to the production of a vast range of intermediates, particularly aryl amines, for many uses. The prominent standing of the US was such that it inspired a young schoolboy, twelve-year-old Robert Burns Woodward, later to become the greatest synthetic organic chemist of the 20th century, to write the following account for his school magazine:

'Coal Tar Dyes

Nearly every girl in this school wears a dress that has many colors upon it. But how many know where those dyes come from. They are coal tar derivatives.

When coal is distilled many products are formed. Among these is aniline, one of the greatest dyestuff intermediates. This compound is the basis of many dyes such as aniline black, Rosaniline, and nearly every color of the rainbow.

FIGURE 17. Advertisement for Calco Chemical Company, Bound Brook, New Jersey, 1925. Edelstein Collection
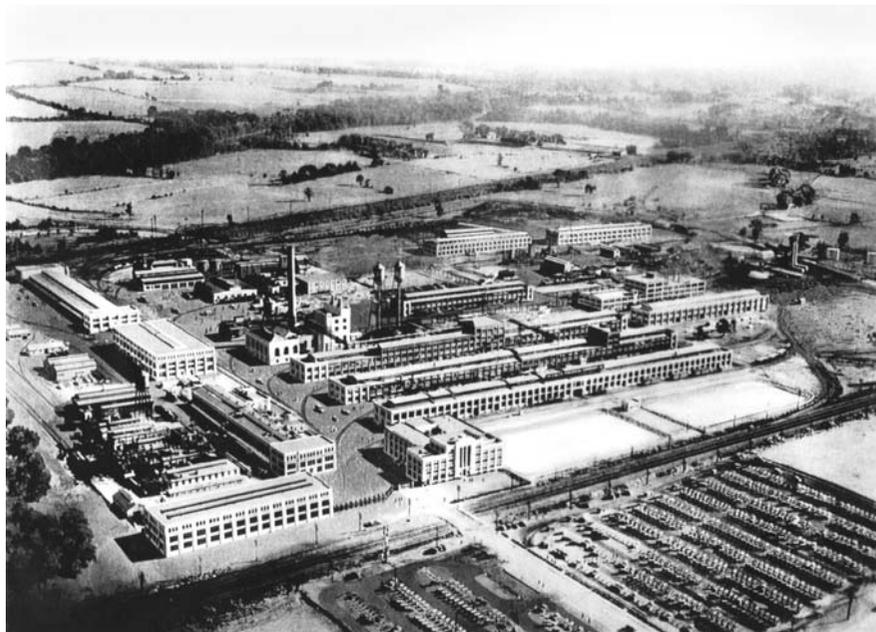
FIGURE 18. Calco Chemical Division, American Cyanamid Company, Bound Brook, New Jersey, 1938. This facility was a major manufacturer of aniline and other aromatic amines, and in the 1950s pioneered the large-scale production of aniline by continuous fluid-bed, vapor-phase reduction of nitrobenzene (Catan process). Edelstein Collection

Then aniline unites indirectly with other compounds, formed more complicated dyes such as methylene blue, aniline green, aniline red, methyl orange, methyl violet, orange II, and primul[i]ne. All of these are biological stains.

Then aniline unites with other substances which form brilliant orange and red dyes'[78].

There were other demonstrations of the importance of the anilines. In Germany Karl Aloys Schenzinger's novel *Anilin*, a somewhat skewed version of the emergence of the aniline-dye industry, served the racial purposes of the Nazi regime. Over 3 million copies would be printed, some after 1945[79].

DuPont was one of the leading American chemical corporations whose business had been transformed by the entry into anilines and dye research. A major manufacturer of aniline and other coal-tar products was the group of firms Schoelkopf, National Aniline, Barrett and Benzol Products that in May 1917 had associated to form what was soon known as National Aniline & Chemical Corporation (NACCO, from 1941 a constituent of Allied Chemical & Dye Corporation). In 1924, Bayer entered into a partnership with Grasselli, that had aquired Bayer's former factory at Rensselaer. In 1928, the joint enterprise was taken over by I.G. Farben and renamed General Aniline Works, Inc. In 1939 it became known as General Aniline & Film Corporation, and supplied around 20% of American-made dyes, some produced from imported German intermediates, particularly anthraquinones. An important development in vat dye production, taken up on a large scale in the US from the mid-1920s, was the building up of anthraquinone from naphthalene-derived phthalic anhydride. This was pioneered industrially in the US during World War

I and removed dependence on imported anthracene, the source of anthraquinone. It also made available a new route to 1-aminoanthraquinone (49), based on condensing phthalic anhydride with chlorobenzene, followed by amination[80].

XIV. OTHER INNOVATIONS

In 1927, as a result of the move into the relative complexity of aromatic organic chemistry, initiated by dyestuffs and intermediates, both Calco and DuPont enhanced their research facilities. The creation of a formal Research Department at Calco was the single most important innovation necessary to ensure the smooth integration of additional products and processes. With this, Calco became one of the first American chemical firms to establish dedicated research and development facilities[81]. DuPont constructed a laboratory complex known as 'Purity Hall', that inaugurated a fundamental research program[82].

In Britain during 1932–1933, a major discovery took place at what would soon be an ICI acquisition, Scottish Dyes. By chance, a blue colorant was obtained during preparation of phthalimide from phthalic anhydride and ammonia. Though not an aromatic amino compound, the stable product is important in the history of dye discovery. It was a phthalocyanine compound, of the type first prepared in 1907. ICI manufactured the copper analogue, known as Monastral fast blue. Introduced in 1934, it represented the first member of the only new structural class of synthetic dye in the 20th century[83].

The Japanese synthetic dye industry emerged during World War I; by 1920 its exports to China were competing with the products of European and US manufacturers. The industry then went into decline, but was revived during the 1930s mainly by Japanese Dyestuffs Manufacturing Co., the largest firm, Mitsui Bussan Kaisah Ltd, Mitsui Kozan Kabushki and Mitsubishi Dye Co. The war also encouraged dye manufacture in Italy and Spain. The Soviet Union relied on newly opened and former German and Swiss factories, that produced 10,000 tons of dyes each year, and also on German imports.

During the 1890s hydroxyanilines were introduced as developers in photography. Oxidation of aniline affords quinone (65), which on reduction gives the important photographic developer hydroquinone, or p-hydroxybenzene (66). Until 1915, the principal source was Europe. After the price increased by 600% in the US, manufacture was attempted by several firms. Though British and German processes involving oxidation of phenol had been developed, DuPont commenced manufacture around 1920 by oxidation of aniline with sodium dichromate, followed by reduction of the quinone with sulfur dioxide. In 1924, Eastman Kodak adapted the same process, using manganese dioxide and sulfuric acid as the source of oxidant (Scheme 23). In 1942, US production of photographic grade hydroquinone, by then of great strategic value, exceeded 3 million lbs.[84]. Derivatives of aromatic amines were employed as the important color formers in the color reversal transparency films first introduced by Kodak (1935) and AGFA (1936).

Triaminobenzene (67) became an important intermediate in production of phloroglucinol, 1,3,5-trihydroxybenzene (1,3,5-benzenetriol) (68), first made by hydrolysis of 67 in the laboratory in 1867[85]. Manufacture, commencing with reduction of trinitrobenzoic acid with tin and hydrochloric acid, was adopted by I.G. Farben for use in the diazo type reproduction processes. This gave a positive image of a line drawing using a light-sensitive diazonium compound and a hydroxy compound, as invented in the mid-1920s. The process was associated with ozalid light-sensitive papers. Phloroglucinol gave a stable jet black background. In 1935, it was first made in the US by Edwal Laboratories, in Chicago, and from 1941 at Ringwood, Illinois. During World War II it was also used in the development of black diazo dyes, particularly on acetate rayon. After 1945, surplus TNT was consumed in the production of phloroglucinol (Scheme 24). For the reduction step, Edwal replaced the expensive tin with iron. The triaminobenzene was also used in the production of antipyretics[86].

(1)   **(65)**

(66)

SCHEME 23

trinitrotoluene (TNT)   trinitrobenzoic acid   triaminobenzene

(67)

phloroglucinol

(68)
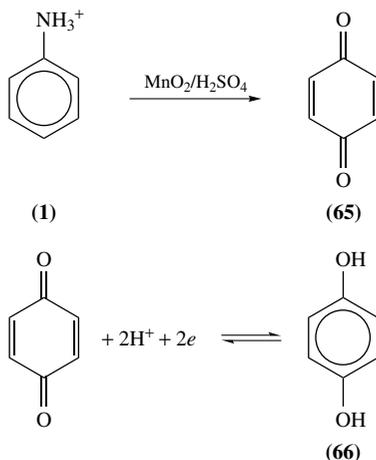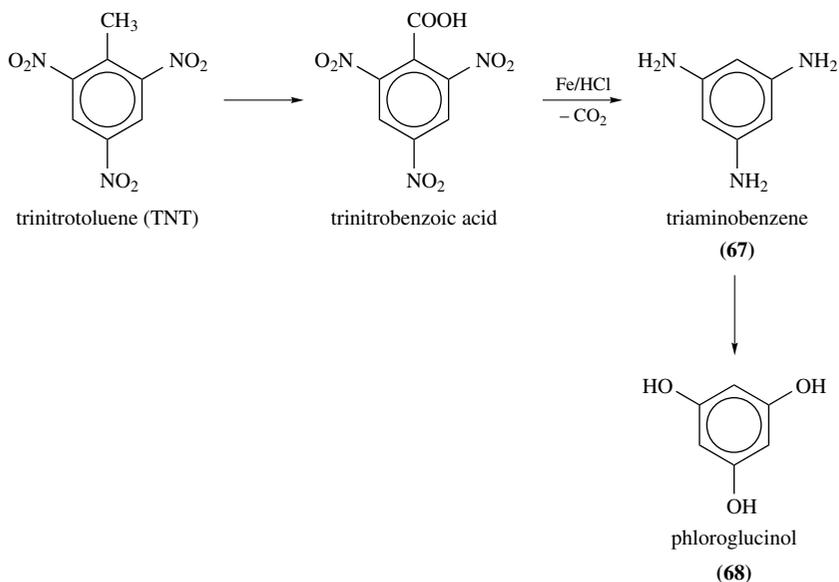
SCHEME 24. Synthesis of phloroglucinol from TNT

XV. MEDICAL RESEARCH AND SULFA DRUGS

Towards the end of the 19th century, the German dye industry embarked on diversification based on its coal-tar intermediates. These became important medicinal products, including Bayer's aspirin, made from the intermediate salicylic acid (*o*-hydroxybenzoic acid). The first local anesthetics were esters of aminobenzoic acid. In 1906, Hoechst introduced the anesthetic novocaine **(45)**, marketed as the hydrochloride of diethylaminoethyl *p*-aminobenzoate, based on the research of Alfred Einhorn. Novocaine was the standard

NHCOCH$_2$N(C$_2$H$_5$)$_2$

H$_3$C   CH$_3$

N=N

H$_2$N   N   NH$_2$
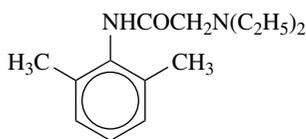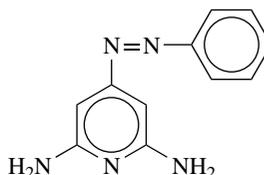
(69)   **(70)**

injectable local anesthetic until the late 1940s, when it was joined by lidocaine **(69)**, another aniline derivative. Some aniline colorants, the medicinal dyes, such as **33** and **44**, and the 2,6-diaminopyridine derivative pyridium **(70)**, were used extensively during World War I and after as antiseptics.

Aniline dyes had been used as models for products that attacked sites of infection within the body by the medical researcher Paul Ehrlich. He employed tissue staining with synthetic dyes at the University of Strasbourg in the early 1870s to develop a new research methodology in the biomedical sciences. Ehrlich followed biological oxidation−reduction processes, using gain and loss of color of stains, and adapted Witt's theory of color and constitution, and aromatic structures, to suggest structural features of living cells. This was then developed into his side chain theory of immunity. Antitoxin behavior was pictorially represented by cartoon-like drawings that demonstrated the combining and toxic components of antigenic toxin. These were named the haptophore and toxophore groups, respectively[87].

Ehrlich sought out dyestuffs that might attack sites of infection within the body. His first success, in 1891, was with the thiazine dye methylene blue **(33)**, used against malaria, though the side effects, including skin coloration, militated against practical application. In 1905, Ehrlich began to employ the aniline derivative atoxyl **(71)**, that had shown action against trypanosome infections. Though the structure of atoxyl was then uncertain, Ehrlich reduced its pentavalent arsenic to the trivalent state. In 1906 with Alfred Bertheim he established that atoxyl was the sodium salt of p-aminophenylarsonic acid. Numerous derivatives were synthesized, including compound 606, arsephenamine, 3,3′-diamino-4,4′-dihydroxyarsenobenzene **(72)**, containing trivalent arsenic, by Ehrlich's Japanese coworker Sahaschiro Hata in 1909. Hata found that it cured chicken spirillosis, relapsing fever and, especially, syphilis. This amino-containing analogue of an azo dye, known as salvarsan, was marketed by the Hoechst dyeworks in 1909. In 1912, an improved preparation, neosalvarsan **(73)**, with a blocked amino group, was marketed. It soon represented one quarter of turnover at Hoechst. (The structures are more complex than as shown here.)

Ehrlich again used Witt's color theory, this time to describe drug action. Ehrlich favored a chemical model for drug action, and suggested that both drugs and poisons formed chemical bonds with the cell. The drug, according to his description, 'fits the biological receptor'. He postulated that drug action was similar to that of antitoxins. His chemoreceptor theory was developed after observations on strains that showed acquired resistance to dyestuffs and their analogues. He defined an ideal drug as one that would contain a haptophore group to enable it to attach specifically to the receptor on the parasite, but that would be harmless to the host. Just as antibodies 'in the manner of magic bullets, seek out the enemy', it was hoped that drugs might be accurately targeted to score a 'bullseye' in a similar way. This became a major tool in medical and agrochemical research. Ehrlich's terminology, like that of Witt, is still in use[88−90].

When in 1925 the main German firms merged their interests to create the behemoth I.G. Farben, the name reflected historical roots rather than the main range of activity. Nevertheless, aromatic amino compounds were at the forefront of research into novel

NH$_2$ ... NH$_2$

HO—[ring]—As=As—[ring]—OH

3,3′-diamino-4, 4′-dihydroxyarsenobenzene
(compound 606)
(salvarsan is the dihydrochloride)

NH$_2$

[ring]

HO—As—ONa
‖
O

atoxyl
(sodium salt of *p*-aminophenyl arsonic acid)
(71)

OH
NH$_2$

[ring]

As ... n

modern formula
(72)

H   O
| ‖
H$_2$N   N—CH$_2$C—O$^-$

Na$^+$

HO—[ring]—As=As—[ring]—OH

neosalvarsan (blocked amino group) (compound 914)

(73)
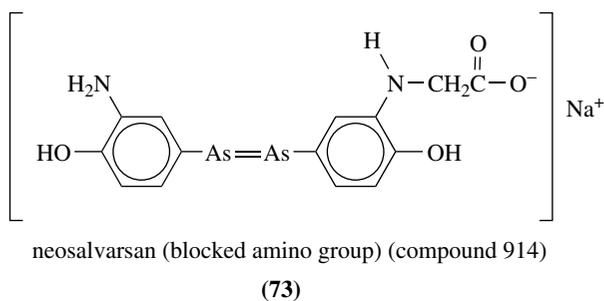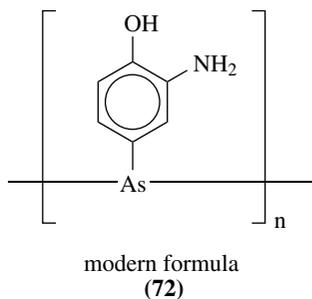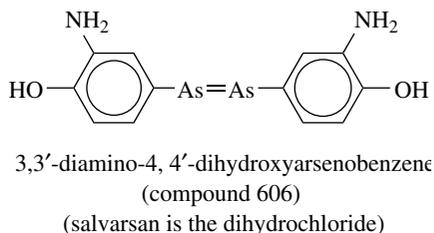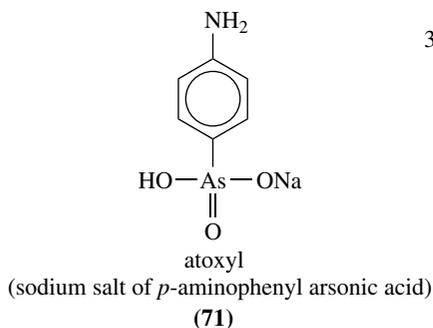
medical products, particularly those required for specific bactericidal use. In the mid-1930s
the curative action of a bright red azo dye led to the discovery of the first antibacterial
sulfonamide, or sulfa, drug at the Bayer division of I.G. Farben. The trade name was
prontosil **(74)**[91].

H$_2$N—[ring]—N=N—[ring]—SO$_2$NH$_2$

H$_2$N

(74)
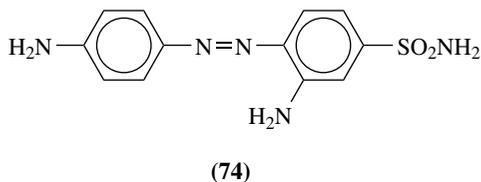
It was a sulfonamide, or sulfamido, derivative of the azo dye chrysoidine **(18)**. French
workers at the Pasteur Institute discovered during a screening campaign that *p*-aminoben-
zenesulfanilamide **(75)**, commonly called sulfanilamide, was an equally effective curative

agent. They quickly established that this compound was in fact a breakdown product of prontosil, formed by cleavage of the azo link in the organism. The preparation of sulfanilamide had been described in 1908 and therefore could not be patented. This enabled several companies to undertake its manufacture and engage in research into what became known as sulfa drugs. American Cyanamid's Calco Chemical Company was the first manufacturer of sulfa drugs in the US.

H_2N—⬡—SO_2NH_2 sulfanilamide (1935)

(75)

H_2N—⬡—SO_2—$\overset{H}{N}$—⬡ (pyridine)   sulfapyridine (1938) (M&B 693)

(76)

H_2N—⬡—SO_2—$\overset{H}{N}$—C (thiazole ring: S—CH, CH, N)   sulfathiazole (1938)

(77)

H_2N—⬡—SO_2—$\overset{H}{N}$—C$\overset{NH}{\underset{NH_2}{}}$ sulfaguanidine (1940) (sulfanilylguanidine)

(78)

H_2N—⬡—SO_2—$\overset{H}{N}$—⬡ (pyrimidine ring: N, N)   sulfadiazine (1940) (sulfapyrimidine)

(79)
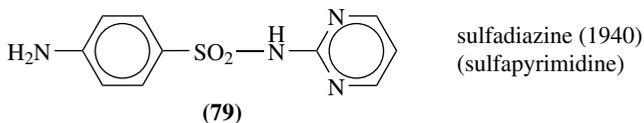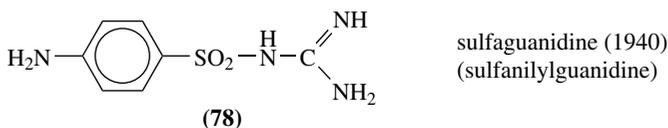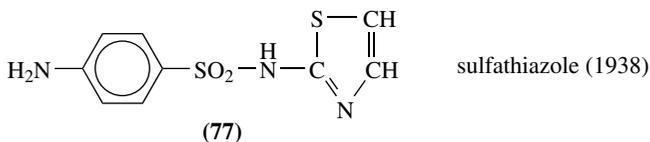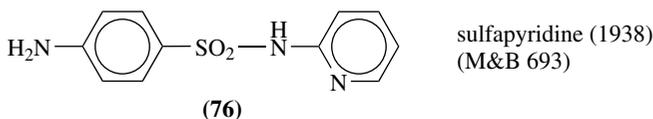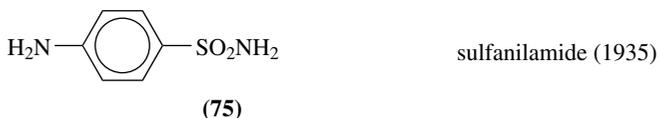
The next major discovery was made in 1938 at May & Baker, of Dagenham, Essex, England. Starting with 2-amination of pyridine, chemists prepared what soon became known as M&B 693, or sulfapyridine **(76)**. Sulfapyridine reduced the death rate from pneumonia from 83.1 per 100,000 in the 1930s to 44.1 in 1946. This was followed by sulfathiazole **(77)**. The poorly absorbed sulfaguanidine **(78)**, discovered in 1940, was introduced in 1941[92]. Sulfadiazine (sulfapyrimidine) **(79)** was also discovered in 1940. Sulfaguanadine was followed by succinylsulfathiazole. Sulfa drugs were important even after the introduction of penicillin, especially for veterinary use. Further research at Bayer stimulated by the success of sulfonamides included the thiosemicarbazone conteben **(80)**, introduced at the end of the 1940s for the first chemical therapy against TB.

Acetanilide **(81)** has long been known to be a useful painkiller, though widespread adoption was restricted by its toxic properties in moderate doses. It was introduced in 1886 by Kalle & Co. as antifebrin, and followed in 1887 by Bayer's *p*-acetophenetidine,

$$NHCOCH_3$$

$$HC=N-NH$$

$$C$$

$$S \quad NH_2$$
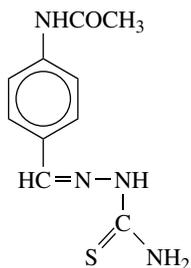
conteben
(*para*-acetamidobenzaldehyde thiosemicarbazone)

(80)

(81)	**(82)**	**(83)**
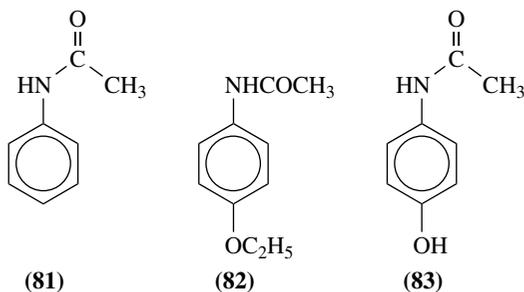
or phenacetin **(82)** (Scheme 25), that had fewer side effects. Unlike quinine, they were antipyretic and analgesic. In 1893, *N*-acetyl-*p*-aminophenol **(83)** was found to possess similar properties and, shortly after, was found to be a metabolite of **81**. After 1948, **83** was developed into the drug Paracetamol, introduced in Britain during 1956. Paracetamol is preferred to acetanilide, since metabolism of the latter affords aniline.
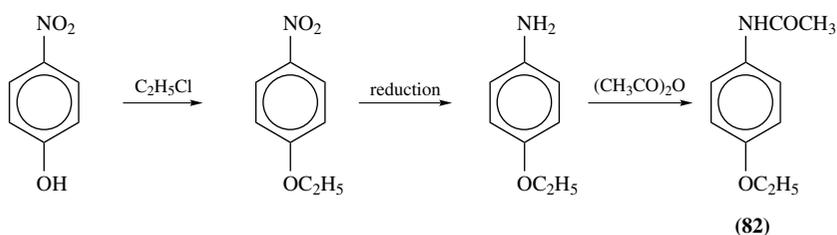
SCHEME 25

XVI. ANTIMALARIALS

The quest to tackle malaria with a synthetic drug was the challenge that led William Perkin to the discovery of his aniline purple, or mauve **(5)**, in 1856. Research into antimalarials continued to attract attention, at first to aid colonial expansion, and later because of shortages in time of war. Research was guided by the fact that quinine was found to be an oxygenated quinoline, a 6-methoxyquinoline derivative **(84)**, as established by Zdenko H. Skraup. The structure became available in 1908, through the research of Paul Rabe[93].

quinine
(84)
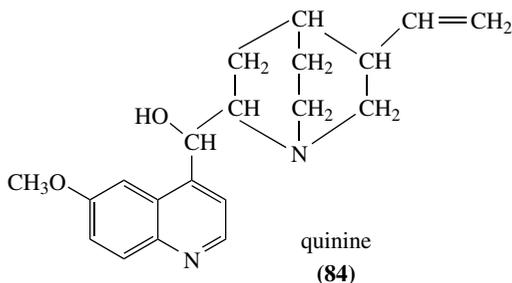
Synthetic antimalarials, derivatives of quinolines and acridines, were investigated in the 1920s at Bayer (and later at I.G. Farben), particularly by the chemotherapist Wilhelm Roehl, and this led to a few successes. Thus 4-methoxyaniline **(85)** was the starting point for the 8-aminoquinoline **86**, synthesized in 1924 by Fritz Schönhöfer and August Winkler, and tested by the pharmacologist Werner Schulemann. The I.G. Farben workers reported its antimalarial activity in 1926, and it was introduced in 1927 as Plasmoquine (known as plasmochin in the US, and pamaquine in the UK) (Scheme 26). However, it turned out to be quite toxic to humans. It was followed in 1930 by the less toxic substituted 9-aminoacridine **87** synthesized by Fritz Mietzsch and Hans Mauss, and introduced in 1932 as Quinaquin (atabrine in the US, mepacrine in the UK). This had the disadvantage that the skin and eyes of patients turned yellow. Further research at Bayer led to the synthesis in 1934 by Hans Andersag and colleagues of the 4-aminoquinoline derivative **88**. Its antimalarial activity was established by Walter Kikuth (Roehl's successor) and the product was patented in 1937, and known as Resochin[94]. However, according to a test procedure devised by Roehl it was quite toxic.
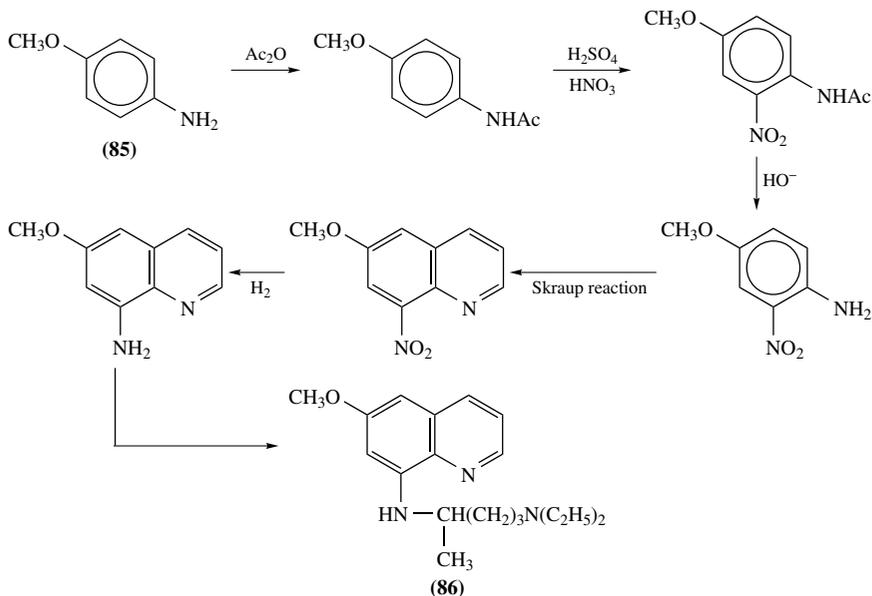
SCHEME 26. Synthesis of Plasmoquine (plasmochin, pamaquine)

CH_3 $(CH_2)_3-N(C_2H_5)_2$
\
CH
NH

OCH₃

Cl

N

2-methoxy-6-chloro-9-(*N*-diethylamino
isopentylamino)-acridine

(87)

CH_3 $(CH_2)_3-N(C_2H_5)_2$
\
CH
NH

Cl

N

4-(*N*-diethylamino isopentylamino)-
6-chloro quinoline (Resochin, chloroquine)
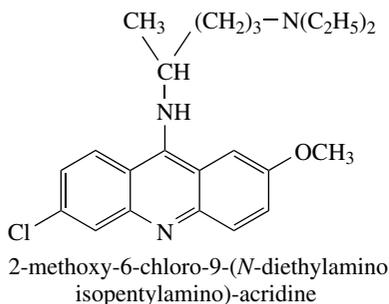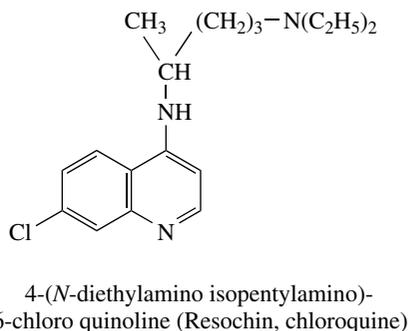
(88)

In 1942, Japan invaded Java, and controlled much of the world supply of quinine. In the US, under the aegis of the Office for Scientific Research and Development, a massive program of research into antimalarials was inaugurated. This was partly aided by tablets of Sontochin, a product found in the possession of German prisoners, and the assistance of the Winthrop Chemical Company, former outlet for I.G. Farben pharmaceuticals, including for atebrine **(87)** (then called Quinacrine in the US). Sontochin, similar to **88**, was 3-methyl-4-(4-diethylamino-1-methylbutylamino)-7-chloroquinoline. In the US, **88**, supplied by Winthrop, was found to be more effective. This was the drug Resochin that had earlier been tested by German workers but was rejected for widespread use, due to its toxicity. The outcome of American research was a multistep process, starting with *m*-chloroaniline, to yield **88**, soon known as chloroquine (Scheme 27). It remained the drug of choice for treatment of malaria for several decades (see Chapter 14)[95,96]. The formal total synthesis of quinine was achieved by Robert Burns Woodward and William von Egers Doering in 1944[97].
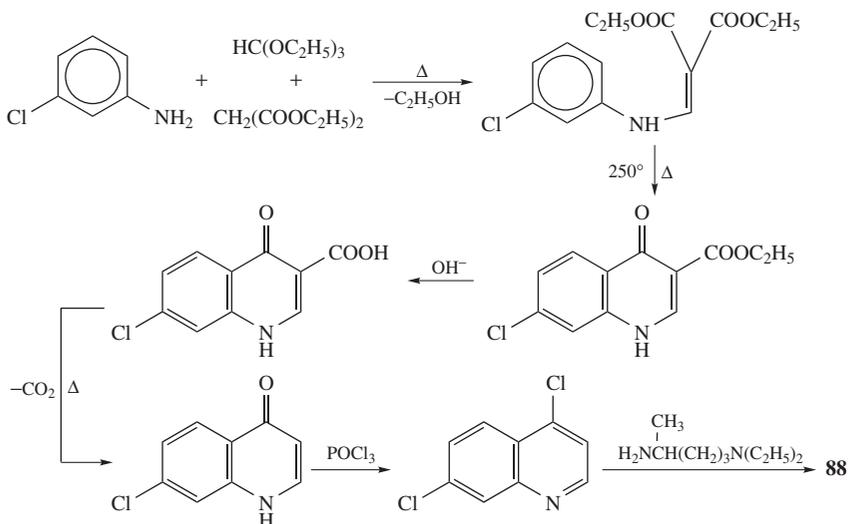
SCHEME 27. Synthesis of chloroquine

During World War II, chemists at ICI, then a newcomer in pharmaceutical research, discovered antimalarials based on biguanidines, including proguanil **(89)** (Paludrine, 1944), prepared from 3-chloroaniline (Scheme 28), and its metabolite dihydrodiazine **(90)**. In 1950, George Hitchings developed the diaminotriazine into what became known as pyrimethamine (Diaprim) **(91)** (Scheme 29)[98].
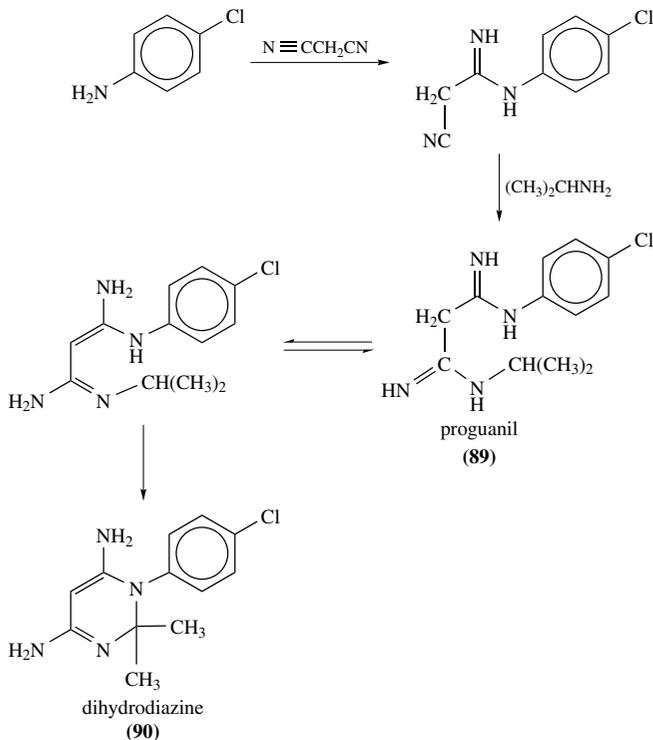
SCHEME 28. Synthesis of proguanil and metabolism to dihydrodiazine
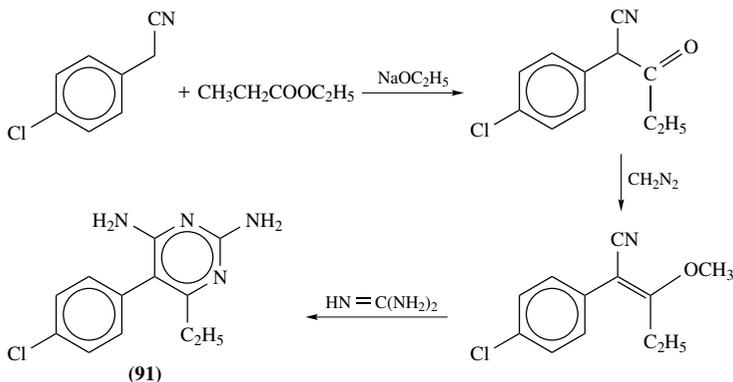
SCHEME 29. Synthesis of pyrimethamine

Research into other antiparasitic drugs included antitrypanosomiasis agents. This work had started with Ehrlich's investigations of benzidine derivatives, including trypan blue (**92a**), trypan red, nagana red (**92b**) and Afridol violet (**92c**). While these products were effective they had the major disadvantages of coloring body fluids and tissues. This led chemists at Bayer in 1920 to remove the chromophore and prepare the aminonaphthalenesulfonic acid derivative suranim (**93**), and then develop the diamidines dimidium (**94**) (Scheme 30) and quinapyramine (**95**).

trypan blue

(**92a**)

nagana red

(**92b**)

Afridol violet

(**92c**)

suranim

(**93**)
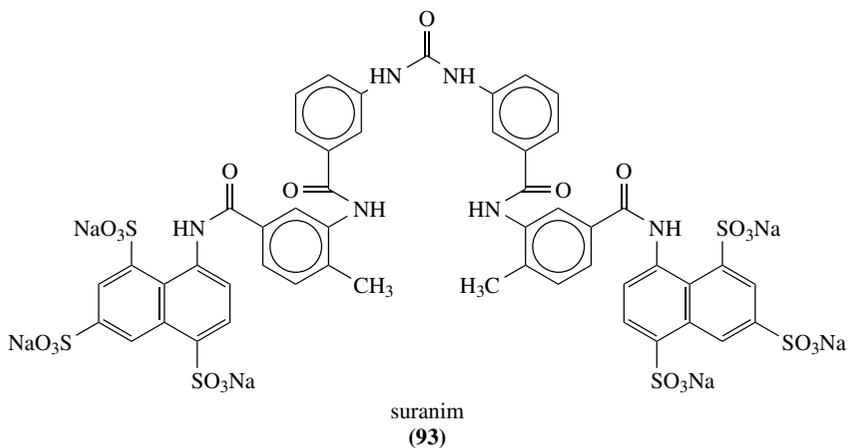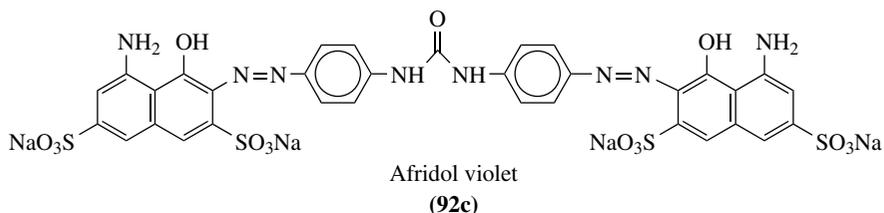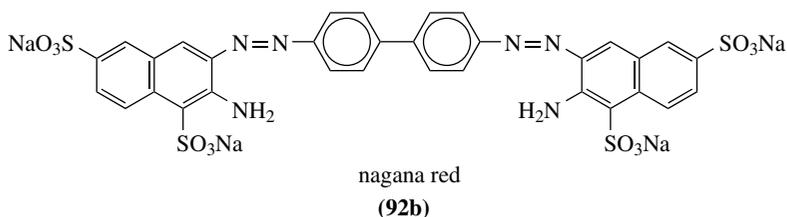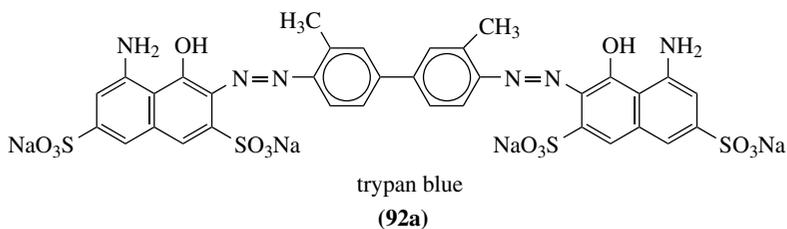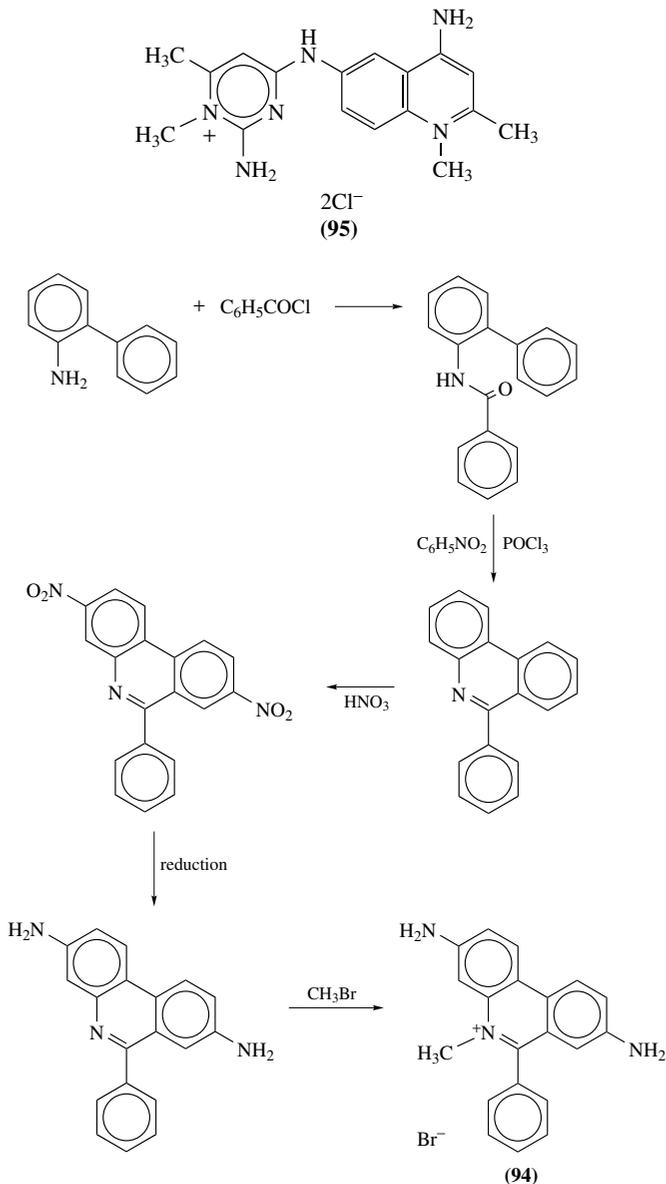
SCHEME 30. Synthesis of **94**

XVII. RUBBER PRODUCTS AND POLYMERS

The growth of the automobile industry and its demand for long-lasting, chemically-resistant rubber products provided an important large-scale use for the coal-tar interme-diates, mainly aniline and ß- or 2-naphthol. This followed George Oenslager's discovery

(96)
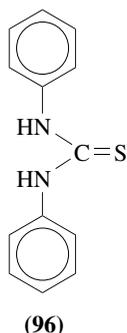
in 1906 at Diamond Rubber in the US that aniline, its less toxic derivative thiocarbanilide (diphenylthiourea) **(96)**, and related organic chemicals containing sulfur accelerated the vulcanization of rubber. Vulcanization enhances cross-linking in rubber that enables restoration of elasticity following deformation. Around 1910, Fritz Hofmann and Kurt Gottlob at Bayer found that ammonium dithiocarbonates made from both aromatic and aliphatic amines were also good accelerators. The patents were licensed to Grasselli for manufacture in the US[99a]. William F. Russell and David Spence introduced *p*-aminodimethylaniline as a rubber accelerator. By 1914 several firms were manufacturing the products invented by Oenslager, for which patents had not been filed. When shortages of imported aniline at the outbreak of World War I affected the production of accelerators as much as it did the manufacture of synthetic dyes, both B. F. Goodrich and United States Rubber erected large in-house aniline production facilities[99b].

In 1921, C. W. Bedford, at Rubber Services Laboratories Co., L. B. Sebrell, for Goodyear Tyre & Rubber, both in the US, and Bruni and Romani at Pirelli, in Italy, developed mercaptobenzothiazole (MBT) **(97)** as an organic accelerator. In 1931, Bayer converted mercaptobenzothiazole into sulfenamides, that contain the grouping =CSNR$_2$. These later became the most important class of accelerators.

In 1933, the Calco Chemical Company began the manufacture of **97** by reacting aniline, carbon disulfide and sulfur together at elevated pressure (Scheme 31), and late in 1936 introduced mercaptobenzothiazyl disulfide (MBTS) **(98)**. Goodyear was the major customer. Zenite 'ultra-accelerators', incorporating zinc **(99)**, that brought about vulcanization in a few minutes, were introduced by Calco in the late 1930s[100].
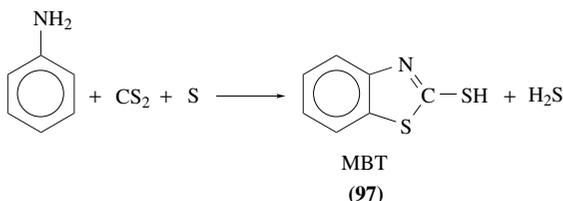
SCHEME 31. Manufacture of mercaptobenzothiazole (MBT)

Dyestuff research based mainly on aromatic amines had brought about large-scale sophisticated research in the US chemical industry. Around 1930, this enabled the rapid move into polymers, resulting at DuPont in the discovery of a successful synthetic rubber process (1930) and nylon (1935). The discovery of polythene at ICI in 1935 arose from research into synthetic dyestuffs and reactions carried out under high pressures,
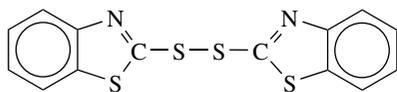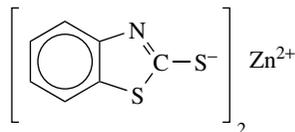
(98)   **(99)**
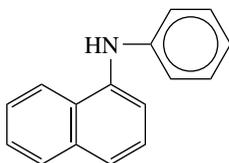
(100)

and academic research at the University of Amsterdam. These and other polymers stimu-
lated new investigations into colorants and, in the case of synthetic rubber, following its
massive development in the US during World War II, into accelerators and antioxidants
based on aromatic amines. Phenyl ß-naphthylamine (phenyl-2-naphthylamine) **(100)** was
the principal antioxidant used in the manufacture of GR-S (Government Rubber-Styrene)
rubber.

XVIII. MELAMINE

The Calco Chemical Division of American Cyanamid, formed in 1939, was synonymous
with the industrial production of the triaminotriazine melamine **(101)**, and of the polymeric
thermosetting resins that also bear its name. Polymeric melamine is converted by the action
of heat or catalysts, or both, into insoluble infusible solids, which are odorless, tasteless
and generally inert chemically.

The triazine compound melamine (2,4,6-triamino-1,3,5-triazine) was first isolated, and
named, in 1834 by Justus Liebig, who obtained it by reacting alkali with melam. A.
Claus in 1875 improved on Liebig's method. S. Cloëz and S. Cannizzaro in 1851, and
E. Dreschel in 1875 and 1876, demonstrated that melamine was formed when cyanamide
or dicyandiamide were heated at elevated temperatures (Scheme 32). In 1885, A. W.
Hofmann made melamine from thiocyanuric esters by heating them in sealed tubes with
concentrated aqueous ammonia[101].

The triazine formula was adopted in 1902, following the work of Otto Diels, and
Frederick D. Chattaway and John M. Wadmore. Though various industrial reactions for
preparing melamine were patented by Henkel and I.G. Farben of Germany, and CIBA,
the industrial process was perfected in 1939 by American Cyanamid which, significantly,
employed its calcium cyanamide. The polymeric melamine resins prepared via trimethy-
lol derivatives **102** and **103** (Scheme 33) became important in the strengthening of paper,
originally for military requirements. While the melamine resins were similar in many
respects to earlier urea-formaldehyde condensates introduced in the late 1920s, they dis-
played greater resistance to moisture and heat. The melamine molding product sold under
the trade name Melmac represented a tremendous advance in the discovery of aminoplas-
tics; it displayed superior molding and mixing properties[102–105]. The addition of fillers
results in resins much less sensitive to moisture, but the transparency is lost.

From 1945, Melmac was adapted for use in plastic tableware and became associated
with the names of leading industrial designers. Melamine was used in the highly suc-
cessful laminates applied to tabletops etc., produced by the Formica Insulation Company,

$$CaC_2 + N_2 \xrightarrow{\text{ca. 1000 °C}} CaCN_2 + C$$

calcium   calcium
carbide   cyanamide

$$CaCN_2 + H_2O + CO_2 \longrightarrow N\equiv CNH_2 + CaCO_3$$

cyanamide

$$2N\equiv CNH_2 \longrightarrow H_2NC=NC\equiv N$$
$$|$$
$$NH_2$$

dicyandiamide
('dicy')

SCHEME 32. Manufacture of melamine

trimethylol melamine
(102)

heat/HCHO

hexamethylol melamine
(103)

melamine resin ⟵ condensation polymerization / −H₂O

SCHEME 33. Manufacture of melamine resin

that had previously turned from Bakelite to urea resins. Melamine offered fast curing times, great durability and the use of light colors for hard-wearing kitchen counter tops, bars and dinettes. The Formica decorative laminates for tables and counters eventually displaced linoleum. Melamine also became important in the coatings and textile finishing industries[106].

XIX. ANILINES AND INSTRUMENTATION

Aromatic amines, and particularly their colored derivatives, were early candidates for industrial instrumental analysis. By the early 20th century the characteristic absorption spectra of synthetic dyes, including those containing amino groups, were available. Spectrophotometers were used in cases where colorimeters and tintometers were of little or no use, such as for examination of solutions containing two or more colorants[107].

Instrumental studies were promoted by Edwin I. Stearns, who joined Calco in 1933. His contributions commenced in 1934, when he adapted instrumental colorimetry to checking the solution-controlled blending of intermediates, particularly picramic acid, which explodes when dry. The safety of the process relied on reliable and rapid monitoring, and was aided by the instrument-based observations of Stearns. The developments at Calco greatly encouraged the wider use of instruments in chemical analysis, color control and research, particularly following the investigations of George L. Royer and Stearns. The first commercial recording spectrophotometer had been introduced in May 1935 by General Electric and was based on the work of MIT professor Arthur C. Hardy. The spectrophotometer, later more generally known as the spectrometer, measured relative amounts of radiant energy as a function of wavelength, and differed from the photometer used in colorimetry since it employed continuously variable monochromatic bands of energy. Standardization of intermediates and colorants moved from instrumental colorimetry to spectrophotometry in the 1940s after Stearns demonstrated the overwhelming superiority of the latter. By this time spectra of anilines, and many azo dyes, were available, and it was possible to discuss the influence of the position of substitution of amino and other groups[108,109].

Stearn's work represented the most successful use in industry of spectrophotometric curves for routine, reliable identification of aromatic molecules, and placed American Cyanamid at the forefront of spectrophotometry. R. Bowling Barnes at American Cyanamid's Stamford laboratories, in Connecticut, also made notable advances in instrumental analysis. Significantly, the first factory of Perkin-Elmer, founded by Richard S. Perkin and Charles W. Elmer in 1938 to manufacture advanced optical systems, was almost adjacent to the Cyanamid Stamford laboratories. The outcome was that the practical application of spectrophotometry was advanced more than in any academic laboratory by American Cyanamid scientists Stearns[110–112] and Barnes.

In 1944, Stearns and Eugene M. Allan achieved the first ever color match using instrumental data. In 1945, Barnes and colleagues, jointly with Richard F. Kinnaird of Perkin-Elmer, for the first time described the latter firm's model 12 infrared spectrophotometer. The outcomes of collaborations involving instrument and chemical manufacturers were widely adopted routine methods for qualitative and quantitative chemicals analysis. Stearns's *The Practice of Absorption Spectrophotometry* remains recommended reading for students[113].

The publications of American Cyanamid investigators included instrumental analysis of chemicals in the industrial environment, including two-component mixtures of nitrobenzene and aniline that were of value in industrial hygiene investigations. Details of this absorbance-ratio method were presented at the 4th Pittsburgh Conference on Analytical Chemistry and Applied Spectroscopy held in March 1953[114].

Aromatic amines are excellent examples of the application of infrared spectra to nitrogen compounds. Primary and secondary amines show moderately weak absorption at 3500 cm^{-1} to 3300 cm^{-1}, corresponding to N−H stretching, with two bands for primary amines and, usually, one for secondary amines. Bands that correspond to N−H bending are seen around 1600 cm^{-1}; they are weak with secondary amines. C−N stretching is observed at 1360 to 1250 cm^{-1} (strong absorption). Tertiary amines are difficult to detect. Though amino groups are transparent in the near-ultraviolet, they and other substituents influence absorption maxima. In fused rings, the absorption maxima make it possible to distinguish between 1- and 2-naphthylamines.

XX. STRATEGIC ANILINES

By the late 1930s, coal-tar intermediates were high on the list of strategic materials in both Europe and the US. In the US, production for 1939 was 605,757,000 lbs., some 50% more than in 1938. Of this figure, 41,775,000 lbs. was represented by aniline oil, 56 percent more than in 1938. This reflected its new uses, particularly in rubber processing. During 1940–1941, the output of aniline as part of the Lend-Lease program to aid Britain and Canada grew to an annual rate of around 12 to 15 million lbs.

The activities of the Calco Chemical Division of American Cyanamid following the entry of the US into World War II in December 1941 included tremendous growth in demand for aromatic amino compounds used in products other than dyes. Calco, unlike many other American firms, offered a diverse range of anilines and their products, covering intermediates for rubber-processing chemicals, synthetic resins and sulfa drugs. Production of aniline at Calco grew to 48 million lbs. at the behest of both the Chemical Advisory Committee of the Army and Navy Munitions Board and the Chemical Warfare Service. The capacity of the N,N-dimethylaniline plant was increased almost 10-fold, and later converted to the production of N-ethylaniline required for the manufacture of Centralite, the stabilizer in smokeless powder. Picatinny Arsenal at Dover, New Jersey, required dinitro-N-methylaniline for tetryl **(40)**, the booster for TNT. Melamine found use in coatings and laminates, plastics and glues, including military map and chart papers, invasion currency, naval electrical panels, aircraft ignition parts of great arc resistance, tableware for the armed forces, and adhesives for plywood planes and boat hulls.

Anthraquinone vat dyes, particularly the amino derivatives, and other colorants were required for coloring uniforms and for camouflage purposes. During 1942, total US dye production reached 152 million lbs., and coal-tar intermediates 1,230 million lbs., as a result of tremendous growth in demand for coal-tar aromatic compounds used in products other than dyes, including rubber-processing chemicals and synthetic resins. When the Office of Strategic Services required a shark chaser, or repellent, it turned to Calco's nigrosine (aniline black) range and induline. A special nigrosine colorant named Calco WBSR was tested during 1943. In 1944, the Naval Research Laboratory asked Calco to undertake further investigations, resulting in the development of a soluble nigrosine-based polyp 'ink' similar to the protective liquid emitted by sharks. The shark repellent and a Calco fluorescein dye used as a sea marker became part of the standard equipment in lifeboat, life-raft and life-jacket survival kits.

In 1943, Calco produced around 97% of the US consumption of sulfadiazine **(79)**, and was the sole American producer of sulfaguanidine **(78)**, both supplied to the Army and Navy Munitions Board. The armed forces also demanded sulfathiazole **(77)**, which cured several common diseases caused by streptococcus, staphylococcus, pneumonococcus and gonococcus, as well as preventing and curing wounds and burns[115]. In Britain, ICI stepped up manufacture of aniline and N,N-dimethylaniline for explosives, as well as for antimalarials and other pharmaceutical products[116,117].

Wartime conditions encouraged the use of waste products and investigations into continuous manufacturing processes. Thus, for example, I.G. Farben manufactured *N*,*N*-dimethylaniline from aniline and dimethyl ether, a waste from the synthetic methanol process, by a continuous autoclave process. Mercaptobenzothiazole **(97)** was also made by a continuous autoclave process. Allied investigators after 1945 were impressed by the great extent to which a number of traditional batch processes for aryl amines and their products had been successfully adapted to automated, continuous operation[118].

$$CH_3CONH-\bigcirc-CH=CH-\bigcirc-NH-N\bigcirc O$$

with SO$_3$H and SO$_3$H substituents

(104)

NHPh ... N N N ... NH—⟨ ⟩—CH=CH—⟨ ⟩—NH ... N N N ... NHPh, with morpholine O groups and SO$_3$Na, SO$_3$Na substituents
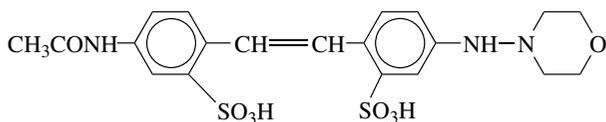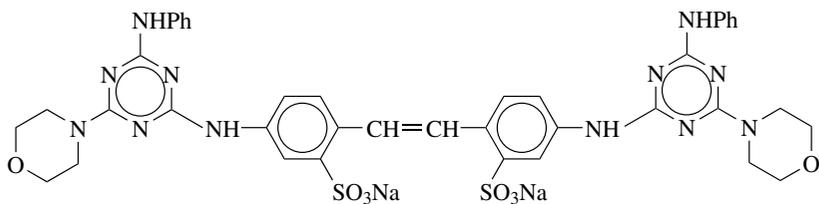
(105)

Novel fluorescent dyes, used as whitening agents (optical brighteners), invented at I.G. Farben, were exploited to great commercial advantage by American and European companies soon after the war. The brighteners, such as **104** and **105**, represented a trend in research away from dyes towards other energy-absorbing compounds, including IR absorbers and plastics additives.

In 1948, with the German chemical industry in disarray, the production of synthetic dyes in the US reached 220 million lbs., the highest figure ever, exceeding production anywhere. The US was now the largest manufacturer and exporter of coal-tar dyes, and would remain so until 1970[119]. The reemergence of the German chemical industry followed the separation of I.G. Farben into its pre-1925 constituent units. During December 1951–January 1952, the new successors were once more known as BASF, Bayer, and Hoechst. AGFA, whose Wolfen plant was in the Soviet zone, was reestablished at Leverkusen, merged with Bayer.

XXI. POLYURETHANES

During the 1950s, a new use for aniline was in the production of the thermoplastic polyurethanes. These relied on derivatives made from either aniline or nitrotoluenes, the latter reduced to toluidines such as **106**, to yield diisocyanates, typically **107** (Schemes 34 and 35). Otto Bayer at I.G. Farben had worked on polyurethane foams during World War II and details of the processes were obtained by the Allied commissions[120].

Drawing on the Allied technical reports, ICI in England began the manufacture of diisocyanates. Production of polyurethanes in the US started in 1954, and by the following year they were available on a commercial scale as adhesives, coatings, foams and elastomers. The main American manufacturers of the intermediate isocyanates were DuPont, Mobay (a joint venture of Mobil and Bayer) and National Aniline.

With the lifting of Allied restrictions on research in German industry, polyurethane applications were advanced by Bayer. This included the important foaming technology,
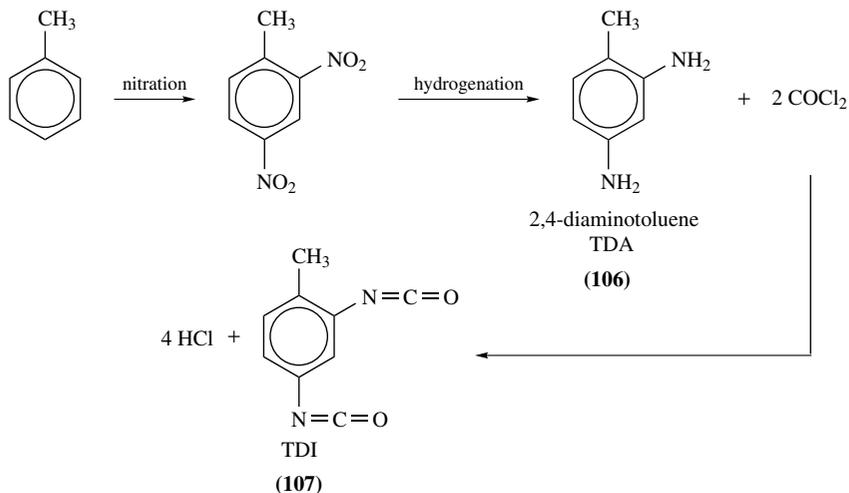
SCHEME 34. Synthesis of toluene diisocyanate (TDI)

discovered, but neglected mainly due to the lack of intermediates, at I.G. Farben during the war. Bayer displayed a lightweight soft foam suitable for upholstery at the 1952 International Plastics Fair, held in Düsseldorf. Allied reports into German science and technology encouraged General Aniline and American Cyanamid to investigate triazenes, such as **108**, as blowing agents for rubber and other polymers in the mid-1950s. These were made from the coupling of sulfonamides to diazotized aniline. The reaction is analogous to the diazonium ion attack on the nitrogen of an aryl amine, rather than on a ring carbon, when conducted under near-neutral conditions. The simplest triazene, containing the grouping $-N=N-N-$, is benzenediazoaminobenzene.
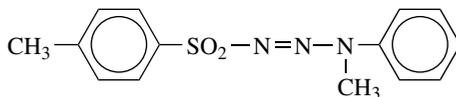
3-methyl-3-phenyl-1-p-toluenesulfonyl triazene

(108)

Spandex stretch fiber, based on polyurethanes, was developed by DuPont and appeared in 1962. From this time, polyurethanes would account for the greater part of demand for anilines. Aniline production alone had more than doubled, to over 100 million lbs. per year, between 1939 and 1957, in part to satisfy demand in products other than dyes. Half the US output was consumed in the production of rubber additives, mainly diphenylamine and cyclohexylamine, the latter used as a chain stopper in manufacture of polyurethanes (also as a boiler water additive and, in the US until banned in 1970, in the manufacture of cyclamate sweeteners). Other polymers, such as epoxy resins, relied on the bulk availability of various aromatic amines (Chapter 14).

```
                        ┌──────────────────┐
                        │     TOLUENE      │
                        └──────────────────┘
                                │
                             nitration
                                │
                    ┌──────────────────────┐
                    │  Mononitro compounds │
                    │     of toluene       │
                    └──────────────────────┘
```

crystallization   crystallization

| o-Nitrotoluene | | p-Nitrotoluene |

nitration   nitration   nitration

| 65% 2,4-Dinitrotoluene | 80% 2,4-Dinitrotoluene | 2,4-Dinitrotoluene |
| 35% 2,6-Dinitrotoluene | 20% 2,6-Dinitrotoluene | |

| reduce to amino compound | reduce to amino compound | reduce to amino compound |

phosgenation   phosgenation   phosgenation

| TOLUENE DIISOCYANATE 65/35 isomer mixture | TOLUENE DIISOCYANATE 80/20 isomer mixture | TOLUENE 2,4-DIISOCYANATE (TDI) |

bimolecular reduction   reduce to amino compound

| benzidine rearrangement | react with formaldehyde

phosgenation   phosgenation

| 3,3'-BITOLUENE 4,4'-DIISOCYANATE (TODI) | 3,3'-DIMETHYLDIPHENYLMETHANE 4,4'-DIISOCYANATE |

| ANILINE | FORMALDEHYDE |

condensation

phosgenation

| DIPHENYLMETHANE 4,4'-DIISOCYANATE (MDI) |

SCHEME 35. Isocyanates from toluene and aniline for polyurethanes

XXII. FIBER-REACTIVE DYES AND AFTER

The first fiber-reactive dyes, those that attached to fibers by covalent bonds rather than by weak intermolecular forces, were announced by ICI in 1956, on the occasion of the 100th anniversary of Perkin's discovery of mauve. This followed from research into wool dyes at the ICI general dyestuffs research laboratory, at Blackley, Manchester. Ian D. Rattee and William E. Stephen were the main contributors at ICI. Stephen modified azo dyes containing free amino groups by incorporation into them of reactive moieties, particularly cyanuric chloride (trichlorotriazine). Dyeing with cotton was successful. The Swiss CIBA had already used the triazine grouping in dye synthesis, and the two firms came to an agreement over its application to the reactive dyes. Introduced commercially as the ICI Procion range, the first fiber-reactive colorants **109**, **110** and **111** exhibited unprecedented fastness. In 1959, Bayer introduced its Permafix reactive dyes, renamed Levafix in 1961. ACNA in Italy made available Reacna dyes in 1965. In 1975, Hoechst introduced a reactive dye with three reactive functional groups, followed in 1979 by Sumito of Japan, which introduced a range of multifunctional colorants. Reactive dyes displaced a number of vat dyes, and reduced the incentive for research into new members of the latter class[121].

Procion brilliant red 2BS
(109)

Procion yellow RS
(110)

Procion blue 3GS

R = NaO$_3$S, R' = H
or
R = H, R' = NaO$_3$S
(111)
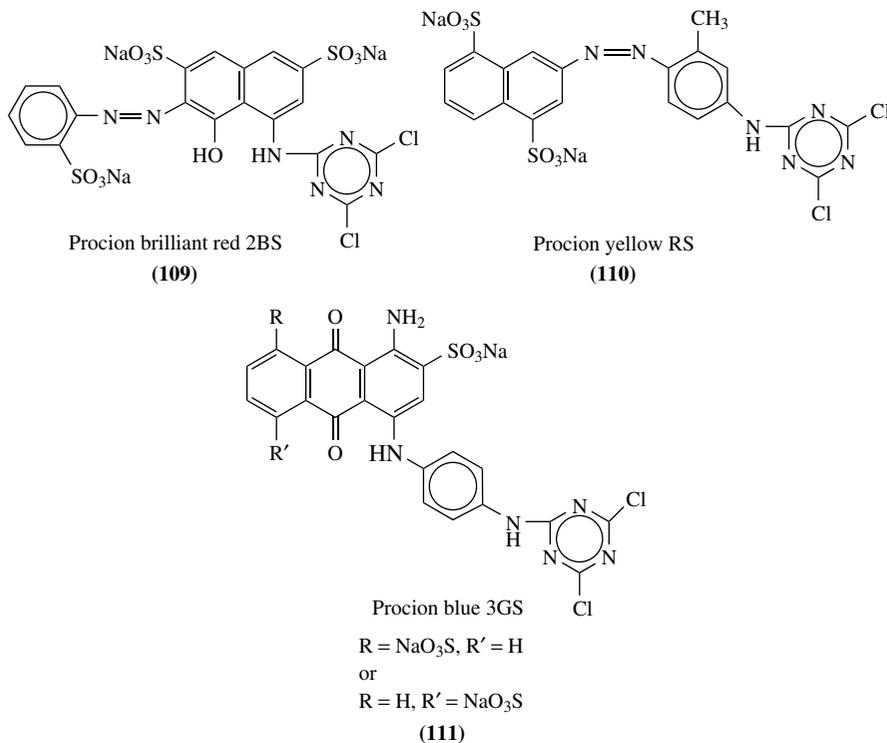
Semisynthetic and synthetic fibers introduced from the 1920s made new demands on the ingenuity of dye-makers. The commercial value of new polymers relied entirely on the ease of coloration. Normal dyeing is accomplished in aqueous solution, often in the presence of a fixing agent, or mordant. This is ideal for cotton, silk and wool, but not for synthetic fibers such as nylon and polyester, that are plastic in nature. They require

disperse dyes. The fiber is heated in an aqueous dispersion of a water-insoluble dye. Basic dyes are employed in the dyeing of polyacrylonitrile fibers.

The blue indigo color, often displaced by other synthetic dyes after around 1920, became popular again from the late 1960s with the swing towards fashionable denim and the faded look. Dyes are mainly used in textile printing and dyeing, but find other uses, including as food colors, for example the black azo colorant **112** in liquorice, and, modified, as pigments, for coloring plastics and synthetic fibers, and for printing on paper. At the end of the 20th century they found new and growing uses in the electronics industries, such as in ink jet printers.
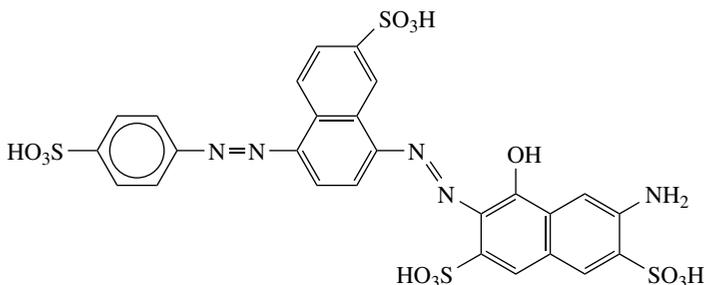
food black 2
(112)

From the 1970s dye-making in the US and Europe went into decline, in part due to tariff reductions in the US (commencing in 1968) and environmental concerns (since many intermediates were toxic). New centers of manufacturers were in Asia, including Japan, Korea, India and China, and Eastern Europe. However, there was considerable expansion in manufacture of anilines in Europe and North America for isocyanates.

XXIII. ORGANIC REACTION MECHANISMS

Just as the anilines had contributed to the development of classical organic chemistry in the second half of the 19th century, they would contribute to cutting edge studies in the first half of the 20th century. This time, however, it was not novel methods and products, but novel theory. The starting point was color and constitution. Witt's theory of color and constitution had been greatly refined by the early 1900s, and was taken up by (Jean) Felix Picard at Laussane and Edwin R. Watson in the province of Bengal, India, among others. Watson believed that tautomeric quinonoid forms were responsible for color. It was in his 1918 monograph, *Colour in Relation to Chemical Constitution*, that he broke new ground[122].

The reason was the first ever use of curly or curved arrows, in this case to represent tautomerism in *N*,*N*-dimethylamino derivatives. While the arrows were not then meant to indicate movement of electrons (as was later universal in the electronic theory of organic reactions), it is most probable that the symbols were adopted by Robert Robinson who, with Watson, worked at British Dyes during World War I[123]. Arthur Lapworth and Alfred Werner had already used arrows in mechanistic studies, the former perhaps influenced by the inventor of the TNA process, Bernard J. Flürscheim, who explained benzene substitution patterns in terms of 'affinity demand', indicated by arrowed bonds[124].

In the 1920s, the debate turned to *ortho–para* and *meta* substitution, at first based on the nitroso group. Christopher K. Ingold, who then favored the Flürscheim approach, predicted, incorrectly as it turned out, *ortho–para* nitration of tertiary benzylamine salt, and *meta* nitration in the free amine. This was based on experimental evidence that was refuted by Robinson. The polemics during the mid-1920s were unpleasant, even acrimonious, but did force both men to review, correct and refine their approaches, with the result that Ingold was enabled to draw up a theory of organic chemistry that has withstood the test of time. Ingold paid attention to competing inductive and electromeric effects in *N*,*N*-dimethylaniline. Dipole measurements made during 1927 and 1928 established that tautomeric effects were at play. In 1928, Ingold introduced the terms nucleophilic, for an electron pair donor, and electrophilic, for an electron pair acceptor. In 1933, he gave the tautomeric effect a new name, mesomerism, and, with Edward D. Hughes, an expert in mechanism, introduced the four terms for reaction types: S_N1, S_N2, for substitution reactions, and E1 and E2, for elimination reactions. A good example of the S_N2 reaction is nucleophilic attack of sodamide on pyridine to yield 2-aminopyridine, required for sulfapyridine (Tschitschibabin reaction). In 1946, Michael Dewar explained the rearrangement of hydrazine into benzidine in terms of a π electron mechanism.

One of the greatest successes of mechanistic organic chemistry concerned explanations of strengths of acids and bases, particularly of aryl amines. As Peter Sykes in 1961 so clearly delineated for undergraduates, this accounted for the feeble basicity of aniline, the weakening when *N*-phenyl groups are introduced, the small effects of *N*-methyl groups, the enhanced base-weakening by the inductive effect when nitro groups are introduced, the mixed effects of electron-donating groups, either base-strengthening in the *o*- and *p*-positions (mesomeric effects) or weakening in the *m*-position, and the massive base strengthening effect in 2,4,6-trinitrodimethylaniline and the small effect in 2,4,6-trinitroaniline[125].

Hofmann's conversion of amides into amines is explained in terms of an electron-deficient nitrogen atom, as is the formation of both *o*- and *m*-toluidines from *o*-chlorotoluene[126]. The Sandmeyer reaction is explained by electron transfer, with loss of nitrogen, to afford aryl radical, as the rate-determining step. Diazo coupling is the result of electrophilic substitution, involving arenediazonium ions that are weak electrophiles acting on primary amines at the nitrogen, though coupling takes place at both carbon and nitrogen in secondary amines, and only at carbon in tertiary amines. The diazonium ions react with phenols that are also activated aromatic compounds.

The amino group is a strong electron-donating group, favoring electrophilic aromatic substitution. While aniline is normally *ortho/para*-directing, in strongly acidic solution protonation of the amino group prevents interaction of the unshared electron pair with delocalized π orbitals of the nucleus, favoring *meta*-substitution, as a result of electrons being drained away from the nucleus by the positively charged nitrogen[127–130]. The outcome of these theoretical advances was that, during the 1960s, the mechanistic classification of reactions displaced classical descriptions of the type long familiar to students. It also displaced traditional aniline chemistry, at least as it applied to synthetic dyes, from textbooks.

XXIV. CELEBRATION AND HISTORY

The manufacture of anilines, the aniline dye industry, and subsequent diversification based on aromatic amines, brought about the emergence of the modern chemical industry. It transformed the world of fashion, the high street and the medical laboratory, facilitated the development of academic chemistry, stimulated the development of industrial research laboratories, made academic and industrial careers, and created enormous prestige and

FIGURE 19. A banquet to celebrate the anilines. This "large and distinguished company" of academic and industrial chemists and others is celebrating the jubilee of the discovery of mauve by William Henry Perkin at the Hotel Mètropole, London, on 26 July 1906. William Perkin, Heinrich Caro, Raphael Meldola, Emil Fischer, and Paul Friedlander are among those at the top table. By this time, the dye industry had developed all the major processes for production of aniline and its congeners, and naphthylamines, and aminoanthraquinones. Edelstein Collection

wealth. Little wonder then that its foundation through William Perkin's 1856 discovery of mauve was celebrated on international scales in London and New York in 1906 (Figure 19) and 1956, as well as in London during 1938 and 1988, the anniversaries of Perkin's birth. On those occasions, chemical industry and the chemical community were the major sponsors. These and other anniversaries, particularly of the foundation of modern corporations, were sources of great pride, as reflected in the popular press and at media events, and in lavish publications[25,72,131–143].

In 2006, the 150th anniversary of mauve and the aniline dye industry was also celebrated, mainly by the Royal Society of Chemistry in London. This time, however, the industrial community played a minor role. The aniline and aniline dyes, in particular, are perceived to be mature technologies, associated more with Asia than western Europe and North America, and certainly with little prestige except among the users. Industry has moved on, mainly to pharmaceuticals and agrochemicals, and is less interested in its aniline heritage, even though many of the new products are based on aromatic amines.

The anilines continue to contribute in other ways, particularly to the historical under-standings of science and technology, to their impacts on patent law, and to their modern interdependence, to our understanding of how scientific knowledge is constructed within a discipline, to technology transfer, and to how new knowledge is applied in related fields of scientific enquiry[62,64,65,144–150]. The anilines also contribute to emerging agendas in environmental, business and economic history[42,151–154]. The history, and historiogra-phy, of the anilines and their applications attract considerable attention among academic historians, biographers and popular science writers[6,12,26,66,155–158]. In the 1980s, at a time when the German aniline dye industry was about to celebrate its 125th anniver-sary, and some were revisiting the Nazi-era history of I.G. Farben, the industrial ani-lines even inspired the German television multipart drama documentary *Fathers and Sons*.

XXV. CONCLUSION

The anilines have played a critical role in the origins of modern chemistry and chemical industry. During the last four decades of the 19th century it was mainly interest in the aryl amine-derived colorants and their intermediates that directed the course of academic research and fostered expansion in education through employment opportunities available in the first theory-based industry. Germany was the greatest beneficiary of the massive expansion in dye manufacture, based mainly on aryl amine intermediates, the growth of classical organic chemistry and the subsequent diversification into biomedical products. Research programs resulted in successes such as the synthesis of indigo, also involving anilines. After 1914, other nations were forced to catch up, particularly Britain and the US, whose industries turned to dye, pharmaceutical and rubber products based on the same coal-tar anilines. During the 1930s, aryl amines found new uses as sulfa drugs and novel polymers for the first colored molded plastic goods and ubiquitous melamine laminates. These were later joined by agrochemical products and colorants for synthetic fibers (see Chapter 14 in this book).

XXVI. REFERENCES

1. J. R. Partington, *A History of Chemistry*, Vol. 4, Macmillan, London, 1964, pp. 389, 397.
2. (a) N. N. Zinin, *Bulletin Scientifique Publie par l'Académie Impériale des Sciences de Saint-Pétersbourg*, **10**, col. 273 (1843).
   (b) N. M. Brooks, *Bull. Hist. Chem.*, **27**, 26 (2002).
   (c) J. S. Muspratt, *Chemistry, Theoretical, Practical & Analytical*, 2 vols., William Mackenzie, Glasgow, Edinburgh, London, 1853–1864, Vol. 1, pp. 598–599.
3. A. W. Hofmann, *Ann. Chem. Pharm.*, **47**, 37 (1843); **48**, 253 (1843).
4. A. W. Hofmann, *Ann. Chem. Pharm.*, **53**, 1 (1845).
5. (a) M. N. Keas, in *Die Allianz von Wissenschaft und Industrie. August Wilhelm Hofmann. 1818–1892. Zeit, Werk, Wirkung* (Eds. C. Meinel and H. Scholz), VCH, Weinheim, 1992, pp. 287–298.
   (b) S. Patai (Ed.), *The Chemistry of the Amino Group*, Interscience, London, 1968.
6. (a) W. H. Perkin, *Proc. Roy Soc.*, **12**, 713 (1862–1863).
   (b) W. H. Perkin, *Proc. Roy. Soc.*, **13**, 170 (1863–1864).
   (c) A. S. Travis, *The Rainbow Makers: The Origins of the Synthetic Dyestuffs Industry in Western Europe*, Lehigh University Press, Bethlehem, Pa., 1993, pp. 31–64.
7. (a) O. Meth-Cohn and M. Smith, *J. Chem. Soc., Perkin Trans. 1*, 5 (1994).
   (b) O. Meth-Cohn and A. S. Travis, *Chem. Br.*, **31**, 547 (1995).
8. A. W. Hofmann, *Comptes Rendus Hebdomadairies des Séances de l'Académie des Sciences*, **47**, 492 (1858).
9. A. W. Hofmann, *Proc. Roy. Soc.*, **12**, 2 (1862–1863).

10. A. W. Hofmann, *Proc. Roy. Soc.*, **13**, 341 (1863–1864).
11. Reference 6c, pp. 67–84, 104–137.
12. C. Reinhardt and A. S. Travis, *Heinrich Caro and the Creation of Modern Chemical Industry*, Kluwer, Dordrecht, 2000.
13. A. S. Travis, *Ambix*, **42**, 1 (1995).
14. A. S. Travis, *Technology and Culture*, **35**, 70 (1994).
15. Reference 12, p. 62.
16. C. Reinhardt and A. S. Travis, *Ambix*, **44**, 11 (1997).
17. Reference 12, pp. 49–88.
18. J. A. Wanklyn, *Report of the Thirty-Fourth Meeting of the British Association for the Advancement of Science (Bath, 1864)*, John Murray, London, 1865, pp. 42–44.
19. *Chemical News*, **10**, 157 (1864).
20. A. S. Travis, in *The Invisible Industrialist: Manufactures and the Construction of Scientific Knowledge* (Eds. Ilana Löwy and Jean-Paul Gaudillière), Macmillan, Basingstoke, 1998, pp. 122–142.
21. C. Reinhardt and A. S. Travis, in *Tools and Modes of Representation in the Laboratory Sciences* (Ed. U. Klein), Kluwer, Dordrecht, 2001, pp. 79–94.
22. Reference 12, pp. 109–123.
23. Reference 6c, pp. 245–254.
24. Reference 12, pp. 125–162.
25. W. Abelhauser, W. von Hippel and J. A. Johnson, *Die BASF: Von 1865 bis zur Gegenwart. Geschichte Unternehmensgeschichte*, C. H. Beck, Munich, 2002; W. Abelhauser, W. von Hippel and J. A. Johnson, *Germany, Industry and Global Enterprise. BASF: The History of a Company*, Cambridge University Press, Cambridge, 2003.
26. J. J. Beer, *The Emergence of the German Dye Industry*, University of Illinois Press, Urbana, 1959.
27. A. Kekulé, *Z. Chem.*, **2**, 689 (1866).
28. Reference 12, pp. 163–167.
29. O. N. Witt, *Chem. Ber.*, **9**, 522 (1876).
30. E. Beckmann, *Chem. Ber.,* **48**, 736 (1915).
31. E. Noelting, *Chem. Ber.*, **49**, 1751 (1916).
32. O. N. Witt, *Chem. Ber.*, **10**, 654 (1877).
33. A. W. Hofmann, *Chem. Ber.*, **10**, 213 (1877).
34. A. W. Hofmann, *Chem. Ber.*, **10**, 389 (1877).
35. W. J. Hornix, Reference 5a, pp. 151–165.
36. Reference 12, pp. 167–168.
37. H. Caro, *Chem. Ber.*, **25**, (Referate), 955 (1892).
38. C. Liebermann and F. Scheiding, *Chem. Ber.*, **8**, 1108 (1875).
39. Reference 12, pp. 175–176.
40. Reference 12, p. 277.
41. Reference 37, p. 1097.
42. J. P. Murmann, *Knowledge and Competitive Advantage: The Coevolution of Firms, Technology and National Institutions*, Cambridge University Press, Cambridge, 2003.
43. A. W. Hofmann, *Chem. Ber.*, **8**, 62 (1875).
44. A. W. Hofmann, *Chem. Ber.*, **10**, 213 (1877).
45. Reference 12, pp. 244–245.
46. H. van den Belt and A. Rip, in *The Social Construction of Technological Systems* (Eds. W. E. Bijker, T. P. Hughes and T. Pinch), MIT Press, Cambridge, Mass., 1987, pp. 135–158.
47. Reference 12, pp. 258–259.
48. Reference 12, pp. 278–280.
49. I. Levinstein *J. Soc. Chem. Ind.*, **21**, 893 (1902).
50. Reference 12, pp. 280–290.
51. Reference 12, pp. 202–208.
52. R. Riedl-Ehrenberg, *Alfred Kern (1850–1893), Edouard Sandoz (1853–1928). Gründer der Sandoz AG, Basel*, Verein für wirtschaftshistoriche Studien, Basel/Zürich, 1986.
53. Reference 12, p. 209.
54. T. Sandmeyer, *J. Soc. Dyers Colour.*, **12**, 154 (1896).

55. A. S. Hester and C. H. Allen, *Modern Chemical Processes*, Vol. 3, Reinhold, New York, 1954, pp. 228–236.
56. J. B. Cohen, *Practical Organic Chemistry*, 3rd edition, Macmillan, London, 1924.
57. A. Bernthsen, revised by J. J. Sudborough, *A Textbook of Organic Chemistry*, new edition, Blackie & Son, London, 1941.
58. L. I. Fieser and M. Fieser, *Organic Chemistry*, D. C. Heath & Company, Boston, 1944.
59. I. L. Finar, *Organic Chemistry: The Fundamental Principles*, Longmans Green & Co., London, 1951.
60. H.-G. Henning, Reference 4, pp. 287–298.
61. B. J. Flürscheim, *J. Soc. Chem. Ind.*, **40**, 97T (1921).
62. C. Reinhardt, *Forschung in der chemischen Industrie. Die Entwicklung synthetischer Farbstoffe bei BASF und Hoechst. 1863–1914*, Technische Universität Bergakademie Freiberg, Freiberg, 1997.
63. Reference 12, pp. 223–228.
64. E. Homburg, *Br. J. Hist. Sci.*, **25**, 91 (1992).
65. G. Meyer-Thurow, *Isis*, **73**, 363 (1982).
66. A. S. Travis, *Dyes Made in America, 1915–1980: The Calco Chemical Company, American Cyanamid, and the Raritan River*, Edelstein Center/Hexagon Press, Jerusalem, 2004, pp. 47–50.
67. Reference 12, pp. 186–201.
68. A. Baeyer, *Chem. Ber.*, **16**, 2188 (1883).
69. Reference 6c, pp. 223–227.
70. P. Kumar, 'Facing Competition: The History of Indigo Experiments in Colonial India, 1897–1920', Ph.D. diss., Georgia Institute of Technology, Atlanta, 2004.
71. P. Reed, *Br. J. Hist. Sci.*, **25**, 113 (1992).
72. E. Verg, G. Plumpe and H. Schultheis, *Milestones: The Bayer Story. 1863–1988*, Bayer AG, Leverkusen, 1988, pp. 170–175.
73. E. Bäumler, *A Century of Chemistry*, Econ Verlag, Düsseldorf, 1968, pp. 302–306.
74. K. Steen, 'Wartime Catalyst and Postwar Reaction: The Making of the United States Synthetic Organic Chemicals Industry, 1910–1930', Ph.D. diss., University of Delaware, 1995, p. 236. UMI Microfilm no. 9610494 (1996).
75. Reference 66, pp. 1–64.
76. D. A. Hounshell and J. K. Smith, *Science and Corporate Strategy: Du Pont R&D, 1902–1980*, Cambridge University Press, Cambridge, 1988.
77. K. Steen, *Isis*, **92**, 91 (2001).
78. R. B. Woodward, *Manet*, North Junior High School, Quincy, Mass., 16 January (1930).
79. M. N. Keas, *Ambix*, **39**, 127 (1992).
80. Reference 66, pp. 76, 77–78.
81. A. Thackray, J. L. Sturchio, P. Carroll and R. Bud, *Chemistry in America 1876–1976. Historical Indicators*, D. Reidel, Dordrecht, 1984, p. 123, note 12.
82. Reference 76, p. 593.
83. M. R. Fox, *Dye-makers of Great Britain, 1856–1976: A History of Chemists, Companies, Products and Changes*, ICI, Manchester, 1987, pp. 191–192.
84. W. H. Shearon, L. G. Davy and H. Von Bramer, *Modern Chemical Processes*, Reinhold, New York, 1954, vol. 3, pp. 90–95.
85. A. Heintzel, *J. prakt. Chem.*, **1**, 230 (1867).
86. M. L. Kastens and J. F. Kaplan, *Modern Chemical Processes*, Vol. 2, Reinhold, New York, 1952, pp. 43–54.
87. A. S. Travis, *Science in Context*, **3**, 383 (1989).
88. *The Collected Papers of Paul Ehrlich* (Eds. F. Himmelweit, M. Marquardt and H. H. Dale), Pergamon, London, (1898) Vol. 1, pp. 596–618 (1956); (1906) Vol. 3, pp. 53–63 (1960); (1913) Vol. 3, pp. 505–518 (1960).
89. J. Parascandola and R. Jasensky, *Bull. Hist. Med.*, **49**, 199 (1974).
90. A. S. Travis, *The Biochemist*, **13**, October–November, 9 (1991).
91. J. E. Lesch, in *Chemical Sciences in the Modern World* (Ed. S. H. Mauskopf), University of Pennsylvania Press, Philadelphia, 1993, pp. 158–215.
92. E. H. Northey, *Ind. Eng. Chem.*, **35**, 829 (1943).
93. P. Rabe, *Chem. Ber*, **41**, 62 (1908).

 94. L. B. Slater, *Ambix*, **51**, 107 (2004).
 95. R. L. Kenyon, J. A. Wiesner and C. E. Kwartler, *Modern Chemical Processes*, Vol. 1, Reinhold, New York, 1950, pp. 110–118.
 96. F. Y. Wiselogie, *Survey of Antimalarial Drugs, 1941–45*, J. W. Edwards, Ann Arbor, Mich., 1946.
 97. O. T. Benfey and P. J. T. Morris (Eds.), *Robert Burns Woodward: Architect and Artist in the World of Molecules*, Chemical Heritage Foundation, Philadelphia, 2001, pp. 57–77.
 98. N. F. Elmore, G. R. Brown and A. T. Greer, in *Basic Organic Chemistry*, part 5, *Industrial Products* (Eds. J. M. Tedder, A. Nechvatal and A. H. Jubb), Wiley, London, 1975, pp. 378–379.
 99. (a) W. Haynes, *American Chemical Industry*, D. Van Nostrand, New York, Vol. 3, *The World War I Period: 1912–1922*, p. 358 (1945); Vol. 4, *The Merger Era*, pp. 408–414 (1948).
     (b) *Technical Notes for the Rubber Industry*, Bayer, Leverkusen, 1966, pp. 18–27.
100. Reference 66, pp. 80–81.
101. T. G. Rochow, R. W. Stafford, D. W. Davis and R. L. Gilbert, *Ind. Eng. Chem.*, **32**, 1187 (1940).
102. *British Plastics and Moulded Products Trader*, **10**, 27 (1939).
103. *British Plastics and Moulded Products Trader*, **11**, 326 (1939).
104. P. P. McClellan, *Ind. Eng. Chem.*, **32**, 1181 (1940).
105. A. S. Travis, *Educ. Chem.*, **37**, 16 (2000).
106. Reference 66, pp. 115–124.
107. J. Formánek, *Untersuchung und Nachweis organischer Farbstoff aufspektroskopschem Wege*, 2nd edn., Springer, Berlin, 1908.
108. W. R. Brode and M. E. Griffith, *Am. Dyest. Rep.*, **26**, 90, (1937).
109. Reference 66, pp. 98–101.
110. E. I. Stearns, in *Analytical Absorption Spectroscopy: Absorptimetry and Colorimetry* (Ed. M. G. Mellon), Wiley, New York, 1950, pp. 306–338.
111. Y. M. Rabkin, *Isis*, **78**, 31 (1987).
112. Reference 66, pp. 192–197.
113. E. I. Stearns, *The Practice of Absorption Spectrophotometry*, Wiley-Interscience, New York, 1969.
114. R. C. Hirt, F. T. King and R. G. Schmitt, *Anal. Chem.*, **26**, 1270 (1954).
115. Reference 66, pp. 136–146.
116. W. J. Reader, *Imperial Chemical Industries: A History*, Oxford University Press, London, Volume 2, *The First Quarter Century 1926–1952*, pp. 262–263 (1975).
117. Reference 83, pp. 185–186.
118. Reference 66, pp. 152–160.
119. K. Venkataraman, *The Chemistry of Synthetic Dyes*, Vol. 1, Academic Press, New York, 1952, p. 13.
120. Reference 66, pp. 284–289.
121. Reference 83, pp. 210–221.
122. E. R. Watson, *Colour in Relation to Chemical Constitution*, Longman & Co., London, 1918.
123. W. H. Brock, *The Fontana History of Chemistry*, Fontana Press, London, 1992, pp. 524–525.
124. J. Shorter, *Ambix*, **50**, 274 (2003).
125. P. Sykes, *A Guidebook to Mechanism in Organic Chemistry*, Longman, London, 1961, pp. 51–54.
126. P. Sykes, *A Guidebook to Mechanism in Organic Chemistry*, 3rd edn., Longman, London, 1970, 153–154.
127. Reference 125, pp. 107, 112–113.
128. G. Chuchani, in Reference 5a, pp. 205–275.
129. B. C. Challis and A. R. Butler, in Reference 5a, pp. 277–347.
130. S. Patai (Ed.), *The Chemistry of the Hydrazo, Azo and Azoxy Groups*, Vol. 2, Wiley, Chichester, 1997.
131. R. Meldola, A. G. Green and J. C. Cain (Eds.), *Jubilee of the Discovery of Mauve and of the Foundation of the Coal-tar Colour Industry by Sir W.H. Perkin, F.R.S., D.Sc., LL.D., Ph.D., Dr.Ing.*, Perkin Memorial Committee, London [1907].
132. H. Pinnow, *75 Jahre Werksgeschichte Hoechst. Zur Erinnerung an die 75. Wiederkehr des Gründungstages der Farbwerke vorm.* Meister Lucius & Brüning, Munich, 1938.

133. H. Pinnow, *Werksgeschichte der Gefolgschaft der Werke Leverkusen, Elberfeld und Dormagen zur Erinnerung an die 75. Wiederkehr des Gründungstages der Farbenfabriken vorm. Friedr. Bayer & Co.*, Frankfurt am Main, 1938.

134. H. Voelcker, *75 Jahre Kalle. Ein Beitrag zur Nassauischen Industriegeschichte. 1863–1938*, Kalle & Co., Wiesbaden-Biebrich, 1938.

135. W. Haynes, *Dyes Made in America, 1915–1940: Calco Chemical Division, American Cyanamid Company*, American Cyanamid Company, Bound Brook, 1940.

136. H. White, Jr. (Ed.), *Proceedings of the Perkin Centennial 1856–1956. Commemorating the Discovery of Aniline Dyes*, sponsored by the American Association of Textile Chemists and Colorists, 1956.

137. *Perkin Centenary London, 100 Years of Synthetic Dyestuffs*, supplement no. 1 to *Tetrahedron*, Pergamon, London, 1956.

138. A. Burgin, *Geschichte des Geigy-Unternehmens von 1758 bis 1939. Ein Beitrag zur Basler Unternehmer–und Wirtschaftsgeschichte. Veröffentlichung zum 200jährigen Bestehen des Geigy-Unternehmens 1958*, Geigy, Basel, 1958.

139. *CIBA Ltd. The Story of the Chemical Industry in Basel*, CIBA and Urs Graf, Olten, 1959.

140. E. N. Abrahart, *The Clayton Aniline Company Limited, 1876–1976*, Clayton Aniline Company Limited, Manchester, 1976.

141. L. Meinzer, K. Dettke, J. Kissener and K.-J. Matz, *125 Jahre BASF. Stationen ihrer Geschichte. Katalog zur Ausstellung im Rathaus-Center Ludwigshafen, 28. April bis 29. Juni 1990*, BASF, Ludwigshafen, 1990.

142. *Chemistry Looks to the Future*, BASF, Ludwigshafen, 1990.

143. P. J. T. Morris and A. S. Travis, *Am. Dyest. Rep.*, **81**, 59, November (1992).

144. P. A. Zimmermann, *Patentwesen in der Chemie. Ursprünge, Anfänge, Entwicklung*, BASF, Ludwigshafen, 1965.

145. (a) C. Schuster, *Vom Farbenhandel zur Farbenindustrie. Die erste Fusion der BASF*, BASF, Ludwigshafen, 1973.
     (b) C. Schuster, *Wissenschaft und Technik. Ihre Begegnung in der BASF während der ersten Jahrzehnte der Unternehmensgeschichte*, BASF, Ludwigshafen, 1976.

146. E. Homburg, *J. Soc. Dyers Colour.*, **99**, 325 (1983).

147. H. van den Belt, E. Homburg and W. J. Hornix (Eds.), *Development of the Dye Industry*, Nijmegen, University of Nijmegen, 1985.

148. W. J. Hornix, in Reference 64, pp. 65–90.

149. C. Reinhardt, in *The Chemical Industry in Europe, 1850–1914: Industrial Growth, Pollution, and Professionalization* (Eds. E. Homburg, A. S. Travis and H. G. Schröter), Kluwer, Dordrecht, 1998, pp. 239–259.

150. A. S. Travis, *Technology and Culture*, **35**, 70 (1994).

151. A. S. Travis, *Environ. Hist.*, **2**, 343 (1997).

152. M. Forter, *Farbenspiel: Ein Jahrhundert Umweltnutzung durch die Basler chemische Industrie*, Chronos Verlag, Zurich, 2000.

153. A. S. Travis, *Ambix*, **49**, 21 (2002).

154. A. S. Travis (Ed.) *History and Technology*, 22, no. 2 2006

155. E. Vaupel, 'Carl Graebe (1841–1927): Leben, Werk und Wirken im Spiegel seines brieflichen Nachlasses', 2 vols, Ph.D. diss., University of Munich, 1987.

156. S. B. McGrayne, *Prometheans in the Lab: Chemistry and the Making of the Modern World*, Mc Graw-Hill, New York, 2001, pp. 15–29.

157. S. Garfield, *Mauve: How One Man Invented a Colour that Changed the World*, Faber & Faber, London, 2000.

158. P. Ball, *Bright Earth: Art and the Invention of Colour*, Penguin, London, 2001, pp. 197–227.

CHAPTER **2**

General and theoretical aspects of anilines

MINH THO NGUYEN

*Department of Chemistry and Institute for Nanoscale Physics and Chemistry,
University of Leuven, Celestijnenlaan 200F, B-3001 Leuven, Belgium
Fax: +32 16 32 7992;   e-mail: minh.nguyen@chem.kuleuven.be*

I. INTRODUCTION

A. General Considerations

Aniline, shown in Figure 1, is a member of the amines family in which the amino group is bound directly to a benzene ring. This simplest primary aromatic amine ($C_6H_5NH_2$) thus belongs to the isoelectronic series of monosubstituted benzenes including toluene ($C_6H_5CH_3$), phenol (C_6H_5OH) and fluorobenzene (C_6H_5F).

Aniline is a colorless oily liquid, heavier than water, boiling at $184\,^\circ C$, melting at $-6\,^\circ C$, little soluble in water (0.32 g$\,l^{-1}$ at $20\,^\circ C$). It is stable under ordinary conditions but can be slowly oxidized and resinified in air. Being a weak base ($pK_b = 4.63$ as compared with that of 9.25 of ammonia), it reacts with strong acids[1]. As an aromatic derivative, it is highly reactive with respect to electrophilic substitution reactions. It can be prepared from chlorobenzene upon heating with ammonia in the presence of a copper catalyst. Commercially, aniline is produced upon reduction of nitrobenzene by a variety of reducing agents such as iron and hydrogen chloride, followed by a steam-distillation of the product. Nitrobenzene is obtained from coal tar which is a by-product of the production of coke from soft coal. Therefore, the purity of aniline is strongly dependent on that of the starting nitrobenzene. In the market, 'aniline oil for blue' stands for pure aniline.
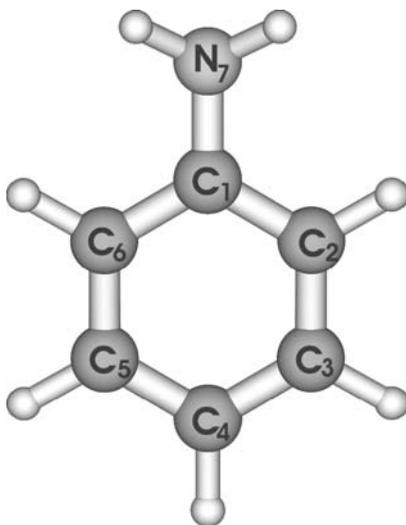
FIGURE 1. Chemical formulae of aniline: $C_6H_5NH_2$. CAS registry number: 62-53-3. Other current names: aminobenzene, phenylamine. The hydrogen atoms, not shown, are bonded as follows: N_7H_8, N_7H_9, C_2H_{10}, C_3H_{11}, C_4H_{12}, C_5H_{13} and C_6H_{14}

Despite a pleasant vinous odor and an aromatic taste, this amine is actually an acrid poison. Without taking necessary precautions, aniline oil could become a dangerous poison for people working with it. The poisoning affects the victim first by an extreme languor, which is followed by dizziness and then by unconsciousness. The poison may be acquired either through the mucous membranes of the lungs and nose, or directly through the skin[2]. Aniline ignites easily and burns with a large smoky flame. Its contamination of the general environment has long been reported.

Aromatic amines form a class of chemical carcinogens for which human exposure has been evidenced[3]. Among the profusion of chemical constituents of tobacco smoke, only aromatic amines have been implicated as human bladder carcinogens[4], and are regarded as determinant etiological factors for the induction of bladder cancer in smokers[5]. In this context, aniline was, for a long time, suspected to be a carcinogen. However, it is actually not classifiable as to its carcinogenicity to humans[6].

The largest use of aniline and its derivatives is in dye production. They are thus important ingredients in color commerce. Every year, thousands of new colors and shades are generated and tested in factories. Polyaniline (PANI) is one of the oldest artificial conducting polymers[7] and its high electrical conductivity among organic compounds has attracted continuing attention[8]. Aromatic amines are also involved in the search for potentially interesting new compounds in materials science[9].

B. A Brief History

The most fascinating episodes of the long history of aniline concern its discovery, and the accidental discovery of its industrial use as a precursor to dyes.

Unverdorben, O. (1806–1873) first discovered aniline in 1826, following a dry and destructive distillation of indigo plant and called it *crystalline*, due to the fact that his new compound easily produced crystals with acids[10].

Runge, F. F., (1795–1867) rediscovered aniline in coal tar oil in 1834, but named it *kyanol*, because a bright blue color appeared whenever it was mixed with a bleaching powder (chloride of lime)[11]. Note that in his pioneer work, Runge also discovered, for the first time, phenol (called then 'carbolic acid'), pyrrole, quinoline, naphthalene, rosolic acid and some other bases[12].

A few years later, Fritzsche, C. J., (1808–1871) isolated in 1840 the same oil when distilling indigo in the presence of a potassium base, and called it *aniline*. The latter was named after an indigo-yielding plant *Indigofera anil*, but also after the Arabic term *al-nil*, which means indigo[13], and the Sanskrit terms *níla* (dark-blue) and *nílá* (indigo plant).

About the same time, Zinin, N. (1812–1880) was able, in 1842, to carry out an original synthesis of aniline, that he named *benzidam*, and of some other aromatic amines by reduction reaction of nitrobenzenes. As for a reducing agent, Zinin utilized a solution of ammonium sulfide to generate molecular hydrogen[14, 15].

At that period, there was a severe lack of a chemical theory which could provide a coherent interpretation of the properties of a seemingly novel class of compounds. For this purpose, Laurent, A. (1808–1853) endeavored to develop further the 'substitution hypothesis', which was originally formulated by his mentor Jean-Baptiste Dumas[16]. Laurent proposed that a substitution reaction did not change the basic formulae of the reactant and the product. Applying this hypothesis, he interpreted the structure of phenol that he was the first chemist to crystallize[17]. He appeared to understand the structural similarity between phenol and aniline, and went on to establish the constitution of aniline[18]. According to Laurent, phenol was a 'hydrate of phenyl radical', whereas aniline was a 'phenamide'. However, the substitution hypothesis was vehemently attacked by Berzélius[19], and the vigorous debate between Laurent, Dumas[20] and Berzélius on a new approach to the

molecular structure of organic compounds went on for some years (cf. Reference 12 for a brief history of this discussion).

In 1843, von Hofmann, A. W., (1818–1892), a student of Justus von Liebig (1803–1873), published a long report on the studies of Laurent, Dumas and Erdmann on the indigo chemistry[21]. He investigated the variously prepared compounds and proved them to be identical. Since then the name *aniline* was definitively adopted. Thanks to this review, he also realized that phenol and aniline were two closely related substances, and thereby supported Laurent's viewpoint. It was in Giessen (Germany) that Hofmann and Laurent were, together, successful in converting a small amount of phenol to aniline[22].

In the middle of the 19th century, the British Empire severely faced malaria in its numerous colonies. The best treatment for malaria was quinine, which at that time was extracted from the bark of the cinchona tree growing wild in the Andes, South America. Obviously, the demand for the antimalarial drug was great, but its supply was limited and the final product was expensive. In a search for a cure for malaria by promoting chemical innovation, the Royal College of Chemistry was founded in London (now the Imperial College), Hofmann was appointed as its first director (1845–1864) and he hired Perkin, W. H., (1838–1907) as an assistant to work on the synthesis of quinine.

In 1856, in an attempt to prepare quinine from coal tar, Perkin oxidized aniline using a strong oxidizing agent as potassium dichromate. He did not obtain quinine at all, but the resulting product made a beautiful purple solution in alcohol. It was a brilliant fuchsia type color which faded easily, and Perkin named it '*mauveine*'[23]. In order to manufacture his new synthetic dye, he built a factory and thenceforth the aniline dye industry in England was begun[24]. It was rapidly expanded and flourished in Europe. Variations of the original synthesis produced dozens of dyes from aniline and most were named after it: aniline reds, aniline violets, greens, yellows, browns, blues etc. Use of phenol and naphthalene (also from coal tar) led to two additional families of colors. Mauve was a huge popular success and it generated much business as in England the purple color had primarily been associated with royalty because of its expense, and it became inexpensive and, more importantly, fashionable. Indeed, Paris fashion houses readily embraced Perkin's colors! It was reported that Queen Victoria appeared at the Royal Exhibition 1862 in wearing a silk gown dyed with mauveine.

In a way, such development profoundly affected the (intrinsically complicated) relationship between people doing pure science and applied sciences, who (eternally) distrusted each other. A change in the chemists' mentality was apparently initiated and university–industry cooperation was timidly put forward. Companies attempted to forge close links with research laboratories, and fundamental science became irrevocably bound up with concrete applications. Such a historical context led to the emergence of industrial research laboratories[25]. In a recent Perkin biography[26], it is written that: 'For the first time, people realized that the study of chemistry could make them rich!'

From an early date, the competition for manufacturing aniline dyes was already stiff. Hofmann's leadership at the Royal College had given the British an edge in synthetic dyes, but after his return to Berlin in 1865[22], British dyestuffs did not remain at the forefront for long. In France, production of synthetic dyes was not competitive and demand there readily shifted to natural and imported products. In Germany, the situation was ideal for dye development. Indeed, in the following decades, the dye industry was mainly developed in Germany thanks to concerted efforts of the government, universities and industries to promote chemical industries in general, and the dye industry in particular. Several companies based on aniline were set up including Badische Anilin und Soda Fabrik (BASF) in 1861, Farbwerke Hoechst in 1862, followed by Freidrich Bayer in 1863 , Kalle&Co in 1864, and Aktien Gesellschafr für Anilin Fabrikation (AGFA) was organized in 1873.

In 1869, BASF filed a patent producing alizarin, a red dye, at the London patent office just one day before that of Perkin arrived. Both parties finally agreed that Perkin would sell alizarin to Britain, and BASF to the rest of the world. Perkin's company did well selling the red dye for a few years, but could not compete with BASF. In 1874, Perkin sold his dyeworks and went back to the laboratory[26]. One of the speakers at a 1914 meeting of the Council of the Leeds Chamber of Commerce (England) stated the situation as follows: 'Some form of protection would be necessary for probably the next fifteen years. In Germany, the capital sunk in this industry amounts to something like $125.000.000; and their concerns have been built-up gradually during the past 25 or 30 years. They have made a scientific study of all branches of the industry, the raw materials for which had come very largely from England. By means of chemical research, they have arrived at the cheapest way of making the intermediate products as well. Thus, the present crisis has found British manufactures unprepared. Practically 90% of the aniline colors consumed in England were imported from Germany, and the same applies more or less to the whole world. . .'[27]. At the end of 1925, the entire German dye industry was consolidated into one firm, I. G. Farbenindustrie (known as IG Farben). The dominance in the dye industry, in turn, carried Germany into world leadership in industrial chemistry, and it is really remarkable that these companies remain at the top of the profession throughout a period of 150 years of wars, depressions, revolutions and mergers!

In the United States of America, it was August Partz, a German chemist, who endeavored in the 1860s to promote the first aniline plant erected on the banks of Gowanus Creek at Green Point, Long Island. Victor G. Bloede, one of the earlier producers of aniline products in the USA, recalled this early attempt in the following terms: 'In those days every thing connected with the manufacture of aniline dyes was held profoundly secret, and I believe Dr. Partz's capital consisted largely in his supposed practical knowledge of the secret processes which had been intrusted to him by the German principals'[28a]. Although they had access to cheaper raw materials and a larger home market, USA dye companies were relatively small before 1914 and could not compete with European imports. This arose from various difficulties leading to the unreliability of their products[28b].

When World War I (WWI) broke out, German supplies of dyes stopped. The '*dye famine*', as it was called, was described as follows: 'The possibility of a complete cessation in shipments was, however, constantly present as a menace, hanging like a sword of Damocles over the head of every consumer of synthetic dyes. . .'[29]. Concerning aniline dyes, the American initiatives were looking up by the mid-1920s when companies such as DuPont, the National Aniline & Chemical Company, Monsanto, Goodyear, Sherwin-Williams etc. were ready to spend a substantial amount of money to begin the production of synthetic dyes, an effort based on German patents regarded by the USA government as the spoils of WWI[30]. DuPont invested heavily in R&D and was in particular aggressively luring German scientists to Delaware with high salary incentives[31]! As a result, when the start of WWII again disrupted the US market, the shortage of imported dyes was less of a problem. With the onset of WWII, Germany lost its position as the world's main producer of dyes. Aided by post-war acquisition of German knowledge, the US dye industry has become a major supplier.

The birth and adolescence of the synthetic dye industry in the late 19th and early 20th centuries prior to WWI has been a case study in international business and economics. Fundamental lessons about building competitive advantages and industry dynamics that led to German companies' ascendance over British, French, European and American rivals have been analyzed meticulously[32].

Nowadays, aniline remains one of the basic starting materials, not only in the dye industry but also in the chemical industry (for polyaniline, polyurethane) and pharmaceutical industry (for the manufacture of drugs such as antipyrine, antifebrin etc.)[33]. World demand for aniline is expected to grow at an impressive rate of several percents per year

and, as a consequence, the short supply of aniline is likely to continue. In the 21st century, a time of globalization of the world economy and market, fierce competition in this pivotal industry is hardly avoidable!

II. MOLECULAR STRUCTURE AND BONDING

A. Equilibrium Structure

Until the mid-1960s, it was assumed that aniline (denoted hereafter as ANI) had a planar geometry in its ground electronic state. The first evidence for its nonplanarity came from an analysis of the electronic (UV) band system near 2940 Å[34]. The first microwave (MW) spectroscopic study[35] clearly demonstrated its nonplanarity. In the MW spectrum, each ground-state rotational transition is accompanied by a vibrational satellite of comparable intensity, showing that the observed rotational transitions are due to structures in both 0^+ and 0^- inversion states, separated from each other by an energy gap smaller than 100 cm^{-1}. Detailed vibrational analysis of the first ultraviolet band system of ANI[36] and subsequent MW[37,38] studies firmly established a pyramidal amino configuration, even though they differed from each other somewhat in the degree of pyramidality around nitrogen. X-ray diffraction analysis also pointed out a nonplanar conformation in the crystal state[39]. Among a subsequent gas-phase electron diffraction study[40] and several rotational studies[41–44], the most recent MW study[44], in which a much larger number of transition lines were recorded (296 for the 0^+ state, 286 for the 0^- state and 190 for the 1^+ state), strongly confirmed the previous gas phase results. *Ab initio* quantum chemical computations[45–56] using different levels of theory also concurred with this finding.

In the singlet ground state, the pyramidal ANI is a nonrigid molecule exhibiting a C_s symmetry point group in which the plane element is perpendicular to the ring plane. The other C_s structures in which the ring plane bisects the pyramidal amino group are the transition structures for internal rotation of NH$_2$ around the C−N bond. The planar C_{2v} structure is the transition structure for nitrogen inversion.

Table 1 lists the calculated geometrical parameters of ANI, that are in quantitative agreement with the available gas-phase r_0 structure[37]. The latter was derived from rotational spectra recorded for 13 isotopic variants. In general, the ring geometry is rather insensitive to the level of calculation. The nitrogen atom is distorted by 2–3° out of the ring plane, whereas the angle between the plane defined by the amino group and the ring plane amounts to around 40°, irrespective of the method employed[55]. The experimental estimates for the latter bond angle varied according to the techniques employed, namely $37.5 \pm 2°$ (MW)[37], $42.4 \pm 0.3°$ (MW)[41a], $38 \pm 3°$ (X-ray)[39], $44.4 \pm 42°$ (ED)[40], 41.7° and 42.2° by vibration−inversion analysis of the far-IR spectra or 46° from analysis of the first UV band[36], and 42° by resonance fluorescence measurements[57]. Because geometrical parameters are not observables, a more direct, and perhaps more rigorous, comparison between experimental and calculated geometries involves rotational constants. As shown in Table 2, the rotational constants of the S_0 state are reproduced to within 0.2% of experiment by the density functional B3LYP method. While the molecular orbital MP2 method and other density functionals provide reasonable data (deviation of 0.4–0.8%), the HF and BLYP result in larger deviations from experiment (1.3%). A similar trend for the performance of the theoretical methods has been observed for the geometry of phenol[12,58].

Results obtained from an X-ray analysis of ANI in a crystalline state[39] pointed out a certain distortion of the ring, and an asymmetry of the amino hydrogen atoms (without C_s symmetry), which is no doubt due to the crystal effect. Otherwise, the C−N distance and amino group bond angles in the crystal structure are quite close to the MW and calculated results.

TABLE 1. Geometry of aniline determined using different levels of quantum chemical theory[a] and experiment

Parameter[b]	HF	MP2	B3LYP	BLYP	BPW91	B3PW91	B3P86	HCTH	MPW1PW91	Exptl.[c]
					Bond lengths (Å)					
C1–C2	1.392	1.405	1.403	1.414	1.410	1.401	1.399	1.404	1.399	1.397
C2–C3	1.383	1.398	1.391	1.401	1.397	1.389	1.388	1.390	1.387	1.394
C3–C4	1.386	1.400	1.395	1.405	1.401	1.392	1.391	1.394	1.390	1.396
C1–N7	1.396	1.407	1.398	1.409	1.402	1.393	1.391	1.391	1.391	1.402
C2–H10	1.077	1.088	1.086	1.092	1.093	1.087	1.086	1.088	1.085	1.082
C3–H11	1.076	1.087	1.085	1.091	1.092	1.086	1.085	1.087	1.084	1.083
C4–H12	1.075	1.086	1.083	1.090	1.090	1.084	1.083	1.085	1.083	1.080
N7–H8	0.996	1.012	1.009	1.017	1.016	1.008	1.008	1.007	1.007	1.001
					Bond angles (deg)					
C1C2C3	120.4	120.5	120.5	120.5	120.5	120.5	120.5	120.6	120.5	120.1
C2C3C4	120.9	120.5	120.8	120.8	120.8	120.8	120.8	120.8	120.8	120.7
C3C4C5	118.7	119.1	118.9	118.9	118.9	118.9	118.9	118.8	118.8	118.9
C1C2H10	119.7	119.4	119.5	119.5	119.5	119.5	119.5	119.5	119.5	119.8
C2C3H11	119.2	119.3	119.2	119.2	119.2	119.2	119.2	119.2	119.2	
C3C4H12	120.6	120.4	120.6	120.5	120.6	120.6	120.6	120.6	120.6	120.5
C4C5H13	119.9	120.1	120.0	120.0	120.0	120.0	120.0	120.0	120.0	
C5C6H14	120.0	120.0	120.0	120.0	120.0	120.0	120.0	119.9	120.0	
C6C1N7	120.6	120.5	120.7	120.7	120.7	120.7	120.7	120.8	120.7	
C1N7H8	114.7	113.5	115.7	115.5	115.3	115.6	115.6	115.7	115.5	115.9
H8N7H9	111.3	110.3	112.2	111.9	111.9	112.3	112.3	112.0	112.2	113.1
γ^d	2.1	3.4	2.3	2.7	2.6	2.3	2.3	2.6	2.3	

[a]HF and MP2 are molecular orbital methods. The others are from density functional theory. Calculations were carried out using the 6-311++G(d,p) basis set.
[b]See Figure 1 for atom numbering.
[c]Experimental values taken from References 37 and 38.
[d] Angle between the C1–N7 bond axis and the C1–C4 axis.

TABLE 2.   Calculated and experimental rotational constants of aniline (MHz)

Method[a]	A_e	B_e	C_e
HF	5712.717(1.7)	2621.807(1.1)	1800.026(1.3)
MP2	5592.166(0.5)	2578.432(0.6)	1768.252(0.5)
B3LYP	5631.892(0.3)	2592.463(0.1)	1777.771(0.0)
BLYP	5548.616(1.2)	2555.608(1.5)	1752.302(1.4)
BPW91	5577.092(0.7)	2571.248(0.9)	1762.535(0.8)
B3PW91	5646.883(0.5)	2602.821(0.3)	1784.164(0.4)
B3P86	5657.854(0.7)	2609.470(0.6)	1788.389(0.6)
HCTH	5636.085(0.3)	2596.715(0.1)	1780.228(0.2)
MPW1PW91	5665.222(0.9)	2610.140(0.6)	1789.458(0.7)
MW[b]	5617.470	2593.868	1777.034
MW[c]	5617.456	2593.867	1777.032
MW[d]	5617.478	2593.859	1777.038

[a] Calculations were using the 6-311++G(d,p) basis set. In parentheses are the ratio (%) of the deviation of the calculated value with respect to the experimental counterpart.
[b,c,d] Rotational constants A_0, B_0, C_0 were determined from MW spectra (References 37, 43 and 44).

The ANI amino group nonplanarity has been investigated in detail[46−56]. There are no significant differences between ring geometries of planar and pyramidal forms. A measure of the degree of nonplanarity, which originates mainly from a balance between the sp^2–sp^3 hybridization of the amino group, is the C−NH_2 bond distance. The value of 1.39–1.40 Å determined for this bond, by either experiment or calculation, is shorter than that of 1.47 Å in methylamine, but rather long as compared with 1.34–1.35 Å in similar 6-membered rings such as cytosine and aminotriazine. This indicates a small but real degree of electron delocalization between the nitrogen lone pair and the ring.

The degree of nonrigidity can usually be quantified by the energy barrier to nitrogen inversion. Although the available experimental estimates for the ANI inversion barrier range from 5 to 18 kJ mol^{-1}, the value of 6–7 kJ mol^{-1} appeared to be the best estimate receiving a large consensus[59−61]. Molecular orbital methods predict a barrier to nitrogen inversion of 7 kJ mol^{-1} by second-order perturbation theory (MP2) and 8 kJ mol^{-1} by coupled-cluster theory (CCSD(T), using in both cases the 6-311++G(d,p) basis set and with ZPE corrections). Compared to ammonia, where the nitrogen inversion barrier amounts to 25 kJ mol^{-1}, the phenyl group thus strongly reduces this parameter. It is worth noting that all current DFT methods predict a too small inversion barrier for aniline (<1 kJ mol^{-1}).

The barrier to internal rotation of the amino group around the C−N bond is more energy-demanding, amounting to 20–25 kJ mol^{-1}[54,55,61].

B. Molecular Orbital Pattern

In the simplest wavefunction describing the closed-shell singlet ground state (S_0) of ANI, its 50 electrons are distributed in twenty-five molecular orbitals (MOs), comprising seven core orbitals and eighteen valence MOs. Due to the C_s symmetry point group, the occupied MOs are divided into two subgroups, namely 16 symmetrical a' and 9 antisymmetrical a'' orbitals. The a' subset approximately includes five core (1s), one N−H, three C−H, five C−C, one C−N and one N lone pair orbitals. The a'' subset contains two core (1s), one N−H, two C−H and four C−C orbitals. Figure 2 displays the three-dimensional pattern of 17 occupied valence orbitals and the LUMO. The HOMO and LUMO are of particular interest. To further illustrate these frontier orbitals, Figure 3

displays another view of their components. The HOMO (25 a') is basically a π-orbital whose p-lobes are centered on the C1, C4 and N7 atoms and lie within the symmetry plane; the *meta*-carbons do not have contributions. The LUMO (26 a'') is a π^*-ring orbital in which the p-components on the symmetry plane at the *ipso*- and *para*-carbon positions vanish and only the p-lobes of the C2, C5 (*ortho*), C4 and C6 (*meta*) ring atoms remain.
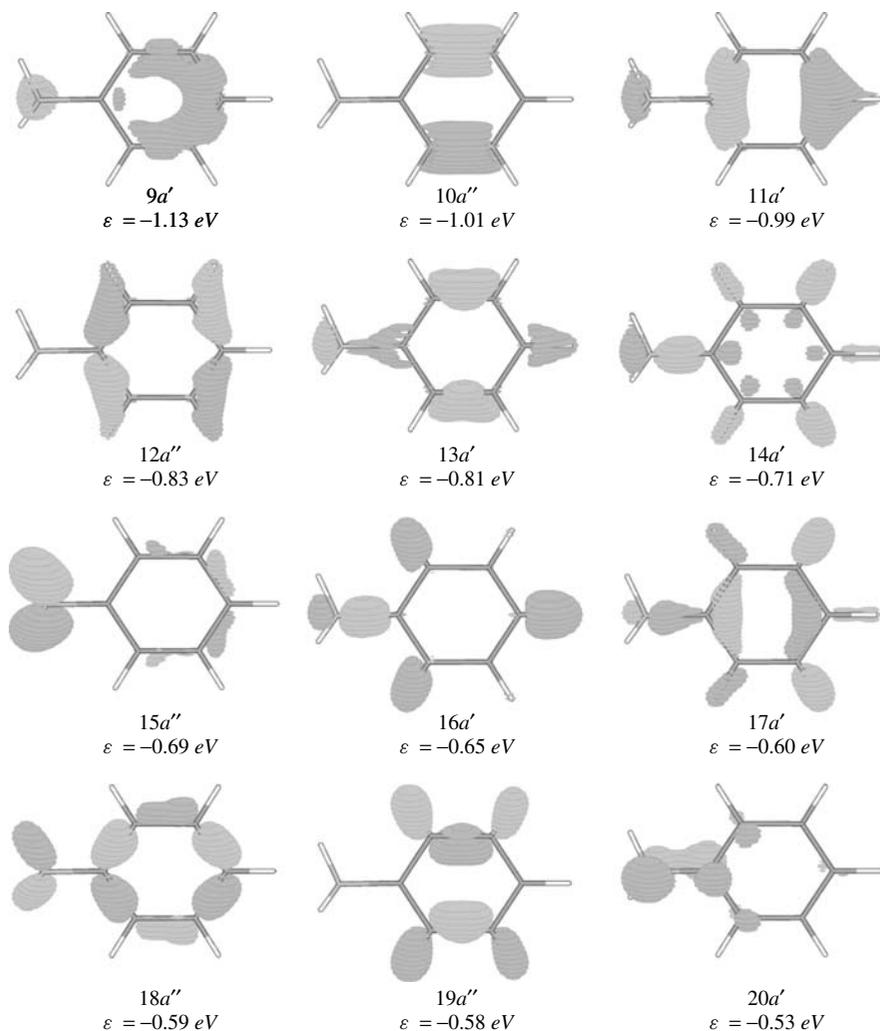
FIGURE 2. Shape of valence molecular orbitals of aniline. Due to its C_s symmetry, the MOs are characterized by a' and a'' irreducible representations, but they are continuously numbered without dividing them into two subsets. ε denotes the orbital energy computed using the HF/6-311++G(d,p) wavefunction

21a′
ε = −0.51 eV

22a″
ε = −0.49 eV

23a′
ε = −0.45 eV

24a″
ε = −0.34 eV

25a′ - HOMO
ε = −0.29 eV

26a″ - LUMO
ε = 0.14 eV

FIGURE 2. (*continued*)

25a′ - HOMO
ε = −0.29 eV

26a″ - LUMO
ε = 0.14 eV
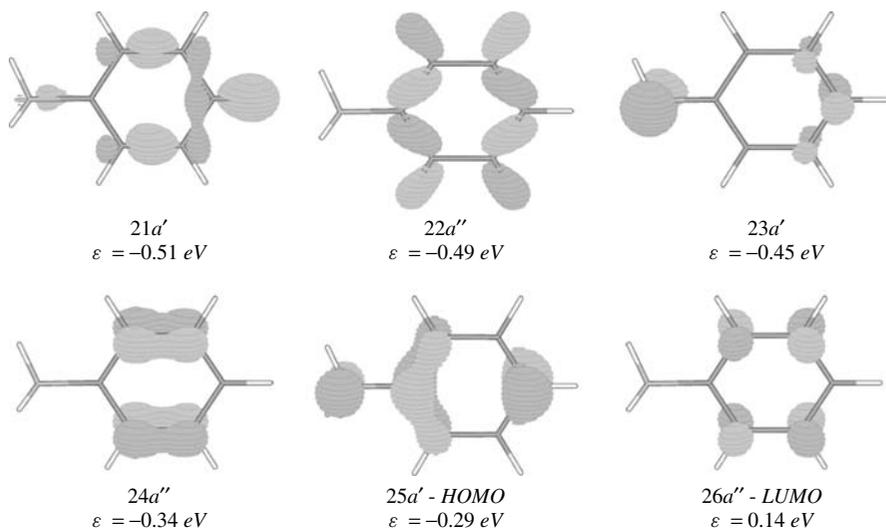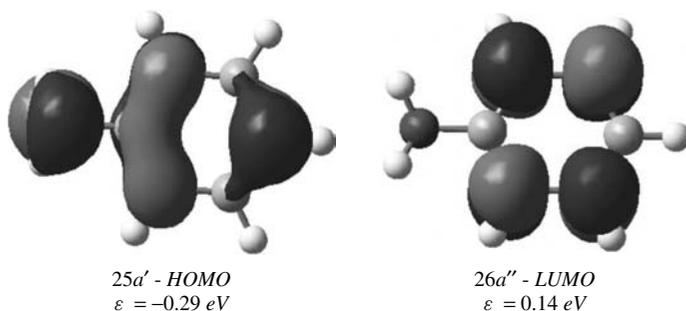
FIGURE 3 (PLATE 1). Another view of the HOMO and LUMO frontier orbitals of aniline

C. Electronic Distribution

Figure 4 lists some selected basic molecular properties related to the electronic repartition in ANI. The charge densities show a substantial π-charge donation from the nitrogen into the ring, namely to the antibonding acceptor π^* (CC) ring orbitals. The nitrogen lone pair n(N) has 91% p-character and is occupied by 1.85 electrons. A strong n(N) $\rightarrow \pi^*$ (CC) interaction, combined with σ-withdrawal, decreases the pyramidal character and flattens the amino group. In the planar form, this stabilizing interaction is maximized and thereby reduces its inversion barrier.

The π-overlap populations between both phenyl and amino moieties are in line with a shorter C−N bond distance. Figure 5 gives a summary of the atomic natural charges and bond indices, computed using the natural bond orbital (NBO) approach. The following bond indices, C1−N7: 1.11, C1−C2: 1.35, C2−C3: 1.45 and C3−C4: 1.42, indicate that the CN bond is slightly more than a single bond and the CC bonds are less than

Dipole moment (D or Debye):

$\mu_X = 0.963 \quad \mu_Y = 1.271 \quad \mu_{Tot} = 1.594$

Quadrupole moment (D.Å):
$Q_{XX} = -47.395 \qquad Q_{YY} = -35.517$
$Q_{ZZ} = -37.017 \qquad Q_{XZ} = -3.1845$

Octapole moment (D. Å^2):
$Q_{XXX} = -0.646 \qquad Q_{YYY} = 15.891$
$Q_{XYY} = -9.489 \qquad Q_{XXY} = 2.619$
$Q_{XZZ} = -0.5660 \qquad Q_{YZZ} = 5.5468$

Hexadecapole moment (D- Å^3):
$Q_{XXXX} = -58.838 \qquad Q_{XXXY} = -1.052$
$Q_{YYYY} = -510.140 \qquad Q_{ZZZZ} = -287.837$
$Q_{YYYX} = -27.426 \qquad Q_{XXYY} = -121.149$
$Q_{XXZZ} = -68.870 \qquad Q_{YYZZ} = -124.887$
$Q_{ZZXY} = -1.909$

Polarizability (a.u.):
$\alpha_{xx} = 48.08$
$\alpha_{yy} = 102.02$
$\alpha_{zz} = 84.98$

FIGURE 4. Some properties of aniline obtained from B3LYP/6-311++G(3df,2p) calculations

double bond. This is manifested in the high barrier to internal rotation of the amino group around the CN bond (>20 kJ mol^{-1} mentioned above). In the perpendicular conformation of the rotational transition structure, the n(N) $\rightarrow \pi^*$ (CC) interaction no longer exists. Overall, the nitrogen is the most negatively charged center. Within the ring, the *ortho*- and *para*-carbons bear the largest negative charges whereas the *meta*-carbon atoms have smaller negative charges; the *ipso*-carbon is positively charged. This is in agreement with those expected on the basis of contributions from the usual valence structures for aniline (Scheme 1) and with the experimentally well known *ortho*- and *para*-directing power of the amino group for electrophilic substitution reactions.

The ANI permanent dipole moment has not yet been well established. Earlier dielectric constant measurements (at a temperature of 459 K in the gas phase) provided a value of $\mu = 1.53$ D[62] (in units of Debye, 1D $= 3.33564 \times 10^{-30}$ C m). An earlier study using the Stark effect determination from the rotational spectroscopy reported a smaller value, $\mu = 1.15 \pm 0.02$ D for $C_6H_5NH_2$ and $\mu = 1.13 \pm 0.02$ D for $C_6H_5ND_2$[38]. However, an independent MW study evaluated the μ_a component at 1.07 D and did not detect any *b*- and *c*-type transitions in the MW spectra[37]. More recent MW studies[43] using also Stark effects in gas-phase electronic spectra pointed out that the values determined from MW spectra are actually the *a*-axis projection of the dipole moment. Therefore, the in-plane component of the dipole moment can be established as $\mu_a(S_0) = 1.13$ D.

Calculated results of μ_a vary: 0.97 (MP2), 1.26 (B3LYP) and 1.20 D (CCSD(T)). The calculated total dipole moment $\mu(S_0)$ amounts to 1.59 (B3LYP), 1.54 (CCSD) and 1.55 D (CCSD(T), using large basis sets). These results tend to support the experimental value of 1.53 D. The dipole moment vector is actually oriented out of the ring plane at an angle of about 45°. The in-plane component is directed with its negative end away from the nitrogen atom toward the aromatic ring (Figure 4). Compared with methylamine, there is a reversal of the dipole moment direction. In CH_3-NH_2 the corresponding component
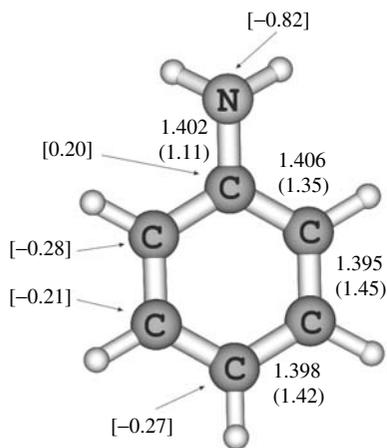
[−0.82]

1.402
(1.11)

1.406
(1.35)

[0.20]

[−0.28]

[−0.21]

1.395
(1.45)

1.398
(1.42)

[−0.27]

Geometry, natural charges and
Wiberg indices

(a)

ρ: 0.298
L: 0.230
ε: 0.064

ρ: 0.300
L: 0.180
ε: 0.226

ρ: 0.305
L: 0.183
ε: 0.231

ρ: 0.020
L: −0.04

ρ: 0.303
L: 0.183
ε: 0.216

Topology of $\rho(\mathbf{r})$

(b)

Laplacian

(c)

1.84

2.74

1.92

2.91

2.77
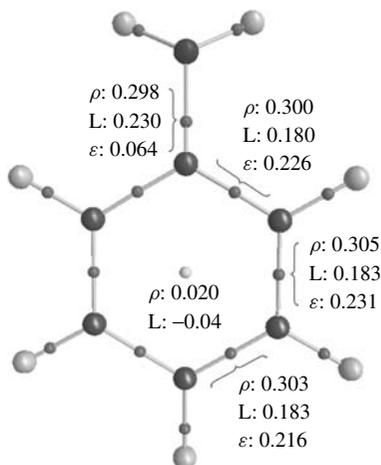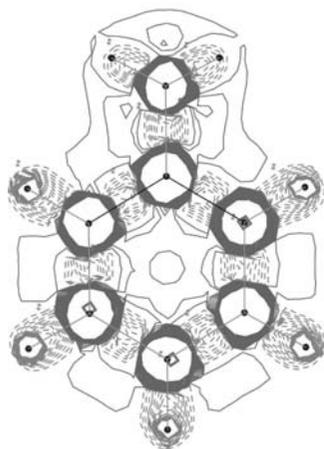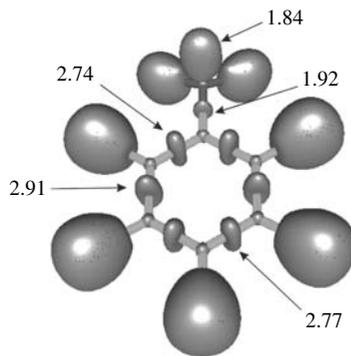
ELF

(d)

FIGURE 5. Summary of electronic distribution in aniline. (a) Bond distances (Å), NBO charges [bracket, in au] and Wiberg indices (parentheses, in au). (b) Topology of the electron density determined from atom-in-molecule calculations: $\rho(\mathbf{r})$ = electron density, L = Laplacian of the density defined as $L(\mathbf{r}) = -\nabla^2\rho(\mathbf{r})$ and ε = ellipticity of the bond critical point. (c) Laplacian map of the density. (d) Iso-surfaces of the electron localization function, ELF = 0.87; the values are the populations of the valence basins
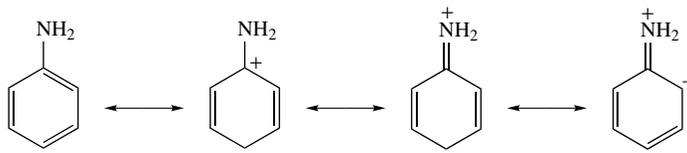
SCHEME 1

along the C−N axis has the negative end toward the nitrogen atom. Using $\mu = 1.53$ D, the out-of-plane component of the ANI dipole moment is evaluated to be $\mu_c = 1.09$ D[37].

The ^{14}N quadrupole hyperfine structure was analyzed from the MW spectrum and the nitrogen nuclear quadrupole coupling constants (NQCC) for aniline-H$_7$ are determined as follows: $\chi_{aa} = 2.34$, $\chi_{bb} = 1.86$ and $\chi_{cc} = -4.20$ MHz[38].

Figure 5 illustrates the Laplacian map of the electron density of ANI ground state on the ring plane and its topology. We would refer to References 12 and 63 for detailed definitions of the terms and their significance. The topology is defined by the $(3, -3)$ attractors (nuclei), bond critical points $(3, -1)$ (BCP), and ring critical points (RCP) maximum electron density (MED) lines and $(3, +1)$ RCP of the one-electron density $\rho(\mathbf{r})$. In the Laplacian map, red regions correspond to those having local charge concentration whereas blue regions indicate those having electron depletion. All the bonds are classically characterized by BCPs having comparable electron density $\rho(\mathbf{r})$ and Laplacian $L(\mathbf{r})$ values. The only noticeable difference concerns the small ellipticity ε of the C−N bond, as compared with those of the CC bonds. As expected, there is a RCP associated with the ring bearing a small density and a negative L value.

Figure 5 equally displays the localization domains of aniline determined using the electron localization function technique (ELF)[12, 64], which defines the electronic basins within a molecular system. The basins correspond to the domains where electrons are localized either in paired bonds or in nonbonding lone pairs. In such a way, the number and nature of bonds between atoms could be determined. The ELF $\eta(\mathbf{r})$ value varies from 0 to 1 ($0 \leqslant \eta(\mathbf{r}) \leqslant 1$), which is chosen to determine the isosurfaces of the domains. Basins can be classified according to their synaptic order, that is, monosynaptic basins belong to the cores (denoted by C) whereas disynaptic basins describe the valence regions (denoted by V).

As in the case of phenol or monosubstituted benzenes[12], ANI exhibits six C(C) and one C(N) core basins, six V(C,C), five V(C,H), one V(C,N), two V(N,H) and one V(N, lone pair) localization domains. Integration of the density over each domain allows the amount of electrons present there to be determined. Thus the C−C bonds are nearly equivalent and each V(C,C) basin classically contains about 2.7–2.9 electrons (close to 3.0), whereas the V(N) and V(C,N) basins have 1.8 and 1.9 electrons, respectively (Figure 5). Relative to benzene, an increase in the population of the V(C$_{ortho}$−C$_{meta}$) basin is noticeable (0.1 e) whereas the populations of other domains remain almost unchanged. Overall, the above analysis is in line with the classical picture that chemists always have about the electron distribution in aniline.

In spite of the lack of a unique and precise definition, aromaticity is one of the most frequently used concepts in (organic) chemistry. This phenomenon, which is classically associated with a cyclic π-electron delocalization, results in a stabilization of the molecular system considered. Benzene is the archetype of the phenomenon of aromaticity. Thus, a question of interest is to what extent the amino substituent influences the electron delocalization in the ring. There are several criteria to evaluate the aromaticity, including the geometry-based (HOMA), energy-based (ASE), magnetism-based (NICS) and electronic delocalization (PDI) models. Recent theoretical evaluations[65] of these parameters

in a series of monosubstituted benzenes pointed out that only very weak influence is noticeable, as shown by the very small variations of the indices. Thus, the nucleus independent chemical shift (NICS) of ANI amounts to -9.8 whereas it is -9.7 in benzene, -9.7 in toluene but -10.8 in phenol. The aromatic stabilization energies (ASE) amount to 135, 136, 139 and 144 kJ mol^{-1} in benzene, toluene, aniline and phenol, respectively. The *para*-delocalization indices (PDI) derived from the atom-in-molecule (AIM) model show that the Ph−X systems are only marginally less aromatic than benzene, and these indices correlate better with more classical substituent constants. Thus, aromatic systems tend to retain their initial electron distribution upon electrophilic substitution. The substituent effect stabilization energy is, however, strongly affected by complexation and solvation[65].

D. Vibrational Modes

The aniline molecule has 14 atoms and therefore contains 36 normal modes of vibration. Their overtone and combination modes are infrared active. Only one complete experimental vibrational study[66] of ANI was carried in the early 1960s with an assignment of the IR spectra in the gas and liquid phases, as well as the Raman spectra in solution. The solid state IR and Raman spectra[67], vapor phase IR[68], far-IR[59,69] low temperature argon matrix[70] and IR-double resonance[71,72] were later reported. Theoretical analyses of the vibrational motions of aniline have also been carried out abundantly[49,54,56,73–80]. The most striking observation was that the characterization depends strongly on the various quantum chemical methods. Thus, the nature of several modes was found to be drastically changed in going from one to another method. Theoretical methods did not predict well absolute vibrational intensities, but the relative intensities are comparable in different methods. Overall, density functional methods with the popular hybrid B3-based functional provide reliable prediction for the calculated wavenumbers.

Table 3 summarizes the experimental and calculated vibrational frequencies along with the calculated IR intensities and potential energy distribution (PED). To simplify the presentation of vibrational modes, mainly for the benefit of the general readers who are not familiar with the labeling according to either the Wilson or Varsányi convention for substituted benzenes, the normal modes illustrated in Figure 6 are simply numbered from Q1 to Q36. Compared with the modes reported in Reference 56, they are identical except for modes Q25 and Q26 that are permuted. We refer to Reference 72 for a full Varsányi labeling of the modes. The experimental values are taken from different vibrational spectroscopic studies. The theoretical values given in Table 3 are calculated using the DFT method and scaled down by different scaling factors. In most cases, the scaled values are quite close to the experimental frequencies recorded either in the gas phase or in the Ar matrix. They are presented as support for the assignments that were not clear-cut on the sole basis of observed data, or were the subject of some discussion in the literature. In the following discussion, only the tabulated experimental values are quoted. After careful analysis, we have adopted the assignment of the important modes as follows:

1. NH$_2$ Vibrations. The modes related to the NH$_2$ group have been extensively investigated and analyzed[73–80]. The antisymmetrical (Q36) and symmetrical (Q35) stretching modes are positioned at 3508 and 3422 cm^{-1}, respectively, with nearly equal IR intensities. According to the calculated PED (Table 3), the NH$_2$ scissoring vibration contributes to two modes, Q28 and in particular with a dominant contribution to Q29. These modes have been assigned to the bands at 1608 and 1618 cm^{-1}, respectively, in the Ar matrix IR spectrum[69,70]. The amino deformation (rocking) is also involved in modes Q18 and Q19 with contributions of 43% and 27%, respectively.

TABLE 3. Fundamental vibrational frequencies (cm^{-1}) and associated potential energy distributions of aniline in its ground electronic (singlet) state. Calculated values were obtained from scaled B3LYP/6-311++G(3df,2p) harmonic frequencies

No.	Calc.	Scale	Expt. [a]	Sym.	Int.	Assignment, PED (% $\geqslant$ 10%) [b]
Q1	219	215	217	A'	5.2	$\delta_{2rg}(63.) + \delta_{1rg}(14.)$
Q2	300	295	277	A''	17.0	$\tau_{[NH_2]}(94.)$
Q3	383	376	390	A''	0.1	$\beta C_2C_6(77.) - \beta_{3rg}(8.) - \beta H_8H_{14}(6.)$
Q4	418	411	415	A''	0.2	$\delta_{3rg}(84.)$
Q5	502	493	501	A'	103.8	$\delta_{2rg}(35.) - \gamma C_1N_7(29.) - \gamma H_8H_{14}(13.)$
Q6	535	526	526	A'	14.3	$\beta_{2rg}(60.) - 9(13.) + \gamma H_8H_{14}(7.)$
Q7	570	560	541	A'	189.1	$\gamma H_8H_{14}(58.)$
Q8	634	623	619	A''	0.3	$\beta_{3rg}(86.)$
Q9	692	680	688	A'	17.2	$\delta_{1rg}(66.) + \gamma C_3H(11.) + \gamma C_5H(11.) - \gamma C_1N_7(10.)$
Q10	761	748	755	A'	71.6	$\gamma C_4H(31.) - \delta_{2rg}(21.) + \gamma C_1N_7(18.)$
Q11	825	811	812	A'	3.9	$\beta_{1rg}(23.) - \nu C_1N_7(20.) - \beta_{2rg}(18.) - \nu C_1C_6(14.) - \nu C_1C_2(14.)$
Q12	832	818	822	A''	0.0	$\gamma C_6H(35.) - \gamma C_2H(35.) - \gamma C_3H(15.) + \beta H_8H(15.)$
Q13	890	875	875	A'	7.4	$\gamma C_2H(28.) + \gamma C_6H(28.) - \gamma C_4H(20.)$
Q14	974	957	957	A''	0.0	$\gamma C_5H(31.) - \gamma C_3H(31.) + \gamma C_2H(14.) - \gamma C_6H(14.)$
Q15	982	965	968	A'	0.1	$\gamma C_4H(26.) - \gamma C_3H(25.) - \gamma C_5H(25.) - \nu C_2C_3(10.)$
Q16	984	967	996	A'	0.4	$\beta_{1rg}(60.) + \nu C_1C_6(10.) + \nu C_1C_2(10.)$
Q17	1047	1029	1028	A'	4.3	$\nu C_4C_5(32.) + \nu C_3C_4(32.)$
Q18	1062	1044	1054	A''	2.7	$\beta H_8H_{14}(42.) - \nu C_1C_6(10.) + \nu C_1C_2(10.)$
Q19	1134	1115	1115	A''	3.9	$\beta H_8H_{14}(30.) + \beta CH(14.) + \beta C_2H(14.)$
Q20	1180	1160	1152	A''	2.0	$\beta C_4H(34.) - \beta C_5H(20.) - \beta C_3H(20.)$
Q21	1201	1181	1176	A'	10.8	$\beta C_2H(21.) - \beta C_6H(21.) - \beta C_3H(19.) + \beta C_5H(19.)$
Q22	1293	1271	1282	A'	72.4	$\nu C_1N_7(54.) + \beta_{1rg}(10.) - \nu C_5C_6(6.) - \nu C_2C_3(6.)$
Q23	1344	1321	1324	A''	6.7	$\nu C_4C_5(14.) - \nu C_3C_4(14.) + \nu C_1C_6(14.) - \nu C_1C_2(14.) - \nu C_5C_6(13.) + \nu C_2C_3(13.)$
Q24	1370	1347	1340	A''	0.0	$\beta C_2H(22.) + \beta C_6H(22.) + \beta C_3H(16.) + \beta C_5H(16.) + \beta C_4H(12.)$
Q25	1501	1475	1470	A''	1.3	$\beta C_4H(25.) - \nu C_2C_3(15.) + \nu C_5C_6(15.)$
Q26	1531	1505	1503	A'	61.1	$\beta C_3H(16.) - \beta C_5H(16.) + \beta C_2H(12.) - \beta C_6H(12.)$
Q27	1624	1596	1594	A''	4.8	$\nu C_4C_5(17.) - \nu C_3C_4(17.) + \nu C_1C_2(17.) - \nu C_1C_6(17.)$
Q28	1642	1614	1608	A'	31.3	$\beta_{[NH_2]}(19.) - \nu C_2C_3(18.) - \nu C_5C_6(18.)$
Q29	1659	1631	1618	A'	135.0	$\beta_{[NH_2]}(70.)$
Q30	3147	3015	3025	A'	16.4	$\nu C_2H(32.) + \nu C_6H(32.) - \nu C_3H(15.) - \nu C_5H(15.)$
Q31	3150	3018		A''	3.5	$\nu C_6H(41.) - \nu C_2H(41.)$
Q32	3166	3033	3037	A'	3.6	$\nu C_4H(27.) - \nu C_5H(20.) - \nu C_3H(20.) - \nu C_6H(16.) - \nu C_2H(16.)$
Q33	3171	3038	3050	A''	31.3	$\nu C_3H(41.) - \nu C_5H(41.)$
Q34	3189	3055	3072	A'	11.6	$\nu C_4H(69.) + \nu C_5H(14.) + \nu C_3H(14.)$
Q35	3568	3418	3422	A'	18.1	$\nu N_7H(50.) + \nu N_7H(50.)$
Q36	3665	3511	3508	A''	16.6	$\nu N_7H(50.) - \nu N_7H(50.)$

[a] Experimental fundamental vibrational frequencies of aniline taken from Reference 56.
[b] ν: stretching, β: bending, γ out-of-plane, β_{1rg}, β_{2rg}, β_{3rg}: bending of 6-membered ring, δ_{1rg}, δ_{2rg}, δ_{3rg}: deformation of 6-membered ring, $\tau_{[NH_2]}$: torsion of NH_2.
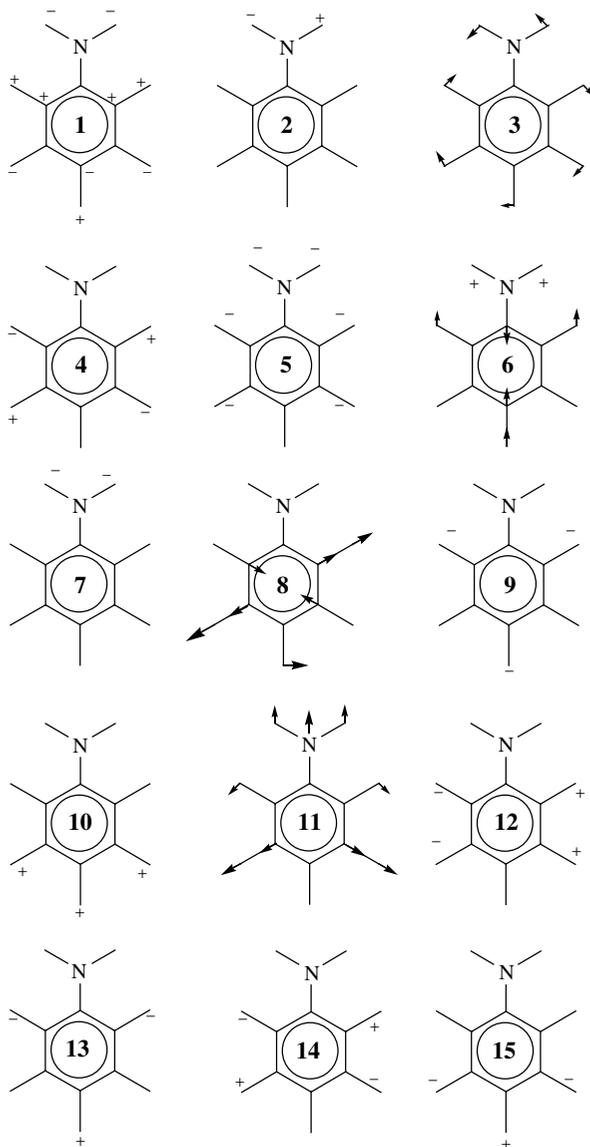
FIGURE 6. Normal displacements of vibrational modes of aniline. The assignment of the normal vibrations and their frequencies is presented in Table 3. The numbers given within the ring correspond to the normal modes numbered from Q1 to Q36 in Table 3 and described in the text
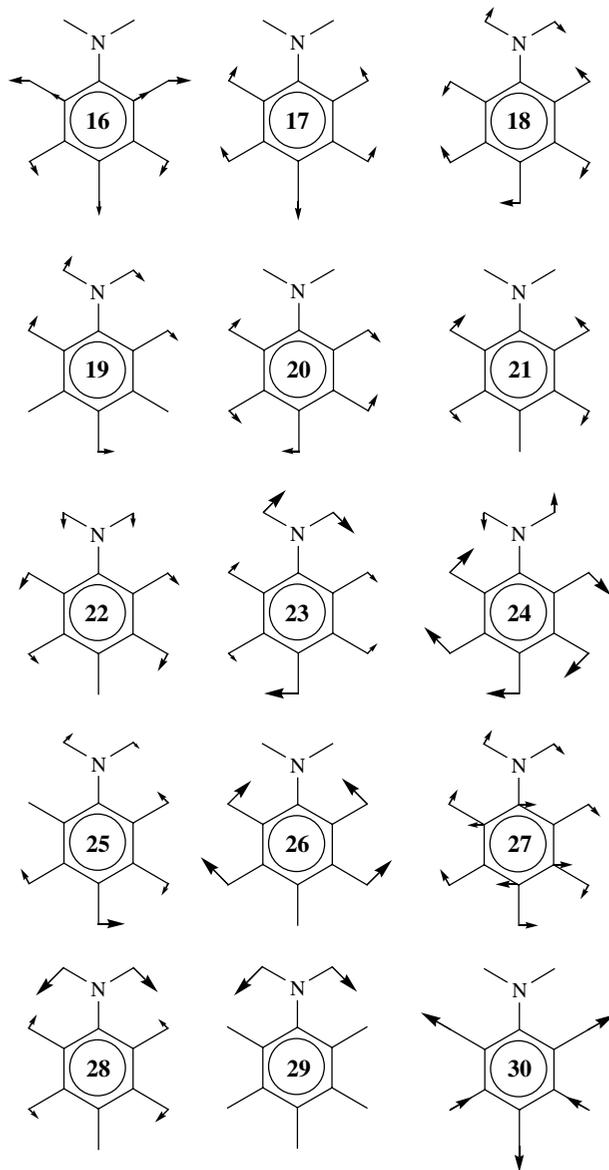
FIGURE 6. (*continued*)
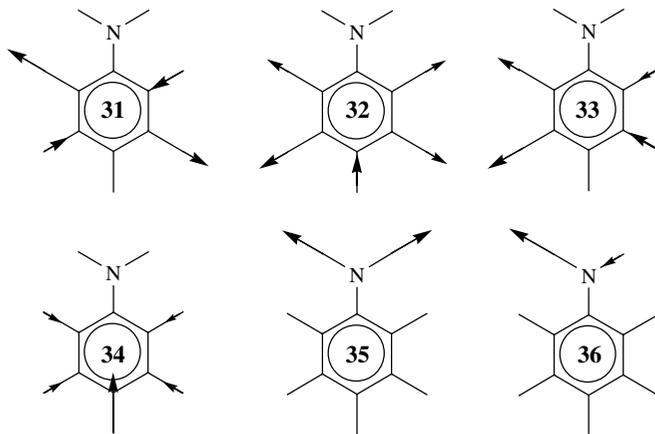
FIGURE 6. (*continued*)

The NH$_2$ wagging, which corresponds to the nitrogen inversion, turns out to be strongly anharmonic in such a way that it is not possible to reproduce its frequency within the harmonic approximation. Use of an asymmetric double minimum potential was necessary to analyze the inversion–rotation coupling of the amino group[54, 67]. The Q7 mode was evaluated to be centered at 541 cm^{-1} (Reference 74). The torsional mode Q2 is associated with a frequency of 277 cm^{-1} (Reference 59). The modes involving a coupling between the phenyl ring and amino group are sensitive to isotopic substitution of NH$_2$ by ND$_2$.

2. C−N Vibrations. The C−N stretching contributes predominantly to mode Q22 (51%) whose frequency at 1282 cm^{-1} (Ar matrix) was obtained. Mode Q12, which contains a significant portion of the CN stretching, was identified at 822 cm^{-1} (Ar matrix). The C−N out-of-plane distortion motion participates in modes Q1 (217 cm^{-1}), Q5 (501 cm^{-1}) and Q10 (755 cm^{-1}).

3. Ring Vibrations. The modes associated with the phenyl ring vibrations are well assigned as they are relatively less sensitive to the nature of the substituent. The following vibrations are noteworthy:

– mode Q9 vibrating at 68 cm^{-1} is an almost pure ring puckering;
– mode Q16 corresponds to a trigonal ring breathing vibration derived from the benzene mode 12 and vibrates at 996 cm^{-1} (Ar matrix);
– mode Q17, absorbed at 1028 cm^{-1}, combines both the CC stretching with the CH in-plane bending vibrations; both modes Q16 and Q17 are weak in IR but strong in Raman spectrum;
– mode Q23 originates from a Kekule-type vibration coupling the ring C−C stretching motions and is located at 1324 cm^{-1};
– mode Q28, which is Raman active, is characterized by the frequency of 1608 cm^{-1};
– the five modes Q30–Q34, dominated by the C−H stretching combinations, vibrate at frequencies of 3072 cm^{-1} (Q34), 3050 cm^{-1} (Q33), 3037 cm^{-1} (Q32) and 3025 cm^{-1} (Q30). Mode Q31 was not observed experimentally but its frequency can be expected at 3022–3024 cm^{-1}.

III. ENERGETICS OF SOME FUNDAMENTAL PROCESSES

A. Unimolecular Rearrangements

Experimental studies of reactions of aniline derivatives[81] suggested that in some cases, it was not the aniline but rather one of its imine isomers that acts as the reactive species. Among the four possible isomers of ANI obtained by placing one H-atom of the NH_2 group on the four ring carbon positions, only the 1,2- and 1,4-tautomers are energetically lower-lying (Figure 7). In the gas phase, the 1,2-tautomer is calculated to be slightly less stable (10 kJ mol^{-1}) than the 1,4 isomer, which is placed at 108 kJ mol^{-1} above ANI. The interconversions between these tautomers are, however, difficult processes, associated with large energy barriers, given in Figure 7, for 1,3-hydrogen shifts. It is well known that in aqueous solution, a chain of solvent water molecules usually acts as catalyst favoring the hydrogen transfer via a concerted relay mechanism[82, 83]. The relative energies between the tautomers are substantially modified upon solvation by hydrogen bonds. It is of interest to note that there is a direct conversion pathway connecting the 1,2-tautomer to itself via a transition structure for 1,5-hydrogen shift. The energy barrier of this H-shift is calculated to be around 200 kJ mol^{-1}.

Photochemistry of aromatic compounds usually leads to a rich variety of rearrangement and dissociation processes. Upon (UV) fluorescence excitation to the S_1 state, the benzene ring undergoes a number of photoisomerizations with formation of the derivatives of fulvene, benzvalene and prismane, etc. Once formed, the latter isomers further undergo re-aromatization. The isomerization processes are usually described in terms of ring permutation[84]. In a molecular beam, aniline was photodissociated experimentally by a 193-nm laser pulse[85] and photofragments were monitored using translational energy distributions. This photon absorption mainly induces a ($\pi^* \leftarrow \pi$) excitation of the phenyl ring. Interconversion of the ring excited state at such a high energy level is usually very fast. As a consequence, the dissociation is expected to occur to a great deal in the ground state, and the channels associated with low energy barriers are the dominant processes. Breaking of the N−H and C−H bonds were found to be favored over other processes. Indeed, the four major dissociation channels, characterized by $m/z = 92, 91, 77$ and 76, correspond to H, H_2, NH_2 and NH_3 channels:

(a) $C_6H_5NH_2 \rightarrow C_6H_5NH + H$
(b) $C_6H_5NH_2 \rightarrow C_6H_3NH_2 + H_2$
(c) $C_6H_5NH_2 \rightarrow C_6H_5 + NH_2$
(d) $C_6H_5NH_2 \rightarrow C_6H_4 + NH_3$
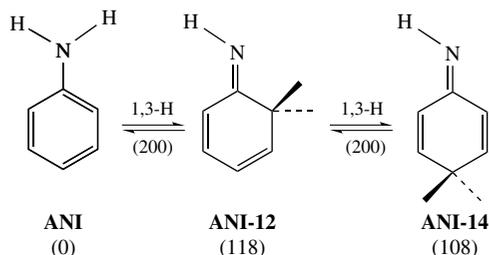
FIGURE 7. Relative energies of aniline and its energetically lower-lying isomers. Values given in parentheses in kJ mol^{-1} were obtained from B3LYP/6-311++G(d,p) + ZPE calculations

The CH$_3$ elimination represents a minor channel:

(e) $C_6H_5NH_2 \rightarrow C_5NH_4 + CH_3$
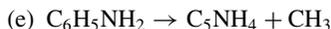
A remarkable feature is the elimination of closed-shell molecules. Because the elimination of an H atom has an exit barrier in the triplet state, dissociation from the T_1 state is also significant (formation of excited states will be discussed in a subsequent paragraph).

Figure 8 illustrates the potential energy surface, constructed at the G3 level of theory[85], schematically showing the different rearrangement and dissociation pathways of ANI in the ground state. Involvement of a lower-energy seven-membered ring isomer constitutes an important feature. Isotope labeling (H/D) experiments showed that 23% of aniline in the S_0 state rearranges to a seven-membered ring[85]. The connection between aniline and 4-methylpyridine is of interest. The barrier for an interconversion connecting both six- and seven-membered rings (around 428 kJ mol^{-1}) is higher than the dissociation limit of the N−H bond cleavage (365 kJ mol^{-1}), but comparable to the barriers of 435 kJ mol^{-1} for H$_2$- and 415 kJ mol^{-1} for NH$_2$-loss. The NH$_3$-loss is characterized by a smaller energy barrier of 301 kJ mol^{-1} (Figure 8). This process starts by a 1,3-H shift from an *ortho*-C atom to N, followed by forming a benzyne−NH$_3$ complex, and then undergoes further a NH$_3$-elimination. There are many possible pathways yielding H$_2$. The photofragment translational energy distribution indicated two different dissociation mechanisms[85].

B. Protonation

Proton transfer is an ubiquitous and fundamental chemical event. The propensity of a molecule to accept (or to donate) a proton is an important descriptor of its reactivity. In the gas phase, protonation of a substrate A is often quantified by its proton affinity (PA), which is conventionally defined as the negative standard enthalpy (ΔH^0) of the reaction $A + H^+ \rightarrow AH^+$. The PA is not solvent-dependent and thus constitutes a measure of the intrinsic basicity of a molecule. This thermochemical parameter can thus be instructive for separating the true electronic effect from the solvation effect. Protonation of aniline has been thoroughly studied both experimentally and theoretically. The main reason for such interest was related to the high dependence of results on experimental conditions[86−94], such as chemical ionization, fast atom bombardment, electrospray etc. On the other hand, inconsistency of quantum chemical methods persists in predicting its most favored protonation site[95−108]. In this section, the protonation of aniline and a series of its halogenated and alkylated derivatives will be examined in some detail.

1. Protonation of aniline: nitrogen versus carbon

This process occurs at either the amine nitrogen or the ring carbon atoms. In solution, the nitrogen atom is the preferred ANI protonation site, due to a higher stabilization by solvent of the *N*-protonated form[86].

In the gas phase, the situation is less clear-cut. Early correlations of PAs with σ_p^+ constants for *para*-substituted anilines led to a conclusion[87] that ANI is protonated on the aromatic ring, yielding either the *ortho* or the *para* protonated isomers, such as in the case of phenol[88]. On the contrary, correlations between PAs of a series of anilines with N(1s) ionization energies suggested that the ANI protonation occurs at the nitrogen[89]. Since then, numerous subsequent mass spectrometric studies[90−98] as well as quantum chemical calculations[98−108], carried out in the past three decades, were unable to decide between both sites.
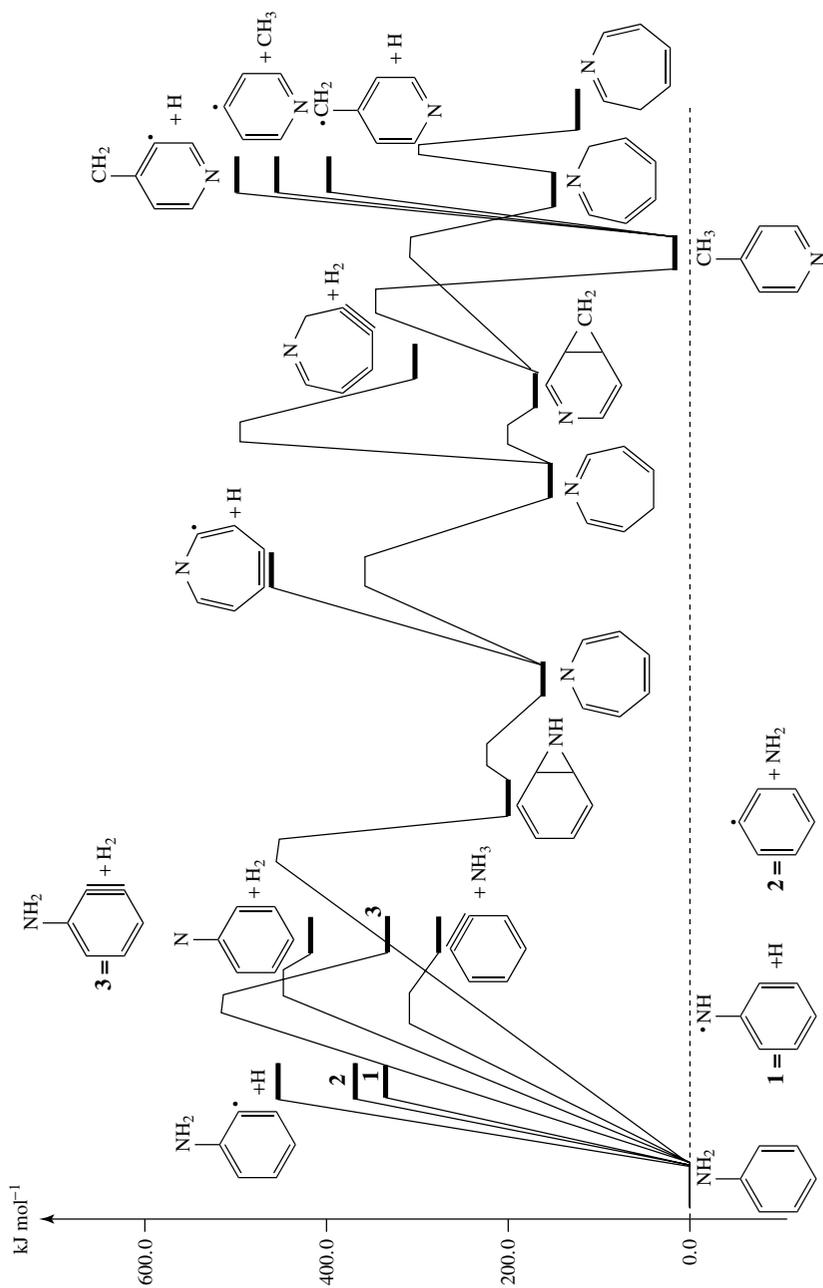
FIGURE 8. Schematic energy profiles showing the unimolecular rearrangements of aniline. Relative energies in kJ mol^{-1} were obtained from G3 calculations based on B3LYP/6-31G(d,p) optimized geometries[85]

It is of interest to mention some detailed mass spectrometric results that were obtained by performing distinct experiments: (a) ion−molecule reactions in mixtures of halobenzenes and ammonia under chemical ionization conditions; (b) ion−molecule reactions of mass-selected ionized halobenzenes toward ammonia in a quadrupole collision cell of a hybrid tandem mass spectrometer; (c) ion−molecule reactions of phenyl diazonium cations with ammonia in the same quadrupole collision cell and, finally, (d) electrospray ionization of anilines in a hybrid quadrupole−time of flight mass spectrometer (QTof). Characterization of the product ions relies on collisional activation experiments in the low or high kinetic energy regime[98].

a. Electron ionization of mixtures of halobenzenes and ammonia under chemical ionization conditions. The ammonia collisional-induced (CI) reaction of chlorobenzene has allowed the characterization of nitrogen-protonated aniline (m/z 94). Based on thermochemical data, the process shown in Scheme 2, namely a direct substitution of a chlorine atom by ammonia, is possible as it is exothermic by about $-20\,\mathrm{kJ\,mol^{-1}}$ (values in Scheme 2 are the standard heats of formation)

$$929 \qquad -46 \qquad\qquad 742 \qquad 121\,\mathrm{kJ\,mol^{-1}}$$
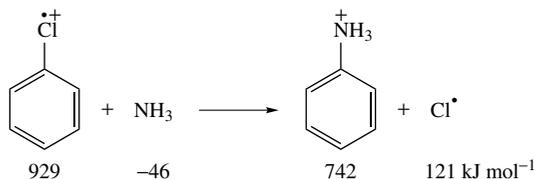
SCHEME 2

The chemistry of mass-selected ionized halobenzenes toward ammonia in a quadrupole collision cell pointed out that the CA spectra of the m/z 94 ions, i.e. protonated aniline, prepared in each of these conditions are qualitatively similar, since all the fragmentations are common. The major observed differences concern the relative intensities of the peaks associated with charge stripping and ammonia loss. In this context, substituted benzenes protonated on a ring carbon atom are more prone to undergo double ionization than substituted benzenes protonated on a substituent.

Applied to experimental data presented in Table 4, these conclusions seem to indicate that (i) mixtures of isomers are produced in all cases, and (ii) ANI itself is mainly protonated on the ring atom under CI conditions, whereas the interaction between ionized iodobenzene and ammonia mainly affords *pure* nitrogen-protonated aniline. Starting with

TABLE 4.   Relative intensities of some significant peaks in the high energy CA spectra of m/z 94 ions generated by ionization of mixtures of ammonia and aniline, chlorobenzene, bromobenzene or iodobenzene in a CI source. The most significant differences are indicated in bold

m/z (%) Samples	93	76	66	51	47[a]	39
Ph-NH$_2$	**100**	**58**	62	86	**31**	47
Ph-Cl	100	83	50	79	21	45
Ph-Br	100	84	51	74	21	43
Ph-I	**86**	**100**	58	67	**11**	37

[a] Charge stripping peaks.

chloro- and bromobenzenes, similar mixtures are generated but the ratios between *N*- and *C*-protonated anilines are intermediate as compared with the two former cases.

   b. Ion–molecule reactions of ionized halobenzenes with pressurized ammonia in the quadrupole collision cell of the hybrid mass spectrometer have been performed in order to increase the selectivity in the measurements. The beams of mass-selected ions were prepared by electron ionization (EI) conditions of chloro-, bromo- and iodobenzenes. All the ionized halobenzenes (PhCl, PhBr, PhI) react with ammonia in the quadrupole collision cell by substitution of the halogen atom by ammonia (m/z 94, see Figure 9a in the chlorobenzene case). The spectrum depicted in Figure 9a also features an intense peak at m/z 77 for phenyl cation that originates from unimolecular and/or collision-induced dissociations of the mass-selected m/z 112 ions. As the phenyl cation is known to react efficiently with nucleophiles such as ammonia, its behavior under the same particular
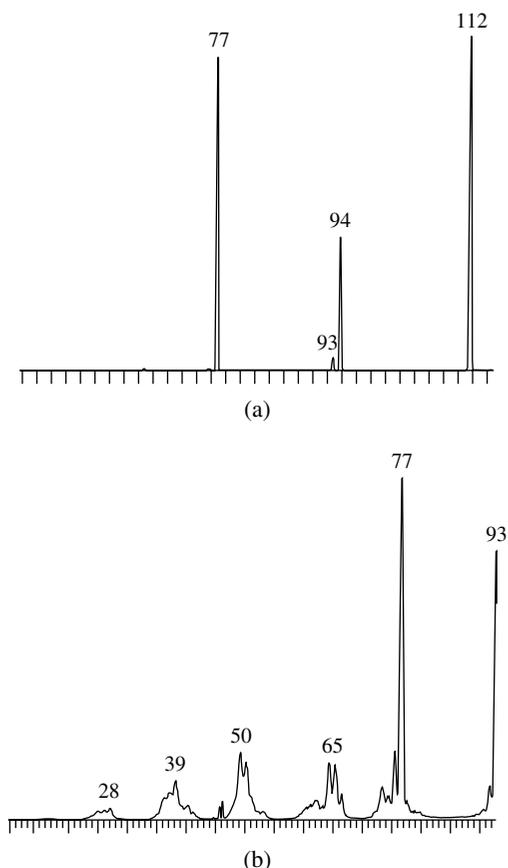
FIGURE 9. Reactions of chlorobenzene radical cations with ammonia: (a) mass spectrum of the ions produced within the quadrupole collision cell (the intensity of the m/z 112 peak is reduced by a factor of 25), and (b) high energy (8 keV, nitrogen collision gas) of the so-produced m/z 94 ions. Spectrum (c) corresponds to the reactions of the m/z 77 phenyl cation, formed in the ion source, with ammonia (the intensity of the m/z 77 peak is reduced by a factor of 40)
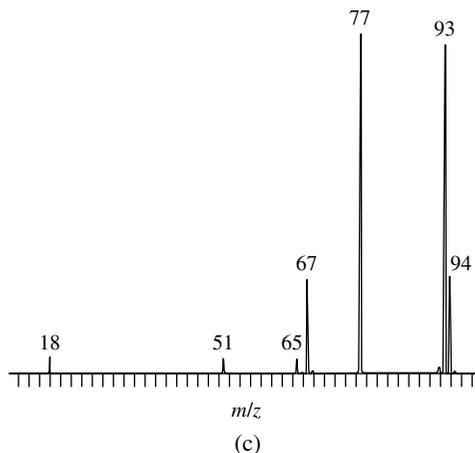
FIGURE 9. (*continued*)

conditions was analyzed. $[C_6H_5{}^+ + NH_3]$ ion is indeed observed, but considering the m/z 77 : m/z 94 branching ratios in Figure 9a and 9c, it is clear that more than 99% of the m/z 94 ions are generated by ion–molecule reactions of the chlorobenzene radical cations with ammonia.

Also noteworthy is the strong intensity of the m/z 93 peak in Figure 9c. These ions were identified as aniline radical cation by a subsequent collisional activation experience (not shown). The production of ionized aniline is not unexpected since the reaction of the phenyl cation with ammonia is strongly exothermic. The heat of the reaction $C_6H_5{}^+ + NH_3 \rightarrow C_6H_5NH_3{}^+$ amounts to $-332\ kJ\,mol^{-1}$. Under these conditions, the kinetic rate constant for collisional stabilization is likely to be too low and most of the adduct $C_6H_5NH_3{}^+$ ions dissociate via the two energetically favorable processes, including the loss of $H^{\bullet}$ (m/z 93) and the loss of NH_3 (m/z 77, a hidden reaction in the present case). The presence of m/z 67 ion (the C_5H_7 composition being deduced from the recorded CA spectrum), which is believed to arise from ring-protonated aniline, indicates that the exothermicity of the reaction could be high enough to convert the initial ammonium ion into an amino carbenium ion (Scheme 3). The energy required for such a [1,3] hydrogen shift is estimated theoretically to be equal to the energy of the nitrogen-protonated aniline ($237\ kJ\,mol^{-1}$, see Scheme 3 and Figure 10), and once the proton is attached on the ring, its migration onto the other positions becomes significantly more favorable.
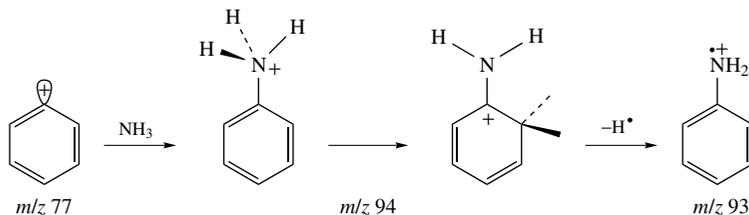
SCHEME 3
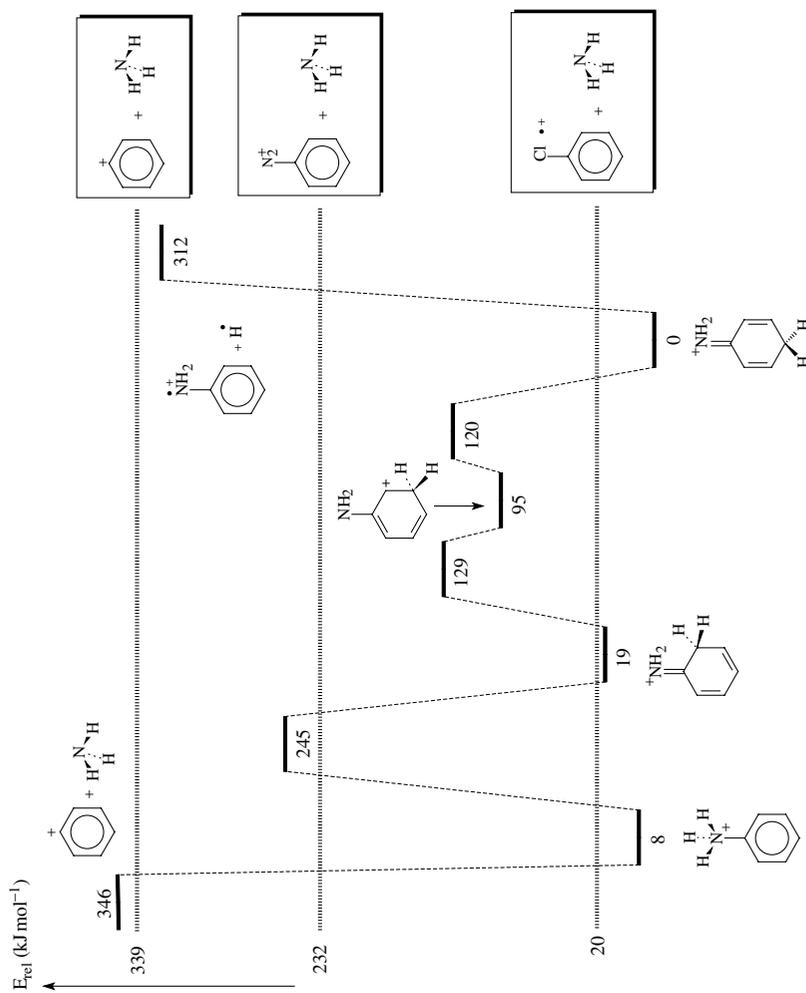
FIGURE 10. Potential energy diagram connecting the various C- and N-protonated anilines and their dissociation products. All values are in kJ mol^{-1}. The levels indicated by values 20, 232 and 339 kJ mol^{-1} correspond to N-protonated aniline produced by ion–molecule reactions (reagents depicted in the insets) in the absence of collisional stabilization: (a) *lower*: ionized chlorobenzene–ammonia, (b) *middle*: phenyldiazonium ion—ammonia and (c) *upper*: phenyl cation–ammonia

Compared with the CA spectra collected in Table 4, the high kinetic energy CA spectrum of the m/z 94 ions, prepared by reacting ionized chlorobenzene with ammonia, is largely dominated by the loss of ammonia (m/z 77) and the loss of a hydrogen atom (m/z 93), the remaining fragments representing less than 20% of the base peak intensities (Figure 9b). The same behavior is noted starting with the bromo and iodo compounds. It can thus be concluded that these ion–molecule reactions produce quasi-specifically beams of N-protonated aniline. The occurrence of C-protonated aniline is thus marginally detected (if at all) and may also result from post-collisional isomerization.

The evolution of the mass spectra of the ion–molecule reaction products of m/z 77 ions with ammonia as a function of the nature of the precursor halobenzene is also of interest. The m/z 94: m/z 93 branching ratio measured as 22:78 for the chlorinated precursor becomes 30:70 for the brominated precursor and 49:51 for the iodinated precursor. Moreover, this ratio is still significantly modified (60:40) if ionized iodobenzene is prepared by charge exchange with methylene chloride in the CI source. The degree of fragmentation of the m/z 94 ions thus appears extremely dependent on the distribution energies of the precursor m/z 77 ions, but the occurrence of isomeric species of the phenyl cation cannot also be ruled out completely.

c. Ion–molecule reactions of phenyl diazonium cations with ammonia in a quadrupole collision cell of a hybrid mass spectrometer. Phenyl diazonium ion was generated by electron ionization of azobenzene. The m/z 105 ions constitute indeed the base peak of the EI mass spectrum. Appearance energy measurement of these ions (AE = 9.8 eV) together with tabulated heats of formation of phenyl radical and neutral azobenzene allow the heat of formation of phenyl diazonium ions to be estimated at about 1020 kJ mol^{-1}. Along with the known heats of formation of ammonia and anilinium ion, the substitution reaction $PhN_2^+ + NH_3 \rightarrow PhNH_3^+ + N_2$ is calculated to be -232 kJ mol^{-1} exothermic and is thus expected to be observed in the gas phase. Decelerated phenyl diazonium ions were allowed to react with ammonia in the quadrupole cell and all the ions generated in the quadrupole are reaccelerated at 8 keV and separated by scanning the field of the second magnet (see Figure 11a). The expected NH_3/N_2 substitution product is clearly detected at m/z 94 in agreement with theoretical estimates. The high energy CA spectrum of the m/z 94 ions (Figure 11b) is found to be quite similar to the spectrum shown in

(a)
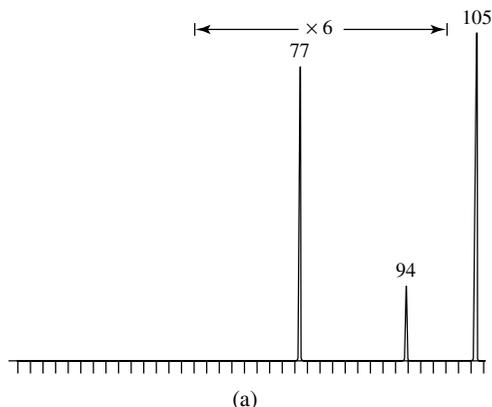
FIGURE 11. Reactions of phenyl diazonium cation with ammonia: (a) mass spectrum of the ions produced within the quadrupole collision cell and (b) high energy (8 keV, nitrogen collision gas) of the so-produced m/z 94 ions. Spectrum (c) corresponds to the reactions of the m/z 77 phenyl cation formed in the ion source with ammonia

(b)

m/z

(c)
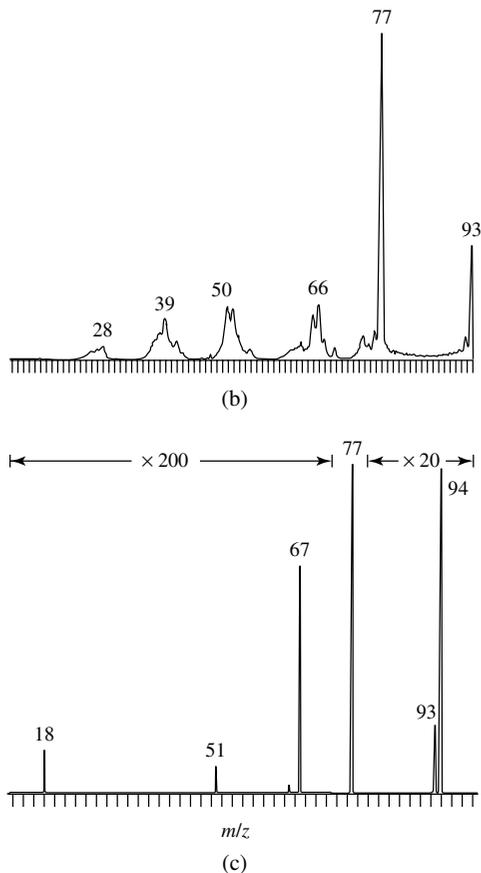
FIGURE 11. (*continued*)

Figure 9b indicating the main formation of ammonium ions in the process. The *m/z* 77 ions generated from azobenzene also react with ammonia, but when compared to the results depicted in Figure 11c, the branching ratio *m/z* 94:*m/z* 93 is now completely inversed.

    d. Electrospray ionization of aniline in a quadrupole–time of flight (Qtof) mass spectrometer. The ESI-MS experiments on aniline lead to the spectra depicted in Figure 12 for different cone voltages starting with an acidified (formic acid) solution of aniline in acetonitrile/water (*ca* 5×10^{-4} M). A protonated ANI is clearly detected at *m/z* 94 together with very small peaks at *m/z* 105, 93 and 77. The peak at *m/z* 95 is also somewhat too intense (13%) to be only ascribed to the ^{13}C -isotopic contribution of the *m/z* 94 ions. Moreover, stepwise increase of the cone voltage to 60 volts (Figure 12b) and to 70 volts (Figure 12c) significantly modifies the relative intensities of these peculiar peaks and the *m/z* 77, 93, 95 and 105 signals become more and more intense when compared to the *m/z* 94 signal. If *m/z* 77 and 93 ions can be readily attributed to collision-induced fragmentations ($H^{\bullet}$ and NH_3 losses, respectively) from protonated anilines, the observation of the *m/z* 95 and 105 was completely unexpected.
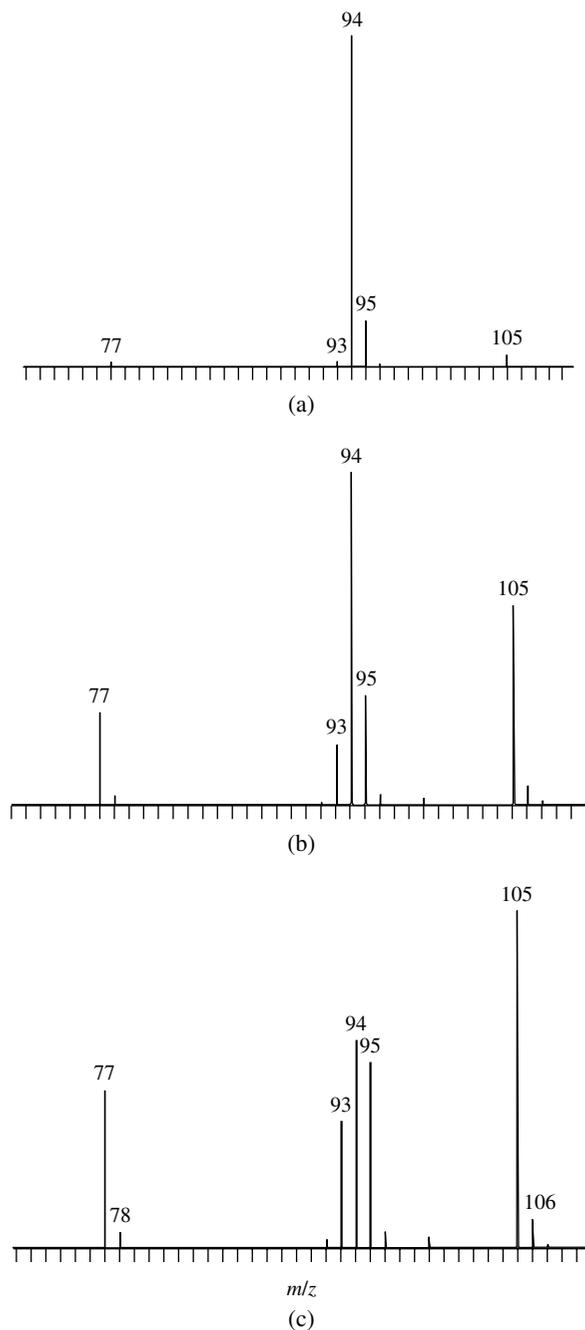
FIGURE 12. ESI mass spectra of aniline at three different cone voltages: (a) 40 volts, (b) 60 volts and (c) 70 volts

The collision-induced dissociation (CID) spectrum of the m/z 94 ions, recorded at 20 eV kinetic energy, features only three peaks associated with the losses of $H^\bullet$ (m/z 93, 12%), NH_3 (m/z 77, 86%) and [$NH_3 + C_2H_2$] (m/z 51, 1.5%); see Figure 13a. The very efficient ammonia loss confirms that we are dealing with the N-protonated
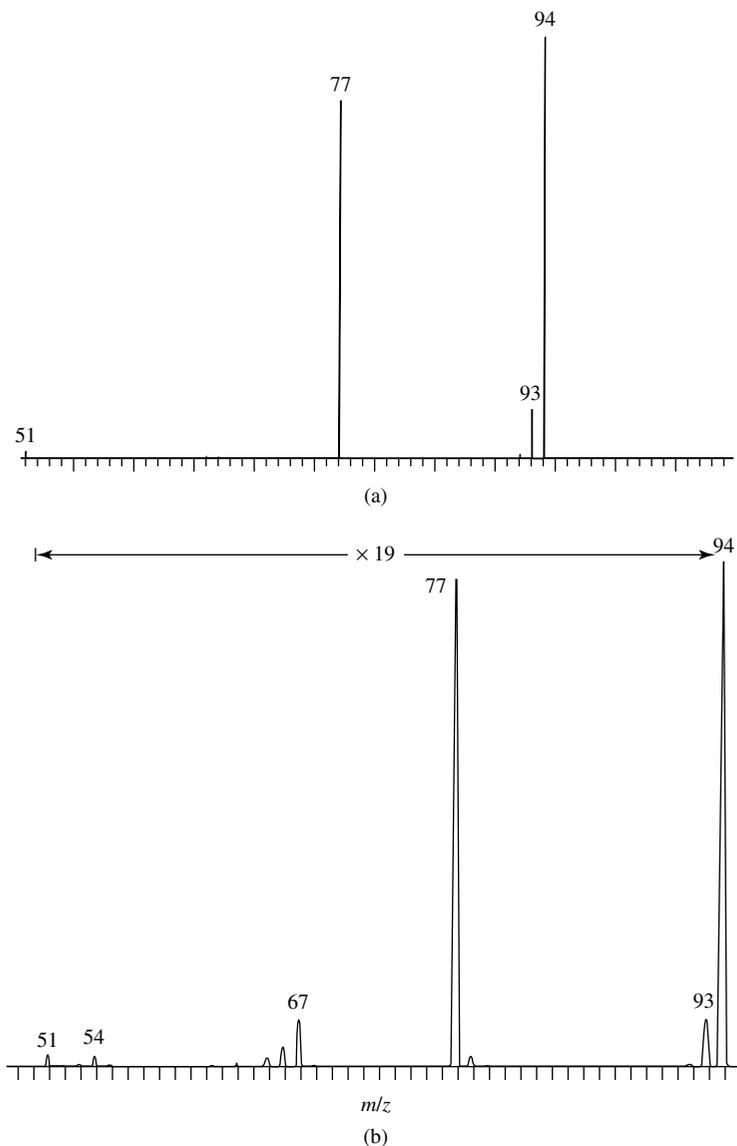
FIGURE 13. (a) CID spectrum of protonated aniline (m/z 94) generated in ESI conditions (20 eV collision energy) and (b) low energy CID spectrum of protonated aniline generated in a chemical ionization source

ANI, and consequently that the condensed-phase ANI protonation mainly occurs at the nitrogen atom, at variance with the gas-phase process (which occurs in the chemical ionization source, *vide supra*). Moreover, use of the tabulated heats of formation of NH_3 (-46 kJ mol^{-1}), $C_6H_5^+$ (1127 kJ mol^{-1}), $H^\bullet$ (218 kJ mol^{-1}) and $C_6H_5NH_2^{\bullet+}$ (829 kJ mol^{-1}) allows one to estimate that the $H^\bullet$ loss requires about 34 kJ mol^{-1} less energy than the NH_3 loss. This demonstrates that the relative abundances of the m/z 93 and 77 peaks also depend on the corresponding frequency factors.

High-energy collisional activation experiments showed the formation of a mixture of *N*- and *C*-protonated molecules under chemical ionization conditions, with a higher population of ring-protonated species. It was therefore of interest to investigate the behavior of a beam of protonated ANI (methane-CI) in low translational energy conditions (quadrupole collision cell, *ca* 20 eV). The result of such an experiment is depicted in Figure 13b. The ammonia loss represents the dominating process; m/z 93 (loss of $H^\bullet$) is also present with a m/z 77:m/z 93 not too different from the ratio measured on Figure 13a (9 vs 7). The most significant difference between both spectra is seen at m/z 67 (loss of CHN from the protonated molecules), not observed in the ESI conditions. The ammonia loss is apparently structure-specific of *N*-protonated aniline, while CHN loss is due to ring-protonated aniline. Although the latter species is probably predominant in the mixture, the lower intensity of the CHN loss is perhaps related to a lower fragmentation cross section.

Ionized aniline possesses an isomeric stable species, the 4- (or 3-) dehydroanilinium distonic ions (m/z 93). It is thus expected that their identification could afford some additional pieces of information related to the localization of the initial site of protonation. The distonic ions can readily be prepared by protonation of iodoanilines followed by collisional deiodination. Such a protonation–deiodination sequence is also readily performed in the quadrupole–time of flight instrument and the CID spectra of all the m/z 93 ions are collected in Table 5. As a reference for aniline radical cations, *N*-methylaniline was used and was observed to intensively expel a methyl radical after protonation and excitation (high cone voltage).

It is clear from the recorded CID data that aniline radical cations are produced in the protonation of aniline, followed by loss of a hydrogen atom. The distonic species are differentiated by a significant signal at m/z 76 for benzyne ions.

e. Quantum chemical calculations of proton affinities of aniline. As far as calculated results are concerned, let us briefly mention that the energy difference between both *N*- and *C*(*para*)-protonated forms turns out to be strongly dependent on the method and basis functions employed. Density functional theory (DFT) and MO-perturbation theory (MP4) methods point to a favored *C*4(*para*)-protonation, whereas coupled-cluster theory (CCSD(T)) and composite G2 and G3 techniques lend a preference for a *N*-protonation. Nevertheless, the energy difference between both protonated forms, in one case or the other, amounts to only a few kJ mol^{-1}.

TABLE 5.   Relative abundance of fragment ions in the CID spectra of m/z 93 ion (70 volts cone voltage, argon collision gas, 25 eV collision energy)

Aniline	*m/z*						
	93	92	78	77	76	66	65
Aniline	100	74	4	1	<1	4	1
N-Me	100	70	5	2	1	6	3
4-Iodo	100	61	4	3	**17**	5	3
3-Iodo	100	60	4	2	**26**	4	2

The calculations[108] carried out at the CCSD(T) level with the large aug-cc-pVTZ basis set provide the following results, with a probable error of ± 4 kJ mol^{-1}:

– at 0 K: PA(N) = 880 kJ mol^{-1}, PA(*para*-C4) = 876 kJ mol^{-1} and PA(*ortho*-C2) = 856 kJ mol^{-1};
– at 298 K: PA(N) = 887 kJ mol^{-1}, PA(*para*-C4) = 884 kJ mol^{-1} and PA(*ortho*-C2) = 863 kJ mol^{-1}.

The current experimental value for PA(aniline) amounts to 877 kJ mol^{-1} at 0 K and 883 kJ mol^{-1} at 298.15 K[109]. High-level molecular orbital methods tend to indicate a slight but consistent preference for *N*-protonation. Such a qualitative change in gas-phase basicities is of fundamental importance in view of the fact that the PA of ammonia is about 85 kJ mol^{-1} larger than that of benzene. The energy gap between both processes, Δ(PA) = PA(N) - PA(*para*-C4), has been found to be reduced following the extension of one-electron basis functions. At a high level such as CCSD(T)/aug-cc-pVTZ, this gap amounts to, at most, 3–4 kJ mol^{-1}, which actually lies within the error bars of the calculated results. Note again that the CCSD(T), G2 and G3 values are derived from single-point electronic energies. Thus, a small change in the geometrical parameters or the zero-point energies used could easily tip the balance in favor of one or another form. This result reinforces the conclusion that both nitrogen- and *para*-carbon-protonated isomers are most likely generated upon protonation of aniline. This is also in line with abundant experimental results discussed above demonstrating the existence of both species under different gas-phase conditions. The PA(ANI) at nitrogen is slightly larger than that of ammonia, PA(NH$_3$) = 853 kJ mol^{-1}, but smaller than that of methylamine[1, 110], PA(CH$_3$NH$_2$) = 891 kJ mol^{-1}.

In the first $\pi^* \leftarrow \pi$ excited state (S_1), the PA(ANI) is reduced by 38 kJ mol^{-1} relative to the ground state PA[111]. The vertical excitation energies in both neutral and protonated forms are comparable, but the adiabatic $S_1 \leftarrow S_0$ transition energy is sharply increased upon protonation, in going from 4.2 to 6.2 eV. The protonated ANI has been found to undergo adiabatic proton-dissociation reactions in aqueous solution, in its excited S_1 state, to produce excited ammonia[111]. The corresponding rate coefficient $k_{diss} = 1.4 \times 10^{10}$ s^{-1} at 298 K was obtained and is the fastest of those reported for protonated aromatic amines. The energy barrier for this process was measured[111a] to be 11 kJ mol^{-1}. Excitation to the S_1 state does not influence the planarity of the aromatic ring, but induces a distortion of 13° of the amino group from the latter. The excited protonated ANI has a fluorescence time of 1530 ps, as compared with that of 930 ps measured for the excited neutral aniline[111b].

2. Proton affinities of halogenated anilines

The PAs of a systematic series of mono-halogenated derivatives XC$_6$H$_4$NH$_2$ (X = F, Cl, Br and I) and *N*-haloanilines have been computed using DFT methods. Note that *N*-haloamines are rather highly unstable species. The effects of two and four substituents on the ring have also been probed. In examining Table 6, a few interesting points could be noted regarding the trends of PAs:

(i) A halogen atom effect results in an overall reduction of the PAs. The largest PA reduction is due to fluorine, followed by chlorine and bromine. The effect is most pronounced in *N*-halo derivatives. When a halogen atom is substituted at nitrogen, *N*-protonation is found to be the preferred electrophilic process but still with a small gap Δ(PA) = 6 kJ mol^{-1}. For the series of mono-halo derivatives, *N*-fluoroaniline presents the smallest PA, with PA(N) = 835 kJ mol^{-1}, whereas 3-bromoaniline exhibits the largest value of PA(C4) = 872 kJ mol^{-1}.

TABLE 6.   Calculated proton affinities (PA, kJ mol^{-1} at 0 K) of halogenated anilines

Substituted aniline	PA ^{a}			Δ(PA) ^{b}
	N	*para*-C4	*ortho*-C2	
H (ANI)	874	882	863	−8
2-Fluoro	857	857	811	0
3-Fluoro	852	869	849	−17
4-Fluoro	862	818	840	44
N-Fluoro	835	829	815	6
2-Chloro	861	858	817	3
3-Chloro	854	871	853	−17
4-Chloro	858	836	840	22
N-Chloro	850	846	840	4
2-Bromo	865	861	814	4
3-Bromo	856	872	854	−16
4-Bromo	858	851	842	7
N-Bromo	864	858	843	6
2,6-Difluoro	839	831	—	8
3,5-Difluoro	830	855	—	−25
2,3,5,6-Tetrafluoro	798	809	—	−11
2,6-Dichloro	847	834	—	13
3,5-Dichloro	835	861	—	−26
2,3,5,6-Tetrachloro	823	833	—	−10
2,6-Dibromo	854	840	—	14
3,5-Dibromo	838	856	—	18
2,3,5,6-Tetrabromo	834	841	—	7

^{a} Using B3LYP/6-311++G(d, p) + ZPE calculations.
^{b} ΔPA = PA(N) − PA(C4) in kJ mol^{-1}.

(ii) In all cases, the *meta* (C3 and C5) positions lead to the smallest PAs (values not shown in Table 6). In contrast, the *ortho* (C2 and C6) positions become in some cases competitive with respect to the *para* (C4) positions. Additional substitutions of halogens either on the ring or at nitrogen tend to further reduce the PAs. The effect of multiple halogen atoms on PAs is more or less additive: for example, the PA(N) amounts to 874 kJ mol^{-1} in aniline, 857 kJ mol^{-1} in 2-F-aniline, 839 kJ mol^{-1} in 2,6-difluoroaniline and 798 kJ mol^{-1} in 2,3,5,6-tetrafluoroaniline; the increment thus amounts to 17–18 kJ mol^{-1} per F atom. The reduction becomes smaller for heavier atoms, being 14 kJ mol^{-1} per Cl atom and 11 kJ mol^{-1} per Br atom. In this case, N remains the preferred protonation site.

(iii) A similar operation at the *meta* position, yielding a 3,5-dihaloaniline, results in a slightly larger reduction of the PA(N), namely by 22 kJ mol^{-1} for F, 19 kJ mol^{-1} for Cl and 18 kJ mol^{-1} for Br, but a smaller reduction of the PA(C4), whose values are decreased by 14 kJ mol^{-1} for F, 10 kJ mol^{-1} for Cl and 17 kJ mol^{-1} for Br. As a consequence, for 3,5-dihaloanilines, PA(C4) is still larger by about 18–25 kJ mol^{-1} than PA(N).

(iv) The preference for C4-protonation is transferred to the 2,3,5,6-tetrahaloanilines but with a smaller Δ(PA) energy gap. Overall, PA(C4) = 809 kJ mol^{-1} for 2,3,5,6-tetrafluoroaniline represents the smallest PA of the whole series considered. Relative to the parent ANI, this value corresponds to a reduction of 73 kJ mol^{-1} of the ring carbon basicity. A comparable amount of 76 kJ mol^{-1} can also be derived for the nitrogen basicity, as measured by PA(N) values, following a tetrafluorination.

3. Proton affinities of alkylanilines

Earlier studies[109] indicated that *N*-alkylanilines are protonated at nitrogen under conditions of thermodynamic equilibrium. More recently, gas-phase protonation of *N*-alkylanilines with Brønsted acid reagents such as CH_4, CH_3OH and $(CH_3)_2CO$ has been demonstrated to lead to significant, if not exclusive, formation of the ring-protonated isomer[110]. By contrast, *N*-protonation has been found by fast atom bombardment (FAB) ionization techniques[110]. It has been concluded that protonation of *N*-alkylanilines under gas-phase chemical ionization conditions is kinetically controlled, and that the added proton samples all ring positions prior to fragmentation of M-H$^+$ cations.

Relatively little is known about the protonation pattern of *C*-alkyl derivatives. Earlier reports[87] pointed out that a number of *meta*-alkylanilines (*m*-anisidine and *m*-toludine) are preferentially ring protonated in the gas phase at equilibrium.

The effects of the methyl groups, in particular those of two and four substituents on the ring, have also been probed (Table 7).

 (i) The methyl group increases the PAs irrespective of its position. When substituted on the ring, the largest methyl effect occurs upon its attachment to the C3(*meta*) position inducing an increase of 21 kJ mol^{-1}, relative to that of the parent aniline, giving PA(C4) = 903 kJ mol^{-1}, and an extension of the Δ(PA) gap up to -20 kJ mol^{-1}. In this case, a preference for C4-protonation is thus clearly indicated. The resulting carbocation at C3 position upon a C4-protonation is largely stabilized by a direct methyl donating effect.
 (ii) The situation is less clear-cut for 2-methylaniline where a gap Δ(PA) = -10 kJ mol^{-1} does not allow a definitive conclusion to be made, in view of the accuracy of the B3LYP method. As in the case of the parent aniline, both *N*- and ring-protonations are expected to occur.
(iii) In contrast, *N*-protonation becomes favored for both 4-methyl and *N*-methyl anilines. Due to the presence of methyl at C4 position, protonation at this site is somewhat disfavored. As expected, the *N*-protonation results in the largest PA(N) = 905 kJ mol^{-1} for *N*-methylaniline. The corresponding C4-protonation also substantially profits from *N*-methyl electron-donating effects yielding PA(C4) = 901 kJ mol^{-1}, which is even 10 kJ mol^{-1} larger than the value of PA(C4) = 891 kJ mol^{-1} in the 2-methyl derivative. This is no doubt the consequence of a strong delocalization of the N-lone pair electrons into the ring.

TABLE 7.   Calculated proton affinities (PA, kJ mol^{-1} at 0 K) of alkylanilines

Substituted aniline	PA ^{a}				Δ(PA) ^{b}
	N	C4	C3	C2	
Aniline	874	882	787	863	-8
2-Methyl	881	891	840	856	-10
3-Methyl	883	903	779	884	-20
4-Methyl	886	877	813	877	9
N-Methyl	905	901	798	887	4
2,6-Dimethyl	889	901	—	—	-12
3,5-Dimethyl	891	924	—	—	-33
2,3,4,6-Tetramethyl	904	937	—	—	-34

^{a} Using B3LYP/6-311++G(d, p) + ZPE calculations.
^{b} ΔPA = PA(N) − PA(C4).

(iv) Additional substitutions of methyl, either on the ring or at nitrogen, consistently increase the PAs. Another methyl group at the second *ortho* position in 2,6-dimethylaniline provides a preferred C4-protonation with PA(C4) = 901 kJ mol^{-1}, implying a positive contribution of 10 kJ mol^{-1} from the second methyl group. The effect is more or less additive, by 10 kJ mol^{-1} per methyl group, in going from aniline (882 kJ mol^{-1}) to 2-methylaniline (891 kJ mol^{-1}) and to 2,6-dimethylaniline (901 kJ mol^{-1}).

The effect becomes substantial when attaching another methyl group at the second *meta* position giving 3,5-dimethylaniline, which results in PA(C4) = 924 kJ mol^{-1}. Thus the methyl effect at this position is again additive by 21 kJ mol^{-1} per methyl group (882 kJ mol^{-1} in aniline, 903 kJ mol^{-1} in 3-methylaniline and 924 kJ mol^{-1} in 3,5-dimethylaniline). Such an additivity is in a great deal found in 2,3,5,6-tetramethylaniline where a value PA(C4) = 937 kJ mol^{-1} has been computed, corresponding to an increase of 55 kJ mol^{-1} relative to aniline, instead of 61 kJ mol^{-1} from pure additivity of four methyl groups. In both 3,5-dimethyl- and 2,3,5,6-tetramethylanilines, the gap Δ(PA) amounts to -33 or -34 kJ mol^{-1}, indicating that the ring sites benefit much more from methyl donation than the nitrogen upon ring substitutions.

(v) In *N,N*-dimethylaniline, *N*-protonation is favored and the relevant PA(N) = 936 kJ mol^{-1} turns out to be the largest PA value for the three dimethyl derivatives considered. However, the C4-protonation is also reinforced by π-electron delocalization resulting in a small gap of Δ(PA) = 5 kJ mol^{-1}.

In summary, it is confirmed that while the nitrogen protonation in the unsubstituted ANI is favored marginally, by about 4 kJ mol^{-1}, over the *para*-C4-protonation, the protonation sites in substituted anilines are essentially determined by the nature and position of the substituents. The halogen atoms consistently reduce the basicity whereas the alkyl groups enhance it. Substitution at *meta* positions induces a larger increment than that at *ortho* positions. The overall effects of substituents on PAs are essentially additive.

The proton-dissociation reaction of alkylated ANIs in the excited S_1 state tends to decrease significantly in *N*-monoalkylanilines but to increase in the *N*-dialkylated derivatives, with much larger activation energies[111]. The differences in the observed k_{diss} rate coefficient between protonated aniline and protonated alkylated derivatives has been explained on the basis of the charge density on the N-atom in the excited S_1 state, the water structure in the vicinity of the amino group which acts as a proton acceptor and steric hindrance of the alkyl groups. As a consequence, the acidity (pK_a values) and fluorescence lifetime of protonated anilines in aqueous solution are remarkably dependent on the substituent position in the ring.

C. Basicities

In solution, the proton transfer of amines is not characterized by the PAs but often by their dissociation constants pK_b. The latter constant refers to the conjugate acid, but in acidic solution, an amine is usually protonated producing an ammonium cation. Therefore, the pK_a dissociation constant measured under this condition for the protonated/neutral RNH$_3^+$/RNH$_2$ (acid/base) couple corresponds to the acidity of the ammonium cation (acid), and conversely to the basicity of the amine molecule (base): pK_a + pK_b = pK_w, where pK_w is the ionization constant of water. The experimental pK_a value of the anilinium Ph-NH$_3^+$ cation amounts to 4.9 in water, 3.6 in DMSO but 10.6 in MeCN. For ammonia and methylamine, pK_a = 9.2 and 10.7 in water, 10.5 and 11.0 in DMSO, but 16.6 and 18.4 in MeCN, respectively[112]. Thus there is a larger change of the two values in acetonitrile solution. The experimental dissociation constants of a large series of

mono- and disubstituted anilines in aqueous solution have been tabulated in different recent papers[113–121].

At the present time, direct computation of the absolute pK_a value of an unknown compound remains a difficult task. However, within a series of homologous compounds, it is possible to evaluate theoretically the relative dissociation constants using a uniform and reliable level of theory. Along with accurate experimental data, there is a correlation between experimental and theoretical constants; the best regression often fits a linear equation: $pK_a(expt) = A \times pK_a(calc) + B$. It is of course most desirable to find a method yielding a linear regression having a correlation coefficient r close to unity, a slope A close to unity and an intercept B close to zero, since that corresponds to a maximum predictive power. However, due to the inherent uncertainties in the evaluation of the proton and ion solvation energies, it appears difficult to attain results having such quality for aqueous solutions[114, 115]. The results determined for nonaqueous solvents (DSMO, acetonitrile etc.) with regression slope in the vicinity of unity are more encouraging.[114]. This enhances the predictive capacity for evaluating the dissociation constant for a new member of the series, and the associated substituent and functional group effects.

For substituted anilines, quantum chemical methods using semiempirical methods[116], or *ab initio* calculations from a rather modest level such as HF/6-31+G(d), B3LYP/6-31G(d,p) to a higher level such as B3LYP/aug-cc-pVTZ or MP2/6-311+G(2df,2p), could provide internally consistent relative pK_a values[117–121]. In other words, it is now possible to predict the pK_a value of a new aniline derivative within experimental accuracy.

In general, in a series of substituted anilines, electron-donating ring substituents increase the pK_a of protonated anilines and electron-withdrawing substituents decrease it. It is known that the latter tend to diminish the pyramidal degree, shorten the C−N bond, increase the dipole moment and lower the HOMO energy. As for an interpretation of the significance of basicity, attempts to correlate dissociation constants (pK_a) of protonated anilines with various thermochemical and quantum chemical parameters have been carried out[116–122]. Let us briefly mention the main correlations found.

(i) Because PA is the main measure of gas-phase basicity, there is obviously a linear relationship[118] with its counterparts in solution: $pK_a = -0.186PA + 4.47$. Specific solvent effects often cause deviations between these two parameters. Similarly, there is an obvious correlation between pK_a and gas-phase Gibbs energies of dissociation equilibria.

(ii) There is a linear relationship between pK_a values and the traditional Hammett σ constants that describe the electronic influence of substituents on equilibria and reactions[117], namely $pK_a = -3.03\sigma + 4.46$.

(iii) As the basicity is commonly associated with the nitrogen atom, its net charge Q_N is also a good indicator: $pK_a = aQ_N + b$, in which the charge Q_N could be evaluated by different theoretical methods. The Q_N values are strongly dependent on the theoretical methods employed, so both coefficients a and b also depend on the method employed. Currently, there are a variety of methods for calculating atomic net charges. The charges derived from the Mulliken, natural orbital (Lowdin, NPA) or atom-in-molecule (AIM) approaches appear to perform better than the others in correlating with the dissociation constants[119].

The change of the dipole moment upon protonation also appears as an additional term in the correlation.

(iv) Another theoretical property related to the charge distribution is the molecular electrostatic potential. Thus the overall potential minimum V_{min} of the molecule is also an index for the dissociation constant: $pK_a = cV_{min} + d$. Again, the V_{min} electrostatic potential and the regression coefficients vary with the quantum chemical method employed.

(v) Electronic indices derived from the atom-in-molecule model (AIM) can also be used to evaluate the basicity. The electron density $\rho(\mathbf{r})$, or its Laplacian $\nabla^2\rho(\mathbf{r})$, at the bond critical point (BCP) of the C−N bond is a measure of the degree of delocalization between both phenyl and amino groups. If the electron density is more segregated, the conjugation is getting smaller, the electron density becomes lower, the BCP(C−N) Laplacian is more positive, the bond becomes more covalent, the lone pair becomes more accessible to accept the proton and, as a consequence, the basicity increases[121, 122]. Any other delocalization index could lead to a similar relationship.

(vi) The nitrogen lone pair corresponds to a local charge concentration characterized by a $(3, -3)$ critical point where the Laplacian is at a maximum. In fact, there is certain correlation between a higher charge concentration and a larger basicity. However, the nitrogen lone pair alone is not a good indicator of the basicity due to the large subsequent loss of delocalization energy in the protonated form[118]. A localization of the nitrogen electron in terms of a localized reactive hybrid orbital leads to a better correlation with PAs[123].

(vii) The ionization energy of a molecule is defined by its chemical potential and polarizability, and therefore it is relevant to the overall reactivity. Because ionization energies can be approximated by HOMO energies by means of the Koopmans theorem, the existence of a linear relationship between pK_a and ε(HOMO) of the neutral substrates is logical[120]. During an aniline protonation, the dominant energy change is caused by the destruction of the frontier orbital whose dominant component is the nitrogen lone pair by an electrophilic (proton) attack. Such a process is controlled by an electron transfer from the HOMO(ANI) to the LUMO(H^+). In such a case, the smaller the aniline ionization energy, the higher its HOMO, the easier the electron transfer, the more basic the aniline and the less acidic its conjugate acid (protonated form)[120].

(viii) It is possible to define a 'local ionization energy' centered at a point in space $I(\mathbf{r})$[124]. The minimum local ionization energy ($I_{S,\mathrm{min}}$) correlates strongly with the experimental pK_a in a linear manner.

(ix) The reactivity indices derived from density functional theory (DFT) including the softness (S), local softness (s) and Fukui functions (f) have also been utilized to rationalize the protonation sites[88, 103−105, 125]. Because the Fukui functions contain information on the frontier orbitals (expressed via the vertical ionization energy and electron affinity in the global softness) and the local net charges, it could be expected that they behave as good protonation indices. In general, the atomic centers with the maximal values of Fukui functions and related indices were found to be the preferred sites for electrophilic or nucleophilic attack. Nevertheless, the obtained results do not always follow the local hard−soft acid base (HSAB) approach. Relative Fukui function values for atomic centers of different types (for example, Fukui functions of carbon and nitrogen centers) cannot be compared with each other. This shortcoming arises from difficulties in evaluating the energies and net charges, in particular for describing the anions, which usually have an expanded charge distribution[88].

(x) Overall, the molecular indices derived solely from quantum chemical calculations of the isolated neutral substrates can now make useful contributions, not only to qualitative understanding of the underlying factors of the basicity, but also to quantitative prediction of the pK_a values of new members. Within the framework of the molecular similarity concept, they offer a multitude of working parameters that are more amenable than the classical and empirical parameters, such as the Hammett constants.

D. Interactions with Metal Ions

Interactions between the Cr^+, Fe^+ and Co^+ metal cations and ANI have been investigated experimentally[126, 127]. The binding energies in the resulting $M(ANI)^+$ complexes have been evaluated to be 187, 226 and 271 kJ mol^{-1}, respectively. Relative to benzene, ANI also binds more strongly to these ions by 17, 18 and 16 kJ mol^{-1}.

As in the protonation, DFT calculations suggested that the binding energies of the Cr^+ cation at both nitrogen and ring sites are comparable to each other, amounting to about 177–181 kJ mol^{-1} (B3LYP results) or 178–188 kJ mol^{-1} (MPW1PW91 results). Within computational uncertainty, the two sites are not resolvable; this was also found to be true for the Cr^+ $(ANI)_2$ isomers.

Results obtained from infrared multiple photon dissociation spectroscopy (IRMPD)[128] allowed the difference in energy between both isomers to be determined. The most diagnostic features from calculations are two distinct peaks in the IR spectra: (i) the peak near 1070 cm^{-1} for the N-bound structure due to a frustrated inversion motion of the amino group, which is destroyed by the presence of Cr, and (ii) the peak near 1310 cm^{-1} for the ring-bound isomer, which is a mixed mode incorporating the C−N stretching and in-plane CH bending motions. This mode is mildly blue-shifted from a vibration centered at 1266 cm^{-1} of bare aniline. The experimental IRMPD spectrum of the complex shows a strong feature at 1300 cm^{-1}, but nothing near 1070 cm^{-1}, thus pointing toward a metal ion−ring interaction. Similarly, interaction in the $Cr(ANI)_2^+$ complexes also leads to a preferred structure with two ring-bound ligands.

Binding energies of alkali cation complexes with one and two ANI molecules have also been determined by threshold collision-induced dissociation and theoretical studies[128–130]. For each alkali cation, both N-bound and ring-bound adducts have been located (Figure 14). In a N-complex, the cation lies above the C−N bond and interacts with the π-electrons as well, indicating that it is also a π-cation complex. The M^+−N distance increases at the B3LYP/6-31G(d,) level in the sequence Li^+ (1.98 Å), Na^+ (2.36 Å), K^+ (2.86 Å), Rb^+ (3.10 Å) and Cs^+ (3.38 Å). Similarly, the distance between the metal ion and the ring centroid also varies in the same sequence: Li^+ (1.87 Å), Na^+ (2.35 Å), K^+ (2.83 Å), Rb^+ (3.13 Å) and Cs^+ (3.39 Å)[130]. At the MP2/6-311++G(2d,2p) level of theory, the N-bound complexes are found to be 8.6, 1.6, 2.8, 1.0 and 1.4 kJ mol^{-1} less stable than the π-complexes for Li^+, Na^+, K^+, Rb^+ and Cs^+, respectively. Such small energy differences suggest that all conformers should have sufficient internal energy at room temperature to freely interconvert. Interaction of the metal ion with nitrogen within the molecular plane turns out to be less favored (by 50 kJ mol^{-1}).

Table 8 lists the experimental bond dissociation energies (BDE) of the alkali M^+−$(ANI)_n$ complexes ($n = 1, 2$)[130]. In general, MO methods (MP2, CCSD(T)) and DFT approaches (B3LYP, BLYP) reproduce the trend and the absolute values with an average deviation of 6 kJ mol^{-1} with respect to the corresponding experimental values[130, 131]. The lithium cation represents the most troublesome case, where the deviation remains large[131]. A few additional points are worth noting:

(i) The BDEs of alkali cations with aniline are consistently smaller than those of the transition metal ions mentioned above.

(ii) Similar to the analogous benzene and monosubstituted benzenes, the BDEs of ANI decrease monotonically as the metal ion size increases from Li^+ to Cs^+. This is due to the fact that the interaction is essentially electrostatic in nature, involving ion−dipole, ion−quadrupole and ion-induced dipole forces, in which the ion−quadrupole interaction is dominant[132]. The binding difference also becomes smaller for adjacent metals as the metal size increases. This is due, on the one hand, to the relative change in the ionic radii of the alkali ions (0.68, 0.97, 1.33, 1.47 and 1.67 for Li^+, Na^+,
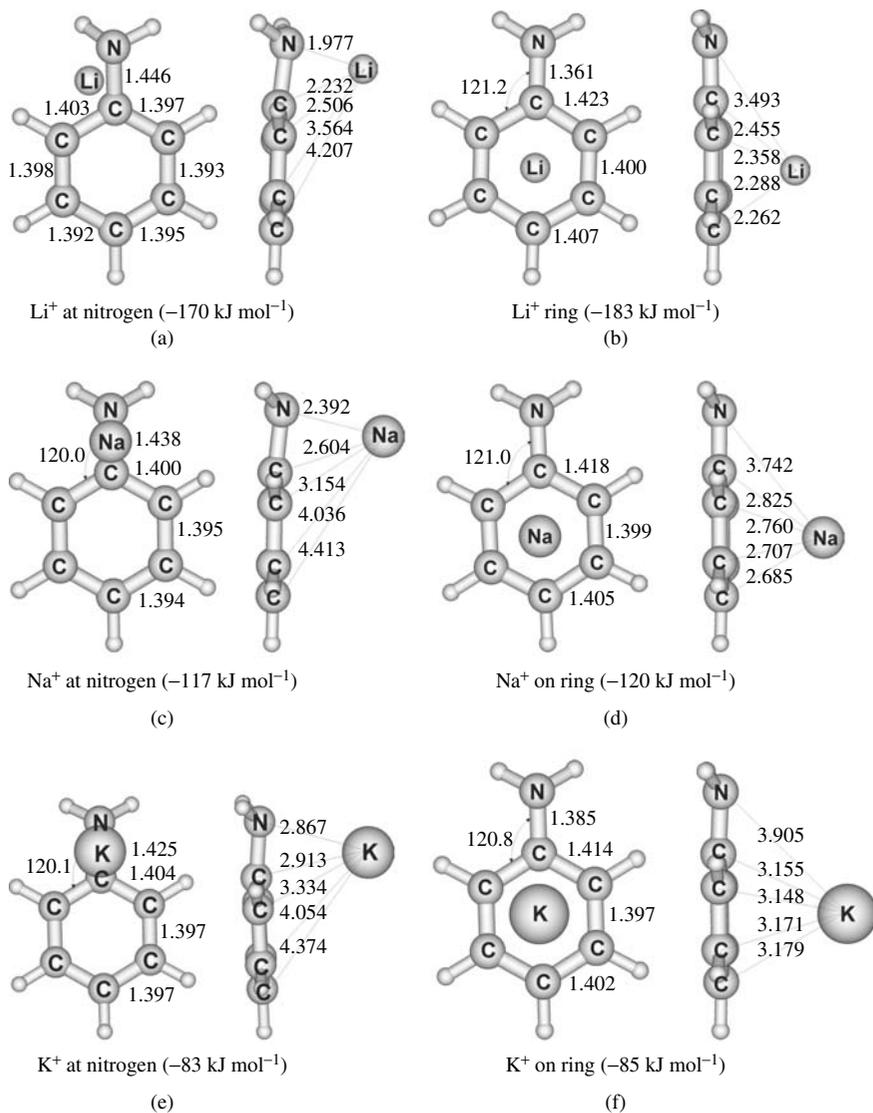
FIGURE 14. Complexes formed by interaction of aniline with alkali metal cations: π-complexes and N-complexes. Bond lengths given in angstroms and bond angles in degrees were obtained from B3LYP/6-311++G(d,p) optimizations. Values given in parentheses are the corresponding complexation energies

K^+, Rb^+ and Cs^+, respectively) and, on the other hand, to the nonlinear distance dependencies of electrostatic interactions. The latter fall off sharply in proportion to R^{-2} for ion–dipole, R^{-3} for ion–quadrupole and R^{-4} for ion-induced dipole interactions.

TABLE 8. BDEs in kJ mol^{-1} of the alkali−aniline cation (X = NH$_2$) and alkali−benzene cation (X = H) complexes

Complex	Experimental[a]	
	X = NH$_2$	X = H
Li$^+$ (C$_6$H$_5$X)	191.5	161.1
Na$^+$ (C$_6$H$_5$X)	119.9	92.6
K$^+$ (C$_6$H$_5$X)	82.5	73.3
Rb$^+$ (C$_6$H$_5$X)	76.3	68.5
Cs$^+$ (C$_6$H$_5$X)	69.3	64.6
Li$^+$ (C$_6$H$_5$X)$_2$	127.9	104.2
Na$^+$ (C$_6$H$_5$X)$_2$	98.8	80.0
K$^+$ (C$_6$H$_5$X)$_2$	75.9	67.5
Rb$^+$ (C$_6$H$_5$X)$_2$	71.8	62.7
Cs$^+$ (C$_6$H$_5$X)$_2$	66.1	58.8

[a] Results obtained using threshold collision-induced dissociation, taken from Reference 130.

(iii) The BDEs of the bis-complexes are systematically smaller. The decrease in the BDEs in going from one to two ANI complexes is largest for Li$^+$ (64.6 kJ mol^{-1}) and becomes substantially smaller for Cs$^+$ (3.2 kJ mol^{-1}).

(iv) Compared with benzene whose interaction energies with alkali ions are also listed in Table 8, the ANI's amino group induces an overall increase in the strength of the π-cation interaction. This is similar to the methyl effect in toluene, but in contrast to that of fluorine in fluorobenzene[133]. As discussed in a preceding section, the ANI dipole moment is oriented about 45° out of the molecular plane. As a consequence, the metal ion−ANI attraction should be enhanced by the ion−dipole interaction, with respect to that of benzene. On the other hand, the polarizability of ANI (11.53 Å^3) is close to that of toluene (12.26 Å^3), but larger than that of benzene (9.99 Å^3) and fluorobenzene (9.86 Å^3). Hence, the ion-induced dipole interaction is invariably stronger in aniline and toluene. In the same vein, the ANI quadrupole moment is also larger than those of the latter monosubstituted benzenes, and thereby induces the largest ion−quadrupole interaction. Note again that the latter is the primary component of the electrostatic stabilization in this type of ion−molecule interaction[132].

E. Deprotonation

According to the Brønsted definition, the acidity of a molecule is associated with its capacity to give up a proton: Ph−NH$_2$ → Ph−NH$^-$ + H$^+$. The change of standard enthalpy or free energy of this deprotonation reaction is a measure of the intrinsic acidity. As discussed above, in solution, the propensity of an aniline derivative is to accept a proton. The measured dissociation constant (pK_a) is related to the basicity of the neutral molecule (or the acidity of the anilinium cations). As a consequence, relatively little is known about their acidity and/or the anilinide anions. However, the NH acidities have been well established in hydroxamic acids even though the latter usually behave as O-acids[134]. It is therefore of interest to get some insight into the deprotonation of aniline in the gas phase.

Figure 15 gives a summary of the calculated deprotonation energies (DPE) at four different sites, and the relative energies of the corresponding anions. It is clear that the amine nitrogen is by far the most preferred deprotonation site. The DPE(N−H) amounts to

DPE	1534	1655	1679	1685
ΔE	0	121	145	151
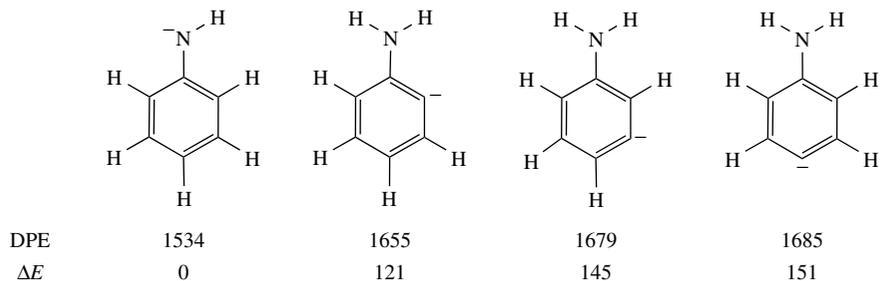
FIGURE 15. Deprotonation energies (DPE) of aniline at different sites and relative energies (ΔE) of the anions. Values given in kJ mol^{-1} were obtained from B3LYP/6-311++G(d,p) + ZPE calculations

about 1534 kJ mol^{-1}, with a probable error of $\pm$ 8 kJ mol^{-1}. This value is much larger than that of 1419 kJ mol^{-1} measured for the gas-phase DPE(N—H) of hydroxamic acid[134], in line with the known fact that aniline is actually a weak acid. Among the ring-deprotonated forms, the *ortho*-C2 position is slightly favored over the *meta*-C3 and *para*-C4 positions. A stabilizing interaction between H(N) atom and the negative charge is likely the factor favoring the *ortho* deprotonation.

Figure 16 displays selected geometrical parameters of both N- and C2(*ortho*)-deprotonated aniline isomers. The fully planar N-anion is isoelectronic with the benzyl (PhCH$_2^-$) and phenolate (PhO$^-$) anions, and their geometries show many similarities. Analysis of Mulliken populations indicates that in the N-anion, *ipso*-C1 bears the most negative charge (-0.88 e), followed by nitrogen (-0.43 e), *meta*-C3 (-0.34 e) and *para*-C4 (-0.18 e). The *ortho*-carbons are positively charged (0.56 e). The p-π delocalization causes a CN bond shortening and a small bond alternation within the ring. These changes lead to the dominance of a quinoidal form in the electronic and geometrical structure. Thus, the C—N distance of 1.33 Å of the N-anion lies between that of 1.40 Å in ANI and 1.25 Å in its isomers (cf. Section II.A). The delocalization of the negative charge from nitrogen to the ring is expected to strongly affect the magnetic properties such as NMR chemical shifts, magnetic susceptibilities etc. A comparable situation has been found in the toluene/benzyl anion and phenol/phenolate anion pairs[135], in which the phenolate anion has a reduced aromaticity, about 60% relative to the neutral phenol. For its part, the C2-anion is not planar but shows a distorted ring and a pyramidal amino group.

The adiabatic ionization energy of the anilinide anion is evaluated to be IE$_a$(PhNH$^-$) = 1.7 $\pm$ 0.1 eV, which is smaller than that of 2.25 eV measured for phenolate anion[135]. TD-DFT computations suggest that the lowest vertical $\pi^* \leftarrow \pi$ excitations of the N-anion are centered at 1.9 eV ($1^1A''$) and 2.1 eV ($1^1A''$). Thus, its excited valence states are expected to be auto-ionizing. Substitution of the H(N) atom by fluorine increases the anion IE by 0.3 eV, whereas substitution by a methyl group slightly reduces it (0.05 eV).

The triplet state of the N-anilinide anion also exhibits a planar structure whose geometrical parameters are quite close to that of the singlet counterpart. The C—N distance amounts to 1.338 Å in the high-spin state. The adiabatic singlet–triplet energy gap amounts to 2.34 eV (B3LYP). Again this is slightly larger than the anion's IE, indicating that it readily undergoes an auto-detachment upon excitation.

As in the case of phenolate anions, it is possible to stabilize anilinide anions by alkali metal cations. Figure 17 displays the selected optimized geometrical parameters of the

(1) 113.6
(2) 122.7
(3) 121.9
(4) 117.0
(5) 122.1
(6) 122.7

(1) 123.9
(2) 113.6
(3) 124.5
(4) 119.2
(5) 119.1
(6) 120.0
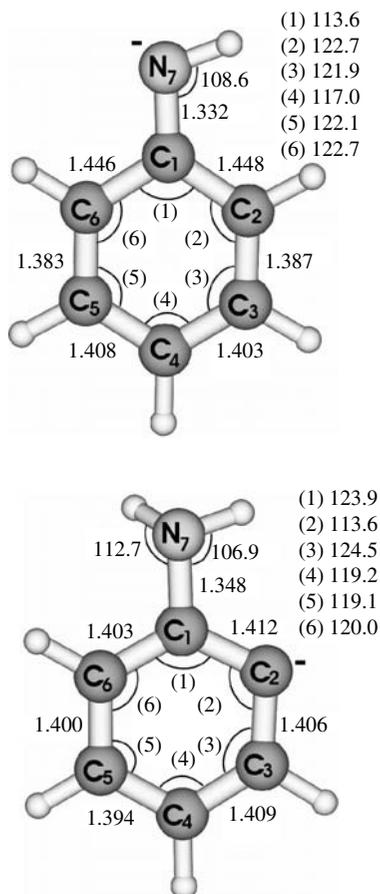
FIGURE 16. Geometries of the N- and *ortho*-C-deprotonated anilines (anions). Bond lengths given in angstroms and bond angles in degrees were obtained from B3LYP/6-311++G(d,p) optimizations

Ph−NHM molecules with M = Li, Na and K, that can be regarded as the products of interaction between Ph−NH⁻ anion and metal cations. While Ph−NHLi and Ph−NHNa are planar, the NHK group in Ph−NHK is slightly pyramidal. The C−N distances are shorter than that in free anion, and the C−N stretching frequencies become larger in going from free anion to Li, Na and K derivatives.

The positive charge is better delocalized in Ph−NHLi (where $q(\text{Li}) = 0.44$ e) than in other metallated species [$q(\text{Na}) = 0.66$ e in Ph−NHNa, and $q(\text{K}) = 0.83$ e in Ph−NHK]. Although charge localization increases the electrostatic energy, it reduces the overall stabilization energy of anilinide anion. The interaction energy between Ph−NH⁻ and M⁺ is calculated to be 640, 538 and 469 kJ mol⁻¹ for Li⁺, Na⁺ and K⁺, respectively (values at the B3LYP/6-311++G(d,p) + ZPE level).
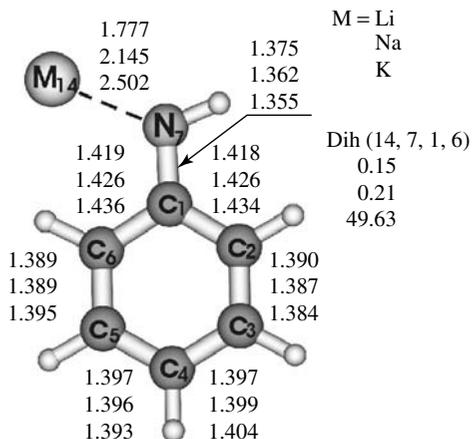
FIGURE 17. Geometries of the Ph—NHM molecules (M = Li, Na and K, denoted by M_{14}). Bond lengths given in angstroms and bond angles in degrees were obtained from B3LYP/6-311++G(d,p) optimizations

Recently, using a soft ionization mass spectrometric technique, known as the atmospheric pressure chemical ionization (APCI), when working in the negative mode, a deprotonation of 2,4-dinitroaniline giving $(M-H)^-$ anion has been observed[136]. Subsequent collisional-induced (CI) decomposition of the $(M-H)^-$ anion gives rise to an elimination of NO radical having an odd number of electrons. A process going from an even to an uneven number of electrons is rather unusual:

$$2, 4\text{-}(O_2N)_2C_6H_3-NH^- \longrightarrow (O_2N)-O^{\bullet}C_6H_3-NH^- + NO^{\bullet}$$
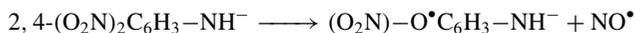
Using the simpler 2-nitroaniline as a model, the N-deprotonation is again found to be favored by 138 kJ mol^{-1} (B3LYP/6-311++G(d,p)) over the proton removal at the *ortho*-C2 site. In an attempt to understand the decomposition mechanism of the resulting N-anion, a portion of the relevant potential energy surface has been constructed and displayed in Figure 18. It appeared that the rate-determining step of the entire process boils down to a nitro−nitrite rearrangement of the N-anion. It is also remarkable that, in the presence of the negative charge, the N−O bond cleavage of the nitrite moiety is characterized by a small but real energy barrier. Such a barrier is a likely reason for the violation of the electron parity[136].

F. Electronic Excitations

The environmental sensitivity of the fluorescence and phosphorescence of phenylalanine, tryptophan and tyrosine, and their side chains, is often examined when considering the macromolecular luminescence of natural peptides and proteins. Therefore, lower-lying singlet and triplet states of toluene, aniline and phenol have been extensively studied as the simplest models of the proteins mentioned above, respectively. Knowledge of the various aspects of electronic spectra of the corresponding aromatic amino acids is often exploited to probe those of the proteins[137]. In other words, accurate information on both
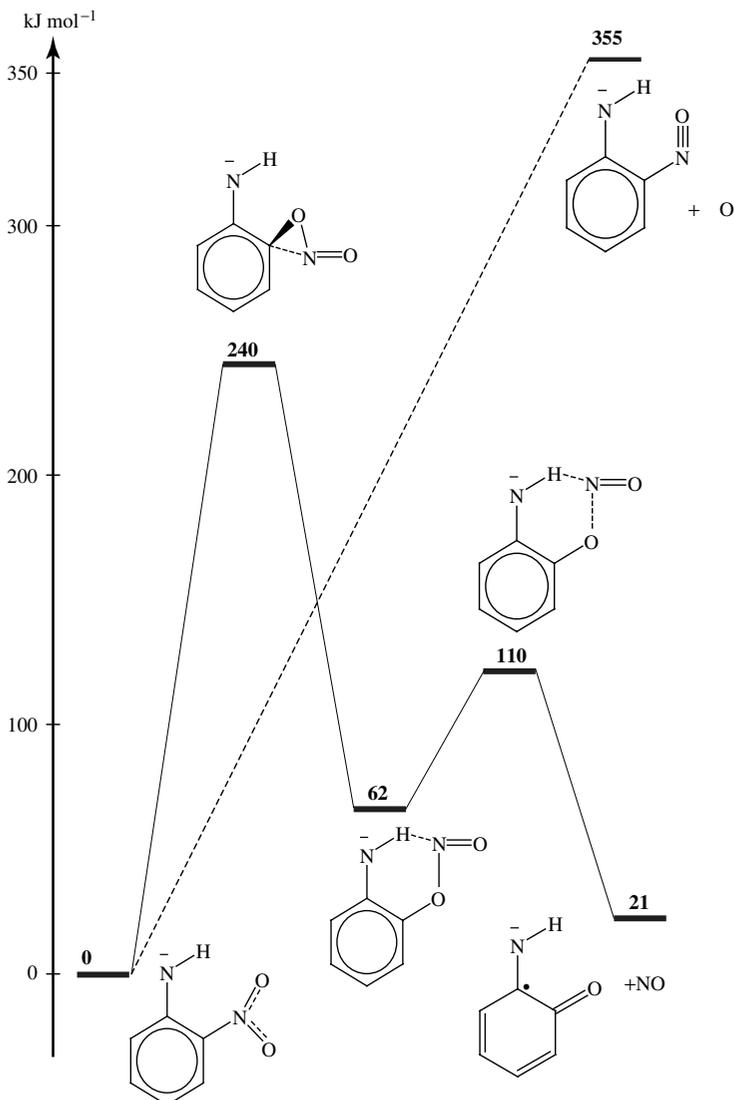
FIGURE 18. Schematic potential energy profiles showing a NO elimination from the 2-nitro-*N*-anilinide anion. Relative energies were obtained from B3LYP/6-311++G(d,p) + ZPE calculations

lower-lying excited states of these benzene derivatives is pivotal for, among other things, the interpretation of photophysical and photochemical properties of proteins. While several studies on the singlet states of ANI have been reported, relatively less is known about its triplet states.

1. Triplet states

The lowest-lying triplet state (T_1) of ANI has been probed using different spectroscopic methods. The values for $T_1 \leftarrow S_0$ electronic transition energy of aniline measured in phosphorescence in different media are quite consistent with each other, varying from 3.41 to 3.45 eV[138]. For the purpose of comparison, let us mention that *ab initio* calculations for both the ground S_0 and lowest-lying triplet T_1 states of phenol (Ph−OH) produced a phosphorescent energy of 3.50 eV[139], which was in good agreement with the experimental value of 3.53 eV[140]. The $T_1 \leftarrow S_0$ transition energies of toluene (Ph−CH$_3$) measured by electron-energy-loss spectroscopy and phosphorescence methods were more scattered, ranging from 3.59 to 3.95 eV[141]. Original experiments on toluene[142] revealed distortions in the T_1 state that were neither anti-quinoidal (two long and four short C−C bonds) nor quinoidal (two short and four long C−C bonds).

The triplet states of ANI and a few derivatives have been investigated in experimental[143–152] and theoretical[153, 154] studies. As seen in a previous section, the dominant configuration for the S_0(ANI) state is

$$X^1 A': \ldots (15a')^2 (9a'')^2 (16a')^2 (17a')^0 (10a'')^0$$

All the three HOMOs are of π-character. Multiconfigurational (CASSCF) and multistate perturbation theory (MS-CASPT2) calculations[153] using the optimized S_0 geometry have predicted the following vertical energies for the three lowest-lying singlet states (excluding the Rydberg states): $S_1(1^1 A'': 4.6$ eV), $S_2(2^1 A': 6.1$ eV) and $S_3(3^1 A': 7.2$ eV), and the four lowest-lying triplet states: $T_1(1^3 A': 3.8$ eV), $T_2(1^3 A'': 4.4$ eV), $T_3(2^3 A': 4.6$ eV) and $T_4(2^3 A'': 5.5$ eV). The dominant configurations for the excited states can be described as single-electron excitations from the latter. Accordingly, the $1^1 A''$, $2^1 A'$ and $3^1 A'$ can be considered to arise from excitations from ($16a'$ to $10a''$), ($16a'$ to $17a'$) and ($16a'$ to $18a'$), respectively, and the $1^3 A'$, $1^3 A''$, $2^3 A'$ and $2^3 A''$ states from excitation from ($16a'$ to $18a'$), ($16a'$ to $10a''$), ($9a''$ to $10a''$) and ($9a''$ to $18a'$), respectively. All of the states correspond to ($\pi^* \leftarrow \pi$) transitions. Under C_s symmetry, transitions from an excited singlet $^1 A'$ state to the ground state $S_0(X^1 A')$ are allowed. Thus, the $S_2(2^1 A')$ state of aniline is most likely responsible for its dual fluorescence observed by experiments[144, 145].

The calculated value of 4.6 eV for the vertical $S_1 \leftarrow S_0$ transition is close to the experimental result of 4.40 eV[143]. Within the expected accuracy of the calculations, namely ± 0.2 eV, it is confirmed that the triplet T_1 (3.8 eV) and T_2 (4.4 eV) states are lower in energy than the singlet S_1 (4.6 eV). The calculated energy gap of 0.8 eV between both S_1 and T_1 compares well with the available experimental value of 0.756 eV (6104 cm^{-1} in Ar matrix)[149].

The ANI triplet state T_1 is generated by a formal HOMO ($16a'$) $\rightarrow$ LUMO + 1 ($18a'$) electronic transition and corresponds to a $^3 A'$ state. Figure 19 displays the geometry of the $T_1(^3 A')$ state of aniline, which becomes more bent. The molecular skeleton keeps the C_s point group, but the amino group is strongly distorted. Although the ring is slightly perturbed (from 1.1 to 4.9°), it possesses a quinoidal form. Relative to the S_0 state, the C−N distance of 1.403 Å is marginally compressed. The NH$_2$ group is obviously distorted from the phenyl ring undergoing a substantial out-of-plane motion (52°). The dihedral angles of HNH$_7$C$_1$ and HHN$_7$C$_1$ in T_1 are 124.3 and 142.0^0, respectively, and the angle between CN and the HNH group amounts to 35°. Note that, except for one bond, the bond distances obtained by a CASSCF(10,10) method differ by 0.002 Å from the corresponding B3LYP values. The barrier to nitrogen inversion in the T_1 state is evaluated to be 8 kJ mol^{-1}, which is marginally larger than that of 6 kJ mol^{-1} for the S_0 counterpart (cf. Section II).
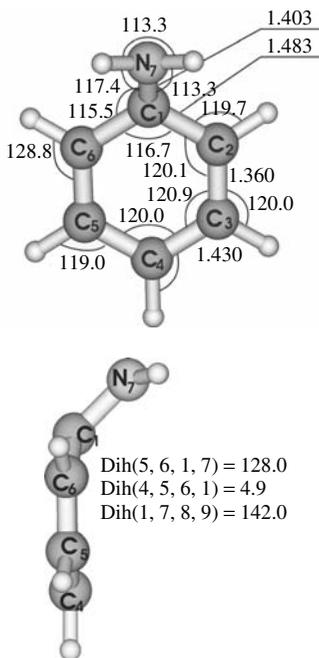
FIGURE 19. Geometry of the lowest-lying triplet aniline ($^3A'$). Bond lengths given in angstroms and bond angles in degrees were obtained from B3LYP/6-311++ G(d,p) optimizations[154]

The vertical singlet–triplet energy gap ($\Delta E_{ST-vert}$) is calculated as the energy difference between total energies of the ground singlet and triplet state at the optimized singlet geometry. Combining both the CASPT2 and B3LYP results, this gap could be predicted as $\Delta E_{ST-vert}(ANI) = 4.0 \pm 0.1$ eV.

The adiabatic energy gap ($\Delta E_{ST-adia}$), which is evaluated as the difference between the energies of both singlet and triplet states at their respective relaxed geometries, has been calculated to be $\Delta E_{ST-adia} = 3.5$ eV[154]. For the $T_1 \leftarrow S_0$ energy gap of ANI, calculated values are thus consistent with the experimental value of 3.41–3.45 eV determined by phosphorescence measurements in different media[140, 148] (27500 cm^{-1} in cyclohexane at 77 K and 27851 cm^{-1} in argon matrices). In general, singlet–triplet energy separations of aromatic compounds can be accurately predicted by DFT computations[155].

Table 9 records the calculated vibrational frequencies of the triplet aniline and scaled with appropriate factors. The ν(C–N) stretch frequency is predicted at 1252 cm^{-1}, which is marginally smaller than that of 1293 cm^{-1} of ANI ground state. However, the corresponding IR intensity is much reduced in the high spin state. The vibronic structure of phosphorescence bands was analyzed, but they are puzzling, very different from those obtained under other experimental conditions. However, the presence of b_1 modes is always observed[149].

The lifetime of the T_1(ANI) state was evaluated at 2 s in Ar matrix, but only 1.2 μs in benzene and 4.3 μs in dioxane. N-Alkyl anilines have shorter lifetimes for their T_1 states, but N-phenyl anilines have longer lifetimes, up to 416 μs in benzene for triphenylamine[146–148]. Ionization of ANI from its T_1 state was also carried out using two-color photoelectron spectroscopy[149].

TABLE 9. Fundamental vibrational frequencies (cm^{-1}) and associated potential energy distributions of aniline in its lowest-lying triplet state. Calculated values were obtained from scaled B3LYP/6-311++G(3df,2p) harmonic frequencies

No.	Freq.	Sym.	Int.	Assignment, PED (%, $\geqslant 10\%$)^{a}
Q1	109	A'	7.6	$\delta_{3rg}(46.) + \delta_{2rg}(26.) - \gamma C_1 N_7(12.)$
Q2	220	A''	19.3	$\delta_{1rg}(55.) + \delta_{4rg}(22.)$
Q3	311	A''	0.4	$\delta_{4rg}(41.) + \beta C_1 N_7(39.)$
Q4	320	A'	9.5	$\gamma C_1 N_7(47.) + \delta_{3rg}(33.)$
Q5	428	A''	2.1	$\delta_{4rg}(53.) - \beta C_1 N_7(19.)$
Q6	502	A'	7.7	$\beta_{2rg}(71.)$
Q7	563	A'	112.8	$\delta_{2rg}(37.) - \gamma H_8 H_{14}(24.)$
Q8	578	A''	0.7	$\beta_{3rg}(70.)$
Q9	589	A'	167.6	$\gamma H_8 H_{14}(56.) + \delta_{2rg}(16.)$
Q10	680	A'	26.9	$\delta_{2rg}(41.) - \gamma C_4 H(38.)$
Q11	714	A''	3.8	$\gamma C_6 H(36.) - \gamma C_2 H(36.)$
Q12	771	A'	7.5	$\nu C_1 C_2(26.) + \nu C_1 C_6(26.) - \gamma C_4 H(11.) + \nu C_1 N_7(11.)$
Q13	787	A'	15.2	$\gamma C_6 H(26.) + \gamma C_2 H(26.) - \gamma C_4 H(17.)$
Q14	905	A''	0.2	$\gamma C_5 H(23.) - \gamma C_3 H(23.)$
Q15	941	A'	9.8	$\nu C_4 C_5(24.) + \nu C_3 C_4(24.) - \beta_{1rg}(14.) - \gamma C_3 H(12.) - 34(12.)$
Q16	957	A'	0.2	$\beta_{1rg}(71.)$
Q17	972	A'	0.4	$\gamma C_3 H(26.) + \gamma C_5 H(26.) - \gamma C_2 H(10.) - \gamma C_6 H(10.)$
Q18	1001	A''	0.0	$\beta_{2[NH_2]}(23.) - \gamma C_5 H(13.) + \gamma C_3 H(13.) - \nu C_1 C_2(13.) + \nu C_1 C_6(13.)$
Q19	1068	A''	0.5	$\nu C_4 C_5(32.) - \nu C_3 C_4(32.) - \beta C_4 H(18.)$
Q20	1147	A''	0.6	$\beta_{2[NH_2]}(26.) - \beta C_2 H(16.) - \beta C_6 H(16.) + \beta C_3 H(12.) + \beta C_5 H(12.)$
Q21	1188	A'	1.3	$\beta C_6 H(25.) - \beta C_2 H(25.) - \beta C_5 H(14.) + \beta C_3 H(14.)$
Q22	1252	A'	4.4	$\nu C_1 N_7(68.)$
Q23	1285	A''	0.4	$\beta C_4 H(26.) + \beta_{2[NH_2]}(17.)$
Q24	1354	A''	1.7	$\nu C_4 C_5(13.) - \nu C_3 C_4(13.) - \beta C_5 H(11.) - \beta C_3 H(11.)$
Q25	1378	A''	3.5	$\beta C_4 H(17.) + \beta C_3 H(16.) + \beta C_5 H(16.) - \nu C_1 C_2(12.) + \nu C_1 C_6(12.)$
Q26	1440	A'	5.3	$\beta C_3 H(22.) - \beta C_5 H(22.) - \beta C_6 H(17.) + \beta C_2 H(17.)$
Q27	1538	A''	0.7	$\nu C_2 C_3(26.) - \nu C_5 C_6(26.) - \beta C_4 H(19.)$
Q28	1595	A'	5.5	$\nu C_5 C_6(29.) + \nu C_2 C_3(29.)$
Q29	1618	A'	32.2	$\beta_{1[NH_2]}(92.)$
Q30	3137	A'	5.8	$\nu C_2 H(30.) + \nu C_6 H(30.) - \nu C_3 H(19.) - \nu C_5 H(19.)$
Q31	3138	A''	0.3	$\nu C_6 H(36.) - \nu C_2 H(36.) - \nu C_5 H(14.) + \nu C_3 H(14.)$
Q32	3155	A'	7.5	$\nu C_3 H(27.) + \nu C_5 H(27.) + \nu C_2 H(19.) + \nu C_6 H(19.)$
Q33	3157	A''	48.0	$\nu C_5 H(36.) - \nu C_3 H(36.) + \nu C_6 H(14.) - \nu C_2 H(14.)$
Q34	3193	A'	13.3	$\nu C_4 H(92.)$
Q35	3449	A'	32.9	$\nu N_7 H(50.) + \nu N_7 H(50.)$
Q36	3583	A''	3.4	$\nu N_7 H(50.) - \nu N_7 H(50.)$

^{a} ν: stretching, β: bending, γ out of plane, β_{1rg}, β_{2rg}, β_{3rg}: bending of six-membered ring, δ_{1rg}, δ_{2rg}, δ_{3rg}, δ_{4rg}: deformation of six-membered ring, $\tau_{[NH2]}$: torsion of NH$_2$
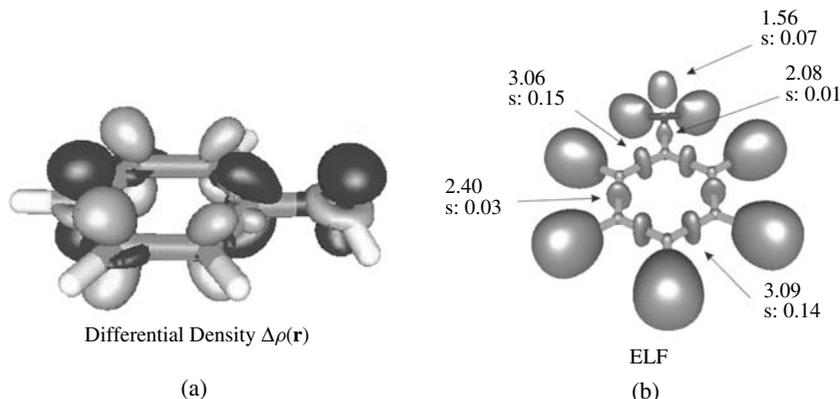
FIGURE 20. Aspects of the electronic distribution in the vertical triplet aniline (triplet state at the singlet ground-state geometry): (a) Differential density; Pink represents the $\Delta\rho(\mathbf{r}) = 0.005$ au, and blue represents the $\Delta\rho(\mathbf{r}) = -0.005$ au isosurface of the differential density. (b) ELF = 0.87 isosurfaces of the electron localization function. Values correspond to basin populations and integrated spin densities (**s** values)

Figure 20 illustrates some aspects of the electronic distribution of the vertical triplet, which is a triplet state of the ANI molecule initially generated at the singlet geometry. Figure 21 summarizes the electronic distribution of the adiabatic triplet aniline, $T_1(\text{ANI})$. The differential density map (Figure 20a) defined by

$$\Delta\rho(\mathbf{r}) = \rho_{\text{vertical triplet}}(\mathbf{r}) - \rho_{\text{singlet}}(\mathbf{r})$$

shows how electrons are moving during vertical excitations. Blue contours show the regions where electron depletion occurs ($\rho_{\text{triplet}}(\mathbf{r}) < \rho_{\text{singlet}}(\mathbf{r})$); pink contours indicate where electron concentration takes place ($\rho_{\text{triplet}}(\mathbf{r}) > \rho_{\text{singlet}}(\mathbf{r})$) during vertical excitation. Natural charges concur with the picture suggested by the differential density, as they amount to 0.31, -0.70 and -0.03 e for nitrogen, *ipso*-C1 and *para*-C4, respectively, whereas they are -0.35 and -0.37 e in the case of *ortho*-C2 and *meta*-C3 atoms.

As suggested by the shape of the HOMO and LUMO of the singlet state, the populations of the $V(C1_{ipso},C2_{ortho})$ and $V(C3_{meta},C4_{para})$ basins are increased during vertical excitation, whereas that of $V(C2_{ortho},C3_{meta})$ decreases, which gives a reversed bond order distribution as compared to the ground state. The integrated spin density shows that the unpaired electrons are mainly located in $V(C1_{ipso},C2_{ortho})$ and $V(C3_{meta},C4_{para})$ basins. The electron localization function of the vertical triplet state emphasizes that during excitation, the lone pair of nitrogen donates electrons to the ring, the sum of the V(C,C) basin populations is now 17.1 e, but it is 16.8 e in the singlet state.

Following geometry relaxation of the triplet state, the nitrogen atom is moving out of the ring plane (Figure 19), and a new lone-pair-type valence basin (with 1.02 e population) on *ipso*-C1 takes place from the excess electron of the ring. As seen on the Laplacian map (Figure 21c), there is a remarkable electron concentration on this basin. According to the integrated spin density values (Figure 21b), the $V(C1_{ipso})$ basin has the largest radical character, whereas the remaining radical electrons are nearly equally distributed on V(N), V(C,N) and V(C,C) basins (Figure 21d). This is reflected in the spin density in the symmetry plane perpendicular to the ring plan (Figure 21e). The population of

the V(C1$_{ipso}$,C$_{ortho}$) basin decreases dramatically, in agreement with the Wiberg indices. Both $\rho(\mathbf{r})$ and ε correspond to the values of a single bond, therefore the ipso-C can be regarded as a sp^3-carbon with a radical on it. On the contrary, the bond order of the ortho-C2—meta-C3 bond actually increases. It is interesting, however, that according to the calculated NICS value, the triplet ANI remains aromatic, although its aromaticity is actually decreased as compared to the singlet ground state.

Geometry, NBO charges and
Wiberg indices

(a)

Topology of $\rho(\mathbf{r})$

(b)

Laplacian

(c)

ELF

(d)
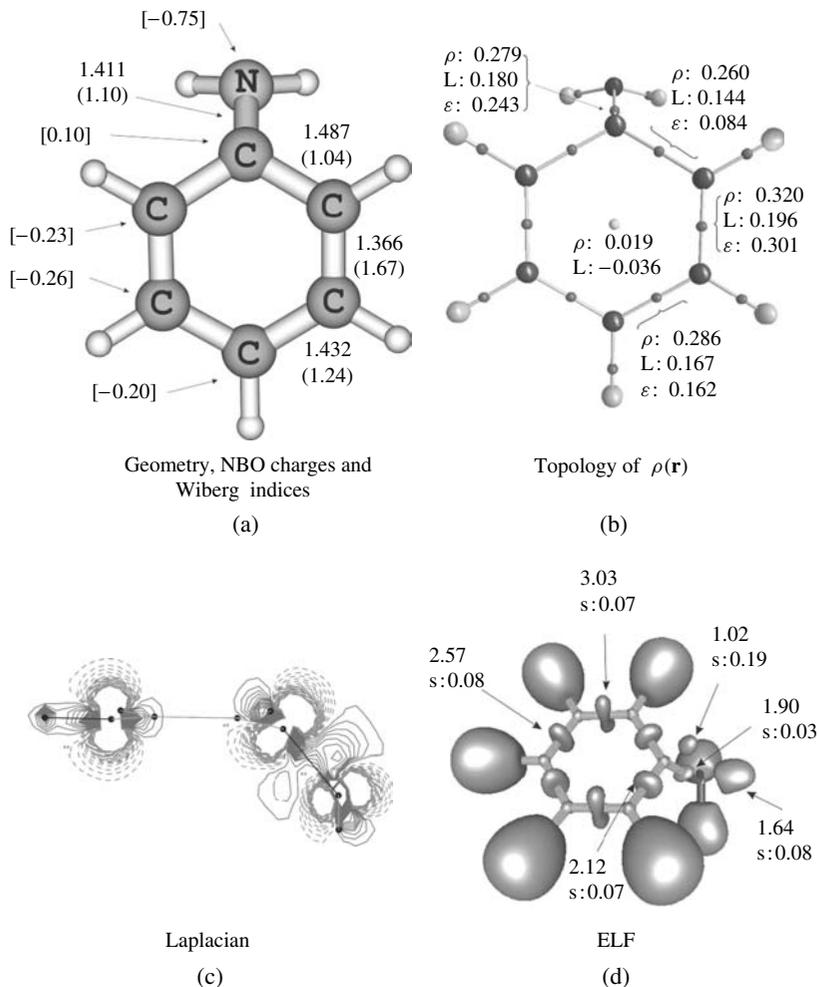
FIGURE 21. Summary of electronic distribution in triplet aniline: (a) Bond distances (Å), NBO charges [bracket, in au] and Wiberg indices (parentheses, in au). (b) Topology of the electron density determined from atom-in-molecule calculations: $\rho(\mathbf{r})$ = electron density, L = Laplacian of the density defined as $L(\mathbf{r}) = -\nabla^2\rho(\mathbf{r})$ and ε = ellipticity of the bond critical point. (c) Laplacian map of the density. (d) Isosurfaces of the electron localization function, ELF = 0.87; the values are the populations of the valence basins. (e) Spin densities in the molecular (CCN) plane

Spin density

(e)
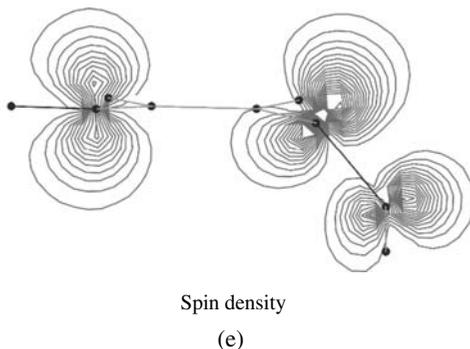
FIGURE 21. (*continued*)

In summary, relative to the S_0 state, the C−C bonds become weaker and the C−N bond is getting stronger. The charge distribution is reorganized to benefit the *ortho* and *meta* ring carbons. The *ipso*- and *para*-carbon and nitrogen atoms experience electron depletion. The *ipso*-carbon enjoys an excess of α-spin electrons. For their part, the topology and the electron localization function (ELF) of T_1 are not basically different from those of the singlet S_0.

In benzene solution, the dipole moment has been measured to be $\mu [T_1(ANI)] = 2.1 \pm 0.2$ D. As discussed in a previous section, the dipole moment lies in the C−N axis. In the triplet T_1 state, the molecule has a more biradical nature, which may cause less contribution of the charge transfer in the C−N direction. Upon excitation, the electron density on the N atom is transferred mostly to the ring carbon atoms; therefore, the dipole moment change in the triplet state is primarily determined by this actual transfer[147].

It has been suggested that ANI higher-lying triplet states are essentially planar[144]. Similarly, the lowest-lying triplet state of *N*,*N*-dialkyl-4-cyanoaniline (4-dialkylaminoben-zonitrile) was determined to be nearly planar and has a biradical character[151]. This is reflected by a high negative charge delocalization on the cyano group, a quinoidal distortion and conjugation of the ring. Photoexcitation of *p*-nitroanilines and its *N*-alkyl derivatives resulted in the formation of triplet states with dipole moments considerably larger than that of the ground state. The lifetime of these triplet species ranges from 54 to 14000 ns[150].

Photophysical and flash photolysis experiments in various solvents showed that the resulting reactions of haloanilines proceed from the triplet state. The latter is involved in the photochemical processes resulting in C−X bond cleavages in which both homolytic and heterolytic pathways are rather competitive with each other[152]. There is also a certain correlation between the BDE(C−N) and activation energy for the C−N bond cleavage in the T_1 state with the BDE(C−N) of the ground S_0 state.

Protonation of triplet aniline has been found to occur preferentially at the *meta*-C3 site[154]. The corresponding PA(C3) = 1017 kJ mol^{-1} is now significantly larger than the PAs of 866, 905, 927 and 995 kJ mol^{-1} at N, *ipso*-C1, *para*-C4 and *ortho*-C2, respectively (UB3LYP/6-311++G(d,p) + ZPE values). Thus the nitrogen becomes the least basic site in the triplet state[154].

2. Singlet states

The ANI singlet excited states have been investigated extensively using different spectroscopic and theoretical methods[36, 42, 43, 61, 72, 150, 156−173]. Electronic spectra due to singlet

excitations have been observed in the gas phase[143], aqueous solution[172], perfluorohexane[145] and in the crystal[174]. The molecular beam, fluorescence excitation spectrum of four rovibronic bands of the $S_1 \leftarrow S_0$ electronic transition has been recorded, and thereby the rotational parameters obtained and its structure resolved[160]. Accordingly, the rotational constants are determined as follows (MHz):

$$A = 5285.102, \ B = 2633.538 \ \text{and} \ C = 1759.162$$

Alternative results are $A = 5276.9$, $B = 2633.8$ and $C = 1759.4$ MHz[162]. Compared with the S_0 constants, the A constant is decreased by 332 MHz whereas the B constant is increased by 38 MHz. This indicates that the overall length along the main axis is reduced upon excitation.

Figure 22 displays the selected geometrical parameters of the lowest-lying singlet state $^1B_2$[163]. Although the latter were determined using a simple quantum chemical method (CIS), they confirmed the planarity of the molecule in the S_1 state[159]. The molecular skeleton is contracting along the in-plane axis, giving rise to a quinoid-like resonance structure. The C–N bond distance of 1.31 Å is much shorter than that of 1.40 Å in the ground state. The planar structure confers a C_{2v} point group and a $^1B_2$ electronic state on the S_1 state.

The calculated net charges indicate that the *ipso*-C1 atom becomes positively charged, whereas all other ring carbon and nitrogen atoms bear negative charge. The net charges on N and C4 are increased upon excitation. As a result, the nitrogen is the most negatively charged center, followed by the *para*-C4 and *meta*-C3 atoms. Overall, the main component of the dipole moment is increased from $\mu_a(S_0) = 1.128$ D to $\mu_a(S_1) = 2.801$ D[43, 61, 165]. The first band has a charge-resonance character with a slight charge-transfer nature. The charge transfer may become more important if the amino group is twisted in an excited state[161]. The pK_a value for S_1(ANI), determined using fluorescence intensity titration, amounts to p$K_a = -0.50$, which is far different from that of 4.5 measured for the ground state (see above)[150].

The vertical $S_1 \leftarrow S_0$ transition energy is identified at $34027-34029$ cm^{-1} (4.219 eV)[34, 159, 160]. The observation of an unfractionated ANI spectrum is in agreement with the high oscillator strength ($f = 0.028$) and the very large fluorescence quantum yield ($\Phi > 0.28$, depending on the vibronic level). This arises from the fact that a direct coupling between the S_1 state and the highly vibrationally excited states of S_0 is of a
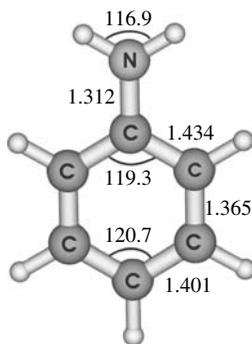
FIGURE 22. Geometry of aniline in its lowest-lying singlet excited $^1B_2$ state. Bond lengths are given in angstroms and bond angles in degrees[163]

higher order process of low efficiency. In addition, because of the relatively large energy gap between the S_1 and T_1 states (about 7200 cm^{-1}, 0.89 eV), the allowed first-order spin−orbit coupling between them is equally inefficient[143]. The fluorescence lifetime of ANI excited by the vibrationless S_1 state was reported as 7.8 ns[168]. Intersystem crossing is the main nonradiative process in the S_1 relaxation. The rate of intersystem crossing is as large as 8.2×10^7 s^{-1}. The decay of the resulting triplet state is very fast; however, no phosphorescence was observed in the gas phase due to the rapid decay from T_1 to S_0.

Rydberg excited states of ANI and its derivatives have been located[72, 143]. A novel band located between the first and second $\pi^* \leftarrow \pi$ transitions, and centered at 37104 cm^{-1} (4.62 eV above the S_0 and 0.38 eV above the S_1 state), has been observed[72]. This singlet $^1B_1$ state has been assigned to a 3s-Rydberg state[161].

Electron redistribution due to a stronger interaction between the ring and amino group, in a planar shape, induces many important changes in the vibrational modes. However, fundamental frequencies of the S_1(ANI) state have been identified only for the modes 6a, 1 and 12 (associated with the symmetric vibrations of the ring) and b_1 (nonsymmetric inversion vibration). These frequencies of the S_1(ANI) are 492 (mode 6a), 761 (mode I^2), 798 (mode 1), 953 (mode 12), 985 (mode 6a) and 1289 (mode 6a) cm^{-1} [160]. Note that the latter labeling of the modes was made according to Varsanyi's notation used for a large variety of benzene derivatives[12].

Due to the fact that vibrational frequencies of excited singlet states were not calculated accurately, a detailed comparison is rather difficult. However, using the CIS/6-31+G(d) vibrational frequencies[163], let us note that the C−H stretch frequencies tend to be increased up to 40−56 cm^{-1} upon excitation. The C−N stretching mode (ν_{14}) exhibits a frequency increase of 123 cm^{-1} in the S_1 state, whereas the two NH$_2$ stretch frequencies are lowered by 176 and 201 cm^{-1}, as a result of a reduction in their force constants. Other modes associated with the amino groups tend to have higher frequencies (up to 50 cm^{-1}). As the excitation involves a transfer of an electron from a π orbital to a π^* orbital, a reduction of the force constants of the out-of-plane vibrations is expected to be larger than those of in-plane modes. Thus the ring puckering (ν_{31}) is characterized by a large frequency decrease (291 cm^{-1}). The most sensitive out-of-plane mode is related to the C−N distortion (ν_{36}), which now has the lowest frequency in the S_1($^1B_2$) state.

G. Dissociation

1. N−H bond dissociation energies

The N−H bond cleavage constitutes the most common photochemical process in NH-containing aromatic compounds. Despite such practical importance[174−176], their accurate thermochemical properties are still scarce. This is in part due to their low stability, low purity and harmful character. Only a limited number of experimental heats of formation of anilines have been reported[177, 178]. In the same vein, until the early 1980s, there was a paucity of data concerning homolytic bond dissociation energies (BDEs) of N−H bonds in the literature. The BDEs provide direct information about the intrinsic strength of chemical bonds.

For decades, the only BDE(N−H) value known was that of the ANI radical cation in aqueous solution[179]. In a 1982 review, only seven values were reported including the values of 368 and 366 kJ mol^{-1} for PhNH−H and PhMeN−H, respectively[180]. In 1991, two more BDE values were determined[181], namely 386 kJ mol^{-1} for PhNH−H and 366 kJ mol^{-1} for Ph$_2$N−H. Since then, both experimental and theoretical results for BDE(N−H) of several series of aniline derivatives have been available[182−198].

In the 1990s, the main electrochemical approach to estimate the BDEs was a combination of the equilibrium acidities (pK_{HA}) and the oxidation potentials of their conjugate

anions ($E_{ox}(A^-)$). For p-substituted anilinide anions, both quantities determined in DMSO were found to be linearly correlated. In addition, both quantities were also linearly correlated with Hammett σ^-/σ^+ constants, indicating that the $E_{ox}(A^-)$ values are mainly dictated by their basicities, and are perturbed to only a minor extent by the radical destabilizing and stabilizing effects of substituents[181–183].

Another electrochemical technique involved combining the reduction potentials of anilinyl radical cations with their pK_a values. The radical cations were generated in water by pulse radiolysis[185]. A value of BDE(PhNH−H) = 373 kJ mol^{-1} was obtained from this electrochemical measurement. Subsequent investigations used the photoacoustic calorimetry (PAC) technique[186, 187], which allows measurements to be performed under conditions relevant to most chemical and biochemical processes. A value of BDE(PhNH−H) = 375 kJ mol^{-1} was obtained from the PAC experiments[188]. Because the latter techniques provided fairly reliable BDEs, there has been a certain consistency in the reported BDE(N−H) values for ANI in solution.

High-level *ab initio* quantum chemical computations[189, 195–198] appeared to converge to a value ranging from 383 to 386 kJ mol^{-1} for the gas-phase BDE(N−H) of aniline. Thus the actual difference of 10 kJ mol^{-1} between measured and calculated results could be accounted for as a medium effect. Significant solvent effects were indeed found among different BDE(N−H) values computed in the gas phase and in heptane, DMSO or aqueous solutions[197]. In this context, it seems reasonable to suggest the following value, BDE(N−H) = 383 ± 4 kJ mol^{-1}, for aniline in the gaseous phase.

For the gaseous-phase N-protonated aniline, a recent quantum chemical study[194] has evaluated the corresponding quantity as BDE(N$^+$−H) = 519 ± 8 kJ mol^{-1} for the Ph−NH$_3^+$ cation. This strength is comparable to that of 523 kJ mol^{-1} for NH$_4^+$, but far larger than that of 460 kJ mol^{-1} for CH$_3$−NH$_3^+$. The theoretical value of 519 kJ mol^{-1} is also substantially larger than an earlier experimental value of 375 kJ mol^{-1} obtained using a linear correlation between BDE(B−H$^+$) and the parameters $pK(HB^+)$ and $E_{ox}(B)$, where B are neutral anilines[180]. In view of the relative accuracy of current quantum chemical methods, such a large discrepancy suggests a reevaluation of the experimental result for the BDE of protonated aniline.

For the ANI radical cation, an acidity constant $pK_a = 6.4$ was obtained[182]; however, no experimental BDE of this ion has been reported. A linear correlation of the oxidation potentials of anilines versus the acidities of the corresponding radical cations was observed. Recent *ab initio* calculations[198] derived a value of BDE(N$^+$−H) = 418 ± 10 kJ mol^{-1} for the aniline radical cation, relative to the Ph−N−H$^+$ cation in its singlet ground state. Removal of an electron reinforces the strength of the N−H bond, due to the electron delocalization.

For the ANI radical anion, an experimental estimate of about 125–180 kJ mol^{-1} has been put forward for the BDE(N−H$^-$) quantity[182]. Thus, addition of an excess electron weakens the N−H bond to a large extent.

For substituted anilines, there has been an apparent variance in the reported results obtained in various solutions (DSMO, water). Such variance likely came from different use of the correlation equation of the type

$$\text{BDE}_{HA} = c_1\, pK_{HA} + c_2 E_{ox}(A^-) + c_3$$

where the coefficient c_3 varies from one study to the other[197]. In some cases, such as *meta*- and *para*-trifluoromethyl- and methoxyanilines, differences might reach up to 28–40 kJ mol^{-1}.

In general, the substituent effects on the BDEs of anilines follow the usual trends observed for aromatic compounds, in line with the Brown−Okamoto σ^+ constants[190, 197].

BDEs computed for both *meta-* and *para-*substituted anilines are linearly correlated with σ_m^+ and σ_p^+ parameters. In a series of p-YC$_6$H$_4$NX-H compounds, it is noted that the strengthening effect on BDE(N−H) of electron-withdrawing (EW) Ys is larger than the weakening effect of electron-donating (ED) Ys. The ED Y groups tend to destabilize the neutral molecule and stabilize the corresponding radical, and thereby lower the BDE as compared with that of ANI. In contrast to phenols, the effects of substituents on the stability of aniline molecules and radicals are of roughly comparable magnitudes. The opposite effect holds true for EW Ys. The effect is much smaller for *meta-*substituted derivatives. For *ortho-*derivatives, similar results to those of the *para-*anilines were obtained (except for a few−OR groups). In these cases, differences between BDE(N−H) values for *ortho* and *para* derivatives are found to be larger than 8 kJ mol^{-1}, and may be attributed to a stabilization effect of the neutral molecules.

A particularly low value, BDE(N−H) = 350 kJ mol^{-1}, has been computed for o-hydroxyaniline, which is due to a peculiar stabilization by the hydrogen bond of the resulting radical[197].

The X substituents also contribute relatively large contributions to BDE(N−H) arising from interactions in the molecules. For X = H, CH$_3$, OH and F, the calculated BDE(N−X) values turn out to have good correlatation with σ_p^+ constants[190]. Effects of remote substituents are also quite significant but rather divergent[196].

In the protonated anilines, electron demand on the system again dictates the substituent effects on BDEs. Accordingly, in a Y−C$_6$H$_4$−NH$_3^+$ series, an EW Y-group destabilizes the YC$_6$H$_4$NH$_2^{\bullet+}$ radical more than the protonated form, whereas an ED Y-group induces a reserve effect. Attempts to correlate the BDEs with the local hard and soft acid base parameters[192, 198] have been made; although less good correlations have been found, this approach certainly deserves to be pursued in future studies.

2. The anilino radical (Ph−N−H$^\bullet$)

In the nonpolar solvent hexane, aniline undergoes a N−H bond cleavage following a 248-nm laser flash photolysis[199−205]. The resulting anilino, or phenylaminyl radical PhNH$^\bullet$, is a well established species having UV absorption maximum at λ_{max} = 308 nm (ε = 3500 M^{-1} cm^{-1}) and λ_{max} = 401 nm (ε = 1250 M^{-1} cm^{-1})[200] in different solvents (water, hexane, cyclohexane, heptane, benzene values are slightly changed with solvent). The electron affinity[206] has been determined experimentally using electron photodetachment spectroscopy: EA(PhNH$^\bullet$) = 164.4 ± 1.2 kJ mol^{-1} (39.3 ± 0.3 kcal mol^{-1}). The radical has also been investigated theoretically using quantum chemical methods[207−211]. The PhNH$^\bullet$ radical can also be generated by hydrogen abstraction from aniline by radicals such as alkoxy radicals[204].

Figure 23 displays selected optimized geometrical parameters of the anilino radical in both lowest-lying doublet ($^2A''$) and quartet ($^4A''$) states. In both electronic states, the C−N bond distances are almost identical. The doublet state exhibits a quinoidal structure, whereas the quartet state geometry is characterized by long C2−C3 and C5−C6 distances (1.51 Å). This basically corresponds to a triradical electronic structure in which two electrons are centered on two allyl-type moieties.

The low-spin $^2A''$ state is the ground electronic state, lying well below the quartet $^4A''$ counterpart, with a doublet−quartet energy gap of ΔE_{DQ}(PhNH$^\bullet$) = 3.72 eV. In the low-spin state, the N-radical is calculated to be 75 kJ mol^{-1} more stable than its ring C-radical isomer. The adiabatic ionization energy and electron affinity are calculated as EA$_a$(PhNH$^\bullet$) = 164 ± 4 kJ mol^{-1} (see above) and IE$_a$(PhNH$^\bullet$) = 8.1 ± 0.1 eV. The calculated EA agrees quite well with the experimental value[206]. The proton affinity amounts to PA(PhNH$^\bullet$) = 965 ± 4 kJ mol^{-1}.
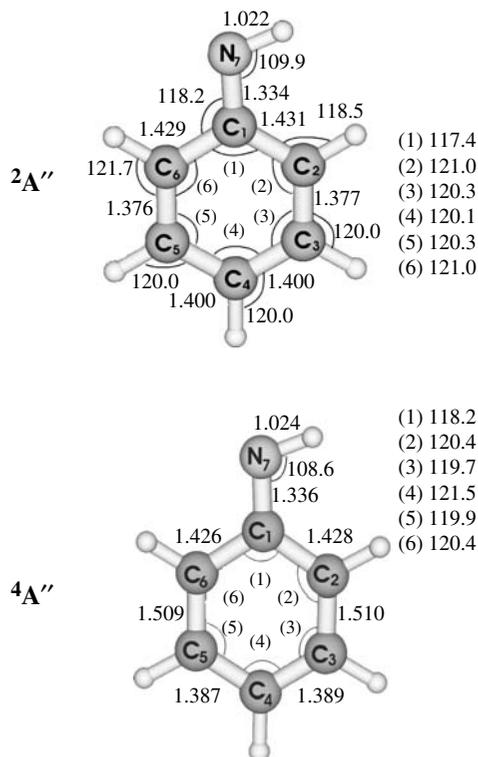
FIGURE 23. Geometry of the anilino radical in both lowest-lying doublet $^2A''$ and quartet $^4A''$ states. Bond lengths given in angstroms and bond angles in degrees were obtained from UB3LYP/6-311++ G(d,p) optimizations

The phenylnitrenium cation (PhNH$^+$), formally generated upon ionization of the anilino radical, exhibits a singlet ground state ($^1A'$), followed by a triplet state ($^3A''$), with a singlet–triplet energy gap of $\Delta E_{ST}(\text{PhNH}^+) = 0.84 \pm 0.1$ eV (81 kJ mol^{-1})[210, 211].

Table 10 records the calculated vibrational frequencies of the anilino radical, and Figure 24 illustrates vividly the associated normal vibrational modes. Note that the modes are again presented without using Varsanyi's labeling. A particular feature concerns the C−N stretching frequency. In an earlier experimental report[200], the band at 1505 cm^{-1} was assigned to this mode. However, in a subsequent theoretical study[209], the band at 1326 cm^{-1} has been assigned to the C−N stretch vibration rather than to the C−C stretch, whereas the band at 1505 cm^{-1} corresponds to the NH bending, combined with a CN stretch. Recent calculations[211], summarized in Table 10 and Figure 24, concur with the latter assignment.

Figure 25 displays various results probing the charge distribution of the anilino radical. Although this molecule has only one N−H bond, the properties of the atoms and bonds in both sides are almost identical (for example, the basin population for V(C1$_{ipso}$,C2$_{ortho}$) is 2.51 e, while it is 2.50 e for V(C1$_{ipso}$,C6$_{ortho}$)). The order of the C1−C2 and C3−C4 bond is reduced due to the resonance structures similar to those of Scheme 1, indicated by the 2.50 and 2.64 e populations of V(C2,C2) and V(C3,C4), respectively, compared

TABLE 10. Vibrational frequencies (cm^{-1}), infrared intensities, normal modes and potential energy distribution of the anilino radical (C$_6$H$_5$N$^{\bullet}$H). Values obtained from scaled UB3LYP/6-311++ G(3df,2p) calculations

No.	Freq.	Sym.	Int.	Modes and potential energy distribution (%, $\geqslant 10\%$)^a
Q1	196	A''	0.3	$\delta_{2rg}(56.) + \delta_{1rg}(16.) - \gamma C_1N_7(10.)$
Q2	388	A''	4.1	$\delta_{3rg}(80.)$
Q3	420	A'	9.0	$\beta C_1N_7(77.) + \beta_{3rg}(13.)$
Q4	485	A''	5.3	$\delta_{2rg}(37.) + \gamma C_5H(29.) - \delta_{1rg}(18.)$
Q5	535	A'	0.1	$\beta_{2rg}(80.)$
Q6	617	A'	0.2	$\beta_{3rg}(80.)$
Q7	662	A''	41.1	$\delta_{1rg}(56.) + \gamma C_5H(17.) + \gamma C_3H(16.)$
Q8	684	A''	38.1	$\tau N_7H(86.)$
Q9	776	A''	56.8	$\delta_{1rg}(31.) - \gamma C_4H(28.) + \gamma C_1N_7(16.)$
Q10	824	A'	1.6	$\nu C_1C_2(26.) + \nu C_1C_6(26.) - \beta_{1rg}(23.)$
Q11	831	A''	2.2	$\gamma C_2H(33.) - \gamma C_6H(27.) - \gamma C_5H(19.) + \gamma C_3H(15.)$
Q12	919	A''	5.0	$\gamma C_4H(30.) - \gamma C_6H(28.) - \gamma C_2H(26.)$
Q13	961	A'	0.2	$\beta_{1rg}(64.) + \nu C_1C_6(13.) + \nu C_1C_2(11.)$
Q14	984	A''	0.0	$\gamma C_3H(57.) - \gamma C_2H(19.) - \gamma C_4H(12.)$
Q15	993	A''	0.1	$\gamma C_5H(53.) - \gamma C_6H(26.)$
Q16	1026	A'	1.6	$\nu C_4C_5(36.) + \nu C_3C_4(33.)$
Q17	1088	A'	17.6	$\nu C_3C_4(11.) - \nu C_2C_3(10.) + \nu C_5C_6(10.) - \beta C_6H(10.) - \beta C_1N_7(10.)$
Q18	1165	A'	10.9	$\beta C_6H(22.) - \nu C_1N_7(20.) + \nu C_1C_6(16.) - \nu C_5C_6(10.)$
Q19	1171	A'	4.9	$\beta C_4H(34.) - \beta C_5H(23.) - \nu C_4C_5(12.)$
Q20	1180	A'	24.2	$\beta C_2H(30.) - \beta C_3H(24.) - \nu C_2C_3(15.) - \nu C_1C_2(12.)$
Q21	1312	A'	0.4	$\nu C_1N_7(63.)$
Q22	1339	A'	4.0	$\nu C_2C_3(17.) + \nu C_4C_5(14.) - \nu C_5C_6(14.) - \nu C_3C_4(13.) + \beta C_4H(12.)$
Q23	1365	A'	16.7	$\beta C_5H(21.) + \beta C_6H(21.) + \beta C_2(18.) + \beta C_3H(11.)$
Q24	1474	A'	6.2	$\beta C_3H(25.) - \beta C_6H(16.) - \nu C_1C_2(15.) + \nu C_1C_2(12.) + \beta C_2H(11.)$
Q25	1490	A'	4.8	$\beta C_5H(22.) + \nu C_1C_6(16.) - \beta C_2H(15.) - \nu C_2C_3(11.)$
Q26	1565	A'	1.3	$\nu C4C5(19.) + \beta C_4H(19.) - \nu C_3C_4(12.) + \nu C_1C_2(10.) - \nu C_1C_6(10.)$
Q27	1586	A'	19.2	$\nu C_5C_6(27.) + \nu C_2C_3(22.) - \beta C_3H(11.)$
Q28	3155	A'	3.5	$\nu C_2H(61.) - \nu C_3H(29.)$
Q29	3166	A'	0.3	$\nu C_5H(48.) - \nu C_4H(25.) + \nu C_2H(18.)$
Q30	3175	A'	14.6	$\nu C_3H(45.) - \nu C_5H(24.) + \nu C_2H(17.)$
Q31	3187	A'	12.5	$\nu C_4H(48.) - \nu C_6H(27.) + \nu C_3H(20.)$
Q32	3195	A'	5.6	$\nu C_6H(61.) + \nu C_5H(22.) + \nu C_4H(13.)$
Q33	3430	A'	2.0	$\nu N_7H(100.)$

^{a} ν: stretching, β: bending, γ: out of plane, τ: torsion, β_{1rg}, β_{2rg}, β_{3rg}: bending of six-membered ring, δ_{1rg}, δ_{2rg}, δ_{3rg}: deformation of six-membered ring.
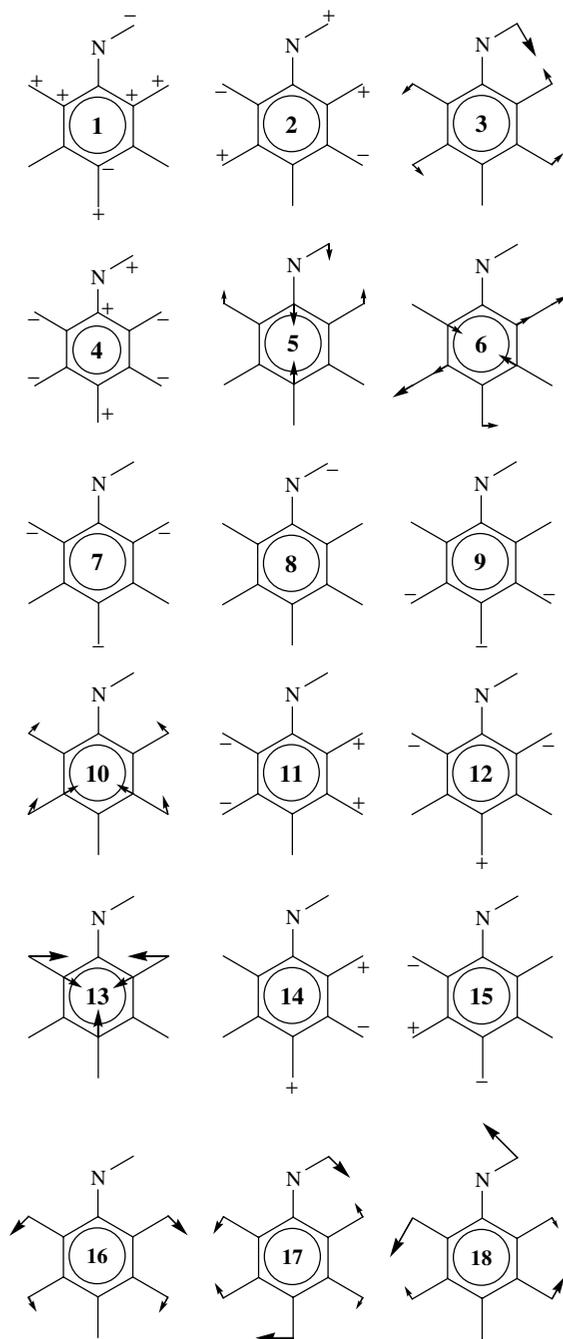
FIGURE 24. Normal displacements of vibrational modes of the anilino radical ($^2A''$). The assignment of the normal vibrations and associated frequencies are presented in Table 10. The numbers given within the ring correspond to the modes Q1–Q33 described in Table 10
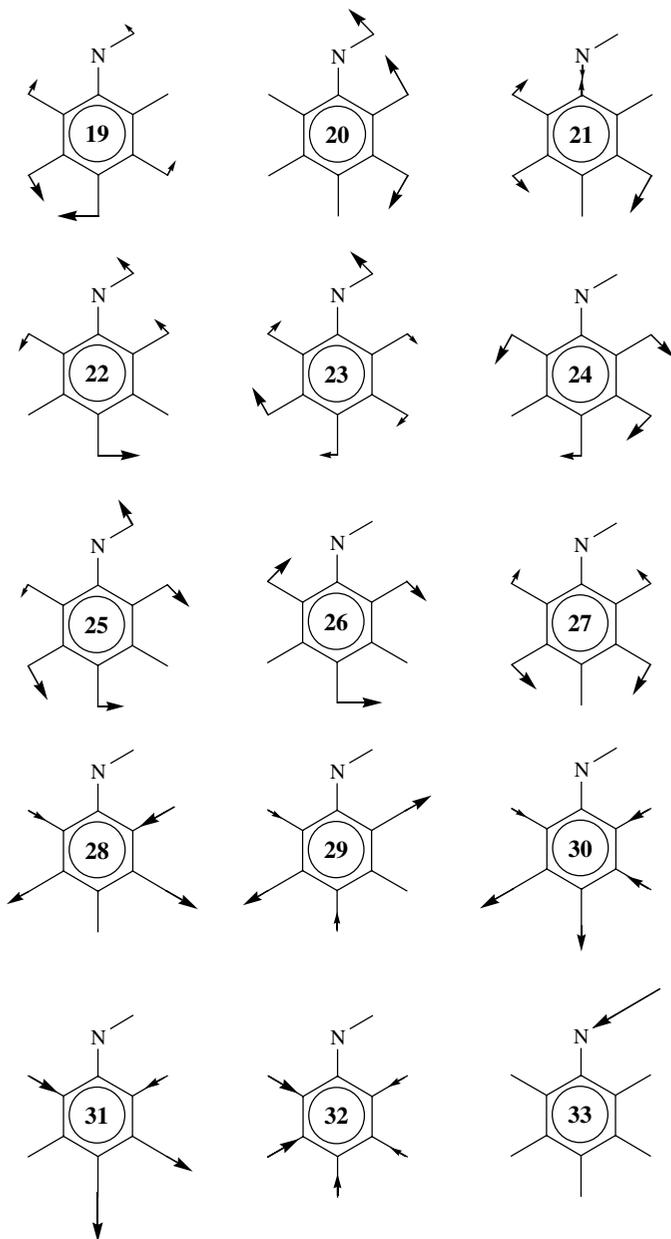
FIGURE 24. (*continued*)

with 2.74 and 2.77 e in the neutral state. The order of the C2−C3 and C1−N bond is enlarged, in accord with the bond indices and bond lengths.

We can find a V(N) lone-pair-like basin in the ELF space which, according to the 2.84 e population, involves the nitrogen lone pair and a large part of the unpaired electron. This latter agrees, by a difference of 0.17 e, with that of the integrated spin density; however, all other valence basins contain a small amount of the radical population. The Laplacian map of the electron density shows that this monosynaptic valence basin is very compact.

In general, the electronic partition in the anilino radical is not much different from that of the isoelectronic benzyl and phenoxy radicals[12]. Figure 25e demonstrates that the *ortho-* and *para-*carbon atoms have positive spin populations (excess of α-spin electrons), whereas the *ipso-* and *meta-*carbons have negative spin populations (excess of β-spin

(a) Geometry, NBO charges and
Wiberg indices

(b) Topology of $\rho(\mathbf{r})$

(c) Laplacian

(d) ELF
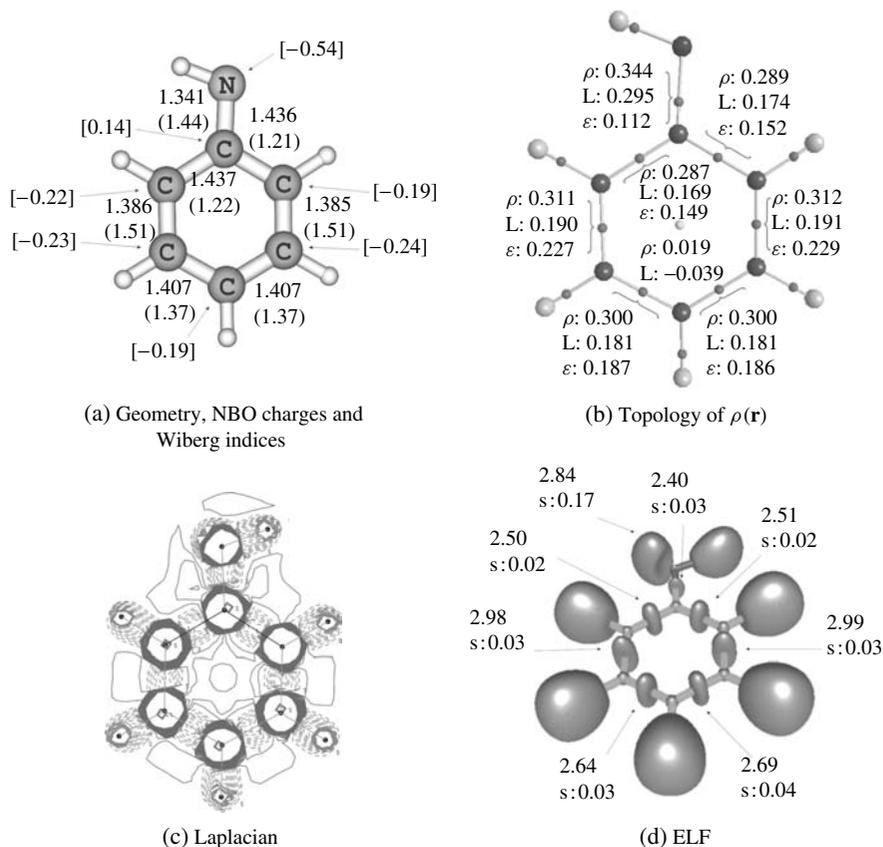
FIGURE 25 (PLATE 2). Summary of electronic distribution in the anilino radical ($^2A''$): (a) Bond distances (Å), NBO charges [bracket, in au] and Wiberg indices (parentheses, in au). (b) Topology of the electron density determined from atom-in-molecule calculations: $\rho(\mathbf{r}) =$ electron density, $L =$ Laplacian of the density defined as $L(\mathbf{r}) = -\nabla^2\rho(\mathbf{r})$ and $\varepsilon =$ ellipticity of the bond critical point. (c) Laplacian map of the density. (d) Isosurfaces of the electron localization function, ELF = 0.87; the values are the populations of the valence basins. (e) Spin density in the molecular plane
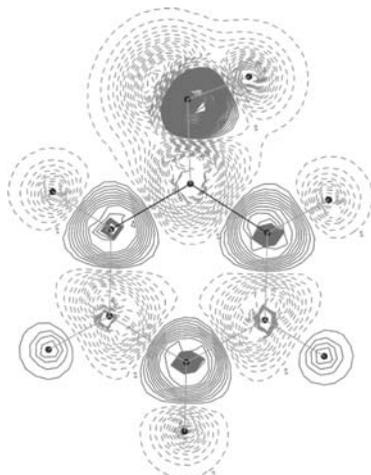
(e) Spin density

FIGURE 25 (PLATE 2). (*continued*)

electrons). However, the excess spin is mainly located on the nitrogen center. The spin distribution has a direct relationship with the magnetic properties of the radical[209, 210]. Effects of the substituents on both the ring and nitrogen sites on the radical stabilities have been analyzed[196]. Accordingly, the p-XC$_6$H$_4$NH−Y radicals are stabilized by electron-withdrawing groups but destabilized by electron-donating groups, a phenomenon just opposite to the observed O-type behavior in other aromatic heteroatomic radicals. The influence of X groups on BDE values originates from polar effects, whereas that on radical stability arises from both spin delocalization and polar effects. The former is important in accounting for the change in radical stabilization of anilino radicals. Overall, the captodative effects are fully operative in these N-centered radicals[196].

H. Ionization

1. Aniline radical cation

The radical cation formed upon ionization of ANI has been studied by different spectrometric techniques, including photoelectron, two-color photoionization, ZEKE[70, 80, 199, 212–226] and mass[107, 227–232] spectrometries. In most cases, the technique used has been coupled with infrared spectroscopy, which allowed the fine vibrational spectrum of the ion to be determined, in both line position and intensity. For example, the ZEKE photoelectron spectrum[216] was recorded by exciting to the neutral $S_1(^1B_2)$ excited state, and well-resolved vibrational bands of the cation were observed. In conjunction with quantum chemical calculations of fundamental frequencies, an assignment of the observed vibrational bands can thus be made. A few theoretical studies[56, 107, 218, 233, 234] have also been devoted to the radical cation.

The vertical ionization energy of aniline amounts to IE$_{vert}$(ANI) = 8.00 eV[1]. The adiabatic ionization energy has been determined experimentally to vary: 62265 ± 18 cm^{-1} [214], 62268 ± 4 cm^{-1} [216], 62271 ± 2 cm^{-1} [218] and 62281 ± 2 cm^{-1} [217]. Accordingly, the value of IE$_a$(ANI) = 7.720 ± 0.005 eV is now well accepted.

There is thus a gain of 0.28 eV for the ion energy following geometry relaxation from its vertical position to its equilibrium structure. Figure 26 displays some selected geometrical parameters of the radical cation ANI$^{\bullet+}$. In its ground state, the ion has a planar geometry, and belongs to the C_{2v} point group and a $^2B_1$ electronic state. This ion is formed upon removal of one (π)-electron of the nitrogen lone pair. The loss of this electron leads to significant changes in the structure and bonding. The remaining electron is coupled with one π-electron forming a C=N double bond (1.33 Å) and causing the ion to be planar. Bonding in the ring is affected. The C2−C3 and C5−C6 bonds now become double bonds, whereas the other CC bonds are stretched. The ANI$^{\bullet+}$ ion has thus a quinoidal form, corresponding to a distonic radical cation in which both charge and radical centers are well separated from each other.

Figure 27 displays the differential electron density map in the vertical position of ANI$^{\bullet+}$. From the shape of the density differences, vertical ionization takes electrons
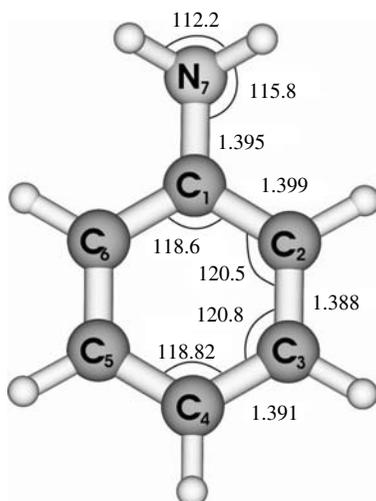
FIGURE 26. Selected geometrical parameters of the aniline radical cation ($^2B_1$). Bond lengths in angstroms and bond angles in degrees were obtained from UB3LYP/6-311++G(d,p) optimization

$$\Delta\rho(\mathbf{r})$$
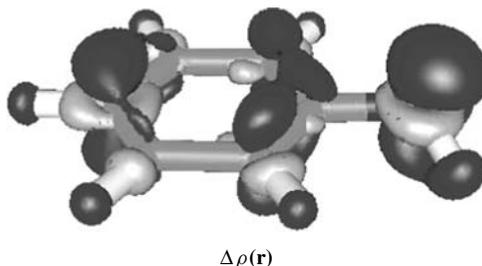
FIGURE 27 (PLATE 3). Differential density $\Delta\rho(\mathbf{r})$ of the vertical aniline radical cation, calculated using UB3LYP/6-311++G(d,p) as the difference between electron densities of both ion and neutral forms at the neutral geometry

mainly from nitrogen, *ortho*-C2, *para*-C4 and, to a lesser extent, *ipso*-C1 and hydrogen atoms. In contrast to the triplet state discussed above, the main difference with respect to the neutral singlet geometry is the planarity of the cation amino group. The nitrogen donation to the C−N bond and the ring is manifested by the lack of the V(N) basin and the enlarged V(C,N) population in the ELF space indicated in Figure 28. This means that the weight of the resonance structures *b* and *c* will be larger than that of *a* (Scheme 4). In agreement with the geometry, both *b* and *c* resonance structures show a double bond between *ortho*-C and *meta*-C, and only *b* has projection on *meta*-C–*para*-C bonds. It follows from the previous discussion that the bond order, bond population and electron density in BCP (Figure 28) increase in the case of *ortho*-C2–*meta*-C3 bonds, as compared to the neutral state, whereas they decrease in the case of *meta*-C3–*para*-C4.
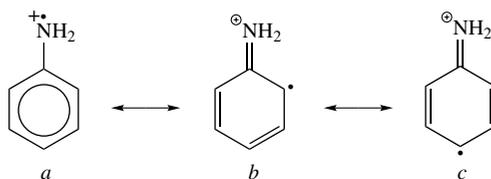
SCHEME 4

The map of spin density illustrated in Figure 29 clearly demonstrates that the excess electron is mainly located on the *para*-C4, *ortho*-C2 and nitrogen centers. It is in line with the image given in Scheme 4, even though the unpaired electron is rather partitioned on different sites than concentrated at one place. It has been shown that the electron pair coupling/decoupling of the oxidized amino $NH_2^{\bullet+}$ group is responsible for effects on the phenyl ring[233]. It removes the quasi-uniform correlation for the neutral ANI, induces regions of high and low spin or charge correlations and also produces a differential localization of electron pairs. In agreement with the argument mentioned above, this invariably gives rise to a quinoidal geometry and distonic character for the ANI radical cation.

It has been noted that alkyl substitution at the C4-position reduces the IE of aniline by 0.25–0.30 eV[225] as the length of the alkyl chain increases, even though the effects on other geometrical properties are not important.

Formation of the radical cation has also been detected in cryogenic 5 K argon matrix and characterized by the IR spectrum[70]. Redox and acidity properties of the ion in solvents have also been carried out[220, 221]. The value $pK_a = 7.05$ was obtained for $ANI^{\bullet+}$ in water[199]. Its one-electron reduction potential (E°) amounts to 0.83, 1.13 and 1.29 V vs. NHE in water, MeCN and DMSO, respectively[220]. The pK_a and E° values of the cation are connected with the N−H bond dissociation energy of the neutral molecule. The one-electron oxidation/reduction potentials in solution could be approached using theoretical methods[234]. Correlation between one-electron oxidation of anilines and HOMO energies of neutrals in aqueous solution have been established.

The $ANI^{\bullet+}$ ion exhibits an electronically excited state whose adiabatic IE was found to be 8.94 eV[212] from He I PES. Two-color laser photoelectron spectroscopy[219] via both the S_0 and S_1 states of ANI revealed that there is an optical transition from the $S_1(^1B_2)$ state to the $^2A_2$ state of $ANI^{\bullet+}$. The IE of the latter state was found at 9.031 eV, which is slightly higher than the PES value. This implies that the $^2A_2$ ($^2\Sigma$) state constitutes the lowest-lying excited state of $ANI^{\bullet+}$, and the $^2A_2 \leftarrow {}^2B_1$ energy gap of $ANI^{\bullet+}$ amounts to 1.22 eV.

Geometry, natural charges
and Wiberg indices

(a)

Topology of $\rho(\mathbf{r})$

(b)

ELF

(c)
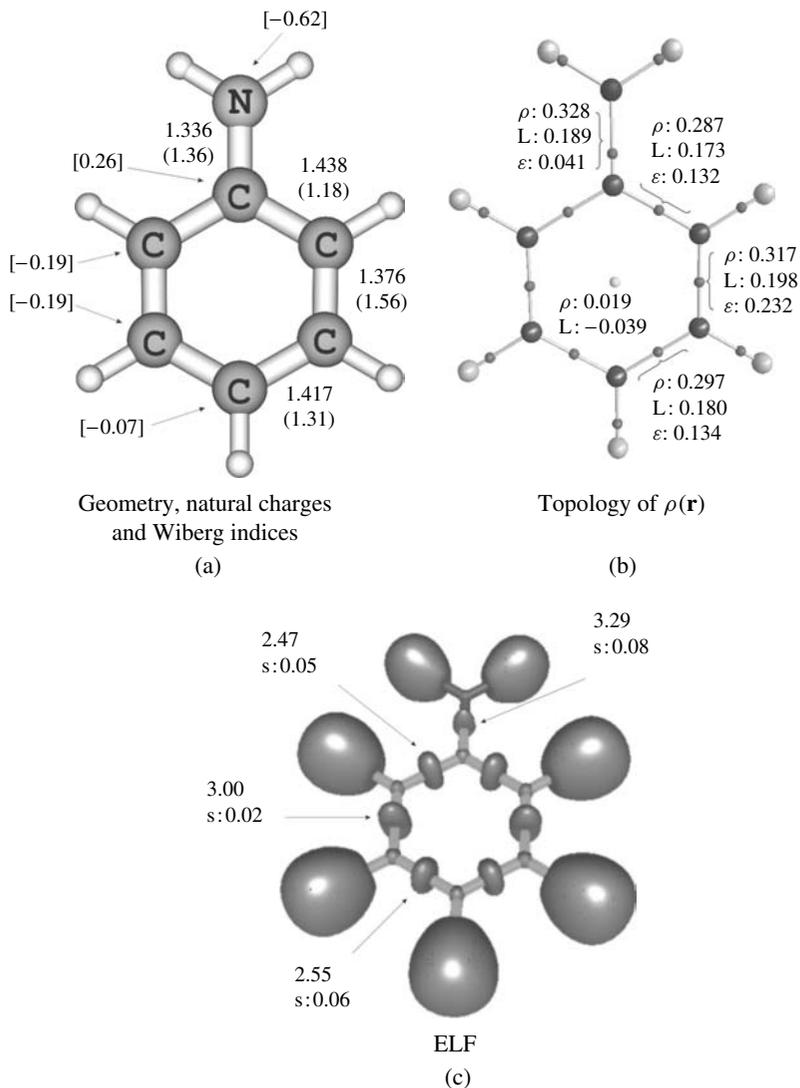
FIGURE 28 (PLATE 4). Summary of electronic distribution in aniline radical cation: (a) Bond distances (Å), NBO charges [bracket, in au] and Wiberg indices (parentheses, in au). (b) Topology of the electron density determined from AIM: $\rho(\mathbf{r})$ = electron density, L = Laplacian of the density defined as $L(\mathbf{r}) = -\nabla^2\rho(\mathbf{r})$ and ε = ellipticity of the bond critical point. (c) Isosurfaces of the electron localization function, ELF = 0.87; the values $\mathbf{s}$ are the populations of the valence basins

Two-photon ionization spectra of ANI measured in several hydrocarbon solvents revealed two thresholds, one at 6.4–6.6 eV and the other at 5.6–6.1 eV. The former was assigned to a direct ANI ionization, whereas the latter was assigned to an unidentified ion-pair formation process between aniline and solvent molecules.
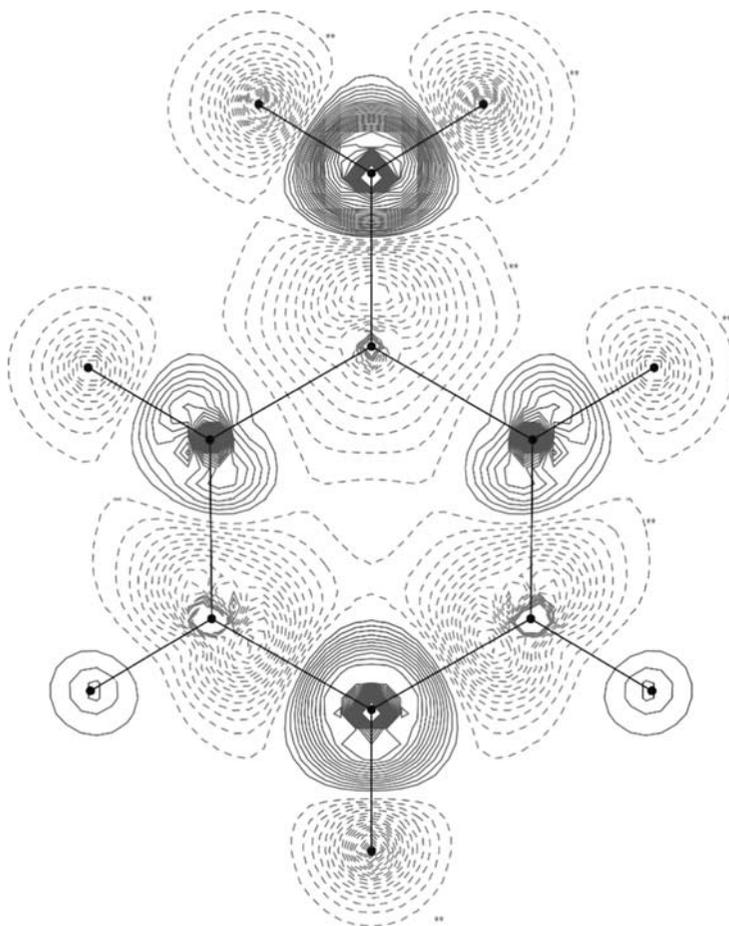
FIGURE 29. Electron spin density of the aniline radical cation in the molecular plane (UB3LYP/6-311++G(d,p))

Table 11 lists the fundamental frequencies of ANI$^{\bullet+}$ and Figure 30 illustrates the main motions of the corresponding normal modes. With respect to the ANI frequencies, the most important changes in the IR and Raman spectra are shown in Figures 31 and 32. The Raman spectrum of the radical cation is characterized by significant changes in the relative intensity pattern of the corresponding bands as compared with the neutral spectrum, particularly in the frequency range of 0—2000 cm^{-1}.

2. Isomers of aniline radical cation

Fourier Transform Ion Cyclotron Resonance (FT-ICR) experiments convincingly demonstrated the formation of dehydroanilinium ion, a distonic isomer of conventional

TABLE 11. Fundamental vibrational frequencies (cm^{-1}) and associated potential energy distributions of the aniline radical cation in its lowest-lying doublet state. Calculated values were obtained from scaled UB3LYP/6-311++G(3df,2p) harmonic frequencies

No	Freq.	Sym.	Int.	Assignment, PED ($\% \geqslant 10\%$) [a]
Q1	185	$B1$	6.7	$\delta_{2rg}(63.) + \delta_{1rg}(13.)$
Q2	367	$A2$	0.0	$\delta_{3rg}(80.)$
Q3	389	$B2$	2.6	$\beta H_8 H_{14}(76.) + \delta_{3rg}(12.)$
Q4	450	$B1$	9.4	$\delta_{1rg}(34.) - \delta_{2rg}(31.) - \gamma C_1 N_7(22.)$
Q5	532	$A1$	1.0	$\beta_{2rg}(84.)$
Q6	573	$A2$	0.0	$\delta_{4rg}(86.)$
Q7	593	$B2$	0.5	$\beta_{3rg}(74.)$
Q8	629	$B1$	156.2	$\delta_{1rg}(40.) + \gamma H_8 H_{14}(27.) + \gamma C_5 H(11.) + \gamma C_3 H(11.)$
Q9	638	$B1$	22.7	$\gamma H_8 H_{14}(42.) - \gamma C_1 N_7(17.) - \delta_{1rg}(16.)$
Q10	793	$B1$	53.2	$\delta_{1rg}(29.) - \gamma C_4 H(21.) + \gamma C_1 N_7(18.) - \gamma C_6 H(12.) - \gamma C_2 H(12.)$
Q11	815	$A2$	0.0	$\gamma C_2 H(34.) - \gamma C_6 H(34.) + \gamma C_3 H(13.) - \gamma C_5 H(13.)$
Q12	819	$A1$	0.2	$\nu C_1 C_6(23.) + \nu C_1 C_2(23.) - \beta_{1rg}(23.) + \gamma C_1 N_7(11.) + \beta_{2rg}(11.)$
Q13	942	$B1$	5.1	$\gamma C_4 H(38.) - \gamma C_6 H(26.) - \gamma C_2 H_9(26.)$
Q14	970	$A1$	0.0	$\beta_{1rg}(70.) + \nu C_1 C_2(11.) + \nu C_1 C_6(11.)$
Q15	1007	$A2$	0.0	$\gamma C_3 H(33.) - \gamma C_5 H(33.) - \gamma C_2 H(14.) + \gamma C_6 H(14.)$
Q16	1008	$A1$	8.8	$\nu C_3 C_4(37.) + \nu C_4 C_5(37.)$
Q17	1012	$B1$	0.8	$\gamma C_5 H(29.) + \gamma C_3 H(29.) - \gamma C_4 H(19.) + \delta_{1rg}(11.)$
Q18	1027	$B2$	0.0	$\beta_{2[NH2]}(58.) + \nu C_1 C_6(14.) - \nu C_1 C_2(14.)$
Q19	1132	$B2$	10.5	$\beta C_4 H(20.) - \nu C_4 C_5(16.) + \nu C_3 C_4(16.) - \beta C_2 H(12.) - \beta C_6 H(12.)$
Q20	1188	$B2$	0.3	$\beta C_5 H(20.) + \beta C_3 H(20.) - \beta C_4 H(18.)$
Q21	1211	$A1$	0.1	$\beta C_2 H(22.) - \beta C_6 H(22.) - \beta C_3 H(16.) + \beta C_5 H(16.)$
Q22	1372	$B2$	2.2	$\beta C_4 H(24.) + \beta C_2 H(19.) + \beta C_6 H(19.)$
Q23	1382	$B2$	9.2	$\nu C_3 C_4(13.) - \nu C_4 C_5(13.) + \nu C_1 C_2(12.) - \nu C_1 C_6(12.) + \nu C_5 C_6(11.) - \nu C_2 C_3(11.)$
Q24	1397	$A1$	0.7	$\nu C_1 N_7(44.)$
Q25	1472	$B2$	5.1	$\nu C_1 C_6(15.) - \nu C_1 C_2(15.) + \beta C_5 H(14.) + \beta C_3 H(14.)$
Q26	1516	$A1$	77.7	$\nu C_1 N_7(23.) + \beta C_3 H(14.) - \beta C_5 H(14.)$
Q27	1549	$B2$	12.7	$\beta C_4 H(27.) + \nu C_5 C_6(14.) - \nu C_2 C_3(14.)$
Q28	1629	$A1$	23.8	$\nu C_2 C_3(24.) + \nu C_5 C_6(24.)$
Q29	1676	$A1$	110.8	$\beta_{[NH2]}(82.) + \nu C_1 N_7(15.)$
Q30	3182	$A1$	0.1	$\nu C_2 H(38.) + \nu C_6 H(38.)$
Q31	3183	$B2$	1.5	$\nu C_6 H(45.) - \nu C_2 H(45.)$
Q32	3194	$A1$	0.0	$\nu C_4 H(62.) - \nu C_3 H(10.) - \nu C_5 H(10.)$
Q33	3204	$B2$	3.7	$\nu C_3 H_{10}(45.) - \nu C_5 C_{12}(45.)$
Q34	3209	$A1$	2.4	$\nu C_4 H(32.) + \nu C_5 H(31.) + \nu C_3 H(31.)$
Q35	3537	$A1$	253.2	$\nu N_7 H(50.) + \nu N_7 H(50.)$
Q36	3648	$B2$	92.2	$\nu N_7 H(50.) - \nu N_7 H(50.)$

[a] ν: stretching, β: bending, γ out of plane, β_{1rg}, β_{2rg}, β_{3rg}: bending of six-membered ring, δ_{1rg}, δ_{2rg}, δ_{3rg}, δ_{4rg}: deformation of six-membered ring, $\tau_{[NH2]}$: torsion of NH_2, $\beta_{1[NH2]}$, $\beta_{2[NH2]}$: bending of NH_2.
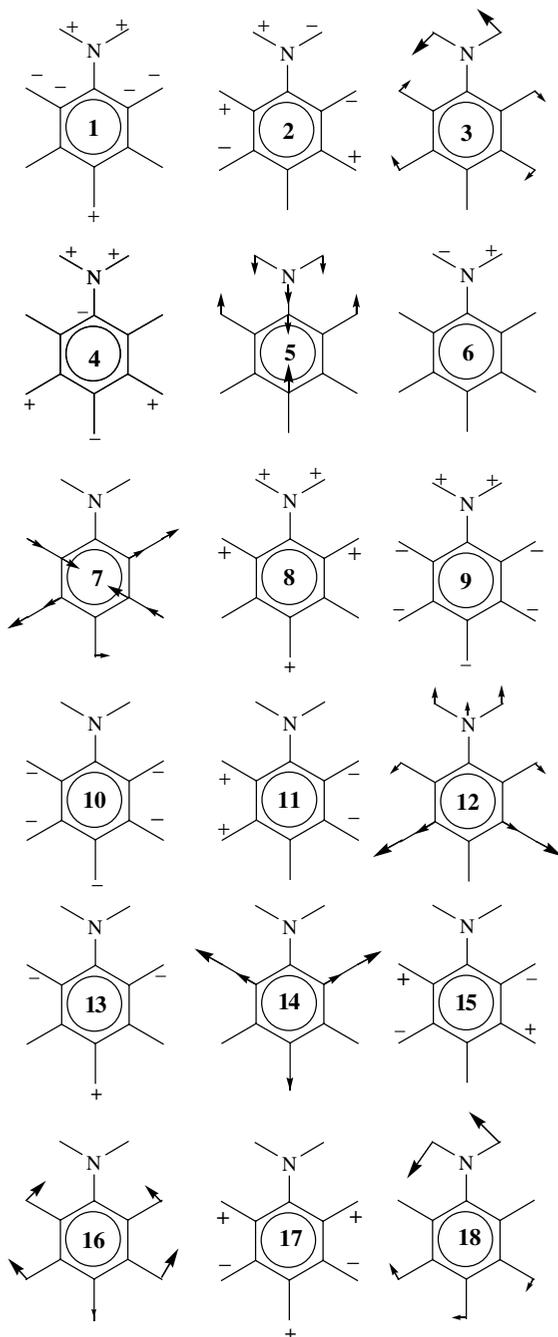
FIGURE 30. Normal displacements of vibrational modes of aniline radical cation ($^2B_1$). The assignment of the normal vibrations and associated frequencies are presented in Table 12. The numbers given within the ring correspond to the normal modes numbered from Q1 to Q36 in Table 11
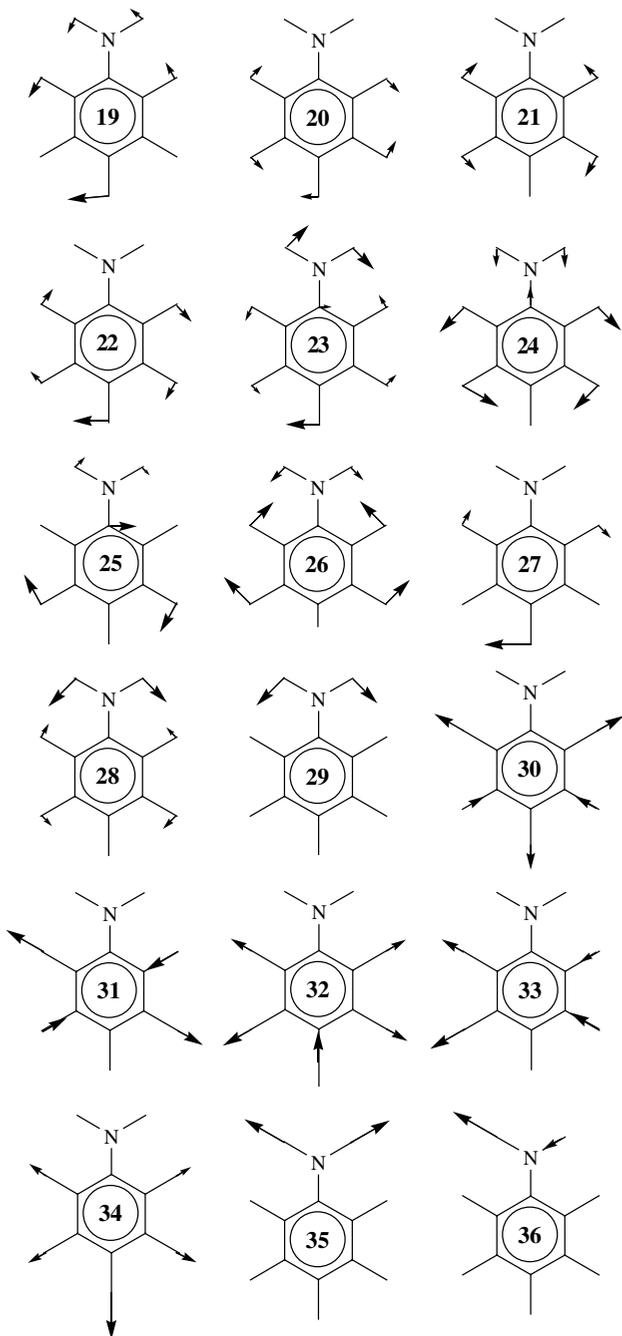
FIGURE 30. (*continued*)
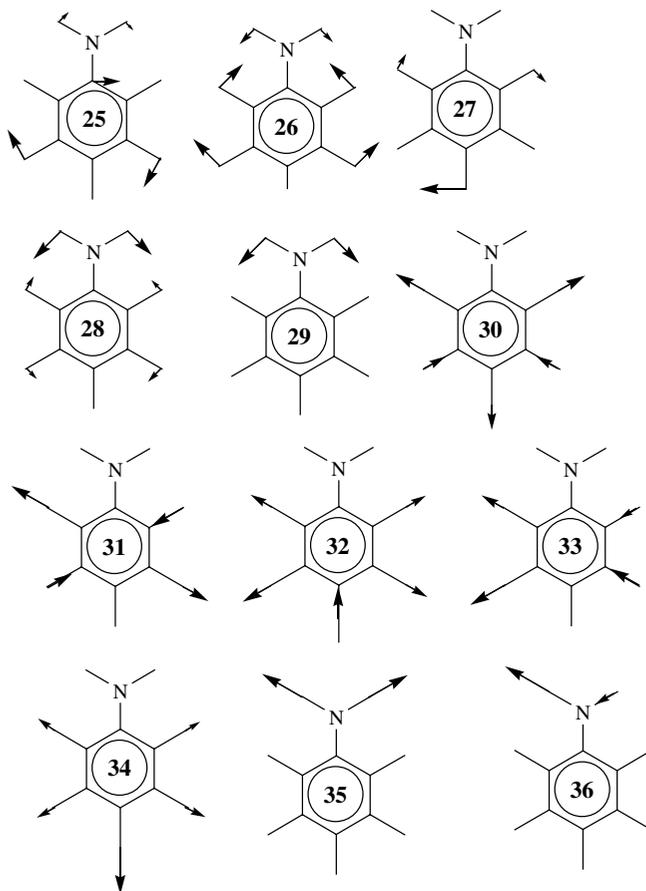
FIGURE 30. (*continued*)

ANI$^{\bullet +}$. Structure identification was based on ion−molecule reactions with dimethyl disulfide: the attachment of a methylthio radical, which usually characterized distonic cations, was detected[232].

The relative stabilities of a series of isomers of aniline radical cation were investigated theoretically[107] and the results are summarized in Figure 33. The distonic isomers **b**, **c** and **d** are 185, 185 and 182 kJ mol^{-1} less stable than the conventional aniline radical cation **a** (= ANI$^{\bullet +}$). The energy of transition structure converting the radical cation **d** into **a** by a 1,3-hydrogen shift is relatively high, being 162 kJ mol^{-1} above **d**. Unimolecular interconversions between **b**, **c** and **d** via 1,2-hydrogen shifts within the ring require higher activation energies. Energy barriers for the **b** → **c** and **c** → **d** isomerizations amount to 266 and 252 kJ mol^{-1}, respectively. There is no dramatic change in the structure of the distonic isomers **b**, **c** and **d**; the C−N bond length increases from 1.32 Å in the conventional ion **a** to 1.49 Å in the distonic structures. A NH$_3$ loss should easily be involved in the dissociation of the distonic ions.
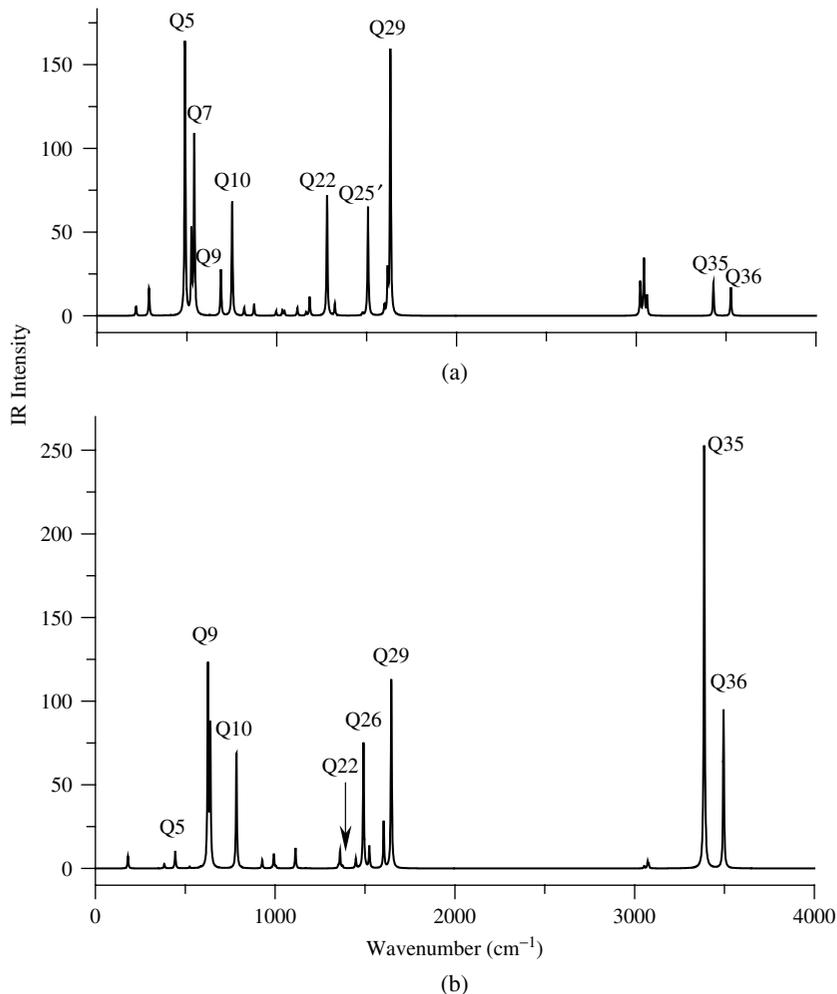
FIGURE 31. Changes of infrared spectrum in going from (a) neutral ANI to (b) radical cation ANI$^{\bullet+}$, calculated at the (U)B3LYP/6-311++G(3df,2p) level of theory

Other isomeric structures of aniline ion, such as ions **e(1−3)**, **f(1−3)** and **g(1−3)** (see Figure 33), have also been considered. The relative energies of these ions are likely to be dependent on the position of the sp^3-carbon within the ring. The largest relative energies (228−275 kJ mol^{-1}) correspond to the isomers **f1, f2** and **f3**, while the smallest ones involve **g2** and **g3** (173−177 kJ mol^{-1}) structures.

In *N*-protonated 4-haloanilines, the C−X bond energies rapidly decrease in going from X = F to X = I. With a bonding energy of just around 224 kJ mol^{-1}, cleavage of a C−I bond in *N*-protonated iodoanilines readily takes place upon collisional activation giving the distonic isomers **b**, **c** or **d**.
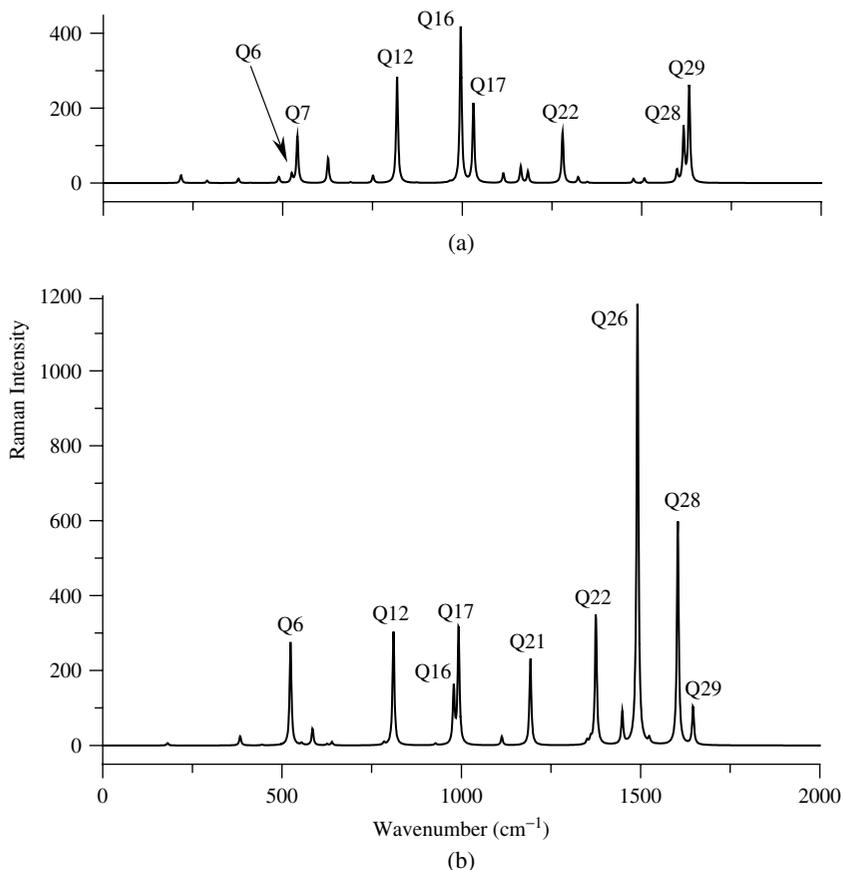
FIGURE 32. Changes of the Raman spectrum in going from (a) neutral ANI to (b) radical cation ANI$^{\bullet+}$, in the range of frequencies 0–2000 cm^{-1}, calculated using the UB3LYP/6-311++G(3df,2p) method

3. MS experiments showing formation of distonic radical cation

Protonated 4-iodoaniline (m/z 220) was readily generated upon chemical ionization using methane as the reagent gas[98]. The collisional activation spectrum of **I-ANI-H$^+$** recorded with argon in the quadrupole collision cell and shown in Figure 34 features, beside the major loss of an iodine atom (m/z 93), structure-significant peaks at m/z 203 for the loss of ammonia and m/z 76 for consecutive eliminations of NH$_3$ and I$^{\bullet}$. It is noteworthy that the extremely efficient iodine loss is also a prominent reaction in the high-energy CA spectrum of the **I-ANI-H$^+$** ions (Figure 34b).

Following isolation of the m/z 220 ions by using the first three sectors and deceleration from 8 keV to some 20–30 eV, collisional deiodination was performed in the Qcell and the product ions reaccelerated up to 8 keV. Mass-selected m/z 93 products were there-after collisionally activated with nitrogen collision gas and the resulting CA spectrum is
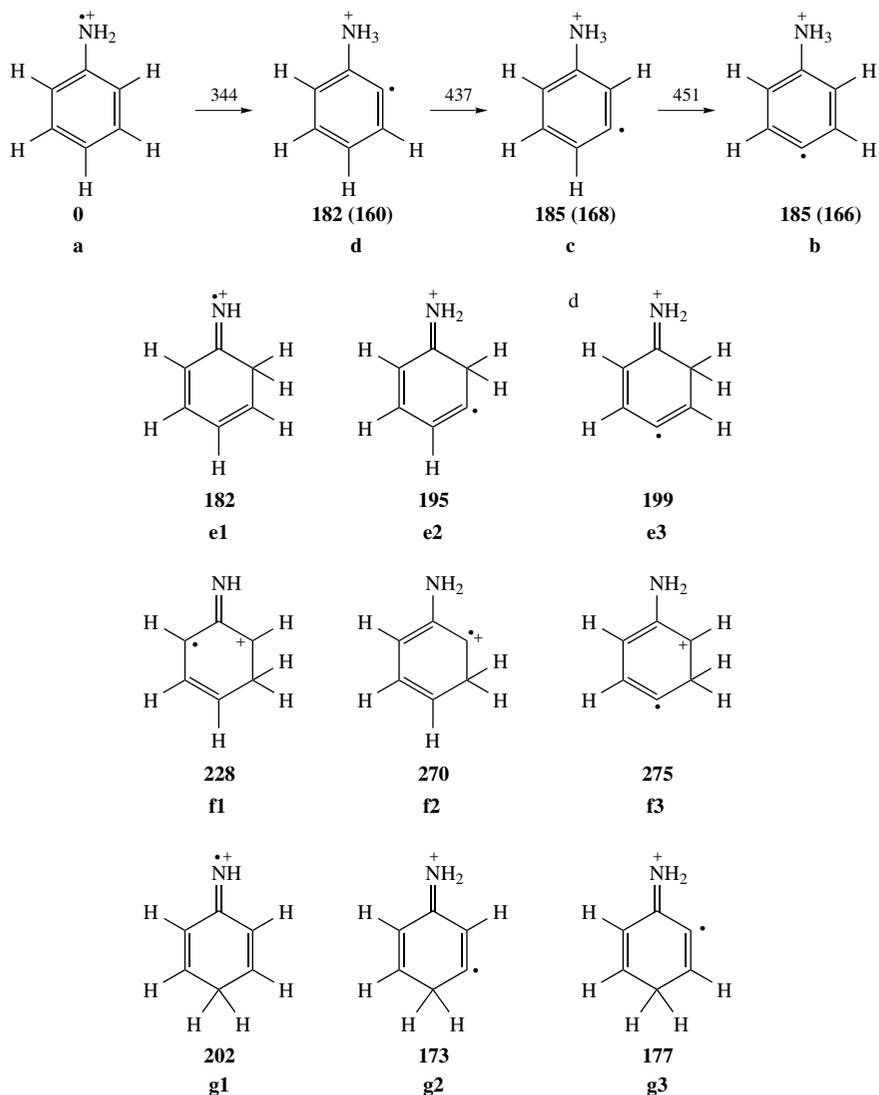
FIGURE 33. Relative energies in kJ mol^{-1} of some isomers of the radical cation ANI$^{\bullet+}$ calculated at the UB3LYP/6-311++G(d,p) + ZPE level. Values in parentheses were derived from UCCSD(T) calculations. The positions of radical and charge sites are given arbitrarily

compared in Figure 35 to the spectrum of 'conventional' aniline molecular ions ANI$^{\bullet+}$ (ions **a**).

Although both spectra were found to be similar, some structurally significant differences can readily be noted: (a) a different distribution of the peak intensities in the m/z 73–78 region, m/z 76 (loss of NH$_3$) being favored for ions **b** and m/z 77 (loss of NH$_2$) for
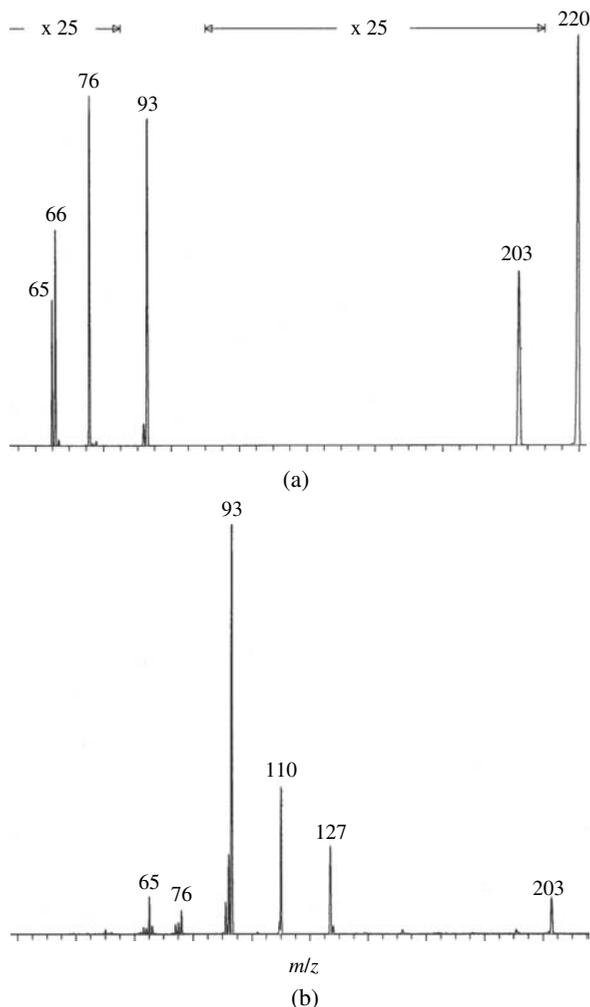
FIGURE 34. Collisional activation spectra of protonated 4-iodoaniline **I-ANI-H**$^+$ in (a) a low kinetic energy regime (Ar, *ca* 20–30 eV) and (b) a high kinetic energy regime (oxygen, 8 keV)

ions **a** and an intensification of the peak at m/z 50 (consecutive loss of ethyne from m/z 76 ions) for ions **b**. These differences are interpreted as resulting from the production, at least partly, of a nonclassical dehydroanilinium structure **b** in the dehalogenation process of protonated 4-iodoaniline **I-ANI-H**$^+$.

Similar results were obtained with protonated 3-iodoaniline **3** and 2-iodoaniline **4** (Scheme 5). Deiodination is again the most intense process upon collisional activation with argon in the Qcell. The CA spectra of the so-produced ions (m/z 93) (Figure 36) are similar but not superimposable on the spectrum of the distonic ions **b**, suggesting that isomeric species such as **c** and **d** are formed in the protonation–deiodination reaction sequence (Scheme 5). The most striking features of the CA spectra are again the increased
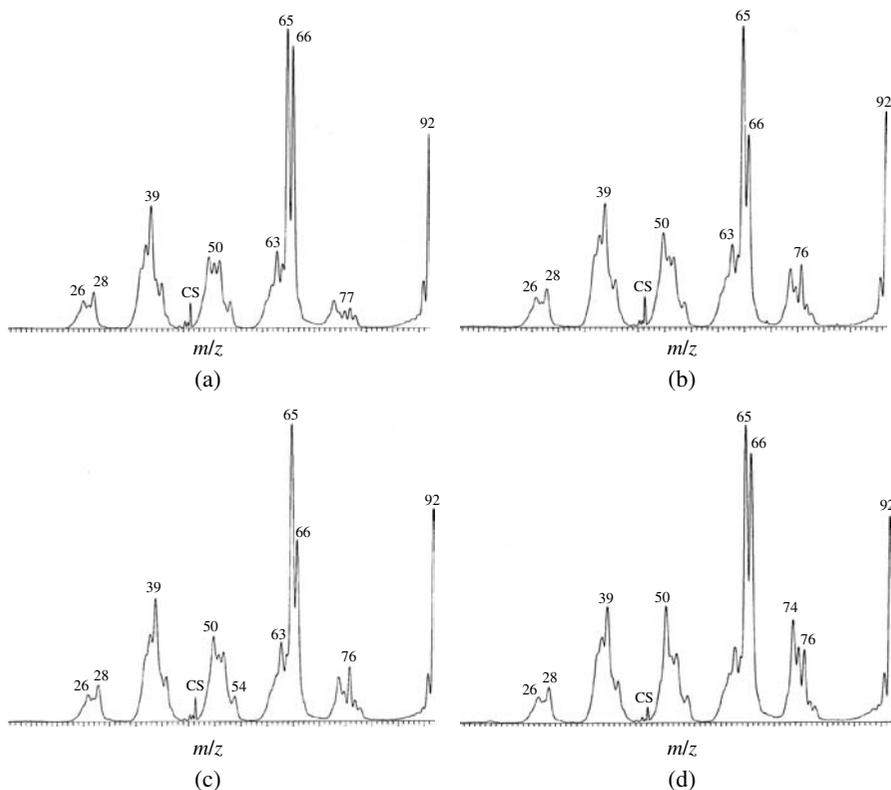
FIGURE 35. Collisional activation spectra (nitrogen collision gas) of the m/z 93 ions produced by electron ionization of aniline (a), and collisional deiodination of protonated 2-, 3- and 4-iodoaniline cations within the quadrupole collision cell (argon collision gas, Figures b–d). CS refers to charge stripping
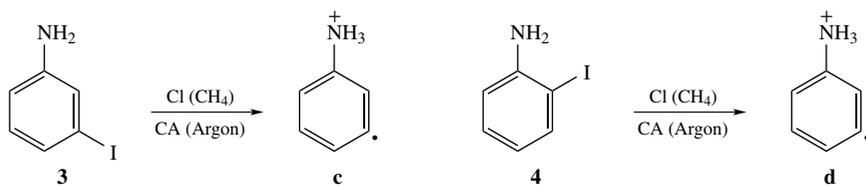
SCHEME 5

intensity of the peaks at m/z 76 and 50 and, albeit of very low intensity, a peak at m/z 17, not detected for aniline molecular ions **a**. The higher intensity of the peak at m/z 74 is also worthy of note.

Neutralization–reionization mass spectrometric (NRMS) experiments demonstrated that the *N*-protonation of aniline is dominant under fast atom bombardment (FAB) conditions. That was indicated by the presence of a very weak recovery signal at m/z 94 in the
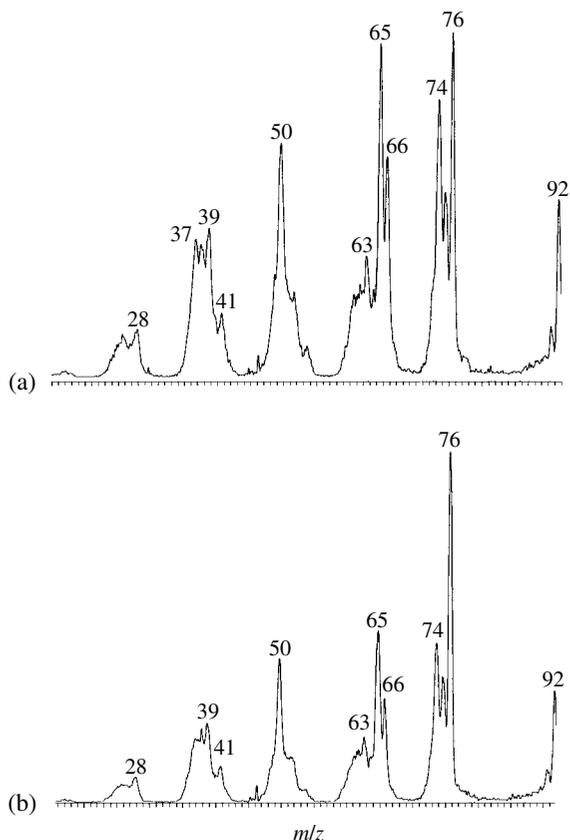
FIGURE 36. Collisional activation spectrum (nitrogen collision gas) of the m/z 93 ions produced by collisional deiodination of (a) protonated 4-iodoaniline and (b) protonated 3-iodoaniline, produced under LSIMS conditions

NR spectrum together with a significant peak at m/z 17 for reionized ammonia. The protonation–deiodination sequence to the 4-iodoaniline and 3-iodoaniline has been applied using the LSIMS ion source. The high-energy CA spectra (Figure 36) of the protonated *para*-iodoaniline (**4-I-ANI-H$^+$**) and *meta*-iodoaniline (**3-I-ANI-H$^+$**) forms obtained in these conditions are indeed completely different from the spectra shown in Figure 35, and feature very intense peaks at m/z 76, 74 and 50. These peaks, associated with the dehydroanilinium structure **b–d** in the CI experiments, are expected for such a distonic ion structure.

In summary, tandem mass spectrometric methodologies demonstrated that the distonic isomers of ionized aniline are stable species in the gas phase and can be generated by a protonation–deiodination sequence on iodoanilines, thanks to the rather weak C−I bonds. Quantum chemical calculations also indicated that, although the distonic isomers are about 160–180 kJ mol^{-1} less stable than ionized aniline, they are protected against unimolecular hydrogen shifts by large energy barriers and are therefore stable under gas-phase conditions.

148
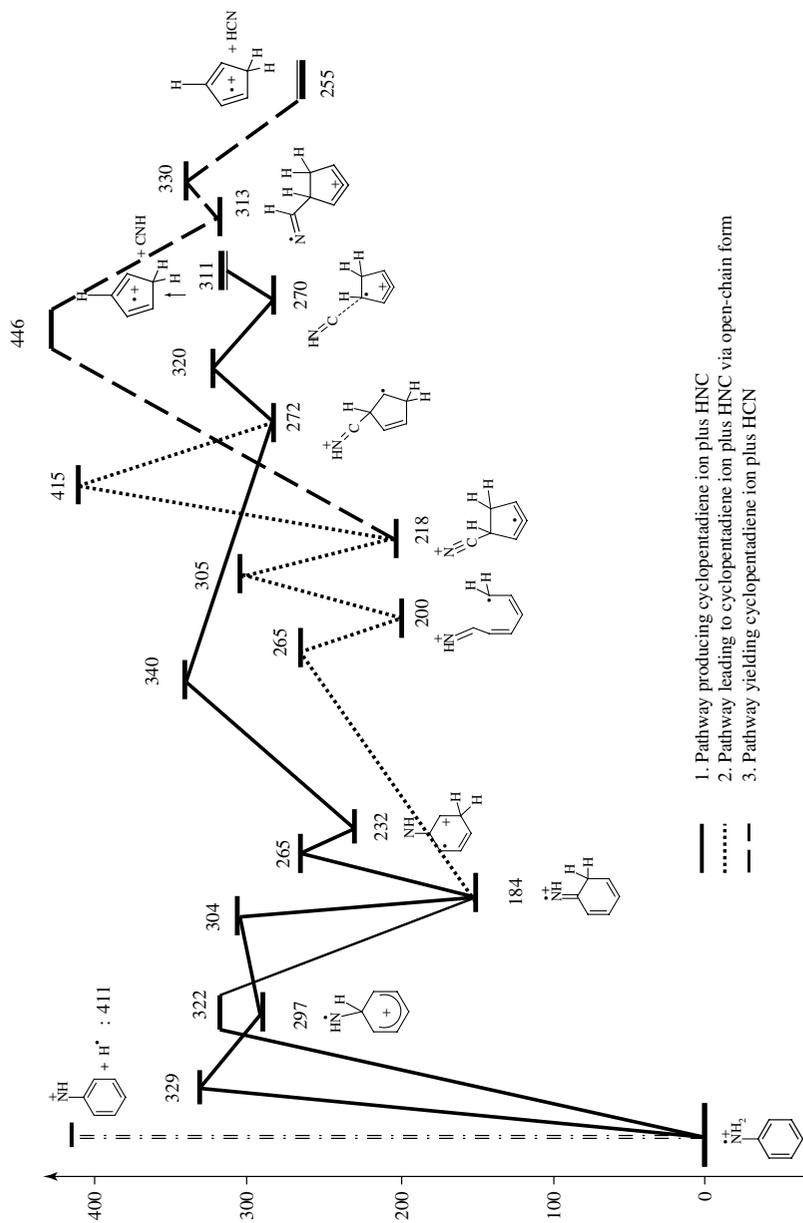
FIGURE 37. Schematic potential energy profiles illustrating the decomposition of aniline radical cation. Relative energies in kJ mol⁻¹ were obtained from UB3LYP/6-311++G(d,p) + ZPE calculations

4. Decomposition of aniline radical cation: HNC versus HCN elimination

The dissociation limit for decomposition of aniline radical cation was first determined from a PEPICO experiment[227]. The main products generated within the microsecond time frame were suggested to be a $C_5H_6^{\bullet+}$ radical cation plus a (HCN) neutral molecule, both formed via a loose transition structure. Energetic considerations established that the cation should have a cyclic rather than an open-chain structure. However, the identity of the (HCN) molecule was not established. Subsequent mass spectrometric experiments[228–235] provided information on the identity of the neutral molecule. Hydrogen isocyanide HNC, not hydrogen cyanide HCN, was eliminated in the fragmentation of the aniline cation[228]. The identification in emission of NH and CN from products constituted the main proof. Metastable aniline ions were accelerated to several kilovolts. When they dissociate in the drift region of the mass spectrometer, both the ionic and neutral fragments are travelling with high velocities. After deflection of the ions, the neutral fragments are collided with He, and they are reionized and fragmented further. No CH^+ peak was observed in the resulting mass spectrum, clearly indicating a HNC formation[229].

A portion of the calculated potential energy surface related to the decomposition of ANI$^{\bullet+}$ is illustrated in Figure 37. Another reaction pathway leading to the formation of pyrrole radical cation + acetylene as products is not shown. Results recorded in Figure 37 basically indicate two distinct reaction pathways, one giving rise to HCN and the other connecting to HNC formation. In both channels, a five-membered cyclic cation is the key intermediate. It is clear that the HNC formation pathway 1, with the rate-determining step at 340 kJ mol^{-1}, is energetically less demanding than the HCN production via pathway 3, which characterized by the highest energy point at 446 kJ mol^{-1}. Figure 38 summarizes the proposed molecular mechanism describing the HNC elimination[235].
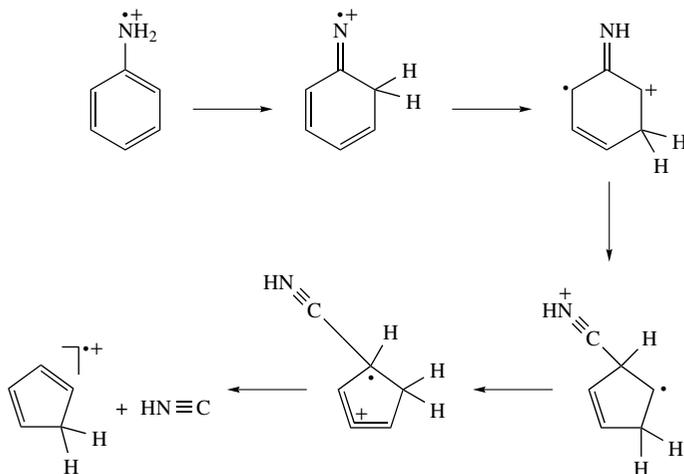
FIGURE 38. The mechanism proposed for the decomposition of aniline radical cation leading to a HNC formation

IV. SOME SPECIAL FEATURES

A. Polyaniline

In 1862, Letheby[236] reported the electrochemical oxidation product of aniline and its color changes upon pH changes. Indeed, in acidic aqueous solution, ANI undergoes oxidative polymerization producing polyaniline (PANI)[237]. More than one century later, in 1968, PANI has been shown to have, among other polymeric properties, a high electrical conductivity and that its electronic character also depends on the acidity, redox level and hydration[238]. A PANI–PANI secondary battery system has been built on the basis of the reversible electrochemical doping and undoping (oxidation and reduction) processes of PANI in acidic media[238]. As a member of the π-conjugated polymers, PANI could be implemented in electronic conductors, light-emitting diodes and chemical sensors[239, 240]. When exploited as active sensing element, the coupling of ligands to its backbone results in physical distortions, or changes in electronic structure, and thereby modifies conductivity.

Nowadays, PANI still receives considerable attention owing to its proton coupled redox chemistry and its resulting pH-dependent properties[237]. As such, it has been used as a pH electrode[241], and coupled to reactions that produce or consume protons to create sensors. In particular, as a dye, PANI also possesses electrochromic effects[237], changing color from pale yellow to green, blue-violet etc. and has been implemented in display devices[242]. It has been utilized in rechargeable lithium–PANI batteries[243]. Interesting electrical and optical properties, in conjunction with the low cost of fabrication and excellent environmental stability, make PANI potential materials in several modern technological applications.

PANI can be synthesized chemically giving a precipitate, or electrochemically in the form of thin films, from aqueous solution. The main problem of PANI is that it is poorly soluble in most common solvents, hampering experimental studies and limiting its industrial exploitation. A new form, o,p-PANI copolymer, has been prepared in attempts to introduce solubilizing and function-enhancing substituents on the conducting polymer backbone without concomitant loss of conductivity[244]. Halogen-capped aniline oligomers have been proposed that are away from the PANI paradigm by isosteric replacement of the amino group[245]. There has been recent interest in chiral PANI nanofibers for applications in chiral separations[246].

PANI is composed of ANI repeat units connected to form a backbone. The existence of a nitrogen atom lying between phenyl rings allows the formation of different oxidation states (doping) that can affect its physical properties. In general, three distinct forms are available, depending on the degree of oxidation of the nitrogens (Figure 39):

(a) A leucoemeraldine base (LB) is a fully reduced form which contains only benzene rings in the polymer chain.
(b) An emeraldine base (EB) is a half oxidized form, where both benzene and quinoidal rings are present.
(c) A pernigraniline (PNB) is a fully oxidized form.

The conducting emeraldine salt (ES) form can be obtained by oxidative doping of LB or by protonation of EB (Figure 40).

The LB forms are basically insulators characterized by large band gaps and the lack of charge carrier, whereas the PNB forms are considered to be semiconducting. The $\pi^* \leftarrow \pi$ maximum absorption band in the LB form is about 3.6–3.8 eV, which is smaller than that of ANI (4.2 eV, see above), but remains large due to an inhibited connection between the ring and the saturated nitrogen linkage[247]. Thanks to a better conjugation between the ring and imine linkage, the $\pi^* \leftarrow \pi$ maximum absorption of the PNB form becomes lower, being 1.7–2.3 eV[248]. In the doped ES form, electrical conductivity is greatly increased by the formation of low-energy hole levels[249]. The low band gap of 1.5 eV in ES is interpreted as arising from excitations to the polaron band[250].
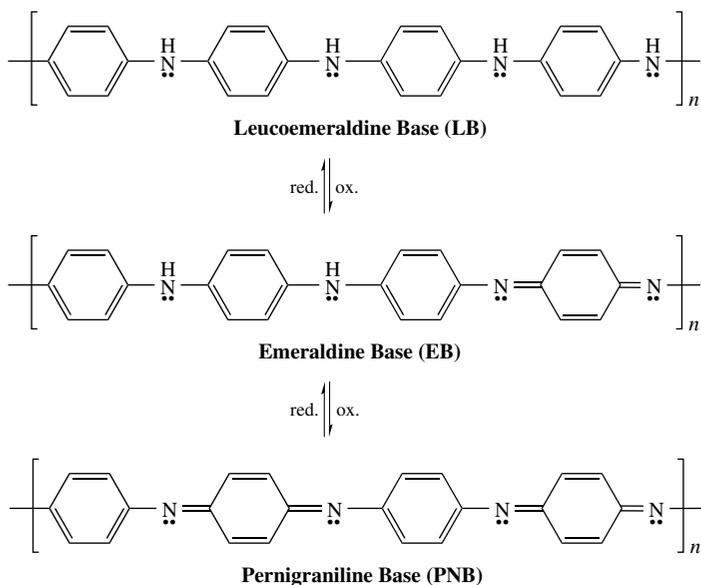
FIGURE 39. Different forms of polyaniline
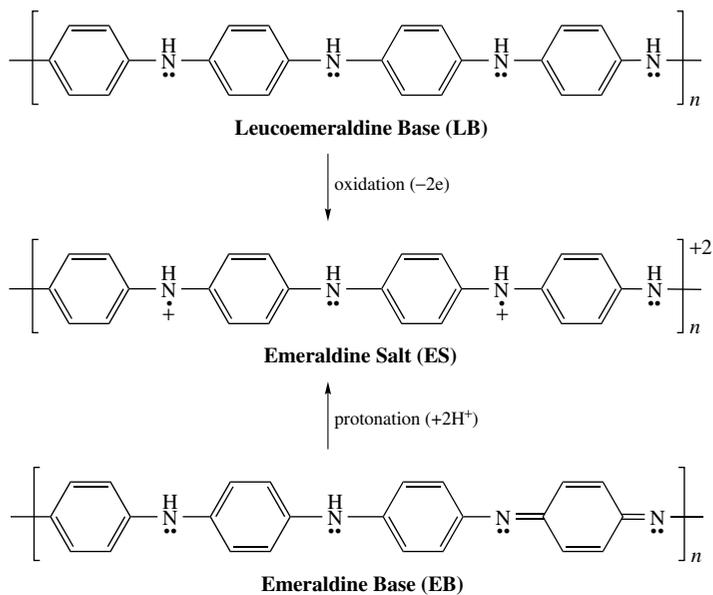
FIGURE 40. Formation of a polyaniline salt following oxidation and protonation of bases

The N_{1s} core-level spectra of both amine LB and imine PNB forms show a difference in electronic structure[251, 252]. While the core ionization of an imine nitrogen results in a high probability for the ionized system to be in an excited state (strong shake-up), the core hole on an amine nitrogen results in very weak coupling to excited states. The difference arises from the shape of the lowest-lying orbital (LUMO), which is mainly localized on the imine nitrogen and on neighboring quinoidal phenyl rings. This results in a strong relaxation of this orbital following creation of a core hole on the imine site, and thereby a substantial coupling between the states of the ionized system. In the amine form, the LUMO has nodes between nitrogen and does not respond to the creation of a core hole on the amine nitrogen.

To theoretically evaluate the band gaps in PANI, geometries and band gaps in small oligomers have been calculated using various levels of theory[253–256]. Excitation energies of the oligomers up to decamer were computed and extrapolated to the band gap value of the infinite chain. The latter were also approximated from the frontier energy HOMO–LUMO gaps of the oligomers. The experimental values mentioned above can be reproduced by these approaches. In particular, DFT methods reproduced well the transitions at 4 eV of LBs and the Peierls gap transition of PNB. The valence band structure and the energy separation of 1.2 eV of nitrogen core levels of LB were also correctly predicted. Helical structures are favored for LB oligomers larger than heptamer, whereas linear structures are preferred for all PNB and ES oligomers. The band gap is smaller in the coplanar form than in the coperpendicular form thanks to greater conjugation between phenyl rings, and it is also lowered by favorable interchain interactions.

The effects of substituents on the band gaps were also investigated[256]. When an electron-acceptor group is attached to the LB benzenoid ring, strong effects over its electronic properties occur. The methoxy and nitro groups induce an interaction between the oxygen of the substituent and the nitrogen of the oligomer through a hydrogen bond. The latter largely modifies the oligomer structure due to strong H–O electrostatic attraction. The cyano and nitro groups (σ-π acceptor) result in an increase of ionization energies. In general, electron-acceptor groups tend to lower the energy of the LUMO more than that of the HOMO, and thus reduce the energy gap. Overall, oligoanilines bearing strong electron-withdrawing groups (such as nitro groups) possess the lowest band gaps and constitute the more promising semiconducting materials.

Protonation of PANI results in a delocalization of protonic charge over a few aromatic rings and tends to stabilize the polaronic hole state[257]. Electron transfer in the oligomer radical cations and interaction between the latter with a water molecule were examined[258]. The charge transfer appears to be dependent on the rotation and position of the water molecule. Hyperpolarizabilities β and γ and magnetic susceptibility of ANI oligomers were also calculated using theoretical methods[259, 260]. *Meta–para* ANI oligomers could be considered to generate high-spin polymers. The corresponding radical cations generated following ionization are in a high-spin state and could be used as building blocks for polaronic ferromagnets[261].

B. Hydrogen Bonding

ANI contains two distinct chromophores, a phenyl ring and an amino group, and is therefore able to form different types of weakly bound aggregates with small molecules at different sites. The van der Waals complexes of ANI with a single, or a cluster of, rare gas atom (Ne, Ar) have attracted much attention[262]. The small binding energies and the usually large amplitude anharmonic motions make the coupling between intramolecular and intermolecular vibrational states possible. These can conveniently be used in the study of the dynamics of photochemical and photophysical processes such as vibrational

predissociation and intramolecular vibrational redistribution (IVR). Extremely sensitive and accurate laser spectroscopy tools, such as the laser induced fluorescence (LIF), resonance enhanced multiphoton ionization (one-color, two-color two-photon, REMPI) mass spectrometry, electron impact (EI) mass spectrometry or zero kinetic energy (ZEKE) photoelectron spectroscopy, usually combined with infrared (IR) spectroscopy, have been developed to observe the cluster properties in a molecular beam[263]. Overall, basic information including the equilibrium structure, intramolecular vibrational frequencies, binding, excitation and ionization energies can be determined for the neutral form in the lower-lying electronic (S_0 and S_1) and ionized states.

Weak complexes of ANI with water molecules were investigated using various IR experiments[264–267]. Infrared depletion spectroscopy induced by the IR multiphoton decomposition (IRMPD) processes allowed the difference between the structure of the neutral and ionized complexes to be differentiated.

The rotational spectra of the ANI–H_2O complex and its ^{18}O isotopomer were recorded in the microwave region and their rotational constants were determined[268]. No indications for large amplitude motions, such as tunneling splittings, were found. Two possible complexes could be formed when ANI interacts with water. While in the first complex ANI is involved as a hydrogen acceptor by the amino group (water as hydrogen donor), it behaves in the second complex as a hydrogen donor yielding a N−H−O hydrogen bond (water as hydrogen acceptor).

According to *ab initio* quantum chemical calculations whose results are summarized in Figure 41, the first possibility actually corresponds to the most stable aniline–water complex, in either the neutral or the ionized form. It is similar to the geometry of the H_3N−HOH complex. Only one equilibrium structure of each complex has been located following geometry optimization. In addition, the identity of the observed complex is confirmed by the good agreement between experimental[268] and calculated rotational constants. The intermolecular distance $r(N−O)$ and the bond angle $\alpha(CNO)$ of the neutral complex are somewhat overestimated by calculations. The hydrogen bond formation energy was evaluated as $\Delta E_{HB}(ANI–H_2O) = −21$ kJ mol^{-1}.

Upon ionization, the second type of complex in which ANI plays the role of hydrogen donor, becomes more stable and in fact the only complex found (Figure 42). Due to the difference between the ionization energies of water and ANI, the complex is formed from interaction of neutral water with ionized aniline. The resulting complexation energy amounts to $\Delta E_{HB}(ANI–H_2O^+) = −72$ kJ mol^{-1}, which represents a substantial stabilization of about 50 kJ mol^{-1}, with respect to the neutral complex formation.

A few fundamental vibrations of the complex radical cation have been detected and assigned[264, 266, 267]. These include the frequencies at 3715 cm^{-1} (OH antisymmetrical stretch), 3630 cm^{-1} (OH symmetrical stretch) and 3440 cm^{-1} (NH stretch)[264]. The NH stretch involved in the H-bond vibrates at a lower frequency of 3105 cm^{-1} [266], which corresponds to a significant red shift due to a N−H−O type of hydrogen bond. A relationship can be established between the red shifts of the NH antisymmetrical stretching vibration of aniline−X$^+$ complexes and the PAs of the partner X molecule[264]. The geometry of the ANI−$H_2O^{\bullet+}$ complex can be understood in considering the difference in PAs of water (697 kJ mol^{-1}) and aniline radical (950 kJ mol^{-1}). In view of such a large magnitude of the difference, the proton is tightly attracted by the N-radical.

The complex formation between ANI and ammonia clusters has been investigated by using mass resolved excitation spectroscopy (MRES), hole burning spectroscopy (HB)[268] and IR spectroscopy coupled to different ionization spectroscopies[269–271]. Rotational spectra of these complexes are not reported yet. Some *ab initio* calculations on both neutral and ionized complexes are available[269, 272–274]. In this case, the most stable form of the neutral ANI–NH_3 complex is a consequence of a hydrogen bond between a NH bond of aniline
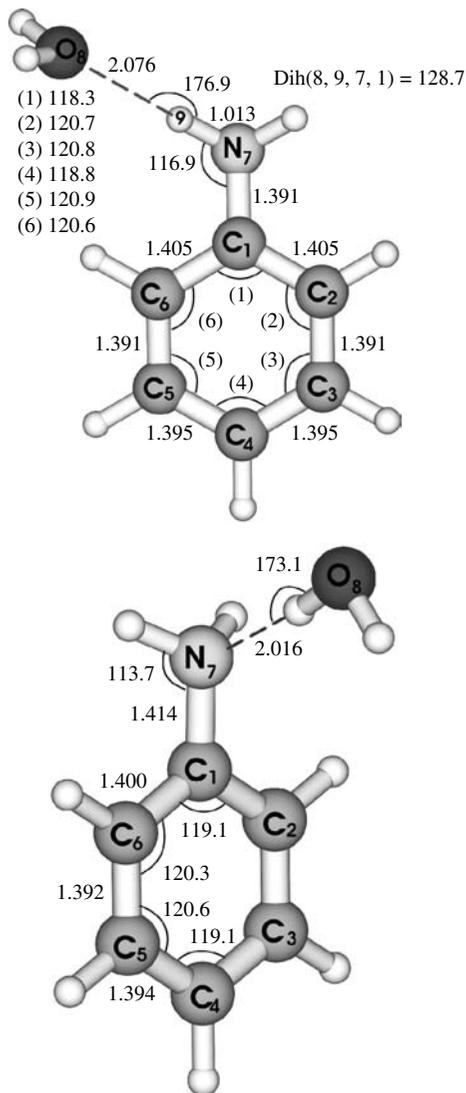
FIGURE 41. Selected geometrical parameters of two aniline–water complexes: *upper*: aniline as hydrogen bond donor; *lower:* aniline as hydrogen bond acceptor. Bond lengths given in angstroms and bond angles in degrees were determined from B3LYP/6-311++G(d,p) optimizations

and the nitrogen lone pair of ammonia (Figure 43). The corresponding hydrogen bond formation energy amounts to $\Delta E_{HB}(\text{ANI}-\text{H}_3\text{N}) = -19$ kJ mol^{-1}, which is of comparable magnitude with that of the neutral water complex mentioned above. Other complexes, resulting from interactions between the ring with NH bonds or between CH bonds with the ammonia nitrogen, are less stable having complexation energies of only 4–5 kJ mol^{-1}.
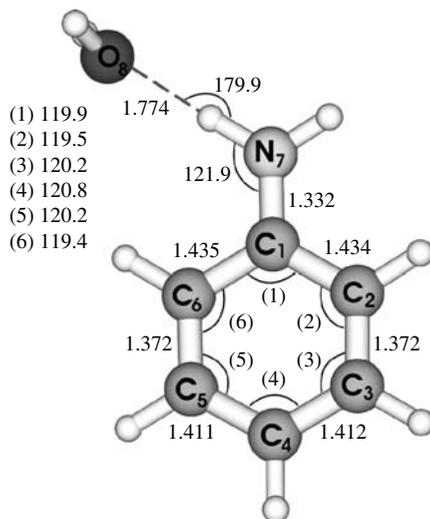
FIGURE 42. Selected geometrical parameters of the radical cation of the aniline−water complex. Bond lengths given in angstroms and bond angles in degrees were obtained from UB3LYP/6-311++ G(d,p) optimizations. Only one complex having aniline as hydrogen bond donor was located
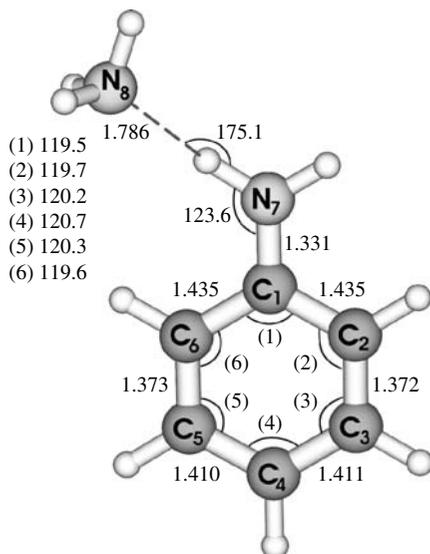
FIGURE 43. Selected geometrical parameters of the neutral and radical cation forms of the aniline−ammonia complex. Bond lengths given in angstroms and bond angles in degrees were obtained from UB3LYP/6-311++G(d,p) optimizations. The H16 atom is bonded to the ammonia nitrogen

Dih(16, 8, 9, 7) = 49.4
Dih(8, 9, 7, 1) = 154.6

(1) 118.1
(2) 120.8
(3) 120.8
(4) 118.7
(5) 120.9
(6) 120.7
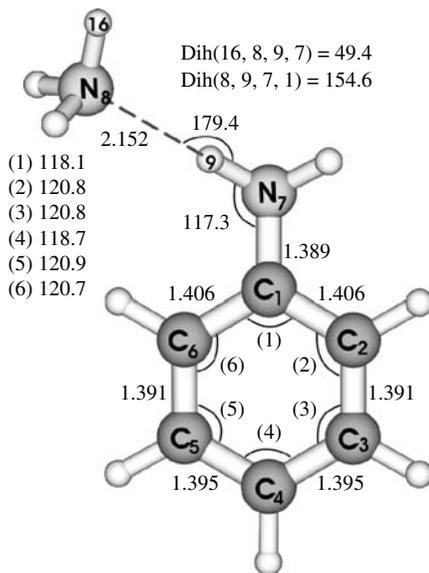
FIGURE 43. (*continued*)

For the ANI−H_3N complex, vibrational bands relevant to the NH stretching modes have been identified and assigned[270], including two strong bands at 3479 and 3354 cm^{-1}. Both correspond to the amino NH stretch, characterized by red frequency shifts of 29 and 68 cm^{-1} following complexation. Accordingly, the vibrational frequency centered at 3354 cm^{-1} is associated with the NH bond involved in the hydrogen bonding with ammonia.

Following ionization, the complex retains its shape in which ammonia acts as the hydrogen bond acceptor, and the main interaction is the hydrogen bond through the ANI−NH bond to the ammonia nitrogen lone pair (Figure 43). The intermolecular N−H distance is, however, compressed in going from 2.1 Å in the neutral form to 1.8 Å in the ionized counterpart.

While the frequencies of 3340 and 3425 cm^{-1} recorded for the ANI−$H_3N^{\bullet+}$ cation complex can be assigned to the free NH stretching modes of ammonia and ANI, respectively, the vibrational frequency at around 2600 cm^{-1} arises from the H-bonded NH bond of aniline. The frequency shift upon ionization is thus substantial. The interaction in the cluster cation is much stronger than that in the neutral cluster. Indeed, quantum chemical calculations provide a hydrogen bonding energy of $\Delta E_{HB}(ANI-H_3N^{\bullet+}) = -80$ kJ mol^{-1}, about four times as large as the energy gained from a neutral association.

In both water and ammonia complexes, the clusters formed by interaction with the ANI molecule become invariably stronger following ionization. Thus, the hydrogen bond pattern involving amine could be modified by controlling its charge.

It is worth noting that in the 1:1 complex of hydroxyaniline (or aminophenol) with a water molecule, the most stable cluster formed arises from an O−H−O interaction, in which water plays the role of hydrogen bond acceptor[275]. It is also remarkable that association of ANI with the CF_3H molecule yields a weak C−H−N complex, but it induces a blue-shift of the CH stretch frequency[276]. The latter is blue-shifted by 30 cm^{-1}, and the

relevant C−H bond distance is shortened by 0.003 Å. In fact, blue-shifted complexes are often detected when monomers interact with halomethane derivatives[277].

V. ACKNOWLEDGMENTS

VI. REFERENCES AND NOTES

1. Different key physicochemical properties of aniline and some of its simple derivatives can be found in (a) the NIST data collections, located at the URL http://webbook.nist.gov/chemistry. (b) S. G. Lias, J. E. Bartmess, J. E. F. Liebman, J. L. Holmes, R. D. Levin and W. G. Mallard, *J. Phys. Chem. Ref. Data*, **17**, Suppl. 1 (1998).
2. A. H. Fiske and E. H. Green, *Ind. Eng. Chem.*, **8**, 573 (1916).
3. C. E. Searle and O. J. Teale, 'Occupational Carcinogens', in *Handbook of Experimental Pharmacology, Carcinogenesis and Mutagenesis*, (Ed. C. S. Cooper), Vol. 94/I, Springer-Verlag, Heidelberg, 1990, pp. 103–151.
4. D. Hoffmann and S. S. Hecht, Advances in Tobacco Carcinogenesis, in *Handbook of Experimental Pharmacology, Carcinogenesis and Mutagenesis*, Springer-Verlag, Heidelberg, Germany, Vol. 94/I, pp. 63–102 (1990).
5. P. Vineis, *Cancer Epidemiol. Biomarkers Prev.*, **1**, 149 (1992).
6. *International Agency for Research on Cancer* (IARC), Monographs, Supplement 7, 99 (1987).
7. A. C. MacDiarmid, J. C. Chiang, M. Halpern, W. L. Mu, N. L. D. Somasiri, W. Wu and S. I. Yaniger, *Mol. Cryst. Liq. Cryst.*, **121**, 121 (1985).
8. A. Petr, N. Neudeck and L. Dunsch, *Chem. Phys. Lett.*, **401**, 130 (2005).
9. A. C. MacDiarmid and A. J. Epstein, in *Photonic and Optophotonic Polymers* (Eds. S. A Jenekhe and K. J. Wynne), American Chemical Society, Washington D.C., 1997, p. 395.
10. O. Unverdorben, *Ann. der Physik*, **8**, 397 (1826).
11. F. F. Runge, *Ann. der Physik*, **31**, 65 and 497 (1834), and **32**, 308 and 331 (1834).
12. See M. T. Nguyen, E. S. Kryachko and L. G. Vanquickenborne, in *The Chemistry of Phenols* (Ed. Z. Rappoport), Part 1, Chap. 1, Wiley, Chichester, 2003, pp. 1–198, for a brief history of the discovery of phenol and a discussion about its structure.
13. (a) C. J. Fritzsche, *Ann. der Chem. Pharm.*, **36**, 84 (1840).
    (b) J. Fritzsche, *J. Prakt. Chem.*, **20**, 453 (1840).
14. B. Pavlov and A. Terentiev, *Chimie Organique*, Editions MIR, Moscow, 1967, p. 454.
15. The synthesis of aminobenzenes from reduction of nitrobenzenes was beyond any doubt a pivotal discovery, and the original preparation of aniline by Nikolaï Zinin is still kept in the Museum of Kazan School of Chemistry (Russia): http://www.kazan.ru/tat_ru/universitet/museums/chmku/eng/s2.php
16. A. Laurent, *J. Prakt. Chem.*, **8**, 201 (1836); *Ann. Chim. Phys.*, **73**, 383 (1839).
17. A. Laurent, *Ann. Chim.*, **iii**, 195 (1841); *J. Prakt. Chem.*, **32**, 286 (1844).
18. A. Laurent, *J. Prakt. Chem.*, **36**, 13 (1845).
19. Letter of Berzélius to Pelouze, *Ann. Chim. Phys.*, **67**, 303 (1838); *Compt. Rend. Acad. Sci.*, **vi**, 629 (1838).
20. J. B. Dumas, *Compt. Rend. Acad. Sci.*, **vi**, 645 (1838).
21. A. W. von Hofmann, *Ann. der Chem. Pharm.*, **48**, 253 and 281 (1843).
22. The support of Hofmann for Laurent was seemingly decisive in this debate, and this episode marked a certain advance of the chemical theory. Hofmann later helped to popularize the atomic model and introduced the concept of valence through his book *An Introduction to*

Modern Chemistry (1865). In fact, this textbook provided a brilliant summary of the emerging theory of chemical structure and strongly influenced the university teaching of chemistry. Hofmann became professor at the University of Bonn in 1864 and at the University of Berlin from 1865, and was a founder (1868) of the Deutsche Chemische Gesellschaft and its journal 'Berichte'. He studied further aniline chemistry and was the first to prepare, among others, rosaniline and its derivatives.

23. A bottle containing the original mauveine made by Perkin is now displayed in the Science Museum, London, UK, which is located next to the Imperial College of Science and Technology.

24. In fact, Perkin dropped out of college at the age of 18 to build a factory to manufacture his new synthetic dye. The original small factory (Perkin & Sons) located on the banks of the Grand Junction Canal, south of the Black Horse Public House, in Greenford, West London, was demolished in 1957.

25. In a way, the performance of German chemical industries owed much to the vision of Justus von Liebig about chemistry: research, invention and application. The URL of the Liebig Museum in Giessen: http://www.uni-giessen.de/~gi04/home1.html.

26. S. Garfield, *Mauve: How One Man Invented a Color that Changed the World*, W. W. Norton, New York, 2001. This author argued that Perkin's fortuitous discovery of a way to mass produce a color changed the world. It gave birth to the synthetic dye industry, revolutionized fashion and sparked popular interest in the commercial applications of chemistry. Before, the organic chemical industry had mainly been confined to manufacturing soap from fats and oils! With his mauveine, Perkin made a fortune. At age 36, he retired as a dyemaker, sold his business and devoted much of the rest of his life to organic chemistry.

27. Statements reported in *J. Gas Lighting*, **128**, 201 (1914) and *Ind. Eng. Chem.*, **7**, 70 (1915),

28. (a) V. G. Bloede, *Ind. Eng. Chem.*, **16**, 409 (1924).
    (b) C. E. Munroe and A. M. Doyle, *Ind. Eng. Chem.*, **16**, 417 (1924).

29. T. H. Norton, *Dyestuff Situation in the United States, November 1915*, US Department of Commerce, Washington DC, 1916.

30. The Chemical Foundation, which was set up by the USA government to manage the German patents, had begun in 1919 the process of selling the patents.

31. D. A. Hounsell and J. K. Smith, *Science and Corporate Strategy. Dupont Research and Development 1902–1980*, Cambridge University Press, New York, USA 1988.

32. J. P. Murmann, *Knowledge and Competitive Advantage: The Coevolution of Firms, Technology, and National Institutions*, Cambridge University Press, New York, USA 2003.

33. See *Ullmann's Encyclopedia of Industrial Chemistry*, Sixth Edition, Wiley-VCH, Weinheim, 2003 for several examples.

34. J. C. D. Brand, D. R. Williams and T. J. Cook, *J. Mol. Spectrosc.*, **20**, 539 (1966).

35. D. G. Lister and J. K. Tyler, *J. Chem. Soc., Chem. Commun.*, 152 (1966).

36. J. C. D. Brand, V. T. Jones, B. J. Forrest and R. J. Pirkle, *J. Mol. Spectrosc.*, **39**, 352 (1971).

37. D. G. Lister, J. K. Tyler, J. H. Hog and N. W. Larsen *J. Mol. Struct.*, **23**, 253 (1974).

38. A. Hatta, M. Suzuki and K. Kozima, *Bull. Chem. Soc. Jpn.*, **46**, 2321 (1973).

39. M. Fukuyo, K. Hirotsu and T. Higuchi, *Acta Crystallog., Sect. B*, **38**, 640 (1982).

40. G. Schulz, G. Portalone, F. Ramondo, A. Domenicano and I. Hargittai, *Struct. Chem.*, **7**, 59 (1996).

41. (a) G. Roussy and A. Nonat, *J. Mol. Spectrosc.*, **118**, 180 (1986).
    (b) B. Kleibömer and D. H. Sutter, *Z. Naturforsch.*, **43a**, 561 (1988).

42. E. R. Th. Kerstel, M. Becucci, G. Pietraperzia and E. Castellucci, *Chem. Phys.*, **199**, 263 (2001).

43. (a) T. M. Korter, D. R. Borst, C. J. Butler and D. W. Pratt, *J. Am. Chem. Soc.*, **123**, 96 (2001).
    (b) D. R. Borst, T. M. Korter and D. W. Pratt, *Chem. Phys. Lett.*, **350**, 485 (2001).

44. E. Ye, K. Chandrasekaran and R. P. A. Bettens, *J. Mol. Spectrosc.*, **229**, 54 (2005).

45. References for articles reporting results of *ab initio* quantum chemical calculations on different properties of aniline and derivatives can be retrieved from the compilation: *Quantum Chemistry Library Data Base* (QCLDB), Japan Association for International Chemical Information, Tokyo, Japan, 2005.

46. W. J. Hehre, L. Radom and J. A. Pople, *J. Chem. Soc., Chem. Commun.*, 669 (1972); *J. Am. Chem. Soc.*, **94**, 1496 (1972).

47. A. Wolf, U. Voets and H. H. Schmidtke, *Theor. Chim. Acta*, **54**, 229 (1980).

48. E. Von Nagy-Felsobuky, R. D. Topsom, S. Polack and R. W. Taft, *J. Mol. Struct. (Theochem)*, **88**, 255 (1982).
49. (a) Z. Niu and J. E. Boggs, *J. Mol. Struct. (Theochem)*, **109**, 381 (1984).
     (b) Z. Niu and J. E. Boggs, *Mol. Phys.*, **55**, 421 (1985).
50. N. V. Riggs and L. Radom, *Int. J. Quantum Chem.*, **31**, 393 (1987).
51. (a) A. D. Gorse and M. Pesquer, *J. Mol. Struct. (Theochem)*, **109**, 381 (1984).
     (b) R. Cervellati, A. D. Esposti and D. G. Lister, *J. Mol. Struct. (Theochem)*, **122**, 173 (1985).
52. Z. H. Yu and M. Q. Jiang, *J. Mol. Struct. (Theochem)*, **251**, 69 (1991).
53. Y. Wang, S. Saebo and C. U. Pittman, *J. Mol. Struct. (Theochem)*, **281**, 91 (1993).
54. O. Bludsky, J. Sponer, J. Leszczynski, V. Spirko and P. Hobza, *J. Chem. Phys.*, **23**, 11042 (1996).
55. M. E. Vaschetto, B. A. Retamal and A. P. Monkman, *J. Mol. Struct. (Theochem)*, **468**, 209 (1999).
56. P. M. Wojciechowski, W. Zierkiewicz, D. Michalska and P. Hobza, *J. Chem. Phys.*, **118**, 10900 (2003).
57. (a) M. Quack and M. Stockburger, *J. Mol. Spectrosc.*, **43**, 87 (1972).
     (b) D. A. Chernoff and S. A. Rice, *J. Chem. Phys.*, **70**, 2511 (1979).
58. The larger deviations of rotational constants arise from the fact that, with respect to the true ones, the Hartree–Fock (HF) method usually predicts too short bond distances (too large rotational constants), whereas the BLYP functional results in too long bond lengths (too small rotational constants). For results of phenol, see Reference 12, pp. 20–21.
59. N. W. Larsen, E. L. Hansen and F. M. Nicolaisen, *Chem. Phys. Lett.*, **43**, 584 (1976).
60. I. Lopez-Tocon, R. G. D. Valle, M. Becucci, E. Castellucci and J. C. Otero, *Chem. Phys. Lett.*, **327**, 45 (2000).
61. J. C. Jiang and C. E. Lin, *J. Mol. Struct. (Theochem)*, **392**, 181 (1997).
62. R. C. West and M. J. Astle (Eds.), *Handbook of Chemistry and Physics*, CRC Press, Florida, 1982, p. E-61.
63. R. F. W Bader, *Atoms in Molecules, A Quantum Theory*, Clarendon, Oxford, 1990.
64. A. D. Becke and K. E. Edgecombe, *J. Chem. Phys.*, **92**, 5397 (1990).
65. (a) T. M. Krygowski, K. Eijsmont, B. T. Stepien, M. K. Cyranski, J. Poater and M. Sola, *J. Org. Chem.*, **69**, 6633 (2004).
     (b) T. M. Krygowski, J. E. Zachara and H. Szatylowicz, *J. Org. Chem.*, **69**, 7038 (2004).
66. J. C. Evans, *Spectrochim. Acta*, **16**, 428 (1960).
67. G. N. R. Tripathi, *J. Chem. Phys.*, **73**, 5521 (1980).
68. R. A. Kydd and P. J. Krueger, *Chem. Phys. Lett.*, **49**, 539 (1977).
69. T. Nakanaga, F. Ito, J. Miyawaki, K. Sugawara and H. Takeo, *Chem. Phys. Lett.*, **261**, 414 (1996).
70. Ch. Gée, S. Douin, C. Crépin and Ph. Bréchignac, *Chem. Phys. Lett.*, **338**, 130 (2001).
71. A. Uskola, F. J. Basterretxea and F. Castano, *J. Mol. Struct.*, **609**, 187 (2002).
72. T. Ebata, C. Minejima and N. Mikami, *J. Phys. Chem. A*, **106**, 11070 (2002).
73. M. Castella-Ventura and E. Kassab, *Spectrochim. Acta*, **50A**, 69 (1994).
74. G. Grahut and P. Pulay, *J. Chem. Phys.*, **99**, 3093 (1995).
75. M. Alcolea Palafox and F. J. Melendez, *J. Mol. Struct. (Theochem)*, **493**, 171 (1999).
76. M. Alcolea Palafox, J. L. Nunez and M. Gil, *J. Mol. Struct. (Theochem)*, **593**, 101 (2002).
77. Y. Tanaka and K. Machida, *J. Mol. Spectrosc.*, **55**, 453 (1975).
78. H. Wolff and W. Hagedorn, *J. Phys. Chem.*, **84**, 2335 (1980).
79. (a) J. Pyka and M. Kreglewski, *J. Mol. Spectrosc.*, **109**, 207 (1985).
     (b) V. E. Borisenko, A. V. Baturin, M. Przeslawska and A. Koll, *J. Mol. Struct.*, **407**, 53 (1997).
80. (a) M. Honda, A. Fujii, E. Fujimaki, T. Ebata and N. Mikami, *J. Phys. Chem. A*, **107**, 3678 (2003).
     (b) D. L. Howard, T. W. Robinson, A. E. Fraser and H. G. Kjaergaard, *Phys. Chem. Chem. Phys.*, **6**, 719 (2004).
81. P. Mulder, I. W. C. E. Arends, D. Santoro and H. G. Korth, *J. Org. Chem.*, **68**, 4247 (2003).
82. (a) M. T. Nguyen and A. F. Hegarty, *J. Am. Chem. Soc.*, **106**, 1552 (1984).
     (b) M. T. Nguyen and T. K. Ha, *J. Am. Chem. Soc.*, **106**, 599 (1984).
83. M. T. Nguyen, G. Raspoet, P. Th. Van Duijnen and L. G. Vanquickenborne, *J Phys. Chem. A*, **103**, 7379 (1999).

84. D. Bryce-Smith and A. Gilbert, in *Rearrangement in Ground and Excited States*, (Ed. P. de Mayo), Volume 3, Academic Press, New York, 1980.

85. C.-M. Tseng, Y. A. Dyakov, C.-L. Huang, A. M. Mebel, S. H. Lin, Y. T. Lee and C.-K. Ni, *J. Am. Chem. Soc.*, **126**, 8760 (2004).

86. J. McMurry, *Organic Chemistry*, Brooks-Cole, Pacific Grove, CA, 2000.

87. (a) I. Dzidic, *J. Am. Chem. Soc.*, **94**, 8333 (1972).
     (b) Y. K. Lau and P. Kebarle, *J. Am. Chem. Soc.*, **98**, 7452 (1976).
     (c) Y. K. Lau, P. P. S. Saluja, P. Kebarle and R. W. Alder, *J. Am. Chem. Soc.*, **100**, 7323 (1978).

88. O. Tishchenko, N. N. Pham-Tran, E. S. Kryachko and M. T. Nguyen, *J. Phys. Chem. A*, **105**, 8709 (2001) and references cited therein.

89. (a) K. D. Summerhays, S. K. Pollack, R. W. Taft and W. J. Hehre, *J. Am. Chem. Soc.*, **99**, 4585 (1977).
     (b) S. K. Pollack, J. L. Devlin, K. D. Summerhays, R. W. Taft and W. J. Hehre, *J. Am. Chem. Soc.*, **99**, 4583 (1977).

90. A. Maquestiau, Y. Van Haverbeke, H. Mispreuve, R. Flammang, J. A. Harris, I. Howe and J. H. Benon, *Org. Mass Spectrom.*, **15**, 144 (1980).

91. K. V. Wood, D. J. Burinsky, D. Cameron and R. G. Cooks, *J. Org. Chem.*, **48**, 5236 (1983).

92. S. J. Pachuta, I. Isern-Flecha and R. G. Cooks, *Org. Mass Spectrom.*, **21**, 1 (1986).

93. Z. Karpas, Z. Berant and R. M. Stimac, *Struct. Chem.*, **1**, 201 (1990).

94. (a) L. J. Chyall and H. I. Kenttämaa, *J. Am. Chem. Soc.*, **116**, 3135 (1994).
     (b) R. L. Smith, L. J. Chyall, B. J. Beasley and H. I. Kenttämaa, *J. Am. Chem. Soc.*, **117**, 7971 (1995).

95. M. J. Nold and C. Wesdemiotis, *J. Mass Spectrom.*, **31**, 1169 (1996).

96. S. W. Lee, H. Cox, W. A. Goddard III and J. L. Beauchamp, *J. Am. Chem. Soc.*, **122**, 9201 (2000).

97. A. G. Harrison and Y. P. Tu, *Int. J. Mass Spectrom.*, **195/196**, 33 (2000).

98. R. Flammang, N. Dechamps, L. Pascal, Y. Van Haverbeke, P. Gerbaux, P. C. Nam and M. T. Nguyen, *Lett. Org. Chem.*, **1**, 21 (2004).

99. M. J. S. Dewar and K. M. Dieter, *J. Am. Chem. Soc.*, **108**, 8075 (1986).

100. P. Sjoberg, J. S. Murray, T. Brinck and P. Politzer, *Can. J. Chem.*, **68**, 1440 (1990).

101. J. P. Ritchie, *J. Mol. Struct. (Theochem)*, **225**, 297 (1992).

102. C. Hillebrand, M. Klessinger, M. Eckert-Maksic and Z. B. Maksič, *J. Phys. Chem.*, **100**, 9698 (1996).

103. R. K. Roy, F. de Proft and P. Geerlings, *J. Phys. Chem. A*, **102**, 7035 (1998).

104. P. Fuentealba, P. Pérez and R. Contreras, *J. Chem. Phys.*, **113**, 2544 (2000).

105. N. Russo, M. Toscana, A. Grand and T. Minerva, *J. Phys. Chem. A*, **104**, 4017 (2000).

106. A. Bagno and F. Terrier, *J. Phys. Chem. A*, **105**, 6537 (2001).

107. H. T. Le, R. Flammang, M. Barbieux-Flammang, P. Gerbaux, and M. T. Nguyen, *Int. J. Mass Spectrom.*, **217**, 45 (2002).

108. P. C. Nam and M. T. Nguyen, unpublished results (2004).

109. Y. K. Lau, K. Nishizawa, A. Tse, R. S. Brown and P. Kebarle, *J. Am. Chem. Soc.*, **103**, 6291 (1981).

110. Y. A. Ranasinghe and G. L. Gish, *Int. J. Mass Spectrom.*, **190/191**, 295 (1999).

111. (a) S. Tajima, S. Shiobara, H. Shizuka and S. Tobita, *Phys. Chem. Chem. Phys.*, **4**, 3376 (2002).
     (b) S. Shiobara, S. Tajima and S. Tobita, *Chem. Phys. Lett.*, **380**, 673 (2002).
     (c) I. Antol, M. Eckert-Maksic and M. Klessinger, *J. Mol. Struct. (Theochem)*, **664**, 309 (2003).

112. W. J. Lyman, W. F. Reehl and D. H. Rosenblatt, *Handbook of Chemical Property Estimation Methods*, Am. Chem. Soc., Washington DC, USA 1990, p. 6–1.

113. C. Karunakaran and R. Kamalam, *J. Org. Chem.*, **67**, 1118 (2002).

114. D. M. Chipman, *J. Phys. Chem. A*, **106**, 7143 (2002).

115. J. R. Pliego and J. M. Riveros, *J. Phys. Chem. A*, **106**, 7434 (2002).

116. B. G. Tehan, E. J. Lloyd, M. G. Wong, W. R. Pitt, E. Gancia and D. T. Manallack, *Quant. Struct. Act. Relat.*, **21**, 473 (2002).

117. K. C. Gross and P. G. Seybold, *Int. J. Quantum Chem.*, **80**, 1107 (2000); *Int. J. Quantum Chem.*, **85**, 569 (2001).

118. (a) K. C. Gross, P. G. Seybold, Z. Peralta-Inga, J. S. Murray and P. Politzer *J. Org. Chem.*, **66**, 6919 (2001).
    (b) K. C. Gross, P. G. Seybold and C. M. Haddad, *Int. J. Quantum Chem.*, **90**, 445 (2002).
119. Y. Fu, L. Liu, R. Q. Li, R. Liu and Q. X. Guo, *J. Am. Chem. Soc.*, **126**, 814 (2004).
120. O. Pytela, M. Otyepka, J. Kulhanek, E. Otyepkova and T. Nevěčná, *J. Phys. Chem. A*, **107**, 11489 (2003).
121. U. A. Chaudry and P. L. A. Popelier, *J. Org. Chem.*, **69**, 233 (2004).
122. (a) M. Mandado, A. N. Grana and R. A. Mosquera, *Chem. Phys. Lett.*, **400**, 169 (2004).
    (b) A. Grana, J. M. Hermida-Ramon and R. A. Mosquera, *Chem. Phys. Lett.*, **412**, 106 (2005).
123. T. Ohwada, H. Hirao and A. Ogawa, *J. Org. Chem.*, **69**, 7486 (2004).
124. P. Politzer, *J. Chem. Phys.*, **86**, 1072 (1987).
125. (a) J. Olah, C. Van Alsenoy and A. B. Sannigrahi, *J. Phys. Chem. A*, **106**, 3885 (2002).
    (b) G. D'Aprano, E. Proynov, M. Leboeuf, M. Leclerc and D. R. Salahub, *J. Am. Chem. Soc.*, **118**, 9736 (1996).
126. K. Schroeter, R. Wesendrup and H. Schwarz, *Eur. J. Org. Chem.*, 565 (1998).
127. J. Oomens, D. T. Moore, G. von Helden, G. Meijer and R. C. Dunbar, *J. Am. Chem. Soc.*, **126**, 724 (2004)
128. T. Fujii, H. Tokiwa, H. Ichikawa and H. Shinoda, *J. Mol. Struct. (Theochem)*, **277**, 251 (1992).
129. S. Mecozzi, P. A. West and D. A. Dougherty, *J. Am. Chem. Soc.*, **118**, 2307 (1996).
130. R. Amunugama and M. T. Rodgers, *Int. J. Mass Spectrom.*, **227**, 339 (2003).
131. P. C. Nam and M. T. Nguyen, unpublished results (2005).
132. D. A. Dougherty, *Science*, **271**, 163 (1996).
133. R. Amunugama and M. T. Rodgers, *J. Phys. Chem. A*, **106**, 5529, 9092 (2002).
134. M. L. Senent, A. Nino, C. M. Caro, S. Ibeas, B. Garcia, J. M. Leal, F. Seco and M. Venturini, *J. Org. Chem.*, **68**, 6535 (2003).
135. See Reference 12, pp. 94–95.
136. V. S. Nguyen, C. Vinckier, T. T. Hue and M. T. Nguyen, *J. Phys. Chem. A*, **109**, 10954 (2005).
137. D. V. Bent and E. Hayon, *J. Am. Chem. Soc.*, **97**, 2599, 2606 and 2612 (1975).
138. R. S. Becker, *Theory and Interpretation of Fluorescence and Phosphorescence*, Wiley-Interscience, New York, 1969.
139. M. Krauss, J. O. Jensen and H. F. Hameka, *J. Phys. Chem.*, **98**, 9955 (1994).
140. S. Sarkar and G. Kastha, *Spectrochim. Acta*, **48A**, 1611 (1992).
141. (a) P. Swiderek, M. Michaud and L. Sanche, *J. Chem. Phys.*, **105**, 6724 (1996).
    (b) E. Yamamoto, T. Yoshidome, T. Ogawa and H. Kawazumi, *J. Electron Spectrosc.*, **63**, 341 (1993).
    (c) Y. Kanda and R. Shimada, *Spectrochim. Acta*, **17**, 279 (1961).
142. (a) P. J. Vergrat and J. H. van der Waals, *Chem. Phys. Lett.*, **26**, 305 (1974).
    (b) H. M. van Noort, P. J. Vergrat, J. Herbich and J. H. van der Waals, *Chem. Phys. Lett.*, **71**, 5 (1980).
    (c) D. M. Haaland and G. C. Nieman, *J. Chem. Phys.*, **59**, 4435 (1973).
143. (a) K. Kimura, H. Tsubomura and S. Nagakura, *Bull. Chem. Soc. Jpn.*, **37**, 1336 (1964).
    (b) K. Kimura and S. Nagakura, *Mol. Phys.*, **9**, 117 (1965).
144. (a) R. Scheps, D. Florida and S. Rice, *J. Chem. Phys.*, **61**, 1730 (1974).
    (b) H. M. van Noort, C. A. Van't Hof, B. Wirnitzer and J. Schmidt, *Chem. Phys. Lett.*, **81**, 251 (1981).
145. (a) K. Fuke and K. Kaya, *Chem. Phys. Lett.*, **94**, 97 (1983).
    (b) K. Fuke and S. Nagakura, *J. Mol. Spectrosc.*, **64**, 139 (1977).
146. O. Sne and O. Cheshnovsky, *Chem. Phys. Lett.*, **146**, 216 (1988).
147. H. Shimomori and A. Sato, *J. Phys. Chem.*, **94**, 13481 (1994).
148. B. Kim, C. P. Schick and P. M. Weber, *J. Chem. Phys.*, **103**, 6903 (1995).
149. C. Gée, A. Cuisset, L. Divay and C. Crépin, *J. Chem. Phys.*, **116**, 4993 (2002).
150. W. Schuddeboom, J. M. Warman, H. A. M. Biemans and E. W. Meijer, *J. Phys. Chem.*, **100**, 12369 (1996).
151. W. M. Kwok, C. Ma, P. Matousek, A. W. Parker, D. Phillips, W. T. Toner, M. Towrie, P. Zuo and D. L. Phillips, *Phys. Chem. Chem. Phys.*, **5**, 3643 (2003).
152. M. Freccero, M. Fagnoni and A. Albini, *J. Am. Chem. Soc.*, **125**, 13182 (2003).

153. O. Rubio-Pons, O. Loboda, R. Minaev, B. Schimmelpfennig, O. Vahtras and H. Agren, *Mol. Phys.*, **101**, 2103 (2003).

154. X. J. Hou, P. Quan, T. Höltzl, T. Veszpremi and M. T. Nguyen, *J. Phys. Chem. A*, **109**, 10396 (2005).

155. M. T. Nguyen, R. Zhang, P. C. Nam and A. Ceulemans, *J. Phys. Chem. A*, **108**, 6554 (2004).

156. M. Ito, *J. Mol. Spectrosc.*, **4**, 106 (1960).

157. J. S. Yadav, P. C. Mishra and D. K. Rai, *Chem. Phys. Lett.*, **31**, 129 (1975).

158. N. Mikami, A. Hiraya, I. Fujiwara and M. Ito, *Chem. Phys. Lett.*, **74**, 531 (1980).

159. (a) J. M. Hollas, M. R. Howson, T. Ridley and L. Halonen, *Chem. Phys. Lett.*, **98**, 611 (1983).
(b) A. R. Bacon and J. M. Hollas, *Faraday Discuss. Chem. Soc.*, **86**, 129 (1988).
(c) J. Christofferson, J. M. Hollas and G. H. Kirby, *Mol. Phys.*, **16**, 441 (1969).

160. (a) E. R. Th. Kerstel, M. Becucci, G. Pietraperzia, D. Consalvo and E. Castellucci, *J. Mol. Spectrosc.*, **177**, 74 (1996).
(b) G. Pietraperzia, M. Becucci, I. Del Pace, I. Lopez-Tocon and E. Castellucci, *Chem. Phys. Lett.*, **335**, 195 (2001).

161. Y. Honda, M. Hada, M. Ehara and H. Nakatsuji, *J. Chem. Phys.*, **117**, 2045 (2002).

162. (a) W. E. Sinclair and D. W. Pratt, *J. Chem. Phys.*, **105**, 7942 (1996).
(b) M. Schäfer and D. W. Pratt, *J. Chem. Phys.*, **115**, 11147 (2001).

163. W. B. Tzeng, K. Narayanan, K. C. Shieh and C. C. Tung, *J. Mol. Struct. (Theochem)*, **428**, 231 (1998).

164. D. M. Upadhyay, M. K. Shukla and P. C. Mishra, *J. Mol. Struct. (Theochem)*, **531**, 249 (2000).

165. J. R. Lombardi, *J. Chem. Phys.*, **50**, 50 (1969); **56**, 2278 (1972); *Chem. Phys.*, **28**, 41 (1978).

166. (a) H. von Weyssenhof and F. Kraus, *J. Chem. Phys.*, **54**, 2387 (1971).
(b) D. E. Powers, J. B. Hopkins and R. E. Smalley, *J. Chem. Phys.*, **72**, 5721 (1980).

167. (a) M. Sonnenshein, A. Amirav and J. Jortner, *J. Phys. Chem.*, **88**, 4214 (1984).
(b) A. Amirav, U. Even and J. Jortner, *Anal. Chem.*,, **54**, 1666 (1982).
(c) A. Amirav, U. Even, J. Jortner and B. Pick, *Mol. Phys.*, **49**, 899 (1983).

168. M. F. Hineman, S. K. Kim, E. R. Berstein and D. F. Kelly, *J. Chem. Phys.*, **96**, 4904 (1992).

169. M. F. Budyka, T. S. Zyubina and A. K. Zarkadis, *J. Mol. Struct. (Theochem)*, **594**, 113 (2002).

170. (a) M. W. Allen, J. R. Unruh, B. D. Slaughter, S. J. Pyszcynski, T. R. Hellwig, T. J. Kamerzell and C. K. Johnson, *J. Phys. Chem. A*, **107**, 5660 (2003).
(b) B. D. Slaughter, M. W. Allen, A. G. H. Lushington and C. K. Johnson, *J. Phys. Chem. A*, **107**, 5670 (2003).

171. K. Pirwska, P. Kolek, J. Goclon and J. Najbar, *Chem. Phys. Lett.*, **387**, 165 (2004).

172. J. M. Leal and B. Garcia, *Z. Phys. Chem. (Leipzig)*, **269**, 26 (1988).

173. F. Bertinelli, A. Brillante, P. Palieri and C. Taliani, *Gazz. Chim. Ital.*, **110**, 321 (1980).

174. P. de Mayo *Rearrangement in Ground and Excited States* (Ed.), Volume 3, Academic Press, New York, 1980.

175. C.-M. Tseng, Y. A. Dyakov, C.-L. Huang, A. M. Mebel, S. H. Lin, Y. T. Lee and C.-K. Ni, *J. Am. Chem. Soc.*, **126**, 8760 (2004).

176. M. Kanzelberger, X. Zhang, T. J. Emge, A. S. Goldman, J. Zhao, C. Incarvito and J. F. Hartwig, *J. Am. Chem. Soc.*, **125**, 13644 (2003).

177. S. P. Verevkin, *J. Chem. Thermodyn.*, **32**, 247 (2000).

178. M. A. V. Ribeiro da Silva, L. M. P. F. Amaral and A. I. M. C. L. Fereira, *J. Chem. Thermodyn.*, **34**, 119 (2002).

179. E. J. Land and G. Porter, *Trans. Faraday Soc.*, **59**, 2027 (1963).

180. D. F. McMillen and D. M. Golden, *Annu. Rev. Phys. Chem.*, **33**, 493 (1982).

181. F. G. Bordwell, J. P. Cheng, G. Z. Ji, A. V. Stish and X.-M. Zhang, *J. Am. Chem. Soc.*, **113**, 9790 (1991).

182. F. G. Bordwell, X.-M. Zhang and J. P. Cheng, *J. Org. Chem.*, **58**, 6410 (1993).

183. W. Z. Liu and F. G. Bordwell, *J. Org. Chem.*, **61**, 4778 (1996).

184. Y. Zhao, F. G. Bordwell, J. P. Cheng and D. Wang, *J. Am. Chem. Soc.*, **119**, 9125 (1997).

185. (a) M. Jonsson, J. Lind, T. E. Eriksen and G. Merenyi, *J. Am. Chem. Soc.*, **116**, 1423 (1994).
(b) M. Jonsson, J. Lind, G. Merenyi and T. E. Eriksen, *J. Chem. Soc., Perkin Trans. 2*, 61 (1995).

186. L. J. Rothenberg, J. D. Simon, M. Bernstein and K. S. Peters, *J. Am. Chem. Soc.*, **105**, 3464 (1983).

187. L. J. J. Laarhoven, P. Mulder and D. D. M. Wayner, *Acc. Chem. Res.*, **32**, 342 (1999).
188. P. A. MacFaul, D. D. M. Wayner and K. U. Ingold, *J. Org. Chem.*, **62**, 3413 (1997).
189. D. A. Pratt, G. A. Dilabio, P. Mulder and K. U. Ingold, *Acc. Chem. Res.*, **37**, 334 (2004).
190. D. A. Pratt, G. A. DiLabio, L. Valgimigli, G. F. Pedulli and K. U. Ingold, *J. Am. Chem. Soc.*, **124**, 11085 (2002).
191. (a) G. P. Bean, *Tetrahedron*, **54**, 15445 (1998).
    (b) G. P. Bean, *Tetrahedron*, **58**, 9941 (2002).
192. Y. R. Luo, *Int. J. Chem. Kinet.*, **34**, 453 (2002).
193. Y. H. Cheng, L. Liu, K. S. Song and Q. X. Guo, *J. Chem. Soc., Perkin Trans. 2*, 1406 (2002).
194. K. S. Song, L. Liu and Q. X. Guo, *J. Org. Chem.*, **68**, 262 (2003).
195. Z. Li and J. P. Cheng, *J. Org. Chem.*, **68**, 7350 (2003).
196. J. R. B. Gomes, M. D. M. C. Ribeiro da Silva and M. A. V. Ribeiro da Silva, *J. Phys. Chem. A*, **108**, 2119 (2004).
197. P. C. Nam, H. T. Le and M. T. Nguyen, unpublished results (2005).
198. M. de L. Romero and F. Mendez, *J. Phys. Chem. A*, **107**, 5874 (2003).
199. (a) L. Quin, G. N. R. Tripathi and R. H. Schuler, *Z. Naturforsch.*, **40a**, 1026 (1985).
    (b) G. N. R. Tripathi and R. H. Schuler, *J. Chem. Phys.*, **86**, 3795 (1987).
200. J. Malkin, *Photochemical and Photophysical Properties of Aromatic Compounds*, CRC Press, Boca Raton, 1992, pp. 117, 201.
201. P. Neta and R. W. Fessenden, *J. Phys. Chem.*, **78**, 523 (1974).
202. F. Saito, S. Tobita and H. Shizuka, *J. Photochem. Photobiol. A*, **106**, 119 (1997).
203. (a) B. D. Wagner, G. Ruel and J. Lusztyk, *J. Am. Chem. Soc.*, **118**, 511 (1996).
    (b) P. A. MacFaul, K. U. Ingold and J. Lusztyk, *J. Org. Chem.*, **61**, 1316 (1996).
204. M. G. Siskos, A. Z. Zarkadis, S. Steenken, N. Karakostas and S. K. Garas, *J. Org. Chem.*, **63**, 3251 (1998).
205. P. S. Drzaic and J. I. Brauman, *J. Phys. Chem.*, **88**, 5285 (1984).
206. R. V. Lloyd and D. E. Wood, *J. Am. Chem. Soc.*, **96**, 659 (1974).
207. D. Maurice and M. Head-Gordon, *J. Phys. Chem.*, **100**, 6131 (1996).
208. C. Adamo, R. Subra, A. Di Matteo and V. Barone, *J. Chem. Phys.*, **109**, 10244 (1998).
209. M. Engström, O. Vahtras and H. Ångren, *Chem. Phys.*, **243**, 263 (1999).
210. P. Quan and M. T. Nguyen, unpublished results (2005).
211. A. H. Winter, D. E. Falvey and C. J. Cramer, *J. Am. Chem. Soc.*, **126**, 9661 (2004).
212. T. P. Debies and R. W. Rabelais, *J. Electron Spectrosc. Relat. Phenom.*, **1**, 355 (1972).
213. J. T. Meek, E. Sekreta, W. Wilson, K. S. Viswanathan and J. P. Kelly, *J. Chem. Phys.*, **82**, 1741 (1985).
214. (a) M. A. Smith, J. Hager and S. C. Wallace, *J. Chem. Phys.*, **80**, 3097 (1984).
    (b) J. Hager, M. A. Smith and S. C. Wallace, *J. Chem. Phys.*, **83**, 4820 (1985).
    (c) J. Hager, M. A. Smith and S. C. Wallace, *J. Chem. Phys.*, **84**, 6771 (1986).
215. G. N. R. Tripathi and R. H. Schuler, *Chem. Phys. Lett.*, **110**, 542 (1984).
216. M. Takahashi, H. Ozeki and K. Kimura, *J. Chem. Phys.*, **96**, 6399 (1992).
217. X. Zhang, J. M. Smith and J. L. Knee, *J. Chem. Phys.*, **97**, 2843 (1992).
218. X. Song, M. Yang, E. R. Davidson and J. P. Reilly, *J. Chem. Phys.*, **99**, 3224 (1993).
219. B. Kim and P. M. Weber, *J. Phys. Chem.*, **99**, 2583 (1995).
220. M. Jonsson, D. D. M. Wayner and J. Lusztyk, *J. Phys. Chem.*, **100**, 17539 (1996).
221. T. Ogawa, T. Ogawa and K. Nakashima, *J. Phys. Chem. A*, **102**, 10608 (1998).
222. H. Piest, G. Vom Helden and G. Meijer, *J. Chem. Phys.*, **110**, 2010 (1999).
223. B. Fehrensen, M. Hippler and M. Quack, *Chem. Phys. Lett.*, **298**, 320 (1998).
224. C. A. Raptis and S. T. Pratt, *J. Chem. Phys.*, **113**, 4190 (2000).
225. (a) J. L. Lin and W. B. Tzeng, *J. Chem. Phys.*, **115**, 743 (2001).
    (b) J. L. Lin and W. B. Tzeng, *Chem. Phys. Lett.*, **362**, 19 (2002).
226. K. Kato and K. Yamanouchi, *Chem. Phys. Lett.*, **397**, 237 (2004).
227. T. Baer and T. E. Carney, *J. Chem. Phys.*, **76**, 1304 (1982).
228. (a) C. Lifshitz, P. Gotchiguian and R. Roller, *Chem. Phys. Lett.*, **95**, 106 (1983).
    (b) C. Lifshitz, M. Goldenberg, Y. Malinovich and M. Peres, *Int. J. Mass Spectrom. Ion Phys.*, **46**, 269 (1983).
    (c) Y. Malinovich, R. Arakawa, G. Haase and C. Lifshitz, *J. Phys. Chem.*, **89**, 2253 (1985).
229. (a) P. C. Burgers, J. H. Holmes, A. A. Mommers and J. K. Terlouw, *Chem. Phys. Lett.*, **102**, 1 (1983).

(b) P. C. Burgers, J. H. Holmes, A. A. Mommers, J. E. Szulejko and J. K. Terlouw, *Org. Mass Spectrom.*, **19**, 442 (1984).

230. J. A. Zimmerman and R. M. O'Malley, *Chem. Phys. Lett.*, **147**, 315 (1988).
231. J. Watanabe, R. Itakura, A. Hishikawa and K. Yamanouchi, *J. Chem. Phys.*, **116**, 9697 (2002).
232. (a) L. J. Chyall and H. I. Kenttämaa, *J. Am. Chem. Soc.*, **116**, 3135 (1994).
     (b) L. J. Chyall and H. I. Kenttämaa, *J. Mass Spectrom.*, **30**, 81 (1995).
233. P. Karafiloglou and J. P. Launay, *J. Phys. Chem. A*, **102**, 8004 (1998).
234. P. Winget, E. J. Weber, C. J. Cramer and D. J. Truhlar, *Phys. Chem. Chem. Phys.*, **2**, 1231 (2000).
235. H. M. T. Nguyen and M. T. Nguyen, unpublished results (2005).
236. H. Letheby, *J. Chem. Soc.*, **15**, 161 (1862).
237. (a) T. A. Skothheim, in *Handbook of Conducting Polymers*, Marcel Dekker, New York, 1986.
     (b) T. A. Skothheim and R. L. Elsenbaumer, *Handbook of Conducting Polymers*, Marcel Dekker, New York, 1998.
238. R. de Surville, M. Jozefowocz, L. T. Lu, J. Berichon and R. Buvet, *Electrochim. Acta*, **13**, 1451 (1968).
239. A. F. Diaz and A. J. Logan, *J. Electroanal. Chem.*, **111**, 111 (1980).
240. A. G. MacDiarmid and A. J. Epstein, *Faraday Discuss. Chem. Soc.*, **88**, 317 (1986).
241. A. Talaie, *Polymer*, **38**, 1145 (1997).
242. N. Kobayashi, K. Yamada and R. Hirohashi, *Electroanal. Acta*, **37**, 2101 (1992).
243. R. B. Kaner and A. G. MacDiarmid, *Sci. Am.*, **258**, 106 (1988).
244. R. E. Ward and T. Y. Meyer, *Macromolecules*, **36**, 4368 (2003).
245. L. T. Sein, Y. Wei and S. A. Jensen, *J. Phys. Chem. A*, **104**, 11371 (2000).
246. W. Li and H. L. Wang, *J. Am. Chem. Soc.*, **126**, 2278 (2004).
247. G. D'Aprano, M. Leclerc and G. Zotti, *Synth. Met.*, **82**, 59 (1996).
248. K. A. Copli, S. Jasty, S. M. Long, S. K. Manohar, Y. Sun, A. G. Macdiarmid and A. J. Epstein, *Phys. Rev. Lett.*, **72**, 3206 (1994).
249. N. S. Saciciftci, A. J. Heeger and Y. Cao, *Phys. Rev. B*, **49**, 5988 (1994).
250. W. Liu, J. Kumar, S. Tripathy, K. J. Senecal and L. Samuelson, *J. Am. Chem. Soc.*, **121**, 71 (1999).
251. P. Snauwart, R. Lazzaroni, J. Riga, J. J. Verbist and D. Gonbeau, *J. Chem. Phys.*, **92**, 2187 (1990).
252. B. Sjogren, W. R. Salaneck and S. Stafstrom, *J. Chem. Phys.*, **97**, 137 (1992).
253. O. Kwon and M. L. McKee, *J. Phys. Chem. B*, **104**, 104 (2000).
254. S. L. Lim, K. L. Tan, E. T. Kang and W. S. Chin, *J. Chem. Phys.*, **112**, 10648 (2000).
255. M. E. Vaschetto, A. P. Monkman and M. Springborg, *J. Mol. Struct. (Theochem)*, **468**, 181 (1999).
256. M. E. Vaschette and B. A. Retamal, *J. Phys. Chem. A*, **101**, 6945 (1997).
257. D. Giri, K. Kundu, D. Majumdar and S. P. Bhattacharyya, *J. Mol. Struct (Theochem)*, **417**, 175 (1997).
258. E. C. Pereira, E. Longo and L. O. S. Bulhoes, *J. Mol. Struct (Theochem)*, **335**, 141 (1995).
259. A. E. de A. Machado, D. V. Petrov, E. H. L. Falcao, A. A. S. De Gama and W. M. de Azevedo, *Chem. Phys. Lett.*, **356**, 451 (2002).
260. A. Petr, A. Neudeck and L. Dunsch, *Chem. Phys. Lett.*, **401**, 130 (2005).
261. M. M. Wienk and R. A. J. Janssen, *J. Am. Chem. Soc.*, **118**, 10626 (1996) and **119**, 4492 (1997).
262. I. Lopez-Tocon, J. C. Otero, J. Soto, M. Becucci, G. Pietraaperzia and E. Castellucci, *Chem. Phys.*, **303**, 143 (2004) and references therein.
263. N. Solco and O. Dopfer, *J. Phys. Chem. A*, **106**, 7261 (2002).
264. T. Nakanaga, K. Kawamata and F. Ito, *Chem. Phys. Lett.*, **279**, 309 (1997).
265. T. Nakanaga and F. Ito, *Chem. Phys. Lett.*, **348**, 270 (2001).
266. Y. Honkawa, Y. Inokuchi, K. Ohashi, N. Nishi and H. Sekiya, *Chem. Phys. Lett.*, **358**, 419 (2002).
267. Y. Inokuchi, K. Ohashi, Y. Honkawa, N. Yamamoto, H. Sekiya and N. Nishi, *J. Phys. Chem. A*, **107**, 4230 (2003).
268. U. Spoerel and W. Stahl, *J. Mol. Spectrosc.*, **190**, 278 (1998) and **198**, 263 (1999).
269. J. A. Fernandez and E. R. Bernstein, *J. Chem. Phys.*, **106**, 3029 (1997).
270. T. Nakanaga, K. Sugawara, K. Kawamata and F. Ito, *Chem. Phys. Lett.*, **267**, 491 (1997).

271. Y. Inokuchi, K. Ohashi, Y. Honkawa, H. Sekiya and N. Nishi, *Chem. Phys. Lett.*, **359**, 283 (2002).
272. J. M. Hermida-Ramon, A. Pena-Gallego, E. Martinez-Nunez, A. A. Fernandez-Ramos and E. M. Cabaleiro, *J. Mol. Struct. (Theochem)*, **497**, 105 (2000).
273. M. Gerhards and C. Unterberg, *Appl. Phys. A: Mater. Sci. Process.*, **72**, 273 (2001).
274. R. Itakura, K. Yamanouchi, T. Yasuike and K. Someda, *Chem. Phys. Lett.*, **396**, 208 (2004).
275. P. S. Meenakshi, N. Biswas and S. Wategaonkar, *J. Chem. Phys.*, **117**, 11146 (2002).
276. J. M. Fan, L. Liu and Q. X. Guo, *Chem. Phys. Lett.*, **365**, 464 (2002).
277. H. M. T. Nguyen, M. T. Nguyen, J. Peteers and Th. Zeegers-Huyskens, *J. Phys. Chem. A*, **108**, 11101 (2004).

CHAPTER **3**

Structural chemistry of anilines

GRAŻYNA MARIA WÓJCIK

Institute of Physical & Theoretical Chemistry, Wrocław University of Technology,
Wyb. Wyspiańskiego 27, 50-370 Wrocław, Poland
Fax: +071 483203364;   e-mail: grazyna.m.wojcik@pwr.wroc.pl

I. INTRODUCTION

Crystal and molecular structures of aniline derivatives have been a frequent objective of research and analysis during the last several years. Especially nitroanilines, model compounds for optically nonlinear materials and their derivatives have been widely studied in order to better understand the mechanism of high molecular hyperpolarizability, as well as the conditions for noncentrosymmetric arrangement of molecules in the crystal, resulting in optically nonlinear materials. For the sake of clarity the problems analyzed may be classified into three groups: the intramolecular charge transfer, the degree of pyramidalization of the amino group and the molecular packing through intermolecular interactions, including hydrogen bonds.

In the external electric field a molecular dipole moment **p** is described by the power series in equation 1,

$$\mathbf{p} = \mathbf{p}_o + \alpha \mathbf{E} + \beta \mathbf{EE} + \cdots \tag{1}$$

where α and β denote molecular polarizability and hyperpolarizability and **E** denotes electric force. The high value of β and the noncentrosymmetric space group enable a nonzero second-order susceptibility of a crystal, which may thus exhibit a nonlinear optical effect, e.g. second harmonic generation (SHG), provided that other exigencies, such as phase-matching angle, are fulfilled[1].

The high molecular hyperpolarizability of p-nitroaniline derivatives is thought to originate from intramolecular charge-transfer between the electron-donating amino group and the electron-withdrawing nitro group. The π electrons of the aromatic ring enhance the charge-transfer as a result of the so-called 'through-conjugation effect'[1]. However, charge distribution within a molecule depends also on other substituents on the aromatic ring and on intermolecular interactions. This distribution has been studied using various methods including quantum-chemical calculations and X-ray and neutron diffraction[2–9].

X-ray diffraction and theoretical study of the charge density in 2-methyl-4-nitroaniline crystal, a nonlinear optical material, showed that the crystal electric field enhances the molecular dipole moment from 9 to 20 D. This enhancement is due to long-range interactions, the intermolecular hydrogen bonds being the strongest[3]. The precise localization of hydrogen atoms is possible from single-crystal neutron diffraction experiment. The results for 2-methyl-5-nitroaniline and m-nitroaniline enabled one to examine such an aggregation of the molecules that optimize the macroscopic nonlinear properties of the materials. Another conclusion from the experiment considered nonplanarity of the amino groups. It facilitates the proton-accepting ability of the amino nitrogen and impacts the molecular aggregation[7–9].

The increasing interest in obtaining efficient organic optically nonlinear materials resulted in a combinational chemistry approach to their synthesis. The structures of several nitroaniline derivatives (including five Schiff bases), the compounds which belong to a chemical class having potential application as nonlinear optical materials, have been reported[4,5].

A detailed X-ray diffraction experiment and quantum-chemical calculations of N,N-dimethyl-4-nitroaniline derivatives, also model compounds for optically nonlinear organic materials, revealed that the introduction of a substituent into the *ortho*- or *meta*-position with respect to the dimethylamino group resulted in decreasing the contribution of the

quinoid form as compared with *para*-isomers and, consequently, decreased the molecular hyperpolarizability[2, 6]. Also, a trigonal–pyramidal configuration of the dimethylamino groups was reported[6]. They are twisted with respect to the ring plane in all the molecules substituted in the *ortho*-position. On the contrary, the dimethylamino group is in the ring plane in the *meta*-substituted molecules[6]. In the case of nonsubstituted amino groups the neutron diffraction experiment was necessary to examine their geometries. Experimental evidence for the amino group nonplanarity in 2-methyl-5-nitroaniline and *m*-nitroaniline has been reported recently[7–9]. The results for the first compound indicate a considerable degree of pyramidalization of the amino group. Its electron configuration seems to be between the planar sp[2] hybridization and regular tetrahedral sp[3] hybridization of the nitrogen atom. This also holds for *m*-nitroaniline. The neutron diffraction studies just mentioned enabled also a detailed analysis of the hydrogen bond network in the crystals. Since the appearance of the papers from Etter's group it is known that molecular recognition between amino and nitro groups in the crystal of *para*- and *meta*-nitroanilines results in a hydrogen bond pattern involving a three-center interaction. One amino proton is located between two 'inside' electron lone pairs of oxygen atoms. This directionality is observed even when the NH$\cdots$O contacts exceed van der Waals distances[10]. Recent combined database studies and *ab initio* calculations have revealed a preference for the asymmetric bifurcated model in which only one O$\cdots$HN distance corresponds to a hydrogen bond[11]. The preferred intermolecular geometry that controls the orientation of adjacent molecules may be drawn schematically as in Figure 1. In the crystals of *para*- and *meta*-nitroanilines and their analogues, infinite molecular chains of hydrogen-bonded molecules are the most significant design element. In the case of *ortho*-isomers a competition between intramolecular and intermolecular hydrogen bonds takes place and sometimes, instead of infinite molecular chains, centric or pseudocentric dimers are formed in the crystals[10].

The problem explored recently in numerous papers concerned conditions under which the molecular chains pack in a parallel or antiparallel way, resulting, respectively, in noncentrosymmetric crystals, indispensable for obtaining nonlinear materials, or centrosymmetric crystals, in which molecular hyperpolarizabilities compensate and the crystals do not exhibit optical nonlinearity. Quantum-chemical semiempirical methods were used to calculate possible aggregates of *para*- and *meta*-nitroaniline molecules which form, respectively, centrosymmetric and noncentrosymmetric networks[12]. The results revealed the importance of second-order interactions, namely the interactions between stacking two-dimensional molecular layers and very weak CH$\cdots$O hydrogen bonds[12]. A new branch of crystal structure chemistry, i.e. crystal engineering, involves various experimental and theoretical methods, such as synthesis, statistical analysis of structural data, theoretical calculations and others, in order to understand how a subtle balance between a multitude of noncovalent forces, including hydrogen bonds, results in infinite crystal architecture built of molecular aggregates[13].

The neutron diffraction study of 2-methyl-5-nitroaniline enlightened the complex hydrogen bond network. It involves not only molecular chains formed by NH$\cdots$O synthons and assembled in a head-to-head way, but also very weak C(aryl)H$\cdots\pi$ interactions between the chains and C(methyl)H$\cdots$O and C(aryl)H$\cdots$O very weak hydrogen bonds[7]. In the case of *meta*-nitroaniline, polar chains induced by NH$\cdots$O synthons and stabilized
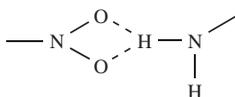
FIGURE 1. Intermolecular contacts between amino and nitro groups in *meta*- and *para*-nitroanilines

by C(aryl)H$\cdots$O interactions are present. The chains are interlinked by very weak NH$\cdots$N(O) hydrogen bonds, thus forming strands, which are localized crosswise on the *bc* plane[9, 14].

The relevant role of hydrogen bonds in the second-order response of the three optically nonlinear nitroaniline analogues, 4-nitro-4′-methylbenzylidene aniline, 5-nitro-2-{[1-phenylethyl]amino}pyridine and 3,5-dinitro-2-{[1-phenylethyl]amino}pyridine, has been reported by Cole and coworkers[15, 16]. In the first crystal, very weak hydrogen bonds between the CH groups as proton donors and the N and O atoms and the π electrons of the aromatic ring as the proton acceptors promote the second harmonic generation signal. The other significant influence on the second-order response seems to result from the stacking arrangement of almost planar molecules with a very short (about 2.6 Å) interplane spacing. In the latter crystal the intramolecular hydrogen bonds influence the molecular packing in such a way that it reduces the macroscopic nonlinear effect as compared with the former crystal[16].

The interplay of intermolecular hydrogen bonds, iodo$\cdots$nitro interactions and aromatic $\pi\cdots\pi$ stacking interactions in three iodonitroanilines has been discussed by Garden and coworkers[17]. Hydrogen exchange along NH$\cdots$O hydrogen bonds within the base pairs in DNA has been calculated in terms of proton conduction repairing bonding defects and stabilizing DNA[18].

Many other phenomena occurring in aniline derivatives have been reported recently. Worth mentioning are, e.g., thermochromism involving proton exchange within intramolecular hydrogen bonds[19], hysteresis-like behavior in *meta*-nitroaniline crystals[20] and relaxation processes corresponding to molecular dynamics in the vicinity of phase transitions[14, 21, 22].

Besides nitroanilines, another group of aniline derivatives, namely aminophenols, has recently drawn attention. Hydroxyl and amino groups are complementary as regards hydrogen bond donors and acceptors, because an amino group has two donors (hydrogen atoms) and one acceptor (a free electron pair). In a hydroxyl group there are one donor and two acceptors. This enables a multitude of possible molecular arrangements through hydrogen bonds and provides an opportunity to study crystal architecture. Molecular recognition between alcohols and amines, leading to supramolecular structures, has been reported by Ermer and Eling[23]. The crystal structure prediction method was used to explore possible modes of molecular assembly in 2-amino-4-nitrophenol that result in three polymorphic structures[24]. The crystal structures and packing features of 13 aminophenols were analyzed and correlated. Three major synthons have been distinguished: molecular sheets, infinite chains and square motifs, which result from a fine balance between several factors, including molecular structure and hydrogen bonds[25].

II. METHODOLOGY

Anilines are organic compounds with an amino group attached to a benzene ring. The Cambridge Structural Database (CSD, July 2004)[26] was used to retrieve and analyze molecular geometries and crystal structures of substituted anilines. Almost, 300,000 entries resulted in many crystal structures retrieved with *QUEST*[26], analyzed statistically with *VISTA*[26] and visualized with *PLUTO*[26]. The objective of the studies has been the statistical analysis of bond lengths and angles in aromatic rings and their correlation with the position of substituents in the ring. The geometry of amino groups and substituted amino groups has been also studied and correlated with the position of the substituents. The occurrence of intramolecular hydrogen bonds has been examined as well. Intermolecular interactions, especially intermolecular hydrogen bonds, have been studied and characterized as 2-, 3-

or 4-center interactions. The mode of molecular packing, the frequency of some motives of molecular aggregation and the preference for crystallization in some space groups will be discussed.

An amino group has strong electron donor and acceptor properties. Due to them anilines easily form various molecular co-crystals in the form of molecular salts (often with halogen anions), metal coordination compounds, charge-transfer and hydrogen-bonded complexes, neutral mixed crystals and hydrates. These crystals have not been considered here because their structure and molecular geometry originate strongly from the properties of other moieties and the interactions between moieties forming a compound. These compounds are beyond the scope of this chapter. The retrieval from the CSD was limited to 'only-organic', 'nonpolymer' crystal structures with reliability factors $R \leqslant 10\%$.

Molecules are characterized through bond lengths and angles. The bond and angle numbering in 3-substituted aniline as an example for ring-substituted anilines is shown in Figure 2. The corresponding values for two aniline molecules in the asymmetric unit cell[27] are shown in Figure 3.

The values are presented below in the form of frequency histograms and through scatter plots visualizing correlation between two values of bonds or/and angles. Frequency histograms show a relationship between the number of occurrences (Y-axis) and a parameter value (X-axis). The characteristics of each histogram, among others the *mean* and *median* value of a parameter and the *skewness* of the histogram, are given in the figure caption.

The *mean* value is the value calculated as the sum of the variable values divided by the number of variables. The *median* value is the value observed in the center of the variable distribution, i.e. there are as many observed variables above and below the median. The *skewness coefficient* is defined in equation 2,

$$\left[n \sum_{i=1}^{n}(x_i - x_{\mathrm{mean}})^3 \right] /(n-1)(n-2)s^3 \qquad (2)$$
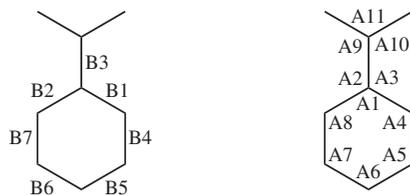
FIGURE 2. Bond and angle numbering in the aniline molecule
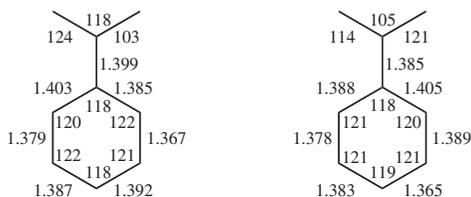
FIGURE 3. Bond and angle values in two aniline molecules in an asymmetric unit cell[27]

where s is a sample standard deviation which is given in equation 3,

$$\left[\sum_{i=1}^{n}(x - x_{\text{mean}})^2/(n - 1)\right]^{0.5} \tag{3}$$

A negative value of the skewness coefficient indicates a left-hand shift of the distribution while a positive skewness indicates a right-hand shift. A skewness value $\geqslant |2.0|$ indicates a significant deviation from the normal distribution. A large discrepancy between the mean and median values corresponds to such a strong deviation. The nonnormality of a distribution may be manifested through *multimodality*, i.e. the presence of two or more peaks, or through the presence of *outliers* in the distribution. The outliers in the frequency histograms in this chapter correspond in general to the bond and angle values in the sterically overcrowded and/or charge perturbed molecules.

The relation between two structural parameters is measured through the *correlation coefficient r*, defined by equation 4,

$$r = \frac{\sum_{i=1}^{n}[(x_i - \overline{x})(y_i - \overline{y})]}{\left\{\left[\sum_{i=1}^{n}(x_i - \overline{x})^2\right]\left[\sum_{i=1}^{n}(y_i - \overline{y})^2\right]\right\}^{0.5}} \tag{4}$$

Its value varies between -1 and 1, corresponding to perfect negative and positive correlations, respectively. A zero value indicates no correlation.

General information and useful definitions concerning statistical and numerical methods of data analysis may by found in the monograph of Bürgi and Dunitz[28] and in earlier monographs of this series[29, 30].

III. STATISTICAL ANALYSIS OF STRUCTURAL DATA RETRIEVED FROM THE CSD

A. *ortho*-Substituted Anilines

A total of 109 structures have been retrieved from the CSD. The frequency histograms of the B1 to B7 bond lengths, the A1, A4 to A8 benzene ring angles and the A9 to A11 amino group angles are shown in Figure 4. An analysis of these histograms leads to the following conclusions:

(1) The B1 bond (between *ortho*-substituents) is longer than other bonds in the benzene ring.
(2) The A1 angle (at the amino group) is smaller than other angles in the ring.
(3) The A9, A10 and A11 angles, which depict the hydrogen positions in the amino groups, have mean and median values about $116°$ and $117°$, respectively. They indicate some degree of amino group pyramidalization. This effect is undoubtedly influenced by the interactions between the substituents in the *ortho*-position. The positive value of skewness in the A9 frequency histogram and the negative skewness in the A10 and A11 histograms corroborate this interpretation.

(4) The outliers in the histograms correspond to the parameter values in the zwitte-rionic molecules (e.g. in the low-temperature, triboluminescent polymorph of 2-aminobenzoic acid[31, 32]) or to values in the molecules with bulky *ortho*-substituents. Also, the multimodality of some histograms results from the unusual parameter values in such molecules.

(5) Correlation coefficients of |0.6| to |0.8| have been found between the A1 and A4 values (negative value), the A4 and A5 values (negative value), the A5 and A6
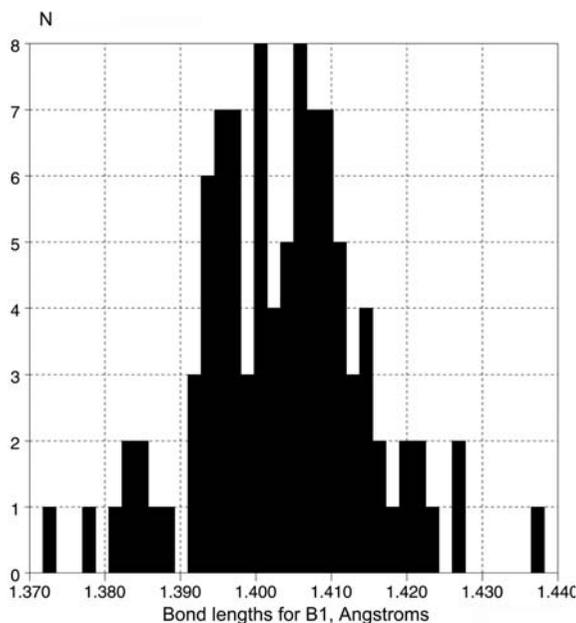
(a)

FIGURE 4. Histograms of number of occurrences (N) for bond (B) and angle (A) values in *ortho*-substituted anilines. For each histogram the number of observations, minimum, maximum, mean and median bond lengths (angles), skewness, mean SE and sample SD are given in the follow-ing order. (a) For B1 (97, 1.373, 1.437, 1.403, 1.404, 0.036, 0.001, 0.011). (b) For B2 (97, 1.350, 1.433, 1.397, 1.397, −0.073, 0.001, 0.012). (c) For B3 (92, 1.337, 1.422, 1.380, 1.379, 0.086, 0.002, 0.017). (d) For B4 (91, 1.343, 1.416, 1.392, 1.394, −1.261, 0.001, 0.012). (e) For B5 (91, 1.348, 1.418, 1.379, 1.380, 0.149, 0.001, 0.012). (f) For B6 (91, 1.304, 1.409, 1.380, 1.381, −2.059, 0.001, 0.014). (g) For B7 (90, 1.329, 1.398, 1.372, 1.373, −0.835, 0.001, 0.013). (h) For A1 (90, 115.382, 120.809, 118.301, 118.271, −0.076, 0.102, 0.967). (i) For A4 (90, 116.747, 122.396, 119.614, 119.547, 0.193, 0.130, 1.233). (j) For A5 (90, 116.685, 123.194, 121.120, 121.161, −0.941, 0.111, 1.053). (k) For A6 (90, 115.504, 122.132, 119.113, 119.054, −0.209, 0.084, 0.796). (l) For A7 (90, 118.445, 123.891, 120.857, 120.753, 0.594, 0.093, 0.887). (m) For A8 (90, 116.000, 122.807, 120.955, 121.057, −2.072, 0.096, 0.909). (n) For A9 (90, 102.085, 135.143, 115.786, 116.303, 0.132, 0.519, 4.924). (o) For A10 (90, 95.893, 138.375, 116.093, 116.545, −0.071, 0.589, 5.592). (p) For A11 (90, 80.722, 141.970, 116.070, 117.468, −1.226, 0.966, 9.168)

(b)

(c)

FIGURE 4. (*continued*)

Bond lengths for B4, Angstroms

(d)

Bond lengths for B5, Angstroms
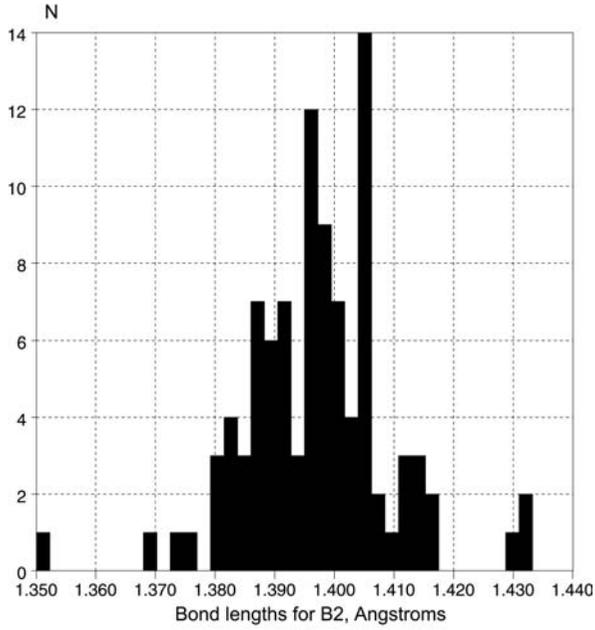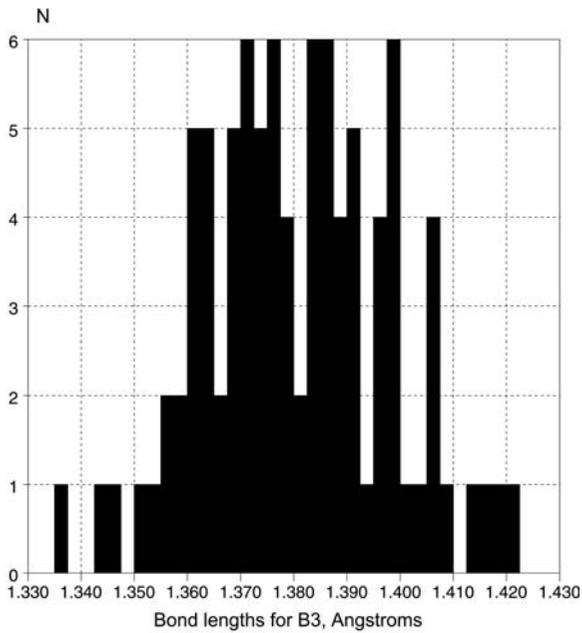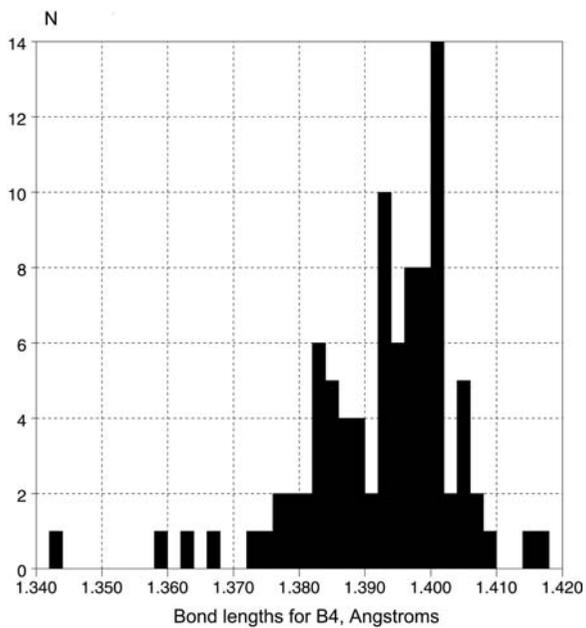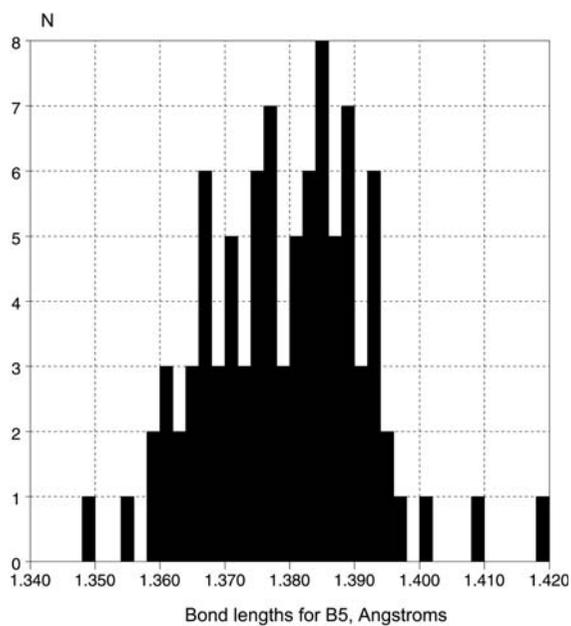
(e)

FIGURE 4. (*continued*)

(f)

(g)

FIGURE 4. (*continued*)

Angles for A1, degrees

(h)

Angles for A4, Angstroms

(i)
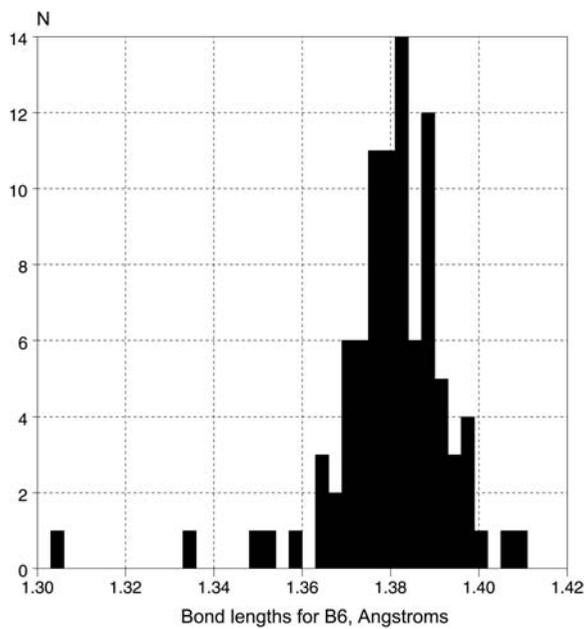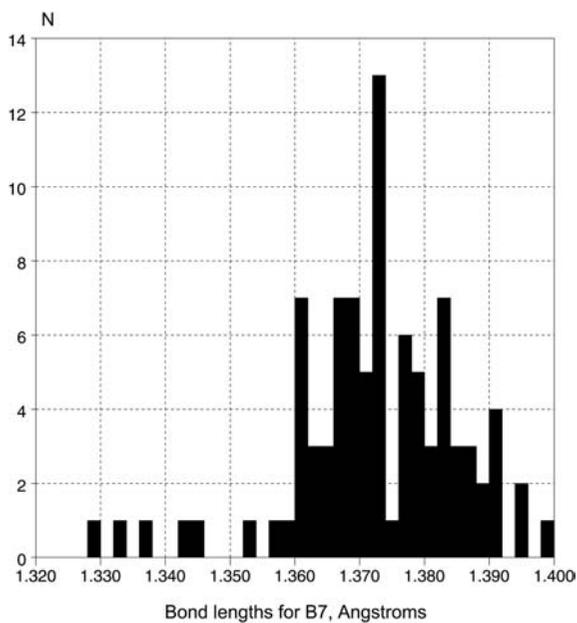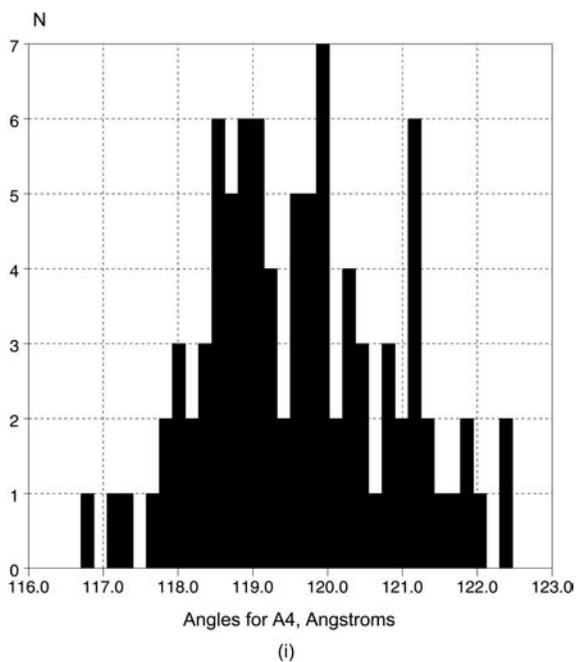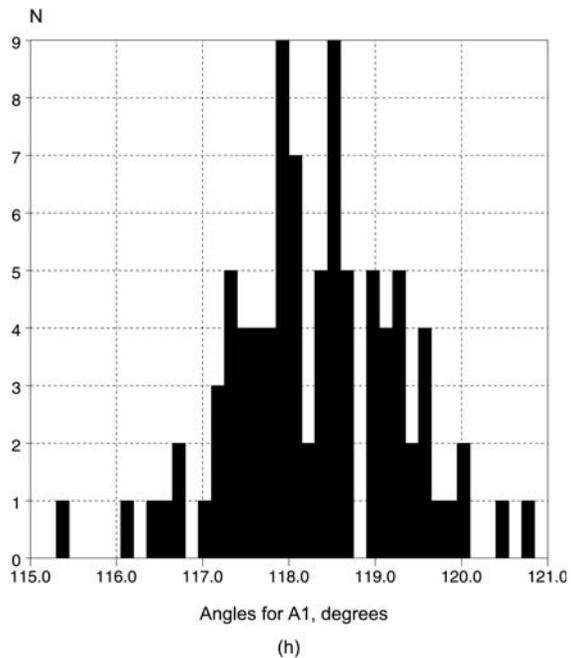
FIGURE 4. (*continued*)

(j)

(k)

FIGURE 4. (*continued*)

Angles for A7, degrees

(l)

Angles for A8, degrees

(m)

FIGURE 4. (*continued*)

Angles for A9, degrees

(n)

Angles for A10, degrees

(o)

FIGURE 4. (*continued*)

N

Angles for A11, degrees

(p)
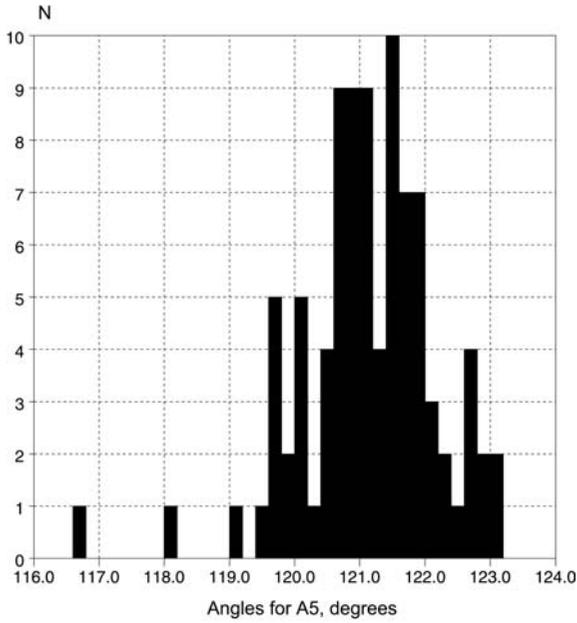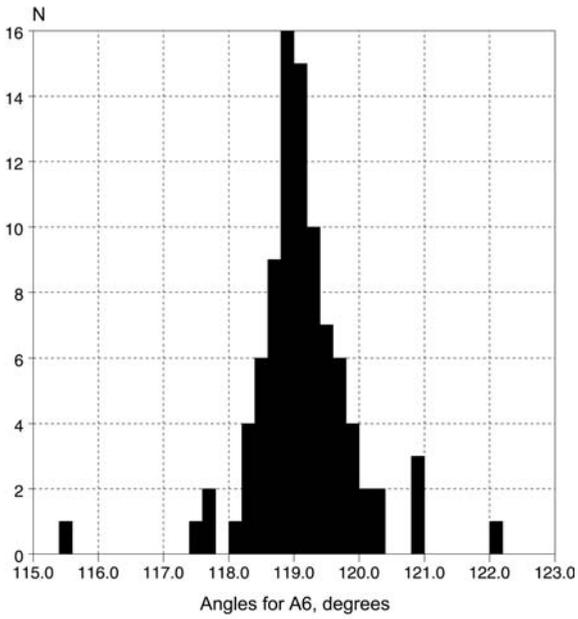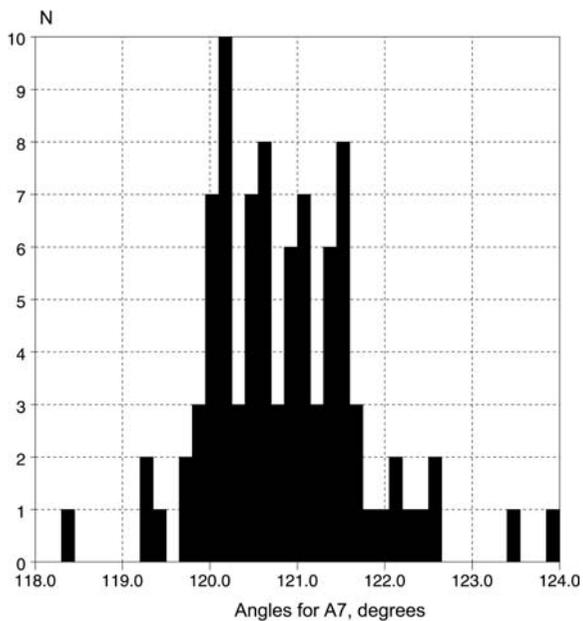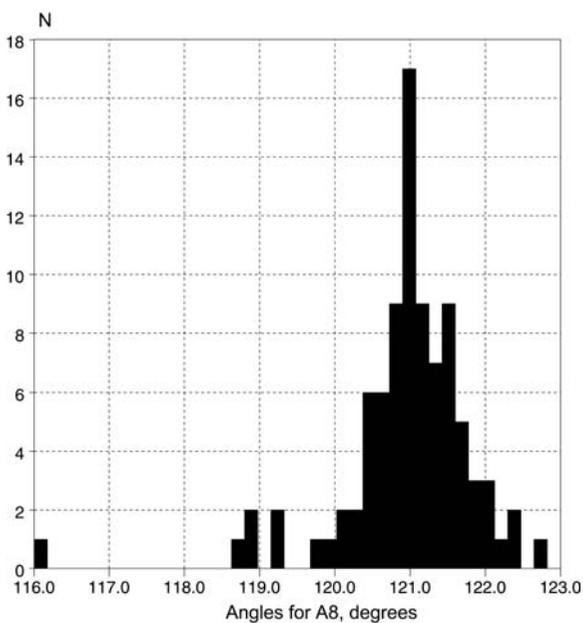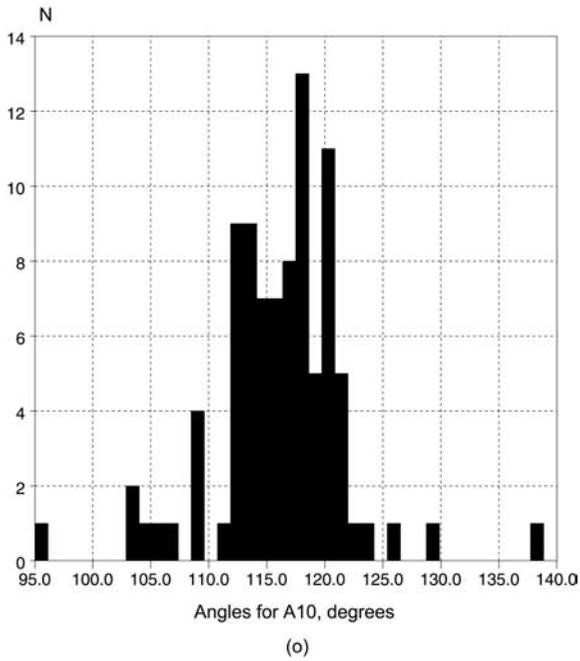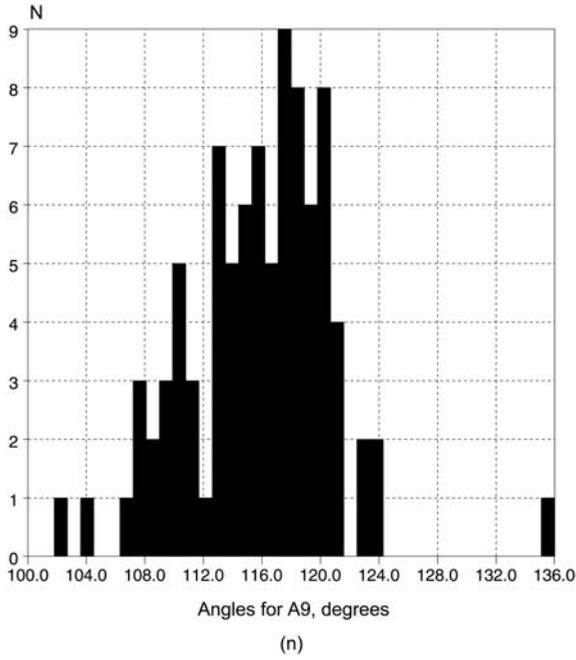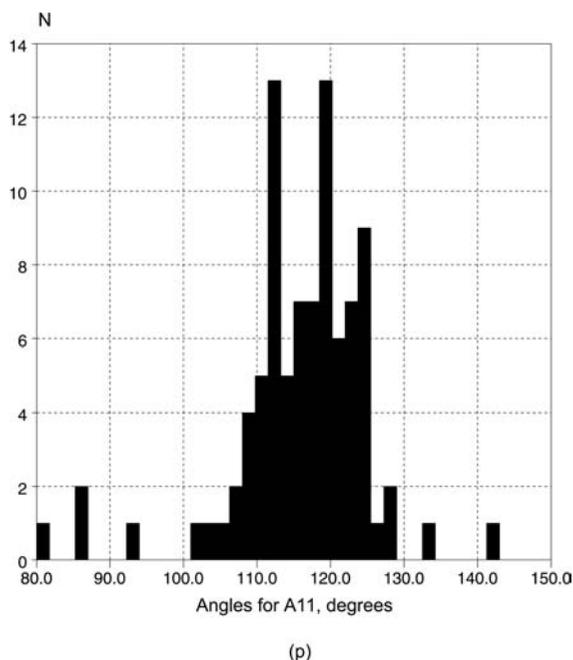
FIGURE 4. (*continued*)

values (negative value) and the A8 and B6 values (positive value). The corresponding scatter plots are shown Figure. 5. These correlation coefficients reflect deformation of aromatic rings in *ortho*-substituted anilines.

B. *meta*-Substituted Anilines

The retrieval from the CSD resulted in 17 crystal structures out of 295,000 entries. The frequency histograms of the molecular bonds and angles are shown in Figure 6. Their analysis leads to the following conclusions:

(1) The A1 angle is distinctly smaller than 120° (the classic value for a regular hexagon).
(2) The values of the A5 angle (at the substituent in the *meta*-position) are often larger than 120° (the median value is 121.2°).
(3) The A6 angle values are smaller than 120°.
(4) The degree of pyramidalization of the amino group is variable, depending on the compound.

Strong correlations with correlation coefficients $\geqslant|0.8|$ have been found between B6 and B1 values, A5 and A4 values and A6 and A5 values. The corresponding scatter plots are shown in Figure 7.

Grażyna Maria Wójcik
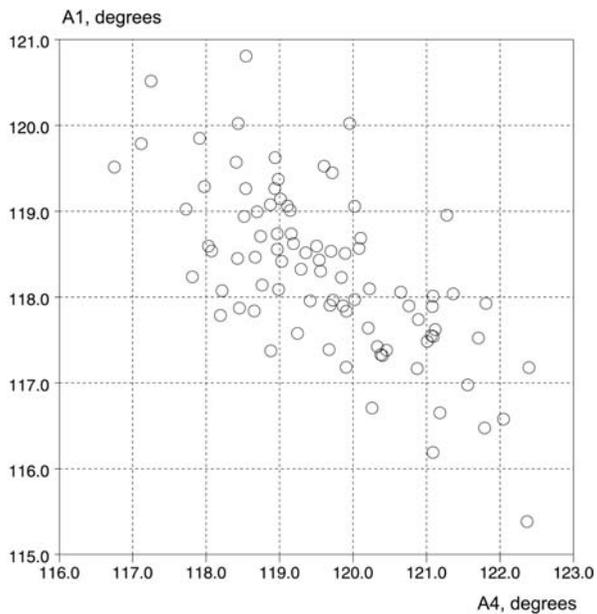
(a)
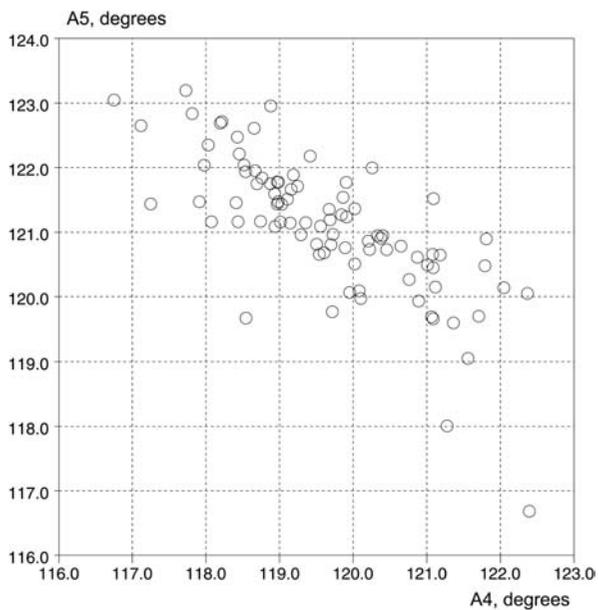
(b)

FIGURE 5. Scatter plots of the correlations between values of (a) A1 vs A4; (b) A5 vs A4; (c) A6 vs A5; (d) B6 vs A8 values in *ortho*-substituted anilines. The *r* values range from |0.6| to |0.8|
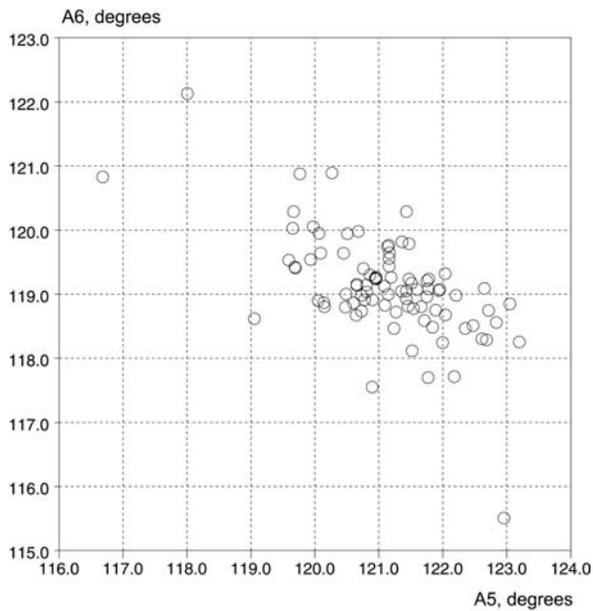
(c)
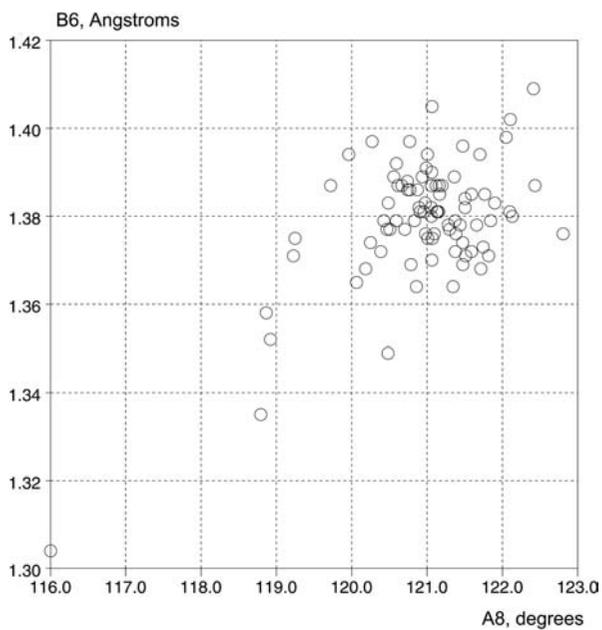
(d)

FIGURE 5. (*continued*)
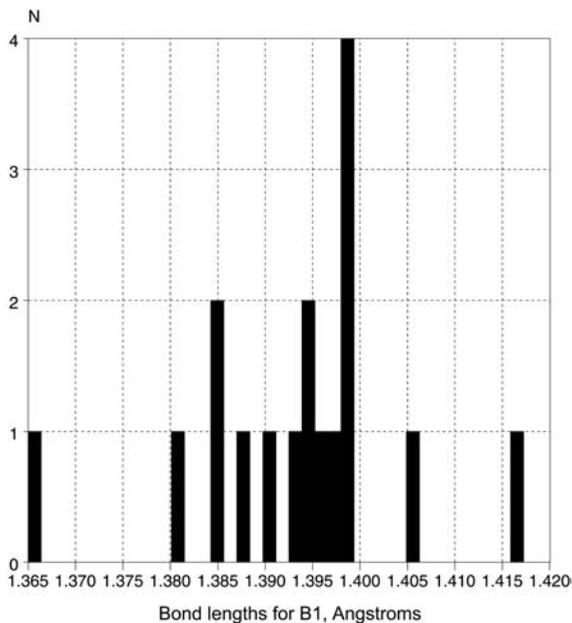
FIGURE 6. Histograms of number of occurrences (N) for bond (B) and angle (A) values in *meta*-substituted anilines. For each histogram the number of observations, minimum, maximum, mean and median bond lengths (angles), skewness, mean SE and sample SD are given in the following order. (a) For B1 (17, 1.366, 1.416, 1.393, 1.395, −0.447, 0.003, 0.011). (b) For B2 (17, 1.370, 1.419, 1.394, 1.395, −0.160, 0.003, 0.011). (c) For B3 (17, 1.365, 1.452, 1.400, 1.395, 0.726, 0.005, 0.022). (d) For B4 (17, 1.367, 1.428, 1.387, 1.384, 1.268, 0.004, 0.015). (e) For B5 (17, 1.368, 1.408, 1.385, 1.387, 0.286, 0.003, 0.011). (f) For B6 (17, 1.348, 1.412, 1.383, 1.385, −0.309, 0.003, 0.014). (g) For B7 (17, 1.366, 1.410, 1.383, 1.383, 1.155, 0.002, 0.009). (h) For A1 (17, 117.819, 120.891, 118.981, 118.917, 0.466, 0.198, 0.817). (i) For A4 (17, 117.987, 122.394, 119.706, 119.341, 0.388, 0.340, 1.402). (j) For A5 (17, 118.233, 124.417, 121.613, 121.189, −0.042, 0.493, 2.032). (k) For A6 (17, 116.739, 121.076, 118.132, 118.021, 0.559, 0321, 1.324). (l) For A7 (17, 119.722, 123.432, 121.365, 121.240, 0.561, 0.187, 0.773). (m) For A8 (17, 118.517, 121.199, 120.164, 120.112, −0.576, 0.184, 0.757). (n) For A9 (17, 106.323, 123.939, 116.619, 119.711, −0.664, 1.334, 5.500). (o) For A10 (17, 103.015, 123.222, 115.648, 116.816, −0.638, 1.362, 5.615). (p) For A11 (17, 91.287, 128.034, 114.475, 117.178, −0.933, 2.181, 8.994)

Bond lengths for B2, Angstroms

(b)

Bond lengths for B3, Angstroms

(c)

FIGURE 6. (*continued*)

Bond lengths for B4, Angstroms

(d)

Bond lengths for B5, Angstroms

(e)

FIGURE 6. (*continued*)

Bond lengths for B6, Angstroms

(f)

Bond lengths for B7, Angstroms
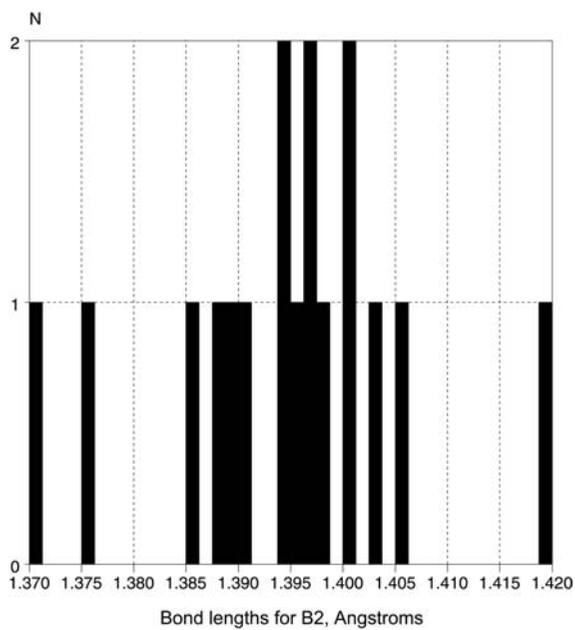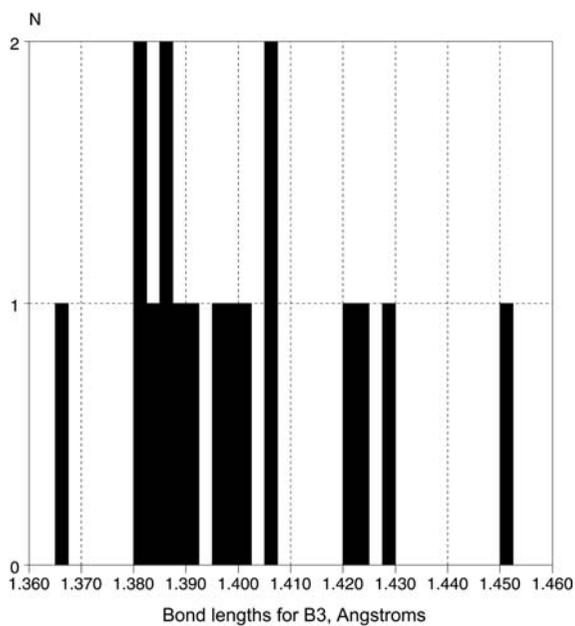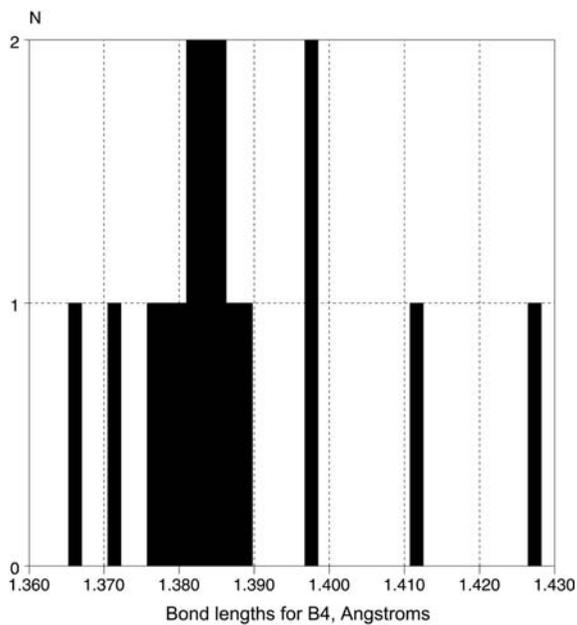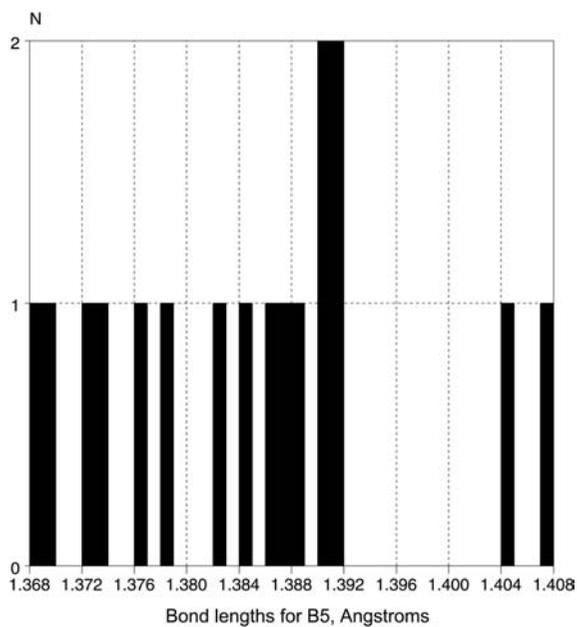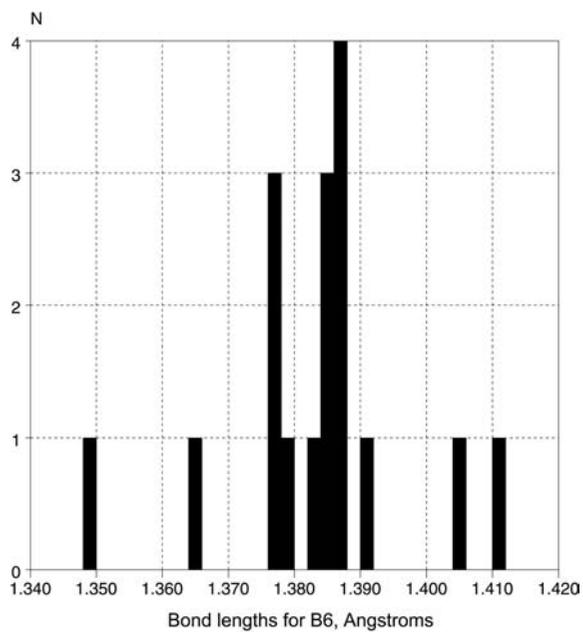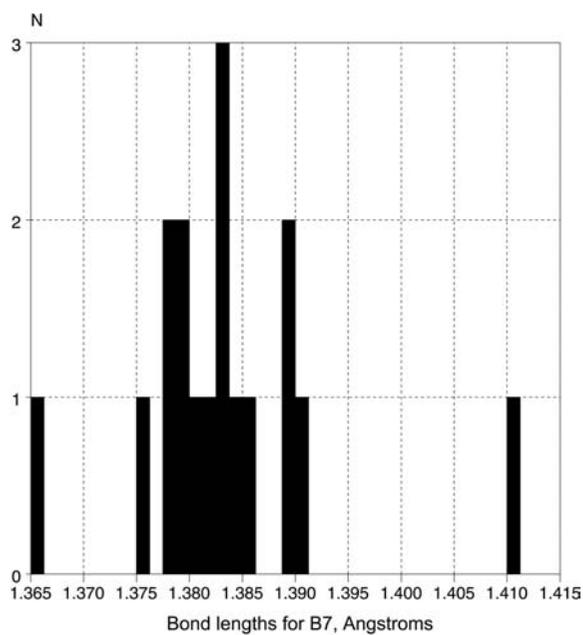
(g)

FIGURE 6. (*continued*)

(h)

(i)

FIGURE 6. (*continued*)

Angles for A5, degrees

(j)

Angles for A6, degrees
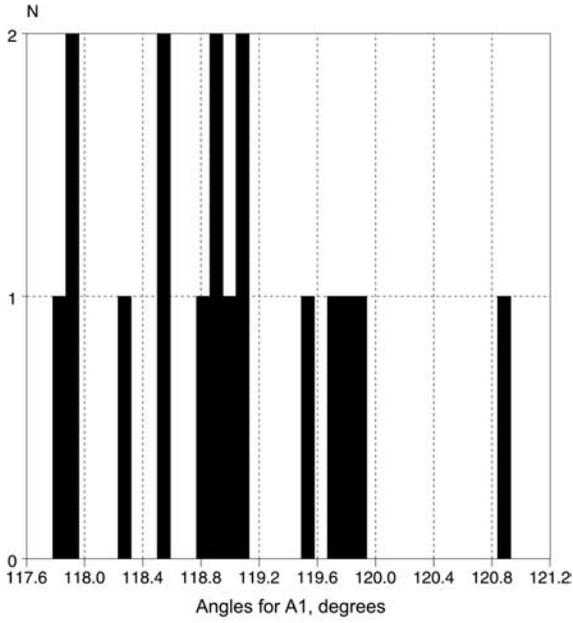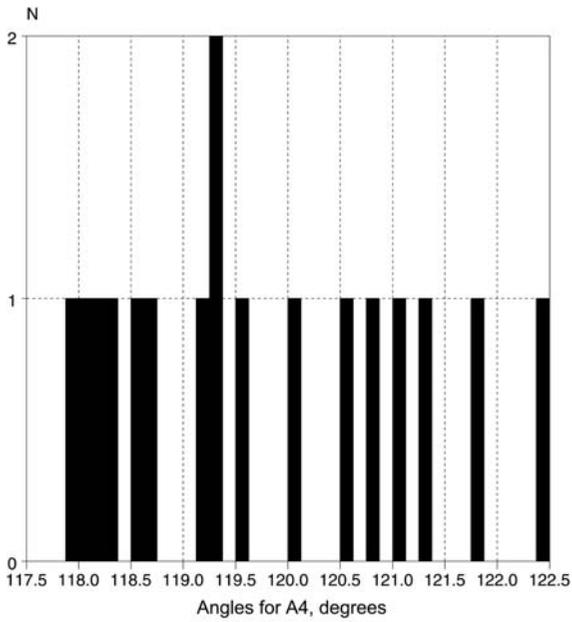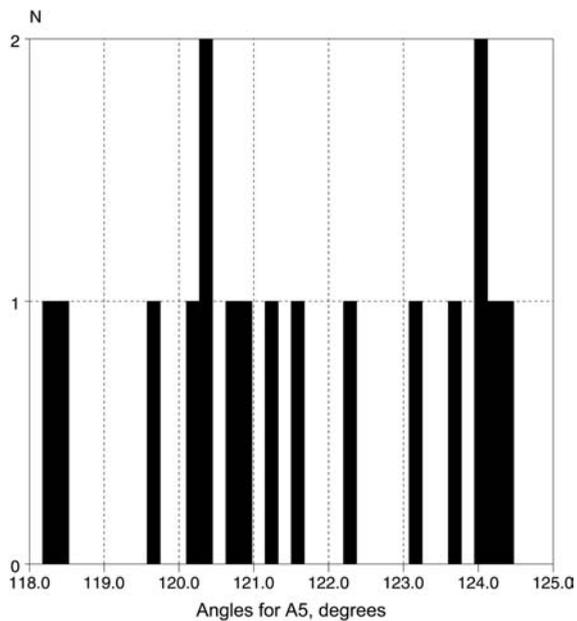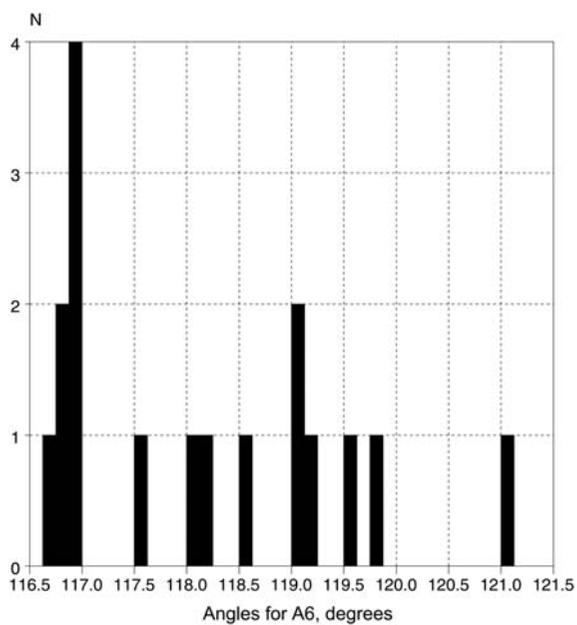
(k)

FIGURE 6. (*continued*)

(l)

(m)

FIGURE 6. (*continued*)

Angles for A9, degrees

(n)

Angles for A10, degrees
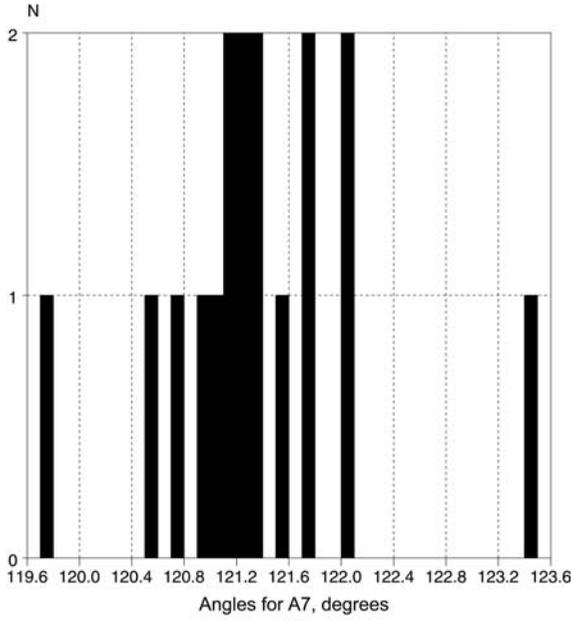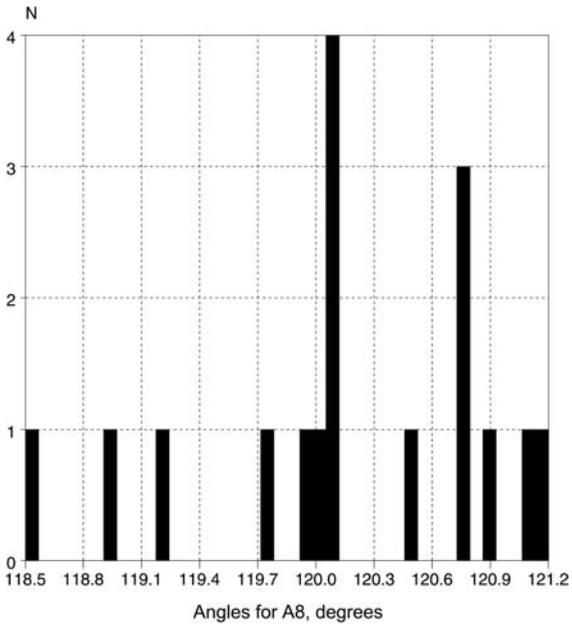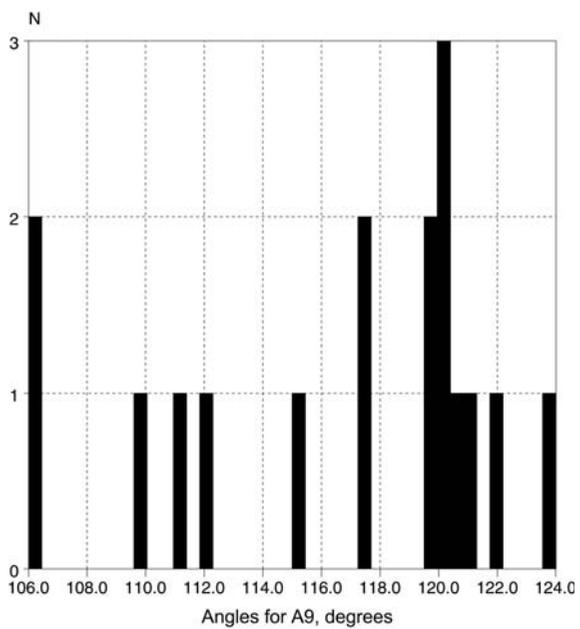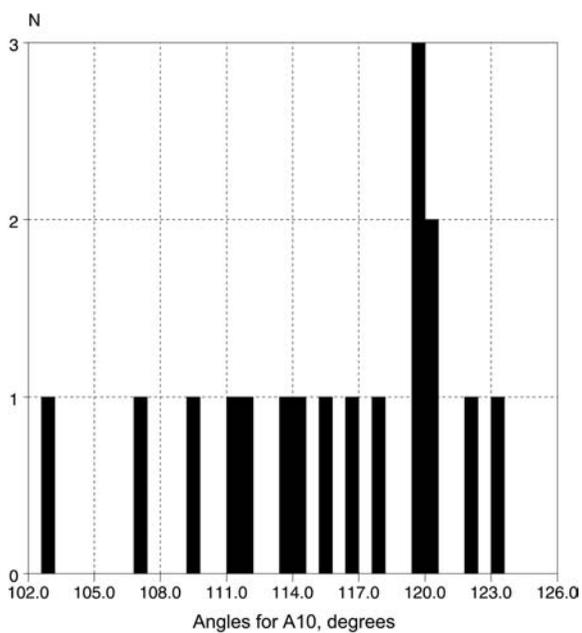
(o)

FIGURE 6. (*continued*)

(p)

FIGURE 6. (*continued*)

(a)
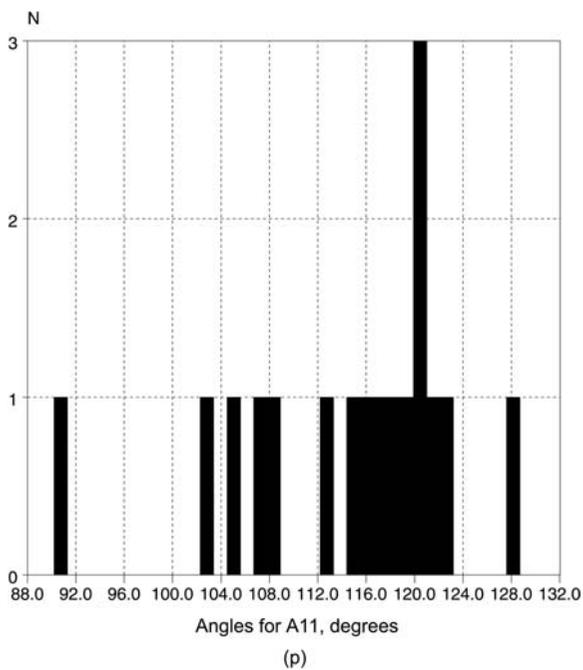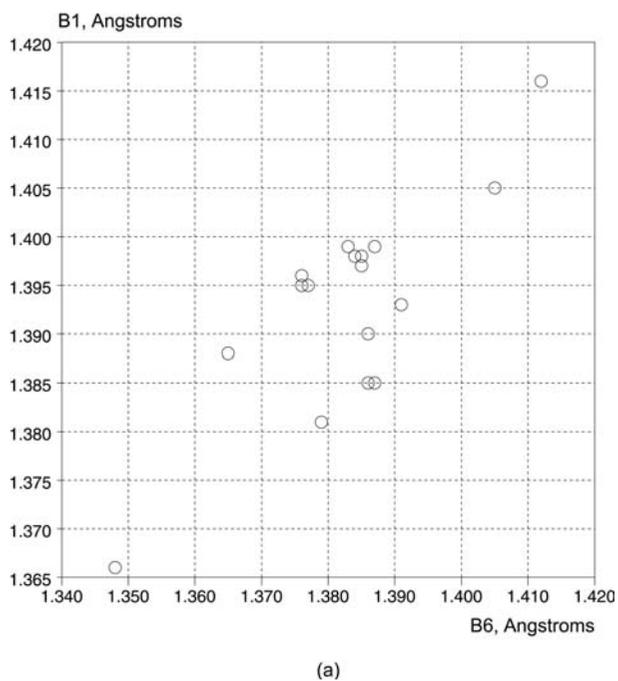
FIGURE 7. Scatter plots of the correlations between values of (a) B1 vs B6, (b) A4 vs A5, (c) A5 vs A6 values in *meta*-substituted anilines. The *r* values are ⩾|0.8|
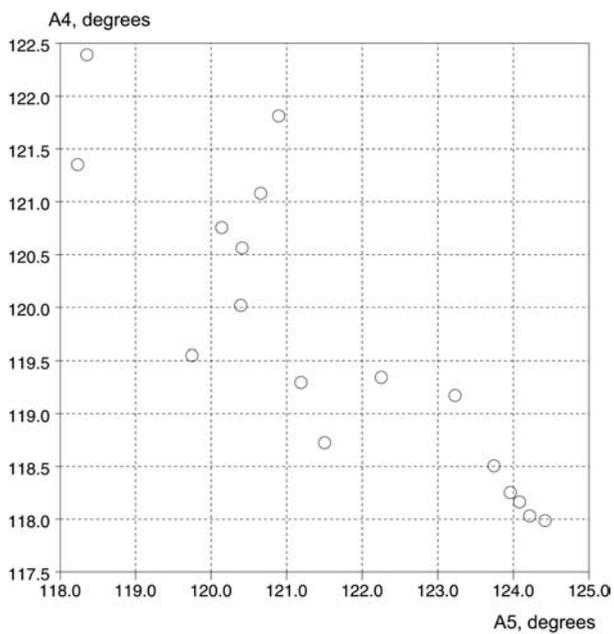
(b)
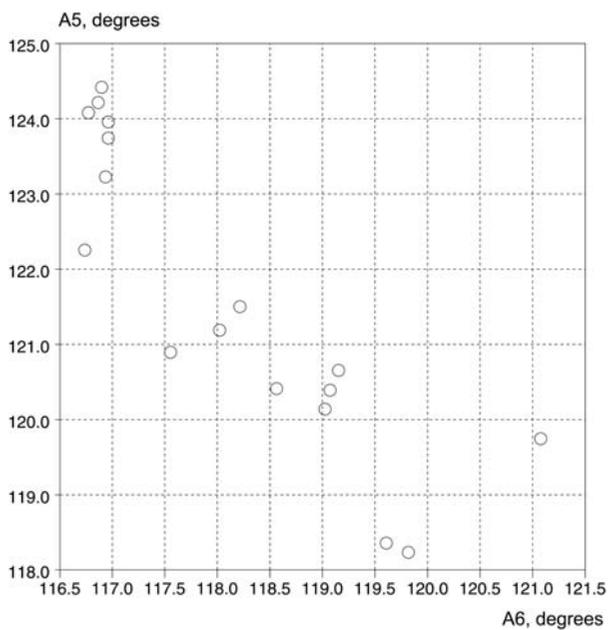
(c)

FIGURE 7. (*continued*)

Significant correlations with correlation coefficients ranging between |0.6| and |0.8| have been found between A6 and A9, A1 and B3, B4 and B6, B4 and A9 and A4 and A6 values.

C. *para*-Substituted Anilines

The retrieval from the CSD resulted in 154 crystal structures out of 295,000 entries. The frequency histograms of the molecular bonds and angles are shown in Figure 8. The detailed analysis of the histograms may be summarized as follows:

(a)
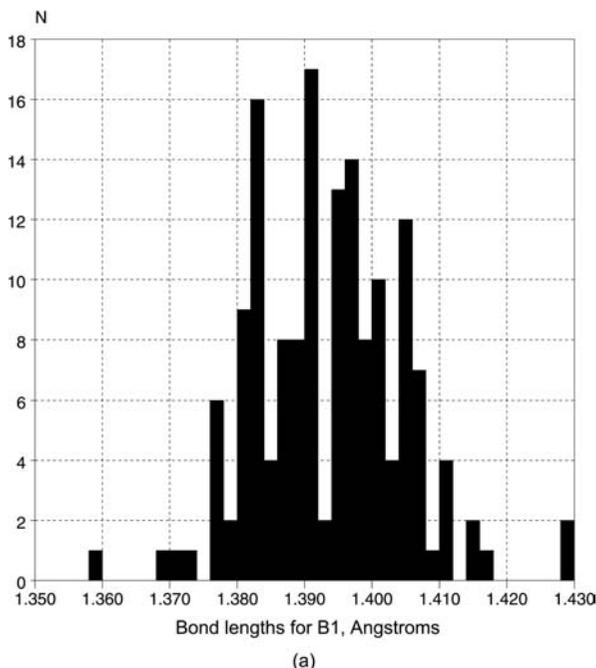
FIGURE 8. Histograms of number of occurrences (N) for bond (B) and angle (A) values in *para*-substituted anilines. For each histogram the number of observations, minimum, maximum, mean and median bond lengths (angles), skewness, mean SE and sample SD are given in the following order. (a) For B1 (154, 1.358, 1.429, 1.393, 1.394, 0.200, 0.001, 0.011). (b) For B2 (154, 1.345, 1.429, 1.393, 1.395, −1.046, 0.001, 0.013). (c) For B3 (151, 1.344, 1.441, 1.381, 1.379, 0.581, 0.001, 0.018). (d) For B4 (151, 1.341, 1.407, 1.377, 1.378, −0.277, 0.001, 0.011). (e) For B5 (150, 1.335, 1.409, 1.387, 1.388, −1.147, 0.001, 0.011). (f) For B6 (147, 1.364, 1.416, 1.390, 1.391, −0.189, 0.001, 0.009). (g) For B7 (147, 1.350, 1.407, 1.376, 1.377, −0.064, 0.001, 0.011). (h) For A1 (147, 115.937, 121.177, 118.418, 118.424, 0.368, 0.063, 0.766). (i) For A4 (146, 119.002, 122.326, 120.735, 120.768, −0.170, 0.050, 0.610). (j) For A5 (146, 118.774, 122.875, 120.579, 120.478, 0.287, 0.077, 0.925). (k) For A6 (146, 115.890, 122.107, 118.954, 119.382, −0.215, 0.115, 1.386). (l) For A7 (146, 117.546, 122.759, 120.540, 120.576, −0.197, 0.079, 0.950). (m) For A8 (146, 118.350, 122.892, 120.753, 120.716, −0.316, 0.060, 0.730). (n) For A9 (146, 89.300, 149.367, 116.559, 117.195, 0.116, 0.593, 7.169). (o) For A10 (146, 78.675, 145.237, 117.480, 118.049, −0.376, 0.649, 7.841). (p) For A11 (146, 46.025, 149.794, 115.252, 116.131, −1.606, 0.999, 12.072)

Bond lengths for B2, Angstroms

(b)

Bond lengths for B3, Angstroms
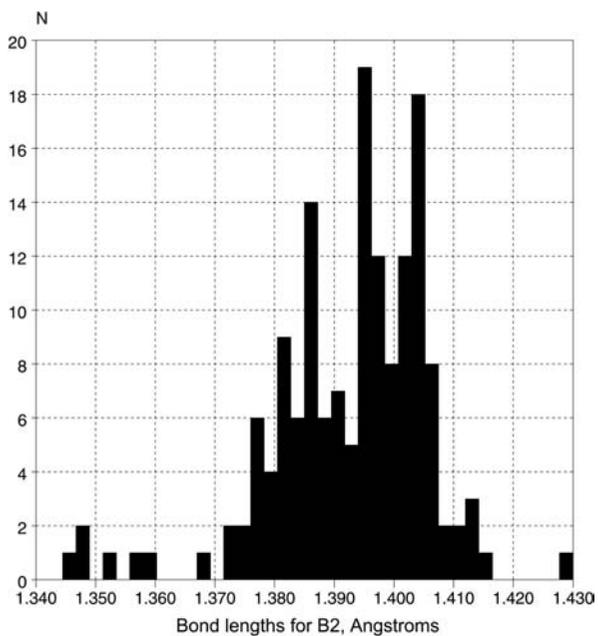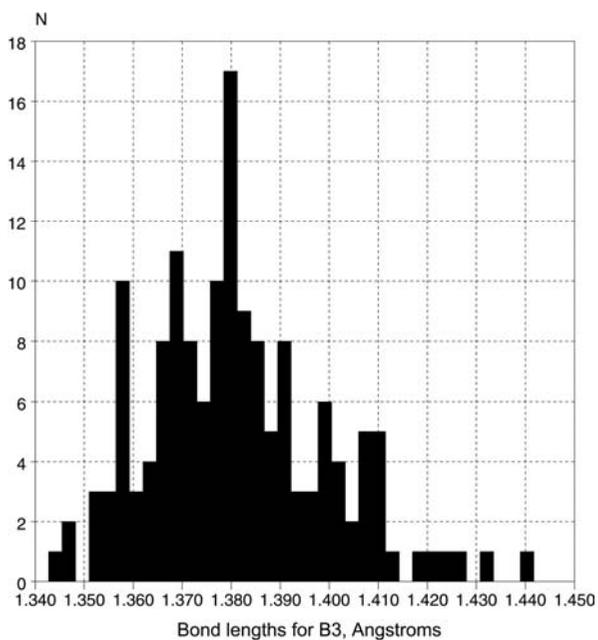
(c)

FIGURE 8. (*continued*)

(d)

(e)

FIGURE 8. (*continued*)

Bond lengths for B6, Angstroms

(f)

Bond lengths for B7, Angstroms

(g)

FIGURE 8. (*continued*)

(h)

(i)

FIGURE 8. (*continued*)

Angles for A5, degrees

(j)

Angles for A6, degrees

(k)

FIGURE 8. (*continued*)

Angles for A7, degrees
(l)

Angles for A8, degrees
(m)

FIGURE 8. (*continued*)

Angles for A9, degrees
(n)

Angles for A10, degrees
(o)
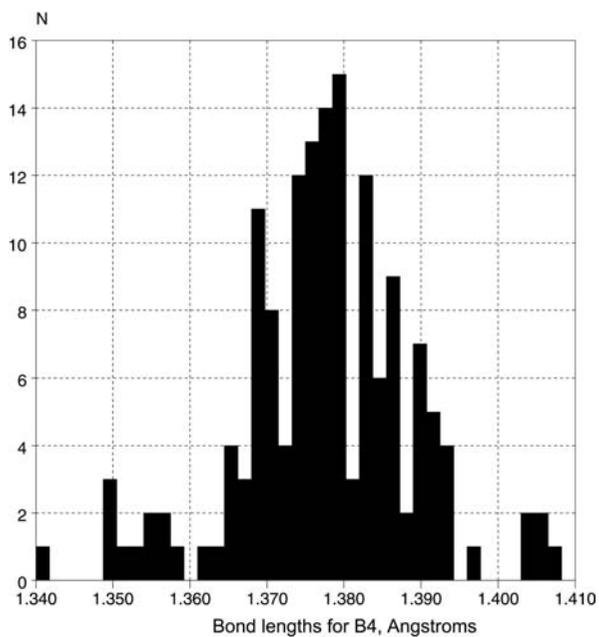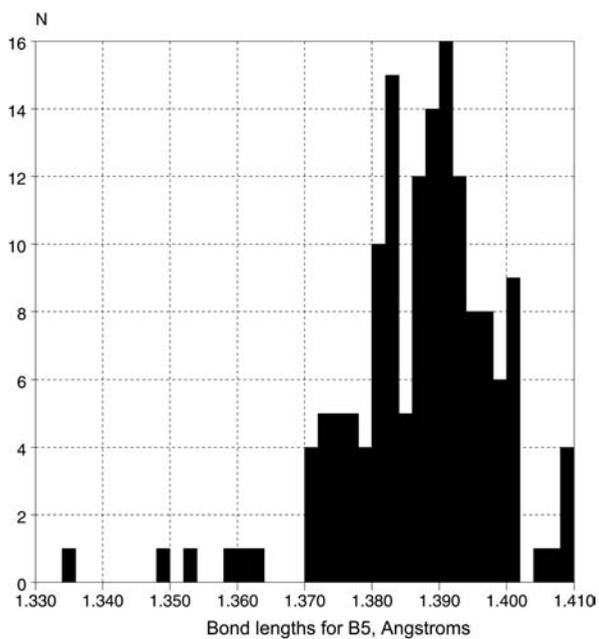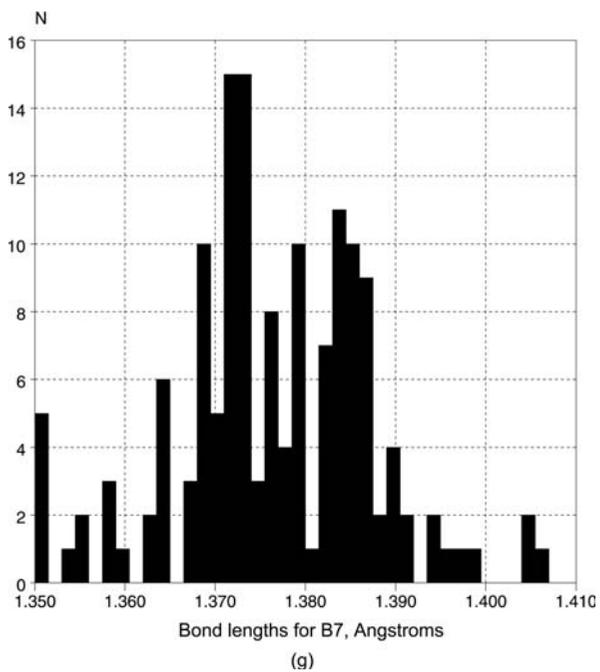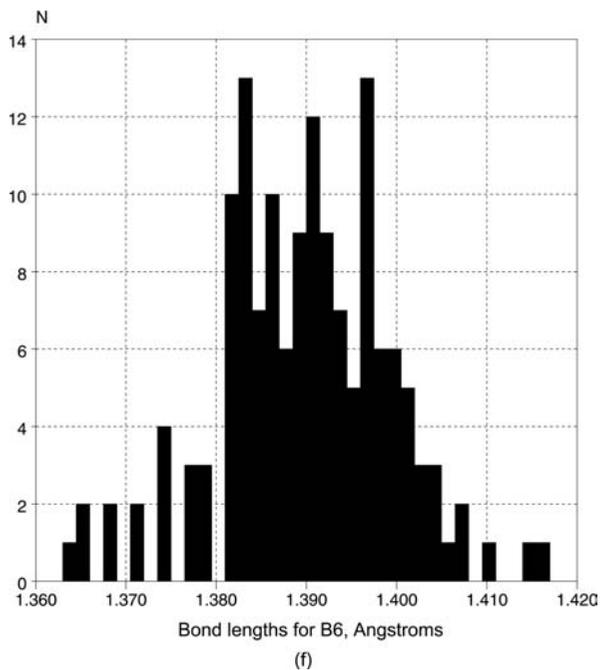
FIGURE 8. (*continued*)
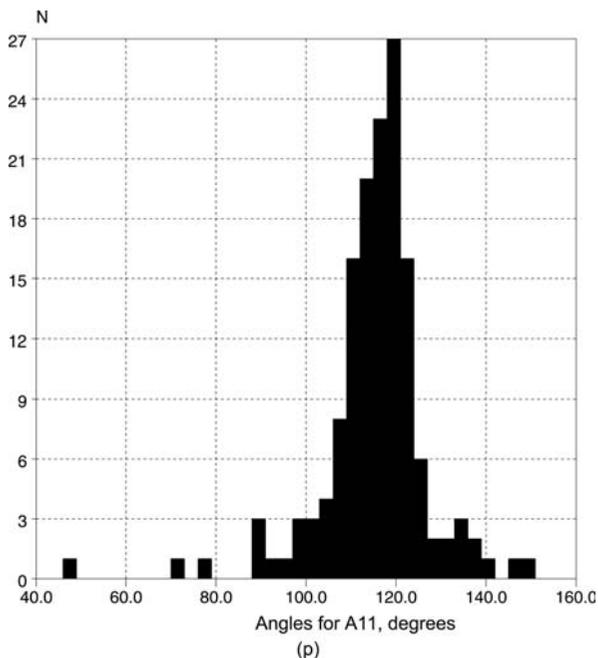
FIGURE 8. (*continued*)

(1) The B4 and B7 bonds are distinctly shorter than other bonds in the ring. Their median values amount to 1.377 Å and 1.378 Å and may be compared with the median values of 1.388 Å, 1.391 Å, 1.395 Å and 1.394 Å of the other bonds. This indicates a significant contribution of quinoid structure in *para*-substituted anilines.
(2) The A1 angle in the ring is distinctly smaller than the other angles in the ring. The median value is 118.42° and the distribution exhibits a small positive skewness. The A6 angle (opposite the A1 angle) has a median value of 119.4° and a mean value of 118.9°. These values are slightly smaller than the values of the A4, A5, A6 and A7 angles and indicate a quinoid charge distribution in the benzene ring.
(3) The A9, A10 and A11 angles reflecting the amino group geometry have median values of 117.2°, 118° and 116.1°, respectively. The degree of pyramidalization is therefore comparable to that in the *ortho*-substituted anilines and is less pronounced than in the *meta*-substituted anilines, with the reservation that the number of retrieved *meta*-anilines is distinctly smaller than the number of *ortho*- and, especially, *para*-anilines.

The outliers and multimodality in the histograms correspond to the parameter values in the molecules with bulky *para*-substituents or zwitterions with NH_3^+ groups in the molecule.

High correlation coefficients of -0.877 and -0.824 for the A5 vs A6 angles and the A6 vs A7 angles, respectively, reflect the high level of correlation. The corresponding scatter plots are shown in Figure 9.
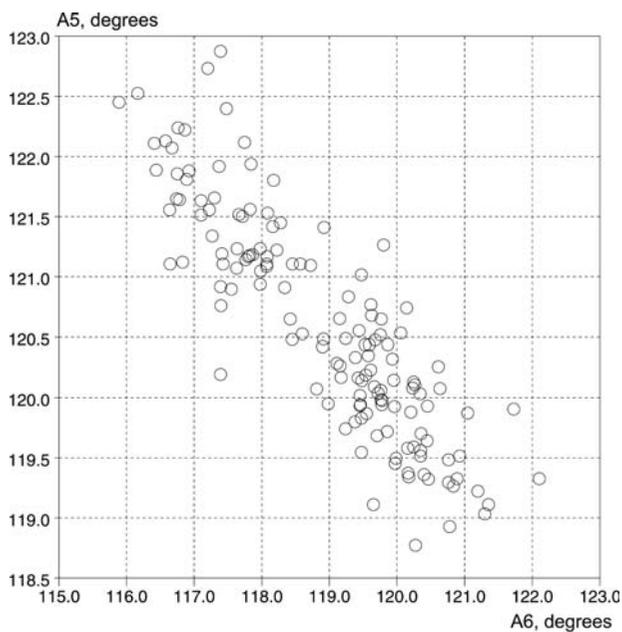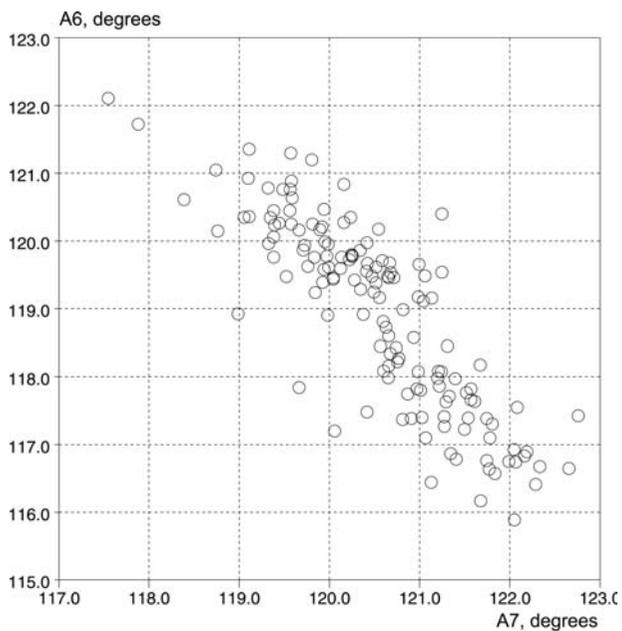
FIGURE 9. Scatter plots of the correlations between values of (a) A5 vs A6 ($r = -0.877$) and (b) A6 vs A7 ($r = -0.824$) in *para*-substituted anilines

D. Disubstituted Anilines

1. 2,4-Disubstituted anilines

A total of 29 crystal structures of 2,4-disubstituted anilines have been retrieved from the CSD. The informative frequency histograms refer to the A9, A10 and A11 angles, which depict the amino group geometry. They are shown in Figure 10.

Most of the angles are equal to 120°, thus indicating the preferred planar configuration of the amino groups. The smallest and largest values of the angles correspond to the molecules with bulky substituents in the 2 and 4 positions with respect to the amino group. They evidently influence the amino hydrogen positions through intramolecular and intermolecular interactions.

Strong correlations with correlation coefficients < -0.8 are observed between the A1 and A8, A6 and A7 and A5 and A6 values. Figure 11 presents the A7 vs A6 scatter plot with a correlation coefficient of -0.914.

(a)
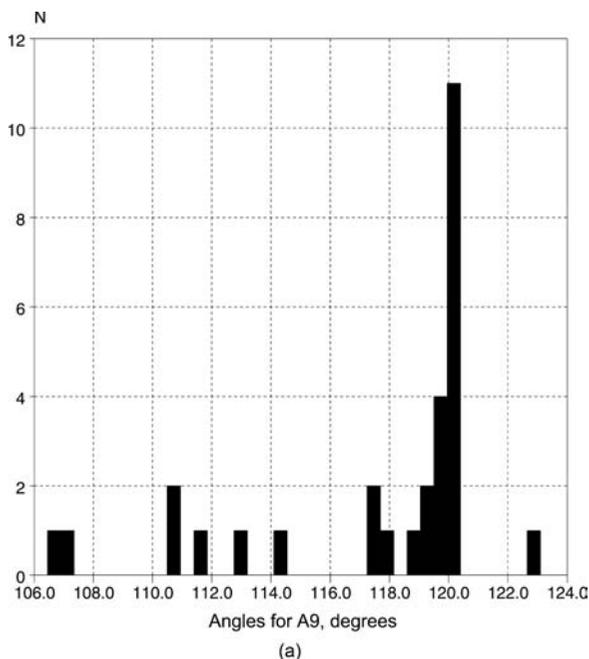
FIGURE 10. Histograms of number of occurrences (N) for bond (B) and angle (A) values in 2,4-disubstituted anilines. For each histogram the number of observations, minimum, maximum, mean and median bond lengths (angles), skewness, mean SE and sample SD are given in the following order. (a) For A9 (29, 106.456, 122.762, 117.438, 119.674, −1.294, 0.794, 4.282). (b) For A10 (29, 114.695, 137.174, 120.417, 119.986, 2.061, 0.774, 4.170). (c) For A11 (29, 107.922, 135.379, 120.004, 120.019, 0.526, 0.976, 5.257)

Angles for A10, degrees

(b)

Angles for A11, degrees

(c)
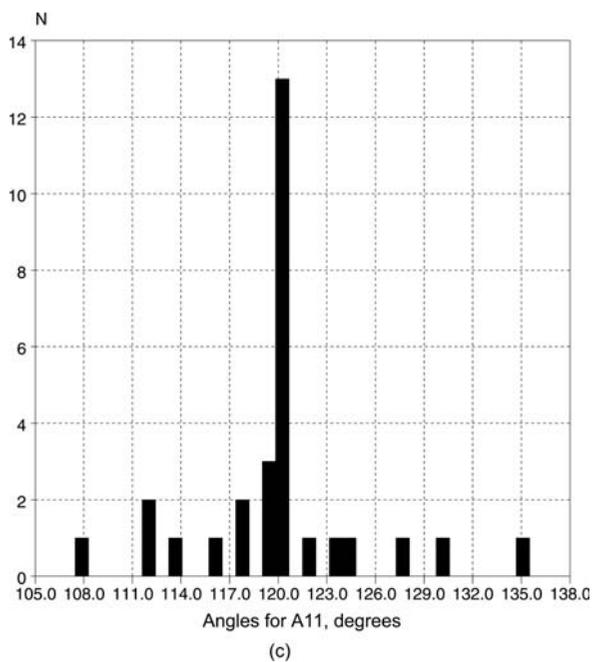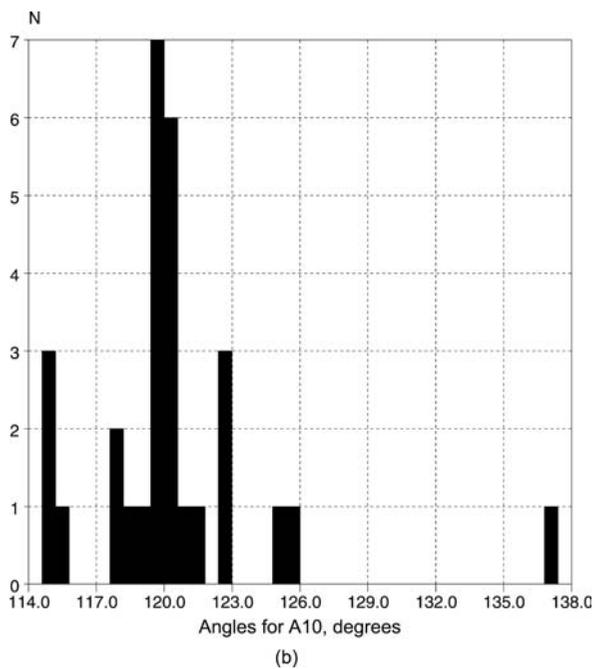
FIGURE 10. (*continued*)

Grażyna Maria Wójcik
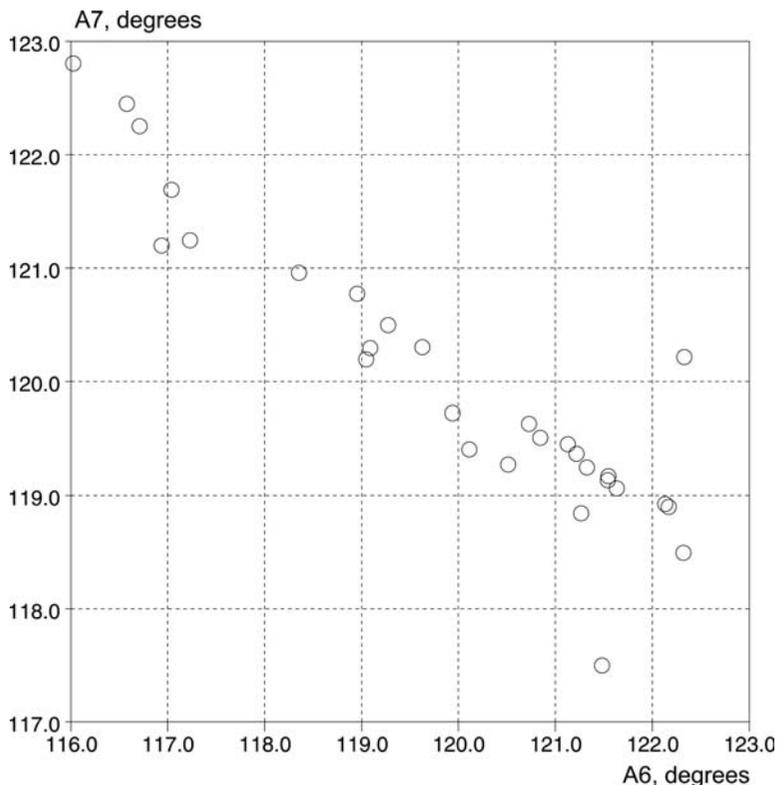
FIGURE 11. A scatter plot of the correlation between values of A7 vs A6 ($r = -0.914$) in 2,4-disubstituted anilines

2. 3,4-Disubstituted anilines

Only 24 crystal structures resulted from 298,097 entries in the CSD. The relevant frequency histograms correspond to the B5, A1, A9, A10 and A11 values and are shown in Figure 12.

The median value of 1.396 Å of B5 is close to the classic bond length in a 3,4-disubstituted aromatic ring (1.397 Å)[33]. The dispersion of the values from 1.374 to 1.416 Å is not very large, bearing in mind the position of the two substituents. The shortest distance, 1.320 Å, results probably from the intramolecular charge transfer and some quinoid contribution in the charge-perturbed molecule of 5-amino-2-nitroaniline[34].

The A1 angle value (at the amino group) is distinctly smaller than the other angles in the aromatic ring. The minimum value, 114.8°, refers to 5-amino-2-nitroaniline[34]. The A9, A10 and A11 angle values indicate a preferred planar configuration of the amino group.

Strong correlations with correlation coefficients >0.8 were found between B4 vs B7 and B3 vs B7 values. This may indicate some contribution of the quinoid structure of the molecules. The corresponding scatter plots are shown in Figure 13.

3. 3,5-Disubstituted anilines

Only 5 crystal structures have been retrieved from the CSD. These are the crystal structures of 3,5-dinitroaniline[34], 3,5-diaminobenzoic acid[35] and 3,5-dichloroaniline[36]. The small number of data makes any meaningful statistical analysis impossible. The A1 angles are smaller than 120°. The values of the A9, A10 and A11 angles are close to 120°, indicating a nearly planar configuration of the amino groups in the crystals.

4. 2,3-Disubstituted anilines

Only one crystal structure, that of 2,3-dichloroaniline[36], has been retrieved from the CSD. The A1 angle is smaller than other angles in the aromatic ring. The amino group exhibits strong pyramidalization, probably due to steric hindrance in the molecule.
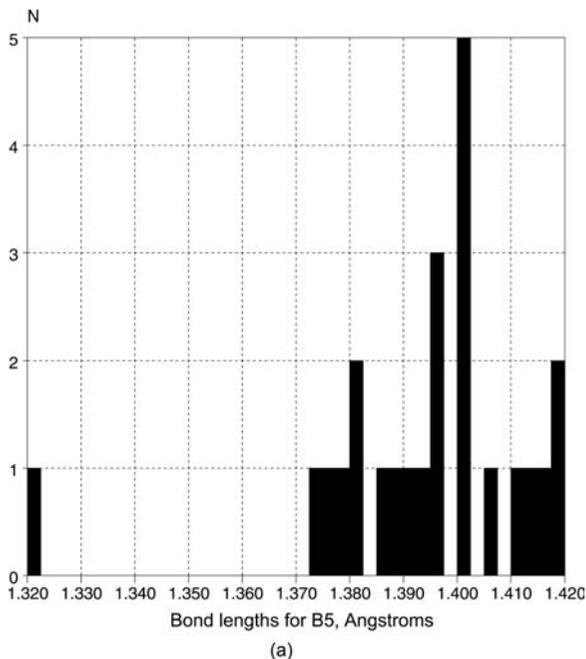
FIGURE 12. Histograms of number of occurrences (N) for bond (B) and angle (A) values in 3,4-disubstituted anilines. For each histogram the number of observations, minimum, maximum, mean and median bond lengths (angles), skewness, mean SE and sample SD are given in the following order. (a) For B5 (24, 1.320, 1.418, 1.394, 1.396, −1.778, 0.004, 0.020). (b) For A1 (24, 114.729, 121.397, 118.553, 118.473, −0.243, 0.275, 1.347). (c) For A9 (24, 108.780, 123.655, 117.074, 119.922, −0.457, 0.804, 3.940). (d) For A10 (24, 106.904, 120.102, 116.659, 117.659, −0.915, 0.809, 3.964). (e) For A11 (24, 102.967, 126.043, 117.591, 119.917, −1.130, 1.079, 5.285)

(b)

(c)

FIGURE 12. (*continued*)

Angles for A10, degrees

(d)

Angles for A11, degrees
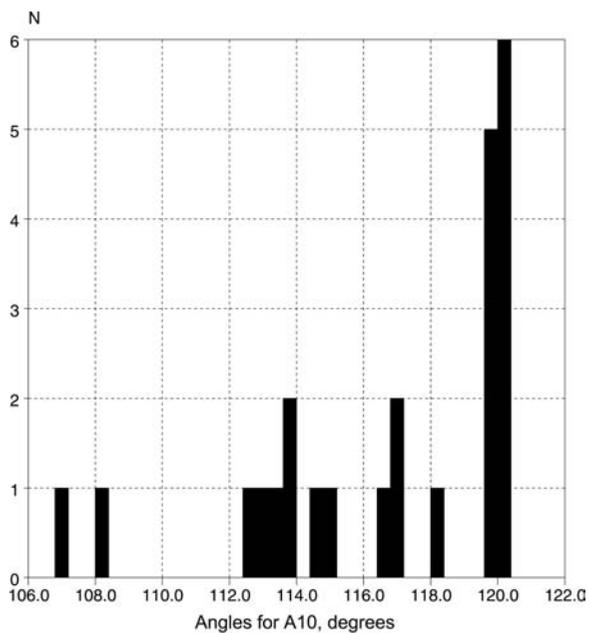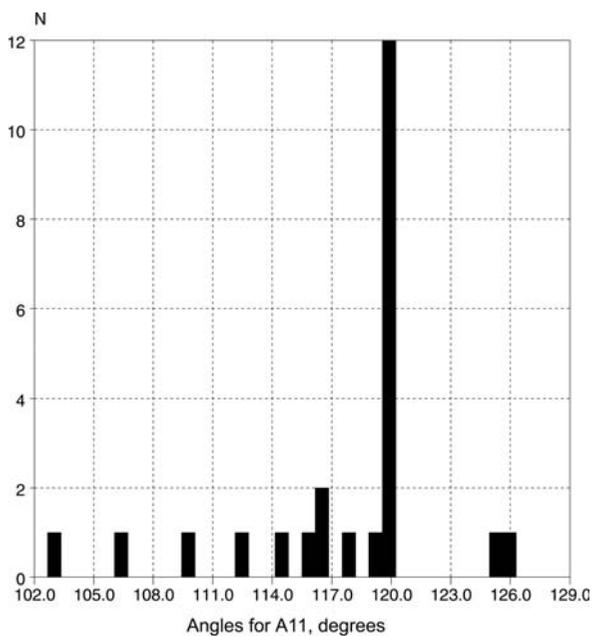
(e)

FIGURE 12. (*continued*)
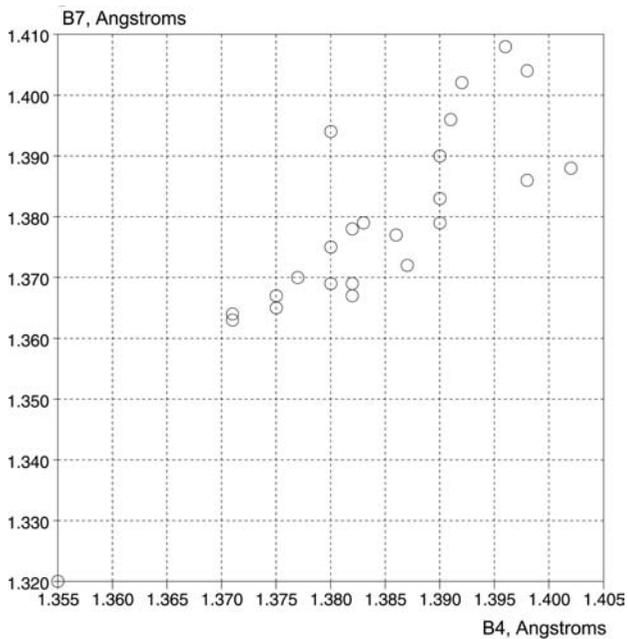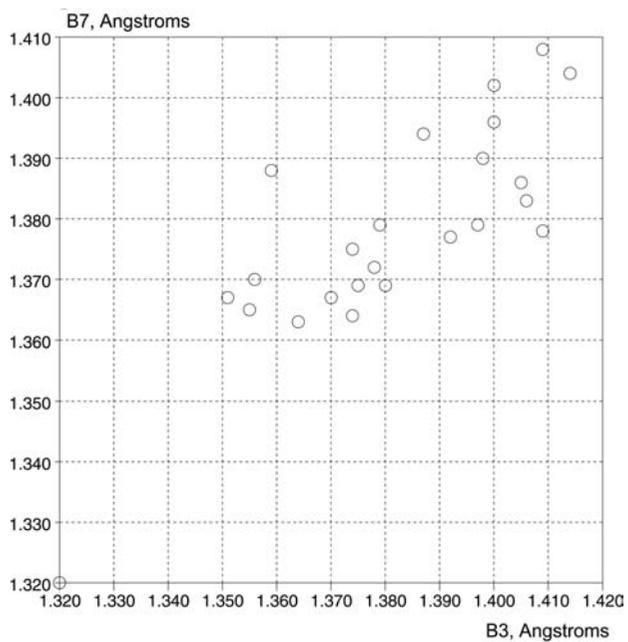
FIGURE 13. Scatter plots of the correlations between values of (a) B7 vs B4 ($r = 0.862$) and (b) B7 vs B3 ($r = 0.821$) in 3,4-disubstituted anilines

5. 2,5-Disubstituted anilines

The retrieval from the CSD resulted in 20 crystal structures. The relevant frequency histograms correspond to the A9, A10 and A11 values and are shown in Figure 14. They indicate a frequent pyramidalization of the amino groups. A relevant correlation with a correlation coefficient of -0.812 was found between the B3 and A10 values occurring in the amino groups.

6. 2,6-Disubstituted anilines

Four crystal structures of 2-amino-3-methylbenzoic acid[37], 2,6-dinitroaniline[38], 2,6-dichloroaniline[36] and 2,6-bis[2,4,6-triisopropylphenyl]aniline[39] were found in the CSD. A preference for a planar amino group configuration seems to occur in the crystals, probably due to inter- and intramolecular hydrogen bonds.

E. Trisubstituted Anilines

1. 2,4,6-Trisubstituted anilines

A total of 17 crystal structures resulted from the CSD retrieval. The relevant frequency histograms refer to the A9, A10 and A11 values and illustrate the preferred planarity of
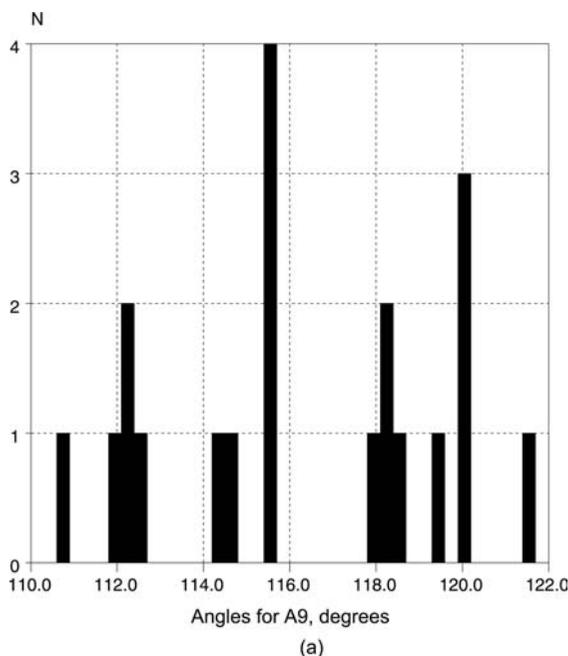
FIGURE 14. Histograms of number of occurrences (N) for angle (A) values in 2,5-disubstituted anilines. For each histogram the number of observations, minimum, maximum, mean and median angles, skewness, mean SE and sample SD are given in the following order. (a) For A9 (20, 110.668, 121.638, 116.240, 115.540, -0.083, 0.728, 3.254). (b) For A10 (20, 106.904, 123.650, 116.162, 116.631, -0.347, 1.073, 4.798). (c) For A11 (20, 102.967, 124.871, 115.916, 118.651, -0.811, 1.341, 5.996)

Angles for A10, degrees

(b)

Angles for A11, degrees

(c)
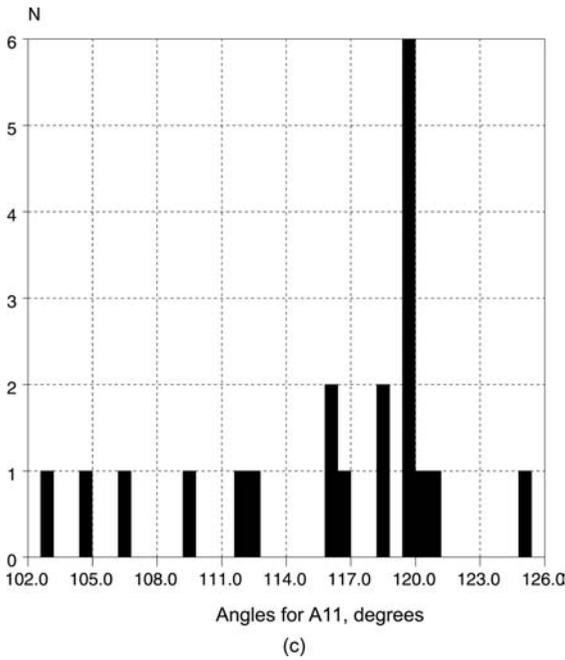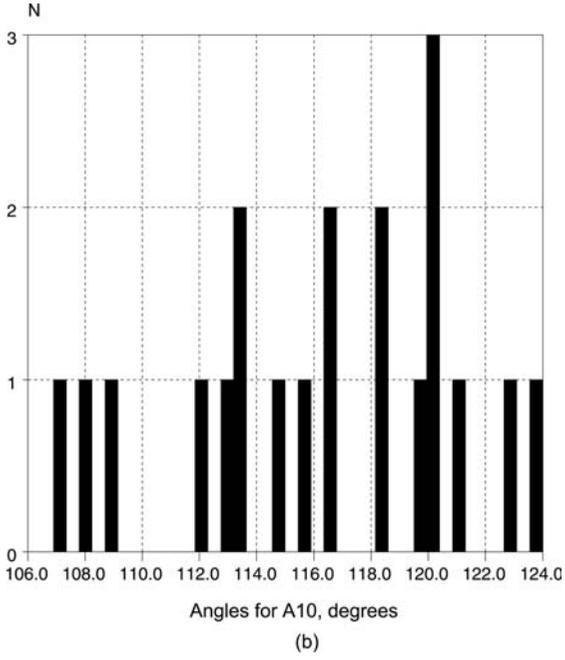
FIGURE 14. (*continued*)

the amino groups. The planarity evidently results from intramolecular hydrogen bonds between amino groups and *ortho*-substituents. The relatively large dispersion of the A11 values corresponds to steric hindrances from bulky substituents in the *ortho*-positions. Figure 15 shows the three histograms.

Strong correlations, with *correlation* coefficients $>|0.8|$ were found between (a) A7 and A8 ($r = -0.867$), (b) A4 and A8 ($r = 0.824$), (c) A1 and A8 ($r = -0.915$), (d) A6 and A7 ($r = -0.931$), (e) A5 and A7 ($r = 0.900$), (f) A5 and A6 ($r = -0.936$), (g) A1 and A4 ($r = -0.907$) and (h) B3 and B7 ($r = 0.818$). There seems to be some contribution of quinoid structure of the aromatic ring. The B1 and B2 bonds are longer than the other bonds in the rings.

2. 2,3,4-Trisubstituted anilines

Only one crystal structure, that of 2,4-diiodo-3-nitroaniline[17], has been retrieved from the CSD. The molecular structure exhibits typical features: the diminished A1 angle (116.7°) and the elongated B1 bond (1.410 Å).
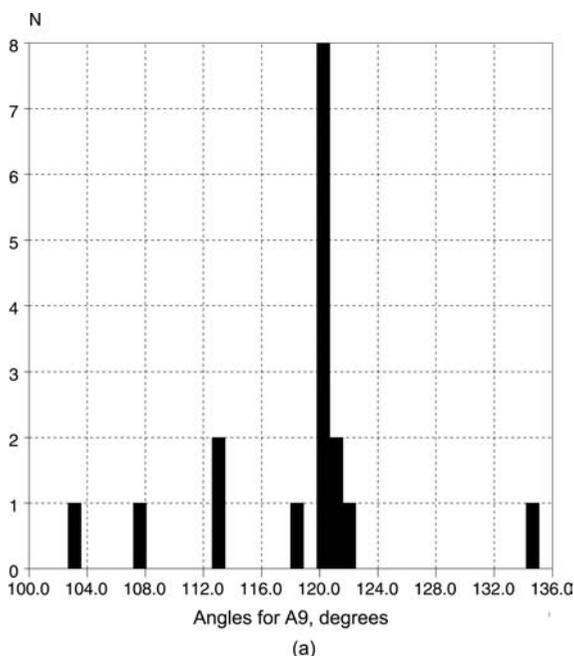
FIGURE 15. Histograms of number of occurrences (N) for angle (A) values in 2,4,6-trisubstituted anilines. For each histogram the number of observations, minimum, maximum, mean and median angles, skewness, mean SE and sample SD are given in the following order. (a) For A9 (17, 103.142, 134.424, 118.555, 120.009, −0.234, 1.621, 6.683). (b) For A10 (17, 103.985, 141.202, 119.547, 119.962, 0.952, 1.719, 7.088). (c) For A11 (17, 109.705, 141.689, 118.892, 119.941, 1.313, 1.840, 7.587)

Angles for A10, degrees

(b)

Angles for A11, degrees

(c)
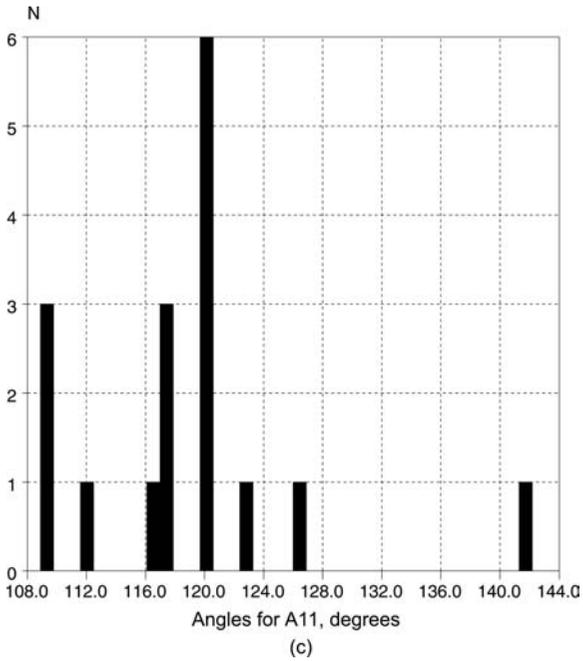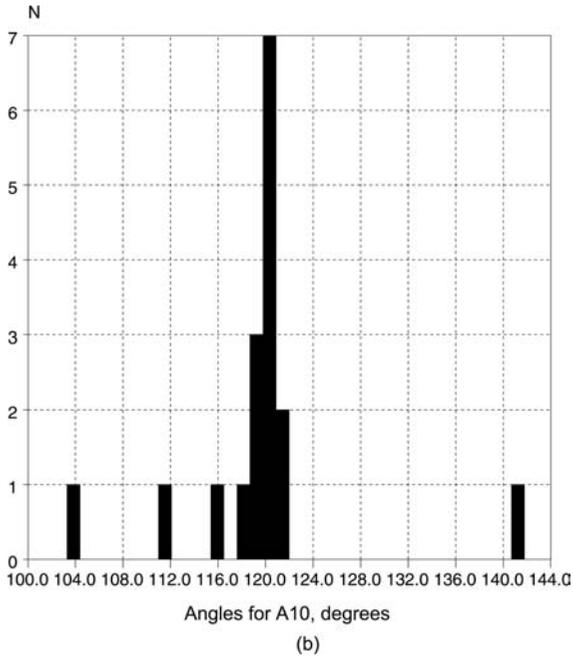
FIGURE 15. (*continued*)

3. 3,4,5-Trisubstituted anilines

No crystal structure has been retrieved from the CSD.

4. 2,4,5-Trisubstituted anilines

A total of 19 crystal structures resulted from 297,000 entries in the CSD. The frequency histograms corresponding to the A1, A9, A10 and A11 values turned out to be relevant and are shown in Figure 16.

The median value of the A1 angle amounts to 117.65° and is comparable to the values in other substituted anilines. The A9, A10 and A11 angles are close to 120°, indicating a preferred planar amino group configuration. The highly asymmetric A9 distribution in the frequency histogram (skewness equal to -1.266) results from interactions between amino groups and bulky *ortho*-substituents.
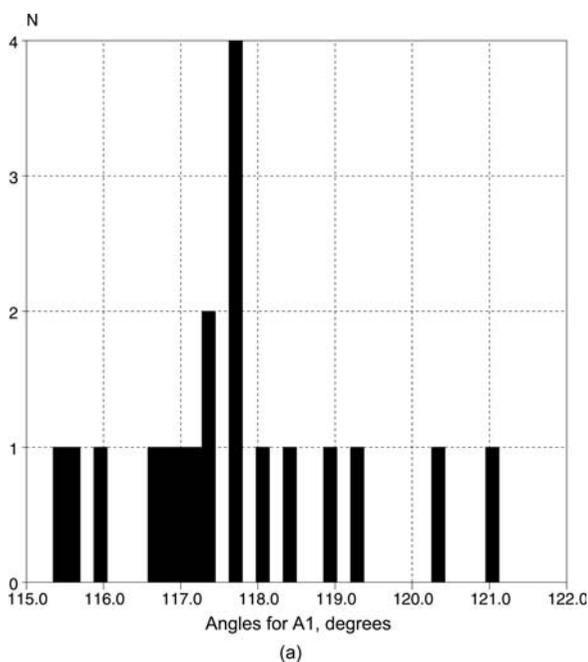
FIGURE 16. Histograms of number of occurrences (N) for angle (A) values in 2,4,5-trisubstituted anilines. For each histogram the number of observations, minimum, maximum, mean and median angles, skewness, mean SE and sample SD are given in the following order. (a) For A1 (19, 115.352, 121.054, 117.694, 117.646, 0.551, 0.333, 1.451). (b) For A9 (19, 102.391, 120.051, 115.940, 116.882, -1.266, 1.108, 4.831). (c) For A10 (19, 109.473, 124.102, 117.573, 119.225, -0.595, 0.880, 3.838). (d) For A11 (19, 101.286, 133.375, 118.718, 119.988, -0.431, 1.780, 7.758)

(b)

(c)
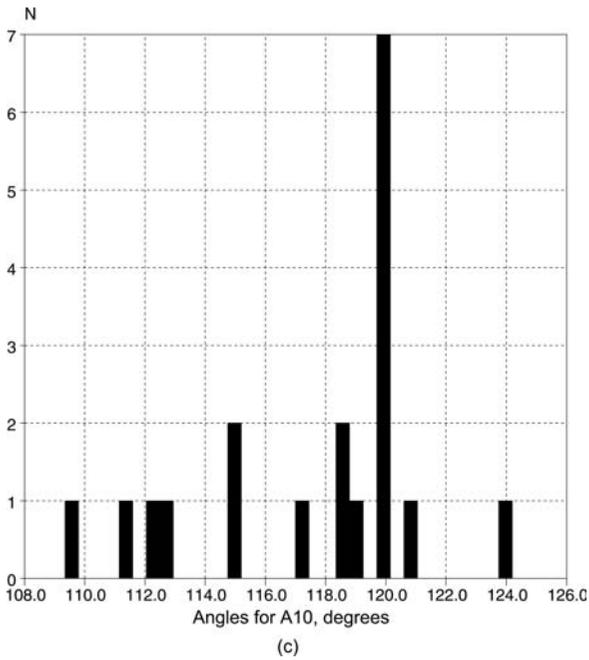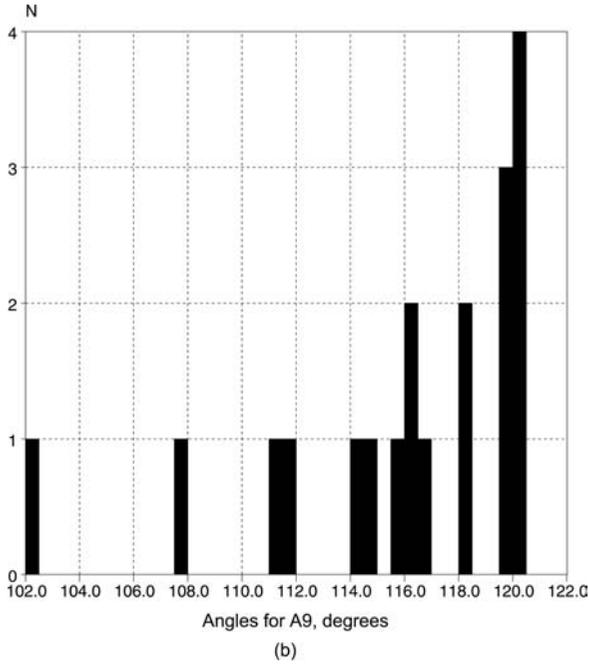
FIGURE 16. (*continued*)
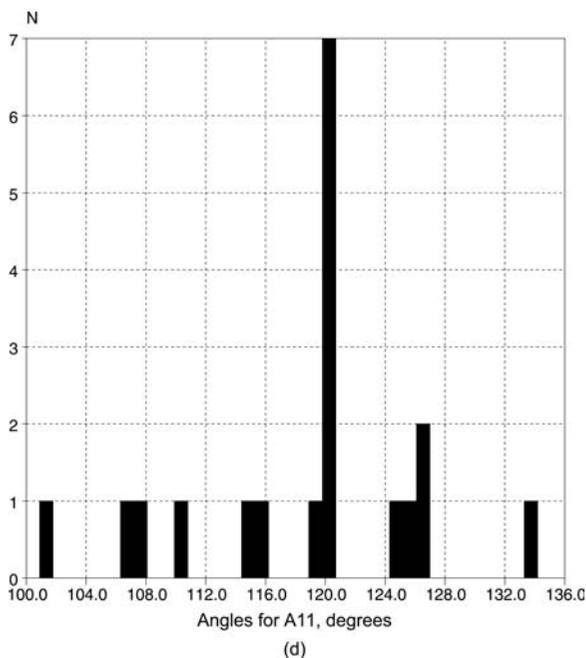
FIGURE 16. (*continued*)

Strong correlations were found between the values of (a) B5 and B6 ($r = -0.821$) and (b) B4 and B6 ($r = 0.894$). The scatter plot for the latter correlation is given in Figure 17.

5. 2,3,5-Trisubstituted anilines

Only two crystal structures were found. These are the structures of 2-hydroxy-3,5-di-*t*-butylaniline[40] and 2-hydroxy-3,5-dinitroaniline[41]. Some degree of amino group pyramidalization is observed in the crystals.

6. 2,3,6-Trisubstituted anilines

No crystal structure has been retrieved from the CSD.

F. Tetrasubstituted Anilines

A total of 12 crystal structures have been retrieved from the CSD. The general features of the molecular structures are in line with those of other substituted anilines. The A1 angle values range between $113°$ and $118°$. The bonds in the ring are slightly elongated, especially between carbon atoms with bulky substituents. Numerous significant correlations between the bonds and angles were found. Correlation coefficients $\geqslant |0.9|$ were found between values of A7 and A4 ($r = 0.932$), A4 and A1 ($r = -0.930$) and A7 and A1 ($r = -0.919$). The scatter plots visualizing the correlations between (a) B4 and B7
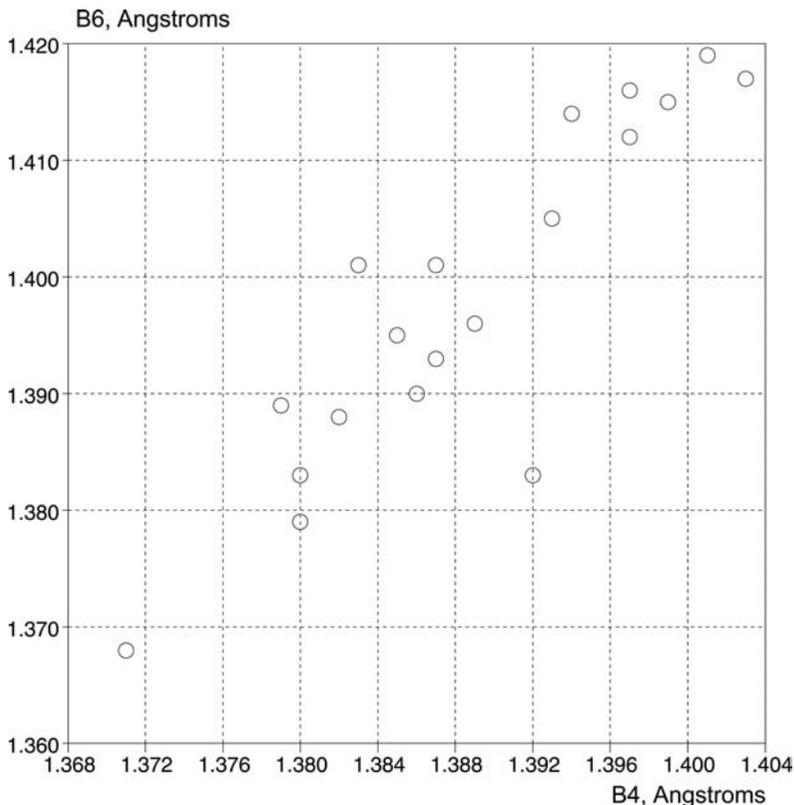
FIGURE 17. A scatter plot of the correlation of values of B6 vs B4 ($r = 0.894$) in 2,4,5-trisubstituted anilines

values ($r = 0.887$) and (b) A7 and A8 values ($r = 0.932$) are shown in Figure 18. The amino group preferably exhibits a planar configuration.

G. Pentasubstituted Anilines

Forty crystal structures have been retrieved from the CSD. In general, the distortion of the aromatic ring is pronounced in the crystals and depends strongly on the substituents on the ring. The same holds for the amino group configuration. Figure 19 shows the frequency histograms of the A9, A10 and A11 values, which reveal wide dispersions of the values. Strong correlations with correlation coefficients $\geqslant |0.9|$ were found between the following values of bonds and angles: (a) B6 vs B7 ($r = 0.894$), (b) B7 vs B3 ($r = -0.894$), (c) B1 vs B7 ($r = 0.820$), (d) B2 vs B6 ($r = 0.822$), (e) B2 vs B3 ($r = -0.869$), (f) B1 vs B3 ($r = -0.828$). Exemplary scatter plots are shown in Figure 20. Both the frequency histograms and the correlation scatter plots indicate that pentasubstituted anilines may be regarded as sterically overcrowded molecules.
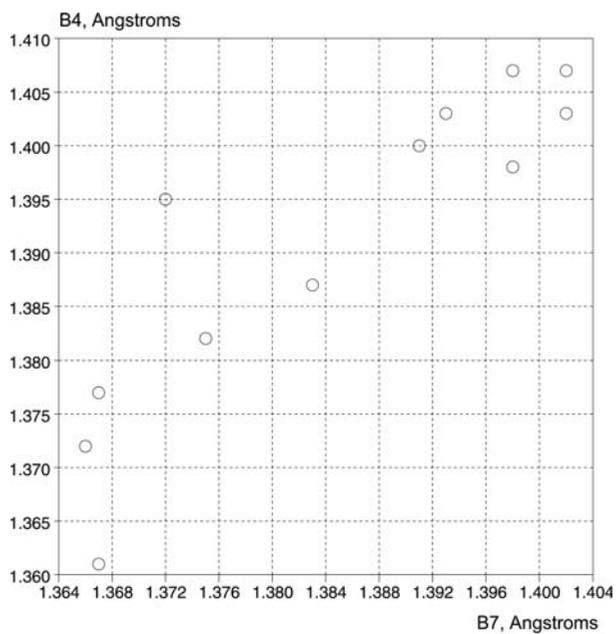
(a)
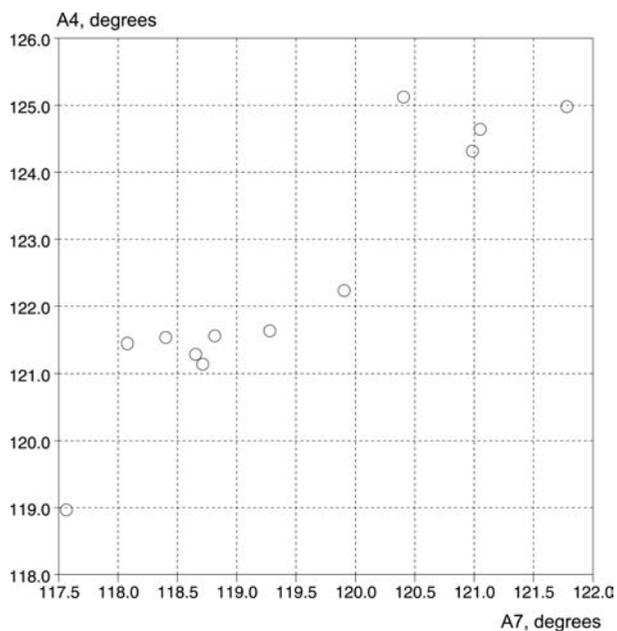
(b)

FIGURE 18. Scatter plots of the correlations of values of (a) B4 vs B7 ($r = 0.887$) and (b) A4 vs A7 ($r = 0.932$) in tetrasubstituted anilines

H. Diaminobiphenyls

Twelve crystal structures of 4,4′-diaminobiphenyls have been retrieved from the CSD. Figure 21 presents the bond and angle numbering in these molecules.

Strong correlations with correlation coefficient $\geqslant |0.8|$ have been found between A4 and A5 ($r = -0.945$), A6 and A13 ($r = 0.828$), A23 and A26 ($r = 0.910$), B4 and B14 ($r = 0.9$), B2 and B4 ($r = 0.937$) and B1 and B9 ($r = -0.905$). Some contribution of quinoid structure is seen by the slight shortening of the B4, B8, B11 and B15 bond lengths. The degree of pyramidalization of the amino groups is pronounced. The A21 to A26 angles are between $115°$ and $117°$. Other perturbations of the molecular structures result from other ring substituents, especially bulky or electron-withdrawing ones. The substituents also influence the twist angle between two moieties of the molecules. Intermolecular and, sometimes, intramolecular hydrogen bonds occur in the crystals. The

(a)
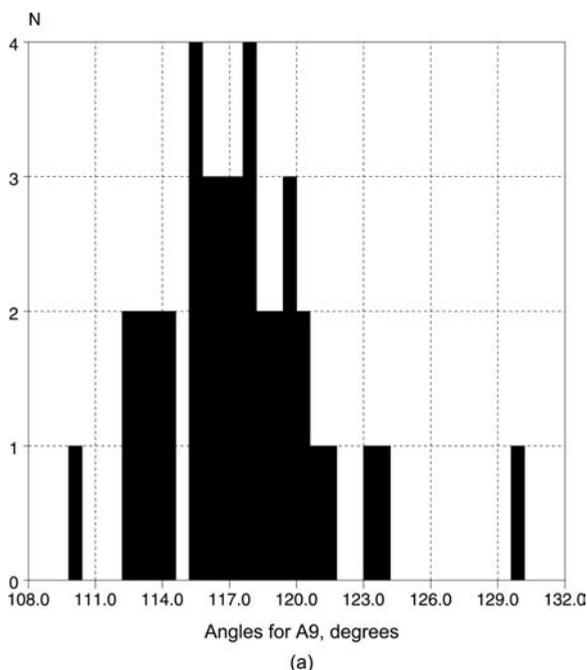
FIGURE 19. Histograms of number of occurrences (N) for angle (A) values in pentasubstituted anilines. For each histogram the number of observations, minimum, maximum, mean and median angles, skewness, mean SE and sample SD are given in the following order. (a) For A9 (40, 109.970, 130.123, 117.359, 117.146, 0.912, 0.578, 3.654). (b) For A10 (40, 113.113, 122.760, 117.683, 118.010, 0.063, 0.379, 2.397). (c) For A11 (40, 107.052, 131.411, 121.414, 122.068, −0.568, 1.086, 6.867)
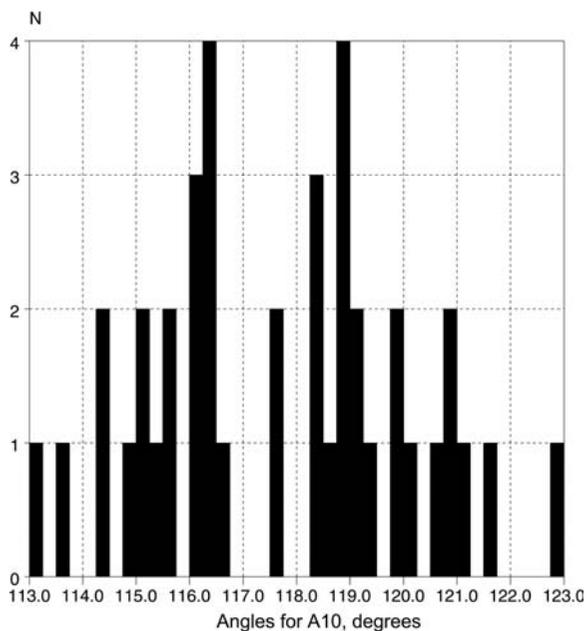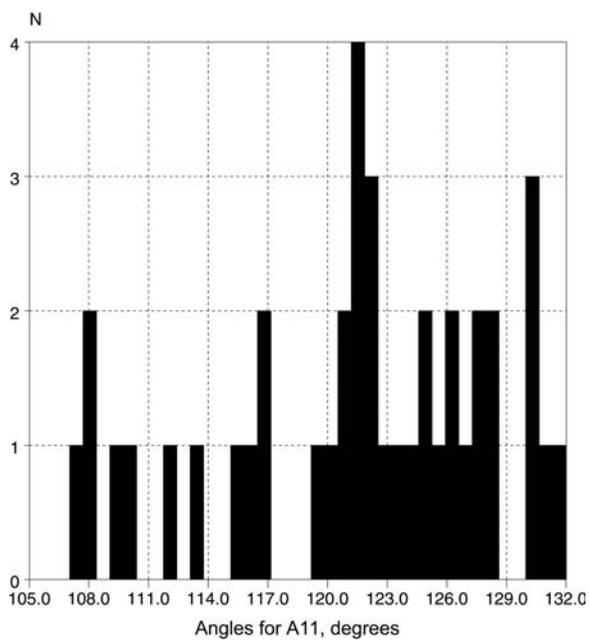
FIGURE 19. (*continued*)

reliability factors R_1 of the structures are often relatively high (around 10%), probably due to pronounced dynamics and some disorder of the positions of the two moieties. Nevertheless, some of the molecules are quite rigid, e.g. 3,3′-dipropyloxy-4,4′-diaminobiphenyl. The intramolecular NH⋯O hydrogen bonds result in planar configuration of the two phenyl rings[42]. Octafluoro-4,4′-diaminobiphenyl is an example of a sterically overcrowded molecule and exhibits a pronounced distortion of both aromatic rings. The values of the ring bond lengths and angles are strongly dispersed (1.18 − 1.57 Å and 109 − 131°). The intramolecular NH⋯F and intermolecular NH⋯N hydrogen bonds occur[43].

Three crystal structures of other diaminobiphenyls have been retrieved from the CSD. The molecules are shown in Figure 22. All the three molecules are nearly planar and exhibit a pronounced degree of the amino group pyramidalization[44−46].

I. Naphthylamines

Six crystal structures of 1-aminonaphthalenes have been retrieved from the CSD. Their bond and angle numbering are given in Figure 23.

Strong correlations with correlation coefficients $\geqslant |0.8|$ have been found between the following values of the bonds and angles: B9 vs B7 ($r = -0.897$), B9 vs B3 ($r = 0.801$), A16 vs B3 ($r = -0.851$), A6 vs A5 ($r = -0.913$) and A15 vs A14 ($r = -0.872$). The pyramidalization of the amino group is most pronounced in 1,8-diaminonaphthalene, probably due to intramolecular hydrogen bonds. On the other hand, intermolecular hydrogen bonds are a common feature of the crystal structure of the naphthylamines architecture.
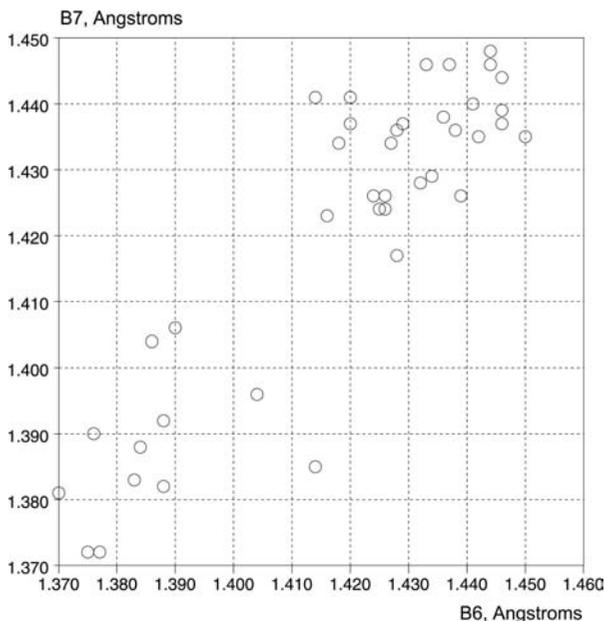
(a)

FIGURE 20. Scatter plots of the correlations of values of (a) B7 vs B6 ($r = 0.894$, (b) B7 vs B3 ($r = -0.894$), (c) B2 vs B3 ($r = -0.869$) in pentasubstituted anilines

(b)

(c)

FIGURE 20. (*continued*)
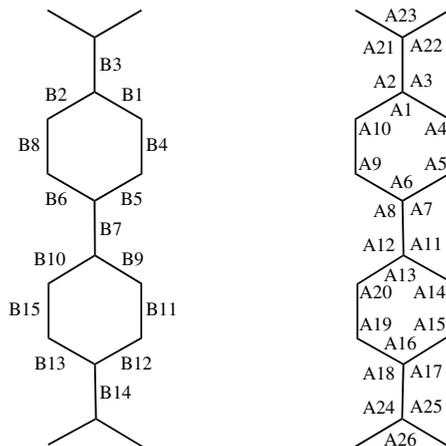
FIGURE 21. Bond and angle numbering in 4,4′-diaminobiphenyl
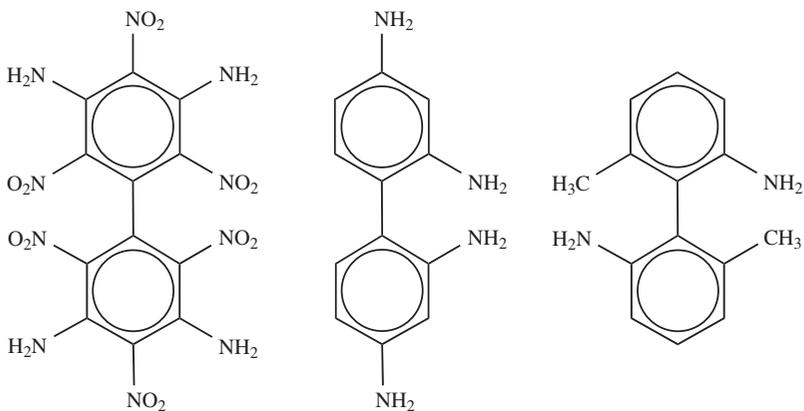
FIGURE 22. Three aminobiphenyls retrieved from the CSD
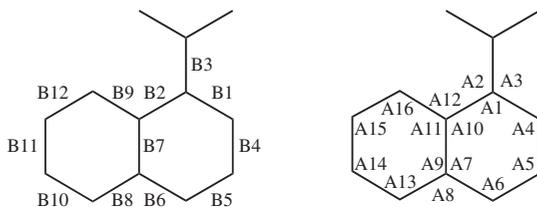
FIGURE 23. Bond and angle numbering in 1-aminonaphthalene
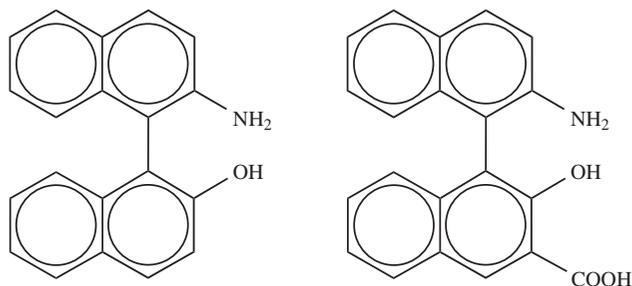
FIGURE 24. Molecules of two aminonaphthalene derivatives exhibiting a planar amino group configuration

Six crystal structures of 2-aminonaphthalenes have been retrieved from the CSD. Generally, a high degree of amino group pyramidalization is observed, with the exception of the two compounds shown in Figure 24. The intramolecular interactions result in the planar amino group configuration in the crystals[47, 48].

J. Anthrylamines

The only crystal structure retrieved from the CSD is that of 9-amino-10-(2′,4′,6′-trinitrophenyl)anthracene, shown schematically in Figure 25.

Both moieties of the molecule are twisted with respect to one another and the corresponding torsional angle amounts to about 90°. The bond lengths and angles in the 9-aminoanthracene moiety exhibit a pronounced distribution of the values. A high degree of the amino group pyramidalization is observed. The two nitro groups in *ortho*-positions to the central bond are strongly twisted out of the phenyl ring plane by 58° and 44° while the third nitro group is only slightly twisted by −6°. The torsional angles result from intramolecular interactions in the sterically overcrowded molecule[49].
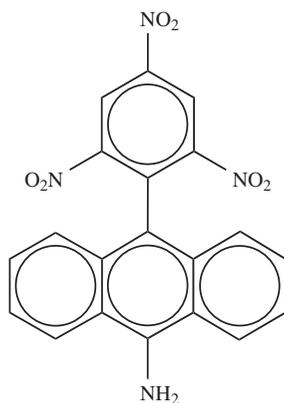
FIGURE 25. The 9-amino-10-(2′,4′,6′-trinitrophenyl)anthracene molecule
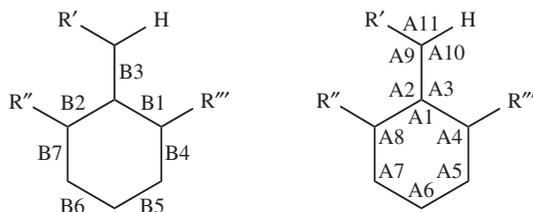
FIGURE 26. Bond and angle numbering in *N*-substituted anilines
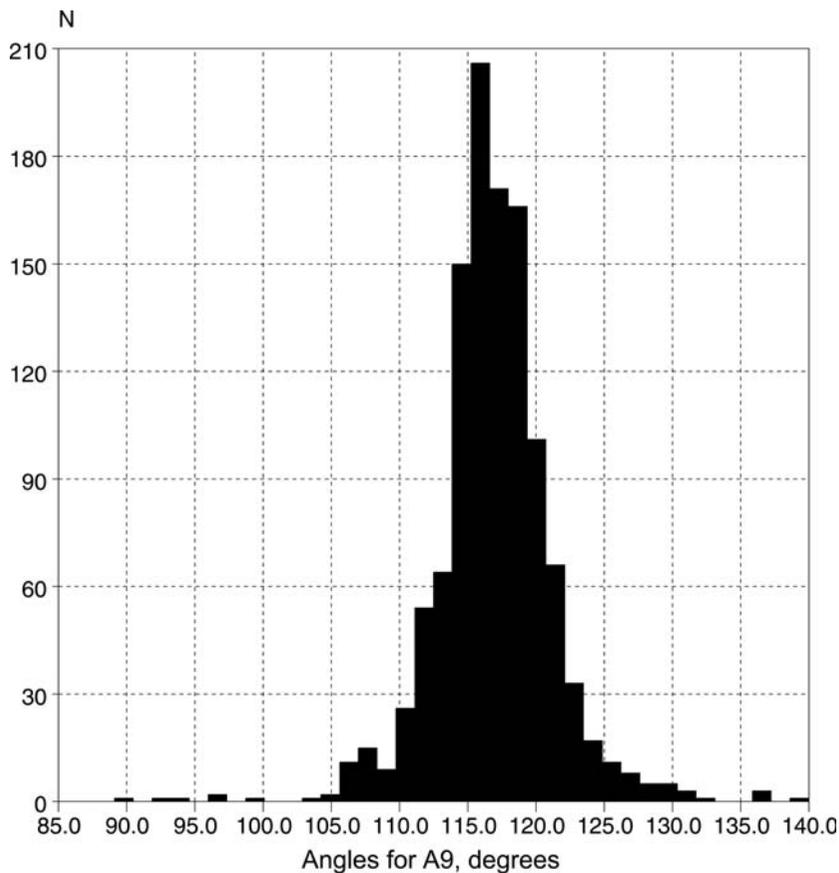
FIGURE 27. A histogram of number of occurrences (N) for angle (A9) value in *N*-substituted anilines. The number of observations, minimum, maximum, mean and median angles, skewness, mean SE and sample SD are given in the following order: 1135, 89.713, 139.437, 116.915, 116.860, −0.220, 0.128, 4.324

K. *N*-Substituted Anilines

Several hundred structures of *N*-monosubstituted anilines have been retrieved from the CSD. Figure 26 shows the schematic drawing with bond and angle numbering of the molecule. The bond lengths exhibit a perfect distribution around the classical value in the aromatic ring. The A1 angle has a median value about 119.2°. The other angles in the aromatic rings exhibit slightly wider dispersion than the bond lengths. Nevertheless, the median values are about 120°. Evidently, the bond angles represent softer parameters than the bond lengths. A rough analysis of the frequency histograms (see Figure 27) showed that the A9 angle has a median value of 116.9°. A significant correlation has been found between the A1 angles and the B3 bond lengths and the corresponding scatter plot is shown in Figure 28.

A more detailed analysis has been performed for ring-2,6-disubstituted *N*-substituted anilines. In these molecules there are possibilities for interactions between a proton on the amino group and a substituent in the *ortho*-position. A total of 106 crystal structures have been retrieved from the CSD. Frequency histograms of bond and angle values are shown in Figure 29.

Outliers and multimodalities in the histograms of the B1, B2 and B3 bonds result from large R″ and R‴ substituents in the *ortho*-position with respect to the amino group or R′
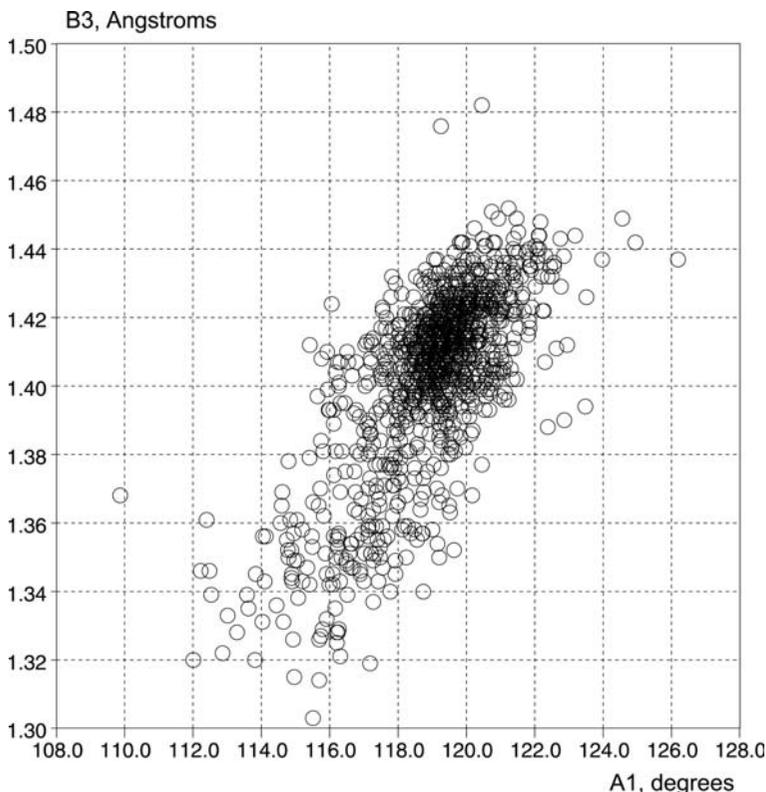
FIGURE 28. A scatter plot of the correlation of values of B3 vs A1 ($r = 0.721$) in *N*-substituted anilines

substituent on the amino group. The very short B2 values correspond to molecules with intramolecular hydrogen bonds. The very short B6 bond lengths refer to molecules with long aliphatic substituents on the ring. The A1 angle has a median value of 120.93°. Its asymmetric distribution with skewness amounting to −0.878 indicates the strong influence of the R′, R″ and R‴ substituents on the molecular geometry. The reverse influence is observed on the A4 value distribution. The A9 angle exhibits a median value of 117.302°. Much smaller values correspond to molecules with long-chain R″ and R‴ substituents. Much larger values may be referred to bulky R′ substituents on the amino group. Consequently, the substitution of one hydrogen atom on the amino group strongly disturbs the molecular geometry of anilines.

(a)
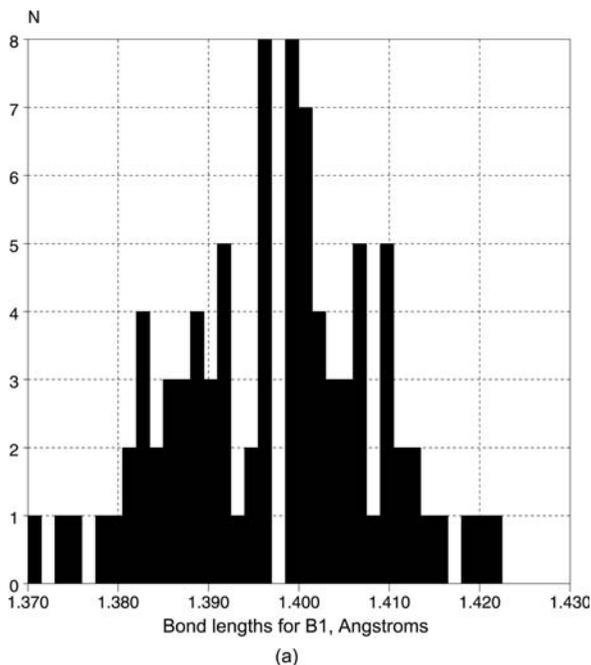
FIGURE 29. Histograms of number of occurrences (N) for bond (B) and angle (A) values in 2,6-substituted *N*-substituted anilines. For each histogram the number of observations, minimum, maximum, mean and median bond lengths (angles), skewness, mean SE and sample SD are given in the following order. (a) For B1 (87, 1.370, 1.421, 1.397, 1.399, −0.122, 0.001, 0.011). (b) For B2 (87, 1.351, 1.422, 1.394, 1.395, −0.806, 0.001, 0.012). (c) For B3 (87, 1.368, 1.523, 1.421, 1.423, 0.555, 0.002, 0.022). (d) For B4 (87, 1.359, 1.416, 1.389, 1.389, −0.110, 0.001, 0.010). (e) For B5 (87, 1.332, 1.398, 1.372, 1.373, −0.836, 0.001, 0.013). (f) For B6 (87, 1.334, 1.399, 1.373, 1.372, −0.494, 0.001, 0.013). (g) For B7 (87, 1.361, 1.408, 1.388, 1.389, −0.355, 0.001, 0.011). (h) For A1 (87, 113.126, 123.383, 119.878, 120.932, −0.878, 0.289, 2.699). (i) For A4 (87, 115.473, 124.057, 119.164, 118.166, 0.685, 0.242, 2.256). (j) For A5 (87, 117.256, 123.790, 120.768, 121.140, −0.395, 0.128, 1.194). (k) For A6 (87, 118.027, 123.280, 120.096, 120.151, 0.281, 0.086, 0.801). (l) For A7 (87, 117.989, 122.307, 120.655, 120.851, −0.449, 0.121, 1.125). (m) For A8 (87, 113.344, 124.496, 119.380, 118.327, 0.442, 0.246, 2.294). (n) For A9 (87, 106.909, 126.541, 116.644, 117.302, −0.174, 0.420, 3.922)
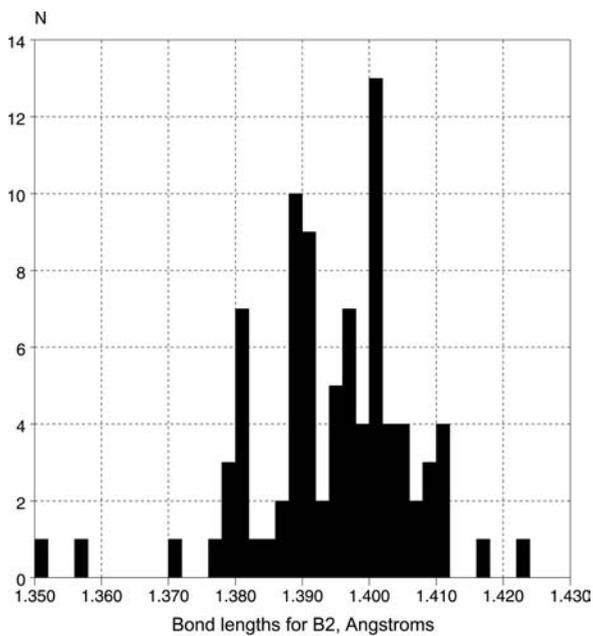
Bond lengths for B2, Angstroms
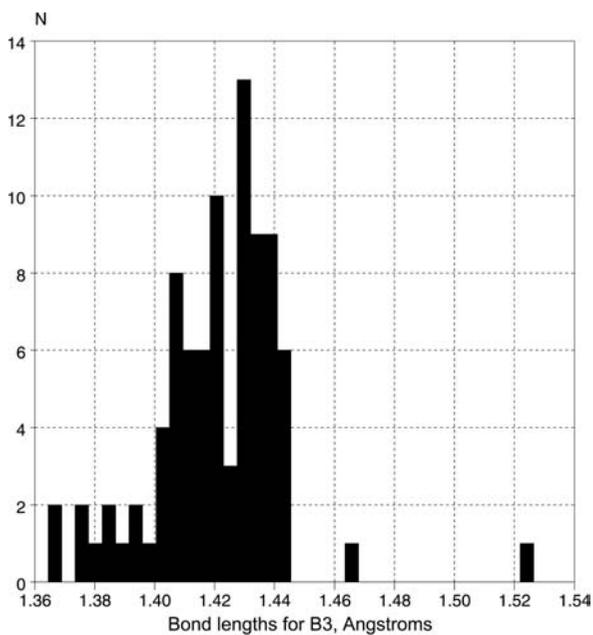
(b)

Bond lengths for B3, Angstroms

(c)

FIGURE 29. (*continued*)

(d)

(e)

FIGURE 29. (*continued*)

Bond lengths for B6, Angstroms

(f)

Bond lengths for B7, Angstroms

(g)

FIGURE 29. (*continued*)

FIGURE 29. (*continued*)

Angles for A5, degrees

(j)

Angles for A6, degrees
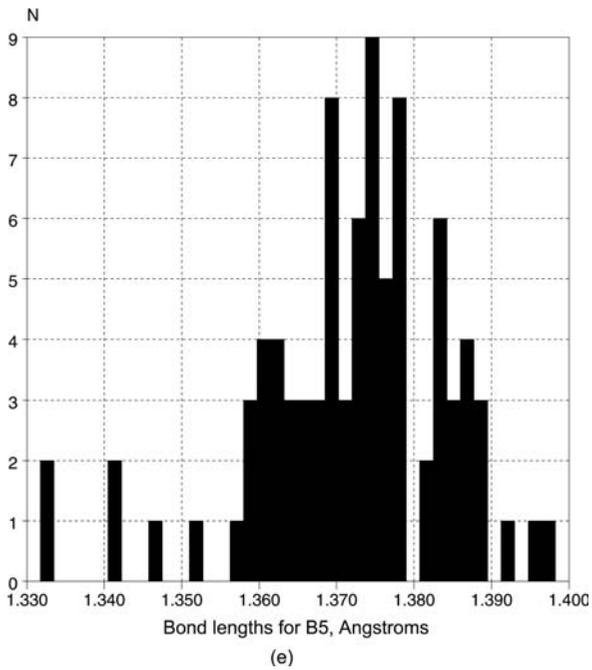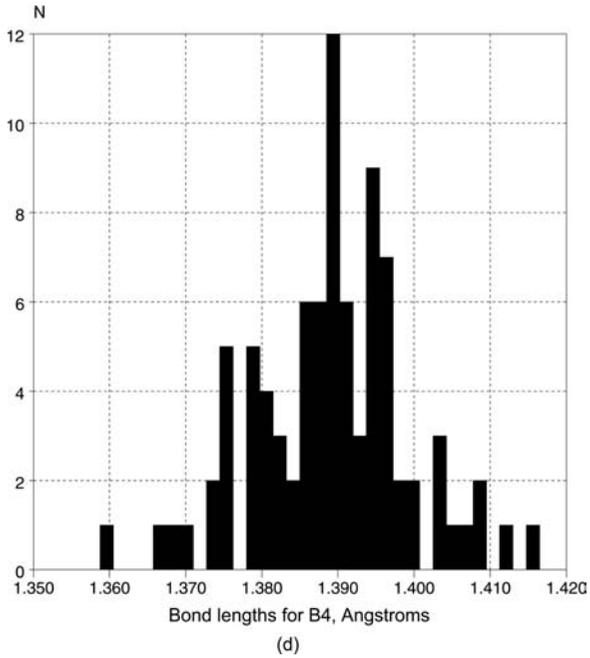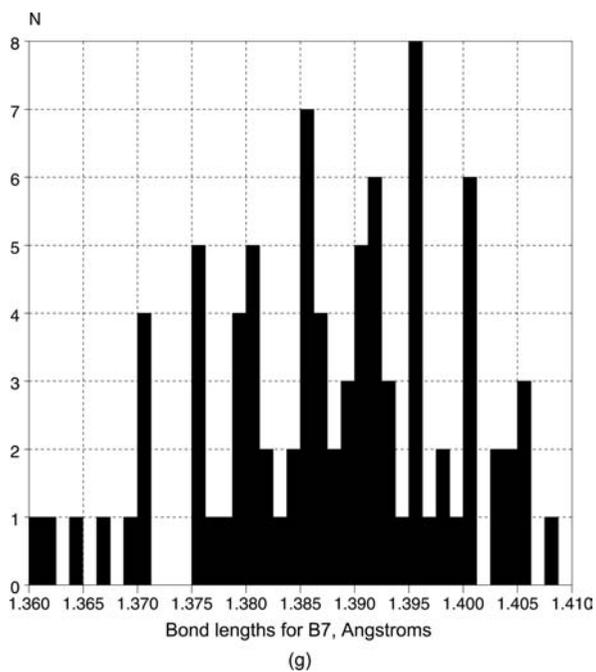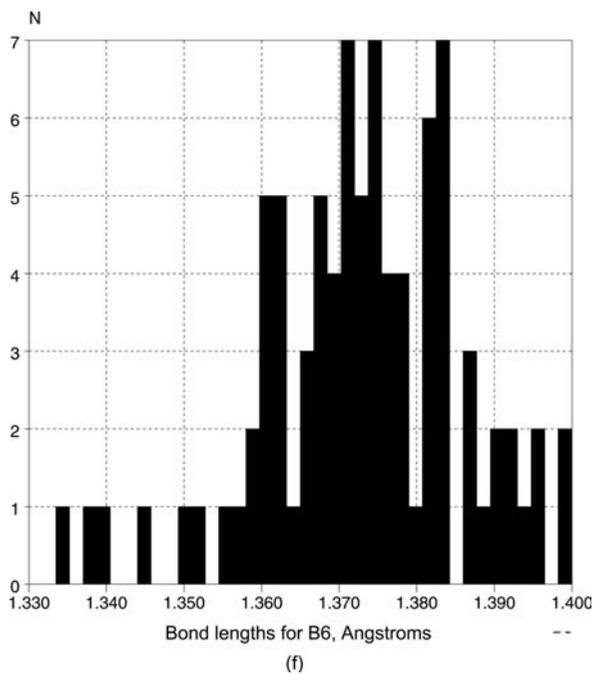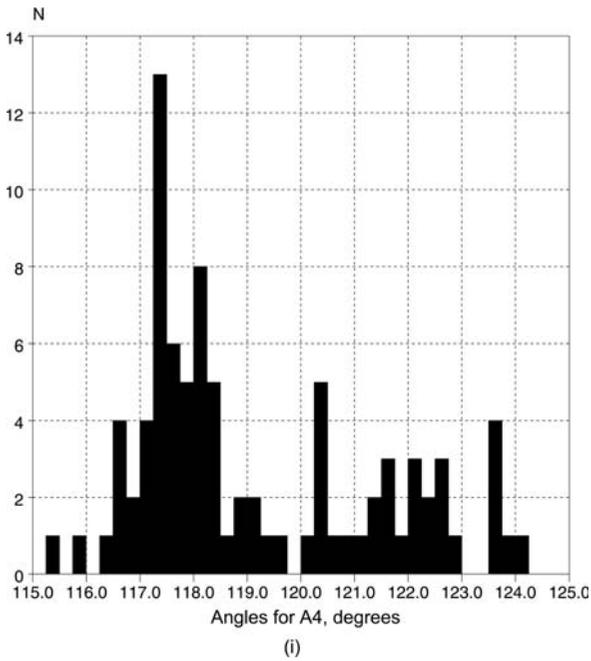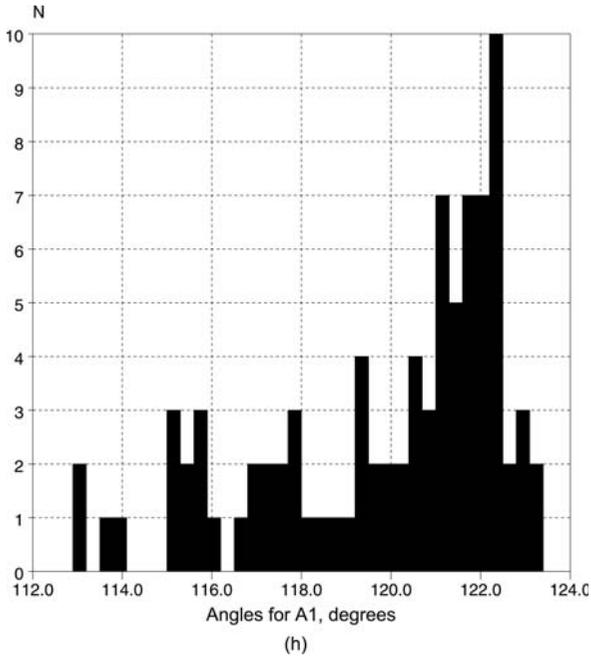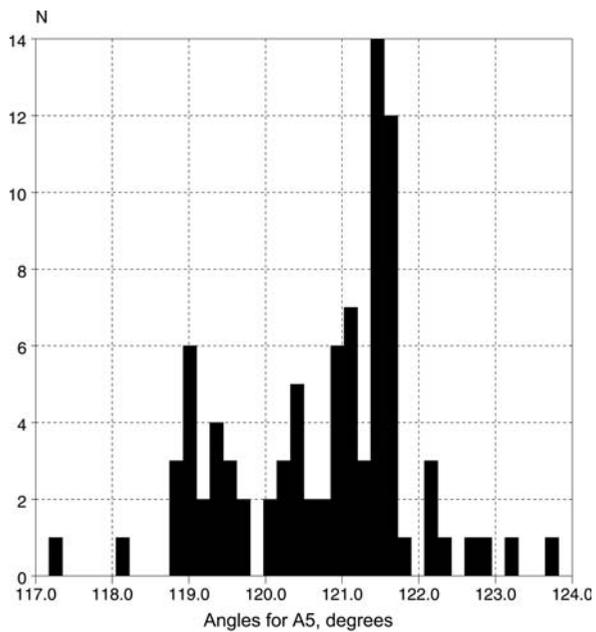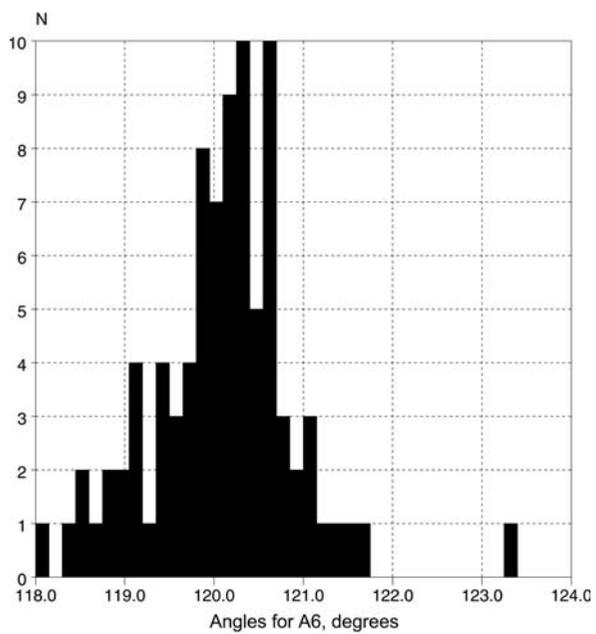
(k)

FIGURE 29. (*continued*)
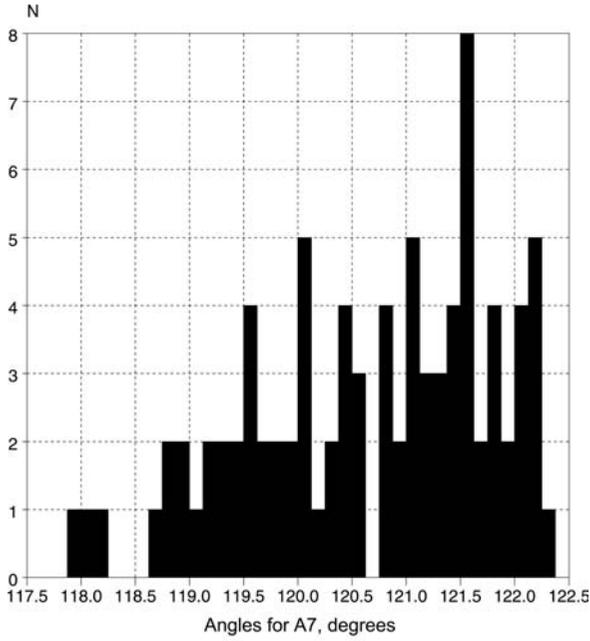
(l)
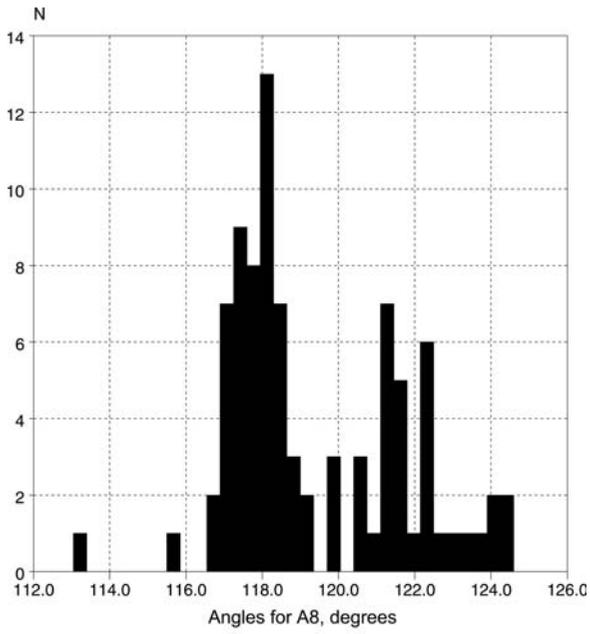
(m)

FIGURE 29. (*continued*)
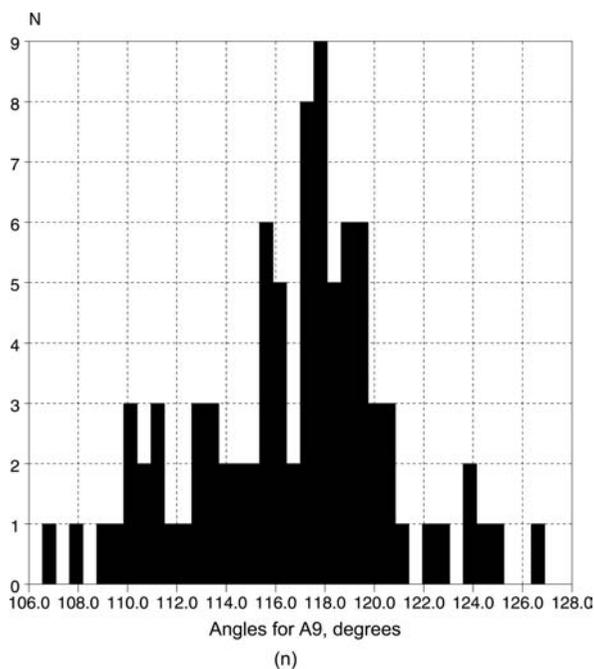
FIGURE 29. (*continued*)

L. Proton Sponges

Proton sponges are 1,8-diaminonaphthalene derivatives in which the amino hydrogens are substituted by methyl groups. The compounds exhibit many interesting properties. The molecule is able to capture a proton which is located between the electron pairs of the two nitrogen atoms, forming a protonated proton sponge. The $N \cdots H \cdots N$ hydrogen bridges are very short[50]. The retrieval from the CSD resulted in 20 crystal structures. Figure 30 shows the bond and angle numbering in an exemplary molecule of 1,8-bis(dimethylamino)naphthalene[51].

The frequency histograms of the bond and angle values are shown in Figure 31. The two aromatic rings are strongly distorted. The B3, B5, B6, B7 and B8 bond lengths are
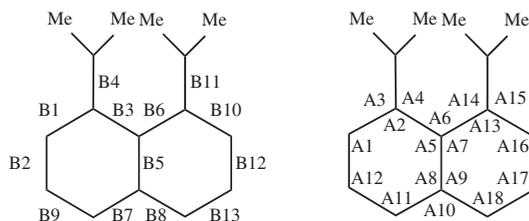
FIGURE 30. Bond and angle numbering in 1,8-bis(dimethylamino)naphthalene
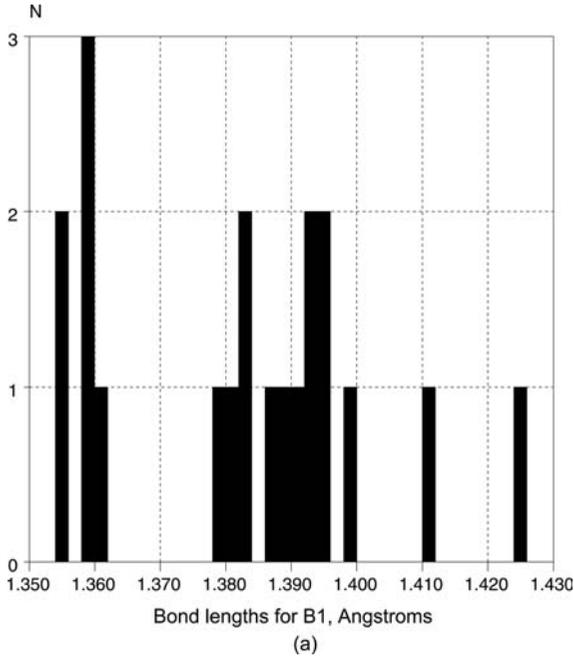
FIGURE 31. Histograms of number of occurrences (N) for bond (B) and angle (A) values in proton sponges. For each histogram the number of observations, minimum, maximum, mean and median bond lengths (angles), skewness, mean SE and sample SD are given in the following order. (a) For B1 (20, 1.355, 1.425, 1.382, 1.385, 0.154, 0.004, 0.019). (b) For B2 (20, 1.366, 1.417, 1.397, 1.398, −0.366, 0.003, 0.015). (c) For B4 (20, 1.360, 1.427, 1.399, 1.401, −0.487, 0.004, 0.016). (d) For B5 (20, 1.403, 1.452, 1.432, 1.437, −0.734, 0.003, 0.014). (e) For B6 (20, 1.425, 1.474, 1.447, 1.447, 0.413, 0.002, 0.009). (f) For B7 (20, 1.403, 1.447, 1.422, 1.423, 0.484, 0.003, 0.013). (g) For B8 (20, 1.383, 1.442, 1.419, 1.421, −0.307, 0.003, 0.015). (h) For B9 (20, 1.332, 1.392, 1.357, 1.359, 0.295, 0.004, 0.017). (i) For B10 (20, 1.363, 1.414, 1.383, 1.384, 0.344, 0.003, 0.015). (j) For B11 (20, 1.362, 1.435, 1.399, 1.402, −0.395, 0.004, 0.016). (k) B12 (20, 1.372, 1.416, 1.394, 1.391, 0.117, 0.003, 0.013). (l) For B13 (20, 1.333, 1.386, 1.359, 1.363, −0.167, 0.004, 0.017). (m) For A1 (20, 119.306, 124.567, 121.923, 121.883, −0.069, 0.299, 1.336). (n) For A2 (20, 116.830, 120.563, 118.467, 118.472, 0.244, 0.198, 0.886). (o) For A3 (20, 118.580, 121.777, 120.448, 120.542, −0.967, 0.177, 0.793). (p) For A4 (20, 120.006, 123.373, 121.065, 120.820, 1.035, 0.194, 0.869). (r) For A5 (20, 113.977, 119.591, 117.492, 117.764, −1.080, 0.295. 1.321). (s) For A6 (20, 123.446, 130.471, 125.211, 124.663, 1.556, 0.435, 1.945). (t) For A7 (20, 115.472, 118.333, 117.285, 117.505, −0.815, 0.202, 0.904). (u) For A8 (20, 116.546, 125.512, 119.880, 119.488, 1.111, 0.505, 2.258). (v) For A9 (20, 117.723, 125.178, 120.076, 120.104, 0.873, 0.448, 2.001). (w) For A10 (20, 109.648, 124.901, 120.018, 120.273, −1.101, 0.922, 4.122). (x) For A11 (20, 117.557, 121.374, 119.920, 120.022, −0.673, 0.236, 1.054). (y) For A12 (20, 118.941, 122.441, 120.631, 120.434, 0.181, 0.228, 1.021). (z) For A13 (20, 116.714, 120.563, 118.541, 118.594, 0.066, 0.189, 0.843). (aa) For A14 (20, 118.960, 121.892, 120.696, 120.755, −0.401, 0.163, 0.728). (bb) For A15 (20, 118.580, 122.112, 120.752, 120.743, −1.086, 0.171, 0.766). (cc) For A16 (20, 119.306, 124.801, 121.890, 121.949, 0.334, 0.292, 1.305). (dd) For A17 (20, 118.671, 122.705, 120.740, 120.695, 0.142, 0.262, 1.173). (ee) For A18 (20, 117.518, 122.435, 119.875, 120.069, 0.059, 0.279, 1.250)
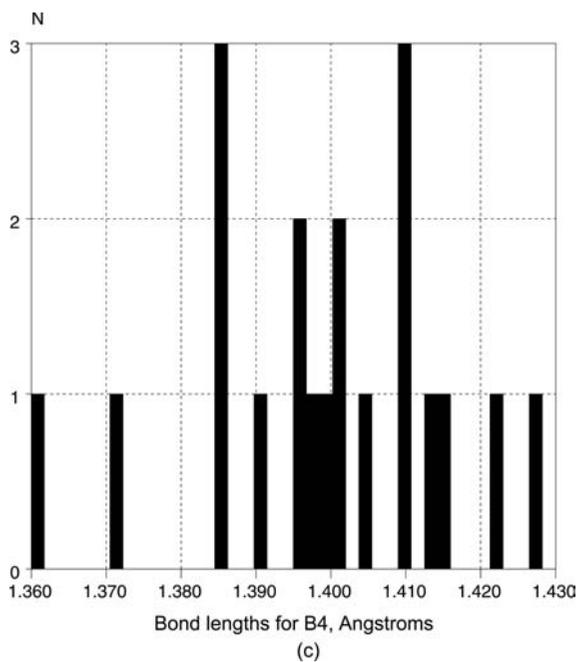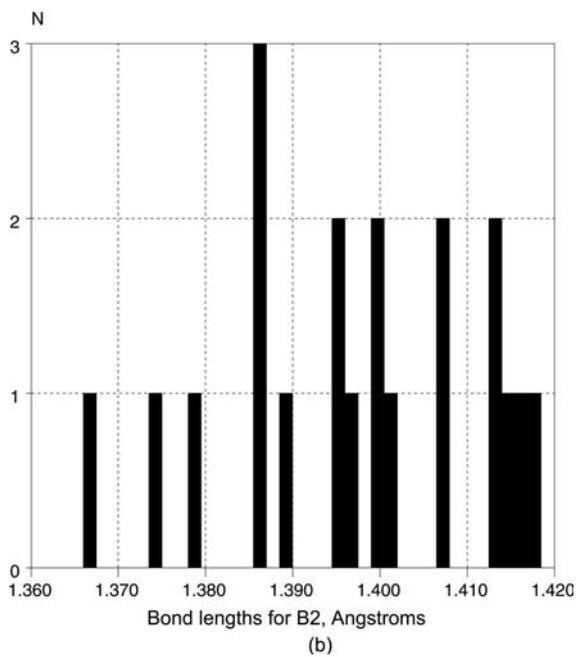
FIGURE 31. (*continued*)
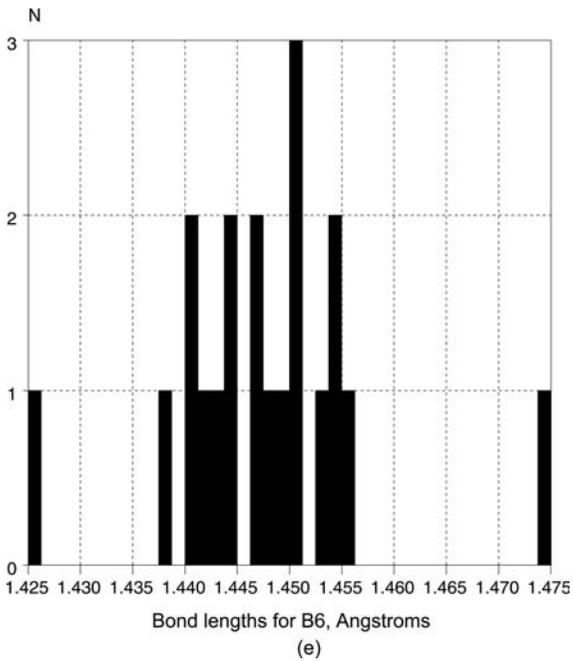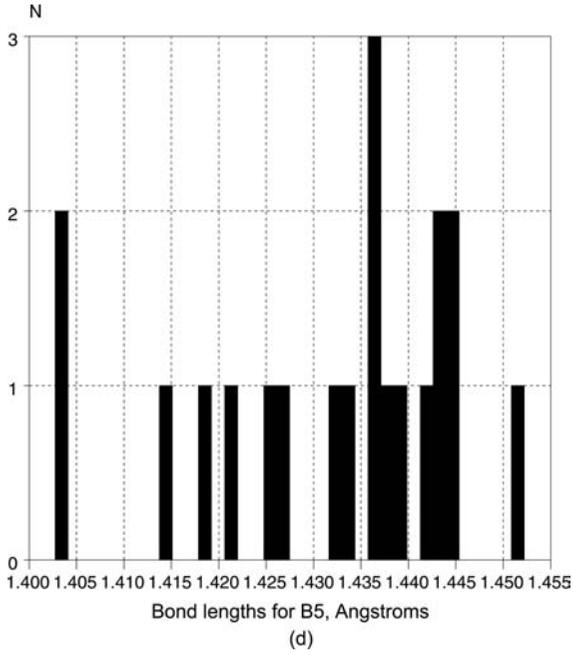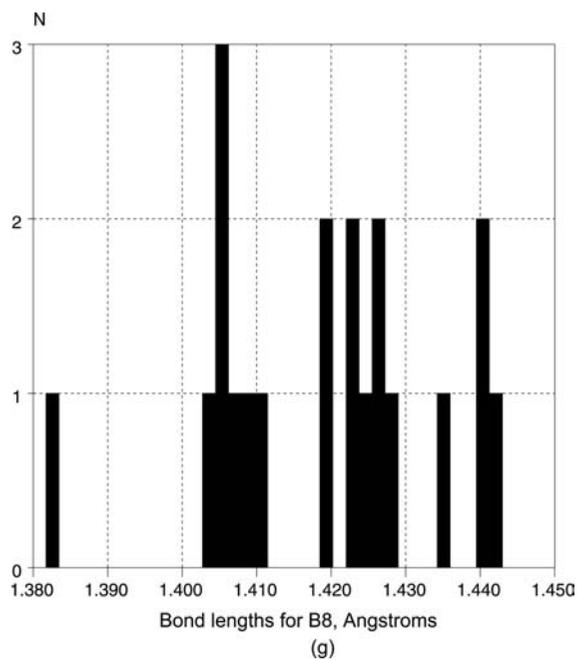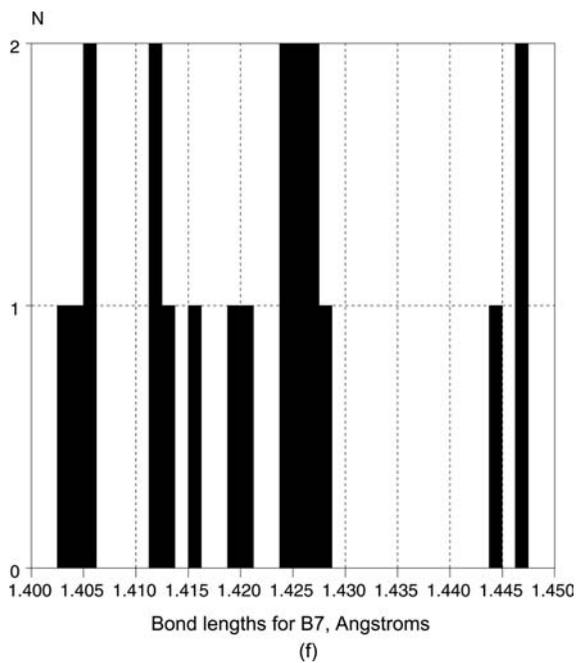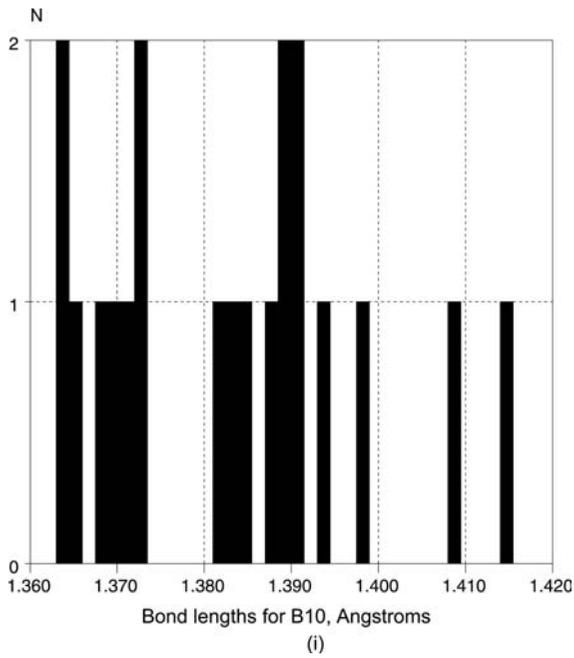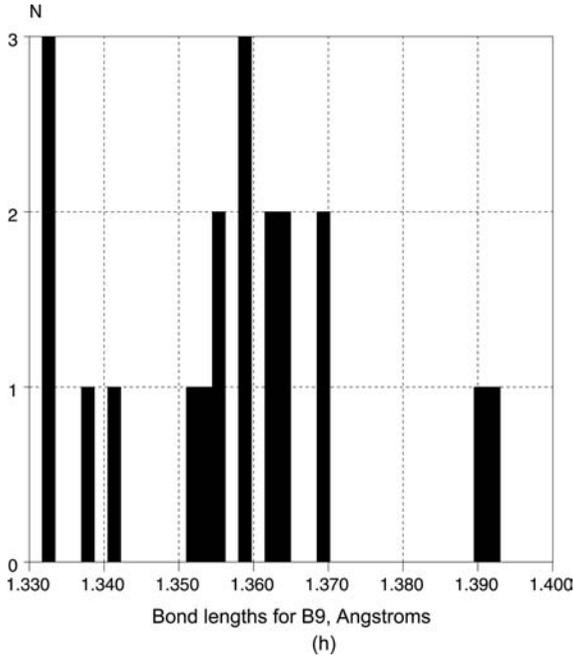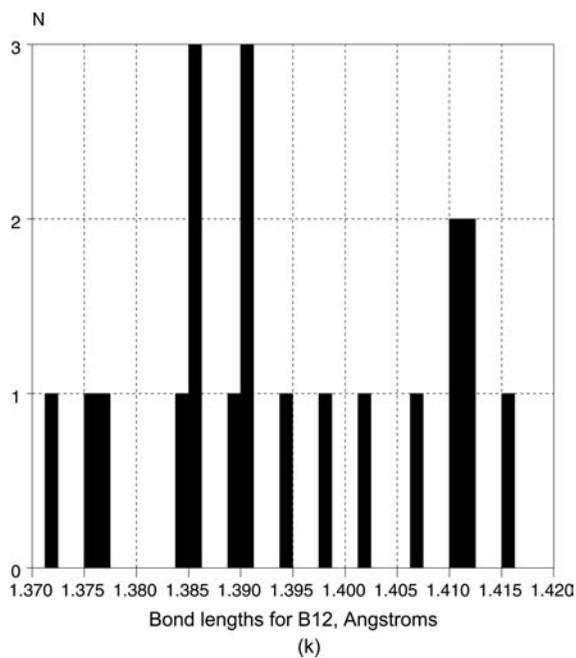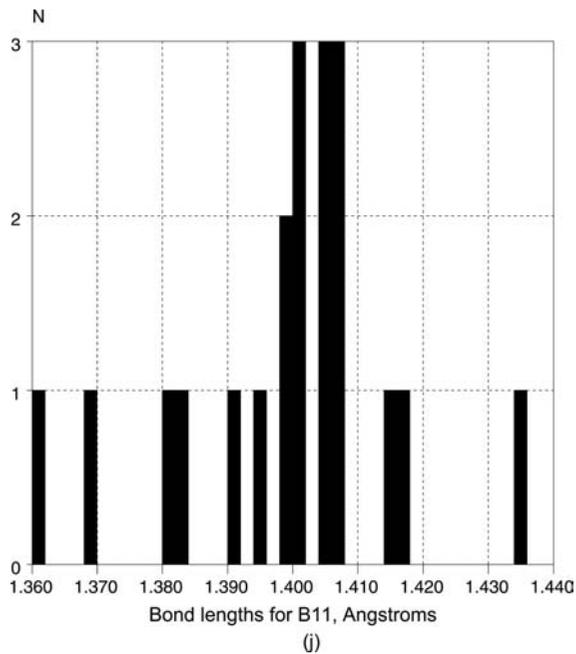
FIGURE 31. (*continued*)

Bond lengths for B7, Angstroms

(f)

Bond lengths for B8, Angstroms

(g)

FIGURE 31. (*continued*)

Bond lengths for B9, Angstroms

(h)

Bond lengths for B10, Angstroms

(i)

FIGURE 31. (*continued*)

FIGURE 31. (*continued*)

Bond lengths for B13, Angstroms

(l)

FIGURE 31. (*continued*)

Angles for A1, degrees

(m)

FIGURE 31. (*continued*)
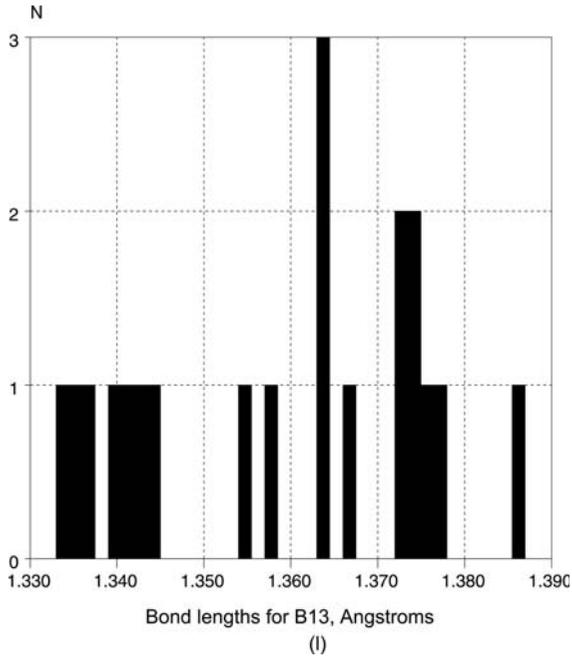
FIGURE 31. (*continued*)
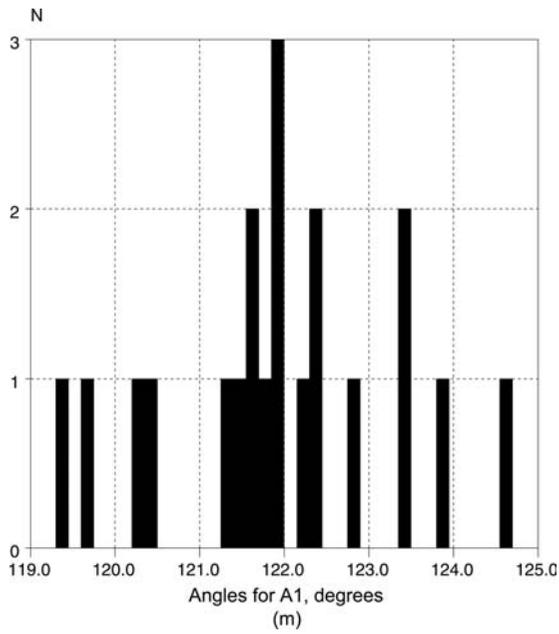
FIGURE 31. (*continued*)
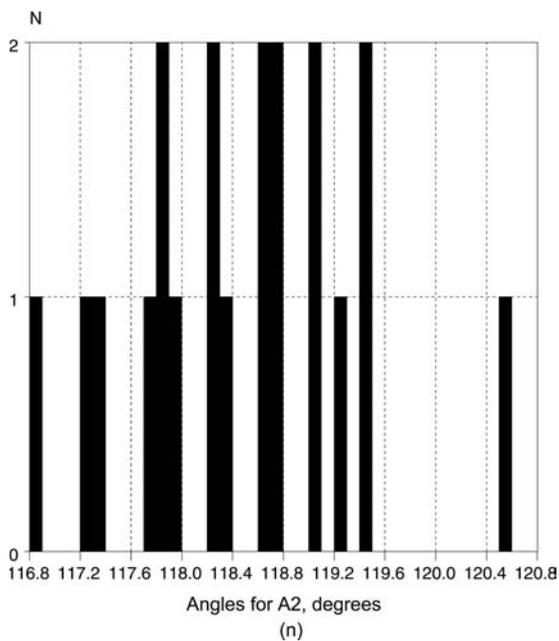
FIGURE 31. (*continued*)
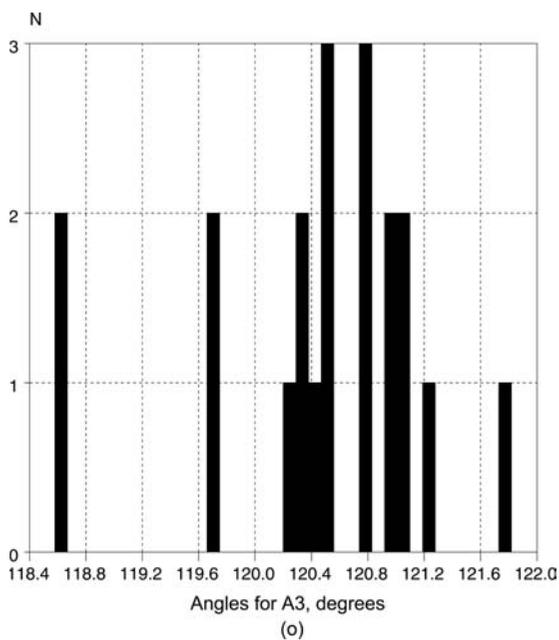
FIGURE 31. (*continued*)
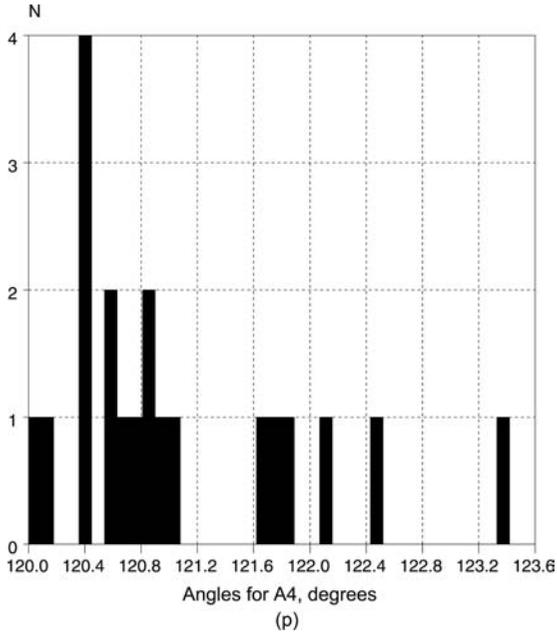
FIGURE 31. (*continued*)
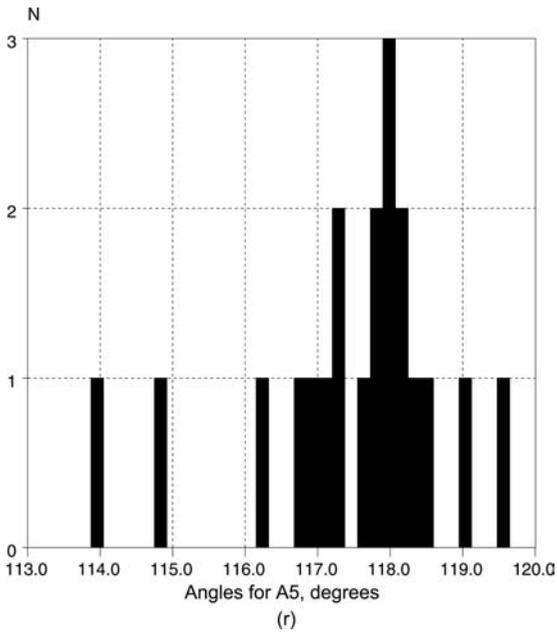
FIGURE 31. (*continued*)
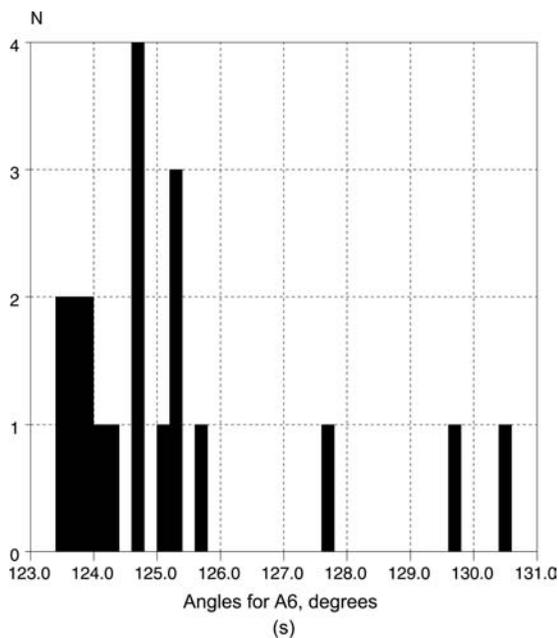
FIGURE 31. (*continued*)
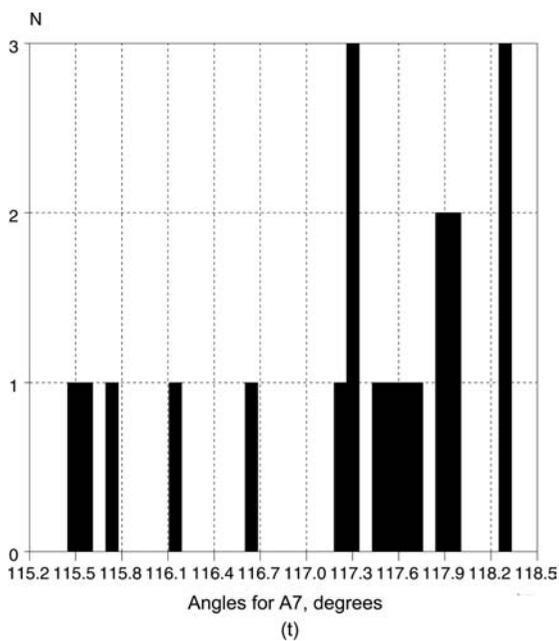
FIGURE 31. (*continued*)
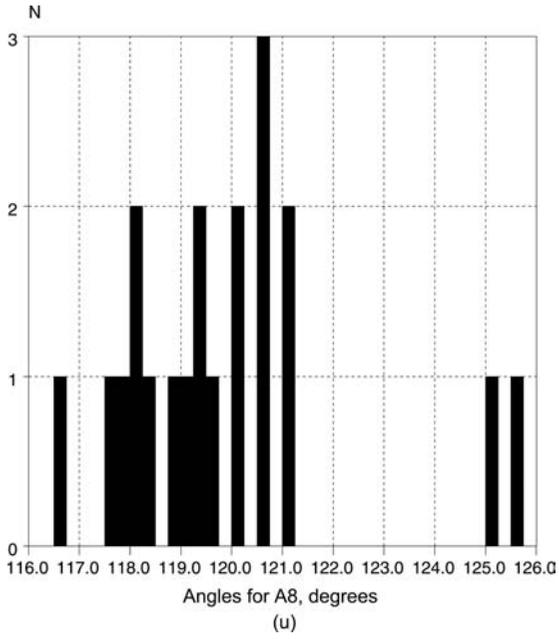
FIGURE 31. (*continued*)
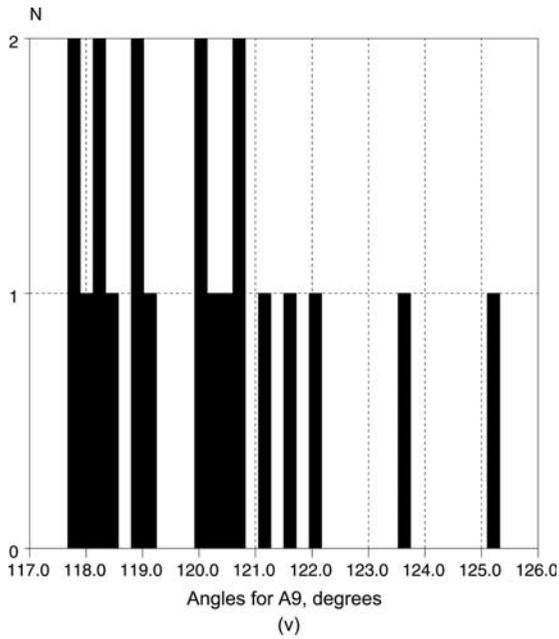
FIGURE 31. (*continued*)
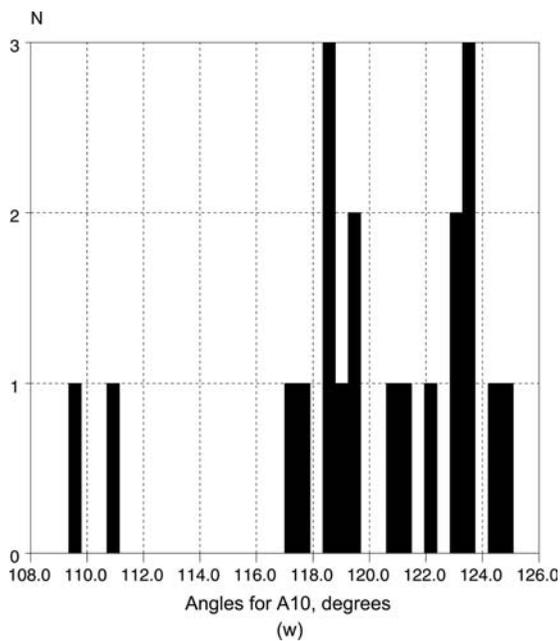
FIGURE 31. (*continued*)
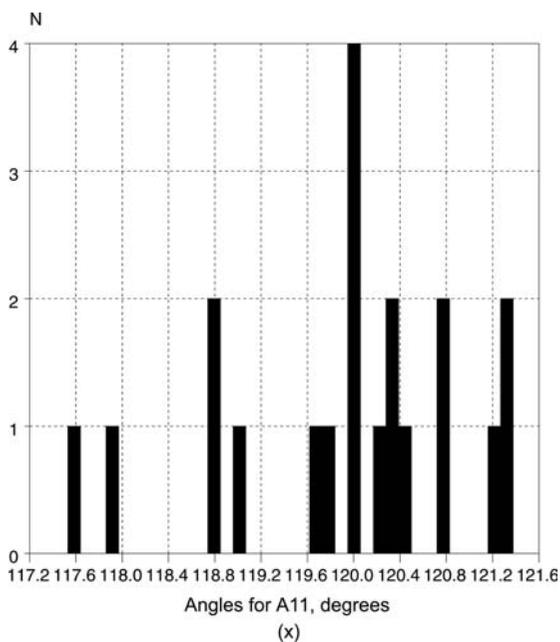
FIGURE 31. (*continued*)
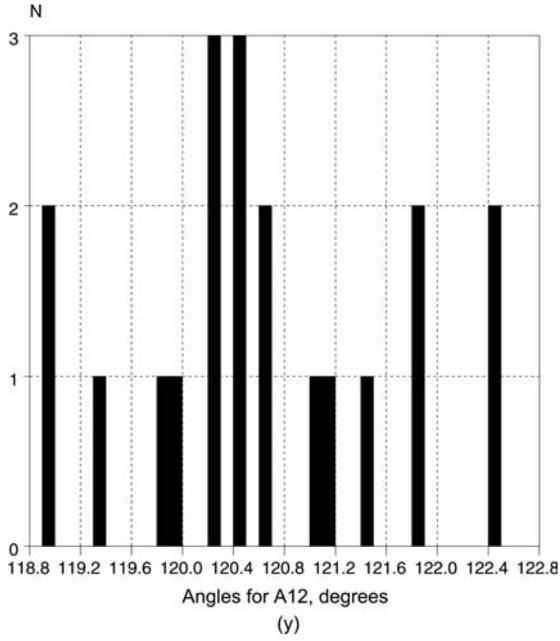
FIGURE 31. (*continued*)
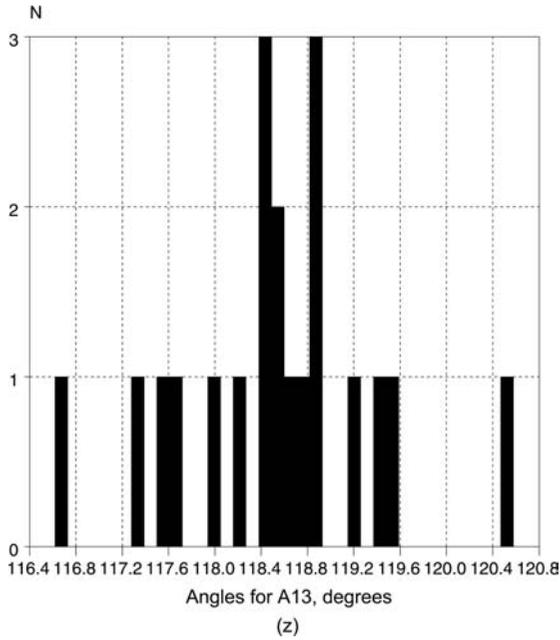
FIGURE 31. (*continued*)
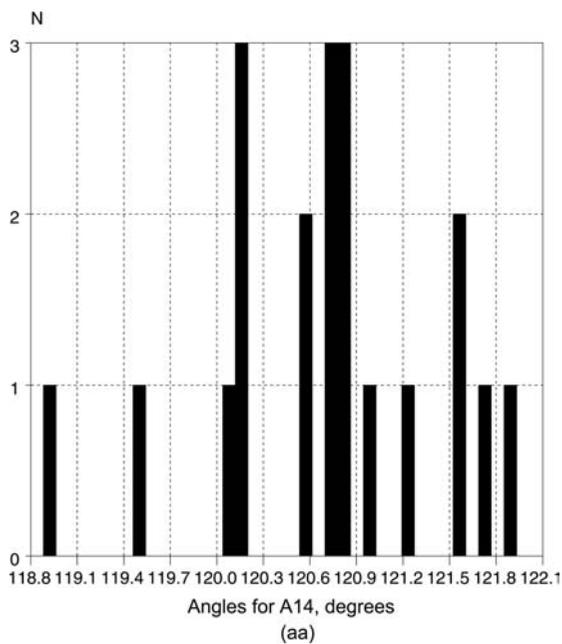
FIGURE 31. (*continued*)
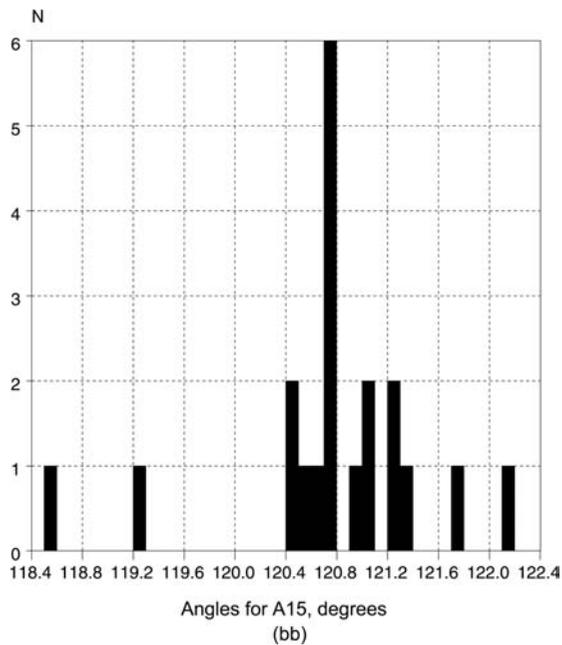
FIGURE 31. (*continued*)
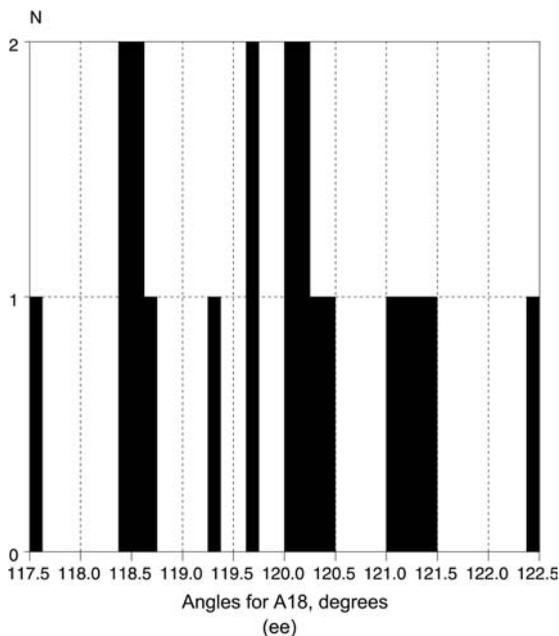
FIGURE 31. (*continued*)

significantly elongated (the median values are 1.448, 1.437, 1.447, 1.423 and 1.421 Å, respectively). The B1, B9, B10 and B13 bond lengths are shortened. Their median values amount to 1.385, 1.359, 1.384 and 1.363 Å, respectively. The median angle values are between 117° and 125°. The A2 and A13 angles (at the amino group) are significantly reduced to *ca* 118°. The A5 and A7 angles are also diminished to *ca* 117.7°. The mean values are very close to the median ones.

Strong correlations, with correlation coefficients $\geqslant|0.8|$, have been found between the following values of the angles: A9 vs A10 ($r = -0.966$), A8 vs A10 ($r = -0.972$), A6 vs A10 ($r = -0.866$), A8 vs A9 ($r = 0.878$), A7 vs A9 ($r = -0.822$), A6 vs A8 ($r = 0.884$), A5 vs A8 ($r = -0.836$), A6 vs A7 ($r = -0.807$) and A5 vs A6 ($r = -0.916$). Significant correlations, with correlation coefficients between $|0.6|$ and $|0.8|$, have been found between A2 vs A13, A11 vs A18, A12 vs A17, A1 vs A16, A7 vs A10, A6 vs A9 and B9 vs B13 (all positive) and A16 vs A17, A9 vs A17, A1 vs A12 and A7 vs A8 (all negative).

IV. MOLECULAR PACKING AND HYDROGEN BONDS IN THE CRYSTALS OF ANILINE DERIVATIVES

Intermolecular hydrogen bonds seem to be a ubiquitous feature in the crystal structures of anilines. The amino groups are the main but not the only proton donor in the crystals. The C(aryl)H groups and (if present) C(aliphatic)H groups are often also involved in very weak hydrogen bondings. Their role as proton donors have been discussed recently in the monograph of Desiraju and Steiner[52]. If other proton donors (e.g. hydroxyl or amino
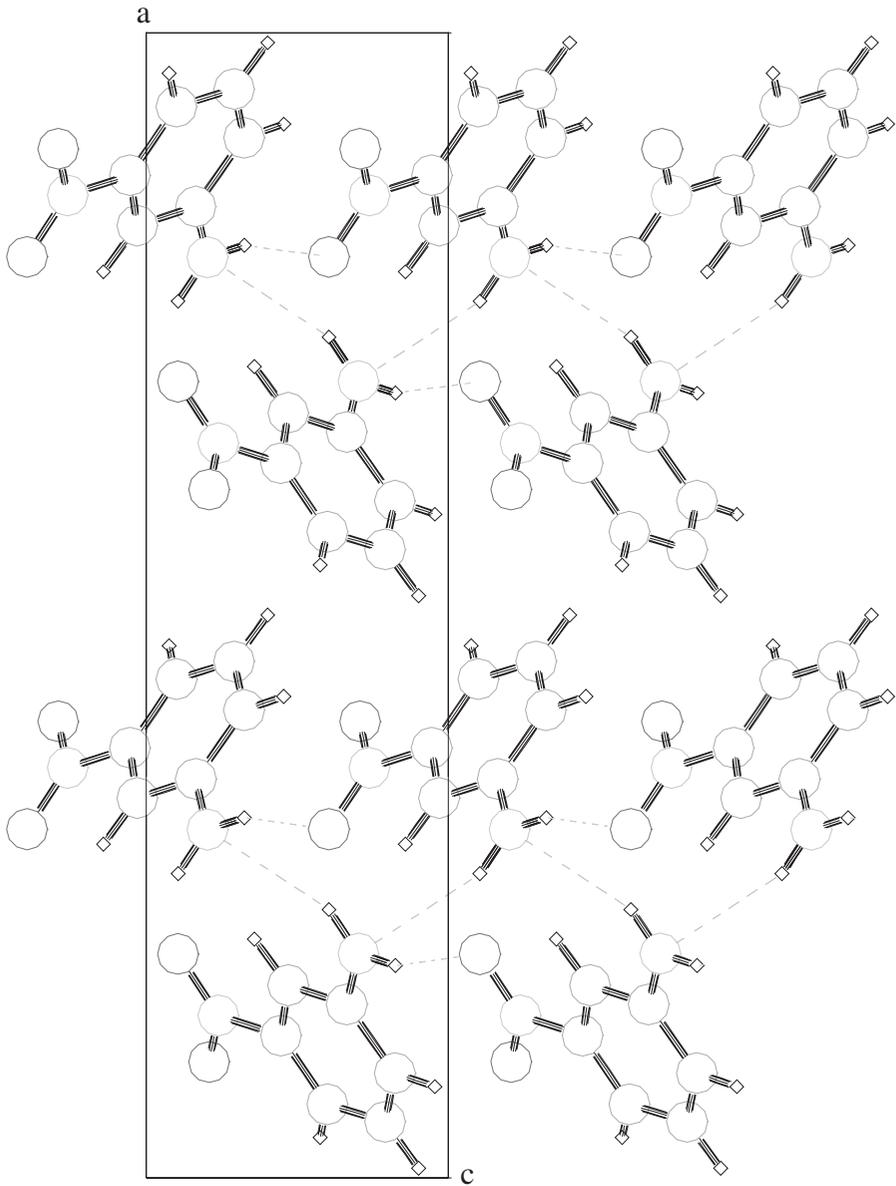
FIGURE 32. Molecular packing with short intermolecular contacts in the *meta*-nitroaniline crystal

groups) are also substituting the benzene ring, they are also involved in the hydrogen bond network. The following substituents on the benzene ring may be proton acceptors: NO_2, F, CN, =O and C=O. If no electron-withdrawing groups substitute the ring, their role may be fulfilled by the free electron pair of the nitrogen atom in the amino group, as it occurs in aniline[27] and *para*-aminoaniline[53].

Chains of hydrogen-bonded molecules are the most common feature of the crystal architecture of anilines. Often, the chains are interlinked by weaker hydrogen bonds, thus forming ribbons or planes or other second-order hydrogen-bonding networks. Figures 32 and 33 present schematically molecules with short intermolecular contacts in *meta*-nitroaniline[14] and in *para*-aminoaniline[53] crystals.

When carboxyl groups substitute a benzene ring, generally centrosymmetric molecular dimers result through COH · · · OC hydrogen bonds. These dimers are then involved in infinite chains through NH · · · O intermolecular hydrogen bonds. Such a molecular packing in the *para*-aminobenzoic acid crystal[54] is shown in Figure 34.

Sometimes, the lack of proton acceptors in a molecule (e.g. in chloroanilines) results in such a molecular arrangement, in which protons of the amino group point toward the Cl atoms and form some kind of molecular chains through very weak 'pseudo' hydrogen bonds, recently called halogen bonds. Figure 35 shows the molecular packing in the *para*-chloroaniline crystal[55].

The substitution on the ring in the *ortho*-positions with respect to the amino group by groups capable of forming hydrogen bonds results in the intramolecular hydrogen bonds. They do not inhibit the formation of intermolecular hydrogen bonds. Thus, the hydrogen bond network in *ortho*-substituted anilines is often more complex and dense in comparison with other isomers. Figure 36 shows the hydrogen bonds in the crystal of 2-aminobenzoic acid[31].

Only very large and bulky substituents make the formation of intermolecular hydrogen bonds impossible. This is not a frequent case and the crystal structure of 4,4′-diamino-3,3′-dipropyloxybiphenyl[42] can be taken as an example. Only intramolecular NH · · · O hydrogen bonds occur in the crystal.

Sometimes, the existence of a few possibilities of different hydrogen bond networks results in polymorph structures. It occurs, for example, in *ortho*-aminobenzoic acid where three crystal structures corresponding to the $P2_1cn$, $Pbca$ and $P2_1/a$ space groups are formed[31, 32, 56–58].
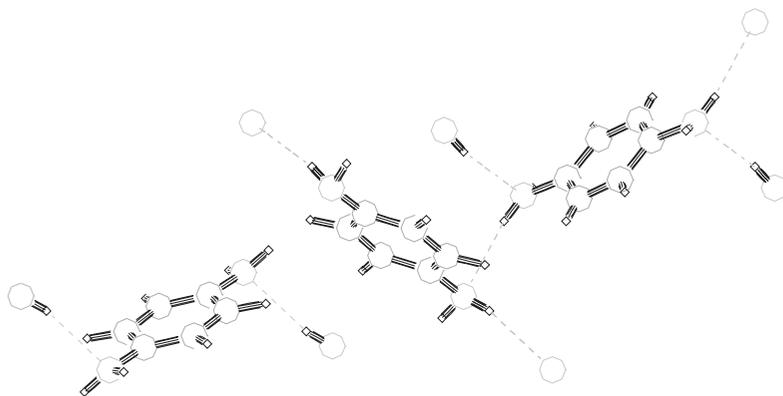
FIGURE 33. Three *para*-aminoaniline molecules in the asymmetric unit cell with short intermolecular contacts
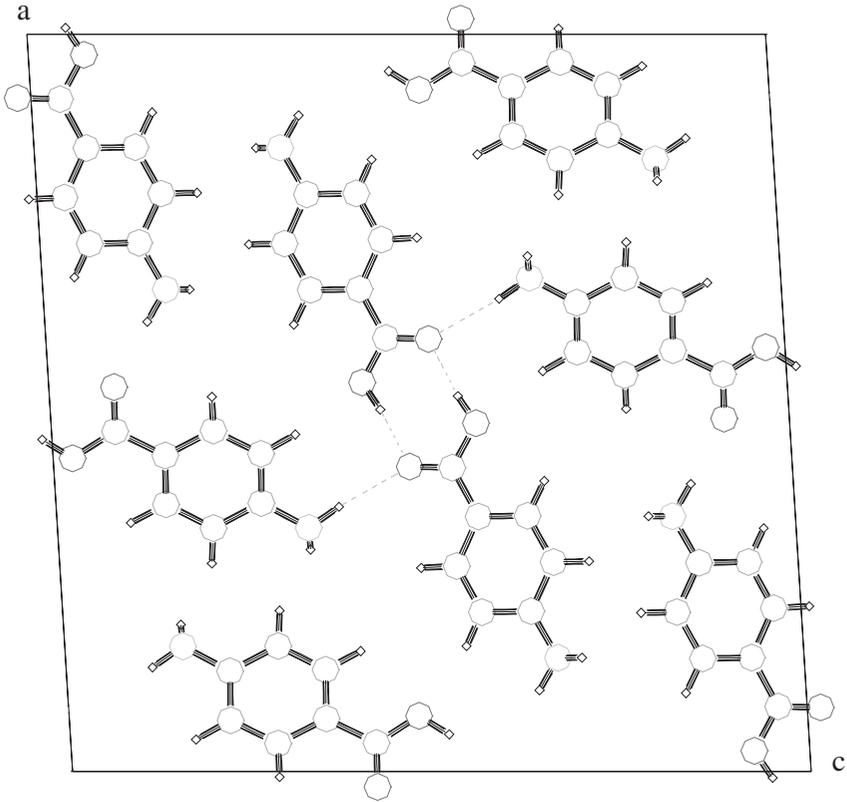
FIGURE 34. Molecular packing and hydrogen bond network in the crystal of *para*-aminobenzoic acid
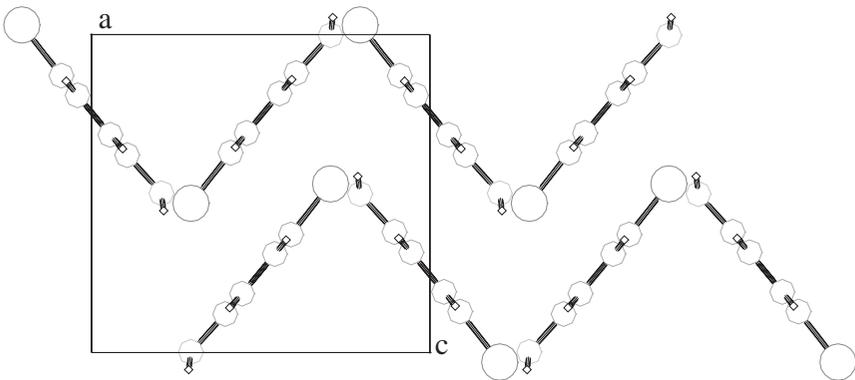
FIGURE 35. Molecular packing in the crystal of *para*-chloroaniline
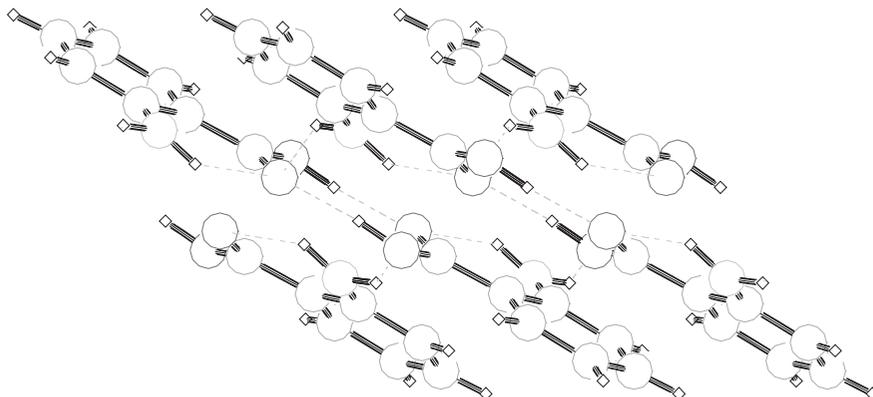
FIGURE 36. Molecular packing and hydrogen bond network in the crystal of *ortho*-aminobenzoic acid
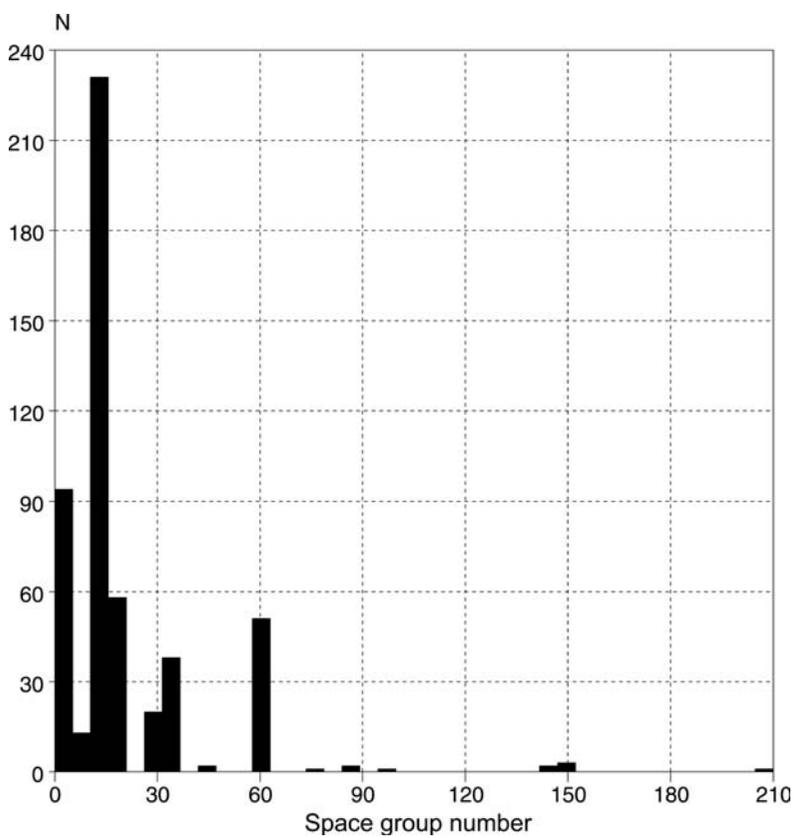
FIGURE 37. Frequency histogram of space groups occurring in the crystals of aniline derivatives; N is number of occurrences

TABLE 1.   Number of occurrences of space groups in the crystals of aniline derivatives

Space group number	Space group symbol	Crystal system	Number of occurrences
1	$P1$	Triclinic	1
2	$P\text{-}1$	Triclinic	73
4	$P2_1$	Monoclinic	19
9	Ia	Monoclinic	13
11	$P2_1/m$	Monoclinic	1
13	$P2/c$	Monoclinic	3
14	$P2_1/c$	Monoclinic	197
15	$C2/c$	Monoclinic	30
19	$P2_12_12_1$	Orthorhombic	58
29	$Pca2_1,\ Pbc2_1,\ P2_1ab$	Orthorhombic	20
33	$Pna2_1,\ P2_1cn$	Orthorhombic	38
43	$Fdd2,\ Iba2$	Orthorhombic	2
60	$Pbcn$	Orthorhombic	4
61	$Pbca$	Orthorhombic	38
62	$Pnma$	Orthorhombic	9
76	$P4_1$	Tetragonal	1
88	$I4_1/a$	Tetragonal	2
96	$P4_32_12$	Tetragonal	1
144	$P3_1$	Trigonal	2
148	$R\text{-}3,\ P\text{-}3$	Trigonal	3
205	$Pa3$	Regular	1

The molecular arrangement in the crystals often occurs around the 2-fold screw axes. Thus, monoclinic and orthorhombic systems are common in the crystals. Additionally, the $P\text{-}1$ space group of a triclinic system often occurs. Symmetry of molecules, especially the large ones, sometimes results in higher crystal symmetries, as in 9-amino-10-(2′,4′,6′-trinitrophenyl)anthracene (space group $P\text{-}3$)[49] and in hexa-aminobenzene (space group $Pa3$)[59]. The frequency of occurrences of space groups in first-order anilines is shown in Figure 37. The most popular is a $P2_1/c(P2_1/n,\ P2_1/a)$ space group (no. 14) occurring in 197 crystal structures. The second most popular space group is $P\text{-}1$ with 73 crystal structures retrieved from the CSD. The third place is occupied by the $P2_12_12_1$ space group (58 occurrences). Table 1 gives a full report of the space group occurrences in the crystals of aniline derivatives. The report is based on 517 crystal structures retrieved from the CSD.

V. CONCLUSIONS

Aniline molecules are relatively rigid. Any flexibility refers to substituents on the aromatic rings and on the amino groups. The configuration of the amino groups exhibits a variable degree of pyramidalization. In general, the molecular structure of aniline derivatives depends strongly on substituents on the aromatic ring and, even more, on substituents on the amino group. Nevertheless, some common structural features have been observed. They may be summarized as follows:

(1) The ring angle at the unsubstituted amino group is distinctly smaller than other angles due to an intramolecular charge transfer.

(2) Anilines substituted at the *para*-position exhibit some contribution from a quinoid structure depending on the other substituents

(3) In general, every second ring bond length and every second angle value in the ring exhibit some positive correlation. The adjacent ring bond lengths and adjacent angles in the ring exhibit a negative correlation.

(4) Unsubstituted amino groups exhibit a tendency toward a pyramidal configuration. However, the degree of pyramidalization is also a consequence of intramolecular and intermolecular hydrogen bonds.

(5) Hydrogen bonds are a ubiquitous feature in the crystals of anilines.

(6) Penta- and hexasubstituted anilines as well as *N*-substituted anilines with large substituents on the amino group may exhibit strong disturbances of their molecular structures due to steric overcrowding and, sometimes, to charge perturbation.

VI. REFERENCES

1. J. Zyss and D. Chemla, *Non-Linear Optical Properties of Organic Molecules and Crystals*, Academic Press, New York, 1987.
2. T. M. Krygowski and J. Maurin, *J. Chem. Soc., Perkin Trans. 2*, 695 (1989).
3. S. T. Howard, M. B. Hursthouse, C. W. Lehmann, P. R. Mallinson and C. S. Frampton, *J. Chem. Phys.*, **97**, 5616 (1992).
4. V. N. Nesterov, T. V. Timofeeva, O. Ya. Borbulevych, M. Yu. Antipin and R. D. Clark, *Acta Crystallogr.*, **C56**, 971 (2000).
5. V. N. Nesterov, T. V. Timofeeva, M. Yu. Antipin and R. D. Clark, *Acta Crystallogr.*, **C56**, 976 (2000).
6. O. Ya. Borbulevych, R. D. Clark, A. Romero, L. Tan, M. Yu. Antipin, V. N. Nesterov, B. H. Cardelino, C. E. Moore, M. Sanghadasa and T. V. Timofeeva, *J. Mol. Struct.*, **604**, 73 (2002).
7. J. Ellena, A. E. Goeta, J. A. K. Howard, C. C. Wilson, J. C. Autino and G. Punte, *Acta Crystallogr.*, **B55**, 209 (1999).
8. A. E. Goeta, C. C. Wilson, J. C. Autino, J. Ellena and G. Punte, *Chem. Mater.*, **12**, 3342 (2000).
9. J. Ellena, A. E. Goeta, J. A. K. Howard and G. Punte, *J. Phys. Chem. A*, **105**, 8696 (2001).
10. T. W. Panunto, Z. Urbańczyk-Lipkowska, R. Johnson and M. C. Etter, *J. Am. Chem. Soc.*, **109**, 7786 (1987).
11. F. H. Allen, C. A. Baalham, J. P. M. Lommerse, P. R. Raithby and E. Sparr, *Acta Crystallogr.*, **B53**, 1017 (1997).
12. L. Turi and J. J. Dannenberg, *J. Phys. Chem.*, **100**, 9638 (1996).
13. C. B. Aakeröy, *Acta Crystallogr.*, **B53**, 569 (1997).
14. G. Wójcik and J. Holband, *Acta Crystallogr.*, **B57**, 346 (2001).
15. J. M. Cole, J. A. K. Howard and G. J. McIntyre, *Acta Crystallogr.*, **B57**, 410 (2001).
16. J. M. Cole, A. E. Goeta, J. A. K. Howard and G. J. McIntyre, *Acta Crystallogr.*, **B58**, 690 (2002).
17. S. J. Garden, S. P. Fontes, J. L. Wardell, J. M. S. Skakle, J. N. Low and C. Glidewell, *Acta Crystallogr.*, **B58**, 701 (2002).
18. P. P. Schmidt, *J. Phys. Chem.*, **99**, 12693 (1995).
19. K. Ogawa, Y. Kasahara, Y. Ohtani and J. Harada, *J. Am. Chem. Soc.*, **120**, 7107 (1998).
20. L. H. Avanci, R. S. Braga, L. P. Cardosolo, D. S. Galvao and J. N. Sherwood, *Phys. Rev. Lett.*, **83**, 5146 (1999).
21. S. Wróbel, B. Thimme Gowda and W. Haase, *J. Chem. Phys.*, **106**, 5904 (1997).
22. M. M. Szostak, G. Wójcik, J. Gallier, M. Berteault, P. Freundlich and H. A. Kołodziej, *Chem. Phys.*, **229**, 275 (1998).
23. O. Ermer and A. Eling, *J. Chem. Soc., Perkin Trans. 2*, 925 (1994).
24. N. Blagden, W. I. Cross, R. J. Davey, M. Broderick, R. G. Pritchard, R. J. Roberts and R. C. Rowe, *Phys. Chem. Chem. Phys.*, **3**, 3819 (2001).
25. V. R. Vangala, B. R. Bhogala, A. Dey, G. R. Desiraju, C. K. Broder, P. S. Smith, R. Mondal, J. A. K. Howard and C. C. Wilson, *J. Am. Chem. Soc.*, **125**, 14495 (2003).
26. F. H. Allen, O. Kennard and R. Taylor, *Acc. Chem. Res.*, **16**, 146 (1983).
27. M. Fukuyo, K. Hirotsu and T. Higuchi, *Acta Crystallogr.*, **B38**, 640 (1982).
28. R. Taylor and F. H. Allen, in *Structure Correlations* (Eds. H.-B. Bürgi and J. D. Dunitz), VCH, Weinheim, 1994.
29. T. M. Krygowski and K. Woźniak, in *The Chemistry of Amidines and Imidates* (Eds. S. Patai and Z. Rappoport), Chap. 2, Wiley, Chichester 1991.

30. B. J. Oleksyszyn, K. Stadnicka and J. Śliwiński, in *The Chemistry of Enamines* (Ed. Z. Rappoport), Chap. 2, Wiley, Chichester, 1994.
31. C. J. Brown, *Proc. R. Soc. London, Ser. A*, **302**, 185 (1968).
32. C. J. Brown and M. Ehrenberg, *Acta Crystallogr.*, **C41**, 441 (1985).
33. A. G. Orpen, L. Brammer, F. H. Allen, O. Kennard, D. G. Watson and R. Taylor, *Appendix A* in *Structure Correlations* (Eds. H.-B. Bürgi and J. D. Dunitz), VCH, Weinheim, 1994.
34. C. Glidewell, D. Cannon, A. Quesada, J. N. Low, S. A. William, J. M. Skakle and L. L. Wardell, *Acta Crystallogr.*, **C57**, 455 (2001).
35. Z. Rzaczyńska, R. Mrozek, J. Lenik, M. Sikorska and T. Głowiak, *J. Chem. Crystallogr.*, **30**, 519 (2000).
36. S.-Q. Dou, N. Weiden and A. Weiss, *Acta Chim. Hung.*, **130**, 497 (1993).
37. G. M. Brown and R. E. Marsh, *Acta Crystallogr.*, **16**, 191 (1963).
38. L. Parkanyi and A. Kalman, *J. Mol. Struct.*, **125**, 315 (1984).
39. B. Twamley, C.-S. Hwang, N. J. Hardman and P. P. Power, *J. Organomet. Chem.*, **609**, 152 (2000).
40. V. M. Jimenez-Perez, C. Camacho-Camacho, M. Guizado-Rodriguez, H. Noth and R. Contreras, *J. Organomet. Chem.*, **614**, 283 (2000).
41. M. A. Menelau, N. H. Fischer and F. R. Fronczek, personal communication (1999).
42. A. El-Shafei, P. D. Boyle, D. Hinks and H. S. Freeman, *Acta Crystallogr.*, **C59**, 71 (2003).
43. S. Ide and A. Topacli, *J. Mol. Struct.*, **526**, 201 (2000).
44. A. J. Bell, E. Eadie, R. W. Read, B. W. Skelton and A. H. White, *Aust. J. Chem.*, **40**, 175 (1987).
45. R. E. Marsh, F. H. Herbstein,, *Acta Crystallogr.*, **B44**, 77 (1988).
46. K. Seno, S. Hagishita, T. Sato and K. Kuriyama, *J. Chem. Soc., Perkin Trans. 1*, 2013 (1984).
47. H. Mahmoud, Y. Han, B. M. Segal and L. Cai, *Tetrahedron:Asymmetry*, **9**, 2035 (1998).
48. M. Smrcina, S. Vyskocil, V. Hanus, M. Polasek, V. Langer, B. G. M. Chew, D. B. Zax, H. Verrier, K. Harper, T. A. Claxon and P. Kocovsky, *J. Am. Chem. Soc.*, **118**, 487 (1996).
49. G. V. Gridunova, V. N. Petrov, Yu. T. Struchkov, I. G. Ilina and O. V. Mikhalev, *Kristallografiya*, **35**, 54 (1990); *Chem. Abstr.*, **112**, 169574g (1990).
50. H. L. Revers, J. A. Kanters and E. Grech, *J. Mol. Struct.*, **271**, 109 (1992).
51. P. R. Mallison, K. Woźniak, C. C. Wilson, K. L. McCormack and D. S. Yufit, *J. Am. Chem. Soc.*, **121**, 4640 (1999).
52. G. R. Desiraju and T. Steiner, *The Weak Hydrogen Bond*, Oxford, University Press, Oxford 1999.
53. Z. P. Poveteva and Z. V. Zvonkova, *Kristallografiya*, **20**, 69 (1975); *Chem. Abstr.*, **83**, 19513e (1975).
54. T. F. Lai and R. E. Marsh, *Acta Crystallogr.*, **22**, 885 (1967).
55. H. Takazawa, S. Ohba and V. Saito, *Acta Crystallogr.*, **B45**, 432 (1989).
56. O. D. G. Boone, J. L. Derissen and J. C. Schoone, *Acta Crystallogr.*, **B33**, 3205 (1977).
57. G. E. Hardy, W. C. Kaska, B. P. Chandra and J. I. Zink, *J. Am. Chem. Soc.*, **103**, 1074 (1981).
58. H. Takazawa, S. Ohba and V. Saito, *Acta Crystallogr.*, **C42**, 1880 (1986).
59. P. A. Dixon, J. C. Calabrese and J. S. Miller, *Angew. Chem., Int. Ed. Engl.*, **28**, 90 (1989).

Thermochemistry of anilines

SUZANNE W. SLAYDEN

Department of Chemistry, George Mason University, 4400 University Drive, Fairfax, Virginia 22030, USA
Fax: +1 703 993 1055; e-mail: sslayden@gmu.edu

and

JOEL F. LIEBMAN

Department of Chemistry and Biochemistry, University of Maryland, Baltimore County, 1000 Hilltop Circle, Baltimore, Maryland 21250, USA
Fax: +1 410 455 2608; e-mail: jliebman@umbc.edu

I. INTRODUCTION: SCOPE AND DEFINITIONS

A. Thermochemistry

As has been the approach for most of the authors' other reviews on organic thermochemistry (see References 1–3 and others that permeate the current text), the current chapter is primarily devoted to the relatively restricted property, the 'molar standard enthalpy of formation' and symbolically written as $\Delta_f H_m^o$. It is also often called the 'heat of formation' and symbolically written as ΔH_f or ΔH_f^o. This chapter foregoes discussion of other thermochemical properties such as Gibbs energy, entropy, heat capacity and excess enthalpy. We also avoid discussion of bond dissociation energies (e.g. of the anilino ArNH−H bond) and gas-phase clustering energies (e.g. with halide or metal ions). Likewise, we ignore questions of base or acid strength (in either solution or gas phase) or of any intermolecular complexation energies except for occasional mention of hydrogen bonding in the pure condensed phase. The temperature and pressure are assumed to be 25 °C ('298 K') and 1 atmosphere or 1 bar (101,325 or 100,000 Pa), respectively. The energy units are kJ mol^{-1} where 4.184 kJ is defined as 1 kcal.

Unreferenced, evaluated enthalpies of formation are taken from the now 'classic' thermochemical archive by Pedley and his coworkers[4]. Other, generally early, data are taken from the archives by Stull, Westrum and Sinke[5]. These archival thermochemical numbers are usually for comparatively simple and well-understood species where we benefit from the data evaluation performed by these authors. Recent data are presented with the original source for more complete attribution although in some cases the data are

readily accessible only from the NIST WebBook[6]. We also include in our discussion old numbers ignored by the archivists when they are the only data for a given species, as well as new numbers that appeared past the archive's cutoff date. Yet other data were ignored by these latter authors for no apparent reason. In most cases, where there are conflicting data, the various values are presented, compared and appraised by the current chapter authors. Those enthalpies of formation that are deemed trustworthy are listed in Tables 1–8. Those that are suspected to be inaccurate are discussed in the text but not included in the tables.

Enthalpies of fusion are taken from Reference 7 and enthalpies of sublimation from Reference 8. Where data for vaporization enthalpies are lacking, we will use the CHLP protocol[9] to estimate them. The derived values assume that the enthalpy of vaporization depends only on the number of carbons in the molecule and the identity of the substituent affixed to the hydrocarbon parent.

B. Definition of Anilines

We restrict our attention to those compounds of the type $ArNR^1R^2$ wherein Ar is a carbocyclic aromatic ring (substituted or not) and R^1 and R^2 are H, some saturated alkyl

TABLE 1.   Enthalpies of formation of alkyl-substituted anilines (kJ mol^{-1})

Compound	Solid	Liquid	Gas	Reference
Aniline	21.4	31.3 ± 1.0	87.1 ± 1.0	4, 7
2-Methylaniline (o-toluidine)		-4.7 ± 1.0	53.6 ± 1.0^a	17
3-Methylaniline (m-toluidine)		-1.3	57.0	5, 17, 20
4-Methylaniline (p-toluidine)	-19.2 ± 1.3		57.0 ± 1.3	17
N-Methylaniline		32.3	85.4	19, 20
		33.4 ± 7.5	83.9 ± 6.3	21
		36.1		18
2,4-Dimethylaniline		-39.2 ± 0.9	23.2 ± 1.1	24
2,5-Dimethylaniline		-38.9 ± 0.5	23.9 ± 0.9	24
2,6-Dimethylaniline		-41.0 ± 1.5	18.6 ± 1.5	25
N,N-Dimethylaniline		47.7 ± 3.2	100.5 ± 4.7	4
		46.0 ± 0.9	100.0 ± 1.0	24
3,N,N-Trimethylaniline		14.4 ± 2.5	72.6 ± 7.5	28
4,N,N-Trimethylaniline		14.4 ± 2.5	68.9 ± 7.4	28
2-Ethylaniline		-24.8 ± 1.8	35.8 ± 2.0	24
N-Ethylaniline		4.0 ± 4.2	56.3 ± 5.9	4
		8.2 ± 0.9	66.5 ± 1.1	24
N-Ethyl-3-methylaniline		-29.5 ± 2.3	30.5 ± 3.8	28
2,6-Diethylaniline		-84.7 ± 1.8	-18.8 ± 1.9	25
N,N-Diethylaniline		-5.3	50.7	26
		1.8 ± 3.2	62.1 ± 7.6	28
2-Isopropylaniline		-53.6 ± 2.1	8.2 ± 2.3	21
2,6-Diisopropylaniline		-139.7 ± 2.4	-70.2 ± 2.4	25
2-t-Butylaniline		-64.2 ± 2.1	-1.5 ± 2.1	25
2,4,6-Tri-t-butylaniline	-268.8 ± 4.2		-194.3 ± 4.3	25
2-Methyl-6-t-butylaniline		-108.6 ± 2.5	-44.8 ± 3.5	34
N-Phenylpiperidine		6.0 ± 1.3	70.3 ± 1.4	35
2,3-Dihydro-1H-indole (indoline)		56.1 ± 3.1	121.5 ± 3.3	36
1,2,3,4-Tetrahydroquinoline		16.7 ± 0.8	82.8 ± 0.8	37

^{a} The enthalpy of vaporization of 2-methylaniline is taken from W. V. Steele, R. D. Chirico, A. Nguyen and S. E. Knipmeyer, *J. Chem. Thermodyn.*, **26**, 515 (1994).

TABLE 2. Enthalpies of formation of arylated anilines (kJ mol^{-1})

Compound	Solid	Liquid	Gas	Reference
1-Naphthylamine	67.7 ± 5.4		157.7 ± 6.8 [a]	4,45
	64.6 ± 5.3		154.6 ± 6.8 [a]	47
2-Naphthylamine	59.7 ± 5.0		133.8 ± 5.1	4
2-Aminobiphenyl	112.0 ± 6.3			4
	93.8 ± 1.1			52
4-Aminobiphenyl	81.0 ± 6.3			4
2,4′-Diaminobiphenyl		103		5
4,4′-Diaminobiphenyl	70.7 ± 1.7			4
Diphenylamine	130.2 ± 1.7		219.3 ± 3.0	4
Triphenylamine	235 ± 3		327 ± 4.2	55
N-Phenyl-2-naphthylamine	159.9 ± 1.9		275.7	4,58
Bis(p-aminophenyl)methane		84 ± 20		67
N,N′-Diphenylmethanediamine	145.4 ± 0.6			68
N,N′,N″-Triphenylhexahydro-1,3,5-triazine	352.7 ± 0.6			68

[a] The enthalpy of sublimation is taken from E. W. Balson, *Trans. Faraday Soc.*, **43**, 54 (1947).

TABLE 3. Enthalpies of formation of polyaminobenzenes (kJ mol^{-1})

Compound	Solid	Liquid	Gas	Reference
o-Phenylenediamine	−0.3 ± 4.2			4
	6.5 ± 1.3	25.1 ± 1.4	92.0 ± 1.3	73
m-Phenylenediamine	−7.8 ± 4.2			4
	−6.4 ± 1.4	18.4 ± 1.4	84.0 ± 1.4	73
p-Phenylenediamine	3.1 ± 0.7			4
	−3.5 ± 1.4	16.6 ± 1.4	88.7 ± 1.4	73
N,N,N′,N′-Tetramethyl-p-phenylenediamine	39.6 ± 3.9			75

TABLE 4. Enthalpies of formation of anilines with oxygen-bonded functional groups (kJ mol^{-1})

Compound	Solid	Gas	Reference
2-Aminophenol	−191.0 ± 0.9	−87.1 ± 1.3	76
	−201.3 ± 1.5	−104.4 ± 1.7	77
3-Aminophenol	−194.1 ± 1.9	−89.4 ± 1.6	76
	−200.2 ± 1.2	−98.6 ± 1.6	77
4-Aminophenol	−190.6 ± 0.9	−81.5 ± 1.7	76
	−194.1 ± 0.9	−90.5 ± 1.2	77
4,6-Dinitro-2-aminophenol (picramic acid)	−243.6		78
	−246.6		79
cis-5a,6,11a, 12-Tetrahydro[1,4]benzoxazino [3,2-b][1,4]benzoxazine	−180.9 ± 6.3	−51.9 ± 6.4	96
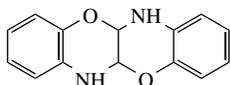
TABLE 5. Enthalpies of formation of anilines with sulfur-containing functional groups (kJ mol^{-1})

Compound	Solid	Gas	Reference
o-Aminobenzenesulfonic acid	−559.6 ± 1.1		93
m-Aminobenzenesulfonic acid	−606.2 ± 1.8		93
p-Aminobenzenesulfonic acid	−612.3 ± 1.0		93
cis-5a,6,11a, 12-Tetrahydro[1,4]benzothiazino [3,2-b][1,4]benzothiazine	123.3 ± 1.2	288.5 ± 6.4	96
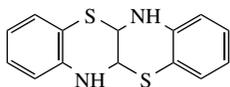
TABLE 6. Enthalpies of formation of anilines with halogen substituents (kJ mol^{-1})

Compound	Solid	Liquid	Gas	Reference
o-Chloroaniline		−3.0 ± 1.6	53.4 ± 3.1	100
m-Chloroaniline		−8.1 ± 1.7	53.0 ± 2.8	100
p-Chloroaniline	−18.5 ± 1.7		59.7 ± 2.3	100
2-Chloro-4-nitroaniline	−74.0 ± 1.4		28.6 ± 2.1	105
2-Chloro-5-nitroaniline	−71.0 ± 1.5		30.0 ± 2.2	105
2,4,6-Trichloroaniline	−80.3 ± 1.8		5.0 ± 2.6	106
2,4,5-Trichloroaniline	−61.4 ± 1.4		28.1 ± 2.9	106
2,3,4-Trichloroaniline	−64.3 ± 2.4		28.1 ± 2.9	106
3,4,5-Trichloroaniline	−67.8 ± 2.0		25.1 ± 3.9	106
2,4,6-Tribromoaniline	57.9 ± 2.4		159.0 ± 2.6	109

TABLE 7. Enthalpies of formation of anilines with π-electron-withdrawing substituents (kJ mol^{-1})

Compound	Solid	Liquid	Gas	Reference
o-Aminobenzoic acid	−400.9 ± 0.9		−296.0 ± 1.3	4
m-Aminobenzoic acid	−411.6 ± 2.3		−293.6 ± 3.9	4
p-Aminobenzoic acid	−412.8 ± 1.0		−296.7 ± 3.8	4
Ethyl p-aminobenzoate	−417.9 ± 0.9			4
3-(N-Anilino)-2-naphthoic acid	−263.6 ± 2.2			4
4-N,N-Dimethylaminobenzaldehyde	−137.6 ± 0.9			4
3-Aminoacetophenone	−173.3 ± 0.5	−161.2 ± 0.7		4
4-Aminoacetophenone	−182.1 ± 0.5	−166.2 ± 0.7		4
o-Nitroaniline	−26.1 ± 0.5	−9.4 ± 1.0	63.8 ± 4.2	4
m-Nitroaniline	−28.2 ± 6.3		59.2 ± 4.2	119
	−38.3 ± 0.5	−14.4 ± 1.0	58.4 ± 1.4	112,4
	−34.2 ± 1.2		62.5 ± 1.8	121
p-Nitroaniline	−42.0 ± 0.8	−20.7 ± 1.2	58.8 ± 1.5	4
N,N-Dimethyl-m-nitroaniline	−20.1 ± 1.8		72.6 ± 1.8	124
N,N-Dimethyl-p-nitroaniline	−35.4 ± 1.4		67.3 ± 1.7	124
	−38.5 ± 1.6		62.8 ± 2.6	125
2,4,6-Trinitroaniline	−72.8			79
2,4,6-Trinitrobenzene-1,3,5-triamine	−154			127
	−140.0			128
N,N-Dimethyl-p-nitrosoaniline	103.0 ± 1.6		185.0 ± 2.3	125

TABLE 8. Enthalpies of formation of biochemical/medicinal relevant anilines (kJ mol^{-1})

Compound	Solid	Gas	Reference
N-Phenylglycine	−396.7 ± 0.6	−268.7 ± 2.1	137
Phenoxazine	−2.1 ± 2.8	94.0 ± 2.8	144
Phenothiazine	166.7 ± 1.9	278.2 ± 1.9	144
1,3,7,9-Tetranitrophenothiazine-S-oxide	−498.0		145

group or another such carbocyclic aromatic ring. The restriction to carbocyclic rings means we have excluded discussion of such species as the isomeric pyridinamines and three of the nucleotide bases cytosine, adenine and guanine. By this definition we also exclude species that are logically considered perhaps more to be enamines than anilines, whether they be indole, 1,5-imino[10]annulene or indigo. We avoid discussion of enamines because they are the subject of generally interesting, complicated but quite extraneous studies. We have also excluded amides such as acetanilide, isatin, benzimidazolone and isatoic anhydride, as well as N-nitrated species such as tetryl. And finally, excepting a brief mention of N-phenylhydroxylamines, no mention is made of any derivative where either of the nitrogen-affixed groups is a heteroatom (i.e. non-H and/or C) and so hydrazines will not be discussed. Therefore, indazolinone and its acetyl derivatives are omitted for multiple reasons. Many of these classes of compounds have been earlier reviewed by the current authors and few new data exist to discuss now. In particular, there are reviews on enamines[10], N- and C-nitrated compounds[11], hydrazines[12] and amides[13].

C. The Enthalpy of Formation of Aniline and Amino/Hydrogen Exchange Reactions

Many of the thermochemical comparisons we make in this chapter are between an aniline and its corresponding denitrogenated counterpart, that is, we consider the effect of replacing a hydrogen atom with the amino group on the aromatic ring, shown as formal reaction 1.

$$\text{Ar−H} + \tfrac{1}{2}\,\text{N}_2 + \tfrac{1}{2}\,\text{H}_2 \longrightarrow \text{Ar−NH}_2 \tag{1}$$

The enthalpy for reaction 1 is the difference between the enthalpies of formation of the two aromatic substances where both species are in the same phase (s, lq or g). The enthalpy of formation of the elements is precisely 0 kJ mol^{-1} by definition. The difference quantity for aniline and benzene is an important benchmark in this review. The enthalpy of formation of aniline[4] is 31.3 ± 1.0 for the liquid and 87.1 ± 1.0 kJ mol^{-1} for the gas. The enthalpy of formation of benzene[4] is 49.0 ± 0.6 and 82.6 ± 0.7 kJ mol^{-1} for the liquid and gas, respectively. The recommended enthalpies of fusion[7] of aniline and benzene are very nearly the same, 10.5 and 9.9 kJ mol^{-1}, resulting in solid-phase enthalpies of formation for the two species of 21.4 and 38.5 kJ mol^{-1}, respectively. Accordingly, the amino/hydrogen difference quantity, or enthalpy of reaction 1, is +4.5 kJ mol^{-1} for the gas. The corresponding liquid- and solid-phase difference quantities are the nearly identical −17.7 and −17.1 kJ mol^{-1}. It is noteworthy that the difference enthalpy is decidedly exothermic in the condensed phases, but slightly endothermic in the gas phase.

Assuming that these are general difference quantities for all aniline derivatives and corresponding 'hydrocarbons', we can use them as simple additive constants to estimate and thereby appraise literature values for the enthalpies of formation of substituted anilines. Alternatively, the enthalpy of reaction 2 is mathematically equivalent to generating the

deviation between the difference quantities for other aromatic rings and those calculated above for benzene and aniline themselves.

$$Ar-H + Ph-NH_2 \longrightarrow Ar-NH_2 + Ph-H \tag{2}$$

D. Resonance Stabilization and Aniline

Because of the interaction between the aromatic ring electrons and the π-electron-donating nitrogen of the affixed amino group, there are additional ionic resonance structures for aniline beyond those of simple (aliphatic or alicyclic) amines and benzene itself. That these contributors sacrifice the aromatic sextet of the benzene certainly minimizes their contribution. One probe of the thermochemical consequences of these resonance structures is to compare the hydrogenation enthalpy of benzene to form cyclohexane with that of aniline to form cyclohexylamine. More generally, we can compare the stabilizing effect of any substituent group X on the aromatic ring by considering the enthalpy of exchange reaction 3. This is equivalent to comparing the hydrogenation enthalpies of the two differently substituted aromatic compounds. The gas-phase enthalpies of reaction for various atoms or groups X are: CH_3, -0.9; OH, -16.2; NH_2, -14.0; SH, 2.5; and Cl, 11.2 kJ mol^{-1}. (The enthalpy of formation of chlorocyclohexane is the average of two values from References 14 and 15.) Aniline 'enjoys' nearly as much resonance-derived enhanced stability over benzene as does phenol[16].

$$\tag{3}$$
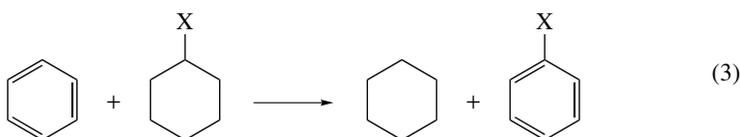
II. ALKYLATED ANILINES AND RELATED SPECIES

Aniline has four different (nonequivalent) sites for possible substitution: the two equivalent sites on nitrogen, the two equivalent *ortho* positions, the two equivalent *meta* positions and the unique *para* position. An alkylated aniline results from the replacement of one or more of these either N—H and/or C—H atoms with a group attached by a saturated carbon.

A. Methylated Anilines

Let us start with the three isomeric C-monomethylated species (the toluidines or methyl-benzenamines) and accept the recent experimental measurements and analysis[17]. This source points out the contradictory and incomplete measurements for these species and uses the expression 'in disarray' to describe the literature. From thermoneutral equation 2, we would predict enthalpies of formation of -12, -5 and 55 kJ mol^{-1} for all three solid, liquid and gaseous toluidines, in reasonable agreement with the experimental values. We note that the *o*-isomer is slightly more stable than its *m*- and *p*-isomers. In comparison, the spread of enthalpy of formation values for the isoelectronic and isosteric xylenes is but 1 kJ mol^{-1} and for the so-related methylphenols[3] (cresols) is but 7 kJ mol^{-1}. As an additional check for thermochemical accuracy, consider the formal methylation reaction 4. For Ar = Ph, the enthalpies of reaction are -36.6 (lq) and -32.2 (g) kJ mol^{-1}. For Ar = $C_6H_4NH_2$, the *ortho, meta* and *para* gas-phase enthalpies of reaction are the

compatible -33.5, -30.1 and -30.1 kJ mol^{-1}. The liquid-phase *ortho* and *meta* reaction enthalpies are -36.0 and -32.6 kJ mol^{-1}.

$$Ar-H \longrightarrow Ar-Me \qquad (4)$$

N-methylation is not expected to result in a nearly identical enthalpy of formation value to that of the C-methylated species. Why should it? Indeed, from a consensus of combustion calorimetry measurements, the liquid[18−21] enthalpy of formation for *N*-methylaniline is 34 ± 2 kJ mol^{-1} and for the gas[19, 21] is 84 ± 2 kJ mol^{-1}. Results from reaction calorimetry[22] are compatible with these values. While methylation of the aromatic ring is quite exothermic, formal methylation of the aniline nitrogen is essentially thermoneutral.

Dimethylation of aniline solely on carbon allows for six isomers of the classically so-called xylidines. For the 2,4-isomer, a 1907 study[23] reports a liquid-phase enthalpy of formation of -88.7 kJ mol^{-1} and a contemporary measurement[24] 90 years later reports values of -39.2 ± 0.9 for the liquid and 23.2 ± 1.1 kJ mol^{-1} for the gaseous species. While we 'naturally' prefer the latter because of greater trust in the reliability of recent values, can we decide on any other grounds? The hydrocarbon counterpart of the dimethylaniline is *m*-xylene, for which the archival enthalpy of formation values are -25.4 ± 0.8 (lq) and 17.3 ± 0.8 (g) kJ mol^{-1}. From equation 2, the derived enthalpies of formation for the 2,4-dimethylaniline are *ca* -43 (lq) and 22 (g) kJ mol^{-1}. The good agreement with the more recent values vindicates our predilection as to choice of values as well as confidence in the applicability of the amino/hydrogen difference quantity.

The contemporarily measured values[24] for liquid and gaseous 2,5-dimethylaniline are -38.9 ± 0.5 and 23.9 ± 0.9 kJ mol^{-1}, respectively. The enthalpy of formation of *p*-xylene is *ca* 1 ± 1 kJ mol^{-1} higher than that of the *m*-isomer in both the liquid and gaseous phases. From equation 2, the predicted enthalpies of formation of 2,5-dimethylaniline are *ca* -42 (lq) and 23 (g) kJ mol^{-1}, respectively, in good agreement with experiment.

What about the 2,6-isomer? In the absence of buttressing effects from adjacent *ortho* substituents (see discussion below), we would think that the enthalpy of formation of this isomer should be the same as that for the 2,4 since both are related by the difference quantity to *m*-xylene. A contemporary Reference 25 gives the enthalpies of formation of -41.0 ± 1.5 for the liquid and 18.6 ± 1.5 kJ mol^{-1} for the gaseous species. The liquid-phase values for the aniline isomers are identical within the error bars, but it would appear that the gas-phase 2,6-isomer is very slightly stabilized relative to its 2,4-isomer—this difference is quite small—although we do not understand why it should be somewhat more, rather than somewhat less, stable.

There are three N,C-substituted dimethylanilines, the N-methyltoluidines. Of these, only the *para* isomer has been studied calorimetrically[26] in the acid-catalyzed liquid-phase disproportionation reaction 5, X = CH$_3$. The reaction is exothermic by only 2 kJ mol^{-1}, essentially thermoneutral, as was the case for the related reaction for *N*-methylaniline[22].

$$(5)$$
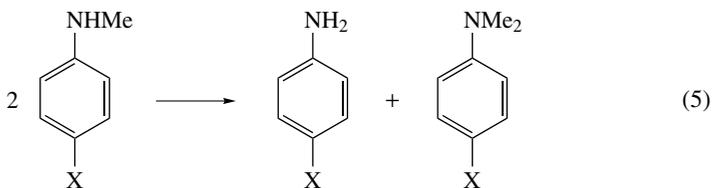
For *N*,*N*-dimethylaniline, the remaining isomer, the enthalpies of formation are 47.7 ± 3.2 kJ mol^{-1} for the liquid and 100.5 ± 4.7 kJ mol^{-1} for the gaseous species[4]. Reference 24

reports the values of 46.0 ± 0.9 and 100.0 ± 1.0 kJ mol^{-1} in fine agreement, but with narrower error bars. Disproportion reaction 5, X = H, is calculated to be quite endothermic, ca 11 (lq) and 20 (g) kJ mol^{-1} when using the average values for the enthalpies of formation of N-methylaniline, given earlier. However, in the aforementioned paragraph, it was found from reaction thermochemistry that this reaction is nearly thermoneutral. We suspect some error in one or more of the enthalpies of formation[27], although errors in enthalpy of reaction measurements or interpretations (e.g. the co-formation of some ring methylated product) cannot be precluded.

There are numerous isomers of the multiply methylated anilines, most of which have been ignored by the thermochemical community. Of the six possible ring-only methylated species, the sole species to be studied is the 2,4,5-trimethylaniline (the earlier-named pseudocumidine) in the very old Reference 23. The solid-phase enthalpy of formation is -110 kJ mol^{-1}. The enthalpy of formation of the corresponding hydrocarbon, 1,2,4-trimethylbenzene (the earlier-named pseudocumene), is -25 kJ mol^{-1} using a temperature-uncorrected fusion enthalpy. The resulting amino/hydrogen difference is 85 kJ mol^{-1}, an altogether unreasonable value.

The enthalpies of formation for the 3,N,N- and 4,N,N-trimethylanilines from contemporary measurements[28] are quite similar. From the average methylation reaction enthalpies of N-methylaniline in equation 4, and the enthalpies of formation of N,N-dimethylaniline, the enthalpies of formation of the trimethylated species are predicted to be ca 14 (lq) and 69 (g) kJ mol^{-1}, in encouraging agreement with the experimental measurements, given the large error bars. No thermochemical data are available for the 2,N,N-isomer. Will it be but ca 5 kJ mol^{-1} less stable as is the case for the isoelectronic liquid-phase isopropyltoluenes? Or, will the difference be more like the 20 kJ mol^{-1} found for the t-butyltoluenes[29] where there are two nearby abutting methyl groups as would be found if the dimethylaniline substructure is forced to be planar[30]?

B. Ethylated Anilines

Of the three isomeric C-ethylated anilines, there are thermochemical data[24] only for the *ortho* isomer. Equation 2 predicts enthalpies of formation of -29.7 (lq) and 34.4 (g) kJ mol^{-1}. Equation 2 also suggests that the difference between enthalpies of formation of 2-ethylaniline and any of the C,C-dimethylanilines would be the same as that between ethylbenzene and any of the dimethylbenzenes, namely ca $11-13$ kJ mol^{-1}. Or said differently, equation 6 is expected to be thermoneutral. The expectation is met for 2,4- and 2,5-dimethylaniline, and nearly so for 2,6-dimethylaniline.

$$PhEt + Me_2C_6H_3NH_2 \longrightarrow 2\text{-}EtC_6H_4NH_2 + Me_2C_6H_4 \qquad (6)$$
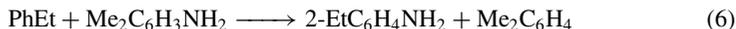
For the N-ethyl isomer there are archival[4] enthalpies of formation (derived from the calculated results presented in Reference 26). There is a much more ancient[23], and very disparate, value of -29 kJ mol^{-1} for the liquid, which is nearly identical to that experimentally determined in Reference 20 and reported in Reference 19. A contemporary measurement[24] reports somewhat more endothermic enthalpies of formation. Our predilection would be to accept the latter measurement. From a recent measurement[28] of the enthalpy of formation of N-ethyl-3-methylaniline, we find values of -29.5 ± 2.3 and 30.5 ± 3.8 kJ mol^{-1} for the liquid and gaseous species, respectively. We would expect reaction 7 to be roughly thermoneutral.

$$PhMe + PhNHEt \longrightarrow PhH + 3\text{-}MeC_6H_4NHEt \qquad (7)$$
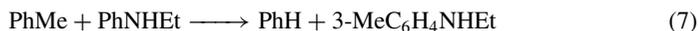
Indeed, within 4 kJ mol^{-1}, and so within the error bars, this is true and so gives us confidence in both the recent measurements of liquid and gaseous N-ethylaniline and its 3-methyl isomer.

Of the plethora of possible diethylanilines species, there are enthalpy of formation data for only 2,6- and N,N-diethylaniline. The enthalpies of formation of the former species are -84.7 ± 1.8 (lq) and -18.8 ± 1.9 (g) kJ mol^{-1} [25]. From the archival value for the liquid enthalpy of formation of the corresponding hydrocarbon, m-diethylbenzene of -73.5 ± 1.5 kJ mol^{-1}, we would have predicted a liquid-phase enthalpy of formation of the aniline of ca -91 kJ mol^{-1} from equation 2. The 6.5 kJ mol^{-1} difference between the experimental and predicted values is suggestive of a 'few' kJ mol^{-1} of buttressing (adjacent o-substitution) derived destabilization. There being no measured enthalpy of formation of the gas-phase m-diethylbenzene species, we may estimate it in two ways. First, using the CHLP protocol to derive the enthalpy of vaporization (50 kJ mol^{-1}), the gas-phase enthalpy of formation is -24 kJ mol^{-1}. Or, assume thermoneutrality for reaction 8 where R = Et, in which case the enthalpy of formation of m-diethylbenzene is -23 kJ mol^{-1}.

$$2\text{PhR} \longrightarrow \text{PhH} + 1,3\text{-C}_6\text{H}_4\text{R}_2 \tag{8}$$

Thus, the predicted gas-phase enthalpy of formation of 2,6-diethylaniline from equation 2 is -19 kJ mol^{-1}, essentially indistinguishable from the experimental value. The above analyses suggested 2,6-dimethylaniline had a small degree of stabilization while the liquid 2,6-diethyl species was likewise slightly destabilized. The latter is suggestive of buttressing (adjacent o-substituents) interactions.

For N,N-diethylaniline, there are two sets of disparate enthalpy of formation values, -5.3 and 1.8 ± 3.2 kJ mol^{-1} (from References 26 and 28, respectively) for the liquid, and 50.7 and 62.1 ± 7.6 kJ mol^{-1} correspondingly for the gas. It appears plausible that reaction 9 should be roughly thermoneutral.

$$\text{PhNMe}_2 + 2/3(\text{Et}_3\text{N}) \longrightarrow \text{PhNEt}_2 + 2/3(\text{Me}_3\text{N}) \tag{9}$$

Trusting the enthalpy of formation values for N,N-dimethylaniline results in an enthalpy of reaction of -7 kJ mol^{-1} for the liquid and 54.4 kJ mol^{-1} for the gas. The older measurement seems better on this basis, but we also wonder if there is some strain energy in N,N-diethylaniline that is unaccounted for.

C. Other Alkylated Anilines and Buttressing Interactions

The measured enthalpies of formation of o-isopropylaniline[21] are -53.6 ± 2.1 and 8.2 ± 2.3 kJ mol^{-1} for the liquid and gaseous species, respectively. From the enthalpies of formation of isopropylbenzene of -41.1 ± 1.0 (lq) and 4.0 ± 1.0 (g) kJ mol^{-1} and the amino/hydrogen difference quantity, the predicted isopropylaniline enthalpies of formation are -59 (lq) and 9 (g) kJ mol^{-1}. Slight destabilization is thus observed for the liquid, ca 5 kJ mol^{-1}, and essentially none for the gas.

For liquid and gaseous 2,6-diisopropylaniline respectively, the measured enthalpies of formation[25] are -139.7 ± 2.4 (lq) and -70.2 ± 2.4 (g) kJ mol^{-1}. There is a measured disproportionation enthalpy of reaction 8 for R = i-Pr[31] of 1.5 ± 0.6 kJ mol^{-1}. The heterogeneously catalyzed reaction enthalpy is assumed to be the same for both the liquid and gas phases, and so enthalpies of formation of liquid and gaseous m-diisopropylbenzene of -129.7 and -73.1 kJ mol^{-1} are derived. The difference between these last two quantities, 56.6 kJ mol^{-1}, is very nearly identical to the enthalpy of vaporization as predicted using the CHLP protocol. Using these derived enthalpies of formation and the amino/hydrogen

difference quantity, the enthalpies of formation of 2,6-diisopropylaniline are predicted to be -147.1 (lq) and -68.6 (gas) kJ mol^{-1}. Again, we find a 'few' kJ mol^{-1} of destabilization in the aniline, 7 kJ mol^{-1} for the liquid and again essentially none for the gas. As before, the estimated destabilization is greater for the liquid than for the gas. This is suggestive of weakening of liquid-phase intermolecular hydrogen bonding, a not unexpected result originating in the steric hindrance for any interaction that is blocked by the two nearby alkyl groups.

The enthalpies of formation of 2-t-butylaniline[25] are -64.2 ± 2.1 and -1.5 ± 2.1 kJ mol^{-1} for the liquid and gas, respectively. The enthalpies of formation of t-butylbenzene are -70.7 ± 1.2 and -22.6 ± 1.2 kJ mol^{-1} for the corresponding phases. The formal reaction enthalpy of equation 2 is endothermic by 24 and 17 kJ mol^{-1} in the liquid and gas phases, respectively. Again we see that the destabilization of the alkyl-substituted amine is larger for the liquid than the gas. That the bulkier t-butyl substituent is more destabilizing than smaller alkyl groups is not unexpected, and the effect is paralleled with various alkylated phenols and toluenes[3, 32].

What about 2,6-di-t-butylated aniline? While enthalpy of formation data are absent for this species, Reference 25 gives us the solid- and gas-phase enthalpies of formation of a surrogate species with the two buttressing t-butyl groups, 2,4,6-tri-t-butylaniline. (If we accept the enthalpy of fusion[25] of 19.4 ± 0.2 kJ mol^{-1} at 426.4 K and do not make temperature corrections, a liquid-phase enthalpy of formation is ca -249 ± 5 kJ mol^{-1}.) The enthalpy of formation of liquid tri-t-butylbenzene[33] is -306.8 ± 2.3 kJ mol^{-1}. The enthalpy of reaction 2 is calculated as ca 75 kJ mol^{-1} and represents the destabilization of the aniline due to the two buttressing t-butyl substituents. Following the same procedure, after estimating the enthalpy of vaporization for the tri-t-butylbenzene (80.5 kJ mol^{-1}), the gas-phase aniline is ca 28 kJ mol^{-1} destabilized.

There is also one 'mixed' alkylated species, 2-methyl-6-t-butylaniline, with liquid- and gas-phase enthalpies of formation[34] of -108.6 ± 2.5 and -44.8 ± 3.5 kJ mol^{-1}. For the corresponding hydrocarbon, m-t-butyltoluene, the gas-phase enthalpy of formation[29] is $-54. \pm 2.$ kJ mol^{-1}, a value corresponding to 5 kJ mol^{-1} of aniline destabilization arising from buttressing. The estimated enthalpy of vaporization of m-t-butyltoluene is 51.1 kJ mol^{-1} and the derived destabilization in the liquid phase is thus 14 kJ mol^{-1}. That it is larger for the liquid than gaseous species is compatible with our earlier observation. However, that it is less than for the monoalkylated species, 2-t-butylaniline, is inexplicable and suggestive of some error in the experimental measurements.

We conclude that buttressing destabilization of anilines applies most strongly to liquid species and gains prominence only for t-butylated species.

D. Carbocyclic Aniline Counterparts

The carbocyclic aniline counterparts are N,N-polymethyleneanilines, that is, cyclic species of the general formula Ph-N(CH$_2$)$_n$ such as N-phenylated aziridine, azetidine, pyrollidine and piperidine ($n = 2$–5). Disappointingly, there are thermochemical data for only the last of these species. The liquid- and gas-phase enthalpies of formation of N-phenylpiperidine have recently been reported[35]. From the same source come the enthalpies of formation of the saturated N-cyclohexylpiperidine, -195.8 ± 0.7 and -135.2 ± 0.9 kJ mol^{-1}, respectively. As was shown in an earlier section, equation 3 reveals the relative extent to which a substituent stabilizes the aromatic ring. The gas-phase formal reaction enthalpy for X $=$ N(CH$_2$)$_5$ is -0.1 kJ mol^{-1} and so we deduce that N-phenylpiperidine has essentially none of the resonance stabilization found in aniline itself. This is surprising at first sight. However, for there to be maximum resonance stabilization of an aniline, the nitrogen should be co-planar with the benzene ring. If the

nitrogen were co-planar in N-phenylpiperidine, there would be steric repulsion between the *ortho* hydrogens on the benzene ring and the alpha hydrogens on the piperidine ring. This enforced arrangement is destabilizing, much as between the *ortho* hydrogens in opposing rings in biphenyl, which is well-established to be nonplanar/twisted in the gas phase despite loss of stabilizing resonance.

N,C-polymethyleneanilines are cyclic species of the general formula 1,2-C_6H_4NH $(CH_2)_n$, such as 2,3-dihydro-1H-indole[36] (indole, $n = 2$) and 1,2,3,4-tetrahydroquino-line[37] ($n = 3$). There are surprisingly few studies of cyclic anilines or their derivatives of this type for which there are enthalpy of formation measurements. The differences between the enthalpies of formation of the aniline and the corresponding hydrocarbon are essentially the same for both $n = 2$ and 3: *ca* 45 (lq) and 61 (g) kJ mol^{-1}.

Finally, we note the reversible solution-phase rearrangement of a collection of 1,3,3-trialkylated derivatives of spiro[indoline-2,3$'$[3H]naphth[2,1-b][1,4]oxazines and the corresponding 2-[2-oxo-1-naphthylidenoiminomethylene]indolines for which the enthalpy of reaction is known[38], but these studies unfortunately fail to provide us any useful thermochemical information, such as enthalpies of formation.

E. Anilines with Unsaturated Hydrocarbyl Substituents

Data on this class of compounds, that are also non-enamines, are surprisingly sparse. The simplest thermochemically characterized species are N,N-dimethyl-p-(2-cyano-2-phenyl)vinylaniline[39] and N,N-dimethyl-p-(2-cyano-2-p-isopropylphenyl)vinylaniline[40] with solid-phase enthalpies of formation of 104 and 68.6 kJ mol^{-1}, respectively. From the same sources we find the enthalpy of formation of 353 kJ mol^{-1} for (2Z)-2,3-diphenyl-2-propenenitrile. One or both of these enthalpies of formation are quite likely incorrect. As just one example, we fail to understand how transformation of dimethylamino into hydrogen can result in an increase of enthalpy of formation of some 250 kJ mol^{-1}, even in the solid phase (only 20 kJ mol^{-1} is found for N,N-dimethylaniline transformed into benzene).

N,N-dimethyl-p-[2-cyano-2-(5,6,7,8-tetrahydronaphthyl)vinyl]aniline and its des(di-amino) derivative, α-benzylidene-5,6,7,8-tetrahydronaphthaleneacetonitrile, have reported solid state enthalpies of formation[41] of 59.0 and 259 kJ mol^{-1}. The corresponding compounds with a 2-substituted benzimidazolyl group replacing the tetrahydronaphthyl, now liquids, have enthalpies of formation[42] of 301.8 and 362 kJ mol^{-1}. Relatedly, N,N-dimethyl-p-(2,2-dicarboxyvinyl)aniline has a solid-phase enthalpy of formation[43] of -769.6 kJ mol^{-1} while its des(diamino) analog, benzylidenemalonic acid, has an enthalpy of formation of -715.0 kJ mol^{-1}. It is seen that loss of the dimethylamino group is accompanied by enthalpy of formation differences of between 55 and 200 kJ mol^{-1}. These differences, and their lack of near constancy, are not readily understandable—the related difference between the enthalpies of formation of liquid N,N-dimethylaniline and benzene is *ca* 35 kJ mol^{-1}.

III. ARYLATED ANILINES AND RELATED SPECIES
A. Amino Derivatives of Polynuclear Aromatic Hydrocarbons

Although not strictly an arylated aniline but rather a benzannelated species, the two isomeric naphthylamines are the simplest polynuclear aromatic hydrocarbon counterparts of aniline. Unfortunately, they are the only such examples with enthalpy of formation data known to the authors. No less than five sets of measurements[23,44–47] with a range of 29 kJ mol^{-1} have been reported for the enthalpy of combustion, and thus of formation, of 1-naphthylamine. Likewise, for the enthalpy of combustion of 2-naphthylamine

there are an analogous diverse set of values[23, 44–46, 48] with a range of 36 kJ mol^{-1}. Of the five enthalpy values for 1-naphthylamine, four were available to archivists[4, 49] who chose only one value[45], corresponding to an enthalpy of formation for the solid of 67.7 ± 5.4 kJ mol^{-1}. A recent measurement[47] gives the compatible enthalpy of formation of 64.6 ± 5.3 kJ mol^{-1}. The average value is 66.2 ± 5.4 kJ mol^{-1}. Of the five enthalpy values for 2-naphthylamine, all were available to the archivists who selected two[45, 48], for a weighted mean of 59.7 ± 5.0 kJ mol^{-1} for the solid.

The difference between the enthalpies of formation of gas-phase 1- and 2-naphthylamine of some 22 kJ mol^{-1} is troubling. It is quite inexplicable when the likewise related differences between 1- and 2-methylnaphthalene, and of 1- and 2-naphthol, all but vanish[50]. The accuracy of the enthalpy of formation values can be assessed with equation 10, which is related to equation 2, and is expected to be thermoneutral when all substances are in the same phase. For the solid or liquid phase and for 1-naphthylamine, and for the solid-phase 2-naphthylamine, the enthalpy of reaction is in the range of -1.1 to 5.4 kJ mol^{-1}. For gas-phase 2-naphthylamine, the enthalpy of reaction is the discrepant -21 kJ mol^{-1}. There being no apparent reason why this reaction should not be approximately thermoneutral also, a calculated enthalpy of formation of gaseous 2-naphthylamine is *ca* 155 kJ mol^{-1}[51]. However, in clear conscience we cannot recommend remeasurement of either (or even better, both) naphthylamines because the 2-isomer is such a powerful carcinogen. Perhaps with appropriate substitution that is simultaneously sterically and electronically innocuous and that also renders the amine toxicologically innocuous, relevant measurements can (and thus should) be made.

$$\text{(10)}$$
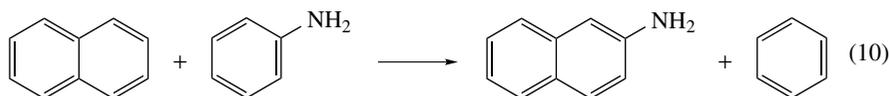
B. C-phenylated Anilines — Derivatives of Biphenyl

The simplest species with but one amino group are the C-phenylated anilines. From Reference 4 there are enthalpies of formation of the isomeric 2- and 4-aminobiphenyl, 112.0 ± 6.3 and 81.0 ± 6.3 kJ mol^{-1}. However, there is a newer measurement for the 2-isomer of 93.8 ± 1.1 kJ mol^{-1}[52]. Still, the 13–31 kJ mol^{-1} enthalpy difference between these two isomers is rather large since the 2-isomer is not expected to be much more strained. The enthalpy of formation difference is less, however, than that found for the corresponding biphenyl carboxylic acids[53] of *ca* 40 kJ mol^{-1}. Equation 2 is essentially thermoneutral for ArNH$_2 =$ 4-aminobiphenyl while it is quite endothermic for ArNH$_2 =$ 2-aminobiphenyl. There is no obvious reason why the 2-derivative should be so different from its 4-isomer, especially since the two phenyl groups in the biphenyl species are not coplanar.

There are numerous isomeric diaminobiphenyls, six with the two amino groups on the same ring and another six with the two amino groups on different rings. However, the only two for which there are enthalpy of formation data are the 4,4$'$ and 2,4$'$ derivatives. The archivally recommended enthalpy of formation of the former is 70.7 ± 1.7 kJ mol^{-1} for the solid: there is an earlier value[54] which differs by some 36 kJ mol^{-1} from the value we accept. The enthalpy of formation of the 2,4$'$-isomer[5], a liquid, is 103 kJ mol^{-1}. The difference of 33 kJ mol^{-1} is partially accounted for by the enthalpy of fusion, which for the 4,4$'$-isomer has been estimated as *ca* 19 kJ mol^{-1} at 400 K, which is similar to that for 2-aminobiphenyl of 14 kJ mol^{-1} at 322 K[6]. The enthalpy of reaction 2 where ArH = 4-aminobiphenyl and ArNH$_2 =$ 4, 4$'$-diaminobiphenyl is 7 kJ mol^{-1} for the solid, a reasonable result given the uncertainty in the measurement of the 4-aminobiphenyl. Acceptable

also is the liquid-phase enthalpy of reaction of 13 kJ mol^{-1} for ArH = 2-aminobiphenyl and $ArNH_2 = 2, 4'$-diaminobiphenyl. This is good, because, once again, we cannot recommend remeasurements of the enthalpies of formation: at least the 4,4'-isomer, known as benzidine, is also generally recognized to be a powerful carcinogen.

C. N-phenylated Anilines

For diphenylamine we find archival values of 130.2 ± 1.7 and $219.3 \pm 3.0 \text{ kJ mol}^{-1}$ for the solid and gaseous species while from Reference 55 we find the values of 235 ± 3 and $327 \pm 4.2 \text{ kJ mol}^{-1}$ for solid and gaseous triphenylamine. The N-phenylation of gas-phase diphenylamine is less endothermic than the phenylation of aniline, 108 vs 132 kJ mol^{-1}, respectively. We would have thought that both steric crowding and saturation of resonance would have destabilized triphenylamine compared to its less phenylated derivatives. Interestingly, the gas-phase phenylation enthalpies of toluene (115 kJ mol^{-1}), diphenylmethane[56] (115 kJ mol^{-1}) and triphenylmethane[57] (107 kJ mol^{-1}) have comparable phenylation enthalpies to each other and to one of the above values. And yet the phenylation enthalpy of gaseous phenol to diphenyl ether is 148 kJ mol^{-1}. The first phenylation enthalpy increases in the order C < N < O.

There are also the N- and 4-methyl, and 4,4'-dimethyl derivatives of diphenylamine with archival enthalpies of formation of 120.5 ± 7.1 (lq), 48.9 ± 7.1 (s) and -11.6 ± 7.5 (s) kJ mol^{-1}, respectively. However, these values are not plausible when compared with the aforementioned value for diphenylamine, $130.2 \pm 1.7 \text{ kJ mol}^{-1}$, and the earlier enunciated methylation enthalpies.

In addition to the enthalpies of formation of the naphthylamines, there are also measured enthalpies of formation for their N-phenyl derivatives. Of the several measurements reported for the two isomers during the first half of the last century, only one was chosen to be included in the archival sources. From this value and that for solid 2-naphthylamine, the N-phenylation enthalpy is calculated as 100 kJ mol^{-1} for the solid. Using our previously calculated enthalpy of formation for gaseous 2-naphthylamine of *ca* 155 kJ mol^{-1}, the N-phenylation enthalpy is *ca* 121 kJ mol^{-1}, compatible with that for gaseous aniline. Assuming the N-phenylation enthalpies are the same for both naphthylamine isomers, the enthalpies of formation of N-phenyl-1-naphthylamine are calculated as 166 (s) and 277 (g) kJ mol^{-1}. The derived enthalpy of sublimation of 111 kJ mol^{-1} at $333–363 \,^\circ\text{C}$ is somewhat higher than the one reported[58] to be 96.5 kJ mol^{-1} at $313–333 \,^\circ\text{C}$.

9,10-Dihydroacridine, a benzannelated 1,2,3,4-tetrahydroquinoline, may be also regarded as an N-phenyl-substituted aniline. The enthalpy of hydrogenation of acridine in a polyether solvent was reported[59] as $-75.3 \text{ kJ mol}^{-1}$. Should we assume that this hydrogenation in a nonpolar solution has the same enthalpy as it would in the gas phase? The assumption of comparability to the gas phase is justified by noting that the calculated enthalpy of hydrogenation of gas-phase anthracene[4] to 9,10-dihydroanthracene is $-71.2 \text{ kJ mol}^{-1}$. (Cf. Reference 60 for hydrocarbon hydrogenation.) If so, from the gas-phase enthalpy of formation of acridine[61] of $273.9 \pm 2.3 \text{ kJ mol}^{-1}$, the enthalpy of formation for 9,10-dihydroacridine is $198.6 \text{ kJ mol}^{-1}$.

D. Polymeric Anilines

Polyanilines, $([(-NH-C_6H_4-NH-C_6H_4)_x-(N=C_6H_4=N-C_6H_4-)_{2-x}]_n)$, like so many other polymers, are stoichiometrically ill-defined. The three stable polyaniline forms are leucoemeraldine ($x = 2$), emeraldine ($x = 1$) and pernigraniline ($x = 0$). Emeraldine is the most important to the chemical and materials science communities because it is

electrically conducting as its doubly protonated counterpart. This polymeric dication has been formulated in various ways, but here we write it as simply Poly-$\{[-C_6H_4NH-]_4^{2+}\}$.

Let us estimate the enthalpy of formation of the leucoemeraldine tetramer, which now is written as Poly$\{[-C_6H_4NH-]_4\}$, by assuming thermoneutrality for the solid phase reaction 11. The result is 367 kJ mol^{-1}.

$$4PhNHPh \longrightarrow Poly\{[-C_6H_4NH-]_4\} + 4C_6H_6 \qquad (11)$$
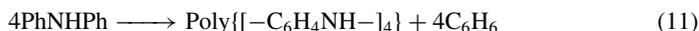
Leucoemeraldine is the formal hydrogenation product of emeraldine. As shown in reaction 12, each tetramer unit contains one reducible quinonediimine moiety.

$$Poly\,[-(C_6H_4N{=}C_6H_4{=}N-)(-C_6H_4NHC_6H_4NH)-] + H_2$$
$$\longrightarrow Poly\{[-C_6H_4NH-]_4\} \qquad (12)$$
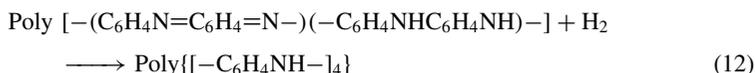
There are two related hydrogenation reactions for which there are requisite enthalpy of formation data: p-benzoquinone to hydroquinone and p-xylylene to p-xylene. For the former reaction, the enthalpies of hydrogenation are -179 kJ mol^{-1} (s) and -142 kJ mol^{-1} (g). For the latter[62], the gas-phase hydrogenation enthalpy is ca -192 kJ mol^{-1}. An interpolated gas-phase hydrogenation enthalpy for p-quinonediimine is ca -167 kJ mol^{-1}. Based on the benzoquinone/hydroquinone example, the solid-phase value presumably would be more negative. The enthalpy of formation of solid emeraldine thus would be at least 534 kJ mol^{-1}.

Estimation of the enthalpy of formation of emeraldine can be approached from a different direction. The standard synthetic reaction using aniline and ammonium perdisulfate has been calorimetrically studied[63] and shown to be exothermic by -439 ± 5 kJ mol^{-1}. Reaction 13 is thus exothermic by -1756 ± 20 kJ mol^{-1} per emeraldine tetramer.

$$4PhNH_2 + 5(NH_4)_2S_2O_8 + 2HCl \longrightarrow Poly\text{-}\{[-C_6H_4NH-]_4^{2+}\ 2Cl^-\} + 10NH_4HSO_4 \qquad (13)$$
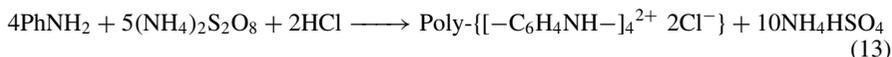
From the necessary inorganic[64] and organic thermochemical data (except for the small enthalpy of solution of the aniline), we derive the enthalpy of formation of the emeraldine salt as 196 ± 25 kJ mol^{-1}. Reaction 14 interrelates the enthalpies of formation of emeraldine and its salt.

$$Poly\text{-}\{[-C_6H_4NH-]_4^{2+}\ 2Cl^-\}$$
$$\longrightarrow Poly\,[-(C_6H_4N{=}C_6H_4{=}N-)(-C_6H_4NHC_6H_4NH)-] + 2HCl \qquad (14)$$
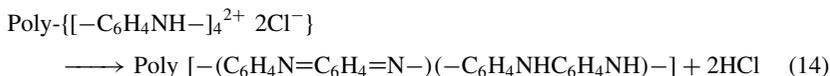
Let us approximate the enthalpy of this reaction by assuming thermoneutrality for the solid-phase reaction 15. Pyridine, with its trigonal nitrogen, is chosen to be the analog for the imino nitrogen of emeraldine.

$$2Py + Poly\text{-}\{[-C_6H_4NH-]_4^{2+}\ 2Cl^-\}$$
$$\longrightarrow 2PyHCl + Poly\,[-(C_6H_4N{=}C_6H_4{=}N-)(-C_6H_4NHC_6H_4NH)-] \qquad (15)$$
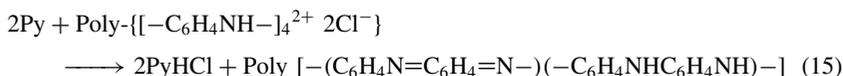
Using a consensus value of the enthalpy of formation of pyridinium chloride of -94 kJ mol^{-1} from References 65 and 66, the resulting enthalpy of formation of emeraldine is predicted to be 568 kJ mol^{-1}. The enthalpies of formation from the two approaches are comparable.

E. Other Anilino Derivatives

In this section we consider derivatives of aniline where the newly introduced aromatic ring is not directly joined to either the phenyl carbon or nitrogen atom of aniline itself. The

first such compound is bis(p-aminophenyl)methane. The enthalpy of combustion for the liquid was reported[67] to be -7200 ± 20 kJ mol^{-1}, while a value of -8744 ± 8 kJ mol^{-1} may be obtained for the solid from Reference 68. This corresponds to a negative enthalpy of fusion and so at least one of these values must be incorrect. The former corresponds to an enthalpy of 84 kJ mol^{-1}, the latter some 1500 kJ mol^{-1} higher and so it can be disregarded.

Accepting the former value, the 'deamination' enthalpy of liquid bis(p-aminophenyl) methane is ca -7 kJ mol^{-1} per NH$_2$ group compared to the -14 kJ mol^{-1} for deamination of p-toluidine[56]. Reference 5 reports a study of the related tris(p-aminophenyl)methane, where the triple p-derivative is assumed given the rich and colorful triphenylmethane/carbinol dye chemistry of the era (e.g. rosaniline, malachite green). The enthalpy of formation given is 200 kJ mol^{-1} for the solid. This value is hard to reconcile with the 171.1 ± 1.4 kJ mol^{-1} for solid triphenylmethane itself[4,57]: why should the tris-aniline have a more positive enthalpy of formation than the parent hydrocarbon?

There are both an enthalpy of formation[68] for solid N,N'-diphenylmethanediamine (bis(phenylamino)methane)) and an enthalpy of rearrangement[69] (aqueous phase) of -60.3 kJ mol^{-1} to the aforementioned bis(p-aminophenyl)methane. Is this difference plausible? We earlier suggested enthalpies of formation of -5 and 55 kJ mol^{-1} for the C-methylated aniline isomers as liquid and gas, and 34 and 84 for their N-methylated isomer. In other words, C-alkylation is energetically preferred over N-alkylation by ca 30 kJ mol^{-1} for a given substituent. Twice this preference is ca 60 kJ mol^{-1}, very nearly identical to the rearrangement enthalpy above. This gives us confidence in the value of 352.7 ± 0.6 kJ mol^{-1} for N,N',N''-triphenylhexahydro-1,3,5-triazine, also from Reference 68. This is encouraging in that there are few other hexahydro-1,3,5-triazines for which thermochemical measurements are available. One such example of hexahydro-1,3,5-triazine thermochemistry is the archivally measured enthalpy of formation of hexamethylenetetramine (1,3,5,7-tetraazaadamantane). Another example is the contemporary[70] solution-phase measurement of the enthalpy of hydrogenolysis (in acetic acid) of the piperidine trimer, dodecahydro-1H,6H,11H-tripyrido[1,2-a:1,2-c:1,2-e][1,3,5]triazine, a process that forms the well-understood piperidine.

Of the highly functionalized 5,10,15,20-tetraphenylporphins, there is 5,10,15,20-tetrakis (o-aminophenyl)porphin. Summing the enthalpy of formation of the solid of 474 ± 17 kJ mol^{-1} with the enthalpy of sublimation of 332 kJ mol^{-1} from Reference 71 results in a gas phase enthalpy of formation of this species of 806 kJ mol^{-1}. Should we assume the applicability of equation 2 as for simpler, lower molecular weight, less hindered anilines, these enthalpy values are incompatible with the values, likewise obtained from Reference 71, of 621.3 ± 6.3 and 865 kJ mol^{-1} for the enthalpies of formation of solid and gaseous 5,10,15,20-tetraphenylporphin. The enthalpy of formation of solid 5,10,15,20-tetrakis(p-(N,N-dimethylamino)phenyl)porphin[72] of -434.8 kJ mol^{-1} is also incompatible with those of both porphyrins cited above.

IV. POLYAMINO BENZENES

While our earlier review on nitro compounds[11] discussed numerous species with multiple nitro groups, the same review on amino compounds discussed few species with multiple amino groups. We don't know of any thermochemical data for any simple benzenetriamine or any species with even more amino groups. The only such species for which there is apparently thermochemical data is 2,4,6-trinitrobenzene-1,3,5-triamine and consideration of it is deferred until nitro-substituted anilines are discussed.

The isomeric diaminobenzenes are more commonly known as the phenylenediamines. In the archive there are enthalpies of formation for the three isomers as solids. The range

is *ca* 11 kJ mol^{-1} and the stability order is *m-* > *o-* > *p-*, although the enthalpies of the *ortho* and *para* overlap within the error bars. There are new enthalpy of combustion, of formation, and phase change measurements[73] for all three phenylenediamines, again with a range of *ca* 13 kJ mol^{-1}. The stability order in the solid and liquid phases is *m* > *p* > *o* where the *para* is unequivocally more stable than the *ortho*. There is also a newer[74], very discordant, value for the first quantity, 39.1 ± 5.7 kJ mol^{-1}. The expected enthalpy of formation values of all three isomers are *ca* 4, 14 and 92 kJ mol^{-1} for the solid, liquid and gaseous species, respectively, by assuming thermoneutrality for equation 2. This is rather surprising as it suggests *m-* and *p-*phenylenediamine are stabilized in the gas phase as well as in the solid, but not liquid, phases The discrepancy tells us that these species are problematic for the thermochemist. In particular, we deduce possibilities for autooxidation to form polymeric (both newly C,N and C,C bonded) and hence ill-defined products. Intersubstituent steric and electronic repulsion should both destabilize the *o-*isomer where, additionally, intermolecular hydrogen bonding is minimized. In the gas phase, the three isomers are now closer in thermochemical stabilities, with enthalpies of formation 92.0 ± 1.3, 84.0 ± 1.4 and 88.7 ± 1.4 kJ mol^{-1}, respectively. This has been explained by the original authors in terms of the absence of intermolecular hydrogen bonding for all three gaseous species and some intramolecular stabilization for the *o-*isomer alone.

Another interesting species is N,N,N',N'-tetramethyl-*p*-phenylenediamine, the parent neutral of the well-known radical cation, Wurster blue. Its enthalpy of formation as a solid[75] is 39.6 ± 3.9 kJ mol^{-1}. Equations 16 and 17 might be expected to be thermoneutral. The calculated enthalpy of reaction of the former is 5.9 kJ mol^{-1} and that of the latter is -7.1 kJ mol^{-1}, adequate indication that the enthalpies of formation are essentially accurate.

(16)

(17)
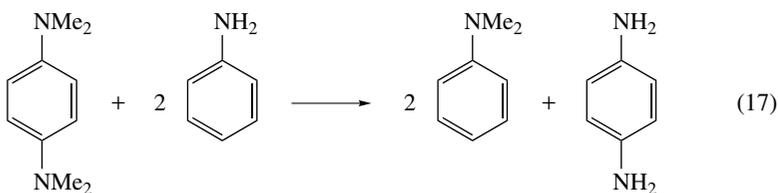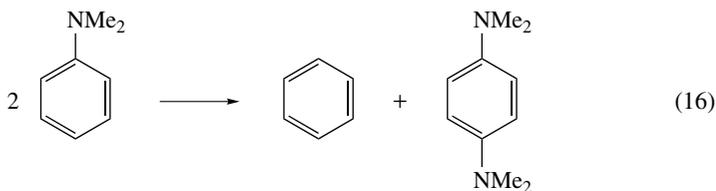
V. ANILINES WITH OXYGEN-BONDED FUNCTIONAL GROUPS

A. Hydroxyanilines (Aminophenols)

The enthalpy of formation of all three aminophenol isomers have been measured twice. Two well-respected contemporary organic thermochemistry groups have studied these species[76, 77]. Although disparate, they are closer than some other pairs of competing values cited in this text. Which set, if either, do we choose? We prefer those of Reference 76. From the archival enthalpy of formation of gaseous phenol of -96.4 ± 0.9 kJ mol^{-1} and equation 2, the enthalpy of formation of any of the isomers is *ca* -92 kJ mol^{-1} in the

absence of any stabilizing or destabilizing features of the molecule. This value is in good agreement with their suggested value for the m-isomer, no stabilizing mechanism being apparent to reconcile the more negative value in Reference 77. The value found in Reference 76 for the o-isomer is essentially the same as for the m-isomer: we can invoke opposing electronic destabilization from the two electron-donating groups and stabilization by hydrogen bonding. The value in Reference 77 requires a much stronger hydrogen bond, unlikely because of its nonlinearity and concurrent weakness. The value for the p-isomer in Reference 76 reflects electronic destabilization in the absence of hydrogen bonding while the result in Reference 77 implies neither effect is operative. Our conclusion is clear. Nonetheless, we are cautious as we recall from our earlier phenol chapter[3] that part of the above discrepancies may arise from problems with sample purity.

B. Other Hydroxyanilines

4,6-Dinitro-2-aminophenol, also known by the trivial name picramic acid, has two nearly identical values reported for the solid[78, 79]. The agreement between them is encouraging. The enthalpy of reaction 2 is ca 5 kJ mol^{-1}, given the -232.7 ± 3.1 kJ mol^{-1} reported for the corresponding deaminated species, 2,4-dinitrophenol.

The enthalpies of formation of N-hydroxyaniline (N-phenylhydroxylamine) and its o-nitro derivative, as liquids, 7 and -13 kJ mol^{-1}, are from Reference 5. That these are almost the only hydroxylamines for which there are reported enthalpy of formation values[80] makes them hard to compare. Nonetheless, we find these data suspect. The o-nitro group in phenylhydroxylamine decreases the enthalpy of formation by ca 20 kJ mol^{-1} while it decreases the enthalpy of formation of aniline by 45 kJ mol^{-1}.

C. Alkoxyanilines

There are surprisingly few alkoxyanilines for which thermochemical data seemingly exist. The simplest compounds are 2- and 4-methoxyaniline, known also as o- and p-anisidine. For the former compound, Reference 81 reports an enthalpy of formation of -46 kJ mol^{-1} for the solid. For the latter, Reference 5 chronicles a value of -172 kJ mol^{-1}, also for the solid. These two values are incomprehensively incompatible with each other. They are also incompatible with an enthalpy of formation derived from equation 2, ca -132 kJ mol^{-1} (using -114.8 kJ mol^{-1} for the enthalpy of formation of liquid anisole).

Reference 81 also reports the solid phase enthalpies of formation of the isomeric 4- and 5-nitro-2-methoxyanilines, -197 and -232 kJ mol^{-1}. These values are disconcertingly disparate. The two isomers should have very nearly identical enthalpies of formation because in both cases there are electron-donating groups $para$ to the nitro group and so there should be comparable stabilization. From equation 18, an estimated value of solid anisole, and the average enthalpy of formation of m- and p-nitroaniline, a calculated enthalpy of formation of the nitro-o-anisidines is ca -210 kJ mol^{-1}.

$$\text{anisole} + \text{nitroaniline} \longrightarrow \text{nitro-}o\text{-anisidine} + \text{benzene} \qquad (18)$$
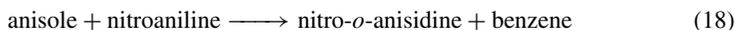
Another, but hardly simple, example is that of the solid 3-amino-4-methoxyacetanilide and 3-(N- (2-cyanoethyl)amino)-4-methoxyacetanilide, with enthalpies of formation[82] of -554 ± 6 and -265.9 ± 1.7 kJ mol^{-1}, respectively. These look suspect in that we do not expect the 2-cyanoethyl substituent in the latter species to decrease the enthalpy of formation by nearly 300 kJ mol^{-1}.

Relevant reaction calorimetric results are available, if not particularly helpful quantitatively. Solution-phase (in benzene) benzoylation of aniline results in exothermicities

some $10-20 \text{ kJ mol}^{-1}$ less than that for p-methoxyaniline[83], the range of values arising from whether benzoyl chloride, bromide or iodide was the acylating reagent. Our intuition suggests that amino and alkoxy substituents that are *para* to one another should result in destabilization. In that the π repulsion of the amino and methoxy lone pairs should be ameliorated in the corresponding amide because of withdrawal of electron density from the amino nitrogen by the carbonyl group of the amide, we conclude that this desta-bilization in methoxyaniline is about the same as the difference in reaction enthalpies, $10-20 \text{ kJ mol}^{-1}$.

Consider now, however, the solution-phase addition reaction[84] of methanol to p-nitrobenzalanilines substituted on the aniline ring; cf. reaction 19. Nearly equal exother-micities of 11 ± 1.3 and $10 \pm 13 \text{ kJ mol}^{-1}$ are found for the parent and p'-methoxylated species in this reaction that produces the correspondingly substituted (α-methoxy-4-nitrobenzyl)anilines. However, the experimental uncertainty of the latter reaction obscures any effect to be documented for the methoxy substituent.

$$O_2N - \underset{}{\bigcirc} - CH = N - \underset{}{\bigcirc} - X \quad + \quad MeOH$$

$$X = H, OMe$$

$$O_2N - \underset{}{\bigcirc} - \underset{\underset{OMe}{|}}{CH} - NH - \underset{}{\bigcirc} - X$$

(19)
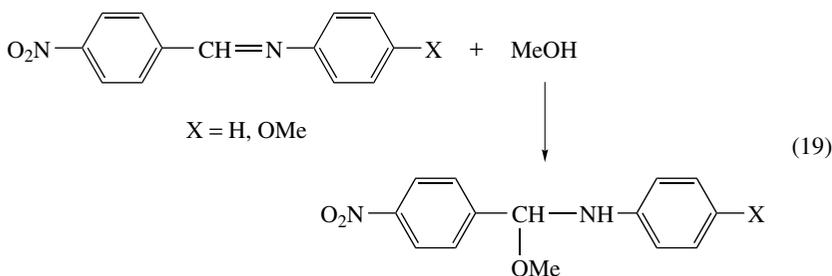
D. Alkoxyalkylanilines

By the term alkoxyalkylanilines, we mean those anilines in which the nitrogen is mono or dialkylated and the ring or nitrogen-substituted alkyl group has an alkoxy sub-stituent. For none of these compounds are there enthalpies of formation for compounds that they could be compared to and so their enthalpies of formation and source are simply recorded here. Following from our definition of anilines, their N-acyl deriva-tives have been ignored. Nonetheless, we include the data for a corresponding 'acetal', N-methyl-N-(dimethoxymethyl)aniline, for which reaction calorimetry[85] resulted in an enthalpy of formation of -296.4 ± 7.6 and $-225.7 \pm 8.4 \text{ kJ mol}^{-1}$ for the liquid and gaseous species, respectively. N-(2-Hydroxy-3-phenoxypropyl)aniline has reported solid- and gas-phase enthalpies of formation of -298 ± 3 and $-185 \pm 3 \text{ kJ mol}^{-1}$ [86]. From the same source there is the related N,N-bis(2-hydroxy-3-phenoxypropyl)aniline with its solid- and gas-phase enthalpies of formation of -582.8 ± 4.2 and $-436.8 \pm 4.2 \text{ kJ mol}^{-1}$. Finally, p-glycidyloxy-N,N-bis(glycidyl)aniline has a solid-phase enthalpy of forma-tion of $-110.5 \pm 1.4 \text{ kJ mol}^{-1}$ [87]. We also note that the aforementioned substituted (α-methoxy-4-nitrobenzyl)anilines belong in this subsection as well.

E. Aryloxyanilines

This class of compounds comprises anilines containing aryloxy groups whether or not it is the ring or the nitrogen that is so substituted. The first two species are 4,4'-diamino diphenyl ether and its 3,3',4,4'-tetraamino analog with their solid-phase enthalpies of for-mation of -17 and -116 kJ mol^{-1} from References 88 and 89, respectively. For compar-ison, the enthalpy of formation of the parent solid diphenyl ether is $-32.1 \pm 1.5 \text{ kJ mol}^{-1}$.

The enthalpies of reaction 2 for these compounds are $+32$ and -67 kJ mol^{-1}, respectively, indicating probably very inaccurate enthalpies of formation. The last compound is 2,2′-bis(*o*-aminophenylbenzimidazol-5-yl) ether with its solid-phase enthalpy of formation[90] of 102 ± 10 kJ mol^{-1}.

VI. ANILINES WITH SULFUR-CONTAINING FUNCTIONAL GROUPS

A. Sulfonic and Sulfonyl Derivatives

There are many sulfur-containing functional groups and the thermochemistry is rich and interesting[91,92] even though there are considerable discrepancies in the early measurements. However, as noted in those earlier reviews, studies concerning anilines and sulfur-containing substituents were limited to *p*-aminobenzenesulfonyl derivatives and the corresponding naphthalene derivatives. It is this medicinal activity of the bacteriostatic 'sulfa' drugs that motivated these investigations. However, there are some new values that are presumably more trustworthy.

The first is the quite contemporary study[93] for the isomeric *o*-, *m*- and *p*-aminobenzenesulfonic acids. The spread of enthalpies of formation, *ca* 53 kJ mol^{-1}, is somewhat larger than we might have expected. However, in that these species are probably the zwitterionic $NH_3^+C_6H_4SO_3^-$, comparisons with other species such as the uncharged benzenesulfonic acid are thwarted.

The second is a comparably contemporary study[94] on both the parent *p*-aminobenzenesulfonamide and *p*-amino-*N*-(3,4-dimethyl-5-isoxazolyl)benzenesulfonamide, known in the medicinal community as sulfanilamide and sulfisoxazole, respectively. As solids, the enthalpies of formation are -458.3 ± 1.6 and -180.1 ± 3.8 kJ mol^{-1}, respectively. The former species may be compared with benzenesulfonamide, for which we cite only the most recent enthalpy of formation[95], -320.1 ± 1.6 kJ mol^{-1}. As has been so often the case, we cannot reconcile the two sets of values. We are immediately thwarted in the comparison of the latter species. We lack the desired data for the desamino species or for any isoxazolamine-containing species.

B. Anilines with Aliphatic Divalent Sulfur Substituents

By this class of compounds we would include such species as *p*-aminothioanisole. However, quite surprisingly, there are no thermochemical data for this or any other simple aliphatic, divalent sulfur substituent containing aniline. Indeed, the only species that qualifies as such a derivative of aniline, albeit hardly simple, is the contemporary measured[96] tetracyclic *cis*-5*a*,6,11*a*,12-tetrahydro[1,4]benzothiazino[3,2-*b*][1,4]benzothiazine. For completeness, we note the enthalpies of formation from the same source for the corresponding dioxygenated (desulfurated) heterocycle, *cis*-5*a*,6,11*a*,12-tetrahydro[1,4]benzoxazino[3,2-*b*][1,4]benzoxazine, -180.9 ± 6.3 and -51.9 ± 6.4 kJ mol^{-1} for the solid and gas, respectively. Is the gas-phase difference of 320 ± 9 kJ mol^{-1} plausible? If we ignore complications from the hemiaminal and hemithioaminal groupings, then the difference should roughly equal twice that of the monocyclic tetrahydrothiopyran and tetrahydropyran. From our archives, we find enthalpies of formation of these species of -63.5 ± 1.0 and -223.4 ± 1.0 kJ mol^{-1}, resulting in a difference of 159.9 ± 1.4 kJ mol^{-1}. Twice this value is 319.8 kJ mol^{-1}, in stunning agreement with that of our tetracyclic species.

VII. ANILINES WITH HALOGEN SUBSTITUENTS

Here, we restrict attention to ring-halogenated compounds as opposed to any hydrogen halide salts, dihalogen complexes, or even N-halogenated species.

A. Fluorinated Anilines

From the nearly century old Reference 97 there are enthalpy of formation values for the three isomeric *o*-, *m*- and *p*-fluoroanilines of -142, -146 and -125 kJ mol^{-1} as liquids. These values initially appear plausible: disubstituted benzenes with two π-donating substituents prefer *meta* orientation and, indeed, *m*-fluoroaniline is the most stable of the three. If intramolecular hydrogen bonding provides stabilization, then the *o*-isomer is rationalized as more stable than the *p*-isomer. Although the measured stability order is reasonable, an enthalpy of formation for any of the fluoroanilines derived from equation 2 is *ca* -168 kJ mol^{-1}. The reason for the large discrepancy evades us, other than to note the general difficulty[98] in measuring the enthalpy of formation of fluorinated species. There are two totally disparate measurements for the enthalpy of formation of *m*-trifluoromethyl-aniline by the same author[97, 99], discouraging us from accepting either of these thermochemical data for fluorinated anilines.

B. Chlorinated Anilines

A very recent set of calorimetric measurements on the isomeric *o*-, *m*- and *p*-chloroanilines has been reported[100]. Although the gas-phase values for the *o*- and *m*-isomers are indistinguishable, they are both more stable than the *p*-isomer. In the liquid phase, the *m*-isomer is somewhat more stable than the *o*-isomer. From equation 2, and the archival values for the enthalpies of formation of liquid and gaseous chlorobenzene of 11.0 ± 1.3 and 52.0 ± 1.3 kJ mol^{-1}, the predicted enthalpy of formation for any liquid chloroaniline is -7 kJ mol^{-1}, while that for any gaseous chloroaniline is 57 kJ mol^{-1}. The predictions are in accord with the experimental results. Earlier measurements are discrepant [101, 102].

The enthalpy of formation of 3-chloro-4-methylaniline has been reported as 26.7 ± 7 and 75.3 ± 7.1 kJ mol^{-1} for the liquid and gas, respectively[103]. The enthalpy of combustion, but not the enthalpy of formation, of 2-chlorotoluene, needed for an analysis by equation 2, has been reported[104] as -3750 ± 10 kJ mol^{-1}. The difference between the enthalpies of combustion of 3-chloro-4-methylaniline (-3607 kJ mol^{-1}, from Reference 103) and 2-chlorotoluene is 143 ± 12 kJ mol^{-1}, while from the archival enthalpies of combustion of aniline and benzene, the difference is 126 kJ mol^{-1}. The 269 kJ mol^{-1} discrepancy is disconcerting.

The enthalpies of formation of the isomeric 2-chloro-4- and 5-nitroanilines have been recently reported[105]. The corresponding de-anilated species, *m*- and *p*-chloronitrobenzene, have reported[102] solid-phase enthalpies of formation of -49 ± 4 and -59 ± 3 kJ mol^{-1}. Although the *p*-chloronitrobenzene is more stable than the *meta* isomer, for the anilated compounds the more stable isomer is the one with the nitro and amino groups *para* to one another and consequently the nitro and chloro groups are *meta*. Accordingly, the enthalpy of reaction 2 for 2-chloro-4-nitroaniline is exothermic (*ca* -8 kJ mol^{-1}) and that for 2-chloro-5-nitroaniline is endothermic (*ca* $+5$ kJ mol^{-1}).

Of the six possible dichloroaniline species, only the 3,4-compound has been reported by calorimetrists[101]. From the archival enthalpy of formation of liquid *o*-dichlorobenzene of -17.5 ± 1.3 kJ mol^{-1}, we would predict a value of *ca* -35 kJ mol^{-1} for the dichloroaniline. The reported value of -89 kJ mol^{-1} for the solid aniline that is most implausible: the enthalpy of fusion of *ca* 50 kJ mol^{-1} that is required for qualitative agreement is inconceivably large.

Of the six possible trichloroaniline isomers, there are enthalpy of formation measurements[106] for four: 2,4,6-, 2,4,5-, 2,3,4- and 3,4,5-trichloroaniline. The 2,4,6-trichloroaniline is very much more stable than any of the other three isomers, which are of comparable stability. To use equation 2, we must consider the enthalpies of formation of the corresponding trichlorobenzenes. All of the enthalpy of formation data come from two sources[107, 108].

Although the gas-phase values from the two sources differ by $4-13$ kJ mol^{-1}, the stability order from each source is consistent: 1, 3, 5- > 1, 2, 4- > 1, 2, 3-trichlorobenzene. From equation 2, the endothermicities of the reactions involving the 2,4,5-, 2,3,4- and 3,4,5-trichloroaniline species are very large, ca $17-36$ kJ mol^{-1}, depending on the isomer pair or the enthalpy values used. The calculated endothermicity is smaller for 2,4,6-trichloroaniline, $3-14$ kJ mol^{-1}. Whether the endothermicities are a consequence of poor calorimetric measurements for either or both sets of isomers or because of the plethora of possible intra- and intermolecular hydrogen bonding sites and considerable molecular polarity is not clear.

C. Brominated Anilines

The sole species for which there are thermochemical data is 2,4,6-tribromoaniline[109]. There are no measurements for the corresponding data for the corresponding tribromobenzene. However, as derived in our corresponding review of the thermochemistry of phenols[3], there are values for the estimated enthalpies of formation of 1,3,5-tribromobenzene of 72 kJ mol^{-1} and 151 kJ mol^{-1} for the solid and gas, respectively. From equation 2, the enthalpies of formation for 2,4,6-tribromoaniline are 155 (s) and 54.9 (g) kJ mol^{-1}, in good agreement.

D. Iodinated Anilines

There is a reported enthalpy of formation for an isomerically unspecified iodoaniline of 175 kJ mol^{-1} for the solid[5]. The archival enthalpy of formation of liquid iodobenzene is given as 117.2 ± 4.2 kJ mol^{-1}. That of the solid value is necessarily smaller. Accordingly, the enthalpy of reaction 2 cannot be any less than 75 kJ mol^{-1}. This is so unreasonable that we therefore ignore the iodoaniline enthalpy of formation value.

VIII. AMIDOANILINES

A. C-bonded Amidoanilines

The only thermochemical examples we know of for aniline compounds where the carbonyl is bonded to a ring carbon are those for p-aminobenzamide[110] (p-carboxamidoaniline) and p-(carboxymethylaminocarbonyl)aniline[111] (p-aminohippuric acid or N-(p-aminobenzoyl)glycine). For the former, we find a solid-phase enthalpy of formation of -187 kJ mol^{-1} while for the latter we find a solid-phase enthalpy of formation of -603.4 ± 1.1 kJ mol^{-1}. Using either the archival value of -202.6 ± 1.1 kJ mol^{-1} or the nearly identical one, -202.1 ± 0.6 kJ mol^{-1}, the recent study[112] for the enthalpy of formation of solid benzamide in reaction 2 results in a predicted value of -219 kJ mol^{-1} for the enthalpy of formation of p-aminobenzamide. We cannot reconcile this with its measured value. From the enthalpy of formation of the relatively recent study of the parent hippuric acid[113], -607.5 ± 1.9 kJ mol^{-1}, and reaction 2, the derived enthalpy of formation of p-aminohippuric acid is -625 kJ mol^{-1}. Again, the disparity is irreconcilable. After all, there have been many measurements of hippuric acid, all of which are quite consonant, and the same source of information for the aminohippuric acid also reports the enthalpy of formation of the solid α-methyl derivative of hippuric acid, N-benzoyl-α-alanine. The enthalpy of formation is -629.2 ± 0.6 kJ mol^{-1}, which is consonant with that of hippuric acid by a plausible 22 kJ mol^{-1} for methylation of the glycine methylene group.

B. N-bonded Amidoanilines

The class of compounds where the carbonyl is bonded to a nitrogen other than the anilino nitrogen is thermochemically poorly represented both in terms of the number of species that have been studied as well as in the qualitative and quantitative understanding of the results derived therefrom. The first species is N-(2-benzamidophenyl)aniline[114], the enthalpy of formation for which as solid is -10 ± 84 kJ mol^{-1}. The large error bar obscures any thermochemical conclusions we could draw. As documented in our archive, the enthalpy of formation of benzidine and its N-mono and N,N'-diacetyl derivatives have all been reported in the same original paper[115]. From that data we deduce that the solid state disproportionation reaction 20 is exothermic by ca -81 kJ mol^{-1}. This is implausible. In a previous section we asserted that the enthalpy of formation of benzidine was substantially accurate. Does the error lie with either or both of the acetyl derivatives?

$$2\ H_2N\!-\!\!\langle\ \rangle\!-\!\!\langle\ \rangle\!-\!NHAc \longrightarrow H_2N\!-\!\!\langle\ \rangle\!-\!\!\langle\ \rangle\!-\!NH_2$$

$$+ \qquad (20)$$

$$AcNH\!-\!\!\langle\ \rangle\!-\!\!\langle\ \rangle\!-\!NHAc$$

Equation 21 represents an acetylation reaction of an aniline, where both the acetic acid and water are liquids and the nitrogen-containing species are solids. For Ar = Ph, the enthalpy of reaction is -32.7 kJ mol^{-1}.

$$\text{ArNH}_2\ +\ \text{CH}_3\text{CO}_2\text{H} \longrightarrow \overset{\displaystyle O}{\overset{\displaystyle \|}{\text{ArNHCCH}_3}}\ +\ \text{H}_2\text{O} \qquad (21)$$

The reaction enthalpy for monoacetylation of benzidine, $\text{ArNH}_2 = p\text{-H}_2\text{NC}_6\text{H}_4\text{C}_6\text{H}_4$ $\text{NH}_2\text{-}p$ is the likewise exothermic -33.1 kJ mol^{-1}. However, per NH$_2$ group, the acetylation of benzidine to diacetyl derivative is -73 kJ mol^{-1}, nearly twice the expected value. In support of this implausible result, the acetylation enthalpy of the monoacetyl to the diacetylbenzidine is -114 kJ mol^{-1}. The enthalpy of formation of N,N'-diacetylbenzidine is likely erroneous.

The solid 5-acetamido-2-methoxyaniline and its N-(2-cyanoethyl) derivative were discussed earlier in the section on alkoxyanilines. Finally, we turn to 5-aminobenzimidazolone with its reported solid-phase enthalpy of formation of -418.0 ± 0.7 kJ mol^{-1} from Reference 74. This value may be contrasted to the -85.1 ± 3.2 and -190.3 ± 1.7 kJ mol^{-1} reported for the solid benzimidazolone in References 74 and 116: neither value is compatible with the aforementioned value for the 5-amino derivative.

C. Related Species

Let us begin with a definition: by related species we mean anilines with substituents related to amides such as amidines and thioamides. We know of one thermochemically relevant species here, N-(tetrazol-5-yl)aniline. This species, studied in Reference 117, has a solid-phase enthalpy of formation of 305 ± 1 kJ mol^{-1}. An interesting comparison for this species involves the energetics of its disproportionation into diphenylamine and

bis(tetrazol-5-yl)amine. From the archival enthalpy of formation of the former, 130.2 kJ mol^{-1}, and the recently reported value[118] for the latter, 128 ± 38 kJ mol^{-1}, we deduce a solid-phase enthalpy of disproportionation of $+27 \pm 23$ kJ mol^{-1} for N-(tetrazol-5-yl)aniline.

IX. ANILINES WITH π-ELECTRON-WITHDRAWING SUBSTITUENTS

Classical chemical reasoning suggests the o- and p-isomers of anilines substituted with π-electron-withdrawing groups should enjoy stabilization because of quinonoid-type resonance that the m-isomer does not have. Additionally, if there should be at least one hydrogen on the amino nitrogen, the o-isomer could be additionally stabilized by intramolecular hydrogen bonding.

A. Carbon-bonded Substituents

1. Carbalkoxy and other carboxylic acid derivatives

For the parent aminobenzoic acids, we accept the consensus archival values. All three isomers have essentially the same gas-phase enthalpies, ca -295 kJ mol^{-1}, somewhat more negative than the value of -290 kJ mol^{-1} one would predict from equation 2. We would have predicted a value of -402 kJ mol^{-1} for the solids, which is the same as for o-aminobenzoic acid. The other two isomers are apparently relatively stabilized.

There are many aniline-related esters. Some are known as sunblocking agents, others as local pain killers, and yet others as food flavorings. Yet however diverse and important these species may be, their thermochemistry is quite sparse. We find only the enthalpy of formation of ethyl p-aminobenzoate from our archive. There is no enthalpy of formation value for ethyl benzoate to compare it to.

There are 14 possible aminonaphthoic acids. The enthalpies of formation of none of them are known. However, the enthalpy of formation of 3-(N-anilino)-2-naphthoic acid, as solid, has been reported to be -263.6 ± 2.2 kJ mol^{-1}. From this datum and others given in our archival source and in this chapter, we find the solid-phase enthalpy of reaction 22 is only 0.5 kJ mol^{-1}, that is, the reaction is thermoneutral.

$$(22)$$
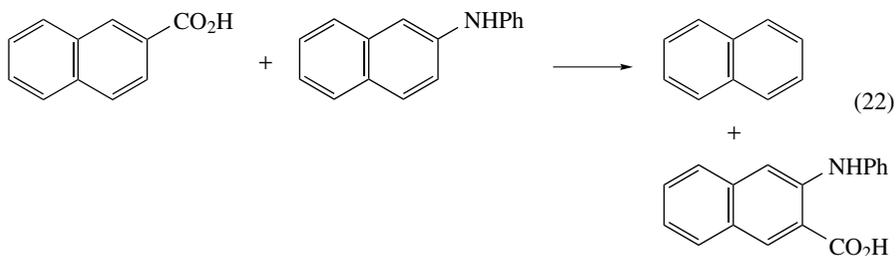
2. Acyl derivatives

Starting with formyl derivatives of any aniline, the only species for which there is enthalpy of formation data is p-N,N-dimethylaminobenzaldehyde, -137 ± 1 kJ mol^{-1}, for the solid from Reference 39b as well as our archive. Likewise, for acetyl derivatives, the data are sparse. They are seemingly limited to the m- and p-acetylanilines, more commonly known as the isomeric 3- and 4-aminoacetophenones. For the former, there is the sole archival value of -173.3 ± 0.5 kJ mol^{-1} for the solid and -161.2 ± 0.7 kJ mol^{-1}

for the liquid. For the latter, we have the corresponding values of -182.1 ± 0.5 and -166.2 ± 0.7 kJ mol^{-1} for the solid and liquid. The *para* isomer is much more stabilized in the solid than in the liquid phase, compared to the *meta* isomer. The predicted value of -160 kJ mol^{-1} is derived from equation 2 and the archival value of -142.5 kJ mol^{-1} for the parent liquid-phase acetophenone. The *m*-isomer shows no stabilization, while the *p*-isomer is but a few kJ mol^{-1} stabilized due to any extended conjugation involving the amino and carbonyl groups.

B. Nitrogen-bonded Substituents

Members of this class of compounds are anilines with the nitro, nitroso, azo or azoxy groups affixed to a ring atom of the aniline.

1. Nitro derivatives

In an earlier chapter on the thermochemistry of nitro derivatives we extensively discussed[11] nitroaniline derivatives and so do not deem it necessary, or even desirable, to discuss these species at length in the current study. The archive presents enthalpies of formation for *o*-nitroaniline in the solid, liquid and gaseous states. Two primary sources are given[119, 120] with reassuringly essentially indistinguishable results. The archive records two enthalpies of formation for the *meta* isomer from the same two sources, but only one of them was chosen as a recommended value[119, 120]. Additionally, there is a newer measurement that is nearly the average of the two previously determined[121]. For the *para* isomer, there are no fewer than four primary publications[119–122] for the solid phase, the latest of which does not appear in the archive.

The first problem encountered in our analysis is the derivation of an enthalpy of formation for any of the nitroanilines from equation 2: -17.6 (s) and 72.0 (g) kJ mol^{-1}. The predicted and the experimental values are clearly very different. We might have expected the *meta* isomer to more closely resemble the calculated enthalpy of formation, since it has no means of resonance stabilization such as is available for the *ortho* and *para* that would account for their deviation from the calculated value. Instead, it is seemingly stabilized by 12 kJ mol^{-1} in the gas phase and 20 kJ mol^{-1} in the solid phase. More disturbing is the isomer stability order. In the solid phase, and using an average enthalpy of formation for each isomer, the stability order is *p*- > *m*- > *o*-. In the gas phase, the isomers' enthalpies of formation are nearly identical. We would have thought that resonance in the *ortho* and *para*, and intramolecular hydrogen-bonding in the *ortho*, would render both of those substantially more stable than the *meta*, at least in the gas phase. Politzer and coworkers have determined computationally the solid-phase enthalpies of formation of *o*- and *m*-nitroaniline[123]. Their computed values of -37.6 (*o*-) and -27.6 (*m*-) are in the expected stability order. Interestingly, these numbers appear to be the reverse of the experimental values that appear in Table 7. The authors claim their calculations could support any of the experimental values, but they did not comment on the reversal of stability order. We note that the gas-phase *meta* isomer's enthalpy of formation as calculated from equation 2 is nearly identical to the computed gas-phase value [123] (using an experimental enthalpy of sublimation) of 68.9 kJ mol^{-1}.

There are enthalpy of formation data for the *meta*[124] and *para*[124, 125] *N*,*N*-dimethylnitroanilines in the solid and gas phases. We know of no data for the *o*-isomer. The *ca* 12 kJ mol^{-1} more positive enthalpy of formation for the gas-phase *meta* dimethyl species parallels the 13 kJ mol^{-1} for the parent *N*,*N*-dimethylaniline. That is, equation 23 is essentially thermoneutral, suggesting little additional interaction between the nitro and amino moieties. It is not surprising that the *p*-isomer is more stable than the *meta*. The

exothermicity of gas-phase reaction 23 for the *para* isomer, *ca* -9 kJ mol^{-1}, shows the expected intersubstituent-derived stabilization.

(23)
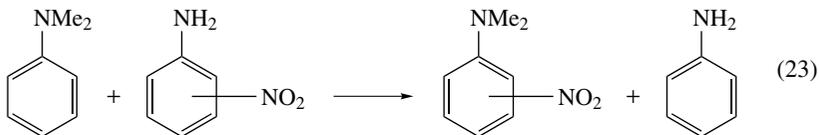
There are six dinitroaniline species with measured enthalpies of formation in the on-line archive[6], but as there are no new measurements or insights since they were last discussed, we forgo mention of them here. We note the two disparate values for 2,4,6-trinitroaniline (also known as picramide) with solid-phase enthalpies of formation of -115.9[126] and -72.8[79] kJ mol^{-1} respectively, because this compound was one of those studied computationally[123]. The conclusion by these authors, from their use of two different homodesmic reactions and a calculated enthalpy of sublimation, is consistent only with the latter enthalpy of formation.

Although it is a triamine, 2,4,6-trinitrobenzene-1,3,5-triamine is discussed here because of its plethora of nitro substituents. There are three very different measurements, -154, -140.0 and -74.7 ± 3.0 kJ mol^{-1} from References 127, 128 and 129, respectively. The computational-study[123] enthalpy of formation of -140 kJ mol^{-1}, using a calculated enthalpy of sublimation, is inconsistent with the last of these values. For the corresponding diamine, we find the discordant values of -98 and 122.3 kJ mol^{-1} from References 128 and 130, respectively. The latter value is not credible. Unfortunately, as is seemingly so often the case, we cannot recommend remeasurements of the enthalpy of formation as these species are explosive.

2. Nitroso derivatives

There are few nitroso anilines for which the enthalpies of formation are seemingly known. The first to be studied was *p*-nitroso-*N*,*N*-dimethylaniline[131] in 1910. A reinvestigation[125] over 80 years later yielded acceptable enthalpy of formation values for the solid and gas. By comparison to the related *p*-nitrodimethylaniline, a formal reaction enthalpy of the gas-phase reaction 24 is found to be 9.5 kJ mol^{-1}, using the enthalpy of formation[132] of monomeric nitrosobenzene of 197 kJ mol^{-1}. Accordingly, the dimethylamino group stabilizes the nitroso species slightly more than the nitro species. However, monomeric nitrosobenzene is thermochemically problematic because it is unisolable, at least in calorimetrically sized samples.

(24)
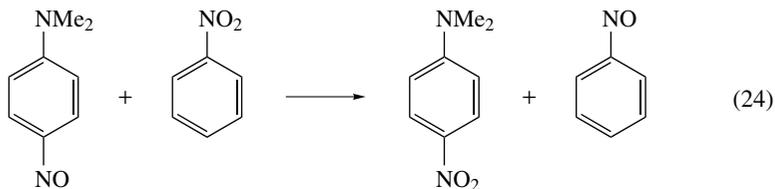
It was found that *p*-nitroso-*N*,*N*-dimethyl and -diethylaniline are similarly stabilized[133]. Using the enthalpy of formation of *p*-nitroso-*N*,*N*-diethylaniline that these authors measured, they noted the near thermoneutrality of the gas-phase reaction 25. It is encouraging,

although not particularly surprising, that diethyl and dimethyl anilines enjoy very much the same stabilization by p-nitroso groups. In that m- and p-nitro groups show comparable stabilization of anilines, we wonder about what will be found for m-nitroso substituents.

(25)
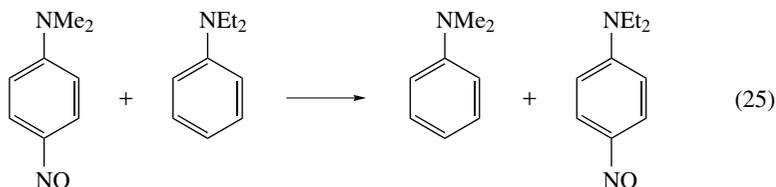
3. Azo species

We recognize many of these azo species as classical dyes and so expect thermochemical data, if available, to be rather old and for the solids. Our expectations are fulfilled: from the nearly century old Reference 134, we find the data for solid 4-aminoazobenzene, 2,4-diaminoazobenzene and 4-dimethylaminoazobenzene. From this early source we find the enthalpy of formation of azobenzene itself of $374 \, \text{kJ} \, \text{mol}^{-1}$ suggesting that reaction 26 is nearly thermoneutral, an altogether reasonable result if it is assumed that the isomeric 2- and 4-aminoazobenzenes have very nearly the same enthalpy of formation. Likewise, reaction 27 is roughly thermoneutral.

(26)

$$\text{azobenzene} + 1, 3\text{-diaminobenzene} \longrightarrow 2, 4\text{-diaminoazobenzene} + \text{benzene} \quad (27)$$
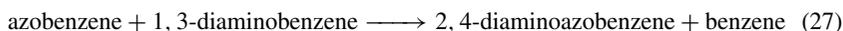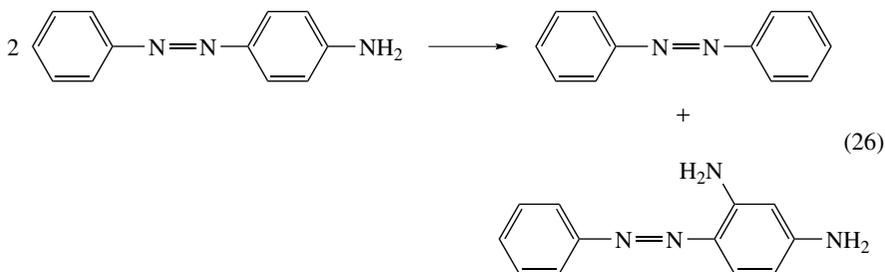
However, it must then be acknowledged that the enthalpy of reaction 2 is $-34 \, \text{kJ} \, \text{mol}^{-1}$, an unlikely quantity. Furthermore, this early enthalpy of formation for azobenzene is painfully disparate from the archival value of $310.2 \pm 3.4 \, \text{kJ} \, \text{mol}^{-1}$, a value recently confirmed by two independent groups[135, 136]. The enthalpies of formation of the amino azo species are also suspect.

Almost no thermochemical data are available for azoxy or azodioxyanilines. Reference 5 reports an enthalpy of formation for only one species, the structurally ill-defined azoxy-m-toluidine, of $174 \, \text{kJ} \, \text{mol}^{-1}$. The above-noted stabilization of nitrosodimethylaniline argues against the formation of the dimeric azodioxyanilines. We recognize them as dimeric nitrosoanilines, and at least the p-derivatives do not dimerize.

X. BIOCHEMICALLY RELEVANT ANILINES

In this section are included anilines that have a biochemical and/or medicinal basis. In this connection we have already mentioned the 'sulfa drugs'.

A. Phenylglycine

N-(Carboxymethyl)aniline is more commonly known as N-phenylglycine. From the contemporary Reference 137 come enthalpies of formation for the solid and the gas. There are also two 100-year-old measurements[138, 139] for the solid that are *ca* 14 kJ mol^{-1} more positive. Also, from Reference 137, we have the enthalpies of formation of its isomer, C-phenylglycine (D-α-phenylglycine), of -445.5 ± 0.6 (s) and -280.5 ± 6.0 (g) kJ mol^{-1}. The C-phenyl isomer is more stable than the N-isomer in both phases. The enthalpies of formation of the corresponding N- and C-methylglycines (more commonly known as sarcosine[4] and alanine[140]) have also been measured and the C-isomer is again found to be more stable. Reaction 28, which interrelates all these species, is some -36 ± 8 kJ mol^{-1} exothermic in the gas phase but essentially thermoneutral in the solid [141].

$$\text{MeNHCH}_2\text{CO}_2\text{H} + \overset{\overset{\text{NH}_2}{|}}{\text{PhCHCO}_2\text{H}} \longrightarrow \overset{\overset{\text{NH}_2}{|}}{\text{MeCHCO}_2\text{H}} + \text{PhNHCH}_2\text{CO}_2\text{H} \qquad (28)$$

The gas-phase exothermicity is due to the enhanced resonance stabilization of aniline compared to benzene for the nonzwitterionic amino acids, as found in the gas phase. On the other hand, the aniline resonance stabilization is lost in the zwitterionic amino acids of the solid phase and thus the reaction is essentially thermoneutral. This is, of course, related to the weak basicity of aniline compared to related nonaromatic bases such as cyclohexylamine, as exhibited by the *ca* 50 kJ mol^{-1} exothermicity of the formal reaction 29.

$$c\text{-HexNH}_2(\text{l}) + \text{PhNH}_3\text{Cl}(\text{s}) \longrightarrow c\text{-HexNH}_3\text{Cl}(\text{s}) + \text{PhNH}_2(\text{l}) \qquad (29)$$
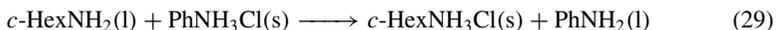
We can model the gas-phase glycines reaction by use of the alternative reaction 30, which is exothermic by -28.1 kJ mol^{-1}, somewhat less than that found for reaction 28.

$$\text{MeNHMe} + \text{PhCH}_2\text{NH}_2 \longrightarrow \text{MeCH}_2\text{NH}_2 + \text{PhNHMe} \qquad (30)$$

How do we model the solid glycines reaction, which plausibly contains the zwitterionic amino acids? A possible reaction is equation 31, where the hydrochloride salts simulate the zwitterions.

$$\text{MeNH}_2\text{Me}^+ \text{ Cl}^-(\text{s}) + \text{PhCH}_2\text{NH}_3{}^+ \text{ Cl}^-(\text{s})$$
$$\longrightarrow \text{MeCH}_2\text{NH}_3{}^+ \text{ Cl}^-(\text{s}) + \text{PhNH}_2\text{Me}^+ \text{ Cl}^-(\text{s}) \qquad (31)$$
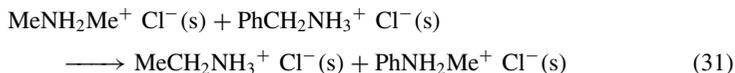
However, we are thwarted in the attempt since we lack most of the necessary enthalpies of formation for these hydrochloride salts, and for that matter for any other salts containing these cations. If we assume a cancellation of the lattice energies on the two sides of the reaction for the solids and thus consider the gas phase, and omit the enthalpy of formation of Cl$^-$ (g) that is common to all species, equation 32 results.

$$\text{MeNH}_2\text{Me}^+ (\text{g}) + \text{PhCH}_2\text{NH}_3{}^+ (\text{g}) \longrightarrow \text{MeCH}_2\text{NH}_3{}^+ (\text{g}) + \text{PhNH}_2\text{Me}^+ (\text{g}) \quad (32)$$
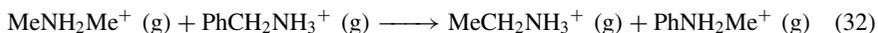
Combining the archival enthalpies of formation for neutrals and recommended proton affinities[143] to obtain the enthalpies of formation of the various ammonium ions, the reaction is calculated to be exothermic by *ca* -18 kJ mol^{-1}. This solid-simulated reaction is enthalpically less favorable than the model gas-phase reaction, just as observed for the amino acids. Let us modify this reaction to simulate the 'larger' $CO_2{}^-$ by using

an affixed methyl group. So, from the preferred value for the enthalpy of formation of *N*-ethylaniline[24], the average of the enthalpies of formation of diethyl and dimethylamine to give the enthalpy of formation of ethylmethylamine, and the proton affinitities[143], reaction 33 is exothermic by only 6 kJ mol^{-1}, in close agreement with the reaction enthalpy of reaction 28 in the solid phase.

$$MeNH_2Et^+ \ (g) + PhCH_2NH_3^+ \ (g) \longrightarrow MeCH_2NH_3^+ \ (g) + PhNH_2Et^+ \ (g) \quad (33)$$
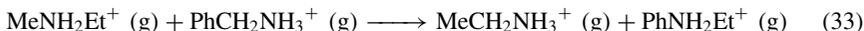
The high resonance energy of anilines and its absence upon protonation both contribute to the significant difference found for the solid and gaseous amino acids.

B. Tricyclic Amines

Many tricyclic amines have been long known as tranquilizers or antidepressants (e.g. thorazine) while others are related to biological stains (e.g. reduced or leuco methylene blue). However, despite these multiple uses, thermochemical data are rare for these species.

We earlier discussed 9,10-dihydroacridine and a recommended gas-phase enthalpy of formation of 198.6 kJ mol^{-1} based on hydrogenation and combustion calorimetric measurements[59–61]. The sole oxygen-containing aniline of this class of compounds that we will discuss is phenoxazine: from Reference 144 we find the solid and gaseous enthalpies of formation of -2.1 ± 2.8 and 94.0 ± 2.8 kJ mol^{-1}, respectively. The two remaining putative anilines are the sulfur-containing phenothiazine and 1,3,7,9-tetranitrophenothiazine-S-oxide. There are two very dissonant measurements of the enthalpy of combustion of phenothiazine as a solid, 49.7 and 166.7 ± 1.9 kJ mol^{-1}, from References 145 and 144 respectively; the latter source also gives us the enthalpy of formation of the gaseous species. From Reference 145 we find a value of -498.0 kJ mol^{-1} for the enthalpy of formation of the tetranitro sulfoxide species as a solid. There are no thermochemical data for the oxygen and sulfur analogs of 9,10-dihydroacridine to compare with any of these diheteroatomic tricyclic species.

C. Penicillins: Thermochemistry to the Rescue

Penicillins are most assuredly not aniline derivatives. It is well-established that they are bicyclic β-lactams. However, as is common for natural products, structural determination followed isolation. Perhaps surprisingly, recognition of this β-lactam functionality arose in part from a thermochemical analysis[146] of a ring-opening reaction involving an aniline derivative as product. Comparison of the enthalpies of formation of *N*-(2-carboethoxy-1-phenylethyl)aniline (i.e. β-phenyl-β-anilinopropionic acid ethyl ester) and the corresponding lactam, with those of methylpenicillin and dimethyl penicilloate (numerically, -346, -15, -977 and -669 kJ mol^{-1}, respectively), provided strong evidence for the now unequivocally established bicyclic β-lactam substructure for penicillins.

XI. REFERENCES AND NOTES

1. J. F. Liebman and S. W. Slayden, in *The Chemistry of Cyclobutanes* (Eds. Z. Rappoport and J. F. Liebman), Wiley, Chichester, 2005, p. 133.
2. S. W. Slayden and J. F. Liebman, in *The Chemistry of Organic Lithium Compounds* (Eds. Z. Rappoport and I. Marek), Wiley, Chichester, 2004, p. 121.
3. S. W. Slayden and J. F. Liebman, in *The Chemistry of Phenols* (Ed. Z. Rappoport), Wiley, Chichester, 2003, p. 223.
4. J. B. Pedley, R. D. Naylor and S. P. Kirby, *Thermochemical Data of Organic Compounds*, 2nd edn., Chapman & Hall, New York, 1986.

5. D. R. Stull, E. F. Westrum, Jr and G. C. Sinke, *The Chemical Thermodynamics of Organic Compounds*, Wiley, New York, 1969.
6. H. Y. Afeefy, J. F. Liebman and S. E. Stein, 'Neutral Thermochemical Data', in *NIST Chemistry WebBook, NIST Standard Reference Database Number 69* (Eds. W. G. Mallard and P. J. Linstrom), National Institute of Standards and Technology, Gaithersburg, MD 20899 (http://webbook.nist.gov), June 2005.
7. J. S. Chickos, W. E. Acree, Jr. and J. F. Liebman, *J. Phys. Chem. Ref. Data*, **28**, 1535 (1999). Strictly, use of these fusion enthalpies are estimates. The quantities should be corrected to 298 K from the melting point. However, the error is generally small because changes in heat capacities of solids and liquids as functions of temperature are generally small.
8. J. S. Chickos and W. E. Acree, Jr., *J. Phys. Chem. Ref. Data*, **31**, 537 (2002).
9. J. S. Chickos, D. G. Hesse and J. F. Liebman, *J. Org. Chem.*, **54**, 5250 (1989); J. S. Chickos, D. G. Hesse, J. F. Liebman and S. Y. Panshin, *J. Org. Chem.*, **53**, 3424 (1988).
10. J. F. Liebman and H. M. Perks, in *The Chemistry of Enamines* (Ed. Z. Rappoport), Wiley, Chichester, 1994, p. 255.
11. J. F. Liebman, M. S. Campbell and S. W. Slayden, in *The Chemistry of Functional Groups, Supplement F2: The Chemistry of Amino, Nitroso, Nitro and Related Groups* (ed. S. Patai), Wiley, Chichester, 1996, p. 337.
12. J. F. Liebman, H. Y. Afeefy and S. W. Slayden, in *The Chemistry of Hydrazo, Azo and Azoxy Groups*, Vol. 2 (Ed. S. Patai), Wiley, Chichester, 1997, p. 79.
13. J. F. Liebman, H. Y. Afeefy and S. W. Slayden, in *The Amide Linkage: Structural Significance in Chemistry, Biochemistry and Materials Science* (Eds. A. Greenberg, C. M. Breneman and J. F. Liebman), Wiley, New York, 2000, p. 115.
14. V. V. Diky, G. J. Kabo, A. A. Kozyro, A. P. Krasulin and V. M. Sevruk *J. Chem. Thermodyn.*, **26**, 1001 (1994).
15. X.-W. An and D.-J. Guo, *Thermochim. Acta*, **253**, 235 (1995).
16. In fact, this value of 14 kJ mol^{-1} may be considered to be significantly underestimated. In that the amino group in aniline is very nearly planar, some 30 kJ mol^{-1} of additional stabilization should be invoked corresponding to the enthalpy of formation difference between planar cyclohexylamine and aniline. (The current analysis, invoking the inversion/planarization energy of cyclohexylamine, assumed that the related barrier is the same as for ammonia and parallels the discussion of the resonance energies of amides and esters presented earlier by A. Greenberg, Y.-Y. Chiu, J. L. Johnson and J. F. Liebman, *Struct. Chem.*, **2**, 117 (1991).)
17. V. N. Emel'yanenko and S. P. Verevkin, *J. Phys. Chem. A*, **109**, 3960 (2005).
18. W. E. Garner and C. L. Abernethy, *Proc. R. Soc. London, Ser. A*, 213 (1921).
19. G. N. Vriens and A. G. Hill, *Ind. Eng. Chem.*, **44**, 2732 (1952). This source reports both the calorimetrically determined and the calculated enthalpies of combustion originally from Reference 20. Only the enthalpies of formation determined from the experimental values are reported here.
20. M. S. Kharasch, *J. Res. Natl. Bur. Stand.*, **2**, 359 (1929).
21. J. P. Guthrie, J. P. Barker, P. A. Cullimore, J. Lu and D. C. Pike, *Can. J. Chem.*, **71**, 2111 (1993).
22. N. M. Matvienko, O. I. Kachurin and V. G. Chekhuta, *Russ. Chem. Rev.*, **48**, 42 (1982).
23. M. P. Lemoult, *Ann. Chim. Phys.*, **12**, 395 (1907).
24. S. P. Verevkin, *J. Chem. Thermodyn.*, **29**, 892 (1997).
25. S. P. Verevkin, *J. Chem. Thermodyn.*, **32**, 247 (2000).
26. O. I. Kachurin, N. M. Matvienko and V. G. Chekhuta, *Russ. Chem. Rev.*, **46**, 64 (1980).
27. See Reference 19, which reports both experimental and calculated enthalpies of combustion of *N*,*N*-dimethylaniline as determined by Kharasch[20]. The corresponding enthalpies of formation are 60.9 and 34.1 kJ mol^{-1}, respectively. Interestingly, the average of these two is the same as the two more recently reported experimental values.
28. M. A. V. Ribeiro da Silva, M. D. M. C. Ribeiro da Silva, M. F. B. M. Monteiro, M. L. A. C. N. Gomes, J. S. Chickos, A. P. Smith and J. F. Liebman, *Struct. Chem.*, **7**, 367 (1996).
29. H. C. Brown and L. Domash, *J. Am. Chem. Soc.*, **78**, 5384 (1956).
30. V. P. Novikov, S. Samdal and L. V. Vilkov, *Russ. J. Gen. Chem. (Engl. Transl.)*, **74**, 1348 (2004).
31. V. E. Popov, A. M. Rozhnov, V. S. Satronov and A. G. Volkova, *Neftekhimiya*, **14**, 364 (1974); *Chem. Abstr.*, **81**, 104496 (1974).

32. S. W. Slayden and J. F. Liebman, *Chem. Rev.*, **101**, 1541 (2001).
33. T. N. Nesterova, S. P. Verevkin, S. Ya. Karaseva, A. M. Rozhnov and V. F. Tsvetkov, *Russ. J. Phys. Chem. (Engl. Transl.)*, **58**, 297 (1984).
34. S. Suradi, J. M. Hacking, G. Pilcher, I. Gumruckcu and M. F. Lappert, *J. Chem. Thermodyn.*, **13**, 857 (1981).
35. S. P. Verevkin, *Struct. Chem.*, **9**, 113 (1998).
36. M. A. R. Matos, M. S. Miranda, V. M. F. Morais and J. F. Liebman, unpublished results.
37. W. V. Steele, R. D. Chirico, I. A. Hossenlopp, A. Nguyen, N. K. Smith and B E. Gammon, *J. Chem. Thermodyn.*, **21**, 1121 (1989).
38. V. I. Minkin, *Chem. Rev.*, **104**, 2751 (2004).
39. (a) D. Zavoianu, S. Perisanu, S. Moga-Gheorghe, C. Bornaz, V. Gaman and A. Radulescu, *Rev. Chim. (Bucharest)*, **33**, 432 (1982).
    (b) D. Zavoianu, I. Contineanu, S. Moga-Gheorghe and D. Marchidan, *Rev. Chim. (Bucharest)*, **37**, 1055 (1986). The enthalpy of formation shown in the table was calculated by NIST from the enthalpy of combustion of -9084 kJ mol^{-1}.
40. D. Zavoianu, I. Ciocazanu, S. Moga-Gheorghe, O. Cuza and C. Bornaz, *Rev. Chim. (Bucharest)*, **36**, 220 (1985).
41. D. Zavoianu, I. Ciocazanu, S. Moga-Gheorghe and C. Bornaz, *Rev. Chim. (Bucharest)*, **37**, 960 (1986).
42. D. Zavoianu, I. Ciocazanu, S. Moga-Gheorghe and C. Bornaz, *Rev. Chim. (Bucharest)*, **41**, 15 (1990).
43. D. Zavoianu, I. Ciocazanu, S. Moga-Gheorghe and C. Bornaz, *Rev. Chim. (Bucharest)*, **39**, 751 (1988).
44. N. A. Pushin, *Bull. Soc. Chim. Belg.*, **9**, 531 (1954).
45. M. Milone and P. Rossignoli, *Gazz. Chim. Ital.*, **62**, 644 (1932).
46. V. A. Schmidt and F. Becker, *Z. Gesamte Schiess Sprengstoffwes.*, **33**, 280 (1933); *Chem. Abstr.*, **28**, 2359 (1934).
47. M. Balcan, S. Arzik and T. Altunata, *Thermochim. Acta,* **278**, 49 (1996).
48. J. B. Willis, *Trans. Faraday Soc.*, **43**, 97 (1947).
49. J. D. Cox and G. Pilcher, *Thermochemistry of Organic and Organometallic Compounds*, Academic Press, London, 1970.
50. S. P. Verevkin, M. V. Roux, R. Notario, D. E. DeMasters and J. F. Liebman, *Mol. Phys.*, **101**, 3231 (2003).
51. The quantum chemically calculated (at the MP2(full)/6-31G(d) level) enthalpy difference, ΔH_{298}, in kJ mol^{-1}, between 1- and 2-naphthylamine is 2.6 kJ mol^{-1} favoring the latter, with directly calculated enthalpies of formation of 156.0 and 153.4 kJ mol^{-1} for the two isomers, respectively. R. Notario and J. F. Liebman, unpublished results.
52. W. V. Steele, R. D. Chirico, S. E. Knipmeyer and A. Nguyen, *J. Chem. Thermodyn.*, **23**, 957 (1991).
53. M. A. R. Matos, M. S. Miranda, D. V. S. S. Martins, N. A. B. Pinto, V. M. F. Morais and J. F. Liebman, *Org. Biomol. Chem.*, **2**, 1353 (2004).
54. M. P. Lemoult, *Compt. Rend.*, **143**, 772 (1906).
55. W. V. Steele, *J. Chem. Thermodyn.*, **10**, 441 (1978).
56. The enthalpies of formation of 97.1 ± 1.4 (lq) and 164.8 ± 1.6 (g) kJ mol^{-1} for diphenylmethane are taken from W. V. Steele, R. D. Chirico and N. K. Smith, *J. Chem. Thermodyn.*, **27**, 671 (1995).
57. The gas-phase enthalpies of formation of 280.3 ± 1.5 for triphenylmethane and of 387.1 ± 2.9 for tetraphenylmethane are taken from S. P. Verevkin, *J. Chem. Eng. Data*, **44**, 557 (1999).
58. R. M. Stephenson and S. Malanowski, *Handbook of the Thermodynamics of Organic Compounds*, Elsevier, New York, 1987.
59. L. M. Jackman and D. I. Packham, *Proc. Chem. Soc. London*, 349 (1957).
60. D. W. Rogers, O. A. Dagdagan and N. L. Allinger, *J. Am. Chem. Soc.*, **101**, 671 (1979).
61. W. V. Steele, R. D. Chirico, I. A. Hossenlopp, A. Nguyen, N. K. Smith and B. E. Gammon, *J. Chem. Thermodyn.*, **21**, 81 (1989).
62. The enthalpy of formation of gaseous *p*-xylylene of 210 ± 20 kJ mol^{-1} was obtained from the energetics of gas-phase ion−molecule reactions from S. K. Pollack, B. C. Raine and W. J. Hehre, *J. Am. Chem. Soc.*, **103**, 6308 (1981). Since gaseous *p*-xylylene polymerizes

in the condensed phase, we are assuming that the phase change enthalpies for *p*-xylylene and
p-xylene would be the same were the former to remain monomeric.

63. Y. Fu and R. L. Elsenbaumer, *Chem. Mater.*, **7**, 671 (1994).
64. D. D. Wagman, W. H. Evans, V. B. Parker, R. H. Schumm, I. Halow, S. M. Bailey, K. L. Churney and R. L. Nuttall, 'The NBS Tables of Chemical Thermodynamic Properties: Selected Values for Inorganic and C_1 and C_2 Organic Substances in SI Units', *J. Phys. Chem. Ref. Data* (1982), **11**, Supplement 2.
65. G. O. Shmeyreva and A. M. Mosin, *Termodin. Org. Soedin.*, 82 (1983); *Chem. Abstr.*, **101**, 199113w (1985).
66. J. Lubkowski and J. Blazejowski, *J. Chem. Soc., Faraday Trans. 1*, **82**, 3069 (1986).
67. A. A. Zalykin and Yu. A. Strepikheev, *J. Appl. Chem. USSR (Engl. Transl.)*, **39**, 2448 (1966).
68. K. Kishore and K. N. Santhanalakshmi, *Thermochim. Acta*, **68**, 59 (1983).
69. J. Santhanalakshmi, *Thermochim. Acta*, **127**, 369 (1988).
70. K. B. Wiberg, D. Y. Nakaji and K. M. Morgan, *J. Am. Chem. Soc.*, **115**, 3527 (1993).
71. D. Wu, G. Xu, S. Qu, R. Xue, C. Gu and F. Zhang, *Thermochim. Acta*, **154**, 233 (1989).
72. X. Hong, W. Dingquan and Q. Songsheng, *Acta Phys. Chim. Sinica*, **5**, 745 (1989).
73. R. Sabbah and L. Perez, *Can. J. Chem.*, **75**, 357 (1997).
74. I. Contineanu, L. Wagner, L. Stanescu and D. I. Marchidan, *Rev. Roum. Chim.*, **27**, 205 (1982).
75. R. M. Metzger and E. S. Arafat, *J. Chem. Phys.*, **78**, 2696 (1983).
76. L. Nunez, L. Barral, S. G. Largo and G. Pilcher, *J. Chem. Thermodyn.*, **18**, 575 (1986).
77. R. Sabbah and M. Gouali, *Can. J. Chem.*, **74**, 500 (1996).
78. W. H. Rinkenbach, *J. Am. Chem. Soc.*, **52**, 115 (1930).
79. L. Medard and M. Thomas, *Mem. Poudres,* **29**, 173 (1949); *Chem. Abstr.*, **46**, 70258 (1952).
80. Discussion of these compounds violates our premise of not having any heteroatom on the nitrogen atom. However, in that there is no 'Patai/Rappoport' volume chapter, or any other review of the thermochemistry of hydroxylamines, we wanted to give these species a thermochemical 'home'.
81. I. Contineanu, T. Ionescu and D. I. Marchidan, *Rev. Roum. Chim.*, **37**, 1111 (1992).
82. I. Contineanu, D. Bretcanu and D. I. Marchidan, *Rev. Roum. Chim.*, **27**, 55 (1982).
83. V. D. Kiselev, D. G. Khuzyasheva and A. I. Konovalov, *J. Gen. Chem. USSR,* **49**, 2273 (1979).
84. Y. Ogata and A. Kawasaki, *J. Org. Chem.*, **39**, 1058 (1974). For reference, the reaction enthalpy for the p'-methylated species is $10 \pm 4 \text{ kJ mol}^{-1}$.
85. J. P. Guthrie, J. P. Barker, P. A. Cullimore, J. Lu and D. C. Pike, *Can. J. Chem.*, **71**, 2111 (1993).
86. V. P. Kuznetsova, E. A. Miroshnichenko, A. N. Zelenetskii, G. V. Rakova, Yu. A. Lebedev and N. S. Enikolopyan, *Dokl. Phys. Chem. (Engl. Transl.)*, **226**, 147 (1976).
87. E. E. Baroody, *Heats of Formation of Propellant Compounds (U)*, Report NSWC-TR-83-250, Naval Surface Weapons Center, Silver Spring, MD, 1983, pp. 1–11.
88. N. V. Karyakin, N. G. Bazhan, V. N. Sapozhnikov, K. G. Shvetsova, G. L. Berestneva, A. N. Lomteva, Yu. B. Zimin and V. V. Korshak, *Vysokomol. Soedin., Ser. A,* **19**, 1541 (1977); *Chem. Abstr.,* **87**, 102811 (1977).
89. N. V. Karyakin, I. B. Rabinovich, V. N. Sapozhnikov, G. P. Kamelova, E. S. Krongauz, V. V. Korshak and A. P. Travnikova, *Vysokomol. Soedin., Ser. B*, **19**, 457 (1977); *Chem. Abstr.*, **87**, 68797 (1977).
90. N. V. Karyakin, N. G. Shvetsova, G. P. Kamelova, A. L. Rusanov, V. V. Korshak and L. K. H. Pliyeva, *Vysokomol. Soedin., Ser. A,* **26**, 36 (1984); *Chem. Abstr.*, **100**, 121670 (1984).
91. J. F. Liebman, in *The Chemistry of the Sulphonic Acids, Esters and their Derivatives* (Eds. S. Patai and Z. Rappoport), Wiley, Chichester, 1991, p. 283.
92. J. F. Liebman, K. S. K. Crawford and S. W. Slayden, in *The Chemistry of Functional Groups, Supplement S: The Chemistry of Sulphur-containing Functional Groups* (Eds. S. Patai and Z. Rappoport), Wiley, Chichester, 1993, p. 147.
93. M.-Y. Yang, G. Pilcher and J. I. Macnab, *J. Chem. Thermodyn.*, **26**, 787 (1994).
94. I. Ciocazanu and V. Meltzer, *J. Therm. Anal.*, **47**, 1755 (1996).
95. M. A. R. Matos, M. S. Miranda, V. M. F. Morais and J. F. Liebman, *Mol. Phys.*, **103**, 221 (2005).

96. R. Gudino, L. A. Torres, M. Campos, R. L. Santillan and N. Farfan, *J. Chem. Thermodyn.*, **29**, 565 (1997).
97. F. Swarts, *J. Chim. Phys.*, **17**, 3 (1919).
98. S. W. Slayden, J. F. Liebman and W. G. Mallard, in *The Chemistry of Functional Groups, Supplement D2: The Chemistry of Organic Halides, Pseudohalides and Azides* (Eds. S. Patai and Z. Rappoport), Wiley, Chichester, 1995, p. 361.
99. F. Swarts, *Recl. Trav. Chim. Pays-Bas*, **28**, 143 (1909).
100. M. A. V. Ribeiro da Silva, J. R. B. Gomes and A. I. M. C. L. Ferreira, *J. Phys. Chem. B*, **109**, 13356 (2005).
101. T. N. Masalitinova, T. P. Oleinikova, V. L. Ryadnenko, N. N. Kiseleva and N. D. Lebedeva, *J. Appl. Chem. USSR (Engl. Transl.)*, **54**, 1551 (1981). The enthalpies of formation(s) and of sublimation for 3,4-dichloroaniline have been recently determined as -49.2 ± 1.2 and 38.3 ± 1.2 kJ mol^{-1}, respectively by M. A. V. Ribeiro da Silva, L. M. P. F. Amaral and J. R. B. Gomes, unpublished results, personal communication from M. A. V. Ribeiro da Silva.
102. A. A. Zalikin, V. L. Kochetkov and Yu. A. Strepikheev, *Khim. Prom. (Moscow)*, **41**, 338 (1965); *Chem. Abstr.*, **63**, 35320 (1965).
103. E. Z. Zhuravlev, T. I. Melent'eva, N. B. Mulyanov, A. I. Kormushehkina and I. I. Konstantinov, Deposited Document, SPSTL 651 Khp-D80; *Chem. Abstr.*, **97**, 12145s (1980).
104. L. Smith, L. Bjellerup, S. Krook and H. Westermark, *Acta Chem. Scand.*, **7**, 65 (1953).
105. M. A. V. Ribeiro Da Silva, L. M. S. S. Lima, L. M. P. F. Amaral, A. I. M. C. L. Ferreira and J. R. B. Gomes, *J. Chem. Thermodyn.*, **35**, 1343 (2003).
106. M. A. V. Ribeiro da Silva, L. M. P. F. Amaral and A. I. M. C. L. Ferreira, *J. Chem. Thermodyn.*, **34**, 119 (2002).
107. V. A. Platonov and Yu. N. Simulin, *Russ. J. Phys. Chem. (Engl. Transl.)*, **59**, 179 (1985); V. A. Platonov and Yu. N. Simulin, *Russ. J. Phys. Chem. (Engl. Transl.)*, **57**, 840 (1983).
108. H. Yan, J. Gu, X. An and R. Hu, *Huaxue Xuebao*, **45**, 1184 (1987); *Chem. Abstr.*, **108**, 138790 (1987).
109. P. H. Allot and A. Finch, *J. Chem Thermodyn.*, **19**, 771 (1987).
110. Z. V. Pushkareva and Z. U. Kokoshko, *Zh. Obshch. Khim.*, **16**, 1269 (1946); *Chem. Abstr.*, **41**, 15153 (1946).
111. I. Contineanu and S. Predescu, *Rev. Roum. Chim.*, **46**, 2303 (2001).
112. W. V. Steele, R. D. Chirico, A. Nguyen, I. A. Hossenlopp and N. K. Smith, *AIChE Symp. Ser.*, 138 (1990).
113. B. N. Oleinik, V. D. Mikina, Yu. I. Aleksandrov, V. F. Ushcevich, T. R. Osipova and K. A. Hrustaleva, *J. Chem. Thermodyn.*, **11**, 145 (1979).
114. N. V. Karyakin, I. B. Rabinovich, V. V. Korshak, A. L. Rusanov, D. S. Tugushi, A. N. Mochalov and V. N. Sapozhnikov, *Polym. Sci. USSR,* **16**, 795 (1974).
115. A. Pongratz, S. Bohmert-Suss and K. Scholtis, *Chem. Ber.*, **77B**, 651 (1944).
116. M. A. R. Matos, M. S. Miranda, V. M. F. Morais and J. F. Liebman, *Mol. Phys.*, **104**, 325 (2006).
117. M. M. Williams, W. S. McEwan and R. A. Henry, *J. Phys. Chem.*, **61**, 261 (1957).
118. M. Friedrich, J. C. Galvez-Ruiz, T. M. Klapotke, P. Mayer, B. Weber and J. J. Weigand, *Inorg. Chem.*, **44**, 8044 (2005).
119. L. Medard and M. Thomas, *Mem. Poudres*, **39**, 195 (1957); *Chem. Abstr.*, **53**, 4102 (1959).
120. N. D. Lebedeva, N. M. Gutner and V. L. Ryadnenko, *Russ. J. Phys. Chem. (Engl. Transl.)*, **45**, 561 (1971).
121. K. Nishiyama, M. Sakiyama and S. Seki, *Bull. Chem. Soc. Jpn.*, **56**, 3171 (1983).
122. L. G. Cole and E. C. Gilbert, *J. Am. Chem. Soc.*, **73**, 5423 (1951).
123. P. Politzer, P. Lane and M. C. Concha, *Struct. Chem.*, **15**, 469 (2004).
124. J. Furukawa, S. Murata, M. Sakiyama and S. Seki, *Bull. Chem. Soc. Jpn.,* **57**, 3058 (1984).
125. W. E. Acree, S. A. Tucker, G. Pilcher and G. Toole, *J. Chem. Thermodyn.*, **26**, 85 (1994).
126. W. H. Rinkenbach, *J. Am. Chem. Soc.*, **52**, 115 (1930).
127. B. T. Fedoroff and O. E. Shefield, in *Encyclopedia of Explosives and Related Items, Part 2700*, Volume 7, Picatinny Arsenal, Dover, NJ, 1975.
128. P. E. Rouse Jr., *J. Chem. Eng. Data*, **21**, 16 (1976). The originally reported experimental uncertainties were later retracted in P. E. Rouse Jr., *J. Chem. Eng. Data*, **23**, 186 (1978).
129. E. E. Baroody and S. T. Peters, *Heats of Formation of Propellant Compounds (U)*, Report IHSP-87-252, Naval Ordnance Station, Indian Head, MD, 1987, p. 1.

130. G. R. Handrick, *Report of the Study of Pure Explosive Compounds. Part IV. Calculation of heat of combustion of organic compounds from structural features and calculation of power of high explosives*, Report C-58247 for the Office of the Chief of Ordnance, contract DA-19-020-ORD-47 by the Arthur D. Little, Inc., Cambridge, MA, 1956.
131. W. Swientoslawski, *Z. Phys. Chem.*, **72**, 49 (1910).
132. This is a consensus value derived from use of the C—N bond energy measurement from K. Y. Choo, D. M. Golden and S. W. Benson, *Int. J. Chem. Kinet.*, **7**, 713 (1975) and the enthalpy of formation of azodioxybenzene (nitrosobenzene dimer) and of its monomerization enthalpy from V. I. Pepekin, V. P. Lebedev, A. A. Balepin and Yu. A. Lebedev, *Dokl. Phys. Chem. (Engl. Transl.)*, **221**, 370 (1975) and K. G. Orrell, V. Sik and D. Stephenson, *Magn. Reson. Chem.*, **25**, 1007 (1987).
133. M. D. M. C. Ribeiro Da Silva, M. A. R. Matos, G. Pilcher and W. E. Acree, Jr., *J. Chem. Thermodyn.,* **30**, 271 (1998).
134. M. P. Lemoult, *Ann. Chim. Phys.*, **14**, 289 (1908).
135. A. R. Dias, M. E. Minas Da Piedade, J. A. Martinho Simões, J. A. Teixeira, C. H. P. Diogo, Y. Meng-Yen and G. Pilcher, *J. Chem. Thermodyn.*, **24**, 4399 (1992).
136. W. V. Steele, R. D. Chirico, S. E. Knipmeyer, A. Nguyen and N. K. Smith, *J. Chem. Eng. Data*, **41**, 1285 (1996).
137. R. Sabbah and S. Skoulika, *Thermochim. Acta*, **36**, 179 (1980).
138. E. Fischer and F. Wrede, *Sitzungsber. Dtsch. Akad. Wiss. Berl., Kl. Math. Phys. Tech.*, 687 (1904).
139. M. P. Lemoult, *Compt. Rend.*, 663 (1904).
140. S. N. Ngauv, R. Sabbah and M. Laffitte, *Thermochim. Acta*, **20**, 371 (1977).
141. The enthalpies of formation of *N*-methylglycine are -513.3 ± 0.3 (s) and -367.2 ± 1.0 (g) kJ mol^{-1} from Reference 4. The enthalpies of formation of *C*-methylglycine (L-alanine) are -559.5 ± 0.5 and -414.7 ± 4.2 (g) from Reference 140 and $-560. \pm 1.7$ (s) from Reference 142. Reference 4 reports enthalpy of formation measurements for the alanines, which are listed as *l*-, *dl*- and *d*-. These symbols were formerly used to indicate the direction of rotation of plane-polarized light and are now replaced by $(-)$, $(\pm)$ and $(+)$, respectively. For alanines, the stereochemical designations and corresponding signs of rotation are D-$(-)$- and L-$(+)$-alanine.
142. I. Contineanu and D. I. Marchidan, *Rev. Roum. Chim.*, **29**, 43 (1984).
143. E. P. L. Hunter and S. G. Lias, *J. Phys. Chem. Ref. Data*, **27**, 413 (1998).
144. R. Sabbah and L. El Watik, *Thermochim. Acta*, **197**, 381 (1992).
145. P. Tavernier and M. Lamouroux, *Mem. Poudres*, **39**, 335 (1957); *Chem. Abstr.*, **54**, 115429 (1960).
146. R. B. Woodward, A. Neuberger and N. R. Trenner, *The Chemistry of Penicillin*, Princeton University Press, New Jersey, 1949, p. 436.

CHAPTER **5**

Mass spectrometry and gas-phase chemistry of anilines

MARCOS N. EBERLIN

ThoMSon Mass Spectrometry Laboratory, Institute of Chemistry, State University of Campinas, 13084 971 Campinas, SP, Brazil
Fax: +55 19 3521 3073;   e-mail: eberlin@iqm.unicamp.br

DANIELLA VASCONCELLOS AUGUSTI

Octávio Magalhães Institute, Ezequiel Diaz Foundation — FUNED, 30510-010 Belo Horizonte, MG, Brazil
Fax: 55-31-33719553;   e-mail: daniella.augusti@funed.mg.gov.br

and

RODINEI AUGUSTI

Department of Chemistry, Federal University of Minas Gerais — UFMG, 31270 901 Belo Horizonte, MG, Brazil
Fax: +55 31 34995700;   e-mail: augusti@ufmg.br

The chemistry of anilines
Edited by Z. Rappoport   © 2007 John Wiley & Sons, Ltd

I. INTRODUCTION

In anilines, the amino group is connected to a benzene ring and thus the nitrogen lone electron pair is considerably delocalized across the aromatic π-system[1]. Despite this delocalization, when subjected to mass spectrometric (MS) analysis, gaseous anilines are readily ionized. Upon electron ionization (EI), they efficiently form radical cations ($M^{+\bullet}$) due to their quite low ionization energies, in the range of 8.6–7.7 eV (Table 1). When subjected to under-vaccum chemical ionization (CI) or atmospheric pressure chemical ionization (APCI), anilines are easily protonated due to their relatively high basicity[1] forming relatively stable anilinium ions $[M + H]^+$. For protonation, proton-transfer reactions with, for instance, CH_5^+ or protonated solvents such as H_3O^+ and $CH_3OH_2^+$ are employed. In solution, anilines are also easily protonated to form solvated $[M + H]^+$ ions; hence, electrospray ionization mass spectrometry (ESI-MS) in the positive ion mode is normally able to transfer these $[M + H]^+$ ions with relatively high efficiency from the solution to the gas-phase environment of mass spectrometers.

Anilines are important in the chemistry of both natural and synthetic compounds, being used in a great variety of applications such as rubber accelerators and antioxidants, dyes and intermediates, photographic chemicals, as isocyanates for urethane foams, in pharmaceuticals, explosives, petroleum refining, and in the production of herbicides and fungicides. Anilines have also been found in tobacco smoke, in effluents from oil shale recovery and oil refineries, and from chemical and coal conversion plants[2]. Anilines, in particular the chlorinated derivatives, represent ubiquitous pollutants being easily degraded in the atmosphere, especially during the daylight hours, primarily by reaction with photochemically-produced hydroxyl radicals. The reaction products include nitrosamines, nitrobenzenes, nitrophenols, phenols, nitrosobenzenes and benzidines[3]. It is therefore of great importance to be able to detect and characterize such a class of fundamental chemicals. For this task, mass spectrometry plays a fundamental role owing to its multitude of techniques for ionization, mass measurements and structural investigations, and with its superior speed, sensitivity and selectivity.

This chapter intends to cover the typical gas-phase ion chemistry of anilines in the dilute gas-phase environment of mass spectrometers mainly under electron ionization (EI) and chemical ionization (CI) conditions. Some representative work dealing with electrospray ionization (ESI) will also be described. We note that, in general, textbooks on mass spectrometry rarely include detailed discussions of the often intricate aspects of the gas-phase ion chemistry of anilines and their relationship with the resulting mass spectra[4,5].

II. IONIZATION ENERGIES (IE) AND PROTON AFFINITIES (PA)
OF ANILINES: THE INFLUENCE OF THE SUBSTITUENTS

Mass spectrometric techniques have been invaluable in measuring the intrinsic properties of anilines, most particularly their ionization energies (IE) and proton affinities (PA). IE is defined as the 0 K enthalpy change required to remove an electron from a neutral molecule[6]. The removal of a single electron from an aniline, usually from the nitrogen atom of the amino group (equation 1), yields the corresponding radical cation and requires energies in the range of *ca* 7.7–8.6 eV (Table 1)[7].

$$\text{(1)}$$
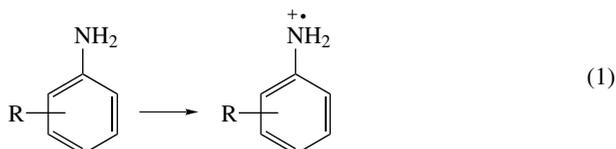
Proton affinity (PA) is the negative of the enthalpy change defined at 298 K for the protonation reaction (equation 2)[6]. As seen from the values of representative monosubstituted anilines (Table 1), PA values of anilines are quite high.

$$\text{(2)}$$
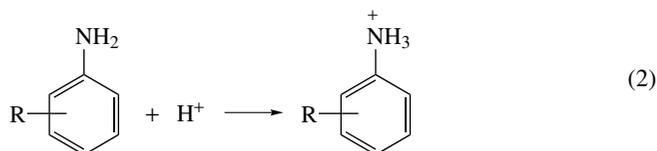
The influence of the ring and the character of the *N*-substituent (electron-donating or withdrawing) on both thermodynamic properties can be evaluated from the data compiled

TABLE 1.   Ionization energies (IE) and proton affinities (PA) of aniline and selected derivatives

Substituent on aniline	Ionization energy (eV) (method)	Proton affinity (kJ mol^{-1})
H	7.72[8]	882.5[9]
2-OCH$_3$	7.5 ± 0.1[10] (CT-MS)	905.2[9]
3-OCH$_3$	7.8 ± 0.1[11] (EI)	913.0[9]
4-OCH$_3$	7.6 ± 0.1[11] (EI)	900.3[9]
2-NO$_2$	8.66[12] (EI)	—
3-NO$_2$	8.80[12] (EI)	—
4-NO$_2$	8.85[12] (EI)	866.0[9]
3-CN	8.61 ± 0.05[13] (EI)	842.3[9]
4-CN	8.64 ± 0.04[13] (EI)	—
2-F	8.50[14] (EI)	—
3-F	8.33[15] (PE)	867.3[9]
4-F	8.18[15] (PE)	871.5[9]
2-OH	—	898.8[9]
3-OH	—	898.8[9]
N-CH$_3$	7.32 ± 0.02[8]	916.6[9]
N-COCH$_3$	8.30 ± 0.10[16] (PE)	—

in Table 1. Because of the diverse methodologies employed in the determination of IE, such as charge transfer mass spectrometry (CT-MS), electron ionization mass spectrometry (EI-MS) and photoelectron spectroscopy (PE), comparison among the IE of the positional isomers must be performed with care. However, it is evident (and expected) that the presence of electron-donating substituents such as hydroxy and methoxy groups markedly decrease the IE of aniline in comparison with anilines substituted by electron-withdrawing ring substituents such as nitro and cyano. Proton affinities are also greatly affected by ring substituents (Table 1). As expected, higher proton affinities are observed for anilines containing electron-donating ring substituents such as methoxy and hydroxy. The presence of electron-withdrawing ring substituents such as fluorine and nitro clearly decreases the PA. *N*-substituents also affect IE and PA considerably. For instance, *N*-methylaniline shows lower IE and higher PA than aniline owing to the electron-donating character of the methyl group, whereas acetanilide, which bears the electron-withdrawing acetyl substituent on the nitrogen, displays a higher IE.

III. 70 eV EI MASS SPECTROMETRY OF ANILINES: THE INFLUENCE OF THE NATURE OF SUBSTITUENTS ON UNIMOLECULAR DISSOCIATION

Electron ionization (EI) was devised first by Dempster[17] and improved later by Bleakney[18] and Nier[19]. EI is widely used in organic mass spectrometry since it works well for many gas-phase molecules. Besides ionization, EI transfers an excess of energy to the ionized molecule, which induces dissociation and the production of fragment ions that are used for compound identification and structural analysis[20]. Attempts to correlate mass spectrometric data with structure can only be described as elegant, though many times it is very complex, puzzling and arbitrary. The insight of the many pioneers in this endeavor, such as those from the groups of McLafferty[21], Beynon[22] and Budzikiewicz[23], led to a number of rational mechanisms for ion dissociation. These rationalizations were masterfully summarized in textbooks and reviews by McLafferty and Turecek[5], Biemann[24], Budzikiewicz, Djerassi and Williams[4, 25] and others.

In EI-MS, the tendency is generally to represent the molecular ion ($M^{+\bullet}$) with an unspecified location for the charge and spin sites. However, Budzikiewicz and coworkers' approach[26] localizes the charge-spin site in a specific σ-bond or preferentially on a lone-pair heteroatom or a π bond (except in conjugated systems). Dissociation is induced by either the charge or spin site and its driving force is provided partially by the interaction between the electron beam and the neutral molecule. Most of the driving force for $M^{+\bullet}$ dissociation is provided, however, by the cation-radical character imposed upon the molecule by ionization (e.g. equation 1). In this chapter, we will discuss several examples of EI-MS of representative anilines that help to establish a rationale for the unimolecular dissociation chemistry of their gaseous ions. In most cases, their molecular ions and other radical cation fragments will be represented with localized spin and radical sites, that is, as if they were formed exclusively by the removal of a specific electron, e.g., a nonbonding nitrogen electron from the amino group (equation 1).

A. Aniline

Figure 1 shows the EI-MS of aniline using electrons with 70 eV of energy. The molecular ion ($M^{+\bullet}$) of m/z 93 (note the odd mass according to the nitrogen rule[20], that is, owing to an odd number of nitrogens) is of great relative abundance, and its stability has been explained[27] by radical delocalization (Scheme 1) across the benzene ring.
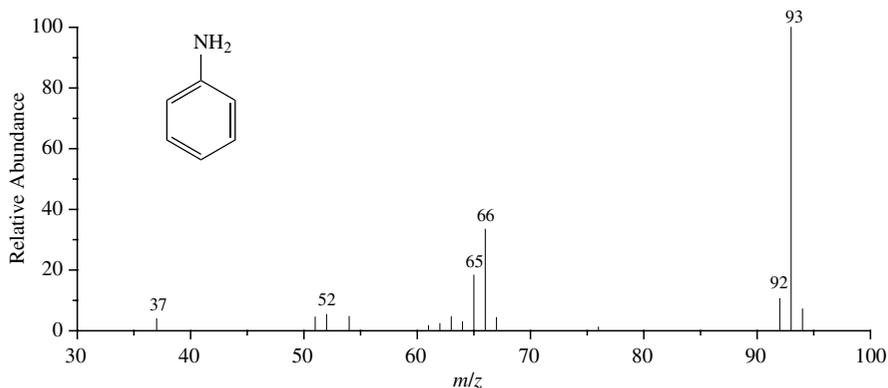
FIGURE 1. 70 eV EI mass spectrum of aniline. Adapted from Reference 40
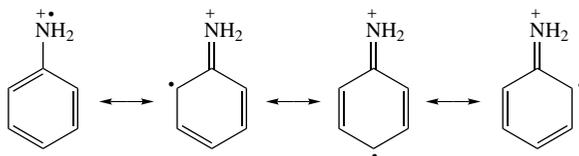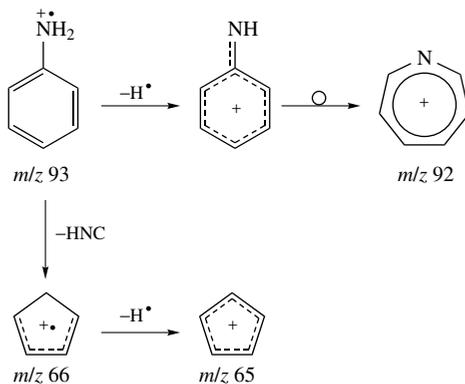
SCHEME 1

SCHEME 2

The loss of one of the amino H atoms[27] yields a moderately abundant $[M - H]^+$ fragment ion of m/z 92, viz. the anilenium ion that may isomerize to the aromatic fully delocalized azatropylium ion (Scheme 2). The subsequent ions $[M - HNC]^{+\bullet}$ of m/z 66 and $[M - HNC - H]^+$ of m/z 65 are also prominent. Note that the aniline molecular ion

preferentially loses HNC (in a one-step process) instead of the more stable HCN isomer[28] as previously assumed[29–31]. Early experiments[27] with labeled ^{15}N had demonstrated the loss of the elements of hydrogen cyanide, and HCN loss was therefore postulated[4]. Furthermore, although the cyclic form for the $[M - HNC]^{+\bullet}$ fragment of m/z 66, likely ionized cyclopentadiene (Scheme 2), is generally assumed to be the exclusive product, we should bear in mind that it has been found by charge stripping (CS) mass spectrometry that these fragments actually consist of a mixture of ions also containing acyclic isomers[32]. Subsequent loss of H$^\bullet$ to give $C_5H_5^+$ ions of m/z 65, probably to be constituted mainly of the cyclopentadiene cation (Scheme 2), is a common secondary dissociation. The formation of $[M - HNC]^{+\bullet}$ and the accompanying fragment $[M - HNC - H]^+$ also occurs for ionized anilines with ring substituents, provided that less energy-demanding channels are unavailable, as will be discussed further in this chapter.

The gaseous molecular ion of the O-analogue of aniline, phenol, has been shown to spontaneously isomerize via a [1,3-H] shift (Scheme 3) to ionized cyclohexa-1,3-dien-5-one (*ortho*-isophenol). The features of this interesting keto–enol equilibrium have been extensively studied by a variety of mass spectrometric methods[33–38]. Similarly, it has also been observed that ionized toluene generates ionized *ortho*-isotoluene in the gas phase (Scheme 3)[39]. By contrast, analogous behavior has not been reported for ionized aniline: EI of aniline seems to generate predominantly ionized aniline which shows no detectable isomerization to ionized *ortho*-isoaniline[16].

$X = O, CH_2$
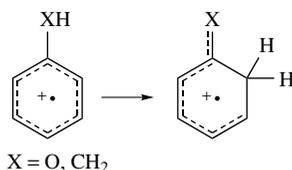
SCHEME 3

B. Methoxyanilines

Figure 2 shows the 70 eV EI-MS of the three positional isomers of methoxyaniline. In all three spectra, the molecular ion of m/z 123 is detected as one of the most abundant ions. A remarkable difference is observed: the ion of m/z 108, formed by the loss of methyl radical, is predominant in the mass spectra of the *ortho* (Figure 2a) and *para* (Figure 2c) isomers but this fragment is not observed at all in the mass spectrum of the *meta* compound (Figure 2b). As Scheme 4 depicts for *ortho*-methoxyaniline, the *ortho*- and *para*-methoxy substituent facilitate the loss of the methyl radical since the resulting product ions are stabilized by charge dispersion via resonance with the properly located amino group. Subsequent dissociation by CO loss generates the fragment ion of m/z 80, probably the energetically favored protonated pyridine[41]. In contrast, almost no $[M - CH_3]^+$ ion is detected in the EI-MS of the *meta* isomer but again a significant $[M - CH_3 - CO]^+$ ion of m/z 80 is seen (Figure 2c). The lack of methyl loss for the *meta* isomer (an interesting example of a '*meta effect*') is therefore attributed to the formation of the energetically unfavorable ion, that is the *meta*-phenoxy cation, which cannot disperse its charge by resonance with the *meta*-amino group. Such a less stable ion thus decomposes rapidly by CO loss to probably yield, after rearrangement, the protonated pyridine ion (Scheme 5).
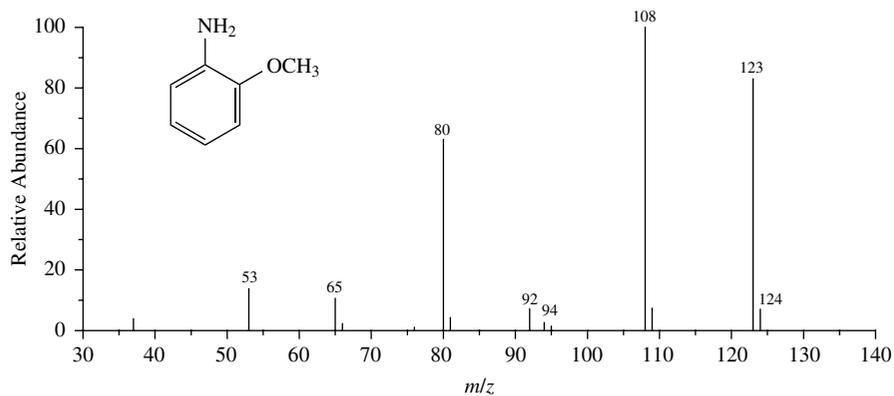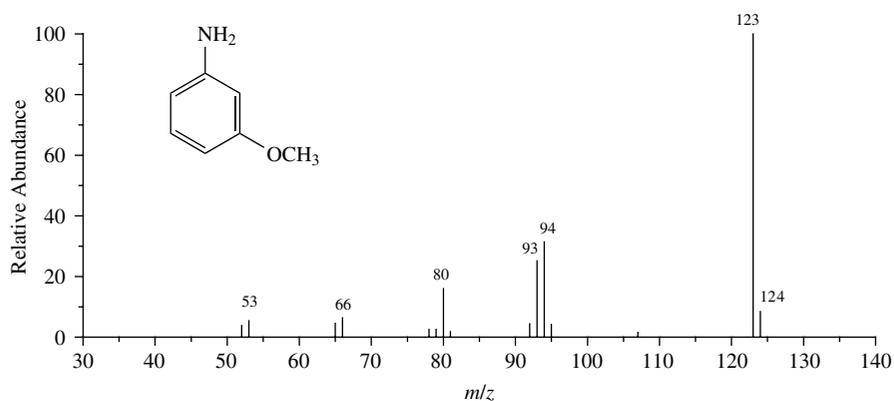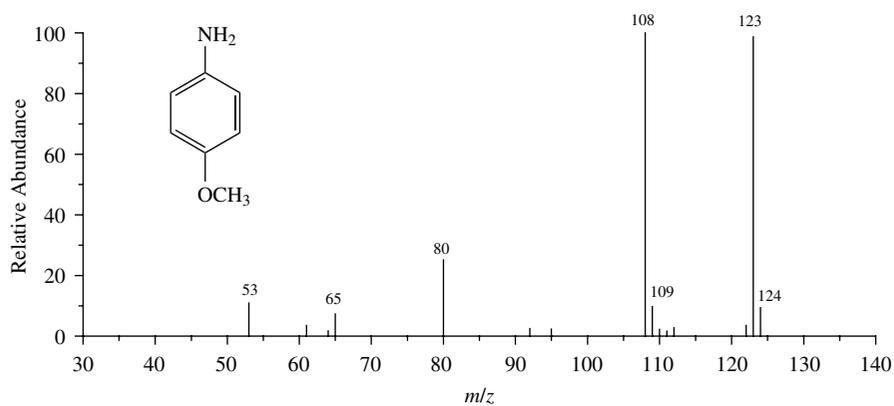
FIGURE 2. 70 eV EI mass spectra of isomeric methoxyanilines: (a) *ortho*, (b) *meta*, (c) *para*. Adapted from Reference 40
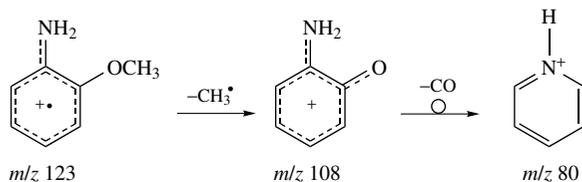
SCHEME 4
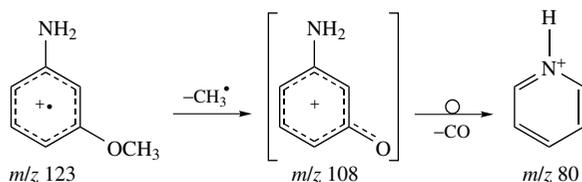
SCHEME 5
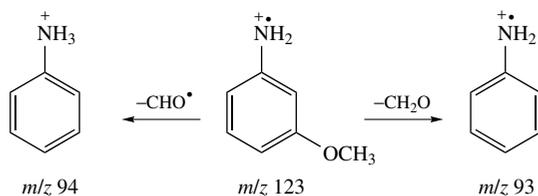
SCHEME 6

In addition, other dissociation processes (Scheme 6) that are probably more energetic than methyl loss (hence not as easily rationalized) become important for the *meta* isomer, such as the loss of a formyl radical (m/z 94) and formaldehyde (m/z 93).

C. Hydroxyanilines

Figure 3 shows the 70 eV EI-MS of the isomeric hydroxyanilines. Unlike the methoxy anilines, for which *ortho, para* and *meta* effects are quite pronounced, the EI-MS of these three positional isomers are very similar. The most abundant ion in the EI-MS of the hydroxyanilines is the molecular ion of m/z 109 whereas, by far the most prominent fragment ion is that of m/z 80, viz. $[M − CO − H]^+$. A substantial contribution of the keto tautomer is suggested for the CO loss process[38, 42, 43], as represented in Scheme 7 for the *ortho* isomer, and this tautomer may account for the weak positional effects.

D. Cyanoanilines

Figure 4 shows the 70 eV EI mass spectra of the three isomeric cyanoanilines. As for the methoxy isomers, the mass spectra of the *ortho-* and *para*-cyanoanilines are
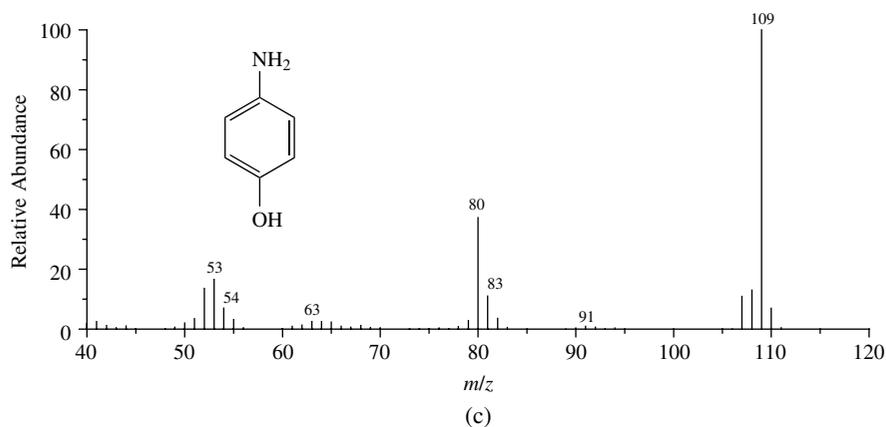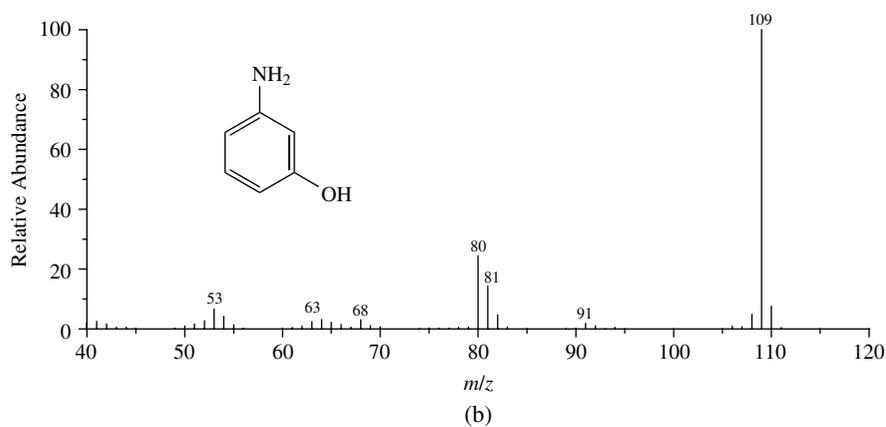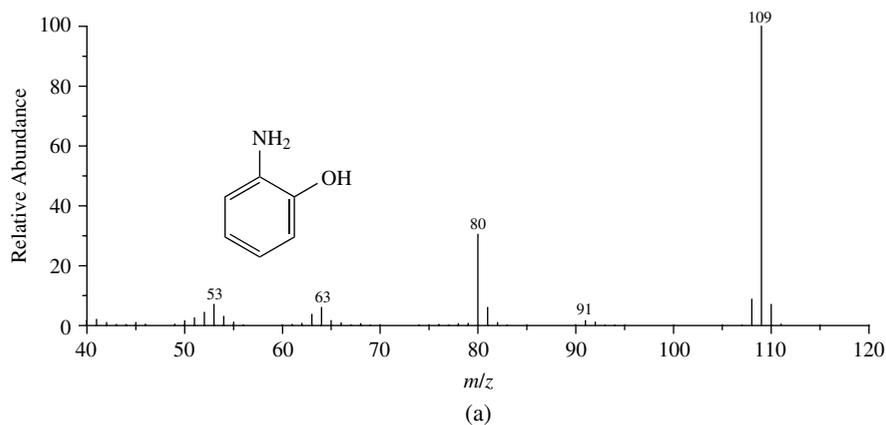
FIGURE 3. 70 eV EI mass spectra of isomeric hydroxyanilines: (a) *ortho*, (b) *meta*, (c) *para*. Adapted from Reference 40
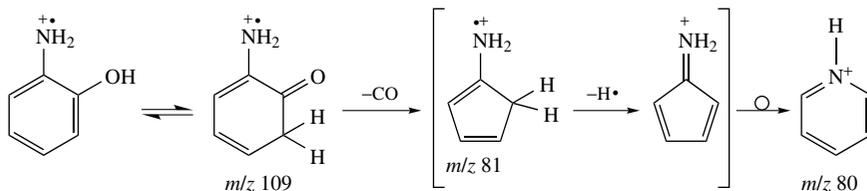
SCHEME 7

considerably different from that of the *meta* isomer. The main difference is related to the detection of an abundant fragment ion of m/z 91 $[M - HNC]^+$ for both the *ortho* and *para* isomers, whereas this fragment ion is nearly absent for the *meta* isomer (Scheme 8). The *meta* isomeric ion of m/z 91 seems therefore to dissociate much more readily by H loss to form the ion of m/z 90 (a '*meta* effect') and this tendency may be interpreted

(a)

(b)
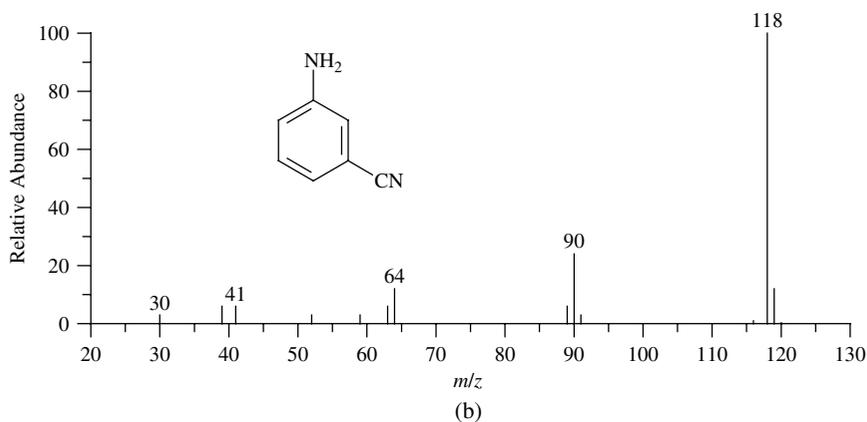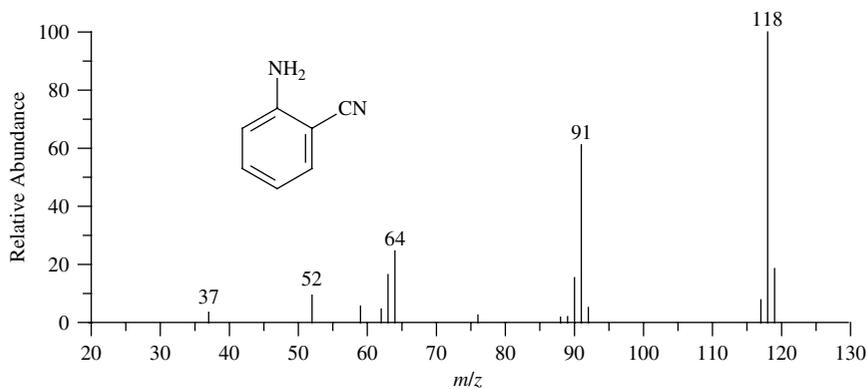
FIGURE 4. 70 eV EI mass spectra of isomeric cyanoanilines: (a) *ortho*, (b) *meta*, (c) *para*. Adapted from Reference 40
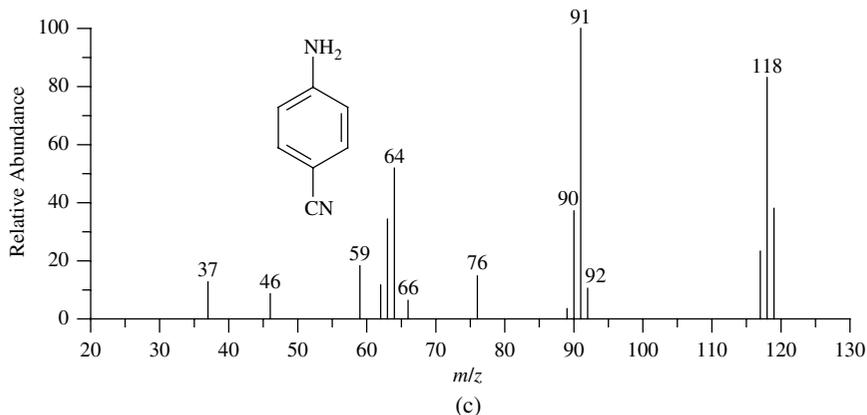
FIGURE 4. (*continued*)

as lack of resonance stabilization with the nitrogen, which is available only for the *ortho* (Scheme 8) and *para* isomers. We suggest that the nascent ion of m/z 90 is likely to be unstable and may isomerize to a more stable species, perhaps to a 'benzyne-like' form of the aza-tropylium ion such as that shown in Scheme 8.
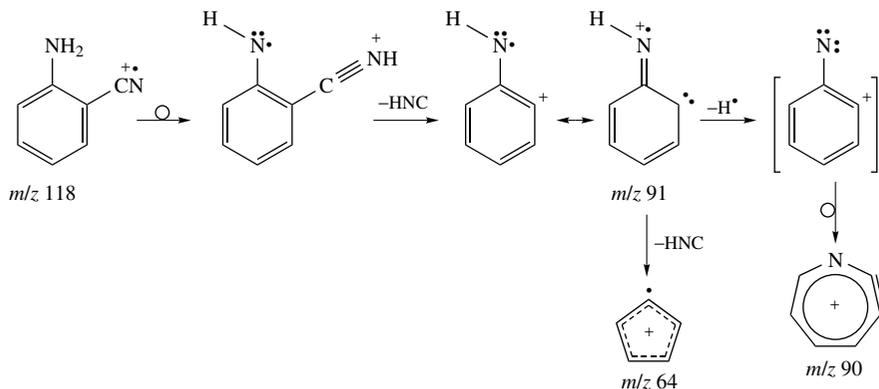
SCHEME 8

E. Halogenated Anilines

The 70 eV EI-MS of the three isomeric *ortho-, meta-* and *para*-halogenated anilines are very similar, and only weak effects are induced by the different positions of the halogen on the aniline ring. To evaluate the effect of the nature of the halogen substituent on dissociation patterns, the spectra of the *para* substituted fluoro, chloro and bromo anilines are collected in Figure 5. Again in these spectra the molecular ion is quite abundant, being detected as characteristic pairs of isotopologue ions for the chloroaniline (^{35}Cl and ^{37}Cl in a ratio of nearly 3:1) and bromoaniline (^{79}Br and ^{81}Br in a ratio of nearly 1:1). The most striking difference is related to the abundance of the fragment ions formed
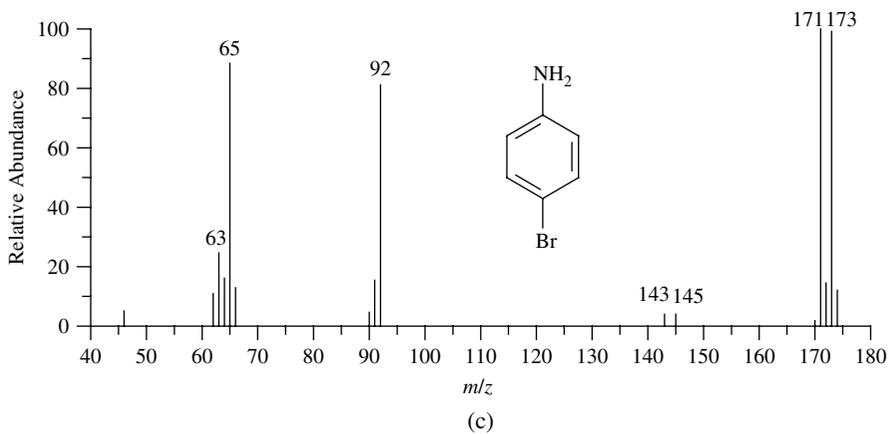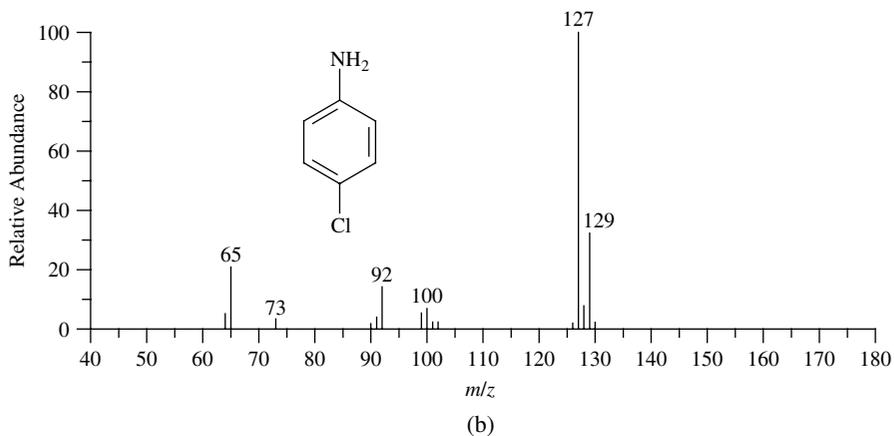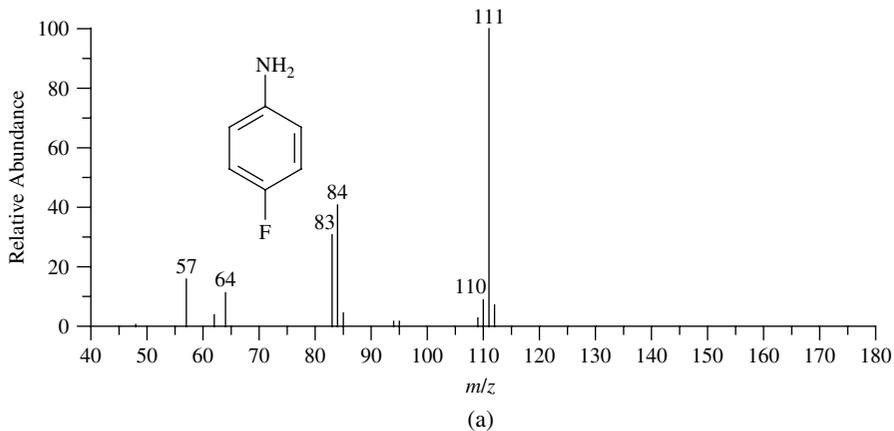
FIGURE 5. 70 eV EI mass spectra of *para*-halogenated anilines: (a) *para*-fluoroaniline, (b) *para*-chloroaniline, (c) *para*-bromoaniline. Adapted from Reference 40
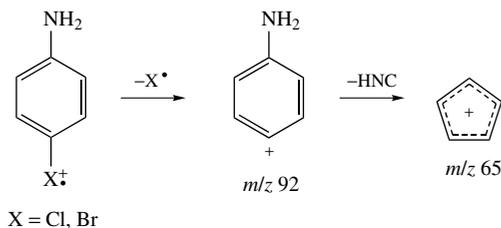
SCHEME 9

upon halogen atom loss, that is, $[M - X]^+$ of m/z 92 as well as $[M - X - HNC]^+$ of m/z 65 (Scheme 9). These fragments are not detected for *p*-fluoroaniline (Figure 5a), are of medium abundance for *p*-chloroaniline (Figure 5b) and quite prominent for the *p*-bromoaniline (Figure 5c). The more facile loss of halogen, in the order Br > Cl > F, can be rationalized by considering the well-known trend in the C−X bond energies, that is C−Br (284 kJ mol^{-1}) < C−Cl$^-$ (339 kJ mol^{-1}) < C−F (485 kJ mol^{-1})[1].

Conversely, the fragment ions formed by losses of HNC (m/z 84) and HNC plus H (m/z 83) are dominant for ionized fluoroaniline (Scheme 10). However, their relative abundance decreases significantly for chloroaniline (m/z 100/102 and 101/99) and bromoaniline (m/z 144/146 and 143/145).
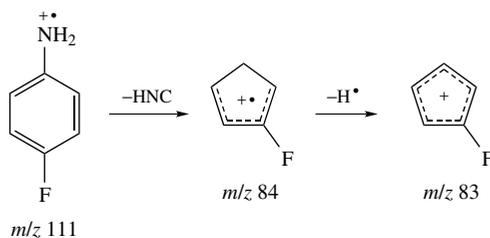
SCHEME 10

F. Alkylanilines

If an aliphatic or alicyclic group is connected to the aniline ring, another typical and frequent dissociation channel is opened, viz. benzylic cleavage[44,45]. This cleavage, which often dominates over or suppresses completely the dissociation pathway leading to the loss of HNC, can prevail regardless of the position of the alkyl substituent. It is, however, particularly favored when the aliphatic group is located *ortho* or *para* to the amino group, allowing for the formation of thermodynamically stable *ortho*- and *para*-aminobenzylic cations. For instance, the loss of H from the molecular ions of *ortho*-, *meta*- and *para*-methylanilines yields the corresponding aminobenzylic cations of m/z 106, an abundant fragment in the respective EI-MS (Figure 6). Furthermore, the *nascent* aminobenzylic cation is likely to isomerize to the ring-expanded aromatic aminotropylium ion (Scheme 11). The isomerization of benzylium-type ions to the more stable, fully aromatic tropylium-type ions depends on the internal energy content of the nascent ion and this intricate process has been extensively studied both experimentally and theoretically[46–50] in a long series of studies on this classic and fundamental dichotomy in gas-phase ion chemistry[51]. A recent theoretical calculation at the B3LYP/6-31G(d,p)
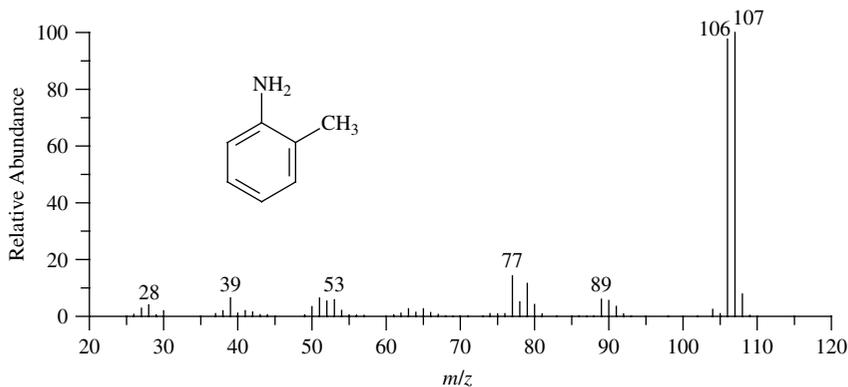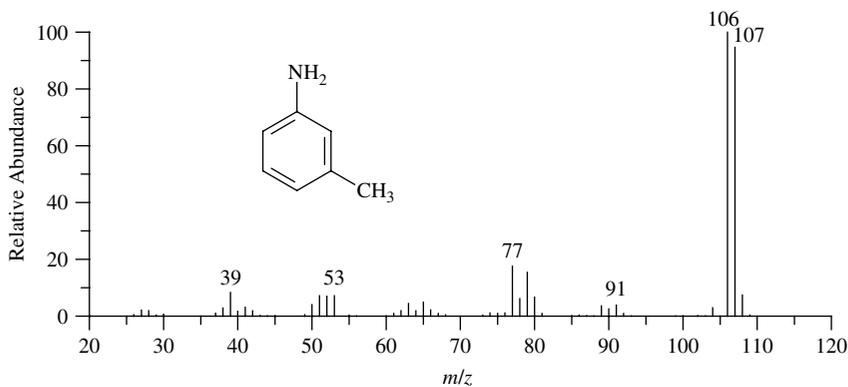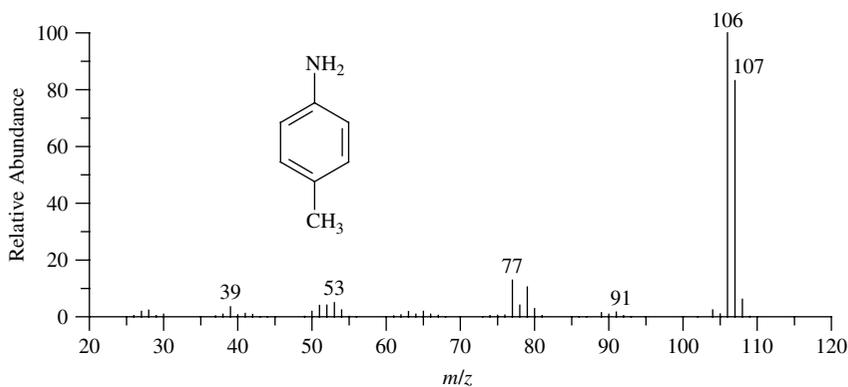
FIGURE 6. 70 eV EI mass spectra of isomeric methylanilines: (a) *ortho*, (b) *meta*, (c) *para*. Adapted from Reference 40

SCHEME 11
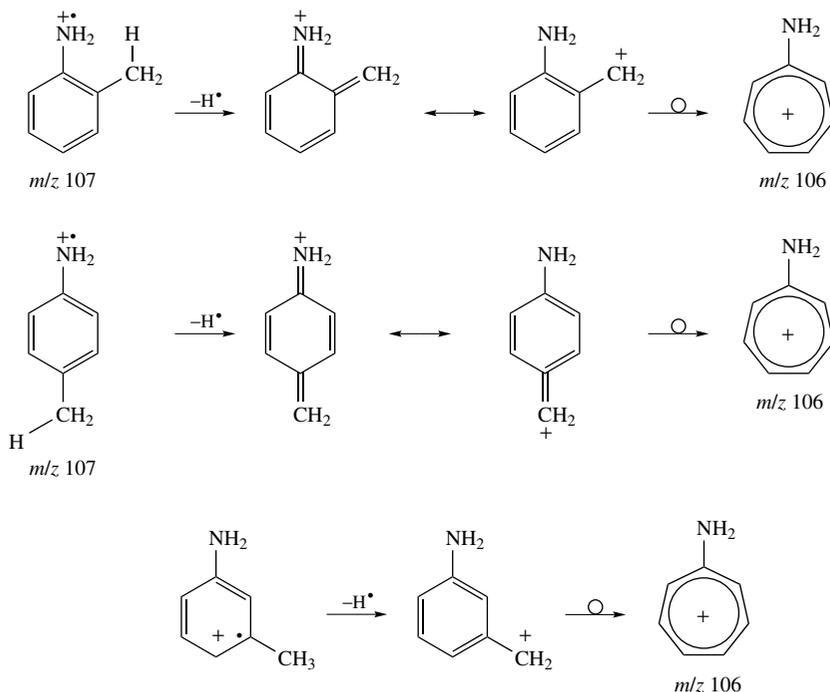
level has estimated this isomerization barrier to lie 287.9 kJ mol^{-1} above the benzylium ion, and the tropylium ion to lie -38.1 kJ mol^{-1} below the benzylium ion[52].

Due to this favored α-cleavage dissociation, branching at the alkyl chain is readily recognized among isomers, as Figure 7 exemplifies by the EI-MS of the pair of 4-n-Bu and 4-t-Bu anilines. Note, however, that α-cleavage is also a dominant process for N-alkylanilines in spite of the formation of the less stable N-phenylimmonium ions (Scheme 12). Consequently, ring and N-substituted isomeric anilines tend to display similar EI-MS. This tendency is exemplified by the EI-MS of the constitutional isomers 4-n-butylaniline (Figure 7a) and N-n-butylaniline (Figure 7c) as well as the EI-MS of N-methyl-n-propylaniline (Figure 8a) and 4-isobutylaniline (Figure 8b). Note that the immonium ions display a chemically saturated nitrogen; hence they cannot disperse the positive charge by resonance with the benzene ring. This similarity makes the location of alkyl substituents in anilines rather less definitive using by EI-MS analysis.

In the EI-MS of N-methylaniline and N,N-dimethylaniline (Figure 9), the most abundant fragment ions are the immonium ions of m/z 106 and m/z 120, respectively. These ions are formed by H loss owing to α-cleavage (Scheme 13), and dissociate further to the phenyl cation of m/z 77. Less abundant fragments of m/z 105 and 104 are also observed in the EI-MS of N,N-dimethylaniline (Figure 9b). The formation of the fragment ion of m/z 105 can be ascribed to result from the elimination of a neutral methane molecule. Additionally, the ion of m/z 105 may lose H to generate the fragment ion of m/z 104 (Scheme 14).
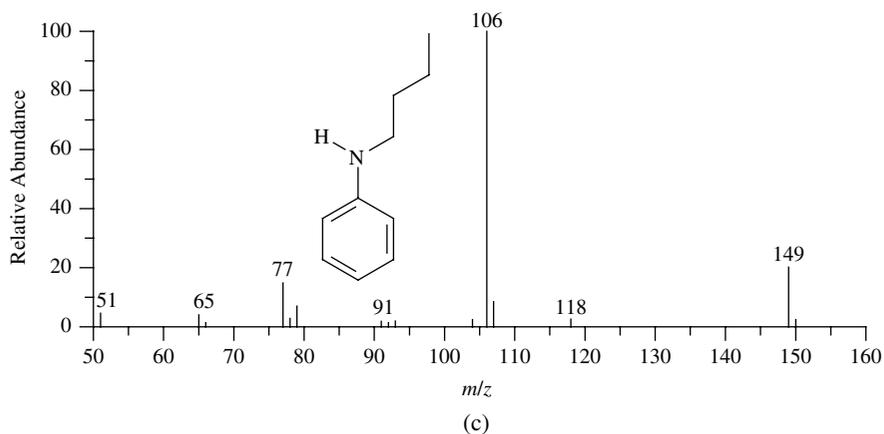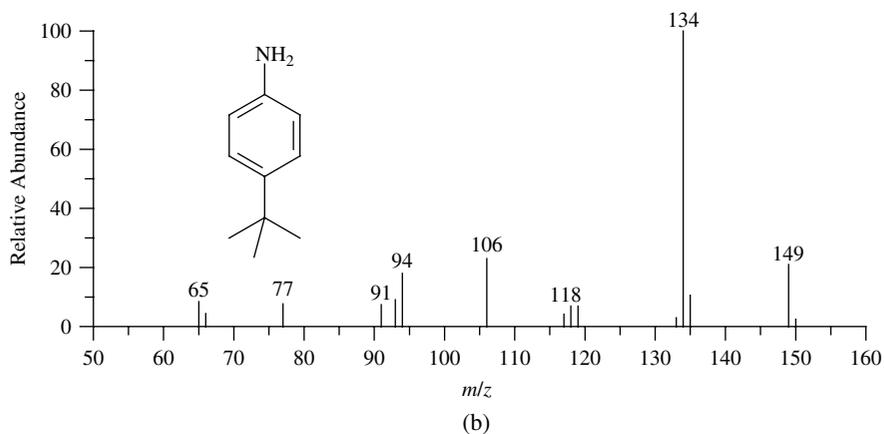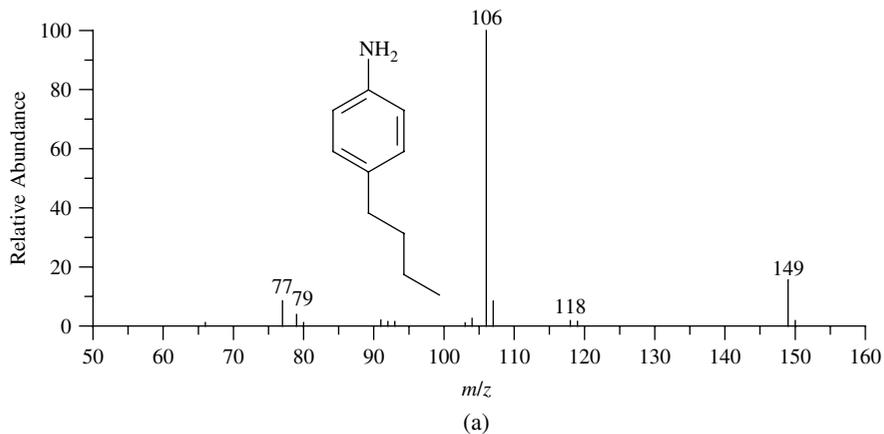
FIGURE 7. 70 eV EI-MS of (a) 4-*n*-butylaniline, (b) 4-tertbutylaniline and (c) *N*-*n*-butylaniline. Adapted from Reference 40

SCHEME 12

(a)
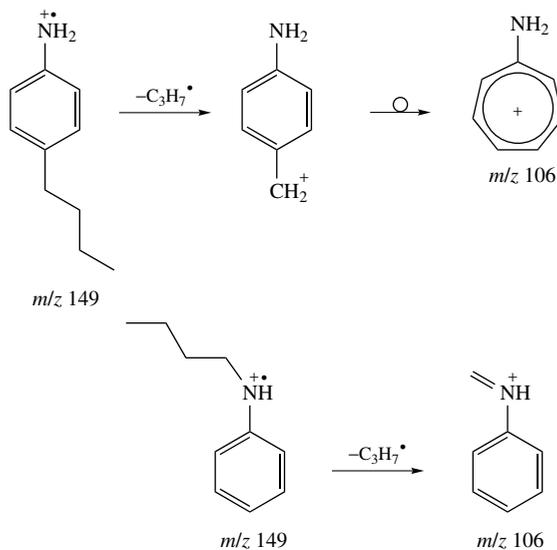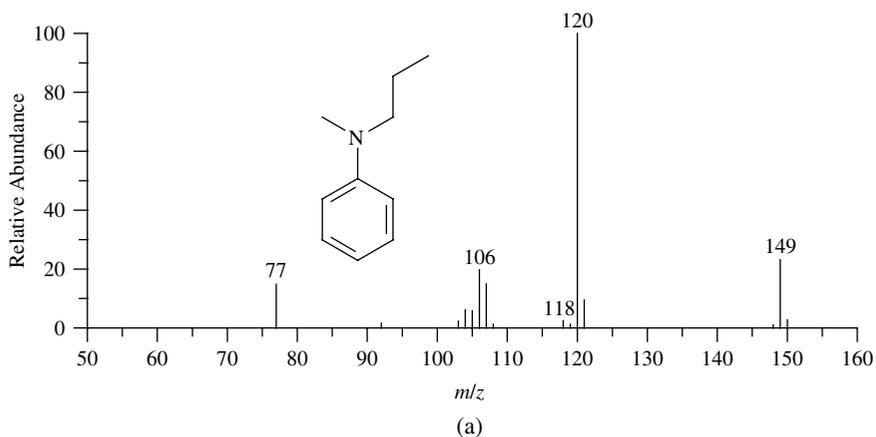
FIGURE 8. 70 eV EI-MS of (a) *N*-methyl-*n*-propylaniline and (b) 4-isobutylaniline. Adapted from Reference 40

(b)

FIGURE 8. (*continued*)

(a)

(b)
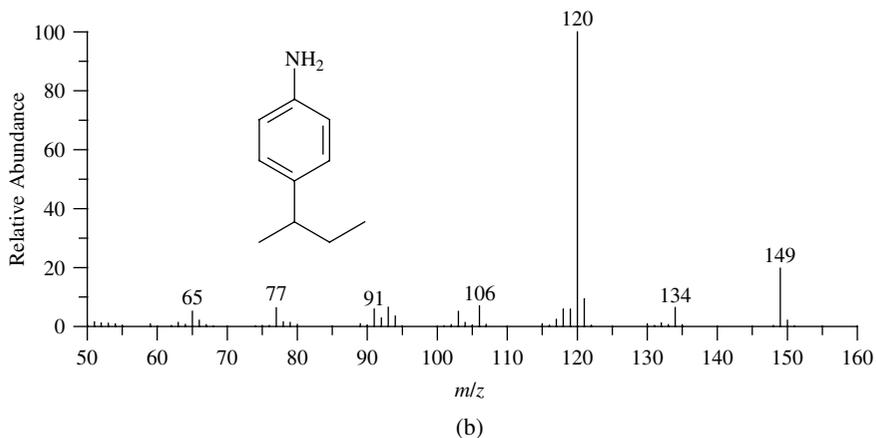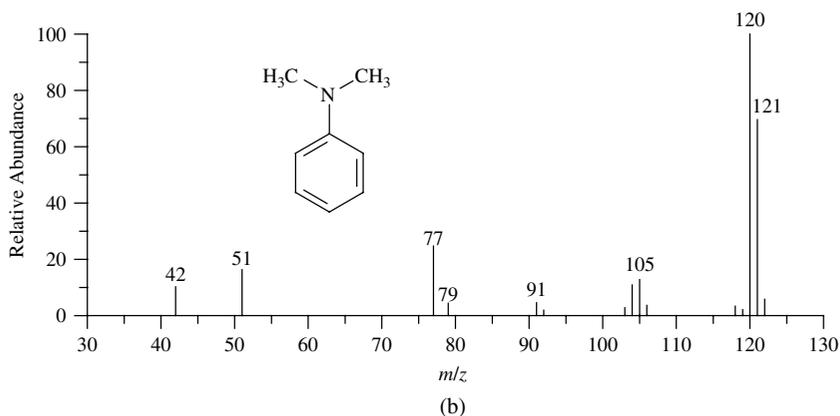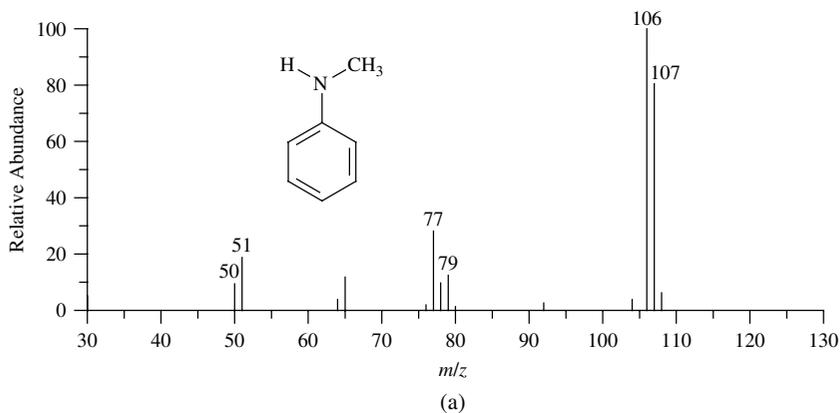
FIGURE 9. 70 eV EI-MS of (a) *N*-methylaniline and (b) *N*,*N*-dimethylaniline. Adapted from Reference 40

$$R = H; \; m/z \; 107 \qquad\qquad R = H; \; m/z \; 106 \qquad\qquad m/z \; 77$$
$$R = CH_3; \; m/z \; 121 \qquad\qquad R = CH_3; \; m/z \; 120$$

SCHEME 13

$$m/z \; 121 \qquad\qquad m/z \; 105 \qquad\qquad m/z \; 104$$
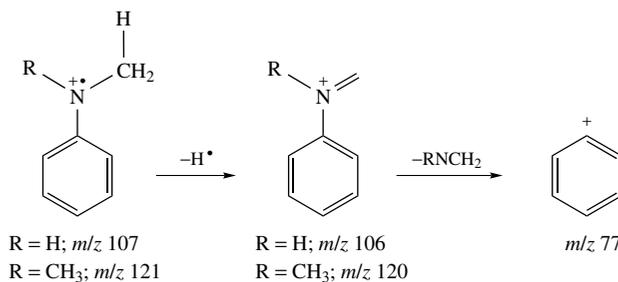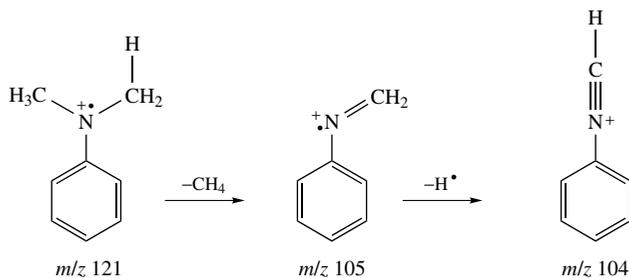
SCHEME 14
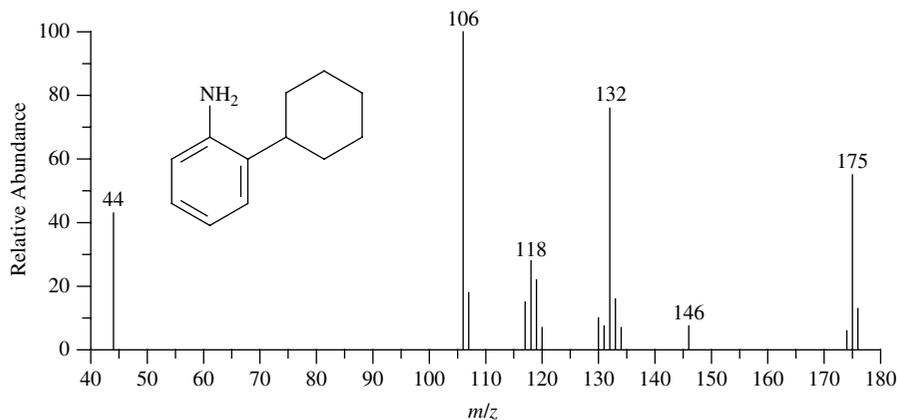
FIGURE 10. 70 eV EI-MS of *ortho*-cyclohexylaniline. Adapted from Reference 40

The EI-induced dissociation of cycloalkyl-substituted anilines, such as *ortho*-cyclohexylaniline (Figure 10), is also governed by the favored benzylic α-cleavage. However, the initial rupture of a benzylic C—C bond forms no fragments leading then to rearrangement of the molecular ion. The nascent rearranged distonic ion suffers subsequent isomerization via a [1,5-H] shift, generating a resonance-stabilized radical cation, which dissociates by the loss of a $C_3H_7^{\bullet}$ radical to form the stabilized fragment ion of m/z 132.
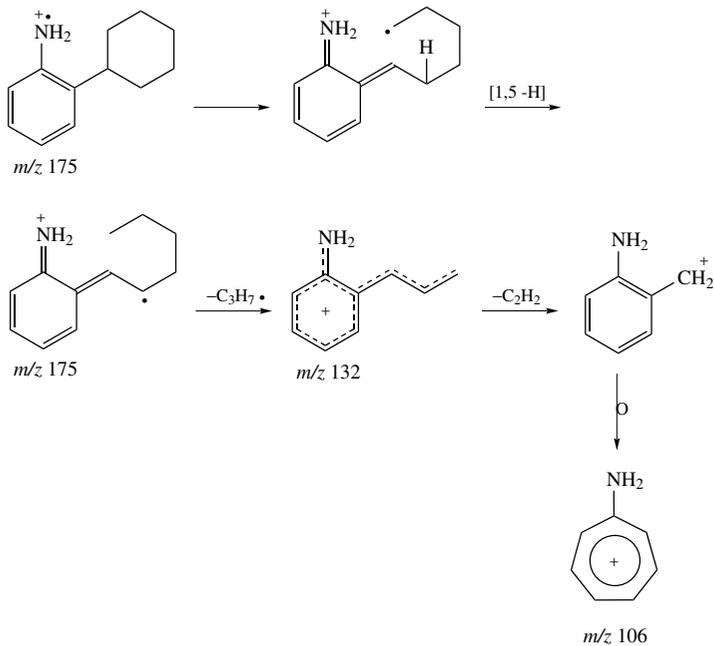
SCHEME 15
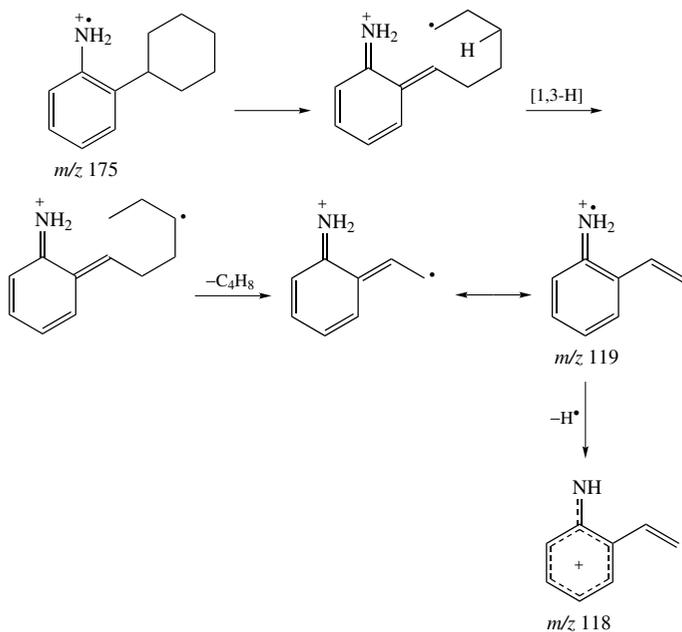
SCHEME 16

This ion probably loses acetylene yielding the aminotropylium ion of m/z 106, which is the most abundant fragment ion (Scheme 15). Furthermore, two less-abundant but also structurally diagnostic ions of m/z 119 and m/z 118 are also detected (Figure 10). These ions are likely produced via an initial [1,3-H] shift followed by the loss of a neutral molecule of C_4H_8 and then H (Scheme 16).

Long-chain *meta*-substituted alkylanilines exhibit, in addition to the benzylic α-cleavage that forms the fragment ion of m/z 106, a highly characteristic dissociation behavior under EI conditions. This structurally diagnostic dissociation allows distinguishing easily the *meta* isomers from the *para* and *ortho* isomers, as Figure 11 illustrates. This process for *n*-hexylanilines is actually an interesting case of a *meta* effect (see Section IV for *ortho* effects), representing a special case of the McLafferty rearrangement[20], and yields an intense fragment ion of m/z 107. It likely involves a [1,5-H] shift from the γ position followed by the elimination of an alkene molecule (Scheme 17). By contrast to the *meta*
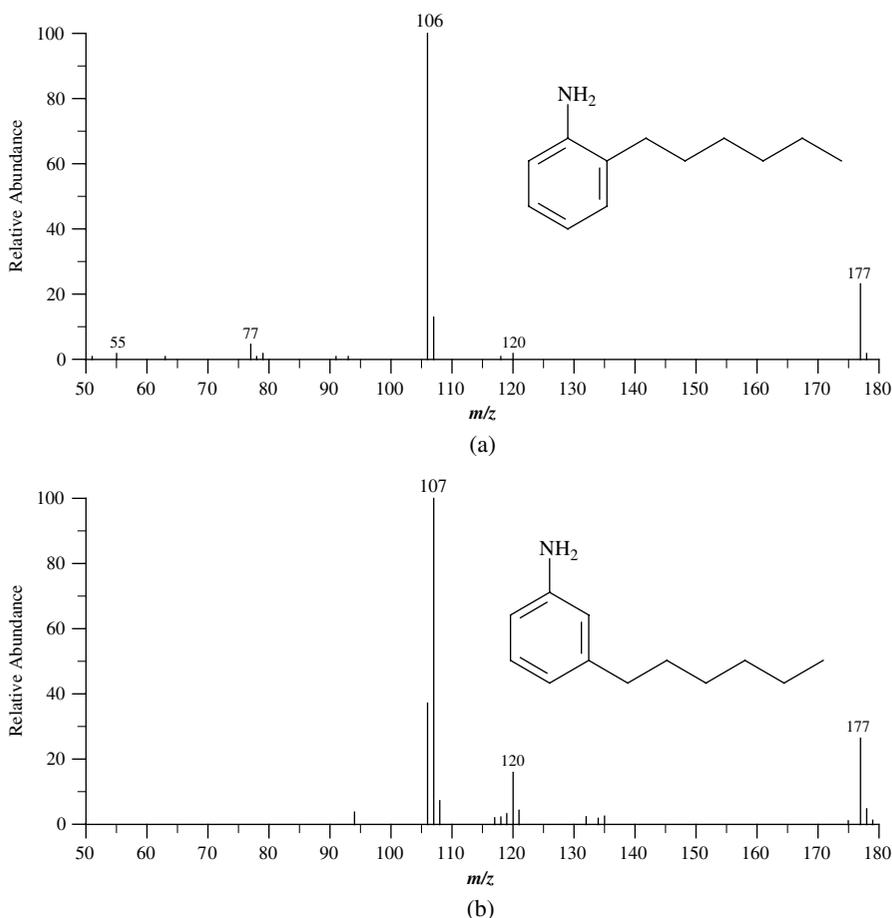
FIGURE 11. 70 eV EI-MS of (a) *ortho-n*-hexylaniline, (b) *meta-n*-hexylaniline, (c) *para-n*-hexylaniline. Adapted from Reference 40
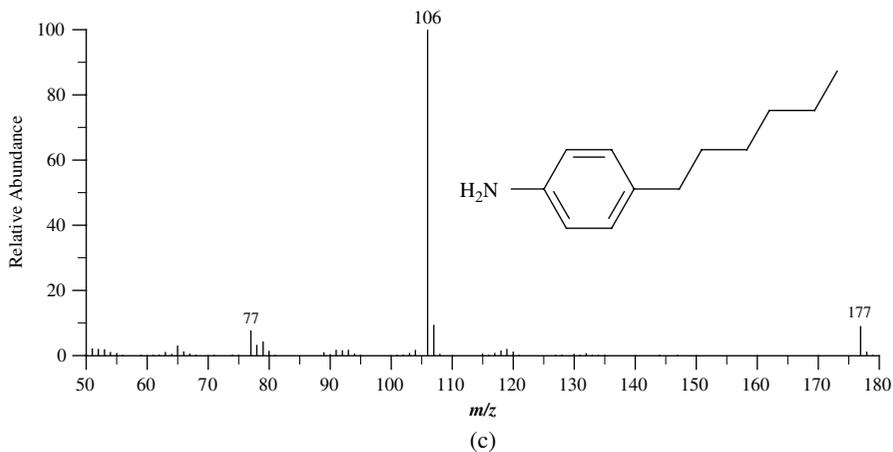
FIGURE 11. (*continued*)
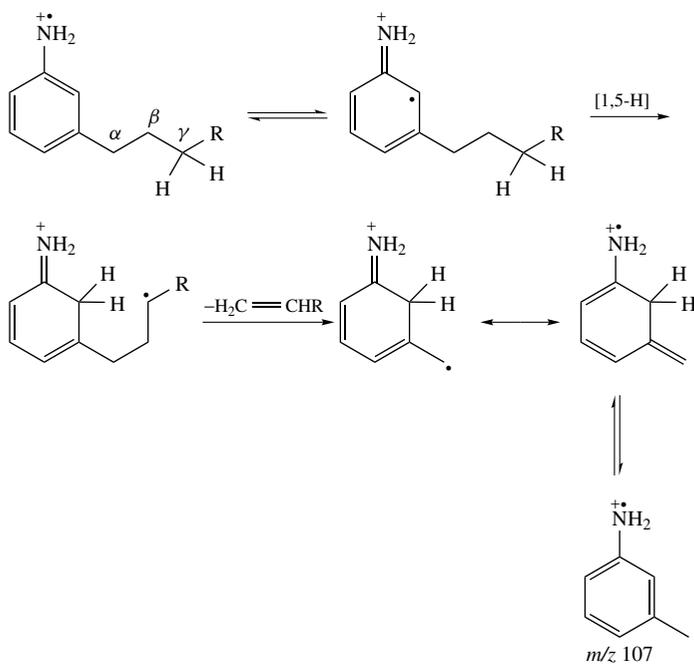
SCHEME 17

isomer, the EI-MS of both the *ortho* and *para* isomers display very abundant ions of
m/z 106 which are likely the highly-stabilized *ortho*- and *para*-aminobenzyl cations (or
the rearranged aminotropylium ion, or a mixture of both) formed by benzylic α-cleavage
(Scheme 12).

IV. *Ortho* EFFECTS IN SUBSTITUTED ANILINES

EI-MS of *ortho*-substituted anilines may differ significantly from those of the *meta* and *para* isomers and, in most cases, by a single and major fragment ion. This *ortho* effect is therefore of great value for structural elucidation and has been studied mechanistically in great detail[53, 54]. The structural assignment is, however, not always unequivocal and comparison with the spectra of all isomers is normally required. We present below a set of representative examples to illustrate the main features of this interesting and important effect in the unimolecular ion chemistry of anilines.

The dissociation of the molecular ions of the isomeric hydroxymethylanilines is used as the first illustrative example (Figure 12). Loss of water from the ionized *ortho* isomer to form the $[M - H_2O]^{+\bullet}$ fragment ion of m/z 105 is greatly favored owing to the *ortho* position of the hydroxyl substituent that allows for intramolecular [1,5-H] shift. This ion subsequently loses either a hydrogen atom or a HNC molecule to yield two equally prominent fragment ions of m/z 104 and 78, respectively. Scheme 18 displays rationalizations for such losses.

(a)

(b)
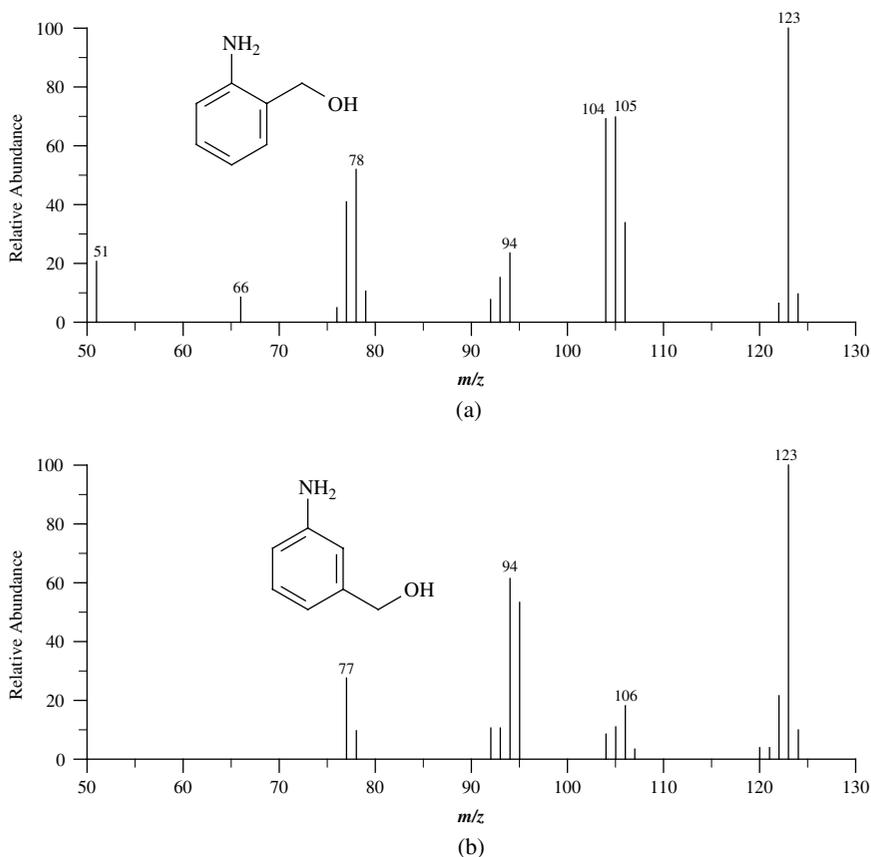
FIGURE 12. 70 eV EI mass spectra of isomeric hydroxymethylanilines: (a) *ortho*, (b) *meta*, (c) *para*. Adapted from Reference 40

(c)
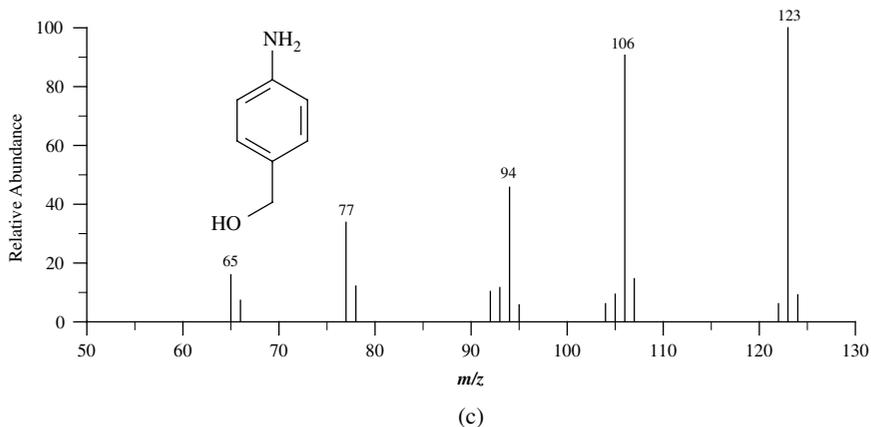
FIGURE 12. (*continued*)
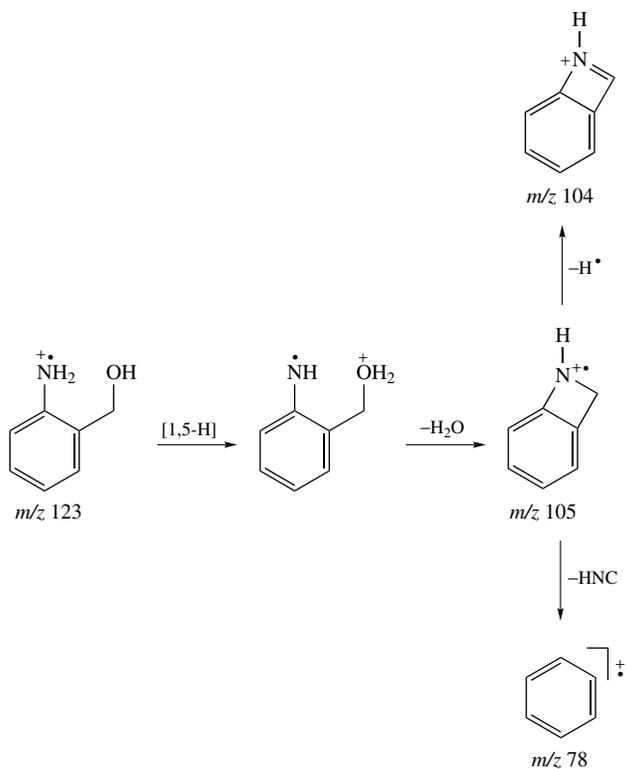
SCHEME 18

The fragment ion of m/z 105 is, by contrast, of much lower abundance in the EI-MS of the *meta* and *para* isomers (Figure 12). The main dissociation pathway for the *para* isomer occurs by OH loss to form the fragment ions of m/z 106, whereas for the *meta* isomer the consecutive losses of CO plus H to form the fragment ion of m/z 94 (assumed to be protonated aniline) dominates (Scheme 19).
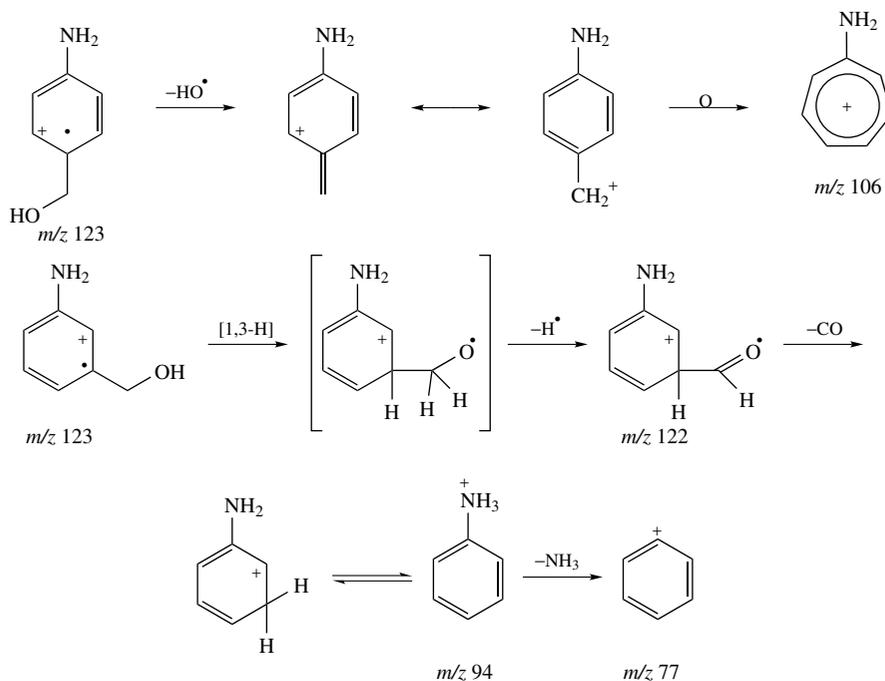
SCHEME 19

The *ortho* specificity is clearly noted in the EI-MS of aminobenzoic acids and aminobenzamides owing to particularly strong *ortho* effects. For instance, the respective losses of H_2O and NH_3 from the molecular ions of *ortho*-aminobenzoic acid (Figure 13a) and *ortho*-aminobenzamide (Figure 14a) are characteristic and greatly favored processes, as rationalized in Scheme 20. The fragments arriving from the concurrent ubiquitous (hence configuration-unspecific) dissociation, viz. the successive losses of $HX^{\bullet}$ and CO to yield the fragments of m/z 120 and mainly m/z 92 (Scheme 20), are clearly seen in the EI-MS of the three isomers (Figures 13 and 14).

Note that a relatively much more abundant fragment ion of m/z 120 is detected in the EI-MS of the *para* isomers owing probably to greater stability (hence less further dissociation by CO loss to form the fragment ion of m/z 92) provided by charge stabilization via resonance with the *para*-amino group (Scheme 21). The *meta*-amino group cannot stabilize the charge and thus destabilizes the ion inductively via its electron-withdrawing effect.

Ortho-benzylanilines fail to display even a moderate *ortho* effect. Although loss of benzene constitutes a characteristic dissociation channel for many arylaliphatic radical
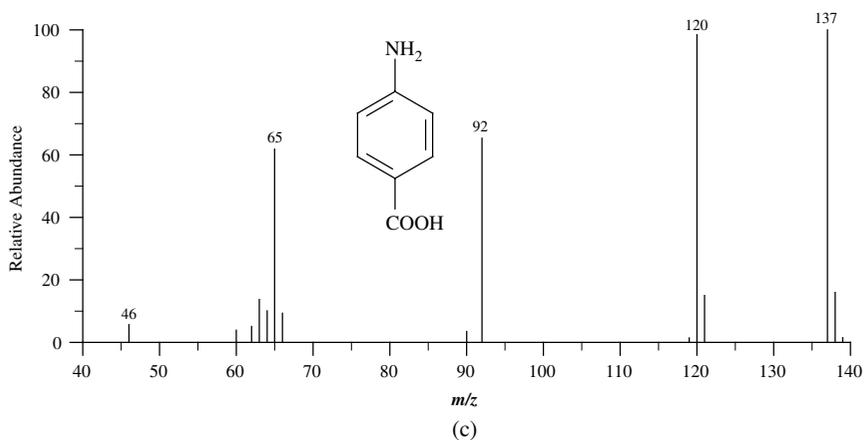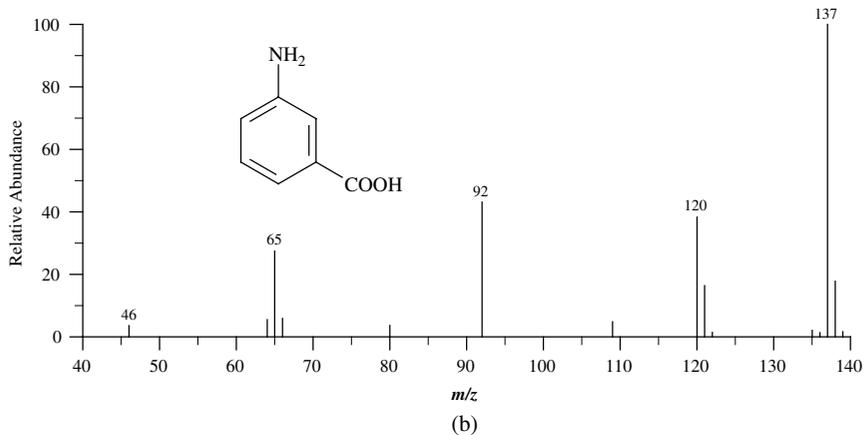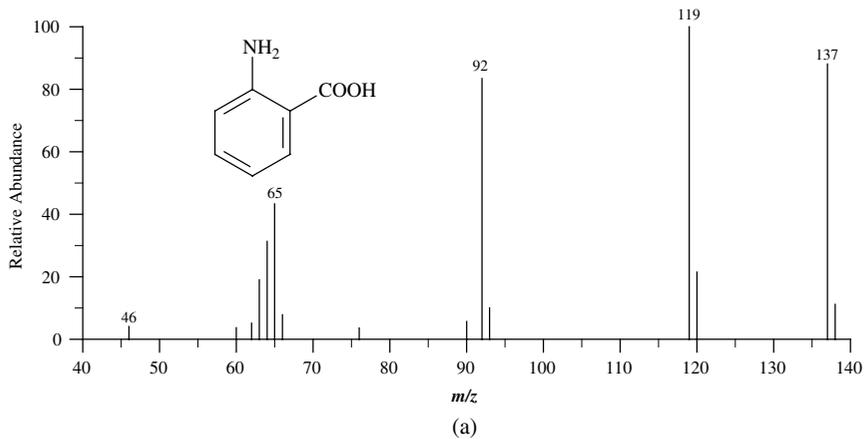
FIGURE 13. 70 eV EI mass spectra of isomeric aminobenzoic acids: (a) *ortho*, (b) *meta*, (c) *para*. Adapted from Reference 40
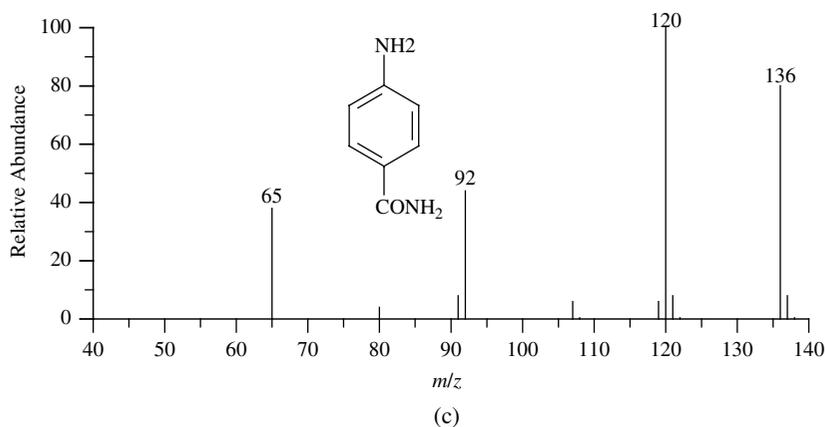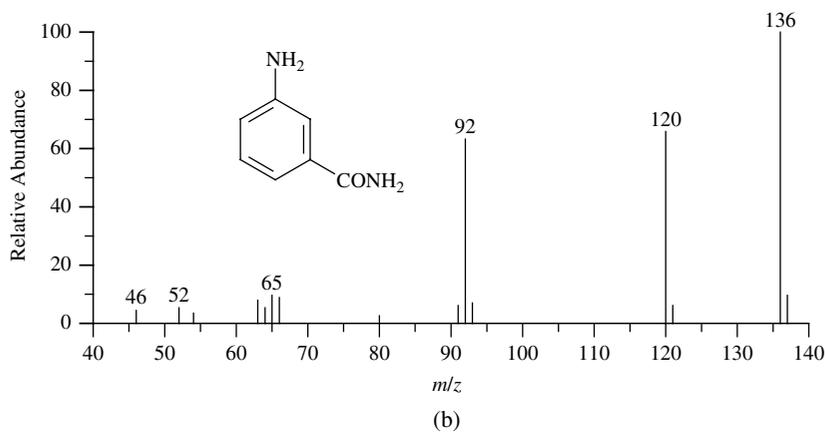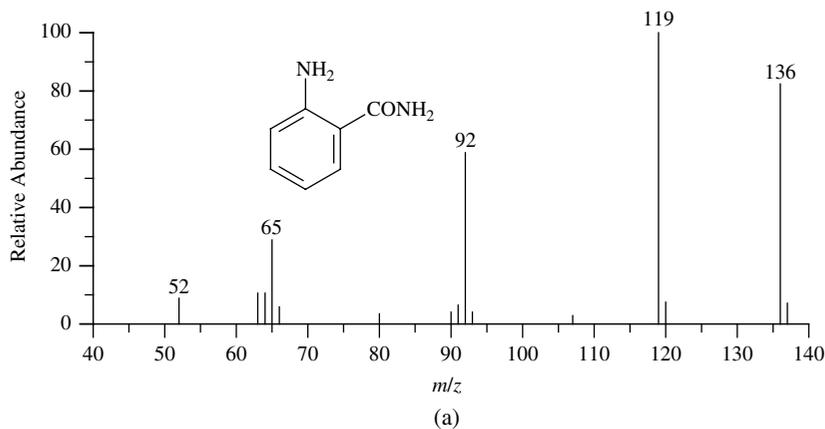
FIGURE 14. 70 eV EI mass spectra of isomeric aminobenzamides: (a) *ortho*, (b) *meta*, (c) *para*. Adapted from Reference 40

X = O; *m/z* 137
X = NH; *m/z* 136
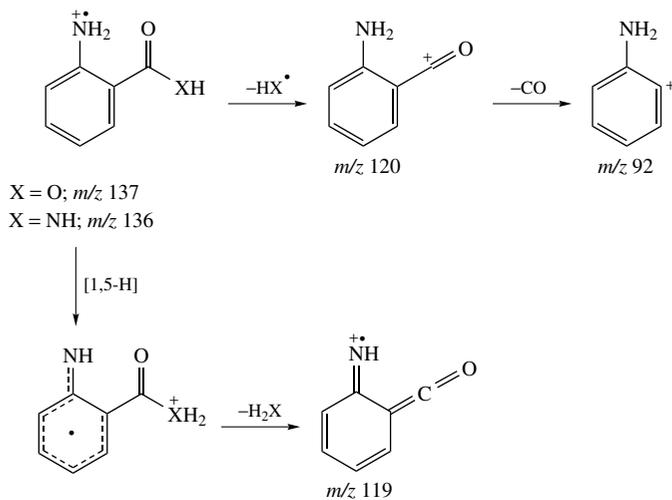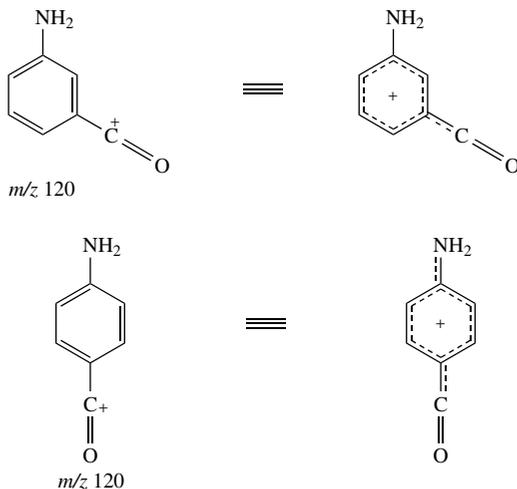
SCHEME 20

SCHEME 21

cations and protonated alkylbenzenes[39, 55−57], benzene is not as good a leaving group as water and ammonia and, as a consequence, competitive dissociation channels usually dominate. Thus, the EI-MS of the *ortho-* and *para*-benzylaniline are quite similar, as Figure 15 exemplifies for *ortho* isomer, in which the $[M − C_6H_6]^{+\bullet}$ fragment of *m/z* 105 is barely detected. The competing dissociation channels yielding the $[M − H]^+$ and
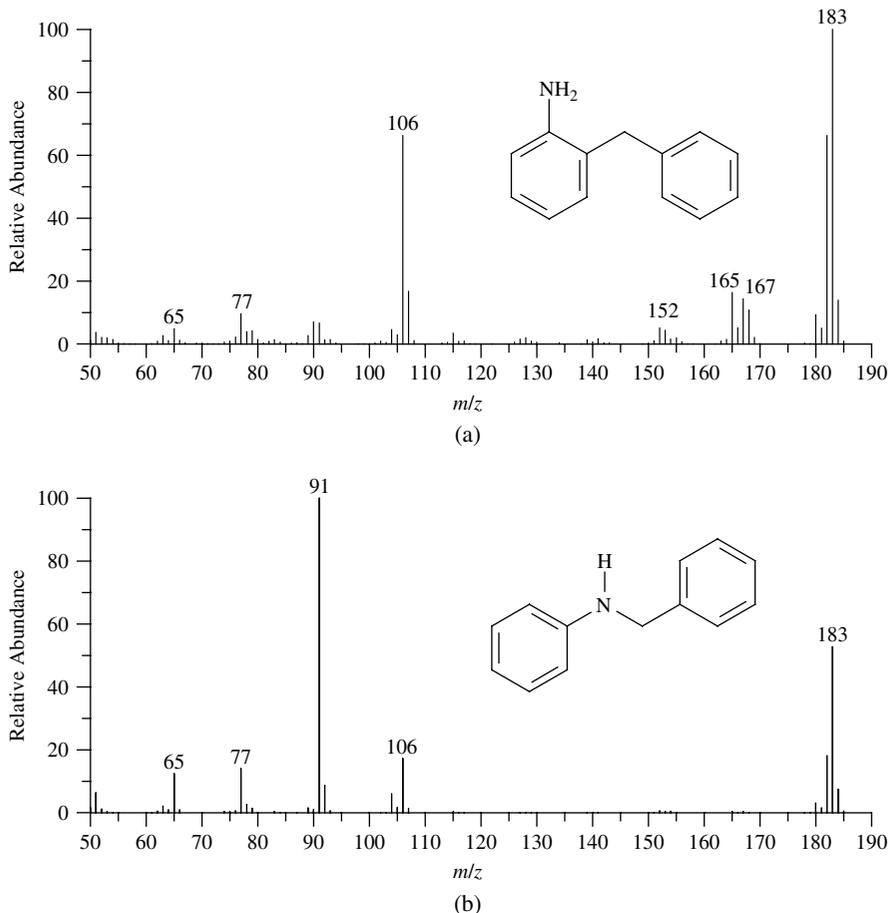
FIGURE 15. 70 eV EI mass spectra of (a) *ortho*-benzylaniline and (b) *N*-benzylaniline. Adapted from Reference 40

$[M - C_6H_5]^+$ fragment ions of m/z 182 and m/z 106 (Scheme 22), respectively, are two of the most important. The nascent benzylic cations may isomerize further to more stable substituted tropylium ions. By contrast, the *N*-benzylic isomer is easily recognized since its EI-MS (Figure 15b) is dominated by the fragment ion of m/z 91 and a reasonably abundant fragment ion of m/z 106 (Scheme 23).

Ortho effects are also very common for nitroanilines[58–64]. For instance, in the EI-MS of the parent nitroanilines, abundant molecular ions of m/z 138 are observed and, aside from differences in relative abundances, the three isomers give similar spectra (Figure 16) in which the fragment ions $[M - NO]^+$ of m/z 108, $[M - NO - CO]^+$ of m/z 80, $[M - NO_2]^+$ of m/z 92 and $[M - NO_2 - HNC]^+$ of m/z 65 are the most abundant. The *ortho*

m/z 106

−Ph•

m/z 183

−H•

m/z 182

m/z 182   and/or   m/z 182

SCHEME 22

m/z 183

−PhNH•

m/z 91

−Ph•

m/z 106
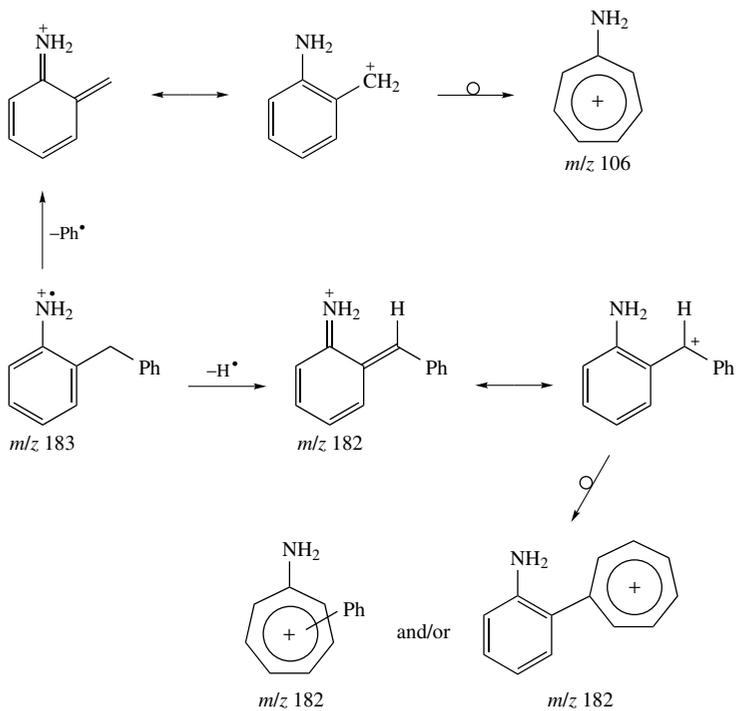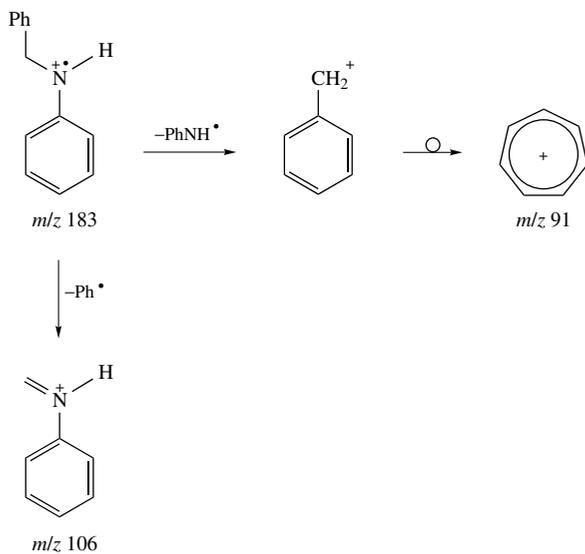
SCHEME 23
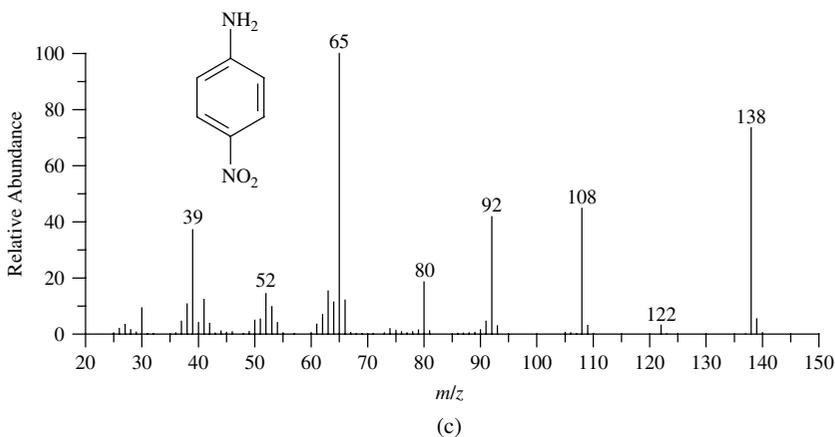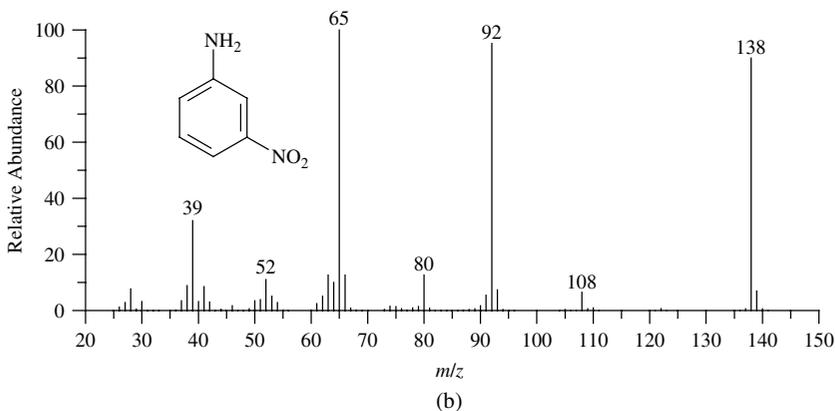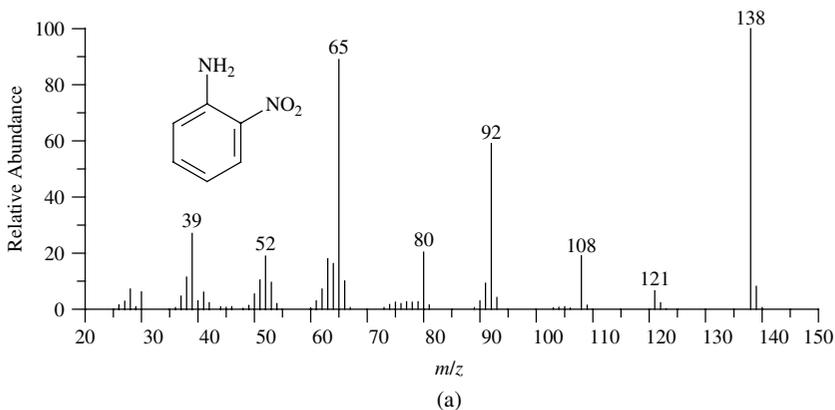
FIGURE 16. EI 70 eV mass spectrum isomeric nitroanilines (a) *ortho*, (b) *meta*, (c) *para*. Adapted from Reference 40

isomer is, however, differentiated by a low abundance but characteristic fragment ion of m/z 121 arising from OH loss. The *meta* and *para* isomers provide a minor fragment ion of m/z 122 via O loss (Scheme 24). Studies performed by using D-labeled substrates at the amino group as well as on the phenyl ring give evidence for a significant preference, enhanced in the metastable decomposition, of HO• loss from the hydrogen of the *ortho* amino group[59].

m/z 138

m/z 121

m/z 138

m/z 122
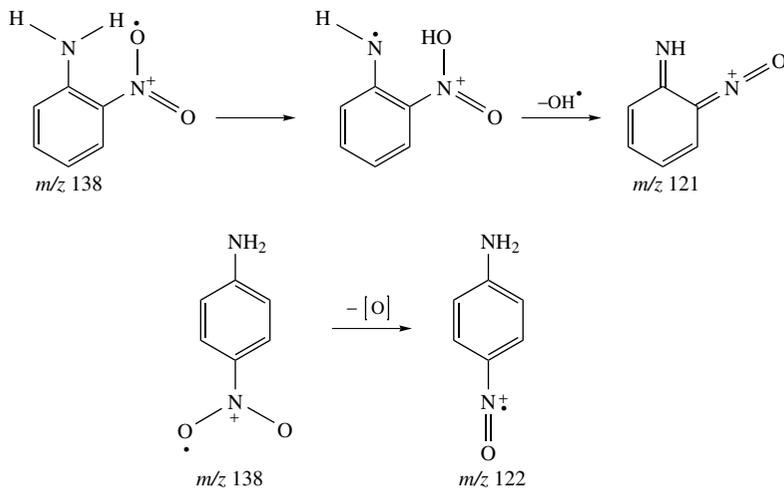
SCHEME 24

Figure 17 shows the EI-MS of the isomeric trifluoromethylanilines. Due to a pronounced *ortho* effect, the *ortho* isomer provides, upon EI-induced dissociation, two very abundant and characteristic fragment ions: $[M - HF]^{+\bullet}$ of m/z 141 and $[M - HF - HNC]^{+\bullet}$ of m/z 114 (Scheme 25). By contrast, the *meta* and *para* isomers are

(a)
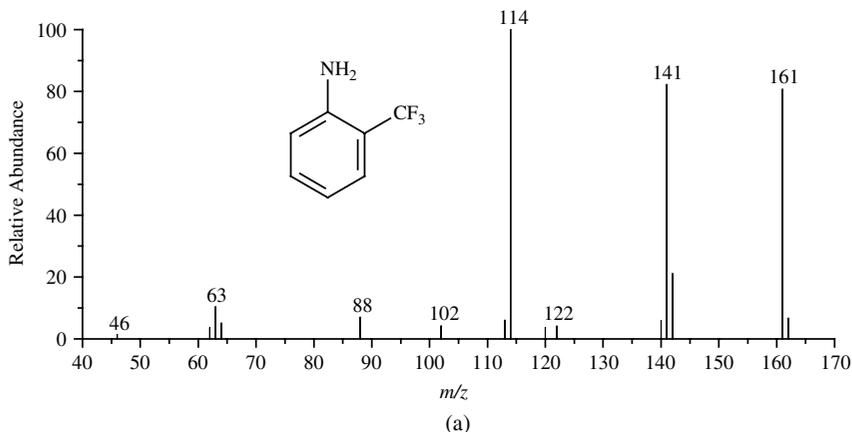
FIGURE 17. 70 eV EI mass spectra of isomeric trifluoromethylanilines: (a) *ortho*, (b) *meta*, (c) *para*. Adapted from Reference 40
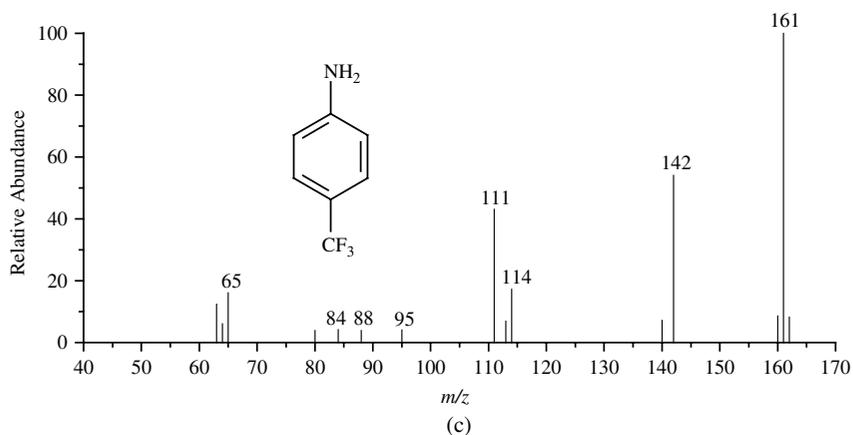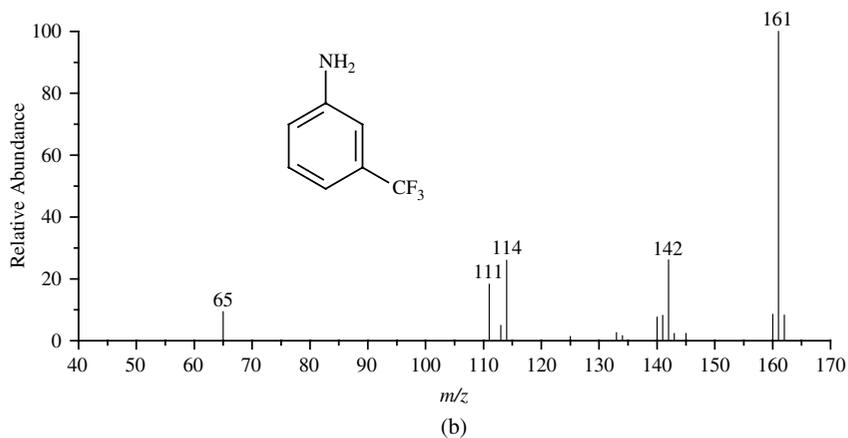
FIGURE 17. (*continued*)
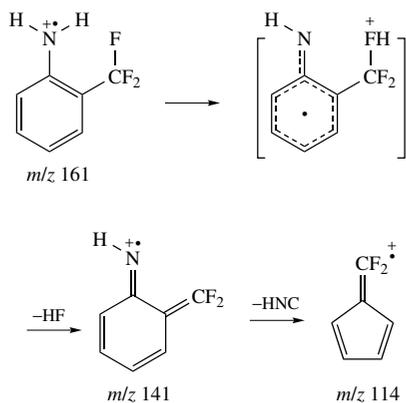
SCHEME 25

characterized by two major fragment ions: $[M - F]^+$ of m/z 142 and $[M - CF_2]^+$ of m/z 111. Loss of difluorocarbene (:CF_2) for the *meta* and *para* isomers (absent for the *ortho* isomer) is rare, and Scheme 26 presents a rationalization for such a remarkable dissociation. A detailed discussion involving several mechanistic aspects of the dissociation of similar systems, i.e. isomeric trifluoromethylphenols, has been given by Matsumoto and coworkers[65] and by Sekiguchi and coworkers[66].
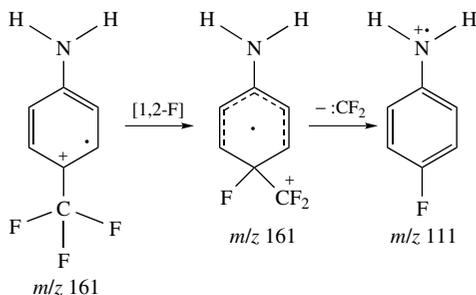
SCHEME 26

V. MISCELLANEOUS DISSOCIATIONS OF IONIZED ANILINES

It seems from the examples already provided that not only *ortho* effects, but in general any relative position of substituents in the aniline ring is often found to profoundly affect the dissociation chemistry of ionized anilines, thus providing distinct EI-MS for structural assignment. The EI-MS of the isomeric benzoylanilines (Figure 18) provide another illustrative set of such characteristic spectra. The EI-MS of the *N*-benzoyl isomer (Figure 18a) is dominated by the benzoyl ion of m/z 105 and its second-generation fragment ion of m/z 77, that is the phenyl cation formed by CO loss (Scheme 27).

(a)
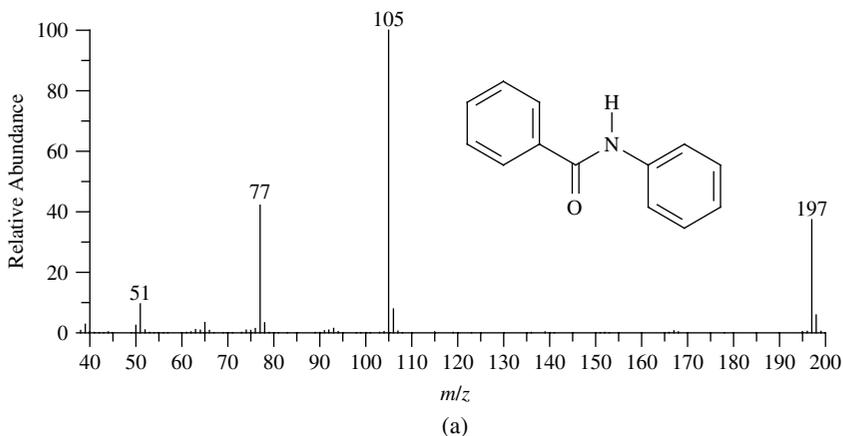
FIGURE 18. 70 eV EI mass spectra of: (a) *N*-phenylbenzamide, (b) *ortho*-aminobenzophenone, (c) *meta*-aminobenzophenone and (d) *para*-aminobenzophenone. Adapted from Reference 40

(b)

(c)

(d)
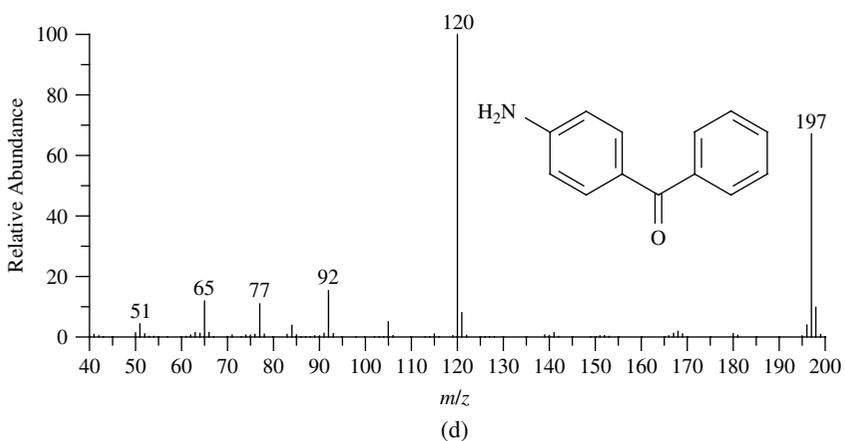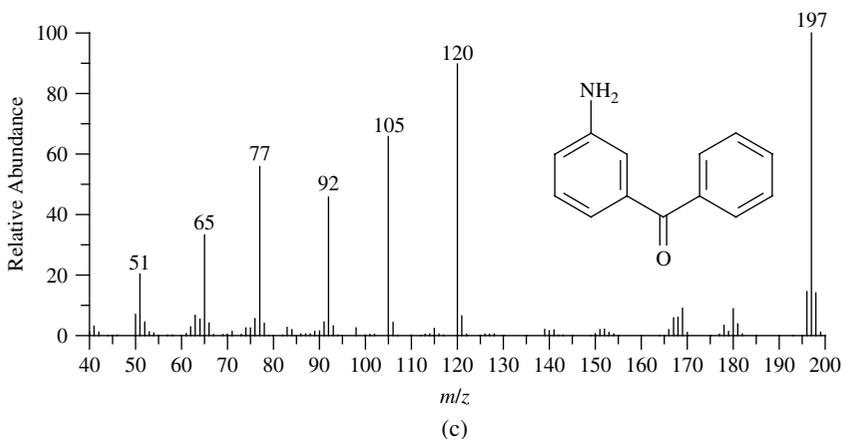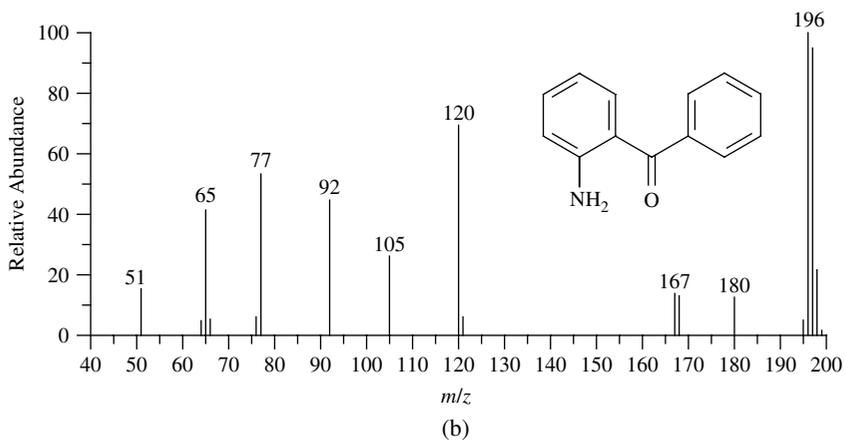
FIGURE 18. (*continued*)
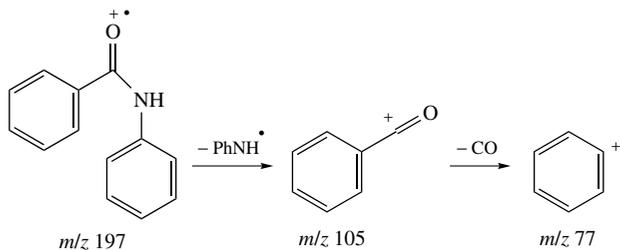
SCHEME 27
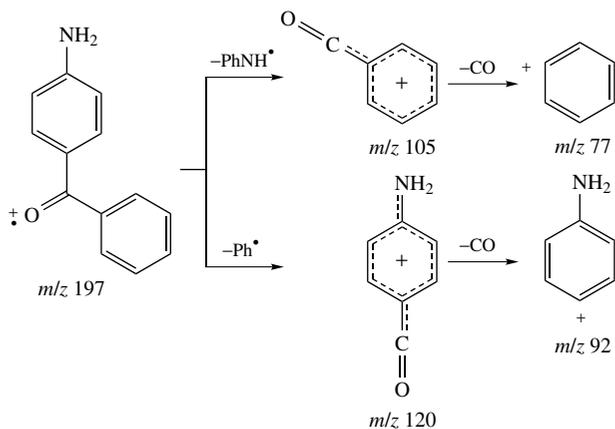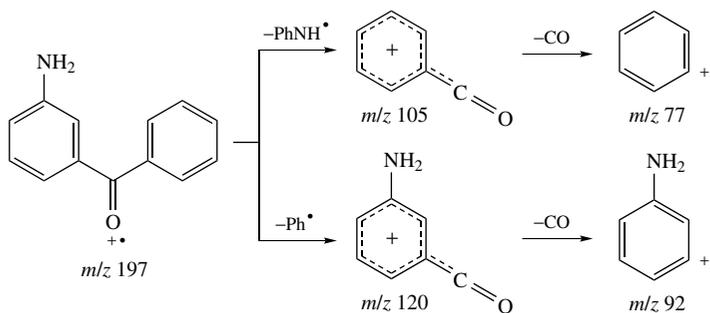
SCHEME 28

For the *ortho, meta* and *para* isomers, however, two dissociation routes compete (Scheme 28), i.e. that forming the pair comprised of the isomeric aminobenzoyl cations of *m/z* 120 and aminophenyl cations of *m/z* 92, and that forming the pair comprised of the benzoyl cation of *m/z* 105 and phenyl cation of *m/z* 77. Note that for the *ortho*

and, most particularly, the *para* isomer, the m/z 120/92 pair dominates owing to charge stabilization provided by resonance with the properly located amino group. For the *meta* isomer, by contrast, charge delocalization via resonance with the amino group is not available. Hence, the electron-withdrawing amino group tends to slightly destabilize the *m*-aminobenzoyl cation by an inductive effect, so that both dissociation channels (m/z 120/92 and 105/77 pairs) are nearly as important.

Cosimelli and coworkers[67] studied the 70 eV EI-MS of the isomeric anilines shown in Scheme 29. The molecular ions were observed to be quite abundant whereas the major fragment ions corresponded to $[M - NO]^{+\bullet}$, $[M - NO_2]^{+\bullet}$, $[M - HNO_2]^{+\bullet}$, $[M - OH]^{+\bullet}$ and $[M - X]^{+}$. Besides these relatively common dissociation modes, they also observed that these ionized anilines form, quite unexpectedly, $XC_6H_4O^{+}$ fragment ions. The formation of significant amounts of such fragments has also recently been observed for anilines bearing a strong electron-withdrawing or electron-donating substituent in the *para* position[64]. Their formation has been demonstrated to result from oxygen migration from the *ortho* nitro group to the aniline ring, as Scheme 30 illustrates for one such aniline derivative. Replacement of an aromatic or heteroaromatic nitrogen by oxygen from other sources such as carbonyl groups have been similarly observed[68–70], and the driving force for such an interesting rearrangement appears to be the stabilization of the *ortho*-quinonid structure[64, 68].

X = OH, NH$_2$, OCH$_3$, CH$_3$, Et, H, F, Cl, Br
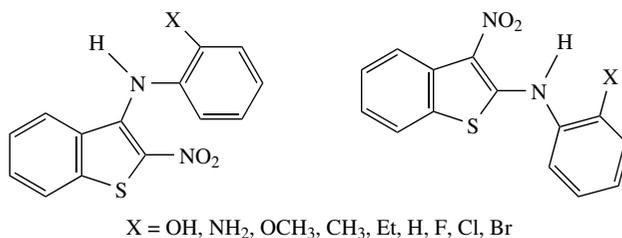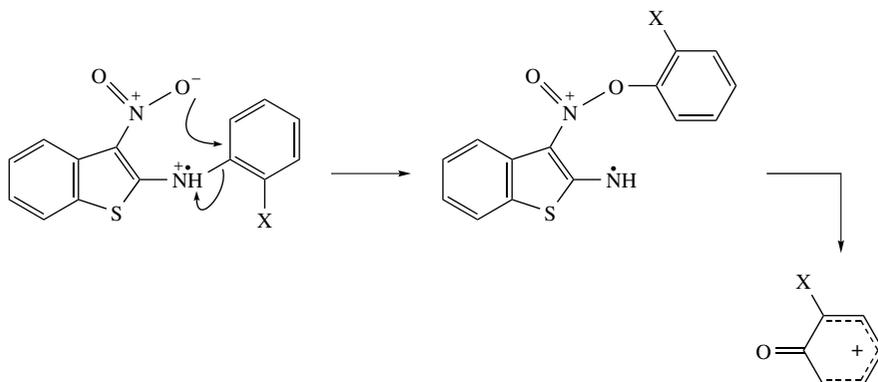
SCHEME 29

SCHEME 30

VI. CHEMICAL IONIZATION AND ELECTROSPRAY IONIZATION MASS SPECTROMETRY OF ANILINES

A. Chemical Ionization (CI-MS)

After the introduction of chemical ionization (CI) as an ionization method in mass spectrometry[71] using CH_4 as the source mainly for the protonating species CH_5^+, numerous other gases have been employed and found to protonate aniline as efficiently[72]. As a general rule, positive ion CI mass spectrometry of anilines is ruled by their diverse response toward proton addition and/or electrophilic attack by reactant ions of the CI plasma.

B. Site of Protonation of Anilines

The parent aniline molecule contains two basic centers that can accept an approaching proton, namely the amino group and the aromatic ring[73]. The exact site of proton attachment for gaseous anilines is frequently not obvious and this has been a topic of lively dispute in gas-phase ion chemistry. *N*-protonation generates the anilinium ion whereas ring C-protonation produces benzenium ions (Scheme 31) with the electron-donating amino group directing the electrophilic H^+ to the *ortho* or (often most favorably) *para* carbons so that the best possible delocalization of the positive charge is achieved[74].
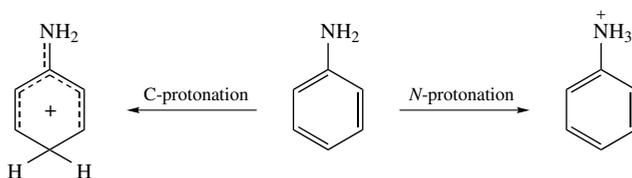
SCHEME 31

According to molecular orbital calculations, the NH_2 substituent and the aromatic *para*-carbon, which is the most basic site of the ring, have quite close PA, the amino group being just slightly more basic by *ca* 4–12 kJ mol^{-1} [75–77]. This proximity is probably the reason why there are so many contrasting reports on protonation sites for gas-phase experiments performed under a wealth of different experimental conditions. When H^+ is added to aniline under kinetic control, as can be true in chemical ionization (CI)[72], the protonation site has been suggested to be not necessarily dictated by the proton affinity (PA)[78]. The structure of CI-generated $[M + H]^+$ has so far been interrogated by several mass spectrometric techniques[79–83], mainly via isotopic labeling followed by collision-induced dissociation (CID)[79–81] and ion/molecule reactions[82, 83]. Based on the behavior of D-isotopologues, these studies have pointed out that CI generates both tautomers, with the predominance of the amino-protonated form[79–83]. Evidence for the production of both forms of protonated aniline comes from the extent of isotope randomization during dissociation or proton transfer[79–83]. For instance, Kenttamaa and coworkers[83] examined the reactions of protonated forms of partially D-labeled aniline with strong bases, and demonstrated that under the conditions employed the amino group is the kinetically favored protonation site of gaseous aniline. They found that almost 90% of the $[M + H]^+$ population is comprised of aniline molecules protonated on the amino group. The possible dependence of a scrambling process on ion lifetime and experimental set-up could explain why dissociative processes[79–81] have suggested mainly C-protonation, whereas H^+ transfer reactions[82, 83] are consistent with mainly *N*-protonation. By using neutralization–reionization mass spectrometry, Nold and Wesdemiotis[84] verified that fast atom bombardment (FAB) ionization

of aniline yields primarily the anilinium ion (*N*-protonation). In contrast, they showed that CI with a variety of reagent gases generates mixtures in which the ring-protonated species dominates[84].

The site of protonation on anilines as well as other substituted benzenes has also been estimated by CI mass spectrometry employing labeled protonating reagents[85]. For instance, using H_2O and D_2O as the CI gases, hence H_3O^+ and D_3O^+ as the major protonating species, extensive exchange of the ring hydrogens with deuteriums was correlated with protonation on the aromatic ring[85, 86].

Intermolecular H^+/D^+ exchange has been shown to be a useful probe for structure elucidation, depending on the relative acidity of the proton-transferring reactant ions. In several cases, this exchange is able to identify isomeric anilines which are indistinguishable by other mass spectrometric methods, such as EI[87].

Beynon and coworkers[79] have investigated the ethylation of a number of anilines using methane as the CI gas, and established via MIKE/CID spectra the positions of H^+ and $C_2H_5^+$ addition under these conditions. Their results indicate that aniline and ring-substituted ethylanilines undergo ethylation on the aromatic ring, whereas *N*-ethylaniline is protonated at the amino group.

C. Competing Sites of Protonation

The presence of an adjacent functional group capable of accepting a proton sometimes provides more favorable protonation sites. For instance, by studying the CID spectrum of protonated acetanilide, Tu and Harrison postulated that dissociation must proceed mainly via ions protonated at the carbonyl oxygen atom (Scheme 32)[88]. Consequently, cleavage of the amide C−N bond that forms the major fragment ions of m/z 94 must be preceded by intramolecular proton transfer[89] that has, however, a high energy barrier[90]. The dissociation of a proton-bound dimer of ketene and aniline formed via an initial acetylium ion/aniline complex[91, 92] was postulated for the formation of protonated aniline of m/z 94 (Scheme 32). Note that the dissociation of such a proton-bound dimer generates exclusively protonated aniline because the proton affinity of aniline (882.5 kJ mol^{-1}) is much larger than that of ketene (834.1 kJ mol^{-1})[9].
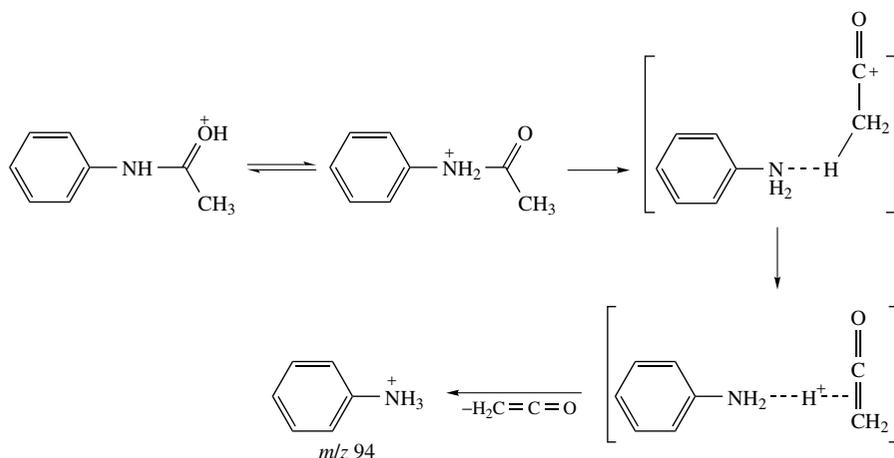
SCHEME 32

With the introduction of an extra functional group capable of accepting a proton, the dissociation of protonated aniline derivatives to form protonated aniline during CI can be dramatically increased. Acetoacetanilide, for example, may be protonated mainly at the amide carbonyl oxygen (**a**) or at the terminal carbonyl oxygen (**b**). The first species (**a**) can hardly isomerize directly to the reacting configuration **c**. However, conversion from **a** to **b** and then to **c** avoids barriers with high energies. As a result, under conventional CI conditions, the dissociation of protonated acetoacetanilide yields protonated aniline in higher abundance (15%) than protonated acetanilide (Scheme 33).

(a)   **(b)**   **(c)**

m/z 94
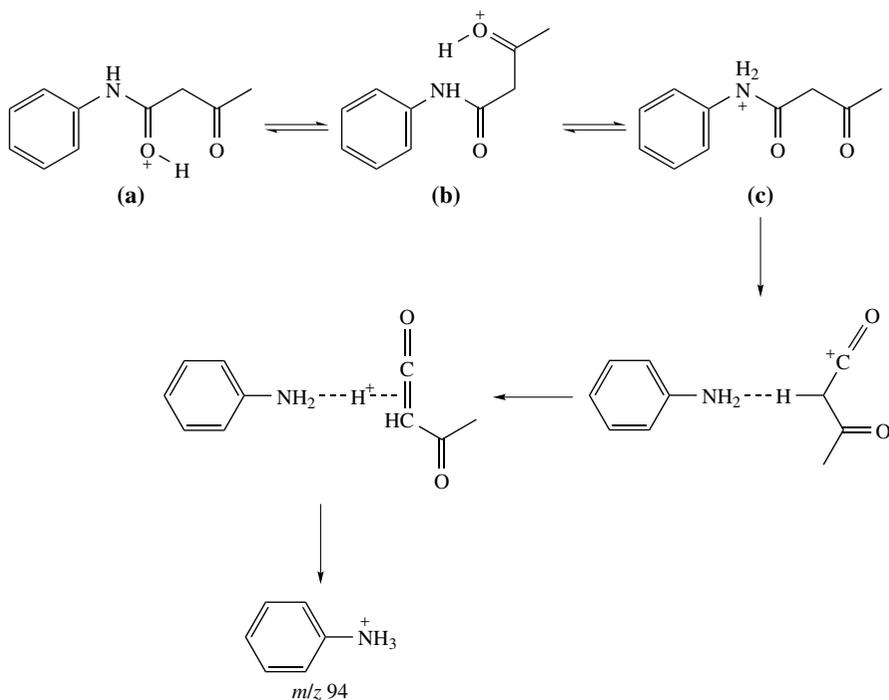
SCHEME 33

A more striking difference in the ease of dissociation of $[M + H]^+$ ions and formation of protonated anilines upon CI is found for the acetanilide derivatives bearing a nitro group. For instance, in the CI mass spectra of *N*-acetyl-*ortho*-nitroaniline, protonated aniline of *m/z* 139 is the most abundant ion. By contrast, the ion of *m/z* 139 drops to only 0.7% relative abundance for the *para* isomer[88]. Protonation of both isomers may occur competitively at the carbonyl and nitro oxygen atoms. Evidently, only the *ortho* isomer is capable of intramolecular proton transfer via a low energy barrier (Scheme 34).

Kingston and coworkers[93] have also postulated that, in the CI of *N*-allylaniline, two protonated isomeric species are formed in ratios varying according to the PA of the reagent gases (Scheme 35). For the reagent gases with higher PA, such as C_4H_{10} and C_3H_6, protonation occurs mainly on the ring. The elimination of ethene from the metastable ions (**a**) yields mainly ions **d** of *m/z* 106. For reagent gases with lower PA, such as CH_4 and H_2, protonation occurs on the nitrogen atom. The metastable ions formed by this reaction
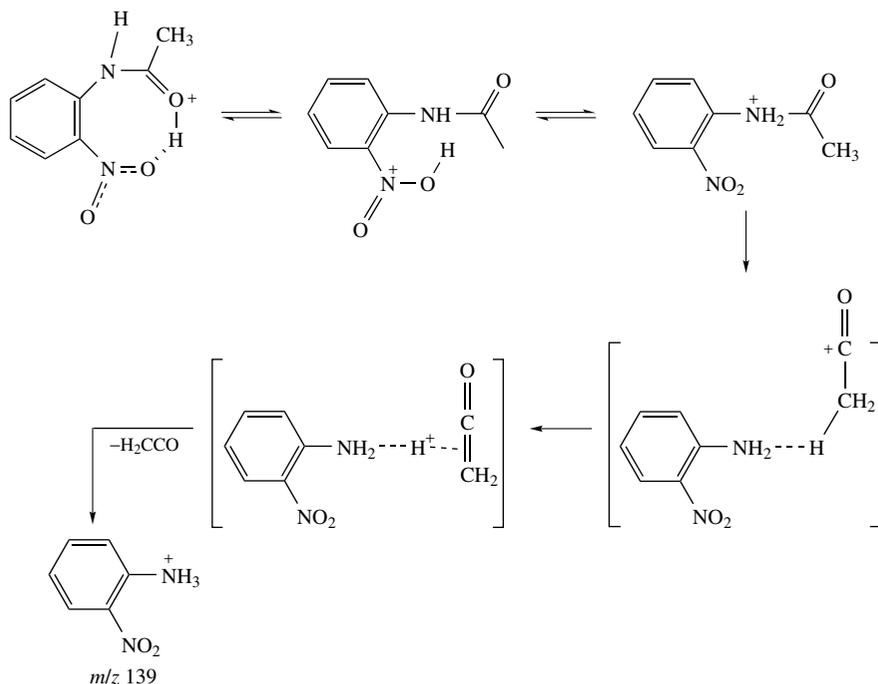
SCHEME 34

(**b**) undergo an amino-Claisen rearrangement[94, 95] yielding ion **c**, which eliminates ethene or ammonia to yield ions **e** of m/z 106 or **f** of m/z 117, respectively.

D. Assorted CI Reagent Gases

Besides those already mentioned, various other reagent gases have also been used in the CI mass spectrometry of anilines. These include chloromethanes, diisopropyl ether[96], benzene[97], acetone[98], acrylonitrile[99], tetramethylsilane[100] and nitric oxide[101]. Chemical ionization with chloromethanes was, for instance, used to study the gas-phase electrophilic addition reactions of chloromethane ions ($CH_{1+x}Cl_{3-x}$; $x = 0, 1, 2$) with aniline and with several monosubstituted benzenes[102]. In the CI (CH_2Cl_2) mass spectrum of aniline only a modest formation of the aminobenzyl cations of m/z 106 is seen, due to electrophilic attack on the ring. The predominant formation of Ph^+ ions of m/z 77 was suggested to occur via an initial electrophilic attack on the nitrogen atom followed by consecutive losses of HCl and $NHCH_2$ (Scheme 36).

Diisopropyl ether, in dilute mixtures with nitrogen, helium or methane, behaves as a selective proton transfer CI reagent gas giving minimal solvation with most protonated species (including anilines) and higher sensitivity than other common reagent gases such as ammonia[96]. Dilute mixtures of benzene in helium also provide a selective chemical ionization system. This methodology can be easily applied to analyze anilines, as demonstrated for alkylanilines[97]. Under these conditions, charge transfer products between the analytes M and $[C_6H_6]^{+\bullet}$ ions yields $M^{+\bullet}$ predominantly. Furthermore, small amounts of the protonated molecule $[M + H]^+$ from proton transfer with $C_7H_7^+$ are also detected.
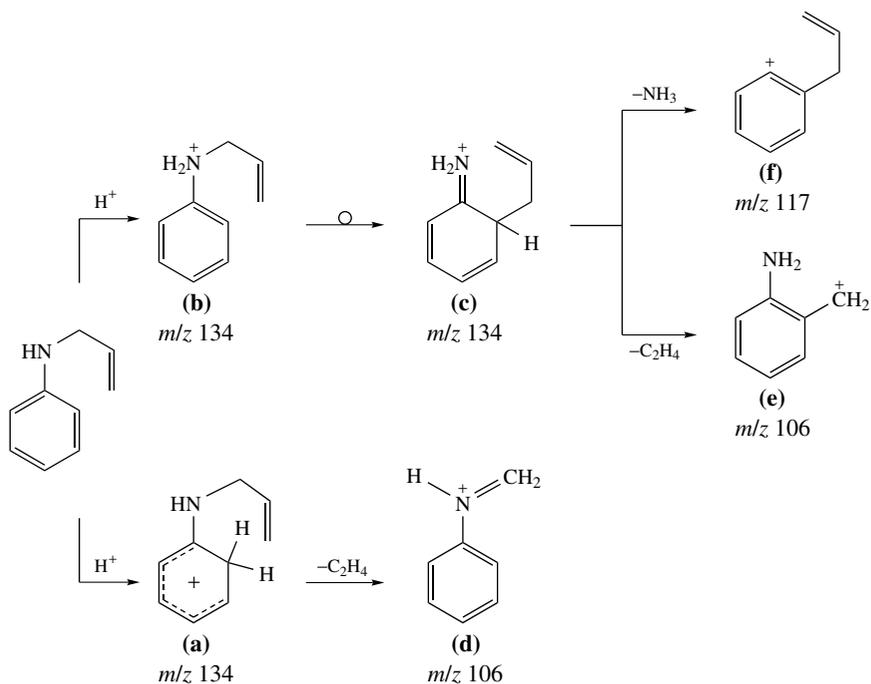
SCHEME 35
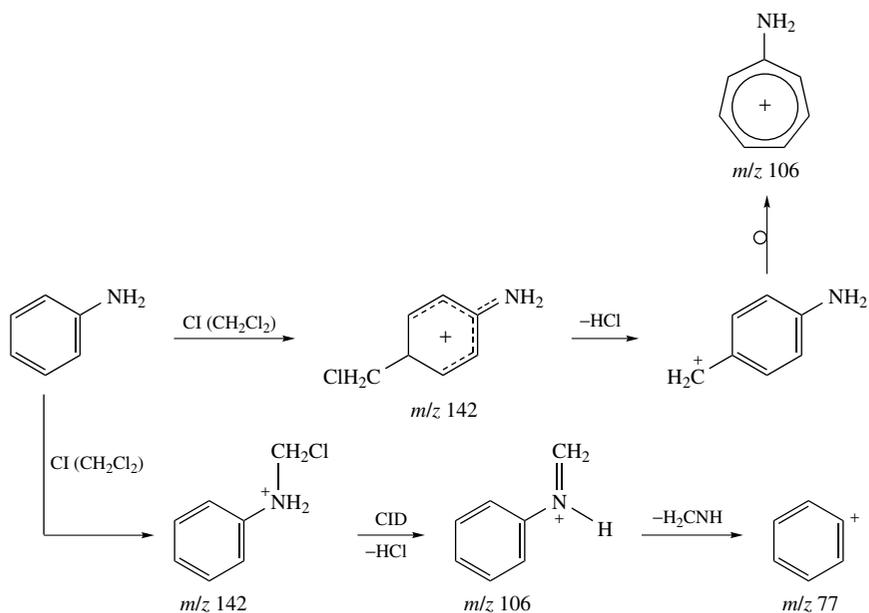
SCHEME 36

Acetone CI mass spectra of aniline and other monosubstituted aromatic compounds were also studied[98]. For aniline, protonation was found to be the main reaction channel, but acetylation is also observed. Typically, the acetylation of aniline occurs mostly at the nitrogen atom.

Among the more rare CI reagent gases, acrylonitrile was employed for aniline and found to produce particularly abundant $[M + C_3H_3N]^+$ and $[M + H]^+$ ions[99]. The use of tetramethylsilane (TMS) as a reagent gas in CI-MS has also enabled the gas-phase trimethylsilylation of aniline as well as other aromatic compounds[100]. The Me_3Si^+ ion generated in the CI plasma gives rise to abundant adduct ions $[M + Me_3Si]^+$ with an m/z increment of 73 units. However, charge transfer also forms large amounts of ionized aniline, whereas $[M + H]^+$ ions are formed only in minor relative abundances. The efficient addition of Me_3Si^+ to various organic molecules has been used to detect compounds of low volatility including aniline derivatives under desorption chemical ionization (DCI) conditions[103].

Several interesting studies have dealt with the use of nitric oxide as the reagent gas in CI-MS. Aniline derivatives tend to show strong responses to electrophilic attack by NO^+ thus yielding abundant $[M + NO]^+$ adducts. However, charge transfer with electron-rich anilines that forms $M^{+\bullet}$ is also frequent. Moreover, CI(NO) mass spectrometry was found to be highly diagnostic with respect to the substituent pattern of arenes[101].

The facile attachment of halide ions to polar organic compounds, and in particular of compounds containing hydrogen bonded to heteroatoms, can be used to generate $[M + X]^-$ adduct ions under negative ion chemical ionization (NCI) conditions[104–108]. Similar to the use of halogen-containing reagent gases in positive ion CI mass spectrometry, gases such as dichloromethane serve as a source of chlorine-containing reactant ions in the CI plasma. Electron bombardment of CH_2Cl_2 under relatively high pressure (*ca* 1 torr) generates Cl^- ions, which are attached to the reagent molecules to give $CH_2Cl_3^-$ ions, which in turn may dissociate to HCl_2^- ions and monochlorocarbene[109]. Owing to the relatively strong bonding interaction between the constituents, the NCI mass spectra of aniline and other polar analytes exhibit the adduct ions $[M + Cl]^-$ as the most abundant, along with anion-bound dimers $[M_2 + Cl]^-$ in varying abundances[109].

Conversely, $NCI(CBr_2Cl_2)$ of aniline and other weak acids was found to produce no or minor yields of the $[M + Br]^-$ anions. Similarly, under $NCI(CH_3I/CH_4)$ conditions, aniline and other weak acids were found to yield minor amounts of $[M + I]^-$ adducts or were unreactive[110]. Furthermore, under $NCI(NF_3)$ conditions, F^- is the major ion formed and constitutes more than 90% of the total ion intensity. Moreover, anilines as well as other amines exhibit only insignificant yields of $[M + F]^-$ adducts[111].

The attachment of halide ions to anilines may therefore afford abundant adduct ions which are valuable for selective detection and molar mass determination of the analytes. For example, Cl^- attachment has proven suitable for the gas chromatography/CI-MS monitoring of human exposure to several aromatic amines[112].

Besides deprotonation and anion addition in the CI plasma, which generate the respective stable $[M - H]^-$ and $[M + X]^-$ ions, the use of electron capture into low-lying p^* orbitals represents the principal approach to generate radical anions. However, if these $M^{\bullet-}$ ions are relatively small, they are too short-lived and decay within $t < 10^{-13}$ s by ejection of an electron, thus suppressing any structure-specific dissociation reaction. However, large $M^{\bullet-}$ ions, in which the excitation energy can be distributed over many internal degrees of freedom, may be sufficiently long-lived ($t > 10^{-6}$ s) to enable their MS detection[113]. When argon or other inert gases are used to decelerate the electrons, the efficiency of the overall electron capture process is much enhanced[105, 113, 114]. As a practical application, the electron-capture negative ion (EC-NI) mass spectra of derivatives (such as perfluoroacyl and pentafluorobenzyl) of chloro-substituted anilines were

obtained[115]. These data revealed that selection of the appropriate derivative is an important consideration in order to carry out trace level analysis by GC/EC-NI-MS[115].

E. Electrospray Ionization (ESI-MS)

Abundant protonated molecules are often formed from anilines upon electrospray ionization[116] in the positive ion mode, although one must be aware that, as observed during CI, dissociation may also occur to considerable extents according to the type and position of the substituents. Structural information is often gained by dissociating the gaseous protonated molecules via tandem mass spectrometric experiments. For instance, high sensitivity in the monitoring of several aniline pesticides was achieved via liquid chromatography coupled to ESI-MS/MS using multiple reaction monitoring (MRM). The pesticide metalachlor (Scheme 37), for instance, was monitored via methanol loss from its protonated molecule (m/z 284 → m/z 252)[117]. The major fragment ion selected for MRM was determined by previous collection of its ESI(+)-MS/MS.

m/z 284 m/z 252 m/z 176
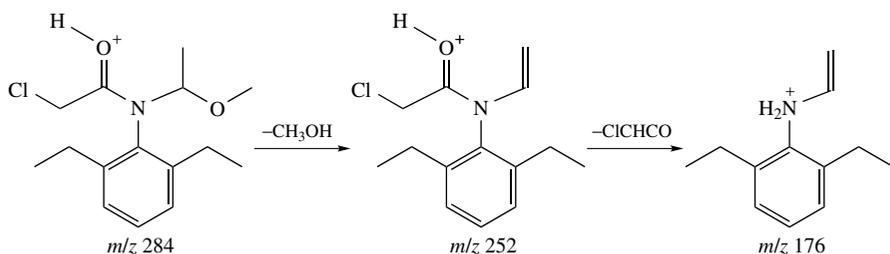
SCHEME 37

In ESI-MS, a wealth of noncovalent ion/molecule adduct ions can be also generated. For instance, the formation of ion/solvent (So) adducts, $[M + So]^+$, were observed during ESI-MS of 3-hydroxyaniline as well as other aromatic molecules. The relative abundances of ions $[M + H]^+$, $[M + So + H]^+$ and $[M + 2 So + H]^+$ were studied as a function of the temperature and pH, with the solvents being mixtures of methanol/water and acetonitrile/water sometimes containing ammonium acetate as additive[118].

Cole and Zhu[119, 120] developed an approach to enable ESI-MS in the negative ion mode to detect analytes that lack acidic sites and thus exhibit weak $[M − H]^-$ signals. This approach relies upon attachment of Cl^- ions, present in electrosprayed solutions of chlorinated solvents, to these analytes. For aniline, the formation of the $[M + Cl]^-$ adduct was observed despite its very low pK_a of 27[121] and low gas-phase acidity of 1502 kJ mol^{-1}[7].

VII. GAS-PHASE REACTIVITY OF ANILINES

Various bimolecular reactions of neutral anilines as well as aniline ions have been found to occur in the gas phase, particularly during CI-MS or via sequential MS^n experiments using preselected isolated ions. In this section, some of these representative bimolecular reactions will be discussed.

For example, Attina and Cacace[122] investigated the intramolecular selectivity of electrophilic reactions of radiolytically formed $C_2H_5^+$, $i\text{-}C_3H_7^+$, $t\text{-}C_4H_9^+$, $(CH_3)_2F^+$ and CH_3CO^+ ions with aniline in the gas phase at nearly atmospheric pressure. Under conditions of kinetic control, the reactivity of the amino group and of the aromatic

ring were comparable, a mixture of ring- and *N*-substituted products were invariably formed in proportions that depended on the nature of the electrophile. The relative rate of *N*-substitution increases in the order: $C_2H_5^+ \sim i\text{-}C_3H_7^+ < (CH_3)_2F^+ < t\text{-}C_4H_9^+ < CH_3CO^+$. The positional selectivity of the gaseous electrophiles, except CH_3CO^+, was characterized by predominant *ortho* substitution.

To investigate competition between radical substitution and addition reactions, Kenttamaa and coworkers[123] performed gas-phase reactions of phenyl radicals bearing a chemically inert, positively charged group and a neutral substituent (CH_3, Cl, or Br), both at the *para* and *meta* position with respect to the radical site, with aniline as well as several other aromatic substrates in a dual-cell Fourier transform ion cyclotron resonance mass spectrometer. The radicals undergo hydrogen abstraction from the substituent and/or addition to the phenyl ring. The presence of the electron-withdrawing substituent Cl or Br on the phenyl ring of the radical slightly increases the rates for both hydrogen atom abstraction and addition due to favorable polarization of the reaction transition states. The extent to which the charged radicals are able to abstract a hydrogen from the aromatic substrate and form stable products via addition to the aromatic ring was found to vary greatly.

Nishimura and coworkers[124] also studied the gas-phase ion/molecule reactions of CH_5^+, $C_2H_5^+$ and $C_3H_5^+$ with aniline and other monosubstituted benzenes using an ion-trap GC/MS system at a low CI gas pressure of CH_4. For aniline, the major product channels were proton and charge transfer. Moreover, small amounts of initial adduct ions, produced by radiative association, and their decomposition products were found in the reactions with $C_2H_5^+$ and $C_3H_5^+$.

Vainiotalo and coworkers[125] investigated the ion/molecule reactions of aniline (and other monoamines) with acetone and pentan-3-one under chemical ionization, using the carbonyl compounds as reagent gas. All the primary monoamines gave rise to nucleophilic addition−elimination reaction products, formed by the reaction of the protonated ketone dimer with a neutral amine. Protonated ketone monomers gave rise only to protonated amines; no addition−elimination products were observed. The structure of the nucleophilic addition−elimination product ion was independent of the structure of the amine but it was considerably dependent on the structure of the ketone. Comparison of the collision-induced dissociation mass spectra of the product ions with those of authentic protonated imines showed that, with acetone as reagent gas, only protonated imines were formed. However, when the size and branching of the ketone increased, enamine formation became clearly more favorable. The formation of protonated amines and enamines must take place through different mechanisms because theoretical calculations show that a high energy barrier separates them from each other, making isomerization improbable.

Nishimura and coworkers[126] also performed the gas-phase ion/molecule reactions of CF_3^+ with aniline and other nitrogen-containing benzene derivatives at near-thermal energy using an ion-beam apparatus. For aniline, the major product channel was charge transfer.

Cooks and coworkers[127] performed electrophilic bromination of aniline and other mono-substituted aromatic compounds using a pentaquadrupole mass spectrometer and $BrCO^+$ and $CH_3NH_2Br^+$ as the reagent ions. Reaction normally occurs at the ring and the brominated product was mass-selected and found to lose mainly Br upon collision-induced dissociation. The electrophilic addition reaction often proceeds via a σ-complex with the ring as suggested by MS^3 experiments. The greater reactivity of $BrCO^+$ is evident since it reacts even with strongly deactivated substrates and this is consistent with a weak Br−CO bond. Competitive protonation occurs when $CH_3NH_2Br^+$ is used.

Cooks and coworkers[128] studied the Cl^+ addition to aniline and other aromatic compounds via isolated NH_3Cl^+, $ClC=O^+$, protonated CH_3Cl, and Cl^+ reagent ions using a pentaquadrupole mass spectrometer. The reactions of protonated monochloramine

(NH_3Cl^+) were followed using a direct insertion membrane probe for sample introduction for product characterization. The main reactions observed for NH_3Cl^+ with aniline and the aromatic compounds were electrophilic Cl^+ and H^+ addition and charge exchange to form the aromatic radical cation. Reactions of $ClC{=}O^+$ include (i) Cl^+ addition, (ii) $CO^{\bullet+}$ substitution for a hydrogen atom and (iii) formation of the molecular ion of the substrate. The naked Cl^+ ion failed to chlorinate aniline and the other aromatic compounds but it underwent charge exchange. Protonated CH_3Cl also fails to add Cl^+, proton transfer being the main reaction observed. MS^3 experiments suggested that both Cl^+ addition and the CO substitution products of aniline are σ-bonded. Comparisons with the MS^2 data of model ions suggested that both Cl^+ and $CO^{\bullet+}$ add principally to the *para* position of aniline.

Gross and coworkers[129] also studied the unimolecular dissociation of protonated acylanilines, viz. *N*-[2-(benzoyloxy)phenyl]benzamides formed via both fast-atom bombardment (FAB) and electrospray ionization (ESI). They found that cyclization occurs upon the loss of a molecule of benzoic acid, and that a similar process occurs for the molecular ion under EI. This gas-phase reaction is analogous to a solution reaction leading to phenylbenzoxazoles. The proposed cyclization process, for which concurrent mechanisms were proposed (Scheme 38 depicts only the displacement reaction route), was corroborated by accurate mass measurements, tandem mass spectrometric experiments with comparison with reference ions, isotopic labeling and theoretical calculations.
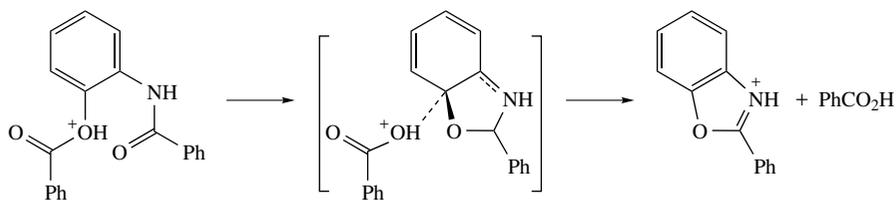
SCHEME 38

Recently, Eberlin and coworkers[130] proposed an EI-MS/MS approach for the direct structural assignment of *ortho*- and *meta/para*-substituted acyl and amidyl anilines in general (as well as phenols). The approach is based on the assertion that most compounds of this class should produce upon EI the respective aminoacylium ion (Scheme 39), and that these diagnostic ions (and hence the position of the ring substituents) could be distinguished via selective ion/molecule reactions.
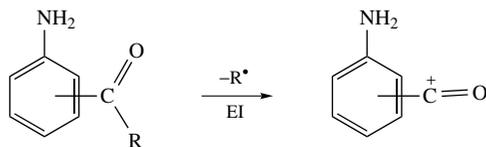
SCHEME 39

As an example of such a reaction, the *ortho*-aminobenzoyl cation of m/z 120 was found to react with acetonitrile to form two abundant product ions of m/z 133 and 161 (Figure 19), assigned as protonated forms of two aromatic heterocyclic compounds
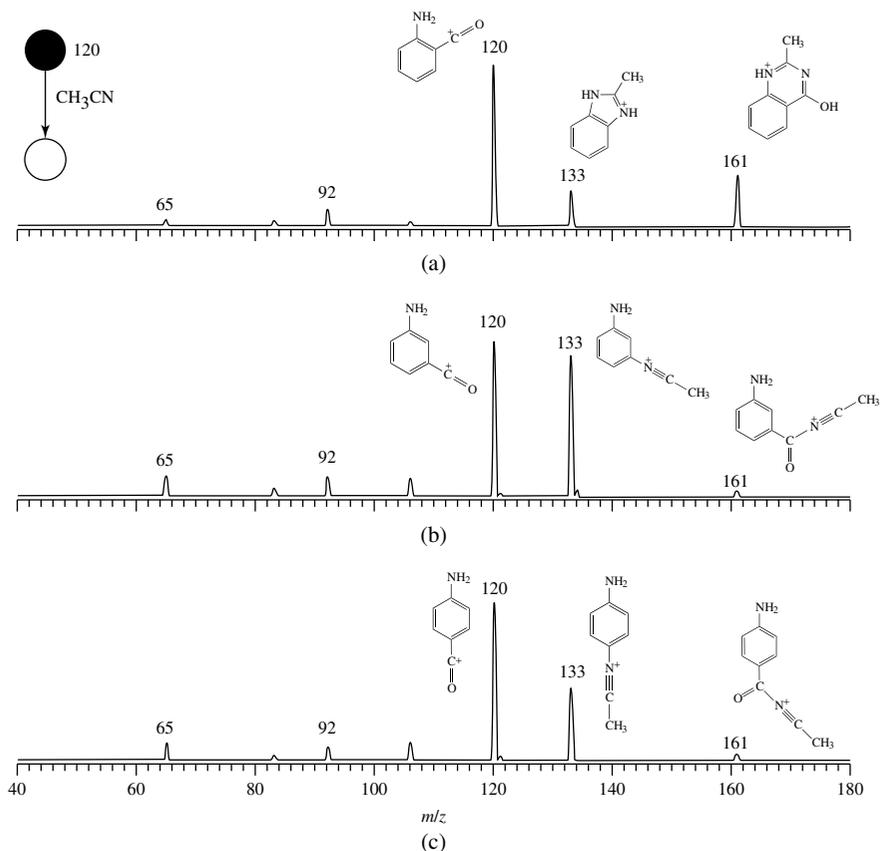
FIGURE 19. Product ion mass spectra for the reactions of isomeric a) *ortho*-, b) *meta*- and c) *para*-aminobenzoyl cations of m/z 120 with acetonitrile. Adapted from Reference 130

(Scheme 40). By contrast, the *meta*- and *para*-aminobenzoyl cations react mainly by a formal CO-by-CH$_3$CN *ipso*-substitution reaction yielding product ions of m/z 133.

Schwarz and coworkers[131] have also studied the gas-phase oxidation of aniline, *N*-methylaniline and *N*,*N*-dimethylaniline by the FeO$^+$ ion via mass spectrometric techniques. Although bare FeO$^+$ is capable of hydroxylating aromatic C−H bonds, the fate of the oxidation of arylamines was found to be governed by FeO$^+$ binding at the amino group. The major reactions observed for the metastable aniline/FeO$^+$ complex were losses of H$_2$, ammonia and water, all involving at least one N−H proton. *N*-alkylation completely shifts the course of the reaction. The unimolecular processes observed were regarded as initial steps of an oxidative dealkylation of the amines mediated by FeO$^+$. Detailed mechanistic insights were obtained by examining the C−H(D) bond activation of *N*-methyl-*N*-([D-3]-methyl)aniline by bare and ligated FeO$^+$ species. The gas-phase reactions of FeO$^+$ with methylanilines showed some similarities to the enzymatic dealkylation of amines by cytochrome P-450.
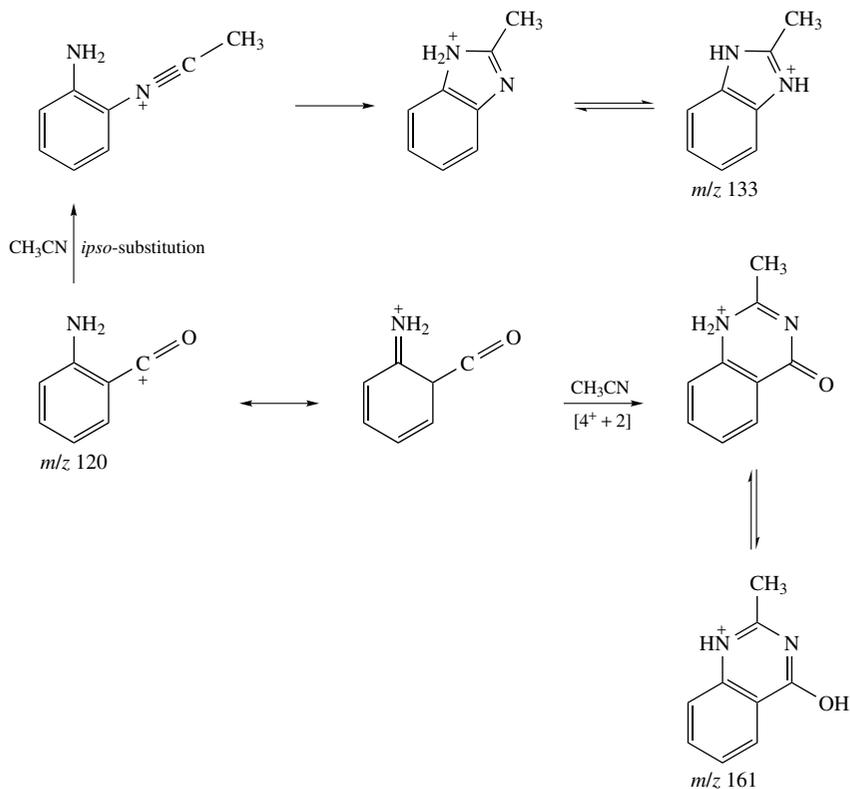
SCHEME 40

Laali and coworkers[132] investigated the reaction of the gaseous 2-*t*-butyl-3-phenyl-phosphirenylium ion (a 2π-Huckel phosphirenylium ion) with aniline and other nucleophiles and dienes via MS^n experiments. In ion/molecule reactions, the ion reacts readily with aniline to form an azonium ion via nucleophilic attack at phosphorus by the amino group, as suggested by calculations and MS^3 experiments.

Freitas and O'Hair[133] studied the gas-phase reactivity of aniline and other nucleophiles toward the methoxymethyl cation, $CH_3 - O^+=CH_2$, an ambident electrophile, using flowing afterglow mass spectrometry. For aniline, two reaction channels were observed: addition followed by elimination of methanol with concomitant $[M + CH]^+$ ion formation and adduct formation, viz. $[M + CH_3OCH_2]^+$.

Ionized aniline may exist in a conventional-ion form as well as in isomeric distonic forms, and gas-phase MS experiments performed by Chyall and Kenttamaa[134, 135] have also been used to form and to study the intrinsic reactivity of these high-energy isomers. Via collision-induced dissociation (CID) of protonated 2-, 3- and 4-iodoanilines in a dual-cell Fourier transform ion cyclotron resonance spectrometer, the 2-, 3- and 4-dehydroanilinium ions were formed as the result of loss of an iodine atom (Scheme 41). Ion/molecule reactions and energy-resolved CID experiments demonstrated that these three ions as well as ionized aniline behave distinctively. The reactivity of three distonic ions
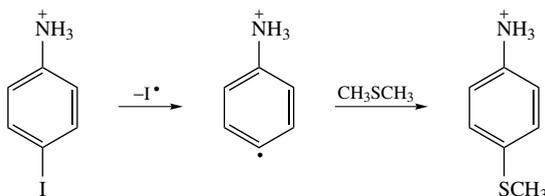
SCHEME 41

(charged phenyl radicals) was found to be largely analogous to that of the phenyl radical. For example, the 4-dehydroanilinium ion abstracts an iodine atom from isopropyl iodide and a thiomethyl group from dimethyl disulfide (Scheme 41), but adds to cyclohexene. Basic molecules were found to induce isomerization of the dehydroanilinium ions to the significantly more stable ionized aniline, by deprotonating the charge site and then donating a hydrogen atom to the radical site.

Cooks and coworkers[136] applied the kinetic method to determine the IE of anilines. They generated the radical cation-bound dimers of substituted anilines under self-CI conditions and examined the dissociation products in a triple quadrupole tandem mass spectrometer. Using N,N-diethylaniline, 3,5-dimethylaniline, N-methylaniline, 2-methylaniline, 3-methylaniline, aniline and benzylamine as reference compounds, a linear correlation was observed in a plot of the natural log of the ratio of the fragment ion abundances versus ionization energy. The average estimated IE values for 4-methoxyaniline, 2-methoxyaniline, 4-methylaniline, 3-chloroaniline and 3-fluoroaniline were determined to be 7.00 ± 0.15 eV, 7.19 ± 0.07 eV, 7.37 ± 0.07 eV, 8.27 ± 0.08 eV and 8.37 ± 0.07 eV, respectively.

Very recently, Cooks and coworkers[137] described a new ionization technique for mass spectrometry and termed it 'atmospheric pressure thermal desorption ionization (APTDI)'. Using this innovative approach, they were able to perform a classical solution reaction between aniline and the 2,4,6-triphenylpyrylium ion (Scheme 42), now in the gas phase at atmospheric pressure, and to detect and characterize the product ions via MS. In solution, the conversion of pyrylium into pyridinium ions is an important route for the conversion of primary amino groups into a variety of other functionalities such as halide, ester, alcohol, nitrate, thiocyanate and azide. Aniline was also 'labeled' with a charge site (Scheme 43) and the resulting aniline organic salt was subjected to APTDI-MS. The gaseous pyridinium ion of m/z 399 so formed was then reacted with benzaldehyde, and the Schiff reaction product ion of m/z 487 was formed promptly (Figure 20).
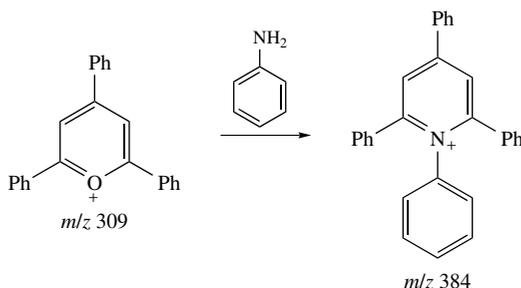
SCHEME 42
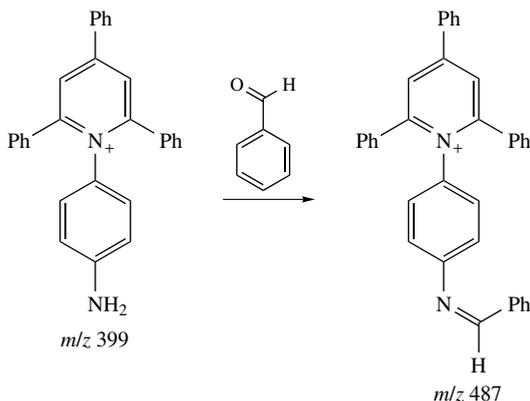
SCHEME 43
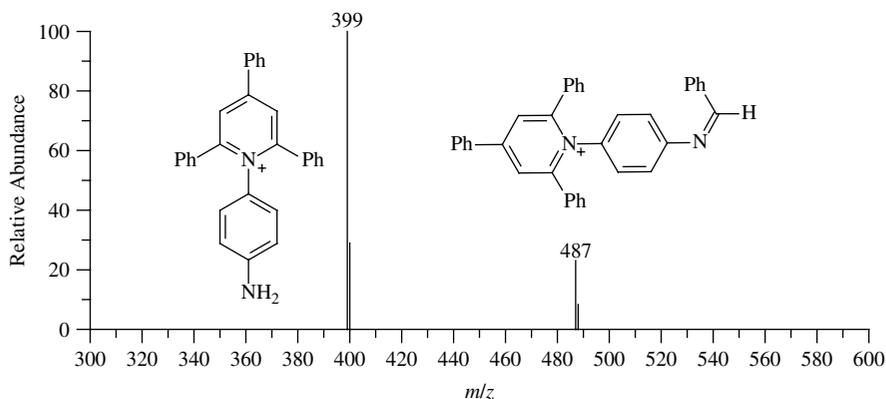
FIGURE 20. Mass spectrum for the ion/molecule reaction of the charge labeled aniline ion of m/z 399 and benzaldehyde in the homogeneous phase at atmospheric pressure. Adapted from Reference 137

IX. REFERENCES

1. S. H. Pine, *Organic Chemistry*, 5th edn., McGraw-Hill, Singapore (1987).
2. N. I. Sax and R. J. Lewis, *Hawley's Condensed Chemical Dictionary*, 11th edn., Van Nostrand Reinhold, New York (1987).
3. A. S. Kao, *Air & Waste*, **44**, 683 (1994).
4. H. Budzikiewicz, C. Djerassi and D. H. Williams, *Mass Spectrometry of Organic Compounds*, Holden-Day, San Francisco (1967).

5. F. W. McLafferty and F. Turecek, *Interpretation of Mass Spectra*, 4th edn., University Scientific Books, Mill Valley (1993).
6. E. de Hoffmann and V. Stroobant, *Mass Spectrometry: Principles and Applications*, 2nd edn., Wiley, New York (2002).
7. S. G. Lias, J. E. Bartmess, J. F. Liebman, J. L. Holmes, R. D. Levin and W. G. Mallard, *Ion Energetics Data*, in *The NIST Chemistry Webbook* (Eds. P. J. Linstromand and W. G. Mallard), National Institute of Standards and Technology, Gaithersburg (2001).
8. S. G. Lias, *Ionization Energy Evaluation*, in *NIST Chemistry Webbook, NIST Standard Reference Database Number 69* (Eds. P. J. Linstromand and W. G. Mallard), National Institute of Standards and Technology, Gaithersburg (2003)
9. E. P. Hunter and S. G. Lias, *J. Phys. Chem. Ref. Data*, **27**, 413 (1998).
10. P. G. Farrell and J. Newton, *Tetrahedron Lett.*, 5517 (1966).
11. P. Brown, *Org. Mass Spectrom.*, **4**, 519 (1970).
12. G. F. Crable and G. L. Kearns, *J. Phys. Chem.*, **66**, 436 (1962).
13. A. Buchs, *Helv. Chim. Acta*, **53**, 2026 (1970).
14. M. A. Baldwin, A. G. Loudon, A. Maccoll and K. S. Webb, *Org. Mass Spectrom.*, **11**, 1181 (1976).
15. G. G. Furin, A. S. Sultanov and I. I. Furlei, *Bull. Acad. Sci. USSR Chem.*, **36**, 530 (1987).
16. G. Bouchoux, *Int. J. Mass Spectrom. Ion Phys.*, **26**, 379 (1978).
17. A. J. Dempster, *Phys. Rev.*, **11**, 316 (1918).
18. W. Bleakney, *Phys. Rev.*, **34**, 157 (1929).
19. A. G. Nier, *Rev. Sci. Instrum.*, **18**, 415 (1947).
20. R. M. Silverstein and F. X. Webster, *Spectrometric Identification of Organic Compounds*, 6th edn., Wiley, New York (1998).
21. F. W. McLafferty, *Pure Appl. Chem.*, **50**, 831 (1978).
22. J. H. Beynon, *Appl. Spectrosc.*, **33**, 339 (1979).
23. H. Budzikiewicz and R. D. Grigsby, *Mass Spectrom. Rev.*, **25**, 146 (2006).
24. K. Biemann, *Mass Spectrometry, Applications to Organic Chemistry*, McGraw-Hill, New York (1962).
25. H. Budzikiewicz, C. Djerassi and D. H. Williams, *Structure Elucidation of Natural Products by Mass Spectrometry*, Holden-Day, San Francisco (1964).
26. H. Budzikiewicz, C. Djerassi and D. H. Williams, *Interpretation of Mass Spectra of Organic Compounds*, Holden-Day, San Francisco (1964).
27. P. N. Rylander, S. Meyerson, E. L. Eliel and J. D. McCollum, *J. Am. Chem. Soc.*, **85**, 2723 (1963).
28. C. F. Pau and W. J. Hehre, *J. Phys. Chem.*, **86**, 321 (1982).
29. C. E. C. A. Hop, M. Dakubu and J. L. Holmes, *Org. Mass Spectrom.*, **23**, 609 (1988).
30. P. C. Burgers, J. L. Holmes, A. A. Mommers and J. K. Terlouw, *Chem. Phys. Lett.*, **102**, 1 (1983).
31. P. O. Danis, C. Wesdemiotis and F. W. McLafferty, *J. Am. Chem. Soc.*, **105**, 7454 (1983).
32. R. Flammang, P. Meyrant, A. Maquestiau, E. E. Kingston and J. H. Beynon, *Org. Mass Spectrom.*, **20**, 253 (1985).
33. P. Longevialle, *Mass Spectrom. Rev.*, **11**, 157 (1992).
34. P. N. T. van Velzen, W. J. van der Hart, J. van der Greef and N. M. M. Nibbering, *J. Am. Chem. Soc.*, **104**, 1208 (1982).
35. A. Maquestiau, Y. V. Haverbeke, R. Flammang, C. D. Meyer, C. G. Das and G. S. Reddy, *Org. Mass Spectrom.*, **12**, 631 (1977).
36. F. W. McLafferty, *Anal. Chem.*, **31**, 82 (1959).
37. F. Borchers, K. Levsen, C. B. Theissling and N. M. M. Nibbering, *Org. Mass Spectrom.*, **12**, 746 (1977).
38. D. H. Russell, M. L. Gross and N. M. M. Nibbering, *J. Am. Chem. Soc.*, **100**, 6133 (1978).
39. D. Kuck, *Mass Spectrom. Rev.*, **9**, 187 (1990).
40. E. Stenhagen, S. Abrahamsson and F. W. McLafferty, *Registry of Mass Spectral Data*, 5th edn., Wiley-Interscience, New York (1974).
41. F. C. Gozzo and M. N. Eberlin, *J. Am. Soc. Mass Spectrom.*, **6**, 554 (1995).

42.   Y. Malinovich and C. Lifshitz, *J. Phys. Chem.*, **90**, 4311 (1986).
43.   M. L. Fraser-Monteiro, L. Fraser-Monteiro, J. de Wit and T. Baer, *J. Phys. Chem.*, **88**, 3622 (1984).
44.   T. Aczel and H. E. Lumpkin, *Anal. Chem.*, **32**, 1819 (1960).
45.   P. Buryan, V. Kubelka, J. Mitera and J. Macak, *Collect. Czech. Chem. Commun.*, **44**, 2798 (1979).
46.   C. Cone, M. J. S. Dewar and D. Landman, *J. Am. Chem. Soc.*, **99**, 372 (1977).
47.   M. Malow, M. Penno and K. M. Weitzel, *J. Phys. Chem. A*, **107**, 10625 (2003).
48.   J. H. Moon, J. C. Choe and M. S. Kim, *J. Phys. Chem. A*, **104**, 458 (2000).
49.   B. J. Smith and N. E. Hall, *Chem. Phys. Lett.*, **279**, 165 (1997).
50.   A. Nicolaides and L. Radom, *J. Am. Chem. Soc.*, **116**, 9769 (1994).
51.   C. Lifshitz, *Acc. Chem. Res.*, **27**, 138 (1994).
52.   I. S. Ignatyev and T. Sundius, *Chem. Phys. Lett.*, **326**, 101 (2000).
53.   H. Schwarz, *Top. Curr. Chem.*, **73**, 231 (1978).
54.   J. T. Bursey, M. M. Bursey and D. G. I. Kingston, *Chem. Rev.*, **73**, 191 (1973).
55.   D. Kuck, *Int. J. Mass Spectrom.*, **213**, 101 (2002).
56.   D. Kuck and U. Fastabend, *Int. J. Mass Spectrom. Ion Processes*, **179/180**, 147 (1998).
57.   D. Kuck, *Mass Spectrom. Rev.*, **9**, 583 (1990).
58.   R. Gawinecki, D. Rasała and T. Bak, *Org. Mass Spectrom.*, **27**, 39 (1992).
59.   H. Budzikiewicz, J. Rullkotter and H. M. Schiebel, *Org. Mass Spectrom.*, **6**, 251 (1972).
60.   D. V. Ramana and M. Vairamani, *Org. Mass Spectrom.*, **12**, 166 (1977).
61.   S. A. McLukey and G. L. Glish, *Org. Mass Spectrom.*, **22**, 224 (1987).
62.   D. N. B. Mallen and J. M. Smit, *Org. Mass Spectrom.*, **14**, 171 (1979).
63.   R. Gawinecki and D. Rasała, *Org. Mass Spectrom.*, **26**, 100 (1991).
64.   G. Avellone, L. Ceraulo, L. Lamartina, B. Cosimelli, D. Spinelli and L. Zuppiroli, *Rapid Commun. Mass Spectrom.*, **13**, 1360 (1999).
65.   T. Yanagisawa, S. Tajima, M. Iizuka, S. Tobita, H. Mitani, H. Sawada and T. Matsumoto, *Int. J. Mass Spectrom.*, **125**, 55 (1993).
66.   S. Tajima, S. Takahashi and O. Sekiguchi, *Rapid Commun. Mass Spectrom.*, **13**, 1458 (1999).
67.   B. Cosimelli, L. Lamartina, C. Z. Lanza, D. Spinelli, R. Spisani and F. Vegna, *Tetrahedron*, **59**, 7189 (2003).
68.   L. Ceraulo, P. de Maria, M. Ferrugia, S. Foti, R. Saletti and D. Spinelli, *J. Mass Spectrom.*, **30**, 257 (1995).
69.   L. Ceraulo, P. Agozzino, M. Ferrugia and R. Rainieri, *Trends Heterocycl. Chem.*, **4**, 115 (1995).
70.   P. Agozzino, L. Ceraulo, M. Ferrugia and R. Rainieri, *J. Mass Spectrom.*, **31**, 1441 (1996).
71.   M. S. B. Munson and F. H. Field, *J. Am. Chem. Soc.*, **87**, 3294 (1965).
72.   A. G. Harrison, *Chemical Ionization Mass Spectrometry*, 2nd edn., CRC Press, Boca Raton (1992).
73.   R. Flammang, N. Dechamps, P. Laurent, Y. Van Haverbeke, P. Gerbaux, N. Pham-Cam and M. T. Nguyen, *Lett. Org. Chem.*, **1**, 23 (2004).
74.   J. McMurry, *Organic Chemistry*, 4th edn., Brooks/Cole, Pacific Grove (1996).
75.   M. J. S. Dewar and K. M. Dieter, *J. Am. Chem. Soc.*, **108**, 8075 (1986).
76.   J. L. Devlin, J. F. Wolf, R. W. Taft and W. J. Hehre, *J. Am. Chem. Soc.*, **98**, 1990 (1976).
77.   S. K. Pollack, J. L. Devlin, K. D. Summerhays, R. W. Taft and W. J. Hehre, *J. Am. Chem. Soc.*, **99**, 4583 (1977).
78.   A. W. McMahon, F. Chadikun, A. G. Harrison and R. E. March, *Int. J. Mass Spectrom. Ion Processes*, **87**, 275 (1989).
79.   A. Maquestiau, Y. Vanhaverbeke, H. Mispreuve, R. Flammang, J. A. Harris, I. Howe and J. H. Beynon, *Org. Mass Spectrom.*, **15**, 144 (1980).
80.   K. V. Wood, D. J. Burinski, D. Cameron and R. G. Cooks, *J. Org. Chem.*, **48**, 5236 (1983).
81.   S. J. Pachuta, I. Isern-Flecha and R. G. Cooks, *Org. Mass Spectrom.*, **21**, 1 (1986).
82.   N. D. Dookeran and A. G. Harrison, *J. Am. Soc. Mass Spectrom.*, **6**, 19 (1995).
83.   R. L. Smith, L. J. Chyall, B. J. Beasley and H. I. Kenttamaa, *J. Am. Chem. Soc.*, **117**, 7971 (1995).
84.   M. J. Nold and C. Wesdemiotis, *J. Mass Spectrom.*, **31**, 1169 (1996).
85.   D. P. Martinsen and S. E. Buttrill Jr., *Org. Mass Spectrom.*, **11**, 762 (1976).

86. D. F. Hunt, C. N. McEwen and R. A. Upham, *Anal. Chem.*, **44**, 1292 (1972).
87. B. S. Freiser, R. L. Woodin and J. L. Beauchamp, *J. Am. Chem. Soc.*, **97**, 6893 (1975).
88. Y. P. Tu and A. G. Harrison, *J. Am. Soc. Mass Spectrom.*, **9**, 454 (1998).
89. M. Vairamani and M. Saraswathi, *Mass Spectrom. Rev.*, **10**, 491 (1991).
90. H. Y. Lin, D. P. Ridge, E. Uggerud and T. Vulpius, *J. Am. Chem. Soc.*, **116**, 2996 (1994).
91. D. J. McAdoo, *Mass Spectrom. Rev.*, **7**, 363 (1988).
92. A. G. Harrison and J.-Y. Wang, *Int. J. Mass Spectrom. Ion Processes*, **160**, 157 (1997).
93. E. E. Kingston, J. H. Beynon, A. Vandezonneville, R. Flammang and A. Maquestiau, *Org. Mass Spectrom.*, **23**, 437 (1988).
94. A. Vandezonneville, R. Flammang, A. Maquestiau, E. Kingston and J. H. Beynon, *Org. Mass Spectrom.*, **21**, 351 (1986).
95. E. E. Kingston, J. H. Beynon, J. G. Liehr, P. Meyrant, R. Flammang and A. Maquestiau, *Org. Mass Spectrom.*, **20**, 351 (1985).
96. R. Barry and B. Munson, *Anal. Chem.*, **59**, 466 (1987).
97. C. Allgood, Y. Lin, Y. C. Ma and B. Munson, *Org. Mass Spectrom.*, **25**, 497 (1990).
98. M. Vairamani, *Org. Mass Spectrom.*, **28**, 1498 (1993).
99. R. Srinivas, M. Vairamani, G. K. V. Rao and U. A. Mirza, *Org. Mass Spectrom.*, **24**, 435 (1989).
100. R. Srinivas, A. R. Devi and G. K. V. Rao, *Rapid Commun. Mass Spectrom.*, **10**, 12 (1996).
101. S. Daishima, Y. Ilda and F. Kanda, *Org. Mass Spectrom.*, **26**, 486 (1991).
102. D. J. Burinski and J. E. Campana, *Org. Mass Spectrom.*, **23**, 613 (1988).
103. R. N. Stillwell, D. I. Carroll, J. G. Nowlin and E. C. Horning, *Anal. Chem.*, **55**, 1313 (1983).
104. R. B. Geerdink, F. A. Maris, G. J. De Jong, R. W. Frei and U. A. T. Brinkman, *J. Chromatogr.*, **394**, 51 (1987).
105. H. Budzikiewicz, *Mass Spectrom. Rev.*, **5**, 345 (1986).
106. R. C. Dougherty, *Anal. Chem.*, **53**, 625A (1981).
107. K. R. Jennings, *Engl. Mass Spectrom.*, **4**, 203 (1977).
108. R. C. Dougherty, J. D. Roberts and F. J. Biros, *Anal. Chem.*, **47**, 54 (1975).
109. H. P. Tannenbaum, J. D. Roberts and R. C. Dougherty, *Anal. Chem.*, **47**, 49 (1975).
110. G. W. Caldwell, J. A. Masucci and M. G. Ikonomou, *Org. Mass Spectrom.*, **24**, 8 (1989).
111. T. O. Tiernan, C. Chang and C. C. Cheng, *Environ. Health Perspect.*, **36**, 47 (1980).
112. W. G. Stillwell, M. S. Bryant and J. S. Wishnok, *Biom. Environ. Mass Spectrom.*, **14**, 221 (1987).
113. H. Budzikiewicz, *Angew. Chem., Int. Ed. Engl.*, **20**, 624 (1981).
114. I. K. Gregor and M. Guilhaus, *Int. J. Mass Spectrom. Ion Processes*, **56**, 167 (1984).
115. T. M. Trainor and P. Vouros, *Anal. Chem.*, **59**, 601 (1987).
116. S. A. McLuckey and G. J. VanBerkel, *Int. J. Mass Spectrom.*, **162**, R9 (1997).
117. A. C. B. da Cunha, M. J. L. de Alda, D. Barceló, T. M. Pizzolato and J. H. Z. dos Santos, *Anal. Bioanal. Chem.*, **378**, 940 (2004).
118. M. Honing, D. Barcelo, B. L. M. vanBaar and U. A. T. Brinkman, *J. Mass Spectrom.*, **31**, 527 (1996).
119. R. B. Cole and J. Zhu, *Rapid Commun. Mass Spectrom.*, **13**, 607 (1999).
120. J. Zhu and R. B. Cole, *J. Am. Soc. Mass Spectrom.*, **11**, 932 (2000).
121. D. Dolman and R. Stewart, *Can. J. Chem.*, **45**, 911 (1967).
122. M. Attina and F. Cacace, *J. Am. Chem. Soc.*, **105**, 1122 (1983).
123. L. E. Ramirez-Arizmendi, L. Guler, J. J. Ferra, K. K. Thoen and H. I. Kenttamaa, *Int. J. Mass Spectrom.*, **210**, 511 (2001).
124. M. Tsuji, T. Arikawa and Y. Nishimura, *Bull. Chem. Soc. Jpn.*, **72**, 293 (1999).
125. M. Pykalainen, A. Vainiotalo, T. A. Pakkanen and P. Vainiotalo, *J. Mass Spectrom.*, **31**, 716 (1996).
126. M. Tsuji, A. M. H. Ujita and Y. Nishimura, *Bull. Chem. Soc. Jpn.*, **68**, 2385 (1995).
127. O. Bortolini, S. S. Yang and R. G. Cooks, *Org. Mass Spectrom.*, **28**, 1313 (1993).
128. T. Kotiaho, B. J. Shay, R. G. Cooks and M. N. Eberlin, *J. Am. Chem. Soc.*, **115**, 1004 (1993).
129. J. T. Moolayil, M. George, S. Srinivas, N. S. Swamy, A. L. Russell, D. E. Giblin and M. L. Gross, *Int. J. Mass Spectrom.*, **249/250**, 21 (2006).
130. L. L. da Rocha, R. Sparrapan, R. Augusti and M. N. Eberlin, *J. Mass Spectrom.*, **39**, 1176 (2004).
131. M. Bronstrup, D. Schroder and H. Schwarz, *Can. J. Chem.*, **77**, 774 (1999).

132. A. A. Sabino, M. N. Eberlin, L. A. B. Moraes and K. K. Laali, *Org. Biomol. Chem.*, **1**, 395 (2003).
133. M. A. Freitas and R. A. J. O'Hair, *Int. J. Mass Spectrom.*, **175**, 107 (1998).
134. L. J. Chyall and H. I. Kenttamaa, *J. Am. Chem. Soc.*, **116**, 3135 (1994).
135. L. J. Chyall and H. I. Kenttamaa, *J. Mass Spectrom.*, **30**, 81 (1995).
136. J. W. Denault, G. D. Chen and R. G. Cooks, *Int. J. Mass Spectrom.*, **175**, 205 (1998).
137. H. Chen, Z. Ouyang and R. G. Cooks, *Angew. Chem.*, **45**, 3656 (2006).

CHAPTER **6**

NMR spectra of anilines

ERKKI KOLEHMAINEN

Department of Chemistry, P.O. Box 35, FIN-40014, University of Jyväskylä, Finland
Fax: +358 14 2602501;   e-mail: ekolehma@jyu.fi

and

RYSZARD GAWINECKI and BORYS OŚMIAŁOWSKI

University of Technology and Life Sciences, Faculty of Chemical Technology and Engineering, Seminaryjna 3, PL 85 326, Bydgoszcz, Poland
Fax: +48 52 3749005;   e-mail: gawiner@utp.edu.pl
borys.osmialowski@people.pl

I. INTRODUCTION

Aniline (aminobenzene, phenylamine) was first isolated from indigo in 1826 by Otto Unverdorben[1a]. In 1845, August Wilhelm von Hofmann separated aniline from coal tar[1b]. The first industrial-scale use of aniline was in the manufacture of mauveine (aniline purple), a dye discovered in 1856 by William Henry Perkin[2]. Later it was shown that mauveine made by Perkin was a mixture of two phenazinium dyes, 3-amino-2-methyl-5-phenyl-7-(*p*-toluidinyl)phenazinium acetate and 3-amino-2,9-dimethyl-5-phenyl-7-(*p*-toluidinyl)phenazinium acetate (Figure 1), which can be formed from aniline and isomeric toluidines as shown by a careful NMR and mass spectral and retrosynthetic analysis of the model compounds and original samples from Perkin collection and from the British Museum[2].
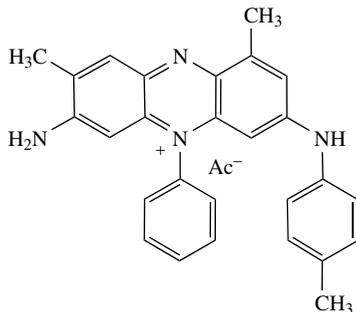
FIGURE 1. 3-Amino-2,9-dimethyl-5-phenyl-7-(p-toluidinyl)phenazinium acetate

Aniline has been one of the most important compounds in the first years of the chemical industry and its importance is still high. Nowadays, the major use of aniline is in the manufacture of polyurethanes. Aniline itself is produced mainly from nitrobenzene by reducing it with iron and dilute hydrochloric acid. Aniline is released from the formed anilinium hydrochloride by sodium carbonate treatment.

The number of known substituted anilines is enormous, owing to the easy electrophilic aromatic substitution of aniline, the rate of which can be even a million times faster than that of benzene[3]. Therefore, there exists a wealth of information on the derivatives of aniline, for example on their electronic effects, in this series of books[4]. It is noteworthy that some important aspects of the electronic effects of the amino group were discussed already more than thirty years ago by Chuchani[5].

From an NMR spectroscopic point of view, aniline itself contains four useful NMR active nuclei: [1]H, ^{13}C, ^{14}N and [15]N. In addition, introducing other NMR sensitive nuclei such as ^{19}F as its substituent(s) or as parts of the substituent can open a still larger scope to the substituted anilines. So it is not surprising that a literature search in Chemical Abstracts of the key words 'nmr' and 'aniline' produces almost 5000 hits. In a continuous wave (CW) period of NMR, the useful nuclei for aniline derivatives at natural abundance were ^{1}H and [19]F. In 1958, Richards and Schaefer published [1]H (at 29.92 MHz) and ^{19}F NMR chemical shifts and coupling constants of neat p-fluoroaniline[6]. In 1961, Spiesecke and Schneider reported the [1]H (at 60 MHz in 5 mol% solution in cyclohexane) and ^{13}C NMR chemical shifts of several monosubstituted benzenes including aniline and N,N-dimethylaniline[7]. The amino substituent chemical shifts (SCSs) for the *ortho*-, *meta*- and *para*-protons were 45.3, 12.2 and 37.5 Hz, and the corresponding N,N-dimethylamino SCSs were 36.0, 6.0 and 36.9 Hz (shielded from the shift of benzene), respectively[7]. The ^{13}C NMR SCSs were -19.2 (C1), $+12.4$ (C2,6), -1.3 (C3,5) and $+9.5$ ppm (C4) in aniline and -22.4 (C1), $+15.7$ (C2,6), -0.8 (C3,5) and $+11.8$ ppm (C4) in N,N-dimethylaniline, respectively[7]. They also reported for the first time the linear relationship between the *para*-effects (both hydrogen and carbon) and Hammett σ-constants for monosubstituted benzenes including aniline and N,N-dimethylaniline[7]. Among *ca* ten monosubstituted benzenes included in this study, amino and N,N-dimethylamino-groups show the strongest electron-donating properties, whereas the nitro-group is the strongest electron acceptor. So already in the early years of NMR the fundamental relationships between the NMR chemical shifts and electronic effects of the substituents of the aromatic ring were discovered by the pioneers of NMR.

The discovery of FT NMR by Ernst and Anderson[8] revolutionized NMR studies with its applicability to insensitive (with low magnetogyric ratio, γ) and nonabundant nuclei such

as carbon-13 and nitrogen-15. Further, polarization transfer techniques such as INEPT (Insensitive Nuclei Enhanced by Polarization Transfer) has further pushed the detection limit for still smaller sample concentrations. Combined with the spin-echo pulse sequence discovered by Hahn[9], INEPT forms a basic module in many two-dimensional heteronuclear chemical shift correlation pulse programs such as HSQC (Heteronuclear Single Quantum Coherence)[10], HMQC (Heteronuclear Multiple Quantum Coherence)[11, 12] and HMBC (Heteronuclear Multiple Bond Correlation)[13]. Further, PFG (Pulsed Field Gradient) techniques[14, 15] used for the selection of coherence transfer pathways and to spoil unwanted magnetization components have still improved the capabilities of liquid state NMR in studying aniline and its derivatives (and other nitrogen-containing compounds).

The discoveries in solid state NMR such as Cross Polarization (CP), which means magnetization transfer from a sensitive and abundant nucleus (such as proton) to an insensitive and nonabundant nucleus (such as carbon-13 and nitrogen-15) obtained by the so-called Hartmann–Hahn condition[16], Dipolar Decoupling (DD) to remove the line broadening caused by dipolar couplings, which do not time-average out in the solid state, differing from the situation in liquids, and Magic Angle Spinning (MAS) to remove chemical shielding anisotropy have made NMR feasible also in studying aniline and its derivatives among the other compounds in solid state at natural abundance.

Also, recent developments in quantum theoretical calculations of NMR parameters have increased their reliability and usefulness, especially in studying the dynamic processes such as conformational equilibria and tautomerism of aniline derivatives. All the above-mentioned items will be included in the following discussion. However, owing to the huge amount of data about ^{1}H NMR parameters, the main focus of this review is directed to ^{13}C, ^{15}N and ^{19}F NMR spectral studies of aniline derivatives. Schiff bases are not included in this review although some of them show an amino−imino tautomerism and can thus be considered as anilines. One reason for this is that a search in Chemical Abstracts using key words 'schiff base' and 'nmr' produced more than 1000 hits.

II. RING AND *N*-SUBSTITUTED ANILINES

The overall screening, σ(tot), of nuclei heavier than hydrogen, such as carbon-13 and nitrogen-15, can be expressed as a sum of three terms (equation 1),

$$\sigma(\text{tot}) = \sigma(\text{diamagnetic}) + \sigma(\text{paramagnetic}) + \sigma(\text{other}) \qquad (1)$$

where σ(diamagnetic) is the local diamagnetic screening of the nucleus, and is caused by magnetically induced local electronic circulations about the nucleus. This term dominates the proton chemical shift and is related directly to the electron density. The local paramagnetic term, σ(paramagnetic), is a descriptor of the deviation from spherical symmetry of the electronic distribution around the nucleus. Contributions to this overall negative term require electrons in orbitals with nonzero angular momentum. The term σ(other) includes all sources of screening other than those at the nucleus, such as anisotropy, field and solvent effects[17].

The paramagnetic term can be expressed by equation 2,

$$\sigma(\text{paramagnetic}) = (1/\Delta E)\langle 1/r^3 \rangle \Sigma Q \qquad (2)$$

where ΔE measures how easily the system can be electronically excited, $\langle 1/r^3 \rangle$ is the average inverse cube of the orbital (in case of nitrogen and carbon it is p or sp^n) and ΣQ is the measure of multiple bonding to nitrogen or carbon (or hybridization of the atom).

The direct observation of the nitrogen-15 spectrum with proton wideband decoupling is problematic due to negative NOE, which decreases the signal intensity. This unwanted

effect can be circumvented by a gated decoupling pulse sequence. Also, paramagnetic relaxation reagents such as $Cr(acac)_3$ have been added to the samples to fasten the slow nitrogen-15 spin relaxation, as in the case of substituted N-nitroanilines[18].

The first systematic ^{15}N NMR studies of aniline derivatives were conducted by Lichter and Roberts[19] and Axenrod and coworkers[20, 21]. In ten ortho- or para-mono-substituted anilines (2-NO$_2$-, 4-NO$_2$-, 2-I-, 2-Br-, 4-I-, 4-Cl-, 2-Cl-, 4-F-, 2-OCH$_3$- and 2-F-) measured for 1 M solutions in acetone, the most deshielded resonances are for 2-NO$_2$- and 4-NO$_2$-aniline, being 71.0 and 70.3 ppm, and the most shielded one that of the 2-F derivative, 43.6 ppm (from the resonance of neat CH_3NH_2), respectively. In the corresponding anilinium ions the ^{15}N NMR chemical shift variation is much smaller, being 44.1 for 2-NO$_2$-, 47.8 for 4-NO$_2$ and 37.0 ppm for the 2-F derivative. This observation can be explained by the fact that protonation (using the nitrogen electron lone pair) removes the effect of the lone-pair delocalization. Differing from the conjugatively interacting substituents, the ring methyl groups appear to possess a much smaller effect. Table 1 presents the ^{15}N NMR chemicals shifts for the ring-substituted monomethyl- (toluidines) and dimethylanilines (xylidines) and the corresponding anilinium ions[22, 23].

As can be seen, di-ortho-substitution seems to have the weakest effect both in the molecule and in the cation. This can be explained by a steric inhibition of the interaction between the lone-pair sp^3-orbital and the aromatic π-system. The same trend can be seen if we compare the ^{15}N NMR chemical shifts of aniline, 56.5 ppm, N-methylaniline, 52.8 ppm and N,N-dimethylaniline, 44.6 ppm. In ortho-substituted N,N-dimethylanilines the shielding effect is related to the number and size of the ortho-substituents (Table 2)[24].

As a general conclusion, an interaction between the nitrogen lone pair and the adjacent π-system deshields the aniline-type nitrogen. It is therefore reasonable to expect that nitrogen chemical shifts can be used as probes for the influence of the ring substituents and the lone-pair delocalization.

A systematic evaluation of the electron donor strengths of different amino groups by using NMR related with UV-Vis, IR and Raman, microwave and photoelectron spectral data, dipole moments, basicity, reactivity, electron and X-ray diffraction data and the results of quantum chemical calculations has been reviewed by Gawinecki and coworkers[25].

Figure 2 presents the geometrical parameters which influence the resonance interaction between the nitrogen electron lone pair and the aromatic π-system. They are $C_{ar}N$ bond length, HNH bond angle α, torsion angle ϕ, bend angle ψ and pyramidalization, i.e. tilt or inversion angle θ. It should be noted that some of these geometrical parameters, such as ψ and θ, are dependent on each other.

TABLE 1. $\delta(^{15}N)$ (in ppm^a) of ring-substituted mono- and dimethylanilines and the corresponding cations

Substituent in aniline	$\delta(^{15}N)$ of molecule	$\delta(^{15}N)$ of anilinium cation
H	56.5	51.1
2-Me	54.2	48.8
3-Me	55.6	50.3
4-Me	53.9	49.6
2,3-Me$_2$	52.9	49.5
2,4-Me$_2$	51.7	47.9
2,5-Me$_2$	53.4	48.7
2,6-Me$_2$	51.0	45.5
3,4-Me$_2$	52.9	50.2
3,5-Me$_2$	55.0	50.7

^{a} Measured as pure liquids from the shift of external nitric acid, $\delta(H^{15}NO_3) = 375.8$ ppm.

TABLE 2. $\delta(^{15}N)$ (in ppm ^{a}) of alkyl substituted
N,N-dimethylanilines

Substituent in N,N-dimethylanilines	$\delta(^{15}N)$
H	44.6
2-Me	33.9
3-Me	43.7
4-Me	42.0
2,3-Me$_2$	33.4
2,6-Me$_2$	17.1
2,6-Et$_2$	13.1
2,6-(i-Pr)$_2$	10.4

^{a} Measured in 10–15% C_6D_6 from the shift of an external
$^{15}NH_4Cl$ in 1 M HCl. $\delta(^{15}NH_4Cl) = 0.0$ ppm
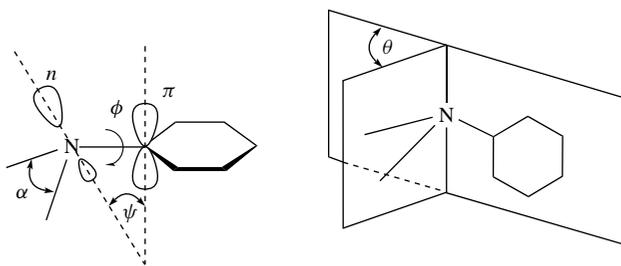
FIGURE 2. Geometrical parameters of aniline molecule
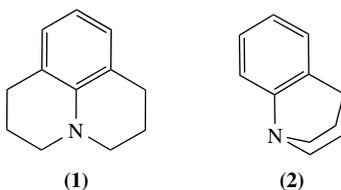
FIGURE 3. Structures of julolidine, **1**, and benzoquinuclidine, **2**

   In most arylamines the angles α, ϕ, ψ and θ are intermediates between those in
julolidine (2,3,6,7-tetrahydro-1H,5H-pyrido[3,2,1-ij]quinoline), **1**, and benzoquinuclidine
(3,4-dihydro-2H-1,4-ethanoquinoline), **2** (Figure 3), both containing the Ar−N< frag-
ments in extreme rigid conformations[26–29].
   However, it should be kept in mind that a high barrier to change in hybridization
of the nitrogen atom may be also expected in other bridged anilines[30]. Little is known
about the ground state conformation of cyclic amines **3** and **4** (Figure 4). The available
molecular geometries of the parent *aza*cycloalkanes, c-$(CH_2)_nNH$, may throw some light
on this problem. Both experiment and theoretical *ab initio* calculations show that the strain
energies in hexamethyleneimine ($n = 6$), piperidine ($n = 5$), pyrrolidine ($n = 4$), azetidine
($n = 3$) and aziridine ($n = 2$) are equal to 7, 0, 5, 25 and 27 kcal mol^{-1}, respectively[31].
This shows that the three- and four-membered rings in such compounds are much more
strained than those in other cyclic amines.
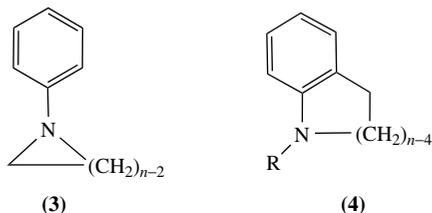
FIGURE 4. Structures of cyclic amines **3** and **4**

All substituents, including amino groups, affect the geometry of the attached aromatic ring. It is noteworthy that valence angles C6C1C2 and C3C4C5 in monosubstituted benzenes where C1 is the *ipso* carbon atom were found to be related to σ_I and σ_R values of the substituent, respectively[32]. Changes in the bond lengths in such compounds are relatively less sensitive to the substituent because of the high force constants involved. At this point it seems noteworthy to mention that the idea of $n-\pi$ conjugation in aromatic amines being discussed throughout the present paper is not commonly accepted. Thus, according to Clark[33], most interactions in aromatic amines arise from repulsion between the unshared electrons and the π-system of the ring rather than from the lone-pair delocalization.

The nitrogen chemical shifts are influenced by the substituent polar[20] and steric effects[24] and thus can be useful when estimating the degree of $n-\pi$ interaction in anilines[34]. Shielding of the nitrogen in N,N-dimethylanilines upon 4-substitution by electron-donating groups is ascribed to decreased electron delocalization. This is evidenced by correlation of the SCS in ^{15}N NMR spectra for 4-substituted anilines and their N,N-dimethyl derivatives with σ_I and σ_R^- values in a dual-substituent-parameter (DSP) analysis[34].

ortho-Substitution in N,N-dimethylaniline causes a considerably large shift of its ^{15}N signal[24]. This has been attributed to the torsional distortion of the NMe$_2$ group from the conformation defined by $\phi = 0°$, which results in a decreased electron delocalization[24]. The shift values correlate with ionization potentials of the aniline π-electrons and thus also become a good measure of nitrogen–benzene ring delocalization, $n_N-\pi_{Ar}$[24]. This relationship shows that the twist angles in 2,6-diethyl- and 2,6-diisopropyl-N,N-dimethylanilines are equal to 77 and 88°, respectively. The range of ^{15}N shifts in the spectra of N-(p-R-phenyl)aziridines, **5** ($n = 3$) (Figure 5), is substantially lower than that for the corresponding N,N-dimethylanilines.

This shows that the lone-pair electrons of the aziridine nitrogen interact less effectively with the benzene ring[34]. A steric effect of the 2,6-dimethyl substitution in N-phenylaziridine on the ^{15}N resonance line position has been found to be much smaller
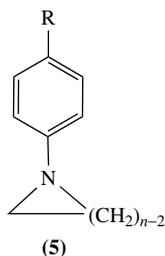
FIGURE 5. Structures of cyclic amines **5**

(6)
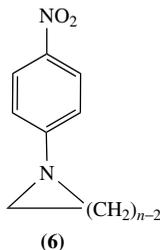
FIGURE 6. Structures of cyclic amines **6**

than that in N,N-dimethylanilines[34]. The analysis of these chemical shifts shows that the angle ϕ in N-phenylaziridine equals $0°$ but the benzene and aziridine rings are not coplanar. The lack of correlation between ionization potentials of substituted N-arylaziridines and ^{15}N shifts has been attributed to direct interactions of the lone-pair orbitals with *para*-substituents that are not reflected in the nitrogen shifts[34].

^{15}N chemical shifts and one-bond $^{15}N-H$ coupling constants in the spectra of anilines show that electron-acceptor substituents in the ring favor the sp^2 hybridization of the amine nitrogen atom[20].

Analysis of the chemical shift values of the ring protons in ^1H NMR spectra of aniline derivatives shows that the donor strength of the amino substituents in the ground state of aromatic amines changes in the following order[35]: 1-pyrrolidino > dimethylamino > 1-piperidino. The amine nitrogen atom in N-(p-nitrophenyl) polymethyleneimines, **6** ($n >$ 3) (Figure 6), as well as in $PhNR_2$, R = Me, Et, was found to be nearly-sp^2 hybridized[30].

However, this is not the case for $n = 3$. Decreased $n_N-\pi_{Ar}$ interaction in **6** ($n = 6$), which reflects the relative rigidity of the chair form of the six-membered ring, is also consistent with the deshielding of the signals of protons 2 and 6 in the spectra of **6** ($n = 5$), **6** ($n = 7$) and $PhNR_2$, where R = Me, Et[36]. Nearly-sp^2 and nearly-sp^3 hybridization of the amino nitrogen atom in **6** ($n = 4-6$) and **6** ($n = 3$), respectively, has also been proved by the solvent-dependent ^1H NMR chemical shifts[37].

The ^1H NMR spectrum of 1-phenylaziridine, **3** ($n = 3$), was found to be strongly temperature-dependent.[38] This means that the $C_{Ar}NCC$ fragment in this compound is nonplanar and that inversion in its molecule occurs rather slowly (the coalescence temperature is less than $-77\,°C$)[38]. Bystrov and coworkers[39] show the methylene protons in this compound to be chemically equivalent. This observation negates low frequency of aziridine ring inversion. Moreover, it proves that n_N electrons in 1-phenylaziridine are not delocalized into the benzene ring[39]. Good quality correlations between ^1H chemical shifts of the methylene protons and σ^- constants for p-substituted N-phenylaziridines indicate that resonance interaction of the amine nitrogen atom with the aromatic ring is important[40]. It is additionally confirmed by the correlations of the ring breathing frequencies with the σ^- values[40].

^{13}C NMR chemical shifts for aniline were found to be quite sensitive to the orientation of the NH_2 group: both theoretical (GIAO, *i.e.* Gauge-Independent Atomic Orbitals) and experimental results show that the amino group is tilted away from the ring plane by $42°$[41]. Calculations show that chemical shift values increase (downfield effect) as the amino group is moved away from the planar orientation, with the largest changes appearing at the *ipso, ortho* and *para* positions[41].

The chemical shifts of the *para* carbon atom in the spectra of N,N-dimethyl- and N,N-diethylanilines and 1-phenylaziridine, 1-phenylpyrrolidine, **3** ($n = 5$), and 1-phenylpiperidine, **3** ($n = 6$), correlate well with other known measures of benzene ring−nitrogen

resonance such as oscillator strength of the UV bands, $\cos^2\phi$ values and exaltation of molar refraction[42, 43]. Moderate quality correlation has also been found between these δ values and pK_a values for various aminobenzenes except N,N-diethylaniline which exhibits an abnormal (high) base strength in hydroxylic solvents, arising from steric inhibition of hydrogen bonding in the free base[36]. Although large differences in basicities were found for N,N-diethylaniline and N-phenylpyrrolidine, close similarity of their ^{13}C NMR spectra shows that electron distributions in the benzene rings are nearly the same in these two compounds[42].

The chemical shifts of the *para* carbon atom with respect to the amino substituent in the ^{13}C NMR spectra of respective *p*-aminobenzaldoximes, **7** (Figure 7), was used to calculate the σ_R^O values for different amino groups[44].

The data presented in Table 3 show that the 1-pyrrolidino group is the most powerful electron donor among all the amino groups studied, as judged by the σ_R^O values.

The π-electron density depends on the twist angle of the substituent at the *para* carbon atom in the aromatic compounds[45] and thus its chemical shift can be used to calculate these angles for the amino groups in anilines. This has been done for compounds of formula **8** (Figure 8)[46]. These data are given in Table 4.

(7)
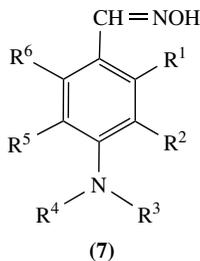
FIGURE 7. Structures of *p*-aminobenzaldoximes **7**

TABLE 3. σ_R^O substituent constants for amino groups (for R^1–R^6, formula **7**)[44]

R^1	R^2	R^3		R^4	R^5	R^6	σ_R^O
H	H	H		H	H	H	−0.48
H	H	Me		H	H	H	−0.52
H	H	Me		Me	H	H	−0.53
H	H	Me		Et	H	H	−0.57
H	H	Et		Et	H	H	−0.57
Me	H	Me		Me	H	H	−0.64
Me	H	Me		Me	H	Me	−0.67
H	Me	Me		Me	H	H	−0.24
H	H		$(CH_2)_4$		H	H	−0.63
H	H		$(CH_2)_5$		H	H	−0.47
H	H		$(CH_2)_6$		H	H	−0.59
H	$(CH_2)_2$			Me	H	H	−0.47
H	$(CH_2)_3$			Me	H	H	−0.48
H	$(CH_2)_4$			Me	H	H	−0.33
H	$(CH_2)_2$			$(CH_2)_3$	H	H	−0.43
H	$(CH_2)_3$			$(CH_2)_3$	H	H	−0.59

(8)
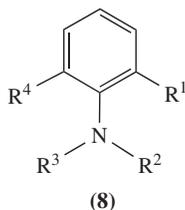
FIGURE 8. Structures of compounds **8**

TABLE 4. Twist angles of the amino group in anilines **8**[46]

R^1	R^2	R^3	R^4	ϕ (deg)
H	H	H	H	12
Me	H	H	H	19
Me	H	H	Me	0
H	H	Me	H	16
Me	H	Me	H	18
Me	H	Me	Me	61
H	Me	Me	H	19
Me	Me	Me	H	68
Me	Me	Me	Me	80
H	Et	Me	H	16
H	Et	Et	H	0
$(CH_2)_2$		H	H	33
$(CH_2)_3$		H	H	0
$(CH_2)_4$		H	H	53
$(CH_2)_5$		H	H	64
$(CH_2)_2$		Me	H	32
$(CH_2)_3$		Me	H	13
$(CH_2)_4$		Me	H	58
$(CH_2)_5$		Me	H	80
$CH(CH_2CH_2)_2$ [a]			H	90

[a] Benzoquinuclidine, **2**.

The effect of the *ortho*-methyl group in *N,N*-dimethylanilines on ^{13}C chemical shift has also been found useful for evaluating the angle ϕ and barrier to rotation of the NMe_2 group[47].

^{13}C NMR spectra show that *N*-phenylaziridine is the least conjugated among the *N*-phenyl cyclic amines. It has been found that the substituent in *p*-substituted *N*-phenylaziridines only slightly affects the electron distribution in the aziridine ring[48]. This proves that $n_N-\pi_{Ar}$ conjugation in these compounds is insignificant, which has been additionally confirmed by the minor temperature effect on the ^{19}F NMR spectrum of 1-(*p*-fluorophenyl)aziridine[48].

^{19}F chemical shifts are very sensitive to very small perturbations in the π-charge density at the fluorine atom produced by the substituent[49]. ^{19}F NMR spectra of *p*-fluoroanilines, *p*-FC$_6$H$_4$NR^{1}R^2, were found useful in evaluating the extent of $n_N-\pi_{Ar}$ conjugation[50]. Substituent constants for the amino, dimethylamino and 1-aziridino groups, based on fluorine chemical shifts of proper fluoroanilines, are equal to $\sigma_R^O = -0.486$, -0.530 and -0.290, respectively[50].

TABLE 5. Polar (σ_I) and resonance (σ_R^O) substituent constants of amino groups based on the ^{19}F chemical shift in the spectra of p-RC_6H_4F[51]

R	σ_I	σ_R^O
$N(CH_2)_2$	0.07	−0.29
NH_2	0.01	−0.48

Analysis of ^{19}F chemical shifts show that the 1-aziridinyl group is not as conjugatively electron-donating as either the NH_2 or NMe_2 group[51]. The polar and resonance substituent constants based on ^{19}F chemical shifts of the respective p-substituted fluorobenzenes are given in Table 5[51].

^{19}F chemical shifts in the NMR spectrum of 4-fluoro 2,N,N-trimethyl-aniline show the *ortho*-methyl group to produce a 56% steric inhibition of the resonance effect[49]. In consequence, the σ_R^O constant for the partially twisted p-dimethylamino substituent is equal to −0.24 (−0.52 compared with the nontwisted NMe_2 group)[49]. ^{19}F chemical shifts of 4-amino-3,5-dimethylfluorobenzene and of its N,N-dimethyl derivative were interpreted in terms of steric inhibition to resonance: two *ortho*-methyl groups are insufficient to push the NH_2 group out of complete conjugation with the benzene ring[52]. Although the N,N-dimethylamino group in 4-amino-3,5,N,N-tetramethyl fluorobenzene is much twisted with respect to the ring plane, there is still a significant resonance interaction between those two parts of the molecule[52].

Analysis of ^1H, ^{13}C and ^{15}N NMR chemical shifts in aminobenzenes and aminopyridines shows that the amine groups are tilted away from the ring plane by 25−45°[41]. Comparison of the calculated and experimental shift values indicates that pyramidalization of the amino nitrogen causes a downfield effect of ^1H, ^{13}C and ^{15}N resonances[41].

It was found that two *ortho*-methyl groups in N-methyl and N,N-dimethylanilines cause a diminution of the N-methyl ^{13}C−^1H coupling constant by about 0.5 and 1.5 Hz, respectively[53]. It is partly attributed to the inductive effect of these groups. Steric inhibition of resonance between the amino group and the benzene ring is responsible for the remainder of this decrease[53].

III. MULTINUCLEAR NMR STUDIES OF *p*-F-ANILINE DERIVATIVES

Owing to its 100% natural abundance, high magnetogyric ratio (good NMR sensitivity) and large chemical shift range of fluorine-19, ^{19}F NMR spectroscopy offers excellent opportunities to observe even small electronic changes in the environment of the fluorine-19 atom produced intramolecularly by a distant p-substituent[49]. Consequently, ^{19}F NMR shieldings of p-substituted fluorobenzenes are more or less directly related to the π-electron density at the fluorine atom[7, 43, 54−57] because the nature of the carbon−fluorine bond is primarily responsible for ^{19}F shielding within a series of such molecules[54−56]. ^{19}F NMR spectra of p-fluoroanilines, p-$FC_6H_4NR^1R^2$, were also found useful in evaluating the extent of n_N−π_{Ar} conjugation[50]. In addition to the above-mentioned intramolecular factors, substantial solvent effects on $\delta(^{19}F)$ have also been observed[58−60].

The intermolecular effects generally involve van der Waals dispersion forces, hydrogen bonding and dipole−dipole interactions[61]. Since $\delta(^{19}F)$ values are also dependent on the sample concentration[50], these were usually extrapolated to infinite dilution when searching for dependencies between $\delta(^{19}F)$ and σ[49, 50, 52, 62].

It has been shown that ^{19}F chemical shifts are linearly correlated quite precisely with the inductive substituent constant, σ_I, for the *meta*-substituted fluorobenzenes[63]. Further,

^{19}F chemical shifts of substituted fluorobenzenes, RC_6H_4F, are correlated with the σ substituent constants[64-66] by a dual substituent constant equation $\delta(^{19}F) = \rho_I\sigma_I + \rho_R\sigma_R +$ const. It is noteworthy that $\rho_I \gg \rho_R$ for the m-substituted and $\rho_I < \rho_R$ for the p-substituted compounds. Taft and coworkers[49, 62, 67, 68] have found that values of $\delta(F_m)$ and $\delta(F_p)$ for substituted fluorobenzenes obey the following equations: $\delta(F_m) = 7.1\sigma_I - 0.05$ and $\delta(F_p) = 7.1\sigma_I + 29.5\sigma_R^O + 0.60$. This indicates that the resonance effect is negligible at the *meta* position and that polar (inductive/field) effects are relatively unimportant at the *para* position. Afterwards, this model was extended[69] and improved equations were introduced[70, 71]: $\delta(F_m) = 5.26\sigma_I + 0.81\sigma_R^O$ and $\delta(F_p) = 7.02\sigma_I + 30.55\sigma_R^O + 0.60$.

^{13}C NMR chemical shifts for C4 in anilines and the corresponding p-fluoroaniline derivatives **9–22** (Figure 9), ^{19}F NMR shifts (relative to an external fluorobenzene) and ^{15}N NMR shifts (relative to an external nitromethane) of p-F-anilines as well as their $^nJ(^1H,^{19}F)$ spin–spin coupling constants are given in Table 6. It should be mentioned that 1:10 dilution of the sample results in at most <0.1 ppm change in $\delta(^{19}F)$. An insignificant concentration effect on their $J(F,H)$ coupling constants has also been observed.

Substitution of the benzene hydrogen by the most electronegative element, fluorine, is expected to have significant effects on the chemical shifts of other nuclei present in the molecule. Thus, the chemical shift of the C4 (with respect to the amino group) atom in p-F-anilines **9–22** (Table 6) and C4 in the corresponding anilines[25] are linearly dependent (correlation coefficient $R = 0.963$, $n = 14$). Similar dependence between $\delta(^{19}F)$ values for p-F-anilines (Table 6) and $\delta(^{13}C4)$ for anilines[25] is of comparable quality ($R = 0.952$, $n = 14$). It is known that $\delta(^{19}F)$ values in a series of p-substituted fluorobenzenes correlate distinctly less well with the corresponding $\delta(^{13}C_p)$ than with $\delta(^{13}C_p)$ for monosubstituted benzenes[72]. The effect of a directly bound fluorine atom on the local π-electron density was believed to be responsible for such a behavior. On the other hand, $\delta(^{15}N)$ in p-F-anilines **9–22** (Table 6) and in the corresponding anilines[25] does not show such a good correlation ($R = 0.814$, $n = 14$).

(9)   (12)   (20)

(10) R^1 = H, R^2 = R^3 = Et
(14) R^1 = H, R^2 = R^3 = Me
(15) R^1 = H, R^2 = Me, R^3 = Et
(16) R^1 = R^3 = H, R^2 = Me
(17) R^1 = R^3 = H, R^2 = Et
(19) R^1 = R^2 = R^3 = H
(21) R^1 = R^2 = R^3 = Me
(22) R^1 = R^2 = Me, R^3 = Et

(11)   (13)   (18)
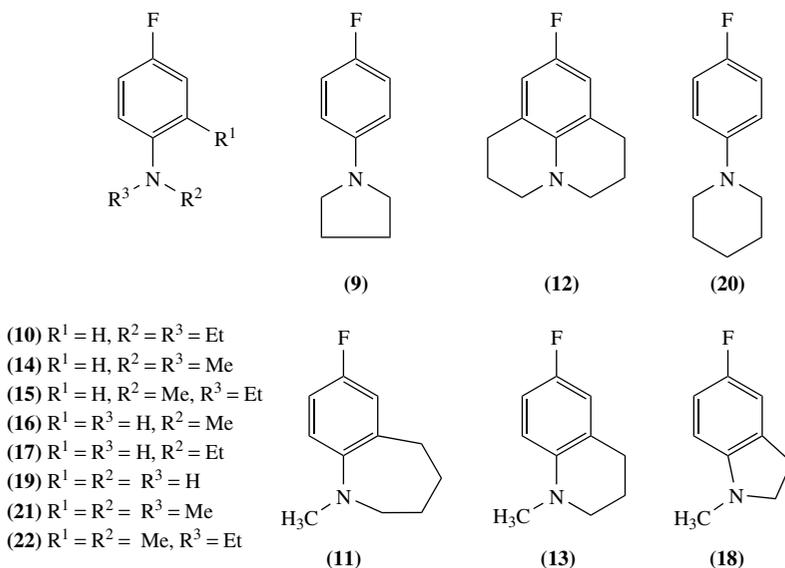
FIGURE 9. Structures of compounds **9–22**

TABLE 6. ^{13}C, ^{15}N and ^{19}F NMR chemical shifts (δ) and ^{1}H,^{19}F coupling constants (Hz) of anilines and their p-F-derivatives **9–22** for 0.1–0.2 M solutions in CDCl$_3$ at 303 K

Compound	$\delta(^{13}C4)$ [a]	$\delta(^{13}C4)$ [b]	$\delta(^{19}F)$ [b]	$\delta(^{15}N)$ [a]	$\delta(^{15}N)$ [b]	$^n J(^1H,^{19}F)$ [c] $n = 3/n = 4$
9	115.20	154.70	−17.64	−308.7	−311.1	8.6/4.3
10	115.32	154.89	−16.82	−309.7	−313.4	8.4/4.2
11	115.33	154.98	−17.25	−319.0	−327.7	8.7/4.7
12	115.61	155.15	−16.14	−318.5	−320.2	9.3/-
13	115.99	155.24	−15.23	−320.8	−321.2	8.9/5.0
14	116.38	155.40	−16.07	−337.7	−339.4	8.5/4.3
15	115.90	155.21	−16.45	−325.0	−327.2	8.5/4.3
16	116.99	155.60	−15.49	−329.2	−332.2	8.8/4.3
17	117.02	155.38	−15.32	−310.4	−313.2	8.6/4.2
18	117.53	155.49	−14.59	−316.2	−318.2	8.4/4.2
19	117.68	155.97	−13.84	−325.5	−329.5	8.8/4.4
20	118.91	156.43	−12.00	−313.2	−315.6	8.7/4.4
21	118.23	156.01	−14.01	−347.3	−325.8	9.3/4.9
22	117.86	156.03	−13.88	−328.1	−331.2	9.3/5.0

[a] $\delta(^{13}C4)$ in corresponding anilines[25].
[b] For 4-fluoroanilines.
[c] Coupling with two different *ortho*-protons.

A known equation, $\sigma_R^O = [\delta(^{19}F) - 7.02\sigma_I - 0.60]/30.55$[70, 71], was used to calculate the resonance substituent constants from $\delta(^{19}F)$ of p-fluoroanilines (Table 7). Table 7 contains also such constants calculated from $\delta(^{13}C4)$ of the respective anilines[25] and p-aminobenzaldoximes[44]. One additional set of the σ_R^O values was obtained by means of the equation $\sigma_R^O = 0.026\delta(^{19}F) - 0.121$, *i.e.* from the linear dependence based on $\delta(^{19}F)$ of the corresponding p-F-anilines (Table 6) and $\sigma_R^O = -0.481$ and -0.539 for NH$_2$ and NMe$_2$[49, 62], respectively (this equation was used to calculate the substituent constants for the remaining substituents). Table 7 presents resonance substituent constants for the different amino groups.

The resonance parameter, σ_R^o, is the difference between the σ^o and σ_I values[67]. It can be seen that the linear dependence, $\sigma_R^O = [\delta(^{19}F) - 7.02\sigma_I - 0.60]/30.55$, and those based on $\delta(^{13}C4)$ of the respective anilines (footnotes *a* and *b* in Table 7) are only moderate ($R = 0.919$, $n = 14$). Further, a similar dependence for the corresponding p-aminobenzaldoximes (footnotes *a* and *c* in Table 7) based on $\delta(^{13}C4)$ is much worse: $R = 0.594$, $n = 11$, $R = 0.672$, $n = 10$ (the point for 1-NMe$_2$, 2-Me is excluded). Unexpectedly, a similar correlation for the numbers in columns marked with footnotes *a* and *d* in Table 7 is excellent: $R = 0.991$, $n = 14$.

Analysis of the ^{1}H NMR shifts of aniline derivatives shows that the donor strength of the amino substituents changes in the following order: 1-pyrrolidino > dimethylamino > 1-piperidino[35]. Based on the $\delta(^{13}C4)$ data for anilines[25], the σ_p substituent constants for different dialkylamino groups change in the following order: NEt$_2$ < NMe$_2$ < N(Me)Et. Further, it seems interesting that $\sigma_{p-N(Me)Et} \approx \sigma_{p-NHMe} = \sigma_{p-NHEt}$[25].

$\delta(^{19}F)$ values suggest the amino nitrogen atom in 6-fluoro-1-methyl-1,2,3,4-tetrahydroquinoline (**11**) to be a stronger donor than that of the nitrogen in NEt$_2$, but other methods do not confirm this conclusion. The properties of that atom in 9-F-julolidine (**12**) are similar (a strong donor), although the substituent constant for the NMe$_2$ group based on $\delta(^{19}F)$ is higher than those obtained by other methods which are comparable to the literature data (Table 7). Similar properties of the *N*-ethyl, *N*-methylamino (**15**) and *N*-methylamino (as

TABLE 7. Resonance substituent constants for the amino groups in nonfluorinated anilines corresponding to the structures of *p*-fluoro derivatives **9–22** (Figure 9)

Substituents on N- and aryl ring	$\sigma_R^{O\ a}$	$\sigma_R^{O\ b}$	$\sigma_R^{O\ c}$	$\sigma_R^{O\ d}$	$\sigma_R^{O\ e}$
N(CH₂)₄	−0.62	−0.57	−0.63	−0.58	0.628[72–74 f]
NEt₂	−0.59	−0.57	−0.57	−0.56	0.571[72–74 f]
N(Me)[2-(CH₂)₃]	−0.61	−0.57	−0.48	−0.57	—
N[2,6-(CH₂)₃]₂	−0.57	−0.56	−0.59	−0.54	—
NH[2-(CH₂)₃]	−0.55	−0.55	—	−0.52	—
NMe₂	−0.57	−0.54	−0.53	−0.54	−0.530[50, 51 g]
					−0.539[49 g]
					−0.533[72–74 f]
					−0.53[75 f]
					−0.52[76 h]
					−0.50[67 i]
N(Me)Et	−0.58	−0.52	−0.57	−0.55	—
NHMe	−0.55	−0.52	−0.52	−0.52	−0.52[72–74 f]
NHEt	−0.55	−0.52	—	−0.52	−0.52[73, 74 f]
N(Me)[2-(CH₂)₂]	−0.52	−0.51	−0.47	−0.50	—
NH₂	−0.50	−0.50	−0.48	−0.48	−0.486[50 g]
					−0.481[49, 51 g]
					−0.47[75 f]
					−0.48[76 g]
N(CH₂)₅	−0.44	−0.47	−0.47	−0.43	−0.474[72–74 f]
1-NMe₂,2-Me	−0.50	−0.49	−0.24	−0.46	−0.24[49, 77 g, j]
1-NH₂,2-Me	−0.51	−0.50	—	−0.48	—

[a] $\sigma_R^O = [\delta(^{19}F) - 7.02\sigma_I - 0.60]/30.55^{70, 71}$.
[b] Based upon $\delta(^{13}C4)$ values of the respective anilines[25].
[c] Based upon $\delta(^{13}C4)$ values of the respective *p*-aminobenzaldoximes[44].
[d] Obtained by means of the equation $\sigma_R^O = 0.026\delta(^{19}F) - 0.121$ (see text).
[e] Literature data.
[f] Based upon the band intensities in the IR spectra of the respective anilines.
[g] The solvent-independent σ_R^O based upon fluorine shielding parameters.
[h] Evaluated statistically.
[i] Evaluated by means of the equation $\sigma_R^O = 2.0\sigma_R^m$.
[j] Based upon σ_R values and upon excitation coefficients for ethyl 3-methyl-4-dimethylaminobenzoate.

well as *N*-ethylamino) groups are suggested only by ^{13}C NMR data of anilines (Table 7). $\delta(^{19}F)$ values suggest the amino nitrogen atom in 5-fluoro-1-methylindoline (**18**) to be a weaker donor than that in julolidine (**12**). A similar conclusion can be drawn by comparing the substituent data for 1-pyrrolidino (**9**) and 1-piperidino groups (**20**). The values for the parent amino group are comparable to or slightly lower than those found in the literature. The *ortho*-methyl group in 4-fluoro-2,*N*,*N*- trimethylaniline diminishes the donor properties of the dimethylamino group but does not do that to the parent amino group.

Molecular models show that in the five-membered ring of indoline and its *N*-methyl derivative, the C$_{Ar}$C$_{Ar}$N valence angle is expected to be much smaller than 120° due to the angle strain. The bicyclic structures of *N*-methylindoline and *N*-methyl-1,2,3,4-tetrahydroquinoline were shown to be planar[78]. The length of the polymethylene bridge between N and C$_{ortho}$ in anilines affects considerably the electronic properties of the nitrogen atom in these compounds[25]. Thus, it is a stronger donor in 1,2,3,4-tetrahydroquinolines than in indolines.

Substitution at the *ortho*-carbon in *N*,*N*-dimethylaniline causes the NMe₂ group to twist out of the ring plane, so the nitrogen becomes more pyramidal[49]. Thus, *ortho*-substitution

decreases the donor properties of the amino group. Due to strong steric interactions, the amino group in 2,N,N-trimethylaniline is a weak electron-donor. The $\delta(^{19}F)$ for 3-methyl-4-N,N-dimethylaminofluorobenzene relative to internal m-fluorotoluene is +7.05 ppm[77]. The normal p-dimethylamino chemical shift is found to be +15.90 ppm, indicating that the *ortho*-methyl substituent produces a 56% steric inhibition to resonance effect[49], which is essentially the same value as that based on σ_R and extinction coefficients for ethyl 3-methyl-4-dimethylaminobenzoate[77]. Thus, $\sigma_R^o = -0.24$ for the twisted p-dimethylamino substituent (compared with -0.52 for the nontwisted NMe$_2$ group)[49].

^{19}F NMR chemical shifts of 4-amino-3,5-dimethylfluorobenzene and of its N,N-dimethyl derivative were interpreted in terms of steric inhibition of resonance: two *ortho*-methyl groups are insufficient to push the NH$_2$ group out of conjugation with the benzene ring[52]. Although the N,N-dimethylamino group in 3,5,N,N-tetramethyl-4-aminofluorobenzene is much twisted with respect to the ring plane, there is still a significant resonance interaction between these two parts of the molecule[52]. The difference between the ^{19}F chemical shift in the NMR spectra of 4-R-3,5-dimethylfluorobenzene and 4-R-fluorobenzene in CCl$_4$ is equal to 1.36 and 11.79 ppm for R = NH$_2$ and NMe$_2$, respectively[52]. This shows that the conformation of Ar-R is only slightly affected by two *ortho*-methyl groups in p-fluoroaniline but it can be significantly affected in N,N-dimethyl-p-fluoroaniline.

As concluding remarks, it can be noted that the ^{19}F NMR chemical shifts of various p-F-anilines were found to be useful in evaluating the resonance substituent constants of different amino groups. Comparison of their $\delta(^{19}F)$ and $\delta(^{13}C4)$ in the corresponding anilines and p-aminobenzaldoximes shows that the substituent constants obtained depend somewhat on the method used. The 1-pyrrolidino group has the highest electron-donor properties among the different amino groups studied. The 1-piperidino group is a rather weak electron-donor. The amino nitrogen atoms in N,N-diethylaniline, 1-methyl-1,2,3,4-tetrahydroquinoline and julolidine are strong electron donors whereas the nitrogen atom in 1-methylindoline is a much weaker donor. *ortho*-Methyl diminishes the donor properties of the N,N-dimethylamino group but does not affect the unsubstituted amino group. The amino nitrogen atom in 1,2,3,4-tetrahydroquinolines is a stronger electron-donor than in indolines.

IV. DYNAMIC NMR OF ANILINE DERIVATIVES

Kleinpeter and coworkers[79] have recently studied restricted rotation and ring inversion in highly substituted anilines, **23–31** (Figure 10), prepared by the reaction of cyclic ylidene malonitriles with acetylene (di)carboxylic acids. Table 8 presents the experimental and calculated activation energies for the restricted rotation of the amino group in **23–31**.

The results are based on variable-temperature (VT) ^1H NMR studies of **23–31**. The results are close to those found for 2-aminoacetophenone, $\Delta G^{\#} = 10.5 \pm 0.5$ kcal mol^{-1} [80]. In addition, for the four compounds **25–28** characterized by the cycloheptene moiety, a slow ring interconversion from chair to chair was evident. For compounds **25, 27** and **28** the experimental $\Delta G^{\#}$ values were 9.4, 10.2 and 10.0 kcal mol^{-1}, and the corresponding coalescence temperatures were 204, 220 and 215 K, respectively. For compound **26** these values are not available.

Lunazzi and coworkers[81] detected a rotational barrier of 7.24 ± 0.02 kcal mol^{-1} for N-methylaniline by low-temperature ^{13}C NMR measurements. Further, shifts of the anisochronous *ortho*- and *meta*-carbons were assigned by *ab initio* calculations. Later on, the same group conducted a systematic study of the substituent effects upon the rotational barrier of alkylanilines[82]. The barriers for C−N internal rotation in 4-substituted N-methylanilines and N-ethyl-, N-isopropyl- and N-tert-butylaniline, respectively, are given in Table 9.

(23) R^1 = Me, R^2 = COOMe, $n = 1$
(24) R^1 = Et, R^2 = COOEt, $n = 1$
(25) R^1 = Me, R^2 = COOMe, $n = 3$
(26) R^1 = Et, R^2 = COOEt, $n = 3$
(27) R^1 = Me, R^2 = H, $n = 3$
(28) R^1 = Et, R^2 = H, $n = 3$
(29) R^1 = Me, R^2 = COOMe, $n = 4$
(30) R^1 = Et, R^2 = H, $n = 4$
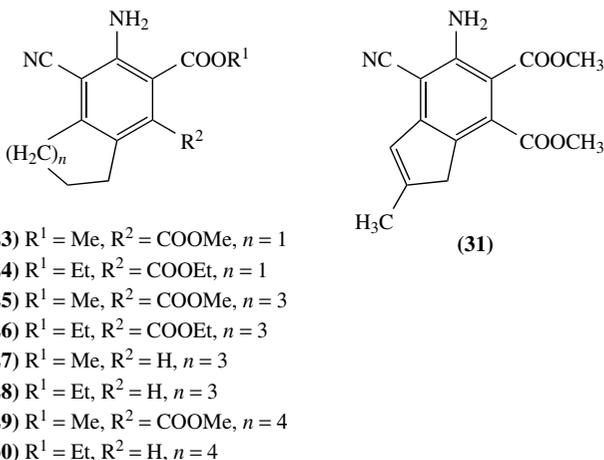
FIGURE 10. Structures of compounds **23–31**

TABLE 8. Experimental and calculated activation energies for the restricted rotation of the amino group in **23–31**

	T (K)	$\Delta G^{\#}$ (kcal mol^{-1})	$\Delta E^{\#}$ (kcal mol^{-1})	$\Delta E^{\#}$ (kcal mol^{-1}) in CH_2Cl_2
23	190	8.1	—	—
24	191	8.1	—	—
25	209	9.0	10.5	8.3
26	205	8.7	10.3	7.7
27	224	9.6	11.1	8.9
28	225	9.6	11.1	9.0
29	206	8.9	—	—
30	229	9.8	—	—
31	183	7.8	—	—

TABLE 9. The barriers, $\Delta G^{\#}$ (kcal mol^{-1}), for the C–N internal rotation in 4-substituted N-methylanilines and N-ethyl-, N-isopropyl- and N-tert-butylaniline

Compound	Solvent	$\Delta G^{\#}$ (kcal mol^{-1})
4-CH$_3$O-N-methylaniline	CHF$_2$Cl	5.7
4-F-N-methylaniline	(CH$_3$)$_2$O	6.9
N-Methylaniline	(CH$_3$)$_2$O	7.2
4-Cl-N-methylaniline	(CH$_3$)$_2$O	7.7
4-CH$_3$CO-N-methylaniline	(CH$_3$)$_2$O	9.4
4-O$_2$N-N-methylaniline	(CD$_3$)$_2$CO	11.1
N-Ethylaniline	(CH$_3$)$_2$O	7.2
N-Isopropylaniline	(CH$_3$)$_2$O	6.8
N-tert-Butylaniline	CCl$_2$F-CHFCl$_2$	6.3

Attempts have also been made to detect rotational isomerism in *ortho*-methyl-*N*-methylaniline. However, even at $-150\,°C$ no rotational isomers were observed, which was explained as due to the fact that only *trans*-isomer was present. A similar investigation was carried out also with 1- and 2-(*N*-methylamino)naphthalenes. Again, no rotational isomers were observed at the lowest attainable temperature. In the case of 1-(*N*-methylamino)naphthalene, the double bond character of the C−N bond should be similar to that of *N*-methylaniline, and the failure to detect two rotamers should be attributed to the much greater stability of the less hindered species. On the other hand, in 2-(*N*-methylamino)naphthalene the negative result should be due to the very low rotation barrier and therefore the slow exchange limit is not achievable. This agrees with the well-known fact that conjugation at the β position of naphthalene is smaller than in the phenyl group.

Anet and Ghiaci[83] have studied how the nitrogen-15 chemical shift is related to the barrier of C−N internal rotation in urea and aniline derivatives. Based on ^{1}H and ^{13}C variable-temperature measurements, they observed a barrier to C−N internal rotation of 6.1 kcal mol^{-1} for *N*-methylaniline, which is in reasonable agreement with barriers predicted by ^{15}N NMR chemical shifts and from the Hammett relationship.

V. ANILINES WITH OTHER (FUSED) AROMATIC RINGS

As described in Section IV, the rotational barrier of isomeric 1-(*N*-methylamino)naphthalenes has been studied by NMR[82]. Zachariasse and coworkers[84] have studied the internal rotation in 4-X-1-aminonaphthalenes (X = CN, Cl, CH$_3$, OCH$_3$) and 4-X-1-(*N,N*-dimethylamino)naphthalenes (X = CN, Cl, CH$_3$) influenced by the electron donor/acceptor character of the substituent. Although the results are based mainly on fluorescence spectral studies, these are also related to ^{1}H NMR data. The amino twist angle can be related to the ^{1}H chemical shift of H2 in the naphthalene ring[85]. Consequently, the twist angle can be measured by monitoring the NMR spectra[86−88]. The shielding of the H2 has been attributed to the electron-donating nature of the methyl substituent in 1-(*N,N*-dimethylamino)naphthalene. The calculated twist angles are 22 and 15° for amino and *N*-methylamino derivatives, respectively. The presence of the *N,N*-dimethylamino group, however, does not result in a further shielding on H2. This finding has been explained by the electronic decoupling of the dimethylamino and naphthyl moieties caused by a larger twist angle, 60°, as compared with amino and methylamino naphthalenes.

Schuster[89] has studied the Substituent-Induced Chemical Shifts (SCS) in 1-aminonaphthalene and 9-aminoanthracenes by ^{13}C NMR spectroscopy. Table 10 presents the ^{13}C SCSs for 1-aminonaphthalene **32**, 9-aminoanthracene **33** and 9-amino-4,5-dichloroanthracene **34** (Figure 11).

TABLE 10.   [13]C SCS [(δ(NH$_2$-derivative) - (δ(H-derivative)] (ppm) for **32, 33** and **34** measured in CDCl$_3$

Compound	C1(8) [a]	C2(7)	C3(6)	C4(5)	C9(1)	C10(4)	C11,12(9)	C13,14(10)
32	−7.14	−1.03	−0.03	0.62	14.17	−8.99	−9.85	0.88
33	−7.08	−1.58	−0.16	0.80	11.70	−9.93	−13.40	0.46
34	−7.06	−1.91	−0.37	0.56	11.78	−10.40	−13.13	0.40
33 [b]	−5.99	−2.20	−0.01	0.55	13.72	−11.68	−13.73	0.91
34 [b]	−5.65	−2.50	0.37	0.80	14.10	−12.80	−13.51	0.32

[a] Numbers in parentheses refer to the corresponding numbering in the naphthalenes.
[b] Measured in 1:1 (CD$_3$)$_2$CO:CDCl$_3$.

FIGURE 11. Structures and numbering of 1-aminonapthalene **32** and 9-aminoanthracene **33**

From the above data the effective values of the substituent constants, σ_I and σ_R, for twisted and hydrogen bonded NH_2 in 9-aminoanthracene in $CDCl_3$ were obtained: $\sigma_I = 0.12$ and $\sigma_R = -0.82$. As a conclusion of these studies, it is stated that the transmission of substituent effects appears to follow similar mechanisms in 9-aminoanthracenes and 1-aminonaphthalenes.

Berger and Diehl[90] have assigned the ^1H and ^{13}C NMR spectra of 2-substituted anthracenes based on ^1H–^{13}C HMQC measurements[11, 12]. The ^1H and ^{13}C NMR chemical shifts for 2-aminoanthracene are given in Table 11.

Sibi has reported the ^{15}N NMR chemical shifts of 1,2-diaminobenzenes, 1,8-diamino-naphthalenes and their monoprotonated species (Table 12)[91].

The above findings are explained as follows. The introduction of an *ortho*-amino substituent in aniline results in shielding of the nitrogen, which can be partly ascribed to γ-effects as is generally observed for carbon and nitrogen[92, 93]. The increased shielding joined with the introduction of a bulky *N,N*-dimethylamino substituent in the benzene series indicates the twisting of one of the *N,N*-dimethylamino groups out of conjugation owing to the steric crowding[24]. The change in the naphthalene series on *peri*-substitution agrees with that observed by Schuster and Roberts[94] in a study of proximity effects on nitrogen chemical shifts of 8-heterosubstituted 1-aminonaphthalenes. The increased shielding observed on the protonation in both the 1,2-diaminobenzenes and 1,8-diaminonaphthalenes may be the result of the proton incorporation into a five- or six-membered ring structure.

TABLE 11. $\delta(^1H)$ and $\delta(^{13}C)$ (in ppm from TMS) of 2-aminoanthracene in $CDCl_3$

H1	7.07	C1	106.1
H3	6.89	C2	144.4
H4	7.84	C3	120.6
H5	7.90	C4	130.6
H6	7.35	C5	128.6
H7	7.40	C6	124.2
H8	7.90	C7	125.8
H9	8.10	C8	127.8
H10	8.27	C9	122.8
		C10	126.6
		C11	130.1
		C12	133.0
		C13	133.9
		C14	127.9

TABLE 12. $\delta(^{15}N)$ (in ppm from external anhydrous ammonia) of aminobenzenes, aminonaphthalenes and their monoprotonated cations

Compound	Molecule [a]	Cation [b]
Aniline	59.76	51.03
2-Methylaniline	57.94	48.73
1,2-Diaminobenzene	52.02	50.70
N,N-Dimethylaniline	44.68	47.53
$2,N,N$-Trimethylaniline	33.83	46.03
1,2-Di(N,N-dimethylamino)benzene	37.87	32.29
1-Aminonaphthalene	62.55	44.39
1-(N,N-Dimethylamino)naphthalene	35.93	35.93
1,8-Diaminonaphthalene	68.10	48.03
1,8-Di(N,N-dimethylamino)naphthalene	45.36	34.13

[a] In 2 M solutions in DMSO-d_6.
[b] As trifluoroacetates in chloroform, [amine]/[TFA] = 1:2.

$R^1 = Me_2N, R^2 = Me_2N$
$R^1 = Me_2N, R^2 = Et_2N$
$R^1 = Me_2N, R^2 = Piperidino$
$R^1 = Me_2N, R^2 = Morpholino$
$R^1 = Pyrrolidino, R^2 = Me_2N$
$R^1 = Piperidino, R^2 = Me_2N$
$R^1 = Morpholino, R^2 = Me_2N$
$R^1 = Me_2N, R^2 = Pyrrolidino$
$R^1 = MeO, R^2 = Me_2N$
$R^1 = Et_2N, R^2 = Me_2N$

$R^1 = Me_2N, R^2 = Me_2N$
$R^1 = Me_2N, R^2 = Et_2N$
$R^1 = Me_2N, R^2 = Piperidino$
$R^1 = Me_2N, R^2 = Morpholino$
$R^1 = Pyrrolidino, R^2 = Me_2N$
$R^1 = Piperidino, R^2 = Me_2N$
$R^1 = Morpholino, R^2 = Me_2N$
$R^1 = Me_2N, R^2 = Pyrrolidino$
$R^1 = MeO, R^2 = Me_2N$
$R^1 = Et_2N, R^2 = Me_2N$
$R^1 = Et_2N, R^2 = Me_2N$

FIGURE 12.   Structures of Victoria Blue cation **35** and corresponding methyl ether **36**

Hepworth and coworkers[95] have studied the effects of N-alkyl and heterocycloalkyl substituents on the light absorption properties of, Victoria Blue **35** and **36** (Figure 12), the 1-naphthyl analogue of Crystal Violet. The steric interaction found between the N-terminal group and the *peri*-hydrogen in the naphthyl residue is correlated with ^1H NMR data.

It has been shown that ^1H NMR spectroscopy can serve as a good measure of the donor strengths of various phenyl-substituted tertiary amino groups[96]. In 1-substituted

TABLE 13. $\delta(^1\text{H2})$ (in ppm) for 1-substituted naphthalenes

Substituent	$\delta(^1\text{H2})$
NH$_2$	6.79
NHEt	6.50
NMe$_2$	7.10
NEt$_2$	7.16
Pyrrolidino	7.02
Piperidino	7.10
Morpholino	7.10

naphthalenes bearing an electron-releasing substituent (such as amino), the signal of H2 is always the most shielded and therefore easy to assign. Therefore, Hepworth and coworkers[95] used 1-substituted naphthalenes as model compounds. Table 13 presents $\delta(^1\text{H2})$ values for some 1-substituted naphthalenes, where the substituents correspond to those in Victoria Blue dyes **35** and **36**.

An increase in the electron-releasing power of the substituent should cause a further shielding of the *ortho*-proton (smaller chemical shift value). This is observed when 1-aminonaphthalene is *N*-ethylated (δ changes from 6.79 ppm to 6.50 ppm). The *peri*-effect causes a relative deshielding of the α-proton in tertiary derivatives. The difference of deshieldings between secondary and tertiary 1-aminonaphthalenes reflects the importance of the deconjugation of the amino group of the latter. Further, ^{1}H NMR spectroscopy confirms that the diethylamino group suffers a larger steric strain, as indicated also by molecular modeling and visible absorption spectra. It also demonstrates that primary and secondary amino substituents can avoid *peri*-hindrance and therefore conjugate effectively with the aromatic system. The signal of the *peri*-proton (H8) is accordingly deshielded by tertiary amino substituents. It appears at 7.85 ppm in 1-aminonaphthalene and 1-(*N*-ethyl)aminonaphthalene and at 8.35 ppm in the *N*,*N*-diethyl derivative, respectively.

VI. NMR RELAXATION STUDIES OF ANILINE DERIVATIVES

Levy and coworkers[97] have measured ^{13}C spin–lattice relaxation times, T_1, for 3- and 4-aminobiphenyls in a number of solvent systems, and of the corresponding ammonium ions in acidic and nonacidic media. The observed T_1 values indicated that the molecular tumbling is anisotropic for these species. In addition, the known biphenyl geometry allowed indentification and semiquantitative evaluation of internal rotation–libration motion. The protonated amine function is motionally more restricted by solvent–solute and ion-pair interactions than the corresponding neutral amine. Thus, in the 3-biphenylammonium ion, the principal axis for molecular reorientation is aligned close to the C3—NH$_3$-bond, whereas in the amine the principal axis lies closer to the biphenyl C_2-symmetry axis. In both 3- and 4-aminobiphenyls, the unsubstituted phenyl rings are less restricted due to rapid phenyl rotation or libration. Table 14 presents ^{13}C T_1-data for 4-aminobiphenyl **37** (NH$_2$ on C4) and 4-biphenylammonium acetate **38** and trifluoroacetate **39**.

In interpreting the above data, two kinds of internal motion should be considered: (1) internal phenyl ring rotation around the CC$'$ bond and (2) torsional vibration (libration), since a full rotation around the CC$'$ bond on the appropriate time scale can be excluded. There is theoretical evidence that the barrier for rotation is 2–5 kcal mol^{-1} while passing the 90$°$ twist angle ($\phi = 90°$)[98–101] and within the range of 0.5–3 kcal mol^{-1} for the $\phi = 0°$ angle[100, 102, 103]. Although the quantitative contributions of hindered full phenyl

TABLE 14.　^{13}C T_1 values (in s^{-1}) for **37**, **38** and **39**

Compound	Solvent	Temp (K)	C4′	C3′	C2′	C2	C3
37	MeCN	312	2.63	4.80	4.89	4.38	4.42
37	$Cl_2C=CCl_2$	309	1.59	3.32	3.38	2.85	2.90
37	CCl_4	315	1.41	3.21	3.29	2.78	2.85
37	MeOH	312	—	4.03	—	3.27	3.25
38	AcOH	315	0.59	1.96	2.08	1.41	1.39
39	DMF	311	0.45	1.42	1.44	1.24	1.22
39	MeOH	306	0.75	2.86	3.02	2.60	2.52
39	MeOH/TFA 19:1 v:v	306	0.60	2.35	2.32	2.03	1.98
39	MeOH/TFA 4:1 v:v	312	0.77	2.92	3.13	2.63	2.68
39	TFA	312	0.30	—	1.09	—	1.00

rotation and librational motion are not known, the authors argue that the librational motion is at least partially effective in the aminobiphenyl system.

In the case of 3-aminobiphenyl, the situation is more complex since there is no longer a simple C_2-molecular symmetry axis. Interpretation of the T_1 for both rings in this system requires several effects to be considered. These are differential internal motion of both rings around the biphenyl axis and the effects of noncoplanarity of the two rings relative to a principal molecular diffusion axis on T_1 values, which is not coincident with the biphenyl axis.

As concluding remarks, the authors mention for aminobiphenyls that the modulation of conjugation due to nonplanarity is small as expected, but for ammonium salts this effect is larger. When 3- and 4-amino derivatives are compared, the influence of the internal motion on T_1 values in the former is stronger.

Bock and coworkers[104] have determined proton spin–lattice relaxation times for N,N-dideuterioaniline in perdeuteriobenzene and perdeuterioaniline solutions as a function of the concentration and temperature at 260–360 K. The activation energies of the intra- and intermolecular relaxation rates were of similar magnitude, namely 4.5 and 4.4 kcal mol^{-1}. At 293 K, the rotational correlation time of the aniline molecule in infinitely dilute perdeuteriobenzene solution was approximately half that of the partially deuteriated aniline molecule, namely 3.0×10^{-12} and 6.3×10^{-12} s^{-1}, respectively. In infinitely dilute perdeuterioaniline the rotational correlation time of N,N-dideuterioaniline was 19×10^{-12} s^{-1}.

VII. SOLID STATE NMR STUDIES

In recent years the molecular and electronic structure of intrinsically conducting polyaniline (PANI) has attracted considerable interest due to its use in optoelectronic applications[105, 106]. There exist some recent papers on that topic where solid state ^{13}C and ^{15}N NMR techniques have been used[107–109]. Sahoo and coworkers[107] studied enzymatically synthesized polyanilines by ^{13}C and ^{15}N CP/MAS NMR techniques. The NMR spectral features indicate that PANI obtained by PEG-hematin (a synthetic biomimetic catalyst) catalysis resembles most chemically synthesized analogues. ^{15}N CP/MAS NMR data were also used for the end-group analysis, providing information on the molecular weight of these enzymatically polymerized PANI samples.

Espe and coworkers[108, 109] have conducted a detailed structural characterization of annealed PANI powder samples by solid state ^{13}C and ^{15}N NMR and FT-IR. Comparing annealed PANI with PANI that has been chemically reduced to Leucoemeraldine Base (LB) **40** form, the solid state ^{13}C and ^{15}N NMR data clearly show the conversion of the quinoid rings to benzenoid rings upon heating at 473 K in vacuum. The structures

LB (**40**)

EB (**41**)

Pernigraniline Base **42**

Cross-linked polyaniline (**43**)
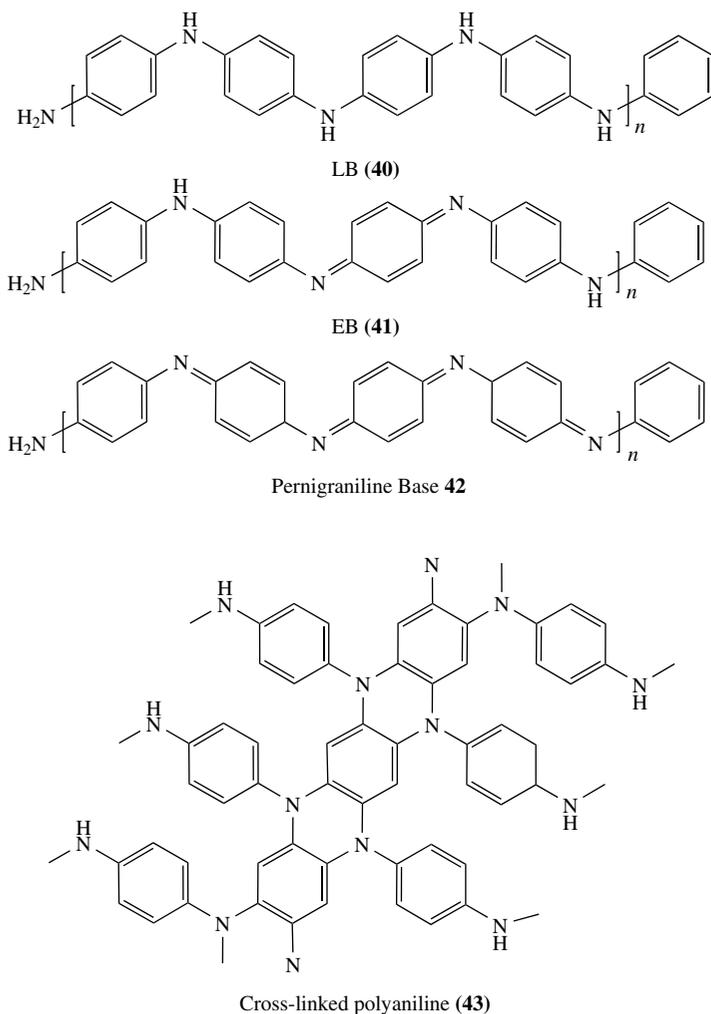
FIGURE 13. Structures of LB **40**, EB **41**, Pernigraniline Base **42** and a cross-linked polyaniline **43**

of PANI at different oxidation levels, i.e. Leucoemeraldine Base (LB) **40**, Emeraldine Base (EB) **41**, Pernigraniline Base **42** and a cross-linked polyaniline **43**, are shown in Figure 13. Combining interrupted-proton decoupling with solid state ^{13}C and ^{15}N NMR reveals the presence of tertiary amine nitrogens generated from the cross-linking of the annealed polymer. The tertiary amine sites occur upon new bond formation between the quinoid rings of one chain with the imine site of an adjacent chain, yielding a *N,N*-diphenylphenazine structure at the site of cross-linking. The NMR data also show that upon heating, cross-linking is a predominant reaction occurring in PANI powder and that it follows a single mechanism. Proton T_1 measurements also reveal that cross-linking is impacting to the chain dynamics with lowering the rate of the chain motion. The ^{1}H T_1

values for EB and LB forms of ^{15}N-enriched PANI are similar, 2.2 and 1.7 ms, while upon annealing the sample the T_1 value drops significantly to 0.36 ms. The shorter spin–lattice relaxation time observed for a heat-treated sample shows that the rate of chain dynamics has been altered, consistent with the cross-linking of the polymer.

Stejskal and coworkers[110] have studied polyaniline–buckminsterfullerene composites by solid state ^{13}C NMR. Their results suggest that the electron density has been transferred from PANI to C_{60}. An indirect proof of the electron density transfer has been obtained with the help of a cross-polarization (CP) experiment, as the appearance of a slight deshielding of the fullerene ^{13}C signal in the composite.

VIII. THEORETICAL CALCULATIONS OF ANILINE NMR PARAMETERS

Barfield and Fagerness[41] have conducted a careful study on the dependence of the ^{13}C, ^{15}N and isotropic ^{1}H NMR chemical shifts on amine substitution of aromatic ring systems both experimentally and by DFT/GIAO (density functional theory/Gauge Independent Atomic Orbitals) methods. The ring atom chemical shifts and $2p_z$-electron densities at *ortho*- and *para*- (but not *meta*) positions are quite sensitive to the orientations of the amino groups, which are pyramidalized as a result of the balance between delocalization with the ring and the use of strongly directed sp^3 orbitals at the nitrogen. The calculated results show that the barriers to amine group torsional and inversion motions are low, but averaging the chemical shifts over these appears to be relatively unimportant. Differences between the DFT and Hartee–Fock-based chemical shifts show that electron correlation effects increase monotonically with the number of NH_2 substituents.

In addition to aniline itself, 1,3-diamino- and 1,3,5-triaminobenzene are included in this study. The structure of aniline has been calculated at MP2/6-311G* and BPW91/6-311G* levels of theory. All magnetic shielding results were based on the GIAO formulation[111–114].

Table 15 presents the experimental and GIAO calculated ^{15}N NMR chemical shifts for aniline, 1,3-diaminobenzene and 1,3,5-triaminobenzene.

Ośmiałowski and Gawinecki[116] have also calculated ^{15}N NMR chemical shifts for aniline derivatives as catalogued in Table 16. The largest differences between experimental and DFT/GIAO calculated ^{15}N NMR chemical shifts can be greatly diminished when medium effects (in the form of aniline–$CHCl_3$ complexes) are taken into account. These calculations are still in progress.

To conclude, we point out that aniline and its numerous derivatives still offer challenges for both experimental and theoretical NMR studies. Especially in the area of solid state NMR, the determination of the components of anisotropic ^{15}N shielding tensors and their quantum chemical calculations can give valuable information on the polymorphism and interactions of aniline derivatives in the solid state.

TABLE 15. Experimental and GIAO calculated ^{15}N NMR chemical shifts for aniline, 1,3-diamino-benzene (DAB) and 1,3,5-triaminobenzene (TAB) relative to neat CH_3NO_2 ($\delta = 0.0$ ppm)

Compound	H*M* [a]	H**M* [b]	B**M* [c]	B*B* [d]	B**B* [e]	Experimental
Aniline	−337.3	−335.8	−312.4	−316.6	−315.4	−320.0/−318.8 [f]
DAB	−335.8	−334.3	−313.1	−317.2	−316.0	−319.1
TAB	−333.8	−332.3	−313.0	−317.9	−316.7	—

[a] Shielding calculated at HF/6-311G* level, structure optimized at MP2/6-311G* level.
[b] Shielding calculated at HF/6-311G** level, structure optimized at MP2/6-311G* level.
[c] Shielding calculated at BPW91/6-311G** level, structure optimized at MP2/6-311G* level.
[d] Shielding calculated at BPW91/6-311G* level, structure optimized at BPW91/6-311G* level.
[e] Shielding calculated at BPW91/6-311G** level, structure optimized at BPW91/6-311G* level.
[f] Taken from Reference 115.

TABLE 16. Calculated and experimental ^{15}N NMR chemical shifts and their differences (in ppm)

Compound	Calculated	Experimental	Difference
Aniline	−325.74	−325.5	−0.24
N,*N*-Dimethylaniline	−329.85	−329.4	−0.45
2,3-Dihydro-1*H*-indole	−309.42	−314.3	4.88
2-Methylaniline	−327.18	−328.1	0.92
2,*N*-Dimethylaniline	−326.10	−327.1	1.00
2-Ethyl-*N*-methylaniline	−327.91	−329.4	1.49
1,2,5,6-Tetrahydro-4*H*-pyrrolo[3,2,1-*ij*]quinoline	−303.69	−307.8	4.11
2-Isopropylaniline	−329.93	−329.4	0.53
N-Ethylaniline	−305.36	−310.4	5.04
N-Methyl-2,3-dihydro-1*H*-indole	−310.52	−316.2	5.68
N-Methylaniline	−323.99	−329.2	5.21
N-Methyl-*N*-ethylaniline	−321.46	−325.0	3.54
N-Phenylpyrrolidine	−307.42	−308.7	1.28
N-Methyl-1,2,3,4-tetrahydroquinoline	−321.48	−319.0	2.48
N-Phenylpiperidine	−311.42	−313.2	1.78

IX. REFERENCES

1. (a) J. Hudson, *The History of Chemistry*, Chap. 15, Chapman and Hall, London, 1992.
   (b) H. Baumgertel, *Pharmazie*, **45**, 133 (1990).
2. O. Meth-Cohn and M. Smith, *J. Chem. Soc., Perkin Trans 2*, 5 (1994).
3. R. J. Fessenden, J. S. Fessenden and M. W. Logue, *Organic Chemistry*, 6th edn., Brooks and Cole Publ. Co., London, 1998, p. 496.
4. J. Shorter, 'Electronic Effects of Nitro, Nitroso, Amino and Related Groups', in *The Chemistry of Amino, Nitroso, Nitro and Related Groups*, Supplement F2, Part 1 (Ed. S. Patai), Wiley, Chichester, 1996.
5. G. Chuchani, in *The Chemistry of the Amino Groups* (Ed. S. Patai), Interscience, London, 1968, p. 205.
6. R. E. Richards and T. Schaefer, *Proc. R. Soc. London, Ser. A*, **246**, 429 (1958).
7. H. Spiesecke and W. G. Schneider, *J. Chem. Phys.*, **35**, 731 (1961).
8. R. R. Ernst and W. A. Anderson, *Rev. Sci. Instrum.*, **37**, 93 (1966).
9. E. L. Hahn, *Phys. Rev.*, **80**, 580 (1950).
10. G. Bodenhausen and D. J. Ruben, *Chem. Phys. Lett.*, **69**, 185 (1980).
11. A. Bax, R. H. Griffey and B. L. Hawkins, *J. Magn. Reson.*, **55**, 301 (1983).
12. A. Bax and S. Subramanian, *J. Magn. Reson.*, **67**, 565 (1986).
13. A. Bax and M. F. Summers, *J. Am. Chem. Soc.*, **108**, 2093 (1986).
14. R. E. Hurd, *J. Magn. Reson.*, **87**, 422 (1990).
15. R. E. Hurd and B. K. John, *J. Magn. Reson.*, **91**, 648 (1991).
16. S. R. Hartmann and E. L. Hahn, *Phys. Rev.*, **128**, 2042 (1962).
17. G. C. Levy and R. L. Lichter, *Nitrogen-15 Nuclear Magnetic Resonance Spectroscopy*, Wiley, New York, 1979, p. 8.
18. E. Kolehmainen, K. Laihia, R. Kauppinen, R. Gawinecki and D. Rasała, *Magn. Reson. Chem.*, **31**, 659 (1993).
19. R. L. Lichter and J. D. Roberts, *Org. Magn. Reson.*, **6**, 636 (1974).
20. T. Axenrod, P. S. Pregosin, M. J. Wieder, E. D. Becker, R. B. Bradley and G. W. A. Milne, *J. Am. Chem. Soc.*, **93**, 6536 (1971).
21. T. Axenrod and M. J. Wieder, *Org. Magn. Reson.*, **8**, 350 (1976).
22. G. Adler and R. L. Lichter, *J. Org. Chem.*, **39**, 3547 (1974).
23. L. Psota, M. Franzen-Sieveking, J. Turnier and R. L. Lichter, *Org. Magn. Reson.*, **11**, 401 (1978).
24. M. F. Sibi and R. L. Lichter, *J. Org. Chem.*, **42**, 2999 (1977).
25. A. Zakrzewska, R. Gawinecki, E. Kolehmainen and B. Ośmiałowski, *Int. J. Mol. Sci.*, **6**, 52 (2005).

26. A. J. Hoefnagel, M. A. Hoefnagel and B. M. Wepster, *J. Org. Chem.*, **46**, 4209 (1981).
27. B. M. Wepster, *Recl. Trav. Chim. Pays-Bas*, **71**, 1159 (1952).
28. K. Rotkiewicz and W. Rubaszewska, *Chem. Phys. Lett.*, **70**, 444 (1980).
29. G. Köhler, K. Rechthaler, G. Grabner, L. Luboradzki, K. Suwińska and K. Rotkiewicz, *J. Phys. Chem.*, **101A**, 8518 (1997).
30. G. L. Butt and R. D. Topsom, *Spectrochim. Acta*, **34A**, 975 (1978).
31. T. Dudev and C. Lim, *J. Am. Chem. Soc.*, **120**, 4450 (1998).
32. A. Domenicano and P. Murray-Rust, *Tetrahedron Lett.*, 2283 (1979) and references cited therein.
33. D. T. Clark, *J. Chem. Soc., Chem. Commun.*, 390 (1966).
34. K. Crimaldi, R. L. Lichter and A. D. Baker, *J. Org. Chem.*, **47**, 3524 (1982).
35. F. Effenberger, P. Fischer, W. W. Schoeller and W.-D. Stohrer, *Tetrahedron*, **34**, 2409 (1978).
36. J. Eastes, M. H. Aldridge, R. R. Minesinger and M. J. Kamlet, *J. Org. Chem.*, **36**, 3847 (1971).
37. M. J. Kamlet, R. R. Minesinger, E. G. Kayser, M. H. Aldridge and J. Eastes, *J. Org. Chem.*, **36**, 3852 (1971).
38. A. T. Bottini and J. D. Roberts, *J. Am. Chem. Soc.*, **80**, 5203 (1958).
39. V. F. Bystrov, R. G. Kostyanovskii, O. A. Pan'shin, A. U. Stepanyants and O. A. Yuzhakova, *Optika i Spektroskopiya*, **19**, 217 (1965); *Chem. Abstr.*, **63**, 480035 (1965).
40. R. F. Severson, J. T. Rudesill, R. G. Zaylskie and J. G. Pomonis, *J. Chem. Eng. Data*, **17**, 392 (1972).
41. M. Barfield and P. Fagerness, *J. Am. Chem. Soc.*, **119**, 8699 (1997).
42. C. P. Nash and G. E. Maciel, *J. Phys. Chem.*, **68**, 832 (1964).
43. P. C. Lauterbur, *J. Chem. Phys.*, **38**, 1415 (1963).
44. R. Gawinecki, E. Kolehmainen and R. Kauppinen, *J. Chem. Soc., Perkin Trans. 2*, 25 (1998).
45. E. G. McRae and L. Goodman, *J. Chem. Phys.*, **29**, 334 (1966).
46. H. Ahlbrecht, E. O. Düber, J. Epsztajn and R. M. K Marcinkowski, *Tetrahedron*, **40**, 1157 (1984).
47. Z. Proba and K. L. Wierzchowski, *J. Chem. Soc., Perkin Trans. 2*, 1119 (1978).
48. E. Liepinsh, A. V. Eremeev, D. A. Tikhomirov and R. S. El'kinson, *Khim. Geterotsykl. Soedin.*, 338 (1978); *Chem. Abstr.*, **89**, 441721 (1978).
49. R. W. Taft, E. Price, I. R. Fox, I. C. Lewis, K. K. Andersen and G. T. Davis, *J. Am. Chem. Soc.*, **85**, 3146 (1963).
50. V. F. Bystrova, O. A. Yuzhakova and R. G. Kostyanovskii, *Dokl. Akad. Nauk SSSR*, **147**, 843 (1962); *Chem. Abstr.*, **59**, 415043 (1963).
51. R. G. Pews, *J. Am. Chem. Soc.*, **89**, 5605 (1967).
52. M. J. S. Dewar and Y. Takeuchi, *J. Am. Chem. Soc.*, **89**, 390 (1967).
53. C. H. Yoder, B. A. Kaduk and R. E. Hess, *Tetrahedron Lett.*, 3711 (1970).
54. M. Karplus and T. P. Das, *J. Chem. Phys.*, **34**, 1683 (1961).
55. F. Prosser and L. Goodman, *J. Chem. Phys.*, **38**, 374 (1963).
56. R. W. Taft, F. Prosser, L. Goodman and G. T. Davies, *J. Chem. Phys.*, **38**, 380 (1963).
57. K. Ito, K. Inukai and T. Isobe, *Bull. Chem. Soc. Jpn.*, **33**, 315 (1960).
58. D. F. Evans, *Proc. Chem. Soc.*, 115 (1958).
59. D. F. Evans, *J. Chem. Soc.*, 877 (1960).
60. R. E. Glick and S. J. Ehrenson, *J. Phys. Chem.*, **62**, 1599 (1958).
61. A. D. Buckingham, T. Schaefer and W. G. Schneider, *J. Chem. Phys.*, **32**, 1227 (1960).
62. R. W. Taft, E. Price, I. R. Fox, I. C. Lewis, K. K. Andersen and G. T. Davis, *J. Am. Chem. Soc.*, **85**, 709 (1963).
63. R. W. Taft, *J. Phys. Chem.*, **64**, 1805 (1960).
64. H. S. Gutowsky, D. W. McCall, B. R. McGarvey and L. H. Meyer, *J. Am. Chem. Soc.*, **74**, 4809 (1952).
65. L. H. Meyer and H. S. Gutowsky, *J. Phys. Chem.*, **57**, 481 (1953).
66. R. T. C. Brownlee and R. W. Taft, *J. Am. Chem. Soc.*, **92**, 7007 (1970).
67. R. W. Taft, S. Ehrenson, I. C. Lewis and R. E. Dlick, *J. Am. Chem. Soc.*, **81**, 5352 (1959).
68. R. W. Taft, *J. Am. Chem. Soc.*, **79**, 1045 (1957).
69. J. W. Emsley and L. Phillips, *Prog. Nucl. Magn. Reson. Spectrosc.*, **7**, 1 (1971).
70. W. J. Hehre, R. W. Taft and R. D. Topsom, *Prog. Phys. Org. Chem.*, **12**, 159 (1976).
71. R. T. C. Brownlee, S. K. Dayal, J. L. Lyle and R. W. Taft, *J. Am. Chem. Soc.*, **94**, 7208 (1972).

72. E. Maciel and J. J. Natterstad, *J. Chem. Phys.*, **42**, 2427 (1965).
73. A. R. Katritzky and R. D. Topsom, *Angew. Chem., Int. Ed. Engl.*, **9**, 87 (1970).
74. R. T. C. Brownlee, A. R. Katritzky and R. D. Topsom, *J. Am. Chem. Soc.*, **88**, 1413 (1966).
75. R. T. C. Brownlee, R. E. J. Hutchinson, A. R. Katritzky, T. T. Tidwell and R. D. Topsom, *J. Am. Chem. Soc.*, **90**, 1757 (1968).
76. S. Ehrenson, R. T. C. Brownlee and R. W. Taft, *Prog. Phys. Org. Chem.*, **10**, 1 (1973).
77. R. W. Taft and H. D. Evans, *J. Chem. Phys.*, **27**, 1427 (1957).
78. W. G. Brown, A. H. Widiger and N. J. Letang, *J. Am. Chem. Soc.*, **61**, 2597 (1939).
79. M. Haydenreich, G. Wolf, J. Voller and E. Kleinpeter, *Tetrahedron*, **60**, 4663 (2004).
80. R. Wasylishen and T. Schaefer, *Can. J. Chem.*, **49**, 3575 (1971).
81. L. Lunazzi, C. Magagnoli, M. Guerra and D. Macciantelli, *Tetrahedron Lett.*, 3031 (1979).
82. L. Lunazzi, C. Magagnoli and D. Macciantelli, *J. Chem. Soc., Perkin Trans. 2*, 1704 (1980) and references cited therein.
83. F. A. Anet and M. Ghiaci, *J. Am. Chem. Soc.*, **101**, 6857 (1979).
84. K. Suzuki, A. Demeter, W. Kühnle, E. Tauer, K. A. Zachariasse, S. Tobita and H. Shizuka, *Phys. Chem. Chem. Phys.*, **2**, 981 (2002).
85. I. Rückert, A. Demeter, O. Morawski, W. Kühnle, E. Tauer and K. A. Zachariasse, *J. Phys. Chem. A*, **103**, 1958 (1999).
86. L. Ernst, *Z. Naturforsch., B*, **30**, 794 (1975).
87. A. Zweig, J. E. Lancaster and M. T. Neglia, *Tetrahedron*, **23**, 2577 (1967).
88. N. J. Bunce, S. R. Cater, J. C. Scaiano and L. J. Johnston, *J. Org. Chem.*, **52**, 4214 (1987).
89. I. I. Schuster, *J. Org. Chem.*, **46**, 5110 (1981).
90. S. Berger and B. W. K. Diehl, *Magn. Reson. Chem.*, **27**, 201 (1989).
91. M. P. Sibi, *Magn. Reson. Chem.*, **29**, 400 (1991).
92. R. L. Lichter and J. D. Roberts, *J. Am. Chem. Soc.*, **94**, 2495 (1972).
93. J. P. Warren and J. D. Roberts, *J. Phys. Chem.*, **78**, 2507 (1974).
94. I. I. Schuster and J. D. Roberts, *J. Org. Chem.*, **45**, 284 (1980).
95. S. G. R. Guinot, J. D. Hepworth and M. Wainwright, *J. Chem. Soc., Perkin Trans. 2*, 297 (1998).
96. C. P. Nash and G. E. Maciel, *J. Phys. Chem.*, **68**, 832 (1964).
97. G. C. Levy, T. Holak and A. Steigel, *J. Am. Chem. Soc.*, **98**, 495 (1976).
98. I. Fischer-Hjalmars, *Tetrahedron*, **19**, 1805 (1963).
99. A. Imamura and R. Hoffman, *J. Am. Chem. Soc.*, **90**, 5379 (1968).
100. D. Perahia and A. Pullman, *Chem. Phys. Lett.*, **19**, 73 (1973).
101. G. Casalone, C. Mariani, A. Mugnoli and M. Simonetta, *Mol. Phys.*, **15**, 339 (1968).
102. A. Golebiewski and A. Parczewski, *Z. Naturforsch., A*, **25**, 1710 (1970).
103. N. L. Allinger and J. T. Sprague, *J. Am. Chem. Soc.*, **95**, 3893 (1973).
104. E. Bock, J. Czubryt and E. Tomchuk, *Can. J. Chem.*, **48**, 2814 (1970).
105. A. G. MacDiarmid, *Angew. Chem., Int. Ed.*, **40**, 2581 (2001).
106. A. G. MacDiarmid, *Synth. Met.*, **84**, 27 (1997).
107. S. K. Sahoo, R. Nagarajan, S. Roy, L. A. Samuelson, J. Kumar and A. L. Cholli, *Macromolecules*, **37**, 4130 (2004).
108. R. Mathew, B. R. Mattes and M. P. Espe, *Synth. Met.*, **131**, 141 (2002).
109. R. Mathew, D. Yang, B. R. Mattes and M. P. Espe, *Macromolecules*, **35**, 7575 (2002).
110. I. Sapurina, M. Mokeev, V. Lavrentjev, V. Zgonnik, M. Trehová, D. Hlatavá and J. Stejskal, *Eur. Polym. J.*, **36**, 2321 (2000).
111. F. London, *J. Phys. Radium (Paris)*, **8**, 397 (1937).
112. R. Ditchfield, *Mol. Phys.*, **27**, 789 (1974).
113. K. Wolinski, J. F. Hinton and P. Pulay, *J. Am. Chem. Soc.*, **112**, 851 (1990).
114. M. Häser, R. Ahlrichs, H. P. Baron, P. Weiss and H. Horn, *Theor. Chim. Acta*, **83**, 455 (1992).
115. J. Dorie, B. Mechin and G. Martin, *Org. Magn. Reson.*, **12**, 229 (1979).
116. B. Ośmiałowski and R. Gawinecki, unpublished results.

CHAPTER **7**

Substituted anilines as solvatochromic probes

YIZHAK MARCUS

*Department of Inorganic and Analytical Chemistry, The Hebrew University of
Jerusalem, Jerusalem 91904, Israel
Fax: +972 2 6585341;   e-mail: ymarcus@vms.huji.ac.il*

I. INTRODUCTION

This chapter examines various derivatives of aniline that have been used as solvatochromic probes of the abilities of solvents and other environments to solvate solutes. It is difficult to delimit what are aniline derivatives proper (aminonaphthalenes are not included, for instance) and not all the derivatives can be discussed in a chapter such as this. Nevertheless, certain dyes that have been extensively used as solvatochromic probes and that have

a substituted amino group bonded to a phenyl ring have been included. The 'chromic' in solvatochromic is taken to include both absorption and emission (i.e. fluorescence) of UV-vis light, but to some extent also infrared radiation and to a small extent also NMR signals.

A. Solvatochromic Probes

The use of solvatochromic probes is based on the postulate that the numerical value obtained from spectroscopic measurements on the probe molecule in a given solvent represents an inherent solvation property of the solvent towards any other solute. This premise in its general form has been refuted long ago, but in a more restrictive sense has been confirmed for practical purposes. There are now two trends concerning the use of the solvatochromic probes. One is to rely on the results from one particular probe in order to arrange solvents in a series with increasing values of the solvating power as measured by this probe. Such is, for example, the Dimroth–Reichardt $E_T(30)$ index[1] that is widely used for indicating the polarity defined as the 'overall solvating ability' of solvents[2]. The other is to employ the converging results from several dissimilar probes, suitably weighted and averaged, in order to express a more restricted aspect of the solvation ability of solvents. Such is, for example, the Kamlet–Taft β parameter that expresses the ability of solvents to act as Lewis bases[3] or the Kamlet–Taft π^* parameter that expresses the polarity/polarizability aspect of the solvents[4].

Both approaches are useful and respond well to queries concerning the solvation abilities of neat solvents with regard to solutes of various types. This is not necessarily the case for solvent mixtures that are widely employed in synthesis, purification and analysis of organic compounds. In solvent mixtures preferential solvation of the solvatochromic probe by one component of the mixture may take place, so that the probe ceases to be representative of the solvation ability towards solutes of different chemical nature. For solvent mixtures, therefore, the averaging of results from several probes, even if providing values with a wider uncertainty than with a single probe, is on the whole the better choice for expressing the solvating power[5].

For a solvatochromic probe to be useful it should have an as large as possible range of signal values, obtained for solvents with extreme solvating properties, from the least to the largest. The signals are generally the wavelengths (or wavenumbers) of a characteristic absorption or fluorescence band in the UV-vis region or, less widely employed, the frequencies of chemical shifts of NMR signals. The values are by and large only slightly dependent on the concentration of the probe molecule in the solvent and the temperature dependence near ambiance is ordinarily ignored.

As the solvating properties in a series of solvents increases, the light absorption band maximum may be shifted towards longer wavelengths (bathochromic or red shifts) or to shorter ones (hypsochromic or blue shifts). The direction of the shift depends on whether the dipole moment of the probe molecule in the excited state is larger or smaller than in the ground state, since the solvating solvent generally interacts with the probe by means of its dipole moment[6].

For many experimentally measured quantities XYZ of solutions (mainly spectroscopic ones) the general Linear Solvation Energy Relationship (LSER) (equation 1)

$$XYZ = XYZ_0 + s\pi^* + a\alpha + b\beta \tag{1}$$

proposed by Kamlet, Taft and coworkers[7] was shown to hold. Here π^*, α and β are the polarity/polarizability, hydrogen bond donation (HBD) and hydrogen bond acceptance/electron pair donation (HBA/EPD) properties of the solvents, respectively, and XYZ_0 is the quantity measurable in the gas phase or in inert solvents without solvation abilities.

The coefficients s, a and b describe the sensitivities of the solute to these properties, as manifested by the measured quantity. In the present context the quantity XYZ is generally the wavenumber of the longest wavelength peak of the light absorption of a solute probe in the UV-vis region, or also its emission wavenumber if fluorescent, its IR characteristic vibration or its NMR chemical shift. For probes that are aniline derivatives the term $a\alpha$ can usually be ignored, since they are less prone to accepting hydrogen bonds from protic solvents, but not quite altogether.

B. Probes for Solvent Basicity

An important property of solvents is their Lewis basicity, or in other words their ability to donate electron density from an unshared pair of electrons towards the formation of a coordinative bond to the solute (EPD solvents), or in a more restrictive sense their ability to accept a proton in a solute-to-solvent hydrogen bond (HBA solvents). The electron density donating atoms in the solvent molecules are generally oxygen or nitrogen atoms and less commonly halogen, sulfur or other electronegative atoms. The solutes used as solvatochromic probes may be inorganic cations or coordinatively unsaturated complexes and molecules, or polar and protic or protogenic organic molecules.

Examples of the former are [N,N,N',N'-tetramethylethylenediamino acetylacetonato Cu(II)]$^+$ and antimony pentachloride. The copper cation is surrounded by two oxygen and two nitrogen donor atoms from the ligands in a square configuration and can still be coordinated by two solvent molecules in a perpendicular direction to the plane of the square in a distorted octahedral configuration. Due to the asymmetrical electric field exerted by the ligands the d−d electronic transition is enhanced and is sensitive to the donor strength of the solvent, hence this probe is useful for measuring the EPD effectiveness of solvents[8]. The tendency of SbCl$_5$ to complete its coordination shell to six ligands by accepting a solvent molecule is reflected by the enthalpy of the formation of the 1:1 donor−acceptor complex with an HBA/EPD solvent molecule in an inert solvent and is the basis of a solvent donicity scale, called the Gutmann donor number, DN[9].

Examples of the use of protogenic (actually protic) probes are those of MeOD and 4-nitrophenol. When MeOD is used as the probe, the shift of the wavenumber of the IR band for the stretching vibration of the O−D bond relative to that in the gas phase is a measure of the HBA effectiveness of the solvent, named the Koppel and Palm B scale[10]. The Kamlet and Taft solvatochromic comparison method is applied[3, 11] by comparing the wavenumbers of the lowest energy (longest wavelength) absorption band of the hydrogen bond donating (HBD) probe 4-nitro*phenol* (**1**) with that of its 'homomorphic' non-HBD probe 4-nitro*anisole* (**2**). The value of the bathochromic shift of the former with respect to the latter in a Lewis base HBA/EPD solvent relative to the shift in cyclohexane (*c*-HexH, regarded as a solvent devoid of donor properties, i.e. a non-HBA/EPD solvent) is the solvent basicity parameter recorded. The solvatochromic comparison method is based on the LSER principle. For a series of solvents S of varying polarity and the non-HBD probe **2**, a reference line is established (with wavenumbers ν in cm^{-1}) (equation 2):

$$-\Delta\nu(\mathbf{2}, \text{S}) = \nu(\mathbf{2}, \text{S}) - \nu(\mathbf{2}, \text{cHexH}) = [a_{1,2}\nu(\mathbf{2}, \text{S}) + b_{1,2}] \tag{2}$$

The HBA/EPD basicity β of any solvent S is then given by the distance of its wavenumber measured with the HBD probe **1** from a linear relationship (equation 3):

$$\beta_{1,2} = -\Delta\Delta(\mathbf{1/2}) = [a_{1,2}\nu(\mathbf{2}, \text{S}) + b_{1,2}] - \nu(\mathbf{1}, \text{S}) \tag{3}$$

The averaged Kamlet−Taft solvent basicity scale β_{KT} was established by averaging similar values of β obtained within narrow limits for several 'homomorphic' HBD and non-HBD

pairs of probes, such as **1** and **2**. Correlations between various scales of solvent basicity have been reported by Marcus[12–14]. For example, the following correlations (equations 4 and 5) have been established:

$$DN(\text{kcal mol}^{-1}) = -5.0 + 0.18895 \ (B/\text{cm}^{-1}) \tag{4}$$

$$DN(\text{kcal mol}^{-1}) = 0.5 + 38.2 \ \beta_{\text{KT}} \tag{5}$$

OH   OMe

NO$_2$ NO$_2$

(1)   **(2)**
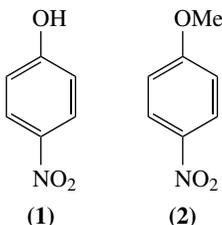
Ring-substituted anilines are HBD probes and have been used to obtain solvent basicity parameters as described in Section II.

C. Probes for Solvent Polarity/Polarizability

The polarity of isolated solvent molecules is given by their dipole moments μ as measured in the gas phase or in inert solvents. The polarizability of solvent molecules α is obtained from measurements of the refractive index n and the density ρ, yielding the molar refraction R, given the relative molar mass M (equation 6):

$$R = (M/\rho)(n^2 - 1)/(n^2 + 2) \tag{6}$$

from which α is obtained as $[3/(4\pi N_A)]R$, where N_A is Avogadro's number. The refractive index is normally measured at the sodium D-line frequency, i.e. n_D, and so R_D results from equation 6, but the frequency and temperature dependences of α are small and generally ignored. The μ and α obtained for isolated solvent molecules are not necessarily suitable measures of the polarity and polarizability of solvents in the bulk, nor of their relevant solvation abilities that depend on these properties. A further quantity that describes the polarity of solvents is the relative permittivity ε, but this again is not a proper measure of the polarity- and polarizability-dependent solvating properties.

Solvatochromic probes, on the other hand, have been widely employed for obtaining values of these properties, and various scales have been proposed for this purpose. The already mentioned $E_T(30)$ scale[1] is one of these as is the scale established by probe **2** according to equation 2. The parameter $E_T(30)$, however, is sensitive to the hydrogen bond donating (HBD) abilities of the solvents besides being sensitive to their polarity and polarizability[15]. It was found expedient to devise a scale based on the averaging of signals from several solvatochromic probes, called the Kamlet–Taft π^* scale, since it was based on the p $\rightarrow \pi^*$ and $\pi \rightarrow \pi^*$ electronic transition in the probe molecules on absorption of light. As originally devised this π^* scale was based on the averaging of the results from seven primary solvatochromic probes: 4-nitroanisole (**2**), N,N-diethyl-3-nitroaniline (**3**), 4-methoxy-β-nitrostyrene, 1-ethyl-4-nitrobenzene, N-methyl-2-nitro-p-toluidine (**4**), N,N-diethyl-4-nitroaniline (**5**) and 4-dimethylaminobenzophenone (**6**) in the analogs of equation 2. See Scheme 1 for the structures of probes **3** to **6** as well as similar ones mentioned further on. The scale was derived from 28 solvents of various types and

$$R^1\diagdown N\diagup R^2$$
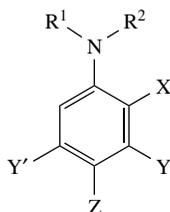
Structure	R^1	R^2	X	Y	Z
3	Et	Et	H	NO_2	H
4	H	Me	NO_2	H	Me
5	Et	Et	H	H	NO_2
6	Me	Me	H	H	C(O)Ph
7	Me	Me	H	H	NO_2
8	H	H	H	H	NO_2
9	H	H	NO_2	H	H
10	H	H	NO_2	H	Me
11	H	H	NO_2	H	MeO
12	Me	Me	NO_2	H	H
13	Me	Me	NO_2	H	Me
14	Me	Me	NO_2	H	MeO
15	H	H	H	NO_2	H
16	H	H	H	NO_2 [a]	H
17	H	H	H	H	C(O)Me
18	Me	Me	H	H	C(O)Me
19	H	H	H	H	CN
24	H	H	H	H	Ph
25	H	H	H	Ph	H
26	H	H	Ph	H	H
27	H	Me	H	H	NO_2
28	H	Me	H	H	NO
29	Et	Et	H	H	NO
30	H	Bu	H	H	NO_2
31	H	Et	H	H	NO_2
32	H	Et	H	NO_2	H
33	H	Me	various [b]	H	various [b]
34	H	C(O)Me	various [b]	H	various [b]
35	H	8-SO_3^--2-Naphthyl	H	H	H
36	Et	Et	H	Me	NO_2
37	Me	Me	H	Me [c]	NO_2
38	Et	Et	H	NO_2	NO_2
39	Et	Et	H	H	HC(O)−
40	Me	Me	H	H	CN
41	Me	Me	H	H	MeOC(O)−
42	Me	Me	H	H	EtOC(O)−
43	Me	Me	H	H	HC(O)−
44	Me	Me	H	Me [c]	CN
45	Me	Me	H	H	R [e]
46	Me	Me	H	NO_2	H
47	Me	Me	H	H	NO
48	−(CH$_2$)$_5$−		NO_2	H	H

SCHEME 1. The structures of some of the substituted anilines used as solvatochromic probes

Structure	R^1	R^2	X	Y	Z
49	n-C$_n$H$_{2n+1}$ ^{d}	n-C$_n$H$_{2n+1}$ ^{d}	H	H	NO$_2$
58	Me	Me	H	H	4-O$_2$NC$_6$H$_4$
60	H	H	H	H	4-O$_2$NC$_6$H$_4$
61	$-$CH$_2$CH$_2-$		H	H	NO$_2$
80	H	H	H	Me	NO$_2$
82	H	Me	NO$_2$	H	H
84	H	H	H	H	8-SO$_3^-$-1-Naphthyl
91	Et	Et	H	H	CN
93	H	H	NO$_2$	H	NO$_2$

^{a} Also Y$'$ = NO$_2$.
^{b} Either X- or Z-substituted by CN, NO$_2$, C(O)Me or C(O)OMe.
^{c} Also Y$'$ = Me.
^{d} With n = 3, 4, 5, 6, 8, 10 and 12.
^{e} R = $-$(CH=CH)$_n$ C$_6$H$_4$NO$_2$-p with n = 1, 2 and 3.

SCHEME 1. (*continued*)

normalized by assigning $\pi^* = 0$ to cyclohexane and $\pi^* = 1$ to DMSO[4]. Fifteen years later the π^* scale was re-examined, and the spectra of **2** and *N*,*N*-dimethyl-4-nitroaniline (**7**) were obtained in the gas phase and in 229 solvents with widely varying properties[16]. It was concluded that the use of **7** is preferable to that of **5**, as described in more detail in Section III.

II. RING-SUBSTITUTED ANILINES WITH AN −NH$_2$ GROUP

Under this heading are discussed solvatochromic probe molecules having the unsubstituted −NH$_2$ group attached to a phenyl group that is substituted on the ring, the primary example being 4-nitroaniline (**8**). Although the hydrogen bond donating (HBD) ability of aniline itself is only moderate, the electron-withdrawing nature of the nitro group in **8** enhances this ability. Therefore, it was proposed by Kamlet and Taft[3] as a suitable solvatochromic probe, together with **1**, for the establishment of the β scale for EPD/HBA solvents. The electronic transition from the non-ionic configuration in the ground state of **8** to an ionic configuration in the excited state (with a partial negative charge on an oxygen atom of the nitro group and a partial positive charge on the amine nitrogen atom) is enhanced by hydrogen bonding of the $-$N$^{\delta+}$ H$_2$ group to the EPD/HBA solvent molecules. This corresponds to a lowering of the transition energy and to a bathochromic effect, as observed. Equation 3 can then be applied to the **8/5** pair (equation 7):

$$\beta_{8,5} = -\Delta\Delta(\mathbf{8/5}) = [a_{8,5}\nu(\mathbf{5}, \text{S}) + b_{8,5}] - \nu(\mathbf{8}, \text{S}) \tag{7}$$

where $a_{8,5} = 1.035$ and $b_{8,5} = 2640$ cm^{-1}. The value of $\beta_{8,5}$ for a given solvent S was found to be proportional to that of $\beta_{1,2}$ as well as to the ^{19}F NMR chemical shifts Δ of 4-fluorophenol within the experimental errors.

   HMPA was thought to be the most basic EPD/HBA solvent available at the time. Hence, it was assigned the value 1.00 for establishing the β_{KT} scale with the normalization factor of $\beta_{8,5} = 2800$ cm^{-1} for this solvent. That is, the β_{KT} scale was constructed by averaging certain quantities, one of which was $\beta_{8,5}/2800$, another $\beta_{1,2}/(2800 \times 0.825)$ and a third Δ^{19}F(2-fluorophenol)/(2800 × 1.365). Later, the corresponding values from 2-nitroanilines[17] (see below) were included in the average for the β_{KT} scale. It was subsequently found[18] that *N*,*N*-dimethyl-4-nitroaniline **7** is a better homomorph of **8**

to use than **5**, since the dimethyl derivative lacks the vibronic structure of the absorption band in the visible region that besets the diethyl one. The corrected normalizing value for HMPA for the use of $\beta_{8,5}$ is thus 2759 cm^{-1}.

In an investigation following the original introduction of the β_{KT} scale the use of 2-nitroanilines as the HBD probes was studied by Yokoyama and coworkers[17]. These probes were 2-nitroaniline (**9**), 2-nitro-4-toluidine (**10**)[19] and 2-nitro-4-anisidine (**11**), compared in the context of the solvatochromic comparison method with their non-HBD *N*,*N*-dimethyl derivatives **12** to **14**, respectively. Whereas for 4-nitroaniline (**8**) there are two hydrogen atoms of the amino group that can form hydrogen bonds with an HBA solvent[20], in the 2-nitroanilines there is only one, since the second is already engaged in an *internal* hydrogen bond with the nitro group. The possible formation of two hydrogen bonds by **8** has the drawback that the strength of the second is affected by the stability of the first[21, 22], and the relative strengths may differ for various HBA solvents. The *a* and *b* parameters in equations corresponding to 3 and 7 of the 2-nitroanilines are $a_{9,12} = 0.874$ and $b_{9,12} = 4510$ cm^{-1}, $a_{10,13} = 0.813$ and $b_{10,13} = 5560$ cm^{-1}, and $a_{11,14} = 0.702$ and $b_{11,14} = 7570$ cm^{-1}. These results correlated very well with the previous ones using 4-nitroaniline, so that the corresponding $-\Delta\Delta\nu$ values could be averaged to yield the β_{KT} scale as finally established[7]. Other 4- and 5-substituted 2-nitroanilines that have been studied by Yokoyama and coworkers in this connection had amino, *N*,*N*-dimethylamino, phenoxy, trifluoromethyl, methylsulfonyl, methoxycarbonyl and ethoxycarbonyl substituents[23, 24]. The ^{15}N NMR chemical shifts caused by these substituents in the 5-position of 2-nitroaniline (as well as in the 4-position of aniline) were also measured in DMSO, but with respect to the substituent effects and not in relation to solvatochromism[25, 26].

The use of **8** as a probe in the solvatochromic comparison method (paired with **7** or **5** for non-HBA solvents) was re-examined by Laurence, Nicolet and Helbert[18]. They used a much wider variety of EPD/HBA bases (68 in all) than those used in the construction of the β_{KT} scale[3, 17] (25 solvents) (equation 8). The coefficients for the expression

$$\beta_{8,7} = -\Delta\Delta(\mathbf{8/7}) = [a_{8,7}\nu(\mathbf{8}, S) + b_{8,7}] - \nu(\mathbf{7}, S) \tag{8}$$

[note the difference with respect to equation 7] were[11] $a_{8,7} = 0.9841$ and $b_{8,7} = 3490$ cm^{-1}. On increasing the temperatures in the range 0 to 105 °C, $\beta_{8,7}$ decreased almost linearly with the reciprocal of the absolute temperature, and the standard error in $\beta_{8,7}$ was 135 cm^{-1} at 25 °C. These attributes make $\beta_{8,7}$ less precise than $\beta_{1,2}$ which is practically temperature independent and has the lower standard error of 100 cm^{-1} at 25 °C. These features, diminishing the attractiveness of using the nitroaniline pair as a solvatochromic probe, were attributed to residual vibronic structure of the absorption band of **7** (even though it is better than **5**), a problem absent in the nitrophenol pair, **1/2**. These authors also found that the correlation of $\beta_{8,7}$ with $\beta_{1,2}$ differs for EPD/HBA solvents of different classes, yielding the family dependencies: (i) oxygen bases (with PO, CO, SO and SO$_2$ donor groups) and nitriles, (ii) ethers, (iii) pyridines and sulfides and (iv) alkylamines. This is demonstrated in Figure 1 for a few solvents belonging to different classes, in particular for alkylamines and pyridines. The EPD/HBA basicity of the trialkylamines is larger than that of HMPA according to the **1/2** pair but lower according to the **8/7** pair or the β_{KT} scale. Laurence and coworkers therefore recommended to avoid the averaging process used by Kamlet, Taft and coworkers[3, 7, 17] and use two separate scales, one based on the **1/2** pair (preferred by Abboud and Notario[27]) and the other based on the **8/7** pair[17]. The deviation of the trialkylamines from the linear correlation (Figure 1) was later explained by Catalán and coworkers[28] by the special properties of the $-$NH$_2$ group of **8** that are due to steric hindrance by the trialkylamine hydrogen bonded to it, an effect absent for **1**.
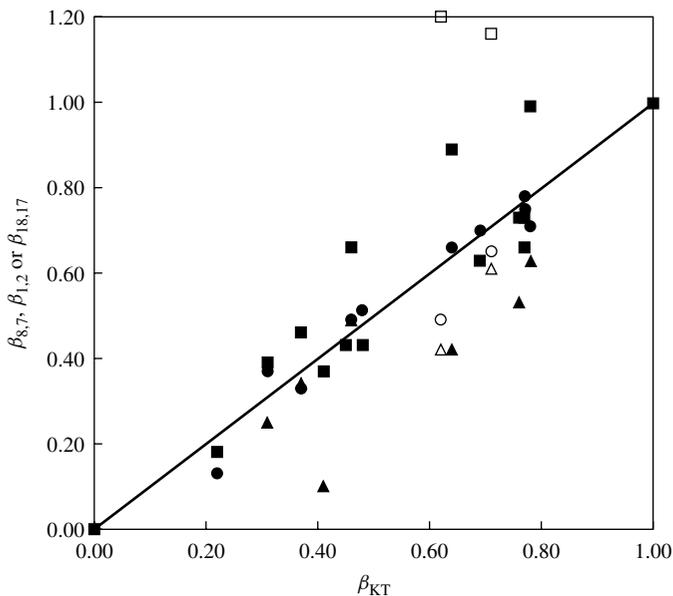
FIGURE 1. Correlation of scales for some common EPD/HBA solvents with solvatochromic comparison probe pairs with the Kamlet–Taft β_{KT} parameters. Circles: pair **8/7**, squares: pair **1/2**, and triangles: pair **17/18** (empty symbols for alkylamines), all normalized with 0.00 for cyclohexane and 1.00 for HMPA

    Nicolet and Laurence[11] studied the temperature dependence of the wavenumber of the lowest energy absorption band of the relevant probes. In the gas phase the effect was negligible, but not so in both non-EPD solvents (perfluorodecalin, n-heptane and 1,2-dichloroethane) and in EPD/HBA solvents (dibutyl ether, HMPA and triethylamine). The hypsochromic effect noted was 5 to 17 cm^{-1} K^{-1} for **8** and 3 to 8 cm^{-1} K^{-1} for **7**. This magnitude (compared with $\beta_{8,7} = 2759$ cm^{-1} at 25 °C for HMPA) is of little consequence for measurements near ambience except for the most precise requirements and is commonly ignored in ordinary work.

    Two further nitroanilines were studied spectroscopically by Drago[29] in various EPD/HBA solvents: 3-nitroaniline (**15**) and 3,5-dinitroaniline (**16**), as well as **8**, but not in the context of the solvatochromic comparison method. Bathochromic shifts were found for both solutes, increasing with the EPD/HBA ability of the solvents studied, but the shifts did not agree with the values calculated by means of Drago's expressions dealing with the covalent and electrostatic contributions to the strengths of the interactions. The discrepancies were attributed to incomplete hydrogen bonding association of the nitroaniline solute with weak HBA solvents. Still, except for the two ethers studied (diethyl ether and dibutyl ether) and triethylamine the spectral shifts in EPD/HBA solvents relative to that in dioxane correlated fairly well with the Kamlet–Taft β_{KT} measures of their basicity as seen in Figure 2.

    Laurence and coworkers[18] studied also the properties of the pair 4-aminoacetophenone (**17**) and 4-N,N-dimethylaminoacetophenone (**18**) as solvatochromic probes, but with regard to 12 solvents only. The imperfect linear correlation of the normalized $\beta_{17,18}$ with $\beta_{8,7}$, β_{KT} and $\beta_{1,2}$ shown in Figure 1 for these solvents indicates the importance not only of the HBD group (−OH for $\beta_{1,2}$ and −NH$_2$ for the other quantities), but also that of the
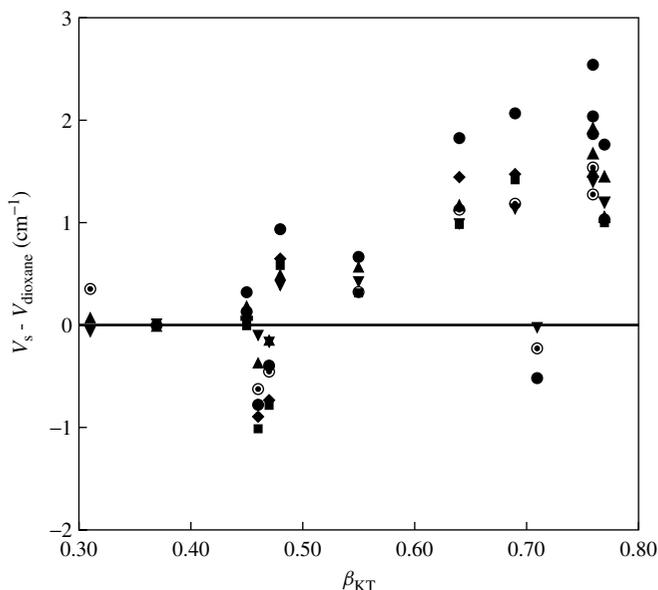
FIGURE 2. Correlation of the (bathochromic) spectral shifts of nitroanilines in EPD/HBA solvents relative to that in dioxane with the β_{KT} scale. The symbols for the probes are: ● for **8**, ▲ for **15**, ▼ for **16**, ♦ for **27**, ■ for **31** and ◉ for **32**. The negative values of the shifts are for dibutyl ether ($\beta_{KT} = 0.46$), diethyl ether ($\beta_{KT} = 0.47$) and triethylamine ($\beta_{KT} = 0.71$)

electron-withdrawing group ($-$MeC(O) for $\beta_{17,18}$ and $-$NO$_2$ for the other pairs). Mirashi and coworkers[30, 31] examined several anilines substituted in the 2-, 3- and 4-positions with methyl, hydroxy, methoxy and nitro groups in various solvents and obtained their specific interaction energies using the Bakhshiev relationships[32], but did not translate them into solvatochromic parameters.

Quantum chemical calculations on the solvatochromic shift of the charge transfer band of **8** in EPD/HBA solvents relative to the gas phase were carried out recently by Wang and coworkers.[33]

The fluorescence intensity of 4-aminobenzonitrile (**19**) in methanol and acetonitrile is comparable with that of the non-solvated probe in the gas phase and the probe exhibits appreciable solvatochromic shifts in polar solvents[34].

Swaminathan and coworkers[35–39] studied the solvatochromic responses of several probes based on two phenyl rings separated by another group: sulfone ($>$SO$_2$), ether ($-$O$-$) and imine ($-$NH$-$); see Scheme 2. The net bathochromic effect of the two amino groups in 4,4'-diaminodiphenyl sulfone (**20**) and its 3, 3' analog was less than that of the single group in 2-aminodiphenyl sulfone (**21**) in any one solvent, but the shift in the emission spectrum of **20** was the larger[35]. The spectral characteristics of 4-aminodiphenyl ether (**22**)[37] and 2-aminodiphenylamine (**23**)[38] in various solvents were also studied. These authors[39] also studied light absorption and fluorescence of aminobiphenyls, where a phenyl group is substituted at positions 2, 3 and 4 in aniline (**24–26**), in 13 solvents of various types. The solvatochromic shifts of the *absorption* did not follow the polarity of the solvents, but the *fluorescence* was red-shifted accordingly, with the Stokes' shifts being largest for the *meta*-substituted isomer **25**.
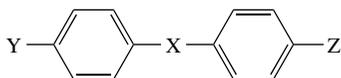
Structure	X	Y	Z
20	$>SO_2$	NH_2	NH_2
21	$>SO_2$	H	NH_2 [b]
22	O	H	NH_2
23	NH	H	NH_2 [b]
50	C=O	NMe_2	NMe_2
51	C=S	NMe_2	NMe_2
52	C=O	NMe_2	$N(C_2H_4OH)_2$
53	C=O	$N(C_2H_4OH)_2$	$N(C_2H_4OH)_2$
54	CH_2 [a]	NO_2	NMe_2
55	CH_2 [a]	NO_2	F
56	CHOH [a]	H	NMe_2 [b]
57	CHOH [a]	H	NEt_2 [b]
59	$-CH=CH-$ [d]	NO_2	NMe_2
62	$-N=CH-$	H	OH [b]
81	C$-$O	H	NH_2
85	$-N=N-$	NMe_2	NO_2
86	$-N=N-$	NMe_2	CF_3 [b]
87	$>SO_2$	NMe_2	NMe_2
94	NH	NO_2	NO_2
95	NH	NO_2	NO_2 [b]
96	NH	NO_2	NO_2 [c]

[a] The positions of the phenyl rings *ortho* to X are bonded together, forming a fluorene structure.
[b] Z is in the 2 position, not the 4 one.
[c] There is also a CF_3 group in position 2.
[d] Not specified[4] whether *cis* or *trans*.

SCHEME 2. Structures of some substituted anilines with two separated phenyl rings

Bekárek and coworkers[40] studied the effects of the medium on the spectrum of 2-nitroaniline and related them to the relative permittivity and refractive index of the solvents. Singh and Manjula[41] studied the fluorescence spectra of 1-(4-aminophenyl)-1,3-butadiene in various solvents.

For correlations[4] of the spectral data of ring substituted anilines having an $-NH_2$ group with the π^* scale, see Section IV.

III. RING-SUBSTITUTED ANILINES WITH AN $-$NHAlk GROUP

Singly *N*-alkyl-substituted anilines with further substitution on the ring have not found any practical use as probes for the solvatochromic comparison method, although some have been studied. Yokoyama and coworkers[17] showed that *N*-methyl-2-nitro-4-toluidine (**4**) was not able to donate a hydrogen bond to HBA solvents, since the lone hydrogen atom on the amine nitrogen was occupied making an internal hydrogen bond with the adjacent nitro group, as was confirmed later[19]. On the contrary, if the nitro group (or a nitroso group) was *para* to the *N*-methyl one, the latter could serve as a probe for HBA solvents by comparison with the corresponding *N*,*N*-dialkyl derivative[18]. Thus, *N*-methyl-4-nitroaniline (**27**) was compared with **7** and *N*-methyl-4-nitrosoaniline (**28**) was compared with *N*,*N*-diethyl-4-nitrosoaniline (**29**). For the 12 solvents for which data were

presented, these probe pairs yielded linear dependences on β_{KT}, but displaced upwards by *ca* 0.06 units, and for the **27/7** pair with somewhat larger slope than, say, the **8/7** pair has. The temperature dependence[11] was a hypsochromic effect of 5 to 13 cm^{-1} K^{-1} for **27** and 3 to 8 cm^{-1} K^{-1} for **28**.

N-Butyl-4-nitroaniline (**30**) was also shown[42] to be able to donate a hydrogen bond to HBA solvents, hence could be used as a solvatochromic probe, but has not been explored further in this respect. Drago[29] reported the wavenumbers of the lowest energy absorption bands of three *N*-alkyl-substituted nitroanilines: **27**, *N*-ethyl-4-nitroaniline (**31**) and *N*-ethyl-3-nitroaniline (**32**). Their spectral shifts relative to that in dioxane are shown in Figure 2 as a function of β_{KT} and a fair correlation is seen.

The infrared spectra of 2- and 4-substituted *N*-methylaniline (**33**) and acetanilide (**34**) were measured by Yokoyama and coworkers[43] in various solvents. The order of susceptibilities of the N−H stretching frequencies to the HBA abilities of the solvents for the various substituents was C(O)OMe < C(O)Me ∼ CN < NO$_2$, in contrast to the corresponding susceptibilities of the UV-vis absorption frequencies that was C(O)Me ∼ CN < NO$_2$ < C(O)OMe.

The ammonium salt of *N*-1-(8-sulfonato)naphthylaniline (**35**) is fluorescent and its emission peaks in 22 polar aprotic and protic solvents were studied by Hüttenhain and coworkers[44]. The solvatochromic shifts (Stokes shifts between absorption and emission peaks) are only moderate, but able to distinguish between protic and aprotic solvents of similar polarity.

For correlations[4] of the spectral data of ring-substituted anilines having an −NHAlk group with the π^* scale, see Section IV.

IV. RING-SUBSTITUTED *N,N*-DIALKYLANILINES

Ring-substituted *N,N*-dialkylanilines, besides serving as the non-hydrogen bonding homomorph of the probes used for establishing the β scales for EPD/HBA solvents, are widely used in order to describe the polarity/polarizability properties of all kinds of solvents. These properties are measured, e.g., by the Kamlet–Taft π^* parameters and are often called the non-specific interaction abilities[16] or just the polarity[4] of the solvents. Kamlet and coworkers[45] noticed the good correlation of the frequencies of the absorption maxima of probes **3** and **2**. The π^* scale was subsequently developed[4] using substituted aniline probes **3**, **4** (an internally hydrogen bonded −NHalkyl solute) and **6** (aceto- rather than nitro-substituted) and four non-aniline probes in twenty-eight non-HBD solvents (some non-hydrogen bonding and some HBA solvents). The scale was normalized by assigning the value $\pi^* = 0.00$ to cyclohexane and $\pi^* = 1.00$ to DMSO. The probes used subsequently for the π^* scale included mostly (besides **2**) *N,N*-dialkylanilines: **3**, **5**, **6**, **7**, *N,N*-diethyl-3-methyl-4-nitroaniline (**36**) and *N,N*-3,5-tetramethyl-4-nitroaniline (**37**)[46]. It turned out that for a large number of anilines, whether having −NH$_2$, −NHAlk or −NAlk$_2$ groups, the wavenumber of their lowest energy absorption band is characterized by a simple linear expression (equation 9):

$$\nu = \nu_0 - s\pi^*$$
(9)

for each probe in up to 60 solvents characterized by their π^* parameters, as is shown in Table 1, adapted from Reference 4. In addition to the nitroanilines shown in Table 1, the same correlation expression was found valid also for many non-nitroanilines and some non-aminophenyl probes. The 4-nitroanilines (whether or not alkyl-substituted on the nitrogen) have, on the average, higher ν_0 values than the 3-nitroanilines and these in turn have higher values than the 2-nitroanilines. The same general trend is seen for the s values in equation 9. The bathochromic effect on ν_0 is −NEt$_2$ > −NMe$_2$ and −NHPr-*i* >

TABLE 1.   Coefficients of the correlation equation 9: $\nu = \nu_0 - s\pi^*$ adapted from Reference 4

Substituted aniline		$(\nu_0/\text{cm}^{-1})/1000$	s
2-Nitroaniline	**9**	26.55	1.536
2-Nitro-p-toluidine	**10**	25.72	1.621
2-Nitro-p-anisidine	**11**	24.33	1.596
3-Nitroaniline	**15**	28.87	1.664
4-Nitroaniline	**8**	31.10	3.138
3-Methyl-4-nitroaniline		31.40	3.377
3,5-Dimethyl-4-nitroaniline		28.68	1.813
Ethyl 4-aminobenzoate		36.85	1.261
4-Aminobenzophenone	**81**	33.09	1.682
3,5-Dinitroaniline	**16**	27.61	1.436
N-Methyl-2-nitroaniline	**82**	24.59	1.593
N-Ethyl-3-nitroaniline	**32**	27.10	2.030
N-Methyl-3-nitro-p-toluidine		23.83	1.632
N-Methyl-4-nitroaniline	**27**	29.37	3.364
N-Ethyl-4-nitroaniline	**31**	29.17	3.327
N-Isopropyl-4-nitroaniline		28.96	3.237
N-Ethyl-3-methyl-4-nitroaniline		29.35	3.341
N,N-Dimethyl-2-nitroaniline	**12**	25.30	2.023
N,N-Dimethyl-2-nitro-p-toluidine	**13**	24.81	2.070
N,N-Dimethyl-2-nitro-p-anisidine	**14**	23.72	2.142
N,N-Diethyl-3-nitroaniline	**3**	25.52	2.212
N,N-Dimethyl-4-nitrosoaniline	**46**	25.39	1.852
N,N-Dimethyl-4-nitroaniline	**7**	28.10	3.436
N,N-Diethyl-4-nitroaniline	**5**	27.52	3.182
N,N-Diethyl-3-methyl-4-nitroaniline	**36**	25.25	3.354
$N,N,3,5$-Tetramethyl-4-nitroaniline		27.69	3.037
4-N,N-Dimethylaminobenzophenone	**6**	30.41	2.013
Ethyl 4-N,N-dimethylaminobenzoate	**42**	27.36	2.747
4-(N,N-Dimethylamino)-β-nitrostyrene		25.25	3.354
4-(N,N-Dimethylamino)benzaldehyde	**43**	30.98	1.682

$-$NHEt $>$ NHMe. Further spectral and structural aspects of these substituted anilines have also been discussed[4].

Nicolet and Laurence[11] studied four phenyl $-$NAlk$_2$ probes not mentioned previously nor included in Table 1: N,N-diethyl-3,4-dinitroaniline (**38**), 4-N,N-diethylaminobenzaldehyde (**39**), N,N-dimethylaminobenzonitrile (**40**) and methyl 4-N,N-dimethylaminobenzoate (**41**), the former two at several temperatures from 0 to 105 °C, the latter two only at 25 °C. The last three probes as well as **6**, **42** and **43** mentioned in Table 1 show that the nitro or nitroso chromophore group is not necessary for obtaining useful solvatochromic probes.

N,N-Dimethylaminobenzonitrile (**40**) is a fluorescing probe, and its emission peak shifts with temperature, pressure and solvent. The emission peaks of **40** in 19 non-polar, polar aprotic and protic solvents was studied by Yoshihara and coworkers[47] and compared with the emission peaks of four N-phenylpyrroles. Its pressure shifts were studied by Hara and Rettig[48] in acetonitrile and hexane. The conformational changes of **40** and its 3,5-dimethyl substituted analog **44** were subsequently studied by Rettig and coworkers[49, 50], showing the excited state to be near-planar, whereas the dimethylamino group is twisted by 60 to 70° in the ground state. Another set of fluorescent probes is α,ω-4-N,N-dimethylanilino-4'-nitrophenylalkylidene, where alkylidene is ethene, 1,3-butadiene and

1,3,5-hexatriene (**45**)[51]. Both the absorption and emission spectra show pronounced solvatochromic shifts in various non-polar, polar and protic solvents, correlating well with the π^* scale.

The empirical treatment of solvent–solute interactions by means of the π^* parameters was re-examined 15 years after their introduction[16]. It was concluded that N,N-dimethyl-4-nitroaniline (**7**), not used in the original introduction of the π^* scale, is superior to N,N-diethyl-4-nitroaniline (**5**) employed originally, since the former is not appreciably affected by differences in band shapes in different solvents as the latter is, due to vibrational structure. An extensive table of ν(**7**) in 229 solvents and the gas phase was provided (and found well correlated linearly with ν(**2**)). New π^* values were obtained for several solvents that differed somewhat from the previously established values[4,7]. The wavenumbers (in cm^{-1}) of **7** were shown to depend on the polarizability (measured by the refractive index n) and the polarity (measured by the relative permittivity ε) of the solvent for 66 non-aromatic solvents as follows (equation 10):

$$\nu(\mathbf{7}) = -12.40[(n^2-1)/(n^2+1)] - 4.46[(\varepsilon-1)/(\varepsilon+1) - (n^2-1)/(n^2+1)] + 32.19 \tag{10}$$

(note the misprint in equation 12 of Reference 16 where $(\varepsilon-1)$ is written instead of $(\varepsilon+1)$). The last term should equal the gas-phase value (31.34 cm^{-1}) but does not exactly do so. For 42 aromatic solvents the coefficients are different (equation 11):

$$\nu(\mathbf{7}) = -9.19[(n^2-1)/(n^2+1)] - 1.64[(\varepsilon-1)/(\varepsilon+1) - (n^2-1)/(n^2+1)] + 29.78 \tag{11}$$

This indicates that the polarity and polarizability contributions to π^* blend differently for aliphatic and alicyclic solvents and aromatic ones. A practical result of this is the necessity to include a $d\delta$ term in certain LSER correlations involving aromatic (and polyhalogenated) solvents[7].

Bekárek and coworkers[40] related the effect of the medium on the spectrum of 2-nitroaniline to the relative permittivity and refractive index of the solvents. In subsequent work, Bekárek and coworkers[52,53] employed several probes, including **5**, **8**, **9**, **10** and **15** as well as some that have not been mentioned previously: 3-nitro-N,N-dimethylaniline (**46**), 4-nitroso-N,N-dimethylaniline (**47**) and N-(2-nitrophenyl)piperidine (**48**), as probes to explore the polarity/polarizability and HBA/EPD properties of a large number of polar and non-polar aprotic aliphatic solvents. The wavenumbers could be fitted to expressions similar to equations 10 and 11, but with a cross-term of the permittivity and refractive index included (equation 12):

$$\nu = A + B[(\varepsilon-1)(n^2-1)/(2\varepsilon+1)(2n^2+1] + C[(n^2-1)/(2n^2+1)] \tag{12}$$

with characteristic values of the coefficients A, B and C. This expression led to better correlations with lower standard deviations than expressions like 10 or 11.

N,N-Dipropyl-4-nitroaniline and N,N-dibutyl-4-nitroaniline (**49**) were prepared by Helburn and coworkers[54] in order to have more lipophilic probes of the polarity of aqueous–organic interface systems. These probes also exhibit the solvent-dependent vibronic structure of the band shapes such as observed for **5**. The value of s in equation 9 decreased in the series **7** > **5** > **49**.

Michler's ketone, 4,4'-bis(dimethylamino)benzophenone (**50**) (Scheme 2), is an example of useful probes; see Scheme 2. It conformed[4] to equation 9 with $\nu_0 = 29960$ cm^{-1} and $s = 2.094$ in 14 solvents at an unspecified temperature and was further studied by Spange and Keutel[55] in 69 solvents at 20 °C. The range of values of the measured bathochromic spectral shift from the least, in n-hexane, to the largest, in 3-methoxyphenol, is 5090 cm^{-1}, among the largest observed for such probes. The carbonyl group in **50** causes it to be

specifically sensitive also to HBD solvents, hence equation 9 needs to be modified in order to accommodate them as $\nu/(10^3 \text{ cm}^{-1}) = 30.010 - 2.18\pi^* - 1.79\alpha$, where α is the Kamlet–Taft hydrogen-bond donation ability of the solvent[7]. Various derivatives of Michler's ketone have also been studied, such as the thio derivative (with a C=S group between the phenyl rings instead of the C=O group) (**51**), examined by Groenen and Koelman[56], and the 4′-[di(hydroxyethyl)amino]-4-dimethylaminobenzophenone (**52**) and 4,4′-bis[di(hydroxyethyl)amino]benzophenone (**53**) studied by El-Sayed and coworkers[57]. The donor–acceptor complex formed between Michler's ketone **50** and tetracyanoethene, studied by Spange and coworkers[58], showed a strong solvatochromic effect, but that of the polarity/polarizability of the solvent was bathochromic whereas that of its HBA/EPD ability was hypsochromic.

V. MORE COMPLEX ANILINES

Under this heading are collected solvatochromic probes which have an amino group attached to a phenyl ring that in turn is bonded by more than one bond to other moieties (Schemes 2 and 3). All these groups are generally further substituted in order to produce chromophores that have a wide solvatochromic amplitude.

A. Various Aniline Derivatives

The probe 2-(dimethylamino)-7-nitrofluorene (**54**) (see Scheme 2) was proposed by Catalán and coworkers[59] as the basis of the *SPP* scale of <u>s</u>olvent <u>p</u>olarity/<u>p</u>olarizability (in conjunction with 2-fluoro-7-nitrofluorene (**55**)). On the assumption that the band shapes are the same for these two probes, they cancel out in the difference $\Delta\nu_{SPP} = \nu(\mathbf{54}) - \nu(\mathbf{55})$. The normalized *SPP* scale was then defined in equation 13:

$$SPP^N(S) = [\Delta\nu_{SPP}(S) - \Delta\nu_{SPP}(g)]/[\Delta\nu_{SPP}(DMSO) - \Delta\nu_{SPP}(g)] \qquad (13)$$

where S is the solvent studied and $\Delta\nu_{SPP}(g)$ is the value calculated for the gas phase, $\nu(\mathbf{54}) - \nu(\mathbf{55}) = 32923 - 28231 = 4692 \text{ cm}^{-1}$. The values of $SPP^N(S)$ were reported for 100 solvents, but this scale does *not* correlate well with the π^* scale, particularly as regards the origin in the gas phase and for slightly polar aromatic solvents[59].

Redzimski and Held[60] studied 2-(dialkylamino)-9-fluorenol, alkyl = methyl or ethyl (**56**, **57**), as fluorescent probes in several solvents, non-polar, polar and protic. The hypsochromic shifts noted were rather modest.

Structurally similar to **54** are 4-nitro-4′-dimethylaminobiphenyl (**58**) and 4-nitro-4′-dimethylaminostilbene (**59**), mentioned in Reference 4 as conforming to equation 9. The probe 4-amino-4′-nitrobiphenyl (**60**) suffers a large red shift in ethanol as the temperature is lowered[61]. N-(4-Nitrophenyl)-polymethylenimines with $n = 2, 3, 4$ and 5 mutually bonded methylene groups in a ring with both end members bonded to the amino nitrogen have also been studied[4, 62, 63]. N-(4-Nitrophenyl)aziridine (**61**), in which the two groups on the amino nitrogen of the nitroaniline are bonded between them in a tight three-membered ring, is the member of the series with $n = 2$. N-(4-Nitrophenyl)aziridine (**61**) conforms to equation 9[4]. The emphasis in the earlier paper[62], however, was on the donation of hydrogen bonds from HBD solvents to the nitro group, and only in the later paper was the behavior according to equation 9 established. If in aziridine the $-(CH_2)_2-$group is replaced by a double bond to a single CH_2 group, then a probe like N-(2-hydroxybenzylidene)aniline (salicylideneaniline, **62**) results. Its Raman spectrum was studied by Turbeville and Dutta[64] in hexane, trifluoroethanol and hexafluoroiso propanol, the hydrogen-bond donating solvents enhancing the alternative zwitterionic conformation. Its absorption (as well as the FTIR) spectrum was later studied by Gegiou and coworkers[65] in the same protic solvents.

(63) $R^1 = R^2 = H$
(89) $R^1 = Et$, $R^2 = H$

(64)

(65a) R = H
(65b) R = p-tolyl

(66)

(67)

Structure	R^1	R^2	R^3	R^4
68	H	H	Me	H
69	H	H	CF$_3$	H
70	Me	Me	CF$_3$	H
71	Et	Et	Me	H
72	Et	Et	CF$_3$	H
73	H	Et	Me	Me
74	H	Et	CF$_3$	Me
75	Me	Me	Me	H
76	H	Et	CF$_3$	H

(77a) $R^1 = H$, $R^2 = Me$;
(77b) $R^1 = H$, $R^2 = Et$;
(77c) $R^1 = R^2 = Me$;
(77d) $R^1 = Me$, $R^2 = Et$

(78)

(79) the NH$_2$ group in positions 2, 3 or 4
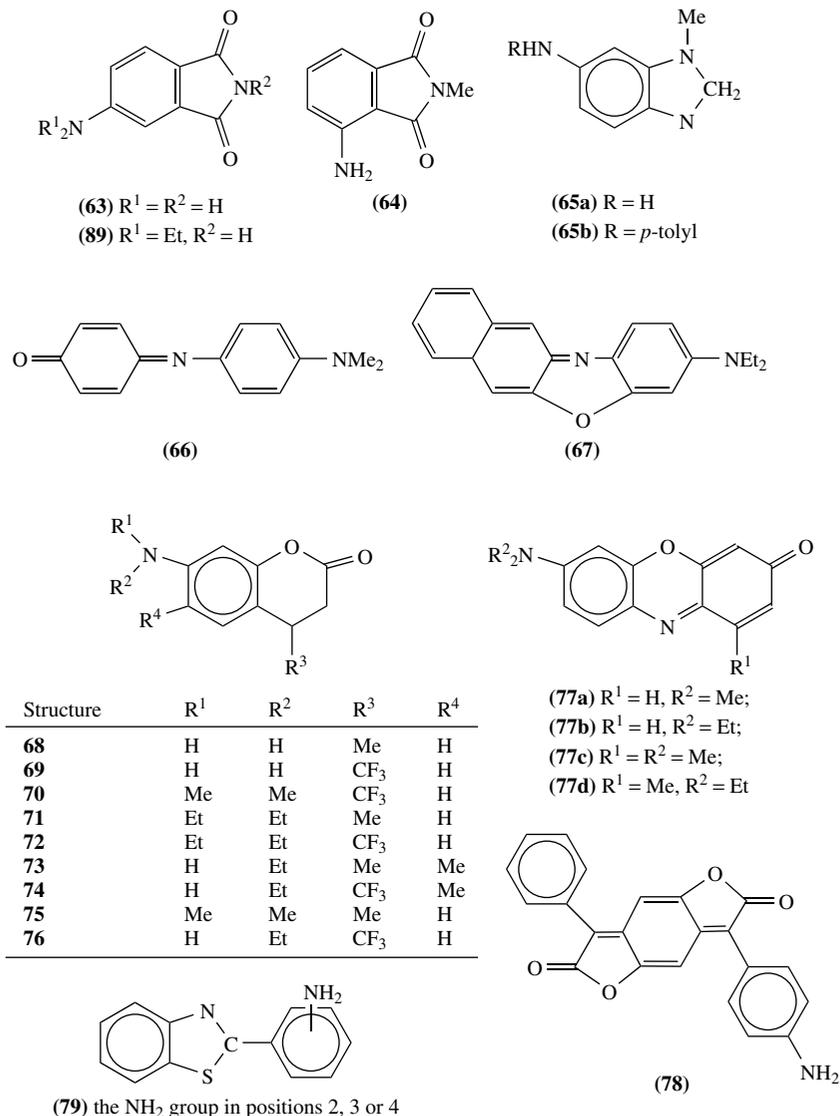
SCHEME 3. Structures of some complex substituted anilines

The solvatochromic fluorescence properties of amino- and imide-N-alkyl-substituted phthalimides were studied by several groups. The response of 4-aminophthalimide (63) in aqueous solutions of various substituted alkanes was used by Saroja and Samanta[66] to monitor their coiling and aggregation. The solvatochromic shifts of 3-amino-N-methyl-phthalimide (64) were studied in mixtures of decalin and propanol by Gorbatsevich and Smirnova[67].

Various other complex anilines have been studied over the years as solvatochromic probes. So have some other probes containing the 4-N,N-dimethylaminophenyl group, including 2-(4-N,N-dimethylaminophenylimino)-3-oxo-2,3-dihydrothionaphthene and 2-(4-N,N-dimethylaminophenylbenzylidine)-3-oxo-2,3-dihydrothionaphthene, studied by Kamlet and coworkers[4]. N-(2′-Hydroxy-4′-N,N-dimethylaminobenzylidene)-4-nitroaniline, having both HBD and HBA properties, was studied by El-Sayed and coworkers[68]. Various polymethylenediamines, substituted on one of the nitrogen atoms with nitrophenyl groups, were studied by Giacomelli and coworkers[42]. Moskal and coworkers[69] studied the solvent effects on the absorption spectrum of α-(4-dimethylaminophenyl)iminoacetoacetanilide, and found it to respond to both the solvent polarity and HBD ability, correlating well with the Dimroth–Reichardt $E_T(30)$ scale. Bekárek and Bekárek[70] studied the solvent effects on the absorption spectrum of 1-nitro-2-(4′-dimethylaminophenyl)ethene and 2-nitro-1-(4′-dimethylaminophenyl)propene. They correlated them, along with similar data for 4-nitro-3-methyl-N,N-diethylaniline, **3**, **5** and **6**, with an expression that depended on the function of the refractive index of the solvents, $(n^2 - 1)/(2n^2 + 1)$.

Amine-substituted benzimidazole was studied with regards to its emission spectra in various solvents[71]. The spectral shifts of 1-methyl-6-aminobenzimidazole (**65a**) from ethyl acetate (peak at 330 nm) to pyridine (peak at 470 nm) are appreciable, but there appears to be no systematic dependence on the polarity or HBA/EPD properties: the peak emissions are at 370 nm for hexane and 362 nm for formic acid, and in many solvents **65a** emits at 354 nm. Substitution of N-p-tolyl instead of the amino group at the 6 position (**65b**) did not improve the solvatochromic performance.

Some more aminophenyl probes with considerable bathochromic shifts between nonpolar and polar solvents were included in a table in Reichardt's book[6]. None of the probes mentioned in this section, except 2-(dimethylamino)-7-nitrofluorene (**54**), has found extensive use for the characterization of the properties of solvents.

B. Aniline-based Dyes

More complex chromophores are produced when the aminophenyl group can take up a quinoid configuration as one of the resonating forms of the molecule. This is the case of Phenol Blue (N-(dimethylaminophenyl)-1,4-benzoquinoneimine) (**66**) (See Scheme 3), and its derivatives that have been studied extensively, also as solvatochromic probes. The solvent dependency of the absorption spectrum of Phenol Blue was first studied by Brooker and Sprague[72], who noted an appreciable bathochromic effect, $\Delta\nu = 3146$ cm^{-1}, as the polarity of the solvent increased from cyclohexane (reddish violet solutions) to water (deep blue solutions). Subsequent work by LeRosen and Reid[73] and by McRae[74] tried to relate the bathochromic spectral shifts to macroscopic properties of the solvents. In the latter work, an expression analogous to equation 10 for 21 non-HBD solvents was presented. McRae's expressions[74] were subsequently used by other authors for the same purpose and to obtain the dipole moment of the excited state of the probe, given that of the ground state. Kolling[75] measured the solvatochromic shifts of **66** in 48 solvents, and found them to be sensitive to the HBD properties of the solvents in addition to their polarity. The transition energy could be described by E_T(kcal) $= 51.82 - 4.26\pi^* - 2.46\alpha$.

Figueras[76] studied the quantitative effect of HBD solvents on the bathochromic shifts of the Phenol Blue probe (**66**) and produced what may be called a Phenol Blue-based solvatochromic scale for hydrogen-bond donation ability, without calling it so. The shifts of HBD solvents relative to tetrachloromethane were approximately proportional to the Kamlet–Taft α values[13] but a two-parameter correlation, involving also π^*, would be better. Figueras tried to separate the hydrogen bonding effect (HBE) from the intrinsic

solvent polarity for m-cresol and 2,2,2-trifluoroethanol, the HBE being about twice that due to the polarity for the former solvent and three times for the latter. He also studied the effects of substitutions of t-butyl groups at the two *ortho* positions of the carbonyl group (also studied by Kamlet and coworkers[4]) as well as of both this and the amine group, and the replacement of the dimethyl groups on the amine nitrogen with only one or none.

Theoretical studies as well as ^{1}H- and ^{13}C-NMR measurements concerning the structure and spectroscopic behavior of Phenol Blue and its N,N-diethyl and its $-NH_2$ analogs were carried out by Morley and Fitton[77]. However, the calculated wavelengths of the solvatochromic band of **66** in non-HBD solvents did not agree at all well with the experimental values. The NMR results suggested that the quinoneimine form of **66** predominated in solution. The resonance Raman spectra of **66** in several liquid and supercritical fluid solvents were measured by Yamaguchi and coworkers[78]. The Raman shifts of the C=N and C=O stretching bands correlated with the solvatochromic band shifts. A somewhat different interpretation of this correlation along with non-resonance Raman spectra in a few solvents were provided by Terenziani and coworkers[79]. A very recent paper, concerning the thermosolvatochromism of **66**, was published by Webb and coworkers[80], looking at the vibrational–electronic coupling from still another point of view. They pointed out that the temperature dependence of the relative permittivity and the refractive index, with an expression similar to equation 10, arising from dielectric continuum theory, are unable to explain the temperature shift and broadening of the absorption band.

Nile Red (**67**) (formerly called Nile Blue A oxazone) is another substituted aniline of complex nature that has been used as a solvatochromic probe. Its structure bears similarities[81] to that of Phenol Blue (**66**), but it is rigidified, in that the quinoid ring (a part of a naphthalene rather than a benzene moiety) is further bound by an oxygen atom *ortho* to its =N− link to the aniline part, *meta* to the diethylamino (not dimethylamino as in **66**) group of the latter. These features make the probe more lipophilic, hence soluble in and applicable for such solvents as supercritical carbon dioxide, as well as stable in hydroxylic solvents, contrary to Phenol Blue[81]. A modified derivative is Nile Blue A base, that has a =NH group instead of the =O group of the quinoid ring. The absorption spectra of the former probe, **67**, have already long ago been studied as a function of the solvent in 23 solvents by Davis and Hetzer[81] and later shown to conform to equation 9 in 17 of them, hence being capable to measure solvent polarity/polarizability properties[4].

A more recent study of Nile Red (**67**) as a solvatochromic probe by Deye and coworkers[82] reported data in 86 liquid solvents. Furthermore, its absorption spectrum in near- and supercritical carbon dioxide, without addends and in the presence of methanol, acetonitrile, dichloromethane or tetrahydrofuran as modifiers, was also measured. The correlation of the transition energy $E_T/kcal = 28590/(\lambda_{max}/nm)$ of **67** with that of the Dimroth and Reichardt betaine, $E_T(30)$, was not linear, since these probes measure a different blend of polarity, polarizability and hydrogen bonding. Nile Red is indeed a strong HBA probe, and is applicable in strongly acidic media, such as formic acid or pentafluorophenol. The Nile Red probe range from the E_T value for water, 48.21, to that for n-hexane, 59.02 kcal, is smaller than that of $E_T(30)$, from 63.1 to 30.9, i.e. it is less sensitive as a probe than the Dimroth–Reichardt betaine. Note the opposite direction of the shift: whereas for the betaine the ground state has a higher dipole moment than the excited state, the opposite is the case for Nile Red.

Sackett and Wolff[83] measured the emission peaks of Nile Red in various polar solvents, ranging from 16260 cm^{-1} for acetone to 15040 cm^{-1} in water. A theoretical study of the absorption and emission solvatochromic properties of Nile Red (**67**) was presented recently by Han and coworkers[84]. The HB strength of the solvents around Nile Red was further studied by means of its fluorescence life time by Cser and coworkers[85]. A fourfold

decrease in the lifetimes was observed on going from 1-decanol (with a Kamlet–Taft $\alpha = 0.70$[13] and a lifetime of *ca* 4 ns like non-HBD solvents) to 1,1,1,3,3,3-hexafluoro-2-propanol, which is a very strong HBD solvent (with a Kamlet–Taft $\alpha = 1.96$[13]). Nile Red featured also in a study by Golini and coworkers[86] concerning its absorption and emission spectra in nine polar solvents as well as its thermochromic behavior in them. The conventional model of Lakowicz[87] was used[86] to interpret the solvatochromic and thermochromic data in terms of the differences between the dipole moments of the ground (8.4 D) and excited (13.4 D) states. Certain derivatives of Nile Red, e.g. *p*-tolyl-di-*n*-propyl Nile Blue base [5-(4-methyl)benzylimino-9-di-*n*-propylaminobenzo(α) phenoxazine], have also been studied with respect to their solvatochromism[4, 81].

Amine-substituted coumarin dyes (**68**–**76**) have also served as fluorescent solvatochromic probes. Solvent effects on the fluorescence of 7-amino-4-methylcoumarin (**68**) and its *N,N*-dimethyl derivative were studied by Kamlet, Dickinson and Taft[88]. The absorption and fluorescence of a series of coumarin laser dyes in various solvents were studied by Jones and coworkers[89]. They all had an amino group in the 7 position and a methyl or trifluoromethyl group in the 4 position. They included one with an unsubstituted amino group (**69**), with an *N,N*-dimethylamino group (**70**) or *N,N*-diethylamino group (**71**, **72**), or with an *N*-ethylamino group, also substituted in the 6-position (**73**, **74**), as well as more complex dyes. The solvents ranged from cyclohexane through ethyl acetate and acetonitrile to ethanol, glycerol and water. The red shifts of the absorption and fluorescence peaks correlated with the π^* values of the solvents. Further solvatochromic properties of 7-aminocoumarins were studied by Rechthaler and Köhler[90]. The amine-substituted coumarin **68** and its *N,N*-diethyl derivative (**71**) were studied by Parkanyi and coworkers in seven polar solvents, and the dipole moments of the ground and excited states were obtained according to the conventional expression[91]. The coumarin derivatives **68** and **71** featured in the study of Antonious and Sabry[92] on their extraction by various solvents in relation to the solvatochromic parameters of the latter. A number of coumarin derivatives: **68**, **70**, **72**, **73**, **75** and **76**, were studied by Kumar and coworkers[93], who calculated the dipole moments of their excited states from solvatochromic data.

Aminophenoxazone dyes were studied by Otsuki and Taguchi[94] with respect to their solvatochromic behavior in non-hydrogen-bonding polar solvents. The absorption spectra of 7-*N,N*-dimethylamino-3-phenoxazone (**77**), its 7-*N,N*-diethylamino analog and its 1-methyl analog were measured in several neat solvents and in aqueous dioxane solutions and the peak positions correlated linearly with the π^* scale. The fluorescence emission peak, however, was not linear with π^*.

Aminobenzodifuranone (**78**) was found by Gorman and coworkers[95] to exhibit a large positive solvatochromic effect. It was sensitive mainly to the HBA/EPD properties in 26 solvents studied but also to their polarity and HBD properties (equation 14):

$$\nu(10^3 \text{ cm}^{-1}) = 18.6 - 0.91\pi^* + 0.97\alpha - 2.93\beta \qquad (14)$$

The absorption peaks ranged from 499 nm for hexafluoroisopropanol (a very strong HBD solvent with high α) to 704 nm for hexamethylphosphoric acid triamide (a very strong EPD solvent with high β).

Dey and Dogra[96] studied the solvatochromic properties of 2-(aminophenyl)benzthiazole (**79**), with the amine group in positions 2, 3 or 4, in 12 solvents ranging from cyclohexane to water in polarity. The largest shift was found for the *meta* isomer: from 26320 cm^{-1} for cyclohexane to 19880 cm^{-1} for water. The 2- and 4-isomers have a quinoid resonance form and smaller spectral shifts, the least being for the 2-isomer that has an internal hydrogen bond.

VI. SOLVATOCHROMIC SCALES BASED ON ANILINES

A. Neat Solvents

As mentioned in the Introduction, Section I.B and Section II, ring-substituted anilines with an $-NH_2$ group can serve as probes for the HBA properties of EPD solvents. An extensive list, for 67 solvents, of the β_{NH_2} values for 4-nitroaniline (**8**) compared with 4-nitro-N,N-dimethylaniline (**7**) as the probe pair was reported by Abboud and Notario[27]. The values were calculated from equation 15:

$$\beta_{NH_2} = [(0.984\nu(\mathbf{7}) + 3.49) - \nu(\mathbf{8})]/2759 \tag{15}$$

where the numerical values pertain to wavenumbers in cm^{-1}. However, it was emphasized that this scale is inferior to the one based on the 4-nitrophenol/4-nitroanisole (**1/2**) probe pair[27]. In spite of this, most workers use in practice the original Kamlet–Taft β scale[7], which is an average of closely agreeing values for the (**1/2**), (**8/7**) and several other probe pairs. This is available for a much larger set of solvents, *ca* 100, although many of the values are 0.00 for non-HBA/EPD solvents. An even larger set of these average β values, for 185 solvents, was given by Marcus[13]. Some of these values were estimated according to rules provided by Kamlet and coworkers[7] rather than determined experimentally.

Section I.C and Section IV describe ring-substituted N,N-dialkylaminophenyl probes used for characterizing the polarity/polarizability properties of solvents. The best among them is N,N-dimethyl-4-nitroaniline (**7**), for which the frequencies at 25 °C in 286 solvents were reported by Dalati[97] and many of them with some values in additional solvents also by Laurence and coworkers[16]. These values were incorporated into the compilation of Abboud and Notario[27] under the heading $\pi^*_{NMe_2}$. Contrary to the solvent-dependent vibronic structure of **5**, the diethyl analog of **7**, the absorption spectrum of **7** does not have such problems. Still, the latter authors preferred the use of π^*_{OMe}, based on probe **2**, over that of $\pi^*_{NMe_2}$ and certainly over the original Kamlet–Taft π^* scale, based on the average of the results from several probes, including **7** as the substituted aniline. Such averaged π^* values for *ca* 180 solvents were reported by Marcus[13], again, some of which were estimated according to rules provided by Kamlet and coworkers[7] rather than determined experimentally.

From time to time more solvents are being added to the lists that have not been included in previous compilations[7, 13, 16, 27]. Such are certain hydroxylic solvents, studied by Gonçalves and coworkers[98] with **5** for solvent polarities and with **8** for their EPD/HBA properties, and alkanolamines studied by Lagalante and coworkers[99] with **7** and **8**, respectively for these properties, as non-exclusive examples.

The ability of aniline derivative solvatochromic probes (**5**, **9**, **27**, **31**, **36**, **61**, **66**, **67** and **80**) to characterize also the HBD abilities of solvents was reviewed by Novaki and El-Seoud[100] on the basis of data from the literature. They determined the sensitivity coefficients of these probes to the π^* and α solvent parameters.

B. Solvent Mixtures

In solvent mixtures the phenomenon of preferential solvation of the solvatochromic probe by one component of the mixed solvent often takes place. Care must therefore be taken when such combinations of mixed solvents and probes are employed for the characterization of the mixed solvent as regards its solvation properties for any arbitrary solute other than the particular probe studied[5]. It has been argued that, contrary to the case of neat solvents, where the use of a single probe can be justified[18, 27], it ought to be more

expedient for mixed solvents to use averaged results of several probes. The provision is that they are chemically sufficiently diversified and the results are converging within a reasonable probable error[5]. This, admittedly, introduces a measure of fuzziness in the parameters used to characterize the solvent mixtures, but should be preferable to the use of a single probe that may not describe properly the relevant solvation property of the solvent mixture for the particular solutes of interest.

Many authors have reported the solvatochromic parameters of aniline probes, or based on aniline probes among others, in solvent mixtures. Kamlet and coworkers[101] undertook 'dilution studies' of **8** and **7** in mixtures of DMSO with tetrachloromethane, chlorobenzene, 1,2-dichloroethane and dichloromethane. The bathochromic shifts were not linear with the volume fraction of the co-solvent, and $-\Delta\Delta(\mathbf{8/5})$ (cf. equation 9) exhibited a maximal value. They called the difference between $-\Delta\Delta(\mathbf{8/5})$ of the solvent mixture and that of neat DMSO the 'cybotactic polarity increment', *CPI*. Such enhancements were also found in mixtures of methanol, tetrahydrofuran and *t*-butanol with tetrachloromethane. The *CPI* of mixtures of DMSO was largest for tetrachloromethane, but depended on the aniline probe: **9**, **16**, **15**, **31**, **32** and 4-aminobenzophenone (**81**), compared with their *N*,*N*-diethyl homomorphs, all producing different values. This means that what was being studied was the near-environment (cybotactic region) of the probe molecule itself, and the results do not provide further information concerning the solvation properties of the mixtures towards any other solute, which should be the purpose of using solvatochromic probes in the first place.

Langhals[102] fitted the results for several probes, including **5**, for mixtures of two solvents differing in polarity (subscript m for the mixture, h for higher and l for lower polarity) to equation 16:

$$E_{\mathrm{m}} - E_{\mathrm{l}} = E_{\mathrm{D}} \ln[(c_{\mathrm{h}}/c^*) + 1] \tag{16}$$

where E is the transition energy, c is the molar concentration, and E_{D} and c^* are two fitting parameters. It was applied with probe **5** to mixtures of ethanol with water and with *n*-heptane, but it does not provide any further insight into the solvation properties of these mixtures.

Carr and coworkers[103–105] used aniline derivatives as solvatochromic probes for diverse purposes. The probes **3** and 2-nitro-*N*-methylaniline (**82**) served as polarity/polarizability probes in aqueous methanol, ethanol (not with **3**) and acetonitrile, with good agreement between them as well as with three other, non-aniline, probes: **2**, 2-nitroanisole and 4-nitroethylbenzene[103, 104]. The latter three were also used in aqueous 2-propanol and tetrahydrofuran. The probes are sufficiently diverse for the resulting π^* values to provide valid characterizations of the polarity/polarizability of the mixtures, applicable to other solutes than the probes used. Under ambient conditions the mole fraction of water in water-saturated 1-octanol (used to mimic biological membranes) is more than one quarter, so that its presence should have profound effects on the phase transfer properties of solutes of many kinds from water to this solvent. Dallas and Carr[105] employed as probes: **5** for the polarity/polarizability, **8/5** for the EPD/HBA properties, and the dyes **66** and **67** for the HBD properties of this medium (all in conjunction with some non-aniline derivative probes). It turned out that the differences between neat 1-octanol and the water-saturated solvent, though consistently measurable by the various probes, is small for all three measures of solvating abilities. The water is engaged in hydrogen bonds with the octanol and thus has no effect on the solvation properties of the bulk mixed solvent.

Bosch, Roses and coworkers explored the use of solvatochromic probes in solvent mixtures involving various alcohols with water as well as with other alcohols, hexane and benzene in a series of papers[106–110]. The aniline derivatives they employed were **5** for the polarity/polarizability and the **8/5** probe pair for the EPD/HBA properties of the mixtures, in conjunction with other suitable non-aniline probes. In order to ensure that what is being

measured is a property of the solvent mixture rather than the specific solute-mixed solvent interactions of the probes, the results from several probes were compared, such as the responses of **8** and **1** in aqueous 2-propanol and 2-methyl-2-propanol (*t*-butanol)[109]. The differences noted were 0.16 to 0.26 units in β, itself ranging from 0.50 (for water) to 0.96 (for the alcohol) on the average. In view of the large differences of the responses between the probes, it is not clear whether the averaging of the results from **8** and **1** is meaningful. Still, the results were interpreted by noting the differences between the averaged values of the parameters and those expected from a linear variation between the neat alcohols and water (and also for these alcohols and ethanol[110]) as an enhancement of the water structure when small amounts of alcohol are added to water. The polarity/polarizability and HBD properties are enhanced and the HBA properties are diminished.

Another set of papers is due to Mancini and coworkers[111–113]. In mixtures of acetonitrile or nitromethane with ethyl acetate, 2-butanone, acetone, DMF and DMSO, the differences between the results for **2** and **5** were much smaller (<0.04) than noted above over the entire composition ranges, hence their averaged π^* values appear to be measures of the polarity/polarizability of the mixtures rather than probe-dependent quantities. The same appears to be the case for the EPD/HBA properties measured by the **2/1** and **8/5** probe pairs of mixtures of acetonitrile with ethyl acetate, DMF and DMSO, but not for acetonitrile-rich mixtures with DMF or DMSO, where the differences between the two probe pairs are considerable[111]. Mixtures of aprotic polar solvents with chloroform showed discrepancies of the results for **2** and **5** of up to 0.15 units, whereas for such mixtures with dichloromethane the differences were smaller, up to 0.05 units in π^*. The **2/1** and **8/5** probe pairs for EPD/HBA properties of these mixtures showed differences for both chloroform and dichloromethane mixed with ethyl acetate, acetonitrile and DMSO, precluding the estimation of reliable β values[111]. The results with HBD solvent components were interpreted in terms of specific interactions with the probes[113].

The probes **7** and 2-nitro-*N*-methylaniline (**82**) were employed by Nigam and coworkers[114] to characterize aqueous methanol and acetonitrile mixtures, and the authors modeled these solutions in terms of the contributions from the water, the co-solvent and the presumed complex formed between them. Mixtures of a non-polar solvent (cyclohexane) and a highly polar one (nitrobenzene) were studied by Nevěčná and Bekárek[115] by means of *N*,*N*-dimethyl-4-nitrosoaniline (**47**). The spectral shifts were found to correlate well with the rate constant for the reaction of triethylamine with ethyl iodide.

Garcia and coworkers[116] applied 4-nitroaniline (**8**) to aqueous mixtures of pyrrolidin-2-one and *N*-methylpyrrolidin-2-one and mixtures of the latter two solvents, but with π^* values measured with 4-nitroanisole (**2**) rather than the homomorph **5** or **7**. Preferential solvation of the probes was invoked as an explanation of the non-ideal dependence of the resulting π^* and β on the composition of the mixed solvent. This again points out the inadequacy of using a single probe to establish generally valid properties of the solvent mixture. Similar conclusions about preferential solvation can be derived from the study by Tabata and coworkers[117] concerning the solvatochromic behavior of 4-(*N*,*N*-dimethylamino)benzonitrile (**40**) in aqueous methanol, ethanol, 1- and 2-propanol, acetone and acetonitrile.

Kauffman and coworkers[118,119] tried to fit the solvatochromic shifts of 1-(9-anthryl)-3-(4-*N*,*N*-dimethylanilino)propane (**83**), relative to the hydrocarbon homomorph with the dimethylamino group replaced by H, to the dielectric non-ideality of solvent mixtures involving hexane with ethanol, tetrahydrofuran and dichloromethane. The shifts were not linear with the mole fraction of the polar component, and Suppan's theory of dielectric enrichment was applied to the data. It was found that the dielectric enrichment that can be calculated from the relative permittivities of the components and of the mixtures is not sufficient to account for the observed solvatochromic shifts, but that preferential solvation of the probe by the polar component is superimposed on this dielectric effect. Earlier,

similar studies were carried out by Cattana and coworkers[120, 121], employing 2-, 3- and 4-nitroaniline as well as several N-alkyl-2-nitroanilines in mixtures of cyclohexane with polar solvents. In non-HBA solvents the preferential solvation can be ascribed predominantly to the independently calculated dielectric enrichment, whereas in HBA solvents it is due in large part to the hydrogen bonding of the probe with the solvent. In the case of the 2-nitroanilines, the intramolecular hydrogen bonding competes with the intermolecular HBE, as noted also in neat solvents.
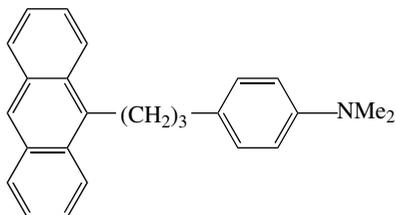
(83)

Another attempt to relate the results from the use of a solvatochromic probe (Phenol Blue (**66**)) to the inherent properties of solvent mixtures was made by Phillips and Brennecke[122]. They obtained the interaction energies (required for the application of the non-random two-liquid (NRTL) approach) of **66** with each of the solvent components from its solubility in the neat solvent. The mixtures studied contained cyclohexane as one component and acetone, triethylamine, ethyl butyrate, cyclohexanone, toluene and acetophenone as the other. Then the local compositions deduced from the solvatochromism of **66** were compared with those calculated by the NRTL equation and reasonable agreement was found.

Wetzler and coworkers[123] employed 4-aminophthalimide (**63**) and 4-amino-N-methylphthalimide (**64**) as solvatochromic (and thermochromic) fluorescent probes in solvent mixtures. A bathochromic shift of the emission spectra was found in mixtures of toluene with ethanol and with acetonitrile[123] when the more polar solvent was added to toluene, but raising the temperature causes a relative hypsochromic effect. Mixtures of benzene and acetonitrile were studied by Nevěčná and coworkers[124] for their polarity by means of the probes **46** and **47** and with respect to the correlation of this with the rate constants of the reaction of triethylamine with ethyl iodide. The fluorescence of the ammonium salt of 4-(1-naphthylsulfonate)aniline (**84**) in dioxane and water mixtures was studied by Hüttenhain and Balzer[125].

In summary, what was learned from these studies was that one generally obtained information on the behavior of the probe molecules themselves in the mixed solvents but not more generally applicable information about the solvent mixtures.

C. Supercritical Fluids

The increased interest in recent years in supercritical fluids as media for chemical reactions produced the need to characterize them in terms of their solvation abilities towards various kinds of solutes. The most widely used supercritical fluid is carbon dioxide, with a critical temperature $T_c = 304.2$ K (31 °C) and pressure $P_c = 7.39$ MPa (74 atm). Being a non-polar solvent, supercritical carbon dioxide (SCCD) can be modified in order to solubilize polar solutes by inclusion of a polar co-solvent, such as methanol. Aniline derivatives have been used as probes for the determination of the polarity of neat and modified supercritical fluids.

In the first paper dealing with the solvatochromic characterization of SCCD, the azo dye probe 4-diethylaminophenyl-4′-nitrophenyldiazene (**85**) and its 2′-trifluoromethyl analog (**86**) were employed by Hyatt[126]. The bathochromic shifts of these probes in several ordinary solvents were linear with their π^* values, so that SCCD could be assigned the value $\pi^* = -0.5$. Another early paper mentioning the application of aniline derivative solvatochromic probes to SCCD is that of Sigman, Lindley and Leffler[127]. They employed **3**, **4**, **5**, **6** and **8**, in SCCD of various densities, and since SCCD is devoid of HBA properties, probe **8** also measures the polarity/polarizability of the medium. The wavenumbers ν were converted to π^* values by inversion of equation 9 using the known ν_0 and s values for the probes, and these π^* values are plotted in Figure 3 for the aniline derivatives and compared with the mean values of five non-aniline derivative probes also employed. It is seen that the former group produces on the average less negative values of π^*, but in all cases the values approach that ($\pi^* = 0$) of the non-polar cyclohexane as the density approaches that of ordinary solvents.

Berger and coworkers[82, 128] used Nile Red (**67**) as the probe for supercritical carbon dioxide, Freon-13 (chlorotrifluoromethane) and Freon-23 (trifluoromethane) without and with modifiers. The earlier work did not specify the pressures employed and reported a temperature below T_c of carbon dioxide as applied to the supercritical fluid, that must be mistaken. However, the trend with the concentration of the modifiers[82] (Figure 4) is interesting. Methanol is able to reduce the E_T values for the Nile Red probe (**67**) considerably, being more efficient in this respect than acetonitrile, dichloromethane (also shown in Figure 3) and tetrahydrofuran, and the values for a few ordinary liquids, ranging from non-polar to highly polar, are shown for comparison. In the later work[128] the composition and density of supercritical mixtures of carbon dioxide and methanol were explored,
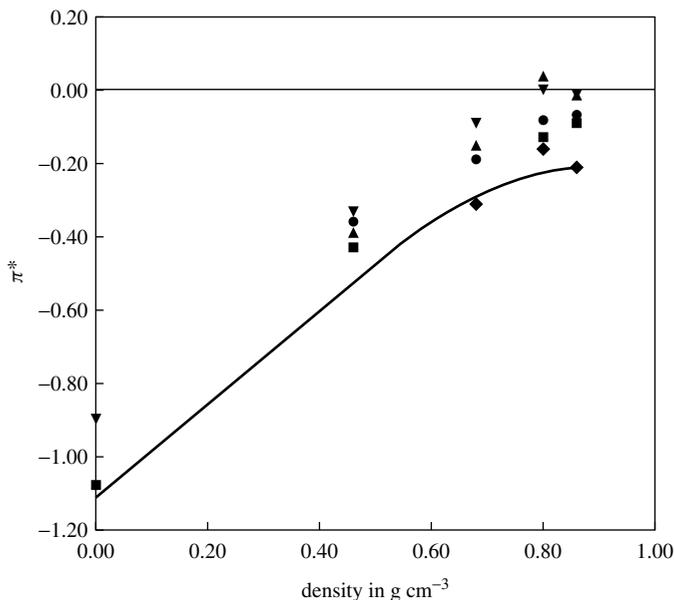
FIGURE 3. The polarity/polarizability π^* parameter of SCCD measured[67] with different aniline derivative probes: ● probe **3**, ▲ probe **4**, ▼ probe **5**, ◆ probe **6**, and ■ probe **8**, and —— averaged for five non-aniline-derivative probes
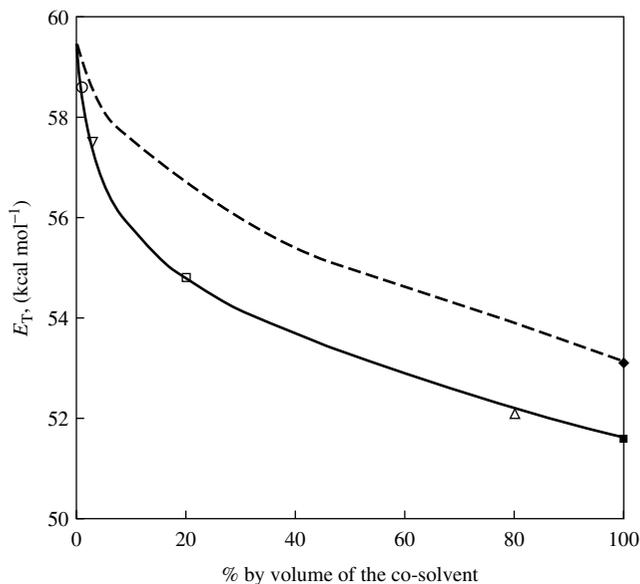
FIGURE 4. The effects of co-solvents of supercritical carbon dioxide on the polarity of the medium[82]. The E_T of Nile Red in supercritical fluids: ■ and the continuous curve: methanol; ♦ and the dashed curve: dichloromethane; and for ordinary liquids: ○: cyclohexane, ▽: tetrachloromethane, □: toluene and △: DMSO

in conjunction with measures of their polarity by means of Nile Red, with regard to chromatographic column performance.

Emission from the twisted intramolecular charge transfer (TICT) state of two fluorescent probes, **40** and **42**, was studied by Sun and coworkers[129, 130] in supercritical ethane, trifluoromethane, SCCD and mixtures of the latter two. The bathochromic shifts increased as the density and content of CHF_3 in the mixtures increased, pointing to the stabilization of the TICT state by the more polar component. Although non-polar and of small polarizability, SCCD caused larger shifts than the equally non-polar ethane, possibly due to the quadrupole moment of CO_2.

Phenol Blue (**66**) was the probe employed by Yamaguchi and coworkers[78] to measure the polarity/polarizability of supercritical trifluoromethane, carbon dioxide, dinitrogen oxide and ethane at 323.2 K (50 °C). These measurements, however, were not used in order to derive more general information on the properties of such supercritical fluids. Kelley and Lemert[131] used this probe in mixtures of solvents saturated with carbon dioxide at high pressures. For example, the polarity of acetone saturated with carbon dioxide at 35 °C and 60 bar is similar to that of neat cyclohexane at ambient conditions (i.e. negligible). Saturation with CO_2 at high pressure is thus tantamount to the addition of an anti-solvent (an admixture that is detrimental to the solvent properties) for the precipitation of solutes from the solvent. Phenol Blue was also used by Sasaki and coworkers to characterize the temperature and pressure dependence of the solvation ability of SCCD[132]. The transition energy decreased as the pressure increased and the temperature decreased, i.e. the density of the SCCD increased. The local density of the SCCD around the probe molecules was estimated from McRae's expression[74] (based on that of Bakhshiev[32]), analogous to equation 10.

Bis(4,4′-N,N-dimethylaminophenyl) sulfone (**87**) was used by Schulte and Kauffman as a fluorescent probe to measure the polarity of mixtures of supercritical carbon dioxide with ethanol[133]. The preferential solvation of the probe by the ethanol in its near environment was confirmed.

Maiwald and Schneider[134] studied the probe pair **8/7** in order to examine the EPD/HBA abilities of supercritical chlorotrifluoromethane, sulfur hexafluoride, dinitrogen oxide and SCCD and found, as expected, that none of these had such abilities (i.e. $\beta \approx 0$). On the contrary, supercritical ammonia had appreciable β values (0.70 at 293 K and 100 MPa), being moderately temperature dependent but with little change on lowering the pressure.

The solvent properties of supercritical carbon dioxide and fluorocarbon mixtures have been studied by several authors using solvatochromic probes based on aniline derivatives. Nile Red (**67**) was employed by Abbott and coworkers[135] to investigate SCCD and its mixtures with pentafluoroethane. The value of $\pi^* = (\nu - \nu_0)/s$ (cf. equation 9) increased moderately at a constant temperature with the pressure in the range 100 to 300 bar but strongly at a given pressure with decreasing temperatures from 120 to 34 °C, the increase being from highly negative values, ca −0.5, to much less negative values, ca −0.1. The admixture of 5.3 and 30.1 mole% of pentafluoroethane raised the π^* values uniformly at all temperatures and pressures studied by about 0.2 and 0.4 units, respectively, thus reaching positive values at high pressures and low temperatures. Hence, the solubilities of polar solutes would be enhanced in such mixtures compared with solubilities in SCCD. The π^* values of supercritical pentafluoroethane and difluoromethane were also determined with Nile Red as the probe, as functions of the temperature and pressure[136]. However, Nile Red is capable of hydrogen bonding, so that this effect has to be compensated for, and measurements using 4-nitroaniline (**8**) and N,N-dimethyl-4-nitroaniline (**7**) were subsequently undertaken[137].

Kho and coworkers[138] took up the study of SCCD-expanded fluorinated solvents, mainly ethoxynonafluorobutane, by means of the probes **8**, 2-nitro-N-methylaniline (**82**) and **7**. Addition of the SCCD decreased the π^* values of the fluoro solvent in a manner paralleling its expansion but affected only little the β values.

Near-critical and supercritical polar HBD solvents have also been studied by means of aniline derivative solvatochromic probes. Eckert and coworkers[139] studied ambient to near-critical water and obtained their β values by means of the probe pair **8/7**. These remained essentially constant and small, approaching that of monomeric water (0.18) at the higher temperatures. Supercritical water (SCW) was studied in this respect by Oka and Kajimoto[140] using probes **8** and **7**. The bathochromic shifts increased with the density of the SCW, but it was concluded that since both probes showed parallel shifts, also parallel to the dielectric function $(\varepsilon - 1)/(2\varepsilon + 1)$, no specific hydrogen bonding takes place between the probes and the water molecules. At temperatures slightly above the critical point ($T_c \leqslant T \leqslant 1.05T_c$) clustering of the water molecules around the probes took place, due to dipolar interactions rather than hydrogen bonds, but such clustering ceased at higher temperatures.

Near-critical and supercritical ethanol were studied by Eckert and coworkers[141] using the probe pair **8/7** to obtain their β values. For liquid ethanol, these declined with increasing temperatures from 0.8 at ambient conditions to 0.3 in ethanol at equilibrium with its vapor at 250 °C. For sub-critical (gaseous) ethanol at 250 °C, β increased somewhat from ca 0.05 at low pressures to ca 0.2 at 17 MPa (170 bar).

D. Room-temperature Ionic Liquids

Room-temperature ionic liquids (RTILs) have become in recent years more widely applied as solvents, hence their solvating properties required investigation. Foremost among

$$
\left[\ \underset{\underset{\text{Me}}{\overset{|}{N}}}{\overset{\overset{R}{\diagdown}}{N}}\ \right]^{+}
$$
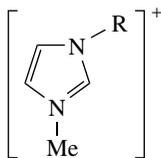
(88)

such liquids are 1-alkyl-3-methylimidazolium salts (**88**). So far, mostly solvatochromic probes other than those based on aniline derivatives have been employed, but some use of the latter probes has been made. Nile Red (**67**) featured in the study of Carmichael and Seddon[142] of 1-alkyl-3-methylimidazolium salts, where alkyl was butyl, hexyl, octyl and decyl and the anions were nitrite, nitrate, tetrafluoroborate, hexafluorophosphate and bis(triflyl)imide. The polarity as measured by this probe (cf. Section VI.A) places these RTILs between N,N-dimethylformamide and 2-aminoethanol, i.e. as highly polar solvents, the polarity decreasing, for a given anion, as the alkyl chain lengthens beyond the hexyl group and for the 1-butyl-3-methylimidazolium in the order of anions given above. The same probe (**67**) was also used by Dzyuba and Bartsch[143] in 1-substituted-3-methylimidazolium bis(triflyl)imides, where the groups at the 1-position were propyl, decyl, benzyl, 2-methoxyethyl and 2-hydroxyethyl. The polarities of these RTILs as far as they are measured by Nile Red are similar to those studied by Carmichael and Seddon[142]. Nile Red (**67**) was used by Fletcher and coworkers[144] in 1-butyl-3-methylimidazolium hexafluorophosphate, with regard to both its absorption and its emission spectra, and compared with its response in normal liquid solvents and the responses of other probes. The polarity of the RTIL was as high as that of water as measured by **67**, whereas other probes placed it nearer acetonitrile. This RTIL was subsequently further studied by Baker, Baker and Bright[145], who used probe **5** to obtain its $\pi^* = 0.92$ and the probe pair **8/5** to obtain its $\beta = 0.21$ at 20 °C, both decreasing moderately as the temperature was raised from 10 to 70 °C. The presence of water (2% by volume) in this RTIL increased both parameters by 0.02 units at all temperatures.

The more conventional probes, N,N-diethyl-4-nitroaniline (**5**) for obtaining π^* values and the probe pair 4-nitroaniline (**8**) and **5** for obtaining β values, were used by Pandey and coworkers[146] in 1-ethyl- and 1-butyl-3-methylimidazolium bis(triflyl)imide and hexafluorophosphate and their mixtures. The β values, ca 0.23, are rather insensitive to the natures of the cation, the anion and the composition, but the π^* values, between 0.96 and 1.04, vary systematically, the hexafluorophosphate salts showing the higher values. The probe N,N-dimethyl-4-nitroaniline (**7**) was used by Eckert and coworkers[147] to study the polarity of 1-butyl-3-methylimidazolium hexafluorophosphate expanded by dissolved carbon dioxide (see also Section VI.C). In the absence of the carbon dioxide the resulting π^* is 0.95 at 35 °C and 0.92 at 50 °C, but the dilution by the carbon dioxide lowers these values gradually with increasing pressure, i.e. amounts of the gas absorbed or the volume expansion.

The fluorescent probe 4-aminophthalimide (**63**) as well as its N,N-diethyl homomorph (**89**) were used by Samanta and coworkers[148, 149] to study the polarity and fluorescence dynamics in 1-alkyl-3-methylimidazolium salts. The alkyl groups were variously ethyl, butyl and octyl and the anions were nitrate, tetrafluoroborate, hexafluorophosphate and bis(triflyl)imide. Similar conclusions were reached concerning the effects of alkyl chain length and anion as those obtained by Carmichael and Seddon[142] using Nile Red. The solvation dynamics were found to depend on the viscosity of the media. Further use of **63** in 1-butyl-3-methylimidazolium hexafluorophosphate was reported by Ingram and

coworkers[150], finding that this RTIL behaves like ordinary highly polar solvents except that it is considerably more viscous.

E. Other Environments

Solvatochromic probes based on aniline derivatives have been used in a host of environments other than liquid solvents and their mixtures, supercritical fluids and room-temperature liquid salts. All these uses cannot be reviewed here and only examples of them are provided.

The polarity of inorganic surfaces, such as silica or alumina, or polymers of natural origin, such as cellulose without and with an organic substance or a linear polymer sorbed on them, has been explored by means of 4,4′-bis(*N*,*N*-dimethylamino) benzophenone (Michler's ketone, **50**) and other probes by Spange and coworkers[151−161]. Cellulose and other native polysaccharides received special attention[151, 152, 157, 159], and the probes **81** and **50**, absorbed on the surface from 1,2-dichloroethane or cyclohexane solutions, could determine the surface HBA/EPD properties and polarities of samples with different crystallinity or other features. Derivatives of Michler's ketone, in which one or two of the *N*,*N*-dimethylamino groups were replaced by di(2-hydroxyethyl)amino groups, have also been used[158]. *N*-(2′-Hydroxy-4′-*N*,*N*-dimethylaminobenzylidene)-2-nitroaniline was used by Spange and coworkers[68] to characterize Aerosil 300 particles in non-HBA solvents. Other authors used other probes for characterizing silica surfaces, partly as reaction media, for which **3** was used by Lindley and coworkers[162] or **40** by Günther and coworkers[163], who studied highly porous silica and alumina surfaces.

The use of solvatochromic probes to explore the solvation abilities of stationary phases in chromatography, based on derivatized silica, was studied by Rutan and coworkers[164−167]. Octadecylsilica with aqueous methanol was studied by means of probes **4** and **5** for its π^* value[167]. Probes such as **9** and **82** have also been used, and it was found that phenyl-derivatized silica is more polar than the octyl-derivatized analog[166]. Silicon-based materials for chromatography (OV type GLC stationary phases) and the low molecular weight analogs, such as hexamethyldisiloxane, were similarly characterized[168]. Other inorganic materials have also been characterized solvatochromically, including 12-tungstophosphoric acid, where **50** and an aminobenzodifuranone dye **90** have been used[169]. Zeolites were characterized by means of salicylideneaniline **62** as the solvatochromic probe[170]. This probe was also used to determine the HBD abilities of silica surfaces[160].

(90)
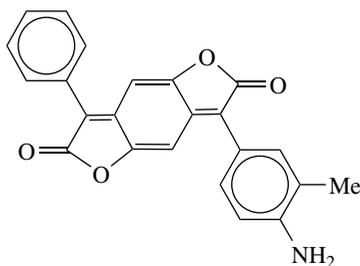
Aniline derivatives have also been employed as solvatochromic probes to characterize the solvation abilities of various polymers and polymer surfaces. Thin films of various polymers were prepared by Paley and coworkers[171] that incorporated the probe **7** for studying the polarity/polarizability and the probe pair **8/7** for studying the HBA/EPD

properties. The surface polarity of poly(α-amino acids) was studied by means of the probes Michler's ketone (**50**), 4-aminobenzophenone (**81**) and an aminobenzodifuranone dye (**78**)[172]. The fluorescence of Phenol Blue (**66**) was used to characterize the polarity of the interior of dendrimers: polyamido amines[173] and poly(propyleneimine)[174]. Other fluorescent probes on the basis of aminobenzonitrile, **40** and **91**, and coumarin dyes, **69** and **92**, were used to study aqueous solutions of α-cyclodextrin[175, 176].
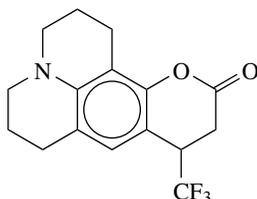
(**92**) Coumarin dye 153

The use of solvatochromic probes to study micelles produced by surfactant solutions has been a popular method. For example, Correa and Silber[177] employed 4-nitroaniline (**8**), 2-nitroaniline (**9**), 2,4-dinitroaniline (**93**) and *N*,*N*-dimethyl-4-nitroaniline (**7**) in reversed micelles produced by solutions of the sodium salt of 1,4-bis(2-ethylhexyl)sulfosuccinate (Aerosol OT, AOT) in hexane at different ratios of water to surfactant. The nitroanilines with a free amino group bind to the surfactant and a new absorption band is seen at longer wavelength, whereas the dimethyl-substituted nitroaniline shows only a shift of the band maximum. Water competes with the nitroanilines for binding sites at the surface of the micelle. In a subsequent paper these authors together with Durantini[178] used further nitroaniline probes: bis(4-nitrophenyl)amine (**94**), *N*-(2-nitrophenyl)-4-nitroaniline (**95**) and *N*-(2-trifluoromethyl-4-nitrophenyl)-4-nitroaniline (**96**), to study the reversed micelles of AOT in hexane and tetrachloromethane. For **94** and **96** again a new absorption band appears, whereas for **95** the internal hydrogen bond precludes hydrogen bonding to the micelles and only dipolar interactions take place. The fluorescent probe 4-(1-naphthylsulfonate)aniline (**84**) was also used to characterize the polarity of inverted micelles of AOT in alkanes and the effect of water and alkanols on them[179, 180]. The maximum of the emission band of the probe shifts to longer wavelengths as the size of the aqueous core of the reversed micelle increases, but the presence of the alkanols quenches the fluorescence. Nile Red (**67**) was used by Datta and coworkers[181] to study the reversed micelles of AOT in heptane, finding a sixfold increase in the lifetime of the excited state of the probe in the aqueous interior of the micelles compared with that in bulk water. The same micelles were studied by Raju and Costa[182] by means of the coumarin dye **72**, but the hydrophobic nature of this probe and its preferential solvation in the heptane make it much less sensitive to the microenvironment in the interior of the inverted micelles.

A series of *N*,*N*-dialkyl-4-nitroaniline probes was employed by Helburn and co-workers[183], with alkyl ranging from methyl (**7**), through ethyl (**5**), propyl, butyl, pentyl, to hexyl (**49**), to study aqueous micelles of sodium dodecyl sulfate (SDS). The *N*,*N*-dipropyl probe was the most sensitive to the critical micelle concentration of aqueous SDS. The longer-chain probes, *N*,*N*-dibutyl to -dihexyl, are more effective for aqueous micelles formed by a non-ionic surfactant, Triton 114, probing the polyoxyethylene portions of these micelles. Even longer chains, octyl, decyl and dodecyl, were attached in order to make the probes more hydrophobic, therefore more soluble in lipids, bilayers, micelles and biological membranes[184]. The micelles formed by block polymers of polystyrene and

poly(acrylic acid) in aqueous solutions were studied by Choucair and Eisenberg[185] using 2-nitrodiphenylamine (**23**). This hydrophobic probe was solubilized at the micellar interface. Micelles of dodecyltrimethylammonium bromide in water were studied by Vitha and Carr[186] by means of the probe **5** for their polarity/polarizability ($\pi^* = 1.02$) and the probe pair **8/5** for their HBA/EPD properties ($\beta = 0.41$). The results with this pair differed significantly from those with the **1/2** pair ($\beta = 0.58$).

Aqueous micelles and phospholipid vesicles were studied by Shin and Whitten[51] by means of a series of polyene-bridged phenyl rings, one ring bearing a dimethylamine group and the other a nitro group *para* to the bridges, **45**. Such probes occupied sites in the structures that corresponded to very high polarities. In essence, the probes are oriented in the bilayers with the amino end in the hydrophobic part and the nitro group in the hydrophilic part.

The fluorescent probe 4-aminophthalimide (**63**) was employed by several authors to study micelles. Samanta and coworkers[187,188] used it to study micellization of common cationic (SDS), anionic (cetyltrimethylammonium bromide) and neutral (Triton-X 100) aqueous surfactants, and the same systems were also studied by Datta, Mandal and coworkers[189,190]. The critical micelle concentration could be determined and it was found that the probe binds to the micelle water interface or to the cyclodextrin cavities that have also been studied[187,188]. Water-in-oil microemulsions of Triton-X 100 in a mixture of benzene and hexane showed[190] the probe to reside in the water core of the reversed micelles, the polarity of which differs much from that of bulk water.

Two rather complex aniline derivatives, 2-[3-(*N*-methyl-*N*-phenylamino)-2-propenylidene]indanone (**97**) and 2,5-bis[3-(*N*-methyl-*N*-phenylamino)-2-propenylidene]cyclopentanone (**98**), were employed as fluorescing probes to characterize the polarity of aqueous micelles and cyclodextrins by Bagchi and coworkers[191].
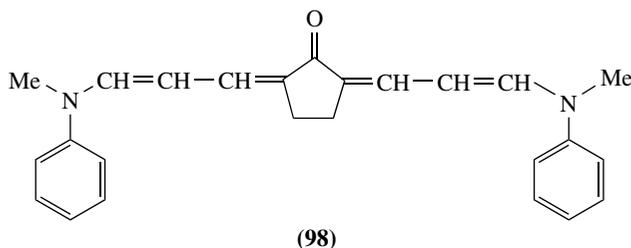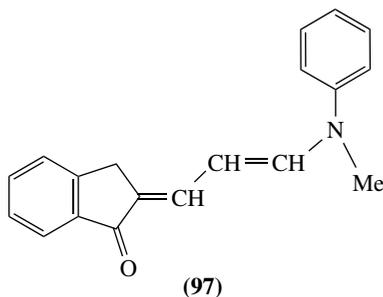
(**97**)

(**98**)

VII. ACKNOWLEDGMENT

VIII. REFERENCES

1. K. Dimroth, C. Reichardt, T. Siepmann and F. Bohlmann, *Liebigs Ann. Chem.*, **661**, 1 (1963).
2. C. Reichardt, *Solvents and Solvent Effects in Organic Chemistry*, 3rd edn., Wiley-VCH, Weinheim, 2003, p. 68.
3. M. J. Kamlet and R. W. Taft, *J. Am. Chem. Soc.*, **98**, 377 (1976).
4. M. J. Kamlet, J.-L. M. Abboud and R. W. Taft, *J. Am. Chem. Soc.*, **99**, 6027 (1977).
5. Y. Marcus, *J. Chem. Soc., Perkin Trans. 2*, 1015, 1751 (1994).
6. C. Reichardt, Chap. 6 in Reference 2.
7. M. J. Kamlet, J.-L. M. Abboud, M. H. Abraham and R. W. Taft, *J. Org. Chem.*, **48**, 2877 (1983).
8. Y. Migron and Y. Marcus, *J. Phys. Org. Chem.*, **4**, 310 (1991).
9. V. Gutmann and E. Wychera, *Inorg. Nucl. Chem. Lett.*, **2**, 257 (1966).
10. I. A. Koppel and V. A. Palm, in *Advances in Linear Free Energy Relationships* (Eds. N. B. Chapman and J. Shorter), Plenum, New York, 1972.
11. P. Nicolet and C. Laurence, *J. Chem. Soc., Perkin Trans 2*, 1071 (1986).
12. Y. Marcus, *J. Solution Chem.*, **13**, 599 (1984).
13. Y. Marcus, *Chem. Soc. Rev.*, **22**, 409 (1993).
14. Y. Marcus, *The Properties of Solvents*, Wiley, Chichester, 1998.
15. Y. Marcus, *J. Solution Chem.*, **20**, 929 (1991).
16. C. Laurence, P. Nicolet, M. T. Dalati, J.-L. M. Abboud and R. Notario, *J. Phys. Chem.*, **98**, 5807 (1994).
17. T. Yokoyama, R. W. Taft and M. J. Kamlet, *J. Am. Chem. Soc.*, **98**, 3233 (1976).
18. C. Laurence, P. Nicolet and M. Helbert, *J. Chem. Soc., Perkin Trans. 2*, 1081 (1986).
19. M. J. Kamlet and R. W. Taft, *J. Org. Chem.*, **47**, 1734 (1982).
20. R. R. Minesinger, E. G. Kaiser and M. J. Kamlet, *J. Org. Chem.*, **36**, 1347 (1971).
21. R. R. Minesinger, M. E. Jones, R. W. Taft and M. J. Kamlet, *J. Org. Chem.*, **42**, 1929 (1977).
22. B. Frange, J.-L. M. Abboud, C. Benamou and L. Bellon, *J. Org. Chem.*, **47**, 4553 (1982).
23. T. Yokoyama, R. W. Taft and M. J. Kamlet, *Spectrochim. Acta A*, **40**, 669 (1984).
24. T. Yokoyama, R. W. Taft and M. J. Kamlet, *J. Org. Chem.*, **51**, 3540 (1986).
25. T. Yokoyama, I. Hanazome, M. Mishima, M. J. Kamlet and R. W. Taft, *J. Org. Chem.*, **52**, 163 (1987).
26. T. Yokoyama, T. Komaki, H. Sato, R. W. Taft and F. Anvia, *J. Org. Chem.*, **54**, 3983 (1989).
27. J.-L. M. Abboud and R. Notario, *Pure Appl. Chem.*, **71**, 645 (1999).
28. J. Catalán, J. Palomar, C. Diaz and J. L. G. de Paz, *J. Phys. Chem. A*, **101**, 5183 (1997).
29. R. S. Drago, *J. Org. Chem.*, **57**, 6547 (1992).
30. L. S. P. Mirashi, R. S. Varkhede and S. S. Kunte, *Indian J. Pure Appl. Phys.*, **28**, 565 (1990).
31. L. S. P. Mirashi, R. S. Varkhede and S. S. Kunte, *Indian J. Pure Appl. Phys.*, **29**, 597 (1991).
32. N. G. Bakhshiev, *Opt. Spectrosc.*, **10**, 379 (1961); **12**, 193 (1962); **13**, 24 (1962).
33. C.-K. Wang, Y.-H. Wang, Y. Su and Y. Luo, *J. Chem. Phys.*, **119**, 4409 (2003).
34. S. Jiang and D. H. Levy, *J. Phys. Chem. A*, **107**, 6785 (2003).
35. N. Rajendiran and M. Swaminathan, *Bull. Chem. Soc. Jpn.*, **68**, 2797 (1995).
36. N. Rajendiran and M. Swaminathan, *J. Photochem. Photobiol. A*, **90**, 109 (1995).
37. N. Rajendiran and M. Swaminathan, *J. Photochem. Photobiol. A*, **93**, 103 (1996).
38. S. K. Nayaki and M. Swaminathan, *Spectrochim. Acta A*, **57**, 1361 (2001).
39. S. K. Nayaki and M. Swaminathan, *Spectrochim. Acta A*, **58**, 2931 (2002).
40. V. Bekárek, J. Jìlek and A. Haviger, *Collect. Czech. Chem. Commun.*, **61**, 155 (1996).
41. A. K. Singh and D. Manjula, *J. Indian Chem. Soc.*, **78**, 635 (2001).
42. L. Giacomelli, R. Cattana, J. Anunziata, M. Hedrera and A. Salerno, *J. Phys. Org. Chem.*, **7**, 162 (1994).
43. T. Yokoyama, R. W. Taft and M. J. Kamlet, *J. Chem. Soc., Perkin Trans. 2*, 875 (1987).
44. S. H. Hüttenhain, W. Balzer and R. Feldmann, *Z. Naturforsch. A*, **49**, 1087 (1994).
45. M. J. Kamlet, E. G. Kayser, J. W. Eastes and W. H. Gilligan, *J. Am. Chem. Soc.*, **95**, 5210 (1973).
46. M. J. Kamlet, T. N. Hall, J. Boykin and R. W. Taft, *J. Org. Chem.*, **44**, 2599 (1979).
47. T. Yoshihara, V. A. Galievsky, S. I. Druzhinin, S. Saha and K. A. Zachariassen, *Photochem. Photobiol. Sci.*, **2**, 342 (2003).
48. K. Hara and W. Rettig, *J. Phys. Chem.*, **96**, 8307 (1992).

49. W. Rettig, D. Braun, P. Suppan, E. Vauthey, K. Rotkiewicz, R. Luboradzki and K. Suwińska, *J. Phys. Chem.*, **97**, 13500 (1993).
50. W. Rettig and S. Lutze, *Chem. Phys. Lett.*, **341**, 263 (2001).
51. D. M. Shin and D. G. Whitten, *J. Phys. Chem.*, **92**, 2945 (1988).
52. V. Bekárek and J. Juřina, *Collect. Czech. Chem. Commun.*, **47**, 1060 (1982).
53. V. Bekárek and J. Ševčik, *Collect. Czech. Chem. Commun.*, **51**, 746 (1986).
54. R. Helburn, N. Ullah, G. Mansour and J. Maxka, *J. Phys. Org. Chem.*, **10**, 42 (1997)
55. S. Spange and D. Keutel, *Liebigs Ann. Chem.*, 423 (1992).
56. E. J. J. Groenen and W. N. Koelman, *J. Chem. Soc., Faraday Trans. 2*, **75**, 58 (1979).
57. M. El-Sayed, H. Müller, G. Rheinwald, H. Lang and S. Spange, *J. Phys. Org. Chem.*, **14**, 247 (2001).
58. S. Spange, E. Vilsmeier, S. Adolphe and A. Fährmann, *J. Phys. Org. Chem.*, **12**, 547 (1999).
59. J. Catalán, V. López, P. Pérez, R. Martin-Villamil and J. G. Rodríguez, *LiebigsAnn.*, 241 (1995).
60. T. Redzimski and J. R. Held, *J. Fluoresc.*, **13**, 393 (2003).
61. K. A. Al-Hassan and M. A. El-Bayoumi, *Chem. Phys. Lett.*, **138**, 594 (1987).
62. M. J. Kamlet, R. R. Minesinger, L. G. Kayser, M. H. Aldrige and J. W. Eastes, *J. Org. Chem.*, **36**, 3852 (1971).
63. M. J. Kamlet, E. G. Kayser, J. W. Eastes and W. H. Gilligan, *J. Am. Chem. Soc.*, **95**, 5210 (1973).
64. W. Turbeville and P. K. Dutta, *J. Phys. Chem.*, **94**, 4060 (1990).
65. D. Gegiou, E. Lambi and E. Hadjoudis, *J. Phys. Chem.*, **100**, 17762 (1996).
66. G. Saroja and A. Samanta, *J. Chem. Soc., Faraday Trans.*, **94**, 3141 (1998).
67. S. K. Gorbatsevich and O. Yu. Smirnova, *J. Chem. Phys.*, **120**, 1369 (2004).
68. M. El-Sayed, H. Müller, G. Rheinwald, H. Lang and S. Spange, *Monatsh. Chem.*, **134**, 361 (2003).
69. J. Moskal, A. Moskal and W. Pietrzycki, *J. Chem. Soc., Perkin Trans. 2*, 1893 (1977).
70. V. Bekárek and V. Bekárek, Jr., *Collect. Czech. Chem. Commun.*, **52**, 287 (1987).
71. G. Verdasco, M. A. Martin, B. del Castilo, P. Lopez-Alvarado and J. C. Menéndez, *Anal. Chim. Acta*, **303**, 73 (1995).
72. L. G. S. Brooker and T. H. Sprague, *J. Am. Chem. Soc.*, **63**, 3214 (1941).
73. A. L. LeRosen and C. E. Reid, *J. Chem. Phys.*, **20**, 233 (1952).
74. E. G. McRae, *J. Phys. Chem.*, **61**, 562 (1957).
75. O. W. Kolling, *Anal. Chem.*, **53**, 54 (1981).
76. J. Figueras, *J. Am. Chem. Soc.*, **93**, 3255 (1971).
77. J. O. Morley and A. L. Fitton, *J. Phys. Chem. A*, **103**, 11442 (1999).
78. T. Yamaguchi, Y. Kimura and N. Hirota, *J. Phys. Chem. A*, **101**, 9050 (1997); *J. Chem. Phys.*, **109**, 9075, 9084 (1998).
79. F. Terenziani, A. Painelli and D. Comoretto, *J. Phys. Chem. A*, **104**, 11049 (2000).
80. M. A. Webb, B. C. Morris, W. D. Edwards, A. Blumenfeld, X. Zhao and J. L. McHale, *J. Phys. Chem. A*, **108**, 1515 (2004).
81. M. M. Davis and H. B. Hetzer, *Anal. Chem.*, **38**, 451 (1966).
82. J. F. Deye, T. A. Berger and A. G. Anderson, *Anal. Chem.*, **62**, 615 (1990).
83. D. L. Sackett and J. Wolff, *Anal. Biochem.*, **167**, 228 (1987).
84. W.-G. Han, T. Liu, F. Himo, A. Touchkine, D. Bashford, K. M. Hahn and L. Noodleman, *ChemPhysChem*, **4**, 1084 (2003).
85. A. Cser, K. Nagy and L. Biczók, *Chem. Phys. Lett.*, **360**, 473 (2002).
86. C. M. Golini, B. W. Williams and J. B. Foresman, *J. Fluoresc.*, **8**, 395 (1998).
87. J. R. Lakowicz, *Principles of Fluorescence Spectroscopy*, Chap. 7, Plenum, New York, 1983.
88. M. J. Kamlet, C. Dickinson and R. W. Taft, *Chem. Phys. Lett.*, **77**, 69 (1981).
89. G. Jones II, W. R. Jackson, C.-Y. Choi and W. R. Bergmark, *J. Phys. Chem.*, **89**, 294 (1985).
90. K. Rechthaler and G. Köhler, *Chem. Phys.*, **189**, 99 (1994).
91. C. Parkanyi, M. S. Antonious, J.-J. Aaron, M. Buna, A. Tine and L. Cissé, *Spectrosc. Lett.*, **27**, 439 (1994).
92. M. S. Antonious and D. Y. Sabry, *Mikrochim. Acta*, **118**, 69 (1995).
93. S. Kumar, R. Giri, S. C. Mishra and M. K. Makhwe, *Indian J. Pure Appl. Phys.*, **33**, 431 (1995).
94. S. Otsuki and T. Taguchi, *J. Photochem. Photobiol. A*, **104**, 189 (1997).

95. A. A. Gorman, M. G. Hutchings and P. D. Wood, *J. Am. Chem. Soc.*, **118**, 8497 (1996).
96. J. K. Dey and S. Dogra, *Bull. Chem. Soc. Jpn.*, **64**, 3142 (1991).
97. M. T. Dalati, Ph.D. Thesis, University of Nantes (1991).
98. R. M. C. Gonçalves, A. M. N. Simões, L. M. P. C. Albuquerque, M. Rosés, C. Ràfols and E. Bosch, *J. Chem. Res. (S)*, 214 (1993); *J. Chem. Res. (M)*, 1380 (1993).
99. A. F. Lagalante, M. Spadi and T. J. Bruno, *J. Chem. Eng. Data*, **45**, 382 (2000).
100. L. P. Novaki and O. A. El-Seoud, *Ber. Bunsenges. Phys. Chem.*, **100**, 648 (1996).
101. M. J. Kamlet, E. G. Kayser, M. E. Jones, J. L. Abboud, J. W. Eastes and R. W. Taft, *J. Phys. Chem.*, **82**, 2477 (1978); M. J. Kamlet, M. E. Jones and R. W. Taft, *J. Chem. Soc., Perkin Trans. 2*, 342 (1979).
102. H. Langhals, *Chem. Ber.*, **114**, 2907 (1981).
103. W. J. Cheong and P. W. Carr, *Anal. Chem.*, **60**, 820 (1988).
104. J. H. Park, M. D. Jang, D. S. Kim and P. W. Carr, *J. Chromatogr.*, **513**, 107 (1990).
105. A. J. Dallas and P. W. Carr, *J. Chem. Soc., Perkin Trans. 2*, 2155 (1992).
106. M. Roses, J. Ortega and E. Bosch, *J. Solution Chem.*, **24**, 51 (1995).
107. E. Bosch, F. Rived and M. Roses, *J. Chem. Soc., Perkin Trans. 2*, 2177 (1996).
108. C. Ràfols, M. Roses and E. Bosch, *J. Chem. Soc., Perkin Trans. 2*, 243 (1997).
109. M. Roses, U. Buhvestov, C. Ràfols, F. Rived and E. Bosch, *J. Chem. Soc., Perkin Trans. 2*, 1341 (1997).
110. U. Buhvestov, F. Rived, C. Ràfols, E. Bosch and M. Roses, *J. Phys. Org. Chem.*, **11**, 185 (1998).
111. P. M. E. Mancini, A. Terenzano, C. Adam, A. Perez and L. R. Vottero, *J. Phys. Org. Chem.*, **12**, 207, 713 (1999).
112. P. M. E. Mancini, A. Terenzano, C. Adam, A. del C. Perez and L. R. Vottero, *J. Phys. Org. Chem.*, **13**, 221 (2000).
113. P. M. E. Mancini, A. del C. Perez and L. R. Vottero, *J. Solution Chem.*, **30**, 695 (2001).
114. S. Nigam, A. de Juan, R. J. Stubbs and S. C. Rutan, *Anal. Chem.*, **72**, 1956 (2000).
115. T. Nevěčná and V. Bekárek, *Collect. Czech. Chem. Commun.*, **51**, 1942 (1986).
116. B. Garcia, A. Aparicio, R. Alcalde, R. Ruiz, M. J. Dávilla and J. M. Leal, *J. Phys. Chem. B*, **108**, 3024 (2004).
117. Y. G. Wu, M. Tabata and T. Takamuku, *J. Solution Chem.*, **31**, 381 (2002).
118. M. H. Khajehpour and J. F. Kauffman, *J. Phys. Chem. A*, **104**, 7151 (2000).
119. M. H. Khajehpour, C. M. Welch, A. Kleiner and J. F. Kauffman, *J. Phys. Chem. A*, **105**, 5372 (2001).
120. R. Cattana, J. J. Silber and J. Anunziata, *Can. J. Chem.*, **70**, 2677 (1992).
121. H. Boggetti, J. D. Anunziata, R. Cattana and J. J. Silber, *Spectrochim. Acta A*, **50**, 719 (1994)
122. D. J. Phillips and J. F. Brennecke, *Ind. Eng. Chem. Res.*, **32**, 943 (1993).
123. D. E. Wetzler, C. Chesta, R. Fernandez-Prini and P. F. Aramendia, *Pure Appl. Chem.*, **73**, 405 (2001); *J. Phys. Chem. A*, **106**, 2390 (2002).
124. T. Nevěčná, J. Vymětalová and V. Bekárek, *Collect. Czech. Chem. Commun.*, **51**, 2071 (1986).
125. S. H. Hüttenhain and W. Balzer, *Z. Naturforsch. A*, **48**, 709 (1993).
126. J. A. Hyatt, *J. Org. Chem.*, **49**, 5097 (1984).
127. M. E. Sigman, S. M. Lindley and J. E. Leffler, *J. Am. Chem. Soc.*, **107**, 1471 (1985).
128. T. A. Berger and J. F. Deye, *Anal. Chem.*, **62**, 1181 (1990).
129. Y.-P. Sun, M. A. Fox and K. P. Johnston, *J. Am. Chem. Soc.*, **114**, 1187 (1992).
130. Y.-P. Sun, G. Bennett, K. P. Johnston and M. A. Fox, *J. Phys. Chem.*, **96**, 10001 (1992).
131. S. P. Kelley and R. M. Lemert, *AIChE J.*, **42**, 2047 (1996).
132. T. Sasaki, H. Takeishi and Z. Yoshida, *J. Supercrit. Fluids*, **15**, 23 (1999).
133. R. D. Schulte and J. F. Kauffman, *Appl. Spectrosc.*, **49**, 31 (1995).
134. M. Maiwald and G. M. Schneider, *Ber. Bunsenges. Phys. Chem.*, **102**, 960 (1998).
135. A. P. Abbott, C. A. Eardley and J. E. Schreier, *J. Phys. Chem. B*, **103**, 8790 (1999).
136. A. P. Abbott and C. A. Eardley, *J. Phys. Chem. B*, **103**, 2504 (1999).
137. A. P. Abbott, S. Corr, N. E. Durling and E. G. Hope, *J. Phys. Chem. B*, **107**, 10628 (1999).
138. Y. W. Kho, D. C. Conrad, R. A. Shik and B. L. Knutson, *Ind. Eng. Chem. Res.*, **42**, 6511 (2003).

139. J. Lu, J. S. Brown, C. L. Liotta and C. A. Eckert, *Chem. Commun.*, 665 (2001); *Ind. Eng. Chem. Res.*, **41**, 2835 (2002).
140. H. Oka and O. Kajimoto, *Phys. Chem. Chem. Phys.*, **5**, 2535 (2003).
141. J. Lu, E. C. Boughner, C. L. Liotta and C. A. Eckert, *Fluid Phase Equil.*, **198**, 37 (2002).
142. A. J. Carmichael and K. R. Seddon, *J. Phys. Org. Chem.*, **13**, 591 (2000).
143. S. V. Dzyuba and R. A. Bartsch, *Tetrahedron Lett.*, **43**, 4657 (2002).
144. K. A. Fletcher, I. A. Storey, A. E. Hendricks, Sh. Pandey and Si. Pandey, *Green Chem.*, **3**, 210 (2001).
145. S. N. Baker, G. A. Baker and F. V. Bright, *Green Chem.*, **4**, 165 (2002).
146. K. A. Fletcher, S. N. Baker, G. A. Baker and S. Pandey, *New J. Chem.*, **27**, 1706 (2003).
147. J. Lu, C. L. Liotta and C. A. Eckert, *J. Phys. Chem. A*, **107**, 3995 (2003).
148. S. N. V. K. Aki, J. F. Brennecke and A. Samanta, *Chem. Commun.*, 413 (2001).
149. R. Karmakar and A. Samanta, *J. Phys. Chem. A*, **107**, 7340 (2003).
150. J. A. Ingram, R. S. Moog, N. To, R. Biswas and M. Maroncelli, *J. Phys. Chem. B*, **107**, 5926 (2003).
151. K. Fischer and S. Spange, *Macromol. Chem. Phys.*, **201**, 1922 (2000).
152. K. Fischer, T. Heinze and S. Spange, *Macromol. Chem. Phys.*, **204**, 1315 (2003).
153. S. Spange, D. Keutel and F. Simon, *J. Chim. Phys.*, **89**, 1615 (1992).
154. S. Spange and D. Keutel, *Liebigs Ann. Chem.*, 981 (1993).
155. S. Spange and A. Reuter, *Langmuir*, **15**, 141 (1999).
156. S. Spange, E. Vilsmeier and Y. Zimmermann, *J. Phys. Chem. B*, **104**, 6417 (2000);
157. K. Fischer, S. Spange, S. Fischer, C. Bellmann and J. Adams, *Cellulose*, **9**, 31 (2002).
158. Y. Zimmermann, M. El-Sayed, S. Prause and S. Spange, *Monatsh. Chem.*, **132**, 1347 (2001).
159. S. Spange, K. Fischer, S. Prause and T. Heinze, *Cellulose*, **10**, 201 (2003).
160. S. Spange, A. Reuter and E. Vilsmeier, *Colloid Polym. Sci.*, **274**, 59 (1996).
161. M. El-Sayed, H. Müller, G. Rheinwald, H. Lang and S. Spange, *Monatsh. Chem.*, **134**, 361 (2003).
162. S. M. Lindley, G. C. Flowers and J. E. Leffler, *J. Org. Chem.*, **50**, 607 (1985).
163. R. Günther, D. Oelkrug and W. Rettig, *J. Phys. Chem.*, **97**, 8512 (1993).
164. J. L. Jones and S. C. Rutan, *Anal. Chem.*, **63**, 1318 (1991).
165. H. Lu and S. C. Rutan, *Anal. Chem.*, **68**, 1387 (1996).
166. S. Nigam, A. de Juan, V. Cui and S. C. Rutan, *Anal. Chem.*, **71**, 5225 (1999).
167. R. S. Helburn, S. C. Rutan, J. Pompano, D. Mitchem and W. T. Patterson, *Anal. Chem.*, **66**, 610 (1994).
168. J. E. Brady, D. Bjorkman, C. D. Herter and P. W. Carr, *Anal. Chem.*, **56**, 278 (1984).
169. Y. Zimmermann and S. Spange, *New J. Chem.*, 1179 (2002).
170. P. K. Dutta and W. Turbeville, *J. Phys. Chem.*, **95**, 4087 (1991).
171. M. S. Paley, R. A. McGill, S. C. Howard, S. E. Wallace and J. M. Harris, *Macromolecules*, **23**, 4557 (1990).
172. S. Spange, C. Schmidt and H. R. Kricheldorf, *Langmuir*, **17**, 856 (2001).
173. D. L. Richter-Egger, J. C. Landry, A. Tesfai and S. A. Tucker, *J. Phys. Chem. A*, **105**, 6828 (2001).
174. D. L. Richter-Egger, A. Tesfai and S. A. Tucker, *Anal. Chem.*, **73**, 5743 (2001).
175. K. A. Al-Hassan, *Chem. Phys. Lett.*, **227**, 527 (1994).
176. K. Fischer, S. Prause, S. Spange, F. Cichos and C. von Borczyskowski, *J. Polym. Sci. B*, **41**, 1210 (2003).
177. N. M. Correa and J. J. Silber, *J. Mol. Liquids*, **72**, 163 (1997).
178. N. M. Correa, E. N. Durantini and J. J. Silber, *J. Colloid Interface Sci.*, **208**, 96 (1998).
179. M. Wong, J. K. Thomas and M. Grätzel, *J. Am. Chem. Soc.*, **98**, 2391 (1976).
180. E. Abuin, E. Lissi, A. Cerón and M. A. Rubio, *J. Colloid Interface Sci.*, **258**, 363 (2003).
181. A. Datta, D. Mandal, S. K. Pal and K. Bhattacharya, *J. Phys. Chem. B*, **101**, 10221 (1997).
182. B. B. Raju and S. M. B. Costa, *J. Phys. Chem. B*, **103**, 4309 (1999).
183. R. Helburn, Y. Dijiba, G. Mansour and J. Maxka, *Langmuir*, **14**, 7147 (1998).
184. G. Mansour, W. Creedon, P. C. Dorrestein, J. Maxka, J. C. MacDonald and R. Helburn, *J. Org. Chem.*, **66**, 4050 (2001).

185.   A. Choucair and A. Eisenberg, *J. Am. Chem. Soc.*, **125**, 11993 (2003).
186.   M. F. Vitha and P. W. Carr, *J. Phys. Chem. B*, **102**, 1888 (1998).
187.   G. Saroja and A. Samanta, *Chem. Phys. Lett.*, **246**, 506 (1995).
188.   G. Saroja, T. Soujanya, B. Ramachandram and A. Samanta, *J. Fluoresc.*, **8**, 405 (1998).
189.   A. Datta, D. Mandal, S. K. Pal, S. Das and K. Bhattacharya, *J. Mol. Liquids*, **77**, 121 (1998).
190.   D. Mandal, S. K. Pal, A. Datta and K. Bhattacharya, *J. Phys. Chem. A*, **102**, 9070 (1998).
191.   M. Shannigrahi, R. Pramanik and S. Bagchi, *Spectrochim. Acta A*, **59**, 2921 (2003).

CHAPTER **8**

Hydrogen bonds of anilines

LUCIANO FORLANI

Dipartimento di Chimica Organica 'A. Mangini', University of Bologna, Viale Risorgimento 4, 40136, Bologna, Italy
Fax: +39 051 2093654;   e-mail: forlani@ms.fci.unibo.it

I. INTRODUCTION

In principle, feeble interactions should be carefully considered in drawing the pathway of a reaction, because they affect the energetic level of reactants and transition states. Consequently, these non-covalent interactions are important for recognizing the actual nature of the reagents (energy levels and geometry, aggregation with solvent or other solutes), in order to explain chemical and biochemical behaviours.

In particular, the non-covalent interactions may be regarded as the starting point for explaining the main phenomena of solvation, i.e. solute/solvent interactions, or the solute/solute interactions with feeble bonds, producing labile species which are often important points on the reaction coordinate of reaction pathways which produce, by a pre-equilibrium, new energetic levels of reactants.

Generally, the solvent cannot be considered as a continuous medium[1, 2] described by the common parameters such as dielectric constant, dipolar moment or polarizability. These parameters certainly offer important information, but they are unable to explain the environment of the solutes and the immediate neighbourhood of solute, in view of the micro situation of solvent around the single molecule of solute.

The great interest regarding the hydrogen bond in investigating solute−solute and solvent−solute interactions is due to several reasons[3]. The main reason (the one usually indicated in the literature) is the low energy of hydrogen bonds which extends[4] from a minimum of $20-30$ kJ mol^{-1} to a maximum of 100 kJ mol^{-1}. It is a weak interaction which plays a central role in biological, non-biological[5] and pre-biotic processes[6] as well as in the structural assessment of biological entities[7]. Recently[8], hydrogen bonds have been indicated to be important in mediating electron transfer at long distance in biological systems such as dichromophore peptides[9].

Self-association of solutes (and, in particular, of amines) arises mainly from hydrogen bonding interactions. The hydrogen bond is responsible for assembling supramolecular systems[10].

It should be emphasized that the hydrogen bond is due to a Lewis acid (the proton), which is the most peculiar acid because it is the least polarizable acid[11]. It is not a fortuitous fact that water is the solvent of biological processes with a very particular behaviour[2]. Consequently, the distinction between a 'protic solvent' and an 'aprotic solvent' is, reasonably, the first rough classification of solvents[1].

From this standpoint a very interesting idea[12, 13] concerns the 'large proton polarizability' in homoconjugated and heteroconjugated hydrogen bonds (see Scheme 1). The equilibria reported in Scheme 1 may be defined as tautomeric equilibrium between molecular and hydrogen bonded ionic-pair species[14].

$$^+B-H--B \quad \rightleftharpoons \quad B--H-^+B \qquad \text{Homoconjugated hydrogen bond}$$

$$A-H---B \quad \rightleftharpoons \quad A^----H-B^+ \qquad \text{Heteroconjugated hydrogen bond}$$
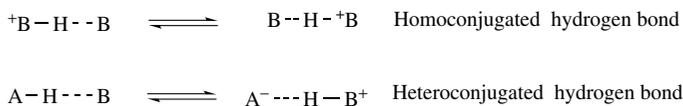
SCHEME 1

Hydrogen bonding interactions are of interest not only in the gas phase and liquid phase, but also in the solid state[10, 15, 16]. Hydrogen bonding interactions compete with other interactions, such as electron donor/acceptor interactions[17]. Both kinds of interactions may be considered to produce true new chemical species which are prone to affect the considered reaction pathway. Anilines (and molecules bearing amino groups in general) act as proton acceptors as well as proton donors. Dimerization of amines is a typical feature of this behaviour.

Self-assembly by hydrogen bonding interactions is a very usual feature (together with the electron donor/acceptor interactions) in natural and unnatural non-covalent assembly of molecules[18].

In particular cases, well-defined structures are detectable as in the case of ribbon or rosette aggregates. A relevant example of N−H groups self-assembling through hydrogen bonding interaction is the production of supramolecular aggregates (rosettes) constituted by some melanine derivatives involving aniline moiety and cyanuric acid[19, 20].

Self-aggregates, such as DNA base rosettes, were indicated to assemble to form nanotubes which, for example, may stop the body rejection of hetero-implants[21].

Historically, the most important methods used to investigate the hydrogen bonds were infrared and uv/vis spectroscopy, X-ray diffraction and ^{1}H NMR spectroscopy. Infrared studies on N−H stretching vibration of aromatic amines started a long time ago by considering all the parameters affecting the position of N−H vibration, such as electronic substituent effects, steric effects, effects of the changes in the aromatic moiety by anellation, and intermolecular and intramolecular hydrogen bonds, which induce some difficulties in assigning the precise frequency for the free N−H vibration in amines[22]. Intramolecular feeble non-covalent interactions are also responsible for structural assessment of structures involving conformational position or tautomer predominance.

Generally, the understanding of non-covalent bonds is very important in identifying molecules able to self-assemble in solution and also to organize themselves in the solid state to obtain particular properties. The two main driving forces in such interactions arise from hydrogen bonds and from electron donor/acceptor interactions involving $n-\pi$ or $\pi-\pi$ interaction[23] until charge transfer complexes are achieved.

Amines (as well as other functional groups such as O−H, S−H and, in general, X−H groups with acidic protons) may act both as proton acceptors (equilibrium **A** of Scheme 2) or as proton donors (equilibrium **B** of Scheme 2), depending on the relative proton acceptor or donor power of the partners.

$$
\begin{array}{c}
\qquad\qquad\qquad\qquad\qquad\qquad \text{H} \\
\qquad\qquad\qquad\qquad\qquad\qquad | \\
\textbf{A)} \quad RNH_2 \; + \; H-X \;\rightleftharpoons\; RN\text{--}H\text{-}X \\
\qquad\qquad\qquad\qquad\qquad\qquad | \\
\qquad\qquad\qquad\qquad\qquad\qquad \text{H}
\end{array}
$$

$$
\begin{array}{c}
\textbf{B)} \quad RNH_2 \; + \; H-X \;\rightleftharpoons\; H\text{-}X\text{--}H-NR \\
\qquad\qquad\qquad\qquad\qquad\qquad\qquad\qquad\; | \\
\qquad\qquad\qquad\qquad\qquad\qquad\qquad\qquad\; \text{H}
\end{array}
$$
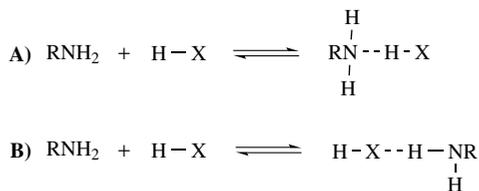
<div align="center">SCHEME 2</div>

Abraham and coworkers attempted to form a scale (in carbon tetrachloride) of solute hydrogen bonding ability[24] taking into account both acidity and basicity by using equation 1,

$$\text{Log } K = L_B \log K_A^H + D_B \tag{1}$$

where K is the equilibrium constant for the hydrogen bonding of a series A of acids against reference base B, the constants L_B and D_B characterize the reference bases, and $\log K_A^H$ values represent the hydrogen bond acidities of acids, i.e. they constitute a scale of solute hydrogen bond acidity. In a similar way, a series of bases forms hydrogen bond ability scale towards a reference acid[25].

When proton donor–acceptor properties are studied, there is a major problem (also from the labelling point of view) arising from the difference between the hydrogen bonding and hydrogen transfer[26]. This distinction is of particular importance in the case of the NH_2 group, when the NH_2 group is the proton acceptor group and the acidic partner is the proton donor (see Scheme 3**A**).

Up to some years ago, this problem was still unsolved and it was left to theoretical chemistry to find a solution. Recent developments in spectroscopy[27,28] (such as rotational spectroscopy of supersonically expanded jets) allows the characterization of associated species (hetero-dimers)[26] between a proton donor and a proton acceptor, before the formation of salts, as shown in Scheme 3.

$$\textbf{A)} \quad RNH_2 \; + \; H-X \; \rightleftharpoons \; \overset{\overset{\displaystyle H}{|}}{\underset{\underset{\displaystyle H}{|}}{RN}}\text{----}H-X \; \rightleftharpoons \; \overset{+}{R}NH_3 \; + \; \overset{-}{X}$$

$$\textbf{B)} \quad RNH_2 \; + \; B \; \rightleftharpoons \; \overset{\overset{\displaystyle H}{|}}{RN}-H\text{---}B \; \rightleftharpoons \; \overset{-}{R}NH \; + \; \overset{+}{B}H$$
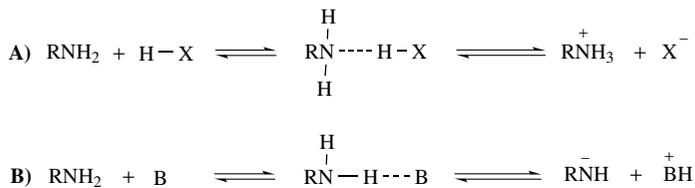
<div align="center">SCHEME 3</div>

Usually, the proton acceptor ability of amines (reaction **A** of Scheme 3) lead to ammonium ion formation, while the N−H bond cleavage (or formation) (reaction **B** of Scheme 3) is a less common process which may be obtained under drastic experimental conditions or via metal aniline complexes[29].

A. Infrared Studies

The near-infrared absorption of primary, secondary and tertiary aliphatic and aromatic amines has been studied extensively since 1925[30, 31] in order to define the spectroscopic properties of the NH bond in a large number of amines.

For a long time, efforts and studies were devoted to the identification of aliphatic and aromatic −NH$_2$ group vibrations and their intensities in the infrared spectrum. One goal was to obtain agreement between experimental and calculated properties of amines[32]. A particular difficulty arises from the presence of hydrogen bonds involving the self-association of the amines or the intermolecular hydrogen bonds with solvent or other solutes.

In solution, the infrared absorption of substituted anilines is greatly influenced by the solvent, which also affects the electronic properties of substituents on the aromatic ring of anilines[33]. In the solid state, infrared spectra of substituted anilines show more than two absorption bands related to the NH$_2$ group due to the intermolecular and intramolecular hydrogen bond[33].

The starting point to investigate the hydrogen bond of proton donor molecules is that the hydrogen bond produces a red shift (or, occasionally, a blue shift) in the vibrational frequency with respect to the frequency of isolated molecule. X-ray diffraction of a single crystal produces information on the relative geometry of molecules and on the non-covalent interactions (mainly van der Waals, electrostatic interactions, charge transfer and hydrogen bonding interactions) in the solid state.

Recently, new spectroscopic techniques[27] have allowed investigation of interactions between two, three or more molecules in order to understand the relative geometry and the kind of interactions which form clusters. Isolated clusters may serve as models for obtaining information on hydrogen bonds in solution as well as in biological systems too.

Particular attention was devoted to hydrogen bonds involving the NH$_2$ group, which are of interest in understanding molecular structure, including that in biological systems. Clusters are mainly formed in supersonic expansion, which may produce different kinds of clusters, depending on the experimental conditions. In this technique the molecules are cooled very efficiently during expansion into a vacuum through a nozzle.

Aniline is a very suitable molecule for investigating the hydrogen bond of the NH group because it is a molecule which may be easily ionized and detected, for example, by resonance enhanced multiphoton ionization (REMPI).

The infrared absorption spectra of neutral clusters (and of corresponding cation clusters) are measured by depletion of the ion signal of the mass spectrometer after absorption of the infrared laser light by the cluster.

Recent new spectroscopic techniques were applied in the fields of spectroscopy and of physical chemistry. One purpose of this chapter is to summarize conclusions relevant to organic chemistry.

II. SELF-ASSOCIATION OF ANILINES

A. Spectroscopic Studies

The position, extinction coefficients and band half-widths of anilines and of polycyclic aromatic amines were studied by infrared spectroscopic measurements a long time ago[34]. One purpose was to understand the hybridization of the nitrogen atom bonded to unsaturated systems[35, 36]. Infrared spectroscopic parameters of the NH_2 group in substituted anilines were correlated with the Hammett sigma substituent constants[37].

Under usual experimental conditions, primary and secondary amines show effects arising from both intermolecular and intramolecular hydrogen bonds.

Self-association of protic solvents, including anilines and aliphatic amines in apolar aprotic solvents, is an important process, because it involves a high percentage of stoichiometric amine as solute, depending on the solute structure, the solvent, the temperature and, obviously, the amine concentration.

In fact, the first effect of intramolecular hydrogen bonds in the condensed phase is the self-association of amines (as well as alcohols), affecting their physical and spectroscopic properties, in particular the N—H frequencies in the infrared spectra.

Although the self-association of amines, and of anilines, and polycyclic aromatic amines in particular, is a complicated process involving 2, 3, 4 or more amine molecules to form aggregated species, the most frequent discussion concerns association equilibrium to form dimeric species (see equation 2). Dimerization is studied extensively for aliphatic amines[38]. In general, aromatic amines are less associated than aliphatic amines. An ^{1}H NMR study[39] of monomer/dimer equilibrium was performed for several amines, including 3-chloroaniline. The δ value for the N—H signal of monomer is obtained by extrapolation of the experimental chemical shift to infinite dilution. Indeed, to avoid complications arising from self-association of aniline, the chemical shift values in the NMR spectra are extrapolated to infinite dilution.

$$\text{Monomer (M)} + \text{Monomer (M)} \rightleftharpoons \text{dimer (D)} \qquad (2)$$

Self-association of anilines was suggested to be responsible for several 'anomalous' kinetic behaviours in nucleophilic aromatic substitution reactions in apolar aprotic solvents[40], but this conclusion was questioned[41].

The self-association of substituted anilines, diphenylamine and N-alkylaniline was studied[42] by infrared spectroscopy a long time ago. By considering the self-association as a dimerization process in carbon tetrachloride and in benzene, aniline is two-fold more associated than N-methylaniline[43]. In carbon tetrachloride, the self-association is higher than in benzene[41]. Studies using the first overtone symmetric stretching band of aniline in cyclohexane revealed[42] the formation of both dimeric and tetrameric species, depending on the aniline concentration and on the temperature. Self-association is considered to occur through hydrogen bonding. Higher multimers are observed for concentration values up to 1.5 M.

The monomer/dimer equilibrium may be studied at very low concentrations. The K_D value (equation 3) ranges from 0.44 M^{-1} at 10 °C to 0.26 M^{-1} at 70 °C, in a concentration range of aniline from 0.03 to 0.2 M. At concentration values of up to 4 M of aniline, the self-association involves monomer, dimer and tetramer species. The tetramer probably exist in a cyclic form.

$$K_D = [D]/[M]^2 \qquad (3)$$

Recently[25], some new tools have offered very important supports to infrared spectroscopy, as reported in the following instances. The infrared depletion spectrum of the aniline dimer, formed in a supersonic jet, indicates[44, 45] that two NH_2 groups are equivalent. One possible structure is a sandwich, with the $N-H\cdots\pi$ hydrogen bonds, with two aniline molecules arranged head to tail, as shown in **1**.

(1)

B. Solid State (X-ray Diffraction)

For many years, substituted anilines were analysed as a single crystal by X-ray diffraction. *p*-Aminophenol was shown[46] by this method to display in the solid state a simple hydrogen bond with a well-ordered head to tail. For 4-ethyl-2,3,5,6-tetracyanoaniline (**2**), the molecular packing shows an intermolecular hydrogen bond pattern, which is depicted in **3** in a simple dimeric form, that is repeated for the second $N-H\cdots NC$ bond[47]. X-ray diffraction of a single crystal of 2,5-dichloroaniline (**4**) shows the absence of hydrogen bonds[48].

(2)   **(3)**   **(4)**

Self-association is a relevant property also for derivatives of aniline, such as anilides[49] or Schiff bases[50]. In anilides, the usual hydrogen bonding interaction involves the NH group of one molecule and a C=O group of a second molecule to produce a cyclic dimer **5**.

(5)

III. INTRAMOLECULAR HYDROGEN BONDS

A. Hydrogen Bonds in Solution

1. Infrared spectroscopic studies

Numerous intermolecular or intramolecular interactions involve formation of $N-H \cdots X$ bonds from amino groups. Intramolecular hydrogen bonds are often responsible for the physical and chemical properties of molecules, and intramolecular hydrogen bonds are usually observed in *ortho*-substituted anilines[51].

In 1960, Bryson and Werner carried out an extensive study on $N-H$ stretching frequencies of substituted 1- and 2-naphthylamines. These frequencies were tentatively related to the pKa values of the naphthylamines[52].

Mononitronaphthylamines, such as 1-nitro-2-naphthylamine (**6**), 3-nitro-2-naphthylamine (**7**) and 2-nitro-1-naphthylamine (**8**), display strong intramolecular hydrogen bonds, as clearly indicated by comparison of the $N-H$ stretching frequencies in CCl_4 and in pyridine. In the latter solvent the main hydrogen bonding interaction is between naphthylamine and pyridine, with the exception of isomers **6–8** where the nitro and the amino groups are bonded in adjacent positions. In these cases, the intramolecular hydrogen bond prevails on the intermolecular hydrogen bond between the amino group and the pyridine solvent[53].

(6)   **(7)**   **(8)**
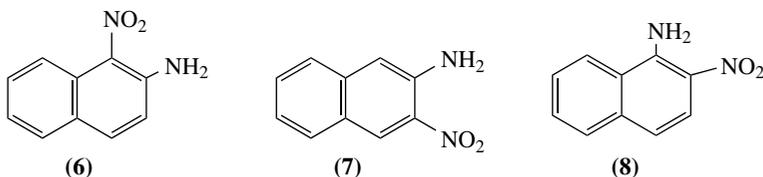
In 1964, Lady and Whetsel focused on the problem of the first overtone $N-H$ stretching bands of 52 *ortho*-substituted anilines, in cyclohexane and in CCl_4, in order to evaluate the intramolecular hydrogen bond between $N-H$ and *ortho* substituents[54]. The $N-H$ stretching frequencies in *ortho*-substituted anilines have also been discussed by G. Moritz[55].

In the same year, Krueger studied the intramolecular hydrogen bonding interaction in 31 *ortho*-substituted anilines and their NHD and ND_2 isotopomers[56]. In fact, the first overtone NH_2 symmetric stretching band is independent of the concentration of aniline and of temperature. A strong intramolecular hydrogen bond is supported also by spectral data of *ortho*-substituted *N*-methylanilines and ND *N*-methylanilines.

The spectral data of monodeuteriated anilines (complete deuteriation to ND_2, and partial deuteriation to NHD, is a popular tool in focusing on these absorption problems and in order to avoid confusion with other overtone bands[57–59]) and the differences in spectral data of corresponding pairs of *ortho*- and *para*-substituted anilines enable evaluation of the effect of the *ortho* substitution on the spectroscopic properties[60]. In the case of 2-trifluoromethylaniline (**9**), there are indications of the presence of an intramolecular hydrogen bond[61–63].

(9)
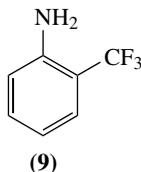
Infrared spectra of a number of *ortho*-aminophenols (and of NHD derivatives) empha-size the importance of the intramolecular hydrogen bond between OH and NH_2 groups, as shown in **10**.
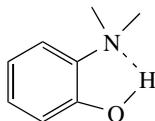
(10)

Infrared spectral data of a partially deuteriated picramide showed[64] that the absorption bands due to the monodeuteriated **11** are single.
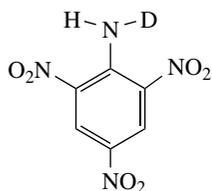
(11)
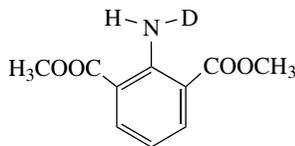
(12)

The investigation[64, 65] on the spectral data of partially deuteriated picramide **11** and 2,6-dicarbomethoxyaniline **12** shows that a double hydrogen bonding interaction is present as illustrated in **13** and **14**.
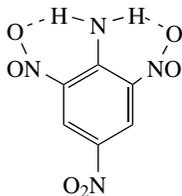
(13)
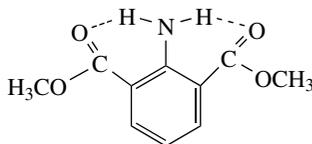
(14)

Infrared spectral data of 4′,5-dimethyl-2-aminoazobenzene (**15**) and 1-phenylazo-2-naphthylamine (**16**) indicate[58] that **15** can exist in CCl_4 in a mixture of tautomers **17** and **18**. **18** may be present with its rotational isomer **19**.

(15)

(16)

(17)   **(18)**

(19)
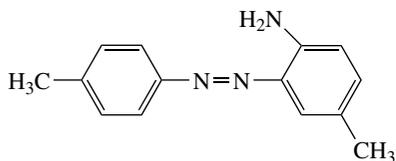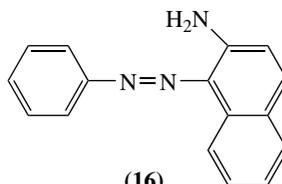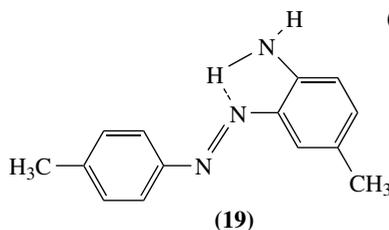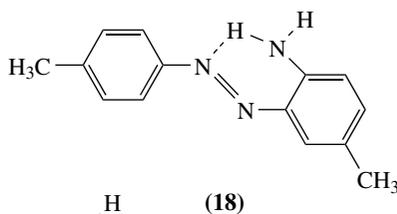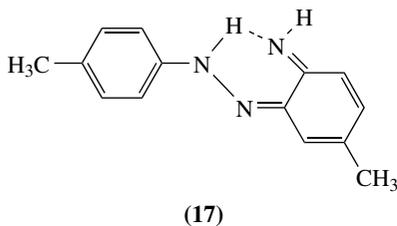
The study of N−H and N−D stretching frequencies of mono- and dideuteriated NH_2 groups agrees with the presence of rotational isomers **20** and **21**.

(20)   **(21)**
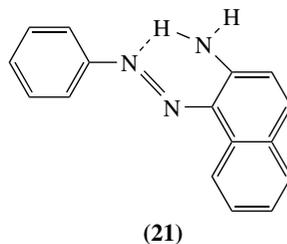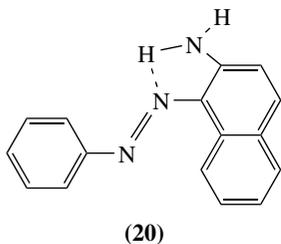
Autoionization-detected infrared spectroscopy (ADIR, which is a new technique)[66] makes it possible to record infrared spectra of isolated bare molecular cations in molecular beams. Conventional time-of-flight mass spectroscopy (at zero kinetic energy) and photoelectron spectroscopy also enable the study of such cations.

Microsolvation structures of the NH_2 group in hydrogen bonded clusters of aniline cations was elucidated by studies of the N−H stretching vibration. The hydrogen bond is stronger in aniline cations than in aniline. N−H frequencies (obtained by infrared spectroscopy applied to jet-cooled substituted aniline) strongly indicate intramolecular hydrogen bond formation between the amino group and *ortho* methyl, cyano, methoxy and fluoro groups. The intramolecular hydrogen bond is remarkably enhanced by the ionization of anilines[66].

N−H stretching vibration of jet-cooled aniline was studied in the neutral and in the cationic ground state. Infrared-ultraviolet double-resonance spectroscopy was used in observation of the neutral ground state, while autoionization-detected infrared spectroscopy was used in observation of the cationic ground state. The N−H frequency shifts of *ortho* cyanoaniline and *ortho* fluoroaniline indicate the presence of an intramolecular hydrogen bond with the neighbouring group. The presence of an intramolecular hydrogen bond was confirmed by spectral data of deuteriated aniline derivatives. An enhancement of the hydrogen bond strength upon ionization was found[66].

2. NMR spectroscopic studies

NMR investigations on several nuclei, of both inter- and intramolecular hydrogen bonds in *ortho*-substituted anilines, start from chemical shift values of the amino group proton.

The ^{15}N−H coupling constant provides further information on the interactions between the NH$_2$ group and *ortho* substituents, involving the solvent effect too[67].

Attempts to deduce an intramolecular hydrogen bond presence from coupling constant values between N−H and H3 in some substituted anilines[68], **22–25**, lead to the conclusion that a coupling constant does not prove the presence of an intramolecular hydrogen bond. On the other hand, the deshielding of the N−H proton in the presence of *ortho* halogen or a nitro group in anilines indicates the intramolecular hydrogen bond with the *ortho* substituent[69], as well as in the acetyl derivatives such as **26**[70].

(22)   **(23)**   **(24)**   **(25)**

(26)   **(26a)**   **(26b)**   **(26c)**
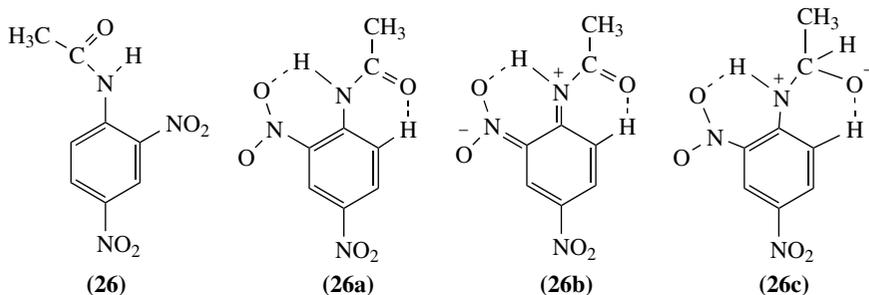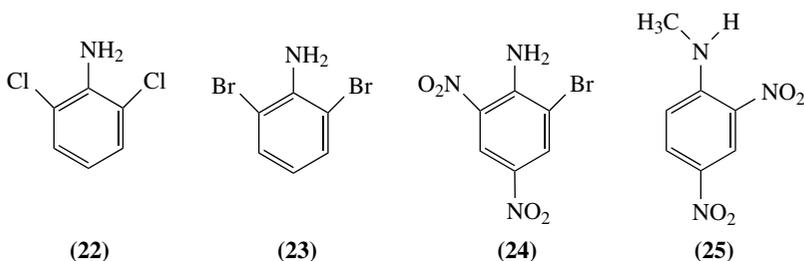
Structures **26a–c** illustrate the hydrogen bond position and the most probable charge distribution of **26**. The presence of the N−H···O bond in 2-nitroanilines can be deduced from the low shielding of the amino proton.

The ^{13}C resonances of atoms bearing a partially deuteriated amino group in aniline and in its derivatives **27–29**, and in *o*-nitroaniline derivative[71], appear as a multiplet.

(27)   **(28)**   **(29)**   **(30)**

R = H, CH$_3$
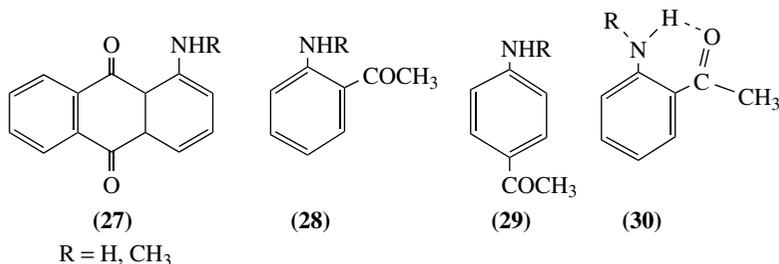
This fact is observed in DMSO, under conditions of slow hydrogen exchange, and the splitting is larger for compounds with an intramolecular hydrogen bond as reported for **30**.

The aminopyrazole derivative (**31**) is indicated[72] by ^{1}H NMR and infrared spectroscopies to have two intramolecular hydrogen bonds: the first with the nitro group on the aniline moiety, and the second with the C=O group of the ester on the pyrazole ring, as depicted in the structure **31**.

(31)
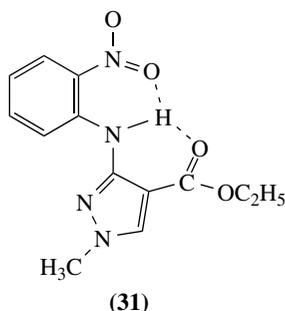
Proton magnetic resonance, infrared spectroscopy and dielectric relaxation measurements, on *ortho*- and *meta*-disubstituted anilines, indicate that (despite what is expected on the basis of the usual steric hindrance arguments) a *meta*-substituted compound such as **32** results in more hindered rotation of the NH$_2$ group than for *ortho*-substituted compounds such as **33**. Solute/solvent and solute/solute intermolecular hydrogen bonding interactions are responsible for this hindered rotation[73].

(32) **(33)**
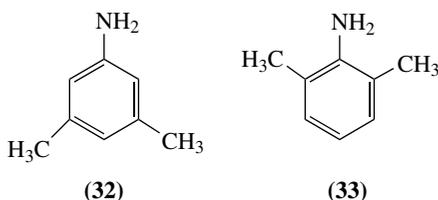
Studies on electro-optical parameters of halogen-substituted anilines indicate the existence of an intramolecular hydrogen bond when the halogen is in the *ortho* position to the amino group. The proton donor ability of the amino group is enhanced by the presence of the halogen atoms, due to their electron-withdrawing inductive effect. A strong influence of hydrogen bonding on the dipole moment and on the electro-optical properties of monobromoanilines is observed for the free amine, while the influence of the halogen in the hydrogen bonded complexes is much smaller[74, 75]. Comparison between inter- and intramolecular hydrogen bonds of some 2-substituted anilines reveals the complexity of this problem[76].

2-Anilinomethylenecyclopentane-1,3-dione[77] (**34**) can exist in several tautomeric forms. Two forms present the C=C double bond in exocyclic (**34A**) or endocyclic (**34B**) positions (Scheme 4). Infrared and ^{13}C NMR spectroscopic data together with quantum mechanical calculations indicate that in the crystal or in CCl$_4$ or CHCl$_3$ solutions, the compound mainly exists in the tautomeric form **34A** due to the participation of an intramolecular hydrogen bond, as illustrated in Scheme 5.
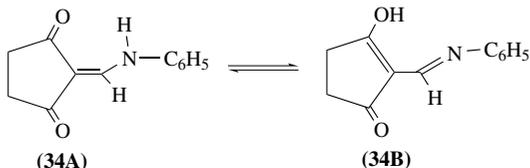
SCHEME 4
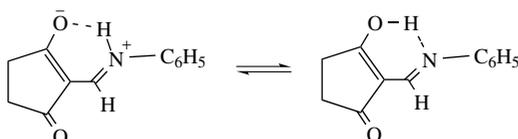
SCHEME 5

The electron donation of anilines towards acids is usually through the nitrogen lone pair, but the *para* carbons (as well as other electron-rich carbon atoms on the aromatic ring) can serve as powerful electron-donating centres towards a positive charge, in some cases by a not reversible process[78-80].

A particular example is the protonation of 1,3,5-tris(N,N-dialkylamino)benzenes (**35**), which are powerful nucleophilic reagents. The reaction between **35** and the proton may occur at a nitrogen atom to afford **36A**, or at a carbon atom to afford the σ cationic complex **36B** (Scheme 6). A particular situation for **36** is that the ^{1}H NMR spectrum of the all-benzene ring protons shows a singlet. This feature may be explained by the formation of a π complex[81] as reported in **37**, or by a dynamic process where the proton quickly shifts from one amino group to another amino group.
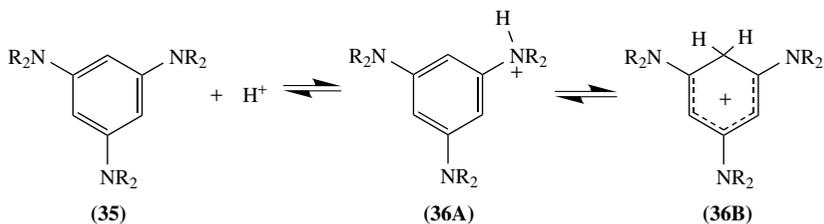
NR$_2$ = piperidino, morpholino, pyrrolidino

SCHEME 6

When substituents, bearing a lone pair able to form an intramolecular hydrogen bond, are present, the proton prefers a fixed position like that reported in **38**, as deduced by NMR spectroscopic data and single crystal X-ray diffraction[82].

B. Solid State (X-ray Diffraction)

Many substituted benzene derivatives show large microscopic second-order non-linear susceptibilities, which probably arise from highly asymmetric charge distribution[83]. Among these, nitroanilines deserve particular attention[84], in view of the considerable number of

(37)   **(38)**
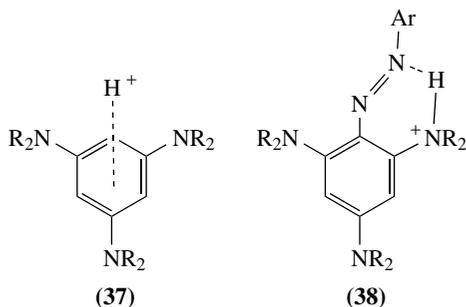
studies carried out by the usual spectroscopic methods, such as NMR, infrared, Raman and uv/visible, and by X-ray diffraction on a single crystal.

Molecular aggregation and supramolecular assembled systems have been extensively investigated in order to understand intermolecular interactions and to predict the modes of molecular assembly. The hydrogen bond is often the major interaction in self-assembly nitroanilines and very frequently it is responsible for the observed assembled patterns[85].

An *ab initio* molecular orbital study on 2-methyl-4-nitroaniline (**39**) pairs in a crystal (which possesses a dimeric form) was conducted in order to ascertain the influence of molecular interaction on its hyperpolarizability of the considered amine. Electrostatic intermolecular interactions were indicated to have a predominant influence on the hyperpolarizability even if no hydrogen bond occurs between molecules[86].

2-Methyl-5-nitroaniline (**40**) was investigated[87] by high-resolution single crystal X-ray diffraction in order to determine the charge distribution and to evaluate the importance of the hydrogen bond in aggregation of nitroanilines[88]. **40** formed a head to tail chain.

(39)   **(40)**   **(41)**
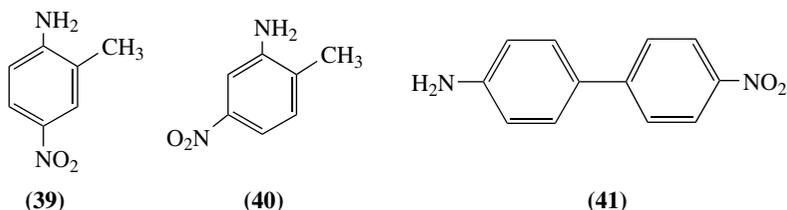
Coppens and coworkers[89, 90] carried out experimental and theoretical investigations on *p*-nitroanilines and *p*-amino-*p'*-nitrobiphenyl (**41**). The Bader atoms in molecules theory (AIM) was used to obtain atomic charges, atomic volumes and dipole moments from the charge density. Topological analysis is an interesting tool for the assessment of radial basis functions. Some discrepancies arise from the different assessments of the geometry[88] of the amino group, which may be considered planar or non-planar.

Infrared and Raman spectral data[91] of 2,2'-dieminodiphenyl in CCl_4 (**42**) and of deuteriated **42** suggest the absence of an intramolecular hydrogen bond, which is indicated by infrared spectral data in the solid phase. In fact, X-ray diffraction of a single crystal[86] of **42** at $-165\,^{\circ}C$ reveals that the two rings are twisted by 58° (one in relation to the other) with both nitrogen atoms in the plane of the respective ring and the two amino groups in a *syn* position with $N \cdots N$ distance of 2.933 Å.

The hydrogen arrangement around the amino groups is disordered. Each amino group is involved as both a donor in an intramolecular hydrogen bonding interaction and as an

(42)   (42A)
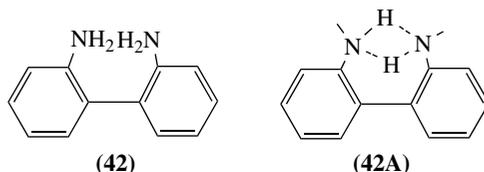
acceptor in an intermolecular hydrogen bond (and *vice versa* as tentatively depicted in
42A)[92].

Nitroanilines are particular and interesting substances for potentially non-linear optical
materials[93, 94], because of their large second order microscopic polarizability[91].

Derivatives of *p*-nitroaniline and of *m*-nitroaniline show a strong second-harmonic
generation[95]. In *m*-nitroaniline, intermolecular hydrogen bonds are responsible for molec-
ular fixation in the plane[96].

Nitroaniline molecules assemble through a bifurcated hydrogen bond (or a three-centre
bond) as reported in **43**, which is a symmetric bond, while **44** represents an asymmet-
ric bond. **45** represents a monocoordinate hydrogen bond. These interactions induce the
formation of an infinite polar chain.

(43)   (44)   (45)
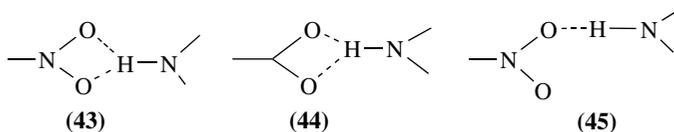
The geometry of the intermolecular interaction between the amino group and a nitro
group for a number of nitro-substituted anilines reveals that the hydrogen bond is a three-
centre interaction[97], which appears to be controlled by the lone-pair directionality of the
nitro groups as shown in **46** for 4-nitro-1-R-aniline. This interaction is mainly explained
by the electron-donating power of the amino group and the electron-withdrawing ability
of the nitro group, thus inducing a strong charge separation.

(46)
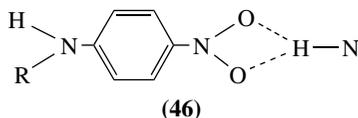
Etter defined empirical hydrogen bond rules[15], mainly regarding the solid state of crys-
tals, and with particular attention to predicting the orientation of neighbouring nitroaniline
molecules[85].

The through-conjugation between nitro and amino groups is an old but very interesting
subject. In fact, to have a strong through-conjugation between the amino group and the
nitro group, the molecular orbital theory requires coplanarity between the nitro group
and the aromatic ring. Frequently, X-ray diffraction data indicate that the nitro group is
twisted from coplanarity.

A substituent at the *ortho* position may exert a 'steric hindrance to the resonance', by
constricting the nitro group to rotate from coplanarity with the phenyl ring. This is reflected
in the different spectroscopic behaviour of nitroanilines **47** and *N*-methylnitroaniline **48**
or *N,N*-dimethylnitroaniline **49**.

(47)   (48)   (49)

(50)   (51)
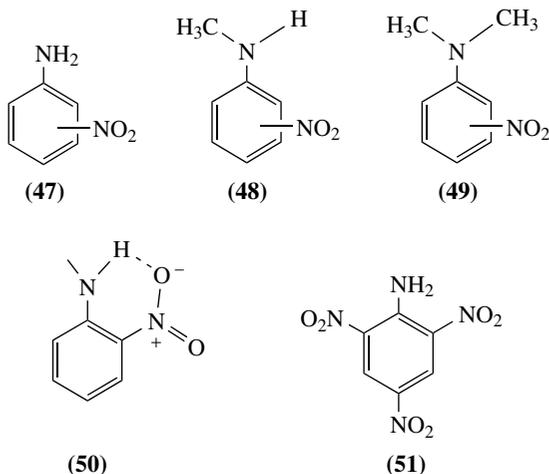
The intramolecular hydrogen bond, as reported in **50**, may have some importance in the hindrance of the resonance. This is the case of picramide **51**. The differences between the spectroscopic properties of nitroanilines and the parent *N*-methylnitroaniline provide, in some cases, interesting conclusions on the geometrical properties of molecules arising from the presence or absence of internal hydrogen bonds. Obviously, intermolecular hydrogen bonds may be of importance in affecting the geometry of the nitro group, particularly not only in the solid state, but also in solution or in gas state. Dimerization of nitroanilines (in the crystal) explains the differences observed in the solid and gas phases[98].

Intramolecular hydrogen bonds in anilines[62] and in naphthylamines affect the HNH angles and the σ-character of the nitrogen bonding orbitals with the consequence of affecting the pKa value of the NH_2 group[99].

The electronic effect of substituents on the N−H stretching frequencies (ν_{N-H}) of anilines[100] or diphenylamines[101] was studied using as a tool linear free-energy relationships (e.g. the Hammett equation). However, the relationship between ν_{N-H} in the infrared spectra and the sigma substituent parameter is not linear because of the change from sp^3 to sp^2 hybridization of the nitrogen atom of the amino group on interaction with the substituent, as shown in structure **52**. In contrast, the NH_2 chemical shift values of aromatic amines in dilute solutions[101, 102] in CDCl$_3$ or in DMSO-d$_6$ are linearly related to the Hammett sigma values. The latter solvent prevents complications[102, 103] such as formation of hydrogen bonds with the amine, self-association of the amines, or intramolecular hydrogen bond as reported in **10**. *N*,*N*-Dimethylanilines behave similarly to the behaviour of anilines[104]. The chemical shifts of 28 substituted anilines are linearly correlated with the sigma values, with a slope of 1.4.

(52)
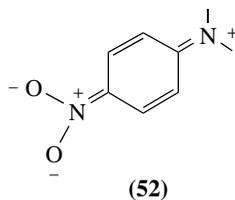
N−H vibrational frequencies of substituted anilines are linearly correlated with the sigma values with a positive slope, while a plot of vibrational frequencies of the anilinium ions (obtained by autoionization-detected infrared spectroscopy) results in a similar plot showing a negative slope[66].

X-ray diffraction of a single crystal offers precise knowledge of the dihedral angle between the nitro group and the aromatic ring plane. Obviously, the geometry of molecules in the solid state cannot be *sic et simpliciter* translated to the other phases, in particular to the solution phase, where the non-covalent specific interactions between the nitro group or the amino group and the solvent may affect the geometry of both groups. Some examples are given below.

In 2,4,6-trinitroaniline (**51**) the 2-, 4- and 6-nitro groups are rotated by 22.4, 4.0 and 8.5° respectively[105], out of the plane of the benzene ring.

X-ray diffraction of 2,4,6-trinitrodiphenyl amine[106] (**53**), 2,4,6-trinitro-*N*-methyldiphenylamine (**54**), 2-*N*-pyridyl-2,4,6-trinitroaniline[106] (**55**) and 2-*N*-pyridyl-*N*-methyl-2,4,6-trinitroaniline[107] (**56**) indicates the non-equivalence in the solid state of the two *ortho*-nitro groups in both **53** and **54**. The presence of the methyl group in **54** produces a significant red shift in the uv/vis spectrum compared with **53**, which probably cannot be related to different torsion angles of the nitro groups: the *ortho*-nitro group is more twisted in **56** than in **53**.
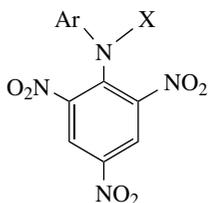
(**53**) Ar = Ph, X = H
(**54**) Ar = Ph, X = Me
(**55**) Ar = 2-pyridyl, X = H
(**56**) Ar = 2-pyridyl, X = Me

The rationalization of the effect of the methyl group is also complicated by the influence of the solvent on the absorption maximum[107] (and on the extinction coefficient).

The infrared spectroscopic investigation on the symmetric and antisymmetric $\nu(NO_2)$ absorption bands of solid dinitroaniline derivatives[108] in KBr matrix shows in the *N*-monosubstituted 2,6-dinitroanilines two different nitro groups. One nitro group lies in the plane of the benzene nucleus due to the hydrogen bond as depicted in **50**. The other nitro group deviates from the benzene ring plane by steric distortion related to the presence of the substituent on the nitrogen of the amino group.

The dihedral angles between the normal and the *ortho* 2 or 6 nitro group in **55**[106] are 39.1 and 17.6° whereas in **56** they are 46.4 and 17.6°. Structure **57** describes the main interactions of this molecules in the solid state.

(**57**)
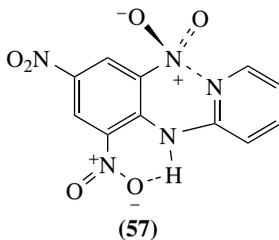
A possible rationalization of the behaviour of nitroanilines must take into account the presence of an internal charge transfer complex, which does not require a parallel of the involved orbitals.

A very particular intramolecular hydrogen bond interaction takes place in rigid systems bearing two amino groups, which are able to trap protons in a structure called a 'proton sponge'[109], as depicted in structures in Scheme 7 which show very high basicity, compared to the basicity of their isomers. From salts **58** it is difficult to remove the proton[110], which is masked by methyl (or other alkyl) groups. The hydrogen bond between the two nitrogen atoms is strong, as homoconjugation requires.
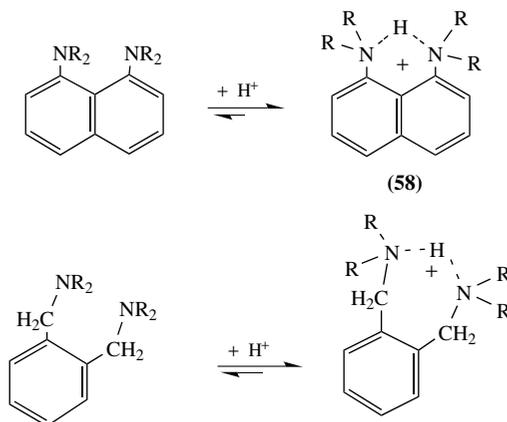
SCHEME 7

The pKa value of some 1,8-diaminonaphthalenes is in the range of 17 to 18 in acetonitrile[111] (whereas the pKa of aniline in acetonitrile is 10.6[112]). The kinetics of proton transfer from proton sponges was also studied[113].

The intramolecular hydrogen bond in protonated **59** and **60** strongly reduces the rate of the proton transfer with respect to the normal proton transfer from an OH and NH_2^+ group. In the series of 1,8-disubstituted naphthalenes, the strength of the hydrogen bond is as reported in Scheme 8[114].

SCHEME 8

$$\overset{+}{N}\!-\!H\cdots O \;<\; O\!-\!H\cdots N \;<\; \overset{+}{N}\!-\!H\cdots N$$
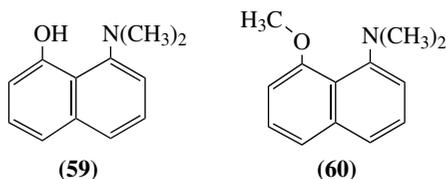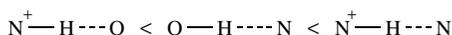
The naphthylamine derivative **59** was investigated[115] by X-ray diffraction analysis of a single crystal, by dipole moment measurements, by ^{1}H NMR and by infrared spectral data.

It displays a strong $O-H \cdots N$ hydrogen bond and, in solution, a feeble self-association produces non-polar dimers. In fact, the absorption maximum of the infrared spectrum, which is related to the ν_{OH} stretching vibration bond, remains unchanged by dilution.

IV. INTERMOLECULAR HYDROGEN BONDS

A. Hydrogen Bonds in Solution

1. Infrared spectroscopic studies

An extensive study[116] of the interaction in complexes between alcohols or phenols and aniline showed the importance of hydrogen bonds in affecting the infrared spectroscopic parameters. When the proton donors are phenols of moderately high acidity, such as the tetrachlorophenols or dinitrophenols, the larger interaction in forming aniline phenol complexes was indicated to be an electron donor/acceptor interaction which predominates over the hydrogen bonding interaction. An instance of competition between the charge transfer complex and hydrogen bonded complex is offered by the 1-naphthylamine/picric acid system[117].

The ternary complex α-naphthylamine/pyridine/picric acid (1:1:1)[118] was studied by infrared spectral data. This complex involves a pyridinium picrate moiety and an interaction between picrate and α-naphthylamine, which is a charge transfer interaction[119].

N,N-Dimethylamine is used to observe[120] interactions with phenols in aprotic solvents such as CD_2Cl_2 by using low temperature ^1H and ^{13}C NMR measurement in the first equilibrium in which the association complex **61A** is formed (Scheme 9), and it then evolves towards the tautomer **61B**. This transformation is slow in solutions cooled below 150 K.

$$\text{PhOH} + \text{NR}_3 \quad \underset{}{\overset{K_{ass}}{\rightleftharpoons}} \quad \text{PhO-H} \text{---} \text{NR}_3 \quad \underset{}{\overset{K_T}{\rightleftharpoons}} \quad \text{PhO} \text{- -} \overset{-}{\text{H}} - \overset{+}{\text{NR}}_3$$

(61A)
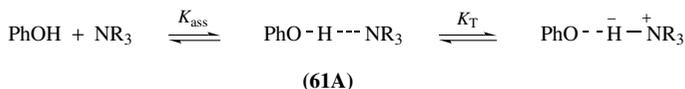
SCHEME 9

Molecular complexes between substituted anilines and some hydroperoxides are mainly due to the $OOH \cdots N$ hydrogen bonding interaction, as tested by infrared absorption spectral data[121]. In CCl_4 solution there is evidence for the presence of both $O-H \cdots N$ and $O \cdots H-N$ interactions. The predominance of one of these types of interaction is affected by the structure of the hydroperoxide and by the substituent bonded to the phenyl ring of aniline. The high acidity of some hydroperoxides, such as 1,1-diphenylhydroperoxide and α-cumyl hydroperoxide, is responsible for the salt character of the formed $N^+-H \cdots O^-$ ion pair.

The effect of the interactions with hydrogen bond acceptors on the infrared spectra of substituted anilines[122] was investigated quantitatively. The first hydrogen bond between the NH_2 group and the solvent CCl_4, with acetonitrile, acetone, diethyl ether, dimethyl sulfoxide and pyridine, causes a larger shift in the symmetric rather than in the antisymmetric NH stretching frequencies. The second hydrogen bond shows a larger effect on the antisymmetric frequency. The relative frequency shifts display an excellent correlation with the Hammett sigma substituent constant. Tentative dissection of the data produces some indication for the presence of intramolecular hydrogen bonds in *ortho*-substituted anilines[123].

Studies on the association[124] of aniline or N-methylaniline with benzene, N,N-dimethylaniline, pyridine and N,N-dimethylcyclohexylamine in forming 1:1 complexes in cyclohexane (taking into account the self association of the protic amine) reveal that formation of

TABLE 1. Selected thermodynamic data (obtained by infrared spectroscopy) for the 1:1 complexes between aniline and proton acceptors or proton donors (chloroform) in cyclohexane at 25°C[124, 125]

Proton donor	Proton acceptor	K (dm^3 mol^{-1})	$-\Delta H$ (kcal mol^{-1})
Aniline	Benzene	0.27	1.64
N-Methylaniline	Benzene	0.14	1.54
Aniline	N,N-Dimethylaniline	0.716	1.63
N-Methylaniline	N,N-Dimethylaniline	0.46	1.83
Aniline	N,N-Dimethylcyclohexylamine	0.69	3.35
N-Methylaniline	N,N-Dimethylcyclohexylamine	0.57	3.76
Aniline	Pyridine	1.65	3.43
N-Methylaniline	Pyridine	1.31	3.77
Aniline	Chloroform	0.51	1.7
Cyclohexylamine	Chloroform	1.10	3.6
Pyrrole	Pyridine	2.5	3.2

the $N-H \cdots \pi$ (Ar) hydrogen bond of the electron-rich aromatic moiety and an $N-H \cdots N$ hydrogen bond may compete, in particular when the proton acceptor partner is N,N-dimethylaniline.

The data in Table 1 clearly indicate that aniline produces more stable complexes than N-methylaniline.

In N,N-dimethylaniline the hydrogen bond may be through either the nitrogen lone pair or the π system of the ring. This latter interaction probably involves an approach via the centre of the aromatic ring, thus forming a discrete hydrogen bond. Other approaches with different directions involve a part of the π system and, consequently, they are less important[100].

The $N-H \cdots \pi$ hydrogen bonding interaction was studied by uv spectrophotometry of the system 1-naphthylamine and the donors reported in Table 2[126]. The equilibrium constant increases by increasing the number of electron donor substituents on the π donor partner. This behaviour parallels that observed extensively for $O-H \cdots \pi$ interaction between phenols, or alcohols with alkenes or aromatic hydrocarbons[127].

Chemical shifts (δ ^{13}C NMR shifts related to C1) of a large number of 3- or 4-substituted anilines are correlated with infrared $N-H$ frequency data and with Hammett sigma values. An intermolecular hydrogen bond, as depicted in **62** and **63** (Scheme 10), was indicated to be present, on the basis of the plots of δ^{13}C1 versus ν_{asym} of NH$_2$ group frequencies in chloroform[100].

TABLE 2. Equilibrium constants for the 1:1 complexes between 1-naphthylamine and substituted benzenes[126]

π Donor	K (dm^3 mol^{-1})
Chlorobenzene	0.109
Benzene	0.147
Toluene	0.245
Ethylbenzene	0.244
Cumene	0.608
p-Xylene	1.30
Mesitylene	2.22
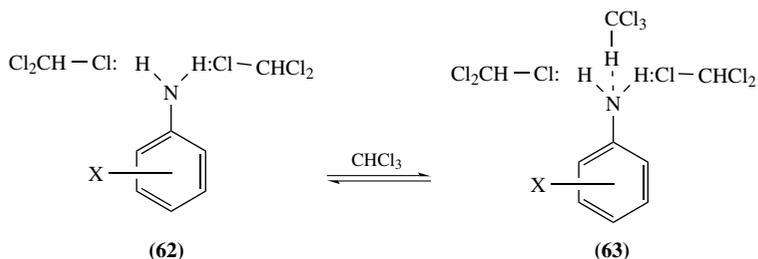
SCHEME 10

TABLE 3. Stability of the 1:1 complexes between sub-
stituted anilines and chloroform in cyclohexane at 35 °C[125]

Amine	K (dm^3 mol^{-1})	pKa
Aniline	0.47	4.58
p-Chloroaniline	0.33	4.05
m-Chloroaniline	0.25	3.52
o-Chloroaniline	0.16	2.71
p-Aminoacetophenone	0.14	2.19
N-Methylaniline	0.25	4.85
N-Ethylaniline	0.23	5.11
p-Phenetidine	0.65	5.25

The stability constants K of the complexes between several substituted anilines and
chloroform (Table 3) are linearly correlated with the pKa values of the anilines by
equation 4[125].

$$\log K = 0.247\text{p}K\text{a} - 1.474 \qquad (4)$$

The linearity of equation 4 agrees with the predominance of the C−H··· N interaction,
where aniline acts as a proton acceptor, even if the interaction involving the π-electrons
may also be operative in the complex formation, but the latter may be considered as a
secondary interaction.

Table 4 reports some thermodynamic properties of hydrogen bonded N−H··· O com-
plexes of aniline and N-methylaniline. Chloroform (Table 3) as proton donor towards

TABLE 4. Selected thermodynamic data[128] (obtained from infrared spectroscopy) for
1:1 complexes between aniline or N-methylaniline and oxygen proton acceptors, in cyclo-
hexane at 25 °C

Proton donor	Proton acceptor	K (dm^3 mol^{-1})	$-\Delta H$ (kcal mol^{-1})
Aniline	Dipropyl ether	0.47	2.77
N-Methylaniline	Dipropyl ether	0.29	3.07
Aniline	THF	1.08	3.04
N-Methylaniline	THF	0.71	3.30
Aniline	Anisole	0.70	1.94
N-Methylaniline	Anisole	0.36	1.82
Aniline	Ethyl acetate	1.50	3.13
N-Methylaniline	Ethyl acetate	0.89	3.49

aniline and *N*-methylaniline forms complexes showing stability comparable to that of *N*-methylaniline and aniline (Table 4) towards oxygenated proton acceptors.

The region of the amino group infrared stretching vibration ($3000–3600$ cm^{-1}) of infrared spectra was investigated for pentafluoroaniline (**64**), 2,3,5,6-tetrafluoroaniline (**65**), 4-methoxytetrafluoroaniline (**66**) and 4-aminotetrafluoropyridine (**67**) both as free amines and 1:1 hydrogen bonded complexes in CCl$_4$ with CH$_3$CN, tetrahydrofuran (THF), dimethylformamide (DMF), dimethyl sulfoxide (DMSO) and hexamethylphosphortriamide (HMPA)[129]. Some data on the equilibrium constants of these complexes are reported in Table 5. High K values for the aminopyridine complexes with respect to the homocyclic parent are observed, as expected on the basis of the electron-withdrawing power of the aza group.

(64)   **(65)**   **(66)**   **(67)**
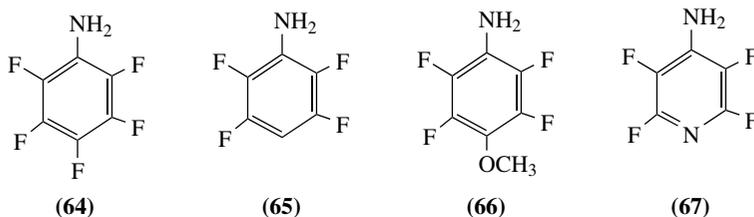
The stretching and bending vibration absorptions of the amino group in the complexes depend also on the presence of heteroatoms in the aromatic ring, such as the 'aza' derivatives[131] aminopyridine and aminopyrimidine (Scheme 11). The relative position of the aza and the amino groups is important. Obviously, the presence of the electron-withdrawing aza nitrogen enhances the proton donor ability of the amino group towards proton acceptor partners (CH$_3$CN, THF, dioxane, DMF, DMSO and HMPA), as shown by the data in Table 5.

TABLE 5. Stability constants[129, 130] of complexes between polyfluoroanilines and some proton acceptors in CCl$_4$ at 25 °C

Proton donor	Proton acceptor	K (dm^3 mol^{-1})
4-Methoxytetrafluoroaniline (**66**)	CH$_3$CN	2.6
	THF	1.4
	DMF	2.8
	DMSO	5.3
	HMPA	8.7
Pentafluoroaniline (**64**)	CH$_3$CN	2.1
	THF	2.0
	DMF	4.3
	DMSO	8.1
	HMPA	25
2,3,5,6-Tetrafluoroaniline (**65**)	CH$_3$CN	2.1
	THF	1.5
	DMF	4.8
	DMSO	9.8
	HMPA	28
4-Aminotetrafluoropyridine (**67**)	CH$_3$CN	2.8
	THF	3.2
	DMF	18
	DMSO	62
	HMPA	204

| 2-aminopyridine | 3-aminopyridine | 4-aminopyridine |

| 2-aminopyrimidine | 4-aminopyrimidine | 5-aminopyrimidine |

SCHEME 11
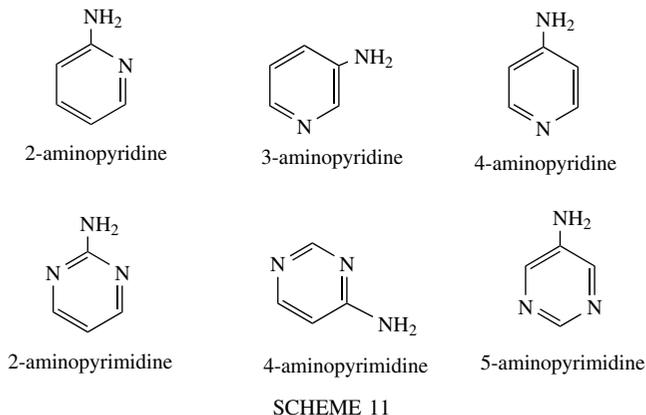
TABLE 6. Stability constants of complexes between aromatic amines and DMSO or hexamethylphosphortriamide HMPA in CCl_4 at $25\,^{\circ}C$

Proton donor	Proton acceptor (DMSO) K ($dm^3\,mol^{-1}$)	Proton acceptor (HMPT) K ($dm^3\,mol^{-1}$)
Aniline	2.5	7
2-Nitroaniline	11	35
3-Nitroaniline	15	65
4-Nitroaniline	22	85
2-Nitro-4-chloroaniline	30	130
2-Chloro-4-nitroaniline	35	140
2-Aminopyridine	5	18
3-Aminopyridine	8	27
4-Aminopyridine	20	65
2-Aminopyrimidine	2.5	9
4-Aminopyrimidine	—	40
5-Aminopyrimidine	—	50
1-Naphthylamine	5	—
2-Naphthylamine	8	—
1-Naphthol	275	—
Phenol	188	—
Pyrrole	12	—
Indole	21	—
Benzyl alcohol	15	—
n-Butyl alcohol	9	—
Chloroform	3	—

Table 6 reports the stability constant of 1:1 complexes between proton acceptors (DMSO and hexamethylphosphortriamide HMPT) and of some heterocyclic amines and of some proton donors involving the O−H group. The electron-withdrawing substituent acts by enhancing the acidity of the NH_2 group[132].

The data in Table 6 confirm the presence of an intramolecular hydrogen bond between one hydrogen atom of the NH_2 group and the oxygen of the nitro group bonded in position 2 to the amino group[132, 133]. The proton donor ability of anilines resembles qualitatively that of alcohols, and it is lower than that of phenols.

The absorption bands ν(NH) of stretching vibrations of N-methyl, N-ethyl and N-phenyl anilines were studied at different temperatures, with the purpose of investigating the N-substituent influence on the spectroscopic properties of free aniline and of H-bonded complexes with hydrogen acceptors, such as DMSO, THF, DMF, CH_3CN and HMPA[132]. From these data too, the 4-nitro group in aniline displays a parallel behaviour to that of the 'aza' group of aminopyridines (Table 5).

As reported in Table 7, diphenylamine forms the more stable complexes with the hydrogen acceptors used. Introduction of a 4-nitro group in N-methylaniline makes the NH group more acidic and results in an increased stability of the complexes.

The absorption bands in the infrared spectra of monobromo-substituted anilines in both the free molecules and the hydrogen bonded complexes with dimethylformamide (DMF), dimethyl sulfoxide (DMSO) and hexamethapol (HMPA) are studied[134]. The temperature effect on the K values in the range of $17-57\,^{\circ}C$ gave the ΔH values (Table 8). As expected, the 1:1 complexes display stronger hydrogen bonds than the 1:2 complexes.

TABLE 7. Stability constants[133] of complexes between N-substituted anilines and some proton acceptors in CCl_4 at $25\,^{\circ}C$

Proton donor	Proton acceptor	K ($dm^3\,mol^{-1}$)
N-Methylaniline	THF	1.3
	DMF	2.0
	DMSO	2.1
	HMPA	2.3
N-Ethylaniline	THF	1.1
	DMF	2.0
	DMSO	2.3
	HMPA	2.6
Diphenylamine	CH_3CN	1.0
	THF	1.1
	DMF	2.5
	DMSO	5.8
	HMPA	6.6
N-Methyl-4-nitroaniline	CH_3CN	2.1
	THF	3.0
	DMF	12.1
	DMSO	21.4
	HMPA	39.1

TABLE 8. Stability constants of complexes between monobromoanilines and proton acceptors in CCl_4 at $25\,^{\circ}C$

Aniline	Proton acceptor	K ($dm^3\,mol^{-1}$)	$-\Delta H$ ($kcal\,mol^{-1}$)
2-Bromoaniline	DMF	4.40	2.6
2-Bromoaniline	DMSO	4.80	3.5
2-Bromoaniline	HMPA	9.09	4.2
3-Bromoaniline	DMF	8.66	2.7
3-Bromoaniline	DMSO	6.98	3.8
3-Bromoaniline	HMPA	20.5	4.4
4-Bromoaniline	DMF	7.12	2.7
4-Bromoaniline	DMSO	6.11	3.6
4-Bromoaniline	HMPA	13.6	4.4

TABLE 9.   Stability constants of complexes between 2,2′-dieminodiphenyl (**42**) and substituted phenols, in CCl_4 at $25\,°C$[91]

Substituted phenols	K ($dm^3\,mol^{-1}$)	$-\Delta H$ ($kcal\,mol^{-1}$)
Phenol	6.2	4.6
4-Bromophenol	12.1	5.2
3-Bromophenol	13.3	5.5
3,4-Dichlorophenol	21.2	6.0
3,5-Dichlorophenol	29.5	6.4
3,4,5-Trichlorophenol	45.5	6.9

The 3-bromoaniline is the best proton donor among the bromoanilines, in agreement with the higher electron-withdrawing effect of the halogen atom in the *meta* position to the reaction centre. The proton acceptor ability shows the usual trend expected by the availability of a lone pair on the heteroatom.

Table 9 reports K values for the complexes between 2,2′-dieminodiphenyl (**42**) and the substituted phenols given in Scheme 12.

(42)
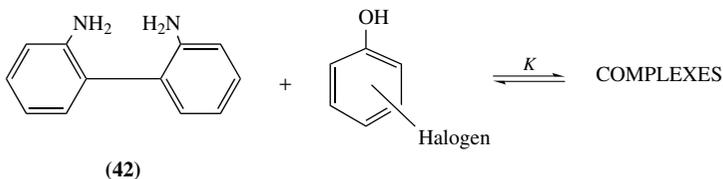
SCHEME 12

The log K values are linearly correlated with the pKa values of phenols by equation 5.

$$\text{Log } K = 4.61 - 0.38 \text{p}K\text{a} \tag{5}$$

The complexes between substituted phenols and aniline show a parallel linearity, reflected by equation 6[135].

$$\text{Log } K = 3.74 - 0.32 \text{p}K\text{a} \tag{6}$$

The dieminodiphenyl shows higher K values than aniline, as judged by the intercepts of equation 5 (for **42**) and equation 6 (for aniline).

The ^{1}H, ^{13}C and ^{15}N NMR chemical shifts of the chloroanilines show that the NH proton in *ortho*-chloroaniline which is close to the chlorine atom is less prone to form an intermolecular hydrogen bond with proton acceptors such as hexamethylphosphoric triamide, as depicted in Scheme 13[136].

The influence of the temperature on the infrared spectrum of several anilines[130] (as well as of other related derivatives), including the position of band maximum, the half-widths and integrated intensity of ν(NH) absorption bands of the free aniline and aniline occupied in hydrogen bond with several proton acceptors, are investigated. This fact enable to investigate the nature of the hydrogen bond, its strength and the relative stabilities of complexes of 1:1 and 1:2 stoichiometry.

Semiempirical quantum chemical calculations[26] on the NH_2 group vibration of aromatic amines were conducted. Some discrepancies between experimental and calculated data were observed.

$$ClC_6H_4NH_2 + O{=}P(N(CH_3)_2)_3 \rightleftharpoons ClC_6H_4N \begin{array}{c} H\text{-}\text{-}O{=}P(N(CH_3)_2)_3 \\ \diagup \\ \diagdown \\ H \end{array}$$

$$\begin{array}{c} O{=}P(N(CH_3)_2)_3 \\ \rightleftharpoons \end{array}$$

$$\rightleftharpoons ClC_6H_4N \begin{array}{c} H\text{-}\text{-}O{=}P(N(CH_3)_2)_3 \\ \diagup \\ \diagdown \\ H\text{-}\text{-}O{=}P(N(CH_3)_2)_3 \end{array}$$
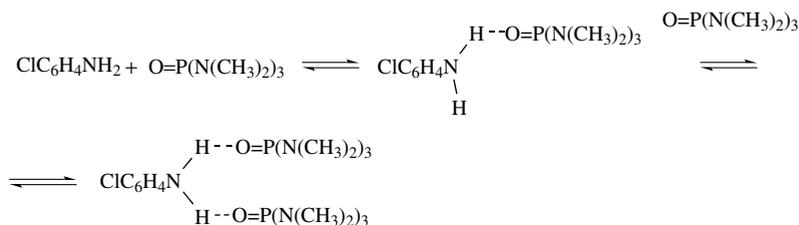
SCHEME 13

Relevant studies concern proton donor/proton acceptor molecular complexes with different stoichiometries of 2:1, 1:1 and 1:2, as depicted in Scheme 14. The 1:2 complexes of pentafluoroaniline, 4-nitrotetrafluoroaniline and 4-aminotetrafluoropyridine in 1:2 complexes with THF and HMPA were investigated. The 1:1 complexes display a different stability[129, 137] from that of 1:2 complexes. As expected, the ΔH values for the 1:1 complexes were higher[137, 138] than for the 1:2 complexes, when calculated for a single $ArNH_2{\bullet}PA$ bond[134].

$$ArNH_2 + PA \rightleftharpoons ArNH_2{\cdot}PA \begin{array}{c} \xrightarrow{+\ PA} ArNH_2{\cdot}(PA)_2 \\ \\ \xrightarrow{+\ ArNH_2} (ArNH_2)_2PA \end{array}$$

PA = proton acceptor
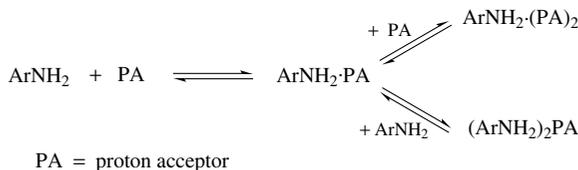
SCHEME 14

Many substituted anilines are investigated[139, 140] as free bases and hydrogen bonded molecules (generally in CCl_4 solutions), in order to identify spectral characteristics of absorption bands of free and 1:1 or 1:2 complexes with several proton acceptor partners; mainly tetrahydrofuran, dimethyl sulfoxide, dimethylformamide and dioxane are used.

The N—H hydrogen bond groups in the 1:1 and 1:2 complexes are not equivalent in dynamics, energetics and electro-optical parameters. The presence of a substituent on the aromatic ring of aniline and its position relative to the NH_2 group influence the non-equivalence of the NH bonds[141]. Anisidines **68–70** are examples of this behaviour[142]. For example, *ortho*-anisidine **68** shows steric inhibition to formation of 1:2 complexes with DMF, DMSO and HMPA[142].

    (68)   (69)   (70)
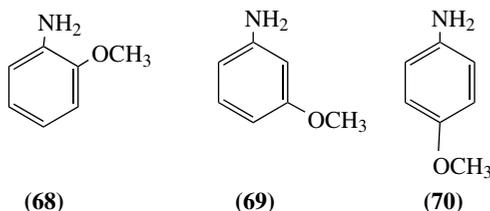
Usually, 2:1 and 1:2 complexes are formed with lower K values than 1:1 complexes[126]. The 2:1 complexes are shown (also by ^1H NMR spectroscopy studies) to be less stable than 1:1 complexes by 10–20%.

Dynamic and electro-optical properties (related to the variation of the dipole moment with respect to the bond length) of aniline, aminotoluenes and many monohalogenoanilines in CCl$_4$ have been studied in order to compare the spectroscopic parameters of the free amino group and of several 1:1 and 1:2 complexes with the proton acceptor CH$_3$CN, THF, DMF, DMSO and HMPA. The electro-optical parameters of the NH$_2$ group are affected by the type and position of the substituent and by the properties of the proton acceptors[139].

The relative strength of hydrogen bonding interactions may be evaluated by diffusion measurements[141]. This method allows the determination of the number of molecules of solvent associated with solutes. Phenols, in ethanol, are associated with 2.5 ethanol molecules, while anilines are associated with 1.1 molecules of ethanol.

The cluster of an aniline/water system (and of the ^{18}O isotopomer) was studied[143]. A linear N−H$\cdots$O hydrogen bond is present: the −NH$_2$ group is the proton acceptor partner (cf. **72**) and H$_2$O is the proton donor partner, as depicted in **71**.

In the cluster 4-aminobenzonitrile/water (1:1) (investigated by uv and infrared spectra), the amino group acts as the proton donor and water is the proton acceptor partner. However, in spite of the fact that the electron-withdrawing electronic effect of the CN group is feeble, a structural isomer of **72** was identified[144], involving the CN group as a proton acceptor (cf. **73**).

(71)   (72)   (73)
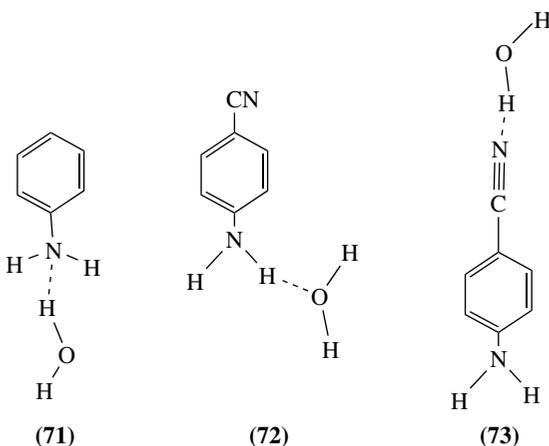
The determination of the NH and OH stretching vibrations of 4-aminophenol and 4-aminophenol bonded to a water molecule, in the neutral and ionic ground state, is carried out by infrared double resonance techniques (infrared-photo-induced Rydberg ionization, IR/R2PI). By means of this method it is possible to state that the more stable structures of the cluster of a 4-aminophenol/water system, as reported in Scheme 15, are **74** and **75** for the neutral species and **76** and **77** in the ionic state[145].

In general, the hydrogen bond produces a spectral shift of the absorbance maximum: the addition of proton acceptor compounds to aniline derivatives changes the λ_{max} value and this variation may be used to calculate the extent of association, i.e. the apparent stability constant of the complex amine/proton acceptor in the ground state. The hydrogen bond also causes fluorescence enhancement of the quenching of amines[146].

Investigation of the fluorescence quenching of 2-aminobenzoic acid (**78**), 1-naphthylamine (**79**), 2-naphthylamine (**80**), *N*-phenyl-1-naphthylamine (**81**) and anilines allows the

(74)   (75)

(76)   (77)

SCHEME 15

(78)   (79)   (80)   (81)
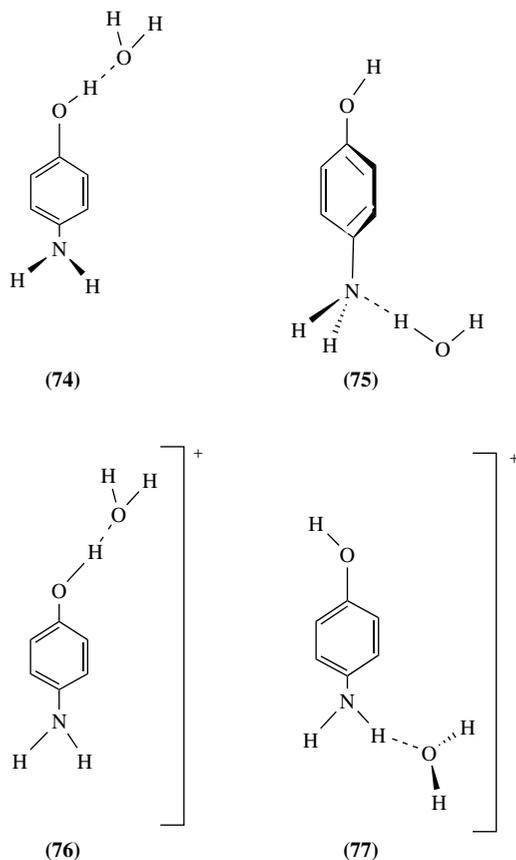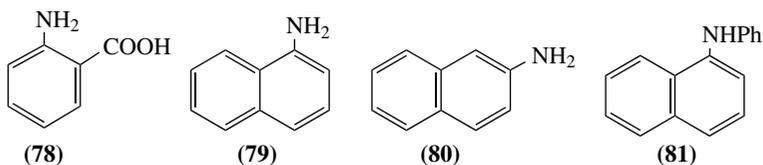
evaluation of the equilibrium constant for the formation of hydrogen bonding complexes in the ground state and the evaluation of the rate of the hydrogen bond formation.

The fluorescence of N-phenyl-1-naphthylamine (**81**) is quenched by proton acceptors such as dioxane, nitriles, esters and amines. Probably a charge transfer interaction between the proton donor and the proton acceptor through the hydrogen bond is the mechanism which accounts for the quenching[147].

Table 10 reports some equilibrium constant values for hydrogen bond formation between **81** and some hydrogen bond acceptors.

TABLE 10. Equilibrium constants for hydrogen bond formation between N-phenyl-1-naphthylamine (**81**) and proton acceptors in cyclohexane at 25 °C[147]

Proton acceptor	K (dm^3 mol^{-1})^a	$-\Delta H$ (kcal mol^{-1})
1,4-Dioxane	1.8	6.2
Benzonitrile	2.0	2.9
Propionitrile	2.5	2.4
Ethyl acetate	1.8	4.1
Methyl acrylate	1.2	4.3
Methyl benzoate	1.4	4.8
Methyl 3,4,5-trimethoxybenzoate	6.3	4.1
Pyridine	3.2	2.2
Triethylamine	0.3	8.4
DABCO^b	2	10

^{a} Calculated from the absorption changes by changing the concentration of the proton acceptor.
^{b} DABCO = 1,4-diazabicyclo[2.2.2]octane.

Even if the rationalization of all the data is a difficult problem, the K values in Table 10 for the amines which serve as proton acceptors show that the availability of the lone pair of the proton acceptor is an important factor in affecting the complex stability. Probably, the mechanism of fluorescence quenching becomes different from the charge transfer mechanism when the hydrogen bond is the main interaction[147].

The system 2-naphthylamine/triethylamine forms proton donor/acceptor interaction, which was investigated in the excited state by measuring time-resolved fluorescence spectra. While the similar 2-naphthol/triethylamine system affords the ion pair interaction, via the hydrogen bond complex, the 2-naphthylamine/triethylamine system presents hydrogen bond interaction which shows a low-temperature absorption with $\lambda_{max} = 370$ nm, and $\lambda_{max} = 370$ nm in the fluorescence spectrum[148].

In general, hydrogen bonds affect fluorescence behaviour. Scheme 16 describes an instance of the equilibrium relationships related to this behaviour.

$$DH^* \;+\; A \;\rightleftharpoons\; (DHA)^*$$

$$DH \;+\; A \;\xrightleftharpoons{K}\; (DH{\cdot}A)$$
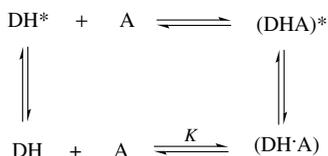
SCHEME 16

In Scheme 16, D and A are proton donor molecules and proton acceptor molecules, respectively. The quantity K represents the stability of the complex DH•A, formed by hydrogen bonding interactions in the ground state. For the 2-naphthylamine/pyridine system, the K value in hexane (obtained by fluorescence quenching measures) is 0.6 dm^3 mol^{-1}. This value is reduced by using benzene as a solvent ($K = 0.2$ dm^3 mol^{-1}) while, in cyclohexane, $K = 12$. The observed variations confirm the importance of solvents in influencing solute/solute interactions[149].

The solvent effect on the uv/vis absorption spectra and the infrared and ^{1}H NMR spectral data of N-(nitrophenyl)alkylenediamines **82** and **83** shows spectroscopic behaviour, indicating the presence of an intramolecular hydrogen bond between the amino groups (cf. Scheme 17) which compete with the intermolecular hydrogen bond between **82** and **83** and the solvents[150].

(82)   (83)   n = 2, 3, 4
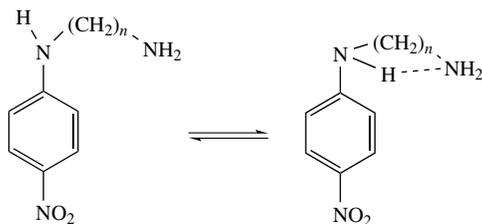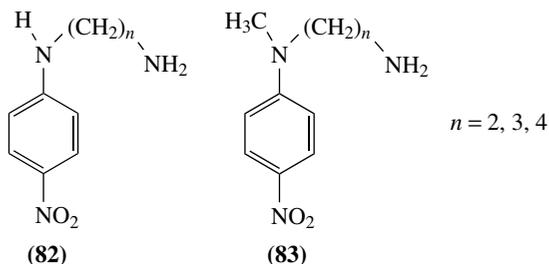
SCHEME 17

2. NMR spectroscopic studies

The proton–proton HNCH spin–spin coupling in N-methylaniline is affected by the pKa value of the proton acceptor partner. Ph_3PO, Ph_3AsO and F^- ions are used in order to elucidate this dependence. The importance of the hydrogen bonding interaction is observed also in aniline reactions. In fact, the addition of potassium fluoride to the reaction mixtures of anilines and alkyl halides strongly enhances the N-alkylation reaction because the nucleophilicity of aromatic amines is increased by hydrogen bond interaction with fluoride ion[151].

The importance of the ability of the proton acceptor partner is confirmed by ^1H NMR spectral data for complexes between aniline or pentafluoroaniline (**64**) and DMSO, acetone and HMPA. These spectral data indicate that the effect of hydrogen bond formation on the chemical shift of the NH_2 group is about the same for both anilines.

The rate of the hydrogen/deuterium exchange in the presence of t-butyl alcohol and 2,6-di-t-butylphenol depends on the strength of both $N-H\cdots O$ and $O-H\cdots N$ bonds[152].

Competition between the charge transfer interaction and hydrogen bond interaction in complexes between 1,2-, 1,3- and 1,4-dinitrobenzene (**84**, **85** and **86**, respectively) and aniline, N-methylaniline and N,N-dimethylaniline is reported to depend on the concentration values used: at low concentrations in the range of the uv/vis spectrophotometric

(84)   (85)   (86)
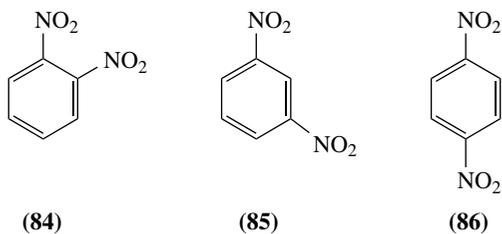
measurements the charge transfer interaction predominates, while in very concentrated solutions the main interaction is a hydrogen bond interaction[153].

B. Solid State (X-ray Diffraction)

X-ray diffraction analysis of a single crystal is a powerful tool for studying the structure of hetero-complexes in the solid state. In particular, complexes between anilines and proton donor molecules are frequently investigated by the usual spectroscopic methods and by X-ray diffraction.

2,3,5-Trichlorophenol (**87**) interacts with aniline to produce complexes[154] (Scheme 18) which involve two pairs of partners, that are arranged to form the hydrogen bonds reported in **88** and in **89**. In **88**, the bond N−H···O is longer than the bond O−H···N[155]. In the crystal the molecule is unionized, while the alternative situation, reported in **89,** is supported by infrared spectra and indicates[155] the presence of hydrogen bonds between ions[116].

$$C_6H_5NH_2 \quad + \quad \text{(87)} \quad \rightleftharpoons \quad \text{COMPLEX}$$

(**87**)

SCHEME 18

O — H - - - N   2.89 Å
N — H - - - O   3.03 Å
(**88**)

$^+$N — H - - O$^-$ 2.84 Å
(**89**)
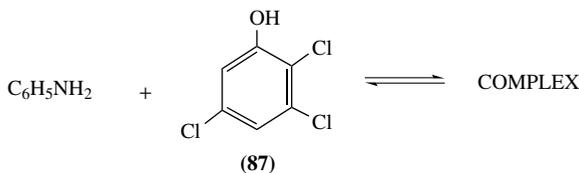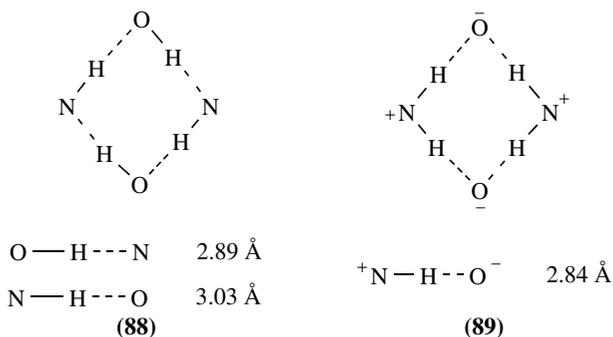
Non-linear optical materials play an important role in several fields, and they are worthy of attention. As a light passes through a non-linear optical material, it produces light waves at harmonics of the frequency of the original light wave. The frequency of an infrared light may be doubled, tripled or quadrupled, providing light in the uv or the visible region of the spectrum.

A non-linear optical material is a molecule in which a non-linear polarization is invoked on application of a strong electric field, which is due to external application of a laser source. Organic compounds with delocalized π electrons (by conjugation) are of interest because of their large non-linear optical properties. Optimization of properties of non-linear optical materials involves molecular design by considering different classes of chromophores and factors able to affect (and enhance) the internal charge transfer interaction, such as intermolecular hydrogen bonding interaction. The study of intermolecular

interactions is focused on the effects of hydrogen bonding interactions. Similar molecules may have very different non-linear optical properties because of their different hydrogen bond pattern.

In order to obtain organic non-linear optical materials, a number of aniliniun L-tartrate salts are prepared. The structure of the complexes between L-tartaric acid and *m*-anisidine or *p*-toluidine was studied by X-ray diffraction of a single crystal. *m*-Anisidinium L-tartrate monohydrate shows pronounced second harmonic generation activity (which is the quadratic term of the equation describing the total polarization of a molecule), while *p*-toluidinium L-tartrate did not show any detectable pronounced second-harmonic generation activity[156].

The hydrogen bond between ions is important for the preparation of solid-state materials prone to show second harmonic generation activity[14, 94]. In the case of anilinium L-tartrate, the presence of hydrogen bonds is important in determining the orientation of components in the lattice[16].

The X-ray diffraction of a single crystal shows that not only is the NH_2 amino group able to form hydrogen bonding interaction, but also the *N,N*-dimethylamino group $N(CH_3)_2$ of *N,N*-dimethyaminoaniline derivatives is able to form N-C−H$\cdots$O hydrogen bonds[157].

Obviously, amino and nitro groups form strong N−H$\cdots$O hydrogen bonds to yield a supramolecular assembly, while the C−H$\cdots$O bond is a weaker interaction potentially able to form supramolecular species. This is the case of *N,N*-dimethylaminoaniline and nitro derivatives, as reported in **90**. 4-*N,N*-Dimethylaminobenzoic acid and 4-nitrobenzoic acid are assessed in the pattern depicted in **91**.

(90)

(91)

(92)
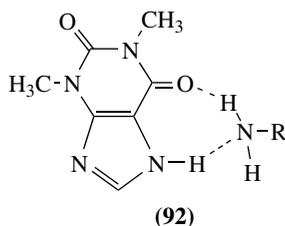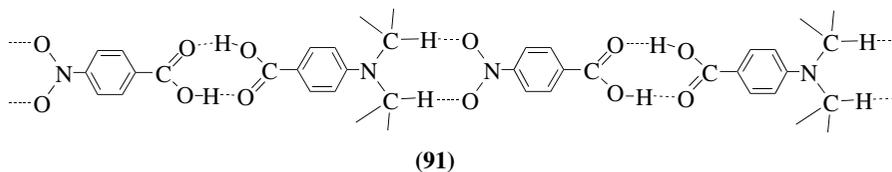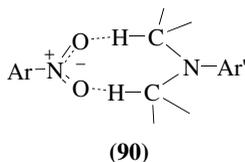
The 1:1 complex between theophylline and benzylamine **92** was prepared and studied by X-ray diffraction. That solid complexes between theophylline and aniline, *N*-methylaniline, and *N,N*-dimethylaniline are not formed was explained by the lower p*K*a values of the

aromatic amines (*ca* 4.5) with respect to the aliphatic amine (pKa benzylamine $= 9.35$ in water at $25\,^\circ$C). Consequently, in complex **92** the proton acceptor ability of the amino nitrogen atom may be considered the driving force in forming the complex[158].

Aniline, *N*,*N*-dimethylaniline and toluene form molecular complexes with (4*a*,8*b*,13*b*)-13-methyl-16-oxo-17-norkaurane-18-carboxylic acid (isosteviol) (**93**) investigated by X-ray diffraction[159]. **93** forms individual 2:1 molecular complexes with aniline or *N*,*N*-dimethylaniline and toluene. The supramolecular crystal structure of these complexes is formed by chiral double helices involving isosteviol molecules. The helices are linked together by intermolecular hydrogen bonds between the carboxy and the carbonyl groups[160].

(93)
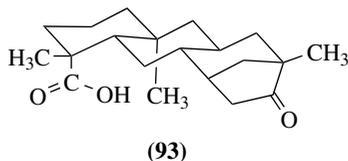
Figure 1 is a drawing of the supramolecular complexes between double helices of isosteviol with aniline (structure **94**) or toluene and *N*,*N*-dimethylaniline (structure **95**).

The co-crystallization of merocyanines (**96** and **97**) and derivatives of aniline or phenol produces non-linear optical organic materials. Merocyanine is a molecule presenting a π

(94)   **(95)**
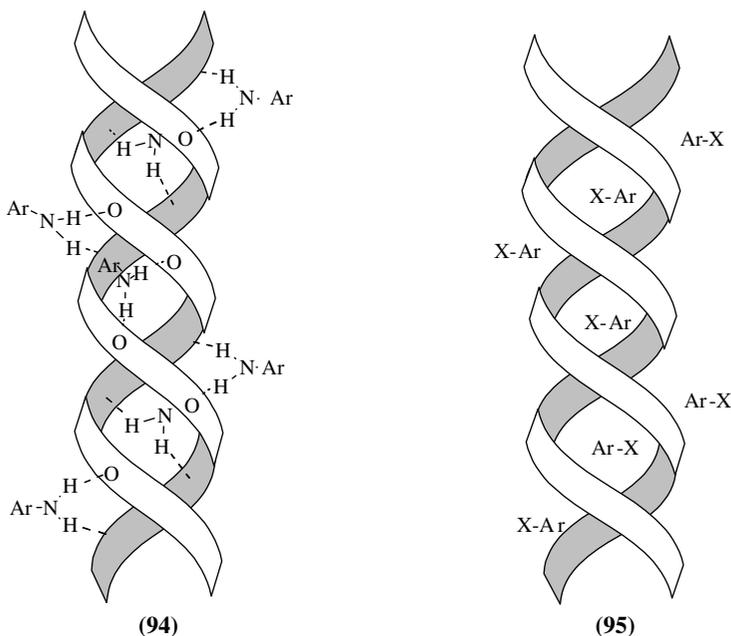
FIGURE 1. Supramolecular structure of the complexes between isosteviol and aniline (**94**), *N*,*N*-dimethylaniline (X $=$ N(CH$_3$)$_2$) or toluene (X $=$ CH$_3$) (**95**). Isosteviol is represented as ribbon helices. Adapted from Reference 159
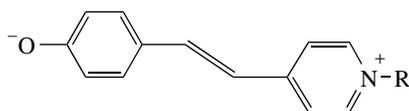
(96) R = CH$_3$

(97) R = CH$_2$CH$_2$OH

electronic system with large molecular hyperpolarizability[161]. Formation of short hydrogen bonds is the driving force of the co-crystallization.

Some particular intermolecular interaction between aromatic amines and different organic and inorganic partners are noteworthy.

Cellulose hydroxyl groups and the amino group of amines form a hydrogen bond which is mainly responsible for the complex formation[162].

The complex between p-phenylenediamine and cotton cellulose is more stable than the complexes of cellulose with aniline, benzylamine and furfurylamine. These complexes were characterized by X-ray diffraction. A 1:1 ratio of the complex furfurylamine/cellulose (referring to the anydroglucose unit) was indicated by a thermogravimetric analysis[162].

A salt between methylphosphonic acid and aniline was investigated by X-ray diffraction of a single crystal[163]. It shows that the hydrogen bond N$-$H$\cdots$OP forms a three-dimensional hydrogen bonded network. The N$\cdots$O distance ranges from 2.7307(12) to 2.8861(11) Å, indicating a strong hydrogen bond with high directionality; the N$-$H$\cdots$O angles are 170$-$177°.

Aniline is also able to form hydrogen bonds with inorganic substances. X-ray or neutron diffraction techniques which were applied on absorption products of aromatic hydrocarbon derivatives (benzene, xylenes, mesitylene, aniline, m-nitroaniline, m-dinitrobenzene) and synthetic zeolites Y indicate that the preferred adsorption sites depend on the formation of hydrogen bonds between the organic partner and the framework oxygen[164].

C. Hydrogen Bonds and Electron Transfer Processes involving Anilines

Aniline and N,N-dimethylaniline are used as donor solvents (or solutes) in order to evaluate the part of the solvent reorganization energy affected by hydrogen bonding interaction in intermolecular electron transfer[165].

Photoinduced electron transfer reactions in hydrogen bonded complexes between electron donor and electron acceptor is an exciting field of investigation of the importance of hydrogen bonds in affecting and, in some cases, in facilitating the electron transfer induced by photon absorption[166, 167].

The coumarin dyes **98** is an ideal system to investigate the importance of the hydrogen bond in an electron transfer process, which involves the carbonyl group of **98**.

(98) R = H, CH$_3$, CF$_3$

The interaction between coumarins and *N*,*N*-dimethylanilines was investigated by measurements of femptosecond optical spectroscopy. In the absence of an amino hydrogen, the main coumarin/aniline interaction is an electron donor/acceptor interaction[168]. A relevant H/D isotope effect[169] (measured on the average fluorescence lifetimes) ranges from 1 to 13 on the rate constant of ultrafast intermolecular electron transfer between coumarin dye **99** or **100** and *N*,*N*-dimethylaniline or aniline is explained by the formation of an intermolecular hydrogen bond with the electron-donating aniline, which is absent in *N*,*N*-dimethylaniline[170].

(99)   **(100)**   **(101)** R = H
                                                         (102) R = CH3
                                                         (103) R = C$_2$H$_5$

The C=O group of coumarin (**98**, R = CH$_3$) is a potential hydrogen bond acceptor. By using subpicosecond time-resolved infrared absorption spectroscopy, following photoexcitation of the cumarin chromophore of **98**, in its complex with aniline, the hydrogen bond dissociation rate is in the order of femtoseconds and the aniline reorients itself by reformation of the hydrogen bond with a new geometry[166].

7-Aminocoumarins **101**–**103** present ultrafast fluorescence quenching by the fluorescence up conversion method when the electron donating partners (aniline or *N*,*N*-dimethylaniline) are present as solvents. An intermolecular electron-transfer process between the coumarins and the anilines is indicated to be active in depressing the quenching rate[171].

Photoreactions between triplet benzophenone **104** and 1-*N*,*N*-dialkylaminonaphthalene (**105**) are studied by means of the laser flash photolysis technique in CH$_3$CN (at λ = 355 nm) in the presence and in the absence of MeOH or H$_2$O. The produced triplet exciplexes ^{3}(**105** ···· **104**)* show electron transfer phenomena which occur due to an increase in the electron affinity of **104** in ^{3}(**105** ···· **104**)* by proton donor molecules, such as methanol or water[172].

(104)   **(105)** R = CH$_3$, C$_2$H$_5$

D. Intermolecular Hydrogen Bonds of Aniline Cation: Infrared Depletion Spectroscopy

The investigation of the structure of ionic complexes between cations and the neutral ligand is important for understanding the solvation of ions by neutral molecules. The

interaction ion–ligand, in general, has a much greater strength than the interaction between the same neutral molecule and the ligand.

To produce ionic clusters, the neutral clusters are ionized by an ultraviolet laser and then irradiated by light from an infrared laser[173].

Extensive attention is devoted to the interactions between aniline and aniline cation and neutral partners to form clusters which are investigated by recent techniques. In particular, van der Waals complexes between aniline and Ar, Kr, N_2, CO, in both neutral and cationic forms, are studied by the technique of zero kinetic energy photoelectronic spectroscopy[174]. Theoretical studies[175] on the aniline and aniline cation, free or complexed with a number of partners (as potential solvents) produce important results about the cluster geometry and the relative importance of different kinds of interactions.

Van der Waals complexes aniline/N_2 are investigated by rotational resolved UV spectra[176].

Interactions between aniline and neutral molecules (N_2, H_2, CH_4 and the rare gas atoms, He, Ne, Ar and Kr) produce van der Waals complexes which are formed in a supersonic jet and are studied by laser-induced fluorescence spectroscopy[177, 178].

Aniline clusters and the corresponding clusters with N_2, CH_4, CHF_3 and CO are studied by detecting the depletion of resonance-enhanced multiphoton ionization spectroscopy (with time-of-flight mass spectrometer) which measures the vibrational spectra of the complexes. The interaction in clusters involving aniline cation is different from that of neutral aniline. The hydrogen bonding interaction is the main interaction in the aniline cation cluster, while neutral aniline clusters are due to van der Waals interaction.

The calculated structure of the [aniline/CO]$^+$ cluster is given in **106**[179].
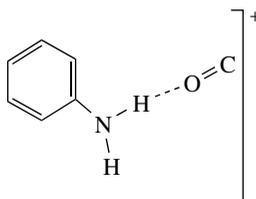
(106)

In a similar way, the clusters between aniline or aniline cation and argon (aniline/Ar$_n$, $n = 1, 2$) are studied by infrared spectra of NH_2 stretching modes in a supersonic jet, by using infrared depletion spectroscopy and time-of-flight mass spectrometry[173].

The complexes between aniline cation and argon are produced in an electron impact ion source. Two main interaction modes, by π bond formation and by hydrogen bond formation, are depicted in **107** (π complex) and **108** (hydrogen bonded complex NH—Ar type) and **109** [hydrogen bonded complex N(H—Ar)$_2$ type], respectively[180, 181]. The symmetric and antisymmetric stretching modes of the NH_2 group are observed[181] for the aniline/argon cluster, at 3422 and 3508 cm^{-1}.
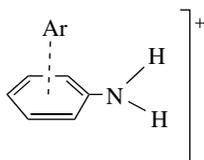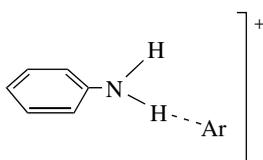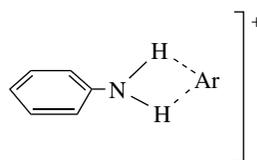
(107)   **(108)**   **(109)**

The 1:1 aniline/argon clusters are usually assumed to have structure **107** while **108** is indicated to be less stable than **107**. The isomeric structures of [aniline/argon$_2$]$^+$ clusters in the cationic ground states are depicted in **110**–**112**[180, 181].

(110)   **(111)**   **(112)**
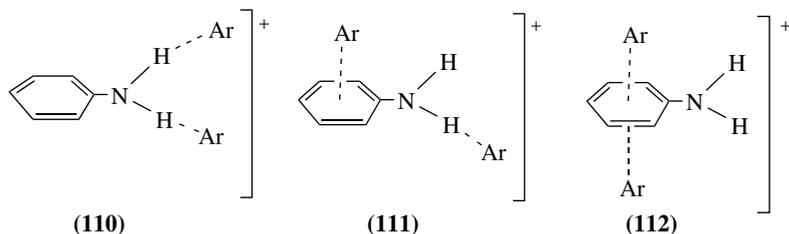
The depletion method allows the measurement of infrared spectra of the amino group stretching vibration of [aniline/(argon)$_n$]$^+$ clusters. Small clusters are like **107**–**110**. Larger [aniline/(argon)$_n$]$^+$ clusters show that the argon atoms in the first solvation shell are in the plane of the aniline ring (three argon atoms on either side of the aromatic ring) and on the aniline ring (six argon atoms surrounding the aromatic ring in the same plane). The second solvation shell involves argon atoms near the NH$_2$ group.

The probable structures of aniline dimer cation are calculated by the *ab initio* MO method: **113** shows the N−H$\cdots\pi$ hydrogen bond and **114** the N−H$\cdots$N hydrogen bond. Spectroscopic data indicate that the structure **113** seems to be preferred, and *ab initio* MO calculations support this conclusion[182].

(113)   **(114)**
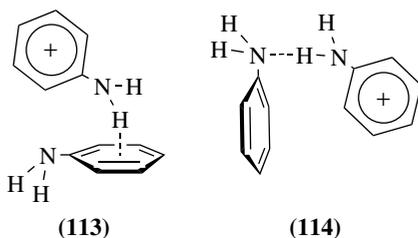
The NH-π type hydrogen bond between the charged aniline and neutral benzene is deduced by the vibrational spectrum of the [aniline/benzene]$^+$ complex. By using a time-of-flight mass spectrometer with an ion reflector, the intermolecular interactions in aniline/benzene trimer ions were investigated. The NH-π and N−H$\cdots$N structures of the [aniline/benzene]$^+$ trimer ions based on theoretical calculations are reported in Scheme 19[183].

New infrared spectroscopic techniques which are used to investigate the benzene/water cluster show an O−H$\cdots\pi$ hydrogen bond[184], similar to that of the NH$_2\cdots\pi$ bond.

The infrared depletion spectroscopy of the aniline/toluene cluster makes it possible to measure the NH$_2$ stretching vibration[185]. The two main possibilities which are derived from the calculated structure of the aniline/toluene and [aniline/toluene]$^+$ clusters are depicted respectively in **115** and **116**. An N−H$\cdots\pi$ hydrogen bond is the main interaction in both cases.

Vibrational spectra of aniline/cyclohexane and aniline/benzene clusters investigated by infrared depletion spectroscopy with selective resonance—enhanced multiphoton ioniza-tion with time-of-flight mass spectrometry (REMPI-TOF mass spectrometry) show[186] an

SCHEME 19

(115)   **(116)**
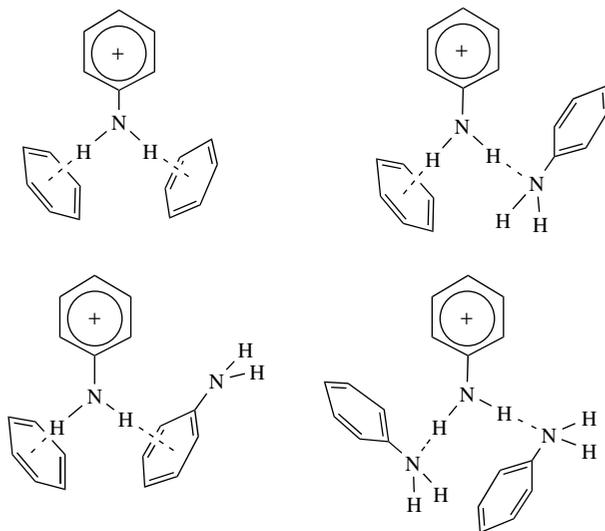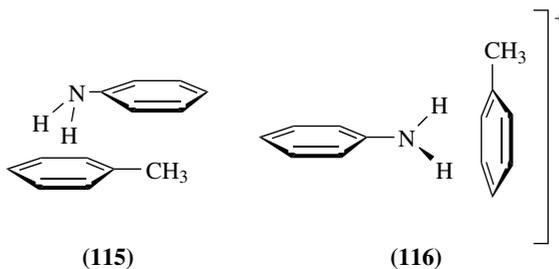
N−H···π hydrogen bond present in the aniline/benzene complex; the two molecules are assessed face to face as depicted in **117**. In this case red shifts of 28.4 and 40.9 cm^{-1} are observed, for symmetric and antisymmetric NH$_2$ stretching bands. As expected, the aniline/cyclohexane cluster presents a smaller red shift.

(117)
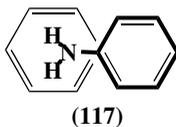
The N−H···π is the main interaction in aniline/alkene (ethene, propene, butene) complex cations[187, 188]. **118** and **119** illustrate the calculated structures of aniline/ethene cluster cation. The aniline cation is bonded to the π electrons of alkene by one (**118**) or two (**119**) hydrogen bonds. Spectroscopic data emphasize that these interactions are different from that observed for the same neutral clusters[44].

Aniline cation and molecular nitrogen undergo intermolecular interaction, which is observed by infrared photodissociation spectroscopy. The cluster system [PhNH$_2$/N$_2$]$^+$ is a model of cation solvation in neutral and hydrophobic medium.

(118)   **(119)**
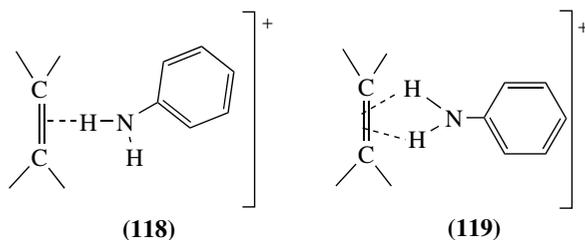
Vibrational dynamics of van der Waals aniline/(N$_2$)$_1$ clusters[189] are compared to those of aniline/(CH$_4$) and aniline/Ar clusters[190]. The experimental results follow the theory prediction (as described by the Fermi rule). Aniline/(N$_2$)$_1$ clusters undergo dynamics which are intermediate with respect to the aniline/(CH$_4$) and aniline/Ar clusters.

The structures of the most stable [PhNH$_2$/(N$_2$)$_n$]$^+$ ($n = 1-4$) clusters which are deduced from infrared spectroscopic data[191] are reported in Scheme 20 with positive charges omitted. The geometries of the hydrogen bonding and of π interactions agree with those obtained by *ab initio* calculations.
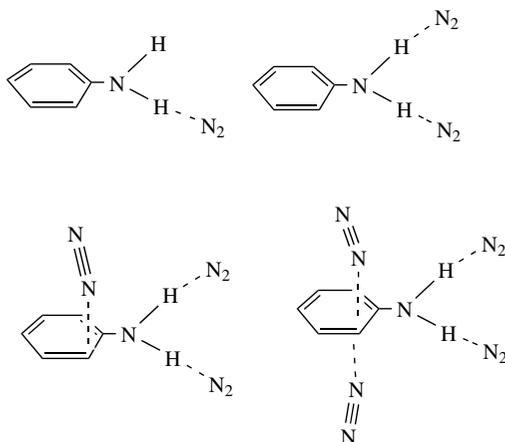
SCHEME 20

Photodissociation of [aniline/thiophene]$^+$, [aniline/furan]$^+$ and [aniline/phenol]$^+$ complexes (which are produced in an ion source of electron impact type), investigated by analysis of infrared spectra, shows that the [aniline/thiophene]$^+$ complex involves a N−H$\cdots\pi$ type hydrogen bond, while with the oxygenated partner, aniline$^+$ interacts via both σ- and π-hydrogen bonding interactions[192].

The NH$_2$ stretching mode of the complex between aniline and furan and its cation indicates[193] that the main intermolecular interaction is due to a weak hydrogen bond of the N−H group and the oxygen of furan as depicted in **120**. On the contrary, for the aniline furan cation complex **121** the main interaction is between the N−H group and the π system of the furan ring.

Of particular interest are studies on the aniline cation with water or methanol clusters investigated by vibrational spectroscopy[194, 195]. In Scheme 21, **122** represents the proposed

(120) **(121)**

(122) **(123)** **(124)**
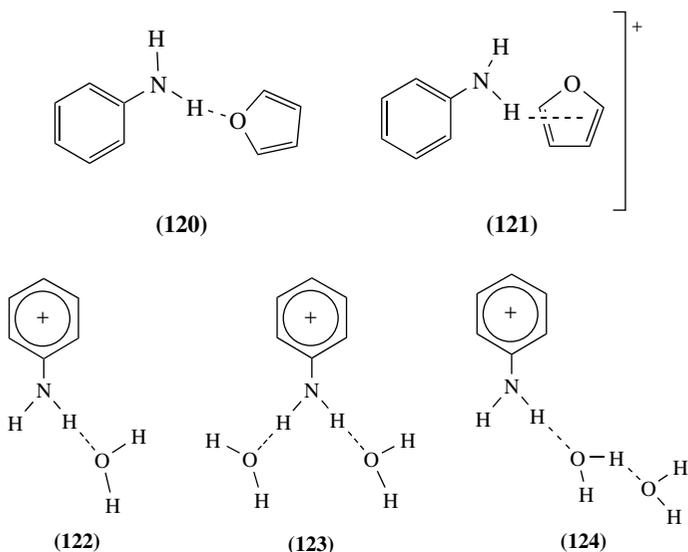
SCHEME 21

structure of the [aniline/(H$_2$O)$_1$]$^+$ complex, while for the [aniline/(H$_2$O)$_2$]$^+$ two main structures, **123** and **124**, are proposed.

These and more complex clusters [aniline/(H$_2$O)$_n$]$^+$, $n = 1$–8 are investigated by infrared photodissociation spectra supplemented by density functional theory calculations[196]. Scheme 22 gives the calculated geometries in the case of $n = 4$.
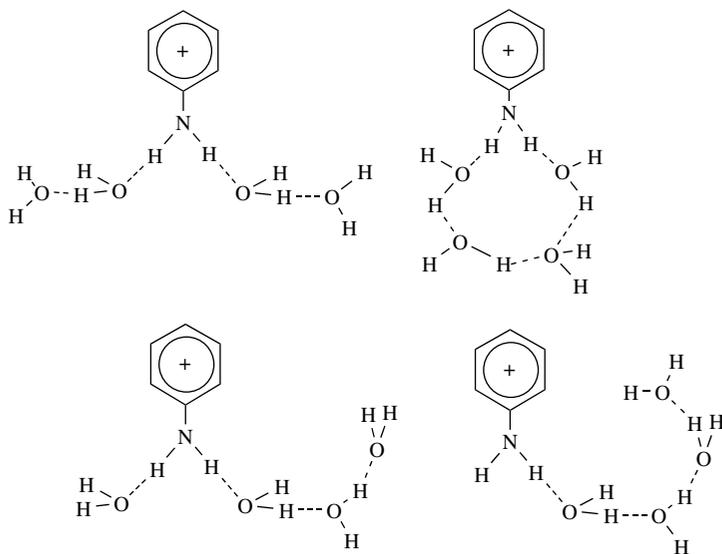
SCHEME 22

The spectra of [aniline/$(H_2O)_2$]$^+$ and [aniline/$(CH_3OH)_2$]$^+$ indicate a large perturbation of both NH oscillators, showing that each NH bond is bound to a solvent molecule in the most populated structure[197].

Infrared depletion spectroscopy of 1:1 hydrogen bonded aniline/Et_2NH cluster shows[198] an N—H$\cdots$N interaction (see **125**) with an energy of about 3.8 kcal mol^{-1}. In **125**, the three bond lengths involving the NH_2 group are N—H (bonded) 1.020 Å, N—H (free) 1.010 Å and N—C 1.399 Å, similar to that reported for the aniline/Et_3N complex[199]. The red shift of the aniline/triethylamine complex with respect to the free aniline is qualitatively reproduced by *ab initio* calculation. The calculated geometry involves one hydrogen bond between the N—H of aniline and the triethylamine nitrogen[199].

The hydrogen bonding interaction between aniline and THF indicates[200] structure **126** with an N—H$\cdots$N hydrogen bond, with a binding energy of 8.8 kcal mol^{-1}.

(125)   **(126)**   **(127)**
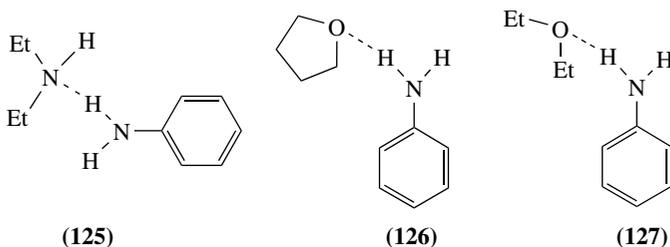
Aniline/NH_3 and [aniline/NH_3]$^+$ clusters are studied by infrared depletion spectroscopy. In both cases the hydrogen bond is between the NH of the aniline and the lone pair of NH_3. In the cation cluster the interaction is much stronger than in the neutral cluster[201].

The 1:1 diethyl ether complex, studied by infrared depletion spectroscopy using cluster-size selective resonance-enhanced multiphoton ionization with time-of-flight mass spectrometry, shows[202] two absorptions at 3372 and 3478 cm^{-1} which are assigned to hydrogen bonded N—H and to free N—H, respectively. The N—H$\cdots$O hydrogen bond energy of structure **127** is calculated to be 3.1 kcal mol^{-1}. The same interaction is involved in the [aniline/$(CH_3)_2O$]$^+$ cluster[203].

The hydrogen bond in methyl 4-*N*,*N*-dimethylaminobenzoate (**128**)/water clusters ($n = 1-3$) is investigated also by infrared depletion spectroscopy in dispersed fluorescence[204]. In the 1:1 cluster between **128** and water, the water molecule is hydrogen bonded to the carbonyl oxygen of the COOMe group. Internal charge transfer in **128** between the amino and ester groups is stabilized by formation of clusters with the water solvent.

(128)
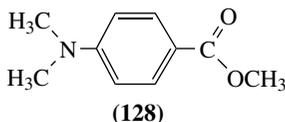
In infrared depletion spectroscopy of the neutral aniline/pyrrole[205] complex, both spectroscopic observation and theoretical calculations indicate the presence of a hydrogen bond between one of the N—H bonds of aniline and the π system of pyrrole, as illustrated in **129**.

Infrared depletion spectroscopy also makes it possible to obtain information about ternary clusters. This is the case of the aniline/water/tetrahydrofuran cluster[206]. Its calculated structure **130** presents a chain-like structure.

(129)

(130)   **(131)**
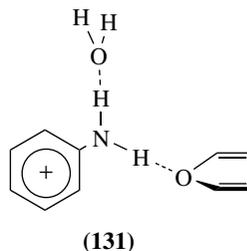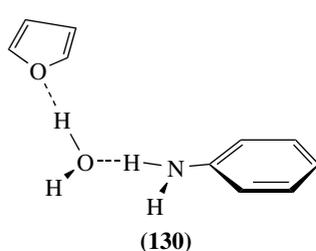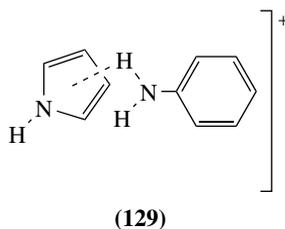
The related cationic cluster has two different hydrogen bonds involving the NH_2 group of aniline cation, as shown in the calculated structure **131**, one with the oxygen atom of tetrahydrofuran and another with the oxygen atom of water. In the same way, the aniline/acetonitrile cation and the aniline/acetonitrile/water cation clusters are studied and their structures are calculated by using the DFT method and displayed by **132** and **133**, respectively[207]. The predissociation of **133** affords only one product channel giving water and **132**. Consequently, the hydrogen bond between CH_3CN and aniline cation may be considered stronger than the hydrogen bond between water and aniline cation.

(132)   **(133)**
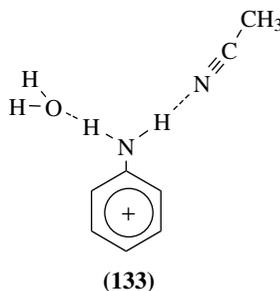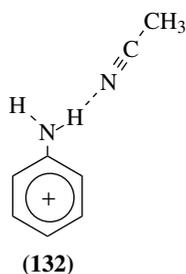
The $N-H\cdots N$ hydrogen bond is responsible for the formation of the complexes between aniline and aliphatic amines (ammonia, methylamine, dimethylamine and tri-methylamine) which act as proton acceptors. Infrared photodissociation spectra and DFT calculation indicate[208] that the clusters [aniline/ammonia]$^+$ and [aniline/methylamine]$^+$ have a non proton transferred (without the proton donation from the aniline moiety to the amine molecule) structure, while the complexes [aniline/dimethylamine]$^+$, [aniline/trimethylamine]$^+$ possess a proton transferred structure. Reasonably, the proton transfer increases on increasing the proton affinity of the amine used as solvent.

The experimental conditions used to obtain the conclusions reported in this section are different from the usual experimental conditions used in organic chemistry of the main

part of experimental organic chemistry. However, the conclusions regarding solute/solvent or solute/solute interactions may be a useful starting point in understanding the actual 'microscopic' situation (in terms of geometry and energetic levels) of reactants and also in performing practical reactions and in explaining reaction mechanisms.

V. HYDROGEN BONDS IN POLYANILINES

Polyaniline (**PANI**) is one of the most important polymeric materials, owing to its electrical, optoelectrical and optical properties[209]. The preparation of polyaniline is very easy. Ammonium persulfate polymerizes monomeric aniline to **PANI** whose repeating moiety is described by **134**. The polymer is stable and environment compatible.
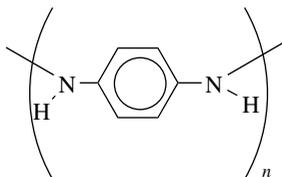
(134)

Different substituents may be present on the homocyclic moiety. The properties of **PANI** depend on the presence of the hydrogen bond (also arising from doping substances, such as salicylic acid) as well as on the protonation to form salts[210].

PANI is deposited on nanocrystalline TiO_2 to form a conductive material, prepared by ultrasonic irradiation. The strong interaction between titanium dioxide and **PANI** is mainly a hydrogen bonding interaction[211]. The hydrogen bond between the OH group present in the doping substance and the nitrogen atom of **PANI** is the driving force for self-assembling hollow microspheres[212].

VI. HALOGEN BONDS IN ANILINES

Finally, we briefly report another interaction not very different from the hydrogen bonding interaction, involving amines and in particular anilines: the halogen bond interaction.

Halogen bonding interaction is a non-covalent interaction involving electron-rich atoms (such as the nitrogen of amines or oxygen of alcohols or phenols) and halogen atoms[213]. Derivatives of aniline (or other nitrogen-containing rings, such as pyridines) may act as an electron donor partner and iodo perfluorocarbons serve as electron acceptors[214].
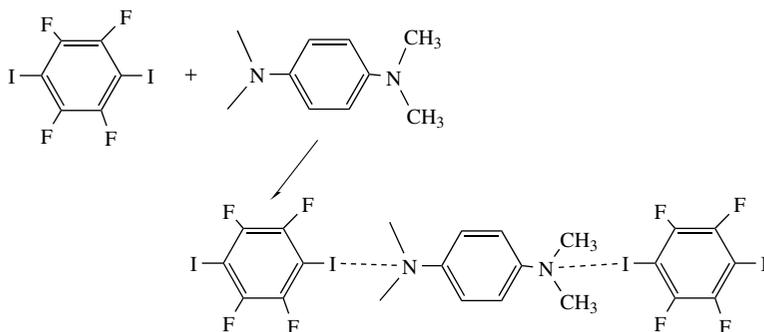
SCHEME 23

Self-assembly of aromatic (and aliphatic) di-iodoperfluorocarbons, with derivatives of anilines which serve as electron donor partners, produces solid crystalline materials. X-ray diffraction agrees with the structure reported in Scheme 23.

The crystal structure of 2,5-dichloroaniline **4**, investigated by X-ray diffraction offers no evidence of the presence of hydrogen bonding interaction, but there is an interesting interaction involving chlorine atoms: the Cl–Cl distance (3.37 Å)[49] is shorter than the usually quoted van der Waals distances (3.6 Å). It may be that this structure represents the first instance of halogen bond interaction[215].

VII. REFERENCES

1. C. Reichardt, *Solvent Effects in Organic Chemistry*, Verlag Chemie, New York, 1979.
2. A. C. Legon and D. J. Millen, *Chem. Soc. Rev.*, **21**, 71 (1992).
3. S. Scheiner, *Molecular Interactions*, Wiley, New York, 1997.
4. J. Emsley, *Chem. Soc. Rev.*, **9**, 91 (1980)
5. G. R. Desiraju, *Crystal Engineering: The Design of Organic Solids*, Elsevier, Amsterdam, 1989.
6. A. Eschenmoser and E. Lowenthal, *Chem. Soc. Rev.*, **21**, 1 (1992).
7. G. A. Jeffrey and W. Soenger, *Hydrogen Bonding in Biological Molecules*, Springer-Verlag, Berlin, 1991.
8. P. Piotrowiak, *Chem. Soc. Rev.*, **28**, 143 (1999).
9. M. A. Fox and E. Galoppini, *J. Am. Chem. Soc.*, **119**, 5277 (1997).
10. G. Desiraju, *J. Chem. Soc., Chem. Commun.*, 1475 (1997).
11. R. G. Pearson (Ed.), *Hard and Soft Acids and Bases*, Dowden, Hutchinson and Ross Inc., Stroudsburg, Pennsylvania, 1973.
12. G. Zundel, *Trends Phys. Chem.*, **3**, 129 (1992).
13. G. Zundel, *Hydrogen Bonds with Large Proton Polarizability and Proton Transfer Process in Electrochemistry and Biology*, in *Advances in Chemical Physics* (Eds. I. Prigogine and S. A. Rice), Vol. III, Wiley, New York, 2000.
14. P. Barczynski, Z. Dega-Szafran and M. Szafran, *J. Chem. Soc., Perkin Trans. 2*, 765 (1985).
15. M. C. Etter, *Acc. Chem. Res.*, **23**, 120 (1990).
16. C. B. Aakeröy and K. R. Seddon, *Chem. Soc. Rev.*, **22**, 397 (1993).
17. L. Forlani, in *The Chemistry of Amino, Nitroso, and Related Groups* (Ed. S. Patai), Chap. 10, Wiley, Chichester, 1996.
18. D. Philip and J. F. Stoddart, *Angew. Chem., Int. Ed. Engl.*, **35**, 1154 (1996).
19. J. P. Mathias, E. E. Simanek and G. M. Whitesides, *J. Am. Chem. Soc.*, **116**, 4326 (1994).
20. J. P. Mathias, C. T. Seto, E. E. Simanek and G. M. Whitesides, *J. Am. Chem. Soc.*, **116**, 1725 (1994).
21. L. Chun, J. G. Morales, H. Fenniri and T. J. Webster, *Nanotechnology*, **15**, 234 (2004).
22. L. J. Bellamy, *The Infrared Spectra of Complex Molecules*, Methuen, London, 1958.
23. C. G. Claessens and J. F. Stoddart, *J. Phys. Org. Chem.*, **10**, 254 (1997).
24. M. H. Abraham, P. L. Grellier, D. V. Prior, P. P. Duce, J. J. Morris and P. J. Taylor, *J. Chem. Soc., Perkin Trans. 2*, 699 (1989).
25. M. H. Abraham, *Chem. Soc. Rev.*, **22**, 73 (1993).
26. A. C. Legon, *Chem. Soc. Rev.*, **22**, 153 (1993).
27. B. Brutschy, *Chem. Rev.*, **92**, 1567 (1992).
28. M. Kanzelberger, X. Zhang, J. Emge, A. S. Goldman, J. Zhao, C. Incarvito and J. F. Hartwig, *J. Am. Chem. Soc.*, **125**, 13644 (2003).
29. J. W. Ellis, *J. Am. Chem. Soc.*, **49**, 347 (1927).
30. F. K. Bell, *J. Am. Chem. Soc.*, **47**, 3039 (1925).
31. J. W. Ellis, *J. Am. Chem. Soc.*, **50**, 685 (1928).
32. V. E. Borisenko, A. V. Baturin, M. Przeslawska and A. Koll, *J. Mol. Struct.*, **407**, 53 (1997).
33. M.-X. Xie and L. Yuan, *Spectrochim. Acta, Part A*, **58A**, 2817 (2002).
34. J. J. Elliott and S. F. Mason, *J. Chem. Soc.*, 1275 (1959).
35. S. Califano and R. Moccia, *Gazz. Chim. Ital.*, **87**, 58 (1957).
36. S. F. Mason, *J. Chem. Soc.*, 3619 (1958).

37. S. Califano and R. Moccia, *Gazz. Chim. Ital.*, **86**, 1014 (1956).
38. H. Wolff and R. Wurtz, *J. Phys. Chem.*, **74**, 1600 (1970).
39. J. L. Mateos, R. Cetina and O. Chao, *J. Chem. Soc., Chem. Commun.*, 519 (1965).
40. N. S. Nudelman, in *The Chemistry of Amino, Nitroso, and Related Groups* (Ed. S. Patai), Chap. 26, Wiley, Chichester, 1996.
41. L. Forlani, *Gazz. Chim. Ital.*, **112**, 205 (1982).
42. N. Fuson, M.-L. Josien, R. L. Powell and E. Utterback, *J. Chem. Phys.*, **20**, 145 (1952).
43. G. Pannetier and L. Abello, *Bull. Soc. Chim. Fr.*, 1646 (1966).
44. K. Sugawara, J. Miyawaki, T. Nakanaga, H. Takeo, G. Lembach, S. Djafari, H. Barth and B. Brutschy, *J. Phys. Chem.*, **100**, 17145 (1996).
45. J. H. Yeh, T. L Shen, D. G. Nocera, G. E. Leroi, I. Suzuka, H. Ozawa and Y. Namuta, *J. Phys. Chem.*, **100**, 4385 (1996).
46. C. J. Brown, *Acta Crystallogr.*, **4**, 100 (1951).
47. K. Folting, J. C. Huffman and L. L. Merritt, *Cryst. Struct. Commun.*, **4**, 705 (1975).
48. B. Sakurai, M. Sundaralingam and G. A. Jeffrey, *Acta Crystallogr.*, **16**, 354 (1963). M. J. Deetz, J. E. Fahey and B. D. Smith, *J. Phys. Org. Chem.*, **14**, 463 (2001).
49. C. J. Brown and D. E. C. Corbridge, *Acta Crystallogr.*, **7**, 711 (1954).
50. Y. Zhou, L. Zhang, X. Zeng, J. J. Vital and X. You, *J. Mol. Struct.*, **553**, 25 (2000).
51. K. B. Whetsel, W. E. Robertson and M. W. Krell, *Anal. Chem.*, **32**, 1281 (1960).
52. A. Bryson and R. L. Werner, *J. Am. Chem. Soc.*, **82**, 4862 (1960).
53. A. Bryson, *Aust. J. Chem.*, **13**, 456 (1960).
54. J. H. Lady and K. B. Whetsel, *J. Phys. Chem.*, **68**, 1001 (1964).
55. G. Moritz, *Spectrochim. Acta*, **20**, 1642 (1964).
56. P. J. Krueger, *Can. J. Chem.*, **42**, 201 (1964).
57. H. Hoyer, *Monatsh. Chem.*, **90**, 357 (1959).
58. G. Moritz, *Spectrochim. Acta*, **18**, 671 (1962).
59. H. Musso and G. Sandrock, *Chem. Ber.*, **97**, 2076 (1964).
60. J. H. Lady and K. B. Whetsel, *Spectrochim. Acta*, **21**, 1669 (1965).
61. P. J. Krueger, *Can. J. Chem.*, **41**, 363 (1963).
62. P. J. Krueger, *Can. J. Chem.*, **40**, 2300 (1962).
63. A. N. Hambly and B. V. O'Grady, *Chem. Ind.*, 86 (1963).
64. A. N. Hambly and B. V. O'Grady, *Chem. Ind.*, 459 (1962).
65. A. N. Hambly and B. V. O'Grady, *Aust. J. Chem.*, **16**, 459 (1963).
66. M. Honda, A. Fujii, E. Fujimaki, T. Ebata and N. Mikami, *J. Phys. Chem. A*, **107**, 3678 (2003).
67. T. Axenrod and M. J. Wieder, *J. Am. Chem. Soc.*, **93**, 3549 (1971).
68. R. Wasylishen and T. Schaefer, *Can. J. Chem.*, **48**, 1263 (1970).
69. J. A. Weil, A. Blum, A. H. Heiss and J. K. Kinnaird, *J. Chem. Phys.*, **46**, 3132 (1967).
70. J. Heidberg, J. A. Weil, G. A. Janusonis and J. K. Anderson, *J. Chem. Phys.*, **41**, 1033 (1964).
71. J. Rueben, *J. Am. Chem. Soc.*, **109**, 316 (1987).
72. D. M. Rackham, S. E. Morgan, J. K. Chabrabarti, K. Jiban and T. M. Hotten, *Spectrosc. Lett.*, **13**, 159 (1980).
73. F. K. Fong, J. P. Mctague, S. K. Grag and C. P. Smyth, *J. Phys. Chem.*, **70**, 3567 (1966).
74. V. E. Borisenko and A. I. Filarovski, *J. Mol. Struct.*, **196**, 353 (1989).
75. V. E. Borisenko and O. N. Grishanova, *J. Mol. Struct.*, **239**, 13 (1990).
76. V. E. Borisenko, N. V. Sokolovskaja, L. A. Kuzina and A. Koll, *Spectrochim. Acta, Part A*, **51**, 1935 (1995).
77. V. V. Gromak, V. G. Avakyan and F. S. Pashkoskii, *J. Appl. Spectrosc.*, **68**, 259 (2001).
78. F. Effenberger and R. Niess, *Angew. Chem., Int. Ed. Engl.*, **6**, 1067 (1967); J. L. Oudar and D. S. Chemia, *J. Chem. Phys.*, **66**, 2664 (1977).
79. W. Knoche, W. W. Shoeller, R. Schomacker and S. Vogel, *J. Am. Chem. Soc.*, **110**, 7484 (1988).
80. W. Sachs, W. Knoche and C. Herrmann, *J. Chem. Soc., Perkin Trans. 2*, 701 (1991).
81. R. S. Mason, C. M. Williams and P. D. J. Anderson, *J. Chem. Soc., Chem. Commun.*, 1027 (1995); N. Solcà and O. Dopfer, *Angew. Chem., Int. Ed.*, **41**, 3628 (2002); N. Solcà and O. Dopfer, *J. Am. Chem. Soc.*, **125**, 1421 (2003).
82. E. Del Vecchio, PhD Thesis, University of Bologna, Italy, 2003.
83. G. F. Lipscomb, A. F. Garito and R. S. Narang, *J. Chem. Phys.*, **75**, 1509 (1981).

84. G. R. Desiraju. *Crystal Engineering. The Design of Organic Solids*, *Material Science Monographs* 54, Elsevier, Amsterdam, 1989.
85. T. W. Panunto, Z. Urbánczyk, R. Johnson and M. C. Etter, *J. Am. Chem. Soc.*, **109**, 7786 (1987).
86. T. Hamada, *J. Phys. Chem.*, **100**, 8777 (1996).
87. J. Ellena, A. E. Goeta, J. A. K. Howard, C. C. Wilson, J. C. Autino and G. Punte, *Acta Crystallogr.*, **B55**, 209 (1999).
88. J. Ellena, A. E. Goeta, J. A. K. Howard and G. Punte, *J. Phys. Chem. A*, **105**, 8696 (2001).
89. A. Volkov, Y. Abramov, P. Coppens and C. Gatti, *Acta Crystallogr.*, **A56**, 332 (2000).
90. A. Volkov, C. Gatti, Y. Abramov and P. Coppens, *Acta Crystallogr.*, **A56**, 252 (2000).
91. K. Platteborze and T. Zeegers-Huyskens, *J. Chim. Phys. Phys.-Chim. Biol.*, **90**, 1667 (1993).
92. T. Ottersen, *Acta Chem. Scand.*, **A31**, 480 (1977).
93. D. J. Williams, *Angew. Chem., Int. Ed. Engl.*, **23**, 690 (1984).
94. A. P. N. Prasad and D. J. Williams, *Introduction to Nonlinear Optical Effects in Molecules and Polymers*, Wiley, New York, 1990; R. Dalven, *Introduction to Applied Solid State Physics*, Plenum Press, New York, 1990.
95. P. D. Southgate and D. S. Hall, *Appl. Phys. Lett.*, **43**, 456 (1971).
96. P. D. Southgate and D. S. Hall, *J. Appl. Phys.*, **43**, 2765 (1972).
97. R. Taylor, O. Kennard and W. Versichel, *J. Am. Chem. Soc.*, **106**, 244 (1984).
98. L. K. Vinson and J. J. Dannenberg, *J. Am. Chem. Soc.*, **111**, 2777 (1989).
99. P. J. Krueger, *Spectrochim. Acta*, **19**, 705 (1963).
100. R. A. Nyquist, *Appl. Spectrosc.*, **47**, 411 (1993).
101. M. Kasai, M. Hirota, Y. Hamada and H. Matsuoka, *Tetrahedron*, **29**, 267 (1973).
102. B. M. Lynch, B. C. Macdonald and J. G. K. Webb, *Tetrahedron*, **24**, 3595 (1968).
103. L. Forlani, *Gazz. Chim. Ital.*, **111**, 159 (1981).
104. I. D. Rae and L. K. Dyall, *Aust. J. Chem.*, **19**, 835 (1966).
105. J. R. Holden, C. Dickinson and C. M. Bock, *J. Phys. Chem.*, **76**, 3597 (1972).
106. L. Forlani, L. P. Battaglia, A. Bonamartini Corradi and G. Pelosi, *J. Cryst. Spectrosc. Res.*, **20**, 499 (1990); L. Forlani, in *Targets in Heterocyclic Systems* (Eds. O. A. Attanasi and D. Spinelli), Vol. 1, Italian Society of Chemistry, Rome, 1997, p. 75.
107. L. Forlani, G. Guastadisegni, L. Raffellini, P. E. Todesco and E. Foresti, *Gazz. Chim. Ital.*, **120**, 493 (1990).
108. J. Majer and V. Kaderabek, *Collect. Czech. Chem. Commun.*, **47**, 1100 (1982).
109. A. L. Llamas-Saiz, C. Foces-Foces and J. Elguero, *J. Mol. Struct.*, **328**, 297 (1994).
110. G. Schroeder, B. Brzeziński, B. Łęska, A. Jarczewski, E. Grech and J. Nowicka-Scheibe, *J. Mol. Struct.*, **354**, 131 (1995).
111. B. Brzeziński, G. Schroeder, E. Grech, Z. Malarski and L. Sobczyk, *J. Mol. Struct.*, **274**, 75 (1992).
112. J. F. Coetzee and G. R. Padmanabham, *J. Am. Chem. Soc.*, **87**, 5005 (1965).
113. B. Brzeziński, G. Schroeder, A. Jarczewski, E. Grech, J. Nowicka-Scheibe, L. Stefaniak and J. Klimkiewicz, *J. Mol. Struct.*, **377**, 149 (1996).
114. A. Awwal and F. Hibbert, *J. Chem. Soc., Perkin Trans. 2*, 152 (1977).
115. E. Grech, J. Nowicka-Scheibe, Z. Olejnik, T. Lis and Z. Pawelka, *J. Chem. Soc., Perkin Trans. 2*, 343 (1996).
116. T. Zeegers-Huyskens, *Spectrochim. Acta*, **23A**, 855 (1967).
117. G. Briegler and H. Delle, *Z. Elektrochem.*, **64**, 347 (1960); P. Huyskens and T. Zeegers-Huyskens, *J. Chim. Phys. Phys.-Chim. Biol.*, **61**, 81 (1964)
118. A. Koffler, *Z. Elektrochem.*, **50**, 200 (1944).
119. Y. Matsunaga and G. Saito, *Bull. Chem. Soc. Jpn.*, **45**, 963 (1972).
120. M. Ilcszszyn, *J. Chem. Soc., Faraday Trans.*, **90**, 1411 (1994).
121. N. N. Vyshinskii, O. S. Morozov, E. I. Solov'eva, B. V. Sul'din and Yu. A. Aleksandrov, *Zh. Obshch. Khim.*, **49**, 2127 (1979).
122. L. K. Dyall, *Spectrochim. Acta*, **25A**, 1423 (1969).
123. L. K. Dyall, *Spectrochim. Acta*, **25A**, 1727 (1969).
124. K. B. Whetsel and J. H. Lady, *J. Phys. Chem.*, **69**, 1596 (1965).
125. K. B. Whetsel and J. H. Lady, *J. Phys. Chem.*, **68**, 1010 (1964).
126. S. Mukherjee, S. R. Palit and S. K. De, *J. Phys. Chem.*, **75**, 2404 (1971).

127. R. West, *J. Am. Chem. Soc.*, **81**, 1614 (1959); W. Beckering, *J. Phys. Chem.*, **65**, 206 (1961); B. Ghosh and S. Basu, *Trans. Faraday Soc.*, **61**, 2097 (1965); M. R. Basilia, E. L. Saier and L. R. Cousins, *J. Am. Chem. Soc.*, **87**, 1665 (1965); Z. Yoshida and E. Ōsawa, *J. Am. Chem. Soc.*, **87**, 1467 (1965); M. Ōki and H. Iwamura, *J. Am. Chem. Soc.*, **89**, 567 (1967).

128. J. H. Lady and K. B. Whetsel, *J. Phys. Chem.*, **71**, 1421 (1967).

129. V. E. Borisenko, G. G. Furin and S. A. Korobeynikova, *Spectrosc. Lett.*, **28**, 715 (1995).

130. V. E. Borisenko, D. S. Kuzmin, A. V. Morev and A. Koll, *J. Mol. Liquids*, **88**, 259 (2000); V. E. Borisenko, G. Y. Blinkova, L. L. Osipova and Y. A. Zavjalova, *J. Mol. Liquids*, **70**, 31 (1996).

131. V. E. Borisenko, S. A. Krekov, A. V. Guzemin and A. Koll, *J. Mol. Struct.*, **646**, 125 (2003).

132. C. Madec, J. Lauransan and P. Saumagne, *J. Phys. Chem.*, **75**, 1157 (1971).

133. V. E. Borisenko, Yu. A. Zavjalova, T. G. Tretjakova, Z. S. Kozlova and A. Koll, *J. Mol. Liquids*, **109**, 125 (2004).

134. A. V. Morev and N. L. Protasova, *J. Appl. Spectrosc.*, **69**, 62 (2002).

135. A. M. Dierkx, P. Huyskens and T. Zeegers-Huyskens, *J. Chim. Phys. Chim-Phys. Biol.*, **61**, 336 (1964).

136. I. Wawer, T. Krysiak and Z. Kęcki, *J. Mol. Struct.*, **326**, 163 (1994).

137. (a) G. S. Denisov, L. A. Kuzina, A. L. Smolyanskii and G. G. Furin, *Z. Prikl. Spektrosk.*, **51**, 476 (1989); *Chem. Abstr.*, **113**, 58411c (1990). (b) G. S. Denisov, L. A. Kuzina, A. O. Miller, A. L. Smolyanskii and G. G. Furin, *Z. Prikl. Spektrosk.*, **51**, 278 (1989); *Chem. Abstr.*, **111**, 204315b (1969).

138. V. E. Borisenko and A. V. Morev, *J. Mol. Struct.*, **322**, 309 (1994).

139. V. E. Borisenko, E. I. Greseva, E. V. Duknova and I. V. Nacheva, *J. Mol. Struct.*, **324**, 199 (1994).

140. V. E. Borisenko, A. V. Morev and A. A. Ponomarev, *Spectrosc. Lett.*, **30**, 107 (1997); V. E. Borisenko, A. V. Morev, I. Faizullin and A. Koll, *J. Mol. Struct.*, **560**, 121 (2001).

141. N. Chen and T. C. Chan, *J. Chem. Soc., Chem. Commun.*, 719 (1997).

142. V. E. Borisenko, A. V. Morev and A. Koll, *J. Mol. Struct.*, **444**, 183 (1998).

143. U. Spoerel and J. Stahal, *J. Mol. Spectrosc.*, **190**, 278 (1998).

144. K. Sakota, N. Yamamoto, K. Ohashi, H. Sekiya, M. Saeki, S. Ishiuchi, M. Sakai and M. Fujii, *Chem. Phys. Lett.*, **341**, 70 (2001).

145. M. Gerhards and C. Unterberg, *Appl. Phys.*, **72**, 273 (2001).

146. S. Mukherjee, *Bull. Chem. Soc. Jpn.*, **60**, 1119 (1987).

147. S. Hamai, *Bull. Chem. Soc. Jpn.*, **60**, 3505 (1987).

148. A. Matsuzaki, S. Nagakura and K. Yoshihara, *Bull. Chem. Soc. Jpn.*, **47**, 1152 (1974).

149. N. Ikeda, T. Okada and N. Mataga, *Bull. Chem. Soc. Jpn.*, **54**, 1025 (1981).

150. L. Giacomelli, R. Cattana, J. Anunziata, J. J. Silber, M. Hedrera, A. Salerno and I. Perillo, *J. Phys. Org. Chem.*, **7**, 162 (1994).

151. J. H. Clark, J. D. Pile, J. M. Miller, S. Paone and S. Y. Tan, *Can. J. Chem.*, **60**, 1815 (1982).

152. I. Wawer, Z. Kęcki and G. S. Denisov, *Spectrosc. Lett.*, **24**, 1363 (1991).

153. M. P. Qureshi, R. K. Varshney and S. B. Singh, *Spectrochim. Acta*, **46A**, 731 (1990).

154. I. Van Bellingen, G. Germain, P. Piret and M. Van Meerssche, *Acta Crystallogr., Sect B*, **27**, 553 (1971).

155. S. C. Wallwork, *Acta Crystallogr.*, **15**, 758 (1962).

156. K. Renuka, T. N. G. Row, B. R. Prasad, C. I. K. Subramanian and S. Bhattacharya, *New J. Chem.*, **19**, 83 (1995).

157. C. V. K. Sharma and G. R. Desiraju, *J. Chem. Soc., Perkin Trans. 2*, 2345 (1994).

158. J. Nishijo, K. Ohno and K. Nishimura, *Chem. Pharm. Bull.*, **10**, 2219 (1982).

159. V. A. Al'fonsov, O. V. Andreeva, G. A. Bakaleinik, D. V. Beskrovnyi, A. T. Gubaidullin, V. E. Kataev, G. I. Kovylyaeva, A. I. Konovalov, M. G. Korochkina, I. A. Litvinov, I. Yu. Strobykina and R. Z. Musin, *Russ. J. Gen. Chem.*, **73**, 1249 (2003).

160. V. A. Al'fonsov, G. A. Bakaleinik, A. T. Gubaidullin, A. T. Kataev, V. E. Kovylyaeva, G. I. Konovalov, A. I. Litvinov, I. Yu. Strobykina, O. V. Andreeva and M. G. Korochkina, *Mendeleev Commun.*, **6**, 227 (1999).

161. C. Bosshard, F. Pan, M. S. Wong, S. Manetta, R. Spreiter, C. Cai, P. Günter and V. Gramlich, *Chem. Phys.*, **245**, 377 (1999).

162. J. J. Creely and R. H. Wade, *Text. Res. J.*, 335 (1978).

163. H. Mahmoudkhani and V. Langer, *J. Mol. Struct.*, **609**, 55 (2002).

164. H. K. Klein, C. Kirschhock and H. Fuess, *J. Phys. Chem.*, **98**, 12345 (1994).
165. Y. Nagasawa, A. P. Yartsen, K. Tominaga, A. E. Johnson and K. Yoshihara, *J. Chem. Phys.*, **101**, 5717 (1994).
166. D. K. Palit, T. Zhang, S. Kumazaki and K. Yoshihara, *J. Phys. Chem. A*, **107**, 10798 (2003).
167. Y. Nagasawa, A. P. Yartsev, K. Tominaga, P. B. Bisht, A. P. Yartsev and K. Tominaga *J. Phys. Chem.*, **99**, 653 (1995).
168. E. W. Castner, D. Kennedy and J. Cave, *J. Phys. Chem. A*, **104**, 2869 (2000).
169. Y. Nagasawa, A. P. Yartsev, K. Tominaga and K. Yoshihara, in *Ultrafast Phenomena IX* (Eds. P. F. Barbara, W. H. Knox, G. A. Mourou and A. H. Zewail), Springer-Verlag, Berlin, 1994.
170. H. Pal, Y. Nagasawa, K. Tominaga and K. Yoshihara, *J. Phys. Chem.*, **100**, 11964 (1996).
171. Y. Nagasawa, A. P. Yartsev, K. Tominaga, A. E. Johnson and K. Yoshihara, *J. Am. Chem. Soc.*, **115**, 7922 (1993).
172. T. Kiyota, M. Yamaji and H. Shizuka, *J. Phys. Chem.*, **100**, 672 (1996).
173. T. Nakanaga and F. Ito, *Chem. Phys. Lett.*, **355**, 109 (2002).
174. J.-G. Jäkel and H. Jones, *Chem. Phys.*, **247**, 321 (1999).
175. P. M. Wojciechowski, W. Zierkiewicz, D. Michalska and P. Hobza, *J. Chem. Phys.*, **118**, 10900 (2003).
176. M. Schäfer and D. W. Pratt, *J. Chem. Phys.*, **115**, 11147 (2001).
177. K. Yamanouchi, H. Watanabe, S. Koda, S. Tsuchiya and K. Kuchitsu, *Chem. Phys. Lett.*, **107**, 209 (1984).
178. K. Yamanouchi, S. Isogai and S. Tsuchiya, *J. Mol. Struct.*, **146**, 349 (1986).
179. R. P. Schmid, P. K. Chowdhury, J. Miyawaki, F. Ito, K. Sugawara, T. Nakanaga, H. Takeo and H. Jones, *Chem. Phys.*, **218**, 291 (1997).
180. N. Solcà and O. Dopfer, *Eur. Phys. J.*, **D20**, 469 (2002).
181. T. Nakanaga, F. Ito, J. Miyawaki, K. Sugawara and H. Takeo, *Chem. Phys. Lett.*, **261**, 414 (1996).
182. T. Nakanaga, K. Chowdhury, F. Ito, K. Sugawara and H. Takeo, *J. Mol. Struct.*, **413–414**, 205 (1997).
183. K. Ohashi, Y. Inokuchi, N. Nishi and H. Sekiya, *Chem. Phys. Lett.*, **357**, 223 (2002).
184. R. N. Pribble and T. S. Zwier, *Science*, **265**, 75 (1994).
185. N. K. Piracha, F. Ito and T. Nakanaga, *Chem. Phys.*, **297**, 133 (2004).
186. P. K. Chowdhury, K. Sugawara, T. Nakanaga and H. Takeo, *Chem. Phys. Lett.*, **285**, 77 (1998).
187. T. Nakanaga, K. Buchhold and F. Ito, *Chem. Phys.*, **277**, 171 (2002).
188. T. Nakanaga, K. Buchhold and F. Ito, *Chem. Phys.*, **288**, 69 (2003).
189. M. F. Hineman, S. K. Kim, E. R. Bernstein and D. F. Kelley, *J. Chem. Phys.*, **96**, 4904 (1992).
190. M. R. Nimlos, M. A. Young, E. R. Bernstein and D. F. Kelley, *J. Chem. Phys.*, **91**, 5268 (1989).
191. N. Solcà and O. Dopfer, *J. Phys. Chem.*, **106**, 7261 (2002).
192. Y. Honkawa, Y. Inokuchi, K. Ohashi, N. Nishi and H. Sekiya, *Chem. Phys. Lett.*, **376**, 244 (2003).
193. T. Nakanaga and F. Ito, *J. Phys. Chem. A*, **103**, 5440 (1999).
194. T. Nakanaga, K. Kawamata and F. Ito, *Chem. Phys. Lett.*, **279**, 309 (1997).
195. T. Nakanaga and F. Ito, *Chem. Phys. Lett.*, **348**, 270 (2001).
196. Y. Inokuchi, K. Ohashi, Y. Honkawa, N. Yamamoto, H. Sekiya and N. Nishi, *J. Phys. Chem.*, **107**, 4230 (2003).
197. Y. Honkawa, Y. Inokuchi, K. Ohashi, N. Nishi and Sekiya, *Chem. Phys. Lett.*, **358**, 419 (2002).
198. P. K. Chowdhury, *J. Phys. Chem.*, **107**, 5692 (2003).
199. P. K. Chowdhury, K. Sugawara, T. Nakanaga and H. Takeo, *J. Mol. Struct.*, **447**, 7 (1998).
200. P. K. Chowdhury, *Chem. Phys. Lett.*, **319**, 501 (2000).
201. T. Nakanaga, K. Sugawara, K. Kawamata and F. Ito, *Chem. Phys. Lett.*, **267**, 491 (1997).
202. P. K. Chowdhury, *J. Phys. Chem. A*, **104**, 7233 (2000).
203. T. Nakanaga and F. Ito, *J. Mol. Struct.*, **649**, 105 (2003).
204. O. Krauss and B. Brutschy, *Chem. Phys. Lett.*, **350**, 427 (2001).
205. K. Kawamata, P. K. Chowdhury, F. Ito, K. Sugawara and T. Nakanaga, *J. Phys. Chem. A*, **102**, 4788 (1998).

206. T. Nakanaga, N. K. Piracha and F. Ito, *J. Phys. Chem. A*, **105**, 4211 (2001).
207. H. Nagai, N. K. Piracha and T. Nakanaga, *Chem. Phys.*, **282**, 75 (2002).
208. Y. Inokuchi, K. Ohashi, Y. Honkawa, H. Sekiya and N. Nishi, *Chem. Phys. Lett.*, **359**, 283 (2002).
209. G. Gustafsson, Y. Cao, G. M. Treacy, F. Klavetter, N. Colaneri and A. J. Heeger, *Nature*, **357**, 477 (1992).
210. P. Colomban, A. Gruger, A. Régis and D. Michel, *J. Chim. Phys.*, **92**, 951 (1995).
211. H. Xia and Q. Wang, *Chem. Mater.*, **14**, 2158 (2002).
212. L. Zhang and M. Wan, *Adv. Funct. Mater.*, **13**, 815 (2003).
213. E. Corradi, S. V. Meille, M. T. Messina, P. Metrangolo and G. Resnati, *Angew. Chem., Int. Ed.*, **39**, 1782 (2000).
214. H. L. Nguyen, P. N. Horton, M. B. Hursthouse, A. C. Legon and D. W. Bruce, *J. Am. Chem. Soc.*, **126**, 16 (2004); P. Metrangolo and G. Resnati, *Chem. Eur. J.*, **7**, 2511 (2001); P. Metrangolo, T. Pilati, G. Resnati and A. Stevenazzi, *Curr. Opin. Coll. & Int. Sci.*, **8**, 215 (2003); R. Bertani, P. Metrangolo, A. Moiana, E. Perez, T. Pilati, G. Resnati, L. Rico-Lattes and A. Sassi, *Adv. Mater.*, **14**, 1197 (2002).
215. P. Metrangolo, H. Neukirch, T. Pilati, G. Resnati and M. Ursini, P 77, *XXIX Convegno Naz. Div. Chimica Organica*, Soc. Chim. Italiana, Potenza (Italy), August 31–September 4 (2004).

CHAPTER **9**

Synthesis of anilines

JOHN F. HARTWIG∗, SHASHANK SHEKHAR, QILONG SHEN and
FABIOLA BARRIOS-LANDEROS

*Department of Chemistry, Yale University, P.O. Box 208107, New Haven, Connecticut
06520 8107, USA*
Fax: 203-432-6144;   e-mail: John.hartwig@yale.edu

∗ Current Address: A410 CLSL, Box 58-6, MC-712, Department of Chemistry, University of
Illinois, 600 South Mathews Av., Urbana, Illinois 61801, USA. Fax: 217-244-8024; e-mail:
jhartwig@uiuc.edu

I. INTRODUCTION

Aromatic amines are found in biologically active natural products, common pharmaceuticals, dyestuffs, materials with conductive and emissive properties, and ligands for transition-metal-catalyzed reactions. For these reasons much effort has been spent for more than a century on methods to prepare aromatic amines. The synthetic methods to obtain these materials range from classical methods, such as nitration and reduction of arenes, direct displacement of the halogens in haloarenes at high temperatures, or copper-mediated chemistry, as well as modern transition-metal-catalyzed processes and improved copper-catalyzed processes. The following sections describe each of these synthetic routes to aromatic amines, including information on the scope and mechanism of most of these routes to anilines and aniline derivatives.

II. UNCATALYZED REACTIONS

A. Direct Nucleophilic Substitution

Anilines can be prepared by direct substitution of a halogenated arene with amine via a nucleophilic aromatic substitution pathway[1,2]. The reactions via this pathway usually require high temperature and/or high pressure to ensure high conversion. Although the reactions occur in the absence of base, reactions in the presence of weak bases, such as alkali hydroxide or carbonate, occur in higher yields. Reactions of electron-poor arenes usually occur in higher yields than reactions of electron-rich arenes (equation 1). Fluoroarenes usually react faster than chloro-, bromo- or iodoarenes[3], although the mechanism of the reaction and the relative activities of these substituents are also affected by the structure of the substrates, the nature of the nucleophiles and the reaction conditions.

$$Y-\text{Ar}-X \;+\; HNR^1R^2 \;\xrightarrow{\;S_N\text{Ar}\;}\; Y-\text{Ar}-NR^1R^2 \tag{1}$$

$$X = F, Cl, Br, I; \; R^1, R^2 = H, \text{alkyl, aryl}$$
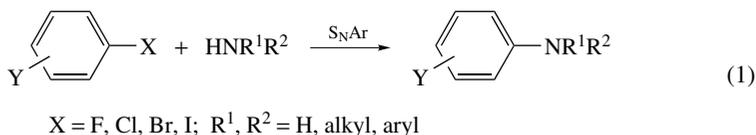
Treatment of chlorobenzene with aqueous ammonia for 8 h at 300 °C generated aniline in 30% yield[3]. Phenol and diphenyl ether were the major side products. The uncatalyzed reactions of o- and p-chloronitrobenzene with ammonia occurred at 200 °C[4]. However, m-chloronitrobenzene did not react under these conditions, presumably due to the weaker stabilization of the charged intermediate. Interestingly, Wohl also found that in the presence of iodide ion, alcoholic ammonia reacts rapidly with o- and p-chloronitrobenzene at 100 °C[5]. 1-Chloro-2,4-dinitrobenzene reacted with alcoholic ammonia even at room temperature.

Most primary and secondary amines replace halogen more rapidly than ammonia[6]. Condensation of amines with 2,4-dinitrophenyl halides was used to prepare derivatives for

identification of unknown compounds many years ago. Because 1-fluoro-2,4-dinitrobenzene reacts with amines at room temperature, this haloarene is used as a 'tagging agent' for free amino groups in proteins.

Generally, reactions with anilines are slower than those with aliphatic amines, in part because anilines are less nucleophilic[7]. Condensation of aromatic amines with unactivated aryl halides usually requires the presence of copper catalysts. Reactions of diarylamines, such as diphenylamine and carbazole, are even slower.

B. Nucleophilic Substitution Through Aryne Intermediates[8,9]

Commercially available alkali amides can also be used in nucleophilic substitution reactions to form anilines, although the reaction mechanisms differ greatly from those of direct nucleophilic substitution reactions conducted with weak bases. The reactions generally occur rapidly at room temperature, and even at temperatures as low as $-33\,^{\circ}$C in the case of amination in liquid ammonia. A mixture of products often results, but the entering amine is rarely found more than one carbon atom away from the leaving halogen (equation 2).

$$
\begin{array}{c}
\text{Y}\!-\!\!\!\text{C}_6\text{H}_4\!-\!\text{X} + \text{MNR}^1\text{R}^2 \longrightarrow \left[\begin{array}{c} \text{aryne} \end{array} \right] \longrightarrow \text{Y}\!-\!\!\!\text{C}_6\text{H}_4\!-\!\text{NR}^1\text{R}^2
\end{array}
\tag{2}
$$

X = F, Cl, Br, I, OTf

R^1, R^2 = H, alkyl, aryl

M = Li, Na, K
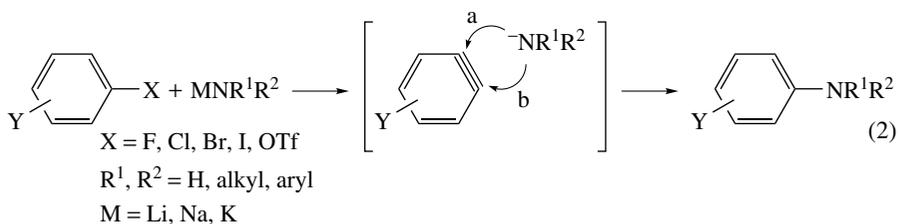
It is believed that such reactions proceed through aryne intermediates. These aryne intermediates have been confirmed by reactions of an isotopically labeled chlorobenzene with potassium amide in liquid ammonia[10,11]. Additionally, aryne intermediates have been observed in flash-photolysis experiments and in mass spectrometry[12] and trapped as a stable nickel complex (Figure 1), which was characterized by ^{1}H NMR spectroscopy[13].

In contrast to the scope of the reactions with weak bases, the scope of reactions with strong bases is not limited to haloarenes with strong electron-withdrawing groups. In the presence of strong bases, substrates without electron-withdrawing groups undergo nucleophilic substitution reactions through aryne intermediates. The regioisomer formed through pathway a or b in equation 2 can be predicted based on consideration of the leaving group and the counter cation of the base: (1) for a given metal, the rate for generation of an aryne follows the order Br > Cl > F; and (2) for a given halogen[14], the ease of elimination of metal halide follows the order Na > Li > MgBr[15].

The degree of rearrangement in the amination of substituted halobenzenes with alkali amides is influenced by the position of the substituent, relative to the halogen. Whereas
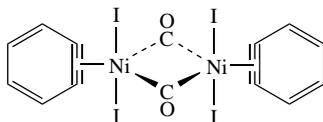
FIGURE 1. Proposed structure of a Ni–benzyne complex

ortho- and *para*-substituted aryl halides can give rise to only 2- and 3-substituted arynes, respectively, *meta*-substituted aryl halides can give rise to either or both isomers. The direction of elimination for a *meta*-substituted halide is determined by which hydrogen (i.e. at 3- or 4-) is more acidic, which in turn is governed largely by the inductive effects of the substituents. In the case of electron-withdrawing substituents, the acidity order is *o* > *m* > *p*; this order is reversed in the case of electron-donating groups[16]. The direction of addition may be predicted by considering the stabilization of the negative charge from the inductive effect of the substituted group[17].

Many papers have been published on the reactions that occur generally with low to moderate yields of alkali amides with aryl halides in liquid ammonia[8]. For example, treatment of *p*-bromoanisole with KNH_2 in liquid ammonia generated a 1:1 ratio of *m*- and *p*-methoxyaniline, in a 31% yield[17]. Perchlorobenzene has been shown to react vigorously with amide ion in liquid ammonia. The major product obtained is a triaminobenzene together with chloride ion.

Reactions of alkali derivatives of aliphatic primary and secondary amines with aryl halides occur in ethereal solution at room temperature, or at reflux[18]. In many cases, free secondary amines, which serve as a proton source, must be added to suppress the secondary reactions. For example, *p*-chlorotoluene reacts with lithium piperidide in boiling ether in the presence of free piperidine to produce a 55:45 mixture of *m*- and *p*-*N*,*N*-disubstituted toluidines in 73% yield. Reactions of *p*-bromo- or fluorotoluene gave a similar product ratio[19]. More recently, Beller and coworkers reported the reactions of aryl chlorides with secondary amines and primary amines. The reactions, carried out at 135 °C using *t*-BuOK instead of lithium alkyl or lithium amide as the base, gave fairly high yield with excellent selectivities[20].

Reactions with alkali derivatives of arylamines are more difficult than those of aliphatic amines. The reactions are generally conducted in a refluxing amine solvent or, in some cases, at room temperature. For example, *p*-bromo- and *p*-iodotoluene were treated with potassium anilide in refluxing aniline to give a 50:50 ratio of isomers in moderate yield[21].

Arynes can also be generated from readily available aryl triflates, and then further reacted with the free amine to form anilines. Wickham and coworkers reported the reaction of substituted phenyl triflates with 2–3 equivalents of lithium diisopropylamide (LDA) in the presence of excess diisopropylamine to generate the corresponding substituted diisopropylaniline in good to excellent yields with a ratio of regioisomers that is similar to that from reaction of the corresponding haloarenes. Reactions were run in DME or THF, even at temperatures as low as −78 °C[22]. If the halogen and triflate functional groups are present in the same arene, elimination of the triflate is faster than elimination of the halogen[23].

Intramolecular aminations of the benzyne intermediates are also possible, although the yields are lower than those of the intermolecular aminations. For example, *N*-methyltetra-hydroquinoline was formed from *N*-methyl-3-(*m*-chlorophenyl)propylamine in 49% yield upon reaction with the combination of phenyl lithium and lithium diethylamide. The yield from the *ortho*-chloro analog was much lower, likely because the formation of the benzyne intermediates is hindered by steric effects in *o*-chloro compounds[24].

C. Nitroarene Reduction

An amino group may be introduced into an aromatic compound by nitration, followed by reduction[25]. Most aromatic compounds, whether of high or low reactivity, undergo nitration with one of a wide variety of nitrating agents[26–28]. The reduction of the nitro compounds to amines can also be effected by a variety of methods (equation 3). This

reaction pathway was the most important method for the preparation of aniline before the introduction of the metal-catalyzed amination reactions.

$$\text{(Y—arene)} \xrightarrow{[NO_2{}^+]} \text{(Y—arene—NO}_2) \xrightarrow{\text{reduction}} \text{(Y—arene—NH}_2) \qquad (3)$$
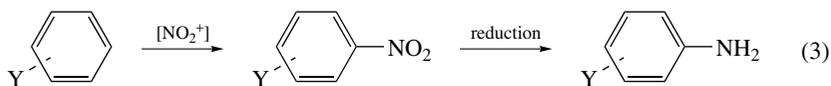
1. Nitration of arenes

The most common reagent for nitration of benzene, simple alkylbenzenes and other less reactive compounds is a mixture of concentrated nitric and sulfuric acids. However, nitration of activated substrates, such as aniline, phenol or pyrrole, occurs with nitric acid alone or in water, acetic acid or acetic anhydride. Concentrated sulfuric acid can oxidize these substrates. A description of the use of other nitrating reagents is outside of the scope of this review, but can be found in Smith and March's *Advanced Organic Chemistry*[29] or Larock's *Comprehensive Organic Transformations*[30].

The nitration mechanism is believed to proceed through an electrophilic aromatic substitution pathway. First, the nitronium ion $NO_2{}^+$ is generated from the nitrating agents, followed by attack of the nitronium ion on the arene to form a cationic arenium ion species. Finally, the conjugate base abstracts the proton from the cationic intermediate to form the final product. The direction of nitration can be predicted by considering the stabilization of the cationic intermediate resulting in the nitronium ion attack. Usually, electron-rich arenes will react at the *ortho* or *para* position while electron-poor arenes will react at the *meta* position. Since the nitro group is deactivating, it is usually easy to stop the reaction after the first nitration. However, the introduction of the second or the third nitro group is possible, particularly when an electron-rich substituent is also present.

2. Reduction of nitroarenes

Many reducing agents have been introduced to reduce aromatic nitro compounds. The most commonly used reducing agents are Zn, Sn or Fe in acid and catalytic hydrogenation[25, 30, 31]. Nearly all nitro compounds can be reduced effectively with tin or iron and hydrochloric acid. Selective reduction of one of two or more nitro groups present in dinitro or polynitro compounds is not possible with iron solutions in HCl. However, the selective reduction of polynitro compounds can be accomplished with stoichiometric amounts of stannous chloride. Nitro compounds containing functional groups that are unstable in acid solution, for example ketones, can be reduced with zinc and hydrochloric acid in alcoholic solution.

The gas-phase catalytic reduction of nitrobenzene by hydrogen gas is a basic industrial method for aniline manufacture[32]. Usually the nitro compounds are smoothly converted to the corresponding amino compounds when their vapors, mixed with hydrogen, are passed over finely divided metals, such as copper or nickel, heated to $200-400\,°C$. Copper is the most effective catalyst, because it resists poisoning and does not affect the aromatic ring structure. The high temperature required for reaction, however, leads to breakdown of the newly created aniline, and hence a decrease in overall aniline yields. Milder reaction conditions can be achieved by reducing nitrobenzene with hydrogen in the presence of solvents. Thus, the liquid-phase reduction provides aniline in a higher yield. The selective reduction of nitro groups in aromatic compounds with hydrogen can be difficult if other functional groups attached to the aromatic ring are reduced faster than the nitro group. Such substituents include carbonyl, cyano, chloro and alkenyl groups.

The deoxygenation of nitroaromatics with CO as reducing agent in the presence of water is an alternative to hydrogenation (equation 4)[33, 34]. The reaction can be run efficiently
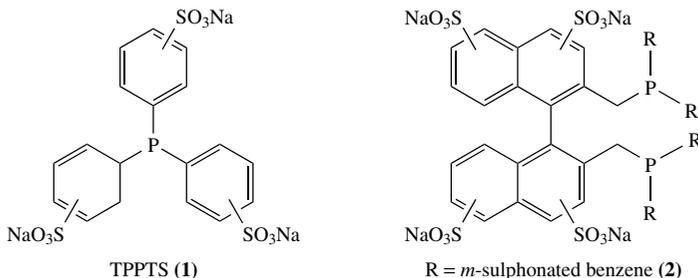
FIGURE 2. Two ligands used for the aqueous reduction of nitrobenzene

using water-soluble ligands such as TPPTS (**1**) and BINAS (**2**) (Figure 2) in a two-phase system[35]. Among dozens of catalyst systems, $Rh_6(CO)_{16}$/TMEDA exhibited a highly chemoselective reduction of aromatic nitro group to the aromatic amino group, even in the presence of ketones, halogens or various substituted double bonds[36].

$$Y = COMe, CN, Cl, C=CH_2 \qquad 50-85\% \qquad (4)$$
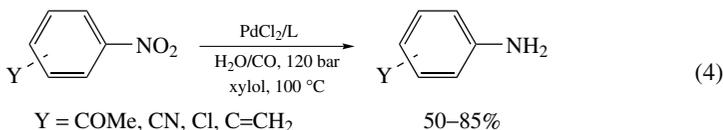
D. Diarylamine from Reaction of Nitrobenzene with Grignard Reagents

The reaction of nitrobenzene with excess aryl magnesium bromides to form diarylamines has been known for many years[37], and the general mechanism of the reaction has been extensively studied. The first step of the reaction is the formation of the nitrosobenzene through 1,2-addition of the Grignard reagent to nitrobenzene[38]. The nitrosobenzene then reacts with another equivalent of Grignard reagent, followed by reduction to generate the desired diarylamine. The possible intermediates (i.e. N,N-diarylhydroxyamines) can be isolated but are sensitive to heat, air, acids and bases. The reaction is limited to aryl magnesium reagents. When alkyl Grignard reagents were used, attack of the aromatic ring rather than the nitro group was observed[39].
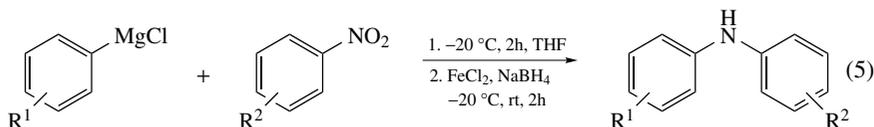
More recently, Sapountzis and Knochel reported a general method for the preparation of polyfunctional diarylamines with excellent yields via the addition of functionalized aryl magnesium compounds to nitroarenes (equation 5)[40]. The functionalized organomagnesium compounds were prepared by a bromine–or iodine–magnesium exchange reaction, a procedure developed by the same group. This reaction can be applied to many functionalized magnesium compounds bearing ester, cyano, methoxy or iodine substituents. Moreover, the nitroarene can have either an electron-poor (e.g. CN, CO_2Et) or electron-rich substituent (e.g. OMe). A drawback of this method is the requirement for two equivalents of Grignard reagent because one equivalent of ArMgX is consumed in the reduction of nitrobenzene to an intermediate arylnitroso species. However, the need to use two equivalents of Grignard reagent has been overcome by conducting the related

addition of aryl Grignard reagents to arylazo tosylates instead of nitrobenzene[41]. Again, excellent functional group tolerance has been observed. Interestingly, by employing the arylazo tosylate pathway, an alkyl magnesium bromide can be used to form a secondary amine with one aryl group and one alkyl group.

E. Miscellaneous

Johnston and coworkers reported a base-free aryl amination method based on radical additions to azomethines through nonconventional addition pathways (equation 6)[42, 43]. By this route, the aryl radical adds to nitrogen, rather than to the carbon of the ketimines. For example, the ketimine prepared from *o*-bromophenethylamine and acetophenone was subjected to tributylstannane and the radical initiator AIBN to give the corresponding indoline in 87% yield. The only side product observed was the directly reduced compound. The fact that only the intramolecular radical addition can afford the high yield limited its application in synthesis of other arylamines.

$$R, R^1 = H, \text{ alkyl, aryl}$$
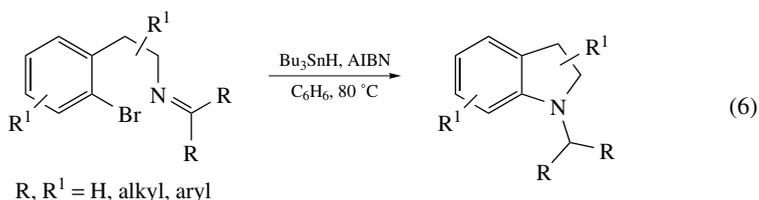
Beller and coworkers recently reported a new strategy for the synthesis of poly-substituted anilines based on a three-component-coupling reaction and a domino deprotection/aromatization reaction (equation 7)[44]. A mixture of *O*-benzyl carbamate, *p*-toluene-sulfonic acid, aldehyde, Ac$_2$O and dienophile in *N*-methylpyrrolidone was allowed to react for 24 h at 120 °C, followed by Pd/C catalyzed dehydrogenation in triglyme at 140 °C. A variety of tri-, tetra- and penta-substituted anilines were efficiently created by this domino process.
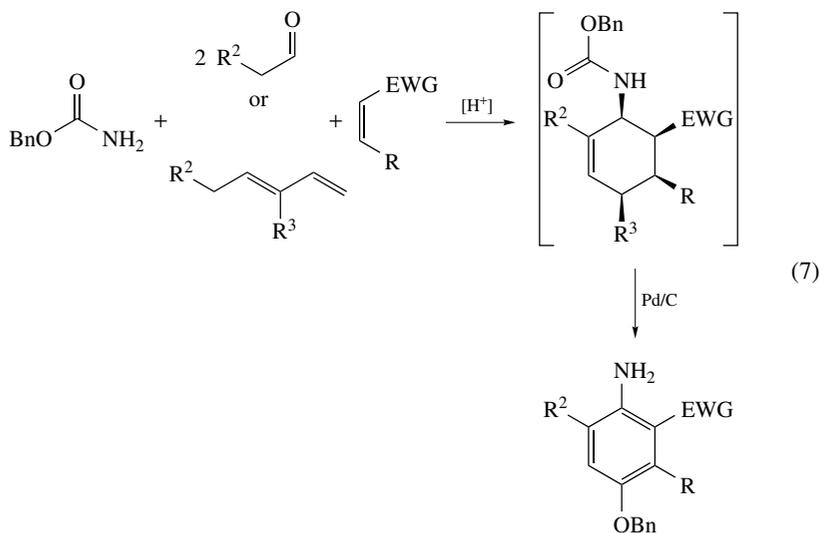
III. PALLADIUM-CATALYZED METHODS

A. Scope of the Palladium-catalyzed Amination

1. Reactions of secondary amines

a. Reactions of secondary alkylamines. This section covers the amination by secondary alkylamines, defined here as amines containing two alkyl groups or one alkyl and one aryl group bound to nitrogen. Specifically, we discuss reactions with aryl bromides, aryl chlorides, aryl triflates and aryl tosylates.

i. Reactions with aryl bromides. The reactions of secondary amines with aryl bromides along with the reaction of primary amines with activated aryl bromides in the presence of stoichiometric amounts of base and a palladium catalyst containing $P(tol-o)_3$ **3** (Figure 3) as ligand were the first aminations of aryl halides without a main-group amido reagent that occurred with useful reaction scope[45, 46]. However, as early as in 1986, several examples of the amination of activated aryl chlorides with electronically poor aryl amines in the presence of $(Ph_3P)_2Pd(Ar)(I)$ as catalyst were reported by Yagupol'skii and coworkers[47]. These reactions produced polynitro and poly(trifluoromethylsulfonyl)-substituted diphenylamines. With a combination of a palladium precursor and $P(tol-o)_3$ as ligand, dialkylanilines form from either cyclic or acyclic secondary amines at 80 °C in aromatic or ether solvents (equation 8). Reactions of cyclic secondary amines occurred in significantly higher yields with some aryl halides. Reactions using *tert*-butoxide as base occurred in higher yields than those with silylamide bases. Sodium counterion was important; reactions conducted with lithium *t*-butoxide gave little amine, and reactions conducted with potassium *t*-butoxide occurred in low yields and generated dark-colored reaction solutions[45].

$$X = o\text{-}, m\text{-}, \text{ or } p\text{-alkyl, phenacyl, amino, alkoxy}$$
$$\text{base} = t\text{-BuONa, or } LiN(SiMe_3)_2$$
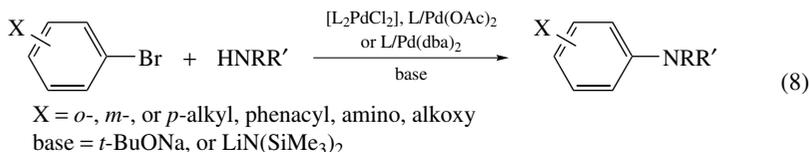
A second development in the formation of dialkylanilines was the use of chelating phosphines. The groups of Hartwig and Buchwald concurrently reported catalysts containing DPPF **4** and BINAP **5** (Figure 3) for the amination chemistry[48, 49]. These ligands are also suitable for some couplings with secondary alkyl amines. In some cases, turnover numbers were improved over the original system for the reactions of secondary amines with aryl bromides[49], but the improvement in yield for reactions of secondary amines
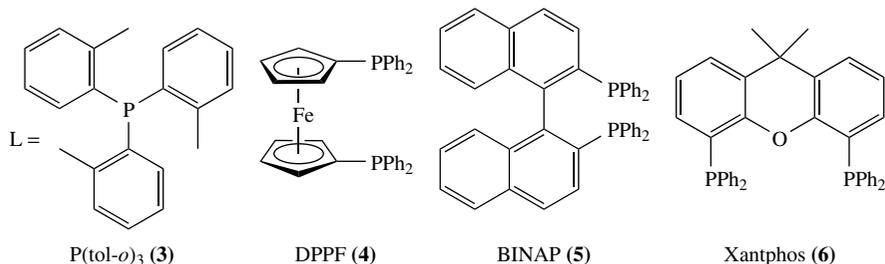
FIGURE 3. Ligands used for the reaction of acyclic secondary amines with aryl halides

over that observed with the original catalyst system was modest. Moreover, the reactions of secondary amines using catalysts derived from BINAP and DPPF typically require higher catalyst loads and are less efficient than those developed subsequently containing *tert*-butylmonophosphines. However, catalysts derived from BINAP and DPPF did allow for reactions of secondary alkylamines with aryl iodides. Even after screening a range of reaction conditions (e.g. variations in temperature and reactant concentrations), the original system with P(tol-o)$_3$ as ligand was relatively ineffective for aminations of aryl iodides[50]. The amination of heteroaryl halides was also improved using catalysts containing BINAP[51] or Xantphos **6**, a ligand with large bite angle[52, 53], but high loading of catalyst was required.

$$73\% \text{ conversion}$$
$$88\% \text{ selectivity}$$
$$100\% \text{ conversion with } 0.02 \text{ mol\%}$$

(9)
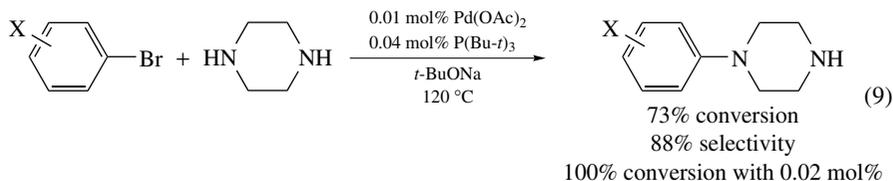
A remarkable advance was reported by Nishiyama and coworkers, which involved the use of P(Bu-t)$_3$ for the amination of cyclic secondary amines with high turnovers (equation 9)[54, 55]. With this simple, commercially available ligand, they obtained roughly 7,000 turnover numbers for the amination of aryl bromides with piperazine at high temperatures. Little cross-coupling with this ligand had been reported previously, and this paper preceded papers describing the use of P(Bu-t)$_3$ in C−C bond-forming cross-coupling chemistry[56−58].

(10)
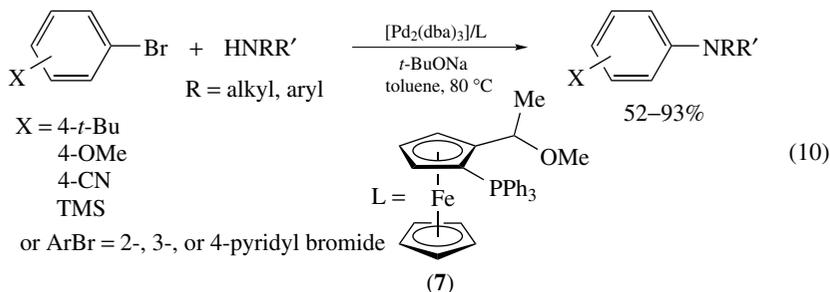
The solution to the problem of finding catalysts for a general reaction of acyclic secondary amines with aryl halides began with the use of Kumada's phosphinoether ligand **7** (equation 10)[59]. With palladium catalysts bearing Kumada's ligand, high yields were observed for this type of amination reaction. Results with this ligand led Buchwald's group, Guram at Symyx, and more recently Singer at Pfizer to prepare more accessible ligands with N and O donor atoms accompanying the phosphine. Additionally, biaryl-based P,N ligands containing alkyl substituents at phosphorus **8** (Figure 4) provided an efficient catalyst for this class of reaction[60]. Along with the work mentioned previously, Guram's group prepared diphenylphosphino and dicyclohexylphosphinoether ligands **9a** and **9b** (Figure 4) with phenyl backbones. These ligands are readily prepared in two steps from inexpensive 2-bromoacetophenone and provide high yields for reactions of cyclic and acyclic secondary amines[61, 62]. Similarly, Singer and coworkers prepared di-i-propylphosphino and di-t-butylphosphinopyrazole ligands **10a** and **10b** (Figure 4)

with phenyl backbones from phenylhydrazine[63]. These ligands were also found to have similar activity to ligands **8** (Figure 4) for reactions of cyclic secondary amines.

Two other groups investigated P,N ligands for amination chemistry with secondary amines. Uemura and coworkers have prepared ligands similar to those of Kumada, but based on arene chromium complexes rather than ferrocenes[64]. Catalysts containing ligand **11** (Figure 4) provide good yields for some aminations with dialkyl amines. For example, reactions of unactivated aryl halides with diethylamine, *N*-ethylaniline or cyclohexyl ethylamine occurred in yields ranging from 73–90%. Arques and coworkers prepared a P,N ligand with an imine nitrogen donor and reported carrying out a single amination reaction run at 160 °C[65].

Although the P,N and P,O ligands structures and potential hemilability of these ligands were part of the design and selection of these ligands, the nitrogen substituent proved to detract rather than enhance the catalytic performance of palladium complexes of the P,N ligands in many cases. Thus, their desamino analogs dialkylphosphino-2-biphenyl ligands **12** and **13** (Figure 5) generated more active catalysts. For example, using 1–5% of the
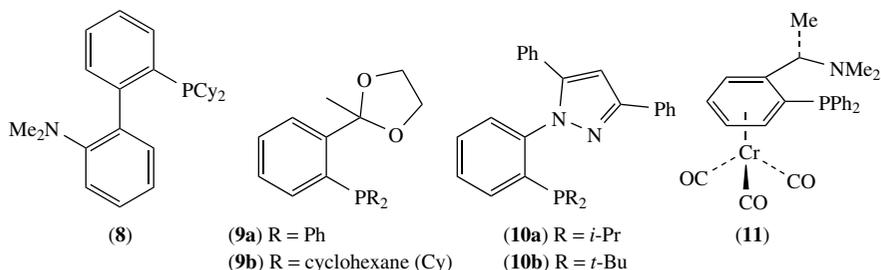
FIGURE 4. Ligands created for the reaction of acyclic secondary amines with aryl halides following the success of Kumada's ligand in catalyzing that reaction, as shown in equation 5
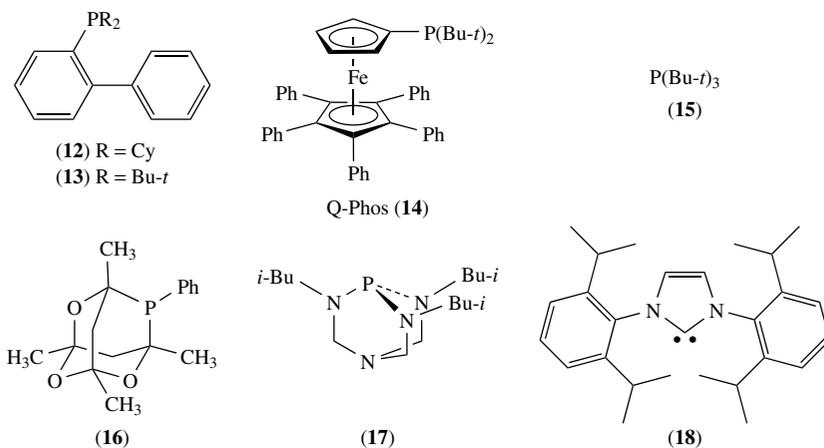
FIGURE 5. Sterically bulky, electronically rich, monodentate alkylphosphines and a carbene for a general reaction of acyclic secondary amines with aryl halides

dicyclohexylphosphino-2-biphenyl and di-*t*-butylphosphino-2-biphenyl ligands allows for room temperature amination of aryl bromides with cyclic and acyclic secondary alkylamines (equation 11). Reactions at 80 °C were generally found most suitable for catalyst loadings of 0.5 mol%[66].

$$R' \overset{Br}{\underset{}{\bigcirc}} + \text{HNRR}' \xrightarrow[\text{t-BuONa, toluene, rt}]{\text{cat. Pd}_2(\text{dba})_3/\text{L}} R' \overset{NRR'}{\underset{}{\bigcirc}} \qquad (11)$$
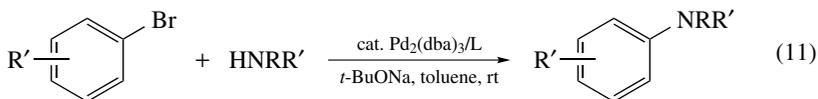
The monophosphine ligand $(\text{Ph}_5\text{Fc})\text{P}(\text{Bu-}t)_2$ (Q-phos) **14** (Figure 5) was formed during the coupling of phenoxide with unactivated aryl halides[67]. This air-stable ligand has a ferrocenyl backbone and forms a highly active palladium catalyst for amination of aryl bromides with a variety of cyclic and acyclic dialkylamines. These reactions proceed with good to excellent yields at 0.05–1% catalytic loading level and 100 °C, though poorer yields have been observed with sterically hindered *ortho*-substituted aryl bromides.

The Tosoh company described the arylation of piperazine using excess of the ligand $\text{P}(\text{Bu-}t)_3$ **15** complexed with Pd(0)[54,55]. During kinetic studies of the same reaction, Hartwig and coworkers discovered that the arylation reaction occurred under much milder conditions when using isolated Pd(0) complexes as catalyst, and even milder conditions when using a 1:1 ratio of ligand to Pd(dba)$_2$. With this catalyst system containing commercially available components, the amination of aryl bromides with cyclic and acyclic secondary alkylamines was conducted at room temperature in quantitative yields (equation 12)[68]. The same reaction can also be conducted in water using sodium hydroxide or potassium hydroxide as the base with a catalytic amount of cetyltrimethylammonium bromide as phase-transfer agent in the presence of 1–2 mol% $\text{Pd}[\text{P}(\text{Bu-}t)_3]_2$[69]. Faster rates still were achieved through the use of a now commercially available Pd(I) dimer [PdBrL, where L = $\text{P}(1\text{-Ad})(\text{Bu-}t)_2$, $\text{P}(\text{Bu-}t)_3$]. For example, using this catalytic complex aminations of aryl bromides with dialkyl amines ran to completion within 15 minutes[70,71].

$$X \overset{}{\underset{}{\bigcirc}} -\text{Br} + \text{HN} \xrightarrow[\text{t-BuONa, rt}]{\substack{1 \text{ mol\% Pd}_n(\text{dba})_m \\ 0.8 \text{ mol\% P}(\text{Bu-}t)_3}} X \overset{}{\underset{}{\bigcirc}} -\text{N} \qquad (12)$$

$$95\%-97\%$$
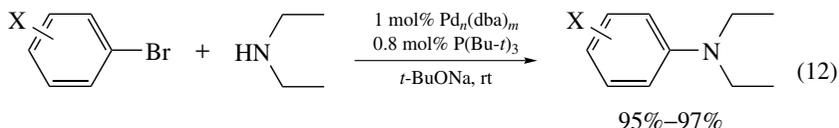
Two other electron-rich, sterically hindered, monodentate phosphine ligands have been prepared and investigated for amination chemistry with cyclic and acyclic amines. Capretta and coworkers prepared a crystalline, air-stable phenyl-phospha-adamantane ligand **16** (Figure 5). Catalysts containing this ligand provided excellent yields for the amination of a variety of aryl bromides with cyclic and acyclic amines[72]. Verkade and coworkers prepared a bicyclic triaminophosphine $\text{P}(i\text{-BuNCH}_2\text{CH}_2)_3\text{N}$ ligand **17** (Figure 5), reasoning that the two planar nitrogens in tris(dialkylamino)phosphines were capable of donating electron density to phosphorus via their unhybridized electron pairs. Further, they reasoned that the basicity of the phosphine would be significantly enhanced by rendering the backbone of the triaminophosphine rigid in a bicyclic framework, and that electronic and steric influences could be readily tailored by introducing suitable organic substituents at each PN$_3$ moiety. Results showed that the combination of Pd(OAc)$_2$, and $\text{P}(i\text{-BuNCH}_2\text{CH}_2)_3\text{N}$ provided similar yields for the amination of aryl bromides with cyclic dialkylamines as reaction with Pd/BINAP and Pd/(*o*-biphenyl)PCy$_2$, but lower yields with acyclic dialkylamines[73,74].

The similarity in steric and electronic properties between the trialkylphosphines and nucleophilic carbenes inspired Nolan and coworkers to employ bulky, electron-donating

carbenes **18** (Figure 5) as ancillary ligands in amination reactions. Reactions of aryl bromides with secondary cyclic and acyclic amines provided high yields at room temperature, but required greater catalyst loading to obtain similar results to those run with the same catalyst and P(Bu-t)$_3$ as the ancillary ligands[75].

ii. Reactions with activated aryl chlorides. The amination of aryl chlorides is significantly more difficult than the amination of aryl bromides because of the decreased reactivity of chloroarenes[76]. The low cost of the aryl chlorides, however, makes them attractive substrates for mild coupling chemistry.

In general, highly activated aryl chlorides (e.g. 4-chlorobenzonitrile or 4-chlorobenzophenone) react similarly to bromobenzene in the oxidative addition step. Thus the standard arylphosphine ligands are suitable for palladium-catalyzed chemistry with these substrates[77].

iii. Reactions with unactivated aryl chlorides. Typically, unactivated aryl chlorides react with amines in palladium-catalyzed reactions using third-generation electron-rich, sterically hindered monophosphines or carbenes as ligands (equation 13). Reddy and Tanaka first employed PCy$_3$ (Cy = cyclohexyl) as the ligand and reported good yields in a few select cases, though the catalyst containing this ligand was not suitable for reactions of most amines[78]. Hamann and Hartwig prepared DtBPF (1,1-bis-di-t-butylphosphinoferrocene) **19** (Figure 6), a t-butyl analog of DPPF, and results with this ligand demonstrated that sterically hindered alkylphosphines were particularly well suited for the amination of aryl bromides and that palladium-catalyzed aminations of aryl chlorides conducted with DtBPF as the ligand occurred at more moderate temperatures than had been used for previous coupling of chloroarenes[79].

Using ligand **8** shown in Figure 4, Buchwald and coworkers reported the amination of unactivated aryl chlorides with secondary amines at temperatures as low as 70–80 °C and the amination of highly activated aryl chlorides at room temperature. Again, with their desamino analogs, dialkylphosphino-2-biphenyl ligands **12** and **13** (Figure 5) generated greater catalytic activity allowing for room-temperature amination of aryl chlorides with cyclic and acyclic secondary alkylamines. However, reactions at 100–110 °C were generally the most suitable for catalyst loading of 0.5 mol%. A limited number of substrate combinations were shown to react with even low catalyst loadings (0.05 mol%)[66]. Although these ligands generate highly reactive catalysts, their synthesis is multi-step in some cases.

Hoping to retain the reactivity but decrease the complexity of the ligand synthesis, Beller and coworkers developed *N*-substituted heteroarylphosphines **20** (Figure 6), an

(**19**)   (**20**)   (**21**)
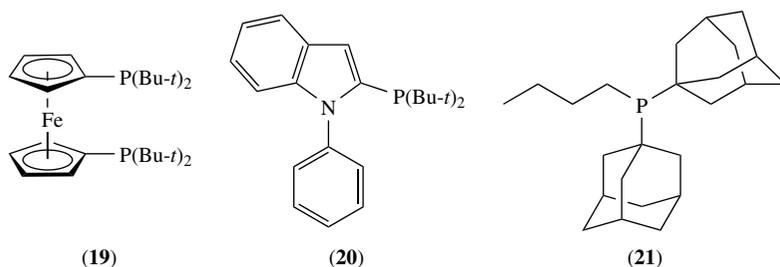
FIGURE 6. Ligands synthesized for amination of unactivated aryl chlorides besides the ligands in Figure 5

analogue to ligands **12** and **13** in a simple two-step process: copper-catalyzed *N*-arylation followed by selective *ortho*-metallation of the corresponding indole and quenching of the resulting anion with R_2PCl. High yields for amination of aryl chlorides were obtained at 120 °C using 0.5 mol% loading of catalyst generated from this ligand. By increasing the ligand concentration (L:Pd = 1:1) and by raising the temperature to 140 °C, high turnover numbers (TON = 8000 based on palladium) for the reaction of 3-chlorotoluene with *N*-methylaniline were obtained[80, 81].

$$X{-}C_6H_4{-}Cl \;+\; HN\!\begin{array}{c}R\\R\end{array} \xrightarrow[\substack{t\text{-BuONa}\\70\,°C}]{\substack{1\text{--}4\ \text{mol\%}\ Pd_n(dba)_m\\L}} X{-}C_6H_4{-}N\!\begin{array}{c}R\\R\end{array} \quad (13)$$

L = **8, 12–20**
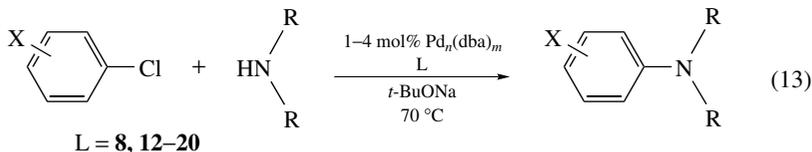
Palladium complexes containing $(Ph_5Fc)P(Bu\text{-}t)_2$ (Q-phos) **14** with a ferrocenyl backbone (Figure 5) were shown to be remarkably general for the amination of aryl chlorides with secondary amines using 0.5–1 mol% catalyst at 100 °C. For example, turnovers of roughly 1000 were also observed for unactivated chlorides with morpholine[67]. Verkade's bicyclic triaminophosphine $P(i\text{-}BuNCH_2CH_2)_3N$ ligand **16** (Figure 5) is also efficient for the amination of aryl chlorides with secondary cyclic amines, although higher loadings (4.0 mol%) were required under similar reaction conditions to achieve similar turnover numbers. Secondary acyclic amines reacted in poor yields[82, 83].

As with aryl bromides, the simple catalyst system of $Pd(dba)_2$ and $P(Bu\text{-}t)_3$ in a 1:1 ratio allowed for the amination of unactivated aryl chlorides with cyclic or acyclic secondary amines (equation 7). Hartwig and coworkers found similar yields for this reaction carried out at 70 °C using 1–5 mol% of catalyst, or 100–110 °C using catalyst loadings that are an order of magnitude lower[68]. The reactions of activated aryl chlorides using this catalyst system occurred at room temperature. The isolated palladium complex $Pd[P(Bu\text{-}t)_3]_2$ was also found to catalyze the amination of unactivated or activated aryl chloride with cyclic or acyclic secondary amines in water using sodium hydroxide or potassium hydroxide as the base with a catalytic amount of cetyltrimethylammonium bromide as phase-transfer agent[69]. Catalysts containing Beller's di(1-adamantyl)-*n*-butylphosphine ligand **21** (Figure 6) were less efficient for amination of aryl chloride with cyclic or acyclic secondary amines compared with the catalyst containing $P(Bu\text{-}t)_3$[80].

The dimeric palladium(I) complex $[\{PdBrL\}_2]$ (L = P(1-Ad)(Bu-*t*)$_2$, P(Bu-*t*)$_3$) catalyzed reactions of aryl chlorides under mild conditions. For example, the amination of aryl chlorides with cyclic or acyclic amines ran to completion *at room temperature within 15 minutes*[70].

Sterically hindered carbenes (**22–26**), discussed previously, are also suitable for amination of aryl chlorides. Complexes of the *N*-alkyl carbene **22** catalyze the coupling of aryl chlorides with amines, but they are less active than the complexes generated from the hindered *N*-aryl carbenes. The most hindered *N*-aryl carbenes **23** and **24** are more reactive than the less hindered **25** and **26**. Nolan and coworkers reported the use of the 2,6-diisopropyl imidazolium system **23** (Figure 7), which contains an unsaturated backbone, for the reaction of aryl chlorides with a variety of amines at 100 °C[75, 84, 85]. Nolan and coworkers also reported the use of carbenes **25–26** as ligands for the amination of aryl chlorides, but the temperature required for these reactions is higher than those typically used with $P(Bu\text{-}t)_3$ or the 2-biphenyl di-*t*-butylphosphines ligands. Hartwig and coworkers showed that using the carbene precursor **24** (Figure 7) with 2,6-diisopropylphenyl groups and a saturated backbone generated complexes that catalyzed the reactions of aryl

Caddick/Cloke (**22**)   IPr/Nolan (**23**)   SIPr/Hartwig (**24**)   IMes/Nolan (**25**) SIMes/Nolan (**26**)

[Pd(IPr)Cl₂]₂ (**27**)   (IPr)Pd(allyl)(Cl) (**28**)   (**29**)

[(IPr)Pd(NQ)]₂ (**30**)
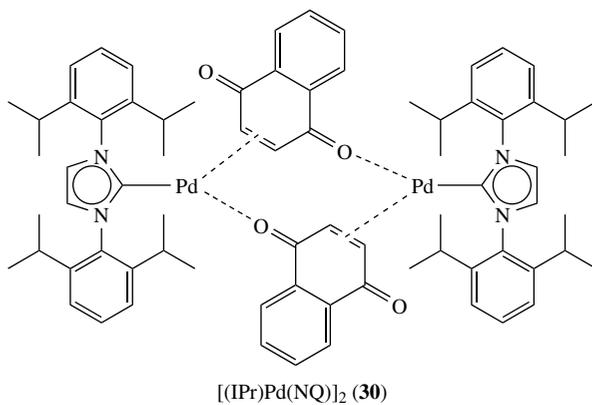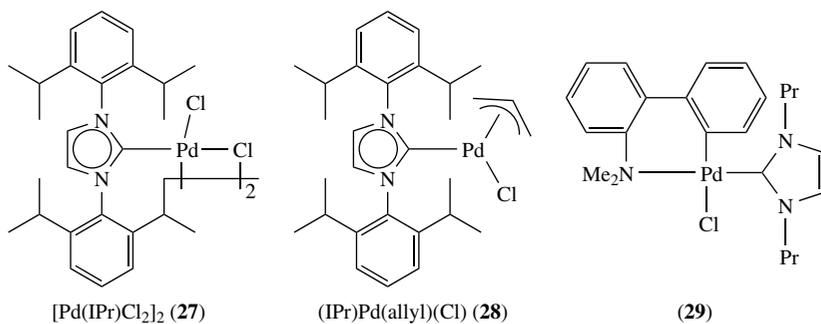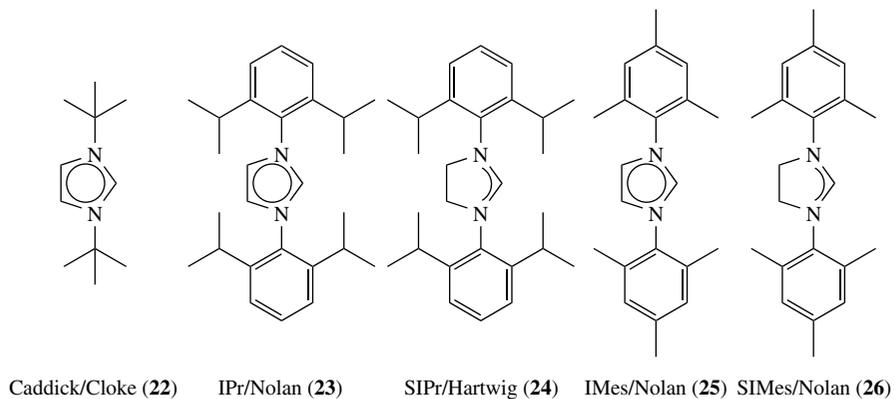
FIGURE 7. Carbenes and complexes with carbene as ancillary ligands synthesized for amination of aryl chlorides

chlorides at room temperature. These fast rates led to reactions with low catalyst loadings and high turnover numbers when reactions were conducted at elevated temperatures[86]. Morpholine, for example, reacted with 4-chlorotoluene in quantitative yields when using 0.02 mol% catalyst. Piperazine, however, reacted more sluggishly, and reaction temperatures of 100 °C were needed to complete conversion even when using 2 mol% catalyst.

The 1:1 ratio of palladium–ligand is crucial for fast rates of the reaction, as was observed with monodentate alkylphosphines[87]. Nolan compared the reactions of *p*-tolyl chloride with *N*-methylaniline, aniline, and dibutylamine using catalysts with different ratios of palladium to ligand. In all of these substrate combinations, the reactions catalyzed by 1:1 ratio of palladium–ligand were at least twice as fast than those catalyzed by 1:2 ratio of palladium–ligand. These observations prompted Nolan's group to synthesize a series of palladium complexes **27–29** bearing a single NHC ligand per palladium (Figure 7). The palladacycle complex **29** is discussed in more detail in Section III.C.1. With these catalysts, the reactions of unactivated aryl chlorides with secondary cyclic and acyclic amines provided high yields at room temperature or 70 °C[75, 85, 88–90]. More recently, Beller and coworkers[91] and shortly after Goossen and coworkers[92] reported that Pd(0)–NHC complexes with naphthoquinone (NQ) **30** (Figure 7) or divinylsiloxane (dvds) as ancillary ligands catalyzed the amination of aryl chlorides with secondary cyclic and acyclic amines in moderate to good yield when *t*-BuONa or KOH was used as the base.

One advantage of these catalysts is the stability of their protonated precursors toward air and moisture. The ligand precursor imidazolium salts are simple to prepare and are now commercially available. Complete conversion of 4-chlorotoluene was observed for a reaction with morpholine conducted without degassing the reagent grade DME[86].

An isolated complex with 1:2 ratio of palladium to NHC was also reported to catalyze the reaction of aryl chlorides with secondary amines. Caddick, Cloke and coworkers[93] recently reported the use of isolated bis(1,3-di-*N*-*t*-butylimidazol-2-ylidne)palladium(0) as a catalyst for the reactions of 4-chlorotoluene with morpholine and piperidine to give 95% and 70% yields, respectively, at 100 °C.

iv. Reactions with aryl triflates. The aryl monophosphines that led to the first catalysts for the amination of aryl bromides did not catalyze the amination of aryl triflates. On the other hand, chelating arylphosphines generated catalysts for the amination of aryl triflates[94–96]. The original procedure in which *tert*-butoxide was used as base and either BINAP or DPPF as the ligand (equation 14) led to the amination of aryl triflates in good yields in many cases. However, cleavage of the triflate to phenol competes with amination, particularly in the case of electron-poor aryl triflates, thereby decreasing the yield of amine.

Y = *o*-, *m*- or *p*-alkyl, CN, COPh, OMe, Ph   53–90%
L$_2$ = DPPF or BINAP

(14)
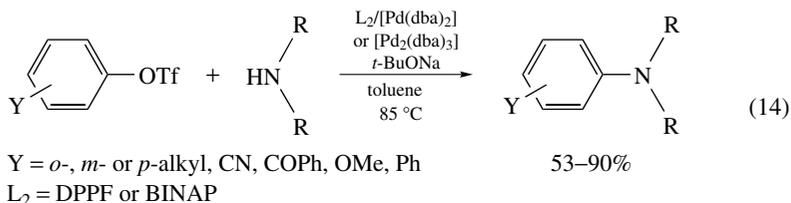
Two reaction modifications have been shown to improve yields. First, Hartwig and coworkers found that slowing the addition of triflate to the reaction mixture ensures low concentrations of this reagent and improves yields in some cases[94]. More generally, Åhman and Buchwald found that the use of Cs$_2$CO$_3$, rather than *t*-butoxide, as the base

allowed for the reaction to occur smoothly without triflate cleavage (equation 15)[96].

$$Y = o\text{-alkyl}, p\text{-CN}, p\text{-COPh},$$
$$p\text{-}, o\text{-alkyl}, p\text{-OMe}$$

$$54\text{--}92\%$$
for dialkylamines
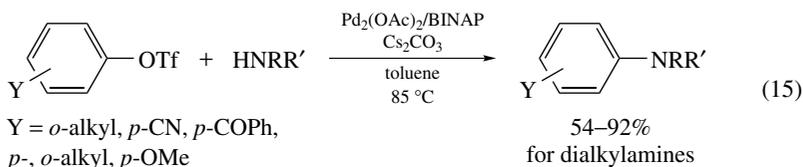
The first room-temperature catalytic aminations of aryl triflates with secondary amines were reported by Buchwald and coworkers using catalysts derived from di-*t*-butylphosphino-2-biphenyl with *t*-BuONa[66]. While reactions of electron-rich and electron-neutral aryl triflates proceeded with high yields, poor results were obtained for electron-deficient aryl triflates, even with the weak bases K_3PO_4 or Cs_2CO_3. At 80 °C, as opposed to room temperature, the yields of amines were considerably greater when K_3PO_4 was used as the stoichiometric base. Electron-rich, electron-neutral and electron-deficient aryl triflates reacted in high yields. Likewise, a complex containing carbene [(IPr)Pd(allyl)(Cl)] **28** (Figure 7) catalyzed the reactions of aryl triflates with cyclic and acyclic secondary amines in high yield[97]. Mechanistically, it appears that the aryl palladium triflate intermediate coordinates amine more readily than the aryl palladium halide complexes due to the lability of the triflate ligand. If this occurs, amine coordination to a cationic metal center will significantly increase the acidity of the N−H bond, and a weaker base can be used.

v. Reactions with aryl tosylates. Aryl tosylates are cheaper, more convenient to prepare from phenols and more stable than aryl triflates. Reactions of aryl tosylates with primary amines will be described in a later section, but only one report of palladium-catalyzed coupling between arene sulfonates and secondary amines has been published[98]. The X-phos ligand **31** (Figure 8), a derivative of ligand **12** (Figure 5), catalyzed the amination of aryl tosylates as shown in equation 16. For unactivated aryl tosylates, these reactions (equation 16) produced high yields with 2 mol% of Pd and 5 mol% of ligand at 110 °C.

X-phos (**31**)
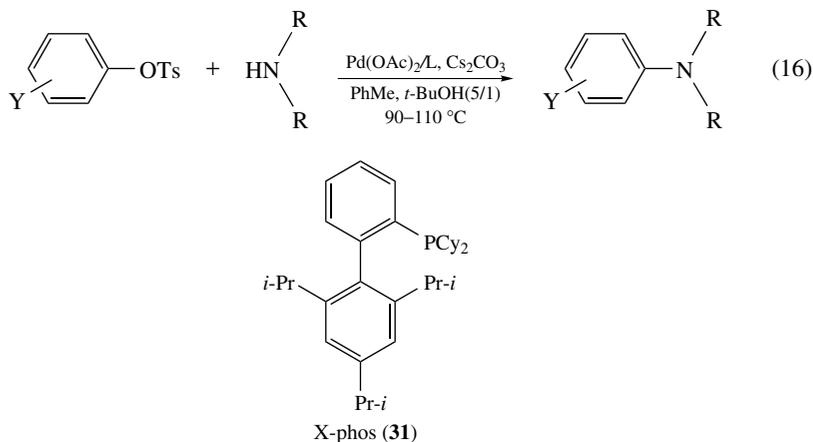
FIGURE 8. X-phos, a derivative of ligand **11** in Figure 5, synthesized for amination of unactivated aryl tosylates

b. Reactions with diarylamines. i. Reactions with aryl halides. The reactions of aryl halides with diarylamines to form triarylamines is more straightforward than the similar reaction with secondary alkylamines because the former substrates cannot generate amido complexes that undergo β-hydrogen elimination. However, the reactions of diarylamines still form some product from reduction of the haloarene by an unknown mechanism. For the most part, the synthesis of triarylamines has focused on the preparation of discrete molecules and polymers that are important for electronic materials applications[99–101].

$$Y = o\text{-},\ m\text{-} \text{ or } p\text{-alkyl, CN, COPh, OMe, Ph}$$
$$L = P(tol\text{-}o)_3, \text{ DPPF or } P(Bu\text{-}t)_3$$

(17)
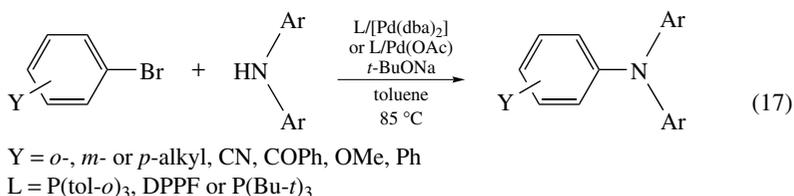
For the reactions of aryl halides with diarylamines (equation 17), the P(tol-o)$_3$ ligand gives good yields in most cases, but catalyst loads of 5–10% were typically required[99]. In some cases, palladium complexes bearing DPPF as ligand are more effective catalysts for the formation of triarylamines, and can even produce unsymmetrical triarylamines in a one-step addition of two aryl halides sequentially to an aniline[100].

Palladium complexes with P(Bu-t)$_3$ as ligand are some of the most active types of catalysts for formation of triarylamines from diarylamines and aryl halides. Workers at Tosoh described the use of this ligand at high temperatures for formation of triarylamines[55]. Hartwig's group subsequently showed that these ligands will form triarylamines at room temperature when a 1:1 ligand:palladium ratio is used (equation 18)[68]. The isolated palladium complex Pd[P(Bu-t)$_3$]$_2$ also catalyzes the amination of unactivated or activated aryl chlorides with diarylamines in water using sodium hydroxide or potassium hydroxide as the base and a catalytic amount of cetyltrimethylammonium bromide as phase-transfer agent.

$$X = Cl, Br$$
$$Y = o\text{-},\ m\text{-} \text{ or } p\text{-alkyl, CN, COPh, OMe, Ph}$$

(18)
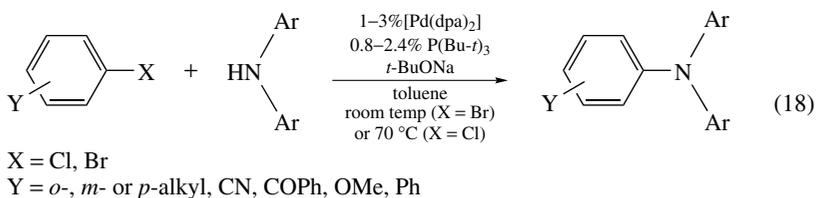
The isolated dimeric [{PdBrL}$_2$] (L = P(1-Ad)(Bu-t)$_2$, P(Bu-t)$_3$) complex catalyzed the reactions of aryl halides with diarylamines with even faster rates, and these rates were similar to those of the aminations of aryl chlorides with cyclic or acyclic amines. For example, the amination of aryl chlorides with diphenylamine was complete within 15 minutes[70].

Palladium complexes of Q-phos (**14**, Figure 5) are also active catalysts for the coupling of aryl bromides with diarylamines[67]. Reactions of aryl bromides occurred at room temperature, even for the somewhat sterically hindered 2-bromotoluene. Reactions of aryl chlorides catalyzed by the same complex required heating at 100 °C, but formed the triarylamine in nearly quantitative yield.

A complex generated from Pd$_2$dba$_3$ and **13** (Figure 5) has also been reported to catalyze the amination of aryl bromides with diarylamines at room temperature, albeit with longer

reaction times than those catalyzed by palladium complexes of Q-phos. The amination of aryl chlorides catalyzed by the combination of Pd_2dba_3 and **13** (Figure 5) occurred at 80 °C with 0.5 mol% catalyst[66]. Complexes containing Verkade's bicyclic triaminophosphine $P(i\text{-}BuNCH_2CH_2)_3N$ ligand **17** (Figure 5), however, were less efficient at catalyzing the same reaction[82, 83].

Increased reaction rates for the coupling of aryl bromide with diphenylamine were also observed with isolated binuclear palladium(I) complexes containing a biphenyl dialkyl-phosphine[102].

ii. Reactions with aryl sulfonates. The reaction of aryl triflates with diarylamines has only been reported with catalysts bearing chelating phosphines. For example, nearly quantitative yields were achieved in the presence of a palladium complex of DPPF as the catalyst[103].

Reaction of diarylamines with aryl nonaflates as part of the synthesis of discrete oligomeric triarylamines has also been reported[104]. Only one paper reports the palladium-catalyzed reactions of diarylamines with aryl tosylates; this reaction was conducted with X-phos **31** (Figure 8) as the ligand in mixed solvents of 5:1 toluene:t-butanol[98].

2. Reactions of primary amines

a. Reactions of primary alkylamines. i. Overview. Like the reactions of acyclic secondary alkylamines with aryl halides, the reactions of primary alkylamines with aryl halides were initially difficult to achieve. As a general rule, the catalysts that give the highest yields for the reactions of aryl halides with primary alkylamines differ from those that give the highest yields for reactions of secondary alkylamines. Palladium complexes containing BINAP as the ligand had been reported to be the most selective catalyst for reactions of primary alkylamines with aryl bromides[49]. More recently, palladium complexes of the hindered Josiphos ligand CyPF-Bu-t **32** (Figure 9) have proven to be highly active and selective for the reactions of primary alkylamines with aryl chlorides[105]. The tight chelation from a rigid backbone, the steric bulk and the electron-rich property of this bisphosphine may explain the higher reactivity of its complexes for this chemistry and its stability toward decomposition. At the time of the preparation of this chapter, the scope and efficiency of the reactions of aryl bromides have not been evaluated with this ligand.

Reactions of primary amines with aryl chlorides are also possible with hindered alkyl-phosphine ligands (e.g. $P(Bu\text{-}t)_3$ or biaryldialkylphosphines), but catalyst loadings tend to be higher and some product from diarylation has been observed when reactions of unhindered aryl halides are run in the absence of an excess amount of the primary amine[68]. In general, reactions of hindered aryl halides occurred in higher yields than reactions of

(**32**) CyPF-Bu-t
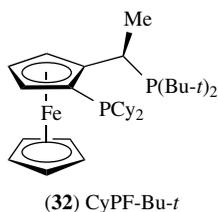
FIGURE 9. Josiphos ligand that generates highly active catalysts for the coupling of primary alkylamines with aryl chlorides

their unhindered counterparts and were achieved over a broader range of catalysts because (a) diarylation of the primary amine does not occur[106] and (b) either reductive elimination occurs more rapidly or β-hydrogen elimination occurs more slowly from these hindered aryl palladium amido complexes.

$$\text{(19)}$$

$$\text{Y} = o\text{-}, p\text{-alkyl, CN, COPh, CONEt}_2$$

X = Br, I   R = alkyl

Y = p-CN, COPh, CONEt₂ 82–96%
Y = o-alkyl 92%, p-alkyl 52%

$$\text{(20)}$$

X = Br, I   R = alkyl
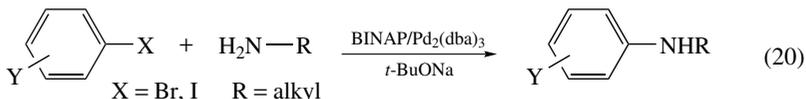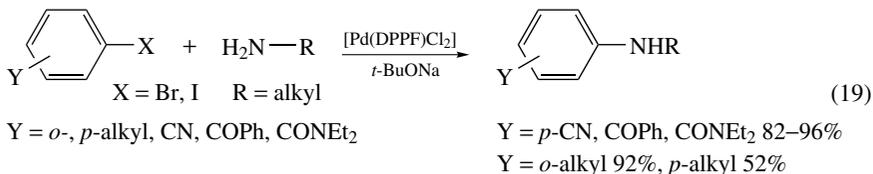
ii. Development of reactions of aryl bromides with primary amines. Hartwig's and Buchwald's groups simultaneously described catalysts that allow high-yield aminations of aryl halides with primary alkylamines (equations 19 and 20)[48, 49]. Palladium complexes of DPPF or BINAP catalyze reactions of primary alkylamines with aryl bromides, although reactions catalyzed by complexes of BINAP often give higher turnover numbers and yields. For example, palladium complexes containing *rac*-BINAP are more effective than those containing DPPF for reactions of primary amines with unhindered aryl halides. With a mixture of Pd(OAc)₂ or Pd₂(dba)₃ and BINAP, high yields and turnover numbers in the range of 100–200 were observed. Rossen and coworkers used phanephos **33** (Figure 10) as the ligand for palladium in the reaction of benzylamine with a dibromocyclophane[107]. Palladium complexes of this ligand reacted similarly to those of BINAP, but only a few reactions were investigated.

$$\text{(21)}$$
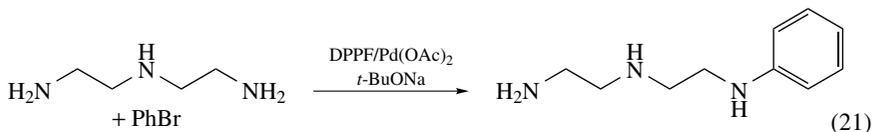
The selectivity for arylation of primary vs. secondary amines using palladium catalysts with chelating ligands has been investigated. Beletskaya, Bessermertnykh and Guilard conducted reactions of polyamines such as that in equation 21, with phenyl bromide using (DPPF)PdCl₂ as catalyst[108]. Good yields of the products resulting from reaction of the primary amine portion of the polyamine were obtained. Senanayake and coworkers reported the high selectivity for arylation of primary over secondary amines using palladium complexes of BINAP in the synthesis of biologically active arylamines, as shown
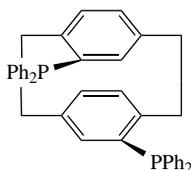
Phanephos **(33)**

FIGURE 10. Phanephos, similar to BINAP, synthesized for amination by primary alkylamines

in equation 22[109].

$$\text{(22)}$$

$$Ar = C_6H_4F\text{-}p$$
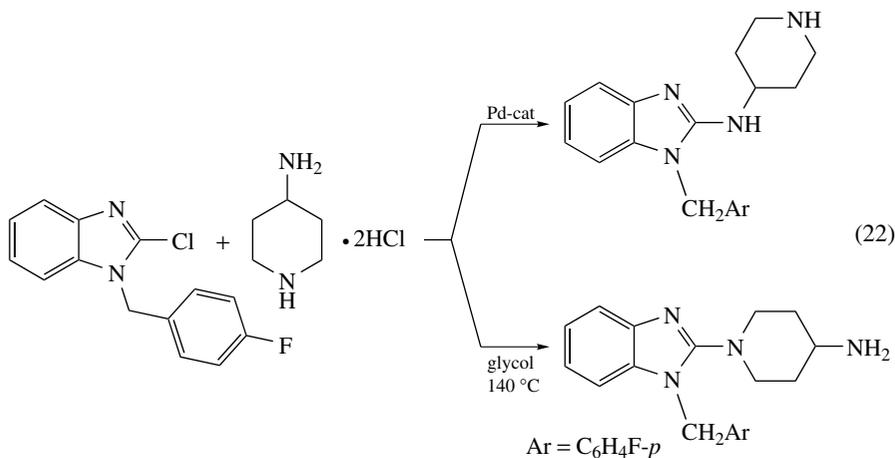
iii. Reactions of primary amines with aryl chlorides. Reactions of unactivated aryl chlorides with primary amines can be conducted with arylphosphines only in special cases because oxidative addition of the aryl chloride is slow. The reactions of primary amines with aryl chlorides catalyzed by complexes of Nolan's unsaturated *N*-heterocyclic carbenes **23–25** (Figure 7) occurred in high yield, but only moderate yield was obtained when the saturated *N*-heterocyclic carbene **30** (Figure 7) was used. Complexes of sterically hindered alkylphosphine ligands catalyze reactions of aryl chlorides, but the catalyst loadings are generally higher than 0.5 mol%, reaction temperatures are high with these loadings and yields are variable.

Complexes of biphenylalkylmonophosphine ligands (e.g. see **12** and **13** in Figure 5) and Beller's heterobiaryl ligand **20** (Figure 6) have been shown to catalyze the reactions of primary amines with unactivated aryl chlorides[60, 66, 81]. Reactions of sterically hindered aryl chlorides with primary amines have been shown to occur in higher yields and with higher selectivity than reactions of unhindered aryl chlorides. Higher yields and selectivity may result from the sterically hindered environment of the metal intermediate, which prevents the formation of diarylalkylamine and competing reduction. The selectivity of catalysts bearing Q-phos **14** (Figure 5) for reaction of primary amines was remarkable[67]. Reactions of unhindered aryl chlorides with primary alkyl amines occurred in good to excellent yields. The ratio of secondary to tertiary amine product was typically greater than 20:1 when a slight excess of alkylamine was used. Complexes containing unsaturated *N*-heterocyclic carbenes **29**[89] or [{Pd(IPr)Cl₂}₂] **27**[75] (Figure 7) were also reported to catalyze the reaction of primary alkyl amines with aryl chlorides in moderate to good yield; formation of tertiary amines was not observed with this system. Use of an ionic liquid also improved the yields of the reaction of unactivated aryl chlorides with cyclohexylamine and cyclopentyl amine when air- and moisture-stable complexes [PdCl₂(*N*-heterocyclic carbene)₂] were used as catalyst[110].

Phosphines that are tightly chelated to the metal center often achieve high selectivity of secondary over tertiary amine products in reactions of primary alkylamines with unhindered aryl halides. The chelation helps prevent competing β-hydrogen elimination of the aryl palladium amido intermediate (*vide infra*). Additionally, the greater steric hindrance of bisphosphine palladium complexes, when compared to mono phosphine palladium complexes, prevents diarylation. Some ligands originally introduced by

Togni, Spindler and Bläser and their coworkers[111, 112] for asymmetric hydrogenation chemistry fit this description of biphosphine. One of these types of ligands, CyPF-Bu-*t* (**32**, Figure 9), is an air-stable, electron-rich bisphosphine that is commercially available from Strem and has a strong conformational preference for chelation because of the benzylic methyl group. Complexes of this ligand are, to date, the most selective catalysts for formation of monoaryl alkylamines from unactivated, sterically unhindered aryl chlorides (equation 23). High turnover numbers between 20,000–100,000 have been observed using catalysts containing this ligand[105].
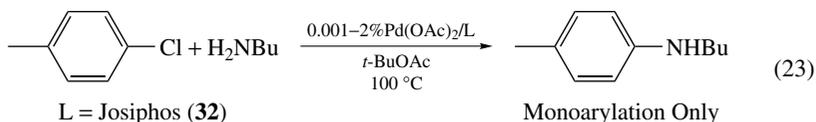
$$\text{—}\langle\text{—}\rangle\text{—Cl} + \text{H}_2\text{NBu} \xrightarrow[\substack{t\text{-BuAc} \\ 100\,°C}]{0.001\text{–}2\%\text{Pd(OAc)}_2/\text{L}} \text{—}\langle\text{—}\rangle\text{—NHBu} \tag{23}$$

L = Josiphos (**32**)   Monoarylation Only

iv. Reactions with aryl triflates. The reactions of primary alkylamines with aryl triflates occur much like the reactions of secondary amines with aryl halides. Specifically, palladium complexes containing BINAP catalyze the reactions of unhindered substrates in the highest yields[95]. Reactions conducted with Cs_2CO_3 as the base would presumably lead to high-yield aminations of aryl triflates with primary alkylamines (equation 24), but these reactions have not been reported for aryl triflates that lack *ortho* substituents[96]. With isolated air- and moisture-stable (IPr)Pd(allyl)Cl complex **28** (Figure 7) as the catalyst and *t*-BuONa as the base, reaction of unhindered aryl triflates with alkylamines also occurred in high yields at 70 °C[97].

$$\text{Y}\text{—}\langle\text{—}\rangle\text{—OTf} + \text{H}_2\text{NR} \xrightarrow[\substack{\text{toluene} \\ 85\,°C}]{\substack{\text{Pd(OAc)}_2/\text{BINAP} \\ \text{Cs}_2\text{CO}_3}} \text{Y}\text{—}\langle\text{—}\rangle\text{—N}\overset{R}{\underset{R}{<}} \tag{24}$$

Y = *o*- and *p*-Me, *p*-CO$_2$Me, *p*-COMe   46–90%
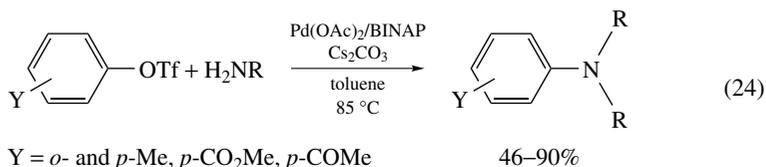
v. Reactions with aryl tosylates. Reactions of aryl tosylates are desirable because of the low cost and greater ease of handling of the reagents used to form tosylates. However, palladium chemistry involving unactivated aryl tosylates is rare[113]. The reactions of *p*-tolyl tosylate with hexylamine in the presence of *t*-BuONa as the base and palladium complexes containing the analog of CyPF-Bu-*t* **32** (Figure 9) PPF-Bu-*t* containing phenyl, instead of cyclohexyl groups, as ligand was the first palladium-catalyzed reaction of an unactivated tosylate (equation 25)[79]. Buchwald later reported that complexes of his group's X-phos ligand (**31**, Figure 8) catalyzed the reactions of unactivated aryl tosylates with primary amines at 110 °C[98]. More recently, milder conditions have been achieved by conducting the reactions of primary amines with aryl tosylates in the presence of the catalyst containing CyPF-Bu-*t* **32** (Figure 9) as ligand. Reactions of phenyl tosylate with hexylamine in the presence of 1 mol% Pd/CyPF-Bu-*t* afforded arylamine in 74% yield after only 2 h at room temperature[114].

$$\text{—}\langle\text{—}\rangle\text{—OTs} + \text{H}_2\text{Nhexyl} \xrightarrow[\substack{t\text{-BuONa} \\ 110\,°C}]{\text{Pd(OAc)}_2/\text{L}} \text{—}\langle\text{—}\rangle\text{—NHhexyl} \tag{25}$$

L = X-phos (**31**) or CyPF-Bu-*t* (**32**)   86%
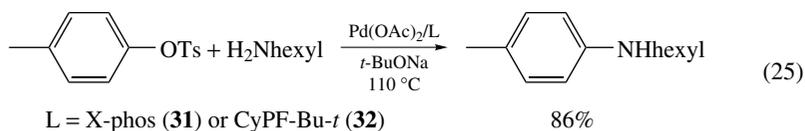
b. Reactions of primary arylamines. i. Reactions with aryl halides. The reactions of primary arylamines with aryl halides are simpler to catalyze than those of primary alkylamines because β-hydrogen elimination will not compete with reductive elimination. However, diarylation of the aniline can be a competing process, and for some reason the original catalyst system containing $P(tol-o)_3$ showed low activity for the reactions of aniline with aryl halides.

Many palladium complexes will catalyze the reaction of an aryl bromide with aniline, but the optimal ligand for a particular reaction is difficult to predict. In the experience of the authors' group during the synthesis of di- and triarylamine precursors to materials, reactions catalyzed by palladium complexes of DPPF and $P(Bu-t)_3$ give high yields[104, 115]. However, small amounts of triarylamine do form from reactions catalyzed by these complexes. Thus, the groups of Meyer[116], Kanbara[117] and Buchwald[118, 119] have used palladium complexes with BINAP for the synthesis of polymeric or discrete oligomeric anilines. Meyer and Kanbara and coworkers presented evidence that the polymeric anilines thus produced have little if any cross-linking. Buchwald and coworkers have also introduced van Leeuwen's DPEphos **34** (Figure 11) as a superior ligand for forming diarylamines under certain reaction conditions[120]. Kocovsky and coworkers have reported that complexes of MAP **35** (Figure 11), a binaphthyl P,N ligand with a dimethylamino and diphenylamino group on the 2 and 2′ positions of the 1,1′-binaphthyl backbone, catalyze the reactions of a binaphthylamine more rapidly than complexes of BINAP[121].

$$(26)$$
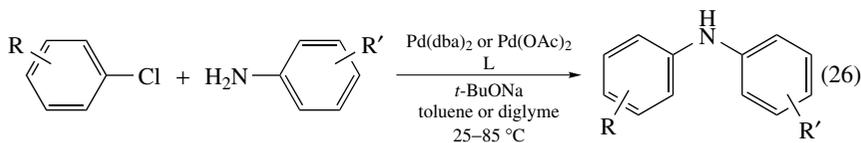
The reactions of unactivated aryl chlorides with primary arylamines, like the reactions with secondary arylamines, require catalysts generated from alkylphosphine ligands or carbenes (equation 26). Palladium complexes with PPF-Bu-*t* and the cyclohexyl analogs of these ligands CyPPF-Bu-*t* **32** catalyze the reactions of diarylamines from unactivated aryl chlorides and anilines in excellent yields[79, 105]. Palladium complexes of the *t*-butyl analog of DPPF, D*t*BPF **19** (Figure 6), also catalyze these reactions in high yields[79]. In addition to complexes of bisphosphines, complexes of alkylmonophosphines catalyze the coupling of primary arylamines with aryl chlorides[60, 67, 68, 70, 81–83]. For example, biaryl-dialkylphosphines, Beller's ligand, $P(Bu-t)_3$, Q-phos and Verkade's ligand (Figures 5 and 6) have been shown to catalyze the amination of unactivated aryl chlorides in good yields at elevated temperature. The isolated palladium complex $Pd[P(Bu-t)_3]_2$ catalyzed the amination of unactivated or activated aryl chloride with primary aryl amines in water using

DPEphos (**34**)   MAP (**35**)
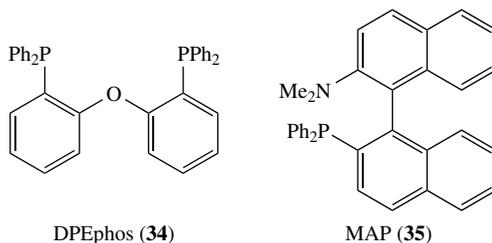
FIGURE 11. Ligands used for arylation of anilines

sodium hydroxide or potassium hydroxide as the base and cetyltrimethylammonium bro-mide as phase-transfer agent[69]. A palladacycle formed from X-phos has also been shown to couple aniline with activated and unactivated aryl chlorides in water[98]. Complexes of the *N*-heterocyclic carbene IPr **23** and SIPr **24** (Figure 7) couple aniline with unactivated aryl chlorides, even at room temperature in excellent yields[68, 75, 85, 88–90].

ii. Reactions of primary arylamines with aryl triflates. The reactions of aryl triflates with primary arylamines have been reported with chelating ligands (equation 27), as well as with hindered alkylphosphines. The reactions of aryl triflates with primary amines catalyzed by complexes of DPPF occur in essentially quantitative yields, most likely because β-hydrogen elimination does not compete with coupling and the amine is more hindered than a linear alkylamine[94]. The turnover numbers were not assessed for these reactions; however, aminations catalyzed by complexes of BINAP **5** (Figure 3) and DPEphos **34** (Figure 11) occur with good turnover numbers[95, 96, 120]. The first reported room-temperature, catalytic amination of aryl triflates with an arylamine was conducted with a palladium complex of a biphenyldialkylphosphine as catalyst[66].

L = DPPF, BINAP   (27)
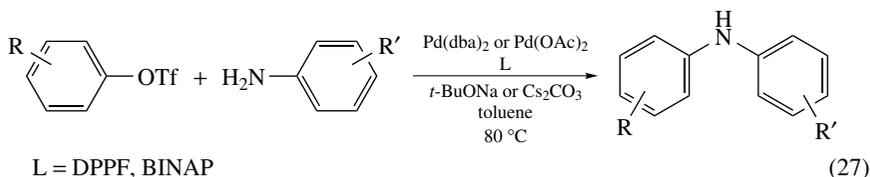
iii. Reactions with aryl tosylates. The reaction of aniline with an activated aryl tosylate has been catalyzed by a combination of palladium and D*t*BPF **19** (Figure 6) to produce a high yield of diarylamine under relatively mild conditions[79]. The reaction of unactivated aryl tosylates with anilines has been more recently reported using catalysts containing X-phos **31** (Figure 8) in the presence of 5% phenylboronic acid[98].

3. Reactions of ammonia equivalents

a. Overview. Although the palladium-catalyzed amination of aryl halides with a variety of primary amines, secondary amines and related nitrogen substrates occurs with broad scope, the analogous reaction with ammonia to form the primary arylamine had not been reported at the time of preparation of the manuscript. Diarylamines were formed in preference to the monoarylamine[122].

Thus, parent anilines have been prepared by palladium-catalyzed reactions from aryl halides and ammonia surrogates. Coupling of the ammonia surrogates with aryl halides or sulfonates under palladium-catalyzed reaction conditions, followed by the cleavage of the protective group, forms the desired arylamine. To date, several types of ammonia surrogates, such as allyl or diallylamines, imines, amides, $LiN(SiMe_3)_2$ and Ph_3SiNH_2, have been used for this type of transformation. More recently, solid-supported reagents based on polystyrene with acid-labile amino groups have been studied. Rink-resins were reported to serve as ammonia equivalents for reactions of activated aryl bromides and chlorides using 10 mol% $Pd_2(dba)_3$ and 30 mol% BINAP. The expected anilines with an electron-withdrawing group in *meta*- or *para*-position were obtained in moderate to good yield after cleavage of the resin using trifluoroacetic acid[123].

b. Reactions of allylamine and diallylamine. One strategy to prepare protected anilines is the reaction of diallylamine with aryl halides in the presence of the complexes that

catalyze reactions of secondary amines (equation 28)[124]. Diallylamine has been reported to react with aryl bromides to produce modest yields of the diallyl-protected aniline in the presence of palladium catalysts ligated by P(tol-o)$_3$. Reactions of allylamine with aryl and heteroaryl bromides catalyzed by (DPPF)PdCl$_2$ occurred in higher yields. Presumably, these reactions can be conducted in a more general fashion with the improved catalysts described in Sections III.A.1 and III.A.2. Cleavage of the allyl group to the parent arylamine was achieved using methanesulfonic acid and Pd/C.

$$L = P(tol\text{-}o)_3, DPPF \qquad\qquad 12\text{--}100\% \tag{28}$$
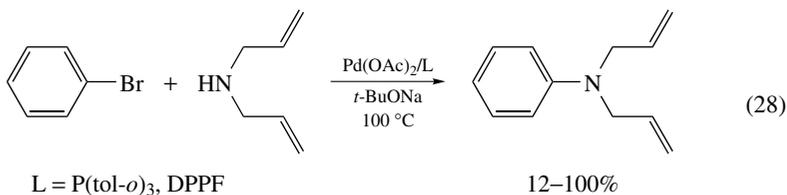
c. Reactions of benzophenone imine. Benzophenone imine is a commercially available ammonia surrogate. *N*-Aryl benzophenone imines are formed by palladium-catalyzed coupling of aryl halides with benzophenone imine[125, 126]. These coupling products are stable to base and mild acid and can be easily isolated and converted to the corresponding aniline under a variety of conditions.

$$R = o\text{-}, m\text{-}, p\text{-alkyl, alkoxy, CN} \tag{29}$$
$$L = DPPF, BINAP$$
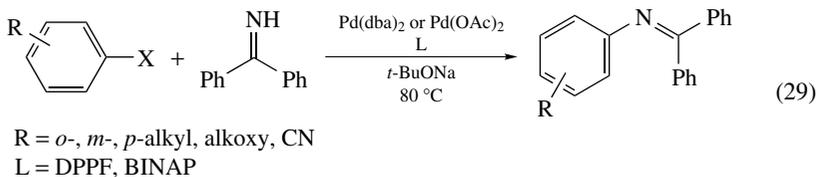
Palladium complexes containing a variety of ligands have been reported as catalysts for coupling of aryl halides and sulfonates with benzophenone imine (equation 29). The reactions occur in nearly quantitative yields with all classes of aryl bromide or iodide tested with catalysts containing BINAP and DPPF. The increased acidity and/or the increased binding constant of imines for transition metals allows this chemistry to be conducted using Cs$_2$CO$_3$ or t-BuONa as the base. Because both ligands are arylphosphines, they will not catalyze the reactions of benzophenone imine with chloroarenes. However, the similarity of the complexes of deprotonated benzophenone imine to complexes of anilides[125] suggested that reactions of benzophenone imine with aryl chlorides can be conducted with the same sterically hindered alkylphosphine ligands. Indeed, reactions of aryl chlorides with benzophenone imine conducted with a combination of Pd$_2$(dba)$_3$ and biphenyldicyclohexylphosphine **12** (Figure 5) as catalyst occurred in good yield[66], but the scope of this process was even broader when catalyzed by complexes of sterically hindered *N*-heterocyclic carbenes **23** (Figure 7)[85]. Reactions of both aryl bromides and aryl chlorides occurred in high yields when the carbene IPr•HCl was used as ligand precursor. In addition, reactions of aryl chlorides with benzophenone imine occurred under milder conditions in the presence of the ferrocene-based, sterically hindered chelating bisphosphine CyPF-Bu-t **32** (Figure 9)[105]. Further, complexes of X-phos **31** (Figure 8) catalyze the reactions of aryl tosylates with benzophenone imine in good yield[98].

d. Reactions of N-trimethylsilylimines. Aldimines are versatile starting materials in synthetic organic chemistry and, because they can be hydrolyzed under very mild conditions,

they can act as an ammonia surrogate. However, the instability of the NH aldimines hampers their use in C−N coupling. Recently, however, N-trimethylsilylimines were introduced by Barluenga and coworkers as equivalents of NH aldimines (equation 30)[127]. The coupling of N-trimethylsilylimines with aryl and vinyl bromides gave N-arylamines or 2-azadienes in excellent yields in the presence of $Pd_2(dba)_3$ and either BINAP or biphenyldialkylphosphine. The major competing side reaction during this process was β-elimination of the aldimines from the palladium(II) complexes to form a nitrile. However, with 4 mol% of this catalyst, complete conversion and less than 5% competing β-elimination were observed.

$$\text{(30)}$$

L = BINAP or **8**   76−97%
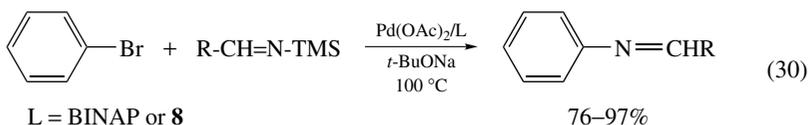
   e. Reactions of amides, sulfonamides, carbamates and sulfoximines.   Palladium-catalyzed amination of aryl halides is more favorable with substrates containing nucleophilic nitrogens. Thus, reagents containing a nitrogen atom located next to a carbonyl or sulfonyl group undergo arylation processes less readily than do more simple amines. The section on copper-catalyzed synthesis of aniline derivatives provides alternative catalysts for the arylation of amides and sulfonamides.

   i. Intramolecular reactions of amides and sulfonamides. Intramolecular reactions of aryl halides with pendant amide or sulfonamide functionality were reported early in the development of palladium-catalyzed aromatic C−N bond formation (equations 31 and 32)[128]. A number of reaction conditions and catalysts were tested. Monophosphines, including PPh_3, were found to be effective ligands for these cyclizations, and carbonate bases proved optimal in most cases tested. The formation of five- and six-membered rings occurred in good yields, but the formation of seven-membered rings occurred in low yields. The cyclization protocols for this early work typically employed high catalyst loading and often required long reaction times. Subsequent work has shown that the same transformations can be achieved with higher yields and with decreased quantities of catalyst when conducted in the presence of complexes of the hemilabile ligand MAP **35** or bidentate ligands with large bite angles, such as DPEphos **34** or Xantphos **6**[129].

$$\text{(31)}$$

R = Me, Bn, t-Bu
L = P(tol-o)$_3$ or P(furyl)$_3$

n = 1, 59−99%
n = 2, 44−82%
n = 3, 5−44%

$$\text{(32)}$$

L = P(tol-o)$_3$
R = o-, m-, p-SO$_2$C$_6$H$_4$Me

n = 1, 88%
n = 2, 87%

ii. Intermolecular reactions of amides and sulfonamides. Many intermolecular reactions of amides or sulfonamides with aryl halides have been conducted with complexes containing chelating phosphines, such as DPPF and Xantphos **6** (Figure 3), and a few examples have been conducted with very hindered biaryl dialkylphosphines. Shakespeare showed that a combination of Pd(OAc)$_2$ and DPPF formed *N*-aryl lactams in good yields from γ-lactams (equation 33)[130]. Reaction times were long for couplings involving electron-neutral aryl halides, but good yields were observed. Four-, six- and seven-membered lactams reacted with unactivated aryl halides in poor yield, but with activated aryl halides in good yields.

$$R = H, CF_3, COPh, CN, OMe$$

Ar = RC$_6$H$_4$Br-*p*

n = 1, 20–52%
n = 2, 70–90%
n = 3, 21–89%
n = 4, 43–94%

(33)

After screening a variety of ligands and reaction variables, Yin and Buchwald found that the combination of Pd(OAc)$_2$ and Xantphos **6** (Figure 3) as catalyst and Cs$_2$CO$_3$ as base induces the intermolecular coupling of a wide range of amides and sulfomides with aryl bromides, iodides and triflates, as well as activated aryl chlorides[131, 132]. Aryl halides with *ortho* or *meta* activating groups were less reactive and required higher reaction temperatures and/or higher quantities of catalysts. The combination of palladium, Xantphos and stoichiometric Cs$_2$CO$_3$ was also shown at 1 mol% Pd loading to catalyze the reaction of bromobenzene and four- to seven-membered ring lactams. Further, this system also promoted the coupling of activated aryl bromides and iodides with ureas.

To accomplish reactions between less reactive aryl chlorides and aryl sulfonates, catalysts containing alkylphosphine ligands were required. For example, Cao and coworkers reported a microwave-promoted, palladium-catalyzed coupling of aryl chlorides with sulfonamides in the presence of palladium and a biphenyl dialkylphosphine ligand[133]. Moderate yields were obtained from reactions of a variety of activated aryl chlorides. The amidation of aryl sulfonates with X-phos (**31**, Figure 8) as the ligand has also been reported[98]. With a combination of 2 mol% palladium and 5 mol% X-phos as catalyst, the coupling of numerous aryl sulfonates with pyrrolidinone, primary amides, *N*-methylformamide and *N*-Boc-amide proceeded in good to excellent yield.

+ NaOPh

62–86%

(34)

iii. Intermolecular reactions of carbamates. Carbamates possess a more electron-rich nitrogen atom than amides or sulfonamides, and thus participate more readily in palladium-catalyzed aminations of aryl halides. For example, *t*-butyl carbamate has been shown to react with aryl halides to form *t*-Boc protected anilines (equation 34)[68]. The catalyst

generated from Pd(dba)$_2$ and P(Bu-t)$_3$ was found to catalyze this arylation. The yields of coupled product from reactions of electron-rich, electron-neutral, sterically hindered or unhindered bromoarenes at 100 °C ranged from 62–86%. Reaction of other carbamates, such as methyl or benzyl carbamate and oxazolinone, occurred in lower yields. Reactions of chloroarenes were slower. Boc-protected toluidine was formed in 59% yield from chlorotoluene at 130 °C. A catalyst generated from X-phos (**30**, Figure 8) also catalyzed the coupling of aryl sulfonates with t-butyl carbamate, but reactions with this catalyst were conducted with a higher loading than the reactions of *tert*-butyl carbamate with chloroarenes catalyzed by Pd(dba)$_2$ and P(Bu-t)$_3$[98].

iv. Intermolecular reactions of sulfoximines. Sulfoximines are less nucleophilic than ketimines, but in some cases sulfoximines react with aryl halides under palladium-catalyzed conditions[134]. For example, DPPF- and BINAP-ligated palladium have been shown to act as catalyst to couple *S*-methyl, *S*-phenyl sulfoximines with electron-poor or electron-neutral aryl halides at 100 °C over long reaction times (equation 35)[134]. The products shown in equation 35 can, in turn, be used as ligands for asymmetric catalysis.

$$R\text{—Ar—Br} + O{=}S(\text{=NH})(\text{Me})(\text{Ph}) \xrightarrow[\substack{t\text{-BuONa} \\ 110\,°C \\ 48\,h}]{\substack{5\%\ \text{Pd(OAc)}_2 \\ L}} R\text{—Ar—N=S(Ph)(Me)(=O)} \qquad (35)$$

R = H, 2-CN, 4-CO$_2$Me, 4-t-Bu   L = DPPF 87%
L = DPPF, BINAP   L = BINAP 67–94%
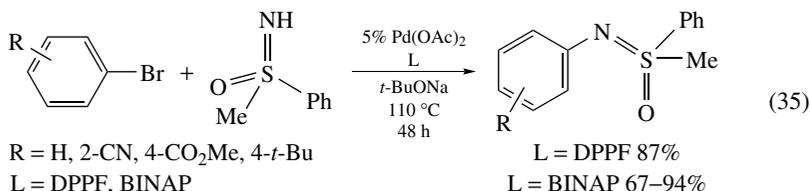
f. Reactions of LiN(SiMe$_3$)$_2$ and Ph$_3$SiNH$_2$. Lithium bis(trimethylsilyl)amide [LiN (SiMe$_3$)$_2$] is a well known, sterically hindered, non-nucleophilic base that is used increasingly in organic synthesis. It is commercially available as solution in hydrocarbon or ether solvents, or as a solid. The low cost of this material and the easy deprotection of a silyl arylamine would make this silylamide a useful ammonia surrogate. The development of conditions to conduct palladium-catalyzed coupling of aryl halides with [LiN(SiMe$_3$)$_2$] was not simple, however.

Hartwig and coworkers first reported conditions to use LiN(SiMe$_3$)$_2$ as an ammonia equivalent for the conversion of aryl halides to anilines[135]. These results stemmed from the observation of the formation of bis(trimethylsilyl)arylamine in competition with the α-arylation of hindered esters in the presence of Pd(dba)$_2$ and P(Bu-t)$_3$ as catalyst. With few exceptions, the reactions of m- and p-substituted aryl bromides and chlorides with [LiN(SiMe$_3$)$_2$] formed the corresponding aniline in high yields after hydrolysis, and palladium loadings as low as 0.2 mol% were sufficient to achieve full conversion. Activated aryl halides reacted at low temperature and generated the protected aniline regiospecifically in high yield. Substrates with *ortho* substituents, however, did not react to form the corresponding aniline, presumably because of the severe steric bulk of the silylamide. Reactions of the less hindered aminotriphenylsilane did occur with *ortho*-substituted aryl halides, and Buchwald and coworkers reported palladium-catalyzed reactions of *ortho*-substituted aryl halides with the combination of this silylamide and [LiN(SiMe$_3$)$_2$] to form the corresponding anilines in high yields (equation 36)[122].

$$R\text{—Ar—X} \xrightarrow[\substack{\text{LHMDS or} \\ \text{Ph}_3\text{SiNH}_2/\text{LHMDS}}]{\text{Pd}_2(\text{dba})_3/L} R\text{—Ar—NH}_2 \qquad (36)$$

X = Cl, Br   64–99%
L = P(Bu-t)$_3$ or **12**
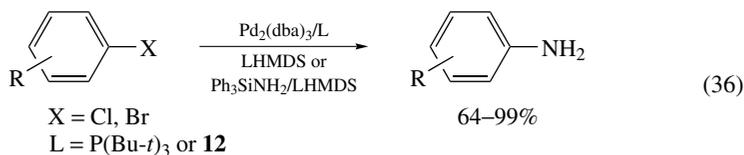
4. Reactions of hydrazones

N-Aryl hydrazones are used in agricultural applications. Additionally, they can be cleaved to form *N*-arylhydrazines for pyrazole synthesis, and the hydrazine portion can be transferred to ketones to generate substrates for the Fischer indole synthesis[136].

a. Intermolecular reactions. The coupling of aryl halides with benzophenone hydrazone has been reported[136, 137]. Complexes of chelating aromatic phosphines (e.g. DPPF and BINAP) were the first to catalyze these reactions (equation 37).

$$X = Br; L = DPPF, BINAP$$
$$X = Cl; CyPF-Bu-t (\mathbf{32})$$

(37)
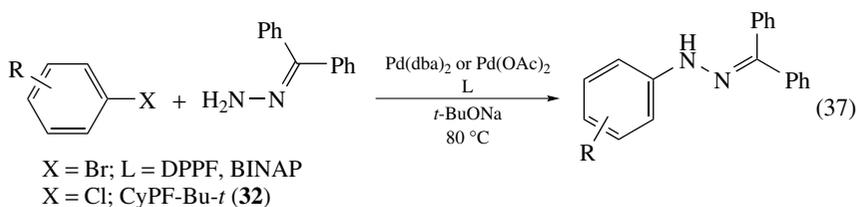
The reactions of benzophenone hydrazone with aryl bromides are remarkably general using either DPPF or BINAP as the ligand for palladium. Sterically hindered or unhindered, electron-rich or electron-poor aryl bromides all react with benzophenone hydrazone to form high yields of *N*-aryl hydrazones. Reactions of hydrazones other than diphenyl hydrazone were less successful. This drawback prompted Buchwald and coworkers to develop a process using the *N*-aryl diphenylhydrazones from the palladium coupling as precursors to other hydrazones that can be used in the Fischer indole syntheses. This transfer of the *N*-aryl hydrazine to a ketone-bearing enolizable hydrogen was conducted in the presence of an acid catalyst[136].

The reactions of benzophenone hydrazone with aryl chlorides are less developed, even with third-generation, hindered alkylphosphines or carbenes. Only one example of the reaction of 2-chloroanisole with benzophenone hydrazone in the presence of a catalyst ligated by biphenyldi-*t*-butylphosphine **13** (Figure 5) has been reported[66]. More recently, reactions of aryl chlorides catalyzed by complexes of CyPF-Bu-*t* **32** (Figure 9) were reported to occur in high yield under mild conditions[105]. In addition, the palladium catalyst generated from X-phos (**31**, Figure 8) has been reported to couple hindered or activated aryl tosylates with benzophenone hydrazone[98].

b. Intramolecular reactions. Palladium catalysts with chelating ligands (e.g. DPPF, BINAP or DPEphos) also catalyze the intramolecular coupling of substituted hydrazones with aryl bromides[138–140](equation 38). By this method, biologically active and pharmaceutically important indazoles have been readily prepared in high yields. In addition to the reactions of halopyridines with *t*-butylcarbazate (H$_2$NNHBoc), Skerlj and coworkers reported the reaction of electron-deficient aryl bromides with this protected hydrazine[141]. Reactions occurred with palladium catalysts ligated by DPPF or the Josiphos ligand CyPF-Bu-*t* **32** (Figure 9), along with Cs$_2$CO$_3$ as the base at temperatures of 100–110 °C.

$$X = Cl; Br$$
$$L = DPPF \text{ or } DPEphos$$

(38)
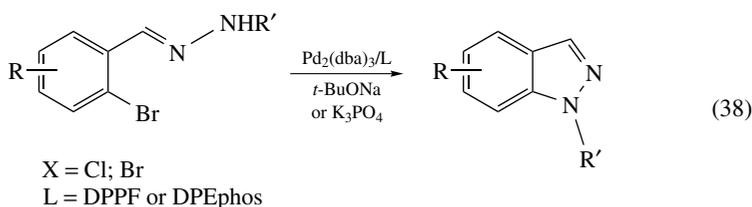
5. Reactions of indoles, pyrroles and carbazoles

The *N*-arylation of certain azoles can be conducted using palladium catalysts. The analogous reactions of pyrazoles and imidazoles have not been reported, and palladium-catalyzed reactions of these azoles with two nitrogens may never compete with classic Ullmann chemistry with copper catalysts. However, azoles containing a single nitrogen atom are suitable substrates for palladium-catalyzed *N*-arylations.

$$(39)$$
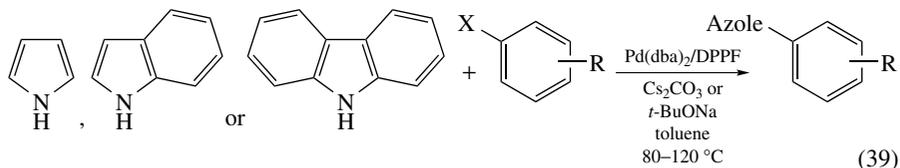
The first reports of palladium-catalyzed arylation (equation 39) of azoles occurred with catalysts bearing DPPF as the ligand[125]. These reactions of indole, pyrrole and carbazole with activated aryl halides were carried out at 80–100 °C. The reactions of indole and pyrrole with unactivated aryl halides such as bromobenzene, 4-bromo-*t*-butylbenzene and 3-bromoanisole occurred in high yields. However, the conditions of these reactions were more severe than those typically necessary to conduct palladium-catalyzed coupling of aryl halides with amines (equation 40).

$$(40)$$
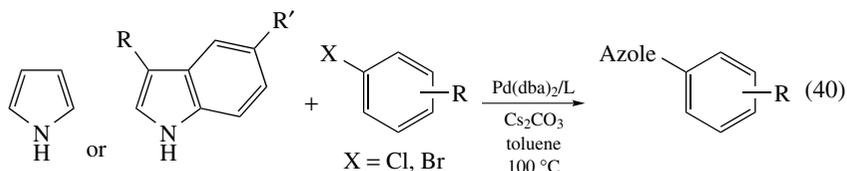
Improved catalysts were necessary for the reactions of indoles, pyrroles and car-bazoles to occur with broader scope under milder conditions. Faster rates for reactions of indole and pyrrole with aryl halides were observed when the reactions were catalyzed by palladium complexes formed by combining a 1:1 ratio of Pd(dba)$_2$ and P(Bu-*t*)$_3$ (equation 40) than when catalyzed by complexes of DPPF[68]. For example, the reaction of 3-bromoanisole with indole catalyzed by 1:1 ratio of Pd(dba)$_2$ and P(Bu-*t*)$_3$ occurred with 3 mol% catalyst at 100 °C over 6 h. In this case, it was necessary to use a weaker base than *t*-BuONa, and the reported chemistry was conducted with Cs$_2$CO$_3$ as base. Mann and coworkers previously demonstrated that high concentrations of azolyl anions can be detrimental to the arylation process by generating stable, anionic bis-azolyl palladium complexes (**36** in Scheme 1), even when the palladium is bound by chelating ligands[125]. The production of these bis-azolyl complexes competes with the formation of neutral complexes (**37** in Scheme 1), which are the species that undergo reductive elimination.

Despite the improved catalyst systems just described, the *N*-arylation of indole, pyrrole and carbazole is not completely general. Competing formation of *N*- and *C*(3)-arylation products has been observed when coupling indole and pyrrole with aryl bromides containing *ortho*-substituents. These hindered aryl halides do, however, undergo clean C−N bond formation with indoles that are substituted in the 3-position. For example, reaction of 2-bromotoluene with 3-methylindole occurred with high yields. Reactions of aryl halides with carbazole were slow and gave low yields of *N*-arylcarbazoles, indicating that palladium complexes formed by combining a 1:1 ratio of Pd(dba)$_2$ and P(Bu-*t*)$_3$ are, indeed, more sensitive to steric effects in this type of C−N bond formation than they are for analogous reactions of amines.
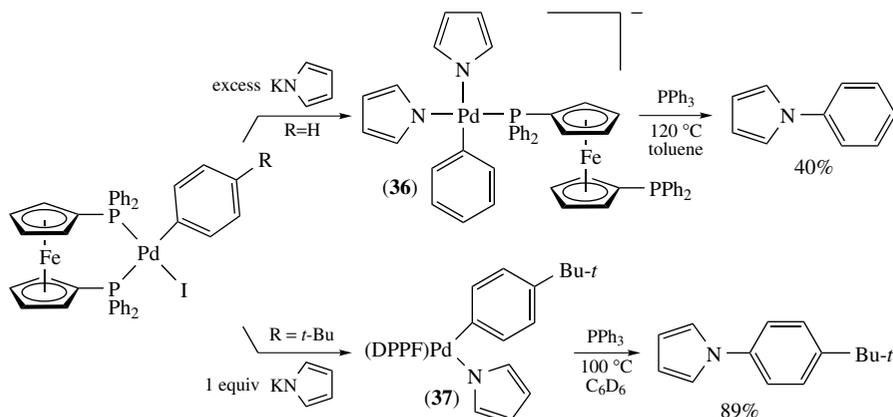
SCHEME 1. Synthesis of the anionic and neutral palladium pyrrolyl complexes and their reactivities

Reactions of indole and pyrrole with chloroarenes also occurred in good yields in many cases when catalyzed by the combination of Pd(dba)$_2$ and P(Bu-t)$_3$. For example, reactions of p-chlorotoluene occurred to give the products of C−N bond formation in yields that were similar to those of the reactions of bromoarenes. However, reactions of indole and pyrrole with aryl chlorides were typically slower than those with aryl bromides. The reactions of deactivated 4-chloroanisole with indole, for example, occurred too slowly under mild conditions to provide useful yields.

Catalysts generated from N-heterocyclic carbenes **23–25** (Figure 7) have been shown to efficiently catalyze the coupling of aryl and heteroaryl halides with indoles. Reactions conducted with the *tert*-butoxide base, which is typically used for the C−N coupling, did not occur, but reactions with NaOH as base occurred to high conversion[85]. Although 4-bromotoluene and bromobenzene reacted with numerous substituted indoles under these conditions, electron-rich and *ortho*-substituted aryl bromides reacted slowly and in low or moderate yields.

The less reactive chlorobenzene and arene sulfonates coupled with phenylindole in the presence of a palladium catalyst generated from X-phos (**31**, Figure 8). For example, 4-*tert*-butylphenyl tosylate reacted to give quantitative yields of N-(4-*tert*-butylphenyl)indole in the presence of 2 mol% Pd, 5 mol% X-phos and K$_3$PO$_4$ as the base[98].

B. Functional Group Tolerance

1. Overview

Most of the coupling of amines and related substrates with aryl halides occurs with the fastest rates and with the highest turnover numbers when the reactions are conducted with t-BuONa as the stoichiometric base. In other cases, however, the strong basicity of this alkoxide greatly limits functional group tolerance. For example, reagents containing nitroarenes, enolizable hydrogens, some free N-H and O-H protic functionality, and labile esters are unsuitable for catalytic aminations using t-BuONa as the base.

Early attempts to solve this problem focused on the use of weaker bases, such as Cs$_2$CO$_3$ or K$_3$PO$_4$[60]. Catalytic aminations conducted with these bases are possible in the presence of esters, aldehydes, enolizable ketones and nitro functional groups on the aryl halide. Alternatively, the functional group tolerance has been shown to be improved

by conducting reactions with the sterically hindered lithium bis(trimethylsilyl)amide as the stoichiometric base[142]. These reactions were conducted with sufficient base, typically 2.2–2.4 equivalents, to deprotonate the protic functionality and to induce the C−N coupling.

2. Reactions with the weaker bases Cs₂CO₃, K₃PO₄, K₂CO₃ and KOH

The weaker base Cs_2CO_3 improved reactions of amines with aryl triflates. In contrast to the high yields obtained from the palladium-catalyzed reactions of amines with electron-rich or electron-neutral aryl triflates in the presence of t-BuONa as the base, modest yields were obtained from the reactions of electron-poor aryl triflates[142]. These lower yields resulted from the greater stability of an electron-deficient phenoxide than of an electron-rich phenoxide, which in turn leads to an increased rate of triflate cleavage. Reactions conducted with Cs_2CO_3 not only occurred in higher yield because of the absence of products from cleavage of the triflate, but occurred with greater functional group tolerance because of the weaker basicity of the system.

Some reactions of functionalized aryl bromides, likewise, can be conducted using Cs_2CO_3 as the base. With catalysts containing monodentate ligands, reactions of amines with electronically diverse aryl halides can be conducted with the weaker carbonate or phosphate bases. With catalysts containing bidentate ligands, reactions of amines with electron-poor aryl halides occur with the weaker bases[60, 67, 142, 143]. Hartwig and coworkers reported that the combination of a phase-transfer catalyst, 1 equivalent of water, and KOH or the combination of phase-transfer catalyst and concentrated aqueous NaOH or KOH led to acceptable reactions and high yield for the formation of arylamines. More importantly, aqueous hydroxide can be used for reactions of substrates bearing reactive nitro, t-butyl ester, enolizable ketones and cyano groups[69]. More recently, Buchwald and coworkers showed that reactions conducted with a catalyst containing X-phos (**31**, Figure 8) and a combination of KOH or K_2CO_3 as base in t-BuOH or H_2O solvent also occur with a higher tolerance for accompanying functional groups[98]. For example, aryl chlorides or sulfonates containing primary amide, amino or free carboxylic acid functional groups all reacted with a variety of amines to give the corresponding products in high yields (equation 41).

$$R\text{—}\underset{}{\underset{}{\bigcirc}}\text{—}X \; + \; HN\underset{R}{\overset{R}{|}} \xrightarrow[\substack{Cs_2CO_3 \text{ or } K_3PO_4 \\ 80-100\,°C}]{\substack{1-4\text{ mol% } Pd_n(dba)_m \\ L = BINAP, \mathbf{7}, \mathbf{13} \text{ or } P(Bu\text{-}t)_3}} X\underset{}{\bigcirc}\text{—}N\underset{R}{\overset{R}{|}}$$

(41)
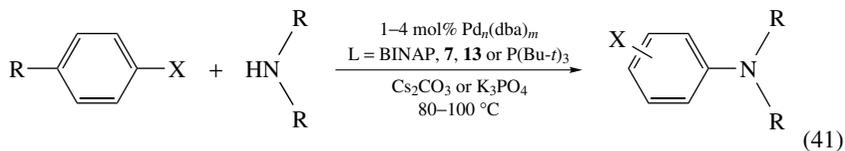
X = Br, R = CN, CHO, COMe, COOMe, base = Cs₂CO₃ for L = BINAP or **7**
X = Cl, R = COOMe, COMe, CN, N₂O, base = K₃PO₄ for L = **13**
         R = Me, base = K₃PO₄ or Cs₂CO₃ for P(Bu-*t*)₃
X = Cl or OTs, R = CONH₂, NH₂, COOH, base = KHO for L = **31**

3. Reactions conducted with LiN(SiMe₃)₂ as base

Although the substrate scope for the palladium-catalyzed aminations of aryl halides was improved by the use of weaker bases, these procedures still had limitations. First, the reactions were typically slower and required higher levels of catalyst than those with t-BuONa as base. Second, reactions of substrates containing alcohol, phenol or amide functional groups have been difficult to accomplish. Recently, Buchwald and coworkers

reported reactions of amines with aryl halides that contain these functional groups with lithium bis(trimethylsilyl)amide as the stoichiometric base (equation 42)[144]. With this simple, commercially available base, the scope of the amination of aryl halides was expanded to include substrates possessing functional groups such as hydroxy, acetanilide and phenoxide. Reactions with catalysts based on Verkade's proazaphosphatrane **14** (Figure 5) also occurred under these conditions[145]. While the transformations occurred in high yield with secondary amines and with primary arylamines, reactions of primary aliphatic amines occurred in low yield, and the couplings of aryl halides containing functional groups *ortho* to the halide did not occur.

$$
R\text{---Ar---}X + HN\begin{matrix}R''\\R'\end{matrix} \xrightarrow[\substack{\text{LHMDS}\\\text{THF/toluene}}]{\text{1--4 mol\% Pd}_n(\text{dba})_m/\text{L}} R\text{---Ar---}N\begin{matrix}R''\\R'\end{matrix}
$$

(42)
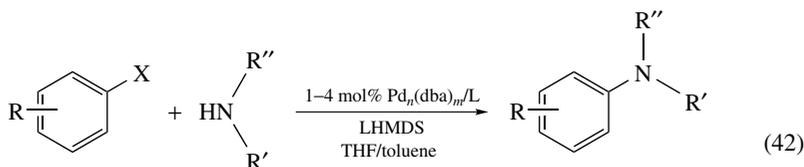
R = NHAc, OH, CH$_2$(CH$_2$)$_n$OH, COOH, CH$_2$COCH$_3$
R′, R″ = alkyl, aryl
L = **8, 12, 17**

As mentioned in Section III.A.2.a.i, reactions of primary amines catalyzed by complexes of chelating phosphines that tightly bind to the metal center can occur with higher selectivity than reactions catalyzed by complexes of hindered monophosphines. Similar trends were observed for reactions of amines with aryl halide bearing a variety of functional groups. Shen, Shekhar, Stambuli and Hartwig reported that reactions of alkylamines with substrates containing multiple functional groups, including primary and secondary alcohols, amides, amines and enolizable ketones, occurred in the presence of catalysts generated from CyPF-Bu-*t* **32** (Figure 9) and with lithium bis(trimethylsilyl)amide as the base. Under these conditions, the reaction of a primary alkylamine with an aryl chloride possessing enolizable hydrogens formed the coupled product in high yield, even with very low (0.05 mol%) catalyst loadings (equation 43)[105].

$$
R\text{---Ar---}X + R'NH_2 \xrightarrow[\substack{\text{LHMDS}\\\text{THF/toluene}}]{\text{0.05--2 mol\% Pd}_n(\text{dba})_m/\text{L}} R\text{---Ar---}NHR'
$$

(43)
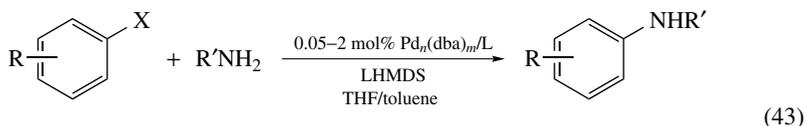
R = NHAc, OH, CH$_2$(CH$_2$)$_n$OH, COOH, CH$_2$COCH$_3$
R′ = alkyl, aryl
L = CyPF-P(Bu-*t*)2 (**32**)

C. Palladacycles, Novel Phosphines and Palladium Dimers

1. Palladacycles and their adducts

Many types of palladacyclic complexes have been used as precursors to catalysts for a variety of coupling processes[146, 147]. Mixtures of dimeric palladacycles containing bridging halide, acetate or trifluoroacetate ions and a phosphine or carbene ligand have been studied as catalysts for the amination of aryl halides. The isolated phosphine adducts can also be applied in catalysis.

These catalysts are more active in some cases than complexes generated from the same ligands and either palladium salts or dba adducts. In general, palladacycles have a higher thermal stability compared to the Pd/phosphine system and precipitation of palladium black is reduced.

The first example of a palladium-catalyzed amination of an aryl chloride, albeit the reaction of a highly activated aryl chloride at a high temperature, was catalyzed by *trans*-di(μ-acetato)bis[*o*-(di-*o*-tolylphosphino)benzyl] dipalladium(II) **38**. *para*-Trifluoromethyl chlorobenzene coupled with piperidine in 98% yield to form a 13:1 mixture of *para* and *meta* regioisomers from a combination of palladium-catalyzed coupling and reactions through benzyne intermediates. Other substrates reacted only in moderate yields[148, 149]. Hartwig and coworkers studied in detail the role of this palladacycle as a source of Pd(0) and proposed a possible mechanism for the formation of the active catalytic species[150] (Scheme 2).
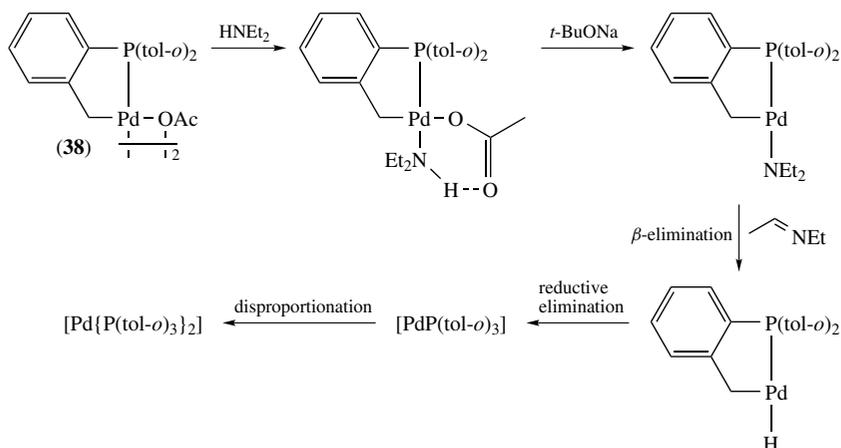
SCHEME 2. Mechanism for the activation of the palladacyclic catalyst precursor **38** to produce [Pd{P(tol-*o*)₃}₂]

Bedford and coworkers studied the catalytic activity of the palladacycles **40** and **41**. These complexes have been isolated, as well as generated *in situ* by cleavage of the cyclometallated palladium dimer with a phosphine (equation 44). The dimeric trifluoroacetate precursor **39** was synthesized by heating *N*,*N*-dimethylbenzylamine with Pd(TFA)₂[151]. The activities of the catalysts generated *in situ* from the combination of palladacycle and phosphine, the combination of Pd(OAc)₂ and phosphine or the isolated phosphine adduct of the palladacycle were ascertained by studying the amination of 4-chloroanisole with morpholine. The order of reactivity of the catalysts generated from Pd(OAc)₂ was PCy₂(*o*-biphenyl) > P(Bu-*t*)₂(*o*-biphenyl) > PCy₃ > P(Bu-*t*)₃. However, the turnover numbers improved significantly for catalysts generated from the *o*-biphenylphosphines and P(Bu-*t*)₃ when the precursor was palladacycle **39**. For example, turnover numbers near 1000 were observed for the reaction of the deactivated 4-chloroanisole with morpholine when catalyzed by a combination of complex **39** and P(Bu-*t*)₃ (entry 9, Table 1).

The *ortho*-palladated phosphinite–phosphine complexes shown in equation 45 are active for Suzuki and Stille coupling of aryl chlorides[152, 153]. Hence, Bedford and coworkers studied the activity of these complexes for the amination of aryl chlorides[151].

TABLE 1.   Amination of 4-chloroanisole with morpholine [a]

Entry	Pd source (mol% Pd)	Added phosphine (mol%)	Conversion [b]	(%) [b] TON
1	Pd(OAc)$_2$ (0.1)	P(Bu-t)$_2$(o-biphenyl) (0.1)	7	70
2	Pd(OAc)$_2$ (0.1)	P(Bu-t)$_2$(o-biphenyl) (0.2)	26	260
3	Pd(OAc)$_2$ (0.1)	PCy$_2$(o-biphenyl) (0.1)	23.5	235
4	Pd(OAc)$_2$ (0.1)	PCy$_2$(o-biphenyl) (0.2)	62.5	625
5	Pd(OAc)$_2$ (0.1)	PCy$_3$ (0.1)	5.5	55
6	Pd(OAc)$_2$ (0.1)	PCy$_3$ (0.2)	7	70
7	Pd(OAc)$_2$ (0.1)	P(Bu-t)$_3$ (0.1)	1	10
8	Pd(OAc)$_2$ (0.1)	P(Bu-t)$_3$ (0.2)	2	20
9	**39** (0.10)	P(Bu-t)$_3$ (0.1)	92	920
10	**39** (0.05)	P(Bu-t)$_3$ (0.1)	17	340
11	**39** (0.05)	PCy$_3$ (0.1)	3.5	70
12	**40** (0.50)		25	50
13	**41** (0.50)		63	126
14	**39** (0.05)	PCy$_2$(o-biphenyl) (0.1)	41	820
15	**39** (0.05)	P(Bu-t)$_2$(o-biphenyl) (0.1)	22.5	450

[a] Conditions: 4-MeOC$_6$H$_4$Cl (1.0 mmol), morpholine (1.26 mmol), t-BuONa (1.39 mmol), toluene (3 mL), 110 °C, 17 h.
[b] Conversion to N-(4-methoxyphenyl)morpholine, average of two reactions, determined by GC (hexadecane standard); TON = turnover number.

The orthometaled dimeric precursor is easily synthesized by the reaction of tris(2,4-di-t-butylphenylphosphite) and PdCl$_2$[154]. The addition of ligand forms the phosphine adducts **42a** and **42b** (equation 45)[152].

$$(44)$$

(**39**)

(**40**) PR$_3$ = PCy$_3$
(**41**) PR$_3$ = PCy$_2$(o-biphenyl)

Y = OC$_6$H$_3$(Bu-t)$_2$-2,4

$$(45)$$

(**42a**) L = PCy$_3$
(**42b**) L = P(Bu-t)$_3$
(**43**) Y = Ph, L = P(Bu-t)$_3$
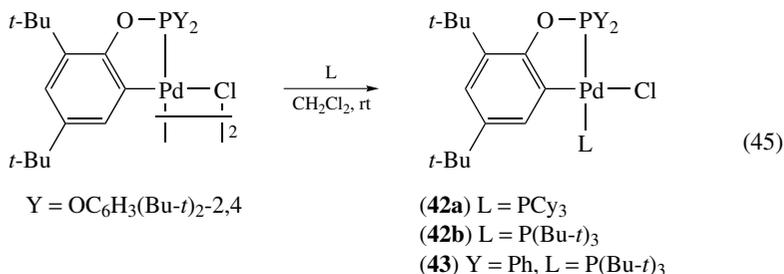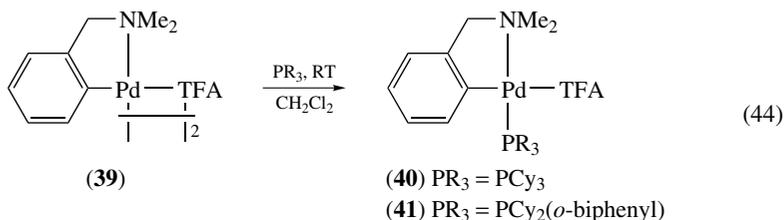
The catalytic activity of **42** and **43** generated *in situ* from mixtures of PCy$_3$ or P(Bu-t)$_3$ and the corresponding cyclometallated chloride dimer were evaluated by studying the reaction of 4-chloroanisole with morpholine[155]. P(Bu-t)$_3$ was found to be the best ligand for this reaction, and turnover numbers as high as 960 were obtained at 100 °C with 0.1% catalyst. The improved performance is thought to be due to the lifetime of the catalyst being lengthened, not due to an increased rate of catalysis. The orthometaled phosphite

is thought to be a 'sacrificial' ligand. The active catalyst is thought to be comprised of a monophosphine Pd(0) complex formed by reductive elimination of the metalated ligand with one of the coupling partners[151, 155].

Nolan and coworkers published a related palladacycle complex containing the N-heterocyclic carbene ligand N,N'-bis((2,6-diisopropylphenyl)imidazol)-2-ylidene[156] (**23**, Figure 7). The complex is air and moisture stable and is obtained by cleaving the cyclometallated dimethylaminobiphenyl chloride dimer with the carbene ligand. The palladacycle carbene adduct catalyzes the coupling of a wide range of aryl chlorides and triflates with morpholines, dialkylamines, aryl alkylamines or primary alkyl amines within 4 h at 70 °C in the presence of 1 mol% of **29**. In addition, 4-chloroanisole and 4-chlorotoluene coupled with morpholine at room temperature within 2 h. The proposed mechanism for the activation of this complex is based on the generation of an aryl alkoxide complex followed by thermal elimination of ether and the formation of a R_3P–Pd(0)–NHC complex.

Zim and Buchwald synthesized the palladacyclic phosphine complex **44** based on their ligand P(Bu-t)$_2$(o-biphenyl) **13** (equation 46)[157]. This air- and moisture-stable palladium complex is a convenient one-component precatalyst for amination of aryl chlorides when combined with sodium *tert*-butoxide or sodium methoxide. For coupling of anilines, the addition of NEt$_3$, which is possibly acting as the reducing agent to produce Pd(0), is necessary.

(46)

(**13**) (**44**)
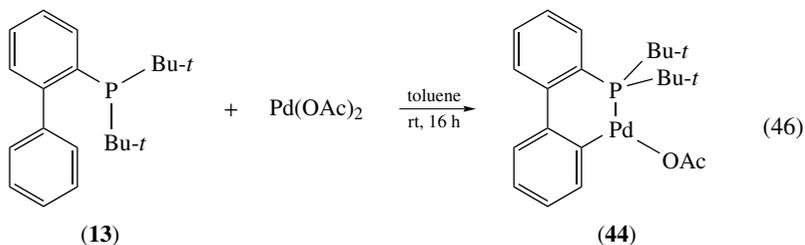
A Solvias research group studied the catalytic activity of a palladacycle formed from dimethylaminobiphenyl, in combination with secondary phosphines. The structures of some of these complexes are shown in Figure 12 (**45a–d**)[158]. The isolated complexes were shown to couple aryl chlorides with N-methylaniline or morpholine in high yields (15 h, 110 °C, 0.5—2 mol% cat). These reactions are rare examples of the use of secondary phosphines in coupling processes. Later, the palladacycle **46** was investigated[159]. The complex containing the ligand with the ferrocene backbone **46** gave higher yields for the

(**45a**) PR$_3$ = HP(norbornyl)$_2$
(**45b**) PR$_3$ = HP(Bu-t)$_2$
(**45c**) PR$_3$ = HPCy$_2$
(**45d**) PR$_3$ = PCy$_3$

(**46**)
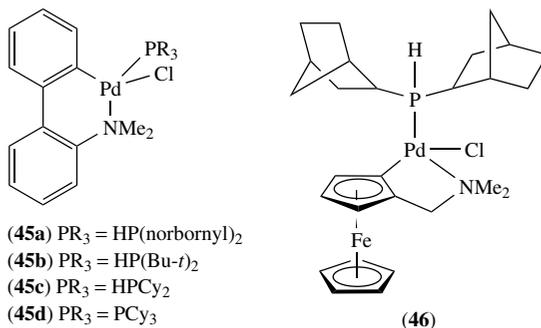
FIGURE 12. Structures of palladacycles developed at Solvias
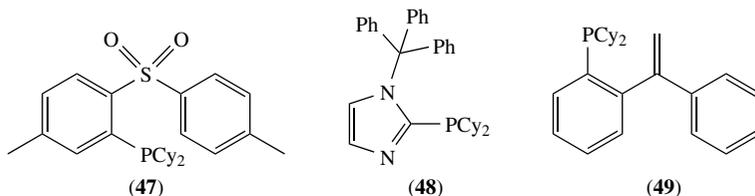
FIGURE 13. Structures of phosphine ligands developed at Pfizer

amination of aryl chlorides (0.5 mol% cat, 2 h, 110 °C) than the related palladacycle **45a** with a biphenyl backbone.

2. Novel phosphines

Tom and coworkers published three new types of phosphines derived from diarylsulfones, tritylimidazole or 2-bromobenzophenone (Figure 13). Their activity in palladium-catalyzed amination of aryl bromides is not general, but they do catalyze the coupling of certain substrates. For example, the coupling of morpholine with 1-bromo-4-nitrobenzene (97% with **47**), 4-bromo-*t*-butylbenzene (81% with **48**) and 4-bromoanisole (96% with **49**) was achieved in high yields[160].

Diphosphinidinecyclobutenes (DPCBs) are good σ donors and strong π acceptors because the phosphorus atoms are sp^2-hybridized with a low-lying LUMO (π*)[161]. The palladium complex **50** is air and moisture stable and was synthesized by treating [Pd(η^3-allyl)Cl]$_2$ with the dpcb ligand, followed by silver triflate (equation 47). The amination of aryl bromides was accomplished at room temperature with 2% catalyst, one equivalent of *t*-BuOK and no solvent[162]. The active catalytic species is believed to be a Pd(0)(dpcb) complex formed by elimination of aminopropene from the catalyst precursor[163, 164].
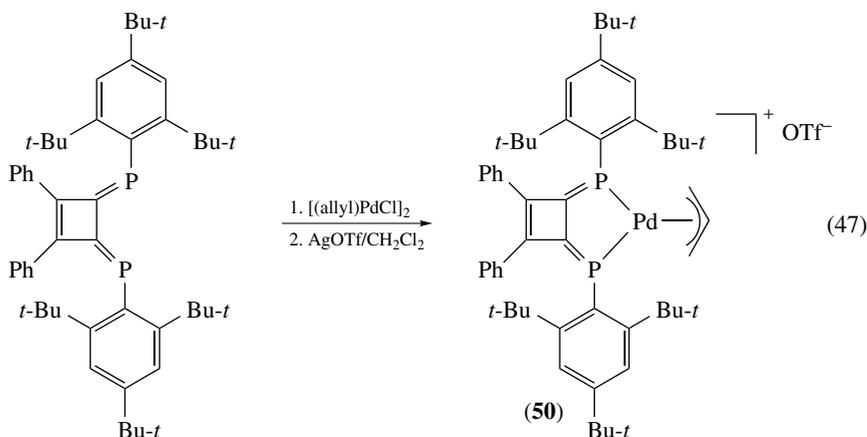
A clever ligand design that makes use of phosphine oxides and their tautomeric phosphinous acids was reported by Li and coworkers at DuPont[165–167]. As shown in Scheme 3, the coordinated di-*t*-butylphosphinous acid **51** makes for a strongly donating ligand when deprotonated, and the ligand is air stable when free in solution. This strategy generated catalysts for a variety of cross-coupling reactions, including aryl halide amination.

Although the substrate scope was not demonstrated to be particularly broad, and coupling of substrate combinations that have been challenging to achieve with other ligands were not studied, the approach to ligand design was a significant departure from conventional systems.
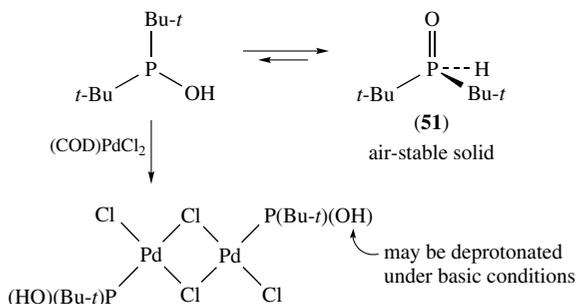
SCHEME 3. Tautomeric phosphine oxides and phosphinous acids used as ligands

3. Phosphine palladium(I) halide dimers

Vilar and coworkers reported the isolation of two new dinuclear Pd(I) dimers containing $P(Bu-t)_2Bph$ (Bph = biphenyl) (equation 48) as ligand[168]. The complexes were prepared by the same conproportionation used to prepare the palladium(I) dimers with trialkylphosphines. The complexes contain a single phosphine, and both metals are coordinated to the terminal phenyl group of the biphenyl unit in a $\mu^2 - \eta^3{:}\eta^3$ fashion. These complexes were tested for the amination of aryl halides with arylamines. The reaction of 4-chlorotoluene with p-tolylamine catalyzed by **52a** or **52b** formed di-p-tolylamine in 78 to 81% yield within 3 h at room temperature, whereas the same reaction conducted with a mixture of $Pd_2(dba)_3$ and $P(Bu-t)_2Bph$ required 80 °C to obtain 90% yield.
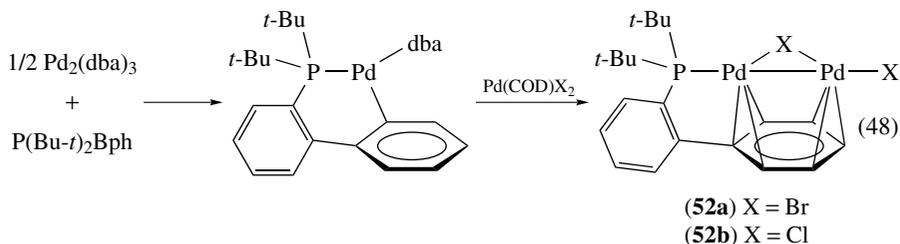
IV. MECHANISM OF PALLADIUM-CATALYZED AMINATION OF ARYL HALIDES

A. Background

The mechanistic aspects of the palladium-catalyzed amination of aryl halides have been studied extensively. This section provides a summary of the conceptual information that has emerged from these studies and that is useful for understanding why a particular catalyst is effective for a certain class of amination reaction and for the design of even more effective catalysts. The three steps of the catalytic cycle have been studied with some of the ligands, typically the ligands used early in the development of this chemistry. Clearly, there will be differences between the mechanism for reactions catalyzed by the

recently developed, highly active systems and those catalyzed by the earlier systems that have been the subject of mechanistic analysis. Nevertheless, basic principles about the catalytic process will apply to all systems. Considering the increased ionic character of the Pd−N or Pd−O bonds vs. Pd−C bonds, and the potential for π-repulsion between the filled metal d- and heteroatom p-orbitals, it is remarkable that these complexes behave as similarly as they do to more classic transition-metal alkyls. Most striking is the ability to conduct C−N bond formation with metal amido complexes bearing β-hydrogens; β-hydrogen elimination from late metal amido complexes was typically believed to be faster than that from transition-metal alkyl complexes. Instead, β-hydrogen elimination from amides may be slower[169].
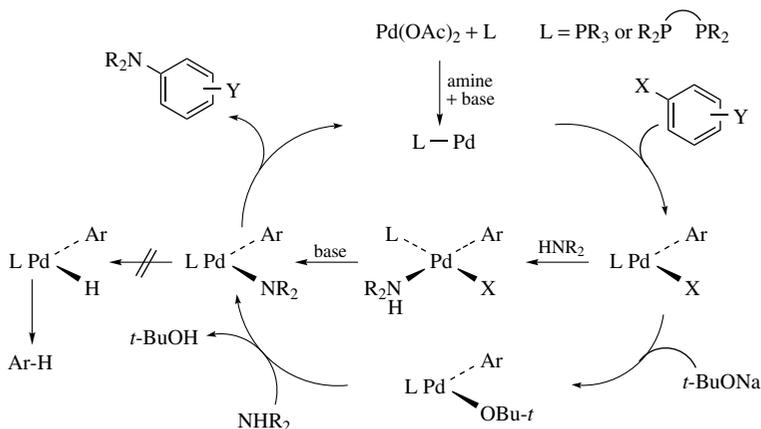
SCHEME 4. General mechanism for palladium-catalyzed amination of aryl halides

The overall mechanism for palladium-catalyzed amination of aryl halides is shown in Scheme 4. Initially, a palladium(0) complex is rapidly formed from Pd(OAc)$_2$ and phosphine ligand in the presence of amine and base. If Pd(dba)$_2$ is used, then either bisphosphine Pd(0) complexes are formed, as with P(Bu-t)$_3$[170], or mixed phosphine/dba palladium(0) complexes are formed as with arylphosphines[171]. When the reactions are initiated with dba complexes, dba is consumed under the reaction conditions, and simple bis-ligand Pd(0) complexes are formed. The mechanism for reduction of Pd(II) to Pd(0) has been studied[172], but the process occurs more rapidly in the presence of amine and base than in the absence of these reagents, even when the amine cannot undergo β-hydrogen elimination.

An unsaturated, Pd(0) complex coordinated by the dative phosphine or carbene ligand undergoes oxidative addition of aryl halide. One set of authors concluded that oxidative addition occurs to a palladium(0) complex [Pd(BINAP)(amine)] with coordinated amine[173]. However, this conclusion has been shown to be invalid, and oxidative addition occurs to [Pd(BINAP)][174]. The resulting arylpalladium halide is converted to an aryl-palladium amide in the presence of amine and base. The arylpalladium amide can then undergo either β-hydrogen elimination to produce arene product and regenerate Pd(0), or it can undergo reductive elimination to form the desired arylamine product and a Pd(0) species. This selectivity for reductive elimination over β-hydrogen elimination is important for determining reaction yields. The pathway by which the immediate product of reductive elimination, most likely a complex of the product amine, converts to the

immediate precursor to carbon–halogen bond cleavage, most likely [Pd(BINAP)(ArBr)] with an intact haloarene, is not well defined for any catalyst at this time.

The step that controls the rate of the overall catalytic cycle is rarely a C−N bond-forming reductive elimination. For reactions of amines with aryl halides in the presence of alkoxide base catalyzed by BINAP or DPPF complexes, the resting state of the catalyst is the Pd(0) species with phosphine ligands. Thus, the oxidative addition portion of the catalytic cycle is the turnover-limiting step. For reactions that employ weak bases, it is likely, although not experimentally verified, that the resting state is the arylpalladium halide. Slower generation of an arylpalladium amide complex from an arylpalladium halide complex is likely to occur with weaker bases. Only in special cases is the reductive elimination turnover limiting. For example, the formation of *N*-aryl azoles and *N*-aryl carbamates may involve reductive elimination processes that are slow enough to act as the turnover-limiting step. The mechanistic discussion below will summarize the experimental data pertaining to the three steps of the cycle involving the palladium complexes that are useful for carbon–heteroatom bond formation.

B. Oxidative Addition

Extensive mechanistic studies have been conducted on the oxidative addition of aryl halides to Pd(0) complexes ligated by PPh$_3$ in different media and with different additives[175, 176]. However, palladium complexes containing these ligands are not active catalysts for amination. Instead, one must consider the addition of aryl halides to palladium complexes bound by ligands relevant to amination. Studies of the mechanism of oxidative addition to palladium(0) complexes of P(tol-*o*)$_3$, DPPF, BINAP, Q-phos, P(Bu-*t*)$_3$ and an *N*-heterocyclic carbene ligand have been reported.

Amatore and coworkers have studied the addition of aryl halides to Pd(0) complexes formed by the addition of chelating phosphines to Pd$_2$(dba)$_3$[171]. Addition of these ligands to Pd$_2$(dba)$_3$ generates mixed phosphine/dba complexes. The kinetic behavior of the complex containing BINAP as phosphine ligand indicated that two competing pathways for addition occur, one by direct reaction of aryl halide with (BINAP)Pd(dba) and one from the (BINAP)Pd intermediate formed by dissociation of dba.

$$\text{L}-\text{Pd}-\text{L} \underset{+\text{L}}{\overset{-\text{L}}{\rightleftharpoons}} \text{L}-\text{Pd} \xrightarrow{\text{ArBr}} \text{L}-\text{Pd}\begin{smallmatrix}\text{Ar}\\\text{Br}\end{smallmatrix} \xrightarrow[\substack{\text{P(tol-}o)_3}]{\text{for L} =} \text{(49)}$$

stable if L is a bulky
or chelating phosphine
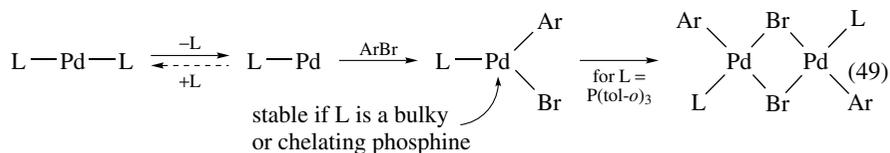
Hartwig has studied the addition of aryl halides to isolated homoleptic Pd(0) complexes containing the phosphines P(tol-*o*)$_3$, DPPF, BINAP and Q-phos (equation 49)[177–179]. Kinetic studies of the reactions of aryl halides with the L$_2$Pd complex containing P(tol-*o*)$_3$ as ligand in aromatic or THF solvent showed that carbon–halogen bond cleavage occurs by a monophosphine Pd(0) species that does not contain solvent directly coordinated to the metal center. An associative mechanism involving reversible displacement of phosphine by aryl halide to make a dative ArX complex prior to carbon–halogen bond cleavage has not been ruled out, but dissociation of ligand clearly precedes the carbon–halogen bond cleavage step.

The palladium complexes (DPPF)$_2$Pd and (BINAP)$_2$Pd also undergo dissociation of ligand, this time to form a (chelate)Pd(0) intermediate that undergoes oxidative addition. Addition of phenyl bromide to (BINAP)$_2$Pd(0), conducted with high ratios of aryl bromide to free phosphine, were close to zero order in phenyl bromide.[178] Under these

conditions, dissociation of phosphine is the major contributor to the rate of the oxidative addition process. However, a second minor pathway for oxidative addition has also been revealed during studies of the oxidative addition of PhBr and PhI to (BINAP)$_2$Pd(0). This mechanism appears to occur by partial dissociation of a BINAP ligand to generate [Pd(κ^1-BINAP)(κ^2-BINAP)], which reacts with the aryl bromide[180].

The additions of aryl halides to PdL$_2$ complexes of Q-phos derivatives were recently reported by Barrios-Landeros and Hartwig[179]. The addition to PhI, PhBr and PhCl takes place through distinct mechanistic pathways (Scheme 5). Iodobenzene reacts by associative displacement of a phosphine, bromobenzene reacts by rate-limiting dissociation of phosphine, and chlorobenzene reacts by reversible dissociation of phosphine, followed by oxidative addition.
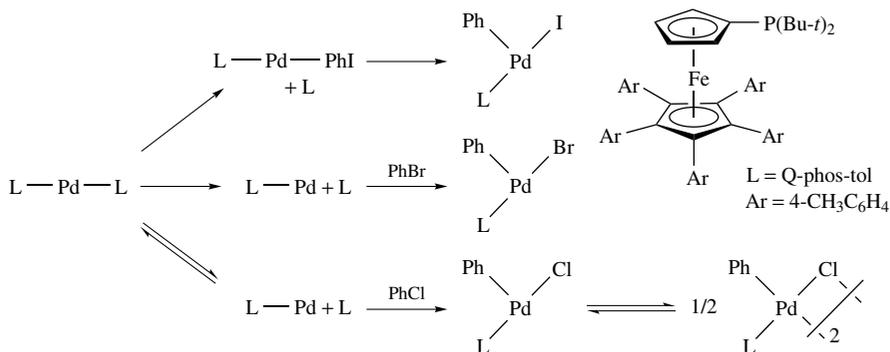
SCHEME 5. Distinct mechanisms for the oxidative addition of ArX (X = I, Br, Cl) to Pd(Q-phos-tol)$_2$

Brown and coworkers reported studies of the addition of aryl iodides to a series of palladium complexes of trialkylphosphines with the general formula Pd[(P(Cy)$_n$(Bu-t)$_{3-n}$)]$_2$ ($n = 0-3$)[181]. They concluded that the complexes of the smaller phosphines ($n = 2, 3$) react with PhI through an associative mechanism and undergo oxidative addition directly to the PdL$_2$ complex. They also concluded that oxidative addition of PhI to complexes of the bulkier phosphines ($n = 0-1$) proceed after dissociation of ligand to generate PdL. In unpublished work, Barrios-Landeros and Hartwig have found that the kinetic behavior of the reactions of these complexes is complex and that these reactions occur with profiles that are characteristic of autocatalysis.

Caddick and Cloke had studied the oxidative addition of aryl chlorides to palladium(0) complexes of the N-heterocyclic carbene with $tert$-butyl groups on the two nitrogens[182, 183]. They isolated and characterized the product of oxidative addition [Pd($cyclo$-C{Nt-BuCH}$_2$)$_2$(4-MeC$_6$H$_4$)Cl] as a square planar complex with a $trans$ configuration. The rate data on the reactions conducted with equal concentrations of the palladium(0) species and the aryl chloride are consistent with oxidative addition after dissociation of ligand. At high concentrations of aryl chloride, the reaction was independent of the concentration of PhCl, presumably because dissociation of ligand becomes the rate-limiting step.

1. Characterization of intermediates

The monoligated [PdL] species has been proposed many times as an intermediate in coupling reactions catalyzed by complexes of hindered monodentate ligand. Oxidative addition to this species would produce an arylpalladium halide complex with only
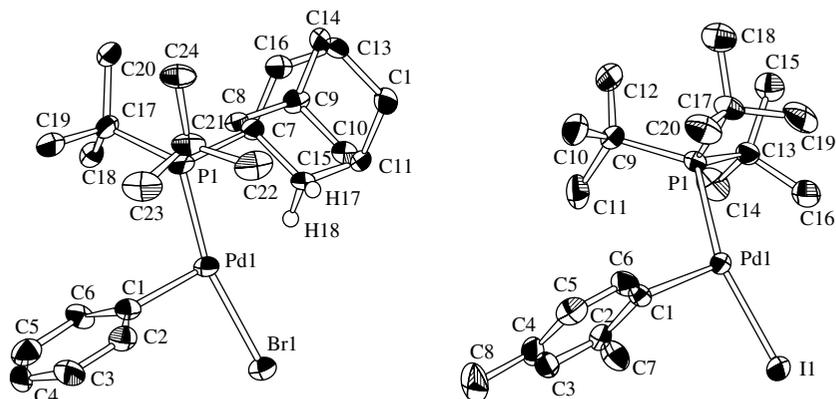
FIGURE 14. [Pd(P(Bu-t)$_2$(1-adamantyl))(Ph)Br] (**53**), [PdP(Bu-t)$_3$(m-xylyl)I] (**54**). Reprinted with permission from (**185**). Copyright 2002 American Chemical Society

three ligands[184]. Stable monomeric complexes of this type have now been isolated, and they have been characterized by many spectroscopic, structural and theoretical methods. The complexes were reported by Stambuli and Hartwig and were prepared by oxidative addition of ArBr and ArI to the Pd(0)L$_2$ complexes or a combination of Pd(dba)$_2$ and ligand. Complexes of this type were prepared with P(Bu-t)$_2$(1-adamantyl) **53**, P(Bu-t)$_3$ **54** (Figure 14) and Q-phos as the phosphine ligand bound to palladium[185, 186]. These complexes contain only three ligands, and they appear to be stabilized by an additional agostic interaction.

C. Reductive Elimination and β-Hydrogen Elimination

1. Fundamental principles

Several studies of the reductive elimination to form C−N bonds and one study on β-hydrogen elimination from late metal amido complexes have been reported. From this work, several principles that control the relative rates for reductive elimination and β-hydrogen elimination have been revealed. First, C−N bond-forming reductive elimination can occur from either 3-coordinate monophosphine or 4-coordinate bis-phosphine complexes[187]. Elimination from the 3-coordinate species appears to be faster[188]. Second, β-hydrogen elimination reactions that start with square planar amido complexes appear to occur predominantly or exclusively from a three-coordinate intermediate formed by phosphine dissociation[169]. Thus, chelating ligands tend to block β-hydrogen elimination, and arylamine products are formed by reductive elimination from a *cis*, four-coordinate species. Third, the rate of reductive elimination is strongly dependent on the nucleophilicity of the heteroatom and electrophilicity of the palladium-bound aryl group[187]. Complexes containing covalent ligands with more nucleophilic heteroatoms bound to palladium undergo reductive elimination more rapidly than those with less nucleophilic heteroatoms bound to palladium. A complementary effect of the aryl group's electronic properties on the rate of reductive elimination is observed. Electron-withdrawing substituents on the aryl group bound to palladium accelerate the rate of reductive elimination[187]. Fourth, steric properties of the phosphine ligand appear to dominate electronic properties. Complexes of sterically hindered alkylphosphine ligands, which are strong electron donors, undergo related reductive eliminations to form the C−O bond in ethers faster than complexes of smaller alkylphosphine ligands or even smaller arylphosphines[189].
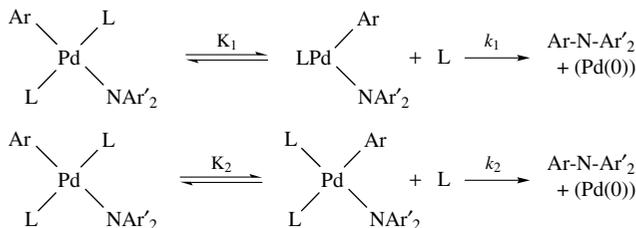
SCHEME 6. Concurrent mechanisms for reductive elimination of amines

2. Studies of the reductive elimination of arylamines

Direct observations of the reductive elimination of arylamines encompass complexes containing PPh_3[187], DPPF[187, 190–192], P(tol-o)$_3$[193], P(Bu-t)$_3$, Q-phos and FcP(Bu-t)$_2$[188] as ligands. Except for complexes of P(tol-o)$_3$, examples of arylpalladium amido complexes that precede reductive elimination were stable enough to isolate and fully characterize. Kinetic studies on the elimination from PPh_3 complexes revealed competing elimination from both three- and four-coordinate intermediates (Scheme 6)[187]. Because some of the arylpalladium amido complexes with PPh_3 as ligand were dimeric and others monomeric, a direct comparison of reaction rates for different types of amido complexes could not be made. However, complexes of DPPF did undergo reductive elimination without prior rearrangements. Thus, one could readily determine that complexes with more electron-rich amide ligands (**55a–55c**) reacted faster, and complexes with more electron-poor aryl groups reacted faster (equation 50). Further, the generation and characterization of DPPF-ligated palladium alkylamido complexes in solution allowed a direct observation of the improved selectivity for reductive elimination over β-hydrogen elimination from complexes containing primary alkylamido ligands[187, 190].

$$NR_2 = \quad \textbf{(55a) NR}_2 = NTol_2\text{: 80 °C, 2 h}$$
$$\textbf{(55b) NR}_2 = NHPh\text{: 25 °C, 1 h}$$
$$\textbf{(55c) NR}_2 = NHBu\text{-}i\text{: 0 °C, 1 h}$$

(50)
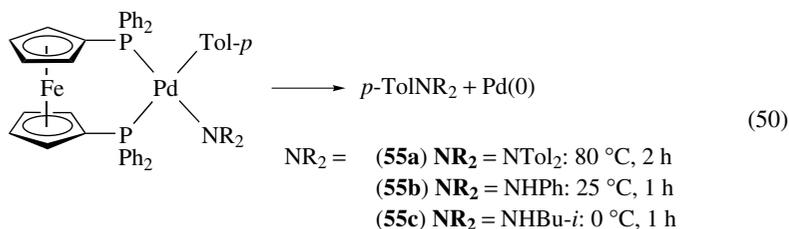
a. Electronic effects on reductive elimination. In order to understand how the relative orientation of ancillary ligands to the aryl and amido groups affects the rate of reductive elimination, Yamashita, Vicario and Hartwig conducted a thorough study of the reductive elimination from palladium amido complexes ligated by symmetrical and unsymmetrical derivatives of DPPF[191] (complexes **56–61**, Figure 15). Systematic variations of the aryl substituents on the ligand, the amine and the metal center led to the conclusion that the orientation of the stronger and weaker phosphine donors, with respect to the amido and aryl groups, can significantly influence the rate of reductive elimination. In fact, the magnitude of the effect of the difference in orientation of the more electron-donating and less electron-donating phosphino groups on the rate of reductive elimination is similar to that from a variation of the overall electron-donating properties of the ligand. In short, the electronic effects of the phosphine *trans* to the amido group were larger than the

(**56a**) Ar = Ph, Ar′ = 4-MeC$_6$H$_4$

(**56b**) Ar = Ar′ = Ph

(**56c**) Ar = Ph, Ar′ = 4-MeOC$_6$H$_4$

(**57**) Ar = 4-MeOC$_6$H$_4$, Ar′ = 4-MeC$_6$H$_4$

(**58**) Ar = 4-CF$_3$C$_6$H$_4$, Ar′ = 4-MeC$_6$H$_4$

(**59**) R = Ph, R′ = 4-MeOC$_6$H$_4$

(**60**) R = 4-CF$_3$C$_6$H$_4$, R′ = Ph

(**61**) R = 4-CF$_3$C$_6$H$_4$, R′ = 4-MeOC$_6$H$_4$
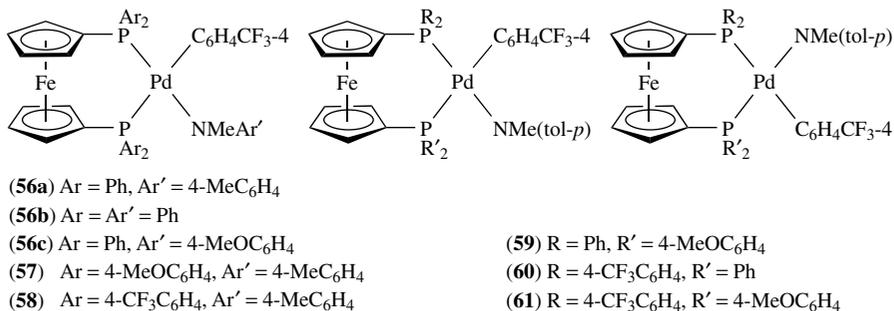
FIGURE 15. DPPF amido complexes with aryl groups of different electronic properties

electronic effects of the phosphine *trans* to the Pd-bound aryl group (**59–61**). These changes in rate as a function of the electronic properties of the ligand *trans* to the aryl and the amido group were best rationalized by ground-state effects. This study also compared the relative magnitudes of the effects of the electronic properties of the groups on the dative ligand (**56a**, **57**, **58**) and the effects of the electronic properties of the groups on the ligands directly involved in the C−N bond formation (**56a–c**). Complexes of electron-donating substituents on the aryl group of the amido ligand react faster than those with electron-withdrawing substituents, and the magnitude of the effect of the substituents on the arylamido group was larger than the effect of the substituents on the arylphosphino groups.

b. Isolation of three-coordinate intermediates. Yamashita and Hartwig isolated three-coordinate arylpalladium amido complexes with the bulky phosphines P(Bu-t)$_3$, Q-phos and FcP(Bu-t)$_2$[188]. Some of these complexes have truly three-coordinate T-shaped geometries and possess no detectable agostic interaction at the empty coordination site. Complexes with an electron-rich *p*-anisyl group and an electron-poor diarylamide with Ar = 3,5-(CF$_3$)$_2$C$_6$H$_3$ were stable enough to be isolated (Figure 16). These complexes underwent reductive elimination of triarylamine directly from the three-coordinate complex upon heating at 60–75 °C.
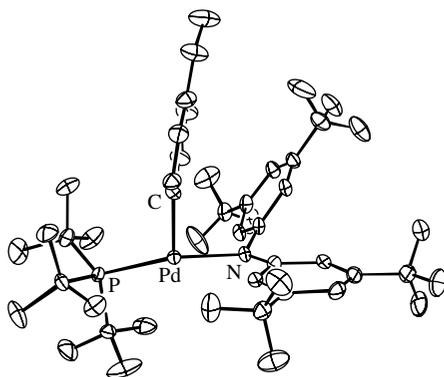
FIGURE 16. [PdP(Bu-t)$_3$(4-OMeC$_6$H$_4$)N(3,5-(CF$_3$)$_2$C$_6$H$_3$)$_2$]

One can assess, at least qualitatively, the relative rates for reductive elimination from three- and four-coordinate complexes by comparing the rate of reductive elimination from the isolated or spectroscopically observed three-coordinate arylpalladium amides and the isolated four-coordinate DPPF complexes. The elimination of N(anisyl)(tol-p)$_2$ from (P(Bu-t)$_3$)Pd(anisyl)[N(tol-p)$_2$] occurs at $-10\,^\circ$C with a half-life of 20 min, while reductive elimination from [(DPPF)Pd(anisyl)[N(tol-p)$_2$] occurs at $75\,^\circ$C with a half-life of 55 min.

3. Relative rates of reductive elimination and β-hydrogen elimination

Several studies have assessed the effect of ligand steric and electronic properties on the relative rates for the two major reactions of arylpalladium amido complexes. In one study, the effects of the structures of chelating ligands on the reductive elimination and β-hydrogen elimination were evaluated. The ratios of products formed from the catalytic process were measured for reactions conducted with bisphosphine ligands with varied bite angles, electronic properties and steric properties[106]. In general, electronic effects produced minor changes in product distribution of the catalytic process[106]. Moreover, the electronic effect on product distribution in the catalytic amination was surprising: complexes of the more electron-rich phosphine formed higher ratios of arylamine to arene than complexes of the less electron-rich phosphine. This trend is the opposite of what one would expect from conventional acceleration of reductive elimination and deceleration of β-hydrogen elimination by reduction of electron density at the metal center[194].

A second study evaluated the effect of the steric properties of a series of monophosphine ligands on the selectivity for formation of products that result from reductive elimination vs. β-hydrogen elimination from arylpalladium dialkylamido intermediates[195]. This study showed that an increased size of the phosphine ligand accelerates the rate of reductive elimination, relative to that of β-hydrogen elimination (equation 51). These results are rationalized by the decrease in coordination number resulting from reductive elimination and increase in coordination number resulting from β-hydrogen elimination, which generates a hydride and imine ligand from an amide.

In addition to these two studies of the partitioning of late metal amide toward reductive elimination and β-hydrogen elimination, a study was published of directly observed β-hydrogen eliminations from Ir(I) primary alkylamido and N-alkyl arylamido complexes that are isoelectronic with the arylpalladium(II) amido complexes of the catalytic amination (equation 52)[169]. This study showed that β-hydrogen elimination from amides can be dramatically slower than β-hydrogen elimination from the analogous alkyl complexes ($70-110\,^\circ$C vs. $0\,^\circ$C). It also showed that β-hydrogen elimination occurred from a three-coordinate intermediate, as is typical for β-hydrogen elimination from alkyl groups of square planar complexes.

$$L = P(\text{tol-}o)_3$$
$$P(\text{tol-}o)_2Ph$$
$$P(\text{tol-}o)Ph_2$$
$$PPh_3$$

Ar-NEt$_2$: Ar-H
9 : 1
8 : 1
3 : 1
1 : 1.2

(51)

$$(52)$$
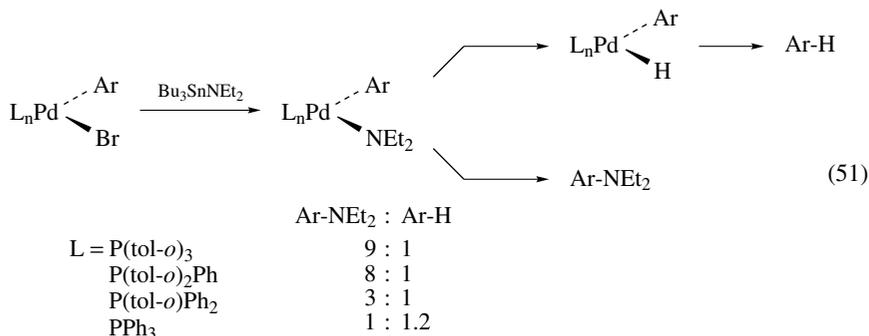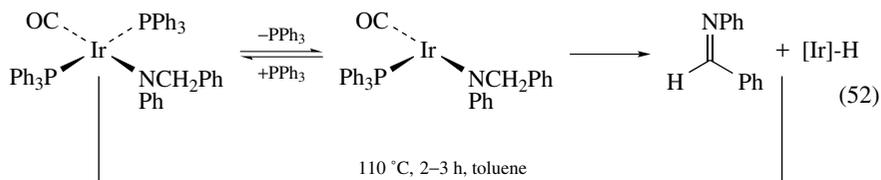
4. Formation of amido complexes in the catalytic process

Three general mechanisms can be envisioned for the formation of amido complexes from arylpalladium halides: direct substitution of halide by alkali amide generated by simple deprotonation of free amine by free base, coordination of amine to the metal center followed by deprotonation of the more acidic coordinated amine, or formation of a palladium alkoxide complex that reacts with amine to form a palladium amide and alcohol. The mechanism followed for this step of the cycle depends on the identity of the catalyst, base and nitrogen substrate. In general, the first mechanism should be avoided because alkali amides react with aryl halides to generate benzyne intermediates and to undergo electron transfer processes[8, 196]. In addition, stabilized nitrogen anions such as pyrrolyl or anilide ions can generate stable ate complexes with palladium[187, 197]. Therefore, a low concentration of most nitrogen anions is desired. In special cases, such as the reactions of diarylamines, palladium-catalyzed amination with anionic amide reagents can provide good yields[99], but there is generally no advantage to this procedure over the use of a weaker base in the presence of amine.

$$(53)$$
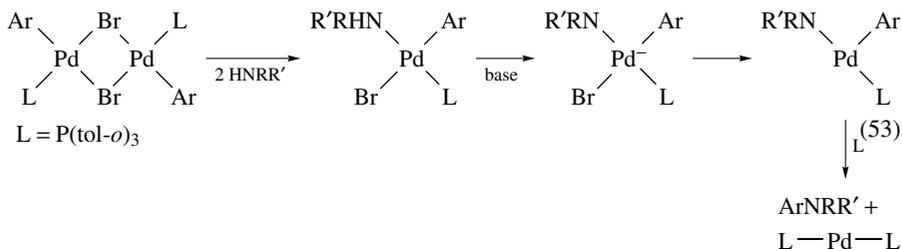
The second mechanism involving deprotonation of coordinated amine is the most likely pathway followed by reactions catalyzed by palladium monophosphine complexes (equation 53). The catalytically active arylpalladium halide intermediates with bulky monophosphine ligands are three-coordinate complexes that can bind amine[198−201]. These mixed amine phosphine complexes can then undergo deprotonation by bases whose conjugate acids are weaker than the amine substrate. For example, alkylamine complexes of arylpalladium halides containing $P(tol\text{-}o)_3$ as ligand have been deprotonated at low temperature by silylamide base to give the coupled product after generation of the palladium amide[193]. Presumably, this general mechanism operates when carbonate or phosphate bases are employed, although the deprotonation process probably occurs at the surface of the solid base in aromatic solvents. The mechanism for the generation of palladium amides during reactions conducted with weak bases or palladium complexes bearing chelating phosphines is less clear. Most likely, deprotonation of a five-coordinate amine complex occurs, but replacement of halide by amine and deprotonation of the resulting cationic amine complex is an alternative pathway. This latter mechanism most likely occurs during catalytic amination of aryl triflates using carbonate or phosphate base because of the lability of the triflate ligand. No mechanistic data have been obtained to

support these pathways involving complexes with chelating ligands, although they have been frequently proposed.

$$(54)$$

R = R' = p-tol
R = H, R' = Ph
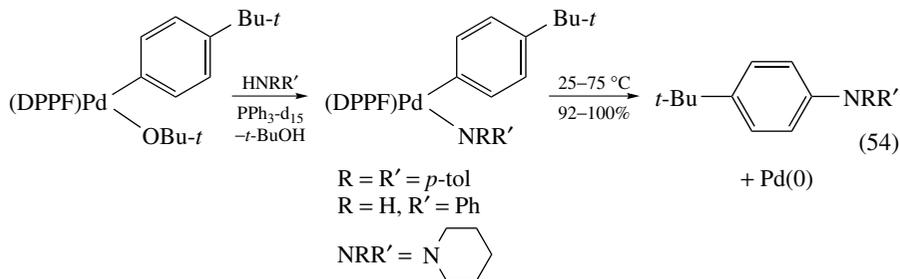
The final pathway, which involves alkoxide intermediates, has been shown to occur when reactions are conducted with t-BuONa as base and DPPF as ligand (equation 54)[192]. DPPF-ligated arylpalladium t-butoxide complexes have been isolated. Reactions of these complexes with arylamines led to rapid formation of the amido complex and subsequent reductive elimination of diarylamine. Reactions with secondary alkylamines led to formation of dialkylanilines, presumably through the intermediacy of an arylpalladium dialkylamido intermediate. Reaction of the DPPF-ligated, arylpalladium halide complexes with alkoxide and dialkylamine together first formed the alkoxide complex. This complex subsequently reacted with amine and reductively eliminated the dialkylaniline. The observation of the alkoxide complex in this reaction strongly suggests the intermediacy of the alkoxide complex in the catalytic reactions[125].

V. COPPER-MEDIATED METHODS

A. Ullmann and Goldberg Reactions: Copper-mediated Amination and Amidation of Aryl Halides

At the beginning of the 20th century, Fritz Ullmann[202–205] started his pioneering work on copper-mediated coupling reactions of aryl halides. He explored new ways to form aryl−C, aryl−N and aryl−O bonds and, thus, paved the way to access a wide range of new products. The formation of biaryls from the copper-mediated reductive coupling of two aryl halides was the first type of coupling reported by Ullmann's laboratory[202]. Two years later he reported that copper compounds could promote the *ipso*-substitution of an aryl halide by nucleophiles such as phenoxides and aryl amines[203] (equation 55). These reactions comprised the first nucleophilic aromatic substitution of unactivated aryl halides. Previous reactions required electron-poor aryl halides in combination with strong nucleophiles. In 1906, Irma Goldberg[206] extended the scope of the reactions that formed C(aryl)−N bonds to include the formation of C(aryl)−N bonds from the reactions of aryl halides with aryl amines or aryl amides in the presence of catalytic amounts of copper (equation 56). A large number of review articles on copper-mediated formation of C−N bonds have appeared[207–214], and this body of literature signals the importance of this work in both academic and industrial laboratories.

$$(55)$$

$$(56)$$
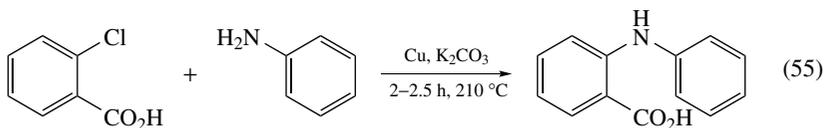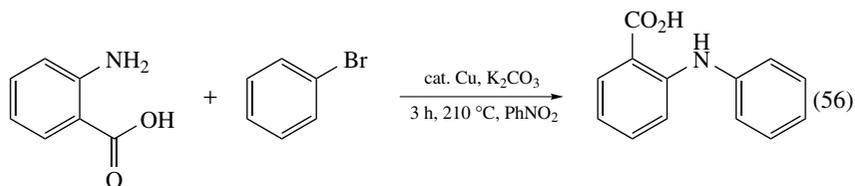
1. Reactions of aryl halides with amines without additives

The first report of copper-mediated C−N bond coupling was published in 1903[203]. In this work, o-chlorobenzoic acid was coupled with aniline without solvent under refluxing conditions in the presence of a stoichiometric amount of copper metal (equation 57). Reactions conducted with added K_2CO_3 occurred in higher yields than reactions without K_2CO_3 because the alkali metal salt of the product N-phenylanthranilic acid was less prone to decarboxylation and resinification in the presence of added base. Later, a variety of anthranilic acids were prepared by condensing anilines with o-chlorobenzoic acids, and other diarylamines were prepared by coupling of anilines with other aryl halides[206, 215−217]. These reactions were generally conducted in refluxing amyl alcohol or nitrobenzene.

$$(57)$$
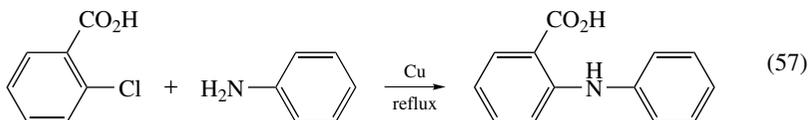
In addition to the drawback of harsh conditions required for these reactions, Ullmann condensations can generate substantial amounts of product from reductive dehalogenation of the aryl halide[218]. Dehalogenation is strongly dependent on the extent to which the halogen atom is activated. Aryl chlorides having electron-withdrawing groups are more sensitive to hydrodehalogenation. Moreover, the reaction is sensitive to the presence of oxidants and added halides. Copper metal itself does not mediate these reactions unless elemental oxygen is also present[215]. The oxygen evidently converts the Cu(0) to a metal salt that mediates the coupling process. CuI is an active catalyst in the presence of KI, and under these conditions Cu(II) is disfavored. This finding suggests that a Cu(I) species is the active catalyst[216].

Traditionally, Ullmann condensation of aryl halides with amines has been conducted by heating ($>150\,^\circ$C) the substrates in the presence of copper powder and a base, such as sodium or potassium carbonate or hydroxide, in a polar solvent[219]. This method has been used extensively for the synthesis of intermediates in pharmaceutical, agro-chemical, fine and polymer chemistry[208]. For example, N-phenylanthranilic acid, an important intermediate in the synthesis of acridinones[220], is synthesized from reactions of o-halobenzoic acids with anilines in water[221] or dimethylformamide[222] with K_2CO_3 as base and Cu powder as catalyst (equation 58). Ultrasonic techniques have been used to improve the yields[222, 223]. Zeide and coworkers condensed o-chlorobenzoic acid and 2-aminopyridine with Cu powder as catalyst under dry conditions to synthesize 11-H-pyrido-[2,1-n]quinazolin-11-one[224], an antiallergic, cell protectant and hypolipemic agent. Later, other derivatives of pyridoquinazolones were also synthesized by Ullmann reactions with Cu powder as catalyst, K_2CO_3 as base, DMF and solvent[225], and ultrasonic treatment[226]. This type of Ullmann coupling is also used extensively for the synthesis

of *o*-arylaminodiarylazo dyes[227], 1-aminoanthraquinones[228] and *N*-arylimidazoles[229–233], important compounds in pharmaceutical research.

$$\text{(58)}$$
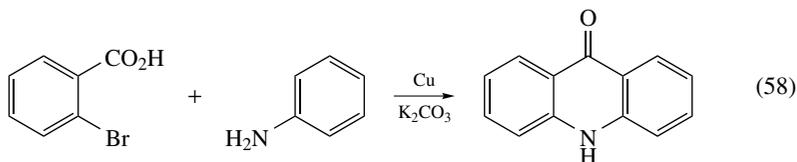
In addition to reactions initiated with copper metal, reactions have been conducted with copper salts, such as copper oxides, alloys and coordination complexes. Reactions with many bases in several polar solvents have also been explored. Diphenylamine and *o*-bromonitrobenzene couple with stoichiometric amounts of copper(I) oxide and copper(I) bromide in DMA (equation 59)[234]. The synthesis of triaryl amines from aryl iodides and arylamines in one-pot proceeds in the presence of CuI and potassium *tert*-butoxide at 135 °C[235]. The highest yields were obtained with aryl iodides and electron-rich arylamines.

$$\text{NHAr}_2 + \text{Ar}'\text{Br} + 0.5\ \text{Cu}_2\text{O} \xrightarrow[\text{165 °C}]{\text{Me}_2\text{NAc}} \text{NAr}_2\text{Ar}' + \text{CuBr} + 0.5\ \text{H}_2\text{O} \qquad \text{(59)}$$
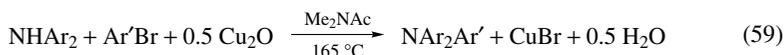
Phase-transfer agents like crown ethers and ethylene oxide oligomers have been used in the preparation of di- and tri-phenylamines with copper catalysts[236–238]. Miller and coworkers[237] reported reactions with 18-crown-6, K_2CO_3, Cu or Cu bronze in a high boiling solvent to synthesize nitroazobenzene dyes by coupling aryl iodides with amino-substituted azo dyes.

Dihydroindoles and tetrahydroquinolines were prepared by an unusually mild version of the Ullmann reaction: intramolecular cyclizations with the combination of CuI (2 equivalents) and CsOAc (5 equivalents) in DMSO[239, 240] over 1–24 h at temperatures ranging from room temperature to 120 °C (equation 60). The scope of this reaction was extended to the preparation of six- and seven-membered fused ring systems. Later, the same authors described the synthesis of *N*-arylalkylamines by an intermolecular reaction between aryl iodides and alkyl amines in the presence of CuI (1.0 equivalent) and CsOAc (2.5 equivalents) in DMSO[241]. Reactions of alkyl amines with aryl iodides having both electron-withdrawing and electron-releasing *para*- and *meta*-substituents occurred in good to excellent yields (70–93%). Selective monoamination of 4-bromoiodobenzene and of 1,4- or 1,3-diiodobenzene occurred. The reactions were strongly hampered by *ortho*-substituents.

$$\text{(60)}$$

$$n = 1\text{–}2$$
$$X = I,\ Br \qquad 39\text{–}98\%$$
$$R = Ns,\ Bn,\ H$$
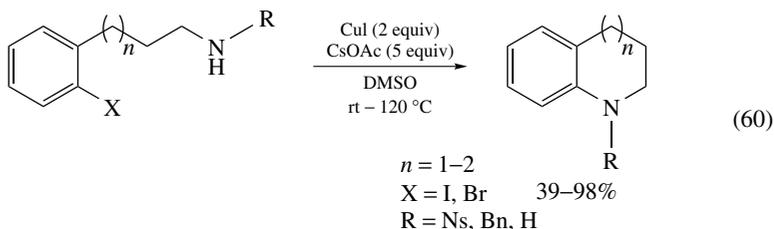
The development of milder intermolecular reactions began with reactions of amino acids. A general *N*-arylation of *α*-amino acids with aryl halides catalyzed by CuI (10 mol %), with K_2CO_3 (1.5 equivalents) as base and DMA as solvent at 90 °C has been reported
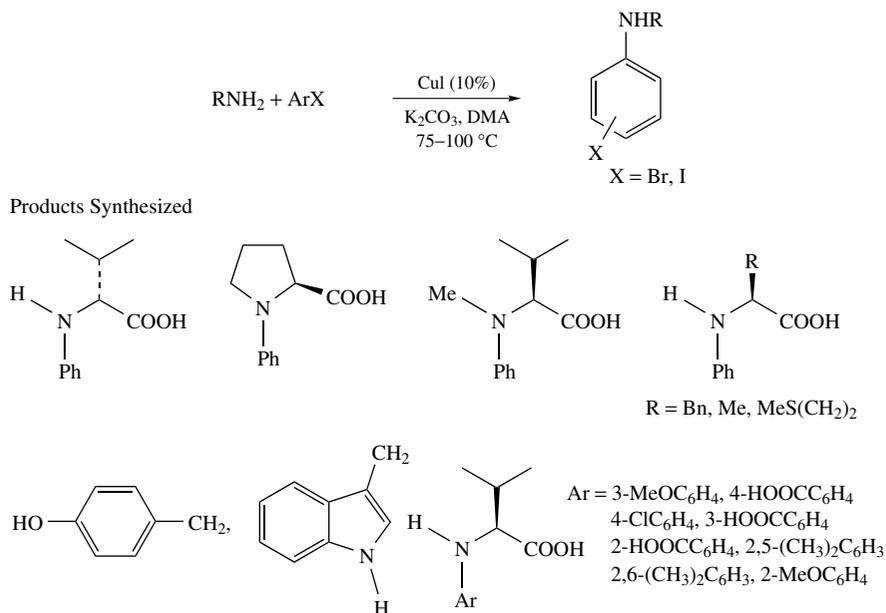
SCHEME 7. *N*-Arylation of α-amino acids with aryl halides

(Scheme 7)[242]. These reactions occurred at lower temperatures than typical Ullmann condensations, even with electron-rich aryl iodides and bromides. No racemization of the amino acid was observed in most cases. Systematic studies of a variety of amino acids as well as different aryl halides and copper ion sources allowed the formation of a wide range of products[243–245]. β-Amino acids and β-amino acid esters were also found to undergo the CuI-catalyzed coupling of aryl iodides and bromides in the absence of any added ligand (equation 61)[243]. To improve the reactivity of amino acids with hydrophilic substituents, tetrabutylammonium hydroxide was added to solubilize the substrates. The products from Ullmann coupling were then obtained in modest yields in the presence of CuI in either MeCN, DMF or DMA[245, 246].

(61)
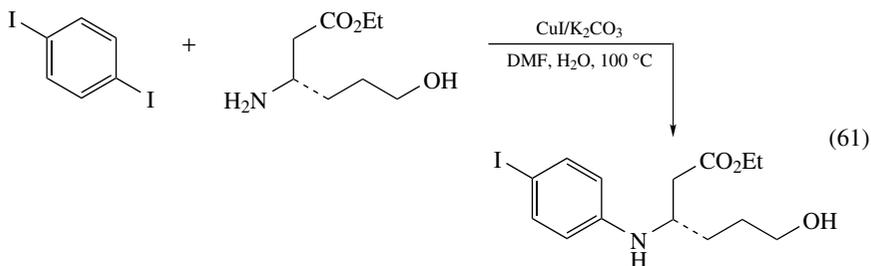
2. Reactions of aryl halides with amines in the presence of additives

Extensive efforts have been made to develop milder conditions for aromatic C−N bond formation with stoichiometric or catalytic amounts of copper. Efforts have also

been made to increase the scope of the classical Ullmann chemistry to allow high-yield reactions with electron-rich aryl iodides and with aryl bromides. Many combinations of copper sources, ligands and bases have now been tested for these reactions. The following sections will provide a survey of the coupling reactions of aryl halides with various nitrogen nucleophiles catalyzed by copper, in combination with additives. These sections are organized by the type of nucleophile.

a. Aromatic amination. The presentation of the reactions of aromatic amines is organized by the type of aryl halide (ArI, ArBr and ArCl) that reacts with the aromatic amine. The reactivity of aryl halides with aromatic amines by copper-mediated coupling reactions follows the order I > Br ≫ Cl. Consequently, most examples of the coupling of aryl halides with arylamines have been reported with ArI and ArBr, and the majority of these reactions have been conducted with aryl iodides. Only a few examples have been reported with ArCl, and these examples are reviewed in a separate section.

i. Copper-mediated reactions of ArI and ArBr with aromatic amines. Aryl iodides are the most common aryl halide used in copper-mediated coupling reactions that form C−N bonds. The most common sources of Cu are CuI, CuBr, $CuBr_2$, [Cu(phen)(PPh$_3$)Br], [Cu(PPh$_3$)$_3$Br] and [Cu(OH)(tmeda)]$_2$Cl$_2$. Many ligands based on nitrogen and oxygen donor atoms for copper have been used and will be included in examples below. The bases used most commonly are KOH, Cs$_2$CO$_3$, t-BuOK, K$_2$CO$_3$, and K$_3$PO$_4$.

Goodbrand and Hu reported reactions of aryl iodides with mono- or diarylamines to form triarylamines in good yields at moderate temperatures in the presence of a catalyst consisting of CuCl and 1,10-phenanthroline (**62**) (equation 62)[247].
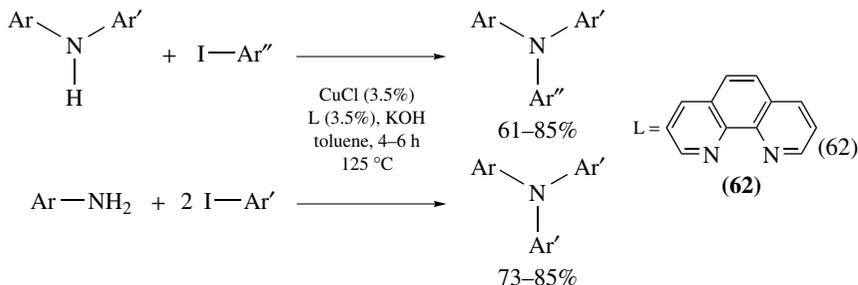
Work by Weingarten[248], Cohen and Crostea[249] and Paine[250] suggested that the active catalytic species in Ullmann reactions are cuprous ions and that the aryl coupling reactions would occur under milder conditions if the solubility of copper salts were increased. Based on this hypothesis, Venkataraman and coworkers studied reactions to form triarylamines from various aryl iodides and aromatic amines catalyzed by Cu(I) complexes, such as Cu(phen)(PPh$_3$)Br and Cu(neocup)(PPh$_3$)Br (neocup = 2,9-dimethyl-1,10-phenanthroline), which are soluble in organic solvents such as dichloromethane, chloroform, toluene, benzene, NMP, DMF and DMSO[251]. A few examples of the coupling of aryl bromides with these catalysts have also been reported. They also reported the synthesis of functionalized diaryl- and triarylamines under mild conditions with the soluble, air-stable copper(I) complex, Cu(PPh$_3$)$_3$Br and Cs$_2$CO$_3$ as base[252]. Chaudhari and coworkers[235] examined a variety of N- and P-containing ligands in combination with CuI as catalyst for the coupling of iodobenzene with aniline catalyzed by CuI with t-BuOK as base. The most efficient chelating ligand was 1,3-bis(diphenylphosphino)propane. However, reactions with 2,2′-bipyridine as ligand for copper gave consistently higher yields

than those with the bisphosphine. Aryl bromides have been reported to react with *ortho*-chloronitrobenzoic acid to form a series of *N*-phenyl-3-nitroanthranilic acids. A mixture of Cu/CuCl was used as catalyst in 2,3-butanediol solvent and *N*-ethylmorpholine as base[253].

Amino acids with secondary amino groups, such as proline or *N*-methylglycine, also generate active copper catalysts for the coupling of aryl iodides with aromatic amines, although the scope of this method for reactions of aromatic amines has not been explored in detail[254]. No examples of the coupling of arylamines with aryl bromides were reported.

ii. Copper-mediated reactions of ArCl with aromatic amines. Few examples of the copper-catalyzed reactions of aryl chlorides with aromatic amines have been reported. The reaction of phenyl chloride with diphenylamine to form triarylamines catalyzed by the soluble complexes of Cu(I) with 1,10-phenanthroline, neocuproine, or 2,2′-bipyridine, CuL(PPh$_3$)Br and K$_2$CO$_3$ as base occurred in about 50% yield[251]. The favorable effect of potentially coordinating *ortho*-substituents on the rates of Ullmann reactions has been exploited to couple *o*-chlorobenzoic acids with anilines to form *N*-arylanthranilic acids in aqueous or DMF solutions in the presence of pyridine[255]. A research group from Bayer screened 80 ligands for the monoarylation of aniline with the activated aryl chloride *para*-chloronitrobenzene. Aniline was used as a neat reagent, CuBr and CuBr$_2$ were found to be the most effective copper sources and K$_2$CO$_3$ was used as base at 190 °C. The chelating biscarbene ligand (**63**) and the biarylphosphine ligand (**12**, Figure 5) shown in Figure 17 were the most effective[256].

b. Aliphatic amination. Whereas the classic Ullmann conditions without added ligands are not suitable for the arylation of aliphatic amines, methods with ligated copper have increased the scope of the arylation of such nucleophiles. The major limitation in the scope of amine in the reactions of aryl halides with aliphatic amines is the low reactivity of acyclic secondary amines. The scope of the reaction typically encompasses reactions of primary aliphatic amines and cyclic secondary amines, such as piperidine, piperazine, pyrrolidine and morpholine. The major limitation in the scope of the aryl electrophile is the lack of reactivity of aryl chlorides. Moreover, reactions of aromatic pseudohalides, such as aryl triflates, have not been reported.

Early progress toward developing copper-catalyzed reactions of aryl halides with aliphatic amines was made with complexes of α- and β-amino acids[242, 244, 245] and β-amino alcohols[257−261]. Volante and coworkers reported the amination of aryl and heteroaryl iodides and bromides in the presence of 0.5 mol% Cu$_2$O at 80 °C with ethylene glycol as additive[262]. Buchwald and coworkers further developed this chemistry by surveying a
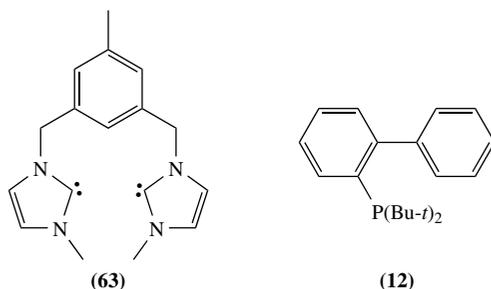
FIGURE 17. Ligands used by Bayer for monoarylation of aniline with activated aryl chlorides
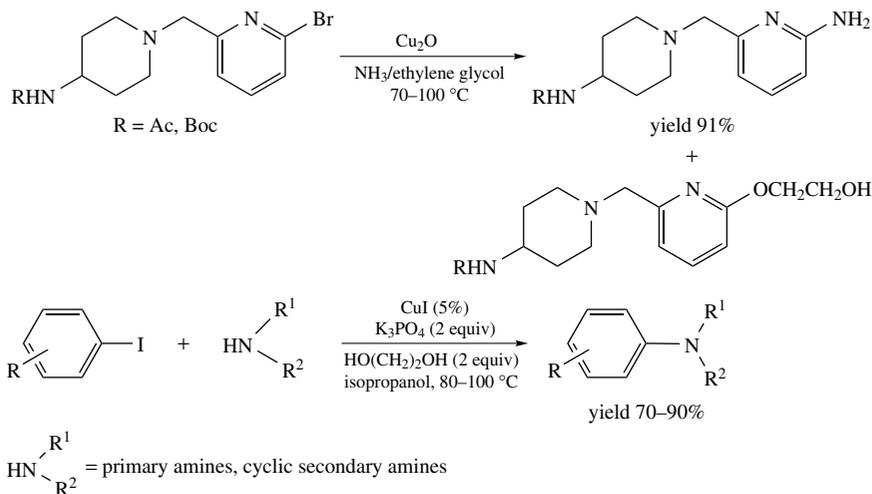
SCHEME 8. Early progress toward reactions of aryl halides with aliphatic amines

variety of diols for amination of aryl iodides with catalytic amounts of CuI[263, 264]. These methods are shown in Scheme 8. The most efficient system involved a combination of CuI (5 mol%), ethylene glycol (2 equivalents) and K_3PO_4 base in 2-propanol at 80 °C. The chelation of the glycols is likely to be a critical factor; both simple alcohols and diols with two remote hydroxyl groups were ineffective at promoting the copper-catalyzed amination. Using this protocol, 4-iodoaniline was successfully coupled with benzylamine; this iodoarene with a free amino group does not efficiently couple with amines in the presence of palladium catalysts. It was also shown that optically active (R)-α-methylbenzylamine reacted with iodobenzene without loss in enantiomeric purity. Aliphatic amines were chemoselectively N-arylated over aromatic amines. Moreover, the amination protocol cleanly affected the selective arylation of the primary amine in the reaction of spermidine with 4-iodotoluene with no reaction observed at the secondary amine moiety. This amination protocol can be performed under air without loss of yield.

The copper-catalyzed reactions of aryl bromides were more effectively conducted with the hindered phenols 2,6-dimethylphenol (**64**) and 2-phenylphenol (**65**) as additive than with ethylene glycol. These reactions were conducted at 100 °C instead of 80 °C, as for the reactions of aryl iodides. Moreover, amine in large excess as solvent was required (equation 63).
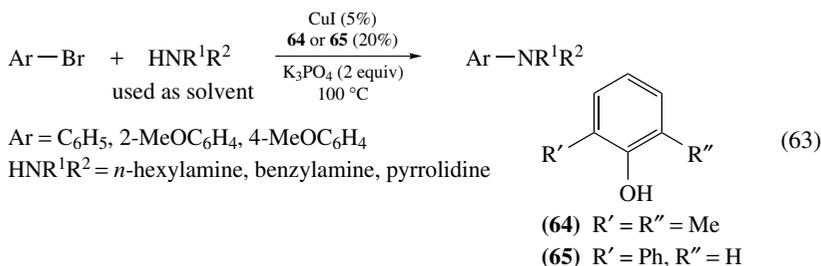
Later, a range of anionic O-donor ligands (**66–79**) were screened to improve the N-arylation of primary alkyl amines using aryl bromides as substrates (Scheme 9)[265].

Ligands Screened

(66)   **(67)**   **(68)**   **(69)**   **(70)**

(71)   **(72)**   **(73)**   **(74)**   **(75)**

(76)   **(77)**   **(78)**   **(79)**
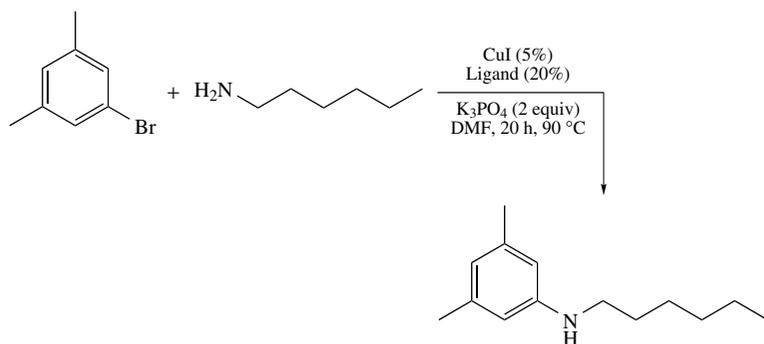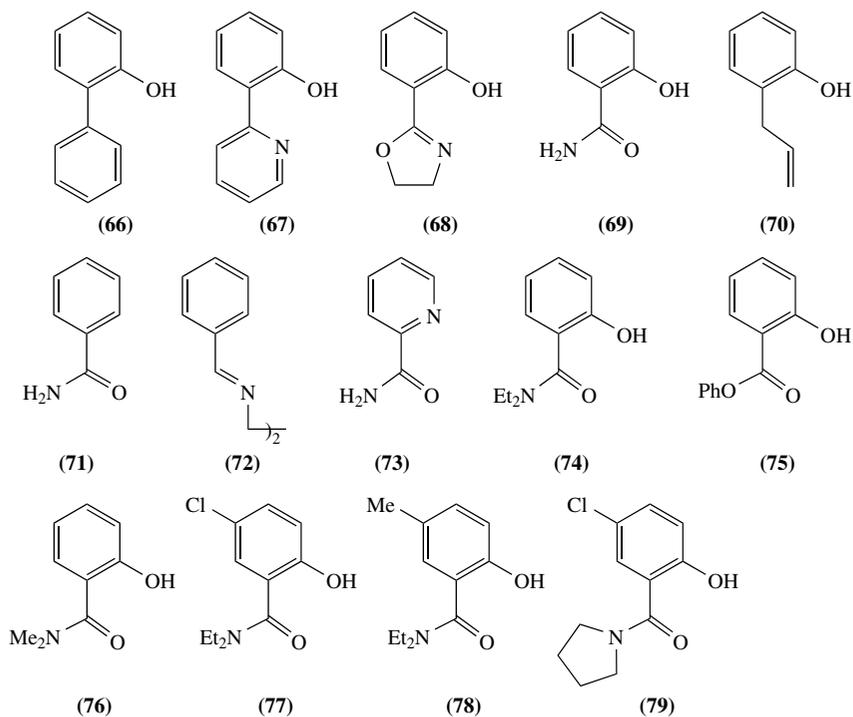
Most effective reaction conditions
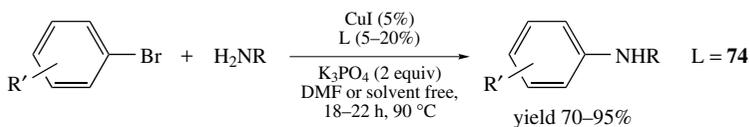
SCHEME 9. Anionic *O*-donors screened for *N*-arylation of primary alkyl amines

The reaction of 5-bromo-*m*-xylene with *n*-hexylamine in the presence of commercially available *N*,*N*-diethylsalicylamide (20 mol%), CuI (5 mol%) and K_3PO_4 (2 equivalents) in DMF at 90 °C produced *N*-aryl hexylamine in 91% yield. The scope of the reaction was expanded to include aryl bromides having thioether, hydroxy, nitrile, keto, nitro and free amino groups. In contrast to palladium-catalyzed couplings, no significant electronic effects were observed in the coupling of *para*-substituted aryl bromides with primary amines. Intramolecular amination of aryl bromides and aryl chlorides were also conducted with a similar protocol, although reactions of aryl chlorides required higher temperatures and longer reaction times than those of aryl bromides. For example, an intramolecular reaction of *ortho*-bromo and *ortho*-chloro aminoalkylarenes catalyzed by CuOAc formed indolines and tetrahydroquinolines[265]. Even with the anionic *O*-donor ligand, the couplings with secondary amines provided poor results. In addition, no examples of the reactions of amides or anilines were reported. Finally, o*rtho*-substituted aryl, as well as heteroaryl substrates, were less reactive than the less hindered *meta*- and *para*-substituted substrates.

The *N*-arylation of amino alcohols has also been studied. Hida and coworkers[258] reported that *β*-amino alcohols are more reactive than amines in the Ullmann condensation with bromoanthraquinones. However, a 100:1 molar ratio of amino alcohol to aryl bromide was used in this initial study. Job and Buchwald[257] then developed a protocol to achieve selective *N*-arylation of primary *β*-amino alcohols with limiting amine. Under Buchwald's conditions, the amino alcohol as limiting reagent reacts with 1.2 equivalents of aryl iodide, CuI (2.5 mol%) and NaOH (2 equivalents) in a mixture of DMSO and H_2O (2:1) or *i*-PrOH at 90 °C (equation 64). Alternatively, the reactions could be conducted with 1 equivalent of ethylene glycol, compared to amine, and the milder base K_3PO_4 (equation 65). The *N* vs. *O* selectivity observed with this second protocol is poorer, compared to the selectivity from the protocol using NaOH as base. Secondary amino alcohols were less reactive than primary amino alcohols using either protocol. For example, the reactions with hydroxide as base effected the *N*-arylation of 2-(ethylamino)ethanol in acceptable yields (63−89%), but *N*-phenyl ephedrine was obtained in only 50% yield, due to incomplete conversion of ephedrine.

$$\text{(64)}$$

R^1 = H, alkyl   R = H, *o*-, *m*-Me, *o*-Br, *o*-, *m*-OMe, *o*-NH$_2$

$$\text{(65)}$$

R = *m*-NO$_2$, *m*-CH$_2$OH, *m*-COMe
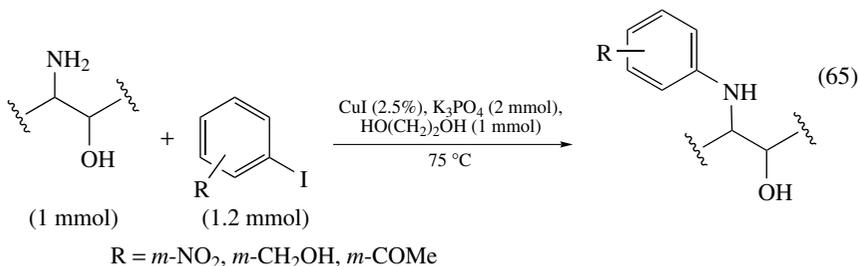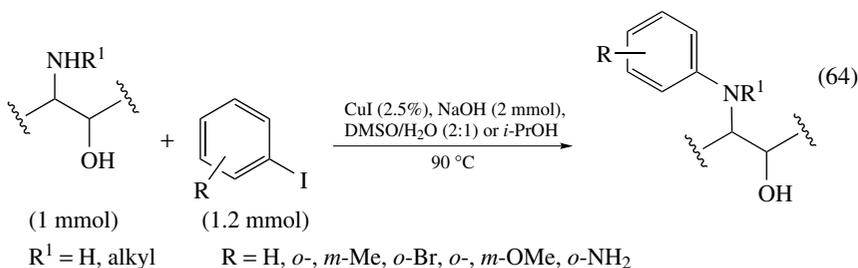
Twieg and coworkers[266] have studied reactions with 2-N,N-dimethylaminoethanol as solvent, and presumably as ligand, for the combination of Cu metal and CuI catalyst. Under these conditions, the reactions of aryl iodides and bromides occurred with unhindered primary amines at 60–90 °C. The reactions of aryl bromides required higher temperatures. Reactions of acyclic secondary amines again occurred much less readily, and aniline was also not found to be a suitable substrate for this protocol.

Recently, Lu and Twieg[267] have also demonstrated that 2-N,N-dimethylaminoethanol (deanol) is an efficient ligand for coupling of aryl iodides with α- and β-amino acids in aqueous medium using CuI as catalyst and K_3PO_4 as base. The optimal reaction conditions employed aryl halide and amine in a 1.0:1.5 ratio, CuI (10%), ligand (2–3 equivalents) and K_3PO_4 (2 equivalents) in water at 80–90 °C (equation 66). Using this protocol the N-arylation of hydrophilic α-amino acids, such as glutamic acid, glycine and serine, was achieved. These substrates had earlier failed to undergo N-arylation. For the first time peptides underwent metal-catalyzed aryl amination reactions. Iodobenzene was coupled with glycylglycine and glycyl-L-leucine using the above protocol to form 40% and 46% yield of the respective arylation products.

$$R = CH_3, i\text{-}Pr, CH_2Ph, CH_2CH_3$$
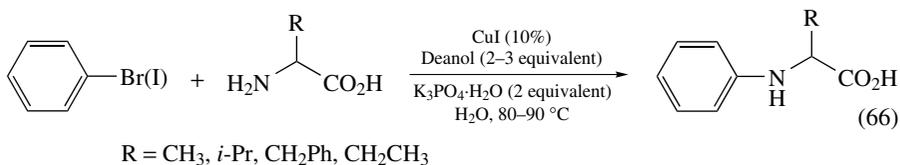
The mildest coupling of aryl halides with aliphatic amines occurs with copper catalysts containing amino acids as ligands (equation 67). These reactions have been conducted between aryl iodides and bromides and primary acyclic amines and secondary cyclic amines[254, 268]. The most effective ligands, among the amino acids screened, were proline and N-methylglycine. This general procedure involves heating a DMSO solution of aryl halide and amine in the presence of 10 mol% CuI, 20 mol% ligand and K_2CO_3 as base at only 40–60 °C. This Ullmann arylation of amines occurs under the mildest conditions reported to date.

$$X = I, Br; R \text{ or } R' = H, \text{alkyl, aryl}$$
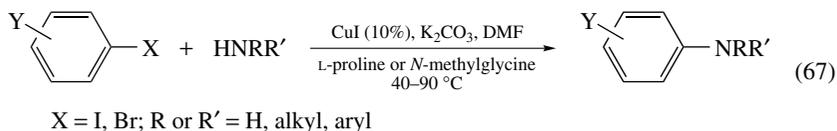
c. N-Heterocyclic amination. Although lying outside the scope of the synthesis of anilines, we note that numerous copper-catalyzed or copper-mediated methods have been published for the coupling of N—H containing heterocycles with aryl halides to form N-aryl heterocycles[269–276]. Although these are significant contributions, the initial procedures involved high reaction temperatures (140 °C or higher) and occurred with narrow scope. No single method was found to be general for each of the major classes of heterocycles (imidazoles, pyrroles, pyrazoles etc.), but many of the heterocycles will undergo reactions with some combination of copper, ligand and base.

B. Copper-mediated Reactions of Arylboronic Acids with Amines

Independent reports by the groups of Chan[277], Evans[278] and Lam[279] in 1998 revealed a new method to conduct copper-mediated arylations that form C(aryl)—O and C(aryl)—N

bonds. Chan and coworkers reported a variety of *N*-arylation reactions using arylboronic acids (2 equivalents) in the presence of copper diacetate (1 equivalent) and a base, such as pyridine or triethylamine. Amines, anilines, amides, ureas, carbamates and sulfonamides underwent *N*-arylation in moderate to excellent yields (equation 68). The commercial availability of boronic acids and the ability to conduct these arylations in air under mild conditions has led this method to be adopted quickly for synthetic applications. These reactions were initially conducted with stoichiometric amounts of copper diacetate. However, in 2000, reactions with catalytic amounts of copper were reported[276]. This summary of the reactions of arylboronic acids with nitrogen substrates will be divided into stoichiometric (copper-mediated) and catalytic processes.

$$X\text{-}H = \text{amine, amide, imide, urea, sulfonamide, carbamate}$$
$$\text{base} = \text{pyridine, triethylamine}$$

(68)
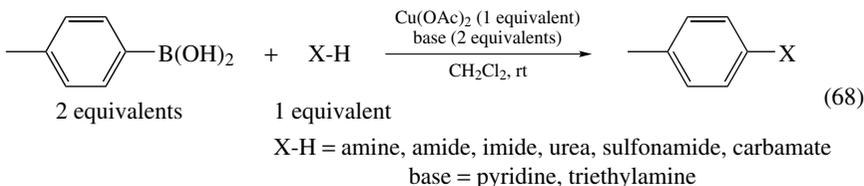
1. Copper-mediated reactions of arylboronic acids with aromatic and aliphatic amines

Only a few examples of the use of stoichiometric amounts of copper to mediate the reaction of arylboronic acids with aromatic or aliphatic amines have been reported. Reports with catalytic amounts of copper are reviewed in a later section. Anilines and cyclohexylamine reacted with *para*-tolylboronic acid to form the *N*-aryl and alkylamine in the original report by Chan and coworkers[277] (equation 68). The reaction employed a 2:1:2:1 ratio of boronic acid:cupric acetate:base:amine in CH_2Cl_2 as solvent at room temperature. Triethylamine or pyridine were used as base. Examples were also reported of the reactions of *para*-tolylboronic acid with amides, ureas, sulfonamides and carbamates. No clear trend was observed for the choice of base for a given amine substrate, and the choice of base was found to be critical for the yield of reaction. For example, pyridine was found to be a suitable base for the coupling of hexylamine, whereas triethylamine was better for coupling of various electron-rich and electron-poor anilines. Cundy and Forsyth[280] reported several additional examples of the arylation of amines. In accordance with Chan's observations, different reaction conditions were developed for each type of *N*-arylation. No strong correlation was observed between the basicity of the amine or the electron-donating property of the arylboronic acids and the reaction yields.

Lam and coworkers[281] also showed that *para*-tolylboronic acid couples with α-aminoesters at room temperature with little or no racemization of the amino acid ester. The yields for the reactions of a series of *para*-tolylboronic acids ranged from 17–67% (equation 69). The general reaction conditions included boronic acid (2 equivalents), triethylamine (2 equivalents), α-aminoester (1 equivalent), $Cu(OAc)_2$ (1.1 equivalents) and 4 Å molecular sieves.

Combs and coworkers[282] conducted the *N*-arylation of primary and secondary aliphatic amines on a solid support in good to excellent yields (68–90%). Chiang and Olsson[283] used a polymer-supported copper complex to mediate the C−N cross-coupling of arylboronic acids with a variety of aromatic and aliphatic amines. The reaction employed arylboronic acid (3 equivalents), amine (1 equivalent), Cu-complex (1.5 equivalents) and NEt_3 (2.6 equivalents). Reactions were conducted in CH_2Cl_2 at room temperature for 24 h (equation 70). The yields were comparable to those catalyzed by homogenous copper[277], but reaction times were shorter. The Cu-complex was recycled twice. Das and Basu[284]

reported simple, microwave-assisted, solvent-free *N*-arylation of primary aliphatic and aromatic amines with arylboronic acids or sodium tetraphenylborate and a stoichiometric amount of cupric acetate on the surface of KF-alumina. Reactions of secondary aliphatic and aromatic amines did not form the coupled product.
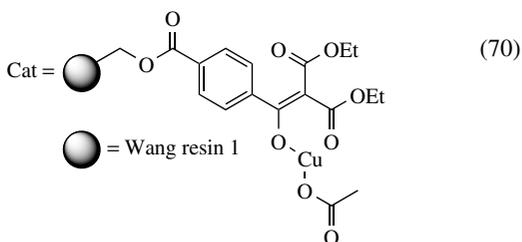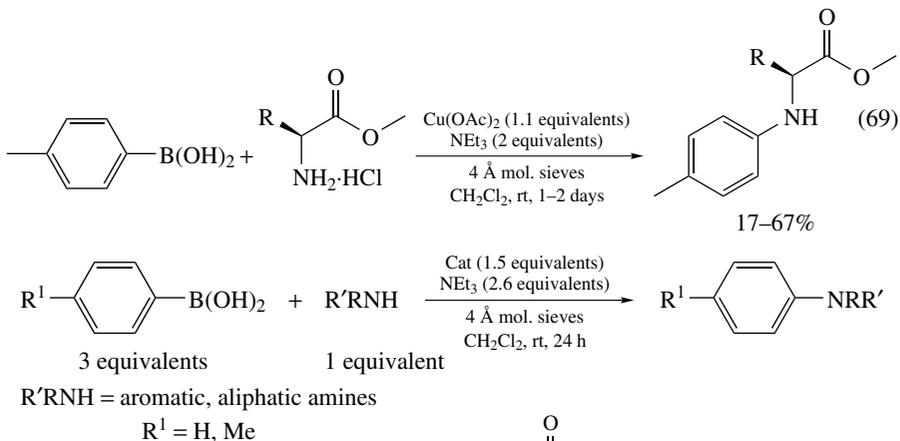
In addition to aliphatic and aromatic amines, amides[275] and sulfonamides[285] have also been used as nitrogen nucleophiles for copper-mediated coupling with arylboronic acids, and these reactions provide protected anilines.

2. Copper-mediated reactions of arylboronic acids with heterocycles containing N−H bonds

Many examples of the arylation of azoles have also been reported. Again, we do not report details of these reactions because these reactions formally lie outside the scope of the synthesis of anilines. However, the reader should note that significant progress has been made on coupling of boronic acids with indazoles[279, 286−288], imidazoles and pyrroles[289] using a stoichiometric amount of copper reagents. Reactions of less nucleophilic heterocycles, such as triazoles and tetrazoles, occur in poor yields. Purines[290], aminopurines and aminopyrimidines[291] have also been coupled with boronic acids using stoichiometric amounts of $Cu(OAc)_2$ and 1,10-phenanthroline as ligand.

The scope of the couplings with heteroaromatic compounds was further expanded by using vinylboronic acids[292]. Benzimidazoline and benzimidazole coupled with vinylboronic acids in the presence of stoichiometric amounts of $Cu(OAc)_2$. Catalytic versions of this reaction have also been reported that utilize TEMPO or pyridine *N*-oxide as co-oxidant[293]. Phenyl and pyridyl boronates have been reported to be more efficient arylating agents than boronic acids[294]. It was speculated that the active arylating agent in the studies

with arylboronic acids might be the anhydride form and not the free acid. The authors also provided the first example of copper-promoted C−N cross-coupling involving a heterocyclic boronic acid.

C. Copper-catalyzed Reactions of Arylboronic Acids with Amines

Collman and Zhong reported the first example of a C−N cross-coupling between an arylboronic acid and a substrate with an N−H bond with catalytic amounts of copper[276]. Using 10 mol% of commercially available [{Cu(OH)•tmeda}$_2$]Cl$_2$ in dichloromethane, imidazole was coupled with phenylboronic acid at room temperature (equation 71). The reaction can be conducted in water, although yields are higher in CH$_2$Cl$_2$[295]. This work also included an investigation of reactions catalyzed by copper ligated by various diamines. Although all ligands gave measurable yields of coupled product (19–68%), reactions catalyzed by a combination of copper and TMEDA were most satisfactory[296].

$$R^1 = o\text{-}, p\text{-Me}, o\text{-}, p\text{-MeO}, p\text{-F}$$
$$R^2 = H, 2\text{-},4\text{-Me}, 4\text{-Ph}$$

(71)
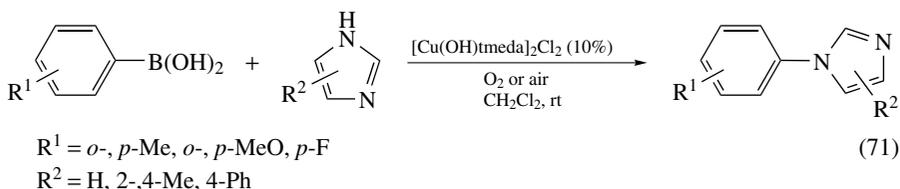
Lam and coworkers[292] and Antilla and Buchwald[297] expanded the scope of this type of catalytic coupling to encompass reactions of amines. Lam reported the coupling of aliphatic and aromatic amines, as well as heterocycles with N−H bonds with a combination of Cu(OAc)$_2$ (10 mol%) and co-oxidants like pyridine N-oxide (PNO) or TEMPO in air. No single set of conditions led to coupling of all substrates. Concurrently, Buchwald reported reactions at room temperature catalyzed by Cu(OAc)$_2$ (5–10 mol%) and myristic acid with stoichiometric amounts of 2,6-lutidine as base. Substituted anilines, as well as primary and secondary amines, reacted with a series of arylboronic acids. Excellent yields of arylated products were obtained for reactions of anilines, but only moderate yields were obtained for reactions of aliphatic amines. Yudin and coworkers employed this protocol to prepare N-aryl aziridines (equation 72)[298].

$$R^1 = H, o\text{-Me}, m\text{-Br}, m\text{-NO}_2, p\text{-MeO}$$

(72)
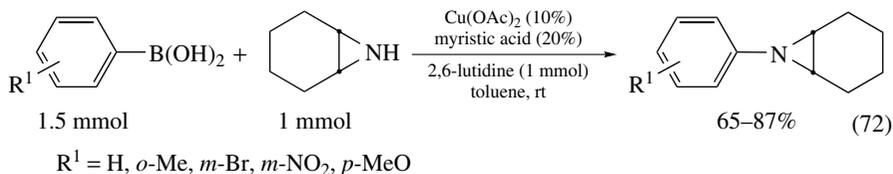
Quach and Batey[299] reported the coupling of primary amines with phenylboronic acids catalyzed by Cu(OAc)$_2$ (10 mol%) without base or ligand but in the presence of 4 Å molecular sieves and air in CH$_2$Cl$_2$ solvent (equation 73). Reactions of potassium phenyl-trifluoroborate also occurred, but in lower yields than reactions of boronic acids. They showed that these reactions occur with a variety of functional groups on the amine, including alkenes, esters, ketones and ketals. α-Amino acid derivatives underwent reaction without detectable epimerization. Anilines were poorer cross-coupling partners under these conditions than were primary and secondary cyclic aliphatic amines.

$$\text{R}^1\text{—C}_6\text{H}_4\text{—BX}_n \;+\; \text{HNR}^2\text{R}^3 \xrightarrow[\text{(ii) amine, rt--40 °C, O}_2\text{, 24 h}]{\substack{\text{(i) Cu(OAc)}_2\cdot\text{H}_2\text{O (10\%)}\\ \text{CH}_2\text{Cl}_2\text{, 4 A mol. sieves, rt, 5 min}}} \text{R}^1\text{—C}_6\text{H}_4\text{—NR}^2\text{R}^3 \tag{73}$$

2 equivalent   1 equivalent   30–98%

$\text{BX}_n = \text{B(OH)}_2, \text{BF}_3{}^-\text{K}^+ \quad \text{R}^2 = \text{alkyl, aryl} \quad \text{R}^3 = \text{alkyl, H}$
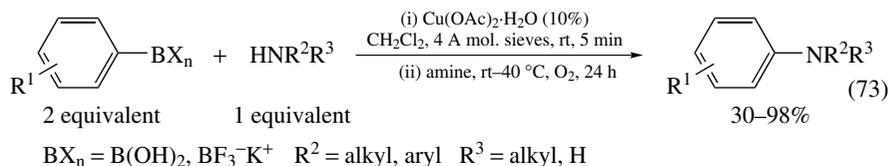
Xie and coworkers[300] reported reactions of imidazoles with arylboronic acids catalyzed by simple copper salts, such as CuCl, CuBr, CuI, CuClO$_4$, CuCl$_2$•H$_2$O, Cu(OAc)$_2$•H$_2$O and Cu(NO$_3$)$_2$•3H$_2$O, in protic solvents without added ligand or base. Reactions catalyzed by 3–5% CuCl in refluxing CH$_3$OH or in a 1:1 mixture of H$_2$O:CH$_3$OH, H$_2$O:C$_2$H$_5$OH or H$_2$O:THF in air occurred in almost quantitative yield, and this procedure encompassed reactions of amines, amides, imides and sulfonamides. While reactions of imides occurred in excellent yield when catalyzed by CuCl, the reactions of amines, amides and sulfon-amides occurred when catalyzed by Cu(OAc)•H$_2$O. The reaction times of 3 h are shorter than those of earlier related processes[301].

In contrast to the apparent need to conduct the copper-catalyzed reactions of arylboronic acids and amines in the presence of oxygen, the *N*-arylation of imidazoles was reported with 5 mol% of [Cu(OH)tmeda]$_2$Cl$_2$ in a mixture of NMP and water under a nitrogen atmosphere (equation 74)[302].

$$\text{C}_6\text{H}_5\text{—B(OH)}_2 \;+\; \underset{\text{1 mmol}}{\text{imidazole}} \xrightarrow[\text{NMP:H}_2\text{O (1:1)}]{\text{[Cu(OH)(tmeda)]}_2\text{Cl}_2\ (5\%)} \text{C}_6\text{H}_5\text{—N-imidazole} \tag{74}$$

1 mmol   1 mmol   99%
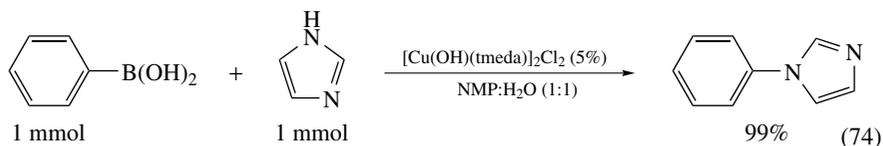
If these reactions truly occur without oxygen, then this result would contradict Collman and coworkers' mechanistic proposal[295]. By this proposal, Cu(II) first reacts with phenyl-boronic acid and then coordinates imidazole. The resulting species undergoes oxidation with dioxygen to generate a Cu(III) complex; reductive elimination generates a Cu(I) species; and the Cu(I) species is then oxidized to Cu(II). In addition to showing that the reaction can be conducted without oxygen, they showed that the first step of the reaction was coordination of imidazole.

D. Copper-mediated Reactions of Arylsiloxanes as Aryl Donors

Lam and coworkers reported that hypervalent arylsiloxanes also react with a variety of substrates containing N−H bonds, in this case in the presence of stoichiometric amounts of copper acetate at room temperature in air without added base (equation 75)[303]. The hypervalent arylsiloxanes are generated by the addition of tetra-*n*-butylammonium fluoride (TBAF) to phenyltrimethoxysilane. The rate of these reactions was an order of magnitude faster than the rate of the corresponding reactions with boronic acids. Aromatic amides with heteroatoms in the α-position also coupled with hypervalent arylsiloxanes[304]. As a function of the α-heteroatom, the rates followed the trend N > S > O. These data are consistent with chelation of the α-substituents.

$$\text{Ar—Si(OMe)}_3 \;+\; \text{HNR}_2 \xrightarrow[\text{CH}_2\text{Cl}_2\text{, air, rt}]{\substack{\text{TBAF (2 equivalents)}\\ \text{Cu(OAc)}_2\text{ (1.1 equivalents)}}} \left[\text{Ar—}\overset{\overset{\text{F}}{|}}{\text{Si}}\text{(OMe)}_3\right]^- \longrightarrow \text{ArNR}_2$$

R = H, alkyl, aryl

$$\tag{75}$$
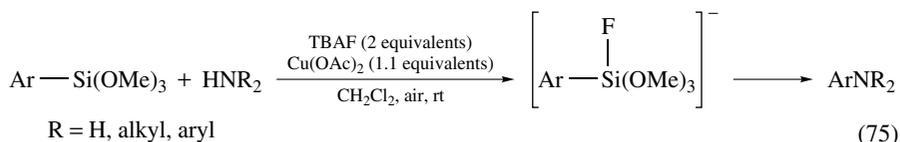
E. Copper-mediated Reactions of Arylbismuth Reagents as Aryl Donors

The *N*-arylations of aliphatic, heterocyclic or aromatic amines is achieved either by treatment with pentavalent triarylbismuth derivatives and catalytic copper species or by treatment with a trivalent triarylbismuthane and stoichiometric amounts of copper diacetate that acts both as an oxidant and as the catalyst[305].

1. Triarylbismuth diacetate — copper-catalyzed arylation

Dodonov and coworkers reported the earliest examples of the reactions of simple aliphatic amines (5–20 equivalents) with triphenylbismuth diacetate (1 equivalent). These reactions were conducted with catalytic amounts of copper diacetate (0.01–0.02 equivalent) in THF and formed the arylamine in 60–85% yields (equation 76)[306–308].

$$\text{Ph}_3\text{Bi(OAc)}_2 \quad + \quad \text{HNR}^1\text{R}^2 \quad \xrightarrow[\text{THF, rt, 60–180 h}]{\text{Cu(OAc)}_2 \ (10\text{–}20\%)} \quad \text{C}_6\text{H}_5\text{—NR}^1\text{R}^2$$

1 equivalent   5–20 equivalents   60–85%

$\text{R}^1, \text{R}^2 = \text{H}, i\text{-Pr}, i\text{-Bu}, t\text{-Bu}, \text{Ph}, \text{Et}$

(76)
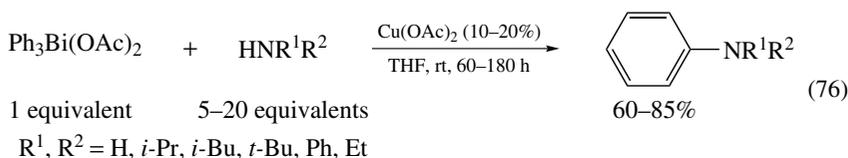
Aniline derivatives were synthesized in methylene chloride in the presence of catalytic amounts of metallic copper (0.1 equivalent) at room temperature[309, 310], but reactions conducted with a soluble Cu(II) catalyst, such as copper (II) dipivalate, occurred in higher yields and in shorter times (5 min–3 h). Yields of arylamine were also higher when the reactions were conducted with added KH[311]. For example, cyclohexylamine reacted to form *N*-phenylcyclohexylamine quantitatively in the presence of KH but in only 66% yield in the absence of KH. Triethylamine also promoted the copper(II)-mediated organobismuth *N*-arylations of amides[312], whereas pyridine more successfully promoted the analogous *N*-arylation of imides and sulfonamides. Sterically hindered arylbismuth reagents reacted in lower yields[306, 313]. Triphenylbismuth bis(trifluoroacetate) was more reactive in these processes than triphenylbismuth diacetate, but the yields from reactions of the trifluoroacetates were modest (15–30%)[314]. Imidazole and other heteroarenes were *N*-arylated in moderate to excellent yield with triphenylbismuth diacetate and catalytic amounts of copper acetate[315–327].

A large number of aniline derivatives have been synthesized using a combination of the procedures discussed above[209, 328–336]. In addition, resin-bound triarylbismuth diacetates (**80a–c**) were used as multidirectional linkers to form arylation products in yields and conditions similar to those reported for the solution-phase *N*-arylations (Figure 18)[337].

Ester derivatives of α-amino acids underwent *N*-arylation with arylbismuth reagents under mild conditions[338–341]. The arylation was performed with both the free amino esters and with the protonated amino ester salts, although most of the latter reacted in only moderate yields. High yields of *N*,*N*-diphenylated products were obtained with 1.2 equivalents of triarylbismuth diacetate; *N*,*N*-diphenylated products were also obtained by a two-step process (equation 77)[339].

In this case, the second *N*-arylation was slow and required 1.5 equivalents of bismuth reagent and 1 equivalent of copper diacetate. For example, the first arylation of (*S*)-valine took place in 1 day at room temperature to yield 85% product, but the second *N*-arylation required 14 days at room temperature to yield 69% product. However, no racemization of the amino acid ester was detected, and for this reason, this procedure offers an advantage over the palladium-mediated arylation of amines that racemize amino acids[342].

80a : 87%, **80b** : 96%, **80c** : 69%

80a : 83%, **80b** : 50%, **80c** : 99%

= chloromethyl polystyrene

(80a) R = H
(80b) R = F
(80c) R = CH$_3$
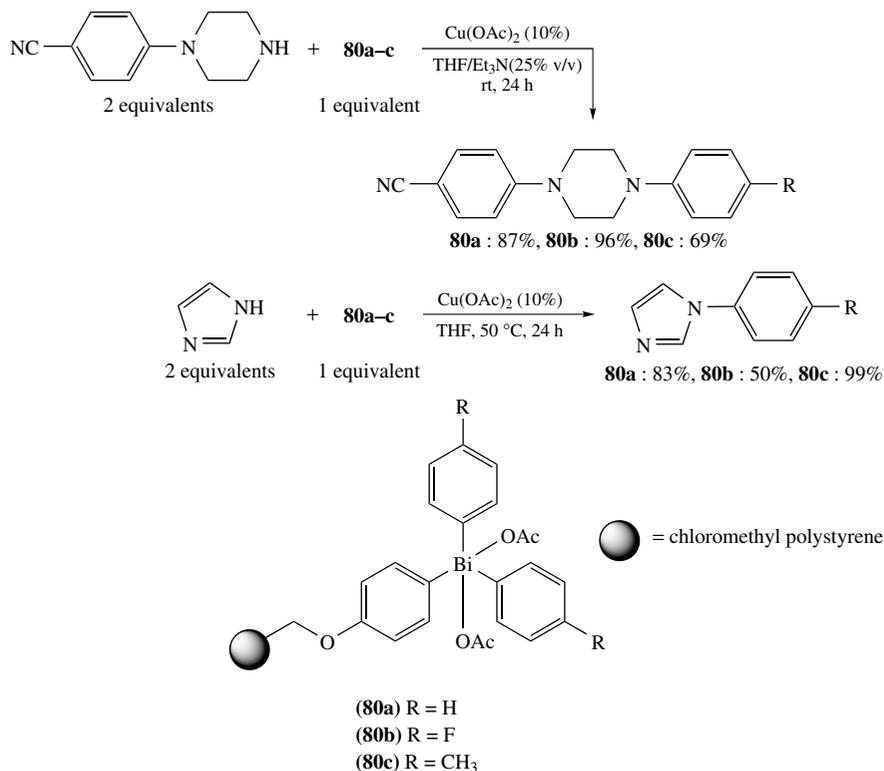
FIGURE 18. Novel resin-bound triarylbismuth diacetate as N-arylation reagent

$$(77)$$
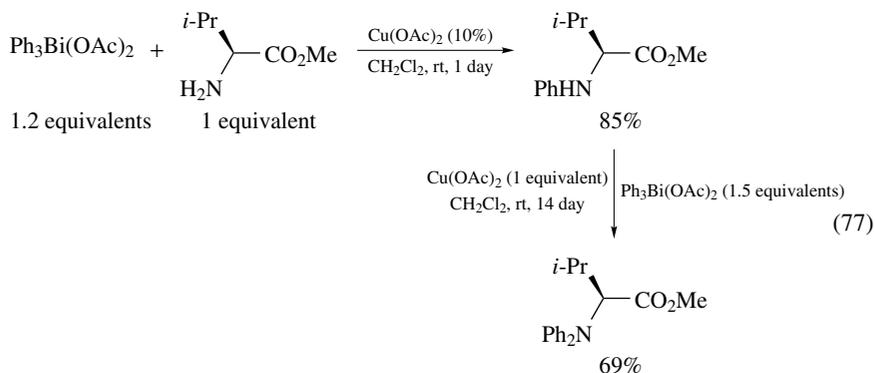
2. Triarylbismuthane — copper diacetate arylation

The reactions of triphenylbismuthane with amines are carried out in the presence of stoichiometric amounts of copper diacetate in methylene chloride for 18–24 h to give

$$RNH_2 \; + \; Ph_3Bi \; + \; Cu(OAc)_2 \quad \xrightarrow[\text{rt}]{CH_2Cl_2} \quad RNHPh$$
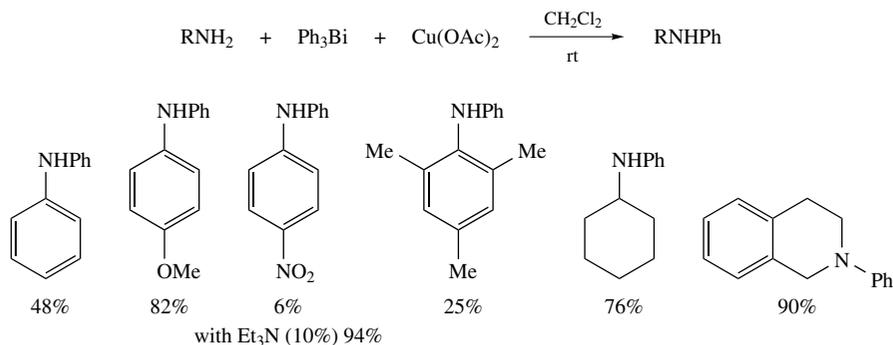
FIGURE 19. Monoarylation products of amines with triphenylbismuthane

N-mono- or *N*,*N*-diphenylamines. The yield of monoarylamines depended on the basicity and steric hindrance of the substrate. For example, 4-nitroaniline reacted to form only 6% of the arylated product, but 4-methoxyaniline reacted to give 82% of the diarylamine. The hindered mesitylamine formed only 25% of the arylation product (Figure 19)[343]. The yields from diarylation were poor. However, the use of 0.1 equivalent of triethylamine improved the yields[312].

Morphine alkaloids reacted to form the *N*-phenyl analogues in modest yields upon reaction with triphenylbismuthane and copper(II) diacetate[344]. Several heterocyclic derivatives, such as piperidines[316, 320], piperazines[319] and benzo-fused-1,5-dithiocines[323], have also been successfully *N*-arylated. A wide range of substituted aminobenzanilides underwent selective *N*-arylation in good yield[336]. Arylbismuthanes have also been used to conduct the arylation of hydrazines[334, 335, 345]. Although arylbismuthanes have been successfully used as arylating reagents, their synthesis has been limited to aryl compounds with substituents that tolerate the formation of organolithium or Grignard reagents.

Resin-bound bismuthanes (**81a−c**) have also been prepared and used as a multidirectional linker for these C−N bond-forming reactions (Figure 20)[337]. The yields were approximately 30% lower than those reported for similar reactions in solution phase.

F. Copper-mediated Reaction of Aryllead Reagents as Aryl Donors

Concurrent with the numerous reports of the reactions of arylbismuth reagents with amines, Barton and coworkers reported reactions with aryllead reagents[346−348]. Although the scope of amination reactions of the aryllead reagents is narrower than that of the amination reactions of organobismuth reagents, *N*-arylations with electron-poor aryl groups were achieved in yields that are useful for preparative purposes[209, 328, 349−350]. The reactions of aryllead reagents with aliphatic amines formed anilines in low yields[348], but a number of heteroarylamines, such as aminoindazole[317, 351], aminobenzodioxole[352] and aminobenzodioxane[331, 353], reacted with aryllead reagents to form the *N*-aryl heteroarylamines in moderate to good yields. Amide nitrogens also underwent *N*-arylation under mild conditions when their sodium salts were treated with *para*-tolyllead triacetate in a mixture of CH_2Cl_2−DMF[354−356].

G. Copper-mediated Reaction of Aryltin Reagents as Aryl Donors

Lam and coworkers[357, 358] explored the reactions of aryltrialkylstannanes as coupling partners in copper-mediated processes because of their air and moisture stability and

2 equivalents 1 equivalent

Cu(OAc)$_2$ (1.5 equivalents)
CH$_2$Cl$_2$, pyridine
40 °C, 24 h

81a : 57%, **81b** : 65%, **81c** : 75%

2 equivalents 1 equivalent

Cu(OAc)$_2$ (10%)
CH$_2$Cl$_2$, Et$_3$N
40 °C, 24 h

81a : 65%, **81b** : 68%, **81c** : 58%

= chloromethyl polystyrene

(81a) R = H
(81b) R = F
(81c) R = CH$_3$
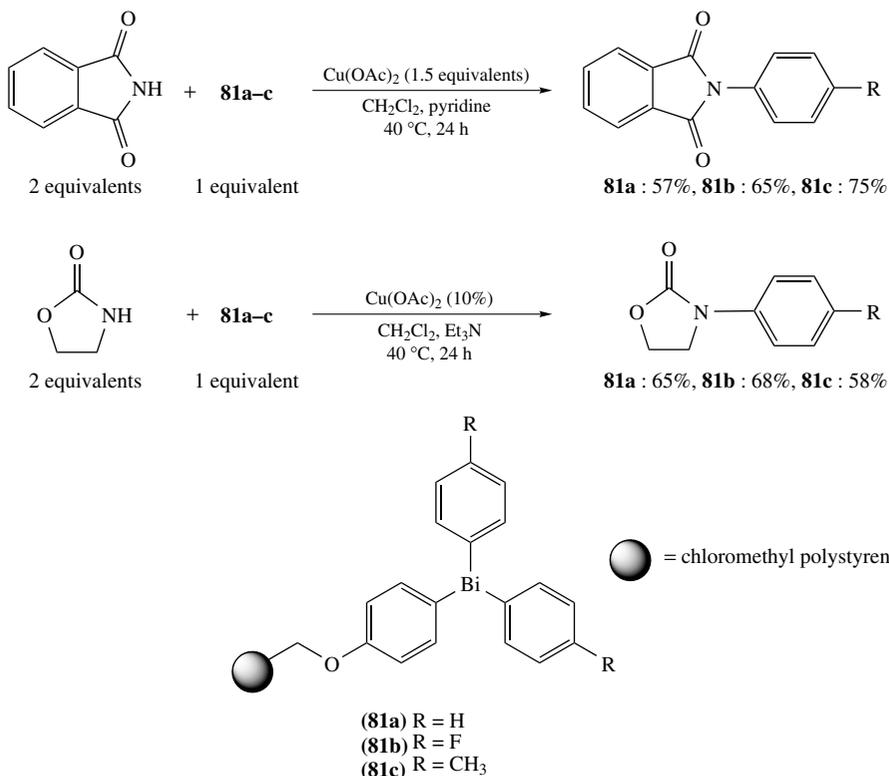
FIGURE 20. Novel resin-bound bismuthanes as *N*-arylation reagents

compatibility with a variety of functional groups. Reactions were conducted most favorably with added TBAF to form a hypervalent stannane anion. Cross-coupling of trimethylphenylstannane (2 equivalents) and benzimidazoline (1 equivalent) at room temperature was achieved in the presence of Cu(OAc)$_2$ (1.1 equivalents) and TBAF (2 equivalents) in CH$_2$Cl$_2$ in 69% yield (equation 78). A number of other compounds with N−H bonds also underwent arylation.

1 equivalent 2 equivalents

Cu(OAc)$_2$ (1.1 equivalents)
TBAF (2 equivalents)
CH$_2$Cl$_2$, rt, 48 h

69%   (78)
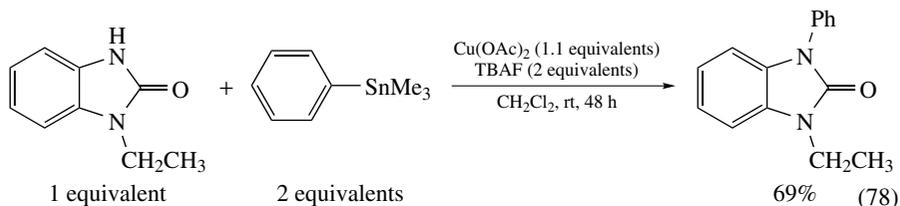
H. Copper-mediated Reaction of Iodonium Salts as Aryl Donors

A mild method for the *N*-arylation of both aromatic amines and cyclic secondary aliphatic amines using aryl iodonium salts was reported by Kang and coworkers[359].

$$R^1R^2NH \quad + \quad Ar_2IBF_4^- \xrightarrow[\text{CH}_2\text{Cl}_2,\ \text{rt, 6 h}]{\overset{\text{CuI (10\%)}}{\text{Na}_2\text{CO}_3}} R^1R^2NAr$$
$$65\text{--}83\%$$

$R^1R^2NH =$ ...

$Ar =$ ...
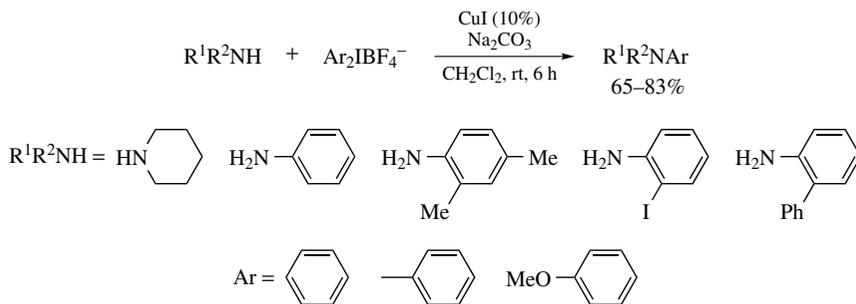
FIGURE 21. *N*-Arylation using aryl iodonium salts

The reactions were conducted with catalytic CuI (10 mol%) and Na_2CO_3 (2 equivalents) in CH_2Cl_2 at room temperature. Moderate to good yields (65–83%) of the *N*-arylated piperidines and anilines were obtained in less than 6 h (Figure 21).

I. Copper-catalyzed Reaction of Amides (Goldberg Reaction)

In 1907, Goldberg[206, 216] reported that the condensation of an aryl bromide and an acetanilide in the presence of K_2CO_3 and CuI yields an *N*-acetyldiarylamine at high temperatures (>200 °C) and that hydrolysis of the resulting amide generates a diarylamine. Since this time, the copper-catalyzed arylation of amides has been used in many laboratories[215, 360–369]. The major limitations of the Goldberg reaction are the high temperatures typically required, the dependence of the yield on purity of reagents[370], the need for highly polar solvents, the need for large amounts of copper reagents and the often modest yields of coupled product.

Buchwald and coworkers have improved upon the traditional Goldberg protocol by focusing on the ability of added ligands to facilitate the copper-catalyzed aryl amidation[371, 372]. They screened a large number of diamines (**82**–**94**) and Cu sources to create a general reaction protocol. *N*,*N*′-Dimethylethylenediamine (**84**) and *trans-N*,*N*′-dimethylcyclohexane-1,2-diamine (**92**) were found to be the most effective ligands when reactions were conducted with CuI (0.2–10 mol%) and K_3PO_4 as base for reactions of aryl iodides and K_2CO_3 as base for reactions of aryl bromides in dioxane as solvent at 60–110 °C (Figure 22). Aryl bromides required longer reaction times at higher temperatures. A variety of functional groups were tolerated in the aryl amidation reaction, including free NH_2 and allyl esters on the nitrogen nucleophile. Intermolecular amidation of aryl chlorides was also achieved using 5 mol% CuI, 11 mol% ligand and an excess (4 equivalents) of the aryl chloride as solvent. For example, the reaction of *para*-chlorotoluene with benzamide occurred in 93% yield after 23 h at 110 °C in neat *para*-chlorotoluene. Intramolecular aryl amidation of an aryl chloride or bromide was also developed.

Hosseinzadeh and coworkers reported a variant of this protocol that involves the use of KF/Al_2O_3 as base in the presence of CuI (10 mol%) and 1,10-phenanthroline (10 mol%) as ligand in refluxing toluene. Quantitative yields of the *N*-arylated products from the reactions of aryl iodides and benzamide, acetamide, acetanilide and δ-valerolactam were obtained in 1.5–12 h[373]. The general reaction protocol developed by Buchwald and coworkers for the amidation of aryl iodides and bromides has been used in several synthetic applications[374–378].
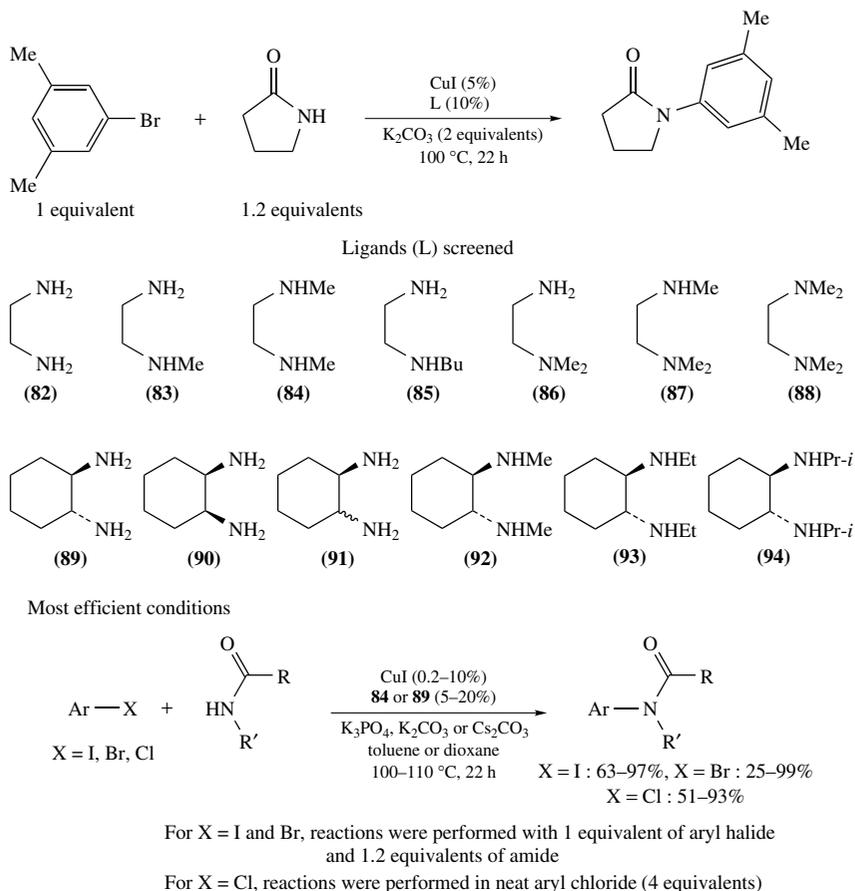
FIGURE 22. Ligands screened by Buchwald and coworkers for improvements of the Goldberg reaction

Recently, a related reaction protocol was developed with an amino acid as ligand[379]. In this protocol various amides were coupled with aryl iodides in the presence of CuI (5 mol%), amino acid (glycine, cystine, cysteine, lysine, arginine, α-alanine, β-alanine) (20 mol%) as ligand and K_3PO_4 as base in dioxane at $100\,^{\circ}C$ (Figure 23).

Amidations of heteroaryl halides have also been reported. Kang and coworkers[380] demonstrated that the cross-coupling of primary and secondary amides, as well as carbamates, with heteroaryl halides can be achieved in the presence of CuI (10 mol%), ethylenediamine as ligand (10 mol%) and K_3PO_4 as base. Various bromofurans, bromothiophenes and bromothioazoles have undergone amidation by this protocol[381, 382]. Arylation of cyclic carbamates with aryl bromides creates a short route to potent antibacterial agents, such as linezolid and toloxatone[383].

Some improvements in the traditional Goldberg reaction have been reported with microwave heating. For example, Lange and coworkers[384] synthesized N-arylpiperazinones, piperazinediones and 3,4-dihydroquinolinones via amidation of aryl bromides. The
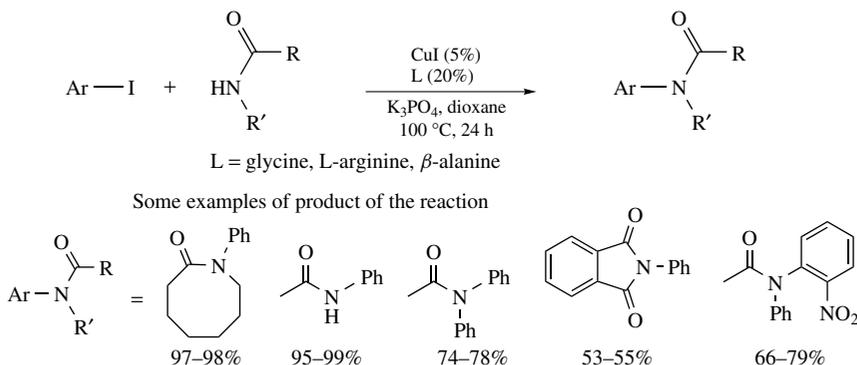
FIGURE 23. Amidation using amino acids as ligands

substrates were combined with CuI (10 mol%) and K₂CO₃ base in NMP and exposed to microwave irradiation to afford the desired products rapidly (20–40 min) in good yield. The reactions have also been performed in the absence of any solvent or in the presence of a small amount of NMP to absorb the microwave energy. Sulfonamides also react with aryl bromides and iodides in NMP[385].

Buchwald and coworkers reported reactions of acyl hydrazides with aryl iodides with CuI (5 mol%) and Cs₂CO₃ in combination with 1,10-phenanthroline as ligand[386]. A large number of functional groups, such as enolizable ketones, primary and phenolic OH, aniline NH₂, ester and cyano groups, were tolerated. Aryl iodides with electron-donating as well as electron-withdrawing substituents in the *meta* or *para* position underwent coupling reactions with *N*-Boc hydrazines in good to excellent yield with excellent regioselectivity. The regioselectivity was reversed with *ortho*-substituted aryl iodides; these reactions formed *N'*-substituted products when benzoic anhydride was used in place of *N*-Boc hydrazine.

VI. MECHANISM OF COPPER-MEDIATED/CATALYZED REACTIONS

Little information is available on the mechanism of the traditional Ullmann condensation reactions. The difficulties in drawing mechanistic conclusions arise from the reactions being conducted at high temperatures ($>150\,^\circ$C) and the typically heterogeneous reaction conditions. Because the mechanism is not yet known in detail, improvements in this reaction have been gained empirically, instead of from theory. The mechanistic proposals for these reactions remain speculative.

In the early 1970s, Tuong and Hida[228, 387, 388] published a set of studies on the mechanism of Ullmann condensations. Kinetic studies were conducted on the condensation of sodium 1-amino-4-bromoanthraquinone-2-sulfonate with aniline in an aqueous buffered solution. Cupric sulfate was used as catalyst because of its solubility in water. The reaction was found to be first order in aryl halide and first order in amine and to depend hyperbolically on the concentration of the catalyst. ESR measurements showed that the copper catalyst exists mainly as cupric species[228]. The reaction rate was unaffected by the ionic strength of the medium but depended heavily on the hydrogen ion concentration. The reaction was retarded by the addition of anions that can coordinate to copper; the retarding effect followed the order: $F^- \ll Cl^- < Br^- < I^- < CN^-$. Halide and cyanide anions form complexes with both cuprous and cupric copper. The order of stability of cupric copper halide and cyanide complexes matches the order of inhibition of the catalytic reaction as

shown above, while the order of stability of cuprous copper halide and cyanide complexes is the opposite of the trend in retarding effect. These correlations pointed toward a Cu(I) compound as the catalytically active species in solution. Molecular oxygen also retarded the rate of the reaction, and these data again point toward a low-oxidation-state copper as catalyst. Consistent with this assertion, 2,2′-biquinolyl (cuproin) and 2,9-dimethyl-1,10-phenthroline (neocuproine), which are known to bind to cuprous copper but not to cupric copper, inhibited the reaction of sodium 1-amino-4-bromoanthraquinone-2-sulfonate with aniline[389, 390].

The rates of reactions with different precatalysts also pointed to Cu(I) species. The initial rate of the reaction initiated with CuI was larger than that of the reaction catalyzed by cupric sulfate. However, a steady state of reactions catalyzed by CuCl was rapidly established (<3 min), and at this steady state, the rate was almost the same as that when cupric sulfate was used. The identity of the steady-state rates was probably observed because cuprous chloride was converted to cupric species, and the reaction took the same course as when the cupric salt was added.

Paine[250] also investigated the mechanism of Ullmann condensations of diarylamines with iodobenzenes under homogeneous and heterogeneous catalytic conditions with cupric and cuprous salts, as well as powdered copper metal. He also concluded that a soluble cuprous ion is the single catalytic species under all conditions. However, in contrast to conclusions drawn by Tuong and Hida[388], a radical mechanism was ruled out. Thus, there is conflicting data on the mechanism of the copper-catalyzed N-arylation, and no clear mechanism has emerged, despite the many years that this chemistry has been known and has been the focus of method development.

A. Mechanism of Reactions of Organometallic Reagents

The remainder of the mechanistic information presented in this review draws from the investigations and proposals by Lockhardt[391] and Barton and coworkers[343] on the intermediacy of hypervalent copper(III) species during the reactions of diaryliodonium salts and pentavalent bismuth reagents. Most of the reactions utilize Cu(I) or Cu(II) salts as the starting copper source. Radical mechanisms are ruled out because the reactions are not inhibited when radical scavengers (such as 1,1-diphenylethylene) are added. It appears that Cu(II) is not the major catalytic species in the reaction.

The mechanistic data on the N-arylations are separated into data on reactions of hypervalent organometallic reagents, reactions of low-valent organometallic reagents, reactions of low-valent organometallic reagents with a co-oxidant, that are catalytic in copper, and reactions of aryl halides (I, Br, Cl).

1. Mechanism of the reactions with hypervalent organometallic reagents

Based on the mechanism of the arylations by diaryliodonium salts Ar_2I^+ X^{-391}, tri-arylbismuth diacetates, $Ar_3Bi(OAc)_2$[343] and aryllead triacetates $ArPb(OAc)_3$[348], a general mechanism is shown (Scheme 10)[392]. The active Cu(I) species is generated in the early stages of the reaction by reduction of the starting Cu(II) diacetate by a nucleophilic component of the reaction system. Because aryllead reagents are known to be inert to $Cu(OAc)_2$, the first step of the catalytic cycle was proposed to form copper amine complexes.

By this mechanism in Scheme 10, the Cu(I) intermediate (**95**) reacts with the substrate with an N−H bond to give a new-Cu(I) intermediate (**96**). No base to neutralize the acid generated by this exchange was included in the published mechanism, but a base was present in the reaction system. Transmetallation between the copper and main group
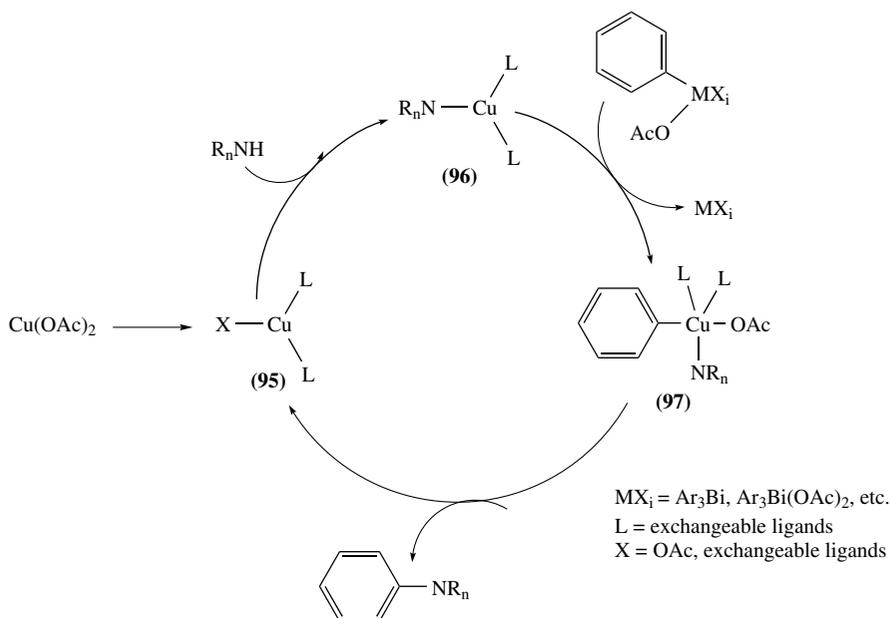
SCHEME 10. General mechanism of copper-catalyzed amination reactions with hypervalent organometallic reagents

reagent is believed to generate a Cu(III) intermediate (**97**), which subsequently undergoes reductive elimination to give the final product and to regenerate the Cu(I) species (**95**).

The above proposal is supported by the lack of reaction of electron-deficient arylamines, such as p-NO$_2$-aniline and p-EtO$_2$C-aniline, in the copper-mediated reactions with lead acetates because of the inability of the amines to reduce Cu(II) to Cu(I). This lack of reduction is indicated by the lack of a color change upon addition of Cu(OAc)$_2$ to a solution of either of the amines. Further, the presence of Cu(III) species may be responsible for the formation of arenes and polymeric species during the N-arylation of anilines that are easily oxidized (Scheme 11).

2. Mechanism of the reactions with low-valent organometallic reagents

Speculations about the mechanism of the N-arylations of low-valent organometallic reagents are based on the studies of reactions of arylbismuth[311, 343], arylboronic acids[278, 357], arylsiloxanes[303] and arylstannanes[357]. Cu(OAc)$_2$ in CH$_2$Cl$_2$ has been the most commonly used source of copper. Cu(OAc)$_2$ is insoluble in CH$_2$Cl$_2$, but upon addition of amine, a deep blue complex is formed that immediately dissolves in CH$_2$Cl$_2$. Thus, the formation of Cu(II)−amine complex (**98** in Scheme 12) is thought to be the first step of the reaction. Transmetallation to form an aryl Cu(II)−amine complex (**99**) is believed to be the second step. This hypothesis is supported by the similarity in yields obtained from the reaction of p-tolylboronic acid with benzimidazole and reaction of p-tolylboronic acid with a preformed Cu(II)−imidazole complex. Addition of TBAF has been proposed to accelerate the transmetallation step by generating a hypervalent organometallic species.
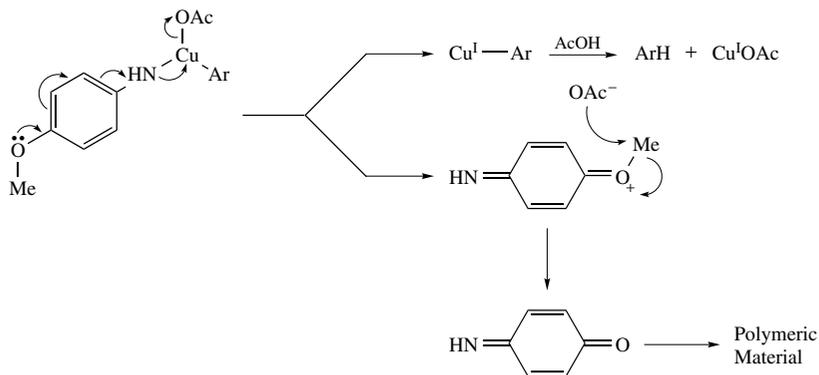
SCHEME 11. Potential mechanism for the formation of arenes and polymeric species during copper-catalyzed *N*-arylation of anilines
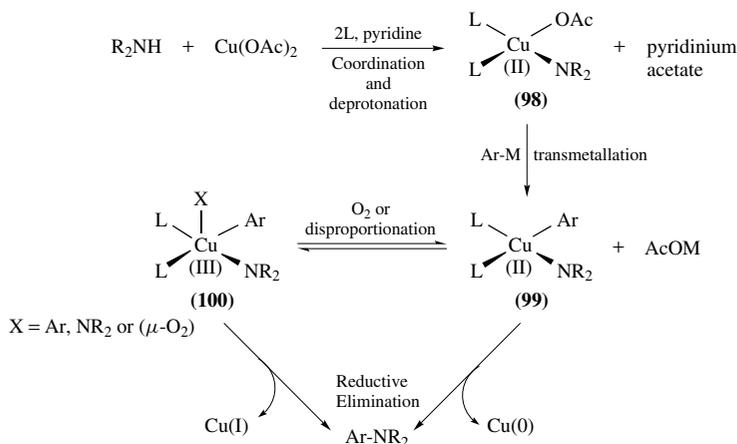
SCHEME 12. Potential mechanisms for copper-catalyzed amination reactions with low-valent organometallic reagents

Complex **99** can either undergo direct reductive elimination to give the products of Cu(0) or can undergo oxidation to a Cu(III) species (**100**)[393], followed by reductive elimination to give the organic products, along with a Cu(I) species. A disproportionation of the Cu(II) complex (**99**) to yield the higher oxidation state Cu(III) complex (**100**) and Cu(I) could also occur. Lower yields of products and substantially slower rates of reactions under anaerobic conditions lend credence to the proposal that complex **99** may be oxidized to complex **100** to facilitate the reductive elimination. The radical pathway was disfavored due to the lack of an effect of a free radical trap.

3. Mechanism of the copper-catalyzed reactions with low-valent organometallic reagents and co-oxidant

Collman and Zhang[276, 296] proposed a mechanism for the coupling of imidazole with arylboronic acids catalyzed by [Cu(OH)•(tmeda)]$_2$Cl$_2$ (Scheme 13) that is similar to the
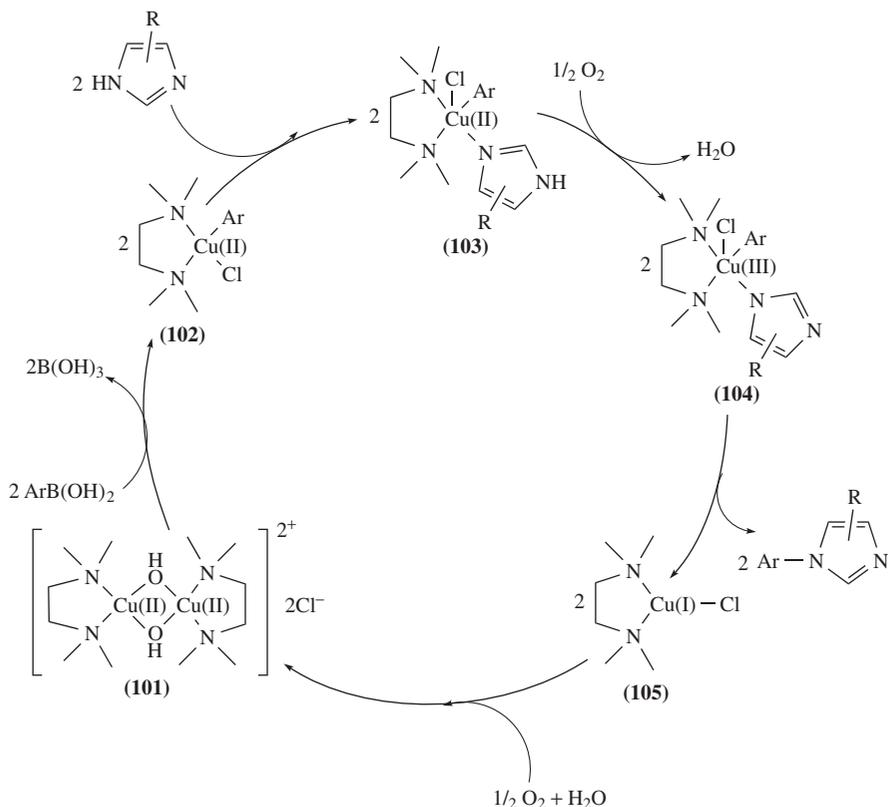
SCHEME 13. Mechanism of coupling of imidazole with arylboronic acids

mechanism proposed by Evans and coworkers[278] for coupling arylboronic acids with phenols. The initial transmetallation of $ArB(OH)_2$ with catalyst **101** would generate copper(II) complex **102**. The imidazole then coordinates to **102** to form another copper(II) complex (**103**). In the presence of O_2, complex **103** could undergo oxidation to form a copper(III) complex (**104**), which would subsequently undergo reductive elimination to give the N-arylimidazole product, along with the copper(I) complex **105**, which would reconvert to the starting species (**101**) in the presence of O_2 and water[394, 395]. The water released in the conversion of **102** to **103** or by the condensation of $ArB(OH)_2$ to generate triarylboroxines[396] would lead to the arylation of water in competition with phenol or the imidazole substrate, thereby diminishing the yield of the desired coupling products. Presumably, during the oxidation of Cu(II) to Cu(III), hydrogen peroxide would also be produced, and this hydrogen peroxide could lead to the oxidation of $ArB(OH)_2$ to $ArOH$[397]. The use of molecular sieves has been shown to increase the yield of the copper-catalyzed reactions. These side reactions can also explain the need for more than 1 equivalent of arylboronic acid to obtain high yields of the arylation products. Lam and coworkers[281] conducted studies with oxygen isotopes to validate the proposal that the arylation of water occurs during the reaction. The use of $^{18}O_2$ showed that the phenolic hydroxyl group is not formed from atmospheric oxygen. This result suggests that phenol

is formed from water produced in the reaction. Indeed, when $H_2^{18}O$ was used, the label was incorporated in the biphenyl phenol product.

It was recently proposed that the first step of the reaction involves the coordination of imidazole and not transmetallation. Also, when the reaction of phenylboronic acid with imidazole was carried out in the presence of $[Cu(OH)L]_2Cl_2$ (L = TMEDA) in NMP/H_2O (1:1) and in the absence of any base, dioxygen was not required as oxidant, and the reaction progressed equally well in the presence or absence of O_2[302].

4. Mechanism of the copper-catalyzed reactions of aryl halides with compounds containing N−H bonds

As summarized in a previous section, the catalytically active species is assumed to be a Cu(I) complex. This Cu(I) complex would then first bind the amine and then undergo oxidative addition to form a transient Cu(III) species. This Cu(III) species would then reductively eliminate the product to regenerate the Cu(I) catalyst[239].

Ma and coworkers[242] noticed the accelerating effect of α-amino acids in the copper-catalyzed coupling reactions of aryl halides with α-amino acids using CuI as catalyst and K_2CO_3 as base. The authors noted that the coupling reaction of bromobenzene with L-
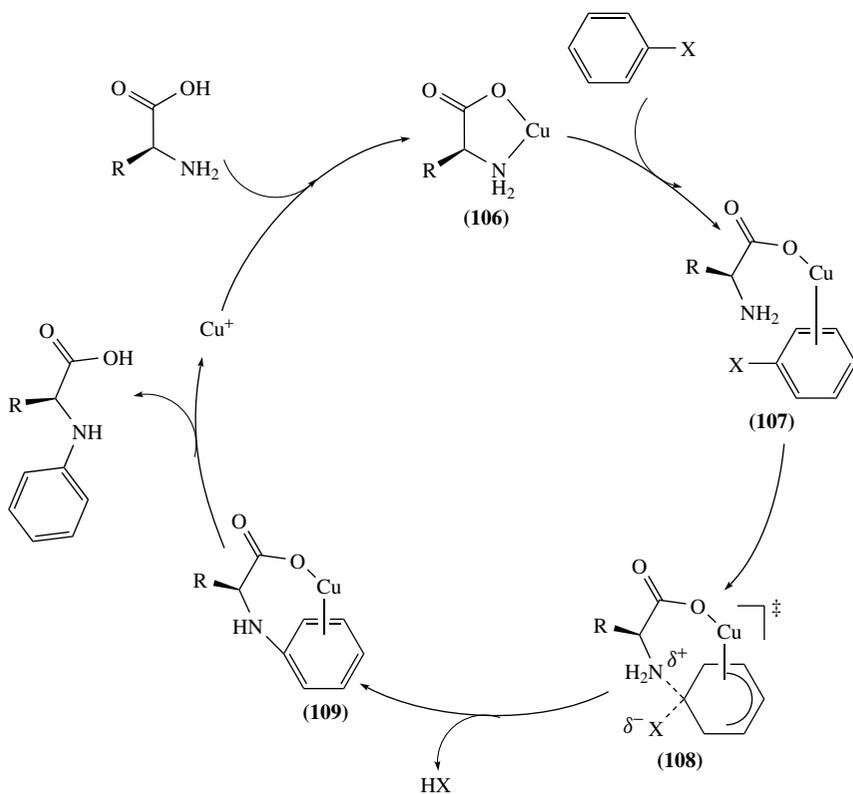
SCHEME 14. Mechanism of copper-catalyzed amination of aryl halides

valine gave 43% conversion at 75 °C in 24 h. In contrast, the coupling of bromobenzene with benzylamine occurred to only 5% conversion at 110 °C after 32 h, and the reaction of (S)-valinol with bromobenzene also occurred to only 5% conversion under similar conditions. Since α-amino acids are poorer nucleophiles than simple amines due to the electron-withdrawing effect of the carboxylate, the coordinating ability of the α-amino acid to copper ions was thought to contribute to the accelerating effect. On the basis of this analysis and the known mechanism of Ullmann condensation by π-complexes (**107**, Scheme 14)[250], they proposed the catalytic cycle shown in Scheme 14. Similarly to the reactions summarized above, cuprous ion was thought to be the catalytically active species. This proposal stems from the observation that CuI, Cu(OAc)$_2$ and Cu(SO$_4$)$_2$ all catalyzed the reaction, but that the rates were much faster for reactions catalyzed by CuI. In Ma's proposed mechanism, Cu(I) reacts with an α-amino acid to form the chelate **106**[398]. Complex **106** coordinates the aryl halide to provide the π-complex **107**. Intramolecular nucleophilic substitution to displace the halogen then occurs at the aromatic ring to give complex **109** via transition state **108**. This step is thought to be rate-limiting, and the intramolecular attack would lower the activation energy to accelerate the reaction.

Support for the proposed mechanism comes from the observation that the L-phenyl-aniline–Cu(II) complex reacted with bromobenzene in the presence of K$_2$CO$_3$ under N$_2$ to yield the product in 43% yield after 48 h, despite low solubility of the complex in the solvent DMA. However, the same reaction carried out with CuI in air did not give the coupled product; only the L-phenylalanine–Cu(II) complex was isolated. This result implies that the major species that forms the C–N bond is the L-phenylalanine–Cu(I) complex.

VII. REFERENCES

1. J. F. Bunnett and R. E. Zahler, *Chem. Rev.*, **49**, 273 (1951).
2. V. M. Vlasov, *Russ. Chem. Rev.*, **72**, 681 (2003).
3. K. H. Lee, F. McPhee, J. J. DeVoss, C. S. Craik and P. R. O. de Montellano, *J. Org. Chem.*, **59**, 6194 (1994).
4. N. N. Vorozhtsov, Jr. and V. A. Kobelev, *Zh. Obshch. Khim.*, **9**, 1043 (1939); *Chem. Abstr.*, **33**, 59696 (1939).
5. A. Wohl, *Ber. Dtsch. Chem. Ges.*, **39**, 1951 (1906).
6. A. Brewin and E. E. Turner, *J. Chem. Soc.*, 332 (1928).
7. E. Wedekind, *Chem. Ber.*, **33**, 426 (1900).
8. H. Heaney, *Chem. Rev.*, **62**, 81 (1962).
9. F. Pietra, *Q. Rev., Chem. Soc.*, **23**, 504 (1969).
10. J. D. Roberts, H. E. Simmons, L. A. Carlsmith and C. W. Vaughan, *J. Am. Chem. Soc.*, **75**, 3290 (1953).
11. M. Panar and J. D. Roberts, *J. Am. Chem. Soc.*, **82**, 3629 (1960).
12. R. W. Hoffman, *Dehydrobenzene and Cycloalkynes*, Academic Press, New York, 1967.
13. E. W. Gowling, S. F. A. Kettle and G. M. Sharpless, *Chem. Commun.*, 21 (1968).
14. I. T. Millar and H. Heaney, *Q. Rev., Chem. Soc.*, **11**, 109 (1957).
15. G. Wittig and F. Bickelhaupt, *Chem. Ber.*, **91**, 883 (1958).
16. G. E. Hall, R. Piccolini and J. D. Roberts, *J. Am. Chem. Soc.*, **77**, 4540 (1955).
17. J. D. Roberts, V. Wheaton, L. A. Carlsmith and D. A. Semenow, *J. Am. Chem. Soc.*, **78**, 611 (1956).
18. R. Huisgen, W. Mack, K. Herbig, N. Ott and E. Anneser, *Chem. Ber.*, **93**, 412 (1960).
19. R. Huisgen and J. Sauer, *Chem. Ber.*, **91**, 1453 (1958).
20. M. Beller, C. Breindl, T. H. Riermeier and A. Tillack, *J. Org. Chem.*, **66**, 1403 (2001).
21. F. Scardiglia and J. D. Roberts, *J. Org. Chem.*, **23**, 629 (1958).
22. P. P. Wickham, K. H. Hazen, H. Guo, G. Jones, K. H. Reuter and W. J. Scott, *J. Org. Chem.*, **56**, 2045 (1991).
23. P. P. Wickham, K. H. Reuter, D. Senanayake, H. Guo, M. Zalesky and W. J. Scott, *Tetrahedron Lett.*, **34**, 7521 (1993).

24. R. Huisgen and H. Konig, *Angew. Chem., Int. Ed. Engl.*, **69**, 268 (1957).
25. J. March, *Advanced Organic Chemistry*, Wiley, New York, 1992.
26. W. M. Weaver, in *The Chemistry of the Nitro and Nitroso Groups*, Part 2 (Ed. H. Feuer), Wiley, New York, 1970, p. 1.
27. G. A. Olah, R. Malhotra and S. C. Narang, *Nitration: Methods and Mechanisms*, VCH, New York, 1989.
28. K. Schofield, *Aromatic Nitration*, Cambridge University Press, Cambridge, 1980.
29. M. B. Smith and J. March, *Advanced Organic Chemistry: Reactions, Mechanism, and Structure*, 5th edn., Wiley, New York, 2001.
30. R. C. Larock, *Comprehensive Organic Transformations: A Guide to Functional Group Preparations*, Wiley-VCH, New York, 1999, p. 823.
31. V. Migrdichian, *Organic Synthesis*, Reinhold, New York, 1957, p. 1422.
32. K. Nomura, *J. Mol. Catal. A: Chem.*, **130**, 1 (1998).
33. A. M. Tafesh and J. Weiguny, *Chem. Rev.*, **96**, 2035 (1996).
34. K. Nomura, *Catalysis Surveys from Japan*, **2**, 59 (1998).
35. A. M. Tafesh and M. Beller, *Tetrahedron Lett.*, **36**, 9305 (1995).
36. K. Kaneda, H. Kuwahara and T. Imanaka, *J. Mol. Catal. A: Chem.*, **88**, L267 (1994).
37. Y. Yost, H. R. Gutmann and C. C. Muscoplat, *J. Chem. Soc., C*, 2119 (1970).
38. H. Gilman and R. McCracken, *J. Am. Chem. Soc.*, **49**, 1052 (1927).
39. G. Bartoli, *Acc. Chem. Res.*, **17**, 109 (1984).
40. I. Sapountzis and P. Knochel, *J. Am. Chem. Soc.*, **124**, 9390 (2002).
41. I. Sapountzis and P. Knochel, *Angew. Chem., Int. Ed.*, **43**, 897 (2004).
42. J. N. Johnston, M. A. Plotkin, R. Viswanathan and E. N. Prabhakaran, *Org. Lett.*, **3**, 1009 (2001).
43. R. Viswanathan, E. N. Prabhakaran, M. A. Plotkin and J. N. Johnston, *J. Am. Chem. Soc.*, **125**, 163 (2003).
44. H. Neumann, A. J. V. Wangelin, S. Klaus, D. Dtrubing, D. Gordes and M. Beller, *Angew. Chem., Int. Ed.*, **42**, 4503 (2003).
45. J. Louie and J. F. Hartwig, *Tetrahedron Lett.*, **36**, 3609 (1995).
46. A. S. Guram, R. A. Rennels and S. L. Buchwald, *Angew. Chem., Int. Ed. Engl.*, **34**, 1348 (1995).
47. N. V. Kondratenko, A. A. Kolomeitsev, V. O. Mogilevskaya, N. M. Varlamova and L. M. Yagupol'skii, *Zh. Org. Khim.*, 1721 (1986); *Chem. Abstr.*, **107**, 39310 (1987).
48. M. S. Driver and J. F. Hartwig, *J. Am. Chem. Soc.*, **118**, 7217 (1996).
49. J. P. Wolfe, S. Wagaw and S. L. Buchwald, *J. Am. Chem. Soc.*, **118**, 7215 (1996).
50. J. P. Wolfe and S. L. Buchwald, *J. Org. Chem.*, **61**, 1133 (1996).
51. S. Wagaw and S. L. Buchwald, *J. Org. Chem.*, **61**, 7240 (1996).
52. J. Yin, M. M. Zhao, M. A. Huffman and J. M. McNamara, *Org. Lett.*, **4**, 3481 (2002).
53. J. Ji, T. Li and W. H. Bunnelle, *Org. Lett.*, **5**, 4611 (2003).
54. M. Nishiyama, T. Yamamoto and Y. Koie, *Tetrahedron Lett.*, **39**, 617 (1998).
55. T. Yamamoto, M. Nishiyama and Y. Koie, *Tetrahedron Lett.*, **39**, 2367 (1998).
56. M. Kawatsura and J. F. Hartwig, *J. Am. Chem. Soc.*, **121**, 1473 (1999).
57. A. F. Littke and G. C. Fu, *Angew. Chem., Int. Ed.*, **37**, 3387 (1998).
58. A. F. Littke and G. C. Fu, *J. Org. Chem.*, **64**, 10 (1999).
59. J.-F. Marcoux, S. Wagaw and S. L. Buchwald, *J. Org. Chem.*, **62**, 1568 (1997).
60. D. W. Old, J. P. Wolfe and S. L. Buchwald, *J. Am. Chem. Soc.*, **120**, 9722 (1998).
61. X. Bei, T. Uno, J. Norris, H. W. Turner, W. H. Weinberg and A. S. Guram, *Organometallics*, **18**, 1840 (1999).
62. X. Bei, A. S. Guram, H. W. Turner and W. H. Weinberg, *Tetrahedron Lett.*, **40**, 1237 (1999).
63. R. A. Singer, S. Caron, R. E. Mcdermott, P. Arpin and N. M. Do, *Synthesis*, 1727 (2003).
64. K. Kamikawa, S. Sugimoto and M. Uemura, *J. Org. Chem.*, **63**, 8407 (1998).
65. P. Molina, A. Arques and A. Garcia, *Tetrahedron Lett.*, **38**, 7613 (1997).
66. J. P. Wolfe, H. Tomori, J. P. Sadighi, J. J. Yin and S. L. Buchwald, *J. Org. Chem.*, **65**, 1158 (2000).
67. N. Kataoka, Q. Shelby, J. P. Stambuli and J. F. Hartwig, *J. Org. Chem.*, **67**, 5553 (2002).
68. J. F. Hartwig, M. Kawatsura, S. I. Hauck, K. H. Shaughnessy and L. M. Alcazar-Roman, *J. Org. Chem.*, **64**, 5575 (1999).
69. R. Kuwano, M. Utsunomiya and J. F. Hartwig, *J. Org. Chem.*, **67**, 6479 (2002).

70. J. P. Stambuli, R. Kuwano and J. F. Hartwig, *Angew. Chem., Int. Ed.*, **41**, 4746 (2002).
71. M. Prashad, X. Y. Mak, Y. G. Liu and O. Repic, *J. Org. Chem.*, **68**, 1163 (2003).
72. D. Gerristma, B. Timothy, J. McNulty and A. Capretta, *Tetrahedron Lett.*, **45**, 8319 (2004).
73. S. Urgaonkar, M. Nagarajan and J. G. Verkade, *J. Org. Chem.*, **68**, 452 (2003).
74. S. Urgaonkar, J.-H. Xu and J. G. Verkade, *J. Org. Chem.*, **68**, 8416 (2003).
75. M. S. Viciu, R. M. Kissling, E. D. Stevens and S. P. Nolan, *Org. Lett.*, **4**, 2229 (2002).
76. V. V. Grushin and H. Alper, *Chem. Rev.*, **94**, 1047 (1994).
77. M. Beller, T. H. Reirmeier, C. Reisinger and W. A. Herrman, *Tetrahedron Lett.*, **38**, 2073 (1997).
78. N. P. Reddy and M. Tanaka, *Tetrahedron Lett.*, **38**, 4807 (1997).
79. B. C. Hamann and J. F. Hartwig, *J. Am. Chem. Soc.*, **120**, 7369 (1998).
80. A. Ehrentraut, A. Zapf and M. Beller, *J. Mol. Catal. A: Chem.*, **182–183**, 515 (2002).
81. F. Rataboul, A. Zapf, R. Jackstell, S. Harkal, T. Riermeier, A. Monsees, U. Dingerdissen and M. Beller, *Chem. Eur. J.*, **10**, 2983 (2004).
82. S. Urgaonkar, J.-H. Xu and J. G. Verkade, *J. Org. Chem.*, **68**, 8416 (2003).
83. S. Urgaonkar, M. Nagarajan and J. G. Verkade, *Org. Lett.*, **5**, 815 (2003).
84. J. Huang, G. Grasa and S. P. Nolan, *Org. Lett.*, **1**, 1307 (1999).
85. G. A. Grasa, M. S. Viciu, J. K. Huang and S. P. Nolan, *J. Org. Chem.*, **66**, 7729 (2001).
86. S. Stauffer, S. I. Hauck, S. Lee, J. Stambuli and J. F. Hartwig, *Org. Lett.*, **2**, 1423 (2000).
87. U. Christmann and R. Vilar, *Angew. Chem., Int. Ed.*, **44**, 366 (2005).
88. M. S. Viciu, R. F. Germaneau, O. Navarro-Fernandez, E. D. Stevens and S. P. Nolan, *Organometallics*, **21**, 5470 (2002).
89. M. S. Viciu, R. A. Kelly, III, E. D. Stevens, F. Naud, M. Studer and S. P. Nolan, *Org. Lett.*, **5**, 1479 (2003).
90. M. S. Viciu, O. Navarro, R. F. Germaneau, R. A. Kelly, III, W. Sommer, N. Marion, E. D. Stevens, L. Cavallo and S. P. Nolan, *Organometallics*, **23**, 1629 (2004).
91. A. Frisch, A. Zapf, O. Briel, B. Kayser, N. Shaikh and M. Beller, *J. Mol. Catal. A: Chem.*, **214**, 231 (2004).
92. L. J. Goossen, J. Paetzold, O. Briel, A. Rivas-Nass, R. Karch and B. Kayser, *Synlett*, 275 (2005).
93. S. Caddick, F. G. N. Cloke, G. K. B. Clentsmith, P. B. Hitchcock, D. McKerrecher, L. R. Titcomb and M. R. V. Williams, *J. Organomet. Chem.*, **617–618**, 635 (2001).
94. J. Louie, M. S. Driver, B. C. Hamann and J. F. Hartwig, *J. Org. Chem.*, **62**, 1268 (1997).
95. J. P. Wolfe and S. L. Buchwald, *J. Org. Chem.*, **62**, 1264 (1997).
96. J. Åhman and S. L. Buchwald, *Tetrahedron Lett.*, **38**, 6363 (1997).
97. O. Navarro, H. Kaur, P. Mahjoor and S. P. Nolan, *J. Org. Chem.*, **69**, 3173 (2004).
98. X. Huang, K. W. Anderson, D. Zim, L. Jiang, A. Klapars and S. L. Buchwald, *J. Am. Chem. Soc.*, **125**, 6653 (2003).
99. J. Louie and J. F. Hartwig, *J. Am. Chem. Soc.*, **119**, 11695 (1997).
100. S. Thayumanavan, S. Barlow and S. R. Marder, *Chem. Mater.*, **9**, 3231 (1997).
101. E. Bellmann, S. Shaheen, S. Thayumanavan, S. Barlow, R. Grubbs, S. Marder, B. Kippelen and N. Peyghambarian, *Chem. Mater.*, **10**, 1668 (1998).
102. U. Christmann, R. Vilar, A. J. P. White and D. J. Williams, *Chem. Commun.*, 1294 (2004).
103. J. Louie, M. S. Driver, B. C. Hamann and J. F. Hartwig, *J. Org. Chem.*, **62**, 1268 (1997).
104. J. Louie and J. F. Hartwig, *Macromolecules*, **31**, 6737 (1998).
105. Q. Shen, S. Shekhar, J. P. Stambuli and J. F. Hartwig, *Angew. Chem. Int. Ed.*, **44**, 1371 (2005).
106. B. C. Hamann and J. F. Hartwig, *J. Am. Chem. Soc.*, **120**, 3694 (1998).
107. K. Rossen, P. J. Pye, A. Maliakal and R. P. Volante, *J. Org. Chem.*, **62**, 6462 (1997).
108. I. P. Beletskaya, A. G. Bessermertnykh and R. Guilard, *Tetrahedron Lett.*, **38**, 2287 (1997).
109. Y. P. Hong, C. H. Senanayake, T. J. Xiang, C. P. Vandenbossche, G. J. Tanoury, R. P. Bakale and S. A. Wald, *Tetrahedron Lett.*, **39**, 3121 (1998).
110. I. Ozdemir, S. Demir, Y. Gok, E. Cetinkaya and B. Cetinkaya, *J. Mol. Catal. A: Chem.*, **222**, 97 (2004).
111. A. Togni, C. Breutel, A. Schnyder, F. Spindler, H. Landert and A. Tijani, *J. Am. Chem. Soc.*, **116**, 4062 (1994).
112. H. Bläser and F. Spindler, *Chimia*, **51**, 297 (1997).
113. Y. Kubota, S. Nakada and Y. Sugi, *Synlett*, 183 (1998).

114.   A. H. Roy and J. F. Hartwig, *J. Am. Chem. Soc.*, **125**, 8704 (2003).
115.   S. I. Hauck, K. V. Lakshmi and J. F. Hartwig, *Org. Lett.*, **1**, 2057 (1999).
116.   N. Spetseris, R. E. Ward and T. Y. Meyer, *Macromolecules*, **31**, 3158 (1998).
117.   T. Kanbara, K. Izumi, Y. Nakadani, T. Narise and K. Hasegawa, *Chem. Lett.*, 1185 (1997).
118.   R. A. Singer, J. P. Sadighi and S. L. Buchwald, *J. Am. Chem. Soc.*, **120**, 213 (1998).
119.   J. P. Sadighi, R. A. Singer and S. L. Buchwald, *J. Am. Chem. Soc.*, **120**, 4960 (1998).
120.   J. P. Sadighi, M. C. Harris and S. L. Buchwald, *Tetrahedron Lett.*, **39**, 5327 (1998).
121.   S. Vyskocil, M. Smrcina and P. Kocovsky, *Tetrahedron Lett.*, **39**, 9289 (1998).
122.   X. H. Huang and S. L. Buchwald, *Org. Lett.*, **3**, 3417 (2001). Noted added in proof: The coupling of ammonia and lithium amide now known. See Q. Shen and J. F. Hartwig *J. Am. Chem. Soc.* **128**, 2180.
123.   K. Weigand and S. Pelka, *Org. Lett.*, **4**, 4689 (2002).
124.   S. Jaime-Figueroa, Y. Liu, J. M. Muchowski and D. G. Putman, *Tetrahedron Lett.*, **39**, 1313 (1998).
125.   G. Mann, J. F. Hartwig, M. S. Driver and C. Fernandez-Rivas, *J. Am. Chem. Soc.*, **120**, 827 (1998).
126.   J. P. Wolfe, J. Åhman, J. P. Sadighi, R. A. Singer and S. L. Buchwald, *Tetrahedron Lett.*, **38**, 6367 (1997).
127.   J. Barluenga, F. Aznar and C. Valdes, *Angew. Chem., Int. Ed.*, **43**, 343 (2004).
128.   J. P. Wolfe, R. A. Rennels and S. L. Buchwald, *Tetrahedron*, **52**, 7525 (1996).
129.   B. H. Yang and S. L. Buchwald, *Org. Lett.*, **1**, 35 (1999).
130.   W. Shakespeare, *Tetrahedron Lett.*, **40**, 2035 (1999).
131.   J. Yin and S. L. Buchwald, *Org. Lett.*, **2**, 1101 (2000).
132.   J. Yin and S. L. Buchwald, *J. Am. Chem. Soc.*, **124**, 6043 (2002).
133.   G. Burton, P. Cao, G. Li and R. Rivero, *Org. Lett.*, **5**, 4373 (2003).
134.   C. Bolm and J. P. Hildebrand, *Tetrahedron Lett.*, **39**, 5731 (1998).
135.   S. Lee, M. Jorgensen and J. F. Hartwig, *Org. Lett.*, **3**, 2729 (2001).
136.   S. Wagaw, B. H. Yang and S. L. Buchwald, *J. Am. Chem. Soc.*, **120**, 6621 (1998).
137.   J. F. Hartwig, *Angew. Chem., Int. Ed.*, **37**, 2090 (1998).
138.   J. J. Song and N. K. Yee, *Org. Lett.*, **2**, 519 (2000).
139.   Y. Zhu, Y. Kiryu and H. Katayama, *Tetrahedron Lett.*, **43**, 3577 (2002).
140.   K. Inamoto, M. Katsuno, T. Yoshino, I. Suzuki, K. Hiroya and T. Sakamoto, *Chem. Lett.*, **33**, 1026 (2004).
141.   Z. Wang, R. T. Skerlj and G. J. Bridger, *Tetrahedron Lett.*, **40**, 3543 (1999).
142.   J. P. Wolfe and S. L. Buchwald, *Tetrahedron Lett.*, **38**, 6359 (1997).
143.   J. P. Wolfe and S. L. Buchwald, *J. Org. Chem.*, **65**, 1144 (2000).
144.   M. C. Harris, X. Huang and S. L. Buchwald, *Org. Lett.*, **4**, 2885 (2002).
145.   S. Urgaonkar and J. G. Verkade, *Adv. Synth. Catal.*, **346**, 611 (2004).
146.   A. D. Ryabov, *Synthesis*, 233 (1985).
147.   R. B. Bedford, *Chem. Commun.*, 1787 (2003).
148.   M. Beller, T. H. Riermeier, C.-P. Reisinger and W. A. Herrmann, *Tetrahedron Lett.*, **38**, 2073 (1997).
149.   T. H. Riermeier, A. Zapf and M. Beller, *Topics in Catalysis*, **4**, 301 (1997).
150.   J. Louie and J. F. Hartwig, *Angew. Chem., Int. Ed. Engl.*, **35**, 2359 (1996).
151.   R. B. Bedford, C. S. J. Cazin, S. J. Coles, T. Gelbrich, P. N. Horton, M. B. Hursthouse and M. E. Light, *Organometallics*, **22**, 987 (2003).
152.   R. B. Bedford, C. S. J. Cazin and S. L. Hazelwood, *Angew. Chem., Int. Ed.*, **41**, 4120 (2002).
153.   R. B. Bedford, C. S. J. Cazin and S. L. Hazelwood, *Chem. Commun.*, 2608 (2002).
154.   D. A. Albisson, R. B. Bedford, P. Noelle Scully and S. E. Lawrence, *Chem. Commun.*, 2095 (1998).
155.   R. B. Bedford and M. E. Blake, *Adv. Synth. Catal.*, **345**, 1107 (2003).
156.   M. S. Viciu, R. A. Kelly, III, E. D. Stevens, F. Naud, M. Studer and S. P. Nolan, *Org. Lett.*, **5**, 1479 (2003).
157.   D. Zim and S. L. Buchwald, *Org. Lett.*, **5**, 2413 (2003).
158.   A. Schnyder, A. F. Indolese, M. Studer and H.-U. Blaser, *Angew. Chem., Int. Ed.*, **41**, 3668 (2002).
159.   U. Nettekoven, F. Naud, A. Schnyder and H.-U. Blaser, *Synlett*, 2549 (2004).
160.   R. A. Singer, N. J. Tom, H. N. Frost and W. M. Simon, *Tetrahedron Lett.*, **45**, 4715 (2004).

161. P. Le Floch and F. Mathey, *Coord. Chem. Rev.*, **179–180**, 771 (1998).
162. A. S. Gajare, K. Toyota, M. Yoshifuji and F. Ozawa, *J. Org. Chem.*, **69**, 6504 (2004).
163. T. Minami, H. Okamoto, S. Ikeda, R. Tanaka, F. Ozawa and M. Yoshifuji, *Angew. Chem., Int. Ed.*, **40**, 4501 (2001).
164. F. Ozawa, T. Ishiyama, S. Yamamoto, S. Kawagishi, H. Murakami and M. Yoshifuji, *Organometallics*, **23**, 1698 (2004).
165. G. Y. Li, *Angew. Chem., Int. Ed. Engl.*, **40**, 1513 (2001).
166. G. Y. Li, P. J. Fagan and P. L. Watson, *Angew. Chem., Int. Ed.*, **40**, 1106 (2001).
167. G. Y. Li, G. Zheng and A. F. Noonan, *J. Org. Chem.*, **66**, 8677 (2001).
168. U. Christmann, R. Vilar, A. J. P. White and D. J. Williams, *Chem. Commun.*, 1294 (2004).
169. J. F. Hartwig, *J. Am. Chem. Soc.*, **118**, 7010 (1996).
170. J. F. Hartwig and S. Stauffer, unpublished results.
171. C. Amatore, G. Broeker, A. Jutand and F. Khalil, *J. Am. Chem. Soc.*, **119**, 5176 (1997).
172. C. Amatore, E. Carre, A. Jutand and M. A. M'Barki, *Organometallics*, **14**, 1818 (1995).
173. U. K. Singh, E. R. Strieter, D. G. Blackmond and S. L. Buchwald, *J. Am. Chem. Soc.*, **124**, 14104 (2002).
174. J. F. Hartwig, Material presented orally at the Thieme-IUPAC Conference on Synthetic Organic Chemistry, Nagoya, Japan, August 2004.
175. C. Amatore, A. Jutand and A. Suarez, *J. Am. Chem. Soc.*, **115**, 9531 (1993).
176. C. Amatore and F. Pfluger, *Organometallics*, **9**, 2276 (1990).
177. J. F. Hartwig and F. Paul, *J. Am. Chem. Soc.*, **117**, 5373 (1995).
178. L. M. Alcazar-Roman, J. F. Hartwig, A. L. Rheingold, L. M. Liable-Sands and I. A. Guzei, *J. Am. Chem. Soc.*, **122**, 4618 (2000).
179. F. Barrios-Landeros and J. F. Hartwig, *J. Am. Chem. Soc.*, **127**, 6944 (2005).
180. L. M. Alcazar-Roman and J. F. Hartwig, *Organometallics*, **21**, 491 (2002).
181. E. Galardon, S. Ramdeehul, J. M. Brown, A. Cowley, K. K. Hii and A. Jutand, *Angew. Chem., Int. Ed.*, **41**, 1760 (2002).
182. A. K. De Lewis, S. Caddick, F. G. N. Cloke, N. C. Billingham, P. B. Hitchcock and J. Leonard, *J. Am. Chem. Soc.*, **125**, 10066 (2003).
183. S. Caddick, F. G. N. Cloke, P. B. Hitchcock, J. Leonard, A. K. de Lewis, D. McKerrecher and L. R. Titcomb, *Organometallics*, **21**, 4318 (2002).
184. U. Christmann and R. Vilar, *Angew. Chem., Int. Ed.*, **44**, 366 (2005).
185. J. P. Stambuli, M. Buehl and J. F. Hartwig, *J. Am. Chem. Soc.*, **124**, 9346 (2002).
186. J. P. Stambuli, C. D. Incarvito, M. Buehl and J. F. Hartwig, *J. Am. Chem. Soc.*, **126**, 1184 (2004).
187. M. S. Driver and J. F. Hartwig, *J. Am. Chem. Soc.*, **119**, 8232 (1997).
188. M. Yamashita and J. F. Hartwig, *J. Am. Chem. Soc.*, **126**, 5344 (2004).
189. G. Mann, C. Incarvito, A. L. Rheingold and J. F. Hartwig, *J. Am. Chem. Soc.*, **121**, 3224 (1999).
190. M. S. Driver and J. F. Hartwig, *J. Am. Chem. Soc.*, **118**, 7217 (1996).
191. M. Yamashita, J. V. C. Vicario and J. F. Hartwig, *J. Am. Chem. Soc.*, **125**, 16347 (2003).
192. G. Mann and J. F. Hartwig, *J. Am. Chem. Soc.*, **118**, 13109 (1996).
193. J. Louie, F. Paul and J. F. Hartwig, *Organometallics*, **15**, 2794 (1996).
194. J. P. Collman, L. S. Hegedus, J. R. Norton and R. G. Finke, *Principles and Applications of Organotransition Metal Chemistry*, University Science Books, Mill Valley, 1987, p. 279.
195. J. F. Hartwig, S. Richards, D. Barañano and F. Paul, *J. Am. Chem. Soc.*, **118**, 3626 (1996).
196. R. Rossi and R. H. de Rossi, *Aromatic Substitution by the $S_{RN}1$ Mechanism*, American Chemical Society, Washington, D.C., 1983.
197. G. Mann, J. F. Hartwig, M. S. Driver and C. Fernandez-Rivas, *J. Am. Chem. Soc.*, **120**, 827 (1998).
198. F. Paul, J. Patt and J. F. Hartwig, *Organometallics*, **14**, 3030 (1995).
199. R. A. Widenhoefer and S. L. Buchwald, *Organometallics*, **15**, 3534 (1996).
200. R. A. Widenhoefer, H. A. Zhong and S. L. Buchwald, *Organometallics*, **15**, 2745 (1996).
201. R. A. Widenhoefer and S. L. Buchwald, *Organometallics*, **15**, 2755 (1996).
202. F. Ullmann, *Ber. Dtsch. Chem. Ges.*, **34**, 2174 (1901).
203. F. Ullmann, *Ber. Dtsch. Chem. Ges.*, **36**, 2382 (1903).
204. F. Ullmann and P. Sponagel, *Ber. Dtsch. Chem. Ges.*, **38**, 2211 (1905).
205. F. Ullmann and R. Maag, *Ber. Dtsch. Chem. Ges.*, **39**, 1693 (1906).

206. I. Goldberg, *Ber. Dtsch. Chem. Ges.*, **39**, 1691 (1906).
207. J. F. Bunnett and R. E. Zahler, *Chem. Rev.*, **49**, 273 (1951).
208. J. Lindley, *Tetrahedron*, **40**, 1433 (1984).
209. G. I. Elliott and J. P. Konopelski, *Tetrahedron*, **57**, 5683 (2001).
210. J.-P. Finet, A. Y. Fedorov, S. Combes and G. Boyer, *Curr. Org. Chem.*, **6**, 597 (2002).
211. K. Kunz, U. Scholz and D. Ganzer, *Synlett*, 2428 (2003).
212. A. W. Thomas and S. V. Ley, *Angew. Chem., Int. Ed.*, **42**, 5400 (2003).
213. B. C. G. Soderberg, *Cord. Chem. Rev.*, **248**, 1085 (2004).
214. I. P. Beletskaya and A. V. Cheprakov, *Cord. Chem. Rev.*, **248**, 2337 (2004).
215. P. E. Weston and H. Adkins, *J. Am. Chem. soc.*, **50**, 859 (1928).
216. I. Goldberg, *Ber. Dtsch. Chem. Ges.*, **40**, 4541 (1907).
217. I. Goldberg and M. Nimerovsky, *Ber. Dtsch. Chem. Ges.*, **40**, 2448 (1907).
218. I. Goldberg and K. Kelley, *J. Chem. Soc.*, 102 (1946).
219. D. Hager, *Organic Synthesis*, Col. Vol. **1**, p. 544, 1948.
220. R. M. Acheson, *Acridines*, Interscience, New York, 1956, p. 122.
221. R. F. Pellon, R. Carrasco and L. Rodes, *Syn. Comm.*, **23**, 1447 (1993).
222. R. Carrasco, R. F. Pellon, J. Elguero and J. A. Paez, *Syn. Comm.*, **19**, 2077 (1989).
223. J.-P. Hanoun, J.-P. Galy and A. Tenaglia, *Syn. Comm.*, **25**, 2443 (1995).
224. O. Zeide, *Ann.*, **440**, 311 (1924).
225. R. F. Pellon, R. Carrasco and L. Rodes, *Syn. Comm.*, **26**, 3869 (1996).
226. D. M. L. Palacios and R. F. P. Comdom, *Syn. Comm.*, **33**, 1777 (2003).
227. B. I. Stepanov and L. B. Aingom, *Zh. Obshch. Khim.*, **29**, 3436 (1959); *Chem. Abstr.*, **54**, 80537 (1960).
228. T. D. Tuong and M. Hida, *Bull. Chem. Soc. Jpn.*, **43**, 1763 (1970).
229. K. Iizuka, K. Akahane, D. Momose and M. Nakazawa, *J. Med. Chem.*, **24**, 1139 (1981).
230. Y. S. Lo, J. C. Nolan, T. H. Maren, J. W. J. Welstead, D. F. Gripshover and D. A. Shamblee, *J. Med. Chem.*, **35**, 4790 (1992).
231. G. R. Martinez, K. A. M. Walker, D. R. Hirshfeld, J. J. Bruno, D. S. Yang and P. J. Maloney, *J. Med. Chem.*, **35**, 620 (1992).
232. J. W. Pavik, R. E. Connors, D. S. Burns and E. M. Kurzweil, *J. Am. Chem. soc.*, **115**, 7645 (1993).
233. M. C. Venuti, R. A. Stephenson, R. Alvarez and J. A. Bruno, *J. Med. Chem.*, **30**, 2136 (1987).
234. R. G. R. Bacon and D. J. Maitland, *J. Chem. Soc., C*, 1973 (1970).
235. A. A. Kelkar, N. M. Patil and R. V. Chaudhari, *Tetrahedron Lett.*, **43**, 7143 (2002).
236. S. Gauthier and J. M. Frechet, *Synthesis*, 383 (1987).
237. R. D. Miller, V. Y. Lee and R. J. Twieg, *J. Chem. Soc., Chem. Comm.*, 245 (1995).
238. S. Suresh, R. J. Gulotty and S. E. Bales, *Polymer*, **44**, 5111 (2003).
239. K. Yamada, T. Kubo, H. Tokuyama and T. Fukuyama, *Synlett*, 231 (2002).
240. K. Yamada, T. Kurokawa, H. Tokuyama and T. Fukuyama, *J. Am. Chem. Soc.*, **125**, 6630 (2003).
241. K. Okano, H. Tokuyama and T. Fukuyama, *Org. Lett.*, **5**, 4987 (2003).
242. D. Ma, Y. Zhang, J. Yao, J. Wu and F. Tao, *J. Am. Chem. Soc.*, **120**, 12459 (1998).
243. D. Ma, C. Xia, J. Jiang, J. Zhang and W. Tang, *J. Org. Chem.*, **68**, 442 (2003).
244. D. Ma and C. Xia, *Org. Lett.*, **3**, 2583 (2001).
245. J.-B. Clement, J. F. Hayes, H. M. Sheldrake, P. W. Shledrake and A. S. Wells, *Synlett*, 1423 (2001).
246. K. Ding, J. Flippen-Anderson, J. R. Deschampsb and S. Wanga, *Tetrahedron Lett.*, **45**, 1027 (2004).
247. H. B. Goodbrand and N.-X. Hu, *J. Org. Chem.*, **64**, 670 (1999).
248. H. Weingarten, *J. Am. Chem. Soc.*, **29**, 3624 (1964).
249. T. Cohen and I. Crostea, *J. Am. Chem. Soc.*, **98**, 748 (1976).
250. A. J. Paine, *J. Am. Chem. Soc.*, **109**, 1496 (1987).
251. R. Gujadhur, C. G. Bates and D. Venkataraman, *Org. Lett.*, **3**, 4315 (2001).
252. R. Gujadhur, D. Venkataraman and J. T. Kintigh, *Tetrahedron Lett.*, **42**, 4791 (2001).
253. G. W. Rewcastle, W. A. Denny and B. C. Baguley, *J. Med. Chem.*, **30**, 843 (1987).
254. D. Ma, Q. Cai and H. Zhang, *Org. Lett.*, **5**, 2453 (2003).
255. R. F. Pellon, T. Mamposo, R. Carrasco and L. Rodes, *Syn. Comm.*, **26**, 3877 (1996).
256. J. Haider, K. Kunz and U. Scholz, *Adv. Synth. Catal.*, **346**, 717 (2004).

257. G. E. Job and S. L. Buchwald, *Org. Lett.*, **4**, 3703 (2002).
258. S. Arai, T. Yamagishi, S. Ototake and M. Hida, *Bull. Chem. Soc. Jpn.*, **50**, 547 (1977).
259. A. V. Kalinin, J. F. Bower, P. Riebel and V. Snieckus, *J. Org. Chem.*, **64**, 2986 (1999).
260. E. Vedejs, P. Trapencieris and E. Suna, *J. Org. Chem.*, **64**, 6724 (1999).
261. J. B. Arterburn, M. Pannala and A. M. Gonzalez, *Tetrahedron Lett.*, **42**, 1475 (2001).
262. F. Lang, D. Zewge, I. N. Houpis and R. P. Volante, *Tetrahedron Lett.*, **42**, 3251 (2001).
263. F. Y. Kwong, A. Klapars and S. L. Buchwald, *Org. Lett.*, **4**, 581 (2002).
264. C. Enguehard, H. Allouchi, A. Gueiffier and S. L. Buchwald, *J. Org. Chem.*, **68**, 4367 (2003).
265. F. Y. Kwong and S. L. Buchwald, *Org. Lett.*, **5**, 793 (2003).
266. Z. Lu, R. J. Twieg and S. D. Huang, *Tetrahedron Lett.*, **44**, 6289 (2003).
267. Z. Lu and R. J. Twieg, *Tetrahedron Lett.*, **46**, 2997 (2005).
268. D. Ma, Y. Li and X. F. Lin, *Chinese Journal of Chemistry*, **22**, 932 (2004).
269. M. A. Khan and J. B. Polya, *J. Chem. Soc., C*, 85 (1970).
270. C. A. Harbert, J. J. Plattner, W. M. Welch, A. Weissmann and B. K. Koe, *J. Med. Chem.*, **23**, 635 (1980).
271. H. Lexy and T. Kauffmann, *Chem. Ber.*, **113**, 2755 (1980).
272. P. C. Unangst, D. T. Connor, S. R. Stabler and R. J. Weikert, *J. Heterocycl. Chem.*, **24**, 811 (1987).
273. Y. Kato, M. M. Conn and J. Rebek, Jr., *J. Am. Chem. Soc.*, **116**, 3279 (1994).
274. Y. Murakami, T. Watanabe, T. Hagiwara, Y. Akiyama and H. Ishii, *Chem. Pharm. Bull.*, **43**, 1281 (1995).
275. W. W. K. R. Mederski, M. Lefort, M. Germann and D. Kux, *Tetrahedron*, **55**, 12757 (1999).
276. J. P. Collman and M. Zhong, *Org. Lett.*, **2**, 1233 (2000).
277. D. M. T. Chan, K. L. Monaco, R.-P. Wang and M. P. Winters, *Tetrahedron Lett.*, **39**, 2933 (1998).
278. D. A. Evans, J. L. Katz and T. R. West, *Tetrahedron Lett.*, **39**, 2937 (1998).
279. P. Y. S. Lam, C. G. Clark, S. Saubern, J. Adams, M. P. Winters, D. M. T. Chan and A. Combs, *Tetrahedron Lett.*, **39**, 2941 (1998).
280. D. J. Cundy and S. A. Forsyth, *Tetrahedron Lett.*, **39**, 7979 (1998).
281. P. Y. S. Lam, D. Bonne, G. Vincent, C. G. Clark and A. P. Combs, *Tetrahedron Lett.*, **44**, 1691 (2003).
282. A. P. Combs, S. Tadesse, M. Rafalski, T. S. Haque and P. Y. S. Lam, *J. Comb. Chem.*, **4**, 179 (2002).
283. G. C. H. Chiang and T. Olsson, *Org. Lett.*, **6**, 3079 (2004).
284. P. Das and B. Basu, *Syn. Comm.*, **34**, 2177 (2004).
285. A. P. Combs and M. Rafalski, *J. Comb. Chem.*, **2**, 29 (2000).
286. V. Collot, P. R. Bovy and S. Rault, *Tetrahedron Lett.*, **41**, 9053 (2000).
287. A. P. Combs, S. Saubern, M. Rafalski and P. Y. S. Lam, *Tetrahedron Lett.*, **40**, 1623 (1999).
288. S. Rossiter, C. K. Woo, B. Hartzoulakis, G. Wishart, L. Stanyer, J. W. Labadie and D. L. Selwood, *J. Comb. Chem.*, **6**, 385 (2004).
289. S. Yu, J. Saenz and J. K. Srirangam, *J. Org. Chem.*, **67**, 1699 (2002).
290. A. K. Bakkestuen and L.-L. Gundersen, *Tetrahedron Lett.*, **44**, 3359 (2003).
291. R. A. Joshi, P. S. Patil, M. Muthukrishnan, C. V. Raman and M. K. Gurjar, *Tetrahedron Lett.*, **45**, 195 (2004).
292. P. Y. S. Lam, G. Vincent, C. G. Clark, S. Deudon and P. K. Jadhav, *Tetrahedron Lett.*, **42**, 3415 (2001).
293. P. Y. S. Lam, G. Vincent, D. Bonne and C. G. Clark, *Tetrahedron Lett.*, **44**, 4927 (2003).
294. D. M. T. Chan, K. L. Monaco and R. H. Li, *Tetrahedron Lett.*, **44**, 3863 (2003).
295. J. P. Collman, M. Zhong, L. Zeng and S. Costanzo, *J. Org. Chem.*, **66**, 1528 (2001).
296. J. P. Collman, M. Zhong, C. Zhang and S. Costanzo, *J. Org. Chem.*, **66**, 7892 (2001).
297. J. C. Antilla and S. L. Buchwald, *Org. Lett.*, **3**, 2077 (2001).
298. M. Sasaki, S. Dalili and A. K. Yudin, *J. Org. Chem.*, **68**, 2045 (2003).
299. T. D. Quach and R. A. Batey, *Org. Lett.*, **5**, 4397 (2003).
300. J.-B. Lan, L. Chen, X.-Q. Yu, J.-S. You and R.-G. Xie, *Chem. Comm.*, 188 (2004).
301. J.-B. Lan, G.-L. Zhang, X.-Q. Yu, J.-S. You, L. Chen, M. Yan and R.-G. Xie, *Synlett*, 1095 (2004).
302. S. S. van Berkel, A. Hoogenband, J. W. Terpstra, M. Tromp, P. W. N. M. van Leeuwen and G. P. F. van Strijdonck, *Tetrahedron Lett.*, **45**, 7659 (2004).

303. P. Y. S. Lam, S. Deudon, K. M. Averill, R. Li, Y. He, P. DeShong and C. G. Clark, *J. Am. Chem. Soc.*, **122**, 7600 (2000).
304. P. Y. S. Lam, S. Deudon, E. Hauptman and C. G. Clark, *Tetrahedron Lett.*, **42**, 2427 (2001).
305. J.-P. Finet, A. Y. Fedorov, S. Combes and G. Boyer, *Curr. Org. Chem.*, **6**, 597 (2002).
306. S. Combes and J.-P. Finet, *Tetrahedron*, **54**, 4313 (1998).
307. V. A. Dodonov, A. V. Guschin and T. G. Brilkina, *Zh. Obshch. Khim.*, **55**, 466 (1985); *Chem. Abstr.*, **103**, 22218 (1985).
308. V. A. Dodonov and A. V. Guschin, *Metalloorg. Khim.*, **3**, 112 (1990); *Chem. Abstr.*, **113**, 22809 (1990).
309. D. H. R. Barton, J.-P. Finet and J. Khamsi, *Tetrahedron Lett.*, **27**, 3615 (1986).
310. A. Miloudi, G. Boyer, D. Al-Abed, J.-P. Finet and J.-P. Galy, *Main Group Met. Chem.*, **24**, 767 (2001).
311. T. Arnauld, D. H. R. Barton and E. Doris, *Tetrahedron*, **53**, 4137 (1997).
312. D. M. T. Chan, *Tetrahedron Lett.*, **37**, 9013 (1996).
313. A. Y. Fedorov, S. Combes and J.-P. Finet, *Tetrahedron*, **55**, 1341 (1999).
314. D. H. R. Barton, J.-P. Finet and J. Khamsi, *Tetrahedron Lett.*, **29**, 1115 (1988).
315. J. E. Dombrowski and P. G. Mattingly, European Pat. Appl., 1989.
316. A. Banfi, M. Bartoletti, E. Bellora, M. Bignoti and M. Turconi, *Synthesis*, 775 (1994).
317. G. Boyer, J.-P. Galy and J. Barbe, *Heterocycles*, **41**, 487 (1995).
318. P. Fan and S. Y. Ablordeppey, *J. Heterocycl. Chem.*, **34**, 1789 (1997).
319. E. Vassileva, M. Shopova, C. Fugier and E. Henry-Basch, *Syn. Comm.*, **27**, 1669 (1997).
320. R. Naito, M. Takeuchi, K. Mrohira, M. Hayakawa, K. Ikeda, T. Shibanuma and Y. Isomura, *Chem. Pharm. Bull.*, **46**, 1274 (1998).
321. S. Y. Ablordeppey, P. Fan, A. M. Clark and A. Nimrod, *Bioorg. Med. Chem.*, **7**, 343 (1999).
322. A. Y. Fedorov and J.-P. Finet, *Tetrahedron Lett.*, **40**, 2747 (1999).
323. I. W. J. Still, R. Natividad-Preya and F. D. Toste, *Can. J. Chem.*, **77**, 113 (1999).
324. Y. Aoki, Y. Saito, T. Sakamoto and Y. Kikugawa, *Syn. Comm.*, **30**, 131 (2000).
325. C. J. Dinsmore, J. M. Bergman, D. D. Wei, C. B. Zartman, J. P. Davide, I. B. Greenberg, D. Liu, T. J. O'Neill, J. B. Gibbs, K. S. Koblan, N. E. Kohl, R. B. Lobell, I.-W. Chen, D. A. McLoughlin, T. V. Olah, S. L. Graham, G. D. Hartman and T. M. Williams, *Bioorg. Med. Chem. Lett.*, **11**, 537 (2001).
326. J.-P. Meigh, M. Alvarez and J. A. Joule, *J. Chem. Soc., Perkin Trans. 1*, 2012 (2001).
327. A. Miloudi, D. El-Abed, G. Boyer, J.-P. Finet, J.-P. Galy and D. Siri, *Eur. J. Org. Chem.*, **7**, 1509 (2004).
328. M. A. Esteves, M. Narander, M. J. Marcelo-Curto and B. Gigante, *J. Nat. Prod.*, **64**, 761 (2001).
329. S. Morel, F. Chatel, G. Boyer and J.-P. Galy, *J. Chem. Res. (S)*, 4 (1998).
330. S. Morel, F. Chatel, G. Boyer and J.-P. Galy, *J. Chem. Res. (M)*, 0115 (1998).
331. F. Chatel, S. Morel, G. Boyer and J.-P. Galy, *Heterocycles*, 2535 (2000).
332. F. Chatel, G. Boyer and J.-P. Galy, *Syn. Comm.*, **32**, 2893 (2002).
333. G. Boyer, F. Chatel and J.-P. Galy, *Arkivoc*, **1**, 563 (2000).
334. O. Loog, U. Maeorg and U. Ragnarsson, *Synthesis*, 1591 (2000).
335. O. Tsubrik, U. Maeorg and U. Ragnarsson, *Tetrahedron Lett.*, **43**, 6213 (2002).
336. R. J. Sorensen, *J. Org. Chem.*, **65**, 7747 (2000).
337. L. K. Rasmussen, M. Begtrup and T. Ruhland, *J. Org. Chem.*, **69**, 6890 (2004).
338. D. H. R. Barton, J.-P. Finet and J. Khamsi, *Tetrahedron Lett.*, **30**, 937 (1989).
339. J. C. Anderson and M. Harding, *Chem. Comm.*, 393 (1998).
340. J. C. Anderson, R. Cubbon, M. Harding and D. S. James, *Tetrahedron: Asymmetry*, **9**, 3461 (1998).
341. C. Balsamini, A. Bedini, G. Spadoni, G. Tarzia, A. Tontini, W. Balduini and M. Cimino, *Il Farmaco*, **53**, 181 (1998).
342. G. A. Doherty, T. Kamenecka, E. McCauley, G. Van Ripper, R. A. Mumford, S. Tong and W. K. Hagmann, *Bioorg. Med. Chem. Lett.*, **12**, 729 (2002).
343. D. H. R. Barton, J.-P. Finet and J. Khamsi, *Tetrahedron Lett.*, **28**, 887 (1987).
344. S. K. Moiseev, I. V. Bakhanova, H. Schimdhammer and V. N. Kalinin, *Russ. Chem. Bull.*, **48**, 589 (1999).
345. O. Loog and U. Maeorg, *Synlett*, **14**, 2537 (2004).

346. D. H. R. Barton, N. Yadav-Bhatnagar, J.-P. Finet and J. Khamsi, *Tetrahedron Lett.*, **28**, 3111 (1987).
347. D. H. R. Barton, D. M. Donnelly, J.-P. Finet and P. J. Guiry, *Tetrahedron Lett.*, **30**, 1377 (1989).
348. D. H. R. Barton, D. M. Donnelly, J.-P. Finet and P. J. Guiry, *J. Chem. Soc., Perkin Trans. 1*, 2095 (1991).
349. R. A. Abramovitch, D. H. R. Barton and J.-P. Finet, *Tetrahedron*, **44**, 3039 (1988).
350. I. Y. Mainagashev, L. S. Klimenko and N. P. Gristan, *Izv. Akad. Nauk, Ser. Khim.*, 2519 (1998); *Chem. Abstr.*, The file has been corrected.
351. S. Morel, G. Boyer, F. Coullet and J.-P. Galy, *Syn. Comm.*, **26**, 2443 (1996).
352. G. Boyer, M. Giorgi, F. Chatel and J.-P. Galy, *J. Chem. Cryst.*, **28**, 735 (1998).
353. G. Boyer and J.-P. Galy, *Molecules*, **3**, M89 (1998).
354. P. Lopez-Alvarado, C. Avendano and J. C. Menéndez, *Tetrahedron Lett.*, **33**, 6875 (1992).
355. P. Lopez-Alvarado, C. Avendano and J. C. Menéndez, *J. Org. Chem.*, **61**, 5865 (1996).
356. P. Lopez-Alvarado, C. Avendano and J. C. Menéndez, *J. Chem. Soc., Perkin Trans. 1*, 229 (1997).
357. P. Y. S. Lam, C. G. Clark, S. Saubern, J. Adams, K. M. Averill, D. M. T. Chan and A. Combs, *Synlett*, 674 (2000).
358. P. Y. S. Lam, G. Vincent, D. Bonne and C. G. Clark, *Tetrahedron Lett.*, **43**, 3091 (2002).
359. S.-K. Kang, S.-G. Lee and D. Lee, *Synlett*, 1022 (2000).
360. T. L. Davis and A. A. Ashdown, *J. Am. Chem. Soc.*, **46**, 1051 (1924).
361. J. Hebky, O. Radek and J. Kejha, *Collect. Czech. Chem. Commun.*, **24**, 3988 (1959).
362. J. Hebky, J. Kejha and M. Karasek, *Collect. Czech. Chem. Commun.*, **26**, 1599 (1961).
363. E. A. Nodiff, S. Lipschutz, P. N. Craig and M. Gordon, *J. Org. Chem.*, **25**, 60 (1960).
364. A. B. Sen and A. K. Sen Gupta, *J. Ind. Chem. Soc.*, **34**, 413 (1957).
365. T. Thu-Cuc, N. P. Buu Hoi and N. D. Xuong, *J. Heterocycl. Chem.*, **1**, 28 (1964).
366. H. Wieland and A. Wecker, *Ber. Dtsch. Chem. Ges.*, **55**, 1804 (1922).
367. P. M. Dharamsena, A. M. F. Oliveira-Campos, M. M. M. Raposo and P. V. R. Shannon, *J. Chem. Res. (S)*, 296 (1994).
368. A. Ito, T. Saito, K. Tanaka and T. Yamabe, *Tetrahedron Lett.*, **36**, 8809 (1995).
369. M. Sugahara and T. Ukita, *Chem. Pharm. Bull.*, **45**, 719 (1997).
370. H. S. Freeman, J. R. Butler and L. D. Freedman, *J. Org. Chem.*, **43**, 4975 (1978).
371. A. Klapars, X. Huang and S. L. Buchwald, *J. Am. Chem. Soc.*, **124**, 7421 (2002).
372. A. Klapars, J. C. Antilla, X. Huang and S. L. Buchwald, *J. Am. Chem. Soc.*, **123**, 7727 (2001).
373. R. Hosseinzadeh, M. Tajbaksh, M. Mohadjerani and H. Mehdunejad, *Synlett*, 1517 (2004).
374. C. S. Li and D. D. Dixon, *Tetrahedron Lett.*, **45**, 4257 (2004).
375. M. V. Nandakumar, *Tetrahedron Lett.*, **45**, 1989 (2004).
376. D. Jaramillo, Q. Liu and J. Aldrich-Wright, *J. Org. Chem.*, **69**, 8151 (2004).
377. S. Z. Wang, J. W. Sun and G. Yu, *Org. Bio. Chem.*, **2**, 1573 (2004).
378. A. Klapars, S. Parris, K. W. Anderson and S. L. Buchwald, *J. Am. Chem. Soc.*, **126**, 3529 (2004).
379. W. Deng, Y. F. Wang and W. Zou, *Tetrahedron Lett.*, **45**, 2311 (2004).
380. S.-K. Kang, D.-H. Kim and J.-N. Park, *Synlett*, 427 (2002).
381. K. R. Crawford and A. Padwa, *Tetrahedron Lett.*, **43**, 7365 (2002).
382. A. Padwa, K. R. Crawford, P. Rashatasakhon and M. Rose, *J. Org. Chem.*, **68**, 2609 (2003).
383. B. Mallesham, B. M. Rajesh, P. R. Reddy, D. Srinivas and S. Trehan, *Org. Lett.*, **5**, 963 (2003).
384. J. H. M. Lange, L. J. F. Hofmeyer, F. A. S. Hout, S. J. M. Osnabrug, P. C. Verveer, C. G. Kruse and R. W. Feenstra, *Tetrahedron Lett.*, **43**, 1101 (2002).
385. H. He and Y.-J. Wu, *Tetrahedron Lett.*, **44**, 3385 (2003).
386. M. Wolter, A. Klapars and S. L. Buchwald, *Org. Lett.*, **3**, 3803 (2001).
387. T. D. Tuong and M. Hida, *Bull. Chem. Soc. Jpn.*, **44**, 765 (1971).
388. T. D. Tuong and M. Hida, *J. Chem. Soc., Perkin Trans. 2*, 676 (1974).
389. R. Flitman and E. Frieden, *J. Am. Chem. Soc.*, **79**, 5198 (1957).
390. M. C. Caserio, D. L. Glusker and J. D. Roberts, *J. Am. Chem. Soc.*, **81**, 336 (1959).
391. T. P. Lockhardt, *J. Am. Chem. Soc.*, **105**, 1940 (1983).
392. A. W. Thomas and S. V. Ley, *Angew. Chem., Int. Ed.*, **42**, 5400 (2003).

393. H. Hayashi, S. Fujinami, S. Nagatomo, S. Ogo, M. Suzuki, A. Uehara, Y. Watanabe and T. Kitagawa, *J. Am. Chem. Soc.*, **122**, 2124 (2000).
394. C. R. H. I. de Dong, *Organic Synthesis by Oxidation with Metal Compounds*, Plenum Press, New York, 1986, p. 423.
395. A. S. Hay, *J. Org. Chem.*, **27**, 332 (1962).
396. L. Santucci and C. Triboulet, *J. Chem. Soc., A*, 392 (1969).
397. M. F. Lappert, *Chem. Rev.*, **56**, 959 (1956).
398. J. P. Greenstein and M. Winitz, *Chemistry of the Amino Acids*, Wiley, New York, 1961, p. 569.

Anilines as nucleophiles

IKCHOON LEE

Department of Chemistry, Inha University, Inchon 402-751, Korea
Fax: +82 32 8654855;   e-mail: ilee@inha.ac.kr

and

DAE DONG SUNG

Department of Chemistry, Dong-A University, Busan 604-714, Korea
Fax: +82 51 2007259;   e-mail: ddsung@dau.ac.kr

I. INTRODUCTION

Aniline nucleophiles were used in the early days in the Menschutkin reaction with alkyl halides in a variety of solvents[1–6] and have made important contributions in the development of the Hammett equation[7]. However, due to the narrow range of basicity ($pK_a = 1.02–6.08$ for 4-NO$_2$–4-NH$_2$ substituted anilines[8], and 0.67–5.89 for 4-NO$_2$–4-

OCH$_3$ substituted N,N-dimethylanilines[9] in water at 25 °C) and the relatively weak nucleophilicity (due to low basicities), the exploitation of anilines as nucleophiles have become somewhat diminished. In recent years, pyridines (pK_a ranges 1.39–9.12 for 4-NO$_2$–4-NH$_2$)[10], secondary alicyclic amines (pK_a ranges *ca* 5.8–11.2 for piperazinium ion–piperidine)[11] and benzylamines (pK_a ranges 8.5–9.64 for 4-NO$_2$–4-OCH$_3$)[12] are preferred to anilines as the nucleophiles in the mechanistic studies of many addition[13] and substitution reactions[14].

Nevertheless, aniline nucleophiles have made continued, important contributions in organic synthesis and in studies of organic reaction mechanisms, which constitute the major subjects of this chapter.

In this chapter, we adopt a few conventions in presenting the reactivity data and mechanistic criteria. Quite a number of nucleophilic reactions are investigated using substituted nucleophiles (nuc), substrates and leaving groups (lg). In these reactions we use X, Y and Z to denote substituents in the nucleophile, substrate and leaving group, respectively. Hence, ρ_{nuc} and β_{nuc} are given as ρ_X and β_X, and similarly ρ_{lg} and β_{lg} are ρ_Z and β_Z, respectively. This convention is convenient since incoming and leaving groups through the substrate are represented in the order X to Y and to Z. Unless otherwise noted, the selectivity parameters are given for X = H and/or Y = H and/or Z = H; thus β_X values are for Y = Z = H and β_Z values are for X = Y = H etc.

As a mechanistic criterion we introduce the cross-interaction constant (CIC) ρ_{ij}, defined in equations 1a and 1b based on the adoption of a convention denoting substituents on the nucleophile, substrate and leaving groups, respectively, as X, Y and Z[15].

$$\log(k_{ij}/k_{HH}) = \rho_i\sigma_i + \rho_j\sigma_j + \rho_{ij}\sigma_i\sigma_j \qquad (1a)$$

$$\rho_{ij} = \partial\rho_j/\partial\sigma_i = \partial\rho_i/\partial\sigma_j \qquad (1b)$$

Thus, the CIC between nucleophile and leaving group is ρ_{XZ} etc.

In discussing the mechanisms of additions and/or substitutions, the sign and magnitude of the CICs are utilized as mechanistic criteria, which have been developed mostly by Lee and coworkers and reviewed in several journals[15].

Due to the difficulties in determining pK_a values in aprotic solvents, e.g. MeCN, DMSO etc., the Brönsted coefficients (β_X) obtained from the plots of log k_2(MeCN) against pK_a(H$_2$O) are used. This procedure is proved to be reliable since the pK_a values in MeCN (and DMSO) change in parallel with those in water for structurally similar amines[16]. The slopes of the plots of pK_a values of anilines in MeOH and in water against σ (σ_p^-) are -3.42[17] [pK_a(MeOH) = $(-3.50 \pm 0.15)\sigma^- - 0.29 \pm 0.10$; $n = 10$, $r = 0.993$] and -2.87[17c,d] [pK_a(H$_2$O) = $(-2.80 \pm 0.10)\sigma^- - 0.11 \pm 0.05$; $n = 10$, $r = 0.995$], respectively, so that the β_X values determined from the plots of log k_2(MeOH) versus pK_a(H$_2$O) should give larger values than those from the plots of log k_2(MeOH) versus pK_a(MeOH) by a factor of 1.25. Thus β_X determined using pK_a(H$_2$O) should be divided by 1.25 or multiplied by 0.80 in order to correct for the pK_a differences in the two solvents[5]. Similarly for anilines in EtOH [pK_a(EtOH) = $(-4.00 \pm 0.15)\sigma^- - 0.17 \pm 0.10$; $n = 10$, $r = 0.995$][17c,d] where the multiplication factor for correction is 0.65.

According to the Marcus equation[18], the reactivity ($\Delta G^{\neq}$) of a group transfer reaction is in many cases controlled either by the thermodynamic barrier (ΔG^o) or by the intrinsic (kinetic) barrier ($\Delta G_o^{\neq}$). A stronger nucleophile ($\delta\sigma_X < 0$) and a better leaving group ($\delta\sigma_Z > 0$) lead to an earlier TS in a thermodynamic barrier controlled reaction series with a lower extent of bond cleavage ($\delta\rho_Z < 0$) and bond making ($\delta|\rho_X| < 0 \rightarrow \delta\rho_X > 0$), respectively, so that the Hammond postulate[19] and Bell–Evans–Polanyi (BEP) principle[20] hold. In this case, the sign of ρ_{XZ} is positive as defined by equation 1b[15b]. Conversely, in an intrinsic barrier controlled reaction series the Thornton rule[21] (anti-Hammond effect)

holds and the sign of ρ_{XZ} becomes negative[15b, 22]. In the former case, a larger reactivity is accompanied by a lower selectivity so that the reactivity–selectivity principle (RSP) holds[22]. In contrast, in the latter case the RSP is violated (anti-RSP)[15g].

In this chapter we will primarily be concerned with the reactivity, selectivity and mechanistic aspects of anilines as nucleophiles in addition and substitution reactions. We will deal with N-substituted as well as ring-substituted anilines. We do not intend to present an exhaustive review of this subject but to survey the more important recent works in this field.

II. NUCLEOPHILIC REACTIONS AT ALIPHATIC CARBONS

A. Primary Carbon Centers

Nucleophilic displacements at alkyl carbons have been studied in MeOH, MeCN and benzene solvents (equation 2, R = Me, Et, *i*-Pr, Me$_3$CCH$_2$ and Me$_3$SiCH$_2$). The rate constants (k_2, M^{-1} s^{-1}), Brönsted β_X (β_{nuc}) and β_Z (β_{lg}) values are summarized in Table 1[23-28] together with ρ_{XZ} values. The rates of nucleophilic substitution listed in Table 1 are in the order of *ca* 10^{-4} M^{-1} s^{-1} irrespective of the reaction media and temperature, despite the notable rate differences which depend on the alkyl group (R), the leaving group (Z) and the solvent. The rate decreases invariably as the alkyl and amino groups become bulkier in the series R = Me < Et < *i*-Pr and NH$_2$ < NMe$_2$ in the aniline[23-25] (entries 1–6). The effects of solvent on the rate vary with the leaving group: k_2 for iodide leaving group (entry 1) is larger in 50% (v/v) MeOH–MeCN than in MeOH, whereas for tosylate leaving group (entry 2) it is opposite, the rate is faster in MeOH than in 50% MeOH–MeCN[23]. Obviously, this is due to a better solvation of the soft I$^-$ ion in the aprotic (MeCN) than in the protic (MeOH) solvent, in contrast to a better solvation of the harder leaving group, tosylate, in MeOH than in MeCN. The Brönsted coefficient is, however, smaller in the mixture than in MeOH for the I$^-$, and *vice versa* for the tosylate. Thus a larger reactivity is accompanied by a lower selectivity so that the reactivity–selectivity principle (RSP) holds. This is a manifestation of the reactivity which is thermodynamic controlled, for which ρ_{XZ} has positive sign, $\rho_{XZ} > 0$. The magnitudes of β_X and β_Z are all within the range of values that are believed to belong to a direct (concerted) displacement (S$_N$2) mechanism. One exception is the somewhat larger β_X values ($\beta_X > 0.8$) obtained for the perchlorate leaving group series in benzene[26] (entries 7, 8 and 9). However, this could be a result of the use of pK_a values for *N,N*-dimethylaniline (DMA) in water rather than in benzene. An interesting case is that while much slower rates are observed for the neopentyl arenesulfonate series[27] (entry 10) due to the steric effect, the rates are almost restored to those expected without the steric effect by replacing a carbon with a silicon in the trimethylsilylmethyl series[28] (entry 11). Insertion of a longer C−Si bond instead of a C−C bond seems to alleviate steric crowding around the reaction center in the S$_N$2 TS. However, in spite of these rate differences between the two series the magnitude of β_X (and ρ_{XZ}) is similar, indicating that the TSs are formed with a similar degree of bond making and bond cleavage in the two reaction series. It is noteworthy that for the anilinolysis of alkyl arenesulfonates the size of ρ_{XZ} is nearly constant at *ca* 0.31 in MeOH (and *ca* 0.33 in MeCN), suggesting that the TS is formed with a nearly constant tightness around the reaction center carbon (*vide infra*).

$$RZ + XC_6H_4NH_2 \longrightarrow XC_6H_4NHR + H^+Z^- \qquad (2)$$

The nucleophilic substitution reactions of anilines at arylmethyl (ArCH$_2$−), arylethyl (ArCH$_2$CH$_2$−), allyl (CH$_2$=CHCH$_2$−) and alkynylmethyl (CH≡CCH$_2$−) carbon centers take place by a direct displacement (S$_N$2) mechanism with Brönsted coefficients, β_X, in the range 0.3–0.8 as can be seen in Table 2[29-48]

TABLE 1. Nucleophilic substitution reactions of anilines at alkyl carbons

Entry	Reaction	$T(^{\circ}C)$	Solvent	$k_2 \times 10^4$ $(M^{-1}\,s^{-1})$	β_X	β_Z	ρ_{XZ}	Reference
1	$MeI + XC_6H_4NH_2$	50	MeOH	4.37	0.62			23
			50%MeCN[a]	8.96	0.42			
2	$MeOTs + XC_6H_4NH_2$	50	MeOH	11.8	0.37			23
			50%MeCN[a]	5.46	0.51			
3	$MeOSO_2C_6H_4Z +$ $XC_6H_4NH_2$	65	MeOH	35.5	0.60	−0.39	0.30	24
4	$EtOSO_2C_6H_4Z +$ $XC_6H_4NH_2$	65	MeCN	7.47	0.66	−0.45	0.32	24
			MeOH	4.50	0.62	−0.37	0.33	
5	$MeOSO_2C_6H_4Z +$ $XC_6H_4NMe_2$	65	MeCN	0.676	0.67	−0.44	0.34	25
			MeOH	26.2	0.66	−0.33	0.24	
6	$EtOSO_2C_6H_4Z +$ $XC_6H_4NMe_2$	65	MeCN	6.11	0.62	−0.44	0.25	25
			MeOH	1.24	0.63	−0.31	0.26	
7	$MeOClO_3 + XC_6H_4NMe_2$	25	benzene	0.207	0.65	−0.44	0.27	26
8	$EtOClO_3 + XC_6H_4NMe_2$	25	benzene	34.4	0.78			26
9	$i\text{-}PrOClO_3 + XC_6H_4NMe_2$	25	benzene	2.16	0.85			26
10	$Me_3CCH_2OSO_2C_6H_4Z +$ $XC_6H_4NH_2$	55	MeOH	0.910	0.83	−0.31	0.31	27
				0.0612	0.59			
11	$Me_3SiCH_2OSO_2C_6H_4Z +$ $XC_6H_4NH_2$	65	MeOH	7.08	0.60	−0.31	0.31	28
			MeCN	1.69	0.77	−0.33	0.33	

[a] 50% MeOH–50% MeCN (v/v).

TABLE 2. Nucleophilic substitution reactions of anilines at arylalkyl-, alkenyl- and alkynylmethyl carbons

Entry	Reaction	Temperature (°C)	Solvent	k_2 ($10^5 \times M^{-1}\,s^{-1}$)	β_X	ρ_{ij}	Reference
1	$YC_6H_4CH_2Cl + XC_6H_4NH_2$	35	MeOH	5.85	0.55	$\rho_{XY} = -0.75$	29a
		55.1	MeOH	22.7	0.38		29b
2	$2\ YC_6H_4CH_2Cl + XC_6H_4NH_2$	50	EtOH	14.2	0.31	$\rho_{XY} = -0.93$	30a,b
3	$YC_6H_4CH_2Br + XC_6H_4NH_2$	50	EtOH	613	0.49	$\rho_{XY} < 0$	30a
4	$YC_6H_4CH_2I + XC_6H_4NH_2$	50	EtOH	1740	0.51		30b
5	$YC_6H_4CH_2Br(I) + XC_6H_4NH_2$	35	MeOH	312 (517)	0.46 (0.43)		31
6	$YC_6H_4CH_2Cl + PhNH_2$	50	MeOH	23.9			32
7	$YC_6H_4CH_2Br + XC_6H_4NMe_2$	45	acetone	181 (k_f)		$\rho_{XY}(f) = -0.26$	33, 34
				102 (k_r)		$\rho_{XY}(r) = 0.77$	34
8	$YC_6H_4CH_2OTs + XC_6H_4NH_2$	35	MeOH	1150	0.28		35
			50%MeCN	445	0.36		
9	$YC_6H_4CH_2OSO_2C_6H_4Z + XC_6H_4NH_2$	35	MeOH	1730	0.29		36
			50%MeCN	683	0.36		
10	$YC_6H_4CH_2OSO_2C_6H_4NO_2\text{-}4 + XC_6H_4NH_2$	35	MeOH	457	0.48		37
			50%MeCN	181	0.54		
11	$YC_6H_4CH_2OSO_2C_6H_4Z + XC_6H_4NMe_2$	35	acetone	129 (Z = 4-Cl)		$\rho_{XY} < 0$	38
12	$YC_6H_4CH_2CH_2OSO_2C_6H_4Z + XC_6H_4NH_2$	65	MeOH	11.0		$\rho_{XY} = -0.12$	39
						$\rho_{YZ} = 0.07$	
						$\rho_{XZ} = -0.45$	
13	$PhCH(Me)CH_2OSO_2C_6H_4Z + XC_6H_4NH_2$	55	MeOH	0.776	0.53	$\rho_{XZ} = -0.39$	40
14	$^a 1\text{-}NaphCH_2CH_2OSO_2C_6H_4Z + XC_6H_4NH_2$	65	MeOH	9.28	0.41	$\rho_{XY} < 0$	41
15	$2\text{-}NaphCH_2CH_2OSO_2C_6H_4Z + XC_6H_4NH_2$	65	MeOH	10.6	0.42	$\rho_{XY} < 0$	41
16	$1\text{-}NaphCH_2OSO_2C_6H_4Z + XC_6H_4NH_2$	25	MeCN	297	0.46	$\rho_{XZ} = -0.12$	42
17	$2\text{-}NaphCH_2OSO_2C_6H_4Z + XC_6H_4NH_2$	25	MeCN	370	0.46	$\rho_{XZ} = -0.13$	42
18	$2\text{-}ThienylCH_2CH_2OSO_2C_6H_4Z + XC_6H_4NH_2$	60	MeCN	3.49	0.58	$\rho_{XZ} = -0.50$	43
19	$3\text{-}ThienylCH_2CH_2OSO_2C_6H_4Z + XC_6H_4NH_2$	60	MeCN	3.47	0.47	$\rho_{XZ} = -0.50$	43
20	$CH_2{=}CHCH_2OSO_2C_6H_4Z + XC_6H_4NH_2$	45	MeCN	282	0.66	$\rho_{XZ} = 0.37$	44
	$^b(+XC_6H_4NMe_2)$			(141)	(0.57)	($\rho_{XZ} = 0.30$)	
21	$CH_2{=}C(Me)CH_2OSO_2C_6H_4Z + XC_6H_4NH_2$	45	MeCN	133	0.68	$\rho_{XZ} = 0.40$	45
	$^b(+XC_6H_4NMe_2)$			(48.5)	(0.65)	($\rho_{XZ} = 0.37$)	

(*continued overleaf*)

TABLE 2. (*continued*)

Entry	Reaction	Temperature (°C)	Solvent	k_2 $(10^{-5} \times M^{-1}\,s^{-1})$	β_X	ρ_{ij}	Reference
22	CH_2=C(Cl)$CH_2OSO_2C_6H_4Z$ + $XC_6H_4NH_2$ [b](+$XC_6H_4NMe_2$)	45	MeCN	13.2 (8.41)	0.68 (0.61)	$\rho_{XZ} < 0$	46
23	CH≡C$CH_2OSO_2C_6H_4Z$ + $XC_6H_4NH_2$ [b](+$XC_6H_4NMe_2$)	45	MeCN	51.9 (20.9)	0.63 (0.57)	$\rho_{XZ} = 0.29$ ($\rho_{XZ} = 0.25$)	47
24	$YC_6H_4N(Me)CH_2SC_6H_4Z$ + $XC_6H_4NH_2$	45	MeOH	170	0.50	$\rho_{XY} = -0.3$	48

[a] Naphthyl.
[b] Corresponding reactions with *N,N*-dimethylanilines, for which the results are given in parentheses.

The rates of reactions at benzylic carbon increase as the leaving group changes from Cl^- to Br^- and to I^- [30] (entries 2–4). This rate increase is also accompanied by an increase in the size of β_X reflecting an increase in the extent of bond formation in the TS. Thus the RSP is violated or anti-RSP holds. In this halide series, the reactivity is not determined by the thermodynamic driving force since the solvation energy is in the order $I^- < Br^- < Cl^-$ [49], but is controlled intrinsically (or kinetically) as the bond energy of the C–halogen bond decreases in the order C–Cl > C–Br > C–I, so that bond breaking in the rate-determining step will be the most facile for C–I and the least facile for C–Cl bond. However, for a given benzyl halide ($PhCH_2Cl$) the rate of nucleophilic substitution reaction of aniline is dependent on the solvation of the halide ion (Cl^-) by the solvent[49]; k_2 increases in the solvent order MeCN (4.04) < i-PrOH (10.8) < DMSO(17.8) < MeOH(23.9) < H_2O (870)[32]. An interesting case is the decomposition reaction of benzylaryldimethylammonium cation ($YC_6H_4CH_2N^+$ $Me_2C_6H_4X$) in acetone[33,34] (entry 7). The decomposition proceeds with a rate constant $k_2 = 10.2 \times 10^{-4}$ $M^{-1} s^{-1}$ with a positive ρ_{XY} ($= 0.77$) whereas the formation step proceeds with a rate constant $k_2 = 18.1 \times 10^{-4}$ $M^{-1} s^{-1}$ with a negative ρ_{XY} ($= -0.26$). It should be noted that in general the bond formation step of an S_N2 reaction leads to a negative ρ_{XY} value while the bond cleavage step exhibits a positive ρ_{XY} value[37].

Ando and coworkers conducted isotope effect studies (entry 11) on the direct displacement reaction of benzyl arenesulfonates with dimethylaniline (DMA)[38]. They found that an electron-withdrawing substituent in the substrate (Y = 3-Br) caused the TS to shift to a later position along the reaction coordinate, which is consistent with that predicted by the Thornton rule (or anti-Hammond effect). The anilinolysis of phenylethyl arenesulfonates (entries 12 and 13) proceeds also by an S_N2 mechanism. The reaction was found to proceed by a dissociative S_N2 mechanism with a relatively small degree of aryl participation. The fraction of the phenonium ion intermediate captured by the aniline nucleophile in the aryl-assisted pathway has been shown to increase with a stronger nucleophile, and a four-center TS in an intermolecular S_Ni mechanism is suggested for the aryl-assisted pathway[39,40]. Under the same reaction conditions, benzylamine nucleophiles react at a rate *ca* two times faster than that of anilines.

The reactions of anilines are faster with the naphthylmethyl series rather than naphthylethyl series[41] (entries 14–17), and 2-naphthyl series is slightly faster than the 1-naphthyl series. In the former case the stabilization of the developing cationic charge in the TS is stronger with naphthylmethyl than with naphthylethyl. In the latter case the steric effect of the H atom at C_9 in the TS causes a slight decrease in the rate of the 1-naphthyl compounds. The extent of bond formation in the TS is similar for 1- and 2-naphthyl series with approximately the same β_X values. Compared to aniline, more basic benzylamine (BnA) nucleophiles react *ca* twice as fast (9.28 vs 18.5 $M^{-1} s^{-1}$ with $PhNH_2$ and $PhCH_2NH_2$ for 1-naphthyl in MeOH at 65 °C) with a larger degree of bond making (larger β_X value) in the TS. This is another case of anti-RSP.

The rates of reactions of anilines with thienylethyl compounds are similar for ethyl groups substituted at the 2- and 3-positions of the thiophene ring (entries 18 and 19), but the rates of reaction with DMA are slightly slower with 3- than with 2-thienylethyl[43].

The reactions of anilines at carbon atoms attached to a vinylic ($CH_2=CHCH_2$) and acetylenic group ($CH\equiv CCH_2$) proceed also by an S_N2 mechanism[44–47] (entries 20–23). Substitution by Me or Cl at the β-carbon of the vinylic system leads to a rate retardation; an electron acceptor group (Cl) retards the rate more than an electron donor (Me), suggesting that a relatively strong cationic charge development occurs at the TS. This is supported by the much slower rate observed with $CH\equiv CCH_2-$ than with $CH_2=CHCH_2-$, since an acetylenic group is a relatively stronger electron acceptor ($\sigma_p = +0.23$)[50] than a vinyl group ($\sigma_p = -0.04$). An electron-withdrawing group substituted at β-carbon destabilizes

the developing cationic charge at the α-carbon reaction center in the TS. The extent of bond formation is similar in all cases with β_X ca 0.6–0.7. A notable difference between this series and the arylmethyl and arylethyl series, for which $\rho_{XZ} < 0$, is that the sign of ρ_{XZ} is positive. Anilino thioethers, $YC_6H_4N(Me)CH_2SC_6H_4Z$ (entry 24), react with anilines in MeOH by an S_N2 mechanism with a late TS[48]. The large negative ρ_{XZ} value obtained suggested a frontside nucleophilic attack.

B. Secondary and Tertiary Carbon Centers

Systematic studies were reported on the nucleophilic substitution reactions of anilines at the alkyl (R^1R^2CH-)[51,52] and cycloalkyl [c-$(CH_2)_nCH$-, $n = 3$–6][53] secondary carbon centers. All the reactions were found to proceed by the S_N2 mechanism. The relevant rate and selectivity data are listed in Tables 3 and 4, respectively. The rate constants (k_2) of the anilinolysis of secondary alkyl compounds in MeCN (Table 3) are of the order of 10^{-5} M^{-1} s^{-1} and are very similar with little difference, depending on the two alkyl groups (R^1, R^2) attached to the reaction center. Interestingly, the β_X and β_Z values in MeCN are also similar with $\beta_X = 0.52$–0.57 and $\beta_Z = -0.32$ to -0.36. The magnitudes of these Brönsted coefficients are somewhat smaller than those ($\beta_X = 0.66$ and $\beta_Z = -0.44$) for the anilinolysis at primary alkyl carbon centers in MeCN. The ρ_{XZ} values are within the range of 0.10–0.13, which is significantly smaller than those for the reactions of anilines with primary alkyl carbon centers, $\rho_{XZ} = 0.31$–0.34 (entries 3, 4 and 10 in Table 1). These comparisons of the magnitude of β_X, β_Z and ρ_{XZ} clearly indicate that the TS for the aniline reactions at secondary alkyl carbon centers is looser than that at primary alkyl carbon centers with a smaller extent of bond making and a larger degree of leaving-group bond scission. There is an important observation that, irrespective of the groups attached (R^1 and R^2) at the secondary carbon atom, the degree of bond formation is similar. The kinetic isotope effects measured with deuterated anilines ($XC_6H_4ND_2$) in Table 3 show that the larger the steric crowding (with a larger negative steric constant, E_s), the smaller the k_H/k_D value, indicating that the $N-H$ vibrational modes of aniline have been interfered with to a larger degree by the larger steric hindrance effect of the R^1 and R^2 groups. In fact, there is a close parallel between the sum of the steric constants (ΣE_s) and the magnitude of the k_H/k_D values. Surprisingly, there is no correlation between the polar substituent constants ($\Sigma \sigma^*$) of R^1 and R^2 groups and the magnitude of k_H/k_D values. Apparently, the polar effect of the secondary carbon has little effect on the approaching aniline nucleophile in the TS, as expected from the relatively loose structure.

The structure of the TS for the nucleophilic reaction of aniline at secondary cycloalkyl carbon centers depends on the size of the cycloalkyl group[53]. We note in Table 4 that although the rate is fastest with the cyclopentyl and slower with the cyclohexyl compound, the TS shifts successively to a later position along the reaction coordinate (more

TABLE 3.   Rates and selectivity parameters for the nucleophilic reactions of anilines at secondary alkyl carbon centers ($R^1R^2CHOSO_2C_6H_4X$) in MeCN at $65.0\,°C$[51,52]

Compound	R^1	R^2	$k_2 \times 10^5$ $(M^{-1}\,s^{-1})$	β_X	β_Z	ρ_{XZ}	$\Sigma \sigma^*$	ΣE_s	k_H/k_D
i-Propyl	Me	Me	4.11	0.53	−0.32	0.10	0.0	0.0	—
2-Butyl	Me	Et	4.51	0.52	−0.36	0.12	−0.100	−0.07	0.93_4
2-Pentyl	Me	Pr	4.98	0.50	−0.36	0.13	−0.115	−0.36	0.90_9
2-Hexyl	Me	Bu	4.63	0.55	−0.35	0.13	−0.130	−0.39	0.89_3
3-Pentyl	Et	Et	4.22	0.57	−0.34	0.12	−0.200	−0.14	0.92
3-Hexyl	Et	Pr	4.51	0.53	−0.35	0.12	−0.215	−0.43	0.88

TABLE 4. Rates and selectivity parameters for the nucleophilic reactions of anilines at cycloalkyl secondary carbon centers (c-$(CH_2)_{n-1}CHOSO_2C_6H_4Z$) in MeCN at $65.0\,^\circ$C[53]

Cycloalkyl	$k_2 \times 10^5$ $(M^{-1}\,s^{-1})$	β_X	β_Z	ρ_{XZ}	k_H/k_D
c-Butyl	1.69	0.33	-0.28	0.11	0.91_3
c-Pentyl	7.41	0.47	-0.31	0.11	0.90_5
c-Hexyl	0.707	0.56	-0.34	0.11	0.89_0
c-Heptyl	6.51	6.51	-0.35	0.11	0.81_8

product-like structure) as the ring becomes larger. Thus the magnitude of β_X and β_Z increases from cyclobutyl to cyclohexyl, indicating a successive increase in the degree of bond formation and bond cleavage. The magnitude of the kinetic isotope effects involving deuteriated anilines ($XC_6H_4ND_2$) also decrease successively due to the closer approach of the aniline nucleophile in the TS. However, the overall tightness of the TS seems to be quite similar with a constant ρ_{XZ} of 0.11.

The reactions of anilines with indan-2-yl arenesulfonates, **1**, in MeOH[54] proceed by an S_N2 mechanism. The rate decreases as the electron-withdrawing power of substituent Y in the ring gets stronger, $k_2 = 5.52$, 4.48 and 3.20 ($\times 10^{-5}$ M^{-1} s^{-1}) at $55.0\,^\circ$C in MeOH for Y = H, Br and NO$_2$ in **1**, respectively. The sign of ρ_Y is therefore negative ($\rho_Y = -0.34$ for X = Z = H) and hence the secondary carbon center becomes more positive in the TS, so that bond cleavage is more advanced than bond making. The sign of ρ_{XZ} changes from positive for the relatively weak electron acceptor Y ($\rho_{XZ} = 0.08$ for Y = Br) to negative for the stronger electron acceptor Y ($\rho_{XZ} = -0.16$). There is a hypothetical substituent with $\sigma_Y = 0.43$ for which $\rho_{XZ} = 0$.

(1)
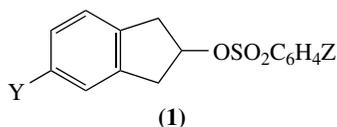
The nucleophilic substitution reactions of anilines with *exo*-2-norbornyl arenesulfonates, **2**, present an interesting example of the preassociation mechanism[55] (Scheme 1). The rate is faster with 2-*exo* ($k_2 = 15.9 \times 10^{-4}$ and 3.24×10^{-5} M^{-1} s^{-1} when X = Z = H in MeOH and MeCN at $60.0\,^\circ$C, respectively) than with 2-*endo* ($k_2 = 0.552 \times 10^{-5}$ M^{-1} s^{-1} with X = Z = H in MeOH at $60.0\,^\circ$C). These reactions are characterized by a large ρ_Z (1.8 and 1.2 for 2-*exo* and 2-*endo*) coupled with a small magnitude of ρ_X (-0.21 and -0.15 for 2-*exo* and 2-*endo*). The ρ_Z values for the aniline reactions are even larger than those for the S_N1 solvolysis in MeOH ($\rho_Z = 1.5$ and 1.0 for solvolysis of 2-*exo* and 2-*endo*). Thus the abnormal substituent effect in the anilinolysis of **2** can only be accounted for by the preassociation mechanism of Scheme 1. The upper route is the normal S_N1 pathway, and the lower route is the preassociation pathway. The preassociation step, K_{ass}, and association of the Nu to the ion pairs, k_n, occur in a diffusion limited or fast process and k'_1 is the rate-limiting step. This mechanism leads to second-order kinetics and therefore is an S_N2 process, but structural effects on rates are very similar to those of S_N1 reactions, since the R$^+$ Z$^-$ pair consists essentially of the two free ions.

Nucleophilic substitution reactions of 1-(trimethylsilyl)ethyl arenesulfonates, **3**, with anilines in MeCN at $65.0\,^\circ$C was found to proceed by an S_N2 mechanism[56]. The ρ_{XZ}

(2-*exo*)

SCHEME 1

(3)
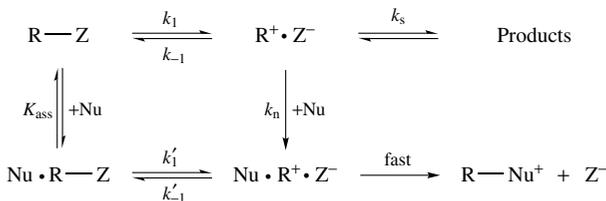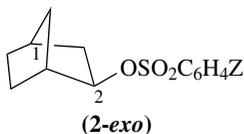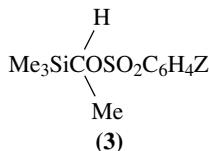
value in MeCN is 0.10, which is similar to those for other S_N2 processes at a secondary carbon atom.

The rate constants, $k_2 = 4.05 \times 10^{-5}$ and 12.3×10^{-5} $M^{-1}\,s^{-1}$ in MeCN and MeOH at 65.0 °C, are *ca* 3–7 times slower than that for the corresponding compound without a Me group bound at the reaction center carbon (entry 11 in Table 1). The β_X and β_Z values are slightly larger in MeCN ($\beta_X = 0.64$ and $\beta_Z = -0.30$) than in MeOH (0.57 and -0.28), so that a somewhat later TS is obtained in MeCN than in MeOH. The reactions of benzylamines instead of anilines gave further increase in the magnitude of β_X (0.65) and β_Z (-0.41) values in MeCN.

The rates of bimolecular substitution reactions of anilines with 1-phenylethyl arenesulfonates $(YC_6H_4CHMeOSO_2C_6H_4Z)^{[57]}$ are relatively fast compared to other aniline reactions at secondary carbon centers: $k_2 = 12.5 \times 10^{-2}$ in MeOH and 8.12×10^{-2} $M^{-1}\,s^{-1}$ in 50% MeCN–MeOH at 25.0 °C when Y = Z = H. The reaction of DMA[58] is much slower, $k_2 = 2.64 \times 10^{-2}$ $M^{-1}\,s^{-1}$ in MeOH at 35.0 °C when Y = Z = H. Relatively large β_X (0.69–0.92) values coupled with large β_Z (-0.2 to -0.4) and large negative ρ_{XZ} (-0.55 to -0.56) values obtained in the aniline reactions are interpreted to indicate a frontside S_N2 attack with an N−H proton hydrogen-bonded to the leaving-group oxygen atom, i.e. an intermolecular S_Ni mechanism (Scheme 2).
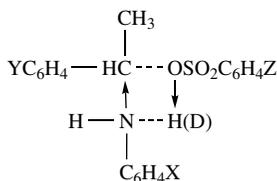
SCHEME 2

The hydrogen bonding of the N—H proton in the TS has been confirmed by the normal kinetic isotope effects, $k_H/k_D > 1.0$, with deuterated anilines (Scheme 2)[15e]. With no hydrogen on the amino group, i.e. in N,N-dimethylaniline (DMA), the magnitude of ρ_{XZ} was diminished to -0.23–-0.25[58], about half of that for anilines. A direct electrostatic interaction between the N and O reaction centers in the frontside attack TS is thought to result in the relatively large magnitude of ρ_{XZ} for the DMAs also.

The reactions of anilines with 1-phenylethyl chloride[59] (YC$_6$H$_4$CHMeCl) in MeOH are much slower ($k_2 = 37.9 \times 10^{-5}$ M^{-1} s^{-1} at 65.0 °C when Y = Z = H) than the corresponding reactions with arenesulfonate leaving groups[57]. This indicates that in the reactions of aniline nucleophiles, arenesulfonates are better leaving groups than the chloride in MeOH[60]. In the reactions of 1-phenylethyl chlorides in MeOH, an unusual selectivity of positive ρ_X was observed. It changes at $\sigma_Y^+ = -0.23$ (where $\rho_X = 0$) from positive for the relatively strong electron-donating Y substituents Y = 4-Me, 4-OMe to negative for the more electron-withdrawing Y substituents. This observation of an isokinetic point ($\hat{\sigma}_Y^+$ at which $\rho_X = 0$) results from a large magnitude of ρ_{XY} (-2.05) coupled with a relatively small ρ_X at Y = 0 ($\rho_X^0 = -0.47$) since the isokinetic point is given by equation 3.

$$\hat{\sigma}_Y^+ = -\rho_X^0/\rho_{XY} \tag{3}$$

In this reaction the TS is considered to have a structure in which nearly complete bond formation occurs between the nucleophile and cation formed in an ion-pair preequilibrium. For relatively strong electron-donating substituent Y, the resonance delocalization of the cationic charge leads to a substantial negative charge accumulation on the reaction center carbon (Scheme 3), which in turn leads to an electron acceptance by the aniline nucleophile, and hence ρ_X becomes positive.
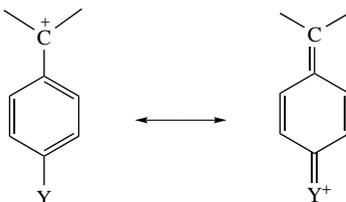
SCHEME 3

The reactivity of 1-methylpropargyl (CH≡CMe-) arenesulfonates with anilines[48] ($k_2 = 0.827 \times 10^{-4}$ M^{-1} s^{-1} in MeCN at 45.0 °C for Y = Z = H) is lower by ca 6 times than the corresponding reactions of propargyl (CH≡CH-) arenesulfonates ($k_2 = 5.19 \times 10^{-4}$ M^{-1} s^{-1})[48]. The corresponding reactivity change is, however, much larger for the reactions with benzylamine nucleophiles; the reactivity drops ca 18-fold ($k_2 = 4.16 \times 10^{-4}$ versus 75.8×10^{-4} M^{-1} s^{-1} for 1-methylpropargyl and propargyl arenesulfonate in MeCN at 45.0 °C), indicating a stronger steric hindrance to approach of benzylamine than of aniline in the TS due to the presence of an additional Me group at the reaction center. The larger steric effect in the benzylamine than in the aniline reactions is also caused by a larger β_X (0.66 versus 0.49) for the benzylamine reaction; a closer approach of the benzylamine than aniline in the TS to the reaction center will increase the steric effect.

In the reactions of anilines with 1-phenyl-2-propyl arenesulfonates[61] (YC$_6$H$_4$CH$_2$ CHMeOSO$_2$C$_6$H$_4$Z), aryl participation (k_Δ) was found with Y = 4-OMe (Scheme 4). The overall rate constant was 3.55×10^{-5} M^{-1} s^{-1} in MeOH at 65.0 °C and the degree of aryl participation as expressed by $100[Fk_\Delta/(k_\Delta + k_s + k_N)]$, where k_N is the rate of
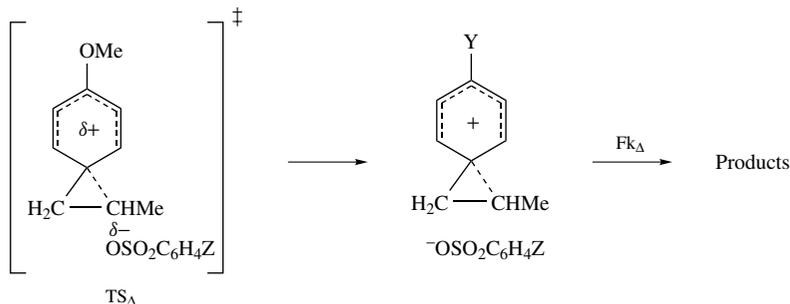
SCHEME 4

direct substitution by the aniline and k_s is the solvolysis rate, ranged for Y = 4-OMe from 21% (X = 4-OMe and Z = 4-Me) to 62% (X = 4-Cl and Z = 4-NO$_2$). Understandably, the aryl participation increases as the nucleophilicity of aniline becomes lower (e.g. when X = 4-Cl) and the leaving ability increases (when Z = 4-NO$_2$). The magnitude of ρ_X (= −0.36) (or β_X = −0.13) is unusually low and that of ρ_Z (= 1.03) (or β_Z = −0.35) is relatively large with Y = 4-OMe, in agreement with an extensive contribution of the aryl-assisted pathway. The magnitude of ρ_{XY} was much larger (−0.71) than that for the 2-phenylethyl system (−0.12)[39], reflecting that the TS becomes tighter by an α-Me substitution. In contrast, the magnitude of ρ_{XZ} is smaller (0.16) than that for the aniline reactions at primary carbon centers (ρ_{XZ} = 0.33, Table 1) and hence the TS is substantially looser than that for typical associative S$_N$2 reactions. The kinetic isotope effects with deuteriated anilines were inverse ($k_H/k_D < 1.0$), but the value approaches 1.0 with Y = 4-OMe (k_H/k_D = 0.987 and 0.906 for Y = 4-OMe and H, respectively, with X = 4-Cl, Z = 4-NO$_2$), since there will be no kinetic isotope effect in the TS$_\Delta$ where the aniline is absent.

Benzhydryl chlorides (YC$_6$H$_4$CHClC$_6$H$_4$) react with anilines in MeCN[62] (k_2 = 8.71 × 10^{-5} M^{-1} s^{-1} at 65.0 °C) and in MeOH (k_2 = 199 × 10^{-5} M^{-1} s^{-1} at 35.0 °C) by the ion-pair mechanism (Scheme 5), in which the nucleophile attacks the preformed carbocation, R$^+$, within a solvent separated ion pair (IP). In this reaction an observable isokinetic point, $\hat{\sigma}_Y^+$, at which ρ_X = 0, was obtained. At this point the rate becomes constant irrespective of the substituent in the aniline (X). This point is dependent on the α-substituent in the benzylic carbocation: $\hat{\sigma}_Y^+$ = −0.23 for 1-phenylethyl (R^1 = H, R^2 = Me) and +0.22 for benzhydryl (R^1 = H, R^2 = Ph) chloride in MeOH. The Marcus equation[18] predicts that at an isokinetic point the intrinsic barrier ($\Delta G_0^{\neq}$) and thermodynamic driving force (ΔG^0) practically completely compensate each other as X is varied. In the latter reaction, the magnitude of ρ_{XY} is large (−2.47 and −1.46 in MeCN and MeOH, respectively) leading to the isokinetic points at $\hat{\sigma}_Y^+$ = 0.13 and 0.22 for the reactions in MeCN and MeOH. Positive ρ_X (negative β_X) values are obtained for Y = 4-Me, H and 4-Cl, and the normal negative ρ_X (positive β_X) values are obtained for Y = 3-Cl, 3,4-Cl$_2$ and 4-NO$_2$. For example, ρ_X = +0.95 (β_X = −0.32) in MeOH at 35.0 °C and ρ_X = +0.92 (β_X = −0.23) in MeCN at 65.0 °C for Y = 4-Me.

Such sign reversal in ρ_X at an isokinetic point is also observed in the reactions of anilines with cumyl (PhCMe$_2$-) arenesulfonates[63] (4-as) and chlorides (4-Cl). Structurally, these systems correspond to R^1 = R^2 = Me in the general α-substituted benzylic compounds so that the reactivity and the reaction mechanism are expected to be related to those of other α-substituted benzylic series discussed above[57,63]. The second-order rate constants for the reactions of aniline are 33.9 × 10^{-3} M^{-1} s^{-1} for cumyl arenesulfonate
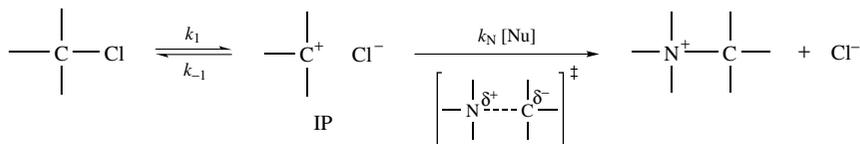
SCHEME 5

(**4-as**) in MeCN[63] at 55.0 °C for Z = H and 6.63×10^{-3} M^{-1} s^{-1} for cumyl chloride (**4-Cl**) in MeOH[64] at 35.0 °C. In the aniline reactions of **4-as** in MeCN, a large negative ρ_{XZ} (= −0.75) is observed and an observable sign reversal of ρ_Z at $\sigma_X = 0.83$ is obtained with a negative ρ_Z value of −0.01 for X = 3,5-(NO$_2$)$_2$. This rather unusual phenomenon is rationalized by a strong interaction between the aniline nucleophile and the sulfonate leaving group due to their close proximity in the frontside attack S$_N$2 TS (Scheme 6).
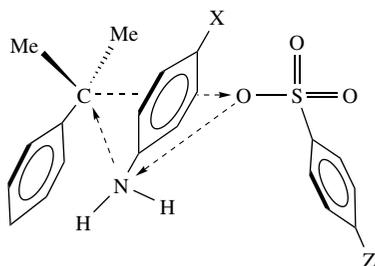
SCHEME 6

The reactions in MeOH indicated that the S$_N$1 channel competes with the S$_N$2 pathway and ion-pair return is observed when the concentration of the aniline nucleophile is low. In the reactions of **4-Cl** derivative with anilines in MeOH, a large magnitude of ρ_Y^+ values and weak chloride common ion depression are observed. This is interpreted to indicate an ion-pair mechanism, discussed above for the aniline reactions with benzhydryl chlorides, in which a preformed benzylic carbocation reacts with the solvent and the aniline nucleophile (Scheme 5). For this reaction series, the sign of ρ_X is always positive for Y = 4-Ph—Y = 3-Cl and a relatively small negative ρ_{XY} (−0.54) gives a large positive isokinetic point at $\hat{\sigma}_Y^+ = +0.72$, which is estimated by equation 3. This large positive value, where $\rho_X = 0$, results from a strongly resonance stabilized cumyl cation. The relationship between the isokinetic point and the stability of the benzylic cation is evident from the data presented in Table 5.

The benzylic carbocation is stabilized by resonance delocalization of the cationic charge into the ring[65] and as a result the benzylic carbon becomes much less positive. As the cation stability increases the isokinetic point shifts to a more positive value.

Nucleophilic substitution reactions of aniline are also studied at tertiary alkyl carbon centers in MeCN[66]. The reactions with 2-cyano-2-propyl, **5**, and 1-cyanooctyl, **6**, arenesulfonates are reported in MeCN at 50.0 °C.

The rates are faster with **5** ($k_2 = 1.76 \times 10^{-4}$ M^{-1} s^{-1} with $\beta_X = 0.62$ and $\beta_Z = -0.32$) than with **6** ($k_2 = 0.636 \times 10^{-4}$ M^{-1} s^{-1} with $\beta_X = 0.59$ and $\beta_Z = -0.48$). In these reactions at tertiary carbon centers the magnitude of ρ_{XZ} is much smaller ($\rho_{XZ} = -0.03$ and −0.05 for **5** and **6**, respectively) than those at primary ($\rho_{XZ} = 0.33$; Table 1) and secondary alkyl carbon centers ($\rho_{XZ} = 0.12$; Tables 3 and 4). The magnitude of ρ_{XZ}

TABLE 5.   Relationship between the isokinetic point $\hat{\sigma}_Y^+$ (where $\rho_X = 0$) and the enthalpy of formation of the benzylic cation (PhC$^+$ R^{1}R^2)

	R^1	R^2	$\rho_X^{0\,a}$	ρ_{XY}	$\hat{\sigma}_Y^{+\,b}$	$\Delta H^{0\,c}$
Benzyl chloride	H	H	−1.61	−0.75	(−2.15)^d	166.7
1-Phenylethyl chloride	H	Me	−0.47	−2.05	−0.23	156.6
Benzhydryl chloride	H	Ph	−0.32	−1.46	+0.22	150.4
Cumyl chloride	Me	Me	−0.39	−0.54	+0.72	147.5

^{a} ρ_X value for Y=H.
^{b} $\hat{\sigma}_Y^+ = -\rho_X^0/\rho_{XY}$, where $\rho_X = 0$.
^{c} The AM1 enthalpies of carbocation formation from chlorides[15], $\Delta H^o = \Delta H_f(R_Y^+) + \Delta H_f(Cl^-) - \Delta H_f(R_YCl)$, in kcal mol^{-1}.
^{d} Value in parentheses is that estimated by $\hat{\sigma}_Y^+ = -\rho_X^0/\rho_{XY}$.

(5)   **(6)**
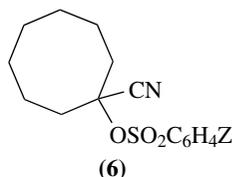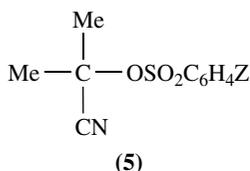
is inversely related to the distance between the nucleophile (X) and the leaving group (Z) in the TS. Thus, the tightness of the TS is approximately constant within this class of compounds, and it becomes successively looser as the reaction center varies from primary to secondary and then to tertiary carbon. *Ab initio* MO calculations were carried out to substantiate these experimental findings[67]. The MP2/6-31+G* geometries and activation barriers, $\Delta E^{\neq}$, were determined for chloride exchange reactions of various alkyl chlorides (RCl) (equation 4).

$$Cl^- + RCl = ClR + Cl^- \tag{4}$$
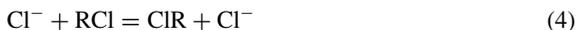
The tightness of the TS expressed as the distance between two Cl atoms in the TS, $r^{\neq}$ (Cl$\cdots$Cl), and the percentage of bond stretching deformation, %CX$^{\neq}$ [$= 100(r^{\neq} - r_0)/r_0$], and activation barrier, $\Delta E^{\neq}$, were determined for 7 primary, 9 secondary and 2 tertiary carbon centers. The averages of ρ_{XZ}, $r^{\neq}_{(Cl\cdots Cl)}$, %CX$^{\neq}$ and $\Delta E^{\neq}$ values are summarized in Table 6. We note that as the TS tightness decreases along the primary $\rightarrow$ secondary $\rightarrow$ tertiary carbon centers, ρ_{XZ} decreases, $r^{\neq}$ increases and the activation energy increases accordingly.

TABLE 6.   Summary of average values of ρ_{XZ}, $r^{\neq}$ (Cl$\cdots$Cl), %CX$^{\neq}$ and $\Delta E^{\neq}$ for primary, secondary and tertiary carbons

Carbon center	$\rho_{XZ}{}^a$	$r^{\neq}$ (Cl$\cdots$Cl)^b	%CX$^{\neq\,b}$	$\Delta E^{\neq}$(kcal mol^{-1})^b
Primary	0.33 ± 0.03	4.67 ± 0.03	32	9.2
Secondary	0.12 ± 0.01	4.80 ± 0.02	36	12.5
Tertiary	−0.04 ± 0.01	4.88 ± 0.03	35	13.4

^{a} Averages of 10 values for primary, 10 values for secondary and 2 values for tertiary centers determined for the nucleophilic substitution reactions of anilines.
^{b} Averages of 7 values for primary, 9 values for secondary and 2 values for tertiary centers determined for chloride exchanges at the MP2/6−31+G*//MP2/6−31+G* level.

III. NUCLEOPHILIC REACTIONS AT UNSATURATED CARBONS

A. Olefinic Carbon Centers

Nucleophilic addition of amines ($XRNH_2$) to olefins ($YC_6H_4CH=CZZ'$) activated by electron- acceptor groups (Z,Z') is known to proceed in aqueous solution through a zwitterionic intermediate, $T^\pm$ (Scheme 7), with an imbalanced TS in which the development of resonance into the activating groups lags behind $C_\alpha - N$ bond formation[13a, 68]. The imbalance in the TS is mainly caused by the poorly developed resonance into Z,Z', and solvation of the negative charge largely localized on carbon (C_β), an exaggerated form of which can be given as in structure **7**[13a, 68].

$$YC_6H_4CH=CZZ' + XRNH_2 \;\underset{k_{-1}}{\overset{k_1}{\rightleftharpoons}}\; \underset{\substack{XR\overset{+}{N}H_2 \\ T^\pm}}{YC_6H_4CH-C\bar{Z}Z'} \;\underset{H^+}{\overset{Ka^\pm}{\rightleftharpoons}}\; \underset{\substack{XRNH \\ T^-}}{YC_6H_4CH-C\bar{Z}Z'}$$

$$\underset{\substack{XRNH}}{YC_6H_4CH-CHZZ'}$$

SCHEME 7

$$\underset{\substack{| \delta+ \\ XRNH_2}}{YC_6H_4\overset{\delta+}{CH}}\cdots\bar{C}\diagdown\substack{Z \\ Z'}$$

(7)
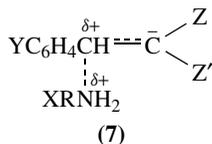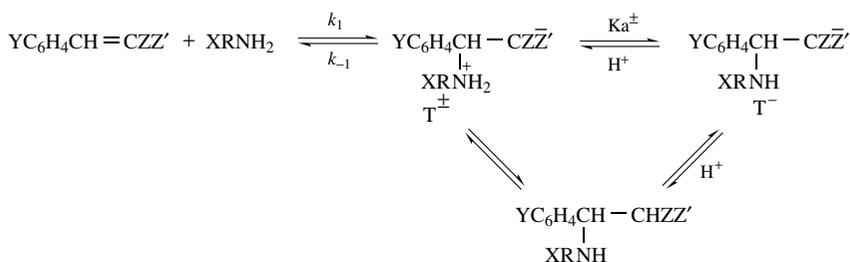
In most cases the acid–base equilibrium, $T^\pm \rightleftharpoons T^-$, is rapidly established and hence the nucleophilic addition step (k_1) is the rate-determining step. However, a number of cases have been reported where decomposition of the zwitterionic intermediate becomes important as a rate-limiting step. Such examples are encountered commonly when the k_{-1} value is unusually high due to a very small equilibrium constant ($K_1 = k_1/k_{-1}$) for $T^\pm$[13a]. The nucleophilic addition of aniline to the activated olefins is such an example. Bernasconi and coworkers[13a, 69] have reported the aniline addition reaction to β-nitrostyrene ($YC_6H_4CH=CHNO_2$) in 50% DMSO–H_2O solution at 20 °C for Y = H. The k_{-1} value (3.8×10^6 s^{-1}) was extremely high compared to k_1 (5.0 M^{-1} s^{-1}) leading to very small K_1 (= 1.3×10^{-6} M^{-1}).

In contrast, for the additions of more basic amines k_1 is larger than k_{-1}; for piperidine and n-butylamine addition, the k_1 and k_{-1} (K_1) values for Y = H are 1.14×10^3 M^{-1} s^{-1}: 36 s^{-1} (31.8 M^{-1}) and 31 M^{-1} s^{-1}: 1.25 s^{-1} (24.8 M^{-1}), respectively[69a].

Similar results are also found in the aniline addition to 1,1-dinitro-2,2-diphenylethylene in 50% DMSO–H_2O at 20 °C. The k_{-1} value ($ca\ 5 \times 10^6$ s^{-1}) is very high relative to k_1 ($ca\ 1.0$ M^{-1} s^{-1}) with $K_1 = ca\ 2 \times 10^{-7}$ M^{-1}. This is again in contrast to the addition reactions of more basic amines; for the addition of piperidine and n-butylamine, the k_1 and k_{-1} (K_1) values are 6.8 M^{-1} s^{-1}: 100 s^{-1} (6.2×10^{-2} M^{-1}) and 40 M^{-1} s^{-1}: 0.36 s^{-1} (1.1×10^2 M^{-1}), respectively[70]. The reports of aniline addition to olefins are very scarce,

mainly due to the very slow overall rate and partly due to difficulties in identifying the UV peaks owing to interference by the olefin peak.

Nucleophilic substitution reactions of highly activated olefins with 2–4 cyano groups $R^1R^2C{=}C(CN)_2$ where R^1 and R^2 are cyano, halogen or aryl groups, by anilines have been extensively studied by Rappoport and his coworkers[71]. In all of the reactions, a zwitterionic complex, $R^1R^2(ArN^+H_2)C{-}C^-(CN)_2$, was formed, and the activation energy was low and was accompanied by a high negative entropy of activation. The formation of an initial π-complex was appreciable in the reaction of tetracyanoethylene ($R^1 = R^2 = CN$) with N-methylaniline and N,N-dimethylaniline[71a,b] in chloroform, but it was very low in the reactions of tricyanovinyl chloride ($R^1 = Cl$, $R^2 = CN$) with N,N-dialkylanilines[71c] in chloroform. In the latter reactions, the order of reactivity was N,N-dibutyl $> N,N$-diethyl $> N,N$-dipropyl $> N,N$-dimethyl-aniline. In the substitution of 1,1-dicyano-substituted halogenoethylenes ($R^1 = F$ or Cl, $R^2 = p$-dimethylaminophenyl) by aromatic amines in acetonitrile, methanol, 2-propanol and t-butyl alcohol, the zwitterionic intermediate $Ar(ArN^+H_2)CX{-}C^-(CN)_2$, where $X = F$ or Cl, was found to form in the initial nucleophilic attack, which is followed by either competition between expulsion of the halide ion followed by N−H bond cleavage, or by amine-catalyzed N−H bond cleavage followed by a carbon–halogen bond cleavage[71d,e]. Reactions of anilines with 1-chloro-(and 1-bromo-) 2,2-dicyano-1-p-nitrophenylethylenes showed very mild catalysis by the amine, while the reactions of 1-chloro (and 1-bromo-) 2-cyano-2-methoxycarbonylethylenes with p-cyanoaniline showed no catalysis[71f].

Nucleophilic addition of amines to the activated olefins in acetonitrile, however, is known to proceed in a single step by concerted formation of the $C_\alpha{-}N$ and $C_\beta{-}H$ bonds[72]. Here again, for the reactions in MeCN the experimental difficulties associated with the aniline addition reaction have resulted in a very limited number of reports. Varghese and coworkers[73] reported the aniline additions to β-nitrostyrene in MeCN at 25 °C. The k_2 value is 4.14×10^{-3} $M^{-1}s^{-1}$ for unsubstituted aniline and the β_X value is 0.44 ± 0.05 ($n = 22$, $r = 0.910$). The same reactions with benzylamines ($XC_6H_4CH_2NH_2$) are, however, reported to proceed by two pathways, an uncatalyzed (k_2) and a catalyzed (k_3) path[72b]. The kinetic isotope effects ($k_H/k_D > 1.0$) involving deuteriated benzylamine ($XC_6H_4CH_2ND_2$) show that the proton transfer from the amine to the β-carbon occurs concurrently with the addition of the amine to the α-carbon. The large β_X ($= 1.36$) value supports the extensive bond formation in the TS.

B. Carbonyl Carbon Centers

Nucleophilic displacements at carbonyl carbon centers have been one of the most extensively investigated subjects in chemistry, especially because of their relevance to the enzymatic catalysis of carbonyl group transfer reactions. The most commonly used criteria for distinguishing the mechanism of aminolysis reactions in solution are the sign and magnitude of the Brönsted coefficients, β_X ($= \beta_{nuc}$) and β_Z ($= \beta_{lg}$). The steady-state treatment of the reactions through an intermediate (equation 5) leads to equation 6, which can be simplified according to the rate-limiting step. For the rate-limiting formation, $k_b > k_{-a}$, and hence, equation 7 applies. For the rate-limiting breakdown of the zwitterionic intertermediate, $T^{\pm}$, $k_b < k_{-a}$, so that equation 8 applies.

$$XC_6H_4NH_2 + RY{-}\overset{\overset{\displaystyle O}{\|}}{C}{-}LZ \underset{k_{-a}}{\overset{k_a}{\rightleftharpoons}} RY{-}\underset{\underset{\displaystyle C_6H_4X}{\overset{\displaystyle |}{\underset{\displaystyle +NH_2}{|}}}}{\overset{\overset{\displaystyle O^-}{|}}{C}}{-}LZ \overset{k_b}{\longrightarrow} XC_6H_4\overset{+}{N}H_2{-}\overset{\overset{\displaystyle O}{\|}}{C}{-}RY + LZ^-$$

$$(5)$$
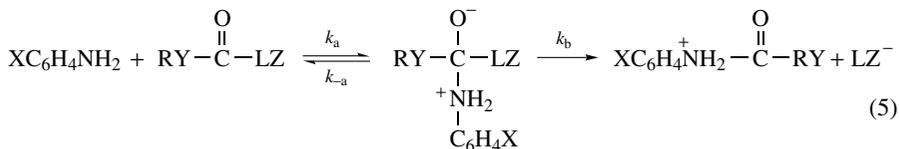
$$k_N = k_a k_b / (k_{-a} + k_b) \tag{6}$$

$$k_N = k_a \tag{7}$$

$$k_N = (k_a / k_{-a})\, k_b = K k_b \tag{8}$$

When $k_{-a} = k_b$, the expulsion rates of the amine and leaving group (LZ) from the intermediate become equal; the rate-limiting step changes from breakdown to formation of the intermediate as the basicity of nucleophile is increased. In a concerted aminolysis, $T^{\pm}$ in equation 5 is a tetrahedral TS, not an intermediate. When breakdown of the intermediate is rate-limiting, the β_X value is larger than ca 0.8, and similarly the β_Z value is also large negative, $-\beta_Z > 0.8$[15g]. In contrast, for rate-limiting formation of the intermediate the β_X and $-\beta_Z$ values are smaller, $\beta_X \leqslant 0.3$ and $-\beta_Z \leqslant 0.4$. For the concerted aminolysis, the magnitude of the Brönsted coefficients exhibits intermediate values, $0.4 \leqslant \beta_X \leqslant 0.7$. These values serve only as general guidelines and there are some exceptional cases[15g].

There are abundant literature reports of the aminolysis of the carbonyl derivatives (esters, carbonates and anhydrides), some of which are summarized in Table 7[74–86].

Acetyl chloride (LZ = Cl) reacts with aniline (entry 1) in 50% dioxane–H_2O solution[74] by a stepwise mechanism with rate-limiting formation of the intermediate ($\beta_X = 0.25$), whereas the anilinolysis of 4-nitrophenyl acetate (LZ = $OC_6H_4NO_2$-4) proceeds in H_2O with rate-limiting breakdown ($\beta_X = 0.85$) of the intermediate (entry 2) due to a decrease in the nucleofugality ($k_{-a} > k_b$) from Cl^- to 4-nitrophenoxide[75]. The reactions of 4-nitrophenyl thioacetate (entry 3) and 2,4-dinitrophenyl methyl carbonate (entry 4) seem to be similar[75, 76]. An interesting case is the aminolysis of O-ethyl S-aryl carbonates[77] (entries 5 and 6). By increasing the nucleofugality from 2,4-dinitrophenoxide to 2,4,6-trinitrophenoxide, the mechanism changes from a stepwise process with rate-limiting breakdown of $T^{\pm}$ to a concerted process. Again, by increasing leaving ability from $T^{\pm}$ from aniline to secondary alicyclic amines the mechanism changes similarly from stepwise to concerted[77]. On the other hand, the reactions of 2,4,6-trinitrophenylthio carbonate with pyridines are stepwise, indicating that anilines kinetically destabilize $T^{\pm}$ in comparison with pyridines as a result of a greater nucleofugality from $T^{\pm}$[87]. Thus the order of expulsion rate (k_{-a}) from $T^{\pm}$ is found to decrease experimentally in the following order: benzylamines > secondary alicyclic amines > anilines > pyridines[15g, 87]. This order is attributed to delocalization of the cationic charge on the amine nitrogen in $T^{\pm}$ for secondary and tertiary amino moieties in $T^{\pm}$, in contrast with the more localized cationic charge on the primary amino nitrogen[15g].

The nucleophilic substitution of anilines at anhydride carbonyl centers[78, 79] (entries 7–9) occurs by the stepwise mechanism with rate-limiting breakdown of $T^{\pm}$. Although the original authors[78] (entries 7 and 8) favored concerted processes for anilinolysis of phthalic and succinic anhydrides, the large β_X values implicate a stepwise mechanism with a rate-limiting expulsion of the leaving group.

The reactions of anilines with benzoyl halides (entries 10 and 11) are simple associative S_N2 processes, albeit the β_X values are large. The sign of ρ_{XY} is negative for both reactions, which is an indication of a concerted process[15g]. The large β_X values are ascribed to a large degree of bond making (an associative S_N2) in the TS. The kinetic isotope effects ($k_H/k_D < 1.0$) involving deuteriated anilines also support concerted displacement[15e, 88]. A similar conclusion was reached by Song and Jencks[89] based on the aminolysis studies of benzoyl fluoride in aqueous solution. Although anilinolysis of phenylacetyl chloride[81] in MeCN exhibits a large β_X value (0.99), the reaction is considered to proceed by a concerted mechanism with a negative ρ_{XY} value (−0.12). For the anilinolysis of phenyl chlorofor-mates in MeCN[82] (entry 13), the magnitudes of β_X (0.77) and k_H/k_D (0.74–0.94) and the negative ρ_{XY} (−0.04) support the concerted mechanism. In contrast, the anilinolysis

554

TABLE 7. Reactions of anilines with carbonyl compounds $XC_6H_4NH_2 + YRCO-LZ \rightarrow YRCO-NHC_6H_4X + H^+ + LZ^-$

Entry	Reactant (YRCO—LZ)	T (°C)	Solvent	k_2 (M^{-1} s^{-1})	β_X	ρ_{ij}	Reference
1	MeCO—Cl	22 ± 2	50% Dioxane–H$_2$O	690	0.25		74
2	MeCO—OC$_6$H$_4$NO$_2$-4	25	H$_2$O	2.1×10^{-4}	0.85		75
3	MeCO—SC$_6$H$_4$NO$_2$-4	25	H$_2$O	1.36×10^{-2}	0.7		75
4	MeOCO—OC$_6$H$_3$(NO$_2$)$_2$-2,4	25	H$_2$O	0.09 ± 0.02	0.9		76
5	EtOCO—SC$_6$H$_3$(NO$_2$)$_2$-2,4	25	H$_2$O	$(1.10 \pm 0.03) \times 10^{-3}$	0.9(0.56)[a]		77
6	EtOCO—SC$_6$H$_2$(NO$_2$)$_3$-2,4,6	25	H$_2$O	$(27 \pm 1) \times 10^{-3}$	0.54(0.48)[a]		77
7	o-C$_6$H$_4$(CO)$_2$O	25	10% Dioxane–H$_2$O	396	0.8		78
8	(CH$_2$)$_2$(CO)$_2$O[b]	25	10% Dioxane–H$_2$O	18.0	0.8		78
9	YC$_6$H$_4$(CO)$_2$—OC$_6$H$_4$Z	40	MeOH	3.47×10^{-2}	1.01	$\rho_{XY} = 0.54, \rho_{XZ} = 1.19$	79
10	YC$_6$H$_4$CO—Cl	35	MeOH	81.8	0.75	$\rho_{XY} = -0.68$	80
11	YC$_6$H$_4$CO—F	55	MeOH	22.0×10^{-3}	1.14	$\rho_{XY} = -1.67$	80
12	YC$_6$H$_4$CH$_2$CO—Cl	−15	MeCN	93.3	0.99	$\rho_{XY} = -0.12$	81
13	YC$_6$H$_4$OCO—Cl	25	MeCN	6.37	0.77	$\rho_{XY} = -0.04$	82
14	YC$_6$H$_4$CH=CHCO—Cl	25	MeOH	13.3	0.83	$\rho_{XY} = 0.88$	83
15	t-BuCO—O—4,6-(MeO)$_2$—1,3,5-triazine	30	MeCN	1×10^{-3}	—	—	84
16	2-ThienylCO—Cl	25	Benzene	2.52×10^{-2}	1.14[c]	—	85
17	2-FurylCO—Cl	25	Benzene	13.3×10^{-2}	1.10[c]	—	86
18	3-FurylCO—Cl	25	Benzene	4.09×10^{-2}	1.11[c]	—	86

[a]The β_X value with secondary alicyclic amines.
[b]Succinic anhydride.
[c]Determined with pK_a(H$_2$O).

of cinnamoyl chloride[83] (entry 14) exhibits larger β_X (0.83) and k_H/k_D (1.02–1.09) values with a positive ρ_{XY} value, which are consistent with a stepwise mechanism with rate-limiting expulsion of the Cl^- leaving group.

Nitrogen isotope effect studies on the acylation of aniline[84] (entry 15) using 2-(4,6-dimethoxy-1,3,5-triazinyl) 2,2-dimethylpropanoate, **8**, in CD_3CN (equation 9) gave a nitrogen isotope effect of 0.996, which lies in between the limiting values of 0.991 for rate-limiting decomposition of the intermediate ($T^{\pm}$) and 1.002 for a rate-limiting formation of $T^{\pm}$. These results indicate a stepwise mechanism with the formation of a tetrahedral intermediate when decomposition of the latter is nearly equally rate-limiting.

$$
\text{Me}-\underset{\underset{\text{Me}}{|}}{\overset{\overset{\text{Me}}{|}}{\text{C}}}-\overset{\overset{\text{O}}{\|}}{\text{C}}-\text{(triazine-OMe)} + H_2NPh \longrightarrow \text{Me}-\underset{\underset{\text{Me}}{|}}{\overset{\overset{\text{Me}}{|}}{\text{C}}}-\overset{\overset{\text{O}}{\|}}{\text{C}}-\overset{\overset{\text{H}}{|}}{\text{N}}-\text{Ph} + HO-\text{(triazine-OMe)} \quad (9)
$$

(8)
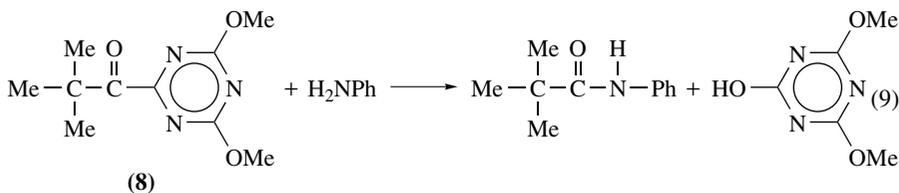
The reactions of 2-thienoyl and 2- and 3-furoyl chlorides with anilines[85, 86] in benzene (entries 16–18) display similar Brönsted coefficients ($\beta_X \cong 1.1$ using pK_a values in H_2O) and Hammett ρ_X values of ca −3.3, which are comparable to those found for benzoylation of 3-thienoyl chloride[86]. Although the β_X values determined by the plots of log k_2 (benzene) against $pK_a(H_2O)$ are large, these reactions most probably proceed by a concerted mechanism, like the benzoylation of anilines (entry 10).

The reactions of anilines with thiocarbonyl derivatives in MeCN, where the leaving groups are thiophenoxides (SAr^-), are summarized in Table 8[90–94]. Based on the mechanistic criteria involving the size of β_X and the sign of ρ_{XZ} values, all the reactions except one (entry 4)[92] proceed by the stepwise mechanism with a rate-limiting expulsion of the leaving group from $T^{\pm}$. It has been pointed out time and again that substitution of O^- (carbonyl) by S^- (thiocarbonyl) in $T^{\pm}$ stabilizes the intermediate[95]. This has been attributed to a much easier formation of a C=O bond in the thiol intermediate relative to the C=S bond in the dithio intermediate due to the weaker π-bonding energy of the C=S group relative to C=O, which results from the lower $\pi_{C=S}^*$ orbital than the $\pi_{C=O}^*$ orbital[96]. The fact that the anilinolysis of O-ethyl dithiocarbonate in MeCN[92] (entry 4) proceeds by a concerted mechanism indicates destabilization of the intermediate by the EtO group relative to other acyl groups listed in Table 8. It should be noted that for the stepwise carbonyl transfer reactions with rate-limiting breakdown of $T^{\pm}$ the sign of ρ_{XZ} (and of ρ_{XY}) is invariably positive whereas for the concerted anilinolysis reactions the sign is negative[15g].

Nucleophilic attack of aniline also occurs at a cyano (nitrile) carbon center. Williams and coworkers[97] have reported on the anilinolysis of dicyanamide (equation 10).

$$
XC_6H_4NH_2 + HN(CN)_2 \longrightarrow XC_6H_4NH-C(NH_2)=N-CN \quad (10)
$$

The reaction in aqueous solution is general acid catalyzed and the Brönsted coefficient for variation in the aniline substituent is constant, being $\beta_X = 0.66$ when the acid is oxonium ion. The Brönsted coefficient for varying the general acid when aniline is kept constant is −0.54 for 4-sulfanilic acid. According to the empirical rate law obeyed (equation 11),

$$
\text{Rate} = k_{HA}[HA][ArNH_2][N(CN)_2^-] \quad (11)
$$

the reaction is acid catalyzed and the nucleophilic attack by aniline occurs at the anion of dicyanamide, $N(CN)_2^-$. The kinetic data are consistent with a mechanism where neutral

TABLE 8.   Reactions of anilines with thiocarbonyl compounds in MeCN: $XC_6H_4NH_2$ + YRCS-LZ $\rightarrow$ YRCS-NHC$_6$H$_4$X + H$^+$ + LZ$^-$

Entry	Reactant	T (°C)	k_2 (M^{-1} s^{-1})	β_X	β_Z	ρ_{ij}	Reference
1	MeCS−SC$_6$H$_4$Z	50	9.46×10^{-4}	0.84	−0.81	$\rho_{XZ} = 0.58$	90
2	EtCS−SC$_6$H$_4$Z	45	3.19×10^{-3}	1.09	−1.10	$\rho_{XZ} = 1.90$	91
3	PhCH$_2$CS−SC$_6$H$_4$Z	45	2.76×10^{-4}	0.93	−1.10	$\rho_{XZ} = 1.41$	91
4	EtOCS−SC$_6$H$_4$Z	30	17.1×10^{-3}, 1.47×10^{-3}(DMA)^a	0.54	−0.19	$\rho_{XZ} = -0.56$, $\rho_{XY} = 0.66$	92
5	YC$_6$H$_4$CS−SC$_6$H$_4$Z	55	2.85×10^{-3}	1.03	−0.76	$\rho_{XZ} = 0.60$	93
6	2-ThienylCS−SC$_6$H$_4$Z	40	3.76×10^{-4}	0.87	—	$\rho_{XZ} = 0.85$	94
7	2-FurylCS−SC$_6$H$_4$Z	15	3.40×10^{-2}	1.40	—	$\rho_{XZ} = 0.75$	94

^{a} Value with N,N-dimethylaniline.
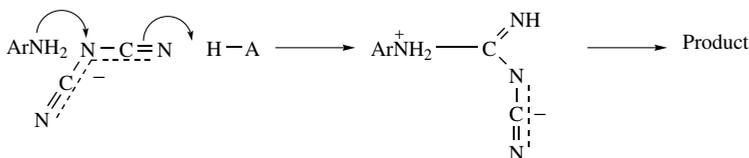
SCHEME 8

aniline attack on the carbon of the dicyanamide anion is assisted by concerted proton transfer from the general acid to the substrate nitrogen (Scheme 8).

The absence of an uncatalyzed addition of aniline to dicyanamide indicates that the direct, or through a water bridge, intramolecular transfer of the proton is not occurring in either a stepwise process or in a concerted process with nucleophilic attack.

Williams and Jencks[98] investigated the aniline reactions with cyanic acid (HN=C=O) and ethyl isothiocyanate (EtN=C=S) in aqueous solution. The reactions of cyanic acid are catalyzed by amine or buffer with $k_2 = 1.55$ M^{-1} s^{-1} (for X = H), and Brönsted-type plots of log k_2 versus pK_a for the nucleophilic reactions of amines show a sharp break at p$K_a = 6$. Basic primary amines and secondary amines lead to a slope $\beta_X = 0.3$, whereas weakly basic amines, mainly anilines, follow a line with slope $\beta_X = 0.8$. The so-called α-effect amines, mainly hydrazine derivatives, generally react more rapidly than simple amines and follow a line with $\beta_X = 0.4$. The change in β_X indicates a change in the rate-determining step with the basicity of the attacking amine, from amine attack for the basic amines to a proton-transfer step (k_t) from the initially formed zwitterionic intermediate to the uncharged urea product for weakly basic amines (Scheme 9).
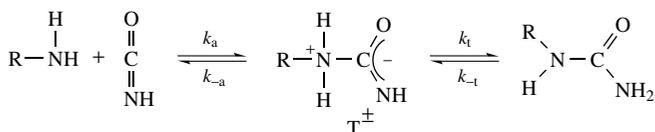
SCHEME 9

The reactions of weakly basic amines (anilines), for which proton transfer is rate-limiting, are catalyzed by a second amine molecule or ammonium ion as well as by

added buffers. There is no break in the Brönsted plot for ethyl isothiocyanate aminolysis, reflecting a relatively small value of k_{-a} in these reactions. As noted previously, in these reactions a relatively small driving force is provided by the conversion of the thiol anion to the C=S from $T^{\pm}$. The value of $\beta_X = 0.28$ is similar to that for the reaction of cyanic acid with basic amines and supports a similar TS.

Satchell and Satchell[99] reported a kinetic study on the aminolysis of *p*-nitrophenyl isothiocyanate with primary amines and anilines in diethyl ether and isooctane as solvents. The detailed analysis reveals that the aminolysis occurs via a zwitterionic intermediate, $T^{\pm}$, which undergoes subsequent proton transfer catalyzed by a second amine molecule (equation 12). Added carboxylic acids form inactive 1:2 amine−acid complexes with strong basic amines and inhibit aminolysis, but with weak bases the acids form only a negligible amount of complex and they catalyze the aminolysis.

$$\text{ArNCS} + \text{RNH}_2 \underset{k_{-a}}{\overset{k_a}{\rightleftharpoons}} \underset{\overset{|}{{}^{+}\text{NH}_2\text{R}}}{\text{ArN}\text{-}\text{C}\text{-}\text{S}} \overset{k_b}{\underset{\text{RNH}_2}{\longrightarrow}} \text{ArNHC}\overset{\text{S}}{\underset{\text{NHR}}{\diagdown}} \qquad (12)$$
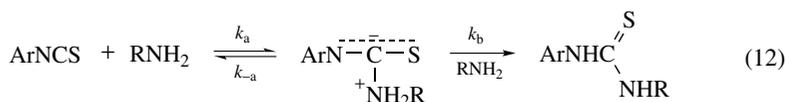
C. Ring Carbons (S$_N$Ar)

Activated nucleophilic aromatic substitutions, S$_N$Ar, take place when the ring bears strongly electron-withdrawing substituents and a good leaving group[100]. In the case of halogen, a wide variety of electron-withdrawing groups such as nitro, trifluoromethyl, sulfonyl and phenylazo have been shown to enhance the substitution rate. Most of the early works involved nucleophilic displacements of the halogen in the 1-halo-2,4-dinitrobenzenes. For example, Hammond and Parks[101] have shown that the order of halogen Y displacement in 1-Y-2,4-dinitrobenzenes with *N*-methylaniline in nitrobenzene and in 99.8% EtOH is F < Cl < Br, indicating that C−X bond breaking is involved in the rate-determining TS.

The importance of bond cleavage in the TS is also found in the nucleophilic displacement of chloride in 4-Y-2,6-dinitrochlorobenzenes with substituted anilines (XC$_6$H$_4$NH$_2$) in a series of MeOH−MeCN mixtures[102]. The β_X values are large (= 0.97) and are practically constant regardless of the Y-substituent, NO$_2$, CN and CF$_3$, and the reaction rate decreases as the MeCN content increases.

The reactions of 1-Y-2,4-dinitrobenzene (Y = Cl and F) with anilines and other amines in acetone[103] show no base catalysis for Y = Cl and the overall second-order rate constant is $k_N = 0.434 \pm 0.011$ M^{-1} s^{-1} with piperidine, which is 10^4-fold higher than with aniline ($k_N = 4.30 \pm 0.25 \times 10^{-5}$ M^{-1} s^{-1}). For Y = F the reaction of aniline is catalyzed by aniline and Dabco (1,4-diazabicyclo[2.2.2]octane) with a linear dependence of k_N on both bases, indicating that $k_{-a} \gg k_b + k_c[B]$ (Scheme 10).
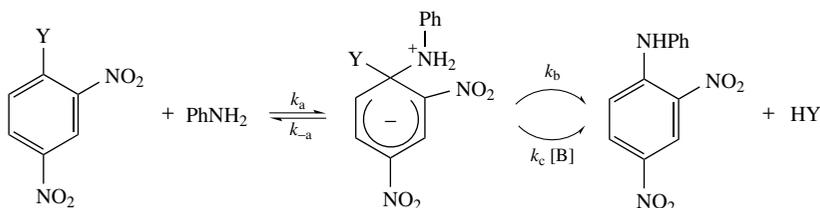
SCHEME 10

On the other hand, Nudelman and Palleros[104a] reported a quadratic dependence of the observed second-order rate constant k_N on the concentration of 2-methoxyaniline in its reaction with 2,4-dinitrofluorobenzene (DNF) in benzene. This behavior is similar to that previously reported in the reaction with 4-methoxyaniline in benzene[104b]. These kinetic results are interpreted in terms of reaction by the *dimer* of the amine which forms a cyclic intermediate with the substrate (Scheme 11).
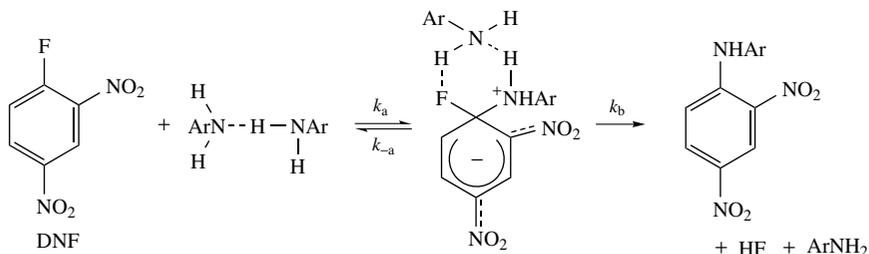
SCHEME 11

This mechanism is also proposed for the reactions between DNF and 2- or 4-methoxyaniline (ArNH$_2$) in the presence of pyridine or Dabco.

Onyido and Hirst[105] have investigated the reactions of 2-methyl- and 4-methylanilines with DNF in DMSO. Based on the base catalysis observed, they concluded that a change in the rate-determining step is induced by the steric effect of the *ortho*-Me group. The rate of reaction is reduced nearly 200-fold when the Me substituent is at *ortho* compared to a *para* position in the aniline nucleophile. That this is due to a mechanistic change was confirmed by the fluorine leaving-group kinetic isotope effects (KIEs)[106]. The $^{18}F/^{19}F$ kinetic isotope effect using isotopically labeled DNF is determined to be 1.0005 ± 0.0030 for 4-Me-aniline and 1.0119 ± 0.0037 for 2-Me-aniline in DMSO at $30\,^\circ$C. The large fluorine leaving-group KIE for sterically hindered 2-Me-aniline suggests a rate-limiting leaving-group departure (k_b), whereas the insignificant fluorine KIE for the less sterically hindered 4-Me-aniline indicates a rate-limiting addition of the nucleophile (k_a).

Evidence for the formation of Meisenheimer, or a σ-complex, involving aniline as a nucleophile has been presented with 1,3,5-trinitrobenzene (TNB) by Buncel and coworkers[107]. Reactions of the TNB−methoxide ion adduct with a series of substituted anilines in DMSO solution yield new TNB−aromatic amine σ-complexes (Scheme 12).

R = H, 3-CF$_3$, 3-NO$_2$, 4-OMe, 4-Me, 4-Cl, 4-Br, 4-CH$_3$CO, 4-CN, 4-NO$_2$ or 3,5-(NO$_2$)$_2$
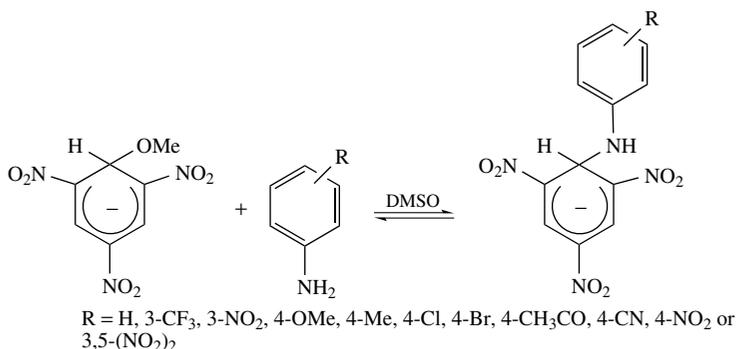
SCHEME 12

The parent TNB–anilide complex is also obtained in the reaction of TNB with potassium anilide in DMSO[108]. The authors found that only the dissociative mechanism is in complete accord with the kinetic behavior exhibited by the conversion of TNB–OMe⁻K⁺ to TNB–NHPh-K⁺ in DMSO[108b]. The mechanistic features involve: (i) a rapidly established equilibrium between the TNB–OMe complex and free TNB, (ii) rate-limiting interconversion of TNB and the protonated anilide complex and (iii) a rapidly established equilibrium between the protonated and unprotonated anilide complexes. When Dabco is involved in the reaction between TNB and aniline in DMSO, the mechanism changes to a rate-limiting deprotonation of the zwitterionic complex, TNB–NH₂Ph±, which was formed in a preequilibrium step[109]. The reactions in DMSO and in MeCN are catalyzed solely by Dabco. Similar studies were extended to the formation of σ-complex between TNB and N-methylaniline in the presence of Dabco in DMSO. Again, the reaction is catalyzed solely by Dabco in a linear fashion, indicating that deprotonation of the zwitterionic intermediate is rate-limiting. The rate-limiting proton transfer in σ-complex formation is considered to provide a strong support for the contention that under certain conditions for S_NAr reactions involving aromatic and aliphatic amines of the same basicity, the reaction involving the aromatic amine is base-catalyzed while that with the aliphatic base is uncatalyzed.

S_NAr reactions involving phenoxide leaving group from Z-aryl 2,4,6-trinitrophenyl ethers (TNB–ArE) in MeCN and DMSO are reported by Crampton and coworkers[110]. The reaction scheme is shown in Scheme 13.
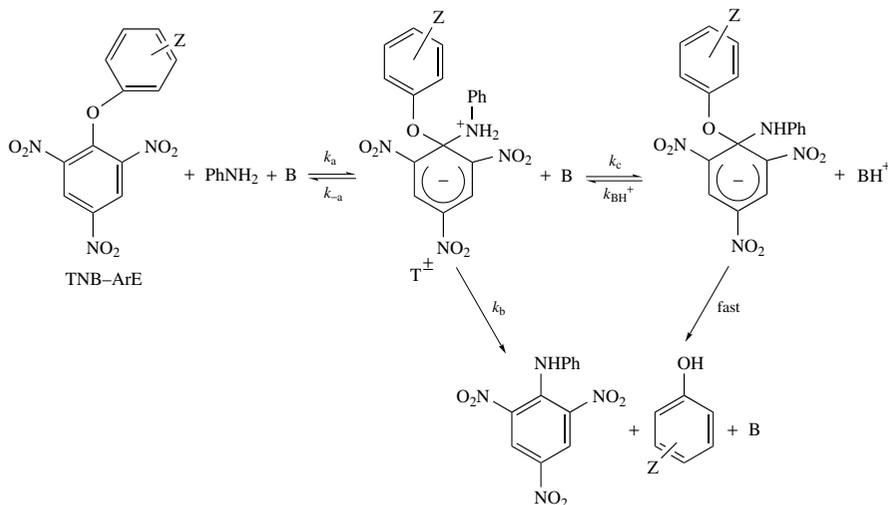
SCHEME 13

The main reaction in MeCN occurs through a base-catalyzed pathway involving formation of a zwitterionic intermediate, equilibrium formation of an anionic intermediate and a rate-limiting proton transfer to base, rate constant k_c, followed by a fast leaving-group expulsion. The corresponding reactions in DMSO, however, are found to proceed by both uncatalyzed (via k_b) and catalyzed pathways. Similar reactions in benzene show that the Hammett coefficient determined with substituted anilines for the catalyzed path is extremely large ($\rho = -7.7$) relative to that for the uncatalyzed path ($\rho = -4.7$). The Brönsted β_X value (which may, however, be unreliable since the $pK_a(H_2O)$ values are

used) is also large (3.0)[111]. The reactions with aniline in MeOH are found to be general base-catalyzed whereas those with *n*-butylamine are not base-catalyzed[112]. The reaction with *N*-methylaniline is much slower, by 10^5-fold relative to that with aniline in both MeCN and DMSO due to increased steric hindrance both in formation of the intermediate and in the proton-transfer step.

The similar reactions involving 4-nitrophenyl 2,4,6-trinitrophenyl ether $(Z = 4\text{-}NO_2$ in TNB$-$ArE) with aniline and *N*-methylaniline are reported in DMSO, MeCN, MeOH and
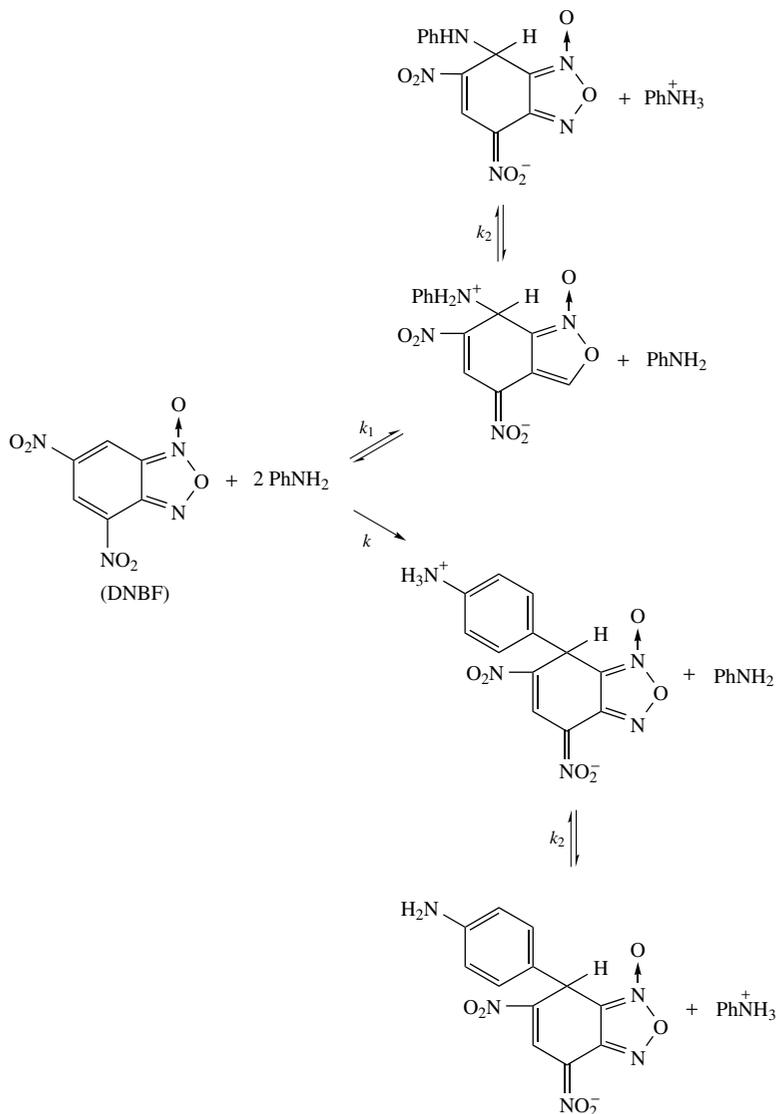
SCHEME 14

benzene[113]. The reactions are base catalyzed in all the solvents. The catalytic efficiency is larger with aniline than with *N*-methylaniline and supports the proton-transfer mechanism of the base-catalyzed step.

S_NAr reactions have been studied mostly with dinitro and trinitro activated benzenes. Recently, the aniline reactions with the highly activated super-electrophile, 4,6-dinitrobenzofuroxan (DNBF), have attracted considerable attention due to its ambient reactivity[114]. In acidic solvent, where aniline is almost completely protonated, the reaction by nitrogen attack is inhibited. However, a carbon–carbon bonded adduct is slowly formed by reaction at the 4-position of the aniline. Kinetic studies in H_2O–DMSO have shown that this adduct formation involves two steps: a carbon–carbon bond formation (k_a), followed by elimination of a proton, K_{dep} (*vide infra*). The reactions of anilines with DNBF in DMSO have shown that the N-bonded adduct (σ-N) is kinetically preferred, but the C-bonded adduct (σ-C), formed in equilibrium with its deprotonated form, is the thermodynamically favored product (Scheme 14).

When the ring position *para* to the amino group in 4-methylaniline is blocked, the adduct (σ-C) is formed by reaction at the 2-position of the aniline. For the C-adduct formation, the β_X value estimated with 4 substituted anilines have a very large negative value of *ca* -3, indicating that formation of the σ-C adduct involves an elimination of a proton from the intermediate. In contrast, the β_X value for the *N*-adduct formation was estimated to be *ca* $+0.98$, which is consistent with an extensive N−C bond formation during the σ-N complex formation.

Nucleophilic displacements on unsubstituted aromatics usually do not occur since H$^-$ is not a good leaving group. However, an example of nucleophilic aromatic substitution of hydrogen (NASH) has been reported on reacting aniline and azobenzene in the presence of base under aerobic conditions to generate 4-(phenylazo)diphenylamine, **9** (equation 13)[115].

$$(13)$$

(9)
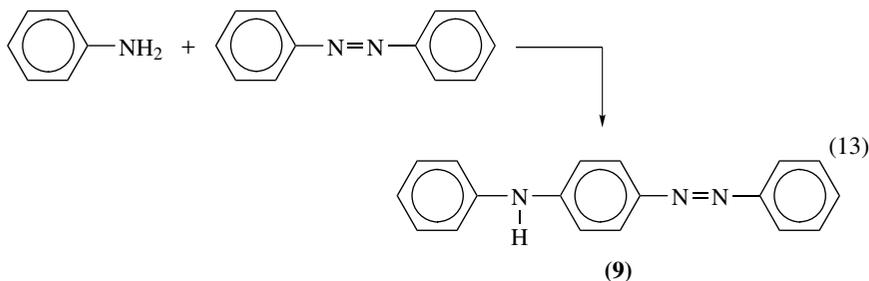
In this reaction the phenylazo moiety functions as the electron-withdrawing group to activate the phenyl ring toward nucleophilic attack of aniline. Like other NASH reactions, a formal oxidation of the σ-complex intermediate is required for product formation. Catalytic hydrogenation of **9** generates 4-aminodiphenylamine (4-ADPA), **10**, and aniline. The 4-ADPA and its derivatives are widely used as antioxidants in rubber products. Thus the NASH reaction involving an azo group as the activating electrophile forms the basis for a novel route to **10** that does not require halogenated intermediates or reagents which ultimately generate waste streams laden with inorganic salts and trace amounts of organic byproducts.

(10)
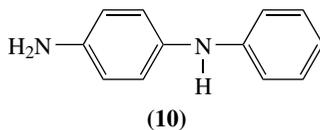
IV. NUCLEOPHILIC REACTIONS AT HETEROATOMS

A. Sulfur Atom Centers

Nucleophilic substitution reactions of anilines at a sulfonyl sulfur (tetra-coordinated sulfur) atom have been widely studied. Some of the works are presented in Table 9.

The reactions of substituted anilines with alkylsulfonyl chlorides (entries 1–3)[116] are investigated in 100, 90, 80, 70 and 50% (v/v) MeOH–MeCN mixtures at 35 and 45 °C. The rates decreased with the increased size of the alkyl group, and also with the increase in MeCN content. The β_X values are found to decrease with the alkyl size, but to increase with the MeCN content ($\beta_X = 0.88$, 0.82 and 0.58 for Me, Et and n-Pr in 50% MeOH–MeCN). Since a faster rate is accompanied by a larger selectivity (β_X), this is an example of the anti-RSP and hence all the reactions are considered to proceed concertedly despite the large β_X (>0.8) values for the Me and Et compounds. The reactions between substituted arylsulfonyl chloride ($YC_6H_4SO_2Cl$) and anilines ($XC_6H_4NH_2$) in MeOH at 15, 25 and 35 °C are reported by Rogne (entry 4)[117]. The β_X values range from 0.78 (Y = 4-NO_2) to 0.55 (Y = 4-MeO) with $\rho_{XY} = -0.67$, which are typical values observed for S_N2 reactions[15]. The rate of the reaction of benzenesulfonyl chloride with N-methylaniline in the aprotic solvents $CHCl_3$ and Me_2CO (entry 5)[118] is strongly accelerated by added salts due to base catalysis. The reactions of arylsulfonyl chlorides with anilines were also studied in 100–50% MeOH–MeCN solutions at 35 °C. The β_X (0.58) and ρ_{XY} (ca -0.5) values indicate an S_N2 mechanism. The β_X value increased with the increased MeCN content, showing an increased degree of N–S bond making in the TS. $Ortho$ substituents in aniline (2-Me and 2,6-Me_2) retard the rate and deviate from the Brönsted plot obtained by 3- and 4-substituted anilines (entry 7)[119]. This is attributed to a steric effect. The reactions of arylsulfonyl fluoride with anilines (entry 8)[120] are much slower than those of the corresponding reactions of arylsulfonyl chlorides in MeOH and the relatively large negative ρ_{XY} (-0.9) but relatively small β_X (0.40) is a typical value for an S_N2 process. The large negative ρ_{XY} thus does not reflect an intermediate formation, but the negative sign (and the magnitude of β_X)[15b, f, g] is a clear indication of the concerted mechanism (with most probably a tight TS). The leaving-group mobility of benzenesulfonyl halides ($PhSO_2Z$ where Z = F, Cl, Br and I) in the reactions of aniline, n-butylamine and hydroxide ion are studied in MeCN–H_2O (9:1) mixture (entries 9 and 10)[121]. Since the reactions proceed by a concerted (S_N2) mechanism, the importance of S–Z bond cleavage in the TS is dependent on the nucleophile; breaking the S–F bond is important for aniline but becomes less important for n-butylamine, and for hydroxide it is almost of no importance. It is, however, unlikely that the reactions of the chloride, bromide and iodide (Z=Cl, Br and I) proceed by a stepwise mechanism with rate-limiting leaving-group expulsion from an intermediate, since the leaving ability of these halides is greater than that of fluoride. When the nucleofugality of the leaving group is high, the intermediate becomes less stable so that the direct displacement mechanism is favored[15g, 95, 120, 122].

The reactions of furansulfonyl chlorides with anilines (entry 11)[123] in MeOH yield a linear Brönsted plot with $\beta_X = 0.51$, which indicates an S_N2 mechanism rather than a stepwise process. This value is quite similar to those found for the reactions of anilines with benzenesulfonyl chloride (0.63)[117], with 2-thiophenesulfonyl chloride (0.53)[124] and with 3-thiophenesulfonyl chloride (0.54)[125]. Thus their anilinolysis mechanism is also expected to be S_N2. The reaction rate therefore depends not only on the nucleophile basicity but also on the substrate reactivity. Comparison of the reaction rates leads to the following reactivity order for the Ar moiety; benzene > 3-thiophene > 3-furan > 2-furan $\geqslant$ 2-thiophene. This reactivity sequence follows the order of the resonance interaction between the

TABLE 9. Reactions of anilines with sulfonyl compound (YRSO$_2$-LZ): XC$_6$H$_4$NH$_2$ + YRSO$_2$ − LZ → YRSO$_2$NHC$_6$H$_4$X + H$^+$ + LZ$^-$

Entry	Reactant[a]	T (°C)	Solvent	$k_2 \times 10^3$ (M^{-1} s^{-1})	β_X	ρ_{XY}	Reference
1	MeSO$_2$–Cl	45	MeOH	13.3	0.84		116
2	EtSO$_2$–Cl	45	MeOH	7.41	0.78		116
3	i-PrSO$_2$–Cl	45	MeOH	0.486	0.50		116
4	YC$_6$H$_4$SO$_2$–Cl	25	MeOH	68.6	0.63	−0.67	117
5	PhSO$_2$–Cl	24.4 ± 0.1	CHCl$_3$, Me$_2$CO	18.3, 40.5			118
6	YC$_6$H$_4$SO$_2$–Cl	35	MeOH	106	0.58	−0.5	119
7	YC$_6$H$_4$SO$_2$–Cl	25	MeOH	16.6(2-Me), 0.959(2,6-(Me$_2$))	0.63	−0.7	119
8	YC$_6$H$_4$SO$_2$–F	45	MeOH	0.266	0.40	−0.9	120
9	PhSO$_2$–F, PhSO$_2$–Cl	25	MeCN–H$_2$O (9:1)	0.00026, 42.7			121
10	PhSO$_2$–Br, PhSO$_2$–I	25	MeCN–H$_2$O (9:1)	312, 35.5			121
11	2-FurylSO$_2$–Cl, 3-FurylSO$_2$–Cl	25	MeOH	6.07, 8.54	0.51		123
12	2-ThienylSO$_2$–Cl	25	MeOH	5.62	0.53		124
13	3-ThienylSO$_2$–Cl	25	MeOH	20.8	0.54		125
14	2-ThienylSO$_2$–F, 2-ThienylSO$_2$–Br	25	MeOH	0.00425, 30.6	~0.53		126
15	2-ThienylSO$_2$–F, 2-ThienylSO$_2$–Cl	25	H$_2$O	0.0350, 709	~0.68		127
16[b]	5-N,N-Me$_2$–NaphSO$_2$–Cl	30	MeOH, MeCN	10.7, 1.37	0.67, 0.72	—	128

[a]All the k_2 values are $k_2 \times 10^3$ M^{-1} s^{-1} except those in parentheses.
[b]5-N,N-Dimethylamino-1-naphthalenesulfonyl chloride (dansyl chloride).

aromatic ring and the sulfonyl group in the substrate. The resonance interaction in five-membered heterocyclic compounds at the 3-position is lower than at the 2-position and hence 3-substituted sulfonyl derivatives are less resonance stabilized in the initial state, leading to a greater reactivity than the corresponding 2-isomers.

Studies of leaving-group effects on the reactivity in the anilinolysis of 2-thiophenesulfonyl halides (F, Cl, Br) in MeOH have led to the observed rate sequence of Br > Cl ≫ F (entry 14)[126]. The corresponding Brönsted coefficients β_Z for the leaving-group variation are -0.31 and -0.38, respectively, with aniline and 4-methoxyaniline. These values are indeed consistent with the concerted displacement mechanism. Similar studies are conducted in water (entry 15)[127] with Y-substituted 2-thiophenesulfonyl halides (Y = 5-MeO, 5-Me, H, 5-Cl, 4-NO$_2$ and 5-NO$_2$). The β_X values increase with the increase in the electron-withdrawing power of the substituent ($\beta_X = 0.50$, 0.68 and 0.75 for Y = 5-MeO, H and 5-NO$_2$, respectively). In contrast, the magnitude of β_Z decreases ($\beta_Z = -0.36$, -0.35 and -0.18 for the corresponding substituent). These changes in the magnitude of β_X and β_Z with the substituent can be interpreted, as the sign of ρ_{XY} is negative and that of ρ_{XZ} is positive ($\rho_{XY} < 0$ and $\rho_{XZ} > 0$), which are indications of a concerted mechanism[15b, f, g, 95]. The second-order rate constants, k_2, for the 5-substituted 2-thiophenesulfonyl chlorides with aniline in MeOH–MeCN mixtures at 25 °C exhibit a maximum rate behavior; for example, for Y = 5-NO$_2$ the rate increases from pure MeOH ($k_2 = 167.1 \times 10^{-3}$ M^{-1} s^{-1}) up to 0.66 mole fraction of MeOH ($k_2 = 583.2 \times 10^{-3}$ M^{-1} s^{-1}) and then decreases down to pure MeCN ($k_2 = 14.8 \times 10^{-3}$ M^{-1} s^{-1}). This rate inversion is accompanied also by the ρ_X-value inversion which increased from $\rho_X = 1.06$ in MeOH to 1.54 in 0.66 mole fraction MeOH and then decreased to 0.88 in MeCN. Thus, the RSP is violated since the greater reactivity is accompanied by the greater selectivity. This is another criterion for the concerted process[15g]. The parallel change of k_2 with ρ_X suggests that bond formation is important in the TS for the reaction.

Nucleophilic substitution reactions of dansyl chloride with anilines (entry 16)[128] are reported in various protic solvents. Interestingly, the β_X values are in parallel with the rates, which are dependent on the dielectric constant (ε)[49] of the solvent as can be seen from the data presented for each solvent in the order [ε; k_2 ($\times 10^4$ M^{-1} s^{-1} at 30 °C for X = H); β_X], MeOH [32.66; 107; 0.67], EtOH [24.55; 37.7; 0.55], n-PrOH [20.45; 8.71; 0.50], 2-PrOH [19.92; 5.33; 0.41], n-BuOH [17.51; 3.07; 0.34], MeCN [35.94; 13.7; 0.72]. In the aprotic solvent MeCN, the rate is somewhat slow despite the largest ε and β_X values. Since the reactivity changes in parallel to the selectivity, the RSP is violated, and a stepwise mechanism through an intermediate can be excluded. Solvatochromic analysis also suggested that the reaction proceeds via an associative S$_N$2 mechanism.

All the reactions of tetracoordinated sulfonyl derivatives with anilines are shown to proceed by a concerted mechanism. This is because the energy gap between $\pi^*_{S=O}$ and σ^*_{S-LG} ($\Delta \varepsilon$) is relatively small. It has been shown[129] that if this energy gap is small, the mixing of the two LUMOs, i.e. $\pi^*_{S=O}$ and σ^*_{S-LG}, is efficient and the incipient n → $\pi^*_{S=O}$ interaction leads to n → σ^*_{S-LG} (concerted process) as a result of the mixing. In contrast, if the energy gap is large, then the mixing becomes inefficient and the incipient n → $\pi^*_{S=O}$ interaction leads to the formation of an intermediate and the reaction proceeds by a stepwise mechanism.

Finally, an example of the reactions at a dicoordinated sulfenyl sulfur is presented. The reactions of (alkoxydichloromethyl)(chlorocarbonyl)polysulfanes (11) with N-methylaniline in CHCl$_3$[130] are rationalized by a carbamoyl route where the alkoxydichloromethyl group loses an alkyl chloride as a masked acid chloride, or by a sulfenyl route which reflects fragmentation of the (alkoxydichloromethyl)polysulfanyl compound into the corresponding alkoxy(thiocarbonyl) and sulfenyl compounds 11 (Scheme 15).

$$\begin{array}{c} \text{Cl} \ \ \text{O} \\ | \ \ \ || \\ \text{ROCSSCCl} \\ | \\ \text{Cl} \\ \textbf{(11)} \end{array} \ + \ \text{PhNMe} \ \longrightarrow \ \left[\begin{array}{c} \text{Cl} \ \ \text{O} \\ | \ \ \ || \\ \text{ROCSSCN(Me)Ph} \\ | \\ \text{Cl} \end{array} \right] \\ \textbf{Int}$$

carbamoyl pathway   sulfenyl pathway

−RCl

$$\begin{array}{c} \text{O} \ \ \text{O} \\ || \ \ \ || \\ \text{Ph(Me)NCSSCN(Me)Ph} \end{array} \qquad\qquad \begin{array}{c} \text{O} \\ || \\ \text{Ph(Me)NSCN(Me)Ph} \\ + \\ \text{S} \\ || \\ \text{ROCN(Me)Ph} \end{array}$$

SCHEME 15

In the sulfenyl pathway, the excess N-methylaniline attacks a sulfenyl sulfur and leads to the fragmentation of the intermediate. A similar reaction mechanism of the competing pathway was also observed with polysulfolanes, $n = 2-4$.

B. Phosphorus and Other Heteroatoms

The reactions of aryl phenyl chlorophosphates with anilines in MeCN (equation 14) are found to proceed by a direct displacement (S_N2) at the phosphorus atom[131].

$$\begin{array}{c} \text{O} \\ || \\ \text{PhO}-\text{P}-\text{Cl} \\ | \\ \text{OC}_6\text{H}_4\text{Y} \end{array} \ + \ 2\text{XC}_6\text{H}_4\text{NH}_2 \ \xrightarrow[\text{55 °C}]{\text{MeCN}} \ \begin{array}{c} \text{O} \\ || \\ \text{PhO}-\text{P}-\text{NHC}_6\text{H}_4\text{X} \\ | \\ \text{OC}_6\text{H}_4\text{Y} \end{array} + \text{XC}_6\text{H}_4\overset{+}{\text{N}}\text{H}_3 \ + \ \text{Cl}^- \qquad (14)$$

The magnitudes of β_X and ρ_{XY} are unusually large with $\beta_X = 1.36$ and $\rho_{XY} = -1.31$, which are most probably due to an extensive bond formation of the amine with the bulky and soft, second-row element, P, in the TS. This proposal is supported by a positive ρ_Y ($= 0.54$ with $X = H$) and by the much smaller k_H/k_D values ($= 0.61-0.87$) involving deuteriated aniline nucleophiles, especially for compounds with an electron-withdrawing ligand ($Y = 4$-Cl). This is apparently a steric isotope effect due to a closer approach of the aniline toward the phosphorus atom which results in a strong hindrance to N−H(D) vibrational modes in the crowded TS. The crowded TS structure is also reflected in a large negative entropy of activation, $-\Delta S^{\neq} = 43-65$ eu. Similar reactions at the phosphorus center of 4-chlorophenyl aryl chlorophosphates with an electron-acceptor ligand, 4-ClC$_6$H$_4$OP(=O)(Cl)OC$_6$H$_4$Y, have been reported in MeCN[132]. In this case, the large β_X ($= 1.45$) and small k_H/k_D (0.64−0.87) values observed are quite similar to those for the substrate lacking a 4-Cl electron-accepting substituent[131], but the magnitude of ρ_Y (0.21) and ρ_{XY} (−0.31) is much smaller. This is attributed to the partial loss of electronic transmission from the aniline (NX in Scheme 16) through P to the Y-substrate ring in the TS due to the electron-acceptor ligand, ClC$_6$H$_4$O. This will result in a weaker intensity of interaction between the substituents X and Y in the TS leading to a smaller magnitude of ρ_{XY}, as was observed. The magnitude of ρ_Y is also reduced due to this partial loss,

or shunt, to the 4-chloro-substituted ring, which occupies an equatorial ligand site as the Y-substituted ring does in a trigonal bipyramidal pentacoordinated (TBP-5C) TS. Here again the low k_H/k_D values and the large negative entropy of activation ($\Delta S^{\neq} = -60$ to -68 eu) reflect the sterically crowded structure of the TS.

SCHEME 16

Kinetic studies of the oxidation reaction of anilines by peroxomonophosphoric acid [$(HO)_2P(=O)OOH$; PMPA] have shown that the reaction takes place by a nucleophilic attack of the aniline lone pair on the electrophilic peroxo oxygen atom[133]. The second-order kinetics, first-order each in the aniline and PMPA, the large negative ρ_X (-1.3 to -1.8), an orderly TS suggested by the low $\Delta H^{\neq}$ (9.4 kcal mol^{-1}) and large negative $\Delta S^{\neq}$ (-32 eu), and the insensitivity of the rates to added acrylamide, Cu^{2+} or Fe^{2+} (which rule out a mechanism involving homolytic scission of the peroxide bond), all constitute strong evidence for a polar TS, **12**. The excellent Brönsted correlation with a slope of $\beta_X = 0.58$ suggests a considerable bond formation in the TS and that the reaction is finally controlled by the nitrogen basicity or nucleophilicity.

(12)
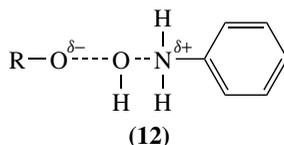
Another example of nucleophilic attack of anilines at an oxygen atom has been reported by Buxton and coworkers[134]. The oxidation of 4-substituted N,N-dimethylanilines by dimethyldioxirane, **13**, in acetone showed a similar qualitative trend as those for the reactions at the MeI and benzoyl peroxide reactions with a reactivity decrease in the order X = MeO > H > Cl $\gg$ NO$_2$. These trends suggest that the oxidation of DMAs by **13** is electrophilic. The ρ_X value of -0.89 shows similarity to the values in the reactions of DMAs with MeI (Menschutkin reaction) which has a ρ_X value of -3.30 at $35\,^{\circ}$C in 90% aqueous acetone. While in the latter reactions the TS is thought to have developed almost a full positive charge, the reactions with **13** have much less charge development partially due to steric crowding in the TS (Scheme 17).
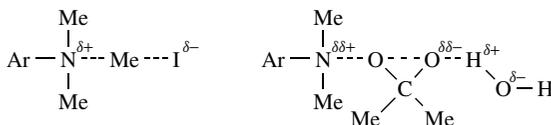
SCHEME 17

Hydrogen bonding is also important. All the data obtained are consistent with a nucleophilic attack by DMA on the oxygen atom (Scheme 17) and do not involve the bis(oxyl)diradical or electron transfer.

The reactions of carcinogens derived from N-arylhydroxylamines with aniline or DMA in MeOH yield diphenylamines or hydrazines by direct nucleophilic attack of the aniline on the nitrogen atom of the model carcinogen[135]. The reactions of N-(sulfonatooxy)-2-(acetylamino)fluorene (**14**) with aniline are quite similar to those of N-(sulfonatooxy)-4-(acetylamino)biphenyl (**15**)[135]. An initial rate-limiting N−O bond cleavage generates the tight ion pair, which in turn generates the free ion by diffusional separation. The latter is then attacked by aniline (or DMA) to yield various N-substituted and C-substituted products (Scheme 18).

(14) **(15)**
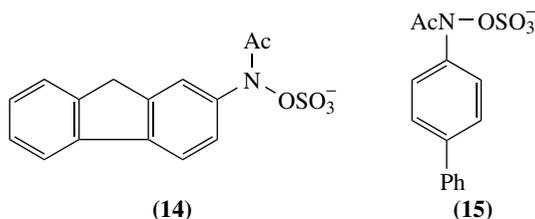
In stoichiometric and catalytic reactions of transition-metal organometallic complexes, ligand substitution reactions are usually an essential first step and sometimes the rate-determining step. The nucleophilic reactions of anilines with transition-metal organometallic complexes can occur by nucleophilic attack at the metal center itself, or at a metal-coordinated organic ligand. Unsaturated ligands such as carbon monoxide, isonitriles, olefins, dienes and arenes are electron-rich species so that they are not normally reactive toward nucleophiles. However, when they are coordinated to electron-deficient transition-metal complexes, they become activated toward nucleophilic attack, completely reversing their normal reactivity. Direct nucleophilic attack at unsaturated ligands is facilitated by strong nucleophilicity, coordination saturation of the metal and a formal positive charge on the metal. The π-acceptor spectator ligands can also facilitate the nucleophilic reaction by accommodating the charge increase experienced at the metal center. Some examples of the nucleophilic reactions of anilines at the transition-metal organometallic complexes are presented below.

The reactions of anilines with 1,5-dialcohols catalyzed by ruthenium catalyst, $RuCl_2$ $(Ph_3)_3$, are important[136] since N-substituted saturated heterocyclic products like piperidines, piperazines or morpholines can be obtained in one step with water as the only side product (equation 15).
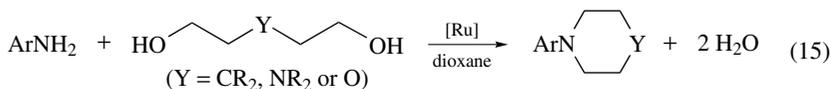
In this reaction, aniline condensation (via initial addition) occurs with a carbonyl group of the aldehyde formed in the ligand by dehydrogenation of alcohol. The imine intermediate formed is then hydrogenated, releasing the monoalkylated secondary amine product.

Anilines with relatively low pK_a values, such as diphenylamine and nitroanilines, are alkylated in the presence of palladium catalyst (Pd(0)) using alkyl carbonates as the alkylating reagents[137]. An example is given in equation 16.

AcN−OSO$_3^-$ AcN·SO$_4^-$

(15)

+ PhNH$_2$ →
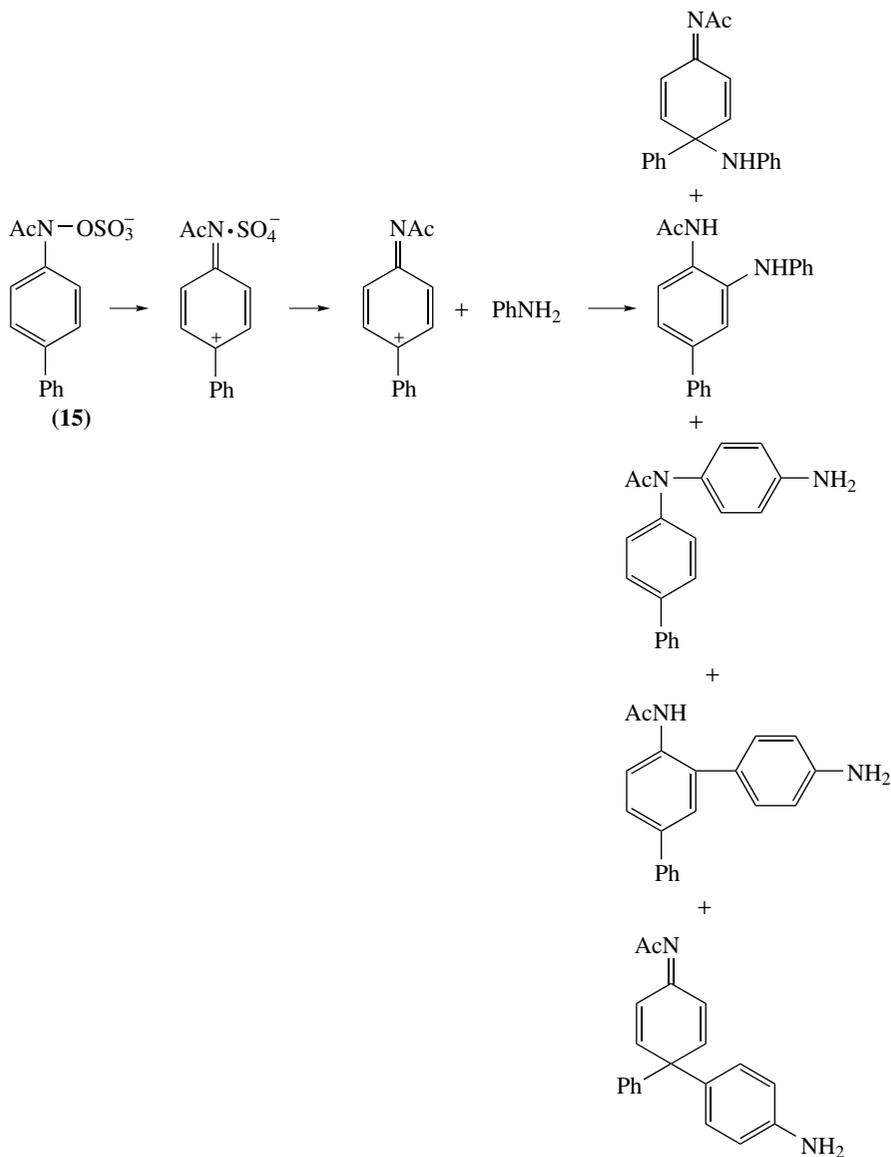
SCHEME 18

The direct nucleophilic attack of anilines occurs at both termini of the allylic system of the cationic η^3-allylpalladium(II) complex **16** generated by oxidative addition of allylic compounds to a Pd(0) complex.

The palladium-catalyzed allylation of anilines can also occur with the allylic alcohol 2-buten-1-ol in benzene[138] (equation 17).

$$NH_2 \quad + \quad 4 \quad Ph \diagdown\diagdown OCO_2Et \quad \xrightarrow[\substack{THF/\ room\ temp.\\ (L = PPh_3)}]{PdL_4}$$

$$N(CH_2CH{=}CHPh)_2 \qquad PhCH{=}CHCH_2 \diagdown NH$$

$$+ \qquad\qquad\qquad (16)$$

$$\underset{NO_2}{} \qquad\qquad \underset{NO_2}{}$$

$$\begin{array}{c} Ph \\ \diagup\diagdown \\ L{-}\overset{+}{Pd}{-}L \\ \mathbf{(16)} \end{array}$$

$$R{-}\!\!\diagdown\!\!\diagup \quad + \quad HO\diagdown\diagdown \quad \xrightarrow[\substack{Ti(OPr\text{-}i)_4\\ A4\ MS}]{Pd(OAc)_2\ /\ PPh_3} \quad \underset{HN}{\overset{R}{}} \quad + \quad \underset{HN}{\overset{R}{}} \quad (17)$$

$$\underset{NH_2}{}$$

R = H, 4-Me, 4-Cl, 4-CO₂, Et
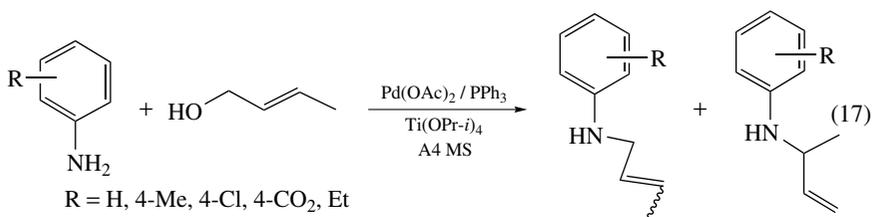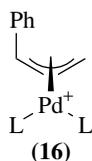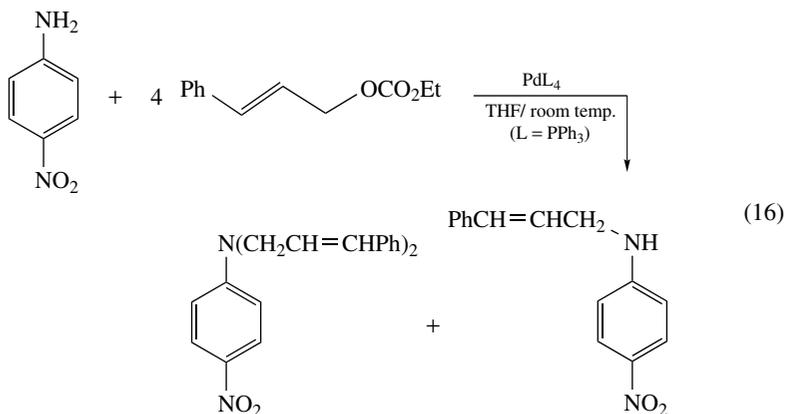
Alcohols react with Pd(0) species to afford a π-allylpalladium intermediate of the type **16** with one L = OH or OTi(OPr-i)$_3$, which reacts subsequently with aniline (ligand exchange leading to **16** with one L = NHAr).

The synthesis of 2,3-disubstituted indoles **17** by the palladium-catalyzed coupling of 2-iodoanilines or its N-methyl, -acetyl and -tosyl derivatives with a wide variety of internal alkynes[139] (equation 18) was reported.

$$\underset{I}{\overset{NH_2}{}} \quad + \quad 3\ R{-}C{\equiv}C{-}R' \quad \xrightarrow[\substack{LiCl,\ AcOK\\ DMF}]{Pd(OAc)_2\ /\ PPh_3} \quad \underset{R'}{\overset{\underset{N}{\overset{H}{}}}{\diagup\diagdown}}{-}R$$

$$\qquad\qquad\qquad\qquad\qquad\qquad (18)$$

(17)

(R, R′ = allyl)
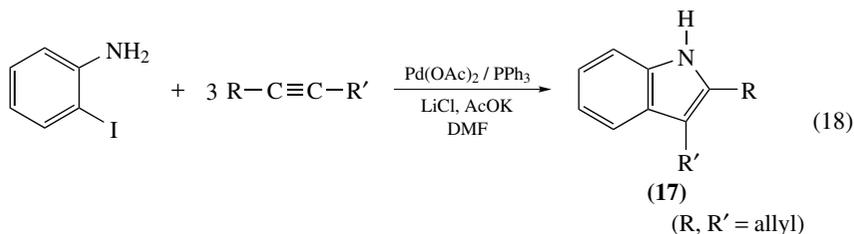
In this reaction, Pd(OAc)$_2$ is first reduced to Pd(0) and then chloride ion is coordinated to form a chloride-ligated Pd(0) species. Oxidative addition of the 2-iodoaniline occurs to Pd(0), which becomes coordinated by the alkyne, leading to the arylpalladium intermediate

(18)   **(19)**
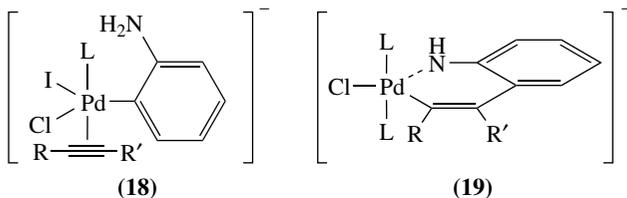
18. The latter undergoes nitrogen displacement of the halide resulting in the vinylic Pd intermediate **19**, to form a six-membered heteroatom-containing palladacycle, which proceeds to form the indole and Pd(0) by reductive elimination.

V. ANILINES AS C-NUCLEOPHILES

The basic center of anilines is normally the nitrogen atom in solution, as it has been well established that the nitrogen-protonated form is much better stabilized by solvation than those protonated on the ring[140]. Anilines are therefore normally N-nucleophiles in solution. However, in principle aniline presents four basic centers, nitrogen and the three (*ortho* and *para*) ring carbons. The resonance interaction of the amino group with the ring enhances the basicity of the *ortho-* and *para*-carbon atoms and the possibility of ring protonation arises. Lately, the question concerning the preferred protonation site of aniline in the gas phase has been a topic of much interest. According to high level *ab initio* calculations (MP4/6-3111++G**//MP2/6-311++G**), the *para* ring carbon is slightly a more favored protonation site than the nitrogen atom[141]. This indicates that the *ortho* and *para* ring carbons of aniline can provide electrophilic centers.

Pollack and coworkers[142] applied experimental pulsed ion cyclotron resonance spectroscopy for identification of the preferred site of protonation in aniline. They found that in the gas phase, aniline is a nitrogen base and protonation on the aromatic ring is $1-3$ kcal mol^{-1} less favorable than the N-protonation. The small magnitude of this difference indicates that both substituent and solvent effects should be capable of bringing about observable shifts in the order of nitrogen and carbon basicities of anilines in solution. They[143] interpreted the deviations of 3-Me and 3-MeO substituted anilines from otherwise linear correlations with the corresponding aqueous-phase quantities in terms of protonation on the aromatic ring rather than at nitrogen as in other substituted anilines.

The simplest type of reaction in which anilines react as C-nucleophiles is the ring hydrogen displacement by H_3O^+ in aqueous acid solution. Acid-catalyzed hydrogen exchange reactions of *N,N*-dialkylanilines (DAAs) with radioactive tritium (T) in aqueous solution were reported by Kendall and coworkers[144]. In all experiments, excess mineral acid (H_2SO_4) is used so that a dynamic equilibrium exists in solution between the conjugate acid ion and basic DAA molecules. It is the latter which undergo the exchange reaction as represented in Scheme 19 for the *para*-hydrogen exchange.

Similar schemes can be presented for the *ortho*-hydrogen exchange. In these circumstances the experimental kinetic data represent both steps of the overall reaction, i.e. deprotonation and exchange, so that the activation free energy, $\Delta G^{\neq}$, includes the free energies of dissociation ($\Delta G_{BH^+}{}^{\neq}$) and for exchange ($\Delta G_B{}^{\neq}$). The experimentally determined number of exchangeable hydrogen atoms in the DAA molecules corresponds well with the predicted number of exchangeable hydrogens in the molecule. For example, DAAs with R=Me, Et, *n*-Pr and *n*-Bu gave 2.7, 3.1, 2.7 and 2.8 hydrogens as the exchanged number of hydrogens corresponding to the predicted 3 (2 *ortho* and 1 *para*) hydrogens. Likewise for 4-Me, 3-Me, 4-Cl and 3-NO$_2$ *N,N*-dimethylanilines (DMAs), 1.7, 2.7, 1.7 and 3 hydrogens were exchanged whereas the predicted numbers are 2, 3,
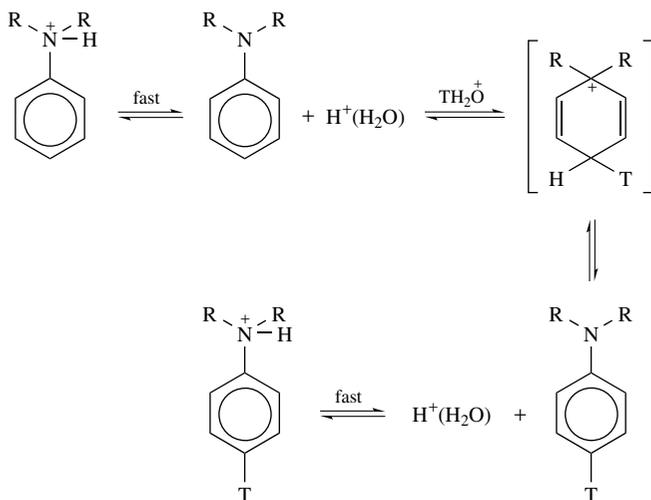
SCHEME 19

2 and 3, respectively. Subtracting the $\Delta G_{BH^+}{}^{\neq}$ part from $\Delta G^{\neq}$, the exchanges within substituted DMAs ($XC_6H_4NMe_2$) have led to a good straight-line Hammett plot for $\log k$ (i.e. $\Delta G_B{}^{\neq}$) vs $\sigma_X{}^+$ with $\rho_X = -3.54$. The relatively large negative Hammett reaction constant reflects a substantial positive charge development in the aniline ring in the TS, supporting an exchange mechanism through a cationic intermediate (Scheme 19). The dependence of rate constant on the acidity and solvent composition in EtOH–H$_2$O mixtures is in line with the proposed AS$_E$2 mechanism, in which exchange occurs on the basic form of the aniline molecule[145].

In general, the reaction of aromatic amines with sources of a positive halogen (chlorine) proceeds to give mixtures of ring-halogenated products (equation 19).

$$C_6H_5NRH + Cl^+ \longrightarrow 2\text{-}ClC_6H_4NRH + 4\text{-}ClC_6H_4NRH + H^+ \qquad (19)$$

For aniline derivatives, the *ortho–para* product ratio is normally 2 and the *N*-chloroaniline intermediate C_6H_5NHCl is generally not isolated or observed. *N*-Chloroanilines undergo acid-catalyzed rearrangement in nonpolar solvents to yield a mixture of 2-Cl, 4-Cl and 2,4-Cl$_2$ anilines. Based on the high *ortho–para* ratio, an intramolecular rearrangement of *N*-chloroanilines was proposed[146]. However, Paul and Haberfield[147] were unable to find conclusive evidence for an *intra*molecular mechanism for the acid-catalyzed rearrangement of *N*-chloroanilines, and the results can be equally interpreted to support an *inter*molecular transfer of chlorine to the *ortho* and *para* ring positions of anilines.

The retro-Menschutkin reaction of *N*-benzyl-*N*,*N*-dimethylanilinium iodide, **20**, produces *N*,*N*-dimethyl 2-, 4- and 2,4-benzylated products[148], which clearly shows the C-nucleophilic reactivity of the DMA.

(20)
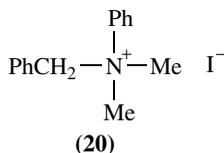
Isolable Meisenheimer complexes between aniline derivatives and an electron-deficient aromatic, DNBF (4,6-dinitrobenzofurazan 1-oxide), were observed (Scheme 14) and reported by three research groups: Read and coworkers[149] in Australia, Buncel's group[150] in Canada and Crampton's group[114] in the U.K. *N*-Methylaniline and *N*,*N*-dimethylaniline react through their *para* positions with the 7-position of the DNBF[149] to give **21**. When the *para* position is blocked by a methyl group, i.e. in 4-methylaniline, the reaction rate with DNBF in $(CD_3)_2SO$ is considerably reduced and the initial π-complex transforms into the *ortho*-substituted complex, **22**. However, the isolation of **22** by reaction in MeOH has been unsuccessful. The initial formation of the π-complex and its slow conversion into the σ-complex during the electrophilic substitutions are consistent with the small deactivating effect of a chloro substituent on the aniline (Scheme 20).

(a) R = R′ = H
(b) R = H, R′ = Me
(c) R = R′ = Me
(21)

(22)
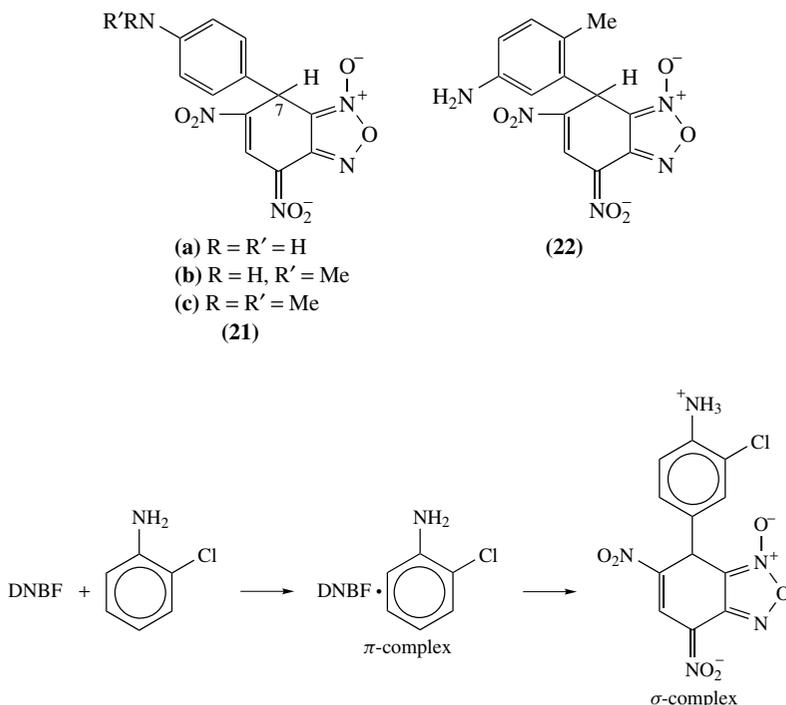
SCHEME 20

Dipolar aprotic solvents such as DMSO stabilize charge intermediates (e.g. σ-complex) much better than hydroxylated solvents, which explains the noticeably faster conversion of the π-complex into the σ-complex in DMSO than in MeOH.

The following observations are reported for product discrimination[150]. (i) The addition of aniline to 1 equivalent of DNBF in $(CD_3)_2SO$ and MeOH results in the rapid formation of the zwitterionic carbon-bonded adduct, **23**. (ii) The addition of 2 equivalents of aniline to a $(CD_3)_2SO$ solution of DNBF results in the formation of both the carbon- and nitrogen-bonded adducts, **24**. (iii) The addition of DNBF to equivalent amounts of aniline and Et_3N in $(CD_3)_2SO$ results in the formation of a greater proportion (*ca* 90%) of **24** and requires a considerably longer time for conversion to **21**.

(23)   **(24)**
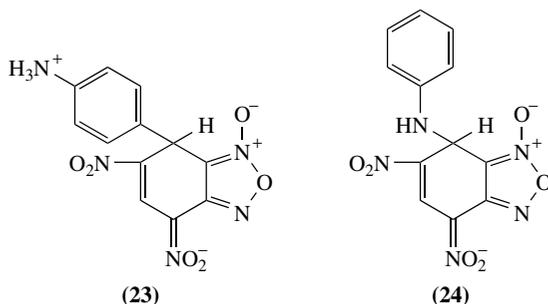
Carbon-bonded adducts are also obtained by the reaction of DNBF in DMSO with
N,*N*-dimethylaniline, 4-methylaniline, 3,5-dimethylaniline and 2,6-dimethylaniline. Several of the carbon-bonded arylamine complexes are isolated as the zwitterions or the potassium salts. Addition of DNBF to **21** in DMSO in the presence of 2 equivalents of Et₃N gave the complex in which aniline is attached to two DNBF moieties via the carbon and nitrogen atoms. The nitrogen-bonded adduct (**24**) is formed in a rapid equilibrium (kinetically favored), whereas formation of the carbon-bonded adducts **21** and **22** is slower but irreversible (thermodynamically favored).

Another highly electrophilic heteroaromatic substrate reported to react with aniline is 4,6-dinitro-2-(2′,4′,6′-trinitrophenyl)benzotriazole 1-oxide[149] (PiDNBT, **25**). In the reactions of **25**, attack by phenoxide and aniline occurs exclusively through oxygen and nitrogen, respectively, in contrast to the case of carbon-bonded adduct formation with DNBF. This failure of formation of carbon-bonded adducts to **25** results from a higher energy barrier for carbon attack than for oxygen or nitrogen attack, due partly to the disruption of aromaticity in the phenoxide and aniline moieties. In addition, attack by more electronegative nucleophilic centers is more favorable in DMSO. When the barrier to oxygen or nitrogen attack at C-1′ of **25** is raised by using 2,6-dimethylaniline and *N*,*N*-dimethylaniline which lead to the transition states with highly sterically hindered structure, very stable C-7 carbon-bonded adducts, **26** and **27**, can be obtained.

(25)

(26)   **(27)**
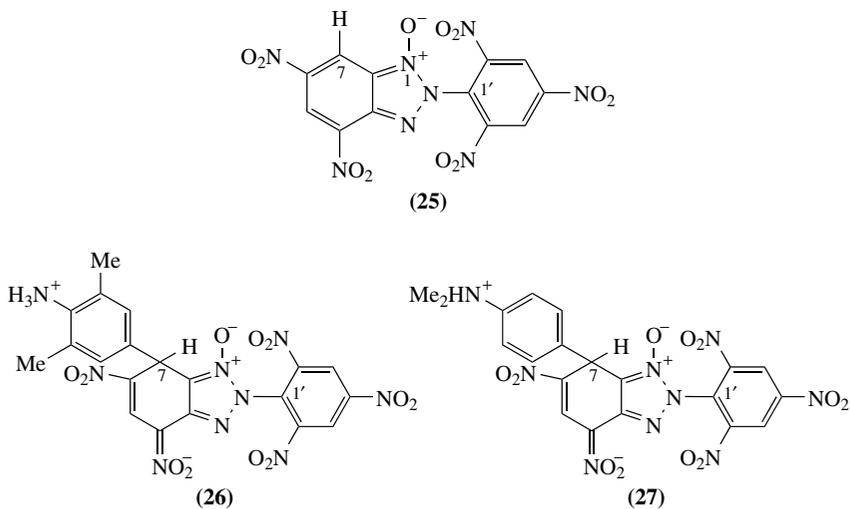
Kinetic studies on the reactions of DNBF with substituted anilines[114] have led to $\beta_X \cong$ 0.98 for the nitrogen-bonded adduct formation, but to a large negative value, $\beta_X = -2.7$, for the carbon-bonded adduct formation. This suggests that in the former process the initial attack of the C7-carbon by the aniline nitrogen atom is the rate-determining step, whereas in the latter process the elimination of a proton, K_{dep}, from the zwitterionic intermediate, which was formed by carbon–carbon bonding, is important in the rate-limiting step. The large negative β_X value for this latter process reflects an appreciable negative charge development on the nitrogen during the rate-limiting deprotonation. For ring-substituted anilines, the value of k_a for the initial C–C bond formation step increases when the solvent is changed from DMSO–water to DMSO. However, for the *N*-methyl derivatives there is little variation in k_a, while with the *N,N*-dimethyl derivatives the value of k_a decreases on transfer to DMSO. This indicates that the rate constant k_a of the initial C–C bond formation is also important in determining the overall rate. Thus, the rate constant for the C-adduct formation, k_C, both the initial attack to form the zwitterionic intermediate, k_a, and the subsequent deprotonation step of the intermediate, K_{dep}, are controlling the rate, i.e. $k_C = k_a K_{dep}$.

Various aminomandelic acid derivatives, **28**, are prepared through highly enantioselective Friedel–Crafts reactions of *N,N*-dimethylanilines with ethyl glyoxylate catalyzed by chiral titanium(IV) complexes[151] (Scheme 21).
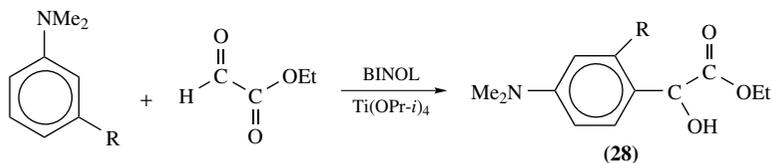
SCHEME 21

In this reaction, 2,2′-dihydroxy binaphthyl derivatives (BINOLs) are used together with Ti(OP-*i*)$_4$ complex. The highly polarized C=O of the formyl group having a δ^+ at the carbon atom is attacked by the most electron-abundant *para* position of *N,N*-dimethylanilines from a less sterically hindered direction (re) to give the product with an (R)-configuration **29**.
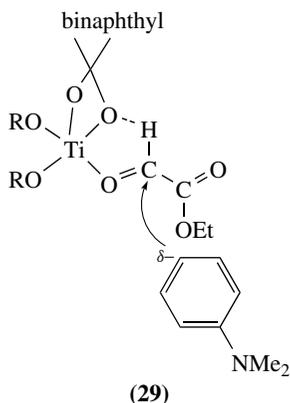
VI. KINETIC ISOTOPE EFFECTS INVOLVING DEUTERIATED ANILINES

The secondary α-deuterium kinetic isotope effects (KIEs) involving deuteriated aniline (or other amine) nucleophiles provide a useful means to determine the TS structures in nucleophilic substitution reactions[15e]. The secondary α-deuterium KIE is related to the space available for the out-of-plane bending vibrations in the TS[152], and is determined by the looseness, i.e. the distance between the nucleophile and leaving group ($d_{XY}^{\neq} + d_{YZ}^{\neq}$) of the S_N2 TS (A in Scheme 22). When a deuteriated aniline nucleophile ($XC_6H_4ND_2$) is used, however, the secondary KIE, k_H/k_D, reflects primarily the extent of bond formation, $d_{XY}^{\neq}$, in the TS (B in Scheme 22). The closer the aniline nucleophile approaches the reaction center (C_Y), the smaller the k_H/k_D value becomes due to the increase in the N−H(D) vibrational frequencies as a result of the crowded space around the amino group in aniline.
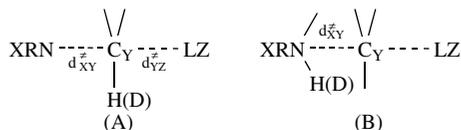
SCHEME 22

The observed k_H/k_D values with deuteriated aniline nucleophiles indeed reflect the variation of the TS structure as predicted by the sign and magnitude of the cross-interaction constant, ρ_{XZ}[15]. A positive ρ_{XZ} ($= \partial\rho_Z/\partial\sigma_X = \partial\rho_X/\partial\sigma_Z > 0$) leads to an earlier TS with a smaller degree of bond cleavage ($\partial\rho_Z < 0$) and bond making ($\partial|\rho_X| < 0 \rightarrow \partial\rho_X > 0$) by a stronger nucleophile ($\partial\sigma_X < 0$) and a stronger nucleofuge ($\partial\sigma_Z > 0$), respectively. This is a consequence of the thermodynamic control of reactivity and selectivity[15g]. In quite contrast, a negative ρ_{XZ} leads to a later TS ($\partial\rho_Z > 0$ and $\partial\rho_X < 0$) with a stronger nucleophile and a stronger nucleofuge, respectively. In this case the reactivity and selectivity are determined intrinsically[15g]. The two reaction series involving the sign reversal in ρ_{XZ} are shown in Table 10. As predicted, the stronger nucleophile (X = 4-MeO) and leaving group (Z = 4-NO_2) lead to the largest k_H/k_D (loosest TS) for the reaction with the positive ρ_{XZ}, and the smallest value (tightest TS) for the reaction with the negative ρ_{XZ}, and vice versa[153].

Furthermore, the magnitude of k_H/k_D is shown to reflect the tightness or distance $d_{XY}^{\neq}$ in Scheme 22. The k_H/k_D values measured in MeCN with deuteriated anilines are presented in Table 3 for secondary alkyl arenesulfonates[52]. For these reactions, the size

TABLE 10. Kinetic isotope effects with deuteriated aniline nucleophiles

Substituents		k_H/k_D	
X	Z	$\rho_{XZ} > 0$[a]	$\rho_{XZ} < 0$[b]
4-MeO	4-NO_2	0.869	0.898
4-MeO	4-Me	0.862	0.955
3-NO_2	4-NO_2	0.858	0.951
3-NO_2	4-Me	0.851	0.973

[a] $XC_6H_4NH_2(D_2) + EtOSO_2C_6H_4Z \rightarrow \rho_{XZ} = +0.33.$
[b] $XC_6H_4NH_2(D_2) + PhCH_2OSO_2C_6H_4Z \rightarrow \rho_{XZ} = -0.12.$

of ρ_{XZ} is practically constant with $\rho_{XZ} = 0.12$ so that the overall TS tightness should be approximately the same. However, the distances of nucleophile approach to the reaction center in the TS, $d^{\neq}_{XY}$, are clearly different due to the different crowdedness around the secondary carbon reaction center, as shown by Taft's steric constants, ΣE_s. We note that as the alkyl group becomes bulkier, the steric constant increases, and the k_H/k_D value decreases, reflecting that the N−H(D) vibrational frequencies increase as the N−H(D) moiety becomes sterically more crowded.

Unusually small k_H/k_D values are observed in the direct displacement reactions of anilines at a phosphorus center[131] (equation 20).

$$(ArO)(PhO)POCl + XC_6H_4NH_2 \longrightarrow (ArO)(PhO)PONHC_6H_4X + HCl \qquad (20)$$
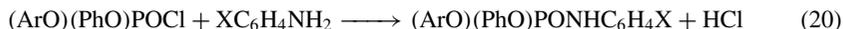
The β_X values are very large (1.24−1.68) and the ρ_{XY} value is large negative (−1.31). The large magnitudes are a clear indication that the bond formation has progressed to a large degree and a tight TS is formed. This prediction is borne out by the unusually small k_H/k_D values (0.61−0.87) observed.

In the reactions of phenyl dithiobenzoates with anilines in MeCN at 55.0 °C[92], the large magnitude of β_X (0.80−1.07) and the signs of the cross-interaction constants, $\rho_{XY} > 0$, $\rho_{YZ} < 0$ and $\rho_{XZ} > 0$, are all consistent with a carbonyl transfer mechanism in which the breakdown of the tetrahedral intermediate, $T^{\pm}$, is rate-limiting. The overall rate constant k_N is given by equation 8 [$k_N = (k_a/k_{-a})k_b$]. Since the equilibrium step, K, should result in an almost negligible KIE due to cancellation of the k_a and k_{-a} terms, the observed k_H/k_D reflects the leaving-group expulsion rate constant k_b from the intermediate. In this step, very little N−H(D) vibrational frequency change is expected since the N−H(D) moiety is slightly relieved as a result of the leaving-group expulsion from $T^{\pm}$. This expectation is indeed realized in the very close k_H/k_D ratio to unity, i.e. $k_H/k_D \cong 1.01$. Unless there is another change involving the N−H(D) bond in the TS, the magnitude of k_H/k_D for the carbonyl transfer reactions with rate-limiting breakdown of the intermediate is similar to the value observed in this reaction.

When, however, hydrogen bonding by the amino hydrogens with the oxygen atom in the leaving group is involved, the k_H/k_D values become very large due to the partial N−H(D) bond cleavage in the TS. Such cases are encountered in the direct displacement by aniline at the α-phenylethyl carbon center[154] (Scheme 2), for which the k_H/k_D values are large (1.70−2.58). A similar example is provided by the anilinolysis of phenyl dithioacetates in MeCN at 50.0 °C[90] when the k_H/k_D values of 1.05−1.36 reflect a weak hydrogen bonding of the amino hydrogen to the leaving-group sulfur atom in the TS for the rate-limiting step in stepwise mechanism.

In the S_N2 reactions the sign of ρ_{XY} is always negative, but the sign of ρ_Y can be either negative or positive. In the former case, bond cleavage is ahead of bond formation in a rather loose TS (dissociative S_N2), while in latter case bond formation has progressed to a greater degree than bond cleavage in a tight TS (associative S_N2). Typical reactions belonging to these two classes of reactions are the reactions of anilines with benzyl halides (Z) (equation 21) and with benzoyl (and benzenesulfonyl) halides (Z) (equation 22).

$$YC_6H_4CH_2Z + XC_6H_4NH_2(D_2) \longrightarrow YC_6H_4CH_2NH(D)C_6H_4X + H^+Z^- \qquad (21)$$

$$YC_6H_4COZ + XC_6H_4NH_2(D_2) \longrightarrow YC_6H_4CONH(D)C_6N_4X + H^+Z^- \qquad (22)$$
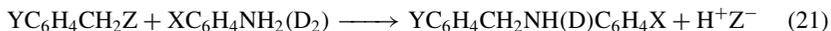
The trends of changes in ρ_X with the variation of the substituent (Y) in the substrate are the same, $\delta\rho_X < 0$ with $\delta\sigma_Y > 0$, since ρ_{XY} is negative (<0) in both cases. However, the changes in k_H/k_D are found to be opposite[155, 156]. For the dissociative S_N2 ($\rho_Y < 0$), the k_H/k_D (<1.0) values decrease, $\delta(k_H/k_D) < 0$, with a more negative ρ_X for a

stronger electron-attracting group in the substrate ($\delta\sigma_Y > 0$), while it is opposite for the associative S_N2 reactions, i.e. $\delta\sigma_Y > 0 \rightarrow \delta\rho_X < 0 \rightarrow \delta(k_H/k_D) > 0$. In the associative S_N2 reactions, a more negative ρ_X does not necessarily reflect the greater degree of bond formation (for which k_H/k_D should decrease) but indicates a smaller extent of bond formation. This is opposite to the normally accepted concept of a greater bond formation for a more negative ρ_X, which applies to the dissociative S_N2 series.

In the initial nucleophilic attack by aniline on the $\pi^*_{C=O}$ orbital in an associative S_N2 reaction, a tetrahedral TS **30** is formed, where an acceptor substituent Y depresses the $\sigma^*_{C-N^+}$ orbital with a consequent stronger charge transfer from a developing lone pair (oriented antiperiplanar to the $C-N^+$ bond) on the carbonyl oxygen atom in the TS[15g, 129]. As a result of this charge transfer into the $\sigma^*_{C-N^+}$ antibonding orbital, the $C-N^+$ bond somewhat stretches[15g, 129], which lead to a lower degree of bond formation despite the larger degree of charge transfer (a more negative ρ_X) for a stronger acceptor Y ($\delta\sigma_Y > 0$). However, we cannot interpret a larger negative ρ_X value as indicating a larger degree of bond formation in the associative S_N2 reactions ($\rho_Y > 0$). Such a detailed TS structure analysis was possible by using the KIEs with deuteriated aniline nucleophiles.

$$
\begin{array}{c}
O^{\delta-} \\
\| \\
XC_6H_4NH_2 \overset{\delta+}{---} C --- Z^{\delta-} \\
| \\
C_6H_4Y
\end{array}
$$

(30)
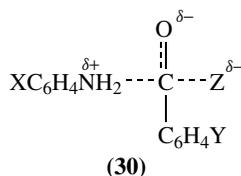
A number of other examples of useful applications of KIEs involving deuteriated aniline nucleophiles are reported[15e-g]. Elucidation of the TS structures is facilitated by means of nucleophile KIEs in conjunction with the sign and magnitude of the cross-interaction constants.

VII. ACKNOWLEDGMENTS

VIII. REFERENCES

1. W. C. Davies and W. P. G. Lewis, *J. Chem. Soc.*, 1599 (1934).
2. W. C. Davies and R. G. Cox, *J. Chem. Soc.*, 614 (1937).
3. K. J. Laidler, *J. Chem. Soc.*, 1786 (1938).
4. W. C. Davies, *J. Chem. Soc.*, 1865 (1938).
5. R. A. Benkeser, C. E. DeBoer, R. G. Robinson and D. M. Sauve, *J. Am. Chem. Soc.*, **78**, 682 (1956).
6. A. D. Harris and K. E. Weale, *J. Chem. Soc.*, 146 (1961).
7. H. H. Jaffe, *Chem. Rev.*, **53**, 191 (1953).
8. K. C. Gross and P. G. Seybold, *J. Org. Chem.*, **66**, 6919 (2001).
9. D. D. Perrin, *Dissociation Constants of Organic Bases in Aqueous Solution*, Butterworths, London, 1965.
10. A. Fischer, W. J. Galloway and J. Vaughan, *J. Chem. Soc.*, 3591 (1964).
11. E. A. Castro, C. A. Araneda and J. G. Santos, *J. Org. Chem.*, **62**, 126 (1997).
12. L. F. Blackwell, A. Fischer, I. J. Miller, R. D. Thompson and J. Vaughan, *J. Chem. Soc.*, 3588 (1964).

13. For example:
   (a) C. F. Bernasconi, *Tetrahedron*, **45**, 4017 (1989).
   (b) H. K. Oh, J. H. Yang, H. W. Lee and I. Lee, *J. Org. Chem.*, **65**, 5391 (2000).
14. For example:
   (a) M. T. Skoog and W. P. Jencks, *J. Am. Chem. Soc.*, **106**, 7595 (1984).
   (b) D. J. Palling and W. P. Jencks, *J. Am. Chem. Soc.*, **106**, 4869 (1984).
   (c) E. A. Castro and F. J. Gil, *J. Am. Chem. Soc.*, **99**, 7611 (1977).
   (d) E. A. Castro and C. Ureta, *J. Org. Chem.*, **54**, 2153 (1989).
   (e) E. A. Castro, L. Leandro, N. Quesieh and J. G. Santos, *J. Org. Chem.*, **66**, 6130 (2001).
   (f) A. K. Guha, H. W. Lee and I. Lee, *J. Org. Chem.*, **65**, 12 (2000).
15. (a) I. Lee, *Chem. Soc. Rev.*, **19**, 317 (1990).
   (b) I. Lee, *Adv. Phys. Org. Chem.*, **27**, 57 (1992).
   (c) I. Lee, *J. Phys. Org. Chem.*, **9**, 661 (1996).
   (d) I. Lee, in *Organic Reactivity. Physical and Biological Aspects* (Eds. B. T. Golding, R. J. Griffin and H. Maskill), Royal Society of Chemistry, London, 1995, p. 361.
   (e) I. Lee, *Chem. Soc. Rev.*, **24**, 223 (1995).
   (f) I. Lee and H. W. Lee, *Collect. Czech. Chem. Commun.*, **64**, 1529 (1999).
   (g) I. Lee and D. D. Sung, *Curr. Org. Chem.*, **8**, 557 (2004).
   (h) N. S. Isaacs, *Physical Organic Chemistry*, 2nd edn., Chap. 4, Longman, Harlow, 1995.
16. (a) J. F. Coetzee, *Prog. Phys. Org. Chem.*, **4**, 54 (1967).
   (b) C. D. Ritchie, in *Solute−Solvent Interactions* (Eds. J. F. Coetzee and C. D. Ritchie), Chap. 4, Marcel Dekker, New York, 1969.
   (c) R. P. T. Tomkins and O. Popovych, *Nonaqueous Solution Chemistry*, Chap. 3, Wiley, New York, 1981.
   (d) W. J. Spillane, G. Hogan, P. McGrath, J. King and C. Brack, *J. Chem. Soc., Perkin Trans. 2*, 2099 (1996).
   (e) N. Foroughifar, K. T. Leffek and Y. G. Lee, *Can. J. Chem.*, **70**, 2856 (1992).
   (f) I. Lee, C. K. Kim, I. S. Han, H. W. Lee, W. K. Kim and Y. B. Kim, *J. Phys. Chem. B*, **103**, 7302 (1999).
17. (a) P. D. Bolton and F. M. Hall, *Aust. J. Chem.*, **20**, 1797 (1967); **21**, 939 (1968); *J. Chem. Soc. B*, 259 (1969).
   (b) J. A. Dean, *Handbook of Organic Chemistry*, Table 4, McGraw-Hill, New York, 1987.
   (c) M. Kilpatrick and C. A. Aremberg, *J. Am. Chem. Soc.*, **75**, 3812 (1953).
   (d) R. P. Bell, *The Proton in Chemistry*, Chap. IV, Methuen, London, 1959.
18. R. A. Marcus, *J. Chem. Phys.*, **24**, 966 (1956); **39**, 1736 (1963).
19. G. S. Hammond, *J. Am. Chem. Soc.*, **77**, 334 (1955).
20. M. J. S. Dewar and R. C. Dougherty, *The PMO Theory of Organic Chemistry*, Chap. 5, Plenum Press, New York, 1975.
21. E. R. Thornton, *J. Am. Chem. Soc.*, **89**, 2915 (1967).
22. (a) A. Pross, *Adv. Phys. Org. Chem.*, **14**, 69 (1977).
   (b) E. Buncel and H. Wilson, *J. Chem. Educ.*, **64**, 475 (1987).
23. I. Lee, B. C. Lee, Y. J. Oh and S. C. Sohn, *Bull. Inst. Basic Sci. Inha Univ.*, **7**, 77 (1986).
24. I. Lee, Y. H. Choi, K. W. Rhyu and C. S. Shim, *J. Chem. Soc., Perkin Trans. 2*, 1881 (1989).
25. I. Lee, K. W. Rhyu, H. W. Lee and C. S. Shim, *J. Phys. Org. Chem.*, **3**, 751 (1990).
26. D. N. Kevill and B. W. Shen, *J. Am. Chem. Soc.*, **103**, 4515 (1981).
27. H. J. Koh, H. W. Lee and I. Lee, *J. Chem. Soc., Perkin Trans. 2*, 253 (1994).
28. H. K. Oh, C. H. Shin and I. Lee, *J. Chem. Soc., Perkin Trans. 2*, 1411 (1993).
29. (a) I. Lee, C. Huh, H. J. Koh and H. W. Lee, *Bull. Korean Chem. Soc.*, **9**, 376 (1988).
   (b) I. Lee, S. C. Sohn, B. C. Lee and H. B. Song, *Bull. Korean Chem. Soc.*, **4**, 208 (1983).
30. (a) F. P. Ballistreri, E. Maccarone and A. Mamo, *J. Org. Chem.*, **41**, 3364 (1976).
   (b) P. R. Young and W. P. Jencks, *J. Am. Chem. Soc.*, **101**, 3288 (1979).
31. I. Lee, S. C. Sohn, H. B. Song and B. C. Lee, *J. Korean Chem. Soc.*, **28**, 155 (1984).
32. F. P. Ballistreri, E. Maccarone, G. Musumara and G. Tomaselli, *J. Org. Chem.*, **42**, 1415 (1977).
33. H. B. Song, M. H. Choi, H. K. Kang and I. Lee, *Bull. Korean Chem. Soc.*, **13**, 216 (1992).
34. I. Lee, Y. K. Park, C. Huh and H. W. Lee, *J. Phys. Org. Chem.*, **7**, 555 (1994).
35. I. Lee, W. H. Lee, S. C. Sohn and C. S. Kim, *Tetrahedron*, **41**, 2635 (1985).
36. I. Lee, S. C. Sohn, C. H. Kang and Y. J. Oh, *J. Chem. Soc., Perkin Trans. 2*, 1631 (1986).

37. I. Lee, S. C. Sohn, Y. J. Oh and B. C. Lee, *Tetrahedron*, **42**, 4713 (1986).
38. T. Ando, H. Tanaka and H. Yamataka, *J. Am. Chem. Soc.*, **106**, 2084 (1984).
39. I. Lee, Y. H. Choi and H. W. Lee, *J. Chem. Soc., Perkin Trans. 2*, 1537 (1988).
40. H. J. Koh, I. V. Shpanko and I. Lee, *Bull. Korean Chem. Soc.*, **15**, 502 (1994).
41. H. K. Oh, S. J. Song, I. H. Cho and I. Lee, *Bull. Korean Chem. Soc.*, **17**, 254 (1996).
42. H. K. Oh, S. J. Song, C. H. Shin and I. Lee, *Bull. Korean Chem. Soc.*, **18**, 161 (1997).
43. H. K. Oh, J. H. Yun, I. H. Cho and I. Lee, *Bull. Korean Chem. Soc.*, **18**, 390 (1997).
44. H. K. Oh, H. J. Koh and I. Lee, *J. Chem. Soc., Perkin Trans. 2*, 1981 (1991).
45. H. K. Oh, C. H. Shin and I. Lee, *J. Phys. Org. Chem.*, **5**, 731 (1992).
46. H. K. Oh, E. M. Jeong and I. Lee, *Bull. Korean Chem. Soc.*, **19**, 1334 (1998).
47. H. K. Oh, J. H. Yang, H. W. Lee and I. Lee, *New J. Chem.*, **24**, 213 (2000).
48. H. K. Oh, J. H. Cho, M. J. Jin and I. Lee, *J. Phys. Org. Chem.*, **7**, 629 (1994).
49. C. Reichardt, *Solvents and Solvent Effects in Organic Chemistry*, Chap. 2, VCH, Weinheim, 1988.
50. C. Hansch, A. Leo and R. W. Taft, *Chem. Rev.*, **91**, 165 (1991).
51. H. K. Oh, Y. B. Kwon and I. Lee, *J. Phys. Org. Chem.*, **6**, 357 (1993).
52. H. K. Oh, Y. B. Kwon, D. S. Chung and I. Lee, *Bull. Korean Chem. Soc.*, **16**, 827 (1995).
53. H. K. Oh, Y. B. Kwon, I. H. Cho and I. Lee, *J. Chem. Soc., Perkin Trans. 2*, 1697 (1994).
54. I. Lee, Y. S. Lee, C. Huh, H. W. Lee and B. C. Lee, *J. Chem. Soc., Perkin Trans. 2*, 2415 (1993).
55. H. K. Oh, E. M. Joung, I. H. Cho, Y. S. Park and I. Lee, *J. Chem. Soc., Perkin Trans. 2*, 2027 (1998).
56. H. K. Oh, C. H. Shin, H. Y. Park and I. Lee, *J. Phys. Org. Chem.*, **7**, 359 (1994).
57. I. Lee, H. Y. Kim, H. K. Kang and H. W. Lee, *J. Org. Chem.*, **53**, 2678 (1988).
58. I. Lee, H. Y. Kim, H. W. Lee and I. C. Kim, *J. Phys. Org. Chem.*, **2**, 35 (1989).
59. I. Lee, W. H. Lee, H. W. Lee and T. W. Bentley, *J. Chem. Soc., Perkin Trans. 2*, 141 (1993).
60. T. H. Lowry and K. S. Richardson, *Mechanism and Theory in Organic Chemistry*, 3rd edn., Harper and Row, New York, 1987, p. 374.
61. I. Lee, W. H. Lee and H. W. Lee, *J. Org. Chem.*, **56**, 4682 (1991).
62. S. Chang, H. K. Koh, B-S. Lee and I. Lee, *J. Org. Chem.*, **60**, 7760 (1995).
63. H. J. Koh, H. W. Lee and I. Lee, *J. Chem. Soc., Perkin Trans. 2*, 125 (1994).
64. I. Lee, H. J. Koh, S. N. Hong and B-S. Lee, *Gazz. Chim. Ital.*, **125**, 347 (1995).
65. I. Lee, D. S. Chung and H. J. Jung, *Tetrahedron*, **50**, 7981 (1994).
66. H. K. Oh, Y. B. Kwon, D. S. Chung and I. Lee, *J. Phys. Org. Chem.*, **9**, 683 (1996).
67. I. Lee, C. K. Kim, D. S. Chung and B-S. Lee, *J. Org. Chem.*, **59**, 4490 (1994).
68. (a) C. F. Bernasconi, *Acc. Chem. Res.*, **20**, 301 (1987).
    (b) C. F. Bernasconi, *Adv. Phys. Org. Chem.*, **27**, 119 (1992).
69. (a) C. F. Bernasconi, R. A. Renfrow and P. R. Tia, *J. Am. Chem. Soc.*, **108**, 4541 (1986).
    (b) C. F. Bernasconi, D. J. Carre and J. P. Fox, In *Techniques and Applications of Fast Reactions in Solution* (Eds. W. J. Gettins and E. Wyn-Jones), Reidel, Dordrecht, 1979, p. 435.
70. H. K. Hall, *J. Org. Chem.*, **29**, 3539 (1964).
71. (a) Z. Rappoport, *J. Chem. Soc.*, 4498 (1963).
    (b) Z. Rappoport and A. Horowitz, *J. Chem. Soc.*, 1348 (1964).
    (c) Z. Rappoport, P. Greenzaid and A. Horowitz, *J. Chem. Soc.*, 1334 (1964).
    (d) Z. Rappoport and R. Ta-Shma, *J. Chem. Soc. (B)*, 871 (1971).
    (e) Z. Rappoport and R. Ta-Shma, *J. Chem. Soc. (B)*, 1461 (1971).
    (f) M. Beit-Yannai, X. Chen and Z. Rappoport, *J. Chem. Soc., Perkin Trans. 2*, 1534 (2001).
    (g) Z. Rappoport and A. Topol, *J. Chem. Soc., Perkin Trans. 2*, 863 (1975).
72. (a) H. K. Oh, T. S. Kim, H. W. Lee and I. Lee, *J. Chem. Soc., Perkin Trans. 2*, 282 (2002).
    (b) H. K. Oh, J. H. Yang, D. D. Sung and I. Lee, *J. Chem. Soc., Perkin Trans. 2*, 101 (2000).
73. B. Varghese, S. Kothari and K. K. Banerji, *J. Chem. Res.* (*S*), 422 (1998); (*M*), 1853 (1998).
74. D. J. Palling and W. P. Jencks, *J. Am. Chem. Soc.*, **106**, 4869 (1984).
75. I-H. Um, K-E. Choi and D-S. Kwon, *Bull. Korean Chem. Soc.*, **11**, 362 (1990).
76. E. A. Castro, F. Ibanez, A. M. Saitua and J. G. Santos, *J. Chem. Res.* (*S*), 56 (1993); (*M*), 317 (1993).
77. E. A. Castro, L. Leandro, P. Millan and J. G. Santos, *J. Org. Chem.*, **64**, 1953 (1999).
78. W. E. Hall, T. Higuchi, I. H. Pitman and K. Uekama, *J. Am. Chem. Soc.*, **94**, 8153 (1972).
79. B. C. Lee, J. H. Yoon, C. G. Lee and I. Lee, *J. Phys. Org. Chem.*, **7**, 273 (1994).

80. I. Lee, C. S. Shim, S. Y. Chung, H. Y. Kim and H. W. Lee, *J. Chem. Soc., Perkin Trans. 2*, 1919 (1988).
81. H. W. Lee, J-W. Lee H. J. Koh and I. Lee, *Bull. Korean Chem. Soc.*, **19**, 642 (1998).
82. K. H. Yew, H. J. Koh, H. W. Lee and I. Lee, *J. Chem. Soc., Perkin Trans. 2*, 2263 (1995).
83. T-H. Kim, C. Huh, B-S. Lee and I. Lee, *J. Chem. Soc., Perkin Trans. 2*, 2257 (1995).
84. Z. J. Kaminski, P. Paneth and M. H. O'Leary, *J. Org. Chem.*, **56**, 5716 (1991).
85. A. Arcoria, S. Fisichella, G. Scarlata and D. Sciotto, *J. Org. Chem.*, **38**, 32 (1973).
86. A. Arcoria, S. Fisichella, G. Scarlata and D. Sciotto, *J. Org. Chem.*, **39**, 3025 (1974).
87. E. A. Castro, M. I. Pizarro and J. G. Santos, *J. Org. Chem.*, **61**, 5982 (1996).
88. L. Melander and W. H. Saunders, Jr., *Reaction Rates of Isotopic Molecules*, Wiley, New York, 1980, p. 170.
89. B. D. Song and W. P. Jencks, *J. Am. Chem. Soc.*, **111**, 8479 (1989).
90. H. K. Oh, S. Y. Woo, C. H. Shin, Y. S. Park and I. Lee, *J. Org. Chem.*, **62**, 5780 (1997).
91. H. K. Oh, S. K. Kim, H. W. Lee and I. Lee, *J. Chem. Soc., Perkin Trans. 2*, 1753 (2001).
92. H. K. Oh, J. Y. Lee, J. H. Yun, Y. S. Park and I. Lee, *Int. J. Chem. Kinet.*, **30**, 419 (1998).
93. H. K. Oh, C. H. Shin and I. Lee, *J. Chem. Soc., Perkin Trans. 2*, 1169 (1995).
94. H. K. Oh, S. Y. Woo, C. H. Shin and I. Lee, *Int. J. Chem. Kinet.*, **30**, 849 (1998).
95. E. A. Castro, *Chem. Rev.*, **99**, 3505 (1999).
96. I. Lee, C. K. Kim, H. G. Li, C. K. Sohn, C. K. Kim, H. W. Lee and B-S. Lee, *J. Am. Chem. Soc.*, **122**, 11162 (2000).
97. S. V. Hill, J. L. Longridge and A. Williams, *J. Org. Chem.*, **49**, 1819 (1984).
98. A. Williams and W. P. Jencks, *J. Chem. Soc., Perkin Trans. 2*, 1753 (1974).
99. D. P. N. Satchell and R. S. Satchell, *J. Chem. Soc., Perkin Trans. 2*, 1415 (1990).
100. F. Terrier, *Aromatic Nucleophilic Substitution (The Influence of the Nitro Group)*, VCH, New York, 1991.
101. G. S. Hammond and L. R. Parks, *J. Am. Chem. Soc.*, **77**, 340 (1955).
102. D. H. Kang, I. S. Koo, J. K. Lee and I. Lee, *J. Korean Chem. Soc.*, **29**, 565 (1985).
103. (a) R. H. de Rossi and R. A. Rossi, *J. Org. Chem.*, **39**, 3486 (1974).
     (b) T. O. Bamkole, J. Hirst and G. Hussain, *J. Chem. Soc., Perkin Trans. 2*, 681 (1984).
     (c) E. T. Akinyele, I. Onyido and J. Hirst, *J. Chem. Soc., Perkin Trans. 2*, 1859 (1988).
104. (a) N. S. Nudelman and D. Palleros, *J. Org. Chem.*, **48**, 1613 (1983).
     (b) C. F. Bernasconi and H. Zollinger, *Helv. Chim. Acta*, **49**, 2570 (1966).
105. I. Onyido and J. Hirst, *J. Phys. Org. Chem.*, **4**, 367 (1991).
106. J. Persson and O. Matsson, *J. Org. Chem.*, **63**, 9348 (1998).
107. (a) E. Buncel and J. G. K. Webb, *Can. J. Chem.*, **50**, 129 (1972).
     (b) E. Buncel and J. G. K. Webb, *Can. J. Chem.*, **52**, 630 (1974).
108. (a) E. Buncel, H. Jarrell, H. W. Leung and J. G. K. Webb, *J. Org. Chem.*, **39**, 272 (1974).
     (b) E. Buncel, J. G. K. Webb and J. F. Wiltshire, *J. Am. Chem. Soc.*, **99**, 4429 (1977).
     (c) F. Terrier, *Chem. Rev.*, **82**, 77 (1982).
109. (a) E. Buncel, C. Innis and I. Onyido, *J. Org. Chem.*, **51**, 3680 (1986).
     (b) E. Buncel and W. Eggimann, *J. Am. Chem. Soc.*, **99**, 5958 (1977).
     (c) T. O. Bamkole, J. Hirst and I. Onyido, *J. Chem. Soc., Perkin Trans. 2*, 1201 (1981).
110. C. Isanbor, T. A. Emokpae and M. R. Crampton, *J. Chem. Soc., Perkin Trans. 2*, 2019 (2002).
111. O. Banjoko and C. Ezeani, *J. Chem. Soc., Perkin Trans. 2*, 1357 (1982).
112. T. A. Emokpae, J. Hirst and P. U. Uwakwe, *J. Chem. Soc., Perkin Trans. 2*, 2191 (1990).
113. T. A. Emokpae and C. Isanbor, *Int. J. Chem. Kinet.*, **36**, 188 (2004).
114. M. R. Crampton and L. C. Rabbitt, *J. Chem. Soc., Perkin Trans. 2*, 1669 (1999).
115. M. K. Stern, B. K. Cheng, F. D. Hileman and J. M. Allman, *J. Org. Chem.*, **59**, 5627 (1994).
116. I. Lee, H. K. Kang and H. W. Lee, *J. Korean Chem. Soc.*, **29**, 478 (1985).
117. O. Rogne, *J. Chem. Soc. B*, 1855 (1971).
118. S. D. Ross, M. Finkelstein and F. S. Dunkl, *J. Org. Chem.*, **39**, 134 (1974).
119. O. Rogne, *J. Chem. Soc., Perkin Trans. 2*, 472 (1972).
120. I. Lee, C. S. Shim, S. Y. Chung, H. Y. Kim and H. W. Lee, *J. Chem. Soc., Perkin Trans. 2*, 1919 (1988).
121. E. Ciuffarin, L. Senatore and M. Isola, *J. Chem. Soc., Perkin Trans. 2*, 468 (1972).
122. I. Lee and I. S. Koo, *Tetrahedron*, **39**, 1803 (1983).
123. A. Arcoria, E. Maccarone, G. Musumara and G. A. Tomaselli, *J. Org. Chem.*, **39**, 3595 (1974).

124. A. Arcoria, E. Maccarone, G. Musumara and G. A. Tomaselli, *J. Org. Chem.*, **38**, 2457 (1973).
125. A. Arcoria, E. Maccarone, G. Musumara and G. A. Tomaselli, *J. Org. Chem.*, **39**, 1689 (1974).
126. E. Maccarone, G. Musumara and G. A. Tomaselli, *J. Org. Chem.*, **39**, 3286 (1974).
127. A. Arcoria, F. P. Ballistreri, G. Musumara and G. A. Tomaselli, *J. Chem. Soc., Perkin Trans. 2*, 221 (1981).
128. S. B. Han, D. D. Sung and I. Lee, *Bull. Korean Chem. Soc.*, **6**, 162 (1985).
129. I. Lee, C. K. Kim, H. G. Li, C. K. Sohn, C. K. Kim, H. W. Lee and B-S. Lee, *J. Am. Chem. Soc.*, **122**, 11162 (2000).
130. A. Schroll and G. Barany, *J. Org. Chem.*, **51**, 1866 (1986).
131. A. K. Guha, H. W. Lee and I. Lee, *J. Chem. Soc., Perkin Trans. 2*, 765 (1999).
132. H. W. Lee, A. K. Guha and I. Lee, *Int. J. Chem. Kinet.*, **34**, 632 (2002).
133. A. K. Panda, S. N. Mahapatro and G. P. Panigrahi, *J. Org. Chem.*, **46**, 4000 (1981).
134. P. C. Buxton, J. N. Ennis, B. A. Marples, V. L. Waddington and T. R. Boehlow, *J. Chem. Soc., Perkin Trans. 2*, 265 (1998).
135. (a) M. Novak, K. A. Martin and J. L. Heinrich, *J. Org. Chem.*, **54**, 5436 (1989).
    (b) J. S. Helmick, K. A. Martin, J. L. Heinrich and M. Novak, *J. Am. Chem. Soc.*, **113**, 3459 (1991).
    (c) M. Novak, K. S. Rangappa and R. K. Manitsas, *J. Org. Chem.* **58**, 7813 (1993).
136. R. A. T. M. Abbenhuis, J. Boersma and G. van Koten, *J. Org. Chem.*, **63**, 4282 (1998).
137. M. Moreno-Manas, L. Morral and R. Pleixats, *J. Org. Chem.*, **63**, 6160 (1998).
138. S-C. Yang and C-W. Hung, *J. Org. Chem.*, **64**, 5000 (1999).
139. R. C. Larock, E. K. Yum and M. D. Refvik, *J. Org. Chem.*, **63**, 7652 (1998).
140. J. McMurry, *Organic Chemistry*, 4th edn., Brooks/Cale, Pacific Grove, CA, 1996.
141. N. Russo, M. Toscano, A. Grand and T. Minerva, *J. Phys. Chem., A*, **104**, 4017, (2000).
142. S. K. Pollack, J. I. Devlin, III, K. D. Summerhays, R. W. Taft and W. J. Hehre, *J. Am. Chem. Soc.*, **99**, 4583 (1977).
143. K. D. Summerhays, S. K. Pollack, R. W. Taft and W. J. Hehre, *J. Am. Chem. Soc.*, **99**, 4585 (1977).
144. B. B. P. Tice, I. Lee and F. H. Kendall, *J. Am. Chem. Soc.*, **85**, 329 (1963).
145. I. Lee and F. H. Kendall, *J. Am. Chem. Soc.*, **88**, 3813 (1966).
146. P. G. Gassman and G. A. Campbell, *J. Am. Chem. Soc.*, **93**, 2567 (1971).
147. D. F. Paul and P. Haberfield, *J. Org. Chem.*, **41**, 3170 (1976).
148. A. G. Giumanini, S. Roveri and D. del Mazza, *J. Org. Chem.*, **40**, 1677 (1975).
149. (a) R. J. Spear, W. P. Norris and R. W. Read, *Tetrahedron Lett.*, **24**, 1555 (1983).
    (b) R. W. Read, R. J. Spear and W. P. Norris, *Aust. J. Chem.*, **37**, 985 (1984).
150. (a) M. J. Strauss, R. A. Renfrow and E. Buncel, *J. Am. Chem. Soc.*, **105**, 2473 (1983).
    (b) E. Buncel, R. A. Renfrow and M. J. Strauss, *J. Org. Chem.*, **52**, 488 (1987).
151. Y. Yuan, X. Wang, X. Li and K. Ding, *J. Org. Chem.*, **69**, 146 (2004).
152. R. A. Poirier, Y. Wang and K. C. Westaway, *J. Am. Chem. Soc.*, **116**, 2526 (1994).
153. I. Lee, H. J. Koh, B-S. Lee, D. S. Sohn and B. C. Lee, *J. Chem. Soc., Perkin Trans. 2*, 1741 (1991).
154. I. Lee, H. J. Koh and H. W. Lee, *J. Chem. Res. (S)*, 282 (1990); *(M)*, 2177 (1990).
155. I. Lee, H. J. Koh and B. C. Lee, *J. Phys. Org. Chem.*, **7**, 50 (1994).
156. B. C. Lee, D. S. Sohn, J. H. Yoon, S. M. Yang and I. Lee, *Bull. Korean Chem. Soc.*, **14**, 621 (1993).

Rearrangements of anilines and their derivatives

SERGEI M. LUKYANOV and ALLA V. KOBLIK

ChemBridge Corporation, Malaya Pirogovskaya str., 1, 119435 Moscow, Russia
Fax: +495 956 49 48; e-mail: semiluk@chembridge.ru

I. INTRODUCTION

Numerous rearrangements are known, in which anilines participate as both starting reactants and final products. The overwhelming majority of these reactions was discovered a long time ago, and many of them became the named reactions that were described in all the courses of organic chemistry as well as in various reviews[1,2]. The literature concerning these rearrangements is very extensive and quite accessible. Therefore, we confine this chapter to a concise survey of these reactions, where most attention is focused on recent publications as well as the most interesting transformations of anilines and their derivatives.

II. REARRANGEMENTS OF ANILINES

Aniline **1** itself can be rearranged into 2-methylpyridine (**4**) upon heating over zeolite catalysts. Amination of phenol with ammonia in the presence of shape-selective zeolites (e.g. ZSM-5) afforded aniline as well as α-picoline as the principal side-product. It was shown that the latter was formed sequentially from aniline[3,4]. Two mechanisms involving the intermediate nitrenium ions **3** (equation 1) (see also Section III.C.1) or ring expansion stage (equation 2) were proposed for this process termed *'benzamine molecular rearrangement'*[3,4]. It should be noted that the ring-opening—ring-closure mechanism (equation 1) assumes a tautomeric equilibrium of aniline as the first step ($\mathbf{1} \rightleftarrows \mathbf{2}$) (*vide infra*).

(1)

(1)

$$(2)$$

(4)
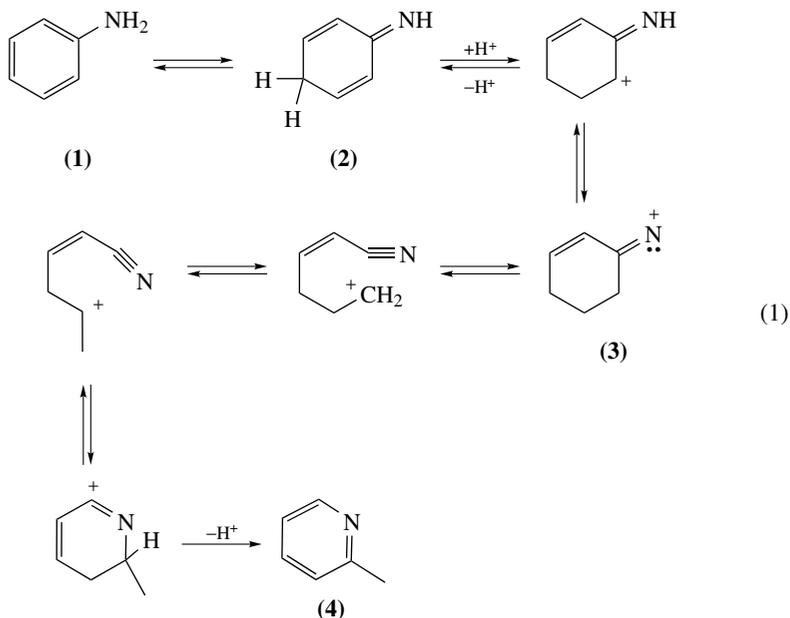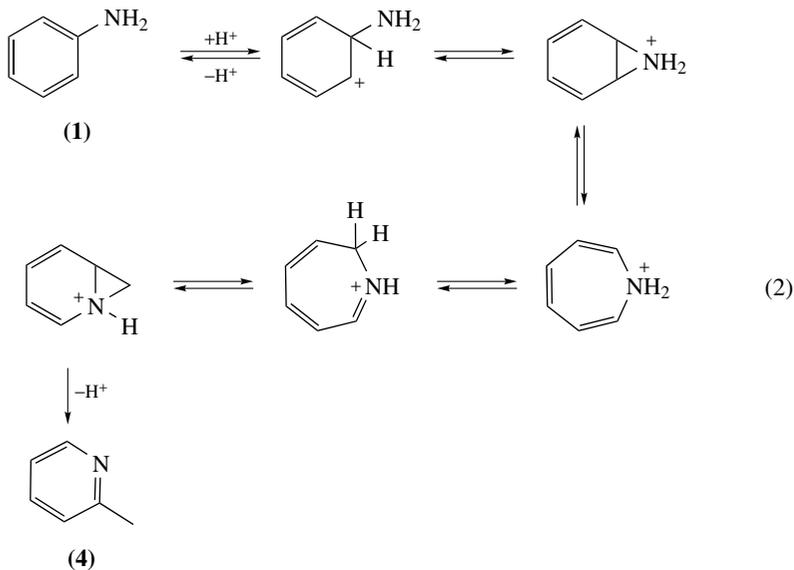
It was shown by thermodynamic[5] and kinetic study[6,7] of the zeolite catalyzed isomerization of aniline **1** to α-picoline **4** that the amounts of the latter in equilibrium gas phase were 12.7%, 15.9% and 18.6% at 600 K, 700 K and 800 K, respectively. The results of investigations in this field have been reviewed[8].

In all the other isomerizations discussed below the aniline derivatives are substituted at the aromatic ring and/or at the nitrogen atom.

Thus, 3-aminopyrocatechols **5a–e** have been rearranged into the corresponding 6-hydroxypicolinic acids **6a–e** in the course of two-stage oxidation[9] (equation 3). A few examples of acyl group migration from the aromatic ring or side chain to the aniline amino group were described, for instance, a conversion of 2-aminobenzophenones **7** into benzanilides **8**[10] (equation 4) (see also Reference 11) (about more known acyl migrations from the amino group to the aromatic nucleus, see Section III.A.4.c). It is interesting that *ortho*-aminophenyl allyl ether **9** undergoes the Claisen rearrangement on heating (see also Section III.A.2.b) without participation of the amino group[12] (equation 5).

A conversion of N-deuteriated aniline hydrochloride into ring-deuteriated anilines can also be regarded as a rearrangement[13]. According to kinetic study, this process follows an intramolecular electrophilic mechanism and should be considered as a transfer of a migrant from the amino group to the aromatic ring.

On the other hand, the *reversible* migrations of hydrogen between amino group and aromatic cycle are uncharacteristic for unsubstituted anilines, although they are postulated sometimes as one of the reaction steps (e.g. equation 1). However, in the case where functional groups such as OH or Cl are attached to the aromatic ring, the tautomerism of anilines becomes the process that can be a key stage of some reactions.

Thus, it was shown that the tautomerization may be of importance in the thermal dehalogenation of chloroaromatics[14]. The formation of diarylamines in this reaction can be also explained by the presence of aniline tautomers in the reaction mixtures[14]. One of the well-known types of aniline tautomerism is the enol-imine–keto-amine equilibrium. In effect, it is a reversible conversion of Schiff bases into enamines that is frequently employed for the synthesis of photochromic compounds, as well as of mesomorphic

compositions[15–19]. The above-mentioned and other kinds of aniline tautomerism were described in detail in several reviews[20, 21].

$$(3)$$
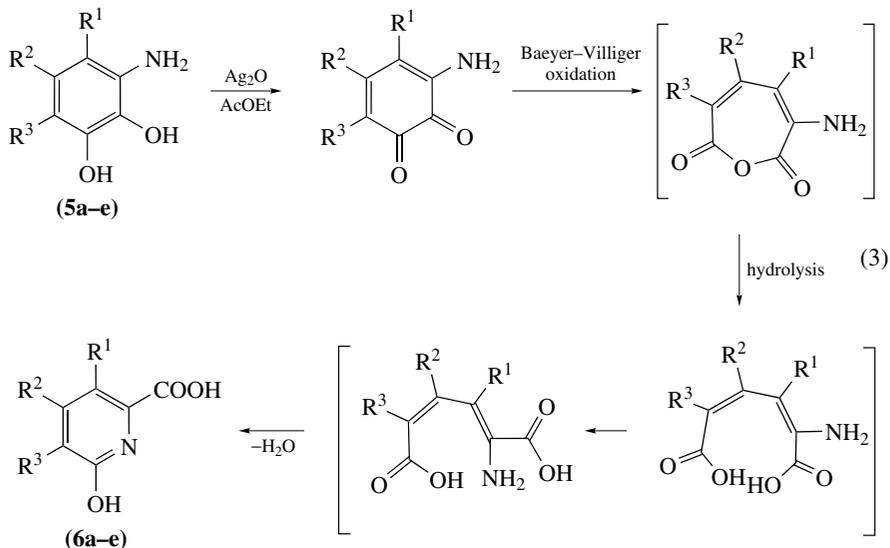
6a–e (a) $R^1 = R^2 = R^3 = H$ (16%); **(b)** $R^1 = COOH$, $R^2 = R^3 = H$ (11%);
(c) $R^1 = NH_2$, $R^2 = Me$, $R^3 = H$ (16%); **(d)** $R^1 = H$, $R^2R^3 = benzo$ (65%);
(e) $R^1 = C_6H_5NH$, $R^2R^3 = benzo$ (31%)

$$(4)$$

$$(5)$$
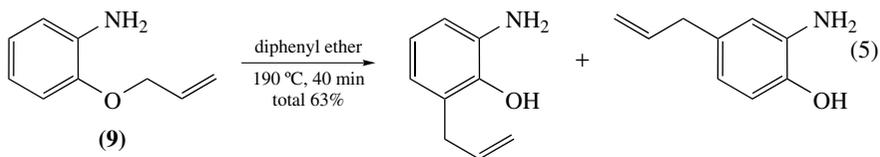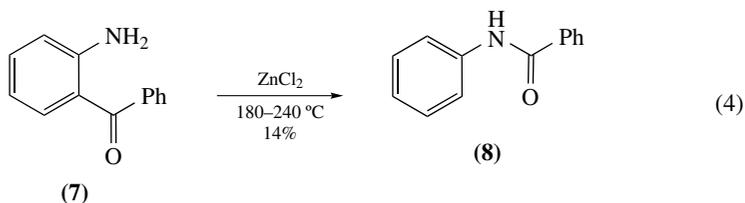
III. REARRANGEMENTS OF N-SUBSTITUTED ANILINES

The majority of aniline rearrangements embraces the transformations of the arylamine derivatives bearing various substituents at the nitrogen atom. These substituents can be connected to the nitrogen atom by the N−C or N−heteroatom (N, O, S, Hal) bond. The rearrangements may occur either by migration of the substituent to the aromatic nucleus or by rebuilding of the N-side chain itself.

A. Aniline Derivatives Containing Ar−N−C Unit

1. Isomerizations of N-alkylanilines

a. Hofmann−Martius and Reilly−Hickinbottom rearrangements. The thermal isomerization of *N*-alkylaniline hydrochlorides **10** as well as the hydrobromides to give ring-alkylated anilines **11** and **12** has been known as the *Hofmann−Martius rearrangement* for more than 130 years and was described in many reviews[2, 22−24] (equation 6).
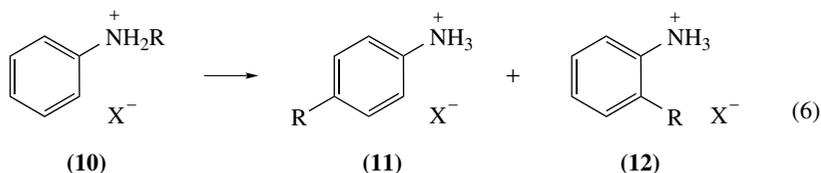
$$R = alkyl; X = Cl, Br$$

This rearrangement proceeds at high temperatures of about 250−300 °C for primary alkyl groups and about 200 °C in the case of secondary and tertiary alkyl migrants. The migration takes place preferably to the *para*-position of the ring, but if this position is occupied, the alkyl group enters the *ortho*-position. The rearrangement is usually accompanied by numerous side reactions such as polyalkylation and formation of alkyl halides as well as olefins, together with isomerization of the migrating alkyl group.

The mechanism of the process is not yet clear. This rearrangement was considered at one time as intramolecular, but it was later concluded that the transformation is rather intermolecular and can occur through formation of a carbenium ion intermediate[25, 26]. However, evidence was obtained more recently in favor of a free radical mechanism involving an *N*-alkyl bond fission[27−29]. An intermolecular free radical isomerization was described also for a thermal decomposition of *N*-benzyl-*N*-methylaniline hydroxides[30, 31].

A dramatic effect of a counterion on the course of the Hofmann−Martius rearrangement was observed upon thermolysis of *N*-benzyl-*N*,*N*-dimethylaniline hydrochloride **13** and hydroiodide **16**[32]. While the thermolysis of compound **13** gave rise to the dealkylation products **14** and **15** (equation 7), the behavior of the hydroiodide **16** under the same experimental conditions was completely different, leading to the three rearranged products **17**−**19** (equation 8).
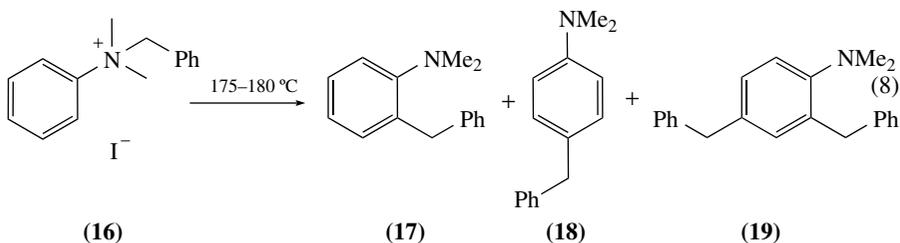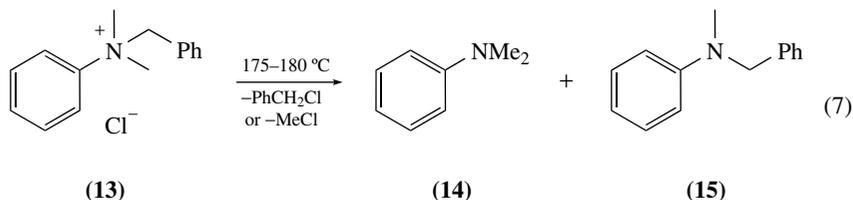
A much more investigated modification of the reaction discussed is known as the *Reilly–Hickinbottom rearrangement*[33]. This isomerization proceeds upon heating of *N*-alkylanilines at 200–250 °C in the presence of metal halides (CoCl$_2$, CdCl$_2$, ZnCl$_2$, ZnBr$_2$) to give the *para*-substituted products in good yields. In contrast to the Hofmann–Martius reaction, the Reilly–Hickinbottom rearrangement occurs without formation of alkyl halides and olefins as well as isomerization of the migrating alkyl groups[22, 23]. The mechanism of this rearrangement has been studied in detail[34].

The isomerizations of *N*-alkylanilines that afford *ortho*-alkylanilines in the presence of heterogeneous acid catalysts such as zeolites, silica/aluminas and γ-alumina have been described recently[35, 36]. The migrating groups in the rearrangements can be triarylmethyl[37–39] or ferrocenylmethyl[40] as well as tricarbonyl(η^5-cyclohexadienylium)iron[41]. Photochemical rearrangements of N-substituted anilines to furnish *ortho*- and *para*-substituted anilines[42, 43] as well as abnormal *meta*-isomers[44] were reported in many publications. It was also found that *N*-alkylanilines rearranged in the plasma of glow discharges to give the corresponding 2- and 4-alkylanilines[45].

b. Stevens and Sommelet rearrangements. Base-catalyzed rearrangements are not typical for *N*-alkylated anilines, while transformations such as Stevens (equation 9) and Sommelet (equation 10) rearrangements are very characteristic for *N*-benzylaniline derivatives **20** and **21** (for reviews see References 46–49; see also References 50 and 51).

$$(9)$$

$$(10)$$
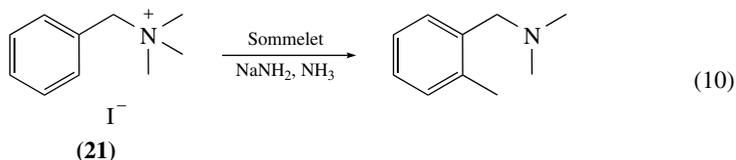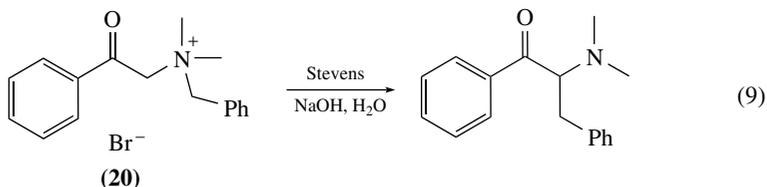
However, participation of aniline derivatives in such rearrangements was also reported in some papers. Thus, fused indolinone **24**[52] and quinoxalinone **27**[53] derivatives were prepared from anilinium salts **22** and **25** through the Stevens rearrangement of the corresponding intermediate carbonyl-stabilized ammonium ylides **23** and **26** (equations 11 and 12). It was shown that these Stevens rearrangements were successful only for ylides **23** and **26** containing an easily migrating benzyl moiety which is linked to the quaternary nitrogen atom. All attempts to conduct such transformations failed when they started from other ammonium derivatives such as **28** or **29**[52, 53].

N-Benzyl-*N*,*N*-dimethylanilinium bromide **30** reacts with sodium amide in liquid ammonia to give both the product of 1,2-shift **33** (Stevens rearrangement) and the *ortho*-substituted compound **34** (Sommelet rearrangement) via the intermediate ylides **31** and **32**[54] (equation 13).

$$R = H, NO_2 \qquad \textbf{(22)}$$

(11)

(12)

(28)   **(29)**
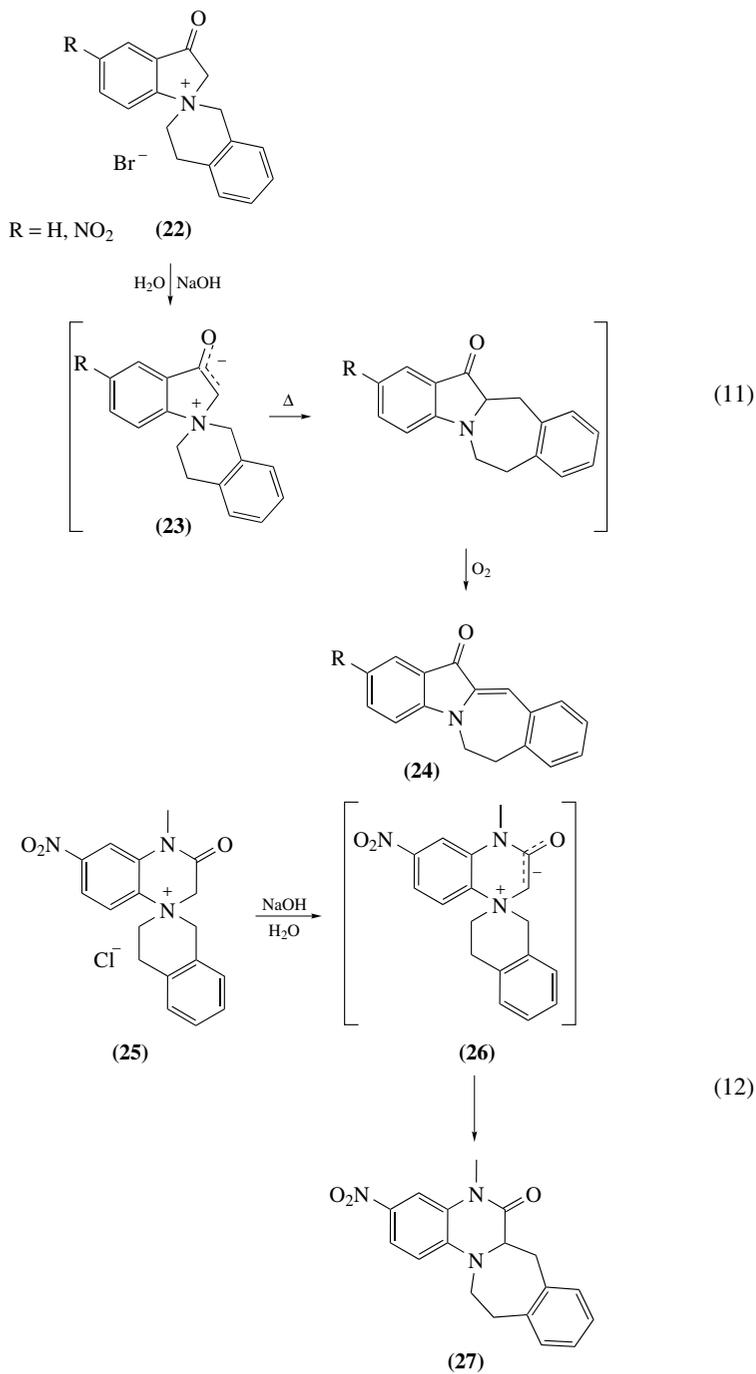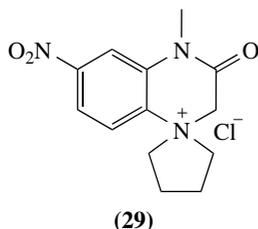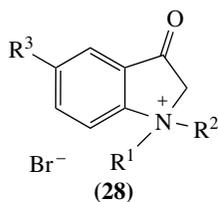
$R^1 = R^2 = Me$; $R^1R^2 = -(CH_2)_4-$, $-(CH_2)_5-$, $-(CH_2)_6-$; $R^3 = H, NO_2$

(34)

Sommelet | 69%

(30)   **(31)**   **(32)**   (13)

(33)
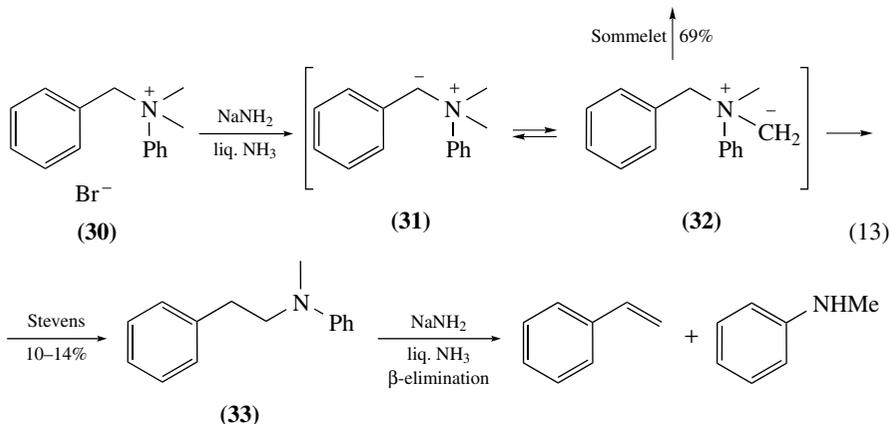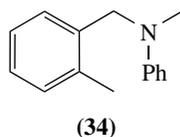
In contrast, when the same anilinium ion **35** is treated with organolithium reagents (MeLi, PhLi, *n*-BuLi) it produces two different products of Stevens rearrangement **33** and **36** as well as *ortho*-methylated benzylamine **34** as a minor product[55] (equation 14). It was also found that the Stevens rearrangement of the anilinium salts can be carried out in the presence of weak bases such as solid sodium carbonate[56].

The ylides **31** and **39**, the key intermediates of both the Stevens and Sommelet rearrangement discussed above, can be generated also by addition of benzyne **38** to *N*-alkylamines. Thus, generation of benzyne **38** in the presence of *N*,*N*-dimethylbenzylamine **37** gave rise to practically a single product **36** of the Stevens rearrangement[57,58] (equation 15).

A Stevens rearrangement of bridged benzodiazabicycloalkane **40** that led to the product **41** of ring expansion was described[59] (equation 16).

The first reported rearrangement involving the 2-thienyl moiety was carried out by the action of potassium hydroxide melt on N-(2-thienyl)-N,N-dimethylanilinium chloride[60].
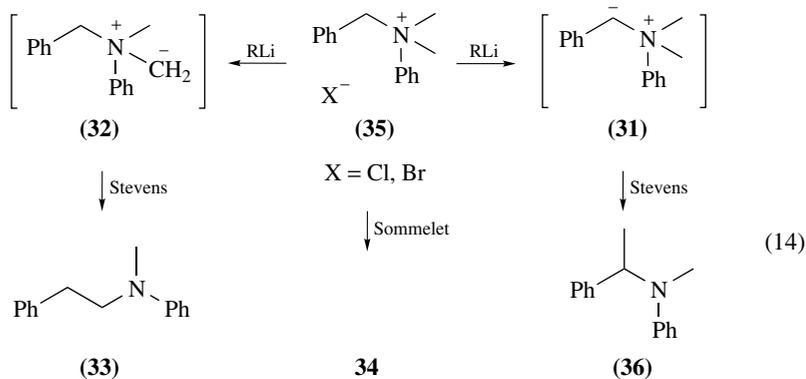
MeLi: 8.4% (**33**), 0% (**34**), 39.5% (**36**);
PhLi: 3.9% (**33**), 0% (**34**), 30% (**36**);
n-BuLi: 8.7–14.3% (**33**), 2–2.5% (**34**), 2.4–6.2% (**36**)

$$39–61\% \qquad (17)$$

(43)
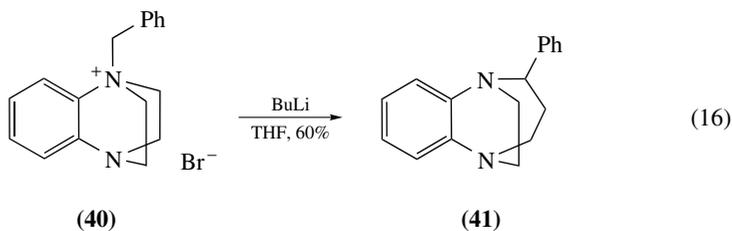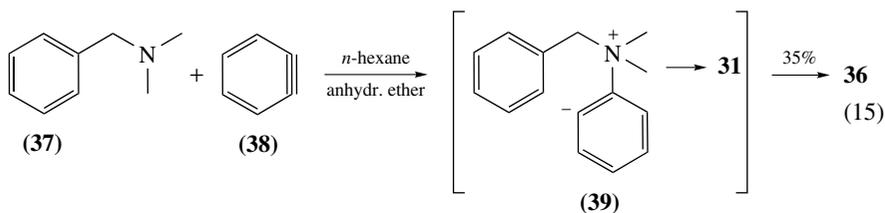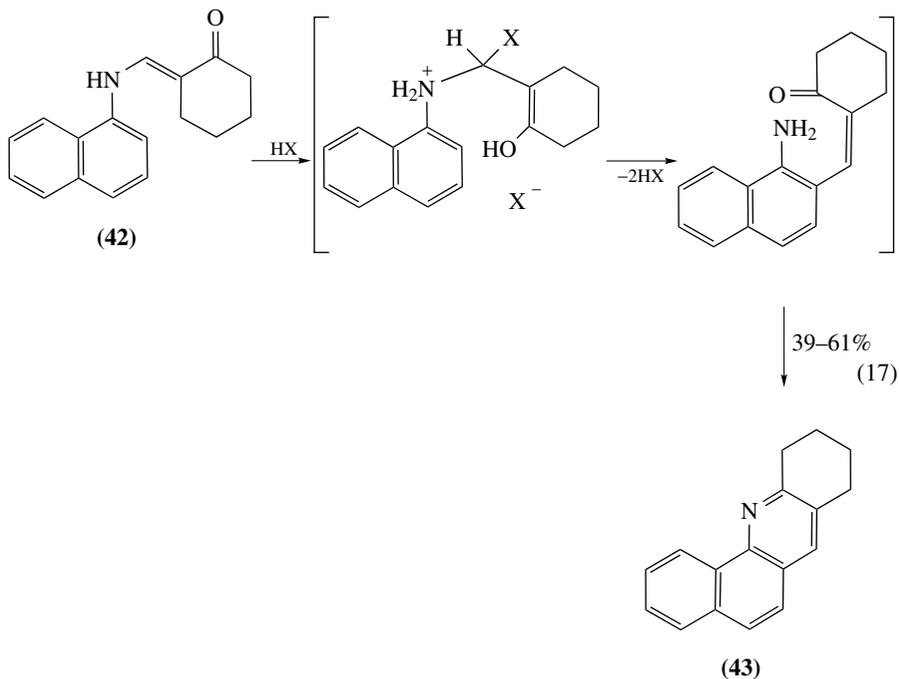
2. Transformations of N-alkenylanilines

a. N-Vinylanilines. A ring-closure of *N*-naphthylenamine **42** in the presence of acids HX (lactic, oxalic or phosphoric acids, ClCH$_2$COOH) afforded an anomalous tetrahydro-benz[*c*]acridine **43**[61] (equation 17). A similar reaction pathway was described for the conversion of *cis*-2-(arylaminomethylene)cyclohexanones into tetrahydroacridines[62]. Some other transformations of aromatic enamines include *cis–trans* isomerizations[63, 64].

b. N-Allylanilines and amino-Claisen rearrangement. An aminomercuration of allenes was reported as a reaction which afforded the easy insertion of the allylic chain both at the nitrogen atom and at the *ortho*-position of secondary aromatic amines[65] (equation 18). Rearrangement of *N*-allylanilines **44** into aromatic enamines **45** includes a shift of the double bond and occurs in liquid ammonia in the presence of NaNH$_2$[66] (equation 19).

However, the most typical transformation of *N*-allylanilines is the [3,3]-sigmatropic rearrangement, known as *the amino-Claisen rearrangement* (**46** → **47** → **48**) that has been described in many reviews[67–70] (equation 20). This process is sometimes also called the 'aza-Claisen rearrangement'[71] as well as the 'aromatic aza-Cope rearrangement'[72].

In contrast to the well-known thermal Claisen rearrangement that enjoyed widespread application in organic synthesis[73], the amino-Claisen rearrangement has received until recently much less attention. This may be due to some limitations such as the relatively low yields, the more drastic reaction conditions as well as the concomitant tendency

toward side reactions[67]. It has been estimated that the thermal amino-Claisen rearrangement has an activation energy requirement of 25 kJ mol^{-1} higher than that for the oxygen analogue[68]. More recently, it was found that the amino-Claisen rearrangement can be successfully carried out in the presence of acid catalysts. The kinetic measurements and detailed investigations of the mechanism of the amino-Claisen rearrangement were described in several fundamental articles[74-76] (see also References 77-79). It was shown that, unlike the *N*-allylanilines, their protonated derivatives rearrange much more easily, being accelerated 10^5–10^7 fold. Nevertheless, both the thermal and the acid catalyzed rearrangement of *N*-allylanilines leads to the 2-allylated anilines with an inverted allylic chain[80]. Semiempirical[71] and *ab initio* calculations[81] supported the chair-like transition state of this rearrangement and predicted that an anionic substituent at the nitrogen atom should reduce the activation energies.

$$\tag{18}$$

$$\tag{19}$$

$R^1 = Me, Et; R^2 = H, Me$

$$\tag{20}$$
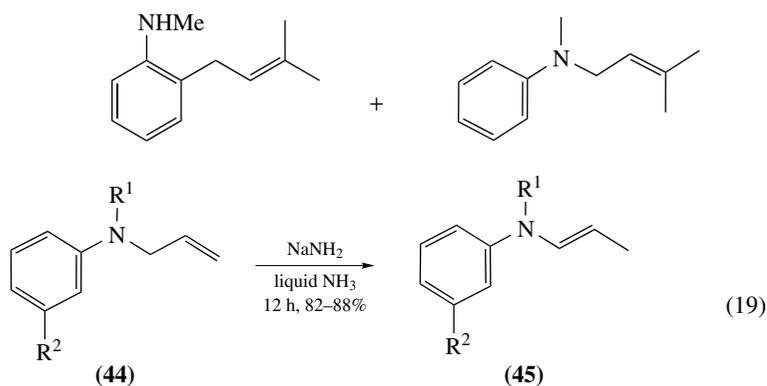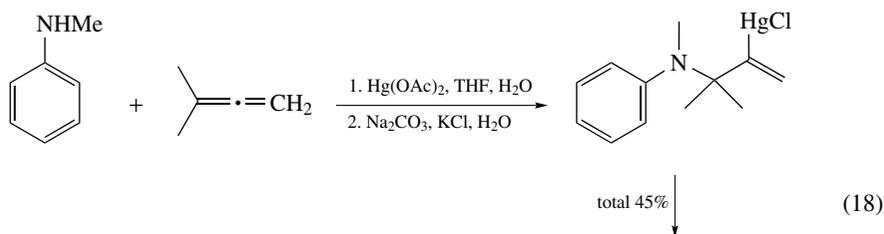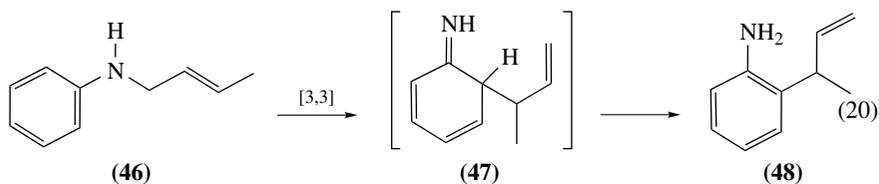
Various acid catalysts such as zinc chloride[74], sulfuric acid[75], HCl[78], *para*-toluenesul-fonic acid[82] as well as aniline hydrochloride[83] have been applied in the amino-Claisen rearrangement. The boron trifluoride—diethyl ether complex was demonstrated to be an efficient catalyst for the transformations of various *N*-allylanilines **49** and **51** into the corresponding 6-allylanilines **50** and the 7-allylindolines **52**[84] (equations 21 and 22). A peculiar two-Claisen rearrangement strategy was employed to prepare the novel indole analogue **57** of mycophenolic acid as a potential antineoplastic agent[85, 86]. In the course of the synthesis, the amino-Claisen rearrangement was carried out at the first step (**53** → **54**) followed by an orthoester Claisen rearrangement (**55** → **56**), followed by three steps to form **57** (equation 23).

$$\text{(21)}$$
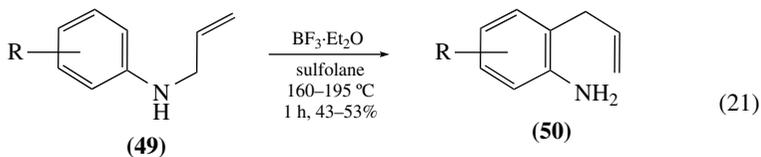
R = 2-NH$_2$, 2-NO$_2$, 2-COOMe, 3-MeO

$$\text{(22)}$$
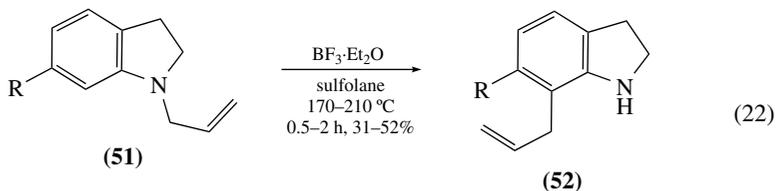
R = H, MeO, NO$_2$

N-Allylanilines undergo the amino-Claisen rearrangement in the presence of Zn^{2+} montmorillonite under microwave irradiation without a solvent to afford indoline deriva-tives in high yields[72]. The amino-Claisen rearrangement occurs with a migration of unsaturated group to the *para*-position of the aromatic nucleus if both *ortho*-positions are occupied[87]. Otherwise, it leads to mixtures of *ortho*- and *para*-isomers when the precursor *N*-allylanilines contain one 2-substituent[88]. In the case of 2,4,6-trisubstituted *N*-allylanilines the migrating groups can enter a *meta*-position[89].

Various sigmatropic rearrangements of 2-hydroxyanilinium ylides bearing allyl moiety at a quaternary nitrogen atom were described in a series of papers[90–92]. The amino-Claisen rearrangements can be carried out as a photochemical reaction[93] or as a process in the gas phase[94]. This rearrangement was often used as a key step in many syntheses to prepare suitable systems for photocyclizations[95], in transformation of 5-arylamino-4-methylene-4,5-dihydroisoxazoles into 4-(2-aminobenzyl)isoxazoles[96] as well as in conversion of *meta*-substituted *N*-allylanilines to 4-substituted indoles[97].

The products of the amino-Claisen rearrangement can in turn be involved in fur-ther isomerizations such as an aromatic di-π-methane (ADPM) rearrangement[98]. Another noteworthy rearrangement is that occurring by treatment of *N*-allylaniline **58** with *tert*-butyllithium to give *N*-(2-methylene-4-pentenyl)aniline **60** via a vinyllithium derivative **59** (so-called 6-*endo* intramolecular carbometallation)[99] (equation 24).

BF₃·Et₂O
sulfolane
200–210 °C, 2 h

$$BF_3 \cdot Et_2O$$

(53) → **(54)** → 3 steps → **(55)**

EtCOOH
105–110 °C | MeC(OMe)₃
12 h, 98%

(56) ← **(23)**

3 steps

(57)

(58) → t-BuLi
−78 °C → **(59)**

1. TMEDA, −78 °C to 0 °C | 2. H₂O   (24)

(60)
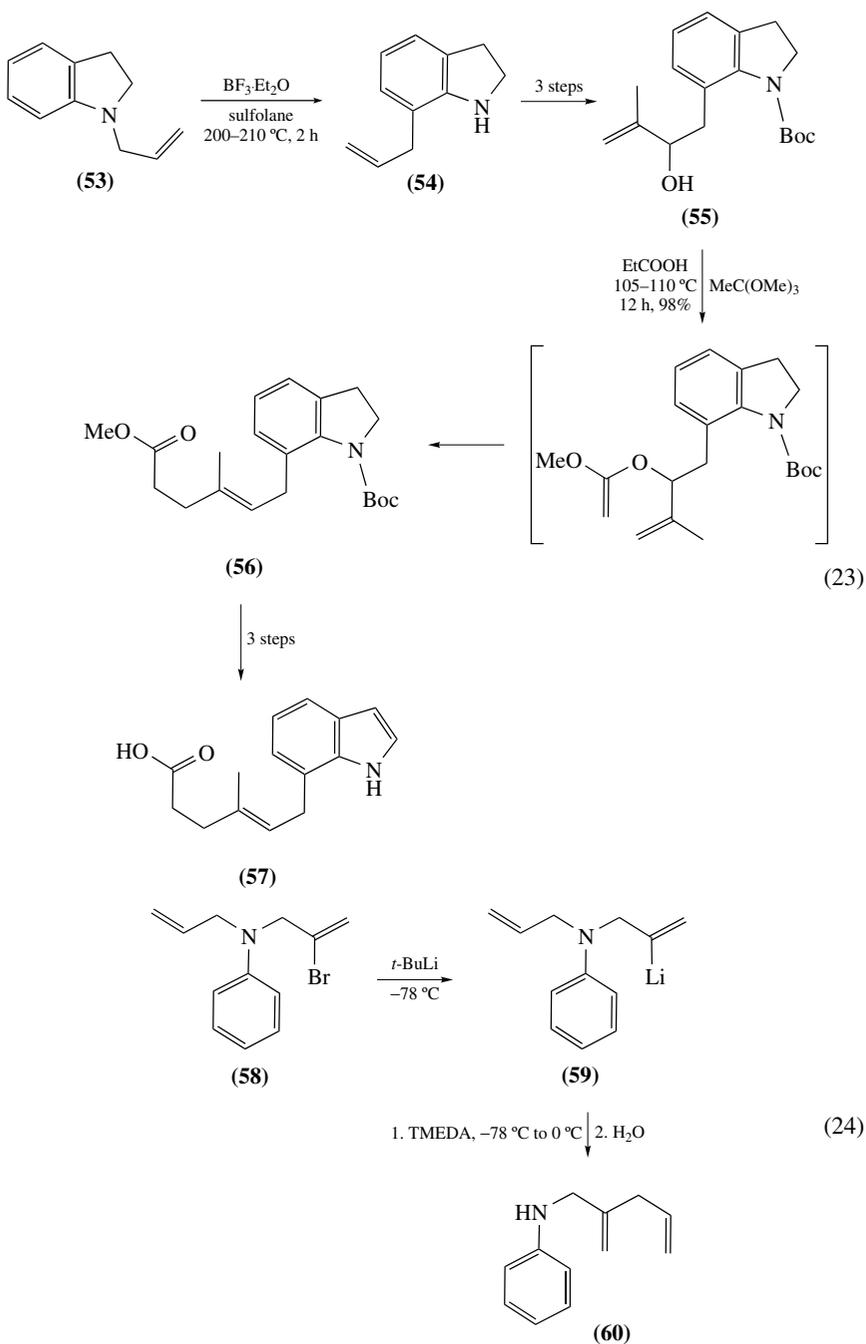
3. N-Alkynylanilines

In contrast to the many examples of amino-Claisen rearrangement of *N*-allylanilines, very scant information can be found in the literature about acid-catalyzed amino-Claisen rearrangements of *N*-propargylanilines and their derivatives. A fundamental investigation that was devoted to rearrangements of various *N*-propargylated arylamines was recently reported[80]. The reactions were carried out under nitrogen in the presence of aqueous H_2SO_4 in various organic solvents (such as primary alcohols or ethylene glycol) in the temperature range 75–250 °C. It was shown that *N*-propynylanilines with unsubstituted *ortho*-positions gave rise to unstable products. The acid-catalyzed rearrangement of *N*-propynyl-2,6-diethylaniline **61** led to the formation of 3-allenylated aniline **62** (21%) and the product of *para*-migration **63** (5%)[80] (equation 25).
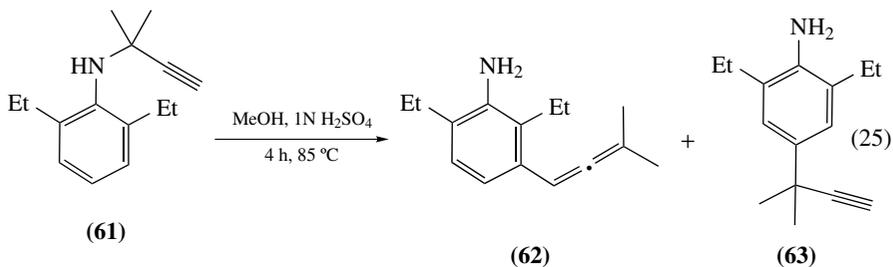
The rearrangements of 2,4,6-trisubstituted *N*-propynylanilines also resulted in 3-allenylated products while a mixture of rearranged products was obtained from *N*-propynyl-2,3,5,6-tetramethylaniline. The main features of the acid-catalyzed amino-Claisen rearrangement of *N*-propargylanilines can be illustrated by a general scheme where the first step is a charge-induced [3,3]-sigmatropic rearrangement of the corresponding anilinium ions **64**[80] (equation 26).
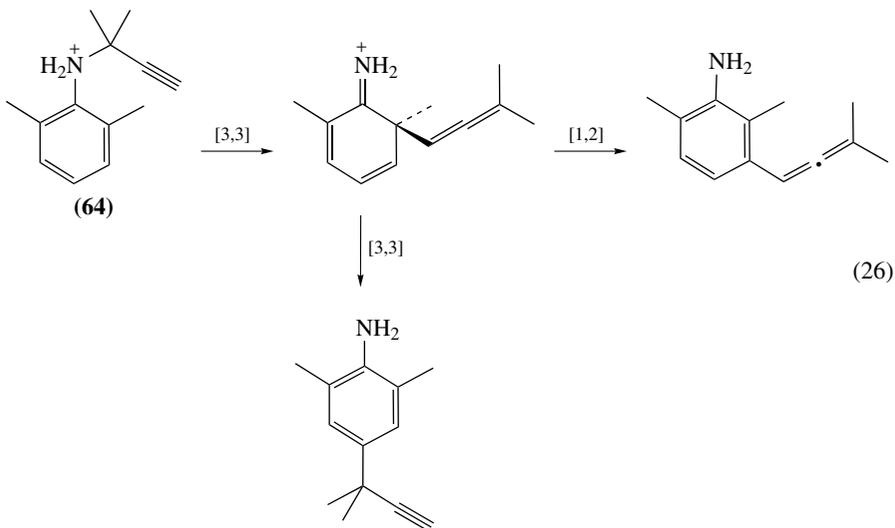
An unusual formation of *N*-arylpyrroles was observed upon thermolysis of *N*-(4-arylsulfenylbut-2-ynyl)anilines that was accompanied by elimination of a benzenethiol unit[100]. Mass-spectral rearrangements of *N*-propynylanilines and related compounds were studied more recently[101, 102].

4. Anilines containing heteroatoms in an N-alkyl chain

a. Smiles rearrangement. The titled base (B⁻)-catalyzed reaction can be characterized as an intramolecular displacement at aromatic nucleus. This rearrangement is initiated by the presence of a nucleophilic center located two or three atoms away from the displaced functional group[103]. The two carbon atoms joining the N and X atoms can be aliphatic or part of an aromatic as well as a heterocyclic ring (equations 27 and 28).

(27)

(28)

X = O, S, NH
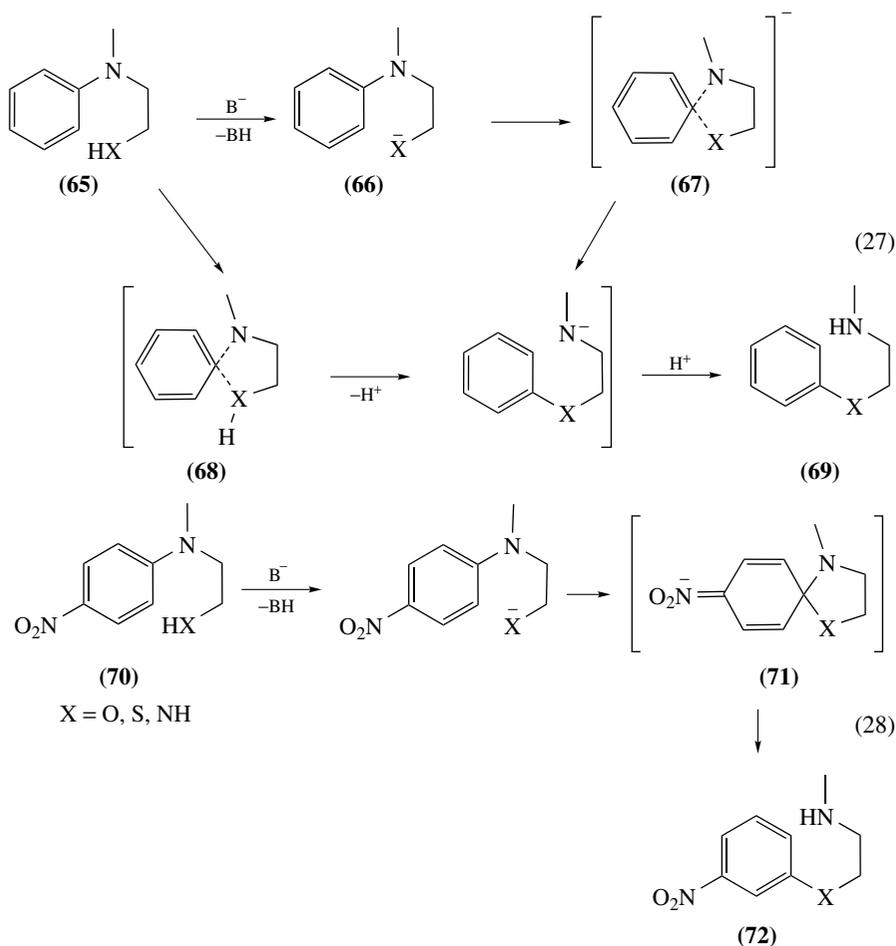
The conversions **65 → 69** and **70 → 72** can proceed by several pathways. An ionization of the nucleophilic function XH in aniline **65** may lead to final product **69** via the transition state **67**. On the other hand, a preliminary **65 → 66** ionization is not always required, and the rearrangement may occur in a concerted fashion through transition state **68**. Besides, in some systems another possibility can be realized when a stabilized intermediate **71** can participate in the rearrangement[103]. Very voluminous information about the Smiles rearrangement has been summarized in detail[103–107].

One of the most known versions of this reaction is a rearrangement of *ortho*-aminodiphenyl ethers **73**[104] (equation 29). The kinetic measurements of the rearrangement of ether **73** [R^1 = H, R^2 = 2,4-$(NO_2)_2$] to form the corresponding 2-hydroxydiphenylamine **74** (with the same R^1 and R^2) were carried out in MeOH-CCl$_4$ solutions[108]. Halogen-activated rearrangements were observed in the examples of polyfluorinated[109] and chlorinated 2-aminodiphenyl ethers[110].

$$(29)$$

(73)   **(74)**
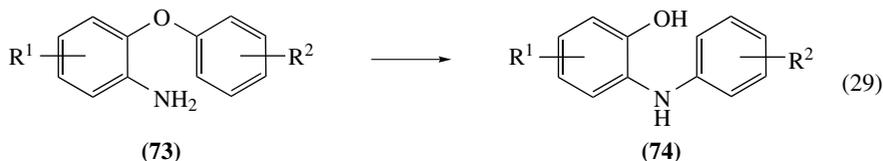
The Smiles rearrangement can be also carried out under acid catalysis conditions. Thus, it was found that the apparent rate constant for the rearrangement of *O*-(*s*-triazinyl) derivatives of 2-aminophenol **75** increased in the pH region above 3, but decreased at pH values below 2[111] (equation 30). The increased rate constant at pH 3 can be explained by a preferential protonation of the ring-nitrogen atom of the triazine nucleus which forms the most reactive intermediate[111].

$$(30)$$

(75)

R = MeO, NMe$_2$
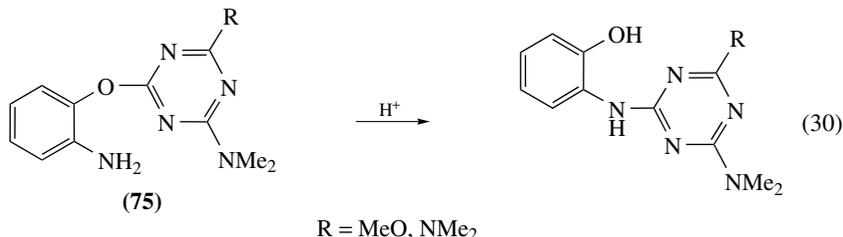
Other aniline derivatives can also take part in the Smiles rearrangement. The base-catalyzed isomerizations of substituted aryloxyacetamides[112, 113], in which a carbonyl group was inserted between oxygen and nitrogen atoms, gave rise to diarylamine and *N*-(hydroxyacyl)anilines, respectively. Many examples of the Smiles rearrangement that proceeded with O → N, S → N as well as N → N migrations have been described as key stages in syntheses of polyfunctional anilines and heterocyclic structures[114–119]. Detailed investigations of photo-Smiles rearrangement were conducted by several research groups[120–126] and summarized in a review[127].

b. Quinamine rearrangement.   One of the most fascinating transformations of *N*-alkylated anilines is the so-called quinamine rearrangement that occurs extremely readily when quinamines **76** are treated with acids[128–130] (equation 31).

$$R^1 = H, Me, Et; R^2, R^3 = Me, Br$$
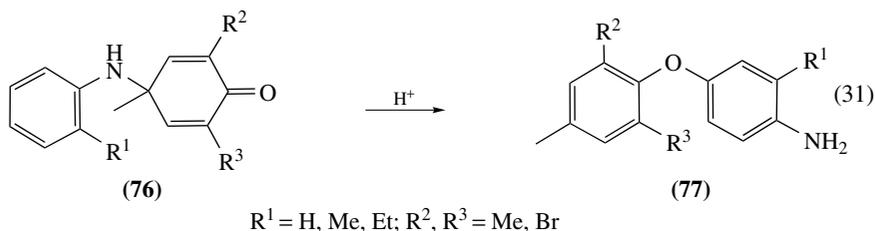
Quinamines having no substituents at the *para*-position of the aniline ring gave 4-aminodiphenyl ethers **77** as the principal products in almost quantitative yields. The behavior of quinamines **76** and their geometric features as well as the kinetic characteristics of the reaction make this transformation very similar to the well-known benzidine rearrangement (Section III.B.1). Like the latter, the mechanism of the quinamine rearrangement involves a transition state that resembles a 'sandwich' of two rings (π-complex)[129].

An interesting reaction that represents a half-way point between the quinamine and benzidine rearrangements can be also mentioned here[129], namely the conversion of *N*-acetyl-*O*,*N*-diphenylhydroxylamine **78** into biphenyls **79** and **80** (equation 32) (see Section III.A.4.c about rearrangements of *N*-acylanilines and Section III.C.1 concerning rearrangements of hydroxylamines).
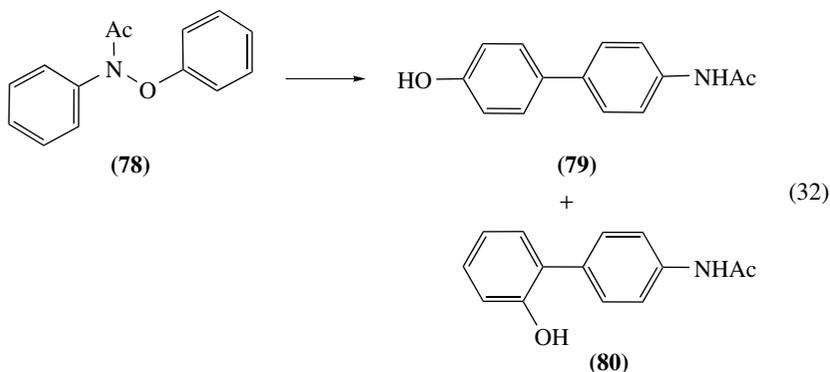
N-Arylaminomethyl aryl sulfides **81** rearrange very readily in acid media to give *para*-aminobenzyl aryl sulfides **82**[131, 132] (equation 33). There is evidence that the reaction is an intermolecular process with participation of a resonance-stabilized sulfonium-carbenium ion.

$$R^1 = H, Me; R^2 = H, Cl, Me, NO_2$$
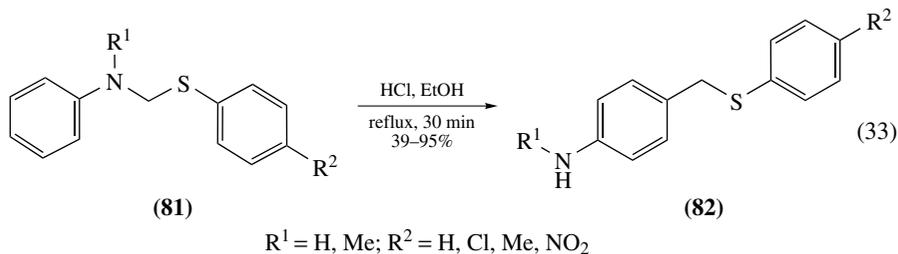
The rearrangement of α-arylaminoketones (**83** → **84**) takes place in the course of the *Möhlau–Bischler indole synthesis* from α-haloketones and anilines[133] (equation 34). Investigations using labeled materials resulted in the proposal of a mechanism involving formation of an epoxide-like intermediate which would allow intramolecular migration of the carbonyl oxygen and require an intermolecular migration of the aniline unit[134].

$$(34)$$
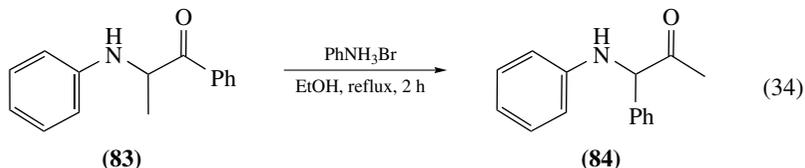
The acid-catalyzed rearrangement of *N*-arylglycosylamines **85** to afford 1-arylamino-1-deoxy-2-ketoses **86** is known as the *Amadori rearrangement* (see reviews in References 135–138) (equation 35). This reaction was used very frequently as a method for modification of natural carbohydrates and was therefore studied intensively for many years[139–144].

$$(35)$$

R = H, Me, MeO, MeS, Br, NO$_2$
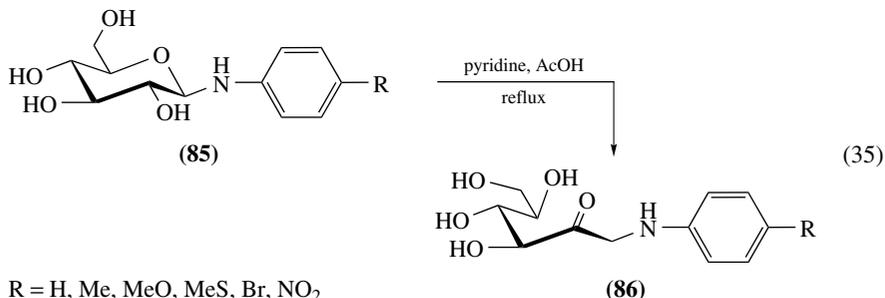
The formation of 2-arylamino-2-deoxyaldoses in the reaction of ketoses with anilines was described as the retro-Amadori reaction (called also the *Heyns rearrangement*)[145].

c. N-Acylanilines. It is well-known that the *N*-acylanilines (i.e. anilides) **87** when treated with polyphosphoric (PPA) as well as with Lewis acids (LA) afford *ortho*- and *para*-acylanilines **88** and **89** (for reviews see References 146 and 147) (equation 36). *N,N*-Diacylanilines (**87**, R^1 = acyl) also rearrange upon heating (150 °C) in the presence of ZnCl$_2$ to give *para*-acylanilines (**89**, R^1 = H, R^2 = Me, Ph)[148].

$$(36)$$
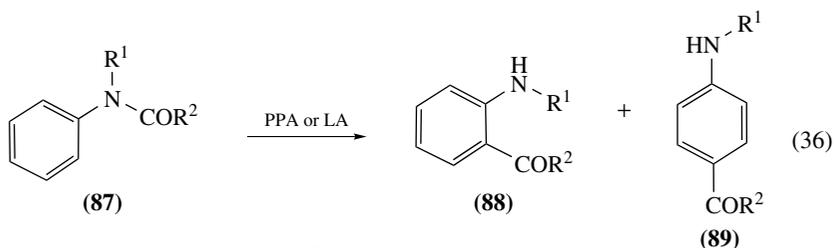
R^1 = H, acyl; R^2 = alkyl, aryl

However, this acid-catalyzed Fries-like rearrangement leads to very low yields of the target products and, therefore, found no serious application for organic synthesis. As a rule, this isomerization was reported as one of the steps in the preparation as well as in the transformations of some N-containing heterocycles[149]. Much more investigated examples of this reaction are the photochemical isomerizations of *N*-acylanilines (so-called 'photo-anilide rearrangements'). An irradiation of acetanilide (**87**, R^1 = H, R^2 = Me) with high pressure mercury vapor lamp in anhydrous ethanol for 8 hours gave rise to *ortho*- and *para*-aminoacetophenones (**88** and **89**, R^1 = H, R^2 = Me) in 20% and 25% yields, respectively[150]. Analogous results were also obtained for other anilides[151−155]. The UV photodegradation of some alkyl *N*-arylcarbamates (**87**, R^1 = H, R^2 = OEt) to give the corresponding *ortho*- and *para*-aminobenzoates (**88** and **89**, R^1 = H, R^2 = OEt) was studied and a mechanism for the rearrangement was proposed[156, 157]. Various rearrangements were observed in the course of electron impact studies on 2-hydroxyimino-*N*-aryl acetamides[158] and *N*-aryl-3-trimethylsilyl-2-propyne-1-carboxamides[159].

A large number of interesting rearrangements was described for which mechanisms including cyclic intermediates were proposed. Samarium diiodide-induced rearrangement of aniline derivatives **90a** and **90b** led to *ipso*-substitution products **92a** and **92b**, probably via the intermediates **91**[160] (equation 37).

(90a) R = Ac
(90b) R = COOCH₂Ph

(91)

(37)

(92a) R = Ac (*t*-BuOH, 19%)
(92b) R = COOCH₂Ph (phenol, 67%)
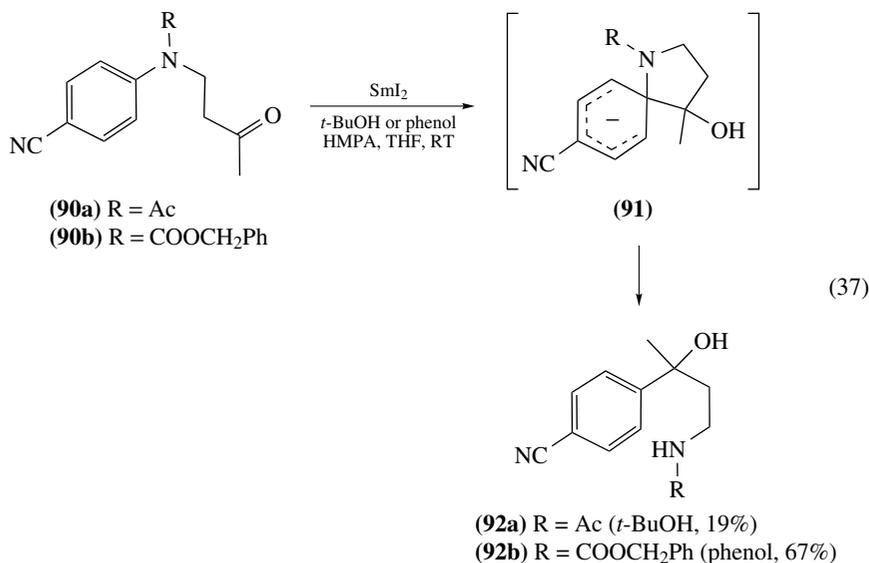
An N → N acyl migration along the side chain occurs slowly on standing of *N*-(2-methylaminoethyl)acetanilide **93** at room temperature and rapidly on heating **93** to give *N*-(2-anilinoethyl)-*N*-methylacetamide **94**[161] (equation 38).

Tandem [1,5]-H, [1,3]-NHPh and [1,5]-NHPh shifts were involved in the formation of pyrimidinones from *N*-arylamino-1,3-diazabuta-1,3-dienes and butadienylketene[162]. Some other interesting rearrangements taking place in a side chain attached to the nitrogen atom were also reported[162−165].

(38)
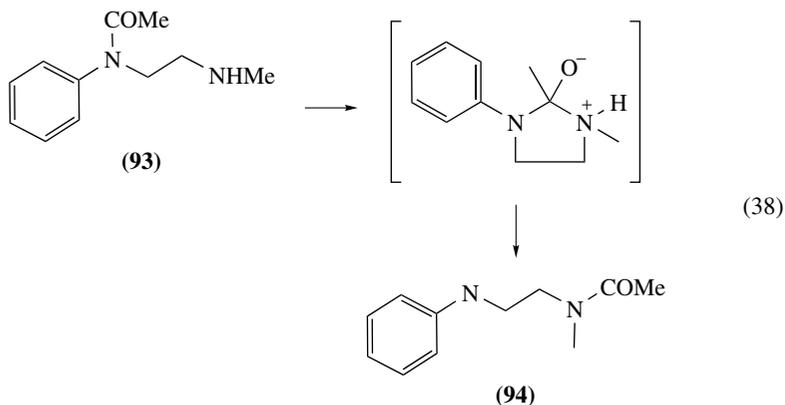
5. Arylimines

The anils (also called azomethines and Schiff bases) are characterized by *syn–anti* isomerizations that were studied in detail using NMR spectroscopy and kinetic measurements[166, 167]. One of the most known reactions of *N*-arylimines is the *Chapman rearrangement* (see reviews in References 168 and 169). This reaction can be represented as the thermal conversion of aryl *N*-arylbenzimidates **95** into *N*-aroyldiphenylamines **97** (equation 39). The intramolecular rearrangement with [1,3] shift of an aryl group from oxygen to nitrogen atom proceeds through a four-membered transition state **96.**

(39)
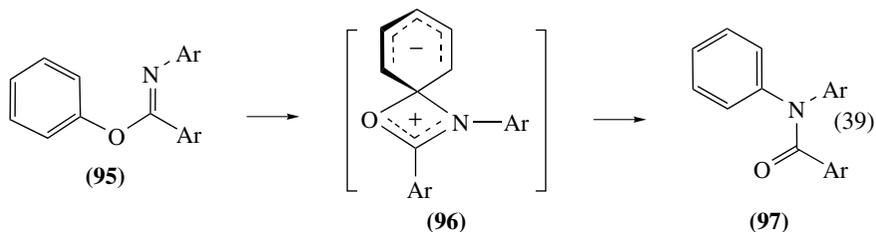
A preparative application of the Chapman rearrangement was used by many authors for the synthesis of diarylamines[170, 171] and *N*-aryl-substituted heterocycles[172] as well as dyes and brighteners[173]. The related Chapman-type *isourea rearrangement* (**98** → **99**) can also be referred to the anionic rearrangements[174] (equation 40).

Another analogous reaction is the *amidine rearrangement* that was also originally described by Chapman[175] and then investigated in detail by others[176–181] (equation 41) (the name 'amidine rearrangement' was used also for the Dimroth rearrangement, see Section IV.C). This N → N shift (**100** → **101**, R = aryl) can be facilitated by introduction of electron-withdrawing substituents into the aryl migrant[179].

The N → N type isomerization as a special version of the amidine rearrangement was described for the 2-arylaminotetrahydro-1,3-diazepine system **102**[176]. The reaction occurred under neutral conditions to form the rearranged products **103** in 24–83% yields (equation 42).

$$(40)$$

(98)   **(99)**
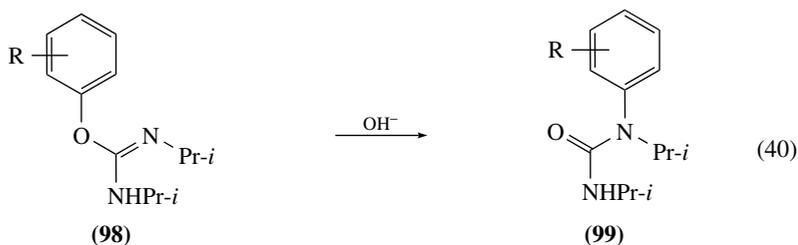
R = H, 2-Me, 3-Me, 4-Me, 2,4-Me$_2$, 2,5-Me$_2$, 3-MeO, 4-Ph, 4-Cl-3-Me

$$(41)$$

(100)   **(101)**
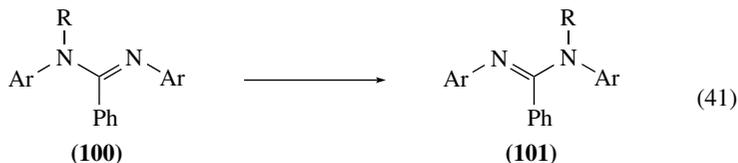
R = 2,4,6-(CF$_3$SO$_2$)$_3$C$_6$H$_2$, MeCO, PhCO, 4-NO$_2$C$_6$H$_4$CO,
    4-BrC$_6$H$_4$CO, CCl$_3$S, 2-NO$_2$C$_6$H$_4$S;
Ar = Ph, 4-MeC$_6$H$_4$, 4-MeOC$_6$H$_4$

$$\xrightarrow{\text{DMF} \atop 100-120\,°C}$$

(102)   **(103)**

$$(42)$$

R^1 = ... , Me— , PhCH$_2$, 3-MeC$_6$H$_4$CH$_2$, ... , H$_2$C—CH$_2$
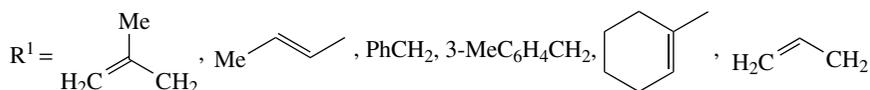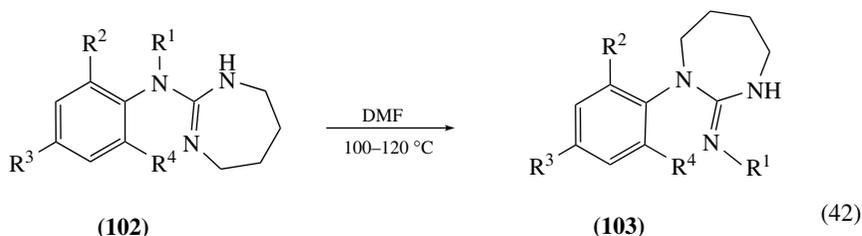
R^2 = Me, Cl; R^3 = H, Cl, NO$_2$; R^4 = Me, Cl

The mesylamides of the 2-arylimino-1,3-thiazolines and -thiazines **104** undergo a thermal isomerization similar to the amidine rearrangement to form the *N*-mesylanilines **105** by N → N shift of the mesyl group as a cation but not as a free radical[182] (equation 43).

Rearrangements of anils were described that proceeded upon oxidation of the starting substrates. Thus, oxidation of furan-2-carboximidamides **106** by (dicarboxyiodo)benzenes **107** resulted in *N*-acyl-*N*-furylureas **108**[183–185] (equation 44). Oxidation of *N*-arylimines **109** by sodium perborate tetrahydrate in CF$_3$COOH led to *N*,*N*-diaryl-substituted formamides **110**[186] (equation 45). Other examples of such oxidative rearrangements including the formation of imidoyl radicals have been reported[187, 188]. Rearrangements of nitrones as oxidized forms of anils were also observed[189, 190].

(104)   **(105)**   (43)
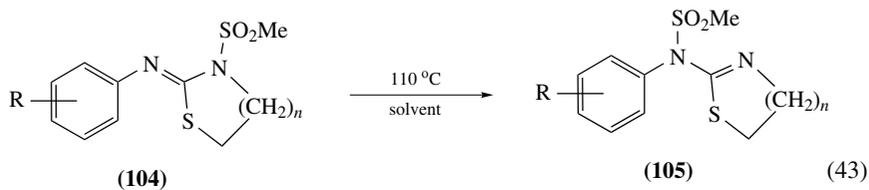
$n = 1, 2$

R = 2,6-Me$_2$, 2,4,6-Me$_3$, 2,6-Me$_2$-4-Br, 2,6-Me$_2$-3-NO$_2$, 2,6-Me$_2$-4-NO$_2$-3-Br

solvent = bromoform, biphenyl, diphenyl ether, nitrobenzene, pyridine

(106)   **(107)**

(108)

(44)
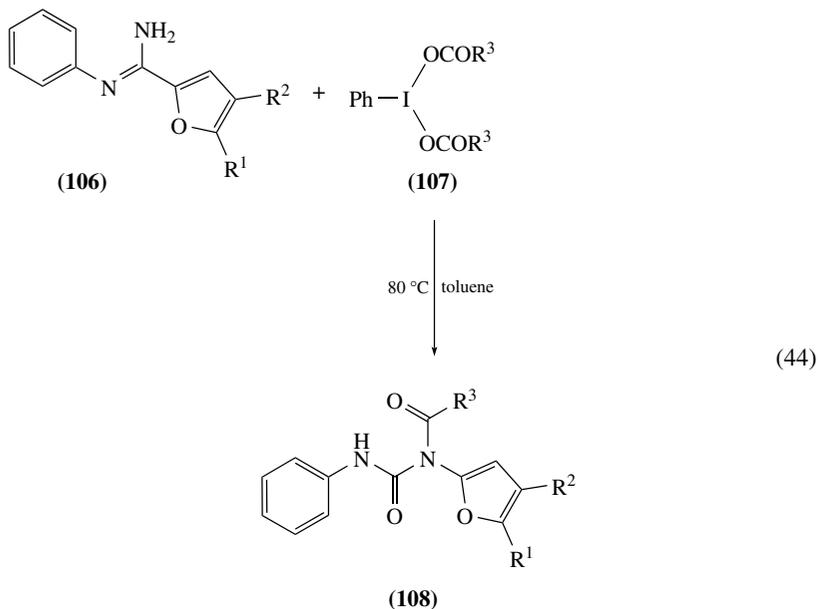
R^1 = H, Me, Ph, 4-MeC$_6$H$_4$, 4-MeOC$_6$H$_4$, 4-NO$_2$C$_6$H$_4$, 4-ClC$_6$H$_4$, 4-BrC$_6$H$_4$

R^2 = H, Me; R^3 = Me, Et, Ph, 2-furanyl

Several papers were devoted to rearrangements of *N*-aryl-β-chloroimines. Treatment of *N*-2-(1,1-dichloroalkylidene)anilines **111** with sodium methoxide in methanol gave rise to *N*-aryl α,β-unsaturated imidates **112** via a new type of Favorskii rearrangement[191]. The same starting compounds **111** were converted into *N*-alkylanilines **113** and **114** in the presence of LiAlH$_4$ in ether[192, 193] (equation 46). A proposed mechanism for these reactions assumed the formation of aziridine as well as azetidine intermediates[194].

The N=C double bond of anils can be a part of 1,5-diene systems that are able to undergo the aza-Claisen rearrangement (see Section III.A.2.b). Such asymmetric isomerization of allylic imidoester enolates **115** was observed upon deprotonation with lithium diethylamide to give the amides **116** in moderate yields but with good stereoselectivity[195] (equation 47).

$$(45)$$
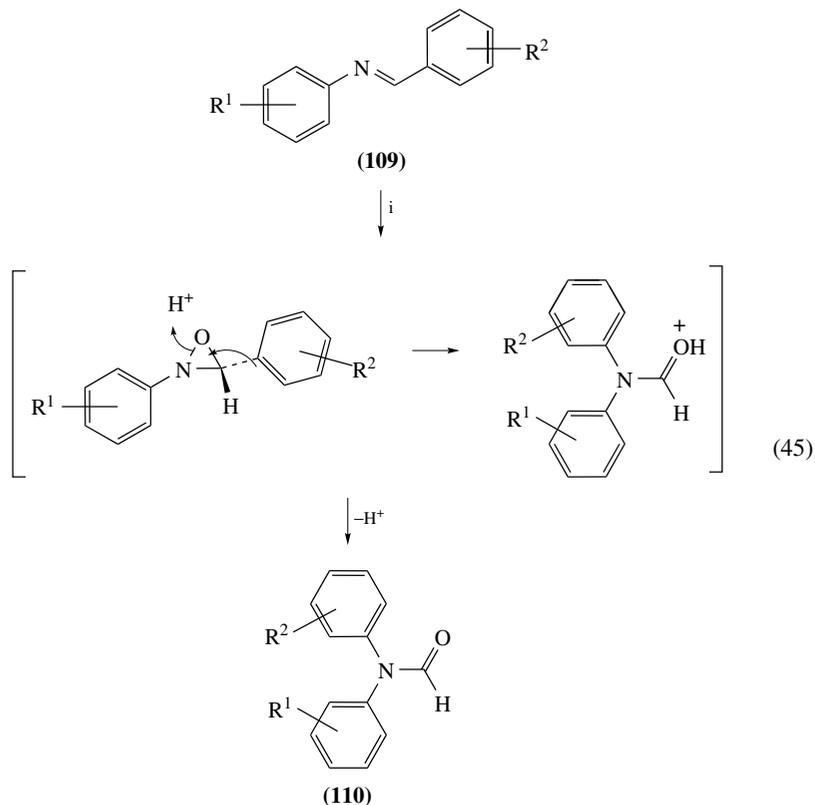
i = NaBO$_3$·4H$_2$O, TFA, 70–80 °C (11–54%)

R^1 = H, 4-Me, 4-Cl, 4-CF$_3$; R^2 = H, 4-Me, 2-Cl, 3-Cl, 4-Cl, 4-CF$_3$

R^1 = H, Me, MeO; R^2 = Et, i-Pr, n-Bu, t-Bu, n-Pen

$$(46)$$

(113) (62–73%)

(114) (24–33%)

R^1 = H, MeO; R^2 = i-Pr, t-Bu

$R^1, R^2 = Me, Et; R^3 = H, Me$

(47)

Ar =
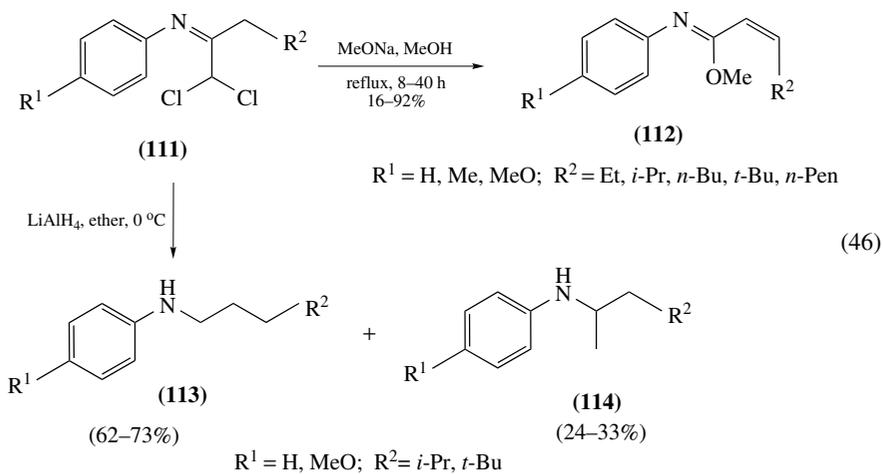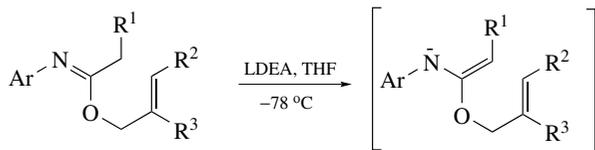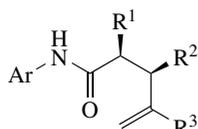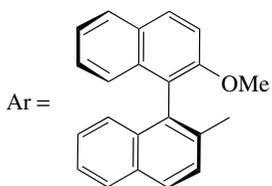
(116)

anti:*syn* = 98:2
de(*anti*) = 82–94%

EtOH
reflux, 2–5 h
42–67%

(117)   **(118)**
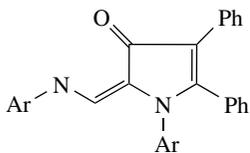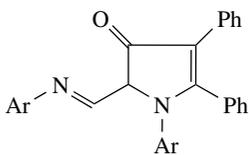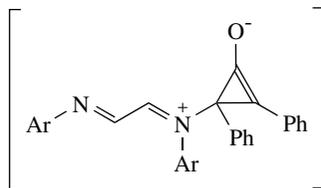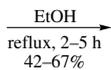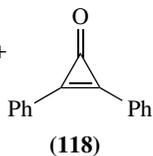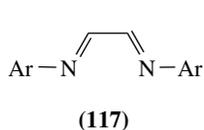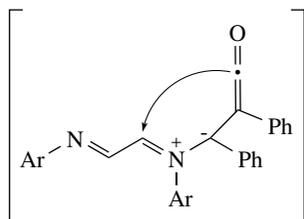
(119)   (48)

Ar = 4-MeC$_6$H$_4$, 4-MeOC$_6$H$_4$

(120)

Some other stereoselective rearrangements of anils were carried out using optically active ferrocene catalysts[196] and silica gel[197].

The synthesis of pyrrolinones **120** from diimines **117** and diphenylcyclopropenone **118** was reported as proceeding via rearrangement of the ketene intermediates **119**[198] (equation 48).

B. Aniline Derivatives Containing Ar−N−N Unit

1. Arylhydrazines

The rearrangement of phenylhydrazine to give *ortho-* and *para-*phenylenediamines was carried out using zeolite catalysts modified by some metals (e.g. Ga, Cr, Sm, V)[199]. However, the overwhelming majority of publications about the isomerizations of *N*-amino substituted anilines was devoted to the *benzidine rearrangement* that has been described in detail[23, 200−205]. The benzidine rearrangement proceeds usually under the action of acids on the hydrazobenzene **121** and its derivatives to afford one or more of five different products such as benzidine **122**, diphenyline **123**, *ortho-*benzidine **124** as well as *ortho-*semidine **125** and *para-*semidine **126** (the products of the so-called *semidine rearrangement*).

(121)   **(122)**   **(123)**

(124)   **(125)**   **(126)**
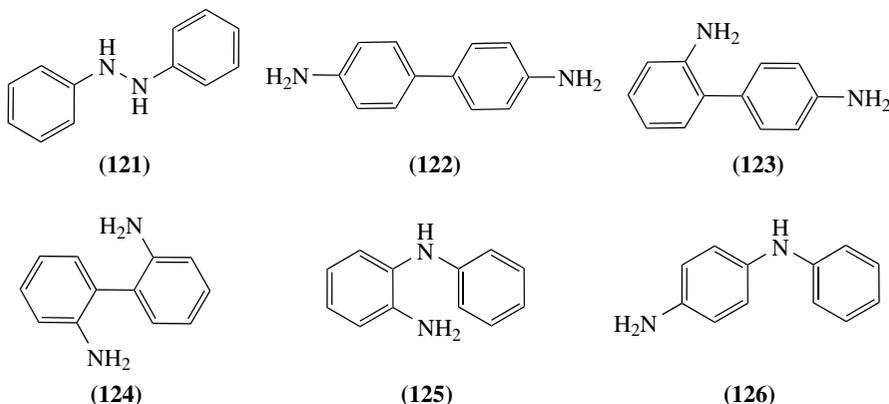
Moreover, the benzidine rearrangement can be performed as a thermal[206] and photochemical[207−209] isomerization. These transformations of arylhydrazines often compete with disproportionation reactions leading to the corresponding anilines and azobenzenes[201, 204]. Although this famous rearrangement is already well-known for over 150 years, its mechanism still remains unclear. It is undoubtedly established now that this reaction is an intramolecular transformation. However, there are several theories involving a π-complex, a caged-radical or polar transition state mechanisms[23, 200, 201, 204], which explain more or less adequately the known results of numerous investigations[210−215].

The benzidine rearrangement found very wide application in synthesis of many aromatic structures. A combination of disproportionation (**127** → **128**) and semidine rearrangement (**128** → **129**) was employed as an approach to some polycyclic systems[216, 217] (equation 49). The benzidine rearrangement was used as the key step in synthesis of benz[*c,d*]indolinones[218], fluorinated polyimides[219], 2,2′,4,4′-tetrasubstituted twisted benzidines[220] and antitumor antibiotic derivatives[221]. Not only diarylhydrazines

but also the corresponding heterocyclic derivatives such as phenylhydrazopyridines[222, 223], arylhydrazoindoles[224] and phenylhydrazothiazoles[225] can react via a benzidine-like rearrangement. It was shown that 1,2-diphenylhydrazine **121** isomerized exclusively to *ortho*-semidine **125** in the presence of square planar rhodium complexes[226].

(49)
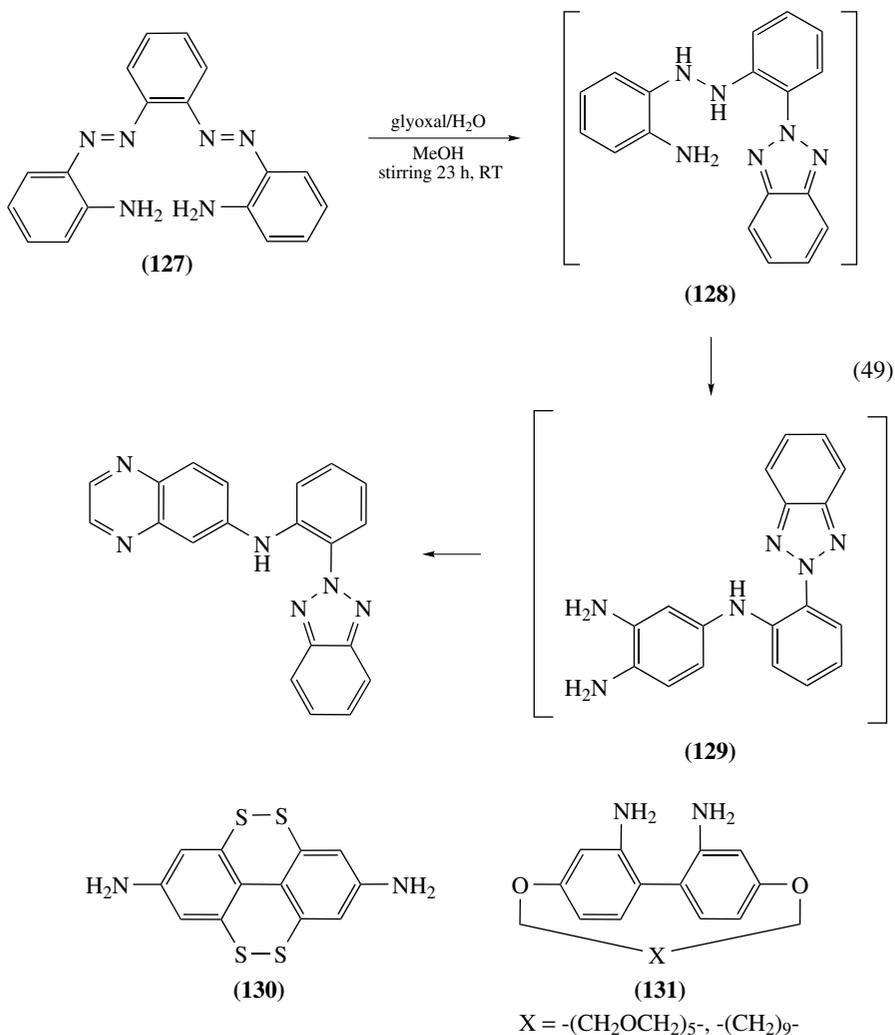
The benzidine rearrangement was employed recently for the preparation of unique bridged diaminodiphenyls **130** and **131**[227, 228]. An unprecedented [9,9]-sigmatropic shift was discovered in the acid-catalyzed benzidine rearrangement of bis[4-(2-furyl)phenyl]

diazane **132**[229] (equation 50). It is interesting that the corresponding *para*-hydrazobiphenyl **133** as well as two bis(3-heterylphenyl)diazanes **135** under the same conditions gave rise to the products of previously reported[212] *ortho*-semidine **134** and *para*-benzidine **136** rearrangements (equations 51 and 52). The authors believe that this result supports the new Shine's formulation that the benzidine rearrangement follows the pattern of sigmatropic processes[229].

(50)

(51)

(52)
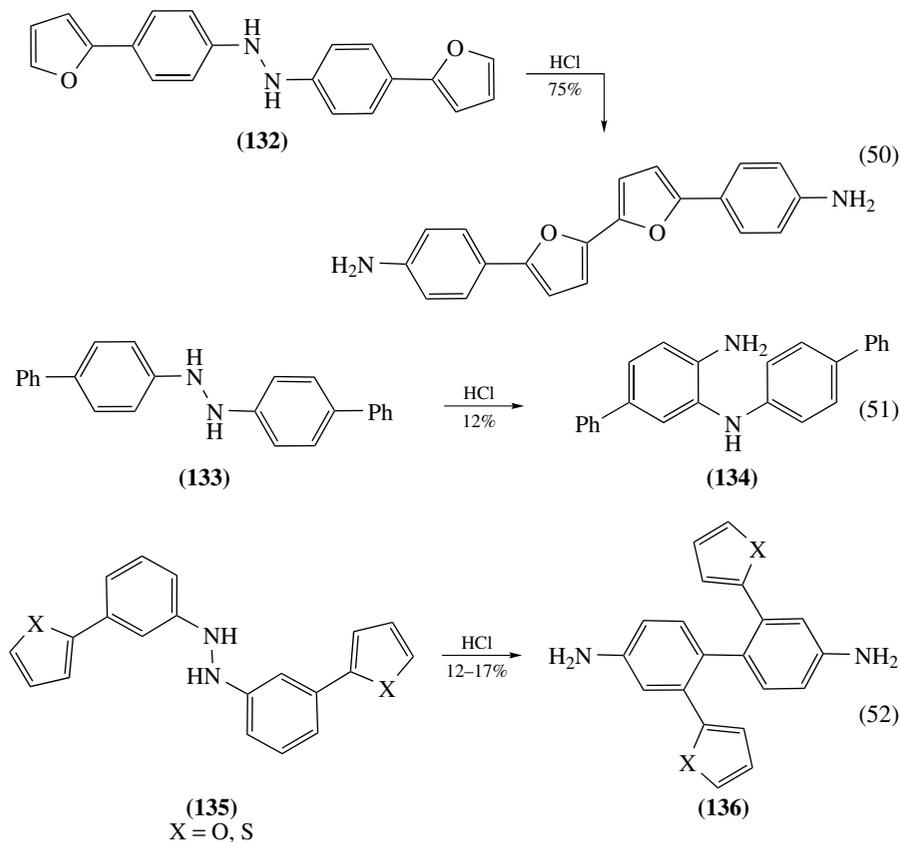
The arylhydrazine derivatives can also participate in other than benzidine isomerizations. Thus, a novel rearrangement of fused *N*-arylamino-substituted 1,4-dihydropyridines **137** resulted in the formation of quinindoline derivatives **139**[230, 231] (equation 53). A proposed mechanism of this reaction assumes a [3,3]-sigmatropic shift like a Cope rearrangement through unstable intermediate **138**.

The hydrazine **140** rearranged when refluxed with HBr in acetic acid solution to furnish the two indole derivatives **141** and **142**[232] (equation 54). The formation of product **141** is in agreement with the mechanism of the Fischer indole synthesis (*vide infra*).

(137) → **(138)** → **(139)**

EtOH
reflux 2–20 h
42–82%

−NH$_3$

(53)
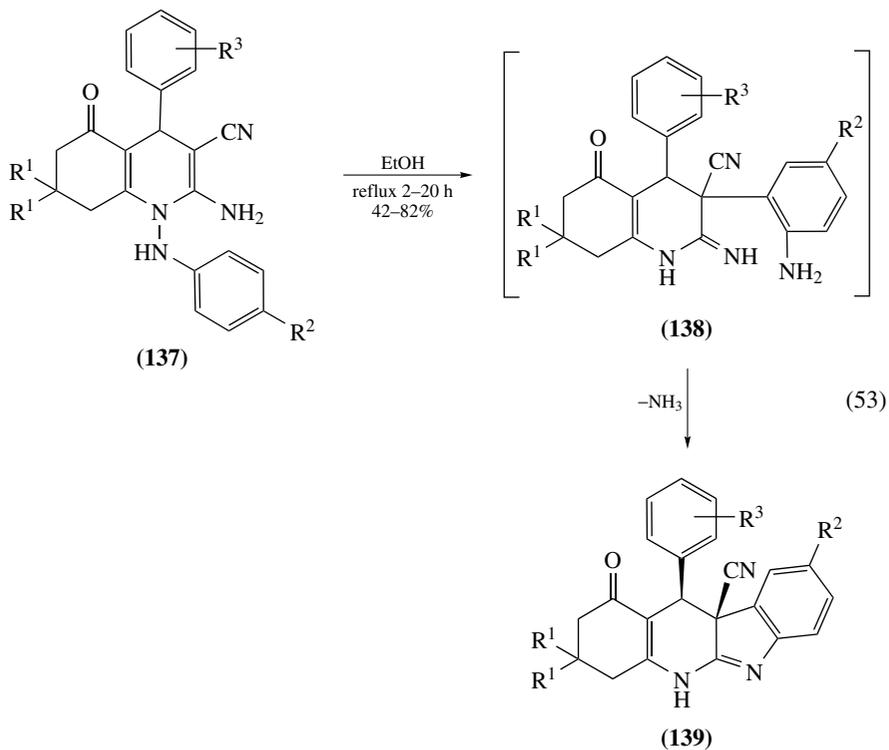
R^1, R^2 = H, Me; R^3 = H, 3-MeO, 4-MeO, 2,5-(MeO)$_2$, 3,4,5-(MeO)$_3$, 4-Br, 4-NO$_2$, 3-NO$_2$

(140) → **(141)** + **(142)**

HBr
AcOH,
100 °C, 1 h

(54)
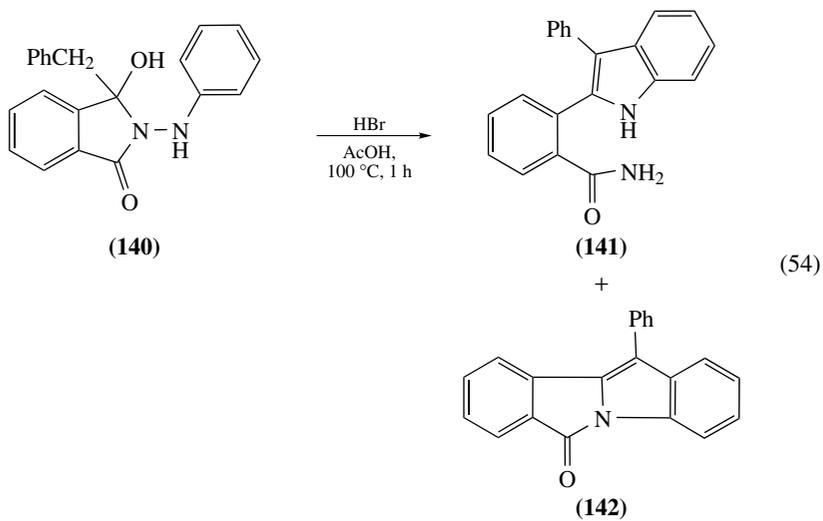
2. Arylhydrazones

The hydrazo rearrangement (the N—N bond cleavage **143** → **144**) is a key step of Fischer's indole synthesis and regarded as a [3,3]-sigmatropic reaction related to the Chapman and Cope rearrangements[233, 234] (equation 55). Within the framework of the Fischer indole synthesis the behavior of some pyrazolines **145**, tetrahydropyridazines **147** and tetrahydro-1,2-diazepines **149** incorporating a hydrazonic unit in the cycles was studied under strongly acidic conditions (polyphosphoric acid)[235]. [3,3]-Sigmatropic rearrangements were observed to occur in all the cases through the corresponding enehydrazine intermediates **146, 148** and **150** (equations 56–58). An interesting variation of the Fischer indole synthesis that consisted of the reaction of arylhydrazines with γ-chloroalkyl ketones was developed (see review in Reference 236). This reaction was employed recently to prepare the tryptamine derivatives **153** starting from the ethyl 4-hydrazinophenylacetates **151** and 3-chloropropyl ketone **152**[237] (equation 59).
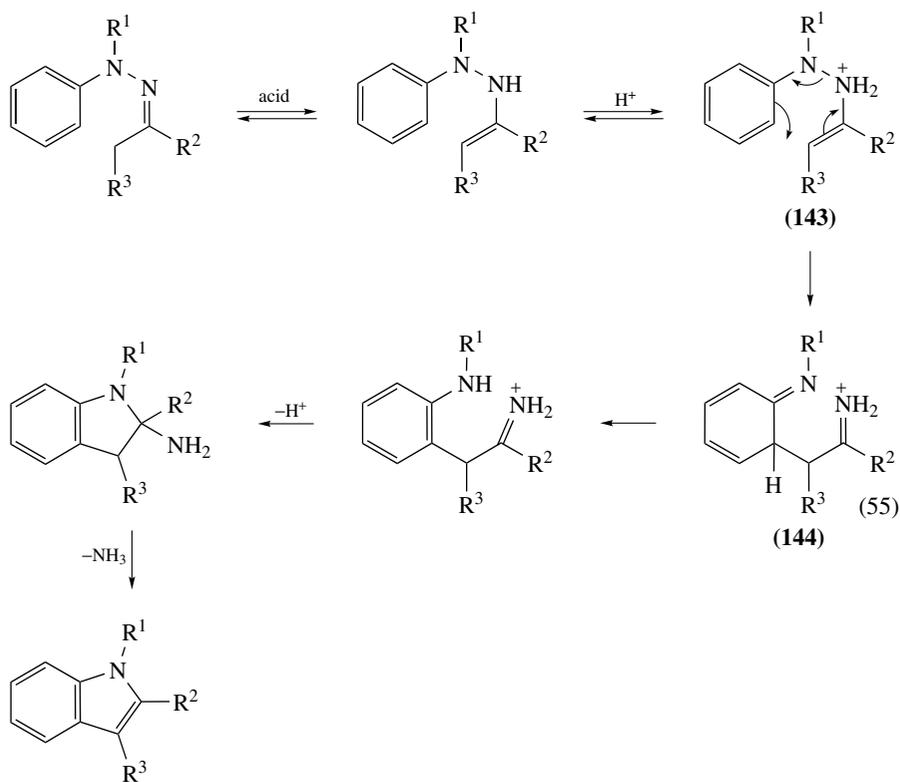
$R^1 = H$, alkyl, acyl; $R^2, R^3 = H$, alkyl, aryl

(56)

(57)

(58)

$$(59)$$

(153)

$$R^1, R^2 = H, Me$$
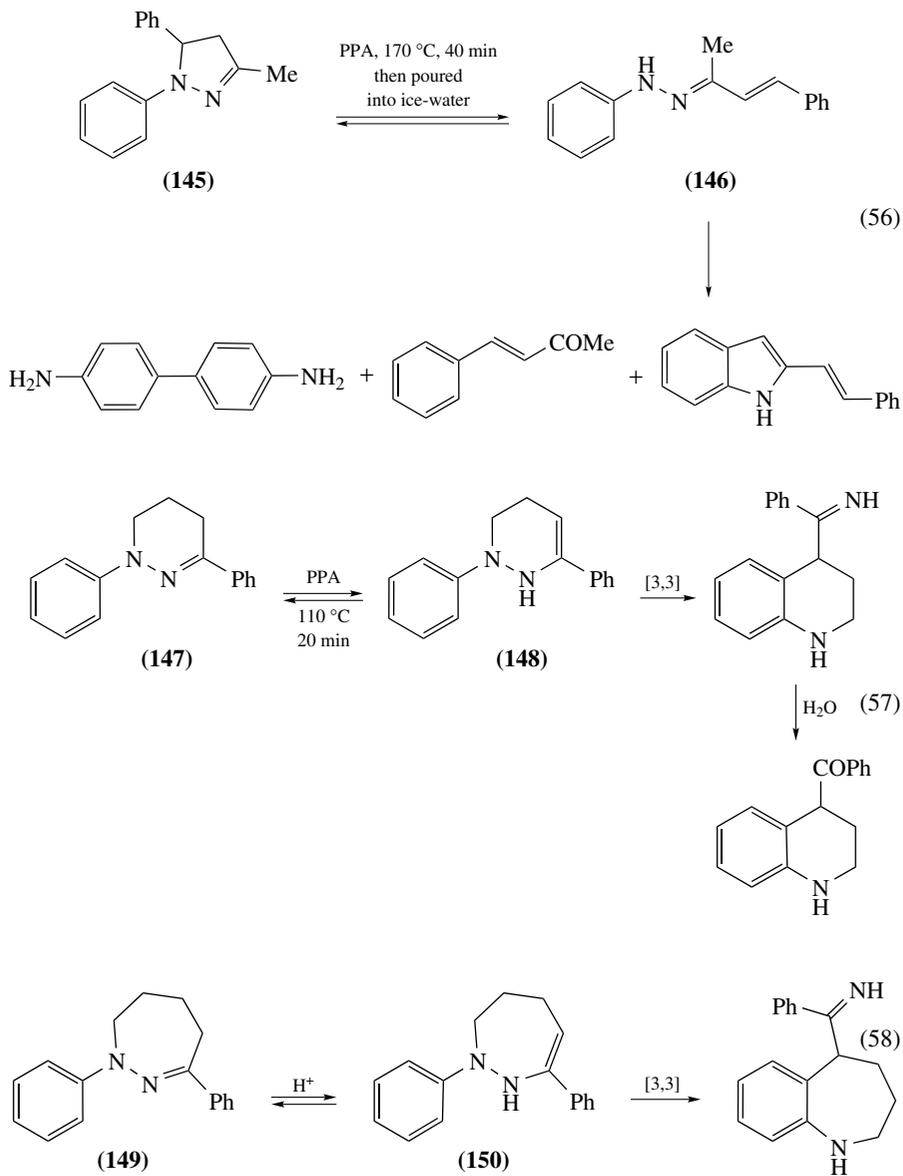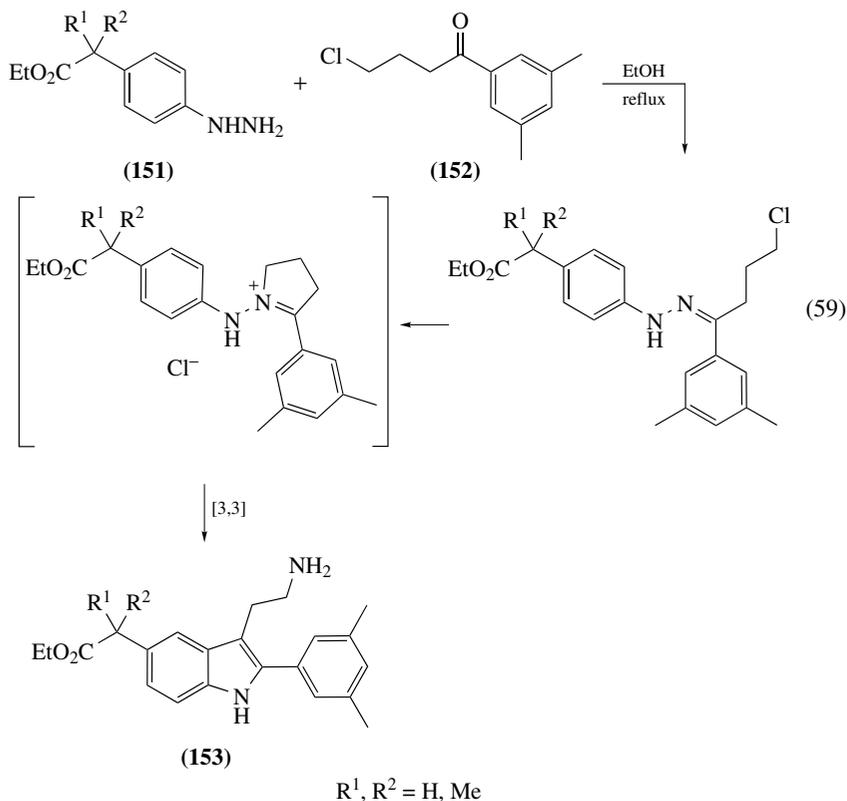
An unprecedented [3,5]-rearrangement was reported to be involved in the conversion of α-(arylthio)acylhydrazones **154** into 4-aminophenyl phenyl sulfide **155**[238] (equation 60). Some other rearrangements of arylhydrazones resulting in indole[239] and triazole derivatives[240] as well as in 3-azapyranosic N-arylaminolactams[241] are also noteworthy.

$$(60)$$

$$R = Me, Ph$$

(155)
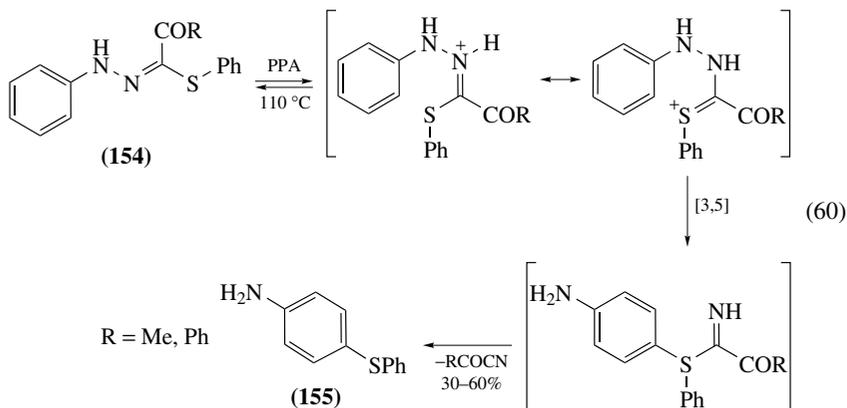
Base-catalyzed isomerization (called 'mononuclear heterocyclic rearrangement') was described for the formation of Z-phenylhydrazone of 3-benzoyl-1,2,4-oxadiazole **156** into 4-benzoylamino-1,2,3-triazole **157**[242, 243] (equation 61).

$$(61)$$

(156)   R = H, NO$_2$ **(157)**
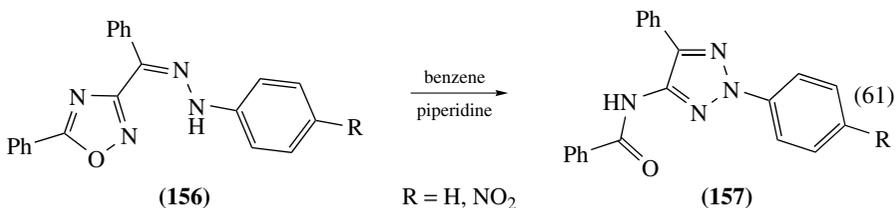
3. Aryltriazenes

The well-known *diazoamino–aminoazo rearrangement* (**158** → **159**) is an inter-molecular reaction occurring stepwise via acidolysis followed by azo coupling[23, 244, 245] (equation 62). This mechanism was supported by isolation of 4-hydroxyazobenzene when the reaction was carried out in the presence of phenol[23].

$$(62)$$

(158)

(159)
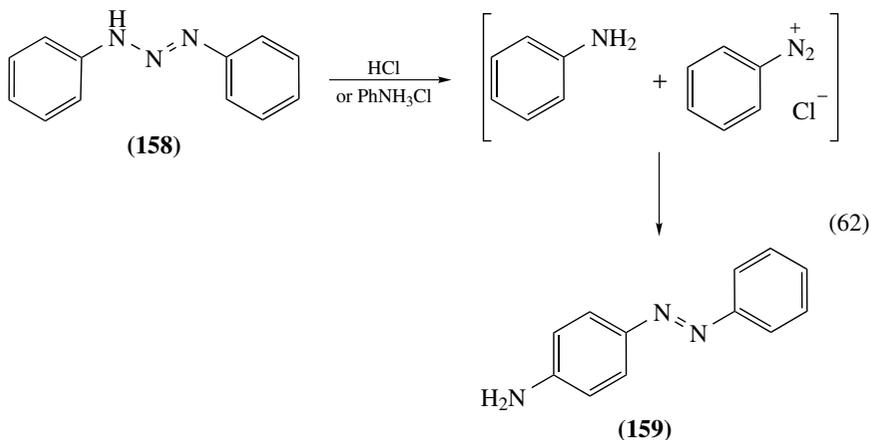
Hydroxytriazolines **160** were rearranged into the corresponding isoquinolinediones **162** upon thermolysis in benzene at 95 °C for 24 hours[246] (equation 63). A probable mechanism assumes a thermal ring-cleavage fragmentation of the starting compounds **160** to the corresponding diazo ketoamides **161** followed by thermal Wolff rearrangement (see also Reference 247).

4. Aryldiazenes

Irradiation of pentacarbonyl iron in the presence of 1-*tert*-butyl-2-aryldiazenes **163** pro-duced in the first step the *ortho*-metallated complexes **164**, which in next thermal step

underwent an *ortho*-semidine rearrangement to give complexes **165**[248] (equation 64). A new thermal rearrangement of sterically crowded α-azo alcohol **166** into bridged bicyclic ring-expanded lactam **168** proceeded via N-protonated intermediate **167**[249] (equation 65).

$R^1 = $ Me, Ph; $R^2 = $ 4-NO$_2$, 4-Cl

(63)

(64)
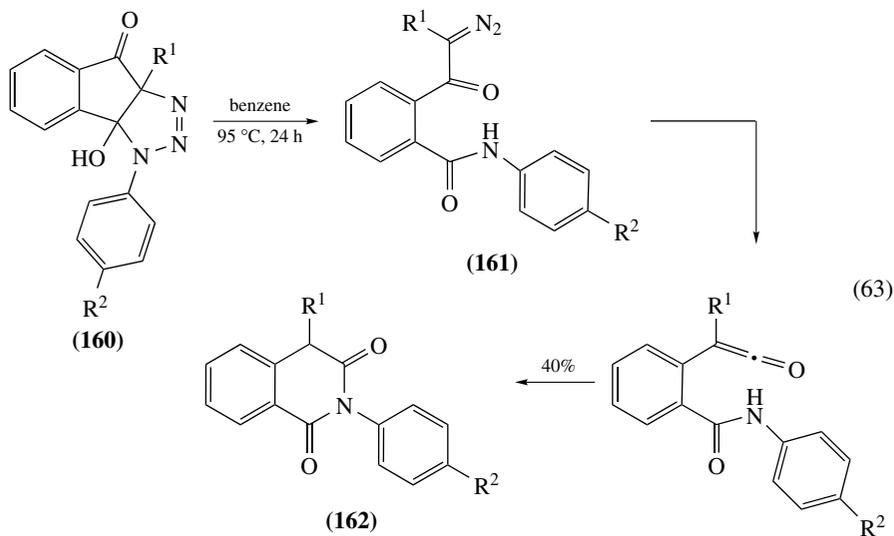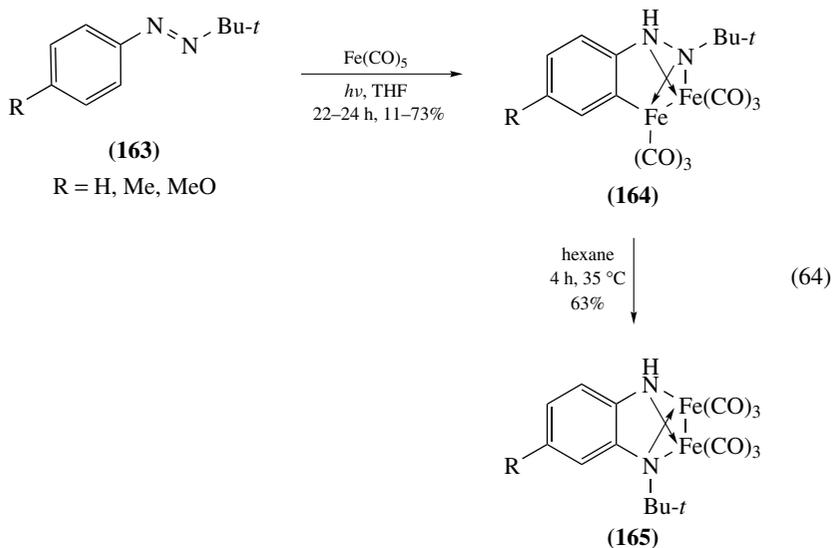
(65)
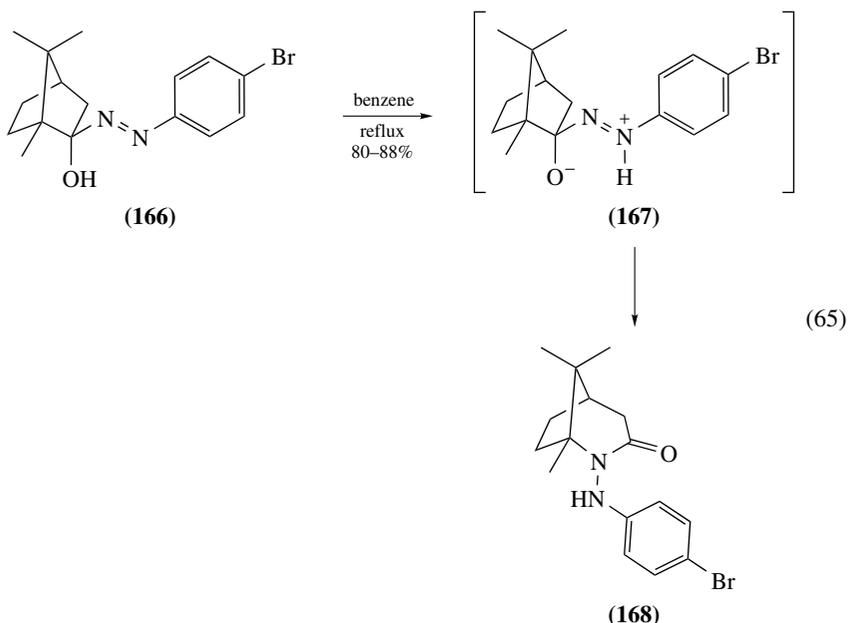
5. N-Nitroanilines

The *aromatic nitramine rearrangement* has been known already for more than 100 years. This reaction can proceed as an acid-catalyzed, thermal and photochemical reaction (see reviews in References 23,250–252). *N*-Nitroaniline **169**, being treated with strong acids, rearranges to give *ortho*-nitroaniline **170** as main product (50–60%), *para*-nitroaniline **171** (5–10%) and some side products (equation 66)[251].

The reaction is considered as an intramolecular process and partially as an intermolecular one, and the 'cation-radical' pathway is regarded as the most reliable mechanism[251, 253] that can be illustrated by the generalized scheme[253] of equation 67. However, more recently an opinion was expressed, that intermediates of the nitramine rearrangement can be formed without any intervention of a proton[254–256].

(66)
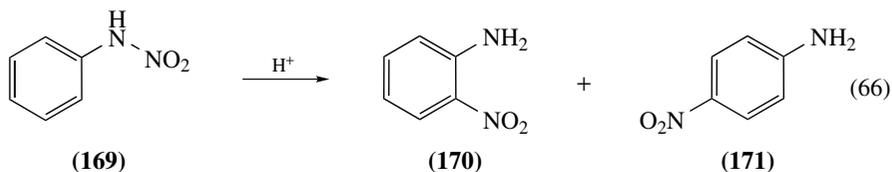
The nitration of a number of anilines **172** in *ca* 70% sulfuric acid was reported as *ipso*-attack followed by a 1,3-rearrangement of the nitro group. The reaction occurs through the *ipso*-intermediate **173** to afford *ortho*-nitroaniline **174**[257] (equation 68).

(67)

(68)

(172)   **(173)**   **(174)**
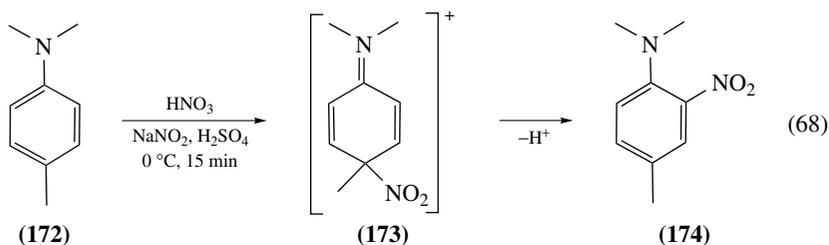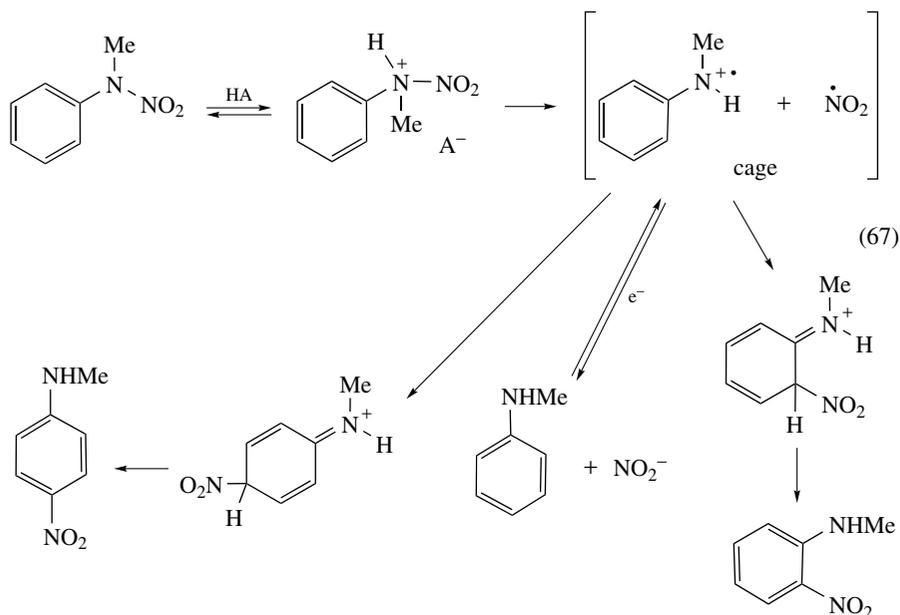
6. N-Nitrosoanilines

The acid-catalyzed isomerization of *N*-nitrosoanilines **175** to *para*-nitrosoanilines **176** is usually called the *Fischer–Hepp rearrangement*[23, 258, 259] (equation 69).

(69)

(175)   **(176)**

R^1 = alkyl, aryl; R^2 = alkyl, Cl, Br, COOH
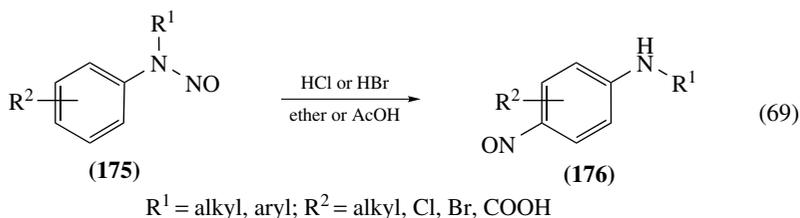
In spite of the fact that this reaction was discovered more than hundred years ago, there is very scanty information concerning its mechanism. Some papers reported evidence in favor of an intermolecular mechanism (i.e. acid-induced denitrosation followed by C-nitrosation of the aromatic nucleus)[23, 258] while other articles describe observations and measurements that support an intramolecular occurrence of the isomerization as in the nitramine rearrangement[260−263]. On the other hand, carrying out the reaction by using three different types of clays (both in the solid state and in a solvent) provided arguments for an intermolecular nature of the rearrangement[264]. It should be noted that the Fischer–Hepp rearrangement found very restricted application in the organic synthesis.

C. Aniline Derivatives Containing Ar−N−O Unit

1. Bamberger rearrangement and other reactions of N-arylhydroxylamines

The acid-catalyzed conversion of *N*-hydroxyanilines **177** into *para*-hydroxyanilines **179** is well-known as the *Bamberger rearrangement* (see reviews in References 23,265−267). It is the opinion now that this intermolecular reaction follows a mechanism of monomolecular S_N1 nucleophilic substitution via intermediate nitrenium ion **178** (see review in Reference 268) (equation 70).
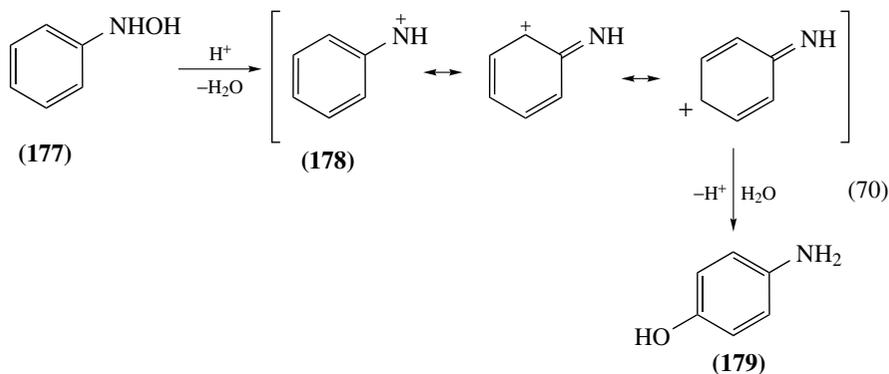
If the reaction mixture contains other nucleophiles in addition to water, such as alcohols, halide anions as well as phenol, the Bamberger rearrangement can lead to the corresponding 4-R-anilines where R = AlkO, PhO, Cl, Br, F[269, 270]. When the reaction is conducted in benzene or toluene in the presence of CF_3SO_3H it gives aminobiphenyls and diphenylamine[271]. The Bamberger rearrangement was studied by the AM1, MNDO and PM3 quantum-chemical methods[272].

Some interesting transformations were described for N-substituted *N*-arylhydroxylamines. The α-aminohydroxamic acids **180** rearranged in the presence of amines to give *N*-acyloxyarylamines **181** (N → O transacylation)[273] (equation 71).

$$(71)$$
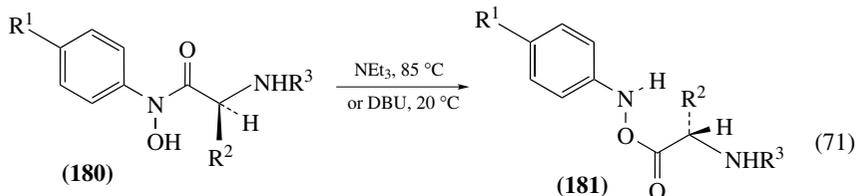
R^1 = H, Me, MeO, Cl; R^2 = H, Me, *i*-Pr, PhCH$_2$, CH$_2$CHMe$_2$, CH(Me)CH$_2$CH$_3$;
R^3 = H, PhCH$_2$

$$(72)$$
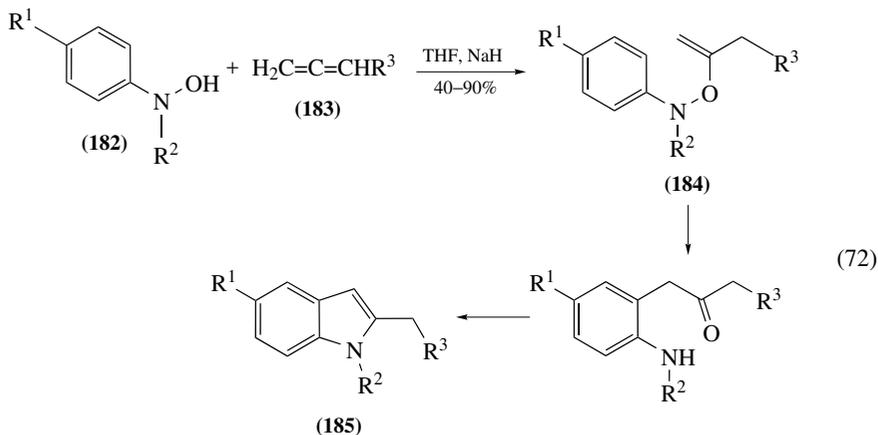
R^1 = H, Me, MeO, Cl, COOMe; R^2 = Et, COMe, COOCH$_2$Ph, PhCH$_2$;
R^3 = CN, COOMe, COOEt, PO(OEt)$_2$, POPh$_2$, SO$_2$Me, SO$_2$Ph, SOMe, SOPh, 4-Me-pyridyl

$$(73)$$
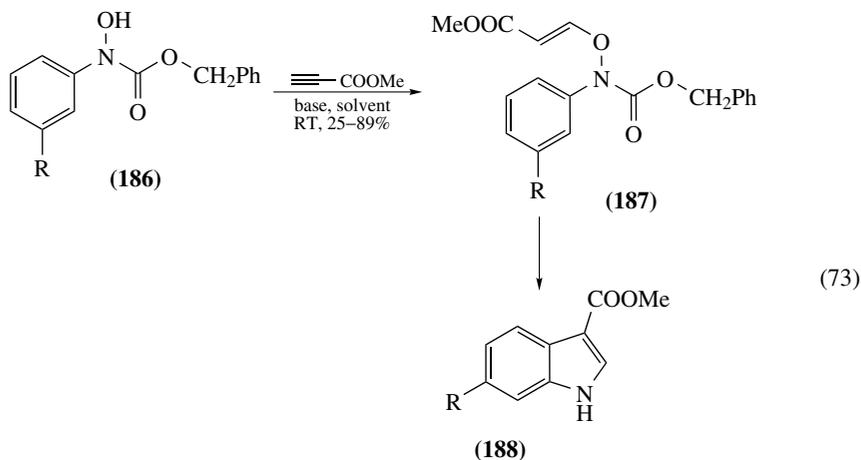
R = H, MeO
base: Et$_3$N, N-methylmorpholine, *i*-Pr$_2$NEt; solvent:C$_6$H$_6$, CH$_2$Cl$_2$, MeCN, MeNO$_2$

The Michael addition of allenes **183**[274] or methyl propiolate[275] to N-substituted *N*-arylhydroxylamines **182** and **186** gave rise to *O*-vinyl-*N*-arylhydroxylamines **184** and **187**, which underwent a hetero-Cope rearrangement resulting in indoles **185** and **188** (equations 72 and 73) (about hetero-Cope rearrangement of *N*-arylhydroxylamines, see also Reference 276). A curious amino group migration was observed on treating *O*-phenylhydroxylamine with trifluoroacetic acid to form 2-aminophenol (50%) and 4-aminophenol (7%)[277].

2. Arylamine N-oxides

The thermal isomerization of arylamine *N*-oxides **189** into substituted hydroxylamines **190** is known as the *Meisenheimer rearrangement* (see review in Reference 278, and Reference 279) (equation 74). In this case[279] the Meisenheimer rearrangement (i.e. the [2,3]-sigmatropic shift **189** → **190**) is followed by [1,3] oxygen shift to carbon (**190** → **191**) on further heating.

$$R^1 = H, Me; \quad R^2 = Me, Ph, CH_2OPh, CH_2OC_6H_4Cl\text{-}4, CH_2OC_6H_4Me\text{-}4$$
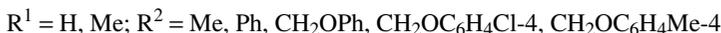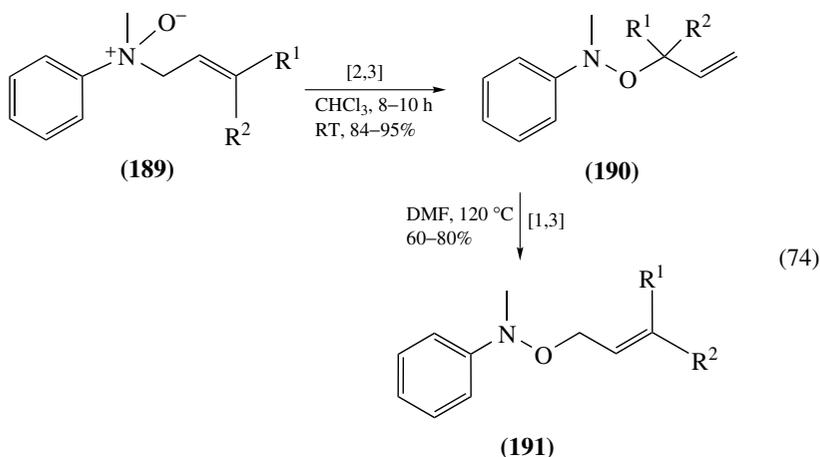
Only certain groups show a tendency for migration from nitrogen to oxygen. These include allyl, benzyl, neopentyl, tetrahalopyridyl and homoadamantyl as well as substituted phenyl groups[280]. An intramolecular cyclic mechanism which proceeds via three-[280] and five-membered[281] transition states was proposed for the reaction. On the other hand, some experimental facts were found in favor of a homolytic scission–recombination mechanism accompanied by a cage effect[282–285].

An introduction of nitrogen substituents to the *ortho-* and *para*-position of *N,N*-dimethylaniline through suitable *N*-oxide derivatives **194** was reported in a related reaction between the *N*-oxide **192** and nitrilium salts **193**, which lead to the acetamides **195** and **196**[286] (equation 75).

(75)

(192)   (193)

(194)

(196)   (195)

15–22%   34–45%

R = Me, Et, i-Pr; X = FSO_3^-, BF_4^-, $SbCl_6^-$
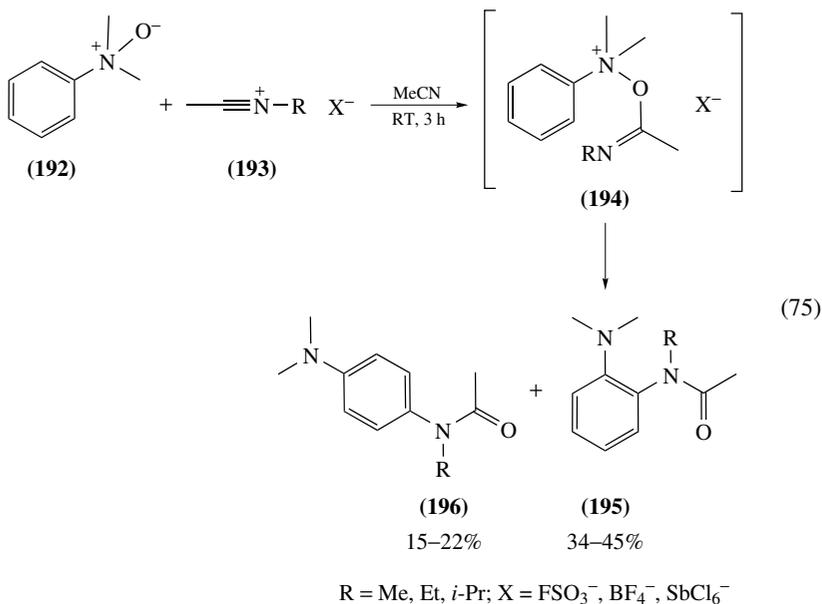
D. Aniline Derivatives Containing Ar−N−S Unit

The *arenesulfenanilide rearrangement* is another member of an important class of rearrangements described above, such as the benzidine, quinamine and nitramine rearrangements. This rearrangement consists of the conversion of arenesulfenanilides **197** into *ortho-* and *para-*aminodiphenyl sulfides **198** and **199**[287, 288] (equation 76). Substitution at the *para-*position generally predominates over *ortho-*substitution[289].

(197)   (198)

+   (76)

(199)
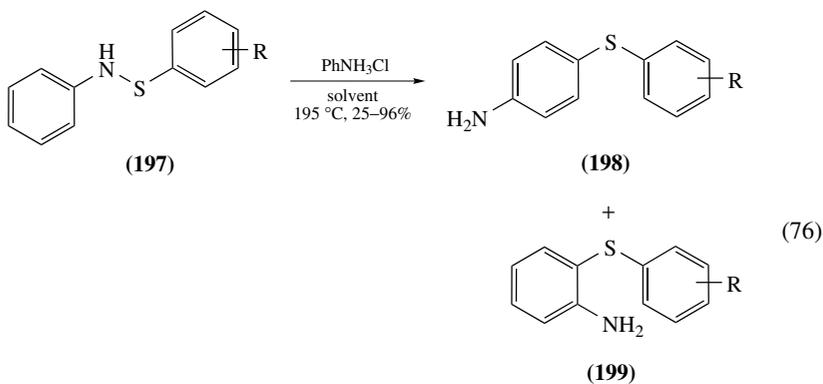
R = H, 4-Me, 4-Cl, 4-Br, 2-NO_2, 3-NO_2, 4-NO_2;
solvent: aniline, anisole, *N,N*-dimethylaniline

The sulfenamides **200** undergo [3,3]-sigmatropic rearrangement followed by cycliza-tion of the intermediate imino-thioaldehydes **201**, which yields the corresponding 1*H*-benz[*g*]indoles **202**[276] (equation 77).

(200) R = H, Me **(201)** **(202)** (77)
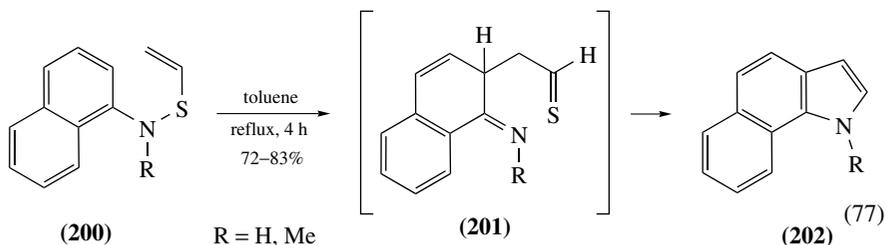
Heating of *N*-aryl-1-alkynesulfenamides **203** in benzene for 3 hours resulted in smooth transformation into the substituted indoline-2-thiones **204**[290] (equation 78).

(203) **(204)** (78)

R = Me, CH$_2$Ph
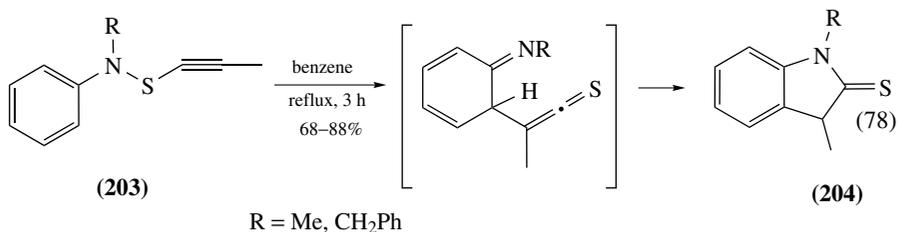
A new synthetic strategy which leads specifically to *ortho*-functionalization of aromatic amines was based on the initial formation of the intermediate aminosulfonium ions **205**, which were converted into ylides **206** in the presence of bases[291] (equation 79). The ylides **206** underwent [2,3]-sigmatropic rearrangement to the *ortho*-substituted anilines **207**.

(205) **(206)** (79)

(207)

Various examples illustrating a synthetic application of this strategy were described[292-295]. The ylides **210** can be obtained by the interaction of sulfides **208** with phenylnitrene **209** generated by thermolysis of phenyl azide[296] (equation 80).

$$R^1 = H; R^2 = Me, Ph; R^1R^2 = -(CH_2)_3-, 2,2'-biphenyl$$

A rearrangement of an *S,N*-ylide in the reaction of 2,5-dihydrothiophene with 4-chloroaniline to afford 2-dihydrothienylaniline was reported recently[297]. The analogous *ortho*-thiomethoxymethylation of the aniline nucleus was observed in the course of rearrangement of *N*-aryl-*S,S*-dimethylsulfimides obtained from anilines by action of DMSO in the presence of P_2O_5 and triethylamine[298, 299].

A method to synthesize amino sulfoxides **212** and **213** was developed based on the rearrangement of sulfinamides **211**[300] (equation 81). The adduct of phenyl sulfonylamine and quadricyclane, i.e. 1,2-thiazetidine-*S*-oxide **214**, underwent smooth rearrangement to furnish the fused 1,4-thiazine-*S*-oxide **215**[301] (equation 82).

The rearrangements of *N*-sulfonylanilines **216** and **218** resulting in the corresponding 2-(arylsulfonyl)anilines **217** and **219** can be carried out in the presence of both acids[302] and bases[303] (equations 83 and 84) as well as by a photochemical reaction upon irradiation with a high-pressure mercury lamp[304].

$$\text{(83)}$$

R = Me, Et, Pr, Bu

(216)   **(217)**

$$\text{(84)}$$

(218)   **(219)**

R^1 = H, 4-MeO; R^2 = Me, Et, Ph; R^3 = H, 2-Me, 4-Me, 4-MeO, 4-NMe$_2$
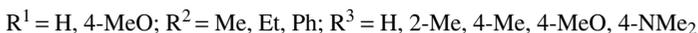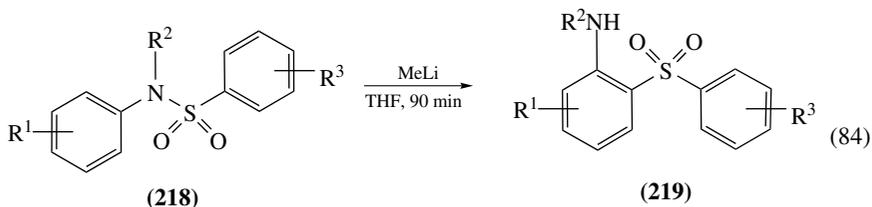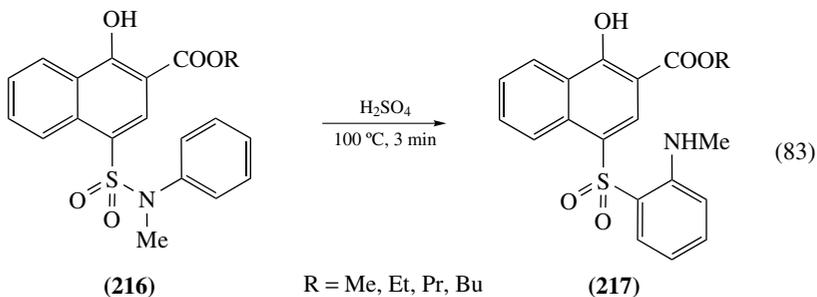
The rearrangement of arylaminosulfuric acids (arylsulfamic acids) **220** to the corresponding ring-sulfonated anilines **221** and **222** was of great interest from both mechanistic and synthetic viewpoints, because these above-named acids have been postulated as intermediates in the sulfonation of aromatic amines with sulfuric acid[305] (equation 85).

$$\text{(85)}$$

(220)   **(221)**   **(222)**
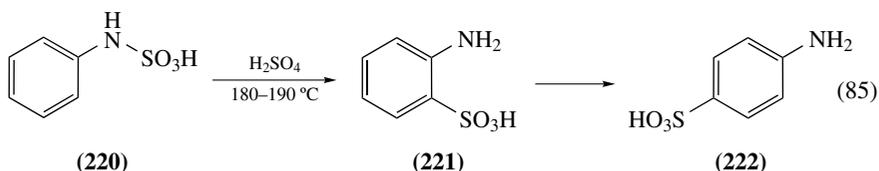
This process is of great practical importance, and therefore many investigations were devoted to optimization of this reaction[306–309].

E. Aniline Derivatives Containing Ar—N—Hal Unit

The mechanism of the thermal and acid-catalyzed rearrangement of *N*-alkyl-*N*-chloroanilines **223** to *ortho-* and *para*-chloroanilines was studied intensively for many years, because this reaction is a part of a large series of related isomerizations that can be characterized by moving a migrant group from the nitrogen atom to the aromatic nucleus[310, 311] (equation 86).

(86)

(223)

R = Me, *t*-Bu

(87)
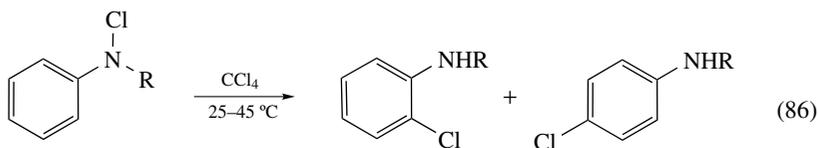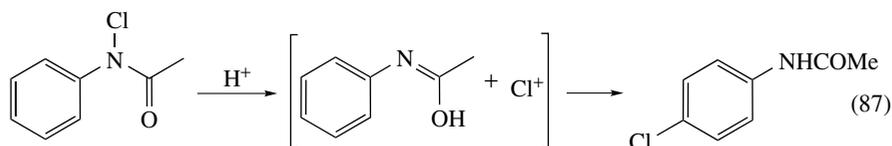
(224)   (225)

However, there is much more information about a rearrangement of *N*-acyl-*N*-chloro-anilines such as **224** into 4-chloroacylanilides **225**[23, 312, 313] (equation 87). This inter-molecular reaction, known as the *Orton rearrangement*, is typical also for N-brominated acetanilides[310]. The theoretical investigations of the transformations of *N*-fluoroaniline were reported recently[314]. A few reports described the rearrangements of anilines con-taining an N−P bond[315, 316].

IV. REARRANGEMENTS OF OTHER COMPOUNDS TO FORM ANILINES

The reactions below are well-known methods for the preparation of anilines from com-pounds other than aromatic amines.

A. Anilines from Phenol Derivatives

The thermal and photochemical Smiles rearrangement (Section III.A.4.a) is most often employed for the transformation of O-substituted phenol derivatives **226** into N-substituted anilines **227** that occurred with aryl migration from oxygen to nitrogen[317] (equation 88).

(88)
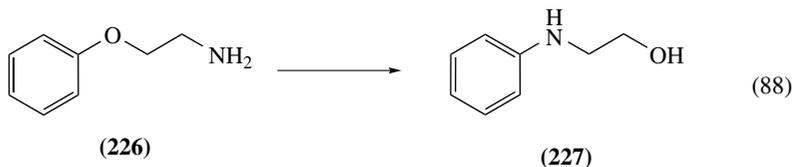
(226)   (227)

Some examples of the Smiles rearrangement that dealt with ring-polyfluorinated phenol derivatives[318] and phenols containing *O*-(acylamino)ethyl groups were published[319]. A most critical step in this transformation of phenols into anilines (called also 'alkylation—rearrangement—hydrolysis sequence') is the final stage, namely the removal of the N-side group. It was found that hydroxyacetyl as well as 2-hydroxy-2-methylpropionyl moieties are the best leaving groups (equation 89), and their preparative application was described repeatedly[320−323]. This rearrangement was used to prepare

alkaloid derivatives[324], polycyclic structures[325] and even phosphate esters[326]. The first example of alkoxide-accelerated Smiles rearrangement was reported some time ago[320].

(89)
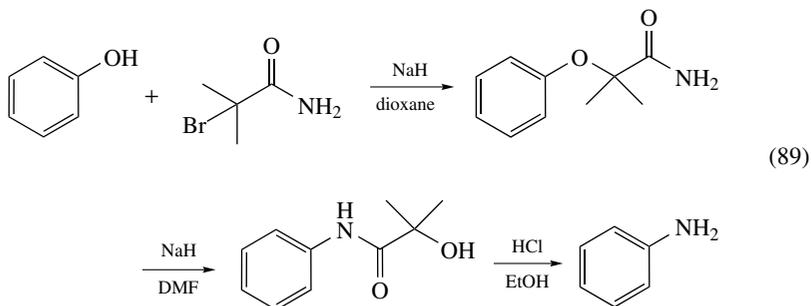
A peculiar method for synthesis of anilines that included as a key step the thermal rearrangement of 4-aryloxy-2-phenylquinazoline **228** to a 3-aryl-2-phenyl-4(*3H*)quinazolinone **229** was described[327] (equation 90).

(228) (90)

(229) R = H, 2,4-Cl$_2$, 2,3,6-Me$_3$, 4-NO$_2$
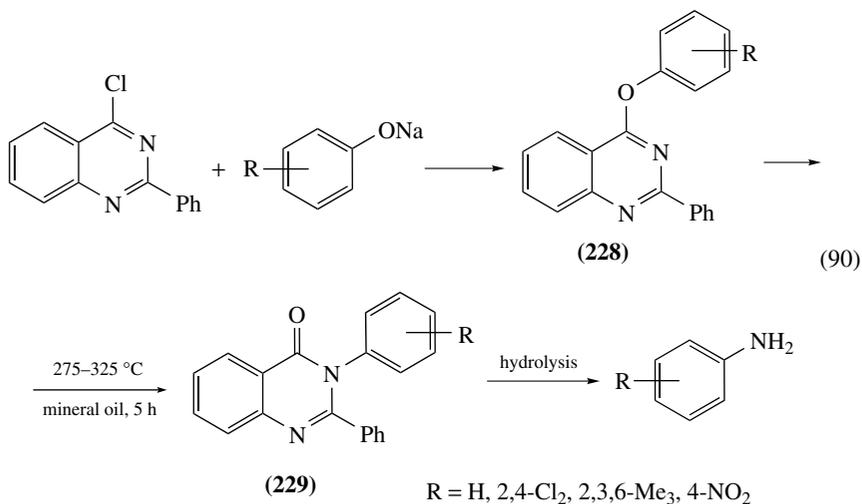
B. Anilines from Carbonyl Compounds

There are also a variety of reactions which involve the migration of an aryl group from carbon to nitrogen[328, 329]. The reactions described below are common knowledge and can be found in any textbook on organic chemistry and widely applicable in synthetic practice. Therefore, these reactions are mentioned very briefly here without discussion of their well-known mechanisms.

The *Hofmann amide rearrangement* is a conversion of a primary carboxamides **230** into amines using aqueous NaOH and bromine (see review in Reference 330). This reaction is, in effect, an elimination of the carbonyl group from the amide and is therefore usually

called a 'Hofmann amide degradation'. Many modifications of the rearrangement have been reported, and one of the recent versions consists of an application of the combination of NBS and sodium methoxide[331] (equation 91).

$$R = H, MeO, Me, CF_3, Cl \qquad (91)$$

$$(92)$$
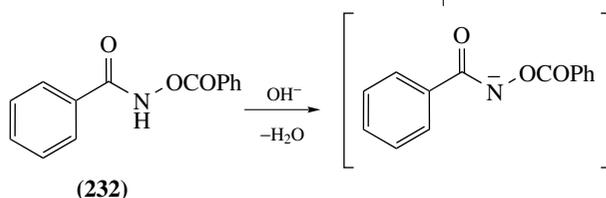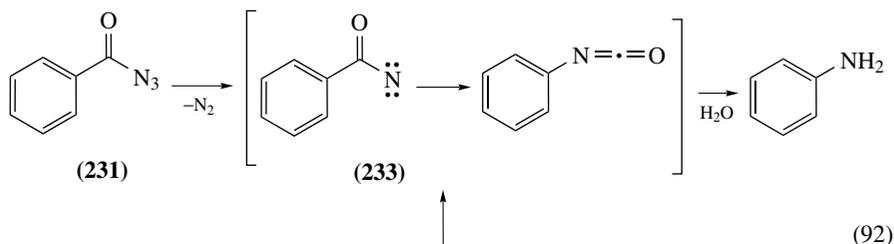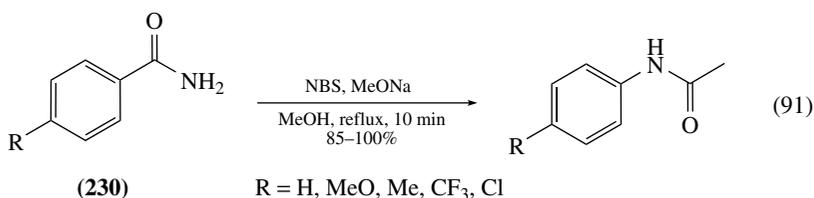
The *Curtius* as well as the *Lossen* rearrangements are transformations of acyl azides **231** and *O*-acylhydroxamic acids **232** to arylamines[328] (equation 92). The reactions proceed through the nitrenium intermediates **233**. The Curtius and Lossen rearrangements of the benzenesulfonyl system gave rise to the phenylsulfamic esters PhNHSO$_2$OR (where R = Me, Et)[332]. An efficient method for the solid-phase synthesis of secondary anilines from aromatic acids was developed using the Curtius rearrangement[333]. It is interesting that aromatic aldehydes can be converted into acyl azides by treatment with iodine azide. Thereby, the Curtius rearrangement was carried out starting from arylaldehydes to give arylamines[334].

$$(93)$$
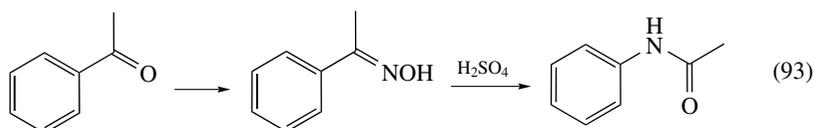
The *Beckmann rearrangement* of oximes to give the corresponding amides (equation 93) is well known and was reviewed in detail[328, 335]. The reaction is usually carried out in the presence of strong acids, although modifications were developed which use much milder conditions, e.g. by application of benzenesulfonyl chloride in alkaline

solutions[336]. These conditions even enable one to retain a protective acetal group in the rearranged molecule. Analogous conditions were used for a synthesis of N-arylureas from amidoximes in the reaction known as the *Tiemann rearrangement*[328].

$$R^2 \quad R^3$$
$$R^1 \underset{(234)}{\underset{\text{ethyl acetate}}{\underset{-78\,°C,\ 20–78\%}{\xrightarrow{p\text{-NBSP}}}}} \underset{(235)}{R^3} \quad (94)$$

$$R^1 = H, 4\text{-MeO}, 3\text{-Me}, 4\text{-Me}, 3\text{-Cl}, 4\text{-Cl}, 3\text{-CF}_3; \quad R^2, R^3 = H, Ph$$
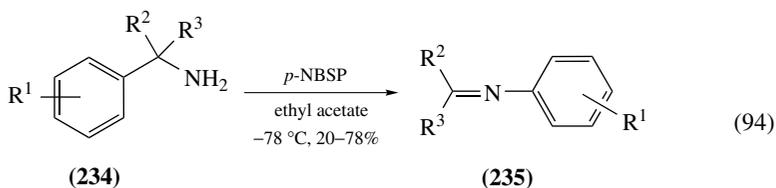
A migration of an aryl group from carbon to nitrogen takes place also in the *Stieglitz rearrangement*. For example, the benzylamine derivatives **234** were converted into anils **235** in a reaction induced by p-nitrobenzenesulfonyl peroxide (p-NBSP)[337] (equation 94).

C. Aniline Derivatives from Heterocycles

The recyclizations of the pyridinium salts **236** to form the aniline derivatives **238**, called the *Kost–Sagitullin rearrangement*, occur in the presence of bases via ring-opened intermediate **237**[338, 339] (equation 95).

$$ (95) $$

$$R^1 = H, 3\text{-Me}, 4\text{-Me}, 5\text{-Me}, 6\text{-Me}, 4,6\text{-Me}_2, 5\text{-Et}; \quad R^2 = Me, Et$$
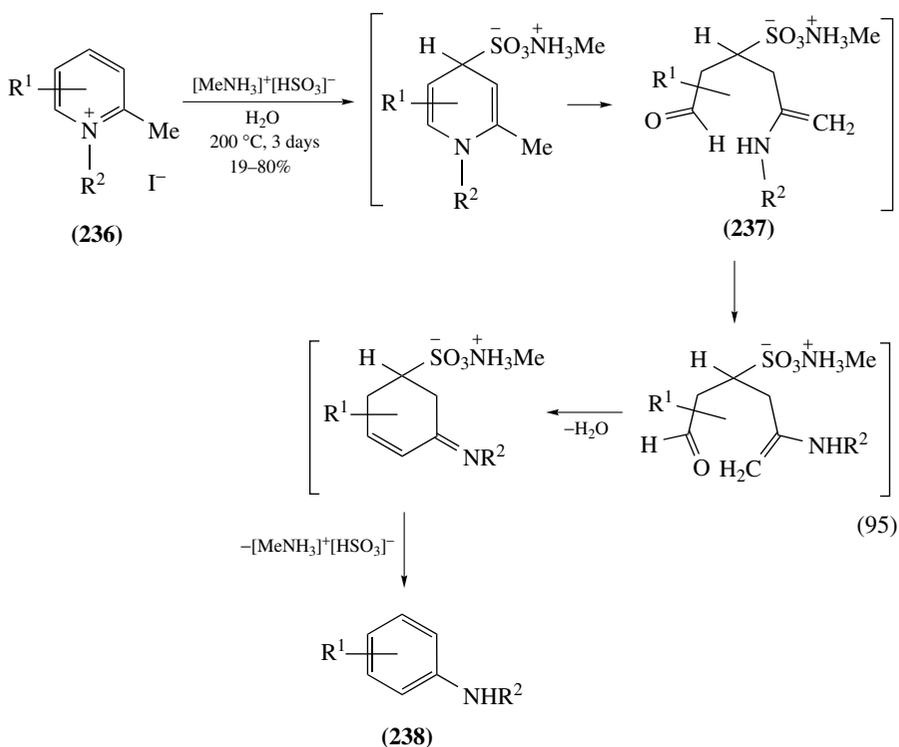
The rearrangement is applicable for synthesis not only of *N*-alkylanilines from pyridines, but also of α-aminopyridines from pyrimidines, α- and β-naphthylamines from isoquinolines, indoles from indolizines as well as carbazoles from β-carbolines[338].

The syntheses of various anilines bearing a heterocyclic unit at a nitrogen atom can be carried out in the framework of the *Dimroth rearrangement* (also called 'amidine rearrangement'). These transformations are, in essence, the recyclizations of N-heterocyclic compounds, mainly pyrimidines **239**, carrying an aryl group at one of the endocyclic nitrogen atoms, with a formal shift of the group to a side imino group at an adjacent position. The rearrangement which proceeds via ring fission and a subsequent cyclization (**240** $\rightarrow$ **241**) results in incorporation of an exocyclic nitrogen into a new cycle, while the aryl group turns out to be connected to the heterocycle through the nitrogen atom[340] (equation 96).

(96)
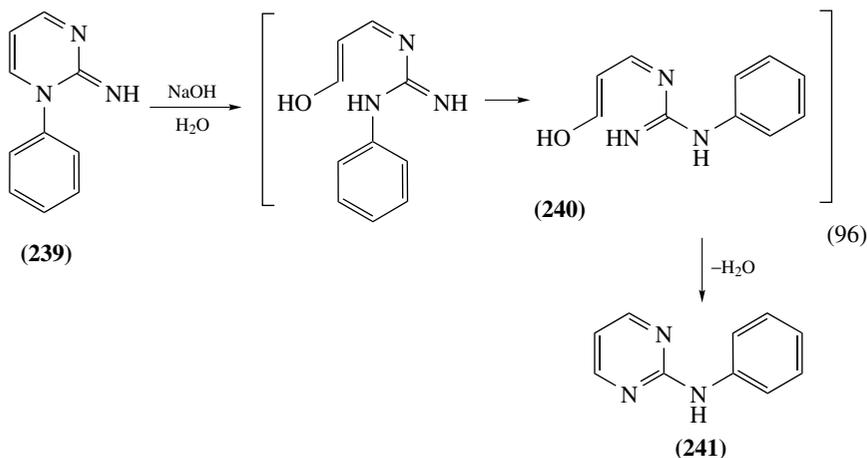
Many papers have appeared that described the syntheses of various heterocyclic systems such as imidazoles[341], 1,2,3-triazoles[342, 343], tetrazoles[344, 345], indanopyridines[346], 5,6-dihydropyridine-2-thiones[347], purines[348], pyrrolopyrimidines[349] and many others.

V. REFERENCES

1. D. V. Banthorpe, 'Rearrangements Involving Amino Groups', in *The Chemistry of the Amino Group* (Ed. S. Patai), Chap. 10, Interscience, London, 1968, pp. 585–667.
2. A. Hassner and C. Stumer, *Organic Syntheses Based on Name Reactions and Unnamed Reactions*, Pergamon, Elsevier, Oxford, 1994.
3. C. D. Chang and P. D. Perkins, *Zeolites*, **3**, 298 (1983).
4. V. A. Tarasevich, M. F. Rusak, A. B. Tereshko and N. G. Kozlov, *Zh. Obshch. Khim.*, **67**, 671 (1997); *Chem. Abstr.*, **128**, 245426h (1998).
5. V. A. Tarasevich, A. B. Tereshko and N. G. Kozlov, *Zh. Obshch. Khim.*, **67**, 457 (1997); *Chem. Abstr.*, **128**, 270275r (1998).
6. A. Tschumper and R. Prins, *Appl. Catal., A*, **174**, 129 (1998).
7. A. Tschumper and R. Prins, *Appl. Catal., A*, **172**, 285 (1998).
8. R. Prins, *Catal. Today*, **37**, 103 (1997).
9. J. H. Boyer and L. R. Morgan, Jr., *J. Am. Chem. Soc.*, **82**, 4748 (1960).
10. K. Isagawa, T. Ishiwaka, M. Kawai and Y. Fushizaki, *Bull. Chem. Soc. Jpn.*, **42**, 2066 (1969).
11. E. E. Glover, K. T. Rowbottom and D. C. Bishop, *J. Chem. Soc., Perkin Trans. 1*, 842 (1973).
12. B. D. Tiffany, *J. Am. Chem. Soc.*, **70**, 592 (1948).
13. N. Okazaki and A. Okumura, *Bull. Chem. Soc. Jpn.*, **34**, 989 (1961).

14. P. Mulder, I. W. C. E. Arends, D. Santoro and H.-G. Korth, *J. Org. Chem.*, **68**, 4247 (2003).
15. E. G. Kozyreva, B. M. Bolotin, V. N. Kokin, A. A. Kozyrev and G. N. Rodionova, *Zh. Org. Khim.*, **30**, 1024 (1994); *Chem. Abstr.*, **123**, 44858y (1995).
16. V. P. Rybalkin, A. D. Dubonosov, E. N. Shepelenko, L. L. Popova, N. I. Makarova, A. V. Tsukanov, V. A. Bren and V. I. Minkin, *Russ. J. Org. Chem.*, **38**, 1326 (2002).
17. V. Vargas and L. Amigo, *J. Chem. Soc., Perkin Trans. 2*, 1124 (2001).
18. K. Ogawa and T. Fujiwara, *Chem. Lett.*, 657 (1999).
19. D. Sanz, M. Perez-Torralba, S. H. Alarcon, R. M. Claramunt, C. Foces-Foces and J. Elguero, *J. Org. Chem.*, **67**, 1462 (2002).
20. E. Chapoteau, B. P. Czech, C. R. Gebauer, A. Kumar, K. Leong, D. T. Mytych, W. Zazulak, D. H. Desai, E. Luboch, J. Krzykawski and R. A. Bartsch, *J. Org. Chem.*, **56**, 2575 (1991) and references cited therein.
21. S. M. Lukyanov and A. V. Koblik, in *The Chemistry of Phenols* (Ed. Z. Rappoport), Part 1, Chap. 11, Wiley, Chichester, 2003, p. 721.
22. F. Möller, in *Methoden der Organischen Chemie (Houben-Weyl)*, Stickstoff-Verbindungen II, Band 11/1, Chap. VII, Georg Thieme Verlag, Stuttgart, 1957, p. 848.
23. C. K. Ingold, *Structure and Mechanism in Organic Chemistry*, Chap. XII, Cornell University Press, Ithaca, 1969.
24. G. F. Grillot, 'The Hofmann–Martius Rearrangement', in *Mechanisms of Molecular Migrations* (Ed. S. B. Thyagarajan), Vol. 3, Wiley-Interscience, New York, 1971, p. 237.
25. J. Thesing, H. Zieg and H. Mayer, *Chem. Ber.*, **88**, 1978 (1955).
26. M. Z. A. Badr and M. M. Aly, *Can. J. Chem.*, **52**, 293 (1974).
27. M. Z. A. Badr and H. A. H. El-Sherief, *Can. J. Chem.*, **53**, 3831 (1975).
28. A. M. Osman, M. Z. A. Badr and A. E. Abdel-Rahman, *Bull. Chem. Soc. Jpn.*, **49**, 2611 (1976).
29. M. Z. A. Badr, A. E. Abdel-Rahman, H. A. H. El-Sherief and M. M. Aly, *Indian J. Chem.*, **20B**, 422 (1981).
30. D. A. Archer and H. Booth, *Chem. Ind. (London)*, 1570 (1962).
31. D. A. Archer, H. Booth and R. D. Stangroom, *J. Chem. Soc., C*, 2276 (1970).
32. A. G. Giumanini, S. Roveri and D. Del Mazza, *J. Org. Chem.*, **40**, 1677 (1975).
33. M. E. Lupes, *Rev. Roum. Chim.*, **17**, 1909 (1972); *Chem. Abstr.*, **78**, 83628v (1973).
34. H. Hart and J. R. Kosak, *J. Org. Chem.*, **27**, 116 (1962).
35. W. F. Burgoyne and D. D. Dixon, *J. Mol. Catal.*, **62**, 61 (1990).
36. R. C. Mordi, J. Dwyer and R. Fields, *J. Catal.*, **143**, 627 (1993).
37. M. G. Siskos, N. Tzerpos and A. Zarkadis, *Bull. Soc. Chim. Belg.*, **105**, 759 (1996).
38. M. Hori, T. Kataoka, H. Shimizu, C. F. Hsu, Y. Hasegawa and N. Eyama, *J. Chem. Soc., Perkin Trans. 1*, 2271 (1988).
39. M. G. Siskos, S. K. Garas, A. K. Zarkadis and E. P. Bokaris, *Chem. Ber.*, **125**, 2477 (1992).
40. J. T. Pennie and T. I. Bieber, *Tetrahedron Lett.*, 3535 (1972).
41. H.-J. Knölker, M. Bauermeister and J.-B. Pannek, *Chem. Ber.*, **125**, 2783 (1992).
42. Y. Ogata and K. Takagi, *J. Org. Chem.*, **35**, 1642 (1970).
43. Y. Ogata and K. Takagi, *Bull. Chem. Soc. Jpn.*, **44**, 2186 (1971).
44. J. Furukawa, K. Omura and S. Sawada, *J. Chem. Soc., Chem. Commun.*, 78 (1974).
45. R. I. Weiss and H. Suhr, *Justus Liebigs Ann. Chem.*, 301 (1973).
46. A. R. Lepley, 'Stevens and Sommelet Rearrangements', in *Mechanisms of Molecular Migrations* (Ed. S. B. Thyagarajan), Vol. 3, Wiley-Interscience, New York, 1971, p. 297.
47. S. H. Pine, *Org. React.*, **18**, 403 (1970).
48. I. E. Marko, 'The Stevens and Related Rearrangements', in *Comprehensive Organic Synthesis* (Eds. B. M. Trost and I. Fleming), Vol. 3, Pergamon Press, Oxford, 1991, p. 913.
49. A. W. Johnson, *Ylid Chemistry*, Chap. 7, Academic Press, New York, 1966.
50. Y. Maeda and Y. Sato, *J. Chem. Soc., Perkin Trans. 1*, 1491 (1997) and references cited therein.
51. F. Möller, in *Methoden der Organischen Chemie (Houben-Weyl)*, Stickstoff-Verbindungen II, Band 11/1, Chap. VII, Georg Thieme Verlag, Stuttgart, 1957, p. 905.
52. J. R. Ruiz, V. J. Aran, J. L. Asensio, M. Flores and M. Stud, *Justus Liebigs Ann. Chem.*, 679 (1994).
53. R. Chicharro, S. de Castro, J. L. Reino and V. J. Aran, *Eur. J. Org. Chem.*, 2314 (2003).
54. G. C. Jones, W. Q. Beard and C. R. Hauser, *J. Org. Chem.*, **28**, 199 (1963).

55. A. R. Lepley and A. G. Giumanini, *J. Org. Chem.*, **36**, 1217 (1971).
56. L. G. Shakhbazyan, A. V. Babakhanyan, D. V. Grigoryan and S. T. Kocharyan, *Russ. J. Gen. Chem.*, **73**, 1608 (2003).
57. A. G. Giumanini and A. R. Lepley, *Bull. Chem. Soc. Jpn.*, **42**, 2359 (1969).
58. A. R. Lepley, R. H. Becker and A. G. Giumanini, *J. Org. Chem.*, **36**, 1222 (1971).
59. S. O. Doronina, A. A. Gall, V. I. Mamatyuk and G. V. Shishkin, *Khim. Geterocycl. Soedin.*, 383 (1993); *Chem. Abstr.*, **120**, 77257t (1994).
60. A. G. Giumanini and G. Lercker, *Gazz. Chim. Ital.*, **104**, 415 (1974).
61. G. E. Hall and J. Walker, *J. Chem. Soc., C*, 2237 (1968).
62. Y. D. Vankar, V. N. Gogte and B. D. Tilak, *Indian J. Chem., Sect. B*, **15B**, 411 (1977).
63. S. Toppet, E. Van Loock, G. L'abbe and G. Smets, *Chem. Ind. (London)*, 703 (1971).
64. N. Hamamichi and T. Miyasaka, *Chem. Pharm. Bull.*, **38**, 3253 (1990).
65. H. Hodjat-Kachani, J. J. Perie and A. Lattes, *Chem. Lett.*, 405 (1976).
66. M. Riviere and A. Lattes, *Bull. Soc. Chim. Fr.*, 2539 (1967).
67. R. P. Lutz, *Chem. Rev.*, **84**, 205 (1984).
68. G. B. Bennett, *Synthesis*, 589 (1977).
69. S. J. Rhoads and N. R. Raulins, *Org. React.*, **22**, 1 (1975).
70. N. M. Przhewalskii and I. I. Grandberg, *Usp. Khim.*, **56**, 814 (1987); *Chem. Abstr.*, **108**, 37675y (1988).
71. J. C. Gilbert and K. R. Cousins, *Tetrahedron*, **50**, 10671 (1994).
72. J. S. Yadav, B. V. S. Reddy, M. A. Rasheed and H. M. S. Kumar, *Synlett*, 487 (2000).
73. S. M. Lukyanov and A. V. Koblik, in *The Chemistry of Phenols* (Ed. Z. Rappoport), Part 1, Chap. 11, Wiley, Chichester, 2003, p. 761.
74. M. Schmid, H.-J. Hansen and H. Schmid, *Helv. Chim. Acta*, **56**, 105 (1973).
75. S. Jolidon and H.-J. Hansen, *Helv. Chim. Acta*, **60**, 978 (1977).
76. H. Katayama, *Chem. Pharm. Bull.*, **26**, 2027 (1978).
77. I. B. Abdrakhmanov, Z. N. Saraeva, N. G. Nigmatullin and G. A. Tolstikov, *Izv. Akad. Nauk SSSR, Ser. Khim.*, 383 (1986); *Chem. Abstr.*, **105**, 225561v (1986).
78. I. B. Abdrakhmanov, V. M. Sharafutdinov, N. G. Nigmatullin, A. G. Mustafin, Z. N. Saraeva and G. A. Tolstikov, *Izv. Akad. Nauk SSSR, Ser. Khim.*, 1273 (1983); *Chem. Abstr.*, **100**, 5529x (1984).
79. I. B. Abdrakhmanov, Z. N. Saraeva, N. G. Nigmatullin, V. D. Komissarov and G. A. Tolstikov, *Izv. Akad. Nauk SSSR, Ser. Khim.*, 2303 (1989); *Chem. Abstr.*, **112**, 97840r (1990).
80. P. Barmettler and H.-J. Hansen, *Helv. Chim. Acta*, **73**, 1515 (1990) and references cited therein.
81. S. Yamabe, S. Okumoto and T. Hayashi, *J. Org. Chem.*, **61**, 6218 (1996).
82. M. A. Cooper, M. A. Lucas, J. M. Taylor, A. D. Ward and N. M. Williamson, *Synthesis*, 621 (2001).
83. I. B. Abdrakhmanov, R. R. Gataullin, A. G. Mustafin, G. A. Tolstikov, I. P. Baikova, A. A. Fatykhov and A. A. Panasenko, *Zh. Org. Khim.*, **26**, 1527 (1990); *Chem. Abstr.*, **114**, 23236t (1991).
84. W. K. Anderson and G. Lai, *Synthesis*, 1287 (1995).
85. G. Lai and W. K. Anderson, *Tetrahedron*, **56**, 2583 (2000).
86. G. Lai and W. K. Anderson, *Tetrahedron Lett.*, **34**, 6849 (1993).
87. I. B. Abdrakhmanov, G. B. Shabaeva and G. A. Tolstikov, *Izv. Akad. Nauk SSSR, Ser. Khim.*, 2411 (1984); *Chem. Abstr.*, **102**, 131598y (1985).
88. H. Katayama and N. Takatsu, *Chem. Pharm. Bull.*, **29**, 2465 (1981).
89. H. Katayama and K. Kaneko, *Heterocycles*, **27**, 1569 (1988).
90. S. Mageswaran, W. D. Ollis, I. O. Sutherland and Y. Thebtaranonth, *J. Chem. Soc., Chem. Commun.*, 651 (1973).
91. W. D. Ollis, I. O. Sutherland and Y. Thebtaranonth, *J. Chem. Soc., Chem. Commun.*, 653 (1973).
92. W. D. Ollis, R. Somanathan and I. O. Sutherland, *J. Chem. Soc., Perkin Trans. 1*, 2930 (1981).
93. N. Paillous and A. Lattes, *Tetrahedron Lett.*, 4945 (1971).
94. E. E. Kingston, J. H. Beynon, A. Vandezonneville, R. Flammang and A. Maquestiau, *Org. Mass Spectrom.*, **23**, 437 (1988).
95. O. Benali, M. A. Miranda, R. Tormos and S. Gil, *J. Org. Chem.*, **67**, 7915 (2002).
96. G. Broggini and G. Zecchi, *J. Chem. Soc., Perkin Trans. 1*, 1843 (1991).

97. S. J. Danishefsky and G. B. Phillips, *Tetrahedron Lett.*, **25**, 3159 (1984).
98. B. Scholl and H.-J. Hansen, *Helv. Chim. Acta*, **69**, 1936 (1986).
99. J. Barluenga, R. Sanz and F. J. Fananas, *Tetrahedron Lett.*, **38**, 6103 (1997).
100. B. S. Thyagarajan and P. E. Glaspy, *J. Chem. Soc., Chem. Commun.*, 515 (1979).
101. P. E. Glaspy, R. A. Hancock and B. S. Thyagarajan, *Org. Mass Spectrom.*, **20**, 228 (1985).
102. P. E. Glaspy, R. A. Hancock and B. S. Thyagarajan, *Org. Mass Spectrom.*, **20**, 281 (1985).
103. W. E. Truce, E. M. Kreider and W. W. Brand, *Org. React.*, **18**, 99 (1970).
104. T. N. Gerasimova and E. F. Kolchina, *Usp. Khim.*, **64**, 142 (1995); *Chem. Abstr.*, **124**, 55823e (1996).
105. T. N. Gerasimova and E. F. Kolchina, *J. Fluorine Chem.*, **66**, 69 (1994).
106. F. Möller, in *Methoden der Organischen Chemie (Houben-Weyl)*, Stickstoff-Verbindungen II, Band 11/1, Chap. VII, Georg Thieme Verlag, Stuttgart, 1957, p. 913.
107. K.-F. Wedemeyer, in *Methoden der Organischen Chemie (Houben-Weyl)*, Phenole, Band VI/1c, Part 1, Georg Thieme Verlag, Stuttgart, 1976, p. 553.
108. F. W. Balfour and T. F. Fagley, *J. Phys. Chem.*, **72**, 1300 (1968).
109. E. F. Kolchina and T. N. Gerasimova, *Izv. Akad. Nauk, Ser. Khim.*, 1101 (1993); *Chem. Abstr.*, **122**, 132357u (1995).
110. D. M. Schmidt and G. E. Bonvicino, *J. Org. Chem.*, **49**, 1664 (1984).
111. T. Shiojima, Y. Hashida and K. Matsui, *Bull. Chem. Soc. Jpn.*, **46**, 2914 (1973).
112. M. S. Wadia and D. V. Patil, *Synth. Commun.*, **33**, 2725 (2003).
113. P. L. Anelli, M. Brocchetta, L. Calabi, C. Secchi, F. Uggeri and S. Verona, *Tetrahedron*, **53**, 11919 (1997).
114. I. Cragg-Hine, M. G. Davidson, O. Kocian, T. Kottke, F. S. Mair, R. Snaith and J. F. Stoddart, *J. Chem. Soc., Chem. Commun.*, 1355 (1993).
115. L. V. Ektova and F. A. Zhuravlev, *Mendeleev Commun.*, 23 (1993).
116. F. A. Davis and R. B. Wetzel, *Tetrahedron Lett.*, 4483 (1969).
117. K. Bowden and P. R. Williams, *J. Chem. Soc., Perkin Trans. 2*, 215 (1991).
118. N. N. Volkova, E. V. Tarasov, L. Van Meervelt, S. Toppet, W. Dehaen and V. A. Bakulev, *J. Chem. Soc., Perkin Trans. 1*, 1574 (2002).
119. A. Borchardt and W. C. Still, *Synlett*, 539 (1995).
120. K. Yokoyama, R. Nakagaki, J. Nakamura, K. Mutai and S. Nagakura, *Bull. Chem. Soc. Jpn.*, **53**, 2472 (1980).
121. K. Mutai, K. Yokoyama, S. Kanno and K. Kobayashi, *Bull. Chem. Soc. Jpn.*, **55**, 1112 (1982).
122. K. Mutai, R. Nakagaki and H. Tukada, *Chem. Lett.*, 2261 (1987).
123. K. Mutai, H. Tukada and R. Nakagaki, *J. Org. Chem.*, **56**, 4896 (1991).
124. G. G. Wubbels, B. R. Sevetson and H. Sanders, *J. Am. Chem. Soc.*, **111**, 1018 (1989).
125. G. G. Wubbels, W. D. Cotter, H. Sanders and C. Pope, *J. Org. Chem.*, **60**, 2960 (1995).
126. I. Ya. Mainagashev, L. S. Klimenko and N. P. Gritsan, *Izv. Akad. Nauk, Ser. Khim.*, 2519 (1998); *Chem. Abstr.*, **130**, 324997q (1999).
127. R. Nakagaki and K. Mutai, *Bull. Chem. Soc. Jpn.*, **69**, 261 (1996).
128. B. Miller, *Tetrahedron Lett.*, 55 (1962).
129. B. Miller, *J. Am. Chem., Soc.*, **86**, 1127 (1964).
130. B. Miller, *J. Am. Chem. Soc.*, **86**, 1135 (1964).
131. P. T. S. Lau and G. F. Grillot, *J. Org. Chem.*, **28**, 2763 (1963).
132. G. F. Grillot and P. T. S. Lau, *J. Org. Chem.*, **30**, 28 (1965).
133. K. L. Nelson and R. L. Seefeld, *J. Am. Chem. Soc.*, **80**, 5957 (1958).
134. K. L. Nelson, J. C. Robertson and J. J. Duvall, *J. Am. Chem. Soc.*, **86**, 684 (1964).
135. R. J. Ferrier, R. Blattner, R. A. Field, R. H. Furneaux, J. M. Gardiner, J. O. Hoberg, K. P. R. Kartha, D. M. G. Tilbrook, P. C. Tyler and R. H. Wightman, *Carbohydr. Chem.*, **33**, 126 (2002).
136. T. Laue and A. Plagens, *Named Organic Reactions*, Wiley, New York, 1998.
137. J. E. Hodge and B. E. Fischer, *Methods in Carbohydrate Chemistry*, Vol. 2, Academic Press, New York, 1963, p. 99.
138. F. Möller, in *Methoden der Organischen Chemie (Houben-Weyl)*, Stickstoff-Verbindungen II, Band 11/1, Chap. VII, Georg Thieme Verlag, Stuttgart, 1957, p. 922.
139. F. Weygand, W. Perkow and P. Kuhner, *Chem. Ber.*, **84**, 594 (1951).
140. F. Micheel, I. Dijong and E. Klevenhausen, *Justus Liebigs Ann. Chem.*, **669**, 136 (1963).
141. T. van Es and R. L. Whistler, *J. Org. Chem.*, **29**, 1087 (1964).

142. S. Kolka, *Polish J. Chem.*, **58**, 689 (1984).
143. L. Azema, F. Bringaud, C. Blonski and J. Perie, *Bioorg. Med. Chem.*, **8**, 717 (2000).
144. L. Shu, P. Wang, Y. Gan and Y. Shi, *Org. Lett.*, **5**, 293 (2003).
145. K. Heyns and W. Beilfuss, *Chem. Ber.*, **106**, 2680 (1973).
146. R. Martin, *Org. Prep. Proc. Int.*, **24**, 373 (1992).
147. F. Möller, in *Methoden der Organischen Chemie (Houben-Weyl)*, Stickstoff-Verbindungen II, Band 11/1, Chap. VII, Georg Thieme Verlag, Stuttgart, 1957, p. 852.
148. J. F. J. Dippy and V. Moss, *J. Chem. Soc.*, 2205 (1952).
149. B. I. Ardashev and V. I. Minkin, *Zh. Obshch. Khim.*, **28**, 1578 (1958); *Chem. Abstr.*, **53**, 1348c (1959).
150. D. Elad, *Tetrahedron Lett.*, 873 (1963).
151. D. Bellus, K. Schaffner and J. Hoigne, *Helv. Chim. Acta*, **51**, 1980 (1968).
152. H. Shizuka, *Bull. Chem. Soc. Jpn.*, **42**, 57 (1969).
153. Y. Katsuhara, H. Maruyama, Y. Shigemitsu and Y. Odaira, *Tetrahedron Lett.*, 1323 (1973).
154. Y. Kanaoka, T. Tsuji, K. Itoh and K. Koyama, *Chem. Pharm. Bull.*, **21**, 453 (1973).
155. I. Datta, T. K. Das and S. Ghosh, *Tetrahedron Lett.*, **30**, 4009 (1989).
156. D. Bellus and K. Schaffner, *Helv. Chim. Acta*, **51**, 221 (1968).
157. J. E. Herweh and C. E. Hoyle, *J. Org. Chem.*, **45**, 2195 (1980).
158. R. K. M. Rao Kallury, A. G. Loudon and A. Maccoll, *Org. Mass Spectrom.*, **13**, 224 (1978).
159. L. P. Safronova, A. S. Medvedeva, L. V. Klyba, V. N. Bochkarev and M. V. Andreev, *Zh. Org. Khim.*, **36**, 208 (2000); *Chem. Abstr.*, **133**, 321930p (2000).
160. S. Gross and H.-U. Reissig, *Synlett*, 2027 (2002).
161. W. B. Wright, Jr. and H. J. Brabander, *J. Org. Chem.*, **26**, 4051 (1961).
162. A. K. Sharma, S. Jayakumar, M. S. Hundal and M. P. Mahajan, *J. Chem. Soc., Perkin Trans. 1*, 774 (2002).
163. S. M. Starling and S. C. Vonwiller, *Tetrahedron Lett.*, **38**, 2159 (1997).
164. J. Rigaudy and J. Baranne-Lafont, *Tetrahedron Lett.*, 1375 (1965).
165. B. Zaleska, T. Bazanek, R. Socha, M. Karelus, J. Grochowski and P. Serda, *J. Org. Chem.*, **67**, 4526 (2002).
166. E. A. Jeffery, A. Meisters and T. Mole, *Tetrahedron*, **25**, 741 (1969).
167. H. Kessler and D. Leibfritz, *Tetrahedron Lett.*, 1423 (1970).
168. J. W. Schulenberg and S. Archer, *Org. React.*, **14**, 1 (1965).
169. F. Möller, in *Methoden der Organischen Chemie (Houben-Weyl)*, Stickstoff-Verbindungen II, Band 11/1, Chap. VII, Georg Thieme Verlag, Stuttgart, 1957, p. 910.
170. O. H. Wheeler, F. Roman, M. V. Santiago and F. Quiles, *Can. J. Chem.*, **47**, 503 (1969).
171. R. Barclay, Jr., *Can. J. Chem.*, **43**, 2125 (1965).
172. A. Marsh, E. G. Nolen, K. M. Gardinier and J.-M. Lehn, *Tetrahedron Lett.*, **35**, 397 (1994).
173. M. D. Bhavsar and S. G. Chiplunkar, *Man-Made Textiles in India*, **35**, 133 (1992); *Chem. Abstr.*, **117**, 253353v (1992).
174. N. A. Suttle and A. Williams, *J. Chem. Soc., Perkin Trans. 2*, 1369 (1983).
175. A. W. Chapman, *J. Chem. Soc.*, 2133 (1929).
176. F. Esser, K. Brandt, K.-H. Pook, H.-J. Förster, H. Köppen, J.-M. Léger and A. Carpy, *J. Chem. Soc., Perkin Trans. 1*, 3311 (1988).
177. V. I. Minkin and I. E. Mikhailov, 'Rearrangements in Amidines and Related Compounds', in *The Chemistry of Amidines and Imidates* (Eds. S. Patai and Z. Rappoport), Vol. 2, Wiley, London, 1991.
178. V. I. Minkin, L. P. Olekhnovich, Yu. A. Zhdanov, I. E. Mikhailov, V. P. Metlushenko, N. M. Ivanchenko and N. I. Borisenko, *Zh. Org. Khim.*, **12**, 1261 (1976); *Chem. Abstr.*, **85**, 123063k (1976).
179. V. I. Minkin, L. P. Olekhnovich, Yu. A. Zhdanov, I. E. Mikhailov, V. P. Metlushenko and N. M. Ivanchenko, *Zh. Org. Khim.*, **12**, 1271 (1976); *Chem. Abstr.*, **85**, 123064m (1976).
180. L. P. Olekhnovich, I. E. Mikhailov, N. M. Ivanchenko, Yu. A. Zhdanov and V. I. Minkin, *Zh. Org. Khim.*, **15**, 1355 (1979); *Chem. Abstr.*, **91**, 210648x (1979).
181. I. E. Mikhailov, V. I. Minkin, L. P. Olekhnovich, V. N. Boiko, N. V. Ignatiev and L. M. Yagupolskii, *Zh. Org. Khim.*, **20**, 454 (1984); *Chem. Abstr.*, **101**, 71979r (1984).
182. G. Toth, L. Toldy, J. Tamas and G. Zolyomi, *Tetrahedron*, **28**, 167 (1972).

183. M. Bobosikova, W. Clegg, S. J. Coles, M. Dandarova, M. B. Hursthouse, T. Kiss, A. Krutosikova, T. Liptaj, N. Pronayova and C. A. Ramsden, *J. Chem. Soc., Perkin Trans. 1*, 680 (2001).
184. C. A. Ramsden and H. L. Rose, *J. Chem. Soc., Perkin Trans. 1*, 2319 (1997).
185. C. A. Ramsden and H. L. Rose, *J. Chem. Soc., Perkin Trans. 1*, 615 (1995).
186. P. Nongkunsarn and C. A. Ramsden, *Tetrahedron*, **53**, 3805 (1997).
187. J.-D. Charrier, C. Landreau, D. Deniaud, F. Reliquet, A. Reliquet and J. C. Meslin, *Tetrahedron*, **57**, 4195 (2001).
188. R. Leardini, H. McNab and D. Nanni, *Tetrahedron*, **51**, 12143 (1995).
189. G. T. Tisue, M. Grassmann and W. Lwowski, *Tetrahedron*, **24**, 999 (1968).
190. G. Singh, R. Singh, N. K. Girdhar and M. P. S. Ishar, *Tetrahedron*, **58**, 2471 (2002).
191. N. De Kimpe and N. Schamp, *J. Org. Chem.*, **40**, 3749 (1975).
192. N. De Kimpe, R. Verhe and N. Schamp, *Bull. Soc. Chim. Belg.*, **84**, 701 (1975).
193. N. De Kimpe, R. Verhe, L. De Buyck and N. Schamp, *Bull. Soc. Chim. Belg.*, **92**, 233 (1983).
194. P. Sulmon, N. De Kimpe and N. Schamp, *Tetrahedron*, **45**, 2937 (1989).
195. D. Enders, M. Knopp and R. Schiffers, *Tetrahedron: Asymmetry*, **7**, 1847 (1996).
196. J. Kang, K. H. Yew, T.-H. Kim and D. H. Choi, *Tetrahedron Lett.*, **43**, 9509 (2002).
197. B. Alcaide, J. Rodriguez-Lopez, A. Monge and V. Perez-Garcia, *Tetrahedron*, **46**, 6799 (1990).
198. M. A.-M. Gomaa, *J. Chem. Soc., Perkin Trans. 1*, 341 (2002).
199. Y. V. S. Rao, S. J. Kulkarni, M. Subrahmanyam and A. V. R. Rao, *Catal. Lett.*, **36**, 267 (1996).
200. H. J. Shine, 'The Benzidine Rearrangement', in *Mechanisms of Molecular Migrations* (Ed. B. S. Thyagarajan), Vol. 2, Wiley-Interscience, New York, 1969, p. 191.
201. R. A. Cox and E. Buncel, in *The Chemistry of the Hydrazo, Azo and Azoxy Groups* (Ed. S. Patai), Vol. 1, Wiley, New York, 1975, p. 775.
202. H. J. Shine, *Bull. Hist. Chem.*, **19**, 77 (1996); *Chem. Abstr.*, **126**, 250676c (1997).
203. E. Bunzel, *Can. J. Chem.*, **78**, 1251 (2000).
204. M. J. S. Dewar, in *Molecular Rearrangements* (Ed. P. de Mayo), Part 1, Wiley-Interscience, New York, 1967, p. 323.
205. F. Möller, in *Methoden der Organischen Chemie (Houben-Weyl)*, Stickstoff-Verbindungen II, Band 11/1, Chap. VII, Georg Thieme Verlag, Stuttgart, 1957, p. 839.
206. H. J. Shine, *Aromatic Rearrangements*, Elsevier, Amsterdam, 1967, p. 126.
207. H. J. Shine and J. D. Cheng, *J. Org. Chem.*, **36**, 2787 (1971).
208. J.-D. Cheng and H. J. Shine, *J. Org. Chem.*, **39**, 2835 (1974).
209. D.-H. Bae and H. J. Shine, *J. Org. Chem.*, **45**, 4448 (1980).
210. L. L. Ferstandig, *Tetrahedron Lett.*, 1235 (1963).
211. J. Rakusan and Z. J. Allan, *Tetrahedron Lett.*, 4955 (1966).
212. H. J. Shine and J. P. Stanley, *J. Org. Chem.*, **32**, 905 (1967).
213. G. A. Olah, K. Dunne, D. P. Kelly and Y. K. Mo, *J. Am. Chem. Soc.*, **94**, 7438 (1972).
214. E. S. Rhee and H. J. Shine, *J. Org. Chem.*, **52**, 5633 (1987).
215. W. Subotkowski, L. Kupczyk-Subotkowska and H. J. Shine, *J. Am. Chem. Soc.*, **115**, 5073 (1993).
216. P. Skrabal and M. Hohl-Blumer, *Helv. Chim. Acta*, **59**, 2906 (1976).
217. P. Luger, J. Malkowski and P. Skrabal, *Helv. Chim. Acta*, **60**, 1545 (1977).
218. N. S. Dokunikhin and G. I. Bystritskii, *Zh. Obshch. Khim.*, **33**, 974 (1963); *Chem. Abstr.*, **59**, 8685c (1963).
219. A. E. Feiring, B. C. Auman and E. R. Wonchoba, *Macromolecules*, **26**, 2779 (1993).
220. H. S. Freeman, D. Hinks and J. Sokolowska-Gajda, US Patent 5,965,717 (1999); *Chem. Abstr.*, **131**, 273148z (1999).
221. Y. Fukuda, S. Seto, H. Furuta, H. Ebisu, Y. Oomori and S. Terashima, *J. Med. Chem.*, **44**, 1396 (2001).
222. K.-S. Cheon, R. A. Cox, S.-R. Keum and E. Buncel, *J. Chem. Soc., Perkin Trans. 2*, 1231 (1998).
223. E. Buncel and K.-S. Cheon, *J. Chem. Soc., Perkin Trans. 2*, 1241 (1998).
224. G. N. Kurilo, N. I. Rostova, A. A. Cherkasova and A. N. Grinev, *Khim. Geterocycl. Soedin.*, 353 (1977); *Chem. Abstr.*, **87**, 22950h (1977).
225. B. W. Lee and S. D. Lee, *Tetrahedron Lett.*, **41**, 3883 (2000).

226. C. J. Davies, B. T. Heaton and C. Jacob, *J. Chem. Soc., Chem. Commun.*, 1177 (1995).
227. Q. Zhu-Ohlbach, R. Gleiter, F. Rominger, H.-L. Schmidt and T. Reda, *Eur. J. Org. Chem.*, 2409 (1998).
228. A. C. Benniston, W. Clegg, A. Harriman, R. W. Harrington, P. Li and C. Sams, *Tetrahedron Lett.*, **44**, 2665 (2003).
229. K. H. Park and J. S. Kang, *J. Org. Chem.*, **62**, 3794 (1997).
230. B. V. Lichitsky, V. N. Nesterov, A. A. Dudinov and M. M. Krayushkin, *Izv. Akad. Nauk, Ser. Khim.*, 1320 (2000); *Chem. Abstr.*, **134**, 42078x (2001).
231. B. V. Lichitsky, D. V. Kozhinov, V. N. Nesterov, L. G. Vorontsova, Z. A. Starikova, A. A. Dudinov and M. M. Krayushkin, *Russ. Chem. Bull.*, 1862 (2002).
232. V. Scartoni, I. Morelli, A. Marsili and S. Catalano, *J. Chem. Soc., Perkin Trans. 1*, 2332 (1977).
233. B. Robinson, *The Fischer Indole Synthesis*, Wiley, Chichester, 1982.
234. K. Bast, T. Durst, R. Huisgen, K. Lindner and R. Temme, *Tetrahedron*, **54**, 3745 (1998).
235. T. Benincori, E. Brenna and F. Sannicolo, *J. Chem. Soc., Perkin Trans. 1*, 2139 (1991).
236. I. I. Grandberg, *Khim. Geterocycl. Soedin.*, 579 (1974); *Chem. Abstr.*, **81**, 63397c (1974).
237. W. T. Ashton, R. M. Sisco, Y. T. Yang, J.-L. Lo, J. B. Yudkovitz, K. Cheng and M. T. Goulet, *Bioorg. Med. Chem. Lett.*, **11**, 1723 (2001).
238. T. Benincori, R. Fusco and F. Sannicolo, *Gazz. Chim. Ital.*, **120**, 635 (1990).
239. C. C. Boido, V. Boido, F. Novelli and F. Sparatore, *J. Heterocycl. Chem.*, **35**, 853 (1998).
240. R. N. Butler and J. P. James, *J. Chem. Soc., Chem. Commun.*, 627 (1983).
241. J. M. J. Tronchet, J. F. Tronchet, F. Rachidzadeh, F. Barbalat-Rey and G. Bernadinelli, *Carbohydr. Res.*, **181**, 97 (1988).
242. V. Frenna, N. Vivona, G. Consiglio and D. Spinelli, *J. Chem. Soc., Perkin Trans. 2*, 1199 (1983).
243. V. Frenna, N. Vivona, A. Caronia, G. Consiglio and D. Spinelli, *J. Chem. Soc., Perkin Trans. 2*, 1203 (1983).
244. K. Clusius and H. R. Weisser, *Helv. Chim. Acta*, **35**, 1524 (1952).
245. V. M. Berezovskii and L. S. Tulchinskaya, *Zh. Obshch. Khim.*, **31**, 2774 (1961); *Chem. Abstr.*, **56**, 11473i (1962).
246. L. Benati, P. C. Montevecchi, P. Spagnolo and E. Foresti, *J. Chem. Soc., Perkin Trans. 1*, 2845 (1992).
247. K. Hirakawa, T. Ito, Y. Okubo and S. Nakazawa, *J. Org. Chem.*, **45**, 1668 (1980).
248. H. Kisch, P. Reisser and F. Knoch, *Chem. Ber.*, **124**, 1143 (1991).
249. T. Otsuka and T. Tezuka, *Heterocycles*, **26**, 2081 (1987).
250. M. J. S. Dewar, in *Molecular Rearrangements* (Ed. P. de Mayo), Part 1, Wiley-Interscience, New York, 1967, p. 311.
251. W. N. White, in *Mechanisms of Molecular Migrations* (Ed. S. B. Thyagarajan), Vol. 3, Wiley-Interscience, New York, 1971, p. 109.
252. F. Möller, in *Methoden der Organischen Chemie (Houben-Weyl)*, Stickstoff-Verbindungen II, Band 11/1, Chap. VII, Georg Thieme Verlag, Stuttgart, 1957, p. 836.
253. W. N. White and J. T. Golden, *J. Org. Chem.*, **35**, 2759 (1970).
254. Z. Daszkiewicz, E. Nowakowska and J. B. Kyziol, *Tetrahedron*, **54**, 5991 (1998).
255. Z. Daszkiewicz, G. Spaleniak and J. B. Kyziol, *J. Phys. Org. Chem.*, **15**, 115 (2002).
256. Z. Daszkiewicz and J. B. Kyziol, *Polish J. Chem.*, **77**, 1217 (2003).
257. P. Helsby and J. H. Ridd, *J. Chem. Soc., Perkin Trans. 2*, 1191 (1983).
258. F. Möller, in *Methoden der Organischen Chemie (Houben-Weyl)*, Stickstoff-Verbindungen II, Band 11/1, Chap. VII, Georg Thieme Verlag, Stuttgart, 1957, p. 834.
259. P. I. Morris, *Chem. Ind. (London)*, 968 (1999).
260. E. Yu. Belyaev and S. V. Petrova, *Zh. Org. Khim.*, **13**, 1220 (1977); *Chem. Abstr.*, **87**, 101704j (1977).
261. G. Steel and D. L. H. Williams, *J. Chem. Soc., Chem. Commun.*, 975 (1969).
262. D. L. H. Williams and J. A. Wilson, *J. Chem. Soc., Perkin Trans. 2*, 13 (1974).
263. D. L. H. Williams, *J. Chem. Soc., Perkin Trans. 2*, 801 (1982).
264. P. Kannan, K. Pitchumani, S. Rajagopal and C. Srinivasan, *J. Mol. Catal. (A)*, **118**, 189 (1997).
265. S. M. Lukyanov and A. V. Koblik, in *The Chemistry of Phenols* (Ed. Z. Rappoport), Part 1, Chap. 11, Wiley, Chichester, 2003, p. 801.

266. F. Möller, in *Methoden der Organischen Chemie (Houben-Weyl)*, Stickstoff-Verbindungen II, Band 11/1, Chap. VII, Georg Thieme Verlag, Stuttgart, 1957, p. 829.
267. K.-F. Wedemeyer, in *Methoden der Organischen Chemie (Houben-Weyl)*, Phenole, Band VI/1c, Part 1, Georg Thieme Verlag, Stuttgart, 1976, p. 85.
268. T. P. Simonova, V. D. Nefedov, M. A. Toropova and N. F. Kirillov, *Usp. Khim.*, **61**, 1061 (1992); *Chem. Abstr.*, **117**, 211715j (1992).
269. M. Tordeux and C. Wakselman, *J. Fluorine Chem.*, **74**, 251 (1995).
270. J. C. Fishbein and R. A. McClelland, *Can. J. Chem.*, **74**, 1321 (1996).
271. T. Okamoto, K. Shudo and T. Ohta, *J. Am. Chem. Soc.*, **97**, 7184 (1975).
272. M. B. Shcherbinin, G. B. Erusalimskii, A. E. Baltser, A. G. Bazanov and V. A. Ostrovskii, *Zh. Org. Khim.*, **31**, 1829 (1995); *Chem. Abstr.*, **125**, 57685f (1996).
273. C. Meier and G. Boche, *Chem. Ber.*, **123**, 1691 (1990).
274. S. Blechert, *Helv. Chim. Acta*, **68**, 1835 (1985).
275. M. Toyota and K. Fukumoto, *Heterocycles*, **31**, 1431 (1990).
276. J.-B. Baudin, S. A. Julia and O. Ruel, *Tetrahedron*, **43**, 881 (1987) and references cited therein.
277. N. Haga, Y. Endo, K. Kataoka, K. Yamaguchi and K. Shudo, *J. Am. Chem. Soc.*, **114**, 9795 (1992).
278. R. A. W. Johnstone, in *Mechanisms of Molecular Migrations* (Ed. S. B. Thyagarajan), Vol. 2, Wiley-Interscience, New York, 1969, p. 249.
279. K. C. Majumdar and G. H. Jana, *J. Org. Chem.*, **62**, 1506 (1997).
280. A.-H. Khuthier, K. Y. Al-Mallah and S. Y. Hanna, *J. Chem. Soc., Perkin Trans. 2*, 413 (1986).
281. M. Moriwaki, Y. Yamamoto, J. Oda and Y. Inouye, *J. Org. Chem.*, **41**, 300 (1976).
282. J. P. Lorand, R. W. Grant, P. A. Samuel, E. O'Connell and J. Zaro, *Tetrahedron Lett.*, 4087 (1969).
283. U. Schöllkopf, U. Ludwig, M. Patsch and W. Franken, *Justus Liebigs Ann. Chem.*, **703**, 77 (1967).
284. U. Schöllkopf and U. Ludwig, *Chem. Ber.*, **101**, 2224 (1968).
285. G. Ostermann and U. Schöllkopf, *Justus Liebigs Ann. Chem.*, **737**, 170 (1970).
286. T. Sheradsky and E. Nov, *J. Chem. Soc., Perkin Trans. 1*, 527 (1983).
287. F. A. Davis, E. R. Fretz and C. J. Horner, *J. Org. Chem.*, **38**, 690 (1973).
288. F. A. Davis, C. J. Horner, E. R. Fretz and J. F. Stackhouse, *J. Org. Chem.*, **38**, 695 (1973).
289. F. Möller, in *Methoden der Organischen Chemie (Houben-Weyl)*, Stickstoff-Verbindungen II, Band 11/1, Chap. VII, Georg Thieme Verlag, Stuttgart, 1957, p. 832.
290. J.-B. Baudin, M. Bekhazi, S. A. Julia, O. Ruel, R. L. P. de Jong and L. Brandsma, *Synthesis*, 956 (1985).
291. P. G. Gassman and H. R. Drewes, *J. Am. Chem. Soc.*, **100**, 7600 (1978).
292. P. G. Gassman, T. J. van Bergen and G. Gruetzmacher, *J. Am. Chem. Soc.*, **95**, 6508 (1973).
293. P. G. Gassman and R. L. Parton, *Tetrahedron Lett.*, 2055 (1977).
294. P. G. Gassman and R. L. Parton, *J. Chem. Soc., Chem. Commun.*, 694 (1977).
295. P. G. Gassman and D. R. Amick, *J. Am. Chem. Soc.*, **100**, 7611 (1978).
296. L. Benati, M. Grossi, P. C. Montevecchi and P. Spagnolo, *J. Chem. Soc., Chem. Commun.*, 763 (1982).
297. M. R. Bryce, J. N. Heaton, P. C. Taylor and M. Anderson, *J. Chem. Soc., Perkin Trans. 1*, 1935 (1994).
298. P. Claus and W. Vycudilik, *Tetrahedron Lett.*, 3607 (1968).
299. P. K. Claus, E. Jäger and A. Setzer, *Monatsh. Chem.*, **116**, 1017 (1985).
300. K. K. Andersen and O. Malver, *J. Org. Chem.*, **48**, 4803 (1983).
301. R. N. Warrener and A. S. Amarasekara, *Synlett*, 167 (1997).
302. S. S. Shrimali, A. Iyer, R. K. Singhal, D. Kishore and B. C. Joshi, *Rev. Roum. Chim.*, **24**, 597 (1979); *Chem. Abstr.*, **92**, 146474d (1980).
303. S. J. Shafer and W. D. Closson, *J. Org. Chem.*, **40**, 889 (1975).
304. H. Nozaki, T. Okada, R. Noyori and M. Kawanisi, *Tetrahedron*, **22**, 2177 (1966).
305. F. Kanetani and H. Yamaguchi, *Bull. Chem. Soc. Jpn.*, **54**, 3048 (1981).
306. Z. Vrba and Z. J. Allan, *Tetrahedron Lett.*, 4507 (1968).
307. Z. J. Allan and Z. Vrba, *Collect. Czech. Chem. Commun.*, **34**, 272 (1969).
308. P. K. Maarsen and H. Cerfontain, *J. Chem. Soc., Perkin Trans. 2*, 921 (1977).
309. R. N. Khelevin, *Zh. Org. Khim.*, **23**, 1925 (1987); *Chem. Abstr.*, **108**, 166776f (1988).

310. D. F. Paul and P. Haberfield, *J. Org. Chem.*, **41**, 3170 (1976).
311. P. G. Gassman and G. A. Campbell, *J. Am. Chem. Soc.*, **94**, 3891 (1972).
312. F. Möller, in *Methoden der Organischen Chemie (Houben-Weyl)*, Stickstoff-Verbindungen II, Band 11/1, Chap. VII, Georg Thieme Verlag, Stuttgart, 1957, p. 827.
313. M. J. S. Dewar, in *Molecular Rearrangements* (Ed. P. de Mayo), Part 1, Wiley-Interscience, New York, 1967, p. 309.
314. K. P. Sudlow and A. A. Woolf, *J. Fluorine Chem.*, **87**, 25 (1998).
315. E. Zbiral, *Tetrahedron Lett.*, 2005 (1966).
316. R. Detsch, E. Niecke, M. Nieger and F. Reichert, *Chem. Ber.*, **125**, 321 (1992).
317. G. G. Wubbels, A. M. Halverson and J. D. Oxman, *J. Am. Chem. Soc.*, **102**, 4848 (1980).
318. S. V. Amosova, V. I. Gostevskaya, G. M. Gavrilova, A. V. Afonin and D.-S. D. Toryashinova, *Zh. Org. Khim.*, **29**, 2416 (1993); *Chem. Abstr.*, **121**, 255329y (1994).
319. S. Sekiguchi, M. Hirai and N. Tomoto, *J. Org. Chem.*, **49**, 2378 (1984).
320. W. R. Baker, *J. Org. Chem.*, **48**, 5140 (1983).
321. R. Bayles, M. C. Johnson, R. F. Maisey and R. W. Turner, *Synthesis*, 33 (1977).
322. J. J. Weidner, P. M. Weintraub, R. A. Schnettler and N. P. Peet, *Tetrahedron*, **53**, 6303 (1997).
323. I. G. C. Coutts and M. R. Southcott, *J. Chem. Soc., Perkin Trans. 1*, 767 (1990).
324. G. R. Geen, I. S. Mann and M. V. Mullane, *Tetrahedron*, **54**, 9875 (1998).
325. N. Selvakumar, D. Srinivas and A. M. Azhagan, *Synthesis*, 2421 (2002).
326. J. B. Domingos, E. Longhinotti, C. A. Bunton and F. Nome, *J. Org. Chem.*, **68**, 7051 (2003).
327. R. A. Scherrer and H. R. Beatty, *J. Org. Chem.*, **37**, 1681 (1972).
328. P. A. S. Smith, in *Molecular Rearrangements* (Ed. P. de Mayo), Part 1, Chap. 8, Wiley-Interscience, New York, 1967, p. 483.
329. F. Möller, in *Methoden der Organischen Chemie (Houben-Weyl)*, Stickstoff-Verbindungen II, Band 11/1, Chap. VII, Georg Thieme Verlag, Stuttgart, 1957, p. 853.
330. E. S. Wallis and J. F. Lane, *Org. React.*, **3**, 267 (1946).
331. X. Huang and J. W. Keillor, *Tetrahedron Lett.*, **38**, 313 (1997).
332. W. Lwowski and E. Scheiffele, *J. Am. Chem. Soc.*, **87**, 4359 (1965).
333. S. Sunami, T. Sagara, M. Ohkubo and H. Morishima, *Tetrahedron Lett.*, **40**, 1721 (1999).
334. L. Marinescu, J. Thinggaard, I. B. Thomsen and M. Bols, *J. Org. Chem.*, **68**, 9453 (2003).
335. L. G. Donaruma and W. Z. Heldt, *Org. React.*, **11**, 1 (1960).
336. D. W. Hansen, Jr., K. B. Peterson, M. Trivedi, S. W. Kramer, R. K. Webber, F. S. Tjoeng, W. M. Moore, G. M. Jerome, C. M. Kornmeier, P. T. Manning, J. R. Connor, T. P. Misko, M. G. Currie and B. S. Pitzele, *J. Med. Chem.*, **41**, 1361 (1998).
337. R. V. Hoffman and D. J. Poelker, *J. Org. Chem.*, **44**, 2364 (1979).
338. R. S. Sagitullin, S. P. Gromov and A. N. Kost, *Tetrahedron*, **34**, 2213 (1978).
339. G. P. Shkil, V. Lusis, D. Muceniece and R. S. Sagitullin, *Tetrahedron*, **51**, 8599 (1995).
340. D. J. Brown, in *Mechanisms of Molecular Migrations* (Ed. S. B. Thyagarajan), Vol. 1, Wiley-Interscience, New York, 1968, p. 209.
341. K. T. Potts and S. Husain, *J. Org. Chem.*, **36**, 3368 (1971).
342. K. M. Baines, T. W. Rourke and K. Vaughan, *J. Org. Chem.*, **46**, 856 (1981).
343. Y. Ogata, K. Takagi and E. Hayashi, *Bull. Chem. Soc. Jpn.*, **50**, 2505 (1977).
344. R. M. Herbst and J. E. Klingbeil, *J. Org. Chem.*, **23**, 1912 (1958).
345. T. Schelenz and W. Schafer, *J. Prakt. Chem.*, **342**, 197 (2000).
346. H. Junek, M. Klade and H. Sterk, *Monatsh. Chem.*, **120**, 781 (1989).
347. R. Weis, K. Schweiger and W. Seebacher, *Tetrahedron*, **57**, 8305 (2001).
348. K. A. M. El-Bayouki, F. E. Nielsen and E. B. Pedersen, *J. Heterocycl. Chem.*, **22**, 853 (1985).
349. M. A. Zahran, E. B. Pedersen and C. Nielsen, *Monatsh. Chem.*, **126**, 1271 (1995).

CHAPTER **12**

Analytical aspects of aromatic amines

JACOB ZABICKY

Department of Chemical Engineering, Ben-Gurion University of the Negev, P.O. Box 653, Beer-Sheva 84105, Israel
Fax: +972 8 6472969;   e-mail: zabicky@bgu.ac.il

I. ACRONYMS

AED	atomic emission detector/detection
AMD	amperometric detector/detection
APCI	atmospheric pressure chemical ionization
APPI	atmospheric pressure photoionization
ATR	attenuated total reflectance
CE	capillary electrophoresis
CMC	critical micelle concentration
COD	chemical oxygen demand
COSY	correlation spectroscopy
CPE	carbon paste electrode
CSEI-sweep	cationic selective exhaustive injection-sweeping
CZE	capillary zone electrophoresis
DA	diode array
DMS	dimethylsiloxane
dsDNA	double stranded DNA
DVB	divinylbenzene
ECD	electron capture detector/detection
ECLD	electrochemiluminescence detector/detection
ELD	electrochemical detector/detection
ELISA	enzyme-linked immunosorbent assay
EOF	electroosmotic flow
EPA	Environmental Protection Agency (USA)
ESCA	electron spectroscopy for chemical analysis
ESI	electrospray ionization
ETSF	electron transfer stopped-flow

FASI	field-amplified sample injection
FIA	flow injection analysis
FLD	fluorescence detector/detection
FPD	flame photometric detector/detection
GC	gas chromatography
GCE	glassy carbon electrode
HAA	heterocyclic aromatic amines
Hb	hemoglobin
HRMS	high resolution mass spectrometry
IARC	International Agency for Research on Cancer
LC	liquid chromatography
LIFD	laser-induced fluorescence detector/detection
LLE	liquid−liquid extraction
LLLME	liquid−liquid−liquid microextraction
LOD	limit/s of detection
LOQ	limit/s of quantitation
MAE	microwave-assisted extraction
MALDI	matrix-assisted laser desorption/ionization
MCS	mainstream cigarette smoke
MEKC	micellar electrokinetic chromatography
MS	mass spectrometry
NICI	negative ion chemical ionization
NIEHS	National Institute of Environmental Health Sciences (USA)
NIH	National Institutes of Health (USA)
NIR	near-infrared
NOESY	nuclear Overhauser enhancement spectroscopy
NPD	nitrogen−phosphorus detector/detection
PAA	primary aromatic amine/s
PAH	polycyclic aromatic hydrocarbon/s
PFF	processed food flavor/s
QSAR	quantitative structure−activity relationship
RAD	radioactivity detector/detection
RSD	relative standard deviation
SAX	strong anion exchanger
SCF	Scientific Committee on Food (EU)
SCX	strong cation exchanger
SDBC	styrene−divinylbenzene copolymer
SDS	sodium dodecyl sulfate
SFE	supercritical fluid extraction
SIM	selected ion monitoring
SNR	signal-to-noise ratio
SPAD	solid-phase analytical derivatizing
SPE	solid-phase extraction
SPME	solid-phase microextraction
SSCE	Ag-AgCl-KCl reference electrode
TNT	2,4,6-trinitrotoluene
TOF	time of flight
UVD	ultraviolet-visible detector/detection
WHO	World Health Organization
XRD	X-ray diffraction

II. INTRODUCTION

A. Scope of the Chapter

This chapter is an updating of the sections dedicated to analytical issues of amines in another volume of *The Chemistry of Functional Groups* series[1]. However, as opposed to a general approach to amines and other N-containing functional groups there, attention is now paid only to compounds bearing one or more amino functional groups attached to an aromatic or heteroaromatic ring system. Analysis of aromatic amines may serve for indirect determination of other functional groups, by previous transformation to amines, such as nitro by reduction or catalytic hydrogenation, isocyanates by hydrolysis and azo groups by reductive cleavage.

B. Aromatic Amines in Nature and Technology

1. General

The main research effort invested in the analysis of aromatic amines is related to environmental and toxicological issues. Various aspect of the analytical chemistry of aromatic amine pollutants have been reviewed[2]. Humans are exposed to aromatic amines released to the environment by industry (dyes, adhesives, pharmaceuticals, explosives, oil refining, synthetic polymers, rubbers, pesticides), forest fires and produced by diverse activities of the modern society (smoking, hair dying, fuel burning, meat cooking). Some relatively simple primary aromatic amines and azaheteroaromatic compounds listed in Table 1 are frequently used for environmental and toxicological studies. In Table 2 are listed more complex structures, such as aza-PAH and HAA found in cooked protein foodstuffs or derived from industrial emissions.

Subsections II.B.2−9 are not mutually exclusive, neither are they comprehensive reviews, but rather structured presentations of subjects that are dealt with from the analytical standpoint in Sections III−V.

2. General toxicological issues

Substituted anilines and benzidines, well known for their high toxicity and suspected carcinogenicity, are widely used in the chemical industry as precursors of dyes, pesticides, pharmaceuticals, etc.[8]. The biological effects of the polycyclic aromatic hydrocarbons (PAH) and their amino derivatives have been reviewed[9]. The QSAR studies on mutagenic and carcinogenic activities of aromatic amines were reviewed[10, 11]. QSAR studies based on the Carcinogenic Potency Database[12] found that aromatic amines are among the major genotoxic biophores for cancer causation in rats and mice[13, 14]; however, there seems to be no specific organs targeted by their carcinogenic action[15]. QSAR modeling was proposed for estimation of carcinogenicity of aromatic amines aiming at the synthesis of safer chemicals, for the estimation of the risk posed by such pollutants in the environment, thus reducing the need for animal experimentation. These calculations pointed to the reliability of *in vivo* experiments on rodents for carcinogenicity assessment[16]. A QSAR study pointed to similarity of the mechanisms of action of aromatic amines for rodent carcinogenicity and *Salmonella* mutagenicity, which are mainly dependent on electronic and steric properties, and being different from those of general toxicity, which are mostly based on hydrophobicity[17]. An estimation of Ames' mutagenicity based on $\ln R$(revertants nmol^{-1}) was made for 95 aromatic and heteroaromatic amines; better estimates were obtained when using a set of indices tailored for this property instead of an arbitrary set of parameters[18].

TABLE 1. Priority pollutants and other simple primary aromatic amines (PAA)

Compound [CAS RN]	pK_a ^{a}	Notes
Aniline (**1a**) [62-53-3]	4.6	b,c
2-Toluidine (**1b**) [636-21-5]	4.4	b,c,d,e,f
3- Toluidine (**1c**) [108-44-1]	4.7	b
4- Toluidine (**1d**) [106-49-0]	5.0	b,d
2-Ethylaniline (**1e**) [578-54-1]	4.4	g
3-Ethylaniline (**1f**) [586-02-0]	4.7	g
4-Ethylaniline (**1g**) [589-16-2]	5.1	g
4-Chloroaniline (**1h**) [106-47-8]	4.0	c,e,f
4-Anisidine (**1i**) [104-94-9]	5.2	c
1,2-Phenylenediamine (**1j**) [95-54-5]	4.5	c
1,3-Phenylenediamine (**1k**) [108-45-2]	4.9	c
1,4-Phenylenediamine (**1l**) [106-50-3]	6.2	c
4-Aminophenol (**1m**) [123-30-8]	5.3	
2-Aminobiphenyl (**1n**) [90-41-5]	3.8	
2,3-Xylidine (**2a**) [87-59-2]	4.6	g
2,4-Xylidine (**2b**) 95-68-1]	4.9	c,g
2,5-Xylidine (**2c**) [95-78-3]	4.6	g
2,6-Xylidine (**2d**) [87-62-7]	4.3	c,f,g
2,4-Diaminotoluene (**2e**) [95-80-7]	5.1	c,e,f
2,6-Diaminotoluene (**2f**) [823-40-5]	4.5	
4-Chloro-2-toluidine (**2g**) [95-69-2]	3.8	c,e,f
5-Nitro-2-toluidine (**2h**) [99-55-8]	2.3	c,e
2,4,5-Trimethylaniline (**3**) [137-17-7]	5.0	c,e
2-Anisidine (**4a**) [90-04-0]	4.5	c,e,f
4-Cresidine (**4b**) [120-71-8]	4.7	c,e
2,4-Diaminoanisole (**4c**) [615-05-4]	5.3	c,e,f
4,4′-Methylenedianiline (**5a**) [101-77-9]	5.3	c,e,f
4,4′-Methylenedi-2-toluidine (**5b**) [838-88-0]	5.2	c,e
2,2′-Dichloro-4,4′-methylenedianiline (**5c**) [101-14-4]	3.3	c,e,f
4,4′-Oxydianiline (**6a**) [101-80-4]	5.5	c,e,f
4,4′-Thiodianiline (**6b**) [139-65-1]	4.6	c,e
4-Aminobiphenyl (**7a**) [92-67-1]	4.3	b,d,e,f
Benzidine (**7b**) [92-87-5]	4.7	c,e,f,h
3,3′-Dichlorobenzidine (**7c**) [91-94-1]	2.7	c,e
3,3′-Dimethylbenzidine (**7d**) [119-93-7]	4.6	c,e,f
3,3′-Dimethoxybenzidine (**7e**) [119-90-4]	4.7	c,e,f
1-Naphthylamine (**8a**) [134-32-7]	3.9	c
1,2-Diaminonaphthalene (**8b**) [938-25-0]	4.5	
1,4-Diaminonaphthalene (**8c**) [2243-61-0]	4.6	
1,5-Diaminonaphthalene (**8d**) [2243-62-1]	4.5	
1,8-Diaminonaphthalene (**8e**) [479-27-6]	4.7	
2-Naphthylamine (**9a**) [91-59-8]	4.2	b,c,d,e,f
2,3-Diaminonaphthalene (**9b**) [771-97-1]	5.0	
1-Fluorenylamine (**10a**) [6344-63-4]	4.4	
2-Fluorenylamine (**10b**) [153-78-6]	4.3	
9-Fluorenylamine (**10c**) [5978-75-6]		i

(*continued overleaf*)

TABLE 1.   (*continued*)

Compound [CAS RN]	pK_a [a]	Notes
1-Anthrylamine (**11a**) [610-49-1]	3.9	
2-Anthrylamine (**11b**) [613-13-8]	4.2	
9-Anthrylamine (**11c**) [779-03-3]	3.9	
9-Phenanthrylamine (**12**) [947-73-9]	3.9	
1-Pyrenamine (**13**) [1606-67-3]	3.9	
3-Fluoranthenamine (**14**) [2693-46-1]	3.9	
6-Chrysylamine (**15**) [2642-98-0]	3.9	
4-Aminoazobenzene (**16a**) [60-09-3]	3.1	*c,e*
4-Amino-2′,3-dimethylazobenzene (**16b**) [97-56-3]	3.0	*c,e*
Pyridine [110-86-1]	5.2	
2-Methylpyridine [109-06-8]	6.0	
3-Methylpyridine [108-99-6]	5.7	
4-Methylpyridine [108-89-4]	6.0	
2,4-Dimethylpyridine [108-47-4]	6.8	
2,6-Dimethylpyridine [108-48-5]	7.4	
3,5-Dimethylpyridine [591-22-0]	6.2	
Quinoline [91-22-5]	4.9	
Isoquinoline [119-65-3].	5.4	

[a] Calculated pK_a. The precision of the published values[3] was reduced by one decimal place to account for the standard deviations.
[b] Found in human blood in ultratrace concentrations.
[c] Mentioned as toxic or carcinogenic in the Toxics Release Inventory (TRI), US EPA, 2001[2,4].
[d] Found in higher concentrations in the blood of smokers than nonsmokers.
[e] Mentioned in Directive 76/769/EEC of the European Community, on the restrictions on marketing and use of dangerous materials[5].
[f] Mentioned in the IARC Evaluation of Carcinogenicity to Humans[6].
[g] Found in the blood of smokers.
[h] Mentioned in the list of Priority Pollutants (Clean Water Act), 1977[7].
[i] Not a PAA. Mentioned in *Chemical Abstracts* as the hydrochloride.
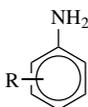
(1) (a) R = H
(b) R = 2-Me
(c) R = 3-Me
(d) R = 4-Me
(e) R = 2-Et
(f) R = 3-Et
(g) R = 4-Et
(h) R = 4-Cl
(i) R = 4-OMe
(j) R = 2-NH$_2$
(k) R = 3-NH$_2$
(l) R = 4-NH$_2$
(m) R = 4-OH
(n) R = 2-Ph
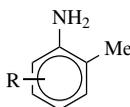
(2) (a) R = 3-Me
(b) R = 4-Me
(c) R = 5-Me
(d) R = 6-Me
(e) R = 5-NH$_2$
(f) R = 3-NH$_2$
(g) R = 4-Cl
(h) R = 4-NO$_2$
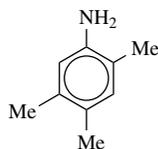
(3)
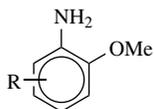
(**4**) (**a**) R = H
   (**b**) R = 5-Me
   (**c**) R = 5-NH$_2$
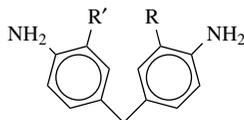
(**5**) (**a**) R = R′ = H
   (**b**) R = R′ = Me
   (**c**) R = R′ = Cl
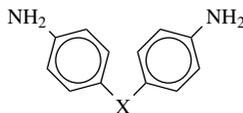
(**6**) (**a**) X = O
   (**b**) X = S
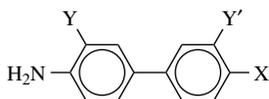
(**7**) (**a**) X = Y = Y′ = H
   (**b**) X = NH$_2$, Y = Y′ = H
   (**c**) X = NH$_2$, Y = Y′ = Cl
   (**d**) X = NH$_2$, Y = Y′ = Me
   (**e**) X = NH$_2$, Y = Y′ = OMe
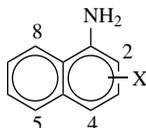
(**8**) (**a**) X = H
   (**b**) X = 2-NH$_2$
   (**c**) X = 4-NH$_2$
   (**d**) X = 5-NH$_2$
   (**e**) X = 8-NH$_2$
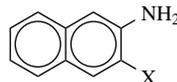
(**9**) (**a**) X = H
   (**b**) X = NH$_2$
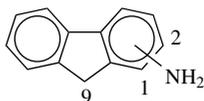
(**10**) (**a**) 1-NH$_2$
   (**b**) 2-NH$_2$
   (**c**) 9-NH$_2$
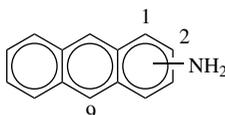
(**11**) (**a**) 1-NH$_2$
   (**b**) 2-NH$_2$
   (**c**) 9-NH$_2$
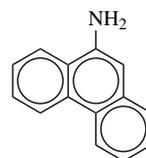
(**12**)

(**13**)
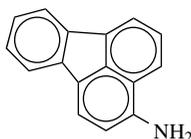
(**14**)
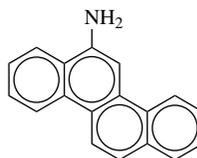
(**15**)
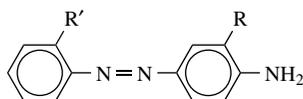
(**16**) (**a**) R = R′ = H
   (**b**) R = R′ = Me

TABLE 2. Major aza-polycyclic aromatic hydrocarbons (PAH) and heterocyclic aromatic amines (HAA) found in cooked meat products and polluted environments

Compound [CAS RN]	$pK_a{}^a$
A. Aza-polycyclic aromatic hydrocarbons	
Benz[*a*]acridine (**17**) [225-11-6]	4.7
Benz[*c*]acridine (**18**) [225-51-4]	4.2
Dibenz[*a*,*c*]acridine (**19**) [215-62-3]	4.7
Dibenz[*a*,*h*]acridine (**20**) [226-36-8]	4.7
Dibenz[*c*,*h*]acridine (**21**) [224-53-3]	4.3
Dibenz[*a*,*j*]acridine (**22**) [224-42-0]	4.7
B. Imidazo-azaarenes	
2-Amino-1-methyl-6-phenylimidazo[4,5-*b*]pyridine (PhIP, **23a**) [105650-23-5]	7.7
2-Amino-l,6-dimethylimidazo[4,5-*b*]pyridine (DMIP, **23b**) [132898-04-5]	8.2
2-Amino-l,5,6-trimethylimidazo[4,5-*b*]pyridine (TMIP, **23c**) [161091-55-0]	8.7
2-Amino-3,5,6-trimethylimidazo[4,5-*b*]pyridine (**24**) [57667-51-3]	8.4
2-Amino-3-methylimidazo[4,5-*f*]quinoline (IQ, **25a**) [76180-96-6]	6.2
2-Amino-3,4-dimethylimidazo[4,5-*f*]quinoline (MeIQ, **25b**) [77094-11-2]	6.5
2-Amino-3,8-dimethylimidazo[4,5-*f*]quinoxaline (MeIQx, **26a**) [77500-04-0]	2.5
2-Amino-3,4,8-trimethylimidazo[4,5-*f*]quinoxaline (4,8-DiMeIQx, **26b**) [95896-78-9]	2.9
2-Amino-3,7,8-trimethylimidazo[4,5-*f*]quinoxaline (7,8-DiMeIQx, **26c**) [92180-79-5]	2.8
2-Amino-3,4,7,8-tetramethylimidazo[4,5-*f*]quinoxaline (TriMeIQx, **26d**) [132898-07-8]	3.2
2-Amino-3-methylimidazo[4,5-*f*]quinoxaline (IQx, **26e**) [108354-47-8]	2.3
2-Amino-1,7,9-trimethylimidazo[4,5-*g*]quinoxaline (**27**)	
C. Carbolines	
3-Amino-1-methyl-5*H*-pyrido[4,3-*b*]indole (Trp-P-2, **28a**) [62450-07-1]	10.6
3-Amino-1,4-dimethyl-5*H*-pyrido[4,3-*b*]indole (Trp-P-1, **28b**) [62450-06-0]	10.9
2-Aminodipyrido[1,2-*a*:3′,2′-*d*]imidazole (Glu-P-2, **29a**) [67730-10-3]	5.8
2-Amino-6-methyldipyrido[1,2-*a*:3′,2′-*d*]imidazole (Glu-P-1, **29b**) [67730-11-4]	6.3
2-Amino-9*H*-pyrido[2,3-*b*]indole (A*α*C, **30a**) [26148-68-5]	6.8
2-Amino-3-methyl-9*H*-pyrido[2,3-*b*]indole (MeA*α*C, **30b**) [68006-83-7]	7.1
9*H*-Pyrido[3,4-*b*]indole (norharman, **31a**) [244-63-3]	7.8
1-Methyl-9*H*-pyrido[3,4-*b*]indole (harman, **31b**) [486-84-0]	8.6
D. 2-Phenylbenzotriazoles	
2-(2-Acetylamino-4-bis(2-methoxyethyl)amino-5-methoxyphenyl)-5-amino-7-bromo-4-chloro-2*H*-benzotriazole (PBTA-1, **32a**) [194590-84-6]	3.3
2-(2-Acetylamino-4-*N*-(2-cyanoethyl)ethylamino-5-methoxyphenyl)-5-amino-7-bromo-4-chloro-2*H*-benzotriazole (PBTA-2, **32b**) [215245-16-2]	3.4
2-(2-Acetylamino-4-2-hydroxyethylamino-5-methoxyphenyl)-5-amino-7-bromo-4-chloro-2*H*-benzotriazole (PBTA-3, **32c**) [270925-57-0]	2.0
2-(2-Acetylamino-4-amino-5-methoxyphenyl)-5-amino-7-bromo-4-chloro-2*H*-benzotriazole (PBTA-4, **32d**) [351995-07-8]	2.4
2-(2-Acetylamino-4-bis(2-acetoxyethyl)amino-5-methoxyphenyl)-5-amino-7-bromo-4-chloro-2*H*-benzotriazole (PBTA-5, **32e**)	
2-(2-Acetylamino-4-bis(2-hydroxyethyl)amino-5-methoxyphenyl)-5-amino-7-bromo-4-chloro-2*H*-benzotriazole (PBTA-6, **32f**) [392274-07-6]	3.1

TABLE 2.   (*continued*)

Compound [CAS RN]	pK_a [a]
2-(2-Acetylamino-4-diethylamino-5-methoxyphenyl)-5-amino-7-bromo-4-chloro-2*H*-benzotriazole (PBTA-7, **32g**)	
2-(2-Acetylamino-4-diallylamino-5-methoxyphenyl)-5-amino-7-bromo-4-chloro-2*H*-benzotriazole (PBTA-8, **32h**)	

[a] Calculated pK_a. The precision of the published values[3] was reduced by one decimal place to account for the standard deviations.
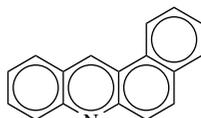
(17)
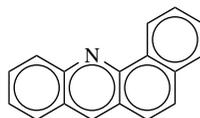
(18)
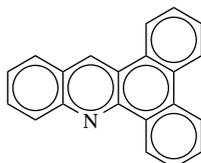
(19)
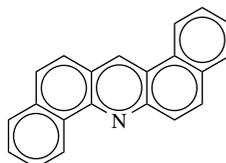
(20)
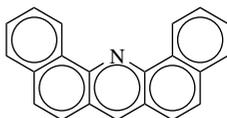
(21)
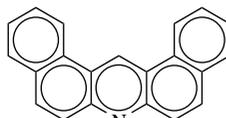
(22)
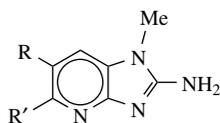
(23) (**a**) R = Ph, R′ = H
(**b**) R = Me, R′ = H
(**c**) R = R′ = Me
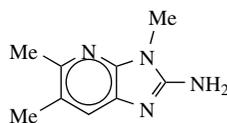
(24)
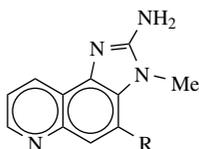
(25) (**a**) R = H
(**b**) R = Me
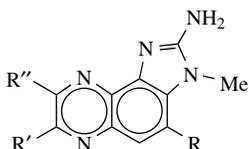
(26) (**a**) R = R′ = H, R″ = Me
(**b**) R = R″ = Me, R′ = H
(**c**) R = H, R′ = R″ = Me
(**d**) R = R′ = R″ = Me
(**e**) R = R′ = R″ = H
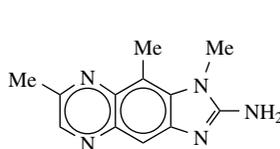
(27)
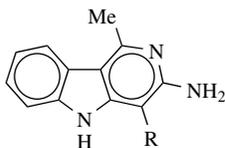
(28) (a) R = H
          (b) R = Me
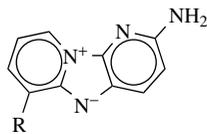
(29) (a) R = H
          (b) R = Me
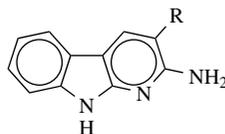
(30) (a) R = H
          (b) R = Me
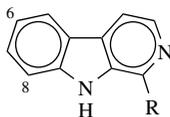
(31) (a) R = H
          (b) R = Me
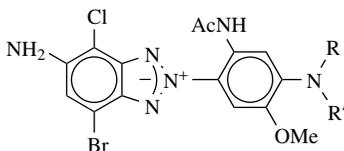
(32) (a) R = R′ = CH$_2$CH$_2$OMe
          (b) R = CH$_2$CH$_2$CN, R′ = Et
          (c) R = CH$_2$CH$_2$OH, R′ = H
          (d) R = R′ = H
          (e) R = R′ = CH$_2$CH$_2$OAc
          (f) R = R′ = CH$_2$CH$_2$OH
          (g) R = R′ = Et
          (h) R = R′ = CH$_2$CH=CH$_2$

The simple aromatic amines in Table 1 carrying note *b* (**1a–d, 7a, 9a**) were found in human blood, of which those carrying note *d* (**1b, 1d, 7a, 9a**) appear on the average with higher concentration for smokers than nonsmokers; in addition, the aniline derivatives carrying note *g* (**1e-g, 2a-d**) have also been detected in smokers' blood. None of the polycondensed aromatic amines **11, 12** and **15** was found in human blood[19]. Aniline, 2-toluidine and *N*-methylaniline were found in human milk, in concentrations from the LOQ to about 10 ppb, of both smoking and nonsmoking lactating women in Ontario, Canada. The aromatic amines may have environmental origin and may be linked with the incidence of breast cancer in the population[20]. DNA adducts of 4-aminobiphenyl (**1n**), PhIP (**23a**) and benzo[*a*]pyrene, taken as model compounds for three different classes of carcinogens, were found in the exfoliated ductal epithelial cells in human breast milk, collected from healthy, nonsmoking mothers. This points to dietary and environmental pollutants as serious risk factors, because breast ductal epithelial cells are the cells from which most breast cancers arise[21]. Formation of DNA adducts on human exposure to the HAA of Table 2.B–C was investigated[22]. The following PAA concentrations ($\mu g\,L^{-1}$, for the median and 95th percentile) were found in the urine excretions of the general population in Germany: aniline (3.5, 79), 2-toluidine (0.12, 2.7), 3-toluidine (0.17, 2.2), 4-toluidine (0.11, 0.43), 2-anisidine (0.22, 0.68), 3-chloroaniline (<0.05, 0.55), 4-chloroaniline (0.11,

0.57), 3,5-dichloroaniline (0.18, 1.5) and 3,4-dichloroaniline (in 20% of the specimens near the LOD, <0.05, 0.12). No 1- or 2-naphthylamine, 4-aminobiphenyl or metabolites of explosives were detected[23].

Reviews appeared on the analytical methods for DNA adducts induced by environmental pollutants such as carcinogens[24] and mutagens[25]. Biomarker monitoring, such as DNA adduct analysis, is a most useful tool for determining mechanisms of activity and assessment of carcinogen effective dose in humans[26]. The DNA adducts are present in very low concentrations (about 1 per 10^7 normal nucleotides), making their analysis in tissues very difficult[27]. PAA undergo enzymatic activation *in vivo* to intermediate nitrenium ions, capable of forming adducts with DNA and proteins by bonding to nucleophilic sites. For example, adducts **33** and **34** can be isolated from DNA in tissues that have been exposed to mutagenic benzidine (**7b**) and 1-aminofluorene (**10a**), respectively. If the altered DNA is not repaired, it may lead to increased rates of sister chromatid exchanges, activation of the aromatic hydrocarbon receptors and ultimately to lung, bladder and skin cancer, transplacental transfer and premature ovarian failure[28].

(33)   **(34)**
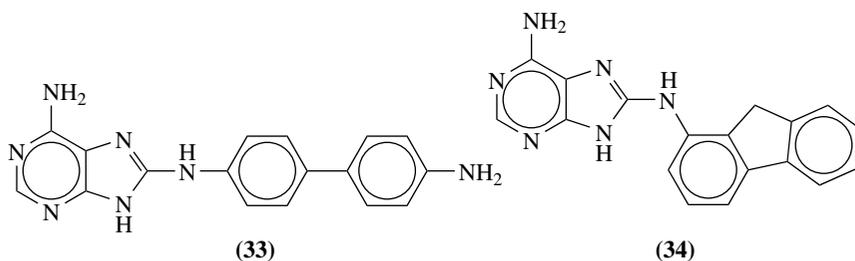
The PAH benzo[*ghi*]fluoranthene (**35**) undergoes metabolism to an epoxide (**36**) which can form adducts with DNA, for example, by binding to a deoxyadenosine residue (equation 1). In Section V.A the structure of four possible diastereoisomers of the deoxyadenosine adduct (**37**) is discussed[29].

(35)   **(36)**   **(37)**   (1)
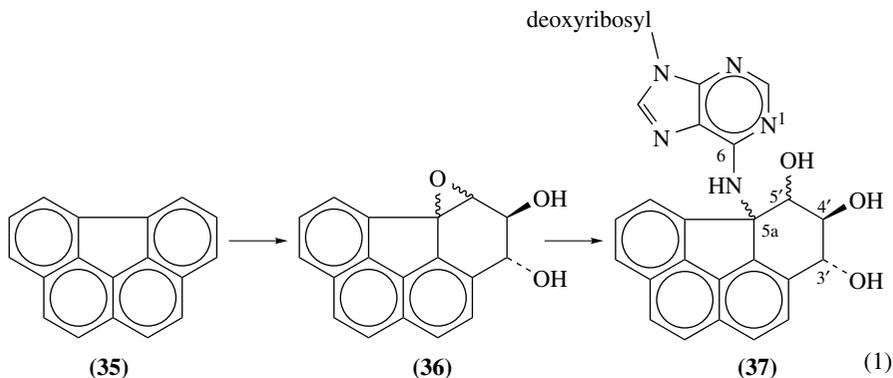
It has been proposed to use hemoglobin adducts in biomonitoring, as a dosimeter for the biologically active dose of arylamines/arylacetamides. This may also provide information about the individual susceptibility to the toxic and carcinogenic effects of these chemicals[30, 31]. Field workers exposed to Propanil (**38**), a major herbicide in rice paddies,

showed the presence of the Hb-**39** adduct derived from a metabolite of **38** (equation 2). No trace of **38** was found in the urine of the workers[32].

$$\text{(2)}$$

(38)   **(39)**
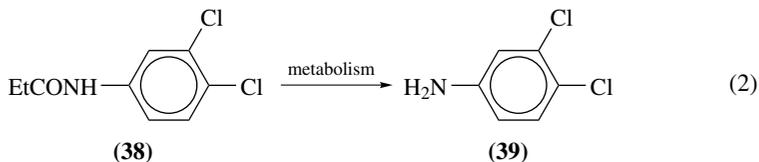
3. Tobacco

Analysis of PAA in MCS pointed to the following main components and average emissions (ng per cigarette) of a low nicotine brand: aniline (**1a**, 69), 2- (**1b**, 11), 3- (**1c**, 23) and 4-toluidine (**1d**, 25), 2- (**1e**, 4), 3- (**1f**, 6) and 4-ethylaniline (**1g**, 8), 2,4- (**2b**, 3), 2,5- (**2c**, 4) and 3,4-xylidine (4), 1- (**8a**, 5) and 2-naphthylamine (**9a**, 9); other components were below 1 ng per cigarette or near the LOD[33]. In another study, where 4-toluidine was added to the collected sample to avoid fast destruction of the PAA (Section III.A.1), results were much higher: **1a** (423), **1b** (240), **1c** (166), **8a** (32) and **9a** (21), 2- (8.2) and 4-aminobiphenyl (**7a**, 3.6), 2-fluorenylamine (**10b**, 3.4), 1-pyrenamine (**13**, 1.3), 3-fluoranthenamine (**14**, 1.2) and 6-chrysylamine (**15**, 0.6). Alkaline tobaccos produced in France and Germany had even larger PAA yields[34]. There seems to be a significant inverse correlation between the levels (*ca* 100 to 450 pg **7a** g^{-1} Hb) of the 4-aminobiphenyl adduct with hemoglobin (**7a**-Hb) caused by smoking and the trolox equivalent antioxidant capacity of the plasma[35]. It has been postulated that the factors affecting aromatic amine yields in MCS are the 'tar' delivery, on an equal 'tar' basis the N content of the tobacco, and, mainly, the combustion temperature. Furthermore, the competing formation of formaldehyde and aromatic amines is controlled by the amount of NH$_2^{\bullet}$ free radicals released on combustion[36]. According to IARC there is only limited evidence for aniline being carcinogenic; however, its acute and long-term exposure toxic effects are well documented. One toxicity pathway for PAA consists of metabolic conversion to the corresponding hydroxylamine, nitrosoarene and sulfinamide adduct formation by reaction with SH groups of cysteine residues on the β-chain of globin, turning hemoglobin to methemoglobin[37].

A group of PAA of special interest are the alkylated anilines because they are the largest fraction of arylamines in tobacco smoke[38]. Analysis of aniline (**1a**), 4-aminobiphenyl (**7a**), 1- (**8a**) and 2-naphthylamine (**9a**) in the urine of smokers, passive smokers and nonsmokers in Germany pointed to a gradual diminution of the levels of the PAA among these groups in that order; however, only **8a** showed a large difference between smokers and nonsmokers. For reference, also the creatinine (**40**) and cotinine (**41**) levels in urine were determined. The levels of the latter were near the LOD for nonsmokers and dramatically increased for smokers. The origins of PAA in the urine of nonsmokers other than tobacco and diesel emissions have to be elucidated, and may be linked to the incidence of bladder cancer in this group[39]. Testing aromatic amines for human bladder carcinogenesis requires animals other than rodents, which seem to be insensitive to this particular feature, whereas studies in dogs show good correlations[40]. The susceptibility to develop cancer derived from tobacco PAA seems to vary much from individual to individual and is related to the *N*-acetyl transferase polymorphism involved in detoxification and activation of the PAA[41]. A principal component analysis study of the distribution of **7a** in blood (as Hb adduct) and various organs of rats (Section III.A.2) pointed to the need of considering also the intake of heavy metal pollutants in pharmacotoxicological investigations of organic pollutants in animals[42].
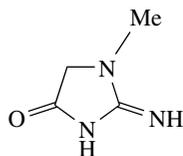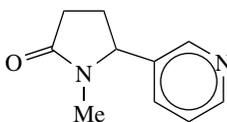
(40)   **(41)**

4. Foodstuffs

Bladder cancer in Chinese women may be linked to the oil fumes in the kitchen air, which were shown to be mutagenic and to contain up to about 50 µg m^{-3} of 4-aminobiphenyl (**7a**) and 2-naphthylamine (**9a**). The concentration of these PAA was substantially reduced on adding the antioxidant catechin (**42**) to the oil[43].
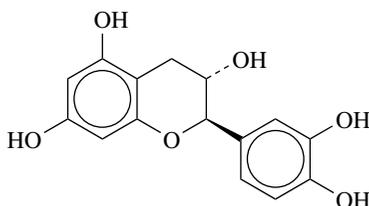
(42)

The problems associated with determination of heterocyclic aromatic amines (HAA, Table 2.B−C) in cooked food were reviewed[44]. HAA are formed on a Maillard-type condensation of amino acids, sugars and creatinine (**40**). They are present in the low ppb range in cooked food of high protein content, such as meat and fish, and have mutagenic and carcinogenic activity[45−47]. The concentration of these trace toxic compounds increases with the time of cooking[48] and varies with the place where the food was prepared, from undetectable amounts in many meats sold in fast food restaurants, to over 10 ng g^{-1} in restaurants that cook food to order, to several hundreds of ng g^{-1} for certain meats cooked in the laboratory or at home[49]. In a project carried out on 'meat cuts' (ready to eat turkey breast, salami, chicken loaf, cooked ham, all beef meat, pepperoni, etc.), randomly purchased from supermarkets and specialty food stores in the Ottawa area, only trace amounts (0.4 ppb) of MeIQx (**26a**) were found in one sample of smoked turkey breast, pointing to the low risk involved in consumption of these products[50a]. Analysis of 25 wines of various regions in Western Europe showed the widespread presence of MeIQx (**26a**) and MeAαC (**30b**) in the low ppt range, as determined by HPLC with tandem ESI-MS-MS detection. The concentrations of these compounds were 2 to 3 orders of magnitude lower than those found in meat products[50b]. Estimations of the daily intake of this type of HAA according to different sources are from 0 to 15 µg[44], but this may vary from place to place: 0.3 to 0.5 µg in USA[51], 1 µg in New Zealand[52], 0 to 7 µg in Sweden[53] and 5 ng kg^{-1} of body weight of Swiss adults[54]. Some caution in the interpretation of toxicological results is in place. Thus, mutagenicity of eight PFF samples, as determined by the Ames test, showed no correlation with the analysis of PhIP (**23a**), IQ (**25a**), MeIQ (**25b**), MeIQx (**26a**) and Trp-P-2 (**28a**). Of two PFF with high mutagenic activity one contained 9.6 ppb of **25a** and traces of **26a** and **28a** whereas in the other all HAA were under the LOD (1 ppb); two samples with high **25a** content (6.7 and 6.8 ppb) showed only

moderate mutagenic activity, while one with moderate content of **25a** (2.1 ppb) showed none; three PFF samples containing no HAA or only traces of **23a** and **28a** were not mutagenic[55].

Among the aminoimidazo-azaarenes listed in Table 2.B, PhIP (**23a**) frequently is the most abundant one. The first step of its metabolism involves hydroxylation at the N^2-position followed by transformations to biologically active species, primarily involving acetyltransferases and sulfotransferases. An alternative hydroxylation path is at the 4′-position. **23a** has been implicated in colon cancer and its activation mechanism has been elucidated[56]. Detoxification processes involve glucoronidation, which may be at the N^2-position on the parent compound (**43**) or of the N^2-hydroxylated compound (**44, 45**), or sulfation of the 4′-hydroxylated compound (**46**), and the metabolites are excreted in the urine (see Section IV.B.1)[57]. Some volatile organic sulfides seem to effectively reduce the concentration of HAA in cooked meat, as was the case for the volatile sulfides of garlic present while frying beef patties, for which a significant reduction in the amounts of **23a** and MeIQx (**26a**) was observed as compared with the patties fried in the absence of garlic[58]. The glucoronide metabolite of **26a** was isolated from urine by SPE and subsequently determined by an immunoaffinity assay, outside the scope of this chapter[59].
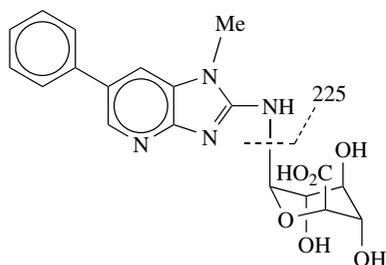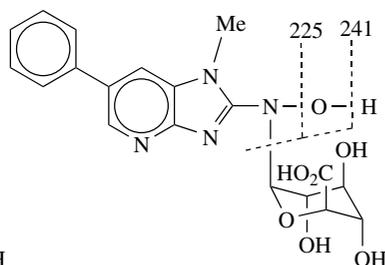
(43)   **(44)**
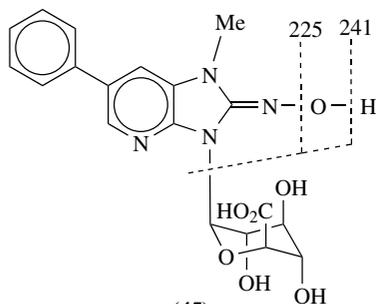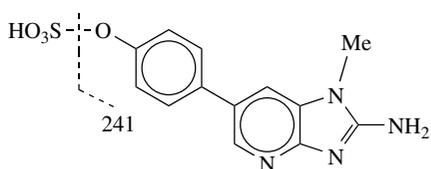
(45)   **(46)**

5. Industrial chemicals

Sterically hindered phenols (e.g. **47a**), aromatic amines (e.g. **48a** = Ar₂NH) and hindered amine light stabilizers (e.g. **49a**) are additives that contribute to the longevity of polymers subjected to strenuous duties, especially under thermal or photochemical oxidative conditions. They degrade by various mechanisms, and they may also regenerate. For example, the phenolic groups of **47a** gradually turn to semiquinones (**47b, 47c, 47d**), **48a** may undergo formylation or even a double condensation with formaldehyde to a dimeric

Ar$_2$NCH$_2$NAr$_2$, and **49a** may undergo gradual transformation to products such as **49b** and **49c**. Although the aromatic amine seems to be more effective than the phenolic compound in its antioxidant ability for polar and nonpolar polymers, a mixture of both types of additives shows a synergism by which the degraded aromatic amine is regenerated by the phenolic compound. A study of the fate of two polymer simulants, the antioxidant additives and their degradation products during thermal oxidation experiments, involved a battery of analytical techniques such as ATR-IR, HPLC-DA-UVD, GC-FID, GC-MS and LC-MS[60]. Sterically hindered aromatic secondary amines serve as antioxidants in fuel and end up in the atmosphere as a result of automotive emissions, both as vapors or in particulates. Five classes of such pollutants have been detected (**50**–**54**) carrying various sterically hindering substituents R and R', as listed beneath **54**. End analysis after appropriate cleanup and preconcentration was by GC-MS[61].
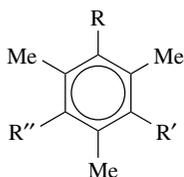
(**47**) (**a**) R = R' = R'' = **47'**

(**b**) R = R' = **47'**, R'' = **47''**

(**c**) R = **47'**, R' = R'' = **47''**
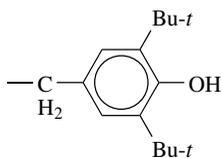
(**d**) R = R' = R'' = **47''**
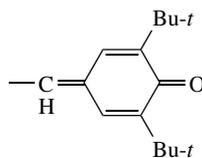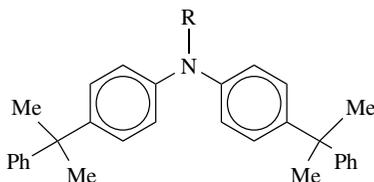
(**48**) (**a**) R = H

(**b**) R = CH=O

(**49**) (**a**) R = H

(**b**) R = Me

(**c**) R = O⌒O⌒Me

(50)   **(51)**

(52)

(53)

(54)

R = R′ = H, *t*-Bu, Bu-*t*, Bu-*s*, Bu-*s*, Bu-*t*, Pr-*i*
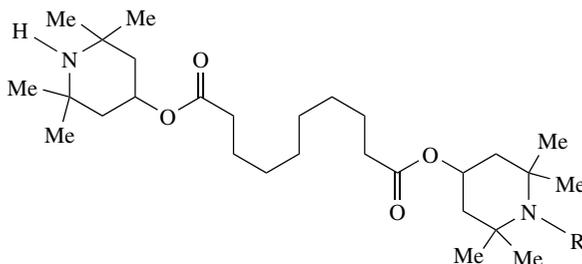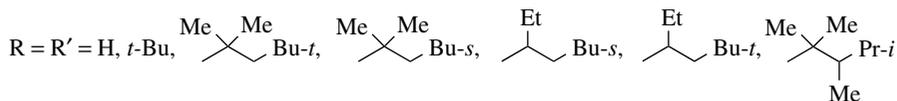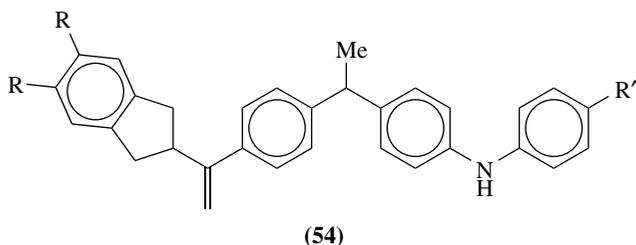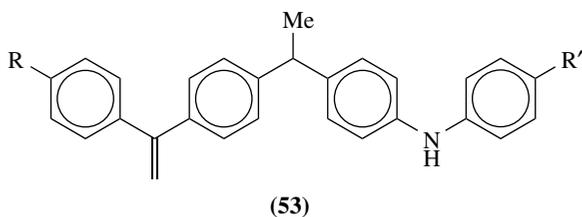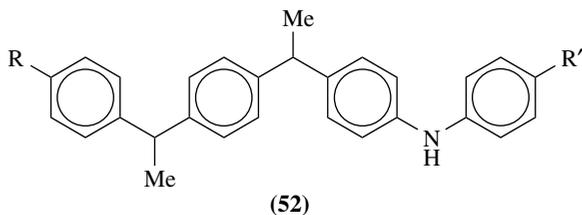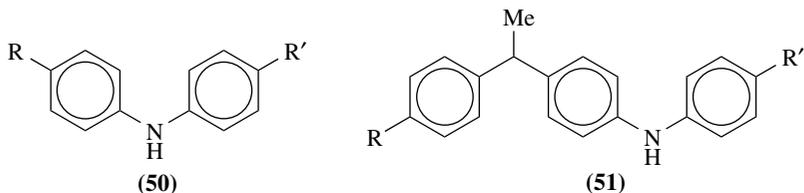
   Polyurethane foams can be recycled. Those derived from methylenebis(4-phenylisocy-anate) may produce 4,4′-methylenedianiline (**5a**), either on pyrolysis or in the recycling process, consisting of heating the foam with glycols, thus adding to potential hazards in the utilization of derived products[62, 63]. Several aromatic isocyanates used in plastics manufacture have been classified as 4A by the SCF of the EU, as being able to hydrolyze to the corresponding amines, some of which are carcinogenic; these include the isocyanate precursors of aniline (**1a**), 2,4- (**2e**) and 2,6-diaminotoluene (**2f**), 4,4′-oxydianiline (**6a**), 4,4′-methylenedianiline (**5a**) and its 2,4′ isomer[64]. Thus, other sources for micropollutants may be corks[65] or flexible multilayered plastic packaging[66] produced with adhesives

containing aromatic isocyanates (ArNCO). In case of incomplete curing, the ArNCO residuals may migrate onto the food and undergo hydrolysis yielding PAA, some of which have been classified as potentially carcinogenic (Table 1, note e). European legislation requires that the overall PAA transferred from the packaging materials into foodstuffs or food simulants should go undetected when the LOD of the analytical method is 20 $\mu g\,kg^{-1}$ foodstuff. At present, the assay for such PAA is based on a coupling reaction to produce an azo dye, followed by spectrophotometric determination[67]. However, in case of a positive result, further tests have to be performed to ascertain whether the measured color is due to the presence of dangerous PAA. To avoid such laborious undertakings, a GC-MS procedure was developed (Section IV.A)[68]. An alternative procedure can be ATR-FTIR (Section IV.E.1)[66].

Various modern products may serve as sources for trace amounts of PAA. The origins, known hazards, release restrictions and environmental fate of PAA derived from azo dyes have been reviewed[2]. The metabolism of nitroarenes is closely linked to that of aromatic amines, as shown in a simplified way in equation 3[69]. *Gloeophyllum trabeum* cultures spiked with TNT show formation of nitroaromatic amines such as 2-amino-4,6-dinitrotoluene, 4-amino-2,6-dinitrotoluene and 2,4-diamino-6-nitrotoluene. Also, autoxidation of the methyl group of TNT or its metabolites may take part in the degradation process, as shown by the presence of Schiff bases and oligomeric and polymeric species; detection and determination of the analytes after LLE and concentration were by HPLC-UVD or GC-MS[70].

$$R = H, Me$$
$$R' = H, NH_2, Cl, etc.$$
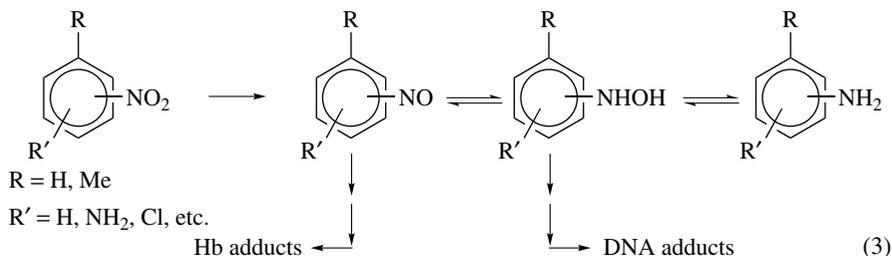
Azo dyes are extensively used in consumer products, such as textiles, leather, paper, gasoline, foodstuffs and cosmetics. When released from their matrix they are reduced by microorganisms present in the environment or on the human skin, producing aromatic amines such as 4-aminobiphenyl (**7a**), benzidine (**7b**) and 2-napthylamine (**9a**), which were classified by IARC[71] as potential human carcinogens. This led to banning certain azo dyes for use in consumer products[5, 72, 73]. Neither chemical or enzymatic degradation of the dyes need be a straightforward process, as shown by the mixtures of aromatic amines obtained in some cases. For example, the extracellular fluid protein of *Streptomyces* sp. was found to catalyze decolorization by reduction of Xylidine Ponceau-2R (**55**) to yield 2,4-xylidine (**2b**), 2,6-xylidine (**2d**) and 2,4,5-trimethylaniline (**3**), and either Direct Black-38 (**56**) or Direct Brown-1 (**57**) to yield 4-aminobiphenyl (**7a**) and benzidine (**7b**)[74]; Acid Black 077 (**58**) yields **7b**[73]. The amines obtained from azo dye degradation were analyzed by UVV spectrophotometry, HPLC-UVD, LC-MS and GC-MS[74]. Methods were proposed for analysis of azo dyes used in toys[75] or leather[76] manufacture, based on cleavage of the azo group with sodium dithionite ($Na_2S_2O_4$) and end analysis of the resulting PAA solutions by RP-HPLC with DA-UVD.

The formula of an azo dye is not sufficient for predicting the causes for its banning under the provisions of the European Community regulations[5], as the commercial product may contain restricted PAA (Table 1, note e) other than those resulting from azo group
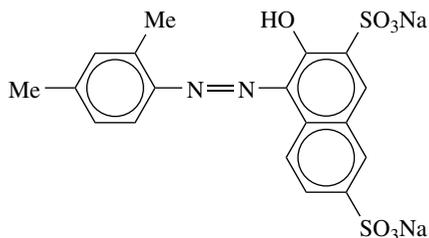
(55)
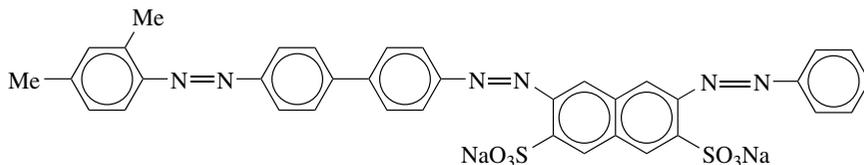
(56)
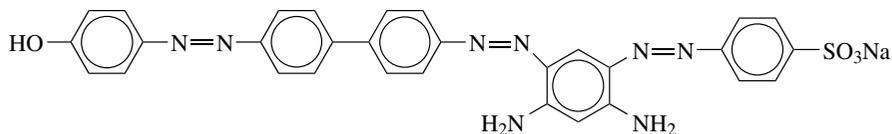
(57)
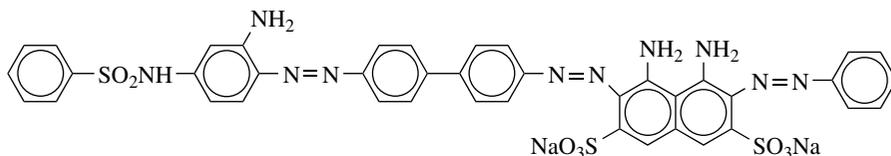
(58)

splitting. This is the case of Acid Black 1 (**59**), containing 4-aminobiphenyl (**7a**) and benzidine (**7b**), which are byproducts of the **59** synthesis, beginning with the so called H acid (**60**)[77].
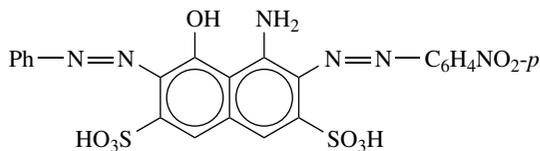
(59)
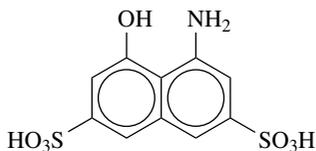
(60)

Purification of effluents with high organic content takes place in two main steps: anaerobic reduction and aerobic oxidation causing mineralization of the organic products. Azo

dyes present in the waters can be decolorized by anaerobic reduction to PAA; however, the resulting PAA are not easily mineralized. Thus, a synthetic wastewater with organic content equivalent to 1925 ± 133 mg L^{-1} COD was subjected to a methanogenesis process in an upflow anaerobic sludge blanket reactor. Spiking 60 to 300 mg L^{-1} of Direct Red 254 (**61**) or Acid Orange 7 (**62**) did not affect the sludge process but brought about fast loss of color, as determined by UVV spectrophotometry. Metabolites such as sulfanilic acid (**63**) and 1-amino-2-naphthol (**64**) were recovered and determined by RP-HPLC, pointing to the presence of toxic residues which could not be mineralized by biodegradation[78, 79]. In fact, many studies address biological decoloration of industrial effluents containing azo dyes; however, only a few pay attention to total removal of the PAA produced in the anaerobic step of the water recycling process. For example, in the case of a reactor and operation design for wool dying effluents, attention is paid mainly to COD diminution and decoloration[80], whereas in the case of Remazol Brilliant Violet 5R (Cu^{2+} complex of **65**), further investigation showed that no aerobic degradation of the aromatic amine was successful after 810 days[81]. The removal of **65** from effluents by flocculation was monitored by UVV spectrophotometry[82]. Quantitative molecular structure–property (QMSP) relationships modeling on more than hundred anionic water-soluble dyes led to the conclusion that concurrence of the following factors is favorable for dye biodegradability: larger molecular size to ionic charge ratio and the presence of more PAA and unsulfonated naphthalene nuclei and fewer aliphatic alcohol groups[83].

(**61**)

(**62**)

(**63**)

(**64**)

(**65**)
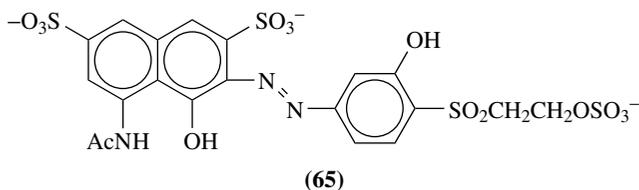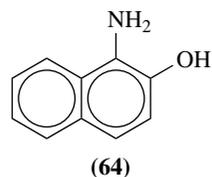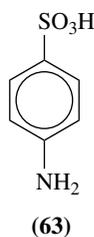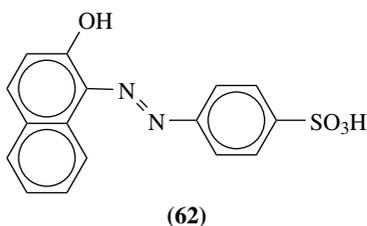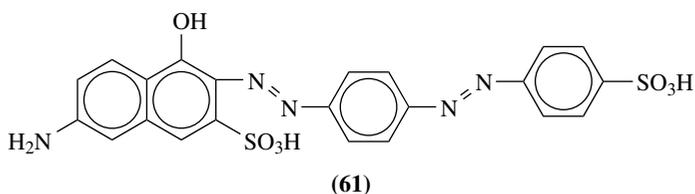
6. General environmental issues

Application of the effect-directed analysis methodology has been reviewed. It consists of the search of toxic compounds present in complex samples, such as those stemming from the environment and industrial effluents, following the simplification operations shown in equation 4, where BA = biological assay, CA = chemical analysis and FR = fractionation. At present it is too expensive for screening applications; however, it is amply justified for identification of specific toxicants near the source of emission, as was the case of mutagens in Table 2.D in river waters[84].

$$(4)$$
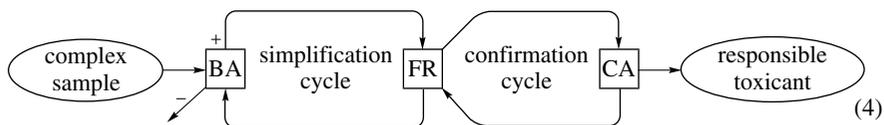
The environmental effects of the polycyclic aromatic hydrocarbons (PAH) and their amino derivatives have been reviewed[85].

7. Air

Determination of atmospheric PAA in Italy showed indoor concentrations from 3 to over 200 ng m^{-3}, without aniline, depending on the absence or presence of cigarette smokers in the room. Outdoors levels without aniline usually were under 40 ng m^{-3}. Indoors aniline levels were more erratic, 53 ng m^{-3} in a nonsmoker's office to 1929 ng m^{-3} in a discotheque, but were not related to cigarette smoke[86].

8. Water

The mutagenic and genotoxic compounds present in surface waters were reviewed. They belong to various classes of compounds: heavy metals, PAH, HAA, pesticides and others, originating in partially treated or untreated discharges from chemical and petrochemical industries, oil refineries, oil spills, rolling steel mills, untreated domestic sludges and pesticides runoff[87]. Owing to their high solubility in water, aromatic amines can easily permeate through soil and contaminate groundwaters[88].

Ozonization for water disinfection is returning instead of chlorination; however, it is not devoid of potential dangers when micropollutants react with ozone. Thus, an aqueous solution of 3-phenylenediamine (**1k**) led to formation of the strongly mutagenic 2-amino-5-[(3-aminophenyl)amino]-4-[(3-aminophenyl)imino]-2,5-cyclohexadien-1-one (**66**)[89].
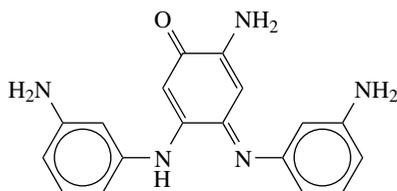
(66)

The presence of mutagens such as nitroarenes and aromatic amines in environmental waters or industrial effluents can be assessed by the Ames test and *in vitro* cytogenetic assay for bacteria (outside the scope of this chapter), involving a combination of toxic

and clastogenic effects[90]. The concentrations of the imidazo-azaarenes Trp-P-2 (**28a**), PhIP (**23a**) and 4,8-DiMeIQx (**26b**) measured in rainwater (85, 35 and 17 $ng\,L^{-1}$, respectively) were attributed to a nearby forest conflagration in Singapore[91]. Norharman (**31a**) and harman (**31b**) are widely distributed in the environment, including water for domestic use, and probably undergo chlorination at the 6 and 8 positions. These two pollutants and their 6-chloro derivatives show comutagenicity with nonmutagenic PAA such as aniline (**1a**) and 2-toluidine (**1b**)[92].

The genotoxicity of human feces and urine is due to the presence of toxic substances ingested with cooked protein food or absorbed from the environment. It persists after biological treatment and ultrafiltration of sewage; however, it is almost totally removed after coagulation–sedimentation treatment[93]. The contributions of genotoxic precursors to the Yodo River in Japan were examined[94]. An observation that water samples of the Yodo River, the main drinking water supply for Osaka, were mutagenic to *Salmonella typhimurium* strains (Ames test) led to the isolation (Section III.A.2) and determination of PBTA-1 (**32a**) and PBTA-2 (**32b**) (Section IV.B.2, 3) at ppb levels, by HPLC with ESI-MS-MS detection (or ELD[95a]). These pollutants are presumably derived from disperse azo dyes in the river by reduction and chlorination[95b]. Eight potent mutagens, PBTA-1 to PBTA-8 (**32a-h**, Table 2.D), were isolated from the waters of several rivers in Japan, downstream from a sewage treatment plant. They are HAA containing Br and Cl stemming from the reduction and chlorination of Br-containing Disperse Blue dyes (**67**) used in the textile industry[96–103], where the R and R′ groups correspond to those of compounds **32a–h**. Compound **32b** shows *in vitro* cytochalasin B-mimetic activity, affecting actin filaments and inducing aberrations in the number of chromosomes of the test cells[104]. Chromosome number aberrations were also shown by action of the analogous pollutant **32a**, the azo dyes **67**, and the intermediate transformation step of the dyes before **32a** and **32b** acquire their chlorine atom[105].

(67)   **(68)**
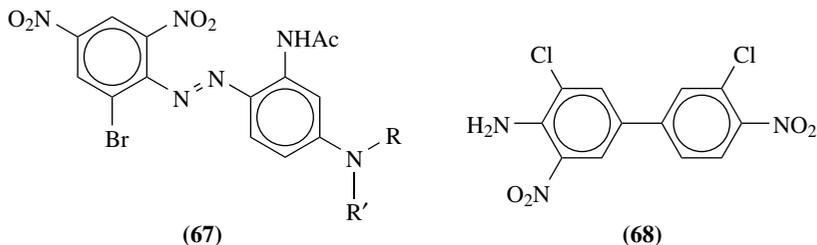
The mutagens IQ (**25a**), Trp-P-1 (**28b**) and AαC (**30a**) were identified in the Danube River in Vienna[106]. Another type of mutagen found in a Japanese river is 4-amino-3,3′-dichloro-5,4′-dinitrobiphenyl (**68**), which presumably originates in the polymer or synthetic dye industries[107].

9. Soil

Soil sorption is an important detoxification process for pollutants of aquifer waters; however, sediment-column experiments to determine the soil sorption capacity are tedious, expensive and their results are affected by various extraneous factors. It was proposed to estimate the adsorption coefficients K_d based on their correlation with the capacity factors, k', measured by isocratic RP-HPLC[108]. A QSAR estimation study was carried out of soil sorption coefficients, K_{oc}, of polar organic chemicals such as substituted anilines and phenols, based on descriptors such as n-octanol–water partition coefficients, K_{ow},

molecular connectivity indices, and quantum chemical parameters. Program development
made use of artificial neural networks for improved results[109].

III. SAMPLE PREPARATION

A. Cleanup and Preconcentration

Analysis at ultratrace levels is full of pitfalls, not only related to the most obvious
reasons, such as choice of separation and detection methods adequate to the matrix, the
analyte and the actual concentrations, but more evasive ones, such as instability of the
analyte when separated from the matrix, losses by evaporation, adsorption on the surface
of vessels and conducts or dissolution in materials that come in contact with the sample.
Some of the works mentioned in this section pay attention to these details too.

1. Sample stabilization

A rapid diminution of recovery with time was noted for the aromatic amines in main-
stream cigarette smoke (MCS), collected in an automatic smoking machine. This is due
to fast reaction of the PAA with other components present in the matrix. Addition of 4-
toluidine (**1d**) to the sample dramatically improved analyte recoveries, as this compound
served as sacrificial reagent[34].

2. Liquid–liquid extraction

A 1000-fold concentration rise was achieved after adjusting to pH 11 a 1 L sam-
ple of groundwater and LLE with three 60 mL aliquots of CH_2Cl_2, which were unified,
filtered, dried and evaporated to a 1 mL volume. This was followed by perfluorobutyry-
lation (Section III.B.1) and end analysis by GC-MS (Section IV.A)[110]. A 125-fold rise
in concentration was achieved in a method for determination of aromatic amines and
nitroarene metabolites in acid hydrolyzed urine. LLE of a 5 mL sample with *n*-hexane
was followed by a series of manipulations including evaporations, centrifuging, deriva-
tizing to the pentafluoropropionamide and final adjustment of the volume to a 40 μL
sample. End analysis was by HPLC-SIM-MS[23]. LLE with ether was applied to recover
the PAA, after alkalinization of the HCl solution used for scrubbing air with Drechsler bot-
tles. End analysis was by GC-MS, after derivatizing with pentafluoropropionic anhydride
(Section III.B.1)[86]. Isolation of PAA in urine was carried out in three steps: (a) Shaking
at 37 °C for 16 h with β-glucuronidase arylsulfatase to decompose certain conjugates fol-
lowed by LLE with benzene, evaporation and dilution with MeOH; (b) SPE of the PAA
with an aromatic sulfonic acid resin, followed by elution with an NH_4OAc solution in
90% MeOH; (c) LLE with benzene and evaporation. The PAA were converted to the
pentafluoropropionamide followed by GC-MS end analysis[39].

A comparison of the efficiency of three extraction methods was made for the detection
of forbidden[5] azo dyes in leather. All procedures included a preliminary degreasing step.
The decoloration with sodium dithionite ($Na_2S_2O_4$) and product recovery steps differed
in each case. According to the German standard for azo dyes in leather[72], the reduction
is carried out in a buffer solution at pH 6 followed by LLE of the released PAA with
t-BuOMe. The second procedure was similar to the German standard but was carried out
in a MAE apparatus; after filtering the buffer solution, the leather matrix was subjected to
MAE twice with MeOH and once with dilute HCl. In the third procedure a small amount
of dithionite solution was added and the suspension was subjected to SFE, followed by
two additional SFE sessions, all with CO_2, and a final one with CO_2-MeOH. The SFE

extracts were collected by SPE on C_{18} and eluted with MeOH. The PAA recoveries for the three procedures were 19, 54 and 38%, respectively. End analysis in all cases was by HPLC-DA-UVD[76].

PAA can be effectively extracted from soil by MeCN containing 1% (v/v) of concentrated NH_4OH with sonication. End analysis is by RP-HPLC. Recoveries from sand spiked at 8.5 to 25 ppb levels were in the 88 to 105% range. The LOD depended on the method of detection, ranging from 0.5 ppb for FLD to 0.5 ppm for UVD[111].

The MCS collected on a Cambridge smoke pad was spiked with internal standards and subjected to simultaneous distillation and extraction by placing it in the distillation flask with 250 mL of a 12% NaCl aqueous solution, while the extract flask contained 15 mL of CH_2Cl_2. Total transfer of the analytes (PAH, PAA and phenols) to the organic solvent was attained after 5 h boiling. The organic extract could be subjected to silylation for the phenols and amidation with heptafluorobutyric anhydride (Section III.B.1) for the aromatic amines, before end analysis by GC-MS[112].

When surfactants in concentrations over the CMC are heated above a certain concentration-dependent temperature (the cloud point), two phases are formed: one is rich in surfactant and the other is aqueous and close to the CMC. The process is reversible on cooling and its mechanism is not completely understood. The surfactant-rich phase can be used for extraction and preconcentration of biomacromolecules, inorganic complexes and organic molecules prior to chromatographic or electrophoretic analysis. The surfactant cloud point extraction method has been reviewed[113–115]. Traces of aromatic amines in the 10 ppm range could be determined in commercial dyes. The aqueous solution of the dye was first cleaned up by passing through a SAX cartridge where the dye was discarded. The aqueous sample was loaded with the nonionic detergent Triton X-114 (**69**) at concentrations from 0.2 to 3.0%, heated to the cloud point ($40\,^\circ$C) and centrifuged at 3500 rpm; the supernatant was discarded and the extract was analyzed by RP-HPLC-UVD, where the detergent was eluted after the PAA[116, 117].

(69)
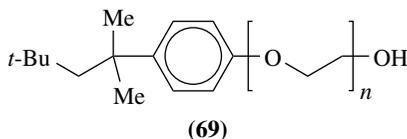
4-Aminobiphenyl (**7a**) was recovered from its hemoglobin (Hb) adduct by centrifuging 10 mL of rat blood to separate the serum, disintegrating the erythrocytes to liberate the Hb, centrifuging the lysate to separate cell debris, dialysing to separate small molecules, determining total Hb by Drobkin's spectrocolorimetric method (addition of a $KCN-K_3Fe(CN)_6-NaHCO_3$ solution, measuring at 540 nm[118]), hydrolyzing the Hb adduct, at pH 11, LLE with hexane, evaporating to dryness, and recovering the analyte into 0.5 mL of MeOH. **7a** was recovered from rat organs after homogenizing, extracting with AcOEt, evaporating to dryness, redissolving in MeOH and applying ultrafiltration to separate solutes over 10^4 Da. End analysis of **7a** was by RP-HPLC-UVD, measuring at 254 nm[42]. A similar procedure was applied for isolation of **7a** from the **7a**-Hb adduct in smokers' blood after spiking the Hb lysate with 4′-fluoro-4-biphenylamine as internal standard; the pentaphenylpropionamide derivatives of the analyte and standard (Section III.B.1) were subjected to end analysis by GC-MS[35]. The lysate of PAA and tobacco-specific nitrosamines recovered by hydrolysis of their Hb adducts in smokers' blood was subjected to SPE on C_{18}, using stainless steel vessels instead of the conventional plastic material, which may dissolve part of the analytes[119].

3. Liquid–liquid–liquid microextraction

In analogy to the relation between SPE and SPME discussed below, a refinement of LLE is achieved by the LLLME method. Analytes in a stirred matrix solution (the donor) are extracted into a thin solvent film filling the pores in the walls of a hollow fiber and diffuse into a collecting solution (the acceptor) filling the inner void of the hollow fiber. The enrichment factor depends not only on the volume ratio between the donor and the acceptor, but also on the operational conditions. The main advantages of the method are simplicity of operation, low cost, the scarce use of organic solvents and avoidance of evaporation operations[120].

LLLME was applied for cleanup and enrichment of trace concentrations of PAA in aqueous solution, using a 4 mL donor sample containing the analytes, about 20% HCl, 2% acetone and 0.1 M NaOH. A 20 mm polypropylene hollow fiber (wall thickness 200 μm, inner diameter 600 μm) is mounted at the tip of a microsyringe holding 4 μL of a 0.5 M solution of each HCl and 18-crown-6 ether, filled with this acceptor and then soaked for 5 s in di-*n*-hexyl ether. Without removing it from the syringe tip, the hollow fiber is dipped into the donor solution, which is magnetically stirred at 1000 rpm for 30 min. When the extraction is finished the fiber is lifted from the donor, the acceptor is sucked back into the syringe and is ready for end analysis by HPLC-UVD, measuring at 254 nm. For quantitative analysis the enrichment factors have to be established for each analyte at a given set of working conditions. For example, at the conditions just described, the LOD (ppb) and enrichment factors were as follows for four PAA: 3-nitroaniline (0.10, 240 ± 5), 4-chloroaniline (0.08, 470 ± 11), 4-bromoaniline (0.05, 510 ± 10) and 3,4-dichloroaniline (0.10, 460 ± 9). The method can be applied to river waters because the humic acids affect only slightly the enrichment factors[121].

A less robust LLLME method was also proposed, without the aid of a hollow fiber, by which the acceptor is a microdrop of 2 μL dipped into an organic layer of ethyl acetate held by a PTFE ring in contact with 2 mL of a stirred donor solution for 15 min. The analytical quality of this procedure is similar to that of the hollow fiber method[122].

4. Supercritical fluid extraction

A study was carried out on the optimization of SFE parameters (temperature, pressure, static time and volume of modifier) for determination of 4-chloro-2-toluidine (**2g**), 4-aminobiphenyl (**7a**), benzidine (**7b**) and 2-naphthylamine (**9a**) in finger paints, which are colored poly(vinyl alcohol) or poly(vinyl acetate)-based pastes or gels for direct application by finger or hand, frequently used by children[123, 124]. SFE yielded significantly higher recoveries and equivalent or better precision than LLE-sonication of aromatic amines from soil samples. Recovery was affected by the percent clay, the specific surface area and the cation exchange capacity of the soil; the latter includes the presence of silanol groups on the surface of the clay materials[125]. In the case of azo dye identification in leather the method was less effective than MAE (Section III.A.2)[76].

5. Solid-phase extraction

SPE methods for organic environmental pollutants, including PAA (Table 1) and HAA (Table 2.B), coupled with electrophoresis end analysis were reviewed[126]. Analysis of PAA in environmental waters requires preconcentration and cleanup to remove interfering substances such as humic acids from the samples. This may be accomplished by several methods, for example: (a) derivatization of the PAA by the Bratton–Marshall method followed by HPLC-UVD measuring at 460 nm (Section III.B.2); (b) flocculation of the water sample with Al^{3+} ions to selectively remove humic compounds before SPE; (c) a

two-step SPE, first at pH 2 with C_{18} material to adsorb the humic compounds, and then at pH 10 on SDBC to extract the PAA; (d) SPE on SDBC and cleanup of the acetonitrile extract on amino-modified silica gel. Method (a) gives good HPLC separations but the sensitivity is lower than with direct detection of the analytes, methods (b) and (c) report substantial losses of analytes, leaving method (d) as the one of choice[108].

SPE can be used to perform analyses of high sensitivity such as GC-MS, or of lower sensitivity such as CZE, without much change in the sample preparation steps. An example of preparation procedure for groundwater: a 1 L sample of filtered and neutralized water (pH 6.5–8) was passed at a rate of 5 mL min^{-1} through an SPE cartridge, made of a 20:80 (w/w) mixture of underivatized and keto-derivatized SDBC. After drying the cartridge under nitrogen for 5 min the retained compounds were eluted with 2 mL of 150 mM H_3PO_4 in water–acetone (80:20), concentrated under a flow of nitrogen, diluted to a final volume of 1 mL and analyzed by CZE-UVD or GC-MS[88].

When an SPE sorbent shows good performance with an analyte its fitness for other analytes, however close in structure, should be experimentally confirmed. A case in point is the forensic analysis of the adrenergic agonists Clenbuterol (**70**) and Compound A (**71**), both forbidden for use as animal feed additives. Four types of sorbents were tested—cyanopropyl resin, sulfonic acid SCX, mixed SCX + C_{18} and nonendcapped C_{18}; only the latter type was found to quantitatively extract **71** although the performance of all four was satisfactory for **70**. End analysis was by GC-MS-MS[127].

(70)　　　　　　　**(71)**
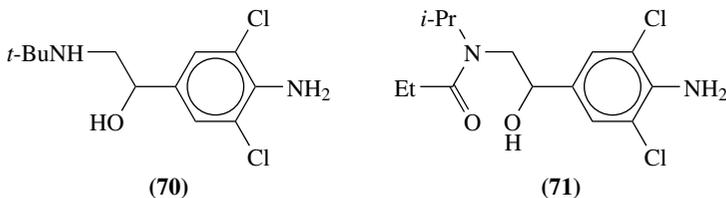
Sorbents based on polymers such as SDBC may be of advantage over silica-based copolymers for SPE application, in that they can discriminate very polar molecules and no loss of adsorbed analytes will occur if the adsorbant is inadvertently dried[68, 128]. A study involving 53 substituted anilines showed excellent recovery of the analyte from SDBC cartridges when the analyte was spiked in water in concentrations of 10 to 20 $\mu g L^{-1}$. Optimization of the pH of drinking water or wastewaters before SPE is necessary to avoid sorption of other solutes with added labor. After elution of the SPE cartridge and concentration, end analysis can be by HPLC-UVD, GC-MS or GC-ECD of the iodo derivatives of the PAA (Section III.B.4)[129]. SPE can be easily performed by passing a sample of water containing PAA through a small SDBC cartridge. This was the first stage of a SPAD scheme for the production of trifluoroacetanilides (Section III.B.1)[68].

Blue rayon or blue cotton consists of a trisulfo-copper-phthalocyanin complex bound to a cellulosic material. The copper complex has high affinity for planar aromatic structures. SPE with blue cotton was part of the cleanup procedure for analysis of HAA (Table 2.B) in fried meat[48]. Blue rayon was used in a portable sampler for SPE of PAH such as bezo[*a*]pyrene in seawater[130] or HAA such as PhIP (**23a**), 7,8-DiMeIQx (**26c**) and Trp-P-2 (**28a**) in rainwater after a forest fire[91] or of IQ (**25a**) and the carbolines Trp-P-1 (**28b**) and AαC (**30a**)[106], or of phenylbenzotriazole mutagens (Table 2.D) in river waters[95a, 96, 99–103]. The analytes were eluted with NH_3/MeOH; end analysis for rainwater was by CZE-UVD[91]. Extraction of HAA in Table 2.D found in polluted river waters was carried out with large blue cotton bales. For example, 1.2 mg of PBTA-2 (**32b**) were isolated from 27 kg of blue cotton immersed for more than a year in the Nishitakase River[131].

Porous polystyrene cross-linked with 1,1′-(methylene-4,4′-phenylene)bismaleimide (**72**) shows good recoveries for aniline (**1a**), 1,2- (**1j**) and 1,3-phenylenediamine (**1k**) in water solution, probably due to adsorption on the imide moieties. Other cross-linked porous aromatic polymers show poor results with these PAA analytes even if they adsorb efficiently similarly substituted nitroaromatic analytes. Recovery of the analytes from the SPE cartridges can be done with MeOH; end analysis was by HPLC-DA-UVD[132].

(72)
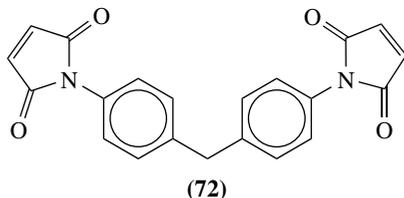
Macroporous *N*-vinylpyrrolidone−DVB copolymers are claimed to offer a balanced measure of hydrophilicity and hydrophobicity in their sorption capacity for a broad range of analytes[133]. This sorbent was applied as the first cleanup step in the determination of four metabolites of PhIP (**23a**) in urine, a few hours after ingestion of cooked chicken. The procedure was followed by elution with MeOH, evaporation to dryness, dissolution in dilute HCl, ultrafiltration and centrifugation to eliminate proteins, SPE on C_{18} and elution with aqueous MeOH. End analysis was by LC-MS-MS (Section IV.B.1)[57].

Organic polymers and silica-based sorbents for SPE are nonspecific and afford very complex chromatograms due to adsorption of multiple trace pollutants present in real samples. It is possible to simplify the chromatographic analysis by immunoextraction, using SPE sorbents endowed with antigen−antibody interactions. Thus, class-selective immunosorbents have been developed for selective extraction of structurally related analytes such as PAH, benzidine and its derivatives, nitroanilines and other aromatic amines. It is also possible to develop high immunoselectivity for a particular compound, instead of a class. Recovery when using the anti-nitroaniline immunosorbent from water spiked with various anilines at the 5 ppb concentration level was poor to fair, for example, 31% for 2-nitroaniline, 58% for 2,4-dinitroaniline, 73% for 4-methyl-2-nitroaniline and 74% for 4-chloro-2-nitroaniline. Selectivity for nitroanilines was good in the case of aniline, with only 6% recovery, but bad in the case of 4-toluidine (35%), 4-chloroaniline (50%) and 2,4-dichloroaniline (58%). End analysis was by HPLC-FLD[134].

A 2000-fold increase in concentration was achieved for traces of the mutagenic HAA PBTA-1 (**32a**) and PBTA-2 (**32b**) in 0.5 L samples of polluted river water by SPE on an Empore disk (C_{18}); after drying the disk it was extracted with 5 mL of MeOH, the solution was evaporated to 0.25 mL and 2.5 ng of diazinon-d_{10} (**73**) was added as internal standard. Quantitative recoveries were observed for both pollutants from spiked river water at 5 to 10 ng L^{-1} levels. Aliquots of 10 µL were analyzed by HPLC-MS (Section IV.B.1)[95].

(73)
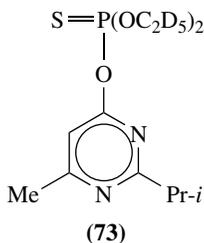
Precolumn preconcentration of aromatic amines and phenolic compounds can be applied instead of derivatizing for HPLC trace analysis, with great labor savings. For aromatic amines the preconcentration column is packed with carboxymethyl-bonded silica. In the case of water analysis, a 5 mL sample is passed through the preconcentration column and the retained analytes are eluted by the mobile phase of the analytical column, consisting of an acetonitrile–acetate buffer (pH 4.66, 40:60, v/v) solution. In the case of anionic dyestuffs analysis for the presence of PAA, 10 mL of solution, containing $1 \, \text{g L}^{-1}$ of the dye at pH 6, is passed through a SAX cartridge where the dyes are retained before the PAA enter the preconcentration column. Excellent recoveries were observed for water samples spiked with 2 ppb of 4-aminobiphenyl (**7a**), benzidine (**7b**), 3,3′-dichlorobenzidine (**7c**), 3,3′-dimethylbenzidine (**7d**), 2-naphthylamine (**9a**) and 4-aminoazobenzene (**16a**) of Table 1, or with the dyestuffs Sunset Yellow FCF (**74**) and Amaranth (**75**), spiked on a dry basis with 10 and 100 ppm of the same aromatic amines, respectively, as determined by HPLC-UVD[135].

(74)   **(75)**
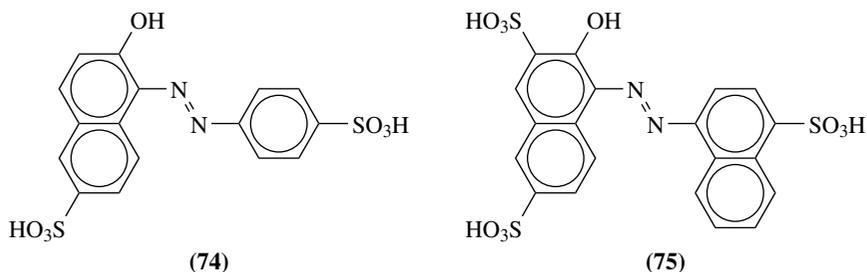
SPE of phenol benzoates and the benzamides derived from aromatic and aliphatic amines and ammonia has been proposed as a cleanup and preconcentration step for the GC-MS simultaneous determination of these classes of compounds in environmental waters. Through an SPE cartridge containing 100 mg SDBC are passed 80 mL out of 100 mL of a water sample which underwent benzoylation (Section III.B.1). After washing and drying the sorbent, the analytes are eluted with 200 μL of ethyl acetate containing 2,4,6-trimethylphenyl 4-nitrobenzoate as internal standard. The eluate is collected over anhydrous sodium sulfate and 1 μL of solution is injected into the GC. The original analytes are present in the 0.1 to 100 ppb concentration range and the LOD are 7 to 39 ppt for most analytes (90 ppt for 2,3,6-trichlorophenol and 20 ppb for ammonia) with linear range from 0.1 to 100 ppb except for ammonia (50 to 4000 ppb)[136].

The recovery of HAA from cooked food matrices was reviewed[44]. Isolation of HAA present in cooked meat is a difficult task due both to the complexity of the matrix and to the low concentration of the analytes, in the ppb range. A complicated cleanup procedure was applied to cooked meat homogenizates after adding internal standards (^{2}H- or ^{13}C-labeled analytes), involving a tandem of cartridges containing diatomaceous earth, propanesulfonic acid (PRS) and C_{18}, to adsorb both polar and nonpolar analytes. After the final recovery from the SPE cartridges the HAA were analyzed by HPLC with APCI-MS-MS detection (Section IV.B.1)[137]. Similar involved procedures with variation of the LLE and SPE media were reported for the analysis of carcinogens generated in cooked food and PFF products[48, 54, 55, 138–145], which may be considered as emulation of the Gross and Grüter technique[146]. For a given sample preparation method the recoveries depend both on the analytes and on the matrix. Thus, the following recoveries, as determined by the method of standard additions, were obtained in a study including four HAA, from fried meat, baked salmon and meat extract, respectively: PhIP (**23a**) (6, 12, 12%), IQ (**25a**) (55,

75, 90%), **25b** (80, 67, 68%) and 4,8-DiMeIQx (**26b**) (78, 62, 91%). End analysis was by CZE-UVD (Section IV.C)[142]. A European interlaboratory project was carried out centered on these four HAA in beef extract, aiming at optimization of the analytical procedures for this type of analytes in food products. The main conclusions concerned the details of the SPE procedures[147]. A comparative study was carried out of various SPE methods for cleanup and preconcentration of HAA in lyophilized meat extract. End analysis was by HPLC-DA-UVD[148].

A variation of the Gross and Grüter SPE method for HAA which are not effectively captured by the PRS column involves homogenization in acid solution, SPE on C_{18} to trap contaminants, followed by SPE on an alternative SCX column, as was used for DMIP (**23b**), TMIP (**23c**) and 2-amino-3,5,6-trimethylimidazo[4,5-*b*]pyridine (**24**) dissolved in acid[141]. In a modification of this method, it is possible to separate the quinoline and quinoxaline type bases in Table 2.B from PhIP (**23a**) and the carbolines in Table 2.C. End analysis was by HPLC-APCI-MS[50]. An almost totally automated system has been proposed, based on this Gross and Grüter SPE technique, in which the alkaline food homogenizate is separated into two fractions containing *apolar* (carbolines) and *polar* (quinoxaline type) HAA. A drawback of the system is the necessity of rinsing with solvents the interconnecting tubing between successive operations. End analysis is by HPLC-MS[149]. PRS cartridges have been applied for separation of PAH from aza-PAH, the latter remaining retained on the SPE medium, to be eluted with $NH_4OH/MeOH$ and analyzed by HPLC-FLD and GC-MS[145, 150].

The low concentrations of HAA in foodstuffs and the complexity of the matrix require cleanup and concentration before end analysis. The sample preparation protocol for chromatographic determination of HAA in beef extract involves selective adsorption and subsequent elution of the analytes on a series of cartridges, including diatomaceous earth, propylsulfonyl silica gel and C_{18}. The dry residue after evaporation of the solvent of the last elution is dissolved in MeOH before end analysis by HPLC-ELD[151]. The complexity of the operations involved in sample preparation for HAA analysis is illustrated by a protocol for meat products: 10 g of sample are subjected to LLE by homogenizing with 6 mL of CH_2Cl_2 and 20 mL of 0.5 M HCl, pH adjustment to *ca* 11, passing through a diatomaceous earth cartridge followed by elution with 60 mL of CH_2Cl_2 and sorption on PRS, elution with 20 mL of $NH_4OH/MeOH$, and evaporation to 200 µL, followed by further cleanup by HPLC-UVD at 265 nm on a SCX column, with a mobile phase gradient from NH_4OAc (pH 4.5)-MeCN to NH_4OAc (pH 6.5)-MeCN, by which the HAA are contained in a mid-fraction of the eluate, which is evaporated to near-dryness and dissolved in 200 µL MeOH. End analysis was similar to the HPLC cleanup, measuring at 265 nm for the aminoimidazo-azaarenes listed in Table 2.B, except for PhIP (**23a**), which was detected at 320 nm. Recoveries of these HAA spiked at 1 to 5 ppb where quantitative except for **23a**, which was about 60%. The method was applied to HAA analysis in Swiss meat products[54]. A similar procedure was found to be the best among seven cleanup methods tested for determination of the aminoimidazo-azaarenes listed in Table 2.B in roasted pork; however, in this case the meat homogenization was carried out in alkaline solution. Recoveries ranged from 46 to 85%[152].

Analysis of aromatic amines in mainstream cigarette smoke (MCS) involves collection of the analytes on a Cambridge filter pad, which is quite effective in retaining particles of diameter larger than 0.1 µm. After extracting the pad with aqueous HCl the aromatic amines can be concentrated by LLE with hexane, derivatized to the pentafluoropropionamide (Section III.B.1) and the end analysis performed by GC-MS-MS (Section IV.A)[36]. The involved precolumn procedures may be simplified to some extent by treating the pad with 5% HCl solution, SPE of the ammonium salt solutions using a cation exchange cartridge, by which neutral and acidic components present in the matrix are eliminated, elution of the neutral amines with ammonium hydroxide solution

in MeOH, and SPE on a cartridge loaded with a nonpolar hydrophobic sorbent from which additional neutral components are rinsed away. The aromatic amines are eluted with toluene, derivatized to the corresponding heptafluorobutyramides (Section III.B.1) followed by GC-MS end analysis (Section IV.A). Excellent recoveries were attained for 100 ng of each of 25 PAA (including five internal standards) spiked on the collecting pad of an automated smoking run of 20 cigarettes[33].

The hydrolysable Hb adducts of PAA were analyzed beginning with basic hydrolysis of Hb in the presence of SDS, centrifugation, SPE on Polysorb MP-1 (C_{18}) and elution with MeCN. The liberated toxic compounds may also include acetylated and oxidized metabolites of the PAA. End analysis was by HPLC-UVD and ELD. The method was applied for determination of Hb adducts of 4-chloroaniline (**1h**), 4-aminobiphenyl (**7a**), benzidine (**7b**), 3,3′-dichlorobenzidine (**7c**) and 2-fluorenylamine (**10b**), after oral administration to rats. In the case of **1h** nonhydrolysable adducts were formed, as shown by radioactive labeling. In cases such as 4-aminobiphenyl (**7a**) and benzidine (**7b**) the hydrolysable Hb adduct returned the original PAA, while in others such as **7b** and 3,3′-dichlorobenzidine (**7c**) also acetylated, deaminated or oxidized metabolites were obtained[31]. The Hb adduct of 3,4-dichloroaniline (**39**) was hydrolyzed in a similar manner and **39** was determined by GC-NICI-MS[32].

6. Solid-phase microextraction

Solid-phase microextraction (SPME) is a modality of SPE consisting of dipping a fiber coated with an effective adsorbent into the fluid containing the analyte. After a suitable accumulation time the fiber is placed in the injection device of a chromatography apparatus, and the mobile phase elutes the adsorbed analyte. The fiber can be reused after a simple cleaning procedure. Although this method has been more extensively applied in GC, its use for HPLC is steadily growing[153]. SPME and its application in chromatography has been reviewed[154]. In a study involving various SPME fibers it was found that Carbowax/templated resin and poly(DMS/DVB) were effective for preconcentration of 4-aminobiphenyl (**7a**), benzidine (**7b**), 3,3′-dichlorobenzidine (**7c**), 3,3′-dimethylbenzidine (**7d**), 1-naphthylamine (**8a**) and 4-aminoazobenzene (**16a**) from aqueous solution. End analysis was by HPLC-UVD. The method was proposed for determination of PAA in environmental waters[155]. Among various commercially available fibers, the one covered with Carbowax/DVB copolymer showed good performance for SPME of 2-toluidine (**1b**), 4-chloroaniline (**1h**), 2,4-, 2,5-, 3,5- and 3,4-dichloroaniline (**39**) from water, at pH 7.6, after addition of NaCl. The LOD for the various analytes varied from 2 to 25 ppt, with good linearity in the 0.05 to 5 ppb range. End analysis was by GC-SIM-MS. The method was applied to analysis of groundwaters in a polluted industrial site north of Milan[156]. A study was carried out on SPME of water containing traces of the carcinogenic PAA 2-toluidine (**1b**), 4-chloro-2-toluidine (**2g**), 5-nitro-2-toluidine (**2h**), 4,4′-methylenedianiline (**5a**), 4,4′-oxydianiline (**6a**) and 4,4′-thiodianiline (**6b**). The results showed that SPME using a fiber coating made of DMS/DVB copolymer is effective in preconcentration for HPLC-UVD analysis, measuring at 242 nm. The LOD for the six amines ranged from 0.6 to 1.4 $\mu g\,L^{-1}$, with RSD lower than 10%[157]. DMS/DVB copolymer fibers were used for SPME of simple aromatic amines in alkaline skimmed human milk. End analysis was by GC with SIM-MS detection[20].

The SPME selectivity of fibers coated with polyacrylate, carbowax-DVB or poly-DMS can be improved by working at pH 2 to extract organic acids such as phenols or at pH 12 to extract organic bases such as aromatic amines and aromatic heterocyclic compounds. The following recoveries of each analyte were attained by a polyacrylate fiber (best overall performance) immersed for 30 min in 2 mL of water, at pH 12, containing 10 μg of

the amine: tributylamine (16%), phenanthridine (**76**, 15%), aniline (**1a**, 0.31%), quinoline (**77**, 0.74%), 2,6-diethylaniline (3.8%), diphenylamine (35%) and 2-nitroaniline (2.5%). The low sorption on the SPME fiber shown by aniline and quinoline is related to the relatively high solubility of these compounds in water; however, other factors may also affect the fiber performance. End analysis was by GC-FID or GC-MS. For best results, the injector temperature had to be programmed to reach 300 °C. Repeated use of the same fiber lowered its performance[158].
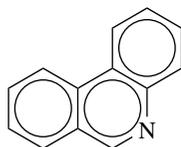
(76)   **(77)**

SPME can be carried out on thin films which can be subsequently analyzed by transmission IR spectroscopy. Parafilm[159], poly-DMS[160] and perfluoroalkoxy-Teflon[161] have been used for SPME-IR of organic analytes in aqueous solution. Thin films mounted on flat stainless steel plates can be used for SPME followed by reflection IR analysis (Section IV.E.1). Acrylonitrile–butadiene copolymer was used to prepare the film for determination of chlorinated PAA in water[162]. A specialized modification of the SPME technique consists of passing the sample through a polyethylene tubing section, 20 mm long and 1.5 mm ID, internally coated with silver and a hydrophobic layer of an appropriate sorbent; the sampler serves afterward as a hollow waveguide for total reflectance determination by FTIR (Section IV.E.1)[163, 164]. For IR end analysis, besides a large partition coefficient for the analytes, the polymeric coating should be stable in the matrix to be analyzed (e.g. water) and should not interfere with the acquisition of a useful IR spectrum of the analytes. In the case of the hollow waveguide the film thickness has to be optimized for the opposing effects of sorption capacity, which increases the signal intensity, and scattering and absorbance of the IR radiation which increases noise. The hollow waveguide sampler method was applied for determination of chlorinated PAA in water, using a layer of acrylonitrile–butadiene copolymer (Section IV.E.1). The hollow waveguide samplers can be regenerated by elution with water[165].

7. In-line preconcentration

Various techniques for in-line concentration enhancement for CE and MEKC have been reviewed, including stacking, FASI and others of more limited application[166]. An alternative approach to the preconcentration methods described above is in-line preconcentration, which is achieved operationally without precolumn intervention of an adsorbant, taking advantage of the dynamics of the CE analytical process. Thus, an effective preconcentration method, such as FASI, is achieved by injecting a plug of low conductivity (e.g. methanol) in the hydrodynamic mode before injecting the sample in the electrokinetic mode. In-line preconcentration was applied for CE combined with highly sensitive MS detection for analysis of HAA present in ultratrace concentrations (Section IV.C)[167].

B. Derivatizing

1. Derivatizing for GC

Phenols, aromatic and aliphatic amines and ammonia in environmental waters undergo easy benzoylation by shaking for 15 min with benzoyl chloride in the presence of $NaHCO_3$,

to yield the corresponding aryl benzoates or benzamides. The reaction mixture is cleaned up and concentrated by SPE (Section III.A.2)[136]. N^1-Methylation (of the sulfonamido group) with diazomethane has been proposed for the volatilization of sulfa drugs. End analysis was by GC-AED (Section IV.A)[168].

N-Pentafluoropropionyl derivatives of aromatic amines ($C_2F_5CONHAr$) are appropriate for ultratrace detection by GC-MS[19] or LC-MS[62]. This derivative has been used for many analytical procedures, e.g. determination of four PAA in MCS[34, 36] and urine[39] and for tracing formation of methemoglobin derived from ingestion of aniline (**1a**) and 2-toluidine (**1b**)[37]. A study was carried out on 73 primary and secondary aromatic amines, including some nitro and chloro derivatives, by which a 100 μL solution of the amine in isooctane was treated with an equal volume of heptafluorobutyric anhydride, at 60 °C for 30 min, followed by elimination of excess reagent and acid byproduct with 2 mL of phosphate buffer at pH 8, LLE with three 1 mL aliquots of CH_2Cl_2, drying and evaporation of the unified extract to 0.5 mL. End analysis was by GC with electron-capture negative-ion chemical ionization (EC-NICI) MS detection (Section IV.A)[110].

Aromatic amines react with dimethyl chlorothiophosphate (**78**) to yield the corresponding thiophosphamide esters (**79**), as shown in equation 5. A sample of material containing 25 to 2000 ng of aromatic amines is heated for 30 min with a large excess of **78**, in the presence of aqueous K_2CO_3 to scavenge the HCl byproduct, the excess reagent is neutralized with cysteic acid ($HO_2CCH(NH_2)CH_2SO_3H$), the **79** derivatives are extracted with n-hexane, and 1 μL aliquot of this solution can serve as sample for end analysis by GC-MS or, more conveniently, by GC-FPD. An advantage of this derivatizing method is that it does not require dry samples. Excellent recoveries were shown for cigarette smoke spiked with aniline (**1a**), 2- (**1b**) and 3-toluidine (**1c**), 3- (**1f**) and 4-ethylaniline (**1g**), 2,3- (**2a**), 2,4- (**2b**) and 2,6-xylidine (**2d**), as determined by GC-FPD[169].

$$ArNH_2 \;+\; \underset{(\textbf{78})}{Cl-\overset{\displaystyle S}{\overset{\|}{P}}\!\!\!<\!\!\overset{OMe}{\underset{OMe}{}}} \longrightarrow \underset{(\textbf{79})}{ArNH-\overset{\displaystyle S}{\overset{\|}{P}}\!\!\!<\!\!\overset{OMe}{\underset{OMe}{}}} \;+\; HCl \qquad (5)$$

The N-dimethylaminomethylene derivatives (**81**) of HAA were prepared by heating these compounds with N,N-dimethylformamide dimethyl acetal (**80**), as shown in equation 6. The reaction was applied for derivatizing HAA listed in Table 2.B–C, with end analysis by GC-MS or GC-NPD[170].

$$\underset{}{Ar-NH_2} \;+\; \underset{(\textbf{80})}{(MeO)_2CHNMe_2} \longrightarrow \underset{(\textbf{81})}{Ar-N=CHNMe_2} \qquad (6)$$

The NH_2 group of PAA can be replaced with an iodine atom on treatment with nitrite in aqueous solution acidified with HI. An alternative halogenation method is aromatic bromination with $Br_2/AcOH$, by which Br atoms occupy *ortho* and *para* positions relative to the amino group. After extraction and concentration, end analysis can be by GC-MS or, more conveniently, by GC-ECD (Section IV.A)[129, 171]. In a study involving 54 PAA, the only analytes failing to yield the corresponding iodobenzene derivatives under the uniformly applied conditions of reaction were dinitroanilines or contained the 1,2-phenylenediamine structure. End analysis was by GC-ECD[172]. In a study involving 54 PAA, N,N-dimethylaniline and diphenylamine, only six of the amines failed to yield a brominated derivative under the uniformly applied conditions of reaction. These included benzidine, two dinitroanilines and three compounds containing the 1,2-phenylenediamine

structure. End analysis was by GC-ECD[173]. The iodination reaction in the presence of I$_2$, (a Sandmayer-like reaction) was applied to the analysis of pollutant metabolites in ground waters sampled on the site of a former ammunition factory, rich in toluidines and their nitro derivatives, which underwent quantitative reaction. The only side reaction observed in a 1 to 2% extent was deamination for 2-amino-4,6-dinitrotoluene, 4-amino-2,6-dinitrotoluene, 2,4-diamino-6-nitrotoluene and 2,6-diamino-4-nitrotoluene. After LLE of the iodotoluenes with pentane or toluene, end analysis was by GC-ECD[174]. The same ground waters were also derivatized by bromination, followed by LLE with pentane and end analysis by GC-ECD. Only three of the analytes failed to yield the expected bromo derivatives: 4-amino-2-nitrotoluene, 2,6-diamino-4-nitrotoluene and 2,4,6-triaminotoluene (no reaction); no interference from nitrotoluenes was observed[175]. See also Section III.B.4.

N-Alkylation with 3,5-bis(trifluoromethyl)benzyl bromide (**82**) in the presence of *N*,*N*-diisopropylethylamine in acetonitrile was proposed for routine GC-MS analysis of HAA of Table 2.B–C present in meat and PFF[143].

CH$_2$Br

F$_3$C   CF$_3$

(**82**)
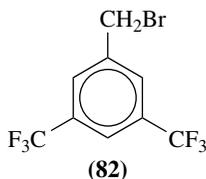
According to the basic idea of SPAD carried out for carboxylic acids, phenols and carbonyl compounds[176], by which derivatizing takes place *in situ* on the cartridge used for SPE, the following procedure will serve to illustrate the case for PAA. A 200 mL aliquot of water at pH 10 (0.5 M K$_2$HPO$_4$ buffer) containing the analytes and 10 µg L^{-1} of 3-chloro-4-fluoroaniline as internal standard is passed through a cartridge containing 100 mg of previously conditioned SDBC adsorbent. After washing with water and drying with N$_2$ at 55 °C for 25 min, the adsorbed PAA are converted to the corresponding trifluoroacetamides on adding to the cartridge 100 µL of a 50% (v/v) solution of trifluoroacetic anhydride in Et$_2$O and drying under N$_2$ at 55 °C for 15 min. This procedure precludes elution of the analytes into the reagent. The excess reagent and the trifluoroacetic acid byproduct are removed with 0.5 M K$_2$HPO$_4$ buffer. The cartridge is washed with water, dried with N$_2$ at 55 °C for 25 min, extracted with 2 mL of *t*-BuOMe and the solution is evaporated to 100 µL. End analysis is by GC-MS (Section IV.A)[68].

2. Formation of azo dyes

Aromatic amines present in water-soluble dyes can be extracted with CHCl$_3$, diazotized to a diazonium salt, coupled with a chromogenic reagent, such as R salt (**83**) or pyrazolone-T (**84**), to obtain a mixture of azo dyes and carry out the end analysis by HPLC-UVD[177–179]. Coupling with 1-naphthol (**85**) has also been proposed for the analysis of PAA by HPLC-UVD[180]. Coupling with 2-anthrylamine (**11b**) has the advantage of producing azo dyes which are soluble in organic solvents such as Et$_2$O or AcOEt, even if the analyte carries the very polar carboxyl or sulfonyl groups. Derivatizing with 1-anthrylamine (**11a**) or according to the Bratton–Marshall method (see below) yields azo dyes which are insoluble in Et$_2$O or AcOEt. The plausible use of 2-naphthylamine (**9a**) was discarded because of the slower reaction. After diazotation, coupling and LLE, end analysis can be by RP-HPLC-UVD, measuring at 279 nm. FLD is not adequate because the fluorescence of **11b** is quenched when forming the azo dye. The method was applied

for determination of sulfanilamide (**86**), 4-aminohippuric acid (**86′**), 4-aminobenzoic acid and 4-aminoacetophenone in urine, as model compounds for various pharmaceuticals. The *N*-acetylated metabolites could also be determined after acid hydrolysis of the urine[181].

(**83**)　　　　　　　(**84**)　　　　　　　(**85**)

(**86**)　　　　　　　(**86′**)
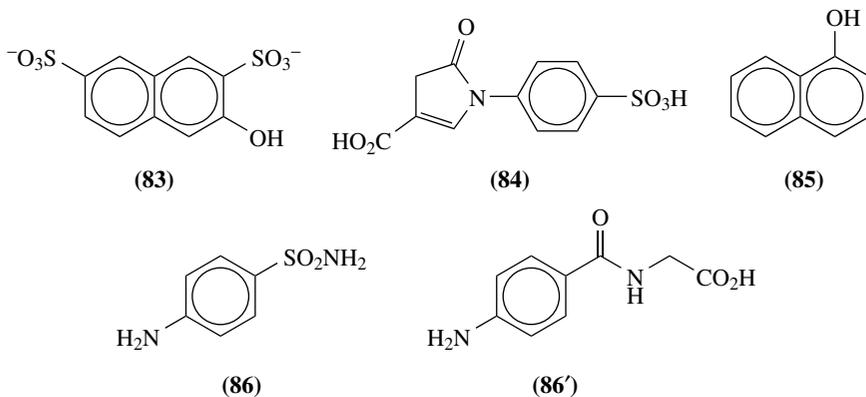
The time-honored Bratton−Marshall method[182] has been an important aid in the development of drugs derived from sulfanilamide (**86**)[183], and is extensively applied in clinical analysis of this type of compounds, even if it is not specific for them. The method continues to stir interest in new developments or as a standard of reference. The procedure consists of two main steps: diazotization of the primary aromatic amine analyte and coupling with *N*-1-naphthylethylenediamine (**87**), to form an azo dye, which is determined colorimetrically or spectrophotometrically. Some uncertainties were observed, such as a positive blank in the absence of sulfanilamide drugs[184], possibly due to the presence of PAA pollutants in the patients' blood[19] (Section II.B.2), or in the determination of sulfamethazine (**88**) levels, due to metabolic *N*-acetylation of the drug[185]. Carrying out the procedure in a micellar SDS medium may be of advantage, inasmuch as the pH for the process is shifted to higher values (e.g. from 1 to 4), the coupling process is accelerated, and no pH adjustment is needed before the spectrophotometric determination at 540 nm. The LOD for the micellar method are in the 0.1 μM range, which is lower than the nonmicellar one by a factor of 2 to 6; linearity is from 2 to 70 μM. This was applied for determination of nitroaromatic compounds in pharmaceuticals, pesticide preparations and environmental waters, after reduction with $SnCl_2$ to the corresponding PAA[186]. Instead of dealing with relatively unstable $NaNO_2$ solutions for diazotation of the analytes, nitrite may be generated online in a FIA system by passing a $NaNO_3$ solution in $NH_3-NH_4Cl-EDTA$ buffer over copperized Cd particles. This process was applied to determination of metoclopramide (**89**) in pharmaceutical preparations, measuring the concentration of the azo dye at 539 nm in a microcell of 1 cm optical path[187].

(**87**)　　　　　　　(**88**)

(89)
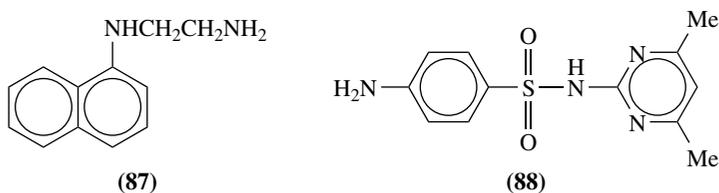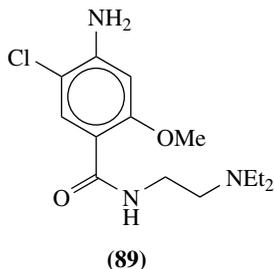
Additional derivatizing methods, based on *in situ* dye production, are mentioned in Sections IV.B.2, IV.E.2 and elsewhere[1].

3. Fluorescent labeling

Labeling primary aromatic amines (ArNH$_2$) with fluorophores may be achieved with the reactive dye 5-(4,6-dichloro-*s*-triazin-2-ylamino)fluorescein (**90a**), in which one of the Cl atoms is replaced by the analyte being attached as an ArNH group (**90b**). In the case of matrices containing several aromatic amines, optimization of the method for the specific analytes is necessary as for the time and temperature of reaction and the pH of the buffer used for the derivatizing solution. The latter factor is necessary to avoid fast hydrolysis of the reactive Cl substituents of **90a** and **90b** while the analytes combine with excess reagent. The carbamate pesticide chlorpropham (**91**) is used for long-term storage of potatoes; it undergoes metabolic oxidation on the aromatic ring. To determine **91** and its metabolites, they may be extracted with dichloromethane from a potato homogenizate, hydrolyzed to chloroanilines (**92a–c**) with hot NaOH, cleaned up by SPE on active carbon, labeled with a fluorescent tag (**90b**) and the end analysis carried out by MEKC-LIFD (Section IV.C)[188].

(90) (**a**) X = Cl
      (**b**) X = NHAr

(91)

(92) (**a**) X = H
      (**b**) X = OH
      (**c**) X = OMe
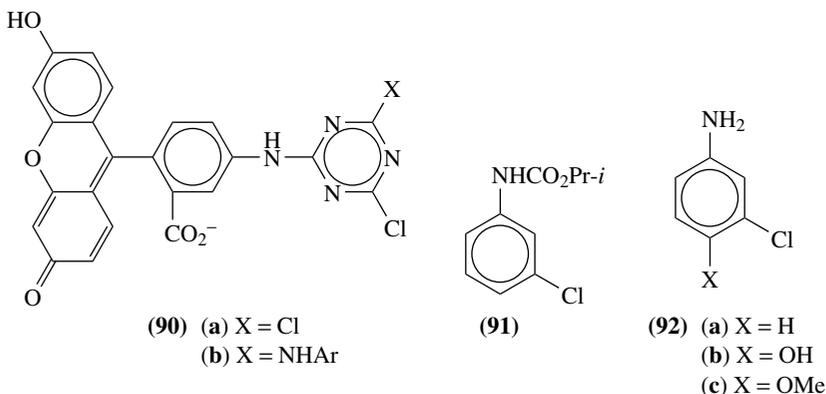
Aromatic amines undergo condensation with fluorescamine (**93**), presumably according to equation 7, to yield fluorescent products (**94**). The process was applied to derivatize PAA mixtures prior to determination by MEKC with FLD (Section IV.C)[189, 190]. This derivatizing procedure was used for detection of unreacted isocyanate residues in the

manufacture of polyurethane, after hydrolysis to the corresponding PAA, by noting a change in color[191].

$$\text{ArNH}_2 \; + \quad \text{(93)} \quad \xrightarrow[\text{pH 5.5}]{} \quad \text{(94)} \tag{7}$$

(93)   **(94)**
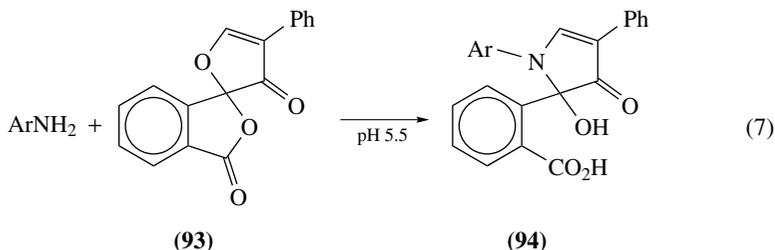
2-(9-Carbazolyl)ethyl chloroformate (**95a**) carries a fluorophore that can easily be attached to primary or secondary amines, and even to the less reactive aromatic amines, to yield the corresponding carbamates (**95b**), as precolumn derivatizing process for immediate injection to RP-HPLC-FLD ($\lambda_{ex} = 293$ nm, $\lambda_{fl} = 360$ nm). The LOD (SNR 3) in fmol units, for 20 μL injection of the derivatized solution of five aromatic amines, in the order of emergence of their corresponding **95b** were: 2-toluidine (3.6), aniline (11.8), 3,4-dimethylaniline (3.6), N-ethyl-4-toluidine (7.2) and 1,4-phenylenediamine (2.0), with linearity over the range from 0.366 to 366 pm. It should be pointed out that good baseline separations were observed for FLD of the derivatives, whereas the original analytes were not well separated (UVD at 254 nm)[192].
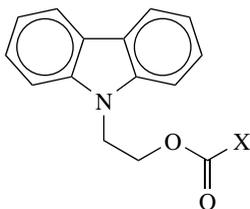
(95)   (**a**) X = Cl
          (**b**) X = NHAr

4. Miscellaneous derivatives

Primary and secondary aliphatic and aromatic amines yield the corresponding acetylacetamides (**97**) on treatment with diketene (**96**) in acetonitrile–borate buffer (pH 7), according to equation 8. Aromatic amines take about 90 min to complete the reaction. Aliquots of the reaction mixture can be analyzed by RP-HPLC-ECLD (Section IV.B.2)[193].

$$\text{Ar-NH}_2 \; + \quad \text{(96)} \quad \longrightarrow \quad \text{(97)} \tag{8}$$

(96)   **(97)**
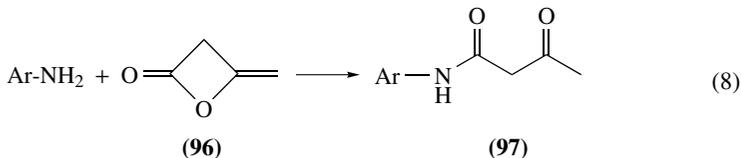
Bromination was applied to the analysis in meat and fish products of ten HAA among those listed in Table 2.B–C. End analysis was by HPLC with tandem ESI-MS-MS detection (Section IV.B.1)[194]. Metallation labeling of a primary amine may be achieved with reagents **98a** or **98b**, which are easily prepared by reaction of 2-acetylpyridine or 2-picolinaldehyde, respectively, with a metallic complex, as shown in equation 9. The metal may be a heavy one (M = Re, X = Br) or a radioactive one (M = ^{99m}Tc, X = Cl). Primary amines undergo condensation with complexes **98** to yield complexed Schiff bases (**99**); the reaction rate is several orders of magnitude faster than with the pyridine derivatives alone. Labeling with Re may be useful for elucidating chirality of amines by XRD crystallographic analysis whereas Tc labeling can be applied for HPLC-RAD[195].

$$(9)$$

(98) **(a)** R = Me
        (b) R = H

(99) **(a)** R = Me
        (b) R = H
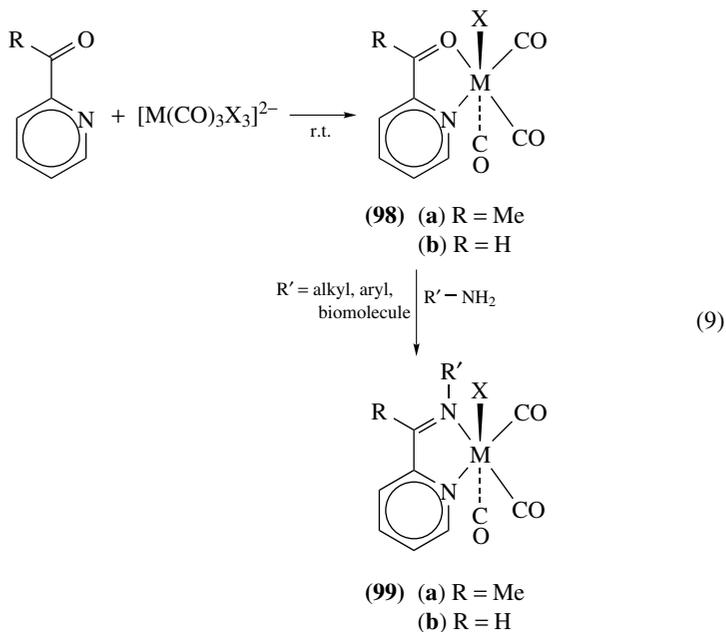
Subjecting the total matrix to chemical treatment may be an effective method for detection of fingerprint derivatives, without actual isolation of the analytes. Thus, for example, colored yarns can be tested for the presence of forbidden azo dyes by subjecting them to partial reduction with sodium dithionite, followed by FTIR of the reduced yarn and detecting the characteristic peaks of restricted PAA. This method was applied to forensic testing of textiles which were dyed with forbidden azo dyes (Section II.B.5)[196].

5. Aromatic amines as analytical reagents

The enantiomeric purity of 2-arylpropionic acids used as pharmaceuticals was determined after derivatizing to the corresponding amides with various PAA and HAA. End analysis was by HPLC-UVD, with simultaneous measurement at 230 and 254 nm, using a cellulose-based stationary phase. The best derivative for routine determinations was chosen in each case after establishing the chromatographic parameters of the enantiomeric pair of derivatives[197].

IV. END ANALYSIS

In Table 3 are summarized the combined separation−detection methods used for end analysis in this chapter.

A. Gas Chromatography

Atomic emission detection (AED) consists of decomposing the analyte emerging from the chromatographic column into excited atomic particles, which on returning to the ground state emit a radiation that can be measured with a DA-UVD. Thus, in the case of sulfa drugs, simultaneous detection of C, N and S can be monitored for each analyte, while detection of H and O requires a separate run for technical reasons. GC-AED was proposed for the analysis of sulfa drugs, such as sulfamethazine (**88**), sulfamethoxazole (**100**), sulfathiazole (**101**), sulfamethoxypyridazine (**102**) and sulfadiazine (**103**), after undergoing *N*-methylation of the sulfonamido group to aid volatilization[168].

The presence of PAA may serve as fingerprints for detection of other functional groups. Unreacted isocyanates used in manufacture of corks may migrate to foodstuffs and hydrolyze there to the corresponding PAA. Thus, cork homogenates in water were extracted with hexane and analyzed by GC-MS for the presence of diamines such as 2,4-diaminotoluene (**2e**), 2,6-diaminotoluene (**2f**) and 4,4′-methylenedianiline (**5a**)[65]. A combination of pyrolysis with GC-MS was applied to qualitative analysis of azo dyes by detection of aromatic amines in the pyrolysate. This fast detection method was applied in

TABLE 3.   Summary of separation−detection combined methods mentioned in this chapter

Method	Section and references
GC-AED	III.B.1[168], IV.A[168].
GC-ECD	III.A.5[129], III.B.1[129, 171, 173, 174], IV.A[129, 171]
GC-FID	II.B.5[60], III.A.4[123, 124], III.A.6[158].
GC-FPD	III.B.1[169], IV.A[169].
GC-MS	II.B.5[60, 61, 68, 70, 74, 86], III.A.5[32, 33, 36, 88, 127, 129, 136, 145, 150], III.A.6[20, 156, 158], III.B.1[19, 36, 37, 68, 129, 143, 169−171], III.B.4[50b], IV.A[33, 36, 65, 68, 129, 171, 198], IV.B.2[145], IV.B.3[199].
GC-NPD	III.B.1[170], IV.A[106, 170].
HPLC-ECLD	III.B.4[193], IV.B.2[193].
HPLC-ELD	II.B.8[95a], III.A.5[31, 48, 151], IV.B.2[48, 139], IV.B.3[48, 151, 200, 201].
HPLC-FLD	III.A.2[111], III.A.5[48, 130, 134, 145, 150], III.B.3[192], IV.B.2[48, 145, 202].
HPLC-MS	II.B.5[60, 74], II.B.8[95b], III.A.5[57, 95, 137, 149, 203], III.B.1[62], III.B.4[194], IV.B.1[28, 57, 62, 95, 137, 143, 194, 199, 203−209].
HPLC-RAD	III.B.4[195].
HPLC-UVD	II.B.5[60, 70, 74−76, 78, 79], II.B.9[108], III.A.2[23, 42, 76, 111], III.A.4[76], III.A.5[31, 54, 68, 96, 108, 128, 129, 132, 135, 148, 152], III.A.6[155, 157], III.B.2[177−181], III.B.3[192], III.B.5[197], IV.B.2[63, 139, 210, 211].
CE-MS	IV.C[166, 167].
CZE-ELD	IV.C[190, 212, 213].
CZE-FLD	IV.C[166].
CZE-UVD	III.A.5[88, 91, 142], IV.C[77, 142, 166, 214, 215].
MEKC-ELD	IV.C[216].
MEKC-FLD	III.B.3[188−190], IV.C[188, 190].
MEKC-UVD	IV.C[217, 218].

(100)

(101)

(102)

(103)
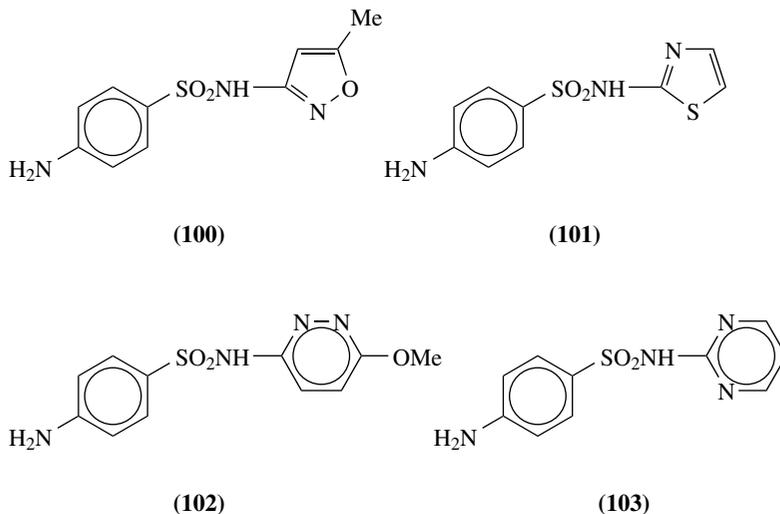
the search for banned azo dyes in textiles made of cotton, wool, polyamide and synthetic leather[198].

The thiophosphamide ester derivatives **79** (Section III.B.1) obtained from samples spiked with standard aromatic amines and 3-phenyl-1-propylamine as internal standard were separated and determined by GC-FPD, using two capillary columns in tandem and a 526 nm filter in the optical path. The LOD (SNR 3) for aniline (**1a**), 2-toluidine (**1b**), 3-toluidine (**1c**), 3-ethylaniline (**1f**), 4-ethylaniline (**1g**), 2,3-xylidine (**2a**), 2,4-xylidine (**2b**) and 2,6-xylidine (**2d**) were 50, 100, 40, 30, 30, 50, 50 and 100 pg, respectively. This method was applied for analysis of smoke collected in the laboratory by burning materials as varied as chicken meat, sausage, sardine, dried squid, bread, black pepper, soy sauce, wood chips, rubber and cigarettes (main-stream and side-stream smoke). All smokes showed the presence of ppm concentrations of the eight standard aromatic amines mentioned above, but none contained detectable concentrations of all of them[169].

GC-MS can be used for determination of *N*-trifluoroacetyl derivatives of PAA. In cases when various analytes are present in the sample, MS detection in the scan mode instead of the SIM mode allows further identification by display of the full MS. A study was carried out of water spiked with aniline (**1a**), toluene-2,4-diamine (**2e**), toluene-2,6-diamine (**2f**), 4,4′-diaminodiphenylmethane (**5a**), 4,4′-oxydianiline (**6a**), 3,3′-dimethylbenzidine (**7d**), 1,5-diaminonaphthalene and 1,3-phenylenediamine (**1k**), which underwent SPAD to the corresponding trifluoroacetamides (Section III.B.1). The LOD were in the 0.1 to 0.4 $\mu g\,L^{-1}$ range, with RSD from 4 to 17%. The method was used for testing the diffusion of PAA into food (simulated by water) which was in contact with laminated flexible food packaging materials. Detectable extracted levels were found for **2e, 2f** and **5a**[68].

End analysis by GC-MS of bromo and iodo derivatives of aromatic amines (Section III.B.4) show easily recognizable ions due to the presence of heavy atoms. A convenient alternative to GC-MS for end analysis of halogenated derivatives is by GC-ECD. The scanning mode acquisition MS of the brominated analytes show characteristic $(n + 1)$-multiplets with two mass unit separations for ions containing *n* Br atoms, stemming from the natural isotope distribution of this element. Analysis of halogenated derivatives showed that about 20 aromatic amines were present at ppb levels in industrial wastewater and ground water from a landfill and a former ammunition plant. In the latter case, most

aromatic amines were degradation products of nitroaromatic explosives. In the other cases aniline and methyl anilines were the main pollutants found[129, 171]. The LOQ for the GC-ECD of the bromination derivatives of fifty aromatic amines recovered from 100 mL water samples were in the range of 1.2 to 40 ppb[173].

Trace analysis of aromatic amine pollutants, with identification and determination of multiple analytes present in the sample, can be conveniently carried out by derivatization to the corresponding heptafluorobutylanilide (104) and GC with electron capture-NICI-MS detection using methane as moderator gas. Identification can be based on the elution time of individual peaks and appearance of the $[M - HF]^-$ ion, which usually is the base peak for derivatives of PAA (104, R = H); only 2,6-dichloroaniline (14%), 2,3,4-trichloroaniline (75%), 2-chloro-4-nitroaniline (44%), 2-chloro-5-nitroaniline (54%) and 4-chloro-3-nitroaniline (58%) were PAA showing the $[M - HF]^-$ ions with relatively less abundance. Also, the heptafluorobutyranilides derived from secondary amines (104, R = Me or Et) had the $[M - HF]^-$ ion with relative intensity less than 100%, as was the case of N-methylaniline (80%), N-ethyl-3-methylaniline (74%) and 4-chloro-N-methylaniline (48%). The LOD were in the range of 0.3 to 66.3 pg injected for the full-scan mode and 0.01 to 0.57 pg injected for the SIM mode. Application of the procedure was attempted for heavily contaminated groundwater samples of an industrial environment[110]. The PAA in mainstream cigarette smoke were preconcentrated by a special SPE procedure (Section III.A.5), converted to 104 derivatives and determined by GC-MS in the SIM-NICI mode, using ring-deuterated PAA as internal standards. The LOD for 20 PAA ranged from 1.4 down to 0.02 ng per cigarette for aniline (1a) and tolidine (7d), respectively, with RSD usually below 10%, except for 2,6-xylidine (2d) and 7d (20%)[33]. A similar investigation of MCS focused on four PAA using the N-pentafluoropropionyl derivative. The reported LOD were 7, 6, 7 and 39 pg per cigarette for 2-toluidine (1b), 2-anisidine (4a), 2-naphthylamine (9a) and 4-aminobiphenyl (7a), respectively[36].

$$F_3C-\underset{\underset{F_2}{|}}{\overset{\overset{F_2}{|}}{C}}-\underset{\underset{O}{\|}}{C}-\underset{\overset{|}{\underset{}{N}}}{\overset{R}{|}}-Ar$$
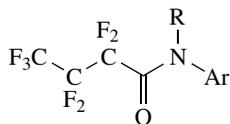
(104) R = H, Me, Et

The N,N-dimethylaminomethylene derivatives (81) of ten HAA listed in Table 2.B–C were analyzed by GC-MS or GC-NPD. All mass spectra showed the $[M]^+$ peak. More convenient was analysis with NPD for which the LOD for injection were in the range of 2 pg for 25a to 15 pg for 23a, with good linearity from 0.5 to 10 ng in all the studied cases[170]. This method was used in detection and estimation of 25a, 28b and 30a in the Danube River[106]. A routine search for the carcinogenic HAA of Table 2.B–C in meat and process flavor products was proposed, based on the cleanup methods for such samples mentioned in Section III.A.5, derivatizing with 3,5-bis(trifluoromethyl)benzyl bromide (82), and capillary GC-SIM-ESI-MS[143].

B. Liquid Chromatography

1. Mass spectrometric detection

Determination of 4,4′-methylenedianiline (5a) in hydrolyzed human urine may serve as a biomarker for exposure to methylenebis(4-phenyl isocyanate) produced on thermal degradation of polyurethane foam. The urine is hydrolyzed with H_2SO_4 and 4,4′-methylenedianiline (5a) is derivatized to the corresponding pentafluoropropionamide.

Analysis by LC with plasma spray-negative ion-MS was most sensitive, using a dideuteriated derivative of **5a** as internal standard. The LOD was about 0.2 $\mu g L^{-1}$ of urine; the overall precision for human urine at 0.5 $\mu g L^{-1}$ was 10% ($n = 5$). The **5a** level found in the urine of a group of exposed workers was 4 $\mu g L^{-1}$ [62].

Three HPLC-ESI MS systems were evaluated for the analysis of heterocyclic aromatic amines (HAA) comparing the performance and quality parameters of electrospray sources and analysers (ion trap, single quadrupole and triple quadrupole) in various acquisition modes (full scan, product ion scan, selected ion monitoring and multiple reaction monitoring). HAA belonging to two types were investigated, the aminoimidazo-azaarenes (Table 2.B), including PhIP (**23a**), DMIP (**23b**), IQ (**25a**), MeIQ (**25b**), MeIQx (**26a**), 4,8-DiMeIQx (**26b**), 7,8-DiMeIQx (**26c**) and TriMeIQx (**26d**), and the carbolines (Table 2.C), including Trp-P-2 (**28a**), Trp-P-1 (**28b**), Glu-P-2 (**29a**), Glu-P-1 (**29b**), AαC (**30a**), MeAαC (**30b**), norharman (**31a**) and harman (**31b**). Similar MS−MS spectra were obtained with the ion trap and the triple quadrupole systems, both in fragmentation and relative abundances; however, adducts were formed in the ion trap for carbolines. Good precision was observed (RSD 12%) and very low LOD were obtained, especially with the triple quadrupole instrument (<1 pg injected). For all tested compounds and instrumental setups, linear response was observed from the LOQ up to 1 ppm, implying a linear range two orders of magnitude larger for the triple quadrupole instrument, because of its lower LOD. The method was applied for HAA determination in lyophilized beef extract[82, 199]. A similar study was carried out by HPLC with multiple ion detection-APCI-MS, which showed high sensitivity on measuring the intensities of the $[M + H]^+$ ions. The method was applied to determination of HAA in beef extract, where the following concentrations were detected in $ng\,g^{-1}$ units, in the order of emergence from the column: **25a** (0.2), **25b** (0.2), **26a** (1.0), **29b** (0.4), **26b** (1.4), **23a** (0.4), **29b** (0.08), **29a** (0.1), **28b** (0.4), **28a** (0.8), **30a** (0.3) and **30b** (0.4)[203, 204]. The optimal conditions for HPLC separation of five aminoimidazo-azaarenes (**25a, 25b, 26a, 26b, 23a**) were achieved with a Supelguard Hypersil ODS precolumn and a TSK gel ODS 80-T-M column, using as mobile phase a gradient of triethylamine−phosphate buffer (pH = 3.3) in acetonitrile. The five HAA were found in charcoal grilled chicken breast and pork fillet[207]. The brominated derivatives (Section III.B.4) of ten HAA from Table 2.B−C in meat and fish products were analyzed by HPLC with tandem ESI-MS-MS detection. The LOD were in the range of 0.1 $ng\,g^{-1}$ of commercial product[194]. In contrast to capillary GC of the HAA in cooked food products, no derivatizing was necessary for good resolution of the analytes by HPLC with ESI-MS-MS detection in the SIM mode[205].

Cooked meat products such as grilled bacon, meat extract pastes and meat extract powders were analyzed for their HAA content. After SPE cleanup and preconcentration (Section III.A.5) the samples were analyzed by HPLC with APCI-MS-MS detection, using nitrogen at 20 psi as sheath gas. The constant neutral loss acquisition mode, looking for $[M + H]^+ - 15$ ions, is well fitted for identifying the presence of compounds such as those listed in Table 2.B, all possessing the N-Me moiety, which is lost yielding quite abundant peaks; the identity of the species can be further confirmed following the fragmentation of such peaks in the product ion mode. All the compounds listed in Table 2.B except for 2-amino-1,7,9-trimethylimidazo[4,5-g]quinoxaline (**27**) were identified and determined in the cooked meat products, the predominant one being IQ (**25a**), reaching over 45 ppb, and the scarcest 7,8-DiMeIQx (**26c**), frequently under 45 ppt. On the average the LOD of the analytical method was 15 ppt, the LOQ 45 ppt and the recovery of HAA 80%[137]. Part of the PhIP (**23a**) ingested with cooked meat undergoes detoxification and elimination in the urine. Analysis of the four metabolites **43**−**46** (Section II.B.4) by LC-MS showed $[M + H]^+$ peaks at m/z 401, 417, 417 and 321, respectively; however, quantitative measurements were carried out on the basis of the MS-MS spectra, with peaks at m/z 425

and/or 441, as the results of fragmentations shown on the structural formulas of these compounds[57].

Potentially mutagenic pollutants PBTA-1 (**32a**) and PBTA-2 (**32b**), after SPE with an Empore disk C_{18} (Section III.A.5), underwent good separation by RP-HPLC without interference by other solutes in the Yodo river waters. Their ESI-MS showed the $[M + H]^+$ ion as the base peak at m/z 543 and 508, respectively. Determination was carried out by ESI-MS-MS based on the main product ion peaks at m/z 511 and 467, resulting from collision induced scission of OMe and CH_2CN, respectively, using calibration curves built from solutions in the 1 to 100 $ng\,L^{-1}$ range. The LOD (SNR 3) were 1 and 2 $ng\,L^{-1}$, and at one sampling site in the river the concentrations were 9.4 and 33 $ng\,L^{-1}$, respectively[95]. The 2-phenylbenzotriazole mutagens listed in Table 2.D were determined by HPLC with tandem APPI-MS-MS detection. The LOD for this type of pollutants using dopant assisted APPI were 0.04 to 0.05 ppt[209], much lower than those obtained using ESI (*ca* 1 ppt)[208].

DNA adducts with PAA, at concentrations of the order of 1 per 10^7 bases, can be determined after hydrolysis of the DNA to adducts such as **33** and **34** (Section II.B.2), by HPLC with tandem ESI-MS-MS detection. The LOD are in the order of 50 fmol on the column, for both analytes. Quantitative analysis of DNA adducts with PAA requires investigation of the MS of each individual adduct to be obtained after hydrolysis of DNA. For example, adducts **33** and **34**, formed on enzymatic condensation of benzidine (**7b**) and 1-aminofluorene (**10a**) with adenine residues of DNA, can be determined by tandem ESI-MS-MS analysis, following the fragmentations depicted in **105** and **106**, which gives optimum intensities when operating under suitable conditions. Additional support for the assignments can be obtained from adducts derived from deuterated **7b** and **10a**[28].

(105)

(106)
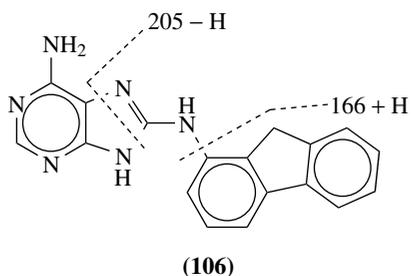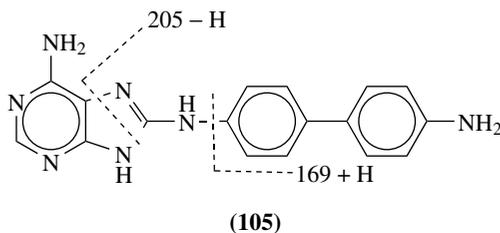
In the case of several isomeric compounds, yielding similar product ion spectra, two characteristics may be useful for identification of the analyte, with the help of a spectral database. The spectral contrast angle θ (equation 10) considers the set of relative intensities of two spectra (a_i of the analyte and b_i taken from the database for the corresponding m/z peaks) as two N-dimensional vectors; the minimal angle found for pairs of spectra points to the most probable identity of the analyte (both vectors have almost the same

direction). Alternatively, the similarity index SI (equation 11) helps in discerning which of the spectra in a database best fits a given spectrum, because the self-SI is the smallest attainable value (ideally, the self-SI should be nil)[219, 220]. Conflicting views were expressed about which of these quantitative molecular similarity analysis approaches works best for MS[38, 220]. A difficult problem attains identification of adduct structures formed by the attachment of isomeric PAA to DNA bases after separation and end analysis by HPLC-MS. Thus, adducts produced on attachment of alkylated aniline residues to the C8 atom of guanine (**107a**–**107e**) or deoxyguanosine (**108a**–**108g**) are difficult to differentiate because their product ion MS are qualitatively identical. It should be pointed out that the $[M + H]^+$ peak of adducts **108** is very prominent under full scan conditions; however, the product ion spectra show the $[BH_2]^+$ peak as the most prominent, after glucosidic cleavage, making the spectra equivalent to those of the **107** adducts. A way to solve the identification difficulty is by calculating the θ or the SI values according to equations 10 or 11 with the aid of a MS database of authentic compounds[38].

$$\theta = \arccos \frac{\sum_{i=1}^{N} a_i b_i}{\sqrt{\sum_{i=1}^{N} a_i^2 \sum_{i=1}^{N} b_i^2}} \tag{10}$$

$$SI = 100 \sqrt{\frac{1}{N} \sum_{i=1}^{N} \left(\frac{a_i - b_i}{a_i + b_i} \right)^2} \tag{11}$$
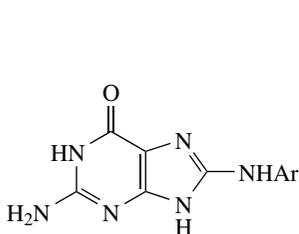
(107)	(108)
(**a**) $ArNH_2 = $ **2d**	(**a**) $ArNH_2 = $ **2d**
(**b**) $ArNH_2 = $ **2a**	(**b**) $ArNH_2 = $ **2a**
(**c**) $ArNH_2 = $ **1b**	(**c**) $ArNH_2 = $ **2c**
(**d**) $ArNH_2 = $ **1c**	(**d**) $ArNH_2 = $ 3,4-xylidine
(**e**) $ArNH_2 = $ **1d**	(**e**) $ArNH_2 = $ **1e**
	(**f**) $ArNH_2 = $ **1f**
	(**g**) $ArNH_2 = $ **1g**
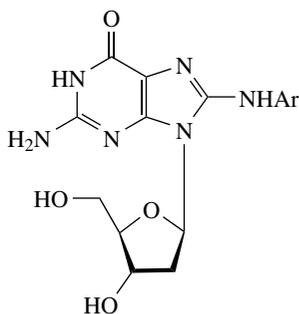
2. Ultraviolet-visible spectrophotometric detection

UVV spectrophotometry is one of the simplest and fastest methods for determination of aromatic amines and may serve also for identification purpose with the aid of diode array detectors. A study was carried out on the performance of direct phase (silica gel) and RP (C_{18}) columns, using a MeOH−0.1 M $NaClO_4$ mobile phase, for the HPLC-UVD (at 256 nm) analysis of five aromatic amines: aniline (**1a**), 1- (**8a**) and 2-napththylamine (**9a**), di- (DPA) and triphenylamine (TPA). Good resolutions and separation factors were observed with the RP column for **1a** vs. the other analytes and for **8a** or **9a** vs. DPA or TPA; however, separation of the **8a**−**9a** or DPA−TPA pairs was poor[210].

The kinetics of four successive *N*-alkylation steps taking place according to equation 12 was followed by HPLC-UVD, measuring at 240 nm, for 4,4′-methylenedianiline (**5a**) exposed to propylene oxide in ethylene glycol solution. It should be pointed out that the relative response factors of the compounds in the reaction mixture gradually decrease from 1.000 for **5a** to 0.289 for the tetraalkylated product. The kinetic behavior as measured chromatographically could be correlated to thermal measurements in a reaction calorimeter[63].

(12)
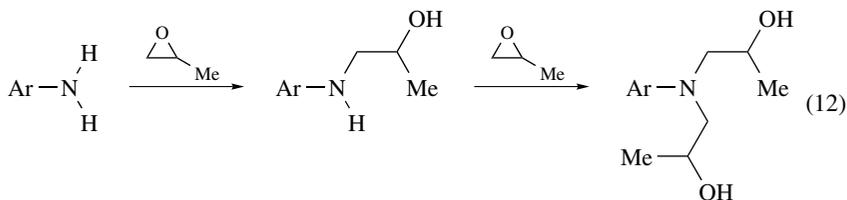
Ion pair RP-HPLC with DA-UVD offers a good alternative for determination of mixtures of PAA which are difficult to resolve by usual RP-HPLC procedures. After optimization as for the pH and anionic component of the isocratic mobile phase, it was opted for phosphate buffer at pH 2.5, containing 5 mM of sodium 1-hexanesulfonate and MeOH in 65:35 volumetric proportion. The method was applied to detection of banned azo dyes, after reduction to PAA, of which the banned ones are denoted by * (entries in Table 1 carrying note *e*). In a study involving 2-, 3- and 4-*chloroaniline (**1h**), 2-* (**1b**) and 4-toluidine (**1d**), 3-, 4-* (**2g**) and 5-chloro-2-toluidine, 3-, 4- and 5-*nitro-2-toluidine (**2h**), 2,3-, 2,4-* (**2e**) and 2,6-diaminotoluene (**2f**), 1- (**8a**) and 2-*naphthylamine (**9a**) under identical conditions, the isomers were well separated from each other, except for 2- and 4-toluidine which had distinct but close retention times with no baseline separation[211].

Nitroarenes can be effectively determined by RP-HPLC-FLD after reduction to the corresponding PAA. Reduction with NaHS was found to be more efficient than with $NaBH_4/CuCl_2$. The method was applied to determination of 2-nitrofluorene and 1-nitropyrene, which were converted to 2-fluorenylamine (**10b**) and 1-pyrenamine (**13**), respectively, and were found to be at *ca* 5 ppm levels in dust collected in the Upper Silesia region[202].

HPLC-DA-UVD was used for confirmation of the presence of HAA from Table 2.A−B, extracted from charcoal-grilled meat by the Gross and Grütter method (Section III.A.5), in parallel with ELD. Due to the complexity of the matrix, the standards addition method was applied, spiking with authentic analytes. The only HAA found in concentrations over the LOD were benz[*a*]acridine (**17**), MeIQ (**25b**) and MeIQx (**26a**)[139]. After suitable extraction and cleanup from fried meat, compound **23a** was determined by HPLC-FLD ($\lambda_{ex} = 316$ nm, $\lambda_{fl} = 370$ nm); other HAA (Table 2.B) also present in the sample

were determined by HPLC-AMD[48]. HPLC-FLD (λ_{ex} = 360 nm, λ_{fl} = 460 nm) served for detection of the aza-PAH listed in Table 2.A. Reconfirmation of structural assignment of isomeric species was by GC-MS. The method was applied to determination of these compounds in the dietary intake of the Upper Sillesia region in Poland, consisting of grilled or fried meats. Four-ring aza-PAH benz[*a*]acridine (**17**) and benz[*c*]acridine (**18**) were more abundant than the five-ring ones dibenz[*a*,*c*]acridine (**19**) and dibenz[*a*,*h*]acridine (**20**), all at levels of 1 ppb or less, making the daily intake of these carcinogens of the order of 0.1 ng[145].

Electroluminescence of ruthenium is attained when Ru(III) is electrochemically reduced to an excited state of Ru(II)*, which decays to the ground state Ru(II) with emission of a photon (λ = 617 nm). Various mechanisms for this process have been reported, some involving a reducing species, which in the present case is the acetylacetamide derivative of an aromatic amine (**97**)[221]. Primary and secondary amines may be determined by RP-HPLC-ECLD after conversion to the **97** derivative according to equation 8. In the electroluminescence detection cell, a stream of the ruthenium(III) complex [Ru(bpy)$_3$]$^{3+}$ (bpy = 2,2′-bispyridine) in H$_2$SO$_4$ solution is introduced, maintaining the pH at *ca* 1.5, and a steady current at 80 μA. The presence of MeCN in the solution helps to enhance the electroluminescence signal. The LOD for the tested PAA [aniline (**1a**), 4-toluidine (**1d**) and 4-chloroaniline (**1h**)] and aliphatic amines were about 0.5 μM in the derivatizing solution[193].

3. Electrochemical detection

Analysis of HAA, mutagens and carcinogenic agents found in ppb levels in cooked protein food can be conveniently carried out by HPLC-ELD, instead of more sophisticated and expensive methods such as HPLC-MS, GC-MS or ELISA. After preconcentration (Section III.A.5), separation of HAA can be carried out on an ion exchange column, taking advantage of differences in their pK_a values. For example, a mixture of MeIQx (**26a**), IQ (**25a**) and MeIQ (**25b**) was eluted in that order from a Spherisorb SCX 5U column, using a 30:70 MeCN–80 mM phosphate buffer (pH 5.6) mobile phase. Although UVD at 263 nm is possible, more sensitive determinations could be achieved by AMD, with a GCE at +1050 mV *vs*. SSCE and an auxiliary electrode. Furthermore, AMD is potentially capable of distinguishing among classes of HAA, because quinoxaline structures such as **26a** have less tendency for oxidation than quinoline structures such as **25a** or **25b**. Figures of merit for **26a, 25a** and **25b** are, respectively: LOD (SNR 3) 35, 37, 70 pg, RSD (*n* = 6) 1.66, 2.20, 2.42%, with linearity from 2.5, 1.0, 2.5 ng up to the maximum tested amount of 20 ng. The method was used for determination of HAA in beef extract[151]. After suitable extraction and cleanup from fried meat, **25a, 25b, 26a** and 4,8-DiMeIQx (**26b**) were determined by HPLC-AMD using a GCE at +0.85 V *vs*. SSCE[48].

Ion chromatography was applied in determination of PAA (in the order of elution): 2,6-diaminotoluene (**2f**), 2,4-diaminotoluene (**2e**), aniline (**1a**), 2-toluidine (**1b**), benzidine (**7b**), 4-chloroaniline (**1h**), 4,4′-methylenedianiline (**5a**), 3-nitroaniline and 1-naphthyl-amine (**8a**) by RP-HPLC-AMD, using as mobile phase a gradient of MeCN and 35 mM H$_2$SO$_4$. Isocyanates are converted on hydrolysis in an acid medium to the corresponding amines, and can be thus determined by the proposed ion chromatographic method. This was applied for determination of 2,4- and 2,6-toluene diisocyanate and 4,4′-methylenedi-phenyl diisocyanate in air, after collection in an impinger, where they were hydrolyzed to 2,4-diaminotoluene (**2e**), 2,6-diaminotoluene (**2f**) and benzidine (**7b**), respectively[201]. Ion pair chromatography of HAA can be carried out in a trichloracetic acid–sodium

acetate buffer at pH 2.5 to avoid peak tailing usually encountered when running chromatograms on silica-based columns, due to the presence of silanol groups on the solid phase. UVD is not sufficiently sensitive for the trace concentrations of HAA found in food. A coulometric array of two electrodes, one for oxidation at +160 mV followed by one for reduction at +10 mV, was proposed for determination of the imidazo-azaarenes in Table 2.B. The method was applied to detection and determination of IQ (**25a**), MeIQx (**26a**), 4,8-DiMeIQx (**26b**) and 7,8-DiMeIQ (**26c**) in a complex matrix such as soup cubes. One of the brands was nearly free of these toxic compounds to the LOD, while the other contained about 1 to 3 ppb of the HAA but was free of **26c** to the LOD[200].

C. Electrophoresis

A most frequent technique for the determination of aromatic amines in environmental samples is GC-MS; however, its application requires cumbersome purification steps before the end analysis. When a rapid throughput would be more convenient and high sensitivity is not required, CZE allows the group separation of cationic amino compounds from both neutral and anionic phenolic compounds, based on different migration times[222–224]. The sensitivity of CZE is sufficient for evaluation of aromatic amines after spills or similar contamination situations; however, it is inadequate for ultratrace situations, which might occur in groundwaters, for which chromatographic methods are called for[88]. Good separation was obtained by CZE of a mixture of PAA listed in Table 1 (all at 10 mg L^{-1} concentration), with a 52 cm effective length capillary recovered with polyimide, working at 22 kV and UVD at 214 nm, using as background electrolyte 50 mM phosphate buffer (pH 3.1). The order of emergence between 5 and 10 min was: 4,4′-methylenedianiline (**5a**), 4,4′-oxydianiline (**6a**), benzidine (**7b**), aniline (**1a**), 2,4-diaminoanisole (**4c**), 2,4-diaminotoluene (**2e**), 2-toluidine (**1b**), 3,3′-dimethylbenzidine (**7d**), 3,3′-dimethoxybenzidine (**7e**), 4-cresidine (**4b**), 1,2-diaminonaphthalene (**8b**), 4-chloroaniline (**1h**), 4-aminobiphenyl (**7a**), 1-naphthylamine (**8a**) and 4-chloro-2-toluidine (**2g**)[77]. The order of emergence in the CZE-AMD determination of a mixture of PAA with acetate buffer at pH 5 was 1,3-phenylenediamine (**1k**), 2-anisidine (**4a**), 4-ethoxyaniline, **7b**, **1b**, 2,4-xylidine (**2b**), 2-ethylaniline (**1e**) and 2,6-xylidine (**2d**). At the working pH the analytes are partially ionized as ammonium cations migrating with the EOF. AMD was performed with a GCE working at +0.7 V vs. SSCE, at which most tested compounds showed maximum sensitivity; however, chloroanilines (not used in the tested mixture) showed low sensitivity in the +0.1 to +0.7 V limiting potential range[190]. A sensitive response to aromatic amines was achieved for CE-AMD, using a carbon fiber microdisk electrode working at +1.0 V vs SCSE with a Pt wire as auxiliary electrode. The placement of the microelectrode at the end of the CE columns is critical. The LOD and linearity range (μM units) achieved for five analytes, in the order of emergence, were: 3,4-dihydroxybenzylamine (0.9, 5 to 1000), 4-phenylenediamine (0.075, 0.5 to 500), 4-aminophenol (1.2, 5 to 500), N,N-dimethylaniline (0.03, 0.1 to 500) and aniline (0.15, 1 to 200)[212]. A series of micromachined, narrow, individually controllable Au band electrodes placed at the end of the CE track allows AMD at several potentials for improved sensitivity and additional voltametric recognition of the emerging analytes. The dimensions of the microelectrode array relative to the capillary diameter and its positioning are crucial for analytical quality. A four-microelectrode array, of which two were working electrodes, was used for determination of various aromatic amines. The microelectrode design needs improvement because its LOD is of the order of 1 μM, which is large as compared to other AMD electrode systems[213].

CZE-UVD, measuring at 210 nm, was applied for separation of a mixture of HAA of the types found in Table 2.B–C, extracted from cooked protein food. After cleanup and preconcentration by the technique described in Section III.A.5, samples were run in solution at pH 2.20 for optimal resolution (better than 1.7). The order of emergence of five such analytes was: MeIQ (**25b**), Trp-P-2 (**28a**), Glu-P-1 (**29b**), MeIQx (**26a**) and PhIP (**23a**). Best overall results were obtained for hydrodynamic injection, with LOD from 35 to 50 ppb, linearity from 0.06 to 10 ppm and good reproducibility[214].

High sensitivity may be achieved with CE for analytes in ultratrace concentrations if the samples undergo suitable preconcentration, for example by SPE and FASI, and if the detection method is highly sensitive. Several technical problems have to be solved in order to achieve the latter desideratum. For example, UVD focusing on a single point of a capillary is precluded by the irradiance phenomenon; this can be solved by illuminating a length of the capillary with an optic fiber bundle and using a charge coupled device camera that can image the full length of the illuminated zone[215]. Various techniques for detection improvement when applying UVD to CE have been reviewed, including use of bubble cells, or Z-shaped cells and the especially sensitive LIFD; MS detection has the advantage of allowing additional identification of the emerging species but needs to be mounted with special adaptors to be coupled with the CE device[166]. CZE-DA-UVD was applied in a study for determination of IQ (**25a**), MeIQ (**25b**), 4,8-DiMeIQx (**26b**) and PhIP (**23a**) in fried meat, baked salmon and meat extract, after suitable cleanup and preconcentration. Except for **23a**, the recoveries and sensitivity of the method were satisfactory[142]. CE with MS detection was applied to separation and determination of mixtures of potentially carcinogenic HAA, including **23a**, DMIP (**23b**), **25a, 25b**, MeIQx (**26a**), **26b**, 7,8-DiMeIQx (**26c**), TriMeIQx (**26d**), Trp-P-2 (**28a**), Trp-P-1 (**28b**), Glu-P-2 (**29a**), Glu-P-1 (**29b**), AαC (**30a**), MeAαC (**30b**), norharman (**31a**) and harman (**31b**). By optimization of the carrier solvent and electrolyte (formic acid–ammonium formate buffer at pH 4.5 and 60% MeOH) it was possible to separate all the sixteen HAA, however, not all to the baseline; here the speciation capabilities of ESI-MS-MS were of great aid; each analyte was monitored by one to three specific fragments. The LOD when applying FASI ranged from 0.75 to 20.8 ng g^{-1}, similar to those obtained for HPLC-MS (Section IV.B.1)[199], and the RSD ($n = 5$) ranged from 0.3 to 1.0% for the migration time and from 3.0 to 11.1% for the concentration at the 0.16 μg g^{-1} level[167].

Micellar electrokinetic chromatography (MEKC) is a variation of the electrophoretic method involving the presence of surfactants in the solution. This may afford a certain advantage over plain electrophoresis as for the time, sensitivity and resolution of the analysis, the avoidance of some technical pitfalls and especially for allowing analysis of nonionic species. Application of this technique requires selection of appropriate surfactants and optimization of the working conditions to achieve good analytical quality. A case in point is the determination of metabolites of Chlorpropham (**91**) after hydrolysis and conversion to fluorescent **90b** by labeling with 5-(4,6-dichloro-s-triazin-2-ylamino)fluorescein (**90a**). CZE did not give satisfactory results. MEKC-LIFD required a mixture of SDS and Triton X-100 in borate buffer at pH 9.5; the excitation was with a laser beam at 488 nm and the fluorescence was measured after an emission band-pass filter of 520 nm. For the chloroanilines **92a**–**c** in aqueous solution or in the original potato matrix, the LOD (SRN 3) varied from 0.3 to 3.1 μg L^{-1} or from 0.8 to 7.2 μg kg^{-1}, with linearity up to about 1000 μg L^{-1} or 1500 μg kg^{-1}, respectively[188]. The **94** fluorescamine derivatives of PAA, obtained according to equation 7, migrated as anions in borate buffer at pH 9, against

the EOF; however, the CZE separation was inefficient. Adding SDS to the background electrolyte turned the technique to MEKC. The order of emergence of a test mixture was aniline (**1a**), 4-chloroaniline (**1h**), 2-toluidine (**1b**), 2,6-xylidine (**2d**), 2-ethylaniline (**1e**) and 2,4-dichloroaniline. The sensitive fluorometric detection allowed low LOD, from 0.5 to 2 ppb. The method was applied to analysis of PAA in effluents from the textile and leather industries[190]. MEKC-DA-UVD in a borate buffer at pH 9.2 with sodium dodecyl sulfate was used for determination of sulfa drugs and their associated compounds in veterinary formulations. The LOD and LOQ were 0.3 and 1 ppm, respectively. The results were confirmed by HPLC analysis[217].

MEKC-AMD, with a carbon fiber disk electrode working at 0.6 V vs. SSCE and a Pt wire auxiliary electrode, was used for the analysis of HAA in cooked meat. The LOD for pan residues collected after frying pork patties were about 10 $\mu g\,L^{-1}$. The following HAA in their order of emergence were detected in pan residues, with the estimates on the basis of ng g^{-1} of fried meat: Glu-P-2 (**29a**, 0.038), MeIQx (**26a**, 1.0), IQ (**25a**, 0.014), 7,8-DiMeIQx (**26c**, 0.054) and 4,8-DiMeIQx (**26b**, 0.51)[216].

CSEI-sweep is an online technique claimed to achieve hundreds-of-thousands-fold preconcentration increases of cationic analytes, consisting of injecting a sample without micelles into a capillary containing a conductive solution separated from the sample by a water plug. On applying a suitable voltage the cationic analytes are swept into a narrow band of much higher concentration, thus allowing for UVD in the subsequent MEKC. The CSEI-sweep-MEKC-UVD technique was applied to determination of environmentally relevant aromatic amines at 0.1 ppb LOD levels, in the order of emergence: *N*-(2-aminoethyl)-1-naphthylamine, 3,4-, 3,5-, 2,4-, 2,3- and 2,5-dichloroaniline, 3-chloroaniline, PhCHMeNH$_2$, *N*-ethylaniline, 2-toluidine (**1b**), 4-anisidine (**1i**), 2- and 4-nitroaniline[218].

D. Electrochemical Methods

Very sensitive differential pulse voltammetry determinations of PAA can be carried out with a system consisting of a modified working CPE, a SSCE and a Pt wire auxiliary electrode. Modification of the CPE is carried out by film development with β-cyclodextrin prepolymer (CDP) or its carboxymethyl derivative (CDPCM) crosslinked with glutaraldehyde. A screen printed version of the triple electrode system was also investigated. At optimal operating conditions of analyte accumulation and pulse application the LOQ were *ca* 9 nM for 1-naphthylamine (**8a**), *ca* 2 nM for 2-naphthylamine (**9a**) and *ca* 1 nM for 2-aminobiphenyl (**1n**), with a better performance for the CDPCM modification over CDP[225].

An indirect electrochemical method developed for nitrite determination may be of general applicability for PAA determination, as shown in equation 13. A nitrite sample is placed into a cell containing a known amount of 3-sulfanilic acid in dilute HCl at pH 3. After 5 min the diazonium ion formation is complete; an excess of catechol (**109**) is added and the concentration of the remaining 3-sulfanilic acid is determined at +0.12 V with a GCE vs. standard calomel electrode, by measuring the adduct (**110**) formed between the aromatic amine and the quinone derived from catechol in the diffusion layer of the electrode. The 3-isomer of sulfanilic acid was chosen among the three isomers, aniline and 4-nitroaniline for its highest sensitivity and its lowest LOD, 0.7 μM, with linearity from 20 to 80 μM. A spectrophotometric assay may be carried out for nitrite by measuring at 516 nm the azo dye derived from catechol and the diazonium ion after 3 h;

however, this reaction is too slow for analytical application[226].

(13)
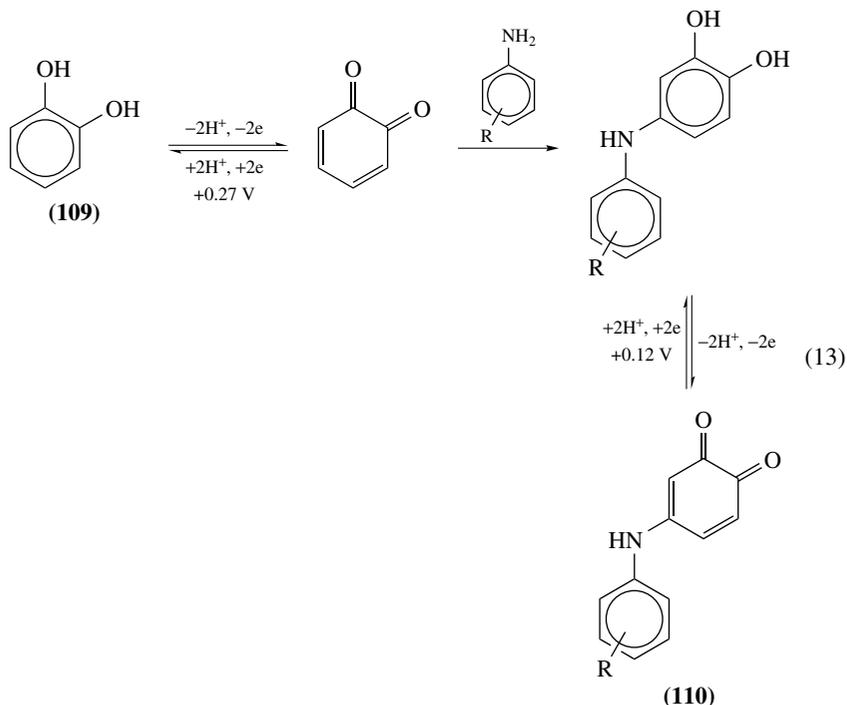
Determination of aromatic amines can be carried out coulometrically in a solution containing bromide ion that is oxidized to bromine, which effects electrophilic substitution at *ortho* or *para* sites relative to the amino group. The titration is carried out in the galvanometric mode, at a constant current of 5 mA, and the end point is determined with a pair of Pt needle electrodes set at 300 mV. The stoichiometry of the bromination has to be established before proceeding to the titration. Thus, drugs derived from 4-aminobenzoic acid, such as benzocaine (**111a**), procaine (**111b**) and procainamide (**111c**), undergo reaction with electrochemically generated Br_2 in a 1:2 proportion; the structurally similar acetaminophen (**111d**) reacts in a 1:1 proportion, as it is more sluggish in its reaction with a second Br_2 molecule. Sulfa drugs such as sulfanilamide (**86**), sulfaguanidine (**112a**), sulfacetamide (**112b**), sulfaethidole (**112c**) and sulfamethoxazole (**100**) undergo 1:2 reactions with electrochemically generated Br_2; sulfathiazole (**101**) shows a 1:4 stoichiometry because, in addition to the benzene ring double bromination, the thiazole group undergoes oxidation to thiazole *N*-oxide (**113**). Determination of such drugs in pharmaceutical preparations had RSD of 5% or lower[227].

A chronopotentiometric method for determination of amino derivatives of PAH is based on the high affinity of DNA for such compounds. In a cell consisting of a DNA-modified CPE, a reference SSCE and a Pt wire auxiliary electrode, an aqueous solution of the PAA is submitted to an accumulation period, during which the analytes are transferred to the working electrode by an intercalation mechanism, after which the solution is changed
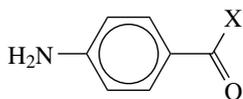
(111)

(a) X = OEt

(b) X = OCH$_2$CH$_2$NEt$_2$

(c) X = NHCH$_2$CH$_2$NEt$_2$

(d) X = Me
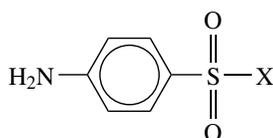
(112)

(a) X = N=C(NH$_2$)$_2$

(b) X = NHAc

(c) X = NH—[thiadiazole]—Et

(113)

X = NH—[thiazole]
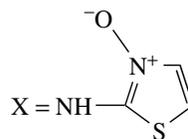
and the analytes are stripped at another potential. The observed LOD (SNR 3) for spiked solutions were approximately 1.8 µM of 2-naphthylamine (**9a**), 80 nM of 2-anthramine (**11b**), 10 nM of 1,2-diaminoanthraquinone (**114**), 20 nM of 9,10-diaminophenanthrene (**115**) and 60 nM for 1-aminopyrene (**13**). These LOD are sufficiently low for application of the method to the analysis of polluted environmental samples[228].
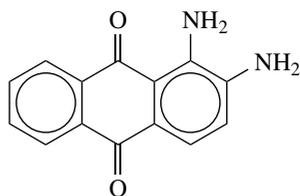
(114)
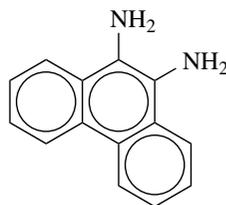
(115)

E. Spectrophotometry and Colorimetry

1. Infrared spectroscopy

SPME on a thin polymeric film supported on a flat stainless steel plate can be used for determination of the sorbed analytes by the reflection IR spectrophotometric method. LOD of the order of 100 ppb with good linearity were found for chlorinated PAA spiked in water, after sorption on a film made of acrylonitrile–butadiene copolymer[162]. ATR-FTIR is a method for analyzing polymer films and their surfaces, well suited for routine analysis[229]. ATR-FTIR was applied for detection of aromatic isocyanates and their derivative PAA impurities in flexible laminates used for food packing, resulting from incomplete polymerization of the isocyanate during production of the packing materials. When toxic isocyanate and PAA are present in the laminate they may diffuse onto the foodstuffs[66].

An alternative to ATR methods is SPME with a hollow waveguide sampler, which may be of advantage because of the higher sensitivity, the shorter analysis times, the absence of practical limitations to sample volume and the possibility of performing mass analyses. The analytes need not penetrate deeply into the plastic layer and it is sufficient that they

become adsorbed on the inner surface of the sampler[163, 164]. The acrylonitrile–butadiene copolymer was found as the best among the commercially available polymers to form the internal coating of the hollow waveguide, both as a good sorbant for the polar aromatic amine analytes and because of its typical CN absorption band at 2237 cm^{-1}, which does not interfere with most intended PAA analytes; the intensity of the CN peak may serve for estimation of the relative thickness of the deposited sorbent film. After passing the solution sample through the hollow waveguide for SPME and drying, a nonimaging IR concentrator is placed on each end of the hollow waveguide sampler for collecting IR radiation from the sample compartment of the FTIR spectrometer into the waveguide and for redirecting the transmitted IR radiation into the detector. The method was applied for determination of 200 mL water samples spiked with 1 to 50 ppm of chlorinated PAA (2- and 4-chloroaniline, 2,4-, 2,5-, 3,4- and 3,6-dichloroaniline, 3-chloro-4-toluidine); on adding the results of 100 scans with 4 cm^{-1} resolution, LOD (3σ) was from 80 to 600 ppb with good linearity[165].

FTIR of the materials used in consumer products can be applied, after a reduction process with $Na_2S_2O_4$, for forensic detection of forbidden azo dyes. Thus, the spectra of yarns which were dyed with Direct Brown 95 (**116**) and Direct Orange G (**117**) showed, respectively, after reduction the strongest peaks of benzidine (**7b**) and 3,3′-dimethylbenzidine (**7d**) protruding over the matrix background[196].

(116)

(117)
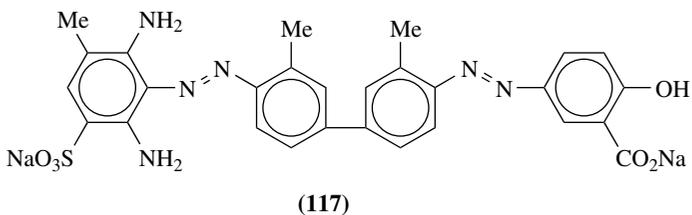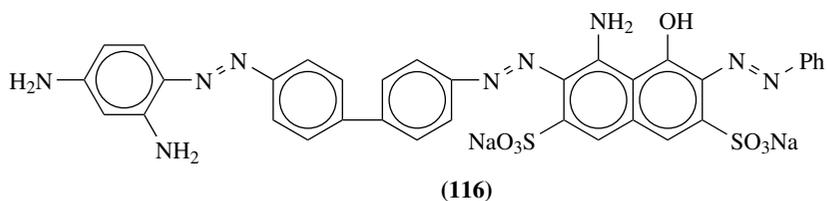
NIR spectrophotometry in the region from 8000 to 4000 cm^{-1} was used to measure the kinetics of copolymerization of an aromatic bismaleimide (**72**) derived from an aromatic diamine (e.g. **5a**), taking place at 160 to 180 °C. The following NIR spectral ranges were useful for this study: primary amine first overtones (ν_{N-H}) at 7000 to 6400 cm^{-1}, double bond first overtone ($\nu_{C=C-H}$) at 6100 cm^{-1}, aromatic first overtones (ν_{C-H}) at 6000 to 5750 cm^{-1}, aliphatic first overtones (ν_{C-H}) at 5750 to 5350 cm^{-1} and primary aromatic amine combination bands first overtones ($\nu_{N-H} + \delta_{NH_2}$) at 5150 to 4800 cm^{-1}. The process consisted mainly of a second-order Michael addition, as depicted in equation 14, and not the plausible imide opening to yield a maleic dianilide (**119**), as shown in equation 15. A Michael addition between maleimide moieties and secondary amine moieties present in the products (**118**) also takes place, however at a rate of about one fourth of that of the primary amine moieties. To improve the SNR of the measurements, usually the results of

32 scans were added; however, with particularly fast or slow reactions, 16 or 64 scans were added[230, 231].

(72) **(118)** (14)

(119) (15)
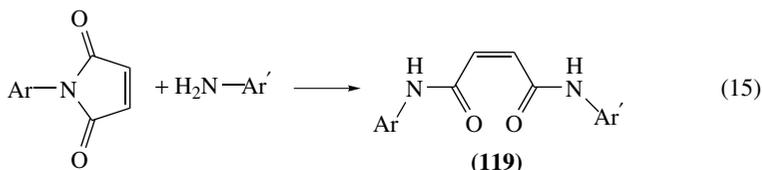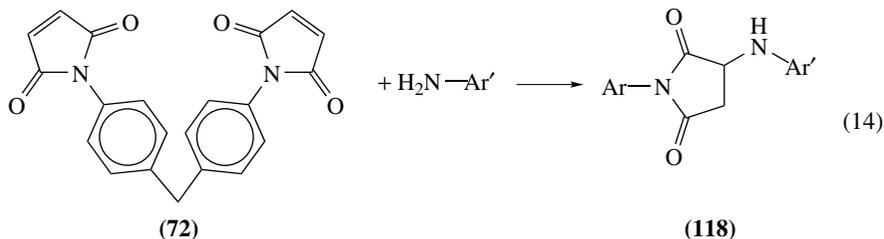
2. Ultraviolet-visible spectroscopy

Many pharmaceuticals contain more than one active ingredient to take advantage of synergistic effects. Chromatographic separations without or with previous derivatizing and first derivative UVV spectrophotometry have been proposed for analyzing such mixtures; however, these procedures involve some technically or computationally complicated steps. The bivariate calibration spectrophotometric method is simpler and of quality similar to that of derivative spectroscopy. The method requires calibrations of the pure analytes in the linearity concentration range, at a set of wavelengths λ_i. Two working wavelengths are chosen according to Kaiser's sensitivity matrix and the concentrations of the analytes are immediately calculated from two simultaneous linear equations. The method was applied for determination of binary preparations of trimethoprim (**120**) and sulfamethoxazole (**100**) and of **120** and sulfamethoxypyridazine (**102**)[232a]. A FIA system for determination of sulfonamides was designed, possessing a solid-phase spectrophotometric microsensing zone inside a flow-through cell, where Sephadex QAE A-25 resin temporarily retains the analyte and the intrinsic absorbance is measured. The LOD were <100 ppm for 40 mL samples and <20 ppm for 600 mL samples, with linear dynamic range from 1 to 45 g L^{-1} (40 mL) and 0.2 to 10 g L^{-1} (600 mL), and RSD ($n = 10$) <2.3%. The method was applied to determination of sulfanilamide (**86**), sulfacetamide (**112b**), sulfamethoxazole (**100**) and sulfadiazine (**103**) in pharmaceutical preparations or urine; potential interferences from compounds such as trimethoprim (**120**) were also investigated[232b].

(120)
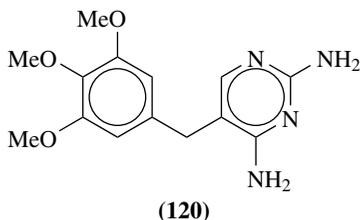
A kinetic method was proposed for the simultaneous determination of 2-, 3- and 4-aminophenol (**1m**), based on the mechanism illustrated in equations 16 and 17 for **1m**. Aminophenols undergo fast oxidation with transition metal ions to a quinone monoimine (**121**), according to equation 16, followed by a slow coupling reaction to yield a diphenylamine (**122**). Two more fast reactions take pace with involvement of **121**, namely an additional coupling of **122** to yield a colorless N,N'-diphenylphenylenediamine intermediate (**123**), which undergoes oxidation to a quinone diimine dye (**124**). The most convenient oxidant from the analytical point of view is $[Mo(CN)_8]^{3-}$; however, care should be taken for this reagent to be in substoichiometric concentration, so that sufficient aminophenol remains for generating the dye. Each one of the aminophenol isomers yields in the presence of 4-aminophenol (**1m**) a dye with a different UVV absorption spectrum and the process takes place at a different rate. This allows simultaneous determination of the three isomers by measuring the kinetics of the oxidation/coupling reaction with a DA-UVV spectrophotometer from 340 to 500 nm. Data processing is by the partial least squares method and requires a previous calibration of the behavior of the oxidant in the presence of various concentrations of the analytes. The measuring ranges are 0.1 to 1.0 mM for 2-aminophenol, 0.3 to 1.0 mM for 3-aminophenol and 0.25 to 3.0 for **1m**, with errors lower than 10%[233].
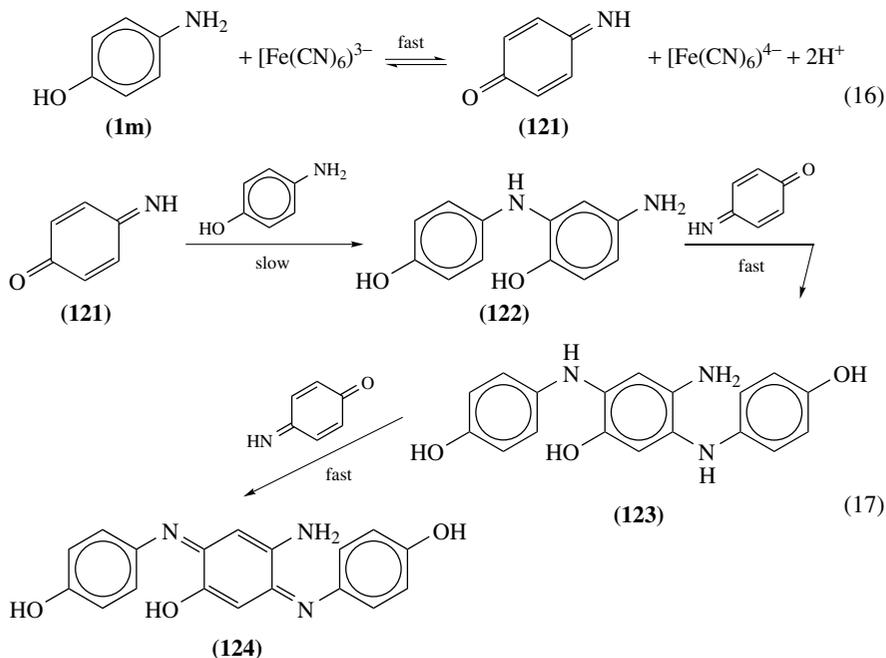
Certain aromatic amines may cause reduction of Fe(III) ions in the presence of FerroZine Iron reagent (**125**), according to equation 18, leading to the formation of a stable violet-colored complex with Fe(II) ions (**126**), the concentration of which is measured at 562 nm. At pH 5, the color develops in a few minutes at room temperature and the absorbance of **126** is proportional to the concentration of the analyte. Neither the oxidation products of the analyte nor the excess of Fe(III) or **125** affect the assay; however, not all aromatic amines undergo this reaction. Thus, compounds such as 1,4-phenylenediamine, 2,4-diaminotoluene, 8-aminoquinoline and 2-amino-3-hydroxypyridine can be determined

by this method, whereas 2-aminopyridine, 3,4-diaminopyridine, 2-amino-5-chloropyridine and 2-amino-3-methylpyridine do not undergo this oxidation[234].

$$+ \text{Fe(III)} \xrightarrow{\text{ArNH}_2} \mathbf{125}_3 \cdot \text{Fe(II)} \qquad (18)$$

$$(\mathbf{126})$$

(125)
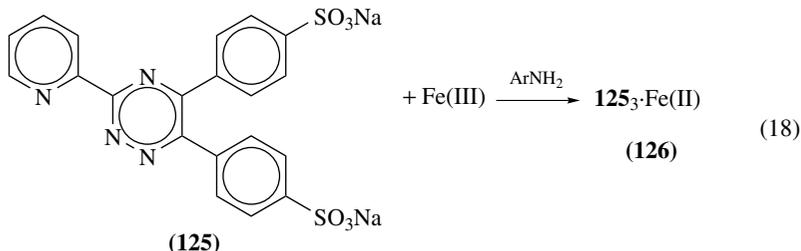
A relatively fast aromatic nucleophilic substitution process takes place with PAA in the presence of 7-chloro-4,6-dinitrobenzofuroxan (**127a**) to yield a colored derivative (**128a**) by displacement of the aromatic chlorine atom, as shown in equation 19. The absorption maximum is pH dependent, and is found at *ca* 510 nm in acidic to neutral solutions. In cases where the absorption peak of the product **128a** overlaps that of the hydrolysis product of **127a** (OH instead of Cl), it is possible to use the alternative reagent 4-chloro-5,7-dinitrobenzofurazan (**127b**). The reaction rate allows carrying out the process in a FIA system. This method was proposed for determination of traces of toxic 4-aminophenol (**1m**) and 1,2-phenylenediamine (**1j**) in pharmaceuticals derived from these aromatic amines, such as acetaminophen (**111d**)[235]. Test strips were developed containing reagents **127a** and **127b** immobilized on nitrocellulose film (10 to 12% N content), using dimethyl phthalate as plasticizer. Although color development for PAA, secondary aromatic amines and hydrazines may be based on the process depicted in equation 19, chromic response was also shown by tertiary aromatic amines such as *N*,*N*-dimethyl- and *N*,*N*-diethylaniline with the **127a** test strips, probably based on color development involving reduction of the *N*-oxide moiety. No interference was observed for alkylamines (which produce hypsochromic shifts), ammonia, phenols, carboxylic acids and inorganic salts. The LOD were in the 10 to 200 ppb range for various classes of tested compounds[236].

$$\qquad (19)$$

(127) (a) X = O   **(128) (a)** X = O
     (b) X = none   **(b)** X = none
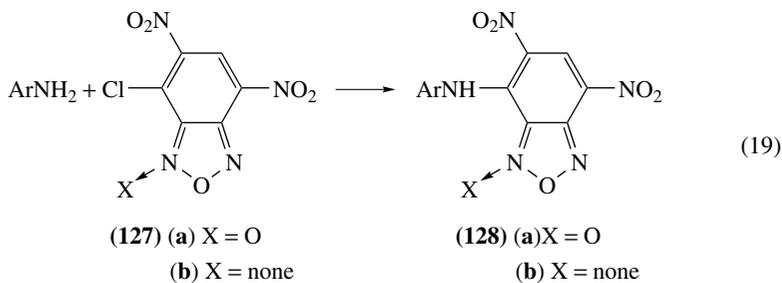
Aromatic nitro compounds can be determined after catalytic hydrogenation to the corresponding PAA, derivatizing with fluorescamine (**93**) according to equation 7 (Section III.B.3) and measuring the luminescence in the 490 to 520 nm region, obtained on excitation at 390 to 410 nm[237,238].

Short-lived free radicals derived from aromatic amines can be generated and detected by the ETSF method. Long-lived free radicals in solution, such as tris(4-bromophenyl)amine radical cation (**129**), react with aromatic amines to yield short-lived radical anions (**130a–d**), as shown in equation 20. Solutions of **129** are generated electrolytically and

are stable for several days. The free radicals **130a–d** can be detected and quantified with a fast scan stopped-flow spectroscopic system. This has the additional advantage over the pulse-electrolysis stopped-flow (PESF) method[239] for generating the free radicals **130a–d** that the reaction is homogeneous, allowing direct observation of the effect of the precursors on the electron transfer processes. The ETSF method was applied to kinetic measurements of the free radical dimerization of **130b–d**[240].

$$\text{(129)} \qquad \text{(130)} \quad \textbf{(a)}\ R = R' = Me$$
$$\textbf{(b)}\ R = H,\ R' = Ph$$
$$\textbf{(c)}\ R = Me,\ R' = Ph$$
$$\textbf{(d)}\ R = R' = Ph \qquad (20)$$

The presence of pending primary aromatic amine groups bound to a solid can be detected according to equation 21, by heating the solid with a DMF solution of chloranil (**131**). Development of color in the solid points to formation of dyes (**132**). A semiquantitative comparimetric method can be developed for various resins based on this reaction. No interference was noted from secondary and tertiary aromatic amines, nor from pyridine and pyrimidine moieties[241].

A kinetic method for determination of aromatic amines was proposed, based on measuring the development of azo dyes (**134**) resulting from coupling a diazonium ion derived from a PAA analyte and the chromophoric substrate 1-(4-hydroxy-6-methylpyrimidin-2-yl)-3-methylpyrazolin-5-one (**133**), as shown in equation 22. After a short induction period initial rate kinetics can be measured; when the process is quite advanced, absorbance reaches a maximum and starts to recede due to oxidation of the azo dye by excess nitrous acid. Each PAA has to be calibrated for its molar absorption coefficient and reaction rate, for optimal measurement. A tenfold excess of **133** over the analytes ensures a pseudo

first-order kinetic dependence on the analyte concentration. The LOD for aniline and its 4-I, 4-Me and 4-Et derivatives were in the range from 0.72 to 1.4 μM, with linearity from *ca* 5 to 80 μM[69].

$$(22)$$
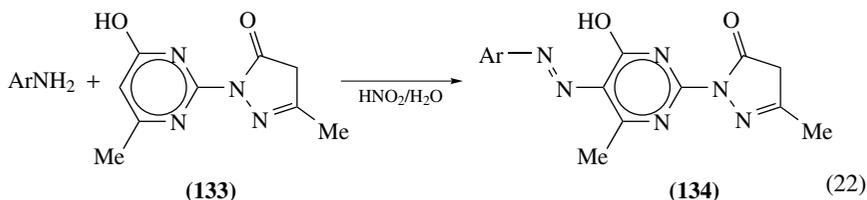
Deterioration of syrups containing the antiemetic metoclopramide (**89**) is due to a Maillard-type process between the active ingredient and the sugar present as sweetener in the preparation. The concentration of 5-methyl-3-phenyl-2-(4′-amino-*s*-triazolo-3′-yl)indole-5′-hydrazide (**135**) was followed by Bratton–Marshall derivatizing (Section III.B.2) and spectrophotometric determination of the azo dye derivative[242]. Care should be taken when using fluorescence detection for possible quenching effects by the presence of certain compounds in the solution. Thus, aniline was found to quench the fluorescence of **135**[243].

(**135**)
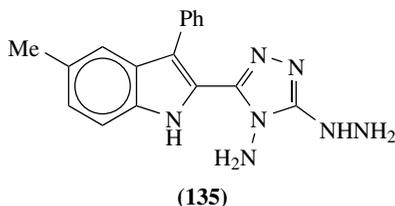
The analysis of amine **136**, present as a residual impurity in the X-ray contrasting media iohexol (**137a**), iopentol (**137b**) and iodixanol (**138**), was carried out in a FIA system equipped with UVD, following the kinetics of development of an azo dye by a modified Bratton–Marshall method (Section III.B.2). Some technical problems attaining the high viscosity and refractive index of the samples had to be solved[244]. Lengthening the light path in the flow cell of a FIA system leads to improved sensitivity and lower LOD; however, optimization of the FIA manifold should be carried out after the path change due to dispersion effects. Such improvements were implemented in the Bratton–Marshall determination of sulfonamide drugs in pharmaceutical preparations containing various active ingredients, such as Abactrim (**139 + 140**) and Bucodrin (**141 + 142 + 143**)[245].

(**136**)   (**137**)   (**a**) R = H
                                         (**b**) R = Me

(138)

(139)

(140)

(141)

(142)

(143)
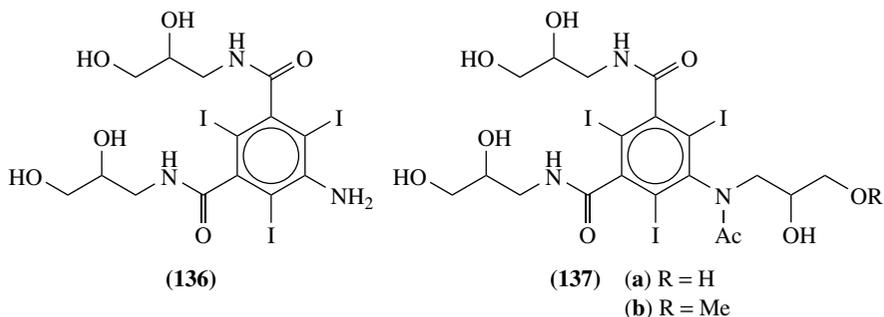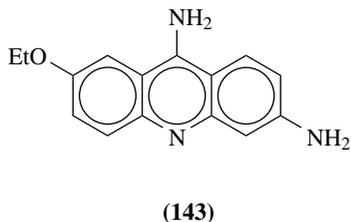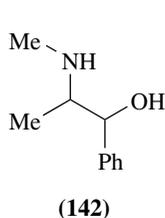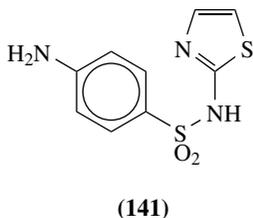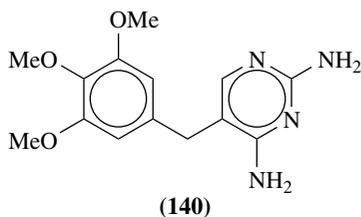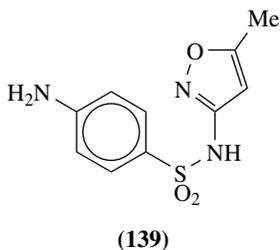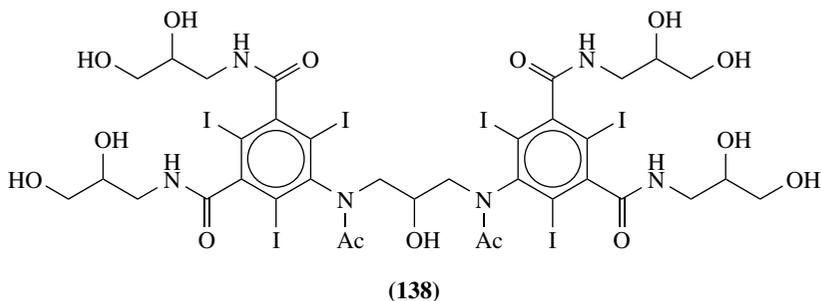
Test strips were prepared by oxidation of cellulose with KIO₄ to a polyaldehyde, followed by condensation with 1-naphthylamine to a poly-Schiff base and reduction with NaBH₄ to an immobilized naphthylamine cellulose derivative, which is mechanically stabilized on a polypropylene sheet. PAA can be detected on addition of nitrite to the test solution and contacting with the strip, where azo dyes are formed. Quantitative analysis can be carried out by diffuse reflectance spectroscopy. The method was applied to pharmaceutical preparations with RSD better than 30%[246].

An evanescent wave biosensor was devised for determination of analytes capable of intercalation in dsDNA in a FIA system. A polyethylene lensed optical fiber is coated with a thin polymeric layer containing dsDNA which is immobilized there. The fiber is placed in a FIA system immersed in a solution of ethidium bromide (**144**), which undergoes intercalation in the dsDNA. The fluorescence signal of **144** is thus enhanced about a 1000-fold relative to the evanescent wave fluorescence measurement without the coating and is dependent on the concentration in solution. If an analyte is present in the same solution, it competes with **144** for intercalation in the DNA and causes fluorescence quenching, which can be measured and correlated to the analyte concentration. This method was applied to determination of various analytes, including 4′,6-diamidino-2-phenylindole dihydrochloride (**145**)[247].

Identification of amino- and nitro-substituted PAH may be effected by Shpol'skii spectroscopy, a technique involving high resolution photoluminescence spectroscopy of the

(144)

(145)
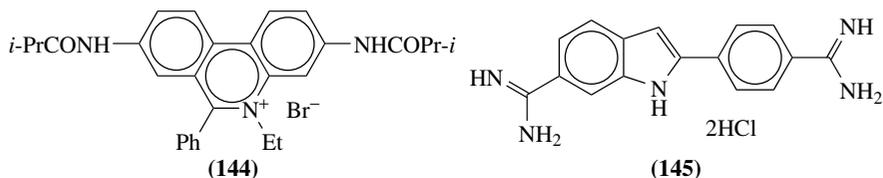
analytes in a solid normal hydrocarbon matrix at low temperatures (15 to 25 K). Identification of individual species is achieved on changing the excitation wavelength and recording the fluorescence spectrum of the analyte with a high resolution diode array. Amino-substituted PAH usually are good fluorophores; however, care should be taken to make the measurements over short exposure times, lest photochemical decomposition will take place, changing the analyte concentration. The feasibility of such proceedings was demonstrated in a study of a series of PAA including 1- (**8a**) and 2-naphthylamine (**9a**), 1,2- (**8b**), 1,5- (**8d**), 1,8- (**8e**) and 2,3-diaminonaphthalene (**9b**), 1- (**10a**), 2- (**10b**) and 9-fluorenylamine (**10c**), 1- (**11a**), 2- (**11b**) and 9-anthrylamine (**11c**), 9-phenanthrylamine (**12**), 1-aminopyrene (**13**), 3-aminofluoranthene (**14**) and 6-aminochrysene (**15**). Furthermore, the method can be extended to determination of nitro-substituted PAH, after conversion to the corresponding amine by reduction with Zn[248].

3. Titration with optical end point

Amines and quaternary ammonium compounds can be determined in the same solution by titration with sodium tetrakis(4-fluorophenyl)borate (**146a**) or sodium tetraphenylborate (**146b**), using as indicator tetrabromophenolphthalein ethyl ester potassium salt (**147**). The analytes are partitioned between the aqueous phase and a 1,2-dichloroethane layer containing the **147** indicator, where they form an ion pair complex, blue with quaternary ammonium compounds and violet-red with other ammonium salts. The titration is carried out with a normalized solution of **146a**, which forms stronger complexes with the analytes than **147**. At the end point the indicator in the organic layer turns a yellow color. **146a** is preferred over **146b** due to its higher selectivity for quaternary ammonium compounds, allowing stepwise titration of mixtures of both types of analytes; in such a case the two end points are denoted by a turn from blue to violet-red and then to yellow. The method was applied to determination of cetylpyridinium chloride (**148**), chlorhexidine dihydrochloride (**149**) and other nonaromatic amines and quaternary ammonium compounds in pharmaceutical preparations[249].

(146)
(**a**) X = F
(**b**) X = H

(147)

(148)

(149)
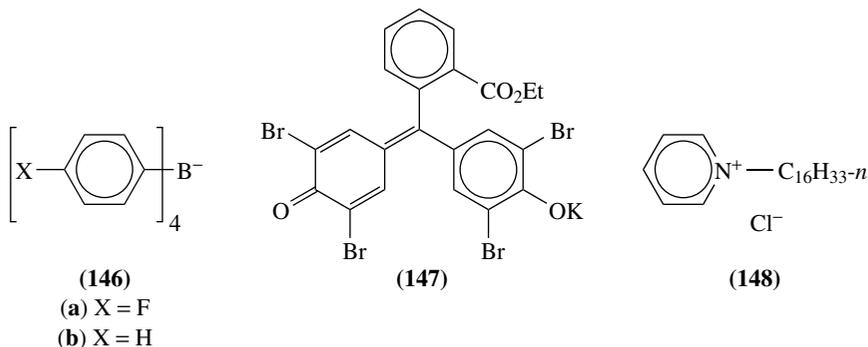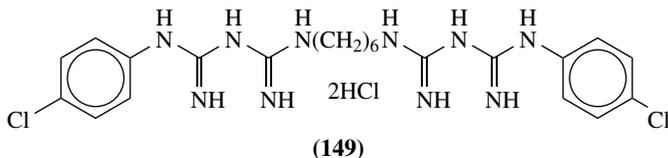
Aromatic amines and epoxy groups may be determined by titration when present in the same sample. The former is carried out with 0.1 M of $HClO_4$ in glacial acetic acid, using Crystal Violet (**150**) as indicator, whereas the latter requires epoxide opening with HCl and the presence of tetraethylammonium bromide[250].

(150)
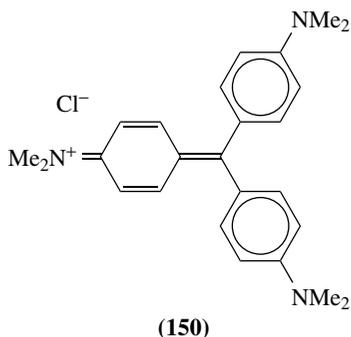
F. Miscellaneous Methods

N,N,N',N'-Tetramethyl-4,4′-methylenedianiline (**151**) is a PVC additive with antioxidant functions. The formation of the amine radical cation $ArN^{\bullet+}Me_2$ and its final transformation to the dimethylanilinium cation ArN^+Me_2 during pulse radiolysis of PVC was followed by ESR spectroscopy. The trace of the amine radical cation was found after subtracting the background due to the macromolecular radicals. The final cation product was determined by UVV spectroscopy[251].

(151)
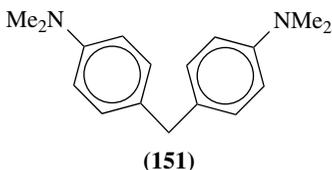
The kinetic behavior of equation 12, as measured chromatographically, could be correlated to thermal measurements in a reaction calorimeter[63]. A method for microdetermination of trimethoprim (**120**) and sulfa drugs was proposed, based on differential scanning calorimetry, by which the heat absorbed by the solid sample in a certain temperature range depends on the relative amounts of the various components in the sample[252].

V. STRUCTURAL CHARACTERIZATION

A. Mass Spectrometry

A study of the ESI-MS fractionation of HAA listed in Table 2.B−C showed structurally related patterns. The most abundant product ion of compounds IQ (**25a**), MeIQ (**25b**)

and MeIQx (**26a**) is derived from the protonated molecular ion; additional product ions may result in a m/z change of -41 and -68 units from loss of the aminoimidazyl substructure. Only one main fragment is shown in the product ion spectrum of PhIP (**23a**), resulting from loss of Me from $[M + H]^+$ (-15 units). Compound Glu-P-2 (**29a**) shows the $[M + H]^+$ peak and either elimination of NH_3 (-17 units) or two stepwise eliminations of HCN (-27 units). The carbolines Trp-P-2 (**28a**), Trp-P-1 (**28b**), norharman (**31a**) and harman (**31b**) followed almost identical fragmentations consisting of $[M + H]^+$ and preponderant loss of NH_3. Besides the loss of Me from $[M + H]^+$ (-15 units) in **31b**, both **31a** and **31b** are characterized by loss of the pyrido moiety, for example $[M + H]^+ - C_4H_6N$ in the case of **31b**. These structural features allow application of tandem selected reaction monitoring-MS detection for determination of these HAA after HPLC separation[253]. The high resolution EI-MS of mutagen **66** (Section II.B.8) showed the M^+ peak at m/z 319.1425, pointing to the formula $C_{18}H_{17}N_5O$ (calc. m/z 319.1433)[89].

Three types of poly(aromatic amine-2,3-pyridinedione) oligomers (**152a–c**) were synthesized; however, they were hard to characterize, due to their low solubility in the usual organic solvents. Samples of each oligomer were incorporated into a matrix of 2,5-dihydroxybenzoic acid, either without or with an alkali metal chloride, and subjected to structural analysis by the MALDI-TOF-MS method. Molecular ions were detected for all three oligomers with n ranging from 1 to 6. However, the most abundant peaks correspond to $n = 1$ or 2, which can be attributed to both lowering of volatilization as the molecular mass grows and steric hindrance to the propagation of the Michael-type condensation taking place in the oligomerization. The MALDI-TOF-MS method can provide information about the end groups of the oligomers. All three oligomers show a normal type of end groups for $n = 1$, $H_2N-Ar-NH$ and H, denoted by 'M*', as shown in formula **152**, with ions $[M^* + H]^+$. For higher oligomers the preferred association is with a sodium ion, showing $[M^* + Na]^+$ peaks; however, **152b** shows $[M^* + H]^+$ peaks for $n = 2$ or 3. Cyclic structures attained on loss of a $C_7H_{10}N_2$ fragment (122 Da), denoted by 'M^', as shown, for example, in **153** and **154**, are also attained for **152a** and **152b**, respectively, for oligomers with $n > 1$, showing the $[M^\wedge + H]^+$ peaks[254].

(152)

(a) Ar =

(b) Ar =

(c) Ar =
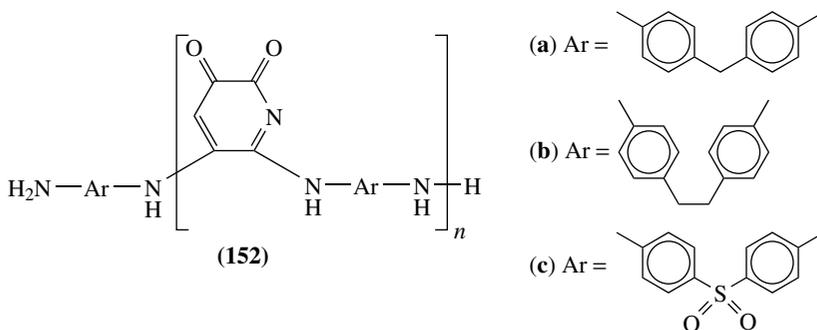
The deoxyadenosidine adduct **37** formed according to equation 1 (Section II.B.2) has four possible configurations, depending on whether the epoxy group in **36** is *cis* or *trans* to the OH on C3′ and on whether attachment of the N atom to the C5a site occurs *syn* or *anti* to the epoxy group. Application of MALDI TOF-MS and postsource decay techniques enables one to discern the configuration of adduct **37**. For example, diastereoisomers **155** and **156** have a different configuration at C5a. The product ion spectra of $[M + H]^+$ at m/z 528 are quite similar, both showing a strong peak at m/z 412 for loss of the deoxyribosyl and a weaker one at m/z 394 for further loss of H_2O. However, **156** shows a peak at m/z

(153)   **(154)**

(155)   **(156)**
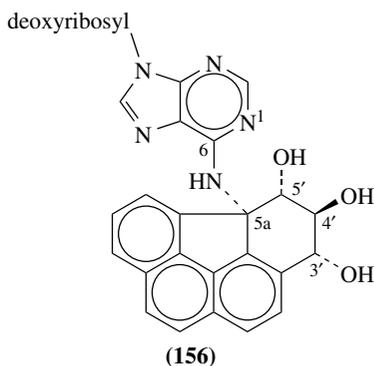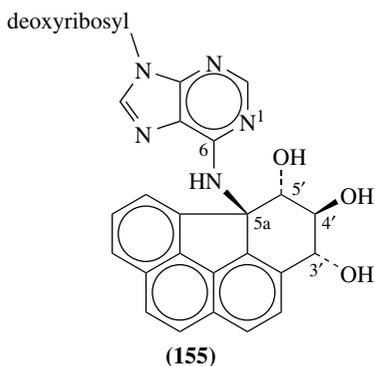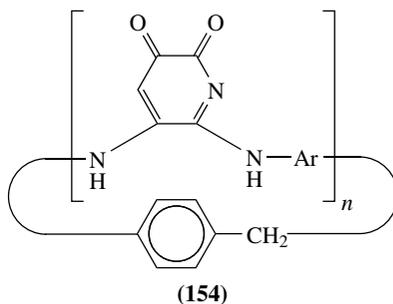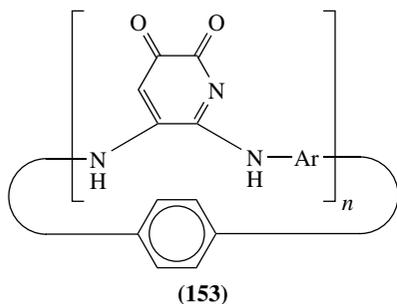
510, corresponding to loss of H_2O from the molecular ion, which is enabled by proton transfer from the protonated N1 position to the OH on C5. A similar mechanism was proposed for one of the other pair of diastereoisomers[29].

B. Electrochemical Properties

Polythiophene randomly grafted with alkyl and aniline tetramer groups (**157**) was synthesized. The tetramer was chosen because it is the minimum oligomer size that mimics the electrochemical behavior of polyaniline, which shows semiconduction and conduction behavior depending on its state of oxidation and the pH. Transition from one structure to the other is illustrated in equation 23, where the electron mobility of quinonoid states (**158**) rearranging to isolated free radicals (**159**) is precluded after reduction to **160**. A correlation was found between the electrochemical behavior and the UVV-NIR spectra of the **157** polymers[255].

(157)

(23)

$$\begin{array}{ccc} (158) & (159) & (160) \end{array}$$
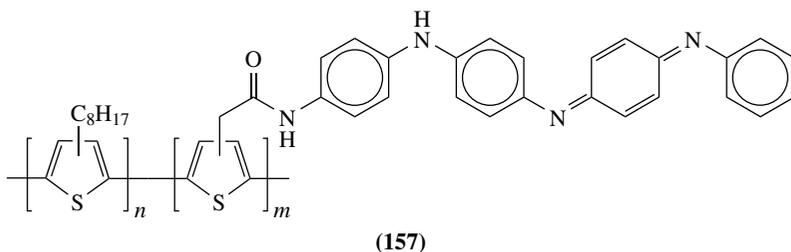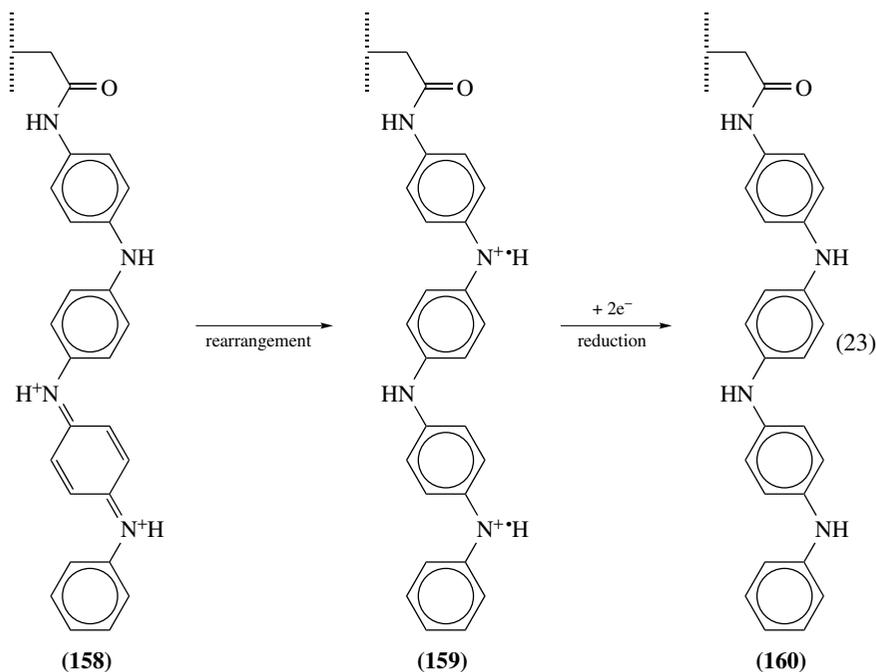
The electrophoretic mobility of a neutral base B in a buffer at a given pH is correlated to its thermodynamic dissociation constant. Such correlations were used for determination of the pK_a of HAA belonging to classes B and C of Table 2, by CZE-UVD (at 214 nm) of these compounds in buffers of pH from 3 to 9. The pK_a values obtained by the CZE method are the same as those obtained from UVV spectrophotometric measurements[256]. The pK_a values derived from these experimental measurements are different from those appearing in Table 2, because the latter values are purely calculated ones (see note a in the table).

C. Nuclear Magnetic Resonance

The structure of PBTA mutagens (**32a–h,** Table 2.D) was determined by various methods, including UVV spectrum, MS, HRMS, single crystal XRD (Section V.D) and ^{1}H NMR. All the protons of **32a** could be assigned by ^{1}H NMR spectroscopy; one of the singlets on the N-phenyl group was confirmed by ^{1}H NOESY[96, 257]; the structure elucidation of compounds **32a–h** was based on stepwise synthesis, starting from the corresponding Disperse Blue dyes (**67**), first by reduction of the nitro groups and finally by chlorination of the 2-phenylbenzotriazole product, each step being confirmed by ^{1}H NMR and other spectral evidence[99–101, 131, 257, 258]. The structural elucidation of mutagen **66** was based on various pieces of evidence, including UVV spectrum and HRMS, but mainly single crystal XRD (Section V.D) and ^{1}H NMR. Of the seventeen protons shown by the MS of **66** seven could be exchanged by D_2O, pointing to NH_2 and NH groups; the other protons could be assigned by ^{1}H–^{1}H COSY as belonging to two aromatic and one aliphatic ring systems. The ^{13}C NMR spectrum shows eighteen C atoms[89]. The structure of the pollutant **68** was demonstrated by ^{1}H NMR and COSY, MS and HRMS[107]. The structure of monochlorinated derivatives at positions 6 and 8 of norharman (**31a**) and

harman (**31b**) could be deduced on assignment of the peaks of the ^{1}H NMR spectrum of these compounds, based on the relative peak area, the chemical shift and the coupling constants[92].

Oligomeric quinolinamides (**161**), where X and Y are convenient end groups to enable addition of one further link to the chain, have been synthesized step by step up to the decamer ($n = 9$). Several structural features have been distinguished for the oligomers. The helical structure shown by XRD analysis (Section V.D) is presumably preserved also in solution, as attested by the ^{1}H NMR spectra of the oligomers. The same functional groups change their environment both according to the length of the oligomer and to their position along the peptidic chain. Thus, in CDCl$_3$ solution, each amide N−H proton of the peptide shows its own resonance peak in the δ 10 to 12.5 ppm region, at slightly different chemical shifts: one singlet for the dimer (**161a**, $n = 1$), δ 11.88 ppm, to nine singlets for the decamer (**161a**, $n = 9$), δ 11.33, 11.23, 10.96, 10.90, 10.79, 10.70, 10.66, 10.63 and 10.60 ppm. As the length of the oligomer grows, both the aromatic and the OC$\underline{H}_2$Pr-i protons show progressively more complex patterns in the 6 to 9 ppm and the 3 to 4 ppm regions, respectively. Even the singlet for the Y = OC$\underline{H}_3$ group, appearing only once in the molecule, progressively shifts upfield from 4.23 ppm for the dimer to 2.93 ppm for the decamer. Addition of the chiral shift reagent Eu(hfc)$_3$ (**162**) to a solution of **161a** ($n = 7$) results in splitting into two equally intense signals, pointing to no preferred helix chirality. The UVV spectrum of **161a** ($n = 1$ to 9) undergoes bathochromic shifts and hypochromic effects as the length of the oligomer increases; furthermore, the fluorescence of the quinoline structure is quenched, presumably by the nitro group[259]. Similar helical foldamers were reported for oligomers resulting from condensation of 2,6-pyridinediamine with 2,6-pyridinedicarboxylic acid (**163a**) and its hydroxy derivative (**163b**). XRD analysis also points to helical conformation (Section V.D)[260, 261]. Seven-ring strands of the **163** oligomer, carrying on both ends NHCO$_2$Bu-t groups, can form double helices of 7.2 Å pitch, both in solution and in crystalline state, as demonstrated by ^{1}H NMR, ^{1}H NOESY and single crystal XRD analysis. Stabilization of such structures is mainly due to π-stacking and, to some extent, to interstrand H-bonding[262, 263].

(161)

(**a**) X = NO$_2$, Y = OMe
(**b**) X = NH$_2$, Y = OMe

(162)
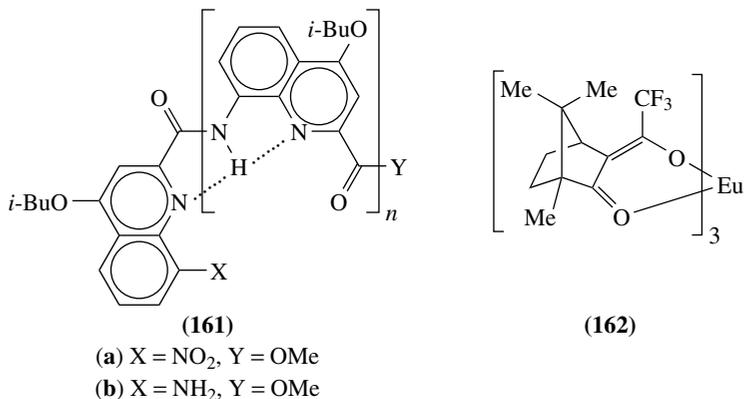
The chiral recognition capability of (+)-(*R*)-18-crown-6-2,3,11,12-tetracarboxylic acid (**164**) was investigated for a variety of amines. It proved to be an effective chiral shift reagent for amines containing aromatic rings. A fivefold equivalent concentration of **164** relative to the analyte is sufficient for chiral recognition; however, the observed shift depends on the deuterated solvent (D$_2$O, CD$_3$OD, CD$_3$CN) used for the ^{1}H NMR spectra. Thus, significant shifts were observed for methine and other protons of enantiomers of
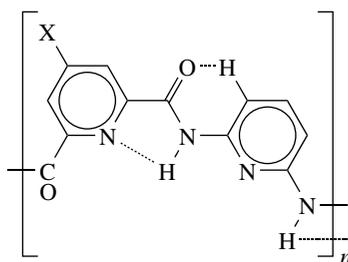
(163)

(**a**) X = H

(**b**) X = OH

nonaromatic amines such as 1-phenylethylamine (**165a**), 1-(1-naphthyl)ethylamine (**165b**), phenylglycine (**165c**), 4-hydroxyephedrine (**166**) or 1-aminoindan (**167**), and aromatic amines such as tryptophan (**168**), α-methyltryptamine (**169**), aminoglutethimide (**170**), primaquine (**171**) or alanine-2-naphthylamide (**172**). The general tendency was for the shift of D enantiomers in the presence of **164** to be more downfield than that of the L enantiomers, thus allowing clear separation of peaks and quantitative estimates of enantiomeric excess. **164** is ineffective for chiral recognition with amines devoid of aromatic rings[264].

(164)   **(165)**   **(166)**
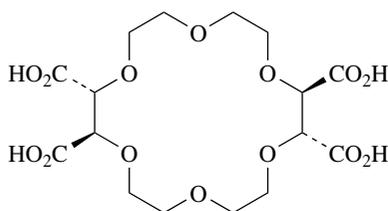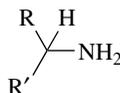
(**a**) R = Me, R′ = Ph

(**b**) R = Me, R′ = 1-Naph

(**c**) R = CO₂H, R′ = Ph
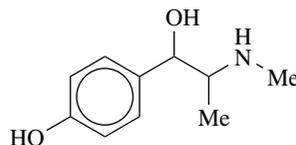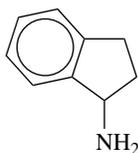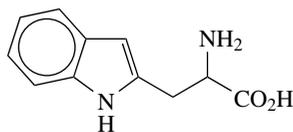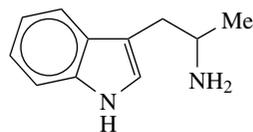
(167)   **(168)**   **(169)**

D. X-Ray Diffraction

The structure of mutagens 2-amino-5-[(3-aminophenyl)amino]-4-[(3-aminophenyl) imino]-2,5-cyclohexadien-1-one (**66**)[89] and PBTA-1 (**32a**)[96] was elucidated by single crystal XRD crystallography, which was supported by additional evidence from MS, UVV

(170)   **(171)**   **(172)**
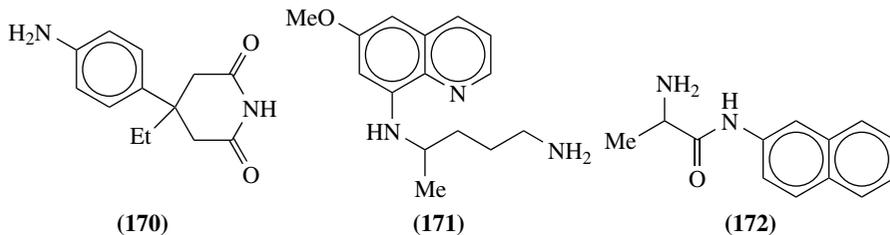
and especially NMR spectroscopies. In the case of **32a** the single crystal was that of the debrominated product, after hydrogenation with a Pd catalyst[96]. The analysis by XRD of the 6,12-epiiminodibenzo[b,f][1,5]diazocines **173a** and **173b** showed interesting features. The crystals of **173a** are assembled by intermolecular van der Waals forces and the configuration is racemic. In the case of **173b** two sets of intermolecular H-bonding exist, NH $\cdots$ NR and NH $\cdots$ OMe, causing distortions in certain bond lengths and bond angles, and the crystal contains a unique enantiomer (the one shown has R,R absolute configuration)[265].
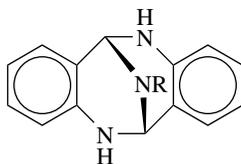
(173)
(**a**) R = Bn
(**b**) R = C$_6$H$_4$OMe-4

   Single crystal XRD analysis of the monomer **161a** ($n = 0$) points to the nitro group sitting in a plane almost perpendicular to that of the aromatic system, due to the strong repulsion between the O atom of the nitro group and the heterocyclic N; on reduction of the monomeric nitro compound to the corresponding amine (**161b**, $n = 0$) a planar configuration is attained with one NH$\cdots$N hydrogen bond between the amino group and the heterocyclic N (0.269 nm, 104°). The dimer (**161a**, $n = 1$) has almost planar configuration but is endowed with two NH$\cdots$N hydrogen bonds, one of dimensions similar to that of the monomeric amine (0.269 nm, 108°) and a slightly longer second one (0.272 nm, 126.5°). The double H-bond causes bending of the δ-aromatic peptide from the trimer ($n = 2$) onwards, leading to a helical conformation, with three peptidic links per turn, as shown by XRD. The pitch of the helix is 0.34 nm, the thickness of an aromatic molecule; from the tetramer ($n = 3$) onwards π-stacking is observed, but the quinoline moieties are not exactly aligned with one another. This leaves no room in the inner space of the helix to accommodate solvent molecules. The helical structure is presumably preserved also in solution, as attested by the ^{1}H NMR spectra of the oligomers (Section V.C). XRD analysis of oligomers **163** points to helical structures with a pitch of 3.5 Å and about 4.5 pyridine rings per turn, with solvent molecules occupying the inner space. The internal H-bonds stabilize the structure so that no tautomerization of **163b** to possible 4-pyridone structures

takes place. The helical conformation is preserved also in solution (Section V.C)[260, 261]. Seven-ring strands of the **163** oligomer, carrying on both ends $NHCO_2Bu$-t groups, can form double helices of 7.2 Å pitch, as shown by single crystal XRD analysis. Stabilization of such structures is due mainly to π-stacking and, to some extent, to interstrand H-bonding[262, 263].

The crystal and molecular structure was determined of the picrates (**174**) of aniline (**1a**), its N-Me derivatives, 1,2- (**1j**), 1,3- (**1k**) and 1,4-phenylenediamine (**1l**). Except for **1j**, combining with two picric acid molecules, the rest show 1:1 stoichiometry. The main structural feature is H-bonding of various strengths, with O−N distances from 267 pm for N-methylaniline to 288 pm for **1j**. The acid proton in these compounds sits on the N atom forming ammonium salts, as shown by the C1−O bond distances near 125 pm for a picrate anion, rather than 130 to 134 pm for picric acid or its π-complexes with benzene and PAH. The picrates of N-methylaniline and **1k** also show π-stacking to some extent, especially in the latter case[266].

(174)

Aniline was polymerized in aqueous solution in the presence of n-dodecylbenzenesulfonic acid (**175**) and ammonium persulfate, $(NH_4)_2S_2O_8$, to yield the corresponding salt of polyaniline (**176**), according to equation 24; at the end of the process, the excess **175** was removed to leave 1 equivalent for each 2 equivalents of aromatic amine. Similarly, the salt of **175** with aniline was treated with formaldehyde according to equation 25, to yield the salt of **175** with aniline-formaldehyde resin (**177**); in this case, however, the acid and base moieties were in a 1 to 1 ratio. After cleanup and removal of the solvent, solid products were obtained, which can be represented schematically as **178** and **179**. Solutions of both **178** and **179** were blended in various proportions and the solvent was evaporated to yield a solid. Evidence from a battery of analytical methods, including FTIR, ^{1}H NMR, ^{13}C cross-polarization−magic-angle spinning−NMR, and UVV spectroscopies, wide-angle XRD, ESCA and optical microscopy, was combined to characterize the structure of the salts of polyaniline (**176**) and aniline-formaldehyde resin (**177**), either alone or in the blend. The structure may contain residues stemming from the condensation of two hydroxymethyl groups to a dibenzyl ether structure (shown in **177**), or other functional groups (not shown). The pure solid has a laminar structure **178**, which can be disturbed on addition of the polymeric electrolyte represented schematically by **179** or the acid **175**[267].

(175 = ArSO₃H)   **(176)**   (24)

(25)

(177)

(178)

(179)

E. Ultraviolet-Visible Spectroscopy

Groups of aromatic amines may be distinguished by their difference absorption spectra, where spectra performed in neutral solution (pH 8) are compared to those taken in acidic solutions (pH 1.5). Thus, the difference spectra of the anilines show a slight hypsochromic shift of the bands from 290 to 280 nm and from 235 to 230 nm. On the other hand, the difference spectra of heterocyclic aromatic amines, such as pyridines, quinolines and isoquinolines, are characterized by the presence of strong negative bands, attributed to a hyperchromic effect caused by protonation[268].

The structural characterization of mutagen **66**, obtained on ozonization of an aqueous solution of 3-phenylenediamine (**1k**), was based mainly on MS, NMR and XRD evidence (Sections V.A, C and D), however the UVV spectrum was helpful in showing that it is not 2,7-phenazinediamine (**180**), another mutagen obtained on treatment of **1k** with hydrogen peroxide, or the plausible 3,3′-diaminoazoxybenzene (**181a**) and 3,3′-diaminoazobenzene (**181b**)[89].

(180)   **(181)** **(a)** X = O
                                  (b) X = nil
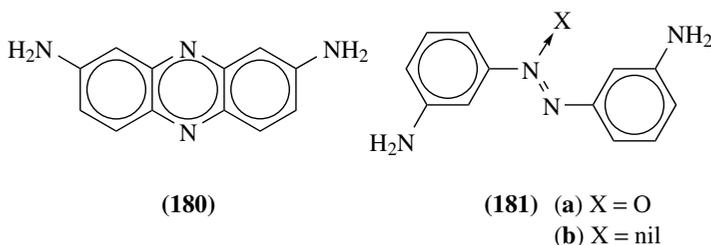
Aromatic amines carrying electronegative groups are proton donors capable of establishing strong H-bonds or even totally transferring the proton to good acceptors. This is illustrated in equations 26 and 27 for the complexes of bis(heptafluoro-4-tolyl)amine (**182**) with aliphatic amines to yield a H-bonded complex (**183**), which on addition of a second equivalent of aliphatic amine turns into a salt (**184**). Formation of the 1:1 and 1:2 species in an aprotic organic solvent can be followed by UVV spectrophotometry, at various temperatures, and K_1, K_2, ΔH and ΔS of the reactions can be determined. On forming the H-bonded complex, a red shift of λ_{max} is observed, from 35840 cm^{-1} for **182** to 34600 cm^{-1} for **183**, with some intensity enhancement; a larger red shift and intensity are observed for **184**, with maximum at 29680 cm^{-1}. The H-bond in **183** can be considered a strong one, with $\Delta H = -(12 \pm 2)$ kcal mol^{-1}. Some peaks related to H-bonding appear in the 500 cm^{-1} region of the IR spectra of these systems; however, they lack analytical value as diagnostic features[269].

(182)   **(183)**

$$(26)$$

(27)
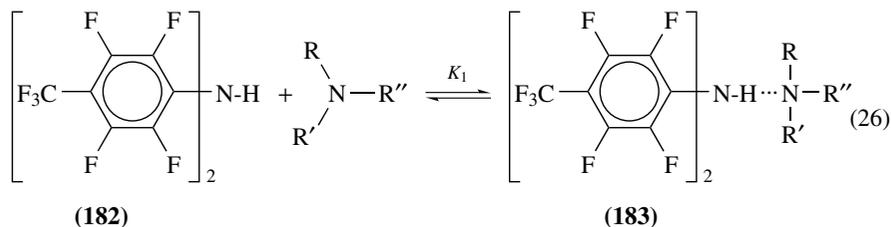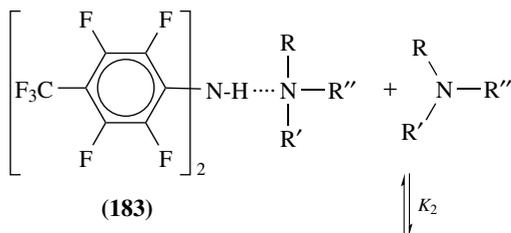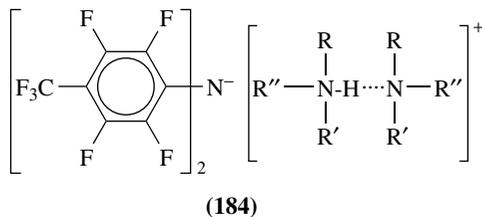
VI. REFERENCES

1. J. Zabicky and S. Bittner, in *The Chemistry of Amino, Nitroso, Nitro and Related Groups* (Ed. S. Patai), Wiley, Chichester, 1996, pp. 1041–1168.
2. H. M. Pinheiro, E. Touraud and O. Thomas, *Dyes Pigments*, **61**, 121 (2004).
3. Advanced Chemistry Development (ACD/Labs) Software V4.67 for Solaris (1994–2006 ACD/Labs), *SciFinder Scholar*, Chemical Abstracts Services, Columbus, OH, USA (2005).
4. EPA, *Toxics Release Inventory (TRI) Program*. (http://www.epa.gov/tri)
5. European Commission, *Off. J. Eur. Commun. L*, **243**, 15 (2002). (http://europa.eu.int/comm/enterprise/chemicals/legislation/markrestr/index_en.htm)
6. IARC, *Overall Evaluations of Carcinogenicity to Humans*, 2004. (http://www-cie.iarc.fr/monoeval/crthall.html)
7. EPA, *Water Quality Standards Database*. (http://oaspub.epa.gov/wqsdatabase/wqsi_epa_criteria.rep_parameter)
8. B. Scholz and N. Palauschek, *Fresenius Z. Anal. Chim.*, **331**, 282 (1988).
9. A. H. Neilson (Ed.), *The Handbook of Environmental Chemistry, Volume 3: Anthropogenic Compounds, Part J: PAHs and Related Compounds: Biology*, Lewis Publishers, Boca Raton, FL, 1997.
10. K.-T. Chung, L. Kirkovsky, A. Kirkovsky and W. P. Purcell, *Mutat. Res.*, **387**, 1 (1997).
11. R. Benigni, A. Giuliani, R. Franke and A. Gruska, *Chem. Rev.*, **100**, 3697 (2000).
12. L. S. Gold, N. B. Manley, T. H. Slone, L. Rohrbach and G. B. Garfinkel, *Toxicol. Sci.*, **85**, 747 (2005). (http://potency.berkeley.edu)
13. A. R. Cunningham, H. S. Rosenkranz, Y. P. Zhang and G. Klopman, *Mutat. Res.*, **398**, 1 (1998).
14. A. R. Cunningham, G. Klopman and H. S. Rosenkranz, *Mutat. Res.*, **405**, 9 (1998).
15. R. Benigni and A. Pino, *Mutat. Res.*, **421**, 93 (1998).
16. R. Franke, A. Gruska, A. Giuliani and R. Benigni, *Carcinogenesis*, **22**, 1561 (2001).
17. R. Benigni and L. Passerini, *Mutat. Res.*, **511**, 191 (2002).
18. S. C. Basak, B. D. Gute, D. Mills and D. M. Hawkins, *J. Mol. Struct. (Theochem)*, **622**, 127 (2003).
19. W. G. Stillwell, M. S. Bryant and J. S. Wishnok, *Biol. Mass Spectrom.*, **14**, 221 (2005).
20. L. S. DeBruin, J. P. Pawliszyn and P. D. Josephy, *Chem. Res. Toxicol.*, **12**, 78 (1999).
21. K. Gorlewska-Roberts, B. Green, M. Fares, C. B. Ambrosone and F. F. Kadlubar, *Environ. Mol. Mutag.*, **39**, 184 (2002).
22. K. Wakabayashi, Y. Totsuka, K. Fukutome, A. Oguri, H. Ushiyama and T. Sugimura, *Mutat. Res.*, **376**, 253 (1997).

23. T. Weiss and J. Angerer, *J. Chromatogr. B*, **778**, 179 (2002).
24. T. M. C. M. de Kok, H. J. J. Moonen, J. van Delft and F. J. van Schooten, *J. Chromatogr. B*, **778**, 345 (2002).
25. H. Sato and Y. Aoki, *Curr. Drug Metab.*, **3**, 311 (2002).
26. G. Talaska, A. Maier, S. Henn, A. Booth-Jones, Y. Tsuneoka, R. Vermeulen and B. L. Schumann, *Toxicol. Lett.*, **134**, 39 (2002).
27. H. Huang, A. Jemal, C. David, S. A. Barker, D. H. Swenson and J. C. Means, *Anal. Biochem.*, **265**, 139 (1998).
28. J. C. Means, P. D. Olsen and E. Schoffers, *J. Am. Soc. Mass Spectrom.*, **14**, 1057 (2003).
29. M. P. Chiarelli, H.-F. Chang, K. W. Olsen, D. Barbacci and B. P. Cho, *Chem. Res. Toxicol.*, **16**, 1236 (2003).
30. I. Zwirner-Baier and H.-G. Neumann, *Arch. Toxicol.*, **68**, 8 (1994).
31. I. Zwirner-Baier and H.-G. Neumann, *Arch. Toxicol.*, **72**, 499 (1998).
32. R. Pastorelli, G. Catenacci, M. Guanci, R. Fanelli, E. Valoti, C. Minoia and L. Airoldi, *Biomarkers*, **3**, 227 (1998).
33. C. J. Smith, G. L. Dooly and S. C. Moldoveanu, *J. Chromatogr. A*, **991**, 99 (2003).
34. G. Grimmer, D. Schneider, K. W. Naujack, G. Dettbarn and J. Jacob, *Polycycl. Aromat. Compd.*, **9**, 85 (1996).
35. J. W. Dallinga, G. R. M. M. Haenen, A. Bast and F. J. Van Schooten, *Biomarkers*, **7**, 291 (2002).
36. R. Stabbert, K.-H. Schäfer, C. Biefel and K. Rustemeier, *Rapid Commun. Mass Spectrom.*, **17**, 2125 (2003).
37. I. Zwirner-Baier, K. Deckart, R. Jäckh and H.-G. Neumann, *Arch. Toxicol.*, **77**, 672 (2003).
38. L. Li, M. P. Chiarelli, P. S. Branco, A. M. Antunes, M. M. Marques, L. L. Gonçalves and F. A. Beland, *J. Am. Soc. Mass Spectrom.*, **14**, 1488 (2003).
39. G. Grimmer, G. Dettbarn, A. Seidel and J. Jacob, *Sci. Total Environ.*, **247**, 81 (2000).
40. R. I. Freudenthal, E. Stephens and D. P. Anderson, *Int. J. Toxicol.*, **18**, 353 (1999).
41. S. Fronhoffs, T. Brüning, E. Ortiz-Pallardo, P. Bröde, B. Koch, V. Harth, A. Sachinidis, H. M. Bolt, C. Haberhold, H. Vetter and Y. Ko, *Carcinogenesis*, **22**, 1405 (2001).
42. H.-M. Chen, T. Qin, L.-X. Zhao and X.-B. Xu, *Ecotoxicology*, **11**, 255 (2002).
43. T.-A. Chiang, W. Pei-Fen, L. S. Ying, L. F. Wang and Y. C. Ko, *Food Chem. Toxicol.*, **37**, 125 (1999).
44. K. Skog, *Food Chem. Toxicol.*, **40**, 1197 (2002).
45. J. S. Felton and M. G. Knize, *Mutat. Res.*, **259**, 205 (1991).
46. K. Wakabayashi, M. Nagao, H. Esumi and T. Sugimura, *Cancer Res.* (Suppl.), **52**, 2092s (1992).
47. R. Vikse, A. Knapstad, L. Klungsoyr and S. Grivas, *Mutat. Res.*, **298**, 207 (1993).
48. M. Murkovic and W. Pfannhauser, *Fresenius J. Anal. Chem.*, **366**, 375 (2000).
49. J. S. Felton, P. Pais, C. P. Salmon and M. G. Knize, *Z. Lebensm. Unters. Forsch. A*, **207**, 434 (1998).
50. (a) B. Stavric, B. P.-Y. Lau, T. I. Matula, R. Klassen, D. Lewis and R. H. Downie, *Food Chem. Toxicol.*, **35**, 199 (1997).
    (b) E. Richling, C. Decker, D. Häring, M. Herderich and P. Schreier, *J. Chromatogr. A*, **791**, 71 (1997).
51. C. Byrne, R. Sinha, E. A. Platz, E. Giovannucci, G. A. Colditz, D. J. Hunter, F. E. Speizer and W. C. Wilett, *Cancer Epidem. Biomark. Prevent.*, **7**, 523 (1998).
52. B. M. Thomson, R. J. Lake, P. J. Cressey and M. G. Knize, *Proc. Nutr. Soc.*, 21 (1996).
53. K. Augustsson, K. Skog, M. Jägerstad and G. Steineck, *Carcinogenesis*, **18**, 1931 (1997).
54. B. Zimmerli, P. Rhyn, O. Zoller and J. Schlatter, *Food Addit. Contam.*, **18**, 533 (2001).
55. B. Stavric, B. P.-Y. Lau, T. I. Matula, R. Klassen, D. Lewis and R. H. Downie, *Food Chem. Toxicol.*, **35**, 185 (1997).
56. S. A. Nowell, J. S. Massengill, S. Williams, A. Radominska-Pandya, T. R. Tephly, Z. Cheng, C. P. Strassburg, R. H. Tukey, S. L. MacLeod, N. P. Lang and F. F. Kadlubar, *Carcinogenesis*, **20**, 1107 (1999).
57. M. G. Knize, K. S. Kulp, M. A. Malfatti, C. P. Salmon and J. S. Felton, *J. Chromatogr. A*, **914**, 95 (2001).
58. H.-S. Shin, W. J. Rodgers, E. A. Gomaa, G. M. Strasburg and J. I. Gray, *J. Food Protect.*, **65**, 1766 (2002).

59.	W. G. Stillwell, R. J. Turesky, R. Sinha, P. L. Skipper and S. R. Tannenbaum, *Cancer Lett.*, **143**, 145 (1999).
60.	J. Barret, P. Gijsman, J. Swagten and R. F. M. Lange, *Polym. Degrad. Stab.*, **76**, 441 (2002).
61.	Z. Moldovan and J. M. Bayona, *Rapid Commun. Mass Spectrom.*, **14**, 379 (2000).
62.	G. Skarping, M. Dalene and P. Brunmark, *Chromatographia*, **39**, 619 (1994).
63.	R. M. Machado, J. W. Mitchell, J. P. Bullock and B. E. Farrell, *Thermochim. Acta*, **289**, 177 (1996).
64.	SCF, *Provisional List of Monomers and Additives Notified to European Commission as Substances Which May Be Used in the Manufacture of Plastics or Coatings Intended to Come into Contact with Foodstuffs*, 2005. (http://europa.eu.int/comm/food/food/chemicalsafety/foodcontact/synoptic_doc_en.pdf)
65.	T. Six and A. Feigenbaum, *Food Addit. Contam.*, **20**, 960 (2003).
66.	K. Ellendt, B. Gutsche and G. Steiner, *Dtsch. Lebensm.-Rundsch.*, **99**, 131 (2003).
67.	B. Brauer and T. Funke, *Dtsch. Lebensm.-Rundsch.*, **87**, 280 (1991).
68.	C. Brede, I. Skjevrak and H. Herikstad, *J. Chromatogr. A*, **983**, 35 (2003).
69.	L. Copolovici and I. Baldea, *Anal. Bioanal. Chem.*, **374**, 13 (2002).
70.	D. Newcombe, A. Paszczynski, W. Gajewska, M. Kröger, G. Feis and R. Crawford, *Enz. Microb. Technol.*, **30**, 506 (2002).
71.	WHO, International Agency for Research on Cancer (IARC). (http://www.iarc.fr)
72.	DIN 53316, *Nachweis Bestimmer Azofarbstoffe in Leder*, Deutsches Institut für Normung, Berlin, 1997.
73.	L.-H. Ahlström, C. Sparr Eskilsson and E. Björklund, *Trends Anal. Chem.*, **24**, 49 (2005).
74.	M. Bhaskar, A. Gnanamani, R. J. Ganeshjeevan, R. Chandrasekar, S. Sadulla and G. Radhakrishnan, *J. Chromatogr. A*, **1018**, 117 (2003).
75.	M. C. Garrigós, F. Reche, M. L. Marín and A. Jiménez, *J. Chromatogr. A*, **976**, 309 (2002).
76.	C. Sparr Eskilsson, R. Davidsson and L. Mathiasson, *J. Chromatogr. A*, **955**, 215 (2002).
77.	S. Borrós, G. Barberá, J. Biada and N. Agulló, *Dyes Pigments*, **43**, 189 (1999).
78.	N. D. Lourenço, J. M. Novais and H. M. Pinheiro, *J. Biotechnol.*, **89**, 163 (2001).
79.	R. Brás, A. Gomes, M. I. A. Ferra, H. M. Pinheiro and I. C. Gonçalves, *J. Biotech.*, **115**, 57 (2005).
80.	I. C. Gonçalves, S. Penha, M. Matos, A. R. Santos, F. Franco and H. M. Pinheiro, *Biodegradation*, **16**, 81 (2005).
81.	N. D. Lourenço, J. M. Novais and H. M. Pinheiro, *Environ. Tech.*, **24**, 679 (2003).
82.	G. Carvalho, W. Delée, J. M. Novais and H. M. Pinheiro, *Color. Technol.*, **118**, 215 (2002).
83.	A. J. Greaves, J. H. Churchley, M. G. Hutchings, D. A. S. Phillips and J. A. Taylor, *Water Res.*, **35**, 1225 (2001).
84.	W. Brack, *Anal. Bioanal. Chem.*, **377**, 397 (2003).
85.	A. H. Neilson (Ed.), *The Handbook of Environmental Chemistry, Volume 3: Anthropogenic Compounds, Part I: PAHs and Related Compounds: Chemistry*, Lewis Publishers, Boca Raton, FL, 1997.
86.	G. Palmiotto, G. Pieraccini, G. Moneti and P. Dolara, *Chemosphere*, **40**, 355 (2001).
87.	T. Ohe, T. Watanabe and K. Wakabayashi, *Mutat. Res.*, **567**, 109 (2004).
88.	A. Cavallaro, V. Piangerelli, F. Nerini, S. Cavalli and C. Reschiotto, *J. Chromatogr. A*, **709**, 361 (1995).
89.	H. Kami, T. Watanabe, S. Takemura, Y. Kameda and T. Hirayama, *Chem. Res. Toxicol.*, **13**, 165 (2000).
90.	M. Černá, A. Pastorková, J. Šmid, H. Bavorová, D. Očadlíková, P. Rössner and J. Zavadil, *Toxicol. Lett.*, **88**, 191 (1996).
91.	J. Wu, M. K. Wong and H. K. Lee, *J. Chromatogr. Sci.*, **33**, 712 (1995).
92.	K. Nakano, K. Suyama, H. Fukazawa, M. Uchida, K. Wakabayashi, T. Shiozawa and Y. Terao, *Mutat. Res.*, **470**, 141 (2000).
93.	Y. Ono, I. Somiya and T. Kawaguchi, *Water Res.*, **30**, 569 (1996).
94.	T. Nobukawa and S. Sanukida, *Water Res.*, **36**, 989 (2002).
95.	(a) T. Ohe, N. Takeuchi, T. Watanabe, A. Tada, H. Nukaya, Y. Terao, H. Sawanishi, T. Hirayama, T. Sagimura and K. Wakabayashi, *Environ. Health Perspect.*, **107**, 701 (1999). (b) H. Moriwaki, H. Harino, H. Hashimoto, R. Arakawa, T. Ohe and T. Yoshikura, *J. Chromatogr. A*, **995**, 239 (2003).

96. H. Nukaya, J. Yamashita, K. Tsuji, Y. Terao, T. Ohe, H. Sawanishi, T. Katsuhara, K. Kiyokawa, M. Tezuka, A. Oguri, T. Sugimura and K. Wakabayashi, *Chem. Res. Toxicol.*, **10**, 1061 (1997).
97. T. Ohe, D. T. Shaughnessy, S. Landi, Y. Terao, H. Sawanishi, H. Nukaya, K. Wakabayashi and D. M. DeMarini, *Mutat. Res.*, **429**, 189 (1999).
98. (a) T. Shiozawa, K. Suyama, K. Nakano, H. Nukaya, H. Sawanishi, A. Oguri, K. Wakayabashi and Y. Terao, *Mutat. Res.*, **442**, 105 (1999).
 (b) T. Shiozawa, A. Tada, H. Nukaya, T. Watanabe, Y. Takahashi, M. Asanoma, T. Ohe, H. Sawanishi, T. Katsuhara, T. Sugimura, K. Wakabayashi and Y. Terao, *Chem. Res. Toxicol.*, **13**, 535 (2000).
99. H. Nukaya, T. Shiozawa, A. Tada, Y. Terao, T. Ohe, T. Watanabe, M. Asanoma, H. Sawanishi, T. Katsuhara, T. Sugimura and K. Wakabayashi, *Mutat. Res.*, **492**, 73 (2001).
100. T. Watanabe, H. Nukaya, Y. Terao, Y. Takahashi, A. Tada, T. Takamura, H. Sawanishi, T. Ohe, T. Hirayama, T. Sugimura and K. Wakabayashi, *Mutat. Res.*, **498**, 107 (2001).
101. T. Watanabe, T. Shiozawa, Y. Takahashi. T. Takahashi, Y. Terao, H. Nukaya, T. Takamura, H. Sawanishi, T. Ohe, T. Hirayama and K. Wakabayashi, *Mutagenesis*, **17**, 203 (2002).
102. T. Watanabe, Y. Takahashi, T. Takahashi, H. Nukaya, Y. Terao, T. Hirayama and K. Wakabayashi, *Mutat. Res.*, **519**, 187 (2002).
103. T. Morisawa, T. Mizuno, T. Ohe, T. Watanabe, T. Hirayama, H. Nukaya, T. Shiozawa, Y. Terao, H. Sawanishi and K. Wakabayashi, *Mutat. Res.*, **534**, 123 (2003).
104. A. Matsuoka, H. Sakamoto, S. Tadokoro, A. Tada, Y. Terao, H. Nukaya and K. Wakabayashi, *Mutat. Res.*, **464**, 161 (2000).
105. A. Matsuoka, A. Tada, Y. Terao, H. Nukaya, A. Önfelt and K. Wakabayashi, *Mutat. Res.*, **493**, 75 (2001).
106. H. Kataoka, T. Hayatsu, G. Hietsch, H. Steinkellner, S. Nishioka, S. Narimatsu, S. Knasmüller and H. Hayatsu, *Mutat. Res.*, **466**, 27 (2000).
107. T. Takamura-Enya, T. Watanabe, A. Tada, T. Hirayama, H. Nukaya, T. Sugimura and K. Wakabayashi, *Chem. Res. Toxicol.*, **15**, 419 (2002).
108. H. Börnick, T. Grischek and E. Worch, *Fresenius J. Anal. Chem.*, **371**, 607 (2001).
109. G. Liu and J. Yu, *Water Res.*, **39**, 2048 (2005).
110. M. Longo and A. Cavallaro, *J. Chromatogr. A*, **753**, 91 (1996).
111. C. M. Pace, J. R. Donnelly and J. L. Jeter, *J. AOAC Int.*, **79**, 777 (1996).
112. J. B. Forehand, G. L. Dooly and S. C. Moldoveanu, *J. Chromatogr. A*, **898**, 111 (2000).
113. W. L. Hinze, E. Pramauro, *CRC Crit. Rev. Anal. Chem.*, **24**, 133 (1993).
114. F. H. Quina and W. L. Hinze, *Ind. Eng. Chem. Res.*, **38**, 4150 (1999).
115. R. Carabias-Martínez, E. Rodríguez-Gonzalo, B. Moreno-Cordero, J. L. Pérez-Pavón, C. García-Pinto and E. Fernández Laespada, *J. Chromatogr. A*, **902**, 251 (2000).
116. Y.-C. Wu and S.-D. Huang, *Anal. Chim. Acta*, **373**, 197 (1998).
117. Y.-C. Wu and S.-D. Huang, *Analyst*, **123**, 1535 (1998).
118. D. L. Drabkin, *Bibliotheca Haematol.*, **21**, 33 (1964) (Pub. 1965).
119. C. Kutzer, B. Branner, W. Zwickenpflug and E. Richter, *J. Chromatogr. Sci.*, **35**, 1 (1997).
120. L. Zhu, L. Zhu and H. K. Lee, *J. Chromatogr. A*, **924**, 407 (2001).
121. L. Zhao, L. Zhu and H. K. Lee, *J. Chromatogr. A*, **963**, 239 (2002).
122. L. Zhu, C. B. Tay and H. K. Lee, *J. Chromatogr. A*, **963**, 231 (2002).
123. M. C. Garrigós, F. Reche, K. Pernías, A. Sánchez and A. Jiménez, *J. Chromatogr. A*, **819**, 259 (1998).
124. M. C. Garrigós, F. Reche, K. Pernías and A. Jiménez, *J. Chromatogr. A*, **896**, 291 (2000).
125. T. S. Oostdyk, R. L. Grob, J. L. Snyder and M. E. McNally, *J. Environ. Sci. Health A*, **30**, 783 (1995).
126. D. Martínez, M. J. Cugat, F. Borrull and M. Calull, *J. Chromatogr. A*, **902**, 65 (2000).
127. M. Fiori, C. Cartoni, B. Bocca and G. Brambilla, *J. Chromatogr. Sci.*, **40**, 92 (2002).
128. M.-C. Hennion, C. Cau-Dit-Coumes and V. Pichon, *J. Chromatogr. A*, **823**, 147 (1998).
129. M. Less, T. C. Schmidt, E. von Löw and G. Stork, *J. Chromatogr. A*, **810**, 173 (1998).
130. S. Kira, H. Horiguchi, Y. Nogami, T. Komatsu, K. Fujisawa, T. Ito and H. Hayatsu, *Bull. Environ. Contam. Toxicol.*, **59**, 941 (1997).
131. A. Oguri, T. Shiozawa, Y. Terao, H. Nukaya, J. Yamashita, T. Ohe, H. Sawanishi, T. Katsuhara, T. Sugimura and K. Wakabayashi, *Chem. Res. Toxicol.*, **11**, 1195 (1998).
132. B. Gawdzik and T. Matynia, *J. Chromatogr. A*, **733**, 491 (1996).

133. Waters, *Oasis Sample Extraction Products.* (http://www.suppliercd.com/scd10/WTRS0001/Attach/m0002399.pdf)
134. M. Bouzige, G. Machtalère, P. Legeay, V. Pichon and M.-C. Hennion, *Waste Manag.*, **19**, 171 (1999).
135. C.-S. Lu and S.-D. Huang, *J. Chromatogr. A*, **696**, 201 (1995).
136. S. Mishra, V. Singh, A. Jain and K. K. Verma, *Analyst*, **126**, 1663 (2001).
137. P. A. Guy, E. Gremaud, J. Richoz and R. J. Turesky, *J. Chromatogr. A*, **883**, 89 (2000).
138. G. A. Perfetti, *J. AOAC Int.*, **79**, 813 (1996).
139. L. Rivera, M. J. C. Curto, P. Pais, M. T. Galceran and L. Puignou, *J. Chromatogr. A*, **731**, 85 (1996).
140. M. G. Knize, C. P. Salmon. S. P. Mehta and J. S. Felton, *Mutat. Res.*, **376**, 129 (1997).
141. M. G. Knize, C. P. Salmon, E. C. Hopmans and J. S. Felton, *J. Chromatogr. A*, **763**, 179 (1997).
142. C. Mardones, L. Arce, A. Ríos and M. Valcárcel, *Chromotographia*, **48**, 700 (1998).
143. E. Richling, M. Kleinschnitz and P. Schreier, *Eur. Food Res. Technol.*, **210**, 68 (1999).
144. F. Toribio, E. Moyano, L. Puignou and M. T. Galceran, *J. Chromatogr. A*, **869**, 307 (2000).
145. B. Janoszka, L. Warzecha, U. Błaszczyk and D. Bodzek, *Acta Chromatogr.*, **14**, 129 (2004).
146. G. A. Gross and G. J. M. Grüter, *J. Chromatogr.*, **592**, 271 (1992).
147. C. De Meester, *Z. Lebensm.-Unters. Forsch. A*, **207**, 441 (1998).
148. F. Toribio, L. Puignou and M. T. Galceran, *J. Chromatogr. A*, **836**, 223 (1999).
149. L. B. Fay, S. Ali and G. A. Gross, *Mutat. Res.*, **376**, 29 (1997).
150. B. Janoszka, L. Warzecha, U. Błaszczyk and D. Bodzek, *Acta Chromatogr.*, **14**, 115 (2004).
151. M. M. C. Van Dyck, B. Rollmann and C. De Meester, *J. Chromatogr. A*, **697**, 377 (1995).
152. B. Janoszka, U. Błaszczyk, L. Warzecha, M. Strózyk, A. Damasiewicz-Bodzek and D. Bodzek, *J. Chromatogr. A*, **938**, 155 (2001).
153. J. O'Reilly, O. Wang, L. Setkova, J. P. Hutchinson, Y. Chen, H. L. Lord, C. M. Linton and J. Pawliszyn, *J. Sep. Sci.*, **28**, 2010 (2005).
154. R. Eisert and J. Pawliszyn, *Crit. Rev. Anal. Chem.*, **27**, 103 (1997).
155. Y.-C. Wu and S.-D. Huang, *Anal. Chem.*, **71**, 310 (1999).
156. L. Müller, E. Fattore and E. Benfenati, *J. Chromatogr. A*, **791**, 221 (1997).
157. W.-Y. Chang, Y.-H. Sung and S.-D. Huang, *Anal. Chim. Acta*, **495**, 109 (2003).
158. H. van Doorn, C. B. Grabanski, D. J. Miller and S. B. Hawthorne, *J. Chromatogr. A*, **829**, 223 (1998).
159. D. L. Heglund and D. C. Tilotta, *Environ. Sci. Technol.*, **30**, 1212 (1996).
160. S. A. Mersham, S. H. Lubbad and D. C. Tilotta, *J. Chromatogr. A*, **829**, 377 (1998).
161. D. C. Stahl and D. C. Tilotta, *Environ. Sci. Technol.*, **33**, 814 (1999).
162. J. Yang and F.-P. Tsai, *Anal. Sci.*, **17**, 751 (2001).
163. J. Yang, J.-W. Her and S.-H. Chen, *Anal. Chem.*, **71**, 3740 (1999).
164. J. Yang and J.-W. Her, *Anal. Chem.*, **72**, 878 (2000).
165. J. Yang and C.-P. Tsui, *Anal. Chim. Acta*, **442**, 267 (2001).
166. G. Hempel, *Electrophoresis*, **21**, 691 (2000).
167. S. Sentellas, E. Moyano, L. Puignou and M. T. Galceran, *Electrophoresis*, **24**, 3075 (2003).
168. B. Chiavarino, M. E. Crestoni, A. Di Marzio and S. Fornarini, *J. Chromatogr. B*, **706**, 269 (1998).
169. K. Kijima, H. Kataoka and M. Makita, *J. Chromatogr. A*, **738**, 83 (1996).
170. H. Kataoka and K. Kijima, *J. Chromatogr. A*, **767**, 187 (1997).
171. T. C. Schmidt, M. Less, R. Haas, E. von Löw and K. Steinbach, *Int. J. Environ. Anal. Chem.*, **74**, 25 (1999).
172. T. C. Schmidt, M. Less, R. Haas, E. von Löw, K. Steinbach and G. Stork, *J. Chromatogr. A*, **810**, 161 (1998).
173. T. C. Schmidt, R. Haas, E. von Löw and K. Steinbach, *Chromatographia*, **48**, 436 (1998).
174. R. Haas, T. C. Schmidt, K. Steinbach and E. von Löw, *Fresenius J. Anal. Chem.*, **359**, 497 (1997).
175. T. C. Schmidt, R. Haas, K. Steinbach and E. von Löw, *Fresenius J. Anal. Chem.*, **357**, 909 (1997).
176. J. M. Rosenfeld, *J. Chromatogr. A*, **843**, 19 (1999).
177. J. E. Bailey, *Anal. Chem.*, **57**, 189 (1985).
178. J. E. Bailey and C. J. Bailey, *Talanta*, **32**, 875 (1985).

179. N. R. Fratz, J. E. Bailey and C. J. Bailey, *J. Chromatogr.*, **331**, 109 (1985)
180. A. Pielesz, I. Baranowska, A. Rybak and A. Wochowicz, *Ecotoxicol. Environ. Safety*, **53**, 42 (2002).
181. T. Hayashi, M. Amino, G. Uchida and M. Sato, *J. Chromatogr. B*, **665**, 209 (1995).
182. A. C. Bratton and E. K. Marshall, Jr., *J. Biochem.*, **128**, 537 (1939).
183. A. J. Glazko, *Ther. Drug Monit.*, **9**, 53 (1987).
184. J. S. Annino, *Clin. Chem.*, **10**, 370 (1964).
185. R. Whelpton, G. Watkins and S. H. Curry, *Clin. Chem.*, **27**, 1911 (1981).
186. I. Escrig-Tena, L. Alvarez Rodríguez, J. Esteve-Romero and M. C. García-Alvarez-Coque, *Talanta*, **47**, 43 (1998).
187. M. Royo Herrero, A. Mellado Romero and J. Martínez Calatayud, *Talanta*, **47**, 223 (1998).
188. E. Orejuela and M. Silva, *Electrophoresis*, **26**, 2991 (2005).
189. J. A. F. de Silva and N. Stojny, *Anal. Chem.*, **47**, 714 (1975).
190. A. Asthana, D. Bose, A. Durgbanshi, S. K. Sanghi and W. T. Kok, *J. Chromatogr. A*, **895**, 197 (2000).
191. N. Ostah, G. Lawson, S. Zafar, G. Harrington and J. Hicks, *Analyst*, **125**, 111 (2000).
192. L. Zhang, J. You, G. Ping, L. Zhang, J. Duana, W. Zhang, Z. Liang and Y. Zhang, *Anal. Chim. Acta*, **494**, 141 (2003).
193. K. Uchikura, *Chem. Lett.*, **32**, 98 (2003).
194. E. Richling, D. Häring, M. Herderich and P. Schreier, *Chromatographia*, **48**, 258 (1998).
195. W. Wang, B. Spingler and R. Alberto, *Inorg. Chim. Acta*, **355**, 386 (2003).
196. A. Pielesz, *J. Mol. Struct.*, **511–512**, 337 (1999).
197. A. Van Overbeke, W. Baeyens and C. Dewaele, *Anal. Chim. Acta*, **321**, 245 (1996).
198. A. Plum, W. Engewald and A. Rehorek, *Chromatographia*, **57**, S243 (2003).
199. E. Barceló-Barrachina, E. Moyano, L. Puignou and M. T. Galceran, *J. Chromatogr. A*, **1023**, 67 (2004).
200. C. Krach and G. Sontag, *Anal. Chim. Acta*, **417**, 77 (2000).
201. Y. Zhu, M. Wang, H. Dua, F. Wang, S. Mou and P. R. Haddad, *J. Chromatogr. A*, **956**, 215 (2002).
202. L. Warzecha and M. Strózyk, *Chem. Anal.*, **43**, 807 (1998).
203. M. T. Galceran, P. Pais and L. Puignou, *J. Chromatogr. A*, **719**, 203 (1996).
204. P. Pais, E. Moyano, L. Puignou and M. T. Galceran, *J. Chromatogr. A*, **778**, 207 (1997).
205. E. Richling, M. Herderich, D. Häring and P. Schreier, *Fresenius J. Anal. Chem.*, **360**, 804 (1998).
206. F. Toribio, E. Moyano, L. Puignou and M. T. Galceran, *J. Chromatogr. A*, **948**, 267 (2002).
207. L. Warzecha, M. Strózyk, B. Janoszka, U. Błaszczyk and D. Bodzek, *Chem. Anal.*, **47**, 539 (2002).
208. H. Moriwaki, H. Harino, H. Hashimoto, R. Arakawa, T. Ohe and T. Yoshikura, *J. Chromatogr. A*, **995**, 239 (2003).
209. H. Moriwaki, H. Harino, T. Yoshikura, T. Ohe, H. Nukaya, Y. Terao, H. Sawanishi, K. Wakabayashi, H. Miyakoda and J.-F. Alary, *J. Environ. Monit.*, **6**, 897 (2004).
210. R. A. K. Rao, M. Ajmal, B. A. Siddiqui and S. Ahmad, *Environ. Monit. Assess.*, **54**, 289 (1999).
211. M. S. Narvekar and A. K. Srivastava, *J. Liq. Chromatogr. Relat. Technol.*, **26**, 85 (2003).
212. X. Huang, T. You, T. Li, X. Yang and E. Wang, *Electroanalysis*, **11**, 969 (1999).
213. F.-M. Matysik, F. Björefors and L. Nyholm, *Anal. Chim. Acta*, **385**, 409 (1999).
214. L. Piugnou, J. Casal, F. J. Santos and M. T. Galceran, *J. Chromatogr. A*, **769**, 293 (1997).
215. E. T. Bergström, D. M. Goodall, B. Pokrić and N. M. Allinson, *Anal. Chem.*, **71**, 4376 (1999).
216. J. C. Olsson, A. Dyremark and B. Karlberg, *J. Chromatogr. A*, **765**, 329 (1997).
217. J. J. Berzas Nevado, G. Castañeda Peñalvo and F. J. Guzmán Bernardo, *J. Liq. Chromatogr. Relat. Technol.*, **22**, 1975 (1999).
218. J. P. Quirino, Y. Iwai, K. Otsuka and S. Terabe, *Electrophoresis*, **21**, 2899 (2000).
219. L. Drahos and K. Vekey, *Rapid Commun. Mass Spectrom.*, **10**, 1309 (1996).
220. K. X. Wan, I. Vidavsky and M. L. Gross, *J. Am. Soc. Mass Spectrom.*, **13**, 85 (2002).
221. R. Wilson, *The Electrochemiluminescence Home Page*. (http://www.liv.ac.uk/Electrochemiluminescence/home1.htm)
222. J. W. Jorgenson and K. D. Lukacs, *Anal. Chem.*, **53**, 1298 (1981).
223. J. W. Jorgenson and K. D. Lukacs, *J. Chromatogr.*, **218**, 209 (1981).

224. J. W. Jorgenson and K. D. Lukacs, *Science*, **222**, 266 (1983).
225. A. Ferancová, E. Korgová, J. Labuda, J. Zima and J. Barek, *Electroanalysis*, **14**, 1668 (2002).
226. E. H. Seymour, N. S. Lawrence, M. Pandurangappa and R. G. Compton, *Microchim. Acta*, **140**, 211 (2002).
227. I. F. Abdullin, N. N. Chernysheva and G. K. Budnikov, *J. Anal. Chem.*, **57**, 629 (2002).
228. J. Wang, G. Rivas, D. Luo, K. Gai, F. S. Valera and N. Dontha, *Anal. Chem.*, **68**, 4365 (1996).
229. M. W. Urban, *Attenuated Total Reflectance Spectroscopy of Polymers*, The American Chemical Society, Columbus, OH, 1996.
230. J. L. Hopewell, G. A. George and D. J. T. Hill, *Polymer*, **41**, 8221 (2000).
231. J. L. Hopewell, G. A. George and D. J. T. Hill, *Polymer*, **41**, 8231 (2000).
232. (a) L. López-Martínez, P. L. López-de-Alba, L. M. de-León-Rodríguez and M. L. Yepez-Murrieta, *J. Pharm. Biomed. Anal.*, **30**, 77 (2002).
     (b) A. Ruiz Medina, M. C. Cano Garcia and A. Molina Diaz, *Anal. Lett.*, **35**, 269 (2002).
233. G. López-Cueto, S. Maspoch, J. J. Rodríguez-Medina and C. Ubide, *Analyst*, **121**, 407 (1996).
234. N. A. Zatar, A. Z. Abu-Zuhri and A. A. Abu-Shaweesh, *Talanta*, **47**, 883 (1998).
235. M. I. Evgen'ev, S. Yu. Garmonov, L. Sh. Shakirova and A. S. Brysaev, *J. Anal. Chem.*, **57**, 1103 (2002).
236. M. I. Evgen'ev, S. Yu. Garmonov and I. I. Evgen'eva, *J. Anal. Chem.*, **57**, 187 (2002).
237. V. N. Ivanova and V. A. Nadolinnyi, *Khim. Interesakh Ustoichivogo Razvitiya*, **11**, 353 (2003); *Chem. Abstr.*, **139**, 142964 (2003).
238. V. A. Nadolinnyi, V. N. Ivanova and S. N. Lunegov, *Khim. Interesakh Ustoichivogo Razvitiya*, **11**, 391 (2003); *Chem. Abstr.*, **139**, 239272 (2003).
239. M. Oyama, M. Yamanuki, T. Sasaki and S. Okazaki, *J. Chem. Soc., Perkin Trans. 2*, 1745 (2000).
240. M. Oyama, T. Higuchi and S. Okazaki, *J. Chem. Soc., Perkin Trans. 2*, 1287 (2001).
241. J. Mařík, A. Song and K. S. Lam, *Tetrahedron Lett.*, **44**, 4319 (2003).
242. B. Resende Freitas and J. Fernandes Magalhaes, *Rev. Bras. Cienc. Farmac.*, **41**, 191 (2005).
243. H. M. Suresh Kumar, R. S. Kunabenchi, J. S. Biradar, N. N. Math, J. S. Kadadevarmath and S. R. Inamdar, *J. Lumin.*, **116**, 35 (2006).
244. G. Johansen, K. Grini, K. Langseth-Manrique and K. H. Karstensen, *Talanta*, **43**, 951 (1996).
245. M. Catalá Icardo, C. Gómez Benito, A. Mellado Romero and J. Martínez Calatayud, *J. Flow Inject. Anal.*, **13**, 160 (1996).
246. V. G. Amelin and I. S. Kolodkin, *J. Anal. Chem.*, **56**, 182 (2001).
247. P. C. Pandey and H. H. Weetall, *Anal. Chem.*, **67**, 787 (1995).
248. I. S. Kozin, C. Gooijer and N. H. Velthorst, *Anal. Chim. Acta*, **333**, 193 (1996).
249. T. Sakai, *Anal. Sci.*, **17**, 1379 (2001).
250. Yu. M. Evtushenko, V. M. Ivanov and B. E. Zaitsev, *J. Anal. Chem.*, **57**, 624 (2002).
251. O. V. Kolninov, V. V. Kolesnikova and V. K. Milinchuk, *Nucl. Inst. and Meth., in Phys. Res. B*, **151**, 330 (1999).
252. Y. M. Issa, A. L. El-Ansary and W. Selim, *Anal. Lett.*, **31**, 131 (1998).
253. E. Richling. M. Herderich and P. Schreier, *Chromatographia*, **42**, 7 (1996).
254. H. Deng, Z. Zhang, Q. Deng and S. Zhao, *Rapid Commun. Mass Spectrom.*, **17**, 2233 (2003)
255. K. Buga, A. Majkowska, R. Pokrop, M. Zagorska, D. Djurado, A. Pron, J.-L. Oddou and S. Lefrant, *Chem. Mater.*, **17**, 5754 (2005).
256. S. D. Mendonsa and R. J. Hurtubise, *J. Chromatogr. A*, **841**, 239 (1999).
257. T. Shiozawa, K. Muraoka, H. Nukaya, T. Ohe, H. Sawanishi, A. Oguri, K. Wakabayashi, T. Sugimura and Y. Terao, *Chem. Res. Toxicol.*, **11**, 375 (1998).
258. T. Watanabe, H. Nukaya, Y. Terao, Y. Takahashi, A. Tada, T. Takamura, H. Sawanishi, T. Ohe, T. Hirayama, T. Sugimura and K. Wakabayashi, *Mutat. Res.*, **498**, 107 (2001).
259. H. Jiang, J.-M. Léger, C. Dolain, P. Guionneau and I. Huc, *Tetrahedron*, **59**, 8365 (2003).
260. V. Berl, I. Huc, R. G. Khoury and J.-M. Lehn, *Chem. Eur. J.*, **7**, 2798 (2001).
261. I. Huc, V. Maurizot, H. Gornitzka and J.-M. Léger, *Chem. Commun.*, 578 (2002).
262. V. Berl, I. Huc, R. G. Khoury, M. J. Krische and J.-M. Lehn, *Nature*, **407**, 720 (2000).
263. V. Berl, I. Huc, R. G. Khoury and J.-M. Lehn, *Chem. Eur. J.*, **7**, 2810 (2001).

264. Y. Machida, M. Kagawa and H. Nishi, *J. Pharm. Biomed. Anal.*, **30**, 1929 (2003).
265. P. Molina, A. Arques, A. Tárraga and M. del R. Obón, *Tetrahedron*, **54**, 997 (1998).
266. H. Takayanagi, T. Kai, S.-i. Yamaguchi, K. Takeda and M. Goto, *Chem. Pharm. Bull.*, **44**, 2199 (1996).
267. K.-S. Ho, T.-H. Hsieh, C.-W. Kuo, S.-W. Lee, J.-J. Lin and Y.-J. Huang, *Polym. Sci. Part A*, **43**, 3116 (2005).
268. A. Łabudzińska and K. Gorczyńska, *J. Mol. Struct.*, **349**, 469 (1995).
269. J. P. Castaneda, G. S. Denisov and V. M. Schreiber, *J. Mol. Struct.*, **560**, 151 (2001).

CHAPTER **13**

Manufacture and uses of the anilines: A vast array of processes and products

ANTHONY S. TRAVIS

Sidney M. Edelstein Center for the History and Philosophy of Science, Technology and Medicine, The Hebrew University of Jerusalem, Edmond J. Safra Campus, Givat Ram, Jerusalem 91904, Israel
Fax: +972 2 6586709;   e-mail: travis@cc.huji.ac.il

I. INTRODUCTION

Coal-tar derived aniline was the first synthetic organic chemical produced in bulk, through processes developed around 1860 by William Henry Perkin and others engaged in the early manufacture of synthetic dyestuffs. Initially it was the basis of the synthetic, or aniline, dye industry that grew mainly in Germany. In the 20th century, aromatic amines were transformed into products for the processing of rubber and synthesis of sulfonamide drugs and other therapeutic agents (see Chapter 1). Aryl amines also contributed to the development of novel polymers. The heterocyclic triaminotriazine melamine became commercially available in 1939, followed in the 1950s by aniline- and toluidine-derived polyurethanes, and later by aramids. Photographic and agricultural products, vulcanizing agents, antioxidants and curing agents for epoxy resins relied, and continue to rely, on the availability of a range of aryl amines. For a century, the manufacture of anilines for colorants was a leading industry, given stability from a spread of business activities. After the late 1970s, the industry reinvented itself, particularly through entry into the life sciences, namely pharmaceuticals, and agrochemicals.

While the consumption of aniline and other aryl amines in textile dye manufacture has fallen, certain products, particularly aniline, and heterocyclic aryl amines, notably melamine, are produced on a vast scale for use in the manufacture of rubber products and polymers. The growth in demand, and the move from coal to petrochemical feedstocks, stimulated the development of novel manufacturing technologies, particularly continuous vapor- and liquid-phase processes for aniline.

Newer uses for anilines include as high performance engineering plastics and organic semiconductors, and for traditional aniline pigments in dye diffusion thermal transfer (D2T2) and the photorealistic ink jet printer.

In this chapter, the emphasis is on manufacture of anilines and their conversions into useful products, including some that retain the aromatic amino group. *Anilines* is used with a broad meaning, to include congeners of anilines, *N*-alkylated and *N*-phenylated anilines, as well as naphthylamines and aminoanthraquinones and their derivatives. Synonyms are given in many instances, since several trade and common names, as well as earlier forms of nomenclature, particularly in cases where names include ring numbering for naphthalene derivatives, are often still in current usage for commercially important products. This is particularly significant due to the revival of interest in colorants and the intermediates from which they are derived for novel applications in new technologies. In a number of cases, the most recent production figures and manufacturing details for intermediates and products reviewed here, often considered proprietary knowledge, are not available.

II. MANUFACTURE OF ANILINE

A. Reduction of Nitrobenzene by Batch Processes

The traditional treatment of nitrobenzene (**1**) with iron and acid, called Béchamp reduction, was employed almost exclusively in the production of aniline (**2**) and many aromatic amines until the 1960s[1,2] (Scheme 1). The reduction is straightforward, and can also be achieved by catalytic hydrogenation, sodium sulfide reduction and zinc reduction with caustic soda. Nitrotoluenes and nitroxylenes are hydrogenated under pressure over a nickel catalyst supported on kieselguhr. The sulfide reduction is useful in selective reduction, such as of *m*-dinitrobenzene to *m*-nitroaniline.

$$4 \; \underset{(1)}{\overset{NO_2}{\bigcirc}} \; + \; 9Fe \; + \; 4H_2O \; \xrightarrow{H^+} \; 4 \; \underset{(2)}{\overset{NH_2}{\bigcirc}} \; + \; \underset{(3)}{3Fe_3O_4}$$
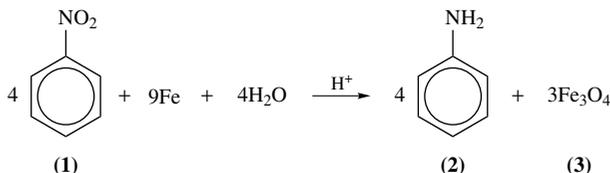
SCHEME 1

The iron–acid batch process continues to be used for certain reductions of nitro compounds. In particular, this process as applied to reduction of **1** to **2** remains viable where the iron is required in the form of the pigment Fe_3O_4 (**3**), as worked by Bayer in Germany since the 1920s. As recently as 2002, Bayer employed the process in the US for iron-oxide pigment manufacture at New Martinsville, using waste iron filings from automobile factories[3]. Additives and different types of iron determine the color of the iron oxide, as does calcination.

The Béchamp reduction of nitrobenzene to afford aniline is generally achieved in 90–95% yield. Reduction is brought about by continuous agitation in a reactor, with hydrochloric acid and iron turnings, and most recently with addition of iron(II) chloride. The rate of reaction is controlled by how deeply the agitator digs into the bed of iron, and the reaction can be followed by observing the color of the refluxing liquid. The removal of spent iron when the operation is conducted on a large scale for aniline alone presents a number of difficulties, both in handling and disposal.

Aniline is isolated by steam distillation. When pure it is a colorless oil. It boils at $184\,^\circ C$, and is slightly soluble in water, with K_b of 4.6×10^{-10}. It has a musty smell, and darkens on exposure to air.

B. Continuous Processes

Process improvements in the manufacture of aniline have been driven by tremendous demand, particularly from the rubber industry, and for use in the manufacture of isocyanates for polyurethanes, dyestuffs, sulfa drugs, agrochemicals, and detonators and stabilizers for explosives. Two widely used catalytic processes have been developed, one vapor phase, the other liquid phase. Both processes are highly exothermic, and the exchange and use of heat is important[4].

1. Continuous vapor-phase catalytic hydrogenation

Continuous vapor-phase catalytic hydrogenation of nitrobenzene, either fixed-bed or fluidized-bed, was originally developed by American firms in the 1950s, particularly American Cyanamid, encouraged by studies carried out at I.G. Farben during World War

II, and developments in petrochemical processes. A variation of the American Cyanamid process is operated by BASF[5].

American Cyanamid's catalytic aniline, or Catan, process for continuous fluid-bed, vapor-phase reduction of nitrobenzene was introduced at Willow Island, West Virginia, in 1958[6]. The Catan process was one of the earliest examples of penetration of fluidized-bed technology into the synthesis of organic chemicals, apart from production of petrochemical intermediates. Fluidization offered the advantages of high heat transfer within the bed and uniform temperature, and ready application to continuous processing[7]. Typically, the nitrobenzene is reduced to aniline by vapor-phase hydrogenation at $200-270\,^\circ C$ (around $300\,^\circ C$ in the BASF process) in a fluidized bed of, for example, copper-on-silica catalyst, promoted with chromium, zinc and barium, or cuproammonium nitrate catalyst (Scheme 2). Hydrogen, made from natural gas, is added in excess. The process can produce over 1,000 lbs. of aniline per hour. The reaction heat is employed in production of steam. Conversion efficiency is high, up to 98% (BASF claims over 99%), and the product is purer than from the iron reduction process, and more easily separated out. Catalyst regeneration involves burning off organic material. Reactivation is achieved by reducing the copper oxide to copper with hydrogen at around 200 to $300\,^\circ C$.

$$\text{NO}_2 \quad + \quad 3\text{H}_2 \quad \xrightarrow{\text{catalyst}} \quad \text{NH}_2 \quad + \quad 2\text{H}_2\text{O}$$

(1)   (2)
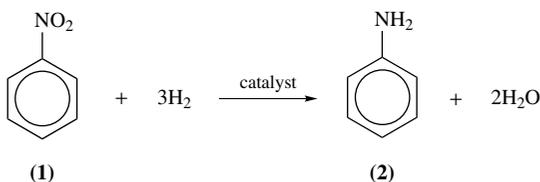
SCHEME 2

Typical catalysts for the fixed-bed vapor-phase hydrogenation include nickel sulfide deposited on alumina. For example, First Chemical Corporation (since 2002 a subsidiary of DuPont) employs the Lonza process, with a fixed-bed catalyst of copper on pumice. First Chemical is the world's second largest merchant producer of aniline, at Pascagoula, Mississippi, and Baytown, Texas, and supplies North American Bayer Corporation with its aniline requirements for polyurethanes[8]. Similar processes are operated by Bayer, with a palladium catalyst on an alumina support, modified with vanadium and lead. A catalyst of nickel sulfide on ammonia has also been revealed.

2. Continuous liquid-phase catalytic hydrogenation

From 1962, Imperial Chemical Industries (ICI), at Wilton, Teesside, England, developed a novel continuous liquid-phase hydrogenation process for aniline. The plant was commissioned in 1964[9]. The process operates at or near the boiling point of aniline, the solvent, which dissipates some heat through evaporation. Effluent vapors carry away water, and aniline is returned to the reactor to ensure steady-state conditions. Supported palladium, nickel or copper catalysts are employed. Liquid-phase catalytic hydrogenation is used to manufacture *p*-toluidine (4), xylidines (5) and benzidine congeners, such as tolidine (3,3′-dimethylbenzidine) (6). DuPont employs a platinum–palladium catalyst on a carbon support, with iron as modifier, providing extended catalyst life, high activity and also ensuring that hydrogenation of the aromatic ring does not take place[10, 11]. While the liquid-phase process has lower energy requirements than the vapor-phase process, it requires product–catalyst separation. Moreover, the vapor-phase process offers longer catalyst life, and efficient use of the heat of reaction.

CH₃

(4) 4-aminotoluene structure

(5) 2,4-dimethylaniline structure

(6) dimethylbenzidine structure

(Note: structures shown)
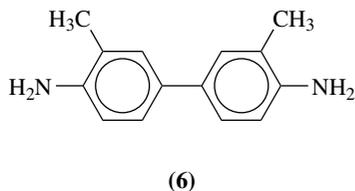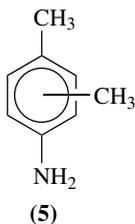
C. Other Processes

Amination (formerly often called ammonolysis) of chlorobenzene with aqueous ammonia, at $210\,^{\circ}$C and $60-70$ atmospheres, with a cuprous salt as catalyst, was employed in the manufacture of aniline until around 1970. Recently, a number of novel catalysts with potential for industrial application have been reported (see Section XXII.D).

Catalytic amination of phenol **(7)** at $425\,^{\circ}$C and around 200 atmospheres has been developed by Mitsui Petrochemical Industries of Tokyo. The nature of the catalyst is unspecified, though various metallic oxides and cocatalysts have been described. One Mitsui process employs a low alkali, weakly acidic alumina catalyst. Mild conditions, high yield and selectivity are claimed. Mitsui operates both the four-step phenol (starting from benzene) and two-step nitrobenzene processes[12].

In the Halcon process, the amination of **7** takes place in the vapor phase with a silica–alumina catalyst (Scheme 3). Amination of phenol has the advantage of reduced capital costs, long catalyst life and high quality product. Excess ammonia favors high conversion of the mildly exothermic ($\Delta H = -544\,\mathrm{kcal\,mol^{-1}}$) and reversible reaction, and also minimizes formation of byproducts. Generally, however, the price of phenol makes this process more expensive than the nitrobenzene routes. The last plant in the US to produce aniline from phenol by amination was operated by Sunoco Chemicals. It produced 140 million lbs./year^{-1}, with diphenylamine, or DPA **(8)** as a coproduct, at Haverhill, Ohio, and ceased production in 2002[13, 14]. Aristech Chemical Corporation at one time operated a phenol-to-aniline process in the US.

$$\text{(7)} + NH_3 \xrightarrow[\text{catalyst}]{\text{alumina-silica}} \text{(2)} + H_2O$$

SCHEME 3

(8) diphenylamine structure
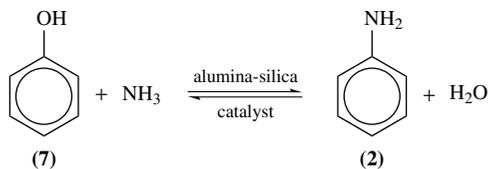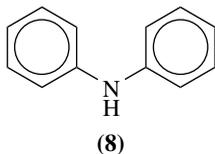
Direct amination of benzene in the presence of catalyst has been investigated by DuPont and Mitsui Toatsu. It has the advantage of the low cost of starting material. However, the process affords only 10% of desired product at each run, and requires high operating temperatures and pressures and excess ammonia[15].

Manufacture of aniline from toluene via benzoic acid has also been investigated for commercial use. A process involving amination of cyclohexanol has been reported[15].

Future trends in reduction of substituted nitrobenzenes will probably be based on novel catalysts. Homogenous transition metal (ruthenium and rhodium) catalysts offer routes to chemospecific reduction of aromatic nitro groups[16]. Novel catalytic methods involving combinatorial chemistry may offer pathways to new industrial hydrogenation processes, where selective reduction is desired. A number of solution- and solid-phase Cr^{II}/Mo^o redox couple reductions of substituted nitroarenes to the corresponding anilines have been proposed[17].

Biocatalytic regioselective reduction of dinitroarenes with baker's yeast has been claimed. However, under the reported conditions the yeast would normally be deactivated[18].

D. Scale of Production

The production of aniline is a major international business, carried on in the US, Europe and Asia, mainly for the conversion, by reaction with formaldehyde under acid-catalyzed conditions, into diaminodiphenylmethanes **9a, 9b** and **9c**, and then into isocyanates, mainly 4,4′-methylenebis(phenylisocyanate) (MDI, also known as 4,4′-methylene-di-paraphenylene isocyanate, 4,4′-diphenylmethane diisocyanate, methylene diphenylene diisocyanate and diisocyanato diphenyl methane) **(9d)**, from which polyurethanes are produced. This accounts for well over 60% of total demand (Figure 1). Aniline is also used in bulk for the production of antioxidants and vulcanization accelerators for rubber. Some 15.5 million lbs. of cyclohexylamine are made each year mainly by catalytic hydrogenation of aniline. Half the demand is for use as a boiler water additive. Other major uses include in the manufacture of herbicides, plasticizers, emulsifying agents, dyes, dry-cleaning soaps, acid gas absorbents and, in Asia, cyclamate sweeteners. Apart from India, the use of aniline for dyestuff manufacture represents about 10% of demand.

(**9a**) $R^1 = R^4 = NH_2$, $R^2 = R^3 = H$
(**9b**) $R^1 = R^2 = NH_2$, $R^3 = R^4 = H$
(**9c**) $R^1 = R^4 = H$, $R^2 = R^3 = NH_2$
(**9d**) $R^1 = R^4 = N-C=O$, $R^2 = R^3 = H$
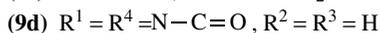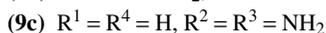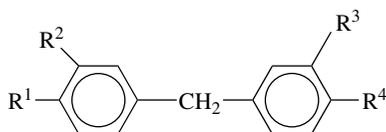
In recent years the aniline-for-isocyanates business has undergone extensive concentration and rationalization. In the US during the late 1990s, First Chemical built and operated a nitrobenzene and aniline facility at Baytown for Bayer's MDI **(9d)** production. Aniline capacity is 250 million lbs., dedicated to Bayer's requirements. A planned second-phase development will add a further 250 million lbs., bringing total capacity to 740 million lbs. Previously, First Chemical sent aniline to Baytown by barge from Mississippi[19]. During 2000, when BASF increased capacity at Geismar, Louisiana, to over 455 million lbs., there were five major domestic US producers of aniline, Huntsman, BASF, First Chemical, DuPont and Sunoco, compared with ten in 1997. The Huntsman aniline facility (Rubicon) at Geismar is the largest producer of aniline in the US, with a capacity of over 870 million lbs. Sunoco and Crompton were the major manufacturers of DPA **(8)**. In
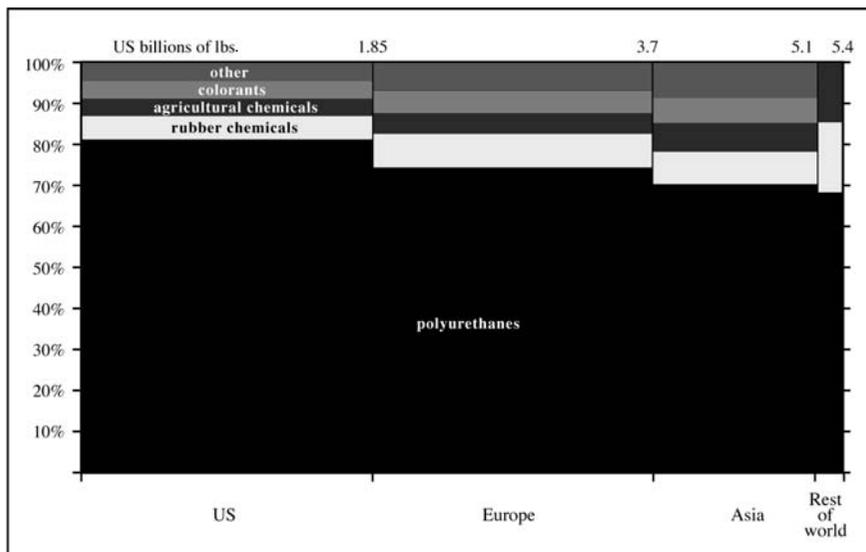
FIGURE 1. Worldwide aniline consumption, 2000

April 2000, Huntsman acquired the polyurethanes business of Imperial Chemical Industries (ICI), at Wilton, Teesside. Subsequent investments in the nitrobenzene and aniline facilities at Wilton brought aniline capacity there to over 300,000 metric tons during 2001, making this the largest aniline plant in the world. Huntsman's aniline is also supplied to its isocyanate facility at Rozenburg, near Rotterdam, the Netherlands. BASF at Antwerp in 1999 tripled aniline capacity there to 180,000 metric tons.

During the second half of the 1990s, annual demand for aniline in the US was 2.3 billion lbs., mainly for MDI. In 2000, US aniline production was 1,866 metric tons, for polyurethanes (80%), rubber chemicals (11%) and agricultural products (5%)[20]. The representative selling price of aniline was $0.27 per pound, relatively low due to the scale of production and competition. In 2003, production increased to 2,137 metric tons, an increase of 5.3% over 2002[21]. The US is a significant exporter of aniline. Except for Sunoco, major producers were aligned or integrated with the four main MDI producers. In 2002, First Chemical reactivated aniline production at its Mississippi site, closed since the opening of the Baytown facility, raising its total capacity to over 1000 million lbs.[22]. Demand for aniline in western Europe was expected to reach 1.2 million metric tons in 2005, based on 4.3% growth.

In Japan, Tosoh Corporation commenced construction in 2003 of a 160,000 metric tons per year plant at Nanyo, to supply Nippon Polyurethane Industry Co. Ltd, manufacturer of 170,000 metric tons per year of MDI (**9d**)[23]. Nippon also manufactures 25,000 metric tons per year of a blend of 2,4- and 2,6-toluene diisocyanates, TDI (**10a** and **10b**), by a process that involves toluidines as intermediates[24]. Tosoh has since embarked on construction of a new $159 million aniline plant. Japan produced 196,000 metric tons of aniline in 2005, based on 1.1% annual growth.

China is a relative latecomer to the aniline business, with extensive growth only in the 1990s. Nevertheless, by 2002, there were some 20 to 25 aniline producers, with total capacity of 280,000 metric tons per year, mainly by vapor-phase hydrogenation[25]. In 2000, Jiln Chemical Industries Corp., the only Chinese producer of MDI-grade aniline,

CH$_3$ CH$_3$ N(CH$_3$)$_2$

N=C=O   O=C=N   N=C=O

N=C=O

(a)   **(b)**

(10)   **(11)**
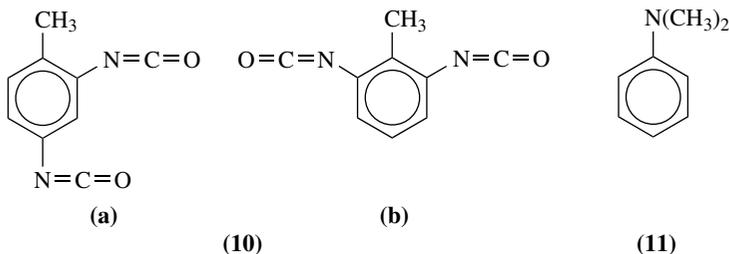
increased capacity to 66,000 tons[26]. In 2003, Lanzhou Chemical Industry Company began construction of a 70,000 ton aniline unit, the second largest of its kind in China[27]. Alkyl anilines are also produced on a large scale. In 2002, the Tianjin Ji County Chemical Industry General Plant increased N,N-dimethylaniline **(11)** production, using an upgraded gas synthesis process, to 6,000 metric tons per annum.

In India during 1995–1996, 29,665 tons of aniline were produced, of which approximately half was probably for the synthetic dye industry, 30% for rubber chemicals and 10% for pharmaceuticals. Other uses include in the textile, paper and metallurgical industries. Estimated Indian aniline demand for 2002–2003 was around 64,000 tons.

World annual production capacity of aniline in 2002 exceeded 2.70 million tons, and in 2005 was around 3.6 million tons, with market demand of 2.90 million tons.

Agrochemical use declined by about 3% in 2005. However, growth projections in 2003 suggested an annual increase of 4 to 5%, until 2010.

III. DIISOCYANATES AND POLYURETHANES

A. Introduction

Polyurethanes are esters of dicarbamic acids and glycols. Their production, by reacting diisocyanates with a dihydroxy alcohol such as ethylene glycol, began in Britain and the US in the mid-1950s, and soon after they were available on a commercial scale as adhesives, coatings (using a polyester resin instead of ethylene glycol), foams and elastomers[28]. The starting points in the manufacture of polyurethanes are nitrotoluenes and aniline, which are converted into isocyanates. The main aromatic isocyanates are what are commonly known as diphenylmethane diisocyanate (MDI) **(9d)**, and toluene diisocyanates (TDI) **(10a** and **10b)**. For polyurethanes, the former is preferred for environmental reasons. Spandex stretch fiber, based on polyurethanes, was first manufactured in the US in 1962 by DuPont, as Lycra.

B. Diphenylmethane Diisocyanate (MDI)

The first stage in the production of MDI **(9d)** is condensation between aniline and formaldehyde, in the presence of HCl, under subatmospheric pressure, at 70–105 °C. This affords 4,4′, 2,4′ and 2,2′ isomers of diaminodiphenylmethane **(9a, 9b** and **9c)**. Reaction with phosgene in an inert solvent, such as chlorobenzene, first at low temperature, and then heating to 120 °C, gives, for the 4,4′ isomer **(9a),** MDI, trimers, tetramers and higher oligomers, the latter known as poly-MDI or PMDI. Continuous liquid-phase phosgenation is favored.

The release of phosgene and toxic solvent has stimulated the development of novel processes. The BASF process for MDI, that employs high temperatures and pressures to increase the rate of reaction, does not release phosgene. Catalytic routes, via oxidative carbonylation of aniline to methyl N-phenyl carbamate **(12)**, using palladium metal

catalyst and alkali iodide promoter, or a cluster catalyst, have been developed in Japan (Scheme 4). The Hüls process (1995) for isophorone diisocyanate involves formation of carbamate from aryl amine, urea and alcohol[29]. MDI is used for rigid foams (insulation, structural components), elastomers and adhesives. Arco Chemicals has developed a process for polyisocyanates that involves selenium-catalyzed carbonylation of nitrobenzene.
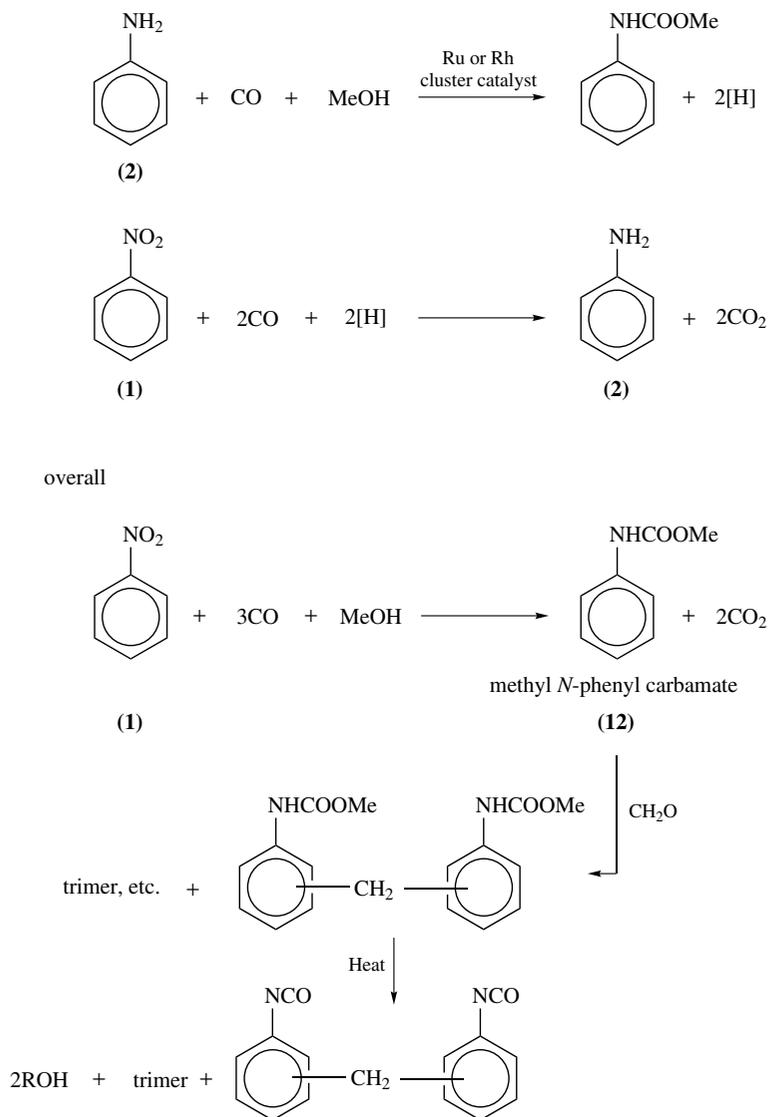
SCHEME 4. Carbonylation of aniline and nitrobenzene to methyl *N*-phenyl carbamate (Catalytica Associates, Nippon Kokan and Haldor Topsoe), and conversion to isocyanates

The Bayer Baytown isocyanate plant received an almost $1 billion investment in the late 1990s, at which time First Chemical constructed the adjacent aniline plant dedicated to Bayer's requirements. Other firms at Baytown supply nitric acid and formaldehyde. This industrial park concept with a full range of support services supplied by the host company, in this case Bayer, has been popular in Europe for several years, and is rapidly gaining favor in the US[30].

C. Toluene Diisocyanate (TDI)

TDI (**10a** and **10b**) is prepared from *o*-nitrotoluene, which is first nitrated to afford 1,4- and 1,5- dinitro isomers. These products are hydrogenated to the corresponding diamines, at 74 °C, over a palladium-on-carbon catalyst. This is the only major use of toluene diamines. On phosgenation, using chlorobenzene as solvent, at around 52 °C, the amines afford the diisocyanates. The TDI is used in the manufacture of flexible foams (upholstery, bedding, seat cushions, etc.), paints, surface coatings, elastomers and adhesives. 1,5-Diaminonaphthalene (**13**) is converted into naphthalene-1,5-diisocyanate (**14**) (Scheme 5), used in specialty polyurethanes.

(13)   **(14)**
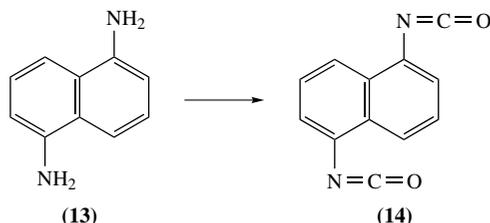
SCHEME 5

The ingredients for polyurethane flexible foam are Freon 11, polyether polyol-triol, polyurethane and TDI. Polyurethane fire-resistant rigid foam is produced from Freon 11, polyether polyol-hexol, polyether polyol-phosphorus, polyisocyanates and polyurethane. MDI foam has advantages over TDI foam, particularly in that it is easier and safer to handle, and for this reason is widely used as a thermal insulation. Flexible foams account for over 60% of the consumption of polyurethanes[31, 32].

IV. INTERMEDIATES FOR DYESTUFFS

A. Introduction

During the 1860s, the manufacture of intermediates based on aniline and its congeners laid the foundations of the synthetic dyestuffs industry. These intermediates were used mainly in the production of triphenylmethane and azo dyes. At the end of the 20th century, the two most important dye classes were azo and anthraquinone vat dyes, though triphenylmethane (more correctly triarylmethane) dyes were, and remain, significant contributors to the overall output. Competition from fiber-reactive dyes has reduced demand for vat dyes.

Dyes may be classified according to chemical constitution or end uses. Those made from aromatic amines, or containing aryl amine moieties, include:

Acid: Anionic: Sodium sulfonates of azo, anthraquinone, triarylmethane, azine, and xanthene.

Basic: Cationic: azo, acridine, anthraquinone, oxazine, thiazine, triarylmethane, and xanthene.

Direct: Anionic and sodium sulfonates of azo, stilbene, oxazine, and thiazole.

Fluorescent brightening agents: Anionic, cationic, or nonionic: stilbene, triazine, coumarin, and oxazole compounds.

Mordant: Anionic, similar to acid dyes, but requiring treatment with a metal salt.

Solvent: Nonionic, free acid or base forms of azo, anthraquinone, xanthene and triarylmethane products.

Sulfur: Anionic, obtained by heating arylamines with sulfur or polysulfides. Indeterminate chemical constitution.

Vat: Derivatives of indigo, anthraquinone and heterocyclic quinones.

The following sections summarize the main routes from anilines to various classes of intermediates, many of which are highly versatile. Following diversification during the era of the coal-tar dye industry, they have been transformed into chemicals vital to the manufacture of agricultural, pharmaceutical and rubber products. While the technologically mature colorants business in Europe and the US has declined, particularly since the 1980s, there has been considerable growth in Asia, most recently in China.

Significant changes in the manufacture of important naphthylamine and aminoanthraquinone intermediates since the 1960s have been stimulated by environmental and toxicity considerations.

B. Intermediates for Triphenylmethane and Azo Dyestuffs

Aryl amine intermediates for azo and triphenylmethane dyes, as well as a number of vat dye (anthraquinone) intermediates, are made from compounds such as benzene, alkyl benzenes (toluene and higher homologues), phenol and naphthalene. A limited number of reactions are used to produce the most important dye intermediates, including nitration, reduction, halogenation, sulfonation, *N*-alkylation, *N*-acylation and alkali fusion[33, 34].

Manufacture of many important amino intermediates used for dyes and other purposes is usually by conversion or replacement of a substituent. For example, as already mentioned, in substituted nitro compounds, the nitro groups may be reduced with iron/hydrochloric acid, hydrogen and catalyst, or zinc in aqueous alkali. Partial reductions can be brought about with sodium sulfide. Amino groups may be introduced by replacing halogens in the aromatic ring. Another approach to amination is by attack on a substituted aromatic compound with ammonia or amines. Thus, for example, direct amination of *p*-chloronitrobenzene **(15a)** in the presence of a copper catalyst affords *p*-nitroaniline **(15b)** in almost quantitative yield; 1,4-dichloro-2-nitrobenzene **(16)** is converted in a similar way to 4-chloro-2-nitroaniline **(17)**. Reactions of ammonia with carboxylic acids or anhydrides are carried out on an industrial scale.
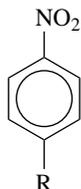
(15a) R = Cl
(15b) R = NH$_2$
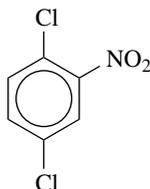
(16)
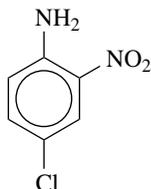
(17)
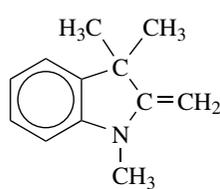
(18)

A typical example of the use of aniline is in the manufacture of Fischer's base, 1,3,3-trimethyl-2-methyleneindoline **(18)**, employed in the manufacture of basic dyes, including Astrazons (Bayer)[35].

Apart from its use in the synthesis of dyes, *m*-aminophenol **(19)** is used in the manufacture of agrochemicals, pharmaceuticals and specialty polymers. *N*,*N*-dimethyl-*m*-aminophenol **(20)** is used in the manufacture of fluorescent dyes and pharmaceuticals.

(19) **(20)**
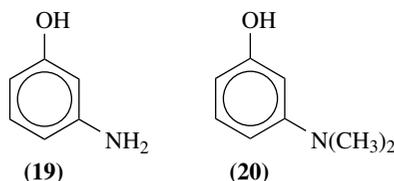
1. Nitroanilines and derivatives

Nitroanilines are employed extensively in dye manufacture. Amination of *o*-chloronitrobenzene, at $175\,^{\circ}C$ and 40 atmospheres, affords *o*-nitroaniline. Partial reduction of *m*-dinitrobenzene gives the corresponding *meta*-derivative. The *para*-isomer **15b** is used more extensively than the other nitroanilines in dye manufacture. In addition to amination of *p*-chloronitrobenzene, it can be made by nitration of acetanilide to yield **(21)**, followed by hydrolysis.

There are two good routes from **15b** to *p*-phenylenediamine **(22)**, namely reduction with Na_2S_3 in aqueous solution, and acid/iron reduction. It is also made by the action of ammonia on *p*-dichlorobenzene under pressure. The *p*-aminoacetanilide **(23)** is made by reduction of the nitro-precursor **21**.

(21) **(22)** **(23)**
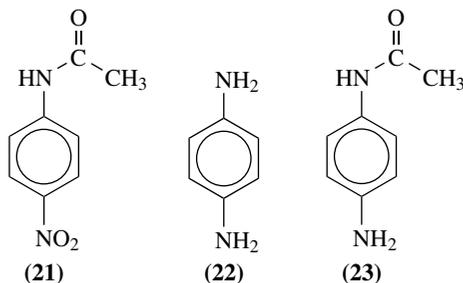
2. Alkoxy derivatives

Alkoxy derivatives of aniline are manufactured for use in dye and pharmaceutical production. Thus the action of methanol and sodium hydroxide on *o*-chloronitrobenzene, followed by reduction, yields *o*-anisidine (*o*-methoxyaniline) **(24a)**. The *para*-isomer **24b** is prepared in a similar way. Both are used for azo dyes and azoic intermediates. The ethoxy derivatives, *o*-phenetidine **(24c)** and *p*-phenetidine **(24d)**, are used in dye manufacture. The amine **24d** is also used to make Phenacetin (acetophenetidine) **(25)**.

3. N-Alkylation and N-arylation

Alkylations of anilines with alcohols, often with acid catalyst, afford *N*-substituted mono-and dialkyl anilines. The monomethyl product *N*-methylaniline is made by heating
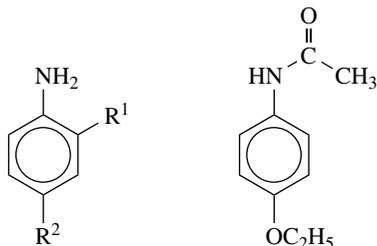
(24a) $R^1 = OCH_3$, $R^2 = H$ (25)
(24b) $R^1 = H$, $R^2 = OCH_3$
(24c) $R^1 = OC_2H_5$, $R^2 = H$
(24d) $R^1 = H$, $R^2 = OC_2H_5$

methanol with aniline and sulfuric acid under pressure. With excess methanol, the dimethyl derivative **11** is formed. The *N*-ethylaniline **26** is obtained by heating aniline hydrochloride with ethanol under pressure. In addition to their widespread uses in dye manufacture, alkyl anilines are employed as promoters for polyester resins, in the production of penicillins and cephalosporins, insecticides and fungicides, and building and construction materials.

(26)

Alkylation of amino group nitrogens can also be brought about with alkyl halides, with ethylene oxide, to yield hydroxyethyl, or with $CH_2=CHCN$, to give cyanoethyl derivatives. An interesting coupling component for a blue dye is made by ethoxylation of 3-amino-4-methoxyacetanilide **(27)** with ethylene oxide, followed by acetylation, to afford the desired 3-diacetoxyethylamino-4-methoxyacetanilide **(28)** (Scheme 6).

New processes include synthesis of *N*-alkylated anilines from olefins and aniline in an inert solvent with at least one catalyst from a range that includes alkali metal alcoholates, alkaline earth metal alcoholates, alkali metal amides and alkaline earth amides[36]. The uses for *N,N*-dimethylaniline **(11)** include in the manufacture of polyester resins, sulfur recovery (in copper refining), insecticides and fungicides, dyes, pharmaceuticals, explosives, rubber products, specialty isocyanates and petroleum additives. The *N*-ethylaniline **(26)** is a dye intermediate and rubber additive, and is used for burn control in explosives, while *N,N*-diethylaniline is used in production of polyester resins, pharmaceuticals, diazo prints (lithographic), and dyes, and as a petroleum additive[37].

Arylation involves the reaction between amines and phenols, aryl halides and aryl amines, including aniline. In arylation, one reactant acts as solvent; acidic catalysts and high temperatures are employed. Diphenylamine (*N*-phenylbenzeneamine, *N*-phenylaniline) **(8)** is made by: condensation of aniline in the presence of a small amount of mineral acid catalyst at around 300 °C; catalytic reaction of chlorobenzene with aniline at high temperature and pressure; and continuous vapor-phase catalytic condensation of aniline. It is a useful intermediate in azo dye manufacture. Crompton is the main US manufacturer of **8**, producing 1.3 billion lbs. in 2000. Applications include as lube additives

SCHEME 6

(45%), in rubber chemicals (45%), as a bridged diphenyl fungicide and in the synthesis of phenothiazine. Annual growth for anilines in the lube business is around 6%.

4. Aniline derivatives from chloronitrobenzene

Monochloroanilines are made by reduction of chloronitrobenzenes with either iron/acid or, nowadays, mainly catalytic hydrogenation. Catalysts include platinum, copper chromite and rhenium in conjunction with palladium[38]. The chloroanilines are used in the manufacture of colorants, agricultural products, pharmaceuticals and polymers. For example, *o*-chloronitrobenzene **(29)** is a source of *o*-nitroaniline, *o*-phenylenediamine (1,2-benzenediamine) **(30)**, *o*-aminophenol **(19b)**, *o*-chloroaniline and 3,3′-dichlorobenzidine **(31a)**. The *o*-phenylenediamine **(30)** is a particularly versatile intermediate, used to prepare thioureidoformates. Ring-substituted *o*-phenylenediamines with cyanoesters yield benzimidazoles that, on condensation with an aldehyde, followed by treatment with H_2S, give a range of thioureas.

(29a) $R^1 = Cl$, $R^2 = H$ (30)
(29b) $R^1 = H$, $R^2 = Cl$

(31a) R = Cl
(31b) R = H

Analogous *para*-isomers are obtained from *p*-chloronitrobenzene **(29b)**. Thus amination with aqueous ammonia at 180 °C and 40 atmospheres gives *p*-nitroaniline **(15a)**, a useful dye intermediate, manufactured by batch or continuous processes. With sodium sulfide, 4,4′-diaminodiphenyl sulfone (4,4′-sulfonyldianiline), also known as dapsone **(32)**, is obtained, a product used in leprosy treatment and in the manufacture of aramides. **15a**

(32)

is also converted into *N*,*N*′-dialkylated *p*-phenylenediamines by condensation with an alkylamine, followed by reductive alkylation.

Chlorination of *p*-nitrochlorobenzene followed by reduction yields 3,4-dichloroaniline, though the process suffers from the presence of *p*-chloroaniline and 2,5-dichloroaniline (from *o*-nitrochlorobenzene in the starting material). A purer product is formed by nitration of *o*-dichlorobenzene followed by reduction.

5. N-Acyl derivatives

Treating aniline with acetic anhydride, or refluxing together aniline with glacial acetic acid, yields acetanilide **(21)**. Nitration with mixed acids affords *p*-nitroacetanilide; hydrolysis of the acetyl group gives *p*-nitroaniline **(15b)**.

6. Aminobenzenesulfonic acids

Sulfonation of anilines is achieved by direct and indirect processes. The direct process is carried out at low temperatures with strong sulfuric acid, or with acid and sulfur trioxide. Substitution at the *para* position is generally favored, though the basicity of the amine and presence of other substituents can lead to formation of isomers. The indirect process requires baking, at high temperature, of amine acid sulfate. The intramolecular rearrangement favors single products, and is useful for introducing substituents at the *para* position when both *ortho* and *para* positions are available.

o-Chloronitrobenzene **(29a)** yields, in four steps, aniline-2-sulfonic acid (orthanilic acid) **(33a)**, that rearranges to sulfanilic acid (aniline-4-sulfonic acid) **(33b)** on heating in sulfuric acid. The product **33b** is also made by baking aniline sulfate at approximately 200 °C. It is used in the manufacture of azo dyes, including tartrazine **(34)** (Scheme 7).

Metanilic acid, the trivial name for *m*-aminobenzenesulfonic acid (aniline-3-sulfonic acid), is made by sulfonation of nitrobenzene, followed by Béchamp reduction. It is used in reactive dyes and optical bleaching agents, or brighteners, that are added to detergents.

7. Benzidine congeners

The highly carcinogenic benzidine, 4,4′-diaminobiphenyl **(31b)**, was formerly made by reduction of nitrobenzene to hydrazobenzene, with subsequent rearrangement. Similar methods are used to prepare substituted benzidines that are believed to be non-mutagenic and non-carcinogenic. The 3,3′-dichloro derivative is a suspected carcinogen.

8. Aminonaphthalenes

These are important coupling components used in the manufacture of azo dyes. While reduction of the nitro precursors can be used to prepare aminonaphthalenes, the Bucherer reaction, replacement of hydroxy by amino group, is often preferred. Thus if 2-naphthol

(29a) ⟶

NH$_2$

SO$_3$H

(33a)

SO$_3$H

NH$_2$

(33b)

SO$_3$H

N$_2^+$Cl$^-$

SO$_3^-$Na$^+$

N

N

O

COO$^-$Na$^+$

N   N

SO$_3^-$Na$^+$

tartrazine (as tri-sodium salt)

(34)

SCHEME 7

OH

(35)

NH$_2$

(36)

NO$_2$

(37)

NH$_2$

(38)
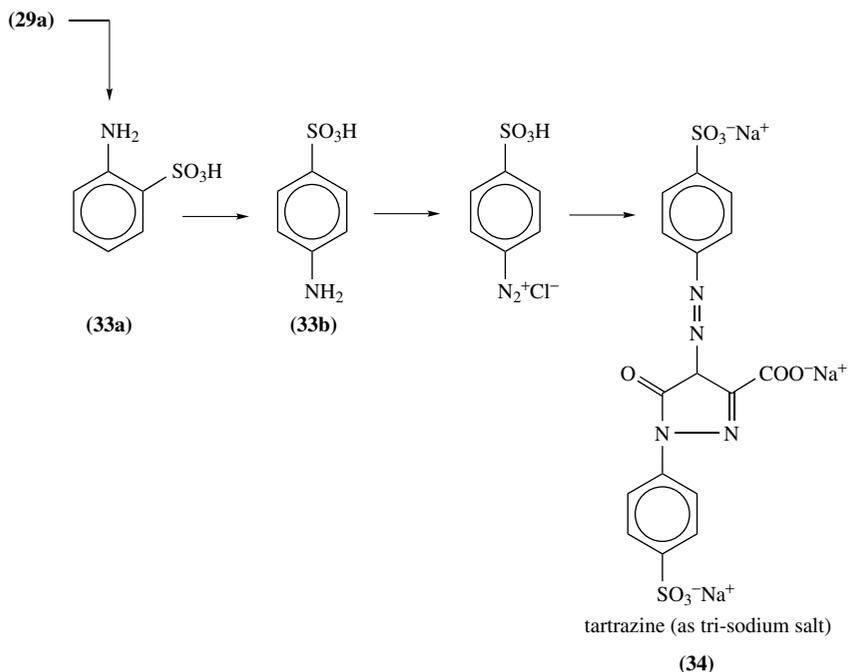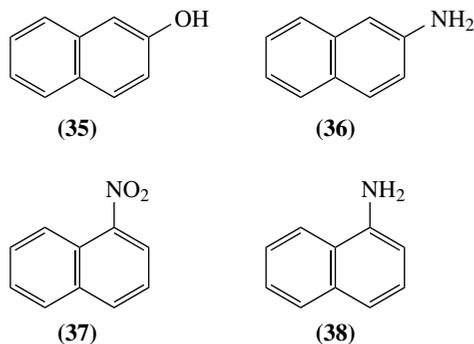
(35) is heated with aqueous ammonium sulfite or bisulfite in an autoclave, the corresponding amine, 2-naphthylamine **(36)**, is produced in high yield. Since **36** is a potent carcinogen, it has not been generally employed in dye manufacture since the 1950s.

Reduction of 1-nitronaphthalene **(37)**, for example with hydrogen and a nickel catalyst, or by amination of 1-chloronaphthalene, yields the 1-amino isomer **38**. It displays the behavior of primary aromatic amines, affording acyl derivatives and salts with strong acids. Coupling with diazo intermediates is mainly at the 4-position. Nitration of 1-nitronaphthalene **(37)** yields mixed 1,5- and 1,8-dinitronaphthalenes, **(39)** and **(40)**, which on reduction in nonaqueous solution with iron and hydrogen give the corresponding 1,5- **(13)** and 1,8- **(41)** diamino isomers (Scheme 8). Of the ten isomeric diamines,
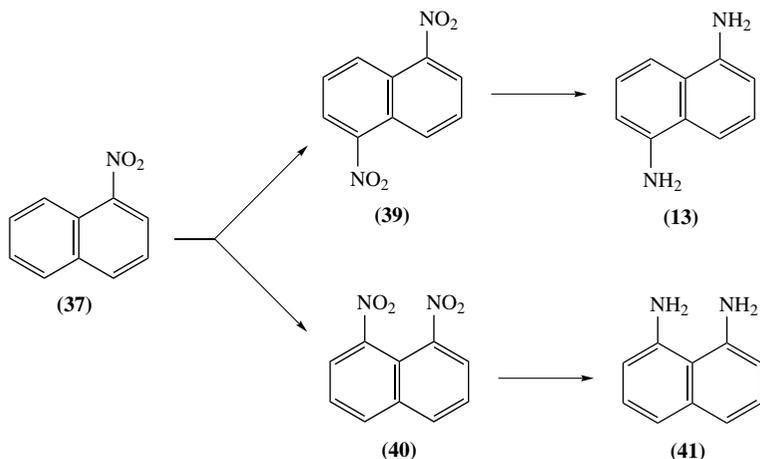
SCHEME 8

only these two are of commercial importance. They are separated by fractional crystallization or solvent extraction. The 1,5-isomer **(13)** can also be made by amination of 1,5-dihydroxynaphthalene with ammonia and sodium bisulfite, a route that is useful if this isomer only is required. It is employed in the manufacture of polyurethanes. Likewise, the 1,8-diamine **(41)** is made by reduction of **40** with iron and acetic acid in xylene, or catalytically. It is used as an antioxidant for lubricating oil, as an analytical reagent for selenium and nitrites, and as a colorant intermediate[39].

Aminonaphthalenesulfonic acids (naphthylaminesulfonic acids) with amino groups in the 1- or 2-positions are also important coupling components for azo dyes and pigments. Their manufacture, particularly work-up stages, deserves a brief description. Thus 2-naphthol **(35)** through reaction with chlorosulfonic acid in a suitable solvent, such as nitrobenzene, benzene or toluene, is converted into the 1-sulfonic acid, known as Armstrong acid **(42)**. The free sulfonic acid is insoluble and may be filtered off, followed by its amination with ammonium hydroxide to yield aminonaphthalene-1-sulfonic acid (2-naphthylamine-1-sulfonic acid) known as Tobias acid **(43)** (Scheme 9). The process is time- and labor-consuming. Typically, sulfonation of 2-naphthol to **42** requires twelve hours, and amination of **42** to **43** a further ten hours. The purification steps include precipitating, filtering, redissolving, reprecipitating, and then drying and grinding (Scheme 10). The acid **43** is used in the preparation of pigments. The difficult, and challenging, development of continuous processes for **43** commenced in the 1970s[40].
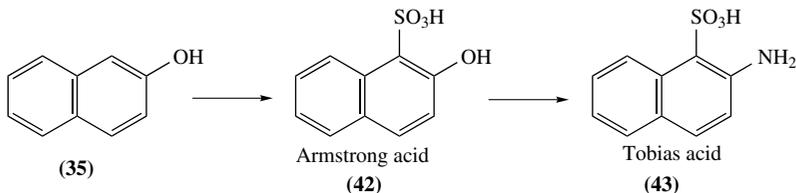
SCHEME 9
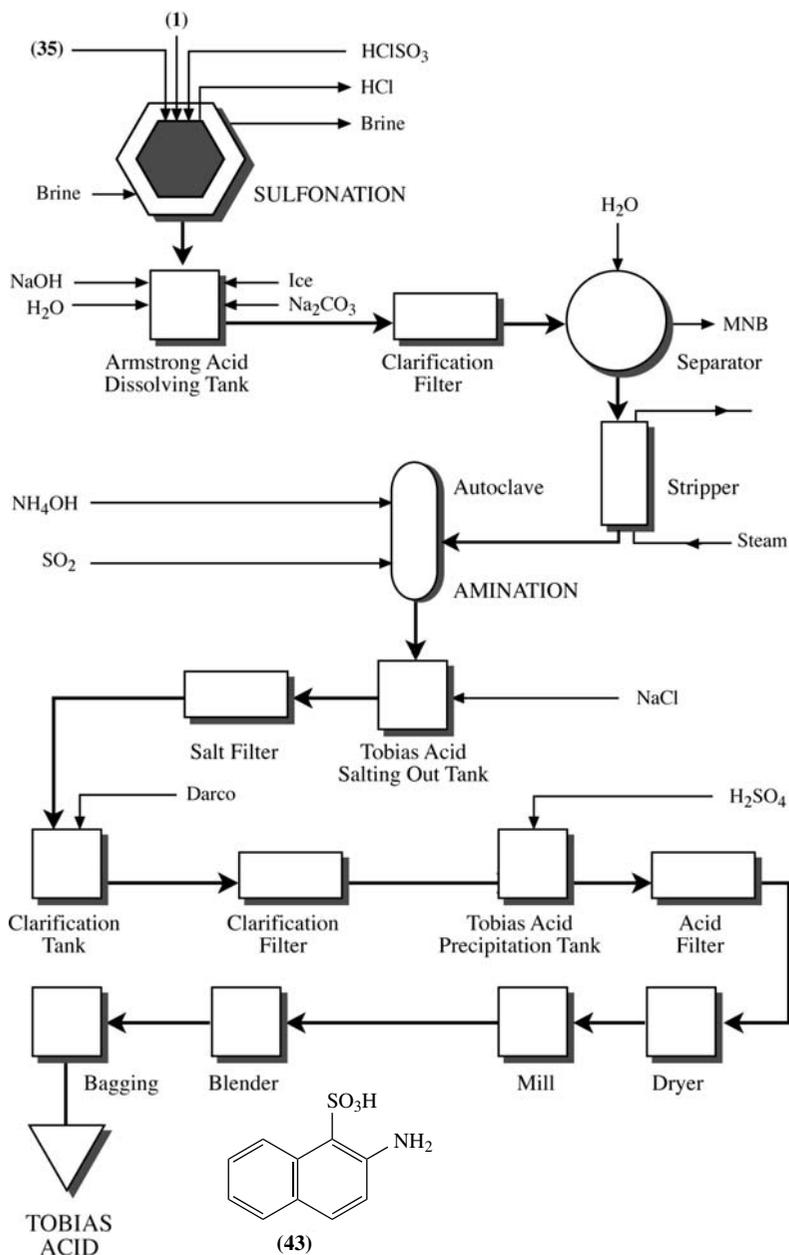
SCHEME 10. Manufacture of Tobias acid (43)

The acid sulfate of 1-naphthylamine rearranges on heating, either dry baking or in a solvent, to yield naphthionic acid, or 1-aminonaphthalene-4-sulfonic acid, 4-amino-naphthalene-1-sulfonic acid (44). It is coupled with diazonium salts of the benzidine congeners. Nitration of 2-naphthalenesulfonic acid (45) yields 5- and 8-nitro compounds that are reduced to the corresponding 5- and 8-amino derivatives (46a and 46b). The 2-amino derivative is Bronner's acid (46c). Mononitration of 45, followed by reduction, yields the important 1-aminonaphthalene-6-sulfonic acid (IUPAC 5-aminonaphthalene-2-sulfonic acid; 1-naphthylamine-6-sulfonic acid) (47a), and 1-aminonaphthalene-7-sulfonic acid (IUPAC 8-aminonaphthalene-2-sulfonic acid; 1-naphthylamine-7-sulfonic acid) (47b) generally called 1,6- and 1,7-Cleve's acids. Good yields of azo dyes are obtained from the mixed acids. Disulfonation of naphthalene, followed by nitration, reduction and fusion with alkali, yields 1-amino-8-naphthol-3,6-disulfonic acid, or H-acid (48). Sodium bisul-fite can be used to reduce the nitro group of 1-nitronaphthalene (37) and introduce sulfonic acid groups in the 2- and 4-positions. Sulfonation of naphthalene, followed by nitration, separation of the products as their sodium salts and then reduction, yields 1-aminonaphthalene-8-sulfonic acid, Peri acid (47c), and 1-aminonaphthalene-5-sulfonic acid, Laurent's acid (47d). Peri acid (47c) is sulfonated to 1-naphthylamine-4,8-disulfonic acid[41].

(44)   (45)

(46a) $R^1 = R^2 = H$, $R^3 = NH_2$
(46b) $R^1 = NH_2$, $R^2 = R^3 = H$
(46c) $R^1 = R^3 = H$, $R^2 = NH_2$

(48)

(47a) $R^1 = R^2 = R^4 = H$, $R^3 = SO_3H$
(47b) $R^1 = R^3 = R^4 = H$, $R^2 = SO_3H$
(47c) $R^1 = SO_3H$, $R^2 = R^3 = R^4 = H$
(47d) $R^1 = R^2 = R^3 = H$, $R^4 = SO_3H$
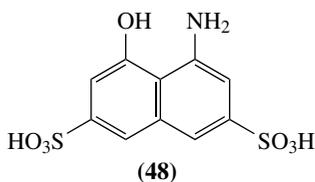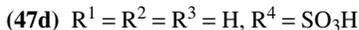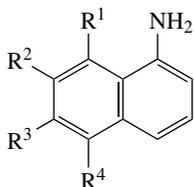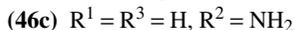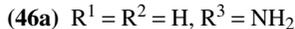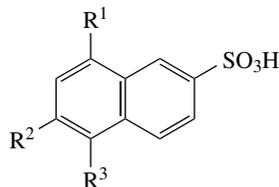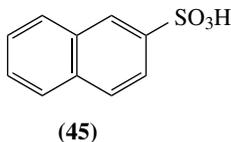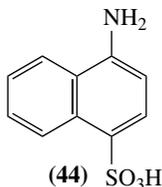
Also useful in dye manufacture are the aminonaphthalenedisulfonic acids 2-amino-naphthalene-5,7-disulfonic acid (6-aminonaphthalene-1,3-disulfonic acid, 6-amino-1,3-naphthalenedisulfonic acid), or amino J acid (49a), and 2-aminonaphthalene-6,8-disulfonic acid (7-aminonaphthalene-1,3-disulfonic acid), or amino G acid (49b).

Amination of Schaeffer's acid (2-naphthol-6-sulfonic acid) (50) as its salt at 150–160 °C yields 2-aminonaphthalene-6-sulfonic acid, Bronner's acid (46c) (Scheme 11).

The N-aryl aminonaphthalenes, including sulfonic acids, are made from reactions involving aniline and a suitable naphthalene derivative. Thus the reaction between ani-line and 2-naphthol (35) in the presence of an acid catalyst, e.g. sulfanilic acid, affords N-phenyl-2-naphthylamine (51).

(**49a**) $R^1 = R^3 = H$, $R^2 = R^4 = SO_3H$
(**49b**) $R^1 = R^3 = SO_3H$, $R^2 = R^4 = H$

β-naphthol	Schaefer's acid β-acid	Bronner's acid
(**35**)	(**50**)	(**46c**)
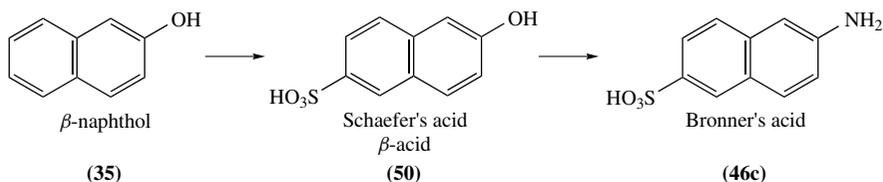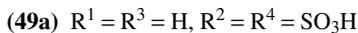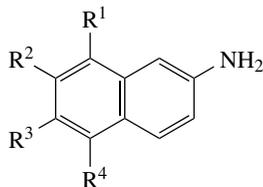
SCHEME 11

(**51**)
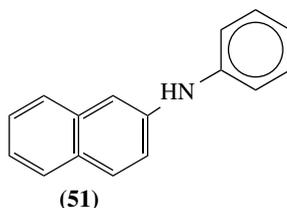
V. AZO DYES

A. Diazotization and Coupling

Aromatic amines react with nitrous acid to afford diazonium salts. The diazotization is carried out at 0 to 5 °C. The salts are used extensively in dye manufacture, mainly by the azo coupling reaction, in which the salts act as electrophilic agents. The azo colorants are characterized by the presence of the atomic grouping made up of two nitrogen atoms, $-N=N-$, the azo group. The general method of preparation involves two steps, the first of which is diazotization of an aromatic or heteroaromatic primary amine. This takes place in diazotization tubs (Scheme 12). The second step is the coupling of the resulting diazonium salt with a coupling component in steel tubs. Typical coupling components include phenols and naphthols, aniline, toluidines, naphthylamines, and their *N*-alkylated and *N*-arylated derivatives, particularly *N*,*N*-diethylaniline (**11**). The coupling reaction of diazonium intermediates (ions) with hydroxyl-containing components is generally carried out in alkaline solution. Aryl amines are coupled in weakly acidic solution. Since low temperatures are employed, tremendous amounts of ice are required in industrial practice. At the end of the reaction, salt is added to precipitate the desired product. Aniline (**2**) and *m*-phenylenediamine (**52a**) are associated with the azo dye chrysoidine (**53**). *o*-Phenylenediamine (**30**) yields benzimidazole precursors. 2,4-Dimethylaniline (**54**) and 2,4-diaminotoluene (**55**) are other examples of the types of intermediates used in the synthesis of azo dyes[42]. A wide range of structural variations is possible with azo dyes.
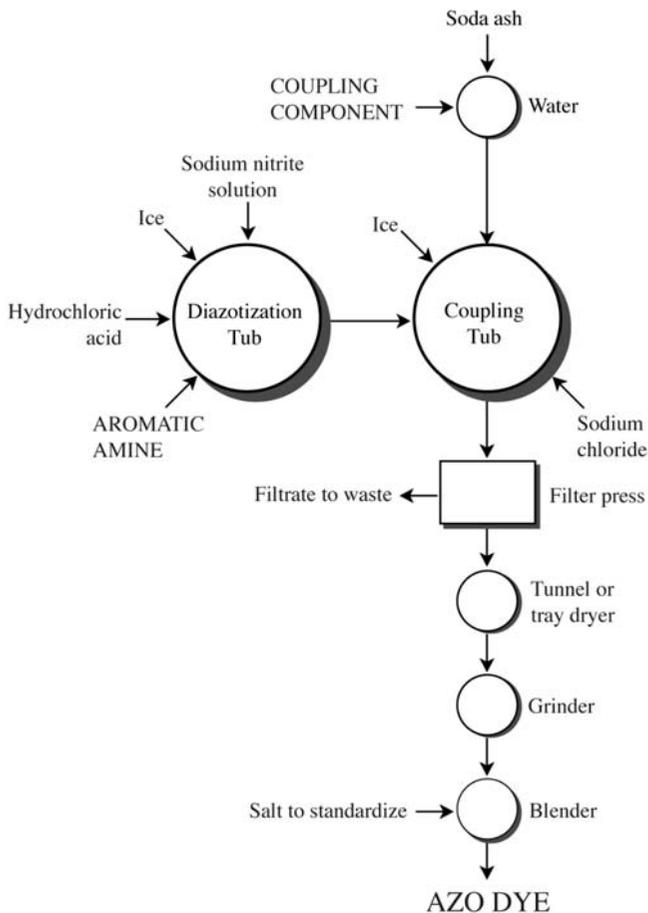
SCHEME 12. Typical steps in production of an azo dye
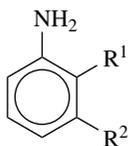
(52a) $R^1 = H, R^2 = NH_2$
(30) $R^1 = NH_2, R^2 = H$
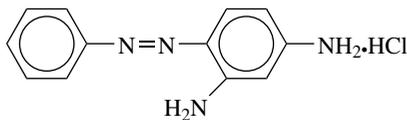
(53)
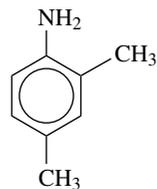
(54)

Automated, computer controlled batch processes were introduced in the 1970s. More recently, continuous azo dye manufacture has become available.

Monoazo dyes are obtained by a single diazotization and coupling sequence A > E, where A is the primary amine and E is the coupling component. The arrow means 'diazotized and coupled with'. Color in part depends on the length of the conjugated chain.

(55)
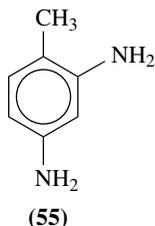
With simple E components, greenish-yellows are obtained; with phenols and anilines, reddish-yellows; with naphthols, oranges; and with certain aminophenols, reds. The diazonium component also contributes to the final color. Naphthylamines give deeper shades than anilines. Diazotization and coupling affords intermediates used in the manufacture of other dyes.

Disazo dyes contain two azo groups, and can be produced with more than one sequence of diazotization and coupling steps. For example, aromatic amines containing two amino groups (D component) can be tetrazotized, that is, both amino groups are diazotized, and coupled with two dissimilar equivalents of coupling components E1<D>E2, making use of differing rates of coupling of the two diazonium salt groupings. These dyes afford deep shades as a result of extensive conjugation. In similar fashion, trisazo, tetrakisoazo, etc. azo groups are introduced into dyes[43, 44].

1. Direct azo dyes

Direct azo dyes for cotton are water-soluble sulfonates possessing elongated co-planar structures. The original members of this class were based on benzidine and its congeners. The trisazo direct black dye **56**, formerly manufactured on a large scale, is an excellent example of selective coupling, and the need for precise control. This colorant is made from benzidine **(31b)**, H-acid **(48)**, aniline **(2)** and *m*-phenylenediamine **(52a)**. The benzidine is first tetrazotized. One diazonium group is then coupled, at low pH, to **48**. In the next step, diazotized **2** is coupled under alkaline conditions to **48**. If the coupling is incomplete, then additional products may form. Next, **52a** is coupled to the second diazonium group of the benzidine moiety. At least four, and possibly six, separate additional products can result from this process alone, unless precise control is maintained. The process is typical of those still used to produce dyes based on less toxic benzidine congeners, including: the *ortho*-tolidine derivative benzopurpurine 4B, Color Index, or CI, Direct Red 2 (CI 23500) **(57)**; and *ortho*-dianisidine azo dyes, CI Direct Blue 80 (CI 31600), CI Direct Blue 98 (CI 23155), CI Direct Blue 1 (CI 24410), CI Direct Blue 76 and CI Direct Blue 100. Azurine G, CI Direct Blue 8 (CI 24140), is also a dianisidine derivative. The use of benzidine was phased out in Western Europe and North America during the 1960s and 1970s, following clear evidence that this compound causes bladder cancer. This is not the case in certain Asian countries, though great care is taken in manufacture, including in the handling of benzidine, ideally as a wet paste.

(56)

1-naphthionic acid   **(57)**
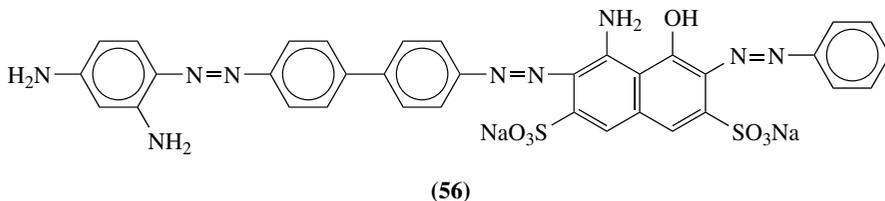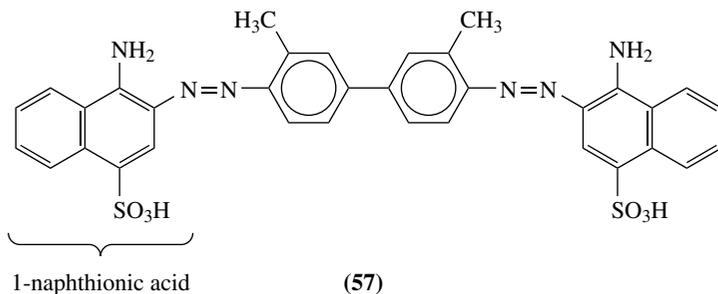
VI. ANTHRAQUINONE VAT DYE INTERMEDIATES

Nitration of anthraquinone **(58)** in mixed concentrated nitric acid/sulfuric acid yields 1-nitroanthraquinone **(59)**. Reduction to the corresponding 1-aminoanthraquinone **(60)** can be carried out with: sodium sulfide or sodium hydrogen sulfide; hydrazine in aqueous sodium hydroxide; metals in sulfuric acid; and by hydrogenation in organic solvent with palladium or Raney nickel (Scheme 13).

(58)   **(59)**   **(60)**
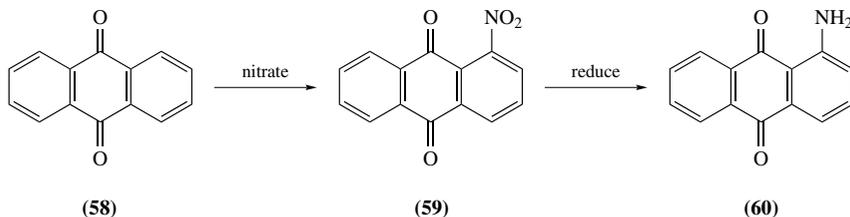
SCHEME 13

The most important derivative employed in vat dye manufacture is the reduction product of 2-nitroanthraquinone, namely 2-aminoanthraquinone **(61)**. It was formerly manufactured from the 2-sulfonic acid of anthraquinone, by reaction with ammonia in the presence of oxygen. However, sulfonation of anthraquinone requires mercury and the subsequent amination requires arsenic, making these processes ecologically unattractive. From the early 1970s, processes for direct nitration of anthraquinone at the 2-position, followed by reduction, were introduced, mainly as a result of research in Japan[45, 46].

(61)
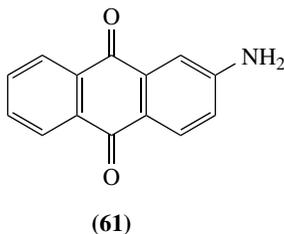
Since nitration of anthraquinone requires a mixture of concentrated nitric and sulfuric acids, which is also ecologically problematic, as well as causing corrosion of reactors, Japanese workers have revealed an alternative method in which nitration of anthraquinone is achieved with nitrogen dioxide in dichloromethane in the presence of methanesulfonic

acid as catalyst. It is claimed that the method can be adapted to the synthesis of other nitroanthraquinones[47].

Aminoanthraquinones undergo acylation with acid chlorides, generally in organic solvent, and with carboxylic acids or anhydrides in oleum. Benzoylation is an important reaction, since many vat dyes contain benzamido groups in the α- (1-) position. The free amino groups may be diazotized to afford biaryl compounds. The great lability of substituents in anthraquinones, as compared with similar benzene and naphthalene compounds, offers a number of routes to aminoanthraquinones.

Chlorobenzene is employed in the synthesis of certain amino-containing vat dye intermediates. When reacted with phthalic anhydride, the product is 2-chloroanthraquinone, which, with ammonia, is converted readily into 2-aminoanthraquinone (**61**). Other routes include replacement of halogen by amino groups, with ammonia or ammonium salts of urea, and alkyl- and aryl amines to afford secondary amines. Modification of the amino group by alkylation, with dimethyl sulfate, alkyl halides or esters of toluenesulfonic acids, is of synthetic value. Arylation of the amino groups is of importance only in the reaction between aminoanthraquinones and nitro- or chloroanthraquinones to yield dianthraquinonylamines, or anthrimides[48]. For example, the reaction between **62** and **63** yields **64,** which can then be converted into carbazole **65**, CI Vat Brown R (Scheme 14). Amination of haloanthraquinones such as 1-amino-4-bromoanthraquinone-2-sulfonic acid (bromamine acid) (**66**), prepared from 1-aminoanthraquinone, is of industrial use.

SCHEME 14

(**66**)
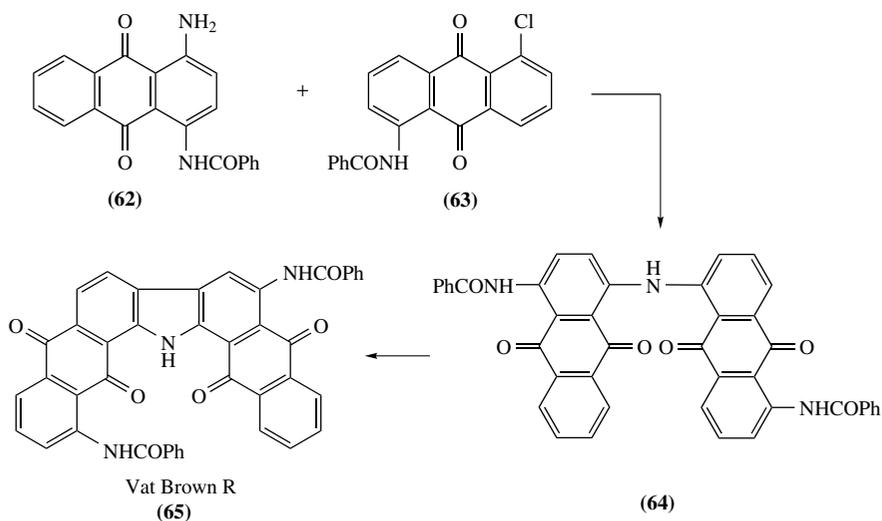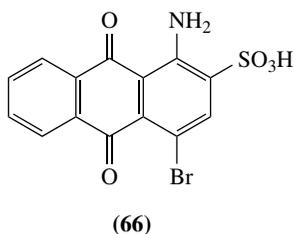
VII. ANTHRAQUINONE VAT DYES

Vat dyes are particularly important in the blue-green region. Their brightness, laundry- and light-fastness render them ideal as colorants for curtains, shirtings, towels and beachwear, despite the multistage syntheses, which make them expensive. Demand for vat dyes is far greater in the US than in Europe. The toxic nature of anthracene and many of its derivatives has led to a decline in their manufacture in Western Europe and the US.

A typical use of **61** is, by fusion with potassium hydroxide at high temperature, in the production of flavanthrone **(67)** (Scheme 15). Fusion of **61** with potassium hydroxide under milder conditions affords the important anthraquinone azines known as indanthrones (Travis Chapter 1). The main vat-dye reactions proceed via anthrimides, which are both dyes and intermediates, since they are readily converted into cyclic carbazole derivatives. For example, benzanthrones, such as **68** and **69**, dibenzanthrones, isodibenzanthrones, and their derivatives and substitution products, are important in vat-dye manufacture. An example of their use is in the synthesis of CI Vat Olive T **(70)** (Scheme 16). Benzanthrone acridones made from 1-aminoanthraquinones are important green dyes. Certain vat-dye reactions require high-boiling organic solvents.
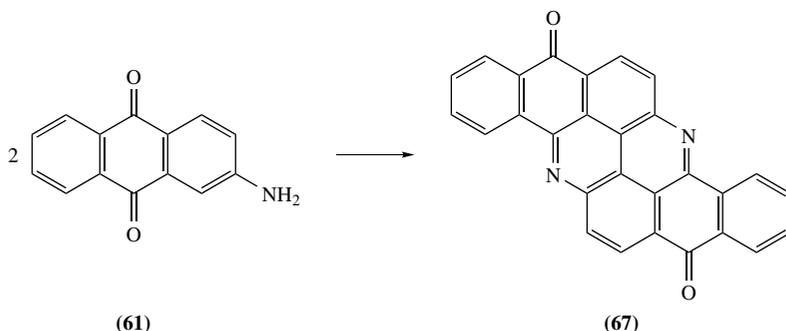
SCHEME 15

Filtration and drying are important steps in the production of dyes. They require time and labor, and filter presses. In the case of vat dyes the presses separate suspended solids, usually the desired product, from liquids, generally in the form of a slurry. This is achieved by forcing the reaction mixture through a suitable filter medium, that supports the solid, under applied pressure. For an acidic slurry, wooden plates and frames are used. The vat dye press cake is washed with water, though in a number of cases organic solvents are used. After filtering, the solids are dried.

VIII. SULFUR DYES

Important sulfur dyes are made by treating aryl amines with sodium polysulfides, or by heating the amines with sulfur, followed by treatment with sodium sulfide. Certain sulfur blacks are made from anilines that include *p*-aminophenol and *p*-phenylenediamine **(22)**. Derivatives of diphenylamine **(8)** yield blue shades. Meta-diamines, such as *m*-phenylenediamine **(52a)**, give brown and yellow colorants. Sulfur dyes are inexpensive, but lack brilliance. There are no red members of this class. They are applied by means of reduction and oxidation processes.

(68)   **(69)**

2   **(60)**

Vat Olive T (Vat Black 25)

(70)
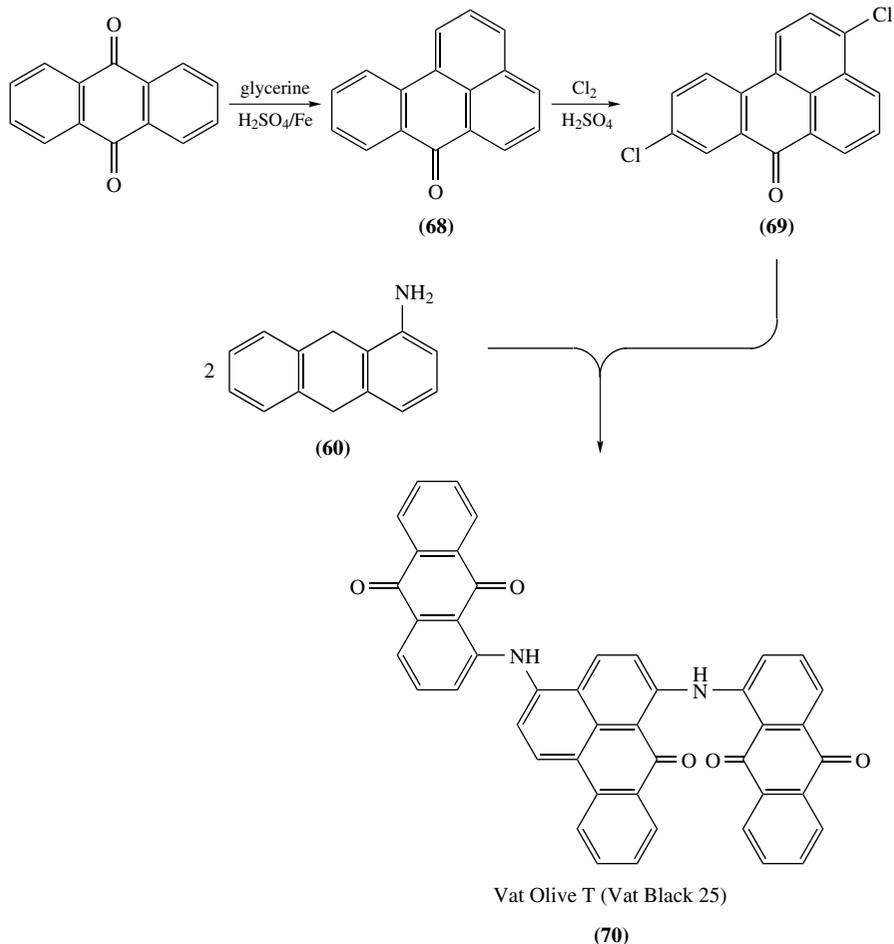
SCHEME 16

IX. INDIGO

The two industrial routes to artificial indigo involve aryl amines, in one case aniline, which is converted to phenylglycine, and in the other case anthranilic acid, from phthalic acid (see Chapter 1). The first route represents the major present use of aniline in synthetic dye manufacture. Global demand exceeds 15,000 tons annually, valued at $200 million. Until 2003, Buffalo Color, of New York, was the main US manufacturer of indigo. This facility was closed as a result of competition from imported synthetic indigo, mainly from China. As with other synthetic dyes, the cost of treatment and disposal of waste in accord with environmental regulations is a major consideration in determining commercial viability at a particular site. Following eco-efficiency analysis, BASF, the main European producer

of indigo, has modified its process to yield 40% pre-reduced indigo in aqueous solution, which is suitable for electrochemical dyeing.

Possible alternative sources of indigo under investigation include the use of genetically-modified *Escherichia coli* (Genencor International), and the cultivation of suitable crops in Europe, part of the $3.2 million sustainable production of the plant-derived indigo project (SPINDIGO), launched by the European Commission in 2001. However, these seem unlikely to displace to any extent the traditional manufacturing processes in the near future. The Genencor method is, so far, more expensive than the existing processes. Moreover, to be competitive new processes would require making available a product that is comparable in consistency and applicability to that obtained from chemical manufacture.

X. APPLICATION OF DYES. ANCHORING DYE ON FIBER

Dyeing is normally readily accomplished in aqueous solution, often in the presence of a fixing agent, or mordant. This is ideal for cotton, silk and wool, but not for certain synthetic fibers, such as nylon and polyester. The latter are plastic in nature, and require disperse dyes. Here the dyeing process involves heating the fiber in an aqueous dispersion of a water-insoluble dye. A solid solution is formed in the fiber. In order to penetrate synthetic fibers, a small dye molecule is required, for which simple water-insoluble mono-azo dyes are ideal. Apart from yellow dyes (where phenolic components are common), these are usually based on *N*,*N*-dialkylated aniline coupling components that permit a wide range of shades to be obtained.

The very hydrophobic cellulosic fibers cotton and viscose do not contain acidic or basic centers. However, certain dyes, such as the bisazo benzidine derivatives, are directly adsorbed on cotton. These are the direct dyes, most of which belong to the azo class. They possess the property of cotton substantivity by hydrogen-bonding with the fiber or with their own kind, accumulating within the fiber pores, and enabling resistance to washing and cleaning treatments[49].

An improved method of dyeing cotton is by using reactive dyes, those that form chemical bonds with the fiber, generally using electrophilic heterocyclic compounds, particularly triazines and pyrimidines. The reactive components, typically cyanuric chloride (2,4,6-trichloro-1,3,5-triazine), are added through the availability of a free amino group in the dye. They were introduced by ICI in England during 1956. The first colorants investigated were dichlorotriazines, based on two naphthalenesulfonic acid azo dyes, and an aminoanthraquinonesulfonic acid, all later introduced as members of the Procion range (see Chapter 1). A successful early Procion colorant is **71**. Reactivity with the hydroxyl of cotton rather than with water is achieved by buffering. In 1957, a monochlorotriazinyl red dye, in which an aminophenyl substituent was present in the triazine ring, appeared, suited
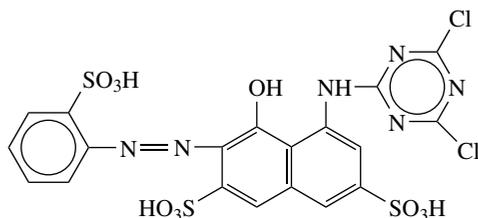
Procion Brilliant Red 2BS

(71)

to cotton and viscose rayon fabrics. Monochlorotriazines had already been exploited by CIBA, though not as components of reactive dyes. Through collaboration with ICI, CIBA introduced Cibacron fiber-reactive dyes in 1957. Hoechst was also active in this area with its vinyl sulfones[43, 50–52].

Aryl amine-derived fluorescent whitening agents, used in detergents, were introduced from the late 1940s, and are based on stilbenes and triazines. Most brightening agents are made from the intermediate 4,4′-diamino-2,2′-stilbenedisulfonic acid, and include incorporation of aminotriazines (see Chapter 1). For example, (Bayer) Phorwites are produced by reacting aniline with cyanuric chloride to afford an intermediate that is then further reacted with the stilbenedisulfonic acid to form the brighteners.

XI. PIGMENTS

Pararosaniline **(72)**, a member of the first major class of synthetic dyes to be invented, is an example of a triarylmethane colorant. It represents a substantial part of the market in lakes and pigments, particularly as phenylated (arylated) blue colorants. Pararosaniline **(72)**, is made by condensation of aniline with formaldehyde in a two-step reaction. The condensation is carried out in an excess of aniline. The product mixture contains pararosaniline and byproducts, and, following removal of excess aniline by steam stripping, is drowned in water at 30 °C and precipitated in the form of hard pellets. The size of the pellets is dependent upon the amount of agitation used in the drowning step. The aqueous layer is separated from the pellets containing the product in a filter press, and the pellets are then treated in an extraction tub. The pure material is obtained by extraction of **72** from the pellets in essentially a two-stage batch process at 95 °C and at a pH of 6.8–7.0. Liquid from a third extraction step is used as feed for the subsequent second-stage extraction. Approximately 10–12 hours are required for the entire extraction operation.
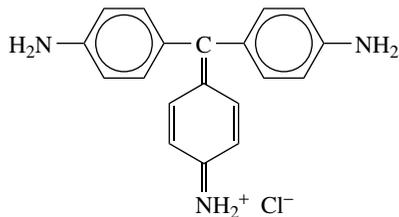
pararosaniline

(72)

Direct reaction of pararosaniline with aniline affords solvent blue, almost identical with the product from the reaction of aniline red (rosaniline) with aniline discovered in 1861 (see Chapter 1). Treatment of solvent blue with sulfuric acid yields the important soluble alkali blue, CI Pigment Blue 61. There are three main manufacturers: BASF, at Huntington, West Virginia, that produces 12 million lbs. each year, representing 40 to 50% of world supply, Clariant, in Germany, and a Hindustan facility in India[53]. CI Pigment Blue 61 is employed as a toner for black inks, and as a blue printing pigment for packaging. The original oxidation of mixed aniline and toluidines with nitrobenzene to afford aniline red is now obsolete. However, the reaction between aniline and nitrobenzene is used to produce the pigment aniline black.

Both 2-naphthol **(35)** and its derivative ß-, or 2-oxynaphthoic acid are important coupling components in the production of azo pigments. The latter is used for several reds,

$$SO_3^-$$
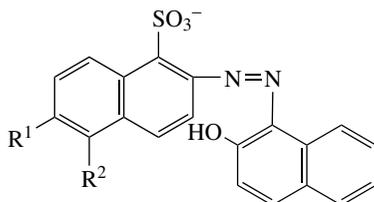
(**73a**) $R^1 = R^2 = H$ (Lithol Red)
(**73b**) $R^1 = Cl, R^2 = C_2H_5$ (Clarion Red)

which represent a large part of consumption of all red pigments. Important products made from **34** are **73a** and **73b**.

The use of color in newspapers and magazines, particularly for advertising, and also for packaging, has trebled since around 1980. There is restricted use of vat colorants as pigments for printing ink, and paint and plastic use, because of the need to ensure that the vat crystals meet the uniformity of the pigment color and strength standard[54]. Cyclization of 1-amino-8-(acetylamino)naphthalene (**74**) yields 2-methylpyrimidine (**75**) from which the orange phthaloperinone pigment **76** is obtained (Scheme 17).

2-methylpyrimidine   orange phthaloperinone
                                              pigment

(**74**)   (**75**)   (**76**)
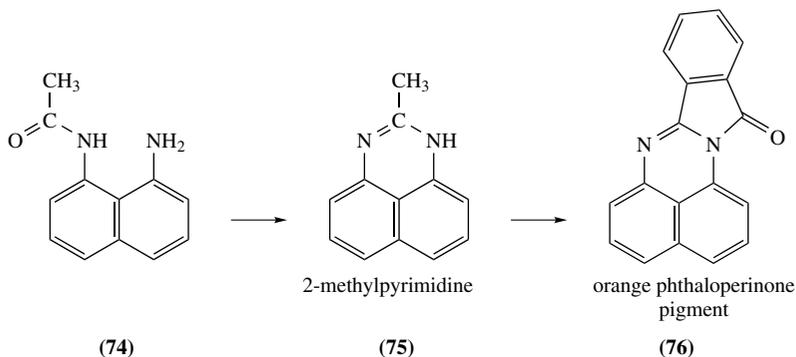
SCHEME 17

A. High-performance Pigments

High-performance organic pigments have displaced red, orange and yellow colorants based on lead, chromium (VI) and cadmium. However, organic pigments require organic solvents, and intermediates such as 3,3′-dichlorobenzidine (**31a**), a suspected carcinogen. Engelhard Corporation in the US has produced a range of environmentally friendly 'Rightfit' azo pigments containing calcium and strontium, and sometimes barium, all manufactured in aqueous media. This enabled Engelhard to phase out its heavy-metal pigments production during 2004. The Rightfit colors range from purple to green-shade yellow, and can be reformulated. In June 2004, Engelhard received the US Environmental Protection Agency 2004 Designing Safer Chemicals Award for these pigments that are approved for indirect food contact applications[55–56]. These pigments have recently been reviewed[57].

B. Digital Printing

The last two decades has witnessed fast-growing and novel applications of some of the traditional dyes and pigments, as well as of new colorants based on existing classes, to a ubiquitous artifact that is connected to the growth of digital technologies, namely the photorealistic ink-jet printer. The first black used in ink jet printing was a food colorant CI Food Black 2 (see Chapter 1), that was modified and employed as its ammonium salt. Particle sizes of 200–300 nm are required in ink jet printing. Suitable small molecules used in the dye diffusion thermal transfer (D2T2) process for color printing are those that adhere to the polyester film. Polyester dyes, a yellow (77), and two azo dyes, a magenta (78), and a cyan, were developed for this purpose[58,59].
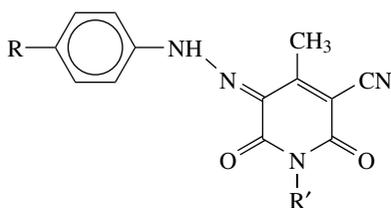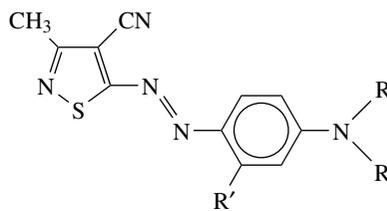
(77)   (78)

R, R′ = alkyl groups

C. The Colorant Industry Today

The European and US colorant industries, particularly for textiles, have declined since the 1980s, due in part to competition from Asian manufacturers. In the US, DuPont and American Cyanamid pulled out around 1980, leaving Crompton & Knowles, merged with Witko, as Crompton Corporation, in 1999, as the main US-owned manufacturer. In 2001, Crompton Colors Inc., specializing in paper and ink-jet printing, was acquired by Sensient Technologies Corporation, of Milwaukee. European corporations have in some cases retained, and expanded, facilities in Asia and South America. In 1995, the textile dyestuff operations of Bayer and Hoechst were merged as DyStar Textilfarben GmbH, based in Frankfurt. In 2000 they were joined by BASF. In August 2004, DyStar, the largest producer of textile dyes in the world, with one production site in China, and other facilities in South America, was acquired by the US private company Platinum Equity, of Los Angeles, California.

Pigment production continues to flourish in the US. Sun Chemical Corporation is the world leader in printing inks and organic pigments. In 2003, it acquired Bayer Polymers high-performance organic pigment facility at Bushey Park, South Carolina, where Bayer Chemicals continued to manufacture brighteners and paper dyes. Several other independent companies, including AGFA and DyStar, have facilities at the Bushey Park complex. Most of the Bayer Chemicals divisions were brought together as Lanxness Corporation, from July 2004. A further corporate divestment, typical of those that have characterized the chemical industry since the 1980s, took place in January 2005 when Bayer spun off Lanxness.

With the overall decline in European and US production since around 1980, there has been massive growth in exports of dyes and pigments from Asia. Exports from China rose 128% during 2003 to $800 million (compared with $324 million in 2000). Nevertheless the growing Chinese economy, and special needs, required the import of colorants valued at $1,763 million during 2003. Exports from Japan and South Korea during 2003 grew

18.8% to \$2,430 million (\$2,493 million in 2000). By 2004, there was around 30 to 40% excess capacity, mainly as a result of growth in Chinese production. Nevertheless in specialties, particularly reactive and disperse dyes, the leaders are Dystar, Ciba Specialty Chemicals and Clariant[60].

XII. AGRICULTURAL CHEMICALS

A. Fungicides

Anilines are used in the manufacture of a wide range of fungicides, including the following classes: anilides; benzanilides; benzimidazole precursors; carbanilate; conazole; formamide (amide fungicides); furanilide; imidazole; nitroaniline; oxazole; pyrazole; pyridine; pyrimidine; sulfonanilide; triazine; triazolone; and urea. Diphenylamine (**8**) is classified as a diphenyl fungicide. Fungicides represent about 20% of the production of agrochemicals. Fungicides and other agrochemicals often have both generic, or non-proprietary, names, and trade, or brand, names, in addition to true chemical names.

The intermediate *o*-phenylenediamine (**30**) yields benzimidazole precursors, including the thioureidoformates originally known as NF44 (**79**) and NF48 (**80**) (Scheme 18). Both are converted into BCM (methyl benzimidazol-2-ylcarbamate) (**81**), a degradation product of the pre-harvest systemic Benomyl (**82**), which contains the benzimidazole ring,
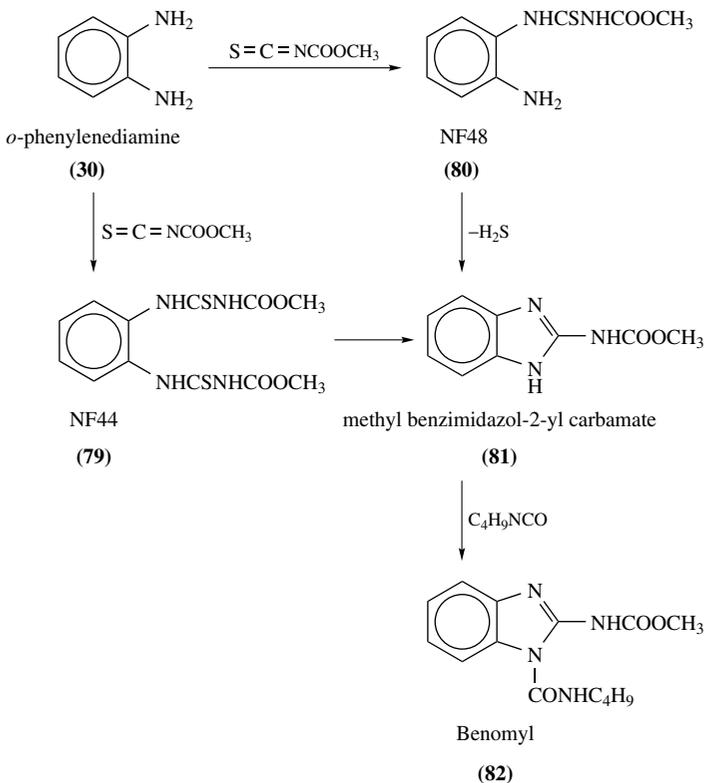
SCHEME 18

suggesting that **79** and **80** act as fungicides in a similar fashion[61]. Benomyl (**82**) was introduced into the UK by DuPont during 1971. Ecological and environmental factors, including resistance to benzimidazole fungicides, have caused decline in manufacture and use. In 1982, its use in Swedish homes and gardens ceased, following studies that indicated fetal and genetic damage when applied in high dosages. From the early 1990s, the use of **82**, also known as Benlate, was restricted in the US, following claims of damage to crops, particularly in Florida. Also, exposure to very high dosages was found to cause eye birth defects (the condition known as anophthalmia), including in Florida, and parts of the UK[62]. Manufacture in the US ceased in 2001, and its use was phased out during 2002. Benomyl is still manufactured in China.

Synthetic versions of the natural product Strobilurin A have found use as valuable fungicides. Various analogs have been investigated by DuPont, including, as lead compound (chemical starting point), a triazolone derivative prepared from a phenoxyaniline-derived semicarbazide. This and similar research carried out elsewhere focuses on retention of the specific toxophore structure, in order to retain biological activity, and variation in the hydrophobic part of the molecule that incorporates a lipophilic moiety[63].

Manufacture of fungicides containing 2,6-dichloro-4-nitroaniline (dicloran) has been discontinued in the US.

B. Herbicides

These make up around 40% of the pesticide market. The range includes amines, amides, carbamates, imides, phenylureas and triazines. They act by direct contact with leaves, translocation and root uptake.

In the 1950s and 1960s, Geigy and other firms developed a series of herbicides based on alkyl and dialkyl triazines, such as the root-herbicide atrazine (**83**)[64]. They are made by stepwise introduction of suitable nucleophiles into precursors. Other members are ametryn, the non-selective simazine (**84**) and the cyanuric chloride-derived methylthio triazine desmetryne (**85**) (Scheme 19). Chlorotoluron is 3-(3-chloro-*p*-tolyl)-1,1-dimethylurea (**86**), a phenylurea herbicide. These products act on the photosynthetic pathway. Both **83** and **84** are used for weed control in maize[65]. Sulfonylureas such as the triazine chlorosulfone (**87**) inhibit the enzyme acetolactate synthase. They offer the major advantage of requiring no more than 10 to 20 g per hectare.

atrazine (**83**)   simazine (**84**)
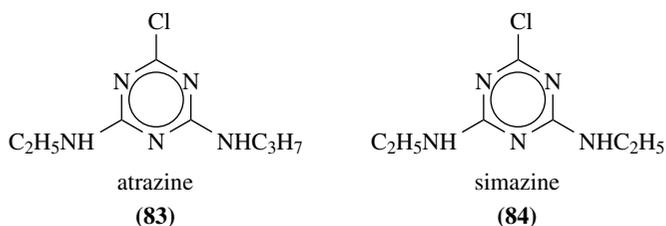
Dinitroaniline herbicides are miotic inhibitors that prevent the growth of roots. They are incorporated into the soil to prevent volatilization and photodegradation. A cotton and corn herbicide introduced by American Cyanamid in the mid-1970s is Prowl, *N*-(1-ethylpropyl)-2,6-dinitro-3,4-xylidine (**88**)[66]. Other trade names include Pendulum and pendimethalin. Catalytic hydrogenation of 3,4-dicholoro-1-nitrobenzene affords 3,4-dichloroaniline (**89**), used in the manufacture of herbicides, for example, by reaction with phosgene. Chloraben (Amiben, metaproterone) is 3-amino-2,5-dichlorobenzoic acid, a pre-emergence weed-control herbicide. Carbamate herbicides include Barban (**90**), though due

SCHEME 19

chlorosulfon

(86)   (87)
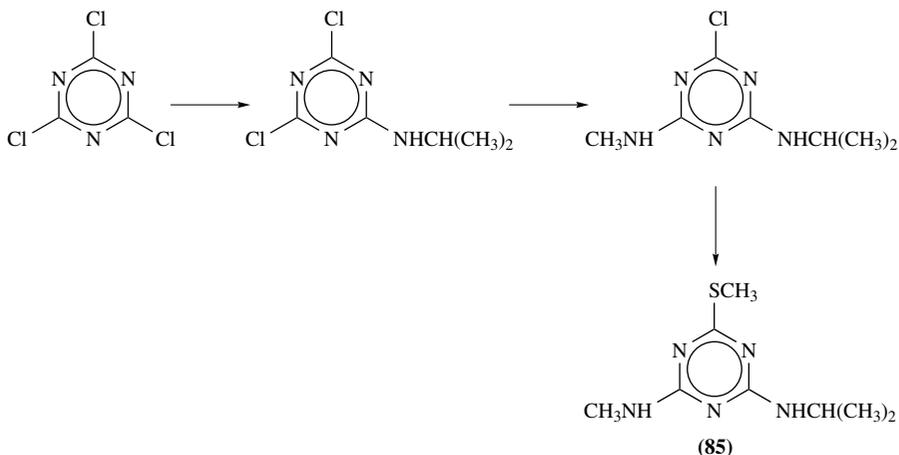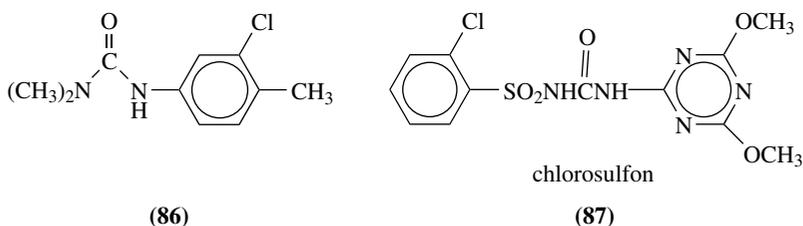
to persistence in the environment its use has declined. Other carbamates include Asulam, or methyl [(4-aminophenyl)sulfonyl]carbamate **(91)**, and Fenasulam, or methyl 4-[2-(4-chloro-*o*-tolyloxy) acetamido]phenylsulfonyl carbamate **(92)**. The *N,N*-dipropyl dinitroaniline herbicide trifluralin **(93)** is useful for weed control in cotton crops (Scheme 20).

Anilides constitute the amide herbicides, such as propanil **(94)**, *N*-(3,4-dichlorophenyl) propionamide, a derivative of **89**, and monuron **(95)**, a derivative of *p*-chloroaniline, which is also employed in the manufacture of carbamate and substituted urea herbicides. Propanil **(94)** was introduced in the 1960s, but was soon found to cause damage to prune trees. It is widely used in rice-growing areas, even though it is hydrolyzed by rice to aniline. Israel's Makhteshim-Agan Industries, the world's largest generic manufacturer of crop-protection chemicals, is a leading producer of the rice herbicide, through its acquisition of a controlling interest in Westrade, of Houston, in 2004. However, at the time of writing, propanil is not licensed for use with rice or other crops in the US, except under emergency conditions, for example in parts of California, where aerial spraying of phenoxy herbicides and related dioxins has been banned. Other aniline-derived herbicides include the 3,4-dichloro dimethylureas diuron and linuron, and the 4-bromophenyl urea metobromuron.

Ortho-alkylated anilines, such as 2-methyl-6-ethylaniline **(96)**, and 2,6-diethylaniline **(97)**, are used in the production of acetanil-like pre-emergence herbicides. applied to corn, soyabeen, etc. The amine **97** is the starting point for the selective systemic alachlor **(98)** (Scheme 21). Acylation of **38** with phthalic anhydride affords the pre-emergence herbicide naptalam (*N*-1-naphthylphthalamic acid) **(99)**.

(88)

(89)

Barban

(90)

Asulam

(91)

Fenasulam

(92)

trifluralin

(93)

SCHEME 20

(94)   **(95)**

(96)

(97)

alachlor

(98)

SCHEME 21

naptalam

(99)

propiconazole

(100)
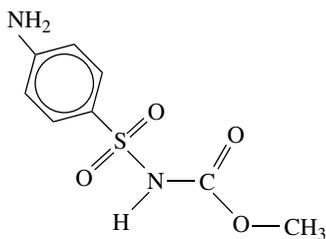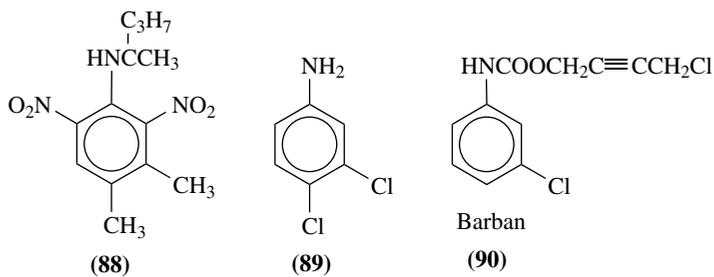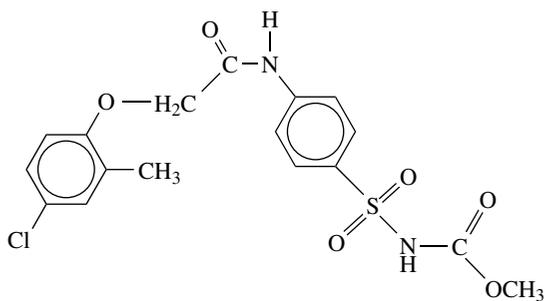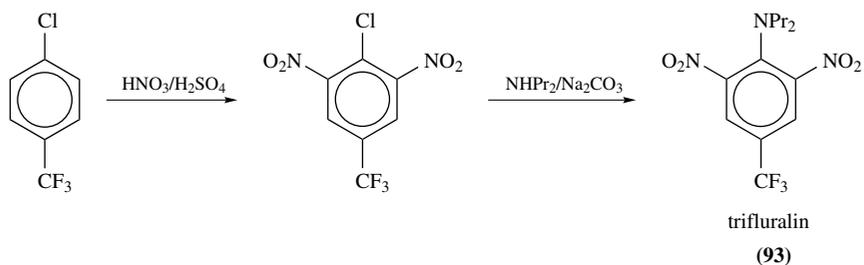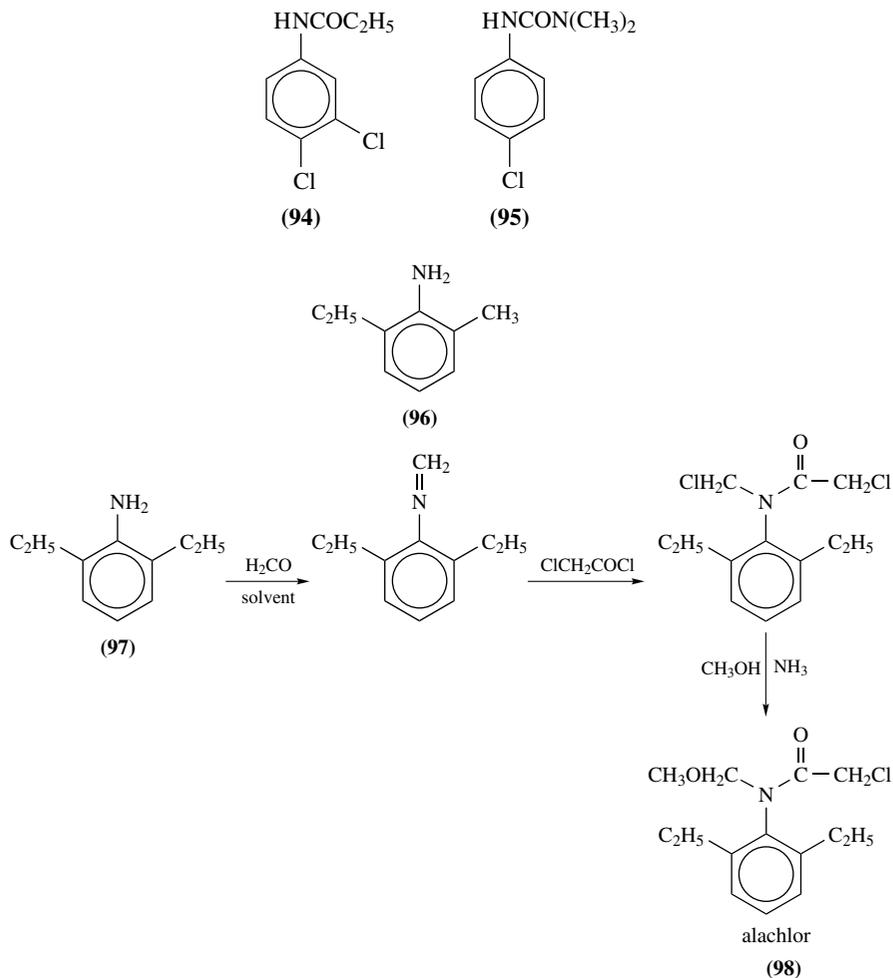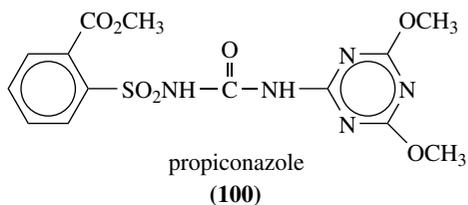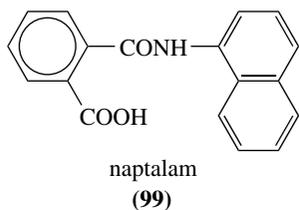
Triazole-sulfonamide herbicides are egosterol biosynthesis inhibitors, and include prop-iconazole **(100)** and flusilazole **(101)**. Apart from a range of sulfonamides introduced in 1992, no further important developments occurred until the introduction of protox-inhibiting herbicides, mainly diphenyl ethers and cyclic imides, the latter including aryl
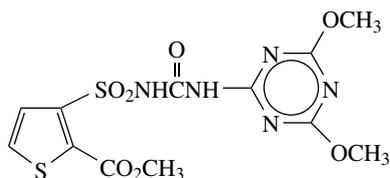
flusilazole
(101)

heterocycles. Protox, or protoporphyrinogen oxidase, is a key enzyme in the biosynthesis of tetrapyrrole. Following a 1996 report that aryloxyphenyl cyanurates exhibit potent herbicidal activity, there has been considerable research into their uses as protox inhibitors. At BASF, conversion of 2,4-dihaloanilines into ureas with methyl isocyanate has been used in preparation of 3-(heterocyclyl)phenyl cyanurates, though the products have not been developed into herbicides[67].

Researchers at FMC Corporation have synthesized 3-(4,6-substituted benzoheterocyclyl)uracil herbicides. The uracil ring synthesis is based on conversion of aryl amines into isocyanates[68]. A useful fluorinated aniline herbicide is fluometuron. Chlorination of 2-methylpyridine **(102)**, followed by amination at the 4-position, and hydrolysis, yields the hormone-weedkiller Picloram **(103)** (Scheme 22).
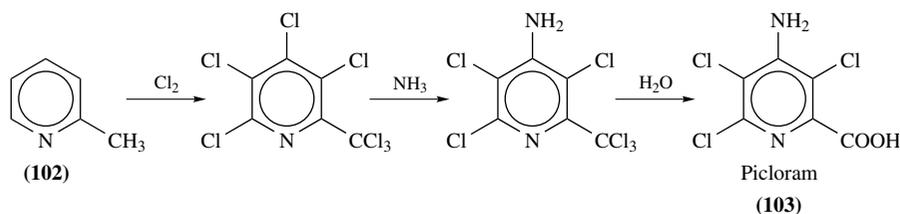
SCHEME 22

C. Insecticides

Typically, insecticides represent about 30% of the market in agrochemicals. Activity depends on the ability to penetrate insects rapidly and reach sites of action in membranes of nerve cells. Insecticides are more soluble in fats than in water. The aryl amine insecticides include carbamic esters, such as pirimicarb **(104)**, a diazine derivative (Scheme 23). It is of short-to-moderate persistence, but more selective than organophosphorus compounds. Acylation of *N*-methyl-1-naphthylamine, or reacting the chloroacetamido derivative with potassium fluoride in glycerol, affords the insecticide and acaricide known as nissol **(105)**.

Conversion of 4-(trifluormethoxy)aniline **(106)** into its methyl carbamate, and then to the corresponding carbamoyl chloride, yields the oxidizine indoxacarb Avaunt **(107)** (DuPont). In the early development work, this was coupled with a hydrazone. However, later it was coupled with an unstable oxadiazine intermediate. Of the two isomers of indoxacarb present in Avaunt, the insectically active isomer represents 75%. The research into a useful product involved novel catalytic asymmetric oxidation chemistry and synthetic strategies[69]. Contributions came from other programs, particularly synthesis of pyrazoline-3-carboxanilides (versions of oxyindazoles) from aryl amines and pyrazoline esters[70]. The reaction of **38** with thiocyanate ion under aqueous conditions yields the rodenticide Antu,1-naphthalenthiourea **(108)**.

SCHEME 23

nissol
(105)

(106)

(107)

Antu
(108)

fenzaquin
(109)
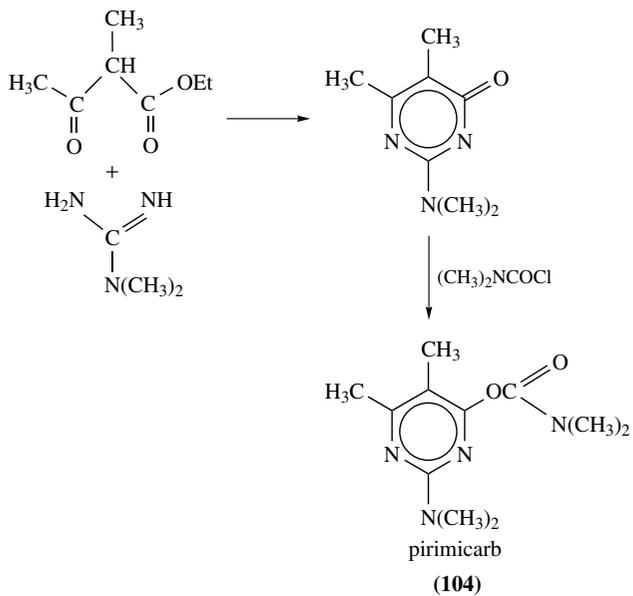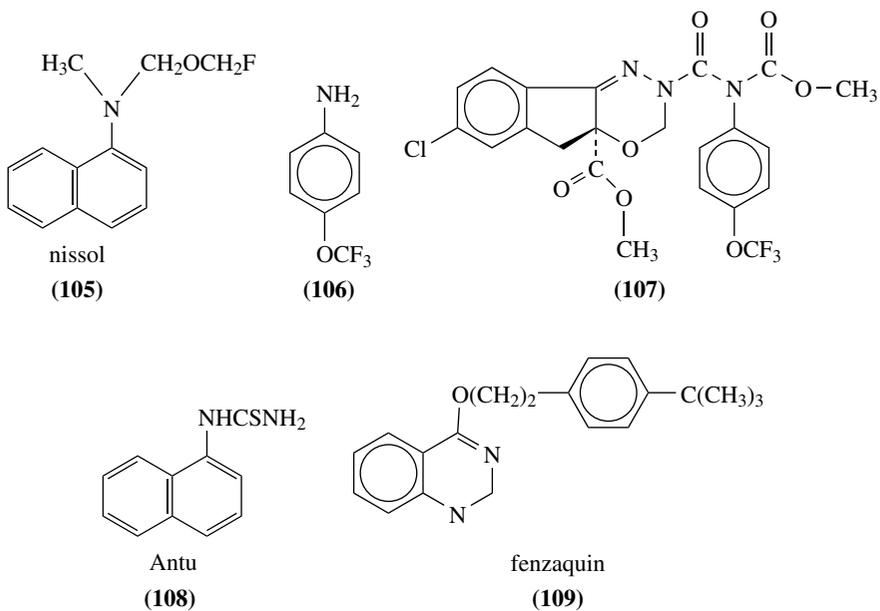
The fused pyrimidine derivatives of fenazaquin (**109**), derived from 1-aminobenzoic acid, are useful miticidal agents[71].

D. Animal Health Products

These include amitraz (**110**), prepared from **54**, a member of the form amidine class, active against mites and ticks, that have replaced organophosphorus compounds. Notably, amitraz is active against newer strains of pyrethroid-resistant ticks. The reaction of diphenylamine (**8**) with sulfur in the presence of iodine as catalyst yields the anthelmintic (worming agent) phenothiazone (phenothiazine) (**111**) (Scheme 24). It is too toxic for human use, though it is an intermediate in the production of antipsychotic drugs.

$$H_3C-\underset{\underset{CH_3}{|}}{\bigcirc}-N{=}CH-\underset{\underset{|}{CH_3}}{N}-C{=}N-\underset{\underset{H_3C}{|}}{\bigcirc}-CH_3$$
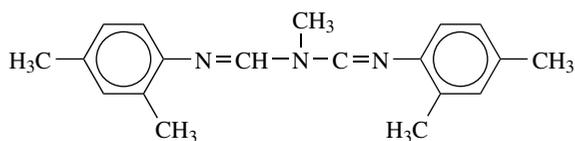
(110)
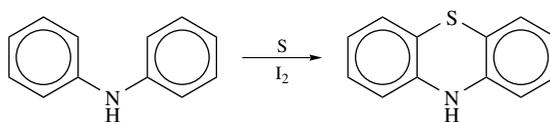
(8)   phenothiazine
(111)

SCHEME 24

Bezimidazole animal health products are often related to crop protection chemicals. The first one, made from *o*-aminoanthranilic acid[72], was thiabendazole (**112**), discovered by Merck in 1961. However, **112** undergoes rapid enzymatic hydroxylation. This is overcome when the thiazole ring is replaced by a 2-methylcarbamate substituent in parbendazole (**113**), patented in 1973. Concerns over tetrogenecity have led to restrictions in the use of **113** and its derivatives in pregnant animals.
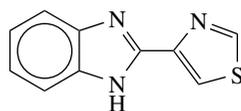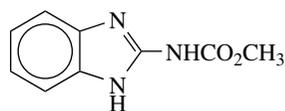
(112)   **(113)**
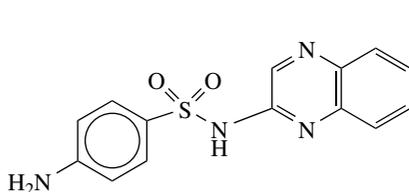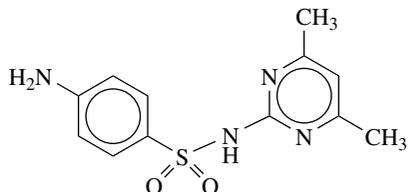
(114)   **(115)**

The poultry industry employs the sulfonamides sulfaquinoxaline **(114)**, also known as Diamprim, and sulfadimidine **(115)** for treatment of coccidiosis. The antimalarial pyrimethamine **(116)** (see Chapter 1) exhibits anti-coccidial properties, as does amprolium, APL, 1-[(4-amino-2-propyl-5-pyrimidinyl)methyl]-2-methylpyridinium chloride hydrochloride **(116a)**, a thiamine antagonist[73].
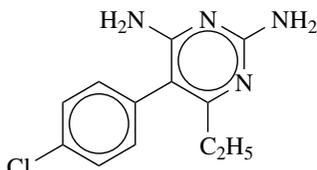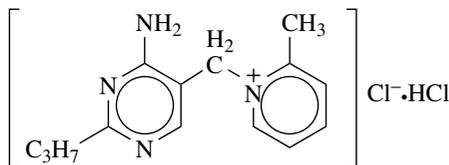
pyrimethamine
(116)   **(116a)**

XIII. PHARMACEUTICAL PRODUCTS

A. Introduction

Organic bulk medicinal products, a large number of which are synthesized from anilines, include: anti-infective agents such as sulfonamides, anthelmintics and urinary antiseptics; analgesics and antipyretics; barbiturate substitutes; and antihistamines. Many retain aromatic amino groups and exhibit a broad spectrum of activity. As with many agrochemicals, pharmaceutical products have both generic and trade names, in addition to true chemical names. Generic manufacture, including of products made from aryl amines, is a major global industry, led by Teva Pharmaceutical Industries Ltd, with headquarters in Israel.

Appropriate analytical techniques are essential for safe and effective use of drugs, and include flow-injection analysis for determinations of those containing primary amine groups, including sulfonamides, novocaine and sulfones[74].

B. Antibacterials

1. Sulfonamide drugs

The first antibacterial sulfonamide, or sulfa, drug was introduced in 1935 by I.G. Farben in Germany. It was known as prontosil, and associated with the Bayer trade name. The next major discovery was made in England during 1938 at May & Baker. It was sulfapyridine, a drug highly effective against pneumonia, soon to be known as M&B 693 (see Chapter 1). Despite the emergence of antibiotics, sulfa drugs are still in use, particularly for veterinary purposes, as well as for human consumption. Commonly used sulfa drugs include the systemic sulfisoxazole **(117)**, for urinary tract and ear infections, sulfamethoxazole **(118)**, for urinary tract infections, and sulfadiazine (sulfapyrimidine, microsulfon) **(119)**. Topical sulfonamide preparations include silver sulfadiazine, and sulfacetamide **(120)**, for treating ocular infections. Aminopyrimidine intermediates are used in the synthesis of sulfadiazine and sulfadimidine.

When the product of reacting chlorobenzene and chlorosulfonic acid is aminated under pressure, the product is dapsone **(32)**, used in control of leprosy[75]. This sulfone was developed as a result of sulfonamide studies undertaken at Bayer that include thiosemi-carbazones active against tuberculosis.
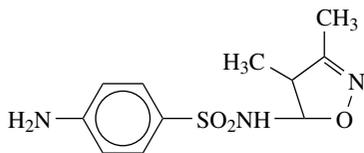
(117)
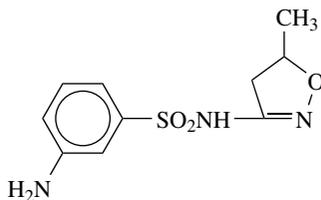
(118)
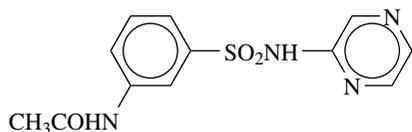
(119)
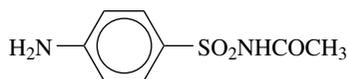
(120)

2. Others

Selective reduction of *m*-dinitrobenzene **(121)** followed by, successively, diazotization, introduction of hydroxyl, reduction of the nitro group and carboxylation, yields the antimycobacterial agent *p*-aminosalicylic acid **(122)** (Scheme 25) used with the antibiotic streptomycin. A three-step synthesis starting with toluene yields the inexpensive drug thioacetazone **(123)**.
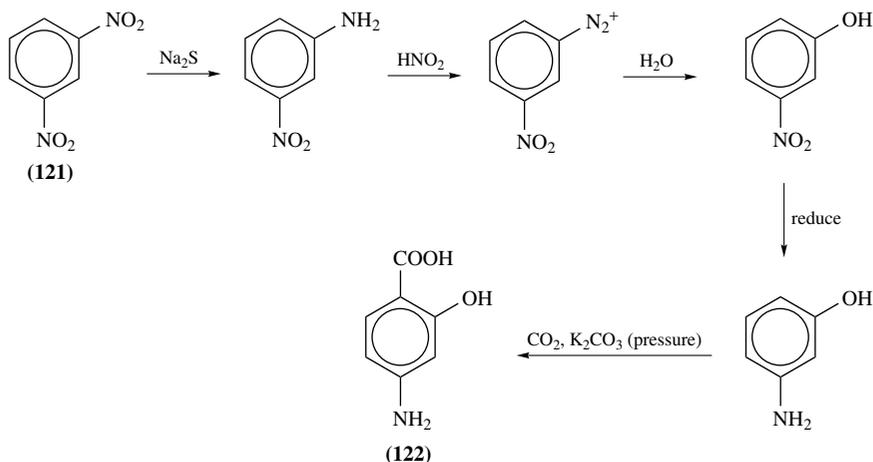
SCHEME 25

An antibacterial agent made from the intermediate 2-amino-6-methylpyridine **(124)** is nalidixic acid **(125)** used for treatment of the urinary tract (Scheme 26)[76]. An aminopyrimidine intermediate is used in the synthesis of trimethoprim, 5-(3,4,5-trimethyoxybenzyl)-2,4-diaminopyrimidine **(126)** (Scheme 27), useful for treatment of infections of the urinary tract and the chest. Unlike antibiotics, there is no build up of bacterial resistance to this drug.

(123)

(124)   **(125)**
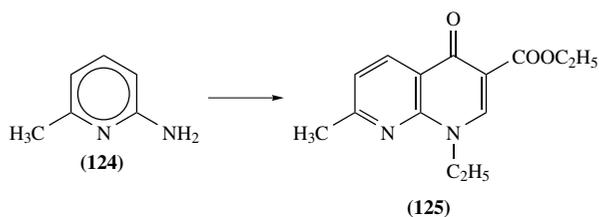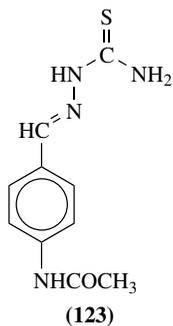
SCHEME 26

(126)
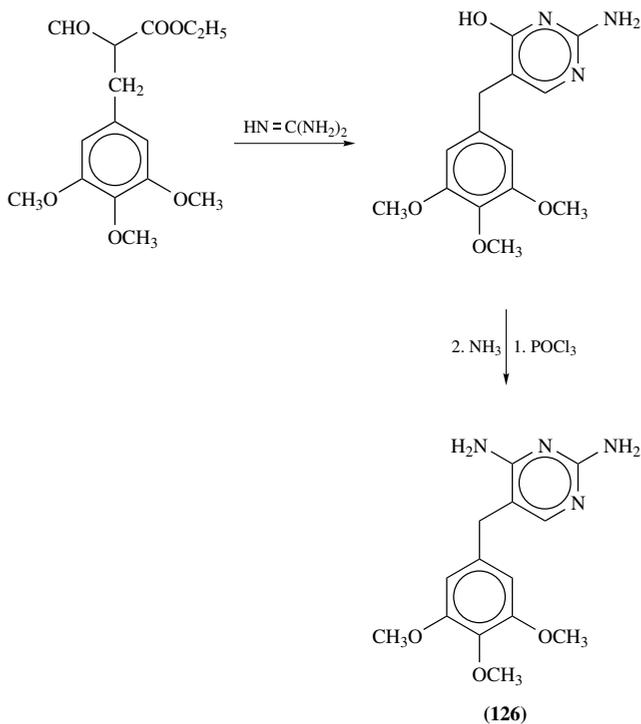
SCHEME 27

C. Antiviral Nucleoside Analogs

The antiviral drug Vidabarine (ARA-A) **(127)** was originally obtained from marine sources, the sponge *Cryptotethia crypta*, and terrestial bacterium *Streptomyces antibioticus*. It is produced by fermentation technology, and is useful in the treatment of herpes infections. Similar nucleosides, prepared from aminopyrimidines, are the antiherpes agents cyclovir (Zovirax), or famciclovir (famvir) **(128a)** and penciclovir (Denavir) **(128b)**. Famciclovir is converted into penciclovir in the body. Abacavrir (Ziagen) is a dideoxynucleoside, containing an aromatic amino group, that inhibits the HIV reverse transcriptase. It is used in combination therapy.
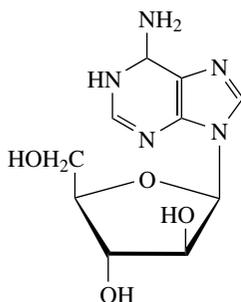
ARA-A, Vidabarine
(127)
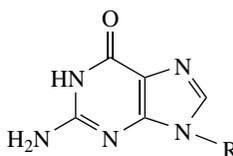
(128a) R = CH$_2$OCH$_2$CH$_2$OH
(128b) R = CH$_2$CH$_2$CH(CH$_2$OH)

D. Antifungal Agents

The first antifungal agents included a number of early triphenylmethane dyes, such as malachite green, gentian violet and basic fuchsin (see Chapter 1). Tolfanate **(129)**, an *N*-alkylated *m*-toluidine derivative, is a topical antifungal agent[77].

Tolfantate
(129)
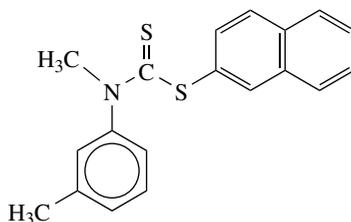
E. Antiparisitics

1. Antimalarials

Despite the emergence of drug-resistant strains of the parasite *Plasmodium falciparum*, the substituted 6-chloro-4-aminoquinoline, which is formally a 3-chloroaniline derivative, known as resochin, or chloroquine **(130)**, and other quinolines, are still widely

used as antimalarials (see Chapter 1). These include primaquine, 8-(4-amino-1-butylamino)-6-methoxyquinoline **(130a)**; and pyrimethamine, 5-(4-chlorophenyl)-6-ethyl-2,4-pyrimidinediamine **(130b)**. In the early 1990s, these quinolines were joined by the 4-methoxyquinoline methanol known as mefloquine, though even with this new drug there were early reports of resistance. Two 4-aminoquinoline Mannich-base derivatives **(131a)** and **(131b)** related to amodiaquine **(131c)** have exhibited more activity than the mother substance. However, in many geographical regions, particularly sub-Saharan Africa, the quinolines are practically useless.

resochin (chloroquine)   primaquine

(130)   **(130a)**   **(130b)**
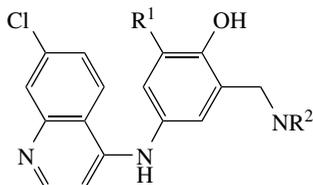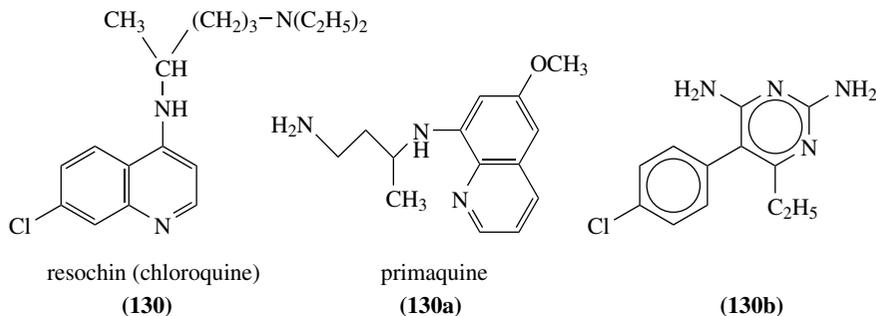
(131a) $R^1 = CH_2CH_2CH_3$, $R^2 = HBu\text{-}t$
(131b) $R^1 = CH(CH_3)_2$, $R^2 = HBu\text{-}t$
(131c) $R^1 = H$, $R^2 = (C_2H_5)_2$

Combinations of drugs, such **115** and sulfadoxine (4-amino-*N*-(5,6-dimethoxy-4-pyrimidinyl)benzenesulfonamide) **(132)**, trade name Fansidar, have been found useful in treatment of malaria[78]. The combination of **115** and **32** is known as Maloprim.

4-Chloroaniline **(133)** is the starting point for biguanidine therapeuticals including the antimalarial proguanil (Paludrine) **(134)**. Metabolism of **134** affords dihydrodiazine **(135)**. Another useful antimalarial is the 4-aminoquinoline known as amodiaquin **(136)**.

Sulfadoxine   proguanil

(132)   **(133)**   **(134)**

dihydrodiazine
(135)

amodiaquin
(136)
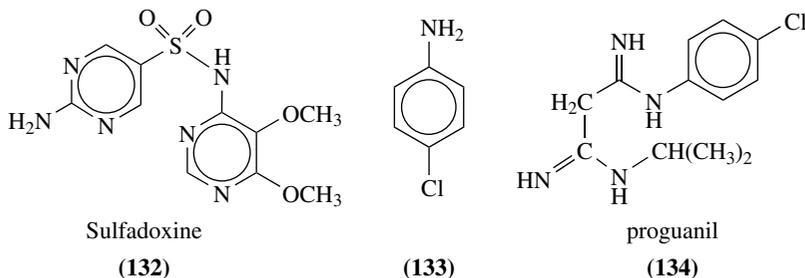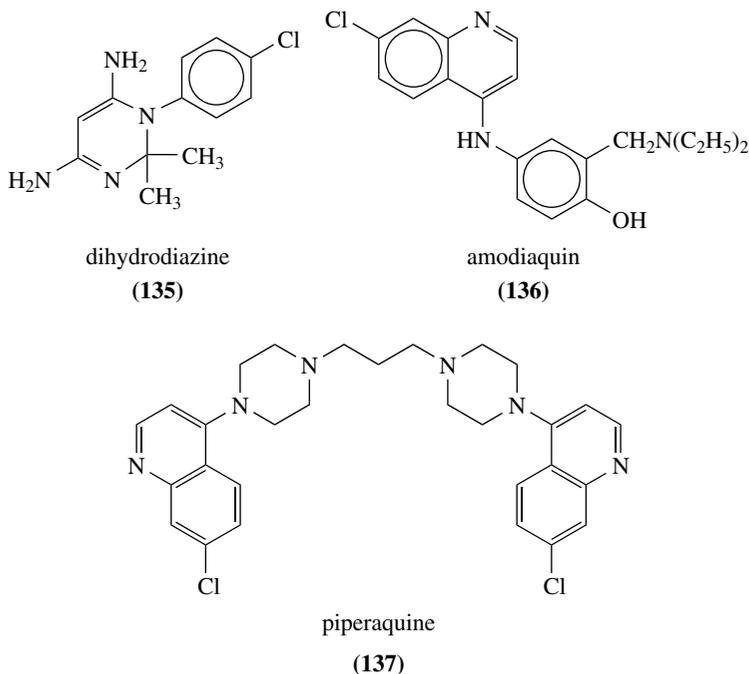
piperaquine
(137)

The bisquinoline known as piperaquine **(137)** was synthesized in 1966 at the Shanghai Pharmaceutical Industry Research Institute. Piperaquine was found to be active against chloroquine-resistant falciparum malaria. In order to delay resistance, it is used in combination therapy, including with dihydroartemisinin, a derivative of the Chinese plant product artemisinin, first isolated in 1972.

Attempts to prevent evolution of resistance have led to investigations of various other combinations of anilines for therapeutic use. Examples include Pyrimethamine **(131)** with sulfadiazine **(119)**, and trimethoprim **(126)** with dapsone **(32)**.

2. Antitrypanosomiasis agents

Earlier antitrypanosomiasis agents included the aminonaphthalenes trypan blue and Afridol violet. They were followed by the amide suramin[79] (see Chapter 1). Heterocyclic aromatic amines include quinapyramine **(138)** and puromycin **(139)**. Starting with 2-aminobiphenyl **(140)**, a five-step reaction yields the phenanthridine dimidium **(141)** (Scheme 28).

3. Anthelmintics

Diphenylamine **(8)** is readily converted into phenothiazine **(111)**, an inexpensive product useful in the treatment of human schistosomiasis (caused by blood and liver flukes), already discussed under animal health products. The salicylanilide oxyclozonide **(142)** came to prominence in the 1970s. Another schistosomal agent is the metabolite of lucanthone **(143a)**, namely hycanthone **(143b)**.

quinapyramine

(138)

puromycin

(139)

(140)

dimidium

(141)

SCHEME 28

(142)

(143a) R = H
(143b) R = OH

F. Products for Treatment of Non-infectious Diseases

Aryl amines are particularly important in the synthesis of central nervous system drugs. The first generation antihistamines reduce allergic reactions by blocking histamine H_1 at receptors in the central nervous system and, through non-selective binding to peripheral receptors, cause sedation. A number are synthesized from 2-aminopyridine, including pyrilamine **(144)**, and methapyrilene hydrochloride **(145)**, a potential carcinogen. Second-generation histamines exhibit no central action and are used for treatment of allergic actions alone[80].

(144)   **(145)**

1. Tranquillizers

These drugs were developed by introducing structural changes into first-generation diphenylmethane histamines that, as side reactions, were observed to cause drowsiness and exhibited sedative effects. *N*-Phenylation of *m*-chloroaniline is the first step in the synthesis of the phenothiazine chlorpromazine **(146)** (Scheme 29), structurally related to methylene blue (see Chapter 1)[81]. It is used for treatment of mental disease, including schizophrenia.

2. Anti-anxiety agents

Roche converted 2-amino-5-chlorobenzophenone **(147)** into the first benzodiazepine antianxiety agent, chlorodiazepoxide **(148)** (Scheme 30). The ring enlargement was unexpected, and was soon incorporated into similar products. The same intermediate, **147**, is the starting point for diazepam **(149)**, and provides one of two routes to oxazepam **(150)** discovered at Wyeth (Scheme 31)[82]. The full range of benzodiazepines exceeds fifteen different drugs used as tranquillizers, and in some case as hypnotics.

3. Hypnotics and sedatives

Anthranilic acid **(151)** and *o*-toluidine are the intermediates used to make Methaqualone **(152)**, an important hypnotic (Scheme 32)[83]. It was introduced as a daytime sedative and

SCHEME 29

for inducing sleep in the UK in 1959, and in the US in 1965 (where it was also known as Quaalude). Though originally considered a safe substitute for barbiturates, its extensive misuse brought about withdrawal from the US market in 1984. Methaqualone remains available in Europe, as the active component of Mandrax.

4. Anesthetics

Local anesthetics make use of the lipophobic property of an aromatic amine moiety, or its acyl derivative, that links with a hydrophilic amino acid. The products include the anilide lidocaine, or 2-(diethylamino)-N-(2,6-dimethylphenyl)acetamide (**153**), the toluidine derivative prilocaine and the century-old procaine, 2-diethylaminoethyl 4-aminobenzoate (**154**)[84]. The ester is prepared by reacting p-aminobenzoic acid with ethylene chlorohydrin and diethylamine.

Many of the medical products reviewed here find multiple applications. Thus procaine compounded with benzylpenicillin, penicillin G is an antimicrobial veterinary drug, approved in the US as a postexposure prophylaxis following inhalation of anthrax, providing that the strains do not have penicillin resistance.
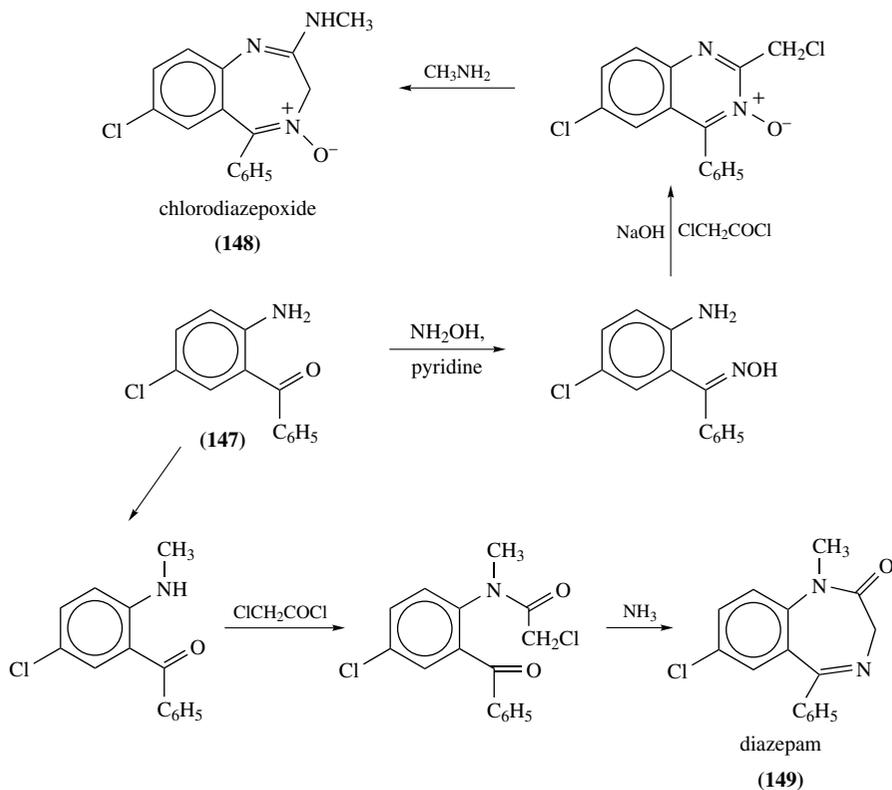
SCHEME 30. Syntheses of chlorodiazepoxide and diazepam
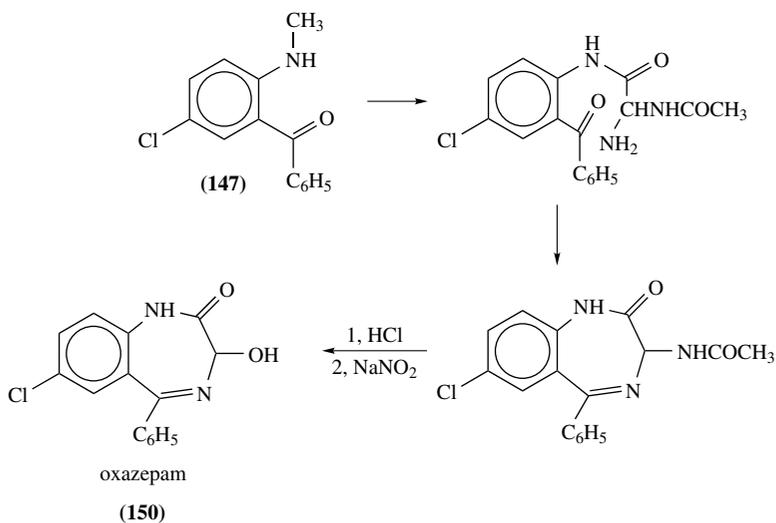
SCHEME 31. Synthesis of oxazepam

SCHEME 32

(153)   (154)

(155)   (156a) R = H
                  (156b) R = COOCH$_3$
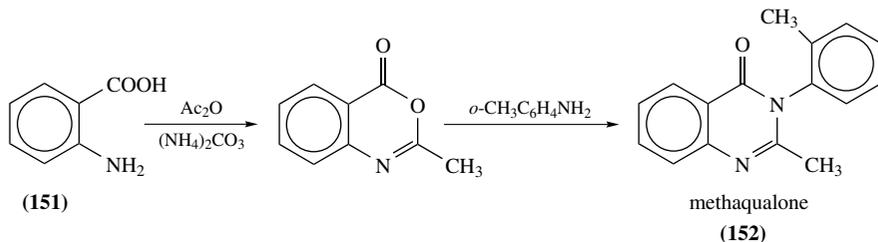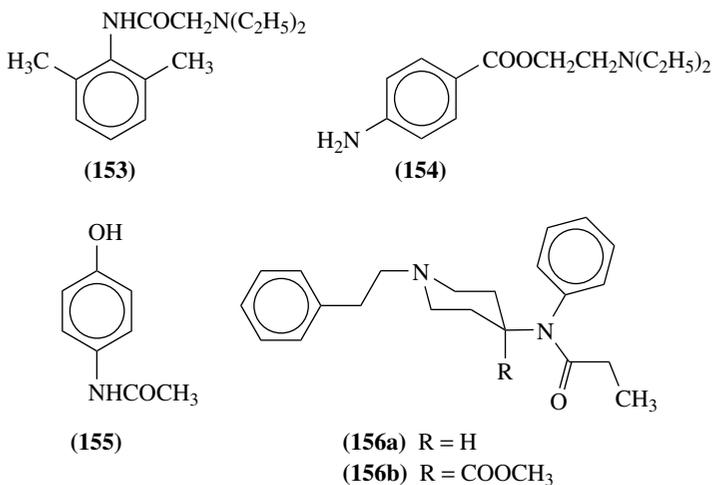
G. Analgesics: Paracetamol, Fentanyl

The most widely used analgesic is Paracetamol, or N-acetyl-p-aminophenol **(155)**, also known as acetaminophen (US), and Tylenol (with codeine), and synthesized from nitrobenzene. Care has to be taken with use; hepatoxicity can develop with overdoses.

Aniline is the starting point for fentanyl, N-(1-phenethyl)-4-piperidinyl)-N'-phenyl propionamide, or N-(1-phenethyl-4-N'-propionanilido)piperidine **(156a)**. This synthetic opiate is approximately 100 times more potent than morphine. It was synthesized in Belgium during the 1950s and introduced into medical practice during the 1960s. Its legal uses include for anesthesia and analgesia in the treatment of chronic cancer pain. A derivative, probably carfentanil **(156b)**, has been developed as an incapacitating agent, and there is speculation that it was used in the October 2002 Moscow theatre siege against Chechen rebels, though with unfortunate deaths caused also to their hostages. Survival following exposure requires rapid application of the opiate antagonist Naloxone.

H. Diuretic Agents

The lead compound in the discovery of diuretics was sulfanilamide. An important product was chlorothiazide **(157)** (Scheme 33), which became the model for the most important thiazide diuretic, furosemide, or frusemide, 4-chloro-N-furfuryl-5-sulfamoylanthranilic acid, or 5-(aminosulfonyl)-4-chloro-2-[(2-furanylmethyl)amino] benzoic acid **(158)**, used

chlorothiazide

(157)

SCHEME 33

(158)

(159)
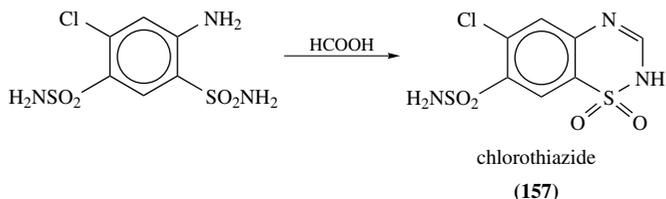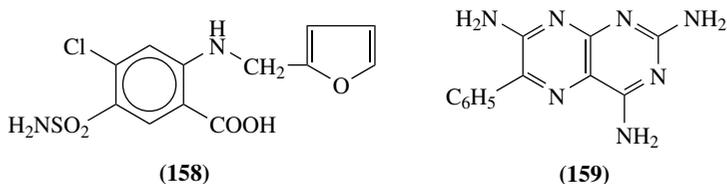
in acute pulmonary oedema[85]. Triamterene, or dyrenium (Dytac) **(159)**, is used with other diuretics, since it reduces potassium loss, particularly when sulfonamides and thiazides are prescribed[86].

I. Vitamin B2 (Riboflavin)

Vitamin B2 is manufactured by a four-step process requiring 3,4-dimethylaniline (3,4-xylidine) and aniline. Ribose, obtained by fermentation of glucose, is first converted into riboside by reaction with the xylidine. Following hydrogenation, the resulting ribamine is reacted with benzenediazonile chloride to afford phenylazoribitylamine. The crystalline, dried product then undergoes cyclocondensation with barbituric acid to afford vitamin B2 in overall yield of 60% or greater. China is a major manufacturer, totaling around 1,000 metric tons per year, two-thirds by this process. A number of fully chemical syntheses have also been employed. More recently, single-stage fermentation processes based on sugar and plant oil have been introduced industrially in Germany, the US and China. These promise to be cheaper and to produce less waste[87].

pteroylglutamic acid (folic acid)

(160)
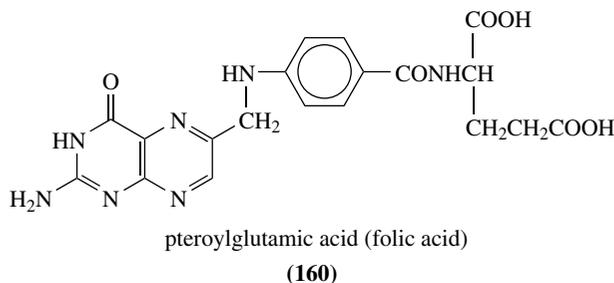
J. Folic Acid

Folic acid **(160)** is a pteroic acid derivative, pteroylglutamic acid, incorporating *p*-aminobenzoic acid. Folates is the generic term for any member, or mixture, of pteroyl-glutamic acids. Synthetic folic acid is manufactured from *p*-aminobenzoyl-L-glutamic acid.

K. Other Important Pharmaceutical Products

The antihypertensive hydrazinophthalizines vasodilators hydralazine **(161a)** and dihydralazine **(161b)** have been used in studies, but they are too toxic for general use. The beta-blocker acebutolol, or Prent (Bayer)[88], Sectral (Wyeth) **(162)**, reduces blood pressure by blocking adreno receptors. As an effective UV absorber, *p*-aminobenzoic acid **(163)** is widely used in sunscreen formulations. Since **163** causes eye irritation and staining of clothes, *p*-aminobenzoic acid is nowadays mainly applied as an ester. The anthranilic acid derivative menthyl anthranilate **(164)** is a UV absorber also added to sunscreen formulations. Some 80% of the market for sunscreens is made up of organic compounds. Newer products include CIBA's benzotriazole derivatives[89−93]. Other uses of *p*-aminobenzoic acid include in the manufacture of aramids and azo dyes.

hydralazine

(161a) R = H
(161b) R = NHNH$_2$

Prent

(162)

(163)

(164)

amascrine

(165)

ethacridine

(166)
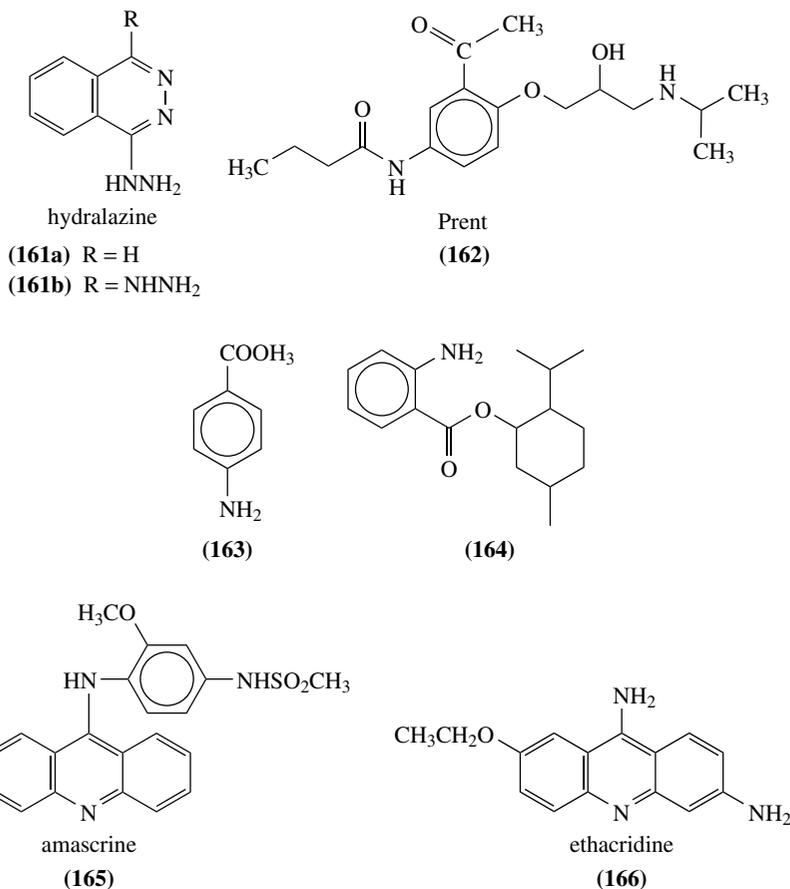
The acridinyl aniside amascrine **(165)** is useful in treatment of some cancers, including acute adult leukemia. The lactate of 7-ethoxy-3,9-acridine diamine, or ethacridine **(166)**, is an abortifacient, used for induction of second trimester abortions. The antitumor drug mitozantrone (mitoxantrone, novantrone) **(167)**, a bis(hydroxy)aminoanthraquinone

HO(CH$_2$)$_2$NH(CH$_2$)$_2$NH   O   OH

HO(CH$_2$)$_2$NH(CH$_2$)$_2$NH   O   OH

mitozantrone (mitoxantrone)

(167)

N(CH$_2$CH$_2$Cl)$_2$

R

(168a) R = CH$_2$CHCOOH
                                  |
                                 NH$_2$

(168b) R = CH$_2$CH$_2$CH$_2$COOH
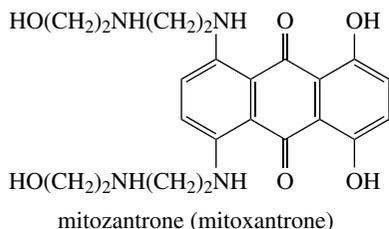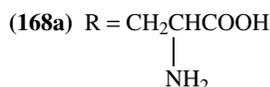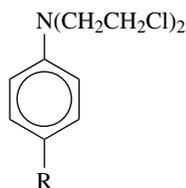
derivative, is effective against some types of breast cancers, and acute leukemia. Mel-phalan **(168a)** and Chlorambucil **(168b)** are employed as alkylating agents in cancer treatment.

XIV. RUBBER PRODUCTS

Activators and vulcanizing agents, including accelerators, mainly derived from aromatic amines, account for around half the consumption of organic rubber-processing chemicals.

A. 2-Mercaptobenzothiazole (MBT) and Derivatives

The vulcanization accelerators include the thiazole 2-mercaptobenzothiazole (MBT) **(169)**, and its derivative benzothiazole disulfide (dibenzoythiazyl disulfide, 2,2′-dithiobis (benzothiazole), MBTS) **(170)**. Organic accelerators enable reduction in time of vulcan-ization, more effective use of sulfur in formation of cross-links and use of low processing temperatures. MBTS delays vulcanization, when compared with MBT alone. They are used in production of conveyor belts, footware, etc. The 2-mercaptobenzothiazole zinc salt (MBTZ) **(171)** is also important, and is used in latex products. Other sulfur donors include 2-morpholinodithiobenzothiazole, 2-(4-morpholinyldithio)benzothiazole (MBSS, MORFAX) **(172)**.
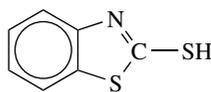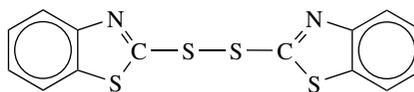
(169)   **(170)**
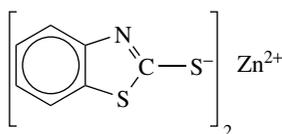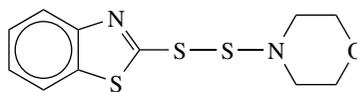
(171)   MBSS
                   (172)

MBT is produced by reacting aniline and carbon disulfide with sulfur at 250 °C and under pressure. The major portion is further processed to MBTS, also an important inter-mediate in the manufacture of various thiazoles for rubber accelerators and plasticizers,

and sulfenamides. MBT is produced by a batch process, though during World War II, I.G. Farben developed a continuous process[94]. The batch process gives a molten crude of 88–90% purity in MBT. An important phase of this process is the purification of the crude MBT, involving a hot caustic extraction and oxidation of the impurities. The crude melt of NaMBT is passed through a packed column in which countercurrent steam stripping removes benzothiazole, H_2S and unreacted aniline. The steam-stripped melt is then extracted with hot alkali. Many of the impurities (comprised essentially of polysulfidic tars) are dissolved hydrotropically or as sodium salts. Most of these dissolved impurities are then precipitated following addition of ammonium or potassium persulfate to the crude solution. The purified NaMBT (97%) is removed by decantation. It is treated with chlorine to yield MBTS, acidified with sulfuric acid to afford purified MBT as a precipitate or reacted with zinc sulfate to produce **171**. Zenite ultra-accelerators, incorporating zinc, bring about vulcanization in a few minutes. MBTS with morpholine and sulfur yields **172**.

Sulfenamides, made from **170**, by reactions involving primary and secondary amines under oxidizing conditions, include *N*-cyclohexyl-2-benzothiazole sulfenamide **(173)** and *N*-oxydiethylene-2-benzothiazole sulfenamide (2-(morpholinothio)benzothiazole) **(174)**. Sulfenamides release 2-mercapto accelerators and amine during vulcanization. The amine is a secondary accelerator that brings about fast vulcanization after a slow start. Applications include in tyres and conveyor belts. They are not applicable to hot-air vulcanization processes[95].
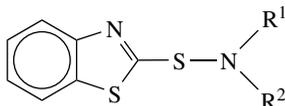
(173) $R^1 = H$, $R^2 = $ cyclohexyl

(174) $R^1R^2 = -(CH_2)_2O(CH_2)_2-$

B. Other Vulcanization Agents

These include: amine-aldehyde products, produced by reacting anilines or *p*-toluidines with aldehydes in the presence of catalyst; aryl-guanidines, such as 1,3-diphenylguanidine, or *N*,*N'*-diphenylguanidine, from reacting cyanogen chloride with hot aqueous aniline, or with toluidine derivatives; dithiocarbamates, from reacting carbon disulfide with primary and secondary amines; a thiuram **(175)**, employed in rapid vulcanization and as a secondary accelerator; and triazine accelerators **(176)**, for special purposes, giving higher cross-linking densities than thiazoles. A useful sulfur donor is **174**. Trichloromethylthio-sulfanilide **(177)** is a vulcanization retarder used with thiazoles.

C. Prevention of Rubber Deterioration

Over half of the remaining market for products used in the processing of rubber is made up of antioxidants, antiozonants and stabilizers, either amino compounds or phenols. Aniline is used to manufacture vulcanization accelerators, antioxidants and antidegradants. Of the latter, several are *N*-substituted derivatives of *p*-phenylenediamine and octyl diphenylamine. Diphenylamines terminate free-radical reactions by donating the amino hydrogen, and are used to protect a wide range of polymers and elastomers. Many synthetic rubbers incorporate alkylated diphenylamine antioxidants. Other antioxidants include aryl amine resinous products from, e.g. condensation of aniline and acetone in the presence of

(175)

x = 2,4

(176)

(177)
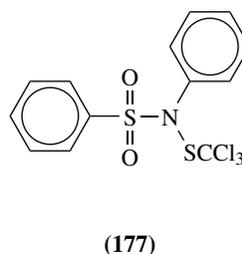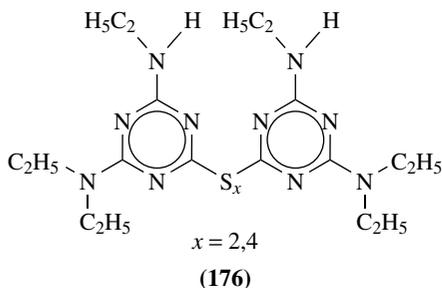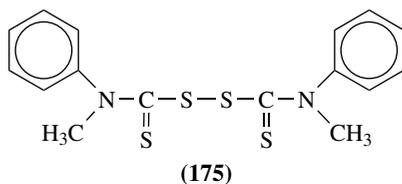
hydrochloric acid. Substituted *p*-phenylenediamines include the product from catalyzed condensation of hydroquinone with aniline, *N*,*N*′-diphenyl-*p*-phenylenediamine **(178)**. However, it suffers from staining of rubber. Reacting aniline with 1-naphthol, in the presence of an acid catalyst such as sulfanilic acid, or, rarely, with 1-naphthylamine, by vapor-phase catalysis with alumina gel at 300 °C, yields the important antioxidant 1-phenylaminonaphthalene, or *N*-phenyl-1-naphthylamine **(179)**. The reaction between aniline and 2-naphthol yields the antioxidant 2-phenylaminonaphthalene, or *N*-phenyl-2-naphthylamine **(51)**. These products protect against oxygen and heat. Liquid-phase catalytic hydrogenation of aniline under pressure yields the antioxidant cyclohexylamine, also employed in manufacture of cyclamates, the sweetening agents; production in the US for this purpose may increase if the ban on their use is lifted. The *p*-phenylenediamines substituted at nitrogen are antioxidants, anti-flex-cracking agents and antiozonants.

(178)

(179)
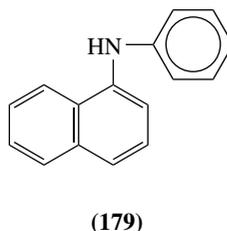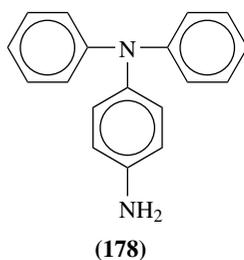
Diphenylamine **(8)** reacts with nitrous acid to yield *N*-nitrosodiphenylamine **(180)**, formerly a useful rubber vulcanization inhibitor. As a toxic nitroso compound, its use is now restricted. The reaction between **8** and acetone yields *N*-phenylbenzeneamine, a rubber antioxidant. 3-Methyl-phenyl-1-benzenesulfonyltriazene **(181)** and its toluene analog, both made from the reaction between the diazonium salt of aniline and the corresponding sulfonamide, have been used as blowing agents for rubber.

The structures (180) and (181) appear here.

(180)   **(181)**
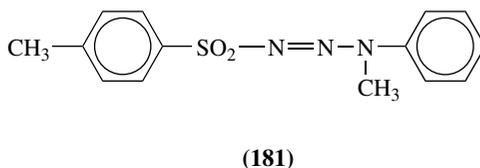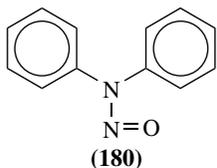
Condensation of aniline with aldehydes and ketones yields 2,2,4-trimethyl-1,2-dihydroquinoline, which polymerizes to give an oxidant employed in the processing of elastomers.

XV. EXPLOSIVES

Nitration of *p*-nitroaniline **(15b)**, or reacting picric acid with phosphorus pentachloride, yields trinitrochlorobenzene, which on amination affords 2,4,6-trinitroaniline, the explosive picramide. Phosgenation of *N*-ethylaniline **(26)** gives a substituted urea used as a stabilizer for explosives. Diphenylamine **(8)** is used as a stabilizer, for nitrocellulose explosives as well as for celluloid, and also as a solid rocket propellant. Ethylaniline **26** is employed in the manufacture of centralite, a stabilizer in smokeless powder. Other uses for **15b**, the largest volume nitroaniline, include in the production of dyes, antioxidants and pharmaceuticals.

XVI. HETEROCYCLIC ANILINES

Heterocyclic aryl amines, such as pyridine and the pyrimidines, are important in the production of colorants and pharmaceutical products and, apart from mention in the relevant sections of this chapter, have received extensive reviews. Here the emphasis is on the industrial applications of aminotriazines, for which industrial interest followed the bulk commercial availability after 1945, particularly from American Cyanamid, of the chlorotriazine cyanuric chloride **(182)**[96]. Reactions of cyanuric chloride with amines and substituted amines afford substituted melamines and various aminotriazines that have found application in pharmaceuticals and herbicides.

The structures (182) and (183) melamine appear here.

(182)   **(183)**
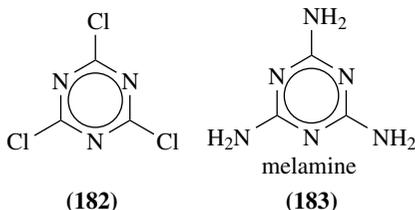
Melamine (2,4,6-triamino-1,3,5-triazine) **(183)** is made by heating dicyandiamide under pressure, mainly by the traditional late-1930s gas-phase technology. It is employed in the manufacture of synthetic resins by condensation with formaldehyde. The product, also called melamine, is used for molding purposes, surface coatings, laminates, fire retardants and in wood-based panels and as wood adhesives (see Chapter 1). Manufacturing processes give both molding compounds and resin syrups.

The furniture, laminate flooring and construction industries are principal users of melamine products. In 1998, Cytec (the 1993 chemicals specialty spin-off from American Cyanamid) in the US began the production of the first formaldehyde-free melamine resins

used in paints and coatings. Important flame-retardants are melamine salts of phosphoric acid, valuable in industrial and electrical applications. The growing interest in non-halogen flame retardants has led to extended applications of melamine phosphates and pyrophosphates[97]. Butylated melamine resins are used in paints and varnishes.

Melamine resins are also important in the strengthening of paper, for use in protecting banknotes, wallpapers and maps. Melamine resins show good resistance to moisture, particularly through addition of fillers, and heat. Melamine offers fast curing times, great durability, and the use of light colors for hard-wearing kitchen and shop counter tops, as, for example, decorative laminates, often called Formica. Domestic appliances, textiles and furniture incorporate melamines. Trimethylol melamine resins are important textile finishing products used in durable press finishing of cellulose fabrics, and for easy-care treatments. More recently, melamine has been found valuable in the dyeing of treated silk fabric[98]. Melamine-treated fiber is stable and offers good heat resistance, particularly in direct flame applications. This property arises from extensive cross-linking and low thermal conductivity. Monodisperse melamine resins are made by polycondensation of methylol melamines. Other uses include as coatings for cans and road vehicles.

DSM Melamine, a division of the Dutch DSM corporation, is the world leader in the melamine business, with, in 2000, capacity of 200,000 metric tons, and around 25% of market share. Since that time, DSM has expanded capacity based on new Shortened Liquid Phase (SLP) high-pressure technology developed in the late 1990s. In 2002, DSM began operation of a 30,000 metric tons-per-year plant at its Geleen facility, supplementing the 115,000-ton gas-phase plant operated there. In July 2004, DSM announced that it was about to commence a joint study with China National Offshore Oil Corp. Chemical Ltd for construction of the world's largest gas-phase technology melamine plant on Hainan Island, making use of local natural gas. Planned annual capacity is 120,000 tons[99]. Agreement was reached in the first quarter of 2005; completion is scheduled for late 2007[99]. China has become a leading global manufacturer of melamine. Production there during 2003 was around 88,000 metric tons, compared with 46,500 metric tons in 1998.

A modern version of an old route to melamine involves treating the guanidine **184** with 1,1,1,3,3,3-hexamethyldisilazine (**185**), the latter acting as both catalyst and solvent. After refluxing for five hours at 120–130 °C, there is quantitative yield of melamine (Scheme 34). Good recovery of catalyst is claimed[100].

SCHEME 34

The methylol and amino functional groups present in melamine resin are available for covalent attachment of antigens, antibodies, enzymes and other ligands of biological importance. Molecularly imprinted polymers that incorporate alkylated aminotriazines have been proposed for analytical purposes[101].

XVII. PHOTOGRAPHIC CHEMICALS

Aniline is converted into hydroquinone, a photographic developer in black and white photography used with metol (*p*-methylaminophenol). Production of hydroquinone commences with oxidation of aniline by manganese dioxide in aqueous sulfuric acid at 0–5 °C,

to yield 1,4-benzoquinone. The product is removed by steam stripping, and is then reduced with iron at $55-65\,^{\circ}$C, or by catalytic hydrogenation. Following crystallization, isolation and drying, the yield of hydroquinone is around 85%[102]. This process is worked in China. Elsewhere, more modern processes are available for manufacture of 1,4-benzoquinone. The photographic developer Amidol M is 2,4-diaminophenol hydrochloride.

Substituted *p*-phenylenediamines are developers used in color photography. They include *N*,*N*-diethyl-*p*-phenylenediamine (*p*-diethylaminoaniline) monohydrochloride, its toluidine analog, *N*-*p*-anilinopyrrolidine, 4-amino-*N*-*β*-methanesulfonamidoethyl-*m*-toluidine sesquisulfate monohydrate and 4-amino-3-methyl-*N*-ethyl-*N*-(*β*-hydroxy-ethyl)aniline sulfate.

XVIII. LIQUID CRYSTALS AND LIQUID-CRYSTAL POLYMERS

Certain aryl amines are endowed with unusual electronic properties. Schiff's bases such as 4-methoxybenzylidene-4-*n*-butylaniline were the original experimental chemicals used in the early development of electrical and electrooptical displays. Liquid crystal display (LCD) technology relies on twisted nematic or supertwisted nematic effects. Later nematogen development was based on cyanobiphenyls[103].

Polyimide films are employed in LCD manufacture. The surface of the film is rubbed to align the molecules. A newer method developed at IBM involves rearrangement of atoms on an amorphous or isotropic surface with a low-energy collimated Ar-ion beam[104]. More recently, the liquid crystalline properties of aniline derivatives, including alkyl anilines[105] and azo compounds, have attracted attention[106]. To date, the development of such liquid crystal polymers has been restricted, despite the success of Kevlar and similar products[107].

Anilines are incorporated into modern chromophores, optical species that offer potential as polymeric electrooptic modulators, possibly as substitutes for lithium niobate crystals, such as **186**. Their large optical non-linearities with extended π-electron systems make possible optical switching and information processing at very low voltages, generally less than 5 volts. The electrooptic modulation depends on redistribution of electrons when externally applied electrical fields disturb internal electrical fields that arise from interactions between electrons and protons. This brings about changes in light intensity or phase and, for example, can be used to encode information onto laser beams. However, application of these organic molecules is dependent upon the availability of crystals in which the chromophores are organized into a non-centrosymmetric lattice[108, 109].

XIX. OTHER POLYMERS

A. Nylon

Caprolactam (6-hexanolactam), used in nylon production, can be made from aniline, by hydrogenation to cyclohexamine in the presence of a nickel–cobalt catalyst. The amine is then converted to cyclohexanone oxime.

B. Polybenzimidazoles

Around 1960 Carl Marvel at Illinois discovered that the reaction between 3,3′,4,4′-tetraaminobiphenyl (diaminobenzidine) **(186)** and diphenyl isophthalate yielded the strong, stable polybenzimidazoles. The thermal and chemical stability of their fibers make them suitable for parachutes, space suits and firefighting clothing. Several novel polymerizations were reported, including with 1,2,5,6-tetraaminoanthraquinones.

(186)
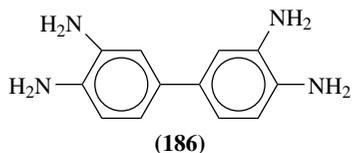
C. Polyimides

The discovery of the polyimide known as Kapton was made in 1965 by Edwards at DuPont. It opened up the high-temperature plastic market. The first stage in manufacture involves the solution-phase reaction between an aromatic diamine with a dianhydride of a tetracarboxylic acid. The amino group nitrogens attack the carbons of the carbonyls in the anhyride. This gives a poly(amic) acid, which is then processed into the required product shape, followed by cyclodehydration to give the polyimide. Typical aromatic diamines are 4,4′-diaminodiphenyl ether (4,4′-oxydianiline), *o*- and *p*-phenylene diamines (**52b** and **22**), 4,4′-methylenedianiline **(9a)** and dapsone **(32)**. Polyimides include the polyesterimides, polyamideimides and polyesteramideimides[110–112].

There are two main methods for synthesis of polyimides. In one, the dianhydride and diamine are separately dissolved in *N*,*N*-dimethylacetamide or *N*-methylpyrrollidinone. The solutions are mixed for 24 h to afford poly(amic) acid. The mixture is then refluxed for a further 24 h, using an azeotroping solvent to distill off water. Alternatively, the diamine is mixed with the dianhydride as its ester-acid, and heated at 190 °C in the presence of *o*-dichlorobenzene as azeotroping solvent. There are reported improvements[113]. A useful intermediate used in the manufacture of polyamide and imide engineering plastics is 1,3-bis(3-aminophenoxybenzene).

Polyimides are high-performance polymers, mainly used as films and as substrates for flexible printed circuits, bar code labels, and transformer and capacitor insulation. The rigid structure is responsible for a T_g greater than 300 °C. Since Kapton is flexible, lightweight and withstands very low and very high temperatures, it is an important aerospace material. Potential uses include as a thin film absorber for solar cells[114].

The optical properties and robust natures offer potential for extensive development of novel devices[115]. Maggioni and colleagues have developed glow discharge vapor deposition polymerization for polyimide coatings, a process that does not involve solvents. This is based on weakly ionized glow discharge using standard radio-frequency magnetron sputtering equipment. Low-energy noble gas ions impinge on a solid organic dianhydride and 4,4′-dioxyaniline, causing them to sublimate and deposit on substrate, where polymerization takes place on heating to yield **187**[116].

(187)
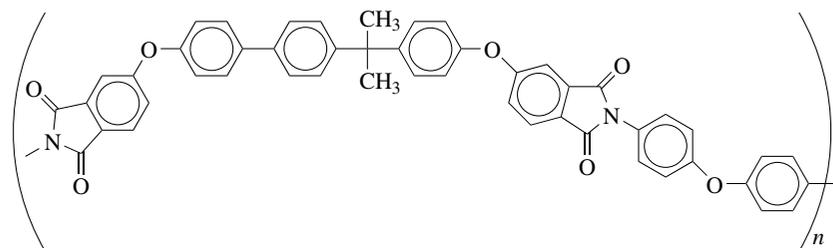
The high refractive indices of polyimides, compared to many other polymers, combined with excellent optical clarity, have been exploited in the development of coatings in optoelectronic applications[117]. Soluble thin-film polyetherimides (OptiNDEX™), such as **188**, with controlled refractive indices for use as optical coatings, have been prepared (Scheme 35). The refractive index is controlled through variation in the dianhydride and diamine composition. The polyimides exhibit good thermal stability at 400 °C, and T_g

diamine

dimethylacetamide, 24 h
25 °C

160 °C, 24 h
−H_2O dimethylacetamide, toluene

(188)
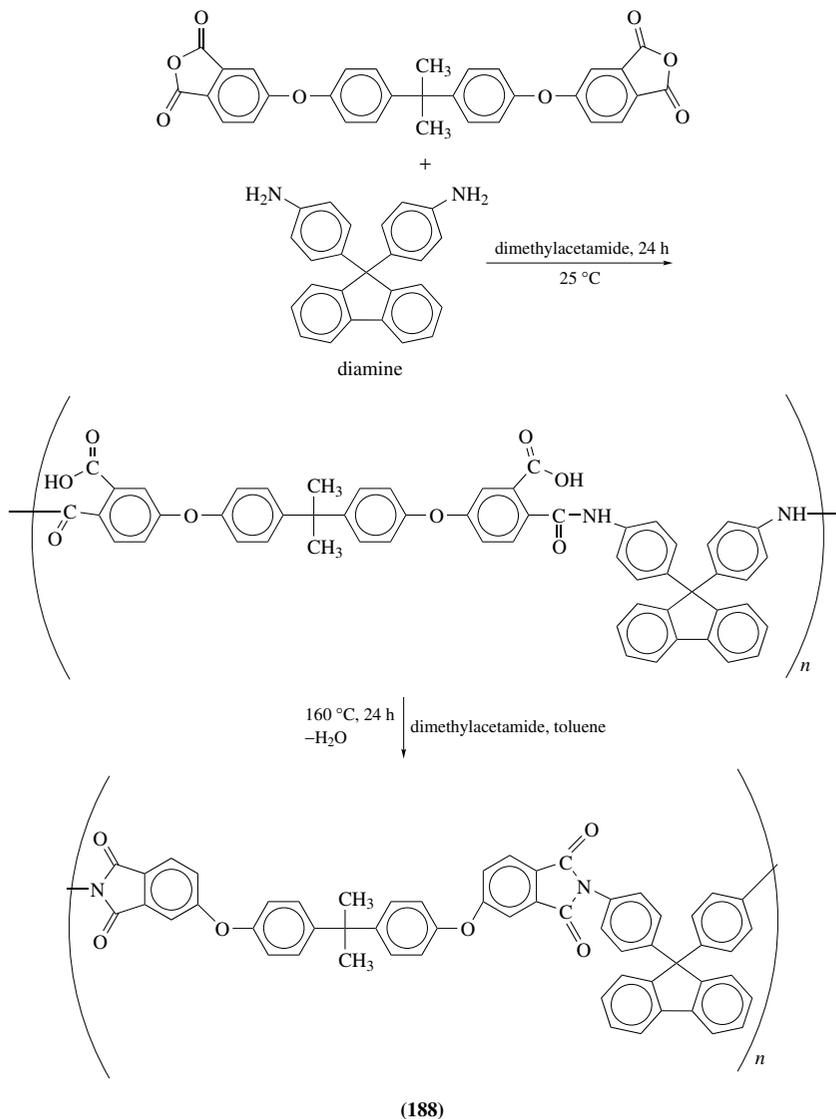
SCHEME 35

above 220 °C. Since they can be spun in thicknesses ranging from a few hundred nanometers to as much as 10 microns, possible uses include as antiglare coatings and various other ophthalmic applications[118].

The process developed by Edwards required elevated temperatures. A low-temperature process uses, instead of the usual dianhydrides, a monomer with two dicyanomethylene groups, which are more reactive toward nucleophiles. Polymerization affords a partially imidized product that readily cyclizes, with loss of malonitrile, to the polyimide[119].

D. Kevlar and PEEK

Nylon is an important engineering plastic because of its toughness, rigidity, abrasion resistance and lack of chemical reactivity. However, polymer relaxation (alignment lost through melting) occurs during the usual industrial process of spinning. In the early 1960s, Kwolek at DuPont's Pioneering Research Laboratory of the Textile Fiber Department discovered liquid-crystalline solutions of an aromatic polyamide (aramid) that for the first time gave aligned, rigid polymer chains during spinning. An improved product, Kevlar, was introduced in 1971 as a super fiber, a low-density straight-chain polymer of great heat stability and stiffness. During extrusion there is an increase in regularity of the liquid crystals. Owing to the packing of the rigid, linear molecule, Kevlar is about five times stronger than steel by weight. Applications include aircraft wings and bullet-resistant helmets and vests. By the late 1970s, aromatic polyamides represented over 50% of the high-temperature plastics market. With polyimides they accounted for almost 90% of total sales in this sector[120].

The *p*-aryl amides are produced from terephthalic acid and *p*-phenylenediamine. They are noted for high strength and thermal resistance that arise from extensive conjugation and linear geometry that enhances chain orientation. High-strength fibers with similar properties can be manufactured from aramids and melamine.

A former application of aniline, now mainly displaced, was conversion to hydroquinone. The hydroquinone is the starting point for a process developed by Rose at ICI's Plastics Division. The outcome, a high melting polymer, resistant to oxidation, is poly(ether-ether-ketone), or PEEK, made from hydroquinone. This high-performance thermoplastic, with fiber reinforcements such as Kevlar, is used in plastic kettles, nose-cones of missiles and engines.

E. Polyanilines

Polyanilines (Scheme 36) are conjugated polymers whose π electrons are delocalized over the whole molecule. They are important conducting polymers that also act as semiconductors, in a similar manner to inorganic semiconductors[121–123]. They are made by chemical or electrochemical (anodic) oxidation of aniline. The product, a poor textile colorant, dates from the 1860s, and is still known by the name given at that time, emeraldine. In the electrochemical process, it is possible to produce thin films directly on conductive substrates. Polyanilines have been used in photoelectrochemical devices[124–126].

Polyaniline coatings provide corrosion protection for aluminum and iron alloys[127]. Electroactive and electronically conductive polyaniline polymethacrylate-silica nanocomposites have been investigated for use in detection of biological warfare agents[128]. Electronic properties have been investigated by MacDiarmid and coworkers[129–130]. The use of polyaniline membranes in gas separations has been reported[131]. Polyaniline **189** mixed with a dimercaptan, such as 2,5-dimercapto-1,3-thiadiazole, has been proposed as a composite organic cathode for use in low-cost, solid-state, rechargeable lithium batteries[132]. Another potential use is as a plastic infrared polarizer[133]. Polyaniline **(189)**, as pseudo-leucoemeraldine, combines with the phenylene sulfide **190** to yield a diphenyl monomer,
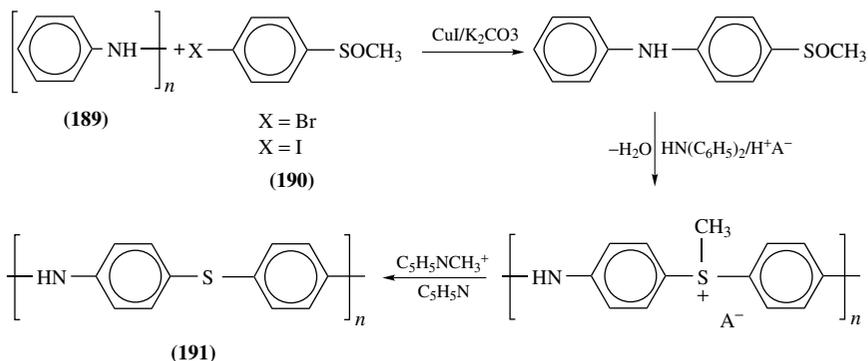
SCHEME 36

that is converted into a soluble, colorless, structurally well defined and thermally stable polymer, poly(phenylenesulfidephenylenamine) (191), with potentially useful optical, mechanical and electronic properties (Scheme 36)[134].

XX. CURING AGENTS FOR EPOXY RESINS

Aromatic amines, particularly 4,4′-methylenedianiline (MDA, 4,4′-diaminodiphenyl-methane) (9a), are extensively employed as curing, or hardening, agents for epoxy resins, the condensation products of epichlorohydrin and bisphenol A. Certain of these amines have high T_g values; others have high viscosities. Blends, comprising mainly of 9a with higher functionality polymethylene polyanilines, have excellent mechanical, thermal and electrical properties. The *m*-phenylenediamine (MPDA) (52a) is another important curing agent. An intermediate employed in the production of curing agents is *o*-ethylaniline (192).
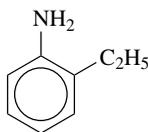
(192)

Epoxy resins are used in cold setting or thermo setting adhesives, in production of industrial composites and films of high resistance and permanence. Over half of production is used in protective coatings. Electrical laminates and filament windings are also important uses, representing about 20% of consumption.

Other aromatic amines are used when exposure to high temperatures and/or corrosive chemicals are required. They are formulated to have convenient mixing ratios, the desired application rheology and adequate pot life, while curing. As coating films or as adhesive bonds they offer, in many cases, better performance than single component systems. The intermediate 4,4′-[1,4-phenylenebis(1-methylethylidene)]bisaniline is used in the production of high-performance epoxy resins and epoxy curing agents[135, 136].

XXI. THE ANILINE POINT

Aniline is employed in an important routine test used in the petroleum industry for the determination of the approximate aromatic content of oils. The aniline point is the lowest

temperature at which an oil is completely miscible with an equal volume of aniline. Instrumental methods are employed, and the aniline point test is also used for evaluating the oil-based drilling fluids known as muds.

XXII. FUTURE DIRECTIONS FOR COMMERCIAL ANILINES
A. Combinatorial Chemistry

Combinatorial chemistry has proved of value in the development of therapeutic agents. A method for solid-state synthesis of an oxalic acid library involving conversion of anthranilic acid derivatives into 2-(oxalylamino)benzoic acids has been reported[137].

Solid-phase (polystyrene) immobilized 2-aminobenzophenones have been converted into a library of 196 1,4-benzodiazepines. Once released from the support, the library was screened in the 96-well ELISA plate format[138].

With the availability of extensive libraries of derivatives made by combinatorial methods, new derivatives of existing colorants are being developed to aid drug discovery by enhancing screening methods.

B. Aromatic Amines and Metallocene Catalysts

Since the early 1990s there has been considerable interest in metallocene-based polyolefines using catalysts incorporating anilines, in which the nitrogen is a preferred heteroatom for ligand attachment[139].

C. Self-assembly of Macromolecules

Substituted anilines have found use in the synthesis of tectons for self-assembly studies in biological systems[140]. The diaminotriazine **193**, a tecton, undergoes molecular self-assembly, offering potential for one-step syntheses of macromolecules (Scheme 37)[141]. A versatile tecton is 2-amino-4,6-dichlorotriazine **(194)**[142].

(193)

SCHEME 37

(194)
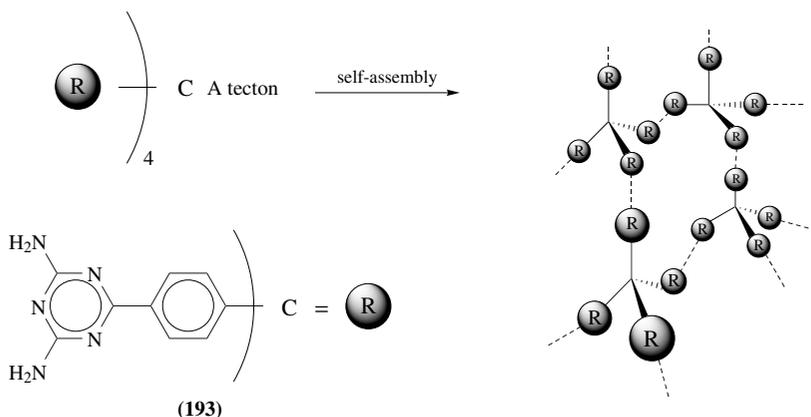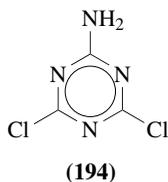
D. Aryl Amines from Aryl Halides

   Ligand-palladium catalyzed aminations of aryl bromides, chlorides and triflates, at ambient temperatures, have been described. High yields are achievable with commercially available catalysts, and product separation is simple[143–145] (see Chapter 14). The mechanism has been elucidated[146]. Greater efficiency has been reported with the palladium catalyst immobilized on a solid phase, particularly silica, permitting its ready recovery and reuse[147]. In contrast, advantages have been claimed for aminations using a heterogeneous nickel-on-charcoal [Ni^0/C] catalyst[148, 149].

XXIII. CONCLUSION

Aromatic amines have a long and varied history of manufacture and application that in terms of diversity is far from closure. The consumption for rubber products and polyurethanes today far outpaces other uses. Since the 1970s, the anilines have taken on new roles as starting points for high-strength polymers with extensive aerospace applications and as lead chemicals in drug and agrochemical developments. Aryl amines serve as starting points for liquid crystals and liquid-crystal polymers. One of the very oldest aniline products, the curious black pigment known as emeraldine, has since the early 1990s become a useful polymer and, almost uniquely, an organic semiconductor. Current trends in research into the anilines suggest growing uses in imaging systems and considerable potential for novel applications such as in molecular self-assembly and in combinatorial chemistry.

XXIV. REFERENCES

1. A. S. Travis, *The Rainbow Makers: The Origins of the Synthetic Dyestuffs Industry in Western Europe*, Lehigh University Press, Bethlehem, Pa., 1993, pp. 88–103.
2. A. S. Travis, *Chem. Ind. (London)*, 15 August, 508 (1988).
3. *Chemical Market Reporter*, February 4, 2002; Robert Baptista, personal communication.
4. T. Kahl and K.-W. Schroder, http://www.mrw.interscience.wiley.com/ueic/articles/a02_303/sect3.html
5. H. A. Wittcoff and B. G. Reuben, *Industrial Organic Chemicals*, Wiley, New York, 1996, p. 255.
6. R. Norris Shreve, *Chemical Process Industries* (International Students Edition), 3rd edn., McGraw Hill, New York, 1967, p. 814.
7. A. S. Travis, *Dyes Made in America: The Calco Chemical Company, American Cyanamid, and the Raritan River*, Edelstein Center/Hexagon Press, Jerusalem, 2004, pp. 222–225.
8. Robert Baptista, personal communication.
9. M. R. Fox, *Dye-makers of Great Britain, 1856–1976: A History of Chemists, Companies, Products and Changes*, ICI, Manchester, 1987, p. 215.
10. A. H. Jubb, in *Basic Organic Chemistry*, part 5, *Industrial Products* (Eds. J. M. Tedder, A. Nechvatal and A. H. Jubb), Wiley, London, 1975, pp. 124–125.
11. E. G. Hancock, *Benzene and Its Industrial Derivatives*, Ernest Benn Ltd, London, 1975, p. 481.
12. M. Yasuhara, Y. Tatsuki, M. Nakamura and F. Matsunaga, US patent 5545753, August 13, 1996, assigned to Mitsui Petrochemical Industries, Tokyo.
13. Sunoco Chemicals, press release, December 2, 2002.
14. Ron Reynolds, personal communication.
15. D. F. Rudd, S. Fathi-Afshar, A. A. Trevino and M. A. Stadtherr, *Petrochemical Technology Assessment*, Wiley, New York, 1981.
16. K. Nomura, *Catalysis Surveys from Japan*, **2**, 56 (1998).
17. A. Hari and B. Miller, *Angew. Chem., Int. Ed.*, **38**, 2777 (1999).
18. N. J. Turner, *Chem. Ind. (London)*, 1 August, 592 (1994).
19. Robert Baptista, personal communication.

20. Ron Reynolds, personal communication.
21. *Chem. Eng. News.*, **82**, no. 27, 51 (2004).
22. *Chemical Processing*, November 11 (2002).
23. *Chemical Market Reporter*, June 9 (2003).
24. *Chemical Week*, January 7 (2004).
25. *China Chemical Reporter*, September 16 (2000).
26. *China Chemical Reporter*, November 26 (2003).
27. *China Chemical Reporter*, May 6 (2002).
28. *Ind. Eng. Chem.*, **48**, 1383 (1956).
29. Reference 5, pp. 257–259.
30. Robert Baptista, personal communication.
31. H. Ulrich, *Chemistry and Technology of Isocyanates*, Wiley, Chichester, 1997.
32. G. Woods, *ICI Polyurethanes Book*, 2nd edn., Wiley, Chichester, 1990.
33. K. Hunger (Ed.), *Industrial Dyes*, Wiley-VCH, Weinheim, 2003.
34. K. Weissermel and H. J. Arpe, *Industrial Organic Chemistry*, 4th edn., VCH, Weinheim, 2003.
35. Robert Baptista, personal communication.
36. http://www.yet2.com/app/utility/external/indextechpak/28257
37. http://www.buffalocolor.com/alkylated.html
38. V. Kratky, M. Kralik, M. Mecarova, M. Stolcova, L. Zalibera and M. Hronec, *Appl. Cat. A: Gen.*, **235**, 225 (2002).
39. G. Booth, http://www.interscience.wiley.com/ueic/articles/a17_009/sect5.html
40. G. Booth, http://www.mrw.interscience.wiley.com/ueic/articles/a_009/sect6.html38
41. H. A. Lubs (Ed.), *The Chemistry of Synthetic Dyes and Pigments*, Reinhold, New York, 1955.
42. H. Zollinger, *Color Chemistry: Syntheses, Properties and Applications of Organic Dyes and Pigments*, VCH, Weinheim, 1987.
43. C. V. Stead, in Reference 10, pp. 315–350.
44. P. Gregory, in *The Chemistry and Application of Dyes* (Eds. D. R. Waring and G. Hallas), Plenum, New York, 1990, p. 22.
45. G. Hartwig, O. Ackermann and H. Eilingsfeld, BASP Ger. Offen. 2039822, February 17, 1972, *Chem. Abstr.*, **76**, 140,338k (1972).
46. E. Yamada, M. Tamada and K. Nobuoka, Sumitomo Ger. Offen. 2248704, April 12, 1973; Japan Appl. 71 79165, October 7, 1971, *Chem. Abstr.*, **79**, 5,178e (1973).
47. H. Suzuki, T. Murashima, K. Shimizu and K. Tsukamato, *Chem. Ind. (London)*, 5 August, 547 (1991).
48. H. S. Bien, J. Stawlitz and K. Wunderlith, http://www.interscience.wiley.com/ueic/articles/a02_355/sect2.html
49. Reference 44, pp. 323–331.
50. H. Zollinger, *Textile Chemist and Colorist*, **23**, December, 19 (1991).
51. P. J. T. Morris and A. S. Travis, *Am. Dyest. Rep.*, **81**, November, 99 (1992).
52. Reference 44, pp. 343–347.
53. B. Withers, *The Herald-Despatch*, March 21, 2004, www.herald-despatch.com.
54. Isaiah Von, personal communication.
55. http://www.epa.gov/greenchemistry/dsca04.html.
56. Robert Baptista, personal communication.
57. H. M. Smith, *High Performance Pigments*, Wiley-VCH, Weinheim, 2002.
58. W. Herbst and K. Hunger, *Industrial Organic Pigments: Production, Properties, Applications*, 3rd edn., Wiley-VCH, Weinheim, 2004.
59. P. Gregory, *Chemistry in Br.*, August, 39 (2000).
60. A. R. Mullin, *Chem. and Eng. News*, **82**, October 11, 26 (2004).
61. I. T. Kay, B. K. Snell and C. D. S. Tomlin, in *Basic Organic Chemistry*, part 5, *Industrial Products* (Eds. J. M. Tedder, A. Nechvatal and A. H. Jubb), Wiley, London, 1975, pp. 438–439.
62. *Night & Day. The Mail on Sunday Review* (UK), August 18, 18 (1996).
63. R. J. Brown, B. Ashworth, J. E. Drumm, D. A. Frazier, M. A. Hanagan, C. Happersett, G. E. Koether, D. J. Robinson, K.-M. Sun and P. Wojtkowski, in *Synthesis and Chemistry of Agrochemicals IV* (Eds. D. R. Baker, J. G. Fenyes, G. P. Lahm, T. P. Selby and T. M. Stevenson), ACS Symposium Series, Washington DC, 2002, pp. 326–339.
64. Reference 10, pp. 444–445.

65. D. A. Evans and K. R. Lawson, in *Milestones in 150 Years of the Chemical Industry* (Eds. P. J. T. Morris, W. A. Campbell and H. L. Roberts), Royal Society of Chemistry, London, 1991, p. 74. For structures of agrochemicals see dhttp://www.uoguelph.ca/OAC/env/bio/PROFILES.pdf

66. Erwin Klingsberg, personal communication.

67. G. M. Karp, A. D. Crews, M. C. Manfredi, A. Kleemann, R. L. Arotin, M. L. Crawley, B. Dahlke and R. Baerg, in Reference 63, pp. 31–40.

68. G. Theodoridis, J. T. Bahr, S. Crawford, B. Dugan, F. W. Hotzman, L. L. Ravetz, S. Sehgel and D. P. Suarez, in Reference 63, pp. 97–107.

69. R. Shapiro, G. D. Annis, C. T. Blaisdell, D. J. Dumas, J. Fuchs, S. M. Griswold, G. W. Higley, Jr., W. C. Holinsed, J. J. Mrowca, J. A. Sternberg and P. Wojtkowski, in Reference 63, pp. 178–185.

70. T. M. Stevenson, C. R. Harrison, P. D. Lowder, B. A. Crouse, R. W. March, M. J. Currie, M. P. Folgar and D. M. T. Chan, in Reference 63, pp. 120–131.

71. R. E. Hackler, R. G. Suhr, J. J. Sheets, C. J. Hatton, P. L. Johnson, L. N. Davis, R. G. Edie, S. V. Kaster, G. P. Jourdain, J. L. Jackson and E. V. Krumkalns, in *Advances in the Chemistry of Insect Control* (Ed. G. G. Briggs), Royal Society of Chemistry, London, 1994, p. 71.

72. R. J. Willis, in Reference 65, p. 99.

73. N. F. Elmore, G. R. Brown and A. T. Greer, in *Basic Organic Chemistry*, part 5, *Industrial Products* (Eds. J. M. Tedder, A. Nechvatal and A. H. Jubb), Wiley, London, 1975, p. 387.

74. M. I. Evgen'ev, S. Yu. Garmonov, L. Sh. Shakirova and E. V. Degterev, *Pharm. Chem. J.*, **36**, 559 (2002).

75. Reference 73, p. 367.

76. Reference 73, p. 360.

77. Reference 73, p. 371.

78. F. E. G. Cox, *Chem. Ind. (London)*, 5 August, 533 (1991).

79. Reference 73, p. 381.

80. B. J. Price and M. G. Dodds, in Reference 65, p. 31.

81. Reference 61, p. 408.

82. Reference 61, p. 413.

83. Reference 61, p. 415.

84. Reference 61, p. 416.

85. B. J. Price and M. G. Dodds, in Reference 65, pp. 31–32.

86. Reference 73, p. 421.

87. K. P. Stahmann, J. L. Revuelta and H. Seulberger, *Appl. Microbiol. Biotechnol.*, **53**, 509 (2000).

88. E. Verg, G. Plumpe and H. Schultheis, *Milestones: The Bayer Story. 1863–1988*, Bayer AG, Leverkusen, 1988, p. 496.

89. M. S. Reisch, *Chem. Eng. News*, **79**, December 3, 25 (2001).

90. L. Y. Matsuoka, L. Ide, J. Worstman, J. A. MacLaughlin and M. F. Holick, *J. Clin. Endocrinol. Metab.*, **64**, 1165 (1987).

91. F. J. Moloney, S. Collins and G. M. Murphy, *Am. J. Clin. Dermatol.*, **3**, 185 (2002).

92. N. P. Patel, A. Highton and R. L. My, *J. Dermatol. Surg. Oncol.*, **18**, 316 (1992).

93. F. P. Gasparro, *Environ. Health Perspect.*, **108**, Suppl. 1, 71 (2002).

94. Benzothiazole-based Thiazoles. Category Justification and Testing Rationale, Rubber and Plastic Additives Panel, American Chemistry Council, November 2001. Reference 7, pp. 80–81, 160.

95. H. W. Engels, http://www.mrw.interscience.wiley.com/ueic/articles/a23_365

96. *Aero Cyanuric Chloride*, American Cyanamid Company, New York, 1958.

97. B. McSwigan, *The Journal of Coatings Technology*, December 1 (1994).

98. Y. Yang and L. Shiqi, *Am. Dyest. Rep.*, **82**, 22 (1993).

99. DSM, Corporate Technology, Heerlen/Ernst Homburg.

100. Y. H. Kim, B. U. Kim and K. Kim, *Chem. Ind. (London)*, 1 October, 622 (1990).

101. M. T. Muldoon and L. H. Stanker, *Chem. Ind. (London)*, 18 March, 204 (1996).

102. W. H. Shearon, L. G. Davy and H. Von Bramer, *Ind. Eng. Chem.*, **44**, 1730 (1952).

103. P. J. Collings and J. S. Patel, *Handbook of Liquid Crystal Research*, Oxford University Press, Oxford, 1997.

104. P. Chaudhari, J. Lacey, J. Doyle, E. Galligan, S.-C. A. Lien, A. Callegari, G. Hougham, N. D. Lang, P. S. Andry, R. John, Y. K.-H. Yana, M. Lu, C. Cai, J. Speidell, S. Purushothaman, R. Ritsko, M. Saman, J. Stöhr, Y. Nakagawa, Y. Katon, Y. Siatoh, K. Sakai, H. Satoh, S. Odahara, H. Nakano, J. Nakagabi and Y. Shiota, *Nature*, **56**, 411 (2001).
105. N. Rao, M. K. Paul, T. R. Rao and A. Prasad, *Liq. Cryst.*, **29**, 1243 (2002).
106. X. Song, J. Li and S. Zhang, *Liq. Cryst.*, **30**, 331 (2003).
107. A. I. Isayev, T. Kyu and S. Z. D. Cheng (Eds.), *Liquid-crystalline Polymer Systems: Technological Advances*, Vol. 632, American Chemical Society, Washington, DC, 1996.
108. L. R. Dalton, *Chem. Ind. (London)*, 7 July, 510 (1977).
109. L. R. Dalton, A. K. Jen, W. H. Steier, B. H. Robinson, S. H. Jang, O. Clot, H. C. Song, Y. H. Kuo, C. Zhang, P. Rabiei, S. W. Ahn and M. C. Oh, *Proc. Soc. Photo-Opt. Instrum. Eng.*, **5351**, 1 (2004).
110. W. M. Edwards, US patent 317614 (1965).
  (a) C. E. Scroog, A. L. Endry, S. V. Abramo, C. E. Berr, W. M. Edwards and K. L. Olivier, *J. Polym. Sci., Part A*, **3**, 1373 (1965).
111. K. L. Mittal (Ed.), Polyimides: Synthesis, Characterization and Applications, Plenum, New York, 1984.
112. D. H. Solomon, G. G. Qiao and M. J. Caulfield, in *The Chemistry of Phenols*, Part 2 (Ed. Z. Rappoport), Wiley, Chichester, 2003, pp. 1493–1502.
113. A. E. Eichstadt, T. C. Ward, M. D. Bagwell, I. V. Farr, D. L. Dunson and J. E. Grath, *Macromolecules*, **35**, 7561 (2002).
114. http://www.grc.nasa.gov/WWW/RT2001/5000/5401hepp2.html
115. M. Hasegawa and K. Horie, *Prog. Polym. Sci.*, **26**, 259 (2001).
116. V. Rigato, G. Maggioni, A. Patelli, V. Antoni, G. Serianni, M. Spolaore, L. Tramontin, L. Depero and E. Bontempi, *Surf. Coat. Technol.*, **156**, 142 (2001).
117. T. D. Flaim, Y. Wang and R. L. Mercado, *Proc. Soc. Photo-Opt. Instrum. Eng., Optical Systems Design 2003*, **5250**, 423 (2004).
118. R. L. Mercado, Y. Wang, T. D. Flaim, W. L. DiMenna and U. Senapati, in *Proc. Soc. Photo-Opt. Instrum. Eng., Organic Photonic Materials and Devices VI* (Eds. J. G. Grote and T. Kiano), **5351**, 276 (2004).
119. J. Kim and J. A. Moore, *Macromolecules*, **26**, 3510 (1996).
120. H. H. Yang, *Kevlar Aramid Fiber*, Wiley, Chichester, 1993.
121. J. C. Michaelson, *Endeavour, New Series*, **17**, 121 (1993).
122. G. G. Wallace, P. C. Dastoor, D. L. Officer and C. O. Too, *Chem. Innovation*, **30**, 14 (2000).
123. M. Angelopoulos, *IBM J. Res. Dev.*, **45** (2001).
124. (a) E. M. Geniès and M. Lapkowski, *Synth. Mater.*, **24**, 69 (1988); A. G. MacDiarmid and A. J. Epstein, in *Conjugated Polymeric Materials* (Eds. J.-L. Brédas and R. R. Chance), Kluwer, Boston, 1990, p. 53.
  (b) F. Lux, *Polymer*, **14**, 2925 (1994).
125. P. K. Shen and Z. Q. Tian, *Electrochim. Acta*, **34**, 1611 (1989).
126. D. Yaohua and N. Shaolin, *Electrochim. Acta*, **36**, 2015 (1991).
127. A. J. Epstein, *Corrosion Protection of Aluminum and its Alloys Using Electroactive Polymers*, Storming Media, Washington DC, 2000.
128. Y. Wei, *Nanocomposite/Hybrid Materials of Electroactive Polymers with Inorganic Oxides for Biosensor Applications*, Storming Media, Washington DC, 2001.
129. W. S. Huang, B. D. Humphrey and A. G. MacDiarmid, *J. Chem. Soc., Faraday Trans. 1*, **82**, 2385 (1986).
130. J. M. Ginder, A. J. Epstein and A. G. MacDiarmid, *Synth. Met.*, **29**, E395 (1989).
131. M. R. Anderson, B. R. Mattes, H. Reiss and R. B. Kaner, *Science*, **252**, 1412 (1991).
132. N. Oyama, T. Tatsuma, T. Sato and T. Sotomura, *Nature*, **373**, 598 (1995).
133. Y. Cao, N. Colaneri, A. J. Heeger and P. Smith, *Appl. Phys. Lett.*, **65**, 2001 (1994).
134. L. X. Wang, T. Soczka-Guth, E. Havinga and K. Müllen, *Angew. Chem., Int. Ed. Engl.*, **35**, 1495 (1996).
135. http://www.mistsuichemicals.com/fin_chem8.htm
136. E. W. Flick, *Epoxy Resins, Curing Agents, Compounds and Modifiers*, 2nd edn., William Andrew Publishing/Noyes, Norwich/New York, 1993.
137. T. M. Georgiadis, N. Baindur and M. R. Player, *J. Comb. Chem.*, **6**, 224 (2004).
138. B. A. Bunin and J. A. Ellman, *J. Am. Chem. Soc.*, **114**, 10997 (1992).

139. K. B. Sinclair and R. B. Wilson, *Chem. Ind. (London)*, 7 November, 857 (1994).
140. P. M. Petersen, W. Wu, E. E. Fenlon, S. Kim and S. C. Zimmerman, *Bioorg. Med. Chem.*, **4**, 1107 (1996).
141. P. Brunet, M. Simard and J. D. Wuest, *J. Am. Chem. Soc.*, **119**, 2737 (1997).
142. E. A. Archer, A. E. Sochia and M. J. Krische, *Chem. Eur. J.*, **7**, 2059 (2001).
143. J. F. Hartwig, M. Kawatsura, S. I. Hauck, K. H. Shaughnessy and L. M. Alcazar-Roman, *J. Org. Chem.*, **64**, 5575 (1999).
144. J. F. Hartwig, *Pure Appl. Chem.*, **71**, 1417 (1999).
145. J. P. Wolfe, H. Tomori, J. P. Sadighi, J. Yin and S. L. Buchwald, *J. Org. Chem.*, **65**, 1158 (2000).
146. L. M. Alcazar-Roman and J. F. Hartwig, *J. Am. Chem. Soc.*, **123**, 12905 (2001).
147. D. Macquarrie, B. Gotov and S. Toma, *Platinum Met. Rev.*, **45**, part 3, 102 (2001).
148. B. H. Lipshutz and H. Ueda, *Angew. Chem., Int. Ed.*, **39**, 4492 (2000).
149. S. Tasler and B. H. Lipshutz, *J. Org. Chem.*, **68**, 1190 (2003).

CHAPTER **14**

The spectroscopy, photophysics and photochemistry of anilines

JYE-SHANE YANG

Department of Chemistry, National Taiwan University, Taipei, Taiwan (ROC), 10617
Fax: +886 2 23636359;   e-mail: jsyang@ntu.edu.tw

I. INTRODUCTION

The presence of strong interactions between the amino lone-pair electrons and the aryl π electrons in the electronically excited states of aromatic amines (anilines) differentiates their spectroscopy and photochemistry from those of saturated amines and aromatic

hydrocarbons[1,2]. Such interactions are characterized as intramolecular charge-transfer (ICT) from the amino nitrogen (electron donor, D) to the arene (electron acceptor, A)[3], which has triggered versatile photochemical reactions for anilines. Like the saturated amines[4,5], anilines and their N-alkyl derivatives are good electron donors in both the ground and excited states and have been widely used in studies of the behavior of photoinduced electron transfer (PET)[6,7]. Although PET could occur between singlet anilines and ground-state acceptors as well as between singlet acceptors and ground-state anilines, most studies employed anilines as ground-state electron donors rather than excited-state donors. This might be associated with the weak long-wavelength absorption and relatively short singlet lifetimes of simple aniline molecules that restrict the choice of ground-state acceptors. Since this chapter dwells only upon the physical and chemical processes that follow the photoexcitation of anilines, the aspects of quenching of singlet acceptors by ground-state anilines will be excluded. Likewise, the topic of photodegradation of anilines by means of photoexcitation of the catalyst rather than that of the aniline molecules will not be included[8,9]. A few monographs[2,10,11] related to the spectroscopy and photochemistry of anilines have previously been published. This chapter will mainly deal with the recent progress of this area with emphasis on the mechanistic aspects of the photochemical reactions of anilines.

II. SPECTROSCOPY AND PHOTOPHYSICS

A. Substituent Effect

The electronic absorption and emission spectra of anilines depend on the nature of the arene and N-substituent[12]. In general, the intense absorption bands are due to π, π^* transitions of the arene with the contribution of the ICT component. The two typical absorption bands for simple aniline molecule (**1a**) are attributed to the $^1A \rightarrow ^1L_b$ (*ca* 290 nm) and $^1A \rightarrow ^1L_a$ (*ca* 240 nm) transitions and correspond to the S_1 and S_2 states, respectively[13,14]. The fluorescence lifetime is about 3 ns, and the fluorescence quantum yield (Φ_f) is 0.1–0.2, depending on the vibronic levels[15,16]. Intersystem crossing (ISC) is the main nonradiative decay process in the S_1 state decay of **1a**. Although the intersystem crossing rate from S_1 to T_1 is fast, no phosphorescence was observed in the gas phase due to the rapid decay from T_1 to S_0[17]. The increase in the size of arene leads to a bathochromic shift for both ^1L_a and ^1L_b bands, as demonstrated by 2-aminonaphthalene (**2a**) (^1L_b *ca* 338 nm)[18], 1-aminonaphthalene (**3a**) (^1L_b *ca* 318 nm) and 9-aminoanthracene (**4a**) (^1L_a *ca* 390 nm)[12]. In addition, the intersystem crossing becomes less important or negligible for anilines with larger arenes. For instance, the fluorescence dominates the decay of **3a** in acetonitrile ($\Phi_f = 0.86$ and $\Phi_{ISC} = 0.16$)[18,19]. N-Alkylation of anilines generally results in a red shift of both absorption and emission maxima. For example, the amount of spectral shift is *ca* 10 nm for N,N-dimethylaniline (**1b**) vs **1a** and for N,N-dimethyl-2-aminonaphthalene (**2b**) vs 2-aminonaphthalene (**2a**)[16,20]. However, a blue shift of absorption spectra could occur when N-alkylation results in a reduction of conjugation between the amino and aryl groups due to a steric reason[15,21]. This could be illustrated by the longer wavelength of absorption maxima for **3a** (318 nm) vs N,N-dimethyl-1-aminonaphthalene (**3b**) (308 nm) and for **4a** (390 nm) vs N,N-dimethyl-9-aminoanthracene (**4b**) (386 nm) in cyclohexane. The increased amino twist angle in **3b** also accounts for its fast internal conversion (IC) in the S_1 state in nonpolar solvents such as cyclohexane ($\Phi_{IC} = 0.97$)[22]. N-Alkylation also lowers the effective ionization potential of the amino group and thus increases the ICT component and the oscillator strength in the $S_0 \rightarrow S_1$ transition.

The fluorescence quantum yield of anilines might depend on the excitation wavelengths, particularly those belonging to different absorption bands. In addition, this effect is generally more pronounced in nonpolar hydrocarbons than in polar hydrogen-bonding solvents,

(1a) R = H
(1b) R = CH$_3$

(2a) R = H
(2b) R = CH$_3$

(3a) R = H
(3b) R = CH$_3$

(4a) R = H
(4b) R = CH$_3$
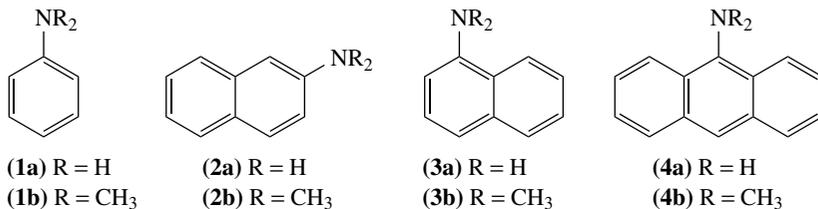
the only exception being water. For **1a** in hexane, a decrease of Φ_f observed for excitation at the second vs the first absorption band has been attributed to the presence of efficient nonradiative deactivation processes that compete with the $S_2 \rightarrow S_1$ transition[13]. The nonradiative deactivation process taken place in S_2 is more likely associated with photochemical N–H cleavage (see Section III.B), since the corresponding wavelength effect on Φ_f is relatively small for **1b**. In aqueous solution, electron ejection becomes the most important deactivation pathway for anilines excited in S_2 and accounts for most of the decrease in Φ_f (see Section III.A).

The fluorescence of anilines generally undergoes substantial positive solvatofluorochromism, namely the fluorescence maximum shifts to the red upon increasing the solvent polarity. For example, the fluorescence maximum for **1a** in cyclohexane is at 315 nm, but it is at 342 nm in water[23]. In contrast, the corresponding absorption spectra are relatively insensitive to the change of solvent polarity. Evidently, the molecular dipole moment is increased on going from the ground (S_0) to the lowest excited (S_1) state, and the equilibrated S_1 state possesses a larger degree of ICT character than the Frank–Condon state. The excited-state dipole moment (μ_e) of anilines could be measured by methods such as the Stark effect[24] and electric dichroism methods[25], but it is often estimated from the slope (m_f) of the Lippert–Mataga plot of the energies of the fluorescence maxima against the orientation polarizability (Δf)[26, 27]. The ground-state dipole moment of **1a** is *ca* 1 D, and the dipole moment becomes 2.45–2.80 D in the S_1 state[18, 28]. The enhancement in dipole moment upon excitation is relatively larger for **2a** ($\Delta\mu_e$ *ca* 2.7 D), **3a** ($\Delta\mu_e$ *ca* 5.6 D) and 4-aminostilbene (**5a**) ($\Delta\mu_e$ *ca* 8 D)[16, 29].
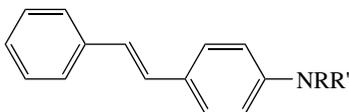
(5a) R = R' = H
(5b) R = R' = CH$_3$
(5c) R = Ph, R' = H
(5d) R = R' = Ph

The differences in spectroscopy and photophysics between *N*-phenyl and *N*-alkyl substituted anilines have been recognized[30, 31]. Due to the π-conjugated nature of the *N*-phenyl group, the size of bathochromic shifts in the electronic spectra of anilines caused by *N*-phenylation is larger than that by *N*-alkylation. This could be illustrated by the case of **5a** in hexane, where the 0–0 transition energy is lowered by *ca* 1200 cm^{-1} upon introducing two *N*-methyl groups (**5b**) or one *N*-phenyl group (**5c**) and by *ca* 2400 cm^{-1} with two *N*-phenyl groups (**5d**)[32]. Thus, the magnitude of the π-conjugation effect of an *N*-phenyl group is nearly equivalent to double the hyperconjugation effect of an *N*-methyl

group. Moreover, in the S_1 state N-phenyl substituted anilines possess a larger ICT character than the N-alkyl substituted counterparts[30, 31]. The N-phenyl vs N-alkyl substituent effects have also been correlated with the geometry of the amino nitrogen[33], the fluorescence efficiency[29, 34], the two-photon absorptivity[35, 36], photoacidity[37], the molecular hyperpolarizability[38] and the optoelectronic properties[39, 40] of functionalized anilines.

A prominent position-dependent substituent effect on the spectroscopic behavior of anilines has been observed when the substituent is a nitro group. Whereas the 2- and 3-isomers of nitroaniline emit only fluorescence in methylcyclohexane and ethanol at 77 K, the 4-isomer emits only phosphorescence under the same condition[41]. The larger tendency to phosphoresce for the 4- vs 2- and 3-isomers might be associated with their relative sizes of excited-state dipole moments. Another example has been provided by aminostilbenes (i.e. the substituent is a styryl group)[29, 42]. The 4-isomer of aminostilbene displays a single intense long-wavelength absorption band, but the 2- and 3-isomers display two less intense bands. In comparison to the 2- and 3-isomers, the 4-isomer displays a larger fluorescence rate constant, shorter singlet lifetime and lower fluorescence quantum yield. Such a substituent effect has been attributed to the difference in the barrier for the central double bond torsion in the S_1 state[29, 43]. Unlike the case of the 4-isomer, both the 2- and 3-isomers have a barrier too high to be overcome, and thus their *trans* → *cis* photoisomerization is through the triplet state. It should also be noted that, as demonstrated by the comparison of **5a–5d** and **6a–6d**, spectroscopic and photochemical differences are also observed in their N-methyl and N-phenyl substituted derivatives[44].
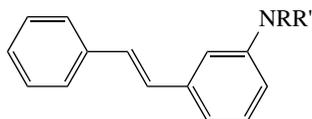
(6a) R = R' = H
(6b) R = R' = CH$_3$
(6c) R = Ph, R' = H
(6d) R = R' = Ph

B. External Electronic Perturbations

General solvent effects on fluorescence spectra refer to the electronic polarization interactions between solvent and solute molecules. However, the electronic structure of a solute could be significantly modified by solvent molecules due to specific solute–solvent interactions[45]. For anilines, specific solvent effects often result from hydrogen bonding, proton transfer and charge-transfer interactions associated with the amino group[16]. This effect has been observed in hydroxylated solvents, where the hydrogen bond could be formed between the hydroxyl hydrogen and the amino lone-pair electrons or between the hydroxyl oxygen and the amino N−H of anilines[46]. The fluorescence quenching of anilines in aqueous vs organic solvents is a well-known phenomenon associated with the hydrogen-bonding interactions between the amino N−H and water molecules[16, 47, 48]. When the hydrogen bond is formed between the amino N−H and proton acceptors such as pyridine, it becomes stronger in the S_1 state and leads to the formation of charge-transfer complexes[49, 50]. This is manifested by the phenomena of red-shifted absorption spectra and fluorescence quenching. Fluorescence quenching of anilines by carbon tetrachloride[51], chlorobenzene[52] and benzonitrile[53] has also been observed.

The spectroscopic perturbation is expected to be larger when the amino lone pair electrons of anilines interact with cations such as protons and metal ions. Protonation of the

aniline nitrogen atom results in a blue shift of the absorption spectrum that is similar to that of the parent arene[54]. This is a consequence of reduced molecular conjugation length and ground-state ICT interactions. For example, the observed absorption bands for **1a** in the low and high pH regime of buffered solutions are at 260 and 254 nm and at 280 and 230 nm, respectively[55]. However, the basicity of anilines in the S_1 state is significantly reduced as a result of photoinduced ICT, and thus the anilinium ion dissociates adiabatically in the excited state. This accounts for the fact that the fluorescence spectrum of anilinium ions is not much different from that of neutral anilines. The mechanistic aspects of the N−H photodissociation of anilinium ions in solutions are presented in the photochemistry Section III.B. It should be noted that in highly alkaline solutions, anilines could also undergo N−H dissociation to generate anilinide ions. For example, a longer-wavelength fluorescence band, corresponding to emission by the anthramide anion, appears in the spectrum for aminoanthracene in highly alkaline solutions[56].

The spectroscopic responses of ionophoric anilines to metal ions resemble the cases of protonation interactions, albeit to a different extent. As demonstrated by many azacrown-derived intrinsic fluoroionophores[57, 58], ion binding leads to a change in both absorption and emission spectra due to the localization of the nitrogen lone-pair electrons by metal ions. However, for simple azacrown-substituted arenes such as compounds **7** and **8**, the ion-binding ability of azacrown is reduced in the S_1 state as a consequence of ICT. This could be envisaged as electrostatic repulsion between the metal ion and the positively charged azacrown nitrogen. Apparently, metal ion coordination is insufficient to inhibit the photoinduced ICT process in anilines. The phenomenon of excited-state ion decoordination often results in a smaller change in the fluorescence than the absorption properties[59, 60]. To avoid the occurrence of excited-state decoordination reaction and thus to ensure a large metal ion-induced fluorescence change for these fluoroionophores, a donor−acceptor−donor (D−A−D) constitution has been suggested (e.g. compound **9**)[61]. The dimethylamino group in **9** is in charge of the photoinduced ICT process so that the azacrown nitrogen is no longer positively charged in the excited state. However, it is not always necessary to have D−A−D systems to display large fluorescence changes. A simple D−A system undergoing D−A decoupling in either the unbound or bound state could display an 'on−off' or 'off−on' type fluorescence switching in response to metal ions. In this context, compound **10** serves as an example of the 'on−off' type fluoroionophoric behavior[62, 63].
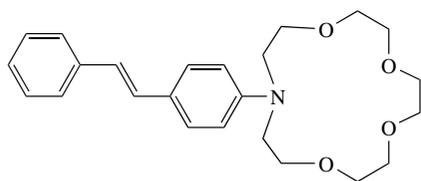
(7)
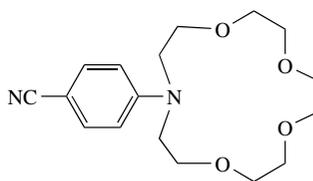
(8)
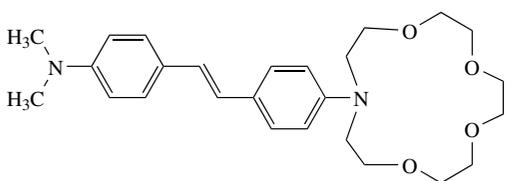
(9)
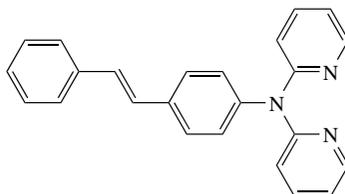
(10)

The excited states of anilines could also be perturbed by ground-state amine, resulting in the formation of Lewis acid–base (LAB) exciplexes and/or triplexes. Unlike common exciplexes, resulting from nonspecific charge-transfer (CT) interactions, the interactions in LAB exciplexes are specific and through space between amine lone-pair orbitals[64, 65]. Fluorescent LAB exciplexes and triplexes have been observed for 3-aminostilbene (**6a**)[66, 67] and 9-aminophenanthrene (**11**)[68] in the presence of aliphatic amines. In these cases, the electronically excited **6a** and **11** are the lone pair acceptors. As depicted in Scheme 1, exciplex formation requires the specific overlap of the amine nonbonded orbital with the electron-deficient p-orbital of the aniline nitrogen, and triplex formation requires a specific interaction with the other lobe of the p-orbital. The interactions between arene–amine exciplexes and ground-state amines to form nonfluorescent triplexes have also been proposed to account for the fluorescence quenching of the former in the presence of amines[69]. Since the factors that determine the stability of excited-state LAB complexes are characteristic of the specific excited-state acceptor, no universal scale of lone-pair donor strength can be expected to describe the formation of such complexes.

(11)
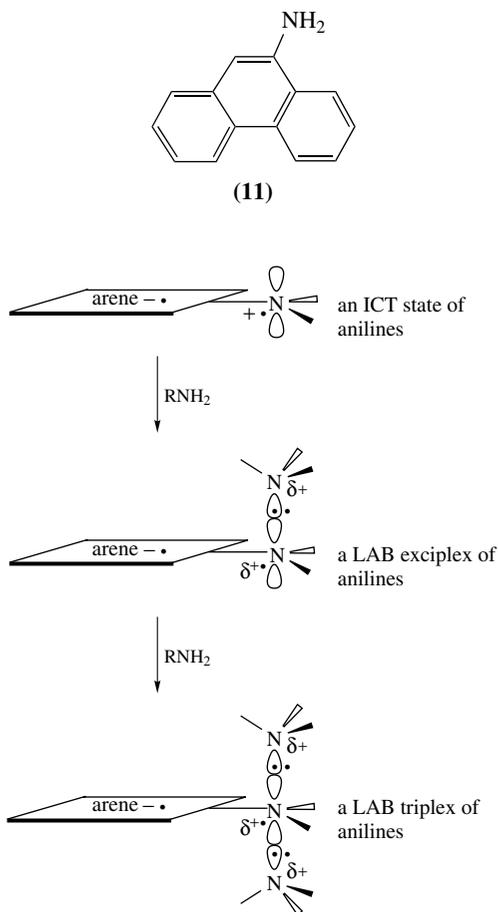
SCHEME 1

C. Excited-state Conformation

The conformational relaxations of anilines followed by electronic excitation have attracted much attention[3, 10, 70]. The increased ICT character of anilines in the S_1 state is generally associated with a conformational change of the amino group from the tetrahedral sp^3 conformation in the ground state to the trigonal sp^2 conformation in the excited state. In contrast, the lowest excited triplet of **1a** and **1b** is nonplanar[71]. Both *N*-alkyl and *N*-phenyl substitutions of anilines result in a more planar structure about the nitrogen atom in the ground state, and the nitrogen is essentially sp^2 hybridized in triphenylamine and its derivatives[30]. Such a change in the conformation of the amino group upon *N*-substitutions has been reflected by the relative Stokes shift and the intensity ratio of the fluorescence 0−1 band vs 0−0 band, corresponding to the Huang−Rhys factor (S)[72], for a series of 4-aminostilbenes (**5a−5d**) in hexane[32]. The gradual decrease of the S value along with the series (i.e. **5a** > **5b** > **5c** > **5d**) is consistent with the assumption of a planar ICT state for 4-aminostilbenes in hexane.

On the other hand, conformational relaxations of anilines, particularly D−A substituted (push−pull) anilines, toward a D−A-deconjugated geometry, called 'twisted intramolecular charge-transfer' (TICT) states, become possible in polar solvents[3]. The concept of TICT[73] originated from the interpretation of the long-wavelength band of the dual fluorescence of 4-(*N,N*-dimethylamino)benzonitrile (**12**) in polar solvents, which was first observed by Lippert and coworkers in 1961[74]. The state responsible for the short-wavelength emission band has been attributed to the locally excited (LE) state, which has a smaller dipole moment. The dimethylamino (D)−benzonitrilo (A) decoupled TICT state allows a full electron transfer, leading to a larger dipole moment and thus a better solvation in polar solvents. In addition to the TICT model, other distinct models have also been proposed, including the in-plane bending of the cyano group (rehybridization by intramolecular charge transfer, RICT)[75], and the pyramidalization (wagged intramolecular charge transfer, WICT)[76] or planarization (planar intramolecular charge transfer, PICT) of the amino group[77] (equation 1). At the current stage, active debates on the PICT[78, 79] vs TICT[80, 81] model for **12** still continue and there is no end in sight in the near future.

(1)
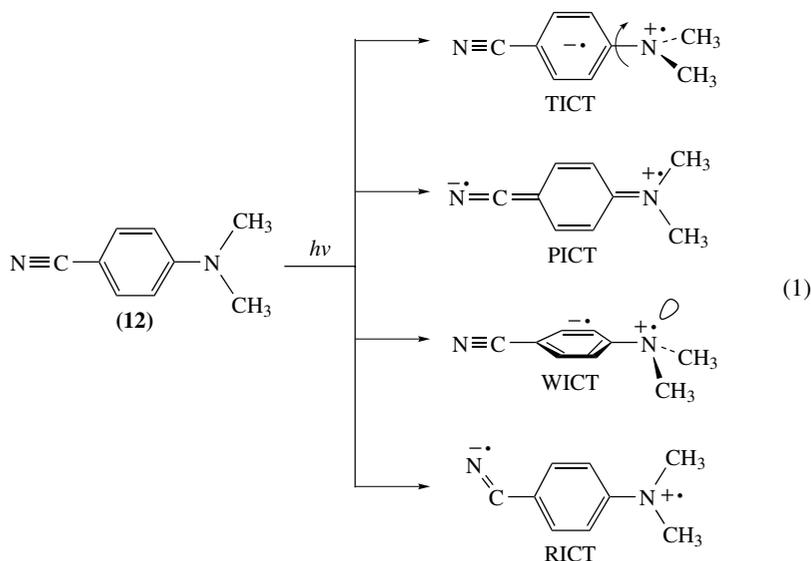
Some important experimental evidence based on fluorescence spectroscopies in favor of the TICT model for **12** is provided as follows. (1) The large dipole moments (13–17 D) deduced from the fluorescence solvatochromic shifts correspond to a state with a full electron transfer. (2) The low fluorescence rate constant (3×10^6 s^{-1}) for the ICT fluorescence indicates a forbidden optical transition. (3) The temperature dependence of the fluorescence quantum yields suggests an equilibrium between the LE and ICT states[82]. (4) The relative intensity ratio of the ICT vs LE fluorescence observed for a series of model compounds **13–16** is consistent with the TICT model[83]. For example, when the C–N bond twisting is restricted (i.e. **13**), only the LE emission is observed. In contrast, when the amino n-orbital is fixed orthogonally to the phenyl p-orbital (i.e. **16**), only the ICT emission is observed. In the cases of **14** and **15**, the larger dihedral angles between the CNC amino plane and the phenyl plane in comparison to that in **12** result in a larger fluorescence intensity ratio of the ICT vs LE band.

(13)   **(14)**   **(15)**   **(16)**
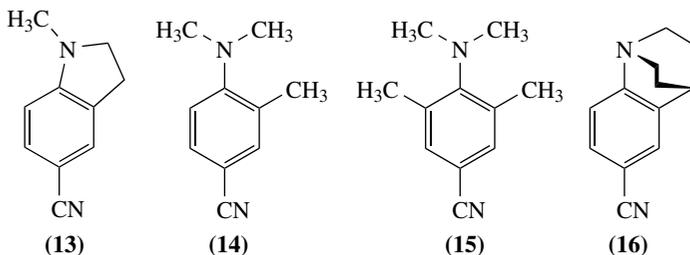
Many other anilines with aromatic donor and/or polycyclic acceptor, including 4-aminodiphenylamines (aniline dimers)[84, 85], have also been proposed to have a TICT state in polar solvents. However, like the case of **12**, the TICT arguments in some systems are controversial, particularly when steady-state dual fluorescence is not present. For example, despite the lack of dual fluorescence in all cases, 4-(N,N-dimethylamino)stilbene (**5b**)[86] and its cyano[87, 88], nitro[89] and dimethylamino[90] derivatives have all been proposed to have a fluorescent TICT state due to the rotation of the styryl-anilino C–C single bond. On the other hand, the corresponding studies on a series of N-arylaminostilbenes (**17a–17f**) have led to a conclusion that the TICT formation depends on the substituent in the N-aryl group and only three of the seven derivatives possess a weakly fluorescent TICT state[91]. In addition, the bond that twists is either the stilbenyl-anilino C–N bond (bond b in **17a**) or the stilbeneamino-phenyl C–N bond (bond a in **17b** and **17c**) instead of the styryl-anilino C–C bond (bond c in **17**). More studies are required to clarify the discrepancies in the proposed TICT geometry for aminostilbenes.

(5c)   R = H
(17a) R = OCH$_3$ **(17d)** R = CH$_3$
(17b) R = CN   **(17e)** R = Cl
(17c) R = CO$_2$CH$_3$ **(17f)** R = CF$_3$
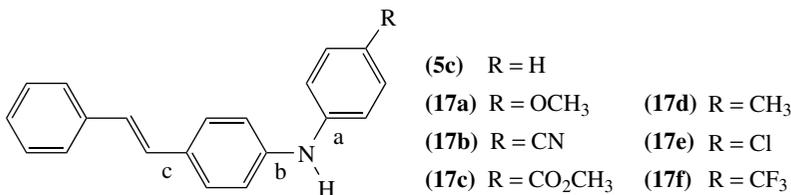
Generally speaking, the increased electron delocalization interactions on going from the ground to the excited state favor a more planar geometry for excited anilines in nonpolar or weakly polar solvents, even when the anilines are pre-twisted in the ground state[92].

The formation of a TICT state is only possible in medium polarity or polar solvents. In addition, the tendency for the TICT state formation is decreased for large vs small D–A systems.

The excited-state conformation of donor–bridge–acceptor (D–σ–A) compounds with anilines as the electron donor and aliphatic groups as the bridge (e.g. compounds **18** and **19**) has also been extensively investigated with respect to the formation of an intramolecular exciplex (or CT excited state)[93, 94]. With different bridges, the exciplex state can be formed with a different geometry. When the bridge is long and flexible, the D–A interactions can result in a sandwiched geometry, called compact CT (CCT) states. In contrast, if the bridge is short or semirigid, the interactions can only result in a loose exciplex or solvent-separated CT with extended conformation (ECT). The D–A interactions also depend on the solvent polarity. In nonpolar alkane solvents, which thermodynamically disfavor a long-range intramolecular electron transfer, the CT exciplex is formed only when the D and A are close enough. However, in polar solvents, the CT exciplex can be formed through conformational change that is facilitated by a long-range electron transfer, namely via the 'harpooning' mechanism[95, 96]. In other words, the initial CT state has an extended conformation (ECT) and the structural relaxed CT state has a more compact form (CCT). In principle, an increase in the D–A separation in the CT state leads to a decrease in the emission maximum[97, 98].

(18)   **(19)**
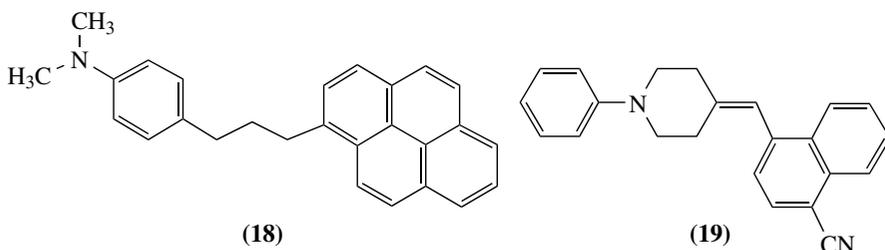
Most of the CT exciplexes for intramolecular D–σ–A systems, such as the cases of **18** and **19**, result from the charge transfer between an excited acceptor and a ground-state aniline (D–σ–A*). The alternative CT interactions from D*–σ–A, albeit relatively rare, have also been reported[99–101]. For example, N-(styrylalkyl)anilines **20** and **21**, where the aniline possesses a lower singlet energy than the styrene chromophore[100], display a solvent-dependent dual emission, attributed to locally excited aniline and intramolecular exciplex fluorescence. The quenching of the aniline donor fluorescence and the appearance of a broad solvatochromic fluorescence band also indicate the occurrence of electron transfer in compounds **22–24**[101]. It is interesting to point out that dual fluorescence corresponding to the emission of the initially ECT (420 nm) and CCT (496 nm) states is observed for **22** in cyclohexane. However, CCT emission is not observed for **23** and **24**, presumably due to a shorter lifetime of their ECT states.

(20)   **(21)**

$$(22) \quad R^1 = R^2 = CN$$

$$(23) \quad R^1 = CN, R^2 = CO_2Me$$

$$(24) \quad R^1 = R^2 = CO_2Me$$
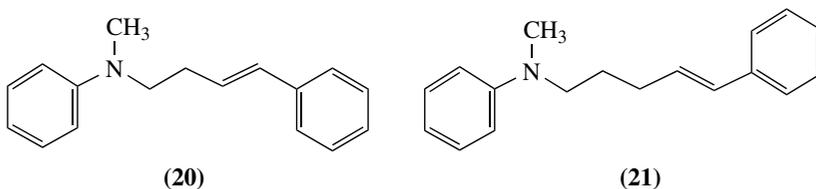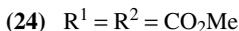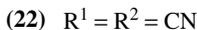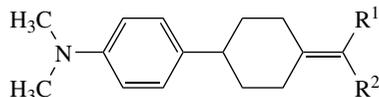
III. PHOTOCHEMISTRY

A. Photoionization

The photoionization process of a molecule is strongly affected by the ambient solvent molecules, so that the ionization mechanism and the ionization potential are significantly different from those in the gas phase. In general, the ionization potential of an aromatic molecule in solution is lower by a few electron volts than that in the gas phase, because of the large solvation energy for the resulting cation and electron even in nonpolar solvents. In polar media, particularly in aqueous solution[102], the photoionization potential becomes sufficiently low, so that the photoionization process can compete with the other decay pathways. Therefore, photoionization in aqueous solution has long been a subject of research interest[103, 104].

Photoionization of anilines in aqueous solution results in the aniline cation radical ($ArNH_2^{+\cdot}$) and hydrated electron (e^-_{aq}), which are stabilized by solvation in water (equation 2).

$$ArNH_{2\,aq}^* + (H_2O)_n \rightarrow ArNH_{2\,aq}^{+\cdot} + e^-_{aq} \qquad (2)$$
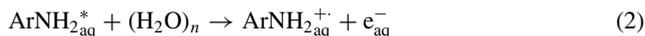
However, the photoionization mechanisms are rather complex, in which not only the solvent polarity but also some specific solute–solvent interactions play an important role. A variety of photoionization mechanisms have been proposed, including one-photon processes with either unimolecular[105] or bimolecular[106] mechanisms and via excited singlet or triplet states, two-photon processes with the singlet or the triplet as intermediate[107] and direct two-photon absorption[108].

For aqueous aniline (**1a**), a relatively high photoionization quantum yield (Φ_e) has been observed upon photolysis with 266 nm ($\Phi_e = 0.18$) and 308 nm ($\Phi_e = 0.16$) laser[109]. The results indicate that the reaction occurs from the nonrelaxed S_1 state by one-photon absorption. Thus, the ionization threshold is less than 4.03 eV. Whereas similar results were also found for its derivatives such as N,N-dimethylaniline (**1b**) and 1,4-diaminobenzene[110], the photoionization of tetramethylphenylenediamine (**25**) in alcohols takes place through the relaxed S_1 state[111]. In addition, 4-aminobenzonitrile undergoes photoionization via a two-photon absorption process[107]. In these cases, the polarization energy of the cation is an important factor determining the photoionization yield of these anilines in aqueous medium.
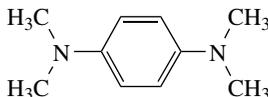
(25)

The dependence of the photoionization process of anilines in aqueous solution on pH could be illustrated by the case of N,N-dimethyl-1-aminonaphthalene (**2b**)[112]. The

photoionization of **2b** does not essentially occur in the pH region <1. In the pH range 2–4, there are two possible ionization processes from both relaxed S_1 and T_1 states of **2b**. The major route is through the proton dissociation of the excited protonated **2b** followed by electron-ejection to water molecules. The minor route is the direct electron transfer from both the S_1 and T_1 states of **2b** to the hydronium ion. Under basic and neutral conditions, the ionization occurs mainly from the nonrelaxed S_1 state of **2b** by one-photon absorption at 266 nm.

B. Photodissociation

1. Photodissociation of the N−H bond

Photodissociation of the N−H bond of anilines could occur, albeit with low quantum yield in most cases, and form hydrogen atoms and aminyl radicals (equation 3)[113].

$$ArNH_2 + h\nu \rightarrow ArNH^\bullet + H \tag{3}$$

It was believed that the homolysis of the N−H bond proceeds at higher electronic excited states that compete with the internal conversion of $S_n \rightarrow S_1$[23, 114]. However, the results of a recent study on the photochemistry of aniline at 193 nm[115], which corresponds to the excitation of electrons of the phenyl ring ($\pi - \pi^*$), reveal that the highly vibrational excited, or 'hot', ground-state aniline molecule after the internal conversion from the initial excited states also undergoes efficient N−H and C−N bond cleavage. The direct dissociation products include hydrogen atoms, hydrogen molecules, NH_2, and NH_3 (Scheme 2). It is also interesting to note that the hot aniline can undergo isomerization to
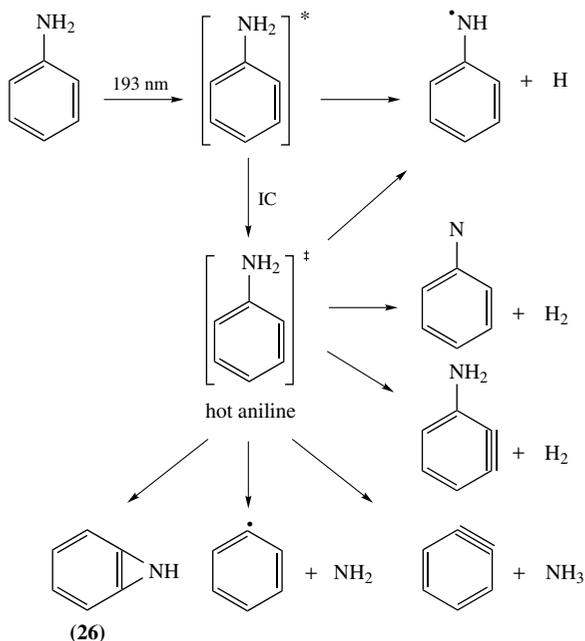
SCHEME 2
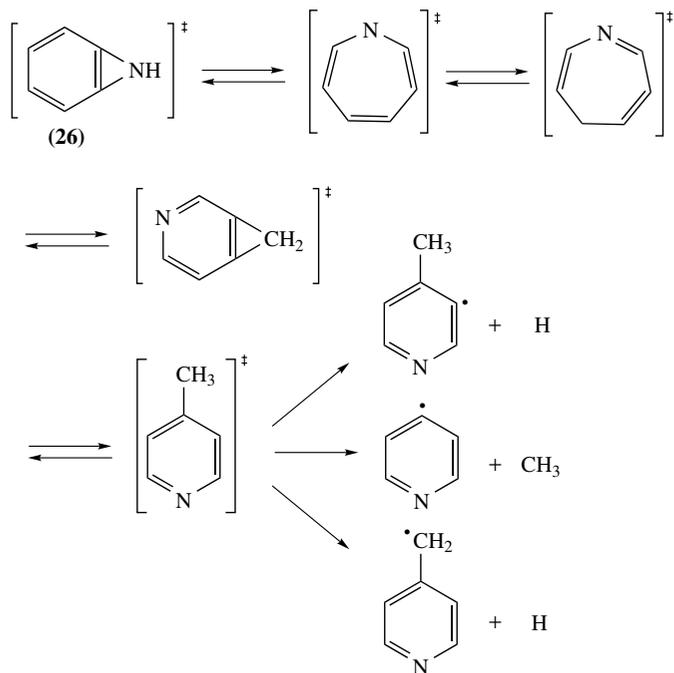
SCHEME 3

form intermediate **26**, followed by a series of isomerization reactions (Scheme 3). More than 23% of hot ground-state aniline produced from the 193-nm excitation has been shown to isomerize to seven-membered-ring isomers, followed by H-atom migration in the seven-membered ring. The seven-membered-ring intermediates then rearomatize to form methyl pyridine or aniline prior to dissociation.

Photodissociation of anilinium ions has been extensively investigated due to the fundamental importance of excited-state proton transfer in chemistry and biochemistry[116, 117]. This reaction is very sensitive to the water environment and thus has been a useful probe for the environment of aqueous solutions. The acid–base equilibria of protonated aniline (**1a**) in aqueous solution in the ground and excited states are depicted in Scheme 4. The acidity constants pK_a^* in the excited states are markedly lower than the ground-state acidity constants (pK_a). The increase in ICT interactions in the excited vs ground state is believed to be responsible for the enhancement of acidity of the anilinium ions upon photoexcitation. This process is also accompanied by the change in configuration for the amino nitrogen from the pyramidal sp^3-like geometry in the ground state to the planar sp^2-like geometry in the S_1 state. The pK_a^* values are often estimated by means of the Förster cycle, the fluorescence titration curve and the triplet–triplet absorbance titration curve[118]. However, it has been recognized that simple acid–base equilibrium cannot be accomplished in the excited state of some anilines, due to the competing process of proton-induced fluorescence quenching ($k_{q'}$). Thus, a dynamic analysis including the quenching process is needed to obtain the correct pK_a^* values. For example, the pK_a^* values for 1-aminonaphthalene (**2a**) determined by the dynamic analyses, the fluorimetric titration and the Förster cycle are -1.0, 2.7 and -5.9, respectively[118]. For

comparison, the pK_a value for **2a** is 3.9. The results of a dynamic analysis for **1a** suggest a large decrease in the pK_a value on going from the S_0 (4.6) to the S_1 state (*ca* -2.2)[119]. The proton dissociation rate of protonated **1a** in aqueous solution at 298 K is 1.4×10^{10} s^{-1}, which is the fastest of those reported for anilinium ions[119]. The proton dissociation rate could be significantly reduced upon introducing substituents into the amino or phenyl groups. For example, the rates are 7.6×10^8 s^{-1}, 4.4×10^7 s^{-1}, 4.1×10^9 s^{-1} and 4.4×10^7 s^{-1} for the protonated form of **1b**, N,N-diethylaniline, 2-toluidine and 2,6-xylidine, respectively[120]. The remarkable decrease of the proton dissociation rate by N-alkyl and *ortho*-alkyl groups has been attributed to the increase in the activation energies as a result of the hydrophobic effects of the alkyl group on the water structure in the vicinity of the amino group.
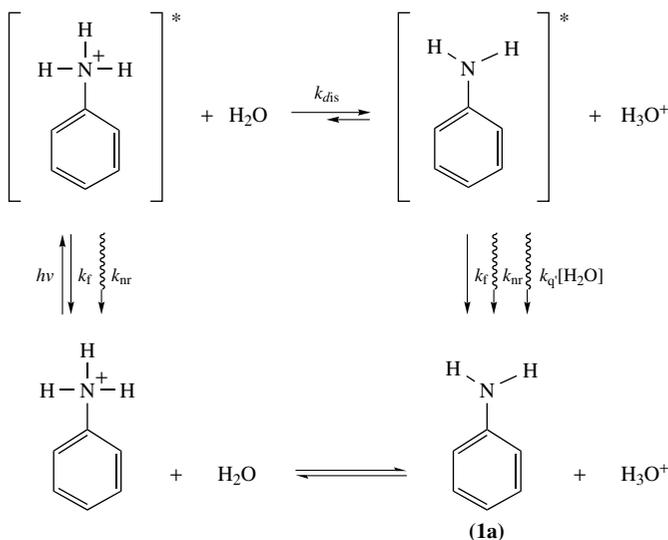
SCHEME 4

Like the case of phenols[121, 122], substituent effects on the proton dissociation of anilinium ions are strongly position-dependent. Examples have been provided by 3- vs 4-cyanoaniline and 3- vs 4-methoxyaniline[123]. Whereas the cyano substitution at the *meta* position of aniline increases the proton dissociation rate by as much as *ca* 29-fold, the rate is reduced by less than 3 times for 4-cyanoaniline vs aniline. In the case of the methoxy substituent, substitution at the *meta* position largely reduces the rate by *ca* 200-fold, but almost no effect was observed when it is at the *para* position.

2. Photodissociation of the C−N bond

Although the hot aniline molecules undergo the aryl-amino C−N bond cleavage (Scheme 2), this reaction is inefficient for anilines in the excited states. In contrast, the anilino-alkyl C−N bond homolysis has been observed for several aniline derivatives. For example, methyl radical (Me$^\bullet$) and anilino radical (PhN$^\bullet$Me) have been detected as the products of the photoirradiation of tetramethylphenylenediamine (**25**) and N,N-dimethylaniline (**1b**), respectively, in 3-methylpentane at 77 K[124, 125].

Homolytic photodissociation of a benzyl-anilino C−N bond has also been observed in a series of *N*-(arylmethyl)anilines. The main products identified for **27** are aniline, triphenylmethane and 9-phenylfluorene (**28**) (equation 4)[126]. The quantum yields for the formation of Ph$_3$C$^\bullet$ are high (0.6–0.8, 248-nm excitation) and independent of solvent. On the basis of the results of laser flash photolysis and ESR studies, the formation of **28** occurs via the intermediate **29** as a result of electrocyclization of Ph$_3$C$^\bullet$ (Scheme 5). In contrast, the dimerization of the benzyl and diphenylmethyl radicals, leading to the formation of 1,2-diphenylethane and 1,1,2,2-tetraphenylethane, respectively, are efficient in the cases of **30** and **31** (equations 5 and 6)[127]. In addition, products resulting from the coupling of the photodissociated benzyl and aniline radicals are also observed for **31**, presumably due to the less sterically hindered PhCH$_2$$^\bullet$ radical when compared with Ph$_2$CH$^\bullet$ and Ph$_3$C$^\bullet$ radicals.

(4)

SCHEME 5

(5)

(30)

(31)

(6)

3. Photodissociation of other chemical bonds

The photodissociation of Malachite Green dyes [(4-Me$_2$NC$_6$H$_4$)$_2$PhCX] has been extensively studied[128]. The amount of heterolytic vs homolytic C—X bond cleavage increases in polar solvents and depends more on the electron affinity of X than on the C—X bond dissociation energy.[129] For Malachite Green leuconitrile (32), the heterolytic C—CN bond cleavage occurs efficiently from the first singlet excited state (equation 7) with a quantum yield of >0.90 in ethanol or acetonitrile, which is independent of light intensity and temperature[130, 131]. The competing decay pathways are fluorescence and intersystem crossing. The photodissociation of 32 could also occur at a higher excited state, which begins with fast ion-pair formation[7]. Recombination competes with vibrational relaxation into a localized contact ion pair. This ion pair then evolves into a contact ion pair with the formation of carbocation 33.

(7)

(32) (33)

When the phenyl group in **32** is substituted with halogen, carbonyl or nitro groups that promote intersystem crossing, the efficiency of photodissociation is significantly reduced[131]. In addition, when the dimethylamino groups in **32** are replaced by monoaza-15-crown-5 (i.e. **34**), the photodissociation rate constant in acetonitrile is significantly influenced by the cation complexation of the crown ether moieties[132, 133]. Two opposite effects could account for the observed changes in the photodissociation rate constant: (1) addition of metal salts increases the polarity of the acetonitrile medium that accelerates the ionization process; (2) coordination of metal ion in the crown ethers suppresses the ionization process due to the intramolecular electrostatic repulsion. The interplays of these two factors might account for the different effects of Na^+ vs K^+ on the rate of photoionization, where it is increased in the presence of 1 equivalent of Na^+ but decreased in the presence of 1 equivalent of K^+. Metal-ion complexation effects are also observed for the mono- (**35**) and tris-crown ether (**36**) substituted analogs, but they show different ion selectivity. The corresponding benzocrown derivatives of **34–36**, namely the replacement products of the *N*-phenyl monoaza-15-crown-5 by benzo-15-crown-5, have also been investigated[134, 135].

(34)   (35)   (36)

1,2-Aminoalcohols[136, 137] and 1,2-diamines[138, 139] are known to undergo an oxidative C−C bond photodissociation with a mechanism that is associated with electron transfer (Scheme 6). In most cases, an excited electron acceptor is required and the amino group functions as a ground-state electron donor. The resulting radical cations then undergo heterolytic C−C bond fragmentation to form an *α*-amino radical and an aldehyde (or ketone) or an iminium ion. To observe such a photodissociation reaction, the rate for bond fragmentation (k_{BF}) must be sufficiently fast that it competes effectively with the back electron transfer process for the charge-transfer state. The hyperconjugation interac-

SCHEME 6

tions between the half-filled N p-orbital and the filled σ_{CC}-orbital presumably weakens the C−C bond, and thus the bond is susceptible to relatively rapid heterolytic fragmentation at ambient temperature[140]. Results have shown that the value of k_{BF} for 1,2-diamines that feature 2° or 3° amines is *ca* 10^5–10^6 s^{-1}, and the rate is slower in the aromatic 1,2-diamine systems[141]. The latter can be attributed to the delocalization of the spin density of the N atom into the aryl ring, which decreases the electrophilicity of the N-centered radical and thus the hyperconjugative interaction. This feature has been applied as a photochemical probe for the photoinduced electron transfer in donor−acceptor substituted organic and organometallic compounds[142, 143]. In the case of compound **37**, no external electron acceptor is required (Scheme 7). The locally excited (^{1}LE) state of the 4-aminobenzonitrile (ABN) group is initially populated by optical excitation, and the bond dissociation reaction occurs from a lower-lying charge transfer (^{1}CT) state that is formed by electron transfer from the piperidine tertiary amine donor to the ABN unit[143]. The forward electron transfer rate constant is larger than 5×10^8 s^{-1}. Since the CT state was not observed by nanosecond transient absorption, the back electron transfer should occur rapidly ($>10^8$ s^{-1}). Accordingly, the C−C bond fragmentation is rapid as well ($>10^8$ s^{-1}) to result in a quantum efficiency of 0.12–0.28.

C. Photocyclization

The photochemical six-electron cyclizations that convert **38** to **39** (equation 8) have been well investigated[144, 145]. The primary synthetic value of this reaction type is the formation of a carbon−carbon bond to an aromatic ring[146]. For *N*-aryl enamines (X = N) derived from cyclic ketones, the stereoselectivity of photocyclization depends on the ring size. While only the *cis*-indoline is obtained for the five-membered-ring enamine (**40**) (equation 9), six- and seven-membered-ring enamines (**41** and **42**) give *trans*-indolines as major products. In addition, the ethyl 2-(*N*-alkylanilino)acetoacetate **43** provides 3-hydroxyindoline **44** in nearly quantitative yield through the enolic form (equation 10)[147]. When **43** is irradiated in protic (acidic) solvent, the reaction leads to the corresponding indole **45**[148]. Similar reactions also take place for *N*-(2-bromophenyl)enaminones **46** and **47** (equation 11)[149].

SCHEME 7

$$X = O, S, Se, NR$$

(38)   **(39)**   (8)

(40) $n = 1$
(41) $n = 2$ (9)
(42) $n = 3$

CH₃ N CO₂Et O CH₃
(43)

CH₃ N CO₂Et HO CH₃

hv

H₃C N H CO₂Et CH₃ HO
(44)

(10)

H^+

H₃C N CO₂Et CH₃
(45)

O Br N H R R
(46) R = H
(47) R = CH₃

$\xrightarrow[\text{MeCN/dioxane}]{hv}$

O N H R R
80–86%

(11)

Since the works of Parker and Barnes[150], the photocyclization of diphenylamines to carbazoles has long been a subject of interest, partly due to the high quantum efficiency[151, 152]. The reaction is more likely to proceed in the T_1 state to form a short-lived intermediate of zwitterionic character[153], which is N-methyl-4a,4b-dihydrocarbazole (**48**) in the case of N-methyldiphenylamine, followed by thermal elimination of two hydrogen atoms (equation 12)[154, 155]. The triplet quantum yields are *ca* 0.57 for diphenylamine and *ca* 0.95 for N-methyldiphenylamine, and the quantum yield for the formation of **48** is *ca* 0.41[156, 157]. In aerobic condition, the conversion of **48** to N-methylcarbazole (**49**) involves little or no side reaction. The quantum yield for the formation of **48** and thus **49** is 0.42 in methylcyclohexane at 20 °C. The activation energies for the forward photocyclization and the backward ring-opening steps are 5.5 and 17.0 kcal mol^{-1}, respectively. It has been shown that O_2 could accelerate the conversion of **48** into N-methylcarbazole[158], but O_2 could also deactivate the T_1 state of diphenylamines[159]. In addition, Ag(I) ions could accelerate the intersystem crossing processes of triplet diphenylamine → ground-state diphenylamine and thus reduce the carbazole product[160].

Me N

hv

Me + N – H H
(48)

[O₂]

Me N
(49)

(12)

Direct photolysis of **50–53** in O_2-saturated acetonitrile solution also leads to the corresponding carbazoles with a quantum yield of *ca* 0.64 in all cases (equation 13)[161]. Apparently, substituents have only a little effect on the chemical yield of carbazole produced by steady-state irradiation in aerated acetonitrile. However, an attempt to carry out such a photocyclization reaction by using photoinduced electron-transfer sensitization has failed, presumably due to fast back electron transfer that quenches the net reaction. It is also interesting to note that chemical oxidation and electrochemical oxidation of **50–53** does not result in carbazoles. Instead, benzidine products are formed. These results are consistent with the AM1 calculations, which suggest that the cyclization reaction is both kinetically and thermodynamically more favorable from the triplet state than from the cation radical or dication.

$$hv = 254 \text{ nm}$$
$$[O_2]$$

(13)

(50) R = R' = H

(51) R = H, R' = F

(52) R = H, R' = OCH$_3$

(53) R = OCH$_3$, R' = H

In the presence of external protic acid, *N*-alkyl-*N*-(4-methoxyphenyl)anilines (**54a–59a**) are converted to *N*-alkyl-1,2,4,9-tetrahydrocarbazol-3-ones (**54b–59b**) (equations 14–16)[162]. A conceivable mechanism is demonstrated for **54a** in Scheme 8, where the dihydrocarbazole intermediate undergoes a successive formal [1,5] and [1,3] hydrogen shift and then acid assisted hydrolysis before the formation of final products.

$$hv = 300 \text{ nm}$$
$$\text{HCl, MeOH}$$

(14)

(54a) R = H, R' = Me   **(54b)** 85%

(55a) R = H, R' = Et   **(55b)** 84%

(56a) R = Me, R' = Me   **(56b)** 72%

(57a) R = OMe, R' = Me   **(57b)** 96%

(15)

(16)

SCHEME 8

The photocyclization reaction of 2-allylanilines, depending on the degree of alkylation at the N atom, has long been a subject of interest. When N,N-dialkylanilines **60a–62a** were irradiated in methanol, the corresponding 2-cyclopropylanilines **60b–62b** were formed in 73, 60 and 47% yield, respectively (equation 17)[163]. This reaction proceeds in the triplet state via a clean aromatic di-π-methane rearrangement. However, no reaction occurs when 2-allyl-1-(N,N-dimethylamino)naphthalene is irradiated in methanol. Thus, this photochemical 'cyclopropanization' of allylated anilines appears to have only a limited scope as preparative method, because it is successful only for a few substrates.

(60a) $R^1 = R^2 = Me$

(61a) $R^1 = Me, R^2 = Et$

(62a) $R^1 = R^2 = Et$

(60b) 73%

(61b) 60%

(62b) 47%

(17)

For secondary 2-allyl-*N*-methylaniline **63** in nonpolar solvents such as cyclohexane and benzene, the photoproducts are different, where indolines are formed along with a minor amount of 1,2,3,4-tetrahydroquinolines (equation 18)[163]. In alcoholic solvents such as methanol, a methoxy derivative is formed in addition to indolines. This transformation has been suggested to occur from the singlet manifold of anilines, because it is not quenched by (*E*)-piperylene or sensitized by acetone[164]. The reaction started with an intramolecular electron transfer from the amino nitrogen to the ethylene group, forming a donor–acceptor complex (Scheme 9). Further H-transfer and diradical coupling reactions of this complex lead to the indoline products or the spirodienimine intermediates (**64**). The cyclopropane ring in intermediate **64** is then opened stereospecifically with inversion of configuration by methanol. The stereochemistry of this reaction is illustrated by the example shown in equation 19[165, 166].

(18)

Irradiation of primary 2-butenylaniline **65** in benzene also gives the indoline products (equation 20). When the reaction was carried out under air, the corresponding indole product, which arises from secondary photoreaction of the primary indoline product, is also formed[167]. When the amino group is substituted with an electron-withdrawing acyl group (i.e. compound **66**), the products of photocyclization are largely reduced (<5%). In conjunction with the observation of exciplex fluorescence for **65** but not for **66**, the photocyclization reaction should take place through an electron-transfer mechanism.

(63)

(64)

SCHEME 9

40%

6%

(19)

29%

14%

(65)

air   79%   21%

argon   94%   6%   (20)

(66)

When 2-allylanilines are irradiated in protic solvents such as H_2O, MeOH and EtOH in the presence of H_2SO_4, the products are *trans*-2-hydroxy- or *trans*-2-alkoxy-1-methylindanes (e.g. **67** in Scheme 10)[168]. The reaction mechanism might involve a tricyclo[4.3.0.0^{1,8}]nona-2,4-diene intermediate from an intramolecular [2s + 2s] cycloaddition reaction between the allylic side chain and the benzene ring of the anilinium group (Scheme 11). Concerted attack of a solvent molecule at C8 of the nonadiene intermediate under ring opening and loss of the ammonium group restores the aromatic system. On the other hand, the aniline **68** and anilinium salt **69** lose the ammonium group reductively under the same conditions (equations 21 and 22).

SCHEME 10

SCHEME 11

(67)

(21)

(68)

(22)

(69)

The potential stereoselectivity of this photocyclization process has recently been investigated for the two rigid 2-allylanilines **70** and **71**[169]. Irradiation of compound **70** at room temperature gives a mixture of diastereomers *trans*-**72** and *cis*-**72** with a little stereoselectivity (equation 23). While a poor stereoselectivity is also observed for **71**, the photocyclization is regioselective, where the products *trans*-**73** and *cis*-**73** are minor (equation 24). However, the diastereoselectivity of *trans*-**72** vs *cis*-**72** is increased in the case of **71** when the temperature is changed, indicating that the reaction is significantly entropy-controlled. In addition, the observation of fluorescent exciplex formation for **70** and **71** supports the electron-transfer mechanism for the photocyclization of 2-allylanilines.

(23)

(**70**)

(*trans*-**72**)
54%

(*cis*-**72**)
46%

An alternative structure participating in this PET-induced photocyclization reaction is exemplified by *N*-(styrylalkyl)anilines **74–76**, where the electron acceptor is linked to the amino group rather than to the *ortho* position of the ring (Scheme 12)[100]. It is noted that

(24)

SCHEME 12

the preparative application of this reaction is limited due to the instability of the adducts **74a−76a** and **74b−76b** under the conditions of irradiation. It is also noted that intramolecular adduct formation was not observed for the corresponding tertiary styrylanilines **20** and **21**.

Other types of *ortho*-substituted anilines could also undergo cyclization reactions upon irradiation[170]. Photocyclization of anthranilonitrile (**77**) in acetonitrile results in indazole (**78**) and benzimidazole (**79**). Analysis of the reaction mixture after short irradiation times revealed that **78** is the initially formed product, which is converted to **79** on further irradiation (equation 25).

$$(25)$$

The corresponding *N*-phenyl derivative **80** forms carbazole with high yield (equation 26)[167].

$$(26)$$

D. Photoisomerization

The photochromism of *N*-salicylideneaniline (**81**) has attracted much attention[171, 172]. Photochromic salicylideneanilines are usually pale yellow and exist in the phenol form in crystals. Upon irradiation with UV light, the proton bonded to the oxygen atom is translocated to the imine nitrogen atom and forms a red photoproduct (equation 27). The activation energies in the forward and backward reactions have been found to be very sensitive to the environment[173]. A question of interest is the structure of the photoproduct, being a *trans*- or a *cis*-ketone[174]. It has been shown that when a single crystal of **81** is irradiated with a UV light at 200 K, 40% of the keto molecules are in the *cis* form and 60% of them are in the *trans* form[175]. The transformation of **82** in the solid state induced by two-photon excitation has been tracked by X-ray analysis (equation 28)[176]. The result reveals that the photoproduct **83** is in a *trans*-keto form. It should be noted that *N*-salicylideneanilines also belong to a class of thermochromic compounds, and the population of the keto form increases on lowering the temperature[177].

A series of *N*-salicylidene-2,6-dialkylanilines (**84a−84e**, **85a−85d**, **86a−86d**, **87a**, **87d**, **88a**, **88b**, **88d**, **89a**, **89d**, **90a**, **90b** and **90d**) has been investigated in order to evaluate the alkyl substituent effects on the crystal packing of molecules and, in turn, their photochromic properties in the solid state[178]. The alkyl groups, particularly the isopropyl group, at the 2,6-positions of the aniline ring can lead to a nonplanar molecular structure, which is effective for the crystals to exhibit photochromism.

(27)

trans-phenol
(81)

cis-keto

trans-keto

(28)

(82)

(83)

R¹
R²
R¹ H
X¹
X²

(84) $X^1 = X^2 = Cl$ **(a)** $R^1 = R^2 = H$
(85) $X^1 = X^2 = Br$ **(b)** $R^1 = Me, \ R^2 = H$
(86) $X^1 = X^2 = I$ **(c)** $R^1 = Et, \ R^2 = H$
(87) $X^1 = X^2 = H$ **(d)** $R^1 = i\text{-}Pr, R^2 = H$
(88) $X^1 = X^2 = t\text{-}Bu$ **(e)** $R^1 = R^2 = t\text{-}Bu$
(89) $X^1 = H, X^2 = Cl$
(90) $X^1 = H, X^2 = Br$

E. Photosubstitution

Anilines themselves do not undergo photosubstitution reactions, but a few of their ring-substituted derivatives such as haloanilines undergo photoreactions that are not observed in the corresponding haloarenes[179]. Apparently, the electron-donating amino group plays an important role in these reactions.

1. 4-Chloroanilines

Chloroanilines are toxic and classified as typical environmental pollutants, resulting from biodegradation of chlorophenylurea-based herbicides[180, 181]. Like the case of parent aniline molecule, photodegradation of chloroanilines continues to be a subject of research interest[182, 183]. Understanding of the subsequent photochemical behavior of chloroanilines is important not only for the purpose of environmental protection but also for exploring new reactions of synthetic values.

4-Chloroaniline (**91a**) and 4-chloro-*N*,*N*-dimethylaniline (**91b**) are weakly fluorescent with quantum yields less than 0.03 and lifetimes less than 1.0 nanosecond, and the latter is not very solvent-dependent[184]. The main deactivation process is intersystem crossing (e.g. $\Phi_{isc} = 0.66$), and it appears to be more efficient in nonpolar hexane solvent than in polar solvents. Both **91a** and **91b** show well-detectable phosphorescence in a glassy matrix with a spectral shape and emission efficiency similar to the nonhalogenated anilines.

NR$_2$

Cl

(**91a**)   R = H
(**91b**)   R = CH$_3$

The photochemistry of 4-chloroanilines in methanol, dioxane–water and dioxane–methanol solvents has been investigated for more than thirty years by Latowski[185, 186]. Large quantum yields of HCl formation (Φ_{HCl}) have been observed for the photolysis of **91a** in protic solvents (e.g. $\Phi_{HCl} = 0.78$ in methanol at 254 nm). However, the values of Φ_{HX} are relatively small for 4-bromoaniline ($\Phi_{HBr} = 0.19$), 4-iodoaniline ($\Phi_{HI} = 0.29$), 2-chloroaniline ($\Phi_{HCl} < 0.02$) and 3-chloroaniline ($\Phi_{HCl} = 0.02$) under the same condition. *N*-Acetylation of **91a** to 4-chloroacetanilide also inhibits the photolytic process. In conjunction with the solvent- and concentration-dependent photolysis rates of **91a**, these results indicate an electron-transfer mechanism for the photochemical reaction: electron transfer occurred from an excited **91a** to an unexcited **91a** molecule, followed by ionization reactions. However, recent analysis of photoproducts from **91a** in water/methanol mixtures has shown that benzidine (**92**) is a major product along with aniline (equation 29)[187]. As a result, a 'carbene' mechanism that leads to the formation of aniline radicals was put forward in analogy to the photochemistry of 4-halophenols[188, 189]. For example, the photolysis of **91a** in aqueous solution first results in the transient species carbene **93** followed by the formation of the aniline radical **94** that was observed as the primary product (Scheme 13)[190]. In addition to **1a** and **92**, other identified secondary products include 4-aminodiphenylamine, 2-aminodiphenylamine, hydrazobenzene, 4-chloronitrosobenzene and 4-chloronitrobenzene, but they are all in low yields[191].

NH$_2$ $\xrightarrow[\text{–HCl}]{hv}$ NH$_2$ + H$_2$N— —NH$_2$

(29)

(**91a**)   (**1a**)   (**92**)

SCHEME 13

   The carbene mechanism for the photolysis of **91a** is modified by Grabner and coworkers according to the results of nanosecond transient absorption spectroscopy and steady-state photoproduct analysis[184]. Product analysis by HPLC for the photolysis of **91a** in aqueous solution indicates the formation of 4-aminophenol, aniline, 4-amino-4′-chlorodiphenylamine (**95**), 2,4′-diamino-5-chlorobiphenyl (**96**) and 4′,5-diamino-2-chlorobiphenyl (**97**) (equation 30). The first transient detectable at nanosecond time resolution was assigned to the protonated imino carbene (**98**), which could interact with O$_2$ (forming intermediate **99**), alcohols, H$_2$O and bromide ions. The reaction between iminoquinone oxide **99** and of **91a** accounts for the formation of **95** (Scheme 14). The estimated quantum yield of carbene formation is 0.53 in neutral aqueous solution. The trend observed in the rate constants for H abstraction from the alcohols increases in the order *tert*-butyl alcohol < methanol < ethanol < 2-propanol. The reaction with bromide is efficient but the corresponding reaction with chloride is slow. Formation of the carbene-substrate adducts **96** and **97** could be interpreted by an electron-transfer reaction between a protonated carbene (acceptor) and an unprotonated **91a** molecule (donor) to form aniline radical and the radical cation of **91a**, followed by in-cage combination. This mechanism is consistent with the observation of more *ortho–para* than *meta–para* coupling.

(30)

SCHEME 14

In acidic medium, the quantum yield of carbene formation is somewhat lower (0.40), and the reactions in equation 30 are slower. It is thus speculated that the difference might be related to the requirement of an additional deprotonation step for generation of the carbene from protonated **91a**. In moderately alkaline solution (pH = 10), the decay of the carbene is accelerated, presumably due to the deprotonation of the imino group by OH$^-$. These reactions suggest a carbene intermediate with a triplet ground state. The photochemical behavior of **91b** parallels that of **91a** in most respects, except for the effect of OH$^-$ on the carbene, which is negligible in the case of **91b**. The differences between the photochemistry of **91a** and 4-chlorophenol might be worth mentioning. First, unlike 4-chlorophenol, **91a** also produces the carbene in aprotic polar solvents such as acetonitrile. Second, contrary to 4-chlorophenol and 4-chloroanisole[192], the reaction mechanisms of **91a** and **91b** are the same. Third, their product distribution in the presence of O$_2$ is different, due to the fact that the iminoquinone oxide **99** is able to add to **91a**.

In acetonitrile, the following reaction has been suggested to account for the observed transient spectra (equation 31)[192]:

More detailed studies of the photolysis of 4-chloroanilines in neat acetonitrile have been carried out by Albini and coworkers, and the results have been intriguing in both synthetic and mechanistic aspects. As is the case in neutral aqueous solution, **91a** and **91b** undergo reductive dechlorination to **1a** and **1b** and coupling reactions to **96a** and **96b** upon irradiation in acetonitrile (equation 32)[193].

$$hv, \text{MeCN} \tag{32}$$

(91a) R = H
(91b) R = Me

(1a) R = H   50%
(1b) R = Me   47%

(96a) R = H   38%
(96b) R = Me   30%

In the presence of NaBH$_4$, the reaction gives a clean reduction of **91a** to **1a** (95%)[194].

When the reaction is carried out in the presence of 1-hexene (1 M), the yield of **1a, 1b, 96a** and **96b** is largely reduced and 4-(β-chloroalkyl)anilines (**100a** and **100b** and **101a** and **101b**) are formed (equation 33)[194]. In the presence of both 1-hexene and NaBH$_4$, the corresponding dechlorinated compounds (**102** and **103**) are the main products.

$$\text{(91)} \xrightarrow{hv, \text{MeCN}} \tag{33}$$

(100a) R = H   48%
(100b) R = Me   35%

(101a) R = H   25%
(101b) R = Me   18%

(102)   39%

(103)   21%

When different alkenes were present, allyl, vinyl or lactone derivatives could be obtained (equation 34)[195].

Photoadducts could also be formed when the alkenes are replaced by benzene and methyl-substituted benzenes (equation 35) and heterocyclic arenes such as furans, pyrrole and thiophene (equation 36)[196]. It should be noted that the arylation took place at the α position of these heterocycles, but at the β position when both the α positions are methylated. In addition, hexamethylbenzene could also lead to photoadducts. The reactions of **91a** and **91b** are efficient with the quantum yields for decomposition of **91a** and **91b** being 0.44 and 0.87, respectively. Thus, these reactions offer alternative methods for the synthesis of biarylamines and 4-alkylanilines.

(34)

(35)

There are some differences in the photochemical reactions of **91a** and **91b** and alkenes when the acetonitrile solvent is replaced by other solvents such as alcohols, ethyl acetate and chlorinated hydrocarbons. These include (1) a change in the product ratio, (2) a change in the reaction quantum yield and (3) the formation of new products by trapping solvent molecules. For example, irradiation of **91b** with 1-hexene in methanol gives the 4-(β-methoxyalkyl)anilines **104** and **105** (equation 37) rather than **100b** and **101b**. It should be noted that with all of the alcohols tested (i.e. methanol, 2-propanol, *tert*-butyl alcohol and TFE) the alkoxyaniline **106** is formed at most in trace amounts.

(36)

(37)

(106)

It should also be noted that in nonpolar solvents such as cyclohexane, the photoreaction is much slower with a quantum efficiency decreased by a factor >20 in comparison to that in acetonitrile[195]. This could be attributed to the efficient process of intersystem crossing ($\Phi_{ISC} = 0.66$) for **91a** in nonpolar solvents.

Instead of using the previously proposed carbene mechanism (Scheme 14), Albini has proposed a 'phenyl cation' mechanism, in which the 4-aminophenyl cation (**107**) is generated by heterolytic photocleavage of the C—Cl bond, followed by electrophilic substitution reactions, to account for the above photochemical reactions of **91** (Scheme 15)[193–197]. This stems from the great similarity in reactivity between **91a** and **91b**, which suggests that the reactions do not require previous deprotonation to a neutral carbene **93**, since

SCHEME 15

it could be formed only from **91a**. Generation of aryl cations has been restricted to a few precursors and methods. Solvolytic generation of aryl cations has been observed for arenediazonium salts[198, 199] and aryl triflates[200] in 2,2,2-trifluoroethanol (TFE). The phenyl cation has been generated by decay of tritium-marked benzene[201] and by the photolysis of benzenediazonium salts in TFE[202] or 1,1,1,3,3,3-hexafluoroisopropyl alcohol[203] and halobenzenes under extremely low temperature (4 K)[204]. An issue that is under debate is the electronic character of the ground state of the phenyl cation, namely whether it is a triplet[205] or a singlet[198, 206]. Previous[207] and recent[208] *ab initio* molecular-orbital calculations have suggested that the ground state of aryl cation is singlet, unless it is substituted with an electron-donating group in the *para* position. The low-temperature transient absorption experiments for 4-(N,N-diethylamino)benzenediazonium salts (**108**) confirm a triplet ground state with a lifetime less than 15 ps in fluid solution at room temperature[202]. However, the initially formed singlet state of **108** upon photolysis in TFE is so active that it is nearly completely consumed before it can intersystem cross to the triplet and leads to alkoxyaniline as the major product (*ca* 90%). The inefficient formation of alkoxyanilines in the photoheterolysis of **91** in alcohols has led to the conclusion that the reaction intermediates are triplet 4-aminophenyl cations. The triplet state was calculated by the CASSCF method to be the ground state and more stable by >10 kcal mol^{-1} than the corresponding singlet state in the gas phase[4, 5]. In addition, the triplet has a mixed carbene–diradical character at the divalent carbon, and the singlet has a σ cation–singlet carbene character. Such a difference in electronic nature for the triplet vs singlet state is in accord with the difference in reactivity toward π vs σ nucleophiles (alkenes vs alcohols).

(108)

2. Other chloroanilines

The photochemistry of the constitutional isomers of **91a** is relatively simple. The maximal absorption of 3-chloroaniline (**109**) in aqueous solution is located at 286 nm. The main photoproduct of **109** in aqueous solution is 3-aminophenol[209]. The transformation is almost quantitative, independent of the presence of oxygen, but secondary photoproducts such as resorcinol could be detected upon prolonged irradiation. These observations suggest that the reaction is initiated by a heterolytic C—Cl bond cleavage, followed by hydrolysis.

(109)

The photochemistry of 2-chloroaniline (**110**) in aqueous solution is less specific than that of 3-chloroaniline. The main photoproducts identified by Ishikawa and coworkers are 2-chloronitrobenzene, 2-chlorophenol and phenol. They suggested that the former results from an initial photooxidation of **110** and the other two species are its secondary photoproducts[210]. However, in a later report the main photoproduct was shown to be 1,3-cyclopentadiene-1-carbonitrile (**111**), and 2-chlorophenol, 2-aminophenol and phenol were detected as minor photoproducts. In addition, 2-chloronitrobenzene was not observed at all[211]. The formation of **111** was also observed in the gas phase phototransformation of **110**, and it might involve the phenylnitrene intermediate[212, 213]. In a recent report, a plausible mechanism for the formation of **111** has been suggested: the heterolysis of the C−Cl bond generates an iminocarbene, which rearranges into ketene iminium ion and then into **111** (Scheme 16)[214]. In addition, diaminochlorobiphenyls have been detected in deoxygenated but not in air-saturated solutions.

SCHEME 16

When compared with monochloroanilines, the photochemistry of dichloroanilines is less explored. The main photochemical reaction of dichloroanilines in aqueous solution is photohydrolysis, namely a substitution of Cl by OH[215]. According to the behavior of the six isomers of dichloroaniline (**112−117**), a priority order in the site of substitution is *meta* > *ortho* > *para*. In other words, *para* and *ortho* substitutions are minor pathways when the *meta* position is chlorinated. This is illustrated by the case of **114** (equation 38). The reaction quantum yields for six dichloroaniline isomers are in the range 0.015−0.060, which is substantially lower than that for 3-chloroaniline (0.12). Apparently, the presence of a second chlorine on the ring disfavors photohydrolysis. Likewise, compound **113** neither reacts as 2-chloroaniline nor as 4-chloroaniline. The formation of **111** observed with 2-chloroaniline does not occur with *ortho*-chlorinated dichloroanilines (**112−115**). In the cases of **113** and **115**, aminochlorophenoxazones are formed as secondary photoproducts, resulting from the initially formed aminochlorophenols and an *o*-benzoquinone monoamine intermediate. With **113**, 2-amino-7-chlorophenoxazin-3-one (**118**) has been identified, and three derivatives (**119−121**) have been identified with **115**. The conversion of **116** to 5-amino-2-chlorophenol at λ > 290 nm is *ca* 78% with a quantum yield 0.052, and the reaction has been suggested to proceed through an aryl cation produced by heterolytic cleavage of the *meta* C−Cl bond[216]. The fact that the reaction is not affected by oxygen is consistent with a heterolytic mechanism. A variety of other photoproducts such as 4-chloroaniline, aniline, chloronitrobenzenes and azobenzene have also been detected for **116**[217]. It should be noted that the main photoreaction of **113, 114** and **116** in methanol is the substitution of Cl by H with a priority order *para* > *meta* > *ortho*[218].

(112)   (113)   (114)   (115)   (116)   (117)

(114)   70%   <5%   <1%

$$(38)$$

(118)   (119)

(120)   (121)

Irradiation of trichloroanilines **122** and **123** also leads to azobenzenes[219].

(122)   (123)

3. Other haloanilines

The photochemical behavior of 4-fluoroaniline (**124**) and 4-bromoaniline (**125**) in aqueous solutions is essentially similar to that of **91a**. The only significant difference is in the quantum yields of halide formation (Φ_X), which is **124** ($\Phi_X = 0.50$) > **91a** ($\Phi_X = 0.43$) > **125** ($\Phi_X = 0.27$)[184]. Although **124** has a larger photochemical reactivity, the values of its fluorescent quantum yields (>0.10) and lifetimes (>1.89 ns) are larger than those for **91a**.

$$NH_2 \qquad\qquad NH_2$$

F
Br

(124)   **(125)**

Little is known about the photochemistry of 4-iodoaniline. It is thought to undergo homolytic C−I bond cleavage to yield a phenylamine radical and an I atom[220]. This has been observed when 4-iodoaniline is adsorbed on the GaN(0001)-(1 × 1) surface. The photodissociation of the C−I bond is more likely to proceed by direct excitation of the molecule rather than through a substrate mediated process involving transfer of excited carriers between adsorbate and substrate[220].

The photochemistry of 2-fluoroaniline and 2-bromoaniline is also similar to that of 2-chloroaniline, but the formation of 2-aminophenol is more efficient with 2-fluoroaniline than with the other two species. In contrast, the formation of biphenyl derivatives is more efficient for 2-bromoaniline than 2-chloroaniline, and it does not occur for 2-fluoroaniline[214]. The absence of biphenyl derivatives in the presence of oxygen indicates that the reaction involves the excited triplet state.

F. Photoaddition

Like the situation in photosubstitution, anilines themselves do not undergo photoaddition reactions. However, methanol solvent molecules photoadd to vinyl-substituted anilines such as dihydroquinolines **126a** and **126b** (equation 39)[221].

OMe   OH

hv
HOR′

R′ = H or CH$_3$ +

(126a) R = H   **(127a)** R = H   **(128a)** R = H
(126b) R = CH$_3$ **(127b)** R = CH$_3$ **(128b)** R = CH$_3$

(39)

The photoaddition of alcohols to **126a** and **126b** depends on the nature of alcohols and the basicity of solutions. The photoaddition of pure ROH to **126a** and **126b** is only

restricted to water and methanol. For other alcohols such as ethanol and propanol, the reaction occurs only in the presence of water and gives mixtures of the corresponding alkoxy and hydroxy adducts. In neutral methanol solutions, only the Markovnikov ether products **127a** and **127b** are obtained. In the presence of KOH, **126a** only results in **127a**, but **126b** leads to a mixture of **127b** and **128b**[222]. It should be noted that **127a, 127b, 128a** and **128b** are not stable in alkaline solutions under the irradiation condition and both can be converted into the corresponding starting materials **126a** and **126b**. It should also be noted that dihydroquinolines are known to undergo photodissociation of the N−H bond and form aminyl radicals in hydrocarbon solvents or dry alcohols[223]. For N-substituted tertiary dihydroquinolines, photodissociation of the C−N bond in isopentane−ethanol−ether glasses at 77 K has also been reported[224].

The photoaddition more likely proceeds in the excited singlet state due to the lack of sensitivity of the reaction to the presence of oxygen. Two transient species have been detected for the case of **126a**, corresponding to cyclic *o*-quinomethane imine **129** and carbocation **130** (**130a** ↔ **130b**) (Scheme 17). The formation of **129** is impossible for **126b**, but the corresponding zwitterionic form **131** could account for the formation of carbocation **132**. Kinetic studies have shown that the attack of methanol molecule on carbocation **130** is a reversible process[225]. Other nucleophiles such as azide ion could compete with methanol in attacking the carbocation, forming new photoadducts[226].

SCHEME 17

Photoinduced regioselective methanol addition has also been observed for **133** (equation 40). The regioselectivity is different from that in 4-methoxystilbene (**134**) (equation 41)[227]. Since the latter has been attributed to a zwitterionic singlet state (**135**) in which the positive charge is stabilized by the 4-methoxy substituent, the former was then rationalized by attack of methanol on a CT state (**136**) in which the positive charge is localized on the aniline ring and the negative charge on the vinyl naphthalene. It is interesting to note that the corresponding 4-amino isomer of **133** does not undergo photoaddition reaction.

(40)

(41)

(135)   **(136)**

G. Photopolymerization

Polyaniline (**137**) is one of the most promising conductive polymers and the conductivity could be reversibly controlled by oxidation or protonic doping mechanisms[228, 229]. In addition, polyaniline displays good environmental and thermal stability, and its undoped form is solution processable from both organic and aqueous acid solutions. The polymerization of aniline is usually carried out by a chemical or electrochemical oxidation reaction[230, 231]. However, photochemical methods toward the preparation of polyaniline have recently been reported[232–240].

(137)

There are two types of photopolymerization processes: (1) photopolymerization with photocatalytic systems and (2) direct photoexcitation of the monomer. The former has been demonstrated by the formation of polythiophene and polypyrrole either by n-type

silicon wafers or by Ru(bpy)$_3$$^{2+}$[232]. The photopolymerization of aniline and its derivatives via PET between Ru(bpy)$_3$$^{2+}$ and anilines has also been reported[232–235]. Since the photopolymerization of aniline in homogeneous solution involves branched and compact coil structures, the reaction has been carried out in the presence of polyelectrolyte as polymerization templates to improve the physicochemical properties of the photopolymerized polyanilines. The templates include a bilayer film composed of Ru(bpy)$_3$$^{2+}$-incorporated Nafion and methyl viologen (MV^{2+}) -pendant poly(siloxane)[233], a single-layer film composed of Ru(bpy)$_3$$^{2+}$- and MV^{2+}-incorporated Flemion film[234], two-dimensional clay interlayers intercalated with Ru(bpy)$_3$$^{2+}$ in acidic aqueous solutions[235] and DNA[236]. The photopolymerization process appears to be more efficient for aniline solutions of lower pH and higher ionic strength[237]. A solution of aniline in acidic KBrO$_3$/KBr can also polymerize to form a thin film at the air–water interface[238]. The polymerization is induced by the BrO$_2$$^{\bullet}$ radical initiator. When the polymerization is carried out in the presence of 320-nm light at the interface, a macroscopic pattern is formed on the film in the shape and size of the incident light beam. The latter has been attributed to the additional radical initiator Br atom resulting from the dissociation of Br$_2$ by light.

For the direct photoexcitation of the aniline monomer itself, a Nd:YAG laser to irradiate an Au electrode in a solution containing aniline under an applied external bias has been used[239]. In addition, photopolymerization of aniline could also be induced in aqueous solution of transition metal salts (i.e. silver nitrate) without the need of oxidative reagents or bias voltage applied to an electrode[240]. This method yields a composite material where silver nano- and microwires are formed along with polyaniline. It has also been shown that the morphology of the polymer strongly depends on the excitation wavelength. While a globular morphology is observed for the UV synthesis, a fibrillar one is found for visible light excitation. The photopolymerization mechanism is proposed to proceed through a PET process from the aniline or anilinium ion to Ag$^+$, and the resulting aniline cation radicals undergo head-to-tail coupling to form polymers (Scheme 18).
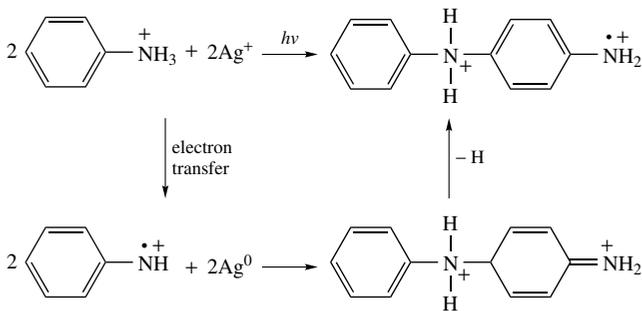
SCHEME 18

The photopolymerization of 4-bromoaniline on the liquid (ethanol) surface beam has been investigated[241]. With a femtosecond UV laser, the pulse photoionizes the molecule, and the parent ion (4-H$_2$NC$_6$H$_4$Br$^+$) then interacts with a neutral aniline molecule to form a dimer ion (H(−NHC$_6$H$_4$−)$_2$Br$^+$). A propagation of this reaction leads to aniline polymer. In contrast, a nanosecond UV laser leads to the formation of aniline radical and a bromine atom, and the former then reacts with one additional aniline molecule to form a dimer product and so on. The propagation is terminated by reacting with an ethanol molecule.

H. Photosensitization

There are only few examples that are initiated or facilitated by the excited singlet of anilines. As mentioned earlier, this could be attributed to its weak absorption at long wavelength that limits the choice of substrates as ground-state acceptors. Previously, photosensitized dechlorination of chlorobenzenes by N,N-dimethylaniline (**1b**) was found to be efficient ($\Phi = 0.2-0.6$)[242, 243]. In accord with the fluorescence quenching behavior of anilines by chlorobenzenes[244], the dechlorination process occurs by electron transfer from the excited **1b** to the chlorobenzene, followed by fast rupture of the C—Cl bond.

The use of singlet anilines as electron-donating sensitizers for improving the photochemical reduction of aromatic sulfoxides has recently been reported[245]. Unimolecular photochemical deoxygenation of sulfoxides is a known process that occurs with low quantum yields[246, 247], although good chemical yields have been observed for some cases. The reaction is improved in the presence of sodium methoxide[248]. The successful use

SCHEME 19

of more classic electron-transfer agents such as anilines establishes the electron-transfer mechanism of the photoreduction reaction[248]. This is demonstrated by the photoreduction of diphenyl sulfoxide (**138**) in methanol. In the presence of NaOMe, the quantum yield for the appearance of diphenyl sulfide (Φ_S) is *ca* 0.04. A replacement of NaOMe by *N*-methylaniline leads to a tenfold enhancement of quantum yield ($\Phi_S = 0.48$). A nearly quantitative yield of aryl sulfides is obtained when the sensitizer is *N*-methylcarbazole ($\Phi_S = 0.95$). *N*-alkylcarbazoles are known to be good electron donors with low photoionization potential in polar solvents[249]. The hydoxysulfuranyl radical (**139**) has been suggested to be a key intermediate, and the S−O bond cleavage is more likely a heterolytic process according to the solvent effects (Scheme 19).

Another reaction triggered by PET from singlet anilines is the C−O bond fragmentation of phenacyl[250] and *N*-methyl-4-picolinium esters[251]. Such photosensitized reactions might be useful in developing photoremovable protecting groups for carboxylic acids. A proposed mechanism for *N*, *N*-dimethylaniline (**1b**)-sensitized deprotection of phenyl phenacylacetate is shown in Scheme 20. Initial electron transfer leads to the cation radical of **1b** along with the anion radical of the phenacyl ester. The latter fragments rapidly and produces the carboxylate anion and the phenacyl radical **140**. A direct transfer of a H atom from the radical cation of **1b** to **140** leads to the formation of the iminium ion **141**. This iminium ion is hydrolyzed either by traces of water in the reaction medium or upon workup to give *N*-methylaniline. Fluorescence quenching experiments have shown that the substrates interact with the excited singlet state of **1b**. In addition, low product yields will be observed when the carboxylic acids contain functional groups (e.g. Br) that react rapidly upon one-electron reduction.

SCHEME 20

A similar mechanism could also be proposed for the 9-methylcarbazole-sensitized $C-O$ bond cleavage of the picolinium esters (**142–144**) (Scheme 21)[251]. The formation of *N*-methyl-4-picolyl radical **145** is verified by the observation of *N*-methylpicolinium ion (**146**) in the presence of 1,4-cyclohexadiene, a good H-atom donor. Other anilines such *N*,*N*,*N′*,*N′*-tetramethylbenzidine and triphenylamine are also efficient sensitizers in this reaction.
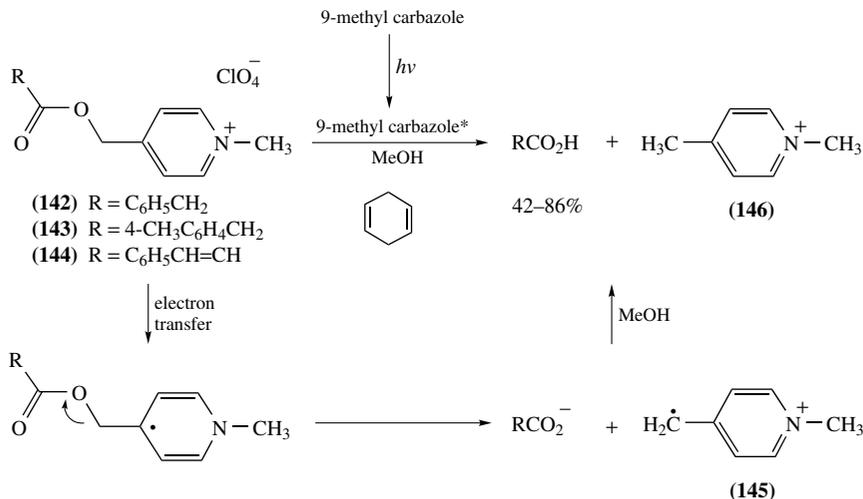
SCHEME 21

IV. REFERENCES

1. A. M. Halpern, in *The Chemistry of Amino, Nitroso, and Nitro Compounds and Their Derivatives, Supplement F, Part 1* (Ed. S. Patai), Wiley, Chichester, 1982, p. 155.
2. J. Malkin, in *Photophysical and Photochemical Properties of Aromatic Compounds*, Chapters 7 and 13, CRC Press, Boca Raton, 1992.
3. Z. R. Grabowski and K. Rotkiewicz, *Chem. Rev.*, **103**, 3899 (2003).
4. F. D. Lewis, *Adv. Electron Transf. Chem.*, **5**, 1 (1996).
5. T.-I. Ho and Y. L. Chow, in *The Chemistry of Amino, Nitroso, and Nitro Compounds and Their Derivatives, Supplement F2, Part 2* (Ed. S. Patai), Wiley, Chichester, 1996, p. 683.
6. N. J. Pienta, in *Photoinduced Electron Transfer, Part C: Organic Substrates* (Eds. M. A. Fox and M. Chanon), Elsevier, Amsterdam, 1988, p. 421.
7. M. R. Wasielewski, *Chem. Rev.*, **92**, 435 (1992).
8. L. Sánchez, J. Peral and X. Domènech, *Electrochim. Acta*, **42**, 1877 (1997).
9. S. P. Kamble, S. B. Sawant, J. C. Schouten and V. G. Pangarkar, *J. Chem. Technol. Biotechnol.*, **78**, 865 (2003).
10. W. Rettig and M. Maus, in *Conformational Analysis of Molecules in Excited States* (Ed. J. Waluk), Wiley-VCH, New York, 2000, p. 1.
11. F. Brouwer, in *Conformational Analysis of Molecules in Excited States* (Ed. J. Waluk), Wiley-VCH, New York, 2000, p. 177.
12. I. B. Berlman, in *Handbook of Fluorescence Spectra of Aromatic Molecules*, 2nd edn., Academic Press, New York, 1971.
13. G. Köhler and N. Getoff, *J. Chem. Soc., Faraday Trans. 1*, **76**, 1576 (1980).
14. B. D. Slaughter, M. W. Allen, G. H. Lushington and C. K. Johnson, *J. Phys. Chem. A*, **107**, 5670 (2003).
15. R. Scheps, D. Florida and S. A. Rice, *J. Chem. Phys.*, **61**, 1730 (1974).

16. G. Köhler, *J. Photochem.*, **38**, 217 (1987).
17. J. L. Knee and P. M. Johnson, *J. Chem. Phys.*, **80**, 13 (1984).
18. F. D. Lewis, J. L. Hougland and S. A. Markarian, *J. Phys. Chem. A*, **104**, 3261 (2000).
19. I. Rückert, A. Demeter, O. Morawski, W. Kühnle, E. Tauer and K. A. Zachariasse, *J. Phys. Chem. A*, **103**, 1958 (1999).
20. W. D. Oosterbaan, M. Koeberg, J. Piris, R. W. A. Havenith, C. A. van Walree, B. R. Wegewijs, L. W. Jenneskens and J. W. Verhoeven, *J. Phys. Chem. A*, **105**, 5984 (2001).
21. J. Dey and I. M. Warner, *J. Phys. Chem. A*, **101**, 4872 (1997).
22. K. Suzuki, H. Tanabe, S. Tobita and H. Shizuka, *J. Phys. Chem. A*, **101**, 4496 (1997).
23. G. Perichet, R. Chapelou and B. Pouyet, *J. Photochem.*, **13**, 67 (1980).
24. T. M. Korter, D. R. Borst, C. J. Butler and D. W. Pratt, *J. Am. Chem. Soc.*, **123**, 96 (2001).
25. W. Liptay, in *Excited States* (Ed. E. C. Lim), Vol 1, Academic Press, New York, 1974, p. 129.
26. E. Z. Lippert, *Z. Electrochem.*, **61**, 962 (1957).
27. N. Mataga, Y. Kaifu and M. Koizumi, *Bull. Chem. Soc. Jpn.*, **29**, 465 (1956).
28. J. R. Lombardi, *J. Chem. Phys.*, **56**, 2278 (1972).
29. F. D. Lewis, R. S. Kalgutkar and J.-S. Yang, *J. Am. Chem. Soc.*, **121**, 12045 (1999).
30. J.-S. Yang, S.-Y. Chiou and K.-L. Liau, *J. Am. Chem. Soc.*, **124**, 2518 (2002).
31. L.-H. Ma, Z.-B. Chen and Y.-B. Jiang, *Chem. Phys. Lett.*, **372**, 104 (2003).
32. J.-S. Yang, C.-M. Wang, C.-Y. Hwang and K.-L. Liau, *Photochem. Photobiol. Sci.*, **2**, 1225 (2003).
33. K. Sakanoue, M. Motoda, M. Sugimoto and S. Sakaki, *J. Phys. Chem. A*, **103**, 5551 (1999).
34. Y.-J. Pu, M. Soma, J. Kido and H. Nishide, *Chem. Mater.*, **13**, 3817 (2001).
35. M. Rumi, J. E. Ehrlich, A. A. Heikal, J. W. Perry, S. Barlow, Z. Hu, D. McCord-Maughon, T. C. Parker, H. Röckel, S. Thayumanavan, S. R. Marder, D. Beljonne and J.-L. Brédas, *J. Am. Chem. Soc.*, **122**, 9500 (2000).
36. B. R. Cho, K. H. Son, S. H. Lee, Y.-S. Song, Y.-K. Lee, S.-J. Jeon, J. H. Choi, H. Lee and M. Cho, *J. Am. Chem. Soc.*, **123**, 10039 (2001).
37. W. Zhou, S. M. Kuebler, D. Carrig, J. W. Perry and S. R. Marder, *J. Am. Chem. Soc.*, **124**, 1897 (2002).
38. C. M. Whitaker, E. V. Patterson, K. L. Kott and R. J. McMahon, *J. Am. Chem. Soc.*, **118**, 9966 (1996).
39. C. L. Lee, K. B. Lee and J. J. Kim, *Appl. Phys. Lett.*, **77**, 2280 (2000).
40. K. Brunner, A. van Dijken, H. Börner, J. J. A. M. Bastiaansen, N. M. M. Kiggen and B. M. W. Langeveld, *J. Am. Chem. Soc.*, **126**, 6035 (2004).
41. O. S. Khalil, C. J. Seliskar and S. P. McGlynn, *J. Chem. Phys.*, **58**, 1607 (1973).
42. F. D. Lewis and J.-S. Yang, *J. Am. Chem. Soc.*, **119**, 3834 (1997).
43. F. D. Lewis, W. Weigel and X. Zuo, *J. Phys. Chem. A*, **105**, 4691 (2001).
44. J.-S. Yang, K.-L. Liau, C.-W. Tu and C.-Y. Hwang, *J. Phys. Chem. A*, **109**, 6450 (2005).
45. J. R. Lakowicz, *Principles of Fluorescence Spectroscopy*, 2nd edn., Chap. 6, Kluwer Academic/Plenum Publishers, New York, 1999.
46. F. D. Lewis and W. Weigel, *J. Phys. Chem. A*, **104**, 8146 (2000).
47. J. Lee and G. W. Robinson, *J. Am. Chem. Soc.*, **107**, 6153 (1985).
48. D. Yuan and R. G. Brown, *J. Phys. Chem. A*, **101**, 3461 (1997).
49. Y. Hirata, N. Mataga and Y. Sakata, *J. Phys. Chem.*, **86**, 1508 (1982).
50. N. Ikeda, H. Miyasaka, T. Okada and N. Mataga, *J. Am. Chem. Soc.*, **105**, 5206 (1983).
51. T. Iwasaki, T. Sawada, M. Okuyama and H. Kamada, *J. Phys. Chem.*, **82**, 371 (1978).
52. V. Avila, J. J. Cosa, C. A. Chesta and C. M. Previtali, *J. Photochem. Photobiol. A: Chem.*, **62**, 83 (1991).
53. E. Schaffner and H. Fischer, *J. Phys. Chem.*, **100**, 1657 (1996).
54. J. C. Joshi and D. D. Pant, *Chem. Phys. Lett.*, **59**, 529 (1978).
55. M. W. Allen, J. R. Unruh, B. D. Slaughter, S. J. Pyszczynski, T. R. Hellwig, T. J. Kamerzell and C. K. Johnson, *J. Phys. Chem. A*, **107**, 5660 (2003).
56. Ya N. Malkin, N. O. Pirogov, M. V. Kopytina and V. I. Nosova, *Bull. Acad. Sci. USSR, Chem. Div. Sci.*, **33**, 1704 (1984).
57. B. Valeur and I. Leray, *Coord. Chem. Rev.*, **205**, 3 (2000).
58. J.-S. Yang, C.-Y. Hwang, C.-C. Hsieh and S.-Y. Chiou, *J. Org. Chem.*, **69**, 719 (2004).
59. P. Dumon, G. Jonusauskas, F. Dupuy, P. Pée, C. Rullière, J.-F. Létard and R. Lapouyade, *J. Phys. Chem.*, **98**, 10391 (1994).

60. J.-F. Létard, S. Delmond, R. Lapouyade, D. Braun, W. Rettig and M. Kreissler, *Recl. Trav. Chim. Pays-Bas*, **114**, 517 (1995).
61. K. Rurack, *Spectrochim. Acta A*, **57**, 2161 (2001).
62. J.-S. Yang, Y.-H. Lin and C.-S. Yang, *Org. Lett.*, **4**, 777 (2002).
63. J.-S. Yang, Y.-D. Lin, Y.-H. Lin and F.-L. Liao, *J. Org. Chem.*, **69**, 3517 (2004).
64. W. Hub, S. Schneider, F. Dörr, J. D. Oxman and F. D. Lewis, *J. Phys. Chem.*, **87**, 4351 (1983).
65. S. Schneider, P. Geiselhart, G. Seel, F. D. Lewis, R. E. Dykstra and M. J. Nepras, *J. Phys. Chem.*, **93**, 3112 (1989).
66. F. D. Lewis, L.-S. Li, T. L. Kurth and R. S. Kalgutkar, *J. Am. Chem. Soc.*, **122**, 8573 (2000).
67. F. D. Lewis, R. S. Kargutkar and T. L. Kurth, *J. Phys. Chem. A*, **108**, 1425 (2004).
68. F. D. Lewis, A. Ahrens and T. L. Kurth, *Photochem. Photobiol. Sci.*, **3**, 341 (2004).
69. F. Fages, J. P. Desvergne and H. Bouas-Laurent, *J. Am. Chem. Soc.*, **111**, 96 (1989).
70. T. Ebata, C. Minejima and N. Mikami, *J. Phys. Chem. A*, **106**, 11070 (2002).
71. R. Scheps, D. Florida and S. A. Rice, *J. Chem. Phys.*, **61**, 1730 (1974).
72. H. Bässler and B. Schweitzer, *Acc. Chem. Res.*, **32**, 173 (1999).
73. K. Rotkiewicz, K. H. Grellmann and Z. R. Grabowski, *Chem. Phys. Lett.*, **19**, 315 (1973).
74. E. Lippert, W. Lüder, F. Moll, W. Nägale, H. Boos, H. Prigge and I. Seibold-Blankenstein, *Angew. Chem.*, **73**, 695 (1961).
75. A. L. Sobolewski and W. Domcke, *Chem. Phys. Lett.*, **259**, 119 (1996).
76. W. Schuddeboom, S. A. Jonker, J. M. Warman, U. Leinhos, W. Kühnle and K. A. Zachariasse, *J. Phys. Chem.*, **96**, 10809 (1992).
77. T. von der Haar, A. Hebecker, Y. Il'ichev, Y.-B. Jiang, W. Kühnle and K. A. Zachariasse, *Recl. Trav. Chim. Pays-Bas*, **114**, 430 (1995).
78. K. A. Zachariasse, S. I. Druzhinin, W. Bosch and R. Machinek, *J. Am. Chem. Soc.*, **126**, 1705 (2004).
79. T. Yoshihara, S. I. Druzhinin and K. A. Zachariasse, *J. Am. Chem. Soc.*, **126**, 8535 (2004).
80. J. Dobkowski, J. Wójcik, W. Kozminski, R. Kolos, J. Waluk and J. Michl. *J. Am. Chem. Soc.*, **124**, 2406 (2002).
81. D. Rappoport and F. Furche, *J. Am. Chem. Soc.*, **126**, 1277 (2004).
82. Z. R. Grabowski, K. Rotkiewicz, A. Siemiarczuk, D. J. Cowley and W. Baumann, *Nouv. J. Chim.*, **3**, 443 (1979).
83. Z. R. Grabowski, K. Rotkiewicz and A. Siemiarczuk, *J. Lumin.*, **18/19**, 420 (1979).
84. S. Kapelle, W. Rettig and R. Lapouyade, *Chem. Phys. Lett.*, **348**, 416 (2001).
85. J. P. Malval, J. P. Morand, R. Lapouyade, W. Rettig, G. Jonusauskas, J. Oberlé, C. Trieflinger and J. Daub, *Photochem. Photobiol. Sci.*, **3**, 939 (2004).
86. J.-F. Létard, R. Lapouyade and W. Rettig, *J. Am. Chem. Soc.*, **115**, 2441 (1993).
87. W. Rettig and W. Majenz, *Chem. Phys. Lett.*, **154**, 335 (1989).
88. D. Pines, E. Pines and W. Rettig, *J. Phys. Chem. A*, **107**, 236 (2003).
89. R. Lapouyade, A. Kuhn, J.-F. Létard and W. Rettig, *Chem. Phys. Lett.*, **208**, 48 (1993).
90. J.-F. Létard, R. Lapouyade and W. Rettig, *Chem. Phys. Lett.*, **222**, 209 (1994).
91. J.-S. Yang, K.-L. Liau, C.-M. Wang and C.-Y. Hwang, *J. Am. Chem. Soc.*, **126**, 12325 (2004).
92. M. M. Martin, P. Plaza, P. Changenet-Barret and A. Siemiarczuk, *J. Phys. Chem. A*, **106**, 2351 (2002).
93. N. Mataga, *Pure Appl. Chem.*, **56**, 1255 (1984).
94. B. Wegewijs, R. M. Hermant, J. W. Verhoeven, A. G. M. Kunst and R. P. H. Rettschnick, *Chem. Phys. Lett.*, **140**, 587 (1987).
95. J. Jortner, M. Bixon, B. Wegewijs, J. W. Verhoeven and R. P. H. Rettschnick, *Chem. Phys. Lett.*, **205**, 451 (1993).
96. M. Kurono and M. Itoh, *J. Phys. Chem.*, **99**, 17113 (1995).
97. J. W. Verhoeven, T. Scherer and R. J. Willemse, *Pure Appl. Chem.*, **65**, 1717 (1993).
98. T. Scherer, I. H. M. van Stokkum, A. M. Brouwer and J. W. Verhoeven, *J. Phys. Chem.*, **98**, 10539 (1994).
99. J.-S. Yang, Y.-D. Lin, Y.-H. Chang and S.-S. Wang, *J. Org. Chem.*, **70**, 6066 (2005).
100. F. D. Lewis, J. W. Wagner-Brennan and A. M. Miller, *Can. J. Chem.*, **77**, 595 (1999).
101. W. D. Oosterbaan, J. Koeberg, J. Piris, R. W. A. Havenith, C. A. van Walree, B. R. Wegewijs, L. W. Jenneskens and J. W. Verhoeven, *J. Phys. Chem. A*, **105**, 5984 (2001).
102. J. Lee and G. W. Robinson, *J. Am. Chem. Soc.*, **107**, 6153 (1985).

103. H. B. Steen, *J. Chem. Phys.*, **61**, 3997 (1974).
104. D. V. Bent and E. Hayon, *J. Am. Chem. Soc.*, **97**, 2612 (1975).
105. Y. He, C. Wu and W. Kong, *J. Chem. Phys.*, **120**, 7497 (2004).
106. G. W. Haggquist, R. D. Burkhart and D. R. Naqvi, *J. Phys. Chem.*, **95**, 7588 (1991).
107. R. Rahn, J. Schroeder, J. Troe and K. H. Grellmann, *J. Phys. Chem.*, **93**, 7841 (1989).
108. T. Ogawa, T. Ogawa and K. Nakashima, *J. Phys. Chem. A*, **102**, 10608 (1998).
109. F. Saito, S. Tobita and H Shizuka, *J. Chem. Soc., Faraday Trans. 1*, **92**, 4177 (1996).
110. F. Saito, S. Tobita and H. Shizuka, *J. Photochem. Photobiol. A: Chem.,* **106**, 119 (1997).
111. Y. Hirata and N. Mataga, *J. Phys. Chem.*, **89**, 4031 (1985).
112. S. Tajima, S. Tobita and H. Shizuka, *J. Phys. Chem. A*, **104**, 11270 (2000).
113. G. Köhler, J. Zechner, N. Getoff and J. Tatischeff, *J. Photochem.*, **9**, 304 (1978).
114. L. Qin, N. R. Tripathi and R. H. Schuler, *Z. Naturforsch.*, **40a**, 1026 (1985).
115. C.-M. Tseng, Y. A. Dyakov, C.-L. Huang, A. M. Mebel, S. H. Lin, Y. T. Lee and C.-K. Ni, *J. Am. Chem. Soc.*, **126**, 8760 (2004).
116. E. Pines and G. R. Fleming, *J. Phys. Chem.*, **95**, 10448 (1991).
117. J. E. Hansen, E. Pines and G. R. Fleming, *J. Phys. Chem.*, **96**, 6904 (1992).
118. H. Shizuka, *Acc. Chem. Res.*, **18**, 141 (1985).
119. S. Tajima, S. Shiobara, H. Shizuka and S. Tobita, *Phys. Chem. Chem. Phys.*, **4**, 3376 (2002).
120. S. Shiobara, R. Kamiyama, S. Tajima, H. Shizuka and S. Tobita, *J. Photochem. Photobiol. A: Chem.*, **154**, 53 (2002).
121. L. G. Arnaut and S. J. Formosinho, *J. Photochem. Photobiol. A: Chem.*, **75**, 1 (1993).
122. L. M. Tolbert and K. M. Solntsev, *Acc. Chem. Res.*, **35**, 19 (2002).
123. S. Shiobara, S. Tajima and S. Tobita, *Chem. Phys. Lett.*, **380**, 673 (2003).
124. P. J. Berkowies and A. C. Albrecht, *J. Phys. Chem.*, **75**, 431 (1971).
125. S. Arimitsu, K. Kimura and H. Tsubomura, *Bull. Chem. Soc. Jpn.*, **42**, 1858 (1969).
126. M. G. Siskos, A. K. Zarkadis, S. Steenken, N. Karakostas and S. K. Garas, *J. Org. Chem.*, **63**, 3251 (1998).
127. M. G. Siskos, A. K. Zarkadis, S. Steenken and N. Karakostas, *J. Org. Chem.*, **64**, 1925 (1999).
128. H. Zollinger, *Color Chemistry—Syntheses, Properties, and Applications of Organic Dyes and Pigments*, 3rd revised edn., Chap. 4, Wiley-VCH Weinheim, 2003.
129. L. E. Manring and K. S. Peters, *J. Phys. Chem.*, **88**, 3516 (1984).
130. M. L. Herz, *J. Am. Chem. Soc.*, **97**, 6777 (1975).
131. K. G. Spears, T. H. Gray and D. Huang, *J. Phys. Chem.*, **90**, 779 (1986).
132. K. Kimura, R. Mizutani, M. Yokoyama, R. Arakawa, G. Matsubayashi, M. Okamoto and H. Doe, *J. Am. Chem. Soc.*, **119**, 2062 (1997).
133. K. Kimura, R. Mizutani, M. Yokoyama, R. Arakawa and Y. Sakurai, *J. Am. Chem. Soc.*, **122**, 5448 (2000).
134. K. Kimura, M. Kaneshige and M. Yokoyama, *J. Chem. Soc., Chem. Commun.*, 1103 (1994).
135. K. Kimura, M. Kaneshige and M. Yokoyama, *Chem. Mater.*, **7**, 945 (1995).
136. X. Ci, L. Y. C. Lee and D. G. Whitten, *J. Am. Chem. Soc.*, **109**, 2536 (1987).
137. X. Ci and D. G. Whitten, *J. Am. Chem. Soc.*, **109**, 7215 (1987).
138. M. A. Kellett and D. G. Whitten, *J. Am. Chem. Soc.*, **111**, 2314 (1989).
139. J. W. Leon and D. G. Whitten, *J. Am. Chem. Soc.*, **115**, 8038 (1993).
140. Y. Wang, B. T. Hauser, M. M. Rooney, R. D. Burton and K. S. Schanze, *J. Am. Chem. Soc.*, **115**, 5675 (1993).
141. X. Ci, M. A. Kellett and D. G. Whitten, *J. Am. Chem. Soc.*, **113**, 3893 (1991).
142. Y. Wang and K. S. Schanze, *J. Phys. Chem.*, **99**, 6876 (1995).
143. Y. Wang, L. A. Lucia and K. S. Schanze, *J. Phys. Chem.*, **99**, 1961 (1995).
144. A. G. Schultz, *Acc. Chem. Res.*, **16**, 210 (1983).
145. A. G. Schultz and L. Motyka, in *Organic Photochemistry* (Ed. A. Padwa), Vol. 6, Marcel Dekker, New York, 1983, p. 1.
146. R. Huisgen, *Angew. Chem., Int. Ed. Engl.*, **19**, 947 (1980).
147. A. G. Schultz and W. K. Hagmann, *J. Chem. Soc., Chem. Commun.*, 726 (1976).
148. A. G. Schultz and W. K. Hagmann, *J. Org. Chem.*, **43**, 4231 (1978).
149. H. Iida, Y. Yuasa and C. Kibayashi, *J. Org. Chem.*, **44**, 1236 (1979).
150. C. A. Parker and W. J. Barnes, *Analyst*, **82**, 606 (1957).
151. H. Shizuka, Y. Takayama, I. Tanaka and T. Morita, *J. Am. Chem. Soc.*, **92**, 7270 (1970).

152. E. I. Mal'tsev, V. A. Takchev and A. V. Vannikov, *J. Photochem. Photobiol. A: Chem.*, **43**, 73 (1988).
153. N. Chattopadhyay, C. Serpa, P. Purkayastha, L. G. Arnaut and S. J. Formosinho, *Phys. Chem. Chem. Phys.*, **3**, 70 (2001).
154. E. W. Förster, K. H. Grellmann and H. Linschitz, *J. Am. Chem. Soc.*, **95**, 3108 (1973).
155. K. H. Grellmann, W. Kühnle, H. Weller and T Wolff, *J. Am. Chem. Soc.*, **103**, 6889 (1981).
156. T. Suzuki, Y. Kajii, K. Shibuya and K. Obi, *Bull. Chem. Soc. Jpn.*, **65**, 1084 (1992).
157. N. Chattopadhyay, C. Serpa, L. G. Arnaut and S. J. Formosinho, *Phys. Chem. Chem. Phys.*, **3**, 3690 (2001).
158. H. Linschitz and K. H. Grellmann, *J. Am. Chem. Soc.*, **86**, 303 (1964).
159. G. Fischer, E. Fischer, K. H. Grellmann, H. Linschitz and A. Temizer, *J. Am. Chem. Soc.*, **96**, 6267 (1974).
160. M. F. Budyka, O. D. Laukhina and T. N. Gavrishova, *J. Photochem. Photobiol. A: Chem.*, **134**, 143 (2000).
161. M. A. Fox, M. T. Dulay and K. Krosley, *J. Am. Chem. Soc.*, **116**, 10992 (1994).
162. J.-H. Ho and T.-I. Ho, *Chem. Commun.*, 270 (2002).
163. U. Koch-Pomeranz, H.-J. Hansen and H. Schmid, *Helv. Chim. Acta*, **58**, 178 (1975).
164. U. Koch-Pomeranz, H. Schmid and H.-J. Hansen, *Helv. Chim. Acta*, **60**, 768 (1977).
165. S. Jolidon and H.-J. Hansen, *Helv. Chim. Acta*, **62**, 2581 (1979).
166. B. Scholl and H.-J. Hansen, *Helv. Chim. Acta*, **63**, 1823 (1980).
167. O. Benali, M. A. Miranda and R. Tormos, *Eur. J. Org. Chem.,* 2317 (2002).
168. B. Scholl, S. Jolidon and H.-J. Hansen, *Helv. Chim. Acta*, **69**, 184 (1986).
169. O. Benali, M. A. Miranda, R. Tormos and S. Gil, *J. Org. Chem.,* **67**, 7915 (2002).
170. J. P. Ferris and F. R. Antonucci, *J. Am. Chem. Soc.*, **96**, 2010 (1974).
171. E. Hadjoudis, M. Vittorakis and I. Moustakali-Mavridis, *Tetrahedron*, **43**, 1345 (1987).
172. E. Hadjoudis, in *Photochromism. Molecules and Systems* (Eds. H. Dürr and H. Bouas-Laurent), Chap. 17, Elsevier, Amsterdam, 1990, p. 685.
173. T. Goto and Y. Tashiro, *J. Lumin.*, **72**, 921 (1997).
174. W. Turbeville and P. K. Dutta, *J. Phys. Chem.*, **94**, 4060 (1990).
175. M. Y. Shen, L. Z. Zhao and T. Goto, *J. Chem. Phys.*, **112**, 2490 (2000).
176. J. Harada, H. Uekusa and Y. Ohashi, *J. Am. Chem. Soc.*, **121**, 5809 (1999).
177. K. Ogawa, Y. Kasahara, Y. Ohtani and J. Harada, *J. Am. Chem. Soc.*, **120**, 7107 (1998).
178. H. Fukuda, K. Amimoto, H. Koyama and T. Kawato, *Org. Biomol. Chem.*, **1**, 1578 (2003).
179. J. Cornelisse and E. Havinga, *Chem. Rev.*, **75**, 353 (1975).
180. K. W. Moilanen and D. G. Crosby, *J. Agric. Food Chem.*, **20**, 950 (1972).
181. K. Othmen and P. Boule, *Bull. Environ. Contam. Toxicol.*, **59**, 924 (1997).
182. M. Sánchez, H. Wolfger and N. Getoff, *Radiat. Phys. Chem.*, **65**, 611 (2002).
183. G. Mailhot, L. Hykrdová, J. Jirkovsky, K. Lemr, G. Grabner and M. Bolte, *Appl. Cat. B: Environ.*, **50**, 25 (2004).
184. K. Othmen, P. Boule, B. Szczepanik, K. Rotkiewicz and G. Grabner, *J. Phys. Chem. A*, **104**, 9525 (2000).
185. T. Latowski, *Ann. Soc. Chim. Pol.*, **40**, 231 (1966).
186. T. Latowski, *Ann. Soc. Chim. Pol.*, **42**, 99 (1968).
187. B. Szczepanik and T. Latowski, *Pol. J. Chem.*, **71**, 807 (1997).
188. A. Ouardaoui, C. A. Steren, H. van Willigen and C. Yang, *J. Am. Chem. Soc.*, **117**, 6803 (1995).
189. A.-P. Durand, R. G. Brown, D. Worrall and F. Wilkinson, *J. Photochem. Photobiol. A: Chem.*, **96**, 35 (1996).
190. J. Zechner, L. S. Prangova, G. Grabner and N. Getoff, *Z. Phys. Chem.*, **102B**, 137 (1976).
191. G. C. Miller and D. G. Crosby, *Chemosphere*, **12**, 1217 (1983).
192. G. Grabner, C. Richard and G. Köhler, *J. Am. Chem. Soc.*, **116**, 11470 (1994).
193. M. Fagnoni, M. Mella and A. Albini, *Org. Lett.*, **1**, 1299 (1999).
194. P. Coppo, M. Fagnoni and A. Albini, *Tetrahedron Lett.*, **42**, 4271 (2001).
195. M. Mella, P. Coppo, B. Guizzardi, M. Fagnoni, M. Freccero and A. Albini, *J. Org. Chem.*, **66**, 6344 (2001).
196. B. Guizzardi, M. Mella, M. Fagnoni and A. Albini, *Tetrahedron*, **56**, 9383 (2000).
197. B. Guizzardi, M. Mella, M. Fagnoni, M. Freccero and A. Albini, *J. Org. Chem.*, **66**, 6353 (2001).

198. C. G. Swain, J. E. Sheats and K. G. Harbison, *J. Am. Chem. Soc.*, **97**, 783 (1975).
199. R. G. Bergstrom, R. G. M. Landells, G. H. Wahl and H. Zollinger, *J. Am. Chem. Soc.*, **98**, 3301 (1976).
200. Y. Himeshima, H. Kobayashi and T. Sonoda, *J. Am. Chem. Soc.*, **107**, 5286 (1985).
201. M. Speranza, *Chem. Rev.*, **93**, 2933 (1993).
202. S. M. Gasper, C. Devadoss and G. B. Schuster, *J. Am. Chem. Soc.*, **117**, 5206 (1995).
203. S. Steenken, M. Ashokkumar, P. Maruthamuthu and R. A. McClelland, *J. Am. Chem. Soc.*, **120**, 11925 (1998).
204. M. Winkler and W. Sander, *Angew. Chem., Int. Ed.*, **39**, 2014 (2000).
205. R. W. Taft, *J. Am. Chem. Soc.*, **83**, 3350 (1961).
206. H. B. Ambroz and T. J. Kemp, *Chem. Soc. Rev.*, **8**, 353 (1979).
207. J. D. Dill, P. v. R. Schleyer and J. A. Pople, *J. Am. Chem. Soc.*, **99**, 1 (1977).
208. A. Nicolaides, D. M. Smith, F. Jensen and L. Radom, *J. Am. Chem. Soc.*, **119**, 8083 (1997).
209. B. David, M. Lhote, V. Faure and P. Boule, *Water Res.*, **32**, 2451 (1998).
210. S. Ishikawa, K. Baba, Y. Hanada, Y. Uchimura and K. Kido, *Bull. Environ. Contam. Toxicol.*, **42**, 65 (1989).
211. K. Othmen and P. Boule, *Bull. Environ. Contam. Toxicol.*, **59**, 924 (1997).
212. D. W. Cullin, N. Soundararajan, M. S. Platz, and T. A. Miller, *J. Phys. Chem.*, **94**, 8890 (1990).
213. T. Ishida, H. Abe, A. Nakajima and K. Kaya, *Chem. Phys. Lett.*, **170**, 425 (1990).
214. K. Othmen and P. Boule, *J. Photochem. Photobiol. A: Chem.*, **136**, 79 (2000).
215. K. Othmen and P. Boule, *J. Photochem. Photobiol. A: Chem.*, **121**, 161 (1999).
216. G. C. Miller, M. J. Miille and D. G. Crosby, *Tetrahedron*, **35**, 1797 (1979).
217. M. Mansour, H. Parlar and F. Korte, *Chemosphere*, **4**, 235 (1975).
218. M. Mansour, S. Wawrik, M. Parlar and F. Korte, *Chem. Z.*, **104**, 339 (1980).
219. M. Mansour and F. Korte, *Chemosphere*, **5**, 383 (1976).
220. V. M. Bermudez, *Surf. Sci.*, **519**, 173 (2002).
221. T. D. Nekipelova, *Photochem. Photobiol. Sci.*, **1**, 204 (2002).
222. T. D. Nekipelova and I. I. Levina, *Russ. Chem. Bull.*, **51**, 2055 (2002).
223. Y. N. Malkin, N. O. Pirogov and V. A. Kuzmin, *J. Photochem.*, **26**, 193 (1984).
224. J. Kolc and R. S. Becker, *J. Am. Chem. Soc.*, **91**, 6513 (1969).
225. T. D. Nekipelova, I. I. Levina and V. S. Shishkov, *Kinet. Catal.*, **45**, 24 (2004).
226. T. D. Nekipelova, I. I. Levina, P. P. Levin and V. A. Kuzmin, *Russ. Chem. Bull.*, **53**, 803 (2004).
227. J. Woning, A. Oudenampsen and W. H. Laarhoven, *J. Chem. Soc., Perkin Trans. 2*, 2147 (1989).
228. A. G. MacDiarmid, J. C. Chiang, A. F. Richter and A. J. Epstein, *Synth. Met.*, **18**, 285 (1987).
229. J. E. Albuquerque, L. H. C. Mattoso, D. T. Balogh, R. M. Faria, J. G. Masters and A. G. MacDiarmid, *Synth. Met.*, **113**, 19 (2000).
230. A. G. MacDiarmid, J. C. Chiang, M. Halpern, W. S. Huang, S. L. Mu and N. L. D. Somasiri, *Mol. Cryst. Liq. Cryst.*, **121**, 173 (1985).
231. E. M. Geniès, A. Boyler, M. Lapkowski and C. Tsintavis, *Synth. Met.*, **36**, 139 (1990).
232. R. Noufi, D. Tench and L. F. Harren, *J. Electrochem. Soc.*, **127**, 2310 (1980).
233. K. Teshima, K. Yamada, N. Kobayashi and R. Hirohashi, *Chem. Commun.*, 829 (1996).
234. S. Uemura, T. Nakahira and N. Kobayashi, *J. Mater. Chem.*, **11**, 1585 (2001).
235. S. Uemura, M. Yoshie, N. Kobayashi and T. Nakahira, *Polym. J.*, **32**, 987 (2000).
236. S. Uemura, T. Shimakawa, K. Kusabuka, T. Nakahira and N. Kobayashi, *J. Mater. Chem.*, **11**, 267 (2001).
237. K. Teshima, S. Uemura, N. Kobayashi and R. Hirohashi, *Macromolecules*, **31**, 6783 (1998).
238. D. Chowdhury, A. Paul and A. Chattopadhyay, *J. Phys. Chem. B*, **106**, 4343 (2002).
239. N. Kobayashi, K. Teshima and R. Hirohashi, *J. Mater. Chem.*, **8**, 497 (1998).
240. R. A. de Barros, W. M. de Azevedo and F. M. de Aguiar, *Mater. Character.*, **50**, 131 (2003).
241. Y. Hashimoto, F. Mafunè and T. Kondow, *J. Phys. Chem. B*, **102**, 4295 (1998).
242. C. A. Chesta, J. J. Cosa and C. M. Previtali, *J. Photochem.*, **32**, 203 (1986).
243. C. A. Chesta, J. J. Cosa, A. Soltermann and C. M. Previtali, *An. Asoc. Quim. Argent.*, **77**, 487 (1989).
244. V. Avila, J. J. Cosa, C. A. Chesta and C. M. Previtali, *J. Photochem. Photobiol. A: Chem.*, **62**, 83 (1991).

245. J. W. Cubbage, T. A. Tetzlaff, H. Groundwater, R. D. McCulla, M. Nag and W. S. Jenks, *J. Org. Chem.*, **66**, 8621 (2001).
246. G. M. Gurria and G. H. Posner, *J. Org. Chem.*, **38**, 2419 (1973).
247. D. D. Gregory, Z. Wan and W. S. Jenks, *J. Am. Chem. Soc.*, **119**, 94 (1997).
248. P. J. Kropp, G. E. Fryxell, M. W. Tubergen, M. W. Hager, G. D. Harris Jr., T. P. McDermott Jr. and R. Tornero-Velez, *J. Am. Chem. Soc.*, **113**, 7300 (1991).
249. G. W. Haggquist, R. D. Burkhart and K. R. Naqvi, *J. Phys. Chem.*, **95**, 7588 (1991).
250. A. Banerjee and D. E. Falvey, *J. Org. Chem.*, **62**, 6245 (1997).
251. C. Sundararaja and D. E. Falvey, *J. Org. Chem.*, **69**, 5547 (2004).

CHAPTER **15**

Toxicological and environmental aspects of anilines

ANTHONY S. TRAVIS

Sidney M. Edelstein Center for the History and Philosophy of Science, Technology and Medicine, The Hebrew University of Jerusalem, Edmond J. Safra Campus, Givat Ram, Jerusalem 91904, Israel
Fax: +972 2 6586709; e-mail: travis@cc.huji.ac.il

The chemistry of anilines
Edited by Z. Rappoport © 2007 John Wiley & Sons, Ltd

I. INTRODUCTION

Aromatic amines were the first synthetic organic chemicals manufactured on a large scale, mainly for use in the coal-tar dye industry. This meant that information on human exposure in the workplace and the impact of environmental releases became known during the last decades of the 19th century, well before similar information was available on other synthetic chemicals. For this reason, the historical background is very instructive for understanding developments in toxicology and industrial hygiene. Studies into aryl amine toxicity were stimulated by the frequent appearance of cyanosis, or methemoglobinemia (that also resulted from exposure to nitro-precursors), and, around 1900, of urinary tract cancer. Subsequently, three specific aromatic amines were identified as a major group of carcinogens through animal experiments. These were 2-naphthylamine, benzidine and 4-aminobiphenyl. The toxicities of these amines attracted major research efforts before 1950, mainly in industrial research laboratories. From among all organic chemicals produced in bulk, 2-naphthylamine was recognized to be one of the most potent carcinogens. Between 1950 and the early 1970s, manufacture and use of these three products either ceased or was reduced in scale. In 1973, they, along with four other aromatic amines, 1-naphthylamine (which contained the 2-isomer as contaminant), 4-diaminoazobenzene, 3,3′-dichlorobenzidine and the fluorene derivative 3-fluorenylacetamide, were among the ten carcinogens for which, in the US, zero tolerance was recommended[1]. Aromatic amines have been heavily implicated in causing malignant disease. The victims of their carcinogenic actions have usually been workers in specific industrial sectors.

Strict regulations regarding the handling and use of aromatic amines have been enforced since the 1960s, notably in Britain, in 1967, and in the US, following the creation of the Environmental Protection Agency (EPA) in 1970. These moves stimulated investigations into toxic, mutagenic and carcinogenic properties of amines of great utility. As a result, several comprehensive literature reviews appeared around 1980. For this reason the works cited here are not intended to be exhaustive, though they do provide concrete examples of the broad research trends at different time periods in academic, industrial and trade laboratories[2, 3].

The study of the mutagenecity and/or carcinogenecity of anilines constitutes a major chapter in cancer research. It includes important contributions to knowledge about epidemiological aspects of exposure, the activation steps that afford mutagenic metabolites and the mechanisms of tumor induction and cell transformation[4−6]. Aromatic amines have been used as powerful tools in studies on the mechanism of chemical carcinogenesis. Experimental and epidemiological investigations, particularly animal-to-human extrapolations, have been used to establish causality relevant to cancer for a number of aryl amines, including in those cases where the latent period between exposure and the appearance of a recognizable tumor is very long. Since breakthroughs in the understanding of the etiology of tumors arising from aromatic amines have contributed to significant advances in the

understanding of the mechanism of carcinogenesis, a survey of developments is not only essential for an understanding of the current status of research. It also provides context to the legislative and regulatory directives. Moreover, the more potent carcinogens of this class have received little attention since their manufacture and use ceased during the third quarter of the 20th century, which further justifies this approach. Recent interest has focused on aromatic amines of less certain toxicity, including aniline and various curing agents for resins, on rubber-processing products, on amines generated by breakdown of azo dyes in the natural environment and during waste treatment and on novel amines generated during the cooking of meat and fish. There has also been renewed interest in the mechanism of benzidine-induced cancers.

Biological mechanisms of carcinogenesis involve single nucleotide polymorphism (alterations in the DNA sequence). The principal fate proposed for aryl amines is Phase I enzymatic oxidation to *N*-hydroxy precarcinogens that are then carried to the bladder, where Phase II enzymatic acetylation affords the carcinogens. Enzymatic deactivation may also occur, with safe removal of amine from the body. For several cases, the carcinogenic potentials have yet to be fully evaluated. However, it is generally agreed that the cytochrome P-450-mediated monooxygenases (cytochrome P-450 1A2 or CYP1A2) metabolically activate aromatic amines. In the following sections, a number of commonly used synonyms are given for aryl amines found frequently in the chemical, trade, toxicological, medical and environmental literature.

II. CYANOSIS

Aniline (**1**) exposure is by both skin contact and inhalation, which should be minimized, or at best avoided. The blue coloration of skin and lips typical of the condition known as cyanosis, or methemoglobinemia, also known as 'blue lip', 'anilism' and 'anilinism', indicates that the ability of blood cells to transport oxygen is destroyed. Cyanosis involves conversion of hemoglobin in blood to methemoglobin. The heme iron is oxidized from Fe(II) to Fe(III); the product methemoglobin is unable to combine with oxygen or carbon monoxide. Other symptoms include headache and dizziness. Animal experiments have shown that cyanosis caused by aryl amines is brought about by oxidation–enzyme systems that promote metabolism. The mechanism is related to that responsible for the first stage leading to mutagenesis (see Section IV). Cyanosis was prevalent until the 1930s, due to poor working conditions in the manufacture and handling of aniline, and of other amines, such as nitroanilines **2a**, **2b** and **2c**, as well as nitrobenzene (**3**)[7].

(**1**)   (**3**)

(**2a**) $R^1 = NO_2$, $R^2 = R^3 = H$
(**2b**) $R^1 = R^3 = H$, $R^2 = NO_2$
(**2c**) $R^1 = R^2 = H$, $R^3 = NO_2$
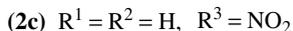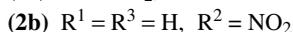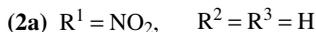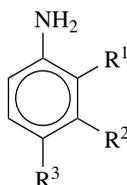
The cause of cyanosis was examined in the late 1930s at the American Cyanamid Company using the then new GE2 Hardy recording spectrophotometer. The results provided a method for measuring the methemoglobin concentration of blood down to 1%

that was valuable in treatment of the condition[8,9]. From the 1950s, methemoglobin and hemoglobin were generally determined with the Pulferich photometer. Improved industrial hygiene, including changes in manufacture introduced from around 1950, and better understanding of processes, have reduced the dangers from cyanosis. Thus for aniline and many other aromatic amines, ingestion, inhalation and skin contact should be prevented, and reactions should be conducted in closed vessels with adequate exhaust ventilation.

A study of the toxicities of 21 aniline derivatives, using rats as test animals, showed that the three nitroanilines (**2a, 2b** and **2c**) and 3,4-dichloroaniline (**4**) were equipotent to aniline, 3-chloroaniline (**5a**) and 4-chloroaniline (**5b**) were more potent than aniline, and the others were less potent or did not bring about changes in methemoglobin levels[10].
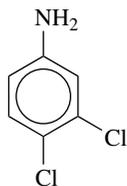
(**4**)
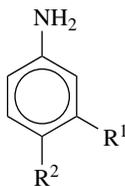
(**5a**) $R^1 = Cl, R^2 = H$
(**5b**) $R^1 = H, R^2 = Cl$

III. ANALYTICAL METHODS FOR ENVIRONMENTAL DETECTION AND SAMPLING OF ANILINES

The need for sensitive methods to detect aniline and other aromatic amines in industrial environments derives from their toxicological properties, particularly cyanosis, and flammability. The recommended threshold limits for aromatic amines range from 0.1 ppm for the methoxyanilines (**6a, 6b and 6c**) to 5 ppm for aniline. Inhalation, ingestion and absorption studies on aryl amines in the workplace environment have been extended to the time-weighted average estimates of exposure during normal activities. For aniline, a workplace threshold limit value (TLV) of 2 ppm as an 8-hour time-weighted average is recommended. Monitoring for aniline in the workplace atmosphere was originally aided by rapid tests for aniline in the air, such as diazotization and coupling with H acid (**7**), which measures concentrations of the amine down to 1 ppm, at which level the odor can also be detected. Concern over levels of exposure led to the development of novel detection and analytical procedures for routine monitoring purposes. Instrumental measurement of atmospheric concentrations in the workplace, in the presence of other contaminants, became available during the early 1950s[11]. Extensive measurements on threshold and toxic levels of aniline have been conducted since the 1950s, including in Eastern Europe[12].
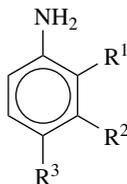
(**6a**) $R^1 = OCH_3, R^2 = R^3 = H$
(**6b**) $R^1 = R^3 = H, R^2 = OCH_3$
(**6c**) $R^1 = R^2 = H, R^3 = OCH_3$
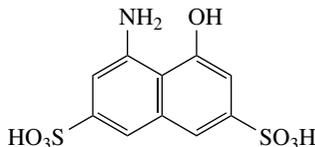
(**7**)

Collection in silica gel columns, followed by UV analysis of ethanol solutions, has been employed for studies in workplace atmospheres[13]. HPLC analysis of around fifty aromatic mono- and diamines has also been achieved with various silica gels using chloroform and/or cyclohexane as mobile phases. The primary separation mechanism depends upon interaction between the amino group and the slightly acidic absorbent[14].

Identification of individual amines by GLC has also proved valuable in environmental analysis. The recommended US EPA method for sampling aniline and congeners involves use of buffered media, and analysis with thermionic nitrogen–phosphorus selective detection[15]. Quantitative recovery has been reported in a two-stage trapping of aryl amines as nonvolatile salts, first in an acidified silica gel-coated glass tube, then with an acid-coated glass-fiber filter[16]. Cryogenic sampling of aniline in air, followed by liquid chromatography, with electrochemical detection, affords almost quantitative collection and recovery, with a detection limit of 4 ppb. The method has been developed for field measurements[17].

Atmospheric sampling does not provide complete quantitative measurement of intake, since occupational exposure occurs by both dermal contact and inhalation. It has been estimated that half of the dose may be absorbed through the skin[18,19]. Skin and surface detection kits are available from commercial sources.

IV. CARCINOMA

A. Introduction

The greatest workplace hazard posed by aromatic amines is bladder cancer. The first aromatic amine found to be responsible for tumor production in the urinary bladder was ß- or 2-naphthylamine (**8**). Papillomous disease of the bladder, often called 'aniline cancer' (after the aniline dye industry), was first observed among dye workers in Frankfurt during the 1890s. Incidences of bladder cancer, in addition to cyanosis and hematuria (abnormal quantities of red blood cells in the urine), among dye-workers working with aromatic amines, particularly the naphthylamines and aniline, as well as in the production of the long-known colorant rosaniline (magenta) (**9**), were reported by Rehn in 1895 at a congress of the German Surgical Society[20]. In 1906 he suggested that bladder tumors developed following exposure to naphthylamines and benzidine (4,4′-diaminobiphenyl) (**10a**), made on a large scale as dye intermediates from the 1880s[21].

B. 2-Naphthylamine and Benzidine

An extensive survey carried out at the Hoechst dyeworks, near Frankfurt, and among dye workers in Basel, led to widespread acknowledgement early in the 20th century of the new hazard to workers in dye factories. The volatility of aromatic amines contributed considerably to the level of skin and lung exposure. Chronic human exposure resulted in toxic symptoms, and in some cases bladder cancer[22]. The long latent period prior to development of a tumor meant that the onset of bladder cancer was generally not observed for at least a decade. This complicated early identification of the causative amines. Hematuria is a typical symptom of bladder cancer. Presumptive evidence for the role of **8** as a principal cause of bladder tumors was reviewed in 1921 by the International Labour Office[23]. In 1926, the first cases in England were described by medical inspectors.

Chemical carcinogenesis emerged as an established field of scientific enquiry after carcinogenic constituents in coal tar were identified by Japanese workers in 1915, and British workers isolated and identified coal-tar 3,4-benzo[*a*]pyrene as a carcinogen. Wignall (1929) reported the prevalence of bladder cancer among workers exposed to **8** and **10a** (studies on **10b, 10c** and **10d** were not reported) and 1-naphthylamine (**11**)[24]. Unlike

2-naphthylamine
(β-naphthylamine)

(8)

rosaniline
(magenta)

(9)

(10a) $R^1 = R^2 = H$
(10b) $R^1 = R^2 = CH_3$
(10c) $R^1 = R^2 = Cl$
(10d) $R^1 = R^2 = OCH_3$
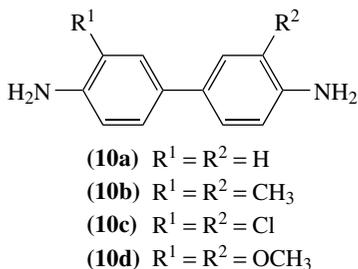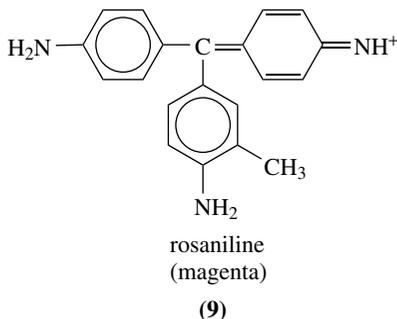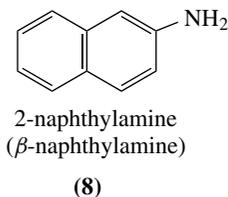
carcinogenic polyaromatic hydrocarbons, whose effects were at the site of application or injection, the target organs for amines were distant from the place of administration. Tumors in test animals arising from contact with aromatic amines appeared in specific organs, according to the test animals. At DuPont, Gehrmann emphasized the role of **8** in bringing about bladder tumors in humans[25, 26].

Rodents such as rats and mice developed liver cancer from exposure to aromatic amines[27]. In contrast, it was found that dogs developed bladder cancer, which is why they were first used as experimental animals at DuPont by Hueper during the 1930s. Hueper induced bladder cancer by injecting and feeding compound **8** to the animals; after two years bladder tumors were identified in many cases, either at autopsy or by cytoscopy. He also drew attention to the fact that commercial **11** contained around 5% of **8**. Hueper did not find tumors among workers who handled aniline[28−30]. Further work was done in the UK by Berenblum and Bonser[31, 32].

1-naphthylamine
(α-naphthylamine)

(11)
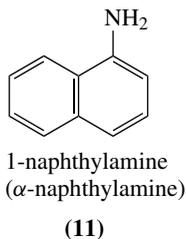
During the late 1940s, German and Italian industrial chemists shared their knowledge of the toxicity of **8** with British and American colleagues. In Germany very high incidences of carcinoma of the bladder were found among workers exposed to benzidine **(10a)**, particularly those engaged in conversion of hydrazobenzene to benzidine. Bladder cancer

was found in almost every worker, sometimes several years after the exposure period, including following retirement[33]. Goldblatt emphasized the connection between aromatic amines and carcinogenesis[34].

A systematic and extensive study into cancer caused by aromatic amines was carried out from the mid-1940s by Scott, at Clayton Aniline Company, in Manchester, England, who worked closely with Williams, at the nearby ICI Dyestuff Division (Blackley). Scott's studies of aromatic amines, particularly **8** and **10a**, became the standard works in the field. He made recommendations for modification of manufacturing plant in order to minimize exposure[35–37]. Benzidine (**10a**) was confirmed as a human carcinogen in 1950[38]. In the following year at a symposium on industrial hygiene, **10a** was placed second after **8** in the list of most potent carcinogens among the aromatic amines produced in bulk[39]. These were, moreover, the most powerful known carcinogens among all organic chemicals.

Case in 1948 began a five-year epidemiological investigation of bladder tumors in the synthetic dye industry for the dyestuff group of the Association of British Chemical Manufacturers (ABCM), eventually covering the entire 1921–1949 period[40]. The probability of contracting cancer was stated to be about 30 times greater for workers engaged in manufacture and use of naphthylamines and benzidine than for the general population. Some twenty companies involved in the ABCM's study discontinued manufacture of 2-naphthylamine (**8**)[41]. The results were reported in the chemical trade press, including in the US[42]. Case went on to provide an epidemiological method for establishing the environmental risk of contracting bladder tumors in other industries where aromatic amines were employed, including the rubber, paint, cable and leather trades. His studies provided unequivocal evidence that **8** was the main carcinogenic amine. The induction time for cancers varied from two years to over a decade for workers exposed to naphthylamines **8** and **11**, and to **10a**. Case and Pearson reported that auramine (**12**) production was associated with tumor of the urinary bladder. Subsequently, this amino-containing dye has become a suspected human carcinogen[43]. The significance of the work of Hueper and Case on the intensive carcinogenic properties of aromatic amines has been reviewed[44].

auramine
(**12**)   (**13**)
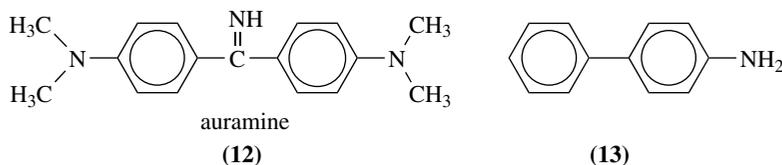
A strong correlation has been suggested between the period and extent of exposure and the period of latency. Moreover, both **8** and **10a** clearly demonstrate that chemicals which are not acutely toxic can cause chronic effects as the result of prolonged intake at dose levels that show no acute symptoms. The increased risk of bladder cancer has not been confined to chemical manufacturers. It has, for example, been reported among Japanese kimono painters and others who use benzidine and naphthylamine colorants. Studies with dogs showed that 4-aminobiphenyl, or 4-biphenylamine (**13**), as contaminant was the probable carcinogen that early in the 20th century caused aniline to be suspected as a principal carcinogen[45, 46].

The large-scale production in Britain and the US of **8** ceased in the 1950s, and of **10a** during the 1960s and 1970s. However, in both countries limited manufacture continued, and it was, and is, also produced elsewhere. Lymphotoxicity arising from **8** has been studied[47]. Production and use of **10a** ceased in Britain during 1962, and in the US during 1972. The application of **10a** as an analytical chromagen (through ready oxidation

to colored quinonoids), and of certain of its congeners, particularly *o*-tolidine, or 3,3′-dimethylbenzidine **(10b)**, in clinical and forensic laboratories, for spot tests, and water analysis, declined during the 1970s. While safer alternative reagents were developed, in most cases certain reagents, such as **10b**, continue to be employed in specific analytical tests, though as dilute (0.1%) solutions.

Epidemiological studies on cause-specific mortality have continued to the present time[48]. The long induction periods observed for aromatic amines—bladder tumors from **10a** were found in the dog after a latent period of seven to nine years, and longer periods for workers exposed to this chemical in the dye-making industry—encouraged monitoring of occupational bladder cancer, and of other studies, long after manufacture and use had ceased. Urine analysis, prostatic alkaline phosphate (PAP) examination and cytoscopy have been recommended for workers engaged in handling these and similar aromatic amines, even after they were no longer exposed[49]. A twofold increase in deaths from all cancers combined and increases in deaths from bladder, kidney and CNS (Central Nervous System) cancer among workers exposed to **8** and **10a** has been reported. The most thorough study was conducted in the US on workers formerly employed at the former CIBA-Geigy Toms River Chemical Corporation dyes and resins factory in Ocean County, New Jersey[50]. This demonstrated that improved conditions of industrial hygiene reduced dramatically the appearance of benzidine metabolites found in urine. Those workers in which bladder cancer was found had, before 1960, when benzidine-dye manufacture commenced at Toms River, worked with the same and similar amines at a facility in Cincinnati where there was less control over exposure during handling and processing.

Initiation of a malignant growth can thus be connected to exposure that is both comparatively short-lasting or to exposure over the course of many years. Invariably there is a long delay between exposure to the carcinogenic agent and development of the malignant growth.

While workplace exposure is normally far higher, and better recorded, than residential exposure, non-occupational clusters of cancer close to the sites of chemical factories are well established. However, the cause and time of exposure, and amount of exposure, are far more difficult to establish. Thus, from 1979 to 1995, childhood leukemia and CNS cancers at Dover Township, close to the Toms River facility, was found to be four times the average for New Jersey. In the mid-1960s, analysis had shown the presence of aromatic amines in a well belonging to the Toms River Water Company, located downstream of the CIBA-Geigy factory. Around the year 2000, these and other industrial releases were among the possible causes studied by the Division of Epidemiology, Environmental and Occupational Health, New Jersey Department of Health and Senior Services, and other interested parties. The latter included two groups of citizens, one group represented by the lawyer who had earlier acted for citizens of Woburn, Massachusetts, in the case made famous in the book *Civil Action*, later a major film.

Similar considerations apply to all aryl amine bladder carcinogens employed in the dye, rubber and leather industries[51]. Between 1930 and 1960, the toxic natures of many other coal-tar (aromatic) amino compounds, particularly azo dyes, were revealed[52].

C. Aminoazo Dyes

Certain aminoazo dyes, as with aromatic amines, induce bladder cancer in dogs. Again, carcinogenesis is found at other organs with other animal species. While before the early 1930s, azo dyes had been found to be toxic, there was no evidence that they were carcinogenic until Yoshida demonstrated that liver tumors could be induced in rats and mice by feeding or injecting the azo dye 4-(*o*-tolylazo)-*o*-toluidine **(14)**[53]. Kinosita showed that

butter yellow, N,N-dimethyl-4-aminoazobenzene (*p*-dimethylaminoazobenzene) **(15)** produces liver tumors in the rat[54]. Orr also reported tumors in animal experiments with **15**; this colorant is now classified as a potential occupational carcinogen. For azo dyes, toxicity arises from enzymatic reduction to afford parent aromatic amines[55]. Subsequently, it was discovered that if one of the two methyl groups in N,N-dimethyl aryl amines was replaced by hydrogen or an ethyl group, carcinogenic activity was maintained; it was lost when both methyl groups were replaced by ethyl or other groups. In 1947, on the basis of experiments with aminoazo dyes that induced cancer, the Millers suggested covalent bonding of metabolites in the liver. This was soon to be accepted as a general precondition for aryl amine-induced carcinogenesis[56].

(14)   **(15)**
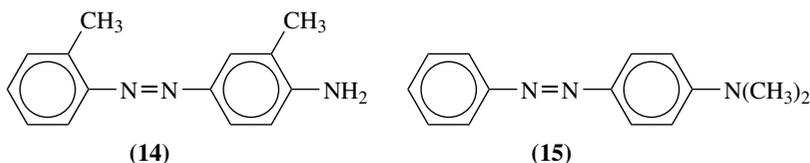
D. Drugs from Aromatic Amines

During the 1940s, aryl amine intermediates employed in the bulk manufacture of sulfonamide (sulfa) drugs caused illness to workers. Animal experiments suggested low toxicity for 2-aminopyrimidine **(16a)**, with a possible toxic effect on the liver after prolonged administration. Toxicity studies, including of 2-amino-4-methylpyrimidine **(16b)**, were conducted at the Kettering Laboratories of Applied Physiology, University of Cincinnati, College of Medicine, and at industrial laboratories[57–59]. The toxicology of a number of the classes of drugs discussed in Chapter 16 have been reviewed[60].

(16a) R = H   **(17a)** R = OH   **(18)**
(16b) R = CH$_3$ **(17b)** R = OC$_2$H$_5$
                        (17c) R = H
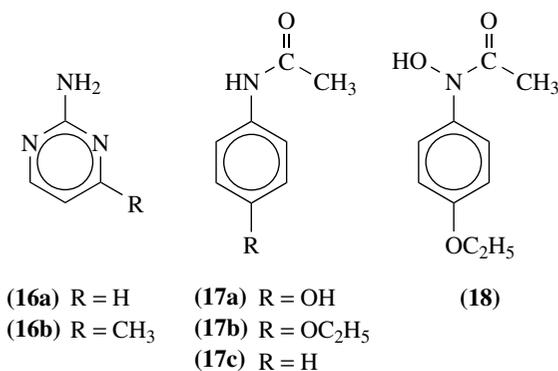
Investigations into drugs suspected of causing cancer in humans have included aryl amine derivatives such as Paracetamol **(17a)**[61] and phenacetin **(17b)**. Metabolism of acetanilide **(17c)** yields aniline, and of **17b** N-hydroxyphenacetin **(18)**[62], in accord with views on mechanisms of toxicity as discussed in the next section. Tumor formation was induced in rats at excessively high dose levels and only under certain conditions. Drugs found to cause methemoglobinemia include antipyrine, acetanilide, sulfanilamide, sulfapyridine, sulfathiazole, sulfonal and thional.

E. 2-Aminofluorene (2-Fluorenamine)

An important area of cancer research involving aromatic amines, with much wider implications, was opened up in 1941 following the finding that tumors were initiated in several organs of rodents by 2-fluorenamine (2-aminofluorene) (19). Extensive studies in the 1950s on rats and other rodents revealed that the derivative 2-acetylaminofluorene, or 2-fluorenylacetamide (2-AAF, or FAA) (20), is considerably more potent than the parent amine. This provided intriguing clues to the metabolic processes[63]. The Millers, following on from their work with azo dyes, in 1960 demonstrated N-hydroxylation of 20 to 21 in rats and rabbits. The product of metabolism was a more potent carcinogen than the parent and caused sarcomas (growths in a solid tissue) at the point of application. The importance of this finding was that the N-hydroxy derivative was one of the first, if not the first, known metabolite of a carcinogenic synthetic organic chemical to be identified. Administration of both 20 and its N-hydroxy derivative 21 led to binding in vivo in the liver. In contrast, 20 showed no reactivity in vitro. This was in accord with the fact that aryl amines require activation in vivo. The tumors appear distant from sites of administration. This suggested a second activation step. The N-hydroxy derivative 21 is thus the precursor, or proximate, carcinogen. Identification of an amino derivative obtained by degradation of protein-bound dyes extracted from rat livers suggested that the ultimate carcinogen was an ester[64]. The new metabolic reaction pathway involving N-hydroxylation was observed in other aromatic amines, particularly 13[65] and 8[66]. Biochemical N-hydroxylation was now believed to be the general reaction in mammary carcinogenesis involving many aromatic amines, including fluorene derivatives[67]. Ring-hydroxylation of 20 was also observed during carcinogenesis in the rat[68].

(19)   (20)

(21)
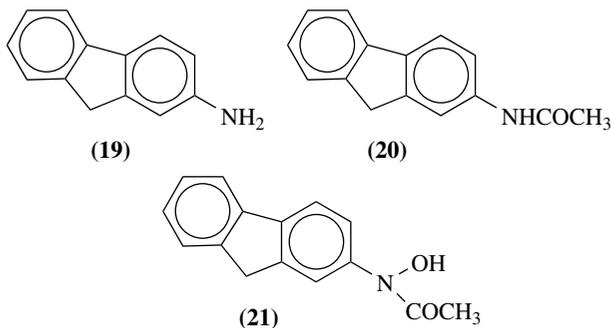
Boyland and colleagues made important contributions following studies of rubber industry workers who had contracted bladder cancer. The glucosiduronic acid of 2-amino-1-naphthol (22) was used to study tumor induction. Manson and Boyland had also suggested that tumors were initiated at sites distant from the point of exposure, and went on to study the metabolism of 2-naphthylamine[69]. This and similar work showed that amines were converted into active metabolites that were then carried to the bladder, where they (or, as later suggested, their esters) were released and promoted tumor formation. Bonser found that aromatic amines were converted to o-hydroxylamines in test animals, and liberated in their urine. Support came from studies on other amines, including 4-biphenylamine[70]. Walpole and Williams showed that 3-methyl-4-aminobiphenyl (23) was a more potent carcinogen than the powerful carcinogen 13, and afforded products that initiated colon cancer[71]. This and other empirical evidence led the Weisburgers and colleagues, after studying single-ring aryl amines, to assert that ortho-methyl derivatives

(22)   **(23)**   **(24)**
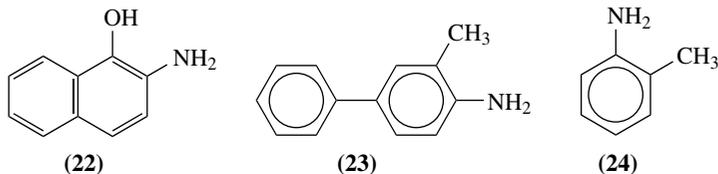
were probably carcinogens, which was supported when *o*-toluidine **(24)** was found to be carcinogenic[72].

After publication of the double helix structure for DNA (1953), attention shifted from binding of carcinogens to proteins to their binding to DNA and RNA with, as a consequence, mutation following modification of DNA. These studies were aided by the availability of labelled carcinogens. By the late 1970s, it was accepted that carcinogenesis induced by aryl amines, and indeed carcinogenesis in general, was initiated by a mutagenic event that led to alteration of DNA: Cancer is a genetic, somatic disease. The assumption is that carcinogenecity is equivalent to mutagenecity. In the case of aryl amines, it is the metabolic products, and not the free amines, that damage DNA, leading to tumor formation.

Though both mutagenic and carcinogenic propensities are related by the extent of binding to DNA, more direct correlation has not been established. Structural features are probably important in determining carcinogenic potential. Aromatic amines that alkylate DNA include *p*-aminoazobenzene **(25)**, **8**, **10a**, **11**, **19**, **20**, aniline mustard (*N*,*N*-bis(2-chloroethyl)aniline) **(26)** and *N*-nitroso-*N*-methylaniline **(27)**. The binding of aniline is very small, as is expected from its apparent low mutagenic and carcinogenic behavior.

(25)   **(26)**   **(27)**
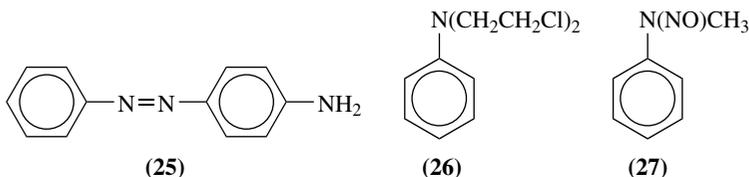
V. MECHANISM OF BLADDER CANCER

A. Introduction

Evidence for the mechanism of bladder cancer derives from correlation of certain structural features of aromatic amines important in carcinogenecity, and knowledge of activation steps and metabolites obtained from laboratory animals[73]. Earlier studies revealed the biochemistry of the carcinogenic aromatic amines: Questions remained as to whether binding to DNA or RNA was causally connected to carcinogenic action.

By the 1970s it was known that aromatic amines and azo dyes are metabolized by specific enzymes. The enzymes require oxygen and reduced NADP and are present in the endoplasmic reticulum membranes of the liver, though the kidney and lung also show activity. *N*-Hydroxylation brought about by these enzymes converts aromatic amines to proximate carcinogens that are converted into ultimate carcinogens in, for example, the bladder[74].

B. Activation

Carcinogenic amines are converted biochemically to *N*-hydroxyaryl amines, mainly in the liver, but also in erythrocytes, the intestine and other organs. This first, or initial,

bioactivation step takes place due to the propensity of aniline to undergo oxidation. The *N*-hydroxylation of **1** to **28** is brought about by the group of membrane-bound enzymes known as cytochrome P-450-mediated monooxygenases (cytochrome P-450 1A2, or CYP1A2), that also metabolize other environmental carcinogens (Scheme 1). This first step, known as phase I, can also be brought about by other cytochrome P-450 enzymes and, in some organs, by prostaglandin H synthases, that favor carcinogenecity and hemoglobin formation. Then a second step, phase II, takes place: conversion of the *N*-hydroxylated metabolite, the proximate carcinogen, to acetate esters, sulfate esters, carbamate esters or phosphate esters. The aglycone conjugate is then transferred from the liver to the bladder[75].
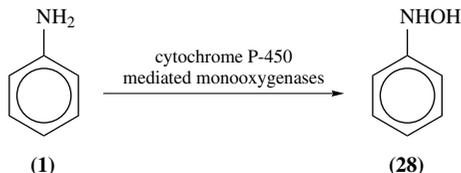
SCHEME 1. Bioactivation of aromatic amines. Phase I

The active compounds are genotoxic, reacting with DNA at specific codons to afford a mutated gene. At the chemical level they are electrophilic, and attack the nucleic acid bases, forming covalent bonds. The activated metabolite reacts only with those proteins and nucleic acids close to the site of activation since either they are unstable, or the activation occurs in the tissues in which tumors are induced. In rats, liver tumors have been linked to sulfate conjugates of the hydroxamic acid derivatives[76]. Note that *N*-hydroxylated 2-naphthylamine **(29)**, obtained in phase I, yields, on rearrangement, 2-amino-1-hydroxynaphthalene **(22)**. Of all genotoxins, 2-AAF **(20)** is probably the most studied, and the most thoroughly reviewed[77–80]. Activation routes involve peroxidation of *N*-hydroxy-*N*-2-AAF **(21)** to afford *N*-acetoxy-*N*-2-AAF **(30)**.
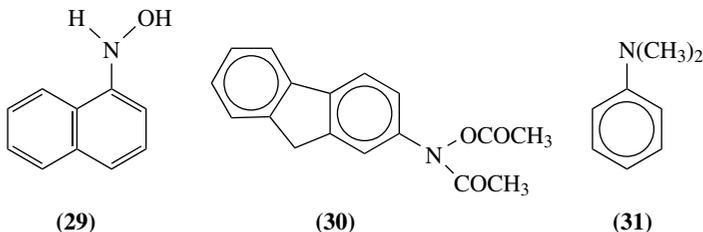
Other proposed mechanisms for metabolic activation include the role of *N*,*O*-acyltransferase in formation of *N*-acetoxyaryl amines[81]. Species and tissue differences as determinants at the sites of tumor induction have been investigated. The connection between amine structure and activity includes empirical evidence indicating that important carcinogenic amines are conjugated aromatic ring systems, with amino groups *para* to the conjugated system.

As mentioned earlier (Section IV. E), single-ring aromatic amines such as *o*-toluidine **(24)** exhibit pronounced carcinogenic properties. When the dimethyl derivative of aniline, *N*,*N*-dimethylaniline **(31),** was fed to Fischer 344 rats and B6C3FI mice, splenic

sarcomas were observed after two years[82, 83]. Cumene hydroperoxide aids demethylation by cytochrome P-450 from adrenal cortex mitochondria[84]. A similar mechanism appears to explain the metabolism of aminoazo dyes.

Studies on carcinogenic azo dyes led to an understanding of possible structure–activity relationships. The Millers's demonstration that metabolites from azo dyes covalently bond in the liver of rats was the first reported case of covalent bonding of a xenobiotic carcinogen derivative to a cellular macromolecule. This reaction leads to an effect on DNA. Thus for N-methyl-4-aminoazobenzene (MAB) **(32)**, its benzoic acid ester, N-benzoyloxy-MAB **(33)**, prepared *in vitro*, reacts with nucleic acids to afford products identical to those obtained *in vivo* following administration of **32**. In like manner, N-hydroxy-MAB was used to show that microsomal N-oxidation takes place. Studies on p-dimethylaminoazobenzene **(15)** and a limited number of its derivatives have been used to examine the impact of N-alkylation on carcinogenic activity. The methyl group may in certain cases be necessary for rat hepatocarcinogenesis. The painting of p-aminoazobenzene on the skins of rats also initiates skin tumors[85].

$$C_6H_5-N{=}N-C_6H_4-N(CH_3)(H)$$

(32)

$$C_6H_5-N{=}N-C_6H_4-N(CH_3)(OC{=}O\,C_6H_5)$$

(33)
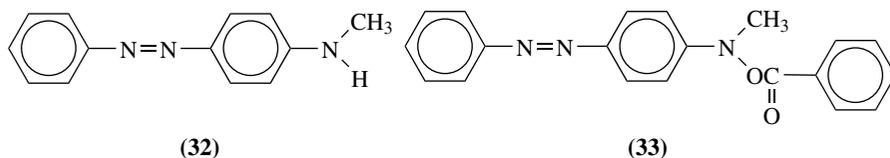
The secondary amine **32** may also exhibit its hepatocarcinogenic character by N-oxidation, followed by secondary conjugation with sulfate to afford the reactive species[86]. Hepatic metabolism of N-hydroxy-N-methyl-4-aminoazobenzene and other N-hydroxy arylamines yield reactive sulfuric acid esters.

A comparison of tumor-producing propensities of aminobiphenyls with nitroso-biphenyls in Syrian golden hamsters confirmed that the former do not induce subcutaneous tumors (unlike the nitroso analogs). The metabolite N-glucuronide can be deconjugated to the corresponding N-hydroxybiphenyl, a probable carcinogen to the bladder epithelium. Single-ring amines and C-nitroso compounds did not induce tumors under the reported conditions[87, 88].

N-Hydroxylation has been correlated with ultimate DNA adduct formation, and initiation of chemical mutagenesis in the reverse mutation assay[89, 90]. Further support derives from esterification by acetyltransferases and sulfotransferases, which facilitates binding with DNA and mutagenesis. As discussed earlier, initial activation, the oxidative N-hydroxylation, occurs through metabolic conversion initiated mainly by microsomal CYP1A2[91, 92].

The genetic toxicity of **20** and of some of its metabolites is significant to these studies[93–95]. Polymorphisms in N-acetyltransferase enzymes (NAT1 and NAT2) link the risk of breast cancer to exposure to aromatic and heterocyclic amines; the mechanism may be similar to that for bladder cancer. Aromatic amines released from dyes and in tobacco smoke have also been included in a recent survey[96]. This revealed empirical evidence for mutation in a specific codon. A polymorphism at codon 105 (Ile/Val) in the GSTP1 gene is linked with higher risk of cancer. Recently, a Chinese group reported evidence of the first association between the GSTP1 AG or GG genotype and higher cytological gradings of exfoliated urothelial cells from workers previously exposed to benzidine **(10a)**. The GSTP1 AA, AG and GG genotypes were determined in occupationally benzidine-exposed Chinese workers in order to assess the role of GSTP1 polymorphisms in bladder cancer[97].

C. Detoxification

An alternative to the enzymatic *N*-hydroxylation, the first stage in carcinogenesis, is *C*-hydroxylation in the aromatic ring. This is an important mode of detoxification.

Most significant, however, is conjugation of the aromatic amine metabolite, the *N*-hydroxy intermediates, to glucuronic acid, though conjugation to sulfate is also important. In the former case, the products from bioactivation by cytochrome P-450 (CYP)-directed oxidation, phase I, are substrates for the uridine diphospho-, or UDP-, glucuronosyltransferases (UGTs). The UGTs bring about a phase II process in which the hydroxyl groups introduced in phase I are further modified, and the product is excreted in the urine. Animal experiments show that *N*-acetylation of primary amines by the *N*-acetyltransferase 1 (NAT1) enzyme, such as of **1** to **34**, is also protective (Scheme 2).
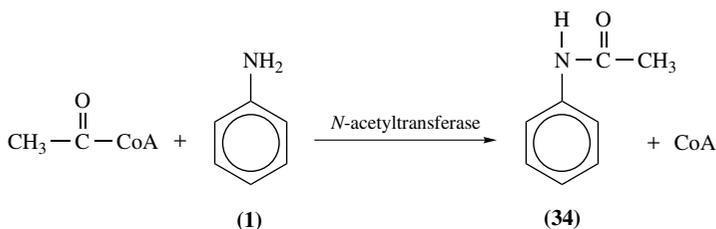
SCHEME 2. Protective acetylation

Metabolic defense against mutagens (chemicals that can change information in genes) is favored by those enzymes that promote conjugation and whose products are eliminated through kidney or biliary excretion. However, since the *N*-acetyltransferase is polymorphic, displaying both slow and rapid acetylator phenotypes, the allele (gene version) that confers a slow acetylator phenotype probably encourages a higher risk of cancer. This acetylation does not occur in dogs[98]. The connection between the much-studied *N*-acetylator phenotype and human disease has stimulated investigations of therapeutic value. This is an important outcome of research into the role of *N*-acetyltransferase activity in aryl amine metabolism.

VI. SPECIFIC AROMATIC AMINES

A. Benzidine and its Congeners

Subcutaneously injected benzidine **(10a)** induces liver tumors, ear duct carcinomas and a few adenocarcinomas of the intestine, in rats. A number of congeners, including *o*-tolidine **(10b)**, 3,3′-dichlorobenzidine **(10c)** and *o*-dianisidine (3,3′-dimethoxybenzidine) **(10d)**, initiate tumors in rats[99–103]. The metabolism of benzidine in the dog has also received attention[104]. The *N*-acetylated metabolites of benzidine have been detected in the urine of monkeys, rats and humans. Metabolism of both *N*,*N′*- and *N*-acetylated derivatives has received extensive coverage[105–117].

Certain benzidine-derived (direct azo) dyes afford, by reduction, generally metabolic degradation in the gut or liver, the free aryl amine. The azo cleavage may be brought about by gut bacteria and mammalian liver azo reductases. In 1978, the US National Institute of Occupational Safety and Health (NIOSH) and the Occupational Safety and Health Administration (OSHA) reported that the benzidine-colorants CI Direct Black 38, CI Direct Blue 6 and CI Direct Brown 95 were all reduced to **10a** by rat liver *in vivo*, though trypan blue **(35)**, Congo red **(36)** and Chicago sky blue were not. However, all six

trypan blue

(35)

Congo red

(36)
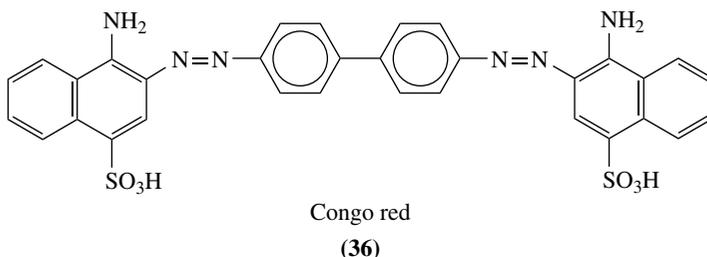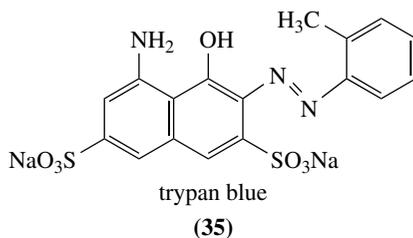
dyes were reduced to various extents in the gut. Since they are all animal liver carcinogens, cleavage in the liver, even if less pronounced, may be more important[118–120].

As already indicated, major preventive measures instituted from around 1950 have reduced the risks of bladder cancer, at least at responsible manufacturers in western countries[121]. Epidemiological surveys in China and Russia show that workers in the 1990s were still exposed to the risks of bladder cancer from **10a**, even after certain controls were introduced. Studies in Shanghai revealed that exposure to **10a** rather than its dyes was the main cause of bladder cancer in the city. The confounding effect of smoking has also been discussed[122]. Another Chinese study emphasized the increased risk to smokers exposed to **10a**, suggesting some level of synergism[123]. The cancer and mortality risk among workers in Moscow exposed to **8** and **10a** was the highest with workers involved in production and handling of **8**. A three-year cancer prevention and control effort involving very low-level exposure to **10a** was not successful[124].

In the US, a workplace study of exposure to benzidine and its congeners, such as **10b, 10c** and **10d**, at the chemical facility of Upjohn (previously Carwin Company), located at North Haven, Connecticut, between 1965 (when benzidine manufacture ceased) and 1989, indicated a statistically significant increase in the standardized incidence ratio[125]. The impact of interindividual variation in NAT2 activity on urinary metabolites and urothelial DNA adducts in workers has been examined[126]. Phenyl-2-naphthylamine **(37)**, and perhaps chemicals used in its manufacture, have been implicated as possible causes of bladder cancer, based on studies of workers at a factory in North Wales. Other amines investigated

(37)
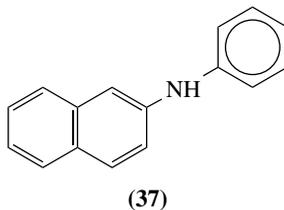
were aniline and *o*-toluidine[127]. Eighty aromatic amines have been classified through quantitative structure–activity relationships, and structural, electronic and hydropathic factors affecting mutagenic potency[128].

B. Aniline

After interest in exposure to benzidine had peaked in the early 1970s, the focus turned to aromatic amines that were either less potent carcinogens, or about which there was some uncertainty regarding their abilities to induce tumors. Aniline came into the latter category, particularly since bulk production far exceeded that of other amines. In 1974, a DuPont study asserted that aniline was the only widely used aromatic amine considered hazardous under normal ambient temperature conditions[129]. Its known toxicity, allied with uncertainty about mutagenic-carcinogenic effects in humans, has led to restrictions in handling and use, and ongoing research into possible significance for the initiation of carcinogenesis. Aniline is toxic to erythrocytes and the spleen. Radiolabeling experiments have indicated that the primary site of aniline-caused damage in the rat is the same as that in cyanosis. The splenic toxicity is possibly secondary to erythrocyte damage, arising from chemically-mediated erythrocyte toxicity; the damage to red blood cells must then be sufficient to cause splenic scavenging of the cells. Evidence derives from decreased blood binding and splenic enlargement, and lower splenic toxicity, in mice, and spleen tumors produced in rats given high doses in two-year bioassay studies. This has been used to support the assertion that splenic injury and carcinogenesis may not take place in workplace environments unless levels of exposure are high enough to cause damage to erythrocytes[130, 131]. Alternatively, it has been argued, since cancer is almost certainly the result of a cell mutation, such as the result of a single molecular interaction of the carcinogen with DNA, it may be that no absolute safe level of carcinogen can exist. Moreover, aniline has been shown to initiate tumors of the spleen in Fischer 344 rats, but not in C57BL/6 X C3H F1 mice. Binding of labelled ^{14}C aniline was found to be greatest in the kidney, large intestine and spleen of rats that had received high doses[132].

As a result of the recognized toxicity of aryl amines, the US EPA has enforced testing consent orders on manufacturers (including importers) of aniline and seven substituted anilines (chloroanilines and nitroanilines)[133]. The most thorough investigation of aniline-induced splenic toxicity in rats through administration of labelled ^{14}C aniline hydrochloride has been undertaken by Khan and coworkers. The iron content of spleen increased by 85% for rats given 3 doses, compared with rats given one dose. Covalent binding to macromolecules in target (spleen) and non-target (liver) organs was observed[134]. Experiments with male Sprague-Dawley [SD] rats has established that aniline induces lipid peroxidation and protein oxidation in the spleen and suggests that oxidative stress played a role in splenic toxicity of aniline[135].

The aniline-related changes in blood were reflected very early, as increases in methemoglobin content, while splenic changes appeared later, characterized by splenic weight changes, followed by protein formation, resulting in malondialdehyde (MDA)–protein adduct formation and morphological changes after a single high-dose exposure. This favors the involvement of free radical-mediated reactions as mechanisms for splenic toxicity, and lipid peroxidation preceding protein oxidation[136].

The *N*-hydroxylated metabolite **(28)** appears to be a splenotoxin, contributing to the toxicity of aniline; at high dose it is cardiotoxic, possibly due to anoxia (absence of oxygen supply) associated with marked methemoglobinemia[137]. Aniline-induced oxidative stress as an early event in the splenic lesions has been suggested following time-dependent subchronic studies in male SD rats that received aniline-contaminated drinking water. Total iron content was greater than in age-matched controls; there were time-dependent increases

in splenic lipid peroxidation (supported by measurement of malondialdehyde–protein adducts); and protein oxidation in the spleen was greater. Analysis for oxidized proteins showed two distinct protein bands at approximately 114 kD and approximately 69 kD in both post-nuclear and mitochondrial fractions of the spleens. Analysis indicated that these proteins were susceptible to aniline-induced oxidative stress. The oxidative stress in the spleen may be ongoing, leading to oxidative modifications of biomolecules, splenic toxicity, capsular hyperplasia and fibrosis, and, possibly, tumor formation with chronic exposure[138].

That iron potentiates the splenic toxicity is suggested by the increased toxicity observed in total iron, low molecular weight chelatable iron, lipid peroxidation and protein oxidation when diets of aniline hydrochloride and carbonyl iron or iron are administered to SD rats[139]. Nitrosobenzene (**38**), the *N*-oxidized metabolite of aniline, contributes to splenic toxicity through decreased erythrocyte counts, and increase in methemoglobin, iron content of spleen, MDA–protein adducts, splenic lipid peroxidation, and protein oxidation[140]. Immunochemical detection, and colocalization with iron in red pulp of the spleen of MDA–protein adducts, indicates that iron-catalyzed lipid peroxidation could be a potential mechanism for splenic toxicity[141]. Khan's group has postulated an association between formation of MDA–protein adducts and overexpression of TGF-beta 1, together promoting splenic injury and fibrogenesis[142]. The contribution of nitric oxide to the oxidative mechanisms of aniline toxicity suggests that oxidative stress leads to nitration of proteins. Immunohistochemical analysis for nitrotyrosine showed intense staining in the red pulp areas of the spleen, localized in macrophages and sinusoidal cells[143].

(38)   (39)
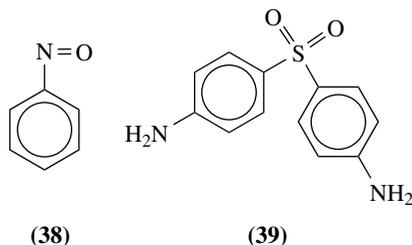
Ciccoli and coworkers have shown that incubation of rat erythrocytes with hydroxylated metabolites of aniline, dapsone (**39**) and the corresponding hydroxylamines brings about enhanced release of iron and methemoglobin formation. This did not occur with parent compounds. That xenobiotics are effective only after biotransformation to metabolites *in vivo* is supported by acute intoxication of rats with aniline or **39** and marked increase in the erythrocyte content of free iron and of methemoglobin[144]. The potent toxicity of aniline-derived aminophenylnorharman in the liver of the *gpt* delta transgenic mouse has been demonstrated[145, 146].

C. *N,N*-Dimethylaniline

Studies on *N*,*N*-dimethylaniline (**31**) have been carried out with Fischer 344 rats and B6C3FI mice. A metabolite, *p*-dimethylaminophenol (**40**), is active in forming hemoglobin *in vitro* and *in vivo*[147]. Efficient environmental analysis for **31** has been hampered by its poor retention on silica tubes. The US OSHA describes experiments involving adsorption in a 10% H_3PO_4-coated XAD-7 tube, followed by GLC. The target concentration is 5 ppm in air, from an air volume of 30 l at 0.2 $l\,min^{-1}$ [148].

$$N(CH_3)_2$$

OH

(40)

D. *ortho*-Toluidine (2-Methylaniline)

The *ortho*-aminotoluene, *o*-toluidine, or 2-methylaniline **(24)** was formerly employed in the manufacture of rosaniline (aniline red, magenta), but not in the manufacture of pararosaniline. It probably accounted for cases of bladder cancer found among workers in aniline dye factories before 1950, by which time new processes had been introduced. However, *o*-toluidine was also used on a large scale as an antioxidant in the rubber industry until at least 1980. As already discussed, it is more toxic than aniline and produces bladder tumors in rats. Support for human bladder cancer arising from occupational exposure derives from various studies[149, 150]. Excess bladder cancer found in workers exposed to both **24** and aniline is expected to arise from the former compound, though the aniline may participate[151]. Further support for **24** as a carcinogen derives from a correlation of the date of onset of worker exposure with increases in bladder cancer[152]. The role of **24** as a general genotoxin has been demonstrated, through metabolism *in vivo* to active genotoxins[153].

An analytical method for **24** and aniline in urine uses HPLC followed by electrochemical detection. The reported limits of detection were 0.6 microgram^{-1} and 1.4 microgram^{-1}, respectively. In order to develop methods for biomarkers of internal dose, binding of **24** to the blood proteins hemoglobin and albumin was investigated *in vivo* (rodent) and *in vitro* (hemoglobin and albumin). Base-hydrolyzable protein adducts were analyzed by HPLC (fluorescence) and/or GC/electron capture (EC). Though GC/EC was more sensitive than HPLC, utility was restricted by interfering peaks. The HPLC method is suggested for determination of exposures to **24** in individuals acutely or chronically exposed to high levels[154].

E. Bis(4-aminophenyl)methane (4,4′-Methylenedianiline; 4,4′-Diaminodiphenylmethane)

Bis(4-aminophenyl)methane, commonly known as 4,4′-methylenedianiline, or MDI **(41)**, is toxic, with an acute oral LD$_{50}$ (rat) of approximately 200 mg kg^{-1}. Occupational exposure occurs by inhalation and dermal contact, particularly from its use as an epoxy resin hardener. Excessive exposure to its dust has resulted in temporary liver damage in workmen. It is a mild eye irritant and can cause cyanosis. Though it is not a primary skin irritant or strong sensitizer, skin irritation can occur with sensitive individuals. It can be handled safely if care is taken to prevent excessive exposure to dust and fumes.

$$H_2N \quad\quad CH_2 \quad\quad NH_2$$

(41)
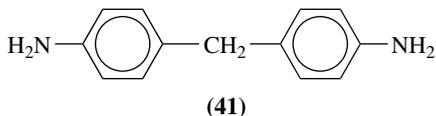
Accidental human exposure to **41** brought widespread awareness of its toxic properties. In February 1965, some of this amine became mixed with flour in a delivery van at Epping,

Essex, in England. The bread made from the contaminated flour caused cholestatic liver damage. In all, there were 84 cases of jaundice and hepatocellular necrosis, subsequently referred to as 'Epping Jaundice'. The hepatoxic response was investigated by Kopelman and coworkers[155, 156], and by Schoental, who confirmed that the cause was contamination of flour with **41**[157, 158].

The amine **41** is an animal carcinogen (mice and rats) and is possibly carcinogenic to humans. High levels of its metabolites were found in the urine of workers employed in using it as a resin hardener in a Swedish study. However, limitations of the study prevented evidence of increased bladder cancer risk. Dermal absorption was emphasized[159]. A Canadian study of a group of workers engaged in similar activities, and who had developed acute jaundice, found one case of bladder cancer[160].

While **41** is a known human hepatotoxin and an animal carcinogen (mice and rats) there is little information regarding its chronic effect in humans. The US EPA regulates **41** under the Clean Air Act (CAA), Superfund Amendments and Reauthorization Act (SARA) and Toxic Substances Control Act (TSCA). The American Conference of Industrial Hygienists recommends a TLV of 0.1 ppm (0.81 mg m^{-3})[161]. Base hydrolysis has been used with GC/MS to measure protein adducts of this amine[162].

F. 4-Biphenylamine (4-Aminobiphenyl)

The formerly widely used rubber antioxidant 4-biphenylamine, 4-ADP (**13**), is, as discussed earlier, a carcinogen comparable in potency to 2-naphthylamine (**8**). This was established through dog experiments in the 1950s. Manufacture in the UK was banned in 1967 in accord with the Carcinogenic Substances Regulations (that also banned manufacture of **8** and **10a**, and placed restrictions on the use of **10b**, **10c** and **10d**). However, **13** continued to be produced as a by-product during the manufacture of diphenylamine (**42**), and concentrates in the refining still. Later studies have been based on mutagenicity assays of mice using *Salmonella typhimurium*[163], and metabolic oxidation by human hepatic chromosomes and purified rat hepatic cytochrome P-450 monooxygenases. Glucuronide conjugates of **13** and its *N*-hydroxy metabolites in human and dog liver have been investigated[164], as has metabolic oxidation by human hepatic microsomes and rat hepatic cytochrome P-450 monooxygenases[165]. Adduct formation with hemoglobin has been used as an index of *N*-oxidation of this arylamine by hepatic P-450 1A2[166]. However, it has been demonstrated that CYP1A2 is not the primary enzyme that brings about hepatocarcinogenesis in mice[167].

(42)
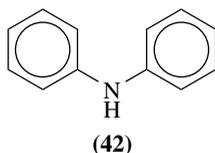
G. Chloroanilines

The chloroanilines are hematoxic, splenotoxic, hepatoxic and nephrotoxic. A German study of 335 male employees engaged in production and processing of 4-chloro-*o*-toluidine (**43**) found no cancer, though later eight of the men developed urothelial cancers. All were working in the production area prior to the implementation of improved hygiene conditions in 1970. This suggested a connection with carcinomas of the urinary bladder[168]. Another German study asserted that **43** may be carcinogenic to humans[169]. Examination of organ-directed toxicity following exposure of Fischer 344 rats to ^{14}C-labeled 2- and
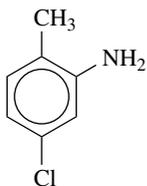
(43)
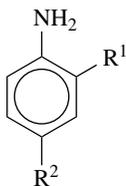
(44a) $R^1 = Cl$, $R^2 = H$
(44b) $R^1 = H$, $R^2 = Cl$
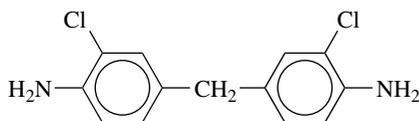
4,4′-methylenebis(2-chloroaniline)
(MBOCA, DACPM)
(45)

4-chloroanilines (**44a** and **44b**) showed accumulation mainly in the liver, as well as in the kidneys. Covalent bonding was detected. The greater toxicity of 4-chloroaniline (**44b**) arises from persistence and longer accumulation[170].

4,4′-Methylenebis(2-chloroaniline) (MBOCA) (**45**), a curing agent for liquid poly-urethane elastomers, has been reported as a carcinogen in mice and rats, and an inducer of transitional cell carcinomas in the urinary bladder of dogs. The International Agency for Research on Cancer (IARC) Working Group found no evidence of carcinogenecity in humans. The US EPA has classified **45** as a Group B2, probable human carcinogen.

H. Aminoanthraquinones and Derivatives

1-Aminoanthraquinone **46a** is widely used in vat dye manufacture. It has induced tumor formation[171]. Some vat black dyes (BB, P2R, 8R, and acridones) made from **46a** have tested positive in the Ames mutagenicity test. Similar considerations apply to 2-aminoanthraquinone (**46b**). Certain aminoanthraquinone-derived vat dyes have been reported as posing little or no risk[172, 173].
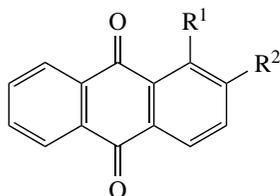
(46a) $R^1 = NH_2$, $R^2 = H$
(46b) $R^1 = H$, $R^2 = NH_2$
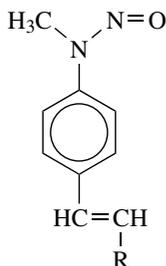
(47a) R =
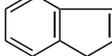
(47b) R =
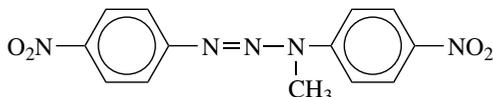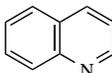
(48)

I. *N*-Nitrosoamines and Triazenes

1-(4-*N*-Nitroso-*N*-methyl-4-aminobenzylidine)indene **(47a)** and 4(4-*N*-Nitroso-*N*-methylstyryl)quinoline **(47b)** have induced tumors in the liver and ear duct of Fischer rats[174]. The nitrosoaniline **27** exhibits esophageal carcinogenecity in rats[175]. The carcinogenecity of triazene (diazoamino) compounds, such as **48**, some of which have been developed as blowing agents for foam rubber, and others used as anticancer drugs, have been reviewed[176].

VII. ENVIRONMENTAL FATE

Releases of aniline in industrialized countries is considerable. According to the US Toxic Release Inventory, during 1998, eighty-two factories in the US released 1,449,754 lbs. of aniline, 217,223 to the atmosphere, 19,549 to surface waters, 1,161,911 by underground injection, 252 to land and 50,819 to disposal sites. While aniline waste is nowadays subjected to recovery, management, energy recovery and waste treatment, this was not so in the past, when anilines caused environmental injuries. The toxic impact of many dyes, e.g. in waste streams and releases to surface waters, arises from the fact that they are degraded, cleaved or reduced to aromatic amines.

A. Waste Treatment

Typical manufacturing processes for dyes and other products made from aromatic amines result in residual materials that include solids, liquids and wastewaters. Wastes in soil become entrained into the site environment, where decomposition reactions, some affording refractory and toxic compounds, take place. Dyes and their by-products appear in wastewaters, including after treatment, and in landfills. Landfilling and dumping of waste aromatic products from dye manufacture has led to reductive release of amines under anaerobic conditions. Extensive reductive splitting of the azo linkage to afford aromatic amines under anaerobic conditions has been observed. Products identified include benzidine **(10a)** and its congeners, that persist in landfills and soils. These cleavage products and metabolites, as aromatic amines and their derivatives, can be more toxic than a parent colorant. For example, CI Direct Blue 15 (CI 24400) degrades to the free amine *o*-dianisidine **(10d)**, a benzidine congener, through cleavage of the two azo linkages[177]. Moreover, in liquid effluents, amines and nitrites react to afford the carcinogenic *N*-nitrosoamines[178]. CI Disperse Blue 79 yields on degradation 6-bromo-2,4-dinitroaniline **(49)**, which is toxic and mutagenic, as is its precursor, 2,4-dinitroaniline. While lipophobic primary amines are generally aerobically degraded, sulfonated arylamines resist degradation.

(49)
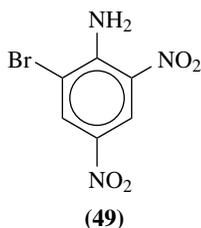
Distribution of aniline and aromatic amines depends on the level of waste treatment, which in turn determines the amount released to the environment. Aniline, unlike secondary and tertiary amines, is moderately soluble, and is released to the environment primarily in wastewater from its manufacture, and at sites where polyurethanes, rubber,

pesticides, dyes, fibers, pigments and pharmaceuticals are produced. Secondary (activated sludge) and tertiary (activated carbon) waste treatment of aromatic amines has met with mixed results. Studies carried out during the 1960s suggested a close correlation between carcinogenic activity and toxicity and resistance towards the action of sludge microorganisms. Aromatic amines were asserted to be quite resistant or even toxic to sludges in aeration tanks. The refractory benzidine (10a) was inhibitory or resistant to sludges, while 2-naphthylamine (8) was both resistant and toxic[179, 180]. Complete removal could be brought about by adsorption[181]. Biodegradability of 10a in aerobic suspended growth reactors has been achieved at low dose levels. For the breakdown to be effective, the concentration should be no greater than around 1 mg^{-1} [182].

Aniline, nitroanilines and halogenated anilines have been measured in treated wastewater from a dye-making factory at 7 to 96 ppb, and in untreated wastewaters at 36 to 480 ppb[183, 184]. Aniline is readily biodegradable and oxidizable in surface water, including in pond water, aided by sewage sludge. GC/MS analysis of biodegradation intermediates shows that initial deamination is followed by formation of identifiable intermediates[185]. 2-Nitroaniline (2a) resists degradation by activated sludge. Chloroanilines biodegrade slower than aniline. Reductive dehalogenation by microorganisms takes place under anaerobic conditions, as demonstrated in aquifers[186]. Azo dyes are considered xenobiotic and resist biodegradation under usual treatment conditions. While colorants are not significantly biodegraded in effluent treatment plants[187] they can be removed by absorption and/or adsorption on activated sewage sludge and precipitation agents[188]. A sequential process, involving anaerobic degradation of azo dyes to free amines, followed by aerobic degradation of the amines, has been proposed[189].

The efficiency of waste treatment is measured by reduction in Biological Oxygen Demand (BOD) and, to a lesser extent, by Chemical Oxygen Demand (COD). However, these measures do not take into account the chemistry of mixed wastes that sometimes, including for aromatic amines, lead to products that are more toxic and refractory than those released from individual manufacturing processes. The principal adsorbant for removal of refractory waste is activated carbon, which has been used on a large scale for treatment of dye-manufacture waste during or following secondary treatment[190–192]. For example, the PACT process developed by DuPont in the 1970s involved addition of powdered activated carbon to activated sludge[193]. The use of powdered activated carbon was investigated by the EPA at its Test and Evaluation Facility in Cincinnati from July 1981 to January 1983. The process, while effective, involves loss of the activated carbon[194]. A continuous activated-carbon process using granulated carbon, with regeneration, was introduced by American Cyanamid, at Bound Brook, New Jersey, mainly for treatment of aromatic waste, including dyes, in 1977. However, it also suffered from loss of carbon during regeneration[195].

The resistance of azo dyes to biodegradation continues to receive considerable attention and is relevant here since color loss is brought about through reductive cleavage of the azo bond with formation of aromatic amines[196]. Typical amino products from anaerobic reduction of azo dyes by microorganisms are mono- and disulfonated naphthalene derivatives with a hydroxy group *ortho* to an amino group. The oxygen-sensitive substituted *o*-aminohydroxybenzenes and *o*-aminohydroxynaphthalenes degrade under aerobic conditions. Autoxidation products from three aminohydroxybenzenes, following exposure to air at neutral pH, were compared to the behavior of the *o*-aminohydroxynaphthalenes and their products in the presence of activated sludge under aerobic conditions. With activated sludge, there was biological conversion of one autoxidation product[197]. Analysis of an aerobic azoreductase on the genetic level has been undertaken, with molecular cloning and characterization of the gene coding for azoreductase from *Bacillus* sp. OY1-2 isolated from soil and from *Xenophilus azovorans* KF46F[198, 199].

Mineralization to carbon dioxide is also possible, generally under anaerobic conditions, with non-specific microorganisms acting on dyes. Redox mediators, such as flavins and quinones, that are enzymatically or chemically reduced, often participate. Other redox mediators include anthraquinone-2,6-disulfonic acid **(50a)** and anthraquinone-2-sulfonic acid **(50b)**, as well as riboflavin[200]. Breakdown under aerobic conditions requires specific microorganisms. Under aerobic conditions, aniline is broken down by activated sludge, or by seeding with sewage, sometimes without acclimation, within four weeks. It is employed as a benchmark for chemical aerobic biodegradability tests, as well as a representative aryl amine pollutant[201–210]. Aniline degrades slowly under anaerobic conditions[211], as observed in reactors[212]. Just 10% biodegradation was found in ten days, including a 28-day lag, with a sewage inoculum[213]. Aniline is completely degraded by bacteria in river mud and sediments in 20 days[214].
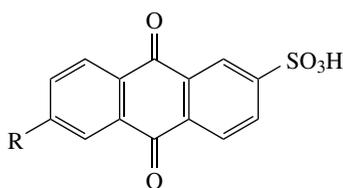
(50a) R = SO$_3$H
(50b) R = H

B. Surface Waters

Aniline in surface waters, including rivers, ponds and lakes, has been detected in concentrations of up to 12 ppb. Adsorption to suspended solids and sediment is expected. In surface waters aniline is broken down by biodegradation and, to a lesser extent, by photooxidation (half-life of the order of days). It does not bioaccumulate in fish. Biodegradation of between 70 and 100% during several days has been reported. While the Henry's Law constant, 2.02×10^{-6} atm-cu m^{-1} mole, suggests ready volatilization from surface waters, the pK_a value of 4.6 indicates that this will be restricted as a result of protonation.

Studies on mechanisms and pathways for aniline degradation and elimination include autoxidation, evaporation, which is very slow from surface waters, formation of nitro products and chemical binding. Degradation in pond water taken from a shallow eutrophic pond at Cook College, New Brunswick, in New Jersey, was followed by GC/MS analysis. Biodegradation was the main destructive mechanism, a process enhanced by addition of activated sewage sludge from a treatment plant adjacent to the former American Cyanamid Bound Brook facility[215]. Degradation has been observed to take place rapidly in surface waters located in industrial areas, but hardly at all in cleaner waters, suggesting that microorganisms can acclimate in the presence of the amine or other contaminants. Aniline has a half-life in distilled water of one week, and in near-black surface water in May sunshine of 4 to 8 h. Photosensitized conversion of aniline to azobenzene, in low yield, 0.2% or less, has been observed. Humic substances act as sensitizers[216].

Strong UV bands at 285 nm, and extension of absorption beyond 290 nm, suggests breakdown by direct photolysis in water[217]. In one study, only 0.7% oxidation was found after 4 h exposure to sunlight[218]. Photodegradation in aquatic environments of chlorinated congeners has been reported for *p*-chloroaniline **(44b)**, 2,4- and 3,4-dichloroanilines, and 2,4,5-trichloroaniline. Much of the research has been stimulated by concern over pesticide degradation of chlorinated anilines. Short-term incubation, of up to 3 days, did not bring

about microbial degradation[219–227]. This indicates that halogens and other substituents reduce the rate of microbial breakdown. Microbial breakdown of 3,4-dichloroaniline has been followed in natural waters[182, 228]. For pure culture and environmental water samples, the rates decrease in the order: aniline (**1**) > 3-bromoaniline > 3-chloroaniline(**4a**) > 3-methylaniline > 3-methoxyaniline(**6b**) > 3-nitroaniline(**2b**) > 3-cyanoaniline[229, 230].

Determinations of degradation of benzidine (**10a**) in wastewater have been undertaken with GC/MS[231]. This has been adapted to general studies of degradation of aromatic amines in water[232]. Diazotization provides a useful test for the presence of free aromatic amines in natural waters and waters destined for human consumption. Quantitative determination of the azo products is measured colorimetrically[233].

Substituted *p*-phenylenediamine photographic developers are discharged to surface waters, particularly during the summer, when the flow of rivers is at their lowest. However, they appear to be lost by biodegradation or capture of breakdown products on sludge.

Quantitative GC/MS analysis, with high recovery, of anilines, including methoxy and chloro derivatives, in river water, sediment and fish samples has been reported. However, recovery was poor for 3,4-xylidine (**51**), and *m*- and *p*-anisidine (**52a** and **52b**)[234]. Analytical methods applicable to colorants and amines have been reviewed[235].

(**51**) (**52a**) R^1 = OMe, R^2 = H
         (**52b**) R^1 = H, R^2 = OMe
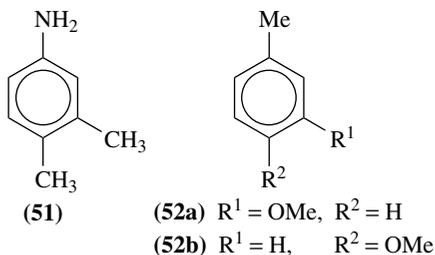
C. Atmospheric Releases

The vapor pressure of aniline (0.67 mm Hg at 25 °C) indicates that if released to the atmosphere, it will exist as a vapor. Aniline is a semivolatile organic compound in the ambient atmosphere, degraded by photochemically-produced hydroxyl radicals. The estimated half-life varies generally from 3.3 to 4 h[236].

D. Soil Contamination

If spilled on land, aniline will undergo a combination of biodegradation, oxidation and chemical binding to components of soil, subject to the condition of the soil. The ratio of the chemical adsorbed per unit weight of organic carbon in the soil or sediment to the concentration of the chemical in solution at equilibrium is K_{oc}. A mean K_{oc} value of 55 for the soil or sediment adsorption coefficient has been calculated for aniline in sewage sludges, which indicates high to moderate mobility in soil. Adsorption is pH-dependent[237]. Aniline bound to humic material will undergo oxidation. Bacteria and fungi cause degradation. The half-life for mineralization to carbon dioxide is less than one week[238a].

Aniline is released in the presence of denitrifying and methanogenic microbial activity[238b]. The pK_a value suggests that in moist soils, aniline will be protonated, and bound to soil, which inhibits degradation. Volatilization does not take place from dry soils, based on the vapor pressure. Studies have been made on the metabolism of aniline-derived products, such as herbicides and fungicides, in soil. Chloroanilines bind to organics in

soil and sediment[239–250]. Reductive deamination of halogenated anilines has been shown to take place during anaerobic microbial degradation[251]. The degradation of 2-nitroaniline (**2a**) to 2-nitrophenol by the bacterium *Nocardai* sp. has been reported. Hydroxylation also occurs with *p*-chloroaniline (**44b**)[252].

Nitroaniline herbicides require for their action incorporation into soil, in order to prevent breakdown. A number of aniline-derived agrochemicals have caused environmental problems, including damage to crops, promotion of resistance and human health difficulties. High doses of the benzimidazole fungicide Benomyl, for example, have caused eye birth defects[253]. The metabolic pathways of amine-derived herbicides have been reviewed[254]. Toxicological aspects of agrochemicals are discussed in Chapter 16.

VIII. REGULATION AND LEGISLATION

A. Britain and the US

In Britain, the 1967 Carcinogenic Substances Regulation placed restrictions on manufacture and use of certain aryl amines[255]. In the US, the toxicity of aromatic amines came under scrutiny after 1970, when Congress passed the Occupational Safety and Health Act. Aromatic amines, including 2-naphthylamine (**8**) and benzidine (**10a**), comprised eight of the fourteen chemicals controlled by the second emergency standard issued by the OSHA[256].

In Europe, similar concerns over the workplace and environmental impacts of dyes and intermediates used in their manufacture led to the founding in 1974 of the Ecological and Toxicological Association of the Dyestuff Manufacturing Industry (ETAD). In 1976, the US EPA implemented the Toxic Substances Control Act. These initiatives led to renewed screening and evaluation campaigns, studies on threshold exposure that caused sensitization, and of effective doses that interact with target organs. The US National Institute of Occupational Safety and Health (NIOSH) chose 58 potentially carcinogenic substances for review and recommendations for workplace standards[257–259]. Of these 58 substances, 23 were dyes and dye intermediates, and of nine classes of chemicals containing known carcinogens and mutagens, aromatic amines and azo dyes were listed as one class.

The American 'Dye Industry ad hoc Committee on NIOSH (carcinogen project)' was established, also in 1976, to determine the significance of the NIOSH project and of the inclusion of a large number of dyes on the list. The dye industry's NIOSH committee and the Synthetic Organic Chemical Manufacturers Association (SOCMA) established a joint Ad Hoc Dyes Ecology Group, in December 1976. The US Dyes Environmental and Toxicology Organization, Inc. (DETO), founded in 1977, established a classification task force. This included an evaluation of the health risks posed by benzidine azo dyes. The starting amines, benzidines **10a**, **10b** and **10d**, and their hydrochloride salts, tested positive in mutagenecity tests, as did a number of the colorants. However, for colorants, the presence of impurities made it impossible to determine the ultimate causes of tumors[260]. A similar study covered a wider range of azo dyes[261].

In 1980, DETO turned its attention to the Fifth Report of the Toxic Substances Control Act Interagency Testing Committee, published in December 1979, which included the recommendation that environmental fate and effects tests be done on **10a**, **10b** and **10d**. Out of over 300 intermediates screened under a US Government carcinogenesis bioassay program, only aromatic amines or their derivatives, six in number, were associated with induction of splenic and peritoneal sarcoma, generally a rare tumor in rats. These six were: aniline hydrochloride, *p*-chloroaniline (**44b**), azobenzene, *o*-toluidine hydrochloride, dapsone (**39**), and the dye known as D & C Red No. 9. In addition, methemoglobinemia was produced by aniline hydrochloride, **38**, **39** and **44b**. No conclusions were drawn on possible mutagenic, cell-transforming and DNA-damaging capabilities[262, 263].

B. Risks to Workers and Consumers

Since the latency period associated with bladder cancer runs into decades, epidemiological studies, screening and occupational monitoring have continued since around 1980[264]. The mortality and risk of bladder cancer among workers previously exposed to 2-naphthylamine has been compared with the general population[265, 266]. A thirty-year follow-up of workers at the former Carwin facility in North Haven, Connecticut, where manufacture of benzidine had been carried out since 1946, found significant excess of bladder cancer, though a decline among those employed after 1950, due to the introduction of preventive measures and the development of a method for rapid determination of benzidine and its metabolites in urine[267].

Risks to consumers of products that incorporate azo colorants have been reviewed, including those with the potential to release any one of 14 aryl amines classified as category 1 or 2 carcinogens according to European Commission Public Health Directive 76/769/EEC[268]. Based on animal data, the risk levels from release of **10a** and its congeners during chronic exposure in a variety of goods, particularly involving entry to the body through the skin, have been considered[269]. Permanent hair dyes, notably those that are darker-colored, and that release amines such as *p*-phenylenediamine (**53**), are associated with increased risk of bladder cancer and adult leukemia through skin adsorption.

$$NH_2$$

$$NH_2$$

(53)

IX. AROMATIC AMINES AS DIETARY CARCINOGENS

In 1977, Sugimura and coworkers found the first of a new class of aromatic heterocyclic amines (HCAs) on cooked fish and meat[270]. This product, 2-amino-1-methylimidazo [4,5 *f*]quinoline (IQ) (**54**), is a carcinogen in animals. It forms a genotoxic *N*-nitroso derivative, N-NO-IQ. Mutagenic activity, as detected by the Ames/*Salmonella* test system, suggests a risk of breast and colon cancer. The HCAs are obtained from foods containing creatine, that afford the *ortho*-aminomethylimidazo ring[271]. This opened a new area for the investigation of aryl amines in the study of cancer.

The mutagenic/carcinogenic food-derived heterocyclic amines appear during pyrolysis of creatine, amino acids and proteins. They are aminoimidazoazaarenes (AIAs), including IQ (**54**), MeIQ (**55**) and MEIQ$_x$ (**56**). *N*-Oxidative metabolism of the glucuronide conjugate of the 2-hydroxyamino derivative of **56** has been shown to take place in human urine[272]. Sulfamate and glucuronide phase II conjugates of **56** appear in the urine of SD rats; metabolism is influenced by dose and cytochrome P-450 induction[273]. Metabolic activation of these carcinogens by human liver and colon has been compared with **13** and **19**[274]. A recent study examines the impact of **56** and of cigarette smoke on cytochrome P-450 mutagenic activation of carcinogens and glucuronidation in rat liver[275].

While the HCA concentration is low, at the ppb level, the carcinogenicity may be enhanced by polyunsaturated oils. Since high-fat western diets may promote aryl amine cancer, considerable importance is attached to the roles of HCAs and the related food-derived PhIP, or 2-amino-1-methyl-6-phenylimidazo[4,5-*b*]pyridine (**57**), in the etiology of cancer. The mechanisms are similar to those encountered with other tumor-forming

IQ
(54)

MeIQ
(55)

MeIQ$_x$
(56)

PhIP
(57)
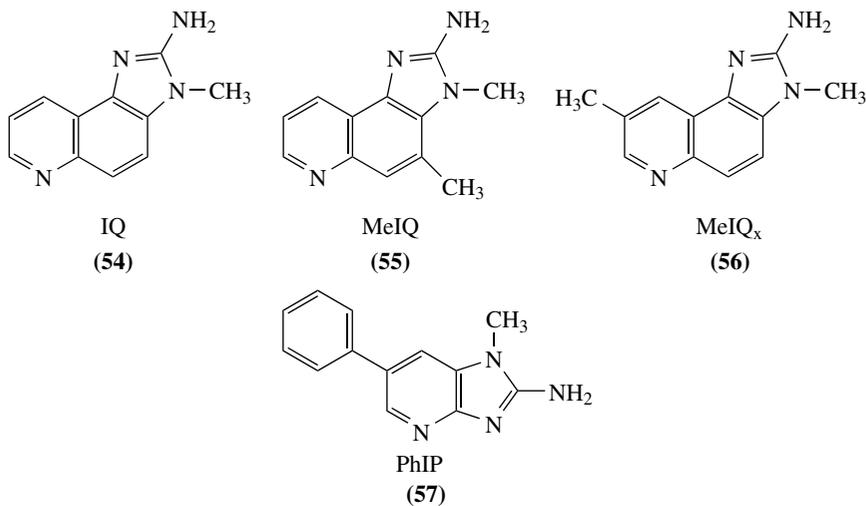
aromatic amines. Both expressed human cytochrome P-450IAI and P-450IA2 enzymes activate these amines by N-hydroxylation to mutagens in the Ames test[94]. P-450IA2 possibly plays a major role in the activation of food-derived amines in the liver[276, 277]. Dietary amines, including **54**, appear to be bioactivated by the enzyme P-450 PA (phenacetindeethylase)[278].

However, carcinogenecity may be reduced by antioxidants, including vegetables, soy and polyphenol teas. Detoxification follows the formation of glucuronides through the action of phase II enzymes, isozymes of UDP-UGTs (glucuronosyltranferases) or of glutathione S-transferases, affording conjugated polar derivatives[279]. Thus glucuronidation may contribute to the elimination of CYP-mediated reactive intermediate metabolites, thereby preventing a toxic event. Yueh and coworkers have analyzed human UGTs for their ability to modulate the carcinogenic actions of N-hydroxyaryl amines formed by CYP1A2. Recombinant human UGT1A9 glucuronidated N-hydroxy-2-AAF **(21)** appears to control the outcome of a genotoxic response. Moreover, the results indicate that while a potential toxicant such as 2-hydroxyamino-1-methyl-6-phenylimidazo(4,5-b)pyridine (N-hydroxy-PhIP) can serve as substrate for glucuronidation, its biological actions can override the detoxification pathway that prevents the mutagenic episode[280]. Aryl amines are strong bacterial mutagens[281, 282].

Metabolic activation, with formation of DNA adducts, induces mutagenecity and carcinogenecity of HCA. There have been numerous studies of DNA adducts of HCAs[283]. Oxidative metabolism through activation of HCAs by rat and human liver microsomes and by purified rat and human cytochrome P-4501A2, followed with esterification by acetyltransferases and sulfotransferases, enables DNA binding and mutagenesis[284]. The nature of HCA–DNA adducts and their connections with mutagenic events has focused on AIA–DNA adducts. A few studies have reported the detection of AIA–DNA adducts in human tissues, though routine detection of these adducts for biomonitoring of exposure to AIAs is not so far possible. AIAs form adducts with the guanine base, mainly at the C8 position. Two AIAs, **54** and **55**, also form minor adducts at the N^2 position of guanine. Mutation spectra induced by AIA–guanine adducts have been reported. The enzyme CYP1A2 has high specificity and catalytic activity in N-hydroxylation of AIAs. However, other metabolizing enzymes may also be involved.

Reversible inhibition of aryl amine *N*-acetyltransferase by S-nitrosothiols has been demonstrated[285]. Aryl amine *N*-acetyltransferase variants generated by random mutagenesis have been identified[286]. Urinary mutagenecity has been correlated with heterocyclic amines and polycyclic aromatic hydrocarbons from fried red meat[287].

Loss of heterozygosity of 8p22 when *N*-acetyltransferase 2 (NAT2) is mapped to 8p22 is associated with increased risk of bladder cancer. The polymorphic NAT2 and chromosome 8 were evaluated in sequential tumors from bladder cancer patients to determine if NAT2 alterations increase the risk of progression in transitional cell carcinoma. Though no association was found between loss of NAT2 and risk of progression, a high rate of polysomy of chromosome 8 implied that other genes on this chromosome influence disease progression[288, 289]. The presence of 4-aminobiphenyl (**13**) in tobacco smoke places smokers at higher risk of bladder cancer[290]. Several recent reviews of food-derived HCAs discuss their roles in mutagenesis and carcinogenesis[291–297].

X. CONCLUSION

The aromatic amines are, in general, toxic chemicals that should be handled with great care. The main acute affect associated with exposure to aniline is increase in methemoglobin level in blood, leading to cyanosis and central nervous system symptoms. For a number of amines, mutagenic injury to humans has been established, particularly in the cases of 2-naphthylamine and benzidine, both formerly produced on a large scale. The latency period for these xenobiotics may last a decade or more. The anilines become genotoxic after first being metabolized by the cytochrome P-450 oxidase family present in tissues such as the liver. The mechanism has been established, based on phase I *N*-hydroxylation and phase II esterification. The enzyme CYP1A2 has the highest specificity and catalytic activity for the phase I process. Mutagenesis invariably, and ultimately, leads to carcinogenesis.

Aromatic amines are released during biodegradation and metabolism of azo dyes. More recently, they have been detected as AIAs following the cooking of meat and fish. Bioactivation of heterocyclic amines leading to AIA–DNA adducts, involving activation through phase I and phase II, and mutations, is almost identical with the processes found with other aromatic amines.

Aniline is photo- and biodegradable and oxidizable in surface waters and sewage sludges. Other aromatic amines, including chloroanilines and benzidine, are less biodegradable, or highly resistant, even when treated with activated sludge. Photodegradation is the main route of aniline degradation in the atmosphere, and of chloroanilines in water.

XI. REFERENCES

1. 'Petition Requesting a Zero Tolerance for Ten Carcinogens Through an Emergency Temporary Standard Issued Under the Authority of the Occupational Safety and Health Act,' Health Research Group, and Oil, Chemical and Atomic Workers, International Union, Washington DC, 1973.
2. *Aromatic Amines: An Assessment of the Biological and Environmental Effects*, Committee on Amines, Board on Toxicology and Environmental Health Hazards, Assembly of Life Sciences, National Research Council, Washington DC, 1981.
3. Toxic profiles database, http://www.atsdr.cdc.gov/toxprofiles/tp62-c9.pdf (for benzidine); National Library of Medicine Hazardous Substances Data Bank; and databases of IRIS, CCRIS and RTECS.
4. H. G. Parkes and A. E. J. Evans, in *Chemical Carcinogens*, 2nd edition, ACS Monograph 182 (Ed. C. E. Searle), American Chemical Society, Washington DC, 1984, pp. 277–301.
5. R. C. Garner, C. N. Martin and D. B. Clayson, in Reference 4, pp. 175–276.

6. P. D. Josephy, B. Mannervik and P. Ortiz de Montellano, *Molecular Toxicology*, Oxford University Press, Oxford, 1997.
7. E. C. Miller and J. A. Miller, in *Chemical Carcinogens*, ACS Monograph 173 (Ed. C. E. Searle), American Chemical Society, Washington DC, 1976, pp. 737–762.
8. A. F. Mangelsdorff, *Ind. Med. Surg.*, **21**, 395 (1956).
9. D. O. Hamblin and A. F. Mangelsdorff, *J. Ind. Hyg.*, **20**, 523 (1938).
10. W. P. Reynolds, M. G. Roell and J. J. Fleming, 'Methemoglobin inducing potential of various substituted anilines in rats'. Toxicology Section of Hoechst-Roussel Pharmaceuticals, Incorporated, unpublished company data (1984). Cited in *Federal Register*, **53**, no. 161, Friday, August 19, 31804 (1988).
11. R. C. Hirt, F. T. King and R. G. Schmitt, *Anal. Chem.*, **26**, 1270 (1954).
12. I. Pacséri, L. Magos and I. A. Bátskor, *A.M.A. Archives of Industrial Health*, **18**, 1 (1957).
13. G. O. Woods and R. G. Anderson, *Am. Ind. Hyg. Assoc. J.*, **46**, 538 (1975).
14. P. R. Young and H. M. McNiar, *J. Chromatogr. A*, **119**, 569 (1976).
15. 'Analytical Procedures for Aniline and Selected Derivatives in Wastewater and Sludge', p. 1, EPA-600/54-84-009 (1984).
16. E. C. Gunderson and C. C. Anderson, *Am. Ind. Hyg. Assoc. J.*, **48**, 634 (1987).
17. T. Otagawa, S. Zaromb and J. R. Stetter, *J. Chromatogr. A*, **408**, 81 (1987).
18. T. Dutkiewicz, *(Medycyna Pracy) Med. Pr.*, **8**, 25 (1957).
19. T. Dutkiewicz and J. K. Piotrowski, *Pure Appl. Chem.*, **3**, 319 (1961).
20. L. Rehn, *Arch. Klin. Chir.*, **50**, 588 (1895).
21. L. Rehn, *Verh. Dtsch. Ges. Chir.*, **35**, 313 (1906).
22. S. C. Leunenberger, *Bruns. Beitr. Klin. Chir.*, **80**, 208 (1912).
23. *International Labour Office. Studies and Reports, Series F., No. 1*, International Labour Office, Geneva, 1921, p. 6.
24. D. A. Hounshell and J. K. Smith, *Science and Corporate Strategy: Du Pont R&D, 1902–1980*, Cambridge University Press, Cambridge, 1988, pp. 555–572.
25. G. H. Gehrmann, *J. Urol.*, **31**, 126 (1934).
26. G. H. Gehrmann, *J. Am. Med. Assoc.*, **107**, 1436 (1936).
27. J. H. Weisburger, *Mutat. Res./Fundamentals and Molecular Mechanisms of Mutagenesis*, **506–507**, 9 (2002).
28. W. C. Hueper, F. H. Wiley and H. D. Wolfe, *J. Ind. Hyg.*, **16**, 255 (1934).
29. W. C. Hueper, *Arch. Pathol.*, **25**, 856 (1938).
30. W. C. Hueper, F. H. Wiley and H. D. Wolfe, *J. Ind. Hyg.*, **20**, 46 (1938).
31. I. Berenblum, *Cancer Review*, **7**, 338 (1932).
32. I. Berenblum and G. M. Bonser, *J. Ind. Hyg.*, **19**, 86 (1937); [I. Berenblum, 'Chemical-Biological Correlation in the Field of Carcinogenesis', in 'First Symposium on Chemical-Biological Correlation', National Research Council, Publication 206, National Academy of Sciences, 1951, 363–369. Draft manuscript, Schoental Archive, Edelstein Center.]
33. *German Dyestuffs and Dyestuffs Intermediates, Including Manufacturing Processes, Plant Design, and Research Data*, FIAT Final Report, no. 1313, PB 85172, Office of Military Government for Germany (US)/Field Information Agency, Technical, Washington, DC, February 1, 1948, p. 401.
34. M. W. Goldblatt, *Br. J. Ind. Med.*, **6**, 65 (1949).
35. T. S. Scott, *Br. J. Ind. Med.*, **9**, 127 (1952).
36. T. S. Scott and M. C. H. Williams, *Br. J. Ind. Med.*, **14**, 150 (1957).
37. T. S. Scott, *Carcinogenic and Chronic Toxic Hazards of Aromatic Amines*, Elsevier, Amsterdam, 1962.
38. S. Spitz, W. H. Maguigan and K. Dobriner, *Cancer*, **3**, 789 (1950).
39. 'Symposium on Industrial Hygiene, Basel, October 11 and 12, 1951', report, Regina Schoental Archive, Edelstein Center, Hebrew University.
40. R. A. M. Case, *Br. J. Ind. Med.*, **10**, 114 (1953).
41. *Chem. Eng. News*, December 28, 31 (1953).
42. *Papilloma of the Bladder in the Chemical Industry*, Association of British Chemical Manufacturers, London, 1953.
43. R. A. Case and J. T. Pearson, *Br. J. Ind. Med.*, **11**, 213 (1954).
44. D. Michaels, *Int. J. Occup. Environ. Health*, **1**, 278 (1995).
45. A. L. Walpole, M. H. C. Williams and D. C. Roberts, *Br. J. Ind. Med.*, **11**, 105 (1954).

46. A. S. Travis, *Dyes Made in America: The Calco Chemical Company, American Cyanamid, and the Raritan River*, Edelstein Center/Hexagon Press, Jerusalem, 2004, pp. 327–332.

47. S. Kumar, G. Taylor, W. Huston, P. Wilson and C. B. Costello, *Br. J. Ind. Med.*, **38**, 167 (1981).

48. L. D. Cassidy, A. O. Youk and G. M. Marsh, *Am. J. Ind. Med.*, **44**, 282 (2003).

49. N. Yamaguchi, H. Tazaki, T. Okubo and T. Toyama, *Am. J. Ind. Med.*, **3**, 139 (1982).

50. E. Delzell, M. Macaluso and P. Cole, *J. Occup. Med.*, **31**, 273 (1989).

51. D. T. Silverman, L. I. Levin, R. N. Hoover and P. Hartage, *J. Natl. Cancer Inst.*, **81**, 1472 (1989).

52. J. H. Weisburger and E. K. Weisburger, *Chem. Eng. News*, February 7, 124 (1966).

53. T. Yoshida, *Trans. Jap. Path. Soc.*, **23**, 636 (1933).

54. R. Kinosita, *Yale J. Biol. Med.*, **12**, 287 (1940).

55. J. W. Orr, *J. Path. Bact.*, **50**, 393 (1940).

56. F. C. Miller and J. A. Miller, *Cancer Res.*, **7**, 468 (1947).

57. R. M. Watrous, *Br. J. Ind. Med.*, **4**, 111 (1947).

58. W. B. Deichmann, K. V. Kitzmiller, F. F. Heyroth and S. Witherup, *J. Ind. Hyg.*, **30**, 71 (1948).

59. I. Nir, in *The Chemistry of the Hydrazo, Azo and Azoxy Groups* (Ed. S. Patai), Vol. 2, Wiley, Chichester, 1997, pp. 701–728.

60. J. F. Treon, H. Wright, K. V. Kitzmiller and W. J. Younker, *J. Ind. Hyg.*, **30**, 79 (1948).

61. A. Wendel, S. Feverstein and K. H. Konz, *Biochem. Pharmacol.*, **28**, 2051 (1979).

62. R. Nery, *Xenobiotica*, **1**, 339 (1971).

63. E. K. Weisburger and J. H. Weisburger, *Adv. Cancer Res.*, **5**, 331 (1958).

64. E. C. Miller and J. A. Miller, in *Accomplishments in Cancer Research 1980* (Eds. J. G. Fortner and J. E. Rhoads), J. B. Lippincott Company, Philadelphia, 1980, pp. 63–98.

65. W. Troll and N. Nelson, *Fed. Proc.*, **20**, 41 (1961).

66. J. A. Miller, C. S. Wyatt, E. C. Miller and H. A. Hartmann, *Cancer Res.*, **21**, 1465 (1961).

67. M. Kiese and H. Uehleke, *Naunyn-Schmiedeberg's Arch. Exp. Path. U. Pharmakol.*, **242**, 117 (1961).

68. (a) J. A. Miller, J. W. Cramer and E. C. Miller, *Cancer Res.*, **20**, 950 (1960).
    (b) E. C. Miller, J. A. Miller and H. A. Hartmann, *Cancer Res.*, **21**, 815 (1961).
    (c) D. Malejka-Giganti and H. R. Gutmann, *Proc. Soc. Exp. Biol. Med.*, **150**, 92 (1975).

69. Cited by Scott, Reference 37, p. 78.

70. (a) Cited by Scott, Reference 37, p. 77.
    (b) G. M. Bonser, D. B. Clayson, J. W. Jull and L. N. Pyrah, *Br. J. Cancer*, **6**, 412 (1952).
    (c) E. Boyland and D. Manson, *Biochem. J.*, **101**, 84 (1966).
    (d) E. Brill and J. L. Radomski, *Life Sci.*, **6**, 2293 (1967).

71. (a) A. L. Walpole and M. H. C. Williams, *Br. Med. Bull.*, **14**, 141 (1958).
    (b) A. L. Walpole, *Acta Unio. Int. Contra Cancrum.*, **19**, 483 (1963).

72. (a) F. Homburger, G. H. Friedell, E. K. Weisburger and J. H. Weisburger, *Toxicol. Appl. Pharmacol.*, **22**, 280 (1972).
    (b) A. B. Russfield, F. Homburger, E. K. Weisburger and J. H. Weisburger, *Toxicol. Appl. Pharmacol.*, **25**, 446 (1973).

73. R. C. Garner, C. N. Martin and D. B. Clayson, in Reference 4, pp. 174–276.

74. G. M. Lower, in *Toxicology and Occupational Medicine, Proceedings of the Tenth Inter-American Conference on Toxicology and Occupational Medicine, Key Biscayne (Miami). Fla, October 22–25, 1978. Developments in Toxicology and Environmental Science*, Elsevier/North-Holland, New York, 1979, pp. 209–219

75. J. L. Radomski, W. L. Hearn, T. Radomski, H. Moreno and W. E. Scott, *Cancer Res.*, **37**, 1757 (1977).

76. C. C. Irving, *Cancer Res.*, **37**, 524 (1977).

77. D. B. Clayson and R. C. Garner, in Reference 7.

78. M. E. McManus, R. F. Minchin, N. D. Sanderson, P. J. Wirth and S. S. Thorgeirsson, *Carcinogenesis*, **4**, 693 (1983).

79. W. E. Durston and B. N. Ames, *Proc. Natl. Acad. Sci.*, **71**, 737 (1974).

80. C. B. Frederick, J. B. Mays, D. M. Ziegler, F. P. Guengerich and F. F. Kadlubar, *Cancer Res.*, **42**, 2671 (1982).

81. C. M. King and W. T. Allaben, in *Conjugation Reactions in Drug Transformation. Proceedings of the Symposium held in Turku, Finland, 1978* (Ed. A. Aitio), Elsevier/North-Holland, New York, 1978, pp. 431–441.
82. K. Abdo, K. M. Wolfe and R. Hiles, *Fed. Proc.*, **43** (3), abstract 1698 (1984).
83. K. M. Abdo, J. Bucher, J. K. Haseman, S. L. Eustis and J. E. Huff, *Proc. Am. Cancer Res., Annu. Meet.*, **30**, 177 (1989).
84. A. A. Akhrem, S. T. Khatyleva, V. M. Shkumatov, V. L. Chashichin and P. A. Kiselev, *Acta Bio. Med. Ger.*, **41**, 1019 (1982).
85. G. Fare and J. W. Orr, *Cancer Res.*, **25**, 1784 (1965).
86. F. F. Kadlubar, J. A. Miller and E. C. Miller, *Cancer Res.*, **36**, 2350 (1976).
87. S. S. Hecht, K. El-Bayoumy, A. Rivenson and E. S. Fialai, *Cancer Lett.*, **20**, 349 (1983).
88. T. Sugimura, *Mutat. Res.*, **376**, 211 (1997).
89. R. C. Gupta, *Proc. Natl. Acad. Sci. U.S.A.*, **81**, 6943 (1984).
90. J. H. Meerman and L. L. van de Poll, *Environ. Health Perspect.*, **102** (suppl. 6), 153 (1994).
91. T. Kamataki, A. Suzuki, H. Kushida, H. Iwata, M. Watanabe, T. Nohmi and K. Fujita, *Cancer Lett.*, **143**, 113 (1999).
92. R. J. Turesky, A. Constable, L. B. Fay and F. P. Guengerich, *Cancer Lett.*, **143**, 109 (1999).
93. R. H. Heflich and R. E. Neft, *Mutat. Res.*, **318**, 73 (1994).
94. M. E. McManus, W. M. Burgess, M. E. Veronese, A. Huggett, L. C. Quattrochi and R. H. Tukey, *Cancer Res.*, **50**, 3367 (1990).
95. M. L. Mendelsohn, L. C. Mohr and J. Peeters, *Biomarkers: Medical and Workplace Applications*, John Henry Press, Washington DC, 1998.
96. G. Talaska and M. Al-Zoughool, *J. Environ. Sci. Health, Part C Environ. Carcinogenesis Ecotoxicol. Rev.*, **21**, 133 (2003).
97. Q. Ma, G. Lin, Y. Qin, D. Lu, K. Golka, F. Geller, J. Chen and J. Shen, *Pharmacogenetics*, **13**, 409 (2003).
98. K. Marshall, *J. Biol. Chem.*, **211**, 499 (1954).
99. G. B. Pliss, *Acta Unio Int. Cancrum*, **19**, 499 (1963).
100. G. B. Pliss, *Gig. Tr. Prof. Zabol.*, **9**, 18 (1965).
101. G. B. Pliss, *Vopr. Onkol.*, **5**, 524 (1959).
102. G. B. Pliss and M. A. Zabezhinsky, *J. Natl. Cancer Inst.*, **45**, 283 (1970).
103. V. M. Lakshmi, N. T. Zenser, F. F. Hsu, M. B. Mattammal, T. V. Zenser and B. B. Davis, *Carcinogenesis*, **17**, 1941 (1996).
104. V. M. Lakshmi, M. B. Mattammal, L. A. Spry, F. F. Kadlubar, T. V. Zenser and B. B. Davis, *Carcinogenesis*, **11**, 139 (1990).
105. K. C. Morton, C. M. King and K. P. Baetcke, *Cancer Res.*, **39**, 3107 (1979).
106. K. C. Morton, F. A. Beland, F. E. Evans, N. F. Fullerton and F. F. Kadlubar, *Cancer Res.*, **40**, 751 (1980).
107. C. N. Martin, F. A. Beland, R. W. Roth and F. F. Kadlubar, *Cancer Res.*, **42**, 2678 (1982).
108. J. C. Kennelly, F. A. Beland, F. F. Kadlubar and C. N. Martin, *Carcinogenesis*, **5**, 407 (1984).
109. C. B. Frederick, C. C. Weiss, T. J. Flammang, C. N. Martin and F. F. Kadlubar, *Carcinogenesis*, **6**, 959 (1985).
110. V. M. Lakshmi, T. V. Zenser, H. D. Goldman, G. G. Spencer, R. C. Gupta, F. F. Hsu and B. B. Davis, *Chem. Res. Toxicol.*, **8**, 711 (1995).
111. S. R. Babu, V. M. Lakshmi, F. F. Hsu, T. V. Zenser and B. B. Davis, *Carcinogenesis*, **16**, 3069 (1995).
112. V. M. Lakshmi, D. A. Bell, M. A. Watson, T. V. Zenser and B. B. Davis, *Carcinogenesis*, **16**, 1565 (1995).
113. V. M. Lakshmi, T. V. Zenser and B. B. Davis, *Drug Metab. Dispos.*, **25**, 481 (1997).
114. T. V. Zenser, V. M. Lakshmi and B. B. Davis, *Drug Metab. Dispos.*, **26**, 856 (1998).
115. T. V. Zenser, V. M. Lakshmi, F. F. Hsu and B. B. Davis, *J. Biol. Chem.*, **274**, 14850 (1999).
116. M. Ciotti, V. M. Lakshmi, N. Basu, B. B. Davis, I. S. Owens and T. V. Zenser, *Carcinogenesis*, **20**, 1963 (1999).
117. T. V. Zenser, V. M. Lakshmi, F. F. Hsu and B. B. Davis, *Drug Metab. Dispos.*, **29**, 401 (2001).
118. E. L. Wynder, J. Onderdouk and N. Mantel, *Cancer*, **16**, 1388 (1963).
119. H. M. Anthony, *J. Soc. Occup. Med.*, **24**, 110 (1974).
120. V. Glezer, in Reference 59, pp. 729–746.

121. J. W. Meigs, L. D. Marrett, F. U. Ulrich and J. T. Flannery, *J. Natl. Cancer Inst.*, **76**, 1 (1986).
122. X. Y. You, J. G. Chen and Y. N. Hu, *Br. J. Ind. Med.*, **47**, 544 (1990).
123. W. Bi, R. B. Hayes, P. Feng, Y. Qi, X. You, J. Zhen, M. Zhang, B. Qu, Z. Fu, M. Chen, H. T. Co Chien and W. J. Blot, *Am. J. Ind. Med.*, **21**, 481 (1992).
124. M. A. Bulbulyan, L. W. Figgs, S. H. Zahm, T. Savitskaya, A. Goldfarb, S. Astashevsky and D. Zaridze, *Int. J. Epidemiol.*, **24**, 266 (1995).
125. R. Ouellet-Hellstrom and J. D. Rench, *J. Occup. Environ. Med.*, **38**, 1239 (1996).
126. N. Rothman, V. K. Bhatnagar, R. B. Hayes, T. V. Zenser, S. K. Kashyap, M. A. Butler, D. A. Bell, V. M. Lakshmi, M. Jaeger, R. Kashyap, A. Hirvonen, P. A. Schultze, M. Dosemeci, F. Hsu, D. J. Parikh, B. B. Davis and G. Talaska, *Proc. Natl. Acad. Sci.*, **93**, 5084 (1996).
127. T. Sorahan, L. Hamilton and J. R. Jackson, *J. Occup. Environ. Med.*, **57**, 106 (2000).
128. F. T. Hatch, M. G. Knize and M. E. Colvin, *Environ. Mol. Mutagen*, **38**, 268 (2001).
129. A. L. Linch, *Am. Ind. Hyg. Assoc. J.*, **35**, 426 (1974). DHHS (NIOSH) Publication No. 90-116 *NIOSH Alert: Preventing Bladder Cancer from Exposure to o-Toluidine and Aniline*, December 1990; http://www.cdc.gov/niosh/90-116.html, updated 3/4/1997.
130. J. S. Bus, *CIIT Activities* (Chemical Industry Institute of Toxicology), **3**, 1 (1983).
131. J. S. Bus and J. A. Popp, *Food Chem. Toxicol.*, August 25, 619 (1987).
132. D. J. McCarthy, W. R. Waud, R. F. Struck and D. L. Hill, *Cancer Res.*, **45**, 174 (1985).
133. Environmental Protection Agency, 40 CFR Part 799, Testing Consent Orders on Aniline and Seven Substituted Anilines, *Federal Register*, **53**, Friday, August 19 (1988).
134. M. F. Khan, B. S. Kaphalia and G. A. Ansari, *J. Toxicol. Environ. Health*, **44**, 415 (1995).
135. M. F. Khan, P. J. Bloor, Y. Gu, N. W. Alcock and G. A. Ansari, *Fundam. Appl. Toxicol.*, **35**, 22 (1997).
136. M. F. Khan, X. Wu, B. S. Kaphalia, P. J. Bloor and G. A. Ansari, *Toxicol. Lett.*, June 16, 31 (1997).
137. M. F. Khan, S. M. Green, G. A. Ansari and P. J. Bloor, *Toxicol. Sci.*, **42**, 64 (1998).
138. M. F. Khan, X. Wu, P. J. Bloor and G. A. Ansari, *Toxicol. Sci.*, **48**, 134 (1999).
139. M. F. Khan, X. Wu, N. W. Alcock, P. J. Bloor and G. A. Ansari, *J. Toxicol. Environ. Health A*, **57**, 173 (1999).
140. M. F. Khan, X. Wu and G. A. Ansari, *J. Toxicol. Environ. Health A*, **60**, 263 (2000).
141. M. F. Khan, X. Wu, G. A. Ansari and P. J. Bloor, *J. Toxicol. Environ. Health A*, **66**, 93 (2003).
142. M. F. Khan, X. Wu and J Wang, *Toxicol. Appl. Pharmacol.*, **187**, 22 (2003).
143. M. F. Khan, X. Wu, B. S. Kaphalia, P. J. Boor and G. A. Ansari, *Toxicology*, **194**, 95 (2003).
144. L. Ciccoli, M. Ferrali, V. Rossi, C. Signorini, C. Alessandrini and M. Comporti, *Toxicol. Lett.*, October 29, 57 (1999).
145. K. I. Masumura, Y. Totsuka, K. Wakabayashi and T. Nohmi, *Carcinogenesis*, **24**, 1985 (2003).
146. T. Kawamori, Y. Totsuka, N. Uchiya, T. Kitamura, H. Shibata, T. Sugimura and K. Wakabayashi, *Carcinogenesis*, **25**, 1967 (2004).
147. M. Kiese, E. Rauscher and W. Nikolaus, *Naunyn-Schmiedebergs Arch. Exp. Pathol. Pharmacol.*, **254**, 253 (1966).
148. US Occupational Safety & Health Administration (OSHA) Method no. PV2064. Occupational Safety & Health Administration, OS Department of Labor, 996, http://www.osha~slc.gov/dts/sltc/methods/partial/pv2064/pv2064.html
149. E. Ward, A. Carpenter, S. Markowitz, D. Roberts and W. Halperin, *J. Natl. Cancer Inst.*, **83**, (1991).
150. C. Sellers and S. Markowitz, *Regul. Toxicol. Pharmacol.*, December 16, 301 (1992).
151. E. M. Ward, G. Sabbioni, D. G. DeBord, A. W. Teass, K. K. Brown, G. G. Talaska, D. R. Roberts, A. M. Ruder and R. P. Streicher, *J. Natl. Cancer Inst.*, **88**, 1046 (1996).
152. S. B. Markowitz and K. Levin, *J. Occup. Environ. Med.*, **46**, 154 (2004).
153. N. Danford, *Mutat. Res. Rev. Genet. Toxicol.*, **258**, 207 (1991).
154. A. W. Teass, D. G. DeBord, K. K. Brown, K. L. Cheever, L. E. Stettler, R. E. Savage, W. W. Weigel, D. Dankovic and E. Ward, *Int. Arch. Occup. Environ. Health*, **65**, S115 (1993).
155. H. Kopelman, M. H. Robertson, P. G. Sanders and I. Ash, *Br. Med. J.*, **1**, 514 (1966).
156. H. Kopelman, P. J. Scheuer and R. Williams, *Q. J. Med.*, **25**, 553 (1966).
157. R. Schoental, *Nature*, **219**, 1162 (1968).

158. R. Schoental, *Isr. J. Med. Sci.*, **4**, 1146 (1968).
159. A. Selden, P. Berg, R. Jakobsson and J. de Laval, *Int. Arch. Occup. Environ. Health*, **63**, 403 (1992).
160. G. M. Liss and S. S. Guirguis, *Am. J. Ind. Med.*, **26**, 117 (1994).
161. *Federal Register*, **57**, 35630, 8 October (1992). http://www.atsdr.cdc.gov/toxprofiles/tp122-c8.pdf
162. E. Bailey, A. G. Brooks, I. Bird, P. B. Farmer and N. B. Street, *Anal. Biochem*, **190**, 17X (1990).
163. E. J. Lazaer and S. C. Louie, *Cancer Lett.*, **4**, 21 (1978).
164. S. R. Babu, V. M. Lakshmi, G. P. W. Huang, T. V. Zenser and B. B. Davis, *Biochem. Pharmacol.*, **51**, 1679 (1996).
165. M. A. Butler, F. P. Guengerich and F. F. Kadlubar, *Cancer Res.*, **49**, 25 (1989).
166. G. J. Hammons, K. L. Dooley and F. F. Kadlubar, *Chem. Res. Toxicol.*, **7**, 829 (1994).
167. S. Kimura, M. Kawabe, J. M. Ward, H. Morishama, F. F. Kadlubar, G. J. Hammons, P. Fernandez-Salguero and F. J. Gonzalez, *Carcinogenesis*, **20**, 1825 (1999).
168. R. P. Bos, R. M. E. Browns, R. Van Dorn, J. L. G. Theuws and P. Henderson, *Toxicology*, **16**, 113 (1980).
169. M. J. Stasik, *Int. Arch. Occup. Environ. Health*, **60**, 21 (1998).
170. W. Popp, W. Schmieding, M. Speck, C. Vahrenholz and K. Norpoth, *Br. J. Ind. Med.*, **49**, 529 (1992).
171. L. D. Dial, D. K. Anestis, S. R. Kennedy and G. O. Rankin, *Toxicology*, **131**, 109 (1998).
172. H. Oettel, H. Frohberg, N. Nothdurft and G. Wilhelm, *Arch. Toxicology*, **21**, 9 (1965).
173. R. Anliker and E. A. Clarke, *Chemosphere*, **9**, 595 (1980).
174. R. S. Yamamoto, H. L. Richardson, E. K. Weisburger, J. H. Weisburger, T. Benjamin and C. T. Bahner, *J. Natl. Cancer Inst.*, **51**, 1313 (1973).
175. H. Druckrey, R. Preussmann, D. Schmähl and G. Blum, *Nauturwissenschaften*, **48**, 722 (1961).
176. G. F. Kolar, in Reference 4, pp. 868–914.
177. (a) D. C. Bomberger and R. L. Boughton, *Wastes from Manufacture of Dyes and Pigments (Benzidine and Its Congeners Subsector)*, SRI International, Menlo Park, California, 1981, p. 43. Citing B. Dieckhues, *Zentralbl. Bakteriol. Parasitenled.*, **180**, 244 (1961).
(b) *Toxicological Profile for Benzidine*, US Department of Health and Human Services. Public Health Service. Agency for Toxic Substances and Disease Registry, Atlanta, Georgia, September 2001.
178. M. L. Richardson, K. Webb and T. Gough, *Ecotoxicol. Environ. Safety*, **4**, 207 (1980).
179. H. W. Malaney, *J. Water Pollut. Control Fed.*, **32**, 1300 (1960).
180. G. W. Malaney, P. A. Lutin, J. J. Cibulka and L. H. Hickerson, *J. Water Pollut. Control Fed.*, **39**, 2020 (1967).
181. H. H. Tabak and E. F. Barth, *J. Water Pollut. Control Fed.*, **50**, 552 (1978).
182. L. A. Games and R. A. Hites, *Anal. Chem.*, **49**, 1433 (1977).
183. P. Pitter, *Water Res.*, **10**, 231 (1976).
184. OECD Chemicals Testing Programme: Degradation/Accumulation Group. Commission of the European Communities Report no. EYR 8631 EN (1983).
185. C. D. Lyons, S. Katz and R. Bartha, *Appl. Environ. Microb.*, **48**, 491 (1984).
186. E. P. Huhn and J. M. Suflita, *Environ. Toxicol. Chem.*, **8**, 1149 (1989).
187. D. A. Gardner, T. J. Holdsworth, G. M. Shaul, K. A. Dostol and L. D. Betowski, *Aerobic and Anaerobic Treatment of C.I. Disperse Blue 79 Report*, EPA, 600/S2-89/051, Washington DC, 1990.
188. D. Brown and P. Laboureur, *Chemosphere*, **12**, 397 (1983).
189. S. Seshadri, P. L. Bishop and A. M. Agha, *Waste Manage.*, **14**, 127 (1994).
190. A. Reife, in *Kirk-Othmer Encyclopedia of Chemical Technology*, 4th edn., Vol. 8, Wiley, New York, 1993, pp. 753–783.
191. A. Reife, D. Betowski and H. S. Freeman, in *Encyclopedia of Environmental Analysis and Remediation* (Ed. R. A. Myers), Wiley, New York, 1998, pp. 1442–1165.
192. A. Reife and H. S. Freeman (Eds.), *Environmental Chemistry of Dyes and Pigments*, Wiley, New York, 1995.
193. D. G. Hutton, 'DuPont PACT Process: Performance and Results from the Chambers Works,' E.I. du Pont de Nemours & Co., Inc., 1979.

194. G. M. Shaul, M. W. Barnett and K. A. Dostal, in *Proceedings of the 37th Industrial Waste Conference, 1981, Purdue University*, Ann Arbor Science Publishers, Ann Arbor, Mich., 1982, pp. 677–689.
195. A. C. Marek Jr. and M. A. Pikulin, in *Proceedings of the 33rd Industrial Waste Conference, 1978, Purdue University*, Ann Arbor Science Publishers, Ann Arbor, Mich., 1979, pp. 105–112.
196. A. Stolz, *Appl. Microb. Biotech.*, **56**, 69 (2001).
197. M. Kudlich, M. J. Hetheridge, H. J. Knackmuss and A. Stolz, *Environ. Sci. Technol.*, **33**, 896 (1999).
198. Y. Suzuki, T. Yoda, A. Ruhul and W. Sugiura, *J. Biol. Chem.*, **276**, 9059 (2001).
199. S. Blümel, H. K. Knackmuss and A. Stolz, *Appl. Environ. Microbiol.*, **68**, 3948 (2002).
200. A. B. Dos Santos, I. A. Bisschops, F. J. Cervantes and J. B. van Lier, *Chemosphere*, **55**, 1149 (2004).
201. P. Pitter, *Water Res.*, **10**, 231 (1976).
202. *An Index of Refractory Organics*, USEPA-600/2-77-174 (1977).
203. P. Gerike and W. K. Fischer, *Ecotoxicol. Environ. Safety*, **3**, 159 (1979).
204. M. Kawasaki, *Ecotoxicol. Environ. Safety*, **4**, 444 (1980).
205. R. Zahn and H. Z. Wellens, *Z. Wasser Abwasser Forsch.*, **13**, 1 (1980).
206. J. L. Means and S. J. Anderson, *Water Air Soil Pollut.*, **16**, 301 (1981).
207. F. Korte and W. Klein, *Ecotox. Environ. Safety*, **6**, 311 (1982).
208. P. A. Gilbert and C. M. Lee, in *Biotransformation and Fate of Chemicals in the Aquatic Environment* (Eds. A. W. Maki, K. L. Dickson and J. Cairns), University of Michigan, Pellston, MI, 1980, pp. 34–45.
209. W. Schefer and O. Walechli, *Z. Wasser Abwasswer Forsch.*, **13**, 205 (1980).
210. D. Freitag, H. Geyer, A. Kraus, R. Viswanathan, D. Kotzias, A. Attar, W. Klein and F. Korte, *Ecotoxicol. Environ. Safety*, **6**, 60 (1982).
211. F. C. Miller, R. Zisook and R. Zepp, *J. Agric. Food Chem.*, **28**, 1053 (1980).
212. R. E. Speece, *Environ. Sci. Technol.*, **2**, 557 (1983).
213. L. E. Hallas and M. Alexander, *Appl. Environ. Microbiol.*, **45**, 1234 (1983).
214. D. Calamari, R. D. Gasso, S. Galassi, A. Provini and M. Vighi, *Chemosphere*, **9**, 753 (1980).
215. C. D. Lyons, S. Katz and R. Bartha, *Appl. Environ. Microbiol.*, **48**, 491 (1984).
216. R. G. Zepp, G. L. Baughman and P. F. Schlotzhauer, *Chemosphere*, **10**, 109 (1981).
217. P. Méallier, *Ann. Chim.*, **4**, 15 (1969).
218. W. M. Draper and D. G. Crosby, *Arch. Environ. Contam. Toxicol.*, **12**, 121 (1983).
219. H.-M. Hwang, R. E. Hodson and R. F. Lee, *Appl. Environ. Microbiol.*, **50**, 1177 (1986).
220. H.-M. Hwang, R. E. Hodson and R. F. Lee, *Water Res.*, **21**, 309 (1987).
221. H.-M. Hwang and S. W. Maloney, *Bull. Environ. Contam. Toxicol.*, **56**, 343 (1996).
222. H.-M. Wang, D. McCullum and L. Slaughter, *Bull. Environ. Contam. Toxicol.*, **60**, 81 (1998).
223. J. D. Rosen, M. Slewierski and G. Winnett, *J. Agric. Food Chem.*, **18**, 494 (1970).
224. G. Engelhardt, P. Wallnofer, G. Fuchsbichler and W. Baumerster, *Chemosphere*, **6**, 85 (1977).
225. R. D. Minard, S. Russel and J.-M. Bollag, *J. Agric. Food Chem.*, **25**, 841 (1977).
226. I.-S. You and R. Bartha, *J. Agric. Food Chem.*, **30**, 274 (1982).
227. D. D. Kaufman, J. R. Plimmer and U. I. Klingebiel, *J. Agric. Food Chem.*, **21**, 127 (1973).
228. P. C. Kearney and J. R. Plimmer, *J. Agric. Food Chem.*, **20**, 584 (1972).
229. D. F. Paris and N. L. Wolfe, *Environ. Microbiol.*, **53**, 911 (1987).
230. H. Reber, V. Helm and N. G. K. Karanth, *Eur. J. Appl. Microbiol.*, **7**, 181 (1979).
231. R. L. Jenkins and R. Baird, *Bull. Environ. Contam. Toxicol.*, **13**, 436 (1975).
232. R. Baird and R. L. Jenkins, *J. Water Pollut. Control Fed.*, **49**, 1609 (1977).
233. M. A. El-Dib, *Journal AOAC*, **54**, 1383 (1971).
234. T. Okumura, K. Imamura and Y. Nishikawa, *J. Chromat. Sci.*, **34**, 190 (1996).
235. K. Venkataraman (Ed.), *The Analytical Chemistry of Synthetic Dyes*, Wiley, New York, 1977.
236. D. Brown and P. Labourer, *Chemosphere*, **12**, 405 (1983).
237. R. L. Swann, D. A. Laskowski, P. J. McCall, K. Vander Kuy and H. J. Dishburger, *Res. Rev.*, **85**, 17 (1983).
238. (a) US EPA (7407). OOPT Chemical Fact Sheets, Aniline Fact Sheet (CAS 62-53-3). EPA 749-F-95-002. December 1994. http://www.epa.gov/opptintr/chemfact/anal-fs.txt
    (b) D. S. Kosson and S. V. Byrne, *Environ. Health Perspect.* **103** (suppl. 5), 1 (1995).
239. L. M. Bordeleau and R. Bartha, *Can. J. Microbiol.*, **18**, 1857 (1972).

240. N. K. Van Alfen and T. Kosuge, *J. Agric. Food Chem.*, **22**, 221 (1974).
241. J.-M. Bollag, P. Blattman and T. Laanio, *J. Agric. Food Chem.*, **26**, 1302 (1978).
242. P. C. Kearney and J. R. Plimmer, *J. Agric. Food Chem.*, **20**, 584 (1972).
243. J.-M. Bollag, R. D. Minard and S. V. Liu, *Environ. Sci. Technol.*, **17**, 72 (1983).
244. A. Saxena and R. Bartha, *Bull. Environ. Contam. Toxicol.*, **30**, 485 (1983).
245. G. E. Parris, *Environ. Sci. Technol.*, **14**, 1099 (1980).
246. I.-S. You, R. A. Jones and R. Bartha, *Bull. Environ. Contam. Toxicol.*, **29**, 476 (1982).
247. T. S. Hsu and R. Bartha, *J. Agric. Food Chem.*, **24**, 118 (1976).
248. D. Freitag, I. Scheunert, W. Klein and F. Korte, *J. Agric. Food Chem.*, **32**, 203 (1984).
249. G. G. Briggs and N. Walker, *Soil Biol. Biochem.*, **5**, 695 (1973).
250. S. Russel and J.-M. Bollag, *Acta Microbiol. Pol.*, **26**, 59 (1977).
251. V. Travkin, B. P. Baskunov, E. L. Golovlev, M. G. Boersma, S. Boeren, J. Vervoort, W. J. H. van Berkel, I. M. C. M. Rietjens and L. A. Golovleva, *FEMS Microbiol. Lett.*, **209**, 307 (2002).
252. B. Ehring, J. Prassler, P. R. Wallnöfer and W. Ziegler, *UWSF Z. Umweltchem. Okotox.*, **4**, 81 (1992).
253. *Pesticides News*, March, no. 35, 20 (1997).
254. T. Roberts (Ed.), *Metabolic Pathways of Agrochemicals*. Part 1. *Herbicides and Plant Growth Regulators*, Royal Society of Chemistry Information Services, Cambridge, 1998. (Contributing editors on title page, D. H. Hutson, P. W. Lee, P. H. Nicholls and J. R. Plimmer.)
255. *Carcinogenic Substances Regulations, Statutory Instrument No. 879*, Her Majesty's Stationery Office, London, 1967.
256. *Federal Register*, **48**, no. 85, May 3, 10929 (1973); *Federal Register*, **39**, no. 20, January 29, 3756 (1974).
257. 'Special Occupational Review for Benzidine-Based Dyes'. HHEW (NIOSH) publication no. 80–109, Government Printing Office, Washington DC, 1980.
258. M. Bueniger, 'Technical Report: The Carcinogenecity and Metabolism of Azo Dyes, Especially Those Derived from Benzidine', DHHS (NIOSH), publication no. 80–119, July (1980).
259. NIOSH, 'Special Occupational Review for Benzidine-Based Dyes'. HHEW (NIOSH) publication no. 80–109, Government Printing Office: Washington DC, 1980.
260. A. W. Burg and M. C. Charest, *An Evaluation of the Literature Concerning the Potential for Carcinogenic Properties of Bisazobiphenyl Compounds Used as Dyes*, Arthur D. Little, Inc., January 1979.
261. A. W. Burg and M. C. Charest, *Azo Dyes: Evaluation of Data Relevant to Human Health and Environmental Safety*, Arthur D. Little, Inc., July 1980.
262. D. G. Goodman, J. M. Ward and W. D. Reichard, *J. Natl. Cancer Inst.*, **73**, 265 (1984).
263. G. F. Rubino, G. Scansetti, G. Piolatto and E. Pira, *Environ. Res.*, **27**, 241 (1982).
264. S. Markowitz and C. Lyons, 'Bladder Cancer at Bound Brook: Malignant Neglect', Montefiore Medical Center Report, New York, 1979.
265. F. B. Stern, L. I. Murphy, J. J. Beaumont, P. A. Schulte and W. E. Halperin, *J. Occup. Med.*, **27**, 495 (1985).
266. T. J. Mason, P. C. Prorok, W. E. Neeld and W. J. Vogler, *J. Occup. Med.*, **28**, 1011 (1986).
267. J. W. Meigs, L. D. Marrett, F. U. Ulrich and J. T. Flannery, *J. Natl. Cancer Inst.*, **76**, 1 (1986).
268. Opinion on risk of cancer caused by textiles and leather goods coloured with azo-dyes expressed at the 7th CSTEE plenary meeting, Brussels, 18 January 1999. Assessment of the Report by LGC [Laboratory of the Government Chemist] 'The risk of cancer caused by textiles and leather goods coloured with azo dyes'. http://europa.eu.int/comm/health/ph_risk/committees/sct/docshtml/sct_out27_en.htm
269. M. J. Zeilmaker, H. J. van Kranen, M. P. Van Veen and J. Janus, *Cancer Risk Assessment of Azo Dyes and Aromatic Amines from Tattoo Bands, Folders of Paper, Toys, Bed Clothes, Watch Straps and Ink*, RIVM Rapport 601503019, 2000. http://www.rivm.nl/bibliotheek/rapporten/601503019.html
270. T. Sugimura, T. Kawachi, M. Nagao, T. Yahagi, Y. Seino, T. Okamoto, K. Shudo, T. Kosuge, K. Tsuji, K. Wakabayashi, Y. Iitaka and A. Itai, *Proc. Jpn. Acad.*, **45**, 58 (1977).
271. (a) N. J. Gooderham, S. Murray, A. M. Lynch, M. Yadollahi-Farsani, K. Zhao, A. R. Boobis and D. S. Davies, *Drug Metab. Dispos.*, **29**, 529 (2001).

(b) J. H. Weisburger, *Mutat. Res./Fundamentals and Molecular Mechanisms of Mutagenesis*, **506–507**, 9 (2002).

272. W. G. Stillwell, R. J. Turesky, R. Sinha and S. R. Tannenbaum, *Cancer Res.*, **59**, 5154 (1999).
273. R. J. Turesky, J. Markovic, I. Bracco-Hammer and L. B. Fay, *Carcinogenesis*, **12**, 1847 (1991).
274. R. J. Turesky, N. P. Lang, M. A. Butler, C. H. Teitel and F. F. Kadlubar, *Carcinogenesis*, **12**, 1839 (1991).
275. Y. Mori, A. Koide, Y. Kobayashi, F. Furukawa, M. Hirose and A. Nishikawa, *Mutagenesis*, **18**, 87 (2003).
276. N. Nagao, M. Honda, Y. Seino, T. Kawachi and T. Sugimura, *Cancer Lett.*, **2**, 230 (1977).
277. Y. Yamazoe, M. Abu-Zeid, K. Yamauchi and R. Kato, *Jpn. J. Cancer Res.*, **79**, 1159 (1988).
278. T. Shimada, M. Iwasaki, M. V. Martin and F. P. Guengerich, *Cancer Res.*, **49**, 3218 (1989).
279. M. Nagao and T. Sugimura (Eds.), *Food Borne Carcinogens: Heterocyclic Amines*, Wiley, New York, 2000.
280. M.-F. Yueh, N. Nguyen, M. Famourzadeh, C. P. Strassburg, Y. Oda, F. P. Guengerich and R. H. Tukey, *Carcinogenesis*, **22**, 943 (2001).
281. T. Sugimura, *Mutat. Res.*, **376**, 211 (1997).
282. H. A. J. Schut and E. G. Snyderwine, *Carcinogenesis*, **20**, 353 (1999).
283. M. E. Moller, I. B. Glowinski and S. S. Thorgeirsson, *Carcinogenesis*, **5**, 797 (1984).
284. R. J. Turesky, A. Constable, J. Richoz, N. Varga, J. Markovic, M. V. Martin and F. P. Guengerich, *Chem. Res. Toxicol.*, **11**, 925 (1998).
285. J. Dairou, N. Atmane, J. M. Dupret and F. Rodrigues-Lima, *Biochem. Biophys. Res. Commun.*, **307**, 1059 (2003).
286. J. E. Summerscales and P. D. Josephy, *Mol. Pharmacol.*, **65**, 220 (2004).
287. U. Peters, R. Sinha, D. A. Bell, N. Rothman, D. J. Grant, M. A. Watson, M. Kulldorff, L. R. Brooks, S. H. Warren and D. M. DeMarina, *Environ. Mol. Mutagen.*, **43**, 53 (2004).
288. A. D. Watters, M. W. Stacey, J. J. Going, K. M. Grigor, T. G. Cooke, E. Sim and J. M. Bartlett, *Urol. Int.*, **67**, 235 (2001).
289. E. Richter and G. Sabbioni, in *Toxicology* (Eds. H. Marquardt, S. G. Schafer, R. McClellan and F. Welsch), Academic Press, San Diego, 1990, pp. 729–741.
290. S. R. Tannenbaum and P. L. Skipper, *Methods Enzymol.*, **231**, 625 (1994).
291. R. H. Dashwood, *Mutat. Res.*, **511**, 89 (2002).
292. J. S. Felton, M. G. Knize, C. P. Salmon, M. A. Malfatti and K. S. Kulp, *Environ. Mol. Mutagen.*, **39**, 112 (2002).
293. M. Nagao, T. Ushijima, N. Watanabe, E. Okochi, M. Ochiai, H. Nakagama and T. Sugimura, *Environ. Mol. Mutagen.*, **39**, 158 (2002).
294. K. Skog, *Food Chem. Toxicol.*, **40**, 1197 (2002).
295. K. Skog and A. Solyakov, *Food Chem. Toxicol.*, **40**, 1213 (2002).
296. R. J. Turesky, *Drug. Metab. Rev.*, **34**, 625 (2002).
297. R. H. Dashwood, *J. Biochem. Mol. Biol.*, **36**, 35 (2003).

CHAPTER **16**

Electrochemistry of anilines

JAN S. JAWORSKI and MAREK K. KALINOWSKI

Faculty of Chemistry, Warsaw University, 02-093 Warszawa, Poland
Fax: +48 22 822 5996; e-mail: jaworski@chem.uw.edu.pl; mkalin@chem.uw.edu.pl

I. INTRODUCTION

Electro-oxidation of aniline and its derivatives has been extensively studied in many laboratories and the early results have been reviewed in detail[1–3]. Thus, this chapter covers the period from approximately 1984 to the beginning of 2004 but some important earlier works considering general mechanisms are also mentioned. It was ascertained in classic investigations that the reaction pathways are strongly dependent on the medium properties, on the nature of substituent and also, to some extent, on the electrode material. A problem that plagues identification of the intermediates is electrode filming by the oxidation products. It is well known, for example, that in aqueous acidic solutions the anodic oxidation of aniline passes through various stages to form finally polyaniline, traditionally called aniline black. The polymer is thought to be of the general formula **1** that consists of alternating reduced (amine nitrogen) and oxidized (imine nitrogen) head-to-tail linked aniline dimeric subunits[4]. The value of y in each individual unit x may be $y = 1$, the fully reduced form, $y = 0.5$, the form that is half-oxidized, and $y = 0$, the fully oxidized form. The net oxidation state of a given polymer has been described as arising from a mixture of various amounts of these free different forms.

(1)
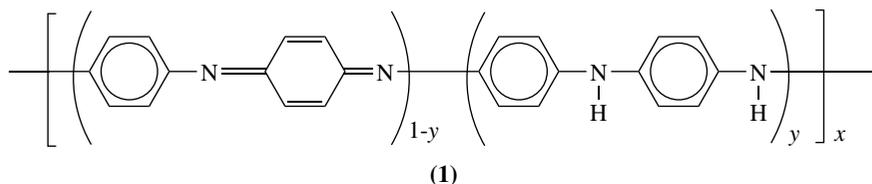
Conductive polymers based on aniline subunits are attractive materials because they have promising applications in a variety of fields, such as charge storage systems[5], sensors[6], electrochromic devices[7] and protector against corrosion[8]. Thus, the electropolymerization of anilines has received considerable attention, but this subject is not considered in this Chapter. However, early stages of electropolymerization followed by many derivatives of aniline are now firmly elucidated and are important from the point of view of the general mechanism of electro-oxidation. Unstable cation radicals, being the products of primary electrode reactions, and other intermediates have been identified by modern spectroelectroanalytical techniques and have contributed to the understanding of these interesting systems. The last mentioned matter will be reported in this Chapter.

In this review, attention is focused primarily on the oxidation mechanisms under the given conditions, which is the essential topic of interest for organic chemists. Reaction pathways will be outlined if they seem to be well established. However, even small differences in medium properties used by different researchers can lead to serious variations as will be shown in some examples. Anodic oxidation of unsubstituted aniline is discussed in Section II and electrode reactions of *N*-substituted and *C*-substituted anilines in Sections III and IV, respectively. In the last case, the oxidation of reactants with monosubstituted ring is presented first (*para*-substituents separately from the effects of *ortho*- and *meta*-substituents), and next the oxidation of di- and trisubstituted anilines. In each part the processes in dipolar aprotic solvents, in particular in acetonitrile (ACN) and *N*,*N*-dimethylformamide (DMF), are compared with those proceeding in aqueous solutions, chiefly in commonly used acidic media.

Electrosynthesis of aniline and its derivatives is very important for practical applications. Although electrolytic hydrogenation of nitrobenzene is a well-known process, a continued development in this area has been observed in recent years. In particular, the application of indirect electrolysis with a titanium complex mediator[9] and a hydrogen-storage alloy electrode[10] for reduction of nitrobenzenes to anilines as well as the use of TiO_2/Ti electrode[11] and Cu–Zr amorphous alloy as an electrocatalyst[12] for electrochemical preparation of *p*-aminophenol can be given as examples. However, this subject is rather related to electrochemical properties of nitrobenzenes and will not be discussed in this Chapter.

A fundamental effect of substituents on the mechanism and products distribution in the anodic oxidation of anilines was pointed out at the beginning of this Introduction. The problem is discussed qualitatively in a few parts of Section III. A more quantitative approach using Linear Free Energy Relationships (LFER), first of all the Hammett equation, is rather difficult because of strong dependences of standard potentials and the mechanism of the oxidation on medium acidity (even in unbuffered aprotic solutions, which is due to the participation of protons from a reactant), on various side reactions as well as the change of the overall mechanism with the nature of substituents. Thus, LFER investigations in the electrochemistry of anilines are scarce, contrary to similar studies on chemical oxidation of substituted anilines in solutions. An important example is the recent investigation of kinetic data for 31 anilines oxidized by sodium percarbonate ($Na_2CO_3 \cdot 1.5\ H_2O_2$) in glacial acetic acid[13]. Careful analysis (taking into account the effects of acid–base equilibrium, the possibility of cross-conjugation with the reaction

center, specific reaction rates of *ortho*-substituted derivatives and assuming that anilines exist in dual forms as free bases and conjugated acids) not only confirmed the validity of structure–reactivity relationships (in particular the isokinetic relationship) but also convincingly showed that the hitherto simple method of correlation is in fact erroneous[13]. Nevertheless, a few electrochemical examples are given below. Nelson and coworkers[14] using chronoamperometry and voltammetry with the platinum rotating disk electrode analyzed the coupling rate constants of 21 substituted triphenylammonium cation radicals in ACN containing 0.1 M tetraethylammonium perchlorate. They found[14] correlations with substituent constants of Hammett σ or Okamoto and Brown σ^+ (better correlations were obtained in the case of σ^+, except for strong electron-donating groups).

Oxidation of trisubstituted N,N',N''-triphenyl-1,3,5-triaminobenzenes (**2a–2e**) showed one to three irreversible cyclic voltammetric peaks. Potentials of the first peak fulfill the Hammett equation (against the $3\sigma^+$ values, according to the additivity rule for three *para*-substituents) giving the slopes, i.e. the reaction constants ρ^+, equal to -1.53, -1.45 and -1.43 V/($3\sigma^+$ unit) in solutions of methylene chloride, ACN and propylene carbonate, respectively (solutions contained 0.1 M tetrabutylammonium perchlorate)[15]. An interpretation of the above reaction constants is rather difficult because of the irreversibility (radical cations formed by the first electron transfer evidently disappear in fast chemical steps). However, relatively small values of ρ^+ may be related[15] to a charge delocalization onto the outer aromatic ring of the radical cation.
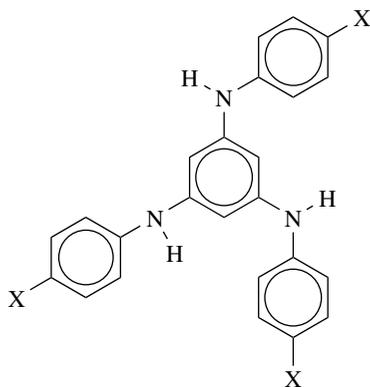
(**2a**) X = MeO
(**2b**) X = Me
(**2c**) X = H
(**2d**) X = F
(**2e**) X = Cl

A substituent effect on electrochemical and xerographic properties of triarylamines has recently been reported[16]. The oxidation potentials correlate with both the Hammett substituent constants and the calculated HOMO energies of the molecules under investigation, and this approach was used[16] to rationalize xerographic properties, including transport phenomena of solid-state solutions in polycarbonate-Z.

In this Chapter the following common abbreviations are used: CV, cyclic voltammetry; RDE, rotating disk electrode; rds, rate-determining step; TBABF$_4$, tetrabutylammonium tetrafluoroborate; TBAPF$_6$, tetrabutylammonium hexafluorophosphate; TEAP, tetraethylammonium perchlorate; TBAP, tetrabutylammonium perchlorate; DMSO, dimethyl

sulfoxide; ACN, acetonitrile; DMF, N,N-dimethylformamide; ITO electrode, transparent iridium-dopped tin oxide coated glass electrode; ETFS, electron-transfer stopped-flow method; SERS, surface-enhanced Raman scattering. The cited potentials are mainly expressed (unless otherwise noted) versus an aqueous saturated calomel electrode (SCE) or versus an Ag/Ag$^+$ couple in ACN for measurements in ACN solutions.

II. ANODIC OXIDATION OF ANILINE

The anodic oxidation of aniline (**3**) to the final product, polyaniline, is quite complex and there is still a controversy as regards the reaction pathway. The main question to be answered concerns the chemical nature of the intermediates. For instance, it was widely believed even in early papers[17] that, in acidic media, the polymerization process involves a coupling of aniline radical cation that is formed in the initial oxidation step. The cation (**4**), being an acid, would be stabilized in acidic conditions, but the redox system **4/3** was not directly observed even in very fast CV experiments (scan rate above 50000 V s^{-1}, glassy carbon electrode) performed in solutions of aniline containing H$_2$SO$_4$[18]. In basic medium **4** can be deprotonated to produce C$_6$H$_5$NH$^\bullet$, the anilino neutral radical (**5**).

resonance structures

(4)
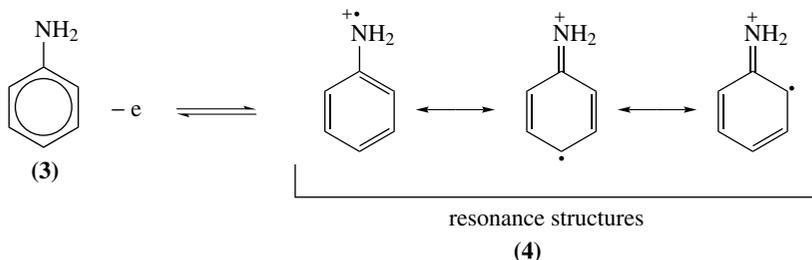
It is possible to suggest further oxidation of **4** yielding the C$_6$H$_5$NH$_2{}^{2+}$ dication (**6**) which, after deprotonation, produces C$_6$H$_5$NH$^+$, the nitrenium cation (**7**). The last one can be alternatively formed as a result of the oxidation of **5**, therefore the oxidation diagram of aniline may be presented as in Scheme 1, where the values of E_1, E_2 and E_3 represent potentials of the corresponding electron transfers. It is worth noting that Scheme 1 corresponds with the well-documented fact that the properties of polyaniline vary depending on the use of aqueous or non-aqueous acidic, neutral or basic conditions[19].
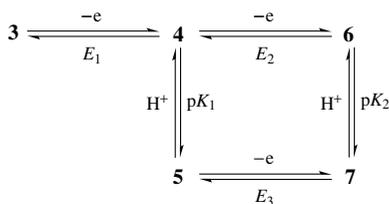
SCHEME 1

In connection with Scheme 1, the results of Mu and Kan[20] are of special interest. In order to prove that intermediates can be generated during electrolysis of aniline, experiments were carried out using a rotating ring-disk platinum electrode. The potential of the ring was controlled at +0.20 V versus Ag/AgCl/saturated KCl electrode, whereas

disk potential was scanned from 0 V in a positive direction (scan rate 48 mV s^{-1}) and stopped at 1.15 V. Experiments with an aqueous solution consisting of 0.2 M aniline and 0.5 M KCl led to the characteristic ring current—time changes; in the first scan the corresponding curve increased rapidly when the disk potential was over 0.75 V and two distinct peaks were formed at 1.0 and 1.1 V, respectively. Thus two intermediate species can exist, and therefore the authors suggested[20] that the first peak (at 1.0 V) corresponds to the **4/3** redox couple. The radical cation (**4**) is not stable in low acidity media and loses proton forming **5**, which is further oxidized at 1.1 V forming the nitrenium cation (**7**). According to that, only one intermediate is produced during electrolysis in solutions of high acidity. Moreover, the majority of radical cations (**4**), which do not deprotonate at high proton activity, catalyze aniline polymerization at the disk electrode, and only a small part of **4** passes from the disk to the ring to form a first peak on the ring current−time curves.

Scheme 1 was first proposed by Geniès and Lapkowski[21] who reported their spectroelectrochemical studies of aniline oxidation in a eutectic mixture of average formula $NH_4F + 2.3$ HF. This mixture is liquid at room temperature and has similar properties to liquid HF, known to be suitable for the stabilization and detection of cation radicals. Using an optically transparent working electrode, which was prepared by gold deposition on polyester, the authors have observed the evolution of optical spectra being the result of oxidation of 40 mM aniline solution. Apart from the 670 nm band characteristic of polyaniline, they have found strong absorption associated with the existence of a soluble intermediate. The last band, located at 420 nm, disappeared gradually with a simultaneous increase of the 670 nm band, indicating that the intermediate is involved in the process of polyaniline formation. What is, however, the nature of this intermediate?

To solve that problem, Geniès and Lapkowski[21] performed an *in situ* EPR measurement. However, no electron spin resonance signal was observed during the oxidation of aniline, and this prompted the authors to suggest that the reputed intermediate must be the nitrenium cation (**7**), formed according to Scheme 1. By that means, the radical cation (**4**), the initial product of anodic oxidation of aniline, has not been identified. Add for completeness that one of the peaks which appears frequently on the CV curves of polyaniline (the so-called 'middle' peak) has been attributed to the presence of a polymer containing phenazine ring **8**. The cation **7** has now been assumed as the intermediate responsible for the process leading to this system according to Scheme 2[22].

Next, Park and coworkers[23] studied electro-oxidation of aniline in 1 M H_2SO_4 by means of the CV and *in situ* spectroelectrochemistry. They argued that the species that is responsible for electronic transition at 430 nm observed during electrolysis should be the nitrenium cation (**7**). This species was seen to disappear rapidly in an aniline solution of high concentrations (e.g. 3 mM), but it was found to live longer when the aniline concentration decreased. This suggests that this species is attacked by aniline in solutions and therefore it was assumed to be a reasonable candidate for an initial species of polymer growth. It should be added, however, that six years later the above suggestions were reinterpreted in one of the papers from this research group[24] (see text below). The problem of the initial stage of anodic oxidation of aniline is very difficult to study indeed.

Just then, it was demonstrated that identification of the cation radical (**4**) generated upon electro-oxidation of aniline is possible but difficult to perform, because its lifetime is very short. Therefore, to study the initial stage of the oxidation of aniline, lower aniline concentrations are desirable in order to decrease the rates of dimerization processes. Accordingly, the reduction peak for the cation **4** was observed for the first time by Yang and Bard[18]; they found that a cyclic voltammogram recorded at a scan rate of 200 V s^{-1} and at very low aniline concentration (0.05 mM) in ACN solution shows a small cathodic signal corresponding to the redox system **4/3**. Note that this result was obtained with a
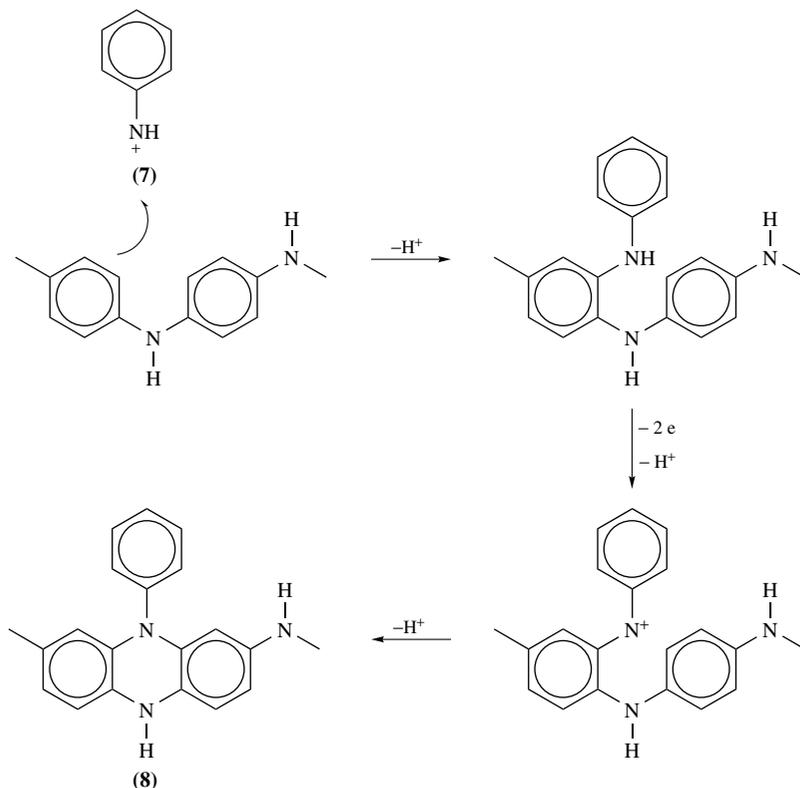
SCHEME 2

25-μm diameter platinum microelectrode and 0.1 M TBAPF$_6$ served as a background elec-
trolyte. The rate constant for the coupling reaction was estimated to be about 10^8 M^{-1} s^{-1},
leading to an approximate lifetime for **4** of 2 ms under the experimental conditions. The
voltammogram is consistent with a formal potential for the redox couple **4/3** of about
0.75 V vs. SCE. Hence the experiments reported in Reference 18 gave the first direct
evidence for the formation of the radical cation (**4**) during an anodic oxidation of aniline.
Those radicals are admittedly too unstable to be observed by ESR spectroscopy but their
role in electro-oxidation of **3** is now commonly accepted. Note that the radical cation (**4**)
is the least stable of the aromatic amines, so many additional arguments are known for
the existence of its substituted derivatives. Also, the dimers were the subject of successful
electrochemical and *in situ* ESR studies but this problem will be treated below.

A substantial number of papers have been published on the primary products of
the decay of **4**. A typical cyclic voltammogram at a slow scan rate (e.g. 50 mV s^{-1})
taken during the oxidation of aniline at a platinum electrode in 1 M H$_2$SO$_4$ is rather
complicated[18, 25–27]. Multiple redox waves show that the anodic process is very com-
plex and involves coupled multiple heterogeneous electron transfers and homogeneous
chemical processes. The species responsible for the pair of peaks at 0.23 V vs. a satu-
rated mercurous sulfate electrode (SMSE) has been identified as resulting from the redox
behavior of benzidine (**9**), whereas the peaks at −0.02 V vs. SMSE[18] were attributed

to *p*-aminodiphenylamine (**10**). This indicates that in aqueous acidic medium the radical cations generated by electro-oxidation of aniline react, through its resonance structures, by tail-to-tail and head-to-tail coupling, to form **9** and **10**, respectively.
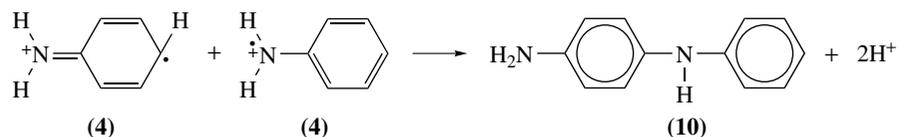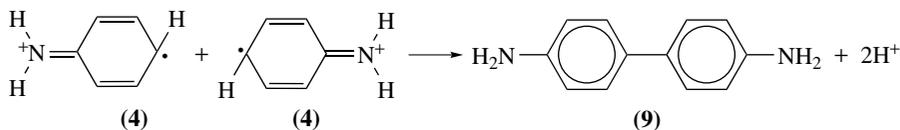
In acidic solutions **10** exists in the singly protonated form (**11**) which oxidizes reversibly with two-electron transfer yielding protonated *N*-phenylquinonediimine (**12**). CV curves recorded in the pH range 1.2–4.8 (scan rate 100 mV s^{-1}, platinum working electrode) indicated that two protons are released during the oxidation and the overall electrochemical process may be written as[28]
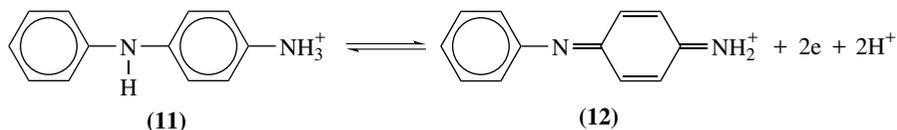
In spite of that, the appearance of the radical cation of **10** was also shown by simultaneous ESR measurements. Thus, it seems to be evident that **11** and **12** comproportionate to form the radical cation **13**.
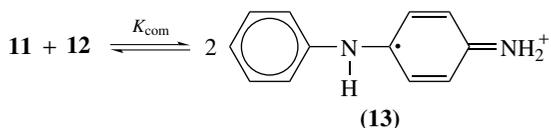
Male and Allendoerfer draw the conclusion[28] from their electrochemical measurements that K_{com}, the comproportionation equilibrium constant, must be less than 1. In a more extensive study[29] the value $K_{com} = 0.027$ was determined in DMSO and found to be independent of the activity of the protons in solution (the concentration of H$_2$SO$_4$ was varied in the range between 0.1 and 0.5 M). It was proved, moreover, that the decay of radical cation **13** could be described by a kinetic equation based on a second-order dimerization process and a pre-equilibrium for the radical formation by comproportionation. The corresponding second-order rate constant was found to be $k = 34$ M^{-1} s^{-1} at room temperature[29].

The ESR spectrum of **13** was also observed during the anodic oxidation of aniline in DMSO solutions containing 0.2 M H$_2$SO$_4$[30]. The concentration of paramagnetic species was very low, therefore the accumulation of 90 spectra was necessary to obtain a fully readable result. Note that the electropolymerization of aniline can be blocked in the solvent used and, of course, this should facilitate the identification of unstable intermediates

in an anodic process[31]. A more recent electrochemical and *in situ* time-resolved FT-IR study indicated that the radical cation **13** is generated in the reaction of anodically generated anilinium radical cation (**4**) with aniline and this is a stage initiating the polymer growth (experimental conditions: aqueous solution containing 0.05 M aniline and 0.5 M H_2SO_4)[32].

Recall here the properties of **12** being the product of oxidation of **11**. It is well established that **12** in acidic media can undergo a relatively slow oxidative decomposition process leading to *N*-phenylquinoneimine (**14**), which may be reversibly reduced to *p*-hydroxydiphenylamine (**15**). Moreover, **14** can undergo slow decomposition with the formation of the anilinium cation (**16**) and *p*-benzoquinone (**17**) forming a reversible redox couple with hydroquinone (**18**) (Scheme 3)[18]. The potentials for some electron transfers mentioned above are very near one another, so that the corresponding peaks merge to form broader waves beginning with the second cycle of the voltammogram. A noticeable feature is the existence of peaks at 0.08 V vs. SMSE corresponding to the **14/15** redox couple; the absence of these on the cyclic voltammetric curve recorded at a scan rate of 20 V s^{-1} confirms that slow oxidative hydrolysis starting from **12** did not occur during the fast potential scan. Assuming that the hydrolysis of **14** is a pseudo-first-order process, the magnitude of the rate constant in 1 M H_2SO_4 was estimated[18] as less than 10 s^{-1}.
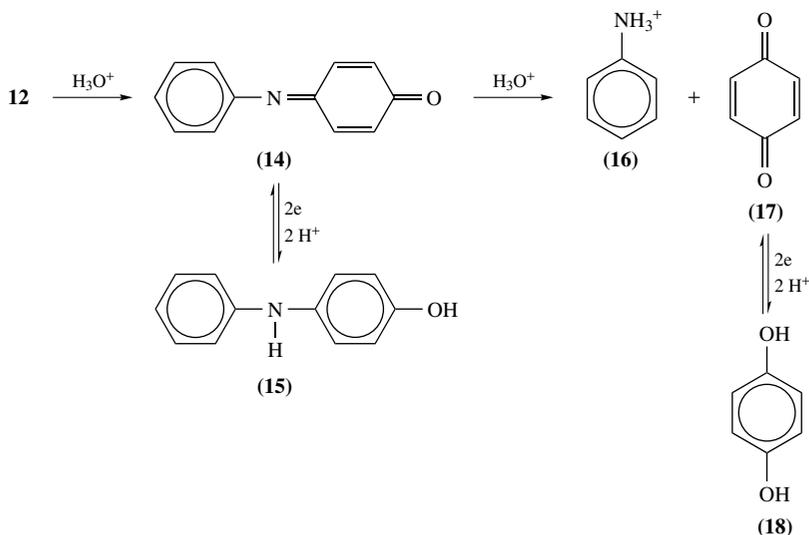
SCHEME 3

Yang and Bard[18] claimed that **9**, similarly to **10**, is also an initial dimerization product for further polymer growth. Benzidine (**9**) undergoes reversible two-electron oxidation forming (1,1′-biphenyl)-4,4′-diimine (**19**). The addition of **9** during anodic oxidation of aniline in DMSO containing 0.2 M H_2SO_4 resulted in some interesting ESR behavior[30]. It was found that the radical **20** with an indamine structure is formed by the reaction of **19** with protonated aniline, and further oxidation of the formed **21** and protonation.

Let us return, however, to the problem of the 'middle' peaks in cyclic voltammograms. As pointed out earlier, Geniès and coworkers[22] assumed that they might be the result of the phenazine nucleus insertion into the growing polymer, but such an interpretation was controversial[25, 32, 33]. On the basis of CV measurements carried out in solutions

containing 1 M H_2SO_4 Duić and coworkers[34] suggested that those peaks be considered as a result of a hydrolysis process, which can be deduced from Scheme 3. Voltammetric and simulation studies of Yang and Bard[18] finally elucidated this question; the authors argued that the interpretation of the middle peak depends on the aniline concentration and on the time scale of the experiment. When a high amine concentration is used at a slow scan rate, the peak may be assumed to be the result of redox processes of *p*-hydroxydiphenylamine and *p*-aminodiphenylamine in the early stages, but that of 1,4-benzoquinone and *p*-aminophenol at later stages. Next, at fast scan rates, when oxidative hydrolysis is suppressed, the peak results from redox behavior of *p*-aminodiphenylamine. Similarly, at a lower aniline concentration, only the last mentioned compound is responsible for the middle peak. In conclusion, **10** is the dominant component with the fastest reaction kinetics. Alternatively, in the presence of small amounts of benzidine in solutions, the middle peak may also result from a small oligomer with the diphenylamine structure. In this case, benzidine, being more easily oxidizable than the parent substance, i.e. aniline, undergoes oxidation at the same potential. The product **19** incorporates presumably aniline forming the trimer **21**, as discussed above, and the resultant chain is again oxidized to incorporate another aniline molecule from the solution phase etc. Note that the trimer **21** has a unit **22** with redox potential similar to that corresponding to **10**. Therefore, the middle peak could be either that of **10** or a small oligomer with **22** unit.

(19)

(20)

(21)

(22)
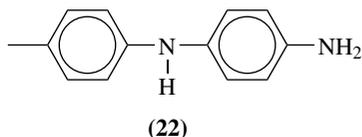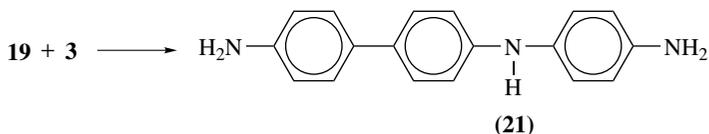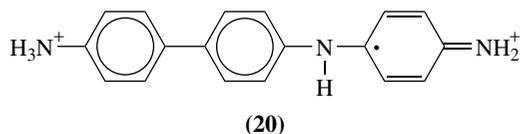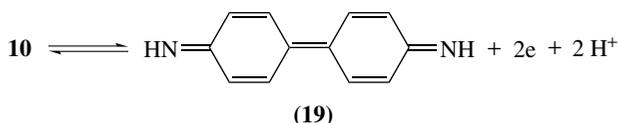
Thus, **9** and **10** are the major coupling products formed upon oxidation of aniline in aqueous H_2SO_4 solution. Theoretically, it is possible to imagine two mechanisms of the reaction pathway: (i) dimers are formed by two radical cations coupling, and (ii) an electrophilic attack of the radical cation on a neutral molecule of aniline produces the corresponding dimer. In the second case it is assumed that the coupling product loses another electron and therefore the total number of electrons transferred in the overall processes would be the same in both mechanisms.

In order to clarify the mechanism of the coupling, digital simulations were carried out and compared with the CV curves recorded at a glassy carbon electrode[18]. The anodic peak of aniline is most useful to discriminate between different possibilities. The effect of scan rate and concentration on this peak current, as well as on the peak potential and the difference between the peak potential and the half-peak potential, is sensitive to the coupling mechanism. Moreover, the ratio of cathodic peak currents for possible dimers to the anodic peak current of aniline depends strongly on the coupling routes and their rates. A comparison of simulation data with the experimental cyclovoltammograms leads to the conclusion that both **9** and **10** are formed by the radical cation—radical cation coupling. The rate constant of the process leading to p-aminodiphenylamine is of the order of $10^7 \ M^{-1} \ s^{-1}$ and is about 2.5 times faster than that for benzidine[18]. It is noteworthy in this context that the SERS studies of aniline adsorbed on the gold electrode surface indicated the radical cation—parent molecule coupling to yield exclusively benzidine[35].

The results reported in Reference 18 need some comments. First, Sharma and co-workers[25], who studied oxidative voltammetry of aniline on graphite electrodes in acidic conditions, observed that in 0.1 M sulfuric acid the radical cation (**4**) undergoes not only head-to-tail and tail-to-tail but also head-to-head coupling to form p-aminodiphenylamine, benzidine and hydrazobenzene (**23**), respectively; **23** is oxidizable to azobenzene (**24**).
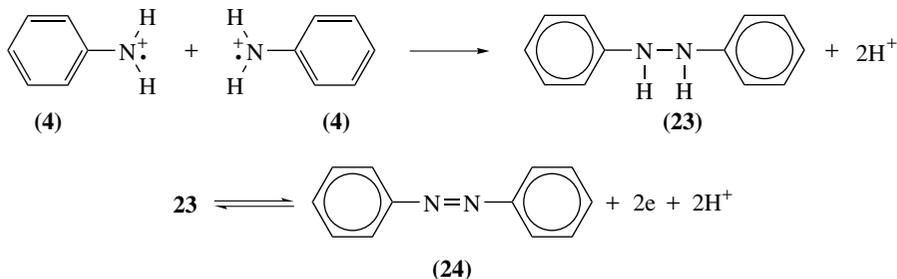
Next, in 2.2 M H_2SO_4, **23** is either not formed at all, or if formed then it undergoes molecular rearrangement giving rise to benzidine. Thus, in 2.2 M sulfuric acid **9** and **10** are the products of coupling, similarly to what was suggested by Yang and Bard[18] for 1 M H_2SO_4 solutions. Secondly, in a more recent paper[36] Stassen and Hambitzer have studied the anodic oxidation of aniline by means of electrochemical thermospray mass spectrometry. The working electrode was a platinum foil with an area of nearly 1 cm^2; the electrolyte solutions consisted of 0.01 M amine and 0.1 M sulfuric acid. During the anodic process, the authors observed in the mass spectrum, as singly charged protonated molecules, the reduced form of the dimer ($m/z = 185$) and, at a factor of 10 lower abundance, the reduced form of the trimer ($m/z = 275$). No oligomers beyond the trimers were observed. It was concluded that higher oligomers were deposited onto the electrode surface because of their insolubility and therefore were not identified in the mass spectra. A question arose as to the structure of the generated dimers: both possible products, p-aminodiphenylamine and benzidine (in their protonated forms), have the same mass and hence are not distinguishable in the mass spectrum. That is why, in order to unequivocally elucidate the mass spectra, measurements were made with d_5-aniline in which all five hydrogens of the ring were exchanged with deuterium. The deuteriated molecules of protonated benzidine (**9a**) and protonated p-aminodiphenylamine (**11a**) differ in their mass by one atomic mass unit, and now differentiation between them is possible. Thermospray mass spectrometry shows only one signal at $m/z = 194$ and this reveals that no benzidine is formed under the experimental conditions. In other words, only **11** has been identified

$$H_2N-\text{C}_6D_4-\text{C}_6D_4-NH_3^+ \quad (9a)$$

$$D-\text{C}_6D_4-\overset{H}{\underset{|}{N}}-\text{C}_6D_4-NH_3^+ \quad (11a)$$
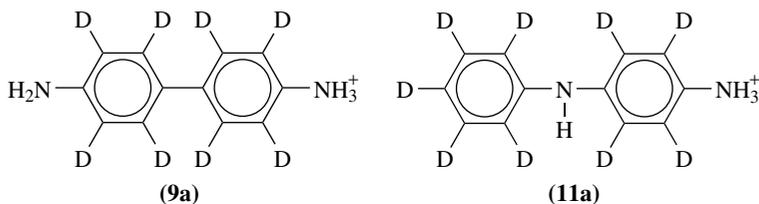
as an exclusive dimerization product[36]. Similarly, **10** has been observed as the only dimer formed during the initial stages of 10^{-3} M aniline oxidation at a platinum electrode with the surface area of about 15 mm^2 in aqueous solutions buffered at pH 5[37]. Both cyclic voltammetry and *in situ* FT-IR spectroscopy confirmed that finding, and no evidence supporting the formation of other dimerization products, such as **9** and **23**, has been found under the experimental conditions. The resulting dimer **10** was found to be poorly soluble in aqueous medium and, consequently, its fraction precipitated on the electrode surface when formed.

The finding reported in these papers[36, 37] is in fact inconsistent with the results of previously mentioned electrochemical studies, the authors of which have found that at least both the head-to-tail and tail-to-tail dimers are formed under very similar experimental conditions. Furthermore, the observation of only the reduced dimer (and, similarly, trimer) is rather intriguing, as it has been demonstrated many times that the dimers, being the products of the initial stages of aniline oxidation, are easier to oxidize than the parent compound.

In that context, the results reported by Deng and Van Berkel[38] seem to be of special interest. A thin-layer electrochemical flow cell (with a working glassy carbon electrode) coupled on-line with electrospray mass spectrometry was used by the authors to study the soluble products from the controlled-potential oxidation of aniline in aqueous and methanol (50 vol%) media. The solutions were buffered at pH 4, 6.5 and 9, respectively. Singly protonated aniline oligomers containing even 10 aniline units were identified in the electrospray mass spectra when electro-oxidation of aniline was carried out at a controlled potential of 1.0 V vs. Ag/AgCl redox couple in methanol solutions at pH 4. The abundance of those higher oligomers decreased at higher solution pH and in water at pH 4. The electrochemically generated dimers (also in singly protonated form) in methanol were observed in two possible redox states, viz. the fully reduced and the fully oxidized ones. Corresponding structures were revealed to vary as a function of pH by comparing their tandem mass spectrometry product ion spectra with the product ion spectra of the dimer standards. Inspection of the spectra of the oxidized species revealed convincingly that only head-to-tail dimeric species **12** is formed at pH 4. Both compounds, deprotonated **12** and **23** (head-to-head dimer), were then identified at pH 9, whereas no tail-to-tail dimer **19** was observed either at pH 4 or at pH 9. Next, from the midst of a group of the reduced dimers protonated **9** and **11** are formed at pH 4, but the formation of **10** and **23** can be observed at pH 9.

Thus, one can conclude that the use of a thin-layer electrochemical flow cell on-line with electrospray mass spectrometry provided important information regarding the products of early stages of the anodic oxidation of aniline. The fact that head-to-head, head-to-tail and tail-to-tail aniline dimers were shown to be present in the electrospray mass spectrum resulting from aniline oxidation indicates that the higher oligomers may be a mixture of linkage sequences. This conclusion is of course important for the electropolymerization pathways. An instrumental setup configured for a simultaneous recording of electrochemical, spectroelectrochemical and mass data (quartz crystal analyzer) on an electrode is

also very powerful in elucidating the details of intermediates and the reaction sequence of those complex processes[39]. Moreover, the original *in situ* technique for measuring electrochemical impedance spectra during the anodic oxidation of aniline gave a number of observations that would not have been obtained without such experiments[40]. However, the results reported in the papers[39, 40] are important in the first place for elucidation of the mechanisms of electropolymerization, so the corresponding details will not be discussed here.

Finally, two questions should be mentioned here. The first of them is connected with the effect of encapsulation of **10** into the hydroxypropyl-β-cyclodextrin cavity on electrochemical behavior of the predominant intermediate dimer observed during the anodic oxidation of aniline. Spectroelectrochemical results indicated[41] that the host−guest interaction increases when the pH of the solution is increased from 0.4 to 5.6. It was found that the interaction is weak for the diprotonated form, a little stronger for the singly protonated one (**11**) and much stronger for the neutral molecule of **10**. The electrochemical oxidation of **10** (only in its neutral form) occurs outside the cyclodextrin cavity; the encapsulated compound does not participate in the anodic process within the time scale of the experiments[41]. The second question is connected with the electrochemical oxidation of aniline in a silica sol-gel matrix[42]. An interesting result of this study is that the pore structure of silica solid electrolyte (prepared by a sol-gel process) leads to the products that were dependent on the aging time and, consequently, on the pore size. When the aging time was limited to one day, the aniline oxidation resulted in the formation of polyaniline, whereas with the aging time of 3−5 days only the formation of dimers and other small oligomers was observed[42].

III. ELECTROCHEMISTRY OF NITROGEN-SUBSTITUTED ANILINE DERIVATIVES

The oxidation mechanisms for *N*-substituted anilines have received great attention for about 40 years[1−3]. One of the main results was the finding that substitution at the nitrogen atom enhances considerably the stability of the radical cation intermediate. The possibility of obtaining quite stable cation radicals of tertiary aromatic amines bearing substituents in the *para* position of phenyl groups is particularly meaningful; these radicals have been used as mediators in several redox catalysis studies of oxidation processes, for example in the oxidation of benzylic alcohols[43]. At the beginning of this Section, let us consider the first stages of the anodic reactions of *N*-alkyl-substituted compounds.

Not long ago relatively little was known about the oxidation process of *N*-alkylanilines. Galus and Adams in their pioneer work described the anodic behavior of *N*-methylaniline in aqueous acidic medium. They have found that the oxidation leads to *N*,*N*′-dimethylbenzidine, which forms together with *N*-methylaniline another reaction product[44]. The structure of these products had remained unknown for a long time and it has been elucidated only recently by the results of electrochemical thermospray mass spectrometry measurements[36]. Subsequently, it has been established that the anodic behavior of *N*-ethylaniline in 0.1 M H_2SO_4 is quite similar and the major coupling product is the analogue of benzidine[25]. Such a result is of course distinctly different from that of aniline for which *p*-aminodiphenylamine was identified as a main dimerization product. However, this observation can be explained in terms of the inductive effect of the alkyl group joined to the nitrogen atom of the molecule. Accordingly, the electron-releasing alkyl group tends to disperse the positive charge on the radical cation formed in the initial stage of electro-oxidation. Such a dispersal tends to increase the stability and hence to decrease the reactivity of the radical cation towards formation of head-to-head and head-to-tail dimers. The predominant coupling is therefore the tail-to-tail coupling resulting in the formation of benzidine derivatives[25].

Malinauskas and Holze convincingly confirmed the supposition that the faster coupling proceeds with unsubstituted aniline, whereas N-alkyl-substituted derivatives react somewhat slower. They have used UV-VIS spectroelectrochemistry for the investigation of the early stage of anodic oxidation of N-methyl[45] and N-ethylaniline[46] at an ITO working electrode; the supporting electrolyte was 0.5 M H_2SO_4 in aqueous solution. The absorbance bands located at $\lambda_{max} = 443$ nm and 450 nm for N-methylaniline and N-ethylaniline, respectively, were ascribed to the formation of intermediate species formed during electrolysis. Once formed, the intermediate undergoes further chemical transformations, forming oligomer or polymer products as an end product of electro-oxidation. It was shown that in contrast to aniline, the intermediate could be observed even on a minute time scale.

A very similar picture was obtained for aniline-N-3-propylsulfonic acid (**25**). During anodic oxidation of this compound on an ITO glass electrode in acidic solution, the formation of an intermediate characterized by the absorption band with $\lambda_{max} = 453$ nm could be observed[47,48]. After interruption of the electrolysis, the band disappeared in a relatively long time scale depending on the concentration of the parent compound. The spectrum finally obtained was typical of polymer species. Also, an intermediate was found to be generated during electrolysis of N-benzylaniline[49]. The intermediate, which shows an absorption band at $\lambda_{max} = 460$ nm, is able to react spontaneously with the substrate forming a polymeric end product, which is deposited on an ITO glass electrode surface.

$$H\diagdown\underset{\displaystyle N}{}\diagup(CH_2)_3SO_3H$$

(25)
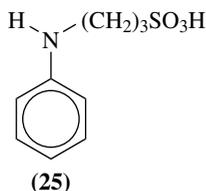
On the basis of the recently reviewed works[45−49] it is difficult to verify the nature of intermediate species described here. In the simplest case one can try to ascribe the bands located at *ca* 440–460 nm to a radical cation, which was postulated many times to be formed in early stages of the anodic oxidation of aniline and its derivatives[50]. However, there are indirect clues[39] that the intermediate should be the product of further transformations of a radical cation (head-to-tail coupling products are oxidizable, yielding a quinoid dication species that is detectable spectrophotometrically around $\lambda = 450$ nm[18]) rather than a simple radical cation of the **4** type. Thereby, the important question concerning the nature of intermediate species still remains unresolved.

Similarly to the case of aniline, Stassen and Hambitzer identified successfully the products of the anodic oxidation of N-methyl and N-ethylaniline in 0.1 M H_2SO_4 with electrochemical thermospray mass spectrometry[36]. In that order a potentiostatic electrolysis in the thin-layer flow cell was carried out and the corresponding mass spectra were recorded. In the case of N-methylaniline four signals were registered: the dimeric product occurred at $m/z = 199$ and 213, whereas the most intense peaks of trimers lay at $m/z = 304$ and 315. It was found that the main dimeric product is protonated N,N'-dimethylbenzidine (**26**), but protonated N,N'-dimethyl-p-aminodiphenylamine (**27**) was also identified as the by-product. The product ratio is 7:3 in favor of the benzidine derivative. Both dimers are formed by recombination of two radical cations and are characterized by $m/z = 213$. When deuterated at the N−H group, the compounds become distinguishable; they have a different number of exchangeable protons and some of their signals in the mass spectra are now separated by one unit.

(26)   (27)

SCHEME 4

(28)   (29)
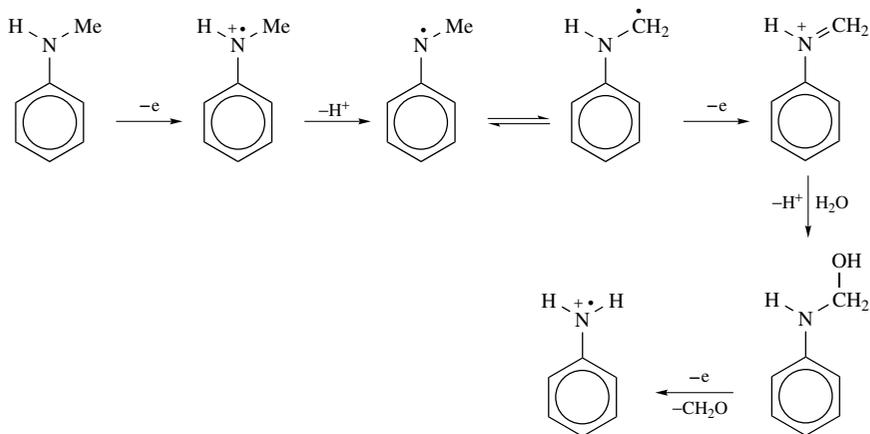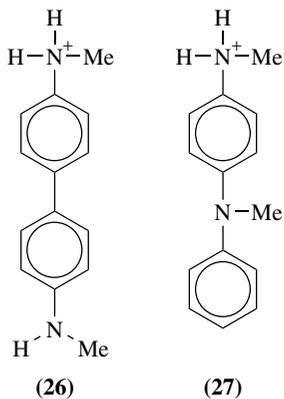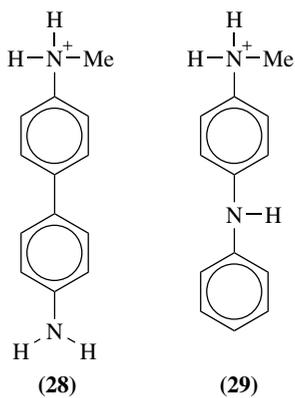
In their study, Stassen and Hambitzer also demonstrated that dimers undergo dealkylation. Scheme 4 illustrates the mechanism of that process, and the resulting aniline radical cation undergoes further reaction to the corresponding dimer. The peaks at $m/z = 199$ were attributed to the dealkylated dimers for which the structures **28** and **29** can be shown.

Dimeric species are precursors of the trimers that were also detected in the mass spectra ($m/z = 318$). The reaction of **26** leads exclusively to the formation of the C-C-N-C-coupled trimer **30**. Starting with **27** two trimers can be formed: the C-C-N-C-coupled compound (**31**) is the main product, whereas the C-N-C-N-coupled species (**32**) is the by-product (an intensity ratio of 9:1 was established). It can be easily seen that the former is strongly favored because of steric interactions. Dealkylated trimers ($m/z = 304$) are also formed.
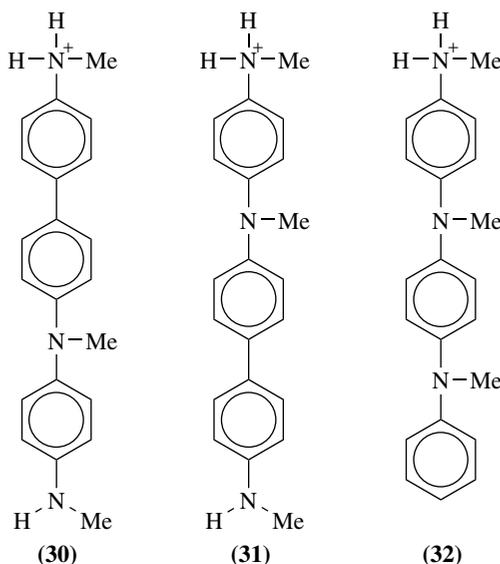
Now, let us consider electro-oxidation of N,N-disubstituted anilines. The cyclic voltam-mograms (scan rate 50 mV s^{-1}) obtained for 0.1 M aqueous solutions of N,N-dimethyl-aniline (DMA), N-ethyl-N-methylaniline (EMA), N,N-diethylaniline (DEA) and N,N-di-n-butylaniline (DBA) at a basal-plane pyrolytic graphite electrode in a 0.5 M Na$_2$SO$_4$ + H$_2$SO$_4$ (pH 1.0) solution exhibit two distinct peaks during the first oxidation scan[51]. In each case, the first and second peaks correspond to one-electron oxidation. The reduction peaks on the reverse scan (50 mV s^{-1}) are rarely observed, indicating fast consumption of oxidation products by the follow-up chemical reaction. The compounds are oxidized more easily in the following order (potentials are given against a sodium chloride saturated calomel electrode): DMA (0.84 V) > EMA (0.86 V) > DEA (0.95 V) > DBA (0.98 V) > aniline (1.02 V). The new reduction–oxidation signals were observed at about 0.5 V on the second scan; they were attributed to the non-identified coupling products of the cation radicals. Because of steric effects of alkyl groups on the N-atom, tail-to-tail coupling and, consequently, the formation of benzidine analogues were anticipated[51]. Note that a similar picture was observed earlier for DMA[52] and DEA[25], and for DEA it was discussed in terms of the inductive effect of ethyl groups at the N-atom[25]. On the other hand, the voltammograms in alkaline media (pH 13) are significantly different from those recorded in acidic media. Only one peak, being due to the one-electron oxidation

of DMA, overlapped with the background current due to the O_2 evolution process, was observed[53] at a scan rate of 50 mV s^{-1}. At the same time, not even the smallest cathodic current corresponding to that anodic peak was recorded. This is not surprising: the stability of DEA$^{+\bullet}$ increases in more acidic media; the aniline radical cations and their substituted derivatives behave after all as the Brønsted N-acids. In aqueous solutions the following pK_a values were obtained: 7.05 (determined by means of pulse radiolysis)[54], 7.6 ± 0.3 and 3.6 ± 0.2 (by means of laser flash photolysis)[55] for the radical cations of aniline, N-methylaniline and diphenylamine, respectively.

Anodic transformations of EMA and DMA in aqueous solutions containing 0.1 M CH_3COONH_4 were studied successfully using electrochemical thermospray mass spectrometry[56, 57]. The first step was the oxidation to radical cations; their recombination formed the corresponding benzidine derivatives, being the chief product of electro-oxidation. The main side reaction was also analyzed. In its starting step, the radical cations that display significant acidity are deprotonated at the α-carbon atom of an alkyl substituent with the formation of neutral radicals. A part of these radicals is oxidized anodically to immonium ions. By follow-up reactions, such as dealkylation, oxidation and recombination with radical cations, dimers that are other than benzidine are formed. They react then to give trimers and higher oligomers. Convincing information on the structure of these products was obtained by measurements in D_2O-based electrolyte solutions[57].

The mechanism of electro-oxidation of DMA in acetonitrile was studied by rapid scan cyclic voltammetry. The reduction peak for the radical cation DMA$^{+\bullet}$ was observed at scan rates above 500 V s^{-1}. It was found that DMA$^{+\bullet}$ underwent a second-order radical cation—radical cation coupling with deprotonation to form N,N,N′,N′-tetramethylbenzidine. A rate constant of 6.3×10^5 M^{-1} s^{-1} was calculated[58]. No evidence of polymerization was detected.

Oyama and coworkers[59] have introduced an electron-transfer stopped-flow (ETFS) method for the UV-VIS monitoring of a cation radical–neutral precursor proton transfer reaction. In this method, unstable cation radicals are formed via the electron transfer processes with stable cation radicals whose oxidation potential is positive relative to that of unstable ones. By mixing an acetonitrile solution of tris(p-bromophenyl)amine cation radical (TBPA$^{+\bullet}$) with an acetonitrile solution of N,N-dimethyl-p-toluidine (**33**), the kinetic analysis could be carried out for the oxidative dimerization of **33**. The experiments clearly show a second-order reaction with a rate constant of 650 M^{-1} s^{-1} at 298 K and N,N,N′N′-tetramethyl-α,α'-bi-p-toluidine (**34**) as the final product[60, 61]. Accordingly, the proposed mechanism[60–62] including the dimerization of radicals **35$^{\bullet}$** is given by Scheme 5.

These processes were also studied by a CV technique using a range of concentrations from 1 to 70 mM of **33** at platinum microdisk electrodes of radii ranging from 10 to 50 μm and using scan rates from 20 mV s^{-1} to 6 V s^{-1}. Theory was developed to simulate the mechanism shown in Scheme 5 using the ADI method made to experimental CV curves. The mechanism was found to be consistent with the observed data[62]. The following rate constants were inferred: $k_1 = 5.9 \times 10^5$ M^{-1} s^{-1} and $k_2 = 9.2 \times 10^8$ M^{-1} s^{-1}. The mechanism of the decay of N,N-dimethyl-p-anisidine radical cation in ACN solutions is similar[63] to that proposed for DMA$^{+\bullet}$. In contrast, the dimerization pathway of 4-bromo-N,N-dimethylaniline radical cation (**36$^{+\bullet}$**) was found to be dependent on the concentration of the parent compound, **36**. When **36$^{+\bullet}$** was generated quantitatively, i.e. **36** was absent in solution, a first-order reaction with a rate constant of 0.20 s^{-1} and leading to tetramethylbenzidine dication was observed. Then, when a large excess of **36** was present, the tetramethylbenzidine radical cation (**37$^{+\bullet}$**) was formed quantitatively in the rapid process[64].
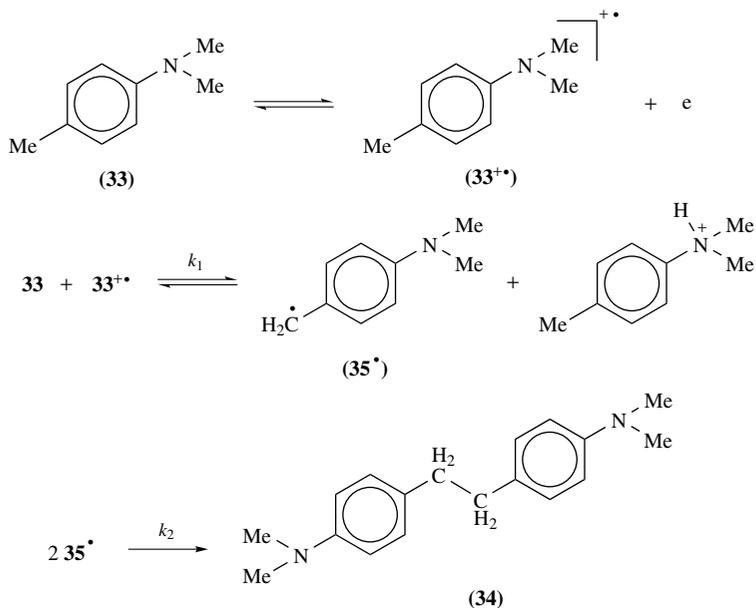
SCHEME 5
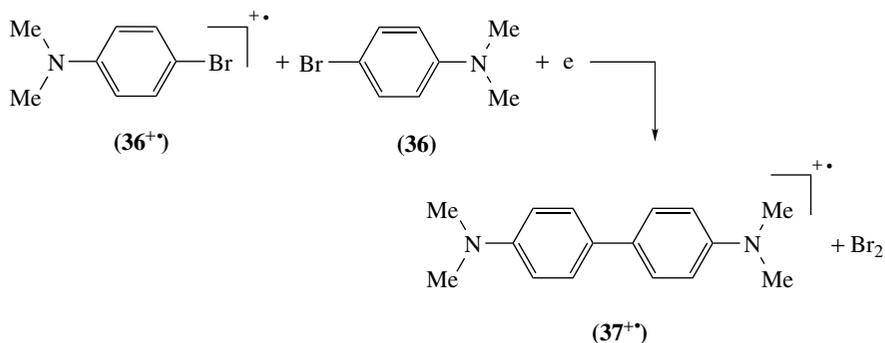
Recall that in the cases of **33** and N,N-dimethyl-p-anisidine, the reaction products were the dimeric compounds formed via the C−C bonding of the carbon atoms of the methyl groups, while the reaction product of p-anisidine is known to be formed via the C−N bonding accompanying elimination of the methoxy group in the *para* position[65]. The p-anisidine and N-methyl-p-anisidine cation radicals were found to be more short-lived than the N,N-dimethyl-p-anisidine cation radical because two methyl groups on the N-atom exhibit a blocking effect to prevent direct C−N bonding[66].

Electro-oxidation of diphenylamine systems has received extensive attention. Recent interest has been associated with the preparation of electronically conductive polymers, such as polyaniline. An important role of p-aminodiphenylamine in the anodic oxidation of aniline is well documented and therefore fundamental electrochemical properties

of this compound were discussed in the previous Section of this Chapter. Now it is important to mention that diphenylamine behaves very similarly: in 4 M H_2SO_4 + 50 vol% C_2H_5OH its CV curve shows an oxidation peak at 0.75 V vs. SCE, which follows a mechanism consisting of a fast one-electron oxidation followed by a coupling of the cation radical to the C−C *para*-coupled dimer diphenylbenzidine, and subsequent two-electron reversible oxidation of diphenylbenzidine itself[67]. Repetitive cycling of the potential over the oxidation peak of diphenylamine indicates the build-up of the polymer with the structure **38**[67, 68]. In addition, the electropolymerizaton processes of diphenylamine have also been studied by cyclic electrochemical quartz crystal microbalance measurements[69] and the results obtained supported the scheme described earlier[67, 68, 70].
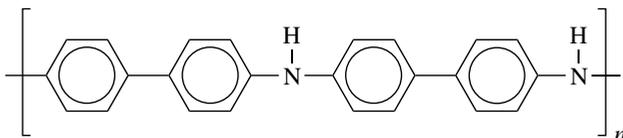
(38)

Cyclic voltammetry, performed with ultramicrodisk platinum electrodes of different diameters (ranging from 5 to 100 µm), was applied to investigate the mechanism of initial stages of electropolymerization of diphenylamine (**39**) in ACN solutions containing $TBAPF_6$, as electrolyte[71]. The diphenylamine radical cation, which is detectable at scan rates above 100 V s^{-1}, undergoes a second-order radical cation—radical cation coupling to form N,N'-diphenylbenzidine (**40**). Digital simulations, performed by the explicit finite-difference method with an exponentially expanding grid, suggested that the dimerization is followed by proton loss and additional electron transfer processes yielding the N,N'-diphenylbenzidine dication.

In very dry acetonitrile the parent diphenylamine molecule acts as a proton acceptor. However, the presence of a small amount of water displaces **39** as the base, and simplifies the interpretation of voltammetric data; under these conditions the net charge passed during the electrode reaction is two electrons per diphenylamine molecule. A rate constant of $k = 2.0 \times 10^5$ M^{-1} s^{-1} for the coupling reaction was determined[71].

The effect of the addition of a base, such as pyridine, in modifying the nature of the electro-oxidation product of aromatic amines has already been noted in early works[72]. More recently, Andrieux and coworkers[73] have investigated both the effect of the changes in structure of aromatic amines and the effect of added bases on the oxidation processes of two secondary and two tertiary amines, with and without methoxy groups in the *para* position of the aromatic rings. Among these, diphenylamine (**39**) and its 4,4′-dimethoxy derivative (i.e. dianisylamine, **41**) were investigated by cyclic voltammetry in ACN on a platinum electrode with the addition of bases of different basicity. It was found that the voltammetric curve of **39** is changed upon the addition of 2,6-lutidine. A new less positive peak appears for a low excess factor of lutidine, γ, which is the ratio of lutidine to amine concentrations, and this is the only wave observed when $\gamma \geqslant 2$. The number of transferred electrons is always 2, but under these conditions a product with only one reversible wave at 0.470 V vs. SCE is formed, as compared with two reversible peaks (at 0.675 and 0.800 V, respectively) recorded in the absence of the base. The wave at 0.470 V was identified as being due to N,N'-diphenylbenzidine, which is formed quantitatively in solutions containing the lutidine. Thus, even in the presence of lutidine the anodic oxidation of **39** leads to the same product in spite of a visible difference in the shape of the CV curves.
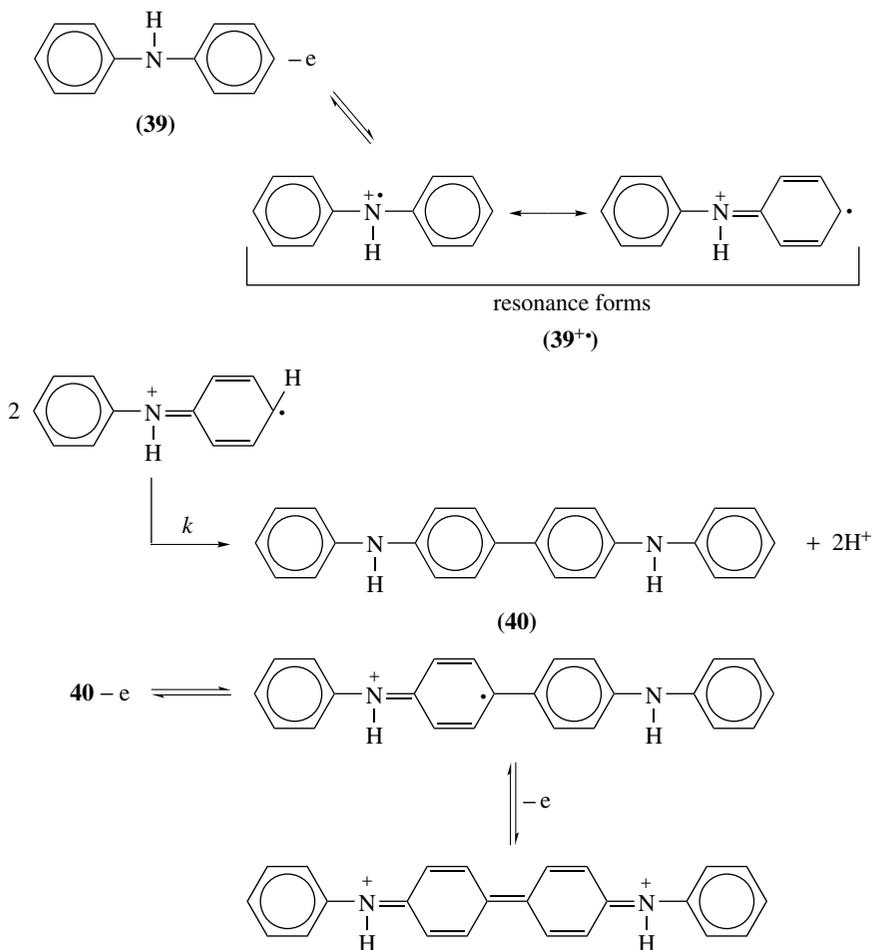
The situation is more complicated in the case of **41**: the shape of voltammograms recorded in the presence of lutidine depends not only on γ but also on scan rates. More-over, at a fast sweep rate, for example at 500 V s^{-1}, the number of electrons transferred is about 2, but it increases to the value of 2.5 at low sweep rates. The results seem to be in agreement with the following oxidation mechanism[73]:

at a fast sweep rate

$$41 + B \longrightarrow 1/2 \ INT^{2+} + BH^+ + 2e$$

at a low sweep rate

$$1/2 \ INT^{2+} + B \longrightarrow 1/2 \ \mathbf{42}$$

$$\mathbf{42} \longrightarrow \mathbf{42}^{+\bullet} + e$$

(41)

(42)

(43)
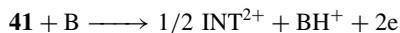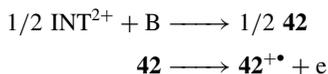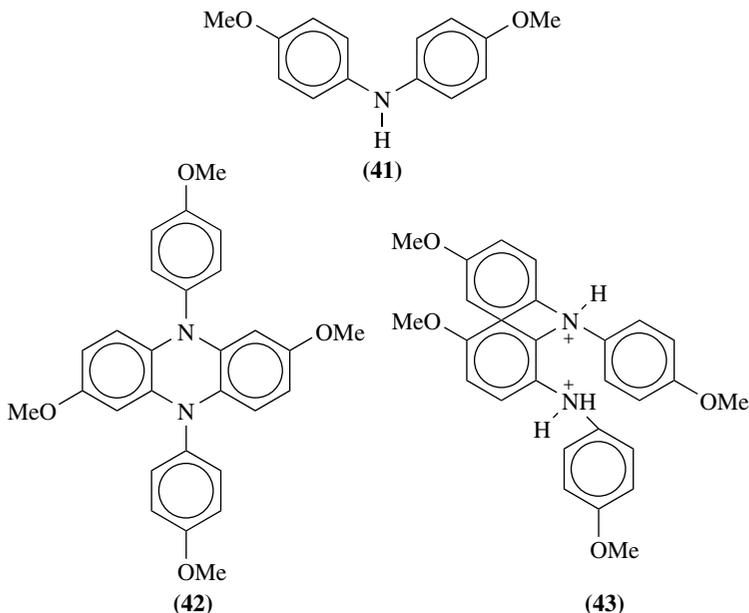
where **B** is the lutidine molecule, **42** is, most probably, 2,6-dimethoxy-9,10-dianisyl-9,10-dihydrophenazine[74, 75] and INT^{2+} marks a non-identified intermediate, probably the dication of 5-methoxy-N,N,N'-trianisyl-o-phenylenediamine (**43**).

Thus, without the p-OCH$_3$ substituents, the coupling of two radical cations through this *para* position is easy, also in the presence of a weak base (lutidine). The formation of **40** is evident during an anodic oxidation of **39** in aprotic conditions even if the voltammetric curve is modified in the presence of the base. With stronger bases (quinuclidine and tetramethylammonium hydroxide) the formation of **40** does not occur because of probable deprotonation of the nitrogen atom. The presence of the $-$OCH$_3$ groups in the *para* position prevents dimerization of two cation radicals. In that case, dianisylamine deprotonation by the base occurs first, leading to a condensation product[73].

The anodic behavior of p-aminodiphenylamine (**10**) in ACN differs considerably from that described above, although the proton-releasing processes play, as before, a decisive role. It was established[76] that **10** is first transformed into its radical cation, which rapidly reacts with the parent molecule forming the neutral radical and the protonated form of **10**. The neutral radical is oxidized at the same potential (Scheme 6), giving rise to a net two-electron oxidation reaction for two molecules of **10**. The experiments performed in the presence of pyridine confirm this mechanism; the proton transfer process seems to be the rate-determining step[76].

Oyama and coworkers analyzed the decay of diphenylamine and N-methyldiphenyl-amine cation radicals in ACN[59, 77] using their ETFS method. Similarly to what was mentioned above, these cation radicals were generated quantitatively by electron transfer with TBPA$^{+\bullet}$ and their absorption spectra ($\lambda_{\max} = 675$ and 639 nm, respectively) could be successfully observed in a time frame of less than a few tens of milliseconds and, as a result, the kinetics of dimerization could be analyzed. In both cases the reactions were found to be of second order in the radical cations concentration, and the corresponding rate

$$10 \; \rightleftharpoons \; 10^{+\bullet} \; + \; e$$
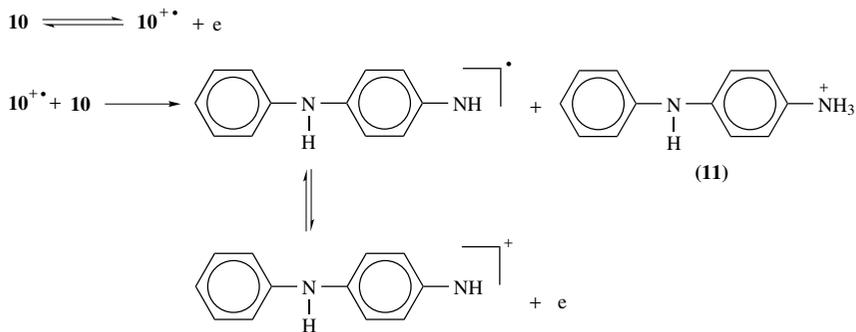
SCHEME 6

constants were determined to be 1.4×10^6 and 1.0×10^6 $M^{-1}\,s^{-1}$ for the cation radicals of methyldiphenylamine and $39^{+\bullet}$, respectively.

In the decay of the radical cation of 4-methyldiphenylamine (**44**), for which an electronic absorption spectrum with $\lambda_{max} = 689$ nm was observed, the main reaction route is the formation of a benzidine-type dimer, similarly to that in the case of $39^{+\bullet}$. The dimerization rate constant is 2.3×10^4 $M^{-1}\,s^{-1}$. However, in the presence of a large excess of parent molecules acting as a base, the formation of cyclized dimers was also suggested. In contrast, the formation of cyclic structures was found to be characteristic of the radical cations of 3′-substituted (**45**) and 3,3′-disubstituted (**46**) derivatives of diphenylamine. On the basis of CV measurements, the formation of dihydrodiphenylphenazine derivatives may be anticipated and, consequently, **47** is assumed to be the product of dimerization of **45**. In both cases the rate constants were as fast as *ca* 1×10^7 $M^{-1}\,s^{-1}$; the 3-methyl substituent promotes visibly the reaction between the 6-position of the phenyl ring of

(44) (45)

(46)

(47)
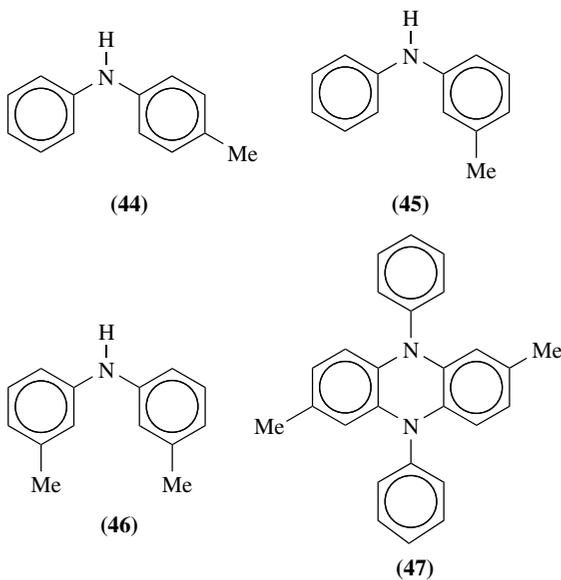
the radical cation and the nitrogen atom of another radical cation. These results were obtained in ACN solutions, again by using an electron transfer stopped-flow method[78]. It can thus be said that the Oyama method permits direct spectrophotometric detection and straightforward kinetic analysis of short-lived cation radicals.

Triarylamines have been the subject of many electrochemical studies. In early works[79–82] much attention was focused on anodic reactions of triphenylamine (**48**), in particular processes producing tetraphenylbenzidine (**49**), which have been shown to proceed via the coupling of radical cations (**48**$^{+\bullet}$). The product, **49**, is oxidizable at more negative potentials than that of **48**, to the radical cation **49**$^{+\bullet}$ and dication **49**$^{2+}$, respectively. A radical—radical dimerization was found to be the rate-determining step[83] and consequently Scheme 7 illustrates the electro-oxidation mechanism of that process[83–85]. This mechanism has recently been used to verify the possibility of applying the concept of the reaction layer to the study of electrode processes coupled with the second-order chemical reactions at microelectrodes under steady-state conditions[86].

The formation of **49**$^{+\bullet}$ and **49**$^{2+}$ in ACN solutions as a function of electrode potential was monitored successfully by electrochemistry combined on-line with mass spectrometry through a particle beam interface[87]. It was also revealed using the Oyama method that in solutions the stability of radical cation **48**$^{+\bullet}$ is only little influenced by an interaction with the parent molecule **48**[84, 88]. This effect is not detectable voltammetrically. Since the electronic spectrum of **48**$^{+\bullet}$ has a sharper absorption maximum at 647 nm and a shoulder at 560 nm, the kinetics of dimerization can be analyzed by following the absorbance decay at 467 nm. As a result, the dimerization rate constant was estimated[84] as 1.8×10^3 M^{-1} s^{-1}, which was in good agreement with the value of 3×10^3 M^{-1} s^{-1} reported independently on the basis of voltammetric data[83].

Cyclic voltammograms of **48** recorded in ACN solutions containing as much as fivefold excess of pyridine are almost identical to those obtained without this base[89]. In both cases the product of the anodic reaction is the dimer **49**. Identical electrochemical responses in the presence and in the absence of pyridine imply that there are no detectable inter-actions between the cation radical **48**$^{+\bullet}$ and the pyridine molecules. However, diverse transformation of the decay profiles of **48**$^{+\bullet}$ depending on the concentration of pyridine was observed using an electron transfer stopped-flow technique. The last observation was ascribed to the interaction between **48**$^{+\bullet}$ and pyridine, in which the proton is extracted by the molecule of the base[89]. One can therefore assume that this is an example of the process for which the voltammetric measurements at conventional scan rates cannot give full information about the pathway of the electrochemical reaction.

Thus, the radical cations **48**$^{+\bullet}$ are relatively stable in ACN solutions; the cathodic current corresponding to their reversible reduction can be observed voltammetrically at scan rates of the order of 20 V s^{-1}. Dimerization is connected with deprotonation that occurs at the phenyl ring, and therefore to make this process difficult the *para* positions of the rings should be blocked. Indeed, the results of Andrieux and coworkers[83] manifest convincingly that the radical cations **50**$^{+\bullet}$–**52**$^{+\bullet}$, which demonstrate reversible redox couples with the parent molecules at a scan rate of 0.1 V s^{-1}, are much more stable than **48**$^{+\bullet}$, and, particularly, than **53**$^{+\bullet}$. In the former case, the reversible voltammograms were recorded at an unusually high scan rate of 20000 V s^{-1}. One can observe at the same time that the stability of radical cations seems to be connected with the formal potentials of redox systems, E^o (the corresponding E^o values[83] are collected in Table 1). In addition, the electrochemical behavior of three triphenylamines mono- (**54**), di- and trisubstituted by boronic ester groups is similar to that obtained for triphenylamine[90].

Interestingly, deprotonation of the cation radical can also occur at the level of the methyl group, as demonstrated in the case of **55**[91].

resonance forms

(48$^{+\bullet}$)

2 **48**$^{+\bullet}$ $\longrightarrow$

+ 2 H$^+$

(49)

$-e$

(49$^{+\bullet}$)

$-e$

(49^{2+})
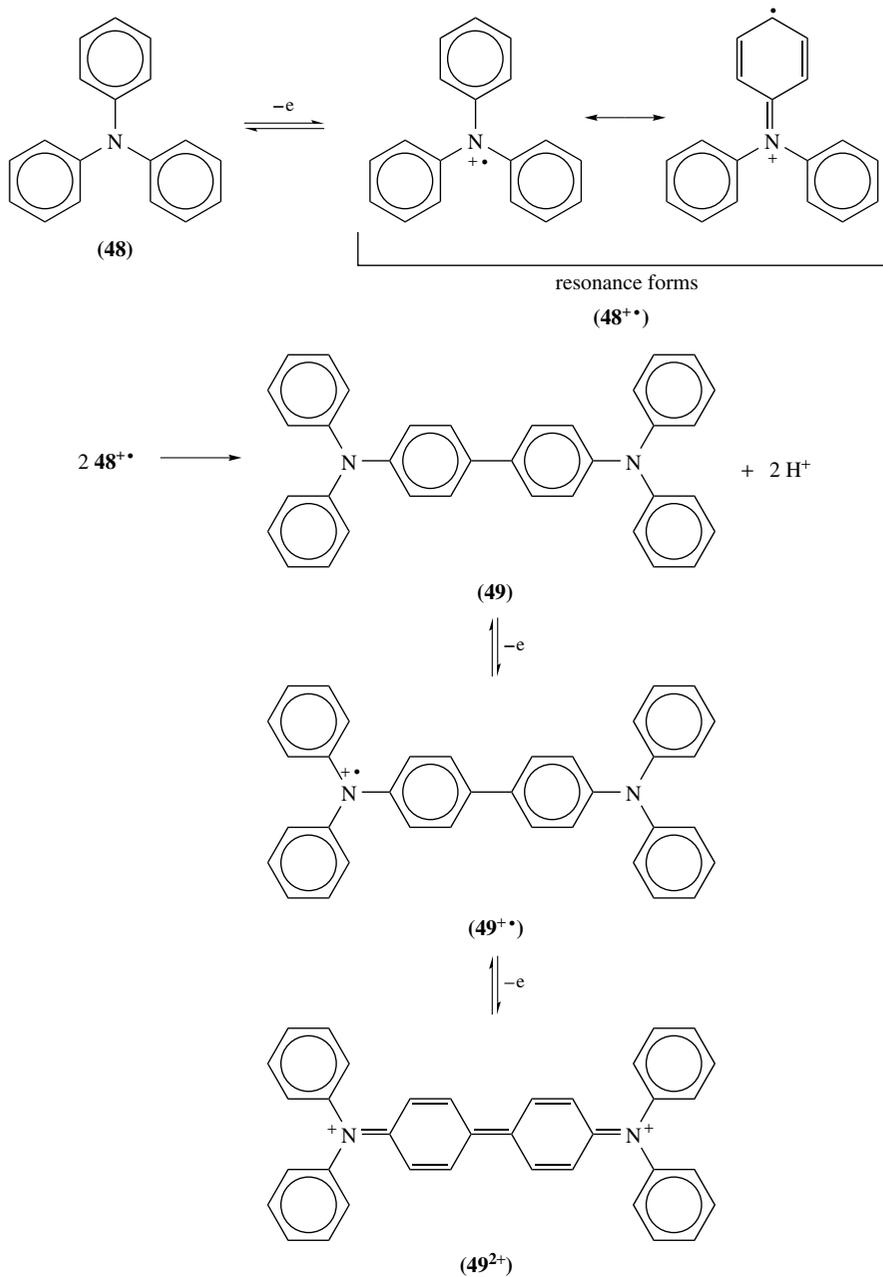
SCHEME 7

TABLE 1. Standard potentials and reversibility of the first electro-oxidation step of tertiary amines in acetonitrile[83]

Compound	Formula	E^o (V) [a]	v (V s^{-1}) [b]
48	Ph$_3$N	0.96	>20
50	(p-BrC$_6$H$_4$)$_3$N	1.09	>0.1
51	(p-MeOC$_6$H$_4$)$_3$N	0.55	>0.1
52	(p-MeC$_6$H$_4$)$_2$PhN	0.82	>0.1
53	PhNMe$_2$	0.90	>20 000

[a] Standard potentials were measured against SCE.
[b] Scan rate at which reversibility was observed.

(54)   (55)
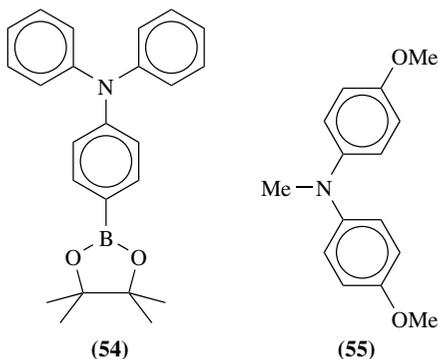
It has been shown very recently that 1,3,5-tris(4-(*N*-phenyl-*N*-3-methylphenyl)phenyl) benzene (**56**), when studied in DMF and dichloromethane solutions, forms two and three reversible one-electron anodic waves, respectively[92]. The kinetics of heterogeneous electron transfers has recently been studied using the high speed microband channel electrode in solutions containing 0.1 M TBAP as electrolyte; it was possible to find standard potentials E^o, transfer coefficients α and, finally, standard rate constants k^o. The obtained data, labeled by subscripts 1, 2 and 3 for the first, second and third electron transfer, respectively, are collected in Table 2.

TABLE 2. Formal potentials E^o, transfer coefficients α and standard rate constants k^o at 20 °C for electro-oxidation of **56** in DMF and dichloromethane solutions[92]

	DMF	CH$_2$Cl$_2$
E^o_1 (V) [a]	0.532 ± 0.002	0.161 ± 0.002
E^o_2 (V) [a]	0.766 ± 0.003	0.495 ± 0.003
E^o_3 (V) [a]		1.128 ± 0.004
α_1	0.48 ± 0.06	0.52 ± 0.02
α_2	0.52 ± 0.02	0.62 ± 0.03
α_3		0.53 ± 0.07
k^o_1 (cm s^{-1})	1.03 ± 0.41	0.44 ± 0.04
k^o_2 (cm s^{-1})	1.02 ± 0.20	0.17 ± 0.03
k^o_3 (cm s^{-1})		0.08 ± 0.02

[a] Standard potentials were determined vs. Ag pseudo-reference electrode.
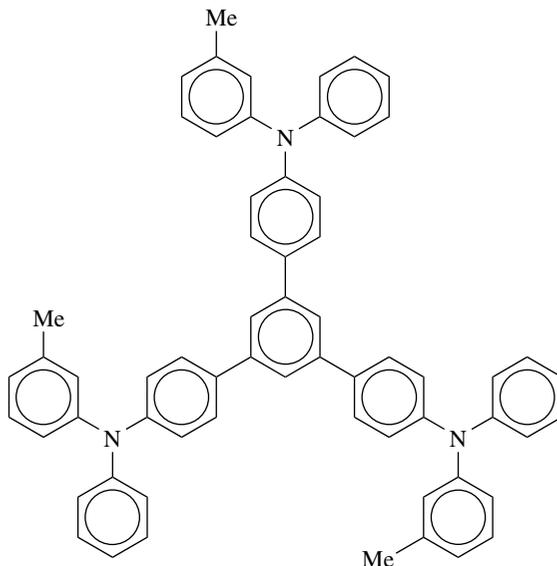
(56)

In recent years, *meta*-connected oligoarylamines have attracted continuing attention as model precursors for positively charged organic high-spin systems. Such molecules are often expected to serve as building blocks for the preparation of bulk magnetic materials[93, 94]. Generally, cyclic voltammograms of these compounds in formally aprotic media reveal consecutive one-electron reversible waves. The measurements demonstrate that up to four and even six electrons can be removed, illustrating the stability of generated cationic species in the time scale of the experiments.

A series of N,N,N',N'-tetraaryl-4,6-dimethyl-1,3-phenylenediamines (**57**) shows a substituent effect on the stability of electro-oxidation products[95]. Cyclic voltammograms of **57a** and **57b** in propionitrile exhibit two reversible one-electron transfers at ambient
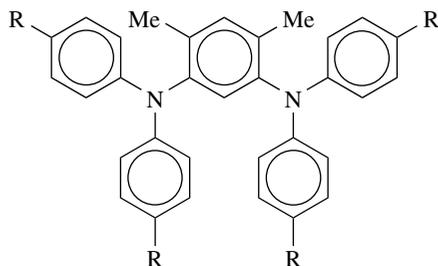
(57a) R = MeO
(57b) R = Me
(57c) R = H
(57d) R = F
(57e) R = Cl

temperature yielding stable radical cations and dicationic species, respectively. A triplet state was unequivocally identified for the ground state of **57a** by an electron-spin transient mutation spectroscopy[96, 97]. Compound **57c** oxidizes in an irreversible one-electron step, indicating instability of the radical cation, while compounds **57d** and **57e** exhibit at $-78\,^\circ$C two reversible one-electron redox systems[95]. Electrochemical and spectroscopic properties of symmetric and asymmetric tetraaryl *m*- and *p*-phenylenediamines, treated as precursors of organic high-spin and mixed valence systems, were also analyzed[98, 99].

Alternating *meta* and *para* oligoanilines also seem to be interesting building blocks for future polaronic ferromagnets. Note, therefore, that a stable di(cation radical) **60** in a triplet ground state is formed in a proton-triggered redox reaction between N,N'-bis(4-diphenylamine)-1,3-phenylenediamine (**58**) and **59**. The reaction occurs in ACN solutions upon addition of 1 vol% trifluoroacetic acid[100, 101].

(58)

+

(59)

(60)
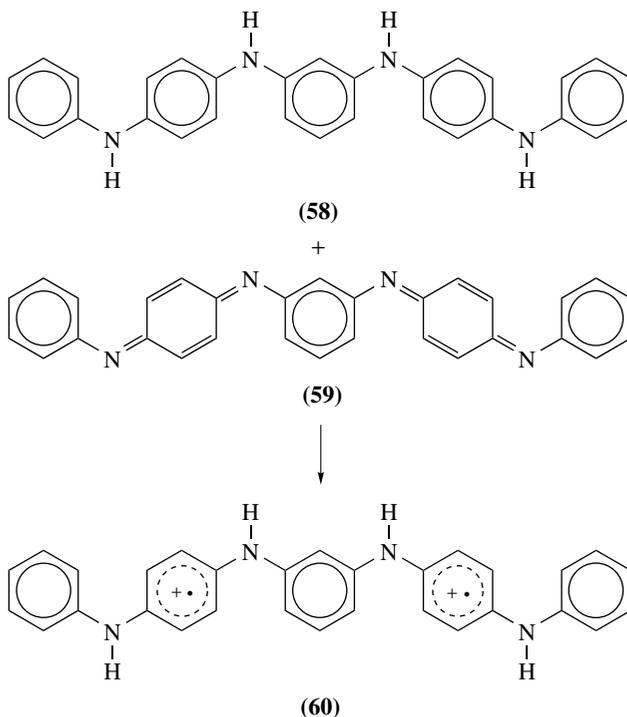
The removal of two electrons from a *p*-phenylenediamine unit with secondary amines leads to deprotonation and gives irreversible oxidation processes. However, cyclic voltammograms of compound **58** were carried out in ACN with 0.01 M $HClO_4$, because in the presence of acid deprotonation is suppressed and the voltammogram reveals two broad reversible oxidations[102]. Cyclic voltammograms of compound **61** in dichloromethane containing 0.1 M $TBAPF_6$ (scan rate 100 mV s^{-1}) indicates that oxidation is a reversible process in which up to four electrons can be removed. The corresponding cation radicals and di(cation radicals) are stable under ambient conditions. Next, in the voltammograms of **62**, **63** and **64** as many as six oxidation waves can be distinguished. Consequently,

the properties of the corresponding tricationic species, which are sufficiently stable in dichloromethane, have been established by UV-VIS and ESR spectroscopy[102].
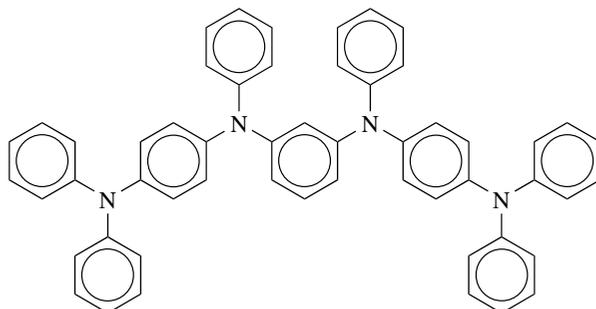
(61)
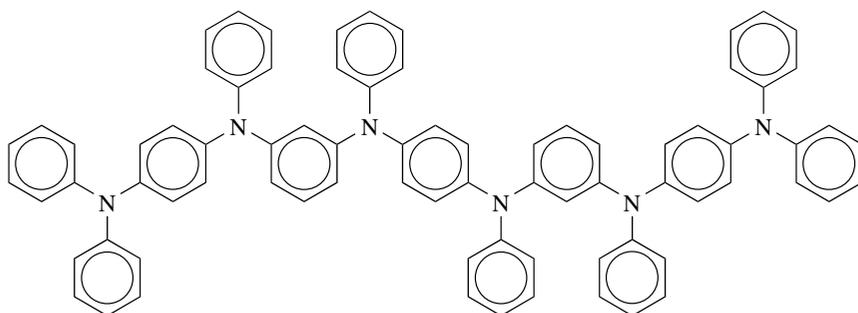
(62)

Formation of mono-, di- and tri(cation radicals) was also observed by cyclic voltammetry of compounds **65a** and **65b** in dichloromethane with 0.1 M TBABF$_4$ (scan rate 50 mV s^{-1}). Both trications were stable in solutions at room temperature for several hours. It is interesting that the tri(cation radical) of **65b** is not reactive towards oxygen, as indicated by no loss of ESR signal intensity upon purging its solution with O$_2$. The mono-, di- and tri(cation radicals) of **65b** all survive isolation and have been prepared as PF$_6^-$ salts by NOPF$_6$ oxidation of the parent compound[103].

The formation of tricationic species of 1,3,5-tris(diphenylamino)benzene (**66**) may be observed by a CV technique in dichloromethane containing TBABF$_4$ at a scan rate of 0.3 V s^{-1}. The tri(cation radical) can be easily obtained by chemical oxidation of **66** in CH$_2$Cl$_2$—trifluoroacetic anhydride mixture containing TBABF$_4$. The species is stable at room temperature in an evacuated sample tube in the presence of an excess of trifluoroacetic anhydride and BF$_4^-$ counter ion. No intensity change in its ESR spectrum was observed over a one-month period. Analysis of the spectrum indicates that the tri(cation radical) exists in a quartet ground state, or the doublet and quartet are nearly degenerated ground state[104].

Reports describing solid state chemistry of cation radicals are decidedly rare. We therefore make a short note of the redox properties of *N*,*N*′-diphenyl-*N*,*N*′-bis(2,4-dimethylphenyl)-(1,1′-biphenyl)-4,4′-diamine (**67**). CV studies of this compound in
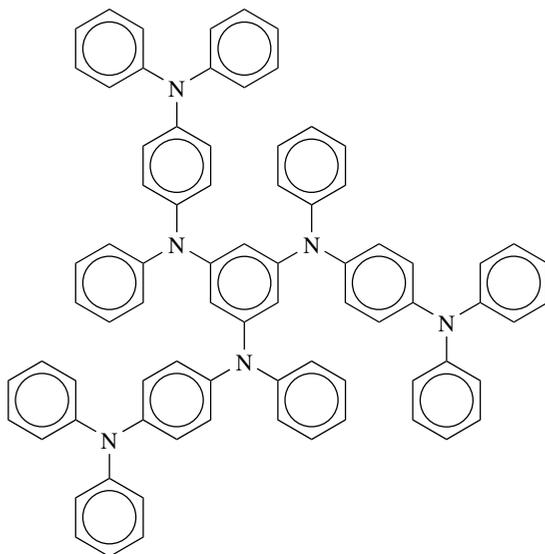
(63)
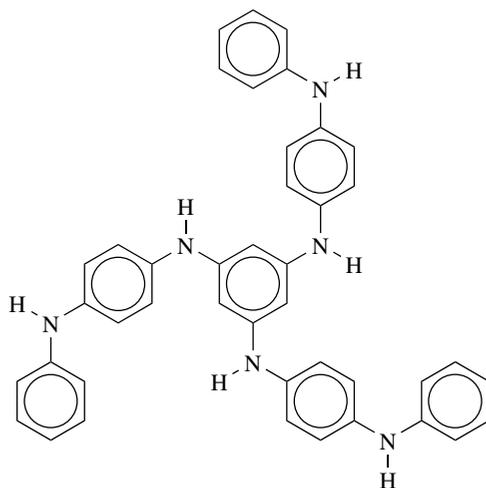
(64)

$CH_2Cl_2 + 0.1$ M TBABF$_4$ (scan rate 0.1 V s^{-1}) revealed two reversible one-electron peaks, associated with the formation of the cation radicals and dications, respectively. Chemical oxidation of **67** with one equivalent of SbCl$_5$ in dichloromethane resulted in immediate formation of a dark orange solution of cation radical, from which dichroic, needle-like crystals (with SbCl$_6^-$ counter ions) with a metallic luster were obtained following the addition of *n*-hexane. The crystallographic, molecular and electronic properties of these crystals were studied exhaustively[105].
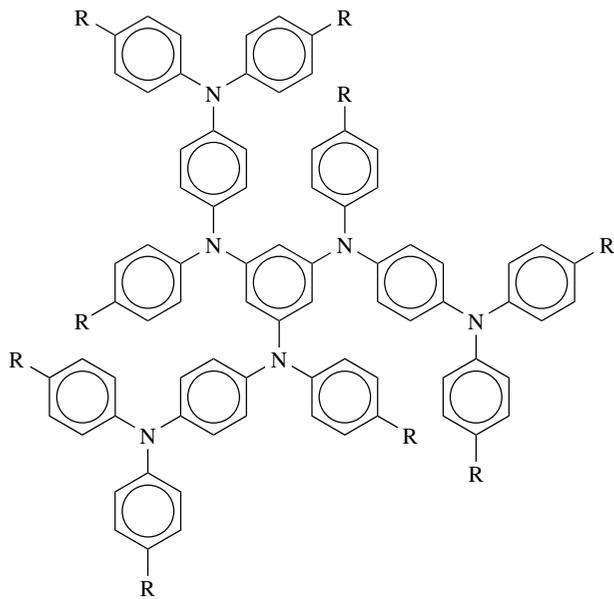
(65a) R = H
(65b) R = MeO
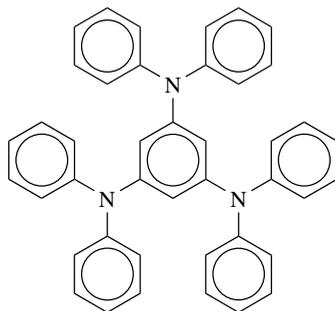
(66)
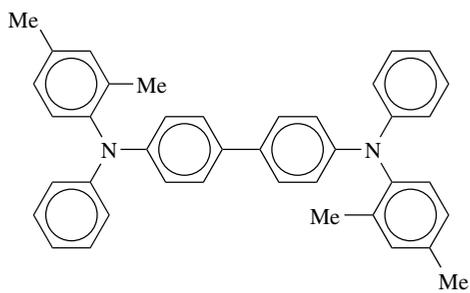
(67)

IV. RING-SUBSTITUTED ANILINES

The general mechanism of anodic oxidation and the main products of dimerization are similar for various C-substituted anilines, but detailed steps for a given reactant and the products distribution depend strongly on the nature and position of the substituent as well as on the medium used. It becomes comprehensible when taking into account that substituents exert a strong influence on the acid–base properties of the neutral reactants as well as on the reactivity of the electrogenerated radical cations, and that protonation/deprotonation steps participate in reaction schemes.

A. Monosubstituted Anilines

1. para-Substituents

The general pattern of anodic behavior of *para*-substituted anilines (**68**) was established in aqueous acidic media by Bacon and Adams[17, 106]. The postulated one-electron oxidation of the substrate to the radical cation **68**$^{+\bullet}$ is followed by rapid head-to-tail coupling of **68**$^{+\bullet}$ with the substrate **68** giving protonated 4′-substituted 4-aminodiphenylamine in the oxidized form (**69**) as the final main product. The product **69** shows reversible redox peaks at more cathodic potentials, supporting its identification beside the spectral and chemical analysis. The product formation is preceded by elimination of one *para*-substituent and, if it leaves as an anion (e.g. halide, methoxide or ethoxide ion), then the overall electrochemical process (equation 1) corresponds to a one-electron (two electrons per two reactant molecules) process. However, if it leaves as a neutral group (e.g. CO_2 in the oxidation of *p*-aminobenzoic acid), a dimer is formed in the reduced form and the overall reaction is a two-electron process.

$$2\,X\!\!-\!\!\text{C}_6\text{H}_4\!\!-\!\!NH_2 \longrightarrow X\!\!-\!\!\text{C}_6\text{H}_4\!\!-\!\!N=\text{C}_6\text{H}_4=\overset{+}{N}H_2 + X^- + 2H^+ + 2e$$

(**68a**) X = OMe	(**69a**) X = OMe
(**68b**) X = Cl	(**69b**) X = Cl
(**68c**) X = Br	(**69c**) X = Br
(**68d**) X = Et	(**69d**) X = Et
(**68e**) X = Me	(**69e**) X = Me
(**68f**) X = Ph	(**69f**) X = Ph
(**68g**) X = I	(**69g**) X = I

(1)
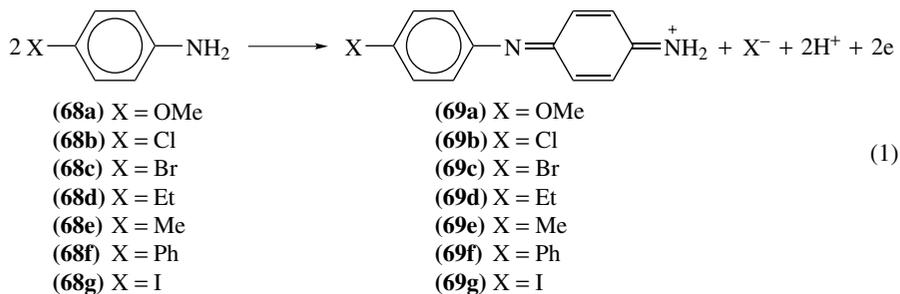
More recently, the same overall reaction was established in aprotic media[65, 107–110], but then the product may exist in the protonated (as shown above) or deprotonated form (**70**, equation 2), depending on the exact pH of the experiment[65, 107].

$$2\,X\!\!-\!\!\text{C}_6\text{H}_4\!\!-\!\!NH_2 \longrightarrow X\!\!-\!\!\text{C}_6\text{H}_4\!\!-\!\!N=\text{C}_6\text{H}_4=NH + X^- + 3H^+ + 2e$$

(**68a**) X = OMe	(**70a**) X = OMe
(**68b**) X = Cl	(**70b**) X = Cl
(**68c**) X = Br	(**70c**) X = Br
(**68g**) X = I	(**70g**) X = I

(2)
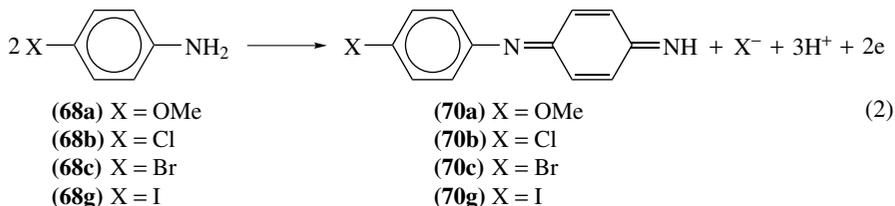
Only the application of fast cyclic voltammetry (in the range of $10–100\ \text{kV s}^{-1}$) at gold ultramicroelectrodes has resulted recently in obtaining[65, 107] in DMF reversible one-electron oxidation peaks of *p*-anisidine (**68a**), *p*-chloroaniline (**68b**) and *p*-bromoaniline

(**68c**) (equation 3). Thus, the formation of radical cations **68$^{+\bullet}$** in the first step of the oxidation of typical *para*-substituted anilines with substituents acting in opposite directions was proved. It was also possible to find transfer coefficients α and standard potentials E^{o} for equation 3, and (in conditions of quasi-reversibility) the standard rate constants k^{o} for this heterogeneous electron transfer. The voltammetric data for the oxidation in unbuffered DMF of **68a–68c** are collected in Table 3.

$$\textbf{68} \;\underset{}{\overset{k^{\mathrm{o}}}{\rightleftharpoons}}\; \mathrm{X}\!-\!\!\left[\bigcirc\!\!-\!\mathrm{NH_2}\right]^{+\bullet} + \; \mathrm{e} \tag{3}$$

(**68a$^{+\bullet}$**) X = OMe
(**68b$^{+\bullet}$**) X = Cl
(**68c$^{+\bullet}$**) X = Br
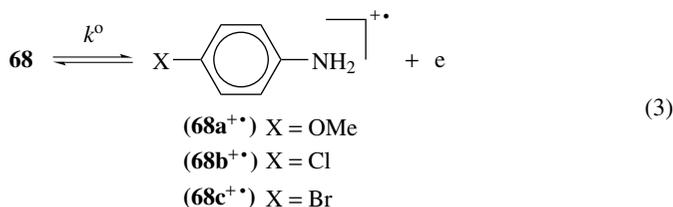
Inspection of these data shows that the standard potential is less positive for **68a** than for **68b** and **68c**, as expected, because the oxidation should be easier in the presence of an electron-releasing than of an electron-withdrawing substituent. The parallel shift of k^{o} values is also well understood as being caused by thermodynamic contribution to the activation barrier, which is in full agreement with the Marcus theory of electron transfer kinetics. The most interesting observations are the quite different slopes of the change of anodic peak potentials with the scan rate $\partial E_{\mathrm{pa}}/\partial \log \nu$ and with the reactant concentration $\partial E_{\mathrm{pa}}/\partial \log c$, which are diagnostic criteria for the reaction mechanism. It is evident that the rate-determining step (rds) is the second-order reaction of dimerization in the case of **68a**, but the behavior is more complicated for **68b** and **68c** where for the overall dimerization there is no dependence on the reactant concentration. The detailed mechanism (DIM2) proposed[65] for **68a** (Scheme 8) includes one-to-one coupling of cation radical **68a$^{+\bullet}$** and substrate **68a** as the rds; the corresponding rate constant is given in Table 3. Thus, the C−N bond formation occurs through an overall *ipso* substitution of

TABLE 3. Electrochemical characteristics of the oxidation of *para*-substituted anilines in DMF + TBABF$_4$ at 25 °C

	68a	**68b**	**68c**
σ ^{a}	−0.27	0.23	0.23
pK_a of **68$^{+\bullet}$** ^{b}	10	5	5
E^{o} (V vs. SCE) ^{c}	0.685 ± 0.005	1.055 ± 0.005	1.057 ± 0.005
k^{o} (cm s^{-1}) ^{d}	ca 0.4	1.1	1.2
α ^{e}	0.45	0.62	0.56
$\partial E_{\mathrm{pa}}/\partial \log \nu$ (mV) ^{f}	30	20	20
$\partial E_{\mathrm{pa}}/\partial \log c$ (mV) ^{g}	30	0	0
$\log k_{\mathrm{rds}}$	7.7 ^{h}	5.34 ^{i}	5.65 ^{i}
Reference	65	107	107

^{a} Hammett substituent constant for X from Reference 111.
^{b} Equilibrium acidity of radical cations **68$^{+\bullet}$** in DMSO from Reference 112.
^{c} Standard potential for the reversible oxidation measured at high scan rates.
^{d} Rate constant for the first electron transfer.
^{e} Transfer coefficient.
^{f} Slope of the shift of anodic peak potential with a scan rate ν.
^{g} Slope of the shift of anodic peak potential with the reactant concentration.
^{h} Rate constant in M^{-1} s^{-1} for the dimerization (rate-determining step).
^{i} Apparent rate constant in s^{-1} for the overall rds.
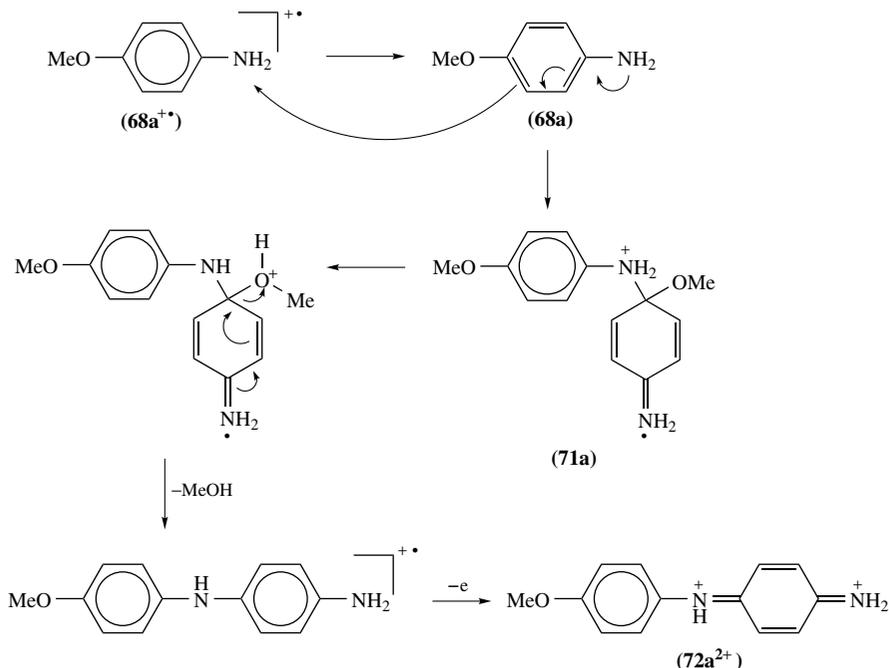
SCHEME 8

the methoxy group in the *para*-substituted position, followed by rearrangement of radical **71a**, elimination of methanol and final oxidation to the 4-amino,4′-methoxydiphenylamine dication (variamine blue dication, **72a^{2+}**, as shown in Scheme 8).

Two alternative routes (with the same final product and electrochemical characteristics) were also considered[65]. They include an irreversible proton transfer from **68a$^{+\bullet}$** to **68a** resulting in the deprotonated radical that is coupled in a subsequent step with parent **68a** or its radical cation **68a$^{+\bullet}$**. However, in further work[107] it was shown that the oxidation peak potential E_{pa} does not depend on the concentration of the added base *sym*-collidine (which is a stronger base in water than **68a**). This indicates that **68a** is not able to deprotonate its radical cation **68a$^{+\bullet}$** and the mechanism involves only a true nucleophilic attack of **68a** onto its radical cation **68a$^{+\bullet}$**, as shown in Scheme 8.

More recently, the detailed kinetics of the decay reaction of *p*-anisidine radical cations **68a$^{+\bullet}$** in ACN was investigated by the ETSF method[66] using spectral analysis of **68a$^{+\bullet}$** (absorption band at 450 nm) and products variamine blue dication **72a^{2+}** (absorbance at 580 nm) and radical cation **72a$^{+\bullet}$** (absorbance at 595 nm). Contrary to previous results of Simon and coworkers[65] in DMF, the formation of dication **72a^{2+}** as well as of radical cation **72a$^{+\bullet}$** was observed with the overall stoichiometry shown in equations 4a and 4b.

$$\textbf{68a}^{+\bullet} + \textbf{68a}^{+\bullet} \longrightarrow \textbf{72a}^{2+} + \text{MeOH} \qquad (4a)$$

$$\textbf{68a}^{+\bullet} + \textbf{68a} \longrightarrow \textbf{72a}^{+\bullet} + \text{MeOH} \qquad (4b)$$

However, it should be emphasized here that in the ETSF experiments decay reactions occur in homogeneous solutions not in the vicinity of the electrode as in the previous work[65].

Nevertheless, the rate law of decay was found[66] to be $-d[\textbf{68a}^{+\bullet}]/dt = k_1[\textbf{68a}^{+\bullet}]^2[\textbf{68a}]$ when radical cations $\textbf{68a}^{+\bullet}$ are formed in the presence of parent molecules $\textbf{68a}$ but $-d[\textbf{68a}^{+\bullet}]/dt = k_2[\textbf{68a}^{+\bullet}]^2$ in the absence of parent molecules. Finally, a mechanism of dimerization was proposed (Scheme 9) corresponding to reactions 4a and 4b and consistent with the rate laws found if $k_1 = 2Kk'$ and $k_2 = 2k''$.
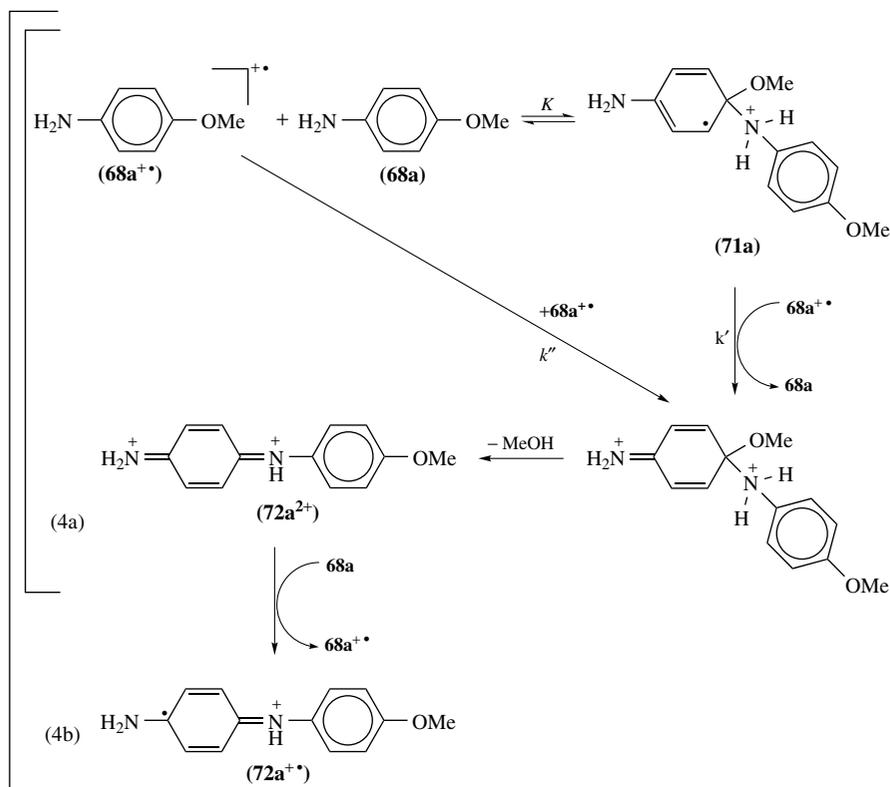
SCHEME 9

On the other hand, a different mechanism than that proposed by Bacon and Adams[106] was suggested by Sharma and coworkers[25] for the oxidation of *p*-toluidine (**68e**) in acidic (0.1 M H_2SO_4) and aprotic (ACN) media on the basis of CV experiments on graphite electrodes. The dimerization of primary radical cations $\textbf{68e}^{+\bullet}$ can occur only by head-to-head coupling (equation 5) and results in 4,4′-dimethylhydrazobenzene (**73e**), which is immediately oxidized to 4,4′-dimethylazobenzene (**74e**). Thus, the overall process is the two-electron exchange and the back reduction of **74e** is restricted because two methyl groups in *para* positions substantially increase the electron density at the $-N=N-$ site.

Absorbance of intermediates formed during the anodic oxidation of **68e** in 0.5 M H_2SO_4 in spectroelectrochemical experiments on ITO glass electrodes was observed in the range 490–520 nm and it was found[46] that the ensuing reactions are slower than those for unsubstituted anilines, but the nature of intermediates was not resolved. However,

in earlier investigations in basic aqueous solutions head-to-head as well as head-to-tail couplings were observed[113, 114] and for **68e** also a coupling in the *ortho*-position was observed[114].

(68e$^{+\bullet}$) X = Me

(68b$^{+\bullet}$) X = Cl

(73e) X = Me

(73b) X = Cl

$-2e$ | $-2H^+$

(5)

(74e) X = Me

(74b) X = Cl
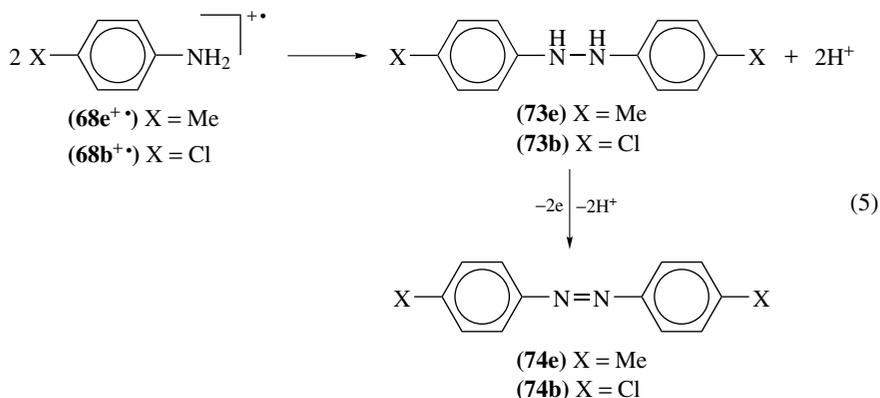
Anodic oxidation of 4-aminobiphenyl (**68f**, X = Ph) in mixtures of hydrochloric acid and ACN results in the same polymer (**38**) as that obtained from diphenylamine, suggesting[68] the conventional head-to-tail coupling, as for other *para*-substituted anilines.

The anodic oxidation of *p*-haloanilines in DMF[107] or ACN[108–110] results in **70** as a main product (equation 6), but the corresponding 2,4-dihaloanilines were also formed as minor products. They are oxidized in ACN giving in the second cycle a 'shoulder' after the main oxidation peak[108, 109]. Their formation was explained[107] by the reaction between the substrate (**68b** or **68c**) with the dihalogens formed by oxidation of halide ions, released as shown in equation 2. It was proved experimentally that Cl$^-$ and Br$^-$ ions are oxidizable in aprotic solvents at potentials corresponding to the oxidation of **68b** and **68c**, respectively, in contrast to the behavior observed in aqueous solutions.

(68b) X = Cl

(68c) X = Br

(68g) X = I

(70b) X = Cl

(70c) X = Br

(70g) X = I

(6)
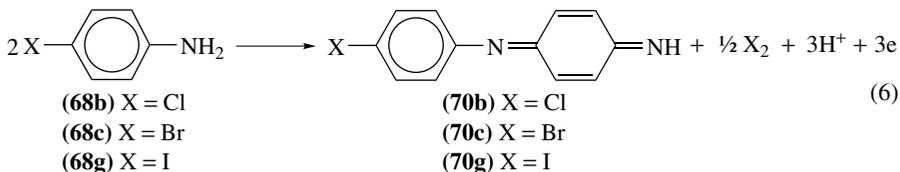
Equations 2 and 6 fully explain the observed[107–110] electron stoichiometry: the apparent number of electrons per molecule changes between $1 \leqslant n_{app} \leqslant 1.5$ depending on the fraction of halide ion that is oxidized.

The detailed mechanism (Scheme 10) proposed[107–110] for the main product formation on the basis of electrochemical characteristics (Table 3) involves, before the coupling step, a fast reversible deprotonation of the primary radical cation (**68b$^{+\bullet}$** or **68c$^{+\bullet}$**) by a base present in the medium. The resulting radical **75** is coupled with radical cation **68$^{+\bullet}$** and the adduct formed releases spontaneously a HX molecule giving the final product 4-imino-4′-halodiphenylamine (**76b** or **76c**). The overall mechanism corresponds to the e-p-RRC-p mechanism according to Savéant nomenclature[115] (e and p denote electron and proton transfer, respectively, and RRC denotes the radical–radical coupling with block capitals indicating the rds). The apparent rate constants, k_{app}, for the overall deprotonation/dimerization sequence were determined[107] (Table 3): for **76b**, $k_{app} = k_{dim} K_H$ and for
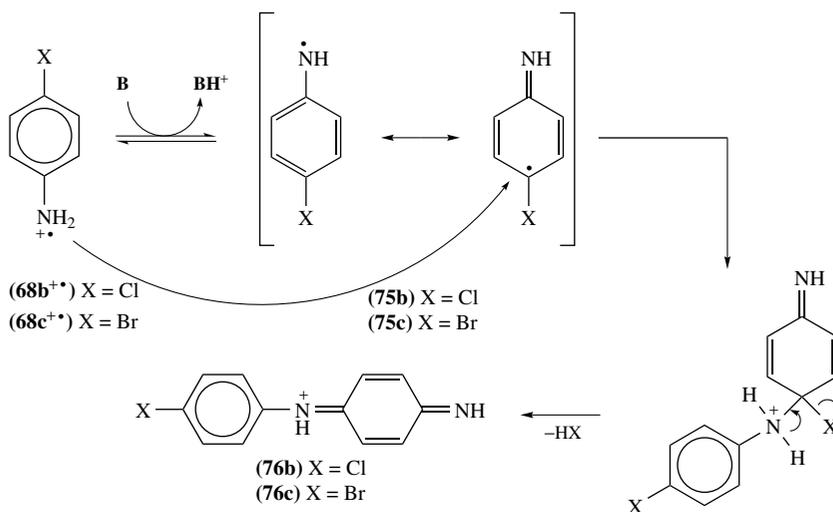
SCHEME 10

76c, $k_{app} = 2/3\ k_{dim} K_H$, where k_{dim} is the dimerization rate constant and K_H the equilibrium constant of the protonation of **75**. The mechanism proposed was confirmed[107] by experiments with the added relatively stronger but non-nucleophilic base 2,6-lutidine. At lower base concentration the electrochemical characteristics remain similar but the shifts of potentials of the oxidation peaks indicate the participation of 2,6-lutidine in the deprotonation step. At higher concentrations $\partial E_{pa}/\partial \log v = 30$ mV per decade, indicating irreversible deprotonation of **68$^{+\bullet}$**, which becomes the rds, and the process corresponds to the e-P-rrc-p mechanism.

In conclusion, the difference in mechanisms for the main oxidation route of **68a** (DIM2 mechanism) and **68b, 68c** (e-p-RRC-p mechanism with fast deprotonation of radical cations) can be easily understood, taking into account that halogenated radical cations **68b$^{+\bullet}$** and **68c$^{+\bullet}$** are much stronger acids than **68a$^{+\bullet}$** due to inductive and mesomeric effects of halogen substituent, as revealed from the equilibrium acidity estimated in DMSO (Table 3).

Detailed analysis of voltammetric results as well as oxidation products prepared by controlled potential electrolysis of **68b** and **68c** in ACN and identified by modern techniques of gas chromatography and electrospray mass spectrometry (GC-ECD, GC-MS and ES-MS) showed[108, 109] that halogen substituents are oxidized after elimination to elemental halogens (equation 6), which substitute the free *ortho* position of the substrate, resulting in the formation of dihalogenated anilines **77b** and **77c** and halodiphenylamines **70** as shown in equation 7. **70b** is the main product for the oxidation of *p*-chloroaniline (**68b**), but **77c** is produced in the greatest amount in the case of *p*-bromoaniline (**68c**), as is evident from Table 4. The halogenation consumes all the expelled halogens (no AgCl or AgBr precipitated after addition of Ag$^+$ ions[108, 109]) and it occurs simultaneously with the main dimerization process taking place in accordance with the Bacon–Adams mechanism. Parallel chlorination of dimers **70** beside substrates was proposed on the basis of voltammetric curves[108]. Electro-oxidation products obtained from **68b** and **68c** are summarized in Table 4. Moreover, the *ortho*-position coupling shown in equation 8, beside head-to-tail coupling, results in **78b**, which was found experimentally among the products

TABLE 4.   Relative intensity (%) from GC-MS peaks of products[108, 109] arising from controlled potential electrolysis of **68b** ($E = 0.800$ V vs. Ag/Ag$^+$) and **68c** ($E = 0.840$ V vs. Ag/Ag$^+$) in unbuffered ACN

Product	X = Cl	X = Br
4-X-aniline **68**	100	100
2,4-X$_2$-aniline **77**	23	58
2,4,6-X$_3$-aniline	0.7	1.2
4,4′-X$_2$-azobenzene	1.1	1.2
4-Amino-4′-X-diphenylamine **70**	78.4	38.8
2-Amino-4,5′-dichlorodiphenylamine **78b** (or 5,10-dihydro-2-hydroxy-7-X-phenazine)	30.4	3.2 ^{a}
4-Amino-3,4′-X$_2$-diphenylamine **79**	8.8	2.4

^{a} 5,10-Dihydro-2-hydroxy-7-bromophenazine.

in the case of the chloro derivative. On the other hand, the *ortho*-coupling is evidently smaller[109] for **68c** (Table 4) because of a steric hindrance of the large bromine atom as well as of less electrophilic properties of radical cation **68c**$^{+\bullet}$. The formation of **79** can be easily explained[108] by the coupling of the substrate radical cation **68b**$^{+\bullet}$ with one of the products **77b**.

$$3 \quad \longrightarrow \quad X\text{—}\bigcirc\text{—N}=\bigcirc=\text{NH} \; + \; \bigcirc \; + \; 4e \; + \; 4H^+ \tag{7}$$

(68b) X = Cl   **(70b)** X = Cl   **(77b)** X = Cl
(68c) X = Br   **(70c)** X = Br   **(77c)** X = Br
(68e) X = Me   **(70e)** X = Me   **(77e)** X = Me

$$2 \; \textbf{68b} \quad \longrightarrow \quad \bigcirc=\text{N}\text{—}\bigcirc\text{—Cl} \; + \; 4e \; + \; 4H^+ \tag{8}$$

(78b)

The overall process is also complicated by the fact that the amino groups of **68b** and **68c** act in ACN as strong proton acceptors consuming protons liberated during the oxidation. The resulting protonated amines cannot be oxidized electrochemically, decreasing the apparent number of electrons exchanged n_{app}[108, 109].

The oxidation of *p*-iodoaniline (**68g**) in ACN occurs in a similar way, according to equation 6 and producing 4-amino-4′-iododiphenylamine (**70g**) and iodine (no AgI precipitated after the addition of Ag$^+$ ions). However, iodine is unable to iodinate the parent aniline **68g** in ACN[109].

On the other hand, the head-to-head coupling giving azobenzene derivatives was negligibly small[108, 109]. However, it should be remembered that in earlier investigations the above coupling was found to be important in basic aqueous solutions[113, 114, 116, 117] as

well as in ACN containing pyridine[72]. The oxidation of **68b** in large-scale electrolysis on the platinum electrode in ACN with 0.1 M pyridine (**80**) resulted[72] in 4,4'-dichloroazobenzene **74b** as the main product (24.3%) and tetra-p-chloroazophenine (**81**), i.e. 2,5-bis(p-chlorophenylamino)benzoquinone di-p-chlorophenylimine (7.8%). A two-electron overall process was observed in the same medium in voltammetric experiments performed at a platinum RDE. Thus, the mechanism proposed (equation 9) involved the deprotonation of primary radical cation **68b**$^{+\bullet}$ by pyridine with the formation of neutral radical **75b** and protonated pyridine (**82**). Next, the radical–radical coupling of **75b** results in 4,4'-dichlorohydrazobenzene (**73b**), which was further oxidized to **74b**.

(9)
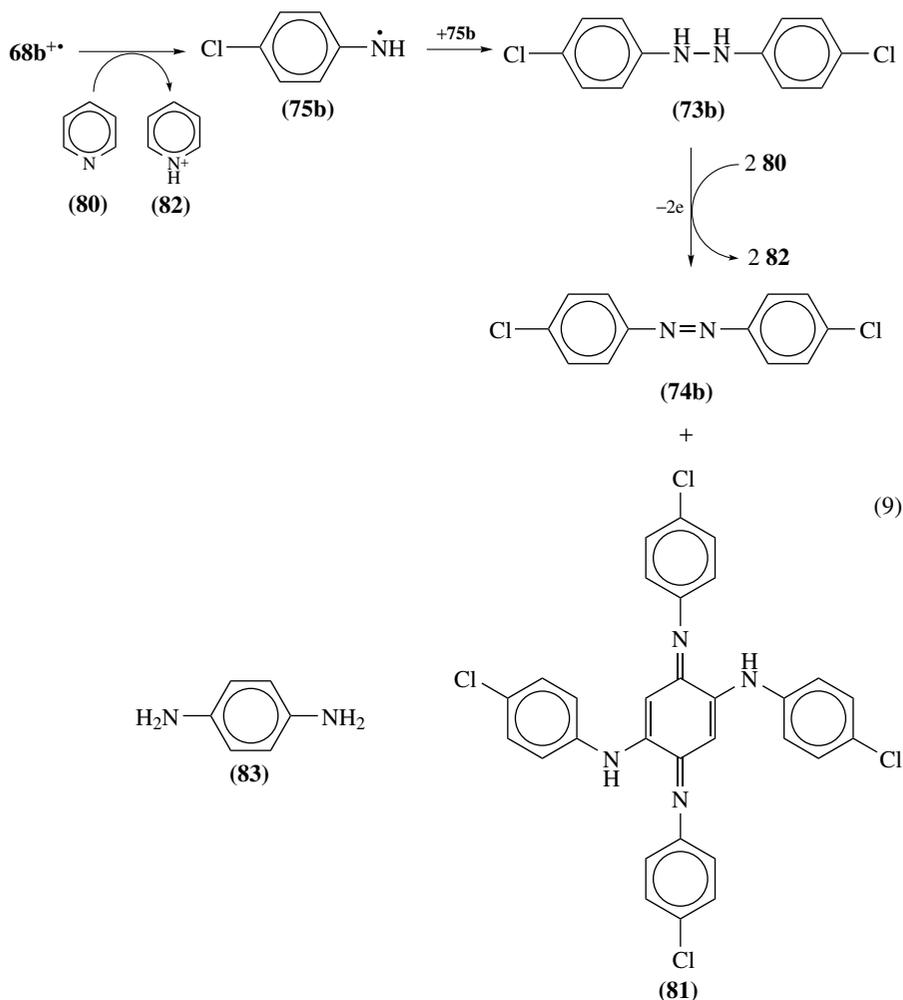
The electrochemical properties of phenylenediamines, in particular of *para*-phenylene-diamine (**83**), have been studied intensively. In aqueous media, the oxidation potentials of these compounds depend upon the pH value, since the amino group can be protonated. In the pH range of 2–6, the radical cation **83**$^{+\bullet}$ can be generated anodically as demonstrated

by Adams and coworkers by the use of an ESR technique[118, 119]. Two-electron oxidation leads to quinonediimine, for which two routes of decomposition are opened. One of these is the hydrolysis yielding the quinoneimine, and the other is a 1,4-addition of a nucleophile to the quinoidal system. The electro-oxidation of **83**[120, 121] and its nitrogen-substituted derivatives[122, 123] in aprotic conditions has also received considerable attention. A reversible process leading to stable radical cations was observed in ACN, DMF, chloroform and other formally aprotic media.

The kinetics of the electro-oxidation of derivatives of **83** has been a subject of long-standing interest. In particular, solvent effects on the standard heterogeneous rate constants k^o and on the corresponding homogeneous rate constants k_{hom} have been investigated and compared. Grampp and Jaenicke[124] determined the rate constants k_{hom} of the half-exchange reactions between derivatives of **83** and the corresponding radical cations in six aprotic solvents with various electric permittivities, ε. The results seemed to be in accordance with the classic Marcus theory: $\ln k_{hom}$ was found to depend linearly on the Pekar factor $\gamma = (1/\varepsilon_o - 1/\varepsilon)$, where ε_o stands for optical electric permittivity. However, the calculated Marcus activation free enthalpies were considerably smaller than the measured ones and temperature dependences of k_{hom} were not in agreement with the Marcus theory. The observed deviations were explained by a temperature-dependent reaction distance and a preceding association between radical cations and counter ions, which increases strongly with a decrease in ε of the solvent[125]. Similar observations were made for all remaining systems under investigation[124, 125].

On the other hand, a different solvent effect has been observed for the electro-oxidation of **83**. It has been shown that the dynamics of solvent reorientation strongly affects the heterogeneous electron transfer rate in the studied case. Opałło has found[126] a satisfactory linear dependence between $\log k^o$ and $-\log \tau_L$, where τ_L is the longitudinal relaxation time of a given solvent. The intriguing fact was the separation of correlation lines for hydrogen-bond donor solvents and aprotic ones, but it can be explained in terms of multiple relaxation behavior of hydrogen-bonded liquids[127]. Next, Kapturkiewicz and Jaenicke[128] have compared the kinetics of homogeneous and heterogeneous electron transfers in **83** systems and have found that the free energies of activation are much greater in the heterogeneous case than in the homogeneous one. This result may be explained by different shapes of the activated complexes, constituting one or two ellipsoidal molecules for heterogeneous and homogeneous transfer, respectively.

An important step forward was made by Fawcett and Foss[129], who proposed on the basis of modern theories the general equation

$$\ln k = K - \theta \ln \tau_L - pP$$

where K is a solvent-independent constant, θ is a fraction between 0 and 1 describing the relative contributions of the solvent frequency factor and inner vibrational frequency of the reactant, P is a solvent parameter describing its solvation ability towards reagents and p marks the response of the system to this parameter. The parameter P can be the Pekar factor γ (as in the original Marcus theory) or the quantities describing solvent basicity (cation solvation) and acidity (anion solvation) when the so-called specific solvation predominates. Accordingly, only a very small dependence of τ_L on the rate of homogeneous electron transfers of **83** systems can be observed ($\theta \approx 0.1$), whereas in the case of anodic oxidation of **83** the $\ln k^o$ values are significantly correlated with $\ln \tau_L (\theta \approx 0.7)$. However, a smaller θ value is expected for lower adiabacity and a higher inner-shell reorganization energy of reactants. It is also interesting to observe that the effect of 12 aprotic and hydrogen-bonded solvents on the kinetics of the electro-oxidation of $N,N,N'N'$-tetramethyl-p-phenylenediamine shows[130] a correlation with both τ_L and γ. In binary solvent mixtures, for which the values of longitudinal relaxation times are not available,

the dependence of k^o on τ_L was verified through the viscosity values measured at different mixture compositions[131]. More details on solvent effects in simple heterogeneous electron transfer reactions can be found in a number of reviews[132-135].

Finally, it should be remembered from earlier works that in acidic media the oxidation of *p*-aminophenol (**84**) and its derivatives results[136] in the formation of *p*-quinone (**17**) formed by hydrolysis of intermediate quinoneimine (**85**, equation 10). This oxidation resembles the analogous process of **83**, as expected from the similar electron-releasing character of the NH$_2$ and OH substituents. A similar reaction is also important in the mechanism of the electro-oxidation of *ortho*- and *meta*-substituted anilines, as discussed below.

$$(10)$$
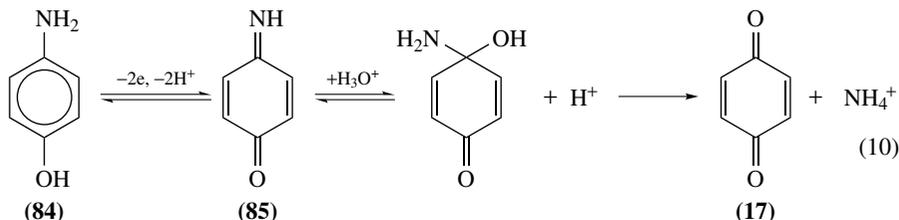
2. ortho- and meta-Substituents

Bacon and Adams in their classic work[106] suggested on the basis of voltammetric peaks that the oxidation of *o*-toluidine occurs similarly to that of aniline, i.e. the subsequent dimerization involves both the head-to-tail and tail-to-tail coupling giving 2′,3-dimethyl-4-aminodiphenylamine and 3,3′-dimethylbenzidine, respectively. However, no experimental identification of products and their ratio were given and the increase in the amount of benzidine with acidity was not explained[106]. The two main routes of radical cation coupling were next confirmed and a detailed mechanism of anodic oxidation of *ortho*- and *meta*-substituted anilines (**86**) in 3M sulfuric acid was proposed by Hand and Nelson[137] (Scheme 11). The primary oxidation product, the radical cation **86**$^{+\bullet}$, forms benzidines (**87**) by tail-to-tail coupling but the amount of **87** decreases when the *ortho*-substituent becomes more electron-withdrawing because the deprotonation of **86**$^{+\bullet}$ is then facilitated due to stronger acidity of the amine nitrogen. Thus, the reaction route shifts to the formation of diphenylamine (**88**). Further oxidation of **87** to chemically inert dications gives characteristic cathodic and anodic peaks on cyclic voltammograms of *ortho*-substituted anilines, but for *meta*-substituted anilines such peaks were observed only for *m*-OMe, *m*-Me and *m*-F substituents indicating probably some steric restrictions for larger substituents. Other peaks observed on voltammetric curves were identified with products of head-to-tail coupling of *ortho*- and *meta*-substituted anilines giving 2′,3-disubstituted- and 2,3′-disubstituted-4-amino-diphenylamines (**88**), respectively (or intermediates of their hydrolysis), which are also oxidized to **89**. However, the oxidation product can undergo a two-step hydrolysis affording the parent aniline **90** or **91** as well as 2-substituted *para*-benzoquinone (**92**). The formation of quinones was supported by voltammetric peaks of *p*-quinone/hydroquinone couples, and also by ESR spectra in the case of methyl derivative. It is interesting to note that the same 2-substituted *para*-benzoquinones (**92**) are the end products of hydrolytic degradation of both *ortho*- and *meta*-substituted anilines but the process occurs by different routes, as was persuasively shown. The faster decomposition of *N-ortho*-X-phenyl benzoquinoneimine (**93**) than *para*-benzoquinoneimine (**94**) was expected because of the effect of *ortho*-substituents, and thus the product of oxidation of **88** should be more stable for *meta*-substituted anilines. This was indeed found

SCHEME 11

in voltammetric behavior as well as in exhaustive electrolysis which produced mainly substituted benzoquinones, indicating complete hydrolysis in the case of *ortho*-substituted anilines and *meta*-compounds with strong electron-withdrawing substituents. However, hydrolysis products were not observed for *m*-OMe and *m*-Me anilines. Moreover, 2-substituted *para*-benzoquinones (**92**) with electron-withdrawing substituents (NO_2, CHO, $COCH_3$, COOH) can undergo a nucleophilic 1,4-addition of water to form substituted trihydroxybenzenes (**95**), which are susceptible to further oxidation to **96** (as observed on voltammetric curves). Thus, the overall four-electron process of decomposition of **89** was observed and a maximum of 6 electrons can be exchanged for the oxidation of parent aniline **86**. The determined number of electrons exchanged as well as a change in the products distribution with the time of experiments (scan rate in voltammetry and the time of preparative electrolysis) supported the above interpretation.

Oxidation of *o*-toluidine (**90a**) and *m*-toluidine (**91a**) in acidic solutions was found[25] to be very similar to that of unsubstituted aniline. Two electrons are involved in the overall process and products of head-to-tail and tail-to-tail coupling were observed on CV curves in 2.0 M sulfuric acid. However, in 0.1 M H_2SO_4 hydrazobenzene formed by head-to-head coupling was also found as the third product. In ACN solutions two one-electron steps of the oxidation were observed separately and the coupling of the dication with the neutral, parent molecule resulted in the formation of hydrazobenzene, which was instantaneously oxidized to azobenzene, similarly to what was described for *p*-toluidine (equation 5). Absorbance transients for intermediates of the anodic oxidation of **90a** and **91a** as well as *o*-anisidine (**90b**) and *m*-anisidine (**91b**) were poorly defined in 0.5 M H_2SO_4 solutions because the intermediates undergo fast consecutive reactions[46].

A more recent investigation of the oxidation products for the same four anilines with electron-donating groups in ACN using the ETSF method[138] also showed that spectroscopic detection of short-lived radical cations and their primary reactions were not possible. However, absorption spectra of the products of their coupling were observed in the case of the most stable radical cations of **90a**. Dimeric products of tail-to-tail coupling (equation 11a) were identified in absorption spectra (maxima at 460 nm and 440 nm) as 3,3′-dimethylbenzidine (**97a**) in the form of radical cation (**97a$^{+\bullet}$**) and dication (**97a^{2+}**). The dication **97a^{2+}** was formed during the oxidation of **90a** at lower concentration of 0.1 mM, but **97a$^{+\bullet}$** was formed at higher concentrations of **90a** of 1.0 and 10 mM, indicating fast equilibria in further electron transfer reactions with the monomer (equations 11b and 11c).

$$\textbf{90a}^{+\bullet} \;+\; \textbf{90a}^{+\bullet} \;\longrightarrow\; \textbf{97a} \;+\; 2\text{H}^+ \tag{11a}$$

$$\textbf{97a} \;+\; \textbf{90a}^{+\bullet} \;\rightleftharpoons\; \textbf{97a}^{+\bullet} \;+\; \textbf{90a} \tag{11b}$$

$$\textbf{97a}^{+\bullet} \;+\; \textbf{90a}^{+\bullet} \;\rightleftharpoons\; \textbf{97a}^{2+} \;+\; \textbf{90a} \tag{11c}$$
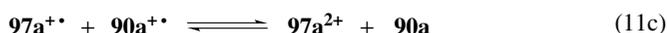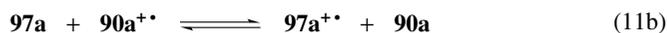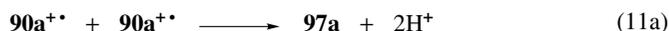
Although **97a$^{+\bullet}$** and **97a^{2+}** are stable in ACN (as proved by reversible peaks on CV curves recorded at 100 mV s^{-1}) their absorbances decrease monotonously in the presence of monomer radical cations **90a$^{+\bullet}$**, indicating relatively slow consecutive reactions, probably the formation of trimers[138]. On the other hand, *o*-anisidine radical cations **90b$^{+\bullet}$** are more reactive, but they undergo no tail-to-tail coupling because the spectra observed[138] are different from those given by *o*-dianisidine (3,3′-dimethoxybenzidine) radical cation or dication. Finally, radical cations of *meta*-substituted anilines **91a** and **91b** show the highest reactivity and for them no changes were observed on absorbance spectra in ETSF experiments[138].

(90a) X = Me
(90b) X = OMe
(90c) X = OH   (91a) X = Me
                 (91b) X = OMe   (97a)
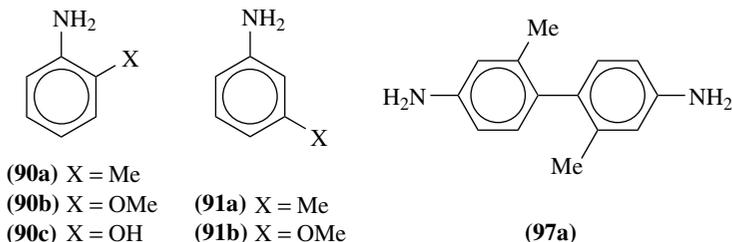
SERS spectra were successfully applied[139-141] in order to elucidate the initial steps of electropolymerization of **90b** and *o*-aminophenol (**90c**). The oxidation of **90c** after immersion of the Ag electrode into the aqueous solution results in at least two products of consecutive reactions of radical cations **90c$^{+\bullet}$** on the electrode surface at open-circuit potential[139, 140]. Detailed examination of CV curves as well as SERS spectra in a wide range of pH (controlled by the addition of $HClO_4$ or KOH) indicated that in neutral and alkaline media (pH = 7 to 9.1) the main product is 2,2′-dihydroxyazobenzene (**98**), formed by the head-to-head coupling of the intermediate **99c** in overall equation 12. The pair of redox peaks corresponding to the two-electron exchange between substituted azo- and hydrazo-compound was observed on the voltammograms. The formation of **98** is facilitated in alkaline solutions.

$$\textbf{90c}^{+\bullet} \ + \ OH^- \ \longrightarrow \ \text{(99c)} \ + \ H_2O$$

$$2 \ \textbf{99c} \ \longrightarrow \ \text{(98)} \ + \ 2e \ + \ 2H^+$$

(12)
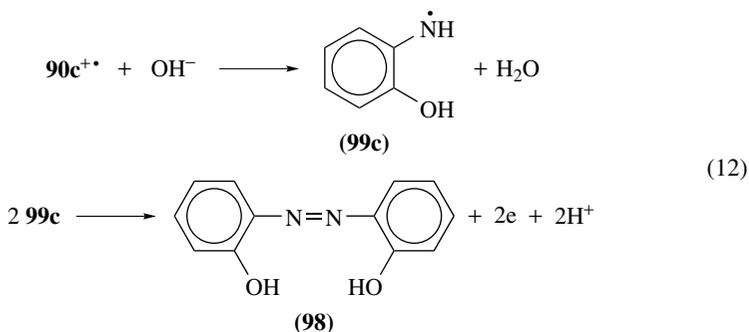
On the other hand, in acidic solutions of pH < 4 the head-to-tail coupling of radical cations **90c$^{+\bullet}$** is favored and the main product is the cyclic dimer 3-aminophenoxazone **100**. It can be reduced (equation 13) giving additional voltammetric peaks and its identification was supported by the IR spectrum in a KBr pellet.

$$\text{(100)} \ \xrightarrow[+2H^+]{+2e} \ \text{product}$$

(13)
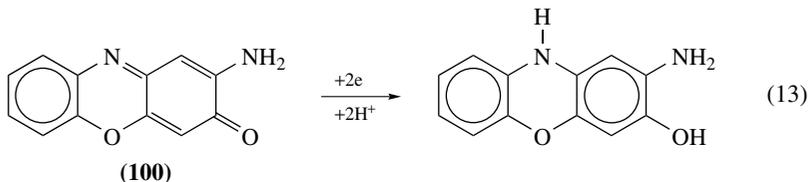
Head-to-tail coupling of radical cations **90b$^{+\bullet}$** was also confirmed and the structure of the product formed at Ag and Au electrodes was investigated by SERS and surface-enhanced resonance Raman (SERRS) spectra[141]. The pair of cathodic and anodic peaks observed at 0.34 V vs. SCE on CV curves after a few cycles during the oxidation of

90b in acidic media (0.2 and 1.0 M HClO$_4$) could not be assigned to the degradation products as described previously[142]. They rather correspond to cyclic compounds **101** or **102** incorporated into the polymer matrix, as suggested[141] on the basis of the spectra showing bands characteristic of the oxazine-type structure.

(101)   **(102)**
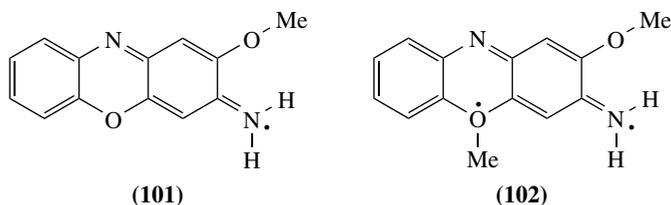
B. Polysubstituted Anilines

The oxidation of polyhalogenated anilines was investigated extensively in ACN[108–110] as well as in acidic aqueous media[143–148]. For 2,4-disubstituted anilines **77** the electro-oxidation mechanism is very similar to that observed for *p*-haloanilines **68**. In ACN the main products are *N*-(2,4-X$_2$-phenyl)-3'-X-quinone diimine **103** formed by the head-to-tail coupling with the elimination of halogen and trihalogenated anilines **104** (equation 14), in full analogy with equation 7.

$$+ 4e + 4H^+ \tag{14}$$

(77b) X = Cl   **(103b)** X = Cl   **(104b)** X = Cl
(77c) X = Br   **(103c)** X = Br   **(104c)** X = Br
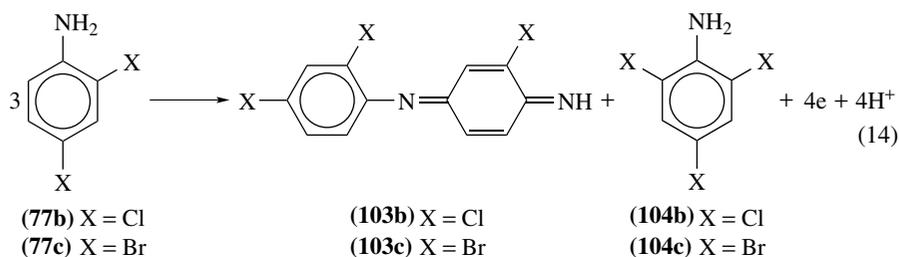
No products of the head-to-head coupling were found[108, 109] in accordance with the fact that halogen is an easily expelled group. The coupling in the *ortho*-position as in equation 8 found for monosubstituted anilines could not take place either. However, poly-halogenated dimers **105** and **106b** were also found among the products (listed in Table 5) of controlled potential electrolysis.

Compounds **105** and **106b** are formed in overall reactions given in equations 15 and 16, respectively, which both correspond to the two-electron oxidation of one molecule of **77**. However, using the gold RDE for the oxidation of **77** (X = Cl, Br or I) in ACN the apparent number of electrons equal to $n_{app} = 1.04$–1.05 was found[110], indicating the simple Bacon–Adams mechanism because at the rotating speed applied the products leave the electrode surface faster than any halogenation could take place.

On the other hand, for the oxidation of 2,4,6-trihaloanilines **104** neither coupling in the *ortho*-position nor further halogenation of the substrate is possible because no free position is available on the parent molecules. However, the peaks of chloride oxidation and elemental chlorine reduction were observed on CV curves of **104b**, and on CV curves recorded after electrolysis of **104c** the peaks of Br$_2$/Br$_3^-$ and Br$_2$/Br$^-$ couples were found[108, 109]. The apparent number of electrons exchanged during the electrolysis at controlled potential was equal[108, 109] to $n_{app} = 1.55$ and 1.52 for **104b** and **104c**, respectively. A similar

TABLE 5. Relative intensity (%) from GC-MS peaks of products arising from controlled potential electrolysis of **77b** ($E = 0.950$ V vs. Ag/Ag$^+$) and **77c** ($E = 1.000$ V vs. Ag/Ag$^+$) in unbuffered ACN[108, 109]

Product	X = Cl	X = Br
2,4-X$_2$-aniline **77**	74.3	79.5
2,4,6-X$_3$-aniline **104**	33.1	31.7
4-Hydroxy-2′,3,4′-X$_3$-diphenylamine	9.0	28.3
N-(2,4-X$_2$-phenyl)-3′-X-quinone diimine **103**	100	100
N-(2,4,6-X$_3$-phenyl)-3′-X-quinone diimine **105**	26	4.6
N-(2,4,6-X$_3$-phenyl)-3′,5′-X$_2$-quinone diimine **106b**	16.5	—
Unknown[a]	5.4	—

[a] Probably a product of the hydrolysis of **103**.

conclusion on $n_{app} \approx 1.5$ was obtained[110] in the voltammetric time scale, although the experimental n_{app} values were a little lower. This indicates the oxidation of halogenides expelled from the *para*-position beside the dimerization of radical cations **104**$^{+\bullet}$, similarly to what was established for monosubstituted *p*-haloanilines (cf. equation 6). Indeed, for the bromo compound the main product **106c** is formed by the head-to-tail coupling according to equation 6, as is evident from the data collected in Table 6. However, for the oxidation of trichloroaniline **104b** the head-to-head coupling is favored and the main product of electrolysis is 2,2′,4,4′,6,6′-hexachlorohydrazobenzene (**107b**)[108] as shown in Table 6. The detailed route of the formation of **107b** was not investigated[108], but it is obvious that head-to-head coupling will be favored for more acidic anilines (because protons are eliminated in the process) as well as for molecules for which expulsion of the *para*-substituent is more difficult. The first suggestion is supported by earlier observations of the formation of azobenzene derivatives during the oxidation of anilines in basic aqueous solutions[113, 114, 116, 117] where they dissociate, and in ACN in the presence of pyridine[72, 149]. The second one is supported by the mechanism found for the oxidation of *p*-toluidine in ACN[25], as discussed previously (cf. equation 5). Assuming a similar radical cations coupling as described by equation 5, the reaction described in equation 17 is favored because the presence of the three electron-withdrawing Cl substituents increases the acidity of **104b** (in DMSO p$K_a = 23.5$ and 29.4 for **104b** and *p*-chloroaniline **68b**, respectively[112]; unfortunately, pK_a for radical cations **104b**$^{+\bullet}$ could not be determined). One can also expect that the increasing number of electron-withdrawing substituents decreases the ability to expel chloride ion in the order of **68b** > **77b** > **104b**[108]. Although pK_a values for trisubstituted bromoanilines are not known[112], they are probably similar to those of the corresponding chloroanilines because of very close values of substituent constants for Cl and Br. Thus, the different main oxidation products of **104b** and **104c** are rather caused by the higher steric restrictions in the bromo analogue of **107b**.

$$2\ \textbf{77} \longrightarrow \text{X}\!\!-\!\!\overset{\overset{\displaystyle X}{|}}{\underset{\underset{\displaystyle X}{|}}{\bigcirc}}\!\!-\!\!N\!\!=\!\!\overset{X}{\bigcirc}\!\!=\!\!NH\ +\ 4e\ +\ 4H^+ \tag{15}$$

(**105b**) X = Cl
(**105c**) X = Br
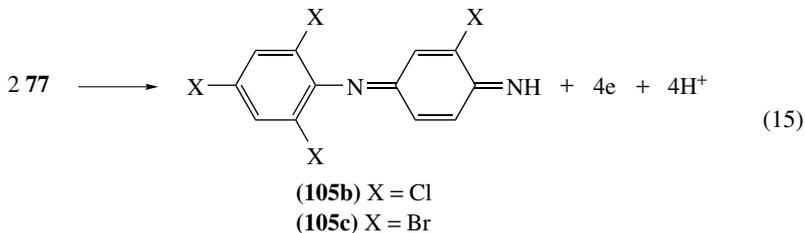
TABLE 6.   Relative intensity (%) from GC-MS peaks of products arising from electrolysis of **104** at controlled potential $E = 1.200$ V vs. Ag/Ag$^+$ in unbuffered ACN[108, 109]

Product	X = Cl	X = Br
2,4,6-X$_3$-aniline **104**	2.9	9.0
N-(2,4,6-X$_3$-phenyl)-3′,5′-X$_2$-quinine diimine **106**	38.9	100
2,2′,4,4′,6,6′-Cl$_6$-hydrazobenzene **107b**	100	—

$$4\ \mathbf{77} \longrightarrow \text{[structure]} + 8e + 8H^+ \tag{16}$$

(**106b**) X = Cl
(**106c**) X = Br

$$2\ \mathbf{104b^{+\bullet}} \longrightarrow \text{[structure (107b)]} + 2\ H^+ \tag{17}$$

(**107b**)
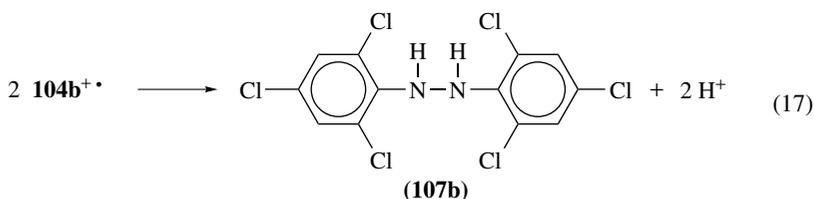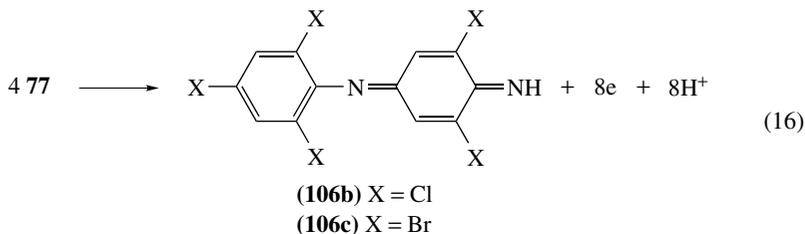
It should also be remembered that the large-scale electrolysis of **77b** resulted in the formation of 2,2′,4,4′-tetrachloroazobenzene **108** with yields of 30.1% if the oxidation was performed in ACN containing 0.1M pyridine[72] and 38% in 2:1 H$_2$O–DMF mixture also with added pyridine[149]. Similar oxidation of 2,4,6-trichloroaniline **104b** in DMF containing pyridine resulted in 2,2′,4,4′,6,6′-hexachloroazobenzene **109** (47.5% yield). Pyridine was added to deprotonate the primary radical cations, which allows a head-to-head coupling similarly to that in equation 9.

(**108**)   (**109**)
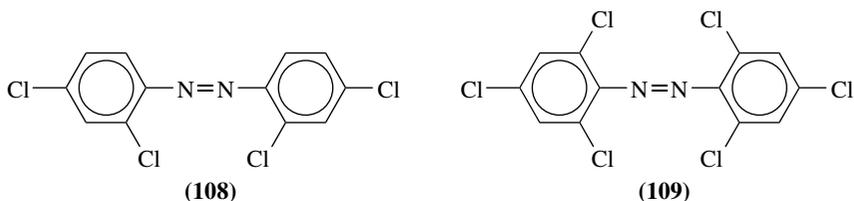
The oxidation of polyhaloanilines in acidic aqueous solutions at a concentration of sulfuric acid higher than 1.0 M is different in two aspects from those found in ACN. Firstly, the electroactive substrate exists in the protonated form, e.g. **110** in the case of 2,4-dihaloanilines, as is evident from pK_a values[150] as well as from the fact that voltammetric peak potentials of the main process (I) are independent of acid concentrations[145, 146]. Secondly, as a consequence, no aniline radical cations are formed and their dimerization is

not observed. However, primary oxidation products undergo hydrolysis with the formation of halobenzoquinoneimine **111** and halobenzoquinone **92**, which are both still electroactive. Although the hydrolysis products are similar to those found for the oxidation of *ortho*-X- and *meta*-X-anilines in acidic media[137], the mechanism and intermediates are very different.

A detailed examination of the oxidation of 2,4-dihaloanilines using CV, RDE voltammetry and controlled potential electrolysis at Pt electrodes indicated[145, 146] the single oxidation process I at lower acid concentrations $c_{acid} < 5.0$ and 6.5 M, respectively for **110b** and **110c**. The separated, second one-electron process II observed at more positive potentials in the case of the chloro compound **110b** (but overlapped with process I for $c_{acid} > 8.0$ M) was identified with the oxidation of the ejected chloride ion to chlorine radical. This process is reversible in RDE voltammetry and quasi-reversible in CV. The last electron transfer is preceded by a fast ionization $HCl \leftrightarrows Cl^- + H^+$ because the half-wave potential of process II shifts with the Hammett acidity function, giving the slope of 65 mV/H_o. A similar reaction was suggested for **110c** but no separate redox peaks were observed on CV curves. At more positive potentials a process III was observed which overlaps with the process II at $c_{acid} = 12.0$ M. Processes I and III are controlled either by diffusion or by adsorption depending on the medium; the adsorption behavior is important for process I at $c_{acid} < 4.0$ M and for process III at $c_{acid} > 9.0$ M. Both processes I and III gave the same two products which showed characteristic cathodic peaks (and anodic in the second cycle) and were identified with **111** and **92** by comparison with CV behavior of authentic samples. Thus, the proposed mechanism for process I (under diffusion conditions) involves[145, 146] two-electron oxidation of the protonated reactant **110** with a rds formation of cation **112** (Scheme 12). **112** is then deprotonated to **77²⁺**, which undergoes subsequent hydrolysis in the *para*-position with a loss of the halide ion and two protons, yielding protonated 2-halo-*p*-benzoquinoneimine **111** and 2-halo-*p*-benzoquinone **92**. Both products showed CV peaks corresponding to redox equilibria of equations 18 and 19, which give **113** and **114**. For the bromo compound **92c**, a further very slow hydration to 3-bromo-1,2,4-benzenetriol (**95c**) was proposed in order to explain the new peaks observed on CV curves recorded after a long-time (24 h) electrolysis of **112c**, which correspond to the reaction in equation 20.

$$X - \bigcirc - NH_2 \; + \; H^+ \; \rightleftharpoons \; X - \bigcirc - \overset{+}{N}H_3$$

(**77b**) X = Cl
(**77c**) X = Br

(**110b**) X = Cl, pKa = 2.02
(**110c**) X = Br, pKa = 1.83
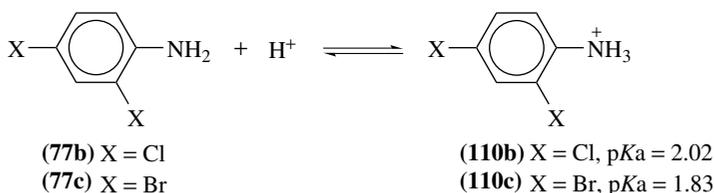
The oxidation process III is an irreversible, two-electron transfer with a half-wave potential depending on the Hammett acidity function with a shift equal to 70 mV/H_o, which indicates a fast loss of two protons before the charge transfer. This process finally results in the formation of **92** as in process I. Thus, it was proposed[145, 146] that the initial cation **112** loses two protons from the benzene ring yielding a monopositive cation, which undergoes a rds two-electron oxidation, but its further decomposition was not investigated. It was only noted that oxidation potentials of the cations formed by the proton loss from **112b** and **112c** in a given medium are the same[146].

SCHEME 12

$$111 \ + \ 2e \ + \ 2H^+ \ \rightleftharpoons \ \text{(113)} \tag{18}$$

$$92 \ + \ 2e \ + \ 2H^+ \ \rightleftharpoons \ \text{(114)} \tag{19}$$

$$92c \ + \ H_2O \ \longrightarrow \ \text{(95c)} \ \rightleftharpoons \ \text{(96c)} \ + \ 2e \ + \ 2H^+ \tag{20}$$
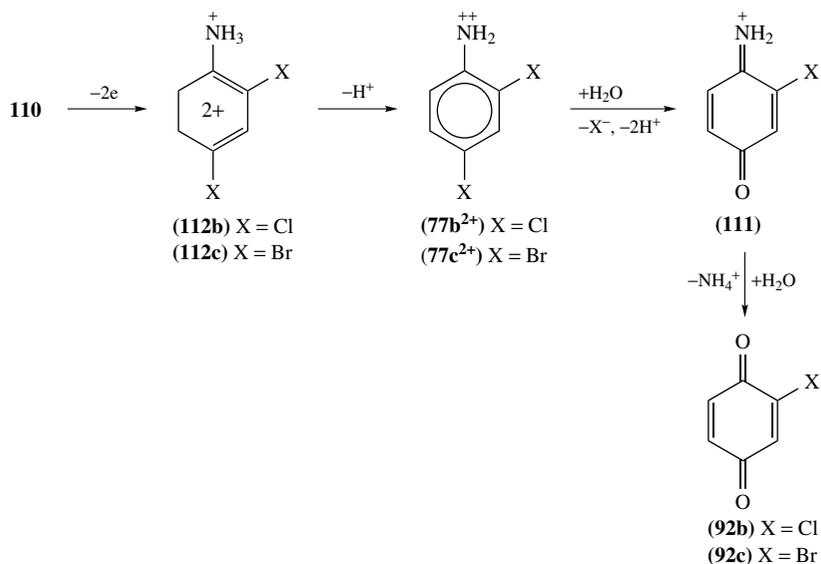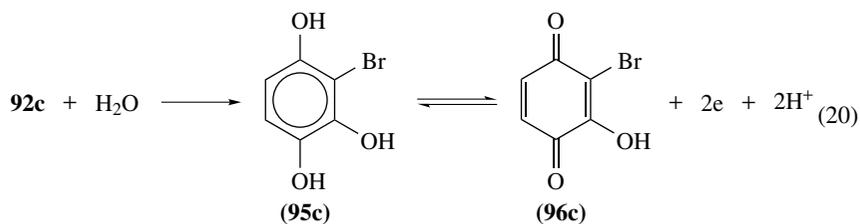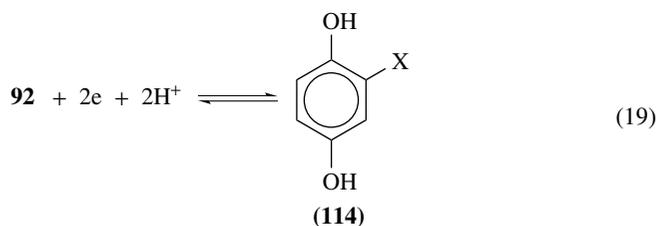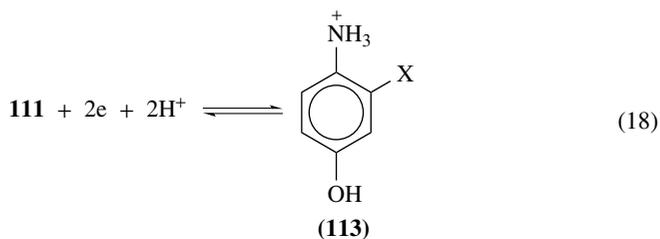
On the other hand, the anodic oxidation of 2,4,6-tribromoaniline **104c** in acidic aqueous media at Pt electrodes resembles[144] the behavior of 2,4-dihaloanilines in the participation of the protonated form of the reactant **115**, which is oxidized in the initial step to the tripositive cation **116** (Scheme 13). However, their further deprotonation results in the formation of two different cations: **117** (an analogue of **77²⁺**) and **118** formed by the loss of only one proton from the benzene ring, contrary to the reaction of **77c²⁺**.

$$104c + H^+ \rightleftharpoons \quad (115) \quad \rightleftharpoons \quad (116) \quad + \; 2e$$

(115) — NH_3^+ ring with Br at 2, 6 positions and Br at 4 position

(116) — NH_3^+ ring (dipositive) with Br at 2, 6 positions and Br at 4 position

$-H^+$ (from 116 to left) $-H^+$ (from 116 to right)

(117) — NH_2^{++} ring with Br at 2, 6 and Br at 4 ⟷ NH_2^+ quinoneimine form with Br

(118) — NH_3^+ ring (monopositive) with Br at 2, 6 and Br at 4
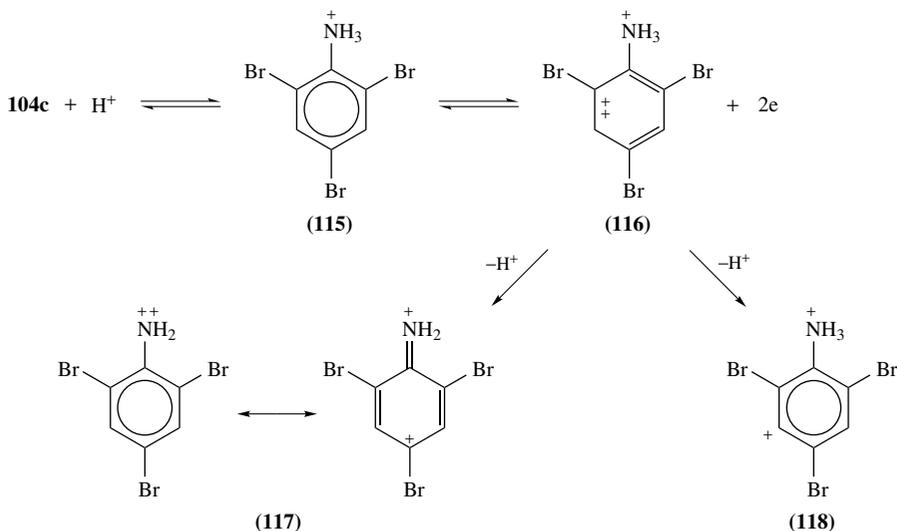
SCHEME 13

The first cation **117** undergoes consecutive hydrolysis in the *para*-position with a loss of HBr molecule giving 2,6-dibromo-*p*-benzoquinoneimine (**119**) and 2,6-dibromobenzoquinone (**120**), as shown in Scheme 14. However, their further reduction was not observed on CV curves, contrary to **111** and **92** giving reactions 18 and 19. Instead of that, **120** is further hydrolyzed to 3,5-dibromo-1,2,4-trihydroxybenzene (**121**), which can be electrochemically oxidized to 3,5-dibromo-2-hydroxybenzoquinone (**122**), and the last process gives a cathodic and anodic pair of peaks observed on CV curves. This means that the hydrolysis of quinone **120** is much faster than the hydrolysis of 2-bromo analogue **92c**. The oxidation of **115** to **116** is the rds responsible for the first, irreversible and diffusion-controlled process observed[144] using CV and RDE voltammetry in solutions of 60% perchloric acid and sulfuric acid of concentrations lower than 12.5 M. At higher H_2SO_4 concentrations the process is kinetically controlled and depends on adsorption phenomena similarly to the second, also irreversible process observed at more positive potentials in solutions of H_2SO_4 with $c_{acid} > 9.0$ M and of 60% $HClO_4$.

The starting reactant of this second process was suggested to be the cation **118**, which is initially oxidized in a two-electron step, and the final product formed in the time scale of CV experiments ($v = 0.010 - 0.100$ V s^{-1}) undergoes cathodic reduction at a potential more positive by about 0.15 V than the reduction of **122**. With the increase of acid concentration this new cathodic peak increases at the cost of the peak corresponding to **122**. This electroactive product was not identified, but from the dependence of half-wave and peak potentials of the second oxidation process on the Hammett function it
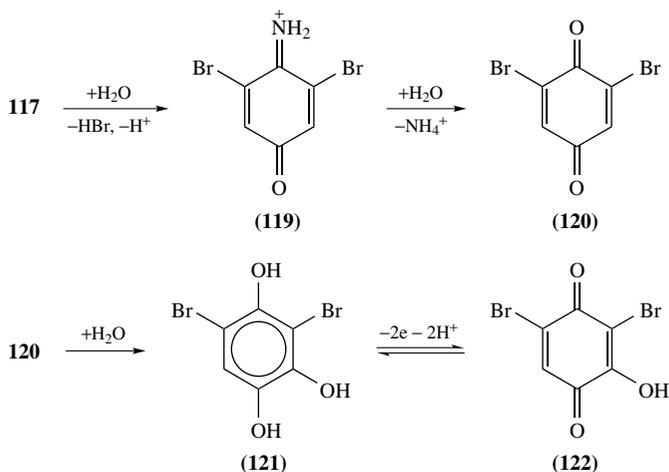
SCHEME 14

was proposed[144] that the process includes the loss of one proton between two electron-transfer steps. Moreover, the electrolysis at the controlled potential of 1.30 V vs. SCE (which lies between the anodic peaks of the first and second processes) resulted[143] in the formation of *N*-(2,3,4-tribromophenyl)-1,3-(2′,4′,6′-tribromo)phenylenediamine (**123**) and their formation was explained[144] by dimerization of the cation **118** in the *meta*-position with the parent aniline **104c**, followed by the interchange of bromo substituent from the position 2 to 5. However, the dimer **123** was not found[143] after the electrolysis at a controlled, more anodic potential than the second oxidation peak. The detailed pathway of the second process was not explained[144].

(123)
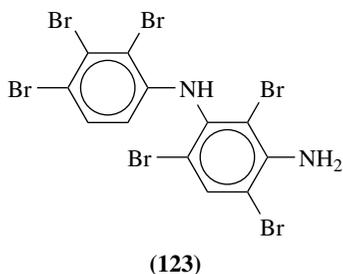
After changing one *ortho*-bromo substituent to the strong electron-withdrawing nitro group, a one-electron oxidation is favored resulting in the formation of a more stable radical cation. This step is followed by deprotonation but the radical cation is not immediately oxidized, leading to the two-electron step as was established for 2,4,6-tribromoaniline **104c**. Thus, the mechanism becomes more similar to that described by Hand and Nelson[137] for the *ortho*- and *meta*-monosubstituted anilines. In sulfuric acid solutions of concentrations in the range 9.0 M $< c_{acid} <$ 13.0 M, 2,4-dibromo-6-nitroaniline (**124**) exists with a protonated amino group **125** (which is the only form at $c_{acid} <$ 11.0 M). However, at higher acidity the nitro group is also protonated, giving **126**[147].

$pK_a = -3.10$

(124)   **(125)**   **(126)**
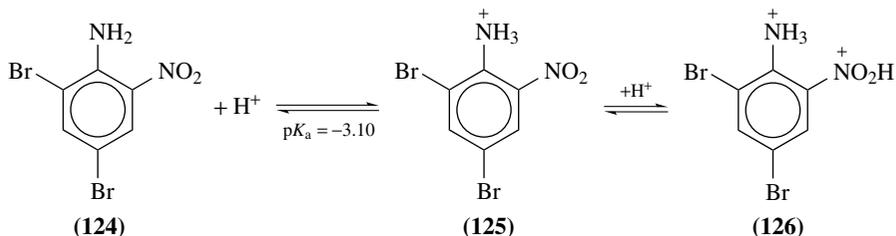
The monocation **125** (as well as the dication **126**) undergoes a single oxidation process (equation 21) resulting in the dication **124^{2+}** and corresponding to the eCe mechanism[147], i.e. two one-electron reversible steps are divided by the irreversible chemical reaction of the first order (the rds) identified as the loss of one proton. The rate constant for that step was determined from RDE voltammetry to be equal to 3.6 s^{-1} for acid concentrations 9.0 M $< c_{acid} <$ 11.0 M. This means, of course, that the oxidation of the benzene ring is more difficult in the presence of the NO$_2$ group of **125** than the analogue process of **115**, which gave two-electron oxidation. Moreover, the last reactant was oxidized at *ca* 200 mV less anodic potential.

125   (21)

(125$^{•2+}$)   **(124^{2+})**
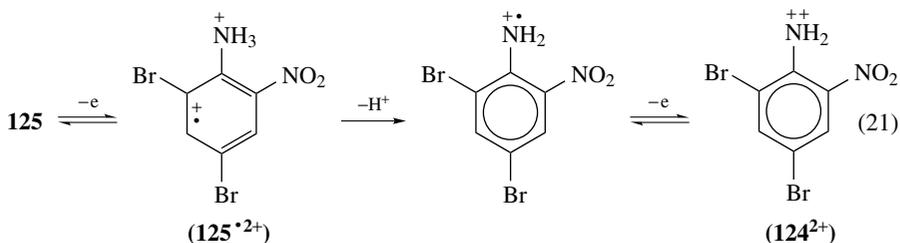
The mechanism proposed[147] was supported by the results of CV and RDE voltammetry. Namely, the reduction peak corresponding to the first oxidation step was observed on CV curves in solutions of $c_{acid} = 12.0$ M at higher scan rates (starting from $v = 10$ V s^{-1}) and the anodic peak potential shifts to more positive values with v. Moreover, the first electron transfer becomes quasi-reversible with the increase in the scan rate v. Thus, from the variation of the difference between anodic and cathodic peak potentials with v it was possible to determine the corresponding standard rate constant $k^o = 4 \times 10^{-2}$ cm s^{-1} but only in media with higher acid concentrations of 13.0–15.0 M, i.e. when **126** participates in the reaction. For the reaction of **125** the k^o value must be lower. It was also found that the apparent number of electrons n_{app} gradually decreases from 2 to 1 with the increase in the rotating speed of RDE, as expected for the eCe mechanism. The CV peaks of the reversible reduction and oxidation corresponding to the second electron transfer were also observed at higher $v \geqslant 5$ V s^{-1}. It was suggested[147] that the reversible reduction and oxidation peaks of the final product observed at less anodic potentials at low acid concentrations and at low scan rates correspond to *p*-benzoquinone/hydroquinone couple **128/129** (equation 22), but 2-bromo-6-nitro-*p*-benzoquinone (**128**) was found to be unstable under the experimental conditions and was not identified after the controlled potential electrolysis. Nevertheless, the overall mechanism proposed[147] includes further hydration of **124^{2+}** in the *para*-position to form 2-bromo-6-nitrobenzoquinoneimine (**127**) and 2-bromo-6-nitrobenzoquinone (**128**), similarly to that observed for 2,4,6-tribromoaniline in the same media[144].

However, the diprotonated cation **126** formed at higher acid concentrations $c_{acid} >$ 11.0 M is also oxidized to the protonated radical cation **126$^{+•}$**, which follows the same mechanism of decomposition, giving protonated 2-bromo-6-nitro-*p*-benzoquinone (**130**) as the final product. **130** can be further reduced to **131**, as observed on CV curves recorded in solutions with higher acid concentrations.

$$\textbf{124}^{2+} \xrightarrow[\mathrm{-Br^-,\ -2H^+}]{\mathrm{+H_2O}} \textbf{(127)} \xrightarrow[\mathrm{-NH_4^+}]{\mathrm{+H_2O}} \textbf{(128)} \quad \Big\updownarrow \substack{+2e\,+\,2H^+} \quad \textbf{(129)} \tag{22}$$

$$\textbf{(126}^{+•}\textbf{)} \xrightarrow[\mathrm{-e,\ -Br^-,\ -NH_4^+}]{\mathrm{+2H_2O,\ -3H^+}} \textbf{(130)} \quad +\ 2e\ +\ 2H^+ \rightleftharpoons \textbf{(131)}$$

Moreover, at $c_{acid} \geqslant 13.0$ M another oxidation reaction at more positive potentials was observed[147] and found to be an irreversible, diffusion-controlled, two-electron process with the peak potential depending on the scan rate (with $\partial E_{pa}/\partial \log \nu = -30$ mV) and half-wave potential in RDE voltammetry depending on the Hammett acidity function (with a slope of 30 mV/H$_o$) indicating the fast one-proton transfer as the preceding step. However, the overall process resulted in the same final product **130**, which is electroactive. Thus, it was proposed that this second process starts from the protonated radical cation **126$^{+•}$** which loses one proton from the benzene ring and next undergoes two-electron irreversible oxidation, which is the rds. However, the further decomposition to **130** was not explained[147].

The oxidation mechanism of polysubstituted anilines with electron-releasing methyl groups is different from that discussed above for polyhaloanilines, because the initially

formed radical cations are more stable due to the inductive effect of the methyl groups. The oxidation of 2,4-dimethylaniline (**77e**) in 0.1 M sulfuric acid occurs[25] by the formation of the radical cation **77e$^{+\bullet}$** and in the next step the dication **77e^{2+}**, showing then two one-electron anodic peaks. The head-to-head coupling of **77e$^{+\bullet}$** as well as **77e^{2+}** with the parent molecule **77e** resulted in the formation of hydrazobenzene, which is instantaneously oxidized to azobenzene in a similar way to that observed for *p*-toluidine **68e** (equation 5). On the other hand, for 2,6-dimethylaniline (**132**) two successive oxidation steps occur, yielding first the radical cation (which is also stabilized by the presence of two *ortho*-methyl groups) and then the dication. However, all three types of coupling take place, similarly to what was observed for unsubstituted aniline as well as for *o*-toluidine **90a** and *m*-toluidine **91a**, since the *para*-position in **132** is vacant. Thus, three additional pairs of peaks were found on CV curves[25]. In a similar manner the oxidation in ACN resembles that of the toluidines: voltammetry of **77e** is similar to that of **68e** and the behavior of **132** is similar to that of **90a**[25].

(77e)   (132)
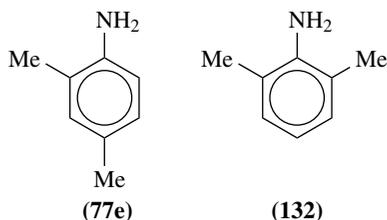
In investigations of the effect of *ortho*-substituents on the oxidation mechanism of *p*-bromoanilines in sulfuric acid solutions, a comparison with electrochemical behavior of 2,4-dibromo-6-methylaniline (**133c**) and 4-bromo-2,6-dimethylaniline (**133e**), i.e. reactants with weak, electron-donating methyl groups, is also interesting[148]. In solutions of acid concentrations $1.0\ \mathrm{M} < c_{\mathrm{acid}} \leqslant 13.0\ \mathrm{M}$, both anilines **133** are present only in the protonated forms **134**, as revealed from the fact that RDE half-wave and CV peak potentials for the first oxidation process were independent of c_{acid}. A single oxidation process was found for **134c** up to the concentration $c_{\mathrm{acid}} = 5.0\ \mathrm{M}$, whereas for **134e** a similar process was observed for $c_{\mathrm{acid}} < 3.0\ \mathrm{M}$ and was followed by the oxidation of the bromide anions expelled in the overall process to bromine (via bromine atom, which is probably adsorbed on the Pt electrode), but at $c_{\mathrm{acid}} > 3.0\ \mathrm{M}$ both processes overlap. The RDE and CV characteristics of this first process indicated the eC mechanism with the first-order chemical reaction as the rds. Namely, the CV peak potential of the diffusion-controlled oxidation process depends on the scan rate (with $\partial E_{\mathrm{pa}}/\partial \log \nu = -30$ mV), and for **133e** it also depends on acid concentration (with the slope of *ca* 30 mV/H$_{\mathrm{o}}$). Thus, the chemical step was assumed to be the deprotonation of dication radical **134$^{\bullet 2+}$** (formed in the

(133c) X = Br   (134c) X = Br
(133e) X = Me   (134e) X = Me
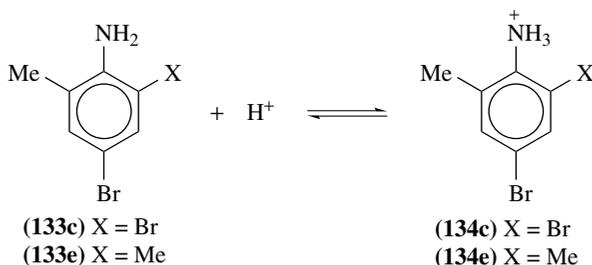
first, reversible electron transfer from **134**), resulting in the formation of the radical cation **135**$^{+\bullet}$ (equation 23).

(23)

(**134c**$^{\bullet 2+}$) X = Br
(**134e**$^{\bullet 2+}$) X = Me

(**135c**$^{+\bullet}$) X = Br
(**135e**$^{+\bullet}$) X = Me
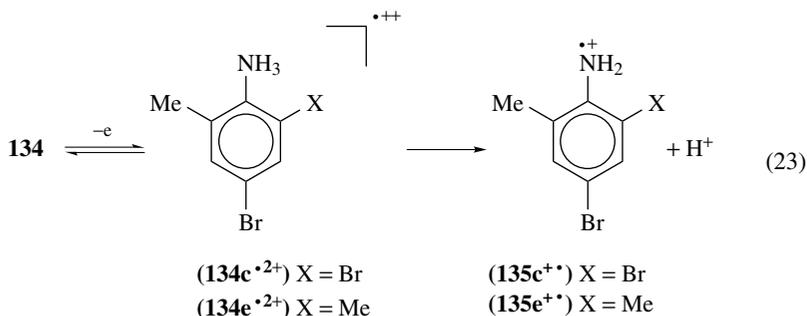
Final products obtained in a crystalline form after the controlled potential electrolysis of **133c** and **133e** were identified as 2,3-dibromo-6-methylbenzoquinone (**140**) and *N*-(4′-bromo-2′,6′-dimethylphenyl)-2,6-dimethylbenzoquinoneimine (**137e**), respectively. Their yields were *ca* 50% and 60–40% depending on c_{acid}, respectively for **140** and **137e**. Thus, the common mechanism (Scheme 15) proposed for the decomposition of both reactants includes the head-to-tail coupling of radical cations **135**$^{+\bullet}$ with the loss of a bromide anion and a proton and the formation of diimine **136**, which is further hydrolyzed to **137**. Both

(**136c**) X = Br
(**136e**) X = Me

(**137c**) X = Br
(**137e**) X = Me

(**138c**) X = Br
(**138e**) X = Me

(**139c**) X = Br
(**139e**) X = Me
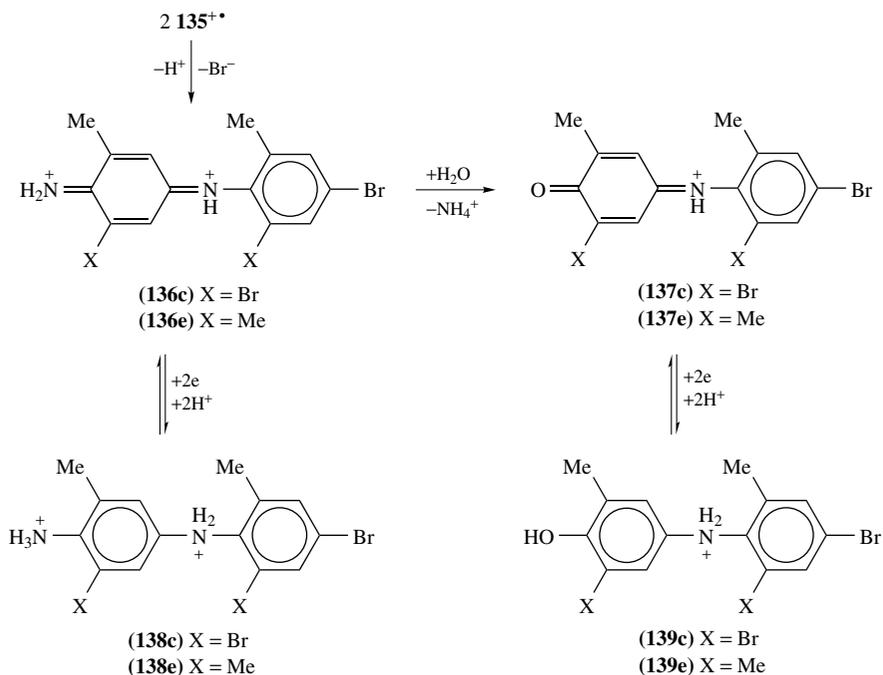
SCHEME 15

products **136** and **137** could be reversibly reduced to protonated *p*-aminodiphenylamine derivatives **138** and **139**, and CV peaks corresponding to these redox couples were observed.

On the other hand, the hydrolysis of **137c** followed by bromination and a further loss of a bromide anion and a proton resulted in the final electrolysis product **140** (equation 24).

$$\textbf{137c} + H_2O + Br_2 \longrightarrow \quad \underset{\textbf{(140)}}{\text{[structure]}} \quad + \textbf{134c} + Br^- + H^+ \tag{24}$$
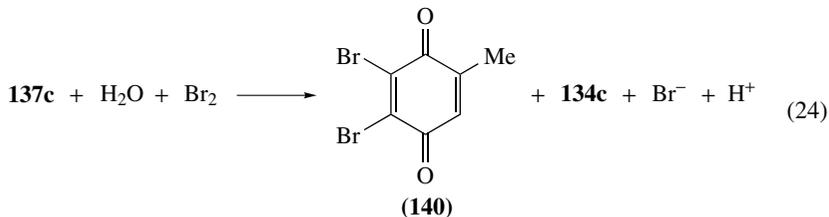
In concentrated acid solutions ($c_{acid} > 5.0$ M and $c_{acid} > 3.0$ M for **133c** and **133e**, respectively) an oxidation peak for the second process was observed at potentials *ca* 0.4 V more positive than for the first process. A similar CV and RDE characteristic (at $c_{acid} < 10.0$ M) was found for both processes; this indicates a similar eC mechanism. The electrolysis at controlled potential corresponding to the second process gave the same products **140** and **137e** with the same yields, but the number of electrons determined by coulommetry ($n = 5$) was higher than that considered for the first process and some polymeric products were also obtained. It was then proposed[148] that the second oxidation process starts from the one-electron reversible transfer to the protonated dimer **137** followed by deprotonation of dication radical (the rds) and further decomposition leading to polymers. On the other hand, in solutions with $c_{acid} > 10.0$ M the dication radical formed in the initial electron transfer was adsorbed on the Pt electrode surface and this phenomenon controls the kinetics of the anodic reaction.

In conclusion, the mechanism of the oxidation of substituted *p*-bromoanilines in strong acidic solutions (where initial reactants are completely protonated) depends strongly on the nature of the *ortho*-substituents. For weak electron-withdrawing substituents (one or two Br atoms) a two-electron irreversible process occurs, followed by deprotonation and a subsequent hydrolysis of the formed dication with loss of bromide ion, finally resulting in the formation of *p*-benzoquinone imine and afterwards *p*-benzoquinone. In the case of two *ortho*-Br substituents, a deprotonation from the benzene ring is also possible yielding the *meta* dimer. For the stronger electron-withdrawing nitro group, the radical cation formed by the first electron transfer is more stable and further oxidation of the benzene ring is then less favored than deprotonation. The oxidation occurs according to a eCe mechanism, but the final product after hydrolysis, *p*-benzoquinone, is the same as previously observed. On the other hand, the introduction of one or two weak electron-donating methyl substituents stabilized the radical ions formed by one-electron and one-proton loss (the eC mechanism) and their head-to-head coupling gives dimeric *N*-phenyl-*p*-benzoquinoneimine, which is the final product in the case of two methyl groups. However, for only one *ortho*-methyl group, i.e. a system with less electron-releasing character, further hydrolysis and deprotonation result in the formation of *p*-benzoquinone.

V. EPILOGUE

Aniline and its derivatives have been used over many years to produce insecticides, fungicides, herbicides, defoliants, animal repellents, drugs and, especially, aniline

dyes. Chemically and electrochemically synthesized polymers and copolymers are also applicable in many fields of current activity (Chapter 14). Of course, all these compounds can enter into the environment, predominantly into water, during any stage of industrial processes and use, as well as from aniline-containing semi-manufactured products such as coal tar. The compounds are toxic (Chapter 16) due to the formation of carcinogenic azo-derivatives and other oxidation products arising from interaction with microflora[151, 152]. It is not surprising, therefore, that the removal of aniline from waste water is of special importance. For this purpose various adsorbents are used, so the adsorptive and electrosorptive phenomena have attracted great interest[153]. Let us consider, consequently, some recent reports.

Adsorption of aniline on minerals, such as kaolinite, montmorillonite and vermiculite as well as on α-alumina and iron powders, has been studied in order to better understand the interaction of the adsorbate with natural adsorbents[154–157]. However, the results, similarly to those obtained on a smooth polycrystalline platinum electrode[158], are not useful for the removal of aniline from waste water. The commonly used activated charcoal is also deficient owing to slow kinetics of the removal of dissolved pollutants. In this situation, activated carbon fibers, woven as a C-cloth, seem to be the ideal adsorbents for removal of aniline from waste streams. The reports of Niu and Conway[159, 160] explained the adsorptive and electrosorptive behavior of aniline on C-cloth electrodes and suggested a methodology for clean-up of industrial waste waters.

The next problem is connected with electroanalytical methods of quantitative determination of aniline. Quite recently, Kusu and coworkers[161] have proposed an original method of voltammetric determination of weak organic bases, such as aniline and N,N-diethylaniline, based on anodic oxidation of α-tocopherol in an unbuffered solution. They have found that voltammograms of α-tocopherol recorded after the addition of a given base exhibit a new oxidation peak (prepeak) at a potential more negative than that of α-tocopherol. The prepeak height was observed to depend linearly on the concentration of base. Hence the prepeak, which is controlled by diffusion of a base to the electrode surface, can be used for quantitative determination of aniline and its N,N-diethyl derivative at concentrations of 0.13–2.5 mM. A suitable medium is methanol containing 0.05 M LiClO$_4$ and 3 mM α-tocopherol. A plastic formed carbon disk electrode with a geometric area of 7.07 mm^2 was used throughout the experiments. The use of a platinum wire coated with a thin layer of polyaniline has been also applied for the determination of aniline in aqueous media[162]. A theoretical equation describing the potential dependence of the electrode on the concentration of aniline in solutions has been derived and shown to be in conformity with the experimental results. The measurements were performed in phosphate buffer at pH 6.9.

Finally, considering the electrochemical properties of aniline, some problems connected with modifications of the electrode surface should not be omitted. It is known that such modifications may result in the enhancement of particular properties of the working electrode, which can be exploited in electroanalytical chemistry. One can say that many times the acceleration of the rate of heterogeneous electron transfer at modified electrodes was observed and reactions at polyaniline-modified electrodes have been among those most frequently investigated This important subject lies just outside the field covered by this Chapter and so only one example is given. It is noteworthy that at the electrodes modified by polymers of aniline-N-3-propylsulfonic acid and p-phenylenediamine, electrocatalysis of 1,4-benzoquinone/hydroquinone redox couple is observed, whereas at the electrode covered by the polymer of m-phenylenediamine an inhibition of the same redox couple is shown[163, 164]. Although this finding is well documented, full explanation of the observed difference is rather unclear.

VI. REFERENCES

1. R. Lines, in *Organic Electrochemistry. An Introduction and a Guide* (Eds. M. M. Baizer and H. Lund), 2nd edn., Chap. 15, M. Dekker, New York, 1983, pp. 469–479.
2. K. Yoshida, *Electrooxidation in Organic Chemistry. The Role of Cation Radicals as Synthetic Intermediates*, Wiley-Interscience, New York, 1984.
3. R. C. Reed and R. M. Wightman, in *Encyclopedia of Electrochemistry of the Elements* (Eds. A. J. Bard and H. Lund), Vol. XV, Chap. XV-1, M. Dekker, New York, 1984, pp. 2–165.
4. A. G. MacDiarmid, in *Conjugated Polymers and Related Materials: The Interconnection of Chemical and Electronic Structure* (Eds. W. R. Salaneck and L. Lundstrom), Chap. 6, Oxford Scientific Press, Oxford, 1993.
5. A. G. MacDiarmid, S. L. Mu, N. L. Somasiri and W. Wu, *Mol. Cryst. Liq. Cryst.*, **121**, 187 (1985).
6. M. V. Deshpande and D. P. Mainerkar, *Prog. Polym. Sci.*, **18**, 623 (1993).
7. T. Kobayashi, H. Yoneyama and H. Tamura, *J. Electroanal. Chem.*, **161**, 419 (1984).
8. R. Noufi, A. J. Nozik, J. White and L. F. Warren, *J. Electrochem. Soc.*, **129**, 2261 (1982).
9. D. Floner. L. Laglaine and C. Moinet, *Electrochim. Acta*, **42**, 525 (1997).
10. S. Lu, Q. Li, C. Lu, Q. Liu and H. Yang, *J. Electroanal. Chem.*, **457**, 149 (1998).
11. K. Polat, *Turk. J. Chem.*, **27**, 501 (2003).
12. J. H. Jiang, R. S. Zhai and X. H. Bao, *J. Alloys Comp.*, **354**, 248 (2003).
13. C. Karunakaran and R. Kamalam, *J. Org. Chem.*, **67**, 1118 (2002).
14. S. C. Creason, J. Wheeler and R. F. Nelson, *J. Org. Chem.*, **37**, 4440 (1972).
15. D. T. Glatzhofer and M. C. Morvant, *J. Phys. Org. Chem.*, **11**, 731 (1998).
16. T. P. Bender, J. F. Graham and J. M. Duff, *Chem. Mater.*, **13**, 4105 (2001).
17. R. N. Adams, *Acc. Chem. Res.*, **2**, 175 (1969).
18. H. Yang and A. J. Bard, *J. Electroanal. Chem.*, **339**, 423 (1992).
19. E. Steckhan, in *Organic Electrochemistry. An Introduction and a Guide* (Eds. M. M. Baizer and H. Lund), 3rd edn., Chap. 15, Marcel Dekker, New York, 1991; E. Steckhan, in *Organic Electrochemistry* (Eds. H. Lund and O. Hammerich), 4th edn., Chap. 15, M. Dekker, New York, 2002, pp. 550–560.
20. S. Mu and J. Kan, *Electrochim. Acta*, **41**, 1593 (1996).
21. E. M. Geniès and M. Lapkowski, *J. Electroanal. Chem.*, **236**, 189 (1987).
22. E. M. Geniès, M. Lapkowski and J. F. Penneau, *J. Electroanal. Chem.*, **249**, 97 (1988).
23. Y. B. Shim, M. S. Won and S. M. Park, *J. Electrochem. Soc.*, **137**, 538 (1990).
24. B. J. Johnson and S. M. Park, *J. Electrochem. Soc.*, **143**, 1277 (1996).
25. L. R. Sharma, A. K. Manchanda, G. Singh and R. S. Verma, *Electrochim. Acta*, **27**, 223 (1982).
26. D. L. Stilwell and S. M. Park, *J. Electrochem. Soc.*, **135**, 2254, 2497 (1988).
27. E. M. Geniès, J. F. Penneau and M. Lapkowski, *J. Electroanal. Chem.*, **260**, 145 (1989).
28. R. Male and R. D. Allendoerfer, *J. Phys. Chem.*, **92**, 6237 (1988).
29. A. Petr and L. Dunsch, *J. Phys. Chem.*, **100**, 4867 (1996).
30. A. Petr and L. Dunsch, *J. Electroanal. Chem.*, **419**, 55 (1996).
31. L. Dunsch and A. Petr, *Ber. Bunsenges. Phys. Chem.*, **97**, 436 (1993).
32. A. Zimmermann, U. Künzelmann and L. Dunsch, *Synth. Metals*, **93**, 17 (1998).
33. A. Kitani, M. Kaya and K. Sasaki, *J. Electrochem. Soc.*, **133**, 1069 (1986).
34. L. Duić, Z. Mandić and S. Kovač, *Electrochim. Acta*, **40**, 1681 (1995).
35. P. Gao, D. Gosztola and M. J. Weaver, *J. Phys. Chem.*, **93**, 3753 (1989).
36. J. Stassen and G. Hambitzer, *J. Electroanal. Chem.*, **440**, 219 (1997).
37. F. Cases, F. Huerta, P. Garcés, E. Morallón and J. L. Vázques, *J. Electroanal. Chem.*, **501**, 186 (2001).
38. H. Deng and G. J. Van Berkel, *Anal. Chem.*, **71**, 4284 (1999).
39. H. S. Shim, I. H. Yeo and S. M. Park, *Anal. Chem.*, **74**, 3540 (2002).
40. J. S. Yoo, I. Song, J. H. Lee and S. M. Park, *Anal. Chem.*, **75**, 3294 (2003).
41. J. F. Bergamini, M. Belabbas, M. Jouini, S. Aeiyach, J. C. Lacroix, K. I. Chane-Ching and P. C. Lacaze, *J. Electroanal. Chem.*, **482**, 156 (2000).
42. J. Widera and J. A. Cox, *Electrochem. Commun.*, **4**, 118 (2002).
43. E. Steckhan, *Top. Curr. Chem.*, **142**, 1 (1987).
44. Z. Galus and R. N. Adams, *J. Phys. Chem.*, **67**, 862 (1963).

45. A. Malinauskas and R. Holze, *Ber. Bunsenges. Phys. Chem.*, **101**, 1859 (1997).
46. A. Malinauskas and R. Holze, *Electrochim. Acta*, **44**, 2613 (1999).
47. A. Malinauskas and R. Holze, *Ber. Bunsenges. Phys. Chem.*, **100**, 1740 (1996).
48. A. Malinauskas and R. Holze, *Electrochim. Acta*, **43**, 2413 (1998).
49. A. Malinauskas and R. Holze, *J. Solid State Electrochem.*, **3**, 429 (1999).
50. G. P. Evans, in *Advances in Electrochemical Science and Engineering* (Eds. H. Gerisher and C. W. Tobias), Vol. 1, Chap. 1, VCH, Weinheim, 1990.
51. T. Ohsaka, T. Okajima and N. Oyama, *J. Electroanal. Chem.*, **200**, 159 (1986).
52. G. Neubert and K. B. Prater, *J. Electrochem. Soc.*, **121**, 745 (1974).
53. N. Oyama, T. Ohsaka and T. Shimizu, *Anal. Chem.*, **57**, 1526 (1985).
54. L. Qin, G. N. R. Tripathi and R. H. Schuler, *Z. Naturforsch.*, **40a**, 1026 (1985).
55. M. Jonsson, D. D. M. Wayner and J. Lusztyk, *J. Phys. Chem.*, **100**, 17539 (1996).
56. G. Hambitzer and J. Heitbaum, *Anal. Chem.*, **58**, 1067 (1986).
57. G. Hambitzer, J. Heitbaum and I. Stassen, *J. Electroanal. Chem.*, **447**, 117 (1998).
58. H. Yang, D. O. Wipf and A. J. Bard, *J. Electroanal. Chem.*, **331**, 913 (1992).
59. M. Oyama, T. Higuchi and S. Okazaki, *Electrochem. Commun.*, **2**, 675 (2000).
60. M. Oyama, M. Goto and H. Park, *Electrochem. Commun.*, **4**, 110 (2002).
61. M. Goto, H. Park, K. Otsuka and M. Oyama, *J. Phys. Chem. A*, **106**, 8103 (2002).
62. N. V. Rees, O. V. Klymenko, R. G. Compton and M. Oyama, *J. Electroanal. Chem.*, **531**, 33 (2002).
63. M. Oyama and M. Goto, *Indian J. Chem. A*, **42**, 733 (2003).
64. M. Oyama and T. Higuchi, *J. Electrochem. Soc.*, **149**, E12 (2002).
65. P. Simon, G. Farsang and C. Amatore, *J. Electroanal. Chem.*, **435**, 165 (1997).
66. M. Goto, K. Otsuka, X. Chen, Y. Tao and M. Oyama, *J. Phys. Chem. A*, **108**, 3980 (2004).
67. N. Comisso, S. Daolio, G. Mengoli, R. Salmaso, S. Zecchin and G. Zotti, *J. Electroanal. Chem.*, **255**, 97 (1988).
68. J. Guay and L. H. Dao, *J. Electroanal. Chem.*, **274**, 135 (1989).
69. K. Fehér and G. Inzelt, *Electrochim. Acta*, **47**, 3551 (2002).
70. C. Y. Chung, T. C. Wen and A. Gopalan, *Electrochim. Acta*, **47**, 423 (2001).
71. H. Yang and A. J. Bard, *J. Electroanal. Chem.*, **306**, 87 (1991).
72. S. Wawzonek and T. W. McIntyre, *J. Electrochem. Soc.*, **114**, 1025 (1967).
73. C. P. Andrieux, I. Gallardo and M. Junca, *J. Electroanal. Chem.*, **354**, 231 (1993).
74. G. Cauquis, H. Delhomme and D. Serve, *Electrochim. Acta*, **20**, 1019 (1975).
75. D. Serve, *Electrochim. Acta*, **21**, 1171 (1976).
76. N. Pekmez, K. Pekmez and A. Yildiz, *J. Electroanal. Chem.*, **348**, 389 (1993).
77. M. Oyama, T. Higuchi and S. Okazaki, *J. Chem. Soc., Perkin Trans. 2*, 1287 (2001).
78. H. Park and M. Oyama, *J. Chem. Soc., Perkin Trans. 2*, 1335 (2002).
79. R. F. Nelson and R. N. Adams, *J. Am. Chem. Soc.*, **90**, 3925 (1968).
80. L. S. Marcoux, R. N. Adams and S. W. Feldberg, *J. Phys. Chem.*, **73**, 2611 (1969).
81. R. F. Nelson and S. W. Feldberg, *J. Phys. Chem.*, **73**, 2623 (1969).
82. R. F. Nelson and R. H. Philp, Jr., *J. Phys. Chem.*, **83**, 713 (1979).
83. D. Larumbe, I. Gallardo and C. P. Andrieux, *J. Electroanal. Chem.*, **304**, 241 (1991).
84. M. Oyama, R. Nozaki and S. Okazaki, *Anal. Chem.*, **63**, 1387 (1991).
85. T. Sumiyoshi, *Chem. Lett.*, 645 (1995).
86. Q. Zhuang and D. Sun, *J. Electroanal. Chem.*, **440**, 103 (1997).
87. T. Zhang and A. Brajter-Toth, *Anal. Chem.*, **72**, 2533 (2000).
88. M. Oyama, T. Higuchi and S. Okazaki, *Electrochem. Solid State Lett.*, **5**, E1 (2002).
89. M. Oyama and M. Kambayashi, *Electrochem. Commun.*, **4**, 759 (2002).
90. M. Nicolas, B. Fabre, J. M. Chapuzet, J. Lessard and J. Simonet, *J. Electroanal. Chem.*, **482**, 211 (2000).
91. J. P. Dinnocenzo and T. E. Banach, *J. Am. Chem. Soc.*, **111**, 8646 (1989).
92. N. V. Rees, J. D. Wadhawan, O. V. Klymenko, B. A. Coles and R. G. Compton, *J. Electroanal. Chem.*, **563**, 191 (2004).
93. K. Itoh and M. Kinoshita (Eds.), *Molecular Magnetism, New Magnetic Materials*, Gordon and Breach, Amsterdam, 2000.
94. A. Rajca, *Chem. Rev.*, **94**, 811 (1994).
95. M. Yano, Y. Ishida, M. Tatsumi, K. Sato, D. Shiomi, M. Oyama and T. Takui, *J. Phys. Chem. Solids*, **65**, 733 (2004).

96. M. Yano, K. Sato, D. Shiomi, A. Ichimura, K. Abe, T. Takui and K. Itoh, *Tetrahedron Lett.*, **37**, 9207 (1996).

97. K. Sato, M. Yano, M. Furuichi, D. Shiomi, K. Abe, T. Takui. K. Itoh, A. Higuchi, K. Katsuma and Y. Shirota, *J. Am. Chem. Soc.*, **119**, 6607 (1997).

98. M. Yano, K. Aoyama, Y. Ishida, M. Tatsumi, K. Sato, D. Shiomi and T. Takui, *Polyhedron*, **22**, 2003 (2003).

99. M. Yano, Y. Ishida, K. Aoyama, M. Tatsumi, K. Sato, D. Shiomi, A. Ichimura and T. Takui, *Synth. Metals*, **137**, 1275 (2003).

100. M. M. Wienk and R. A. J. Janssen, *Chem. Commun.*, 267 (1996).

101. M. M. Wienk and R. A. J. Janssen, *J. Am. Chem. Soc.*, **118**, 10626 (1996).

102. M. M. Wienk and R. A. J. Janssen, *J. Am. Chem. Soc.*, **119**, 4492 (1997).

103. K. R. Stickley, T. D. Selby and S. C. Blackstock, *J. Org. Chem.*, **62**, 448 (1997).

104. K. Yoshizawa, A. Chano, A. Ito, K. Tanaka, T. Yamabe, H. Fujita, J. Yamauchi and M. Shiro, *J. Am. Chem. Soc.*, **114**, 5994 (1992).

105. P. J. Low, M. A. J. Paterson, H. Puschmann, A. E. Goeta, J. A. K. Howard, C. Lambert, J. C. Cherryman, D. R. Tackley, S. Leeming and B. Brown, *Chem. Eur. J.*, **10**, 83 (2004).

106. J. Bacon and R. N. Adams, *J. Am. Chem. Soc.*, **90**, 6596 (1968).

107. C. Amatore, G. Farsang, E. Maisonhaute and P. Simon, *J. Electroanal. Chem.*, **462**, 55 (1999).

108. M. Kádár, Z. Nagy, T. Karancsi and G. Farsang, *Electrochim. Acta*, **46**, 1297 (2001).

109. M. Kádár, Z. Nagy, T. Karancsi and G. Farsang, *Electrochim. Acta*, **46**, 3405 (2001).

110. S. Pusztai, T. Dankházi and G. Farsang, *Electroanal.*, **15**, 539 (2003).

111. C. Hansch, A. Leo and R. W. Taft, *Chem. Rev.*, **91**, 165 (1991).

112. F. G. Bordwell, X.-M. Zhang and J.-P. Cheng, *J. Org. Chem.*, **58**, 6410 (1993).

113. P. G. Desideri, L. Lepri and D. Heimler, *J. Electroanal. Chem.*, **32**, 225 (1971).

114. P. G. Desideri, L. Lepri and D. Heimler, *J. Electroanal. Chem.*, **43**, 387 (1973).

115. L. Nadjo and J.-M. Savéant, *J. Electroanal. Chem.*, **44**, 327 (1973).

116. P. G. Desideri, L. Lepri and D. Heimler, *J. Electroanal. Chem.*, **52**, 93 (1974).

117. P. G. Desideri, L. Lepri and D. Heimler, *J. Electroanal. Chem.*, **52**, 105 (1974).

118. L. H. Piette, P. Ludwig and R. N. Adams, *J. Am. Chem. Soc.*, **83**, 3909 (1961).

119. L. H. Piette, P. Ludwig and R. N. Adams, *Anal. Chem.*, **34**, 916 (1962).

120. R. L. Bent, J. C. Dessloch, F. C. Duennebier, D. W. Fassett, D. B. Class, T. H. James, D. B. Julian, W. R. Ruby, J. M. Snell, J. H. Sterner, J. R. Thirtle, P. W. Vittum and A. Weisberger, *J. Am. Chem. Soc.*, **83**, 3100 (1961).

121. O. Fisher and V. Komarek, *Collect. Czech. Chem. Commun.*, **41**, 2320 (1976).

122. G. Cauquis, H. Delhomme and D. Serve, *Tetrahedron Lett.*, 1965 (1972).

123. G. Cauquis and D. Serve, *Anal. Chem.*, **44**, 2222 (1972).

124. G. Grampp and W. Jaenicke, *Ber. Bunsenges. Phys. Chem.*, **88**, 325 (1984).

125. G. Grampp and W. Jaenicke, *Ber. Bunsenges. Phys. Chem.*, **88**, 335 (1984).

126. M. Opałło, *J. Chem. Soc., Faraday Trans. 1*, **82**, 339 (1986).

127. L. D. Zusman, *Sov. Electrochem.*, **24**, 1125 (1988).

128. A. Kapturkiewicz and W. Jaenicke, *J. Chem. Soc., Faraday Trans. 1*, **83**, 2727 (1987).

129. W. R. Fawcett and C. A. Foss, Jr., *J. Electroanal. Chem.*, **270**, 103 (1989).

130. H. Fernández and M. A. Zón, *J. Electroanal. Chem.*, **332**, 237 (1992).

131. M. B. Moressi, M. A. Zón and H. Fernández, *Electrochim. Acta*, **45**, 1669 (2000).

132. M. J. Weaver, *Chem. Rev.*, **92**, 463 (1992).

133. W. R. Fawcett, *Langmuir*, **5**, 661 (1989).

134. W. R. Fawcett, *Electrochim. Acta*, **42**, 833 (1997).

135. J. S. Jaworski and M. K. Kalinowski, in *Similarity Models in Organic Chemistry, Biochemistry and Related Fields* (Eds. R. I. Zalewski, T. M. Krygowski and J. Shorter), Chap. 8, Elsevier, Amsterdam, 1991, pp. 387–454.

136. D. Hawley and R. N. Adams, *J. Electroanal. Chem.*, **10**, 376 (1965).

137. R. L. Hand and R. F. Nelson, *J. Electrochem. Soc.*, **125**, 1059 (1978).

138. M. Oyama and K. Kirihara, *Electrochim. Acta*, **49**, 3801 (2004).

139. A. Kudelski and J. Bukowska, *J. Mol. Struct.*, **275**, 145 (1992).

140. K. Jackowska, J. Bukowska and A. Kudelski, *J. Electroanal. Chem.*, **350**, 177 (1993).

141. J. Widera, W. Grochala, K. Jackowska and J. Bukowska, *Synth. Metals*, **89**, 29 (1997).

142. D. Goncalves, L. H. C. Matosso and L. O. S. Bulhoes, *Electrochim. Acta*, **39**, 2271 (1994).

143. E. Brillas, J. M. Costa and E. Pastor, *An. Quim.*, **79**, 211 (1983).

144. E. Brillas, J. M. Costa and E. Pastor, *J. Electroanal. Chem.*, **160**, 185 (1984).
145. S. Arias and E. Brillas, *Electrochim. Acta*, **30**, 1441 (1985).
146. S. Arias and E. Brillas, *J. Electroanal. Chem.*, **198**, 303 (1986).
147. S. Arias, E. Brillas and J. M. Costa, *J. Chem. Soc., Faraday Trans. 1*, **83**, 2619 (1987).
148. S. Arias, E. Brillas and J. M. Costa, *J. Electroanal. Chem.*, **283**, 231 (1990).
149. S. Wawzonek and T. W. McIntyre, *J. Electrochem. Soc.*, **119**, 1350 (1972).
150. A. D. Courville, *C. R. Acad. Sci.*, **262**C, 1196 (1966).
151. G. E. Parris, *Residue Rev.*, **76**, 1 (1980).
152. M. Raupach and L. J. Janik, *J. Colloid Interface Sci.*, **121**, 449 (1988).
153. K. Rajeshwar and J. G. Ibanez, *Environmental Electrochemistry*, Academic Press, New York, 1997.
154. A. Moreale and R. van Bladel, *Clay Miner.*, **14**, 1 (1979).
155. O. P. Homenauth and M. B. McBride, *Soil Sci. Soc. Am. J.*, **58**, 347 (1994).
156. M. E. Essington, *Soil Sci.*, **158**, 181 (1994).
157. S. Ardizzone, H. Høiland, C. Lagioni and E. Sivieri, *J. Electroanal. Chem.*, **447**, 17 (1998).
158. F. Fiçicioğlu, S. Kuliyev and F. Kadirgan, *J. Electroanal. Chem.*, **408**, 231 (1996).
159. J. Niu and B. E. Conway, *J. Electroanal. Chem.*, **536**, 83 (2002).
160. J. Niu and B. E. Conway, *J. Electroanal. Chem.*, **546**, 59 (2003).
161. J. Taguchi, S. Ohtsuki and F. Kusu, *J. Electroanal. Chem.*, **557**, 91 (2003).
162. I. A. Vinokurov and J. Kankare, *J. Electroanal. Chem.*, **543**, 101 (2003).
163. R. Mazeikiene and A. Malinauskas, *ACH-Models Chem.*, **136**, 363 (1999).
164. R. Mazeikiene and A. Malinauskas, *Reactive Functional Polymers*, **45**, 45 (2000).

CHAPTER **17**

Proton sponges

ALEXANDER F. POZHARSKII and VALERY A. OZERYANSKII

Department of Organic Chemistry, Rostov State University, Zorge str., 7, 344090, Rostov-on-Don, Russian Federation
Fax: +7 863 2975146;   e-mails: apozharskii@rsu.ru, vv_ozer2@rsu.ru

I. INTRODUCTION

Neutral organic bases possessing anomalously high thermodynamic basicity in conjunction with lowered proton addition–elimination rates (low kinetic basicity and acidity) are called

TABLE 1. pK_a values^a of N-methylated 1,8-diaminonaphthalenes at 25 °C

(1–6)
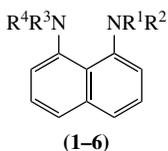
Compound	R^1	R^2	R^3	R^4	pK$_a$	
					H$_2$O[1]	MeCN[2]
2	H	H	H	H	4.61	10.99
3	Me	H	H	H	—	11.64
4	Me	H	Me	H	5.61	11.95
5	Me	Me	H	H	—	12.87
6	Me	Me	Me	H	6.43	12.91
1	Me	Me	Me	Me	12.34	18.18

^{a} For the sake of simplicity, the term pK_a is used throughout the text rather than pK_{BH}^+. pK_a is a measure of the acid dissociation of the conjugate acid of the nitrogen bases.

'proton sponges'. The archetypal 'proton sponge' is 1,8-bis(dimethylamino)naphthalene (**1**), for which the Aldrich company in the early 1970s gave this trade mark. The name arose due to the appealing similarity in the behaviour of such compounds and genuine sponges, which slowly absorb water, retain it firmly and are difficult to be wrung out. The fact that the basicity of **1** is astonishingly high for aromatic amines was recognized in 1968 by Alder and coworkers[1]. They found that whereas the pK_a values for 1,8-diaminonaphthalene **2**, its mono-, di- and trimethyl derivatives **3–6** fall in the range typical of ordinary aryl amines, the basicity of **1** increases at once by almost six powers of ten reaching pK_a = 12.34 (Table 1). It is noteworthy that this correlation is characteristic not only for aqueous media, but also for non-aqueous solutions (e.g. acetonitrile[2]) and the gas phase[3].

It is believed[1,4–6] that the abnormally high basicity of compound **1** is caused by two main factors: (1) destabilization of the base due to severe repulsion between nitrogen lone electron pairs and (2) formation of a strong intramolecular hydrogen bond (IHB) in the protonated form **1·H$^+$** (equation 1).

(1)
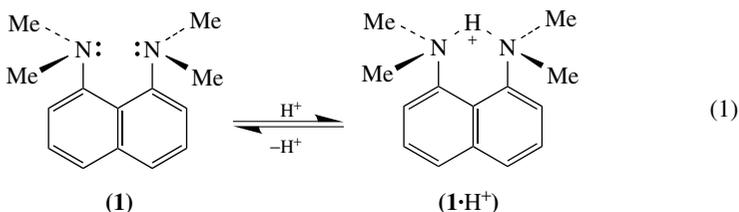
Since the mid-1980s, for the sake of more deeply understanding these factors, Staab and coworkers have synthesized a series of related diamines on the basis of fluorene **7**[7], heterofluorenes **8–10**[8], phenanthrenes **11** and **12**[9], benzo[c]phenanthrene **13**[10] and polynuclear diazaarenes **14**[11,12], **15**[13] and **16**[14]. The polycyclic vinamidines **17** and **18**, possessing even stronger basicity than compounds **1** and **7–16**, were synthesized by Schwesinger and coworkers[15].

(7) X = CH$_2$
(8) X = S
(9) X = Se
(10) X = Te

(11) X—X = CH$_2$—CH$_2$
(12) X—X = CH=CH

(13)

(14)   (15)   (16)

(17)   (18) R = H, Me
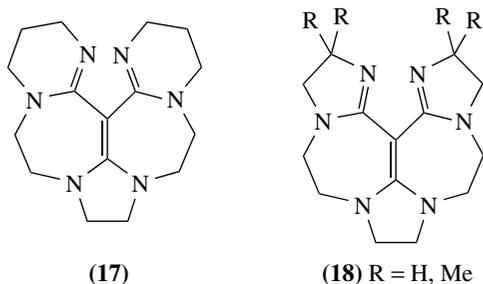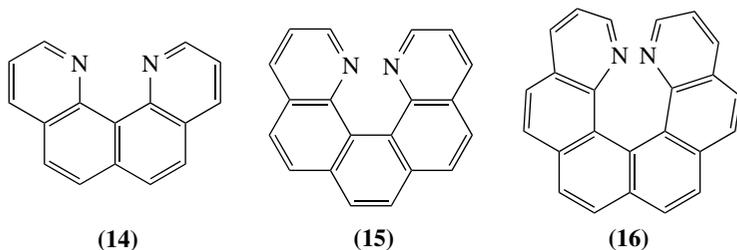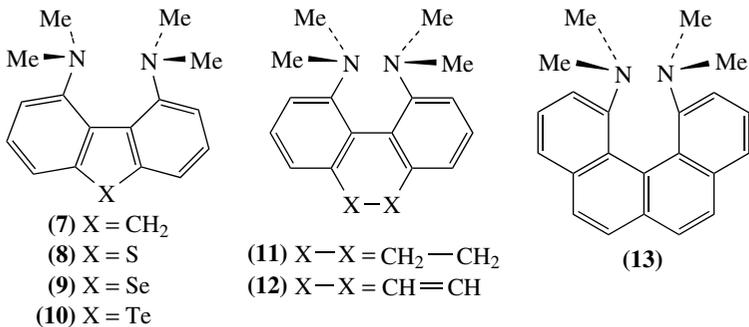
Further progress in this direction has gradually brought about the concept establishing the criteria of which compounds can be referred to as proton sponges. The main principles of this concept are a number of structural requirements, the most important of which are: (1) a proper spatial organization of the molecule providing rigid fixation of two nitrogen atoms at a sufficiently close distance from each other; (2) the presence of a destabilizing effect due to the nitrogen lone electron pair repulsion in the non-protonated molecule; (3) the existence of a strong IHB in the protonated molecule that relieves steric and electronic strain characteristic for the conjugated base; (4) the presence of a hydrophobic environment at the nitrogen atoms, mostly alkyl groups, which actually accounts for the sponge effect (low rates of proton addition−elimination and low *N*-nucleophilicity, displaying difficulty to coordinate with all Lewis acids except the proton). Unfortunately, not all of these principles are commonly taken into consideration and many publications still appear where target compounds are mistakenly referred to as proton sponges. To name but a few, mostly due to violation of the last criterion, are compounds **14**−**18**, iminophosphorane **19**[16], bis-guanidine **20**[17] and 1,8-bis(dimethylaminomethyl)naphthalene
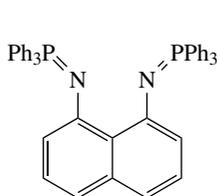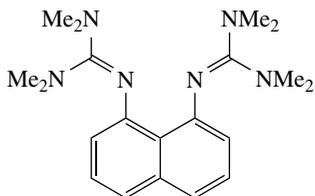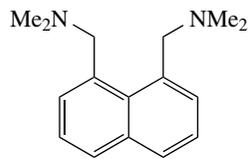
(19)   **(20)**   **(21)**

(**21**)[18]. For other similar cases of incorrect assignment, see References 19–26. Actually, all these bases should be more correctly named 'proton sponge-like compounds'[27].

For a long time researchers paid attention mainly to the basicity and structure of the proton sponges, as reflected in the first reviews on this topic[4–6, 28]. However, later studies have shown that the reactivity of proton sponges is, at least, no less interesting and allows one to understand all their specifics on a firm grounding. With this in mind and in keeping with the title, in this chapter the main aspects of aniline proton sponges of type **1** and **7–13** are generalized, including methods of preparation, structural and physicochemical characteristics, reactivity and practical application data. The majority of the chapter is devoted to naphthalene proton sponges. Aside from **1** and other tetraalkylated derivatives of 1,8-diaminonaphthalene, these include compounds in which the amino groups are incorporated into cycles (**22–27**) or linked by different bridges (**28–34**). The so-called 'double proton sponges' **35–37** and other polykis(dialkylamino)naphthalenes also form a peculiar group of compounds. The earlier review on naphthalene proton sponges[29] now requires updating since the amount of new information has almost doubled.
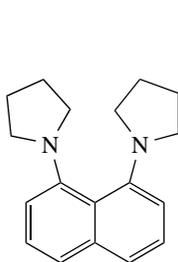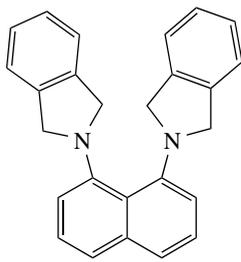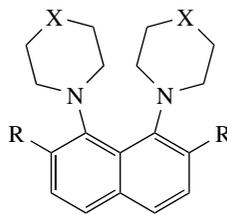
(22)   **(23)**   **(24)**   X = CH$_2$, R = H
       (25a) X = O, R = H
       (25b) X = O, R = OMe
       (25c) X = O, R = OEt
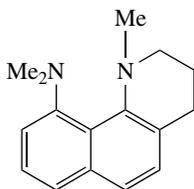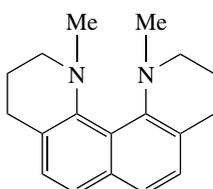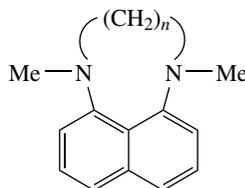
(26)   **(27)**   **(28a)** n = 1
       (28b) n = 2
       (28c) n = 3
       (28d) n = 4
       (28e) n = 5

(29)   (30)   (31)   (32)

(33)   (34)   (35)

(36) $n = 0$
(37) $n = 1$
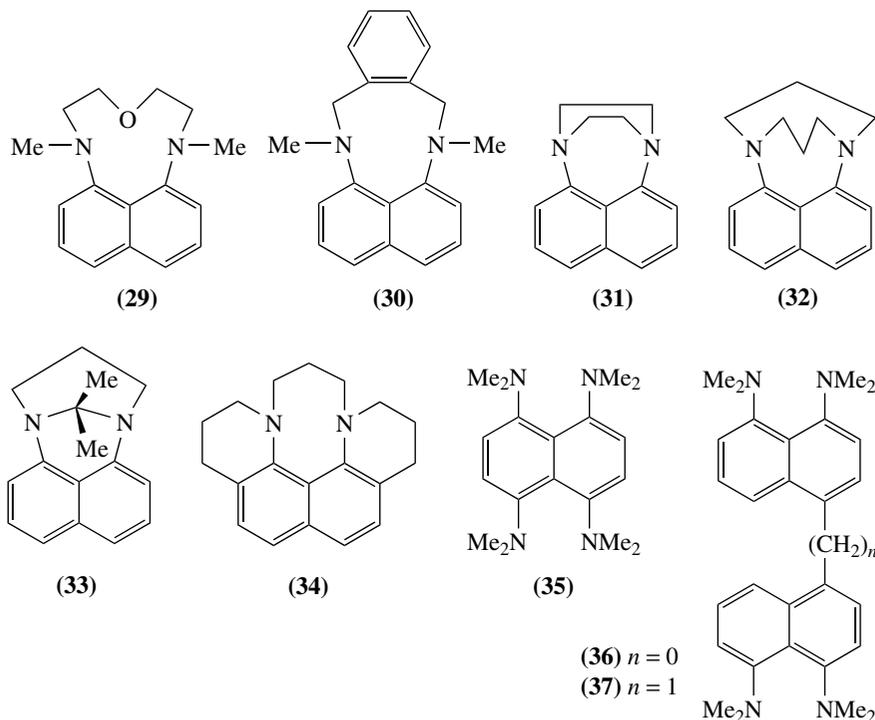
II. SYNTHESIS OF PROTON SPONGES

A. 1,8-Bis(dialkylamino)naphthalenes

There are two common approaches to the synthesis of these compounds, fruitfully complementing each other. The first is based on the alkylation of 1,8-diaminonaphthalene or its partially alkylated derivatives. In the second, 1,1,3-trialkyl-2,3-dihydroperimidinium salts are used as the starting material.

1. From 1,8-diaminonaphthalenes

There are three ways, almost equal in their efficiency, for the exhaustive alkylation (commonly methylation) of diamine 2 and its derivatives. Two of them require the use of a strong base such as sodium or potassium hydride in anhydrous THF[30] or KOH in DMSO[31] for the ionization of N−H bonds. The N-anions of the starting and partially alkylated amines are apparently the active species under these conditions. The N−H bond ionization is favoured by the relatively high NH-acidity of 2 ($pK_a = 24.5$, DMSO, 25 °C) ascribed to the stabilization of the anion 38 through IHB (Scheme 1)[32]. The yield of proton sponge 1 or its acenaphthene analogue 40[33] is commonly high, but it may decrease in the case of some ring-substituted derivatives (Table 2). In the preparation of 1,8-bis(diethylamino)naphthalene (39), the use of HMPA as a solvent instead of DMSO was recommended[31].
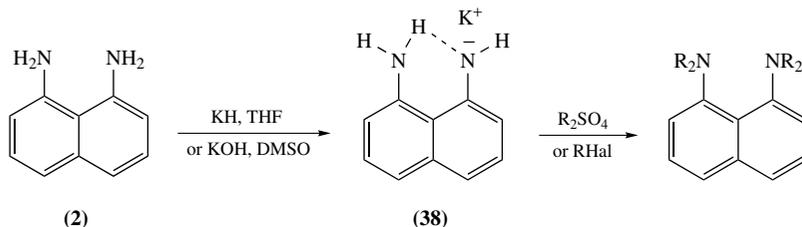
SCHEME 1

The third protocol for exhaustive methylation includes exploitation of the Me_2SO_4- $Na_2CO_3-H_2O$ system and is especially suitable for polyamines with low NH-acidity. Obviously, alkylation in this case proceeds by means of a quaternization–deprotonation sequence. The reaction occurs in a two-phase mode at room temperature and provides remarkably high yields (Section II.B.1).

The alkylation of diamine **2** with α,ω-dihaloalkanes in non-aqueous solvents in the presence of sodium carbonate gives diverse results, depending on the alkylene chain length (Table 2). If the halogens are separated by 4 or 5 atoms, 1,8-dipyrrolidino- **22** and **23**, 1,8-dipiperidino- **24** or 1,8-dimorpholinonaphthalenes **25a–c** are formed, respectively. With a closer disposition of the halogens, bridged sponges like **31–33** are normally formed. Interestingly, the alkylation with 1,3-dibromopropane yields, along with compound **32**, a small amount of pentacyclic by-product **34**. Apparently, its precursor is naphtho[1,8-*b*,*c*]-1,5-diazacyclooctane (also isolated in low yield), which on reacting with 1,3-dibromopropane first undergoes *N*- and then intramolecular *C*-alkylation.

Some kinds of proton sponges are best prepared starting from accessible 1,8-bis(methylamino)naphthalene (**4**) or its derivatives[2,40–43]. For example, the optimal synthesis of 1,8-bis(dimethylamino)-4,5-dinitronaphthalene (**51**) consists in methylation of compound **50**, which in turn can be prepared from perimidone **49** (Scheme 2)[44,45].

Alder and coworkers have synthesized proton sponges **28–30** with moderate to high yield by treating diamine **4** with α,ω-dihaloalkanes[35].

The alkylation of *N*,*N*,*N*′-trialkyl-substituted 1,8-diaminonaphthalenes proceeds very smoothly. The reaction is usually conducted on heating the substrate with an excess of alkyl halide in an appropriate solvent or without solvent. The proton sponge salt initially formed is then converted into the base on treatment with aqueous alkali[33,46,47].

Recently, there has been research activity in the area of chiral proton sponges, in particular, those containing nitrogens with pairs of different substituents. The molecular asymmetry of such sponges, especially well pronounced in the cationic forms, arises as a result of the arrangement of bulkier functions at opposite sides of the naphthalene ring plane. Synthesis of these compounds, e.g. **52**[48], **53**[33] and **54**[49], is also achieved via alkylation of the corresponding *N*,*N*′-dialkyl- or *N*,*N*,*N*′-trialkyl-1,8-diaminonaphthalenes (Scheme 3).

The preparation of 'isotopomers' of **1** with CD_3 groups from 1,8-diaminonaphthalene and Me_2SO_4-d_6 is also described[50,51].

2. From 2,3-dihydroperimidinium salts

This method, advanced primarily in the authors' laboratory[33], can be especially recommended in two cases: (1) for proton sponges with non-standard combinations of

TABLE 2. Synthesis of proton sponges by exhaustive *N*-alkylation of the corresponding 1,8-diaminonaphthalenes

Proton sponge	Alkylating agent	Reaction conditions	Yield (%)	References
1	Me_2SO_4	NaH, THF, reflux, 3.5 h	87	30
1	MeI	KOH, DMSO, 100 °C, 3 h	95	31
1	Me_2SO_4	Na_2CO_3, H_2O, RT, 2 h	92	34
22	$Br(CH_2)_4Br$	Na_2CO_3, 160 °C, 0.7 h	60	35
23	o-$C_6H_4(CH_2Br)_2$	Na_2CO_3, DMF, reflux, 1 h	5	35
24	$Br(CH_2)_5Br$	Na_2CO_3, 150 °C, 1 h	20	35
25a	$O(CH_2CH_2Cl)_2$	Na_2CO_3, 150 °C, 1.5 h	10	35
25b	$O(CH_2CH_2Cl)_2$	Na_2CO_3, 170 °C, 1.5 h	3	36
25c	$O(CH_2CH_2Cl)_2$	Na_2CO_3, 170 °C, 1.5 h	15	36
28b	$Br(CH_2)_2Br$	$NaHCO_3$, DMF, reflux, 1 h	20	35
28b	$Br(CH_2)_2Br$	NaH, THF, reflux, 24 h	80	35
28c	$Br(CH_2)_3Br$	$NaHCO_3$, diglyme, 190 °C, 1 h	43	35
28c	$Br(CH_2)_3Br$	NaH, THF, reflux, 36 h	1	35
28d	$Br(CH_2)_4Br$	$NaHCO_3$, diglyme, reflux, 46 h	58	35
28e	$Br(CH_2)_5Br$	Na_2CO_3, diglyme, reflux, 26 h	25	35
29	$O(CH_2CH_2Cl)_2$	Na_2CO_3, diglyme, reflux, 150 h	77	35
30	o-$C_6H_4(CH_2Br)_2$	Na_2CO_3, DMF, reflux, 24 h	13	35
31	$Br(CH_2)_2Br$	Na_2CO_3, DMF, reflux, 1 h	42	35
32	$Br(CH_2)_3Br$	Na_2CO_3, sulpholane, 150 °C, 52 h	5	35
33	$Br(CH_2)_3Br$	Na_2CO_3, acetone, reflux, 8 h	34	35
39	EtI	KOH, HMPA, 100 °C, 8 h	99	31
40	MeI	KOH, DMSO, 100 °C, 4 h	94–98	37, 38
40	Me_2SO_4	Na_2CO_3, H_2O, RT, 2 h	90	34
41	Me_2SO_4	NaH, THF, reflux, 4 h	71	39
42	MeI	K_2CO_3, DMF, reflux, 30 h	42	37
43	MeI	K_2CO_3, DMF, reflux, 30 h	76	37
44	MeI	NaH, THF, reflux, 20 h	40	35
44	Me_2SO_4	Na_2CO_3, H_2O, RT, 5 h	70	34
45	EtBr	KH, THF, reflux, 20 h	21	35
46	MeBr	KH, THF, reflux, 72 h	8	36
47	EtBr	KH, THF, reflux, 72 h	6	36
48	MeI	NaH, THF, reflux, 24 h	27	35
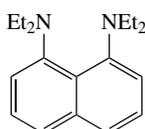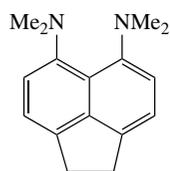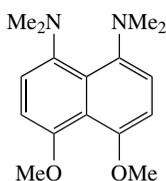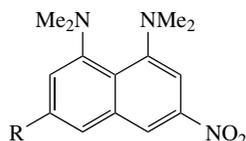
(39)   **(40)**   **(41)**   **(42)** R = H
                                    (43) R = NO₂
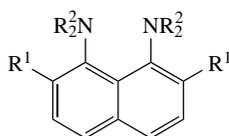
(44) R¹ = OMe, R² = Me
(45) R¹ = OMe, R² = Et
(46) R¹ = OEt, R² = Me
(47) R¹ = OEt, R² = Et
(48) R¹ = R² = Me
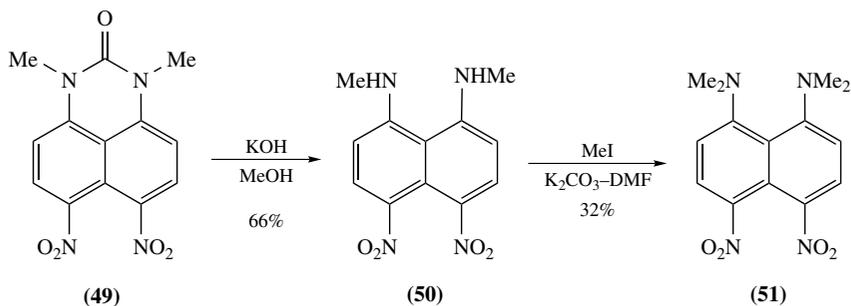
SCHEME 2
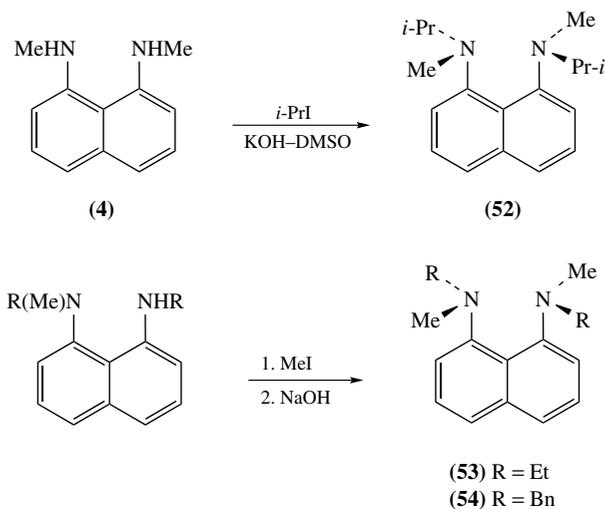
SCHEME 3

N-substituents and (2) for proton sponges with naphthalene ring substituents, which are introduced with difficultly by direct functionalization. Preparation of 4,5-dibromo-1,8-bis(dimethylamino)naphthalene (**59**) can serve as a typical illustration (Scheme 4)[52]. The starting compound is 1,3-dimethylperimidone **55**, which is susceptible, unlike naphthalene and compound **1**, to selective *peri*-dibromination with NBS in THF solution. The further straightforward reduction of the amide carbonyl in the 6,7-dibromoperimidone gives 6,7-dibromo-1,3-dimethyl-2,3-dihydroperimidine (**56**). Subsequent quaternization with methyl iodide offers a route to the 2,3-dihydroperimidinium salt **57**, which is smoothly cleaved in aqueous alkali to form 4,5-dibromo-1-dimethylamino-8-methylaminonaphthalene (**58**). Further methylation of the latter provides the desired product **59**. The yields at all steps are good to excellent. Notably, 2,3-dihydroperimidinium salts can be converted directly into the corresponding proton sponge by using reductive scission with LiAlH₄ or NaBH₄[41], though if employed to **57** this process is complicated by partial debromination. More details on this method can be found in a review[29].
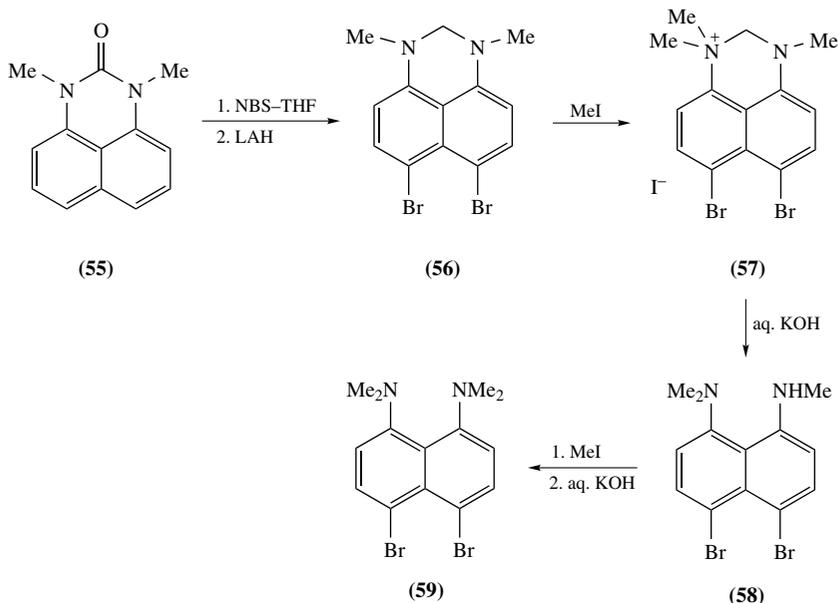
SCHEME 4

3. From 1,8-dihalonaphthalenes

In one instance, the proton sponge derivatives **61** were prepared by nucleophilic displacement of the activated chlorine atoms in *peri*-dichloroacenaphthene **60** on heating with excess of dimethyl- or diethylamine (equation 2)[53]. Regrettably, the structure of all compounds reported in this work was elucidated without NMR analysis, utilizing only combustion analysis and IR spectroscopy.

(2)

R = Me 85%
R = Et 57%
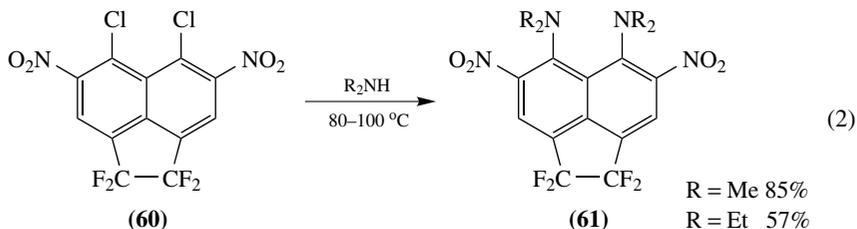
4. By functionalization of already existing proton sponges

A considerable number of proton sponges can be prepared by functionalizing the parent sponge **1** or its suitable derivatives. Thus, the 1,1′-binaphthyl sponge **36**, which possesses interesting properties, is formed by treatment of **1** with some oxidants. This and many other reactions are discussed in Section IV.

B. Polykis(dialkylamino)naphthalenes

In this section, the derivatives of 1,8-bis(dialkylamino)naphthalenes with at least one additional dialkylamino group will be covered. There exist two approaches to the synthesis of such compounds. The first consists of reduction and successive alkylation of the corresponding nitro- or polynitronaphthalenes. Until recently, this approach was successful only for the preparation of tris- and tetrakis(dialkylamino)naphthalenes. For the introduction of more dialkylamino groups, the nucleophilic substitution of fluorine atoms in octafluoronaphthalene is the method of choice.

1. From polyaminonaphthalenes

This method was successfully employed for the preparation of the tris(dialkylamino) derivatives **62**–**64** and tetraamines **35** and **65**–**68**. Some details are given in Table 3. For the synthesis of **63** and **65**–**67**, the *ortho*-dialkylamino groups were introduced by means of nucleophilic substitution of one or both of the methoxy groups in compound **69** with the appropriate dialkylamine (Scheme 5). In other cases this was achieved via exhaustive methylation of the amino groups in mono-, di- or polyamines.

(62) R = H
(63) R = OMe

(64)

(65) R = NMe$_2$

(66) R = N ⟨pyrrolidine⟩

(67) R = N ⟨piperidine⟩

(68)
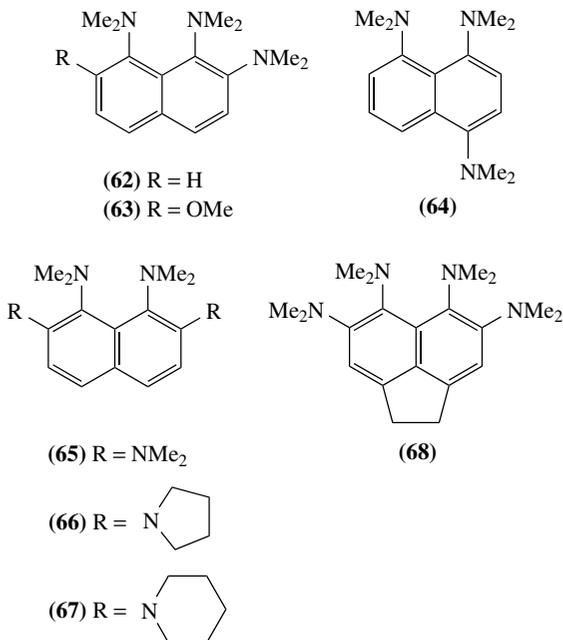
2. From octafluoronaphthalene

The successful synthesis of octakis(phenylthio)- **70a**[59], octakis(aryloxy)- **70b**[60] and octapyrrolyl naphthalenes **70c**[61] has demonstrated a possibility of multiple substitution of fluorine atoms in octafluoronaphthalene (OFN) under the action of relatively mild nucleophiles. This approach has been recently tested for the preparation of polykis(dialkylamino)naphthalenes.

TABLE 3. Synthesis of tris- and tetrakis(dialkylamino)naphthalenes from (nitro)naphthylamines

Proton sponge	Starting material and reaction conditions	Yield (%)	References
35	1,8-Bis(dimethylamino)-4,5-dinitronaphthalene (**51**); 1) H$_2$, Pd-C, 2) Me$_2$SO$_4$, NaH, THF, reflux, 5 h	31	45, 54
35	1,8-Bis(methylamino)-4,5-dinitronaphthalene (**50**) or 1,4,5,8-tetranitronaphthalene; 1) SnCl$_2$, HCl, 2) Me$_2$SO$_4$, NaH, THF, reflux, 10 h	9–14	44
62	1,8-Bis(dimethylamino)-2-nitronaphthalene; 1) H$_2$, Pd-C, 2) MeI, KOH, DMF, 100 °C, 2 h	81	55
63	7-Dimethylamino-2-methoxy-1,8-dinitronaphthalene; 1) H$_2$, Pd-C, 2) Me$_2$SO$_4$, Na$_2$CO$_3$, H$_2$O, RT, 5 h	61	56
64	1,8-Bis(dimethylamino)-4-nitronaphthalene; 1) H$_2$, Pd-C, 2) MeI, KOH, DMF, 100 °C, 1 h	87	57
64	1,4,5-Trinitronaphthalene; 1) SnCl$_2$, HCl, 2) Me$_2$SO$_4$, NaH, THF, reflux, 3 h	60	44
64	1,4,5-Trinitronaphthalene; 1) SnCl$_2$, HCl, 2) Me$_2$SO$_4$, Na$_2$CO$_3$, H$_2$O, RT, 2 h	52	34
65	2,7-Bis(dimethylamino)-1,8-dinitronaphthalene; 1) H$_2$, Pd-C, 2) Me$_2$SO$_4$, NaH, THF, reflux, 17 h	7	54, 58
65	2,7-Bis(dimethylamino)-1,8-dinitronaphthalene; 1) H$_2$, Pd-C, 2) Me$_2$SO$_4$, Na$_2$CO$_3$, H$_2$O, RT, 5 h	57	34, 56
65	2,7-Diamino-1,8-dinitronaphthalene; 1) SnCl$_2$, HCl, 2) Me$_2$SO$_4$, Na$_2$CO$_3$, H$_2$O, RT, 10 h	5–10	34, 56
66	1,8-Dinitro-2,7-dipyrrolidinonaphthalene; 1) H$_2$, Pd-C, 2) Me$_2$SO$_4$, Na$_2$CO$_3$, H$_2$O, RT, 5 h	48	56
67	1,8-Dinitro-2,7-dipiperidinonaphthalene; 1) H$_2$, Pd-C, 2) Me$_2$SO$_4$, Na$_2$CO$_3$, H$_2$O, RT, 5 h	39	34
68	5,6-Bis(dimethylamino)-4,7-dinitroacenaphthene; 1) H$_2$, Pd-C, 2) Me$_2$SO$_4$, Na$_2$CO$_3$, H$_2$O, RT, 5 h	63	56
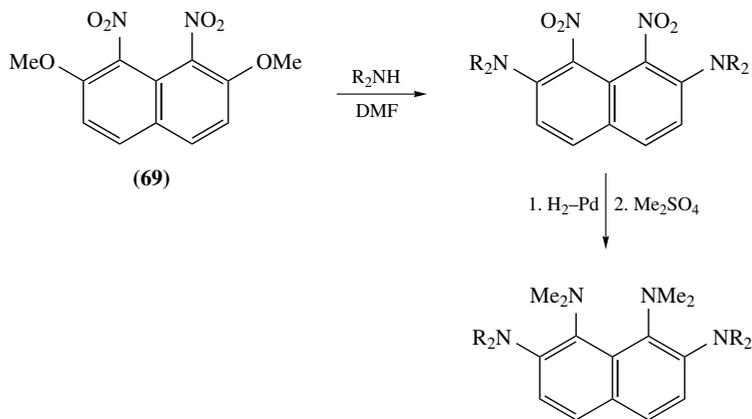
SCHEME 5

(70a) R = SPh
(70b) R = OAr

(70c) R = N (pyrrole)

(71) R = NMe$_2$

(72) R = N (piperidine)

(73) R = NMe$_2$

(74) R = N (pyrrolidine)

(75) R = N (piperidine)

(76) R = NMe$_2$

(77) R = N (pyrrolidine)
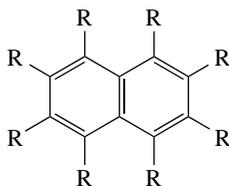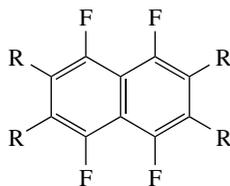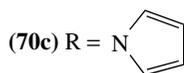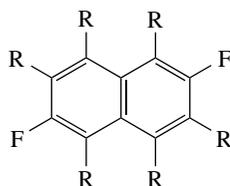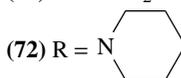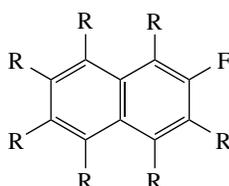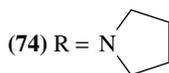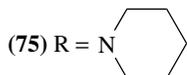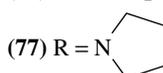
It turned out that heating of OFN with secondary amines in sealed tubes and in a dipolar aprotic solvent leads exclusively to β-substitution to produce tetrakis(dialkylamino)tetra-fluoronaphthalenes, e.g. 71 and 72, in a high yield. An attempt to replace other fluorines failed even under drastic conditions (10-fold excess of dialkylamine, sealed tubes, 190 °C, 14 days)[62].

Unlike this reaction, the reaction of OFN with lithium dialkylamides easily proceeds at ambient temperature and results in the formation of hexa- 73–75 or heptaamines 76 and 77 in 41–46% yield[63]. The reaction occurs smoothly and selectively in dioxane or THF with two-fold excess of lithium dialkylamide per each fluorine atom. It is also recommended that HMPA be added to the reaction mixture (2 equivalents per 1 equivalent of the lithium amide), since cyclic ether solvents are prone to interact with non-solvated lithium amides and thus to form ring-opening products that then react with OFN. Lithium piperidide in either dioxane or THF gives exclusively the hexa-substituted derivative 75. Lithium dimethylamide produces hexaamine 73 in dioxane and heptaamine 76 in THF, whereas the most reactive lithium pyrrolidide forms in dioxane almost a 1:1 mixture of polyamines 74 and 77, and the only product in THF is 77.

The reaction of tetraamines 71 and 72 with lithium dialkylamides has also been inves-tigated. Under a wide range of conditions (dioxane or THF, heating up to 95 °C for 48 h) the pairs 72/lithium piperidide and 71/lithium dimethylamide remain intact in dioxane. However, using THF instead of dioxane in the last case enables one to introduce three

additional dimethylamino groups, resulting in the isomeric heptaamine **78** (equation 3)[64].

$$\mathbf{71} \xrightarrow[\substack{\text{THF, RT, 24 h} \\ 42\%}]{\text{LiNMe}_2} \quad \mathbf{(78)} \tag{3}$$
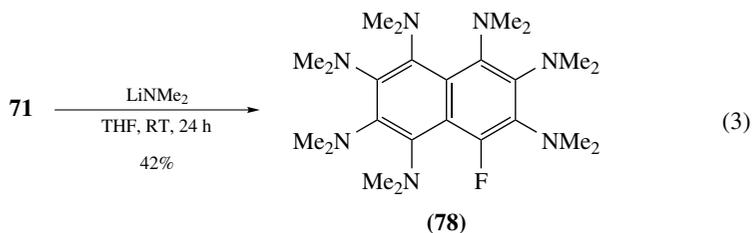
Treatment of fluorinated polykis(dialkylamino)naphthalenes with small excess of LiAlH$_4$ in boiling THF results in exhaustive hydrodefluorination. This route, starting from **71**, **73** and **75**, provides high yields of tetrakis(dimethylamino)naphthalene **79**[62] and proton sponges **80** and **81**[64].

(79)

(80) R = NMe$_2$

(81) R= N
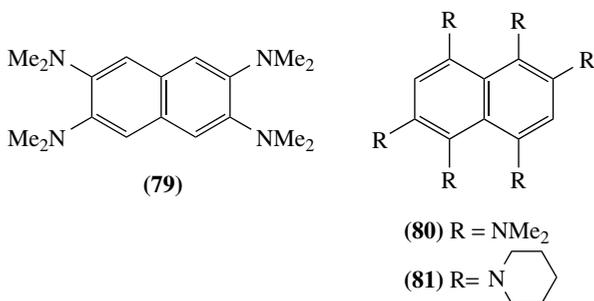
The properties of compounds **73–78**, **80** and **81** are considered in more detail in Sections III.A and IV.A.1.

C. Analogues of the Naphthalene Proton Sponge with *N*-Substituents Other than Alkyl Groups

All known proton sponge analogues of this type contain *N*-phenyl, *N*-acyl, *N*-amino or *N*-nitroso groups. Though the majority of these compounds is not characterized by increased basicity, consideration of their structural and physicochemical features gives additional insight into the *peri*-interaction of the amino groups.

1. Proton sponges with N-aryl and N-acyl groups

So far only derivatives with two (**83**) and four (**84**) *N*-phenyl groups have been described using 1,8-bis(phenylamino)naphthalene (**82**) as their precursor[65]. In the preparation of **83** it was methylated through its dilithium salt, whereas in the case of **84** it was successively arylated with dehydrobenzene generated from *o*-bromofluorobenzene and Mg, and then with iodobenzene according to the Ullmann reaction conditions (Scheme 6).

Proton sponge analogues with *N*-acyl substituents are commonly prepared by treatment of 1-dimethylamino-8-methylaminonaphthalene (**6**) with the corresponding carboxylic acid anhydride, as in the case of **85**[43], or with acyl chloride, as for **86** and **87**[66].

SCHEME 6

(82)

(83)

(84)

(85) R = Me
(86) R = Ph
(87) R = 2-FC$_6$H$_4$

(88a)

(88b)

(89)

(90) R = H
(91) R = NO$_2$

(92)
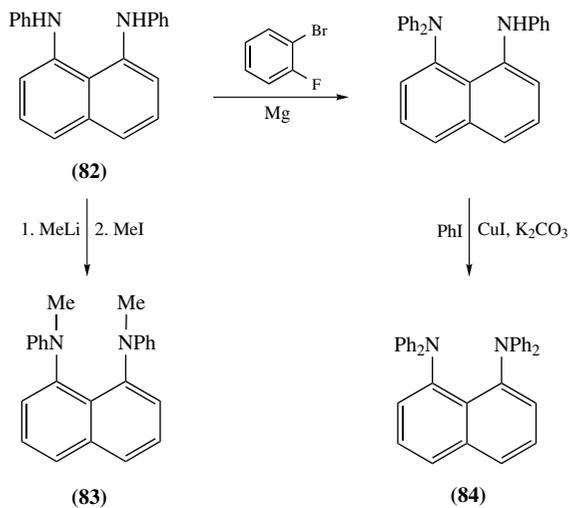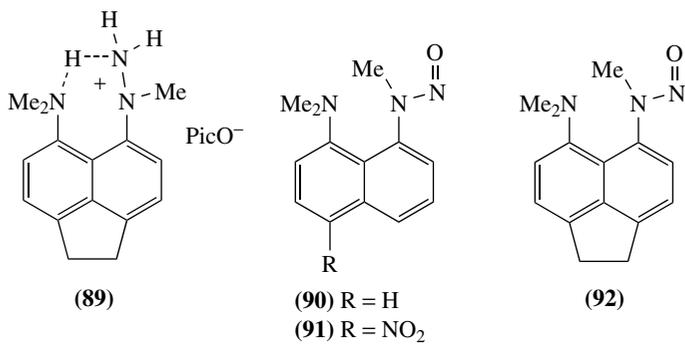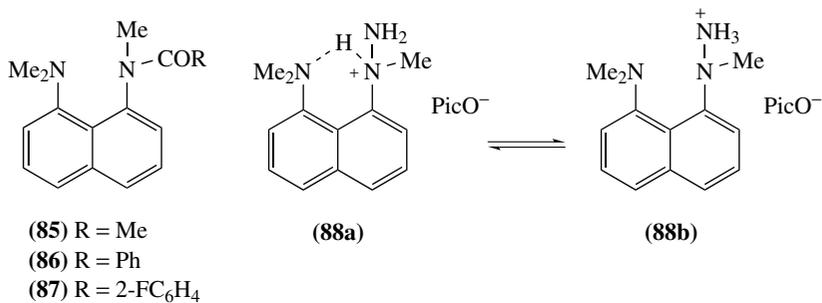
2. Compounds with N-amino and N-nitroso groups

Electrophilic amination of compound **6** and its acenaphthene counterpart with *O*-picrylhydroxylamine has led to the monohydrazine proton sponges **88a**, **88b** and **89** isolated as their picrates (PicO⁻)[67]. During an attempt to prepare the corresponding free bases by alkaline treatment of the picrates, a significant degradation took place, though it was possible to record the ^{1}H NMR spectra of the bases when 1,8-bis(dimethylamino)-2,7-dimethoxynaphthalene (**44**) was used as deprotonation agent right in the NMR ampoule[67].

N-Nitroso compounds **90**–**92** were prepared in a good yield by nitrosation of the corresponding *N*,*N*,*N*′-trimethyl derivatives with nitrous acid[43], and the structures of

(93)

(94)
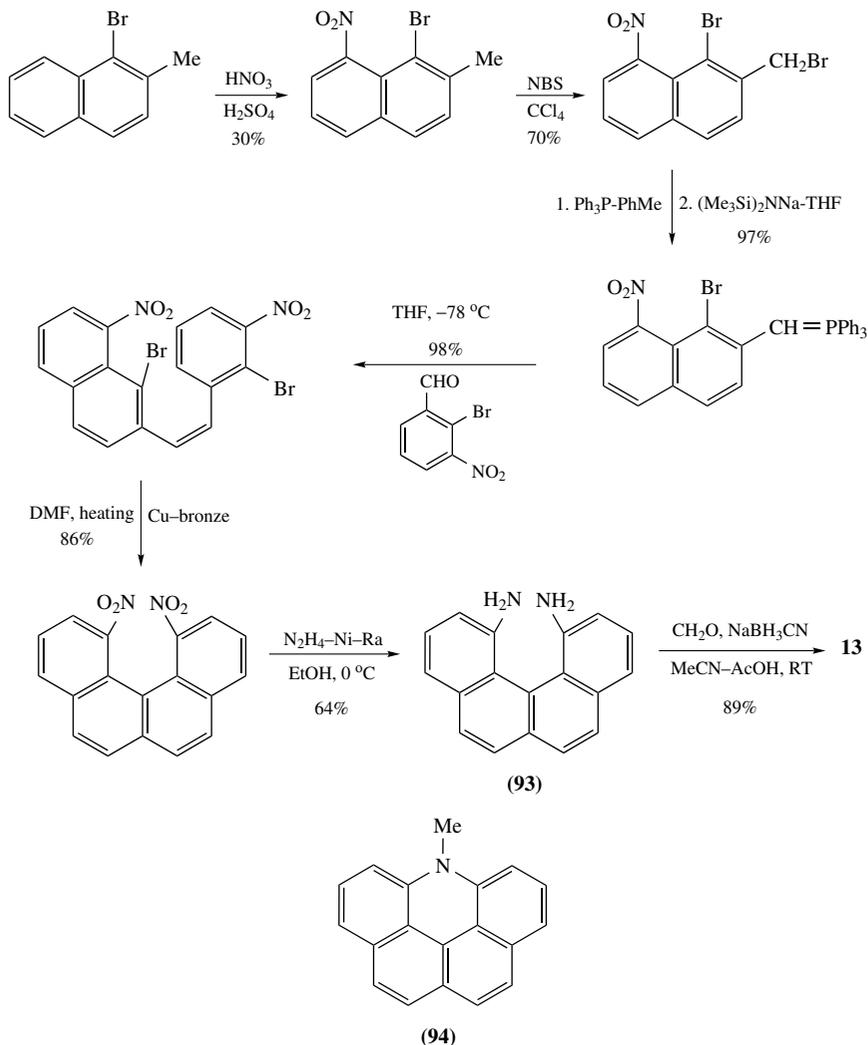
SCHEME 7

nitrosamines **90** and **91** were determined by X-ray diffraction. The isolation of salts of the protonated **90**–**92** is not straightforward, since on treatment with acids, denitrosation occurs.

D. Other Arene and Hetarene Proton Sponges

The main corner-stone in synthesizing these compounds, e.g. **7**–**13**, is the construction of an appropriate carbon skeleton, containing nitro or amino groups fixed in a due manner. A typical example is the multi-step synthesis of 1,12-bis(dimethylamino)benzo[*c*]phenanthrene (**13**) from 1-bromo-2-methylnaphthalene (Scheme 7)[10]. Interestingly, in the final stage of this route, the majority of methylation procedures, when applied to diamine **93**, resulted in the loss of one amino group to form compound **94**, and only the use of the Borch and Hassid CH_2O–$NaBH_3CN$[68] methylating system allowed one to isolate the target substance.

The synthesis of fluorene, heterofluorene, and phenanthrene proton sponges together with related compounds **95**–**99** has been reviewed[4]. Some properties of dibenzofuran **100** are described in Reference 69. As a rule, a synthetic path starts with a suitable 2,2′-dinitrodiphenyl derivative, which is reduced, making an exhaustive alkylation of the amino groups either at the last stage (e.g. for **7**) or at some intermediate stage (for **8**–**12**). The methylating agent is usually a Me_2SO_4–NaH–THF system.
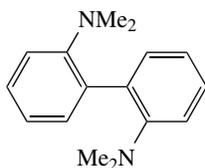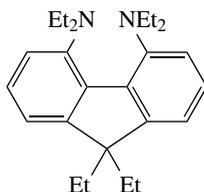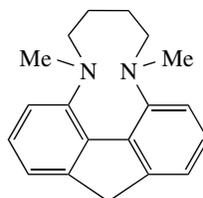
(**95**)   (**96**)   (**97**)
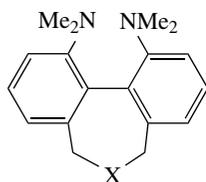
(**98**) X = O
(**99**) X = S
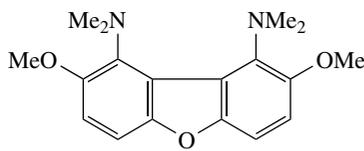
(**100**)

III. PHYSICOCHEMICAL PROPERTIES

A. Molecular Structure

Analysis of the molecular structure of proton sponges serves as a key for understanding their high basicity and unusual reactivity. The most important parameters here are: (1) the conformation of the dialkylamino groups and their orientation relative to the aromatic system and each other and (2) distortions occurring in the aromatic system. Additionally, in the case of cations, the geometry of the hydrogen bridge, including its symmetry, N···N distance and linearization of the N–H···N angle, are of particular interest.

1. Bases

In principle, all structural features of the proton sponges are due to a strong steric and electrostatic repulsion of the *peri*-dialkylamino groups, superimposed on their tendency to conjugate, as effectively as possible, with the ring π-system. There are several mechanisms to diminish such repulsion: (1) distortions of the aromatic ring causing the amino groups to be more distant, (2) deviation of the amino groups from normal geometry, mainly via increasing the N–C(1)(8)–C(9) angles (α and β, Table 4), (3) optimal mutual orientation of the methyl groups and the unshared electron pairs, (4) planarization of the nitrogen atoms. Let us examine these mechanisms in detail.

a. Distortions of the aromatic system and changing the $N \cdots N$ distance. A considerable distortion of the aromatic system planarity is the most important feature of proton sponge bases. For example, in molecule **1**, according to X-ray data, the fragments C(1)C(9)C(10)C(4) and C(8)C(9)C(10)C(5) are symmetrically twisted relative to

TABLE 4. Internitrogen distance, $r(N \cdots N)$, sum of valence angles at nitrogen atoms, $\Sigma\theta$, angles α, β and γ and the angle between NR_2 groups and mean ring plane, φ, in proton sponge molecules
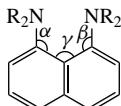
Compound	$r(N \cdots N)$ (Å)	$\Sigma\theta$ (deg)[a]	α (deg)	β (deg)	γ (deg)	φ (deg)[a]	References
2	2.72; 2.74	333.5	120.5	122.3	124.7	22	70
1	2.79	347.1	120.1	120.8	125.8	40	71
8	2.86	347.9	121.1	121.2	—	34	8
9	2.82	349.2	119.1	120.5	—	34	8
12	2.78	352.9	121.1	121.9	—	—	4
13	2.96	345.8	119.9	120.1	—	37	10
24	2.89	339.0	120.6	121.1	126.8	39	72
25a	2.86	337.3	120.7	120.7	127.1	42.5	72
32	2.89	355.8	—	—	—	—	73
35	2.75	344.5	120.4	120.8	123.6	40	45
40	2.88	339.1	120.0	120.8	130.5	43	74
44	2.76	346.2	120.1	121.2	125.3	74	75
48	2.75	352.6	120.2	120.7	125.3	70	76
65	2.77	356.2	119.0	121.0	124.6	55	54
66	2.85	357.6	120.9	120.9	127.7	61	54
68	2.82	352.4	119.0	120.5	129.1	63	56
101	2.77	352.9	121.7	121.9	125.4	71	77
102	2.775	353.9	120.7	121.0	125.1	69	78
103	2.82	356.7	116.2	120.5	133.6	80	76
104	2.83	356.1	120.9	124.7	125.5	84	76
105	2.925	350.4; 355.3[b]	116.8	124.8	126.9	73; 83	76
106	2.92	350.0; 350.7[b]	114.3	123.8	125.7	69; 78	79
107	2.955	348.3	121.0	121.1	129.8	36	74
108	2.86	351.6; 357.0	120.2	122.4	123.5	36; 27	80
109	2.95	354.7; 360.0	121.7	120.7	124.7	25; 41	81
110	3.03	357.9	121.7	121.9	124.0	20	81

[a] Average values for two NR_2 groups. For **105**, **106**, **108** and **109** with different geometries of the NMe_2 functions both values are given for $\Sigma\theta$ and φ.
[b] NMe_2 group with inverted nitrogen pyramid.

(101) R = Cl
(102) R = Br
(103) R = I
(104) R = SMe
(105) R = SiMe₃
(106) R = C(OH)Ph₂

(107)

(108) R¹ = R³ = H, R² = NO₂
(109) R¹ = R³ = CHO, R² = H
(110) R¹ = H, R² = R³ = CHO
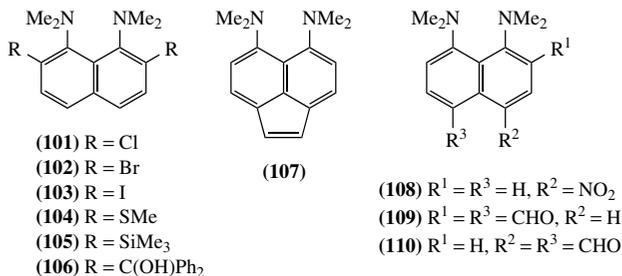
the central C(9)−C(10) bond: the torsion angles are equal to 8.9 and 10.5° (compare Figures 1a and 1b). The mean ring plane is formed by the atoms C(2), C(3), C(9), C(10), C(6), C(7), while C(1) and C(8) and also the nitrogen atoms deviate from the plane (the nitrogens by as much as 0.4 Å) in opposite directions. This increases both the C(1)−C(8) distance to 2.56 Å (2.45 Å in the naphthalene molecule) and the N · · · N distance to 2.79 Å (2.72−2.74 Å in 1,8-diaminonaphthalene). The inter-nitrogen distance can become even bigger on increasing the bulk of the dialkylamino group (Table 4, compounds **24** and **25a**), through the tightening influence of the bridging groups (e.g. CH₂CH₂ and CH=CH in the acenaphthene **40** and acenaphthylene **107** sponges) and especially by effective conjugation between the amino groups and electron-withdrawing substituents. The latter require significant planarization of the NMe₂ groups and increase in their coplanarity with the ring π-system. Anyhow, a larger space is necessary for these changes. Indeed, among all known proton sponges, a record N · · · N distance (3.03 Å) was found for the *peri*-dialdehyde **110**, the aromatic moiety of which is the most twisted (Figure 1c).

Surprisingly, another possible mechanism for removing the dialkylamino groups from one another, consisting of enlargement of the angles α and β, is not realized in practice, and the 120−121° values of these angles (Table 4) are evident of that; an exception are compounds **105** and **106**, which are discussed below. Concerning the angle γ, its noticeable increase (up to 124−130°) can be ascribed to a pure mechanical stretching,

(a)　　　　　　　　(b)　　　　　　　　(c)

(d)　　　　　　　　(e)　　　　　　　　(f)
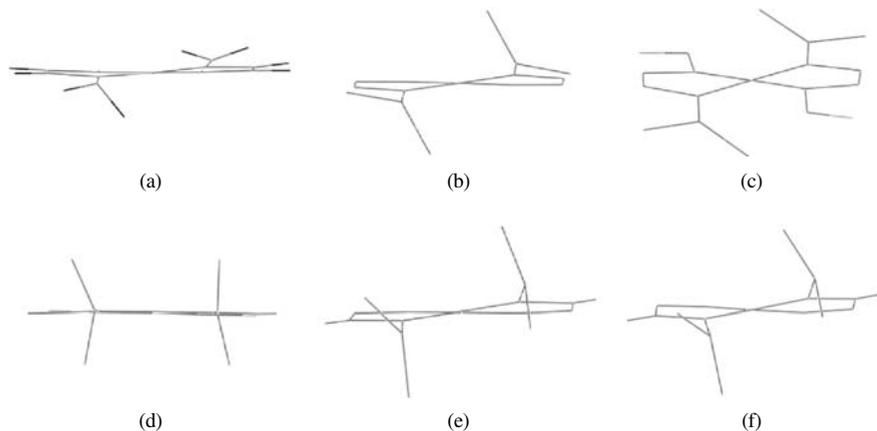
FIGURE 1. View of some proton sponge molecules along the average ring plane with the amino groups directed to the viewer as wireframe CIF generated models (2,7-substituents, if any, are excluded; hydrogens are shown for **2** only): (a) **2**, (b) **1**, (c) **110**, (d) **104**, (e) **105** and (f) **106**
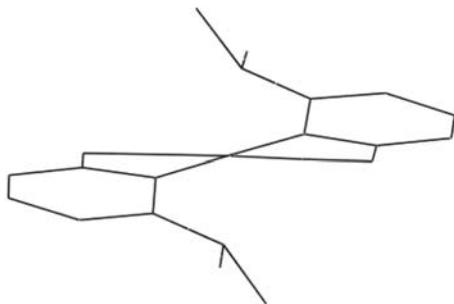
FIGURE 2. Side view of the 1,12-bis(dimethylamino)benzo[*c*]phenathrene molecule (**13**) (only C and N atoms are shown)

caused by deviation of the dialkylamino groups, or from their repulsion with *ortho*-substituents (Section III.A.1.b).

The example of 1,12-bis(dimethylamino)benzo[*c*]phenanthrene (**13**) is also informative. Here, the interaction of the NMe$_2$ groups leads to a strong spiralization (helical deformation) of the aromatic moiety, resulting in increasing the N$\cdots$N distance to almost 3 Å (Figure 2).

b. Conformations, planarization and orientation of the dialkylamino groups.   The dimethylamino groups of the parent proton sponge **1** interact to form the conformation shown in Figure 3a (see also Figure 1b). This conformation may be called 'in-in' (*trans*) since the lone electron pair axes are pointed inside the inter-nitrogen space and in opposite directions with regard to the mean ring plane. Such orientation results in a non-equivalence of the *N*-methyls: while two of them (conditionally equatorial) are situated near the ring plane and oriented outside, the other two (axial) lie inside the inter-nitrogen space and are approximately perpendicular to the ring plane. Another structural feature of diamine **1** is a considerable planarization of the nitrogen atoms that, to some degree, also relieves the repulsion between the methyls and especially between the unshared electrons. Thus the valence angles sum at the nitrogens in **1** is 347° against 333.5° for 1,8-diaminonaphthalene.
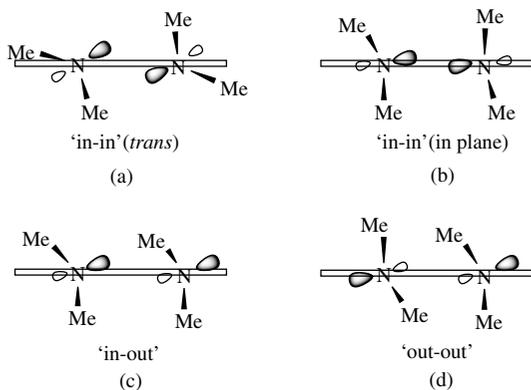
FIGURE 3. Various types of dimethylamino group conformations in naphthalene proton sponges (white rectangles denote the side view of the mean ring plane)

Especially strong planarization of the NMe$_2$ groups accompanied by their turning to be almost perpendicular to the ring plane (the angle φ reaches 80–84°) is observed in 2,7-disubstituted proton sponges. The 'in-in' (in plane) conformation (Figures 1d, 3b) thus arising is characterized with almost pure sp^2-hybridization of the nitrogen atoms and, consequently, high (>95%) p-character of the lone electron pairs[76]. As seen from Table 4, the degree of planarization of *peri*-NMe$_2$ groups and the angle of their rotation around the C$_{ar}$−N bond are qualitatively proportional to the volume of the *ortho*-substituents.

A remarkable feature of the 2,7-bis(trimethylsilyl) derivative **105** and *o,o*-dialcohol **106** is the inversion of one of the NMe$_2$ groups, so that its unshared electron-pair axis is oriented towards the *ortho*-substituent ('in-out' conformation, Figures 1e, 1f and 3c). It is believed, for **105**, that this is favoured by p,d-interaction between the amino nitrogen and the silicon atom, and for **106**, is due to formation of IHB with participation of the alcoholic hydroxyl. Both these interactions (electron and H-bond induced) are accompanied by a strong inclination of the inverted NMe$_2$ group towards the *ortho*-substituent ('leaning effect') that increases the N $\cdots$ N distance to 2.93 Å and the β angle to 124–125°. It is noteworthy that the second NMe$_2$ group in compounds **105** and **106** retains its 'in' conformation, though the leaning effect towards the inverted amino group is also detectable. More details on the structure of 2,7-disubstituted proton sponges can be found elsewhere[76].

The only known compound with 'out-out' conformation (Figure 3d) is probably bridged diamine **31**.

c. Conjugation of dialkylamino groups with the aromatic π-system. The X-ray data are also helpful for estimating the degree of conjugation between the *peri*-dialkylamino groups in the proton sponges and the aromatic π-system. Since the rotation angle, φ, for each NMe$_2$ group relative to the mean ring plane in the parent compound **1** is equal to 40° (Table 4), one can calculate, using the well known ratio $M = M_o \cos^2 \varphi$, that the remaining conjugation in **1** (M) is 59% of that (M_o) in an ideally flat and coplanar model[76]. In 2,7-disubstituted proton sponges, the conjugation weakens seriously, retaining only 2–7% of its value in the case of such voluminous *ortho*-substituents as I, SMe and SiMe$_3$. On the contrary, the introduction of electron-withdrawing groups in the naphthalene ring, particularly in positions 4 and 5, allows the NMe$_2$ groups to participate in through-conjugation. This is indirectly manifested in increasing the N $\cdots$ N distance, flattening and coplanarization of the functional groups, though, owing to those, the aromatic ring undergoes additional twisting (Figure 1c, see data for compounds **107–110** in Table 4).

2. Cations

On transition from proton sponge bases to the corresponding cations, the molecular structure changes sharply. In particular, this is reflected by a significant planarization of the aromatic system, formation of strong IHB between dialkylamino groups, forcing the nitrogen atoms to be closer in space (average separation is 2.59 Å for naphthalene sponges). For all that, the NAlk$_2$ groups are pyramidalized and oriented with their electron pairs facing each other. At the same time, as shown in Table 5, the details of these changes vary greatly depending on the type of aromatic system, counter ion, the nature and the position of the substituents.

a. Naphthalene proton sponges. Up to now, X-ray investigations have been conducted for more than 100 proton sponge salts with different anions and substituents. Their results were analysed selectively in review papers[4, 6, 29, 90, 91]. We shall consider here only general points, as well as a number of new data.

TABLE 5. X-ray geometrical characteristics of the N−H···N hydrogen bridge in proton sponge proton complexes

Cation	Anion	T (K)	Distance (Å)			∠NHN (deg)	$\Sigma\theta$ (deg) [a]	References
			N···N	N−H	H···N			
1•H+	Br−	RT	2.56	1.31	1.31	153	337.8	82
1•H+	SCN−	RT	2.57	1.30	1.30	160	339.5	83
1•H+	SCN−	188	2.57	1.32	1.32	156	336.6	83
1•H+	4,5-dichlorophthalate	100	2.58	1.20	1.43	156	336.2	84
1•H+	CuCl4²−	RT	2.58	1.21	1.43	158	336.5	85
1•H+	BPh4−	RT	2.55	1.17	1.57	136	335.2	86
1•H+ [b]	—	—	2.59	—	—	155	336.4	—
7•H+	ClO4−	RT	2.63	1.31	1.31	177	334.8	7
8•H+	BF4−	RT	2.59	1.30	1.30	173	334.1	8
9•H+	BF4−	RT	2.57	1.29	1.29	175	336.1	8
12•H+	ClO4−	RT	2.54	1.20	1.36	167	337.7	9
13•H+	I−	RT	2.70	1.35	1.35	177	339.6	10
35•2H+	2Br−	RT	2.57	1.22	1.39	158	336.1	45
40•H+	Br−	200	2.67	0.99	1.72	159	337.2	74
41•H+	Br−	RT	2.55	1.28	1.28	170	336.5	39
44•H+	Br−	100	2.57	1.30	1.30	160	340.5	87
87•H+	CF3SO3−	173	2.87	0.88	2.17	136	334.2; 349.3	66
95•H+	Br−	RT	2.65	1.33	1.33	175	337.0	88
101•H+	Br−	RT	2.56	1.29	1.29	165	342.7	77
102•H+	Br−	100	2.55	0.85	1.73	162	342.9	78
105•H+	ClO4−	163	2.52	1.28	1.28	163	341.6	89
107•H+	Br−	200	2.67	0.98	1.75	156	336.9	74
108•H+	ClO4−	RT	2.57	0.99	1.65	153	336.3; 337.4	80
111	—	RT	2.57	1.27	1.34	160	336.2	39
112•H+	Cl−	RT	2.57	1.30	1.34	154	343.0	89
113•H+	Br−	100	2.56	1.02	1.59	157	337.5; 337.2	90

[a] Average values for two NR2 groups. For **87•H+**, **108•H+** and **113•H+** with apparently different NMe2 geometries, both values are given.
[b] Average data for all up-to-date known structures with **1•H+** cations
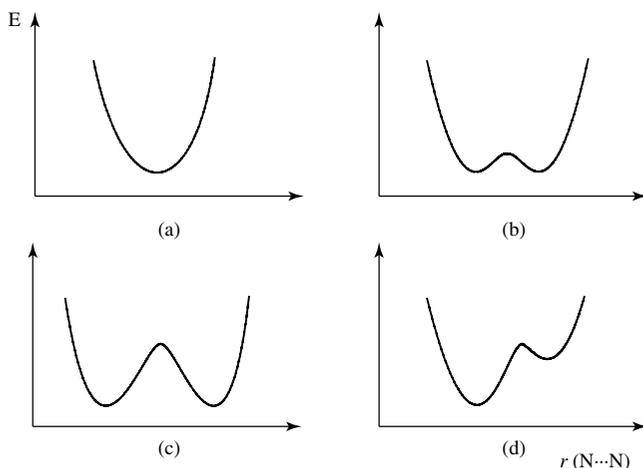
FIGURE 4. Possible types of IHB potential energy profiles in proton sponge cations

Theoretically, there can be four hydrogen bridge types in the proton sponge cations; they are commonly described by the energy profiles shown in Figure 4. Profile (a) with one minimum corresponds to a completely symmetrical bridge, whereas profiles (b) and (c) are both characteristic for equilibrium of two equivalent asymmetric structures (equation 4) strongly differing by the barrier, and therefore by the rate of this process. The question as to which of the profiles are indeed realized in cation $1 \cdot H^+$ was a focus of investigations. Additionally, for cations with intrinsic asymmetry, such as $108 \cdot H^+$, profile (d) becomes possible.

$$\text{Me}_2\text{N}_+ \overset{\text{H}}{\cdots} \text{NMe}_2 \qquad \rightleftharpoons \qquad \text{Me}_2\text{N} \overset{\text{H}}{\cdots} {}_+\text{NMe}_2 \tag{4}$$

$$(1 \cdot H^+\text{--a}) \qquad\qquad\qquad (1 \cdot H^+\text{--b})$$
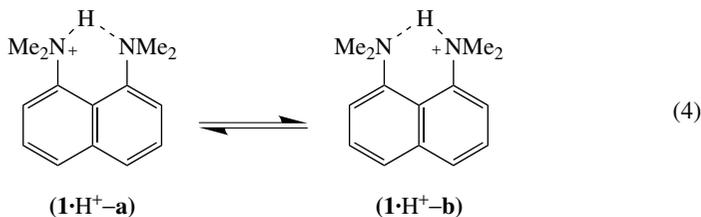
Theoretical calculations of an $[H_3N \cdots H \cdots NH_3]^+$ system have shown that when the $N \cdots N$ distance is 2.75 Å, the potential curve has two minima with a barrier of 10.9 kJ mol^{-1}; with a decrease in the distance to *ca* 2.50 Å, the barrier disappears. As seen in Table 5, the minimal $N \cdots N$ distance for proton sponge cations is 2.54–2.55 Å, i.e. none of the compounds has a symmetrical barrier-free H-bond. Indeed, in 80% of cases, the X-ray studies on salts of proton sponge **1** have revealed an asymmetric hydrogen bridge with the distances N—H and $N \cdots H$ in the ranges 0.84–1.27 Å and 1.42–1.86 Å, respectively. It is believed that such strong variations are due to the influence of the anion, either by an electric field effect or by structural changes in the crystal lattice.

Only in a few measurements of salts $1 \cdot H^+ X^-$ was the NH proton found to lie strictly in a symmetry plane of the cation with averaged N—H bond lengths of *ca* 1.3 Å. Nevertheless, the current standpoint is prone to accept that these results reflect a disordered position of the proton equilibrating rapidly between the two nitrogen atoms. This is supported by the fact that symmetrical H-bridges were mainly recorded when the measurements were conducted at ambient rather than at low temperature[92].

The geometry of the hydrogen bridge is essentially influenced by the substituents. For instance, in the acenaphthene $40 \cdot H^+$ and acenaphthylene $107 \cdot H^+$ proton sponge cations, the tightening influence of the CH$_2$CH$_2$ and CH=CH bridges leads to a noticeable enlargement of the $N \cdots N$ distance, and consequently the hydrogen bond becomes quite asymmetric. In cations of the non-symmetric bases $108 \cdot H^+$ and $113 \cdot H^+$ the proton is preferentially localized at the N(8) atom, i.e. more distant from the substituent (Figure 4d). If, however, for $108 \cdot H^+$, considering the electron-withdrawing character of the nitro group, this is quite clear, in the case of amino derivative $113 \cdot H^+$ such an H-bridge structure is hard to explain[90].

An interesting situation occurs in the dication of the doubly protonated proton sponge $35 \cdot 2H^+$ and in the zwitterion of 4,5-dihydroxy-1,8-bis(dimethylamino)naphthalene (**111**). The asymmetry of both hydrogen bridges in these systems is clearly controlled by electrostatic factors in order to obtain maximal separation of the two positively charged centres in $35 \cdot 2H^+$ and, in reverse, to gain an attraction between the cationic and anionic centres in **111**.

There are very specific changes of the hydrogen bridge geometry in the cations of 2,7-disubstituted proton sponges. The measurements of such systems were performed for five salts with cations $44 \cdot H^+$, $101 \cdot H^+$, $102 \cdot H^+$, $105 \cdot H^+$ and $112 \cdot H^+$. The *ortho*-substituents in these cations display a distinct 'steric pressure' on the adjacent *N*-methyl groups, pushing

(**40·H⁺**) X—X = CH₂CH₂   (**108·H⁺**) R = NO₂   (**35·2H⁺**)   (**111**)
(**107·H⁺**) X—X = CH=CH   (**113·H⁺**) R = NH₂

(**112·H⁺**)   (**87·H⁺**)
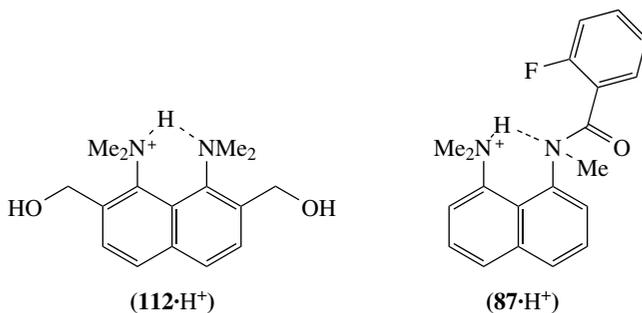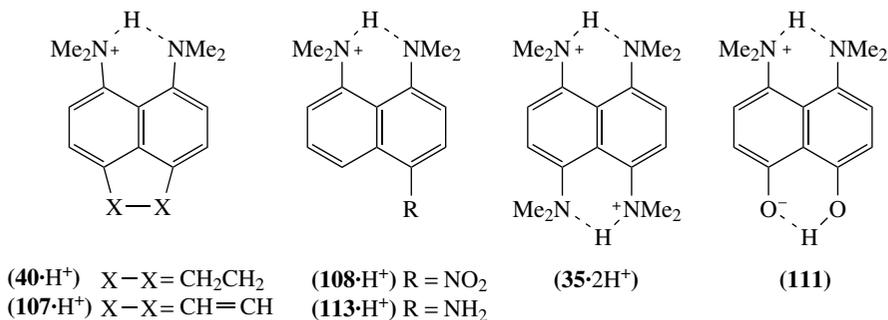
them above the molecular plane. This, in turn, forces the NH proton to move deeper into the inter-nitrogen space (Scheme 8). Clear-cut evidence for this process is an essential planarization of the N-atoms in the cations of all *ortho*-disubstituted proton sponges (cf. $\Sigma\theta$ indices, Table 5), as well as linearization of the N—H···N angle in cations **44·H⁺**, **101·H⁺**, **102·H⁺** and **105·H⁺** in comparison with, e.g., cation **1·H⁺**.
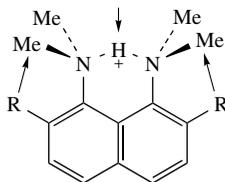
SCHEME 8

As expected, the N···N distance in cation **105·H⁺** is significantly shorter than in all other proton sponge cations and equals 2.530 Å at room temperature and 2.524 Å at 163 K[89]. It is at the same level as the N···N distance (2.526 Å) in the inside protonated 1,6-diazabicyclo[4.4.4]tetradecane (**114**), whose hydrogen bridge was hitherto considered to be the shortest one[93]. The hydrogen bridge in cation **105·H⁺** is perfectly symmetric and this symmetry is retained on lowering the temperature; the N—H bond lengths (1.28 Å) are also the shortest in the series of proton sponge cations. At the same time, unlike cation **1**, steric strain in cation **105·H⁺** is not completely released and yet remains notable.

Structural investigations of the NH-deuteriated salts **44·DBr**[87] and **102·DBr**[78] revealed no geometrical isotope effect within the experimental error.

(114)

X-ray data collected for the chiral proton sponge **54**•H⁺ cation and for the picrates of monohydrazine sponges **88** and **89** are also informative[49, 67]. In the case of **88**, the NH proton is disordered and the data may be interpreted in favour of the presence of two tautomeric forms **88a** and **88b** in the crystal lattice. In cation **89**, the proton is entirely located at the β-nitrogen atom of the hydrazino group, forming a hydrogen bond with the NMe₂ group, and closing up a seven-membered cycle. This is the only example of such a type in the naphthalene proton sponge series[67]. Another case of unusual chelation was brought to light by an X-ray study of protonated *N*-(*o*-fluorobenzoyl)-*N*,*N*′,*N*′-trimethyl-1,8-diaminonaphthalene **87**•H⁺ (Table 5). In this salt, an IHB with a record degree of asymmetry is realized. More interesting is the participation in the chelation of the amide nitrogen, rather than the carbonyl, which is known as the common nucleophilic centre in the amides.

b. Other arene and hetarene proton sponges. The main feature of these proton sponge cations is the almost complete linearity of the hydrogen bridge (Table 5). Thus the N—H···N angle for the cations of fluorene **7**•H⁺ and benzo[*c*]phenanthrene **13**•H⁺ sponges reaches 177°. Interestingly, in **13**•H⁺ a helical deformation of the benzene rings is retained, i.e. the transition from the base to the cation is not accompanied by steric relief. In nearly all cations of this series, **7**•H⁺, **8**•H⁺, **9**•H⁺, **13**•H⁺ and **95**•H⁺ (with the partial exception of **12**•H⁺), a symmetrical hydrogen bond is recorded. This result is likely affected by the temperature since all the measurements were conducted at 298–302 K.

B. NMR spectra

¹H, ¹³C and ¹⁵N NMR spectra of the proton sponges and their cations were investigated both in solutions and in the solid state. These were used to establish structural and electronic characteristics of the molecules and to investigate the proton exchange between the cations and bases[94].

1. Bases

In the ¹H NMR spectrum of the parent proton sponge **1**, the signals for all the aromatic protons are at higher field than those for naphthalene (δ 7.81 and 7.46 ppm for α- and β-protons, respectively). The largest shielding from the NMe₂ groups is of the *ortho*-protons, and then come *meta*- and *para*-protons. The difference in the chemical shifts between *meta*- and *para*-protons is very little (Table 6). The signals of the *N*-methyl groups in **1**, as in the majority of other unsubstituted proton sponges, are located at 2.7–2.8 ppm. In the 2,7-disubstituted compounds they are, however, shifted up to 3.0 ppm as a result of the nitrogen atom flattening, and consequently the increase in the *s*-character of the N—C bond orbitals. The influence of other substituents on the chemical shift values is within the expected region. Regrettably, the literature data do not cite any ¹H NMR spectroscopic information for non-naphthalene proton sponges.

TABLE 6. ^{1}H NMR spectra in CDCl$_3$ of selected proton sponge bases
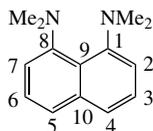
Compound	Substituents	Chemical shifts, δ, (ppm)				Coupling constants, J (Hz)			References
		H-2(7)	H-3(6)	H-4(5)	NMe$_2$	$J_{2,3}$	$J_{3,4}$	$J_{2,4}$	
1	—	6.97	7.31	7.37	2.81	7.3	7.9	1.5	76
35	4,5-(NMe$_2$)$_2$	6.79	6.79	—	2.76	—	—	—	44
40	4,5-CH$_2$CH$_2$	6.96	7.17	—	2.83	7.5	—	—	74
44	2,7-(OMe)$_2$	—	7.06	7.48	2.89	—	9.0	—	35
65	2,7-(NMe$_2$)$_2$	—	7.19	7.40	2.97	—	8.6	—	56
107	4,5-CH=CH	6.89	7.53	—	2.91	7.6	—	—	74
110	4,5-(CHO)$_2$	6.80	7.93	—	2.93	8.4	—	—	29

TABLE 7.   Solution and solid ^{13}C and ^{15}N NMR spectra for proton sponge **1** in neutral and protonated forms (δ, ppm)

Atom	**1** in CD$_3$CN	**1**•HClO$_4$ in CD$_3$CN	**1** in the solid state	**1**•HBF$_4$ in the solid state
C(1)	151.33	145.12	119.8	117.40
C(2)	113.57	122.36	112.10	120.70
C(3)	126.30	127.86	124.60	128.30
C(4)	122.28	130.04	120.90	126.50
C(5)	122.28	130.04	122.10	126.50
C(6)	126.30	127.86	123.90	128.30
C(7)	113.57	122.36	113.30	120.70
C(8)	151.33	145.12	121.80	117.40
C(9)	121.13	120.02	149.70	143.40
C(10)	138.58	136.19	136.50	134.80
CH$_3$	44.68	46.73	41.0; 41.8; 44.2; 45.1	43.6; 46.4
N(1), N(8)	-336.8 [a]	-346.7 [a]	—	—
References	95, 96	95, 96	97	97

[a] vs MeNO$_2$.

^{13}C and ^{15}N NMR spectra of proton sponge **1** (Table 7) and its derivatives have been recorded. ^{1}H MAS and ^{13}C NMR spectra of a solid sample of the diamine **1** have revealed a strong asymmetry of the molecule. All the four CH$_3$ groups, like all the ring carbon atoms, appear as separate signals, i.e. they are non-equivalent (Table 7). This has been interpreted in terms of electrostatic interactions between neighbouring molecules in the crystal lattice.

Rather useful information is given by the spin−spin coupling constants, J (Table 6). For the H−H interactions, as a rule $J_{3,4}$ is larger than $J_{2,3}$, and in some 2,7-disubstituted proton sponges, e.g. **44**, the $J_{3,4}$ value reaches 9 Hz. The $J_{2,3}$ values, in turn, increase on substituting positions 4 and 5 by mesomeric acceptors, such as CHO, apparently due

to an increased contribution of structures of type **110a** and **110b** in the resonance hybrid (equation 5).

(5)
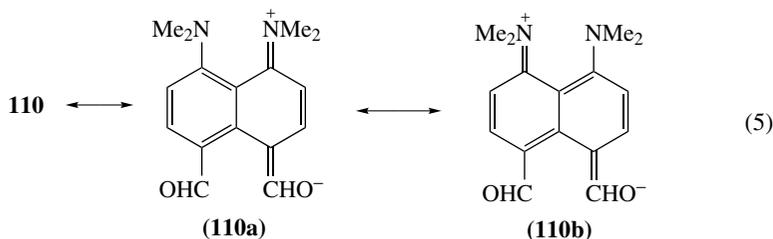
It is remarkable that in the high-resolution ^{13}C NMR spectra of compound **1**, the carbon atom of each CH_3 group couples not only with the neighbouring nitrogen atom ($^1 J_{C(Me)-N(1)} = 8.3$ Hz) but also with the distant one. The latter coupling ($^{2h} J_{C(Me)-N(8)} = 0.8$ Hz) was referred to an interaction through a weak IHB of the type $C-H \cdots N$[96].

2. Cations

On going from the base **1** to the cation **1•H$^+$**, the signals for the H-2(7), H-3(6), H-4(5) and CH_3 protons are shifted downfield by 1.1, 0.4, 0.7 and 0.3 ppm, respectively[95]. Although it would be logical to expect that the *ortho*-proton signals were at the lowest field, it is not always the case. Depending on the solvent and, to a lesser extent, on the counter ion, the signals of *ortho*- and *para*-protons may overlap, and sometimes the H-4(5) protons turned out to be even more deshielded[95]. The signals of both types of protons can be distinguished since the $J_{3,4}$ values are larger when compared with $J_{2,3}$.

Yet, the main feature of the ^{1}H NMR spectra of proton sponge cations is the unusually large chemical shift of the NH proton (δ 18–20 ppm), which is indicative of strong chelation (Table 8). For the cations of symmetrical proton sponges, e.g. **1•H$^+$**, the NH signal in a high-resolution spectrum has 13 lines due to spin–spin interaction with the protons of the four methyl groups. Accordingly, the signal of the latter is split into a doublet with an intensity of 12 proton units and with $J_{NMe,NH} = ca$ 2.6 Hz[98]. It is assumed that the symmetry of the IHB for the symmetrical cations is illusive at room temperature, since it reflects fast motion of the NH proton relative to the plane of symmetry on the NMR time scale (equation 4)[50, 99]. As it is postulated, the frequency of this motion, during which the proton jumps via a tunneling mechanism within the inter-nitrogen space, may be over 10^{10} Hz[100].

In asymmetrically substituted cations, the NMe_2 groups are non-equivalent and they are observed as two doublets with different values of the $J_{NMe,NH}$ coupling constants (Table 8). It was suggested that the relationship between these constants can be used for estimating the IHB asymmetry via the 'proton localization index' (PL)[98], which is calculated in accordance with equation 6.

$$PL = [J_{1(8)-NMe,NH}/(J_{1-NMe,NH} + J_{8-NMe,NH})] \cdot 100\% \qquad (6)$$

For example, the most asymmetrical is the hydrogen bridge in the cations of 2-halogeno-**115•H$^+$** and especially 2-nitro-1,8-bis(dimethylamino)naphthalenes **116•H$^+$** (Scheme 9; compare with the corresponding *para*-derivatives, **117•H$^+$** and **108•H$^+$**). In DMSO-d$_6$,

TABLE 8. ^{1}H NMR parameters of the atoms participating in IHB for some proton sponge cations

Cation	Solvent	δ, NMe$_2$ (ppm) ^{a}	δ, N$\cdots$H$\cdots$N (ppm)	$J_{\text{NMe,NH}}$ (Hz) ^{a}	References
1•H$^+$	DMSO-d$_6$	3.12	18.33	2.63	98
1•H$^+$	CD$_3$CN	3.11	18.69	2.64	98
7•H$^+$	DMSO-d$_6$	3.19	18.25	2.03	7
8•H$^+$	DMSO-d$_6$	—	19.06	—	8
9•H$^+$	DMSO-d$_6$	—	19.28	—	8
10•H$^+$	DMSO-d$_6$	3.08	18.86	2.3	8
11•H$^+$	DMSO-d$_6$	—	16.50	—	9
12•H$^+$	DMSO-d$_6$	—	18.37	2.17	9
35•2H$^+$	DMSO-d$_6$	3.14	18.80	—	45
40•H$^+$	DMSO-d$_6$	3.09	16.35	2.41	38
67•H$^+$	DMSO-d$_6$	3.29	19.88	1.86	56
67•H$^+$	CD$_3$CN	3.30	20.11	2.60	56
95•H$^+$	DMSO-d$_6$	—	11.20	—	88
98•H$^+$	DMSO-d$_6$	—	11.76	—	4
102•H$^+$	DMSO-d$_6$	3.40	20.09	2.41	98
102•H$^+$	CD$_3$CN	3.41	20.33	2.64	98
103•H$^+$	DMSO-d$_6$	3.43	20.21	2.24	76
103•H$^+$	CD$_3$CN	3.43	20.46	2.48	76
105•H$^+$	DMSO-d$_6$	3.26	20.44	2.34	76
105•H$^+$	CD$_3$CN	3.26	20.69	2.58	76
107•H$^+$	DMSO-d$_6$	3.15	15.77	2.31	38
108•H$^+$	DMSO-d$_6$	3.17; 3.28	18.50	1.72; 3.19	98
108•H$^+$	CD$_3$CN	3.08; 3.19	18.72	2.13; 3.36	98
111	DMSO-d$_6$	2.93	18.10	2.2	39
115•H$^+$	DMSO-d$_6$	3.22; 3.33	18.09	<1; 3.95	98
115•H$^+$	CD$_3$CN	3.26; 3.27	18.87	1.65; 3.84	98
116•H$^+$	DMSO-d$_6$	3.04; 3.41	16.16	<0.5; 4.40	98
116•H$^+$	CD$_3$CN	3.11; 3.36	16.96	0.88; 4.39	98
117•H$^+$	DMSO-d$_6$	3.11; 3.14	18.56	2.31; 2.53	98

^{a} There are two values for asymmetrical cations

the $J_{1-\text{NMe,NH}}$ value in **116•H$^+$** is so small that it could hardly be detected, i.e. the proton localization at the N(1) atom does not exceed 7–10%. At the same time, in the cation of 4-bromo derivative **117•H$^+$**, the PL-1 and PL-8 indices are almost equal, indicating a low IHB asymmetry. It was established that the transition from DMSO to the less proton-accepting solvent, acetonitrile, favours the symmetrization of the hydrogen bridge[98]. The degree of the IHB asymmetry may be also estimated using the difference between the coupling constants of the NH proton with the ^{15}N nitrogen atoms, $^1J_{\text{NH,N(1)}}$ and $^1J_{\text{NH,N(8)}}$[101–104]. It should be noted that both methods give quite similar results: differences between PL indices are within 2%.

The above-mentioned asymmetry of the IHB in the crystals of the dication of the double proton sponge **35** (Section III.A.2) is practically not seen in the NMR spectra. Thus, the NH protons, as well as the methyl groups of dication **35•2H$^+$**, are equivalent in solution and display singlet peaks at $\delta = 18.8$ and 3.14, respectively[45]. In the formally symmetrical dication of the double sponge **118•2H$^+$**, the NMe$_2$ groups are non-equivalent in pairs and display different singlet peaks, evidently because of a general desymmetrization of the molecule, caused by distortion of the eight-membered cycle[105]. In contrast, in the monocations **35•H$^+$** and **118•H$^+$**, prepared in solution from the corresponding dication and one equivalent of a base, the signal of each of the NMe$_2$ groups participating in IHB

	PL-8	PL-1		PL-8	PL-1		PL-8	PL-1		PL-8	PL-1
DMSO	84%	16%		*ca* 100%	*ca* 0%		52%	48%		65%	35%
MeCN	70%	30%		83%	17%		–	–		61%	39%
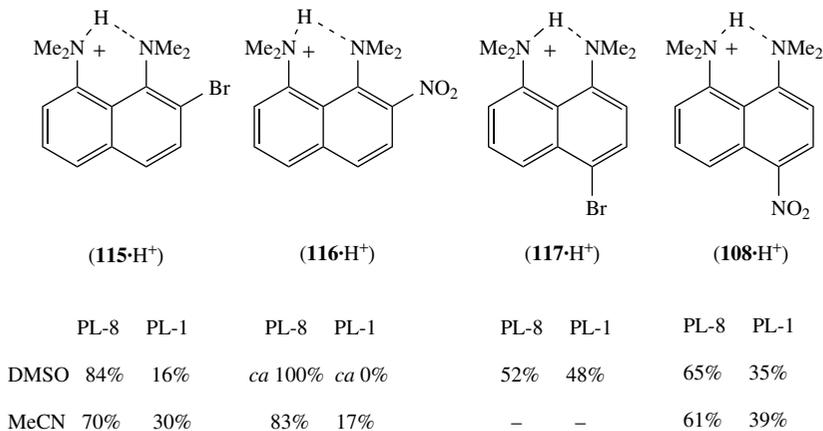
SCHEME 9

is split into a doublet with the constant $J_{NMe,NH} = 1.8-2.0$ Hz (Scheme 10)[45, 105]. The ^{1}H NMR spectra of the dication $36 \cdot 2H^+$ of the binaphthyl sponge are even more complex[106].

For a series of compounds of the same type, there exists no apparent correlation between the stability of the IHB and the chemical shift of the NH proton. This follows, for example, from the comparison of cations $1 \cdot H^+$ and $108 \cdot H^+$. Though in the spectrum of the latter, the NH signal is shifted somewhat downfield, the hydrogen bridge of $108 \cdot H^+$ is easily cleaved with DMSO and other dipolar solvents (Section III.C), whereas in the cation $1 \cdot H^+$, no signs of the cleavage were observed. Apparently, the stability of the IHB is largely determined by the basicity of the corresponding proton sponge, while the δ_{NH} value depends mainly on such factors as the distance between the nitrogen atoms, the extent of the aromatic π-system and the position of the NH proton relative to this system. Thus, increasing the $N \cdots N$ distance weakens the NH proton deshielding and results in its shift to a higher field. This situation is distinctly reflected in cations of the acenaphthene $40 \cdot H^+$ ($\delta_{NH} = 16.4$ ppm) and acenaphthylene $107 \cdot H^+$ ($\delta_{NH} = 15.8$ ppm) proton sponges, and also in the highly non-coplanar cations $11 \cdot H^+$, $95 \cdot H^+$ and $98 \cdot H^+$ (Table 8, compare with data of Table 5).

For the chelated polynuclear monocation $15 \cdot H^{+\ 13}$, the record value of $\delta_{NH} = 23.9$ ppm is striking evidence for the influence of the extent of the π-system. The NH proton deshielding is also favoured by linearization of the hydrogen bridge, as confirmed by the data of Tables 5 and 8 for 2,7-disubstituted proton sponges. Obviously, the larger the $N-H \cdots N$ angle, the deeper the chelated proton moves into the diamagnetic field area.

^{13}C and ^{15}N NMR spectra of cation $1 \cdot H^+$ (Table 7) and its 2- and 4-substituted derivatives with different anions (tetrazolide[107], hydrosquarate[108], BF_4^-, BPh_4^-, CNS^- [50], ClO_4^- [96], $CF_3CO_2^-$ [101]) were recorded both for solutions and crystalline samples. The signals of ^{13}C(2) and ^{13}C(4) nuclei are the most sensitive to salt formation: they shift 4–5 ppm downfield. However, the largest changes in the chemical shifts (by 6–12 ppm for both solutions and the solid state) are observed for ^{15}N nuclei in the ^{15}N NMR spectra upon transition from the base to the cation.

Perrin and Ohta[50, 99] have employed a method of isotopic perturbation of the C(1)−C(8) chemical shifts on measuring the ^{13}C NMR spectra of cations $1 \cdot H^+$ and $44 \cdot H^+$ with different anions and with certain combinations of CH_3 and CD_3 groups. It was concluded from the data that the IHB in these salts is asymmetrical and, in solutions, there is a

18.80 (br.s)   18.75 (br.s)

H   3.14 (s)   H   3.04 (d)

Me$_2$N   NMe$_2$ Me$_2$N $\overset{+}{\cdots}$ NMe$_2$ Me$_2$N $\overset{+}{\cdots}$ NMe$_2$

HBF$_4$ 35

2

Me$_2$N   NMe$_2$ Me$_2$N $\overset{+}{\cdots}$ NMe$_2$ 2BF$_4^-$ Me$_2$N   NMe$_2$ BF$_4^-$

H

(35)   **(35·2HBF$_4$)**   **(35·HBF$_4$)**

18.45 (br.s)   18.52 (br.s)

3.12 (s)   H   3.05 (s)   3.10 (d)   H   3.05 (d)

Me$_2$N   NMe$_2$ Me$_2$N $\overset{+}{\cdots}$ NMe$_2$ Me$_2$N $\overset{+}{\cdots}$ NMe$_2$

F$_3$C   O   CF$_3$ F$_3$C   O   CF$_3$ F$_3$C   O   CF$_3$

HClO$_4$ 118

2

Me$_2$N   NMe$_2$ Me$_2$N $\overset{+}{\cdots}$ NMe$_2$ 2ClO$_4^-$ Me$_2$N   NMe$_2$ ClO$_4^-$

H

(118)   **(118·2HClO$_4^-$)**   **(118·HClO$_4$)**
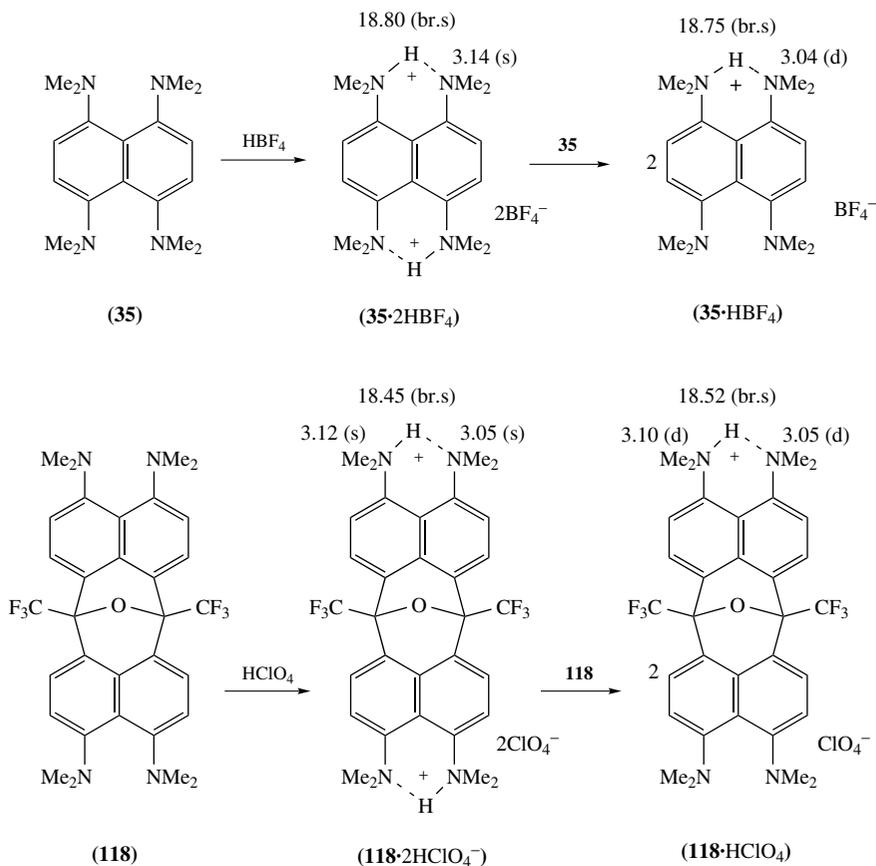
SCHEME 10. Protonation of some double proton sponges in ^{1}H NMR (δ in ppm in DMSO-d$_6$)

fast equilibration between the two equivalent tautomeric forms (see equation 4). Using deuterium isotope effects on chemical shifts of the N–D···N bridged proton sponges, it has been recently demonstrated that upon deuteriation this equilibrium is shifted towards the predominant form in the case of non-symmetrical cations (Figure 4d)[104]. A method of desymmetrization (by labelling one of the methyl groups by ^{13}C) was applied for identification of the *dl* and *meso* isomers of chiral sponge **54** and its cation, with the help of the differing Overhauser enhancements using rapid temperature drop methods and selective magnetization transfer experiments in ^{13}C NMR (Scheme 11)[49, 109, 110]. The thermodynamic diastereomer ratios for **54** and **54•H$^+$** at 293 K in DMF-d$_7$ are 73.4:26.6 and 89.7:10.3, respectively[49]. Notably, the equilibration between *meso* and *dl* isomers of **54•H$^+$ I$^-$** is fast at ambient temperature on the real time scale (even in CD$_2$Cl$_2$) but is much slower on the NMR.

Selective displacement of one CH$_3$ by the CD$_3$ group was employed to establish the structure of IHB in the cations of non-symmetrically substituted naphthalene proton sponges by ^{1}H NMR[111]. This direct method is simple and does not require NMR on other nuclei such as deuterium, carbon or nitrogen.

(dl)-(54)   (meso)-(54)

+H+

(dl)-(54·H+)   (meso)-(54·H+)
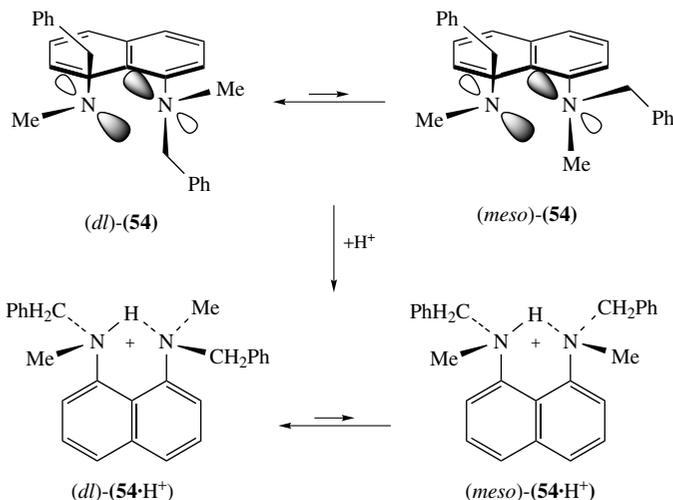
SCHEME 11

Recently, using ^{13}C NMR, for the perchlorate **1**·HClO$_4$ with both nitrogens being ^{15}N, a scalar coupling across the IHB with $^{2h}J_{NN} = 8.7$ Hz was recorded[96]. A careful comparison of these data with parallel data for the free base **1** has confirmed a transmission of the effect through the hydrogen bridge and excluded a $^4J_{NN}$ interaction (see also similar data for partially ^{15}N-methylated 1,8-diaminonaphthalenes[112]).

^{1}H and ^{13}C NMR spectral data of solid samples of **1**·H$^+$ with thiocyanate and tetrafluoroborate anions have revealed two types of N-methyl groups, presumably located close to the ring plane and remote from it[97]. However, the naphthalene ring of cation **1**·H$^+$, unlike its base, did not reveal any asymmetry (see Table 7).

3. NMR spectra and molecular dynamics

A vast number of the proton sponges are sterically strained compounds. That is why many of them exist in different conformations due to hindered rotation of the dialkylamino groups around the C_{ar}−N bonds, inversion of the nitrogen atoms or distortion of the aromatic ring. The corresponding transitions can be followed by NMR spectroscopy under a broad range of conditions. Sometimes, the dynamic processes manifest themselves even at room temperature as a widening of peaks of the N-alkyl groups or aromatic protons.

Although the solution ^{1}H and ^{13}C NMR spectra of the proton sponge **1** demonstrate the equivalence of all four N-methyl groups at room temperature, this was shown to result from fast reversible equilibrations that average the corresponding conformations on the NMR time scale. It turned out that the singlet of the CH$_3$ groups in the ^{1}H NMR spectrum of **1** in CF$_2$Cl$_2$ splits into a doublet upon cooling down to $-120\,^\circ$C[46]. The free energy of activation, $\Delta G^{\#}$, for this conformational change was estimated to be *ca* 31 kJ mol^{-1}. It was assumed that the interconversion of the methyl groups has a synchronous character and occurs via a planar transition state with a C_{2v} symmetry (Scheme 12).

In the case of the sterically more demanding 1-benzylmethylamino-8-dimethylaminonaphthalene (**119**), the conversion of the NMe$_2$ group singlet into the doublet occurs at $-38\,^\circ$C; simultaneously, the methylene group singlet splits into a quartet. In this case, the $\Delta G^{\#}$ value is nearly doubled. Similar dynamic processes of different complexity
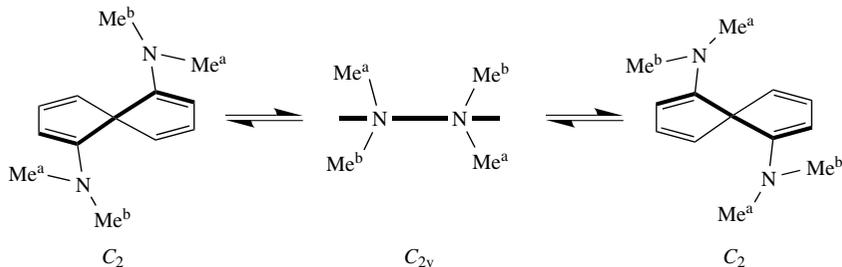
SCHEME 12

TABLE 9. Activation barriers, $\Delta G^{\#}$, for the interconversion of N-methyl groups, and coalescence temperatures, T_c, for some proton sponges and their analogues

Compound	Solvent	$\Delta G^{\#}$ (kJ mol^{-1})	T_c, (K)	References
1	CF$_2$Cl$_2$	31.4	203	46
11	CD$_2$Cl$_2$	45.7	243	4
85	DMSO-d$_6$	58.4	306	43
90	DMSO-d$_6$	66.3	333	43
92	DMSO-d$_6$	61.4	308	43
118	CDCl$_3$	61.9	283	105
119	CDCl$_3$	57.3	265	46
120	CDCl$_3$	65.0	313	41
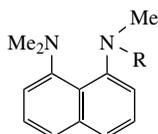
(**119**) R = CH$_2$Ph
(**120**) R = i-Pr

TABLE 10. UV longwave absorption bands of 1,8-diaminonaph-thalenes (CHCl$_3$) and dihedral angles φ in their molecules[2]

Compound	λ_{max}, (nm)	lg ε	φ (deg)
28a	344	4.27	0
1	341	4.09	35
2	337	4.02	42
3	339	3.95	46
4	351	3.78	55
5	341	3.94	90 [a]; 14 [b]
6	351	3.98	81 [a]; 0 [b]

[a] For the NMe$_2$ group.
[b] For the NH$_2$ group in **5** and NHMe group in **6**.

were observed for compounds **11**, **85**, **90**, **92**, **118** and **120** (Table 9), and the binaphthyl proton sponge **36**[106]. ^{1}H NMR line-shape analysis and, hence, the determination of T_c of the interconversion of *dl*-**54** and *meso*-**54** could not be conducted because of the unequal population of the diastereomers and small chemical shift difference of the methyl groups[49]. This was, however, determined from a series of ^{13}C spectra in DMF-d$_7$, thus giving barriers as high as *ca* 61 kJ mol^{-1} for *dl*-**54** $\rightleftarrows$ *meso*-**54** and *ca* 87 kJ mol^{-1} for *dl*-**54•**H$^+$ $\rightleftarrows$ *meso*-**54•**H$^+$; the *dl*-sponge is 2.5 kJ mol^{-1} more stable than the *meso*-isomer and so is the *dl*-salt, which is 5.4 kJ mol^{-1} lower in energy than its *meso* counterpart[109, 110].

C. Electronic Absorption Spectra, Colouration and Solvatochromism

UV spectra provide valuable information concerning electronic interaction of dialkylamino groups with the aromatic π-system. The longwave absorption band in the UV spectra of 1,8-diaminonaphthalene and its *N*-alkyl derivatives lies in the region 340–350 nm (Table 10). As in the case of other aryl amines, it is ascribed to electron transfer from the *n*-orbital of the nitrogen atoms to the π-antibonding orbital of the naphthalene ring. The intensity of this band depends strongly on the twist angle of the amino group around the C$_{ar}$−N bond. This was used to determine the value of the dihedral angle φ between the plane passing through the C$_{ar}$−N bond perpendicularly to the aromatic system and the plane passing through the same bond and the symmetry axis of the lone electron pair of the nitrogen atom. The angle φ was determined from the known correlation $\varepsilon/\varepsilon_o = \cos^2\varphi$, where ε is the extinction coefficient at the absorption maximum for the amine under question, and ε_o is the same for a planar model with $\varphi = 0°$, when the conjugation is maximal. 1,3-Dimethyl-2,3-dihydroperimidine (**28a**) was chosen as the model for which the longwave absorption band did have the maximum intensity. The calculated values of φ are listed in Table 10.

For the proton sponge **1**, the value of $\varphi = 35°$ agrees well with the X-ray data ($\varphi = 40°$)[71] and other estimates[1], and indicates the good ability of the NMe$_2$ groups to conjugate with the ring π-system and the substituents (cf. Section III.A.1.c). The conjugation is especially effective when there are electron-withdrawing groups in position 4 of the naphthalene ring. Indeed unlike the colourless **1**, the corresponding 4(5)-substituted derivatives display colours from yellow to violet (Table 11).

The long wavelength absorption band, due to the cross-conjugation, is very sensitive to the solvent polarity. For example, 1,8-bis(dimethylamino)-4-nitronaphthalene (**108**) reveals a positive solvatochromism with λ_{max} values of 411, 444, 463 and 484 nm in *n*-hexane, benzene, methanol and DMSO, respectively[80]. On the other hand, 4-[2-{4′,5′-bis(dimethylamino)naphth-1′-yl}-vinyl]-1-methylpyridinium perchlorate (**128**) displays a negative solvatochromism, reminiscent in this respect of the known solvatochromic betaine **129** (Table 12).

An interesting situation occurs in 2,7-disubstituted derivatives of proton sponge **1**. As noted earlier (Section III.A.1), here the NMe$_2$ groups are twisted out almost perpendicularly to the ring plane and are not capable of effective conjugation. Nevertheless, nearly all of them, regardless of the substituent, display different shades of yellow. We have suggested recently[76] that the nature of this colour is connected with the splitting of the near adjacent *n*-orbitals of the two *peri*-dimethylamino groups, resulting in a decrease in the energetic gap between the highest occupied molecular orbital, n$_-$, and the π-antibonding orbital (Figure 5).

Alexander F. Pozharskii and Valery A. Ozeryanskii

TABLE 11.   UV longwave absorption bands and colours of some proton sponges in MeOH

Compound	$\lambda_{max}(\lg \varepsilon)$	Colour	References
107	418 (3.91)	Orange	38
108	463 (4.02)	Dark cherry	80
110	449 (3.52)	Brown	81
121	353 (3.62)	Pale yellow	113
122	516 (4.02)	Dark violet	114
123	363 (3.79); 370 $(-)$ [a]	Yellow	81, 115
124	407 (3.84)	Yellow	81
125	389 (3.68)	Yellow	114
126	431 (3.68)	Red	114
127	521 (4.00)	Maroon	114

[a] In MeCN.

(**121**) R = CH=CH$_2$
(**122**) R = CH=C(CN)$_2$
(**123**) R = CN
(**124**) R = CHO
(**125**) R = COMe
(**126**) R = COCF$_3$

(**127**)
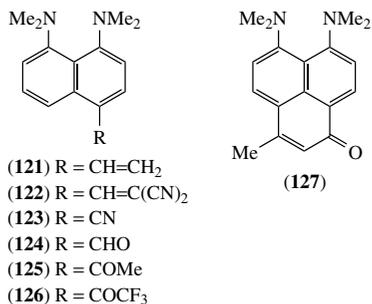
TABLE 12.   Solvatochromism of salt **128** and betaine **129** (λ_{max} and colour)
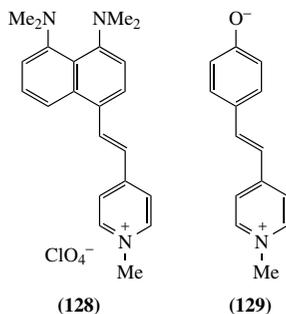
(**128**)   (**129**)

Solvent	**128**		**129**	
References	116		117	
H$_2$O	362	Yellow	442	Yellow
DMSO	522	Dark red	572	Violet-blue
DMF	526	Dark red	—	—
MeCN	528	Dark red	—	—
EtOH	528	Dark red	510	Red
CHCl$_3$	570	Violet-blue	620	Dark blue
CH$_2$Cl$_2$	613	Violet-blue	—	—
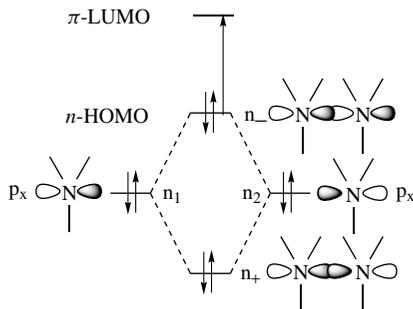
FIGURE 5. Schematic representation of the possible energy levels and the electronic transition of the nitrogen lone pairs occupying bonding and antibonding molecular orbitals on two spatially close nitrogen atoms in compound **32** and 2,7-disubstituted naphthalene proton sponges

A comparison of the bridged diamines **31** and **32** supports this assumption[35]. For **32**, the orientation of the aminonitrogens and their almost perfect planarity resembles that of the 2,7-disubstituted proton sponges. In fact, compound **32** was described as yellow needles with low intensive longwave band centred at 379 nm (lg ε 2.37). In **31**, the nitrogen atoms are pyramidalized, their electron pairs are pointed outside and they do not interact strongly with each other. Not surprisingly, this compound is colourless with λ_{max} 280 nm (3.85) and its UV/vis spectrum is quite similar to that of naphthalene.

Along with the influence of the bridged groups as in **31** and **32**, or the *ortho*-substituents as in compounds **101**–**105**, the nitrogen atoms of proton sponges could be completely taken out of conjugation by protonation. For instance, the absorption spectra of cations **1•H**$^+$ [29] and **108•H**$^+$ in 0.1 M HCl[80] resemble closely the spectra of naphthalene and 1-nitronaphthalene, respectively. However, remarkable variations in colour were observed for cation **108•H**$^+$ on changing the solvent. When the colourless perchlorate **108•HClO$_4$** is dissolved in DMSO, DMF or pyridine, the solution immediately turns deep red or orange-red, whereas in the majority of other solvents, colourless, yellowish or pink solutions are formed. The reason for such solvatochromism is the decreased basicity of **108** and the pronounced IHB asymmetry of its cation, so that solvents with high proton-acceptor ability disrupt the IHB, thereby enabling conjugation of the NMe$_2$ groups. This kind of solvatochromism is characteristic also for cations of other low-basicity proton sponges[118]; it can be used effectively for lecture demonstrations when discussing topics such as conjugation, solvation and hydrogen bonding.

D. Infrared Spectra

The IR spectra of the proton sponge **1** and its cation have been studied in details by Polish chemists and were briefly summarized in a review[29]. Since then, new investigations were conducted on the salts **1•H**$^+$ of some new anions[92, 119], and the salts of 2,7-dimethoxy- (**44**)[87], 2,7-dichloro- (**101**)[77], 2,7-dibromo- (**102**)[78] and 4-amino-1,8-bis(dimethylamino)naphthalenes (**113**)[90]. The most interesting feature of the spectra is the appearance of stretching vibration bands of the hydrogen bridge, ν(NHN). In MeCN, CH$_2$Cl$_2$ and ClCH$_2$CH$_2$Cl solutions the band looks like a very broad 'continuum' at the background level extending from 3000 to about 300 cm^{-1}. In the solid, the nature of the absorption changes drastically and the band shifts towards 800–250 cm^{-1}, displaying a fine structure. This phenomenon is typical of very strong hydrogen bridges with a short N$\cdots$N distance (2.55–2.65 Å). The dependence of the position of the ν(NHN) band

on the aggregate state of the sample[120], the pressure[121], the counter ion structure[122] and deuteriation[123] was studied. In the last case, an isotopic ratio, $\nu(NHN)/\nu(NDN)$, which in some instances reaches 1.80–2.05 (for weak IHBs, the ratio is usually <1.45), was determined. For the pair of salts **44•HBr/44•DBr** this ratio reaches 2.08, the largest value published to date, reflecting exceptionally high polarizability of the hydrogen bridge in protonated **44**[87]. On the basis of the IR spectral data of proton sponge salts, most authors conclude that the potential energy curve for the hydrogen bridge corresponds to a potential either with two minima and a very low barrier or with one minimum with a flat bottom (Figure 4a,b). Incoherent inelastic neutron scattering (IINS) and Raman absorption spectra, recently performed for **1** and its protonated forms, turned out to be very informative in studies of low-frequency vibrations involving the methyl and dimethylamino groups[119]. However, the intense band in IR spectra at *ca* 500 cm^{-1}, ascribed to the (NHN) protonic vibrations, was observed neither in the Raman nor in the IINS spectra.

A sharp high-frequency shift of the $\nu_{C=O}$ stretching band for the change **87** → **87•H$^+$** ($\Delta \nu = 47$ cm^{-1}) is evident for the unusual participation of the amide nitrogen, rather than the carbonyl oxygen, in proton binding[66].

E. Nuclear Quadrupole Resonance Spectra

Contrary to the original[124] interpretation of the ^{14}N NQR spectrum with cross-relaxation of the base **1**, later measurements[125] revealed the presence in this spectrum of four (rather than two) resonance peaks from two nitrogen atoms. This is convincing evidence for their non-equivalence, which thus agrees with the NMR data on the asymmetry of the proton sponge molecule in crystals.

F. Electron Spectroscopy for Chemical Analysis

The ESCA spectrum recorded for the salt **1•HBF$_4$** in the N1s energy region revealed two maxima of equal height, formally indicating the non-equivalence of the nitrogen atoms in the cation[126]. However, the splitting of the peaks was relatively small. This was interpreted in favour of a nearly symmetrical hydrogen bridge in cation **1•H$^+$**. ESCA spectra of salts **1•H$^+$** with some other anions have also been studied[127, 128].

G. Fluorescence Spectroscopy

An advantage of this type of spectroscopy, as of the preceding one, is its time-independence, i.e. the method enables one to follow processes occurring within *ca* 10^{-16} s. Szemik-Hojniak and coworkers have applied fluorescence excitation spectroscopy on supersonic beam expansions to investigate the photophysical properties of the proton sponge **1**[129]. From the vibronic intensities in the excitation spectrum and the temperature dependence of this spectrum, they concluded that **1** in the gas phase adopts two main conformations in its electronic ground state. *Ab initio* calculations using 6-31G* basis set have shown that while the more stable one, called DMAN-1, closely resembles the classical 'in-in' structure (Figures 1b and 3a), the second conformer (DMAN-2) is actually a structure of 'in-out' type (Figures 1e and 3c), two examples of which, **105** and **106**, have been recently discovered[76, 79]. Interestingly, theoretical estimations predict for DMAN-2 an N···N distance of 2.96 Å, in fair agreement with the X-ray data for **105** (2.93 Å) and **106** (2.92 Å).

The $S_1 \leftrightarrow S_0$ transitions of conformers DMAN-1 and DMAN-2 as well as the properties of their excited states have been also studied by semi-empirical AM1 calculations[130].

H. Mass Spectra

The fragmentation of the molecular ion of the ring-unsubstituted proton sponges is determined by the 'proximity effect' of dimethylamino groups and at early stages involves practically only these groups. The fragmentation processes include isomerization and elimination of $MeNH_2$, Me_2NH and H• fragments giving rise to stable heterocyclic ions. For more details, see reviews published elsewhere[4, 29]. The main fragmentation path of the sterically overloaded molecular ions of compounds **73** and **76** is an elimination of dimethylmethyleneimmonium ion, $Me_2N^+=CH_2$ (m/z 58)[63]. Accurate liquid secondary ion mass spectrometric investigation of the salts **100**•HI and **100**•DI has revealed their perfect stability (MH^+ and MD^+ = 100%, $M^{+•}$ = 0%)[69]. **100**•DI, placed in a liquid matrix of m-nitrobenzyl alcohol containing 1% of CF_3CO_2H, does not exchange its deuterium. Under such conditions, the monoperchlorate salt of **1** remains protonated (or deuteriated) only to a little extent. This is indicative for the conservation of 'buttressing effects' in the gas phase of the *ortho*-disubstituted proton sponges (Section IV.A.1.d).

I. Dipole Moments

Dipole moments in benzene were measured for only three compounds: the proton sponge **1**, its 4-formyl- **124** and 4,5-diformyl **110** derivatives[81]. The dipole moment of compound **1** (μ = 1.19 D) is precisely equal to that of 1-dimethylaminonaphthalene. This is below the expected value, since the conjugation of both NMe_2 groups with the ring would result in the addition of the vectors of the corresponding moments. Evidently, due to violation of the molecular planarity (Section III.A.1.a), both vectors are directed at a considerable angle to each other. In contrast, the dipole moments of the aldehyde **124** (μ = 5.44 D), and especially the dialdehyde **110** (μ = 9.21 D), appeared to be unexpectedly high. This is indicative of a very efficient conjugation of the CHO and the NMe_2 groups and corresponds to the X-ray data for compound **110** (Figure 1c, equation 5). The high dipole moment makes this compound closer to ionic substances and, unlike many other derivatives of proton sponge, the dialdehyde **110** possesses metal lustre and is rather soluble in water. The photoexcited molecule of **1** as a result of internal charge transfer acquires a dipole moment of 9.5 D, which was proved by a combination of electron and fluorescent spectroscopic techniques[131].

Howard has calculated the dipole moments using the B3LYP/6-31+G**//HF/6-31G** level of theory for a series of proton sponges: **1** (μ = 1.13 D), **7** (μ = 0.96 D), **8** (μ = 2.57 D) and **12** (μ = 0.84 D)[132]. Attention should be drawn to the fairly good agreement between experimental and theoretical values of μ for compound **1**.

J. Electron-donating and Electron-accepting Properties

The gas-phase ionization potentials, IP, of 1,8-diaminonaphthalenes **1**–**6** measured by electron impact lie in the range 7.38–7.47 eV[2]. This could indicate that the first electron is ejected from the π-orbital of compounds **1**–**6**. Indeed, if these values characterize the ejection of an n-electron, then, due to the significant difference in the basicities, the IP_1 value of the sponge **1** would be much lower than that of the diamines **2**–**6**. Maier[133], who used photoelectron spectroscopy to measure the ionization potentials of compounds **1** and **2**, also assigned the IP_1 value for 1,8-diaminonaphthalene **2** (7.10 eV) to the π-ionization potential. In the case of proton sponge **1**, however, on the basis of theoretical calculations, the value IP_1 = 7.05 eV was ascribed to electron ejection from the n-orbital. According to these calculations, the highest occupied π-MO of compound **1** correlated better with the second ionization potential, IP_2 = 7.47 eV. Photoionization potentials of the fluorene proton sponge **7** and bridged diamines **31** and **32** (Table 13) have also been measured; they

were interpreted from the standpoint of splitting of the levels occupied by the unshared electron pairs of the two nitrogen atoms (Figure 5).

Electrochemical oxidation of the proton sponge **1** on a platinum disk electrode in MeCN has been shown to proceed via two reversible one-electron waves with $E_{ox}^{1/2} = +0.36$ and $+1.02$ V (Table 13)[134]. Presumably, the radical cation **1**$^{+\bullet}$ is formed in the first step and the dication **130** with a σ-bond between the nitrogens in the second step (equation 7). The radical cation **1**$^{+\bullet}$ was also generated by oxidation of compound **1** with lead dioxide. Its ESR spectrum represents a non-resolved singlet with a width ΔH of *ca* 23 E ($g = 2.0043$). From this, it was concluded that the conjugation of the NMe$_2$ groups with the naphthalene ring in molecule **1** is significant and its electron-donor properties lie between those of *N*,*N*-dimethylaniline (**131**) ($E_{ox}^{1/2}$ +0.68) and *N*,*N*,*N'*,*N'*-tetramethyl-*p*-phenylenediamine (**132**) (+0.015 V)[134].

$$(7)$$
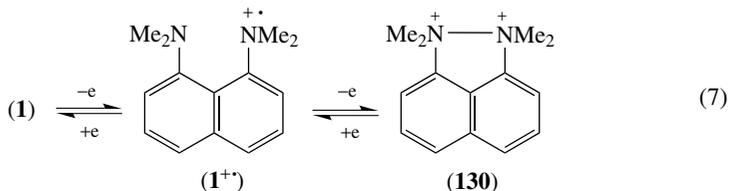
The oxidation of compound **32** occurs in a similar manner but even more easily[136]. Its radical cation can be stored unchanged in acetonitrile for months. The UV spectrum of **32**$^{+\bullet}$ ($\lambda_{max} = 480$ nm, lg $\varepsilon = 3.1$) is very close to that of neutral **32** itself, from which one can conclude that the naphthalene moiety does not take part in the oxidation. As found by cyclovoltammetry, the double proton sponge **35**, unlike its isomer **79**, is oxidized with reversible two-electron transition, composed of two superimposed one-electron steps at $E_{ox}^{1/2}$ -0.50 V (Table 13)[45]. Apparently, the driving force for this process is the formation of the resonance-stabilized dication **133** (equation 8), which was isolated in the form of black crystals with I$_3$$^-$ anions ($\lambda_{max} = 643$ nm, lg $\varepsilon = 4.02$) and investigated in

TABLE 13. Ionization potentials (IP$_1$) and electrochemical oxidation potentials ($E_{ox}^{1/2}$) for some aminonaphthalenes and proton sponges

Compound	IP$_1$ (eV)		$E_{ox}^{1/2}$ (V) (in MeCN) [a]
	EI	PE	
1	7.38[2]	7.05; $\Delta E = 2.0$ eV[133]	0.36, 1.02[134]
2	7.47[2]	7.10[133]	—
7	—	7.1; $\Delta E = 2.2$ eV[135]	—
12	—	—; $\Delta E = 2.6$ eV[4]	—
31	—	7.56; $\Delta E = 1.2$ eV[73]	—
32	—	6.90; $\Delta E = 0.9$ eV[73]	0.11, 0.72[136]
35	—	—	(−0.50)[45]
63	—	—	(−0.33)[58]
79	—	—	(−0.01), (+0.07)[58]
131	—	—	0.68[134]
132	—	—	0.015[134] (−0.30), (+0.29)[137]
134	—	—	(−0.13)[58]

[a] vs SCE (Hg$_2$Cl$_2$ electrode). The data in parentheses are referred to ferrocene standard Fc/Fc$^+$ = 0.00 V.

detail[45, 137]. The radical cation $35^{+\bullet}$ giving the ESR spectrum with hyperfine structure can be obtained by chemical oxidation of compound 35[45].

(133)   (8)

Similarly, non-separable two-electron transitions were also observed for proton sponges 65, 66 and tetraamine 134[54, 58]. As seen from Table 13, compound 35 is the strongest electron donor among all known tetrakis(dimethylamino)naphthalenes. The oxidation of 65 with four mole equivalents of iodine at low temperature also led to the formation of a black-brown salt ($\lambda_{max} = 723$ nm, lg $\varepsilon = 4.31$) of the dication 135[58].

(134)   (135)

The inclination of diamines $1-6$ to form 1:1 molecular complexes (MC) with 1,3,5-trinitrobenzene (TNB) has been pointed out[2]. The corresponding measurements reveal a lack of any correlation between the basicity of 1,8-diaminonaphthalenes and the ease of MC formation. This would seem to indicate that compounds $1-6$ act as π-donors, and the differences in MC stability, the least stable of which is the $1 \cdot$TNB complex, are mainly determined by steric factors and the inductive effect of the methyl groups[2].

There is only one report on the ability of proton sponges to undergo one-electron reduction[138]. Thus treatment of compound 1 with sodium in 1,2-dimethoxyethane gave a stable radical anion, for which the EPR spectrum was recorded at $-20\,^{\circ}$C. The hyperfine splitting constants (HFS) for the unpaired electron with ring protons, $a_{H(4),H(5)}$, $a_{H(3),H(6)}$ and $a_{H(2),H(7)}$ are 4.46, 1.77 and 1.39 Gs, respectively, values which are somewhat smaller in comparison with that for the naphthalene radical anion. The HFS constants with the protons of the methyl groups and ^{14}N nuclei are very small. This was interpreted as reflecting the non-coplanarity of the dimethylamino groups and the naphthalene ring. The magnitude of the dihedral angle between the axes of unshared electron pairs of the N atoms and the $2p\,\pi$-orbitals of the ring C-atoms in the radical anion $1^{-\bullet}$ was estimated to be $60-70^{\circ}$.

K. Quantum-chemical Calculations

Quantum-chemical calculations at different levels of theory have been widely used for estimating various structural and energetic parameters of proton sponges (Table 14).

TABLE 14. Survey of quantum-chemical calculations on proton sponge molecules

Calculated parameter	Compounds	Calculation method, basis set	References
Enthalpy of formation, H-bonding	**1**, **1•H$^+$**, **2**	Semi-empirical, AM1, MNDO/M	139
Structure by geometry optimization	**1**, **1•H$^+$**	*Ab initio*, 6-31G	140
	1, **1•H$^+$**, **44**, **44•H$^+$**	MP2/6-31G*	141
	1, **7**, **12**, **44**	HF/6-31G**, BLYP/6-31G**	142
	1, **1•H$^+$**, **7**, **7•H$^+$**, **8**, **8•H$^+$**, **12**, **12•H$^+$**	B3LYP/6-31+G**//HF/6-31G**	132
	Two conformers of **1**	6-31G*	129
	40, **107**, **123**, **123•H$^+$**	B3LYP/6-31G**	38, 115
	44•I$^+$, **102•I$^+$**	DFT and *ab initio* MP2/6-31G(d,p)	78, 87
Energy of IHB	**1•H$^+$**, **7•H$^+$**, **8•H$^+$**, **12•H$^+$**	*Ab initio*, B3LYP/6-31+G**//HF/6-31G**	132
Strain energy	**1**, **1•H$^+$**, **7**, **7•H$^+$**, **8**, **8•H$^+$**, **12**, **12•H$^+$**	*Ab initio*, B3LYP/6-31+G**//HF/6-31G**	132
	1, **7**, **12**, **44**	HF/6-31G**, BLYP/6-31G**	142
	40, **107**	B3LYP/6-31G**	38
Solvation energy	**1**, **44**	Polarizable continuum model, HF/6-31G*	141
Proton affinity	**1**, **7**	*Ab initio*, MP2/RHF/6-31G*	143
	1, **44**	MP2/6-31G*//HF/6-31G*	141
	1, **2**	B3LYP/6-31G*	144
	1, **7**, **8**, **12**	B3LYP/6-31+G**//HF/6-31G**	132
	1, **44**, **48**	DFT, BP/DZVP	145
	40, **107**	*Ab initio*, B3LYP/6-31G**	38
	88	B3LYP/6-31+G**//HF/6-31G**	67
Barrier for proton transfer	**1**, **7**	*Ab initio*, MP2/RHF/6-31G*	143
	1, **44**	MP2/6-31G*//HF/6-31G*	141
	1, **2**	B3LYP/6-31G*	144
	1, **7**, **8**, **12**	B3LYP/6-31+G**//HF/6-31G**	129
	44, **102**	DFT and *ab initio* MP2/6-31G(d,p)	78, 87
Electron-donating potential on protonation	**1**, **7**	*Ab initio*, MP2/RHF/6-31G*	143
$S_1 \leftrightarrow S_o$ transitions and maxima of absorption and emission	Two conformers of **1**	Semi-empirical, AM1	130
Dipole moments	**1**, **7**, **8**, **12**, **123**	*Ab initio*, B3LYP/6-31+G**//HF/6-31G**	115, 132

Good to satisfactory agreement between theory and experiment has been obtained for proton affinity values, absorption maxima in the electronic spectra and dipole moments. As for geometrical characteristics, a noted trend is that the B3LYP[132] and MP2[78] structures are generally closer to the experimental structure than the HF structures. Practically all the calculations are consistent with the fact that the asymmetrical hydrogen bond in $\mathbf{1}$•H$^+$ and other similar cations is energetically preferable over the symmetrical bond[140, 141, 143]. The barrier for intramolecular proton transfer in cation $\mathbf{1}$•H$^+$ is estimated to be $15.9-21.8$ kJ mol^{-1} at the HF/6-31G* level, but it essentially disappears at the B3LYP/6-31+G**/HF/6-31G** level[132]. The energy of the IHB and the strain energies for different types of proton sponges have been mostly estimated by Howard[132]. These data are discussed in Section IV.A.1.a. Attempts to employ the *ab initio* method for calculating the IR spectra of compounds $\mathbf{1}$, $\mathbf{1}$•H$^+$, $\mathbf{44}$•H$^+$ and $\mathbf{102}$•H$^+$ showed more success only in the last two cases[78, 87, 119].

IV. REACTIVITY

A. Reactions Involving Dialkylamino Groups

1. Protonation and basicity

a. General survey of basicity. Certainly, the most important property of all proton sponges is their exceptionally high basicity. Analysis of the pK_a values facilitates understanding both the reactivity and structural properties of these compounds. At present, the basicity constants (determined as pK_a values of the corresponding conjugate acids of the amines) for more than 100 proton sponges, mostly of the naphthalene type, are known. Owing to solubility problems, relatively few of the values have been determined in water or water–DMSO mixtures by spectrometry. For the majority of compounds, measurements were performed in non-aqueous solvents by potentiometric titration (in acetonitrile) or by competitive trans-protonation (commonly in DMSO) between two compounds close in basicity. In the last case, the measurement of concentrations is usually conducted by NMR that gives somewhat less precise results. Only for two proton sponges were the pK_a values calculated theoretically (Table 15). As for the gas-phase basicities, the only experimental proton affinity value is known for the archetypal sponge $\mathbf{1}$; for many other compounds, the PA values were calculated theoretically (Table 15). Herewith it is accepted that superbases have PA $\geqslant 1005$ kJ mol^{-1} [146]. Hence, 1,8-bis(dimethylamino)naphthalene and other proton sponges can be regarded as superbases. Recently, Streitwieser and Kim[148] have reported the ion-pair basicity of proton sponge $\mathbf{1}$ and compared it with those of several other amines in THF. Tables 16 and 17 embrace selected data on basicities of unsubstituted proton sponges, their analogues and derivatives with N- and ring-substituents.

We have already outlined the two general reasons for the high basicity of proton sponges, namely (1) steric strain and electrostatic repulsion relief upon the protonation and (2) the formation of a strong IHB in the cation. It is now known that the relative contribution of each of these factors varies with the structure[132, 141]. Besides, the basicity depends on a number of other factors. Among them are the changes in the nitrogen hybridization state[151], the incomplete relief of steric strain in cations[4, 76], the loss in conjugation energy of the dialkylamino groups with the π-system on protonation etc. Taking into account the objective difficulties of the problem, it is not surprising that opinions on the importance of each of the factors differ so drastically.

On the basis of *ab initio* calculations using HF/6-31G** and BLYP/G-31G** levels, Howard has concluded that for naphthalene $\mathbf{1}$ and phenanthrene $\mathbf{12}$ proton sponges, the IHB contribution in the overall increase of basicity is not less than 65%, whereas the other 35% are equally divided between the relief of steric strain and the electronic repulsion on

TABLE 15.   Calculated gas-phase proton affinities, PA and theoretical solution pK_a values of some proton sponges

Compound	PA (kJ mol^{-1})	pK_a (solvent)
1	1030.1 (exp.)[3], 1077.2[143], 1040.4[144], 1028.7[145], 1020.3[146], 1027.4[147], 1030.7[22, 38, 132]	8.5 (DMSO)[149], 11.9 (H$_2$O)[149], 18.1 (MeCN)[149], 18.3 (MeCN)[150]
7	1090.6[143], 1039.3[132]	—
8	1028.9[132]	—
12	1041.0[132]	—
40	1038.7[38]	—
44	1096.9[145]	11.1 (DMSO)[149], 20.1 (H$_2$O)[149], 23.2 (MeCN)[149]
48	1055.0[145]	—
88	1001.5[67]	—
107	1013.1[38]	—

TABLE 16.   Ionization constants, pK_a, of proton sponges without substituents in the arene moiety

Compound	Solvent (method of measurement)^a	pK_a	References
1	H$_2$O (S)	12.10	152
1	MeCN (PT)	18.50	153
1	DMSO (CE)	7.5	154
7	H$_2$O–DMSO (6.5:3.5) (S)	12.8^b	4, 9
8	DMSO (CE)	11.9^b	4, 8
9	DMSO (CE)	11.8^b	4, 8
11	DMSO (CE)	10.9^b	4, 8
12	H$_2$O–DMSO (6.5:3.5) (S)	11.5^b	4, 9
13	MeCN (CE)	5.8^b	10
39	MeCN (PT)	18.95	33
39	H$_2$O–DMSO (7:3) (S)	13.0^b	155
52	DMSO (CE)	7.9	48
22	H$_2$O (S)	9.97	156
25a	H$_2$O (S)	7.49	36
26	MeCN (PT)	17.50	157
27	MeCN (PT)	17.60	157
28a	H$_2$O–EtOH (1:1) (PT)	3.77	158
28b	H$_2$O (S)	4.62	156
28c	H$_2$O (S)	10.27	156
28d	H$_2$O–DMSO (7:3) (S)	13.6^b	156
28e	H$_2$O–DMSO (7:3) (S)	13.0^b	156
96	H$_2$O–DMSO (6:4) (S)	13.6^b	4

^{a} (S)—spectrophotometry, (PT)—potentiometric titration, (CE)—competitive experiment.
^{b} Extrapolation to the H$_2$O scale.

the transition to the cation[132]. The gas-phase hydrogen bond energy was estimated to be in the range of 50–100 kJ mol^{-1}. For calculating the proton sponge strain energy, she has used the 'all-encompassing' definition of this parameter as the sum of the lone pair–lone pair repulsion energy, $E(LP \cdots LP)$, and the distortion energy, E(distortion), including the energy loss caused by the aromatic destabilization (equation 9).

$$\text{'Strain energy'} = E(LP \cdots LP) + E(\text{distortion}) + E(\text{aromatic destabilization}) \qquad (9)$$

The 'strain energy' values obtained for naphthalenes **1** and **44**, and for fluorene **7** and phenanthrene **12** proton sponges, of 18.1, 40.5, 12.3 and 61.0 kJ mol^{-1} respectively, led to the conclusion that '... the strain energy rarely, if ever, makes a larger contribution to proton sponge basicity than the intramolecular hydrogen bond (often *ca* 100 kJ mol^{-1})'[142]. Howard indicated also that the 'proton sponge strain can not be estimated from structural parameters and *ab initio* calculations provide the only route to its estimation'. An opinion on the prevailing role of the IHB was also expressed by Pachkovskii and Voityuk[139].

Another point of view, based on calculations at the MP2/6-31G*//HF/6-31G* level[141], says that the main factor (*ca* 50%) for the increase in the basicity of proton sponges is the destabilization of the base due to the nitrogen lone-pair repulsion, and the hydrogen bond contribution is at most 30%. An even smaller value of the stabilization effect of the hydrogen bond results from experimental work of Perrin and Ohta[50, 99] and Lloyd-Jones and coworkers[109]. In our opinion, in solution, the truth lies between these extreme standpoints.

For example, the basicity of 2,2′-bis(dimethylamino)diphenyl (**95**) (pK_a = 7.9) is higher by 2.8 powers of ten than that of *N,N*-dimethylaniline (pK_a = 5.1)[4, 88]. Since the benzene rings in **95** are twisted by an angle of 125° relative to one another, the compound is free from both noticeable repulsion of the nitrogen unshared electron pairs and steric strain due to this repulsion. Thus, this difference in basicity can be ascribed, with a fair degree of confidence, to the stabilizing effect of the IHB in cation **95•H$^+$** (equation 10). In the case of proton sponge **1**, the IHB contribution has to be even higher, perhaps 3.2–3.5 pK_a units, i.e. about 50% of the overall increase in the basicity, since **1**, unlike **95**, is as yet pre-organized for protonation.

$$ \text{(10)} $$

(95)   **(95•H$^+$)**

By using the correlation, $\Delta G^{\circ} = 2.3RT\text{p}K_a$, one can calculate that the cation **1•H$^+$** is by 40 kJ mol^{-1} more stable than the dimethylanilinium cation. One half of this value (approximately 20 kJ mol^{-1}) is the hydrogen bond energy in cation **1•H$^+$** in water. Though this is much smaller than the above-mentioned theoretical estimates of 50–100 kJ mol^{-1} in the gas phase, this value agrees quite well with the average energies for such hydrogen bridges[99, 159]. The 20 kJ mol^{-1} value makes also understandable the easiness of some processes, requiring a preliminary IHB breaking of the cation **1•H$^+$**, e.g. electrophilic substitution in **1** in acidic media (Sections IV.B and IV.D) or mutual transformations of the stereoisomeric cations of chiral sponges (Scheme 11).

Another important feature of proton sponges is their exceptionally difficult diprotonation. Thus, the pK_a^2 value of −9.0 found in H$_2$O–H$_2$SO$_4$ mixtures[154] for compound **1** is very much lower than the value for the first protonation, pK_a^1 = 12.1 (Table 16). It is not surprising that in contrast to 1,8-diaminonaphthalene (**2**), which gives quite a stable crystalline dihydrochloride, the corresponding salts of the diprotonated proton sponge cannot be obtained even with excess of strong acids (HClO$_4$, HBF$_4$ etc.). Clearly, breaking the hydrogen bond in the monoprotonated sponges is energetically unfavourable. In accord with these data is the fact that the *N*-methylated cation of the proton sponge **136**, free of the IHB, under the action of HClO$_4$ or CF$_3$SO$_3$H, forms the dication **137a** which equilibrates with CH-tautomers **137b** and **137c** (Scheme 13)[160, 161]. For the same

reason, the chelated cations **28d•H⁺** and **28e•H⁺** do not undergo second N-protonation under similar conditions, whereas their non-chelated analogues **31•H⁺** and **32•H⁺** form the N(1),N(8)-dications[161].

SCHEME 13

(28d·H⁺)   (28e·H⁺)   (31·H⁺)   (32·H⁺)

b. Unsubstituted proton sponges. Among unsubstituted proton sponges, only the fluorene sponge **7** (pK_a 12.8) is more basic than compound **1**. It is believed that the reason for this is the formation of more stable IHB in the cation **7•H⁺** [4]. Although the bridge is longer (2.63 Å) than that in the **1•H⁺** (2.57 Å), this can be well overweighted by its nearly perfect linearity. According to Howard's theoretical calculations[132], the IHB energetic contribution in the overall increase of basicity of fluorene **7** and dibenzothiophene **8** sponges reaches 96%.

From these data, further basicity increase should be expected for the phenanthrene sponge **12**. This expectation, however, is not justified and the pK_a value of **12** is only 11.5, despite its being rather short (2.54 Å) and linearity of the IHB (167°) in the cation **12•H⁺** (Table 5). It is assumed that the principal reason for the reduced basicity of diamine **12** lies in its helicene-like structure, which is retained in the corresponding cation, i.e. the protonation in this case does not result in steric relief[4]. Even more pronounced helicene strain is manifested in the cation of benzophenanthrene sponge **13•H⁺**, having a basicity (pK_a = 5.8) only a little higher than that of dimethylaniline.

It should be emphasized that unlike the initial theoretical suggestion[143], there is no obvious relationship between the proton sponge basicities and the electrostatic repulsion of the unshared electron pairs of the NMe₂ groups. This conclusion follows from comparison of values of the n_+/n_- splitting (Figure 5) whose magnitude, ΔE (Table 13), could serve as a measure of such repulsion.

c. Influence of the N-substituents. As expected, successive substitution of the N-methyl groups by ethyl[33] or isopropyl[41,48] groups slightly increases the basicity. For instance, the pK_a value of the tetraethyl sponge **39** is 0.5 units higher than that of the parent compound **1** (cf. also compounds **52** and **96** in Table 16). In contrast, if the nitrogen atoms are incorporated into the saturated rings, as in compounds **22**, **25a**, **26** and **27**, the basicity

often drops down, probably due to the non-optimal directionality of the lone-pair axes and the formation of less tight IHB.

It follows from Table 16 that, of the diamines **28**, only compounds **28c–e** can be regarded as proton sponges. The basicities of **28a** and **28b** are characteristic of ordinary arylamines. It is clear that the methylene and ethylene bridges in these molecules fix rigidly the nitrogen atoms in a configuration which excludes the formation of a fixed IHB. Strictly speaking, for this reason, the bridged diamines **31** and **32** are not proton sponges.

d. Proton sponges with substituents in the arene moiety. One of the most intriguing phenomena in the chemistry of proton sponges is a sharp increase in their basicity upon the introduction of alkoxy groups at *ortho*-positions to the dialkylamino groups. Thus, the change from diamine **1** to its 2,7-dimethoxy derivative **44** is accompanied by a basicity increase of four powers of ten. The pK_a value of dimethoxydibenzofuran **100** was estimated to be 14.37 (H_2O)[69]. Compounds **44–47** were hitherto the strongest bases among all naphthalene and arene proton sponges. There are many speculations as to why their basicity becomes so high. Almost all of them, are reduced to the so-called 'buttressing effect'. It is supposed that the latter forces the $NAlk_2$ groups to be closer in space with a consequent increase in their repulsion, which additionally destabilizes the base. From this standpoint, one may propose that the bulkier the *ortho*-substituents are, the greater the basicity should be, but, as was recently demonstrated with a series of 2,7-disubstituted 1,8-bis(dimethylamino)naphthalenes (Table 17), there is no such a dependence[76]. This is

TABLE 17.   Ionization constants, pK_a, of proton sponges with substituents in the naphthalene moiety

(A)   (B)   (C)

Type of structure	Compound	R^1	R^2	Solvent (CE)[a]	pK_a	References
A	**101**	Cl	Cl	DMSO	6.8[b]	76
A	**102**	Br	Br	DMSO	6.5[b]	76
A	**103**	I	I	DMSO	6.7	76
A	**104**	SMe	SMe	DMSO	8.1	76
A	**105**	SiMe$_3$	SiMe$_3$	DMSO	7.0	76
A	**48**	Me	Me	DMSO	9.8	76
A	**65**	NMe$_2$	NMe$_2$	DMSO	11.2	56, 58
A	**44**	OMe	OMe	DMSO	11.5[c]	56, 58
B	**113**	NH$_2$	H	DMSO	9.8	57
B	**138**	NHMe	H	DMSO	10.1	57
B	**64**	NMe$_2$	H	DMSO	8.0[b]	57
B	**117**	Br	H	DMSO	6.5[b]	163
B	**108**	NO$_2$	H	DMSO	3.5[d]	47
B	**59**	Br	Br	MeCN (PT)	16.40	153
C	**42**	—	—	DMSO	5.2	37

[a] For abbreviation see Table 16. [b] For pK_a in MeCN see Reference 153. [c] 16.1 in the H_2O scale; see Reference 162.
[d] For pK_a in MeCN see Reference 164.

because the 'buttressing effect' is actually a complex combination of various interactions between the *ortho*-substituents and the dimethylamino groups in both bases and cations. A contradictory directionality of these interactions strongly reduces the importance of the 'buttressing effect' in compounds with very voluminous *ortho*-substituents (Br, I, SMe, SiMe₃), the basicity of which is close to that of parent compound **1**. In the case of less bulky electron-donating *ortho*-functions (OMe, NMe₂, Me), their buttressing and polar effects act in the same direction, explaining why compounds of this type (e.g. **44**, **48**, **65**) are remarkably basic[56, 76]. Notably, the chelated cation **65·H⁺** (as well as the proton salts of compounds **66**–**68**), on treatment with mineral acids in MeCN solution, can be further protonated at both *ortho*-NMe₂ groups[56].

The influence of distant substituents in *meta*- and *para*-substituted proton sponges is predictable in general: the electron-donating groups increase and the electron-withdrawing groups decrease the basicity, in accordance with their Hammett's σ-constants and space orientation. For instance, the ionization constant of 4-dimethylamino derivative **64** is noticeably lower than that of its monomethylated **138** and non-methylated **113** analogues, in spite of the greater electron-releasing properties of the NMe₂ group when compared to NHMe and NH₂. Evidently, there is a spatial interaction of the NMe₂ group with the neighbouring *peri*-proton, resulting in some twisting of the group out of the naphthalene plane with a consequent decrease in its effective electron donation.

There are some other specific manifestations of basicity of substituted proton sponges which are worthy of close consideration. For example, the protonation of compound **127**

(**127·H⁺**)   pK_a = 14.60 (MeCN)

(**139·H⁺-a**)   (**139**)   (**139·H⁺-b**)

SCHEME 14

occurs at the carbonyl oxygen, apparently due to the formation of resonance-stabilized hydroxyphenalenium ion **127·H⁺** [118]. In a similar way, a diazafluoranthene sponge is protonated in dimethyl sulfoxide at the pyridazine ring giving the deep coloured (λ_{max} = 560 nm) salt of cation **139·H⁺-b**, but in CD$_3$CN the proton is attached to the NMe$_2$ groups producing the chelated cation **139·H⁺-a** (λ_{max} = 397 nm) (Scheme 14) [118].

It was already mentioned (Section III.A.2) that 4,5-dihydroxy-1,8-bis(dimethylamino) naphthalene actually exists in the form of the internal salt **111** [39]. Somewhat similar is the situation with 2,7-dihydroxynaphthalene **140**, also behaving in solution as a betaine [165]. The latter, on treatment with acids, gives the cation **140·H⁺**, while the action of alkali results in protonated dianion **141** (Scheme 15). All attempts to deprotonate **141** (even with the KOH–DMSO system at 100 °C or with LiH–DMSO) failed. This implies that the basicity of still unisolated dianion **142** lies in the limit of pK_a = 25–26 (H$_2$O scale). Thus, dianion **142** can be presently considered as the strongest base among all proton sponge and aniline derivatives.

SCHEME 15

It was recognized that acenaphthene **40** and acenaphthylene **107** proton sponges, unlike the pair of compounds **11** and **12** [4], easily interconvert by oxidation and reduction, respectively [38]. Since in the course of this transformation, the basicity change amounts to over four pK_a units (equation 11), these compounds form a redox system with easily modified basicity. It is believed that such properties may be of use in creating molecular devices [38].

(11)

TABLE 18. Ionization constants for double proton sponges at 25 °C

Compound	Solvent [a]	pK_a^1	pK_a^2	References
35	DMSO (CE)	9.8	4.9	45
36	MeCN (PT)	18.10	18.10	153
37	MeCN (PT)	18.30	18.30	153
118	MeCN (PT)	16.60	14.0	105

[a] For abbreviations see Table 16.

e. Double and polyfunctional proton sponges. All double proton sponges, on treatment with acids, give dications, e.g. **35**•2H$^+$ and **118**•2H$^+$ (Scheme 10). For the bases **35** and **118**, both the pK_a^1 and pK_a^2 values were determined; they differ about by 5 and 2.5 units, respectively (Table 18). In the case of the 1,1'-binaphthyl- **36** and 1,1'-binaphthylmethane- **37** proton sponges, the first and second ionization constants turned out to be very close and could not be separated. Notably, treatment of both these bases even with one half of an equivalent of an acid resulted in isolation of the diprotonated salt exclusively. The monoprotonated species for all known double proton sponges were observed only in an NMR tube after the addition of one equivalent of the same base to the corresponding dication (Scheme 10).

It follows from Tables 17 and 18 that tetrakis(dimethylamino)naphthalenes **35** and especially **65** possess higher basicity in comparison with parent compound **1**. It was hoped that a further increase in the number of NMe$_2$ groups would increase the basicity even higher. Unfortunately, the first representatives of such compounds, namely hexa- and heptakis(dialkylamino)naphthalenes (Section II.B.2), turned out to be scarcely soluble in MeCN, DMSO, EtOH and H$_2$O. Yet, their pK_a values were measured in 80% aqueous dioxane by a potentiometric titration technique[166]. The acid ionization constants are summarized in Table 19 together with the pK_a values of tetrakis(dimethylamino)naphthalenes **35** and **65** determined under the same conditions.

Though the polykis(dialkylamino)naphthalenes are notably stronger bases than compound **1** ($pK_a = 9.89$ in this solvent system[63]), they are still less basic than 1,2,7,8-tetrakis(dimethylamino)naphthalene (**65**). Certainly, the reason for that is the spatial overcrowding of the molecules forcing the dialkylamino groups to be twisted out of the naphthalene plane by a large angle and strongly decreasing their +M-effect. In addition, the X-ray data for salt **75**•2HClO$_4$ has shown that protonation of compounds of such a type does not result in an essential steric relief[63]. Consequently, there is little doubt that the basicity of the as yet unknown octakis(dimethylamino)naphthalene should not be extraordinarily high.

f. Mechanism and rates for deprotonation of cations. As has already been mentioned, the high basicity of proton sponges is accompanied by low rates of their protonation–deprotonation. Indeed, whereas the deprotonation of common ammonium salts

TABLE 19. Ionization constants for some polykis(dialkylamino)naphthalenes in 4:1 (v/v) dioxane—water at 25 °C[63, 64]

Compound	pK_a^1	pK_a^2	Compound	pK_a^1	pK_a^2
73	12.23	8.23	**80**	13.11	8.70
75	11.23	6.93	**81**	11.90	7.22
76	12.90	7.63	**35**	12.71	8.23
78	13.90	—	**65**	14.87	—

is limited only by diffusion ($k = 3 \times 10^{10}$ l mol^{-1} s^{-1})[167], for cations **1**•H$^+$ and **39**•H$^+$, the process occurs by 5–6 orders more slowly[152, 168–171]. In the case of the cations of 2,7-dialkoxy-1,8-bis(dialkylamino)naphthalenes, **44**•H$^+$–**47**•H$^+$, the deprotonation has been slowed so much that it can be followed spectrophotometrically[172]. Herewith, owing to high basicity of compounds **44**–**47**, their cations are deprotonated only in alkaline DMSO solutions[162]. Presumably, there are two reasons for the low deprotonation rates: first, the necessity to break-up a rather strong IHB in the cations, and second, the steric factors: the proton in the cation is in a hydrophobic pocket to which the access of a base must be hindered (see References 36 and 156 for details). Further increase in the hydrophobic environment at the N atoms (e.g. transition from **1**•H$^+$ to **39**•H$^+$), results not so much in increasing pK_a as in decreasing (*ca* 38-fold with OH$^-$ as a base) the kinetic basicity (Table 16)[155]. A similar picture, though affected by the 'buttressing effect', was observed for cations with *ortho*-substituents (e.g. **44**•H$^+$ and **45**•H$^+$)[172].

In several cases, IR and NMR methods were used to investigate the interaction of compound **1** with phenols[122, 173–175], carboxylic acids[174], SH and SeH acids[176, 177]. As proved by NMR experiments, **1** is not protonated by aliphatic alcohols and thiols[177]. Unexpectedly it was found that phenol (pK_a = 9.99) hardly protonates proton sponge, despite the fact that the basicity of the latter is more than two orders of magnitude higher than that of the phenolate anion. Distinct protonation is observed only with phenols having pK_a < 8.4. The interaction gives two types of proton complexes with 1:1 and 1:2 compositions, the latter being much more stable. This is rationalized in terms of formation of homoconjugated anions, ArOH $\cdots^-$ OAr. Evidence for their stability can be deduced from the fact that the 1:1 salt between the base **1** and pentachlorophenol disproportionates in acetonitrile to give a new 1:2 salt and a non-protonated proton sponge (equation 12)[122].

$$2(\mathbf{1}{\cdot}H^+C_6Cl_5O^-) \rightleftarrows (\mathbf{1}) + (\mathbf{1}{\cdot}H^+C_6Cl_5O^{-\cdots}HOC_6Cl_5) \qquad (12)$$

Vivid debates in the literature were concerned with the mechanism of the deprotonation of proton sponge cations. Virtually all the data indicate that this process occurs in two steps: first, the IHB is cleaved under the influence of a base, and then deprotonation of the non-chelated cation takes place. Apparently, the first stage is rate-determining and therefore the equilibrium concentration of the non-chelated cation at each moment of time should be low[172]. However, in one case, all the three species participating in equilibrium were recorded[80]. It was found that the ^{1}H NMR spectrum of the perchlorate **108**•HClO$_4$ in DMSO-d$_6$ displayed peaks not only of the chelated cation, but also those of the free base **108** and the non-chelated cation **108**•H$^+$-**a** (Scheme 16). At an initial concentration of the dissolved salt **108**•HClO$_4$ of 5×10^{-2} M, the ratio **108**•H$^+$: **108**•H$^+$-**a**:**108** is 68:19:13. If the concentration of the original salt decreases by one power of ten, this ratio changes drastically to 26:5:69 and the deprotonated base becomes the predominant form. The cation **108**•H$^+$ does not undergo any noticeable changes in acetonitrile. Similarly, the cation of the proton sponge **1**•H$^+$ is the only species that is present in DMSO-d$_6$. Apparently, there are three reasons for the abnormal behaviour of cation **108**•H$^+$ in dimethyl sulfoxide: (1) considerable asymmetry of the IHB (Scheme 9, see Section III.B.2), (2) decreased basicity of the nitro derivative **108** and (3) optimal basicity of the solvent (pK_a = 0) which is sufficient to induce partial scission of the IHB and subsequent deprotonation.

2. Reactions with other Lewis acids

In contrast to the original report[1], it was established that on treatment with methyl fluorosulfate, compound **1** gives the non-crystalline fluorosulfonate, which is converted into the crystalline tetrafluoroborate **136** under the action of NaBF$_4$[161]. An attempt to

SCHEME 16

synthesize the borate complex **143** by treating the cation **1·H$^+$** with pyridine-borane was unsuccessful (equation 13), although tetramethyl-*o*-phenylenediamine and 2,2′-bipyridyl easily form complexes of this type[178].

$$(13)$$

At the same time, interaction of the neutral base **1** with polyboranes or boron trifluoride does occur even at low temperatures (Scheme 17)[179]. NMR monitoring showed that while **1** with diborane or BF$_3$ gave salts of similar type, **144** and **145**, interaction between **1** and decaborane resulted in proton transfer, and reaction with pentaborane led to the formation of ionic compound X$^+$ B$_9$H$_{14}$$^-$, whose cationic part (X$^+$) remained unidentified.
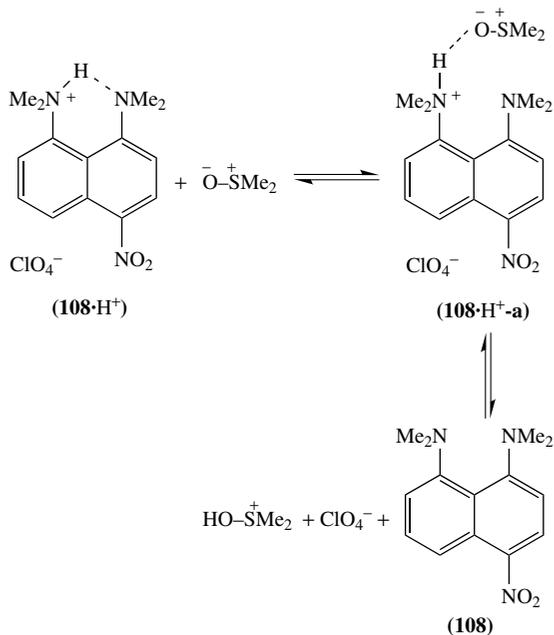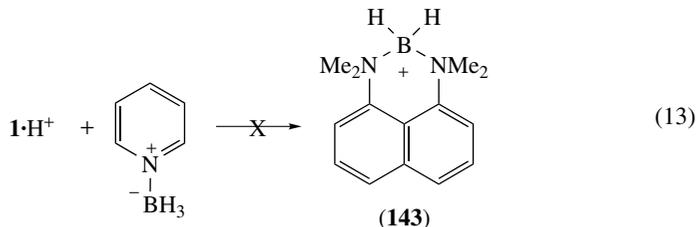
Product **145** was also obtained when diamine **1** reacted with complexes of boron trifluoride/diethyl ether or boron trifluoride/isoxazole in benzene[180]. 1,10-Phenanthroline, but not 2,2′-bipyridyl, behaves similarly. Though the proton sponge cannot replace pyridine from the (Py)$_2$BF$_2$$^+$ PF$_6$$^-$ salt[180], the above results proved that **1** can, in principle, serve as a chelating ligand for boron-containing cations.

In rare cases the proton sponge can react with Lewis acids as a monodentate ligand. Thus, reaction of **1** with highly electrophilic borane B(C$_6$F$_5$)$_3$ in CD$_2$Cl$_2$ led to the

SCHEME 17

(146)
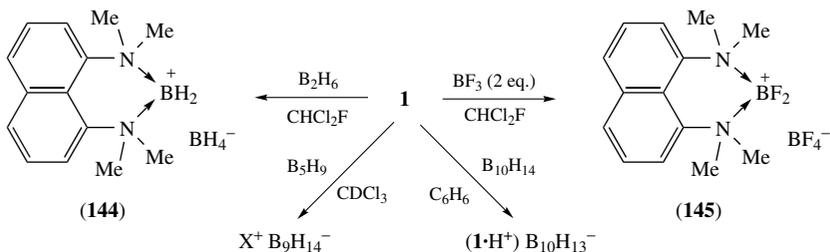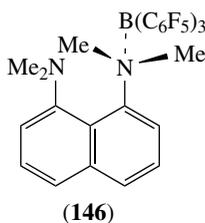
formation of a complex with hypothetical structure **146**[177]. This was proved by multinuclear magnetic resonance, and in particular by the observation of non-equivalence of the dimethylamino groups and the asymmetry of the naphthalene core.

For a long time it was thought that metallic complexes of proton sponges cannot exist because of steric hindrance and a too small N $\cdots$ N ligand distance. However, Japanese chemists have recently reported the successful preparation of the first such compounds[181]. They have found that the parent sponge **1** reacts with bis(hexafluoroacetylacetonato) palladium(II) in hexane solution with immediate deposition of dark violet crystals of a 1:1 molecular complex **1**•Pd(hfac)$_2$ with unknown structure. After standing for a week, this complex is transformed into the red complex **147**, which easily undergoes ligand exchange on treatment with other β-diketones (e.g. acetylacetone and dibenzoylmethane) to produce complexes **148** (Scheme 18). X-ray study of the latter has confirmed that severe distortions of the naphthalene ring system (e.g. the N $\cdots$ N distance is 2.94 Å) is a price the ligand **1** pays for the possibility to form such complexes. Therefore, it is not surprising that complex **147** gradually reacts with traces of water to form a new salt with protonated (**1**•H$^+$) proton sponge moiety[181]. Some earlier, transition metal complexes similar to **147** were also described for the 4,9-dichloro derivative of quinoquinoline **14**[182].

3. Dealkylation

Since the NMe$_2$ groups are in a crowded environment, it seems reasonable that under certain conditions the proton sponges can be demethylated. Two mechanisms for the demethylation should be considered: (1) a pure nucleophilic mechanism and (2) an oxidative mechanism in which an interaction with a nucleophile is also possible. The first mechanism is realized on heating the proton sponge salts with soft nucleophiles such as thiocyanate[46], phenylthiolate, phenylselenolate[183] or iodide ions[184] (Scheme 19). In addition to the steric strain, an additional driving force for this process seems to be the formation of *N,N,N'*-trimethyl-1,8-diaminonaphthalenes, which are stabilized by both IHB and a rather effective conjugation between the NHMe group and the ring system. Consequently, such demethylation reaction can serve as a good method for obtaining
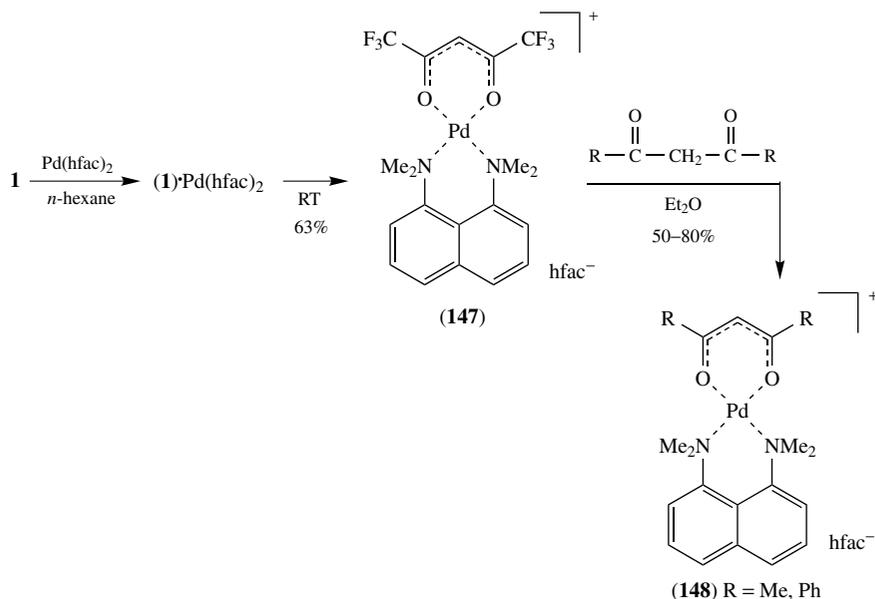
SCHEME 18

compounds of type **6**. Notably, in a paradoxical way this approach can be employed even for exhaustive realkylation of naphthalene proton sponges (e.g. **1** → **39**) elaborated as a one-pot process[184]!
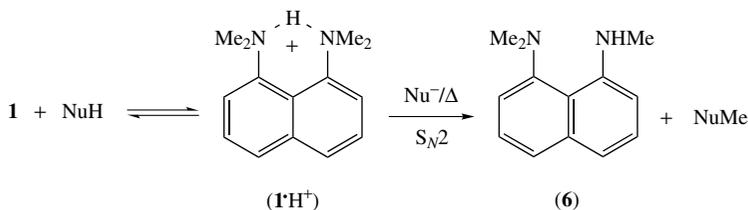
SCHEME 19

Nucleophilic demethylation of neutral sponges occurs only if the ring contains strong electron-withdrawing groups and if the reaction is carried out in a superbasic medium[185]. Thus, treatment of the nitro derivative **108** with a solution of KOH in DMSO resulted in the formation of compound **149** (yield 40%), together with the naphthol **150** (7%) and the lactam **151** (11%) (Scheme 20).

The formation of **150** seems a result of nucleophilic substitution of the dimethylamino group in the more activated C1 position. A presumable mechanism of formation of the lactam **151** includes an intramolecular nucleophilic displacement of the NMe$_2$ group (Scheme 21).

Some complex reactions also entail hydrolytic substitution of the NMe$_2$ group by the carbonyl (Section IV.D).
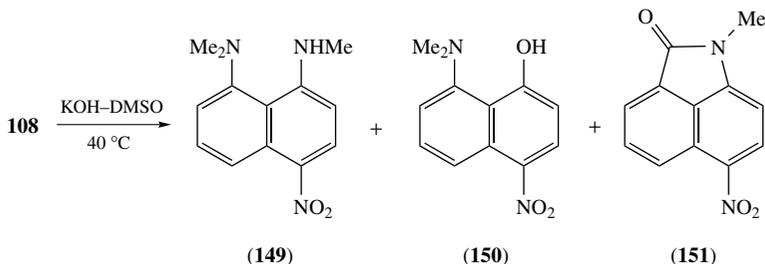
SCHEME 20
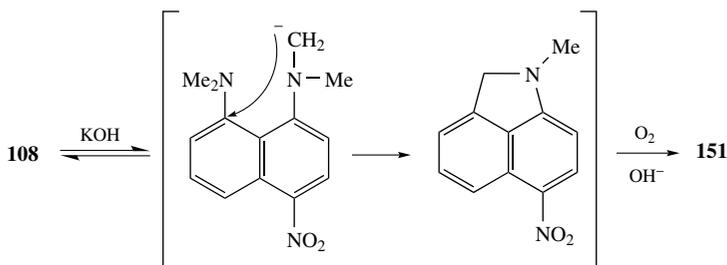
SCHEME 21

The oxidative demethylation mechanism was observed in a series of acenaphthene proton sponges. Thus, on oxidation of compound **40** with manganese dioxide, apart from the acenaphthylene proton sponge **107** (equation 11), 5-dimethylamino-6-methylamino-acenaphthylene (**154**) is formed in 33% yield[38]. Neglecting the question of the sequence of demethylation and CH_2CH_2 bridge oxidation steps, it would be sensible to suggest that the reaction proceeds through two successive one-electron transfers generating first the radical cation **152** and then the methyleneimmonium cation **153**, which cleave hydrolytically to the diamine **154** (Scheme 22). The extent of demethylation reaction was found to be even higher during the nitration of **40** with HNO_3-AcOH mixture or especially with nitronium tetrafluoroborate in acetonitrile, producing compounds **155** and **156** (Scheme 23)[47].

4. Conversion to 2,3-dihydroperimidinium salts

In the presence of transition metal complexes, such as those of Ir^{3+} (Scheme 24), Rh^{3+} and Ru^{3+}, the proton sponge **1** behaves as a hydride donor from one of its methyl groups[51, 186]. The methyleneimmonium cation **157** thus formed undergoes immediate cyclization to a 1,1,3-trimethyl-2,3-dihydroperimidinium salt **158**.

Occasional formation of such salts in a small amount on nitration of compound **1**, e.g. with N_2O_4 in 1,2-dichloroethane, indicates that the process could be initiated with common oxidants[47]. However, a question arises here as to why a similar cyclization is not observed for acenaphthene sponges (cf. Scheme 22)? The answer may be that the $N \cdots N$ distance in these sponges is remarkably longer (Table 4) and thus the cyclization becomes unfavourable. That the double proton sponge **35** with an $N \cdots N$ distance yet shorter than **1** (Table 4) is very prone to cyclize to dihydroperimidinium salts[44, 64, 137], confirms this explanation (Section IV.B.8).

(152)   **(153)**

(154)

SCHEME 22

(155) (52%)   **(156)** (4%)
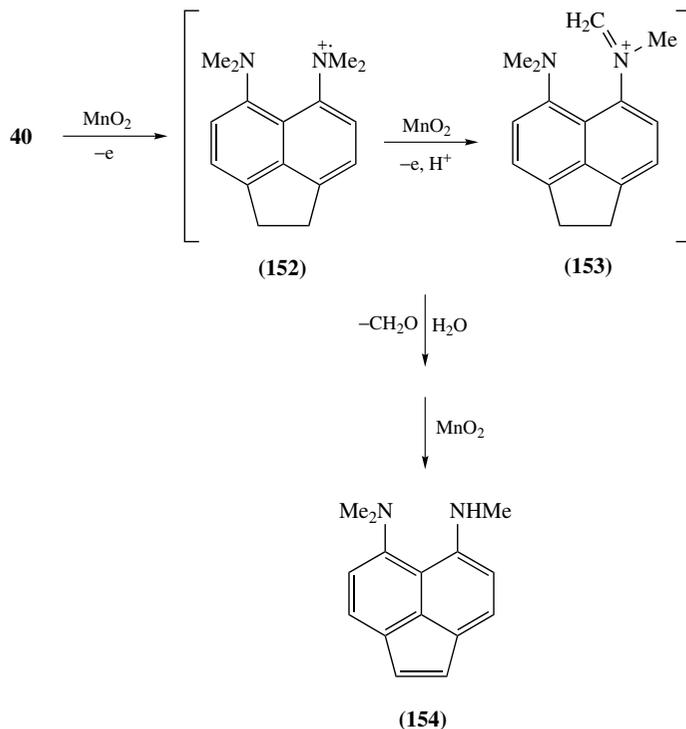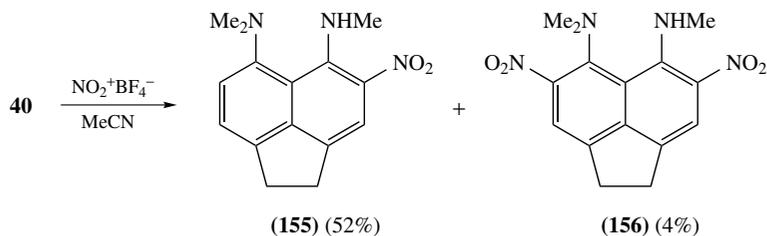
SCHEME 23

Some dihydroperimidinium salts are unstable due to steric crowding and exist exclusively in the open-chain methyleneimmonium form. An example is provided by 1,2,2,3-tetramethyl-2,3-dihydroperimidine (**159**), which on heating with iodomethane in a water-free medium gives salt **160**, which according to NMR data has structure **161**[41]. More important, if the reaction is conducted in wet DMF, then a high yield of proton sponge **1** is formed. Evidently, the salt **161** is hydrolysed under these conditions to N,N,N'-trimethyl-1,8-diaminonaphthalene (**6**), which is further methylated to **1** (Scheme 25). On the other hand, reduction of **161** enables one to isolate the isopropylated proton sponge **120**[41].

1   +

SCHEME 24

(157)   **(158)**

(159)   **(160)**   **(161)**

DMF/H₂O | MeI

(1)
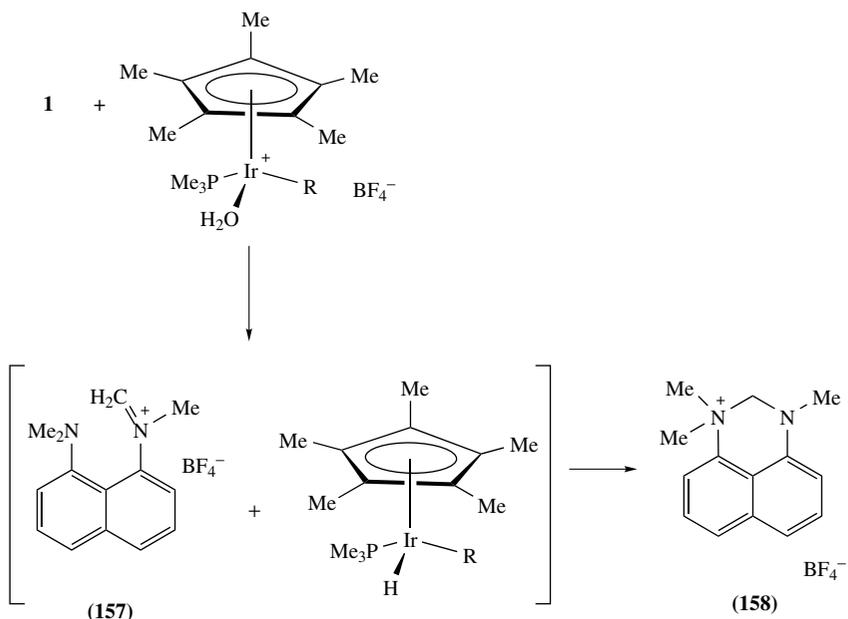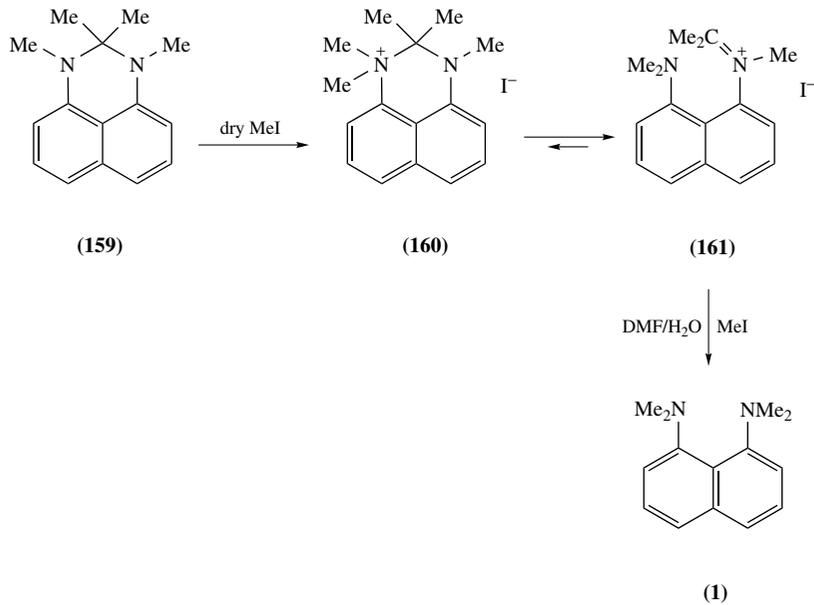
SCHEME 25

5. Reductive elimination of the dimethylamino groups

In several cases, a reductive displacement of the NMe_2 groups by hydrogen was observed. For instance, treatment of the binaphthyl proton sponge **36** with excess of lithium metal in THF followed by bubbling oxygen at $-15\,^\circ$C resulted in the formation of 4,4′-bis(dimethylamino)-1,1′-binaphthyl (**162**) (Scheme 26). When the reaction was conducted with heating, the sole reaction product was perylene **163**, rather than the expected perylene sponge[106]. Apparently, the elimination of NMe_2 groups already occurs at the stage of formation of the radical anion **36⁻•**. An additional example of such conversion can be found in Reference 57.
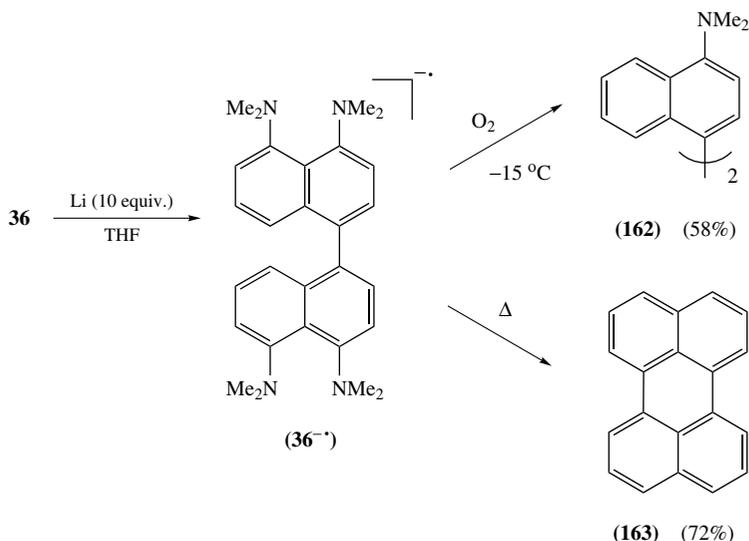
SCHEME 26

B. Reactions at the Aromatic Rings

Owing to the effective conjugation of the *peri*-dimethylamino groups with the aromatic system (Section III.A.1.c), the naphthalene sponges reveal quite a considerable π-excessive character with the negative π-charge being localized at the *ortho*- and *para*-positions. Therefore, it is not surprising that the most typical reactions of the naphthalene sponges are electrophilic substitutions and oxidative transformations. It is probable that some reactions, such as chlorination with *N*-chlorobenzotriazole, occur through a radical mechanism, but convincing evidence for this is absent.

1. Oxidation and reduction

As mentioned above, a number of proton sponge oxidative conversions are connected with the formation of radical cations and dications, as well as with the elimination of hydride ion from the methyl group (Sections III.J and IV.A.4). Additionally, we note that oxidation of compound **1** with thallium triacetate or lead tetraacetate in CH_2Cl_2 at low temperature[106] or, better, with iodine in boiling acetonitrile[187] gives the 1,1′-binaphthyl proton sponge **36** in moderate to good yields. The latter is also formed as a by-product in the nitration of proton sponge **1** (Section IV.B.2).

There is little information on reduction of the aromatic system in proton sponges (Section III.J), whereas a lot of data exist concerning functional group reduction (Sections IV.A.5 and IV.C).

2. Nitration

In the nitration reactions, all the main properties of the proton sponges, such as the high basicity, the facile oxidation and the effective conjugation of the NMe_2 groups and the ring system, are clearly displayed. The nitration of compounds **1** and **40** has been studied in most detail. The nitrating agents used were nitric acid in concentrated H_2SO_4 or acetic acid, nitrogen dioxide, tetranitromethane and nitronium tetrafluoroborate. Let us start with the data on naphthalene proton sponge **1**.

The nitration of **1** with one equivalent of HNO_3 in H_2SO_4 gave two products: the 4-nitro derivative **108** and the binaphthyl proton sponge **36** in 70 and 10% yield, respectively[164, 187]. The reaction proceeds even at $-20\,°C$ and is completed within 5 min. These conditions are essentially milder than those for the naphthalene nitration. This is somewhat astonishing, since in such an acidic medium the diamine **1** seems to exist entirely as cation **1•H+**, which should be more inert towards electrophiles than the naphthalene itself. One of the reasonable explanations of this discrepancy is that the reaction proceeds via very small equilibrium amounts of the non-protonated **1** or the non-chelated cation **1•H+-c**. Any of them, under the action of the nitronium cation, is oxidized to the radical cation **1+•**, which either dimerises or reacts with $•NO_2$ to give the reaction products **36** and **108** (Scheme 27). There are several indirect pieces of evidence in favour of this. One of them
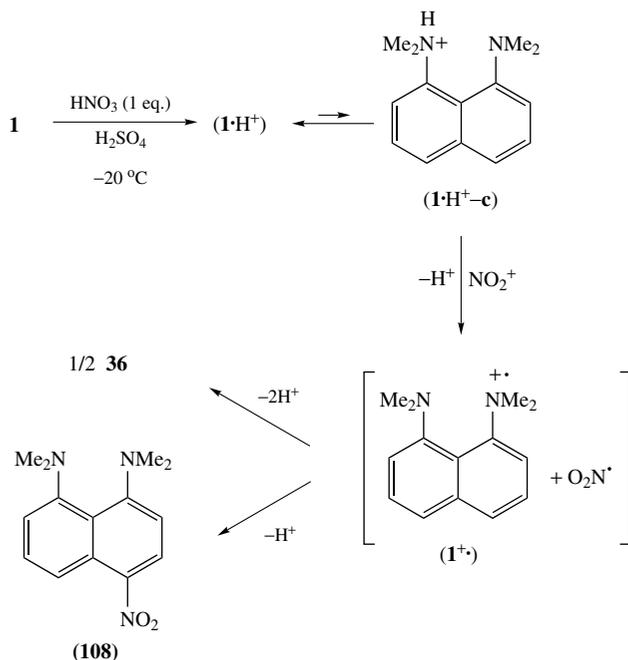
SCHEME 27

is the almost complete inertness of the highly basic 2,7-disubstituted proton sponges **44** and **65** towards electrophiles. Obviously, in the presence of an acid, these compounds are fully protonated to give the chelated cations. On the other hand, in the form of neutral bases, they are still non-reactive owing to the orthogonality of the ring plane and the NMe₂ groups (Section III.A.1.c).

In an attempt to introduce the second nitro group into compound **108**, even using one equivalent of HNO₃ in H₂SO₄, the tetranitro derivative **165** was isolated as the only product (Scheme 28)[164]. This implies that every subsequent nitration step under these conditions proceeds more easily than the previous one since the basicity decreases on increasing the number of NO₂ groups. Consequently, the concentration of the more reactive non-protonated base is gradually increased. Notably, this phenomenon is also observed on nitration of unsubstituted compound **1** with one equivalent of HNO₃ in acetic acid[164].
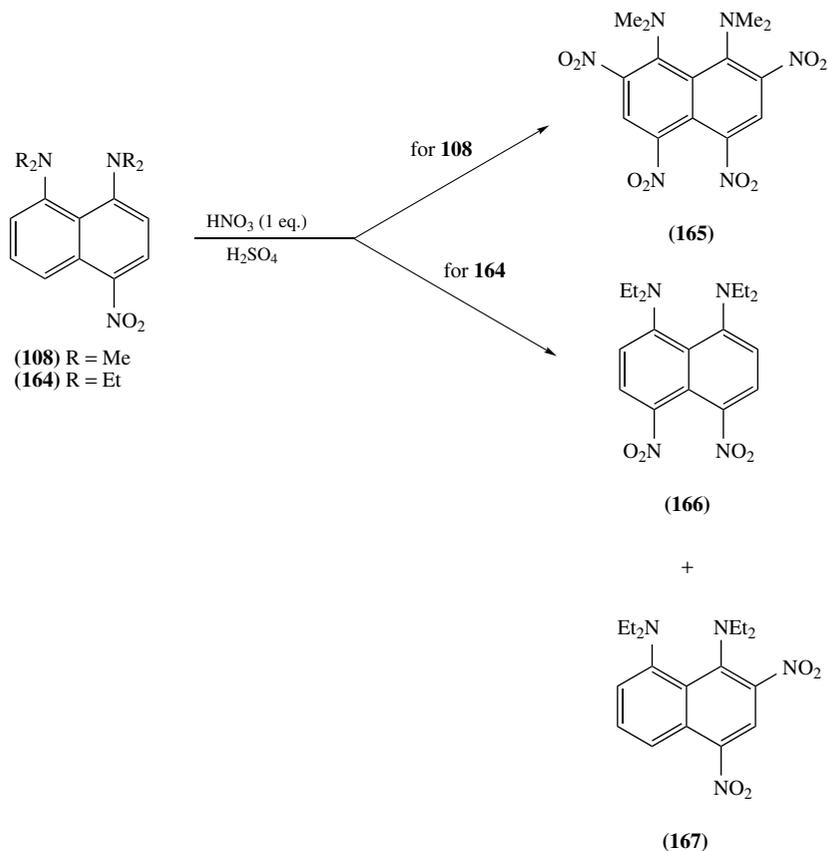
SCHEME 28

The naphthalene ring activation with the NMe₂ groups is so high that the nitration of 1,8-bis(dimethylamino)-3,6-dinitronaphthalene (**43**) proceeds further, enabling one to isolate the hexanitro proton sponge **168** in a good yield (equation 14)[37]. The second

and following nitrations of the proton sponges are unlikely to proceed through a radical cation pathway; most likely, they proceed by the conventional addition−elimination S_E2Ar mechanism.

$$(14)$$

(43)　　　　　　　　　　　　　　　　　　　　(168)
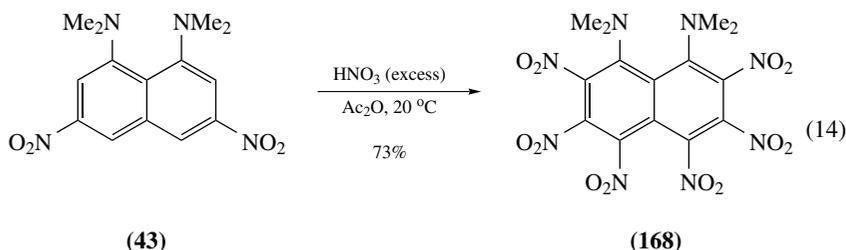
In contrast to the 4-nitro derivative **108**, its tetraethyl counterpart **164** could be mono-nitrated to form a mixture of compounds **166** and **167** (Scheme 28)[164]. Probably, in this case, owing to higher basicity of the tetraethyl sponge (Table 16), both dinitro derivatives in sulfuric acid are present mainly in the form of cations and their further nitration occurs relatively slowly. The nitration of 4-bromo-1,8-bis(dimethylamino)- (**117**)[52] and 1,4,5-tris(dimethylamino)naphthalenes (**64**)[44] in H_2SO_4 led to compounds **169**, **170** and **171**.

(169)　　　　　　　　　(170)　　　　　　　　　(171)
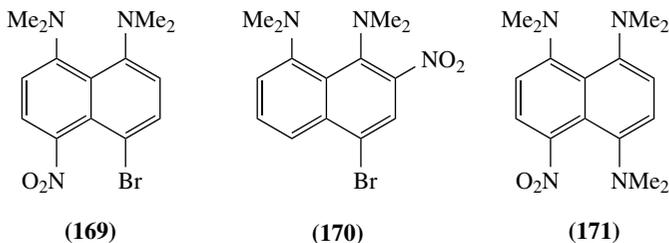
Nitration of compound **1** with nitrogen dioxide or tetranitromethane in $CHCl_3$ and especially in CCl_4 occurs with low selectivity and with strong tarring[47,187]. Nevertheless, thus obtained complex mixtures of all possible *ortho*(*para*)-mono-, di-, tri- and tetrani-tro derivatives can be separated chromatographically. The nitration apparently proceeds through a radical ion mechanism, since some of the binaphthyl proton sponge **36** could also be detected in the reaction mixtures.

A distinct feature of the acenaphthene proton sponge **40** is that the *para*-positions are already occupied and the nitration may proceed at either the sterically hindered *ortho*-positions or the poorly activated *meta*-positions. As noted above (Schemes 22 and 23), the *ortho*-nitration is complicated by demethylation of one of the NMe$_2$ groups. Still, selective mono-*ortho*-nitration without demethylation under comparatively mild condi-tions (tetranitromethane/CCl_4/0 °C) has been reported to proceed in a good yield[47]. Even more important is the possibility to perform a regioselective *meta*-nitration of compound **40** in sulfuric acid to the derivatives **172**−**174** (Scheme 29). Obviously, the reaction occurs in this case via the cation **40**•H$^+$ [37].

3. Halogenation

Treatment of the proton sponge **1** with one equivalent of bromine in AcOH or CCl_4 has been shown to lead to a crimson-coloured complex of unknown structure, which
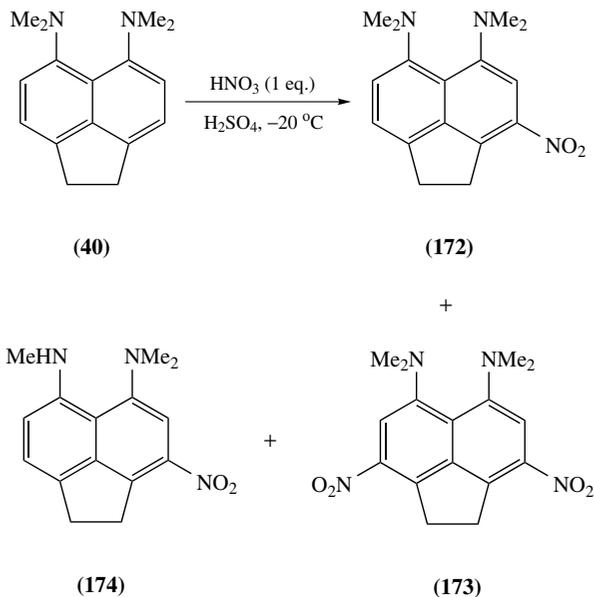
SCHEME 29

on addition of conc. H_2SO_4 is transformed into the 4-bromide **117** in good yield[188]. A simpler way to **117** is monobromination of **1** with the NBS/THF system[163]. 4-Chloro-1,8-bis(dimethylamino)naphthalene can be prepared in nearly quantitative yield by the action of sodium nitrite in hydrochloric acid on **1**[187]. Apparently, the process is realized through interaction of the radical cation $1^{+\bullet}$ with chloride ion. In hydrobromic acid, the bromide **117** could also be obtained, though in *ca* 20% yield. The use of the $NaNO_2$/HF system gives rise to nitration or dimerisation of the radical cation $1^{+\bullet}$ [187].

From the preparative point of view, most valuable are the chlorination and bromination of proton sponge **1** at positions 2 and 7 with, respectively, *N*-chlorobenzotriazole (CBT)[189] and *N*-bromosuccinimide[98] (Scheme 30). The method is useful for the preparation of *ortho*-dihalides **101**, **102** and monochloride **175**. The monobromide **115**, even using one equivalent of NBS, is rarely formed free of significant amounts of the disubstituted **102**, which are hard to separate. Consequently, an alternative way to **115** is monolithiation of the corresponding dibromide with butyllithium followed by quenching the reaction mixture with water.
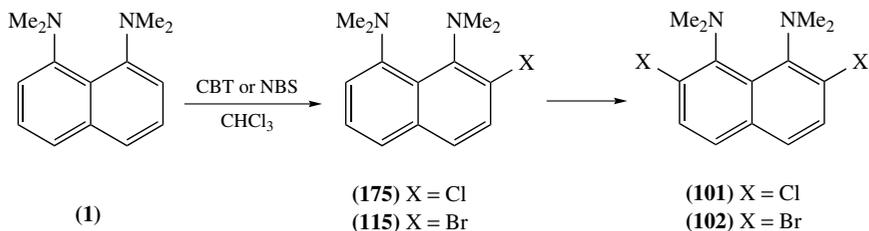
SCHEME 30

The *ortho*-halogenation probably proceeds via participation of the neutral proton sponge, rather than its cation. According to calculations, the π-electron density at positions 2 and 7 of **1** is greater than at the *para*- and *meta*-positions. Again, the radical mechanism of substitution cannot be ruled out[190].

With one equivalent of NBS, the 4-bromide **117** gives a mixture of 2,4- and 2,5-dibromo derivatives in a 54:46 ratio. Further bromination of this mixture with 1 equivalent of NBS gives 2,4,7-tribromo-1,8-bis(dimethylamino)naphthalene as the only product. An attempt to convert it to a tetrabromo derivative by introducing the fourth bromine atom at position 5 was unsuccessful[52].

4. Formylation and acylation

Compound **1** easily undergoes a Vilsmeier formylation[188, 191] and a Friedel–Crafts acylation[114]. The products of the first reaction, depending on the conditions, are the 4-carboxaldehyde **124** or the dialdehydes **109** and **110**. The acylation occurs exclusively at positions 4 and 5 to form the corresponding mono- or diketones. Both reactions have been reviewed[29]. Since then, new data were obtained for the Friedel–Crafts acylation of **1** with oxalyl chloride which gave 1,1′-dinaphthyl ketone **176** in a good yield[163].

(176)
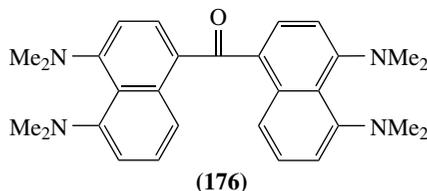
More interesting results have been obtained for the trifluoroacetylation of **1**. The reaction with trifluoroacetic anhydride depends dramatically on the solvent, the duration of the experiment and the molar ratio **1**:$(CF_3CO)_2O$. In CH_2Cl_2 at $-30\,°C$, at a 1:0.6 ratio, 1,8-bis(dimethylamino)-4-trifluoroacetylnaphthalene (**126**) was isolated as the sole product in 48% yield[114]. However, on increasing the amount of $(CF_3CO)_2O$ to 1.5 equivalents and keeping the reaction mixture at room temperature for 48 hours, the main product, isolated in 53% yield, is 7,14-epoxidinaphtho[1,8-*a,b*;1′,8′-*e,f*]cyclooctane (**118**), while only traces of the ketone **126** were found. Under similar conditions, but in 1,2-dichloroethane as solvent, the yield of **126** reaches 57% and the 2,4-diketone **177** and the *trans*- **178a** and *cis*-isomers **178b** of 1,3-dihydroxy-6,7-bis(dimethylamino)-1,3-bis(trifluoromethyl)-1*H*,3*H*-naphtho[1,8-*c,d*]pyranes are also formed in small amounts (Scheme 31)[105].

There is some evidence that the diols **178** are the hydration products of the intermediate and highly electrophilic 1,8-bis(dimethylamino)-4,5-bis(trifluoroacetyl)naphthalene[105]. The double proton sponge **118** is apparently formed by a cyclodimerisation of monoketone **126** catalysed by trifluoroacetic anhydride (Scheme 32). Obviously, this nice reaction, previously unknown in the naphthalene series, is a consequence of high *C*-nucleophilicity of the proton sponge.

5. Hydroxymethylation and Mannich reaction

Proton sponges **1** and **39** are hydroxymethylated by paraform in polyphosphoric acid at position 4 to the alcohols **179a** and **179b** (Scheme 33)[191, 192]. At higher temperature, **1** is converted in a good yield into naphthopyrane **181**, evidently via dehydration of the consecutively formed dialcohol **180**. Alcohols **179**[191], as well as 2(7)-hydroxymethyl
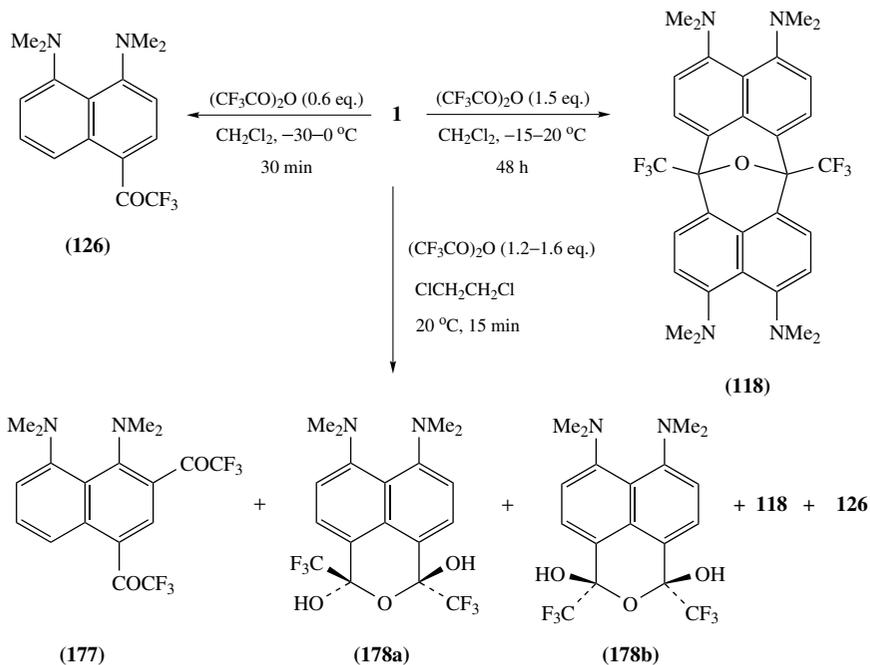
SCHEME 31
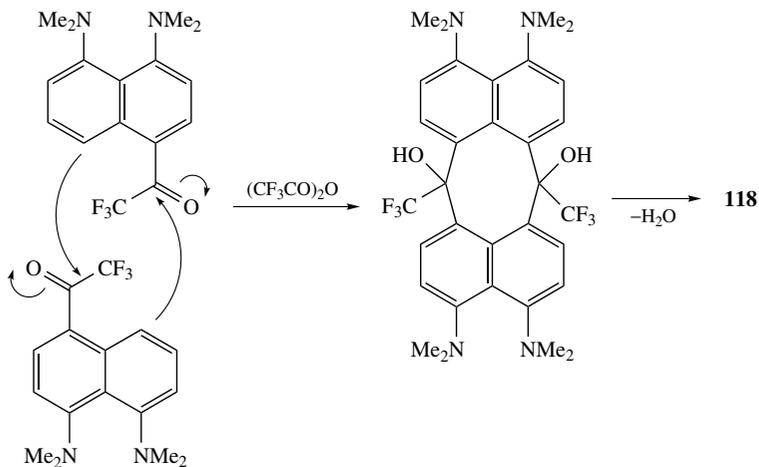
SCHEME 32
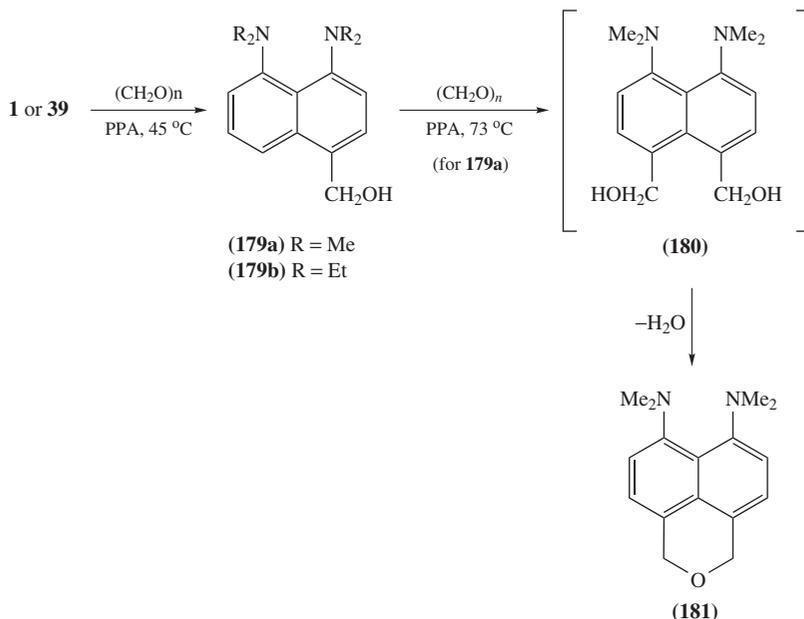
SCHEME 33

derivatives of type **112**[89], can be prepared by reduction of corresponding aldehydes or ethoxycarbonyl derivatives with LiAlH$_4$.

On treatment of **1** with equimolar quantities of formaldehyde and piperidine, morpholine or diethylamine in acetic acid, the Mannich bases **182a–c** were synthesized in good yield. Their analogue, **182d**, was obtained in the reaction of **1** with one equivalent of bis(dimethylamino)methane in AcOH or with N,N-dimethylmethyleneimmonium chloride in dry acetonitrile (yields are 79 and 47%, respectively)[193]. The introduction of the second dialkylaminomethyl group into compounds **182** is discussed in Section IV.D.
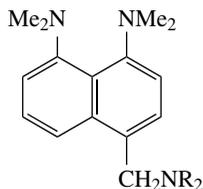
(**182a**) NR$_2$ = NEt$_2$
(**182b**) NR$_2$ = piperidino
(**182c**) NR$_2$ = morpholino
(**182d**) NR$_2$ = NMe$_2$

6. Reactions with other carbon electrophiles

As *C*-nucleophile, proton sponge **1** is easily added to coordinated[194] and perfluorinated[195] alkenes to produce compounds of type **183** and **184** (Scheme 34). Other reactions of this type include arylation and hetarylation with compounds containing active halogen, e.g. picryl chloride[196] or trifluoro-1,3,5-triazine[197], giving 4(5)-aryl- and hetaryl derivatives **185** and **186** (Scheme 35).
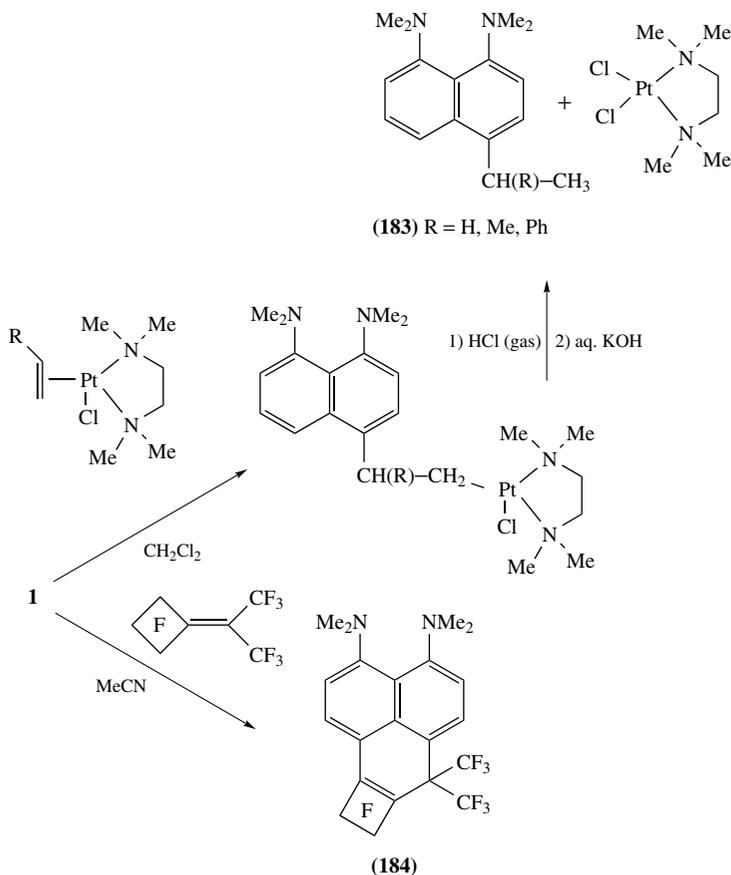
SCHEME 34

The reaction of the proton sponge with electron-deficient azomethines[198] or 4,6-dinitro derivatives of benzofuroxan and benzofurazan[196] results in the formation of adducts **187** (Scheme 35) and **188**. It has been recently reported that alkylated C_{60} chlorides 1,4-$RC_{60}Cl$ undergo nucleophilic substitution with **1** affording fullerene proton sponges **189** in a good yield[199]. An $S_{RN}1$ mechanism, initiated by a single-electron transfer from **1** to the C_{60} chlorides, was proposed on the basis of the enhanced rates compared with the rate of S_N1 reaction for anisole. For more details on inter- or intramolecular electron transfer in mixtures of **1** and C_{60} or in adducts **189**, see Reference 200. Also, in attempting to use the proton sponge as a deprotonating agent, the formation of zwitterionic adduct

(185)

1

(186)

ArSO$_2$N=CHCCl$_3$ | AlCl$_3$

(187) Ar = Ph, 4-MeC$_6$H$_4$, 4-ClC$_6$H$_4$

SCHEME 35

(188) X = N, N→O

(189) R = CH$_2$Cl, CHCl$_2$, CCl$_3$
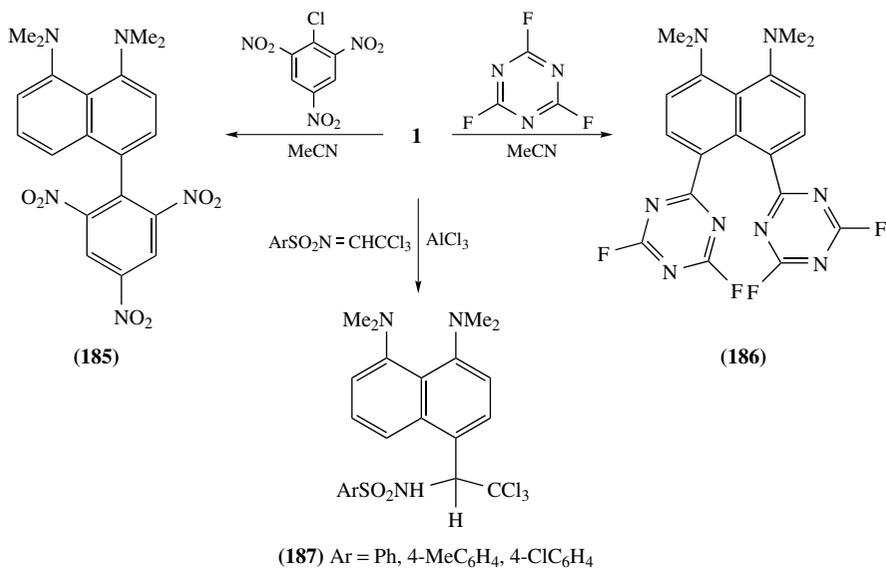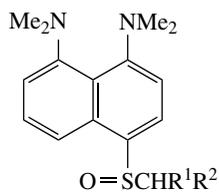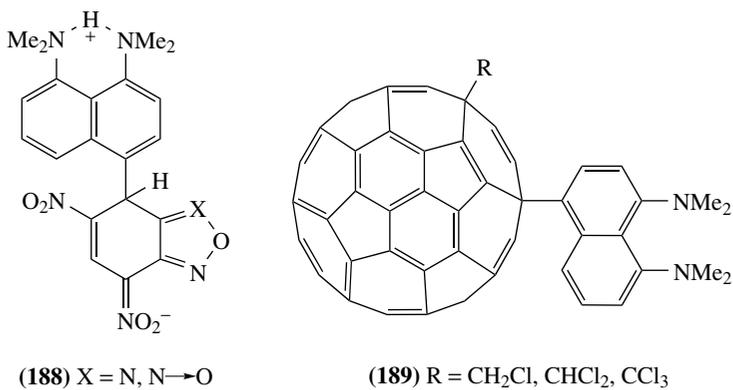
(190) R^1 = H, Cl; R^2 = H, Ph

with a $C(sp^2)-C(sp^3)$ bond linking position 4 of **1** and a dicarbacobaltaborane cage is observed[201].

7. Miscellaneous reactions

An example of proton sponge reaction with sulfur electrophiles is known. The interaction of compound **1** with alkanesulfenyl chlorides led to a series of 4-alkylsulfenyl derivatives **190**[202]. The proton sponge **1** can participate in an azo-coupling reaction, also proceeding at position 4[56].

8. Reactivity features of double and 2,7-disubstituted naphthalene proton sponges

In the course of functionalization reactions, performed recently with the double proton sponges **35** and **118**, and *ortho*-disubstituted derivatives **44** and **65**, some properties worthy of consideration have been revealed.

Trifluoroacetylation of tetraamine **118** is the only definite example of electrophilic substitution on a double proton sponges[203]. The products of this reaction were di- **191** and tetraketones **192** isolated with 5 and 8% yields, respectively (equation 15).

(191) R = H
(192) R = COCF$_3$
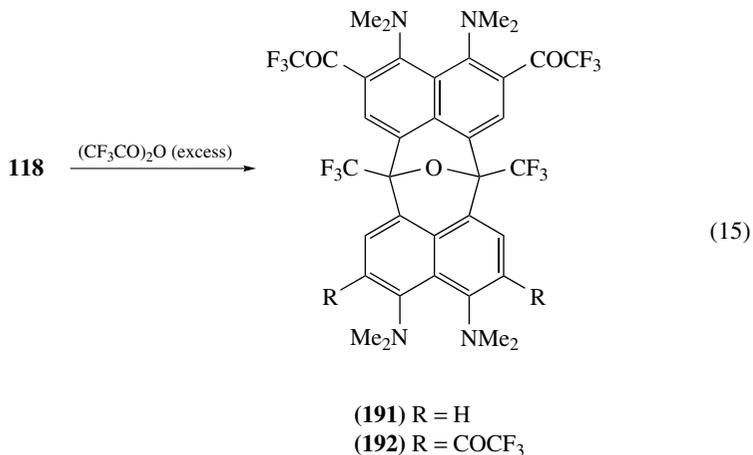
The formation of compounds with only an even number of CF$_3$CO groups was explained as follows. After introducing the first substituent, the two halves of the molecule become sharply distinct in their basicity. The acid, produced in the reaction, would protonate the still unsubstituted fragment and make it unreactive, whereas due to its decreased basicity the monosubstituted fragment would take part in the reaction in its non-protonated form. Consequently, the second substituent will enter into the substituted naphthalene ring. Further substitution is probably governed by similar factors, reminiscent in this respect of the tetranitration of proton sponge **1** (cf. Scheme 28)[203].

Although the trend of protonation of the double proton sponge **35** resembles that of compound **118** (Section III.B.2, Scheme 10), its low oxidative potential and essentially higher basicity (Tables 13 and 18) strongly hinder the substitution in both acidic and neutral media. Treatment of compound **35** with nitrating, nitrosating and halogenating agents as well as with diazonium salts or trichloroethyl azodicarboxylate (E$^+$) leaves the substrate

either unchanged (in the presence of acids) or converts it quantitatively into the dihydroperimidinium salt **193** (Section IV.A.4). The latter is unreactive towards electrophiles and can be reduced again to proton sponge **35** with NaBH$_4$ (equation 16)[44, 64, 137].

$$\text{(35)} \qquad\qquad\qquad \text{(193)} \tag{16}$$
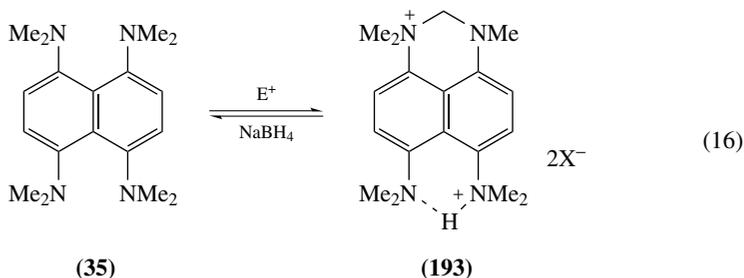
2,7-Disubstituted proton sponges, due to increased basicity coupled with poor conjugation of the NMe$_2$ groups with the ring π-system (Section III.A.1.c), are also remarkably inert towards electrophiles. For example, compound **65**, independent of the medium acidity, stays intact on treatment with nitrating agents or diazonium salts[56]. The only exception is, in part, 2,7-dimethoxynaphthalene **44**, giving the nitro derivatives **194** and **195** in moderate yield in excess of HNO$_3$/H$_2$SO$_4$ mixture[56]. Thus, the *ortho*-disubstituted proton sponges **44** and **65** (and, probably, **45**–**48**, **63**, **66**–**68**) possess weak *C*-nucleophilicity, which in combination with increased basicity makes them very prominent reagents for organic synthesis (Section V).

(194)   **(195)**
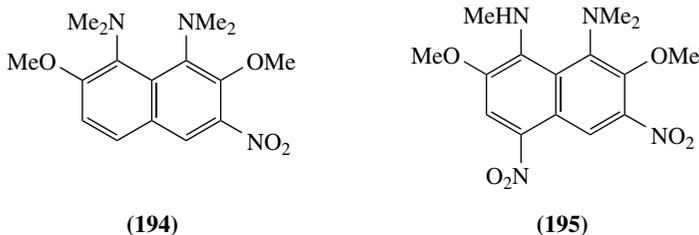
C. Reactions of Functional Groups

1. Carbonyl functionalities

A large number of proton sponge **1** derivatives (azomethines, hydrazones, oxime, nitrile) were synthesized from the 4-aldehyde **124**[188]. The latter was also converted by the Wittig reaction into vinyl derivatives **121**[113] and **196**[188]. Additional alkene derivatives such as **122** were synthesized by condensation of the aldehyde **124** with CH-acids[114]. The conversion of aldehydes[89, 163, 191], ketones[163, 204] and ethoxycarbonyl derivatives[89, 204] of proton sponge to the corresponding alcohols, e.g. **106**, **112** and **197**, during the action of lithium aluminium hydride or organometallic reagents has also been described.

An interesting reactivity is displayed by *peri*-dialdehyde **110**. On boiling in water solution it undergoes an intramolecular Cannizzaro reaction to form the naphtho[1,8-*c,d*]pyranone derivative **198**. It is noteworthy that the reaction does not require an addition of alkali, probably because the necessary basicity of the medium is provided by the substrate itself[188].

Me$_2$N NMe$_2$ Me$_2$N NMe$_2$ Me$_2$N NMe$_2$

CH=CHCO$_2$Et CHOH

(196) **(197)** **(198)**

Me$_2$N NMe$_2$ Me$_2$N NMe$_2$

O$_2$N NO$_2$

CO$_2^-$ K$^+$

(199) **(200)**
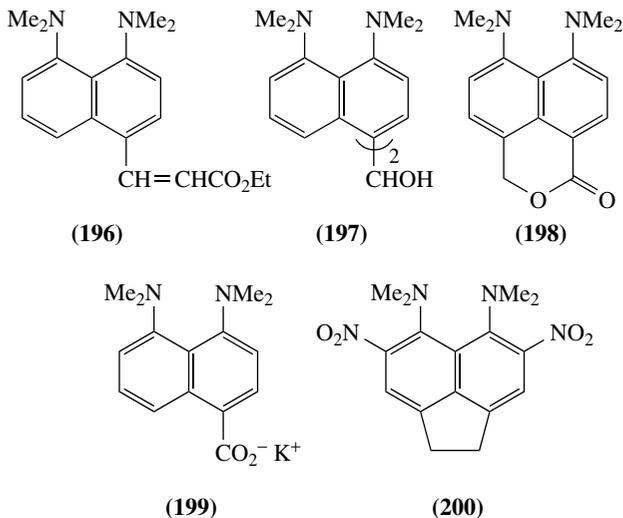
1,8-Bis(dimethylamino)-4-trifluoroacetylnaphthalene (**126**) on reflux in a H$_2$O–EtOH basic solution is transformed almost quantitatively to a carboxylic acid, isolated as the potassium salt **199**[114].

2. Nitro and amino groups

The reduction of *para*- **51**, **108**, **171**[44, 45, 54, 57] and *ortho*-nitro derivatives **116** and **200**[55, 56] of proton sponges to the corresponding amines was reported. These are air-sensitive compounds, the *ortho*-amines being somewhat more stable than their *para*-isomers. The amino groups, especially in the case of *para*-derivatives, are readily acylated[55, 57], methylated[34, 44, 45, 55–57], diazotized[57] and produce Schiff bases on action with aldehydes[57]. The investigation of azomethines of type **201** prepared from amine **113** and specially chosen substituted salicylic aldehydes has confirmed high electron-donating and proton-accepting properties of the 4,5-bis(dimethylamino)-1-naphthyl group assisting the OH-proton to shift to the imine nitrogen atom or even to jump to the proton sponge fragment[205].

X OH NMe$_2$

N NMe$_2$

Y

(201) X = H, NO$_2$; Y = Br, NO$_2$
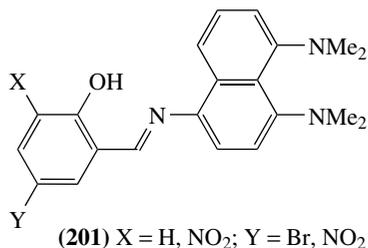
3. Halogeno functions

Proton sponge halides play an important role in organometallic synthesis of many valuable derivatives of this series. This can be illustrated by Scheme 36, showing the

preparation of a number of 2,7-disubstituted 1,8-bis(dimethylamino)naphthalenes by treatment of the corresponding organometallic compounds **202a** and **202b** with diverse electrophiles. The yields of proton sponges **48**, **103**, **104** and **203**–**205** are high, but those for **105** and **106** are low (10–15%) for steric reasons. Notably, in two instances, when iodine and diethyl carbonate were used as electrophiles, up to 20% of monosubstituted derivatives **206** and **207** were also isolated[76]. A similar approach was employed for the preparation of 4-R-1,8-bis(dimethylamino)naphthalenes (R = I, SMe, CO$_2$Et, SiMe$_3$, CHO) from the 4-bromide **117**[163, 188].

Me$_2$N   NMe$_2$

M   M

102 $\xrightarrow[\text{or Mg/Et}_2\text{O}]{n\text{-BuLi/Et}_2\text{O}}$

(202a) M = Li
(202b) M = MgBr

Electrophile

Me$_2$N   NMe$_2$ Me$_2$N   NMe$_2$

E   E   +   E

(48) E = Me   **(206)** E = I
(103) E = I   **(207)** E = CO$_2$Et
(104) E = SMe
(105) E = SiMe$_3$
(106) E = C(OH)Ph$_2$
(203) E = CO$_2$Et
(204) E = CHO
(205) E = D
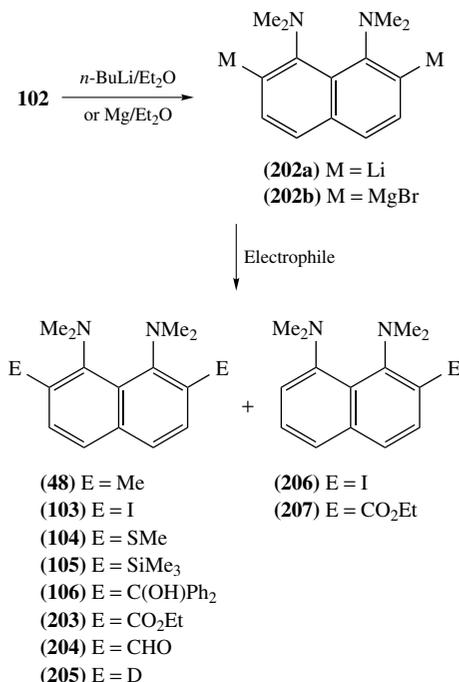
SCHEME 36

As already emphasized (Section II.B.2), the fluorine atoms in fluorinated polykis (dialkylamino)naphthalenes can be reductively eliminated by treatment with LiAlH$_4$.

4. Alkene functions

When 1,8-bis(dimethylamino)-4-vinylnaphthalene (**121**) is heated with 3,6-diphenyl-s-tetrazine (DFT), a [4 + 2]-cycloaddition reaction with reverse electron demands takes place to give the 1,4-dihydropyridazine derivative **208** (Scheme 37). The latter could be oxidized with chloranil or with excess of DFT to pyridazine **209**[118]. A similar reaction with acenaphthylene proton sponge **107** gives directly the annelated pyridazine **139**, since the intermediate dihydropyridazine is readily oxidized in air. It was established that the reactivity ratio of compounds **107**, **121**, 5-dimethylaminoacenaphthylene and acenaphthylene in the reaction with DFT is equal to 32:17:14:1, respectively. These data are in

(121)

(208)

(209)
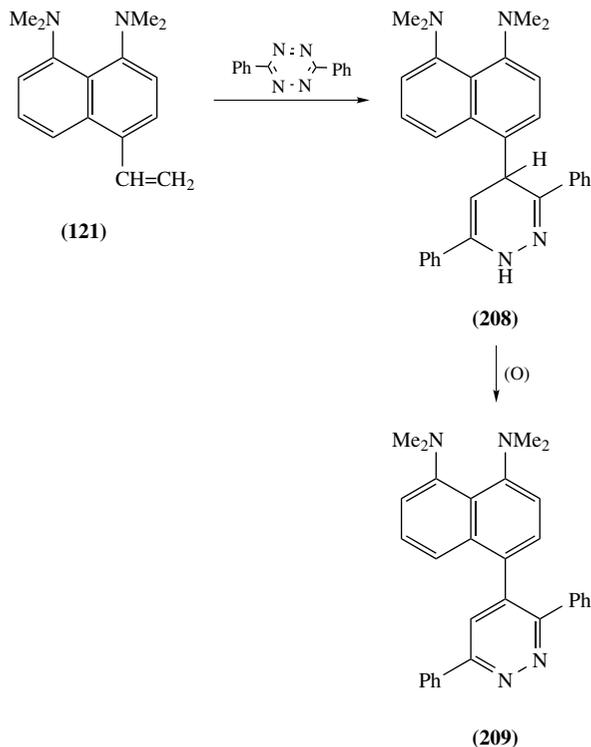
SCHEME 37

accord with activation of the alkene bond by the electron-releasing effect of the NMe$_2$ groups[118].

For other information on this subject, including hydrogenation and polymerization of the alkene function, see References 38 and 113.

D. Transformations of Naphthylmethyl Carbocations Derived from Naphthalene Proton Sponges

One of the interesting properties of proton sponges consists in the unusual reactivity of the corresponding 1-naphthylmethyl carbocations and in their easy formation from different precursors. Thus, treatment of the 4-hydroxymethyl derivative **179a** with concentrated HCl furnishes spiro compound **214** in a good yield[192, 206]. It was established that the process proceeds according to Scheme 38 and begins with a fast formation of cation **179a•H$^+$**, followed by a slow conversion of the hydroxyl into chlorine or other functionality, depending on the acid used. The cation **210•H$^+$** thus formed stays unchangeable in a strongly acidic medium for a long time. However, at basification near pH = 0, a sharp change in colour from pale yellow to orange-red occurs. Probably, at this stage cation **210•H$^+$** is deprotonated and the neutral base **210** undergoes a rapid heterolysis of the C−Cl bond leading to the formation of 4,5-bis(dimethyalmino)-1-naphthylmethyl carbocation **211**. Effective resonance stabilization of the latter is the driving force of this process. Owing to the conjugation of the carbenium centre and the NMe$_2$ groups (cf.
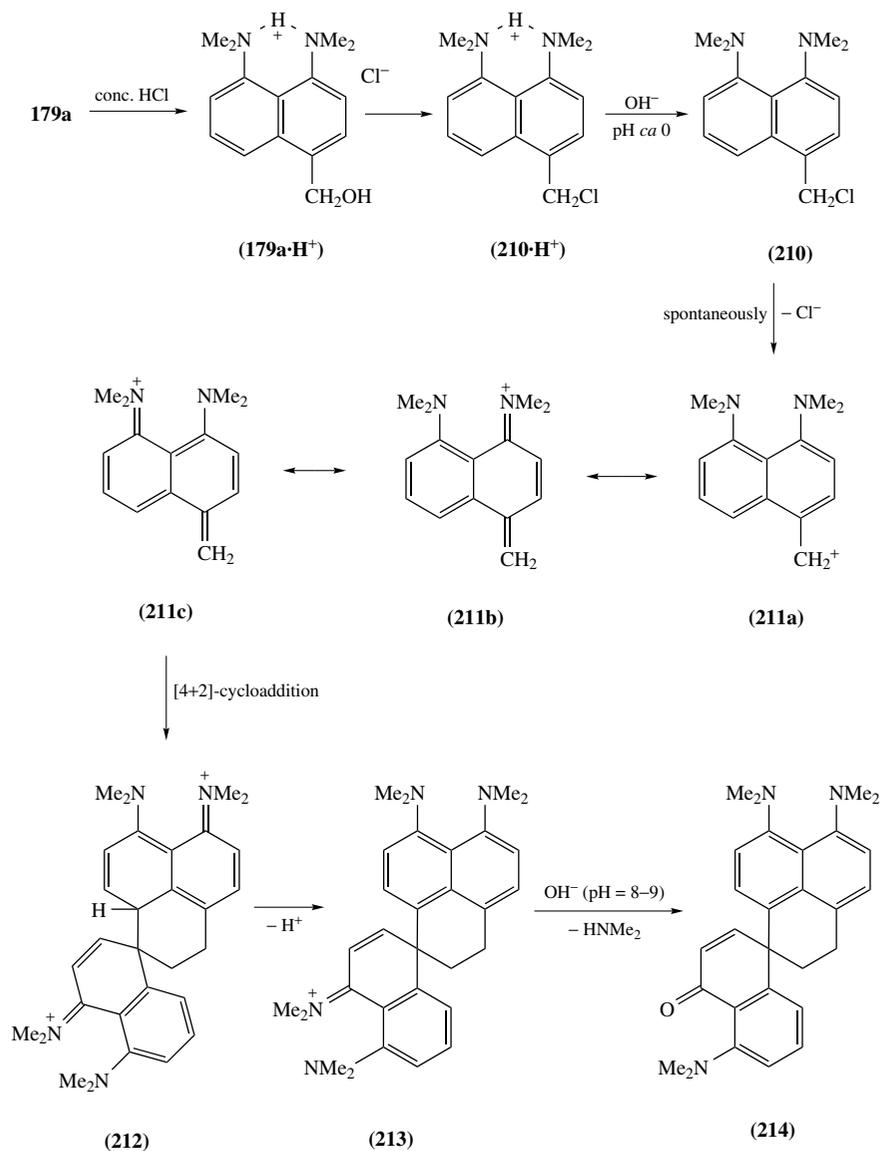
SCHEME 38

canonical structures **211b** and **211c**) this cation can be considered as an *exo-endo*-1,3-diene. Compound **211** further undergoes immediate [4 + 2]-cyclodimerisation to **212**, in which one molecule of the cation displays the properties of 1,3-diene while another acts as dienophile. The primary cyclodimerisation product is the orange-coloured immonium salt **213**. Its basic hydrolysis gives the yellow spiro compound **214**. A similar product has been derived from tetraethyl sponge alcohol **179b**[191].

The type of conversions of cation **211** is changed dramatically on treating the alcohol
179a with Lewis acids (Al$_2$O$_3$, SiO$_2$ or TiO$_2$)[191, 207]. In this case, the main reaction products were the binaphthylmethane proton sponge **37** (10%), the 4-aldehyde **124** (19%), the
4-dimethylaminomethyl-1,8-bis(dimethylamino)naphthalene **182d** (22%) and the symmetrical spiro compound **215** (23%), an isomer to **214** (the yields are given for Al$_2$O$_3$; for
other oxides they vary somewhat) (Scheme 39). The formation of aldehyde **124** can be
ascribed to the well-known ability of carbenium ions to oxidize alcohols to aldehydes via
elimination of a hydride ion. Formation of the binaphthylmethane derivative **37** seems to
be due to the *ipso*-substitution of the CH$_2$OH group in the precursor alcohol by carbocation **211**. An attack by the carbocation at the unsubstituted *peri*-position 5 in **179a** should
lead to the formation of the binaphthylmethane alcohol **216**, which further generates the
carbocation **217**. Subsequent intramolecular *ipso*-attack by the carbenium centre on the
other residue of the proton sponge at position 4 gives ultimately the spiro product **215** via
the immonium salt **218**. The dimethylamine liberated in the hydrolysis of the immonium
group reacts with the carbocation **211** to give the Mannich base **182d**.

Thus, the formation of symmetrical (caused by perpendicular arrangement of the naphthalene and cyclohexadienone ring systems) cyclohexadienone **215** proceeds not as a
[4 + 2]-cycloaddition of two carbocation species but rather as a two-step electrophilic
substitution, the first stage of which is intermolecular and the second intramolecular. The
reasons for the different direction of the cyclodimerisation reactions of carbocation **211** in
protic media and in the presence of Lewis catalysts have been discussed elsewhere[29, 207].

SCHEME 39

Possible mechanism for formation of **215**:

(216) (217) (218)

(219)

SCHEME 39. (*continued*)

An intriguing question is why, in cation **217**, the second possible path of intramolecular attack to give dinaphthocyclooctane **219** is not realized? One can suggest that this is caused by the special geometry of this cation, in which both naphthalene rings are strongly rotated in relation to each other. This is indirectly confirmed by the X-ray data of the binaphthylmethane proton sponge **37**, showing an angle of 85.5° between the two naphthalene planes[208]. Thus, the only instance of a cyclodimerisation reaction leading to dinaphthocyclooctanes remains the formation of compound **118** (Schemes 31 and 32).

Proton-sponge-based secondary and tertiary alcohols behave differently towards acids. For instance, 4-α-hydroxyethyl derivatives **220a–c** are transformed in good yields to the corresponding alkenes **121** and **222a** and **222b** as a result of a fast E1-elimination from the intermediary formed carbocations **221a–c** (Scheme 40)[204]. The alcohol **223a** having

(220a) R = H
(220b) R = Me
(220c) R = Ph

(221a) R = H
(221b) R = Me
(221c) R = Ph

(121) R = H
(222a) R = Me
(222b) R = Ph

SCHEME 40

an α-trifluoromethyl group remains unchanged by reaction with protic or Lewis acids. Apparently, the corresponding carbocation **224a** is not formed due to the destabilization caused by the electron-withdrawing CF$_3$ group. In contrast, the cation **224b**, generated from the α-hydroxybenzyl derivative **223b**, cyclodimerises by 'head-to-tail' reaction to the symmetrical spiro compound **225** in high yield (Scheme 41)[206, 209]. The structure **225** has been confirmed by X-ray measurements[209].

The tertiary alcohol **226** demonstrates a highly specific reactivity[204]. On heating with concentrated HCl, it produces the benzo[*a*]fluorene derivative **229** as the sole product in 65% yield. It was proposed that a key stage of this complex conversion is the Friedel–Crafts intramolecular arylation of cation **227** (**227a** ↔ **227b**) (Scheme 42). Apparently, the reaction proceeds through the enamine intermediate **228** with hydrolytic displacement of the NMe$_2$ group for a carbonyl (presumably via the enol). Interestingly, above 135 °C ketone **229** isomerizes to the IHB stabilized phenol **230** via two 1,3-sigmatropic shifts[204].

The tendency to generate the resonance-stabilized 1-naphthylmethyl carbocations in the proton sponge series is so pronounced that it sometimes modifies well-known reactions. The Mannich reaction can serve as a typical example. As indicated above (Section IV.B.5), the proton sponge **1** easily forms monosubstituted Mannich bases **182a**–**d**. However, on

(223a) R = CF$_3$
(223b) R = Ph

(224a) R = CF$_3$
(224b) R = Ph

(R = Ph)

(225)
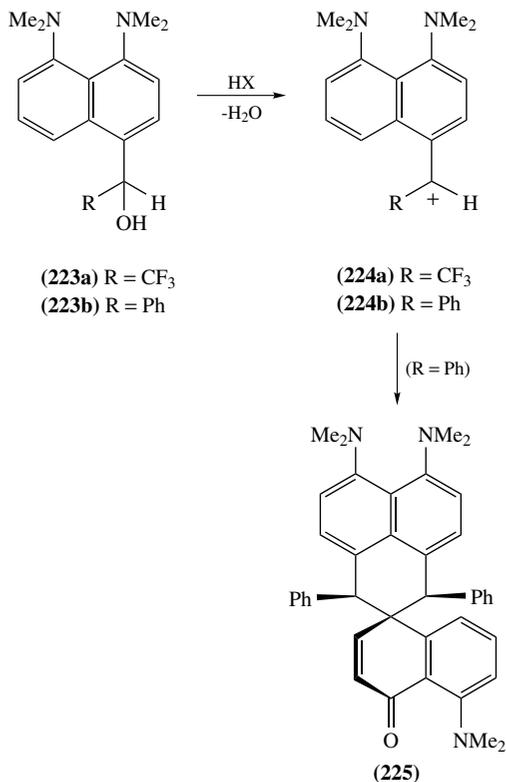
SCHEME 41

attempting to prepare the bis-Mannich bases **231** by aminomethylation of compounds **182** with Eschenmoser's reagent, the piperidinium salts **235a**, **235b** and **236** were unexpectedly obtained, depending on the structure of the dialkylaminomethyl group (Scheme 43)[193]. Presumably, the transient bis-Mannich bases are protonated *in situ* on the CH$_2$NMe$_2$ (for **231b–d**) or CH$_2$NEt$_2$ (for **231a**) group with spontaneous loss of dialkylamine molecule from the ammonium salts **232a–d**. A successive intramolecular nucleophilic addition in carbocations **233b**, **233c** and **234** affords the corresponding piperidinium salts.

It is noteworthy that under certain conditions the mono-Mannich bases are also capable of generating carbocations. Thus on heating compound **182b** with methyl iodide, it is converted into the spiro compound **215**. The possible mechanism involves a spontaneous elimination of *N*-methylpiperidine from the intermediate ammonium salts, e.g. **237**, and formation of carbocations **211** and **217** as shown in Scheme 44 (cf. Scheme 39)[193]. Due to the anhydrous media, the immonium salt **238** can be isolated before its hydrolysis.

It is instructive to compare the behaviour of the proton-sponge-based naphthylmethyl carbocations with analogues stabilized by other electron-donating groups, such as methoxyls. Thus on treatment with hydrochloric acid, 4,5-dimethoxynaphthyl-1-methanol (**239**) undergoes complete oligomerization, possibly into a mixture of oligomers with the general structure **241**. However, in the presence of Al$_2$O$_3$, the alcohol **239** forms
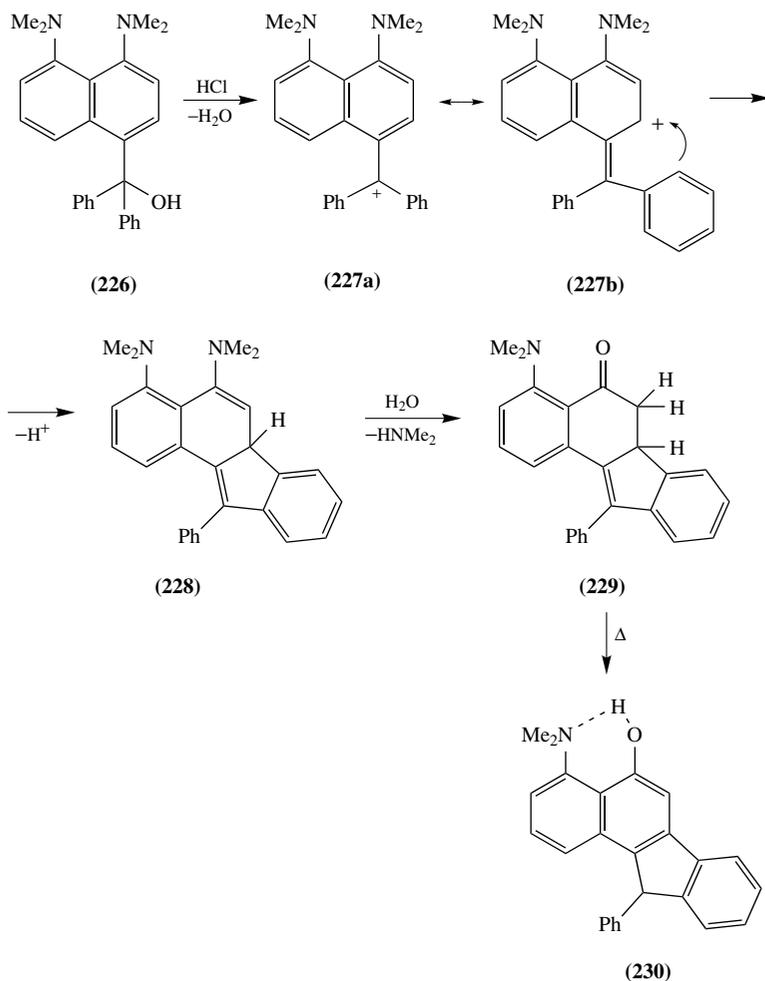
SCHEME 42

spirocyclohexadienone **242** in moderate yield (Scheme 45)[207]. The symmetrical structure of the latter testifies to a two-step electrophilic substitution mechanism via carbocation **240**, similar to that shown in Scheme 39.

The behaviour of the 'mixed' alcohol **243** with *peri* NMe$_2$ and OMe groups is somewhat reminiscent of its proton sponge counterpart **179a**. On heating with trifluoroacetic acid, **243** is converted in moderate yields, evidently via cation **244**, into a mixture of the non-symmetrical spiro compound **245** and the binaphthylmethane derivative **246** (Scheme 46)[210]. On alumina, 20% of aldehyde **247** and 35% of binaphthylmethane **246** were obtained.

An acidic treatment of 1-dimethylamino-4-hydroxymethylnaphthalene (**248**) leads to the formation of binaphthylmethane derivative **250** in quite good yield. Two other products were the spirocyclohexadienone **251** and 1-dimethylamino-4-methylnaphthalene **252**

182a–d

$$CH_2=\overset{+}{N}Me_2 \ Cl^-$$

$$H^+ \qquad \qquad H^+$$

(232b,c) $\qquad$ **(231a–d)** $\qquad$ **(232a,d)**

$-HNMe_2 \qquad \qquad -HNR_2$

(a) $NR_2 = NEt_2$

(b) $NR_2 = -N$ piperidine

(c) $NR_2 = -N$ morpholine O

(d) $NR_2 = NMe_2$

(233b,c) $\qquad \qquad$ **(234)**

(235a) Y = CH$_2$
(235b) Y = O

(236)
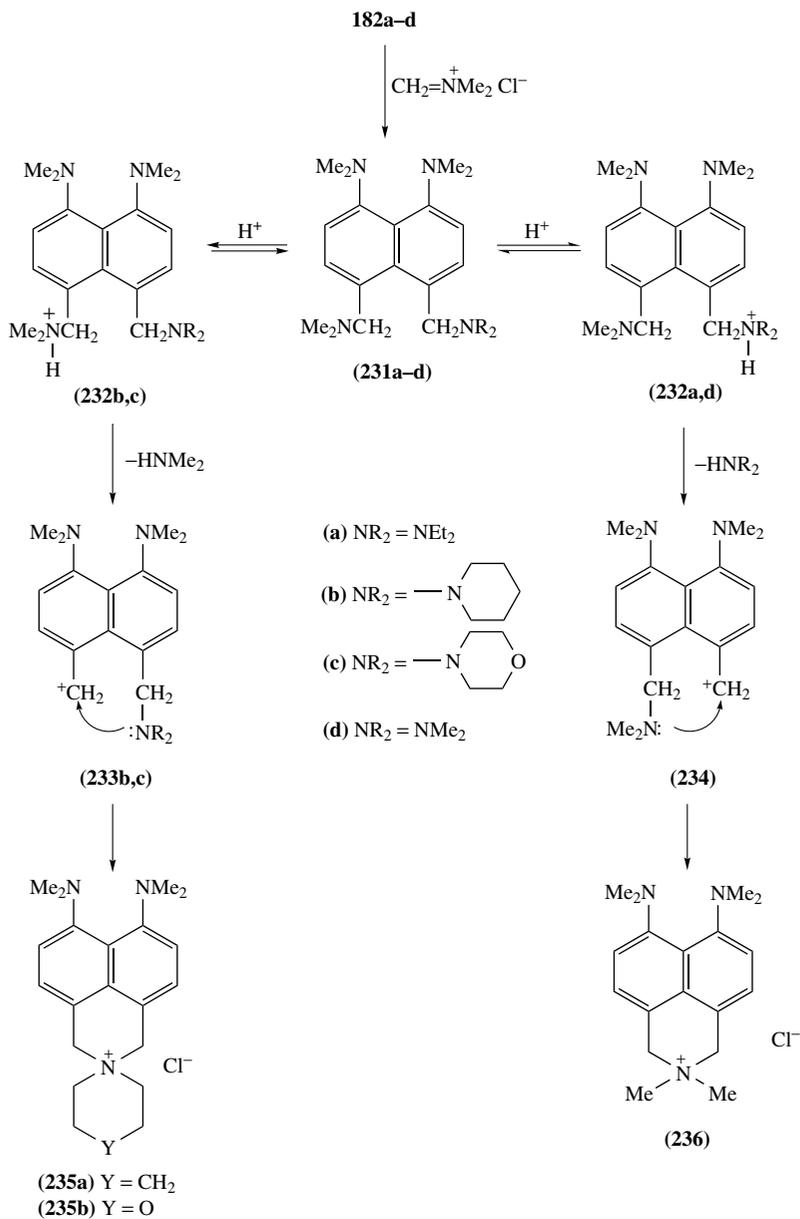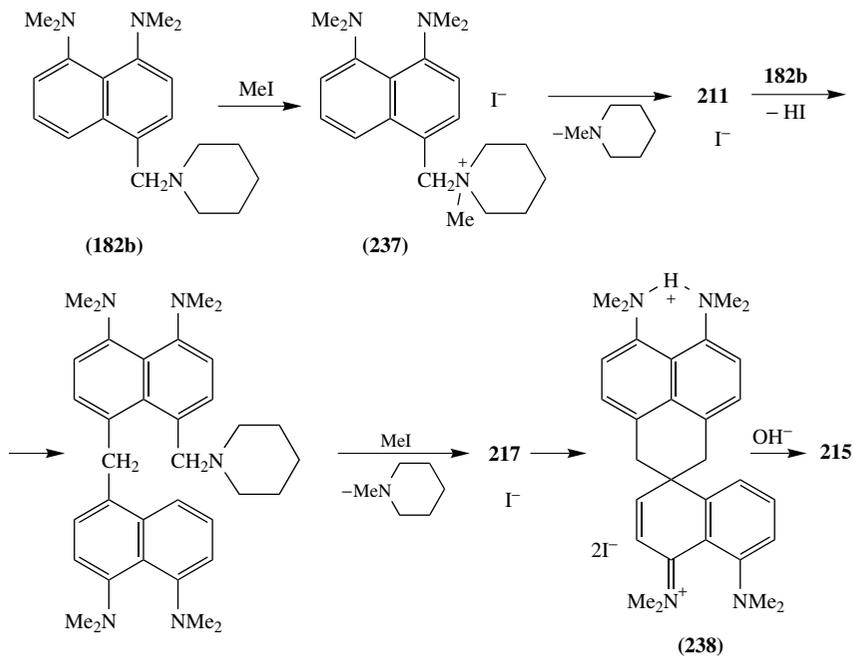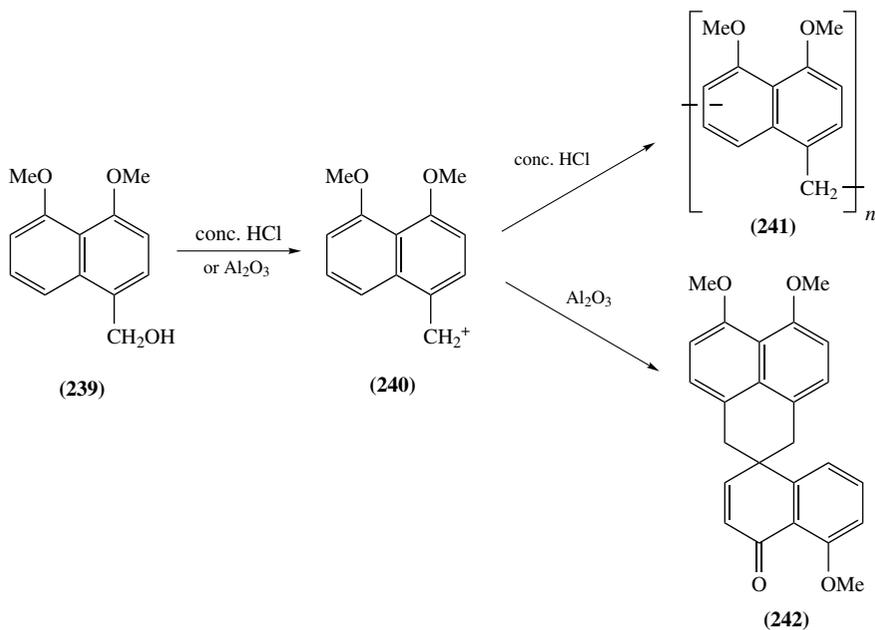
SCHEME 43

SCHEME 44

SCHEME 45
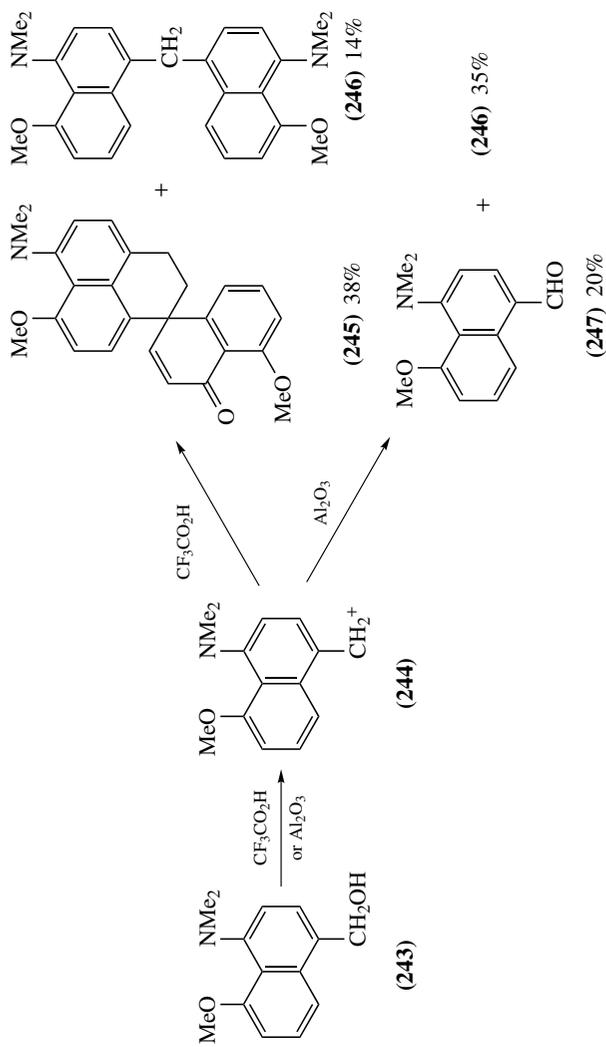
SCHEME 46
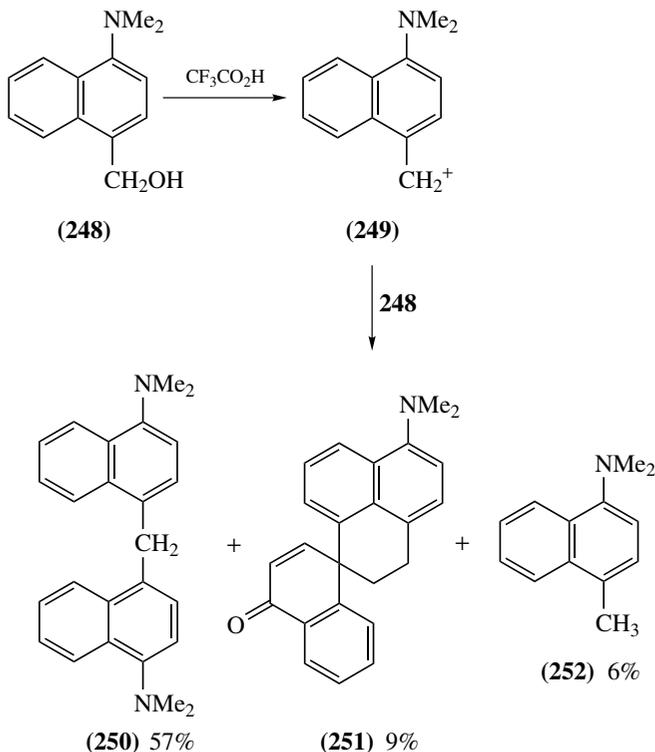
SCHEME 47

(Scheme 47)[208]. Notably, even one NMe$_2$ group in cation **249** is sufficient to promote a [4 + 2]-cyclodimerisation.

These results show that the formation of asymmetrical spiro compounds **214**, **245** and **251** is favoured by the presence of a basic NMe$_2$ functionality in the starting alcohol. Apparently, in an acidic media the NMe$_2$ exists mainly in the protonated form that minimizes the oligomerization, as well as the formation of the binaphthylmethane products. Consequently, the carbocation species can interact preferentially with each other via [4 + 2]-cycloaddition. The cyclodimerisation is especially prominent for the proton sponges due to their enhanced basicity.

Most surprising is the formation of spiro compounds of type **214** when, contrary to electrostatic laws, formally two positively charged carbon atoms of the methylene groups combine. Quantum-mechanical calculations[206, 211, 212] suggest that this process is favoured by the symmetry of molecule frontier orbitals and it may be asynchronous, occurring via the intermediary formation of a biradicaloid species.

V. APPLICATION OF PROTON SPONGES

The main area of application of proton sponges, primarily compound **1**, is in organic synthesis as strong but low-nucleophilicity bases. Besides, the proton sponges and their salts are a favourite model of physical chemists and theoreticians for investigating hydrogen bonds and a number of other interesting phenomena.

A. In Organic Synthesis

The nature of proton sponges does not allow them to be used directly as kinetically active bases, e.g. in $E2$ elimination reactions, involving the ionization of C−H bonds[213]. However, due to the low nucleophilicity, the proton sponges are useful reagents when it is necessary to bind an acid liberated in the course of the reaction without any effect on other base-sensitive groups. As a rule, in such cases, a proton transfer from substrate to the proton sponge requires an additional carrier, which most frequently is the solvent molecule (such as alcohol, THF, DMSO, acetone)[57, 214, 215]. Let us consider some typical examples.

Utilization of **1** in the conversion of imidazoles **253** into 2-sila-3H-imidazo[2,1-b] thiazoles **254** affords over 80% yield of the desired products (equation 17)[216]. In contrast, replacement of compound **1** by ordinary bases (e.g. OH⁻, MeO⁻) leads to the cleavage of the S−Si bond.

(253) **(254)** R = H, Ph

(17)
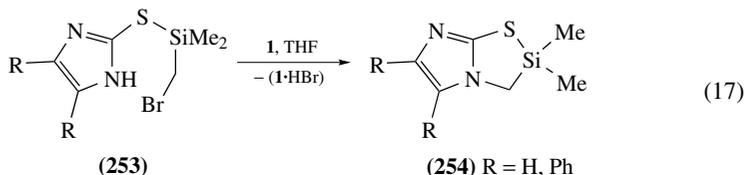
Similarly, the *cis−trans* isomerization of pyrazolines (**255a** → **255b**), proceeding through an open-chain anion, can be achieved in the presence of compound **1**, while common bases interact with the electrophilic substituents (equation 18)[217].

(255a)

(18)

R = CO₂Me

(255b)
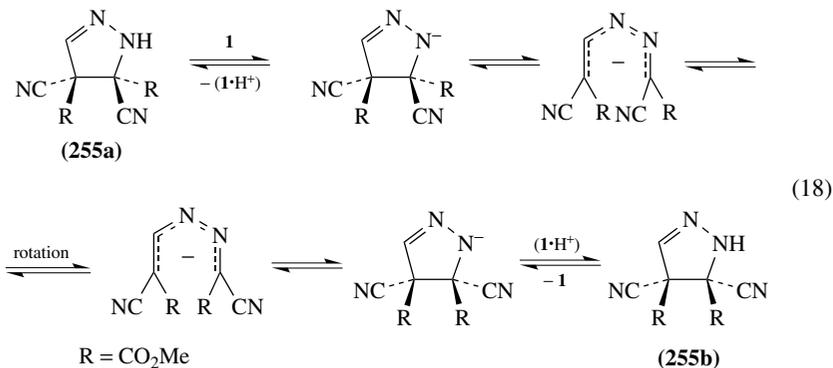
In reactions of chiral compounds requiring the use of a base, the proton sponge practically causes no racemisation and favours the retention of high optical purity. An example is the conversion of optically active alcohols into ethers under the action of trialkyloxonium tetrafluoroborates (equation 19)[218−220].

(19)
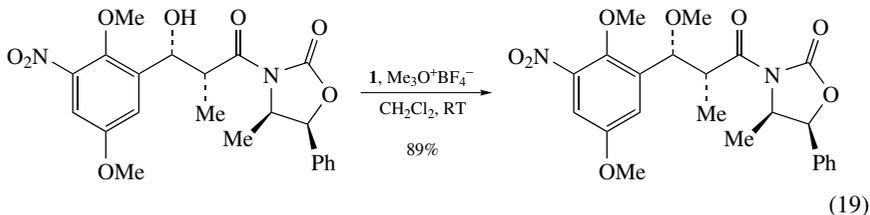
Diamine **1** was used in a mild and simple preparation of isocyanates from aliphatic amines and diphosgene (equation 20)[221].

$$R-NH_2 \ + \ \underset{Cl \qquad OCCl_3}{\overset{O}{\diagup\diagdown}} \xrightarrow[\substack{CH_2Cl_2, \ 0\ ^{\circ}C \\ 39–81\%}]{\textbf{1}} \ R-NCO \qquad (20)$$
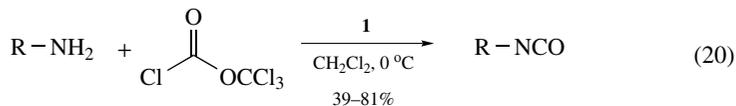
Phosgene-free synthesis of isocyanates directly from carboxylic acids and diphenylphosphonic azide $(PhO)_2P(O)N_3$ in combination with proton sponge **1** followed by Curtius rearrangement has been also described[222].

There are reports on utilizing diamine **1** as auxiliary base during alkylation of imines in DMF[223] and NH-heterocycles in MeCN[224].

In conjunction with proton sponge, the activated phosphate **256** turned out to be an effective reagent in the direct synthesis of peptides and branched amides from carboxylic acids (equation 21). In this process, diamine **1** surpassed in its efficiency for such bases as triethylamine, N,N-dimethylaniline, 2,6-lutidine and Hünig bases[225].

$$\underset{R}{\overset{R^1}{\diagdown}}NH \ + \ R_2-CO_2H \xrightarrow[CH_2Cl_2, \ RT]{\substack{PhN\diagdown\overset{SO_2CF_3}{\underset{PO(OEt)_2}{}} \\ \textbf{1} \ / \ \textbf{(256)}}} \underset{R \qquad O}{\overset{R^1 \qquad R^2}{\diagdown N \diagup}} \qquad (21)$$

$$\text{77–99\%}$$
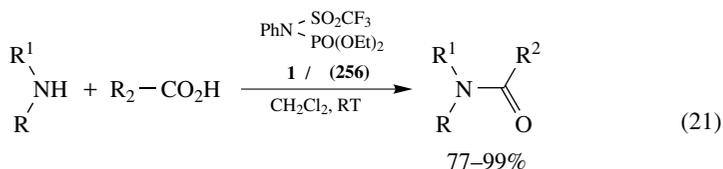
$$R = t\text{-Bu, Ph, CH}_2\text{Ph, CH(Me)Ph}$$
$$R^1 = H, Me; \ R^2 = Me, i\text{-Pr, } t\text{-Bu, Ph}$$

Along with amidines DBU and DBN, **1** affords moderate yields (30–47%) of 2,6-dichloropurine, an important pharmaceutical intermediate, during its preparation from xanthine in boiling $POCl_3$[226]. Aside from yield and selectivity enhancement, these bases improve the solubility of the starting xanthine.

The catalytic activity of proton sponge in the Knoevenagel reaction has been studied[227]. It was shown that benzaldehyde, in the presence of 2 mol% of **1**, reacts with ethyl cyanoacetate and ethyl acetoacetate (equation 22). The condensation is accelerated in polar solvents (especially in DMSO) and does not occur in the case of diethyl malonate, as its CH-acidity is too low ($pK_a = 13.3$).

$$PhCHO \ + \ H_2C\underset{CO_2Et}{\overset{R}{\diagdown}} \xrightarrow[-H_2O]{\textbf{1}, RT} PhCH=\underset{CO_2Et}{\overset{R}{\diagup}} \qquad (22)$$

$$R = CN, Ac$$
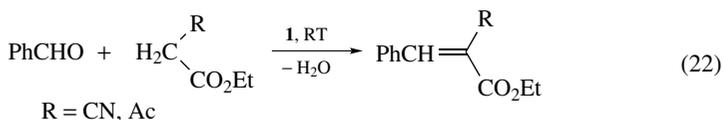
If the proton sponge fragment is chemically connected to an inorganic support (like silica gel in **257**), it proved to be an effective and useful heterogeneous catalyst, displaying its activity in a wide range of solvents. With 0.5–1 mol% of the anchored proton sponge **257**, it is possible to perform the Knoevenagel and Claisen–Schmidt condensations in 20–100% yields[228].

There are some other examples of base catalysis with participation of 1,8-bis(dimethylamino)naphthalene in the preparation of N-substituted trichloroacetamides from amines

Me$_2$N   NMe$_2$

(257)
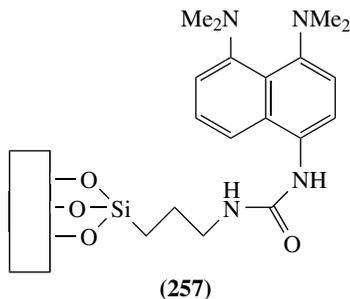
and hexachloroacetone[229], Michael addition of malonodinitrile[230] and ketene imine dimerisation[231]. In the last case the dimerisation is presumably launched by NC−CH$_2^-$ and CCl$_3^-$ anions, generated in a small equilibrium concentration in the **1**/MeCN and **1**/CHCl$_3$ systems. In particular, 0.06 M solution of base **1** in acetonitrile affords 2×10^{-6} M concentration of the NC−CH$_2^-$ anion and this is quite enough for the catalytic reaction to be carried out[231].

Dehydrochlorination of acid chlorides of type RCH$_2$COCl by proton sponge **1** in order to produce monoketenes is not directly realized[232, 233], but proceeds in the presence of benzoylquinine (BQ) as a 'shuttle base'. The *in situ* generated ketenes were used further for the synthesis of optically active β-lactams **258** (Scheme 48). Additionally, a method providing *trans*-isomers of **258** with the help of diamine **1** has recently been elaborated[234].

R = Ph, Et, OPh, OAc, OBn

(258) 95–98% ee
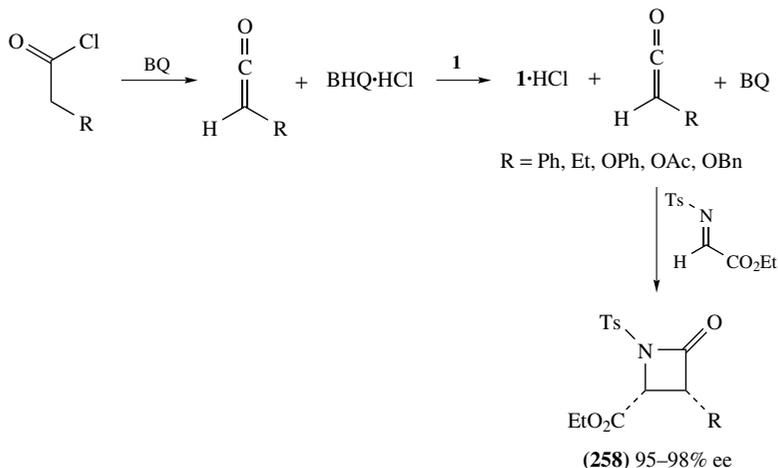
SCHEME 48

The **1**/BQ system alone or with Lewis acid additives was also employed for asymmetric catalysis in the synthesis of β-amino acids[235]. During an elaboration of the tandem catalytic asymmetric chlorination/esterification process, Lectka and coworkers found that proton sponge **1** competes with ketenes in the reaction with halogenating agents, such

as chloroquinone **259**[236]. Hence, alongside the main reaction leading to chloroester **260** (equation 23), the by-product **261** (up to 30%) was also isolated as a result of ketene alcoholysis with the pentachlorophenol formed (equation 24).

(23)

(24)
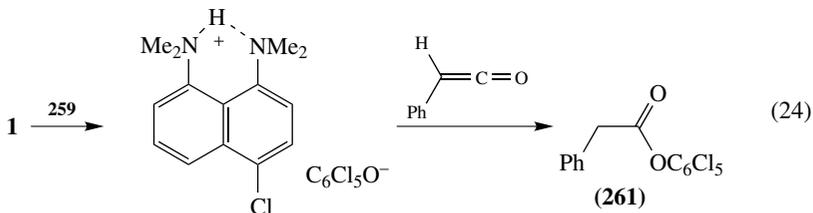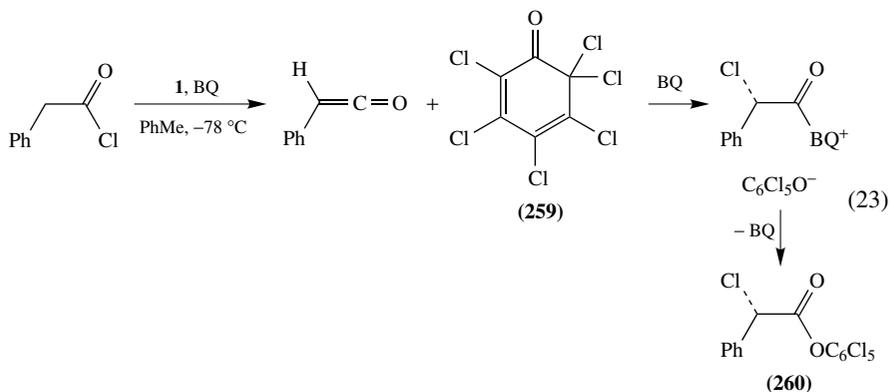
The proton sponge **1** has been offered as an auxiliary base in a variety of cross-coupling reactions. For instance, the palladium-catalysed alkoxycarbonylation of aryl and benzyl halides on treatment with CO in MeOH gave methyl carboxylates in a high yield (equation 25)[237]. The yields are lower with other bases and the reaction is not so clean.

$$\text{PhCH}_2\text{Cl} \xrightarrow[\text{(PPh}_3)_2\text{PdCl}_2,\ \mathbf{1}]{\text{MeOH, CO}} \text{PhCH}_2\text{CO}_2\text{Me}$$

91%

(25)
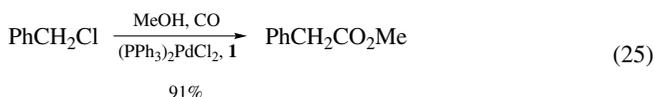
Compound **1** has been successfully employed in controlling the high enantioselectivity of Pd-catalysed arylation and alkenylation of olefines using aryl(alkenyl) triflates (e.g. equation 26)[238, 239]. The yields and optical purity of the products are distinctively lower with aliphatic amines (Et$_3$N, i-Pr$_2$NEt), pyridines (2,6-dimethyl-, 2,6-di-t-butyl-4-methyl-) and inorganic salts (AcONa, Na$_2$CO$_3$) as bases.

R = H, CO$_2$Et
X = O, N-CO$_2$Me

45–95%

87–99% ee

(26)
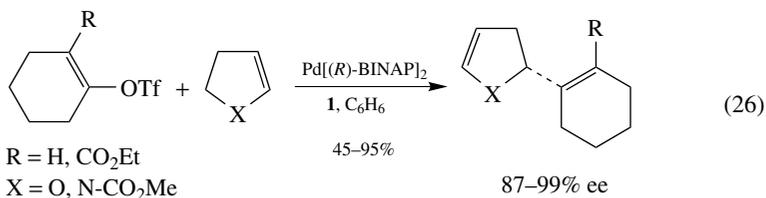
On treatment with proton sponge **1**, cationic rhodium complexes of type **262** have been shown to undergo double intramolecular dehydrofluorinative/C–C coupling to produce quantitatively rhodium complexes of hybrid cyclopentadienyl-phosphine ligands **263** (equation 27)[240].
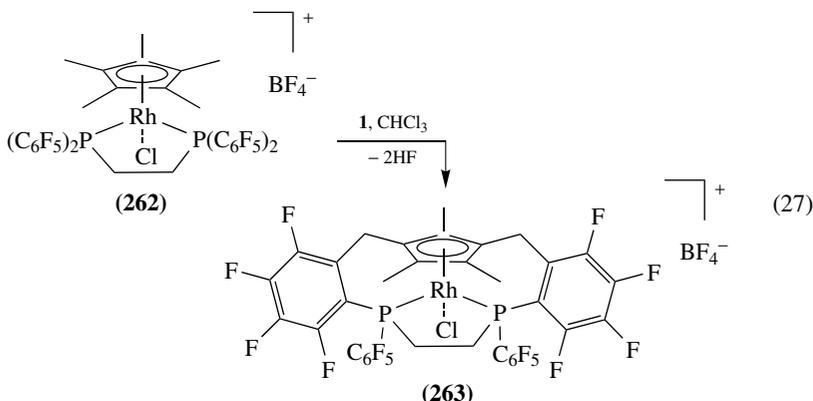
This transformation is one of the most convenient syntheses of chelating polyfunctional ligands, studied extensively in organometallic chemistry. In this reaction, the practically non-coordinating nature of proton sponges (cf. equation 13) is effectively used. In the case of other bases, the process does not proceed (Et$_3$N) or results in the formation of complex mixtures (*t*-BuOK).

Proton sponge **1** has also found application in the introduction and elimination of different protecting groups. Thus, in order to protect the carboxylic function, it has been suggested to use *N*-acyl-5,6-dihydrophenanthridines **265**[241]. The latter can be prepared in accordance with equation 28 by treating a mixture of carboxylic acid and 5,6-dihydrophenanthridine with 2-chloropyridinium salt **264** in the presence of 4-dimethylaminopyridine and proton sponge **1**. Amides **265** are stable towards acidic or basic hydrolysis, as well as to Grignard reagents, but upon the action of Ce(NH$_4$)$_2$(NO$_3$)$_6$ in acetonitrile they are converted back into the carboxylic acids.
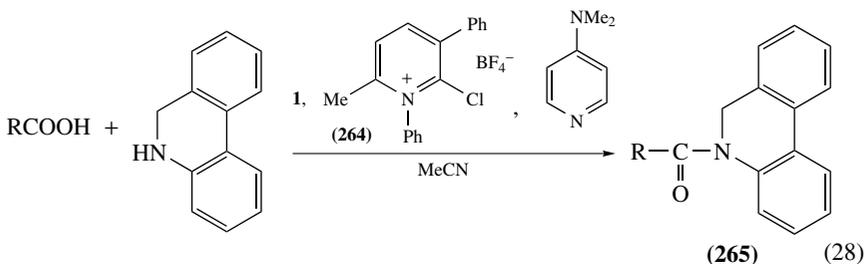
In another case, **1** was used to deprotect the 2-(allyloxy)phenylacetyl group, employed as a protecting functionality in carbohydrate chemistry[242]. Thus, heating compound **266** with a palladium catalyst/proton sponge system results in an almost quantitative yield of compound **268** (equation 29). In accordance with a postulated relay mechanism, the phenolic allyl ether is cleaved by the transition metal followed by intramolecular ester cleavage by nucleophilic attack of the released hydroxyl. The aforementioned conditions

do not affect acetyl, benzoyl and levulinoyl esters and this is especially important in oligosaccharide synthesis. In the presence of triethylamine, the process stops before its completion, affording a mixture of **268** and deallylated intermediate **267** (up to 25%). The high basicity and non-inclination of the proton sponge to coordinate with metals (for the single case, see Section IV.A.2) afford almost quantitative yield of **268**.

$$(29)$$
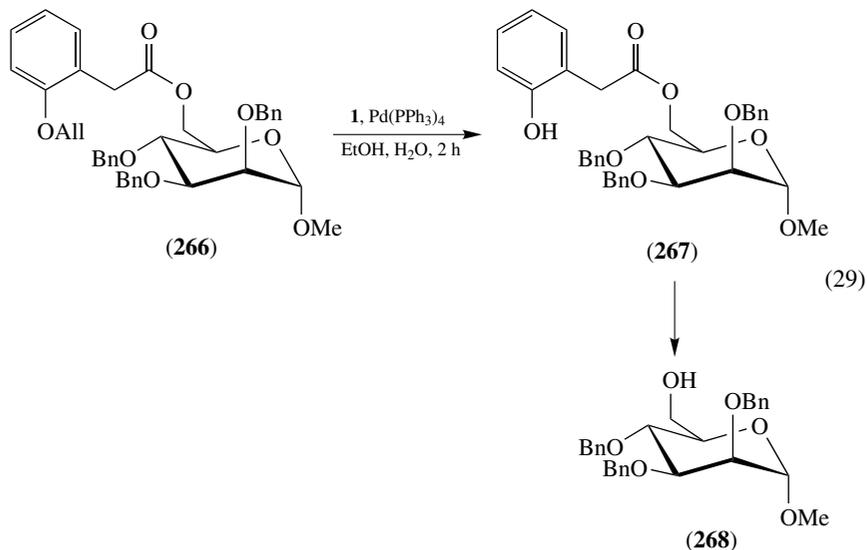
Chambers and coworkers[243, 244] suggested proton sponge hydrofluoride as a soluble and effective fluoride ion source. Thus, the **1**/HF/MeCN system was successfully employed for generating carbanions from perfluoroalkenes and for halogen exchange reaction with substrates such as 2,4,6-trichloropyrimidine or benzoyl chloride. In the last case, the insolubility of the produced hydrochloride **1**•HCl in acetonitrile facilitated the products separation and allowed recycling of the proton sponge. A more suitable system, **1**/Et$_3$N•3HF, was proposed later for the selective nucleophilic fluorination of dichlorodiazines and chloronitropyridines[245, 246]. Recent application of the system **1**/H^{18}F/MeCN/H$_2$O in nucleophilic substitution reactions expanded the number of available and fast radiofluorination methods, allowing one to introduce a radioisotopic ^{18}F-label into pharmacophore substrates[247].

Until recently, there had been no reports on the application of 2,7-disubstituted proton sponges like **44** and **65** in organic synthesis. Their advantage in comparison with compound **1** is their increased basicity coupled with their extremely low *C*-nucleophilicity. Lately, the 2,7-dimethoxy compound **44** was used for deprotonation of salts of other proton sponges, in particular of **88** and **89** (Section II.C.2)[67]. In another example, when the proton sponge **1** participated in the azo-coupling reaction, the addition of base **44** increased the degree of interaction (equation 30)[56]. The yield of the azo compound **269** was nearly quantitative, and the base **44** could be easily recovered.

Proton sponge **1** was recommended as an unusual debrominating agent in the conversion of *vic*-dibromides into alkenes. Thus, heating **1** with 1,2-dibromoacenaphthene in dimethoxyethane gives acenaphthylene in a nearly quantitative yield[248]. The debromination of dibromo derivatives of coumarin, isocoumarin and chalcone occurs similarly. Though the mechanism of this reaction is still under investigation, its driving force can

be the above-mentioned high *C*-nucleophilicity of **1** which results, in particular, in the formation of a π-complex with molecular bromine (Section IV.B.3).

(30)
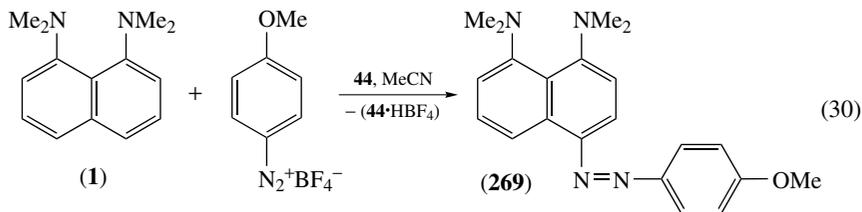
A kind of technical application of *N*-alkylated 1,5- and 1,8-diaminonaphthalenes was also reported. In particular, tetraallyl proton sponge **270**, prepared in accord with equation 31, has demonstrated significant antioxidant activity in lubricant compositions. Though the yield of **270** was not mentioned, it was emphasized that its antioxidant properties and its lesser-alkylated precursors work at a concentration of only 0.5%[249].

(31)
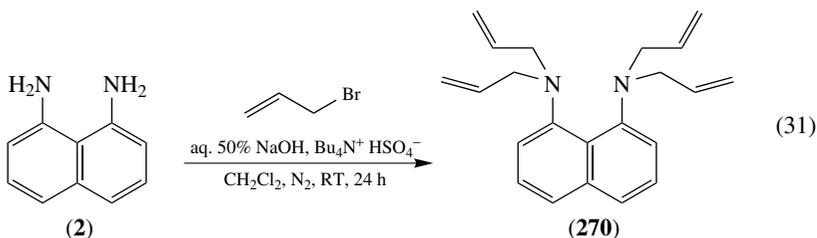
B. In Theoretical and Physicochemical Studies

Proton sponges, mostly compound **1**, have found wide application as models in studying low-barrier IHB[50, 84], performing isotopic desymmetrization for estimating the IHB stability[110] and for disclosing weak interatomic interactions such as $C-H\cdots O$, $C-H\cdots N$ and $C\pi \cdots C\pi$ in solution[96] and in the solid[84, 215, 250]. Proton sponge-based highly-conjugated molecules of potential importance for non-linear optics have been reported[118, 197] and organic bases with easily-adjustable basicity were devised[38]. Application of the proton sponge as deprotonating agent in crystal engineering for investigating sulfonylamide anions[251] or strongly asymmetric anions of type $[HO-H\cdots OH]^-$ is also well documented[252]. Here are some other examples.

On the basis of the extrathermodynamic assumption ΔH_t° (**1**) $= \Delta H_t^\circ$ (**1·H$^+$**), provided that **1·H$^+$** is a large cation with non-specific solvation[154], conjugated systems of type **1/1·H$^+$** were used for calculating single-ion enthalpies of transfer. Using the heats of solvation of the base **1**, the salt **1·CF$_3$SO$_3$H** and the acid CF_3SO_3H, a thermodynamic scale of solvent basicity (in kJ mol^{-1}) based on the enthalpy of proton transfer has been constructed: Py (-63) > DMF (-32) > Me$_2$SO (-27) > EtOH (-1) $\approx$ H$_2$O (0) $\approx$ MeOH (2) > propylene carbonate (44) > MeCN (55) > sulfolane (69)[253]. These values are in good agreement with the enthalpies of complex formation with gaseous BF$_3$ and also reflect the solvent Lewis basicity (for non-protonic solvents).

Careful measurements of the heat of solvation of naphthalene, 1-dimethylaminonaphthalene and 1,8-bis(dimethylamino)naphthalene in 16 organic solvents, differing strongly in their properties, led to the conclusion that the presence of NMe$_2$ groups on the naphthalene does not significantly contribute to solute–solvent interactions[254].

TABLE 20.   Conductometrically estimated K_r and K_d values for the products of some acid–base reactions of carbon acids **271**–**273**

		X	(**271**) X = CN, Y = H
O_2N-	$-CH$		(**272**) X = NO$_2$, Y = H
		Y	(**273**) X = CN, Y = Ph
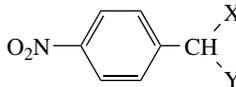
AH	B	K_r (mol l^{-1})	K_d (mol l^{-1})
271	DBU	4	3×10^{-2}
272	**1**	1.36	1.3×10^{-3}
273	**1**	1.91	6.7×10^{-5}

The conductometric investigation of hydrogen transfer reactions between nitro- or cyano-group activated C-acids and some amine bases (including proton sponge) in MeCN at 25 °C has shown their large degree of dissociation into free ions ($K_d > 1 \times 10^{-4}$ mol l^{-1})[255]. Therefore, the salt-like products of these reactions in acetonitrile are in fact not the ion pairs as was postulated previously. For illustration, this follows from the K_r and K_d values for the products of some reactions (equation 32 and Table 20).

$$AH + B \; \underset{K_r}{\overset{}{\rightleftharpoons}} \; A^-, BH^+ \; \underset{K_d}{\overset{}{\rightleftharpoons}} \; A^- + BH \qquad (32)$$

The behaviour of proton sponge in water–heptane reverse micelles in the presence of a surfactant was reported[256]. The neutral and protonated form of the proton sponge

(**274**)   no fluorescence

pH < 10 | H$^+$

(**275**)   strong fluorescence
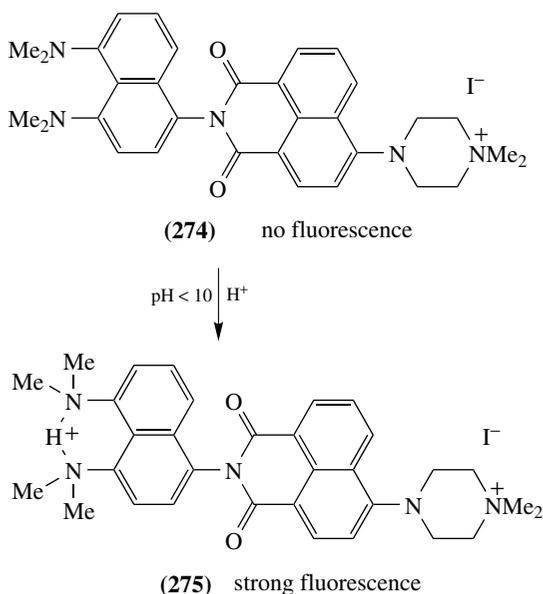
is solubilized respectively in heptane and in the water core of the micelle, both forms being in equilibrium. It was emphasized that simultaneously diamine **1** is able to create a rather high basicity inside the micro-drops of water with concentration of OH^- ions within $5 \times 10^{-4} - 10^{-3}$ M.

Recently, proton sponge was used as a fluorescent indicator for protons[257]. By incorporating the residue of **1** into the structure of the known fluorophore, 4-aminonaphthalimide, the researchers designed the fluorescent switch **274**, whose synthesis was conducted in 5 steps with overall yield *ca* 10%.

The action of sensor **274** is based on a photoinduced electron transfer (PET) mechanism. Whereas the PET process from the neutral proton sponge residue to the 4-aminonaphthalimide part quenches the fluorescence of **274**, upon protonation to **275**, the fluorescence intensity is strongly enhanced due to inhibition of the PET process. The switch **274**, having a quaternary ammonium fragment, works both in organic and in water solutions and displays an intense fluorescence already at pH < 10, i.e. in strongly alkaline media. This is apparently due to the high basicity of the proton sponge.

VI. CONCLUSION

The preceding discussion has shown that the concept of proton sponges appears extremely fruitful for the chemistry of arenes and aromatic amines. They contribute significantly to acid–base theory, to the theory of the hydrogen bond, to general structural theory and to preparative organic chemistry. There is no doubt that the application of proton sponges in organic synthesis may increase due to the creation of useful reagents on polymer supports, new chiral bases and reagents with low *N*- and *C*-nucleophilicity. There are also some perspectives in making proton-sponge-based switchable molecular devices, effective catalysts or biomimetic systems. Investigations of 1,8-bis(dimethylamino)naphthalene have demonstrated that the chemistry of proton sponges is as highly specific as their physicochemical and structural characteristics, and many reactions have no analogies in the naphthalene series. There is much interest in conducting similar studies for other proton sponge types, such as fluorene, phenanthrene and heterocyclic sponges; however, many of the latter compounds have yet to be synthesized.

VII. ACKNOWLEDGEMENT

VIII. REFERENCES

1. R. W. Alder, P. S. Bowman, W. R. S. Steele and D. R. Winterman, *J. Chem. Soc., Chem. Commun.*, 723 (1968).
2. A. F. Pozharskii, A. N. Suslov, N. M. Starshikov, L. L. Popova, N. A. Klyuev and V. A. Adanin, *Zh. Org. Khim.*, **16**, 2216 (1980); *Chem. Abstr.*, **94**, 120385s (1981).
3. Y. K. Lau, P. P. S. Saluja, P. Kebarle and R. W. Alder, *J. Am. Chem. Soc.*, **100**, 7328 (1978).
4. H. A. Staab and T. Saupe, *Angew. Chem., Int. Ed. Engl.*, **27**, 865 (1988).
5. R. W. Alder, *Chem. Rev.*, **89**, 1215 (1989).
6. A. L. Llamas-Saiz, C. Foces-Foces and J. Elguero, *J. Mol. Struct.*, **328**, 297 (1994).
7. H. A. Staab, T. Saupe and C. Krieger, *Angew. Chem., Int. Ed. Engl.*, **22**, 731 (1983).
8. H. A. Staab, M. Höne and C. Krieger, *Tetrahedron Lett.*, **29**, 1905 (1988).
9. T. Saupe, C. Krieger and H. A. Staab, *Angew. Chem., Int. Ed. Engl.*, **25**, 451 (1986).
10. H. A. Staab, M. Diehm and C. Krieger, *Tetrahedron Lett.*, **36**, 2967 (1995).
11. M. A. Zirnstein and H. A. Staab, *Angew. Chem.*, **99**, 460 (1987).

12. C. Krieger, I. Newsom, M. A. Zirnstein and H. A. Staab, *Angew. Chem., Int. Ed. Engl.*, **28**, 84 (1989).
13. H. A. Staab, M. A. Zirnstein and C. Krieger, *Angew. Chem., Int. Ed. Engl.*, **28**, 86 (1989).
14. H. A. Staab, M. Diehm and C. Krieger, *Tetrahedron Lett.*, **35**, 8357 (1994).
15. R. Schwesinger, M. Misfeldt, K. Peters and H. G. von Schnering, *Angew. Chem., Int. Ed. Engl.*, **26**, 1165 (1987).
16. A. L. Llamas-Saiz, C. Foces-Foces, J. Elguero, P. Molina, M. Alajarin and A. Vidal, *J. Chem. Soc., Perkin Trans. 2*, 1667 (1991).
17. V. Raab, J. Kipke, R. M. Gschwind and J. Sundermeyer, *Chem. Eur. J.*, **8**, 1682 (2002).
18. B. Brzezinski, T. Głowiak, E. Grech, Z. Malarski and L. Sobczyk, *J. Chem. Soc., Perkin Trans. 2*, 1643 (1991).
19. M. Ciampolini, N. Nardi, B. Valtacoli and M. Micheloni, *Coord. Chem. Rev.*, **120**, 223 (1992).
20. T. J. Hubin, J. M. McCormick, S. R. Collinson, N. W. Alcock and D. H. Busch, *J. Chem. Soc., Chem. Commun.*, 1675 (1998).
21. Y. Miyahara, K. Goto and T. Inazu, *Tetrahedron Lett.*, **42**, 3097 (2001).
22. M. C. Elliott, E. Williams and S. T. Howard, *J. Chem. Soc., Perkin Trans. 2*, 201 (2002).
23. V. Raab, K. Harms, J. Sundermeyer, B. Kovačevič and Z. B. Maksič, *J. Org. Chem.*, **68**, 8790 (2003).
24. G. Bucher, *Angew. Chem., Int. Ed.*, **42**, 4039 (2003).
25. V. Raab, E. Gauchenova, A. Merkoulov, K. Harms, J. Sundermeyer, B. Kovačeviç and Z. B. Maksič, *J. Am. Chem. Soc.*, **127**, 15738 (2005).
26. E. Estrada and Y. Simon-Manso, *Angew. Chem., Int. Ed.*, **45**, 1719 (2006).
27. T. Kanbara, Y. Suzuki and T. Yamamoto, *Eur. J. Org. Chem.*, 3314 (2006).
28. F. Hibbert and J. Emsley, *Adv. Phys. Org. Chem.*, **26**, 255 (1990).
29. A. F. Pozharskii, *Russ. Chem. Rev.*, **67**, 1 (1998).
30. H. Quast, W. Risler and G. Döllscheir, *Synthesis*, 558 (1972).
31. L. A. Kurasov, A. F. Pozharskii and V. V. Kuz'menko, *Zh. Org. Khim.*, **17**, 1944 (1981); *Chem. Abstr.*, **95**, 203877a (1981).
32. E. M. Arnett, K. G. Venkatasubramanian, R. T. McIver, E. K. Fukuda, F. G. Bordwell and R. D. Press, *J. Am. Chem. Soc.*, **104**, 325 (1982).
33. A. F. Pozharskii, L. A. Kurasov, V. V. Kuz'menko and L. L. Popova, *Zh. Org. Khim.*, **17**, 1005 (1981); *Chem. Abstr.*, **95**, 187185r (1981).
34. V. I. Sorokin, V. A. Ozeryanskii and A. F. Pozharskii, *Eur. J. Org. Chem.*, 496 (2003).
35. R. W. Alder, M. R. Bryce, N. C. Goode, N. Miller and J. Owen, *J. Chem. Soc., Perkin Trans. 1*, 2840 (1981).
36. F. Hibbert and G. R. Simpson, *J. Chem. Soc., Perkin Trans. 2*, 243 (1987).
37. V. A. Ozeryanskii and A. F. Pozharskii, *Russ. Chem. Bull.*, **49**, 1399 (2000).
38. V. A. Ozeryanskii, A. F. Pozharskii, G. R. Milgizina and S. T. Howard, *J. Org. Chem.*, **65**, 7707 (2000).
39. H. A. Staab, C. Krieger, G. Hieber and K. Oberdorf, *Angew. Chem., Int. Ed. Engl.*, **36**, 1884 (1997).
40. G. Bar-Haim and M. Kol, *J. Org. Chem.*, **62**, 6682 (1997).
41. V. A. Ozeryanskii, E. A. Filatova, V. I. Sorokin and A. F. Pozharskii, *Russ. Chem. Bull.*, **50**, 846 (2001).
42. A. A. Konstantinchenko, A. F. Pozharskii and V. N. Stepanova, *Zh. Org. Khim.*, **29**, 1437 (1993); *Chem. Abstr.*, **121**, 157255b (1994).
43. M. G. Koroleva, O. V. Dyablo, A. F. Pozharskii, E. V. Sennikova and Z. A. Starikova, *Russ. J. Org. Chem. (Engl. Transl.)*, **41**, 997 (2005).
44. V. I. Sorokin, V. A. Ozeryanskii and A. F. Pozharskii, *Russ. J. Org. Chem. (Engl. Transl.)*, **38**, 699 (2002).
45. T. Barth, C. Krieger, F. A. Neugebauer and H. A. Staab, *Angew. Chem., Int. Ed. Engl.*, **30**, 1028 (1991).
46. R. W. Alder and J. E. Anderson, *J. Chem. Soc., Perkin Trans. 1*, 2086 (1973).
47. V. A. Ozeryanskii, A. F. Pozharskii and N. V. Vistorobskii, *Russ. Chem. Bull.*, **49**, 1212 (2000).
48. V. A. Ozeryanskii and A. F. Pozharskii, *Russ. Chem. Bull.*, **52**, 271 (2003).
49. J. P. H. Charmant, G. C. Lloyd-Jones, T. M. Peakman and R. L. Woodward, *Eur. J. Org. Chem.*, 2501 (1999).

50. C. L. Perrin and B. K. Ohta, *J. Am. Chem. Soc.*, **123**, 6520 (2001).
51. R. P. Hughes, I. Kovacik, D. Lindner, J. M. Smith, S. Willemsen, D. Zhang, I. A. Guzei and A. L. Rheingold, *Organometallics*, **20**, 3190 (2001).
52. N. V. Vistorobskii and A. F. Pozharskii, *Russ. J. Org. Chem. (Engl. Transl.)*, **32**, 61 (1996).
53. B. V. Kunshenko, L. A. Alekseeva and L. M. Yagupolskii, *Zh. Org. Khim.*, **6**, 1286 (1970); *Chem. Abstr.*, **73**, 66313t (1970).
54. H. A. Staab, A. Kirsch, T. Barth, C. Krieger and F. A. Neugebauer, *Eur. J. Org. Chem.*, 1617 (2000).
55. V. A. Ozeryanskii and A. F. Pozharskii, *Russ. Chem. Bull.*, **49**, 1406 (2000).
56. V. A. Ozeryanskii, V. I. Sorokin and A. F. Pozharskii, *Russ. Chem. Bull.*, **53**, 404 (2004).
57. V. A. Ozeryanskii and A. F. Pozharskii, *Russ. Chem. Bull.*, **46**, 1437 (1997).
58. A. Kirsch, C. Krieger, H. A. Staab and F. A. Neugebauer, *Tetrahedron Lett.*, **35**, 8365 (1994).
59. R. H. Barbour, A. A. Freer and D. D. MacNicol, *J. Chem. Soc., Chem. Commun.*, 362 (1983).
60. A. A. Freer, D. D. McNicol, P. R. Mallinson and C. D. Robertson, *Tetrahedron Lett.*, **30**, 5787 (1989).
61. H. A. M. Biemans, C. Zhang, P. Smith, H. Koojiman, W. J. J. Smeets, A. L. Spek and E. W. Meijer, *J. Org. Chem.*, **61**, 9012 (1996).
62. V. I. Sorokin, V. A. Ozeryanskii and A. F. Pozharskii, *Eur. J. Org. Chem.*, 766 (2004).
63. V. I. Sorokin, V. A. Ozeryanskii, A. F. Pozharskii and Z. A. Starikova, *Mendeleev Commun.*, **14**, 14 (2004).
64. V. I. Sorokin, *Candidate Thesis in Chemical Sciences*, Rostov State University, Rostov-on-Don (2003).
65. G. Rimmler, C. Krieger and F. A. Neugebauer, *Chem. Ber.*, **125**, 723 (1992).
66. C. Cox, H. Wack and T. Lectka, *Angew. Chem., Int. Ed.*, **38**, 798 (1999).
67. A. F. Pozharskii, O. V. Dyablo, M. G. Koroleva, E. V. Sennikova, Z. A. Starikova and S. T. Howard, *Mendeleev Commun.*, **13**, 180 (2003).
68. R. F. Borch and A. I. Hassid, *J. Org. Chem.*, **37**, 1673 (1972).
69. M. Rentzea, F. Kühn and H. A. Staab, *Org. Mass Spectrom.*, **28**, 490 (1993).
70. A. L. Llamas-Saiz, C. Foces-Foces, P. Molina, M. Alajarin, A. Vidal, R. M. Claramunt and J. Elguero, *J. Chem. Soc., Perkin Trans. 2*, 1025 (1991).
71. H. Einspahr, J.-B. Robert, R. E. Marsh and J. D. Roberts, *Acta Crystallogr.*, **B29**, 1611 (1973).
72. W. Wong-Ng, S. C. Nyburg, A. Awwal, R. Jankie and A. J. Kresge, *Acta Crystallogr.*, **B38**, 559 (1982).
73. R. W. Alder, N. C. Goode, T. J. King, J. M. Mellor and B. W. Miller, *J. Chem. Soc., Chem. Commun.*, 173 (1976).
74. A. F. Pozharskii, V. A. Ozeryanskii and Z. A. Starikova, *J. Chem. Soc., Perkin Trans. 2*, 318 (2002).
75. A. A. Woolf, cited in F. Hibbert, *Adv. Phys. Org. Chem.*, **22**, 166 (1986).
76. A. F. Pozharskii, O. V. Ryabtsova, V. A. Ozeryanskii, A. V. Degtyarev, O. N. Kazheva, G. G. Alexandrov and O. A. Dyachenko, *J. Org. Chem.*, **68**, 10109 (2003).
77. T. Głowiak, I. Majerz, Z. Malarskii, L. Sobczyk, A. F. Pozharskii, V. A. Ozeryanskii and E. Grech, *J. Phys. Org. Chem.*, **12**, 895 (1999).
78. A. J. Bienko, Z. Latajka, W. Sawka-Dobrowolska, L. Sobczyk, V. A. Ozeryanskii, A. F. Pozharskii, E. Grech and J. Nowicka-Scheibe, *J. Chem. Phys.*, **119**, 4313 (2003).
79. A. F. Pozharskii, O. V. Ryabtsova, V. A. Ozeryanskii, A. V. Degtyarev, Z. A. Starikova, L. Sobczyk and A. Filarowski, *Tetrahedron Lett.*, **46**, 3973 (2005).
80. A. F. Pozharskii, V. V. Kuz'menko, G. G. Alexandrov and D. V. Dmitrienko, *Zh. Org. Khim.*, **31**, 570 (1995); *Chem. Abstr.*, **124**, 260232c (1996).
81. A. F. Pozharskii, G. G. Alexandrov and N. V. Vistorobskii, *Zh. Org. Khim.*, **27**, 1536 (1991); *Chem. Abstr.*, **116**, 173682r (1992).
82. D. Pyzalska, R. Pyzalski and T. Borowiak, *J. Crystallogr. Spectrosc. Res.*, **13**, 211 (1983).
83. E. Bartoszak, M. Jaskolski, E. Grech, T. Gustafsson and I. Olovsson, *Acta Crystallogr.*, **B50**, 358 (1994).
84. P. R. Mallinson, G. T. Smith, C. C. Wilson, E. Grech and K. Wozniak, *J. Am. Chem. Soc.*, **125**, 4259 (2003).
85. J. Valdes-Martinez, M. D. Rio-Ramirez, S. Hernandez-Ortega, C. B. Aakeröy and B. Helfrich, *Cryst. Growth Des.*, **1**, 485 (2001).

86. K. N. Robertson, P. K. Bakshi, S. D. Lantos, T. S. Cameron and O. Knop, *Can. J. Chem.*, **76**, 583 (1998).
87. V. A. Ozeryanskii, A. F. Pozharskii, A. J. Bieńko, W. Sawka-Dobrowolska and L. Sobczyk, *J. Phys. Chem. A*, **109**, 1637 (2005).
88. H. A. Staab, C. Krieger and M. Höne, *Tetrahedron Lett.*, **29**, 5629 (1988).
89. A. F. Pozharskii, A. V. Degtyarev, O. V. Ryabtsova, V. A. Ozeryanskii, Z. A. Starikova, L. Sobczyk and A. Filarowski, unpublished results.
90. V. A. Ozeryanskii, A. F. Pozharskii, T. Głowiak, I. Majerz, L. Sobczyk, E. Grech and J. Nowicka-Scheibe, *J. Mol. Struct.*, **607**, 1 (2002).
91. P. K. Bakshi, T. S. Cameron and O. Knop, *Can. J. Chem.*, **74**, 201 (1996).
92. E. Grech, Z. Malarski, W. Sawka-Dobrowolska and L. Sobczyk, *J. Phys. Org. Chem.*, **12**, 313 (1999).
93. R. W. Alder, A. G. Orpen and R. B. Sessions, *J. Chem. Soc., Chem. Commun.*, 999 (1983).
94. R. L. de Groot and D. J. Sikkema, *J. R. Neth. Chem. Soc.*, **95**, 10 (1976).
95. Z. Dega-Szafran, B. Nowak-Wydra and M. Szafran, *Magn. Reson. Chem.*, **31**, 726 (1993).
96. M. Pietrzak, J. Wehling, H.-H. Limbach, N. S. Golubev, C. Lopez, R. M. Claramunt and J. Elguero, *J. Am. Chem. Soc.*, **123**, 4338 (2001).
97. K. Wozniak, H. He, J. Klinowski and E. Grech, *J. Phys. Chem.*, **99**, 1403 (1995).
98. A. F. Pozharskii and V. A. Ozeryanskii, *Russ. Chem. Bull.*, **47**, 66 (1998).
99. C. L. Perrin and B. K. Ohta, *J. Mol. Struct.*, **644**, 1 (2003).
100. P. Bernatowicz, J. Kowalewski and D. Sandström, *J. Phys. Chem. A*, **109**, 57 (2005).
101. J. Klimkiewicz, M. Koprowski, L. Stefaniak, E. Grech and G. A. Webb, *J. Mol. Struct.*, **403**, 163 (1997).
102. J. Klimkiewicz, L. Stefaniak, E. Grech and G. A. Webb, *J. Mol. Struct.*, **412**, 47 (1997).
103. M. Pietrzak, L. Stefaniak, A. F. Pozharskii, V. A. Ozeryanskii, J. Nowicka-Scheibe, E. Grech and G. A. Webb, *J. Phys. Org. Chem.*, **13**, 35 (2000).
104. E. Grech, J. Klimkiewicz, J. Nowicka-Scheibe, M. Pietrzak, W. Schief, A. F. Pozharskii, V. A. Ozeryanskii, S. Bolvig, J. Abildgaard and P. E. Hansen, *J. Mol. Struct.*, **615**, 121 (2002).
105. A. F. Pozharskii, N. G. Tregub, N. V. Vistorobskii, E. Yu. Romanova, Z. A. Starikova and A. I. Yanovsky, *Russ. Chem. Bull.*, **48**, 1299 (1999).
106. N. V. Vistorobskii, A. F. Pozharskii and M. I. Rudnev, *Russ. Chem. Bull.*, **47**, 91 (1998).
107. E. Grech, L. Stefaniak, I. Ando, H. Yoshimizu, G. A. Webb and L. Sobczyk, *Bull. Chem. Soc. Jpn.*, **63**, 2716 (1990).
108. E. Grech, L. Stefaniak, I. Ando, H. Yoshimizu and G. A. Webb, *Bull. Chem. Soc. Jpn.*, **64**, 3761 (1991).
109. P. Hodgson, G. C. Lloyd-Jones, M. Murray, T. M. Peakman and R. L. Woodward, *Chem. Eur. J.*, **6**, 4451 (2000).
110. G. C. Lloyd-Jones, *Synlett.*, 161 (2001).
111. V. A. Ozeryanskii and A. F. Pozharskii, *Russ. Chem. Bull.*, **55**, 164 (2006).
112. G. C. Lloyd-Jones, J. N. Harvey, P. Hodgson, M. Murray and R. L. Woodward, *Chem. Eur. J.*, **9**, 4523 (2003).
113. N. V. Vistorobskii and A. F. Pozharskii, *Russ. Chem. Bull.*, **45**, 2297 (1996).
114. N. V. Vistorobskii and A. F. Pozharskii, *Zh. Org. Khim.*, **27**, 1543 (1991); *Chem. Abstr.*, **116**, 193866g (1992).
115. A. Szemik-Hojniak, I. Deparasinska, W. J. Buma, G. Balkowski, A. F. Pozharskii, N. V. Vistorobskii and X. Allonas, *Chem. Phys. Lett.*, **401**, 189 (2005).
116. A. F. Pozharskii, N. V. Vistorobskii, A. A. Bardin and E. A. Filatova, *Russ. J. Org. Chem. (Engl. Transl.)*, **42**, 131 (2006).
117. C. Reichardt, *Angew. Chem.*, **77**, 30 (1965).
118. A. F. Pozharskii, V. A. Ozeryanskii and N. V. Vistorobskii, *Russ. Chem. Bull.*, **52**, 218 (2003).
119. A. Pawlukojc, I. Natkaniec, E. Grech, J. Baran, Z. Malarski and L. Sobczyk, *Spectrochim. Acta*, **A54**, 439 (1998).
120. B. Brzezinski, E. Grech, Z. Malarski and L. Sobczyk, *J. Chem. Soc., Faraday Trans.*, **86**, 1777 (1990).
121. S. D. Hamann and M. Linton, *Aust. J. Chem.*, **29**, 1641 (1976).
122. E. Grech, Z. Malarski and L. Sobczyk, *J. Mol. Struct.*, **129**, 35 (1985).
123. E. Grech, Z. Malarski and L. Sobczyk, *Chem. Phys. Lett.*, **128**, 259 (1986).

124. D. Stephenson and J. A. S. Smith, *Proc. R. Soc. London, Ser. A: Math. Phys. Sci.*, **416**, 149 (1988).
125. B. Nogaj, K. Wozniak, D. Lemanski, M. Ostafin and E. Grech, *Solid State Nucl. Magn. Reson.*, **4**, 187 (1995).
126. E. Haselbach, A. Henriksson, F. Jachimowicz and J. Wirz, *Helv. Chim. Acta*, **55**, 1757 (1972).
127. K. Wozniak, H. He, J. Klinowski, W. Jones and T. L. Barr, *J. Phys. Chem.*, **99**, 14667 (1995).
128. K. Wozniak, H. He, J. Klinowski, T. L. Barr and P. Milart, *J. Phys. Chem.*, **100**, 11420 (1996).
129. A. Szemik-Hojniak, J. M. Zwier, W. J. Buma, R. Bursi and J. H. Van der Waals, *J. Am. Chem. Soc.*, **120**, 4840 (1998).
130. A. Szemik-Hojniak, I. Deperasinska, X. Allonas and P. Jacques, *J. Mol. Struct.*, **526**, 219 (2000).
131. A. Szemik-Hojniak, G. Balkowski, G. W. H. Wurpel, J. Herbich, J. H. van der Waals and W. J. Buma, *J. Phys. Chem. A*, **108**, 10623 (2004).
132. S. T. Howard, *J. Am. Chem. Soc.*, **122**, 8238 (2000).
133. J. P. Maier, *Helv. Chim. Acta*, **57**, 994 (1974).
134. N. T. Berberova and O. Yu. Okhlobystin, *Zh. Org. Khim.*, **19**, 1114 (1983); *Chem. Abstr.*, **99**, 175024g (1983)
135. R. Gleiter, W. Schäfer, H. A. Staab and T. Saupe, *J. Org. Chem.*, **49**, 4463 (1984).
136. R. W. Alder, R. Gill and N. C. Goode, *J. Chem. Soc., Chem. Commun.*, 973 (1976).
137. T. Barth, C. Krieger, H. A. Staab and F. A. Neugebauer, *J. Chem. Soc., Chem. Commun.*, 1129 (1991).
138. F. Gerson, E. Haselbach and G. Plattner, *Chem. Phys. Lett.*, **12**, 316 (1971).
139. S. S. Pachkovskii and A. A. Voityuk, *Zh. Fiz. Khim.*, **64**, 1592 (1990); *Chem. Abstr.*, **113**, 131282t (1990).
140. J. A. Platts, S. T. Howard and K. Wozniak, *J. Org. Chem.*, **59**, 4647 (1994).
141. M. Peräkylä, *J. Org. Chem.*, **61**, 7420 (1996).
142. S. T. Howard and J. A. Platts, *J. Org. Chem.*, **63**, 3568 (1998).
143. E. Fujiwara, K. Omoto and H. Fujimoto, *J. Org. Chem.*, **62**, 7234 (1997).
144. I. Alkorta and J. Elguero, *Struct. Chem.*, **11**, 335 (2000).
145. H. Guo and D. R. Salahub, *J. Mol. Struct. (Theochem)*, **547**, 113 (2001).
146. D. Suares, J. A. Menendez, E. Fuente and M. A. Montes-Moran, *Angew. Chem., Int. Ed.*, **39**, 1320 (2000).
147. B. Kovačević, Z. B. Maksič and R. Vianello, *J. Chem. Soc., Perkin Trans. 2*, 886 (2001).
148. A. Streitwieser and Y.-J. Kim, *J. Am. Chem. Soc.*, **122**, 11783 (2000).
149. R. W. Alder, *J. Am. Chem. Soc.*, **127**, 7924 (2005).
150. M. Mascal, M. Lera, A. J. Blake, M. Czaja, A. Kozak, M. Makowski and L. Chmurzynski, *Angew. Chem., Int. Ed.*, **40**, 3696 (2001).
151. N. G. Korzhenevskaya, V. I. Rybachenko and G. Schroeder, *Tetrahedron Lett.*, **43**, 6043 (2002).
152. F. Hibbert, *J. Chem. Soc., Perkin Trans. 2*, 1862 (1974).
153. A. F. Pozharskii, N. L. Chikina, N. V. Vistorobskii and V. A. Ozeryanskii, *Russ. J. Org. Chem. (Engl. Transl.)*, **33**, 1727 (1997).
154. R. L. Benoit, D. Lefebvre and M. Frechette, *Can. J. Chem.*, **65**, 996 (1987).
155. A. Awwal and F. Hibbert, *J. Chem. Soc., Perkin Trans. 2*, 1589 (1977).
156. F. Hibbert and G. R. Simpson, *J. Chem. Soc., Perkin Trans. 2*, 613 (1987).
157. L. A. Kurasov, A. F. Pozharskii and V. V. Kuz'menko, *Zh. Org. Khim.*, **19**, 859 (1983); *Chem. Abstr.*, **99**, 194907p (1983)
158. V. I. Sokolov, A. F. Pozharskii, I. S. Kashparov, A. G. Ivanov and B. I. Ardashev, *Khim. Geterotsikl. Soedin.*, 558 (1974); *Chem. Abstr.*, **81**, 49650y (1974).
159. J. A. Gerlt, M. M. Kreevoy, W. W. Cleland and P. A. Frey, *Chem. Biol.*, **4**, 259 (1997).
160. R. W. Alder and N. C. Goode, *J. Chem. Soc., Chem. Commun.*, 108 (1976).
161. R. W. Alder, M. R. Bryce and N. C. Goode, *J. Chem. Soc., Perkin Trans. 2*, 477 (1982).
162. F. Hibbert and K. P. P. Hunte, *J. Chem. Soc., Perkin Trans. 2*, 1895 (1983).
163. O. V. Ryabtsova, A. F. Pozharskii, V. A. Ozeryanskii and N. V. Vistorobskii, *Russ. Chem. Bull.*, **50**, 854 (2001).
164. L. A. Kurasov, A. F. Pozharskii, V. V. Kuz'menko, N. A. Klyuev, A. I. Chernyshev, S. S. Goryaev and N. L. Chikina, *Zh. Org. Khim.*, **19**, 590 (1983); *Chem. Abstr.*, **99**, 22064v (1983).

165. V. A. Ozeryanskii, A. A. Milov, V. I. Minkin and A. F. Pozharskii, *Angew. Chem., Int. Ed.*, **45**, 1453 (2006).
166. L. G. Van Uitert and C. G. Haas, *J. Am. Chem. Soc.*, **75**, 451 (1953).
167. M. Eigen, *Angew. Chem., Int. Ed. Engl.*, **3**, 1 (1964).
168. F. Hibbert, *Acc. Chem. Res.*, **17**, 115 (1984).
169. F. Hibbert and K. P. P. Hunte, *J. Chem. Soc., Perkin Trans. 2*, 1562 (1981).
170. F. Hibbert, *J. Chem. Soc., Chem. Commun.*, 463 (1973).
171. A. Awwal, R. Burt and A. J. Kresge, *J. Chem. Soc., Perkin Trans. 2*, 1566 (1981).
172. G. H. Barnett and F. Hibbert, *J. Am. Chem. Soc.*, **106**, 2080 (1984).
173. Z. Pawelka and T. Zeegers-Huyskens, *J. Mol. Struct. (Theochem)*, **200**, 565 (1989).
174. B. Brzezinski, E. Grech, Z. Malarski and L. Sobczyk, *J. Chem. Soc., Perkin Trans. 2*, 857 (1991).
175. S. Toppet, K. Platteborze and T. Zeegers-Huyskens, *J. Chem. Soc., Perkin Trans. 2*, 831 (1995).
176. B. Brzezinski, E. Grech, Z. Malarski and L. Sobczyk, *Pol. J. Chem.*, **68**, 261 (1994).
177. M. J. Drewitt, M. Niedermann, R. Kumar and M. C. Baird, *Inorg. Chim. Acta*, **335**, 43 (2002).
178. J. E. Douglass, H. Shih, R. E. Fraas and D. E. Craig, *J. Heterocycl. Chem.*, **7**, 1185 (1970).
179. T. Onak, H. Rosendo, G. Siwapinyoyos, R. Kubo and L. Liauw, *Inorg. Chem.*, **18**, 2943 (1979).
180. J. S. Hartman and J. A. W. Shoemaker, *Polyhedron*, **19**, 165 (2000).
181. T. Yamasaki, N. Ozaki, Y. Saika, K. Ohta, K. Goboh, F. Nakamura, M. Hashimoto and S. Okeya, *Chem. Lett.*, **33**, 928 (2004).
182. H.-U. Wüstefeld, W. C. Kaska, F. Schüth, G. D. Stucky, X. Bu and B. Krebs, *Angew. Chem., Int. Ed.*, **40**, 3182 (2001).
183. H. J. Reich and M. L. Cohen, *J. Org. Chem.*, **44**, 3148 (1979).
184. V. A. Ozeryanskii, A. F. Pozharskii, M. G. Koroleva, D. A. Shevchuk, O. N. Kazheva, A. N. Chekhlov, G. V. Shilov and O. A. Dyachenko, *Tetrahedron*, **61**, 4221 (2005).
185. A. F. Pozharskii, V. A. Ozeryanskii and V. V. Kuz'menko, *Russ. J. Org. Chem. (Engl. Transl.)*, **32**, 66 (1996).
186. S. N. Gamage, R. H. Morris, S. J. Rettig, D. C. Thackray, I. S. Thornburn and B. R. James, *J. Chem. Soc., Chem. Commun.*, 894 (1987).
187. V. A. Ozeryanskii, A. F. Pozharskii and A. M. Fomchenkov, *Russ. Chem. Bull.*, **47**, 313 (1998).
188. N. V. Vistorobskii and A. F. Pozharskii, *Zh. Org. Khim.*, **25**, 2154 (1989); *Chem. Abstr.*, **112**, 234930m (1990).
189. V. A. Ozeryanskii, A. F. Pozharskii and N. V. Vistorobskii, *Russ. J. Org. Chem. (Engl. Transl.)*, **33**, 251 (1997).
190. P. Carloni, L. Eberson, L. Greci, P. Stipa and G. Tosi, *J. Chem. Soc., Perkin Trans. 2*, 1779 (1991).
191. N. V. Vistorobskii, O. V. Vinogradova and A. F. Pozharskii, *Russ. Chem. Bull.*, **46**, 348 (1997).
192. N. V. Vistorobskii, A. F. Pozharskii, A. I. Chernyshev and S. V. Shorshnev, *Zh. Org. Khim.*, **27**, 1036 (1991); *Chem. Abstr.*, **116**, 6221h (1992).
193. O. V. Vinogradova, A. F. Pozharskii and Z. A. Starikova, *Russ. Chem. Bull.*, **52**, 208 (2003).
194. L. Maresca, G. Natile and F. P. Fanizzi, *J. Chem. Soc., Dalton Trans.*, 1867 (1992).
195. R. D. Chambers, S. R. Korn and G. Sandford, *J. Chem. Soc., Chem. Commun.*, 856 (1993).
196. F. Terrier, J.-C. Halle, M.-J. Pouet and M.-P. Simonnin, *J. Org. Chem.*, **51**, 409 (1986).
197. R. D. Chambers, S. R. Korn and G. Sandford, *Tetrahedron*, **48**, 7939 (1992).
198. I. B. Rozentsveig, G. G. Levkovskaya, A. N. Mirskova and O. B. Kozyreva, *Russ. J. Org. Chem. (Engl. Transl.)*, **33**, 565 (1997).
199. Y. Lee, T. Kitagawa and K. Komatsu, *J. Org. Chem.*, **69**, 263 (2004).
200. R. Horie, Y. Araki, O. Ito, Y. Lee, T. Kitagawa and K. Komatsu, *J. Phys. Chem. A*, **109**, 6140 (2005).
201. F. S. McQuillan, T. A. Hamor, R. Tanna, P. R. Ashton, M. S. Tolley and C. J. Jones, *J. Organometal. Chem.*, **549**, 233 (1997).
202. G. Opitz, K. Rieth and G. Rimmler, *Tetrahedron Lett.*, **27**, 167 (1986).
203. E. Yu. Romanova, A. F. Pozharskii and G. S. Borodkin, *Russ. Chem. Bull.*, **50**, 860 (2001).

204. A. F. Pozharskii, O. V. Ryabtsova, N. V. Vistorobskii and Z. A. Starikova, *Russ. Chem. Bull.*, **49**, 1097 (2000).
205. V. A. Ozeryanskii, A. F. Pozharskii, W. Schilf, B. Kamieński, W. Sawka-Dobrowolska, L. Sobczyk and E. Grech, *Eur. J. Org. Chem.*, 782 (2006).
206. N. V. Vistorobskii, A. F. Pozharskii, S. V. Shorshnev and A. I. Chernyshev, *Mendeleev Commun.*, 10 (1991).
207. A. F. Pozharskii and N. V. Vistorobskii, *Russ. Chem. Bull.*, **45**, 971 (1996).
208. O. V. Vinogradova, E. A. Filatova, N. V. Vistorobskii, A. F. Pozharskii, I. V. Borovlev and Z. A. Starikova, *Russ. J. Org. Chem. (Engl. Transl.)*, **42**, 338 (2006).
209. A. F. Pozharskii, G. G. Alexandrov and N. V. Vistorobskii, *Russ. J. Org. Chem. (Engl. Transl.)*, **32**, 1009 (1996).
210. A. F. Pozharskii, N. V. Vistorobskii, M. I. Rudnev and A. I. Chernyshev, *Russ. Chem. Bull.*, **45**, 2039 (1996).
211. M. E. Kletskii and A. F. Pozharskii, in *Proceedings of the 7th International Symposium on Chiral Discrimination*, Jerusalem, 1995, p. 12.
212. M. E. Kletskii and A. F. Pozharskii, In *Proceedings of the 7th Meeting on Stereochemistry*, Trest Castle, 1995, p. 116.
213. R. W. Alder, N. C. Goode, N. Miller, F. Hibbert, K. P. P. Hunte and H. J. Robbins, *J. Chem. Soc., Chem. Commun.*, 89 (1978).
214. S. Özkar and R. G. Finke, *Langmuir*, **18**, 7653 (2002).
215. G. S. Nichol and W. Clegg, *Cryst. Growth Des.*, **6**, 451 (2006).
216. H. Alper and M. S. Wolin, *J. Org. Chem.*, **40**, 437 (1975).
217. R. Huisgen, A. Mitra and J. R. Moran, *Chem. Ber.*, **120**, 159 (1987).
218. M. Jo Diem, D. F. Burow and J. L. Fry, *J. Org. Chem.*, **42**, 1801 (1977).
219. D. A. Evans and A. E. Weber, *J. Am. Chem. Soc.*, **108**, 6757 (1986).
220. D. A. Evans, S. J. Miller and M. D. Ennis, *J. Org. Chem.*, **58**, 471 (1993).
221. S. T. Sigurdsson, B. Seeger, U. Kutzke and F. Eckstein, *J. Org. Chem.*, **61**, 3883 (1996).
222. J. W. Gilman and Y. A. Otonari, *Synth. Commun.*, **23**, 335 (1993).
223. A. Flamini, V. Fares, A. Capobianchi and V. Valentini, *J. Chem. Soc., Perkin Trans. 1*, 3069 (2001).
224. L. Beer, J. L. Brusso, R. C. Haddon, M. E. Itkis, H. Kleinke, A. A. Leitch, R. T. Oakley, R. W. Reed, J. F. Richardson, R. A. Secco and X. Yu, *J. Am. Chem. Soc.*, **127**, 18159 (2005).
225. T. Yasuhara, Y. Nagaoka and K. Tomioka, *J. Chem. Soc., Perkin Trans. 1*, 2901 (2000).
226. Q. Zeng, B. Huang, K. Danielsen, R. Shukla and T. Nagy, *Org. Process Res. Develop.*, **8**, 962 (2004).
227. I. Rodriguez, G. Sastre, A. Corma and S. Iborra, *J. Catal.*, **183**, 14 (1999).
228. A. Corma, S. Iborra, I. Rodriguez and F. Sanchez, *J. Catal.*, **211**, 208 (2002).
229. C. Bew, V. Oterode Joshi, J. Gray, P. T. Kaye and G. D. Meakins, *J. Chem. Soc., Perkin Trans. 1*, 945 (1982).
230. K. Itoh, Y. Oderaotoshi and S. Kanemasa, *Tetrahedron: Asymm.*, **14**, 635 (2003).
231. E. Langhals, R. Huisgen and K. Polborn, *Chem. Eur. J.*, **10**, 4353 (2004).
232. A. E. Taggi, A. M. Hafez, H. Wack, B. Young, W. J. Drury, III and T. Lectka, *J. Am. Chem. Soc.*, **122**, 7831 (2000).
233. A. E. Taggi, A. M. Hafez, H. Wack, B. Young, D. Ferraris and T. Lectka, *J. Am. Chem. Soc.*, **124**, 6626 (2002).
234. A. Weatherwax, C. J. Abraham and T. Lectka, *Org. Lett.*, **7**, 3461 (2005).
235. A. M. Hafez, T. Dudding, T. R. Wagerle, M. H. Shah, A. E. Taggi and T. Lectka, *J. Org. Chem.*, **68**, 5819 (2003) and references cited therein.
236. S. France, H. Wack, A. E. Taggi, A. M. Hafez, T. R. Wagerle, M. H. Shah, C. L. Dusich and T. Lectka, *J. Am. Chem. Soc.*, **126**, 4245 (2004).
237. J. K. Stille and P. K. Wong, *J. Org. Chem.*, **40**, 532 (1975).
238. F. Ozawa, A. Kubo and T. Hayashi, *Tetrahedron Lett.*, **33**, 1485 (1992).
239. F. Ozawa, Y. Kobatake and T. Hayashi, *Tetrahedron Lett.*, **34**, 2505 (1993).
240. R. M. Bellabarba and G. C. Saunders, *J. Fluorine Chem.*, **112**, 139 (2001).
241. T. Uchimaru, K. Narasaka and T. Mukaiyama, *Chem. Lett.*, 1551 (1981).
242. E. Arranz and G.-J. Boons, *Tetrahedron Lett.*, **42**, 6469 (2001).
243. R. D. Chambers, T. F. Holmes, S. R. Korn and G. Sandford, *J. Chem. Soc., Chem. Commun.*, 855 (1993).

244. R. D. Chambers, S. R. Korn and G. Sandford, *J. Fluorine Chem.*, **69**, 103 (1994).
245. M. Darabantu, T. Lequeux, J.-C. Pommelet, N. Ple, A. Turck and L. Toupet, *Tetrahedron Lett.*, **41**, 6763 (2000).
246. M. Darabantu, T. Lequeux, J.-C. Pommelet, N. Ple and A. Turck, *Tetrahedron*, **57**, 739 (2001).
247. G. Pascali, D. O. Kiesewetter, P. A. Salvadori and W. C. Eckelman, *J. Label. Compd. Radiopharm.*, **47**, 373 (2004).
248. T.-L. Ho and C. M. Wong, *Synth. Commun.*, **5**, 87 (1975).
249. D. H. Steinberg and J. J. Luzzi, *Eur. Pat. Appl.*, No. 0512954A1, 13 p. (1992); *Chem. Abstr.*, **118**, 84238 (1993).
250. P. R. Mallinson, K. Wozniak, C. C. Wilson, K. L. McCormack and D. S. Yufit, *J. Am. Chem. Soc.*, **121**, 4640 (1999).
251. Z. Malarski, T. Lis, Z. Olejnik, E. Grech, J. Nowicka-Scheibe, I. Majerz and L. Sobczyk, *J. Mol. Struct.*, **552**, 249 (2000).
252. M. J. Drewitt, M. Niedermann and M. C. Baird, *Inorg. Chim. Acta*, **340**, 207 (2002).
253. R. L. Benoit and D. Figeys, *Can. J. Chem.*, **69**, 1985 (1991).
254. D. Figeys, M. Koschmidder and R. L. Benoit, *Can. J. Chem.*, **70**, 1586 (1992).
255. W. Galezowski and A. Jarczewski, *Can. J. Chem.*, **70**, 935 (1992).
256. E. Bardez and B. Valeur, *Chem. Phys. Lett.*, **141**, 261 (1987).
257. Y. Xiao, M. Fu, X. Qian and J. Cui, *Tetrahedron Lett.*, **46**, 6289 (2005).

Author Index

This author index is designed to enable the reader to locate an author's name and work with the aid of the reference numbers appearing in the text. The page numbers are printed in normal type in ascending numerical order, followed by the reference numbers in parentheses. The numbers in *italics* refer to the pages on which the references are actually listed.

Subject Index

Entries are in letter-by-letter alphabetical order ignoring spaces and punctuation marks. Page numbers in *italic* refer to Figures and Tables not included in the relevant page ranges.

2-AAF (2-fluorenylacetamide), 844, 861
Abactrim, UV−visible spectroscopy, 693, 694
Absorption spectra, proton sponges, *962*,
  963−965
Acenaphthene, proton sponge analogue, 936,
  938, 989
Acenaphthylene, proton sponges, 949, 983
Acetaminophen, electrochemical analysis, 686
Acetoacetanilide, protonation, 332
Acetone, CI−MS, 335, 337
Acetonitrile (ACN), anodic oxidation, 913
Acetylacetamides, diketene treatment, 673
N-Acetyltransferase enzymes (NAT1 and
  NAT2), 650, 652, 847, 848
Acid Black 1, synthesis, 655
Acid Black 077, reduction, 655
Acid-catalyzed hydrogen exchange,
  N,*N*-dialkylanilines, 570
Acidic aqueous solutions, anodic oxidation,
  915−924
Acidity
  deprotonation energetics, 113
  NH-acidity, 936−937
  photoacidity, 786
Acid Orange 7, decolorization, 657
ACN (acetonitrile), 913
ACNA, fiber-reactive dyes, 65
Acrylonitrile, CI−MS reagent, 335
Acrylonitrile−butadiene copolymer,
  solid-phase microextraction, 668, 688
Actin filaments, cytochalasin B-mimetic
  activity, 659
Activated carbon
  solid-phase extraction, 672
  waste treatment, 856
Activation energies
  amino group restricted rotation, 360, *361*

intra- and intermolecular relaxation, 366
  photocyclization, 801
Acylanilines
  ortho, *meta/para*-substituted, 338
  protonated, 338
N-Acylanilines, rearrangement, 600−602
Acylation
  Friedel−Crafts acylation, 991
  proton sponges, 991, 992
Acyl derivatives
  N-acyl dyestuff intermediates, 730
  N-acyl proton sponges, 944, 945
  thermochemistry, 282−283
Addition reactions
  Michael addition, 688−689
  nucleophilic, 537−581
  oxidative, 493, 494−496
  photoaddition, 821−823
  solution-phase, 277
Adenine, liquid chromatography, 679
Adhesives, aromatic isocyanates, 654−655
Adiabatic ionization energy, anilinide anion,
  114
ADIR (autoionization-detected infrared
  spectroscopy), 415
ADPA (4-aminodiphenylamine), 561
Adrenergic agonists, solid-phase extraction,
  663
Adsorption
  of aniline, 925
  soil coefficients, 659
Aerobic oxidation, effluents, 656−657
Aetna, 35
AGFA (Aktiengesellschaft für
  Anilinfabrikation), 2, 43
  dye synthesis, 12, 19, 23, 24, 38, 62, 78, 745
  photography, 46

25a′ - HOMO
ε = −0.29 eV

26a″ - LUMO
ε = 0.14 eV

PLATE 1

(a) Geometry, NBO charges and
Wiberg indices
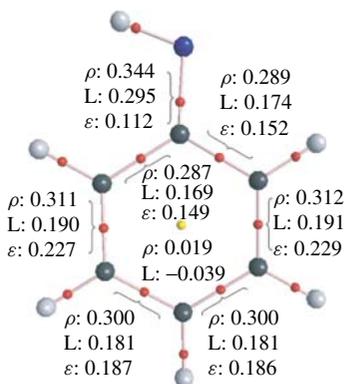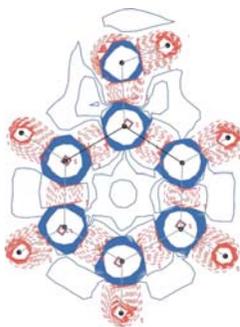
(b) Topology of ρ(**r**)

(c) Laplacian
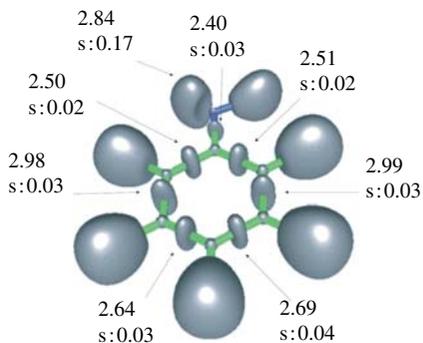
(d) ELF

PLATE 2
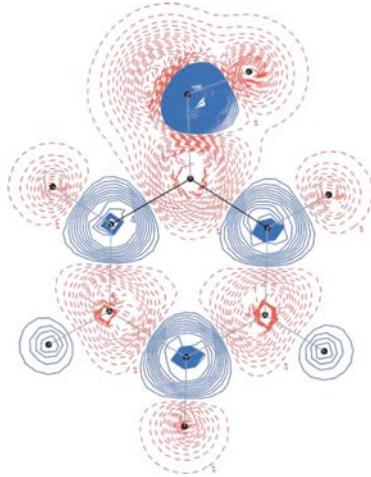
(e) Spin density

PLATE 2 (*continued*)
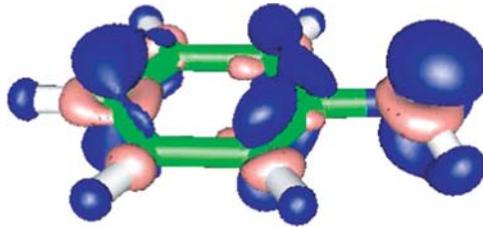
$\Delta\rho(\mathbf{r})$

PLATE 3

Geometry, natural charges
and Wiberg indices

(a)

Topology of $\rho(\mathbf{r})$

(b)

ELF

(c)

PLATE 4